Lipids (2010) 45:1–10
DOI 10.1007/s11745-009-3364-9

ORIGINAL ARTICLE

Early and Sustained Enrichment of Serum n-3 Long Chain Polyunsaturated Fatty Acids in Dogs Fed a Flaxseed Supplemented Diet

Brent L. Dunbar · Karen E. Bigley · John E. Bauer

Received: 15 September 2009 / Accepted: 13 October 2009 / Published online: 5 November 2009

Abstract A study was conducted in dogs to assess n-3 long chain polyunsaturated fatty acid incorporation after feeding an α-linolenic (ALA)-rich flaxseed supplemented diet (FLX) for 84 days. Serum total phospholipids (PL), triacylglycerol (TG), and cholesteryl esters (CE) were isolated at selected times and fatty acid methyl esters were analyzed. Increased LA was seen in the FLX-PL fraction after 28 days and an expected decrease in PL–AA. Enrichment of ALA, eicosapentaenoic acid (EPA) and docosapentaenoic acid n-3 (DPAn-3) in the FLX-group occurred early on (day 4) in both PL and TG fractions but no docosahexaenoic acid (DHA) was found, consistent with data from other species including humans. In contrast, no accumulation of DPAn-3 was seen in serum-CE, suggesting that this fatty acid does not participate in reverse-cholesterol transport. The accumulation of DPAn-3 in fasting PL and TG fractions is likely due to post-absorptive secretion after tissue synthesis. Because conversion of DPAn-3 to DHA occurs in canine neurologic tissues, this DPAn-3 may provide a circulating reservoir for DHA synthesis in such tissues. The absence of DPAn-3 in serum-CE suggests that such transport may be unidirectional. Although conversion of DPAn-3 to DHA is slow in most species, one-way transport of DPAn-3 in the circulation may help conserve this fatty acid as a substrate for DHA synthesis in brain and retinal tissues especially when dietary intakes of DHA are low.

Keywords Gas–liquid chromatography · Lipid analysis · Thin layer chromatography · Mammalian lipid biochemistry · Plasma lipids · Cholesteryl ester formation · Metabolism · n-3 Fatty acids · Nutrition

Abbreviations

AA	Arachidonic acid
ALA	Alpha-linolenic acid
CE	Serum cholesteryl ester fraction
DHA	Docosahexaenoic acid
DPAn-3	Docosapentaenoic acid, n-3
EDTA	Ethylenediaminetetraacetic acid
EPA	Eicosapentaenoic acid
FLX	Flax seed supplemented diet
LA	Linoleic acid
PL	Serum phospholipid fraction
SUN	Sunflower seed supplemented diet
TG	Serum triacylglycerol fraction

Introduction

Long chain n-3 fatty acids, notably eicosapentaenoic acid (EPA) and docosapentaenoic acid (DHA), are documented to have important health benefits including cardioprotective effects [1–3] as well as roles in neurological development [4–6] and the inflammatory response [7–9]. While many studies have emphasized EPA and DHA, naturally occurring fish oils are additionally enriched in docosapentaenoic acid (DPAn-3), an important intermediate in

A portion of this study was presented in abstract form at The Waltham International Symposium: Pet Nutrition and Health in the 21st Century, 26–29 May 1997, Orlando, FL, USA.

B. L. Dunbar · K. E. Bigley · J. E. Bauer (✉)
Companion Animal Nutrition Lab, Department of Veterinary Small Animal and Clinical Sciences, College of Veterinary Medicine, Texas A&M University, 4474 TAMU, College Station, TX 77843-4474, USA
e-mail: jbauer@cvm.tamu.edu

DHA synthesis [10]. Consequently, recommendations have been made for the general public to increase their dietary intakes of fatty fish rich in these compounds [11]. However, cost, availability, heavy metal concerns, and dietary preferences may limit fish and fish-oil intake among certain populations [12]. Metabolically, α-linolenic acid (ALA) is a precursor of EPA, DPAn-3, and DHA. Studies in several mammalian species have found that DPAn-3 is the main ALA metabolite in cell membranes of most herbivores and carnivores [13]. As such it may be an important plasma or tissue reservoir for either EPA or DHA synthesis.

Dietary ALA has been shown to increase blood concentrations of cardioprotective fatty acids in humans and to exert benefits in post-myocardial infarction patients [2]. High ALA diet also reduces lipid and inflammatory cardiovascular disease risk factors in patients with hypercholesterolemia [14] and certain inflammatory mediators in free-living subjects [15]. The cardioprotective effects of ALA appear to be due, in part, by reduction in the production of inflammatory cytokines [16]. It is unknown whether ALA is cardioprotective in its own right although there is an ever growing body of research supporting this possibility (reviewed in [17]).

The canine species has served as a model demonstrating that intravenously infused EPA and DHA reduces the risk of cardiac arrhythmias [18]. Because dogs, like humans, can convert either ALA or stearidonic acid to longer chain n-3 derivatives [19, 20], the ability of dietary ALA to provide enough EPA to be similarly cardioprotective is unknown. Knowledge of dietary ALA metabolism in dogs will therefore provide a basis for future investigations of the canine arrhythmic model using dietary interventions with n-3 fatty acids.

It should also be mentioned that dogs, although relatively expensive, are a species of choice for human drug development including compounds affecting lipid metabolism and especially where serial blood sampling is performed. Furthermore, because many of the commercial foods fed these animals during such testing now contain increased amounts of flaxseed or linseed oil, it has become necessary to understand effects that such background diets may have on lipid metabolism per se. Thus, the canine species is an important animal species with which to investigate the time course and extent of incorporation of long chain n-3 fatty acids in plasma or tissues when ALA-enriched diets are fed. Seed oils rich in ALA such as flaxseed, canola, or corn show promise for providing functional enrichment of cell membranes with EPA, DPAn3, and, under some conditions, DHA. They may provide an alternative to fish and fish oil, which may be less available and sustainable globally.

The present study was performed to evaluate the early time course and extent of accumulation of long chain n-3 derived fatty acids in the major serum lipid subfractions of dogs fed an ALA enriched diet over a 12 week feeding period. Serum total phospholipid fatty acids are generally used as a biomarker of tissue enrichment; serum triglyceride fatty acids reflect the post-absorptive state of fasted samples; and cholesteryl ester fatty acid profiles demonstrate important metabolic preferences during their return to the liver via reverse cholesterol transport. Analysis of each of these serum lipid subfractions under conditions of a single dietary modification provides a complete metabolic picture of the dynamics of fatty acid metabolism and allows a thorough evaluation of lipid metabolic alterations in this canine model.

Experimental Procedures

Flaxseed and Sunflower Seed Supplements

Whole flax and sunflower seeds were ground and screened (200 mesh, ENRECO, Manitowoc, WI, USA) to improve digestibilities. The composition of the ground seeds is shown (Table 1). The flaxseed contained 52.7% ALA and the sunflower seed contained 68.2% LA while the other fatty acids were distributed nearly equivalently between these two oilseeds.

Animals and Diets

A commercially available canine dry, extruded diet (basal diet; Hill's®, Canine Senior, single lot number) was lightly sprayed with up to 1% (w/w) distilled water in a bakery mixer (Model L800, Hobart Industries, Inc, Troy, OH, USA) and the ground seeds were coated onto the expanded food particles at 3% by weight of the basal diet. Two diets were thus produced varying in fatty acid composition reflecting the supplement used. The diets were allowed to dry completely, stored at 4°C in their original bags, then placed in plastic drums fitted with lids until the time of

Table 1 Fatty acid composition of flax and sunflower seed oils (relative %)

Fatty acid	Sunflower	Flax
12:0	0.5	–
14:0	0.2	–
16:0	6.8	4.8
16:1	0.1	–
18:0	4.7	4.7
18:1n-9	18.6	19.9
18:2n-6	68.2	15.9
18:3n-3	0.5	52.7
20:4n-6	0.4	–

Values are the average of two determinations

feeding. Complete fatty acid profiles of the two supplemented diets have been previously reported [21]. Dietary treatments were such that the fatty acid profiles of the two supplemented diets varied predominately between 18-carbon n-6 and n-3 fatty acid series.

The basal diet contained approximately 23.8% energy as fat (about 97 g fat/kg diet), 7.8% energy as linoleic acid (LA). On an as-fed basis this diet contained 17.0% protein, 58.5% carbohydrate, 3.0% fiber, 10.8% moisture and 3552 kcal/kg diet. The supplemented diets contained 25% of energy total fat (about 102 g fat/kg diet). The sunflower seed supplemented diet (SUN) contained 9.3% kcal as LA and 0.43% kcal as ALA. It also contained 17.0% protein, 56.9% carbohydrate, 4.2% fiber, and 10.8% moisture (as-fed). By contrast, the flaxseed supplemented diet (FLX) contained 7.3% kcal as LA and 2.5% kcal as ALA with 17.2% protein, 57.0% carbohydrate, 3.7% fiber, and 10.8% moisture on an as-fed basis. Because the LA contents of each diet were between 7.3 and 9.3% energy, it was anticipated that tissue levels would be saturated with LA [22, 23]. Thus, a comparison between a low ALA (0.43% kcal) diet (SUN) and an enriched ALA (2.5% kcal) diet (FLX) was made at saturating dietary concentrations of LA.

The protocol for this study was approved by the Texas A&M University Laboratory Animal Use Committee. Dogs were individually maintained in kennels according to the American Physiological Society Guidelines for Animal Research. Eighteen adult, mixed breed dogs, ranging in body weight from 10 to 20 kg were divided into 2 groups of 9 each. To begin the study, feeding periods were staggered over three successive days so that 3 animals from each group (6 animals per day) were fed the supplemented diets assuring feeding and sample collections in a timely manner.

The basal diet was fed, unsupplemented, for a 2 week diet acclimation period prior to blood sample collection on day 0. The dogs were then randomly assigned to either the SUN or FLX group and fed their respective diets for 84 days. Because the animals were fed to maintain their starting body weights and monitored weekly, all animals were observed to readily and consistently consume all food offered. All dogs were weighed weekly during the feeding period. Blood samples were obtained via jugular vena puncture with no anticoagulant after withholding food overnight (day 0) just prior to starting the feeding period. Thereafter, the animals were fed their respective diet and blood samples again collected after withholding food at 4, 7, 14, 28, 56, and 84 days.

Sample Analyses

Serum was freshly harvested from the blood samples on the day of collection and total lipids were extracted and sub-fractionated via thin layer chromatography [21]. After visualization with iodine vapor, the phospholipids (PL), triacylglycerol (TG), and cholesteryl ester (CE) fractions were scraped from the plates, placed in screw-capped glass tubes fitted with Teflon caps, and 4% sulfuric acid in methanol added for trans-methylation prior to capillary gas chromatography [21]. Fatty acid profiles were determined using an Omegawax^{TM} 320 fused silica capillary column (0.25 μm thickness, 30 m long, and 0.32 mm ID) (Supelco, Inc. Bellafonte, PA) with a Hewlett Packard Series II 5890 Gas Chromatograph (Hewlett Packard Co., Palo Alto, CA) with a 50:1 split ratio and helium as carrier gas at 30 ml/min initial velocity. The column oven was temperature programmed starting at 180°C, held for 15.5 min, then heated to 210°C at 12°C/min and held for 19 min. The injection and detector temperatures were held constant at 250 and 260°C respectively. Flame ionization detection was used and results generated with HP Chem Station® software package (Hewlett Packard Co, Palo Alto, CA, USA). Authentic fatty acid methyl ester standards (68-B, 20-A, Nu-Check Prep, Elysian, MN, USA) and fish oil standards were used to identify the samples via retention time comparisons. [21]. In addition, a standard for 20:3n5 (Δ5,8,11) via lipid extraction and trans-methylation of *Podocarpus nagi* seeds rich in this fatty acid was prepared and used to provide a preliminary identification of this fatty acid triene when observed in the samples. When present, it was tentatively identified as a 20:3n-6 isomer that awaits confirmation of its more precise molecular configuration. The seeds were generously provided by Shigeru Matsutani (Kyoto Botanical Garden, Kyoto, Japan).

Statistics

Statistical analyses of all data were performed using the Microsoft Windows® version of SAS/STAT Version 6 (SAS Institute, Cary, NC, USA). The Shapiro–Wilks test was performed and nearly all the data were normally distributed. Repeated measures ANOVA using a general linear model was performed with the diet as a between-subject factor and time as a within-subject factor. Friedman's test was used for the non-normally distributed data. Main effects of time and diet as well as the interaction of time with diet were therefore determined. When diet or diet × time effects were found, student's *t* test was used to identify differences between the two dietary treatments at the same time.

In all cases, significance was set at $P < 0.05$. Fatty acid profiles of lipid fractions obtained on Days 0, 4 and 84 have been previously reported in abstract form [21]. Results of the complete repeated measures ANOVA analyses of samples collected at all sample times are now presented.

Results

Statistically significant time effects were seen with the majority of fatty acids in this study. This finding was not unexpected due to lipid modification of the basal diet in which the day 0 values were compared with those obtained at subsequent sampling periods after feeding the two supplements. Also, it should be noted that the fatty acid profiles of the serum PL, TG, and CE in the SUN group were essentially unchanged over time after day 4 (Tables 2, 3, and 4). These findings were not unexpected because the relative fatty acid compositions of both the basal diet and SUN supplemented basal diet were nearly identical. However, where diet and diet × time interactions were observed, comparisons between the SUN and FLX groups were made and a number of important differences were observed. The diet*time interactions are shown in the footnotes to Tables 2, 3, and 4 and included the n-3 polyunsaturated fatty acids except for DHA in all fractions and 22:4n-6 in the PL fraction (Table 2). Interactions between diet and time indicated that the duration of feeding interacts with the diet per se to provide an additional effect on a particular fatty acid beyond any main diet effect seen.

Enrichment of serum n-3 polyunsaturated fatty acids in the FLX group occurred early on (day 4) in each lipid subclass examined. Specifically, PL fractions were significantly enriched in ALA and EPA beginning on day 4 and remained so during the entire feeding period (Table 2). At the end of the feeding period, serum PL fatty acid changes included significant elevations of ALA (254% increase), EPA (195% increase), and DPAn-3 (68% increase) and significant decreases of AA, in the FLX group (Fig. 1). It is especially noteworthy, however, in the FLX group, that PL–DHA was unchanged during the entire period demonstrating the lack of serum DHA accumulation in the FLX (i.e. ALA) supplemented dogs. Also, increased PL–LA was seen in the FLX group and this increase reached statistical significance on days 28 and 84 while numerical elevations of PL–LA in this group were also seen at every sample time after day 0 (Table 2). On day 28 the anticipated decrease in PL–AA was observed within the FLX group which remained so for the duration of the study. Of additional interest was that when the FLX diet was fed, 22:4n-6 was decreased as early as 7 days relative to the SUN group which appeared to be modestly increased, but not significantly so, with time. Serum TG fractions of FLX fed dogs were similarly enriched in ALA (217% increase), EPA (171% increase), and DPAn-3 (122% increase) and again no DHA was found (Table 3).

In the serum CE fraction, flaxseed supplementation resulted in a significant increase in ALA at day 4 and throughout the feeding period. This change was followed beginning on day 7 with a statistically significant accumulation of EPA (Table 4). Percentage increases of ALA and EPA were greatest among all lipid fractions analyzed with 300% increases seen in ALA at day 7 and in EPA at day 14. These statistically significant accumulations culminated on day 84 with a 423% increase of ALA and 410% increase in EPA (Table 4). However, no appreciable accumulation of either DPAn-3 or DHA was seen in this fraction at any time point studied.

Discussion

Rapid accumulation of EPA, but not DHA, was seen in serum PL and TG lipid fractions in the canine model when a 3% (w/w) whole ground flaxseed supplement was added to a moderately high LA containing diet (7.3% of energy as LA). Notably, early and significant increases in ALA, EPA, and DPAn-3 were all seen with the exception of DHA. Similar enrichments of EPA and DPAn-3 have been observed in human plasma using a 4 week feeding period [24]. For that matter, this phenomenon has been observed in humans and various other animal species (reviewed in [25]) and is consistent with other evidence that plasma enrichment of DHA after ALA supplementation is less efficacious than providing smaller dietary amounts of preformed DHA per se [25, 26]. It should be noted that studies in rats have shown the conversion of ALA all the way to DHA to be effective in liver and plasma [27]. By contrast, however, there is resistance for serum DHA levels to increase in dogs fed ALA at the dietary amounts employed in this study given the observation that PL–DHA was unchanged in the FLX group during the entire dietary period. This finding is more similar to results seen in humans [25].

The accumulation of DPAn-3 seen in both fasting PL and TG fractions is consistent with secretion after tissue synthesis from dietary ALA. Conversion of DPAn-3 to DHA has been reported in canine neurologic tissues [28] and likely occurs after uptake of fatty acid precursors from the circulation. These findings suggest that production of DPAn-3 from ALA may serve as an important circulating reservoir for tissue DHA synthesis as DPAn-3 is transported via plasma lipids to neurological tissues [29].

It should be noted that conversion of ALA to longer chain derivatives is largely affected by the relative amounts of LA present in the diet and thus the LA/ALA ratio [25]. However, many human studies using n-3 fatty acid supplementation have been unable to accurately document n-6 intakes which may explain, in part, variability of results seen. In the present study, using dogs, the LA/ALA ratio of the FLX supplemented diet was 3.1:1 while that of the SUN group was 23.3:1 both of which are within the range

Table 2 Serum phospholipid fatty acid composition during the feeding period

FA	Days														FLX SD[b]	SUN SD[b]
	0		4		7		14		28		56		84			
	FLX	SUN	FLX	SUN	FLX	SUN	FLX	SUN	FLX	SUN	FLX	SUN	FLX	SUN		
14:0	0.12	0.13	0.15	0.17	0.13	0.14	0.14	0.16	0.15	0.15	0.13	0.15	0.15	0.18	0.03	0.06
14:1	0.00	0.00	0.01	0.00	0.00	0.00	0.00	0.00	0.00	0.00	0.00	0.00	0.00	0.00	0.00	0.00
15:0	0.08	0.07	0.08	0.08	0.07	0.08	0.08	0.08	0.08	0.08	0.07	0.08	0.07	0.09	0.01	0.01
16:0	14.37	14.31	14.28	14.42	13.50	13.78	13.80	13.84	13.89	13.91	13.53	13.91	14.04	14.74	1.18	1.58
16:1n-7	0.39	0.42	0.39	0.42	0.36	0.42	0.37	0.42	0.33	0.33	0.31	0.33	0.31	0.33	0.11	0.13
17:0	0.62	0.56	0.56	0.56	0.59	0.56	0.59	0.57	0.59	0.59	0.59	0.59	0.58	0.64	0.07	0.06
17:1n-7	0.22	0.30	0.24	0.26	0.24	0.28	0.23	0.26	0.25	0.19	0.23	0.19	0.20	0.23	0.05	0.06
18:0	29.94	29.07	29.23	28.29	28.48	28.47	28.82	28.18	29.11	29.01	29.57	29.01	29.07	28.54	1.58	2.20
18:1n-9	5.25	5.28	5.26	5.15	5.38	5.16	5.31	5.30	5.09	4.85	5.05	4.85	5.19	5.02	0.40	0.54
18:1n-7	2.21	2.27	2.19	2.27	2.09	2.31	2.19	2.26	2.06	2.00	2.04	2.00	1.92	1.80	0.44	0.43
18:2n-6	16.04	16.31	17.37	16.99	17.60	16.53	17.81	17.26	17.64[a]	16.22	18.16	17.43	18.46[a]	16.86	1.77	2.25
18:3n-6	0.18	0.17	0.19	0.17	0.19	0.17	0.19	0.18	0.19	0.19	0.21	0.19	0.19	0.16	0.05	0.05
18:3n-3	0.11	0.08	0.35[a]	0.08	0.38[a]	0.06	0.40[a]	0.08	0.34[a]	0.08	0.38[a]	0.08	0.39[a]	0.09	0.11	0.04
20:0	0.21	0.22	0.21	0.24	0.22	0.23	0.21	0.24	0.21	0.23	0.21	0.23	0.22	0.22	0.03	0.06
20:1n-9	0.12	0.17	0.12	0.13	0.13	0.14	0.12	0.14	0.12	0.14	0.13	0.14	0.12	0.13	0.02	0.05
20:2n-6	0.26	0.27	0.26	0.27	0.27	0.29	0.30	0.33	0.26	0.34	0.33	0.34	0.32	0.32	0.07	0.10
20:3n-9	0.10	0.11	0.06	0.10	0.04	0.05	0.07	0.12	0.10	0.07	0.06	0.07	0.06	0.14	0.09	0.10
20:3 isomer	0.23	0.22	0.19	0.20	0.17	0.17	0.23	0.22	0.25	0.22	0.24	0.22	0.25	0.33	0.11	0.10
20:3n-6[c]	1.31	1.24	1.16	1.22	1.07	1.08	1.19	1.32	1.24	1.26	1.22	1.26	1.30	1.41	0.38	0.49
20:3n-3	0.01	0.01	0.02	0.00	0.04	0.00	0.05	0.00	0.04	0.00	0.05	0.00	0.06	0.00	0.04	0.00
20:4n-6	21.20	21.86	20.27	21.83	21.49	23.01	19.86	21.68	20.01[a]	21.88	19.57[a]	21.88	19.23[a]	21.08	2.30	2.34
20:4n-3	0.00	0.00	0.00	0.00	0.01	0.00	0.02	0.00	0.02	0.00	0.01	0.00	0.02	0.00	0.02	0.00
20:5n-3	0.20	0.14	0.35[a]	0.13	0.36[a]	0.09	0.49[a]	0.14	0.46[a]	0.14	0.50[a]	0.14	0.59[a]	0.16	0.22	0.06
22:0	0.26	0.27	0.24	0.30	0.28	0.30	0.26	0.30	0.25	0.31	0.27	0.31	0.28	0.30	0.05	0.09
22:1n-9	0.00	0.00	0.00	0.00	0.00	0.00	0.00	0.00	0.00	0.00	0.00	0.00	0.00	0.00	0.00	0.00
22:2n-6	0.00	0.01	0.01	0.01	0.00	0.00	0.01	0.01	0.00	0.01	0.02	0.01	0.00	0.01	0.02	0.02
23:0	0.25	0.25	0.27	0.29	0.29	0.26	0.26	0.29	0.26	0.27	0.31	0.27	0.27	0.27	0.06	0.08
22:4n-6	1.42	1.58	1.19	1.70	1.07[a]	1.71	1.02[a]	1.76	0.97[a]	1.95	0.86[a]	1.95	0.80[a]	1.99	0.51	0.71
22:5n-6	0.23	0.26	0.19	0.25	0.18	0.25	0.19	0.26	0.16	0.27	0.17	0.27	0.15	0.28	0.07	0.09
22:5n-3	1.99	1.65	2.37[a]	1.66	2.55[a]	1.61	3.02[a]	1.60	3.21[a]	1.65	3.45[a]	1.65	3.34[a]	1.58	0.70	0.32
24:0	0.28	0.29	0.29	0.33	0.31	0.39	0.29	0.32	0.29	0.33	0.29	0.33	0.31	0.33	0.05	0.12
22:6n-3	0.65	0.68	0.65	0.75	0.68	0.76	0.63	0.70	0.63	0.71	0.62	0.63	0.59	0.63	0.29	0.29
24:1n-9	0.54	0.56	0.56	0.66	0.63	0.62	0.55	0.61	0.53	0.60	0.54	0.55	0.55	0.50	0.13	0.21

Values represent relative % ($n = 9$)

Diet × time interactions were found as follows

18:3n-3, $p < 0.001$; 20:5n-3, $p < 0.01$; 22:4n-6, $p < 0.03$; 22:5n-3, $p < 0.04$

[a] Significantly different from SUN group at same time period, $p < 0.05$; by student's t test after repeated measures ANOVA

[b] Combined standard deviation among all sample times

[c] Δ8,11,14 isomer

of values recommended by the 2006 National Research Council for canine diets [30]. The recent report by Marangoni et al. found similar increases of EPA and DPAn-3 in a small group of normal humans supplemented with walnuts containing 4.4 g LA/day and 1.2 g ALA per day at a LA/ALA ratio of 3.6:1 [24]. In that study, amounts of LA and ALA from other dietary sources were not strictly controlled although participants were instructed to specifically limit their consumption of other ALA containing foods and fish during the short study period. Given these similar findings, it is of interest that the FLX group LA/ALA ratio in the present study is essentially equivalent to

Table 3 Serum triacylglycerol fatty acid composition during the feeding period

FA	Days														FLX SD[b]	SUN SD[b]
	0		4		7		14		28		56		84			
	FLX	SUN	FLX	SUN	FLX	SUN	FLX	SUN	FLX	SUN	FLX	SUN	FLX	SUN		
14:0	1.07	0.98	1.02	1.26	0.97	0.97	1.04	1.13	1.19	1.17	0.98	1.40	1.29	1.60	0.31	0.63
14:1	0.44	0.27	0.51	0.30	0.60	0.31	0.50	0.30	0.48	0.34	0.46	0.21	0.56	0.20	0.49	0.29
15:0	0.23	0.21	0.23	0.24	0.24	0.25	0.22	0.22	0.24	0.23	0.23	0.24	0.23	0.30	0.06	0.05
16:0	19.03	18.89	17.10	17.86	15.94	17.02	17.63	16.84	16.90	18.03	16.80	18.41	16.71	19.03	2.13	2.33
16:1n-7	2.95	2.52	2.85	2.63	2.45	2.63	2.64	2.59	2.56	3.05	2.37	2.27	2.32	2.78	1.01	1.30
17:0	0.55	0.46	0.52	0.54	0.51	0.49	0.51	0.53	0.55	0.51	0.48	0.49	0.56	0.70	0.14	0.14
17:1n-7	0.31	0.22	0.27	0.25	0.23	0.21	0.28	0.21	0.24	0.22	0.26	0.20	0.26	0.32	0.06	0.12
18:0	6.20	6.63	6.52	6.71	6.62	7.05	6.56	5.90	6.56	5.38	6.08	6.20	6.57	6.70	1.72	2.16
18:1n-9	28.02	28.46	28.17	26.62	29.07	27.38	27.89	27.54	28.13	27.93	26.41	25.91	27.86	28.01	2.62	2.35
18:1n-7	4.29	3.61	3.90	4.04	3.73	3.93	3.75	4.06	3.86	4.30	3.51	3.54	3.51	4.30	0.64	0.78
18:2n-6	22.72	24.57	23.79	25.44	23.97	25.98	23.92	26.23	23.72	24.98	26.15	27.67	23.98	24.09	2.73	3.67
18:3n-6	0.60	0.55	0.51	0.70	0.58	0.64	0.53	0.75	0.57	0.75	0.57	0.69	0.50	0.49	0.28	0.29
18:3n-3	1.06	0.74	2.75[a]	0.62	2.90[a]	0.68	2.90[a]	0.62	2.72[a]	0.65	3.44[a]	0.74	3.36[a]	0.60	0.92	0.18
20:0	0.06	0.12	0.09	0.07	0.07	0.10	0.08	0.06	0.08	0.01	0.10	0.12	0.11	0.06	0.08	0.09
20:1n-9	0.37	0.31	0.38	0.39	0.34	0.44	0.38	0.41	0.41	0.33	0.38	0.39	0.41	0.45	0.11	0.16
20:2n-6	0.29	0.31	0.37	0.40	0.29	0.42	0.34	0.44	0.38	0.38	0.39	0.45	0.42	0.47	0.11	0.12
20:3n-9	0.63	0.55	0.51	0.64	0.52	0.54	0.45	0.75	0.54	0.73	0.45	0.61	0.51	0.72	0.38	0.48
20:3 isomer	0.07	0.07	0.04	0.01	0.03	0.00	0.01	0.01	0.02	0.02	0.03	0.03	0.04	0.05	0.08	0.06
20:3n-6[c]	0.57	0.58	0.54	0.63	0.59	0.66	0.50	0.72	0.53	0.64	0.53	0.64	0.51	0.59	0.13	0.20
20:3n-3	0.00	0.00	0.04	0.00	0.04	0.00	0.04	0.00	0.06	0.01	0.11	0.00	0.09	0.00	0.08	0.01
20:4n-6	4.46	4.90	3.90	5.46	4.25	5.64	3.80	5.35	3.77	4.91	4.13	4.70	3.36	3.44	1.97	2.02
20:4n-3	0.00	0.01	0.05	0.01	0.01	0.00	0.01	0.00	0.02	0.00	0.02	0.01	0.06	0.01	0.05	0.01
20:5 n-3	0.28	0.21	0.49[a]	0.21	0.53[a]	0.13	0.56[a]	0.19	0.60[a]	0.21	0.76[a]	0.23	0.76[a]	0.05	0.31	0.16
22:0	0.05	0.06	0.02	0.07	0.04	0.11	0.03	0.05	0.04	0.02	0.02	0.06	0.00	0.02	0.06	0.08
22:1n-9	0.00	0.00	0.00	0.00	0.00	0.00	0.00	0.00	0.00	0.00	0.00	0.00	0.00	0.01	0.00	0.00
22:2n-6	0.00	0.00	0.00	0.00	0.06	0.04	0.08	0.01	0.00	0.01	0.04	0.06	0.00	0.00	0.06	0.05
23:0	0.00	0.00	0.00	0.01	0.00	0.00	0.00	0.00	0.00	0.02	0.00	0.00	0.00	0.00	0.00	0.01
22:4n-6	0.73	0.86	0.74	1.09	0.61	0.97	0.51	1.14	0.60	1.04	0.57	1.11	0.52	1.04	0.37	0.61
22:5n-6	0.02	0.00	0.00	0.01	0.00	0.00	0.00	0.00	0.00	0.01	0.00	0.00	0.00	0.00	0.01	0.01
22:5n-3	0.60	0.47	0.93[a]	0.57	0.89[a]	0.49	1.08[a]	0.59	1.18[a]	0.52	1.38[a]	0.60	1.33[a]	0.43	0.35	0.26
24:0	0.00	0.01	0.00	0.01	0.00	0.00	0.00	0.00	0.00	0.00	0.00	0.00	0.00	0.00	0.00	0.01
22:6n-3	0.03	0.01	0.04	0.01	0.00	0.00	0.00	0.00	0.00	0.00	0.00	0.01	0.00	0.02	0.03	0.02
24:1n-9	0.00	0.00	0.00	0.00	0.00	0.00	0.00	0.00	0.00	0.00	0.00	0.00	0.00	0.00	0.00	0.00

Values represent relative % ($n = 9$)

Diet × time interactions were found as follows

18:3n-3, $p < 0.001$; 20:5n-3, $p < 0.020$; 22:5n-3, $p < 0.016$

[a] Significantly different from SUN group at same time period, $p < 0.05$

[b] Combined standard deviation among all sample times

[c] Δ8,11,14 isomer

human recommendations from a 1999 National Institutes of Health Workshop that diets contain no more than 6.7 g of LA and 2.2 g of ALA per day yielding an LA/ALA ratio of 3.0:1 [31] as well as those from the International Society for the Study of Fatty Acids and Lipids in which diets containing 2% of energy from LA and 0.7% energy from ALA are noted resulting in an LA/ALA ratio of 2.9:1 [32]. Hence, the canine data presented here may provide a reasonable model to study the effects of LA and ALA, per se or in combination, with incremental amounts of EPA and/or DHA for human lipid metabolism. Future investigations of canine responses to n-3 fatty acids are thus warranted.

Table 4 Serum cholesteryl ester fatty acid composition during the feeding period

FA	Days														FLX SD[b]	SUN SD[b]
	0		4		7		14		28		56		84			
	FLX	SUN	FLX	SUN	FLX	SUN	FLX	SUN	FLX	SUN	FLX	SUN	FLX	SUN		
14:0	0.31	0.32	0.29	0.28	0.28	0.26	0.29	0.27	0.30	0.27	0.30	0.28	0.29	0.31	0.06	0.08
14:1	0.29	0.25	0.22	0.22	0.22	0.15	0.21	0.18	0.16	0.12	0.20	0.16	0.20	0.14	0.09	0.10
15:0	0.11	0.10	0.10	0.10	0.11	0.11	0.09	0.10	0.10	0.10	0.11	0.11	0.10	0.11	0.02	0.02
16:0	9.34	9.43	8.70	8.55	8.70	8.58	8.44	8.34	8.31	7.93	8.39	8.20	8.05	7.76	1.11	1.36
16:1n-7	1.37	1.36	1.22	1.21	1.24	1.28	1.13	1.18	1.07	1.11	1.03	0.98	1.00	0.99	0.37	0.33
17:0	0.12	0.10	0.12	0.12	0.12	0.13	0.12	0.12	0.10	0.12	0.12	0.12	0.12	0.13	0.03	0.03
17:1n-7	0.13	0.12	0.09	0.15	0.12	0.13	0.13	0.15	0.09	0.15	0.11	0.14	0.12	0.16	0.06	0.04
18:0	1.70	1.71	1.67	1.57	1.65	1.73	1.55	1.60	1.55	1.47	1.52	1.54	1.52	1.57	0.23	0.26
18:1n-9	12.20	12.31	11.05	10.74	11.05	10.65	10.91	11.10	10.59	10.16	10.62	9.76	10.25	10.39	1.23	1.87
18:1n-7	3.19	3.21	3.01	3.02	3.16	3.21	2.97	3.01	2.90	2.77	2.84	2.77	2.70	2.49	0.75	0.61
18:2n-6	54.19	52.73	54.99	54.73	53.68	52.77	56.15	55.31	57.08	56.18	57.60	56.34	57.48	56.36	3.42	6.09
18:3n-6	0.39	0.35	0.36	0.39	0.31	0.37	0.35	0.44	0.36	0.45	0.33	0.41	0.34	0.41	0.07	0.11
18:3n-3	0.13	0.08	0.46[a]	0.10	0.51[a]	0.07	0.64[a]	0.12	0.56[a]	0.10	0.61[a]	0.11	0.68[a]	0.15	0.19	0.06
20:0	0.02	0.00	0.02	0.00	0.00	0.01	0.00	0.00	0.00	0.00	0.00	0.00	0.00	0.00	0.02	0.01
20:1n-9	0.00	0.00	0.01	0.04	0.01	0.00	0.00	0.00	0.03	0.01	0.03	0.00	0.00	0.00	0.02	0.02
20:2n-6	0.00	0.00	0.01	0.00	0.00	0.00	0.00	0.00	0.00	0.00	0.00	0.00	0.00	0.00	0.00	0.00
20:3n-9	0.04	0.04	0.03	0.02	0.00	0.01	0.02	0.02	0.02	0.03	0.01	0.02	0.01	0.02	0.05	0.06
20:3 isomer	0.05	0.05	0.05	0.06	0.06	0.06	0.03	0.04	0.06	0.06	0.06	0.07	0.11	0.12	0.09	0.06
20:3n-6[c]	0.36	0.36	0.37	0.36	0.34	0.36	0.33	0.37	0.36	0.39	0.34	0.38	0.37	0.37	0.09	0.14
20:3n-3	0.00	0.04	0.00	0.00	0.00	0.00	0.00	0.00	0.00	0.02	0.00	0.00	0.00	0.05	0.00	0.04
20:4n-6	13.38	15.02	15.37	16.39	15.73	17.70	14.33	16.01	14.41[a]	16.88	13.93	16.07	14.37	15.79	2.44	2.82
20:4 n3	0.05	0.02	0.00	0.00	0.01	0.00	0.02	0.00	0.00	0.00	0.00	0.00	0.00	0.02	0.02	0.01
20:5n-3	0.10	0.10	0.23	0.06	0.25[a]	0.05	0.40[a]	0.09	0.37[a]	0.10	0.39[a]	0.10	0.51[a]	0.17	0.20	0.09
22:0	0.26	0.18	0.10	0.15	0.27	0.22	0.23	0.14	0.23	0.19	0.17	0.14	0.24	0.24	0.12	0.12
22:1n-9	0.02	–	0.00	–	0.00	0.04	0.00	0.00	0.00	–	0.00	–	0.00	0.00	0.01	0.04
22:2n-6	0.02	–	0.00	–	0.00	0.04	0.00	0.04	0.00	0.00	0.02	0.00	0.00	0.00	0.02	0.03
23:0	0.00	0.02	0.00	0.00	0.00	0.00	0.00	0.00	0.00	0.00	0.00	0.00	0.00	0.00	0.00	0.00
22:4n-6	0.00	0.04	0.00	0.00	0.00	0.00	0.00	0.00	0.00	0.00	0.00	0.00	0.00	0.03	0.00	0.01
22:5n-6	0.00	0.00	0.00	0.00	0.00	0.00	0.00	0.00	0.00	0.00	0.00	0.00	0.00	0.00	0.00	0.00
22:5n-3	0.00	0.00	0.00	0.01	0.00	0.00	0.00	0.00	0.03	0.00	0.02	0.00	0.04	0.00	0.03	0.02
24:0	0.00	0.00	0.00	0.00	0.00	0.00	0.00	0.00	0.00	0.00	0.00	0.00	0.00	0.00	0.00	0.00
22:6n-3	0.00	0.00	0.00	0.04	0.03	0.00	0.02	0.00	0.02	0.00	0.00	0.01	0.00	0.05	0.00	0.00
24:1n-9	0.00	0.00	0.00	0.00	0.00	0.00	0.00	0.00	0.00	0.00	0.00	0.00	0.00	0.00	0.00	0.00

Values represent relative % ($n = 9$)

Diet × time interactions were found as follows

18:3n-3, $p < 0.001$; 20:5n-3, $p < 0.0013$

[a] Significantly different from SUN group at same time period, $p < 0.05$

[b] Combined standard deviation among all sample times

[c] Δ8,11,14 isomer

As in the other lipid fractions, the observed changes in the CE fraction appeared to achieve a steady state after approximately 28 days of supplementation. It is of interest, however, that while there were significant increases of EPA in the flaxseed group, essentially no DPAn-3 or DHA was found in the serum CE fraction of these dogs. By contrast, in an earlier study, when we fed fish oil to dogs, we also observed that DPAn-3 was not present in the CE fraction. DHA was found, but only to a small extent relative to the PL and TG fractions [33]. Previous studies investigating lecithin:cholesterol acyl transferase (LCAT) in various species have also reported CE-DPAn-3 to be absent in

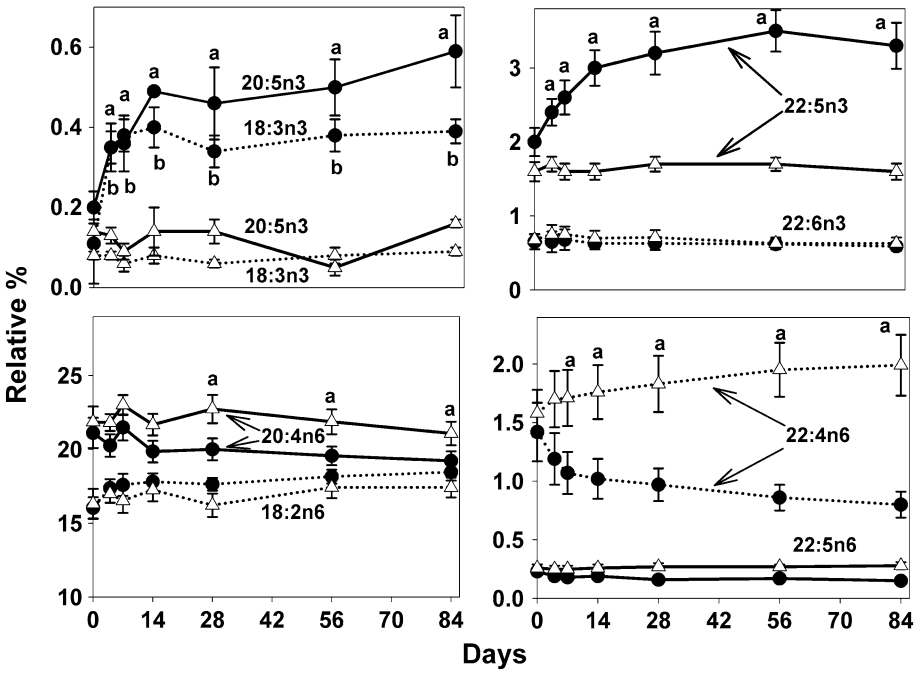

Fig. 1 Time course of the accumulation of selected n-3 and n-6 fatty acids in the serum phospholipid fractions of dogs fed diets supplemented with whole ground sunflower and whole ground flax seed. *Filled circles* represent values from dogs fed the flax seed supplement; *open triangles* correspond to those animals fed the sunflower seed supplement. Fatty acid species are as indicated on each plot; values are relative % ± SD; letters *a* and *b* each indicate a statistically significant difference between diet groups for the same fatty acid at time points indicated, $p < 0.05$

canines [34, 35]. Taken together, these findings indicate that this fatty acid, and perhaps 22 carbon fatty acids in general, may not be preferred substrates for cholesterol esterification via reverse cholesterol transport as mediated by the LCAT enzyme. Also because no appreciable accumulation of DHA occurred in the CE fraction with flaxseed feeding, this fatty acid is apparently seen only in the presence of a sufficient preformed dietary source. Given that DHA in human plasma CE is present in low concentrations as well, the importance of this finding in the canine model is that CE-DHA may serve as a potential biomarker of dietary DHA sufficiency in both dogs and humans and should be investigated further.

It is particularly noteworthy that the fatty acid profiles in the present work show differential metabolic enrichment of lipid fractions with the derived n-3 LCPUFA after ALA feeding in the canine. Enrichment of post-absorptive serum PL and TG with DPAn-3 suggests the possibility of transport and delivery of this fatty acid into tissues without its return via reverse cholesterol transport in the CE fraction. We hypothesize that while conversion of DPAn-3 to DHA is slow in dogs, humans, and other species, one-way transport of DPAn-3 via the circulation may serve to physiologically conserve this fatty acid as a substrate for DHA synthesis in tissues such as brain and retina and especially when dietary sources of DHA are scarce. Furthermore, because DPAn-3 is absent in serum CE, such transport may be unidirectional.

Observations relating to the metabolism of n-6 fatty acids in dogs were also made in this study. The significant increase of PL–LA in the FLX group, even at lower total LA dietary content, may be the result of a reported preference of delta-6 desaturase for ALA versus LA [18]. As such, competition between these two fatty acids for conversion to longer chain derivatives may result in LA accumulation providing a sparing effect when ALA is fed. Alternatively, this finding may be a consequence of the reduction of AA in this fraction due not only to n-3 polyunsaturated fatty acid incorporation but also some competition between LA and AA in the process of phospholipid esterification. In any case, this accumulation of LA in fur-bearing animals such as dogs may subsequently participate in skin and hair coat improvements previously observed in canine species fed polyunsaturated fatty acid supplements [36, 37]. Finally, decreased amounts of 22:4n-6 seen with flaxseed supplementation resulted in a statistically significant difference as early as 7 days which remained decreased thereafter. By contrast, a nearly constant amount of PL–AA was seen in the SUN group providing substrate for chain elongation to 22:4n-6. Competition between n-3 and n-6 fatty acids for incorporation into the serum PL pool may have made more AA available for 22:4n-6 synthesis thereby resulting in the modest increase in this fatty acid species. Such AA chain elongation may, in part, help minimize the accumulation of excessive amounts of AA in cell membranes for eicosanoid synthesis when high n-6 diets are fed.

Overall, the results of this study have demonstrated that aspects of canine fatty acid metabolism are more similar to humans than rodent species and thus offer a useful model for investigations in several areas including not only cardiac arrhythmia studies but also spontaneous models of

carcinogenesis and cognitive decline which develop more rapidly due to shorter canine life spans. One direct finding of relevance to human health from this study is the potential for CE-DHA as a biomarker of DHA status for human health. Furthermore, establishment of a metabolic steady state with respect to serum fatty acid accumulation appeared as early as 28 days Knowledge of these phenomena permits future investigations of the canine model, where appropriate, to take advantage of shorter term feeding studies in which a metabolic steady state is desired given the expense and sometimes ethical concerns with this species.

Acknowledgments This work was supported in part by Essential Nutrient Research Corp., Manitowoc, WI, USA and the Mark L. Morris Professorship in Clinical Nutrition at Texas A&M University.

References

1. Burr ML, Fehily AM, Gilbert JF, Rogers S, Holliday RM, Sweetnam PM, Elwod PC, Deadman NM (1989) Effects of changes in fat, fish, and fibre intakes on death and myocardial reinfarction: diet and reinfarction trial (DART). Lancet 2:757–761
2. DeLorgeril M, Salen P, Martin JL, Monjaud I, Delaye J, Mamelle N (1999) Mediterranean diet, traditional risk factors, and the rate of cardiovascular complications after myocardial infarction; final report of the Lyon Diet Heart Study. Circulation 99:779–785
3. Wang C, Harris WS, Chung MM, Lichtenstein AH, Balk EM, Kupelnick B, Jordan HS, Lau J (2006) Fatty acids from fish or fish-oil supplements, but not linolenic acid, benefit cardiovascular disease outcomes in primary and secondary prevention studies; a systematic review. Am J Clin Nutr 83:5–17
4. Sinclair AJ (1975) Long chain polyunsaturated fatty acids in the mammalian brain. Proc Nutr Soc 34:287–291
5. Anderson GJ, Connor WE, Corliss JD (1990) Docosahexaenoic acid is the preferred dietary n-3 fatty acid for the development of the brain, retina. Pediatr Res 27:89–97
6. Jeffrey BG, Mitchell DC, Gibson RA, Neuringer M (2002) n-3 Fatty acid deficiency alters recovery of the rod photoresponse in rhesus monkeys. Invest Ophthalmol Vis Sci 43:2806–2814
7. James MJ, Gibson RA, Cleland LG (2000) Dietary polyunsaturated fatty acids and inflammatory mediator production. Am J Clin Nutr 71:343S–348S
8. Calder PC (2002) Dietary modification of inflammation with lipids. Proc Nutr Soc 61:345–358
9. Lee TH, Hoover RL, Williams JD, Sperling RI, Ravalese J 3rd, Spur BW, Robinson DR, Corey EJ, Lewis RA, Austen KF (1985) Effect of dietary enrichment with eicosapentaenoic and docosahexaenoic acids on in vitro neutrophil and monocyte leukotriene generation and neutrophil function. New Eng J Med 312:1217–1224
10. Voss A, Reinhart M, Sankarappa S, Sprecher H (1991) The metabolism of 7, 10, 13, 16, 19-docosapentaenoic acid to 4, 7, 10, 13, 16, 19-docosahexaenoic acid in rat liver is independent of a 4-desaturase. J Biol Chem 266:19995–20000
11. Kris-Etherton PM, Harris WS, Appel LJ (2002) Fish consumption, fish oil, n-3 fatty acids, and cardiovascular disease. Circulation 106:2747–2757
12. Krauss RM, Eckel RH, Howard B, Appel LJ, Daniels SR, Deckelbaum RJ, Erdman JW Jr, Kris-Etherton P, Goldberg IJ, Kotchen TA, Lichtenstein AH, Mitch WE, Mullis R, Robinson K, Wylie-Rosett J, Jeor S, Suttie J, Tribble DL, Bazzarre TL (2000) AHA dietary guidelines: revision 2000: a statement for healthcare professionals from the Nutrition Committee of the American Heart Association. Stroke 31:2751–2766
13. Crawford MA, Casperal NM, Sinclair AJ (1978) The long chain metabolites of linoleic and linolenic acids in liver and brain in herbivores and carnivores. Comp Biochem Physiol 54B:395–401
14. Zhao G, Etherton TD, Martin KR, West SG, Gillies PJ, Kris-Etherton PM (2004) Dietary alpha-linolenic acid reduces inflammatory and lipid cardiovascular risk factors in hypercholesterolemic men and women. J Nutr 134:2991–2997
15. Caughey GE, Mantzioris E, Gibson RA, Cleland LG, James MJ (1996) The effect on human tumor necrosis factor α and interleukin 1β production of diets enriched in n-3 fatty acids from vegetable or fish oil. Am J Clin Nutr 63:116–122
16. Zhao G, Etherton TD, Martin KR, Gillies PJ, West SG, Kris-Etherton PM (2007) Dietary α-linolenic acid inhibits proinflammatory cytokine production by peripheral blood mononuclear cells in hypercholesterolemic subjects. Am J Clin Nutr 85:385–391
17. Stark AH, Crawford MA, Reifen R (2008) Update on alpha-linolenic acid. Nutr Rev 66:326–332
18. Leaf A, Kang JX, Xiao YF, Billman GE (2003) Clinical prevention of sudden cardiac death by n-3 polyunsaturated fatty acids and mechanism of prevention of arrhythmias by n-3 fish oils. Circulation 107:2646–2652
19. Dunbar BL, Bauer JE (2002) Conversion of essential fatty acid by delta-6 desaturase in dog liver microsomes. J Nutr 132:1701S–1703S
20. Harris WS, DiRienzo MA, Sands SA, George C, Jones PG, Eapen AK (2007) Stearidonic acid increases the red blood cell and heart eicosapentaenoic acid content in dogs. Lipids 42:325–333
21. Bauer JE, Dunbar BL, Bigley KE (1998) Dietary flaxseed in dogs results in differential transport and metabolism of (n-3) polyunsaturated fatty acids. J Nutr 128:2641S–2644S
22. Lands WEM, Libelt B, Morris A, Kramer NC, Prewitt TE, Bowen P, Schmeisser D, Davidson MH, Burns JH (1992) Maintenance of lower proportions of (*n*-6) eicosanoid precursors in phospholipids of human plasma in response to added dietary (n-3) fatty acids. Biochim Biophys Acta 1180:147–162
23. Bauer JE, Waldron MK, Spencer AL, Hannah SS (2002) Predictive equations for the quantitation of polyunsaturated fats in dog plasma and neutrophils from dietary fatty acid profiles. J Nutr 132:1642S–1645S
24. Marangoni F, Colombo C, Martiello A, Poli A, Paoletti R, Galli C (2007) Level of the n-3 fatty acid eicosapentaenoic acid in addition to those of alpha linolenic acid are significantly raised in blood lipids by the intake of four walnuts a day in humans. Nutr Metab Cardiovasc Dis 17:457–461
25. Brenna JT, Salem N Jr, Sinclair AJ, Cunnane SC, International Society for the Study of Fatty Acids, Lipids, ISSFAL (2009) Alpha-linolenic acid supplementation and conversion to n-3 long-chain polyunsaturated fatty acids in humans. Prostaglandins Leukot Essent Fatty Acids 80:85–91
26. Heinemann KM, Waldron MK, Bigley KE, Lees GE, Bauer JE (2005) Long-chain (n-3) polyunsaturated fatty acids are more efficient than α-linolenic acid in improving electroretinogram response of puppies exposed during gestation, lactation, and weaning. J Nutr 135:1960–1966
27. Rapoport SI, Rao JS, Igarashi M (2007) Brain metabolism of nutritionally essential polyunsaturated fatty acids depends on both the diet and the liver. Prostaglandins Leukot Essent Fatty Acids 77:251–261
28. Alvarez RA, Aguirre GD, Acland GM, Andreson RE (1994) Docosapentaenoic acid is converted to docosahexaenoic acid in the retinas of normal and *prcd*-affected Miniature Poodle dogs. Invest Vis Sci 35:402–408

29. Pawlosky R, Barnes A, Salem N Jr (1994) Essential fatty acid metabolism in the feline: relationship between liver and brain production of long-chain polyunsaturated fatty acids. J Lipid Res 35:2032–2040
30. National Research Council (NRC) (2006) Nutrient requirements of dogs and cats. National Academy Press, Washington, DC
31. Simopoulos AP, Leaf A, Salem N Jr (2000) Workshop statement on the essentiality of and recommended dietary intakes for n-6 and n-3 fatty acids. Prostaglandins Leukot Essent Fatty Acids 63:119–121
32. Executive Committee Report: (2004) Recommendation for intake of polyunsaturated fatty acids in healthy adults. International Society for the Study of Fatty Acids and Lipids. http://www.issfal.org.uk
33. Bauer JE, McAlister KG, Rawlings JM, Markwell P (1997) Molecular species of cholesteryl esters formed via plasma lecithin:cholesterol acyltransferase in fish oil supplemented dogs. Nutr Res 17:861–872
34. Subbaiah PV, Liu M (1996) Comparative studies on the substrate specificity of lecithin:cholesterol acyl transferase towards the molecular species of phosphatidyl choline in the plasm of 14 vertebrates. J Lipid Res 37:113–120
35. Liu M, Bagdade JD, Subbaiah PV (1995) Specificity of lecithin:cholesterol acyl transferase and atherogenic risk: comparative studies on the plasma composition and in vitro synthesis of cholesteryl esters in 14 vertebrate species. J Lipid Res 36:1813–1824
36. Kirby NA, Hester SL, Rees CA, Kennis RA, Zoran DL, Bauer JE (2009) Skin surface lipids and skin and hair coat condition in dogs fed increased total fat diets containing polyunsaturated fatty acids. J An Phys An Nutr 93:505–511
37. Rees CA, Bauer JE, Burkholder WJ, Kennis RA, Dunbar BL, Bigley KE (2001) Effects of dietary flax seed and sunflower seed supplementation on normal canine serum polyunsaturated fatty acids and skin and hair coat condition scores. Vet Derm 12:111–117

Lipids (2010) 45:11–19
DOI 10.1007/s11745-009-3376-5

ORIGINAL ARTICLE

The Consumption of Food Products from Linseed-Fed Animals Maintains Erythrocyte Omega-3 Fatty Acids in Obese Humans

Philippe Legrand · B. Schmitt · J. Mourot · D. Catheline · G. Chesneau · M. Mireaux · N. Kerhoas · P. Weill

Received: 18 June 2009 / Accepted: 17 November 2009 / Published online: 11 December 2009

Abstract Based on mechanistic and epidemiological data, we raise the question of the relationship between qualitative dietary polyunsaturated fatty acids (PUFA) changes and increase in obesity. In this double-blind trial, we studied the effects on 160 overweight volunteers (body mass index, BMI >30) of a 90 days experimental diet rich principally in animal fat with a low PUFA/saturated fatty acid (SFA) ratio but a low n-6/n-3 ratio, using animal products obtained from linseed-fed animals. The control diet provided less animal fat, a higher PUFA/SFA ratio and a higher n-6/n-3 ratio. Both diets excluded seafood. In the experimental group, we observed a significant increase in red blood cell (RBC) α-linolenic acid content and a slight increase in EPA and DHA derivatives, while in the control group we observed a significant reduction in EPA and DHA content. Between groups now, the difference in the three n-3 fatty acids changes in RBC was significant. This demonstrates that plasma EPA and DHA levels can be maintained without fish if products from linseed-fed animals are used. During the diets, we noted a significant reduction in weight, BMI and hip circumference within both groups of volunteers. However, no significant difference was observed between the control group and the experimental group. Interestingly, 150 days after the end of the trial (i.e., day 240), we noted a significant weight gain in the control group, whereas no significant weight gain was observed in the experimental group. This was also observed for the BMI and hip circumference. Moreover, significant differences in BMI ($P < 0.05$) and weight ($P = 0.05$) appeared between the two groups, showing in both cases a smaller increase in the experimental group. During the 90 days trial, we did not observe any differences between groups in terms of total cholesterol, HDL cholesterol, LDL cholesterol or triglycerides, suggesting that the saturate content and the P/S ratio are not as important as the n-6 and n-3 fatty acid composition.

Keywords n-3 Fatty acids · Linseed · Red blood cell · Fatty acid composition · Obese

Abbreviations

BMI	Body mass index
PUFA	Polyunsaturated fatty acids
FA	Fatty acid
SFA	Saturated fatty acid
LNA	Linoleic acid
ALA	α-Linolenic acid

Introduction

In only a few decades, obesity has become a major health concern, which also increases the risk of type 2 diabetes

P. Legrand (✉) · D. Catheline
Biochimie-Nutrition Humaine Agrocampus-INRA, Rennes, France
e-mail: philippe.legrand@agrocampus-ouest.fr

B. Schmitt · M. Mireaux
CERN, Centre Hospitalier Lorient, Lorient, France

J. Mourot
INRA-Senah, Rennes, France

G. Chesneau · N. Kerhoas
Bleu Blanc Coeur, Combourtillé, France

P. Weill
Valorex, Combourtillé, France

and cardiovascular disease. Obesity is a multifactorial disease. Excessive adipose tissue development is primarily due to an imbalance between caloric intake and caloric expenditure, this imbalance being related to changes in dietary habits and to more sedentary lifestyles. However, in addition to the energy imbalance, different aspects of lipid metabolism such as lipid synthesis, transport, storage and catabolism are also implied in obesity development. Amongst nutrients involved in this metabolism, all fatty acids play obviously a major role from a quantitative point of view, but polyunsaturated fatty acids (PUFA) may also play a qualitative role, which is less well established. Indeed, recent data show that PUFA from the n-6 or n-3 series do not play identical roles. While n-6 PUFA are now well known as activators of adipose tissue development [1] and their dietary excess is suspected to favor childhood adiposity [2] and adult adiposity [3–5], n-3 PUFA seem to play a more favorable role, acting against different mechanisms leading to obesity. Thus in humans, n-3 PUFA seem somewhat to limit metabolic syndrome and type 2 diabetes [6–8]. A negative correlation has been described between abdominal obesity and n-3 PUFA content of adipose tissue [9]. Moreover, n-3 fatty acid intake limits fat accumulation in mice [10] and rats [11].

The fatty acid (FA) composition of the diet has changed significantly since the 1960s, when obesity began to increase. The first change was the increase in the PUFA/(saturated fatty acid) SFA ratio, due to the increase in consumption of vegetable oils rich in PUFA rather than animal fat which are richer in SFA. The second change was the subsequent increase in n-6 PUFA content, while n-3 PUFA content decreased or remained constant. This is due to the very high levels of n-6 PUFA in the most common vegetable oils (soybean, corn, sunflower, etc.) used in human nutrition as well as in animal feeds. Consumption data show that the linoleic acid (LNA) to α-linolenic acid (ALA) ratio increased by approximately three times to reach a range of 12–25 in most of the western diets during this period [12, 13]. These dietary ratio values are consistent with other values in humans, measured in breast milk [14, 15] and in subcutaneous adipose tissue [16, 17].

Thus, based on both mechanistic and epidemiological data, we raise the question of the relationship between these qualitative changes in dietary PUFA and increase in obesity, and more precisely when the increase in the dietary PUFA/SFA ratio is always associated with a large increase in the dietary n-6/n-3 FA ratio.

In this double-blind trial, we studied the effects on volunteers of a 90 days experimental diet rich in animal fat with both low PUFA/SFA and low n-6/n-3 ratios, using principally animal products obtained from linseed-fed animals. The control diet provided less animal fat, a higher value for the PUFA/SFA ratio and a higher value for the n-6/n-3 ratio. The volunteers were overweight or obese (body mass index, BMI $\approx$ 31). The main results were: (1) Plasma EPA and DHA levels can be maintained without fish, if using products from linseed-fed terrestrial animals. (2) During the diets, we noted a significant reduction in weight, BMI, and hip circumference within both groups of volunteers, but no significant difference was observed between the control group and the experimental group. However, the experimental diet limited weight recovery after the end of the trial. (3) No comparative deleterious effect (on plasma lipid parameters) was observed between diets, suggesting that the n-6/n-3 ratio is as important as the SFA level.

Materials and Methods

Volunteers

One hundred and sixty volunteers with metabolic syndrome (78 men and 82 post-menopausal women) between 18 and 65 years old were selected from those responding to local press recruitment (293 volunteers were evaluated). Inclusion criteria were waist circumference $\geq$80 cm for women and $\geq$94 cm for men, plus at least two other risk factors: triglycerides (TG) $\geq$1.5 g/l; fasting plasma glucose (FPG) $\geq$1.0 g/l; HDL cholesterol $\leq$0.4 g/l for men and $\leq$0.5 g/l for women; systolic blood pressure (BP) $\geq$130 mmHg; diastolic BP $\geq$85 mmHg or treatment for hypertension. The average body weight, BMI and hip circumference were respectively, 88.5 $\pm$ 15.6 kg, 31.5 $\pm$ 4.3 kg/m^2 and 109 $\pm$ 7.6 cm. Exclusion criteria included diabetes, any treatment for hypercholesterolemia and any disease judged incompatible with the study by the investigator. During a visit, the purpose and method of the study was explained to the selected volunteers; written informed consent was obtained from those willing to participate and a prescription was given. Inclusion and exclusion criteria were checked during a medical visit. The proposed diets were then explained to the volunteers and some menu examples were given to help them to adhere to the nutritional advice given during an individual consultation with a dietitian. The diets were given to volunteers from day 0 to day 90. At day (D) 90, 137 volunteers remained in the trial: 72 in the experimental group and 65 in the control group. The others decided to stop the trial between D0 and D90. All statistical analyses at D90 were carried out with these 137 volunteers. At day 240, 98 volunteers (72%) came back for the last anthropometric measurements: 50 in the experimental group (69%) and 48 in the control group (74%).

Study Design

Subjects were randomly assigned to one of two different diets. As regards animal products, the experimental diet included products with a high level of n-3 originating from linseed-fed animals while the control group diet included standard animal products. The feeds of animals that supplied the experimental products (dairy products, meats and eggs) contained an average of 5% of extruded linseed and are described in details in other publications [18]. As regards plant products, the experimental group volunteers received 5 g/day of extruded linseed flour, while the control group volunteers received the same amount of extruded wheat/soybean (90/10) flour. Moreover, the experimental group's bread included 4% extruded linseed flour. In the experimental diet, flour plus bread represent 40% of the total ALA intake while animal products provide long-chain derivatives (EPA plus DHA), and account for 60% of ALA. The control group volunteers received margarine with a high n-6 content (rich in sunflower oil) instead of the butter that the experimental group received.

The macronutrient content of the two diets was similar. The overall composition and energy intake of the two diets did not differ. The proposed energy intake was 1,667 kcal for women and 1,931 kcal for men. Subjects were asked not to consume any fish or seafood products or products containing more than 5% fat. Products containing linseed or products with a high n-3 content were also forbidden. The only authorized oil was olive oil (10 g a day). Male and female diets only differed by the amount of carbohydrates and meat (+50 g and +40 g for men, respectively).

The fat spread was butter for the experimental group and margarine for the control group, which mainly explains the difference in the proportion of lipids of animal origin between the two diets. The recommended weekly intake of eggs was ten. Sugar (sucrose) was requested to be reduced or excluded from the diet in order to reduce total calorie intake and reduce weight.

Subjects undertook an adjustment period of 2 weeks during which they had to follow the prescribed diet, consuming their own usual products (usual meats, eggs, dairy products, and fat spread). Afterward, at day 0, experimental or control products were provided for the whole family. They were delivered every week to a local shop where subjects collected them, presenting their volunteer card. Compliance was verified by checking the collection of the products with the help of local shop managers. Each member of the family was given 1,050 ml of milk, 10 eggs, 250 g of fat spread, 210 g of hard cheese, 7 slices of ham, 50 g of diced bacon fat, 2 sausages, 2 loaves of bread, 2 pork chops plus occasionally beef, chicken or veal. Small quantity adaptations were necessary according to the number of persons in the family and the packaging size. Flour (linseed or wheat/soybean) were provided for the volunteers only and not for the whole family.

During the experimental period, from D0 to D90, the volunteers met a dietitian to receive nutritional advice at least once a month. Compliance with the diet was evaluated by weekly recording of consumption. From D90 to D240, the volunteers returned to a free diet with the reintroduction of fish and previously forbidden products and had no visits with any member of the dietitian's team.

Anthropometry and Assays

The following anthropometric and plasma lipids parameters were measured at the hospital at D0 and D90: body weight and BMI were measured by TANITA TBF 300 MA, and hip circumferences were measured with an automatic rubber band. Blood lipids (total cholesterol, HDL cholesterol and triglycerides) were analyzed with an enzymatic technique using Advia1650-Siemens, and LDL cholesterol was calculated by the Friedwald formula [19]. After the end of the trial (D90), volunteers were requested to come back 5 months later (D240) for additional anthropometric measurements only.

Lipid Extraction and Fatty Acid (FA) Analysis

RBC lipids were extracted from 0.5 ml of samples with a mixture of hexane/isopropanol (3:2 v/v), after acidification with 1 ml HCl 3 M [20]. Total lipid extracts were saponified for 30 min at 70 °C with 1 ml of 0.5 M NaOH in methanol and methylated with 1 ml BF_3 (14% w/v in methanol) for 15 min at 70 °C. Fatty acid methyl esters were extracted twice with pentane and analyzed by GC using an Agilent Technologies 6890N (Bios Analytic, Toulouse, France) with a split injector (20:1) at 250 °C and a bonded silica capillary column (BPX 70, 30 m × 0.25 mm; SGE, Villeneuve-St Georges, France) with a polar stationary phase of 70% cyanopropyl polysilphenylene-siloxane (0.25 µm film thickness). Helium was used as a carrier gas (average velocity 24 cm/s). The column temperature program started at 150 °C, increased by 2 °C/min to 220 °C and held at 220 °C for 10 min. The flame ionization detector temperature was 250 °C. Identification of FA methyl ester was based on retention times obtained for FA methyl esters prepared from FA standards.

Statistical Analysis

Analyses of covariance, with terms for the treatment group and the baseline value were used to compare least square means and to test for differences in baseline to endpoint changes between treatments. Paired *t*-tests are also performed within each treatment group. Different analyses

were performed using stratifications by sex and the value of each metabolic syndrome risk factor. All analyses were conducted using SAS® version 8.2. The study was designed as an intend-to-treat analysis. The difference was considered significant when $P < 0.05$ and a tendency when $0.05 < P < 0.10$.

Results

Effects of Changes in Animal Feeding on Animal Products Composition and on FA Composition of Volunteers Diets

The main lipid sources used in the volunteers' diets are shown in Table 1. In the two diets, lipids provided 33% of the total caloric intake. Animal products used in the experimental diet originated from animals fed 5% extruded linseed, which provides C18:3n-3 (ALA) to the animals. In the control diet, animal products came from standard French breeding farms. This variable fraction represents 77% of the volunteers' lipid intake. The diets given to the volunteers are described in Tables 2 and 3. The real consumption of each volunteer is not known very precisely as meals were taken at home. The two diets were iso-caloric and iso-lipidic. In addition to the animal lipids presented above, margarine was used in the control diet. This margarine is a commercial product, the composition of which is close to the composition of French lipid intakes (Table 1). The experimental diet was rich in animal lipids (76% of total lipids). It provided high levels of n-3 PUFA, (not only ALA but also long-chain derivatives EPA and DHA) and low levels of n-6 PUFA. 40% of ALA is provided by linseed flour plus bread, in the experimental diet. Compared with the experimental diet, the control diet was richer in plant lipids (animal fats provided only 49% of lipids) and was richer in total PUFA (17.3 vs. 9.1 g/day in the experimental diet). Moreover, LNA content was much higher in the control diet (16.0 vs. 5.5 g/day in the experimental diet). As a result, the following ratios were very different between the two diets: PUFA/SFA values were 0.7 in the control diet versus 0.3 in the experimental diet, and C18:2n-6/C18:3n-3 values were 22.9 in the control diet versus 2.3 in the experimental diet.

Change in Volunteers' RBC FA Composition

The two diets produced clear changes in the content and ratios of numerous FAs in the RBC (Table 4). For n-3 PUFA, we observed in the volunteers receiving the experimental diet (animal products from linseed-fed animals plus a small amount of linseed flour and bread) a significant increase in ALA content between day 0 and day 90 and a significant increase in the total n-3 fatty acids. In the control group of volunteers, no effect was observed as regards ALA content, but the EPA and DHA content and total n-3 fatty acids decreased significantly. Between groups, the differences in the ALA, EPA and DHA changes (D90-D0) were significant.

Table 1 Fatty acid (FA) composition (% of total FA) of main lipid sources given to volunteers

FA composition (% of total FA)	Standard Margarine[a]	Standard dairy products[b]	Dairy products from "linseed industry"[b]	Standard eggs	Eggs from "linseed industry"	Standard pork[c]	Pork from "linseed industry"[c]
C14:0	1.7	11.6 ± 0.1	10.4 ± 0.3	0.4 ± 0.0	0.3 ± 0.0	1.3 ± 0.1	1.3 ± 0.2
C16:0	9.7	33.3 ± 0.9	26.0 ± 1.5	25.3 ± 0.8	21.0 ± 0.8	24.9 ± 1.0	24.6 ± 1.2
C18:0	8.2	8.7 ± 0.3	11.0 ± 0.4	7.7 ± 0.2	7.8 ± 0.4	13.5 ± 1.4	14.3 ± 1.3
C18:1n-9	21.1	17.4 ± 0.5	20.4 ± 0.6	46.7 ± 2.7	45.9 ± 2.5	43.3 ± 3.1	39.7 ± 3.1
C18:2n-6	51.5	1.5 ± 0.1	1.8 ± 0.0	12.0 ± 2.6	12.7 ± 1.3	10.0 ± 1.9	10.7 ± 2.1
C20:4n-6		0.1 ± 0.0	0.1 ± 0.0	1.5 ± 0.2	0.8 ± 0.1	1.1 ± 0.9	1.5 ± 1.2
∑n-6 PUFA	51.5	1.6 ± 0.1	2.0 ± 0.1	13.6 ± 2.6	13.6 ± 1.4	11.5 ± 2.6	12.6 ± 3.0
C18:3n-3	0.2	0.3 ± 0.0	0.9 ± 0.3	0.5 ± 0.2	6.5 ± 0.8	0.6 ± 0.1	2.3 ± 0.9
C20:5n-3					0.2 ± 0.0	0.1 ± 0.1	0.3 ± 0.3
C22:5n-3		0.1 ± 0.0	0.1 ± 0.0	0.1 ± 0.0	0.2 ± 0.0	0.2 ± 0.2	0.6 ± 0.4
C22:6n-3				0.7 ± 0.1	1.3 ± 0.2	0.1 ± 0.1	0.2 ± 0.1
∑n-3 PUFA	0.2	0.4 ± 0.1	1.2 ± 0.4	1.5 ± 0.3	8.2 ± 0.7	1.2 ± 0.4	3.5 ± 0.9
C18:2n-6/C18:3n-3	257.5	5.2 ± 1.1	2.1 ± 0.6	24.4 ± 4.9	2.0 ± 0.1	16.5 ± 4.5	5.6 ± 2.9

[a] Margarine was chosen because of its high similarity with the mean FA acid profile of vegetable oils consumed in France

[b] Lipids from butter, milk and cheeses

[c] Lipids from cooked meats (bacon pieces, sausage and ham) and fresh meat

Table 2 Estimation of the consumption of products and fatty acids (g/volunteer/day) by volunteers

	Control group		Experimental group	
	Products	Fatty acids	Products	Fatty acids
Margarine	25	20.0	0	0.0
Butter*	0	0.0	25	20.0
Semi-skimmed milk*	155	2.6	155	2.6
Cheese*	32	9.1	32	9.1
Eggs*	82	9.1	82	8.2
Cooked meats[a]*		9.9		9.9
Pork*		1.2		1.2
Bread*	100	0.5	100	1.0
Linseed meal	0	0.0	10	1.4
Soya/wheatmeal[b]	10	0.3	0	0.0
Olive oil	10	9.4	10	9.4
Other animal lipids[c]		1.6		1.6
Other vegetable oils[d]		4.8		4.8
Fish[e]	0	0.0	0	0.0
Total		68.5		69.2
Animal lipids (% of total lipids)		49		76

[a] Bacon pieces, sausage and ham

[b] Wheatmeal (90%) and soybean meal (10%)

[c] Beef, lamb, chicken (no qualitative difference between both groups)

[d] Fatty acids from industrial products, starchy vegetables and fruits (no qualitative difference between both groups)

[e] Consumption of fish and seafood products was prohibited during the experiment

* Products in the standard group were standard products, while products in the experimental group came from (1) animals (beef, chicken and pork) fed a linseed-enriched diet (5% of cooked linseed) or (2) linseed-enriched bread (5% of cooked linseed)

The n-6 PUFA content increased between D0 and D90 in the RBC of the control group, the increase being significant for LNA and for total n-6 fatty acids, but not significant for arachidonic acid (C20:4n-6). In the experimental group, we did not observe any significant change in the n-6 fatty acid content of the RBC. Between groups, the difference in the LNA and total n-6 fatty acid changes (D90–D0) was significant.

We noted also that the LNA/ALA ratio increased significantly in the control group and decreased significantly in the experimental group. The difference in changes between groups was also significant. This was equally true for the Σn-6/Σn-3 ratio.

More generally, the total PUFA content increased significantly in the control group and did not change in the experimental group. Furthermore, an increase in stearic acid content was noted in the experimental group, whereas oleic acid content was reduced in both groups.

Changes in Anthropometric Parameters

From D0 to D90, i.e., over the period of the diets, we noted a significant reduction in weight, BMI, and hip circumference in both groups of volunteers (Table 5). However, no significant difference was observed between the control group and the experimental group. Interestingly, from D90 to D240, i.e., after the end of the trial, we noted a significant weight gain in the control group, whereas no significant weight gain was observed in the experimental group. This was equally true for the BMI and hip circumference, which both increased solely in the control group. Between the two groups, from D90 to D240 we showed a significant difference for the BMI ($P < 0.05$), and a difference at the limit of significance for weight ($P < 0.06$), showing in both cases a smaller increase in the experimental group.

Changes in Plasma Lipid Parameters

These parameters were studied at D0 and D90. In Table 6, we first observed within each of the two groups a general deterioration in all the parameters, with an increase in LDL cholesterol in both groups and an increase in TG in the experimental group. However, the main result was that no significant difference between the groups was noted in total cholesterol, HDL cholesterol, LDL cholesterol or triglycerides over the period from D0 to D90. These parameters were not measured at D240. This is an interesting and novel result when considering the dietary characteristics

Table 3 Estimation of the mean fatty acid consumption by volunteers (g/volunteer/day)

	Control group (standard products)	Experimental group (products from "linseed industry")
Total FA	68.5	69.2
C4 to C12	2.8	4.3
C14:0	1.6	3.4
C16:0	12.9	14.8
C18:0	5.5	6.4
∑Saturated FA (SFA)	24.3	30.9
C16:1n-7	0.6	0.7
C18:1n-9 cis	24.4	25.0
Others C18:1 (*cis*/*trans*)	0.2	1.9
∑Monounsaturated FA (MUFA)	26.9	29.1
C18:2n-6	16.0	5.5
C20:4n-6	0.21	0.17
∑n-6 PUFA	16.2	5.7
C18:3n-3	0.7	2.4
C20:5n-3	0.01	0.07
C22:5n-3	0.03	0.07
C22:6n-3	0.07	0.13
∑n-3 PUFA	0.8	2.7
∑Polyunsaturated FA (PUFA)	17.3	9.1
PUFA/SFA	0.7	0.3
C18:2n-6/C18:3n-3	22.9	2.3

other than the n-3 fatty acids. Indeed, the high level of SFA (44% fatty acid = 14.6% energy) in the experimental diet did not lead to any deleterious effect on plasma lipid parameters, as compared with the control diet (35% fatty acid = 12% energy). Moreover, the experimental diet was also low in n-6 fatty acids (8.2 vs. 23.6% fatty acid), low in total PUFA (13.1 vs. 25.2% fatty acid) and none of these characteristics caused any deleterious effect on the plasma lipid parameters.

Discussion

The fatty acid content of RBC is considered to be a tissue marker for dietary fatty acid composition [21, 22]. The first result of this study is the increase in the ALA content of RBC in the experimental group, whereas it did not vary in the control group. This increase in ALA is mainly due to the dietary animal products obtained from linseed-fed animals but also from linseed flour and bread included in the experimental diet. All together the ALA supply was about 2.4 g/day, which is a little higher than the French recommended intake [23]. We noted in the control group that ALA intake corresponded to the French average consumption [13, 17] and that this intake was sufficient to maintain its levels in the RBC during the study. More interesting is the effect of the diet on EPA and DHA content in the RBC. These contents decreased significantly

Table 4 Red blood cell fatty acid composition in volunteers (% of total FA)

	Control group			Experimental group	
	Day 0	Day 90		Day 0	Day 90
C16:0	20.2 ± 1.4	20.0 ± 1.8		20.0 ± 1.6	20.3 ± 1.7
C18:0	10.5 ± 2.9	11.5 ± 3.5		10.5 ± 3.4	12.1 ± 3.5**
∑Saturated FA (SFA)	32.5 ± 2.9	33.2 ± 4.1		32.2 ± 3.7	34.2 ± 4.0**
C18:1n-9	23.5 ± 2.55	21.0 ± 4.3***		22.8 ± 2.8	21.8 ± 3.3*
∑Monounsaturated FA (MUFA)	29.7 ± 3.2	25.9 ± 4.4***	##	28.5 ± 3.5	27.1 ± 3.8*
C18:2n-6	20.9 ± 4.0	24.0 ± 5.5***	###	22.2 ± 5.0	20.6 ± 5.2
C20:4n-6	8.9 ± 2.1	9.5 ± 2.8		9.0 ± 2.2	9.4 ± 2.4
∑n-6 PUFA	32.7 ± 3.3	36.5 ± 5.1***	###	34.1 ± 3.7	32.9 ± 4.3
C18:3n-3	0.43 ± 0.2	0.46 ± 0.7	#	0.42 ± 0.1	0.68 ± 0.4***
C20:5n-3	0.62 ± 0.2	0.40 ± 0.2***	###	0.73 ± 0.3	0.77 ± 0.3
C22:6n-3	2.6 ± 0.8	2.3 ± 0.8*	#	2.6 ± 0.8	2.7 ± 0.9
∑n-3 PUFA	4.6 ± 1.2	4.0 ± 0.9***		4.7 ± 1.2	5.3 ± 1.3**
C18:2n-6/C18:3n-3	55.4 ± 19.9	77.0 ± 28.7***	###	58.0 ± 19.8	35.6 ± 14.1***
∑n-6 PUFA/∑n-3 PUFA	7.6 ± 2.0	9.8 ± 3.6***	###	7.6 ± 2.1	6.6 ± 2.0**

Significant intra-group difference: $P < 0.05$ (*), $P < 0.01$ (**), $P < 0.001$ (***)

Significant inter-group difference: $P < 0.05$ (#), $P < 0.01$ (##), $P < 0.001$ (###)

Table 5 Change in anthropometric parameters in volunteers

	Control group		Experimental group	
	Day 90–Day 0	Day 240–Day 90	Day 90–Day 0	Day 240–Day 90
Weight (kg)	−3.5 ± 3.0*	+1.7 ± 2.6**	−2.9 ± 2.6*	+0.4 ± 3.0†
BMI (kg/m^2)	−1.3 ± 1.0*	+0.6 ± 0.9**	−1.0 ± 0.9*	+0.1 ± 1.1#
Hip circumference (cm)	−2.5 ± 3.4*	+0.9 ± 2.7*	−2.0 ± 2.6*	0 ± 2.8

Significant intra-group difference: $P < 0.05$ (*), $P < 0.01$ (**)

Significant inter-group difference: $P < 0.06$ (†), $P < 0.05$ (#)

Table 6 Plasma lipid parameters (mmol/l) in volunteers

	Control group		Experimental group	
	Day 0	Day 90	Day 0	Day 90
Triglycerides	1.44 ± 0.59	1.48 ± 0.92	1.46 ± 0.76	1.62 ± 0.86*
Total cholesterol	5.47 ± 0.99	5.58 ± 0.94†	5.67 ± 1.09	5.76 ± 0.99
HDL cholesterol	1.36 ± 0.33	1.31 ± 0.30†	1.41 ± 0.32	1.32 ± 0.28**
LDL cholesterol	3.47 ± 0.82	3.63 ± 0.82**	3.57 ± 0.85	3.72 ± 0.88*

Significant intra-group difference: $P < 0.06$ (†), $P < 0.05$ (*), $P < 0.01$ (**)

No significant inter-group difference

in the control group, whereas they were maintained in the experimental group. Maintaining the EPA and DHA levels in the RBC in the experimental group, without consuming fish and other seafood during the trial, constitutes the major result of this study. This demonstrate the efficiency of the terrestrial animal vector for providing EPA and DHA to humans, when the animals receive small amounts of the precursor ALA alone (linseed-fed animals). This can be mainly explained by the direct intake of EPA + DHA contained in the animal products of the experimental diet (Table 3), since these derivatives are synthesized from ALA by the linseed-fed animals during their growth. In addition, it is likely that low conversion of ALA to EPA + DHA also took place in the volunteers during the trial, but conversion in humans is known to be very low to EPA, and extremely low (less than 0.5% ALA) to DHA [24](for a review on ALA conversion and supplementation). Moreover, for these reasons, ALA provided by flour and bread in the experimental diet, could account only modestly for EPA synthesis and not for DHA synthesis, in volunteers.

Before the trial, the volunteers consumed a varied diet including fish and other seafood, and were recruited in a marine area (large fishing harbor) where a high consumption of n-3 fatty acids from fish and other seafood was described in a previous study [25]. Although fish and other seafood remain the main source of n-3 derivatives (EPA + DHA) for the population, the supplies of fish are limited whereas people have been encouraged to increase their intake [26]. We show here that improving the feeds of terrestrial animals by incorporating linseed is quantitatively capable of maintaining the EPA and DHA levels in the RBC of a population. In an earlier study, only EPA was increased by a similar experimental diet [18], but this previous study was performed with healthy volunteers exhibiting a high level of DHA in the RBC (4.8%), whereas the present study was performed with obese subjects having only 2.6% DHA in the RBC. This low level of DHA observed here also suggests a low DHA consumption by obese volunteers or a reduced conversion of α-linolenic precursor or even a higher catabolism (β-oxidation) of this fatty acid, and raises the question of larger requirement of n-3 to maintain tissues in obese. Finally, we showed here a decrease in EPA and DHA derivatives in the control group, suggesting (at least in the absence of fish consumption) that the average ALA intake in France is not sufficient to maintain correct EPA + DHA levels by ALA conversion alone, especially with a high dietary LNA/ALA ratio .

As regards n-6 fatty acids, we observed an increase in LNA content in the RBC of the control group, which reflects the control diet, characterized by standard animal products and sunflower-margarine. This increase inside the control group explains the significant difference observed for LNA between the two groups, since no significant change in LNA content was observed inside the experimental group. Although the dietary LNA content was three times lower in the experimental group than in the control group, it was sufficient to maintain the LNA and arachidonic acid levels in the RBC.

One of the goals of this work was: to evaluate the effect of the experimental diet, rich in n-3 fatty acids, on various anthropometric parameters of obesity. The results showed clearly that the volunteers from both groups lost weight and that no significant difference of weight was observed between the two groups over the period of the diets. This is probably due to the fact that both diets were normo-caloric; in other words probably hypo-caloric (for obese individuals) when compared with the diet consumed before the trial. This suggests that the reduction in caloric intake may have masked any qualitative effects relating to the diet's fatty acid composition. However, the results obtained at day 240 (in only 72% of the day 90 population) showed a weight gain in the control group, whereas no weight gain was determined in the experimental group. This interesting result suggests that the experimental diet, provided between day 0 and day 90, was able to limit the weight gain recovery. The changes in BMI and hip circumference confirmed the effect on weight, between day 90 and day 240, within the groups. Between groups, the BMI was significantly lower at day 240 in the experimental group and weight tended to be lower in the experimental group than in the control group. Our results suggest that n-3 fatty acids may have several metabolic effects. More precisely, we can suppose that the enrichment of the tissues in n-3 fatty acids improves various metabolic syndrome parameters, which is consistent with the literature [10, 11, 27–29], and reduces the weight gain recovery phenomenon. One can also suggest a different energy expenditure, implying membrane processes, which are known to be modulated by membrane fatty acid composition [30, 31]. A very recent study showed that plasma n-3 PUFA were negatively associated with obesity [32]. Finally, we can also suppose that the high n-6 fatty acid levels in the control diet could also explain the difference between groups, since LNA is considered to be very adipogenic [1, 4, 5]. Moreover, the weight gain observed in the control group is in good agreement with the work by Dayton et al. [3] showing an even stronger effect but with longer exposure to the same type of diet rich in LNA. In any case, the n-6/n-3 balance seems to be involved, whereas the proportion of saturated fatty acids does not appear to be a determinant of weight gain, since the experimental diet was the richest in saturated fatty acids. Lastly, observing the inhibiting effect on weight gain recovery in the long term after the end of the trial is a new and very interesting observation, since this long-term period is frequently subject to dramatic weight recovery as is often described in the literature in humans [33]. However, the effects reported here on anthropometric parameters at D240 can be considered only as preliminary results for further investigations.

Finally, we studied the plasma lipid parameters in the volunteers. Surprisingly, the plasma lipid parameters tended to worsen within each group although volunteers lost weight. In the literature, weight loss generally improves plasma lipid parameters [34–37] but this occurs after caloric restriction, which is not the case in the present study. However, our results suggest at least that content and duration of both diets are unable to stop the lipid parameter evolution in obese persons. Interestingly, between groups, we observed no significant difference in total cholesterol, HDL cholesterol, LDL cholesterol or triglycerides during the trial (D0–D90). In other words, the experimental diet was much richer in saturated fatty acids, but did not alter the plasma lipid parameters during the 90 days as compared with the control group. This suggests that the level where saturated fatty acids are deleterious remains to be determined and probably should be re-evaluated [38], depending on the diet composition in n-3 and n-6 PUFA. If we consider the PUFA/SFA ratio, the experimental diet exhibited the lower value, without any deleterious effects on the plasma lipid parameters (as compared with the control diet), which is in good agreement with a previous work with different values of the PUFA/SFA ratio in humans [39]. This suggests that the PUFA/SFA ratio is less relevant than the balanced composition of the experimental diet in both n-6 and n-3 fatty acids, as compared with the excess of n-6 fatty acid in the control diet. Finally, the results in terms of plasma lipid parameters also suggest that a diet containing 76% animal lipids (experimental diet) does not appear to be more deleterious than a diet containing 49% animal lipids only (control diet).

References

1. Massiera F, Saint-Marc P, Seydoux J, Murata T, Kobayashi T, Narumiya S, Guesnet P, Amri EZ, Negrel R, Ailhaud G (2003) Arachidonic acid and prostacyclin signaling promote adipose tissue development: a human health concern? J Lipid Res 44:271–279
2. Ailhaud G, Guesnet P (2004) Fatty acid composition of fats is an early determinant of childhood obesity: a short review and an opinion. Obes Rev 5:21–26
3. Dayton S, Hashimoto S, Dixon W, Pearce ML (1966) Composition of lipids in human serum and adipose tissue during prolonged feeding of a diet high in unsaturated fat. J Lipid Res 7:103–111
4. Ailhaud G, Massiera F, Weill P, Legrand P, Alessandri JM, Guesnet P (2006) Temporal changes in dietary fats: role of n-6 polyunsaturated fatty acids in excessive adipose tissue development and relationship to obesity. Prog Lipid Res 45:203–236
5. Ailhaud G, Guesnet P, Cunnane SC (2008) An emerging risk factor for obesity: does disequilibrium of polyunsaturated fatty acid metabolism contribute to excessive adipose tissue development? Br J Nutr 100:461–470
6. Feskens EJ, Bowles CH, Kromhout D (1991) Inverse association between fish intake and risk of glucose intolerance in normoglycemic elderly men and women. Diabetes Care 14:935–941

7. Feskens EJ, Virtanen SM, Rasanen L, Tuomilehto J, Stengard J, Pekkanen J, Nissinen A, Kromhout D (1995) Dietary factors determining diabetes and impaired glucose tolerance. A 20-year follow-up of the Finnish and Dutch cohorts of the seven countries study. Diabetes Care 18:1104–1112
8. Nkondjock A, Receveur O (2003) Fish-seafood consumption, obesity, and risk of type 2 diabetes: an ecological study. Diabetes Metab 29:635–642
9. Garaulet M, Perez-Llamas F, Perez-Ayala M, Martinez P, de Medina FS, Tebar FJ, Zamora S (2001) Site-specific differences in the fatty acid composition of abdominal adipose tissue in an obese population from a Mediterranean area: relation with dietary fatty acids, plasma lipid profile, serum insulin, and central obesity. Am J Clin Nutr 74:585–591
10. Wang H, Storlien LH, Huang XF (2002) Effects of dietary fat types on body fatness, leptin, and ARC leptin receptor, NPY, and AgRP mRNA expression. Am J Physiol Endocrinol Metab 282:E1352–E1359
11. Baillie RA, Takada R, Nakamura M, Clarke SD (1999) Coordinate induction of peroxisomal acyl-CoA oxidase and UCP-3 by dietary fish oil: a mechanism for decreased body fat deposition. Prostaglandins Leukot Essent Fatty Acids 60:351–356
12. Simopoulos A (2001) n-3 Fatty acids and human health: defining strategies for public policy. Lipids 36:S83–S89
13. Astorg P, Arnault N, Czernichow S, Noisette N, Galan P, Hercberg S (2004) Dietary intakes and food sources of n-6 and n-3 PUFA in French adult men and women. Lipids 39:527–535
14. Guesnet P, Antoine JM, Rochette de Lempdes JB, Galent A, Durand G (1993) Polyunsaturated fatty acid composition of human milk in France: changes during the course of lactation and regional differences. Eur J Clin Nutr 47:700–710
15. Guesnet P, Couet C, Alessandri JM, Antoine JM, Durand G (1995) Variabilité de la teneur en acide linoléique (18:2n-6) et du rapport 18:2n-6/18:3n-3 des lipides dans le lait de femme en France. Ann Pédiatr 42:289–294
16. Dubnov G, Berry EM (2004) Omega-6 fatty acids and coronary artery disease: the pros and cons. Curr Atheroscler Rep 6:441–446
17. Combe N, Boué N (2001) Apports alimentaires en acides linoléique et alpha-linolénique d'une population d'Aquitaine. Oléagineux Corps gras Lipides 8:118–121
18. Weill P, Schmitt B, Chesneau G, Daniel N, Safraou F, Legrand P (2002) Effects of introducing linseed in livestock diet on blood fatty acid composition of consumers of animal products. Ann Nutr Metab 46:182–191
19. Friedwald WT, Levy RI, Fredrickson DS (1972) Estimation of the concentration of low-density lipoprotein cholesterol in plasma without use of the preparative ultracentrifuge. Clin Chem 18:499–502
20. Rioux V, Lemarchal P, Legrand P (2000) Myristic acid, unlike palmitic acid, is rapidly metabolized in cultured rat hepatocytes. J Nutr Biochem 11:198–207
21. Sands SA, Reid KJ, Windsor SL, Harris WS (2005) The impact of age, body mass index and fish intake on the EPA and DHA content of human erythrocytes. Lipids 40:343–347
22. Cao J, Schwichtenberg KA, Hanson NQ, Tsai MY (2006) Incorporation and clearance of omega-3 fatty acids in erythrocytes, membranes and plasma phospholipids. Clin Chem 52:2265–2272
23. Legrand P, Bourre JM, Descomps B, Durand G, Renaud S (2001) Lipides. In: Martin A, AFSSA-CNERNA-CNRS (eds) Apports nutritionnels conseillés pour la population française. Tec et Doc Lavoisier, Paris, pp 63–82
24. Brenna JT, Salem N, Sinclair A, Cunnane S (2009) Alpha-linolenic acid supplementation and conversion to n-3 long-chain polyunsaturated fatty acids in humans. Prostaglandins Leukot Essent Fatty Acids 80:85–91
25. Leblanc JC, Sirot V, Volatier JL, Bemrah-Aouachria N (2006) Etude des Consommations Alimentaires de Produits de la mer et Impregnation aux éléments traces, Polluants et Omega-3 (CALIPSO). AFSSA-INRA (ed), pp 1–160
26. Jenkins D, Sievenpiper J, Pauly D, Sumaila U, Kendall C, Mowat F (2009) Are dietary recommendations for the use of fish oils sustainable? CMAJ 180:633–637
27. Delarue J, Couet C, Cohen R, Brechot JF, Antoine JM, Lamisse F (1996) Effects of fish oil on metabolic responses to oral fructose and glucose loads in healthy humans. Am J Physiol 270:E353–E362
28. Couet C, Delarue J, Ritz P, Antoine JM, Lamisse F (1997) Effect of dietary fish oil on body fat mass and basal fat oxidation in healthy adults. Int J Obes Relat Metab Disord 1:7–43
29. Moussavi N, Gavino V, Receveur O (2008) Could the quality of dietary fat, and not just its quantity, be related to risk of obesity? Obesity (Silver Spring) 16:7–15
30. Storlien LH, Hulbert AJ, Else PL (1998) Polyunsaturated fatty acids, membrane function and metabolic diseases such as diabetes and obesity. Curr Opin Clin Nutr Metab Care 1:559–563
31. Hulbert AJ (2007) Membrane fatty acids as pacemakers of animal metabolism. Lipids 42:811–819
32. Micallef M, Munro I, Phang M and Garg M (2009): Plasma n-3 polyunsaturated fatty acids are negatively associated with obesity. Br J Nutr (in press). doi:10.1017/S0007114509382173
33. Turk MW, Yang K, Hravnak M, Sereika SM, Ewing LJ, Burke LE (2009) Randomized clinical trials of weight loss maintenance: a review. J Cardiovasc Nurs 24:58–80
34. Watts GF, Chan DC, Ooi EM, Nestel PJ, Bellin LJ, Barrett PH (2006) Fish oils, phytosterols and weight loss in the regulation of lipoprotein transport in the metabolic syndrome: lessons from stable isotope tracer studies. Clin Exp Pharmacol Physiol 33:877–882
35. Ng TW, Watts GF, Barrett PH, Rye KA, Chan DC (2007) Effect of weight loss on LDL and HDL kinetics in the metabolic syndrom: associations with changes in plasma retinol-binding protein-4 and adiponectin levels. Diabetes Care 30:2945–2950
36. Chan DC, Watts GF, Ng TW, Yamashita S, Barrett PH (2008) Effect of weight loss on markers of triglyceride-rich lipoprotein metabolism in the metabolic syndrome. Eur J Clin Invest 38:743–751
37. Ueki K, Sakurai N, Tochikubo O (2009) Weight loss and blood pressure reduction in obese subjects in response to nutritional guidance using information communication technology. Clin Exp Hypertens 31:231–240
38. Knopp RH, Retzlaff BM (2004) Saturated fat prevents coronary artery disease? An American paradox. Am J Clin Nutr 80:1102–1103
39. Chan JK, Bruce VM, McDonald BE (1991) Dietary alpha-linolenic acid is as effective as oleic acid and linoleic acid in lowering blood cholesterol in normolipidemic men. Am J Clin Nutr 53:1230–1234

Lipids (2010) 45:21–27
DOI 10.1007/s11745-009-3372-9

ORIGINAL ARTICLE

Dietary Source of Stearidonic Acid Promotes Higher Muscle DHA Concentrations than Linolenic Acid in Hybrid Striped Bass

Anant S. Bharadwaj · Steven D. Hart · Billie J. Brown · Yong Li · Bruce A. Watkins · Paul B. Brown

Received: 29 June 2009 / Accepted: 30 October 2009 / Published online: 22 November 2009

Abstract Rapid expansion of aquacultural production is placing increasing demand on fish oil supplies and intensified the search for alternative lipid sources. Many of the potential alternative sources contain low concentrations of long chain n-3 fatty acids and the conversion of dietary linolenic acid to longer chain highly unsaturated fatty acids is a relatively inefficient process in some species. A 6-week study was conducted to compare tissue fatty acid (FA) concentrations in hybrid striped bass fed either 18:3n-3 (α-linolenic acid; ALA) or 18:4n-3 (stearidonic acid; SDA). Hybrid striped bass were fed either a control diet containing fish oil, or diets containing ALA or SDA at three different levels (0.5, 1 and 2% of the diet). There were no significant differences in whole animal responses between fish fed ALA or SDA. Liver and muscle concentrations of ALA and SDA were responsive to dosages fed. However, only 22:6n-3 concentrations in muscle were significantly affected by dietary source of 18 carbon precursors. Muscle 22:6n-3 concentrations were significantly higher in fish fed SDA compared to fish fed ALA. Based on these data, it appears that feeding SDA can increase long chain n-3 fatty acid concentrations in fish muscle.

Keywords Hybrid striped bass · Fish · Muscle · Stearidonic acid · Linolenic acid

A. S. Bharadwaj · S. D. Hart · B. J. Brown · P. B. Brown (✉)
Department of Forestry and Natural Resources,
Purdue University, 715 West State Street,
West Lafayette, IN 47907-2061, USA
e-mail: pb@purdue.edu

Y. Li · B. A. Watkins
Lipid Chemistry and Molecular Biology Laboratory,
Department of Basic Medical Science, Purdue University,
West Lafayette, IN 47907, USA

Present Address:
A. S. Bharadwaj
Novus International, 20 Research Park Drive,
St. Charles, MO 63304, USA

Present Address:
S. D. Hart
Indiana Soybean Alliance, 5730 West 74th Street,
Indianapolis, IN 46278, USA

Abbreviations

ALA	Linolenic acid
ANOVA	Analysis of variance
AA	Arachidonic acid
DHA	Docosahexaenoic acid
DPA	Docosapentaenoic acid
EPA	Eicosapentaenoic acid
EFA	Essential fatty acid
FAME	Fatty acid methyl esters
FA	Fatty acid
FID	Flame ionization detector
GC	Gas chromatograph
HUFA	Highly unsaturated fatty acid
IPF	Intraperitoneal fat
LC-n-3 HUFA	Long chain n-3 highly unsaturated fatty acids
MONO	Total monounsaturated fatty acids
PSEM	Pooled standard error of the mean
RLW	Relative liver weight
SAT	Total saturated fatty acid
SDA	Stearidonic acid

Introduction

A significant proportion of the global fish oil supply is used as a dietary lipid and fatty acid (FA) source for propagation

of aquatic animals [1]. The rapid increase in aquacultural production and the associated demand for fish oil may create a shortage of this commodity in the near future. The supply of lipid sources from oilseed crops is larger than the supply of fish oil and regarded as a logical choice for replacing fish oil, either partially or completely, in dietary formulations [2]. Plant-derived lipid sources have been fed to fish without significantly compromising growth or health, but their use has generally resulted in lower muscle concentrations of n-3 fatty acids, thereby reducing the potential health benefits to humans from the consumption of fish [2, 3]. Terrestrial plant-based lipids contain relatively high concentrations of linoleic acid (18:2n-6), oleic acid (18:1n-9) and to a lesser extent, linolenic acid (ALA; 18:3n-3), and do not contain long chain highly unsaturated fatty acids of the n-3 family (LC-n-3 HUFA; ≥20 C) [4].

Fish are unable to synthesize either linoleic or ALA acid and have a dietary requirement for n-3 and/or n-6 FA [5]. Turchini et al. [5] recently reviewed most of the published data on EFA requirements in fish and concluded that, in general, marine fish require a dietary supply of LC-n-3 HUFA such as 20:5n-3 (eicosapentaenoic acid; EPA) or 22:6n-3 (docosahexaenoic acid; DHA), whereas species with a freshwater life history stage require either ALA, ALA and 18:2n-6 or only 18:2n-6 to satisfy their essential fatty acid (EFA) requirements [5–7]. The n-3 family remains a focal point for research efforts because they can have significant impacts on human health. ALA is metabolized through a series of desaturation and elongation reactions to form long chain n-3 HUFA. In the first step, ALA is converted to 18:4n-3 (stearidonic acid; SDA) by the action of Δ6 desaturase, which is considered an inefficient and rate limiting process in vertebrates [8–10]. Providing a dietary source of SDA might be a viable method of increasing n-3 FA concentrations in fish [11].

Metabolism of n-3 FA varies among fish species. Marine fish such as gilthead seabream *Sparus aurata*, turbot *Scophthalmus maximus*, golden gray mullet *Liza aurata* and European sea bass *Dicentrarchus labrax* have limited ability to convert 18 C FA to LC-n-3 HUFA [12–17]. Freshwater fish, or those with a freshwater life history stage, such as tilapia *Oreochromis niloticus*, zebrafish *Danio rerio*, brown trout *Salmo trutta*, rainbow trout *Oncorhynchus mykiss*, and Atlantic salmon *Salmo salar* are able to elongate and desaturate ALA to EPA and DHA [12, 13, 18–21].

Stearidonic acid has been evaluated in both mammals and fish. In humans, ingestion of SDA increased plasma and erythrocyte EPA and 22:5n-3 (docosapentaenoic acid; DPA) [22]. In rats fed SDA, an increase in liver and plasma EPA was observed [9], whereas in mice an increase in plasma and splenocyte 20:4n-3 (eicosatetraenoic acid; ETA), EPA, and DHA concentrations were reported [23]. Similarly, increases in red blood cell and heart EPA concentrations were observed in beagles fed SDA [24]. In turbot and Atlantic salmon cell lines, SDA was metabolized to EPA and DPA, with only low concentrations of DHA being formed [25, 26]. Echium oil, a rich source of SDA, has been fed to Atlantic cod *Gadus morhua*, Arctic charr *Salvelinus alpines*, and Atlantic salmon, but the comparisons were with fish oil [27–29]. There does not appear to be a formal comparison of ALA to SDA as a source of n-3 FA in fish.

The hybrid striped bass is a cross between the anadromous striped bass and strictly freshwater white bass with a reported requirement for LC-n-3 HUFA [30]. However, there is little information on n-3 FA metabolism in this hybrid. Lane et al. [31] and Trushenski et al. [32, 33] reported effects of feeding various lipid sources on fillet composition over time and effects on various lipid classes, but there have been no reports of feeding selected n-3 precursors and resulting downsteam effects on LC-n-3 HUFA. We hypothesized that the hybrid striped bass would efficiently use SDA as a source of n-3 FA as both parental species have a freshwater life history stage and this hybrid might be a good model for formal comparison of ALA to SDA. Specific objectives were to: (1) determine if dietary SDA would promote higher concentrations of LC-n-3 HUFA than dietary ALA; and, (2) determine if high dietary concentrations of SDA and ALA would promote increased tissue retention of n-3 HUFA.

Experimental Procedures

Fish Husbandry

Juvenile hybrid striped bass (*Morone saxatilis* × *M. chrysops*) were obtained from Keo Fish Farms (Keo, AR, USA), and transported to the Purdue University Aquaculture Facility. Procedures used during transport, quarantine, and the experimental period were approved by the Purdue Animal Care and Use Committee. Fish were acclimated to laboratory conditions for 10 weeks before being used in the study and fed a commercial diet during that period (Nelson and Sons, Murray, UT, USA).

A semi-closed, recirculating system comprising 32 individual, 190-L aquaria were used in this study. Each aquarium was constantly aerated via an airstone connected to a regenerative blower. The experimental system was equipped with four submerged filtration tanks for solid material removal and a submerged biological filtration tank for oxidation of nitrogenous waste products. Water was pumped through a sand filter to each aquarium at a rate of ~4 L/min. Water temperature was maintained at 26 ± 1 °C during the study.

Groups of 10 fish were randomly stocked into individual aquaria and acclimated to the experimental system for 2 weeks prior to the experiment. Fish were fed a commercial diet (Nelson and Sons, Murray, UT, USA) for the first week and their respective experimental diets for 1 week thereafter. Triplicate groups of fish were randomly assigned a dietary treatment. Fish were fed to satiation twice daily during both the acclimation and experimental portions of the study. Before the start of the study, the number of fish per tank was reduced to five. The average initial weight in each tank was 208 g/fish. Water quality was monitored daily throughout the study and maintained within acceptable limits. Ammonia- and nitrite-N concentrations did not exceed 0.5 and 0.05 mg/L, respectively. Dissolved oxygen concentrations did not fall below 7 mg/L. The study was conducted for 6 weeks.

Diets

The basal diet was formulated to contain 40 g/100 g crude protein and 10 g/100 g lipid. All diets contained 400 g/kg solvent extracted, dehulled soybean meal, 150 g/kg corn gluten meal, 150 g/kg fish meal, 100 g/kg ground, whole wheat, 20 g/kg mineral premix, 30 g/kg vitamin premix, 1 g/kg ascorbyl-polyphosphate, 1 g/kg choline-Cl, 10 g/kg soybean lecithin, and 38 g/kg α-cellulose. Seven different experimental diets were formulated by varying the dietary lipid source (Table 1). The control diet contained 10 g/100 g menhaden oil and the remaining diets contained either flaxseed oil as a source of ALA (55% wt:wt) or a purified source of SDA (60% ethyl ester, wt:wt) at 0.5, 1 and 2 g/100 g of the diet. High-oleic acid safflower oil was used to balance the lipid content of the ALA and SDA containing diets.

Stearidonic acid, flaxseed oil, and high-oleic safflower oil were obtained from commercial producers (K. D. Pharma Bexbach GmbH, Bexbach, Germany; U.S. Soy, Mattoon, IL, USA; and, Oilseeds International, San Francisco, CA, USA, respectively). Soybean meal, and fish meal were obtained from the Purdue University Animal Sciences Research and Education Facility Feed Mill (Montmorenci, IN, USA). Corn gluten meal, menhaden oil, and flax oil were obtained from commercial suppliers (A. E. Staley Mfg. Co., Lafayette, IN, USA; Omega Protein, Reedville, VA, USA; and, U.S. Soy, Mattoon, IL, USA, respectively). L-ascorbyl polyphosphate (a source of vitamin C, 35% active ingredient) was obtained from Roche Inc. (Nutley, NJ, USA). Vitamin (U.S. Fish and Wildlife Service #30) and mineral (U.S. Fish and Wildlife Service #3) premixes were obtained from feed manufacturers (Zeigler Bros., Inc., Gardners, PA, USA, and Nelson and Sons, Inc., Murray, UT, USA, respectively). All diets used in this study were manufactured at the Purdue University Aquaculture Facility [34]. Dry ingredients were mixed in a V-mixer (Patterson-Kelley, East Stroudsburg, PA, USA), then transferred to a Hobart mixer (Hobart Corporation, Troy, OH, USA) and mixed with water and lipid. Choline chloride was dissolved in water and mixed into each of the diets [35]. Diets were adjusted to pH 7 ± 0.2 with saturated sodium hydroxide. Diets were pelleted with a 3.1-mm die attached to the Hobart mixer. The resulting strands were chopped into pellets of uniform length and air dried for 72 h. The dried diets were sealed in airtight bags, flushed with nitrogen gas and stored at −20 °C.

Sample Collection

At the end of 6 weeks, fish were euthanized with tricaine methanosulfonate (Argent Chemicals, Redmond, WA, USA) and weighed. The final weights of fish were used along with initial weights to calculate weight gain over the duration of the study. Three fish from each replicate were weighed and livers and intraperitoneal fat (IPF) dissected and weighed. Muscle samples were collected from the region below the dorsal fin, ~1 cm anterior to the center of the fish.

Livers and IPF weights were used to calculate relative liver weights (RLW) and IPF ratio, respectively. Muscle and liver samples were stored in polyethylene bags containing water. All sample bags were flushed with nitrogen gas, sealed and stored at −20 °C. All fatty acid analyses were completed within 4 weeks of sample collection.

Lipid Extraction and Fatty Acid Analysis

Diet, liver, and muscle samples were homogenized in a 2:1 chloroform–methanol solution and lipids extracted [36]. Total lipids were then saponified and fatty acid methyl esters (FAME) synthesized by esterification with boron trifluoride (BF_3) in methanol (14% w/v; Supelco, Bellfonte,

Table 1 Lipid composition of experimental diets (g/kg) fed to hybrid striped bass

Ingredient	Control	ALA0.5	ALA1	ALA2	SDA0.5	SDA1	SDA2
Menhaden oil	100						
High oleic safflower oil		90.9	81.8	63.6	91.6	83.2	66.4
Flaxseed oil (55% ALA)		9.1	18.2	36.4			
Stearidonic acid (60% SDA)					8.4	16.8	33.6

PA, USA). These FAME were analyzed using a GC (Agilent 6890 Series GC System, 7683 Series Injector; Agilent Technologies, Palo Alto, CA, USA), equipped with a DB-23 column (30 m, 0.53 mm i.d., 0.5 μm film thickness; J&W Scientific, Folsom, CA, USA). The GC was operated at 140 °C for 2 min and temperature was increased 1.5 °C/min to 198 °C and held for 7 min. Helium was used as carrier gas. The injector and FID temperatures were 225 and 250 °C, respectively. The FAME were identified by comparison of retention times with those of pure standards (GLC-422, GLC-87, GLC-68A, GLC 76; Nu-Chek-Prep, Elysian, MN, USA) and FAME prepared from menhaden oil. The fatty acid composition of total lipids in diets was determined as described above. The fatty acid composition of diet, liver and muscle samples was identified in terms of area % and reported as g/100 g of fatty acids in lipids.

Statistical Analysis

All data were analyzed as both an unbalanced (with control diet) and balanced (without control diet) 2 × 3 factorial design using each aquarium as the experimental unit and dietary treatment as the independent variable. All tabular presentations were of the balanced statistical analysis with designated symbols indicating differences between fish fed the control diet and those fed the experimental diets. All percentage data were arc sine transformed prior to analysis [37]. All data were subjected to two-way ANOVA using Statistical Analysis System release 8.0 Software (SAS Institute, Cary, NC, USA). Main effects were dietary fatty acid type and dietary fatty acid level. If significant differences were detected, Student–Newman–Keuls test was used to separate means. Differences were considered significant at $p < 0.05$.

Results

Relatively low concentrations of ALA and SDA (1.6 and 1.7 g/100 g total lipids, respectively) were found in the control diet (Table 2). The ALA and SDA diets both contained lower concentrations of saturated fatty acids than the control diet, but contained higher concentrations of monounsaturated fatty acids. The ALA diets (ALA0.5, ALA1 and ALA2) contained 5.2, 10.2, and 20.1 g/100 g ALA, respectively. The SDA diets (SDA0.5, SDA1, and SDA2) contained 5.0, 10.0 and 19.9 g/100 g SDA, respectively.

There were no mortalities during the study. Weight gain, feed intake and feed conversion ratio were not significantly affected by dietary treatment, FA level or the interaction of the two main effects (Table 3). Relative liver weights and IPF ratios were also not significantly affected by dietary treatment, FA level or interaction.

Table 2 Fatty acid composition (g/100 g) of experimental diets fed to hybrid striped bass

Fatty acid	Control	ALA0.5	ALA1	ALA2	SDA0.5	SDA1	SDA2
14:0	8.6	0.7	0.7	0.6	0.7	0.7	0.7
15:0	0.7	0.1	0.1	0.1	0.1	0.1	0.1
16:0	21.6	8.0	7.9	7.9	7.7	7.2	6.8
16:1n-7	10.5	0.9	0.8	0.8	0.9	0.9	0.9
18:0	4.6	2.7	2.9	2.1	2.6	2.4	2.4
18:1n-9	11.1	56.9	52.2	46.0	58.7	53.4	44.2
18:2n-6	10.7	19.8	19.6	18.3	19.0	18.8	17.6
18:3n-3	1.6	5.2	10.2	20.1	0.4	0.4	0.5
18:4n-3	1.7	ND[2]	ND	ND	5.0	10.1	19.9
20:0	0.4	0.4	0.4	0.3	0.1	0.1	0.1
20:1n-9	1.1	0.4	0.4	0.3	0.4	0.3	0.3
20:4n-6	0.5	0.2	0.2	0.2	0.2	0.2	0.2
20:5n-3	6.5	1.2	1.2	1.1	1.2	1.2	1.3
22:1n-9	0.7	0.2	0.2	0.2	0.2	0.1	0.1
22:5n-3	1.2	0.2	0.1	0.2	0.2	0.2	0.2
22:6n-3	6.9	1.0	0.9	0.9	0.9	0.9	1.0
SAT	35.9	11.9	11.8	11.1	11.1	10.5	10.1
MONO	23.4	58.1	53.0	46.9	59.5	54.6	45.1

Values are means of duplicate analyses

Total saturated fatty acids

Total monounsaturated fatty acids

ND not detected

Dietary sources of ALA and SDA significantly affected liver concentrations of ALA and SDA (Table 4) Liver ALA concentrations were significantly higher in fish fed the ALA series of diets and liver SDA concentrations were significantly higher in fish fed the SDA series of diets. Further, increasing dietary concentrations resulted in increasing concentrations in liver samples. Concentrations (and range of mean values) of 14:0 (1.3–1.4), 15:0 (0.1–0.2), 16:1n-7 (2.4–2.6), 17:0 (0.3), 18:0 (3.0–3.4), 18:1n-9 (44.5–47.6), 18:2n-6 (13.8–14.2), 20:1n-9 (1.6–2.0), 20:4n-6 (0.5–0.6), 20:5n-3 (1.8–2.2), 22:5n-6 (0.2), 22:5n-3 (0.6–0.7), 22:6n-3 (4.1–5.3), total monounsaturates (50.7–53.9), total n-6 HUFA (1.4–1.5), the n-6/n-3 HUFA ratio (0.2) and ARA/DHA ratio (0.1) in liver were not significantly affected by dietary lipid source, level or the interaction of the two variables (data not shown). Concentrations (and mean value) of 14:0 (4.2), 16:0 (15.0), 16:1n-7 (7.5), 20:4n-6 (1.3), 20:4n-3 (1.1), 20:5n-3 (7.6), 22:5n-6 (0.5), 22:5n-3 (2.3), 22:6n-3 (23.2), total, n-6 HUFA (2.9), and total n-3 HUFA (0.1) in liver of fish fed the control diet were significantly higher than in fish fed other dietary treatments.

Table 3 Mean initial weight (W_i, g/fish), weight gain (W_g g/fish/6 weeks), feed intake (FI, g/fish/6 weeks), feed conversion ratio (FCR), relative liver weight (RLW), and intraperitoneal fat index (IPF) of juvenile hybrid striped bass fed varying concentrations of linoleic acid (ALA) or stearidonic acid (SDA)

	W_i	W_g	FI	FCR	RLW	IPF
Control	208.4 ± 0.8	46.8 ± 6.1	123.9 ± 2.0	2.7 ± 0.3	1.0 ± 0.2	3.1 ± 0.8
0.5 ALA	208.4 ± 1.2	52.6 ± 13.2	124.9 ± 11.9	2.4 ± 0.4	1.1 ± 0.1	3.4 ± 0.7
1 ALA	209.4 ± 0.4	54.0 ± 20.9	124.3 ± 10.1	2.5 ± 0.8	1.1 ± 0.1	4.4 ± 0.9
2 ALA	208.3 ± 1.0	60.5 ± 6.3	120.6 ± 9.2	2.0 ± 0.4	1.0 ± 0.1	4.0 ± 0.8
0.5 SDA	207.9 ± 1.5	64.5 ± 3.2	136.7 ± 6.1	2.1 ± 0.4	1.0 ± 0.2	4.5 ± 0.8
1 SDA	207.6 ± 1.5	53.5 ± 9.2	120.6 ± 6.8	2.3 ± 0.2	1.2 ± 0.2	3.4 ± 0.7
2 SDA	208.5 ± 1.9	58.3 ± 2.8	124.6 ± 3.8	2.2 ± 0.3	1.1 ± 0.2	3.4 ± 0.9
ANOVA p values						
Source	0.9441	0.2749	0.4455	0.3276	0.6021	0.2921
Level	0.3333	0.4559	0.0546	0.4396	0.8393	0.3621
S × L	0.6000	0.4382	0.0903	0.6735	0.4325	0.2126

Values are means of 3 replicates

Probability ($p > F$) of treatment differences as determined by ANOVA

Table 4 Fatty acid composition of liver from hybrid striped bass fed a control diet and diets containing linolenic acid and stearidonic acid at different levels

Fatty acid	Diets							ANOVA p values		
	CTRL	0.5LNA	1LNA	2LNA	0.5SDA	1SDA	2SDA	FA Type	Level	T × L
18:3n-3	1.5 ± 0.1	2.0 ± 0.4c	4.1 ± 0.2b	6.1 ± 1.3a	1.0 ± 0.2c	1.0 ± 0.2c	1.4 ± 0.2c	<0.0001	<0.0001	0.0006
18:4n-3	1.0 ± 0.2	0.4 ± 0.2d	0.5 ± 0.1d	0.8 ± 0.1d	1.3 ± 0.1c	2.4 ± 0.4b	5.5 ± 0.4a	<0.0001	<0.0001	<0.0001
20:4n-3	1.1 ± 0.1	0.2 ± 0.1	0.2 ± 0.1	0.2 ± 0.1	0.2 ± 0.1	0.2 ± 0.1	0.3 ± 0.1	0.1276	0.8109	0.2569
20:5n-3	7.6 ± 0.2	2.1 ± 0.3	1.6 ± 0.4	1.8 ± 0.4	2.3 ± 0.5	2.1 ± 0.5	2.0 ± 0.4	0.4567	0.3153	0.8351
22:5n-3	2.3 ± 0.2	0.7 ± 0.2	0.5 ± 0.1	0.5 ± 0.1	0.7 ± 0.2	0.8 ± 0.4	0.6 ± 0.2	0.7083	0.8846	0.8128
22:6n-3	23.2 ± 1.4	5.3 ± 1.1	3.4 ± 0.9	4.3 ± 0.6	5.2 ± 1.4	4.8 ± 1.6	4.9 ± 0.1	0.3455	0.2097	0.2884

Muscle concentrations of ALA and SDA were significantly affected by the interaction of FA type and level (Table 5). There were no other significant interactions in muscle samples. Mean muscle concentrations of SDA and DHA were significantly higher in fish fed SDA compared to fish fed ALA. There were no other significant affects of FA type. Mean concentrations of ALA and SDA were significantly affected by FA levels in diets.

Mean concentrations (and range of mean values) of 14:0 (1.1–1.5), 15:0 (0.2), 16:0 (16.1–17.5), 16:1n-7 (2.2–3.0), 17:0 (0.2–0.3), 18:0 (4.8–5.5), 18:1n-9 (19.1–24.4), 18:1n-7 (1.5–1.6), 20:1n-9 (0.9–1.1), 20:3n-6 (0.7), 20:4n-6 (2.0–2.2), 20:4n-3 (0.3–0.4), 20:5n-3 (6.6–7.1), 22:5n-6 (0.5–0.6), 22:5n-3 (1.3–1.4), total unsaturates (22.9–23.7), total monounsaturates (27.3–29.9), total n-6 HUFA (3.4–3.6), and the ratios of ARA/EPA and ARA/DHA in muscle samples were not significantly affected by dietary FA source or level (data not shown).

Discussion

These data indicate that feeding hybrid striped bass a dietary source of SDA promotes higher muscle SDA and DHA concentrations than fish fed a dietary source of ALA. Further, concentrations in both liver and muscle were responsive to the dosage fed. However, increases in DHA or other LC-n-3 HUFA were not of the same magnitude as the increases in ALA and SDA. Thus, while the increased DHA concentrations in muscle of fish fed SDA appears consistent with the inefficient rate limiting step associated with the Δ-6 desaturase, there are other factors contributing to LC-n-3 HUFA concentrations in the muscle of hybrid striped bass. This appears to be the first evaluation of a concentrated source of SDA in diets fed to fish compared to a source of ALA; thus, there are no direct comparisons with other studies. However, there are comparisons to in vitro studies.

Table 5 Fatty acid composition of muscle total lipids from hybrid striped bass fed a control diet and diets containing linolenic acid and stearidonic acid at different levels

Fatty acid	Diets							ANOVA *p* values		
	CTRL	0.5 LNA	1 LNA	2 LNA	0.5 SDA	1 SDA	2 SDA	FA Type	Level	T × L
18:3n-3	0.7 ± 0.2	1.8 ± 0.2c	2.4 ± 0.2b	4.3 ± 0.1a	0.9 ± 0.1d	1.1 ± 0.4d	1.3 ± 0.1d	<0.0001	<0.0001	<0.0001
18:4n-3	0.5 ± 0.1	0.8 ± 0.5c	0.5 ± 0.2c	0.5 ± 0.1c	0.8 ± 0.1c	1.4 ± 0.1b	2.8 ± 0.3a	<0.0001	0.0002	<0.0001
20:4n-3	0.5 ± 0.1	0.3 ± 0.1	0.4 ± 0.2	0.3 ± 0.1	0.3 ± 0.1	0.3 ± 0.1	0.3 ± 0.1	0.6539	0.8921	0.7659
20:5n-3	10.7 ± 1.1	6.4 ± 0.8	7.1 ± 0.6	6.3 ± 1.0	7.0 ± 0.9	7.0 ± 0.9	6.9 ± 0.5	0.9641	0.8590	0.8932
22:5n-3	1.7 ± 0.1	1.3 ± 0.1	1.5 ± 0.2	1.2 ± 0.1	1.4 ± 0.1	1.3 ± 0.1	1.3 ± 0.1	0.7603	0.8239	0.8118
22:6n-3	25.7 ± 1.3	15.3 ± 3.0	15.1 ± 2.5	14.1 ± 1.8	17.9 ± 1.1	15.4 ± 2.5	18.1 ± 0.2	0.0111	0.8957	0.7230

Atlantic salmon cells treated with SDA contained higher concentrations of SDA, 20:4n-3 and EPA compared to cells that were supplemented with ALA [38]. In a separate study, SDA was metabolized to EPA in both Atlantic salmon and turbot cell lines, but more efficiently in salmon [25]. In both cell lines, only a small amount of DHA was detected, although there was significant production of DPA in both. In another study with Atlantic salmon cell cultures, SDA was converted to EPA and DPA, but not to DHA [26]. The developing picture in fish appears to support the inefficient Δ-6 desaturase step in FA metabolism, but also appears to indicate considerable variation in further metabolism of n-3 FA across species. The Atlantic salmon and hybrid striped bass have qualitatively different FA requirements [39], which may be influencing this comparison.

Mean muscle concentrations of ALA were 1.8, 2.4 and 4.3 g/100 g FA in fish fed the ALA series of diets, respectively and 0.9, 1.1 and 1.3 g/100 g FA in fish fed the SDA series, respectively. Mean SDA concentrations in muscle of fish fed the SDA series of diets were 0.8, 1.4 and 2.8 g/100 g, respectively and 0.8, 0.5 and 0.5 g/100 g FA in fish fed the ALA series of diets, respectively. Thus, differences appear related to dose. It is not known if higher dietary levels of ALA and SDA would promote higher muscle retention of n-3 HUFA and is an area for future study.

Neither dietary fatty acid type nor level significantly affected weight gain, feed intake, FCR, HSI, or IPF in the present study. Similar results have been reported in fish fed echium oil compared to fish and other lipid sources. In Arctic charr fed either fish oil or echium oil, no significant differences in growth, mortality, feed efficiency, or tissue lipids were observed [28]. Similarly, cod fed either fish oil or echium oil did not exhibit significant differences in growth, feed efficiency, RLW, or liver and muscle lipid concentrations [27]. Lipid classes in muscle or liver were not affected by dietary lipid type in cod. In Atlantic salmon parr fed fish oil, echium oil, canola oil or a 1:1 mixture of canola and echium oils, dietary lipid did not significantly affect growth, feed efficiency, feed consumption or RLW [29]. Lipid classes of red and white muscle were also not affected by dietary lipid. However, the FA composition of liver and muscle lipids in these species of fish, as with the hybrid striped bass in the present study, was affected by dietary lipid source. In all previous studies with fish fed echium oil, the comparison was with fish oil and virtually all fatty acids were significantly affected by lipid source, whereas the minority of fatty acids were significantly changed in this study.

Results from our study lead us to speculate that the initial Δ-6 desaturase reaction step may be rate limiting in the metabolism of 18 C FA in muscle of the hybrid striped bass as DHA concentrations are higher when a dietary source of SDA was provided compared to a source of ALA. However, other steps in the elongation and desaturation of SDA appear to be influencing LC-n-3 HUFA concentrations as the dose dependent increases from dietary SDA did not result in dose dependent increases in DHA or any other n-3 FA.

Acknowledgments This study was supported by Purdue Agriculture Research Programs.

References

1. New MB, Wijkstroem UN (2002) Use of fishmeal and fish oil in aquafeeds: further thoughts on the fishmeal trap. FAO circular no. 975. Food and Agriculture Organization of the United Nations Rome
2. Rosenlund G, Obach A, Sandberg MG, Standal H, Tveit K (2001) Effect of alternative lipid sources on long-term growth performance and quality of Atlantic salmon (*Salmo salar* L.). Aquacult Res 32:323–328
3. Torstentsen BE, Bell JG, Rosenlund G, Henderson RJ, Graff IE, Tocher DR, Lie Ø, Sargent JR (2005) Tailoring of Atlantic salmon (*Salmo salar* L.) flesh lipid composition and sensory quality by replacing fish oil with a vegetable oil blend. J Agric Food Chem 53:10166–10178
4. NRC (1998) Nutrient requirements of swine. National Academy Press, Washington
5. Turchini GM, Torstensen BE, Ng WK (2009) Fish oil replacement in finfish nutrition. Rev Aquacult 1:10–57

6. Sargent JR, Bell JG, Bell MV, Henderson RJ, Tocher DR (1995) Requirement criteria for essential fatty acids. J Appl Ichthyol 11: 183–198
7. Takeuchi T (1997) Essential fatty acid requirements of aquatic animals with emphasis on fish larvae and fingerlings. Rev Fish Sci 5:1–25
8. Sargent JR, Tocher DR, Bell JG (2002) The lipids. In: Halver JE, Hardy RW (eds) Fish nutrition. Academic Press, San Diego
9. Huang YS, Smith RS, Redden PR, Cantrill RC, Horrobin DF (1991) Modification of liver fatty acid metabolism in mice by n-3 and n-6 Δ6-desaturase substrates and products. Biochim Biophys Acta 1082:319–327
10. Yamazaki K, Fujikawa M, Hamazaki T, Yano S, Shono T (1992) Comparison of the conversion rates of α-linolenic acid (18:3(n-3)) and stearidonic acid (18:4(n-3)) to longer polyunsaturated fatty acids in rats. Biochim Biophys Acta 1123:18–26
11. Ursin VM (2003) Modification of plant lipids for human health: development of functional land-based omega-3 fatty acids. J Nutr 133:4271–4274
12. Owen JM, Adron JW, Middleton C, Cowey CB (1975) Elongation and desaturation of dietary fatty acids in turbot *Scophthalmus maximus* L., and rainbow trout, *Salmo gairdneri*. Lipids 10:528–531
13. Tocher DR, Carr J, Sargent JR (1989) Polyunsaturated fatty acid metabolism in fish cells: differential metabolism of (n-3) and (n-6) series acids by cultured cells originating from a freshwater teleost fish and from a marine teleost fish. Comp Biochem Physiol 94B:367–374
14. Mourente G, Tocher DR (1993) Incorporation and metabolism of ^{14}C-labelled polyunsaturated fatty acids in wild-caught juveniles of golden grey mullet, *Liza aurata*, in vivo. Fish Physiol Biochem 12:119–130
15. Mourente G, Tocher DR (1994) In vivo metabolism of [1–^{14}C] linolenic acid (18:3(n-3)) and [1–^{14}C] eicosapentaenoic acid (20:5(n-3)) in a marine fish: time-course of the desaturation/elongation pathway. Biochim Biophys Acta 1212:109–118
16. Tocher DR, Ghioni C (1999) Fatty acid metabolism in marine fish: low activity of fatty acyl Δ5 desaturation in gilthead sea bream (*Sparus aurata*) cells. Lipids 34:433–440
17. Mourente G, Dick JR, Bell JG, Tocher DR (2005) Effect of partial substitution of dietary fish oil by vegetable oils on desaturation and *β*-oxidation of [1–^{14}C]18:3n–3 (LNA) and [1–^{14}C] 20:5n–3 (EPA) in hepatocytes and enterocytes of European sea bass (*Dicentrarchus labrax* L.). Aquaculture 248:173–186
18. Henderson RJ (1996) Fatty acid metabolism in freshwater fish with particular reference to polyunsaturated fatty acids. Arch Anim Nutr 49:5–22
19. Tocher DR, Bell JG, MacGlaughlin P, McGhee F, Dick JR (2001) Hepatocyte fatty acid desaturation and polyunsaturated fatty acid composition of liver in salmonids: effects of dietary vegetable oil. Comp Biochem Physiol 130B:257–270
20. Tocher DR, Agaba M, Hastings N, Bell JG, Dick JR, Teale AJ (2002) Nutritional regulation of hepatocyte fatty acid desaturation and polyunsaturated fatty acid composition in zebrafish (*Danio rerio*) and tilapia (*Oreochromis niloticus*). Fish Physiol Biochem 24:309–320
21. Hagve TA, Christopherson BO, Dannevig BH (1986) Desaturation and chain elongation of essential fatty acids in isolated liver cells from rat and rainbow trout. Lipids 21:202–205
22. James MJ, Ursin VM, Cleland LG (2003) Metabolism of stearidonic acid in human subjects: comparison with the metabolism of other n-3 fatty acids. Am J Clin Nutr 77:1140–1145
23. Ishihara K, Komatsu W, Saito H, Shinohara K (2002) Comparison of the effects of dietary α-linolenic, stearidonic, and eicosapentaenoic acids on production of inflammatory mediators in mice. Lipids 37:481–486
24. Harris WS, DiRienzo MA, Sands SA, George C, Jones PG, Eapen AK (2007) Stearidonic acid increases the red blood cell and heart eicosapentaenoic acid content in dogs. Lipids 42:325–333
25. Ghioni C, Tocher DR, Bell MV, Dick JR, Sargent JR (1999) Low C18 to C20 fatty acid elongase activity and limited conversion of stearidonic acid, 18:4(n-3), to eicosapentaenoic acid, 20:5(n-3), in a cell line from the turbot, *Scophthalmus maximus*. Biochim Biophys Acta 1437:170–181
26. Ghioni C, Porter AEA, Taylor GW, Tocher DR (2002) Metabolism of 18:4n–3 (stearidonic acid) and 20:4n–3 in salmonid cells in culture and inhibition of the production of prostaglandin F2α (PGF2α) from 20:4n–6 (arachidonic acid). Fish Physiol Biochem 27:81–96
27. Bell JG, Strachan F, Good JE, Tocher DR (2006) Effect of dietary echium oil on growth, fatty acid composition and metabolism, gill prostaglandin production and macrophage activity in Atlantic cod (*Gadus morhua* L.). Aquacult Res 37:606–617
28. Tocher DR, Dick JR, MacGlaughlin P, Bell JG (2006) Effect of diets enriched in Δ6 desaturated fatty acids (18:3n-6 and 18:4n-3), on growth, fatty acid composition and highly unsaturated fatty acid synthesis in two populations of Arctic charr (*Salvelinus alpinus* L.). Comp Biochem Physiol 144B:245–253
29. Miller MR, Nichols PD, Carter CG (2007) Replacement of dietary fish oil for Atlantic salmon parr (*Salmo salar* L.) with a stearidonic acid containing oil has no effect on omega-3 long-chain polyunsaturated fatty acid concentrations. Comp Biochem Physiol 146B:197–206
30. Nematipour GR, Gatlin DM (1993) Requirement of hybrid striped bass for dietary (n-3) highly unsaturated fatty acids. J Nutr 744–753
31. Lane RL, Trushenski JT, Kohler CC (2006) Modification of fillet composition and evidence of differential fatty acid turnover in sunshine bass *Morone chrysops* × *M. saxatilis* following change in dietary lipid source. Lipids 41:1029–1038
32. Trushenski JT, Lewis HA, Kohler CC (2008) Fatty acid profile of sunshine bass: I. profile change is affected by initial composition and differs among tissues. Lipids 43:629–641
33. Trushenski JT, Lewis HA, Kohler CC (2008) Fatty acid profile of sunshine bass: II. Profile change differs among fillet lipid class. Lipids 43:643–653
34. Twibell RG, Watkins BA, Rogers L, Brown PB (2000) Dietary conjugated linoleic acids alter hepatic and muscle lipids in hybrid striped bass. Lipids 35:155–161
35. Halver JE (1989) The vitamins. In: Halver JE (ed) Fish nutrition, 2nd edn. Academic Press, San Diego
36. Li Y, Watkins BA (2001) Analysis of fatty acids in food lipids. In: Wrolstad RE (ed-in-chief) Current protocols in food analytical chemistry. Wiley, New York
37. Zar JH (1984) Biostatistical analysis, 2nd edn. Prentice-Hall, Trenton
38. Tocher DR, Dick JR (1990) Polyunsaturated fatty acid metabolism in cultured fish cells: incorporation and metabolism of (n-3) and (n-6) series acids by Atlantic salmon (*Salmo salar*) cells. Fish Physiol Biochem 8:311–319
39. Ruyter B, Rosjo C, Einen O, Thomassen M (2000) Essential fatty acids in Atlantic salmon: effects of increasing dietary doses of n-6 and n-3 fatty acids on growth, survival and fatty acid composition of liver, blood and carcass. Aqua Nutr 6:119–127

Lipids (2010) 45:29–36
DOI 10.1007/s11745-009-3375-6

ORIGINAL ARTICLE

Mitochondrial Cholesterol Transporter, StAR, Inhibits Human THP-1 Monocyte-Derived Macrophage Apoptosis

Qianming Bai · Xiaobo Li · Yanxia Ning · Fengdi Zhao · Lianhua Yin

Received: 13 October 2009 / Accepted: 10 November 2009 / Published online: 28 November 2009

Abstract Steroidogenic acute regulatory protein (StAR) plays an important role in the maintenance of intracellular lipid homeostasis. Macrophages are the key cellular player in the pathophysiology of atherosclerosis. Imbalance of macrophage lipid homeostasis causes cellular apoptosis, which is the key process in the initiation of atherosclerosis. The present study has investigated the effects of StAR in the apoptotic process of human THP-1 derived macrophages induced by serum withdrawal or Ox-LDL. Overexpression of StAR significantly decreased the number of apoptotic macrophages by decreasing the expression of pro-apoptotic genes Caspase-3 and Bax mRNA and protein levels, as well as through increasing expression of anti-apoptotic gene Bcl-2 mRNA and protein levels in the absence and presence of Ox-LDL. The results indicate that StAR plays an important role in macrophage and foam cell apoptotic processing, which may provide a potential method for preventing atherosclerosis.

Keywords Steroidogenic acute regulatory protein · Apoptosis · Macrophages · Caspase-3 · Bax · Bcl-2 · Atherosclerosis

Abbreviations

ABCG1	ATP-binding cassette transporter G1
ApoE−/−	Apolipoprotein E-deficient
Bax	BCL2-associated X protein
Bcl-2	B cell lymphoma/leukemia-2
CYP27A1	Sterol 27-hydroxylase
EGFP	Enhanced green fluorescence protein
FC	Free cholesterol
FCM	Flow cytometry
GAPDH	Glyceraldehyde-3-phosphate dehydrogenase
IMM	Inner mitochondrial membrane
LDL	Low-density lipoprotein
LXRα	Liver X receptor alpha
MOI	Multiplicity of infection
OMM	Outer mitochondrial membrane
Ox-LDL	Oxidized low-density lipoprotein
PE	Phycoerythrin
PMA	Phorbol 12-myristate 13-acetate
PPARγ	Proliferation peroxysome activator receptor gamma
P450scc	Side-chain cleavage cytochrome P450
StAR	Steroidogenic acute regulatory protein
THP-1	Human, peripheral blood, leukemia, acute monocytic
TUNEL	Terminal deoxynucleotidyl transferase-mediated dUTP nick end labeling
7-ADD	7-Amino-actinomycin
25HC	25-Hydroxycholesterol
25HC3S	Sulfated 25-hydroxycholesterol
27HC	27-Hydroxycholesterol

Q. Bai · X. Li · Y. Ning · F. Zhao · L. Yin (✉)
Department of Physiology and Pathophysiology,
Shanghai Medical College, Fudan University, P.O. Box 224,
138 Yixueyuan Road, 200032 Shanghai
People's Republic of China
e-mail: lhyin@shmu.edu.cn

Introduction

Macrophages are central to the initiation and progression of atherosclerosis. In certain circumstances, macrophages accumulate modified low-density lipoproteins (LDLs), especially oxidized LDL (Ox-LDL). These modified LDLs can be metabolized into free cholesterol and cholesterol

esters leading to foam cell formation, which is a critical step for macrophage apoptosis and atherosclerosis progression [1–4]. Intracellular free cholesterol is considered to be a potent inducer of macrophage apoptosis, and subsequently necrosis, which could contribute to lesion necrosis, plaque destabilization, and disruption leading to acute atherothrombotic cardiovascular events [5–7]. Apoptotic and necrotic death of macrophages and foam cells lead to accumulation of insoluble lipids and other cellular contents, a characteristic of advanced lesions [8]. Therefore, decreasing intracellular cholesterol and cholesterol ester levels may prevent macrophages from foam cell formation and apoptosis.

Steroidogenic acute regulatory protein (StAR), one of the mitochondrial cholesterol delivery proteins, could deliver cholesterol from the outer mitochondrial membrane (OMM) into the inner mitochondrial membrane (IMM), which plays an important role in the maintenance of intracellular lipid homeostasis [9–11]. Our previous studies demonstrated that overexpression of StAR in THP-1 macrophages activates liver X receptor alpha (LXRα) and proliferation peroxysome activator receptor gamma (PPARγ), and increases ATP-binding cassette transporter G1 (ABCG1) and sterol 27-hydroxylase (CYP27A1) expression. Subsequently, it decreases intracellular lipid levels and the secretion of inflammatory factors, such as TNFα [12]. Furthermore, overexpression of StAR in ApoE−/− mice also decreases serum and tissue lipids [13]. Both free cholesterol accumulation and inflammatory factors are major pathogens for macrophage apoptosis [5, 14, 15]. Thus, StAR or StAR-like cholesterol transporters may be involved in the regulation of apoptosis. We hypothesized that StAR inhibits macrophage and foam cell apoptosis and necrosis.

In the present study, we provided convincing evidence that StAR plays an important role in the prevention of macrophage apoptosis, which may have therapeutic value for the prevention of atherosclerosis.

Experimental Procedure

Materials and Reagents

Culture media and reagents, TRIZOL reagent and a SuperScript™ III First-Strand Synthesis System for RT-PCR were purchased from Invitrogen (Carlsbad, CA). The SYBR® Green real-time PCR Master Mix was from the Toyobo Company (Osaka, JP). Primary antibodies against StAR and β-actin were purchased from Abcam Ltd. (Cambridge Science Park, Cambridge, UK). Antibodies against Caspase-3, Bax and Bcl-2 were purchased from SantaCruz Biotechnology, Inc (Santa Cruz, CA). Second antibodies against rabbit and mouse IgG were obtained from Kirkegaard and Perry Laboratories (Guildford, UK). The Annexin V-PE apoptosis detection kit (containing PE-conjugated Annexin V, 7-AAD and 10× binding buffer) was purchased from BD Biosciences (San Jose, CA). Lipoproteins were prepared from 80 ml blood of healthy donors by gradient ultracentrifugation as previously described [16]. The recombinant adenovirus encoding StAR (Ad-StAR) was prepared as described [17]. The control adenovirus expressing the enhanced green fluorescence protein (Ad-EGFP) was purchased from Vector Gene Technology Company Ltd. (Beijing, China). All other reagents were from Sigma-Aldrich Chemical Co (St. Louis, MO) unless stated otherwise.

Cell Line and Cell Culture

THP-1, a human monocytic cell line, was purchased from the American Type Culture Collection (Manassas, VA). Cells were cultured in RPMI 1640 medium with 25 mM HEPES buffer (supplemented with 10% fetal bovine serum, 2 mM L-glutamine (Invitrogen), 100 U/ml of penicillin, and 100 μg/ml of streptomycin) at 37 °C in a humidified incubator with 5% CO_2. THP-1 monocytic cells were differentiated to macrophages by addition of 50 nM phorbol 12-myristate 13-acetate (PMA) for 48 h. After being differentiated to macrophages, the PMA-containing medium was removed, and replaced with serum-free media, the cells were cultured for another 24 h before treatment. The macrophages were converted to foam cells by incubation with Ox-LDL (25 μg/ml) for 48 h as previously described [3].

Infection of Macrophages with Adenovirus Encoding Human StAR

THP-1 derived macrophages were infected with recombinant adenovirus encoding Ad-StAR at a multiplicity of 50 pfu/cell for 48 h in the absence and presence of Ox-LDL as previously described [18]. The adenovirus encoding Ad-EGFP were used as controls.

Morphological Assessment of Apoptosis by Electron Microscopy

A method of uranyl acetate and lead citrate staining was used to detect morphological changes as previously described [19]. In short, THP-1 derived macrophages were infected with Ad-StAR or Ad-EGFP in the absence and presence of Ox-LDL for 48 h. The cells were digested with pancreatin and fixed with 3% glutaraldehyde precooled at 4 °C for 2 h. After washed with PBS twice, the cells were fixed with 1% osmic acid for one more hour, dehydrated by acetone, and embedded in epoxide resin. After stained with

Table 1 Primer pairs used to amplify PCR products

Gene	Sequence (5′→3′)	Product size (bp)	Annealing temperature (°C)	GenBank accession no.
StAR	Forward: CTGAGGCAACAGGCTGTGAT	122	60	NM_000349
	Reverse: AGCCGAGAACCGAGTAGAGAG			
Caspase-3	Forward: ATGGAAGCGAATCAATGGACTC	138	60	NM_032991
	Reverse: CTGTACCAGACCGAGATGTCA			
Bcl-2	Forward: GAACTGGGGGAGGATTGTGG	124	60	NM_000633
	Reverse: CCGGTTCAGGTACTCAGTCA			
Bax	Forward: GGGTGGTTGGGTGAGACTC	191	60	NM_004324
	Reverse: AGACACGTAAGGAAAACGCATTA			
GAPDH	Forward: CATGAGAAGTATGACAACAGCCT	113	60	NM_002046
	Reverse: AGTCCTTCCACGATACCAAAGT			

uranyl acetate and lead citrate, the cells were observed under transmission electron microscope.

Agarose Gel Electrophoresis for DNA Fragmentation Detection

Selected apoptotic DNA was extracted from the treated cells and analyzed by agarose gel electrophoresis according to the manufacturer's instructions. In short, 4 μg of specific DNA was loaded to 1% agarose gel, and fragments were visualized by ethidium bromide staining.

Quantification of Apoptosis by Flow Cytometry

THP-1 cells were seeded in a six-well plate at 1×10^6 cells/well density, differentiated, and infected as described above. The media were changed with fresh serum-free RPMI 1640 media in the presence or absence of 25 μg/ml Ox-LDL. Forty eight hours after the change, apoptotic cells were assessed by flow cytometry as previously published [20]. In brief, the harvested cells were washed twice with cold PBS, then resuspended in 1× binding buffer at a concentration of 1×10^6 cells/ml, incubated with Annexin V-PE (Phycoerythrin) and 7-ADD (7-amino-actinomycin) for 15 min at room temperature in the dark. The positive cells were analyzed by flow cytometry within one hour.

Determination of Total mRNA by Real-Time Fluorescent Quantitative RT-PCR

Total RNA was extracted according to the manufacturer's instructions. 2 μg of total RNA were reversely transcribed and amplified. The relative mRNA levels were measured by real-time PCR using SYBR-Green real-time PCR Master Mix (Toyobo, Osaka, Japan) with SYBR-Green I. Specific primer pairs for StAR, Caspase-3, Bax, Bcl-2, GAPDH were designed based on published sequences in GenBank and are listed in Table 1.

Determination of Relative Protein Levels

After infection or treatment, total cell lysates were harvested in RIPA sample buffer. Thirty micrograms of protein was loaded to 12% SDS-PAGE to detect Caspase-3, Bax, Bcl-2 using β-actin as loading control, and Western blot analysis was performed as previously described [21].

Statistic Analysis

Data are expressed as means ± SD and evaluated by independent-samples t test and the Games–Howell post-test using SPSS 11.5 software. A value of $P < 0.05$ was considered statistically significant.

Results

StAR Gene was Successfully Overexpressed in THP-1 Derived Macrophages by Infection with Recombinant Adenovirus

THP-1 derived macrophages were infected with recombinant adenovirus encoding Ad-EGFP at a multiplicity of 0, 10, and 50 pfu/cell respectively. All of these cells were incubated for another 48 h. Transfection efficiency was detected by fluorescence microscope and flow cytometry as shown in Fig. 1a–d. The cells infected with Ad-EGFP at a multiplicity of 50 pfu/cell for 48 h had the highest infection efficiency (about 50%). This condition was used in the following experiments unless otherwise mentioned.

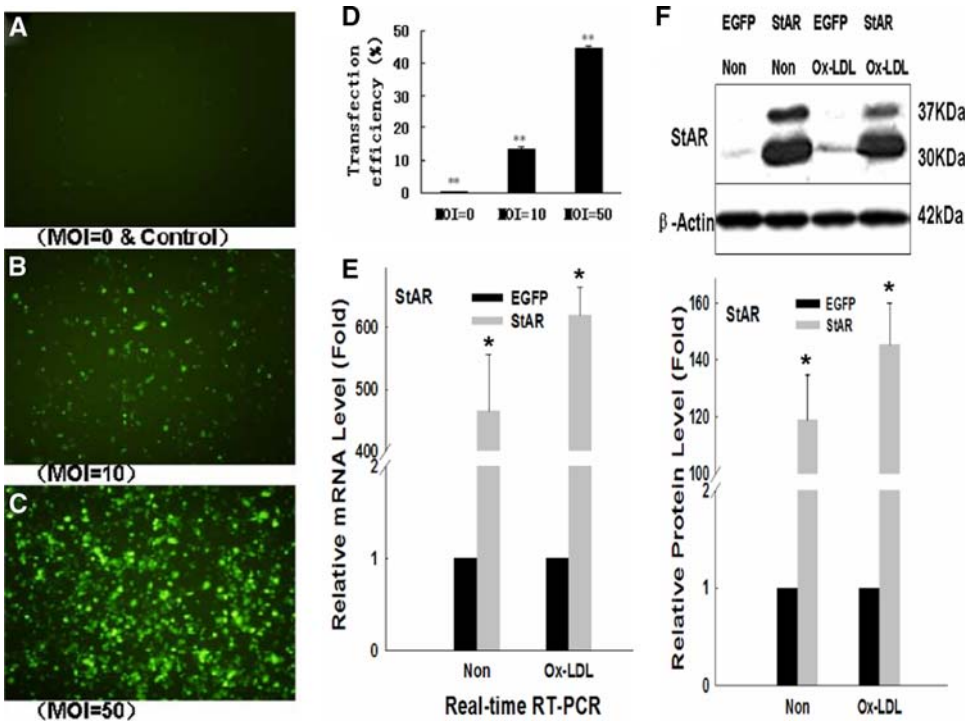

Fig. 1 StAR gene was successfully overexpressed in THP-1 derived macrophages. THP-1 derived macrophages were transfected with recombinant adenovirus encoding Ad-StAR and Ad-EGFP. Then, the transfection efficiency of StAR gene in THP-1 macrophages was detected by fluorescence microscope (**a**–**c**) and flow cytometry (**d**). The levels of StAR mRNA (**e**) and protein (**f**) were determined by real-time RT-PCR and Western blot. Cells infected with Ad-EGFP were the controls; *Non* cells incubated in serum-free media without Ox-LDL; *Ox-LDL* with 25 μg/ml Ox-LDL in serum-free media. $*P < 0.05$; $**P < 0.01$

THP-1 derived macrophages that were infected with recombinant adenovirus encoding Ad-StAR at a multiplicity of 50 pfu/cell for 48 h expressed high levels of StAR mRNA and protein but did not exhibit evidence of cell toxicity. Real-time RT-PCR analysis showed that infection with Ad-StAR increased StAR mRNA levels by 460-fold in the absence of Ox-LDL and 620-fold in the presence of Ox-LDL respectively in the THP-1 cells (Fig. 1e). Western blot analysis showed one major immunoreactive band with a molecular weight of 30 kDa (lower band), which was consistent with StAR mature protein, and a second band with the molecular weight of 37 kDa (upper band), which was consistent with a precursor form (Fig. 1f). It showed that Ad-StAR infection increased the StAR protein levels about 120-fold in the absence of Ox-LDL and 145-fold in the presence of Ox-LDL respectively. A summary of the data normalized to β-actin is shown in the lower panel of Fig. 1f.

Effect of StAR Overexpression on Morphology of THP-1 Derived Macrophages and Foam Cells

Morphology changes of the cells with StAR overexpression in the presence or absence of Ox-LDL were assessed by electron microscope. As shown in Fig. 2a–d, compared with the cells infected with Ad-EGFP, chromatin condensation, margination, apoptotic body and lipid droplet in the cells infected with Ad-StAR were significantly decreased.

Effect of StAR Overexpression on Apoptosis in THP-1 Macrophages and Foam Cells Detected by DNA Fragmentation

As shown in Fig. 2e, overexpression of StAR in THP-1 derived macrophages with or without Ox-LDL showed much weaker "DNA laddering" representing integer multiples of the internucleosomal DNA length (about 180–200 bp), which is indicative of apoptosis, compared with the control cells infected with Ad-EGFP. It suggested that StAR could inhibit THP-1 macrophage apoptosis.

Effect of StAR Overexpression on Apoptosis and Necrosis in THP-1 Derived Macrophages Detected by Flow Cytometric

THP-1 derived macrophages were randomized into the following groups: negative control (no infection and no staining); negative control used for detection of transfection efficiency (infected with Ad-EGFP but no staining); control groups (infected with Ad-EGFP in the presence or absence Ox-LDL, and staining with Annexin V-PE and 7-AAD); experiment groups (infected with Ad-StAR in the presence or absence of Ox-LDL, and stained with Annexin V-PE and 7-AAD). The number of apoptotic cells was determined by flow cytometry as shown in Fig. 2f. Ad-StAR infected cells without Ox-LDL dramatically inhibited the apoptosis both in the early and end stage of apoptosis (Fig. 2g). However, Ad-StAR infected cells

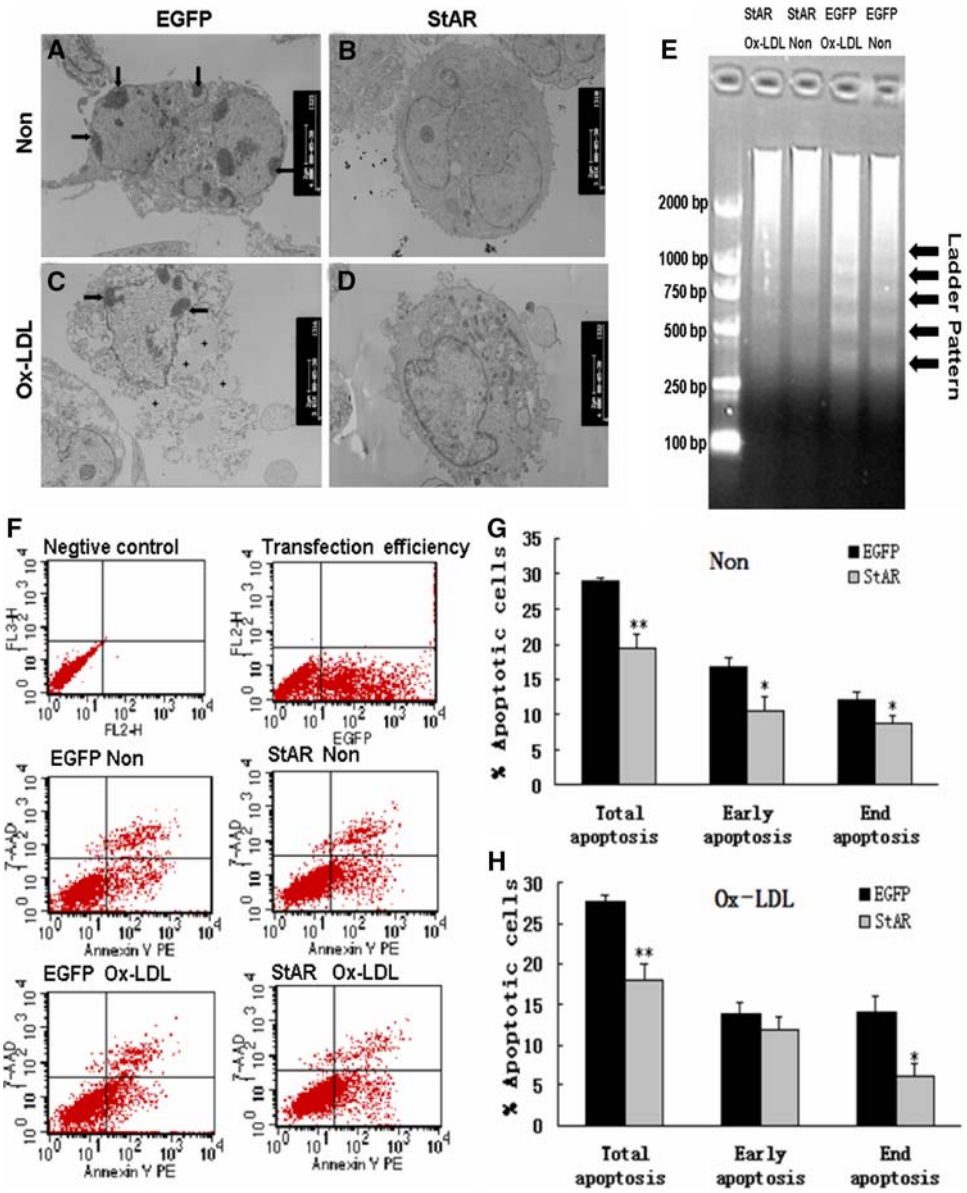

Fig. 2 Effect of StAR on THP-1 macrophages and foam cells apoptosis. THP-1 derived macrophages were incubated with or without 25 μg/ml Ox-LDL for 24 h following infection with recombinant adenovirus encoding Ad-CMV-EGFP and Ad-CMV-StAR at a multiplicity of 50 pfu/cell. Then, THP-1 macrophages and foam cells morphological changes were analyzed by electron microscope (**a**–**d**) and DNA ladder fragmentation was detected on 1% agarose gel electrophoresis (**e**). The number of THP-1 macrophages apoptosis was assessed by FCM (**f**–**h**). *Arrow* chromatin condensation, margination and apoptosis body. *Plus* lipid droplet or blebbing. *Non* cells incubated in serum-free media without Ox-LDL; *Ox-LDL* with 25 μg/ml Ox-LDL in serum-free media. $^{*}P < 0.05$ versus EGFP. $^{**}P < 0.01$ versus EGFP

treated with 25 μg/ml Ox-LDL mainly inhibited apoptosis at the end stage (Fig. 2h).

Effect of StAR Overexpression on Pro- and Anti-Apoptotic Genes' Protein Expression

The protein levels of Caspase-3 (Fig. 3b), Bax (Fig. 3c), Bcl-2 (Fig. 3d) following StAR overexpression in THP-1 derived macrophages were detected by Western blot analysis as shown in Fig. 3a. The pro-apoptosis protein Caspase-3 and Bax were decreased consistently by 0.6- (Non), 0.5- (Ox-LDL), and 0.7- (Non), 0.6- (Ox-LDL) fold respectively, while anti-apoptosis protein Bcl-2 was increased by 1.6- (Non) and 2.1- (Ox-LDL) fold in Ad-StAR infected macrophages in the presence or absence of Ox-LDL.

Effect of StAR Overexpression on Pro- and Anti-Apoptotic Genes' mRNA Expression

The mRNA levels of the genes related to apoptosis were determined by real-time RT-PCR after the cells had been infected with the recombinant adenovirus for 48 h as indicated. As shown in Fig. 4, the pro-apoptosis gene Caspase-3 (Fig. 4a) and Bax (Fig. 4b) were decreased by 0.6- (Non), 0.7- (Ox-LDL), and 1.0- (Non), 0.4- (Ox-LDL) fold respectively, while anti-apoptosis protein Bcl-2 (Fig. 4c) was increased by 1.4- (Non) and 1.5- (Ox-LDL) fold in the Ad-StAR infected macrophages with or without Ox-LDL. Because the Bax gene in the Ad-StAR infected macrophages without Ox-LDL had no dramatic change, the Bax/Bcl-2 ratio was assessed, and the result was shown in

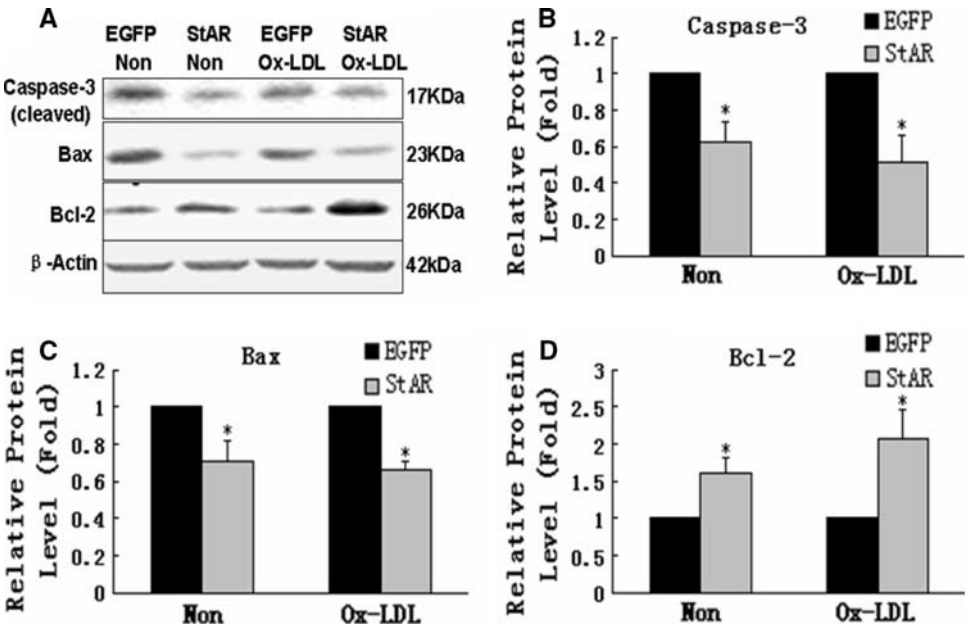

Fig. 3 Effect of StAR on Caspase-3, Bax and Bcl-2 protein expression. After transfection and treatment with or without Ox-LDL, total cell lysates of THP-1 derived macrophage were extracted for determination the protein levels of Caspase-3, Bax and Bcl-2. *Non* cells incubated in serum-free media without Ox-LDL; *Ox-LDL* with 25 μg/ml Ox-LDL in serum-free media. $*P < 0.05$ versus EGFP

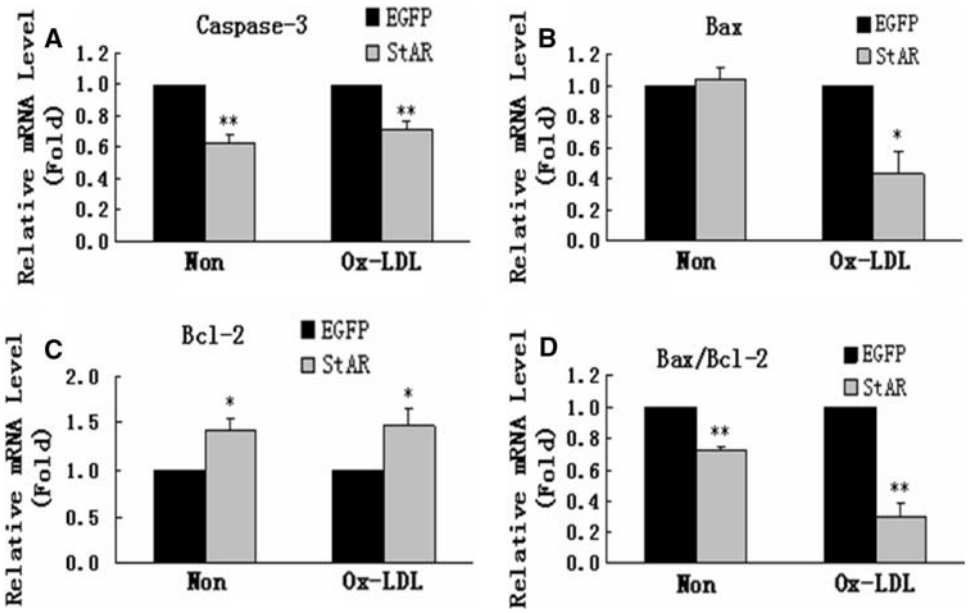

Fig. 4 Effect of StAR on Caspase-3, Bax and Bcl-2 mRNA expression. After transfection and treatment with or without Ox-LDL, total RNA of THP-1 derived macrophage was extracted for determination the mRNA levels of Caspase-3, Bax and Bcl-2. *Non* cells incubated in serum-free media without Ox-LDL; *Ox-LDL* with 25 μg/ml Ox-LDL in serum-free media. $*P < 0.05$ versus EGFP. $**P < 0.01$ versus EGFP

Fig. 4d. The Bax/Bcl-2 ratio was decreased to 0.7- (Non) and 0.3- (Ox-LDL) in the Ad-StAR infected macrophages with or without Ox-LDL.

Discussion

Macrophages play a key role in the initiation and progression of atherosclerosis. Lipid-laden cells (foam cells), predominantly of monocytic origin, are a hallmark feature of atherosclerotic plaques [4, 22, 23]. In advanced plaques, necrotic lipid-filled cores are formed following the death of macrophages and foam cells. Cytotoxic substances released from these cells are thought to contribute to plaque destabilization, which could then result in a clinical event such as a heart attack or stroke [22, 24]. Therefore, targeting the inhibition of apoptosis and necrosis of macrophages and foam cells may present a therapeutic strategy for atherosclerosis.

The StAR was first found in steroidogenic tissues. It could transport cholesterol from the OMM into the IMM, where the cholesterol side-chain cleavage enzyme, P450scc, is located. This enzyme catalyzes the first and rate-limiting step in steroidogenesis converting insoluble cholesterol to soluble pregnenolone [11, 25, 26]. In recent years, it was reported that StAR was also expressed in the non-steroidogenic tissues such

as liver, vascular endothelial cells and macrophages, and it plays an important role in the maintenance of intracellular lipid homeostasis [10, 21, 27]. Overexpression of StAR in these tissues decreases lipid levels (both cholesterol and triglyceride) and inflammatory factors. However, the effect of StAR on apoptosis is still not clear yet.

In the current research, we provided convincing evidence that StAR inhibits macrophage and foam cell apoptosis, the number of apoptotic cells was significantly lower compared with the control groups after overexpression of StAR, which was consistent with the TUNEL results of Ning et al. [12]. Apoptotic cells had typical morphological and biochemical characteristics, including shrinkage of the cells, chromatin condensation, margination, apoptosis body, and oligonucleosomal fragmentation of nuclear DNA as shown in Fig. 2a–d [28, 29].

Ox-LDL is taken up by macrophages, leading to the accumulation of high levels of intracellular cholesterol and the transformation of macrophages into lipid-laden foam cells [1, 4, 30]. Increasing numbers of reports indicate that Ox-LDL is cytotoxic to macrophages and contributes to macrophage apoptosis [31–33], which may relate to down-regulating expression of the anti-apoptotic genes Bcl-2 and up-regulating the pro-apoptotic genes Bax and Caspases [34–37]. However, in the present study, the apoptotic index, including morphology, DNA ladder, and the quantity of apoptotic and necrotic cells, in groups treated with or without Ox-LDL were not obviously different. Fewer THP-1 macrophages undergoing apoptosis both in the early and the end stage were observed in the cells infected with Ad-StAR without Ox-LDL. However, the apoptosis in the cells infected with Ad-StAR with Ox-LDL only occurred in the end stage (Fig. 2f–h), which can partly be explained by the difference in transfection efficiency between the groups with and without Ox-LDL.

To better understand the mechanism of StAR overexpression inhibiting apoptosis in the THP-1 macrophages and foam cells, we determined the protein and mRNA expression of the genes related to apoptosis by Western blot and real-time RT-PCR. The results showed that compared with the control groups, the expression of pro-apoptotic proteins including Caspase-3 and Bax were lowered 0.6- (without Ox-LDL), 0.5- (with Ox-LDL) and 0.7- (without Ox-LDL), 0.6- (with Ox-LDL) fold respectively, while the anti-apoptotic protein Bcl-2 level increased to 1.6- (without Ox-LDL) and 2.1- (with Ox-LDL) fold. The change of mRNA levels was consistent with that of protein levels.

As a cholesterol delivery protein, StAR regulates the formation of oxysterols in the mitochondria [38]. The generated oxysterols, including 27-hydroxycholesterol (27HC) and 25-hydroxycholesterol (25HC), have been implicated in the regulation of lipid metabolism. Li et al. [39] reported cholesterol was delivered into mitochondria and hydroxylated to 25HC and subsequently 3β-sulfated to form sulfated 25-hydroxycholesterol (25HC3S). Ma et al. has shown that the 25HC3S increased cell proliferation and decreased apoptosis in macrophages [40, 41]. Taking other reports and our results together, we can state that the mechanism of StAR inhibiting apoptosis in THP-1 macrophages and foam cells is as follows: when cellular cholesterol levels are increased in cells, cholesterol is delivered by StAR protein to mitochondria, where it is hydroxylated to 25HC, then sulfated to 25HC3S, which decreases apoptosis by decreasing the expression of pro-apoptotic genes including Caspase-3 and Bax and increasing the expression of the anti-apoptotic gene Bcl-2.

Acknowledgments This work was supported by the National Natural Science Foundation of China (NSFC 30871021 and NSFC 30800547).

References

1. Bobryshev YV (2006) Monocyte recruitment and foam cell formation in atherosclerosis. Micron 37:208–222
2. Hansson GK (2005) Inflammation, atherosclerosis, and coronary artery disease. N Engl J Med 352:1685–1695
3. Yamada Y, Doi T, Hamakubo T, Kodama T (1998) Scavenger receptor family proteins: roles for atherosclerosis, host defence and disorders of the central nervous system. Cell Mol Life Sci 54:628–640
4. Pennings M, Meurs I, Ye D et al (2006) Regulation of cholesterol homeostasis in macrophages and consequences for atherosclerotic lesion development. FEBS Lett 580:5588–5596
5. Tabas I (2002) Consequences of cellular cholesterol accumulation: basic concepts and physiological implications. J Clin Investig 110:905–911
6. Zhou J, Chew M, Ravn HB, Falk E (1999) Plaque pathology and coronary thrombosis in the pathogenesis of acute coronary syndromes. Scand J Clin Lab Investig Suppl 230:3–11
7. Corsten MF, Reutelingsperger CP, Hofstra L (2007) Imaging apoptosis for detecting plaque instability: rendering death a brighter facade. Curr Opin Biotechnol 18:83–89
8. Glass CK, Witztum JL (2001) Atherosclerosis. The road ahead. Cell 104:503–516
9. Miller WL (2007) Steroidogenic acute regulatory protein (StAR), a novel mitochondrial cholesterol transporter. Biochim Biophys Acta 1771:663–676
10. Hall EA, Ren S, Hylemon PB et al (2005) Detection of the steroidogenic acute regulatory protein, StAR, in human liver cells. Biochim Biophys Acta 1733:111–119
11. Pandak WM, Ren S, Marques D et al (2002) Transport of cholesterol into mitochondria is rate-limiting for bile acid synthesis via the alternative pathway in primary rat hepatocytes. J Biol Chem 277:48158–48164
12. Ning Y, Bai Q, Lu H et al (2009) Overexpression of mitochondrial cholesterol delivery protein, StAR, decreases intracellular lipids and inflammatory factors secretion in macrophages. Atherosclerosis 204:114–120
13. Ning Y, Xu L, Ren S et al (2009) StAR overexpression decreases serum and tissue lipids in apolipoprotein E-deficient mice. Lipids 44(6):511–519

14. Bjorkerud S, Bjorkerud B (1996) Apoptosis is abundant in human atherosclerotic lesions, especially in inflammatory cells (macrophages and T cells), and may contribute to the accumulation of gruel and plaque instability. Am J Pathol 149:367–380
15. Harada-Shiba M, Kinoshita M, Kamido H, Shimokado K (1998) Oxidized low density lipoprotein induces apoptosis in cultured human umbilical vein endothelial cells by common and unique mechanisms. J Biol Chem 273:9681–9687
16. Schulz T, Schiffl H, Scheithe R, Hrboticky N, Lorenz R (1995) Preserved antioxidative defense of lipoproteins in renal failure and during hemodialysis. Am J Kidney Dis 25:564–571
17. Pandak WM, Bohdan P, Franklund C et al (2001) Expression of sterol 12alpha-hydroxylase alters bile acid pool composition in primary rat hepatocytes and in vivo. Gastroenterology 120:1801–1809
18. Ren S, Hylemon P, Marques D et al (2004) Effect of increasing the expression of cholesterol transporters (StAR, MLN64, and SCP-2) on bile acid synthesis. J Lipid Res 45:2123–2131
19. Dai ZJ, Gao J, Ji ZZ, Wang XJ, Ren HT, Liu XX, Wu WY, Kang HF, Guan HT (2009) Matrine induces apoptosis in gastric carcinoma cells via alteration of Fas/FasL and activation of caspase-3. J Ethnopharmacol 123(1):91–96
20. Vermes I, Haanen C, Steffens-Nakken H, Reutelingsperger C (1995) A novel assay for apoptosis. Flow cytometric detection of phosphatidylserine expression on early apoptotic cells using fluorescein labelled Annexin V. J Immunol Methods 184:39–51
21. Ning Y, Chen S, Li X, Ma Y, Zhao F, Yin L (2006) Cholesterol, LDL, and 25-hydroxycholesterol regulate expression of the steroidogenic acute regulatory protein in microvascular endothelial cell line (bEnd.3). Biochem Biophys Res Commun 342: 1249–1256
22. Ross R, Rous-Whipple Award Lecture (1993) Atherosclerosis: a defense mechanism gone awry. Am J Pathol 143:987–1002
23. Stary HC, Chandler AB, Dinsmore RE et al (1995) A definition of advanced types of atherosclerotic lesions and a histological classification of atherosclerosis. A report from the Committee on Vascular Lesions of the Council on Arteriosclerosis, American Heart Association. Arterioscler Thromb Vasc Biol 15:1512–1531
24. Libby P, Geng YJ, Aikawa M et al (1996) Macrophages and atherosclerotic plaque stability. Curr Opin Lipidol 7:330–335
25. Miller WL (1988) Molecular biology of steroid hormone synthesis. Endocr Rev 9:295–318
26. Miller WL (2007) StAR search—what we know about how the steroidogenic acute regulatory protein mediates mitochondrial cholesterol import. Mol Endocrinol 21:589–601
27. Ma Y, Ren S, Pandak WM et al (2007) The effects of inflammatory cytokines on steroidogenic acute regulatory protein expression in macrophages. Inflamm Res 56:495–501
28. Wyllie AH (1980) Glucocorticoid-induced thymocyte apoptosis is associated with endogenous endonuclease activation. Nature 284:555–556
29. Falcieri E, Gobbi P, Zamai L, Vitale M (1994) Ultrastructural features of apoptosis. Scanning Microsc 8:653–665 (discussion 665–666)
30. Brown MS, Goldstein JL (1983) Lipoprotein metabolism in the macrophage: implications for cholesterol deposition in atherosclerosis. Annu Rev Biochem 52:223–261
31. Clare K, Hardwick SJ, Carpenter KL, Weeratunge N, Mitchinson MJ (1995) Toxicity of oxysterols to human monocyte-macrophages. Atherosclerosis 118:67–75
32. Hardwick SJ, Hegyi L, Clare K et al (1996) Apoptosis in human monocyte-macrophages exposed to oxidized low density lipoprotein. J Pathol 179:294–302
33. Li W, Yuan XM, Brunk UT (1998) OxLDL-induced macrophage cytotoxicity is mediated by lysosomal rupture and modified by intralysosomal redox-active iron. Free Radic Res 29:389–398
34. Li D, Yang B, Mehta JL (1998) Ox-LDL induces apoptosis in human coronary artery endothelial cells: role of PKC, PTK, bcl-2, and Fas. Am J Physiol 275:H568–H576
35. Siow RC, Richards JP, Pedley KC, Leake DS, Mann GE (1999) Vitamin C protects human vascular smooth muscle cells against apoptosis induced by moderately oxidized LDL containing high levels of lipid hydroperoxides. Arterioscler Thromb Vasc Biol 19:2387–2394
36. de Nigris F, Franconi F, Maida I, Palumbo G, Anania V, Napoli C (2000) Modulation by alpha- and gamma-tocopherol and oxidized low-density lipoprotein of apoptotic signaling in human coronary smooth muscle cells. Biochem Pharmacol 59:1477–1487
37. Haendeler J, Zeiher AM, Dimmeler S (1996) Vitamin C and E prevent lipopolysaccharide-induced apoptosis in human endothelial cells by modulation of Bcl-2 and Bax. Eur J Pharmacol 317:407–411
38. Schroepfer GJ Jr (2000) Oxysterols: modulators of cholesterol metabolism and other processes. Physiol Rev 80:361–554
39. Li X, Pandak WM, Erickson SK et al (2007) Biosynthesis of the regulatory oxysterol, 5-cholesten-3beta, 25-diol 3-sulfate, in hepatocytes. J Lipid Res 48:2587–2596
40. Ren S, Hylemon P, Zhang ZP et al (2006) Identification of a novel sulfonated oxysterol, 5-cholesten-3beta, 25-diol 3-sulfonate, in hepatocyte nuclei and mitochondria. J Lipid Res 47:1081–1090
41. Ma Y, Xu L, Rodriguez-Agudo D et al (2008) 25-Hydroxycholesterol-3-sulfate (25HC3S) regulates macrophage lipid metabolism via the LXR/SREBP-1 signaling pathway. Am J Physiol Endocrinol Metab 295:E1369–E1379

Lipids (2010) 45:37–51
DOI 10.1007/s11745-009-3365-8

ORIGINAL ARTICLE

HOCl-Mediated Glycerophosphocholine and Glycerophosphoethanolamine Generation from Plasmalogens in Phospholipid Mixtures

Jacqueline Leßig · Beate Fuchs

Received: 21 October 2008 / Accepted: 3 July 2009 / Published online: 25 November 2009

Abstract Many mammalian tissues and cells contain, in addition to (diacyl) phospholipids, considerable amounts of plasmalogens, which may function as important antioxidants. Apart from the "scavenger" function mediated by the high sensitivity of the vinyl-ether bond, the functional role of plasmalogens is so far widely unknown. Furthermore, there is increasing evidence that plasmalogen degradation products have harmful effects in inflammatory processes. In a previous investigation glycerophosphocholine (GPC) formation was verified as a novel plasmalogen degradation pathway upon oxidation with hypochlorous acid (HOCl), however these investigations were performed in simple model systems. Herein, we examine plasmalogen degradation in a more complex system in order to evaluate if GPC generation is also a major pathway in the presence of other highly unsaturated glycerophospholipids (GPL) representing an additional reaction site of HOCl targets. Using MALDI–TOF mass spectrometry and ^{31}P NMR spectroscopy, we confirmed that the first step of the HOCl-induced degradation of GPL mixtures containing plasmalogens is the attack of the vinyl-ether bond resulting in the generation of 1-lysophosphatidylcholine (lysoPtdCho) or 1-lysophosphatidylethanolamine. In the second step HOCl reacts with the fatty acyl residue in the *sn*-2 position of 1-lysoPtdCho. This reaction is about three times faster in comparison to comparable diacyl-GPL. Thus, the generation of GPC and glycerophosphoethanolamine (GPE) from plasmalogens are relevant products formed from HOCl attack on the vinyl-ether bond of plasmalogens under pathological conditions.

J. Leßig · B. Fuchs (✉)
Medical Faculty, Institute of Medical Physics and Biophysics, University of Leipzig, Härtelstraße 16-18, 04107 Leipzig, Germany
e-mail: Beate.Fuchs@medizin.uni-leipzig.de

Keywords Boar spermatozoa · Glycerophosphocholine · Glycerophosphoethanolamine · Hypochlorous acid · Lysophosphatidylcholine · Lysophosphatidylethanolamine · MALDI-TOF MS · Plasmalogen · ^{31}P NMR spectroscopy

Abbreviations

amu	Atomic mass unit
DHA	Docosahexaenoic acid
DPA	Docosapentaenoic acid
2-DH-1-LPC	1-Lyso-2-docosahexaenoyl-*sn*-glycero-3-phosphocholine
2-DH-1-LPE	1-Lyso-2-docosahexaenoyl-*sn*-glycero-3-phosphoethanolamine
CerPCho	Sphingomyelin
DPPA	1,2-Dipalmitoyl-*sn*-glycero-3-phosphate
DPPC	1,2-Dipalmitoyl-*sn*-glycero-3-phosphocholine
GPC	Glycerophosphocholine
GPE	Glycerophosphoethanolamine
ChoGpl	Choline glycerophospholipids
EtnGpl	Ethanolamine glycerophospholipids
GPL	Glycerophospholipid
$PDHPC_{ether}$	1-*O*-1′-Palmityl-2-docosahexaenoyl-*sn*-glycero-3-phosphocholine
$PDHPC_{plasm}$	1-*O*-1′-Palmitenyl-2-docosahexaenoyl-*sn*-glycero-3-phosphocholine
$PDHPE_{plasm}$	1-*O*-1′-Palmitenyl-2-docosahexaenoyl-*sn*-glycero-3-phosphoethanolamine
$PDPPE_{ether}$	1-*O*-1′-Palmityl-2-docosapentaenoyl-*sn*-glycero-3-phosphoethanolamine

$PDPPC_{ether}$	1-*O*-1′-Palmityl-2-docosapentaenoyl-*sn*-glycero-3-phosphocholine
$PDPPC_{plasm}$	1-*O*-1′-Palmitenyl-2-docosapentaenoyl-*sn*-glycero-3-phosphocholine
HOCl	Hypochlorous acid
lysoPtdCho	Lysophosphatidylcholine
lysoPtdEtn	Lysophosphatidylethanolamine
LPL	Lysophospholipid
MALDI-TOF MS	Matrix-assisted laser desorption & ionization time-of-flight mass spectrometry
1-M-2-LPC	1-Myristoyl-2-lyso-*sn*-glycero-3-phosphocholine
MPO	Myeloperoxidase
$MPO–H_2O_2–Cl^-$	Myeloperoxidase-hydrogen peroxide-chloride
$SAPC_{plasm}$	1-*O*-1′-Stearenyl-2-arachidonoyl-*sn*-glycero-3-phosphocholine
$SDHPC_{plasm}$	1-*O*-1′-Stearenyl-2-docosahexaenoyl-*sn*-glycero-3-phosphocholine
$SDHPE_{plasm}$	1-*O*-1′-Stearenyl-2-docosahexaenoyl-*sn*-glycero-3-phosphoethanolamine
PakCho	Plasmanyl choline
PakEtn	Plasmanyl ethanolamine
PlsCho	Plasmenyl choline
PlsEtn	Plasmenyl ethanolamine
PtdCho	Phosphatidylcholine
PtdEtn	Phosphatidylethanolamine
PMNL	Polymorphonuclear leukocytes
PNA	*para*-nitroaniline
^{31}P NMR	^{31}P nuclear magnetic resonance spectroscopy
POPC	1-Palmitoyl-2-oleoyl-*sn*-glycero-3-phosphocholine
ROS	Reactive oxygen species
SDHPC	1-Stearoyl-2-docosahexaenoyl-*sn*-glycero-3-phosphocholine
1-*S*-2-LPC	1-Stearoyl-2-lyso-*sn*-glycero-3-phosphocholine

Introduction

Plasmalogens represent a glycerophospholipid (GPL) class with a vinyl-ether moiety in the *sn*-1-position of the glycerol backbone [1]. The marked reactivity of this group renders plasmalogens subject to oxidation and imparts potentially strong antioxidative properties to these phospholipids [1, 2]. Compared to their 1-acyl analogues, plasmalogens are more susceptible to oxidative damage [3, 4]. Therefore, their supposed function as "scavengers" [5] can be explained by the direct reaction between atmospheric oxygen or—in particular—reactive oxygen species (ROS) and the vinyl-ether moiety [5, 6]. In binary mixtures of plasmenylcholine (PlsCho) and phosphatidylcholine (PtdCho), selective oxidation of PlsCho by hypochlorous acid (HOCl) followed by the formation of lysophosphatidylcholine (lysoPtdCho) is obvious. The rate constant of the reaction of plasmalogens with HOCl is approximately ten times higher than the rate constant of the reaction of alkenes with HOCl [7]. Double bonds of the fatty acyl residue present in the *sn*-2 position of the resulting lysoPtdCho are secondary HOCl targets leading to the production of lysoPtdCho-chlorohydrins. Unsaturated lysoPtdCho species are also more susceptible to oxidative attack than unsaturated PtdCho [4].

The preferred destruction of plasmenyl-phospholipids in membranes under oxidative stress is one possible explanation of the physiological function of these compounds in membranes: Plasmalogens are supposed to protect animal cells against oxidative damage [2, 5, 6, 8–11], and are regarded as natural antioxidants in lipoproteins [2].

Plasmalogens are also lipids involved in brain signal transduction and synaptic function [12]. It has been shown that a plasmalogen-selective phospholipase A_2 (PLA_2) exists in the brain and that it is probably involved in the regulation of the K^+ channels [13, 14]. The contribution of plasmalogens to signal transduction was also demonstrated in the heart where a special PLA_2 selectively hydrolyzes plasmalogen substrates [15], resulting in the production of lysoplasmalogens and prostacyclin, important bioactive products [16]. Furthermore, PlsCho vesicles are characterized by changed molecular dynamic properties in comparison to their diacyl analogues underscoring the biological significance of plasmalogens [17]. Experiments using ethanolamine glycerophospholipids containing either an ester or a vinyl-ether linkage at the *sn*-1 position indicated that introduction of the vinyl-ether group increased the tendency to give hexagonal phases [18].

Cellular membranes contain often 20%, in some cases even more than 50%, of plasmalogen glycerophospholipids [10]. There is a preponderance of plasmalogens in cardiac sarcolemma [19]. In some sperm plasma membranes, highly unsaturated compounds, such as 1-*O*-1′-palmitenyl-2-docosahexaenoyl-*sn*-glycero-3-phosphocholine ($PDHPC_{plasm}$) and 1-*O*-1′-palmitenyl-2-docosapentaenoyl-*sn*-glycero-3-phosphocholine ($PDPPC_{plasm}$) are very abundant [20, 21].

In different mammalian tissues, the plasmalogen concentration decreases upon aging. A similar behaviour has also been observed in patients with Alzheimer's disease (AD) [10, 22–25]. Plasmalogen deficiency may, thus, play an important role in AD pathogenesis and altered plasmalogen content may contribute to neurodegeneration, synapse loss and synaptic dysfunction in AD [25].

Concomitantly, an accumulation of plasmalogen oxidation products such as α-hydroxyaldehydes and plasmalogen epoxides is detectable [10, 24, 26, 27]. Finally, neuropathological conditions (e.g. ischemia, spinal cord injury) and chronic diseases such as atherosclerosis and myocardial infarction are also characterized by membrane instability and increased oxidative damage [9, 23].

Although plasmalogen GPL can be basically regarded as efficient antioxidants in vivo [11, 28–30], it is not known so far, if the removal of reactive oxygen species compensates the negative effects mediated by the plasmalogen decrease and the related accumulation of plasmalogen oxidation products [31].

At an inflammatory locus, HOCl is generated by myeloperoxidase (MPO), a heme-enzyme released from polymorphonuclear leukocytes (PMNL) [32]. HOCl reacts with a variety of molecules including amino acids, proteins, carbohydrates, nucleic acids and lipids [33–38]. Chlorohydrins are generated as the primary products when HOCl reacts with the double bonds of unsaturated PtdCho [38–40]. Additionally, α-chlorofatty aldehydes and 2-lysophosphatidylcholines (2-lysoPtdCho) are characteristic products of reactive chlorinating species produced by MPO (or its products) targeting the vinyl-ether bond of plasmalogens in cellular membranes [41–45].

Plasmalogens containing a polyunsaturated fatty acyl residue at the *sn*-2 position are more sensitive to oxidative modifications than their monounsaturated counterparts [7, 11, 46]. Free radical-induced oxidation of plasmalogen GPL with esterified docosahexaenoic acid (DHA) at the *sn*-2 position occurs at both, the *sn*-1 and *sn*-2 position, accompanied by the formation of glycerophosphocholine (GPC) [47]. Combined plasmalogen and 1-lysoPtdCho degradation and subsequent GPC generation could be demonstrated in artificial plasmalogens after HOCl-treatment, whereby marked GPC formation occurred only in the case of highly unsaturated 1-*O*-1′-stearenyl-2-docosahexaenoyl-*sn*-glycero-3-phosphocholine ($SDHPC_{plasm}$) and 1-*O*-1′-stearenyl-2-arachidonoyl-*sn*-glycero-3-phosphocholine ($SAPC_{plasm}$) [47]. However, these investigations are limited because there was only a single artificial plasmalogen as target for HOCl whereas under in vivo conditions there are many targets [47].

Therefore, the aim of this study was to extend the results of our previous study [47], where the preferred reactivity of the plasmalogen vinyl-ether group in comparison to olefinic residues was demonstrated. It is not yet known, whether the unsaturated 1-lysoPtdCho or an intact diacyl PtdCho exhibits a higher reactivity against HOCl. It was also not known which role phosphatidylethanolamine (PtdEtn) species—that are normally present in biological systems—presumably play and which products may be expected in their presence. To address these questions, we examined the HOCl-induced plasmalogen degradation in an artificial model mixture of polyunsaturated plasmalogen-ChoGpl and PtdCho using a combination of MALDI–TOF mass spectrometry and high resolution ^{31}P-NMR spectroscopy. We confirmed our results using a complex biological lipid mixture from boar spermatozoa. Boar spermatozoa were chosen because they contain large amounts of polyunsaturated GPL (particularly DHA and docosapentaenoic acid, DPA) as well as plasmalogens. Under conditions of HOCl attack, we demonstrated a marked increase in GPC formation from PlsCho in boar spermatozoa, confirming that our model system is replicated in a lipid mixture mimicking in vivo conditions.

Experimental Procedures

Chemicals and Samples

All chemicals for NMR spectroscopy (sodium cholate, EDTA, and deuterated water with an isotopic purity of 99.6%), buffer preparation ($NaH_2PO_4 \times H_2O$, $Na_2HPO_4 \times 2H_2O$ and trishydroxymethylaminomethane, TRIS), and matrix preparation (*p*-nitroaniline, PNA) as well as all solvents (chloroform and methanol) and taurine (2-aminoethane-1-sulfonic acid) were obtained in the highest commercially available purity from Fluka Feinchemikalien GmbH (Taufkirchen, Germany). 1-*O*-1′-stearenyl-2-docosahexaenoyl-*sn*-glycero-3-phosphocholine ($SDHPC_{plasm}$), 1-stearoyl-2-docosahexaenoyl-*sn*-glycero-3-phosphocholine (SDHPC) and 1-*O*-1′-stearenyl-2-docosahexaenoyl-*sn*-glycero-3-phosphoethanolamine ($SDHPE_{plasm}$), 1-stearoyl-2-docosahexaenoyl-*sn*-glycero-3-phosphoethanolamine (SDHPE) as well as the internal standards 1-myristoyl-2-lyso-*sn*-glycero-3-phosphocholine (1-M-2-LPC), 1,2-dipalmitoyl-*sn*-glycero-3-phosphocholine (DPPC), 1-palmitoyl-2-oleoyl-*sn*-glycero-3-phosphocholine (POPC) and 1,2-dipalmitoyl-*sn*-glycero-3-phosphate (DPPA) were purchased from Avanti Polar Lipids (Alabaster, MA, USA) as solutions in $CHCl_3$ and used without further purification.

Boar spermatozoa lipid extracts were kindly provided by Dr. Karin Müller and co workers from the Leibnitz Institute for Zoo and Wildlife Research (Berlin, Germany). Boar semen was obtained from different fertile animals of a breeding station (Hermitage Deutschland GmbH Besamungseberstation Golzow, Germany). After the removal of seminal fluid by centrifugation (8 min, 700×*g*, 22 °C), the sperm pellets were pooled and extracted according to the method of Bligh and Dyer [48].

HOCl Incubation and Lipid Extraction

Two aliquots of the phosphatidylcholine (SDHPC) and the corresponding plasmalogen glycerophosphocholine

($SDHPC_{plasm}$) dissolved in chloroform were mixed in an equimolar ratio (each lipid 2 mM) and evaporated to dryness. Vesicles (4 mM GPL in total) were prepared by suspending the lipid film in a 50-mM phosphate buffer (pH 7.4) and vortexing vigorously for 30 s. A stock solution of NaOCl was kept in the dark at 4 °C. Its concentration was determined at pH 12 using $\varepsilon_{290} = 350\ M^{-1}\ cm^{-1}$ for ^{-}OCl [49]. NaOCl was diluted with phosphate buffered saline (50 mM) immediately prior to use. Liposomes were incubated with varying concentrations of $HOCl/ClO^{-}$ for 1 h at pH 7.4. Adding an excess of taurine stopped the reaction. Subsequently, twice the volume of a chloroform/methanol mixture (2:1, v/v) was added in comparison to the aqueous phase in order to extract the lipids [48]. Both, the organic and the aqueous layer were used for further analysis. Experiments with plasmalogen glycerophosphoethanolamine were performed in the same way. For the investigation of the boar spermatozoa lipid extracts 4 mM lipid vesicles (whole lipid extract; corresponding to approximately 0.6 mM plasmalogen-ChoGpl) were incubated with NaOCl and processed as described above.

MALDI–TOF Mass Spectrometric Measurements

Positive ion MALDI–TOF mass spectra were acquired on a Bruker Daltonics Autoflex workstation (Bremen, Germany). The system utilizes a pulsed nitrogen laser emitting at 337 nm. The extraction voltage was 20 kV and 200 single laser shots were averaged for each mass spectrum. In order to enhance the spectral resolution, spectra were recorded in the reflector mode under "delayed extraction" conditions [50, 51]. Internal standards were added for quantitative analysis [50–52]. Known amounts of DPPC and 1-M-2-LPC were added to the organic phases of interest prior to MALDI–TOF MS. Furthermore, GPC amounts were estimated by comparison with the intensities of selected matrix peaks [51, 53]. The organic or aqueous phases of the reaction mixtures were applied to the MALDI target using PNA as matrix [54]. For the investigation of the organic and aqueous phases the "low mass gate" (matrix suppression) was set to $m/z = 400$ and 150, respectively. All spectra were processed using the software "Flex analysis" version 2.2 provided by Bruker Daltonics.

^{31}P-NMR Spectroscopic Measurements

The dried organic and aqueous layers of the reaction mixtures were combined and solubilized [55, 56] in 50 mM TRIS (pH 7.65) containing 200 mM sodium cholate and 5 mM EDTA. DPPA was added as the concentration and frequency standard. After intense vortexing of the 0.5-ml samples ^{31}P-NMR spectra were recorded in 5-mm NMR tubes on a Bruker DRX-600 spectrometer operating at 242.88 MHz for ^{31}P. All measurements were performed using a direct $^{31}P/^{1}H$-NMR probe at 30 °C (303 K) with composite pulse decoupling (Waltz-16) to eliminate ^{31}P-^{1}H coupling. ^{31}P-NMR spectra of the boar spermatozoa extracts were additionally recorded at 60 °C (333 K). At this temperature the sphingomyelin (CerPCho) resonance is shifted to lower ppm values [57] and the GPC resonance can be clearly resolved whereas the GPC and CerPCho resonances overlap in the spectra recorded at 30 °C.

Other NMR parameters were as follows: experiment time: 2–8 h, data size: 8 k, 60° pulse (6.7 μs), pulse delay 2 s, and a line broadening of 1 Hz.

All peak assignments were confirmed by comparison with the shift of commercially available reference compounds. Spectra were processed using the software "1D WIN NMR" version 6.2® (Bruker Analytische Messtechnik GmbH, Rheinstetten, Germany) including the deconvolution (II) routine for peak area determination [58].

Results

Artificial Lipid Model System

In order to start with a simple model system, an artificial mixture of different commercially available GPL was used.

Artificial Mixture of Choline Glycerophospholipids

The plasmalogen glycerophosphocholine 1-*O*-1′-stearenyl-2-docosahexaenoyl-*sn*-glycero-3-phosphocholine ($SDHPC_{plasm}$) and the PtdCho 1-stearoyl-2-docosahexaenoyl-*sn*-glycero-3-phosphocholine (SDHPC) were investigated in the presence of different amounts of hypochlorous acid. Plasmalogens and PtdCho with highly unsaturated fatty acyl residues in the *sn*-2-position were chosen because of their extreme sensitivities to oxidative stress and their significant abundance in many cells, particularly spermatozoa. Both species possess six double bonds in the *sn*-2 position of their glycerol backbones but have different linkage types in the *sn*-1 position.

Selected examples of the positive ion MALDI–TOF mass spectra of the extracts of the reaction mixture are shown in Fig. 1. Spectra of untreated ChoGpl are shown in trace 1a. $SDHPC_{plasm}$ gives two major peaks at $m/z = 818.6$ and 840.6 corresponding to the H^{+} and Na^{+} adducts, respectively. Similarly, SDHPC shows also two peaks at $m/z = 834.6$ and 856.6 corresponding to the H^{+} and Na^{+} adducts. Spectra in Fig. 1 also exhibit additional peaks at $m/z = 468.3$ and 490.3 corresponding to 1-M-2-LPC. This compound was added to the organic phase as internal standard to allow reliable quantitative evaluation of the reaction products. POPC ($m/z = 760.6$ and 782.6)

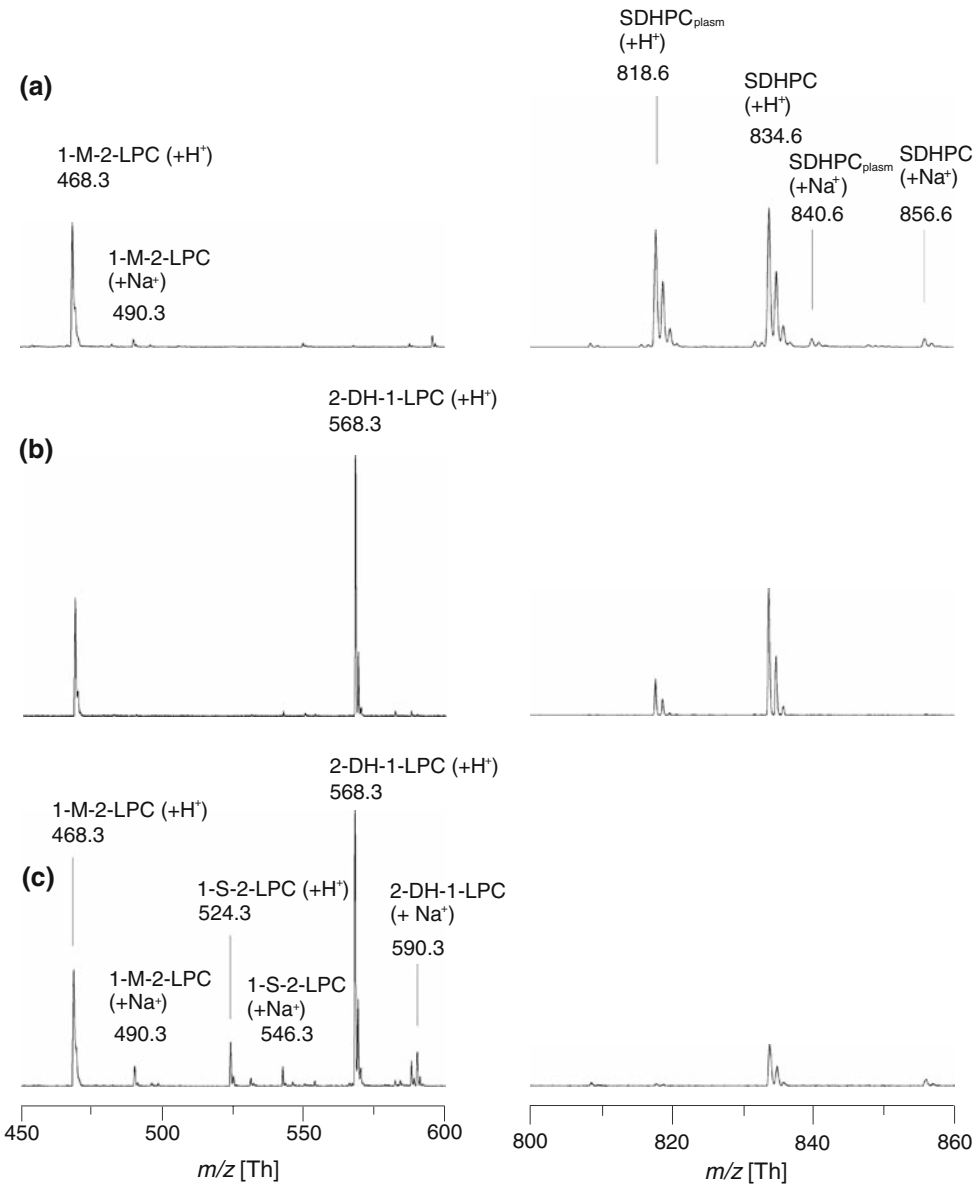

Fig. 1 Positive ion MALDI–TOF mass spectra of the organic extracts of a mixture of $SDHPC_{plasm}$ and SDHPC (2 mM each) after incubation with **a** buffer, **b** 2.5 and **c** 10 mM HOCl for 1 h at room temperature (~25 °C). The decrease of the plasmalogen-ChoGpl ($SDHPC_{plasm}$) and the phosphatidylcholine (SDHPC) with increasing HOCl concentrations is shown at the right hand side while the lysophosphatidylcholine generation (2-DH-1-LPC and 1-S-2-LPC) is shown at the left hand side. Spectra were scaled according to the integral intensity of the 1-M-2-LPC standard and the *m/z* values as well as the peak assignments are indicated. Spectra were split for clarity

was also added as internal standard for the quantitative assessment of the higher mass range (data not shown). Two different standards were used because compounds with higher masses are characterized by more marked contributions of heavier isotopes that lead to diminished peak intensities. Spectra were scaled along the *y* axis with respect to the intensity of 1-M-2-LPC. The POPC standard is not shown because spectra were split to emphasize the mass regions of interest.

The plasmalogen peaks were strongly diminished upon treatment with 2.5 mM HOCl, whereas the peak intensities of SDHPC remained nearly constant (trace 1b). Additional peaks became detectable in the low mass region at $m/z = 568.3$ and 590.3 corresponding to the H^+ and Na^+ adduct of 1-lyso-2-docosahexaenoyl-*sn*-glycero-3-phosphocholine (2-DH-1-LPC).

After treatment with 10 mM HOCl (i.e. a fivefold molar excess over the plasmalogen) the plasmalogen peaks (trace 1c) disappeared completely whereas the SDHPC peak is still detectable. The peak intensities of the 2-DH-1-LPC remained nearly constant, whereas additional peaks at $m/z = 524.3$ and 546.3 corresponding to the H^+ and Na^+ adduct of 1-stearoyl-2-lyso-*sn*-glycero-3-phosphocholine (1-S-2-LPC) were generated. However, the intensities of 2-DH-1-LPC were much higher in comparison to 1-S-2-LPC. This is a clear indication of the much higher reactivity of the vinyl-ether bond of the plasmalogens in comparison to the ester linkages of common GPL. Chlorohydrin formation (indicated by various 52 amu shifts as there are several reaction sites [38]) is marginally observed from SDHPC using HOCl concentrations of 5 mM and higher (data not shown).

The aqueous phases of the extracts of the incubation mixture were also analyzed by MALDI–TOF MS (data not shown). New peaks corresponding to GPC appeared at m/z = 258.1 and 280.1 in the HOCl-treated samples [47] but were completely absent in the control sample (data not shown). This clearly indicates that GPC is a major oxidation product of plasmalogens particularly if an excess of HOCl is used. The GPC generation will be discussed below in more detail.

In order to evaluate the relative contributions of 1-S-2-LPC, 2-DH-1-LPC and GPC, these products were quantified in dependence on the concentrations of HOCl used (data not shown, but see data obtained by ^{31}P-NMR as given below). Intensities of the peaks of interest were related to the intensities of the internal standards, i.e. the sum of the intensities of the H^+ and Na^+ adducts of 1-myristoyl-2-lyso-*sn*-glycero-3-phosphocholine (m/z = 468.3 and 490.3) for 1-lyso-2-acyl-glycerophosphocholines (Fig. 1), and the sum of the intensities of the H^+ and Na^+ adducts of 1-palmitoyl-2-oleoyl-*sn*-glycero-phosphocholine (m/z = 760.6 and 782.6) for the plasmalogen-ChoGpl and the PtdCho.

There are significant reactivity differences between $SDHPC_{plasm}$ and SDHPC with HOCl. The peaks of the plasmalogen $SDHPC_{plasm}$ decrease continuously with increasing HOCl concentrations whereby the contribution of 2-DH-1-LPC increases (Fig. 1). No plasmalogen could be detected anymore at HOCl concentrations higher than 7.5 mM, whereas the SDHPC peaks did not decrease significantly up to HOCl concentrations of 2.5 mM (Fig. 1, trace b). The conversion of SDHPC into the chlorohydrinated fatty acid and 1-S-2-LPC started at HOCl concentrations of about 5 mM, whereas the formation of GPC from plasmalogen was observed already at smaller HOCl concentrations and increased continuously if higher HOCl concentrations were used (data not shown). The proposed three-stage pathway of the reactions of HOCl with the PlsCho/PtdCho mixture relevant to Fig. 1 is schematically shown in Fig. 2. The sequential oxidation of plasmalogens to lysoPtdCho, which are important targets for the subsequent HOCl-attack leading to the generation of lysoPtdCho-chlorohydrins, is illustrated in this schema [4].

The reaction products of the $SDHPC_{plasm}$/SDHPC mixture subsequent to incubation with HOCl were additionally analyzed by ^{31}P-NMR spectroscopy. For that purpose, the aqueous and the organic phases were evaporated to dryness, recombined and solubilized in aqueous sodium cholate. Selected ^{31}P-NMR spectra of the mixture of $SDHPC_{plasm}$ and SDHPC after incubation with different amounts of HOCl are shown in Fig. 3. In trace a, the ^{31}P-NMR spectrum of the mixture of both GPLs (incubated with pure buffer in the absence of HOCl) is shown as reference. There is only one peak representing the combined resonances of $SDHPC_{plasm}$ and SDHPC at $\delta = -0.62$ ppm because no differentiation in dependence on the acyl or alkenyl residues can be made under the applied experimental conditions. A survey of the spectral resolution achievable by ^{31}P NMR using the mixed micelle approach is available in [58]. This spectrum (3a) unequivocally proves the absence of even small amounts of lysoPtdCho and GPC in the starting material.

^{31}P-NMR spectra of the $SDHPC_{plasm}$/SDHPC mixture after treatment with HOCl are shown in traces b and c. The intensities of the resonances of 2-DH-1-LPC and GPC detected at −0.18 and 0.03 ppm, respectively, are increasing in the presence of 2.5 mM HOCl (trace b). A further increase of the 2-DH-1-LPC and GPC resonances was observed if an increased excess of HOCl was used and an additional peak corresponding to 1-S-2-LPC appeared at −0.15 ppm (trace c). This compound is generated by the release of oxidatively-modified docosahexaenoic acid from the *sn*-2-position of SDHPC. Please note that a partial migration of the fatty acyl residue from the *sn*-2 to the *sn*-1 position (minor peak at −0.33 ppm) takes place in mixed detergent-GPL micelles [59]. Thus, a second very minor resonance of the corresponding lysoPtdCho isomer is detectable at −0.33 ppm but with much lower intensity than the "real" lysoPtdCho. This has nothing to do with the HOCl effect but is caused by a methodological reason [59].

The quantitative evaluation of the ^{31}P-NMR data is given in Fig. 4 whereby 0.5 mM DPPA was used as internal standard (the ^{31}P-NMR chemical shift is $\delta = 3.15$ ppm i.e. this resonance is outside the presented spectral range in Fig. 3). With increasing HOCl concentrations, the concentration of the $SDHPC_{plasm}$/SDHPC mixture decreases slowly (Fig. 4a, triangles). The concentration of 2-DH-1-LPC (Fig. 4a, rectangles) reaches a maximum at about 5 mM HOCl. The decrease of the $SDHPC_{plasm}$/SDHPC resonance for about 1.25 mM correlates with the 1.25 mM increase of the 2-DH-1-LPC at 5 mM HOCl. The subsequent slight decrease of the 2-DH-1-LPC resonance at HOCl concentrations of 7.5 and 10 mM is consistent with the simultaneously detected GPC generation (Fig. 4, trace b) and confirms the sequential formation of 2-DH-1-LPC and GPC even in the presence of an additional highly unsaturated PtdCho target. At the highest HOCl concentrations (7.5 and 10 mM), the generation of small amounts of 1-S-2-LPC derived from SDHPC is evident (Fig. 4a, circles). The loss of $SDHPC_{plasm}$/SDHPC (1.9 mM) at 10 mM HOCl is consistent with the sum of the concentration increase of 2-DH-1-LPC (1 mM), 1-S-2-LPC (0.3 mM) and GPC (0.6 mM). Thus, NMR data indicate a comparable behaviour as already evidenced by MALDI–TOF MS (cf. Fig. 1). Even if the detailed reasons of slight deviations between both methods are not yet clear, it seems likely that chlorohydrin

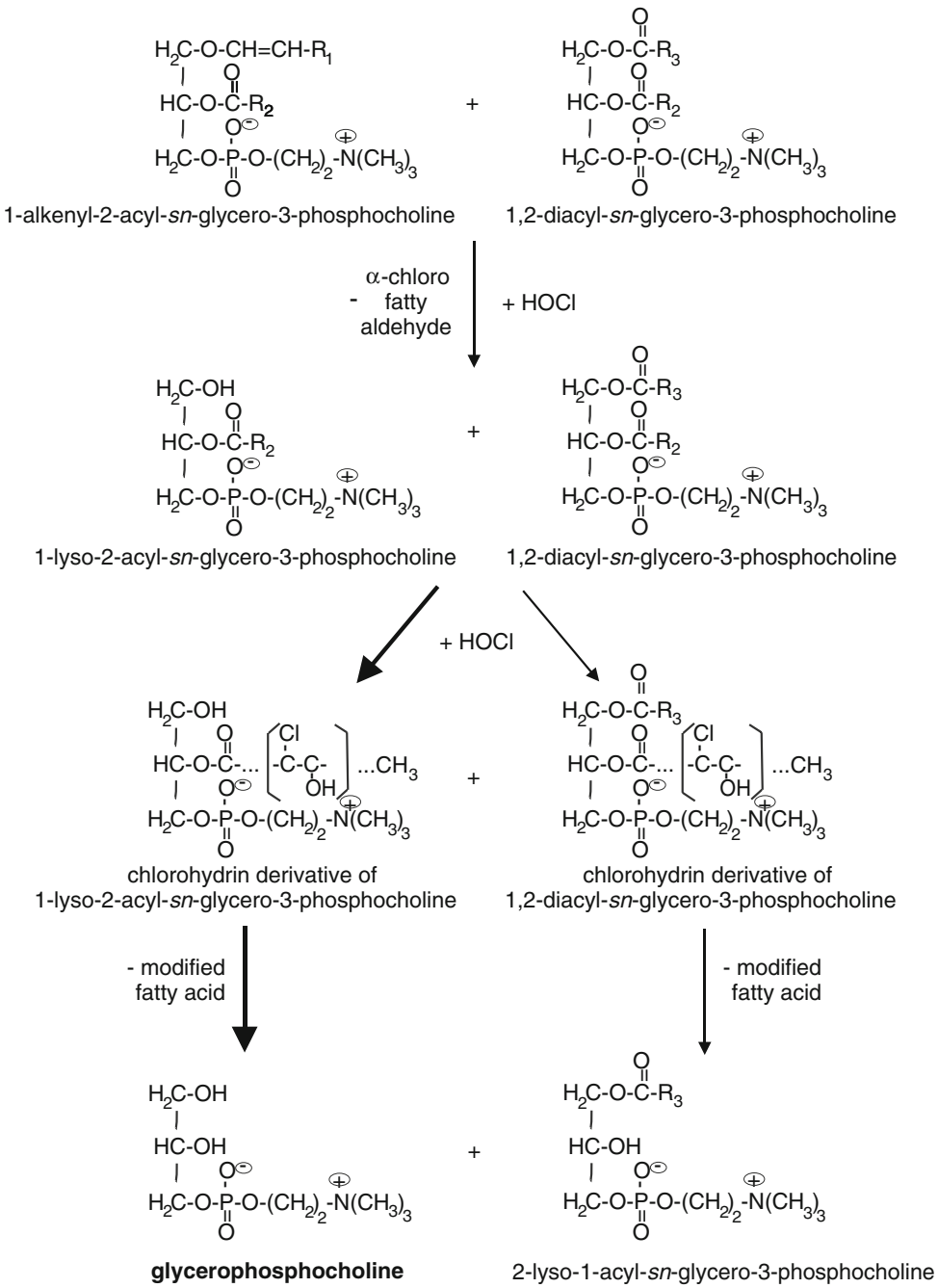

Fig. 2 Proposed three-stage pathway of the preferred cleavage of the *sn*-1 plasmalogen ChoGpl accompanied by the generation of 1-lyso-2-acyl ChoGpl and α-chloro fatty aldehydes in a plasmalogen/phosphatidylcholine mixture. In the second step, the formation of chlorohydrin derivatives of the polyunsaturated fatty acyl residues in the *sn*-2 position takes place leading finally (in the third step) to the generation of GPC in the case of the plasmalogen and 2-lyso-1-acyl glycerophosphocholine in the case of the phosphatidylcholine. R_1 stearenyl residue, R_2 docosahexaenoyl residue, R_3 palmityl residue

formation contributes to the observed differences: As previously shown [44], chlorohydrin formation is reflected by many different peaks of rather low intensities if MALDI–TOF MS is used, whereas in the case of NMR only broadening of the GPL resonance under retention of the integral intensity is observed.

Artificial Mixture of Phosphatidylethanolamines

For initial investigations of the HOCl-induced degradation of GPL of boar spermatozoa lipid extracts that contain a mixture of GPL, including PlsCho and PlsEtn, some selected plasmalogen species were also investigated on a model level after HOCl incubation by ^{31}P-NMR spectroscopy. Selected ^{31}P-NMR spectra of 1-*O*-1′-stearenyl-2-docosahexaenoyl-*sn*-glycero-3-phosphoethanolamine ($SDHPE_{plasm}$) after incubation with different concentrations of HOCl are shown in Fig. 5. In order to prevent the aggregation of the PlsEtn in the reaction mixture, these incubations were performed in the presence of completely saturated DPPC ($\delta = -0.61$ ppm) that does not react at all with HOCl. In trace a, the ^{31}P-NMR spectrum of $SDHPE_{plasm}$ incubated with pure buffer in the absence of HOCl is shown as control and the resonance of $SDHPE_{plasm}$ is obvious at $\delta = -0.04$ ppm.

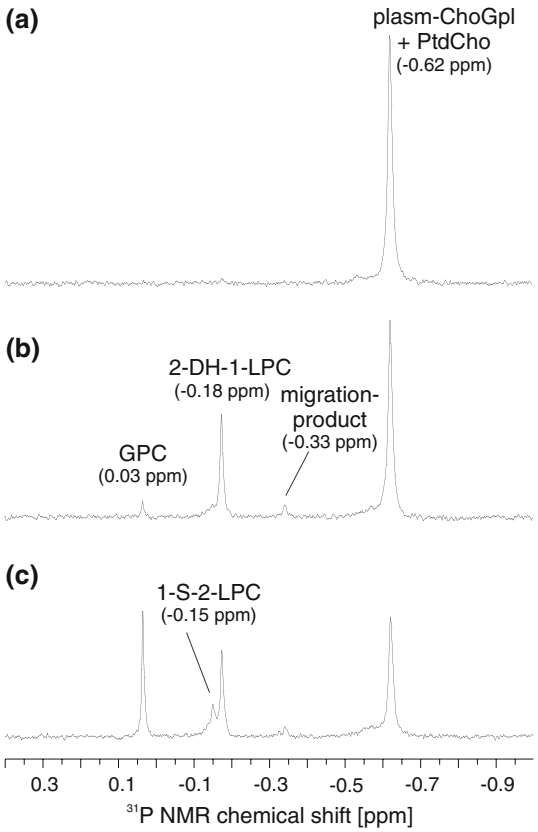

Fig. 3 242.88 MHz ^{31}P-NMR spectra of the combined organic and aqueous extracts of an $SDHPC_{plasm}$/SDHPC mixture after incubation with **a** buffer, **b** 2.5 mM and **c** 10 mM HOCl for 1 h at room temperature. The plasmalogen and PtdCho concentrations were each 2 mM in all cases. Spectra were scaled according to the intensity of the DPPA standard resonance (peak outside the shown chemical shift range at 3.15 ppm). Peak assignments and the related chemical shifts are indicated. Further methodological details are available in [58]

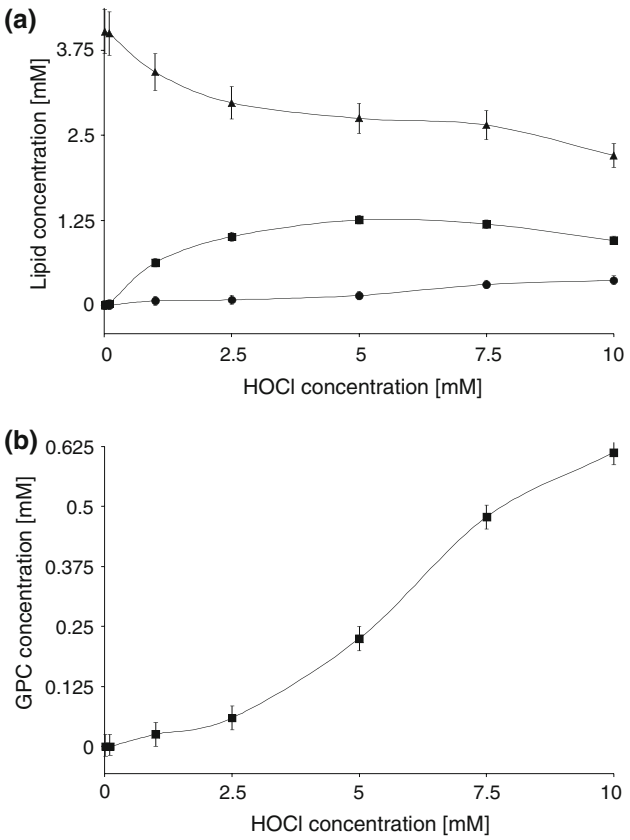

Fig. 4 Quantitative analysis of the integral peak intensities determined from the ^{31}P-NMR spectra provided in Fig. 3: The absolute $SDHPC_{plasm}$/SDHPC (*triangles*), 2-DH-1-LPC (*rectangles*) and 1-S-2-LPC (*circles*) concentrations (**a**) as well as the GPC concentrations (**b**) calculated by comparison with the integral intensity of the internal standard (DPPA) are shown. *Error bars* represent standard deviations of three independent measurements. The *drawn lines* were not derived from a mathematical model but only represent spline curves to guide the eye

With increasing HOCl concentrations (2.5 mM) the intensity of the $SDHPE_{plasm}$ resonance decreases continuously whereby 2-DH-1-LPE (0.37 ppm) and GPE (0.57 ppm) are generated (trace b). At the highest HOCl concentration (10 mM, trace c) the $SDHPE_{plasm}$ resonance has completely disappeared whereas the GPE resonance increased concomitantly with a decrease of the 2-DH-1-LPE resonance. This is in agreement with the sequential formation of 2-DH-1-LPE and GPE upon HOCl-treatment of polyunsaturated fatty acid containing PlsEtn.

It is rather surprising that basically the same products are obtained equally if plasmalogen-ChoGpl or -EtnGpl species react with HOCl. In contrast to the plasmalogen-ChoGpl, the -EtnGpl (as well as the lysoPtdEtn and the GPE) contain an additional "free" amino group that possesses high reactivity with HOCl [60]. The resulting mono- and dichloramines, however, are not very stable compounds and decompose slowly under generation of further compounds such as aldehydes or nitriles [60]. As the chemical shifts of lysoPtdEtn and GPE do not markedly change under the influence of HOCl, the question whether there is the intact plasmalogen-EtnGpl and/or potentially chlorinated species cannot be convincingly answered by means of ^{31}P NMR. Unfortunately, however, the detectability of chloramines by MALDI–TOF MS is also difficult [61]. Therefore, this question was not further addressed in this work.

ChoGpls and EtnGpls in a Model Mixture

For more detailed investigations of the HOCl-induced degradation of GPLs in complex lipid mixtures such as spermatozoa extracts, which contain not only plasmalogen-ChoGpls and plasmalogen-EtnGpls but also their GPLs mixtures mimicking a more complex lipid system, were finally investigated by ^{31}P-NMR spectroscopy. Selected ^{31}P-NMR spectra of an equimolar mixture of $SDHPE_{plasm}$, $SDHPC_{plasm}$, 1-stearoyl-2-docosahexaenoyl-*sn*-glycero-3-phosphoethanolamine (SDHPE) and SDHPC after

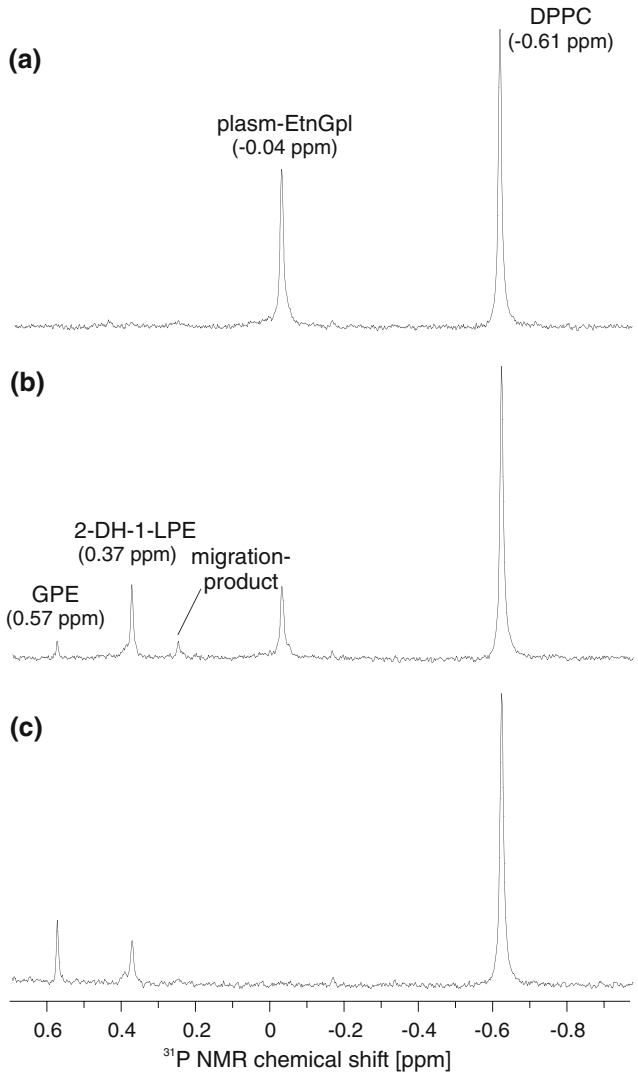

Fig. 5 242.88 MHz ^{31}P-NMR spectra of the combined organic and aqueous extracts of plasmalogen glycerophosphoethanolamine (in combination with DPPC that was added to suppress the aggregation of large EtnGpl aggregates) after incubation with **a** buffer, **b** 2.5 mM and **c** 10 mM HOCl for 1 h at room temperature. The plasmalogen concentration was 2 mM in all cases. Spectra were scaled according to the intensity of the DPPA standard resonance (peak outside the shown range at 3.15 ppm). All peak assignments and the corresponding ^{31}P-NMR chemical shifts are indicated

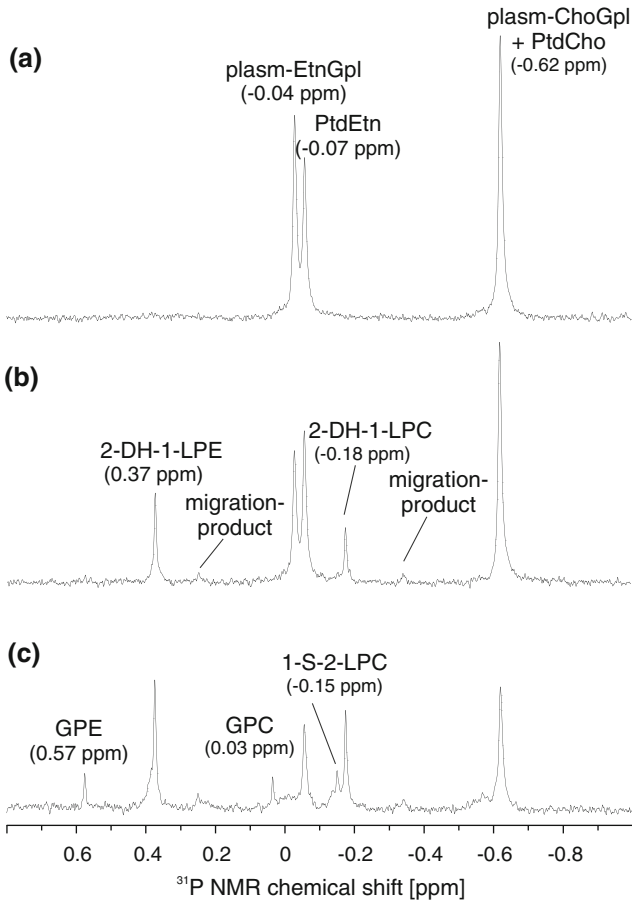

Fig. 6 242.88 MHz ^{31}P-NMR spectra of the combined organic and aqueous extracts of an $SDHPC_{plasm}$/SDHPC and $SDHPE_{plasm}$/SDHPE mixture after incubation with **a** buffer, **b** 2.5 mM and **c** 10 mM HOCl for 1 h at room temperature. The plasmalogen, PtdCho and PtdEtn concentrations accounted for 1 mM in all cases. Further methodological details are available in [58]

incubation with different concentrations of HOCl are shown in Fig. 6. In trace a, the ^{31}P-NMR spectrum of the reaction mixture incubated with pure buffer in the absence of HOCl is shown as control. The peaks appearing beside the resonances of $SDHPC_{plasm}$ and SDHPC at $\delta = -0.62$ ppm represent the resonances of $SDHPE_{plasm}$ (−0.04 ppm) and SCPE (−0.07 ppm). With increasing HOCl concentrations (2.5 mM) the intensities of the $SDHPE_{plasm}$ and the $SDHPC_{plasm}$/SDHPC resonance decrease continuously whereby 2-DH-1-LPE (0.37 ppm) and 2-DH-1-LPC (−0.18 ppm) are generated (trace b). At the highest HOCl concentration (10 mM, trace c) the $SDHPE_{plasm}$ resonance has completely disappeared whereas the GPE resonance increased concomitantly with the GPC resonance. This proves the sequential formation of 2-DH-1-LPE and GPE concomitantly with 2-DH-1-LPC and GPC upon HOCl-treatment of polyunsaturated plasmalogen-EtnGpls and ChoGpls in the same reaction mixture.

A quantitative evaluation of the ^{31}P-NMR data is given in Fig. 7. As already outlined above, 0.5 mM DPPA served as internal reference. With increasing HOCl concentrations, the concentration of the $SDHPC_{plasm}$/SDHPC resonance decreases slowly (Fig. 7a, black triangles). The concentration of 2-DH-1-LPC (Fig. 7a, black rectangles) reaches a maximum at about 5 mM HOCl. The decrease of the $SDHPC_{plasm}$/SDHPC resonance for about 0.7 mM correlates with the 0.7 mM increase of the 2-DH-1-LPC in the presence of 5 mM HOCl. The subsequent decrease in the 2-DH-1-LPC resonance at HOCl concentrations of 7.5 and 10 mM is consistent with the pronounced GPC

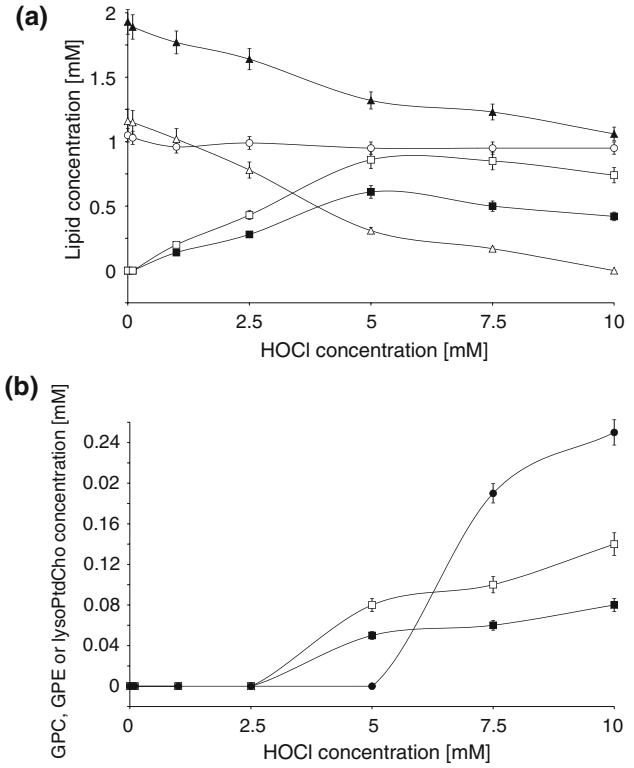

Fig. 7 Quantitative analysis of the integral peak intensities of the ^{31}P NMR resonances provided in Fig. 6: The absolute $SDHPC_{plasm}$/SDHPC (*black triangles*) and 2-DH-1-LPC (*black rectangles*) concentrations as well as the absolute $SDHPE_{plasm}$ (*white triangles*), SCPE (*white circles*) and 2-DH-1-LPE (*white rectangles*) concentrations (**a**) as well as the GPC (*black rectangles*), GPE (*white rectangles*) and 1-S-2-LPC (*black circles*) concentrations (**b**) calculated by comparison with the integral intensity of the internal standard (DPPA) are shown. *Error bars* represent standard deviations of three independent measurements. The *drawn lines* were not derived from a mathematical model but do only represent spline curves to guide the eye

generation (Fig. 7, trace b, black rectangles) and confirms the sequential formation of 2-DH-1-LPC and GPC from the plasmalogen even in the presence of additional highly unsaturated GPLs. At the highest HOCl concentrations (7.5 and 10 mM) the generation of small amounts of 1-S-2-LPC derived from SDHPC is also evident (Fig. 7b, black circles). The $SDHPC_{plasm}$/SDHPC concentration decrease by 0.8 mM at 10 mM HOCl concentration agrees well with the sum of the concentration increase of 2-DH-1-LPC (0.5 mM), 1-S-2-LPC (0.25 mM) and GPC (0.07 mM).

Furthermore, the concentration of the $SDHPE_{plasm}$ resonance decreases with increasing HOCl concentrations (Fig. 7a, white triangles). The concentration of 2-DH-1-LPE (Fig. 7a, white rectangles) reaches a maximum at about 5 mM HOCl. The decrease of the $SDHPE_{plasm}$ resonance by about 0.8 mM correlates with the 0.8 mM increase of the 2-DH-1-LPE at 5 mM HOCl. The subsequent decrease of the 2-DH-1-LPE resonance at the highest HOCl concentrations of 7.5 and 10 mM is consistent with the pronounced GPE generation (Fig. 7, trace b, white rectangles) and confirms the sequential formation of 2-DH-1-LPE and GPE even in the presence of further highly unsaturated GPLs. The intensity of the SDHPE resonance remains nearly constant upon HOCl treatment (Fig. 7a, white circles). The $SDHPE_{plasm}$ concentration decrease by 1 mM at 10 mM HOCl concentration agrees well with the sum of the concentration increase of 2-DH-1-LPE (0.85 mM) and GPE (0.14 mM).

Overall, the NMR data indicate only a slightly higher reactivity of $SDHPE_{plasm}$ in comparison to $SCPC_{plasm}$.

Boar Spermatozoa Extracts

Boar spermatozoa are characterized by a very high content of ether linked and plasmalogen GPL. The most important constituents are 1-*O*-1′-palmitenyl-2-docosahexaenoyl-*sn*-glycero-3-phosphocholine ($PDHPC_{plasm}$) and 1-*O*-1′-palmitenyl-2-docosahexaenoyl-*sn*-glycero-3-phosphoethanolamine ($PDHPE_{plasm}$) [20, 62].

Important ether-linked glycerophospholipids are 1-*O*-1′-palmityl-2-docosahexaenoyl-*sn*-glycero-3-phosphocholine ($PDHPC_{ether}$), 1-*O*-1′-palmityl-2-docosapentaenoyl-*sn*-glycero-3-phosphocholine ($PDPPC_{ether}$) and 1-*O*-1′-palmityl-2-docosapentaenoyl-*sn*-glycero-3-phosphoethanolamine ($PDPPE_{ether}$) [20]. Furthermore, boar spermatozoa contain significant amounts of sphingomyelin (CerPCho) and diacyl-PtdChos. However, a detailed investigation of the reactivity of these compounds with HOCl was outside the scope of this paper.

The ^{31}P-NMR spectra of boar spermatozoa lipid extracts after incubation with different concentrations of HOCl measured at 303 K (left hand side) and 333 K (right hand side) are shown in Fig. 8. These different temperatures were chosen in order to demonstrate the significant resolution increase under slightly different conditions. In trace a, the spectrum of a boar spermatozoa lipid extract incubated with pure buffer in the absence of HOCl is shown as reference. This spectrum exhibits six major resonances representing PlsCho and PtdCho (−0.62 ppm), PakCho (−0.56 ppm), two different CerPCho resonances (CerPCho 14:0 $\delta = -0.06$ and CerPCho 16:0 $\delta = 0.01$ ppm), plasmalogen–EtnGpl (−0.03 ppm) and ether–EtnGpl (0.02 ppm). This is in agreement with the known GPL composition of boar spermatozoa [20].

After incubation of the spermatozoa extracts with increasing HOCl concentrations (2.5 mM, i.e. about fourfold excess over the PlsCho, the PlsCho and PlsEtn resonances decreased significantly and resonances corresponding to the expected degradation products, the 2-DH-1-LPC (−0.18 ppm) and 2-DH-1-LPE (0.37 ppm), became detectable (Fig. 8, trace b). Furthermore, the PakCho resonance (−0.56 ppm) decreases slightly and ether-lysoPtdCho

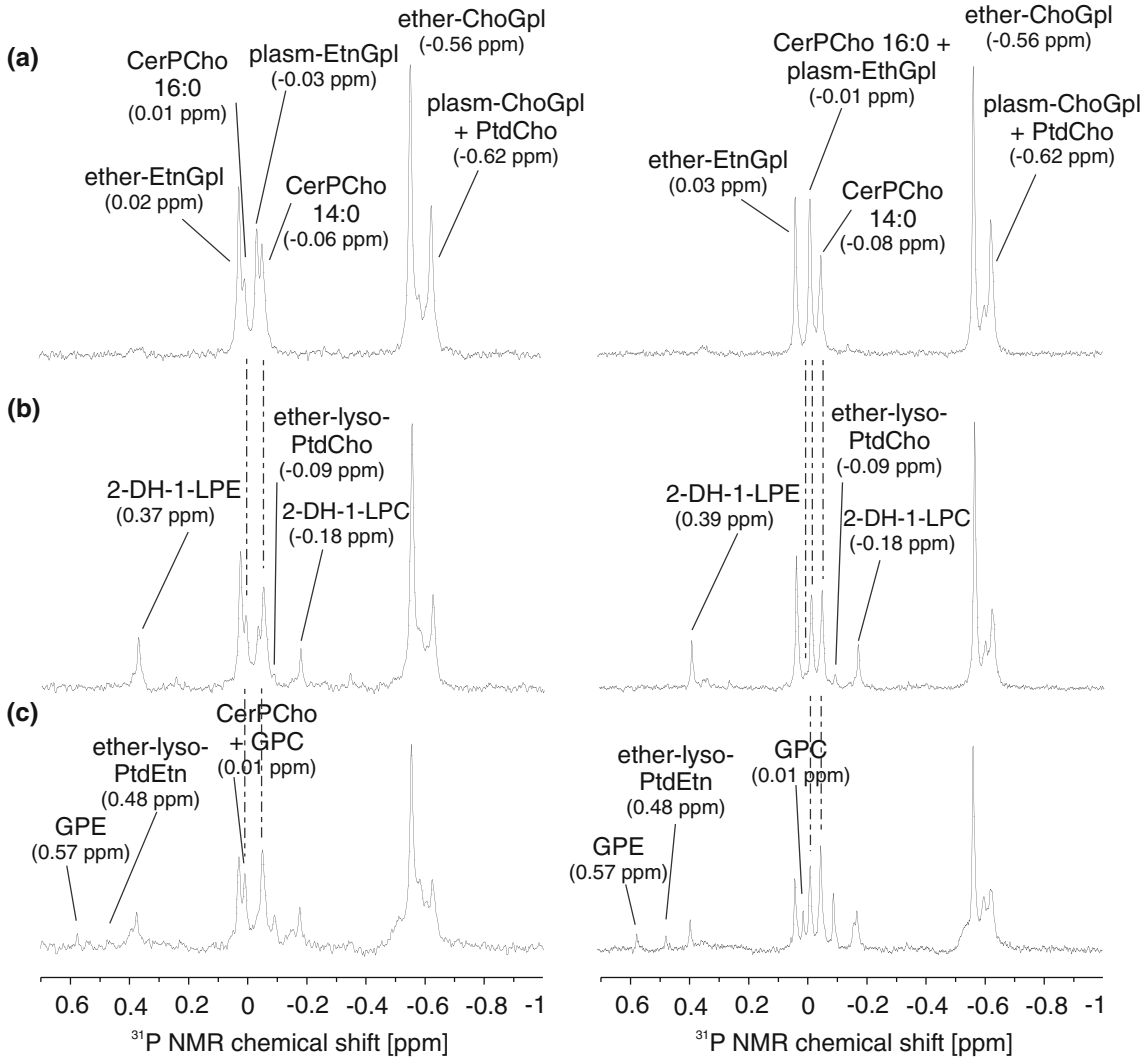

Fig. 8 242.88 MHz ^{31}P-NMR spectra of the combined organic and aqueous extracts of boar spermatozoa after incubation with **a** buffer, **b** 2.5 mM and **c** 10 mM HOCl for 1 h at room temperature. The spectra at the left side were acquired at 303 K whereas spectra at the right side were recorded at 333 K. The boar phospholipid concentration was about 4 mM in all cases. Spectra were scaled according to the resonance of the used DPPA standard (peak outside the shown frequency range at 3.15 ppm) and all peak assignments and the chemical shifts are indicated. *Vertical dotted lines* indicate the resonances undergoing the most pronounced changes

(−0.09 ppm) appears as a weak resonance. The intensities of PlsCho and PlsEtn as well as PakCho and PakEtn were additionally diminished after incubation with 10 mM HOCl (Fig. 8, trace c), whereby the intensities of the ether derived lysoPtdCho and lysoPtdEtn resonances increased slightly. In contrast, the 2-DH-1-LPC and 2-DH-1-LPE resonances remain nearly constant or decrease only slightly, respectively. This observation can be explained by the formation of GPC (0.01 ppm) and GPE (0.57 ppm) from unsaturated 1-lysoPtdCho and 1-lysoPtdEtn. Unfortunately, the resonance of GPC overlaps with the peak of CerPCho 16:0 if the ^{31}P-NMR spectra are recorded at 303 K. Therefore, all ^{31}P-NMR spectra were additionally acquired at 333 K (Fig. 8 right hand side). At 333 K the GPC peak can be differentiated from the resonance of CerPCho containing 16:0, whereby, however CerPCho containing 16:0 overlaps with PlsEtn (Fig. 8, trace a, right hand side). From the spectra recorded at 333 K it is evident that weak GPC formation is observed already after incubation with 2.5 mM HOCl (trace b, right hand side). At HOCl concentrations of 10 mM the GPC resonance reaches its maximum intensity (trace c, right hand side). This confirms the sequential formation of 2-DH-1-LPC and GPC as well as of 2-DH-1-LPE and GPE also upon HOCl-treatment of biologically relevant boar spermatozoa lipid extracts, not only in simplified model systems.

Additionally, the incubation of boar spermatozoa lipid extracts with different HOCl concentrations was also studied by MALDI–TOF MS. We focussed on $PDHPC_{plasm}$ in order to confirm the ^{31}P-NMR data. The $PDHPC_{plasm}$

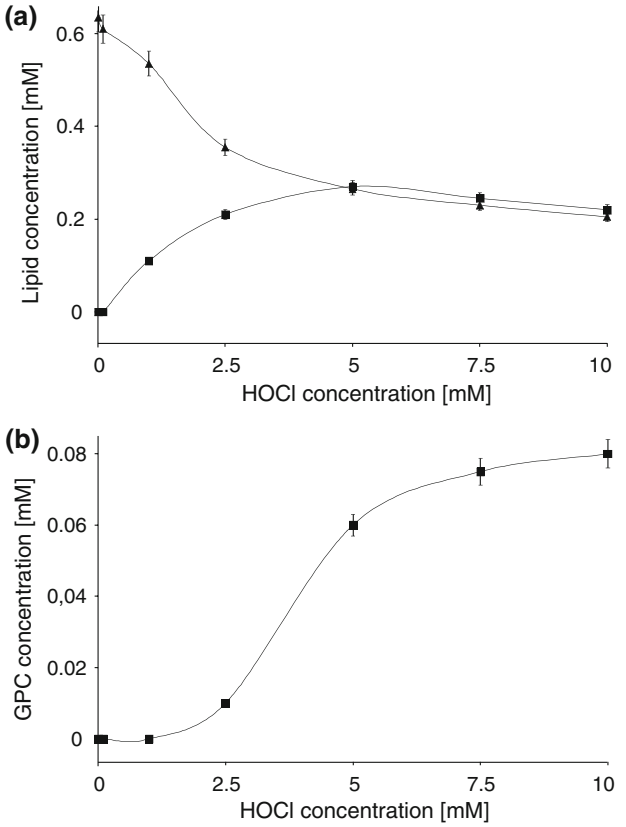

Fig. 9 Quantitative analysis of the integral peak intensities of the ^{31}P NMR spectra shown in Fig. 8. The absolute plasmalogen-ChoGpl (*triangles*) and the 2-DH-1-LPC concentrations (*rectangles*) (trace a) as well as the absolute GPC concentrations (*rectangles*) (trace b) determined by ^{31}P-NMR spectroscopy and calculated according to the known concentration of the DPPA internal standard are shown in dependence on the HOCl concentration. *Error bars* represent standard deviations of three independent measurements. In the case of the 2-DH-1-LPC the *error bars* are in the range of the symbol size. The *drawn lines* were not derived from a mathematical model but do only represent spline curves to guide the eye

peaks at $m/z = 790.6$ and 812.6 (initial concentration about 0.6 mM) disappeared nearly completely upon treatment with 2.5 mM HOCl (data not shown). New peaks were detectable in the low mass range at $m/z = 568.3$ and 590.3 corresponding to the H^+ and Na^+ adduct of 1-lyso-2-docosahexaenoyl-*sn*-glycero-3-phosphocholine (2-DH-1-LPC). After incubation with 10 mM HOCl the 2-C-1-LPC peaks disappeared. Concomitantly, the peaks of GPC ($m/z = 258.1$ and 280.1) appeared in the spectra of the aqueous phases and increased with increasing HOCl concentrations (data not shown).

A quantitative evaluation of the data obtained by ^{31}P NMR is shown in Fig. 9. Only the fate of the PlsCho and their related degradation products were quantitatively analyzed. Unfortunately, however, the PlsCho resonance overlaps with the PtdCho resonance in the ^{31}P-NMR spectra and, thus, both compounds can not be individually analyzed. However, the intensity loss of PlsCho was accompanied by an increase of the corresponding 2-DH-1-LPC resonance. With increasing HOCl concentrations, the PlsCho concentration decreases slowly (trace a, triangles), whereby HOCl concentrations of 2.5 mM and higher lead to marked degradation of PlsCho. The concentration of 2-DH-1-LPC (trace a, rectangles) reaches a maximum at about 5 mM HOCl. The subsequent decrease of the 2-DH-1-LPC concentration in the presence of 7.5 and 10 mM HOCl is consistent with marked GPC generation (trace 9b). However, please note that GPC formation starts already at HOCl concentrations of about 2.5 mM. This result unequivocally proves the degradation of the initially formed 2-DH-1-LPC from plasmalogen-ChoGpl and the subsequent formation of GPC under the influence of HOCl. This obviously also holds for complex biological lipid mixtures where highly unsaturated GPL "substrates" are additionally available for reaction with HOCl.

Discussion

The high sensitivity of plasmalogens—in particular their vinyl-ether bond—to different ROS has been well documented [3]. In a previous study the degradation of PlsCho by HOCl, a highly oxidative and chlorinating reagent produced by MPO, a heme-enzyme which is released by stimulated PMNL under inflammatory conditions could be demonstrated. PlsCho containing highly unsaturated fatty acyl residues (e.g. DHA) at the *sn*-2-position of the glycerol backbone are degraded by HOCl to a higher extent than PtdCho resulting in 1-lysoPtdCho as well as glycerophosphocholine [47]. This confirms that the vinyl-ether bond is the most oxidation-sensitive double bond in GPL leading to 1-lysoPtdCho, whereas the highly unsaturated acyl residue in the *sn*-2 position is less sensitive to ROS and results in GPC generation. This holds at least for isolated PlsCho model systems.

However, oxidative stress affects not only one substrate or one particular GPL class. From the chemical view of lipid oxidation all highly unsaturated acyl residues are sensitive targets for HOCl. Consequently, the aim of this study was to investigate which highly unsaturated acyl chain is oxidatively modified to which extent by HOCl treatment of a PlsCho and PtdCho mixture containing both the same highly unsaturated fatty acyl residue, DHA, in *sn*-2 position.

In addition to the expected 2-DH-1-LPC generation from $SDHPC_{plasm}$ in a $SDHPC_{plasm}$/SDHPC mixture, a secondary reaction product—GPC—resulting from further degradation of 2-DH-1-LPC can be easily observed if only a slight excess of HOCl is used. In contrast, only minor 1-S-2-LPC generation (resulting from HOCl-induced degradation of

SDHPC) could be detected. The GPC generation from $SDHPC_{plasm}$ or its degradation product, 2-DH-1-LPC, is about three times more pronounced than the 1-S-2-LPC generation from SDHPC in an equimolar mixture of $SDHPC_{plasm}$/SDHPC. This is remarkable because both contain the same fatty acyl residue in the *sn*-2 position but in complete agreement with former investigations [63].

Obviously, HOCl cleaves the unsaturated fatty acyl chain preferentially in 2-DH-1-LPC rather than in SDHPC. One possible explanation is the fact that the fatty acyl chain in the *sn*-2 position of SDHPC is sterically shielded against ROS attacks in comparison to the acyl chain in the *sn*-2 position of 2-DH-1-LPC. In contrast, the *sn*-2 position of 2-DH-1-LPC seems easily accessible for HOCl (leading finally to GPC generation) when the residue in *sn*-1 position is previously hydrolyzed by HOCl. However, it is so far unknown if this in vitro effect is primarily caused by the much smaller vesicular size of 2-DH-1-LPC in comparison to SDHPC [58]. The generation of chlorohydrins as transients between the educt and the corresponding lyso compound was also expected. As lipids with polyunsaturated fatty acyl residues were exclusively used in this study, many different chlorinated products can be expected. High numbers of chlorination sites induce the cleavage of the modified fatty acyl residues due to the considerable electronegativity of the added chlorine [44]. Therefore, the negligible generation of chlorohydrins is caused by simultaneous generation of lysolipids. Additionally, the large variety of chlorinated products results in very low peak intensities per single product and, thus, poor detectability.

Additionally, PlsEtn exhibited a similar reaction behavior as PlsCho upon HOCl-treatment leading to 2-DH-1-LPE and further GPE generation, whereby PlsEtn exhibited apparently slightly higher reactivity than ChoGpl.

Subsequent to the evaluation of artificial GPL systems, a more complex lipid system mimicking the complex lipid mixtures of biological membranes was also investigated. Many tissues and cellular membranes contain significant amounts of plasmalogens. Spermatozoa membranes, especially boar spermatozoa [20], contain elevated amounts of PlsCho and PlsEtn. Furthermore, they contain considerable amounts of other highly unsaturated GPL, for instance PakCho and PakEtn. The detection of alterations in the concentration of selected lipid-derived metabolites can be beneficial in the management of various pathological conditions, including infertility in males [64], whereby the GPC concentration in mammalian semen is considerable and much higher than in other body fluids [65]. For this reason, boar spermatozoa membrane lipid extracts were investigated to translate the results of the PlsCho/PtdCho mixture into a more complex, but also more relevant biological lipid mixture.

GPC is known as a water-soluble phosphodiester acting as lysophospholipase inhibitor and represents, therefore, a compound that decreases the phospholipid turnover [65, 66]. The GPL content of spermatozoa does not significantly change but the GPC concentration increases during their passage through the female genital tract [65]. Thus, decreased plasmalogen levels are likely to result in enhanced GPC concentrations that in turn enable lysophospholipid reacylation and reduce the need of de novo GPL synthesis [65]. Nevertheless, GPC accumulation is efficiently regulated by the enzyme GPC: choline phosphodiesterase [67].

Aging or chronic inflammatory processes are characterized by a significant decrease in the plasmalogen content and concomitantly an accumulation of oxidation products that are likely to disturb the sensitive balance between apoptosis and necrosis [22, 68]. Exceedingly high necrosis rates may result in spermatozoa damage and infertility. Thus, the role of accumulated plasmalogen degradation products under conditions of oxidative stress must be studied in more detail. GPC and GPE are presumably also relevant but so far underestimated oxidation products.

Summarizing, we were able to demonstrate that the formation of GPC and GPE from PlsCho and PlsEtn, respectively, occurs under in vitro and in vivo conditions also in the presence of further highly unsaturated GPL. The first step of the HOCl-induced degradation of GPL mixtures containing plasmalogens is surely the oxidation of the vinyl-ether group resulting in the generation of 1-lysoPtdCho and 1-lysoPtdEtn. It could be shown that HOCl subsequently affects the fatty acyl residue in the *sn*-2 position of 1-lysoPtdCho about three times more efficiently than that of diacyl-GPLs.

Consequently, the generation of GPC and GPE from plasmalogen-ChoGpls and -EtnGpl and their degradation products (1-lysoPtdCho and 1-lysoPtdEtn) must be considered as highly relevant in biological membranes and particularly under inflammatory conditions.

Acknowledgment This work was supported by the German Research Council (DFG Schi 476/5-1, FU 771/1-1 and Gl 199/4-3) and the Federal Ministry of Education and Research (Grant BMBF 0313836). The kind gift of boar spermatozoa samples by Dr. Karin Müller and Ulrike Jakop is gratefully acknowledged. We would also like to thank the Translational Centre for Regenerative Medicine (TRM) Leipzig for the possibility to use the selective ^{31}P dual NMR probe. Finally, we are greatly indebted to Dr. Jürgen Schiller for careful proof-reading of the final manuscript version.

References

1. Zommara M, Tachibana N, Mitsui K, Nakatani N, Sakono M, Ikeda I, Imaizumi K (1995) Inhibitory effect of ethanolamine plasmalogen on iron- and copper-dependent lipid peroxidation. Free Radic Biol Med 18:599–602

2. Vance JE (1990) Lipoproteins secreted by cultured rat hepatocytes contain the antioxidant 1-alk-1-enyl-2-acylglycerophosphoethanolamine. Biochim Biophys Acta 1045:128–134
3. Brites P, Waterham HR, Wanders RJA (2004) Functions and biosynthesis of plasmalogens in health and disease. Biochim Biophys Acta 1636:219–231
4. Messner MC, Albert CJ, Hsu F-F, Ford DA (2006) Selective plasmenyl choline oxidation by hypochlorous acid: formation of lysophosphatidylcholine chlorohydrins. Chem Phys Lipids 144:34–44
5. Morand OH, Zoeller RA, Raetz CRH (1988) Disappearance of plasmalogens from membranes of animal cells subjected to photosensitized oxidation. J Biol Chem 263:11597–11606
6. Zoeller RA, Morand OH, Raetz CRH (1988) A possible role for plasmalogens in protecting animal cells against photosensitized killing. J Biol Chem 263:11590–11596
7. Skaff O, Pattison DI, Davies MJ (2008) The vinyl ether linkages of plasmalogens are favored targets for myeloperoxidase-derived oxidants: a kinetic study. Biochemistry 47:8237–8245
8. Thai T-P, Rodemer C, Worsch J, Hunziker A, Gorgas K, Just WW (1999) Synthesis of plasmalogens in eye lens epithelial cells. FEBS Lett 456:263–268
9. Spiteller G (1993) Review: on the chemistry of oxidative stress. J Lipid Mediat 7:199–221
10. Brosche T, Platt D (1998) The biological significance of plasmalogens in defense against oxidative damage. Exp Gerontol 33:363–369
11. Khaselev N, Murphy RC (1998) Susceptibility of plasmenyl glycerophosphatidylethanolamine lipids containing arachidonate to oxidative degradation. Free Radic Biol Med 26:275–284
12. Rosenberger TA, Oki J, Purdon D, Rapoport SI, Murphy EJ (2002) Rapid synthesis and turnover of brain microsomal ether phospholipids in the adult rat. J Lipid Res 43:59–68
13. Farooqui AA, Yang H-C, Horrocks LA (1995) Plasmalogens, phospholipase A_2 and signal transduction. Brain Res Rev 21:152–161
14. Farooqui AA, Ong W-Y, Horrocks LA (2006) Inhibitors of brain phospholipase A_2 activity: their neuropharmacological effects and therapeutic importance for the treatment of neurological disorders. Pharmacol Rev 58:591–620
15. McHowat J, Liu S, Creer MH (1998) Selective hydrolysis of plasmalogen phospholipids by Ca^{2+}-independent PLA_2 in hypoxic ventricular myocytes. Am J Physiol 274:C1727–C1737
16. McHowat J, Creer MH (2000) Selective plasmalogen substrate utilization by thrombin-stimulated Ca^{2+}-independent PLA_2 in cardiomyocytes. Am J Physiol Heart Circ Physiol 278:H1933–H1940
17. Scherrer LA, Gross RW (1989) Subcellular distribution, molecular dynamics and catabolism of plasmalogens in myocardium. Mol Cell Biochem 88:97–105
18. Han X, Gross RW (1992) Nonmonotonic alterations in the fluorescence anisotropy of polar head group labeled fluorophores during the lamellar to hexagonal phase transition of phospholipids. Biophys J 63:309–316
19. Gross RW (1984) High plasmalogen and arachidonic acid content of canine myocardial sarcolemma: a fast atom bombardment mass spectroscopic and gas chromatography-mass spectroscopic characterization. Biochemistry 23:158–165
20. Leßig J, Gey C, Süß R, Schiller J, Glander H-J, Arnhold J (2004) Analysis of the lipid composition of human and boar spermatozoa by MALDI–TOF mass spectrometry, thin layer chromatography and ^{31}P NMR spectroscopy. Comp Biochem Physiol Biochem Mol Biol 137B:265–277
21. Lenzi A, Picardo M, Gandini L, Dondero F (1996) Lipids of the sperm plasma membrane: from polyunsaturated fatty acids considered as markers of sperm function to possible scavenger therapy. Hum Reprod Update 2:246–256
22. Goodenowe DB, Cook LL, Liu J, Lu Y, Jayasinghe DA, Ahiahonu PWK, Heath Y, Flax J, Krenitzky KF, Sparks DL, Lerner A, Friedland RP, Kudo T, Kamino K, Morihara T, Takeda M, Wood P (2007) Peripheral ethanolamine plasmalogen deficiency: a logical causative factor in Alzheimer's disease and dementia. J Lipid Res 48:2485–2498
23. Hartmann T, Kuchenbecker J, Grimm MOW (2007) Alzheimer's disease: the lipid connection. J Neurochem 103(Suppl 1):159–170
24. Weisser M, Vieth M, Stolte M, Riederer P, Pfeuffer R, Leblhuber F, Spiteller G (1997) Dramatic increase of alpha-hydroxyaldehydes derived from plasmalogens in the aged human brain. Chem Phys Lipids 90:135–142
25. Han X, Holtzman DM, McKeel D Jr (2001) Plasmalogen deficiency in early Alzheimer's disease subjects and in animal models: molecular characterization using electrospray ionization mass spectrometry. J Neurochem 77:1168–1180
26. Farooqui AA, Horrocks LA (2001) Plasmalogens: workhouse lipids of membranes in normal and injured neurons and glia. Neuroscientist 7:232–245
27. Dudda A, Spiteller G, Kobelt F (1996) Lipid oxidation products in ischemic porcine heart tissue. Chem Phys Lipids 82:39–51
28. André A, Juanéda P, Sébédio JL, Chardigny JM (2005) Effects of aging and dietary n-3 fatty acids on rat brain phospholipids: focus on plasmalogens. Lipids 40:799–806
29. Kuczynski B, Reo NV (2006) Evidence that plasmalogen is protective against oxidative stress in the rat brain. Neurochem Res 31:639–656
30. Brosche T, Brueckmann M, Haase KK, Sieber C, Bertsch T (2007) Decreased plasmalogen concentration as a surrogate marker of oxidative stress in patients presenting with acute coronary syndromes or supraventricular tachycardias. Clin Chem Lab Med 45:689–691
31. Leβig J, Fuchs B (2009) Plasmalogens in biological systems: their role in oxidative processes in biological membranes, their contribution to pathological processes and aging and plasmalogen analysis. Curr Med Chem 16:2021–2041
32. Klebanoff SJ (1991) Myeloperoxidase: occurrence and biological function. In: Everse J, Everse KE, Grisham MB (eds) Peroxidases in chemistry and biology, vol 1. CRC Press, Boca Raton
33. Winterbourn CC (1985) Comparative reactivities of various biological compounds with myeloperoxidase-hydrogen peroxide-chloride, and similarity of oxidant to hypochlorite. Biochim Biophys Acta 840:204–210
34. Pattison DI, Davies MJ (2001) Absolute rate constant for the reaction of hypochlorous acid with protein side chains and peptide bonds. Chem Res Toxicol 14:1453–1464
35. Hawkins CL, Pattison DI, Davies MJ (2002) Hypochlorite-induced oxidation of amino acids, peptides and proteins. Amino Acids 25:259–274
36. Schiller J, Arnhold J, Gründer W, Arnold K (1994) The action of hypochlorous acid on polymeric components of cartilage. Biol Chem Hoppe-Seyler 375:167–172
37. Prütz WA (1996) Hypochlorous acid interactions with thiols, nucleotides, DNA, and other biological substrates. Arch Biochem Biophys 332:110–120
38. Arnhold J, Osipov AN, Spalteholz H, Panasenko OM, Schiller J (2001) Effects of hypochlorous acid on unsaturated phosphatidylcholines. Free Radic Biol Med 31:1111–1119
39. Winterbourn CC, van den Berg JJM, Roitman E, Kuypers FA (1992) Chlorohydrin-formation from unsaturated fatty acids reacted with hypochlorous acid. Arch Biochem Biophys 296:547–555
40. Van den Berg JJM, Winterbourn CC, Kuypers FA (1993) Hypochlorous-acid mediated modification of cholesterol and phospholipids: analysis by gas chromatography-mass spectrometry. J Lipid Res 34:2005–2012

41. Thukkani AK, Hsu F-F, Crowley JR, Wysolmerski RB, Albert CJ, Ford DA (2002) Reactive chlorinating species produced during neutrophil activation target tissue plasmalogens. J Biol Chem 277:3842–3849
42. Albert CJ, Crowley JR, Hsu F-F, Thukkani AK, Ford DA (2001) Reactive chlorinating species produced by myeloperoxidase target the vinyl ether bond of plasmalogens. J Biol Chem 276:23733–23741
43. Thukkani AK, Albert CJ, Wildsmith KR, Messner MC, Martinson BD, Hsu F-F, Ford DA (2003) Myeloperoxidase-derived reactive chlorinating species from human monocytes target plasmalogens in low density lipoprotein. J Biol Chem 278:36365–36372
44. Arnhold J, Osipov AN, Spalteholz H, Panasenko OM, Schiller J (2002) Formation of lysophospholipids from unsaturated phosphatidylcholines under the influence of hypochlorous acid. Biochim Biophys Acta 1572:91–100
45. Panasenko OM, Schiller J, Spalteholz H, Arnhold J (2003) Myeloperoxidase-induced formation of chlorohydrins and lysophospholipids from unsaturated phosphatidylcholines. Free Radic Biol Med 34:553–562
46. Khaselev N, Murphy RC (2000) Structural characterization of oxidized phospholipid products derived from arachidonate: containing plasmenyl glycerophosphocholine. J Lipid Res 41:564–572
47. Leßig J, Schiller J, Arnhold J, Fuchs B (2007) Hypochlorous acid-mediated generation of glycerophosphocholine from unsaturated plasmalogen glycerophosphocholine lipids. J Lipid Res 48:1316–1324
48. Bligh EG, Dyer WJ (1959) A rapid method of total lipid extraction and purification. Can J Biochem Physiol 37:911–917
49. Morris JC (1966) Acid ionization constant of HOCl from 5 to 35 degrees. J Phys Chem 70:133–140
50. Fuchs B, Arnold K, Schiller J (2008) Mass spectrometry of biological molecules. In: Meyers RA (ed) Encyclopedia of analytical chemistry. Wiley, Chichester
51. Schiller J, Süß R, Arnhold J, Fuchs B, Leßig J, Müller M, Petković M, Spalteholz H, Zschörnig O, Arnold K (2004) Matrix-assisted laser desorption and ionization time-of-flight (MALDI-TOF) mass spectrometry in lipid and phospholipid research. Prog Lipid Res 43:443–478
52. Benard S, Arnhold J, Lehnert M, Schiller J, Arnold K (1999) Experiments towards quantification of saturated and polyunsaturated diacylglycerols by matrix-assisted laser desorption and ionization time-of-flight mass spectrometry. Chem Phys Lipids 100:115–125
53. Asbury GR, Al-Saad K, Siems WF, Hannan RM, Hill HH (1999) Analysis of triacylglycerols and whole oils by matrix-assisted laser desorption/ionization time-of-flight mass spectrometry. J Am Soc Mass Spectrom 10:983–991
54. Estrada R, Yappert MC (2004) Alternative approaches for the detection of various phospholipid classes by matrix-assisted laser desorption/ionization time-of-flight mass spectrometry. J Mass Spectrom 39:412–422
55. Pearce JM, Komoroski RA (2000) Analysis of phospholipid molecular species in brain by ^{31}P NMR spectroscopy. Magn Reson Med 44:215–223
56. London E, Feigenson GW (1979) Phosphorous NMR analysis of phospholipids in detergents. J Lipid Res 20:408–412
57. Puppato A, DuPré DB, Stolowich N, Yappert MC (2007) Effect of temperature and pH on ^{31}P nuclear magnetic resonances of phospholipids in cholate micelles. Chem Phys Lipids 150:176–185
58. Schiller J, Müller M, Fuchs B, Arnold K, Huster D (2007) ^{31}P NMR spectroscopy of phospholipids: from micelles to membranes. Curr Anal Chem 3:283–301
59. Plückthun A, Dennis EA (1982) Acyl and phosphoryl migration in lysophospholipids: importance in phospholipid synthesis and phospholipase specificity. Biochemistry 21:1743–1750
60. Fuchs B, Schober C, Richter G, Nimptsch A, Süß R, Schiller J (2008) The reactions between HOCl and differently saturated phospholipids: physiological relevance, products and methods of evaluation. Mini Rev Org Chem 5:254–261
61. Richter G, Schober C, Süß R, Fuchs B, Birkemeyer C, Schiller J (2008) Comparison of the positive and negative ion electrospray ionization and matrix-assisted laser desorption ionization time-of-flight mass spectra of the reaction products of phosphatidylethanolamines and hypochlorous acid. Anal Biochem 376:157–159
62. Fuchs B, Jakop U, Göritz F, Hermes R, Hildebrandt T, Schiller J, Müller K (2009) MALDI-TOF "fingerprint" phospholipid mass spectra allow the differentiation between ruminantia and feloideae spermatozoa. Theriogenology 71:568–575
63. Reiss D, Beyer K, Engelmann B (1997) Delayed oxidative degradation of polyunsaturated diacyl phospholipids in the presence of plasmalogen phospholipids in vitro. Biochem J 323:807–814
64. Deepinder F, Chowdary HT, Agarwal A (2007) Role of metabolomic analysis of biomarkers in the management of male infertility. Expert Rev Mol Diagn 7:351–358
65. Burt CT, Ribolow H (1994) Glycerol phosphorylcholine (GPC) and serine ethanolamine phosphodiester (SEP): evolutionary mirrored metabolites and their potential metabolic roles. Comp Biochem Physiol Biochem Mol Biol 108B:11–20
66. Ribolow H, Burt C (1987) Analysis of lipid metabolism in semen and its implications. In: McCarthy S, Hazeline F (eds) Magnetic resonance of the reproductive system, Slack, Thorofare
67. Burg MB (1995) Molecular basis of osmotic regulation. Am J Physiol 268:F983–F996
68. Maeba R, Maeda T, Kinoshita M, Takao K, Takenaka H, Kusano J, Yoshimura N, Takeoka Y, Yasuda D, Okazaki T, Teramoto T (2007) Plasmalogens in human serum positively correlate with high-density lipoprotein and decrease with aging. J Atheroscler Thromb 14:12–18

Lipids (2010) 45:53–61
DOI 10.1007/s11745-009-3370-y

ORIGINAL ARTICLE

Olive Oils Modulate Fatty Acid Content and Signaling Protein Expression in Apolipoprotein E Knockout Mice Brain

Regina Alemany · María A. Navarro · Oliver Vögler · Javier S. Perona · Jesús Osada · Valentina Ruiz-Gutiérrez

Received: 24 July 2009 / Accepted: 19 October 2009 / Published online: 19 November 2009

Abstract Atherosclerosis contributes to disruption of neuronal signaling pathways by producing lipid-dependent modifications of brain plasma membranes, neuroinflammation and oxidative stress. We investigated whether long-term (11 weeks) consumption of refined- (ROO) and pomace- (POO) olive oil modulated the fatty acid composition and the levels of membrane signaling proteins in the brain of apolipoprotein E (apoE) knockout (KO) mice, an animal model of atherosclerosis. Both of these oils are rich in bioactive molecules with anti-inflammatory and antioxidant effects. ROO and POO long-term consumption increased the proportion of monounsaturated fatty acids (MUFAs), particularly of oleic acid, while reducing the level of the saturated fatty acids (SFAs) palmitic and stearic acid. As a result, the MUFA:SFA ratio was higher in apoE KO mice brain fed with ROO and POO. Furthermore, both oils reduced the level of arachidonic and eicosapentaenoic acid, suggesting a decrease in the generation of pro- and anti-inflammatory eicosanoids. Finally, ROO and POO induced an increase in the density of membrane proteins implicated in both the Gαs/PKA and Gαq/PLCβ1/PKCα signaling pathways. The combined effects of long-term ROO and POO consumption on fatty acid composition and the level of signaling proteins involved in PKA and PKC activation, suggest positive effects on neuroinflammation and brain function in apoE KO mice brain, and convert these oils into promising functional foods in diseases involving apoE deficiency.

Keywords Apolipoprotein E knockout mice · Dietary olive oils · Brain · Fatty acid composition · Signaling proteins

Abbreviations

AA	Arachidonic acid
apoE	Apolipoprotein E
BHT	2,6-di-*tert*-butyl-*p*-cresol
COX	cyclooxygenase
CNS	Central nervous system
DHA	Docosapentaenoic acid
EPA	Eicosapentaenoic acid
FAMEs	Fatty acid methyl esters
KO	Knockout
MUFA	Monounsaturated fatty acid
PKA	Protein kinase A
PKC	Protein kinase C
PLA2	Phospholipase A2
PLC	Phospholipase C
POO	Pomace olive oil
PUFA	Polyunsaturated fatty acid
ROO	Refined olive oil
SDS	Sodium dodecyl sulfate
SFA	Saturated fatty acid

R. Alemany (✉) · O. Vögler
Section of Cell Biology, Department of Biology, Institut Universitari d'Investigacions en Ciències de la Salut (IUNICS), University of the Balearic Islands, Ctra. Valldemossa Km 7.5, 07122 Palma de Mallorca, Spain
e-mail: regina.alemany@uib.es

M. A. Navarro · J. Osada
Department of Biochemistry and Molecular and Cellular Biology, University of Zaragoza, C/Pedro Cerbuna, 12, 50009 Zaragoza, Spain

J. S. Perona · V. Ruiz-Gutiérrez
Instituto de la Grasa, Consejo Superior de Investigaciones Científicas (CSIC), Av. Padre García Tejero, 4, 41012 Seville, Spain

Introduction

Atherosclerosis, a main risk factor for ischemic stroke, is today considered as a chronic inflammatory state [1]. A critical event promoting atherosclerosis involves accumulation and oxidation of LDL-derived lipids in the vascular wall triggering a subsequent inflammatory response. The release of pro-inflammatory cytokines and activation of phospholipase A2 (PLA2) by macrophage foam cells in developing atherosclerotic lesions alters brain lipid metabolism and stimulates production of eicosanoids and reactive oxygen species thereby favoring injuries in the central nervous system (CNS) [2, 3].

Apolipoprotein E (apoE) is the main lipoprotein transporter of cholesterol, phospholipids and polyunsaturated fatty acids in the brain and mediates the binding of lipoproteins to cell surface receptors. Deregulated lipid metabolism due to deficiencies in apoE may be of particular importance for CNS injuries and disorders, such as Alzheimer's disease (AD), as abnormalities in lipid metabolism and peroxidation may contribute to the progression of neurodegeneration [4]. For this reason, apoE knockout (KO) mice, originally developed for studies on the pathogenesis of atherosclerosis, have become an attractive animal model for studying the consequences of an imbalance in lipid metabolism on brain function [5, 6]. Accordingly, brains from apoE KO mice show alterations in the phospholipid and fatty acid composition when compared with control mice [7], which could in part explain the impairment in neurotransmitter-associated signaling reported in these mice [8]. In this context, impaired coupling of neurotransmitter receptors (e.g., muscarinic M1 receptors) to G proteins as well as reductions in protein kinase A (PKA), phospholipase C (PLC) and protein kinase C (PKC) activities have been observed in brain tissues from both patients with AD [9, 10] and apoE KO mice [11].

The Mediterranean diet is characterized by the consumption of olive oil (OO), which contains a high proportion of the natural monounsaturated fatty acid (MUFA) oleic acid (about 80%). The so-called "orujo" or pomace olive oil (POO) is a sub-product of OO that is traditionally commercialized in Spain and also rich in oleic acid (about 74%). The importance of high-oleic acid oils as an integral component of the Mediterranean diet and its beneficial influence on cardiovascular parameters is well known [12]. Indeed, there is evidence to suggest that OO is fundamental for the beneficial influence of this diet on inflammatory parameters [13]. In addition to fatty acids, ROO and POO contain also minor quantities of other compounds in their unsaponifiable fraction, such as tetra- and penta-cyclic triterpenes (e.g., oleanolic and maslinic acid, erythrodiol and uvaol), sterols and tocopherols. Several important biological activities, e.g., antioxidant, anti-inflammatory, vasodilatory and anti-tumoral effects, have been recently attributed to these minor nutritional components [14–17]. Moreover, new improved procedures for POO extraction, through centrifugation and additional refining, permit us to concentrate significant amounts of them in the final product [18]. Accordingly, long-term consumption (>8 weeks) of diets enriched in OO and POO delayed the progression of atherosclerosis in apoE KO mice by modifying plasma lipids and pro-inflammatory parameters as well as by increasing antioxidant defenses [19–22]. Nevertheless, little is known about the influence of these dietary oils on the pathologically altered fatty acid composition in the brain and the signaling proteins implicated in neurotransmission in this animal model.

Therefore, the purpose of the present study was to examine the changes in lipid composition and pivotal signaling proteins in the brain of apoE KO mice. The content of the different fatty acid types was measured in this model after long-term consumption of refined OO (ROO) and POO (Table 1). Furthermore, we also analyzed whether the observed changes in lipid composition were accompanied by variations in membrane proteins implicated in G protein signaling pathways that lead to activation of PKA and PKC in the brain.

Table 1 Composition of the refined (ROO) and pomace olive oil (POO)

Component	ROO	POO
Erythrodiol + Uvaol	0.0017	0.050
Maslinic acid	0	0.011
Squalene	0.26	0.25
Total phytosterols	0.112	0.224
Total tocopherols	0.022	0.098
Waxes	0.012	0.34
Fatty acids		
Myristic (14:0)	0.02	0.02
Palmitic (16:0)	10.98	10.29
Stearic (18:0)	3.53	2.95
Arachidic (20:0)	0.42	0.45
Behenic (22:0)	0.12	0.17
Lignoceric (24:0)	0.05	0.07
Palmitoleic (16:1)	0.82	0.76
Oleic (18:1)	77.80	74.27
Gadoleic (20:1)	0.25	0.33
Linoleic (18:2n-6)	4.52	8.07
Linolenic (18:3n-3)	0.62	0.70
Saturated	15.12	13.95
Monosaturated	78.87	75.36

Dietary components are expressed as g% (w/w). Values are means ± SEM of three determinations. SEM values were less than 0.01%

Experimental Procedures

Animals and Diets

Homozygous apolipoprotein E knockout mice (apoE KO), hybrids of C57BL/6J and 129Ola strains, were bred at the 'Unidad Mixta de Investigación', Zaragoza. Twenty-six males, aged two months were fasted overnight, anesthetized with isofluorane, and blood samples were obtained by retroorbital bleeding to estimate the initial plasma cholesterol and triglycerides. Three random groups with equivalent plasma cholesterol and triglycerides were housed in sterile filter-top cages in rooms maintained on a 12-h light/12-h dark cycle. Animals had ad libitum access to food and water. The study protocol was approved by the Animal Research Ethical Committee at the University of Zaragoza. Body weights and food intake were recorded throughout the experiment.

Mice were maintained on normal chow: Teklad Mouse/Rat Diet no. 2014 (Harlan Teklad, Harlan Ibérica, Barcelona, Spain). Three study groups were set up: (a) a control group fed on chow alone (n = 9), (b) a group that received freshly prepared refined olive oil (ROO, 10% w/w) from our pilot plant along with chow diet ($n = 9$), and (c) a group that received pomace olive oil (POO, 10% w/w) in their diet (also called "orujo olive oil") ($n = 8$) as described previously [20]. All diets were prepared weekly and stored in N_2 atmosphere at −20 °C, fresh food was provided daily. Animals were fed on experimental diets for 11 weeks and all diets were well tolerated. To determine their composition, both olive oils were analyzed following the standard regulations of the European Union [23]. Briefly, phytosterols and triterpenic dialcohols (erythrodiol + uvaol) were separated by thin-layer chromatography, whereas the pentacyclic triterpene acid fraction (maslinic acid) was isolated by solid-phase extraction [18]. Afterwards, the compounds were analyzed by gas chromatography. Total tocopherols were determined by the IUPAC 2432 method [24]. Table 1 shows the composition of the different olive oils. At the end of the experimental period and after fasting overnight, animals were sacrificed by suffocation in CO_2 and left brain tissue was rapidly frozen in liquid N_2.

Analysis of Total Brain Fatty Acids

To analyze fatty acids, lipids were extracted from 100 mg of brain tissue as described elsewhere [25] using 2,6-di-*tert*-butyl-*p*-cresol (BHT) as an antioxidant. The extracted lipids were redissolved in 1 mL of chloroform:methanol (2:1, v/v) and maintained at −20 °C until use. Lipids were transmethylated and the resulting fatty acid methyl esters (FAMEs) were analyzed by gas chromatography as described previously [26]. Individual FAMEs were identified by comparing the retention times with that of standards.

Immunoblot Analysis and Quantification of Membrane-Associated Signaling Proteins in the Brain

Quantitative immunoblotting of G proteins, PLCβ1 and protein kinases (PKA and PKCα) was carried out in brain homogenates. Briefly, total brain proteins were solubilized and fractionated by SDS–polyacrylamide (10%) gel electrophoresis, and then transferred to membranes by western blotting. The following primary antibodies were used to detect the distinct proteins: anti-Gαs (1:350), anti-Gαq/11 (1:5,000) and anti-Gαo (1:5,000) all from Santa Cruz Biotechnology (USA), and anti-PKAcatα (1:1,000), PKARIIα (1:1,000), PKARIIβ (1:5,000), anti-PLCβ1 (1:1,000) and anti-PKCα all from BD Transduction Laboratories (Heidelberg, Germany). The quantification of the labelling was performed by image analysis using at least four standard curves of different protein contents loaded on the same gels (i.e., total protein loaded vs integrated optical density) [see 27, 28]. This quantification procedure was repeated at least three times for each sample on different gels. Values obtained from the groups supplemented with ROO and POO were normalized to the protein content of the control group (taken as 100%).

Statistical Analysis

Results are expressed as means ± SEM. One-way analysis of variance (ANOVA) followed by Bonferroni's test was used for the statistical evaluations. Differences between experimental groups were considered statistically significant at a value of $P < 0.05$.

Results

Effect of Chronic ROO and POO Consumption on Brain Fatty Acid Composition

Long-term consumption of ROO and POO induced changes in the fatty acid content of total lipids isolated from apoE KO mice brain. After the 11-week period of ROO and POO consumption, MUFA proportion had increased by 5.7 and 2.9%, respectively. When compared to control animals, these changes meant relative increases of 23 and 12% in the ROO and POO groups, respectively (Table 2). The difference was mainly due to an increase in the proportion of oleic acid (18:1n-9). In contrast, ROO and POO consumption decreased the amount of polyunsaturated fatty acids

Table 2 Fatty acid composition of the brain (% of total fatty acids)

Fatty Acid	Control	ROO	POO
14:0	3.39 ± 0.02	3.17 ± 2.59	6.76 ± 5.17
14:1	2.09 ± 0.01	2.32 ± 0.02$^{***\#\#}$	2.16 ± 0.09
16:0	19.55 ± 0.09	16.85 ± 0.50**	16.91 ± 1.58**
16:1n-9 + n-7	4.33 ± 0.00	5.10 ± 0.00$^{***\#\#}$	4.68 ± 0.24**
16:2n-7	2.69 ± 0.02	4.15 ± 0.05$^{***\#\#\#}$	3.58 ± 0.27***
18:0	18.65 ± 0.05	17.12 ± 0.75*	17.10 ± 1.08*
18:1n-9 + n-7	17.94 ± 0.00	22.30 ± 0.81$^{***\#\#}$	20.17 ± 1.16**
18:2n-6	0.80 ± 0.01	0.51 ± 0.00	0.57 ± 0.05
18:3n-3	ND	0.39 ± 0.03	0.37 ± 0.03
20:0	1.06 ± 0.01	3.06 ± 0.07***	2.37 ± 0.49***
20:1n-9 + n-7	ND	0.33 ± 0.01	0.33 ± 0.01
20:4n-6	10.85 ± 0.05	8.77 ± 0.19***	8.81 ± 0.88***
20:5n-3	3.20 ± 0.05	2.78 ± 0.02***	2.90 ± 0.18**
22:6n-3	15.39 ± 0.13	12.84 ± 0.05***	13.36 ± 1.21**
Total SFA	42.65 ± 0.15	40.19 ± 1.26	42.92 ± 2.83
Total MUFA	24.36 ± 0.01	30.05 ± 0.81$^{***\#\#}$	27.23 ± 1.53***
Total PUFA	32.94 ± 0.14	29.44 ± 0.42**	29.59 ± 2.11**
MUFA:SFA	0.57 ± 0.002	0.75 ± 0.04$^{***\#}$	0.64 ± 0.07
PUFA:SFA	0.77 ± 0.01	0.73 ± 0.03	0.70 ± 0.09
MUFA:PUFA	0.74 ± 0.003	1.02 ± 0.01$^{***\#\#\#}$	0.92 ± 0.06***

The values of total brain fatty acids from apoE KO mice are expressed as the means ± SEM (n = 8–9)

ND Non detectable

* $P < 0.05$

** $P < 0.01$

*** $P < 0.001$ versus control

$^{\#}$ $P < 0.05$

$^{\#\#}$ $P < 0.01$

$^{\#\#\#}$ $P < 0.001$ versus POO

(PUFAs) by about 3.4%. This corresponded to a relative decrease of at least 10% in both experimental groups when compared to control animals (Table 2). Moreover, ROO and POO consumption significantly decreased the content of the saturated fatty acids (SFAs), stearic (18:0) and palmitic (16:0) acid. These SFA's diminished in the order of 1.5–2.7%, respectively, which represented a relative change of 8–14% when compared to the control group. As a result, after ROO and POO consumption the ratios of MUFAs:PUFAs and MUFAs:SFAs were higher in apoE KO mice brain (Table 2). Prior to ROO and POO consumption, the proportion of araquidonic acid (AA) (20:4n-6), a precursor in the production of pro-inflammatory eicosanoids, was 10.85 ± 0.05% of the total fatty acids. In contrast, ROO and POO consumption decreased AA proportion by 19%, when compared to control animals. Interestingly, the proportion of eicosapentaenoic acid (EPA) (20:5n-3) and docosapentaenoic acid (DHA) (22:6n-3), which are metabolized to potent anti-inflammatory mediators, also decreased by around 10 and 16%, respectively, in both experimental groups (Table 2).

Effects of Chronic ROO and POO Consumption on Membrane Signaling Proteins in the Brain

To determine whether the changes in lipid composition induced by long-term ROO and POO consumption affected membrane-associated proteins, we measured the brain levels of G proteins, PKA (IIα and IIβ), PLCβ1 and PKCα by quantitative immunoblotting. These proteins are major intracellular signaling proteins regulating brain function and their interaction with membranes is sensitive to membrane lipid composition. Long-term ROO consumption induced a significant increase in the overall levels of Gαs and Gαq/11 in apoE KO mice brain when compared to controls (75 ± 15 and 27 ± 5%, respectively, Fig. 1a, b). Likewise, POO consumption also produced a significant increase of these G protein levels (60 ± 10% for Gαs, Fig. 1a; and 59 ± 4% for Gαq/11, Fig. 1b). Interestingly, a further increase in the levels of Gαq/11 was observed when the diet was supplemented with POO (26 ± 3% when compared to the ROO group, Fig. 1b). In contrast, no significant changes were observed in brain Gαo levels after ROO or POO consumption (Fig. 1c).

Having observed that ROO and POO consumption increased Gαs and Gαq/11 levels, we set out to determine whether proteins downstream of these G proteins were also influenced by these dietary supplements. Hence, we analyzed the effects of ROO and POO consumption on PKA (downstream of Gαs), and on PLCβ1 and PKCα (downstream of Gαq/11) levels. In agreement with the Gαs protein data, we observed increased levels of the catalytic (catα; 141 ± 7%) and the regulatory RIIα (134–141%) and RIIβ (149–152%) PKA subunits after chronic ROO and POO consumption, when compared to control animals (Fig. 2). Similarly, brain PLCβ1 and PKCα levels also increased significantly in both groups. The levels of PLCβ1 augmented by 16 ± 6% in the ROO group and 21 ± 6% in the POO group when compared to control animals (Fig. 3a). Finally, PKCα levels were equally up-regulated, albeit to a much higher extent, increasing 61 ± 9 and 109 ± 8% in ROO and POO groups, respectively (Fig. 3b). As observed for Gαq/11 (Fig. 1b), long-term POO consumption further increased brain PKCα levels (30 ± 5%) when compared to ROO group (Fig. 3b).

Discussion

Deficiencies in apolipoprotein E (apoE) alter lipid homeostasis and produce lipid modifications of plasma membranes in the brain, in this way contributing to

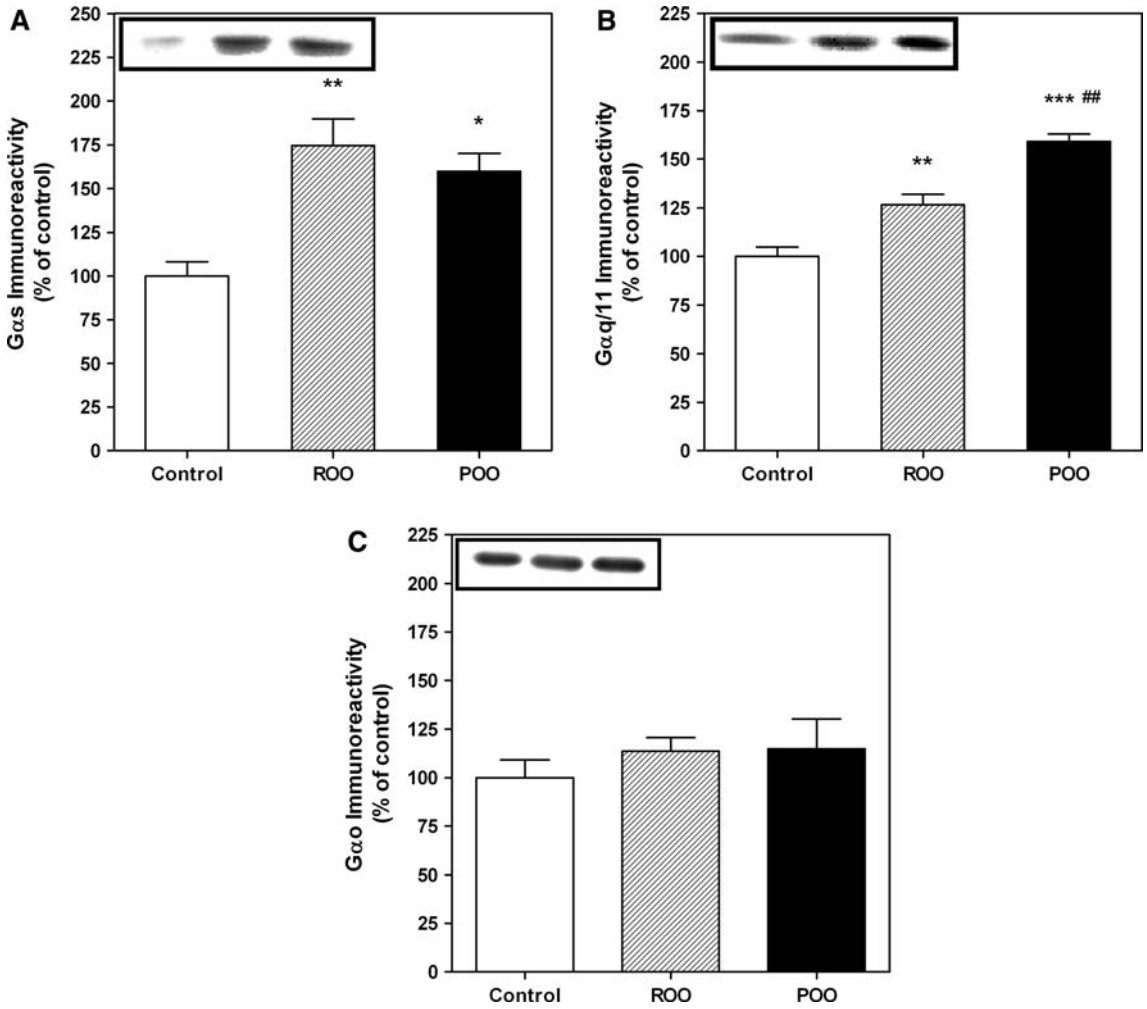

Fig. 1 G protein levels in apoE KO mice brain. *Upper panels* show the levels of Gαs (**a**), Gαq/11 (**b**) and Gα*o* (**c**) in representative immunoblots. Immunoreactive bands are representative of 8–9 animals per group. The *columns* show brain Gα subunit levels quantified against standard curves and normalized to the protein content of the control group (taken as 100%). *ROO* indicates values in apoE KO mice after long-term ROO consumption and *POO*, values in apoE KO mice after long-term POO consumption. $^{*}P < 0.05$, $^{**}P < 0.01$ and $^{***}P < 0.001$ versus control; $^{\#\#}P < 0.01$ versus ROO group

neurodegeneration [4]. ApoE knockout (KO) mice, an animal model for studies on the pathogenesis of atherosclerosis, develop cognitive deficits resembling those of Alzheimer's disease (AD) and have become an attractive animal model for studying the consequences of an imbalance in the lipid metabolism on brain function [6, 29]. Indeed, important changes in cholesterol or phospholipid membrane content, cholesterol membrane leaflet distribution, and degree of FA saturation, have been reported in apoE KO mice brain [7, 30]. Interestingly, these alterations could in turn affect cognitive performance of these mice [8]. Furthermore, the brain of atherosclerotic apoE KO mice is believed to be particularly vulnerable to oxidative stress as it has lower antioxidant and anti-inflammatory defenses, which leads to progressive brain cell damage and decline in cerebral function [31].

In this work, we have analyzed the changes in both fatty acid composition and membrane-signaling protein levels induced by long-term (11 weeks) ROO and POO consumption in apoE KO mice brain. These two olive oils contained high concentrations of bioactive molecules, such as tetra- and penta-cyclic triterpenes (erythrodiol + uvaol and maslinic acid), tocopherols and phytosterols (Table 1), which are known to be essential for the beneficial influence of the Mediterranean diet on inflammatory [15, 32] and cardiovascular parameters [33], and which were recently associated with a delay of atherosclerosis development in apoE KO mice [20, 34]. In this context, particularly triterpenes, such as oleanolic acid, improved not only brain anti-inflammatory defenses but also ameliorated malfunctioning neurological signs in an experimental animal model for multiple sclerosis [35]. For these reasons, we

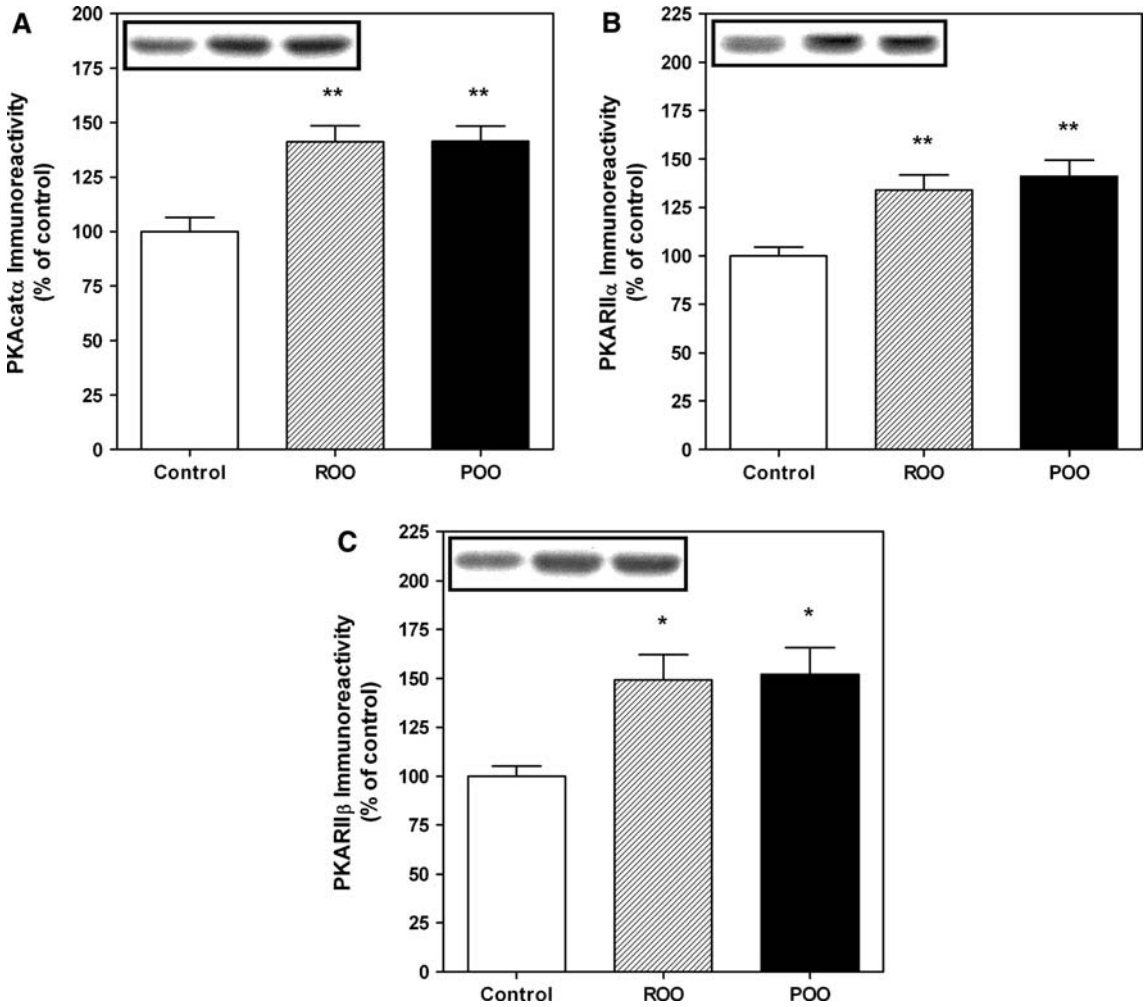

Fig. 2 PKA levels in apoE KO mice brain. *Upper panels* show representative immunoblots for catalytic (PKAcatα) (**a**) and regulatory IIα (PKARIIα) (**b**) and IIβ (PKARIIβ) (**c**) PKA subunit levels. Immunoreactive bands are representative of 8–9 animals per group. The *columns* show brain PKA subunit levels quantified against standard curves and normalized to the protein content from controls (taken as 100%). *ROO* indicates values in apoE KO mice after long-term ROO consumption and *POO*, values in apoE KO mice after long-term POO consumption. $*P < 0.05$ and $**P < 0.01$ versus control

hypothesized that dietary ROO and POO supplementation may also have positive effects on neuroinflammation and brain function by modulating lipid composition and the levels of signaling proteins in apoE KO mice brain.

After long-term ROO and POO consumption, the most apparent difference in brain fatty acid composition was a significant increase in the total amount of MUFA. This increase was mostly due to a rise in the proportion of oleic acid (Table 2), probably as a result of the high amount of oleic acid present in both olive oils (Table 1). It is known that higher MUFA:SFA ratio reduces membrane microviscosity (i.e., increase membrane fluidity), thereby enabling proteins involved in cellular signaling to function together. In this context, the increase in the MUFA:SFA ratio observed after ROO and POO could account for some cognitive benefits by reverting the pathologically altered membrane fluidity seen in the brain of apoE KO mice [30]. On the other hand, dietary fatty acids can also influence the production of eicosanoids, which are implicated in inflammatory processes. The activation of PLA2 in atherosclerotic lesions releases arachidonic acid (AA), eicosapentaenoic acid (EPA), and docosapentaenoic acid (DHA). Whereas AA is metabolized to pro-inflammatory eicosanoids through the COX pathway, a major pathway promoting inflammation, EPA and DHA are mainly processed to molecules that have important roles as inflammation inhibitors (e.g., resolvins) [36]. Interestingly, ROO and POO consumption decreased not only the level of AA, but also that of EPA and DHA (Table 2), which most probably result in a decline of the production of pro-inflammatory and compensatory anti-inflammatory eicosanoids, suggesting a general reduction in the degree of neuroinflammation in apoE KO mice brain.

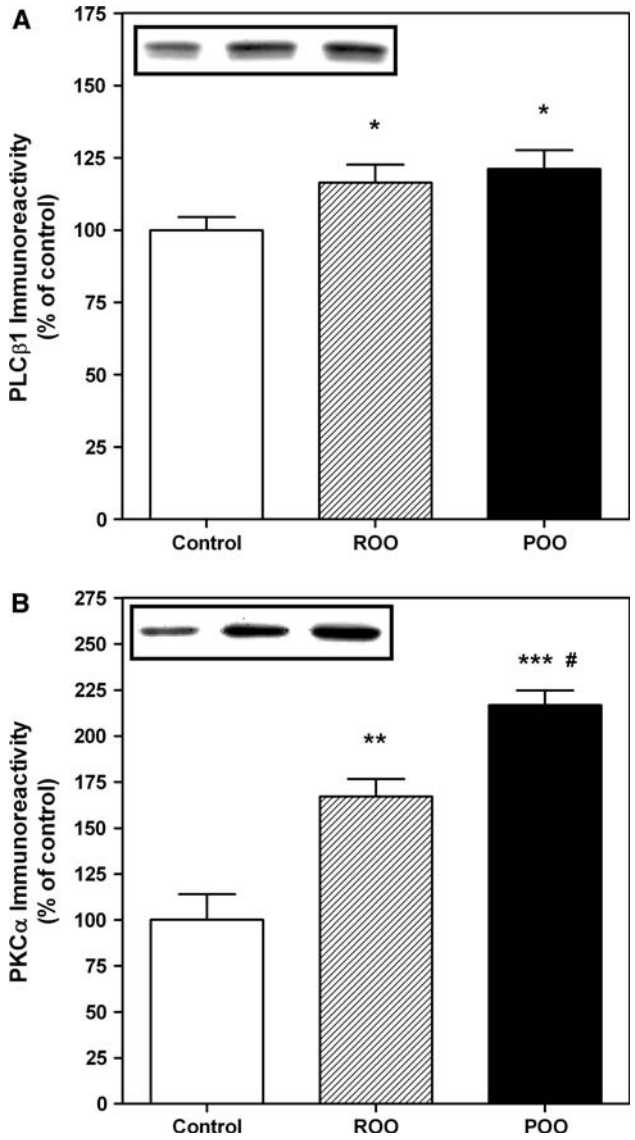

Fig. 3 PLCβ1 and PKCα levels in apoE KO mice brain. *Upper panels* show representative immunoblots for PLCβ1 (**a**) and PKCα (**b**) levels. Immunoreactive bands are representative of 8–9 animals per group. The columns show brain protein levels quantified against standard curves and normalized to the protein content of controls (taken as 100%). *ROO* indicates values in apoE KO mice after long-term ROO consumption and *POO*, values in apoE KO mice after long-term POO consumption. $^{*}P < 0.05$, $^{**}P < 0.01$ and $^{***}P < 0.001$ versus control; $^{\#}P < 0.05$ versus ROO group

The effects on lipid composition observed in apoE KO mice brain fed with ROO and POO enriched diets were accompanied by alterations in membrane-associated proteins that influence the activation of brain PKA and PKC. Significant increases in Gαs/PKA levels were found in apoE KO mice brain of both dietary groups (Figs. 1, 2). Likewise, the levels of proteins, which participate in the phosphoinositide signaling cascade, namely the Gαq/11 protein and the enzymes PLCβ1 and PKCα, were also up-regulated after long-term ROO and POO consumption. Interestingly, POO increased brain Gαq/11 and PKCα levels to a higher extent than ROO, which could be related to the higher concentrations of triterpenes in POO [37]. PKA and PKC have been implicated in the phosphorylation of many proteins, as well as in neurotransmitter release and dopaminergic neurotransmission. Thus, the effect of the intake of both oils on the levels of membrane proteins that participate in cellular signaling (including G proteins, PKA, PLCβ1 and PKCα), suggests that they should improve GPCR-induced neuronal signaling in apoE KO mice. This would counteract the impaired neurotransmitter-mediated signal transduction that has been reported in apoE KO mice [8]. Indeed, reductions in the level and/or activity of GPCR and their corresponding G proteins, as well as of their down-stream effectors, such as PLC/PKC have been reported in both neurodegenerative disorders associated with apoE deficiency [9, 10] and in apoE KO mice [11]. Nevertheless, the participation of additional mechanisms in these processes cannot be excluded.

In summary, long-term ROO and POO consumption modulates brain fatty acid composition in apoE KO mice and influences the levels of pivotal membrane proteins implicated in the activation of PKA and PKC, suggesting positive effects on neuroinflammation and brain function. The combination of these two molecular effects might convert ROO and POO oils into valuable functional foods in diseases involving apoE deficiency. Further studies are needed to evaluate in a direct way the efficacy of olive oil consumption on cognitive function in such neurodegenerative diseases.

Acknowledgments We thank Angel Beltrán, Jesús Navarro, Carmen Navarro and Elena Santa Clotilde of the *Unidad Mixta de Investigación* for their invaluable help in maintaining the animals and Dr. Pablo V. Escribá of the University of the Balearic Islands for the helpful discussions. This work was supported by grants from the 'Comision Interministerial de Ciencia y Tecnologia' (AGL2005-00572), Red FIS de investigación cooperativa G03-140 (Instituto de Salud Carlos III, Ministerio de Sanidad y Consumo, Spain), and SAF2007-60173 (Ministerio de Educación y Ciencia, Spain). Regina Alemany and Oliver Vögler hold contracts from the Spanish I3 Programme ("Programa de Incentivación de la Incorporación e Intensificación de la Actividad Investigadora").

Conflict of Interest Statement The authors declare that there does not exist any conflict of interest.

References

1. Stoll G, Bendszus M (2006) Inflammation and atherosclerosis: novel insights into plaque formation and destabilization. Stroke 37:1923–1932
2. Fan J, Watanabe T (2003) Inflammatory reactions in the pathogenesis of atherosclerosis. J Atheroscler Thromb 10:63–71

3. Adibhatla RM, Hatcher JF (2008) Altered lipid metabolism in brain injury and disorders. Subcell Biochem 49:241–268
4. Lane RM, Farlow MR (2005) Lipid homeostasis and apolipoprotein E in the development and progression of Alzheimer's disease. J Lipid Res 46:949–968
5. Moghadasian MH, McManus BM, Nguyen LB, Shefer S, Nadji M, Godin DV, Green TJ, Hill J, Yang Y, Scudamore CH, Frohlich JJ (2001) Pathophysiology of apolipoprotein E deficiency in mice: relevance to apo E-related disorders in humans. Faseb J 15:2623–2630
6. Crisby M, Rahman SM, Sylven C, Winblad B, Schultzberg M (2004) Effects of high cholesterol diet on gliosis in apolipoprotein E knockout mice. Implications for Alzheimer's disease and stroke. Neurosci Lett 369:87–92
7. Lomnitski L, Oron L, Sklan D, Michaelson DM (1999) Distinct alterations in phospholipid metabolism in brains of apolipoprotein E-deficient mice. J Neurosci Res 58:586–592
8. Krzywkowski P, Ghribi O, Gagne J, Chabot C, Kar S, Rochford J, Massicotte G, Poirier J (1999) Cholinergic systems and long-term potentiation in memory-impaired apolipoprotein E-deficient mice. Neuroscience 92:1273–1286
9. Cowburn RF, O'Neill C, Bonkale WL, Ohm TG, Fastbom J (2001) Receptor-G-protein signalling in Alzheimer's disease. Biochem Soc Symp 67:163–175
10. Tsang SW, Lai MK, Kirvell S, Francis PT, Esiri MM, Hope T, Chen CP, Wong PT (2006) Impaired coupling of muscarinic M1 receptors to G-proteins in the neocortex is associated with severity of dementia in Alzheimer's disease. Neurobiol Aging 27:1216–1223
11. Hung MC, Hayase K, Yoshida R, Sato M, Imaizumi K (2001) Cerebral protein kinase C and its mRNA level in apolipoprotein E-deficient mice. Life Sci 69:1419–1427
12. Estruch R, Martinez-Gonzalez MA, Corella D, Salas-Salvado J, Ruiz-Gutierrez V, Covas MI, Fiol M, Gomez-Gracia E, Lopez-Sabater MC, Vinyoles E, Aros F, Conde M, Lahoz C, Lapetra J, Saez G, Ros E (2006) Effects of a Mediterranean-style diet on cardiovascular risk factors: a randomized trial. Ann Intern Med 145:1–11
13. De La Puerta Vazquez R, Martinez-Dominguez E, Sanchez Perona J, Ruiz-Gutierrez V (2004) Effects of different dietary oils on inflammatory mediator generation and fatty acid composition in rat neutrophils. Metabolism 53:59–65
14. Rodriguez-Rodriguez R, Herrera MD, Perona JS, Ruiz-Gutierrez V (2004) Potential vasorelaxant effects of oleanolic acid and erythrodiol, two triterpenoids contained in 'orujo' olive oil, on rat aorta. Br J Nutr 92:635–642
15. Marquez Martin A, de la Puetra Vazquez R, Fernandez-Arche A, Ruiz-Gutierrez V (2006) Supressive effect of maslinic acid from pomace olive oil on oxidative stress and cytokine production in stimulated murine macrophages. Free Radic Res 40:295–302
16. Martin R, Carvalho-Tavares J, Ibeas E, Hernandez M, Ruiz-Gutierrez V, Nieto ML (2007) Acidic triterpenes compromise growth and survival of astrocytoma cell lines by regulating reactive oxygen species accumulation. Cancer Res 67:3741–3751
17. Martin R, Ibeas E, Carvalho-Tavares J, Hernandez M, Ruiz-Gutierrez V, Nieto ML (2009) Natural triterpenic diols promote apoptosis in astrocytoma cells through ROS-mediated mitochondrial depolarization and JNK activation. PLoS One 4:e5975
18. Perez-Camino MC, Cert A (1999) Quantitative determination of hydroxy pentacyclic triterpene acids in vegetable oils. J Agric Food Chem 47:1558–1562
19. Ferre N, Camps J, Paul A, Cabre M, Calleja L, Osada J, Joven J (2001) Effects of high-fat, low-cholesterol diets on hepatic lipid peroxidation and antioxidants in apolipoprotein E-deficient mice. Mol Cell Biochem 218:165–169
20. Acin S, Navarro MA, Perona JS, Arbones-Mainar JM, Surra JC, Guzman MA, Carnicer R, Arnal C, Orman I, Segovia JC, Osada J, Ruiz-Gutierrez V (2007) Olive oil preparation determines the atherosclerotic protection in apolipoprotein E knockout mice. J Nutr Biochem 18:418–424
21. Arbones-Mainar JM, Navarro MA, Carnicer R, Guillen N, Surra JC, Acin S, Guzman MA, Sarria AJ, Arnal C, Aguilera MP, Jimenez A, Beltran G, Uceda M, Osada J (2007) Accelerated atherosclerosis in apolipoprotein E-deficient mice fed Western diets containing palm oil compared with extra virgin olive oils: a role for small, dense high-density lipoproteins. Atherosclerosis 194:372–382
22. Arbones-Mainar JM, Ross K, Rucklidge GJ, Reid M, Duncan G, Arthur JR, Horgan GW, Navarro MA, Carnicer R, Arnal C, Osada J, de Roos B (2007) Extra virgin olive oils increase hepatic fat accumulation and hepatic antioxidant protein levels in APOE-/- mice. J Proteome Res 6:4041–4054
23. European Union Commission (1991) Regulation (EEC) No 2568/91 of 11 July 1991 on the characteristics of olive oil and olive-residue oil and on the relevant methods of analysis. Official Journal of the Commission of the European Communities L248:1–83
24. IUPAC (1992) Determination of tocopherols and tocotrienols in vegetable oils and fats by HPLC. Method 2.432. In: Paquot C, Hautfenne A (eds) Standard methods for analysis of oils, fats and derivatives, 7th edn. (revised and enlarged). Blackwell Scientific, Oxford
25. Folch J, Lees M, Sloane Stanley GH (1957) A simple method for the isolation and purification of total lipides from animal tissues. J Biol Chem 226:497–509
26. Ruiz-Gutierrez V, Montero E, Villar J (1992) Determination of fatty acid and triacylglycerol composition of human adipose tissue. J Chromatogr 581:171–178
27. Alemany R, Terés S, Baamonde C, Benet M, Vögler O, Escribá PV (2004) 2-Hydroxyoleic acid: a new hypotensive molecule. Hypertension 43:249–254
28. Alemany R, Vögler O, Terés S, Egea C, Baamonde C, Barceló F, Delgado C, Jakobs KH, Escribá PV (2006) Antihypertensive action of 2-hydroxyoleic acid in SHRs via modulation of the protein kinase A pathway and Rho kinase. J Lipid Res 47:1762–1770
29. Choi J, Forster MJ, McDonald SR, Weintraub ST, Carroll CA, Gracy RW (2004) Proteomic identification of specific oxidized proteins in ApoE-knockout mice: relevance to Alzheimer's disease. Free Radic Biol Med 36:1155–1162
30. Igbavboa U, Avdulov NA, Chochina SV, Wood WG (1997) Transbilayer distribution of cholesterol is modified in brain synaptic plasma membranes of knockout mice deficient in the low-density lipoprotein receptor, apolipoprotein E, or both proteins. J Neurochem 69:1661–1667
31. Ramassamy C, Krzywkowski P, Averill D, Lussier-Cacan S, Theroux L, Christen Y, Davignon J, Poirier J (2001) Impact of apoE deficiency on oxidative insults and antioxidant levels in the brain. Brain Res Mol Brain Res 86:76–83
32. Marquez-Martin A, De La Puerta R, Fernandez-Arche A, Ruiz-Gutierrez V, Yaqoob P (2006) Modulation of cytokine secretion by pentacyclic triterpenes from olive pomace oil in human mononuclear cells. Cytokine 36:211–217
33. Rodriguez-Rodriguez R, Perona JS, Herrera MD, Ruiz-Gutierrez V (2006) Triterpenic compounds from "orujo" olive oil elicit vasorelaxation in aorta from spontaneously hypertensive rats. J Agric Food Chem 54:2096–2102
34. Acin S, Navarro MA, Carnicer R, Arbones-Mainar JM, Guzman MA, Arnal C, Beltran G, Uceda M, Maeda N, Osada J (2005) Dietary cholesterol suppresses the ability of olive oil to delay the

development of atherosclerotic lesions in apolipoprotein E knockout mice. Atherosclerosis 182:17–28
35. Martin R, Carvalho-Tavares J, Hernandez M, Arnes M, Ruiz-Gutierrez V, Nieto ML (2009) Beneficial actions of oleanolic acid in an experimental model of multiple sclerosis: a potential therapeutic role. Biochem Pharmacol (epub ahead of print)
36. Das UN (2006) Essential fatty acids: biochemistry, physiology and pathology. Biotechnol J 1:420–439
37. Takahashi K, Suzuki S, Hano Y, Nomura T (2002) Protein kinase C activation by iridal type triterpenoids. Biol Pharm Bull 25:432–436

Lipids (2010) 45:63–71
DOI 10.1007/s11745-009-3371-x

ORIGINAL ARTICLE

The Spectrum of Plant and Animal Sterols in Different Oil-Derived Intravenous Emulsions

Maria Luisa Forchielli · Germana Bersani · Sara Tala · Gabriele Grossi · Cristina Puggioli · Massimo Masi

Received: 28 February 2009 / Accepted: 27 October 2009 / Published online: 22 November 2009

Abstract Intravenous lipid constituents have different effects on various biological processes. Some of these effects are protective, while others are potentially adverse. Phytosterols, in particular, seem to be implicated with parenteral nutrition-associated cholestasis. The aim of this study is to determine the amount of plant and animal sterols present in lipid formulations derived from different oil sources. To this end, animal (cholesterol) and plant (β-sitosterol, campesterol, and stigmasterol) sterols in seven different commercially available intravenous lipid emulsions (ILEs) were quantified by capillary gas chromatography after performing a lipid extraction procedure. The two major constituents of the lipid emulsions were cholesterol (range 14–57% of total lipids) and β-sitosterol (range 24–55%), followed by campesterol (range 8–18%) and stigmasterol (range 5–16%). The fish oil-derived formulation was an exception, as it contained only cholesterol. The mean values of the different sterols were statistically different across ILEs ($P = 0.0000$). A large percentage of pairwise comparisons were also statistically significant ($P = 0.000$), most notably for cholesterol and stigmasterol (14 out of 21 for both), followed by campesterol (12 out 21) and β-sitosterol (11 out 21). In conclusion, most ILEs combined significant amounts of phytosterols and cholesterol. However, their phytosterols:cholesterol ratios were reversed compared to the normal human diet.

Keywords Phytosterols · Cholesterol · Intravenous lipid emulsions · Cholestasis · Gas chromatography

Abbreviations

ILEs	Intravenous lipid emulsions
TPN	Total parenteral nutrition
PNAC	Parenteral nutrition-associated cholestasis
LCT	Long-chain triglycerides
MCT	Medium-chain triglycerides
GC	Gas chromatography
cGC	Capillary gas chromatography

Introduction

Intravenous lipid emulsions (ILEs) are the source of fat within total parenteral nutrition (TPN). The principal idea behind their use is the prevention of essential fatty acid deficiency. Only recently, due to the increasing interest in lipids for therapeutic purposes, have new ILEs been essayed and marketed, to offer potential new health benefits or to modify metabolic derangements in diseases. ILEs have been found to have positive effects in gastrointestinal, pulmonary, cardiovascular, autoimmune, oncologic, and critical care diseases. At the same time, they have been blamed as possible causes of TPN-associated complications. Phytosterols, in particular, have been included in the

M. L. Forchielli (✉) · M. Masi
Department of Pediatrics, S Orsola-Malpighi, Medical School of Bologna, Via Massarenti 11, 40138 Bologna, Italy
e-mail: luisa.forchielli@unibo.it

G. Bersani · C. Puggioli
Department of Pharmacy, S Orsola-Malpighi, Medical School of Bologna, Bologna, Italy

S. Tala · G. Grossi
Department of Clinical Biochemistry, S Orsola-Malpighi, Medical School of Bologna, Bologna, Italy

list of toxic substances responsible for parenteral nutrition-associated cholestasis (PNAC) [1–5].

So far, little is known on the main sterol components of commercially available ILEs. The literature and the manufacturers have focused on fatty acid composition and possibly on other lipophilic substances such as diacylglycerols, egg phosphatide, and α-tocopherol. Phytosterols, in contrast, are often not even included in the list of main ILE components, as their amounts have been reported as minimal.

The aim of this study is to analyze the contents of the most representative ILEs in great detail and to identify their sterol profiles, including phytosterols.

Materials and Methods

Samples

Seven ILEs were selected based on their principal lipid constituents (soy, safflower, olive oil, and fish oil): Structolipid®, Intralipid®, Lipovenos®, Omegaven® (Fresenius Kabi AG, Germany), Clinoleic® (Clintec, France), Lipofundin MCT,® and Lipofundin S® (Braun, Germany), all at 20% lipid concentration with the exception of Omegaven®, which contains a 10% lipid amount. All the ILEs have various long-chain triglycerides (LCT) from plant or marine sources. In Lipofundin MCT®, medium-chain triglycerides (MCT) are combined with LCT. Table 1 shows the composition of each product.

Reagents, Solvents, and Standards

Chloroform (analytical reagent grade), *n*-hexane (analytical reagent grade), methanol (Lichrosolv), diethyl ether, anhydrous sodium sulphate, potassium chloride, and potassium hydroxide were supplied by Merck (Darmstadt, Germany). Acetone (AnalaR®) was purchased from BDH (VWR International Ltd., Leicestershire, UK). Bidistilled water and silylating agents (pyridine, hexamethyldisilazane and trimethylchlorosilane) were supplied by Carlo Erba (Milano, Italy).

(24*R*)-Ethylcholest-5-en-3β-ol (β-sitosterol) (purity: 60% β-sitosterol and 30% (24*R*)-methylcholest-5-en-3β-ol (campesterol)) was purchased from Research Plus (Bayonne, NJ, USA). (24*S*)-Ethylcholest-5, 22-dien-3β-ol (stigmasterol) (purity: 93%), cholest-5-en-3β-ol (cholesterol) (purity: 99%), and 5α-cholestane (purity: 97%) were purchased from Sigma (St. Louis, MO, USA). The purity of the standards was controlled by gas chromatography (GC).

Lipid Extraction

Lipid extraction was performed using a modified version [6] of the method by Folch et al. [7]. Two 10-ml volumes of each ILE were sampled and homogenized with 200 ml

Table 1 Composition of the tested intravenous lipid emulsions

Name	Composition
Structolipid® 20%	Purified soy bean oil structured triglycerides 200 g/1,000 ml
	Excipients: purified egg phospholipids, glycerol
Intralipid® 20%	Soybean oil 200 g/1,000 ml
	Egg yolk phospholipids 12 g/1,000 ml
	Excipients: glycerol 22.5 g/1,000 ml
Clinoleic® 20%	Mixture of purified olive oil (approximately 80%) and purified soybean oil (approximately 20%) 200 g/1,000 ml
	Excipients: purified egg phosphatides 12 g/1,000 ml, glycerol 22.50 g/1,000 ml, sodium oleate 0.30 g/1,000 ml
Lipovenos® 20%	Soybean oil 200 g/1,000 ml
	Egg phospholipids 12 g/1,000 ml [75–81%(3-*sn*-phosphatidylcholin)]
	Glycerol 25 g/1,000 ml
	Excipients: sodium oleate
Lipofundin MCT® 20%	Soybean oil 100 g/1,000 ml, α-tocopherol
	Medium-chain triglycerides (coconut) 100 g/1,000 ml
	Excipients: egg yolk lecithin, sodium oleate, α-tocopherol
Lipofundin S® 20%	Soybean oil 200 g/1,000 ml
	Excipients: egg yolk lecithin, glycerol, sodium oleate, α-tocopherol
Omegaven 10%	Purified fish oil 100 g/1,000 ml
	Excipients: egg yolk lecithin, glycerol, sodium oleate, α-tocopherol

of a chloroform:methanol solution (1:1, v/v) in a glass bottle with screw-cap. Successively, the bottle was placed at 60 °C for 20 min before adding 100 ml of chloroform. After a 3-min homogenization, the content of the bottle was filtered through filter paper. The filtrate was mixed thoroughly with 100 ml of a 1 M KCl solution and left overnight at 4 °C in order to achieve phase separation. The lower phase was collected and transferred into another Sovirel bottle. To dry the sample completely, 3–4 spoons of anhydrous sodium sulfate were added. The bottle was sealed and placed in darkness for 2 h at 4 °C. The organic phase was further filtered through a layer of anhydrous sodium sulfate with chloroform on filter paper, collected into a pre-weighed flask, and dried using a vacuum rotary evaporator (Buchi Rotavapor R, Switzerland) with a water bath at 40 °C. The fat content was determined gravimetrically. The extracted fat was dissolved in hexane:isopropanol (4:1, v/v) and was held at −20 °C until analysis. The lipid extraction procedure was performed three times per sample.

Determination of Sterols

A 50-µl amount of the internal standard solution (1 mg of 5α-cholestane/ml) was added to a 250-mg lipid subfraction of the Folch extract. Subsequently, the sample was dried under nitrogen and treated with 10 ml of 1 N KOH solution in methanol, in order to obtain a saponification at room temperature for 18 h, in darkness and under continuous agitation [8]. To extract the unsaponifiable matter, 10 ml of water and 10 ml of diethyl ether were added to the samples, which were vigorously shaken. The diethyl ether fraction was then separated; the extraction with 10 ml of diethyl ether was repeated three times.

The three portions of diethyl ether were pooled, washed twice with 5 ml of a 0.5 N KOH solution, washed once with 5 ml of a 20% NaCl solution to remove any residual emulsion, and extracted. A correct washing procedure must lead to washing water having a pH <8. The ether extract was added with anhydrous sodium sulfate, kept at 4 °C for 2 h, filtered using Whatman No. 1 filter paper, and extracted again with 10 ml diethyl ether. The resulting ether extract was evaporated using a vacuum rotary evaporator, dissolved in 1 ml of hexane:isopropanol (4:1, v/v) and held at −20 °C until analysis.

One-fifth of the unsaponifiable matter was dried and silylated, according to Sweeley et al. [9]. After 20 min at 40 °C, the sample was dried under a nitrogen stream and dissolved in 100 µl of hexane. One microliter of the silylated sample was analyzed by capillary gas chromatography (cGC) for the sterol determination. The gas chromatograph (HRGC 5300 Mega Series, Fisons, Rodano, Italy) was equipped with a split/splitless injector and a flame ionization detector. A fused-silica capillary column (30 m × 0.32 mm i.d. × 0.25 µm film thickness) coated with 100% dimethyl-polysiloxane (CP-Sil 5 CB Low Bleed/MS, Chrompack-Varian, Middelburg, The Netherlands) was used. The oven temperature was programmed to rise from 250 to 325 °C at a rate of 3 °C/min and held for 10 min at 325 °C. The injector and detector temperatures were both set at 325 °C. Helium was used as the carrier gas at a flow rate of 3 ml/min; the split ratio was 1:15.

Sterols were identified by comparing their retention times with those of commercial sterol standards and by spiking the silylated samples with a small amount of silylated sterol standards.

Sterols were then quantified by comparing the peak areas of the internal standard (5α-cholestane) and its concentration with the peak areas of the sample sterols. The GC response factors of sterols with respect to the internal standard were considered equal to 1.

Data Analysis

Two samples of each ILE underwent lipid extraction. For each lipid extraction, in turn, sterol determination was performed three times. GC data were stored and processed with a Turbochrom Navigator acquisition system (Ver. 6.1.1.0.0:K20) (Perkin Elmer Instruments, Norwalk, CT, USA). The means, standard deviations (SD), and coefficients of variability (CV) were then computed for the sterol contents.

STATA Software v.3 (Santa Monica, CA, USA) was used to perform one-way analysis of variance (ANOVA) with multiple-comparison tests (using both the Bonferroni and Scheffe' options to validate results) at a 95% confidence level ($P < 0.05$) to identify differences among ILEs.

Results

The amount of extracted lipids was quantified and classified by type of sterols (animal: cholesterol, and plant: β-sitosterol, campesterol, and stigmasterol). Animal and plant sterols were differently represented across solutions, with the latter generally accounting for a greater share than the former. Chromatograms of the identified sterols are shown in Fig. 1. For each ILE, Table 2 reports the presence of each sterol as a percentage of the total amount of sterols; Table 3 does the same with respect to phytosterols only; Table 4 reports the presence of each sterol relative to the overall quantity of fat as well as the ratio of plant to animal sterols. Finally, Table 5 shows the mean content of each sterol in each ILE, as well as the standard deviation and the percent coefficient variation.

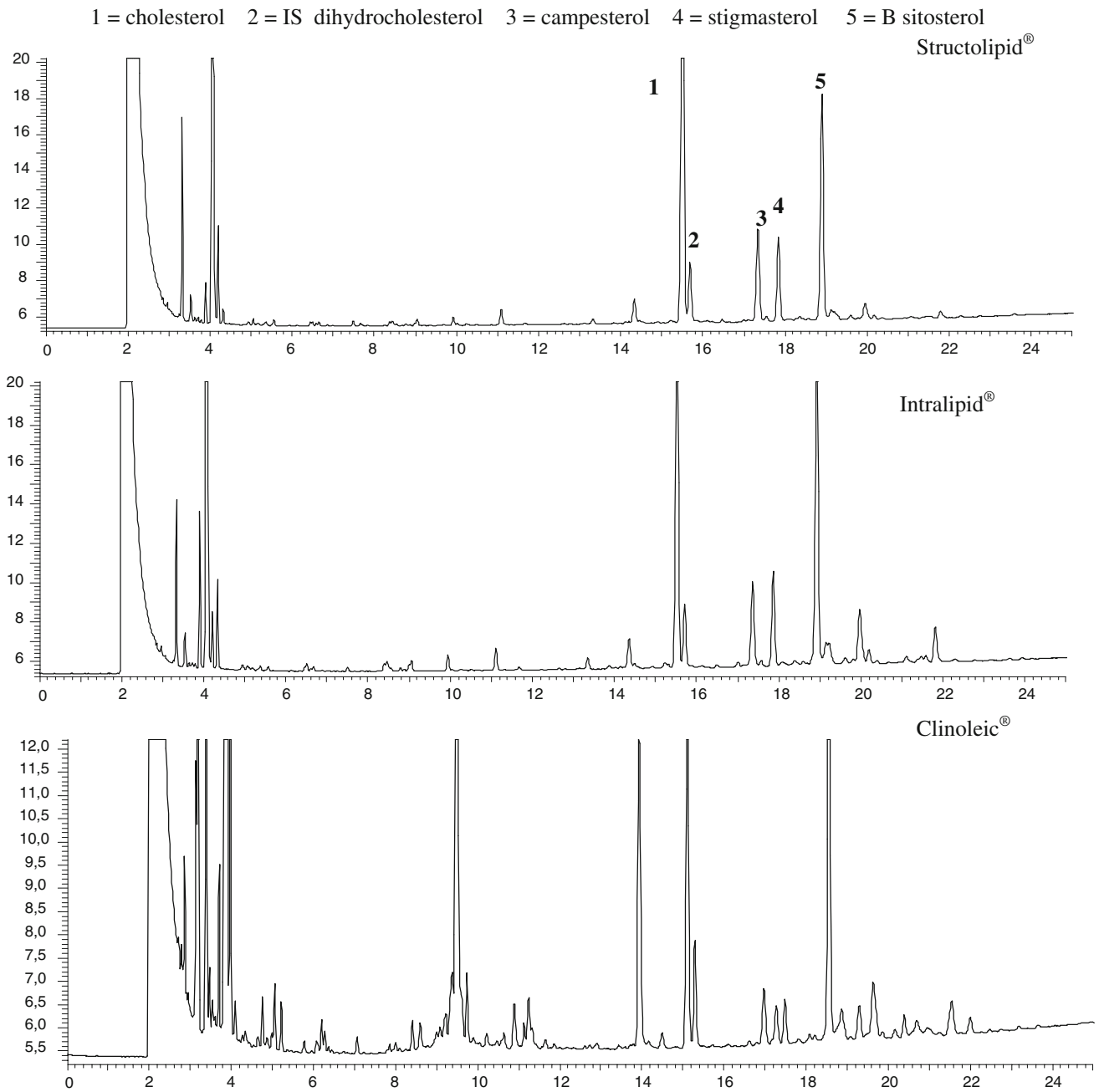

Fig. 1 Chromatograms of plant and animal sterols identified in the intravenous lipid emulsions *1* cholesterol *2* IS dihydrocholesterol, *3* campesterol, *4* stigmasterol, *5* B sitosterol

Of the seven ILEs, Omegaven® is peculiar in that it contains only cholesterol. Among the other six, cholesterol and β-sitosterol were the main components, followed by campesterol and stigmasterol, with the only exception being Lipofundin S®. Structolipid® was the only solution with more animal sterols than plant ones (56.6 vs. 43.4%). Structolipid® and Intralipid® were the two ILEs with the highest percentages of cholesterol (56.6 and 43.4%, respectively) and the lowest percentages of β-sitosterol (24.2 and 36.5%, respectively). Conversely, the ILEs with the lowest percentages of cholesterol and the highest percentages of β-sitosterol were Clinoleic® (32.2 and 55.2%, respectively), Lipovenos® (21.8 and 50.6%) and Lipofundin S® (14 and 52%). Clinoleic® had the lowest quantities of campesterol (7.8%) and stigmasterol (4.9%).

The average quantities of each sterol were found to be statistically different across the ILEs (P 0.0000). The coefficients of variation were small for all ILEs with the exception of Lipofundin S®, whose variation coefficients were large for all animal and plant sterols. With respect to

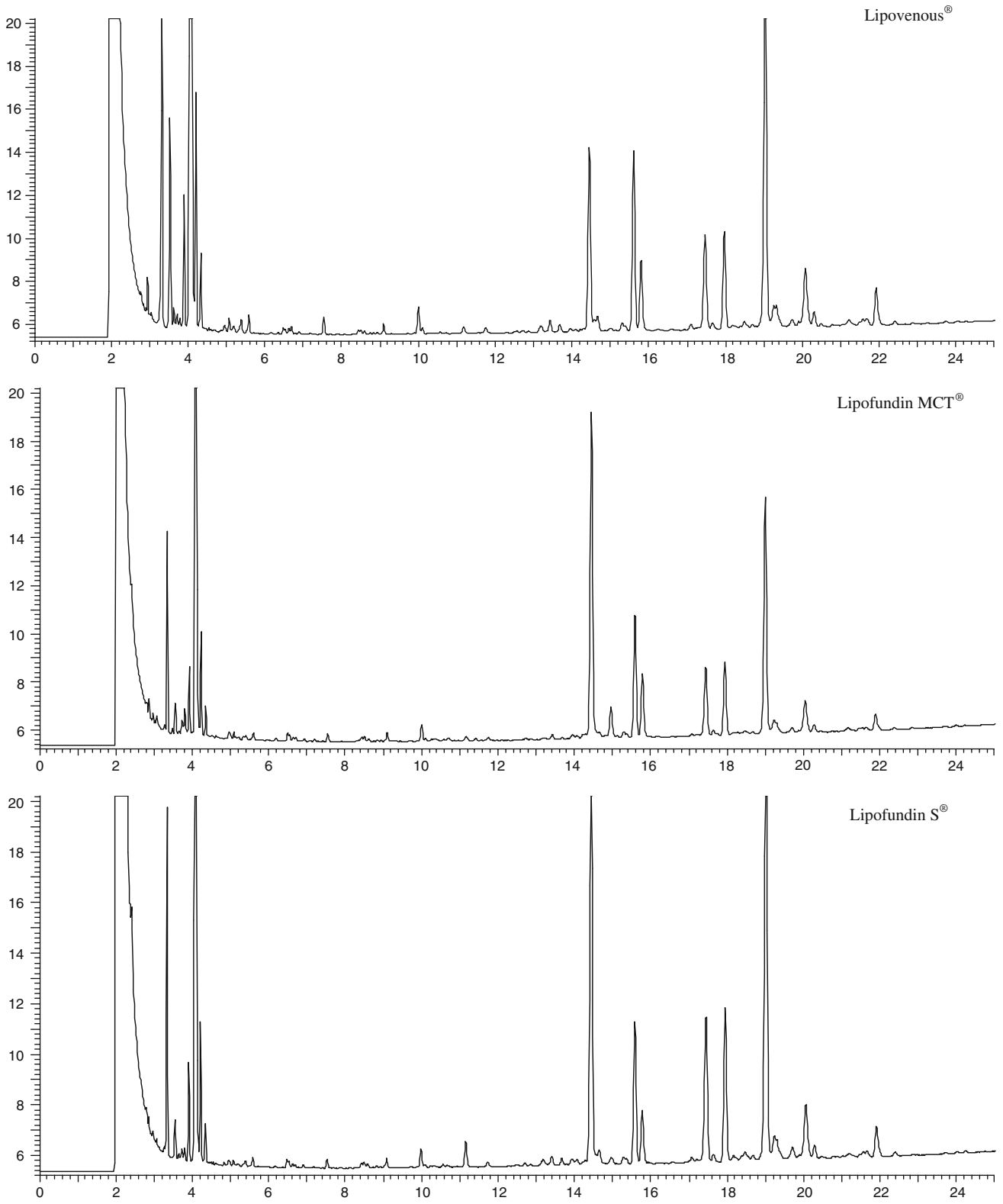

Fig. 1 continued

each sterol, a multiple pairwise comparison between ILEs confirmed statistically significant pairwise differences (P 0.000) with few exceptions. Nonstatistically significant pairwise comparisons between ILE means were particularly frequent for β-sitosterol (10 out of 21, involving Structolipid® Intralipid® Clinoleic® Lipovenos® and Lipofundin MCT®),

Table 2 Distribution of animal and plant sterols in intravenous lipid emulsions (average amounts)

Name	% Cholesterol (over total sterols)	% Campesterol (over total sterols)	% Stigmasterol (over total sterols)	% β-Sitosterol (over total sterols)
Structolipid® 20%	56.6	10.5	8.7	24.2
Intralipid® 20%	43.4	9.8	10.2	36.5
Clinoleic® 20%	32.2	7.8	4.9	55.2
Lipovenos® 20%	21.8	14.3	13.3	50.6
Lipofundin MCT® 20%	22.5	14.7	15.0	47.9
Lipofundin S® 20%	14.0	17.7	16.3	52.0
Omegaven 10%	100	0	0	0

Table 3 Distribution of plant sterols in intravenous lipid emulsions

Name	% Campesterol (over total phytosterols)	% Stigmasterol (over total phytosterols)	% β-Sitosterol (over total phytosterols)
Structolipid® 20 g/100 ml	24.3	20.0	55.8
Intralipid® 20 g/100 ml	17.4	18.0	64.6
Clinoleic® 20 g/100 ml	11.5	7.2	81.4
Lipovenos® 20 g/100 ml	18.2	17.0	64.8
Lipofundin MCT® 20 g/100 ml	18.9	19.3	61.7
Lipofundin S® 20 g/100 ml	20.6	19.0	60.4

Table 4 Overall fat composition of the intravenous lipid emulsions

Name	Fat %	Cholesterol mg/kg of fat (mg/100 ml solution)	Campesterol mg/kg of fat (mg/100 ml solution)	Stigmasterol mg/kg of fat (mg/100 ml solution)	β-Sitosterol mg/kg of fat (mg/100 ml solution)	All plant sterols mg/kg of fat (mg/100 ml solution)	Ratio animal to plant sterols	Plant sterols + cholesterol mg/kg of fat (mg/100 ml solution)
Structolipid® 20%	20.8	1,795 (37.3)	334 (6.9)	275 (5.7)	768 (16.0)	1,376 (28.6)	1:0.8	3,171 (66.0)
Intralipid® 20%	20.8	1,209 (25.1)	274 (5.7)	283 (5.9)	1,017 (21.1)	1,574 (32.7)	1:1.3	2,783 (57.9)
Clinoleic® 20%	20.6	524 (10.8)	127 (2.6)	79 (1.6)	899 (18.5)	1,105 (22.7)	1:2.1	1,629 (33.6)
Lipovenos® 20%	21.0	452 (9.5)	295 (6.2)	275 (5.8)	1,049 (22.0)	1,619 (34.0)	1:3.6	2,071 (43.5)
Lipofundin MCT® 20%	21.1	357 (7.5)	233 (4.9)	238 (5.0)	761 (16.1)	1,233 (26.0)	1:3.5	1,590 (33.6)
Lipofundin S® 20%	21.0	458 (9.6)	582 (12.2)	537 (11.3)	1,706 (35.8)	2,825 (59.3)	1:6.2	3,283 (68.9)
Omegaven 10%	11.2	1,914 (21.5)	0	0	0	0	1:0	1,914 (21.5)

followed by campesterol (9 out 21) and by cholesterol and stigmasterol (both 7 out 21). The pairwise comparisons which did not reach statistical significance are summarized and included in Table 5.

Discussion

Scattered reports in the literature have linked PNAC to the vegetable sterol components of ILEs [1–5]. Information on the sterol contents of ILEs, however, is currently scanty. The purpose of this paper has thus been to collect and present some data on the sterols contained in the most representative ILEs.

To this end, seven ILE formulations were selected as being representative in terms of their main oil component (soy, olive oil, fish oil variably combined with medium- or long-chain fatty acids, and purified triglycerides). These products were chemically analyzed to identify and quantify their animal and plant sterol contents.

Table 5 Summary statistics for sterol content in the intravenous lipid emulsions

Name	Cholesterol		Campesterol		Stigmasterol		β-Sitosterol	
	Mean (SD) (mg/100 ml solution)	CV (%)	Mean (SD) (mg/100 ml solution)	CV (%)	Mean (SD) (mg/100 ml solution)	CV (%)	Mean (SD) (mg/100 ml solution)	CV (%)
Structolipid® 20%	37.3 (0.3)	0.9	6.9 (0.1)	1.2	5.7 (0)	0.6	16 (0.1)	0.7
Intralipid® 20%	25.1 (0.3)	1.0	5.7 (0.1)[a]	1.3	5.9 (0.4)[a]	6.2	21.1 (0.4)[a]	1.8
Clinoleic® 20%	10.8 (2.2)	20.6	2.6 (0.1)[b]	2.8	1.6 (0.1)	6.6	18.5 [1][a,b]	5.7
Lipovenos® 20%	9.5 (0.3)[c]	2.8	6.2 (0.1)[a,b]	2.0	5.8 (0.2)[a,b]	2.9	22 (0.6)[a,b,c]	2.8
Lipofundin MCT® 20%	7.5 (0.1)[c,d]	1.1	4.9 (0.1)[a,b,c,d]	4.1	5.0 (0.1)[a,b,d]	1.3	16 (0.6)[a,b,c,d]	3.5
Lipofundin S® 20%	9.6 (1.3)[c,d,e]	13	12.2 (1.8)	14.9	11.3 (1.5)	13.50	35.8 (4.5)	12.6
Omegaven® 10%	21.5 (0.9)[b]	4	0[c]	0	0[c]	0	0	0
Number of nonstatistically significant pairwise comparison	7 out 21		9 out 21		7 out 21		10 out 21	

SD standard deviation

%CV percent coefficient of variation

The symbols identify nonstatistically significant pairwise comparisons between ILE means for each sterol with

[a] Compared to Structolipid®

[b] Compared to Intralipid®

[c] Compared to Clinoleic®

[d] Compared to Lipovenos®

[e] Compared to Lipofundin MCT®

All formulations had both animal and plant sterols, with the exception of Omegaven®, which contained only cholesterol. The source of cholesterol in these ILEs is egg yolk. The relative weight of each sterol varied significantly across formulations ($P = 0.0000$), with a large percentage of pairwise comparisons being statistically significant ($P = 0.000$), most notably for cholesterol and stigmasterol (14 out of 21 for both). Only one solution (Structolipid®) was found to have more animal (56.6%) than plant sterols, but a large presence of cholesterol (43.4%) was also detected in Intralipid®. Overall, the detection of large cholesterol contents was a surprise, since egg phospholipids were intended as a minor constituent of ILEs. Conversely, Clinoleic®, Lipofundin S®, Lipovenos®, and Lipofundin MCT® showed to be rich in β-sitosterol, with quantities ranging between 47.9 and 55.2% of total sterols.

The phytosterol contents of some ILEs differed from those detected in other studies, in which a smaller range of products and/or sterols was looked at. For Intralipid®, the plant sterol concentrations we found are similar to Ellegard's [10], but lower than those reported in two other studies [3, 11]. For Clinoleic®, phytosterols and cholesterol quantities were once again similar to Ellegard's. For Structolipid®, however, we found twice as much cholesterol as Ellegard (373 vs. 200 mg/l). No comparisons were possible for the other ILEs due to lack of data in the literature.

Within each set of extractions and determinations, the measurements were highly consistent, although some minimal differences did emerge. The small values of most coefficients of variation suggest that the analyses were executed appropriately. The occasionally high variation coefficient can thus be ascribed not to methodological issues, but to actual differences in quantities of sterols, unsaturated fat, and tocopherols across batches of the same product. Cross-batch variability may stem from both the quality of the oil source and the extraction process itself. Overall time and year of harvest, geographical source, and climate may affect the amount of sterols present in the ILEs. This amount may be further modified by refinement, with a reduction of free sterols by up to 30% of their original quantity [12]. Quantities of unsaturated fat and tocopherols may change the ratio of free to esterified sterols. The relatively high variation coefficient found in Clinoleic® and Lipofundin S® may stem respectively from the high content of oleic acid, which has been proven to be unstable [13], and of tocopherols. Conversely, those ILEs which are fully synthetized in a laboratory (e.g. Structolipid®) or semisynthetic (e.g. Lipofundin MCT®) are more stable. This is again reflected by the low variation coefficient. In addition, final cholesterol content of ILEs seems to be strongly affected by the amount of egg phospholipids added to the ILEs. This quantity has never been specified by producers. Appropriate storage is another key factor in

the fat variability of ILEs, which must be kept at a temperature below 25 °C. In our case, the ILEs tested were maintained below this temperature at all times. For this reason, we did not check for sterol variability and peroxidation over time. Finally, it is possible that the use of ethyl ether in the lipid extraction may have caused sterol peroxidation. This possibility was not further investigated because we believe that, ethyl ether being part of a cold saponification, the use of low temperatures should have prevented sterol oxidation.

We had an excellent separation of fats and the quantification of stigmasterol, which previous studies had left undetermined. In Plat et al. [14], the presence of stigmasterol was considered insignificant, and only sitosterol and campesterol were identified. On the contrary,in our study, stigmasterol was very well represented, to the point that its level was close to that of campesterol in most solutions. Stigmasterol is a potent antagonist of some hepatic nuclear receptor families, leading to the development of biliary injuries, while sitosterol and campesterol had minimal or insignificant inhibitory effects in a human-derived liver cell line HepG2 [15]. In addition, stigmasterol disrupts cholesterol homeostasis. Whether ILEs with a high content of stigmasterol are crucial to the development of PNAC is yet to be proven.

In humans, there is evidence of wide individual variations in plant sterols [16]. Plasma levels of campesterol and sitosterol (24-methyl and 24-ethyl analogue of cholesterol, respectively) are high, followed by minimal amounts of stigmasterol, ergosterol, avenasterol, and brassicasterol. β-sitosterol is secreted as neutral sterol into bile more rapidly than cholesterol and other plant sterols [17]. This more rapid fractional turnover of β-sitosterol may indirectly indicate that the rigorous exclusion of sterols other than cholesterol in vertebrates may be essential for the maintenance of normal cholesterol homeostasis. It is therefore particularly critical that, in all the solutions we analyzed, the ratio of cholesterol to phytosterols is highly skewed toward phytosterols, when compared to the amounts absorbed by a healthy person on a standard diet. For a 70-kg adult on a standard diet, the content of sterols is approximately 200–400 mg/day for phytosterols and 1,200–1,700 mg/day for cholesterol. Of these, only 10–20 mg/day of phytosterols and 300–500 mg/day of cholesterol are taken up by the gastrointestinal system and brought to the liver, where they are secreted into the bile. When the recommended intake of 1 g/(kg day) of fat is provided intravenously to a 70-kg adult, on the other hand, the data presented in Table 4 translate into an intake of phytosterols in the range of 119–241 mg/day (about 10 times the normal amount absorbed through the diet) and an intake of cholesterol in the range of 26–129 mg/day (about one tenth of the amount absorbed through the diet). This may explain why, in a study performed in short-bowel patients with and without parenteral nutrition and in controls, higher serum levels of phytosterols were detected in those on parenteral nutrition compared to those on oral intake or the controls [10]. Compared to controls, all the patients with short-bowel syndrome appeared to have lower serum levels of cholesterol, but higher endogenous cholesterol and bile acid synthesis. In another case, a person with short-bowel syndrome who had received home-parenteral nutrition for over 27 years with soy-based ILE [18], serum cholesterol remained surprisingly low (80–140 mg/dL; normal range <200) even though phytosterols had not been determined.

The fish oil-based ILE is the only formulation without plant sterols. This could explain its beneficial effects on liver functions, in terms of the reversal of PNAC in humans, regularity of bile flow, and prevention of hepatic lipogenesis in animals [19, 20]. These beneficial effects, however, may also stem from the presence of cholesterol, which may be more naturally suited to the human body. Another explanation could be the lower supplementation of lipids, in line with the recommended dosage of 1 g/(kg day). If cholesterol is indeed beneficial, structured lipids could be another option in the presence of PNAC. In our analysis, we found a cholesterol to plant sterol ratio of 1:0.8, confirming a cholesterol predominence. However, the absolute values of both sterols were high.

Our study is the first to determine the animal and plant sterol quantities in ILEs originating from different oils. The quanti-qualitative determinations of animal and plant sterols will require further confirmation, especially in terms of sample type and storage time, but they already suggest the need for future research looking at the phytosterols:cholesterol ratio and its association to liver dysfunction during ILE infusions.

Acknowledgments We are particularly grateful to Dr. Maria Rodriguez Estrada and Mr Stefano Savioli at the Food Science Department directed by Prof. Lerker, University of Bologna, for their expertise and technical assistance offered for accurate laboratory determinations.

References

1. Bindl L, Lütjohann D, Buderus S, Lentze MJ, Bergmann KV (2000) High plasma levels of phytosterols in patients on parenteral nutrition: a marker of liver dysfunction. J Pediatr Gastr Nutr 31:313–316
2. Llop JM, Virgili N, Moreno-Villares JM et al (2008) Phytosterolemia in parenteral nutrition patients: implications for liver disease development. Nutrition 24:1145–1152
3. Clayton PT, Bowron A, Mills KA et al (1993) Phytosterolemia in children with parenteral nutrition-associated cholestatic liver disease. Gastroenterology 105:1806–1813
4. Iyer KR, Clayton P (1998) New insight into mechanisms of parenteral nutrition-associated cholestasis: role of plant sterols. J Pediatr Surg 33:1–6

5. Lascala GC, Le Coultre C, Roche BG et al (1993) The addition of lipids increases the TPN-associated cholestasis in the rat. Eur J Pediatr Surg 3:224–227
6. Boselli E, Velazco V, Caboni MF, Lercker G (2001) Pressurized liquid extraction of lipids for the determination of oxysterols in egg-containing food. J Chromatogr 917:239–244
7. Folch J, Lees M, Sloane-Stanley GH (1957) A simple method for the isolation and purification of total lipids from animal tissues. J Biol Chem 226:497–509
8. Sander BD, Addis PB, Park SW, Smith DE (1989) Quantification of cholesterol oxidation products in a variety of foods. J Food Protect 52:109–114
9. Sweeley CC, Bentley R, Makita M, Wells WW (1963) Gas–liquid chromatography of trimethylsilyl derivatives of sugars and related substances. J Am Chem Soc 85:2497–2507
10. Ellegard L, Sunesson A, Bosaeus I (2005) Higher serum phytosterol levels in short bowel patients on parenteral nutrition support. Clin Nutr 24:415–420
11. Saubion JL, Hazane C, Jalabert M (1998) The role of sterols in lipid emulsions for parenteral nutrition. Nutrition 14:477–478
12. Ferrari RA, Esteves W, Mukherjee KD, Schulte E (1997) Alteration of sterol and sterol esters in vegetable oils during industrial refining. J Agric Food Chem 45:4753–4757
13. Pironi L, Guidetti MC, Zolezzi C, Fasani C, Bersani G et al (2003) Peroxidation potential of lipid emulsions after compounding in All-In-One solutions. Nutrition 19:784–788
14. Plat J, Brzezinka H, Lütjohann D, Mensink RP, von Bergmann K (2001) Oxidized plant sterols in human serum and lipid infusions as measured by combined gas-liquid chromatography-mass spectrometry. J Lipid Res 42:2030–2038
15. Carter BA, Taylor OA, Prendergast DR et al (2007) Stigmasterol, a so lipid-derived phytosterol, is an antagonist of the bile acid nuclear receptor FXR. Pediatr Res 62:301–306
16. Berge KE, von Bergmann K, Lutjohann D et al (2002) Heritability of plasma noncholesterol sterols and relationship to DNA sequence polymorphism in ABCG5 and ABCG8. J Lipid Res 43:486–494
17. Salen G, Ahrens EH, Grundy SM (1970) Metabolism of β-sitosterol in men. J Clin Invest 49:952–967
18. Forchielli ML, Richardson D, Gura K, Folkman J, Lo CW (2008) Better living through chemistry, constant monitoring, and prompt interventions: 26 years on home parenteral nutrition without major complications. Nutrition 24:103–107
19. Alwayn IP, Gura K, Nose V et al (2005) Omega-3 fatty acid supplementation prevents hepatic steatosis in a murine model of nonalcoholic fatty liver disease. Pediatr Res 57:445–452
20. Gura KM, Lee S, Valim C et al (2008) Safety and efficacy of a fish-oil-based fat emulsion in the treatment of parenteral nutrition-associated liver disease. Pediatrics 121:678–686

Lipids (2010) 45:73–80
DOI 10.1007/s11745-009-3369-4

ORIGINAL ARTICLE

Lipid Abnormalities in a Never-Treated HIV-1 Subtype C-Infected African Population

Carla Maria T. Fourie · Johannes M. Van Rooyen · Annamarie Kruger · Aletta E. Schutte

Received: 7 August 2009 / Accepted: 23 October 2009 / Published online: 15 November 2009

Abstract Dyslipidemia has been documented worldwide among human immunodeficiency virus-infected (HIV) individuals and these changes are reminiscent of the metabolic syndrome (MetS). In South Africa, with the highest number of HIV infections worldwide, HIV-1 subtype C is prevalent, while HIV-1 subtype B (genetically different from C) prevails in Europe and the United States. We aimed to evaluate if HIV infection (subtype C) is associated with dyslipidemia, inflammation and the occurrence of the MetS in Africans. Three hundred newly diagnosed HIV-infected participants were compared to 300 age, gender, body mass index and locality matched uninfected controls. MetS was defined according to the Adult Treatment Panel III (ATP III) and International Diabetes Federation (IDF) criteria. The HIV-infected group showed lower high density lipoprotein cholesterol (1.23 vs. 1.70 mmol/L) and low density lipoprotein cholesterol (2.60 vs. 2.80 mmol/L) and higher triglycerides (1.29 vs. 1.15 mmol/L), C-reactive protein (3.31 vs. 2.13 mg/L) and interleukin 6 (4.70 vs. 3.72 pg/L) levels compared to the uninfected group. No difference in the prevalence of the MetS was seen between the two groups (ATP III, 15.2 vs. 11.5%; IDF, 21.1 vs. 22.6%). This study shows that HIV-1 subtype C is associated with dyslipidemia, but not with a higher incidence of MetS in never antiretroviral-treated HIV-infected Africans.

Keywords HIV-1 subtype C · South Africa · African · Metabolic syndrome · Dyslipidemia · Never-treated · Inflammation

Abbreviations

AIDS	Acquired immunodeficiency syndrome
ARV	Antiretroviral
ATP III	Adult Treatment Panel III
BMI	Body mass index
CI	Confidence intervals
CVD	Cardiovascular disease
DBP	Diastolic blood pressure
FG	Fasting glucose
HDL-C	High-density lipoprotein cholesterol
HIV	Human immunodeficiency virus
HR	Heart rate
hs-CRP	High sensitivity C-reactive protein
hs-IL-6	High sensitivity interleukin-6
IDF	International Diabetes Federation
LDL-C	Low-density lipoprotein cholesterol
MetS	Metabolic syndrome
OR	Odds ratios
PP	Pulse pressure
PURE	Prospective urban and rural epidemiological
SBP	Systolic blood pressure
TC	Total cholesterol
TG	Triglycerides
WC	Waist circumference

C. M. T. Fourie (✉) · J. M. Van Rooyen · A. E. Schutte
HART (Hypertension in Africa Research Team),
Subject Group Physiology, North-West University,
Potchefstroom, South Africa
e-mail: carla.fourie@nwu.ac.za

A. Kruger
AUTHeR (Africa Unit for Transdisciplinary Health Research),
Faculty of Health Science, North-West University,
Potchefstroom, South Africa

Introduction

Southern Africa accounts for almost a third of all new human immunodeficiency virus (HIV) infections and acquired immunodeficiency syndrome (AIDS) related deaths worldwide, and an estimated 5.5 million people are living with HIV in South Africa [1]. The predominant virus responsible for these infections in South Africa is HIV-1, group M (major), subtype C [2, 3], which accounts for 55–60% of all HIV-1 infections worldwide [4, 5], and differ as much as 30% in its genomes from HIV-1 subtype B, responsible for the infections in North America, Europe and Australia [2, 5, 6]. The clinical consequences of these subtype variations still remain unclear [7].

Cardiovascular involvement in various forms, such as dyslipidemia [8], lipodystrophy [9, 10], endothelial dysfunction [11], accelerated atherosclerosis [12] and coagulation disorders [13] have been documented worldwide among HIV-infected individuals. This involvement can be associated with various factors, such as the infection itself, opportunistic infections, the therapy or non HIV related cardiovascular risk factors like smoking and age [14]. It is well known that the lipid profile of HIV-infected individuals changes, and these changes include increased levels of triglycerides (TG), and decreased levels of total cholesterol (TC), low-density lipoprotein cholesterol (LDL-C) and high-density lipoprotein cholesterol (HDL-C) [12, 15–18]. It remains unclear what the relative contribution of the HIV infection and the ongoing inflammation are to the blood lipids [7, 19].

Some of the changes seen in HIV-infected individuals—in particular low HDL-C levels, hypertriglyceridemia, increased levels of visceral adipose tissue, plasma glucose and insulin—are reminiscent of the metabolic syndrome (MetS) [10]. The MetS has been identified as a significant and multifaceted risk factor for cardiovascular disease (CVD) [10, 20]. The above metabolic abnormalities are among the most significant side effects experienced with highly active antiretroviral (ARV) therapy, in particular with protease inhibitors [10, 14, 21]. On the other hand, the long term effects of the infection itself (as ARV therapy can not completely eradicate HIV-1) have become increasingly challenging [22] and may play a role in these metabolic changes. This is seen in the study of Bonfanti et al. [23] where the prevalence of the MetS was higher in the HIV-infected individuals compared to the general population, but was similar in treated and untreated HIV-infected individuals.

Even though South Africa is the country with the largest number of HIV infections in the world [1], to the best of the authors's knowledge, no study to date has been done to specifically evaluate whether the HIV-1 (subtype C) infection itself, prevalent in South Africa [3], leads to the same metabolic changes and inflammatory state seen in HIV-1 (subtype B), prevalent in Europe, United States, Australia and South America [5].

The aim of this study was therefore to evaluate whether HIV-1 (subtype C) infection itself is associated with dyslipidemia, inflammation and the occurrence of the MetS in newly identified HIV-infected participants who had never received ARV therapy.

Methods

Study Design and Participants

This sub-study is embedded in the larger international PURE (Prospective Urban and Rural Epidemiological) study. The overarching PURE study is a longitudinal multi national study that will track changes in lifestyles, CVD risk factors and chronic diseases over a period of 12 years, using periodic standardized data collection in urban and rural areas of developing countries in transition, including South Africa. The South African leg of the study was performed in the North West province where a total of 2,000 black South Africans (1,000 urban and 1,000 rural) were randomly recruited from a rural and urban setting and screened during the baseline phase in 2005. The inclusion criteria were volunteers older than 35 years that were non users of any chronic medication and with no self-reported diseases. For this sub-study the 300 newly identified HIV-infected participants of the baseline PURE study population were individually matched with 300 HIV-uninfected participants (case-control design), according to age, gender, body mass index (BMI) and locality (urban and rural). The methodology appropriate to this sub-study will be discussed.

Ethical Considerations

All participants provided signed informed consent after all the procedures had been explained to them in their home language. The study protocol complies with the Declaration of Helsinki as revised in 2004 [24] and was approved by the Ethics Committee of the North-West University, Potchefstroom, South Africa.

Experimental Protocol

Permission to execute the PURE study was obtained from the provincial Department of Health, local authorities and from the Tribal Chief in the rural area. For about 12 weeks 30–35 participants arrived at the research locality of the rural or urban areas at about 07:00 each morning after a 10–15 min drive (provided by the research team) from their

communities. The participants were introduced to the setup and after the procedures were explained they signed the informed consent forms and received HIV pre-counseling given by trained counselors. The HIV status of the participants was revealed during post-counseling and the infected participants were referred to their local clinic or hospital for follow-up and CD4 cell count determination. During the course of the morning demographic, lifestyle and food frequency questionnaires were completed with the help of the specially trained field workers in the subject's home language. Lifestyle data included self reported current tobacco use, alcohol intake as well as medical history.

Anthropometric Measurements

Height, weight, hip and waist circumference (WC) were measured (Precision Health Scale, A & D Company, Japan; Invicta Stadiometer, IP 1465, UK; Holtain unstretchable metal tape) using standardized procedures [25].

Cardiovascular Measurements

Systolic blood pressure (SBP), diastolic blood pressure and heart rate were obtained with a validated OMRON HEM-757 device. After a 10-min rest period, blood pressure measurements were performed twice (5 min apart) on the right arm (brachial artery), while the participants were seated upright and relaxed with his/her right arm supported at heart level. Appropriate cuffs were used for obese participants.

Blood, Serum and Plasma Samples

Blood was drawn from the antebrachial vein using a sterile winged infusion set and syringes. Serum was prepared according to appropriate methods and stored at −80 °C in the laboratory. In the rural area serum was stored at −18°C (no longer than 5 days) until it could be transported to the laboratory facility and was then stored at −80 °C until analysis.

Biochemical Analyses

Quantitative determination of the cholesterol, HDL-C, TG, glucose (GOD-POD), high sensitivity C-reactive protein (hs-CRP) and creatinine concentration in the serum of the participants was done with the Konelab20i™ auto analyzer (Thermo Fisher Scientific Oy, Vantaa, Finland), a clinical chemistry analyzer for colorimetric, immunoturbidimetric and ion-selective electrode measurements. LDL-C was calculated by using the Friedewald formula [26]. The creatinine clearance rate was estimated using the Cockcroft-Gault formula [27]. Serum concentrations of high sensitivity interleukin-6 (hs-IL-6) were measured using human enzyme-linked immunosorbent assays (Quantikine® HS ELISA, R&D Systems, Minneapolis, USA). HIV status was determined with the First Response (PMC Medical, India) rapid HIV card test using whole blood. If tested positive, the test was repeated with the Pareeshak (BHAT Bio-tech India) card test. The card test distinguishes between HIV-1 and HIV-2, but not between subtypes. The HIV-1 subtype C epidemic prevalent in South Africa has been established by serotyping and genotyping [1–3].

The Metabolic Syndrome

The MetS in the sub-study was identified according to the definition of the Third Report of the National Education Program Expert Panel on Detection, Evaluation and Treatment of High Blood Cholesterol in Adults (ATP III) [20], and according to the definition of the International Diabetes Federation (IDF) [28].

Statistical Analysis

All data were statistically analyzed by means of Statistica v.8 (Statsoft Inc., OK, USA, 2008). Mean values and standard deviations were calculated. The distribution of hs-CRP, CRP:HDL ratio and hs-IL-6 were normalized by logarithmic transformation before analysis, reporting the geometric mean and 5–95% percentiles. Independent *t* tests were used to compare the characteristics of the continuous variables of the HIV-infected and uninfected groups. The Chi-square tests were done to compare data of categorical variables. An analysis of covariance (ANCOVA) was performed to compare the cardiovascular parameters, lipid profile, glucose, hs-CRP and hs-IL-6 of the HIV-infected and uninfected participants, whilst adjusting for tobacco and alcohol use.

Odds ratios (OR), as estimates of risk, with 95% confidence intervals (CI), were calculated using 2×2 frequency tables for HIV-infected versus uninfected participants. Since very few participants met the cut-off values for the MetS (for both the ATP III and IDF definitions), especially for WC in African men, the median was used as cut-off value for the calculation of OR. Frequency tables were used to determine the number of subjects that were classified according to each specific MetS definition (ATP III and IDF), thereby determining the prevalence of the MetS in both the HIV-infected and control groups. The Chi-square test was used to obtain the *P* values. *P* values ≤ 0.05 are regarded as significant.

Results

Characteristics of HIV-infected participants and matching controls are reported in Table 1. Due to individual

Table 1 Characteristics of the HIV-infected and uninfected African participants ($N = 600$)

	HIV infected ($N = 300$)	HIV uninfected ($N = 300$)	P
Age (years)	44.0 ± 8.04	44.0 ± 7.81	0.97
Height (cm)	161 ± 9.88	161 ± 8.37	0.62
Weight (kg)	59.5 ± 13.5	58.9 ± 13.9	0.61
BMI (kg/m^2)	22.9 ± 5.59	22.8 ± 5.48	0.92
Waist (cm)	75.9 ± 10.6	75.9 ± 10.1	0.98
Hip (cm)	92.6 ± 13.8	93.0 ± 13.9	0.71
Waist:hip ratio	0.83 ± 0.11	0.82 ± 0.10	0.62
SBP (mm Hg)	124 ± 21.8	129 ± 21.8	0.003
DBP (mm Hg)	84.0 ± 14.7	85.9 ± 14.3	0.09
PP (mm Hg)	40.2 ± 11.5	43.7 ± 13.1	0.0005
HR (beats/min)	76.4 ± 15.0	72.2 ± 15.2	0.0009
TC (mmol/L)	4.42 ± 1.25	5.02 ± 1.33	<0.0001
HDL-C (mmol/L)	1.23 ± 0.58	1.70 ± 0.71	<0.0001
LDL-C (mmol/L)	2.60 ± 1.01	2.80 ± 1.14	0.01
TG (mmol/L)	1.29 ± 0.77	1.15 ± 0.75	0.03
TG:HDL-C ratio	1.41 ± 1.47	0.86 ± 1.21	<0.0001
Glucose (mmol/L)	5.35 ± 1.26	5.50 ± 1.10	0.13
hs-CRP (mg/L)	3.31 (0.32–50.4)	2.13 (0.23–29.2)	0.0006
CRP:HDL-C ratio	2.94 (0.21–62.0)	1.36 (0.13–18.5)	<0.0001
hs-IL-6 (pg/ml)	4.70 (1.29–20.9)	3.72 (1.11–16.9)	0.0004
Creatinine (μmol/L)	83.8 (46.0–376)	76.5 (46.4–372)	0.83
eCrCl (ml/min)	73.5 (15.1–160)	79.7 (16.1–157)	0.15
Calorie intake (kJ)	1,879.0 ± 953	1,836.1 ± 1,003	0.59
Total fat intake (g/day)	51.3 ± 33.4	50.4 ± 38.4	0.78
Tobacco users N (%)	127 (42.3)	137 (45.6)	0.41
Alcohol users N (%)	96 (32.0)	103 (34.3)	0.54

Data are expressed as arrhythmic means ± standard deviation, geometric mean (5–95 percentiles) or % of N

N indicates number of participants, *BMI* body mass index, *SBP* systolic blood pressure, *DBP* diastolic blood pressure, *PP* pulse pressure, *HR* heart rate, *TC* total cholesterol, *HDL-C* high-density lipoprotein cholesterol, *LDL-C* low-density lipoprotein cholesterol, *TG* triglycerides, *hs-CRP* high-sensitivity C-reactive protein, *hs-IL-6* high-sensitivity interleukin 6, *eCrCl* estimated creatinine clearance

All *P* values were obtained with independent *t* tests, except for tobacco and alcohol users where the Chi-square test was used

matching, age and BMI values, as well as the other anthropometric measurements were almost identical in the two groups. HIV-infected participants had a lower SBP, pulse pressure, TC, HDL-C and LDL-C, whereas the heart rate, TG, TG:HDL-C ratio, hs-CRP, CRP:HDL-C ratio and hs-IL-6 were higher in the HIV-infected group. After adjusting for tobacco and alcohol use, similar results were obtained, which were expected as the percentage tobacco and alcohol users did not differ. There were no differences in the calorie and fat intake between the HIV-infected and uninfected groups. Separate analyses as in Table 1 were performed for each gender and similar results were obtained.

The OR of the HIV-infected group versus the uninfected group is shown in Table 2. In this study population having a lower HDL-C is five times more likely when being a HIV-infected man and three times more likely in women. The Odds ratio for having a higher TG, hs-CRP and hs-IL-6 level is respectively 1.7, 1.8 and 1.7 times more when being HIV infected.

The MetS defined according to the ATP III and IDF criteria are shown for HIV-infected and uninfected participants in Table 3. In comparison with the controls no difference (15.2 vs. 11.5%; $P = 0.18$) in the MetS was seen in the HIV-infected, never-ARV-treated participants according to the ATP III definition. Similar results were shown for the IDF definition (21.1 vs. 22.6%; $P = 0.65$).

Discussion

In this study HIV-1- (subtype C) infected, never-ARV-treated, participants showed dyslipidemia and inflammation. These results are in agreement with documented data on HIV-infected individuals of other population groups [12, 18, 29] where HIV-1 (subtype B) prevails [5].

A low HDL-C concentration increases the risk for coronary heart disease [30] and for every 1 mg/dl increase in serum HDL-C, a 2% reduction in CVD is estimated [31]. Duprez et al. found that lower HDL levels were associated with a higher risk of CVD in HIV-infected patients and Jericó et al. found smoking and HDL cholesterol to be the main cardiovascular risk factors in their HIV-infected study population [32, 33]. In our study population a HIV-infected man is seven times, and a woman three times more likely to have low HDL-C levels which should increase

Table 2 Odds Ratios of HIV-infected ($N = 300$: M = 116, F = 184) participants versus uninfected ($N = 300$: M = 116, F = 184) participants

	OR	
	HIV infected versus HIV uninfected	95% CI
WC		
M (≥73 cm)	0.93	0.6–1.6
F (≥75 cm)	0.94	0.6–1.4
TG (≥1.0 mmol/L)	1.70	1.2–2.3*
HDL-C		
M (<1.4 mmol/L)	5.25	2.9–9.2*
F (<1.3 mmol/L)	2.92	1.9–4.5*
SBP (≥124 mm Hg)	0.72	0.5–1.0*
DBP (≥84 mm Hg)	0.72	0.5–1.0*
FG (≥5.3 mmol/L)	0.64	0.5–0.9*
hs-CRP (≥2.7 mg/L)	1.78	1.3–2.5*
hs-IL-6 (4.2 pg/ml)	1.67	1.2–2.3*

N indicates number of participants, *M* male, *F* female, *WC* waist circumference, *TG* triglycerides, *HDL-C* high-density lipoprotein cholesterol, *SBP* systolic blood pressure, *DBP* diastolic blood pressure, *FG* fasting glucose, *hs-CRP* high sensitivity C-reactive protein, *hs-IL-6* high sensitivity interleukin 6

Median of the total group was used as cut-off value. Significance is indicated by *

their risk for CVD. Even though Africans normally exhibit lower fasting triglyceride and higher HDL-C levels than Caucasians [34], HDL-C levels of our HIV-infected participants (1.23 ± 0.58 mmol/L) were below the level of 1.28 mmol/L (50 mg/dl), which is seen as an increased risk for CVD [35].

Because the contribution of HIV to dyslipidemia is difficult to distinguish from those of classic cardiovascular risk factors, control participants were carefully matched by gender, age, BMI and locality to minimize the confounding effect of these non HIV related conditions on the results of this study. Furthermore, the participants in this study were newly identified and had never received ARV therapy. It could therefore be speculated that the metabolic changes seen have been influenced by HIV-1, subtype C, infection itself.

To identify the MetS in our study population, the criteria of the most frequently used ATP III definition and more recent IDF definition were used. Although our infected participants never received ARV treatment, the prevalence of MetS of 15% (ATP III definition) and 21% (IDF definition) is higher of that found by Badiou et al. [36] in HIV-positive individuals (7.3 vs. 11.2%; 80% treated by combined ARV therapy) and in agreement with the study by Samaras et al. [37] (14 vs. 18%), where 93% of the participants had received ARV therapy at some time. The TG:HDL-C ratio, which is closely linked to lipid disorders associated with MetS, was higher in our HIV-infected participants, as observed previously in HIV-infected individuals [38] and in type 2 diabetes patients [39]. The most prevalent lipid abnormalities seen in our study were the low HDL-C levels and higher TG levels exhibited by the HIV-infected participants. This was also seen in the SIMONE study where the diagnosis of MetS in HIV-infected individuals was mainly due to reduced HDL-C and high serum TG levels [40].

Much controversy still exist whether HIV-infected individuals have a higher prevalence of MetS (with or without therapy). In the study of Mondy et al. [41] the researchers found the prevalence of MetS to be similar among the HIV-infected participants (25.5%), who received ARV therapy, and the matched NHANES control participants (26.5%). On the other hand, in the cohort of HIV-infected individuals of Samaras et al. [37], the prevalence of the MetS was less in HIV positive adults (all received ARV therapy at some time) than in the general population. Our study, where the participants never received ARV therapy, shows that the prevalence of the MetS (both according to the ATP III and IDF definition) does not differ between the HIV-infected and the matched uninfected participants. This finding is in contrast with the finding of Bonfanti et al. [23] which reported a higher prevalence of MetS in never-treated HIV-infected individuals than in the general population.

Abdominal obesity, an essential component of the MetS, seems to occur less frequently in HIV-infected individuals (treated), and they seldom meet the cut-off value of the MetS criteria [37, 42]. Furthermore, there are no specific population group WC cut-off value available for sub-Saharan Africans and in this study the cut-off value for Europeans were used, as suggested by the IDF definition, when identifying the prevalence of MetS using the IDF criteria. It is known that abdominal obesity is more prevalent among African women than men [43] and very few male participants met the WC cut-off value whether HIV infected (0.88% ATP III and 2.63% IDF) or not (0% ATP III and 0.88% IDF), suggesting that these WC cut-off values might influence the outcome of the prevalence of the MetS in our study. The fact that the participants of our study were matched according to BMI to differentiate between the contribution of the infection itself and classical risk factors, could therefore not address this problem. Although more women met the WC cut-off value, it has also been shown that there is a clear difference regarding body composition between African and Caucasian women and Schutte et al. [44] suggested that these differences should be incorporated by the IDF definition when establishing a WC cut-off value for Africans. They also suggested that different HDL-C and TG cut-off values be used

Table 3 Comparison of the prevalence of the MetS between the HIV-infected ($N = 300$: M = 116, F = 184) and uninfected participants ($N = 300$: M = 116, F = 184)

	ATP III			IDF		
	HIV infected	HIV uninfected	*P*	HIV infected	HIV uninfected	*P*
WC						
M	0.88	0.00	0.32	2.63	0.88	0.31
F	18.33	18.68	0.93	33.9	40.1	0.22
TG	18.2	14.3	0.19	17.6	14.3	0.28
HDL-C						
M	47.4	12.1	<0.0001	46.5	11.2	<0.0001
F	62.6	33.7	<0.0001	62.6	33.7	<0.0001
BP	50.0	59.0	0.03	50.0	59.0	0.03
FG	22.7	25.1	0.49	36.6	43.7	0.08
MetS	15.2	11.5	0.18	21.1	22.6	0.65

Data are expressed as % of *N*

ATP III definition of MetS requires three or more of the following criteria: abdominal obesity, WC, men > 102 cm, women > 88 cm; hypertriglyceridemia ≥ 1.69 mmol/L; low HDL-C, men < 1.04 mmol/L, women < 1.29 mmol/L; blood pressure ≥ 130/85 mm Hg, or fasting glucose ≥ 6.1 mmol/L

IDF definition of MetS requires abdominal obesity, WC, men ≥ 94 cm, women ≥ 80 cm, and two or more of the following criteria: hypertriglyceridemia ≥ 1.7 mmol/L; low HDL-C, men < 1.03 mmol/L; women < 1.29 mmol/L; blood pressure ≥ 130/85 mm Hg, or fasting glucose ≥ 5.6 mmol/L

N indicates number of participants, *M* male, *F* female, *WC* waist circumference, *TG* triglycerides, *HDL-C* high density lipoprotein cholesterol, *BP* blood pressure, *FG* fasting glucose, *MetS* metabolic syndrome

All *P* values were obtained via the Chi-square test

for Africans to determine the prevalence of MetS in an African population as they mostly show more favorable lipid values than Caucasians [44].

HIV lipodystrophy is characterized by dyslipidemia, visceral adiposity and a loss of abdominal and peripheral subcutaneous fat [45]. Lipodystrophy is seen in only a small portion of HIV-infected individuals not receiving ARV therapy [46]. The HIV-infected and uninfected participants in this study were matched according to BMI and no differences were seen in waist or hip circumference or waist:hip ratio. Odds ratios also showed no increase in risk for an increase in WC when being HIV infected. The participants were newly identified as being HIV infected and therefore it is not known how long the participants have been infected. However, it seems that no fat redistribution took place in our never-treated HIV-infected participants.

The fasting glucose levels were similar between the HIV-infected and the control groups. The use of fasting glucose level alone to diagnose impaired tolerance is likely to underestimate the prevalence of insulin resistance, advocated as a causative factor of the MetS [47].

Both low serum HDL-C levels and high serum hs-CRP levels are seen as independent risk factors for CVD [37, 48], and the concentration of CRP is seen as a predictor of cardiovascular events [49]. A study by Wadham et al. [50] showed that HDL-C inhibits the inflammatory effect of CRP. In the general population the MetS is associated with inflammation and the IDF consensus group has highlighted elevated CRP as apparently being related to the MetS. The hs-CRP levels differ between the HIV-infected and control group (3.31 vs. 2.13 mg/L; $P = 0.0006$) and the OR for having a higher hs-CRP is 1.78 when HIV infected. The latter did not seem to influence the risk for MetS in this study. However, it is not known for how long the participants have been infected, and the duration of infection might be an important determinant of inflammatory status and its consequences.

Although hypertension is very common in black South Africans [51, 52] and 59% of the HIV uninfected participants had a high blood pressure (according to both the ATP and IDF definition for MetS), the SBP as well as the prevalence of high blood pressure were lower in the HIV-infected group. This seems to be consistent with previous studies [53], as hypertension in the HIV population is mostly associated with the use of ARV therapy, the MetS, insulin resistance and/or anthropometric disorders [54].

Kidney function is often compromised in the HIV-infected population, and HIV-associated nephropathy is frequently seen in immunosuppressed individuals of black ethnicity [55]. In our study no difference in serum creatinine or estimated creatinine clearance rate was seen between the HIV-infected and uninfected participants.

These results suggest that identification of the MetS in HIV-1 subtype C infected Africans should not be the main focus for the identification of individuals at risk for CVD. Low HDL-C and elevated TG levels seem to be the most prevalent abnormalities and therefore emphasis should be placed on determining the HDL-C and TG levels and to treat the metabolic abnormalities present, thereby reducing the probable cardiovascular risk faced by these individuals.

This study should be interpreted within the context of its strengths and limitations. We applied a case–control design and carefully matched the control subjects according to age, gender, BMI and locality. When viewing previous studies regarding HIV and cardiovascular risk, our study population is unique in specifically two aspects: they were infected with the subtype C virus instead of subtype B, and they were unaware of their infected status and therefore have never received ARV treatment. Thus the differences found could probably be attributed to the infection itself. Furthermore, the data as obtained in this study is limited in HIV-infected South Africans. A limitation of the study is that the duration of the HIV infection is unknown as the participants were newly identified being HIV infected. Also, some of the participants chose not to visit the local clinic or hospital for follow-up (CD4 cell count determination and possible subsequent treatment) after they were informed of their HIV-infected status. This is probably due to stigmatization which still exists among South African individuals [56, 57]. Thus, we were only able to obtain CD4 cell count data from a limited group of participants ($N = 72$) and those results were not used in the study due to the small sample size.

In conclusion, the results of this study provide evidence that HIV-1, specifically subtype C, is associated with dyslipidemia and an inflammatory state of newly identified HIV-infected, never-treated, African individuals that may increase their risk for CVD. The study therefore shows that HIV-1 subtype C, though genetically different from subtype B, seems to influence the MetS components in the same way as HIV-1 subtype B, but does not increase the prevalence of the MetS in Africans.

Acknowledgments The authors would like to thank the PURE-SA research team, especially Dr. M Watson, who was responsible for the HIV testing and counseling, the field workers and office staff in the Africa Unit for Transdisciplinary Health Research (AUTHeR), North-West University, South Africa. PURE International, Dr. S Yusuf and the PURE project staff at the PHRI, Hamilton Health Sciences and McMaster University, ON, Canada. This work was financially supported by SANPAD (South Africa—Netherlands Research Program on Alternatives in Development), South African National Research Foundation (NRF GUN numbers 2069139 and FA2006040700010), North-West University, Population Health Research Institute (PHRI), and the Medical Research Council (MRC) of South Africa.

References

1. UNAIDS (2008) Sub-Saharan Africa. Aids epidemic update. Regional Summary. http://data.unaids.org/pub/Report/2008/jc1526_epibriefs_ssafrica_en.pdf. Accessed March 2009
2. Peeters M (2001) The genetic variability of HIV-1 and its implications. Transfus Clin Biol 8:222–225
3. Jacobs GB, de Beer C, Fincham JE, Adams V, Dhansay MA, van Rensburg EJ, Engelbrecht S (2006) Serotyping and genotyping of HIV-1 infection in residents of Khayelitsha, Cape Town, South Africa. J Med Virol 78:1529–1536
4. Thomson MM, Najera R (2005) Molecular epidemiology of HIV-1 variants in the global AIDS pandemic: an update. AIDS Rev 7:210–224
5. Freire E (2006) Overcoming HIV-1 resistance to protease inhibitors. Drug Discov Today 3(2):281–286
6. Gaschen B, Taylor J, Yusim K, Foley B, Gao F, Lang D, Novitsky V, Haynes B, Hahn BH, Bhattacharya T, Korber B (2002) Diversity considerations in HIV-1 vaccine selection. Science 296:2354–2360
7. Simon V, Ho DD, Abdool KQ (2006) HIV/AIDS epidemiology, pathogenesis, prevention, and treatment. Lancet 368:489–504
8. Riddler SA, Smit E, Cole SR, Li R, Chmiel JS, Dobs A, Palella F, Visscher B, Evans R, Kingsley LA (2003) Impact of HIV infection and HAART on serum lipids in men. JAMA 289:2978–2982
9. Carr A, Cooper DA (1998) Images in clinical medicine Lipodystrophy associated with an HIV-protease inhibitor. N Engl J Med 339:1296
10. Grinspoon SK (2005) Metabolic syndrome and cardiovascular disease in patients with human immunodeficiency virus. Am J Med 118(Suppl 2):23S–28S
11. Constans J, Conri C (2006) Circulating markers of endothelial function in cardiovascular disease. Clin Chim Acta 368:33–47
12. Hsue PY, Lo JC, Franklin A, Bolger AF, Martin JN, Deeks SG, Waters DD (2004) Progression of atherosclerosis as assessed by carotid intima-media thickness in patients with HIV infection. Circulation 109:1603–1608
13. Glazier JJ, Spears JR, Murphy MC (2006) Interventional approach to recurrent myocardial infarction in HIV-1 infection. J Interv Cardiol 19:93–98
14. Sudano I, Spieker LE, Noll G, Corti R, Weber R, Luscher TF (2006) Cardiovascular disease in HIV infection. Am Heart J 151:1147–1155
15. Rose H, Woolley I, Hoy J, Dart A, Bryant B, Mijch A, Sviridov D (2006) HIV infection and high-density lipoprotein: the effect of the disease vs the effect of treatment. Metabolism 55:90–95
16. Asztalos BF, Schaefer EJ, Horvath KV, Cox CE, Skinner S, Gerrior J, Gorbach SL, Wanke C (2006) Protease inhibitor-based HAART, HDL, and CHD-risk in HIV-infected patients. Atherosclerosis 184:72–77
17. Tershakovec AM, Frank I, Rader D (2004) HIV-related lipodystrophy and related factors. Atherosclerosis 174:1–10
18. Fisher SD, Miller TL, Lipshultz SE (2006) Impact of HIV and highly active antiretroviral therapy on leukocyte adhesion molecules, arterial inflammation, dyslipidemia, and atherosclerosis. Atherosclerosis 185:1–11
19. de Gaetano DK, Rabagliati R, Iacoviello L, Cauda R (2004) HIV infection, HAART, and endothelial adhesion molecules: current perspectives. Lancet Infect Dis 4:213–222
20. National Cholesterol Education Program (NCEP) Expert Panel on Detection, Evaluation, and Treatment of High Blood Cholesterol in Adults (Adult Treatment Panel III) (2002) Third Report of the National Cholesterol Education Program (NCEP) Expert Panel on Detection, Evaluation, and Treatment of High Blood Cholesterol

in Adults (Adult Treatment Panel III) final report. Circulation 106(25):3143–3421
21. Martin LS, Pasquier E, Roudaut N, Vandhuick O, Vallet S, Bellein V, Bressollette L (2008) Metabolic syndrome: a major risk factor for atherosclerosis in HIV-infected patients (SHIVA study). Presse Med 37:579–584
22. Salyer J, Lyon DE, Settle J, Elswick RK, Rackley D (2006) Coronary heart disease risks and lifestyle behaviors in persons with HIV infection. J Assoc Nurses AIDS Care 17:3–17
23. Bonfanti P, Giannattasio C, Ricci E, Facchetti R, Rosella E, Franzetti M, Cordier L, Pusterla L, Bombelli M, Sega R, Quirino T, Mancia G (2007) HIV and metabolic syndrome: a comparison with the general population. J Acquir Immune Defic Syndr 45:426–431
24. World Medical Association Declaration of Helsinki (accessed February. 2009) Ethical principals for Medical Research Involving Human Subjects. http://www.wma.net/e/policy/b3.htm
25. Jones M (2001) International Society for the Advancement of Kinanthropometry (ISAK). International standards for anthropometric assessment, Adelaide, National Library of Australia
26. Johnson R, McNutt P, MacMahon S, Robson R (1997) Use of the Friedewald formula to estimate LDL-cholesterol in patients with chronic renal failure on dialysis. Clin Chem 43:2183–2184
27. Cockcroft DW, Gault MH (1976) Prediction of creatinine clearance from serum creatinine. Nephron 16(1):31–41
28. International Diabetes Federation (2009) The IDF consensus worldwide definition of the metabolic syndrome. http://www.idf.org/webdata/docs/Metabolic_syndrome_definition.pdf. Accessed March 2009
29. Rose H, Hoy J, Woolley I, Tchoua U, Bukrinsky M, Dart A, Sviridov D (2007) HIV infection and high density lipoprotein metabolism. Atherosclerosis 199(1):79–86
30. Gordon T, Castelli WP, Hjortland MC, Kannel WB, Dawber TR (1977) High density lipoprotein as a protective factor against coronary heart disease. The Framingham Study. Am J Med 62:707–714
31. Castelli WP, Anderson K, Wilson PW, Levy D (1992) Lipids and risk of coronary heart disease. The Framingham Study. Ann Epidemiol 2:23–28
32. Duprez DA, Kuller LH, Tracy R, Otvas J, Cooper DA, Hoy J, Neuhaus J, Paton NI, Friis-Moller N, Lampe F, Liappis AP, Neaton JD (2009) Lipoprotein particle subclasses, cardiovascular disease and HIV infection. Doi:10.1016/j.atherosclerosis.2009.05.001
33. Jericó C, Knobel H, Sorli ML, Montero M, Guelar A, Pedro-Botet J (2006) Prevalence of cardiovascular risk factors in HIV-infected patients. Rev Clin Esp 206(11):556–559
34. Seedat YK (1999) Hypertension in black South Africans. J Hum Hypertens 13:96–103
35. Miller NE, Thelle DS, Forde OH, Mjos OD (1977) The Tromso heart-study. High-density lipoprotein and coronary heart-disease: a prospective case-control study. Lancet 1:965–968
36. Badiou S, Thiebaut R, urillac-Lavignolle V, Dabis F, Laporte F, Cristol JP, Mercie P (2008) Association of non-HDL cholesterol with subclinical atherosclerosis in HIV-positive patients. J Infect 57:47–54
37. Samaras K, Wand H, Law M, Emery S, Cooper D, Carr A (2007) Prevalence of metabolic syndrome in HIV-infected patients receiving highly active antiretroviral therapy using International Diabetes Foundation and Adult Treatment Panel III criteria: associations with insulin resistance, disturbed body fat compartmentalization, elevated C-reactive protein, and [corrected] hypoadiponectinemia. Diabetes Care 30:113-119
38. Carpentier A, Patterson BW, Uffelman KD, Salit I, Lewis GF (2005) Mechanism of highly active anti-retroviral therapy-induced hyperlipidemia in HIV-infected individuals. Atherosclerosis 178:165–172
39. Krauss RM (2004) Lipids and lipoproteins in patients with type 2 diabetes. Diabetes Care 27:1496–1504
40. Bonfanti P, Ricci E, de Socio G, Zeme D, Carradori S, Penco G, Parruti G, Grosso C, Madeddu G, Vichi F, Bini T, Martinelli C, Melzi S, Quirino T (2006) Metabolic syndrome: a real threat for HIV-positive patients? Results from the SIMONE study. J Acquir Immune Defic Syndr 42:128–131
41. Mondy K, Overton ET, Grubb J, Tong S, Seyfried W, Powderly W, Yarasheski K (2007) Metabolic syndrome in HIV-infected patients from an urban, Midwestern US outpatient population. Clin Infect Dis 44:726–734
42. Pao V, Lee GA, Grunfeld C (2008) HIV therapy, metabolic syndrome, and cardiovascular risk. Curr Atheroscler Rep 10:61–70
43. Puoane T, Steyn K, Bradshaw D, Laubscher R, Fourie J, Lambert V, Mbananga N (2002) Obesity in South Africa: the South African demographic and health survey. Obes Res 10:1038–1048
44. Schutte AE, Schutte R, Huisman HW, Rooyen JM, Malan L, Olckers A, Malan NT (2009) Classifying Africans with the metabolic syndrome. Horm Metab Res 41:79–85
45. Grinspoon S, Carr A (2005) Cardiovascular risk and body-fat abnormalities in HIV-infected adults. N Engl J Med 352:48–62
46. Lichtenstein KA, Ward DJ, Moorman AC, Delaney KM, Young B, Palella FJ Jr, Rhodes PH, Wood KC, Holmberg SD (2001) Clinical assessment of HIV-associated lipodystrophy in an ambulatory population. AIDS 15:1389–1398
47. Abbasi F, Brown BW Jr, Lamendola C, McLaughlin T, Reaven GM (2002) Relationship between obesity, insulin resistance, and coronary heart disease risk. J Am Coll Cardiol 40:937–943
48. Ridker PM, Buring JE, Cook NR, Rifai N (2003) C-reactive protein, the metabolic syndrome, and risk of incident cardiovascular events: an 8-year follow-up of 14 719 initially healthy American women. Circulation 107:391–397
49. Pasceri V, Willerson JT, Yeh ET (2000) Direct proinflammatory effect of C-reactive protein on human endothelial cells. Circulation 102:2165–2168
50. Wadham C, Albanese N, Roberts J, Wang L, Bagley CJ, Gamble JR, Rye KA, Barter PJ, Vadas MA, Xia P (2004) High-density lipoproteins neutralize C-reactive protein proinflammatory activity. Circulation 109:2116–2122
51. Opie LH, Seedat YK (2005) Hypertension in sub-Saharan African populations. Circulation 112:3562–3568
52. van Rooyen JM, Kruger HS, Huisman HW, Wissing MP, Margetts BM, Venter CS, Vorster HH (2000) An epidemiological study of hypertension and its determinants in a population in transition: the THUSA study. J Hum Hypertens 14:779–787
53. Jericó C, Knobel H, Montero M, Sorli ML, Guelar A, Gimeno JL, Saballs P, Lopez-Colomes JL, Pedro-Botet J (2005) Hypertension in HIV-infected patients: prevalence and related factors. Am J Hypertens 18:1396–1401
54. Gazzaruso C, Bruno R, Garzaniti A, Giordanetti S, Frantino P, Sacchi P, Filice G (2003) Hypertension among HIV patients: prevalence and relationships to insulin resistance and metabolic syndrome. J Hypertens 21(7):1377–1382
55. Winston J, Deray G, Hawkins T, Szczech L, Wyatt C, Young B (2008) Kidney disease in patients with HIV infection and AIDS. Clin Infect Dis 47:1449–1457
56. Holzemer WL, Uys LR (2004) Managing AIDS stigma. SAHARA J 1:165–174
57. Greeff M, Phetlhu R (2007) The meaning and effect of HIV/AIDS stigma for people living with AIDS and nurses involved in their care in the North West Province, South Africa. Curationis 30:12–23

Lipids (2010) 45:81–89
DOI 10.1007/s11745-009-3373-8

ORIGINAL ARTICLE

Use of Comparative Proteomics to Identify Key Proteins Related to Hepatic Lipid Metabolism in Broiler Chickens: Evidence Accounting for Differential Fat Deposition Between Strains

Jianzhen Huang · Xue Tang · Jiming Ruan · Haitian Ma · Sixiang Zou

Received: 7 August 2009 / Accepted: 28 October 2009 / Published online: 29 November 2009

Abstract In order to investigate differences in fat metabolism during embryonic development, a comparative proteomics strategy was employed using Arbor Acres (AA) and San Huang (SH) broiler chickens with different growth and fat deposition characteristics. These birds were floor-reared and fed identical diets, and embryonic livers were collected from AA and SH chicken embryos on days 9, 14 and 19 of incubation and hatching. Proteins were extracted and fractionated by two-dimensional electrophoresis (2-DE), Neuhoff's colloidal Coomassie Blue G-250 staining was carried out, and stained gels were scanned and analyzed using PDQuest7.3 software (Bio-Rad). In-gel trypsin digestion of the differential protein spots and matrix-assisted laser desorption/ionization-time of flight mass spectrometry (MALDI-TOF-MS) were subsequently assessed. Peptide mass fingerprinting of the differentially expressed proteins was performed using the server from MASCOT or either Prospector or ProFound, and 37 proteins were successfully identified. In the present study, embryo and liver weights showed a trend toward enhanced growth during embryonic development. Of the 37 identified differential proteins, phosphoenolpyruvate carboxykinase (PEPCK), apolipoprotein A-I (Apo A-I), fatty acid-binding protein (L-FABP) and 3-hydroxy-3-methylglutaryl-Coenzyme A synthase (HMG-CoA synthase) were up-regulated in SH chickens to a greater extent than they were in AA chickens. These observations suggest that the lipid metabolic proteins and enzymes are inherent characteristics that contribute to the apparent differences in fat deposition between the two strains.

Keywords Embryonic development · Broilers · Proteomics · Lipid metabolism

Abbreviations

AA	Arbor Acres
SH	San Huang
2-DE	Two-dimensional electrophoresis
MALDI-TOF-MS	Matrix-assisted laser desorption/ionization-time of flight mass spectrometry
Apo	Apolipoprotein
L-FABP	Fatty acid-binding protein
PEPCK	Phosphoenolpyruvate carboxykinase
HMG-CoA synthase	3-Hydroxy-3-methylglutaryl-Coenzyme A synthase
ME	Malic enzyme
FAS	Fatty acid synthetase
ACC	Acetyl-CoA carboxylase
DTT	Dithiothreitol
PMSF	Phenylmethanesulfonyl
CHAPS	3-(3-Cholamidopropyl-dimethylammonio)-1-propanesulfonate

J. Huang · H. Ma (✉) · S. Zou
Key Laboratory of Animal Physiology and Biochemistry, Nanjing Agricultural University, 210095 Nanjing, China
e-mail: mahaitian@njau.edu.cn

J. Huang
e-mail: hjzh0722@yahoo.com.cn

J. Huang · J. Ruan
College of Animal Science, Jiangxi Agricultural University, 330045 Nanchang, China

X. Tang
State Key Laboratory of Food Science and Technology, School of Food Science and Technology, Jiangnan University, 214122 Wuxi, China

IPG	Immobilized pH gradient gel
SDS-PAGE	SDS-polyacrylamide gel electrophoresis
BSA	Bovine serum albumin
HDL	High density lipoprotein
LCAT	Lecithin: cholesterol acyl transferase

Introduction

Over the past several decades, an unintended consequence of the increased growth rates that have been achieved in commercial poultry production has been the development of excessive abdominal fat deposits. This trait represents a major drawback for the industry, as it reflects reduced feed efficiency during rearing and decreases the yield of lean meat after processing [1]. It is, therefore, of particular interest to better understand avian lipid metabolism and to further elucidate the genetic mechanisms involved in the regulation of fat deposition in poultry. Unlike mammalian species, in birds, the liver is the main site of de novo fatty acid synthesis, accounting for 95% of all lipid production in young chicks, with the adipose tissue serving only as a lipid storage site [2, 3].

Considerable metabolic and physiological research has been conducted on liver tissue, and some studies have shown that the main source of variability between fat- and lean-type chicken lines can be attributed to differences in liver fatty acid metabolism [1, 4–6]. It is known that gene expression and the activity of lipogenic enzymes differ between fat- and lean-line chickens during fat deposition. Some of the genes involved in fatty acid synthesis, such as malic enzyme (ME), ATP citrate lyase and Acetyl-CoA carboxylase (ACC), have been found to be differentially expressed in the two lines [7].

The San Huang (SH) broiler chicken is a well-known Chinese indigenous breed that displays uniform body fat, high intramuscular fat, and excellent meat quality, while Arbor Acres (AA) chickens display less favorable meat quality characteristics, caused by excessive abdominal fat deposition. Thus, these two species of broiler chickens provide good models for the study of hepatic lipid metabolism differences. Zhao et al. [8, 9] reported that genes related to lipid metabolism, such as fatty acid synthetase (FAS), ACC and apolipoprotein B100 (ApoB100), display different mRNA expression profiles during embryonic liver development in the two lines. However, little information is available relative to liver protein expression in the pathways and mechanisms that contribute to adiposity variability in both lean and fat lines, especially in chicken embryos. To date, the proteomic approach provides a powerful tool to study various biological and medical mechanistic phenomena and has been focused on characterizing the diseased liver [10, 11]. A global protein expression analysis of the chicken embryo liver will aid in the identification of differentially expressed proteins involved in lipid metabolism, provide new insight into the mechanism of fat deposition in embryonic broiler chickens, and pave the way toward a new framework for future studies.

Therefore, the aim of the current study was to identify differences in fat deposition between AA and SH chicken lines, to describe and compare protein profiles in the embryonic livers, and to identify those differential proteins that are of particular importance in the control of hepatic lipid metabolism and fat deposition. Achievement of this latter goal will provide the basic molecular information necessary to understand the regulation of fat deposition in embryonic broiler chickens.

Materials and Methods

Reagents

Immobilized pH gradient gel (IPG) strips, urea, thiolurea, dithiothreitol (DTT), 3-(3-cholamidopropyl-dimethylammonio)-1-propanesulfonate (CHAPS), ampharmalyte pH 3–10, phenylmethanesulfonyl (PMSF), and iodoacetamide were all purchased from Bio-Rad (Richmond, CA, USA), while Coomassie Brilliant Blue G-250 was purchased from Amresco (Solon, OH, USA) and trypsin was purchased from Promega (Madison, WI, USA). All chemicals for SDS-PAGE were of electrophoresis grade.

Animals

A total of 120 AA and SH female broilers (42-weeks-old) were obtained and housed in the Wuxi Breeding Company (Jiangsu, China). The birds were divided into two groups (AA and SH, 60 birds per group), and each group was kept in three pens, with 20 broilers per pen. All birds were fed identical diets and floor-reared under natural lighting at constant temperature (20 ± 3 °C) and humidity (50 ± 3%). They were placed under dietary restriction but they had free access to drinking water. Nutrient levels within the diet (Table 1) were based on NRC (1994) recommendations. Animal care and use were approved by the Institutional Animal Care and Use Committee of Nanjing Agricultural University.

Before the initiation of the experiment, the birds were acclimatized to the environmental conditions for at least 2 weeks. Eggs from each of three pens for each group were collected, numbered and weighed, and placed in an electric forced-draft incubator at 37.5 ± 0.5 °C and 60% relative

Table 1 Ingredient composition and nutrient content of diets

Ingredient (%)	
Corn	67.3
Wheat bran	2.0
Soybean meal	16.0
Salt	0.4
Calcium phosphate	2.3
Limestone	6.8
DL-Methionine	0.1
Vitamin–mineral	1.0
Premix[a]	2.0
Calculated nutrient composition	
ME[b] (kJ/kg)	2,750
Crude protein (%)	19.74
Lysine (%)	0.1
Methionine + cystine (%)	0.93
Calcium (%)	3.0
Total phosphorus (%)	0.88
Available phosphorus (%)	0.53

[a] Vitamin–mineral premix supplied the following per kg of diet: *vitamin A* 1,500 IU; *vitamin D3* 200 IU; *vitamin E* 10 mg; *vitamin K3* 0.5 mg; *thiamine* 1.8 mg; *riboflavin* 3.6 mg; *D-pantothenic acid* 10 mg; *folic acid* 0.55 mg; *pyridoxine* 3.5 mg; *niacin* 35 mg; *cobalamin* 0.01 mg; *biotin* 0.15 mg; *Fe* 80 mg; *Cu* 8 mg; *Mn* 60 mg; *Zn* 40 mg; *I* 0.35 mg; and *Se* 0.15 mg

[b] Metabolizable energy in kilojoules per kilogram

humidity. Only un-chipped and intact eggs were used in the experiment prior to incubation. The start of the incubation period was referred to as "E1d" (1-day-old embryos), and after hatching, the term used was "H1" (1-day-old birds). Embryonic livers were collected from AA and SH chicken embryos on days 9, 14 and 19 of incubation and hatching, and then washed twice with cold physiological saline (0.9% NaCl solution) to remove blood and other possible contaminants. Samples were then flash-frozen in liquid nitrogen and stored at −80 °C prior to homogenization.

Protein Sample Preparation and Two Dimensional Gel Electrophoresis

Tissues were homogenized in a lysis buffer consisting of 7 mol/L urea, 2 mol/L thiolurea, 2% (w/v) CHAPS, 50 mmol/L DTT, 0.8% (w/v) ampharmalyte pH 3–10 and 1 mmol/L PMSF, using a glass homogenization vessel in an ice bath. The resultant homogenate was swirled for 20 min and centrifuged for 20 min at 15,000×*g* at 4 °C. Supernatant was collected and fractionated into aliquots. The protein concentration for each of the final supernatants was measured by the Bradford assay [12] using bovine serum albumin (BSA) as the standard. Eight hundred micrograms of each protein extract were separated by iso-electrophoresis using IPG strips (pH 3.0–10.0 NL, 17 cm) in the protean system (Bio-Rad). Focusing was performed through 1 h at 250 V, 1 h at 500 V, 1 h at 2,000 V, 2 h at 8,000 V, and then holding at 8,000 V until a total of at least 60,000 Vh was reached. The second dimension was run on a 12.5% polyacrylamide SDS gel using the Multiphor system (Amersham Biosciences). The 2-DE for each sample was repeated four times. Neuhoff's colloidal Coomassie Blue G-250 stain was carried out according to the method described by Candiano et al. [13]. Stained gels were scanned and analyzed using PDQuest7.3 software (Bio-Rad). After alignment, spots between gels were first automatically matched. The matched spots were then re-examined manually to ensure accuracy. Generally, only those spots, with a quality of over 50, were chosen for further analysis. Spot quantity normalization was conducted in the 'total quantity of valid spots' mode.

MALDI-TOF-MS Analysis and Database Queries

In-gel trypsin digestion of protein spots, and MALDI-TOF-MS (Reflex III, Bruker-Daltonics, Germany) analyses were based on procedures described by Wang et al. [14]. MS fingerprinting data searches were performed by search engines of ProFound (http://129.85.19.192/ profound_ bin/WebProFound.exe) and MS-fit (http://prospector.ucsf.edu/uscfhtml3.4/ms-fit.htm) against the NCBInr database in the taxa of *Gallus gallus* (Chicken) with the parameter sets of trypsin digestion, two missed cleavages, complete modification of iodoacetamide (Cys), partial modification of methionine oxidation, protein mass = ±20% of the observed protein mass, *p*I = ±1 of observed *p*I, and a mass tolerance for monoisotopic data of 100 ppm. Protein identification was assigned when the following criteria were met: at least four matching peptides and >20% sequence coverage.

Functional Annotation of Identified Proteins

Functions of proteins identified through MS fingerprinting data were annotated by querying against the protein function database Pfam (http://www.sanger.ac.uk/Software/Pfam/; [15]) or Inter-Pro (http://www.ebi.ac.uk/interpro/; [16]).

Statistical Analysis

The effect of embryonic development age (days) on embryo weight and liver weight were analyzed by two-way ANOVA (with developmental age as the main effect) using the general linear models approach. Differences among individual means were evaluated. Analysis of variance (ANOVA) and correlation coefficient estimates for protein

expression changes were conducted using JMP 5.1 (SAS Institute). The statistical significance level was set at $P < 0.05$.

Results

Changes in Embryo Weight and Liver Weight in AA and SH Broiler Chickens at Various Embryonic Stages and at Hatching

Both body weight and absolute liver weight were significantly higher in AA broiler chickens than in SH broiler chickens starting on day 14 of embryonic development and continuing to hatching ($P < 0.05$). However, body weight and absolute liver weight both exhibited trends toward increases in both species.

Comparative Analysis of Liver Proteins between AA and SH Broiler Chickens

Good separation of protein spots was apparent in the 2D gel electrophoresis, except in the base area (Fig. 1). After auto-matching and a manual quality check of the detected spots, 326 valid spots were identified in this experimental series. To determine the repeatability among gels of the same sample, spot to spot correlation coefficients were estimated. Results showed that they varied from 0.81 to 0.92, with all being significant at $P \geq 0.0001$. In each sample, at least one of the three correlation coefficients was over 0.85, while the difference in spot volume among replicates was not significant, based on ANOVA.

In general, the protein profiles in embryo livers from AA and SH broiler chickens during the four development stages were similar. However, certain spots displayed obvious differences in volume or abundance. A total of 40 spots, which reflected a two-fold difference in volume as compared to the two breeds during the four development stages, were subjected to detailed identification. Spots 1, 2, 3, 4, 5, 6, 7, 13, 15, 16, 17, 23, 24, 25, 28, 29, 30, 31, 32, 33, 35 and 36 displayed down-regulation in SH broiler chicken embryo liver, among which, spots 6, 7, 13, 15, 16, 17, 23, 24, 25, 33 and 36 showed a greater than three-fold difference in volume. The remainder of the 40 spots displayed up-regulation in SH broiler chicken embryo liver, and spots 8, 9, 11, 12, 18, 20, 21, 22, 34 and 39 showed a greater than three-fold difference in volume.

Proteins from all 40 spots were subjected to in-gel digestion and analyzed by MALDI-TOF-MS. Protein identification using the MS fingerprint data was conducted by querying the Swiss-Prot, NCBInr protein and chicken polypeptide databases. Positive identifications were obtained for all 40 spots, except for spots 3, 6 and 23. Thus, only the data for the remaining 37 spots were used for further analysis, and the protein identity for each of the 37 spots is listed in Table 2.

Proteins identified successfully were sorted into six main functional classes based on the KOG database comparison. A large group of proteins (spots 17, 27, 29, 34, 35, 36, 38, 39 and 40) were categorized as important in metabolism, such as PEPCK, ApoA-I, L-FABP, HMG-CoA synthase, enolase, sulfotransferase, etc. Some proteins (spots 7, 8, 9 and 28) were found to be involved in signal transduction, while others (spots 11, 12, 14, 30, 32, 34 and 37) are known to participate in energy metabolism, protein synthesis and disease/defense. The remaining proteins were not related to any KOG based function (Table 3).

Discussion

Hamburger and Hamilton [17] described a series of stages to categorize the entire 21-day development period of the chicken embryo, based on external characteristics. These stages can be divided into three phases. The two earlier phases form a period during which the organs and systems of the body are formed, while the last phase, from day 13 until hatching, is characterized by the maturation and growth of the organ systems. Embryonic development is an energy consuming process. During the two earlier phases, glucose within the yolk sac supplies energy, but about 90% of the total energy required by the embryo for growth comes from β-oxidation of fatty acids derived from yolk lipids [18, 19]. Previous studies have indicated that differences in lipid metabolism exist during the embryonic stage of development among the different lines of broiler breeders [20, 21]. In the current study, we found that body weight and absolute liver weight in AA broiler chickens were slightly higher than in SH birds during the last phase of embryonic development, which indicates that there was a difference in lipid metabolism between the breeds.

Using a proteomic approach, 37 proteins that exhibited differential changes in profile when taken from AA and SH chicken embryonic livers were identified. Some of these were involved in important aspects of metabolism and, in particular, lipid metabolism.

Phosphoenolpyruvate carboxykinase (PEPCK) is a rate-controlling enzyme in gluconeogenesis which catalyzes the synthesis of phosphoenolpyruvate (PEP) from oxaloacetate (OAA). It is expressed primarily in liver, kidney and adipose tissue, where its synthesis is highly regulated by insulin, glucocorticoids, thyroid hormone and glucagon at the level of transcription. PEPCK exists as two different isozymes in vertebrate tissues (PEPCK-C and PEPCK-M), which show remarkable similarity in protein secondary structure. PEPCK-C is the major form evident in

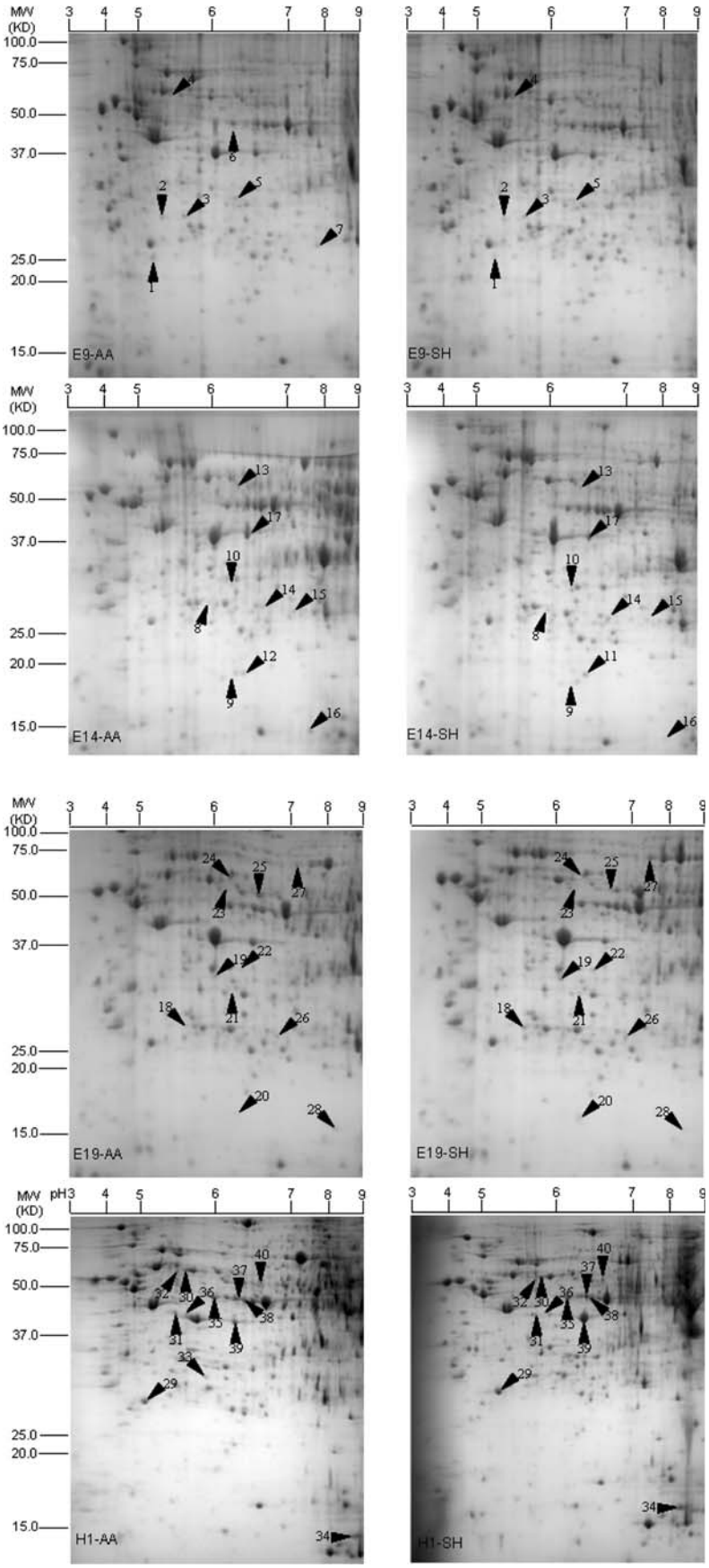

Fig. 1 Proteins profiles of AA chicken and SH chicken embryo liver at the stage of E9, E14, E19, H1. *Arrows* indicate the proteins with at least a 2.0-fold change in the four development stages

Table 2 Changes in embryo weight, liver weight in AA broiler and SH broiler during embryonic development

		E9	E14	E19	H1
Body weight (g)	AA	$1.86 \pm 0.03^{a*}$	$13.87 \pm 0.13^{b*}$	$33.33 \pm 0.46^{c*}$	$46.57 \pm 0.83^{d*}$
	SH	1.66 ± 0.02^{a}	10.45 ± 0.14^{b}	23.05 ± 0.41^{c}	35.35 ± 0.79^{d}
Liver weight (g)	AA	$0.051 \pm 0.001^{a*}$	$1.19 \pm 0.012^{b*}$	$1.65 \pm 0.02^{c*}$	$1.97 \pm 0.025^{d*}$
	SH	0.049 ± 0.004^{a}	1.14 ± 0.01^{b}	1.56 ± 0.03^{c}	1.83 ± 0.027^{d}

Means without common letter differ significantly between age groups

* Breed differences at the same age ($P < 0.05$) ($n = 15$)

embryonic chicken liver tissue, while PEPCK-M only exists in the liver of adult chickens [22]. Tordjman et al. [23] have reported that fatty acids stimulate PEPCK-C gene expression, and recent studies have suggested that PEPCK is also important in the maintenance of blood glucose concentration and insulin resistance. In this paper, PEPCK resulted from up-regulation in SH chicken embryonic liver, which indicates that gluconeogenesis was more pronounced in SH chicken embryonic liver than in AA chicken embryonic liver, indirectly suggesting that fatty acid oxidation in SH chicken embryos provides enhanced levels of non-carbohydrate substrate for gluconeogenesis.

ApoA-I, the major protein component of high-density lipoprotein (HDL), has diverse physiological functions, including lipid binding and solubilization, activation of lecithin: cholesterol acyl transferase (LCAT), modulation of HDL rearrangement during metabolism and lipid transfer, and interaction with HDL receptors on cell surfaces. Douaire et al. [24] reported that the mRNA levels of genes coding for lipogenic enzymes (acetyl-coenzyme A carboxylase, fatty acid synthase, malic enzyme, Δ9-desaturase) and apoproteins (apoB and apoPVLDL-II) did not differ significantly between fat and lean birds, while the mRNA levels for genes coding for apoA-I were significantly different. We found that apoA-I was expressed to a greater extent in SH chicken embryonic liver than in AA birds. This observation could indicate that cholesterol metabolism was enhanced by higher levels of apoA-I in SH chicken embryonic liver.

HMG-CoA synthase is the rate-limiting enzyme for ketone body formation and the catalyst for the condensation of acetoacetyl-CoA and acetyl-CoA to form HMG-CoA plus free CoA. The activity of HMG-CoA synthase is located in both the cell cytosol and in the mitochondria. The HMG-CoA produced by cytosolic HMG-CoA synthase is the starting point for the isoprenoid pathway which, in addition to producing cholesterol as its main end product, yields other important isoprenoids. Control of ketogenesis is exerted by transcriptional regulation of mitochondrial HMG-CoA synthase. Mitochondrial and cytosolic HMG-CoA synthase are encoded by two different genes. Hegardt [25] reported that fasting, cAMP, and fatty acids increase the transcriptional rate of mitochondrial HMG-CoA synthase, while re-feeding and insulin repress it. In the present study, we observed that HMG-CoA synthase protein levels were significantly higher in SH broiler chickens than they were in AA broiler chickens. Therefore, ketogenesis was enhanced, and this reflected, at least in part, an increased acetyl-CoA level in the liver, which resulted from the high rate of fatty acid beta oxidation in SH broiler chickens.

Fatty acid-binding proteins (L-FABP) are small molecular weight proteins with high binding affinities for long-chain fatty acids [26], and they are members of a super family of lipid-binding proteins that occur intra-cellularly in invertebrates and vertebrates. In mammals, the intracellular or cytoplasmic FABP form a group of at least nine distinct proteins, with molecular weights ranging from 14 to 15 kDa. They are named according to the tissues from which they are isolated [26], and they are involved in intracellular fatty acid movement, cell growth and differentiation, cellular signaling, gene transcription, and protection of enzymes from the toxic effects of free fatty acids [27]. Ceciliani et al. [28] isolated a FABP from chicken liver which had an isoelectric point of 9.0, whereas other L-FABPs have isoelectric points near 6.0. It has been documented that the ontogeny of FABP in turkey liver is associated with fatty acid metabolism in turkey embryos and poults [29]. Martin et al. [30] reported that L-FABP gene ablation dramatically enhances many of the effects of dietary cholesterol to significantly induce hepatic cholesterol and triacylglycerol accumulation as well as to potentiate BW gain (primarily as fat tissue mass). Cogburn et al. [31] reported that L-FABP gene expression was higher (1.66-fold) in hyperthyroid (lean) chickens than in hypothyroid (fat) chickens. Wang et al. [32] have also reported that chicken liver tissue L-FABP mRNA levels vary among different breeds, with the Baier layers (a Chinese local breed) having higher levels than meat-type broilers. They indicated that L-FABP gene assessment was used as an important candidate gene in chicken QTL detection programs, focusing on phenotypes related to fat traits. In this study, the results showed that L-FABP protein expression was significantly higher in SH broiler chickens

Table 3 Differentially expressed proteins of SH chicken embryo' liver identified by PMF query

Spot no.	Up or down in SH chicken	Protein name	Exp. MW (KDa)/*p*I	Theor. MW (KDa)/*p*I	Sequence coverage (%)	Functional classification	Accession no.
1	Down	Hypothetical protein	23/5.0	22.53/5.3	57	Unknown	CAG32430
2	Down	PREDICTED: hypothetical protein	30/5.1	32.44/5.2	30	Unknown	XP_414311
4	Down	Hypothetical protein	62/5.1	67.05/5.2	21	Unknown	CAG31507
5	Down	PREDICTED: hypothetical protein	31.5/6.0	33.20/5.8	66	Unknown	XP_416283
7	Down	Glutathione S-transferases CL2	25/7.4	26.05/6.9	75	Signal transduction	NP_990421
8	Up	PREDICTED: similar to sepiapterin reductase	27/6.0	29.28/5.8	60	Signal transduction	XP_423038
9	Up	Signal transducer and activator of transcription 5B	26.5/6.0	90.57/5.9	21	Signal transduction	NP_990110
10	Up	Hypothetical protein	30/6.0	36.84/6.0	28	Unknown	CAG32095
11	Up	Parkinson disease (autosomal recessive, early onset) 7	19/6.3	19.93/6.3	69	Neurodegenerative diseases	NP_989916
12	Up	Parkinson disease (autosomal recessive, early onset) 7	18.2/6.2	19.93/6.3	69	Neurodegenerative diseases	NP_989916
13	Down	Hypothetical protein	57.7/6.1	60.66/6.0	28	Unknown	CAG32042
14	Up	PREDICTED: similar to prosomal P27K protein	27/6.5	27.85/6.1	28	Unknown	XP_421242
15	Down	PREDICTED: hypothetical protein	26/7.8	24.24/8.1	35	Unknown	XP_422398
16	Down	Non-metastatic cells 2, protein (NM23B) expressed in *Gallus gallus*	16.5/8.2	17.44/7.9	83	Unknown	NP_990378
17	Down	Sulfotransferase	38/6.5	36.34/5.9	57	Drug development	NP_990391
18	Up	PREDICTED: similar to Prohibitin isoform 2	28.5/5.2	29.94/5.6	64	Unknown	XP_418103
19	Up	PREDICTED: hypothetical protein	32/5.8	33.20/5.8	70	Unknown	XP_416283
20	Up	Hypothetical protein	17/6.1	17.21/6.0	32	Unknown	CAG32130
21	Up	Hypothetical protein	29/6.0	29.48/6.0	48	Unknown	CAG31370
22	Up	PREDICTED: hypothetical protein	31/6.2	35.24/6.5	37	Unknown	XP_420181
24	Down	Formiminotransferase cyclodeaminase	61/6.1	59.76/5.9	46		NP_990234
25	Down	PREDICTED: hypothetical protein	55/6.5	53.14/6.0	27	Unknown	XP_414831
26	Up	Hypothetical protein	27/6.7	25.24/6.5	39	Unknown	CAG32709
27	Up	Phosphoenolpyruvate carboxykinase [GTP], mitochondrial precursor	70.8/7.6	71.75/8.6	66	Glycolysis/ gluconeogenesis	P21642
28	Down	Phospholipid hydroperoxide glutathione peroxidase	18/8.3	19.23/7.8	73	Signal transduction	AAM18080
29	Down	Apolipoprotein A-I	28.2/5.2	30.66/5.6	69	Lipid metabolism	NP_990856
30	Down	Chaperonin containing TCP1, subunit 8 (theta)	59.7/5.3	59.36/5.3	49	Chaperones and folding catalysts	NP_001004389
31	Down	Hypothetical protein	41.1/5.7	41.41/6.1	57	Unknown	CAG32388

Table 3 continued

Spot no.	Up or down in SH chicken	Protein name	Exp. MW (KDa)/*p*I	Theor. MW (KDa)/*p*I	Sequence coverage (%)	Functional classification	Accession no.
32	Down	Protein disulfide isomerase-associated 3 precursor	59/5.7	56.56/5.8	35	Chaperones and folding catalysts	NP_989441
33	Down	PREDICTED: hypothetical protein isoform 2	30/6.1	30.64/6.0	50	Unknown	XP_421871
34	Up	Fatty acid-binding protein, liver (L-FABP)	14/9.0	14.25/8.7	44	Lipid metabolism	P80226
35	Down	Enolase 1	49.5/6.0	47.63/6.2	43	Carbohydrate metabolism	NP_990451
36	Down	Sulfotransferase	36.34/5.9	36.34/5.9	53	Drug development	NP_990391
37	Up	Similar to ubiquinol–cytochrome *c* reductase	50.63/6.1	53.43/6.6	47	Energy metabolism	XP_414356
38	Up	Enolase 1	49/6.2	47.63/6.2	43	Carbohydrate metabolism	NP_990451
39	Up	Sulfotransferase	37/6.5	36.34/5.9	53	Drug development	NP_990391
40	Up	3-Hydroxy-3-methylglutaryl-Coenzyme A synthase 1	59.5/6.5	57.5/5.4	27	Synthesis and degradation of ketone bodies	NP_990742

than in AA birds. The higher expression level for L-FABP in the embryonic liver of SH broiler chickens might result in increased fatty acid transportation into the mitochondria or peroxisomes and, thus, enhanced fatty acid oxidation and reduced fat deposition.

Taken together, it can be concluded that PEPCK, apoA-I, FABP, HMG-CoA synthase were up-regulated in the embryonic liver of SH broiler chickens, which suggests that gluconeogenesis, cholesterol metabolism and fatty acid oxidation were functional in the embryonic liver of SH broiler chickens prior to their occurrence in the embryonic livers of AA broiler chickens. It also suggests that the observed differences in lipid metabolism between AA and SH birds might, in part, be attributed to this differential expression of proteins in embryonic liver. However, given the limitations of the proteomics approach relative to immobilized pH gradients and pH intervals, we cannot extrapolate this conclusion to total protein synthesis and/or degradation without further study.

In conclusion, expression of the proteins and enzymes related to hepatic lipid metabolism in broiler chickens exhibited specific breed characteristics during embryogenesis. The data suggest that these proteins were associated with fat traits and that they contributed to the apparent differences in fat deposition observed between SH and AA broiler chickens. The data also strongly suggest that the regulation of adiposity in chickens derived from lean and fat lines was linked to the regulation of the key proteins and enzymes screened in the present study.

Acknowledgments This work was supported by the National Key Basic Research Development Program of China, 973 Program (Project No. 2004CB117505). We are also grateful to Dr. William W. Riley, General Manager, International Division, Hinapharm Pharmaceutical Co., Ltd. Foshan for his critical reading of the manuscript.

References

1. Leclercq B, Hermier D, Guy G (1990) Metabolism of very low density lipoproteins in genetically lean or fat lines of chicken. Reprod Nutr Dev 30(6):701–715
2. Leveille GA (1969) In vitro hepatic lipogenesis in the hen and chick. Comp Biochem Physiol 28(1):431–435
3. Griffin HD, Guo K, Windsor D, Butterwith SC (1992) Adipose tissue lipogenesis and fat deposition in leaner broiler chickens. J Nutr 122(2):363–368
4. Legrand P, Hermier D (1992) Hepatic Δ9 desaturation and plasma VLDL level in genetically lean and fat chickens. Int J Obes Relat Metab Disord 16(4):289–294
5. Saadoun A, Leclercq B (1983) Comparison of in vivo fatty acid synthesis of the genetically lean and fat chickens. Comp Biochem Physiol B 75(4):641–644
6. Hermier D, Chapman MJ (1985) Plasma lipoproteins and fattening: description of a model in the domestic chicken, *Gallus domesticus*. Reprod Nutr Dev 25(1B):235–241
7. Daval S, Lagarrigue S, Douaire M (2000) Messenger. RNA levels and transcription rates of hepatic lipogenesis genes in genetically lean and fat chickens. Genet Sel Evol 32(5):521–531
8. Zhao S, Ma H, Zou S, Chen W, Zhao R (2007) Hepatic lipogenesis in broiler chickens with different fat deposition during embryonic development. J Vet Med A Physiol Pathol Clin Med 54(1):1–6
9. Zhao S, Ma H, Zou S, Chen W (2007) Effects of in ovo administration of DHEA on lipid metabolism and hepatic

lipogenetic gene expression in broiler chickens during embryonic development. Lipids 42(8):749–757
10. Parent R, Beretta L (2005) Proteomics in the study of liver pathology. J Hepatol 43(1):177–183
11. El-Aneed A, Banoub J (2006) Proteomics in the diagnosis of hepatocellular carcinoma: focus on high risk hepatitis B and C patients. Anticancer Res 26(5A):3293–3300
12. Bradford MM (1976) A rapid and sensitive method for the quantitation of microgram quantities of protein utilizing the principle of protein-dye binding. Anal Biochem 72:248–254
13. Candiano G, Bruschi M, Musante L et al (2004) Blue silver: a very sensitive colloidal Coomassie G-250 staining for proteome analysis. Electrophoresis 25(9):1327–1333
14. Wang Y, Yang L, Xu H, Li Q, Ma Z, Chu C (2005) Differential proteomic analysis of proteins in wheat spikes induced by *Fusarium graminearum*. Proteomics 5(17):4496–4503
15. Bateman A, Birney E, Cerruti L et al (2002) The Pfam protein families database. Nucleic Acids Res 30(1):276–280
16. Apweiler R, Attwood TK, Bairoch A et al (2001) The InterPro database, an integrated documentation resource for protein families, domains and functional sites. Nucleic Acids Res 29(1):37–40
17. Hamburger V, Hamilton HL (1992) A series of normal stages in the development of the chick embryo. 1951. Dev Dyn 195(4):231–272
18. Noble RC, Cocchi M (1990) Lipid metabolism and the neonatal chicken. Prog Lipid Res 29(2):107–140
19. Speake BK, Murray AM, Noble RC (1998) Transport and transformations of yolk lipids during development of the avian embryo. Prog Lipid Res 37(1):1–32
20. Tona K, Onagbesan OM, Jego Y, Kamers B, Decuypere E, Bruggeman V (2004) Comparison of embryo physiological parameters during incubation, chick quality, and growth performance of three lines of broiler breeders differing in genetic composition and growth rate. Poult Sci 83(3):507–513
21. Zhao R, Muehlbauer E, Decuypere E, Grossmann R (2004) Effect of genotype-nutrition interaction on growth and somatotropic gene expression in the chicken. Gen Comp Endocrinol 136(1):2–11
22. Monteil C, Fillastre JP, Morin JP (1995) Expression and subcellular distribution of phosphoenolpyruvate carboxykinase in primary cultures of rabbit kidney proximal tubule cells: comparative study with renal and hepatic PEPCK in vivo. Biochim Biophys Acta 1243(3):437–445
23. Tordjman J, Khazen W, Antoine B et al (2003) Regulation of glyceroneogenesis and phosphoenolpyruvate carboxykinase by fatty acids, retinoic acids and thiazolidinediones: potential relevance to type 2 diabetes. Biochimie 85(12):1213–1218
24. Douaire M, Le Fur N, el Khadir-Mounier C, Langlois P, Flamant F, Mallard J (1992) Identifying genes involved in the variability of genetic fatness in the growing chicken. Poult Sci 71(11):1911–1920
25. Hegardt FG (1998) Transcriptional regulation of mitochondrial HMG-CoA synthase in the control of ketogenesis. Biochimie 80(10):803–806
26. Ockner RK, Manning JA, Poppenhausen RB, Ho WK (1972) A binding protein for fatty acids in cytosol of intestinal mucosa, liver, myocardium, and other tissues. Science (New York, NY) 177(43):56–58
27. Besnard P, Niot I, Poirier H, Clement L, Bernard A (2002) New insights into the fatty acid-binding protein (FABP) family in the small intestine. Mol Cell Biochem 239(1–2):139–147
28. Ceciliani F, Monaco HL, Ronchi S, Faotto L, Spadon P (1994) The primary structure of a basic (*p*I 9.0) fatty acid-binding protein from liver of *Gallus domesticus*. Comp Biochem Physiol B Biochem Mol Biol 109(2–3):261–271
29. Ding ST, Bacon WL, Lilburn MS (2002) The development of an immunoblotting assay for the quantification of liver fatty acid-binding protein during embryonic and early posthatch development of turkeys (*Meleagridis gallopavo*). Poult Sci 81(7):1057–1064
30. Martin GG, Atshaves BP, McIntosh AL, Mackie JT, Kier AB, Schroeder F (2006) Liver fatty acid binding protein gene ablation potentiates hepatic cholesterol accumulation in cholesterol-fed female mice. Am J Physiol 290(1):G36–G48
31. Cogburn LA, Wang X, Carre W, Rejto L, Porter TE, Aggrey SE, Simon J (2003) Systems-wide chicken DNA microarrays, gene expression profiling, and discovery of functional genes. Poult Sci 82(6):939–951
32. Wang Q, Li H, Li N, Leng L, Wang Y (2006) Tissue expression and association with fatness traits of liver fatty acid-binding protein gene in chicken. Poult Sci 85(11):1890–1895

Lipids (2010) 45:91–96
DOI 10.1007/s11745-009-3374-7

ORIGINAL ARTICLE

Electron Paramagnetic Resonance Investigation of Stratum Corneum Lipid Structure

Kouichi Nakagawa

Received: 14 September 2009 / Accepted: 6 November 2009 / Published online: 29 November 2009

Abstract Electron paramagnetic resonance (EPR) in conjunction with a slow-tumbling simulation was utilized for defining stratum corneum (SC) lipid structure. We found that ordering calculated from the simulation is an appropriate index for evaluating SC lipids structure. The SC from two sites (mid-volar forearm and lower-leg) of human volunteers was stripped consecutively from one to three times using a glass plate coated with a cyanoacrylate resin. Aliphatic spin probes, 5-doxylstearic acid (5-DSA) and 3β-doxyl-5α-cholestane (CHL), were used to monitor SC ordering. EPR spectrum of 5-DSA incorporated in the SC demonstrated a characteristic peak for the first strip. However, EPR spectra of CHL in the SC did not show a clear difference for each strip, except for the peak intensity. The results imply that CHL is not incorporated into the lipid phase as easily as 5-DSA is. A slow-tumbling simulation of the EPR spectrum was performed to analyze the detailed lipid structure. The simulation results for 5-DSA show differences in values of the SC ordering as a function of depth. Thus, these results along with the simulation analysis provide a detailed SC layer structure.

Keywords EPR · ESR · Skin lipid · Order parameter · Spin probe · Stratum corneum · Simulation · Lipid structure

Abbreviations

EPR	Electron paramagnetic resonance
ESR	Electron spin resonance
SC	Stratum corneum
5-DSA	5-Doxylstearic acid
CHL	3β-Doxyl-5α-cholestane
TEWL	Transepidermal water loss
S	Conventional order parameter
MOMD	Microscopically ordered but macroscopically disordered
S_0	Simulated order parameter

K. Nakagawa (✉)
RI Research Center, Fukushima Medical University,
1 Hikarigaoka, Fukushima 960-1295, Japan
e-mail: nakagawa@fmu.ac.jp

Introduction

Electron paramagnetic resonance (EPR) is useful for elucidating structural aspects of stratum corneum (SC) [1–5]. Non-invasive spectroscopic characterization of the outermost layer of the SC is an important subject in dermatology and cosmetology. The SC, a heterogeneous structure composed of corneocytes embedded in the intercellular lamellar lipid bilayer, acts as the main epidermal barrier against chemicals, oxidative stress, the UV component of sunlight, and other invasive environmental factors, as well as regulating transepidermal water loss (TEWL) to prevent dehydration of viable cells underneath the SC. The intercellular lamellar lipid bilayers play a critical role in these barrier functions.

It is essential to know the composition of SC lipids as well as their structure in relation to depth. The various components, such as ceramides, cholesterol, and free fatty acids of SC lipids have been investigated by thin-layer chromatography (TLC) [6, 7]. It was also pointed out that the levels of SC lipids in a group of women aged 41–50 showed a decrease in SC lipid levels [8].

At present, no quantitative method is available to evaluate the structures and motions of the molecular components of the intercellular lamellar lipid bilayers. TEWL

measurement is the only non-invasive method which indirectly provides knowledge of the status of the lipid layers in relation to water permeation, but the measurement itself does not provide direct information regarding the state of the SC. The ordering of the lipid bilayer can be studied by X-ray analysis only for in vitro SC specimens or model lipid membranes composed of water. Structural information can be obtained by analysis of aliphatic spin probes incorporated into the lamellar lipids using EPR [1–5]. Therefore, EPR can potentially detect the skin-lipid structures as well as their dynamics.

The EPR spin probe method has been utilized to characterize the skin-lipid structures [1, 2], as well as fluidity [3]. The physicochemical properties of intercellular lipids of SC were investigated as a function of various surfactants [4], and water content [5]. These studies provided information about the fluidity-related behavior of SC under various conditions by measuring EPR signal intensities and hyperfine values. Recently, we recognized that the conventional method of calculating the chain ordering using hyperfine values cannot differentiate subtle EPR spectral changes [1, 2]. Changes in the probe behavior are reflected in the EPR line width as well as the line shape, besides the hyperfine values. Precise analysis of EPR spectra can be performed by spectral simulation to extract quantitative ordering of the lipid structures [9, 10]. Therefore, EPR in conjunction with a simulation method should be useful to obtain direct information regarding skin-lipid structures. Such knowledge of the SC structural changes and mobility would be important in understanding the mechanism of irritant dermatitis and other SC diseases.

This paper describes an EPR investigation of the lipid ordering of SC using aliphatic spin probes together with a slow-tumbling simulation. EPR spectra were analyzed both by conventional calculation and slow-tumbling simulation. The obtained values of the order parameter are discussed in terms of EPR spectral changes in relation to the lipid moieties.

Experimental Section

Sample Preparations of Stripped SC from Volunteers and Spin Labeling of the SC

The Fukushima Medical University Internal Review Board approved all protocols used herein. The ethical principles for non-clinical biomedical research involving human subjects as stated in the Declaration of Helsinki Guidelines were adhered to in every respect. SC was removed from the mid-volar forearm of volunteers, who had given informed consent to the procedure, with a single drop of cyanoacrylate resin, and placed on quartz glass (7×37 mm^2; Matsunami Glass Ind. Ltd., Japan). The time interval was approximately 2 min between successive strippings. The spin probe agents, 5-doxylstearic acid (5-DSA) and 3β-doxyl-5α-cholestane (CHL), were purchased from Aldrich-Sigma Chemical Co. Inc. and used as received. A schematic representation of the configuration of the spin probes in a membrane is shown in Fig. 1. SC samples were incubated in $\sim$50 μM probe aqueous (H_2O) solutions for $\sim$60 min at 37 °C. After rinsing with deionized water to remove excess spin probe, the SC sample was mounted in the EPR cavity. Sample preparation has been described in detail elsewhere [1, 2].

EPR Measurements

EPR measurements were performed with an EMX EPR spectrometer from Bruker Instruments Inc. (Billerica, MA). First derivative, X-band spectra were recorded in a high sensitivity microwave cavity using a microwave power, 5 mW; time constant, 0.1 s; sweep time, 120 s; modulation, 0.1 mT; sweep width, 12.5 mT. Each spectrum used in the data analysis is an average of 2–5 scans. All measurements were performed at ambient temperature. The

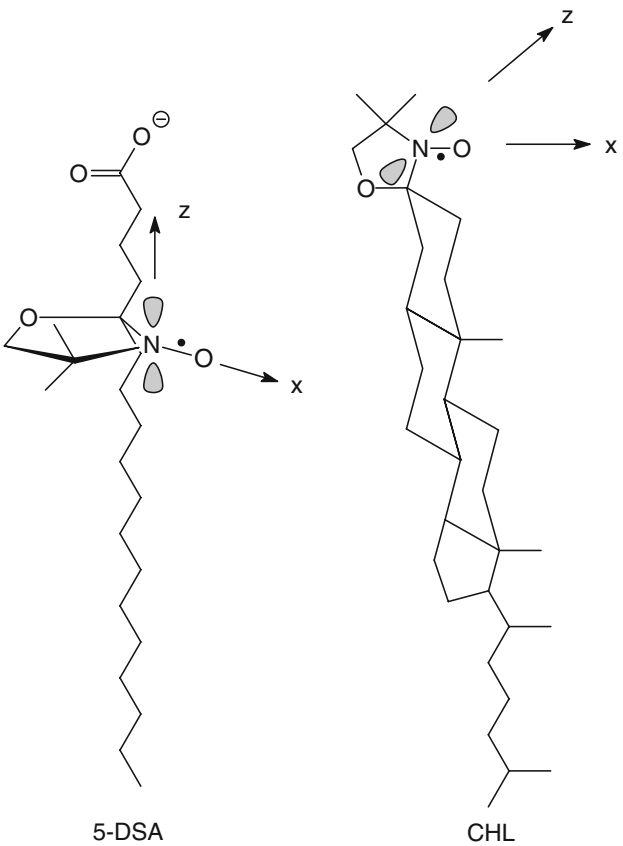

Fig. 1 A schematic representation of the configuration of the aliphatic spin probes in a membrane, where the *Z*-axis of the acyl chain is parallel to the *z*-axis of the membrane

resulting EPR spectra of 5-DSA in the SC samples were analyzed using two methods: conventional calculation of the order parameter and spectral simulation [9].

Conventional EPR Analysis

The inclination of the principal axis of the nitroxide radical to the rotational axis of the long-chain probe molecule represents a measure of the order–disorder of the molecular assemblies of a membrane. The order parameter indicates the membrane chain dynamics and microenvironment of the medium in which the spin probe is incorporated. The conventional order parameter (S) is determined from the hyperfine coupling of the EPR signals according to the following relations [11]:

$$S = \frac{A_{\parallel} - A_{\perp}}{A_{ZZ} - \frac{1}{2}(A_{XX} + A_{YY})} \times \frac{a}{a'}, \tag{1}$$

$$a' = \frac{A_{\parallel} + 2A_{\perp}}{3}, \tag{2}$$

where a is the isotropic hyperfine value, $(A_{XX} + A_{YY} + A_{ZZ})/3$; A_{XX}, A_{YY}, and A_{ZZ} are the principal values of the spin probe. In calculation based on the experimental spectra, the following principal components were used for 5-DSA [12].

$$A_{XX}, A_{YY}, A_{ZZ} = (0.66, 0.55, 3.45)\ \text{mT} \tag{3}$$

$$g_{XX}, g_{YY}, g_{ZZ} = (2.0086, 2.0063, 2.0025) \tag{4}$$

The experimental hyperfine couplings of $2A_{\parallel}$ and $2A_{\perp}$ are obtained from the EPR spectrum. The order parameter indicates that the S value increases with increasing anisotropy of the probe site in the membrane. On the other hand, the S value becomes zero for completely isotropic rotation of the nitroxide radical. Since the spin probe is incorporated into the highly oriented intercellular lipid structure in normal skin, in which the probe cannot move freely due to the rigidity of the lipid structure, its EPR spectrum represents the microscopically oriented profile. When the normal structure is completely destroyed by chemical and/or physical stress, the EPR spectral profiles changes to three sharp lines because the probe mobility is unrestricted. Therefore, the EPR spectral profile reflects the rigidity of the environment of the probe moiety. However, the conventional analysis measuring $2A_{\parallel}$ and $2A_{\perp}$ gives limited information concerning the probe moiety in the membrane, and may not reveal subtle differences in the overall spectra related to the membrane chain ordering [9].

EPR Slow-Tumbling Simulation Analysis

The slow-tumbling motions of the aliphatic spin probes were calculated using the nonlinear least-squares fitting program called NLSL (2000 version for Windows) to analyze the EPR spectra based on the stochastic Liouville equation [13–15]. The simulation of the EPR spectra for spin probes incorporated into multilamellar vesicles was performed using a microscopically ordered but macroscopically disordered (MOMD) model introduced by Meirovitch et al. [16]. This model is based on the characteristics of the dynamic structure of lipid dispersions. For example, lipid molecules are preferentially oriented by the local structure of the bilayer, but the lipid bilayer fragments are overall distributed randomly. The spectrum from the sample can be regarded as a superposition of the spectra from all of the fragments.

The lipid and DSA molecules in the bilayer membrane experience ordering potentials, which restrict the amplitude of the rotational motion. The orienting potential in a lipid bilayer, $U(\Omega)$, determines the orientational distribution of molecules with respect to the local ordering axis of the membrane bilayer. It can be expressed as an expansion in generalized spherical harmonics [17, 18],

$$-U/kT = c_0^2 D_{00}^2(\Omega) + c_2^2\left(D_{02}^2(\Omega) + D_{0-2}^2(\Omega)\right) + \cdots, \tag{5}$$

where $\Omega = (\alpha, \beta, \gamma)$ are the Euler angles between the molecular frame of the rotational diffusion tensor and the local director frame. The c_0^2 and c_2^2 are dimensionless potential energy coefficients, k is the Boltzmann constant, and T is the absolute temperature.

The order parameter, S_0, is defined as

$$S_0 = \langle D_{00}^2 \rangle = \left\langle \frac{1}{2}(3\cos^2\gamma - 1) \right\rangle = \frac{\int d\Omega \exp(-U/kT) D_{00}^2}{\int d\Omega \exp(-U/kT)}, \tag{6}$$

which measures the angular extent of the rotational diffusion of the nitroxide moiety. Gamma (γ) is the angle between the rotational diffusion symmetry axis and the z-axis of the nitroxide axis system; z is the axis of the nitrogen $2p_z$ atomic orbital, and the x-axis lies along the N–O bond, as shown in Fig. 2. The local or microscopic ordering of the nitroxide spin probe in the membrane is characterized by the S_0 value. A larger S_0 value indicates more restricted motion. Therefore, S_0 reflects the local ordering of bilayer molecules in the membrane. The A and g of Eqs. 3 and 4 were used for the simulation of 5-DSA, respectively.

Results

Figure 3 shows the experimental and simulated EPR spectra of 5-DSA in the SC. The reasonable agreement of the experimental and simulated spectra suggests that

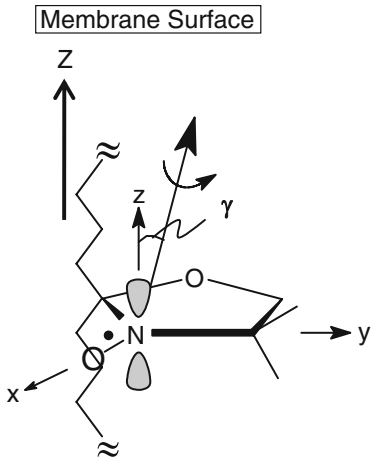

Fig. 2 A schematic representation of a conformation of DSA spin probe in the SC membrane, where *Z*-axis of the acyl chain is parallel to *z*-axis of the nitrogen $2P_z$ orbital

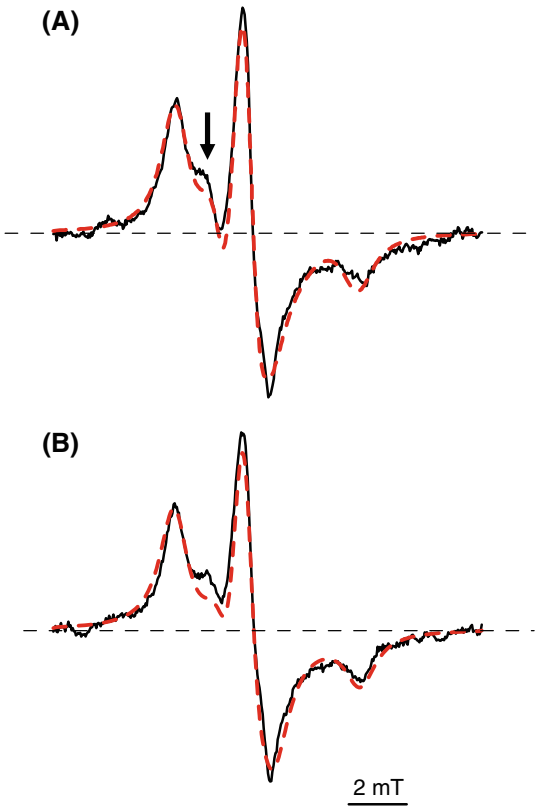

Fig. 3 The experimental (*solid line*) and simulated (*dotted line*) EPR spectra of 5-DSA in stripped SC from human mid-volar forearm (M, 79). The *arrow* indicates the characteristic peak for the first strip. The S_0 values obtained by the simulation were **a** 0.25 and **b** 0.74

simulation analysis can provide detailed information regarding the SC lipids. The S_0 value changes from 0.25 to 0.74, while the *S* value is in the range of 0.56–0.59. The conventional *S* value was calculated using the hyperfine values ($2A_{\|}$ and $2A_{\perp}$) from the observed spectrum in Eq. 1.

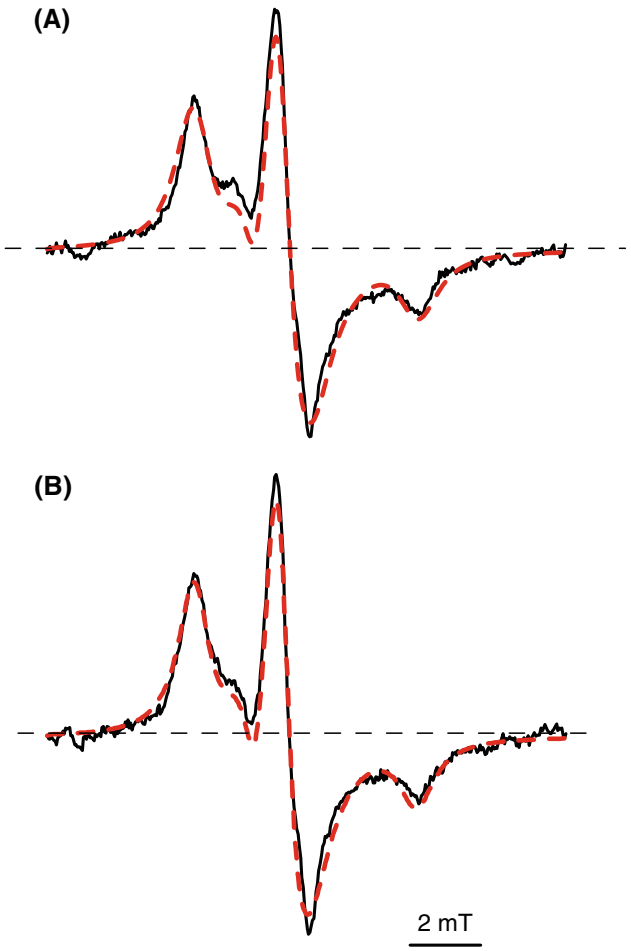

Fig. 4 The experimental (*solid line*) and simulated (*dotted line*) EPR spectra of 5-DSA in stripped SC from human lower-leg. Parallel and perpendicular hyperfine components are indicated for the conventional calculation. The S_0 values obtained by the simulation were **a** 0.28 and **b** 0.60

The arrow in the spectrum (**a**) indicates the characteristic peak, which is prominent only for the first strip (Fig. 3). This peak mainly does not belong to the slow probe motion in the SC. The peak diminishes in intensity with increasing depth in the SC. The marked peak appears near the center of the spectrum because the probe embedded in the first sample stripped has greater freedom of motion. The other two lines of the nitroxide probe overlaid the central region of the spectrum. The results imply that the probe signal can originate from sebaceous secretion where the probe is relatively mobile [2].

Figure 4 shows that human SC stripped from lower-leg presents typical EPR spectra of 5-DSA incorporated in the SC lipids. The EPR spectrum of stripping number 1 slightly differs from number 3. The characteristic peak indicated the arrow in the spectrum is prominent only for the first strip. This peak diminishes in intensity with increasing depth in the SC. Satisfactory agreement between the

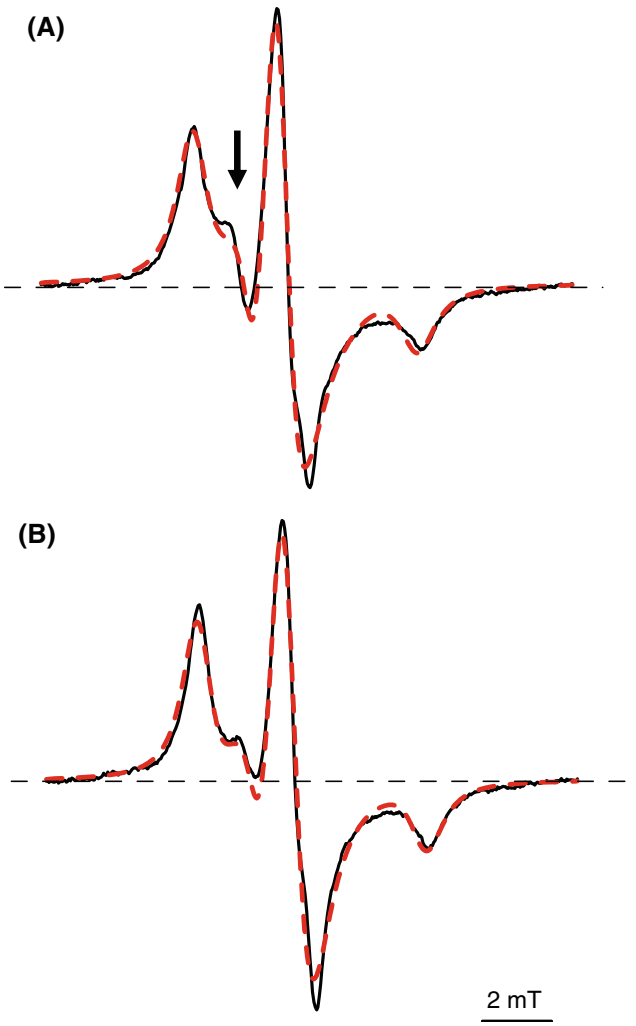

Fig. 5 The experimental (*solid line*) and simulated (*dotted line*) EPR spectra of 5-DSA probe in stripped SC from human mid-volar forearm (F, 51). The *arrow* indicates the characteristic peak for the first strip. The S_0 values obtained by the simulation were **a** 0.34 and **b** 0.36

experimental and calculated spectra can provide a quantitative S_0, which reveals the microscopic ordering in association with the structure of the SC lipids.

Figure 5 presents typical EPR spectra of 5-DSA incorporated in the SC lipids from human mid-volar forearm (F, age 51). The characteristic peak indicated by the arrow is prominent only for the first strip. The reasonable agreement of the simulated and experimental spectra suggests that simulation analysis can provide comprehensive information regarding the SC lipids.

Discussion

The modern EPR slow-tumbling simulation reveals detailed SC lipid structure. Significant differences exist

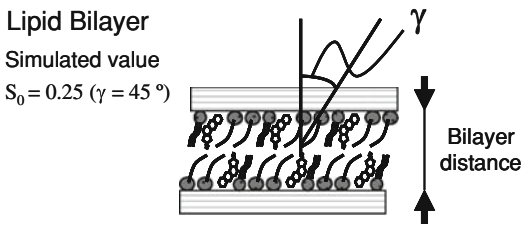

Fig. 6 Schematic illustration of relative lipid bilayer distances and the values of simulated order parameter related to the angles between the bilayer surface and the single-chain probe. The angle (γ) reflects the bilayer distance

between the conventional and simulated order parameters in Fig. 3. Because the slow-tumbling simulation calculates the total line-shape of the spectrum, it is able to extract more detailed information about the SC structure than the conventional analysis, which is normally ambiguous in distinguishing the two hyperfine components (parallel and perpendicular) from the experimental spectrum due to the presence of weak and broad signals [5]. Thus, the S_0 values (0.2–0.9) obtained by the simulation suggest that the outermost SC layers are less rigid (or more mobile), while the deeper lipid layers (S_0–0.9) have more rigid and oriented structures.

One can calculate the angle (γ in Fig. 2) between the rotational diffusion symmetry axis (the lipid in SC) and the z-axis of the nitroxide axis system [19]. Figure 6 represents the schematic illustration of the bilayer distance in relation to the angle. The simulated S_0 value of 0.25 can be the angle of 45°. The value of 0.74 is the angle of 25°. The angle suggests that the SC lipids align nearly perpendicularly to the bilayer surface. The larger S_0 value yields larger distance between the lipid bilayer. The analysis implies that the longer distance of the lipid bilayer can be related to the oriented SC structure.

The S_0 value changes from 0.28 to 0.60, while the S value is in the range of 0.63–0.64 in Fig. 4. The S_0 value of 0.60 is the angle of 31°. The higher S_0 value implies that the lower SC lipids have better-ordered structure than those of the upper SC lipids. Similarly, the S_0 value was 0.34, while the S value was 0.54. The simulated S_0 value of 0.34 can be the angle of 42° in Fig. 5.

Figure 7 shows EPR spectra of CHL from the mid-volar forearm of a male subject. A relatively broad 3 line pattern was obtained. The spectral pattern was very similar to that of the first strip, except for the intensity. The intensity of the second stripped sample was weak under the same experimental procedure for the probes. The weaker intensity than that of 5-DSA and the broad 3 line signal suggest that CHL probe may not be easy to incorporate with the SC lipid. Moreover, the weak intensity implies that the broadening may not be due to the spin–spin interaction.

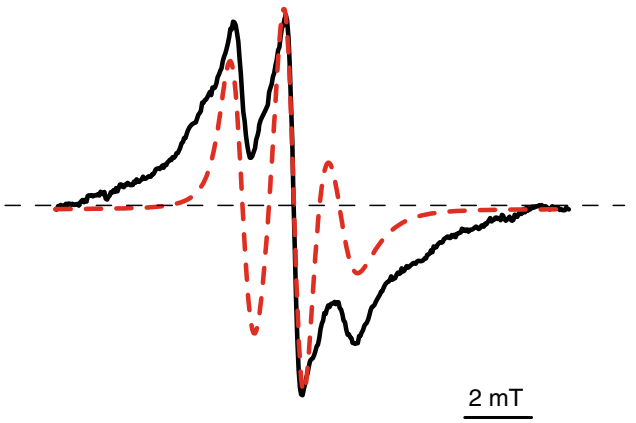

Fig. 7 The in vitro experimental (*solid line*) and simulated (*dotted line*) EPR spectra of CHL probe from human mid-volar forearm (M, 79)

The dotted line is the slow-tumbling simulation of the CHL spectrum in Fig. 7. There is a clear difference between the observed and the simulated spectrum. The discrepancy suggests that CHL moieties might be quite different orientations as well as motions in the SC. The EPR and the simulation results imply that CHL probe is difficult to incorporate into the SC lipids and the probe may locate into different parts in the SC.

EPR spectroscopy along with a modern computational analysis provides quantitative insight into the SC structure as a function of the depth. The EPR spectral pattern contains information regarding the probe mobility as well as the lipid structure. Satisfactory agreement between the experimental and calculated spectra can provide a quantitative S_0, which reveals the microscopic lipid chain ordering in the SC. In addition, the EPR method recognizes sebaceous exudates [2]. Thus, EPR together with computational analysis could in turn provide more comprehensive information, which would result in the understanding of various SC.

Acknowledgments The authors thanks Mr. E. Yagi of Shiseido Research Center, Dr. N. Naber, Prof. R. Cooke, and Prof. H. I. Maibach of University of California at San Francisco for his useful suggestions. Part of this research was supported by a Grant-in-Aid for Scientific Research (C) (21500410) from JSPS (K.N.).

References

1. Nakagawa K, Mizushima J, Takino Y, Sakamoto K, Maibach HI (2006) Chain ordering of stratum corneum lipids investigated by EPR slow-tumbling simulation. Spectrochim Acta Part A 63:816–820
2. Yagi E, Sakamoto K, Nakagawa K (2007) Depth dependence of stratum corneum lipid ordering: a slow-tumbling simulation for electron paramagnetic resonance. J Invest Dermatol 127:895–899
3. Kitagawa S, Ikarashi A (2001) Analysis of electron spin resonance spectra of alkyl spin labels in excised guinea pig dorsal skin, its stratum corneum, delipidized skin and stratum corneum model lipid liposomes. Chem Pharm Bull 49:165–168
4. Kawasaki Y, Quan D, Sakamoto K, Cook R, Maibach HI (1997) Electron spin resonance studies on the influence of anionic surfactants on human skin. Skin Res Technol 194:238–242
5. Alonso A, Meirelles NC, Yushmanov VE, Tabak M (1996) Water increases the fluidity of intercellular membranes of stratum corneum: correlation with water permeability, elastic, and electrical resistance properties. J Invest Dermatol 106:1058–1063
6. Bonté F, Saunois A, Pinguet P, Meybeck A (1997) Existence of a lipid gradient in the upper stratum corneum and its possible biological significance. Arch Dermatol Res 289:78–82
7. Weerheim A, Ponec M (2001) Determination of stratum corneum lipid profile by tape stripping in combination with high-performance thin-layer chromatography. Arch Dermatol Res 293:191–199
8. Rogers J, Harding C, Mayo A, Banks J, Rawlings A (1996) Stratum corneum lipids: the effect of ageing and the seasons. Arch Dermatol Res 288:765–770
9. Nakagawa K (2004) ESR spin probe investigation of chain ordering of a triglycerol membrane. Bull Chem Soc Jpn 77:269–273
10. Nakagawa K (2003) Diffusion coefficient and relaxation time of aliphatic spin probes in a Unique Triglyceride Membrane. Langmuir 19:5078–5082
11. Hubbell WL, McConnell HM (1971) Molecular motion in spin-labeled phospholipids and membranes. J Am Chem Soc 93:314–326
12. Ge M, Rananavare SB, Freed JH (1990) ESR studies of stearic acid binding to bovine serum albumin. Biochim Biophys Acta 1036:228–236
13. Meirovitch E, Igner D, Igner E, Moro G, Feed JH (1982) Electron-spin relaxation and ordering in smectic and supercooled nematic liquid crystals. J Chem Phys 77:3915–3938
14. Schneider DJ, Freed JH (1989) Slow motional magnetic resonance spectra: a user's guide, chap. 1. In: Berliner LJ, Reuben J (eds) Biological magnetic resonance, vol 8. Plenum, New York, pp 1–76
15. Budil DE, Lee S, Saxena S, Freed JH (1996) Nonlinear-least-squares analysis of slow-motion EPR spectra in one and two dimensions using a modified Levenberg Marquardt algorithm. J Magn Reson Ser A 120:155–189
16. Meirovitch E, Nayeem A, Freed JH (1984) Analysis of protein–lipid interactions based on model simulations of spin resonance spectra. J Phys Chem 88:3451–3465
17. Crepeau RH, Saxena S, Lee S, Patyal BR, Freed JH (1994) Studies on lipid membranes by two-dimensional Fourier transform ESR: enhancement of resolution to ordering and dynamics. Biophys J 66:1489–1504
18. Ge M, Field KA, Aneja R, Holowka D, Baird BA, Freed JH (1999) Electron spin resonance characterization of liquid ordered phase of detergent-resistant membranes from RBL-2H3 cells. Biophys J 77:925–933
19. Nakagawa K (2009) Electron paramagnetic resonance studies of skin lipid structure, chap. 19. In: Barel AO, Paye M, Maibach HI (eds) Handbook of cosmetic science and technology, 3rd edn. Informa Healthcare, New York, pp 207–215

Lipids (2010) 45:97–110
DOI 10.1007/s11745-009-3379-2

ORIGINAL ARTICLE

High Dietary Fat Exacerbates Weight Gain and Obesity in Female Liver Fatty Acid Binding Protein Gene-Ablated Mice

Barbara P. Atshaves · Avery L. McIntosh · Stephen M. Storey · Kerstin K. Landrock · Ann B. Kier · Friedhelm Schroeder

Received: 21 August 2009 / Accepted: 24 November 2009 / Published online: 25 December 2009

Abstract Since liver fatty acid binding protein (L-FABP) facilitates uptake/oxidation of long-chain fatty acids in cultured transfected cells and primary hepatocytes, loss of L-FABP was expected to exacerbate weight gain and/or obesity in response to high dietary fat. Male and female wild-type (WT) and L-FABP gene-ablated mice, pair-fed a defined isocaloric control or high fat diet for 12 weeks, consumed equal amounts of food by weight and kcal. Male WT mice gained weight faster than their female WT counterparts regardless of diet. L-FABP gene ablation enhanced weight gain more in female than male mice—an effect exacerbated by high fat diet. Dual emission X-ray absorptiometry revealed high-fat fed male and female WT mice gained mostly fat tissue mass (FTM). L-FABP gene ablation increased FTM in female, but not male, mice—an effect also exacerbated by high fat diet. Concomitantly, L-FABP gene ablation decreased serum β-hydroxybutyrate in male and female mice fed the control diet and, even more so, on the high-fat diet. Thus, L-FABP gene ablation decreased fat oxidation and sensitized all mice to weight gain as whole body FTM and LTM—with the most gain observed in FTM of control vs high-fat fed female L-FABP null mice. Taken together, these results indicate loss of L-FABP exacerbates weight gain and/or obesity in response to high dietary fat.

B. P. Atshaves · A. L. McIntosh · S. M. Storey · K. K. Landrock · F. Schroeder (✉)
Department of Physiology and Pharmacology, Texas A&M University, TVMC, College Station, TX 77843-4466, USA
e-mail: fschroeder@cvm.tamu.edu

A. B. Kier
Department of Pathobiology, Texas A&M University, TVMC, College Station, TX 77843, USA

Keywords Liver · Fatty acid binding protein · Fat · Oxidation · Body weight · Fat/lean tissue mass

Abbreviations

L-FABP	Liver fatty acid binding protein
FTM	Fat tissue mass
LTM	Lean tissue mass
WT	Wild-type
DEXA	Dual emission X-ray absorptiometry
LCFA	Long chain fatty acids
rtPCR	Real-time PCR
ACO-1	Palmitoyl CoA oxidase-1
ACO-2	Branched chain CoA oxidase-2
ACO-3	Pristanoyl CoA oxidase-3
PBE	L-peroxisomal bifunctional enzyme
CpT1-l	Carnitine palmitoyl CoA acyltransferase-1
MCAD	Mitochondrial medium chain acyl CoA dehydrogenase
HMG-CoA Syn	HMG-CoA synthase
CYP4A3	Cytochrome p450, family 4, subfamily A, polypeptide 3

Introduction

Liver fatty acid binding protein (L-FABP) is a small 14-kDa soluble protein highly expressed in tissues active in long chain fatty acid (LCFA) uptake, oxidation and metabolism—especially liver, intestine, and kidney (0.1–0.4 mM; rev. in [1]). L-FABP is unique among the fatty acid binding protein family in that it has two known (rather than one) ligand binding sites, a broad

range/promiscuity for a variety of ligands, and high affinity for long chain fatty acids (LCFAs) or their CoA thioesters (LCFA-CoAs) [1–6]. Demonstration of LCFA and LCFA-CoA binding to L-FABP provided the first insight that this protein may be involved in LCFA uptake and intracellular targeting to metabolic organelles for oxidation and esterification. This expectation has since been borne out by multiple studies performed in vitro, in cultured cells, and mice as follows:

Purified L-FABP extracts LCFA/LCFA-CoA from membranes and protects LCFA-CoAs from hydrolysis [7–11]. Also in vitro, L-FABP removes palmitoyl CoA induced substrate inhibition of carnitine palmitoyltransferase-1, the rate limiting step in mitochondrial LCFA oxidation [12, 13], and serves as a LCFA donor protein for peroxisomal and LCFA-CoA donor protein for mitochondrial LCFA oxidation [14, 15]. Finally, L-FABP facilitates presentation of bound LCFA-CoA for esterification to phosphatidic acid and cholesteryl ester by purified liver microsomes [7–11]. Thus it was expected that L-FABP should alter LCFA oxidation and esterification in living cells and in animals.

In L-FABP overexpressing transformed cells, L-FABP enhanced LCFA uptake [1, 16–19], intracellular transport/diffusion [1, 17], oxidation (especially with branched-chain fatty acids selectively oxidized in peroxisomes [20], and esterification [16, 18, 21]. Initial physiologic studies suggested that L-FABP may function in LCFA metabolism. For example, L-FABP concentration in rat tissues was directly related to the oxidative capacity (liver or other L-FABP expressing tissues) [22, 23]. Further, peroxisomal proliferators induced expression of L-FABP and peroxisomal β-oxidation in primary rat hepatocyte cultures [24, 25]. More recently, the relevance of L-FABP to LCFA/LCFA-CoA oxidation and esterification was more firmly established by studies with genetically engineered mice, in which L-FABP gene ablation inhibited hepatic LCFA uptake and LCFA oxidation in vivo, and reduced hepatic cytosol binding capacity for LCFA and LCFA-CoA [26–29]. Cultured primary mouse hepatocytes from L-FABP knockout (KO) and wild-type (WT) mice also confirmed that loss of L-FABP reduced LCFA uptake, intracellular transport/diffusion, and oxidation [30].

Thus in-vitro, cultured-cell, and animal studies have indicated that L-FABP is involved in hepatic uptake of LCFAs derived from diet or adipose tissue. In the liver, L-FABP may target bound LCFA and/or LCFA-CoA to intracellular organelles for oxidation (mitochondria, peroxisomes) or esterification [endoplasmic reticulum (ER)] for storage (lipid droplets) or secretion (VLDL). Since the net effect of L-FABP would elicit rapid hepatic uptake and removal of LCFAs—primarily by oxidation since hepatic storage of esterified LCFAs is limited—it was hypothesized that L-FABP gene ablation would enhance high fat diet induced weight gain and obesity. This hypothesis was tested in male and female and L-FABP KO and WT mice pair-fed a defined isocaloric high fat versus control diet. Absence of L-FABP exacerbated weight gain and obesity induced by high dietary fat.

Materials and Methods

Materials

RNeasy mini kits were from Qiagen (Valencia, CA). Probes and primers used in the real-time PCR experiments on mouse liver RNA were purchased from Applied Biosystems (Foster City, CA). Protein was quantified by Protein Assay Dye Reagent (Bio-Rad Laboratories, Hercules, CA).

Animals

L-FABP gene-ablated mice were generated using a construct strategy that deleted all four exons of the L-FABP gene as described earlier [26]. Since the L-FABP KO mice were backcrossed to normal C57BL/6NCr mice (Charles River Wilmington, MA obtained through the National Cancer Institute, Frederick Cancer Research and Development Center, Frederick, MD) to the N6 generation (98.4% genetic homogeneity), C57BL/6NCr mice of matching sex/age were used as control animals for the feeding studies. Mice were housed in ventilated microisolator cages, temperature was maintained at 25 °C, and lighting was a constant 12-h light/dark cycle. For the first 7 weeks of life mice were given water and fed standard chow (4.4% gm% fat, Harlan Teklad Rodent Diet 8604, Madison, WI) ad libitum. The Animal Care and Use Committee of Texas A&M University approved all animal protocols.

Composition of Experimental Diets

Defined high fat and control pelleted diets were obtained commercially (Research Diets, Inc., New Brunswick, NJ). The defined control diet (# D12450B, Research Diets, Inc., New Brunswick, NJ) was comprised of 20, 70, and 10 kcal% protein, carbohydrate and fat, respectively, with caloric value of 4,057 kcal/1,055 g or 3.85 kcal/g diet (Table 1). The control diet contained 10 kcal% (4.3 gm%) as fat comprised of soybean oil and lard in nearly equal weight proportions. The isocaloric high-fat diet (# D12451, Research Diets, New Brunswick, NJ) was comprised of 20, 35, and 45 kcal% protein, carbohydrate and fat, respectively, with caloric value of 4,057 kcal/858 g or 4.73 kcal/g

Table 1 Ingredient and fatty acid group percent composition in control and high fat diets

Group	Control diet	High fat diet
Ingredient gm% (kcal%)		
Protein	19.2 (20)	24 (20)
Carbohydrate	67.3 (70)	41 (35)
Fat	4.3 (10)	24 (45)
Fatty acid (%)		
Saturated	25.1	36.3
Monounsaturated	34.7	45.3
Polyunsaturated	40.2	18.5

(Table 1). Fat was increased to 45 kcal% (24 gm%) by increasing the amount of lard (but not soybean oil) and decreasing the amount of carbohydrate. Both control and high-fat diets had very low cholesterol, 0.002 and 0.02%, respectively, by weight. Fatty acids in the control diet were 25.1, 34.7, and 40.2% saturated, monounsaturated, and polyunsaturated fatty acids, respectively (Table 1), while fatty acid composition in the high-fat diet was comprised of 36.3, 45.3, and 18.5% saturated, monounsaturated, and polyunsaturated fatty acids, respectively (Table 1). Thus, the high-fat diet had more saturated and monounsaturated concomitant with less polyunsaturated fatty acids.

Dietary Study

One week before beginning the dietary studies, male and female mice (7 weeks old, 20–30 g) were switched to a pelleted defined control diet (10 kcal% fat; # D12450B, Research Diets, Inc., New Brunswick, NJ) described above (Table 1), a diet free of significant amounts of phytoestrogens or cholesterol [31] that could complicate any high-fat effect and sex-based comparisons [32]. Each mouse was housed individually in Tecniplast Sealsafe IVC cages equipped with external water bottles and lid holders with wire bars for holding food pellets. After 1 week of acclimation on the control diet, pair-feeding of the high-fat diet for 12 weeks was accomplished as follows: male and female WT and L-FABP KO mice were divided into four groups of 14 mice each: male L-FABP KO, male L-FABP WT, female L-FABP KO, and female L-FABP WT mice. On day one of the feeding study, the amount of control diet consumed as determined by weight and calorie content was measured in one half of the mice in each group. On day two, the other half of each group were pair-fed (1 day offset) the defined high-fat diet based on the amount of control diet consumed by the first half. Each day in the 12-week study body weights of mice from each group were recorded and the amount of high fat and control diet consumed was measured to ensure that each paired group was given food that by weight and calorie was similar to within a non-significant margin of the control group from the previous day. Briefly, at mid-morning daily, each mouse was weighed, and food intake was measured by weighing remaining pellets in the food holder plus any gathered from bedding. The latter were easily recovered since the food was color-coded (yellow for control food, red for high-fat food). At the end of 12 weeks, mice were fasted overnight 12 h, to assure that liver was not influenced by recent digestion and to give more uniform liver weights. Mice were then anesthetized by intraperitoneal (IP) injection of a mixture of ketamine and xylazine (0.01 mL/g body weight; 10 mg ketamine/mL and 1 mg xylazine/mL in 0.9% saline solution), weighed, and examined for whole body phenotype (see below). The anesthetized mice were then euthanized by cervical dislocation, serum collected, and livers harvested, weighed, snap-frozen on dry ice, and stored at −80 °C for mRNA analyses as described [33].

Whole-Body Phenotype

The whole body phenotype was analyzed at the beginning and end of the study by dual-energy X-ray absorptiometry (DEXA) utilizing a Lunar PIXImus densitometer (Lunar Corp., Madison, WI). DEXA determined the relative proportion of fat tissue mass (FTM) and bone-free lean tissue mass (LTM) as described earlier [34]. Prior to PIXImus analysis each mouse was anesthetized as described in the previous section. To facilitate recovery after the procedure, mice were injected with yohimbine (0.11 μg/g body weight), as well as with warm saline solution for rehydration. Mice were kept warm during recovery with heat pads to minimize heat loss, and checked every 10 min until recovery was complete. Whole body composition was determined by exposing the mouse (except the head region) to sequential beams of low- and high-energy X-rays with image acquisition of the X-rays impacting a luminescent panel. Bone mass was separated from soft tissue mass by measurement of the ratios of signal attenuation at the different energy levels. Soft tissue mass was further resolved into lean tissue mass (LTM) and fat tissue mass (FTM) for accurate measurement of whole body composition. Calibration was performed using a phantom mouse with known bone mineral density and FTM as described in Refs. [33, 34]. Data were expressed as gain in FTM and LTM at the end of the dietary study compared to the beginning as described earlier [34].

Serum β-Hydroxybutyrate Measurement

Serum levels of the ketone body β-hydroxybutyrate, a product of acetyl CoA produced from fatty oxidation, can be used to measure fatty acid oxidation in the liver [26, 28,

29, 34]. Serum levels of β-hydroxybutyrate (3-HB) were measured with high sensitivity and specificity according to the manufacturer's directions (Autokit 3HB, Wako Diagnostics, Richmond, VA) by measuring the rate of Thio-NADH (β-thionicotinamide adenine dinucleotide) production spectrophotometrically at 405 nm upon oxidation of 3-HB.

Liver Lipid Content

Liver lipids were extracted, resolved into individual lipid classes, and quantitated as described earlier [34].

Real-Time PCR of Mouse Liver RNA

Real-time PCR (rtPCR) was performed on total RNA from liver isolated and purified with RNeasy mini kits (Qiagen, Valencia, CA) according to the manufacturer's instructions. Total concentration of RNA extracts was determined spectrophotometrically followed by confirmation of RNA integrity by agarose electrophoresis and ethidium bromide staining. Expression patterns were analyzed by quantitative real-time PCR using an ABI PRISM 7000 Sequence Detection System (Applied Biosystems, Foster City, CA), TaqMan® One Step PCR Master Mix Reagent kit, as well as gene specific TaqMan® PCR probes and primers. Thermal cycler protocol was as follows: 48 °C for 30 min, 95 °C for 10 min before the first cycle, 95 °C for 15 s, and 60 °C for 1 min, repeated 40 times. TaqMan® One Step chemistry was used for total RNA reverse-transcription in the first step of the thermal cycler protocol (48 °C for 30 min) prior to amplification. Specific probes and primers were Assay-on-Demand® products for mouse: (i) Peroxisomal fatty acid oxidative enzymes: palmitoyl CoA oxidase-1 (ACO-1, Mm00443579_m1), branched chain CoA oxidase-2 (ACO-2, Mm00446408_m1), pristanoyl CoA oxidase-3 (ACO-3, Mm00446122_m1), and L-peroxisomal bifunctional enzyme (PBE, Mm00470091_m1); (ii) Mitochondrial fatty acid oxidative enzymes: carnitine palmitoyl CoA acyltransferase 1 (CpT1, Mm00550438_m1) and mitochondrial medium chain acyl CoA dehydrogenase (MCAD; Mm00431617_m1); and (iii) ER lipid metabolic enzymes including cytochrome p450, family 4, subfamily A, polypeptide 3 (CYP4A3, Mm00484132_m1). Probes and primers were from Applied Biosystems (Foster City, CA). Experiments were performed in triplicate and analyzed with ABI Prism 7000 SDS software (Applied Biosystems) to determine the threshold cycle (C_T) from each well. Primer concentrations and cycle number were optimized to ensure that reactions were analyzed in the linear phase of amplification. The mRNA expression levels of ACO-1, ACO-2, ACO-3, PBE, CPT-1, MCAD, and CYP4A3 determined in all groups were normalized to the housekeeping gene coding for 18S RNA. All mRNA data were expressed relative to the control male wild type mouse group on control diet). Relative expression levels were determined by the comparative $2^{-\Delta\Delta C_T}$ method [35] where $\Delta\Delta C_T = [C_T \text{ of target gene} - C_T \text{ of 18 s}]_{\text{different mice groups}} - [C_T \text{ of target gene} - C_T \text{ of 18 s}]_{\text{control mouse group}}$ as described in User Bulletin 2, ABI Prism 7000 Sequence Detection System (Applied Biosystems, Foster City, CA).

Statistical Analysis

Data analysis was performed on eight dietary groups consisting of seven mice/group: male control-fed WT, female control-fed WT, male control-fed L-FABP KO, female control-fed L-FABP KO, male high fat control WT, female high fat control WT, male high fat L-FABP KO, and female high fat L-FABP KO mice. All data were analyzed by analysis of variance (ANOVA) combined with the Newman-Keuls multiple comparisons test (GraphPad Prism, San Diego, CA). Values represent the mean ± SEM, with $p < 0.05$ considered statistically significant.

Results

Effect of High-Fat Diet and L-FABP Gene Ablation on Food Consumption

To ensure that any alterations in weight gain were not due to potential differences in food preference, mice were pair-fed as described in "Materials and Methods". Under pair-feeding conditions, one half of the mice in each group were provided access to the same amount of the high-fat diet as consumed each previous day by the other half of the mice on the control diet. The overall result was that total food consumption was similar whether the mice were fed the high-fat or the control diet.

Since the caloric densities of the control and high fat diet were similar, each paired group was given food that by weight and calorie content was similar to within a non-significant margin of the control group from the previous day. Total food consumption of each mouse was measured daily and summed over the 12-week dietary to show that total gram mass and kcal of control or high-fat diets consumed by WT males did not differ from that of WT females (data not shown). Likewise, L-FABP gene ablation did not significantly affect total gram mass or total kcal of control or high-fat diet consumed by either male or females. Thus, all groups consumed the same amount of food and any differences in weight gain or obesity were not due to differences in food consumption.

Effect of High-Fat Diet and Sex on Weight Gain and Body Weight in Wild-Type Mice

While control-fed WT male (Fig. 1a, solid circles) and female (Fig. 1c, solid circles) mice gained weight with increasing time on the control defined diet, weights were higher for males (0.093 ± 0.008 g/day) than females (0.067 ± 0.007 g/day). The final body weight of WT males (Fig. 2a) was 1.3-fold significantly higher than that of females (Fig. 2b), but males started with higher initial body weights such that there was only a slight difference in weight gain when expressed as a percent gain (Fig. 2c).

On the high-fat diet, both WT males (Fig. 1b, solid circles) and females (Fig. 1d, solid circles) also gained weight with increasing time, with males gaining markedly more weight than on control food. WT males on the high-fat diet gained weight at nearly twofold faster rate (0.18 ± 0.01 g/day) than on the control diet (0.09 ± 0.01 g/day). In contrast, WT females on the high-fat diet gained weight at a similar rate (0.063 ± 0.004 g/day) to control diet (0.067 ± 0.007 g/day). Consequently, at the end of the 12-week study, WT males weighed much more, regardless of whether expressed as total body weight (Fig. 2a) or as % change in weight (Fig. 2c), than their WT female counterparts (Fig. 2b, d). However, these changes were not due to differences in food consumption (data not shown). Thus, WT males gained weight faster, regardless of control or high-fat diet, and were more sensitive to weight gain induced by high-fat diet than their WT female counterparts.

Effect of High-Fat Diet and Sex on Weight Gain and Body Weight in L-FABP Knockout Mice

L-FABP gene ablation did not significantly affect the rate of weight gain in males (Fig. 1a, solid triangles) fed the control diet. While L-FABP gene ablation trended to slightly decrease the rate of weight gain in females (Fig. 1c, solid triangles) on the control diet, this effect did not achieve statistical significance. The lack of effect of L-FABP gene ablation on rate of weight gain on control diet was reflected in only slight or no differences in final body weight (Fig. 2a, b) and % change in body weight (Fig. 2c, d) in male or female L-FABP KO mice as compared to their WT counterparts. In contrast, L-FABP gene ablation significantly increased weight gain in response to the high fat diet, most prominently in females (Fig. 1d, solid triangles) where significant differences were observed in weeks 9–12 between the high-fat fed female KO versus WT mice. However, while weight gain in L-FABP KO males trended higher than for WT males, the rate did not achieve statistical significance at $p < 0.05$ (Fig. 1b). In contrast, L-FABP KO females gained weight nearly 1.8-fold faster than WT females on the same high fat, 12-week diet (Fig. 1d). As a result, at the end of the 12-week high-fat diet, L-FABP KO females weighed significantly

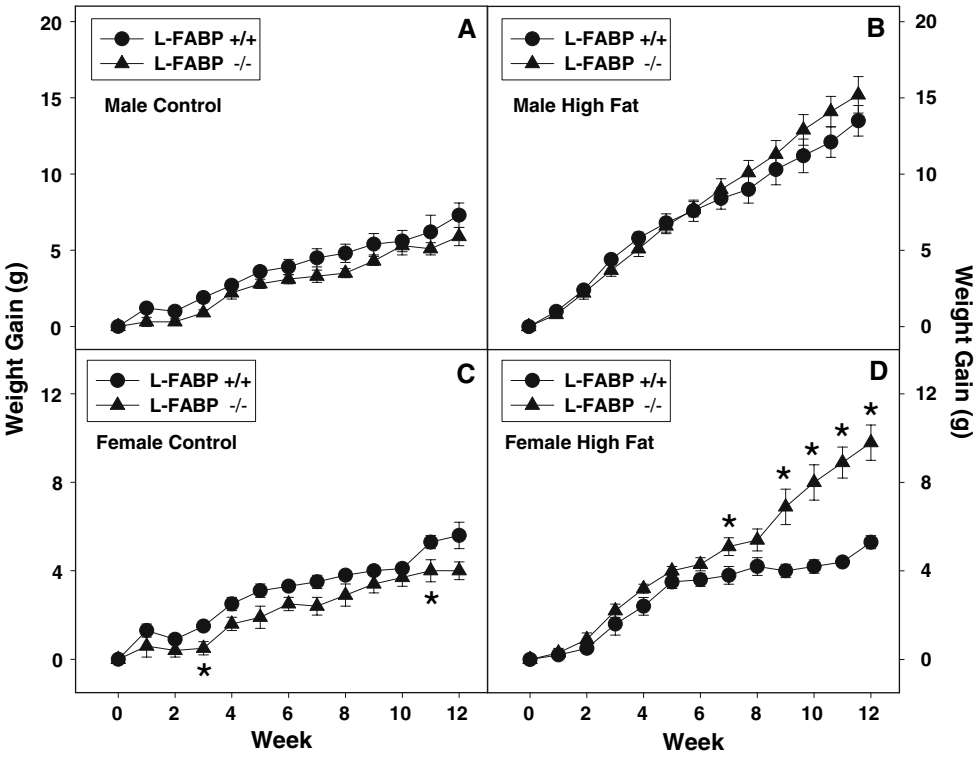

Fig. 1 Weekly weight gain in response to high-fat diet and L-FABP gene ablation. Weight gain of male (**a**, **b**) and female (**c**, **d**) WT and L-FABP KO mice fed a defined control-diet (**a**, **c**) or high-fat diet (**b**, **d**) was measured daily and summed weekly as described in "Materials and Methods". Solid circles refer to WT mice while solid triangles refer to L-FABP KO mice. Values represent the mean ± sem, $n = 5$–7. Statistical analysis was as follows: * $p \leq 0.05$ versus WT mice on high fat diet

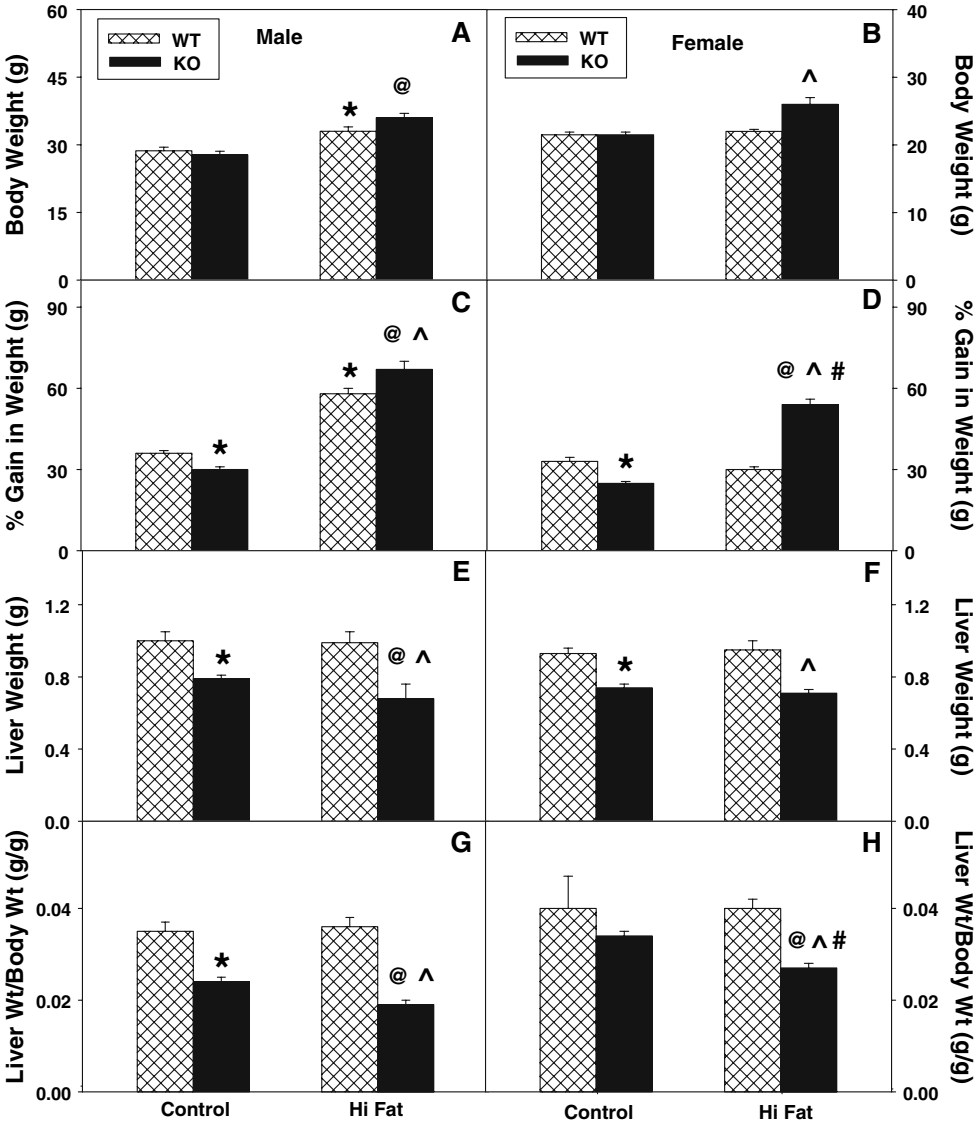

Fig. 2 Effect of L-FABP gene ablation and high-fat diet on final body weight and liver weight. Final body weight (**a**, **b**) and % gain in body weight (**c**, **d**) were determined for male (**a**, **c**) and female (**b**, **d**) WT (*hatched bar*) and L-FABP KO (*solid bar*) mice fed defined control-diet or high-fat diet for 12 weeks as described in "Materials and Methods". After killing, liver weights (**e**, **f**) and liver weight/body weight (**g**, **h**) were determined for male (**e**, **g**) and female (**f**, **h**) WT and L-FABP KO mice as in "Materials and Methods". Values represent the mean ± sem, $n = 5$–7. Statistical analysis was as follows: * $p \leq 0.05$ versus WT mice on control-diet; @ $p \leq 0.001$ versus L-FABP KO mice on control-diet; ^ $p \leq 0.001$ versus WT mice on high-fat diet; and # $p \leq 0.003$ versus male L-FABP KO on high-fat diet

more than their WT female counterparts, expressed as total body weight (Fig. 2b) and as % change in weight (Fig. 2d). However, as previously noted, because the dietary study was pair-fed, weight gain differences were not due to differences in food consumption.

Taken together, these data indicate that L-FABP gene ablation increases sensitivity, particularly of female mice, to high-fat diet induced weight gain.

Effect of High-Fat Diet and Sex on Liver Weight

While high-fat diet did not affect liver weights (Fig. 2e, f) or the ratio of liver weight/body weight (Fig. 2g, h) in either male or female WT mice, L-FABP gene ablation significantly altered these parameters. In control-fed mice, L-FABP gene ablation decreased the liver weight in both males and females (Fig. 2e, f), and the ratio of liver weight/body weight was also decreased in males (Fig. 2g) as compared to their WT counterparts. The high-fat diet further decreased liver weight (Fig. 2e, f) slightly and decreased the ratio of liver weight/body weight (Fig. 2g, h) in both L-FABP KO males and females as compared to their respective control-fed groups. Thus, L-FABP gene ablation decreased absolute liver mass (g) in both males and females on the control diet. The high-fat diet exacerbated these decreases in both L-FABP KO males and females.

Although high fat diet and/or L-FABP gene ablation elicited small changes in content of several individual lipid classes, there was little effect on the total level of liver lipids indicative of steatosis, primarily the neutral lipids (triglyceride + cholesterol ester). Neither isocaloric pair feeding of high fat diet nor L-FABP gene ablation significantly elevated the total level of neutral lipids indicative of steatosis in male mice (Table 2). Neutral lipid content of

Table 2 Effect of high fat diet and L-FABP gene ablation on liver lipid content

Sex	Gene type	Diet	Lipid mass (nmol/mg protein)					
			PL	C	FFA	TG	CE	Neutral lipids
Male	WT	Control	433 ± 23	32 ± 3	45 ± 4	454 ± 45	30 ± 4	484 ± 45
Male	KO	Control	392 ± 30	25 ± 4	30 ± 5	353 ± 33	28 ± 4	381 ± 33
Male	WT	High fat	417 ± 22	36 ± 4	23 ± 2	429 ± 28	46 ± 5	476 ± 29
Male	KO	High fat	446 ± 43	37 ± 3	25 ± 2	469 ± 37	46 ± 6	515 ± 38
Female	WT	Control	486 ± 45	30 ± 3	35 ± 5	907 ± 144	104 ± 14	1,012 ± 145
Female	KO	Control	546 ± 63	43 ± 5	31 ± 4	720 ± 62	135 ± 25	856 ± 67
Female	WT	High fat	467 ± 33	37 ± 3	19 ± 2	885 ± 53	101 ± 8	987 ± 54
Female	KO	High fat	459 ± 22	43 ± 3	24 ± 2	1,069 ± 112	143 ± 14	1,212 ± 113

Lipids were extracted and composition determined as described in "Materials and Methods". Values represent the mean ± SE (n = 5–8)
PL phospholipid, *C* cholesterol, *FFA* unesterified (free) fatty acid, *TG* triacylglyceride, *CE* cholesterol ester, *Neutral Lipids* TG + CE

livers from female mice, regardless of diet or genotype, was generally about twofold higher in female than male mice (Table 2). However, neither isocaloric pair feeding of high fat diet nor L-FABP gene ablation significantly elevated these lipids in female mice (Table 2). Thus, pair-feeding of isocaloric high fat diet did not induce hepatic steatosis in either male or female mice. Likewise, L-FABP gene ablation did not induce hepatic steatosis—regardless of the diet.

Effect of High-Fat Diet and Sex on Fat and Lean Tissue Mass in Wild-Type Mice

To determine if the above changes in body weight were due to altered fat tissue mass (FTM), lean tissue mass (LTM), or both, dual emission X-ray absorptiometry (DEXA) was performed on each mouse at the beginning and end of the dietary study as described in "Materials and Methods". Quantitative analysis and comparison of multiple DEXA images taken at the end versus the beginning of the dietary study showed that control-fed male WT mice (Fig. 3a) exhibited a greater proportion of weight gain as FTM than their female counterparts (Fig. 3b). Furthermore, high-fat fed WT males and females had 3.6- and 3.7-fold higher fat gain, respectively (Fig. 3a), as compared to control diet animals. In addition, the control-fed wild-type males gained much more LTM than their female counterparts (Fig. 3d).

In summary, these data indicated that both WT male and female mice were more susceptible to fat weight gain on a high-fat diet than control diet.

Effect of L-FABP Gene Ablation on Fat and Lean Tissue Mass in Response to A High-Fat Diet

DEXA analysis revealed that the gain in FTM in L-FABP KO male and female mice exhibited a similar qualitative pattern as their WT counterparts on the control diet (Fig. 3), but L-FABP gene ablation increased FTM in control and high-fat fed female mice with a trend towards increase observed for the male KO mice (Fig. 3a). LTM was also increased in the control and high-fat female (Fig. 3d) but not male (Fig 3c) KO mice.

Thus with a control diet, L-FABP gene ablation increased both fat and lean tissue mass in both males and females as compared to WT mice on the same diet. In response to high-fat diet, both L-FABP KO males and females gained more weight as fat, as well as lean tissue mass than their WT counterparts, with more gain observed in females (Fig. 3b) than males (Fig. 3a). The absolute gain observed in FTM was highest for high-fat fed WT and L-FABP KO males (Fig. 3a). In contrast, the largest fold increase in FTM was measured in high-fat fed L-FABP null females (4.5-fold) when compared to fold increases observed with male counterparts (3.4–3.7-fold). In LTM, the high-fat fed L-FABP KO males and females gained similar amounts as compared to control-fed L-FABP KO counterparts.

Effect of High Fat Diet and L-FABP Gene Ablation on Fatty Acid Oxidation: Serum β-Hydroxybutyrate Level

In control-fed WT females, serum β-hydroxybutyrate levels were about 50% higher than males (Fig. 4a), indicating higher hepatic fatty acid oxidation. The high-fat diet increased serum β-hydroxybutyrate levels in male mice to levels indistinguishable from control-fed WT female mice, but similar results were not observed with high-fat fed WT females (Fig. 4b). In control-fed mice, L-FABP gene ablation resulted in decreased serum β-hydroxybutyrate levels in both males and females (Fig. 4), and the high-fat diet produced further decreases, most markedly in females.

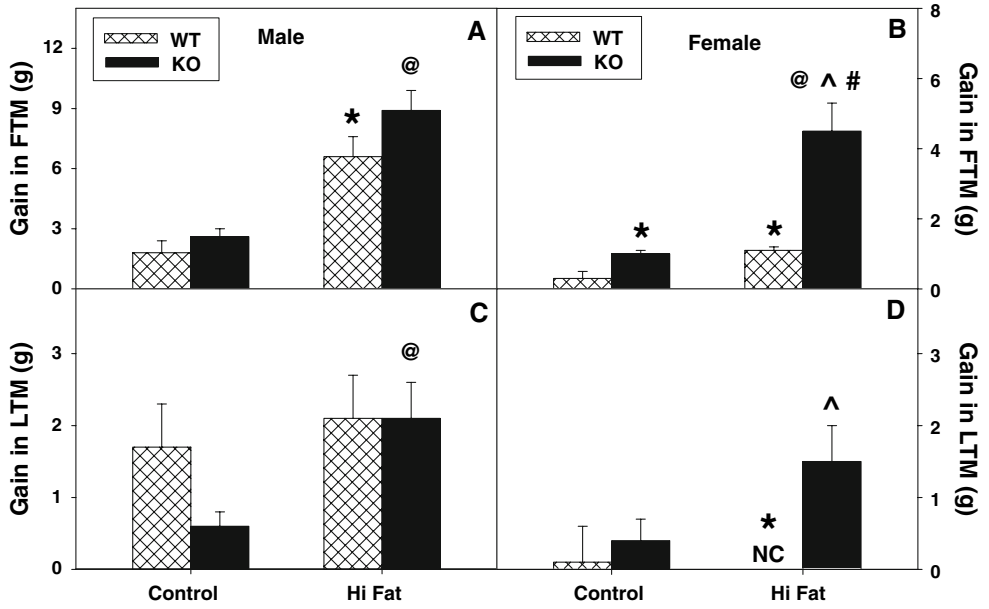

Fig. 3 Effect of L-FABP gene ablation and high-fat diet on whole body phenotype: Gain and percent gain in fat tissue mass (FTM) and lean tissue mass (LTM). At the beginning and end of the 12-week dietary study, FTM and LTM was determined by dual emission X-ray absorptiometry (DEXA) in male and female WT (*hatched bar*) and L-FABP KO (*solid bar*) mice fed control- and high-fat diets as described in "Materials and Methods". Changes in initial and final FTM (**a**, **b**) and LTM (**c**, **d**) for male (**a**, **c**) and female (**b**, **d**) WT and L-FABP KO mice were reported as gain in respective tissue mass. Values represent the mean ± sem, $n = 5$–7. Statistical analysis was as follows: * $p \leq 0.02$ versus WT mice on control-diet; @ $p \leq 0.02$ versus L-FABP KO mice on control-diet; ^ $p \leq 0.006$ versus WT mice on high-fat diet; and # $p \leq 0.001$ versus male L-FABP KO mice on high-fat diet

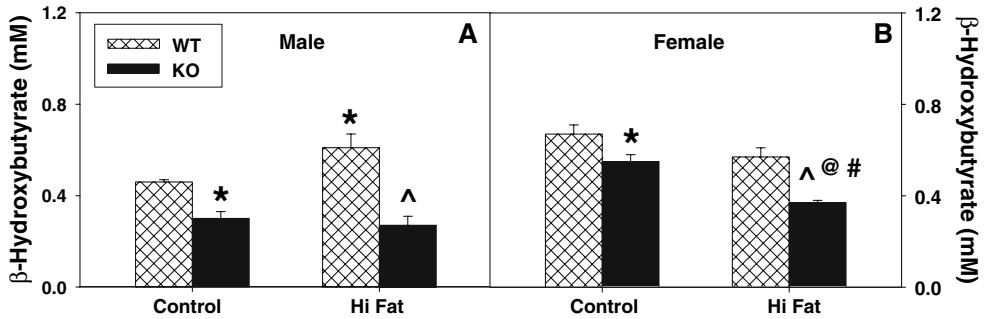

Fig. 4 Effect of L-FABP gene ablation and high-fat diet on serum β-hydroxybutyrate levels. At the end of the dietary study, serum was collected and levels of β-hydroxybutyrate were determined for male (**a**) and female (**b**) WT and L-FABP KO mice as described in "Materials and Methods". *Cross-hatched* and *solid bars* refer to WT and KO mice, respectively. Values represent the mean ± sem, $n = 5$–7. Statistical analysis was as follows: * $p \leq 0.03$ versus WT mice on control-diet; @ $p \leq 0.002$ versus L-FABP KO mice on control-diet; ^ $p \leq 0.007$ versus WT mice on high-fat diet; and # $p \leq 0.05$ versus male L-FABP KO mice on high-fat diet

Taken together, these data indicated that L-FABP gene ablation decreased fatty acid oxidation—an effect magnified by a high-fat diet.

Effect of High-Fat Diet and L-FABP Gene Ablation on Hepatic Levels of Peroxisomal Enzymes Involved in Fatty Acid Oxidation

Since decreased serum levels of β-hydroxybutyrate indicated that L-FABP gene ablation reduced fatty acid oxidation, especially in response to high-fat diet, mRNA levels of four key enzymes involved in peroxisomal fatty acid oxidation were examined: acyl CoA oxidase-1 (ACO-1, the key enzyme in peroxisomal β-oxidation of straight-chain fatty acids); acyl CoA oxidase-2 (ACO-2, involved in branched-chain fatty acid oxidation); acyl CoA oxidase-3 (ACO-3, involved in oxidation of pristanoyl-CoA—a branched-chain acyl CoA), and peroxisomal bifunctional enzyme (PBE). In control-fed wild-type mice, peroxisomal levels of ACO-1 (Fig. 5a, b), ACO-3 (Fig. 5c, d) and PBE (Fig. 5g, h) were significantly lower (about twofold each) in females versus males. The high-fat diet did not increase

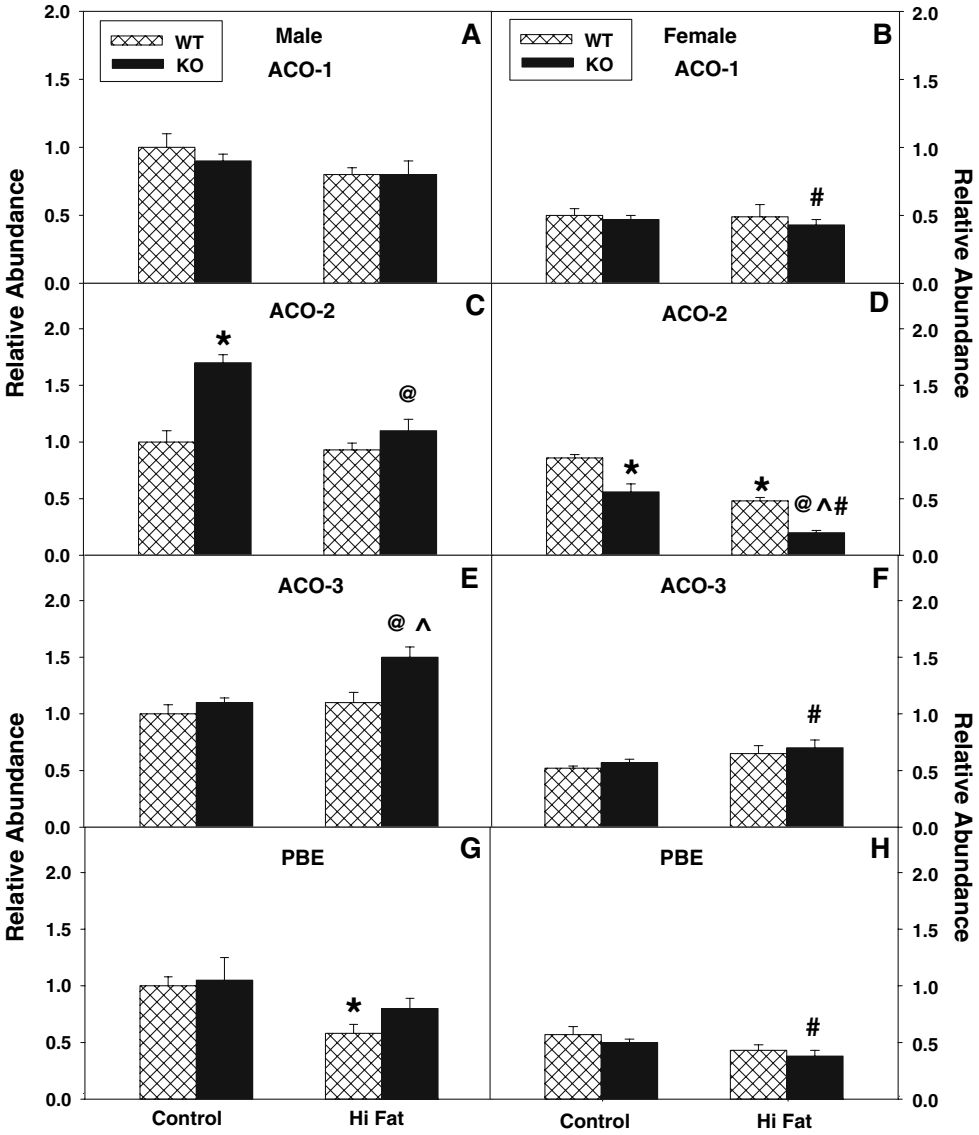

Fig. 5 Effect of L-FABP gene ablation and high-fat diet on key enzymes in hepatic peroxisomal fatty acid oxidation. At the end of the 12-week dietary study, livers were harvested and expression of the key peroxisomal enzymes involved in peroxisomal fatty acid oxidation was measured by real time PCR as described in "Materials and Methods". Acyl CoA oxidase-1 (ACO-1, **a**, **b**); acyl CoA oxidase-2 (ACO-2, **c**, **d**); acyl CoA oxidase-3 (ACO-3, **e**, **f**); and bifunctional enzyme (PBE, **g**, **h**) were determined for male (**a**, **c**, **e**, **g**) and female (**b**, **d**, **f**, **h**) mice as described in "Materials and Methods". *Cross-hatched* and *solid bars* refer to WT and KO mice, respectively. Values represent the mean ± sem, $n = 5$–7. Statistical analysis was as follows: * $p \leq 0.02$ versus WT mice on control-diet; @ $p \leq 0.002$ versus L-FABP KO mice on control-diet; ^ $p \leq 0.03$ versus WT mice on high-fat diet; and # $p \leq 0.01$ versus male L-FABP KO mice on high-fat diet

the levels of these proteins in either sex as compared to their control-fed, sex-matched counterparts.

L-FABP gene ablation did not significantly alter levels of ACO1 in control-fed or high-fat fed mice (Fig. 5a, b). In contrast, L-FABP gene ablation increased the level of ACO-2 in control-fed male mice (Fig. 5c), but decreased the level of ACO-2 in control-fed and high-fat fed females (Fig. 5d) when compared to the correspondingly fed WT mice. ACO-3 level was increased by L-FABP gene ablation in high-fat fed L-FABP KO male mice (Fig. 5e). Levels of PBE were not significantly altered by L-FABP gene ablation in either male (Fig. 5g) or female (Fig. 5h) mice fed control (or high-fat) diet as compared to similar diet fed wild-type mice.

Taken together, these data indicated that, regardless of diet, the male WT and L-FABP KO mice exhibited a greater abundance of several key peroxisomal enzymes (ACO-1, ACO3, PBE) involved in fatty acid oxidation as compared to their female counterparts. L-FABP gene ablation upregulated the expression of several of these oxidative enzymes (ACO-2 in control-fed males; ACO-3 in high-fat fed males), but did not change or slightly decreased the levels of these and other fatty acid oxidative enzymes depending on diet. Thus, the decreased fatty acid oxidation indicated by decreased serum levels of β-hydroxybutyrate in L-FABP KO mice was not associated with decreased expression of most peroxisomal proteins involved in fatty acid oxidation.

Effect of High-Fat Diet and L-FABP Gene Ablation on Hepatic Levels of Mitochondrial Enzymes Involved in Fatty Acid Oxidation

Carnitine palmitoyl transferase-1 (CPT-1, located at the outer mitochondrial membrane), is the rate-limiting enzyme involved in import of straight-chain fatty acids into

mitochondria for β-oxidation, while medium chain acyl CoA dehydrogenase (MCAD) is a key enzyme involved in β-oxidation of straight-chain fatty acids within mitochondria. MCAD (Fig. 6a, b) and CPT-1 (Fig. 6c, d) levels were substantially lower in control-fed WT females than males. The high-fat diet decreased expression of MCAD (Fig. 6a) and CPT1 (Fig. 6c) in males, but not females. L-FABP gene ablation did not significantly affect MCAD (Fig. 6a, b) or CPT-1 (Fig. 6c, d) in control-fed males or females. On the high-fat diet, similar findings were obtained with L-FABP KO females, while MCAD (Fig. 6a), but not CPT-1 (Fig. 6c), was increased in the L-FABP KO males. Therefore, decreased fatty acid oxidation shown as decreased serum levels of β-hydroxybutyrate in L-FABP gene-ablated mice on control and high-fat diets was also not associated with diminution of key enzymes involved in mitochondrial fatty acid β-oxidation.

Effect of High-Fat Diet and L-FABP Gene Ablation on Hepatic Levels of Microsomal Enzymes Involved in Lipid Metabolism

The relative abundance of Cytochrome P450 4A3 (CYP4A3), an important ER enzyme participating in microsomal lipid oxidation, was also measured. High-fat diet and L-FABP gene ablation decreased levels of CYP4A3 in both male and female mice (Fig. 6e, f) showing that L-FABP gene ablation did not increase levels of a key ER enzyme involved in lipid oxidation.

Discussion

A major role of liver is to take up and effectively metabolize dietary long chain fatty acids (LCFAs) after intestinal absorption (rev. in [1, 22, 23]). LCFAs as well as their CoA thioesters are known to be potent detergents that dissolve membranes and inhibit the action of multiple receptors and enzymes (rev. in [1, 7, 36, 37]). To prevent these adverse effects, mammals have evolved a family of cytosolic proteins with sufficiently high affinity for these ligands that intracellular levels of unbound free fatty acid and fatty acyl CoA are maintained at a low level, i.e. nM range (rev. in [1, 37–40]). High levels of liver fatty acid binding protein (L-FABP) representing 2–5% of cytosolic protein (0.1–0.4 mM) are expressed in tissues very active in long chain fatty acid (LCFA) uptake, oxidation and metabolism—especially liver, intestine, and kidney (rev. in [1]). Studies performed in vitro show that L-FABP facilitates uptake of fatty acids from membranes [7–11], removes

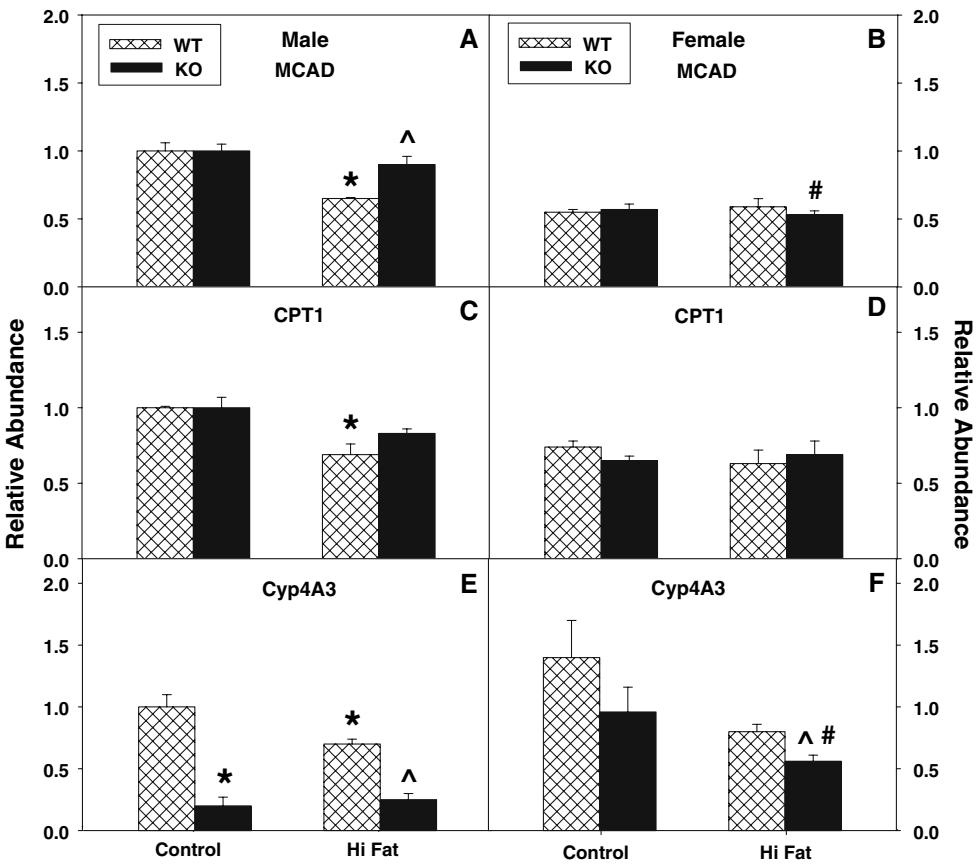

Fig. 6 Effect of L-FABP gene ablation and high-fat diet on liver levels of key enzymes in mitochondrial fatty acid oxidation and microsomal lipid oxidation. At the end of the 12-week dietary study, livers were harvested and expression levels of two key enzymes involved in mitochondrial fatty acid oxidation: medium chain acyl CoA dehydrogenase (MCAD, **a**, **b**), carnitine palmitoyl transferase-1 (CPT-1, **c**, **d**), and a key microsomal enzyme involved in lipid oxidation: cytochrome p4A3 (CYP4A3, **e**, **f**) were measured by real time PCR in male (**a**, **c**, **e**) and female (**b**, **d**, **f**) mice as described in "Materials and Methods". *Cross-hatched* and *solid bars* refer to WT and KO mice, respectively. Values represent the mean ± sem, $n = 5$–7. Statistical analysis was as follows: * $p \leq 0.04$ versus WT mice on control-diet; ^ $p \leq 0.009$ versus WT mice on high-fat diet; and # $p \leq 0.005$ versus male L-FABP KO mice on high-fat diet

substrate inhibition of carnitine palmitoyltransferase-1 (rate limiting step in mitochondrial LCFA oxidation) by palmitoyl CoA [12, 13], and functions as a LCFA donor protein for both peroxisomal and mitochondrial LCFA oxidation in vitro [14, 15]. Other studies with L-FABP overexpressing transformed cells have further established the potential functional significance of L-FABP in facilitating LCFA uptake [1, 16–19], intracellular transport/diffusion [1, 17], oxidation [20], and esterification [16, 18, 21]. The physiological significance and relevance of L-FABP to LCFA and LCFA-CoA oxidation and esterification was confirmed by numerous studies utilizing L-FABP gene-ablated mice where hepatic LCFA uptake in vivo and in cultured hepatocytes exhibited reduced hepatic cytosolic binding capacity for LCFAs and LCFA-CoAs, reduced intracellular LCFA transport/diffusion, and decreased hepatic LCFA oxidation [26–30]. Since liver stores relatively little esterified LCFA as lipid droplets, the net effect of these actions of L-FABP would be to facilitate rapid removal and oxidation. On this basis it was hypothesized that L-FABP gene ablation would enhance weight gain and obesity in a high-fat diet situation. To avoid potential complications due to preference for high fat diet, this hypothesis was addressed by pair feeding L-FABP KO mice compared to WT mice on a defined control diet versus isocaloric high-fat diet for 12 weeks as described in "Materials and Methods". The results provided the following new insights:

First, isocaloric pair feeding of high fat diet elicited sex-dependent body weight gain in male, but not female, mice. Because the mice were pair fed, the greater weight gain of male vs female mice was not due to differences in food consumption. While it was previously established that ad libitum feeding high fat diet itself markedly increases food consumption (as much as 40%) and consequently body weight gain [41–47], the present findings clearly established that weight gain was also greater (at least in males) when the mice were pair fed an isocaloric high fat diet. Thus, consuming the same number of calories as fat (high fat diet) rather than carbohydrate (low fat diet) resulted in increased weight gain in male mice. The greater increase in male mouse body mass was associated with about threefold greater increase in FTM than LTM while female mice isocaloric pair fed high fat diet exhibited increased FTM but not LTM. The molecular basis for the differential response of male versus female mice to isocaloric pair fed high fat diet may be related in part to the sex dependent difference in hepatic L-FABP expression in rodents [31, 48]. Consistent with these findings, sex dependent differences in response to other types of diet (e.g. phytol rich, cholesterol rich, cholestatic, etc.) have also been observed in mice [31, 42–45, 49]. Taken together, these data indicated that the male wild type mice were more efficient in converting both control diet and isocaloric pair fed high fat diet into increased body mass, both FTM and less so LTM.

Second, L-FABP gene ablation elicited sex-dependent body weight gain in female more than male mice. L-FABP gene ablation modestly increased weight gain (primarily as FTM) in control-fed female, but not male, mice. A similar pattern of increased weight gain was also observed in older (>6 mo) female L-FABP KO mice fed ad libitum standard rodent chow [43, 45] or pair-fed a different defined control-diet [42, 43]. Isocaloric pair feeding high fat diet dramatically exacerbated this effect in female, but not male, mice. The increased weight gain in high-fat fed female L-FABP KO mice was not due to differences in food consumption. The molecular basis for the gender dependent effect of L-FABP gene ablation may be related in part to the inter-dependent relationship between L-FABP and PPARα. The promoter of L-FABP contains a PPRE, L-FABP induces expression of PPARα, and L-FABP transports fatty acids into the nucleus to ligand activate PPARα and induce expression of more L-FABP [39, 40, 50, 51]. Roles for PPARs in sex dependent differences in mouse lipid metabolism have also been shown with PPARα null and PPARβ null mice [50, 52, 53].

Third, the effect of L-FABP gene ablation on diet induced obesity and hepatic steatosis appears to be dependent on both feeding regimen and susceptibility of the mouse background strain to diet induced obesity. Isocaloric pair feeding high fat diet (current study) as well as ad libitum feeding standard rodent chow (low fat) or isocaloric pair-feeding different types of low fat defined control diets [42–45] indicated that L-FABP gene ablation did not protect mice from high-fat diet induced weight gain. In addition, isocaloric pair fed high fat diet mice, regardless of sex of L-FABP expression, did not exhibit hepatic steatosis. In contrast to these studies with wild type C57BL/6NJ mice and L-FABP KO mice backcrossed to the C57BL/6NJ mice, ad libitum feeding of high fat diet to the more obesity susceptible C57BL6J strain induced hepatic steatosis [46, 47]. Surprisingly, ad libitum feeding of high fat diet to L-FABP KO mice backcrossed to the more obesity susceptible C57BL6J strain resulted in protection from high fat diet induced obesity and from hepatic steatosis [46, 47]. The marked differences in response to high fat diet between the two L-FABP KO mouse models were not due to differences in back-cross generation number [54]. Instead, these difference in phenotype may be attributed in part to several factors: (i) Wild type mice fed high fat diet ad libitum consume up to 40% more food and gain as much as 50% more weight [46, 47]. While isocaloric pair feeding high fat diet did not upregulate L-FABP in wild type mice determined by western blotting (data not shown), ad libitum feeding high fat diet is known to

activate PPARα—a nuclear receptor that induces transcription of multiple genes in fatty acid metabolism including L-FABP (rev. in [50, 55, 56]). Thus, ad libitum feeding high fat diet may upregulate L-FABP expression in the wild type mice, but not the L-FABP KO mice. (ii) The two independently generated L-FABP KO mice were backcrossed to a different C57BL/6 mouse strains differing markedly in susceptibility to high fat diet induced obesity. The C57BL/6J (Jackson Labs) used to backcross independently generated L-FABP KO mice are more susceptible to high fat diet induced obesity (higher weight gain, impaired glucose tolerance) than mice used for backcrossing in the current study (C57BL/SNJ from Charles River) (JAX NOTES, Issue 511, Fall, 2008, http://jaxmice.jax.org/jaxnotes/511/511n.html) [57–59]. The mechanistic basis for the difference in obesity susceptible of these strains is partly due to the C57BL/6J mouse strain exhibiting a null mutation in the NAD nucleotide transhydrogenase (Nnt) gene which codes for an enzyme that regulates NADH/NAD ratio—an important contributor to LCFA synthesis (JAX NOTES, Issue 511, Fall, 2008, http://jaxmice.jax.org/jaxnotes/511/511n.html). (iii) Overexpression of the green fluorescent protein (GFP) in the independently generated L-FABP KO mouse, but not the wild type control [29, 46, 47]. GFP was recently shown to function as a potent electron donor to several cofactors important in lipid metabolism including cytochrome c, FAD, FMN, and NAD in vitro [60]. Taken together, these findings demonstrate the importance of sex, high fat dietary regimen (pair fed, ad libitum fed), L-FABP KO background strain, and overexpression of GFP as each being important potential contributors to the whole body and hepatic phenotype of L-FABP KO mice fed high fat diet.

Fourth, the finding that L-FABP gene ablation did not induce hepatic steatosis in mice fed either control diet or pair fed high fat diet was consistent with the existing literature of known functions established for L-FABP in vitro, in cultured transformed cells, in cultured primary hepatocytes, and mice. L-FABP KO reduces hepatic uptake of dietary LCFA in vivo [26, 28] and in cultured L-FABP KO hepatocytes [30]. LCFA uptake directly correlates with L-FABP expression level in cultured transfected transformed cell lines [16, 19]. Further support comes from the fact that L-FABP gene ablation reduces LCFA oxidation in vivo as shown by reduced serum β-hydroxybutyrate in mice pair fed high fat diet (current study) and in L-FABP KO mice fed control chow [26, 28, 29], by reduced LCFA oxidation in cultured primary hepatocytes from L-FABP KO [30], and by increased LCFA oxidation in cultured transfected transformed cell lines [16, 19]. Regardless of the back-cross strain utilized to generate the two distinct L-FABP KO mice, inhibition of LCFA β-oxidation was observed in response to L-FABP gene ablation and this inhibition was not associated with major changes in levels of most of the key proteins/enzymes involved in peroxisomal and mitochondrial oxidation.

In summary, the present findings demonstrated that ablation of all four exons of the L-FABP gene and backcrossing to the C57BL/6NJ strain (resistant to high fat diet induced obesity) decreased fatty acid β-oxidation and increased weight gain (especially in fat tissue mass)—effects exacerbated by pair-feeding a defined isocaloric high-fat diet. This phenotype was consistent with predictions based on in vitro and cultured cell studies demonstrating L-FABP increases LCFA uptake (rev. in [1, 26]), LCFA intracellular transport [1, 17, 30, 61, 62], and both mitochondrial and peroxisomal LCFA oxidation [20, 30]. Thus, L-FABP gene ablation did not protect mice from weight gain and obesity induced when fed either control diet or isocaloric pair fed high fat diet, but instead exacerbated weight gain and obesity. While L-FABP gene ablation appeared to protect mice fed high fat diet ad libitum, interpretation of this phenotype is more complex due to much greater food consumption and weight gain concomitant with likely L-FABP upregulation in wild type mice, more obesity sensitive background strain, and presence of GFP in the KO but not wild type mice. Resolving the relative contributions of these factors is an important challenge. It is of interest to note that the pattern of higher weight gain and obesity in L-FABP mice fed high fat diet was also exhibited by adipocyte fatty acid binding protein (A-FABP) gene-ablated mice, which show increased body weight gain as compared with their WT counterparts when fed a high-fat diet [63]. Likewise, intestinal fatty acid binding protein (I-FABP) gene ablation resulted in mice with a higher weight gain than their WT counterparts when fed either a low-fat or a high-fat diet [64]. These findings suggested that in L-FABP KO mice pair fed a high-fat diet, LCFAs are more available for storage (weight gain) rather than hepatic uptake and oxidation (or storage).

Acknowledgments This work was supported in part by the United States Public Health Service National Institutes of Health grants DK41402 (FS and ABK), GM31651 (FS and ABK), and DK70965 (BPA).

References

1. McArthur MJ, Atshaves BP, Frolov A, Foxworth WD, Kier AB, Schroeder F (1999) Cellular uptake and intracellular trafficking of long chain fatty acids. J Lipid Res 40:1371–1383
2. Richieri GV, Ogata RT, Kleinfeld AM (1994) Equilibrium constants for the binding of fatty acids with fatty acid binding proteins from adipocyte, intestine, heart and liver measured with the fluorescent probe ADIFAB. J Biol Chem 269:23918–23930
3. Frolov A, Cho TH, Murphy EJ, Schroeder F (1997) Isoforms of rat liver fatty acid binding protein differ in structure and affinity for fatty acids and fatty acyl CoAs. Biochemistry 36:6545–6555

4. Thompson J, Ory J, Reese-Wagoner A, Banaszak L (1999) The liver fatty acid binding protein-comparison of cavity properties of intracellular lipid binding proteins. Mol Cell Biochem 192:9–16
5. Haunerland NH, Spener F (2004) Fatty acid binding proteins–insights from genetic manipulations. Prog Lipid Res 43:328–349
6. He Y, Yang X, Wang H, Estephan R, Francis F, Kodukula S, Storch J, Stark RE (2007) Solution-state molecular structure of apo and oleate-liganded liver fatty acid binding protein. Biochemistry 46:12543–12556
7. Jolly CA, Hubbell T, Behnke WD, Schroeder F (1997) Fatty acid binding protein: stimulation of microsomal phosphatidic acid formation. Arch Biochem Biophys 341:112–121
8. Jolly CA, Wilton DA, Schroeder F (2000) Microsomal fatty acyl CoA transacylation and hydrolysis: fatty acyl CoA species dependent modulation by liver fatty acyl CoA binding proteins. Biochim Biophys Acta 1483:185–197
9. Schroeder F, Jolly CA, Cho TH, Frolov AA (1998) Fatty acid binding protein isoforms: structure and function. Chem Phys Lipids 92:1–25
10. Chao H, Zhou M, McIntosh A, Schroeder F, Kier AB (2003) Acyl CoA binding protein and cholesterol differentially alter fatty acyl CoA utilization by microsomal acyl CoA: cholesterol transferase. J Lipid Res 44:72–83
11. Nemecz G, Schroeder F (1991) Selective binding of cholesterol by recombinant fatty acid-binding proteins. J Biol Chem 266:17180–17186
12. Woldegiorgis G, Bremer J, Shrago E (1985) Substrate inhibition of carnitine palmitoyltransferase by palmitoyl-CoA and activation by phospholipids and proteins. Biochim Biophys Acta 837:135–140
13. Bhuiyan AKMJ, Pande SV (1994) Carnitine palmitoyltransferase activities: effects of serum albumin, acyl-CoA binding protein and fatty acid binding protein. Mol Cell Biochem 139:109–116
14. Reubsaet FA, Veerkamp JH, Bruckwilder ML, Trijbels JM, Monnens LA (1990) The involvement of fatty acid-binding protein in peroxisomal fatty acid oxidation. FEBS Lett 267:229–230
15. Rasmussen JT, Faergeman NJ, Kristiansen K, Knudsen J (1994) Acyl-CoA-binding protein (ACBP) can mediate intermembrane acyl-CoA transport and donate acyl-CoA for beta-oxidation and glycerolipid synthesis. Biochem J 299:165–170
16. Murphy EJ, Prows DR, Jefferson JR, Schroeder F (1996) Liver fatty acid binding protein expression in transfected fibroblasts stimulates fatty acid uptake and metabolism. Biochim Biophys Acta 1301:191–198
17. Murphy EJ (1998) L-FABP and I-FABP expression increase NBD-stearate uptake and cytoplasmic diffusion in L-cells. Am J Physiol 275:G244–G249
18. Prows DR, Murphy EJ, Schroeder F (1995) Intestinal and liver fatty acid binding proteins differentially affect fatty acid uptake and esterification in L-Cells. Lipids 30:907–910
19. Wolfrum C, Buhlman C, Rolf B, Borchers T, Spener F (1999) Variation of liver fatty acid binding protein content in the human hepatoma cell line HepG2 by peroxisome proliferators and antisense RNA affects the rate of fatty acid uptake. Biochim Biophys Acta 1437:194–201
20. Atshaves BP, Storey S, Huang H, Schroeder F (2004) Liver fatty acid binding protein expression enhances branched-chain fatty acid metabolism. Mol Cell Biochem 259:115–129
21. Jefferson JR, Slotte JP, Nemecz G, Pastuszyn A, Scallen TJ, Schroeder F (1991) Intracellular sterol distribution in transfected mouse L-cell fibroblasts expressing rat liver fatty acid binding protein. J Biol Chem 266:5486–5496
22. Veerkamp JH, van Moerkerk HT (1993) Fatty acid-binding protein and its relation to fatty acid oxidation. Mol Cell Biochem 123:101–106
23. Veerkamp JH, van Moerkerk HT (1992) The fatty acid-binding protein content and fatty acid oxidation capacity of rat tissues. Prog Clin Biol Res 375:205–210
24. Vanden Heuvel JP, Sterchele PF, Nesbit DJ, Peterson RE (1993) Coordinate induction of acyl-CoA binding protein, fatty acid binding protein and peroxisomal β-oxidation by peroxisome proliferators. Biochem. Biophys. Acta 1177:183–190
25. Brandes R, Kaikaus RM, Lysenko N, Ockner RK, Bass NM (1990) Induction of fatty acid binding protein by peroxisome proliferators in primary hepatocyte cultures and its relationship to the induction of peroxisomal beta-oxidation. Biochim Biophys Acta 1034:53–61
26. Martin GG, Danneberg H, Kumar LS, Atshaves BP, Erol E, Bader M, Schroeder F, Binas B (2003) Decreased liver fatty acid binding capacity and altered liver lipid distribution in mice lacking the liver fatty acid binding protein (L-FABP) gene. J Biol Chem 278:21429–21438
27. Martin GG, Huang H, Atshaves BP, Binas B, Schroeder F (2003) Ablation of the liver fatty acid binding protein gene decreases fatty acyl CoA binding capacity and alters fatty acyl CoA pool distribution in mouse liver. Biochemistry 42:11520–11532
28. Erol E, Kumar LS, Cline GW, Shulman GI, Kelly DP, Binas B (2004) Liver fatty acid-binding protein is required for high rates of hepatic fatty acid oxidation but not for the action of PPAR-a in fasting mice. FASEB J 18:347–349
29. Newberry EP, Xie Y, Kennedy S, Buhman KK, Luo J, Gross RW, Davidson NO (2003) Decreased hepatic triglyceride accumulation and altered fatty acid uptake in mice with deletion of the liver fatty acid binding protein gene. J Biol Chem 278:51664–51672
30. Atshaves BP, McIntosh AL, Lyuksyutova OI, Zipfel WR, Webb WW, Schroeder F (2004) Liver fatty acid binding protein gene ablation inhibits branched-chain fatty acid metabolism in cultured primary hepatocytes. J Biol Chem 279:30954–30965
31. Atshaves BP, McIntosh AL, Payne HR, Mackie J, Kier AB, Schroeder F (2005) Effect of branched-chain fatty acid on lipid dynamics in mice lacking liver fatty acid binding protein gene. Am J Physiol 288:C543–C558
32. Thigpen JE, Setchell KD, Goelz MF, Forsythe DB (1999) The phyto estrogen content of rodent diets. Envron Health Persp 107:A182–A183
33. Atshaves BP, McIntosh AL, Martin GG, Landrock D, Payne HR, Bhuvanendran S, Landrock K, Lyuksyutova OI, Johnson JD, Macfarlane RD, Kier AB, Schroeder F (2009) Overexpression of sterol carrier protein-2 differentially alters hepatic cholesterol accumulation in cholesterol-fed mice. J Lipid Res 50:1429–1447
34. Atshaves BP, Payne HR, McIntosh AL, Tichy SE, Russell D, Kier AB, Schroeder F (2004) Sexually dimorphic metabolism of branched chain lipids in C57BL/6J mice. J Lipid Res 45:812–830
35. Livak KJ, Schmittgen TD (2001) Analysis of relative gene expression data using real-time quantitative PCR and the $2^{-\Delta\Delta CT}$ method. Methods 25:402–408
36. Powell GL, Tippett PS, Kiorpes TC, McMillin-Wood J, Coll KE, Schultz H, Tanaka K, Kang ES, Shrago E (1985) Fatty acyl CoA as an effector molecule in metabolism. Fed Proc 44:81–84
37. Gossett RE, Frolov AA, Roths JB, Behnke WD, Kier AB, Schroeder F (1996) Acyl CoA binding proteins: multiplicity and function. Lipids 31:895–918
38. Faergeman NJ, Knudsen J (1997) Role of long-chain fatty acyl-CoA esters in the regulation of metabolism and in cell signalling. Biochem J 323:1–12
39. Huang H, Starodub O, McIntosh A, Kier AB, Schroeder F (2002) Liver fatty acid binding protein targets fatty acids to the nucleus: real-time confocal and multiphoton fluorescence imaging in living cells. J Biol Chem 277:29139–29151
40. Huang H, Starodub O, McIntosh A, Atshaves BP, Woldegiorgis G, Kier AB, Schroeder F (2004) Liver fatty acid binding protein

colocalizes with peroxisome proliferator receptor alpha and enhances ligand distribution to nuclei of living cells. Biochemistry 43:2484–2500
41. Wang Y, Botolin D, Xu J, Christian B, Mitchell E, Jayaprakasam B, Nair M, Peters JM, Busik J, Olson LK, Jump DB (2006) Regulation of fatty acid elongase and desaturase expression in diabetes and obesity. J Lipid Res 47:2028–2041
42. Martin GG, Atshaves BP, McIntosh AL, Mackie JT, Kier AB, Schroeder F (2005) Liver fatty acid binding protein (L-FABP) gene ablation alters liver bile acid metabolism in male mice. Biochem J 391:549–560
43. Martin GG, Atshaves BP, McIntosh AL, Mackie JT, Kier AB, Schroeder F (2006) Liver fatty acid binding protein (L-FABP) gene ablation potentiates hepatic cholesterol accumulation in cholesterol-fed female mice. Am J Physiol 290:G36–G48
44. Martin GG, Atshaves BP, McIntosh AL, Mackie JT, Kier AB, Schroeder F (2008) Liver fatty acid binding protein gene ablated female mice exhibit increased age dependent obesity. J Nutr 138:1859–1865
45. Martin GG, Atshaves BP, McIntosh AL, Mackie JT, Kier AB, Schroeder F (2009) Liver fatty acid binding protein gene ablation enhances age-dependent weight gain in male mice. Mol Cell Biochem 324:101–115
46. Newberry EP, Kennedy SM, Xie Y, Sternard BT, Luo J, Davidson NO (2008) Diet-induced obesity and hepatic steatosis in L-FABP-/- mice is abrogated with SF, but not PUFA, feeding and attenuated after cholesterol supplementation. Am J Physiol Gastrointest Liver Physiol 294:G307–G314
47. Newberry EP, Xie Y, Kennedy SM, Luo J, Davidson NO (2006) Protection against western diet-induced obesity and hepatic steatosis in liver fatty acid binding protein knockout mice. Hepatology 44:1191–1205
48. Pignon J-P, Bailey NC, Baraona E, Lieber CS (1987) Fatty acid-binding protein: a major contributor to the ethanol-induced increase in liver cytosolic proteins in the rat. Hepatology 7:865–871
49. Mackie JT, Atshaves BP, Payne HR, McIntosh AL, Schroeder F, Kier AB (2009) Phytol-induced hepatotoxicity in mice. Toxicol Pathol 37:201–208
50. Schroeder F, Petrescu AD, Huang H, Atshaves BP, McIntosh AL, Martin GG, Hostetler HA, Vespa A, Landrock K, Landrock D, Payne HR, Kier AB (2008) Role of fatty acid binding proteins and long chain fatty acids in modulating nuclear receptors and gene transcription. Lipids 43:1–17
51. McIntosh AL, Atshaves BP, Hostetler HA, Huang H, Davis J, Lyuksyutova OI, Landrock D, Kier AB, Schroeder F (2009) Liver type fatty acid binding protein (L-FABP) gene ablation reduces nuclear ligand distribution and peroxisome proliferator activated receptor-alpha activity in cultured primary hepatocytes. Arch Biochem Biophys 485:160–173
52. Djouadi F, Weinheimer CJ, Saffitz JE, Pitchford C, Bastin J, Gonzalez FJ (1998) A gender-related defect in lipid metabolism and glucose homeostasis in PPARalpha deficient mice. J Clin Inv 102:1083–1091
53. Rosenberger TA, Hovda JT, Peters JM (2002) Targeted disruption of peroxisome proliferator activated receptor beta (delta) results in distinct gender differences in mouse brain phospholipid and esterified fatty acid levels. Lipids 37:495–500
54. Martin GG, Atshaves BP, Huang H, McIntosh AL, Williams BW, Russell DH, Kier AB and Schroeder F (2009) Hepatic phenotype of liver fatty acid binding protein (L-FABP) gene ablated mice. Am J Physiol (submitted)
55. Hostetler HA, Petrescu AD, Kier AB, Schroeder F (2005) Peroxisome proliferator activated receptor alpha (PPARalpha) interacts with high affinity and is conformationally responsive to endogenous ligands. J Biol Chem 280:18667–18682
56. Hostetler HA, Kier AB, Schroeder F (2006) Very-long-chain and branched-chain fatty acyl CoAs are high affinity ligands for the peroxisome proliferator-activated receptor alpha (PPARalpha). Biochemistry 45:7669–7681
57. Tallman DL, Noto AD, Taylor CG (2009) Low and high fat diets inconsistently induce obesity in C57BL/6J mice and obesity compromises n-3 fatty acid status. Lipids 44:577–580
58. Koza RA, Nikonova L, Hogan J, Rim JS, Mendoza T, Faulk C, Skaf J, Kozak LP (2006) Changes in gene expression foreshadow diet-induced obesity in genetically identical mice. PLoS Genet 2:e81
59. Burcelin R, Crivelli V, Dacosta A, Roy-Tirelli A, Thorens B (2002) Heterogeneous metabolic adaptation of C57BL/6J mice to high fat diet. Am J Physiol Endocrinol Metab 282:E834–E842
60. Bogdanov AM, Mishin AS, Yampolsky IV, Belousov VV, Chudakov DM, Subach FV, Verkhusha VV, Lukyanov S, Lukyonov KA (2009) Green fluorescent proteins are light-induced electron donors. Nat Chem Biol 5:459–461. doi:10.1038/nchembio.174
61. Luxon BA, Weisiger RA (1993) Sex differences in intracellular fatty acid transport: role of cytoplasmic binding proteins. Am J Physiol 265:G831–G841
62. Weisiger RA (2005) Cytosolic fatty acid binding proteins catalyze two distinct steps in intracellular transport of their ligands. Mol Cell Biochem 239:35–42
63. Hotamisligl GS, Johnson RS, Distel RJ, Ellis RF, Papaioannou VE, Spiegelman BM (1996) Uncoupling of obesity from insulin resistance through a targeted mutation in aP2, the adipocyte fatty acid binding protein. Science 274:1377–1379
64. Vassileva G, Huwyler L, Poirer K, Agellon LB, Toth MJ (2000) The intestinal fatty acid binding protein is not essential for dietary fat absorption in mice. FASEB J 14:2040–2046

Lipids (2010) 45:111–128
DOI 10.1007/s11745-009-3377-4

ORIGINAL ARTICLE

Rapid Development of Fasting-Induced Hepatic Lipidosis in the American Mink (*Neovison vison*): Effects of Food Deprivation and Re-Alimentation on Body Fat Depots, Tissue Fatty Acid Profiles, Hematology and Endocrinology

Kirsti Rouvinen-Watt · Anne-Mari Mustonen · Rebecca Conway · Catherine Pal · Lora Harris · Seppo Saarela · Ursula Strandberg · Petteri Nieminen

Received: 30 September 2009 / Accepted: 24 November 2009 / Published online: 18 December 2009

Abstract Hepatic lipidosis is a common pathological finding in the American mink (*Neovison vison*) and can be caused by nutritional imbalance due to obesity or rapid body weight loss. The objectives of the present study were to investigate the timeline and characterize the development of hepatic lipidosis in mink in response to 0–7 days of food deprivation and liver recovery after 28 days of re-feeding. We report here the effects on hematological and endocrine variables, body fat mobilization, the development of hepatic lipidosis and the alterations in the liver lipid classes and tissue fatty acid (FA) sums. Food deprivation resulted in the rapid mobilization of body fat, most notably visceral, causing elevated hepatosomatic index and increased liver triacylglycerol content. The increased absolute amounts of liver total phospholipids and phosphatidylcholine suggested endoplasmic reticulum stress. The hepatic lipid infiltration and the altered liver lipid profiles were associated with a significantly reduced proportion of n-3 polyunsaturated FA (PUFA) in the livers and the decrease was more evident in the females. Likewise, re-feeding of the female mink resulted in a more pronounced recovery of the liver n-3 PUFA. The rapid decrease in the n-3/n-6 PUFA ratio in response to food deprivation could trigger an inflammatory response in the liver. This could be a key contributor to the pathophysiology of fatty liver disease in mink influencing disease progression.

Keywords Adipose tissue · Fatty liver disease · Hepatic lipidosis · Liver steatosis · NAFLD · n-3 PUFA · n-6 PUFA

K. Rouvinen-Watt (✉) · R. Conway · C. Pal · L. Harris
Department of Plant and Animal Sciences,
Nova Scotia Agricultural College, P.O. Box 550,
Truro, NS B2N 5E3, Canada
e-mail: krouvinen@nsac.ca

A.-M. Mustonen · U. Strandberg · P. Nieminen
Faculty of Biosciences, University of Joensuu,
P.O. Box 111, 80101 Joensuu, Finland

S. Saarela
Department of Biology, University of Oulu,
P.O. Box 3000, 90014 Oulu, Finland

P. Nieminen
Department of Anatomy and Cell Biology,
Faculty of Medicine, Institute of Biomedicine,
University of Oulu, P.O. Box 5000, 90014 Oulu, Finland

P. Nieminen
Department of Biomedicine, Institute of Anatomy,
University of Kuopio, P.O. Box 1627, 70211 Kuopio, Finland

Abbreviations

ADR	Adrenal
ALT	Alanine aminotransferase
BMI	Body mass index
BW	Body weight
CE	Cholesteryl esters
CerPCho	Sphingomyelin
CHOL	Cholesterol
DG	Diacylglycerols
ER	Endoplasmic reticulum
FA	Fatty acid
FFA	Free fatty acids
HOMA	Homeostasis model assessment
HSI	Hepatosomatic index
MUFA	Monounsaturated fatty acids
NAFLD	Non-alcoholic fatty liver disease
P	Plasma

PL	Phospholipids
PtdCho	Phosphatidylcholine
PUFA	Polyunsaturated fatty acids
RF	Re-fed
SFA	Saturated fatty acids
T_3	Triiodothyronine
T_4	Thyroxine
TAG	Triacylglycerol
UFA	Unsaturated fatty acids
UPR	Unfolded protein response
VLDL	Very-low-density lipoprotein

Introduction

Fatty liver or hepatic lipidosis is a common pathological finding in carnivores such as the American mink (*Neovison vison*), where fat accumulation in the liver often occurs due to metabolic or nutritional causes [1]. Fatty liver is also frequently found in mink dams diagnosed with nursing sickness [2], which is often fatal and only diagnosed post-mortem [3]. In mink, the hepatic lipid infiltration may be caused by several factors, including amino acid or fatty acid (FA) imbalances, excess dietary carbohydrate intake, choline and vitamin B deficiency, poor feed quality, obesity, restricted feeding or food deprivation [1, 4–6]. The body weight (BW) of the mink fluctuates greatly over the production cycle due to seasonal changes in the plane of nutrition [7] as well as hormonal status [8]. However, food deprivation aggravates these normal metabolic responses resulting in the rapid mobilization of body fat and lipid infiltration in the liver [5, 6]. During the production cycle, the risk of development of fatty liver may be elevated due to excessive fattening during the fall, rapid slimming prior to breeding, stress during pregnancy and mid-late lactation and rapid mobilization of body fat reserves for milk production [1, 7].

In humans, hepatic steatosis (lipidosis) is a common finding in (visceral) obesity and type 2 diabetes and it is considered to be the hepatic manifestation of the metabolic syndrome with strong evidence of an unfavorable n-3/n-6 polyunsaturated FA (PUFA) ratio [9, 10]. The FA manifestations and liver histology of mink nursing sickness and the associated fatty liver syndrome show evident similarity to type 2 diabetes [11] and the non-alcoholic fatty liver disease (NAFLD) of humans [10]. It has recently been shown in members of the *Mustelidae* family (e.g. mink, European polecat *Mustela putorius*) that during rapid BW loss the intra-abdominal body fat depots are more efficiently hydrolyzed in relation to adipose tissue mass than subcutaneous fat [6, 12, 13] with the preferential mobilization of n-3 PUFA leading to a potentially unfavorable n-3/n-6 PUFA ratio [14, 15]. The depletion of n-3 PUFA has been proposed to favor FA and triacylglycerol (TAG) synthesis over hydrolysis and FA oxidation, and may impair lipid export from the liver by suppressing very-low-density lipoprotein (VLDL) secretion [9]. The most consistent endocrine responses associated with food deprivation in mustelids include decreased concentrations of plasma leptin, insulin and triiodothyronine (T_3) [12, 16], while hematological changes suggesting immunosuppression have been reported [6, 17]. The human NAFLD presents significant similarities in phenotype to the fasting-induced fatty liver in mustelids [15], despite the different principal correlates, i.e. obesity versus rapid BW loss. Therefore, the mink may serve as a useful animal model to study the biochemical manifestations of human liver steatosis with potential applications to NAFLD.

Previously, the precise time scale of the biochemical manifestations in the development of fasting-induced hepatic lipidosis has not been described in mustelids. It can be hypothesized that the manifestations of lipidosis would appear at specific points of time during fasting and that the induced fatty liver would be reversible after a recovery period. The objectives of the present study were to investigate the development and characterize the fatty liver syndrome in mink in response to 0–7 days of food deprivation and liver recovery with the normal feeding regime resumed for 4 weeks. This study reports the effects on the mobilization of body fat depots, the development of hepatic lipidosis and the subsequent alterations in the liver lipid classes and tissue and plasma FA profiles as well as in the hematological and endocrine variables.

Experimental Procedures

The time scale of the development of hepatic lipidosis in the mink was studied by exposing 60 standard black mink (5 males, 5 females per group, age 9 months) to 0, 1, 3, 5, or 7 days of fasting. In addition, one group was fasted for 7 days followed by a normal feeding regime for 4 weeks [re-fed (RF)]. The fasting experiment was carried out from 10 January through 16 January and re-feeding from 16 January until 13 February 2007. The animals were weighed prior to the study and at the end of each experimental procedure. The RF group was also weighed prior to re-feeding at the end of the fasting period. The experiment was carried out at the Canadian Centre for Fur Animal Research, Nova Scotia Agricultural College, in Truro, Nova Scotia, Canada (45.37°N, 63.27°W). The mink were housed individually in standard-sized cages, provided with a nest box and adequate bedding. The experimental protocols were approved by the Animal Care and Use Committee of the

Nova Scotia Agricultural College and carried out in accordance with the guidelines of the Canadian Council on Animal Care [18]. During the fasting regimes the mink were isolated from the rest of the herd and therefore not subjected to the normal daily feeding routines in order to alleviate potential stress due to food deprivation. Post-approval monitoring during the experiment included twice daily general health checks and a veterinary inspection by two licensed veterinarians of all mink on the morning of the designated days of the fasting regimes. No morbidity or mortality occurred during the course of the experiment. However, based on veterinary consultation, two female mink were sampled on day 6 of fasting due to their rapidly declining BW during the unexpectedly cold weather. Also, for the remaining females in the RF group the normal feeding routine was resumed on day 6 of fasting. The post-fast diet was the same as was fed to all experimental mink before the start of the experiment and contained 32.31% dry matter, 3.34% ash, 13.54% protein, 6.73% lipid and 8.70% carbohydrate of fresh weight, and 5.65 MJ metabolizable energy kg^{-1}. The FA composition (mol%, mean ± SD, $n = 6$) of the lipid fraction was as follows: saturated FA (SFA) 30.85 ± 0.96; monounsaturated FA (MUFA) 49.75 ± 0.94; n-6 PUFA 14.11 ± 0.70; n-3 PUFA 4.91 ± 0.40. The diet was stored frozen in −20 °C and thawed in the refrigerator prior to feeding.

The control group (0 day) was fasted for 12 h prior to euthanasia. To accomplish this, the feeding and feed removal were staggered for mink in this test group according to their planned sampling schedule. At the end of the fasting periods, the animals were anaesthetized with a combination of xylazine (Rompun 3.4 mg kg BW^{-1}) and ketamine hydrochloride (Ketalean 8.5 mg kg BW^{-1}) given as intramuscular injections. The mink were sampled for blood using cardiac punctures (Vacutainer EDTA tubes) and euthanized with an intracardiac injection of pentobarbital sodium (Euthanyl 105.6 mg kg BW^{-1}). Immediately following euthanasia, samples were obtained from various internal organs and tissues. The intermuscular fat sample was obtained from the region of the gluteal muscle and the skeletal muscle tissue from the gastrocnemius muscle. The excised tissues were placed in cryovials and plastic bags and snap-frozen in liquid nitrogen. The samples were kept on dry ice until transferred to long-term storage at −80 °C. The organ and fat depot masses were determined using quantitative dissection. The body mass indices (BMI) indicating adiposity of mustelids [6] were calculated with the formula: BMI = BW (kg) [body $length^3$ (m)]$^{-1}$ and the hepatosomatic indices (HSI) as liver weight in percent of final BW.

The whole blood was analyzed for hematological parameters (SCIL Vet abc Animal Blood Counter; Vet Novations Canada Inc., ON, Canada) by the diagnostic services laboratory of Fundy Veterinarians (Murray Siding, NS, Canada). The plasma glucose, total cholesterol, creatinine, TAG, total protein, urea and total bilirubin concentrations and creatine kinase and alanine aminotransferase (ALT) activities were determined as previously outlined in Mustonen et al. [6, 19]. The glucagon, ghrelin and total T_3 analyses were determined as described in Mustonen et al. [12] and the rest of the endocrinological assays and catecholamines as in Mustonen et al. [16]. The instrument used was a Wizard 1480 Gamma Counter by Wallac (Turku, Finland). The homeostasis model assessment (HOMA) index, as a measure of insulin resistance applied also previously to mustelids [12], was calculated based on the fasting plasma insulin and glucose concentrations [20]; where HOMA = fasting insulin ($\mu U\ mL^{-1}$) × fasting glucose (mmol L^{-1})/22.5.

The liver lipids were extracted according to Folch et al. [21]. The liver lipid classes were analyzed with thin layer chromatography (TLC–FID, Iatroscan new Mark V, Iatron Laboratories Inc., Tokyo, Japan [22]), and the tissue FA composition using gas chromatography mass spectrometry (GC–FID and GC–MS, 6890N network GC-system, Agilent Technologies Inc., Palo Alto, CA, USA). For a more detailed description of FA analyses, see Nieminen et al. [14, 23].

Statistical Analysis

The experimental design used was 2 × 6 factorial with two sexes and six treatment groups. The data were analyzed using the General Linear Models procedure in SAS® v.9.1 (SAS Institute Inc., Cary, NC, USA) to examine the effects of the sex and the fasting regimes and their interaction on the measured variables. A multiple means comparison test (PDiff) was used to identify where differences existed when these effects were found significant. Statistical significance was set at $P < 0.05$. The results are presented as lsmeans ± standard error of the mean (SEM).

Results

BW Loss, Liver Lipid Content and Body Fat Mobilization

In comparison to the non-fasted control, both males and females had significantly lower final BW during 5–7 days of fasting, whereas the 1- to 3-day groups did not differ from the control (0 day; Table 1). Also, the final BW of the RF group were not different during the preceding fast from the mink fasted for 7 days. During the 4-week re-feeding period, the mink recovered some of their BW; at the end of the experiment the RF males weighed 2396.8 ± 130.8 g and the RF females 1148.8 ± 146.2 g. The females

Table 1 Body weight (BW), body length, body mass index (BMI), liver weight, and the weights of the body fat depots in male and female mink in response to fasting for 0 (control), 1, 3, 5, and 7 days, and re-feeding (RF) for 28 days after a 7-day fast

Variable	Fasting regime						*P* value		
Sex	0 day	1 day	3 days	5 days	7 days	RF	Fasting	Sex	F × S
$BW_{initial}$ (g)							0.995	<0.001	1.000
Males	2753.6 ± 112.5	2789.2 ± 112.5	2761.6 ± 112.5	2732.0 ± 112.5	2776.2 ± 112.5	2766.8 ± 112.5			
Females	1293.0 ± 112.5	1368.0 ± 112.5	1345.8 ± 112.5	1303.4 ± 112.5	1326.2 ± 102.7	1345.8 ± 125.8			
BW_{final} (g)							0.003	<0.001	0.860
All mink	1990.4^{a} ± 78.6	2006.0^{a} ± 78.6	1848.3^{abc} ± 78.6	1723.0^{bc} ± 78.6	1659.2^{c} ± 75.3	1650.9^{cf} ± 83.4			
Males	2724.0 ± 111.2	2708.0 ± 111.2	2527.4 ± 111.2	2379.2 ± 111.2	2270.8 ± 111.2	2265.0^{f} ± 111.2			
Females	1256.8 ± 111.2	1304.0 ± 111.2	1169.2 ± 111.2	1066.8 ± 111.2	1047.7 ± 101.5	1036.8^{f} ± 124.3			
ΔBW (g)							<0.001	<0.001	<0.001
Males	-29.6^{e} ± 15.7	-81.2^{d} ± 15.7	-234.2^{c} ± 15.7	-352.8^{b} ± 15.7	-505.4^{a} ± 15.7	-501.8^{af} ± 15.7			
Females	-36.2^{d} ± 15.7	-64.0^{d} ± 15.7	-176.6^{c} ± 15.7	-236.6^{b} ± 15.7	-278.5^{a} ± 14.3	-309.0^{af} ± 17.5			
ΔBW (%)							<0.001	<0.001	0.307
All mink	-1.94^{d} ± 0.71	-3.85^{d} ± 0.71	-11.00^{c} ± 0.71	-15.70^{b} ± 0.71	-19.67^{a} ± 0.68	-20.71^{af} ± 0.75			
Males	−1.06 ± 1.01	−2.94 ± 1.01	−8.66 ± 1.01	−12.99 ± 1.01	−18.23 ± 1.01	-18.40^{f} ± 1.01			
Females	−2.82 ± 1.01	−4.76 ± 1.01	−13.35 ± 1.01	−18.42 ± 1.01	−21.12 ± 0.92	-23.02^{f} ± 1.13			
Body length (cm)							0.338	<0.001	0.839
Males	47.3 ± 0.8	48.9 ± 0.8	49.0 ± 0.8	48.5 ± 0.8	47.5 ± 0.8	47.1 ± 0.8			
Females	39.3 ± 0.8	39.9 ± 0.8	40.1 ± 0.8	38.8 ± 0.8	39.8 ± 0.7	38.8 ± 0.9			
ΔBMI [kg $(m^3)^{-1}$]							<0.001	0.004	0.007
Males	-0.24^{d} ± 0.18	-0.70^{d} ± 0.18	-2.00^{c} ± 0.18	-3.08^{b} ± 0.18	-4.73^{a} ± 0.18	-3.56^{bf} ± 0.18			
Females	-0.60^{d} ± 0.18	-1.00^{d} ± 0.18	-2.72^{c} ± 0.18	-4.04^{a} ± 0.18	-4.45^{a} ± 0.16	-3.37^{bf} ± 0.20			
Liver (g)							0.043	<0.001	0.560
All mink	44.99^{c} ± 2.22	46.40^{bc} ± 2.22	46.07^{c} ± 2.22	52.63^{ab} ± 2.22	53.04^{a} ± 2.13	48.90^{abc} ± 2.36			
Males	57.99 ± 3.14	61.36 ± 3.14	63.00 ± 3.14	71.52 ± 3.14	69.51 ± 3.14	65.07 ± 3.14			
Females	32.00 ± 3.14	31.43 ± 3.14	29.15 ± 3.14	33.73 ± 3.14	36.58 ± 2.87	32.72 ± 3.51			
Subcutaneous fat (g)							0.017	<0.001	0.859
All mink	430^{ab} ± 34	522^{a} ± 34	459^{ab} ± 34	379^{b} ± 34	370^{b} ± 33	380^{b} ± 36			
Males	631 ± 48	733 ± 48	662 ± 48	549 ± 48	532 ± 48	553 ± 48			
Females	229 ± 48	310 ± 48	256 ± 48	209 ± 48	209 ± 44	207 ± 54			
Intra-abdominal fat[g] (g)							<0.001	<0.001	0.947
All mink	175.2^{a} ± 12.9	178.1^{a} ± 12.9	152.6^{ab} ± 12.9	109.3^{c} ± 12.9	107.9^{c} ± 12.4	116.1^{bc} ± 13.7			
Males	232.0 ± 18.3	233.4 ± 18.3	198.9 ± 18.3	133.6 ± 18.3	144.6 ± 18.3	154.9 ± 18.3			
Females	118.4 ± 18.3	122.7 ± 18.3	106.2 ± 18.3	85.0 ± 18.3	71.2 ± 16.7	77.4 ± 20.4			

Table 1 continued

Variable	Fasting regime						*P* value		
Sex	0 day	1 day	3 days	5 days	7 days	RF	Fasting	Sex	F × S
Intermuscular fat (g)							0.187	<0.001	0.617
Males	107.3 ± 10.7	86.6 ± 10.7	95.4 ± 10.7	72.0 ± 10.7	77.2 ± 10.7	72.5 ± 10.7			
Females	44.8 ± 10.7	45.4 ± 10.7	36.2 ± 10.7	43.6 ± 10.7	26.9 ± 9.7	31.2 ± 11.9			
Subcutaneous fat (% BW)							0.016	<0.001	0.992
All mink	20.7^{b} ± 1.1	25.3^{a} ± 1.1	23.6^{ab} ± 1.1	21.1^{b} ± 1.1	21.6^{b} ± 1.0	20.4^{b} ± 1.1			
Males	23.0 ± 1.5	26.9 ± 1.5	25.9 ± 1.5	23.1 ± 1.5	23.5 ± 1.5	22.9 ± 1.5			
Females	18.3 ± 1.5	23.7 ± 1.5	21.3 ± 1.5	19.0 ± 1.5	19.7 ± 1.4	17.9 ± 1.7			
Intra-abdominal fat[g] (% BW)							<0.001	0.038	0.795
All mink	8.9^{a} ± 0.5	9.0^{a} ± 0.5	8.4^{a} ± 0.5	6.7^{b} ± 0.5	6.5^{b} ± 0.5	6.6^{b} ± 0.6			
Males	8.5 ± 0.8	8.6 ± 0.8	7.9 ± 0.8	5.6 ± 0.8	6.3 ± 0.8	6.5 ± 0.8			
Females	9.4 ± 0.8	9.5 ± 0.8	9.0 ± 0.8	7.8 ± 0.8	6.7 ± 0.7	6.7 ± 0.9			
Intermuscular fat (% BW)							0.586	0.379	0.536
Males	3.9 ± 0.5	3.2 ± 0.5	3.9 ± 0.5	3.0 ± 0.5	3.4 ± 0.5	3.1 ± 0.5			
Females	3.5 ± 0.5	3.4 ± 0.5	2.9 ± 0.5	3.9 ± 0.5	2.5 ± 0.5	2.7 ± 0.6			

Presented are lsmeans ± SEM

[a–e] Fasting regimes differ within row ($P < 0.05$)

[f] For RF group calculated after the 7-day fast. All other values of RF group measured after the re-feeding period

[g] Calculated as the sum of mesenteric, omental, diaphragmatic and perirenal fats

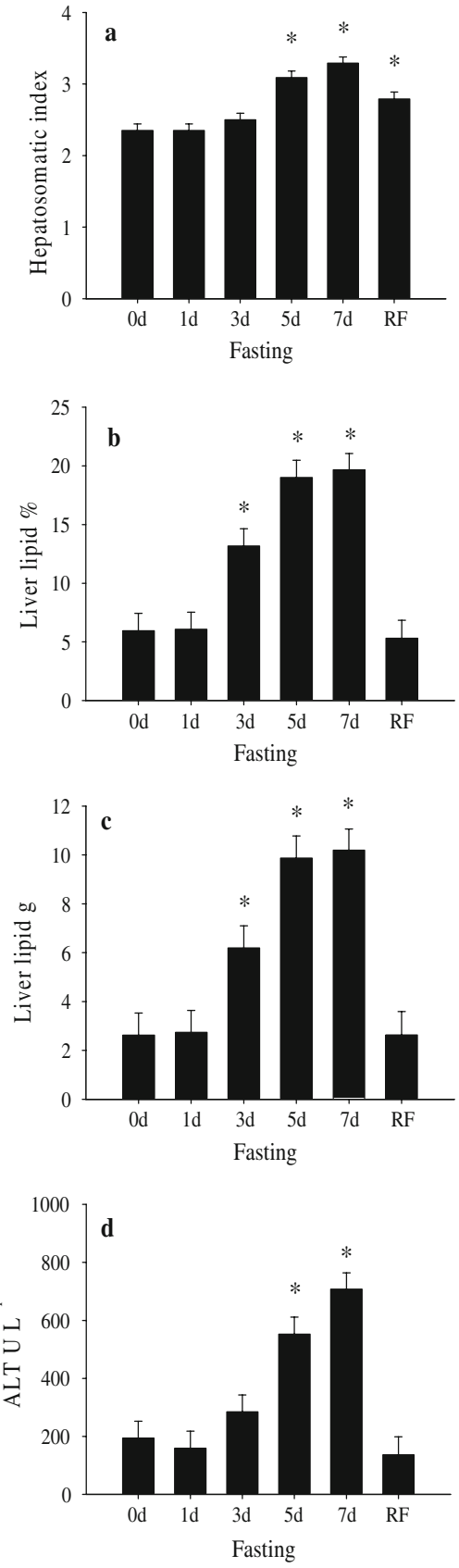

Fig. 1 Changes in the **a** hepatosomatic index, **b** liver lipid %, **c** liver lipid mass (g), and **d** plasma alanine aminotransferase (*ALT*) activity (U L^{-1}) in mink in response to fasting for 0 (control), 1, 3, 5, and 7 days, and re-feeding (*RF*) for 28 days after a 7-day fast. Reported are lsmeans + SEM, both sexes combined. *Asterisk* differs from control ($P < 0.05$). Total $n = 60$. *P* values: **a** fasting <0.001, sex 0.003, F × S 0.471; **b** fasting <0.001, sex 0.384, F × S 0.630; **c** fasting <0.001, sex <0.001, F × S 0.490; and **d** fasting <0.001, sex 0.038, F × S 0.028

showed a more pronounced loss in % BW and BMI. Overall, the HSI was elevated in comparison to the control in the 5-, 7-day and RF groups, whereas the 0- to 3-day groups did not differ (Fig. 1). The females exhibited significantly higher HSI values than the males (2.84 vs. 2.62%, SEM = 0.05). Food deprivation of 3–7 days increased the liver lipid percentage and liver lipid mass (g) in comparison to the control animals in both male and female mink. The liver lipid percentages for the 0-, 1-, 3-, 5-, 7-day, and RF groups were on average 5.9 ± 1.5, 6.1 ± 1.5, 13.2 ± 1.5, 19.0 ± 1.5, 19.7 ± 1.4, and 5.3 ± 1.6%, respectively. The test groups had the following absolute amounts of total liver lipids: 0 day, 2.6 ± 0.9 g; 1 day, 2.7 ± 0.9 g; 3 days, 6.2 ± 0.9 g; 5 days, 9.9 ± 0.9 g; 7 days, 10.2 ± 0.9 g; and RF, 2.6 ± 1.0 g; the males had higher absolute amounts (7.4 ± 0.5 g) than the females (4.1 ± 0.5 g).

In response to food deprivation, the following internal organs reduced in absolute mass: pancreas, small intestine, kidneys, testes and the female reproductive organs, whereas no change was observed in the masses of the spleen, stomach, heart, and the thyroid and adrenal glands (data not shown). The absolute and relative weights of the total intra-abdominal body fat depots declined significantly in response to food deprivation, however, they did not attain the levels of the non-fasted control animals after the re-feeding period (Table 1). Notably, the relative (% BW) combined weight of the omental and mesenteric adipose depots declined in response to the fasting regimes as follows: 0 day, 7.4 ± 0.5%; 1 day, 7.2 ± 0.5%; 3 days, 6.8 ± 0.5%; 5 days, 5.4 ± 0.5%; and 7 days, 5.0 ± 0.4%; while these two visceral fat depots did not recover once normal feeding was resumed (RF, 5.0 ± 0.5%; $P < 0.001$). The females had less subcutaneous fat in absolute and relative mass, however, the relative mass of the total intra-abdominal adipose depots was higher in the female mink in comparison to the males (8.2 ± 0.3% vs. 7.2 ± 0.3%). Overall, the male mink had an average estimated body fat content (% BW) of 34.8% and the females 31.3% (SEM = 0.86; $P < 0.005$). The body fat content ranged between 33.3 and 37.6 ± 1.5% during 0–3 days of fasting, declined to 31.1–31.2 ± 1.4% during 5–7 days, and was 29.9 ± 1.6% after re-alimentation ($P < 0.006$).

Liver Lipid Classes

The majority of liver lipids were in the form of TAG, the relative amount of which increased during 1–7 days of fasting (Fig. 2). The absolute quantities of TAG within the livers in the non-fasted control (0 day) and 1 day fasted mink were on average 1.2–1.5 g, while the total liver TAG contents were 3.9 g at 3 days and 6.7–6.9 g at 5–7 days, and declined to 0.8 g upon re-feeding. On the contrary, the relative amounts of phosphatidylcholine (PtdCho) and total phospholipids (PL) were lower within 3–7 days of fasting. However, when taking into account the liver mass and lipid content, the absolute quantities of total PL were the lowest during 0–1 days (0.93–1.03 g), and elevated within 3 days of fasting (3 days, 1.58 g; 5 days, 2.12 g; 7 days, 2.57 g), while at the end of the 4-week re-feeding period 1.27 g of total PL was present in the liver (SEM = 0.20, $P < 0.001$). The total quantities of PtdCho were the lowest during 0–3 days (0.85–0.99 g), elevated during 5–7 days of food deprivation (5 days, 1.76 g; 7 days, 2.09 g), and returned to pre-fasting levels after re-feeding (0.92 g; SEM = 0.20; $P < 0.001$). Lower relative percentages were also observed in free FA (FFA), diacylglycerols and cholesterol during fasting. In response to re-alimentation, significantly higher percentages of cholesteryl esters, diacylglycerols, cholesterol, sphingomyelin, and total PL were present in the liver lipids in comparison to the control animals. Concomitantly, the RF mink exhibited a significantly lower fraction of TAG in the total liver lipids.

Hematology, Clinical Chemistry and Endocrinology

Overall, the red blood cell count showed lower levels after the re-feeding period (Table 2). This differed from all other treatments except 0 day. The males had on average higher red blood cell counts than the females (9.2 ± 0.1 vs. 8.7 ± 0.1 10^{12} L^{-1}). The hemoglobin concentrations were elevated on day 5 of food deprivation and the males showed higher hemoglobin levels than the females (18.7 ± 0.2 vs. 17.8 ± 0.2 g dL^{-1}) throughout the study. The mean corpuscular hemoglobin concentration increased in both sexes during fasting returning to day 0–1 levels after re-alimentation while the red cell distribution width declined and the mean platelet volume showed minor changes during the fasting regimes. A significant response to food deprivation was observed in the white blood cells, where the lymphocyte percentage declined significantly over the duration of 7 days of fasting with recovery to pre-fasting levels during the re-feeding period, and the granulocyte percentage showed an overall increase during the

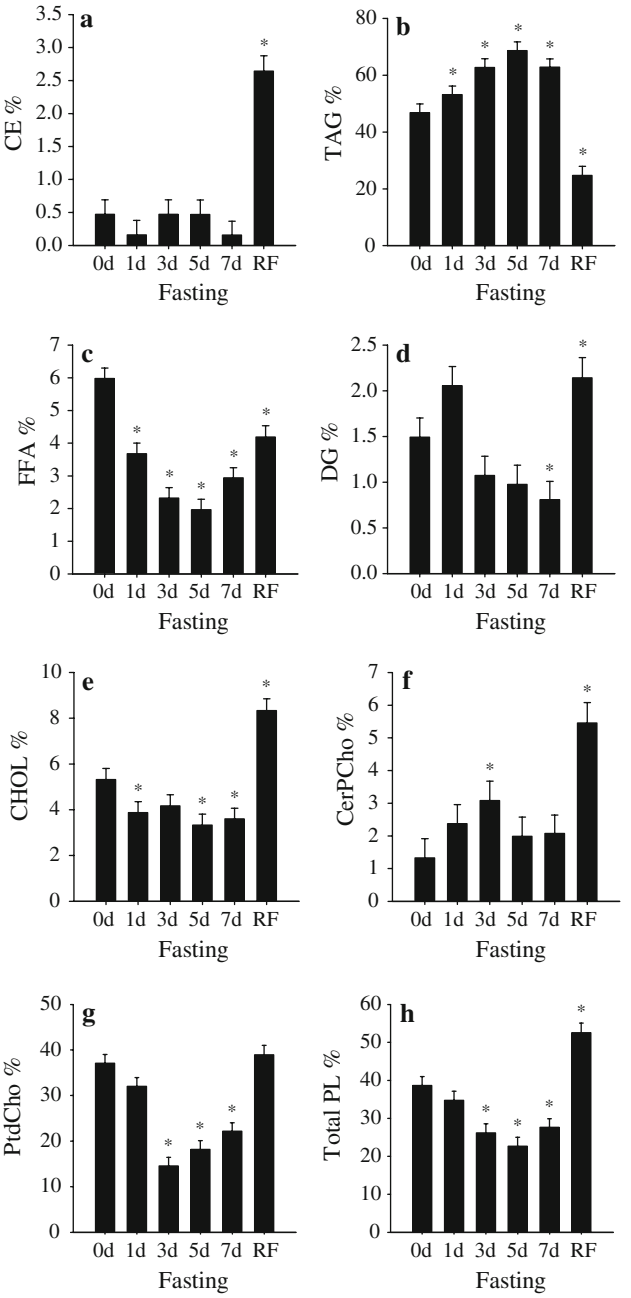

Fig. 2 Alterations in the proportions (%, lsmeans + SEM, both sexes combined) of mink liver lipid classes **a** cholesteryl esters (*CE*) **b** triacylglycerols (*TAG*) **c** free fatty acids (*FFA*) **d** diacylglycerols (*DG*) **e** cholesterol (*CHOL*) **f** sphingomyelin (*CerPCho*) **g** phosphatidylcholine (*PtdCho*) and **h** phospholipids (*PL*) in response to fasting for 0 (control), 1, 3, 5, and 7 days, and re-feeding (*RF*) for 28 days after a 7-day fast. *Asterisk* differs from control ($P < 0.05$). Total $n = 60$. *P* values: **a** fasting <0.001, sex 0.600, F × S 0.988; **b** fasting <0.001, sex 0.235, F × S 0.018; **c** fasting <0.001, sex 0.363, F × S 0.870; **d** fasting <0.001, sex 0.189, F × S 0.892; **e** fasting <0.001, sex 0.032, F × S 0.016; **f** fasting <0.001, sex 0.651, F × S 0.168; **g** fasting <0.001, sex 0.228, F × S <0.001; and **h** fasting <0.001, sex 0.249, F × S 0.015

Table 2 Hematological variables in male and female mink in response to fasting for 0 (control), 1, 3, 5, and 7 days, and re-feeding (RF) for 28 days after a 7-day fast

Variable	Fasting regime						*P* value		
Sex	0 day	1 day	3 days	5 days	7 days	RF	Fasting	Sex	F × S
White blood cells (10^9 L^{-1})							0.803	0.303	0.017
Males	$5.6^{abc} \pm 0.7$	$6.5^{a} \pm 0.7$	$6.4^{ab} \pm 0.7$	$4.3^{c} \pm 0.7$	$5.4^{abc} \pm 0.7$	$4.5^{bc} \pm 0.7$			
Females	$5.1^{b} \pm 0.7$	$6.3^{ab} \pm 0.7$	$4.8^{b} \pm 0.7$	$7.1^{a} \pm 0.7$	$5.6^{ab} \pm 0.6$	$6.3^{ab} \pm 0.8$			
Red blood cells (10^{12} L^{-1})							0.039	0.008	0.683
All mink	$8.8^{ab} \pm 0.2$	$9.2^{a} \pm 0.2$	$9.1^{a} \pm 0.2$	$9.3^{a} \pm 0.2$	$8.9^{a} \pm 0.2$	$8.3^{b} \pm 0.2$			
Males	9.2 ± 0.3	9.4 ± 0.3	9.3 ± 0.3	9.5 ± 0.3	9.4 ± 0.3	8.3 ± 0.3			
Females	8.4 ± 0.3	9.0 ± 0.3	8.9 ± 0.3	9.0 ± 0.3	8.4 ± 0.3	8.3 ± 0.3			
Hemoglobin (g dL^{-1})							0.004	0.003	0.677
All mink	$18.0^{bc} \pm 0.3$	$18.1^{bc} \pm 0.3$	$18.3^{b} \pm 0.3$	$19.4^{a} \pm 0.3$	$18.5^{ab} \pm 0.3$	$17.3^{c} \pm 0.4$			
Males	18.5 ± 0.5	18.5 ± 0.5	18.5 ± 0.5	19.7 ± 0.5	19.4 ± 0.5	17.5 ± 0.5			
Females	17.4 ± 0.5	17.7 ± 0.5	18.1 ± 0.5	19.0 ± 0.5	17.6 ± 0.4	17.1 ± 0.5			
Hematocrit (%)							0.120	0.007	0.713
Males	60.1 ± 1.6	61.4 ± 1.6	60.3 ± 1.6	62.8 ± 1.6	61.8 ± 1.6	57.8 ± 1.6			
Females	57.8 ± 1.6	59.7 ± 1.6	58.3 ± 1.6	60.6 ± 1.6	56.0 ± 1.4	56.6 ± 1.7			
Mean corpuscular volume (μm^3)							0.199	0.410	0.733
Males	65.6 ± 1.4	65.8 ± 1.4	65.4 ± 1.4	66.2 ± 1.4	65.4 ± 1.4	69.8 ± 1.4			
Females	68.8 ± 1.4	66.2 ± 1.4	65.4 ± 1.4	67.4 ± 1.4	66.3 ± 1.3	68.3 ± 1.6			
Mean corpuscular hemoglobin (pg)							0.152	0.645	0.911
Males	20.2 ± 0.5	19.9 ± 0.5	20.1 ± 0.5	20.8 ± 0.5	20.7 ± 0.5	21.1 ± 0.5			
Females	20.8 ± 0.5	19.7 ± 0.5	20.3 ± 0.5	21.1 ± 0.5	20.9 ± 0.4	20.7 ± 0.5			
Mean corpuscular hemoglobin concentration (g dL^{-1})							<0.001	0.333	0.212
All mink	$30.5^{c} \pm 0.1$	$30.0^{d} \pm 0.1$	$30.9^{b} \pm 0.1$	$31.4^{a} \pm 0.1$	$31.4^{a} \pm 0.1$	$30.2^{cd} \pm 0.1$			
Males	30.7 ± 0.2	30.2 ± 0.2	30.7 ± 0.2	31.4 ± 0.2	31.4 ± 0.2	30.3 ± 0.2			
Females	30.2 ± 0.2	29.8 ± 0.2	31.1 ± 0.2	31.4 ± 0.2	31.5 ± 0.2	30.2 ± 0.2			
Red cell distribution width (%)							<0.001	0.547	0.151
All mink	$13.8^{ab} \pm 0.2$	$13.9^{ab} \pm 0.2$	$13.5^{bc} \pm 0.2$	$13.3^{c} \pm 0.2$	$13.2^{c} \pm 0.1$	$14.1^{a} \pm 0.2$			
Males	13.9 ± 0.2	13.8 ± 0.2	13.7 ± 0.2	13.4 ± 0.2	12.9 ± 0.2	13.9 ± 0.2			
Females	13.8 ± 0.2	14.0 ± 0.2	13.2 ± 0.2	13.2 ± 0.2	13.5 ± 0.2	14.4 ± 0.2			
Platelets (10^9 L^{-1})							0.248	0.020	0.392
Males	675 ± 59	605 ± 59	621 ± 59	601 ± 59	589 ± 59	528 ± 59			
Females	723 ± 59	739 ± 59	752 ± 59	594 ± 59	576 ± 54	732 ± 66			

Table 2 continued

Variable	Fasting regime						*P* value		
Sex	0 day	1 day	3 days	5 days	7 days	RF	Fasting	Sex	F × S
Mean platelet volume (μm^3)							0.024	0.940	0.119
All mink	$9.8^{bc} \pm 0.3$	$10.5^{ab} \pm 0.3$	$9.7^{bc} \pm 0.3$	$9.6^{c} \pm 0.3$	$9.7^{bc} \pm 0.3$	$10.8^{a} \pm 0.3$			
Males	9.7 ± 0.4	10.4 ± 0.4	10.4 ± 0.4	9.3 ± 0.4	9.2 ± 0.4	11.1 ± 0.4			
Females	9.8 ± 0.4	10.6 ± 0.4	9.0 ± 0.4	9.8 ± 0.4	10.3 ± 0.4	10.6 ± 0.5			
Lymphocytes (%)							<0.001	<0.001	0.764
All mink	$31.0^{ab} \pm 2.0$	$31.8^{a} \pm 2.0$	$29.2^{ab} \pm 2.0$	$25.8^{bc} \pm 2.0$	$21.3^{c} \pm 1.9$	$33.7^{a} \pm 2.3$			
Males	38.0 ± 2.8	38.7 ± 2.8	33.1 ± 2.8	30.4 ± 2.8	25.0 ± 2.8	38.9 ± 2.8			
Females	24.0 ± 2.8	25.0 ± 2.8	25.2 ± 2.8	21.2 ± 2.8	17.6 ± 2.6	28.5 ± 3.7			
Monocytes (%)							<0.001	<0.001	0.142
All mink	$5.6^{bc} \pm 0.3$	$4.7^{c} \pm 0.3$	$6.6^{a} \pm 0.3$	$5.4^{bc} \pm 0.3$	$6.1^{ab} \pm 0.3$	$4.4^{c} \pm 0.4$			
Males	6.4 ± 0.5	5.2 ± 0.5	6.4 ± 0.5	6.3 ± 0.5	7.3 ± 0.5	5.0 ± 0.5			
Females	4.8 ± 0.5	4.2 ± 0.5	6.7 ± 0.5	4.5 ± 0.5	4.9 ± 0.4	3.8 ± 0.6			
Granulocytes (%)							0.008	<0.001	0.686
All mink	$63.4^{bc} \pm 2.2$	$63.5^{bc} \pm 2.2$	$64.3^{bc} \pm 2.2$	$68.8^{ab} \pm 2.2$	$72.6^{a} \pm 2.1$	$61.8^{c} \pm 2.5$			
Males	55.6 ± 3.0	56.1 ± 3.0	60.5 ± 3.0	63.3 ± 3.0	67.7 ± 3.0	56.1 ± 3.0			
Females	71.2 ± 3.0	70.8 ± 3.0	68.0 ± 3.0	74.3 ± 3.0	77.5 ± 2.8	67.6 ± 3.9			

Presented are lsmeans ± SEM

[a–d] Fasting regimes differ within row ($P < 0.05$)

Table 3 Variables of clinical chemistry and endocrinology in male and female mink in response to fasting for 0 (control), 1, 3, 5, and 7 days, and re-feeding (RF) for 28 days after a 7-day fast

Variable	Fasting regime						*P* value		
Sex	0 day	1 day	3 days	5 days	7 days	RF	Fasting	Sex	F × S
P glucose (mmol L^{-1})							0.032	0.174	0.534
All mink	$9.13^{ab} \pm 0.43$	$7.90^{c} \pm 0.43$	$8.24^{abc} \pm 0.43$	$7.81^{c} \pm 0.43$	$8.01^{bc} \pm 0.41$	$9.45^{a} \pm 0.46$			
Males	8.96 ± 0.61	7.71 ± 0.61	7.50 ± 0.61	7.31 ± 0.61	7.80 ± 0.61	10.06 ± 0.61			
Females	9.30 ± 0.61	8.09 ± 0.61	8.98 ± 0.61	8.30 ± 0.61	8.22 ± 0.56	8.84 ± 0.68			
P triacylglycerols (mmol L^{-1})							<0.001	0.057	0.260
All mink	$0.96^{d} \pm 0.07$	$1.22^{c} \pm 0.07$	$1.60^{a} \pm 0.07$	$1.52^{ab} \pm 0.07$	$1.34^{bc} \pm 0.07$	$0.87^{d} \pm 0.07$			
Males	0.97 ± 0.10	1.18 ± 0.10	1.65 ± 0.10	1.32 ± 0.10	1.24 ± 0.10	0.80 ± 0.10			
Females	0.94 ± 0.10	1.26 ± 0.10	1.56 ± 0.10	1.71 ± 0.10	1.44 ± 0.09	0.95 ± 0.11			
P cholesterol (mmol L^{-1})							0.045	0.108	0.283
All mink	$4.9^{ab} \pm 0.2$	$4.7^{ab} \pm 0.2$	$4.5^{b} \pm 0.2$	$4.7^{ab} \pm 0.2$	$4.4^{b} \pm 0.2$	$5.2^{a} \pm 0.2$			
Males	5.0 ± 0.2	4.8 ± 0.2	4.3 ± 0.2	4.5 ± 0.2	4.5 ± 0.2	4.8 ± 0.2			
Females	4.8 ± 0.2	4.6 ± 0.2	4.6 ± 0.2	4.9 ± 0.2	4.7 ± 0.2	5.5 ± 0.2			
P creatinine (μmol L^{-1})							0.243	0.946	0.249
Males	85 ± 9	84 ± 9	82 ± 9	78 ± 9	86 ± 9	66 ± 9			
Females	71 ± 9	77 ± 9	97 ± 9	88 ± 9	64 ± 8	72 ± 10			
P total protein (g L^{-1})							<0.001	0.017	0.328
All mink	$67.1^{a} \pm 1.2$	$67.6^{a} \pm 1.2$	$60.9^{b} \pm 1.2$	$62.0^{b} \pm 1.2$	$60.1^{b} \pm 1.1$	$62.4^{b} \pm 1.3$			
Males	68.1 ± 1.7	68.0 ± 1.7	63.4 ± 1.7	61.9 ± 1.7	63.1 ± 1.7	62.8 ± 1.7			
Females	66.1 ± 1.7	67.2 ± 1.7	58.3 ± 1.7	62.1 ± 1.7	57.0 ± 1.5	62.0 ± 1.9			
P urea (mmol L^{-1})							0.308	0.906	0.838
Males	2.4 ± 0.5	2.9 ± 0.5	2.5 ± 0.5	2.2 ± 0.5	1.9 ± 0.5	2.7 ± 0.5			
Females	2.8 ± 0.5	3.2 ± 0.5	2.2 ± 0.5	2.8 ± 0.5	1.6 ± 0.5	2.1 ± 0.6			
P total bilirubin (μmol L^{-1})							0.110	0.606	0.479
Males	7.6 ± 0.9	6.6 ± 0.9	7.1 ± 0.9	6.0 ± 0.9	6.5 ± 0.9	5.5 ± 0.9			
Females	7.7 ± 0.9	5.1 ± 0.9	6.3 ± 0.9	8.2 ± 0.9	5.7 ± 0.9	4.6 ± 1.1			
P creatine kinase (U L^{-1})							0.096	0.966	0.202
Males	270.9 ± 64.8	233.7 ± 64.8	114.5 ± 64.8	196.0 ± 64.8	424.4 ± 64.8	197.3 ± 64.8			
Females	250.6 ± 64.8	192.0 ± 64.8	217.0 ± 64.8	171.0 ± 64.8	257.7 ± 59.2	157.4 ± 72.4			
P ALT (U L^{-1})							<0.001	0.038	0.028
Males	$133^{c} \pm 83$	$164^{bc} \pm 83$	$313^{b} \pm 83$	$328^{b} \pm 83$	$616^{a} \pm 83$	$174^{bc} \pm 83$			
Females	$255^{bc} \pm 83$	$155^{cd} \pm 83$	$256^{b} \pm 83$	$777^{a} \pm 83$	$799^{a} \pm 75$	$99^{d} \pm 92$			
P estradiol (pmol L^{-1})							0.104	0.006	0.237
Males	39.727 ± 9.481	40.016 ± 9.481	46.424 ± 9.481	44.209 ± 9.481	44.420 ± 9.481	48.803 ± 9.481			
Females	41.874 ± 9.481	47.260 ± 9.481	50.327 ± 9.481	77.603 ± 9.481	88.877 ± 8.655	46.934 ± 10.600			

Table 3 continued

Variable	Fasting regime						*P* value		
Sex	0 day	1 day	3 days	5 days	7 days	RF	Fasting	Sex	F × S
P progesterone (nmol L^{-1})							0.881	0.636	0.181
Males	0.907 ± 0.226	1.024 ± 0.226	0.872 ± 0.226	1.628 ± 0.226	0.986 ± 0.226	0.794 ± 0.226			
Females	1.195 ± 0.226	0.788 ± 0.226	1.132 ± 0.226	0.855 ± 0.226	0.949 ± 0.226	1.180 ± 0.253			
P cortisol (nmol L^{-1})							0.078	0.688	0.185
Males	106.4 ± 21.5	122.9 ± 21.5	64.7 ± 21.5	78.6 ± 21.5	97.1 ± 21.5	95.5 ± 21.5			
Females	110.5 ± 21.5	110.0 ± 21.5	117.3 ± 21.5	42.6 ± 21.5	44.2 ± 19.6	110.4 ± 24.0			
P insulin (μU mL^{-1})							<0.001	0.272	0.322
All mink	8.994^{a} ± 0.654	6.118^{b} ± 0.617	5.016^{b} ± 0.617	4.557^{b} ± 0.617	4.676^{b} ± 0.590	5.100^{b} ± 0.654			
Males	10.237 ± 0.975	7.062 ± 0.872	4.930 ± 0.872	4.073 ± 0.872	5.141 ± 0.872	5.107 ± 0.872			
Females	7.752 ± 0.872	5.174 ± 0.872	5.101 ± 0.872	5.041 ± 0.872	4.210 ± 0.796	5.093 ± 0.975			
P HOMA index							<0.001	0.581	0.173
All mink	3.693^{a} ± 0.266	2.127^{b} ± 0.251	1.830^{b} ± 0.251	1.576^{b} ± 0.251	1.675^{b} ± 0.240	2.154^{b} ± 0.266			
Males	4.313 ± 0.397	2.406 ± 0.355	1.636 ± 0.355	1.324 ± 0.355	1.780 ± 0.355	2.328 ± 0.355			
Females	3.074 ± 0.355	1.848 ± 0.355	2.024 ± 0.355	1.828 ± 0.355	1.570 ± 0.324	1.980 ± 0.397			
P leptin (ng mL^{-1})							<0.001	0.011	0.052
All mink	3.422^{a} ± 0.147	3.190^{a} ± 0.127	1.955^{cd} ± 0.127	1.970^{bcd} ± 0.127	1.617^{d} ± 0.122	2.171^{bc} ± 0.147			
Males	3.981 ± 0.232	3.444 ± 0.180	2.079 ± 0.180	1.815 ± 0.180	1.649 ± 0.180	2.361 ± 0.180			
Females	2.862 ± 0.180	2.937 ± 0.180	1.832 ± 0.180	2.125 ± 0.180	1.584 ± 0.164	1.982 ± 0.232			
P ghrelin (pg mL^{-1})							0.033	0.968	0.020
Males	421.82^{bc} ± 104.21	512.05^{bc} ± 104.21	312.78^{c} ± 104.21	607.57^{ab} ± 104.21	812.86^{a} ± 104.21	615.64^{ab} ± 104.21			
Females	883.02^{a} ± 104.21	432.36^{b} ± 104.21	431.69^{b} ± 104.21	409.14^{b} ± 104.21	534.75^{b} ± 95.13	549.34^{ab} ± 116.52			
P adiponectin (μg mL^{-1})							0.679	0.172	0.730
Males	2.916 ± 0.401	2.945 ± 0.401	2.952 ± 0.401	3.198 ± 0.401	3.842 ± 0.401	3.194 ± 0.401			
Females	3.374 ± 0.401	3.792 ± 0.401	3.148 ± 0.401	3.599 ± 0.401	3.351 ± 0.366	3.720 ± 0.448			
P glucagon (pg mL^{-1})							0.435	0.403	0.325
Males	44.249 ± 8.274	47.404 ± 8.274	28.150 ± 8.274	26.141 ± 9.251	42.086 ± 9.251	45.071 ± 8.274			
Females	56.368 ± 8.274	42.357 ± 8.274	47.403 ± 10.682	42.570 ± 8.274	44.923 ± 13.083	26.900 ± 10.682			
P growth hormone (ng mL^{-1})							0.385	0.241	0.776
Males	3.259 ± 1.091	2.456 ± 1.091	3.398 ± 1.091	1.930 ± 1.091	5.263 ± 1.091	1.980 ± 1.219			
Females	1.084 ± 1.091	3.052 ± 1.408	2.302 ± 1.091	1.557 ± 1.091	2.306 ± 0.996	1.637 ± 1.219			
P triiodothyronine (nmol L^{-1})							<0.001	0.090	0.131
All mink	0.753^{ab} ± 0.053	0.736^{ab} ± 0.061	0.732^{ab} ± 0.053	0.612^{bc} ± 0.053	0.500^{c} ± 0.053	0.878^{a} ± 0.056			
Males	0.745 ± 0.075	0.776 ± 0.075	0.581 ± 0.075	0.583 ± 0.075	0.519 ± 0.075	0.775 ± 0.075			
Females	0.762 ± 0.075	0.697 ± 0.097	0.884 ± 0.075	0.642 ± 0.075	0.480 ± 0.075	0.980 ± 0.084			

Table 3 continued

Variable	Fasting regime						*P* value		
Sex	0 day	1 day	3 days	5 days	7 days	RF	Fasting	Sex	F × S
ADR dopamine (μg g^{-1})							0.512	0.001	0.321
Males	7.85 ± 1.37	7.77 ± 1.37	6.80 ± 1.37	7.58 ± 1.37	7.52 ± 1.37	7.14 ± 1.37			
Females	11.27 ± 1.37	8.04 ± 1.37	8.62 ± 1.37	11.98 ± 1.37	9.68 ± 1.25	12.18 ± 1.53			
ADR noradrenaline (μg g^{-1})							0.953	0.003	0.482
Males	117.90 ± 16.33	127.35 ± 16.33	119.02 ± 16.33	107.07 ± 16.33	115.81 ± 16.33	106.10 ± 16.33			
Females	147.42 ± 16.33	136.91 ± 16.33	136.16 ± 16.33	159.38 ± 16.33	124.62 ± 14.91	165.57 ± 18.26			
ADR adrenaline (μg g^{-1})							0.355	0.564	0.490
Males	1493.95 ± 175.59	1446.80 ± 175.59	1287.57 ± 175.59	1223.72 ± 175.59	1442.67 ± 175.59	1442.67 ± 175.59			
Females	1577.00 ± 175.59	1330.67 ± 175.59	1307.22 ± 175.59	1475.79 ± 175.59	1318.36 ± 160.29	1880.24 ± 196.32			

Presented are lsmeans ± SEM

[a–d] Fasting regimes differ within row ($P < 0.05$)

P plasma, *ADR* adrenal

fasting regimes with return to day 0–3 levels in response to re-alimentation. The monocyte percentage, on the other hand, showed a more variable response with peak values on days 3 and 7 of fasting.

The plasma TAG concentrations showed a significant increase in response to food deprivation during days 1–7 in comparison to the non-fasted control animals and the RF mink (Table 3). The cholesterol levels varied in the different experimental regimes with the highest values observed in the RF group. Lowest values for both sexes were observed on days 3 and 7 of fasting. Overall, the males had higher plasma total protein concentrations than the females (64.5 ± 0.7 vs. 62.1 ± 0.7 g L^{-1}). In both sexes, the plasma protein levels declined during 3–7 days of food deprivation and remained low upon re-feeding. Concurrently, no change was observed in the plasma urea levels throughout the experimental regimes. For plasma ALT, a significant fasting × sex regime interaction was found, where the female mink showed higher values on day 5 of fasting than the males. The plasma ALT levels increased during 5–7 days of fasting and returned to 0- to 3-day levels in response to re-alimentation (Fig. 1).

A significant decline was observed in the plasma insulin levels during fasting and the concentration remained low thereafter (Table 3). This was accompanied by a decrease in the HOMA index. The plasma leptin concentrations were significantly lower during days 3–7 of fasting in comparison to the 0- to 1-day groups; they also remained low after feeding was resumed. The females had on average lower circulating plasma leptin levels than the males (2.220 ± 0.077 vs. 2.555 ± 0.076 ng mL^{-1}). For plasma ghrelin a significant fasting × sex interaction was found indicating the highest levels in the female mink fasted overnight (0 day), whereas for the males the highest plasma ghrelin concentrations were seen on day 7 of fasting and the lowest on day 3. The plasma T_3 levels declined within 7 days of fasting and returned to pre-fasting levels when feeding was resumed. Generally, the females exhibited higher concentrations of dopamine (10.29 ± 0.56 μg g^{-1}) and noradrenaline (145.00 ± 6.71 μg g^{-1}) in their adrenal glands in comparison to the males (7.44 ± 0.56 μg g^{-1}; 115.54 ± 6.67 μg g^{-1}).

Tissue FA Profiles

A rapid shift was observed in the liver FA profiles in response to food deprivation and re-feeding (Fig. 3; Table 4). In the female mink, significantly lower hepatic n-3/n-6 PUFA ratio was present within 1 day of food deprivation, whereas the males responded within 3 days. The RF mink showed complete recovery of the hepatic total n-3 PUFA and n-3/n-6 PUFA ratio, with the females having significantly higher values compared to the males.

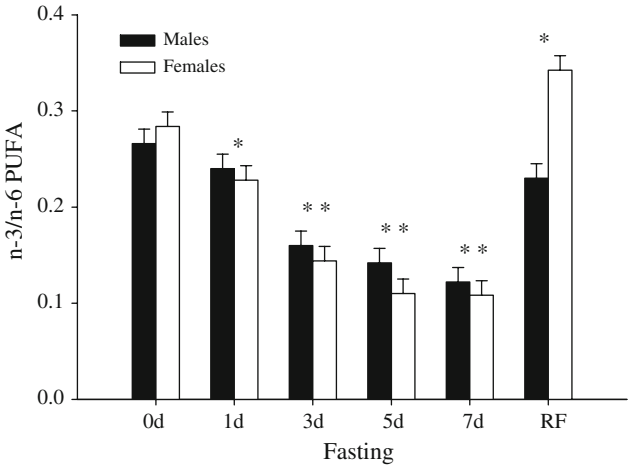

Fig. 3 Changes in the hepatic n-3/n-6 polyunsaturated fatty acid (*PUFA*) ratio (lsmeans + SEM) in male and female mink in response to fasting for 0 (control), 1, 3, 5, and 7 days, and re-feeding (*RF*) for 28 days after a 7-day fast. *Asterisk* females differ from control, *double asterisk* both sexes differ from control ($P < 0.05$). Total $n = 60$. P values: fasting <0.001, sex 0.231, F × S <0.001

In addition, a significant decline was observed in the liver SFA levels after 1 day of fasting, while total MUFA and the unsaturated FA (UFA)/SFA ratio increased during 3–7 days. For these variables, the RF group did not differ from the 0-day mink.

For the other tissues, the FA data (Table 4) are presented by fasting regime only as no interaction (fasting × sex) was observed. The intermuscular adipose tissue exhibited lower concentrations of n-3 PUFA and n-3/n-6 PUFA ratios during food deprivation. Overall, the females had lower n-3 PUFA % ($P = 0.013$) and n-3/n-6 PUFA ratios ($P = 0.008$) than the males in their intermuscular adipose tissue. In the mesenteric fat during the fasting regimes, total SFA were shown to decline while total MUFA increased. Although the UFA/SFA ratio increased in response to food deprivation, the n-3 PUFA % and n-3/n-6 PUFA ratios declined. These changes in the FA composition were reversed when feeding was resumed for 4 weeks. In the perirenal fat, total SFA declined during fasting and subsequently the UFA/SFA ratio increased. Again, a significant decrease was observed in n-3 PUFA as well as n-3/n-6 PUFA ratios during the course of food deprivation. The RF animals were not significantly different in their perirenal PUFA profiles from the controls. However, the SFA proportions of perirenal adipose tissue depots remained low in the RF group while the UFA/SFA ratio remained high. Overall, the females had lower n-3 PUFA % in this adipose depot than the males ($P = 0.036$). In the ventral subcutaneous adipose tissue, a significant decline was once again observed in n-3 PUFA as well as in the n-3/n-6 PUFA ratios during the course of food deprivation.

The typical decline in the n-3/n-6 PUFA ratio in response to food deprivation was also observed in the FA profiles of the skeletal muscle (Table 4). Overall, the females had higher levels of total SFA ($P = 0.019$), total n-3 PUFA ($P = 0.009$) and higher n-3/n-6 PUFA ratios ($P = 0.002$), but lower total MUFA ($P = 0.039$) and UFA/SFA ratios ($P = 0.016$) than the males. Finally, regarding the plasma FA profiles, total MUFA increased while total n-6 and n-3 PUFA declined in response to food deprivation. A significant sex difference was observed ($P = 0.034$) where the female mink had higher plasma n-3/n-6 PUFA ratios in comparison to the males.

Discussion

BW Loss, Fat Mobilization, HSI and Liver Fat Content

It is evident from the current study that fasting of mink for as few as 3 days results in considerable BW loss and a significantly increased liver lipid content primarily present as TAG. These findings are in agreement with previous studies on the effects of food deprivation in mink [5, 6], polecats [15] and sables (*Martes zibellina*) [17]. Furthermore, a 28-day period of re-feeding after a 7-day fast resulted in moderate recuperation of BW and return to normal liver fat percentage, indicating liver recovery. The rapid BW loss during fasting [6, 12] is most likely an outcome of (1) the energetically demanding body shape with a high surface-area-to-volume ratio [24] and (2) the inability of small mustelids to utilize, e.g., torpor or related hypometabolic adaptations [12, 25]. This necessitates rapid mobilization of the adipose tissue depots during food deprivation.

On average, the females lost more % BW than the males. This is likely caused by the significant sexual dimorphism exhibited by the species [26] where, due to its smaller body size, the female mink would be energetically more challenged during times of food deprivation, especially in cold weather. In addition to their smaller BW, the anatomic difference that the female mink seem to deposit relatively more adipose tissue in the intra-abdominal depots may be worth considering. Having more intra-abdominal adipose tissue may, under conditions of preceding obesity, e.g., as a result of autumnal fattening, predispose the female mink to a more rapid onset of hepatic lipidosis. In this regard, the visceral (omental, mesenteric) adipose tissue poses a far greater health risk than subcutaneous fat in humans [27], as the FFA hydrolyzed from these depots are released directly into the hepatic portal circulation [28]. Based on the estimated body fat content (>33% BW), the mink in this study could be considered obese at the start of the food deprivation period. It is also

Table 4 Changes in the tissue fatty acid composition in mink in response to fasting for 0 (control), 1, 3, 5, and 7 days, and re-feeding (RF) for 28 days after a 7-day fast

Tissue variable	Fasting regime						*P* value
	0 day	1 day	3 days	5 days	7 days	RF	
Liver							
SFA_{SUM} (mol%)	$40.03^{a} \pm 0.58$	$37.97^{b} \pm 0.58$	$32.75^{c} \pm 0.58$	$31.37^{cd} \pm 0.58$	$30.10^{d} \pm 0.55$	$39.05^{ab} \pm 0.61$	<0.001
$MUFA_{SUM}$ (mol%)	$33.79^{c} \pm 1.10$	$37.09^{c} \pm 1.10$	$47.24^{b} \pm 1.10$	$50.75^{a} \pm 1.10$	$52.27^{a} \pm 1.15$	$34.82^{c} \pm 1.17$	<0.001
n-6_{SUM} (mol%)	$20.33^{a} \pm 0.43$	$19.95^{a} \pm 0.43$	$17.12^{b} \pm 0.43$	$15.62^{c} \pm 0.43$	$15.59^{c} \pm 0.41$	$20.03^{a} \pm 0.46$	<0.001
n-3_{SUM} (mol%)							<0.001
All mink	$5.64^{a} \pm 0.30$	$4.73^{b} \pm 0.30$	$2.62^{c} \pm 0.30$	$2.00^{d} \pm 0.30$	$1.80^{d} \pm 0.28$	$5.87^{a} \pm 0.31$	
Males	$5.51^{a} \pm 0.42$	$4.88^{a} \pm 0.42$	$2.87^{b} \pm 0.42$	$2.42^{bc} \pm 0.42$	$1.97^{c} \pm 0.42$	$4.52^{a} \pm 0.42$	0.002[e]
Females	$5.78^{ab} \pm 0.42$	$4.58^{b} \pm 0.42$	$2.37^{c} \pm 0.42$	$1.59^{d} \pm 0.42$	$1.63^{d} \pm 0.38$	$7.22^{a} \pm 0.47$	
UFA/SFA ratio	$1.50^{c} \pm 0.05$	$1.64^{c} \pm 0.05$	$2.07^{b} \pm 0.05$	$2.19^{ab} \pm 0.05$	$2.34^{a} \pm 0.05$	$1.56^{c} \pm 0.05$	<0.001
n-3/n-6 ratio	$0.28^{a} \pm 0.01$	$0.24^{b} \pm 0.01$	$0.15^{c} \pm 0.01$	$0.13^{cd} \pm 0.01$	$0.11^{d} \pm 0.01$	$0.29^{a} \pm 0.01$	<0.001
Intermuscular fat							
SFA_{SUM} (mol%)	24.97 ± 0.63	24.75 ± 0.63	25.25 ± 0.63	24.52 ± 0.63	23.37 ± 0.60	23.74 ± 0.67	0.357
$MUFA_{SUM}$ (mol%)	61.32 ± 0.65	61.79 ± 0.65	61.73 ± 0.65	62.63 ± 0.65	63.30 ± 0.62	62.00 ± 0.69	0.289
n-6_{SUM} (mol%)	12.02 ± 0.18	11.85 ± 0.18	11.63 ± 0.18	11.61 ± 0.18	12.00 ± 0.17	11.52 ± 0.19	0.247
n-3_{SUM} (mol%)	$1.43^{a} \pm 0.07$	$1.37^{a} \pm 0.07$	$1.16^{b} \pm 0.07$	$1.02^{b} \pm 0.07$	$1.11^{b} \pm 0.09$	$1.46^{a} \pm 0.07$	<0.001
UFA/SFA ratio	3.02 ± 0.11	3.07 ± 0.11	2.98 ± 0.11	3.11 ± 0.11	3.30 ± 0.11	3.07 ± 0.12	0.396
n-3/n-6 ratio	$0.12^{a} \pm 0.005$	$0.12^{a} \pm 0.005$	$0.10^{b} \pm 0.005$	$0.09^{b} \pm 0.005$	$0.09^{b} \pm 0.004$	$0.13^{a} \pm 0.005$	<0.001
Mesenteric fat							
SFA_{SUM} (mol%)	$28.75^{a} \pm 0.49$	$27.99^{ab} \pm 0.46$	$28.02^{ab} \pm 0.46$	$27.08^{bc} \pm 0.49$	$26.14^{c} \pm 0.44$	$27.62^{ab} \pm 0.49$	0.005
$MUFA_{SUM}$ (mol%)	$58.24^{c} \pm 0.56$	$58.85^{c} \pm 0.53$	$59.55^{bc} \pm 0.53$	$60.57^{ab} \pm 0.56$	$61.49^{a} \pm 0.51$	$59.67^{bc} \pm 0.56$	0.001
n-6_{SUM} (mol%)	11.65 ± 0.14	11.81 ± 0.13	11.39 ± 0.13	11.42 ± 0.14	11.44 ± 0.12	11.32 ± 0.14	0.100
n-3_{SUM} (mol%)	$1.14^{a} \pm 0.06$	$1.12^{a} \pm 0.05$	$0.83^{b} \pm 0.05$	$0.74^{b} \pm 0.06$	$0.75^{b} \pm 0.05$	$1.14^{a} \pm 0.06$	<0.001
UFA/SFA ratio	$2.49^{c} \pm 0.07$	$2.58^{bc} \pm 0.06$	$2.58^{bc} \pm 0.06$	$2.70^{ab} \pm 0.07$	$2.84^{a} \pm 0.06$	$2.62^{bc} \pm 0.07$	0.005
n-3/n-6 ratio	$0.10^{a} \pm 0.004$	$0.10^{a} \pm 0.004$	$0.07^{b} \pm 0.004$	$0.06^{b} \pm 0.004$	$0.07^{b} \pm 0.004$	$0.10^{a} \pm 0.004$	<0.001
Perirenal fat							
SFA_{SUM} (mol%)	$28.63^{a} \pm 0.56$	$27.75^{ab} \pm 0.56$	$26.87^{b} \pm 0.56$	$26.30^{bc} \pm 0.56$	$25.33^{c} \pm 0.51$	$26.70^{bc} \pm 0.56$	0.002
$MUFA_{SUM}$ (mol%)	58.67 ± 0.80	58.97 ± 0.80	60.44 ± 0.80	61.05 ± 0.80	61.35 ± 0.72	60.30 ± 0.80	0.102
n-6_{SUM} (mol%)	11.30 ± 0.43	11.96 ± 0.43	11.59 ± 0.43	11.74 ± 0.43	12.33 ± 0.39	11.62 ± 0.43	0.587
n-3_{SUM} (mol%)	$1.19^{a} \pm 0.06$	$1.10^{a} \pm 0.06$	$0.90^{b} \pm 0.06$	$0.74^{b} \pm 0.06$	$0.81^{b} \pm 0.05$	$1.14^{a} \pm 0.06$	<0.001
UFA/SFA ratio	$2.51^{d} \pm 0.08$	$2.61^{bcd} \pm 0.08$	$2.74^{bcd} \pm 0.08$	$2.81^{abc} \pm 0.08$	$3.00^{a} \pm 0.07$	$2.75^{bc} \pm 0.08$	0.002
n-3/n-6 ratio	$0.11^{a} \pm 0.006$	$0.09^{ab} \pm 0.006$	$0.08^{bc} \pm 0.006$	$0.06^{c} \pm 0.006$	$0.07^{c} \pm 0.006$	$0.10^{ab} \pm 0.006$	<0.001
Ventral fat							
SFA_{SUM} (mol%)	25.93 ± 0.65	25.31 ± 0.65	25.62 ± 0.65	24.64 ± 0.65	23.77 ± 0.65	24.97 ± 0.69	0.238
$MUFA_{SUM}$ (mol%)	61.28 ± 0.69	61.71 ± 0.69	61.71 ± 0.69	63.11 ± 0.69	63.37 ± 0.69	62.50 ± 0.73	0.203
n-6_{SUM} (mol%)	11.26 ± 0.18	11.33 ± 0.18	11.32 ± 0.18	10.96 ± 0.18	11.51 ± 0.18	11.04 ± 0.19	0.318
n-3_{SUM} (mol%)	$1.25^{ab} \pm 0.07$	$1.35^{a} \pm 0.07$	$1.08^{bc} \pm 0.07$	$1.01^{c} \pm 0.07$	$1.08^{bc} \pm 0.07$	$1.22^{ab} \pm 0.08$	0.014
UFA/SFA ratio	2.88 ± 0.10	2.97 ± 0.10	2.94 ± 0.10	3.07 ± 0.10	3.23 ± 0.10	3.03 ± 0.11	0.253
n-3/n-6 ratio	$0.11^{abc} \pm 0.006$	$0.12^{a} \pm 0.006$	$0.09^{bcd} \pm 0.006$	$0.09^{d} \pm 0.006$	$0.09^{cd} \pm 0.006$	$0.11^{abc} \pm 0.006$	0.005
Skeletal muscle							
SFA_{SUM} (mol%)	28.55 ± 0.94	28.99 ± 0.94	28.16 ± 0.94	28.21 ± 0.94	27.66 ± 0.90	28.79 ± 1.00	0.929
$MUFA_{SUM}$ (mol%)	38.31 ± 2.89	37.51 ± 2.89	39.76 ± 2.89	39.55 ± 2.89	37.76 ± 2.77	34.96 ± 3.07	0.888
n-6_{SUM} (mol%)	23.99 ± 1.35	24.11 ± 1.35	23.97 ± 1.35	24.34 ± 1.35	26.25 ± 1.30	25.43 ± 1.43	0.773
n-3_{SUM} (mol%)	8.95 ± 0.73	9.19 ± 0.73	7.91 ± 0.73	7.70 ± 0.73	8.13 ± 0.70	10.62 ± 0.77	0.081
UFA/SFA ratio	2.52 ± 0.14	2.47 ± 0.14	2.58 ± 0.14	2.60 ± 0.14	2.66 ± 0.13	2.55 ± 0.15	0.948
n-3/n-6 ratio	$0.37^{a} \pm 0.02$	$0.37^{a} \pm 0.02$	$0.32^{b} \pm 0.02$	$0.31^{b} \pm 0.02$	$0.31^{b} \pm 0.02$	$0.41^{a} \pm 0.03$	<0.001

Table 4 continued

Tissue variable	Fasting regime						*P* value
	0 day	1 day	3 days	5 days	7 days	RF	
Plasma							
SFA_{SUM} (mol%)	38.79 ± 0.85	39.30 ± 0.85	37.32 ± 0.85	38.04 ± 0.85	36.23 ± 0.85	38.09 ± 0.90	0.164
$MUFA_{SUM}$ (mol%)	19.51^{c} ± 0.73	19.84^{c} ± 0.73	23.49^{b} ± 0.73	24.93^{ab} ± 0.73	25.76^{a} ± 0.70	20.78^{c} ± 0.78	<0.001
n-6_{SUM} (mol%)	32.53^{a} ± 0.66	31.26^{abc} ± 0.66	31.58^{bc} ± 0.66	29.38^{cd} ± 0.66	30.46^{cd} ± 0.63	32.43^{ab} ± 0.70	0.012
n-3_{SUM} (mol%)	9.01^{ab} ± 0.32	9.46^{a} ± 0.32	8.45^{bc} ± 0.32	7.47^{d} ± 0.32	7.88^{cd} ± 0.31	8.74^{abc} ± 0.34	<0.001
UFA/SFA ratio	1.59 ± 0.06	1.56 ± 0.06	1.69 ± 0.06	1.64 ± 0.06	1.76 ± 0.06	1.63 ± 0.06	0.158
n-3/n-6 ratio	0.28 ± 0.01	0.30 ± 0.01	0.28 ± 0.01	0.26 ± 0.01	0.26 ± 0.01	0.27 ± 0.01	0.080

Presented are lsmeans ± SEM

SFA_{SUM} sum of saturated fatty acids, *$MUFA_{SUM}$* sum of monounsaturated fatty acids, *n-6_{SUM}* sum of n-6 fatty acids, *n-3_{SUM}* sum of n-3 fatty acids, *UFA* unsaturated fatty acids

[a–d] Fasting regimes differ within row ($P < 0.05$)

[e] *P* values for F × S

evident from the current data that the mink were largely unable to recover their body fat depots during winter once they had been mobilized due to food deprivation.

Hematology, Endocrinology and Clinical Chemistry

Similar to earlier findings in mink [6], sables [17] and American marten (*Martes americana*) [13] the blood lymphocyte percentage declined in response to 7 days of food deprivation, while in the RF group, the lymphocyte percentage did not differ from the pre-fasted levels. This suggests that prolonged food deprivation could lead to immunosuppression in mink and that this would be reversed once normal feed intake is resumed.

The plasma leptin concentrations were significantly lowered in the mink in response to 3–7 days of food deprivation not dissimilar to earlier observations [16] and remained low thereafter. Our results are also in a close agreement with findings by Mustonen et al. [12] on the European polecat where a drastic decline was observed in plasma leptin concentrations in response to 5-day food deprivation. It is noteworthy that in the American marten and the sable, food deprivation of 2 and 4 days, respectively, did not influence the plasma leptin levels [13, 17]. In these species, the plasma ghrelin concentrations increased in response to short-term food deprivation, whereas no clear response was observed in the current study, where the female mink showed the highest levels when fasted overnight and the males after 7 days. Likewise, the plasma ghrelin levels of the European polecat and male American mink remained unaffected by food deprivation [12, 16]. The different responses observed in these two key endocrine regulators of body energy homeostasis may reflect the different degrees of adiposity among the members of the weasel family. The mink [6] and the European polecat [12] represent species with a propensity to unnatural obesity under captive conditions, whereas the American marten [23] and the sable [17] do not have a tendency to accumulate excessive adipose tissue depots.

During food deprivation, the observed lower T_3 concentration could contribute to the down-regulation of metabolism resulting in reduced energy expenditure when food supply is limited [29]. Since insulin is required for the conversion of thyroxine (T_4) to T_3, the down-regulation of metabolism is a direct outcome of suppression of insulin release in response to food deprivation and the accompanying low blood glucose levels [30]. The characteristic decline in the insulin levels was observed in the mink in the current study similar to our recent findings in the polecats and male American mink, where the plasma insulin levels decreased markedly in response to fasting and coincided with the lower T_3 concentrations and T_3/T_4 ratios [12, 16].

The elevated circulating TAG concentrations may reflect the rapid mobilization of body fat reserves during food deprivation. The increased influx of FFA from the visceral fat depots into the liver may promote hepatic insulin resistance which leads to an accelerated synthesis of VLDL causing elevated plasma TAG levels [27]. This increases the hepatic TAG influx posing an overwhelming challenge to the liver's ability to metabolize these lipids [9, 10] resulting in a perpetuating cycle. The liver lipid metabolism is further challenged in strictly carnivorous mammals [31–33], which rely on gluconeogenesis for blood sugar provision and are unable to conserve nitrogen by down-regulating the urea cycle during fasting [34]. In mustelids, food deprivation is accompanied by decreased plasma arginine levels [12, 35], causing the accumulation of orotic acid [33]. Orotic acid is an intermediary metabolite in the pyrimidine ribonucleotide synthesis, the first step of which is the formation of carbamoyl phosphate, and

it is directly hepatotoxic interfering with the liver's ability to assemble and secrete VLDL [36]. Carbamoyl phosphate, formed from ammonia and bicarbonate, is also required for the urea cycle where it participates in the important step of citrulline synthesis from ornithine maintaining the cycle [37].

In carnivores, a dietary source of arginine is required for the proper functioning of the urea cycle, where arginine is converted to urea yielding ornithine [38]. Shortage of arginine may further compromise the liver lipid metabolism in carnivores as the urea cycle function declines. Arginine is also required for the synthesis of apolipoprotein E, which has a facilitating role in hepatic lipid mobilization increasing the number of VLDL particles secreted by the liver [39]. The rapid depletion of arginine [35] may be an outcome of competing requirements coinciding at the time of extensive body fat mobilization; namely meeting the demands for accelerated VLDL synthesis and eliminating increasing amounts of waste nitrogen resulting from augmented gluconeogenesis. Arginine deficiency, therefore, appears to be a significant constraint for the liver lipoprotein metabolism during food deprivation, when there is no dietary supply of arginine, its synthesis is inadequate [32] and its amount in muscles diminishes as a result of stimulated proteolysis [35]. It is evident that complex biochemical interactions exist among the different physiological systems during food deprivation exerting pathophysiological linkages between the liver lipid metabolism, gluconeogenetic pathways and the urea cycle function. This may help explain the rapidity by which hepatic lipidosis develops in carnivores.

The severity of the fatty liver disease is further exacerbated due to the effects it may have on the central nervous system. It is not known if urinary orotic acid or blood ammonia levels are increased in mink females diagnosed with nursing sickness (DB Hunter, personal communication). However, hepatic lipidosis and coma are among the most prevalent findings in the advanced stage of the disease [2, 40, 41]. In humans [42] and carnivore companion animals [34], hepatic encephalopathy and hyperammonemic coma are commonly associated with fulminant liver failure. The human hepatic encephalopathy is also characterized by low-grade cerebral edema, swelling of astrocytes, hyponatremia and the depletion of organic osmolytes in the brain cells [43]. It is probable that the mortality that often accompanies nursing sickness and the associated hepatic lipidosis in the mink may be an outcome of the decline in the urea cycle function, and ultimately caused by the accumulation of toxic levels of ammonia leading to suppression of the functions of the central nervous system. The hyponatremia in mink dams [41] may also be a significant contributor to mortality as it further exacerbates the pathogenesis of hepatic encephalopathy as seen in humans [43]. In mink farming, electrolyte therapy has been successfully used to treat mink dams in the early stages of nursing sickness [3, 44]. This, in addition to maintaining kidney function [11], may help prevent the development of cerebral edema in subjects with impaired liver function effectively reducing mortality.

Liver Lipids and Tissue FA Profiles

It is evident based on our findings that the significant increase in the HSI would be caused by TAG accumulation as a result of fat mobilization and increased FFA influx into the liver. On the other hand, the relative decrease of lipid components mostly present in cellular membranes may be indicative of liver cell damage supported by the elevated ALT activities, while their relative increase in the RF group may be evidence for hepatocyte regeneration. However, the significantly elevated absolute quantities of total PL during 3–7 days, and of PtdCho during 5–7 days, suggest that as the liver enlarges in size there would be also accelerated synthesis of membrane PL in the endoplasmic reticulum (ER) most likely triggered by ER stress and the unfolded protein response (UPR) [45]. Chronic ER stress has been shown to underlie the physiological responses in obesity, including inflammation and insulin resistance [46]. In liver disease, oxidative stress and ER dysfunction have been proposed as causative factors in the formation of Mallory-Denk bodies [47]; a morphologic hallmark in the transition from simple steatosis (lipidosis) to the more severe steatohepatitis. Possibly, the observed alterations in the liver lipid composition of the 3–7 days fasted mink could be associated with ER stress and the UPR contributing to the development of liver pathology.

The FA data of the various adipose tissue depots clearly show a rapid loss of the n-3 PUFA and a significant decline in the n-3/n-6 PUFA ratio in response to food deprivation. The over-representation of the n-6 PUFA in the body, caused by the selective mobilization of n-3 PUFA during fasting [14, 15], is known to result in increased percentages of these FA in the cell membranes of blood cells and hepatocytes [48]. This in turn results in augmented synthesis of the arachidonic acid (20:4n-6)-derived eicosanoids shifting the physiological state of the body to pro-inflammatory and pro-thrombotic and increasing blood clotting, vasospasms and vasoconstriction. The findings of the present experiment are similar to previous studies on carnivores [14, 15, 19, 23] where the FA profiles indicated lower n-3 PUFA proportions in the livers of fasted animals. The complete recovery of the hepatic n-3/n-6 PUFA ratio in response to re-feeding as seen for the first time in the current experiment is clear evidence of the liver's ability to regenerate and recover from injury caused by lipid accumulation when normal feeding is resumed. The rapid

decrease in the n-3/n-6 PUFA ratio in response to food deprivation could be significant in triggering an inflammatory response in the liver tissue [48]. This could be a key contributor to the pathophysiology of fatty liver disease in mink and may influence the disease progression.

It is noteworthy that the plasma n-3/n-6 PUFA ratio appeared relatively constant throughout the experiment and did not respond to the fasting and re-feeding regimes. The higher circulating levels of the n-3 in relation to the n-6 PUFA indicate augmented mobilization of n-3 PUFA in the female mink, suggesting an elevated physiological demand compared to the males. The resulting more pronounced depletion of the n-3 FA from the adipose tissue depots and the liver may predispose the female mink to the development of metabolic disorders arising from such FA imbalance, such as poor glycemic regulation [49, 50], nursing sickness [11] and fatty liver disease [9].

Mustelids would be suitable models to study NAFLD, as several similarities have been observed in the manifestations of hepatic lipidosis between these species and NAFLD patients. The most obvious are the increased liver TAG content, histological findings of steatosis and potentially increased plasma transaminases [9, 10, 15, 48]. Both NAFLD patients and fasted mustelids display decreased tissue n-3 PUFA proportions and n-3/n-6 ratios [9, 15, 48]. Additional similarities could be liver inflammation [10, 48], oxidative stress [9, 10] and ER stress [47], but these remain to be confirmed in further studies. Finally, mustelids could also be very useful models to study liver recovery avoiding the logistical challenges associated with human subjects, e.g., liver biopsies and long follow-up periods [10]. In the mink, the recovery was relatively rapid, as most of the manifestations of lipidosis had disappeared after 28 days of re-feeding.

The key findings of our study are that (1) the development of hepatic lipidosis in mink is rapid and occurs within only a few days of fasting, (2) the principal manifestations in mink are similar to the human NAFLD making the mink a potentially useful animal model for studies on liver steatosis, and that (3) the hepatic lipidosis and the associated biochemical manifestations are reversible when normal feeding is resumed for 4 weeks. In summary, food deprivation of mink resulted in the rapid mobilization of body fat, most notably visceral, causing elevated HSI, liver TAG content and plasma ALT activities. The hepatic lipid infiltration and the altered liver lipid profiles were associated with a significantly reduced n-3 PUFA proportion in the livers and this decrease was more evident in the females. Likewise, re-feeding of the female mink resulted in a more pronounced recovery of the liver n-3 PUFA. The rapid decrease in the n-3/n-6 PUFA ratio in response to food deprivation could trigger an inflammatory response in the liver tissue. This could be a key contributor to the pathophysiology of fatty liver disease in mink and may influence the disease progression.

Acknowledgments This study was supported by the Natural Sciences and Engineering Research Council of Canada (Discovery Grant to KRW, NSERC Undergraduate Student Research Award to CP and RC), the Canada Mink Breeders' Association, the Nutricia Research Foundation, the Finnish Fur Breeders' Association, the Academy of Finland (A-MM and PN), the Mink Farmer's Research Foundation, Fur Commission USA and the Heger Company. We thank Rae MacInnis, Annette Murphy and Cindy Crossman, the staff of the Canadian Centre for Fur Animal Research, as well as Dr. Tess Astatkie, Dr. Gordon Finley, DVM, Dr. Bruce Ramsay, DVM, Lana Crewe, Jody Muise, Jennifer Dobson, Rauni Kojo and Marja-Liisa Martimo-Halmetoja for the skillful logistical support during this study.

References

1. Hunter DB, Barker IK (1996) Digestive system of mink. In: Hunter DB, Lemieux N (eds) Mink… biology, health and disease. Canada Mink Breeders' Association, University of Guelph, Graphic and Print Services, Guelph
2. Clausen TN, Olesen CR, Hansen O, Wamberg S (1992) Nursing sickness in lactating mink (*Mustela vison*). I. Epidemiological and pathological observations. Can J Vet Res 56:89–94
3. Schneider RR (1996) Diseases of the lactation period. In: Hunter DB, Lemieux N (eds) Mink… biology, health and disease. Canada Mink Breeders' Association, University of Guelph, Graphic and Print Services, Guelph
4. Damgaard BM, Clausen TN, Henriksen P (1994) Effect of protein and fat content in feed on plasma alanine aminotransferase and hepatic fatty infiltration in mink. J Vet Med 41A:620–629
5. Bjornvad CR, Elnif J, Sangild PT (2004) Short-term fasting induces intra-hepatic lipid accumulation and decreases intestinal mass without reduced brush-border enzyme activity in mink (*Mustela vison*) small intestine. J Comp Physiol 174B:625–632
6. Mustonen A-M, Pyykönen T, Paakkonen T, Ryökkynen A, Asikainen J, Aho J, Mononen J, Nieminen P (2005) Adaptations to fasting in the American mink (*Mustela vison*): carbohydrate and lipid metabolism. Comp Biochem Physiol 140A:195–202
7. Rouvinen-Watt K, White MB, Campbell R (2005) Mink feeds and feeding, applied feeding guide and mink feed ingredient database. CD-ROM. Ontario Ministry of Agriculture and Food through the Agricultural Research Institute of Ontario and the Nova Scotia Agricultural College
8. Mustonen A-M, Nieminen P, Hyvärinen H, Asikainen J (2000) Exogenous melatonin elevates the plasma leptin and thyroxine concentrations of the mink (*Mustela vison*). Z Naturforsch 55C:806–813
9. Videla LA, Rodrigo R, Araya J, Poniachik J (2004) Oxidative stress and depletion of hepatic long-chain polyunsaturated fatty acids may contribute to non-alcoholic fatty liver disease. Free Radic Biol Med 37:1499–1507
10. Adams LA, Angulo P, Lindor KD (2005) Nonalcoholic fatty liver disease. Can Med Ass J 172:899–905
11. Rouvinen-Watt K (2003) Nursing sickness in the mink (*Mustela vison*)—a metabolic mystery or a familiar foe? Can J Vet Res 67:161–168
12. Mustonen A-M, Puukka M, Rouvinen-Watt K, Aho J, Asikainen J, Nieminen P (2009) Response to fasting in an unnaturally obese carnivore, the captive European polecat *Mustela putorius*. Exp Biol Med 234:1287–1295

13. Nieminen P, Rouvinen-Watt K, Saarela S, Mustonen A-M (2007) Fasting in the American marten (*Martes americana*): a physiological model of the adaptations of a lean-bodied animal. J Comp Physiol 177B:787–795
14. Nieminen P, Käkelä R, Pyykönen T, Mustonen A-M (2006) Selective fatty acid mobilization in the American mink (*Mustela vison*) during food deprivation. Comp Biochem Physiol 145B:81–93
15. Nieminen P, Mustonen A-M, Kärjä V, Asikainen J, Rouvinen-Watt K (2009) Fatty acid composition and development of hepatic lipidosis during food deprivation—mustelids as a potential animal model for liver steatosis. Exp Biol Med 234:278–286
16. Mustonen A-M, Saarela S, Pyykönen T, Nieminen P (2005) Endocrinologic adaptations to wintertime fasting in the male American mink (*Mustela vison*). Exp Biol Med 230:612–620
17. Mustonen A-M, Puukka M, Saarela S, Paakkonen T, Aho J, Nieminen P (2006) Adaptations to fasting in a terrestrial mustelid, the sable (*Martes zibellina*). Comp Biochem Physiol 144A:444–450
18. Canadian Council on Animal Care (1993) The care and use of experimental animals, vol 1. Olfert ED, Cross BM, McWilliam AA (eds). CCAC, Ottawa
19. Mustonen A-M, Käkelä R, Käkelä A, Pyykönen T, Aho J, Nieminen P (2007) Lipid metabolism in the adipose tissues of a carnivore, the raccoon dog, during prolonged fasting. Exp Biol Med 232:58–69
20. Matthews DR, Hosker JP, Rudenski AS, Naylor BA, Treacher DF, Turner RC (1985) Homeostasis model assessment: insulin resistance and β-cell function from fasting plasma glucose and insulin concentrations in man. Diabetologia 28:412–419
21. Folch J, Lees M, Sloane Stanley GH (1957) A simple method for the isolation and purification of total lipides from animal tissues. J Biol Chem 226:497–509
22. Mustonen A-M, Nieminen P, Hyvärinen H (2002) Liver and plasma lipids of spawning burbot. J Fish Biol 61:1318–1322
23. Nieminen P, Rouvinen-Watt K, Collins D, Grant J, Mustonen A-M (2006) Fatty acid profiles and relative mobilization during fasting in adipose tissue depots of the American marten (*Martes americana*). Lipids 41:231–240
24. Brown JH, Lasiewski RC (1972) Metabolism of weasels: the cost of being long and thin. Ecology 53:939–943
25. Mustonen A-M, Pyykönen T, Aho J, Nieminen P (2006) Hyperthermia and increased physical activity in the fasting American mink *Mustela vison*. J Exp Zool 305A:489–498
26. Thom MD, Harrington LA, Mcdonald DW (2004) Why are American mink sexually dimorphic? A role for niche separation. Oikos 105:525–535
27. Westphal SA (2008) Obesity, abdominal obesity, and insulin resistance. Clin Cornerstone 9:23–31
28. Smith DG, Schenk MP (2000) Dissection guide and atlas to the mink. Morton Publishing Company, Colorado
29. Remillard RL, Armstrong PJ, Davenport DJ (2000) Assisted feeding in hospitalized patients: enteral and parenteral nutrition. In: Hand MS, Thatcher CD, Remillard RL, Roudebush P (eds) Small animal clinical nutrition, 4th edn. Walworth Publishing Company, Mark Morris Institute, Marceline, Missouri
30. Powers MA, Pappas TN (1989) Physiologic approaches to the control of obesity. Ann Surg 209:255–260
31. MacDonald ML, Rogers QR, Morris JG (1984) Nutrition of the domestic cat, a mammalian carnivore. Ann Rev Nutr 4:521–562
32. Deshmukh DR, Sarnaik AP, Mukhopadhyay A, Portoles M (1991) Effect of arginine-free diet on plasma and tissue amino acids in young and adult ferrets. J Nutr Biochem 2:72–78
33. Damgaard BM (1998) Effects of dietary supply of arginine on urinary orotic acid excretion, growth performance and blood parameters in growing mink (*Mustela vison*) kits fed low-protein diets. Acta Agric Scand 48A:113–121
34. Roudebush P, Davenport DJ, Dimski DS (2000) Hepatobiliary disease. In: Hand MS, Thatcher CD, Remillard RL, Roudebush P (eds) Small animal clinical nutrition, 4th edn. Walworth Publishing Company, Mark Morris Institute, Marceline, Missouri
35. Mustonen A-M, Puukka M, Pyykönen T, Nieminen P (2005) Adaptations to fasting in the American mink (*Mustela vison*): nitrogen metabolism. J Comp Physiol 175B:357–363
36. Cornelius LM, Jacobs G (1989) Feline hepatic lipidosis. In: Kirk RW (ed) Current veterinary therapy X: small animal practice. WB Saunders, Philadelphia
37. Ganong WF (2005) Review of medical physiology, 22nd edn. Lange Medical Books, McGraw-Hill, New York
38. Elliott WH, Elliott DC (2005) Biochemistry and molecular biology, 3rd edn. Oxford University Press, New York
39. Maugeais C, Tietge UJF, Tsukamoto K, Glick JM, Rader DJ (2000) Hepatic apolipoprotein E expression promotes very low density lipoprotein-apolipoprotein B production in vivo in mice. J Lipid Res 41:1673–1679
40. Schneider RR, Hunter DB (1992) Nursing disease in the mink. Scientifur 16:239–242
41. Wamberg S, Clausen TN, Olesen CR, Hansen O (1992) Nursing sickness in lactating mink (*Mustela vison*): II. Pathophysiology and changes in body fluid composition. Can J Vet Res 56:95–101
42. Ott P, Clemmesen O, Larsen FS (2005) Cerebral metabolic disturbances in the brain during acute liver failure: from hyperammonemia to energy failure and proteolysis. Neurochem Int 47:13–18
43. Guevara M, Baccaro ME, Torre A, Gómez-Ansón B, Ríos J, Torres F, Rami L, Monté-Rubio GC, Martín-Llahí M, Arroyo V, Ginès P (2009) Hyponatremia is a risk factor of hepatic encephalopathy in patients with cirrhosis: a prospective study with time-dependent analysis. Am J Gastroenterol 104:1382–1389
44. Clausen TN, Hansen O (1989) Electrolytes in mink with nursing sickness. Acta Physiol Scand 136A:P9
45. Sriburi R, Jackowski S, Mori K, Brewer JW (2004) XBP1: a link between the unfolded protein response, lipid biosynthesis, and biogenesis of the endoplasmic reticulum. J Cell Biol 167:35–41
46. Özcan U, Cao Q, Yilmaz E, Lee A-H, Iwakoshi NN, Özdelen E, Tuncman G, Görgün C, Glimcher LH, Hotamisligil GS (2004) Endoplasmic reticulum stress links obesity, insulin action, and type 2 diabetes. Science 306:457–461
47. Hanada S, Harada M, Kumemura H, Omary MB, Koga H, Kawaguchi T, Taniguchi E, Yoshida T, Hisamoto T, Yanagimoto C, Maeyama M, Ueno T, Sata M (2007) Oxidative stress induces the endoplasmic reticulum stress and facilitates inclusion formation in cultured cells. J Hepatol 47:93–102
48. El-Badry AM, Graf R, Clavien PA (2007) Omega 3–Omega 6: what is right for the liver? J Hepatol 47:718–725
49. Hynes AM, Rouvinen-Watt K (2007) Monitoring blood glucose levels in female mink during the reproductive cycle: prevention of hyperglycemia during the nursing period. Can J Vet Res 71:241–248
50. Hynes AM, Rouvinen-Watt K (2007) Monitoring blood glucose levels in female mink during the reproductive cycle: effects of short-term fish oil, chromium picolinate and acetyl-salicylic acid supplementation during late lactation. Can J Vet Res 71:249–255

Lipids (2010) 45:129–135
DOI 10.1007/s11745-010-3384-5

ORIGINAL ARTICLE

Serum Phospholipid Transfer Protein Activity After a High Fat Meal in Patients with Insulin-Treated Type 2 Diabetes

Axel Schlitt · Bernhard Schwaab · Kirsten Fingscheidt · Karl J. Lackner · Gunnar H. Heine · Alexander Vogt · Michael Buerke · Lars Maegdefessel · Uwe Raaz · Karl Werdan · Xian-Cheng Jiang

Received: 23 October 2009 / Accepted: 4 January 2010 / Published online: 27 January 2010

Abstract Plasma phospholipid transfer protein (PLTP) mediates both net transfer and exchange of phospholipids between different lipoproteins. Animal studies have shown that it is closely related to the development of atherosclerosis. Although many studies have indicated that PLTP activity is increased in diabetes mellitus, the role of PLTP in diabetes is still unclear. To evaluate the influence of a high-fat meal on PLTP activity, 50 non-diabetic patients with coronary heart disease (CHD), 50 insulin-treated Type 2 diabetics, and 50 healthy controls were included. We determined PLTP activity before and 4 and 8 h after a high-fat meal. As expected, serum PLTP activity was significantly higher in CHD patients than in healthy controls (71.0 ± 46.2 vs. 54.0 ± 33.8 pmol/μl/h, $P = 0.032$) at baseline. More importantly, we found that serum PLTP activity increased to its maximum 4 h after fat loading and then decreased to nearly basal levels after 8 h both in controls and CHD patients. In contrast, PLTP activity continuously increased during this time period in the diabetic patients. With regards to the data from this study we hypothesize that serum PLTP is involved in the clearance of postprandial lipoproteins and this process is attenuated in diabetes. Since postprandial lipoproteins are atherogenic, the delay in clearance of these particles could play an important role in the development of atherosclerosis in patients with diabetes mellitus.

Keywords Phospholipid transfer protein · Diabetes mellitus

Abbreviations

ACE	Angiotensin converting enzyme
BLp	ApoB-containing lipoprotein
CAD	Coronary artery disease
CHD	Coronary heart disease
CRP	C-reactive protein
HDL	High density lipoprotein
HDL-C	High density lipoprotein-cholesterol
OGTT	Oral glucose tolerance test
PLTP	Phospholipid transfer protein
RLP	Remnant-like particle
TG	Triglycerides
VLDL	Very low density lipoprotein

A. Schlitt and B. Schwaab contributed equally to the submitted work.

A. Schlitt (✉) · A. Vogt · M. Buerke · L. Maegdefessel · U. Raaz · K. Werdan
Department of Medicine III, Martin Luther-University, Ernst-Grube-Str 40, 06120 Halle, Germany
e-mail: axel.schlitt@medizin.uni-halle.de

A. Vogt
e-mail: Vogt.Alex@gmx.net

B. Schwaab · K. Fingscheidt
Curschmann-Clinic, Timmendorfer Strand, Germany

K. J. Lackner
Institute of Clinical Chemistry and Laboratory Medicine, Johannes Gutenberg University, Mainz, Germany

G. H. Heine
Department of Medicine IV, University of the Saarland, Homburg/Saar, Germany

X.-C. Jiang
Department of Anatomy and Cell Biology, Downstate Medical Center Brooklyn, State University of New York, New York, USA

Introduction

The plasma phospholipid transfer protein (PLTP) is primarily involved in high density lipoprotein (HDL) metabolism. PLTP mediates both net transfer and exchange of phospholipids between lipoproteins [1].

PLTP's proatherogenic potency has been clearly demonstrated in atherogenic mouse models: PLTP deficiency resulted in markedly decreased atherosclerosis due in part to decreased production and lower levels of apoB-containing lipoproteins (BLp) [2] and increased bioavailability of vitamin E in atherogenic lipoproteins [3]. PLTP overexpression resulted in markedly increased atherosclerosis due in part to decreased HDL levels [4] and increased VLDL secretion [5].

The role of PLTP in atherosclerosis in humans is still the subject of controversy, however. We have previously shown that high plasma PLTP activity is a risk factor for coronary heart disease (CHD) [6]. In contrast, other authors showed that low PLTP activity was a risk factor for peripheral atherosclerosis [7]. Furthermore, we found that serum PLTP activity was higher in hemodialysis patients than in matched controls and represents a further aspect of uremic dyslipidemia in end-stage kidney disease. However, PLTP activity was not related to survival in this patient group [8]. On the other hand, we found in a recent publication that PLTP is a not only a risk marker but a risk factor for CAD-patients under statin treatment [9]. Thus, the significance of PLTP in atherogenesis is still an open issue.

Patients suffering from diabetes mellitus are at high risk for atherosclerotic diseases. Interestingly, several reports have shown that plasma PLTP activity is elevated in Type 2 [10–12] and Type 1 [13] diabetes mellitus. Furthermore, plasma PLTP decreased in response to exogenous insulin and these effects of insulin were impaired in obese type II diabetic patients. This forms the basis for the hypothesis that plasma PLTP is regulated by insulin [14].

To further investigate possible linkages among PLTP activity, diabetes, and atherosclerosis, we measured serum PLTP activity in insulin-treated patients with diabetes mellitus, patients suffering from coronary heart disease, and healthy controls at baseline and 4 and 8 h after eating a high-fat meal.

Experimental Procedure

Study Population

This prospective study was designed to evaluate postprandial lipoprotein metabolism with a focus on the postprandial kinetics of PLTP activity. We included 50 patients with insulin-treated Type 2 diabetes mellitus (approximately 2/3 of patients suffered from CHD and patients with Type 1 diabetes were excluded), 50 patients with angiographically proven CHD without diabetes mellitus, and 50 subjects with no clinical or anamnestic evidence of atherosclerosis or diabetes mellitus recruited in a general practitioner's office in Timmendorfer Strand. A diabetes mellitus or impaired glucose tolerance in patients with CHD and controls was excluded by standard methods of the Curschmann Clinic Timmendorfer Strand (measurement of fasting glucose, OGTT).

All study subjects were of German nationality and the patients were recruited in the Curschmann Clinic for Rehabilitation, Timmendorfer Strand, Germany. The study was approved by the ethics committee of the University of Lübeck, Germany. Participation was voluntary and each participant gave written informed consent.

Laboratory Methods

Blood samples were taken from all subjects under standardized conditions after an overnight period of fasting. After this first blood sample was taken, subjects ate in a period of approximately 15 min, a meal high in fat, consisting of a total of 1,265 kcal/m^2 body surface area (105 g of fat, consisting of 52 g saturated fat and 300 mg cholesterol, with 48 g carbohydrates and 32 g protein). Subjects were instructed not to eat any other food until after the last blood sample was taken. Further blood samples were taken after 4 and 8 h. All blood samples were immediately centrifuged at 4,000 rpm for 10 min and divided into aliquots. All aliquots were stored at −80 °C until analysis.

Before eating the meal, patients with diabetes mellitus received a dosage of subcutaneous insulin individually adapted to the meal described above. Glucose levels were measured every 2 h until the end of study period to diagnose severe hypo- or hyperglycemia. Indeed, additional insulin administration was required to treat blood glucose levels above 250 mg/dl in three patients (each 4 IU of rapid-acting insulin after 4 h). In another three patients additional carbohydrates were administered to increase blood glucose levels that were lower than 80 mg/dl (all asymptomatic).

PLTP activity was measured by using an assay kit (Cardiovascular Target, NY, USA). Basically, the kit includes donor and acceptor particles. Upon incubating donor and acceptor with 3 µl of human plasma PLTP mediates the transfer of fluorescent phospholipid, which is present in a self-quenched state when associated with the donor. The transfer is determined by the increase in fluorescence intensity as the fluorescent lipid is removed from the donor and transferred to the acceptor. The interassay coefficient of variation in PLTP activity was 3.3 ± 0.5%.

The linear range of PLTP activity in this assay was between 1 and 7 μl of plasma. Three freeze–thaw cycles of plasma did not influence the assay. The PLTP activity was analyzed concurrently in cases and controls, and the laboratory personnel was unaware of the individual group allocation.

C-reactive protein and serum lipoprotein levels were measured by standard methods used at the Institute of Clinical Chemistry and Laboratory Medicine, Johannes Gutenberg University, Mainz, Germany (Roche Diagnostics GmbH, Germany and Rolf Greiner GmbH, Germany).

Statistical Analysis

Continuous variables are presented as mean ± standard deviation, categorical variables in %. The distributions for serum concentrations of triglycerides, HDL-C and CRP were skewed and all analyses were calculated with log-transformed values; however, exponential values were presented. For all analyses log-transformed values of triglycerides, HDL-C and CRP for each group individually were used. Mean levels of variables were compared by ANOVA with post hoc analyses. Pearson's correlation coefficient was used to perform correlation analysis. All analyses were carried out using SPSS 11.5 (SAS Institute Inc., Cary, NC).

Results

Baseline Data

BMI and sex did not differ between insulin-treated diabetic patients and CHD patients and controls; however, the diabetics were older. As expected, active smokers were found more frequently among the controls than in the two patient groups, and medical treatment with statins, ACE inhibitors, β-blockers, diuretics, angiotensin-receptor—blockers, and classic risk factors were more often found in the two patient groups (Table 1). In 33 diabetics (66%) a history of coronary heart disease was known.

Pre- and Post-Prandial PLTP Activity, Total Cholesterol, HDL Cholesterol, Triglycerides, and CRP

As shown in Fig. 1a, at basal level, serum PLTP activity was significantly higher in CHD patients than in controls (71.0 ± 46.22 vs. 54.0 ± 33.8 pmol/μl/h, $P = 0.032$). This result confirmed our previous observations [6]. Furthermore, such a difference is also found when comparing CHD patients and insulin-treated diabetic patients (71.0 ± 46.2 vs. 46.6 ± 35.2 pmol/μl/h, $P = 0.007$).

Table 1 Baseline variables in healthy controls, patients with coronary heart disease, and patients with insulin-treated diabetes are shown. Continuous variables are presented as mean ± standard deviation (statistical comparison by ANOVA), categorical variables in % (statistical comparison by chi-square test)

	Controls	CHD patients	Diabetics
Age (years)	52.7 ± 11	55.5 ± 9	64.0 ± 8.7
Sex (male), %	82	84	78
BMI (kg/m^2)	26.6 ± 4.6	26.8 ± 3.6	28.2 ± 5.0
Hypertension (%)	20	98	90
FH of CHD (%)	6	42	18
Active smokers (%)	34	2	10
CHD (%)	0	100	66
Statins (%)	4	96	96
β-blockers (%)	10	98	68
ACE Inhibitors (%)	8	56	62
ARB (%)	2	16	14
Diuretics (%)	10	20	42

FH of CHD family history of coronary heart disease, *CHD* coronary heart disease, *Diabetics* patients with insulin-treated diabetes

To investigate the influence of potential confounders on group comparison of PLTP activity we adjusted the analysis regarding group comparisons of PLTP activity at baseline and found also in a regression analysis including the variables age, sex and BMI that PLTP at baseline was significantly different in the comparison of subgroups independent on these potential confounders ($P < 0.001$) as presented above.

Four hours after the high-fat meal, serum PLTP activity had more than doubled in both controls (134.0 ± 66.0 vs. 54.0 ± 33.8 pmol/μl/h, $P < 0.001$) and CHD patients (149.3 ± 81.3 vs. 71.0 + 46.22 pmol/μl/h; $P < 0.001$). In contrast, PLTP activity had only increased by 23% in diabetic patients and this effect was not statistically significant (62.1 ± 39.8 vs. 46.6 ± 35.2 pmol/μl/h, $P = 0.051$). Eight hours after the high-fat meal, serum PLTP activity was significantly decreased both in controls and CHD patients ($P < 0.001$ in both groups compared to 4 h after the meal), whereas in diabetics serum PLTP activity tended to increase as compared to measurements 4 h after the meal (72.3 ± 42.5 vs. 62.1 ± 39.8 pmol/μl/h, $P = 0.198$. In other words, postprandial serum PLTP activity was blunted in insulin-treated diabetes patients (see Fig. 1a).

We showed in an additional analysis that the prolonged increase of PLTP activity in insulin-treated diabetic patients during the study period could have been shown both in insulin-treated diabetic patients with or without known CHD (see Table 2). Interestingly, serum PLTP activity was not significantly increased in insulin-treated diabetic patients with known CHD in comparison to insulin-treated diabetic patients without known CHD, which is

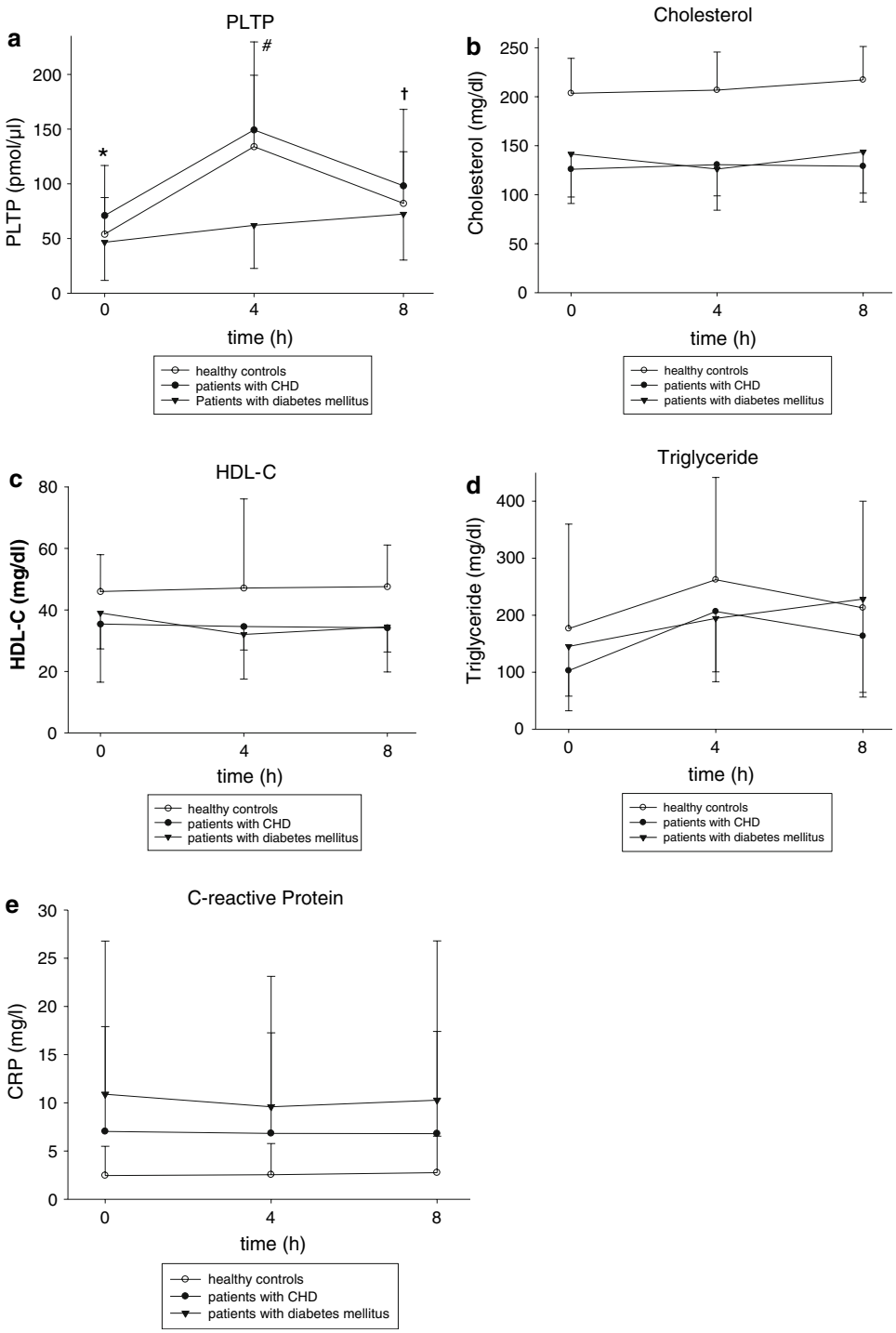

Fig. 1 Pre- and postprandial PLTP activity (**a**), total cholesterol (**b**), HDL cholesterol (**c**), triglyceride (**d**), and CRP (**e**) levels 4 and 8 h after intake of a high-fat meal as described in the material and methods section. All results are presented as mean ± standard deviation. **a** *Asterisk* CHD versus control $P = 0.032$. CHD versus insulin treated diabetic patients $P = 0.007$. *Hash* PLTP activity in CHD and control patients at 0 versus 4 h $P < 0.001$. *Dagger* PLTP activity in CHD and control patients at 4 versus 8 h $P < 0.001$. **b** Control vs. CHD and Control versus insulin treated diabetic patients $P < 0.05$ at 0, 4 and 8 h. **c** Control versus CHD and Control versus insulin treated diabetic patients $P < 0.05$ at 0, 4 and 8 h. **d**, **e** CHD versus control and insulin treated diabetic patients versus control $P < 0.05$ at 0, 4 and 8 h

in concordance with the increase of PLTP activity shown in CHD patients in comparison to insulin-treated diabetic patients in our study (see Table 2).

Next, we measured triglyceride levels, a well-known marker of postprandial lipoprotein catabolism. As expected, both controls and CHD patients showed a bell-shaped curve, indicating accumulation and clearance of postprandial lipoproteins in the circulation after a high-fat loading. To our surprise, such a curve did not exist in insulin-treated Type 2 diabetes patients (Fig. 1d). Like PLTP activity, triglyceride levels were continuously increased in the period of 8 h after the high-fat meal, suggesting that PLTP activity may be responsible for the clearance of postprandial lipoprotein clearance.

We also measured HDL cholesterol and total cholesterol levels. Here, no bell-shaped curve could be observed,

Table 2 Serum PLTP activity in comparison of insulin dependent diabetic patients with or without known CHD. Statistical comparison by *T* test

	PLTP0 pmol/μl/h, mean ± SD	PLTP4 pmol/μl/h, mean ± SD	PLTP8 pmol/μl/h, mean ± SD
Insulin dependent diabetics without known CHD ($n = 17$)	35.8 ± 37.7	47.6 ± 39.6	58.9 ± 38.6
Insulin dependent diabetics with known CHD ($n = 33$)	52.1 ± 33.0	69.1 ± 38.6	78.9 ± 43.4
P-value	0.121	0.076	0.124

0 fasting, *4* 4 h after a high-fat meal, *8* 8 h after a high-fat meal, *SD* standard deviation

which we also reported previously in another study [15]. Moreover, controls had significantly higher HDL cholesterol and total cholesterol levels at all time points than the patients in both groups (Fig. 1c, d all P-values < 0.05). We also measured CRP levels and found that CRP was significantly increased in both patient groups at all time points in comparison to healthy controls (Fig. 1e, all P-values < 0.05).

Correlation Analyses

Interestingly, PLTP was not correlated to triglycerides in any subject at any time point (all P-values > 0.05, data not presented). However, we found a significant association between fasting triglycerides and PLTP activity 8 h after the meal in diabetics or 4 h afterwards in CHD patients, but not in other subgroups (Table 3).

Glucose Levels

Glucose levels were measured in insulin-treated diabetic patients during the study period. We found at baseline a fasting glucose of 145.7 ± 29.7 mg/dl (mean ± SD). Then, glucose levels increased to its maximum 2 h after the meal (182.9 ± 42.0 mg/dl) and continuously decreased during the next 6 h (162.3 ± 58.9 mg/dl 4 h, 128.8 ± 43.9 mg/dl 6 h, 108.9 ± 33.3 mg/dl 8 h after the high fat meal, respectively).

Moreover, we found no significant correlation of PLTP with glucose levels at all time points. Correlations were: PLTP0-Gluc0: $r = -0.207$, $P = 0.222$, PLTP4-Gluc4: $r = -0.272$, $P = 0.094$, PLTP8-Gluc8: $r = -0.204$, $P = 0.213$.

Discussion

In the present study we confirmed our previous observation that plasma PLTP activity is significantly higher in CAD patients than in controls [6]. Furthermore, we demonstrated the following for the first time: (1) postprandial serum PLTP activity levels, like serum TG levels, show a bell-shaped curve with a peak at 4 h in healthy controls and CHD-patients; (2) in insulin-treated patients with diabetes mellitus, postprandial PLTP activity, with a linear line, was significantly lower than that in controls and CAD patients; and (3) postprandial PLTP activity correlates with serum TG levels 8 h after the high-fat meal in diabetic patients. Thus, we hypothesize that serum PLTP is involved in the clearance of postprandial lipoproteins, which is attenuated in insulin-treated Type 2 diabetes.

Table 3 Pearsons coefficients of correlation between PLTP activity and fasting triglycerides in all subgroups. For all analyses, log-transformed values of triglycerides were used

	PLTP0	PLTP4	PLTP8
Controls	$r = -0.231$	$r = 0.014$	$r = 0.088$
TRIGL0	$P = 0.118$	$P = 0.942$	$P = 0.655$
CHD patients	$r = 0.207$	$r = -0.293$	$r = -0.226$
TRIGL0	$P = 0.154$	$P = 0.041$*	$P = 0.123$
Diabetics	$r = 0.085$	$r = 0.071$	$r = -0.298$
TRIGL0	$P = 0.556$	$P = 0.631$	$P = 0.039$*

TRIG triglyceride, *0* fasting, *4* 4 h after a high-fat meal, *8* 8 h after a high-fat meal

*$P < 0.05$ was considered as significant

Based on our observation, serum PLTP activity levels have a typical postprandial rhythm after a high-fat loading, which is mainly affected by the predisposing metabolic conditions. However, our results are different from those published in two previous reports [16, 17], in which postprandial PLTP activity remained nearly unchanged. The obvious difference between the present study and the others is the size of the population. We included 150 persons, whereas not even 15 persons were included in the two previous studies. Moreover, in another study with healthy controls an infusion highly concentrated with triglycerides increased PLTP from 8 h to its maximum after 24 h [15], which may further underline the hypothesis of a regulatory effect of postprandial triglycerides on PLTP.

Furthermore, PLTP mediates the net transfer of phospholipids from apoB-containing particles (postprandial lipoproteins are a major part of them) to HDL, promotes transfer of phospholipids from VLDL and chylomicron into HDL-particles [18], and without PLTP activity HDL levels are dramatically reduced [18]. Thus, it is conceivable that

PLTP activity is necessary to catabolize postprandial lipoproteins.

Although the risk factors for atherosclerotic diseases are well established in diabetes mellitus [19, 20], we hypothesize that PLTP may represent an additional one in these patients.

In diabetes mellitus PLTP is considered to be a determinant of carotid intima-media thickness, an important prognostic marker for patients with CHD [21]. Furthermore, PLTP is increased in patients with impaired glucose tolerance, type II diabetes, and type I diabetes [10–14, 22, 23]. However, in the present study we could not confirm these observations. We found that PLTP activity was not different in diabetics in comparison to healthy controls (54.0 ± 33.8 vs. 46.6 ± 35.2 pmol/μl/h, $P = 0.339$) (Fig. 1a). This may be partly explained by the quiescent disease state predominant in our rehabilitation patients.

The topic of PLTP regulation has been discussed extensively. On the one hand, PLTP secretion may be up-regulated by glucose in vitro; on the other, plasma PLTP activity is decreased by exogenous hyperinsulinemia and glucose-induced hyperinsulinemia in vivo [14, 24, 25].

In our study PLTP increased in the subgroup of insulin-treated diabetics from the fasting state to 4 and 8 h after the meal, although insulin in an adapted dosage was subcutaneously administered before eating the high-fat meal. This means that all diabetics in our study had a peak glucose level accompanied by a peak insulin level approximately 1–2 h after the meal. Then, blood glucose levels decreased slightly in all patients, which was accompanied by a short peak after administering long-acting insulin and also followed by a slight decrease in plasma insulin levels until the end of the 8-hour study period without taking any other food. This underlines the hypothesis that PLTP is not regulated by hyperglycemia and hyperinsulinemia [26]; otherwise, we would expect the same increase in PLTP after 4 h followed by a decrease to 8 h in the diabetic patients that was found in nondiabetic CHD patients and healthy controls in our study.

This finding is supported by correlation analyses in the diabetic subgroup: we found no significant correlation of PLTP with glucose levels at all time points (see "Results" section). However, the interpretation of these data is limited by the fact that we didn't measured glucose in the other groups. On the other hand the different results of our and the previous studies regarding association of PTLP with glucose may be explained by different designs [14, 24–26].

In a subanalysis comparing the diabetics with unknown CHD with diabetics suffering from CHD, the increase of PLTP activity from baseline to 4 and 8 h after the high fat meal was found in both subgroups. Thus, increase of PLTP in the diabetic subgroup was independent on CHD.

Regulation of PLTP under physiological or pathophysiological conditions is still an open issue. As PLTP plays a key role in (postprandial) lipoprotein metabolism [27], other factors related to lipoprotein markers may regulate PLTP activity. Triglycerides are markers of proatherogenic postprandial remnant-like particles (RLP) [28]. Furthermore, it is well known that RLP receptors are downregulated in diabetics and atherosclerotic diseases [28], and in the present study triglycerides increased from fasting to 4 and 8 h after the high-fat meal in the diabetic subgroup; therefore, we hypothesize that serum PLTP activity is related to abnormal RLP metabolism. To confirm this hypothesis, we performed correlation analyses but we found no correlation between fasting triglycerides and PLTP in the total cohort or in healthy controls. However, we did find a significant and negative association between fasting triglycerides and postprandial PLTP activity after eight hours in diabetics ($r = -0.293$, $P = 0.041$) and postprandial PLTP activity after 4 h in CHD patients ($r = -0.298$, $P = 0.039$). Thus, we hypothesize that serum triglycerides and, as a consequence, RLP concentrations may be involved in PLTP regulation under atherosclerotic conditions, which is more prolonged in diabetics than in patients with CHD in our study. However, the negative correlations between PLTP activity and TG levels found in patient groups (at 0 and 8 h) reflects the known alteration of postprandial triglyceride lipolysis in patients with Type 2 diabetes mellitus and CHD rather than RLP clearance [29, 30].

In summary, our study suggests that PLTP is involved in postprandial lipoprotein clearance and this ability is diminished in insulin-treated diabetes. This phenomenon is possibly related to abnormal postprandial clearance of remnant-like particles in these patients.

Acknowledgments Part of this study was taken from the thesis of Kirsten Fingscheidt. The study was partially supported by National Institute of Health grant HL69817.

References

1. Tall AR, Krumholz S, Olivecrona T, Deckelbaum RJ (1985) Plasma phospholipid transfer protein enhances transfer and exchange of phospholipids between very low density lipoproteins and high density lipoproteins during lipolysis. J Lipid Res 26:842–851
2. Jiang XC, Qin S, Qiao C, Kawano K, Lin M, Skold A, Xiao X, Tall AR (2001) Apolipoprotein B secretion and atherosclerosis are decreased in mice with phospholipid-transfer protein deficiency. Nat Med 7:847–852
3. Jiang XC, Tall AR, Qin S, Lin M, Schneider M, Lalanne F, Deckert V, Desrumaux C, Athias A, Witztum JL, Lagrost L (2002) Phospholipid transfer protein deficiency protects circulating lipo- proteins from oxidation due to the enhanced accumulation of vitamin E. J Biol Chem 277:31850–31856
4. van Haperen R, van Tol A, van Gent T, Scheek L, Visser P, van der Kamp A, Grosveld F, de Crom R (2002) Increased risk of

atherosclerosis by elevated plasma levels of phospholipid transfer protein. J Biol Chem 277:48938–48943
5. Lie J, de Crom R, van Gent T, van Haperen R, Scheek L, Lankhuizen I, van Tol A (2002) Elevation of plasma phospholipid transfer protein in transgenic mice increases VLDL secretion. J Lipid Res 43:1875–1880
6. Schlitt A, Bickel C, Thumma P, Blankenberg S, Rupprecht HJ, Meyer J, Jiang XC (2003) High plasma phospholipid transfer protein levels as a risk factor for coronary artery disease. Arterioscler Thromb Vasc Biol 23:1857–1862
7. Schgoer W, Mueller T, Jauhiainen M, Wehinger A, Gander R, Tancevski I, Salzmann K, Eller P, Ritsch A, Haltmayer M, Ehnholm C, Patsch JR, Foeger B (2008) Low phospholipid transfer protein (PLTP) is a risk factor for peripheral atherosclerosis. Atherosclerosis 196:219–226
8. Schlitt A, Heine GH, Jiang XC, Messow M, Blankenberg S, Rupprecht HJ, Ulrich C, Buerke M, Werdan K, Lackner KJ, Köhler H, Girndt M (2007) Phospholipid transfer protein (PLTP) in hemodialysis patients. Am J Nephrol 27:138–143
9. Schlitt A, Blankenberg S, Bickel C, Lackner KJ, Heine GH, Buerke M, Werdan K, Maegdefessel L, Raaz U, Rupprecht HJ, Munzel T, Jiang XC (2009) PLTP activity is a risk factor for subsequent cardiovascular events in CAD patients under statin therapy: the AtheroGene Study. J Lipid Res 50:723–729
10. Riemens SC, Van Tol A, Sluiter WJ, Dullaart RPF (1998) Elevated plasma cholesteryl ester transfer in NIDDM: relationships with apolipoprotein B-containing lipoproteins and phospholipids transfer protein. Atherosclerosis 140:71–79
11. Desrumaux C, Athias A, Bessède G, Vergès B, Farnier M, Perségol L, Gambert P, Lagrost L (1999) Mass concentration of plasma phospholipid transfer protein in normolipidemic, type IIa hyperlipidemic, type IIb hyperlipidemic, and non-insulin-treated diabetic subjects as measured by a specific ELISA. Arterioscler Thromb Vasc Biol 19:266–275
12. Tan KC, Shiu SW, Wong Y, Tam S (2005) Plasma phospholipids transfer protein activity and subclinical inflammation in Type 2 diabetes mellitus. Atherosclerosis 178:365–370
13. Colhoun HM, Taskinen MR, Otvos JD, Van Den Berg P, O'Connor J, Van Tol A (2002) Relationship of phospholipid transfer protein activity to HDL and apolipoprotein B-containing lipoproteins in subjects with and without Type 1 diabetes. Diabetes 51:3300–3305
14. Riemens SC, van Tol A, SluiterE WJ, Dullaart RPF (1998) Plasma phospholipid transfer protein activity is related to insulin resistance: impaired acute lowering by insulin in obese Type II diabetic patients. Diabetologia 41:929–934
15. Riemens SC, Van Tol A, Sluiter WJ, Dullaart RP (1999) Acute and chronic effects of a 24-hour intravenous triglyceride emulsion challenge on plasma lecithin: cholesterol acyltransferase, phospholipid transfer protein, and cholesteryl ester transfer protein activities. J Lipid Res 40:1459–1466
16. Syeda F, Senault C, Delplanque B, Le Roy B, Thaminy A, Gripois D, Blouquit MF, Ruelland A, Mendy F, Lutton C (2003) Postprandial variations in the cholesteryl ester transfer protein activity, phospholipid transfer protein activity and plasma cholesterol efflux capacity in normolipidemic men. Nutr Metab Cardiovasc Dis 13:28–36
17. Mero N, Van Tol A, Scheek LM, Van Gent T, Labeur C, Rosseneu M, Taskinen MR (1998) Decreased postprandial high density lipoprotein cholesterol and apolipoproteins A-I and E in normolipidemic smoking men: relations with lipid transfer proteins and LCAT activities. J Lipid Res 39:1493–1502
18. Jiang XC, Bruce C, Mar J, Lin M, Ji Y, Francone OL, Tall AR (1999) Targeted mutation of plasma phospholipid transfer protein gene markedly reduces high-density lipoprotein levels. J Clin Invest 103:907–914
19. McFarlane SI, Banerji M, Sowers JR (2001) Insulin resistance and cardiovascular disease. J Clin Endocrinol Metab 86:713–718
20. Haffner SM, Lehto S, Ronnemaa T, Pyorala K, Laakso M (1998) Mortality from coronary heart disease in subjects with Type 2 diabetes and in nondiabetic subjects with and without prior myocardial infarction. N Engl J Med 339:229–234
21. de Vries R, Dallinga-Thie G, Smit A, Wolffenbuttel B, van Tol A, Dullaart R (2006) Elevated plasma phospholipid transfer protein activity is a determinant of carotid intima-media thickness in Type 2 diabetes mellitus. Diabetologia 49:398–404
22. Julius U, Jauhiainen M, Ehnholm C, Pietzsch J (2007) Lipid transfer protein activities in subjects with impaired glucose tolerance. Clin Chem Lab Med 45:237–243
23. Dullaart RP, de Vries R, Dallinga-Thie GM, Sluiter WJ, van Tol A (2008) Phospholipid transfer protein activity is determined by Type 2 diabetes mellitus and metabolic syndrome, and is positively associated with serum transaminases. Clin Endocrinol (Oxf) 68:375–381
24. Oomen PH, van Tol A, Hattori H, Smit AJ, Scheek LM, Dullaart RP (2005) Human plasma phospholipid transfer protein activity is decreased by acute hyperglycaemia: studies without and with hyperinsulinaemia in Type 1 diabetes mellitus. Diabet Med 22:768–774
25. Riemens SC, Van Tol A, Sluiter WJ, Dullaart RPF (1999) Plasma phospholipids transfer protein activity is lowered by 24-h insulin and acipimox administration: blunted response to insulin in Type 2 diabetic patients. Diabetes 48:1631–1637
26. Colhoun HM, Scheek LM, Rubens MB, Van Gent T, Underwood SR, Fuller JH, Van Tol A (2001) Lipid transfer protein activities in Type 1 diabetic patients without renal failure and non-diabetic control subjects and the association with coronary artery calcification. Diabetes 50:652–659
27. Tall AR, Lalanne F (2003) Phospholipid transfer protein and atherosclerosis. Arterioscler Thromb Vasc Biol 23:1484–1485
28. Schlitt A, Hojjati MR, von Gizycki H, Lackner KJ, Blankenberg S, Schwaab B, Meyer J, Rupprecht HJ, Jiang XC (2005) Serum sphingomyelin levels are related to the clearance of postprandial remnant-like particles. J Lipid Res 46:196–200
29. Syvänne M, Hilden H, Taskinen MR (1994) Abnormal metabolism of postprandial lipoproteins in patients with non-insulin-dependent diabetes mellitus is not related to coronary artery disease. J Lipid Res 35:15–26
30. Durlach V, Attia N, Zahouani A, Leutenegger M, Girard-Globa A (1996) Postprandial cholesteryl ester transfer and high density lipoprotein composition in normotriglyceridemic non-insulin-dependent diabetic patients. Atherosclerosis 120:155–165

Lipids (2010) 45:137–144
DOI 10.1007/s11745-010-3386-3

ORIGINAL ARTICLE

Fatty Acid Composition of Plasma, Erythrocytes and Adipose: Their Correlations and Effects of Age and Sex

Tokuhiro Ogura · Hideho Takada · Masashi Okuno · Hiroaki Kitade · Takashi Matsuura · Masanori Kwon · Seizaburo Arita · Kei Hamazaki · Miho Itomura · Tomohito Hamazaki

Received: 17 September 2009 / Accepted: 4 January 2010 / Published online: 22 January 2010

Abstract The composition of fatty acids in abdominal subcutaneous adipose tissue and the correlation of fatty acid values of plasma and erythrocytes had not been reported in Japan. The aim of the present study was to investigate the fatty acid composition and correlation of plasma and erythrocyte phospholipids (PL) and adipose triacylglycerols (TG) in 75 adult patients admitted for non-malignant diseases. We also examined the relationship of n-3 and n-6 polyunsaturated fatty acid (PUFA) with patients' characteristics. The total n-3 PUFA were 11.2, 11.8 and 1.9%, and the ratios of n-6/n-3 were 2.41, 1.87 and 8.20 in plasma and erythrocyte PL and adipose TG, respectively. There were the highest correlations for total n-3 PUFA and the n-6/n-3 ratio between plasma and erythrocyte PL and adipose TG. There was a positive correlation between n-3 PUFAs and age, but a negative correlation was found between n-6 PUFAs and age. There was no significant difference in the values of PUFAs in plasma and erythrocyte PL and adipose TG between men and women. The patients with cholesterol cholecystolithiasis showed a significantly lower proportion of eicosapentaenoic acid in plasma and erythrocyte PL than those of the other patients. Our findings suggest that PUFA in plasma and erythrocyte PL may be good biomarkers and more acceptable for studying participants than adipose TG.

Keywords Fatty acid composition · Plasma phospholipids · Erythrocyte phospholipids · Adipose triacylglycerols · Age · Sex · Body mass index · Cholesterol cholecystolithiasis

Abbreviations

ARA	Arachidonic acid
BMI	Body mass index
DHA	Docosahexaenoic acid
EPA	Eicosapentaenoic acid
LA	Linoleic acid
PL	Phospholipid
PUFA	Polyunsaturated fatty acid
TG	Triacylglycerol

T. Ogura · H. Takada (✉) · M. Okuno · H. Kitade · T. Matsuura
Division of Surgery, Takii Hospital of Kansai Medical University, 10-15 Fumizono, Moriguchi, Osaka 570-8507, Japan
e-mail: takadahi@takii.kmu.ac.jp

M. Kwon
Department of Surgery, Hirakata Hospital of Kansai Medical University, 2-3-1 Shinmachi, Hirakata, Osaka 573-1192, Japan

S. Arita
Department of Biostatics, Kansai Medical University, 18-89 Uyamahigashi, Hirakata, Osaka 573-1136, Japan

K. Hamazaki · M. Itomura · T. Hamazaki
Division of Clinical Application, Department of Clinical Science, Institute of Natural Medicine, University of Toyama, 2630 Sugitani, Toyama, Japan

Introduction

In Japan, dietary habits and lifestyle have changed greatly, and nutritionally related diseases are rapidly approaching the levels of Western countries [1–7]. A review of data published by the Japan Ministry of Health, Labour and Welfare for the national nutritional survey in Japan for the years between 1955 and 2004 [6] showed that the total energy intake had changed little. However, the intake of fat has been increasing markedly. In 1955, carbohydrates

accounted for nearly 80% of the total energy intake, but there has been a gradual decrease year by year, and the decrease in the percentage of energy from carbohydrates was balanced by an increase in the percentage of energy from fat intake. Furthermore, the components of dietary fat also changed in Japan between 1955 and 2004. The presence of sea foods rich in eicosapentaenoic acid (EPA) and docosahexaenoic acid (DHA) in the traditional Japanese diet helped to provide a diet with relatively low ratios of n-6 to n-3 polyunsaturated fatty acids (PUFAs). The fat intake from those sources has remained almost the same since 1955, while the intake of animal and vegetable fats rapidly increased up to 1975, with a further slow increase being evident from 1975 to 1995, and a relatively slow decrease afterward. Clearly, the increased fat intake in Japan has been due to the increased consumption of animal and vegetable fats, and not fish oil. This is an obvious reflection of the westernization of Japanese dietary habits, and it has had a negative impact. Dietary intake of fat is related to cardiovascular disease [4, 7, 8], obesity [9, 10] and some cancers [2, 3]. Greater emphasis has been placed on the potential health benefit of maintaining good nutritional practices.

The fatty acid composition of serum lipids has been considered a reliable index reflecting dietary intake of fatty acids over periods of weeks or months [11, 12]. The rate at which fatty acid changes occur in red blood cells is slower than that for plasma lipids [13, 14]. The fatty acid composition of subcutaneous adipose tissue changes much more slowly than that of the other lipid fractions, e.g., plasma lipids and the erythrocyte membrane. The individual level of fatty acid composition of adipose tissue is a valid index for the habitual dietary fatty acid composition over the preceding two and half years in free living adults [15, 16], and this means that subcutaneous adipose tissue biopsies can be particularly useful for studying the long-term effects of dietary fat quality [17]. However, taking blood samples is more acceptable to study patients than adipose tissue excision or aspiration, and fatty acid measurement in plasma or erythrocyte membrane lipids may be more feasible in large-scale epidemiological studies if plasma or red blood cells could be substituted for subcutaneous fat.

In Japan, there is a long history of eating fish, but the Japanese diet continues to become more westernized, especially among the younger generation. We therefore examined the fatty acid composition of these lipids and the association between plasma and erythrocyte phospholipid (PL) and abdominal subcutaneous adipose triacylglycerol (TG) in adults patients admitted for non-malignant diseases. We also examined the role of several personal characteristics (such as age, sex, BMI and patients with cholesterol gallstones etc.) in terms of fatty acid composition of plasma and erythrocyte PL and adipose TG.

Experimental Procedures

Subjects

Seventy-five adult patients who had been admitted for elective surgery to Kansai Medical University Hospital for non-malignant disease; 39 inguinal hernia, 28 cholesterol cholecystolithiasis, 6 abdominal aortic aneurysm, and 2 varicosis patients were entered into this study, of whom 48 were men and 27 were women. Patients with previously reported metabolically important disease (diabetes, hepatic or renal dysfunction, and those undergoing drug treatment for hyperlipidemia) were excluded. Body mass index (BMI) was calculated as weight in kilograms divided by the square of the height in meters.

The protocol was approved by the ethical committee of Kansai Medical University, and all study participants gave their informed consent for use of blood samples and subcutaneous fat for research purposes.

Fasting blood samples obtained after 12–14 h overnight fasting were collected and placed in plastic tubes containing EDTA as an anticoagulant, mixed, and centrifuged for 15 min at room temperature. Plasma and packed red blood cells were obtained from EDTA-anticoagulated blood. Plasma was then transferred to smaller tubes for storage at −80 °C until analysis. RBCs were washed twice with saline and frozen at −80 °C until analysis.

A fragment of adipose tissue was removed from abdominal subcutaneous fat during surgery. Each fragment was rinsed with saline, immediately frozen on dry ice and stored at −80 °C until analysis.

Fatty Acid Analysis

The fatty acid composition of the total phospholipid fraction of washed red blood cells and plasma was determined as follows: Total lipids were extracted by the method of Bligh and Dyer [18]. The total phospholipid fraction was separated by thin-layer chromatography and after transmethylation with HCL–methanol, the fatty acid composition was analyzed by gas chromatography (GC14A Shimadzu Corporation, Kyoto, Japan) with a capillary column DB-225 (0.25 mm, 30 m length id, 0.25 μm; J&M Scientific, Folsom, CA, USA). The column temperature was kept at 170 °C for the first 1 min, raised to 220 °C at a rate of 4 °C/min, and kept at this temperature for 22 min. The whole system was controlled with gas chromatography software, CLSS-GC10 ver. 1.3 (Shimadzu Corporation, Kyoto, Japan).

The fatty acid composition of the triacylglycerol fraction of subcutaneous adipose tissue was determined in a similar manner, except that the TG fraction separated by thin-layer chromatography was used. We adopted the area

percentage of each fatty acid in all detected fatty acids as a measurement value.

The laboratory was blind to the sample origin (disease, sex, age etc.).

Statistical Analysis

Data are expressed as means ± SD. Statistical analysis for the subject characteristics between sex and age groups was performed by the Mann–Whitney test. The correlation for some PUFAs between plasma and erythrocyte PL and adipose TG was calculated using Spearman's method. Univariate regression and multivariate analyses were performed to assess the relationship between plasma PL EPA + DHA, erythrocyte PL EPA + DHA and adipose TG EPA + DHA and characteristics (age and BMI) of participants. Associations between plasma PL linoleic acid (LA) + arachidonic acid (ARA), erythrocyte PL LA + AA and adipose TG LA + AA and some characteristics of the subjects were also analyzed in the same way. In the case of multivariate analysis, age and BMI were included into the calculation as independent predictors. The association of the area percentage of PUFAs for plasma and erythrocyte PL and adipose TG in men and women was analyzed by the ratio test. All statistical analyses were performed with JMP 2005 by the SAS institute Inc., Cary, NC., USA. Significance was taken as $P < 0.05$.

Results

Subjects

The mean age of the men was 58 years (range 27–81 years) and that of the women 58 years (range 33–74 years). The mean BMI value of patients was 23.3 ± 3.7 (range 16.5–37.8). There were no significant differences in the number of the patients and BMI between sex and age groups. Characteristics of the study subjects and body mass indices are shown in Table 1.

Table 1 Characteristics of study subjects

Age (years)	Male		Female	
	n	BMI	*n*	BMI
≤49	14	24.0 ± 4.4[a]	5	21.1 ± 3.1
50–69	22	22.4 ± 2.7	17	25.1 ± 4.5
≥70	12	22.1 ± 2.5	5	24.3 ± 3.6
	48	22.8 ± 3.3	27	24.2 ± 4.3

[a] All values are expressed as means ± SD. *BMI* Body mass index (kg/m^2)

There were no significant difference in the number of the patients and BMI between sex and age groups

Fatty Acid Analysis

The mean fatty acid compositions of plasma and erythrocyte PL and adipose TG fractions are presented in Table 2. In plasma and erythrocyte PL fractions, the greatest proportion of fatty acids was saturated fatty acids, 47.7 ± 1.4 and 45.1 ± 1.4%, respectively, followed by polyunsaturated ones (38.2 ± 1.5 and 33.9 ± 1.4%, respectively). However, in adipose TG fraction the highest proportion of fatty acids was monounsaturated (53.2%), followed by saturated (29.6%) and polyunsaturated fatty acids (17.2%). Palmitic acid (16:0) had the highest proportion of all fatty acids in plasma and erythrocyte PL fraction, and oleic acid (18:1n-9) had the highest in adipose TG fraction. Among PUFA, linoleic acid (LA 18:2n-6, 16.3%), arachidonic acid (AA 20:4n-6, 10.5%) and LA (18:2n-6, 14.2%) accounted for the greatest proportions in plasma PL, erythrocyte PL and adipose TG fractions, respectively. The total n-6 fatty acids were 27.0, 22.1 and 15.3% in plasma PL, erythrocyte PL and adipose TG fractions, respectively. As for the total n-3 fatty acids, they were 11.2, 11.8, and 1.9% in plasma PL, erythrocyte PL and adipose TG fractions, respectively. The ratios of n-6/n-3 were 2.4, 1.9 and 8.2 in plasma PL, erythrocyte PL and adipose TG fractions, respectively.

Fatty Acid Analysis for Cholesterol Gallstone Patients

The fatty acid composition of plasma and erythrocyte PL and adipose TG fractions was compared between the patients with cholesterol cholecystolithiasis and those with inguinal hernia or varicosis. The proportion of plasma PL EPA was 2.0 ± 0.9 and 2.8 ± 1.7 in cholesterol gallstone patients and other patients, respectively ($P < 0.05$). The EPA proportion in the erythrocyte PL fraction was 1.6 ± 0.6 and 2.1 ± 0.9 in cholesterol gallstone patients and the other patients, respectively ($P < 0.001$). However, there were no differences in the EPA proportion in adipose TG fraction in either group. There were no particular differences in the other fatty acids between the groups.

Correlations of Fatty Acid Profile in Plasma and the Erythrocyte PL and Adipose TG Fraction

Significant positive correlations were found for several fatty acids. The correlations were highest for EPA in all three types of comparison. A strong significant positive correlation was found for nearly all PUFAs; LA ($r = 0.81$, $P < 0.001$), AA ($r = 0.74$, $P < 0.001$), EPA ($r = 0.84$, $P < 0.001$), DHA ($r = 0.74$, $P < 0.001$) and total saturated fatty acids in a comparison between plasma and erythrocyte

Table 2 Fatty acid composition of plasma and erythrocyte phospholipids and adipose triacylglycerols

Fatty acid	Plasma phospholipids	Erythrocyte phospholipids	Adipose triacylglycerols
Saturated			
16:0	29.8 ± 1.5	24.6 ± 1.4	21.8 ± 2.2
18:0	14.9 ± 1.2	13.9 ± 1.2	5.3 ± 1.4
20:0	0.5 ± 0.1	0.4 ± 0.0	0.2 ± 0.1
22:0	1.2 ± 0.3	1.5 ± 0.2	0.1 ± 0.2
24:0	1.0 ± 0.2	4.5 ± 0.5	0.0 ± 0.0
Monounsaturated			
16:1n-7	0.5 ± 0.2	0.4 ± 0.2	4.3 ± 1.7
18:1n-9	8.8 ± 1.2	13.6 ± 1.0	44.4 ± 2.3
18:1n-7	2.0 ± 0.4	1.6 ± 0.2	3.4 ± 0.6
20:1n-9	0.2 ± 0.1	0.2 ± 0.1	0.9 ± 0.2
24:1n-9	2.6 ± 0.6	5.2 ± 0.7	0.0 ± 0.0
Polyunsaturated			
n-3 PUFA			
18:3	0.2 ± 0.1	0.1 ± 0.1	0.9 ± 0.3
20:5 (EPA)	2.5 ± 1.5	1.9 ± 0.8	0.1 ± 0.1
22:5	1.0 ± 0.2	2.0 ± 0.3	0.2 ± 0.2
22:6 (DHA)	7.5 ± 1.6	7.7 ± 1.2	0.6 ± 0.4
n-6 PUFA			
18:2 (LA)	16.3 ± 2.8	8.7 ± 1.3	14.2 ± 2.1
18:3	0.0 ± 0.0	0.0 ± 0.1	0.4 ± 0.4
20:3	2.0 ± 0.5	1.1 ± 0.2	0.2 ± 0.1
20:4 (AA)	8.3 ± 1.3	10.4 ± 1.3	0.2 ± 0.1
22:4	0.1 ± 0.1	1.4 ± 0.4	0.0 ± 0.0
22:5	0.0 ± 0.0	0.2 ± 0.1	0.0 ± 0.0
Total n-6[a]	27.0 ± 2.8	22.1 ± 2.3	15.3 ± 2.2
Total n-3[b]	11.2 ± 2.8	11.8 ± 2.0	1.9 ± 0.5
n-6/n-3	2.6 ± 1.0	2.0 ± 0.5	8.7 ± 2.2
LA + AA	24.5 ± 2.6	19.1 ± 1.9	14.4 ± 2.1
EPA + DHA	10.1 ± 2.7	9.6 ± 1.8	0.7 ± 0.4
PUFA	38.0 ± 1.5	33.9 ± 1.3	17.2 ± 2.3
Total saturated[c]	47.7 ± 1.4	45.1 ± 1.4	29.6 ± 2.9

All values are expressed as means ± SD

AA arachidonic acid, *EPA* eicosapentaenoic acid, *DHA* docosahexaenoic acid, *LA* linoleic acid, *PUFA* polyunsaturated fatty acid

[a] Total n-6 is the sum of 18:2n-6, 18:3n-6, 20:3n-6, 20:4n-6, 22:4n-6 and 22:5n-6

[b] Total n-3 is the sum of 18:3n-3, 20:5n-3, 22:5n-3 and 22:6n-3

[c] Total saturated is the sum of 16:0, 18:0, 20:0, 22:0 and 24:0

PL fractions. In a comparison between erythrocyte PL and adipose TG fractions, correlation coefficients were weak or absent for LA (18:2n-6), AA (20:4n-6), DHA (22:6n-3) and saturated fatty acids. Likewise, in a comparison between plasma PL and adipose TG fractions, significant positive correlations were found only for EPA ($r = 0.57$, $P < 0.001$), AA ($r = 0.32$, $P < 0.001$) and LA ($r = 0.27$, $P < 0.05$), but not for DHA or saturated fatty acids. The highest correlations in all three types of comparison were found for the total n-3 fatty acids, the ratio of n-6/n-3 and EPA/PUFA.

Differences in Fatty Acid Composition Due to Sex

The differences in the values of PUFAs in plasma and erythrocyte PL and adipose TG fractions due to sex are shown in Fig. 1. There was no significant difference in the values of PUFAs in plasma and erythrocyte PL and adipose TG fractions between men and women.

Changes in PUFAs with Age

Univariate and multivariate analyses of EPA + DHA in plasma and erythrocyte PL and adipose TG fractions and age are shown in Table 3. Those of LA + AA are shown in Table 4. There was a significantly positive correlation between EPA + DHA in plasma and erythrocyte PL fractions and age, but not n-3 PUFA in the adipose TG fraction and age on both univariate and multivariate analyses, respectively. LA + AA in plasma and erythrocyte PL fractions showed a significant inverse correlation with age, but not between those in the adipose TG fraction and age.

Correlations Between EPA + DHA, and Age and BMI

Univariate and multivariate analyses of EPA + DHA values, and age and BMI are shown in Table 3. There were significantly positive correlations between EPA + DHA in the plasma and erythrocyte PL fractions and age. No significant correlations were found between EPA + DHA and BMI.

Correlations Between LA + AA, and Age and BMI

Univariate and multivariate analyses of LA + AA values, and age and BMI are shown in Table 4. LA + AA values in both PL fractions were inversely correlated with age. Those values in the plasma PL fraction were also inversely correlated with BMI. Otherwise no correlations were found

Discussion

Because monounsaturated and saturated fatty acids are endogenously synthesized, their proportions are not expected to represent the proportion of dietary fatty acids, but at least the essential fatty acids in plasma [19–22], the erythrocyte membrane [22, 23] and adipose tissue [23–26] provide useful information on fatty acid intake. James et al. [27] investigated the relationship between dietary linoleic

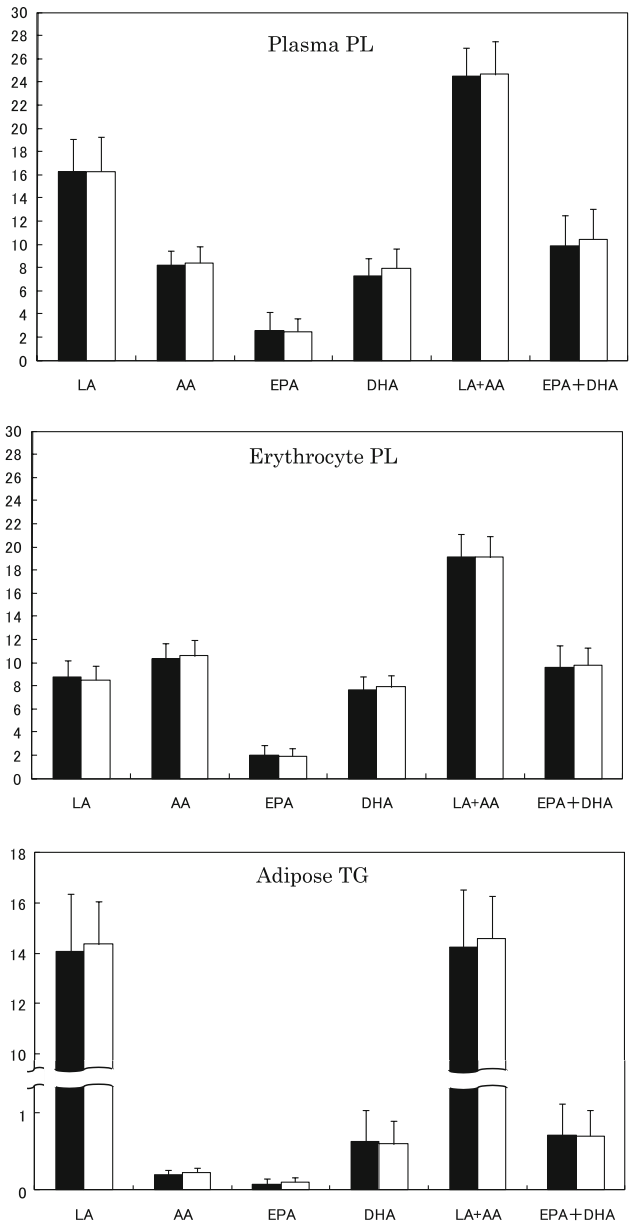

Fig. 1 Area percentage contents of some PUFA for plasma and erythrocyte PL and adipose TG in men and women. *LA* linoleic acid, *AA* arachidonic acid, *EPA* eicosapentaenoic acid, *DHA* docosahexaenoic acid, *PL* phospholipid, *TG* triacylglycerol. *Men* closed columns, *women* open columns. All values are expressed as means ± SD and *bars* indicate one SD. Statistical analysis were done using the ratio test. There were no significant difference between men and women in the values of PUFAs of plasma and erythrocyte PL and adipose TG fractions

acid intake of 2.5–17.5% of energy and the tissue concentration of arachidonic acid in healthy male volunteers. They found a positive linear relationship between dietary LA and the LA concentration in neutrophil phospholipids, plasma triacylglycerols, and plasma cholesteryl esters. By contrast, differences in dietary LA within a broad range were not associated with differences in concentrations of AA in those neutrophil and plasma fractions. They also investigated the effects of n-3 PUFA on AA concentration in neutrophil and plasma PL. The AA concentrations in neutrophil and plasma PL were lowered by 17.6 and 18.1% on supplementation of the diet with 4 g fish oil (1.6 g EPA, 0.3 g DHA), respectively. They concluded that a reduction in dietary linoleic acid by using standard dietary strategies is not likely to lead to a reduction in tissue AA, whereas this can be accomplished by EPA-rich fish-oil supplementation. On the other hand, Harris et al. [28] reported the effects of 16 weeks' intake of fish or fish-oil capsules on the fatty acid composition of erythrocyte and plasma phospholipids. They found that DHA-rich fish oil from either oily fish or fish-oil capsules enriched blood lipids with n-3 fatty acids, but that arachidonic acid concentrations decreased in plasma phospholipids only by 6–7% during the first month, and did not change noticeably thereafter or in erythrocytes at any time. In Japan the average intakes of EPA and DHA are about 0.4 and 0.7 g per day, respectively [29]. Although we did not measure fatty acid intake, considerable intake of EPA in our subjects appeared to affect AA contents in both erythrocyte and plasma PL fractions. This is why we found a very significant correlation in AA values between erythrocyte and plasma PL fractions ($r = 0.74$).

Recently, Beydoun et al. [30] reported the fatty acid composition of plasma phospholipids in 2,251 adults aged 50–65 years in the USA. The percentage of women and age distribution of the subjects were similar to those of our study. Comparing their data with our results, the proportion of total saturated fatty acids, oleic acid, the highest proportion in monounsaturated fatty acids and total unsaturated fatty acids were essentially the same. However, the proportions of n-3 and n-6 fatty acids in plasma phospholipids were very different. Total n-6 PUFA, LA and AA values in their study were 1.4 times, 1.4 times and 1.3 times higher than ours, respectively. Total n-3 PUFA, alpha-linolenate EPA and DHA values in our subjects were 3.1 times, 2.6 times, 4.4 times and 2.6 times higher, respectively, than theirs. The Japanese diet has become more westernized, but Japanese still consume more fish than Western countries such as the USA where the median EPA and DHA intake is 0.25 g per day [31].

Hodson et al. [32] calculated the mean values of 13 fatty acids in various blood fatty acid fractions using 9–19 studies in Western countries. The mean fatty acid composition of adipose tissue was surprisingly similar to our data. The n-3 fatty acids do not accumulate in the adipose tissue, probably because those fatty acids are too "soft" (non-viscous) [33] to keep the adipose tissue more or less solid. A very small accumulation of n-3 fatty acids in the adipose

Table 3 Relation between EPA + DHA in plasma PL, erythrocyte PL and adipose TG and patients' characteristics

Independent variable	Univariate analysis				Multivariate analysis			
	95% CI				95% CI			
	r	Lower	Upper	*P* value	Standardized β	Lower	Upper	*P* value
Plasma PL								
Age	0.33	0.11	0.52	0.004	0.07	0.02	0.11	0.003
BMI	0.13	−0.10	0.35	0.26	0.11	−0.04	0.27	0.15
Erythrocyte PL								
Age	0.42	0.22	0.59	0.0002	0.06	0.03	0.09	0.0001
BMI	0.09	−0.14	0.31	0.46	0.06	−0.04	0.16	0.26
Adipose TG								
Age	0.003	−0.22	0.23	0.98	0.0004	−0.01	0.01	0.90
BMI	0.15	−0.08	0.36	0.20	0.02	−0.01	0.04	0.20

EPA + DHA is the area percentage of EPA + DHA in the total PL fraction in plasma and erythrocyte, and total TG fraction in subcutaneous adipose tissue

BMI body mass index (kg/m^2), *EPA* eicosapentaenoic acid, *DHA* docosahexaenoic acid, *PL* phospholipid, *TG* triacylglycerol

Table 4 Relation between LA + AA in plasma PL, erythrocyte PL and adipose TG and patients' characteristics

Independent variable	Univariate analysis				Multivariate analysis			
	95% CI				95% CI			
	r	Lower	Upper	*P* value	Standardized β	Lower	Upper	*P* value
Plasma PL								
Age	−0.26	−0.46	−0.04	0.02	−0.06	−0.10	−0.01	0.01
BMI	−0.25	−0.45	−0.03	0.03	−0.19	−0.35	−0.04	0.01
Erythrocyte PL								
Age	−0.42	−0.59	−0.21	0.0002	−0.06	−0.09	−0.03	0.0001
BMI	−0.10	−0.32	0.13	0.42	−0.07	−0.17	0.04	0.23
Adipose TG								
Age	0.21	−0.02	0.41	0.07	0.0318	0.00	0.07	0.08
BMI	−0.03	−0.26	0.19	0.77	−0.01	−0.14	0.12	0.88

LA + AA is the area percentage of LA and AA in the total PL fraction in plasma and erythrocyte, and total TG fraction in subcutaneous adipose tissue

AA arachidonic acid, *BMI* body mass index (kg/m^2), *LA* linoleic acid, *PL* phospholipid, *TG* triacylglycerol

tissue in our Japanese subjects appeared to exert no sizable competitive effects on n-6 PUFA value. As expected, in the plasma and erythrocyte PL fractions, increased n-3 fatty acids and decreased n-6 fatty acids were found in our subjects compared with those of Hodson et al. [32].

Cholesterol gallstone disease is a common disease in western countries and also in Japan. A number of dietary factors are involved in the pathogenesis of cholesterol cholelithiasis [34, 35]. It has been reported that populations consuming a diet rich in n-3 FUPA exhibit a low incidence of cholesterol cholelithiasis [36]. In our study, the patients with cholesterol gallstones showed a significantly lower level of EPA in the plasma and erythrocyte PL fraction than those in the other patients.

Concerning sex-related differences in fatty acid composition, a higher proportion of LA and DHA in subcutaneous adipose tissue was reported in Scottish women than in Scottish men [37]. Similar results were also found in serum in middle-aged Finnish [38] and Dutch (>20 years younger than our subjects) [39] subjects. In the present study, there were no significant differences between men and women in any PUFAs of the plasma and erythrocyte PL and adipose TG fractions. Similarly, no sex difference in long chain n-3 PUFAs in serum among over 1,200 Japanese subjects aged 40–79 years was reported [40]. These differences among various studies may be due to differences in hormonal balance, age, dietary intake or disease status.

In the present study, age was positively correlated with n-3 PUFAs in the plasma and erythrocyte PL and adipose TG fractions, but negatively correlated with n-6 FUFAs, especially in the plasma and erythrocyte PL fractions. Itomura et al. [41] investigated the factors influencing EPA + DHA levels in the erythrocyte PL fraction in Japan. They found a significant positive relationship between EPA + DHA in erythrocytes and dietary EPA + DHA %, and also a significant positive relationship between EPA + DHA in the erythrocyte PL fraction and age. Furthermore, in a national nutrition survey in Japan [42], a positive correlation between n-3 PUFAs intake and age was reported, while a negative correlation between n-6 PUFAs intake and age was also reported. Consequently, these correlations were mainly explained by dietary factors.

Not many fatty acid values correlated with BMI in our measured fractions, as reported by Itomura et al. [41]. However, n-3 PUFAs were found to be negatively associated with obesity in Australia [43]. In the Australian study, the exclusion criteria for participation induced consumption of fish-oil supplements and consumption of more than two fatty fish meals per week. On the other hand, almost 60% of people in Japan eat fresh fish more than 3 times per week [40]. Furthermore, there was a big difference in average BMIs between the two studies' subjects. These might explain the different results.

The relationship between types of fat intake and BMI were investigated in Spain [44]. It was reported that energy from fat does not play an important role in the development of obesity. On the other hand, the Nurses' Health Study Cohort showed that dietary lipids other than vegetable fat were positively associated with BMI, and vegetable fat was inversely related to BMI [45]. Waresjo et al. [46] investigated the relationship between the fatty acid composition of serum cholesteryl esters and obesity. They found a positive and significant association between BMI and 20:4n-6 and 20:5n-3, and a strong and inverse association of LA. Taking into consideration that fish oils reduced obesity in rats but had no effects in humans [47], the positive relationship between EPA and BMI was surprising. In our study, an inverse correlation was found between LA + AA in the plasma PL fraction and BMI. The reason for this is not clear.

Adipose tissue PUFA may best reflect the long-term PUFA composition in the diet, but is rarely used as a biomarker because of the invasive sample collection protocol. In our study, PUFAs showed significant and strong correlations between the plasma and erythrocyte PL and adipose TG fractions.

In conclusion, our findings suggest that PUFA in plasma and erythrocyte PL may be a good biomarker and a more acceptable method to study participants than adipose tissue TG.

Acknowledgments We thank all the participants in this study and the staff at the Hematological Examination Section, Central Laboratory for Clinical Investigation, Kansai Medical University Hospital for expert laboratory assistance. We are grateful to Ms. Hiroko Hamatani (University of Toyama) and Ms. Shizuko Takebe (University of Toyama) for their technical assistance in fatty acid analysis.

References

1. Lands WEM, Hamazaki T, Yamazaki K, Okuyama H, Sakai K, Goto Y, Hubbard VS (1990) Changing dietary patterns. Am J Clin Nutr 51:991–993
2. Kotake K, Koyama Y, Nasu J, Fukutomi T, Yamaguchi N (1995) Relation of family history of cancer and environmental factors to the risk of colorectal cancer: a case–control study. Jpn J Clin Oncol 25:195–202
3. Tajima K, Tominaga S (1985) Dietary habits and gastrointestinal cancers: a comparative case-control study in Nagoya, Japan. Jpn J Cancer Res 76:705–716
4. Kagamimori S, Kitagawa T, Nasermoaddeli A, Wang H, Kanayama H, Sekine M, Dilixat Y (2004) Differences in mortality rates due to major specific causes between Japanese male occupational groups over a recent 30-year period. Ind Health 42:328–335
5. Annual Statistical Report of National Health Conditions (2006) Health and Welfare statistics association, Tokyo, Japan (in Japanese)
6. The national health and nutrition survey in Japan (1955–2004) Ministry of Health, Labour and Welfare of Japan (in Japanese)
7. Kubo M, Kiyohara Y, Kato I, Tanizaki Y, Arima H, Tanaka K, Nakamura H, Okubo K, Iida M (2003) Trends in the incidence, mortality, and survival rate of cardiovascular disease in a Japanese community. The Hisayama Study Stroke 34:2349–2354
8. Lifestyle and health conditions based on data from 163 countries. Integrated nutrition, lifestyle and health database: epidemiological information for an improved understanding of diseases of civilization. 21 March 2009. Internet: http://www.canibaiseris.com/2009/03/21/nutrition-and-health-database/. Accessed 15 April 2009
9. Brady LM, Williams CM, Lovegrove JA (2004) Dietary PUFA and the metabolic syndrome in Indian Asians living in the UK. Proc Nutr Soc 63:115–125
10. Ailhaud G, Massiera F, Weill P, Legrand P, Alessandri JM, Guesnet P (2006) Temporal changes in dietary fats: role of n-3 polyunsaturated fatty acids in excessive adipose tissue development and relationship to obesity. Prog Lipid Res 45:203–236
11. Arab L, Akbar J (2002) Biomarkers and the measurement of fatty acids. Health Nutr 5:865–871
12. Zeleniuch-Jacquotte A, Chajès V, Van Kappel AL, Riboli E, Toniolo P (2000) Reliability of fatty acid composition in human serum phospholipids. Eur J Clin Nutr 54:367–372
13. Farquhar JW, Ahrens ED Jr (1963) Effect of dietary fats on human erythrocyte fatty acid patterns. J Clin Invest 42:675–685
14. Katan MB, van Birgelen A, Deslypere JP, Penders M, van Staveren WA (1991) Biological markers of dietary intake with emphasis on fatty acids. Ann Nutr Metab 35:249–252
15. van Staveren WA, Deurenberg P, Katan MB, Burema J, de Groot LCPGM, Hoffmans MDAF (1986) Validity of the fatty acid composition of subcutaneous fat tissue microbiopsies as an estimate of the long-term average fatty acid composition of the diet of separate individuals. Am J Epidemiol 123:455–463
16. Riboli E, Ronnholm H, Saracci R (1987) Biological markers of diet. Cancer Surv 6:685–718

17. Marckmann P (1999) Footprint of fish: docosahexaenoic acid (DHA) in adipose tissue (Editorial). Nutrition 15:407–408
18. Bligh EG, Dyer Wl (1959) A rapid method for total lipid extraction and purification. Can J Biochem Physiol 37:911–917
19. Ma J, Folsom AR, Shahar E, Eckfeldt JH, for the Atherosclerosis Risk in Communities (ARIC) Study Investigators (1995) Plasma fatty acid composition as an indicator of habitual dietary fat intake in middle-aged adults. Am J Clin Nutr 62:564–571
20. Hodge AM, Simpson JA, Gibson RA, Gibson RA, Sinclair AJ, Makrides M, O'Dea K, English DR, Giles GG (2007) Plasma phospholipid fatty acid composition as a biomarker of habitual dietary fat intake in an ethnically diverse cohort. Nutr Metab Cardiovas 17:415–426
21. Arab L (2003) Biomarkers of fat and fatty acid intake. J Nutr 133(Suppl. 3):9255–9325
22. Von Schacky C, Fisher S, Weber PC (1985) Long-term effects on dietary marine ω-3 fatty acids upon plasma and cellular lipids, platelet function, and eicosanoid formation in humans. J Clin Invest 76:1626–1631
23. Neoptolemos JP, Clayton H, Heagerty AM, Nicholson MJ, Johnson B, Mason J, Manson K, James RFL, Bell PRF (1988) Dietary fat in relation to fatty acid composition of red cells and adipose tissue in colorectal cancer. Br J Cancer 58:575–579
24. Hunter DJ, Rimm EB, Sacks FM, Stampfer MJ, Colditz GA, Litin LB, Willett WC (1992) Comparison of measures of fatty acid intake by subcutaneous fat aspirate, food frequency questionnaire, and diet records in a free-living population of US men. Am J Epidemiol 135:418–427
25. London SJ, Sacks FM, Caesar J, Stampfer MJ, Siguel E, Willett WC (1991) Fatty acid composition of subcutaneous adipose tissue and diet in postmenopausal US women. Am J Clin Nutr 54:340–345
26. Yli-Jama P, Haugen TS, Rebnord HM, Ringstad J, Pedersen JI (2001) Selective mobilization of fatty acids from human adipose tissue. Eur J Intern Med 12:107–115
27. James MJ, Gibson RA, D'Angelo M, Neumann MA, Cleland LG (1993) Simple relationships exist between dietary linoleate and the n-6 fatty acids of human neutrophils and plasma. Am J Clin Nutr 58:497–500
28. Harris WS, Pottala JV, Sands SA, Jones PG (2007) Comparison of the effects of fish and fish-oil capsules on the n-3 fatty acid content of blood cells and plasma phospholipids. Am J Clin Nutr 86:1621–1625
29. Kobayashi M, Sasaki S, Kawabata T, Hasegawa K, Tsugane S (2003) Validity of a self-administered food frequency questionnaire used in the 5-year follow up survey of the JPHC study cohort 1 to assess fatty acid intake: comparison with dietary records and serum phospholipid level. J Epidemiol 13(Suppl):S64–S81
30. Beydoun MA, Kaufman JS, Satia JA, Rosamond W, Folsom A (2007) Plasma n-3 fatty acids and the risk of cognitive decline in older adults: the atherosclerosis risk in communities study. Am J Clin Nutr 85:1103–1111
31. Mozaffarian D, Ascherio A, Hu FB, Stampfer MJ, Willett WC, Siscovick DS, Rimm EB (2005) Interplay between different polyunsaturated fatty acids and risk of coronary heart disease in men. Circulation 111:157–164
32. Hodson L, Skeaff CM, Fielding BA (2008) Fatty acid composition of adipose tissue and blood in human and its use as a biomarker of dietary intake. Prog Lipid Res 47:348–380
33. Hamazaki T, Kobayashi S, Urakaze M, Yano S, Fujita T (1985) Viscosities of some triglycerides and ethylester of fatty acids frequently found in cell membranes—a possible effect of viscosity of fatty acids in phospholipids on hemorheology. Biorheology 22:221–226
34. Cuevas A, Miquel JF, Reyes MS, Zanlungo S, Nevi F (2004) Diet as a risk factor for cholesterol gallstone disease. J Am Coll Nutr 23:187–196
35. Yago MD, González V, Serrano P, Calpena R, Martínez MA, Martínez-Victoria E, Mañas M (2005) Effect of the type of dietary fat on biliary lipid composition and bile lithogenicity in humans with cholesterol gallstone disease. Nutrition 21:339–347
36. Schaefer O (1971) When the Eskimo comes to town. Nutr Today 6:8–16
37. Tavendale R, Lee AJ, Smith WCS, Tunstall-Pedoe H (1992) Adipose tissue fatty acids in Scottish men and women: results from the Scottish Heart Study. Atherosclerosis 94:161–169
38. Nikkari T, Luukkainen P, Pietinen P, Puska P (1995) Fatty acid composition of serum lipid fractions in relation to gender and quality of dietary fat. Ann Med 27:491–498
39. Giltay EJ, Gooren LJG, Toorians AWFT, Katan MB, Zock PL (2004) Docosahexaenoic acid concentrations are higher in women than in men because of estrogen effects. Am J Clin Nutr 80:1167–1174
40. Wakai K, Ito Y, Kojima M, Tokudome S, Ozawa K, Inaba Y, Yagyu K, Tamakoshi A, for the JACC Study Group (2005) Intake frequency of fish and serum levels of long-chain n-3 fatty acids: a cross-sectional study within the Japan Collaborative Cohort Study. J Epidemiol 15:211–218
41. Itomura M, Fujioka S, Hamazaki K, Kobayashi K, Nagasawa T, Sawazaki S, Kirihara Y, Hamazaki T (2008) Factors influencing EPA + DHA levels in red blood cells in Japan. In vivo 22:131–136
42. Dietary Reference Intakes for Japanese (2005) Ministry of health, labour and welfare of Japan. Daiichi Press Japan, Tokyo, Japan (in Japanese)
43. Micallef M, Munro I, Phang M, Garg M (2009) Plasma n-3 polyunsaturated fatty acids are negatively associated with obesity. Br J Nutr 19:1–5
44. González CA, Pera G, Quirós JR, Lasheras C, Tormo MJ, Rodriguez M, Navarro C, Martinez C, Dorronsoro M, Chirlaque MD, Beguiristain JM, Barricarte A, Amiano P, Agudo A (2000) Types of fat intake and body mass index in a Mediterranean country. Public Health Nutr 3:329–336
45. Colditz GA, Willett W, Stampfer MJ, London SJ, Segal MR, Speizer FE (1990) Patterns of weight change and their relation to diet in a cohort of healthy women. Am J Clin Nutr 51:1100–1105
46. Waresjo E, Ohrvall M, Vessby B (2006) Fatty acid composition and estimated desaturase activities are associated with obesity and lifestyle variables in men and women. Nutr Metab Cardiovas 16:128–136
47. Li JJ, Huang CJ, Xie D (2008) Anti-obesity effects of conjugated linoleic acid, docosahexaenoic acid, and eicosapentaenoic acid. Mol Nutr Food Res 52:631–645

Lipids (2010) 45:145–157
DOI 10.1007/s11745-010-3385-4

ORIGINAL ARTICLE

DGAT1, DGAT2 and *PDAT* Expression in Seeds and Other Tissues of Epoxy and Hydroxy Fatty Acid Accumulating Plants

Runzhi Li · Keshun Yu · David F. Hildebrand

Received: 12 December 2008 / Accepted: 1 January 2010 / Published online: 27 January 2010

Abstract Triacylglycerol (TAG) is the main storage lipid in plants. Acyl-CoA: diacylglycerol acyltransferase (DGAT1 and DGAT2) and phospholipid: diacylglycerol acyltransferase (PDAT) can catalyze TAG synthesis. It is unclear how these three independent genes are regulated in developing seeds, and particularly if they have specific functions in the high accumulation of unusual fatty acids in seed oil. The expression patterns of *DGAT1*, *DGAT2* and a *PDAT* in relation to the accumulation of oil and epoxy and hydroxy fatty acids in developing seeds of the plant species *Vernonia galamensis*, *Euphorbia lagascae*, *Stokesia laevis* and castor that accumulate high levels of these fatty acids in comparison with soybean and *Arabidopsis* were investigated. The expression patterns of *DGAT1, DGAT2* and the *PDAT* are consistent with all three enzymes playing a role in the high epoxy or hydroxy fatty acid accumulation in developing seeds of these plants. *PDAT* and *DGAT2* transcript levels are present at much higher levels in developing seeds of epoxy and hydroxy fatty acid accumulating plants than in soybeans or *Arabidopsis*. Moreover, *PDAT, DGAT1* and *DGAT2* are found to be expressed in many different plant tissues, suggesting that these enzymes may have other roles in addition to seed oil accumulation. *DGAT1* appears to be a major enzyme for seed oil accumulation at least in *Arabidopsis* and soybeans. For the epoxy and hydroxy fatty acid accumulating plants, *DGAT2* and *PDAT* also show expression patterns consistent with a role in the selective accumulation of these unusual fatty acids in seed oil.

Keywords *Vernonia galamensis* · *Stokesia laevis* · *Euphorbia lagascae* · Castor (*Ricinus communis*) · *Arabidopsis thaliana* · Soybean · Diacylglycerol acyltransferase · Phospholipid: diacylglycerol acyltransferase · Epoxy and hydroxy fatty acids · Oil accumulation · Seed development

Abbreviations

AtDGAT1/2	*Arabidopsis thaliana* DGAT1/2
AtPDAT	*Arabidopsis thaliana* PDAT
BHT	Butylated hydroxytoluene or butylhydroxytoluene
DAF	Days after flowering
DAG	*sn*-1,2-diacylglycerol
DGAT1	Type 1 acyl-CoA: diacylglycerol acyltransferase
DGAT2	Type 2 acyl-CoA: diacylglycerol acyltransferase
ER	Endoplasmic reticulum
LCAT	Lecithin: cholesterol acyltransferase
PDAT	Phospholipid: diacylglycerol acyltransferase
RcDGAT1/2	*Ricinus communis* DGAT1/2
RcPDAT1A	*Ricinus communis* PDAT1A
ScPDAT	*Saccharomyces cerevisiae* PDAT
TAG	Triacylglycerol

Introduction

Seed oils are an important source of fatty acids for human nutrition and hydrocarbon chains for industrial products.

R. Li and K. Yu contributed equally to this work.

R. Li · K. Yu · D. F. Hildebrand (✉)
Department of Plant and Soil Science, University of Kentucky, 1405 Veterans Dr., Lexington, KY 40546, USA
e-mail: dhild@uky.edu

Most seed oils of plants such as soybean, canola, sunflower, oil palm and maize are stored largely in the form of triacylglycerol (TAG), as the major carbon and energy reserve [1]. TAG in common oilseeds is predominantly composed of five fatty acids, the saturated palmitic (C16:0) and stearic (C18:0) acids, monounsaturated oleic acid (C18:1), the polyunsaturated linoleic (C18:2) and α-linolenic (C18:3) acids. However, a very large diversity of fatty acids exists in the reserve TAG of seeds. A number of plant species have been found to contain high levels of unusual fatty acids such as hydroxy, epoxy and acetylenic fatty acids [2]. For example, castor (*Ricinus communis*) oil is as much as 90% ricinoleate, a hydroxy fatty acid (12-hydroxy-octadec-*cis*-9-enoic acid). The seed oils from *Vernonia galamensis*, *Euphorbia lagascae* and *Stokesia laevis* can accumulate 60–80% of an epoxy fatty acid known as vernolic acid (*cis*-12-epoxyoctadeca-*cis*-9-enoic acid) [3–6]. These unusual fatty acids have properties that make them valuable as renewable raw materials for the chemical industry, being used in making plastics, paints, other coatings, adhesives and composites.

The synthesis of TAG and the high accumulation of a single unusual fatty acid in seed oils have attracted considerable interest, both in functional and applied areas of plant biology. In seeds, TAG biosynthesis occurs in certain membranes of the endoplasmic reticulum (ER) and accumulates in oil bodies, which are generated through budding of the outer ER membrane [7]. TAGs are synthesized by the enzymes of the Kennedy pathway, which sequentially transfer acyl chains from acyl-CoAs to *sn*-1, -2 and -3 positions of a glycerol backbone [8]. Acyl-CoA: diacylglycerol acyltransferase (DGAT; EC 2.3.1.20), a transmembrane enzyme, functions in the final step of the pathway by catalyzing the acylation of *sn*-1,2-diacylglycerol (DAG) at the *sn*-3 position using an acyl-CoA substrate. DGAT has been proposed to be the rate-limiting enzyme in plant storage lipid accumulation [9, 10]. It was discovered that many organisms have two distinct classes of DGATs with no homology to each other, designated DGAT1 and DGAT2 [11–14] and a third soluble DGAT has also been described [15]. Genes encoding DGAT1 have been cloned and characterized from several plant species [16–19]. In addition to DGAT, another mechanism of TAG synthesis has been recently reported in plants and yeast [20, 21]. This is an acyl-CoA independent reaction where a phospholipid such as phosphatidylcholine or phosphatidylethanolamine can donate its *sn*-2 acyl group to DAG, resulting in the formation of TAG. This transacylase activity is termed phospholipid: diacylglycerol acyltransferase (PDAT; E.C.2.3.1.158). *PDAT* genes have also been isolated and identified in plants [22, 23].

Although the current literature shows that DGAT1, DGAT2 and PDAT, encoded by three separate gene families, are all capable of catalyzing the final acylation step during TAG synthesis, it remains poorly understood as to how they contribute to the overall accumulation of TAG in seed oils and how they are regulated in developing seeds. The specific functions of DGAT1, DGAT2 and PDAT in the high accumulation of unusual fatty acids such as epoxy and hydroxyl fatty acids in seed oils are only recently beginning to be elucidated and recent studies indicate an important role for DGAT2. In 2006 [24] reported that DGAT2 appeared to be of importance in castor oil biosynthesis and [25] presented good evidence that DGAT2 may be involved in the selective accumulation of the unusual fatty acid, eleostearic acid, in tung (*Vernicia fordii*) oil. Subsequently [26] showed that castor DGAT2 can nearly double hydroxy fatty acid accumulation in *Arabidopsis* seeds (from ~17 to ~30%) co-expressing this gene along with the castor hydroxylase compared to the hydroxylase gene alone.

In the present paper, we report our studies on transcript levels of *DGAT1, DGAT2* and *PDAT* expression during the seed development of *Vernonia galamensis*, *Euphorbia lagascae*, *Stokesia laevis,* castor (*Ricinus communis*), soybeans (*Glycine max* cv. Jack) and *Arabidopsis.* We also examined the correlation between these three gene expression patterns and oil/target fatty acid accumulation in the seeds. Our current data suggest that DGAT2 and PDAT play important roles in epoxy and hydroxy fatty acid accumulation in seed oils of source plants, although DGAT1 appears to be a major enzyme for oil accumulation in all the plants studied, especially soybean and *Arabidopsis*.

Materials and Methods

Plant Materials

Developing seed samples were collected from both the source plants and common oilseed plants. The source plants included *Vernonia galamensis, Euphorbia lagascae, Stokesia laevis* and castor (*Ricinus communis*), which can accumulate high levels of epoxy and hydroxy fatty acids in their seed oils. Soybean and *Arabidopsis thaliana* represent a common oilseed and a model plant for comparison in this study. *Arabidopsis* plants were grown in a growth chamber under a 16 h light 20 °C/8 h dark 15 °C cycle. *Euphorbia*, castor and soybean plants were grown in a greenhouse at 16/8 day/night and 25/21 °C. *Vernonia* and *Stokesia* plants were grown in outdoor plots in Lexington, KY.

Dicot embryogenesis is divided into five general stages: globular, heart, cotyledon, maturation, and dormancy [27–30]. In this study, we focused on cotyledon to maturation stages and further classified them based on six different developmental phases, including: days after flowering (DAF), seed size (length), seed coat color, fresh weight and other morphological traits of seeds. Simply, the days after

Table 1 Classification of 6 different stages of the developing seeds. The numbers indicate days after flowering (DAF) and single seed fresh weight (wt), DAF/seed (wt)

Species	Stage 1	Stage 2	Stage 3	Stage 4	Stage 5	Stage 6
Vernonia (mg)	10	17	24	31	38	45
	<1.9	2.0–2.7	2.8–3.3	3.4–4.4	4.5–5.5	5.3–4.9
Stokesia (mg)	14	21	28	35	42	49
	2–3	3.5–4.5	5.5–7.5	8.5–11.5	10.0–9.0	8.6–7.0
Euphorbia (mg)	12	19	26	33	40	47
	<6.0	7.0–10.0	11.0–14.0	14–15.0	15.5–16.0	15.5–14.0
Castor (mg)	10	20	30	40	50	60
	<0.20	0.25–0.35	0.4–0.45	0.5–0.6	0.65–7.5	0.8–1.0
Soybean (mg)	12	25	35	45	55	65
	30–70	100–150	200–250	300–350	400–480	360–300
Arabidopsis (mg)	6	9	12	15	18	21

For *Arabidopsis*, the seed weight was not measured

flowering/pollination, which represent each developmental stage of the tested plant seeds, are listed in Table 1.

Northern Blots

Total RNA was isolated from roots, stems, leaves, young developing embryos (between stage 1 and 3) and mid-late maturation seeds (between stage 3 and 4) of all the test plants. The Trizol reagent was used for this isolation according to manufacturer's instructions (Invitrogen). Based on the alignment of the known sequences for each *DGAT1*, *DGAT2* and *PDAT* gene, a conserved region was identified for each gene. Then, conserved regions of *Arabidopsis DGAT1* (At2g19450), *DGAT2* (At3g51520) and *PDAT* (At5g13640) cDNAs were amplified and labeled with digoxigenin (DIG)-UPT by a PCR DIG Probe Synthesis Kit (Roche Applied Science). RNA was separated on 1% denaturing formaldehyde gel and transferred onto a Zeta-Probe Blotting Membrane (Bio-Rad Laboratories). Equalized loading of RNA was checked by ethidium bromide staining of rRNAs. The hybridization was performed at 60 °C overnight using the DIG Easy Hyb kit (Roche Applied Science). The final washing step was performed at 65 °C in 0.1 × SSC and 0.1% SDS under constant agitation. The hybridized mRNA was detected with alkaline phosphatase conjugated anti-DIG antibody (Roche Applied Science) and its chemiluminescent substrate, CDP-Star (Roche Applied science), following the manufacturer's protocol.

Real-Time PCR Quantification

Total RNA was extracted from the developing seeds at six developmental stages using the methods described above. After extraction, RNA samples were treated with DNaseI (Promega Co.) to remove contaminating DNA. First-strand cDNA was synthesized with the SuperScript II RT kit (Invitrogen), using equal amounts of oligo (dT) and random primers, according to the manufacturer's instructions. All Real-time reactions were performed in an iCycler iQ detection system (Bio-Rad) using the intercalation dye SYBR Green I master mix kit (Applied Biosystems) as a fluorescent reporter.

PCR reactions were performed in triplicate in 25-μL volumes using 1 μL of each forward and reverse primers (500 nM), 12.5 μL of SYBR green master mix, 5 μL of a 1:10 (v/v) dilution of cDNA and 5.5 μL of DEPC treated water. Reactions were performed in MicroAmp 96-well plates (Applied Biosystems) covered with optical adhesive covers (Applied Biosystems). The following program was applied: initial polymerase activation at 95 °C for 10 min; then a two-temperature thermal cycle consisting of denaturation at 95 °C for 15 s, followed by anneal extension at 60 °C for 1 min, totally 40 cycles.

The quantification of PCR products was performed via a calibration curve procedure using 18S RNA as an internal standard. PCR products were analyzed using melting curves as well as agarose gel electrophoresis to ensure single product amplification. The ratio of gene-specific expression to 18S signal was defined as relative expression. PCR controls were performed in the absence of added reverse transcriptase to ensure RNA samples were free of DNA contamination. Primers for specific amplification of each cDNA were designed using the Primer Express software (Applied Biosystems), taking into account criteria such as product length (around 500 bp), optimal PCR annealing temperature, and likelihood of primer self-annealing (Table 2).

Fatty Acid Analysis

Seed samples collected at the six different development stages were frozen in liquid N_2, stored at −80 °C and then

Table 2 Sets of real-time RT–PCR primers used to amplify gene-specific regions

Gene	Primer Sequence (5′–3′)	
Arabidopsis		
At*DGAT1*	Sense	TTGGCCGCTTTTCATGTG
	Antisense	GCAGTAGAACATGCAGAGCC
At*DGAT2*	Sense	GTCTTTGGTTATGAACCAC
	Antisense	TATTGGTTTACCAACGAC
At*PDAT*	Sense	GGGCTCGAGCTTTGGGAAGG
	Antisense	GCAACAGCTTTTGGAACACC
18 sRNA	Sense	CGGCTACCACATCCAAGGAA
	Antisense	GCTGGAATTACCGCGGCT
Castor (*Ricinus communis*)		
Rc*DGAT1* (*AY366496*)	Sense	TGTTAACAGCAGGCTCATCATT
	Antisense	CCATACAAGCAAGTTCCATCAA
RcDGAT2 (*EU391592*)	Sense	TTTGGTTATGAGCCACATTCAG
	Antisense	CAAGGGTTTACCCATCTCCATA
RcPDAT1A [70]	Sense	GACATCAGTGTGCTGATGGTTT
	Antisense	TGCTCAAACTTTGGTCCCTAAT

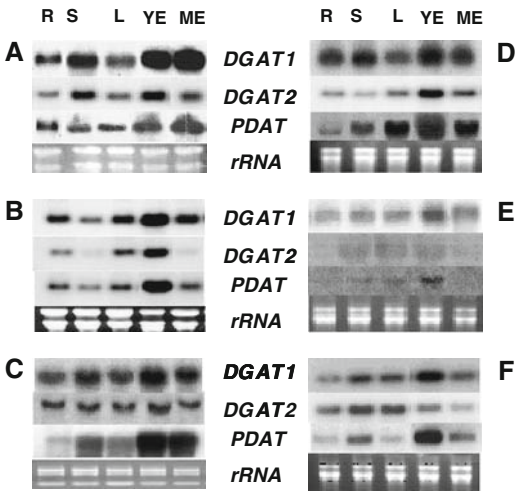

Fig. 1 Northern blot analysis of *DGAT1, DGAT2* and *PDAT* expression in different tissues of plants. Total RNA was extracted from root (*R*), stem (*S*), leaf (*L*), young developing embryo (*YE*) and early maturing seed (*ME*). Total RNA (15 μg) was loaded for Northern blot and hybridized separately to the DIG-labeled cDNA probes of *DGAT1, DGAT2* and *PDAT*. Ethidium bromide staining (*lowest panel*) is shown for equalized loading. The figure shows results typical of those obtained in three independent experiments. **a** *Vernonia galamensis*, **b** *Euphorbia lagascae*, **c** *Stokesia laevis*, **d** Castor (*Ricinus communis*), **e** Soybean (*Glycine max*) (cv. Jack), **f** *Arabidopsis thaliana*. In **a**, the same membrane was used for the blotting (exposure for 5–5 min 15 s), and the same was in **b**. In **d**, DGAT1 and PDAT blots were performed using the same membrane (exposure for 5 min 30 s), and DGAT2 using another membrane (exposed for 5 min). In **e**, the same membrane was used for DGAT2 (exposure for 5 min 30 s) and PDAT (exposure for 6 min), but another membrane for DGAT1 (exposure for 5 min). In **f**, a membrane was used for DGAT1 (5 min exposure), and another membrane for both DGAT2 and PDAT (5 min 20 s exposure)

lyophilized. Weighed samples were transferred the samples to glass test tubes containing 0.5 mL of sodium methoxide after addition of tri-heptadecanoin (tri-17:0) (25 μg/mg in chloroform) as a standard. The seed samples were finely ground and the samples incubated for at least 15 min with shaking. 0.5 mL of isooctane containing 0.001% BHT was added to each tube and mixed well. Phase separation was obtained with centrifugation. The top layer was extracted and transferred into GC auto-sampler vials. The fatty acid methyl esters were analyzed with gas chromatography on a Varian CP-3800 GC with a 24 m × 0.25 mm ID CP-Select CB for FAME (http://www.varianinc.com/cgi-bin/nav?products/consum/gccolumns/select/selfame&cid=KLOJINIPFP) fused silica column with a 0.25 μm film thickness. The temperature program was 90 °C for 1 min., then to 155 °C at 20 °C/min. with no hold, then to 175 °C at 3.6 °C/min. with no hold and finally to 250 °C at 12 °C/min. holding for one min. The areas for each fatty acid including tri-17:0 standard was collected and then used to calculate total oil content (μg/mg) and each fatty acid level (% total fatty acids).

Results

Expression of *DGAT1, DGAT2* and *PDAT* in Different Plant Tissues

To obtain information about the expression patterns of *DGAT1, DGAT2* and *PDAT* genes through a range of tissue types, total RNA was isolated from root, stem, leaf, young developing embryos (between stage 2 and 3) and early maturing seeds (between stage 3 and 4). Northern blot was performed using the conserved regions of *Arabidopsis DGAT1, DGAT2* and *PDAT* cDNA as probes. All three genes were highly expressed in young developing embryos and/or early maturing seeds from the tested epoxy and hydroxy fatty acid accumulating plant species (*Vernonia galamensis*, *Euphorbia lagascae*, *Stokesia laevis* and castor) although they showed variable expression in root, stem and leaf tissues (Fig. 1a–d). For soybeans (Fig. 1e), a common oil crop, stronger expression of *DGAT1* was found in developing seeds (between stage 2 and 4) compared to the level in other tissues. The weak expression of *DGAT2* and *PDAT* was present in stem, leaf and young developing embryos (between stage 2 and 3). No *DGAT2* and *PDAT* transcript was detected in roots, and only trace signals were found in the late maturing seeds (between stage 3 and 4). In *Arabidopsis* (Fig. 1f), a model plant, both *DGAT1* and *PDAT* were clearly expressed in all tissues tested, although their levels were slightly higher in young developing seeds

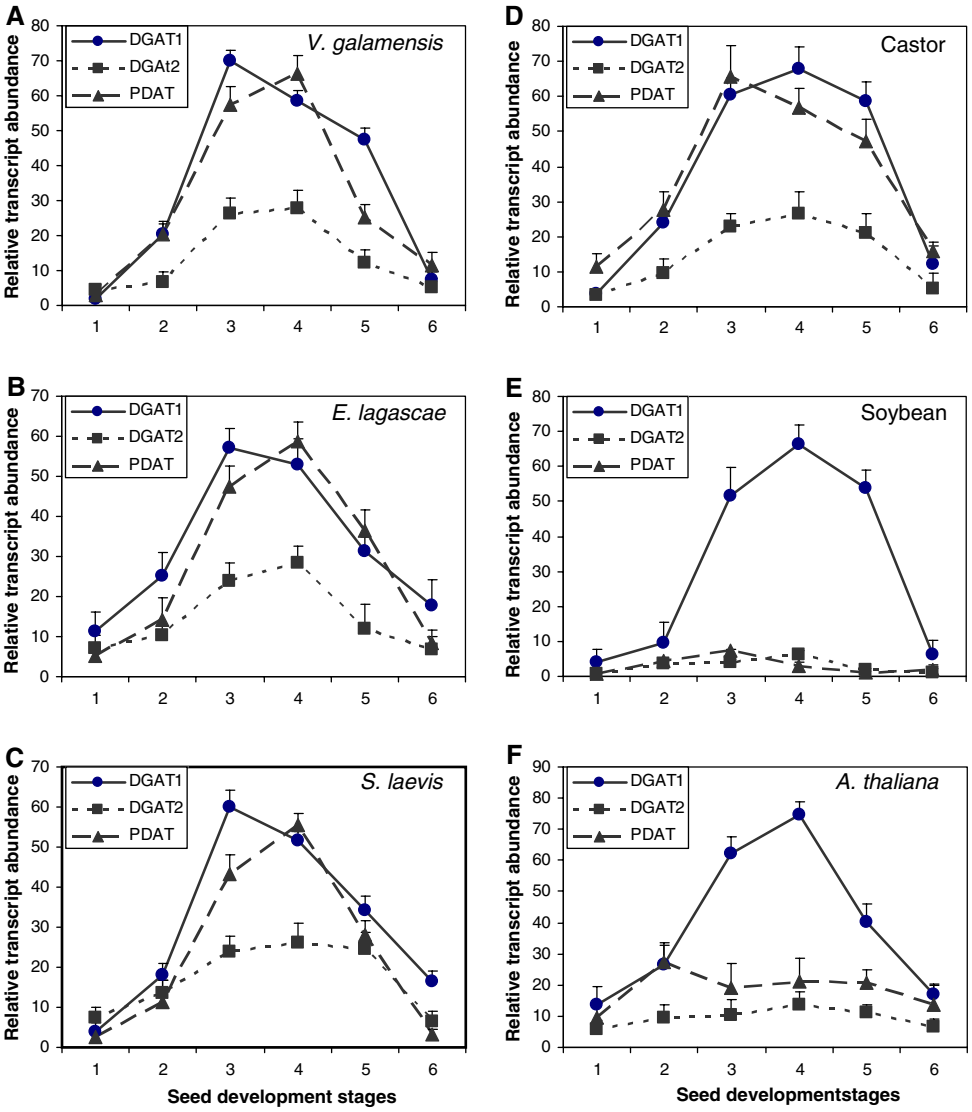

Fig. 2 Expression patterns of *DGAT1, 2* and *PDAT* transcripts during seed development. Expression levels were normalized with respect to the internal control *18 s RNA*. *Data bars* represent the mean ± STD level of relative transcript abundance from five experiments with independent RNA extractions. **a** *Vernonia galamensis*, **b** *Euphorbia lagascae*, **c** *Stokesia laevis*, **d**. Castor, **e**. Soybean (cv. Jack), **f**. *Arabidopsis thaliana*

(between stage 2 and 3). The level of *DGAT2* mRNA was less in seeds than in other tissues.

Temporal Expression Patterns of *DGAT1, DGAT2* and *PDAT* Transcripts During Seed Development

The RNA blots above show that *DGAT1, DGAT2* and *PDAT* are highly expressed in the young developing seeds of the tested plants, except for the weak expression of *DGAT2* in the seeds of soybean and *Arabidopsis*. To determine the relative transcript abundance of these three genes during seed development stages and maturation, relative mRNA expression patterns of these three genes were investigated by quantitative real-time PCR. RNA samples were extracted from seeds at six different developmental stages (stage 1–6) and gene-specific primers were designed to amplify the conserved region (about 400–500 bp) for each gene.

As shown in Fig. 2, the mRNAs of *DGAT1, DGAT2* and *PDAT* accumulated basically in a coordinated manner during seed development of *Vernonia galamensis*, *Euphorbia lagascae*, *Stokesia laevis* and castor. Their transcripts were clearly detectable at an early embryonic phase (stage 2), increased to a maximum at late embryonic phase (stage 3) or early seed maturing phase (stage 4), and declined thereafter, suggesting that the mRNAs have similar stabilities and kinetics of synthesis. Furthermore, the transcript levels were different from each other at their peaks (Fig. 2a–d). The *DGAT1* expression level was similar to that of *PDAT*, and both of them were approximately two to threefold higher than *DGAT2*. These findings suggest that the increased expression of these three genes at late embryonic phase and early seed maturing stage might functionally contribute to seed oil accumulation in these high epoxy or hydroxy source plants. These gene expression studies were repeated with gene specific primers for

DGAT1, *DGAT2* and *PDAT* in castor (Fig. 4) and *DGAT1* and *DGAT2* in *Vernonia* [68] and the same expression patterns were seen as reported in this manuscript.

However, only the *DGAT1* transcript accumulated to high levels with a peak at stage 4 in soybean developing seeds (Fig. 2e), while the transcripts of *PDAT* and *DGAT2* were present at very low levels throughout seed development. For *Arabidopsis* (Fig. 2f), the mRNA accumulation of *DGAT1* reached its maximum at stage 4 while the *PDAT* transcripts peaked at stage 2. *DGAT1* expression was three- to four-folds higher than that of *PDAT* in seed development. Again, *DGAT2* expression was very low during seed development.

Taken together, *DGAT1* had the highest transcript level of these three genes in all tested plant seed development. *PDAT* and *DGAT2* transcripts are present at much higher levels in epoxy and hydroxy accumulating plants than in soybean and *Arabidopsis*.

Developmental Changes in Seed Oil Content

For the purpose of examining the time course of oil accumulation during developing and maturing seeds, the total oil content and fatty acid composition at each stage was determined. As shown in Fig. 3, total oil content (μg/mg) started to increase at stage 3, and reached its peak at stage 6 in the seeds of *Vernonia* (Fig. 3a), *Stokesia* (Fig. 3b), *Euphorbia* (Fig. 3c) and castor (Fig. 3d). The maximum rate of oil accumulation occurred from stage 4 to stage 5 or from stage 3 to stage 4; after that, oil accumulation slowed.

In soybean seed (Fig. 3e), oil accumulation increased at the most rapid rate between stage 2 (25 DAF) and stage 4 (45 DAF), which was followed by a slow increase through stage 6 (65 DAF). Similarly, the rate of oil synthesis began to increase at stage 2 (9 DAF), peaked from stage 3 (12 DAF) to stage 4 (15 DAF), and then gradually declined in *Arabidopsis* seed development (Fig. 3f).

Fatty Acid Profiles Through Seed Development

The fatty acid of particular interest is vernolic acid for *Stokesia*, *Vernonia* and *Euphorbia*, and ricinoleic acid for castor. To understand how the accumulation of these unusual fatty acids is regulated in seeds, we measured fatty acid profiles at each stage of seed development using soybean and *Arabidopsis* for comparison.

Fatty acid profiles were determined for each stage of the developing seeds. Like total oil content, the unusual fatty acid levels also began to elevate sharply from stage 4 to stage 5 or from stage 3 to stage 4, and approached its maximum level at stage 6, whereas the relative amounts of common fatty acids such as 16:0, 18:1 and 18:2 were reduced after stage 3 in the seed development of these source plants (Fig. 3a1, b1, c1, d1).

Following seed development (Fig. 3e1), 18:2, a major fatty acid in soybean seed oil, began to increase from stage 2 though stage 6 at a stable rate while other fatty acids exhibited no dramatic changes, except for 18:3 which decreased. In *Arabidopsis* (Fig. 3f1), 18:1 and 18:2 levels increased by the same pattern with the maximum rate between stage 3 and stage 4. However, levels of other fatty acids declined throughout seed development and maturation.

Coordinate Expression of *DGAT1, 2* and *PDAT* is Consistent with High Epoxy and Hydroxy Fatty Acid Accumulation in Seeds

In this study, we investigated whether the developmental regulation of *DGAT1*, *DGAT2* and *PDAT* expression had functions in the accumulation of oil and target fatty acids of the source plants which contain high levels of unusual fatty acids in seed oil. In Fig 2, it is clearly seen that the three genes were concomitantly expressed throughout the seed development of *Vernonia*, *Stokesia*, *Euphorbia* and castor, with the highest rate of expression between stage 2 and 3. As shown in Fig 3, the temporal patterns of total oil content were basically consistent with the accumulation patterns of the target fatty acids in the source plant seeds. Their maximum rate of increase in vivo was between stages 3 and 5 in seed development. In comparison of patterns of the mRNA levels and oil/fatty acid accumulation, it was found that the maximum expression rate of the three genes was in close parallel to the maximum increased rate of oil and target fatty acid accumulation in the seed development, although the former was one or two developmental stage ahead of the latter. It is understood that accumulation of the transcripts precedes accumulation of the enzymes and enzymatic products. However, only the *DGAT1* transcript was largely increased during the active period of TAG and major fatty acid accumulation in the seeds of soybeans and *Arabidopsis* (Figs. 2, 3). A relationship between oil accumulation and *DGAT2* and *PDAT* function in soybean seeds is unlikely, because these two genes are expressed at low levels at stages of high oil synthesis. In *Arabidopsis* seeds, *DGAT2* also exhibited weak expression. The *PDAT* transcript peaked at an early stage (DAF 9), and was much lower than the maximum *DGAT1* level, suggesting that *PDAT* expression is not closely related to oil accumulation during *Arabidopsis* seed development.

Overall, the present data indicate that *DGAT1*, *DGAT2* and *PDAT* all show expression patterns consistent with roles in oil accumulation in high epoxy or hydroxy fatty acid accumulators.

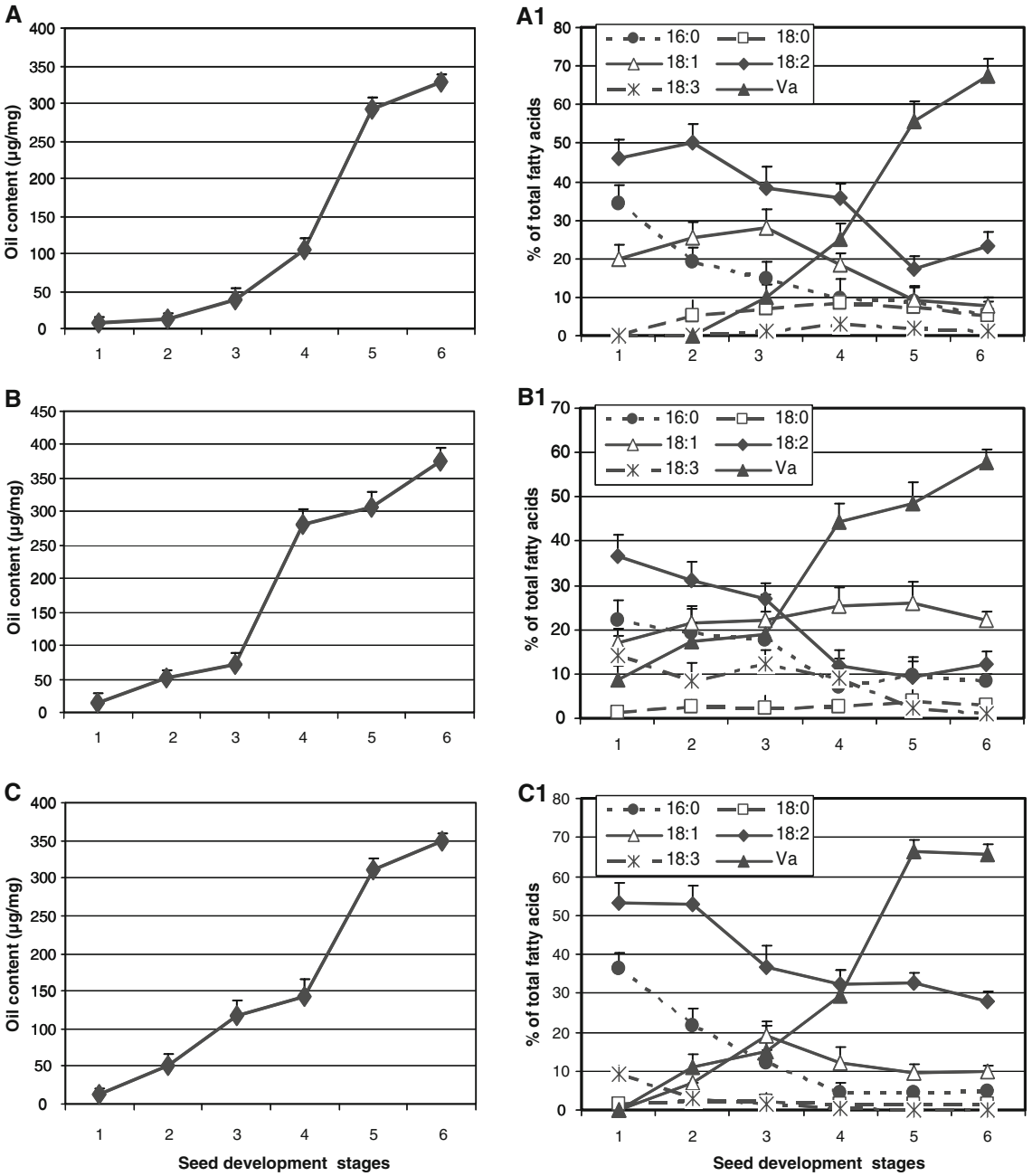

Fig. 3 Oil content and fatty acid profiles during seed development. Fatty acid compositions and total contents in developing seed were performed as described in the materials and methods. Data represent mean values of five independent experiments, and *error bars* indicate STD. **a**, **a1** *Vernonia galamensis*, **b**, **b1** *Euphorbia lagascae*, **c**, **c1** *Stokesia laevis*, **d**, **d1** Castor, **e**, **e1** soybean (cv. Jack), **f**, **f1** *Arabidopsis thaliana*

Discussion

Triacylglycerols (TAGs) are quantitatively the most important storage form of energy for eukaryotic cells. During the past few years, the biosynthesis of TAG has received much attention. To date, three independent gene families, *DGAT1, DGAT2* and *PDAT* have been described and encode unique proteins with the capacity to form TAG, and all three genes are present in the genomes of eukaryotes [16, 17, 20, 22, 23, 31, 32]. It has also been reported that these three genes could contribute to oil accumulation in plant seeds [33, 34]. However, it is still unclear how they determine the final TAG accumulation in seeds.

DGAT1 has been quite extensively studied in *Arabidopsis*. Two mutants, AS11 [13, 35, 36] and ABX45 [12] have been analyzed, and these studies show that a

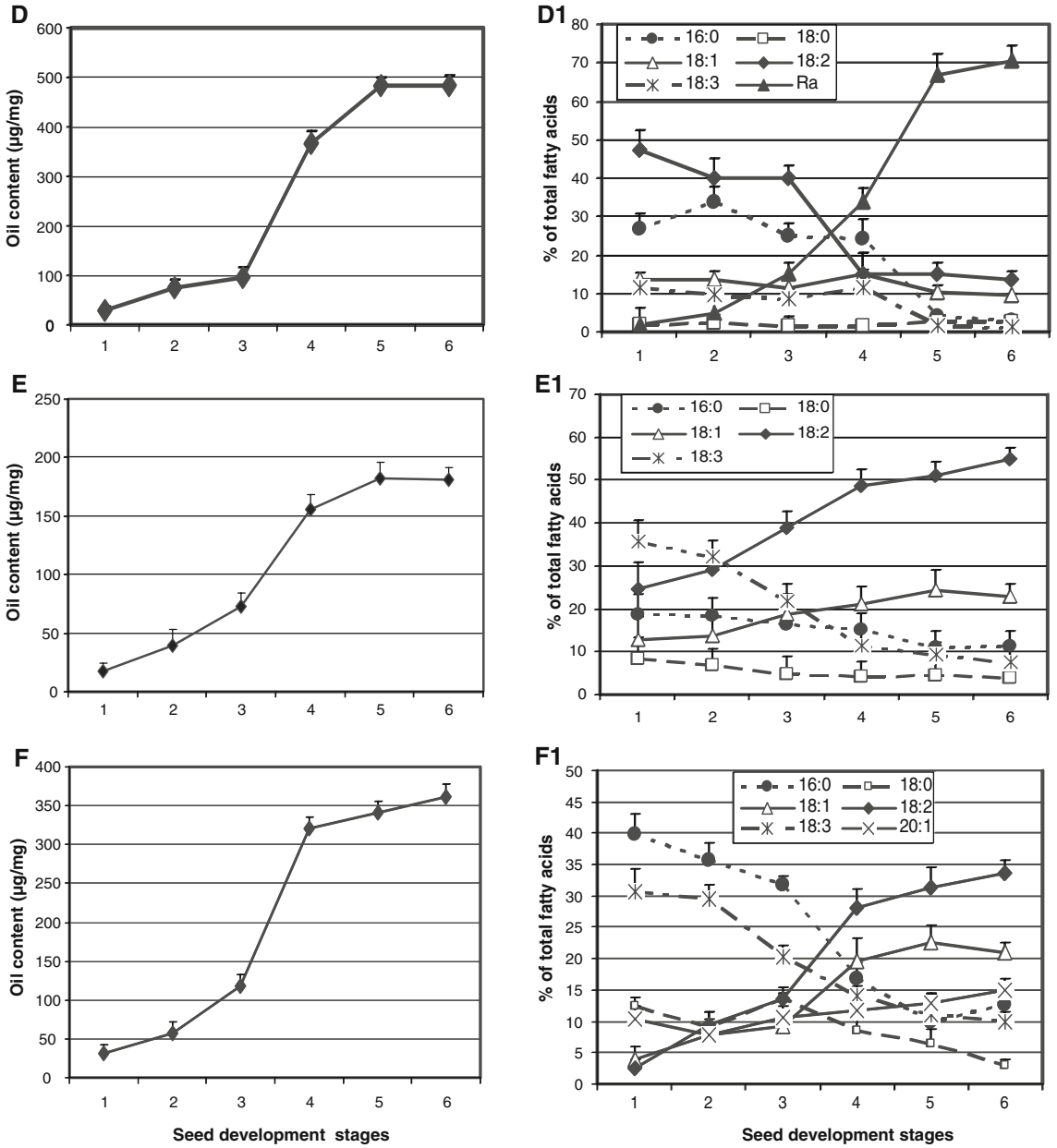

Fig. 3 continued

dysfunctional DGAT1 protein results in a decrease in stored TAG and a modified TAG fatty acid profile. Seed-specific over-expression of an *Arabidopsis DGAT1* gene enhances oil deposition and average seed weight, suggesting that DGAT1 catalyzes a rate-limiting step in TAG biosynthesis [35]. These results provide strong evidence that DGAT1 is an important enzyme in catalyzing TAG formation in plant seeds. However, the seeds of these two mutants still synthesize TAGs at 55–75% of the normal level, indicating that other enzymes also contribute to TAG accumulation in *Arabidopsis* seeds [12, 20, 31, 37].

Research on other oil plants also indicates an important role of DGAT1 for oil synthesis and accumulation in seeds. It is found that the critical stage for castor oil biosynthesis is between 19 DAP and 26 DAP, where castor DGAT1 (RcDGAT) protein and activity significantly increases. The close correlation between profiles of RcDGAT activity and oil accumulation is consistent with a role of RcDGAT in castor oil biosynthesis [38, 39]. Kroon et al. [24] indicate this is apparently mainly due to DGAT2. High expression of *DGAT1* is reported during development of oilseed rape (*Brassica napus*) seeds [16]. A tight correlation between

DGAT activity and oil deposition is also reported by other groups [40, 41]. By silencing the expression of *DGAT1* in tobacco, Zhang et al. [42] found that the expression level of *DGAT1* is correlated with oil content in the seeds, and reduction of *DGAT1* transcript also results in decreased seed weight. In addition, the seeds with *DGAT1* silenced still accumulate some TAG.

During soybean (cv. Amsoy 71) seed development, the rate of lipid biosynthesis was reported to increase markedly between 15 and 45 DAF [43] or from 20 to 50 DAF [44]. Our data show that the period of highest oil accumulation in soybean cv 'Jack' grown under the conditions stated in the materials and methods is between 25 and 45 DAF (Fig 3e, e1), a period where *DGAT1* transcript levels were maximal (Fig 2e). For *Arabidopsis*, the rate of oil synthesis peaked at 9–15 DAF (Fig. 3f, f1), and the highest level of *DGAT1* transcript occurs at this period of seed development (Fig. 2f). It has previously been reported that oil is synthesized at maximum rates between 7 and 13 DAF [45], and that the DGAT1 protein peaks at 7–9 DAF during *Arabidopsis* embryo development [46]. Moreover, our current data also shows that *DGAT1* transcript levels accumulate to a higher level than *DGAT2* and *PDAT*, and the peak of the *DGAT1* transcript level is consistent with the maximum increase of oil and fatty acid accumulation during seed development of *Vernonia, Euphorbia, Stokesia,* castor, soybeans and *Arabidopsis*.

Many of the more than 300 naturally occurring unusual fatty acids that have been described in seeds to date have high-valued properties for industrial utilization. The main component of seed oil in *Vernonia galamensis*, *Crepis palaestina*, *Euphorbia lagascae* and *Stokesia laevis* is the epoxy fatty acid vernolic acid whereas a hydroxy fatty acid, ricinoleic acid, is the major component in castor seed oil. The accumulation of unusual fatty acids in TAG can be divided into two major steps. First is the insertion of the functional group into the acyl chain, followed by the incorporation of the unusual fatty acid into TAG. In unusual fatty acid accumulating plants, these fatty acids are found almost exclusively in TAG and are excluded from membrane lipids, most likely because they are deleterious to membrane function [47]. Therefore, at least two enzymes are needed for these unusual fatty acids to accumulate in seed oil. One is for the synthesis of the unusual fatty acid and others are for specifically incorporating the unusual fatty acid into TAG. Several genes have been identified that code for enzymes involved in the synthesis of some unusual fatty acids [48]. For example, epoxygenase genes responsible for epoxidizing linoleic acid have been cloned from several accumulators of vernolic acid [49–52]. However, transgenically expressing these synthesis enzymes only result in low levels of the unusual fatty acid accumulation in seed oil [50, 52–55]. Low-level accumulation of unusual fatty acids in transgenic plants may be from the failure to efficiently incorporate them into TAGs, leading to their rapid degradation through the β-oxidation cycle [56–58]. These findings suggest that besides the synthesis enzyme, the enzymes catalyzing the final acylation step of TAG synthesis such as DGAT1, DGAT2 and PDAT might be other major contributors for selective accumulation of unusual fatty acids in native plant seed oil.

PDAT activity has been identified in microsomal preparations from castor and *Crepis palaestina* plants [20]. It is proposed that PDAT is involved in the transfer of the oxygenated acyl groups from phospholipids into TAGs. Stahl et al. [22] demonstrated that *Arabidopsis* PDAT (AtPDAT, At5g13640) utilized different phospholipids as acyl donor and accepted acyl groups ranging from C10 to C22. AtPDAT exhibited highest activity for acyl groups containing several double bonds, epoxy, or hydroxyl groups. AtPDAT has similar acyl specificity for vernoloyl and ricinoleoyl groups as the PDAT activity assayed in the microsomal preparations from developing castor endosperm, indicating that the plant PDAT acyl specificities are general and not limited to plants producing unusual fatty acids. Furthermore, the transformants over-expressing *AtPDAT cDNA* had tenfold higher PDAT activity than the wild type, and did not have any alteration in fatty acid composition in either vegetative parts or in the oil accumulating seeds. Expression of *PDATs* from other plants may show specificity not seen with this *Arabidopsis PDAT*. Mhaske et al.'s [23] work on a knockout mutant of *Arabidopsis* in the *PDAT* gene (locus At5g13640) shows that this knockout has no effect on either the fatty acid content or composition of seed. PDAT activity encoded by this gene is not a major determinant of TAG synthesis in *Arabidopsis* seeds. This is contrary to the situation in yeast where PDAT is a major contributor to TAG accumulation in exponential growth phase [59]. Stahl et al. [22] reported that *Arabidopsis* has six ORFs with significant homology to either lecithin: cholesterol acyltransferase (LCAT) or ScPDAT. They demonstrated that At5g13640 has PDAT activity but At3g44830 is mainly expressed in developing seeds. This has lead Stahl et al. (2004) to hypothesize that At3g44830 has a specific role in TAG deposition in developing seeds but confirmation of this awaits further experimentation.

Several *DGAT2* genes have been recently cloned and characterized from animal [32], fungi [31] and plants [19, 31]. In yeast, the DGAT2 enzyme is dominant in the stationary growth phase when the yeast is storing significant amounts of TAG [59, 60]. In animals, the temporal-spatial expression of the *DGAT2* gene is different from *DGAT1*, and therefore has different physiological functions in vivo [61–63]. Recent experiments indicate a particularly

important role for *DGAT2* expression and conjugated and hydroxy fatty acid accumulation in seed oil and that DGAT2 can function different from DGAT1 in plants [24–26].

In our present study, the expression pattern of *DGAT2* was consistent with a role in the accumulation of oil and epoxy or hydroxy fatty acids during seed development. Only very low levels of *DGAT2* transcript were detected in soybean and *Arabidopsis* developing seeds, suggesting a correspondingly small role (if any) in TAG synthesis. Similarly, *PDAT* expression in developing seeds is high for epoxy and hydroxy fatty acid accumulating plants and weak for soybean and *Arabidopsis.* The *PDAT* expression data in this study also suggest that *PDAT* might play an important role in epoxy and hydroxyl fatty acid accumulation, which is consistent with the results obtained in the functional analysis of PDAT from castor and *Crepis palaestina* plants [20].

The primary role of DGAT1, DGAT2 and PDAT is to catalyze the final step of storage TAG synthesis. It is expected that these three genes would mainly be expressed in developing seeds of oil plants. However, it has been suggested that their expression is not restricted to the embryos. DGAT activity has been found in spinach leaves [64] and germinating soybean cotyledons [65]. *DGAT1* transcripts have been detected in many tissues in *Arabidopsis* including developing siliques, flowers, germinating seeds and young seedlings [13]. Using RNA gel blot analysis, Hobbs et al. [16] detected low levels of *DGAT1* expression in leaves and stems as well as its strong expression in embryos and flowers in *Brassica napus*. In *Arabidopsis* seedlings, *DGAT1* is expressed in shoot and root apical regions, correlating with rapid cell division and growth [46]. In addition, *DGAT1* gene expression is up-regulated by glucose and associated with glucose-induced changes in seedling development [46]. *DGAT1* transcripts are expressed in different tobacco tissues including leaves, stems, roots, petals and developing seeds [42]. Roles in fatty acid mobilization and senescence in leaves have also been reported [66, 67]. These observations suggest that the *DGAT1* gene may also be involved in physiological activities other than its "classical" role for storage fatty acid accumulation in plants or TAG synthesis occurs at least transiently in many plant tissues.

The *AtPDAT* (At5g13640) gene is also found to express in leaves, root, flowers and developing seeds of *Arabidopsis* [22]. Some PDATs may possibly play a general protective role by removing oxidized fatty acids from phospholipids, or function in the removal of DAG, a product of the phosphatidylinositol signaling pathway [23]. Preliminary information on *DGAT2* expression in plant tissues is just emerging. In animals extensive information on its expression in different types of cells and tissues has already been reported.[24–26, 61, 62, 68].

Our data provide evidence that *DGAT1*, *DGAT2* and *PDAT* expression in leaves, stems and roots as well as in developing seeds is different between unusual and normal fatty acid accumulating oilseeds. Consistent with previous knowledge, our results also suggest that *DGAT1, DGAT2* and *PDAT* genes might be involved in other physiological activities of plants.

It should be noted that *Arabidopsis* genome contains only one *DGAT1* [15], one *DGAT2* (NM_115011) and six *PDATs* [21]. The other species tested here may contain one or multiple isoforms for each of the three classes of genes. We previously isolated two *DGAT1* cDNA clones from *Vernonia* (EF653277 and EF653276) [69] and soybean (AF257589 and AF257590). We also cloned one full-length cDNA of Vernonia *DGAT2* (FJ652577). It was reported that the castor genome contains one *DGAT1* [37], one *DGAT2* [23] and two *PDATs* [70]. In the present study, the conserved region of each gene family was used for the probe and primer design, which allows detection of the expression levels of each gene family or at least one isoform expression (if one more isoforms present in the genome). The three gene expression patterns in *Arabidopsis* and DGTA1 expression pattern in castor obtained by this study are in agreement with the previous reports [15, 21, 23, 34, 45], indicating our experiments provide useful information on expression of TAG biosynthetic genes in these plants although the primers are heterologous for some plants tested here. In castor seeds, our data shows *DGAT1* expression is higher than *DGAT2*, whereas *DGAT2* level is higher than *DGAT1* reported by Kroon et al. [23]. This discrepancy might be due to differences in castor genotype and sampling. Interestingly, compared to *DGAT2* expressions in soybean and *Arabidopsis*, we concluded DGAT2 is important for unusual fatty acid accumulation that is consistent with their conclusion, supported by transgenic experiments in *Arabidopsis* [25]. We also characterized *DGAT1* and *DGAT2* cDNA clones [69] and conducted the transgenic experiments [71], which confirms the suggestion from this study that both DGATs function in unusual fatty acid accumulation in *Vernonia* seeds. Further QPCR was also performed with castor gene specific primers for *DGAT1*, *DGAT2* and *PDAT* (Fig. 4) and *Vernonia DGAT1* and *DGAT2* specific primers in Li et al. [68] and the same expression patterns were seen as reported in this manuscript.

Developing an understanding of the control of TAG synthesis in seeds and how plants can accumulate high levels of certain fatty acids (particularly unusual fatty acids) in seed oil is a significant challenge if yields are to be increased and unusual fatty acids are to be engineered for high production in common oilseed plants. The present study was carried out with the aim of investigating *DGAT1*, *DGAT* and *PDAT* transcript levels in relation to the

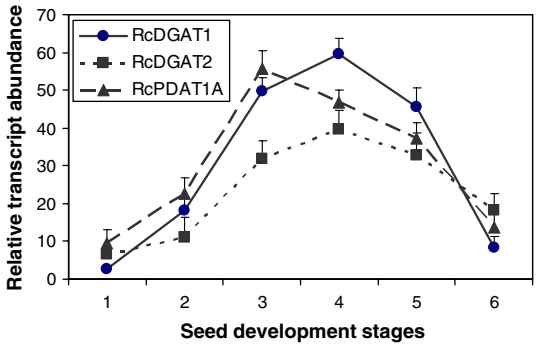

Fig. 4 Expression patterns of *DGAT1, 2* and *PDAT* transcripts during castor (*Ricinus communis*) seed development using castor gene specific primers. Expression levels were normalized with respect to the internal control *18 s RNA*. *Data bars* represent the mean ± STD level of relative transcript abundance from five experiments with independent RNA extractions. Real-time PCR was performed as described in "Materials and Methods" (and legend of Fig. 2). Gene-specific primers were designed based on the ORF of each gene. Primers for *RcDGAT1 (AY366496)* were 5′-tgttaacagcaggctcatcatt-3′ (*forward*) and 5′-ccatacaagcaagttccatcaa-3′ (*reverse*). Primers for *RcDGAT2 (EU391592)* were 5′-tttggttatgagccacattcag-3′ (*forward*) and 5′-caagggtttacccatctccata-3′ (*reverse*). Primers for *RcPDAT1A* [70] were 5′-gacatcagtgtgctgatggttt-3′ (*forward*) and 5′-tgctcaaacttt ggtccctaat-3′ (*reverse*)

accumulation of oil and epoxy and hydroxy fatty acids in developing seeds of *Vernonia galamensis*, *Euphorbia lagascae*, *Stokesia* and castor in comparison with soybean and *Arabidopsis*. For all plants examined, *DGAT1* appears to be a major enzyme gene for seed oil accumulation. For the epoxy and hydroxy fatty acid accumulating plants, *PDAT* and *DGAT2* also appear to play significant roles in the selective accumulation of these unusual fatty acids in the seed oil. We provide the first evidence that *DGAT2* is expressed in different tissues including developing seeds of the tested plants. Consistent with other reports, *PDAT* and *DGAT1* are found to be expressed in different plant tissues.

Acknowledgments This research was supported by the United Soybean Board, Ashland Chemicals, the Kentucky Science and Engineering Foundation, the Consortium for Plant Biotechnology Research, and the Kentucky Soybean Promotion Board. We gratefully acknowledge John Johnson for his technical support.

References

1. Bewley J, Black M (1994) Seeds: Physiology of Development and Germination, 2nd edn. Plenum, New York
2. van de Loo FJ, Fox BG, Somerville C (1993) Unusual fatty acids. In: Moore JTS (ed) Lipid metabolism in plants. CRC, Boca Raton, pp 91–126
3. Perdue RE (1989) Vernonia: bursting with potential. Agric Eng 70:11–13
4. Pascual MJ, Correal E (1992) Mutation studies of an oilseed spurge rich in vernolic acid. Crop Sci 32:95–98
5. Bafor M, Smith MA, Jonsson L, Stobart K, Stymme S (1993) Biosynthesis of vernoleate (*cis*-12-epoxyoctadeca-*cis*-9-enoate) in microsomal preparations from developing endosperm of *Euphorbia lagascae*. Arch Biochem Biophys 303:145–151
6. Thompson AE, Dierig DA, Kleiman R (1994) Variation in *Vernonia galamensis* flowering characteristics, seed oil and vernolic acid contents. Ind Crop Prod 3:175–183
7. Huang AHC (1992) Oil bodies and oleosins in seeds. Annu Rev Plant Physiol Plant Mol Biol 43:177–200
8. Ohlrogge JB, Browse J (1995) Lipid biosynthesis. Plant Cell 7:957–970
9. Ichihara K, Takahashi T, Fujii S (1988) Diacylglycerol acyltransferase in maturing safflower seeds: its influences on the fatty acid composition of triacylglycerol and on the rate of triacylglycerol synthesis. Biochim Biophys Acta 958:125–129
10. Perry H, Harwood J (1993) Changes in the lipid content of developing seeds of *Brassica napus*. Phytochemistry 32:1411–1415
11. Cases S, Smith SJ, Zheng Y, Myers HM, Lear SR, Sande E, Novak S, Collins C, Welch CB, Lusis AJ, Erickson SK, Farese RV Jr (1998) Identification of a gene encoding an acyl CoA:diacylglycerol acyltransferase, a key enzyme in triacylglycerol synthesis. Proc Natl Acad Sci USA 95:13018–13023
12. Routaboul J-M, Benning C, Bechtold N, Caboche M, Lepiniec L (1999) The TAG1 locus of *Arabidopsis* encodes for a diacylglycerol acyltransferase. Plant Physiol Biochem 37:831–840
13. Zou J, Wei Y, Taylor DC (1999) The *Arabidopsis thaliana* TAG1 mutant has a mutation in a diacylglycerol acyl transferase gene. Plant J 19:645–654
14. Oelkers P, Behar A, Cromley D, Billheimer J, Sturley S (1998) Characterization of two human genes encoding acyl coenzyme A: cholesterol acyltransferase-related enzymes. J Biol Chem 273:26765–26771
15. Saha S, Enugutti B, Rajakumari S, Rajasekharan R (2006) Cytosolic triacylglycerol biosynthetic pathway in oilseeds: molecular cloning and expression of peanut cytosolic diacylglycerol acyltransferase. Plant Physiol 141:1533–1543
16. Hobbs DH, Lu C, Hills MJ (1999) Cloning of a cDNA encoding diacylglycerol acyltransferase from *Arabidopsis thaliana* and its functional expression. FEBS Lett 452:145–149
17. Bouvier-Nave P, Benvenise P, Oelkers P, Sturley S, Schaller H (2000) Expression in yeast and tobacco of plant cDNAs encoding acyl CoA:diacylglycerol acyltransferase. Eur J Biochem 267:85–96
18. Nykiforuk CL, Furukawa-Stoffer TL, Huff PW, Sarna M, Laroche A, Moloney MM, Weselake RJ (2002) Characterization of cDNAs encoding diacylglycerol acyltransferase from cultures of *Brassica napus* and sucrose-mediated induction of enzyme biosynthesis. Biochimica Biophysica Acta Mol Cell Biol Lipid 1580:95–109
19. Beisson F, Koo AJK, Ruuska S, Schwender J, Pollard M, Thelen JJ, Paddock T, Salas JJ, Savage L, Milcamps A, Mhaske VB, Cho Y, Ohlrogge JB (2003) *Arabidopsis* genes involved in acyl lipid metabolism: a census of the candidates, a study of the distribution of expressed sequence tags in organs, and a web-based database. Plant Physiol 132: 681–97 (updated version at http://www.plantbiology.msn/lipids/genesurvey/)
20. Dahlqvist A, Ståhl U, Lenman M, Banas A, Lee M, Sandager L, Ronne H, Stymne S (2000) Phospholipid:diacylglycerol acyltransferase: an enzyme that catalyzes the acyl-CoA-independent formation of triacylglycerol in yeast and plants. Proc Natl Acad Sci USA 97:6487–6492
21. Oelkers P, Tinkelenberg A, Erdeniz N, Cromley D, Billheimer JT, Sturley SL (2000) A lecithin cholesterol acyltransferase-like gene mediates diacylglycerol esterification in yeast. J Biol Chem 275:15609–15612
22. Ståhl U, Carlsson A, Lenman M, Dahlqvist A, Huang B, Bana W, Bana A, Stymne S (2004) Cloning and functional characterization

of a phospholipid:diacylglycerol acyltransferase from *Arabidopsis*. Plant Physiol 135:1324–1335
23. Mhaske V, Beldjilali K, Ohlrogge J, Pollard M (2005) Isolation and characterization of an *Arabidopsis thaliana* knockout line for phospholipid: diacylglycerol transacylase gene (At5g13640). Plant Physiol Biochem 43:413–417
24. Kroon JTM, Wei W, Simon WJ, Slabas AR (2006) Identification and functional expression of a type 2 acyl-CoA:diacylglycerol acyltransferase (DGAT2) in developing castor bean seeds which has high homology to the major triglyceride biosynthetic enzyme of fungi and animals. Phytochemistry 67:2541–2549
25. Shockey JM, Gidda SK, Chapital DC, Kuan J-C, Dhanoa PK, Bland JM, Rothstein SJ, Mullen RT, Dyer JM (2006) Tung tree DGAT1 and DGAT2 have nonredundant functions in triacylglycerol biosynthesis and are localized to different subdomains of the endoplasmic reticulum. Plant Cell 18:2294–2313
26. Burgal J, Shockey J, Lu C, Dyer J, Larson T, Graham I, Browse J (2008) Metabolic engineering of hydroxy fatty acid production in plants: RcDGAT2 drives dramatic increases in ricinoleate levels in seed oil. Plant Biotechnol J 6:819–831
27. Verdier J, Thompson RD (2008) Transcriptional regulation of storage protein synthesis during dicotyledon seed filling. Plant Cell Physiol 49:1263–1271
28. Le BH, Wagmaister JA, Kawashima T, Bui AQ, Harada JJ, Goldberg RB (2007) Using genomics to study legume seed development. Plant Physiol 144:562–574
29. Goldberg RB, de Paiva G, Yadegari R (1994) Plant embryogenesis: zygote to seed. Science 266:605–614
30. Dahmer ML, Hildebrand DF, Collins GB (1992) Comparative protein accumulation patterns in soybean somatic and zygotic embryos. In Vitro Cell Dev Biol Plant 28P:106–114
31. Lardizabal KD, Mai JT, Wagner NW, Wyrick A, Voelker T, Hawkins DJ (2001) DGAT2 Is a new diacylglycerol acyltransferase gene family: purification, cloning, and expression in insect sells of two polypeptides from *Mortierella ramanniana* with diacylglycerol acyltransferase activity. J Biol Chem 276:38862–38869
32. Cases S, Stone SJ, Zhou P, Yen E, Tow B, Lardizabal KD, Voelker T, Farese RV Jr (2001) Cloning of DGAT2, a second mammalian diacylglycerol acyltransferase, and related family members. J Biol Chem 276:38870–38876
33. Hobbs D, Flintham J, Hills M (2004) Genetic control of storage oil synthesis in seeds of *Arabidopsis*. Plant Physiol 136:3341–3349
34. Jako C, Kumar A, Wei Y, Zou J, Barton DL, Giblin EM, Taylor DC, Covello PS (2001) Seed-specific over-expression of an *Arabidopsis* cDNA encoding a diacylglycerol acyltransferase enhances seed oil content and seed weight. Plant Physiol 126:861–874
35. Jako C, Kumar A, Wei Y, Zou J, Barton DL, Giblin EM, Covello PS, Taylor DC (2001) Seed-specific over-expression of an *Arabidopsis* cdna encoding a diacylglycerol acyltransferase enhances seed oil content and seed weight. Plant Physiol 126:861–874
36. Katavic V, Reed DW, Taylor DC, Giblin EM, Barton DL, Zou J, Mackenzie SL, Covello PS, Kunst L (1995) Alteration of seed fatty acid composition by an ethyl methanesulfonate-induced mutation in *Arabidopsis thaliana* affecting diacylglycerol acyltransferase activity. Plant Physiol 108:399–409
37. Lu C, Hills MJ (2002) *Arabidopsis* mutants deficient in diacylglycerol acyltransferase display increased sensitivity to abscisic acid, sugars, and osmotic stress during germination and seedling development. Plant Physiol 129:1352–1358
38. He X, Turner C, Chen G, Lin J-T, Mckeon T (2004) Cloning and characterization of a cDNA encoding diacylglycerol acyltransferase from castor bean. Lipids 39:311–318
39. He X, Chen G, Lin J-T, Mckeon T (2004) Regulation of diacylglycerol acyltransferase in developing seeds of castor. Lipids 39:865–871
40. Tzen J, Cao Y, Laurent P, Ratnayake C, Huang A (1993) Lipids, proteins, and structure of seed oil bodies from diverse species. Plant Physiol 101:267–276
41. Weselake R, Pomeroy M, Furukawa T, Golden J, Little D, Laroche A (1993) Development profile of diacylglycerol acyltransferase in maturing seeds of oilseed rape and safflower and microspore-derived cultures of oilseed rape. Plant Physiol 102:565–571
42. Zhang F-Y, Yang M-F, Xu Y-N (2005) Silencing of *DGAT1* in tobacco causes a reduction in seed oil content. Plant Sci 169:689–694
43. Privett OS, Dougherty KA, Erdahl WL, Stolyhwo A (1973) Studies on the lipid composition of developing soybean seeds. J Am Oil Chem Soc 50:516–520
44. Ohlrogge JB, Kuo T-m (1984) control of lipid synthesis during soybean seed development: enzymic and immunochemical assay of acyl carrier protein. Plant Physiol 74:622–625
45. Focks N, Benning C (1998) A novel, low-seed-oil mutant of *Arabidopsis* with a deficiency in the seed-specific regulation of carbohydrate metabolism. Plant Physiol 118:91–101
46. Lu CL, de Noyer SB, Hobbs DH, Kang J, Wen Y, Krachtus D, Hills MJ (2003) Expression pattern of diacylglycerol acyltransferase-1, an enzyme involved in triacylglycerol biosynthesis, in *Arabidopsis thaliana*. Plant Mol Biol 52:31–41
47. Millar A, Smith MA, Kunst L (2000) All fatty acids are not equal: discrimination in plant membrane lipids. Trends Plant Sci 5:95–101
48. Jaworski J, Cahoon EB (2003) Industrial oils from transgenic plants. Curr Opin Plant Biol 6:178–184
49. Hitz WD (1998) Fatty acid modifying enzymes from developing seeds of *Vernonia galamensis*. DuPont, USA
50. Lee M, Lenman M, Banas A, Bafor M, Singh S, Schweizer M, Nilsson R, Liljenberg C, Dahlqvist A, Gummeson PO, Sjodahl S, Green A, Stymne S (1998) Identification of non-heme diiron proteins that catalyze triple bond and epoxy group formation. Science 280:915–918
51. Cahoon EB, Ripp KG, Hall SE, McGonigle B (2002) Transgenic production of epoxy fatty acids by expression of a cytochrome P450 enzyme from *Euphorbia lagascae* seed. Plant Physiol 128:615–624
52. Hatanaka T, Shimizu R, Hildebrand D (2004) Expression of a *Stokesia laevis* epoxygenase gene. Phytochemistry 65:2189–2196
53. Eccleston V, Cranmer A, Voelker T, Ohlrogge J (1996) Medium-chain fatty acid biosynthesis and utilization in *Brassica napus* plants expressing lauroyl-acyl carrier protein thioesterase. Planta 198:46–53
54. Kinney AJ (2001) Perspectives on the production of industrial oils in genetically engineered oilseeds. In: Kuo TM, Gardner HW (eds) Lipid biotechnology. Marcel Dekker, New York, pp 85–93
55. Singh S, Thomaeus S, Lee M, Stymne S, Green A (2001) Transgenic expression of a Δ12-epoxygenase gene in *Arabidopsis* seeds inhibits accumulation of linoleic acid. Planta 212:872–879
56. Eccleston VS, Ohlrogge JB (1998) Expression of lauroyl-acyl carrier protein thioesterase in *Brassica napus* seeds induces pathways for both fatty acid oxidation and biosynthesis and implies a set point for triacylglycerol accumulation. Plant Cell 10:613–622
57. Poirier Y, Ventre G, Calelari D (1999) Increased flow of fatty acids toward β-oxidation in developing seeds of *Arabidopsis* deficient in diacylglycerol acyltransferase activity or synthesizing medium-chain-length fatty acids. Plant Physiol 121:1366–1459
58. Moire L, Rezzonico E, Goepfert S, Poirier Y (2004) Impact of unusual fatty acid synthesis on futile cycling through β-oxidation and on gene expression in transgenic plants. Plant Physiol 134:432–442

59. Oelkers P, Cromley D, Padamsee M, Billheimer J, Sturley S (2002) The *DGA1* gene determines a second triglyceride synthetic pathway in yeast. J Biol Chem 277:8877–8881
60. Sandager L, Gustavsson M, Ståhl U, Dahlqvist A, Wiberg E, Banas A, Lenman M, Ronne H, Stymne S (2002) Storage lipid synthesis is non-essential in yeast. J Biol Chem 277:6478–6482
61. Yu XX, Murray SF, Pandey SK, Booten SL, Bao D, Song X-Z, Kelly S, Chen S, McKay R, Monia BP, Bhanot S (2005) Antisense oligonucleotide reduction of DGAT2 expression improves hepatic steatosis and hyperlipidemia in obese mice. Hepatology 42:362–371
62. Stone SJ, Myers HM, Watkins SM, Brown BE, Feingold KR, Elias|| PM, Farese RV (2004) Lipopenia and skin barrier abnormalities in DGAT2-deficient mice. J Biol Chem 279:11767–11776
63. Orland MD, Anwar K, Cromley D, Chu C-H, Chen L, Billheimer JT, Hussain MM, Cheng D (2005) Acyl coenzyme A dependent retinol esterification by acyl coenzyme A:diacylglycerol acyltransferase 1. Biochim Biophys Acta 1737:76–82
64. Martin B, Wilson R (1983) Sub-cellular location of triacylglycerol synthesis in spinach leaves. Lipids 19:117–121
65. Wilson R, Kwanyuen P (1986) Triacylglycerol synthesis and metabolism in germinating soybean cotyledons. Biochim Biophys Acta 877:231–237
66. Slocombe SP, Cornah J, Pinfield-Wells H, Soady K, Zhang Q, Gilday A, Dyer JM, Graham IA (2009) Oil accumulation in leaves directed by modification of fatty acid breakdown and lipid synthesis pathways. Plant Biotechnol J 7:694–703
67. Kaup MT, Froese CD, Thompson JE (2002) A role for diacylglycerol acyltransferase during leaf senescence. Plant Physiol 129:1616–1626
68. Turkish AR, Henneberry AL, Cromley D, Padamsee M, Oelkers P, Bazzi H, Christiano AM, Billheimer JT, Sturley SL (2005) Identification of two novel human acyl-coa wax alcohol acyltransferases: members of the diacylglycerol acyltransferase 2 (DGAT2) gene superfamily. J Biol Chem 280:14755–14764
69. Yu K, Li R, Hatanaka T, Hildebrand D (2008) Cloning and functional analysis of two type 1 diacylglycerol acyltransferases from *Vernonia galamensis*. Phytochemistry 69:1119–1127
70. Browse J, Shockey J, Burgal J (2008) Enhancement of hydroxy fatty acid accumulation in oilseed plants. US Patent Application #20080282427
71. Li R, Yu K, Hatanaka T, Hildebrand DF (2010) Vernonia DGATs increase accumulation of epoxy fatty acids in oil. Plant Biotechnol J 8:184–195

Lipids (2010) 45:159–165
DOI 10.1007/s11745-009-3378-3

ORIGINAL ARTICLE

Facile and Stereoselective Synthesis of (*Z*)-15-Octadecenoic Acid and (*Z*)-16-Nonadecenoic Acid: Monounsaturated Omega-3 Fatty Acids

Tristan Rawling · Colin C. Duke · Pei H. Cui · Michael Murray

Received: 29 October 2009 / Accepted: 25 November 2009 / Published online: 13 January 2010

Abstract Facile syntheses of the monounsaturated omega-3 fatty acids, (*Z*)-15-octadecenoic acid and (*Z*)-16-nonadecenoic acid, are presented. Commercially available hydroxy fatty acids were esterified and oxidised, followed by the Wittig reaction to introduce the omega-3 olefinic bond; hydrolysis yielded the omega-3 fatty acids in high purity. An examination of different reaction conditions for the Wittig step found that THF as solvent and coupling temperatures of −78 °C gave optimal stereoselectivity, affording the omega-3 olefins in *Z*:*E* ratios ≥97:3. The syntheses have overall yields of ∼43%, and utilise straightforward, robust chemistry, that may be readily scaled up and reproduced. Also presented is a method for accurately determining the double bond geometry and isomeric purity of the fatty acid products using ^{1}H–^{13}C-HSQC NMR and GC–MS, respectively.

Keywords Omega-3 · Fatty acid · Wittig reaction · Stereoselectivity

Abbreviations

DCM	Dichloromethane
DMF	*N*,*N*-dimethylformamide
FAME	Fatty acid methyl ester
$NaN(TMS)_2$	Sodium bis(trimethylsilyl)amide
PCC	Pyridinium chlorochromate
PUFA	Polyunsaturated fatty acid
THF	Tetrahydrofuran

T. Rawling (✉) · P. H. Cui · M. Murray
Pharmacogenomics and Drug Development Group, Faculty of Pharmacy A15, University of Sydney, Sydney, NSW 2006, Australia
e-mail: trawling@pharm.usyd.edu.au

C. C. Duke
Pharmaceutical Chemistry, Faculty of Pharmacy, University of Sydney, Sydney, NSW 2006, Australia

Introduction

Omega-3 polyunsaturated fatty acids (PUFAs) have been the subject of intense recent interest because their beneficial actions in cells and in vivo are biologically distinct from those of their omega-6 counterparts. Thus, omega-3 fatty acids possess anti-inflammatory and anti-cancer effects, and have also been shown to inhibit platelet aggregation, promote neuronal cell survival, increase membrane fluidity and to modulate the expression of genes that regulate lipid metabolism [1]. Populations with a high intake of omega-6 PUFAs exhibit an increased risk of breast, colon and prostate cancer, compared to those with a high consumption of omega-3-containing oils [2–5]. Moreover, in vivo and in vitro studies have shown that omega-6 PUFAs stimulate carcinogenesis and tumour growth and metastasis, while omega-3 PUFAs repress tumourigenesis [2, 6, 7]. PUFAs undergo biotransformation to eicosanoid derivatives catalysed by cyclooxygenase, lipoxygenase and cytochrome P450 enzymes; these eicosanoids mediate many of the cellular effects of PUFAs [8, 9]. Because omega-3 and omega-6 PUFAs give rise to parallel series of eicosanoids with differing potency, the omega-3 olefinic bond is strongly implicated in the beneficial properties of the parent omega-3 PUFAs.

Most studies of the biological effects of omega-3 fatty acids have focussed on naturally occurring PUFAs, such as α-linolenic acid and eicosapentaenoic acid. However, the

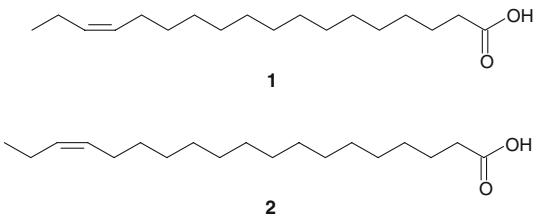

Fig. 1 The (*Z*)-monounsaturated omega-3 fatty acids prepared in this work

assignment of particular cellular actions to the omega-3 bond is confounded by possible interference from other double bonds in these molecules. Indeed, with the exception of the omega-3 double bond, the olefinic bonds in eicosapentaenoic acid are analogous to those in the major omega-6 PUFA arachidonic acid. Surprisingly, there has been little work done to date on the synthesis of monounsaturated omega-3 fatty acids, which may serve as probes to clarify some of the biological properties of the omega-3 double bond.

Syntheses of the monounsaturated omega-3 fatty acid (*Z*)-15-octadecenoic acid (**1**) (Fig. 1) have been reported. Klok et al. [10] reported a seven step synthesis starting from 1,12-dodecanediol, in which hydrogenation of 15-octadecynoic acid is used to prepare the omega-3 bond. An alternative eleven step synthesis has been reported by Gunstone et al. [11], starting from undec-10-enoic acid. In the present article, we describe a four step synthesis of (*Z*)-15-octadecenoic acid (**1**), as well as (*Z*)-16-nonadecenoic acid (**2**), in high isomeric purity. The synthetic procedure employs straightforward, robust, quick and inexpensive reactions, and may be readily scaled up. **1** occurs naturally and has been detected in, but not isolated from, animal products including beef [12], pork [13], cows milk and butter [14], and in human blood [15] and human milk [16, 17]. As well as being useful probes for studying the properties of the omega-3 double bond in fatty acids of naturally and non-naturally occurring chain lengths, these compounds may permit the convenient synthesis of metabolites, such as epoxides derived from reactions of the omega-3 bond. The preparation of corresponding metabolites from polyunsaturated fatty acids leads to complex mixtures that require extensive purification [18].

Experimental Procedures

Instrumentation

Preparative liquid chromatography was performed using Dry Column Vacuum Chromatography (DCVC) with Merck Silica Gel 60H (5–25 μm) as the stationary phase. A 70-mm (ID) column was used, and 50-mL fractions were collected. TLC was carried out on Merck silica gel 60 F_{254} TLC plates. ^{1}H-NMR (400 MHz), ^{13}C-NMR (100.5 MHz), and ^{1}H–^{13}C-HSQC-NMR spectra were recorded using a Varian 400-MR instrument. Spectra were referenced internally to NMR solvent ($CDCl_3$; ^{1}H δ 7.26 ppm, ^{13}C δ 77.10 ppm). High Resolution Mass Spectra (HRMS) were obtained by the Mass Spectrometry Unit at the School of Chemistry, The University of Sydney, on a Bruker 7T Fourier Transform Ion Cyclotron Resonance Mass Spectrometer. Melting points were measured on a Stuart SMP10 melting point apparatus.

GC–MS was performed on a PolarisQ GC–MS–MS ion trap mass spectrometer coupled to a Trace GC, which was fitted with a ZB Wax column (30 m × 0.25 mm × 0.25 μm). Automated injections were performed on an AS2000 Autosampler. The injection port temperature was 190 °C and 1.0-μL injections were made in splitless mode, with the split valve opened after 1 min. Helium was used as carrier gas, at a flow rate of 1 mL/min. The GC oven temperature was programmed as follows: initial temperature of 100 °C for 2.5 min, then ramped at 5 °C/min to 280 °C, and held for 6.5 min giving a total run time of 45 min. Eluted compounds were subjected to methane chemical ionisation and detection was made in full scan mode scanning the MS from 100 to 600 amu in 2 μs. Compounds **1** and **2** were converted to their methyl esters using acetyl chloride/methanol prior to GC–MS analysis.

Chemicals

The following were purchased from the indicated commercial suppliers and were used as received: 15-hydroxypentadecanoic acid (97%), 16-hydroxyhexadecanoic acid (98%), 1 M sodium bis(trimethylsilyl)amide in THF, *n*-propyltriphenylphosphonium bromide, anhydrous THF and acetyl chloride (Aldrich, Castle Hill, NSW, Australia); pyridinium chlorochromate (PCC) and iodomethane (Fluka, Castle Hill, NSW, Australia), and potassium carbonate and sodium hydroxide (Ajax Finechem, Taren Point, NSW, Australia).

General Procedure for the Synthesis of the Methyl Esters **5** and **6**

To a solution of the hydroxy fatty acid (**3** or **4**, 7.87 mmol) in acetone (160 mL) was added water (8 mL), potassium carbonate (23.60 mmol) and iodomethane (39.33 mmol). The resulting mixture was refluxed for 4 h, and then concentrated in vacuo. The residue was dissolved in water (60 mL), and the solution was acidified with 1 M HCl. The aqueous phase was extracted with DCM (3 × 60 mL), and the combined extracts were washed with brine (100 mL), dried over Na_2SO_4, and concentrated in vacuo, affording methyl esters **5** and **6**.

Methyl 15-hydroxypentadecanoate (**5**)

White solid (72%). m.p. 49–50 °C (lit. m.p. 49.8 °C (19)). CI–MS: *m/z* (%): 273 ($[M + H]^+$, 6), 255 (39), 241 (29), 223 (95), 205 (100), 163 (14), 149 (39), 135 (39), 121 (42), 107 (26). The ^{1}H- and ^{13}C-NMR spectra of the product were in good agreement with previously reported data [19].

Methyl 16-hydroxyhexadecanoate (**6**)

White solid (70%). m.p. 53–54 °C (lit. m.p. 54.5–56 °C (20)). The ^{1}H- and ^{13}C-NMR, and MS spectra of the product were in good agreement with previously reported data [20].

General Procedure for the Synthesis of Aldehydes **7** and **8**

To a suspension of PCC (6.68 mmol) and Celite (1.440 g) in anhydrous DCM (20 mL) under nitrogen, was slowly added the methyl ester (**5** or **6**, 3.93 mmol) in anhydrous DCM (6 mL). The mixture was stirred for 2 h under nitrogen, after which diethyl ether (50 mL) was slowly added. The resulting mixture was stirred for 10 min, and then filtered over Celite. The Celite was washed with ether (2 × 20 mL), and the filtrate concentrated in vacuo. The residue was purified on silica gel by stepwise gradient elution with dichloromethane/hexane (40:60 to 100:0).

Methyl 15-oxopentadecanoate (**7**)

White solid (86%). m.p. 39–41 °C. CI–MS: *m/z* (%): 271 ($[M + H]^+$, 8), 239 (36), 221 (68), 203 (100), 175 (11), 161 (21), 147 (39), 133 (40), 121 (46), 107 (28). The ^{1}H- and ^{13}C-NMR spectra of the product were in good agreement with previously reported data [21, 22].

Methyl 16-oxohexadecanoate (**8**)

White solid (78%). m.p. 41–43 °C. ^{1}H NMR (400 MHz, $CDCl_3$): δ 9.76 (t, J_{HH} = 2.0 Hz, 1H, C**H**O), 3.67 (s, 3H, C**H**$_3$O), 2.42 (td, J_{HH} = 7.6, 2.0 Hz, 2H, CHOC**H**$_2$), 2.30 (t, J_{HH} = 7.2 Hz, 2H, C**H**$_2$COO), 1.66–1.58 (m, 4H, C**H**$_2$CH$_2$COO and C**H**$_2$CH$_2$CHO), 1.36–1.24 (m, 20H, C**H**$_2$). CI–MS: *m/z* (%): 285 ($[M + H]^+$, 8), 253 (52), 235 (96), 217 (100), 175 (16), 151 (16), 147 (34), 135 (43), 121 (47), 107 (24). The ^{13}C-NMR spectrum of the product was in good agreement with previously reported data for a crude product [23].

General Procedure for the Synthesis of Omega-3 Fatty Acid Methyl Esters **9** and **10**

To a suspension of *n*-propyltriphenylphosphonium bromide (7.07 mmol) in anhydrous THF (10 mL) at 0 °C under a nitrogen atmosphere, was added NaN(TMS)$_2$ (1.0 M in THF, 6.43 mmol). The resulting orange mixture was stirred for 40 min at room temperature. The mixture was then cooled to −78 °C, and the aldehyde (**7** or **8**, 3.21 mmol) in THF (5 mL) was added dropwise by syringe. Stirring at −78 °C was continued for 30 min after which the reaction mixture was allowed to warm to room temperature. After further stirring for 2 h the reaction was quenched with saturated aqueous NH_4Cl (20 mL), and extracted with DCM (3 × 40 mL). The combined extracts were dried over Na_2SO_4, and the DCM removed in vacuo. The residue was purified on silica gel by stepwise gradient elution with dichloromethane/hexane (20:80 to 50:50).

Methyl (*Z*)-15-octadecenoate (**9**)

Colorless oil (80%). ^{1}H NMR (400 MHz, $CDCl_3$): δ 5.40–5.28 (m, 2H, C**H**C**H**), 3.66 (s, 3H, OC**H**$_3$), 2.30 (t, J_{HH} = 7.6 Hz, 2H, C**H**$_2$COO), 2.08–1.98 (m, 4H, C**H**$_2$CHCHC**H**$_2$), 1.62 (quin, J_{HH} = 7.6 Hz, 2H, C**H**$_2$CH$_2$COO), 1.38–1.20 (m, 20H, C**H**$_2$), 0.95 (t, J_{HH} = 7.6 Hz, 3H, C**H**$_3$). ^{13}C NMR (100.5 MHz, $CDCl_3$): δ 174.32 (**C**OO), 131.47 (**C**H), 129.34 (**C**H), 51.40 (O**C**H$_3$), 34.10 (**C**H$_2$COO), 29.77, 29.62 (3C), 29.56, 29.53, 29.43, 29.28, 29.24, 29.14, 27.08 (CH**C**H$_2$), 24.95 (**C**H$_2$CH$_2$COO), 20.48 (CH**C**H$_2$), 14.37 (**C**H$_3$). CI–MS: *m/z* (%): 297 ($[M + H]^+$, 100), 265 (94), 247 (68), 191 (10), 178 (12), 163 (17), 149 (24), 135 (24), 121 (25), 107 (15). R_t = 25.43 min. *Z*:*E* ratio = 97.0:3.0. HRMS (APCI) calculated for $C_{18}H_{33}O$ ($[M + H–MeOH]^+$) 265.25259, found 265.25307.

Methyl (*Z*)-16-nonadecenoate (**10**)

Colorless oil (76%). ^{1}H NMR (400 MHz, $CDCl_3$): δ 5.40–5.28 (m, 2H, C**H**C**H**), 3.66 (s, 3H, OC**H**$_3$), 2.30 (t, J_{HH} = 7.6 Hz, 2H, C**H**$_2$COO), 2.06–1.98 (m, 4H, C**H**$_2$CHCHC**H**$_2$), 1.62 (quin, J_{HH} = 7.2 Hz, 2H, C**H**$_2$CH$_2$COO), 1.38–1.22 (m, 22H, C**H**$_2$), 0.95 (t, J_{HH} = 7.6 Hz, 3H, C**H**$_3$). ^{13}C NMR (100.5 MHz, $CDCl_3$): δ 174.33 (**C**OO), 131.48 (**C**H), 129.35 (**C**H), 51.41 (O**C**H$_3$), 34.11 (**C**H$_2$COO), 29.77, 29.65 (2C), 29.62 (2C), 29.58, 29.54, 29.44, 29.29, 29.24, 29.14, 27.09 (CH**C**H$_2$), 24.95 (**C**H$_2$CH$_2$COO), 20.49 (CH**C**H$_2$), 14.38 (**C**H$_3$). CI–MS: *m/z* (%): 311 ($[M + H]^+$, 97), 279 (100), 261 (68), 191 (12), 177 (15), 163 (18), 149 (23), 135 (28), 121 (27), 109 (19). R_t = 26.98 min. *Z*:*E* ratio = 98.5:2.5. HRMS (APCI) calculated for $C_{19}H_{35}O$ ($[M + H–MeOH]^+$) 279.26824, found 279.26856.

General Procedure for the Synthesis of Omega-3 Fatty Acids **1** and **2**

To a solution of the omega-3 fatty acid methyl ester (**9** or **10**, 1.66 mmol) in ethanol (25 mL) was added 1.5 M

NaOH (12 mL). The mixture was heated to 40 °C for 5 min to obtain a clear solution. Stirring was continued at room temperature for 2 h. The volume of the reaction mixture was reduced to 20 mL by rotary evaporation, and the solution was adjusted to pH 3 with 1.0 M HCl. The white solid was collected by filtration, thoroughly washed with water, and dried under vacuum to yield the omega-3 fatty acids **1** and **2**.

(*Z*)-15-octadecenoic acid (**1**)

White solid (96%). m.p. 41–42 °C (lit. m.p. 40.5–41.5 °C (11)). ^{1}H NMR (400 MHz, $CDCl_3$): δ 5.43–5.27 (m, 2H, C**H**C**H**), 2.35 (t, $J_{HH} = 7.6$ Hz, 2H, C$\mathbf{H}_2$COO), 2.08–1.98 (m, 4H, C$\mathbf{H}_2$CHCHC$\mathbf{H}_2$), 1.63 (quin, $J_{HH} = 7.2$ Hz, 2H, C$\mathbf{H}_2$CH$_2$COO), 1.38–1.22 (m, 20H, C$\mathbf{H}_2$), 0.95 (t, $J_{HH} = 7.4$ Hz, 3H, C$\mathbf{H}_3$). ^{13}C NMR (100.5 MHz, $CDCl_3$): δ 179.94 (**C**OO), 131.48 (**C**H), 129.35 (**C**H), 34.03 (**C**H$_2$COO), 29.77, 29.62 (3C), 29.57, 29.54, 29.42, 29.29, 29.23, 29.05, 27.09 (CH**C**H$_2$), 24.68 (**C**H$_2$CH$_2$COO), 20.49 (CH**C**H$_2$), 14.38 (**C**H$_3$). CI–MS (FAME derivative): *m/z* (%): 297 ([M + H]$^+$, 92), 265 (100), 247 (80), 191 (13), 178 (16), 163 (24), 149 (32), 135 (33), 121 (33), 107 (19). R_t (FAME derivative) = 25.54 min. *Z*:*E* ratio = 97.0:3.0. HRMS (ESI) calculated for $C_{18}H_{33}O_2$ ([M–H]$^-$) 281.24751, found 281.24832.

(*Z*)-16-nonadecenoic acid (**2**)

White solid (94%). m.p. 52–53 °C. ^{1}H NMR (400 MHz, $CDCl_3$): δ 5.43–5.28 (m, 2H, C**H**C**H**), 2.34 (t, $J_{HH} = 7.6$ Hz, 2H, C$\mathbf{H}_2$COO), 2.08–1.96 (m, 4H, C$\mathbf{H}_2$CHCHC$\mathbf{H}_2$), 1.61 (quin, $J_{HH} = 7.2$ Hz, 2H, C$\mathbf{H}_2$CH$_2$COO), 1.38–1.20 (m, 22H, C$\mathbf{H}_2$), 0.95 (t, $J_{HH} = 7.6$ Hz, 3H, C$\mathbf{H}_3$). ^{13}C NMR (100.5 MHz, $CDCl_3$): δ 179.81 (**C**OO), 131.48 (**C**H), 129.35 (**C**H), 34.07 (**C**H$_2$COO), 29.77, 29.65 (2C), 29.63 (2C), 29.58, 29.55, 29.43, 29.29, 29.24, 29.07, 27.09 (CH**C**H$_2$), 24.70 (**C**H$_2$CH$_2$COO), 20.49 (CH**C**H$_2$), 14.38 (**C**H$_3$). CI–MS (FAME derivative): *m/z* (%): 311 ([M + H]$^+$, 94), 279 (100), 261 (68), 191 (10), 177 (15), 163 (17), 149 (24), 135 (24), 121 (27), 109 (15). R_t (FAME derivative) = 27.24 min. *Z*:*E* ratio = 98.5:2.5. HRMS (ESI) calculated for ([M–H]$^-$) $C_{19}H_{35}O_2$ 295.26316, found 295.26399.

Results and Discussion

Synthesis

The synthesis of compounds **1**–**2** is shown in Scheme 1. An important step in the synthesis was the Wittig reaction of aldehydes **7** and **8** with *n*-propyltriphenylphosphonium bromide to form the omega-3 double bond. The Wittig reaction was selected as there is no ambiguity as to the positioning of the double bond and, through careful control of the reaction conditions, high stereoselectivity may be achieved. This allowed for the preparation of fatty acids in high isomeric purity, without the need for time-consuming preparative HPLC purification.

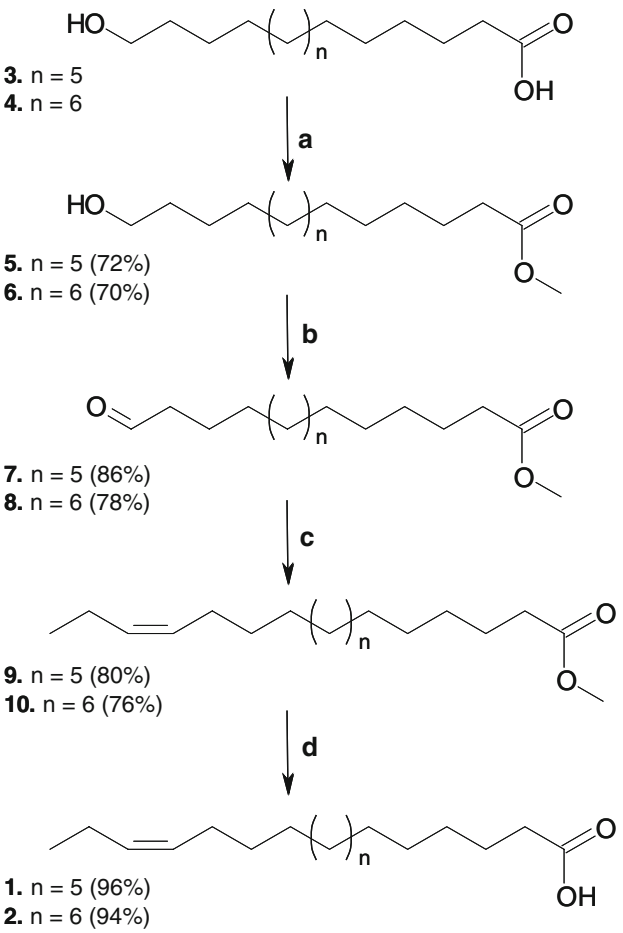

Scheme 1 Synthesis of the model (*Z*)-monounsaturated omega-3 fatty acids. Reaction conditions: **a** MeI, K_2CO_3, acetone/water, reflux, 4 h; **b** PCC, DCM, rt, 2 h; **c** [Ph_3PPr]Br, NaN(TMS)$_2$, THF, −78 °C to rt, 2.5 h; **d** NaOH, ethanol/water, rt, 2 h

The first step in the synthesis was esterification of 15-hydroxypentadecanoic acid (**3**) and 16-hydroxyhexadecanoic acid (**4**), which was done to facilitate the purification of subsequent compounds by chromatography on silica gel. Initially, esterification of **3** and **4** was attempted following the Fischer protocol (1 g of **3** or **4**, 5 equiv acetyl chloride, 50 mL methanol). ^{1}H-NMR spectra of the products isolated after liquid–liquid extraction contained a weak triplet at 4.05 ppm that was attributed to a methylene ester group i.e. –COOC$\mathbf{H}_2$CH$_2$–, from the product of intermolecular esterification of two hydroxyfatty acid molecules. Additional resonances attributable to this product were not observed, possibly because they may be obscured by the stronger resonances of the target products. The

intermolecular esterification products could not be removed by silica gel chromatography. Subsequent attempts using more dilute reaction conditions (1 g of **3** or **4** in 200 mL of methanol), which might reduce the rate of intermolecular esterification, also failed to yield a pure product. Reaction conditions were therefore sought under which intermolecular esterification could not occur. Thus, **3** and **4** were esterified using iodomethane, and the triplet attributed to the intermolecular esterification product was absent from the ^{1}H-NMR spectra of the isolated products. Oxidation of the thus obtained **5** and **6** with PCC proceeded smoothly, affording the aldehydes **7** and **8,** respectively, in good yield.

With **7** and **8** in hand we set out to prepare the (*Z*)-omega-3 double bond. Wittig reactions using amide bases such as $NaN(TMS)_2$ are reported to yield exclusively the (*Z*)-isomer [24–26]. The reaction was initially performed following a literature procedure [24] (Table 1, entry 2), however GC–MS and ^{13}C-NMR analysis of the product isolated from silica chromatography indicated that the reaction had not proceeded with absolute (*Z*) selectivity (*Z*:*E* = 95.5:4.5). The stereoselectivity of the Wittig reaction is dependent on several factors, including the nature of the aldehyde and ylide, and the reaction conditions [27, 28]. Thus, the influence of the temperature at which the ylide and aldehyde were combined and the role of different solvent systems were tested in attempts to improve the stereoselectivity (Table 1). It emerged that dimethylformamide (DMF) decreased the reaction yield and, consistent with previous findings, THF was found to give optimum (*Z*) selectivity [27, 28]. Higher reaction temperatures improved the reaction yield, however a concurrent increase in formation of the (*E*) isomer was observed. Thus, to obtain optimal stereoselectivity, the Wittig reaction was performed in THF at −78 °C, to afford **9** and **10** (*Z*:*E* ≥ 97.0:3.0).

Table 1 Yield and *Z*:*E* ratio obtained from the Wittig reaction of **7** and *n*-propyltriphenylphosphonium bromide[a]

Solvent	Temperature (°C)[b]	*Z*:*E* ratio[c]	Yield (%)[d]
THF + DMF (12:1)	Room Temperature	92.5:7.5	70
THF + DMF (12:1)	0	95.5:4.5	65
THF	0	95.5:4.5	75
THF	−78	97.0:3.0	69
Toluene	−78	95.5:4.5	69

[a] All reactions performed under conditions analogous to those reported in the general procedure used to prepare **9** and **10**. Only the solvent system and temperature at which **7** was added to the ylide were changed

[b] Temperature at which **7** was added to ylide

[c] *Z*:*E* ratio determined by GC–MS

[d] Isolated yield based on the aldehyde

Hydrolysis of **9** and **10**, to afford the omega-3 fatty acids **1** and **2** in excellent yields, was achieved using NaOH. Under the mild reaction conditions employed, pure products were obtained without the need for subsequent chromatography. In addition, no change in the *Z*:*E* ratio was observed upon de-esterification, indicating base catalysed isomerisation [29] of (*Z*) double bonds did not occur under the reaction conditions.

Omega-3 Olefinic Bond Characterisation

Previously, identification of double bond geometry and isomeric purity of synthetically prepared, unsaturated fatty acid derivatives has been achieved using ^{1}H-NMR spectroscopy [10, 26, 30, 31]. In the ^{1}H-NMR spectra of **1** and **2**, as well as their precursors **9** and **10**, the olefinic proton resonances were found to be coincident. Consequently, ^{1}H-NMR spectroscopy did not provide reliable data regarding the double bond geometry or isomeric purity of these compounds. A similar observation had been made in the synthesis of (*E*)-vaccenic acid [32].

The double bond configurations in **1**, **2**, **9,** and **10** were identified using the chemical shifts of the signals arising from the carbons adjacent to the double bond. Assignment of these resonances was achieved using ^{1}H–^{13}C-HSQC NMR spectroscopy, where coupling of these signals to the proton resonances at 2.02 ppm, which arise from the protons adjacent to the double bond, was observed. Using this approach, resonances arising from the carbon atoms adjacent to the double bond in the ^{13}C-NMR spectra of **1**, **2**, **9**, and **10** were identified at ∼27 and 20 ppm. Similar shifts have been reported in the ^{13}C-NMR spectra of a series of unbranched omega-3 (*Z*)-alkenes [33], and the chemical shifts of these resonances may be considered diagnostic for the omega-3 (*Z*) configuration. In the case of the (*E*) isomers, deshielding shifts these resonances to ∼32 and 25 ppm, respectively [33]. Weak resonances at ∼32 and 25 ppm, attributed to the (*E*) isomers, were observed in the ^{13}C-NMR spectra of **1**, **2**, **9**, and **10**.

In addition to the configurations of double bonds, the chemical shifts of the adjacent carbons atoms indicate the position of the double bond. Thus, chemical shifts of ∼20 and 27 ppm are typical for omega-3 (*Z*) compounds [33] but shift significantly when the position of the double bond is changed. For example, they appear at ∼29 and 27 ppm in the ^{13}C-NMR spectra of omega-4 (*Z*) alkenes [33]. The double bond position is also confirmed by the chemical shift of the methyl group protons which appear at 0.95 ppm in the ^{1}H-NMR spectra of **1**, **2**, **9**, and **10**; these lie within the 0.93–1.03 ppm range reported to be characteristic of omega-3 fatty acids [34].

The isomeric purity of the olefinic compounds was determined by GC–MS. Gas chromatograms of **9** and **10**,

and the FAME derivatives of **1** and **2**, displayed two peaks with identical mass spectra. Based on order of elution [35], the first minor compound to elute was identified as the (*E*) isomer, and the second major compound as the (*Z*) isomer. That the (*Z*) isomer is the major constituent of the olefinic compounds is supported by the ^{13}C-NMR data. Using a Zebron ZB-Wax column and relatively long run times of 45 min, baseline separation was achieved, and the *Z*:*E* ratio was then calculated from the peak areas. Under the GC conditions described, the FAME derivatives of **1** and **2** had retentions times of 25.54 and 27.24 min, respectively, with those of the corresponding (*E*) isomers at 25.25 and 26.94 min, respectively.

Conclusions

This article presents a convenient synthesis of two (*Z*)-monounsaturated omega-3 fatty acids with a high degree of isomeric purity. The four-step synthetic procedure beginning with the hydroxy fatty acids has an overall yield of ~43%, and may be readily scaled up to prepare gram quantities. The fatty acids described will be valuable model compounds for researchers to evaluate the functional importance of the omega-3 double bond in the cellular actions of naturally-occurring omega-3 PUFAs.

Acknowledgments The present work was supported by a grant from the Australian National Health and Medical Research Council. The authors wish to acknowledge Bruce Tattam for his expertise and assistance with the GC–MS analysis.

References

1. Schmitz G, Ecker J (2008) The opposing effects of n-3 and n-6 fatty acids. Prog Lipid Res 47:147–155
2. Xia S-H, Wang J, Kang JX (2005) Decreased n-6/n-3 fatty acid ratio reduces the invasive potential of human lung cancer cells by downregulation of cell adhesion/invasion-related genes. Carcinogenesis 26:779–784
3. Bartsch H, Nair J, Owen RW (1999) Dietary polyunsaturated fatty acids and cancers of the breast and colorectum: emerging evidence for their role as risk modifiers. Carcinogenesis 20:2209–2218
4. Larsson SC, Kumlin M, Ingelman-Sundberg M, Wolk A (2004) Dietary long-chain n-3 fatty acids for the prevention of cancer: a review of potential mechanisms. Am J Clin Nutr 79:935–945
5. Schumacher MC, Laven B, Wolk A, Brendler CB, Ekman P (2007) Do omega-3 dietary fatty acids lower prostate cancer risk? A review of the literature. Curr Urol 1:2–10
6. Funahashi H, Satake M, Hasan S, Sawai H, Newman Robert A, Reber Howard A, Hines Oscar J, Eibl G (2008) Opposing effects of n-6 and n-3 polyunsaturated fatty acids on pancreatic cancer growth. Pancreas 36:353–362
7. Yam D, Peled A, Huszar M, Shinitzky M (1997) Dietary fish oil suppresses tumor growth and metastasis of Lewis lung carcinoma in mice. J Nutr Biochem 8:619–622
8. Smith WL (1989) The eicosanoids and their biochemical mechanisms of action. Biochem J 259:315–324
9. Fitzpatrick FA, Murphy RC (1988) Cytochrome P-450 metabolism of arachidonic acid: formation and biological actions of "epoxygenase"-derived eicosanoids. Pharmacol Rev 40:229–241
10. Klok R, Egmond GJN, Pabon HJJ (1974) Synthesis of 19-cis-docosenoic, 17-cis-eicosenoic, and 15-cis-octadecenoic acid. Recl Trav Chim Pays Bas 93:222–224
11. Gunstone FD, Ismail IA (1967) Fatty acids. XIII. Synthesis of all the cis-*n*-octadecenonic acids. Chem Phys Lipids 1:209–224
12. Leheska JM, Thompson LD, Howe JC, Hentges E, Boyce J, Brooks JC, Shriver B, Hoover L, Miller MF (2008) Effects of conventional and grass-feeding systems on the nutrient composition of beef. J Anim Sci 86:3575–3585
13. Bragagnolo N, Rodriguez-Amaya DB (2002) Simultaneous determination of total lipid, cholesterol and fatty acids in meat and backfat of suckling and adult pigs. Food Chem 79:255–260
14. Couvreur S, Hurtaud C, Lopez C, Delaby L, Peyraud JL (2006) The linear relationship between the proportion of fresh grass in the cow diet, milk fatty acid composition, and butter properties. J Dairy Sci 89:1956–1969
15. Bicalho B, David F, Rumplel K, Kindt E, Sandra P (2008) Creating a fatty acid methyl ester database for lipid profiling in a single drop of human blood using high resolution capillary gas chromatography and mass spectrometry. J Chromatogr A 1211:120–128
16. Li J, Fan Y, Zhang Z, Yu H, An Y, Kramer JKG, Deng Z (2009) Evaluating the trans fatty acid, CLA, PUFA and erucic acid diversity in human milk from five regions in China. Lipids 44:257–271
17. Mosley EE, Wright AL, McGuire MK, McGuire MA (2005) Trans fatty acids in milk produced by women in the United States. Am J Clin Nutr 82:1292–1297
18. Cui PH, Zhang WV, Hook J, Tattam BN, Duke CC, Murray M (2009) Synthesis and NMR characterization of the methyl esters of eicosapentaenoic acid monoepoxides. Chem Phys Lipids 159:30–37
19. Kamitakahara H, Nakatsubo F (2005) Synthesis of diblock copolymers with cellulose derivatives. 1. Model study with azidoalkyl carboxylic acid and cellobiosylamine derivative. Cellulose 12:209–219
20. Kraft ML, Moore JS (2004) Multitechnique characterization of fatty acid-modified microgels. Langmuir 20:1111–1119
21. Ballini R, Bosica G, Gigli F (1998) alpha-Nitrocycloalkanones as a new source for the one-pot synthesis of functionalized 1, 4-diketones, gamma-oxoaldehydes, gamma-ketoesters, and methyl w-oxoalkanoates. Tetrahedron 54:7573–7580
22. Wang G, Hollingsworth RI (1999) Synthesis and properties of a bipolar, bisphosphatidyl ethanolamine that forms stable 2-dimensional self-assembled bilayer systems and liposomes. J Org Chem 64:4140–4147
23. Waugh KM, Berlin KD (1984) Studies in lipid mimics. Synthesis and carbon-13 relaxation time measurements (T1 values) of methyl esters of w-(2-anthryl)alkanoic acids. J Org Chem 49:873–878
24. Ainai T, Matsuumi M, Kobayashi Y (2003) Efficient total synthesis of 12-oxo-PDA and OPC-8:0. J Org Chem 68:7825–7832
25. Bestmann HJ, Stransky W, Vostrowsky O (1976) Reactions of alkylidene triphenylphosphoranes, XXXIII. Pheromones, VIII. Preparations of lithium salt-free ylide solutions with sodium bis(trimethylsilyl)amide as base. Chem Ber 109:1694–1700
26. Magrioti V, Constantinou-Kokotou V (2002) Synthesis of (S)-alpha-amino oleic acid. Lipids 37:223–228
27. Maryanoff BE, Reitz AB (1989) The Wittig olefination reaction and modifications involving phosphoryl-stabilized carbanions.

Stereochemistry, mechanism, and selected synthetic aspects. Chem Rev 89:863–927
28. Schlosser M, Schaub B, De Oliveira-Neto J, Jeganathan S (1986) Practical guidance for obtaining optimum cis-selectivities in Wittig reactions with triphenylphosphonio-alkanides. Chimia 40:244–245
29. Kuklev DV, Smith WL (2004) Synthesis of four isomers of parinaric acid. Chem Phys Lipids 131:215–222
30. Karagiozov SK, Abbott FS (2004) Practical stereoselective synthesis of (2E)- and (2Z)-4-Cycloalkylidenebut-2-enoic Acids. Synth Commun 34:871–888
31. Quesada E, Acuna AU, Amat-Guerri F (2003) Synthesis of carboxyl-tethered symmetric conjugated polyenes as fluorescent transmembrane probes of lipid bilayers. Eur J Org Chem 1308–1318
32. Duffy PE, Quinn SM, Roche HM, Evans P (2006) Synthesis of trans-vaccenic acid and cis-9-trans-11-conjugated linoleic acid. Tetrahedron 62:4838–4843
33. De Haan JW, Van de Ven LJM (1973) Configurations and conformations in acyclic, unsaturated hydrocarbons. Carbon-13 NMR study. Org Magn Reson 5:147–153
34. Guillen MD, Ruiz A (2003) Rapid simultaneous determination by proton NMR of unsaturation and composition of acyl groups in vegetable oils. Eur J Lipid Sci Technol 105:688–696
35. Aro A, Kosmeijer-Schuil T, van de Bovenkamp P, Hulshof P, Zock P, Katan MB (1998) Analysis of C18:1 cis and trans fatty acid isomers by the combination of gas-liquid chromatography of 4, 4-dimethyloxazoline derivatives and methyl esters. J Am Oil Chem Soc 75:977–985

Lipids (2010) 45:167–177
DOI 10.1007/s11745-009-3380-9

ORIGINAL ARTICLE

Possible Biosynthetic Pathways for all *cis*-3,6,9,12,15,19,22,25,28-Hentriacontanonaene in Bacteria

Shinji Sugihara · Ryuji Hori · Hitomi Nakanowatari · Yasuhiro Takada · Isao Yumoto · Naoki Morita · Yutaka Yano · Kazuo Watanabe · Hidetoshi Okuyama

Received: 4 August 2009 / Accepted: 25 November 2009 / Published online: 27 December 2009

Abstract A very long chain polyunsaturated hydrocarbon, hentriacontanonaene (C31:9), was detected in an eicosapentaenoic acid (EPA)-producing marine bacterium, which was isolated from the mid-latitude seashore of Hokkaido, Japan, and was tentatively identified as mesophilic *Shewanella* sp. strain osh08 from 16S rRNA gene sequencing. The geometry and position of the double bonds in this compound were determined physicochemically to be all *cis* at positions 3, 6, 9, 12, 15, 19, 22, 25, and 28. Although C31:9 was detected in all of the seven EPA- or/and docosahexaenoic acid-producing bacteria tested, an EPA-deficient mutant (strain IK-1Δ8) of one of these bacteria had no C31:9. Strain IK-1Δ8 had defects in the *pfaD* gene, one of the five *pfa* genes responsible for the biosynthesis of EPA. Although *Escherichia coli* DH5α does not produce EPA or DHA inherently, cells transformed with the *pfa* genes responsible for the biosynthesis of EPA and DHA produced EPA and DHA, respectively, but not C31:9. These results suggest that the Pfa protein complex is involved in the biosynthesis of C31:9 and that *pfa* genes must not be the only genes responsible for the formation of C31:9. In this report, we determined for the first time the molecular structure of the C31:9 and discuss the possible biosynthetic pathways of this compound.

Keywords Decarboxylation · Eicosapentaenoic acid · Head-to-head condensation · Hentriacontanonaene · *pfa* Genes · Polyunsaturated fatty acid · Polyunsaturated hydrocarbon · *Shewanella* sp.

S. Sugihara · H. Nakanowatari · H. Okuyama
Course in Environmental Molecular Biology and Microbial Ecology, Division of Biosphere Science, Graduate School of Environmental Science, Hokkaido University, Kita-ku, Sapporo 060-0810, Japan

R. Hori · H. Okuyama
Department of Biological Sciences, Faculty of Science, Hokkaido University, Kita-ku, Sapporo 060-0810, Japan

R. Hori · H. Okuyama (✉)
Laboratory of Environmental Molecular Biology, Faculty of Environmental Earth Science, Hokkaido University, Kitaku-ku, Sapporo 060-0810, Japan
e-mail: hoku@ees.hokudai.ac.jp

Y. Takada
Division of Cellular Life Science, Faculty of Advanced Life Science, Hokkaido University, Kita-ku, Sapporo 060-0810, Japan

I. Yumoto · N. Morita
Research Institute of Genome-Based Biofactory, National Institute of Advanced Industrial Science and Technology (AIST), Toyohira-ku, Sapporo 062-8517, Japan

Y. Yano
National Research Institute of Fisheries Science, Fisheries Research Agency, Kanazawa-ku, Yokohama 236-8648, Japan

K. Watanabe
Microbial Engineering Group, Sagami Chemical Research Center, Hayakawa, Ayase 252-1193, Japan

Present Address:
K. Watanabe
WysiWyg Co., Ltd., Haccobori, Chuo-ku, Tokyo 104-0032, Japan

Abbreviations

CI	Chemical ionization
CI-GC/MS	Chemical ionization–mass spectrometry
DHA	Docosahexaenoic acid
EI	Electron impact ionization
EI-GC/MS	Electron impact ionization–mass spectrometry
EPA	Eicosapentaenoic acid
FAME	Fatty acid methyl ester
GC/MS	Gas chromatography–mass spectrometry
GLC	Gas–liquid chromatography
HPLC	High-performance liquid chromatography
PUHC	Polyunsaturated hydrocarbon
PUFA	Polyunsaturated fatty acid

Introduction

A unique very long straight-chain polyunsaturated hydrocarbon (PUHC) with an odd number of carbon atoms, hentriacontanonaene (C31:9), was first discovered in marine Antarctic bacteria [1]. The same compound was reported in a deep-sea bacterium [2]. These C31:9-producing bacteria are psychrophilic and produce eicosapentaenoic acid (EPA) and/or docosahexaenoic acid (DHA) [1]. However, the molecular structure of C31:9 has not been determined, and the relationship between these *n*-3 polyunsaturated fatty acids (PUFAs) and C31:9 biosynthesis is not clear, although bacterial EPA and DHA are synthesized by the Pfa protein complex encoded by the *pfaA, pfaB, pfaC, pfaD*, and *pfaE* genes [3].

Another straight-chain PUHC with an odd number of carbons, all *cis*-3,6,9,12,15,18-heneicosahexaene (C21:6), is distributed in marine planktonic algae and animals [4, 5]. The biosynthesis of C21:6 may occur through the decarboxylation of DHA [4] because the marine organisms possessing C21:6 contain DHA [4, 5] as well as the hydrocarbon derived from DHA (Δ4, 7, 10, 13, 16, 19) by decarboxylation. C21:6 from DHA should have double bonds at 3, 6, 9, 12, 15, and 18. Eukaryotes have a decarboxylation pathway to synthesize odd-carbon-number alkanes from even-carbon-number counterpart fatty acids via fatty aldehyde formation [6]. However, no biochemical or molecular evidence on the biosynthesis of C21:6 is available, and information about C31:9, which is recognized as a biomarker of Antarctic bacteria [1], is limited.

We isolated an EPA-producing bacterium from the surface of seaweed collected at the mid-latitude seashore of Hokkaido, Japan. This isolate (designated strain osh08) included, in addition to low levels of EPA, a hydrocarbon suspected to be C31:9. In this study, we describe the physicochemical determination of the molecular structure of this compound including the position and geometry of the double bonds. We investigated the distribution of C31:9 using various types of marine and nonmarine microorganisms, including EPA- or DHA-producing bacteria and eukaryotes, a genetically engineered EPA-deficient mutant of *Shewanella* species, and *Escherichia coli* that had been transformed with the *pfa* genes responsible for the biosynthesis of EPA or DHA. We discuss the possible biosynthetic pathways of C31:9 with regard to the distribution of EPA, DHA, C31:9, and *pfa* genes in bacteria.

Experimental Procedures

Strains and Culture Conditions of Bacteria and Eukaryotes

Bacterial strains isolated from seaweed samples that had been collected at the mid-latitude seashore of Oshoro, Hokkaido, Japan (43.19N, 141.00E) were screened for their ability to produce long-chain PUFAs such as EPA and DHA in moderate-temperature environments. The seaweed fragments (approximately 2 × 3 cm) soaked in seawater were vortexed. Portions (200 μL) of the seawater sample were spread on the plates containing ZoBell agar medium (1 g/L peptone, 1 g/L yeast extract, 0.1 g/L $Fe_3(PO_4)_2$, and 0.15 g/L agar in 50% (by vol) seawater; [7]). Sea water used in this study was natural seawater that had been filtered using filter paper (type No. 02, Advantec, Tokyo, Japan). Plates were then incubated at 20 °C for several days. Bacterial colonies were subjected to methanolysis using 10% (by vol) acetyl chloride in methanol, as described below. One strain (osh08) capable of producing EPA was isolated, purified by repeated streaking of cells on the agar plates, and utilized for further investigations.

Strain osh08 was cultivated in the ZoBell liquid medium with shaking at 180 rpm at 25 °C for 1 day, unless otherwise stated. To investigate effects of temperature on growth and production of C31:9, strain osh08 was cultivated at 0, 4, 15, 20, 25, 30, 37, 40, and 43 °C.

The following strains were used: *Colwellia maris* ABE-1^T [8], *Moritella marina* MP-1^T (ATCC15381^T), *Shewanella marinintestina* IK-1^T [9], *Shewanella pneumatophori* SCRC-2738^T [10], *Shewanella benthica* (ATCC43992), *Pseudomonas alcaliphila* AL15-21^T [11] as marine bacteria; *Pseudomonas psychrophila* E-3^T [12], *Vibrio rumoiensis* S-1^T [13], *Shewanella oneidensis* MR-1^T (ATCC 700550^T), *Pseudomonas aeruginosa* WatG [14], *Rhodococcus erythropolis* (laboratory strain isolated from soil), *E. coli* DH5α (Takara Bio, Tokyo, Japan), and *Stenotrophomonas maltophilia* (laboratory strain from soil) as nonmarine bacteria; a thraustochytrid-like microorganism

strain 12B [15] and *Schizochitrium limacinum* SR21 [16] as marine eukaryotes; and a terrestrial eukaryote, *Saccharomyces cerevisiae* (baker's yeast). Nonmarine and marine bacteria were grown in a Luria–Bertani (LB) medium and a LB medium containing 30 g/L NaCl, respectively. Strain 12B, *S. limacinum* SR21, and yeast were grown in F medium, as described previously [15].

Extraction and Analysis of Lipids

Hydrocarbons of osh08 were first extracted with hexane from the fatty acid methyl ester (FAME) fraction after methanolysis of dry cells (approximately 15 mg) using 1 mL of 10% (by vol) acetyl chloride in methanol at 100 °C for 1 h. A mixture of 10 μg each of heneicosanoic acid (21:0, Sigma–Aldrich, Tokyo) and *n*-tetracosane (C24:0, Sigma–Aldrich) was used as an internal standard. To avoid coextraction of FAMEs, hydrocarbons were directly extracted from dry cells (approximately 10 mg) with 20 mL of a mixture of methanol/hexane (1:1, by vol) after sonic oscillation at 70 watts for 10 s in an ice bath using a sonic disruptor (model, W-185; Branson, Danbury, CT). This procedure was repeated three times. The combined hexane extracts were used as crude hydrocarbon fraction.

The crude hydrocarbon fraction was applied to thin-layer chromatography (TLC) on silica gel plates (type 5721, Merck, Darmstadt, Germany) using a mixture of hexane/ethyl ether/acetic acid (90:10:1, by vol) as solvent. Squalene (Kanto Chemical, Tokyo), and squalane (Tokyo Kasei Kogyo, Tokyo), were used as standards.

Purification of C31:9 was performed by reversed-phase high-performance liquid chromatography (HPLC). Crude hydrocarbon extracts (1.5 mg aliquots) were dissolved in 1 mL of acetonitrile. The solution was filtered through a Millex-HV filter (pore size 0.45 μm, Millipore, Billerica, MA). A 300-μL aliquot of the filtrate was subjected to HPLC on a liquid chromatography system (model CCMP, Tosoh, Tokyo) equipped with an ODS column (type TSKgel ODS-80Ts, 15 cm long, 2.0 mm I.D., Tosoh) and an ultraviolet detector (model UV-8010, Tosoh), which had been equilibrated with acetonitrile. C31:9 was eluted with the same solvent at a flow rate of 1.0 mL/min, and absorbance at 210 nm of the eluate was monitored. The retention time of C31:9 was around 16.2 min. C31:9 with a purity of more than 99%, which was evaluated by gas-liquid chromatography (GLC; see below), was subjected to further analysis.

The *cis* and *trans* configurations of double bonds of C31:9 were determined using HPLC-purified hydrocarbon fraction (approximately 500 μg) by infrared spectrometry (IR; model FT/IR 660 Plus, Jasco, Tokyo) by the potassium bromide method. Assignment of individual peaks of C31:9 in IR was referred to [17–19].

The purified hydrocarbon fraction dissolved in hexane at 3.5 μg/mL was fully hydrogenated using H_2 gas at room temperature for 40 min. Platinum(IV) oxide at 5 mg/mL was used as a catalyst. Hydrogenated hydrocarbon was extracted with hexane. Partial hydrogenation was performed using hydrazine [20]. The hydrocarbon fraction (approximately 20 μg) was dissolved in 1 mL methanol and then mixed with 0.1 mL hydrazine and 0.1 mL 30% H_2O_2 (by vol). The reaction mixture was stirred for 90 min at 50 °C. To stop the reaction, 1 mL 5 M HCl was added, and the mixture was extracted with hexane. The extract was applied to silver nitrate TLC on silica gel (no. 5721, Merck), as described previously [21] with a solvent system composed of hexane/benzene (1:1, by vol). Silica gels corresponding to spots whose mobility was close to that of authentic 1-dodecene (C12:1, Sigma–Aldrich) were scraped off the plate and extracted with a mixture of methanol/water/hexane (1:1:2, by vol). A hexane fraction containing hydrocarbons with one double bond was recovered. The location of double bonds in each monounsaturated hydrocarbon was determined by chemical ionization (CI) ion-trap mass spectrometry using acetonitrile as a regent gas (see below and [22–24]).

The FAME fraction including hydrocarbon, crude and purified hydrocarbons, and hydrogenated hydrocarbons were analyzed by GLC as described [25] on a gas chromatograph (model GC-353B, GL Sciences, Tokyo) equipped with a polar capillary column (type BPX70, 25 m long, 0.22 mm I.D., 0.25 μm film thickness, SGE Japan, Yokohama, Japan) unless otherwise stated, and flame ionization detection with nitrogen as the carrier gas. The GLC oven temperature was 80 °C initially and programmed up to 240 °C at a rate of 4.0 °C/min. The oven temperature was held at the maximum for 60 min. The injector and detector temperatures were set at 221 °C. The data were analyzed using a D-2500 Chromato-Integrator (Hitachi, Tokyo). In order to detect PUFAs and PUHCs with very long retention times, GLC analysis was also performed using a nonpolar capillary column (type TC-1, 30 m long, 0.25 mm I.D., 0.1 μm film thickness) obtained from GL Science. The injector and detector temperatures were set at 250 and 340 °C, respectively. The oven temperature was first set at 50 °C, and then raised to 330 °C at the rate of 10 °C/min. The maximum oven temperature was held for 10 min. Triacontanoic acid methyl ester (30:0) and tetratriacontane (C34:0) from Sigma–Aldrich were used as internal standards.

Relative fatty acid and hydrocarbon composition was expressed as weight percentage of the total combined weight of these compounds. The hydrocarbons and FAMEs were also analyzed by ion-trap mode gas chromatography–mass spectrometry (GC/MS) on a Varian system (model CP-3800 gas chromatograph and Saturn 2200 ion trap mass

spectrometer, Varian Technologies Japan, Tokyo) under the same conditions as described previously [25]. Data were analyzed using a Saturn™ Software Workstation Version 5.52. In GC/MS analysis, two modes of electron impact ionization (EI) and CI were utilized and abbreviated as EI-GC/MS and CI-GC/MS, respectively. In CI-GC/MS, acetonitrile was used as an ionization reagent.

FAMEs were identified by comparing their retention times with those of authentic standards in GLC and by their EI-GC/MS analysis. To determine the position of double bonds of monounsaturated fatty acids, the FAME fraction was subjected to the I_2-catalyzed reaction for the formation of adducts with dimethyl disulfide according to the procedure of Shibahara et al. [26] The resultant dimethyl disulfide adducts were analyzed by EI-GC/MS, as described above. The position of double bonds of EPA was determined by EI-GC/MS analysis of its pyrrolidide derivative prepared, as previously [27].

DNA Procedures

For PCR amplification of 16S rRNA genes, osh08 cells were cultivated as described above. Genomic DNA was isolated by the method of Marmur [28]. PCR was performed using a Mastercycler® ep gradient Thermal Cycler (Eppendorf AG, Hamburg, Germany) in a total volume of 50 μL using *Ex Taq* DNA polymerase (Takara Bio) in the supplied buffer. For the amplification of the full length of 16S rRNA genes, primers 9F (5′-GAGTTTGATCCTGG CTCAG-3′) and 1541R (5′-AAGGAGGTGATCCAGCC-3′) were used. PCR was carried out according to the following program, an initial denaturation at 95 °C for 5 min followed by 30 cycles of 1 min at 95 °C, 1 min at 57 °C, and 2 min at 72 °C, concluding with a 5 min extension at 72 °C for the amplification of the 16S rRNA gene. PCR products were analyzed by electrophoresis on 10 g/L agarose gels and were visualized by a UV transilluminator after staining with ethidium bromide (Nippon Gene, Tokyo).

PCR products that had been ligated to the pCR2.1-TOPO® vector using the TOPO TA cloning® Kit (Invitrogen) were subjected to cycle sequencing according to the manufacturer's protocol. Recombinant vectors were used to transform *E. coli* DH5α and transformants were selected by blue/white colony screening. Individual white colonies were grown at 37 °C overnight with rotary shaking in LB medium. Plasmid pCR2.1-TOPO carrying 16S rRNA gene from osh08 was isolated with the mini-preparation method [29]. Cycle sequencing was performed as described previously [30]. The sequence comparative searches were performed using the NCBI (http://www.ncbi.nlm.nih.gov/) databases. The osh08 16S rRNA gene sequence has been deposited in DDBJ/GenBank/EMBL with the accession number of AB447987.

Table 1 Fatty acid and hydrocarbon composition in osh08 grown at 25 °C

Fatty acid and hydrocarbon[a]	Content (w/w, % total[b])
12:0	3.4 ± 0.3
iso13:0	2.8 ± 0.1
13:0	1.5 ± 0.3
14:0	3.3 ± 0.2
iso15:0	8.8 ± 0.5
15:0	8.0 ± 1.1
15:1(7)	1.2 ± 0.1
15:1(9)	1.0 ± 0.2
16:0	14.5 ± 1.0
16:1(7)	0.7 ± 0.1
16:1(9)	28.8 ± 0.7
17:0	3.5 ± 0.5
17:1(9)	9.3 ± 0.7
17:1(11)	0.7 ± 0.2
18:0	1.4 ± 0.1
18:1(9)	0.9 ± 0.1
18:1(11)	4.0 ± 1.0
20:5(5,8,11,14,17)	0.5 ± 0.2
C31:9	3.0 ± 0.6
Others	2.7 ± 0.5
Total	100

[a] Fatty acids are abbreviated, as in 16:1(9), where the number before the colon shows the number of carbon atoms and after the number of double bonds in the fatty acid. The distance of the double bond from the carboxylic end of the fatty acid is indicated in parenthesis. iso13:0 and iso15:0 are iso-branched fatty acids. C31:9 is hentriacontanonaene

[b] Fatty acids and hydrocarbons were separately quantified using 21:0 and C24:0, respectively, as internal standards, and the sum of these compounds was regarded as 100%. The data indicated are mean ± standard errors for three independent experiments

Results

Extraction and Cellular Contents of Polyunsaturated Hydrocarbons and Fatty Acids

The compound suspected to be a very long chain hydrocarbon with multiple double bonds was extracted with hexane in the FAME fraction after methanolysis of osh08 cells grown at 25 °C. As described below, this compound was identified as a PUHC with 31 carbons and 9 double bonds (hentriacontanonaene; C31:9). Δ9-Hexadecenoic acid (28.8 ± 0.7%) and hexadecanoic acid (14.5 ± 1.0%) were the major fatty acids and pentadecenoic, hexadecenoic, heptadecenoic and octadecenoic acids included two isomers with a double bond at different positions (Table 1). C31:9 was the sole hydrocarbon detected in the fraction. The contents of C31:9 and EPA (20:5) were 3.0 ± 0.6 and 0.5 ± 0.2%, respectively.

C31:9 was extracted directly from dry cells in the hexane fraction with a mixture of hexane and methanol (1:1, by vol). The content of this compound was 0.63 ± 0.02 μg/mg of dry cells for cells grown at 20 °C for 18 h (3.15 μg/mL of culture). The content of C31:9 after methanolysis was calculated to be 0.49 ± 0.01 μg/mg of dry cells (2.45 μg/mL of culture) for cells grown under the same conditions.

Effects of Temperature on the Growth of Strain osh08 and Content of EPA and C31:9

The osh08 cell grew in the temperature range of 4 to 40 °C, and the optimum growth occurred at 30 °C. No growth was observed at 0 °C or 43 °C. According to Wiegel's definition [31], this type of strain should be regarded as mesophilic bacteria that are tolerant to a temperature around 5 °C rather than as psychrotrophs, which can grow at 0 °C.

Table 2 shows the contents of C31:9 and EPA in the total FAME fraction including hydrocarbons after methanolysis of osh08 cells grown at various temperatures. The maximum production of C31:9 and EPA was at 25 and 4 °C, respectively. It is interesting that the content of C31:9 and EPA changed in an antiparallel mode with regard to their biosynthetic pathways (see below). To our knowledge, the highest temperature at which EPA is produced in bacteria is 28 °C for *Shewanella japonica* [32] and *S. pacifica* [33]. Although EPA comprises around 0.2% of total fatty acids, osh08 produced EPA at 37 °C, and the maximum temperature at which C31:9 was produced was also 37 °C (Table 2).

Physicochemical Analysis of C31:9

In EI-gas chromatographic analysis of the FAME fraction including hydrocarbons, C31:9 occurred at a retention time of about 34 min (Fig. 1a), and no peak was detected after C31:9. The mass spectrum of C31:9 in EI-GC/MS was similar to that of the methyl esters of PUFAs such as arachidonic acid, EPA, and DHA, where fragment ions at an *m/z* of 79 and 91 were dominant (Fig. 2a), suggesting that the hydrocarbon contained multiple methylene-interrupted double bonds in the straight aliphatic chain. In CI/MS analysis of the C31:9 peak, an ion of $[M + 54 + H]^+$ at *m/z* 473 was prominent (Fig. 2b). The molecular weight of H_2-hydrogenated C31:9 (C31:0), whose retention time was around 30 min in an EI-gas chromatogram (Fig. 1b), was determined to be 436 by the occurrence of an $[M + 40 + H]^+$ ion at *m/z* 477 in CI/MS (Fig. 2c). These results indicate that the hydrocarbon comprises 31 carbon atoms with 9 double bonds (C31:9, molecular weight, 418).

In GLC analysis of the total FAME fraction using a nonpolar capillary column, EPA and C31:9 appeared around 22 and 28.5 min, respectively, and the retention times of 30:0 and C34:0 used as internal standards were about 26 and 34 min, respectively. However, no peaks suspected to be 32:9 fatty acid were detected (data not shown).

The EI-gas chromatogram of partially hydrogenated hydrocarbons gave five peaks (peaks 1, 2, 3, 4, and 5 in Fig. 3) with the same molecular weight of 434, suggesting that the fraction was a mixture of hydrocarbons with one double bond at different positions.

The CI-mass spectrum of one isomer (peak 1 in Fig. 3) was shown in Fig. 4a, where fragment ions at *m/z* 264 (a) and 278 (b) were evident. This result indicates the location of a double bond at 15 (or 16 when counted from the opposite end). Peak 2 was that of an isomer having a double bond at 12 or 19, because fragment ions at *m/z* 222 (a) and 320 (b) were detected (Fig. 4b). Peaks 3, 4, and 5 were determined to be isomers having double bonds at 9 or

Table 2 Eicosapentaenoic acid and hentriacontanonaene contents in osh08 cells grown at various temperatures

Growth temperature (°C)	EPA (w/w, % total[a])	C31:9 (w/w, % total[a])
4	1.9 ± 0.2	1.1 ± 0.1
15	0.9 ± 0.4	2.0 ± 0.2
20	0.6 ± 0.1	2.4 ± 0.2
25	0.5 ± 0.2	3.0 ± 0.6
30	0.3 ± 0.1	1.7 ± 0.1
37	0.2 ± 0.1	1.4 ± 0.2
40	ND	ND

ND not detected

[a] Fatty acids and hydrocarbons were separately quantified using 21:0 and C24:0, respectively, as internal standards. The data indicated are mean ± standard errors for three independent experiments

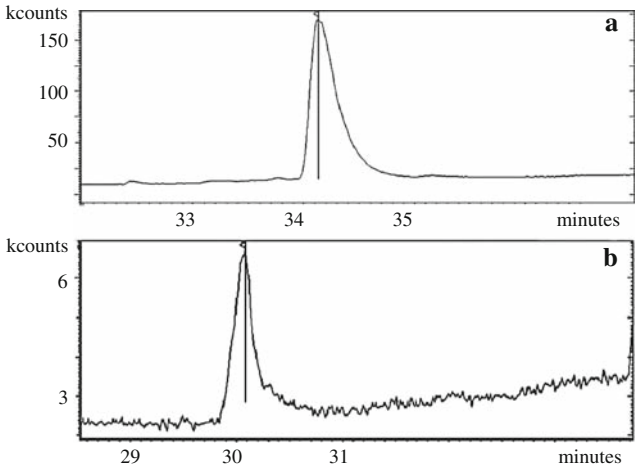

Fig. 1 EI-gas chromatograms of native hentriacontanonaene (C31:9; **a**) and its fully hydrogenated derivative, hentriacontane (C31:0; **b**)

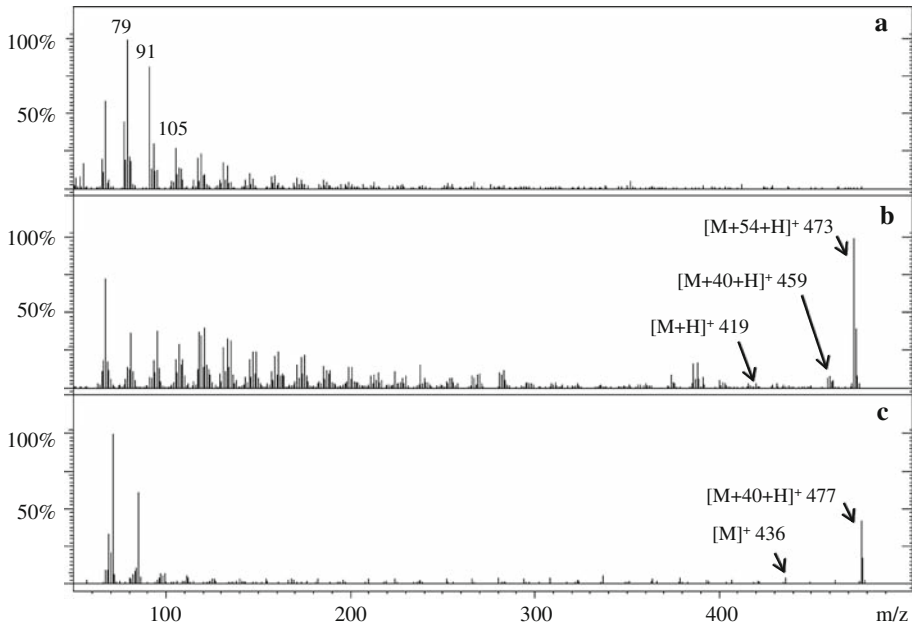

Fig. 2 EI-mass spectrum of native C31:9 (**a**), and CI-mass spectra of C31:9 (**b**) and C31:0 (**c**). Acetonitrile was used as the ionization reagent in CI/MS

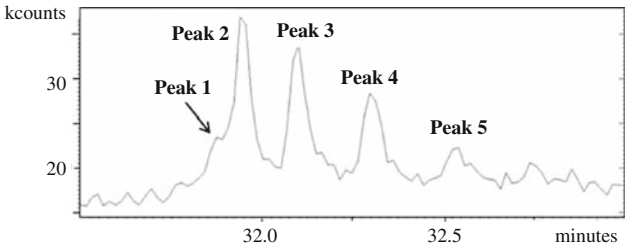

Fig. 3 EI-gas chromatogram of a C31:1 mixture prepared from partially hydrogenated C31:9. Five peaks of the C31:1 isomers were numbered

22, 6 or 25, and 3 or 28, respectively (Fig. 4c–e). The results are summarized together with the relative intensity of each diagnostic ion in Table 3. The double bonds at 3, 6, 9, and 12 are equivalent to the locations at 28, 25, 22, and 19, respectively.

The infrared spectrum of HPLC-purified C31:9 is shown in Fig. 5. There were intense peaks at 2,963 and 2,855 cm^{-1} corresponding to C–H stretching of CH_3 groups, intense peaks at 2,921 and 2,360 cm^{-1} corresponding to C–H stretching of CH_2 groups, and peaks at 1,457 and 1,337 cm^{-1} corresponding to C-CH_2 and C-CH_3 groups, respectively [18]. A peak at 1,391 cm^{-1} corresponded to CH bending of the HC=CH *cis* double bond [19]. However, there was no peak at 970 cm^{-1} corresponding to CH bending of the HC=CH *trans* double bond. The intense peaks around 3,015 and 1,670 cm^{-1} are regarded as those corresponding to CH stretching and C=C stretching, respectively, of the HC=CH *cis* double bond [17, 19]. The relatively intense peak at 1,731 cm^{-1} is considered to correspond to C=O and C–O stretching of

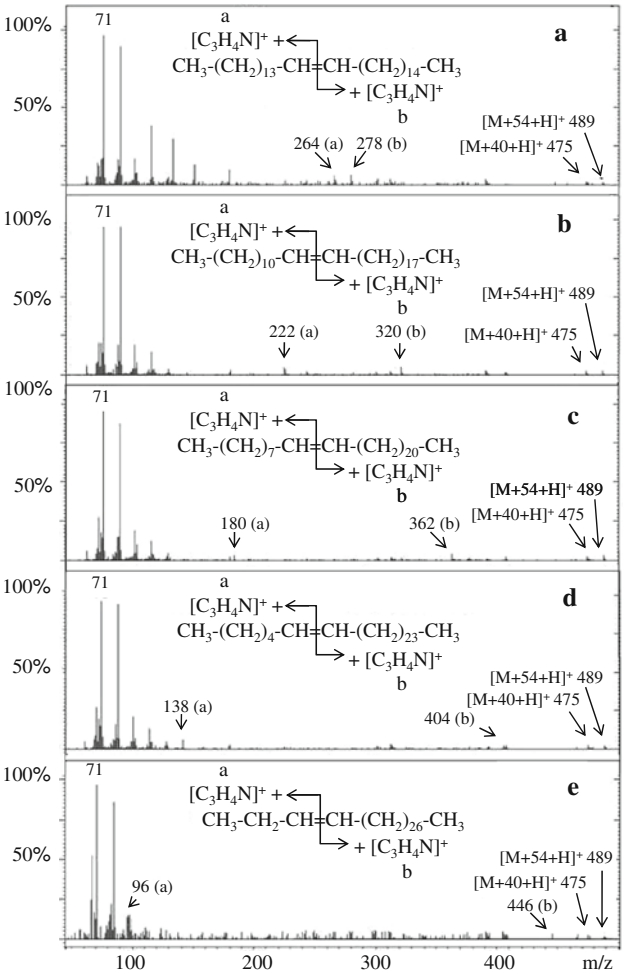

Fig. 4 CI-mass spectra of the C31:1 isomers. Panels a, b, c, d, and e are a spectrum of peaks 1, 2, 3, 4, and 5, respectively, in Fig. 3

Table 3 Summary of diagnostic ions in the acetonitrile CI mass spectra of hentriacontamonoene isomers

C31:1 isomer	Peak no. in Fig. 3	*m/z* of fragment (relative intensity)	
		a[a]	b[a]
15(16)-C31:1	1	264 (7.3)	278 (6.9)
12(19)-C31:1	2	222 (8.9)	320 (6.2)
9(22)-C31:1	3	180 (5.9)	362 (4.2)
6(25)-C31:1	4	138 (7.7)	404 (2.8)
3(28)-C31:1	5	96 (8.3)	446 (3.0)

[a] A fragment shown in Fig. 4

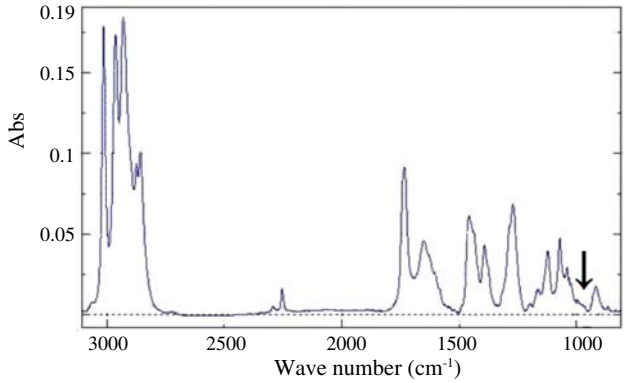

Fig. 5 IR spectrum of C31:9. There was no characteristic peak at 970 cm^{-1} corresponding to CH bending of the HC=CH *trans* double bond (a region indicated by *arrow*)

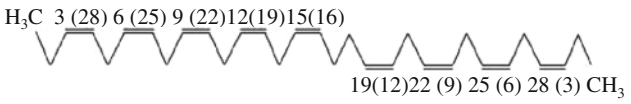

Fig. 6 Proposed structure of C31:9. The position of the double bonds of C31:9 (product) was counted from both methyl ends

carboxylate ester of the contaminating fatty acid methyl esters [17, 19]. Considering all these data together, we identified the compound as all *cis*-3, 6, 9, 12, 15, 19, 22, 25, 28-hentriacontanonaene (C31:9) (Fig. 6). The position and geometry of double bonds of C31:9 were determined for the first time in this study.

Distribution of C31:9 in Various Microorganisms and its Possible Biosynthetic Pathways

Table 4 shows the distribution of EPA, DHA, C31:9, and *pfa* genes in bacteria and some eukaryotic microorganisms. C31:9 was found in all tested marine bacteria that produce EPA or DHA, as also found by Nichols et al. [1]. The *pfa* genes responsible for the biosynthesis of EPA and DHA have been cloned from *S. pneumatophori* SCRC-2738, *S. marinintestina* IK-1, and *M. marina* MP-1 [3]. *Shewanella oneidensis* MR-1^T grown at 20 °C for 18 h contained both EPA and C31:9 at 0.2 ± 0.1 and $2.0 \pm 0.7\%$, respectively, of the total FAME and hydrocarbon fraction, although this strain, which was isolated from sediments of a freshwater lake, does not require NaCl for growth [34] and is recognized as mesophilic [35]. The chromosome of this bacterium (AE014299; see [36]) included *pfa* genes (Table 4). However, the marine bacterium *P. alcaliphila* AL15-21^T and nonmarine yeast produced neither PUFA nor C31:9. Two marine eukaryotes, which are known to produce very high levels of DHA and other PUFAs [15, 16], produced no C31:9. These eukaryotic microorganisms are expected to have *pfa*-like genes that are responsible for the biosynthesis of PUFAs because such genes have been cloned from *Schizochytrium* sp. ([37] and see accession numbers AF378327, AF378328, and AF378329). Although *E. coli* DH5α does not inherently produce EPA or DHA, the cells transformed with the *pfa* genes responsible for the biosynthesis of EPA and DHA produced EPA and DHA, respectively, but not C31:9 (Table 4 and see [3]). In contrast, the EPA-deficient mutant (strain IK-1Δ8) of *S. marinintestina* IK-1, in which one of the five *pfa* genes, *pfaD* gene, responsible for biosynthesis of EPA is defective [38], produced neither EPA nor C31:9. These results suggest that five *pfa* genes are involved in the biosynthesis of C31:9. However, *pfa* genes must not be the only genes responsible for the formation of C31:9 because *E. coli* recombinants carrying *pfa* genes had no C31:9 (Table 4).

Tentative Identification of Strain osh08

The 1,534 bp nucleic acid sequence of the 16S rRNA gene of osh08 was determined and was 99.8 and 98.4% similar to that of *Shewanella basaltis*^{T} (EU143361) and *S. hafniensis*^{T} (AB205566), respectively. The strain was identified tentatively as *Shewanella* sp. strain osh08. Detailed characterization of this strain is in progress.

Discussion

In this study, an EPA-producing mesophilic strain (*Shewanella* sp. strain osh08) was isolated from the mid-latitude seashore of Hokkaido, Japan. This strain included a long-chain PUHC, hentriacontanonaene (C31:9), which has never been reported in bacteria other than psychrophiles [1, 2]. The geometry and position of the double bonds in this compound were determined to be all *cis* (Fig. 5) at positions 3, 6, 9, 12, 15, 19, 22, 25, and 28 (Table 3 and see Fig. 6). The same compound (C31:9) was detected in marine and nonmarine, and psychrophilc and mesophilic bacteria, which contained EPA and/or DHA (Table 4).

Table 4 Distribution of eicosapentaenoic and docosahexaenoic acids, hentriacontanonaene, and *pfa* genes in various microorganisms

Organisms	Temperature (°C)	EPA	DHA	C31:9	*pfa* Genes (Reference)
Marine bacteria					
Shewanella sp. osh08	20	+[a]	−[b]	+	ND
Colwellia maris ABE-1^T	15	+	+	+	ND
Moritella marina MP-1	15	+	+	+	+ [3]
Shewanella benthica	15	+	−	+	ND
Shewanella pneumatophori SCRC2738^T	20	+	−	+	+ [3]
Shewanella marinintestina IK-1^T	20	+	−	+	+ [3]
Shewanella marinintestina IK-1Δ8	20	−	−	−	±[c] [38]
Pseudomonas alcaliphila AL15-21^T	20	−	−	−	ND
Nonmarine bacteria					
Pseudomonas psychrophila E-3^T	20	−	−	−	ND
Pseudomonas aeruginosa WatG	20	−	−	−	ND
Rhodococcus erythropolis	20	−	−	−	ND
Stenotrophomonas maltophilia	20	−	−	−	ND
Shewanella oneidensis MR-1^T	20	+	−	+	+ [36]
Escherichia coli DH5α	20	−	−	−	−
E. coli DH5α/pEPAΔ1[d]	20	+	−	−	+ [3, 44]
E. coli DH5α/pDHA3 plus pET21a::*pfaE*[e]	15	−	+	−	+ [3, 44]
Marine eukaryotes					
Thraustochytrid-like microorganism strain 12B	30	+	+	−	ND
Schizochitrium limacinum SR21	30	+	+	−	ND
Nonmarine eukaryotes					
Saccharomyces cerevisiae	30	−	−	−	−

For microorganisms other than osh08, the fatty acid and hydrocarbon fraction was prepared by methanolysis of wet or dry cells in the presence of only 21:0 as internal standard, as described in Materials and Methods

ND not determined

[a,b] Present and absent, respectively

[c] Present but only the *pfaD* gene is deficient

[d,e] *E. coli* DH5α carrying pEPAΔ1 that contains *pfaA–E* genes responsible for the biosynthesis of EPA and *E. coli* DH5α carrying pDHA3 that contains *pfaA–pfaD* genes and *pfaE* gene responsible for the biosynthesis of DHA, respectively

Based on our present results, previous studies on the bacterial distribution of PUFAs and *pfa* genes [3], and data on the predicted biosynthetic pathway of PUFAs in the polyketide synthesis mode [37, 39, 40], we will discuss the biosynthetic routes of C31:9.

When hydrocarbons are produced from fatty acids, decarboxylation of the precursor is necessary. Aliphatic hydrocarbons can be produced in eukaryotes by decarboxylation of corresponding fatty acids [6]. Some marine and freshwater algae produce a C21:6 hydrocarbon with double bonds at 3, 6, 9, 12, 15, and 18, and this PUHC is thought to be formed by decarboxylation of DHA [5], although no biochemical or molecular evidence is available. This speculation is acceptable because (1) the positions of the double bonds of C21:6 are consistent with the view of the decarboxylation of DHA with double bonds at Δ4, 7, 10, 13, 16, and 19; and (2) most organisms that have C21:6 also contain DHA [5].

Two biosynthetic routes can be proposed for the formation of C31:9 (see Fig. 7). One pathway is that C31:9 is synthesized by a head-to-head condensation mechanism, in which two molecules of Δ4, 7, 10, 13-hexadecatetraenoic acid (16:4) are condensed in a head-to-head mode. An additional double bond can be formed by the condensation of two fatty acid molecules, which releases CO_2 (Fig. 7a). The head-to-head formation of long chain nonisoprenoid hydrocarbons from fatty acids has been reported in both in vivo [41] and in vitro [42] systems of *Sarcina lutea*, where a monounsaturated long chain hydrocarbon can be formed from two saturated fatty acid molecules by the following equation [41–43].

$$RCH_2COOH + R'CH_2COOH \rightarrow RCH = CHCH_2R' + CO_2$$

In the in vitro system, the head-to-head condensation requires coenzyme A, Mg^{2+}, ATP, NADPH, and either

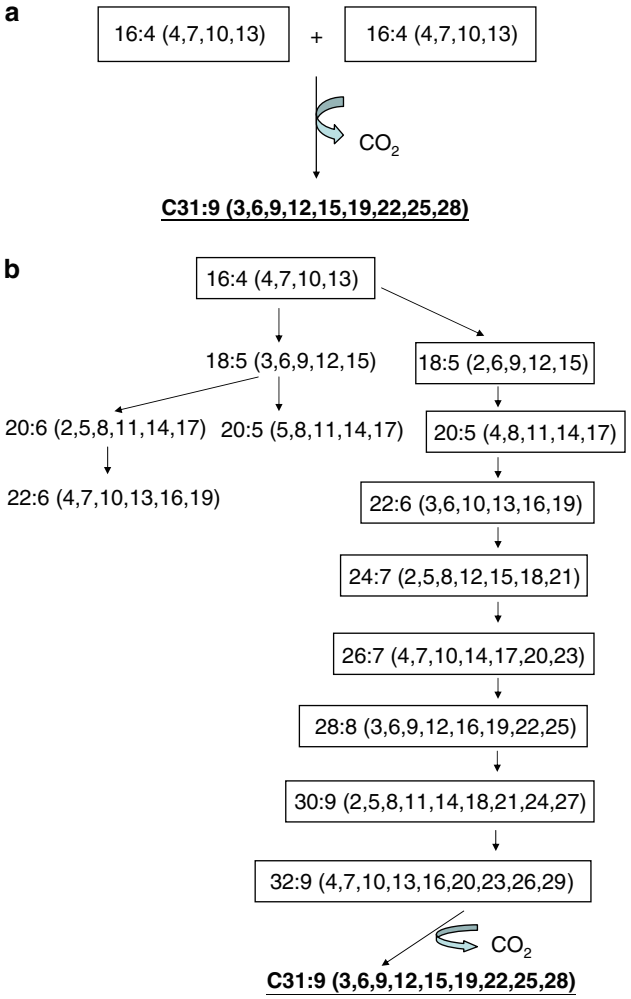

Fig. 7 Possible biosynthetic pathways of C31:9. **a** C31:9 formation by head-to-head condensation of two Δ4,7,10,13-hexadecatetraenoic acid (16:4) molecules. **b** C31:9 formation by decarboxylation of a hypothetical very long chain polyunsaturated fatty acid, Δ4,7,10,13,16,20,23,26,29-dotriacontanonaenoic acid (32:9), which may be synthesized by the Pfa protein complex using 16:4 as a precursor. Fatty acids in this figure are abbreviated, as in 16:4(4,7,10,13), where the number before the colon shows the number of carbon atoms and after the number of double bonds in the fatty acid. The distances of the double bonds from the carboxylic end of the fatty acid are indicated in parentheses. Fatty acid intermediates before 16:4 (4,7,10,13) are not shown. Compounds other than 16:4(4,7,10,13), 20:5(4,8,11,14,17) (EPA), 22:6(4,7,10,13,16,19) (DHA), and hentriacontanonaene (C31:9) are hypothetical. Boxed fatty acids are regarded as intermediates in the formation of C31:9

pyridoxal phosphate or pyridoxamine phosphate as cofactors [43]. Although we have no direct biochemical evidence on the role of this mechanism in the formation of C31:9, the number and positions of double bonds in C31:9, the antiparallel occurrence of EPA and C31:9 in osh08 cells (below 25 °C, Table 2), and the detection of 16:4 in EPA-producing recombinant *E. coli* [44] support this hypothetical pathway.

The other proposed biosynthetic pathway of C31:9 may occur by decarboxylation of a hypothetical very long chain PUFA, Δ4, 7, 10, 13, 16, 20, 23, 26, 29-dotriacontanonaenoic acid (32:9), which may be synthesized by the Pfa protein complex using 16:4 as a precursor (Fig. 7b). At the final step in this hypothetical biosynthetic process of C31:9, decarboxylation of the 32:9 fatty acid is necessary. No intermediate fatty acids other than 16:4 would be overlapped after 16:4 in the biosynthetic pathways of 32:9 and EPA (and DHA) because of the antiparallel occurrence of EPA and C31:9 in osh08 cells grown at various temperatures. However, no fatty acid corresponding 32:9 has been detected in the FAME fraction of osh08 under different GLC conditions using polar and non polar columns (see above). In both proposed pathways, the C31:9 molecule could have an ethylene-interrupted double bond between C15 and C19 (or C12 and C16) (see Figs. 6 and 7). With regard to the decarboxylation activity to synthesize C31:9, such activity would be present only in bacteria carrying *pfa* genes, because there was no C31:9 detected in two PUFA-producing marine eukaryotes, which are expected to have eukaryote type *pfa* genes ([37] and Table 4).

Acknowledgments The infrared analysis of C31:9 was carried out using the apparatus of the OPEN FACILITY, Hokkaido University Sousei Hall with extensive assistance by and discussion with Dr. Y. Matsuo. The authors would like to express their appreciation to Drs. K. Shimazu and K. Nakata of the Faculty of Environmental Earth Science, Hokkaido University for their discussions throughout the work. This work was partly supported by a grant from the National Institute of Polar Research and a Grant-in-Aid from Hokkaido Innovation through Nanotechnology Support (HINTS).

References

1. Nichols DS, Nichols PD, McMeekin TA (1995) A new *n*-$C_{31:9}$ polyene hydrocarbon from Antarctic bacteria. FEMS Microbiol Lett 125:281–285
2. Tamaoka J, Yanagibayashi M, Kato C, Horikoshi K (1998) A polyunsaturated hydrocarbon hentriacontanonaene (C31H46) from a deep-sea bacterium strain DSS12. In: Atlantic Canada Society for Microbial Ecology and International Committee on Microbial Ecology (eds) Program & Abstracts. Eighth international symposium on microbial ecology, Halifax, p 319
3. Okuyama H, Orikasa Y, Nishida T, Morita N (2007) Bacterial genes responsible for the biosynthesis of eicosapentaenoic and docosahexaenoic acids and their heterologous expression. Appl Environ Microbiol 73:665–670
4. Blumer M, Mullin MM, Guillard RRC (1970) A polyunsaturated hydrocarbon (3, 6, 9, 12, 15, 18-heneicosahexaene) in the marine food web. Marine Biol 6:226–235
5. Lee RF, Loeblich AR III (1971) Distribution of 21:6 hydrocarbon and its relationship to 22:6 fatty acid in algae. Phytochemistry 10:593–602
6. Kolattukudy PE, Croteau R, Brown L (1974) Structure and biosynthesis of cuticular lipids. Plant Physiol 53:670–677
7. ZoBell CE (1946) Marine microbiology, a monograph on hydrobacteriology. Chronica Botanica Co., Waltham

8. Yumoto I, Kawasaki K, Iwata H, Matsuyama H, Okuyama H (1998) Assignment of *Vibrio* sp. strain ABE-1 to *Colwellia maris* sp. nov., a new psychrophilic bacterium. Int J Syst Bacteriol 48:1357–1362
9. Satomi M, Oikawa H, Yano Y (2003) *Shewanella marinintestina* sp. nov., *Shewanella schlegeliana* sp. nov. and *Shewanella sairae* sp. nov., novel eicosapentaenoic-acid-producing marine bacteria isolated from sea-animal intestines. Int J Syst Evol Microbiol 53:491–499
10. Hirota K, Nodasaka Y, Orikasa Y, Okuyama H, Yumoto I (2005) *Shewanella pneumatophori* sp. nov., eicosapentanoic-acid-producing marine bacterium isolated from pacific mackerel (*Pneumatophorus japonicus*) intestine. Int J Syst Evol Microbiol 55:2355–2359
11. Yumoto I, Yamazaki K, Hishinuma M, Nodasaka Y, Suemori A, Nakajima K, Inoue N, Kawasaki K (2001) *Pseudomonas alcaliphila* sp. nov., a novel facultatively psychrophilic alkaliphile isolated from seawater. Int J Syst Evol Microbiol 51:349–355
12. Yumoto I, Kusano T, Shingyo T, Nodasaka Y, Matsuyama H, Okuyama H (2001) Assignment of *Pseudomonas* sp. strain E-3 to *Pseudomonas psychrophila* sp. nov., a new facultatively psychrophilic bacterium. Extremophiles 5:343–349
13. Yumoto I, Iwata H, Sawabe T, Ueno K, Ichise N, Matsuyama H, Okuyama H, Kawasaki K (1999) Characterization of a facultatively psychrophilic bacterium, *Vibrio rumoiensis* sp. nov., that exhibits high catalase activity. Appl Environ Microbiol 65:67–72
14. Wongsa P, Tanaka M, Ueno A, Hasanuzzaman M, Yumoto I, Okuyama H (2004) Isolation and characterization of novel strains of *Pseudomonas aeruginosa* and *Serratia marcescens* possessing high efficiency to degrade gasoline, kerosene, diesel oil, and lubricating oil. Curr Microbiol 49:415–422
15. Perveen Z, Ando H, Ueno A, Ito Y, Yamamoto M, Yamada Y, Takagi T, Kaneko T, Kogame K, Okuyama H (2006) Isolation and characterization of a novel thraustochytrid–like microorganism that efficiently produces docosahexaenoic acid. Biotechnol Lett 28:197–202
16. Yaguchi T, Tanaka S, Yokochi T, Nakahara T, Higashihara T (1997) Production of high yields of docosahexaenoic acid by *Schizochytrium limacinum* strain SR21. J Am Oil Chem 74:1431–1434
17. Chapman D (1965) Infrared spectroscopy of lipids. 15th Annual summer program symposium on quantitative methodology in lipid research. Part II. J Am Oil Chem Soc 42:353–371
18. Park MO, Tanabe M, Hirata K, Miyamoto K (2001) Isolation and characterization of a bacterium that produces hydrocarbons extracellularly which a equivalent to light oil. Appl Microbiol Biotechnol 56:448–452
19. Ueda N, Ando S, Hayashi A, Yano I, Hayashi M (1974) Analysis and identification of lipids. In: The Japanese Biochemical Society (ed) Collection of articles on experiments in biochemistry, 1st series, 3. Chemistry of lipids. Tokyo Kagaku Dozin Co., Ltd., Tokyo, pp 75–178 (in Japanese)
20. Sato D, Ando Y, Tsujimoto R, Kawasaki K (2001) Identification of novel nonmethylene-interrupted fatty acids, 7E, 13E-20:2, 7E, 13E, 17Z-20:3, 9E, 15E, 19Z-22:3, and 4Z, 9E, 15E, 19Z-22:4, in Ophiuroidea (brittle star) lipids. Lipids 36:1371–1375
21. Okuyama H, Sasaki S, Higashi S, Murata N (1990) A *trans*-unsaturated fatty acid in a psychrophilic bacterium, *Vibrio* sp. strain ABE-1. J Bacteriol 172:3515–3518
22. Oldham NJ, Svatoš A (1999) Determination of the double bond position in functionalized monoenes by chemical ionization ion-trap mass spectrometry using acetonitrile as a reagent gas. Rapid Commun Mass Spectrom 13:331–336
23. Moneti G, Pieraccini G, Dani F, Catinella S, Traldi P (1996) Acetonitrile as an effective reactant species for positive-ion chemical ionization of hydrocarbons by ion-trap mass spectrometry. Rapid Commun Mass Spectrom 10:167–170
24. Moneti G, Pieraccini G, Dani F, Turillazzi S, Favretto D, Traldi P (1997) Ion-molecule reactions of ionic species from acetonitrile with unsaturated hydrocarbons for the identification of the double-bond position using an ion trap. J Mass Spectrom 32:1371–1373
25. Orikasa Y, Nishida T, Hase A, Watanabe K, Morita N, Okuyama H (2006) A phosphopantetheinyl transferase gene responsible for biosynthesis of *n*-3 polyunsaturated fatty acids from *Moritella marina* strain MP-1. FEBS Lett 580:4423–4429
26. Shibahara A, Yamamoto K, Nakayama T, Kajimoto G (1985) Rapid determination of double bond positions in monounsaturated fatty acids by GC–MS and its application of fatty acid analysis. J Jpn Oil Chem Soc 34:618–625
27. Watanabe K, Ishikawa C, Yazawa K, Kondo K, Kawaguchi A (1996) Fatty acid and lipid composition of an eicosapentaenoic acid-producing marine bacterium. J Mar Biotechnol 4:104–112
28. Marmur J (1961) A procedure for the isolation of deoxyribonucleic acid from microorganisms. J Mol Biol 3:208–218
29. Sambrook J, Russell DW (2001) Molecular Cloning: a laboratory manual, 3rd edn. Cold Spring Harbor Laboratory Press, Cold Spring Harbor
30. Ito H, Hosokawa R, Morikawa M, Okuyama H (2008) A turbine oil-degrading bacterial consortium from soils of oil fields and its characteristics. Int Biodeterior Biodegradation 61:223–232
31. Wiegel J (1990) Temperature spans for growth: hypothesis and discussion. FEMS Microbiol Lett 75:155–169
32. Ivanova EP, Sawabe T, Gorshkova NM, Svetashev VI, Mikhailov VV, Hicolau DV, Christen R (2001) *Shewanella japonica* sp. nov. Int J Syst Evol Microbiol 51:1027–1033
33. Ivanova EP, Gorshkova NM, Bowman JP, Lysenko AM, Zhukova NV, Sergeev AF, Mikhailov VV, Nicolau DV (2004) *Shewanella pacifica* sp. nov., a polyunsaturated fatty acid-producing bacterium isolated from sea water. Int J Syst Evol Microbiol 54:1083–1087
34. Venkateswaran K, Moser DP, Dollhopf ME, Lies DP, Saffarini DA, MacGregor BJ, Ringelberg DB, White DC, Nishijima M, Sana H, Burghardt J, Stackebrandt E, Nelson KH (1999) Polyphasic taxonomy of the genus *Shewanella* and description of *Shewanella oneidensis* sp. nov. Int J Syst Bacteriol 2:705–724
35. Abboud R, Popa R, Souza-Egipsy V, Giometti CS, Tollaksen S, Mosher JJ, Findlay RH, Nealson KH (2005) Low-temperature growth of *Shewanella oneidensis* MR-1. Appl Environ Microbiol 71:811–816
36. Heidelberg J, Paulsen I, Nelson K, Gaidos E, Nelson WC, Read TD, Eisen JA, Seshadri R, Ward N, Methe B, Clayton RA, Meyer T, Tsapin A, Scott J, Beanan M, Brinkac L, Daugherty S, DeBoy RT, Dodson RJ, Durkin AS, Haft DH, Kolonay JF, Madupu R, Peterson JD, Umayam LA, White O, Wolf AM, Vamathevan J, Weidman J, Impraim M, Lee K, Berry K, Lee C, Mueller J, Khouri H, Gill J, Utterback TR, McDonald LA, Feldblyum TV, Smith HO, Venter JC, Nealson KH, Fraser CM (2002) Genome sequence of the dissimilatory metal ion-reducing bacterium *Shewanella oneidensis*. Nat Biotechnol 20:1118–1123
37. Metz JG, Roessler P, Facciotti D, Levering C, Dittrich F, Lassner M, Valentine R, Lardizabal K, Domergue F, Yamada A, Yazawa K, Knauf V, Browse J (2001) Production of polyunsaturated fatty acids by polyketide synthases in both prokaryotes and eukaryotes. Science 293:290–293
38. Nishida T, Morita N, Yano Y, Orikasa Y, Okuyama H (2007) The antioxidative function of eicosapentaenoic acid in a marine bacterium, *Shewanella marinintestina* IK-1. FEBS Lett 581:4212–4216
39. Ootaki M, Morita N, Nishida T, Tanaka M, Hase A, Yano Y, Yamada A, Yu R, Watanabe K, Okuyama H (2003) Genes and

pathways involved in biosynthesis of eicosapentaenoic and docosahexaenoic acids in bacteria. In: Murata N, Nishida I, Yamada M, Sekiya J, Okuyama H, Wada H (eds) Advanced Researches of Plant Lipids. Kluwer, Tokyo, pp 49–52
40. Orikasa Y, Tanaka M, Sugihara S, Hori R, Nishida T, Ueno A, Morita N, Yano Y, Yamamoto K, Shibahara A, Hayashi H, Yamada Y, Yamada A, Yu R, Watanabe K, Okuyama H (2009) *pfaB* Products determine the molecular species produced in bacterial polyunsaturated fatty acid biosynthesis. FEMS Microbiol Lett 295:170–176
41. Albro PW, Dittmer JC (1969) Biochemistry of long-chain, non-isoprenoid hydrocarbons. III. Metabolic relation of long-chain fatty acids and hydrocarbons and other aspects of hydrocarbon metabolism in *Sarcina lutea*. Biochemistry 8:1913–1918
42. Ladygina N, Dedyukhina EG, Vainshtein MB (2006) A review on microbial synthesis of hydrocarbons. Process Biochem 41:1001–1014
43. Albro PW, Dittmer JC (1969) Biochemistry of long-chain, non-isoprenoid hydrocarbons. IV. Characteristics of synthesis by a cell-free preparation of *Sarcina lutea*. Biochemistry 8:3317–3324
44. Orikasa Y (2007) Molecular biological and biochemical studies on microbial genes responsible for the biosynthesis of long chain *n*-3 polyunsaturated fatty acids. PhD thesis, Hokkaido University, Sapporo, Japan

Lipids (2010) 45:179–187
DOI 10.1007/s11745-009-3381-8

ORIGINAL ARTICLE

Isolation and Characterization of a Stress-Dependent Plastidial Δ^{12} Fatty Acid Desaturase from the Antarctic Microalga *Chlorella vulgaris* NJ-7

Yandu Lu · Xiaoyuan Chi · Zhaoxin Li · Qingli Yang · Fuchao Li · Shaofang Liu · Qinhua Gan · Song Qin

Received: 11 August 2009 / Accepted: 7 December 2009 / Published online: 20 January 2010

Abstract An acclimation to the changing physicochemical conditions and high amount of Δ^{12}-unsaturated fatty acids of the Antarctic *Chlorella vulgaris* NJ-7 prompted us to speculate about the involvement of Δ^{12}-fatty acid desaturases (FAD) in its adaptation to the extremely unfavorable ambience. A full-length cDNA sequence, designated CvFAD6, was isolated from *C. vulgaris* NJ-7 via RT-PCR and RACE methods. Sequence alignment showed that the gene was homologous to corresponding Δ^{12}-FAD from other eukaryotes. Phylogenetic analysis showed that it was grouped with plastidial Δ^{12}-FAD with conserved histidine boxes. Yeast cells transformed with a plasmid construct containing CvFAD6 coding region accumulated a considerable amount of linoleic acid ($18{:}2\Delta^{9,12}$), normally not present in wild-type yeast cells, suggesting that the isolated gene encodes a functional Δ^{12} enzyme. The correlation between the accumulation of CvFAD6 and temperature has been examined by real time PCR. The analysis showed a constant expression of CvFAD6 from 25 to 15 °C whereas a fourfold increased from 25 to 4 °C. Moreover, CvFAD6 transcription was more sensitive to saline stress since a 20-fold increase at 6% NaCl was detected. Our data demonstrate that CvFAD6 is the enzyme responsible for the Δ^{12} fatty acids desaturation involved in low temperature and high salinity acclimation for Antarctic *C. vulgaris* NJ-7.

Keywords Antarctic *Chlorella* · Cold stress · Δ^{12} fatty acid desaturation · Gene regulation · Salt stress

Abbreviations
FAD Fatty acid desaturase
UFA Unsaturated fatty acid

Y. Lu · S. Qin (✉)
YanTai Institute of Coastal Zone Research, Chinese Academy of Sciences, 264003 Yantai, People's Republic of China
e-mail: sqin@yic.ac.cn

Y. Lu · F. Li · S. Liu
Institute of Oceanology, Chinese Academy of Sciences, 266071 Qingdao, People's Republic of China
e-mail: ydlu@live.cn

Y. Lu · S. Liu
Graduate School of the Chinese Academy of Sciences, 100049 Beijing, People's Republic of China

X. Chi · Q. Yang
Shandong Peanut Research Institute, 266100 Qingdao, People's Republic of China

Z. Li
Yellow Sea Fisheries Research Institute, Chinese Academy of Fishery Sciences, 266071 Qingdao, People's Republic of China

Q. Gan
Shandong Entry-Exit Inspection and Quarantine Bureau, 266001 Qingdao, People's Republic of China

Introduction

Cold-adapted organisms are able to acclimate rapidly to the changing physicochemical conditions within the brine channel systems. The capability of responding to rapid changes in a host of external stresses including, temperature and salinity, is therefore an intrinsic characteristic of life in sea ice and just as important as being able to survive freezing temperatures [1]. *Chlorella vulgaris* NJ-7 grow

well at temperatures between 4 and 30 °C [2]. Compared with other well studied cold-adapted chlorophytes that failed to grow at temperatures above 20 °C [3, 4], it has retained a higher versatility in response to environmental changes. *C. vulgaris* NJ-7 would seem to be the first candidate for research on acclimation to dramatic temperature and salinity shifts.

Organisms have evolved a number of adaptive mechanisms to counteract the effects of temperature change such as, loss of membrane fluidity, decrease in enzymatic activity, and a decline in protein stability [5]. Total fatty acids of *C. vulgaris* NJ-7 showed variations for different treatments. It is highest at 4 °C (71.09 ± 2.09 mg/g) while lowest at 25 °C (53.99 ± 3.07 mg/g). They are 70.14 ± 2.740020, 60.87 ± 2.82 and 60.73 ± 1.48 mg/g at 15 °C, 25 °C + 3% NaCl and 25 °C + 6% NaCl, respectively (our data). Cold adaptation has always been linked to high levels of membrane-associated polyunsaturated fatty acids (PUFA). Moreover a higher degree of unsaturated fatty acids (UFA) in the membrane lipids is also an adaptive advantage under high-salinity stress [6]. The total amount of Δ^{12} UFA (16:2, 16:3, 18:2 and 18:3) was 37.49 and 34.53% in Antarctic microalgae *Chlamydomonas raudensis* Ettl (UWO241) and *Chlorella* BI, respectively [4]. Otherwise, it was about twice as much in *C. vulgaris* NJ-7 (73.7%) [7]. C18:2, normally 20–30 mg/g (our data), is high while the amount of C18:1 is only a trace (0.03 mg/g) in *C. vulgaris* NJ-7. On the other hand, researches on fatty acid distributions of *C. vulgaris* NJ-7 under different treatments revealed the linkage between fatty acids alteration and stresses. Percentages of 18:2 in total fatty acids by mass increased in response to exposure to lower temperature and higher salinity [7].

Fatty acid desaturases (FAD) play an essential role in fatty acid metabolism and the maintenance of biological membranes [8]. High amount of Δ^{12}-UFA of *C. vulgaris* NJ-7 prompted us to speculate about the involvement of Δ^{12}-FAD in its adaptation to the extreme unfavorable ambience. FAD can be divided into two groups: soluble and membrane-bound desaturases. Of the latter, Δ^{12} FAD catalyze the desaturation at Δ^{12} position to introduce the second hydrogen bond and anchor to the endoplasmic reticulum (ER) and plastidial membrane as two different isoforms: FAD2 and FAD6 [9, 10].

In order to clarify the involvement of Δ^{12} FAD in freezing and salt tolerance and further explore the regulatory mechanism of oleate desaturation, we isolated a novel plastidial oleate desaturase (FAD6) gene in Antarctic microalga, *C. vulgaris* NJ-7 and demonstrated its function by expression in yeast. Meanwhile, the expression pattern of this gene was investigated at different temperature or salt stresses.

Materials and Methods

Strains and Growth Conditions

Chlorella vulgaris NJ-7 was grown in batch cultures in a salt medium (BG11) [11], and initially maintained at a temperature of 25 °C with 12 h of incandescent light and 12 h of darkness.

DNA and RNA Isolation and cDNA Synthesis

Chlorella vulgaris NJ-7 in the exponential growth phase were harvested. The dried mass was frozen in liquid nitrogen, ground with a mortar and pestle into a fine powder. Genomic DNA was isolated following the protocol described by Sambrook et al. [12]. Total RNA was extracted from the powder according to the method of Li et al. [13]. The RNA samples were used for the first-strand cDNA synthesis after being treated with DNaseI to remove DNA. It was synthesized with a reverse transcription polymerase chain (RT-PCR) reaction kit (Takara) according to the manufacturer's instructions. A 500-μg amount of total RNA was used in a 20-μL reaction system. Controls received water instead of reverse transcriptase to assess any contamination from genomic DNA as described by Zhou et al. [14].

PCR with Degenerate Primers

First-strand cDNA was used as a template. Available sequences of Δ^{12}-acyl lipid desaturases from the GenBank database [15] were used to design two degenerate primers, F1/R1 (Table 1). F1 and R1 corresponded to the highly conserved regions FVVGHDC and FWMSTF.

PCR contained 1 × PCR Ex Taq buffer (Mg^{2+} plus), 0.2 mM of each dNTP, 0.4 μM of each primer, and 1 U of Ex-Taq (Takara) per 25 μL reaction. Amplification run on a Tpersonal Thermocycler 118 (Biometra, Germany) following parameters: an initial 5-min denaturation step at 94 °C, followed by 30 cycles of 94 °C for 30 s, 55 °C for 30 s, and 72 °C for 1 min, finally extended at 72 °C for 7 min. The PCR fragments were cloned into a pMD-18-T vector (Takara) and sequenced.

Full-Length cDNA and Genomic Sequences Isolation

The nucleotide sequences of the 3′ and 5′-ends of CvFAD6 were amplified by the RACE method [12]. Amplifications were carried out using the SMART RACE cDNA Amplification Kit (BD-Clontech) according to the manual. 3′ and 5′RACE were performed using gene-specific primers (3GSP1, 3GSP2, 5GSP1 and 5GSP2, Table 1). PCR was carried out using the formulation described in the manual.

Table 1 Primers used in experiment

Aim	Oligonucleotide sequence 5′–3′	Product size (bp)
Partial cDNA cloning		
F1	TTYGTRGTNGGNCAYGACTG	470
R1	GTRAANGTRCTCATCCARAA	
5′RACE		
5GSP1	GCGGCTTCTGCTGCTCGGTGTAC	
5GSP2	TCCACCAGCTTGTTGGTGTG	640
3′RACE		
3GSP1	GCAGAAGGAGACGATGGACAAGTGG	
3GSP2	GAGCAAGTACACCGAGCAGCAGAAGCC	834
Full-length cDNA and genomic sequences cloning		
F2	GTTCTAAGCATACCTACGGGAGTCA	1,406/ 3,112
R2	GGGTTTGCCAAGTCACTCACA	
Real-time PCR		
F3	GTGTGAGTGACTTGGCAAACCC	108
R3	GACATCAGCAGTGGAGAAGAGGA	
F4	ACATCCGCAAGGACCTGTACTC	163
R4	CCGATCCACACGCTGTACTTG	
pYFAD6 construction		
F5	GAATTCACC**ATG**CAGGCAACAGTCGCGT	1,293
R5	CTCGAG**TTA**CATGTTGTTGGGCAGCACC	

F Forward, *R* reverse

The program was performed as follows: 5 min at 94 °C, followed by 30 s at 94 °C, 3 min at 72 °C, for 5 cycles, 30 s at 94 °C, 30 s at 70 °C and 3 min at 72 °C, for 5 cycles, 30 s at 94 °C, 30 s at 68 °C and 3 min at 72 °C, for 25 cycles, finally extended at 72 °C for 7 min. Nested PCR was carried out using the nested universal primers and gene-specific primers. Secondary PCR fragments were subcloned into pMD-18-T vector and nucleotide sequences were determined.

Based on the information of 3′- and 5′-ends sequences, two gene-specific primers F2 and R2 (Table 1) were designed to amplify the full-length cDNA and genomic sequence. PCR was performed with the GC-Rich PCR system (Takara) using 1 × GC buffer (Mg^{2+} plus), 0.2 mM dNTP, 0.5 μM F2 and R2, 1 U of LA-Taq per 25 μL reaction. Reaction conditions were as follows: 5 min denaturation at 94 °C, followed by 30 cycles of 94 °C for 30 s, 55 °C for 30 s and 72 °C for 1 min/kb, finally extended at 72 °C for 7 min. The PCR fragments of the expected length (1.4 and 3.1 kb) were cloned into pMD-18-T vector and sequenced.

Sequence Analysis

A BLAST search program (http://www.ncbi.nlm.nih.gov/blast/) was used. Multiple sequence alignment of putative CvFAD6 was performed with Clustalx1.81 [16]. The distribution of the hydrophobic amino acids was analyzed using the Kyte-Doolittle hydropathy scale [17]. Transmembrane (TM) regions of the protein were predicted with TMHMM (Transmembrane Hidden Markov Model) [18]. The signal sequence analysis was done using a signal peptide prediction server [19].

Phylogenetic affiliation of the CvFAD6 was examined by comparing it to the confirmed and putative plastidial and microsomal Δ^{12} FAD obtained from public databases. Amino acid sequences were aligned using the ClustalX program with the implanted BioEdit [16, 20]. Phylogenetic trees were constructed using neighbor-joining methods, as implemented in the program MEGA4 [21]. Minimum evolution and maximum parsimony analyses were also performed. Bootstrap support was estimated using 1,000 replicates for distance analyses. Default program parameters were used.

Expression in Yeast

The open reading frames was amplified with specific primers, F5 and R5 (Table 1), and subcloned behind the GAL1 promoter of the yeast expression vector pYES2.0 (Invitrogen). The 5′ ends of the F5 and R5 contain an *Eco*RI or an *Xho*I restriction site (underlined) respectively to facilitate subsequent manipulation. The sequence orientation and identity were confirmed by sequencing and the resulted plasmid was designated pYFAD6.

Saccharomyces cerevisiae INVSc1 was transformed and selected according to the manual. Yeast cultures were grown to logarithmic phase at 30 °C in synthetic minimal medium (SC-Ura). The cells were then induced as described by Robert et al. [22], and were incubated at 15 °C for a further 48 h. The cells were harvested by centrifugation, and washed three times with sterile distilled water and then dried by lyophilization. The total lipids were extracted and analyzed according to the method described by Hsiao [23].

Growth Under Various Stresses and Quantification Real Time PCR (qRT-PCR)

Algae at the logarithmic phase were divided into five treatments for a further 14 days. The treatments are as follow: 25 °C, 0% (w/v) NaCl (control); 15 °C, 0% NaCl; 4 °C, 0% NaCl; 25 °C, 3% NaCl; 25 °C, 6% NaCl. Turbulence was monitored by determining OD_{730} every 24 h. Values were calculated with the mean of three independent samples. For real-time PCR, algae at the logarithmic phase were divided into the same five treatments. After an interval of 36 h, algae were harvested by centrifugation at 5,000 rpm for 5 min at 4 °C and washed with sterile,

distilled, deionized water to remove salts before they were centrifuged again.

Two pairs of gene-specific primers were designed according to the CvFAD6 cDNA (F3 and R3) and β-actin sequences (F4 and R4, Table 1). Standard curves for CvFAD6 and β-actin genes were generated by tenfold serial dilutions (10^5–10^{10} copies/μL) of each plasmid DNA to select the optimum dilution degree for qRT-PCR. PCR products were quantified continuously with ABI 7900 Real-Time PCR System (Applied Biosystems) using SYBR Green fluorescence (Takara) according to the manufacturer's instruction. Control reactions were amplified with an RNA template but without reverse transcriptase. The relative amounts of CvFAD6 RNA were normalized to the respective β-actin transcripts. The $2^{-\text{delta delta CT}}$ method [24] was used to analyze qRT-PCR data.

Nucleotide Sequencing and Accession Number

The nucleotide sequences of CvFAD6 genomic and cDNA have been deposited and assigned the accession number GQ175317 and FJ774004 in the EMBL/GenBank/DDBJ database.

Results

Cloning and Characterization of the CvFAD6 Gene

A 470 bp cDNA fragment was generated by RT-PCR with degenerate primers. The amplicon shared a 69% sequence similarity to chloroplast Δ^{12} FAD genes from *Chlamydomonas* sp. W80 and *Polytomella parva*. It indicated that a partial putative FAD6 had been isolated. Gene-specific primers were further designed to obtain the full-length CvFAD6. A 640 bp 5′-RACE product and an 843 bp 3′-RACE product were amplified. The nucleotide sequences of both products from RACE experiments shared an overlap on flanking regions of the 5′ or 3′ ends of the partial putative CvFAD6 cDNA fragment, suggesting that these fragments are portions of the same gene. Sequence analysis revealed that the cloned CvFAD6 cDNA was 1,615 bp in length, which contained a 1,272 bp open reading frame, a 56 bp 5′-untranslated region, and a 287 bp 3′-untranslated region with the characteristics of the poly (A) tail. An ATG translation initiation codon was identified in the sequence of the 5′ terminus (57–59 bp), and a TAA termination codon was found 1,270 nucleotides downstream of the initiation site.

BlastX and BlastN searches combined with alignments between CvFAD6 genome and CvFAD6 cDNA sequences allowed us to identify the genomic organization. The result indicated that CvFAD6 genomic sequence of 3,112 bp was interrupted by nine introns. The sizes and splicing sites of the exons were summarized in Fig. 1. There were canonical GT/AG splicing signals at the ends of the putative introns. The 3′ acceptor splice site is also preceded by pyrimidine-rich sequences as is a common feature of mRNA 3′ splice sites.

Comparison with Other Desaturases

CvFAD6 encoded 423 amino acid residues with an estimated molecular mass of 48.3 kDa and a theoretical isoelectric point of 8.78. A Blast search revealed that the primary structure of CvFAD6 showed 29 and 32% similarity to its (EU596474) [7] and *Chlorella* C-27 microsomal Δ^{12} FAD (BAB78716) [25], respectively. However, it was more similar to these of known plastidial Δ^{12} FAD, with a 65% identity to *C. reinhardtii* (XP_001693068), 63% to *Mesostigma viride* (ABD58898), 53% to *Descurainia Sophia* (ABI73993) and 54% to *Arabidopsis thaliana* (NP_194824). Thus, we deduced that CvFAD6 encoded a plastidial Δ^{12} desaturase rather than a microsomal one.

The distribution of the hydrophobic amino acids of CvFAD6 was typical for a membrane protein, as identified using the Kyte-Doolittle hydropathy scale [17]. The prediction of TM helices by TMHMM indicated that the deduced protein contained five hydrophobic domains between amino acids 102–124, 129–148, 218–240, 255–277 and 282–304, which would be long enough to span the membrane bilayer twice, with the N-terminus facing the cytosol. In addition, CvFAD6 had a transit peptide at the N-terminus, which was a feature of plastidial desaturases as represented by soybean gmFAD6 [26]. All these observations suggested that CvFAD6 encoded a plastidial, rather than a microsomal, Δ^{12} FAD.

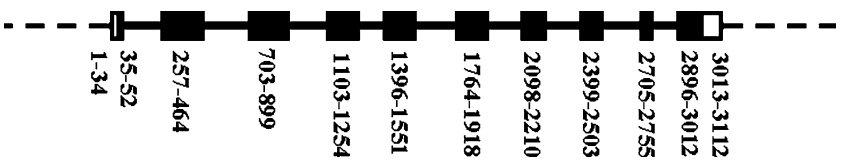

Fig. 1 The complete gene structures of *C. vulgaris* NJ-7 FAD6. Exons are shown as *boxes*: *black boxes* are open reading frames, *empty boxes* are 5′- or 3′-untranslated regions

A multiple sequence alignment of CvFAD6 against similar plastidial Δ^{12} FAD highlighted conserved motifs including FVVGHDC and FWMSTF against which the degenerate primers were designed. Otherwise conserved histidine boxes, HXXXXH (147–151), HXXHH (183–187, 345–349), HXXXXXH (234–239) and HHXXXH (302–307), were found to located in hydrophilic regions separated by long hydrophobic or membrane spanning regions. The histidine-rich motifs, which were highly conserved among membrane-bound acyl-CoA and acyl-lipid desaturases, were proposed as forming the potential diiron active site [27].

Phylogenetic Analysis

All tree topologies were highly congruent. Two major clades were very well supported based on bootstrap values (Fig. 2). All of the microsomal Δ^{12} FAD were grouped. CvFAD6 was clustered within plastidial Δ^{12} FAD group.

Functional Analysis in *S. cerevisiae*

To validate the protein activity, pYFAD6 and empty vector, pYES2.0 (control), were expressed in *S. cerevisiae* INVSc1. Compared with fatty acid profiles derived from the control, pYFAD6 transformants showed a novel peak. The novel peak corresponded to 18:2 which was produced by Δ^{12} desaturation of 18:1Δ^{9}. No 16:2 was detected, indicating that CvFAD6 recognized only one substrate (18:1) in yeast (Fig. 3). Different TM topologies of Δ^{12}-FAD were proposed which lead to different regioselectivity [28]. Δ^{12}-FAD from the *Lentinula edodes* [29] and *Rhizopus arrhizus* [28] recognized only one substrate (18:1)

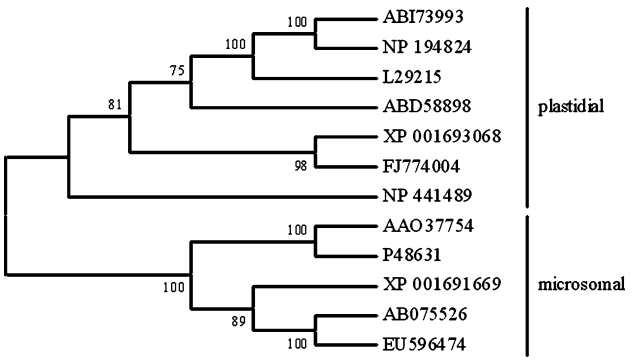

Fig. 2 Neighbor-joining phylogram showing relation of Δ^{12} FAD and related desaturases based on amino acid sequences. Bootstrap analysis of 1,000 randomized sequence replicates was performed; Sequences shown are: ABI73993-*D. Sophia*, NP_194824-*A. thaliana*, L29215-*Glycine max*, ABD58898-*M. viride*, XP_001693068-*C. reinhardtii*, FJ774004-CvFAD6, NP_441489-*Synechocystis* sp. PCC 6803 DesA, AAO37754-*Punica granatum*, P48631-*Glycine max*, XP_001691669-*C. reinhardtii*, AB075526-*Chlorella* C-27, EU596474-CvFAD2

whereas Δ^{12}-FAD from *Phaeodactylum tricornutum* [30], *Sapium sebiferum* [31] and *Chlorella* C-27 [25] recognized two substrates (16:1 and 18:1) while 18:1 was the preferred substrate. Furthermore, the amount of 18:1 was found to be reduced which can be explained by the conversion of 18:1 into 18:2 (Table 2). These results demonstrate directly that CvFAD6 gene encodes a Δ^{12} fatty acid desaturase, which converts 18:1 to 18:2.

Yeast is known to be the model of choice for the functional characterization of microsomal FAD, because it contains a physiological electron donor system (cytochrome b5 and NADH-cytochrome b5 reductase) required by such desaturases. However, it is surprising that a plastidial oleate desaturase (FAD6), that uses ferredoxin as the physiological electron donor, can be functionally expressed in *S. cerevisiae*, where no ferredoxin is present. Nevertheless, the low desaturation levels evident from Fig. 3b suggest activity of desaturases of plastidial origin. The possible reason is that ferredoxin and NADPH-ferredoxin reductase, are supplied to some extent with reducing equivalents in yeast cells. It is consistent with the finding in *P. tricornutum* [30].

Effects of Temperature and Salt Stress on the Growth of *C. Vulgaris* and CvFAD6 Expression

Algal cells at the logarithmic phase were transformed with different treatments: 4 °C + 0% NaCl, 15 °C + 0% NaCl, 25 °C + 0% NaCl, 25 °C + 3% NaCl, and 25 °C + 6% NaCl, with the starting optical density $OD_{730} = 0.8$, each of these in triplicate. Cell density was monitored turbidometrically at 730 nm daily, and specific growth rates were calculated using the equation $\mu = (\ln Xt - \ln X0)/t$, where $X0$ is the initial cell density, and Xt is the cell density after t days [2]. The results signified that low temperature and high salinity slowed down the growth of *C. vulgaris* NJ-7. The growth rate at 4 °C + 0% NaCl was lower than that at 15 °C + 0% NaCl, and the latter was lower than that at 25 °C + 0% NaCl (Fig. 4a); meanwhile, the growth rate at 25 °C + 6% NaCl was lower than that at 25 °C + 3% NaCl while the latter was lower than that at 25 °C + 0% NaCl (Fig. 4b). And 25 °C + 6% NaCl had the most serious effects on its growth. Next were 4 °C + 0% NaCl, and 25 °C + 3% NaCl (Fig. 4c).

Considering the changing profiles of 18:2 fatty acid and the preliminary experiments [7], we chose an interval of 36 h for stress treatment. Then algae were harvested for first strand cDNA synthesis.

The gene expression patterns of CvFAD6 in *C. vulgaris* NJ-7 were analyzed by qRT-PCR. β-Actin [7] was used as a reference for total RNA. β-Actin PCR product was not detected when reverse transcriptase was omitted, indicating that the RNA template was free of genomic DNA. The data

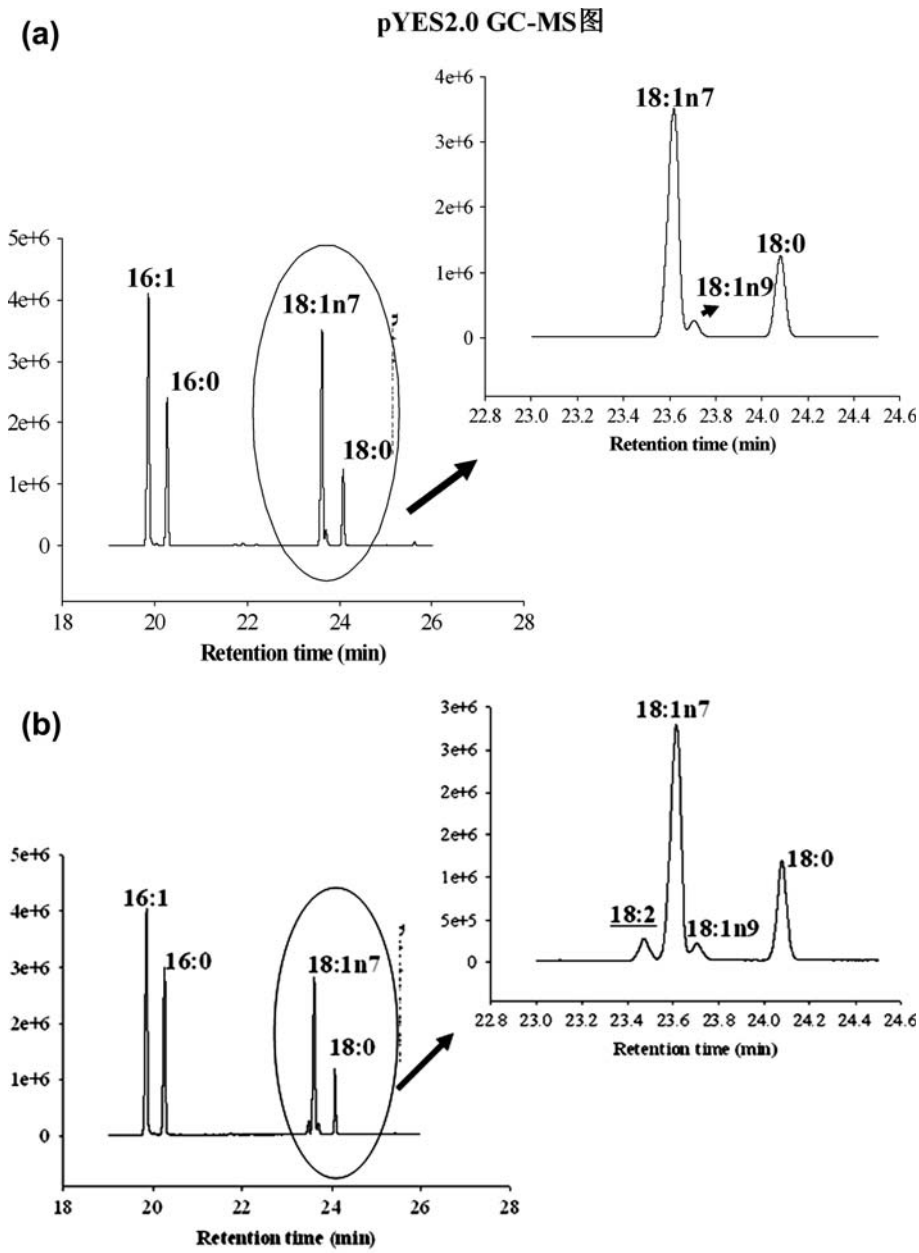

Fig. 3 GC of FAME of recombinant yeast harboring pYES2 (control, **a**) and pYFAD6 containing the CvFAD6 gene (**b**). The transformants at logarithmic phase were grown for 48 h at 15 °C, and FAME from whole cells were prepared and analyzed by gas chromatography (GC) as indicated in "Materials and Methods". The experiment was repeated twice and results of a representative experiment are shown

Table 2 Composition of the major fatty acids (% w/w) of pYES2 and pYFAD6 yeast transformants by GC–MS analysis

Transformant	14:0	16:0	16:1	16:2	18:0	18:1	18:2	21:1
pYES2	0.67	19.19	34.84	ND	9.86	31.86	ND	2.63
pYFAD6	1.13	25.45	35.77	ND	9.78	25.78	2.08	ND

ND Not detected

revealed that temperature and salt concentration regulated the accumulation of CvFAD6 gene transcripts. Transcript accumulations remained relatively constant when algae at 25 °C were transferred to 15 °C. However, transcript accumulation increased significantly at 4 °C, more than fourfold than that at 25 °C (Fig. 5). CvFAD6 was expressed abundantly under salt stress, twofold at 3% NaCl and 20-fold at 6% NaCl (Fig. 5). Thus NaCl was related to the upregulation of CvFAD6 mRNA levels. A higher expression pattern under salt stress suggested a correlation between the level of membrane desaturation and salt concentration.

Discussion

A novel plastidial Δ^{12} fatty acid desaturase from Antarctic *C. vulgaris* NJ-7 was isolated using RT-PCR with degenerate primers designed from conserved motifs and RACE methods. The isolated protein was found to contain features

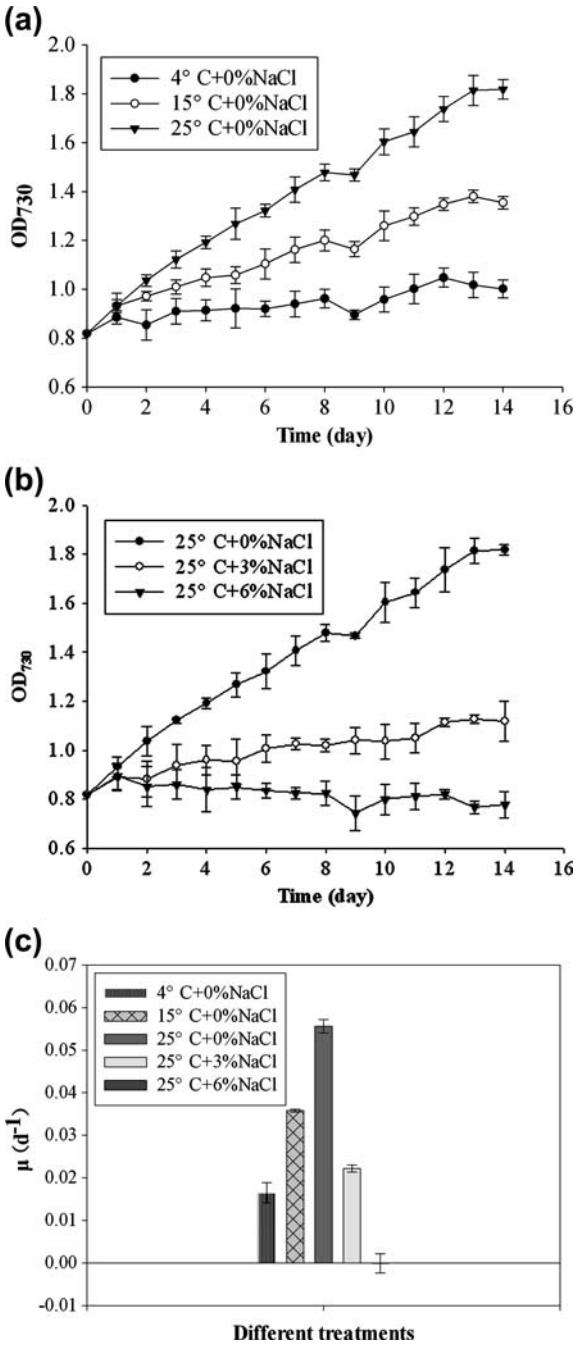

Fig. 4 Effects of temperature and salinity on the growth of *C. vulgaris* NJ-7. Algae at the logarithmic phase were divided into five treatments. The treatments are as follow: 25 °C, 0% (w/v) NaCl (control); 15 °C, 0% NaCl; 4 °C, 0% NaCl; 25 °C, 3% NaCl; 25 °C, 6% NaCl. Turbulence was monitored by determining OD_{730} every 24 h. **a** growth curve at different temperature; **b** growth curve at different concentration of NaCl; **c** growth rates of *C. vulgaris* NJ-7 which were calculated using the equation $\mu = (\ln Xt - \ln X0)/t$, $X0$ is the initial cell density, and Xt is the cell density after t days. Data are presented as means ± SDs ($n = 3$). See "Materials and Methods" for details

characterizing membrane-bound Δ^{12} FAD including membrane-spanning regions separating conserved histidine boxes.

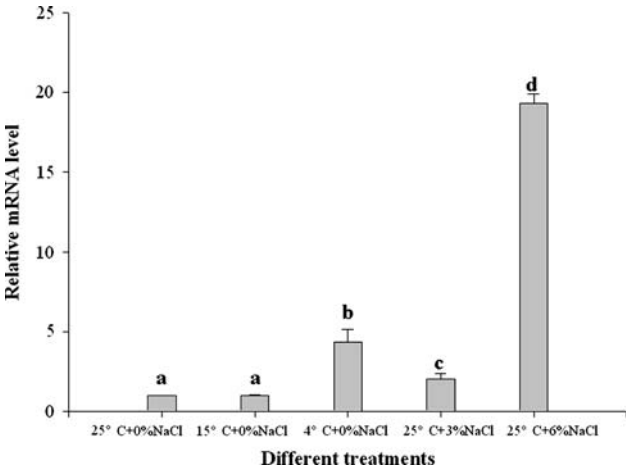

Fig. 5 Real-time-PCR quantification of the CvFAD6 mRNA levels under different stresses. Algae at logarithmic phase were divided into five treatments: 25 °C, 0% (w/v) NaCl (control); 15 °C, 0% NaCl; 4 °C, 0% NaCl; 25 °C, 3% NaCl; 25 °C, 6% NaCl. After an interval of 36 h, algae were harvested and the real-time PCRs were employed to quantify the relative amounts of CvFAD6 transcripts. Data are presented as the mean ± SD ($n = 3$). *Bars* with *different letter* indicate that means are significantly different ($P < 0.05$)

Phylogenic analysis suggested that CvFAD6 was a group with confirmed and putative plastidial Δ^{12} FAD. The result was further supported by the predication of a transit peptide at the N-terminus. Moreover DesA from *Synechocystis* sp. PCC 6803 was found to be closely related with plastidial Δ^{12} FAD (Fig. 2). Though the peptide length of DesA was dramatically shortened, FVVGHDC and FWMSTF motifs and four of the five histidine boxes were conserved. Thus we believe that plastidial Δ^{12} FAD in eukaryotes have a prokaryotic origin.

To validate the protein activity, the putative Δ^{12} FAD was expressed in *S. cerevisiae*. Linoleic acid (18:2), normally not present in wild-type yeast cells, was detected in pYFAD6 transformants. It indicated that the isolated gene encodes a functional Δ^{12} enzyme.

qRT-PCR analysis clarified that the transcripts of CvFAD6 accumulated at different rates during the changes of temperature and salinity. Both cold and high salinity stress led to a higher amount of transcripts. Although the temperature change from 25 to 4 °C resulted in fourfold increase of transcripts, 25 to 15 °C had no effects on the accumulation of CvFAD6. It signified that CvFAD6 played roles in lower temperature around the freezing point. Additionally it implied that the microalga employed other mechanisms to overcome intermediate temperature shifts [7]. The response profile of CvFAD6 is different from that of the microsomal Δ^{12} FAD, CvFAD2 [7]. Its mRNA increased when alga was transfer from 25 to 15 °C or 4 °C after 36 h. Moreover, growth of *C. vulgaris* NJ-7 was most seriously affected by 6% NaCl whereas CvFAD6 mRNA

accumulated more than 20-fold at 6% NaCl. mRNA of CvFAD6 accumulated more dramatically than CvFAD2 (8.5-fold) for 6% NaCl induction. It signifies that they respond differently to stresses, at least in different degree. CvFAD2 initiates transcription accumulation in response to major or intermediate temperature shifts whereas CvFAD6 was only upregulated under freezing temperature stress [7]. Otherwise, the latter is more sensitive to salinity change. In addition, high salinity showed more notably stimulative to CvFAD6 expression than low temperature though the change of 18:2 was not so dramatic. It may be because of low translation rate or a decrease of enzyme activity at high salinity. Sea water freezes at approximately −1.8 °C (salinity of 3.4%), and the salts contained within the water are expelled from the growing ice crystal matrix. When ice forms from freshwater, the result is a hard brittle solid with the primary inclusions being gas bubbles. In contrast when sea water freezes the resultant ice is a semisolid matrix, permeated by a labyrinth of brine filled channels and pores. The volume of ice occupied by the brine channels is directly proportional to the temperature of the ice, as are the brine concentrations within the channels. The higher concentration the salt is, the lower the ice-point is. Brine channel walls constitute large surface areas that can be colonized by algae and used as sites for attachment and locomotion [1]. Thus high salinity slows down the ice formation of ambient sea water meanwhile high salinity impedes the formation of an ice crystal matrix within Antarctic *C. vulgaris* NJ-7. Salt stress induced increases in the UFA was also observed in fungus for the sake of adaptation to a wide range of NaCl concentrations [32]. Decreases in the palmitic fatty acid (C16:0), together with increases in the linoleic fatty acid resulted in the maintenance the correct membrane fluidity at high salinity [33]. To our knowledge, it is the first time that a plastidial Δ^{12} desaturase gene has been found that is induced by both low temperature and high salinity. Therefore the CvFAD6 of plasma membrane involved in the acclimation to the dramatically changing ambience of Antarctic *Chlorella* NJ-7. Moreover, CvFAD6 could be further utilized in plant genetic engineering to enhance cold and high salinity tolerance [34] and improve the oleic acid content [35–37].

In conclusion, we isolated the salinity- and cold-inducible fatty acid desaturase CvFAD6. CvFAD6-expressing transgenic yeast showed a novel peak of 18:2. Real-time PCR analysis revealed that CvFAD6 was involved in different stress responses in a different manner. The changing profile of CvFAD6 mRNA levels is not coincident with the change of 18:2 fatty acid. We believe that the response process of *C. vulgaris* NJ-7 to stresses is a network where CvFAD6 is involved. Stresses alter gene expression positively or negatively in a regulatory network with synergistic and antagonistic effects. Stress responses require the coordinated interaction of many factors. Several players regulate crosstalk and allow the alga to fine-tune specific responses to different stimuli. The functions of stress-related genes are not unvaried and are stress- and time-dependent. However, we only concentrated on transcripts accumulation, the result cannot be used to determine the change of enzyme activity. Further research should consider the FAD profiles from post-transcription and translation levels. Large scale studies of the genome sequences of cold or high salinity-adapted organisms [38–42] will step up the clarification of the role of fatty acids in freezing and salt tolerance.

Acknowledgments We thank Pro. Xu Xudong (Institute of Hydrobiology, Chinese Academy of Sciences) for providing the Antarctic microalga strain *C. vulgaris* NJ-7. This work was supported by the Key Innovative Project of Chinese Academy of Science (KSCX2-YW-G-002, KZCX2-YW-209, KZCX2-YW-225), the National Science Foundation of China (30870247, 30670165, 40876082), the High-Tech Research and Development Program of China (No.2006AA10A114), the National Key Basic Research and Development Project of China (No.2007CB116212) and the Key Technology Research Project of Qingdao (No.07-1-4-16-nsh).

References

1. Mock T, Thomas DN (2005) Recent advances in sea-ice microbiology. Environ Microbiol 7:605–619
2. Hu HH, Li HY, Xu XD (2008) Alternative cold response modes in *Chlorella* (Chlorophyta, Trebouxiophyceae) from Antarctica. Phycologia 47:28–34
3. Morgan-Kiss RM, Ivanov AG, Huner NP (2002) The Antarctic psychrophile, *Chlamydomonas subcaudata* is deficient in state I-state II transitions. Planta 214:435–445
4. Morgan-Kiss RM, Ivanov AG, Modla S, Czymmek K, Huner NPA, Priscu JC, Lisle JT, Hanson TE (2008) Identity and physiology of a new psychrophilic eukaryotic green alga. Chlorella sp., strain BI, isolated from a transitory pond near Bratina Island, Antarctica. Extremophiles 12:701–711
5. D'amico S, Collins T, Marx JC, Feller G, Gerday C (2006) Psychrophilic microorganisms: challenges for life. EMBO Rep 7:385–389
6. Morgan-Kiss RM, Priscu JC, Pocock T, Gudynaite-Savitch L, Huner NPA (2006) Adaptation and acclimation of photosynthetic microorganisms to permanently cold environments. Microbiol Mol Biol Rev 70:222–252
7. Lu YD, Chi XY, Yang QL, Li ZX, Liu SF, Gan QH, Qin S (2009) Molecular cloning and stress-dependent expression of a gene encoding Δ12-fatty acid desaturase in the Antarctic microalga *Chlorella vulgaris* NJ-7. Extremophiles 13:875–884
8. Chi XY, Zhang XW, Guan XY, Ding L, Li YX, Wang MQ, Lin HZ, Qin S (2008) Fatty acid biosynthesis in eukaryotic photosynthetic microalgae: identification of a microsomal Δ12 desaturase in *Chlamydomonas reinhardtii*. J Microbiol 46:189–201
9. Shanklin J, Cahoon EB (1998) Desaturation and related modifications of fatty acids. Annu Rev Plant Physiol 49:611–641
10. Sakuradani E, Kobayashi M, Ashikari T, Shimizu S (1999) Identification of Δ12-fatty acid desaturase from arachidonic acid-producing *Mortierella* fungus by heterologous expression in the yeast *Saccharomyces cerevisiae* and the fungus *Aspergillus oryzae*. Eur J Biochem 261:812–820

11. Stanier RY, Kunisawa R, Mandel M, Cohen-Bazire G (1971) Purification and properties of unicellular blue-green algae. Bacteriol Rev 35:171–205
12. Sambrook J, Fritsch EF, Maniatis T et al (2001) Molecular cloning: a laboratory manual. Cold Spring Harbor Laboratory Press, New York
13. Li Y, Sommerfeld M, Chen F, Hu Q (2008) Consumption of oxygen by astaxanthin biosynthesis: a protective mechanism against oxidative stress in *Haematococcus pluvialis* (Chlorophyceae). J Plant Physiol 165:1783–1797
14. Zhou XR, Robert SS, Petrie JR, Frampton DM, Mansour PM, Blackburn SI, Nichols PD, Green AG, Singh SP (2007) Isolation and characterization of genes from the marine microalga *Pavlova salina* encoding three front-end desaturases involved in docosahexaenoic acid biosynthesis. Phytochemistry 68:785–796
15. Benson DA, Karsch-Mizrachi I, Lipman DJ, Ostell J, Wheeler DL (2005) GenBank. Nucleic Acids Res 33:D34–D38
16. Thompson JD, Gibson TJ, Plewniak F, Jeanmougin F, Higgins DG (1997) The CLUSTAL_X windows interface: flexible strategies for multiple sequence alignment aided by quality analysis tools. Nucleic Acids Res 25:4876–4882
17. Kyte J, Doolittle RF (1982) A simple method for displaying the hydropathic character of a protein. J Mol Biol 157:105–132
18. Moller S, Croning MD, Apweiler R (2001) Evaluation of methods for the prediction of membrane spanning regions. Bioinformatics 17:646–653
19. Bendtsen JD, Nielsen H, von Heijne G, Brunak S (2004) Improved prediction of signal peptides: SignalP 3.0. J Mol Biol 340:783–795
20. Chenna R, Sugawara H, Koike T, Lopez R, Gibson TJ, Higgins DG, Thompson JD (2003) Multiple sequences alignment with the Clustal series of programs. Nucleic Acids Res 31:3497–3500
21. Tamura K, Dudley J, Nei M, Kumar S (2007) MEGA4: molecular evolutionary genetics analysis (MEGA) software version 4.0. Mol Biol Evol 24:1596–1599
22. Robert SS, Petrie JR, Zhou XR, Mansour MP, Blackburn SI, Green AG, Singh SP, Nichols PD (2009) Isolation and characterisation of a Δ5-fatty acid elongase from the marine microalga *Pavlova salina*. Mar Biotechnol 11:410–418. doi:10.1007/s10126-008-9157-y
23. Hsiao TY, Holmes B, Blanch HW (2007) Identification and functional analysis of a Δ-6 desaturase from the marine microalga *Glossomastix chrysoplasta*. Mar Biotechnol 9:154–165
24. Livak KJ, Schmittgen TD (2001) Analysis of relative gene expression data using real-time quantitative PCR and the $2^{-\text{delta delta CT}}$ method. Methods 25:402–408
25. Suga K, Honjoh K, Furuya N, Shimizu H, Nishi K, Shinohara F, Hirabaru Y, Maruyama I, Miyamoto T, Hatano S, Iio M (2002) Two low-temperature-inducible *Chlorella* genes for delta12 and omega-3 fatty acid desaturase (FAD): isolation of delta12 and omega-3 fad cDNA clones, expression of delta12 fad in *Saccharomyces cerevisiae*, and expression of omega-3 fad in *Nicotiana tabacum*. Biosci Biotechnol Biochem 66:1314–1327
26. Hitz WD, Carlson TJ, Booth JR Jr, Kinney AJ, Stecca KL, Yadav NS (1994) Cloning of a higher-plant plastid omega-6 fatty acid desaturase cDNA and its expression in a cyanobacterium. Plant Physiol 105:635–641
27. Shanklin J, Whittle E, Fox BG (1994) Eight histidine residues are catalytically essential in a membrane-associated iron enzyme, stearoyl-CoA desaturase, and are conserved in alkane hydroxylase and xylene monooxygenase. Biochemistry 33:12787–12794
28. Wei DS, Li MC, Zhang XX, Ren Y, Xing LJ (2004) Identification and characterization of a novel Δ12 -fatty acid desaturase gene from *Rhizopus arrhizus*. FEBS Lett 573:45–50
29. Sakai H, Kajiwara S (2005) Cloning and functional characterization of a Δ12 fatty acid desaturase gene from the basidiomycete *Lentinula edodes*. Mol Genet Genomics 273:336–341
30. Domergue F, Spiekermann P, Lerchl J, Beckmann C, Kilian O, Kroth PG, Boland W, Zähringer U, Heinz E (2003) New insight into *Phaeodactylum tricornutum* fatty acid metabolism. Cloning and functional characterization of plastidial and microsomal Δ12-fatty acid desaturases. Plant Physiol 131:1648–1660
31. Niu B, Ye H, Xu Y, Wang S, Chen P, Peng S, Ou Y, Tang L, Chen F (2007) Cloning and characterization of a novel Δ12-fatty acid desaturase gene from the tree *Sapium sebiferum*. Biotechnol Lett 29:959–964
32. Turk M, Abramovi′c Z, Plemenitaš A, Gunde-Cimerman N (2007) Salt stress and plasma-membrane fluidity in selected extremophilic yeasts and yeast-like fungi. FEMS Yeast Res 7:550–557
33. Turk M, Mejanelle L, Šentjurc M, Grimalt JO, Gunde-Cimerman N, Plemenitaš A (2004) Salt-induced changes in lipid composition and membrane fluidity of halophilic yeast-like melanized fungi. Extremophiles 8:53–61
34. Yokotani N, Ichikawa T, Kondou Y, Matsui M, Hirochika H, Iwabuchi M, Oda K (2009) Tolerance to various environmental stresses conferred by the salt-responsive rice gene *ONAC*063 in transgenic *Arabidopsis*. Planta 229:1065–1075. doi:10.1007/s00425-009-0895-5
35. Despeghel J, Granier C, Monsanto SAS (2007) Fad-2 mutants and high oleic plants. EP1806398
36. Patel M, Jung S, Moore K, Powell G, Ainsworth C, Abbott A (2004) High-oleate peanut mutants result from a MITE insertion into the FAD2 gene. Theor Appl Genet 108:1492–1502
37. Zhou XR, Singh S, Liu Q, Green A (2006) Combined transgenic expression of Δ12-desaturase and Δ12-epoxygenase in high linoleic acid seeds leads to increased accumulation of vernolic acid. Funct Plant Biol 33:585–592
38. Rabus R, Ruepp A, Frickey T et al (2004) The genome of *Desulfotalea psychrophila*, a sulfate-reducing bacterium from permanently cold Arctic sediments. Environ Microbiol 6:887–902
39. Saunders NFW, Thomas T, Curmi PMG et al (2003) Mechanisms of thermal adaptation revealed from the genomes of the Antarctic Archaea *Methanogenium frigidum* and *Methanococcoides burtonii*. Genome Res 13:1580–1588
40. Medigue C, Krin E, Pascal G et al (2005) Coping with cold: the genome of the versatile marine Antarctica bacterium *Pseudoalteromonas haloplanktis* TAC125. Genome Res 15:1325–1335
41. Methe BA, Nelson KE, Deming JW et al (2005) The psychrophilic lifestyle as revealed by the genome sequence of *Colwellia psychrerythraea* 34H through genomic and proteomic analyses. Proc Natl Acad Sci USA 102:10913–10918
42. Thorvaldsen S, Hjerde E, Fenton C, Willassen NP (2007) Molecular characterization of cold adaptation based on ortholog protein sequences from *Vibrionaceae* species. Extremophiles 11:719–732. doi:10.1007/s00792-007-0093-y

Lipids (2010) 45:189–198
DOI 10.1007/s11745-010-3383-6

ORIGINAL ARTICLE

Chemical Structure of *Bacteriovorax stolpii* Lipid A

Sebastian Beck · Frederic D. Müller · Eckhard Strauch · Lothar Brecker · Michael W. Linscheid

Received: 16 December 2009 / Accepted: 4 January 2010 / Published online: 22 January 2010

Abstract *Bdellovibrionales* is a phylogenetically diverse group of predatory prokaryotes, which consists of the two families *Bdellovibrionaceae* and *Bacteriovoracaceae*. We describe LPS and lipid A of the type strain *Bacteriovorax stolpii* DSM 12778, representing the first characterized endotoxin of a *Bacteriovoracaceae* member. It has a smooth form LPS, which was identified by SDS-polyacrylamide gel electrophoresis. The lipid A structure was determined by combined gas chromatography–mass spectrometry, electrospray ionization mass spectrometry and NMR spectroscopy. Its backbone consists of two β-(1 → 6)-linked 2,3-diamino-2,3-dideoxy-D-glucopyranoses (Glc*p*N3N) carrying a pyrophosphoethanolamine at O-4′ of the non-reducing sugar and a phosphate group linked to O-1 of the reducing Glc*p*N3N. Positions 2, 3, 2′ and 3′ of the two Glc*p*N3N are acylated with primary 3-hydroxy fatty acids and one of those carries a secondary fatty acid.

S. Beck and F. D. Müller contributed equally to this work.

Electronic supplementary material The online version of this article (doi:10.1007/s11745-010-3383-6) contains supplementary material, which is available to authorized users.

S. Beck · F. D. Müller · M. W. Linscheid (✉)
Department of Chemistry, Humboldt-Universität zu Berlin, Brook-Taylor-Str. 2, 12489 Berlin, Germany
e-mail: m.linscheid@chemie.hu-berlin.de

S. Beck · F. D. Müller · E. Strauch
Department of Biological Safety, Federal Institute for Risk Assessment, Diedersdorfer Weg 1, 12277 Berlin, Germany

L. Brecker
Department of Organic Chemistry, University of Vienna, Währinger Straße 38, 1090 Vienna, Austria

Keywords *Bdellovibrionales* · *Bacteriovorax* · Endotoxin · Lipid A · Mass spectrometry · NMR spectroscopy · Predatory prokaryotes

Abbreviations

BALOs	*Bdellovibrio*-and-like organisms
CID	Collision induced dissociation
COSY	Correlation spectroscopy
ESI–MS	Electrospray ionization–mass spectrometry
EXSY	Exchange spectroscopy
FTICR MS	Fourier transform ion cyclotron resonance mass spectrometry
GC–MS	Gas chromatography–mass spectrometry
Glc*p*N3N	2,3-diamino-2,3-dideoxy-D-glucopyranose
HMBC	Heteronuclear multiple bond coherence
HMQC	Heteronuclear multiple quantum coherence
LPS	Lipopolysaccharide
MALDI-ToF	Matrix assisted laser desorption/ionisation-time of flight mass spectrometry
NMR	Nuclear magnetic resonance
NOESY	Nuclear Overhauser effect spectroscopy
P^{I}	Phosphate residue at C-1 of the reducing sugar Glc*p*N3N^{I}
P^{II}	Phosphate residue at C-4 of the non-reducing sugar Glc*p*N3N^{II}
*P*EtN	Phosphoethanolamine
R-form LPS	Rough form lipopolysaccharide
ROESY	Rotating frame nuclear Overhauser effect spectroscopy
SDS-PAGE	Sodium dodecylsulfate polyacrylamide gel electrophoresis
S-form LPS	Smooth form lipopolysaccharide
TOCSY	Total correlation spectroscopy

Introduction

Bdellovibrionales, also referred to as *Bdellovibrio*-and-like organisms (BALOs), are predatory prokaryotes causing lysis of other Gram-negative bacteria by invading and replicating within their periplasm [1–3]. Despite this unique and similar predatory lifestyle as well as common morphological features among predatory prokaryotes, genetic analyses revealed distinct differences. At present the two families Bdellovibrionaceae and Bacteriovoracaceae constitute the order *Bdellovibrionales* [4–8]. The type strain *Bdellovibrio bacteriovorus* HD100 (DSM 50701) is a well-studied representative of Bdellovibrionaceae [3, 6–10]. It is an obligate predator with an essential requirement of living prey cells for growth and replication [9]. Its lipid A is very different from other bacteria, since charged groups are completely lacking. This uncommon structure is supposed to be the main reason for the unique biophysical properties and a decreased endotoxic activity of the lipopolysaccharide (LPS) [10]. As the encounter of predators with prey bacteria occurs through surface structures of the outer membrane, the unusual lipid A could also be a prerequisite for the predatory lifestyle.

In contrast, the type strain *Bacteriovorax stolpii* (DSM 12778), a typical representative of the family *Bacteriovoracaceae*, is a facultative predator capable of growing intracellularly within prey bacteria or extracellularly in rich media [11, 12]. Without the obligate need of living prey cells, *B. stolpii* is an interesting candidate for therapeutic applications. It has been shown that the cell wall of *B. stolpii* possesses unusual sphingophosphonolipids [13–15]. Furthermore, outer membrane proteins show some high strain specificities in comparison to other predators like *B. bacteriovorus* or *Peredibacter starrii* [16]. Thus, structure determination of the *B. stolpii* lipid A is of special interest. In particular, comparison with the *B. bacteriovorus* lipid A might allow identification of specific motives in taxonomically distinct groups of predatory bacteria and enable a better understanding of processes involved in the attachment and penetration of predatory prokaryotes. In continuation of our previous work we now examined the LPS and lipid A of the facultative predatory strain *B. stolpii*.

Experimental Procedures

Bacterial Growth and Lipopolysaccharide Extraction

Bacteriovorax stolpii (DSM 12778, ATCC 27052) was grown in peptone yeast extract medium (ATCC 526) at 30 °C for 3–5 days. Each batch was checked by 16S rDNA amplification, followed by restriction pattern analyses of the resulting amplicons [8]. Cells were harvested by centrifugation, washed twice in 2% phenol, ethanol and acetone and dried in a rotary concentrator. The yield was 12.8 g bacteria (dry weight) from 27 L culture. The pellet was resuspended in 100 mL bidistilled water and nucleic acids were degraded by addition of RNAse A, DNAse I and incubation at 37 °C for 16 h with gentle stirring. Additionally, Proteinase K was added and the mixture was incubated for 8 h at 37 °C. The resulting suspension was dialyzed for 48 h at room temperature and lyophilized. The phenol/chloroform/light petrol ether (2:5:8, v/v/v) method was used for LPS extraction [17]. Crude LPS was precipitated from the extract by dropwise addition of ethanol. The precipitate was further purified by addition of RNase A, DNase I and incubation at 37 °C for 16 h and additionally treated with Proteinase K. The resulting suspension was dialyzed against bidistilled water and lyophilized to yield 645 mg of LPS.

Gel Electrophoresis of LPS

For gel electrophoresis of LPS, the gel system according to Laemmli was used [18]. Samples were suspended in loading buffer, boiled for 10 min, and separated at 20 mA on a 12% (w/v) polyacrylamide gel at 8 °C. Gels were stained by the oxidative silver staining protocol [19].

Isolation and Derivatisation of Lipid A

Lipid A of *B. stolpii* was obtained by mild acidic hydrolysis of LPS. One hundred and eighty milligrams of LPS were suspended in 1% acetic acid to a final concentration of 7 mg mL^{-1} and heated to 100 °C for 120 min. The mixture was cooled on ice, followed by centrifugation at 4 °C for 10 min at 12,000×*g*. The precipitate was washed in bidistilled water and acetone, resuspended in bidistilled water and lyophilized to yield 63 mg of lipid A. Dephosphorylated lipid A was obtained by suspending 50 mg of lipid A in 10 mL of hydrofluoric acid (48%) and stirring for 48 h at 4 °C. The reaction mixture was directly dialyzed against bidistilled water and lyophilized to yield 38 mg of dephosphorylated lipid A.

Fatty Acid Analysis

Fatty acids were analyzed as their corresponding methyl esters. A 1-mg sample of lipid A or LPS was dissolved in 2 M HCl in methanol (500 µL) and heated to 100 °C for 16 h. The mixture was dried using a gentle stream of compressed nitrogen and fatty acid methyl esters were extracted by partitioning between bidistilled water (50 µL) and chloroform and extraction with chloroform (three

times, 100 μL each). The combined extracts were dried and redissolved in 50 μL chloroform. A 1-μL sample was analyzed by gas chromatography–mass spectrometry (GC–MS).

Gas chromatography–mass spectrometry was performed on an electron impact ionization Hewlett Packard mass spectrometer G1800A with a fused silica capillary column (HP-5MS, 30 m, inner diameter 0.25 mm, film thickness 0.25 μm). Hydrogen was used as the carrier gas at a flow rate of 1 L h^{-1} and the initial GC temperature was 150 °C for 3 min, then raised to 320 °C at 5 °C min^{-1}. Relative abundances were determined from the corresponding peak areas, while the fatty acid methyl ester Mix GLC-80 (Supelco) was used as external standard.

Sugar Analyses

For qualitative analyses, the sugars were converted into their alditol acetates after hydrolysis of lipid A, reduction with sodium borohydride and peracetylation, according to previously described procedures [20]. Determination of the absolute configuration of sugars was carried out by analyses of the corresponding acetylated (*S*)-2-butylglycosides [21, 22]. The temperature program for sugar analyses was identical as in the case of fatty acid methyl ester analyses.

Mass Spectrometry

Matrix-assisted laser desorption ionization time-of-flight mass spectrometry (MALDI-ToF MS) of intact LPS was performed on a Voyager DE mass spectrometer (Applied Biosystems) in delayed extraction mode. LPS was dispersed in bidistilled water to a concentration of 10 mg mL^{-1} and directly mixed on target with an equal volume of saturated dihydroxy benzoic acid solution in water/acetonitrile (1:1, v/v). Mass spectra were calibrated externally by using LPS preparations from *Escherichia coli* K-12 (DSM 423) with known chemical structure [23].

Electrospray ionization-Fourier transform ion cyclotron resonance mass spectrometry (ESI-FTICR MS) was performed on a Finnigan LTQ FTMS (Thermo Electron) equipped with a 6-T superconducting magnet. Samples were dissolved in a mixture of chloroform/methanol/water (100:75:15, v/v/v) to a concentration of about 10–20 μg mL^{-1}, treated with Amberlite IR-120 cation exchanger, a flow rate of 3 μL min^{-1} was used. The spray voltage was 4.3 kV (positive ESI) or 4.0 kV (negative ESI). The nitrogen sheath gas flow rate was 15 arb and the transfer capillary temperature remained at 200 °C during all measurements. Transfer optics and lenses were optimized by automatic tuning. All spectra were acquired with a resolution of 100,000.

Nuclear Magnetic Resonance Spectroscopy

Fully protonated lipid A was obtained by suspending 2.0 mg lipid A in 2 mL distilled water, increasing the pH to ~9 by addition of 0.36 M aqueous triethylamine, and decreasing of the pH to ~2 by addition of 0.1 M HCl. The precipitate was isolated by centrifugation (2,000×*g*, 10 min) and dissolved in 3 mL chloroform/methanol (4:1, v/v). After washing three times with 5 mL distilled water and removal of the solvent at ~20 mbar, all exchangeable protons were replaced by deuterium dissolving lipid A in 3.0 mL of chloroform-*d*/methanol-d_4 (2:1, v/v) and drying in a stream of nitrogen. The lipid A was dried over P_4O_{10} (~0.1 mbar) and dissolved in 0.5 mL chloroform-*d*/methanol-d_4 (2:1, v/v). The dephosphorylated lipid A was treated in the same way and dissolved in 0.5 mL pyridine-d_5/methanol-d_4 (2:1, v/v).

NMR spectra were measured at 315 K ± 0.05 K on Bruker AV600 and DRX600 spectrometers using the XWINNMR 2.6 and Topspin 1.3 software, respectively. Irradiation and measurement frequencies were 600.13 MHz (^{1}H), 242.94 MHz (^{31}P) and 150.1 MHz (^{13}C). One dimensional ^{1}H, ^{31}P, and ^{13}C spectra were recorded and Fourier transformed to spectra with 7,250 Hz (^{1}H), 25,000 Hz (^{31}P), and 32,000 Hz (^{13}C). Two dimensional spectra (COSY, NOESY, ROESY, TOCSY and HMQC) were recorded with a spectral width of 7,250 Hz for ^{1}H and 32,000 Hz for ^{13}C. Selected parameters for 2D NMR experiments: TOCSY, mixing time 70–100 ms. NOESY, mixing time 200 and 400 ms. ROESY, mixing time 225 ms. Tetramethylsilane (δ_H 0.00 ppm, δ_C 0.0 ppm), methanol (δ_H 3.35 ppm, δ_C 49.0 ppm) or DMSO (δ_H 2.25 ppm, δ_C 39.4 ppm) were used as internal standards.

Results

SDS-PAGE and Mass Spectrometry of LPS

The *B. stolpii* lipopolysaccharides (LPS) showed an S-form pattern in SDS-PAGE analyses (see Supplementary Material). In addition to the typical O-antigen ladder, two major abundant bands were apparent from the gel separation. These two bands likely correspond to R-forms of the isolated LPS. Furthermore, the LPS was subjected to ESI-FTICR MS, however, no conclusive data was obtained in positive as well as in negative ionization mode. This was most likely caused by the high chemical diversity of the LPS, as apparent from the SDS-PAGE analyses. The negative MALDI-ToF spectrum of the LPS (see Supplementary Material) showed lipid A derived signals in the range of *m*/*z* 1,500–1,800 as the most abundant signals, as identified by ESI–MS experiments of lipid A (see below).

The high abundance of lipid A derived signals in MALDI-ToF analyses most probably resulted from laser-induced fragmentations of LPS species.

Compositional Analysis of *B. stolpii* Lipid A

The analyses of alditol acetates in combination with the analyses of acetylated (*S*)-2-butylglycosides of sugars revealed that the lipid A exclusively harbors 2,3-diamino-2,3-dideoxy-D-glucopyranoses (Glc*p*N3N) as sugar moieties, similar to the lipid A of *B. bacteriovorus* [10]. The GC–MS analyses of fatty acid methyl esters confirmed that non-hydroxylated and 3-hydroxy fatty acids are present in the LPS of *B. stolpii*. No unsaturated fatty acids or other hydroxy fatty acids were present in the LPS. For the non-hydroxylated fatty acids, dodecanoic acid (12:0), 11-methyl dodecanoic acid (*iso*-13:0), tetradecanoic acid (14:0) and 13-methyl tetradecanoic acid (*iso*-15:0) were identified. While 11-methyl dodecanoic acid is the most abundant non-hydroxylated fatty acid, a wider distribution was found for the 3-hydroxylated fatty acids (Table 1). No 3-hydroxy dodecanoic acid was found in these experiments. All fatty acid analyses were performed with lipid A and LPS of *B. stolpii*, while no differences were detected.

Mass Spectrometry of *B. stolpii* Lipid A

In the mass spectrum of negative ions (Fig. 1a) several groups of signals differing in the mass of one methylene group (CH_2, 14.015 u) were detected. The most intense signals, those of the singly charged ($[M–H]^-$) group of signals around *m/z* 1,612.075, were assigned to lipid A consisting of a 2,3-diamino-2,3-dideoxyglucopyranose (Glc*p*N3N) disaccharide carrying two phosphate groups and five fatty acids ($LA_{penta}P^{I}P^{II}$). The signals around *m/z* 1,735.085 correspond to the deprotonated species ($[M–H]^-$) of the penta-acylated lipid A carrying two phosphate groups and one phosphoethanolamine (*P*EtN) group ($LA_{penta}P^{I}P^{II}$*P*EtN). The fatty acid distribution for the $LA_{penta}P^{I}P^{II}$*P*EtN species is shown in Table 2. A series of ions around *m/z* 1,627.090 could be identified as penta-acylated lipid A with one phosphate group and a *P*EtN group ($LA_{penta}P^{II}$*P*EtN). The signals around *m/z* 1,532.114 resulted from penta-acylated lipid A species substituted with one phosphate group only ($LA_{penta}P^{I}$ or $LA_{penta}P^{II}$). $LA_{penta}P^{I}P^{II}$, $LA_{penta}P^{II}$*P*EtN and $LA_{penta}P^{I}P^{II}$*P*EtN could also be detected as doubly charged ions. The base signals for these three groups were *m/z* 805.538 for $LA_{penta}P^{I}P^{II}$, *m/z* 813.047 for $LA_{penta}P^{II}$*P*EtN and *m/z* 867.042 for $LA_{penta}P^{I}P^{II}$*P*EtN.

Collision induced dissociation (CID) of the negatively charged species at *m/z* 1,735.086 ($LA_{penta}P^{I}P^{II}$*P*EtN) resulted in the loss of a phosphoethanolamine residue (*P*EtN, $C_2H_6NO_3P$, 123.008 u) or of a phosphate group (H_3PO_4, 97.976 u), while fragmentation of the species around *m/z* 1,612.075 ($LA_{penta}P^{I}P^{II}$) only resulted in the dominant loss of a phosphate group (H_3PO_4, 97.976 u). Additionally, in all these fragmentation experiments the loss of 214.193 u, corresponding to the elimination of a 13:0 fatty acid, was observed. For CID of the cluster at *m/z* 1,532.114 ($LA_{penta}P^{I}$/$LA_{penta}P^{II}$) the elimination of a 13:0 fatty acid residue has been the most abundant fragmentation, while in no cases additional fragmentations were apparent that allowed the unambiguous determination of the fatty acid distribution.

In the positive ion spectrum (Fig. 1b), the same molecular species, apart from $LA_{penta}P^{I}$/$LA_{penta}P^{II}$, could be identified as protonated $[M + H]^+$ or sodiated ions $[M + Na]^+$. The signals around *m/z* 1,516.117 originated from fragmentation of the $LA_{penta}P^{I}P^{II}$ ions [loss of a phosphate group (H_3PO_4, 97.976 u)]. Additionally to these signals, singly charged ions in the range of *m/z* 850–1,050 could be detected and were assigned to the corresponding B-ions. The ions around *m/z* 1,026.652 represented the non-reducing sugar part of the lipid A of *B. stolpii*, consisting of the Glc*p*N3N^{II} sugar moiety carrying three fatty acids, one phosphate and one *P*EtN group ($B_{tri}P^{II}$*P*EtN). Based on these findings the *P*EtN group of the lipid A of *B. stolpii* could clearly be located at the non-reducing sugar of the disaccharide backbone. The signals around *m/z* 903.643 originated from B-ion fragment ions carrying one phosphate group and three fatty acids ($B_{tri}P^{II}$) (B-fragment nomenclature according to Domon et al. [24]).

MS/MS experiments of B-ions in positive ESI–MS proved that a secondary fatty acid, which is linked to the 3-hydroxy group of a primary fatty acid, is present at the non-reducing sugar part of the lipid A. Furthermore, these analyses showed that 11-methyl dodecanoic acid (*iso*-13:0) is the dominant secondary fatty acid in the investigated lipid A, since in all these experiments the loss of 196.182 or 214.193 u has been the most abundant fragmentation for

Table 1 Relative abundances of fatty acids in LPS of *B. stolpii* as determined by GC–MS analyses of fatty acid methyl esters

	Relative abundance (%)
Non-hydroxy fatty acids	
12:0	3
iso-13:0	77
14:0	12
iso-15:0	9
Hydroxy fatty acids	
3-OH *iso*-13:0	18
3-OH 14:0	46
3-OH *iso*-15:0	37

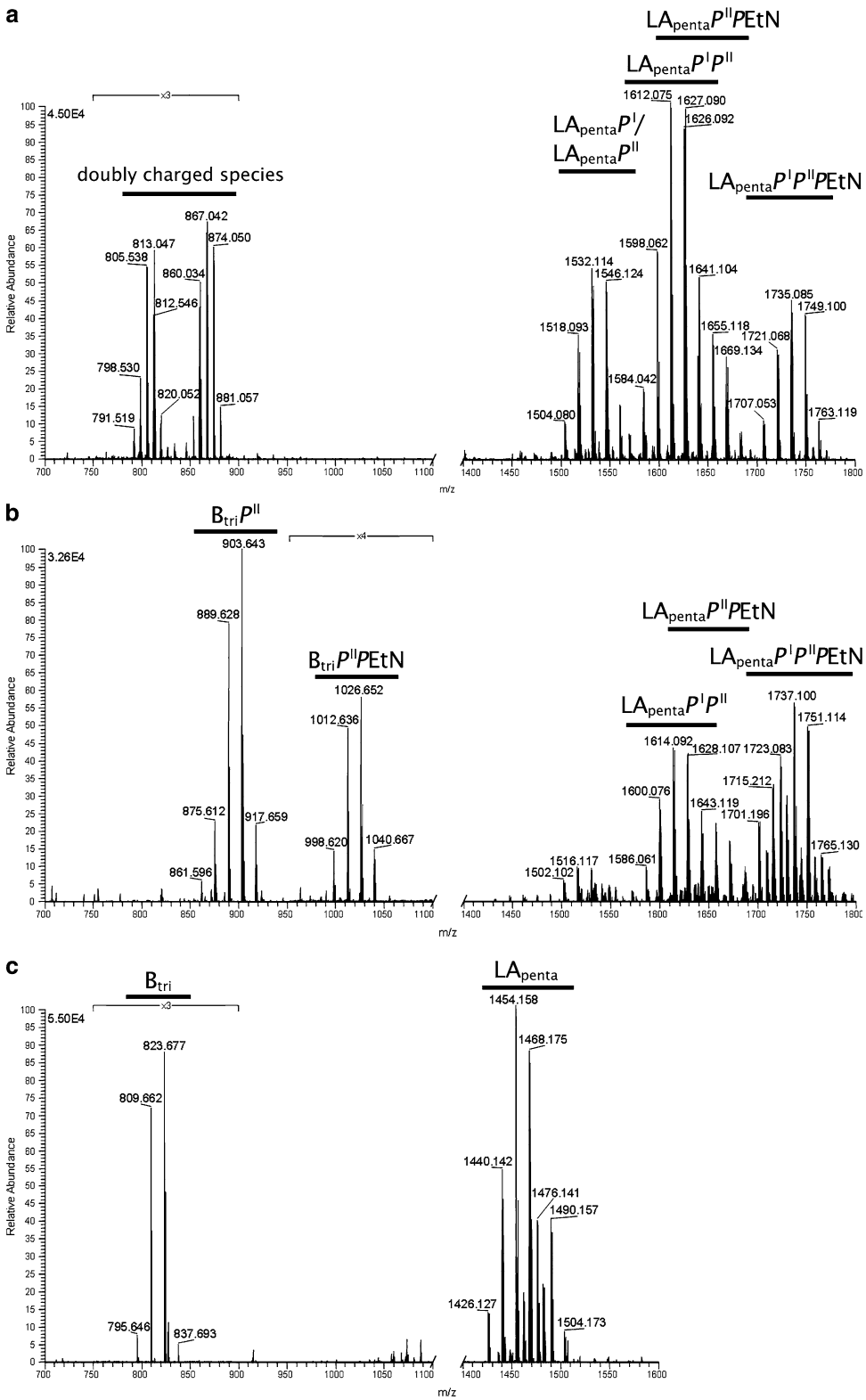

Fig. 1 ESI-FTICR mass spectra of *B. stolpii* lipid A: negative (**a**) and positive (**b**) ions, as well as the positive ions ESI-FTICR mass spectrum of dephosphorylated lipid A of *B. stolpii* (**c**)

B-ions. Fragmentation experiments of the $[M + H]^+$ signals around *m/z* 1,737.100 ($LA_{penta}P^{I}P^{II}PEtN$) resulted in the dominant formation of the corresponding B-ions (Table 2). In the positive ion spectrum of the dephosphorylated lipid A of *B. stolpii* (Fig. 1c), only two groups of ions were present: LA_{penta} (*m/z* 1,454.158) and B_{tri} (*m/z* 823.677).

An unambiguous assignment of the primary fatty acid residues linked to the amino groups at positions 2 and 3 of the two Glc*p*N3N was not possible as previously reported

Table 2 Fatty acid distributions and relative abundances of monophosphorylated B-ions (BtriP^{II}) of molecular species of lipid A of *B. stolpii*

Molecular species[a]		Relative abundances of observed monophosphorylated B-ions[b]					Fatty acid distributions[c]		
m/z $[M + H]^+$	*m/z* $[M–H]^-$	*m/z* 861.60 (%)	*m/z* 875.61 (%)	*m/z* 889.63 (%)	*m/z* 903.64 (%)	*m/z* 917.66 (%)	Secondary fatty acid bound to Glc*p*N3N^{II}	Primary fatty acids bound to Glc*p*N3N^{II}	Primary fatty acids bound to Glc*p*N3N^{I}
1709.069 (1709.069)	1707.053 (1707.053)	21	*58*	20	0	0	*iso*-13:0	3-OH *iso*-13:0	3-OH 14:0
								3-OH 14:0	3-OH 14:0
1723.083 (1723.084)	1721.068 (1721.069)	8	29	*54*	10	0	*iso*-13:0	3-OH 14:0	3-OH 14:0
								3-OH 14:0	3-OH 14:0
1737.100 (1737.100)	1735.085 (1735.084)	2	11	*49*	36	2	*iso*-13:0	3-OH 14:0	3-OH 14:0
								3-OH 14:0	3-OH *iso*-15:0
1751.114 (1751.116)	1749.100 (1749.100)	3	9	14	*62*	12	*iso*-13:0	3-OH 14:0	3-OH 14:0
								3-OH *iso*-15:0	3-OH *iso*-15:0
1765.130 (1765.131)	1763.119 (1763.116)	0	12	32	*36*	19	*iso*-13:0	3-OH 14:0	3-OH *iso*-15:0
								3-OH *iso*-15:0	3-OH *iso*-15:0

[a] Experimental and theoretical values (in *brackets*) are given

[b] Relative abundances of B-ions were estimated from MS/MS experiments of positive ions

[c] Secondary fatty acid distributions were deduced from fragmentation experiments of B-ions, primary fatty acid distributions of Glc*p*N3N^{II} were calculated from most abundant B-ions (*italics*) of the corresponding molecular species and the fatty acid distribution of Glc*p*N3N^{I} was determined from neutral losses in MS/MS experiments

[25, 26]. Nevertheless, an assignment of fatty acid residues according to accurate masses from ESI-FTICR MS measurements could be made (Table 2). In agreement with the GC–MS analyses of fatty acid methyl esters (Table 1), the two primary fatty acids bound to Glc*p*N3N^{II} were assigned from the masses of B-ions in FTICR MS experiments. Additionally, the two primary fatty acids bound to Glc*p*N3N^{I} were assigned from the determined neutral losses in MS/MS experiments, being in good agreement with the data of the chemical component analyses.

NMR Spectroscopy of *B. stolpii* Lipid A

NMR spectra of unmodified lipid A showed relative poor line resolution independent of the used solvent systems [27, 28]. In particular, solvents generally suitable for measurements of lipid A carrying phosphoethanolamine groups (*P*EtN) caused signals with relatively large line widths at half height (>10 Hz) [29, 30]. In order to circumvent this problem, the sugar moiety and the fatty acid substitution pattern have been analyzed on dephosphorylated lipid A, prepared by reaction with hydrofluoric acid. The dephosphorylation was verified by ESI-FTICR MS (Fig. 1c) and the NMR spectra have been performed in pyridine-d_5/methanol-d_4 (2:1, v/v) at 315 K with reasonable resolution. The sugar moiety of *B. stolpii* lipid A was proven to consist of two Glc*p*N3Ns with a β-(1 → 6) interglycosidic linkage. ^{1}H and ^{13}C chemical shifts of Glc*p*N3N^{II} indicated a 2,3-diamino-2,3-dideoxy glucopyranose structure, which is diacylated in positions 2 and 3 (Table 3). The $^3J_{H–H}$ coupling constants of H-2′, H-3′, H-4′ and H-5′ in Glc*p*N3N^{II} were in the range of 10–12 ppm, thus, proving the β-glucopyranose configuration. The β-anomeric conformation was assigned from the $^3J_{H1'–H2'}$ coupling constant (8.7 Hz) and the (1 → 6) interglycosidic linkage was determined by ^{13}C chemical shift of C-6 in Glc*p*N3N^{I} (Table 3). The reducing Glc*p*N3N^{I} also showed typical shifts (Table 3) and $^3J_{H–H}$ coupling constants of a 2,3-diacylated 2,3-diamino-2,3-dideoxy glucopyranose structure. Remarkable, although the anomeric position of Glc*p*N3N^{I} was dephosphorylated, over 90% of the lipid A was present in the α-anomeric form ($^3J_{H1–H2}$ = 3.2 Hz). ^{1}H and ^{13}C chemical shifts of the Glc*p*N3N^{II} (1 → 6)Glc*p*N3N^{I} sugar moiety are listed in Table 3 and spectra are shown in Fig. 2.

The integral of ca. 150 aliphatic protons in the ^{1}H spectrum indicated the presence of five fatty acids which correlated with results from GC–MS and ESI-FTICR MS. An assignment of the complete fatty acids by NMR was not possible due to overlapping signals. However, ^{1}H NMR shifts of protons in position 2, 3, and 4 of all 3-hydroxy fatty acids were assigned (Table 4). Thereby the absolute configuration of position 3 is most likely to be (*R*) in all cases, comparable to all other yet studied lipid As [31]. Integrals over the signals of the hydroxy fatty acids of the dephosphorylated lipid A indicated about 60% to be 3-hydroxy fatty acids with a free OH-group, ~20% to be 3-hydroxy fatty acids carrying a secondary fatty acid,

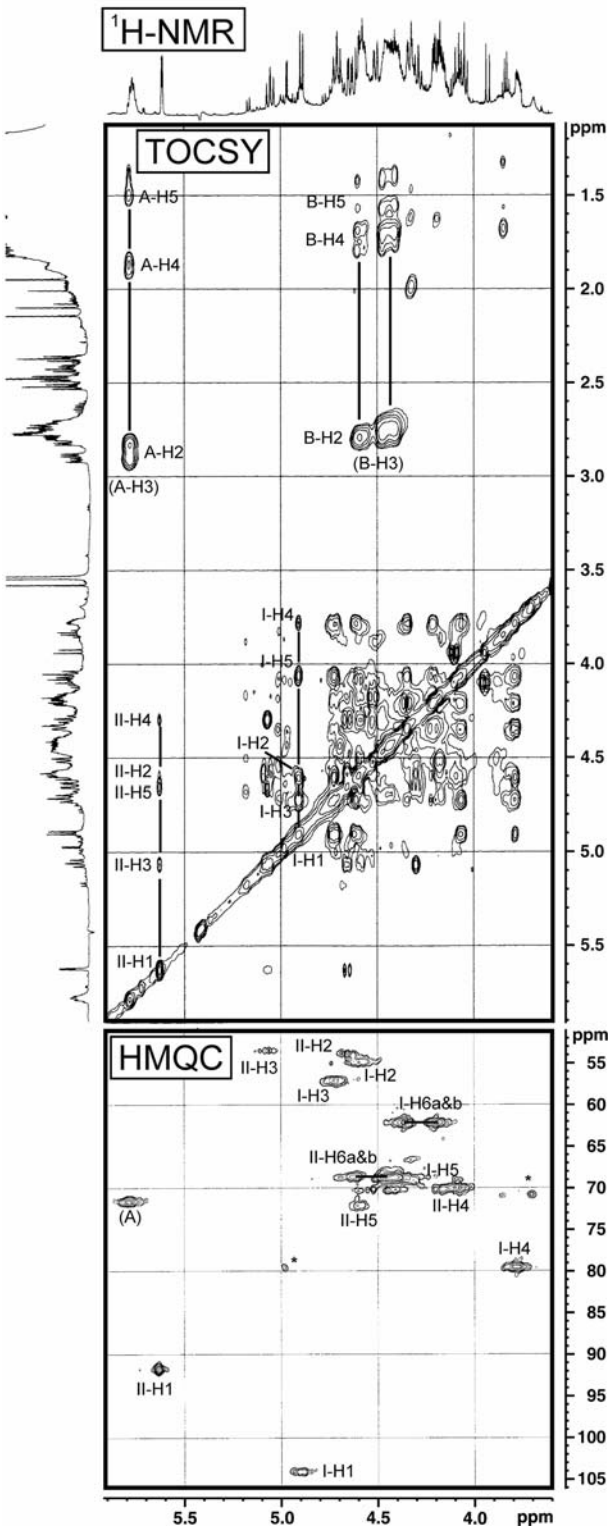

Fig. 2 Parts of ^{1}H, TOCSY, and $^{1}H/^{13}C$ HMQC spectra of dephosphorylated *B. stolpii* lipid A. Assignment of the signals are given according the common carbohydrate nomenclature (I = Glc*p*N3N^{I}; II = Glc*p*N3N^{II}). Signals of hydroxy fatty acids with acylated OH-group are indicated with "*A*" and signals of hydroxy fatty acids with free OH-group are indicated with "*B*". The according shift values are listed in Tables 3 and 4

Table 3 Proton and carbon chemical shifts of the sugar backbone of the dephosphorylated lipid A of *B. stolpii*

	H1/C1	H2/C2	H3/C3	H4/C4	H5/C5	H6a/C6	H6b
Glc*p*N3N^{I}							
δ ^{1}H (ppm)	4.89	4.59	4.72	3.79	4.08	4.21	4.36
δ ^{13}C (ppm)	104.0	54.9	57.3	79.5	70.1	62.1	
Glc*p*N3N^{II}							
δ ^{1}H (ppm)	5.63	4.62	5.07	4.32	4.59	4.62	4.44
δ ^{13}C (ppm)	91.7	54.0	53.8	68.7	72.3	68.8	

Table 4 Proton chemical shifts [δ ^{1}H (ppm)] of position 2, 3, 4, and 5 in all primary 3-hydroxy fatty acids (FA-1–FA-4) of the dephosphorylated lipid A of *B. stolpii*

	H2a/b	H3	H4a/b	H5a&b
3-OH fatty acids carrying a secondary fatty acid				
FA-1	2.91/2.81	5.78	1.87/1.83	1.52
3-OH fatty acids with free OH functionalities				
FA-2	2.71/2.70	4.58	1.79/1.70	1.43
FA-3	2.70/2.64	4.48	1.76/1.70	1.43
FA-4	2.69/2.63	4.40	1.76/1.70	1.42

and ~20% to be non-hydroxy fatty acids. This is in good agreement with the mass spectrometric results. The non-hydroxy fatty acids showed four different signal groups, which indicated variations in their conformation and configuration.

Additionally, chemical shifts of the different terminal ends of the fatty acids were determined. In branched fatty acids the CH_3 groups (ω) had $\delta_H = 0.80$ ppm and $\delta_C = 13.4$ ppm, while the neighboring CH groups ($\omega - 1$) had a $\delta_H = 1.19$ ppm and $\delta_C = 38.1$ ppm. These shifts differed from the ones of the unbranched fatty acids (CH_3 (ω): $\delta_H = 0.78$ ppm and $\delta_C = 13.2$ ppm; CH_2 ($\omega - 1$): $\delta_H = 1.44$ ppm and $\delta_C = 37.0$ ppm). Comparison of the different ^{1}H NMR signal intensities of these partly overlapping signal groups proved the nearly equal occurrence of branched and unbranched fatty acids (Table 1, Fig. 3).

1D and 2D ^{1}H spectra as well as 1D ^{31}P spectra have been recorded in $CDCl_3$/methanol-d_4 (4:1) at 305 K for further analysis of the intact lipid A. Although spectra showed a relatively poor line resolution, they allowed completion of the structure determination. The anomeric signal of Glc*p*N3N^{I}, identified in COSY had the characteristic down field shift of a phosphorylated α-anomeric form (~5.5 ppm) and the phosphate group (P^{I}, –O–PO_3H) had therefore to be located in this position (α-D-Glc*p*N3N^{I}-(1 → P^{I})). In Glc*p*N3N^{II} the positions 1, 2 and 3 were occupied by the interglycosidic linkage to Glc*p*N3N^{I} and

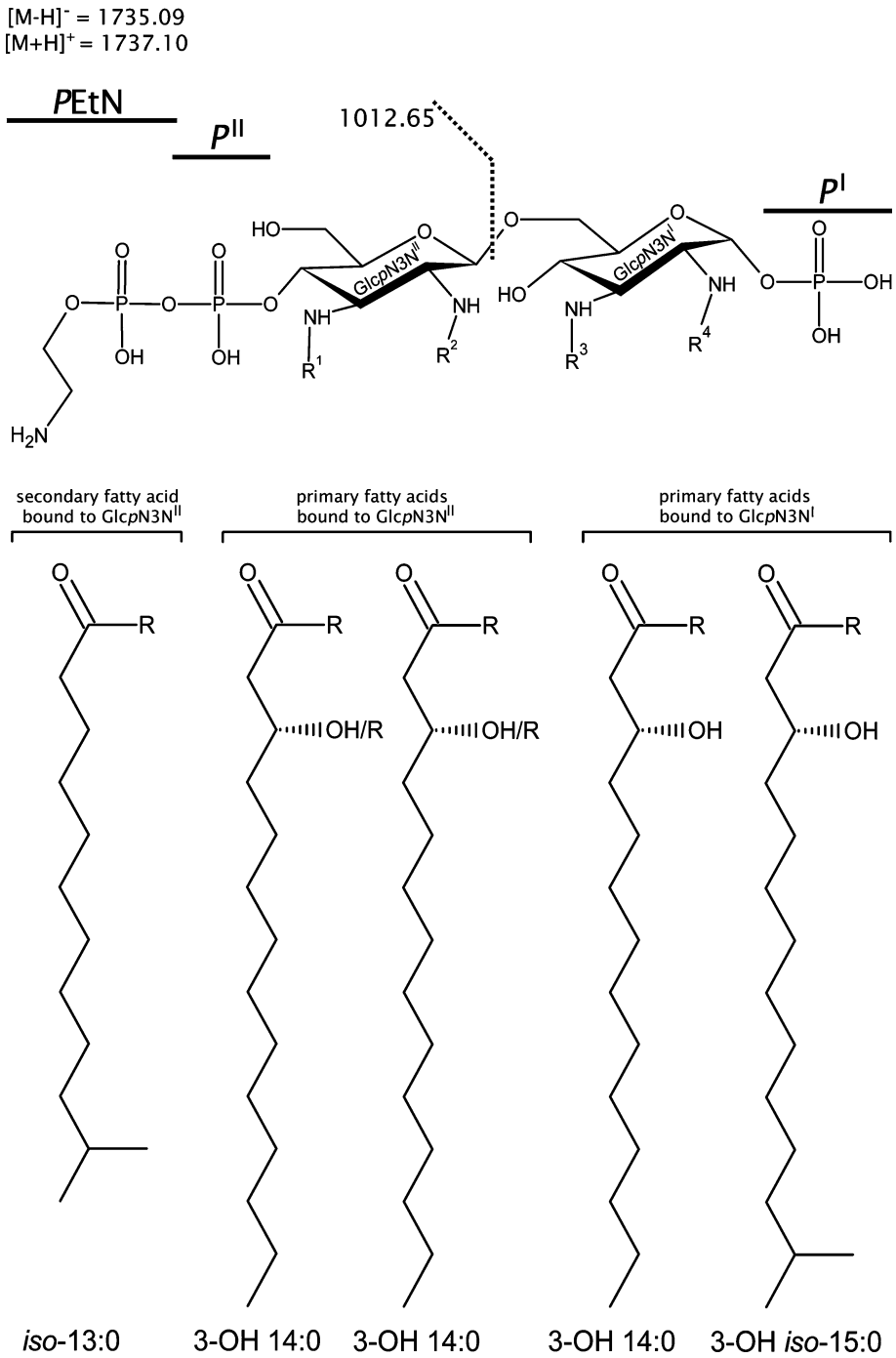

Fig. 3 Chemical structure of the lipid A of *B. stolpii*. *Upper part* structure of the backbone with two β-(1 → 6)-linked D-Glc*p*N3Ns, being substituted at C1 and C4′ with a phosphate group (P^{I}) and a pyrophosphoethanolamine (P^{II}*P*EtN) group, respectively. Corresponding *m*/*z* value for B-ion fragments in positive ionization mode is given. *Lower part* structure and distribution of the fatty acid residues. The exact position of each fatty acid residue could not be determined from the results of the analyses

by two acyl groups, respectively. A hydroxy function in position 6 represented the binding position for the O-specific chain. Thus, the remaining position 4 is carrying the two phosphate groups and the ethanolamine. ^{31}P spectra indicated these groups to be pyrophosphoethanolamine ($\delta(^{31}P)$ = ca. −10 ppm), as it has been reported in a few other lipid A structures.[23, 30, 32–34].

The resulting lipid A backbone structure was determined to (*P*EtNP^{II} → 4)-β-D-Glc*p*N3N^{II}-(1 → 6)-α-D-Glc*p*N3N^{I}-(1 → P^{I}), as shown in Fig. 3 for the species with highest molecular weight ($LA_{penta}P^{I}P^{II}$*P*EtN) observed in mass spectra (*m*/*z* 1,737.100 $[M + H]^+$ and *m*/*z* 1,735.085 $[M–H]^-$). Therein, each 2,3-diamino-2,3-dideoxy-glucopyranose is substituted with two primary 3-hydroxy fatty acids linked to the amino groups at positions 2 and 3. The non-reducing sugar (Glc*p*N3N^{II}) additionally carries a non-hydroxy secondary fatty acid linked to the 3-hydroxy group of a primary fatty acid.

Discussion

The two *B. stolpii* and *B. bacteriovorus* strains possess a S-form LPS [10]. Lipid As of both *Bdellovibrionales*, however, harbor only a few common structural features, which set them apart from most other lipid A structures. They possess β-(1 → 6)-linked 2,3-diamino-2,3-dideoxy-D-glucopyranoses in their backbone. Similar structures have been found in *Brucella*, *Rhodopseudomonas*, *Leptospira*, and *Mesorhizobium* species [35–37], while lipid A of most other Gram-negative bacteria have two β-(1 → 6)-linked 2-amino-2-deoxy-D-glucopyranoses in their backbone [38–40]. Another common feature of the two lipid As is the presence of *iso*-branched fatty acids [10], which are also rarely found in other bacteria. It remains to be determined, whether these structural features are related to the distinct biological activity of the *Bdellovibrionales* and could be important for their unique lifecycle.

The significant differences between the lipid A structures are numerous. *B. bacteriovorus* possesses the only yet isolated uncharged lipid A [10]. In contrary, the now investigated lipid A of taxonomically related *B. stolpii* has a phosphate and a *PP*EtN group in its backbone. Hence it owns several functionalities, which are able to carry negative as well as positive charges. A further difference between the lipid As is the absence of unsaturated fatty acids or dihydroxy fatty acids in *B. stolpii*. These variations coincide with genetic differences and might portend variations in their mechanisms to penetrate other bacteria [4–8].

Bacteriovorax stolpii lipid A has a strong amphiphilic character, likely caused by intermolecular ionic interactions between protonated primary amines and deprotonated phosphate functionalities. This strong tendency of forming aggregates is accompanied by a molecular dynamic between different conformations. Such chemical exchanges were indicated by weak and broad in phase EXSY cross peaks in ROESY spectra. Aggregation due to the strong amphiphilic character of *B. stolpii* lipid A and the resulting short transversal relaxation times (T_2) have hence not been the only reason for the line broadening in NMR spectra. The dynamic effects of the molecules rather cause the presence of more than one conformation in energetic minima. Disaggregation of *B. stolpii* lipid A in non-natural environments as reported for some other lipid As does hence not automatically lead to enhancement of NMR-spectral resolution [27–30].

Such molecular motion of pyrophosphoethanolamine (*PP*EtN) groups has been described to cause stability changes in the outer membrane under different environmental conditions. The possibility of having different lipid A conformations might be applied by the *B. stolpii* to change the outer membrane structure. These variations might be used to change forms from a non-predatory style to a predatory style, when necessary or possible. Hence, it is of interest to discover the *B. stolpii* lipid A structures and dynamics in membranes, in particular in dependence on the presence of other lipid A membranes. An investigation of the endotoxic potential of *B. stolpii* lipid A in different environments is also interesting in this context [41].

More analyses of other *Bdellovibrionales* (e.g. *Peredibacter* or other *Bacteriovorax*/*Bdellovibrio* species) are necessary for the assignment of conserved structures within the lipid As and LPS of predatory prokaryotes. Such studies will help to identify building blocks or conserved components of the outer membrane and will increase the understanding of the mechanisms involved in prey cell recognition and invasion. The current study resolves the second structure of an endotoxin of a predatory bacterium and confirms once again that the unique predatory lifestyle is associated with special structures.

Acknowledgments The authors gratefully acknowledge financial support by the Deutsche Forschungsgemeinschaft Grant LI309/29-1 (to F. M.).

References

1. Snyder AR, Williams HN, Baer ML, Walker KE, Stine OC (2002) 16S rDNA sequence analysis of environmental *Bdellovibrio*-and-like organisms (BALO) reveals extensive diversity. Int J Syst Evol Microbiol 52:2089–2094
2. Stolp H, Petzold H (1962) Untersuchungen über einen obligat parasitischen Mikroorganismus mit lytischer Aktivität für *Pseudomonas*-Bakterien. Phytopathol Z 45:364–390
3. Stolp H, Starr MP (1963) *Bdellovibrio bacteriovorus* gen et sp. n., a predatory, ectoparasitic, and bacteriolytic microorganism. Antonie Van Leeuwenhoek 29:217–248
4. Baer ML, Ravel J, Chun J, Hill RT, Williams HN (2000) A proposal for the reclassification of *Bdellovibrio stolpii* and *Bdellovibrio starrii* into a new genus, *Bacteriovorax* gen. nov. as *Bacteriovorax stolpii* comb. nov. and *Bacteriovorax starrii* comb. nov., respectively. Int J Syst Evol Microbiol 50(Pt 1):219–224
5. Baer ML, Ravel J, Pineiro SA, Guether-Borg D, Williams HN (2004) Reclassification of salt-water *Bdellovibrio* sp. as *Bacteriovorax marinus* sp. nov. and *Bacteriovorax litoralis* sp. nov. Int J Syst Evol Microbiol 54(Pt 4):1011–1016
6. Davidov Y, Jurkevitch E (2004) Diversity and evolution of Bdellovibrio-and-like organisms(BALOs), reclassification of *Bacteriovorax starrii* as *Peredibacter starrii* gen. nov., comb. nov., and description of the *Bacteriovorax-Peredibacter* clade as *Bacteriovoracaceae* fam. nov. Int J Syst Evol Microbiol 54(Pt 5): 1439–1452
7. Jurkevitch E, Minz D, Ramati B, Barel G (2000) Prey range characterization, ribotyping, and diversity of soil and rhizosphere *Bdellovibrio* spp isolated on phytopathogenic bacteria. Appl Environ Microbiol 66:2365–2371
8. Schwudke D, Strauch E, Krueger M, Appel B (2001) Taxonomic studies of predatory bdellovibrios based on 16S rRNA analysis, ribotyping and the hit locus and characterization of isolates from the gut of animals. Syst Appl Microbiol 24:385–394

9. Rendulic S, Jagtap P, Rosinus A, Eppinger M, Baar C, Lanz C, Keller H, Lambert C, Evans KJ, Goesmann A et al (2004) A predator unmasked: life cycle of *Bdellovibrio bacteriovorus* from a genomic perspective. Science 303:689–692
10. Schwudke D, Linscheid M, Strauch E, Appel B, Zahringer U, Moll H, Muller M, Brecker L, Gronow S, Lindner B (2003) The obligate predatory *Bdellovibrio bacteriovorus* possesses a neutral lipid A containing alpha-D-mannoses that replace phosphate residues: similarities and differences between the lipid As and the lipopolysaccharides of the wild type strain *B. bacteriovorus* HD100 and its host-independent derivative HI100. J Biol Chem 278:27502–27512
11. Diedrich DL, Denny CF, Hashimoto T, Conti SF (1970) Facultatively parasitic strain of *Bdellovibrio bacteriovorus*. J Bacteriol 101:989–996
12. Seidler RJ, Mandel M, Babtist JN (1972) Molecular heterogeneity of the bdellovibrios: evidence of two new species. J Bacteriol 109:209–217
13. Steiner S, Conti SF, Lester RL (1973) Occurrence of phosphonosphingolipids in *Bdellovibrio bacteriovorus* strain UKi2. J Bacteriol 116:1199–1211
14. Watanabe Y, Nakajima M, Hoshino T, Jayasimhulu K, Brooks EE, Kaneshiro ES (2001) A novel sphingophosphonolipid head group 1-hydroxy-2-aminoethyl phosphonate in *Bdellovibrio stolpii*. Lipids 36:513–519
15. Jayasimhulu K, Hunt SM, Kaneshiro ES, Watanabe Y, Giner J-L (2006) Detection and identification of *Bacteriovorax stolpii* UKi2 sphingophosphonolipid molecular species. J Am Soc Mass Spectrom 18:394–403
16. Beck S, Schwudke D, Appel B, Linscheid M, Strauch E (2005) Characterization of outer membrane protein fractions of *Bdellovibrionales*. FEMS Microbiol Lett 243:211–217
17. Galanos C, Luderitz O, Westphal O (1969) A new method for the extraction of R lipopolysaccharides. Eur J Biochem 9:245–249
18. Laemmli UK (1970) Cleavage of structural proteins during the 455 assembly of the head of bacteriophage T4. Nature 227:680–685
19. Tsai CM, Frasch CE (1982) A sensitive silver stain for detecting lipopolysaccharides in polyacrylamide gels. Anal Biochem 119:115–119
20. Bryn K, Jantzen E (1982) Analysis of lipopolysaccharides by methanolysis, trifluoroacetylation, and gas chromatography on a fused-silica capillary column. J Chromatogr 240:405–413
21. Gerwig GJ, Kamerling JP, Vliegenthart JF (1978) Determination of the D and L configuration of neutral monosaccharides by high-resolution capillary G.L.C. Carbohydr Res 62:349–357
22. Gerwig GJ, Kamerling JP, Vliegenthart JF (1979) Determination of the absolute configuration of mono-saccharides in complex carbohydrates by capillary G.L.C. Carbohydr Res 77:1–17
23. Raetz CRH (1990) Biochemistry of endotoxins. Annu Rev Biochem 59:129–170
24. Domon B, Costello CE (1988) A systematic nomenclature of carbohydrate fragmentation in FAB-MS/MS spectra of glycoconjugates. Glycoconj J 5:397–409
25. Sforza S, Silipo A, Molinaro A, Marchelli R, Parrilli M, Lanzetta R (2004) Determination of fatty acid positions in native lipid A by positive and negative electrospray ionization mass spectrometry. J Mass Spectrom 39:378–383
26. Corsaro MM, Piaz FD, Lanzetta R, Naldi T, Parrilli M (2004) Structure of lipid A from *Pseudomonas corrugata* by electrospray ionization quadrupole time-of-flight tandem mass spectrometry. Rapid Commun Mass Spectrom 18:853–858
27. Brecker L (2003) Nuclear magnetic resonance of lipid A—the influence of solvents on spin relaxation and spectral quality. Chem Phys Lipids 125:27–39
28. Wang Y, Hollingsworth RI (1995) A solvent system for the 479 high-resolution proton nuclear magnetic resonance spectroscopy of membrane lipids. Anal Biochem 225:242–251
29. Ribeiro AA, Zhou ZM, Raetz CRH (1999) Multi-dimensional NMR structural analyses of purified Lipid X and Lipid A (endotoxin). Magn Reson Chem 37:620–630
30. Zhou Z, Ribeiro AA, Raetz CRH (2000) High-resolution NMR spectroscopy of lipid A molecules containing 4-amino-4-deoxy-L-arabinose and phosphoethanolamine substituents. Different attachment sites on lipid A molecules from NH_4VO_3-treated *Escherichia coli* versus kdsA mutants of *Salmonella typhimurium*. J Biol Chem 275:13542–13551
31. Rietschel ET (1976) Absolute configuration of 3-hydroxy fatty acids present in lipopolysaccharides from various bacterial groups. Eur J Biochem 64:423–428
32. Touzé T, Tran AX, Hankins JV, Mengin-Lecreulx D, Trent SM (2008) Periplasmic phosphorylation of lipid A is linked to the synthesis of undecaprenyl phosphate. Mol Microbiol 67:264–277
33. Zughaier SM, Lindner B, Howe J, Garidel P, Koch MHJ, Brandenburg K, Stephens DS (2007) Physicochemical characterization and biological activity of lipooligosaccharides and lipid A from *Neisseria meningitidis*. J Endotoxin Res 13:343–357
34. Kulshin VA, Zaehringer U, Lindner B, Frasch CE, Tsai CM, Dmitriev BA, Rietschel ET (1992) Structural characterization of the lipid A component of pathogenic *Neisseria meningitidis*. J Bacteriol 174:1793–1800
35. Choma A, Sowinski P (2004) Characterization of *Mesorhizobium huakuii* lipid A containing both D-galacturonic acid and phosphate residues. Eur J Biochem 271:1310–1322
36. Que-Gewirth NL, Ribeiro AA, Kalb SR, Cotter RJ, Bulach DM, Adler B, Girons IS, Werts C, Raetz CR (2004) A methylated phosphate group and four amide-linked acyl chains in *Leptospira interrogans* lipid A. The membrane anchor of an unusual lipopolysaccharide that activates TLR2. J Biol Chem 279:25420–25429
37. Varbanets LD (1994) The endotoxins of Gram-negative bacteria: their structure and biological role. Mikrobiol Z 56:76–97
38. Alexander C, Rietschel ET (2001) Bacterial lipopolysaccharides and innate immunity. J Endotoxin Res 7:167–202
39. Rietschel ET, Kirikae T, Schade FU, Mamat U, Schmidt G, Loppnow H, Ulmer AJ, Zahringer U, Seydel U, Di Padova F et al (1994) Bacterial endotoxin: molecular relationships of structure to activity and function. FASEB J 8:217–225
40. Hase S, Rietschel ET (1976) Isolation and analysis of the lipid A backbone. Lipid A structure of lipopolysaccharides from various bacterial groups. Eur J Biochem 63:101–107
41. Rietschel ET, Brade L, Schade FU, Seydel U, Zahringer U, Mamat U, Schmidt G, Ulmer AJ, Loppnow H, Flad HD et al (1993) Bacterial endotoxins: relationship between chemical structure and biological effect. Immun Infekt 21:26–35

Lipids (2010) 45:199–208
DOI 10.1007/s11745-009-3382-7

METHODS

An Improved Method for Determining Medium- and Long-Chain FAMEs Using Gas Chromatography

Zhidong Xu · Kevin Harvey · Thomas Pavlina · Guy Dutot · Gary Zaloga · Rafat Siddiqui

Received: 24 November 2009 / Accepted: 21 December 2009 / Published online: 16 January 2010

Abstract The existing protocols for analyzing fatty acid methyl esters (FAMEs) using a one-step acetyl chloride (AC) catalyzed transesterification and extraction procedure cannot accurately determine the medium- and long-chain fatty acids simultaneously in clinical (enteral, parenteral) formulations. For example: (1) addition of AC at room temperature generates an exothermic reaction that often results in loss of sample and possible injury to the analyst; (2) certain polyunsaturated fatty acids (PUFAs) are less stable at elevated temperatures during the transesterification and contribute to the over-estimation of the C16:0 and C18:1 fatty acids; and (3) the flame-ionization detector (FID) response varies depending on the carbon chain length of the fatty acids, that consequently impacts the underestimation of medium-chain fatty acid (C6–C10) recoveries. To overcome these deficiencies and accurately determine FAMEs, we have developed an improved one-step transesterification method that employs the addition of AC in tubes kept on a dry ice bath, the transesterification at room temperature, and the data analysis using relative response factors. Using this modified protocol, we determined the fatty acid composition of lipid emulsions (Omegaven® and Lipidem®) on a Shimadzu GC2010 gas chromatography (GC) system using a capillary GC column (Zebron ZB-WAX plus, 30 m, 0.25 mm ID, 0.25 μm). Our data suggest that the improved method can be easily used to accurately determine fatty acids (C6–C24) in functional foods and lipid emulsions.

Keywords Medium-chain fatty acids · Long-chain fatty acids · Relative response factor · Lipid emulsion · Transesterification

Abbreviations

AC	Acetyl chloride
AOAC	Association of Analytical Chemists
Calc.	Calculations
Exp	Experimental
FAME	Fatty acid methyl esters
FAs	Fatty acids
FID	Flame ionization detector
GC	Gas chromatography
IS	Internal standard
PUFAs	Polyunsaturated fatty acids
REF	Relative response factor
Theo	Theoretical

Introduction

Absolute accuracy is important when analyzing the fatty acid (FA) composition of functional foods and clinical dietary formulations. Lipids in functional food and dietary

Z. Xu · K. Harvey · R. Siddiqui
Methodist Research Institute, Clarian Health,
Indiana University School of Medicine,
Indianapolis, IN 46202, USA

T. Pavlina · G. Zaloga
Baxter Healthcare Corporation, Deerfield, IL, USA

G. Dutot
Baxter SAS, Maurepas Cedex, France

R. Siddiqui
Department of Medicine, Indiana University School
of Medicine, Indianapolis, IN 46202, USA

R. Siddiqui (✉)
Cellular Biochemistry Laboratory,
Methodist Research Institute,
E504D, 1800N Capitol Ave, Indianapolis, IN 46202, USA
e-mail: rsiddiqu@clarian.org

formulations contain a wide variety of fatty acids differing in chain length, degree of unsaturation and position, and configuration of double bonds. Although a gas chromatography/mass spectrometry method has been developed to quantitatively determine C8–C26 chain length fatty acids [1], the GC analysis of FAMEs with FID remains the most frequently used method [2, 3]. The results from GC/FID are often expressed as a relative percentage of total fatty acids, which may potentially contribute to error in data interpretation [1]. The accurate quantification of FAs in biological samples depends on proper extraction, methylation of FAs into FAMEs, optimized GC run conditions and calculation of their concentration using internal and external standards [4–6].

The one-step digestion, extraction and esterification of biological samples, which is referred to as "direct transesterification," is widely used because of its simplicity, rapidity and higher accuracy [7–9]. This method has some complications. For example: addition of acetyl chloride at room temperature generates an exothermic reaction that often results in loss of sample and possible injury to the analyst; adding the acetyl chloride slowly with stirring is often cumbersome for large numbers of samples; certain polyunsaturated fatty acids are less stable at temperatures of 100 °C during the transesterification process; and the generation of molecular species that may contribute to the over-estimation of fatty acids [10]. Furthermore, the FID response varies with carbon-chain variation. The FID response is based on ionization of alkyl carbon entities, whereas the carboxyl carbon is not ionized during the combustion [11, 12]. To accurately determine FAMEs with a FID, a correction factor is normally applied based on a theoretical relative response factor ($RRF_{(Theo)}$) to compensate for the unionized carboxyl carbon [11, 13]. The widely used $RRF_{(Theo)}$ was originally calculated based on "active atom" theory without considering the instrument conditions [6, 14]. However, it has been realized that the instrument parameters, sample running conditions and the fatty acid composition in samples can influence the RRF and hence may affect the analysis [15–20].

To overcome these deficiencies and accurately determine medium- and long-chain FAMEs, we have developed an improved one-step transesterification method that employs the addition of acetyl chloride in a dry ice bath, transesterification at room temperature and data analysis using the experimental relative response factor ($RRF_{(Exp)}$) based on relative peak area ratios of the individual fatty acid to the internal standard (IS), C23:0, under optimized GC run conditions. Our data suggest that our improved protocol for FAME analysis accurately determines both medium- and long-chain fatty acids in a one-step transesterification and extraction procedure. This procedure can easily be adopted to perform an accurate FAME analysis on large numbers of clinical and research samples on a routine basis in less time and without any threat of hazards to the analyst.

Materials and Methods

Materials

Fatty acid standards, the internal standard, and FAME mixture (GLC-461A) were purchased from Nu-Chek (Nu-Chek Prep, Inc., USA). The purity of all fatty acid standards was at least 99%. Benzene (CHROMASOLV® Plus, for HPLC, ≥99.9%), hexane (CHROMASOLV®, for HPLC, ≥97.0%), chloroform (anhydrous, ≥99%), methanol (anhydrous, 99.8%) and acetyl chloride (Puriss. p.a., ≥99.0%) were purchased from Sigma–Aldrich (St Louis, MO, USA). A FocusLiner for the GC-2010 system was purchased from Supelco (Sigma–Aldrich), and a Zebron ZB-WAX plus (30 m, 0.25 mm ID, 0.25-μm film thickness) capillary GC column was purchased from Phenomenex (Torrance, CA, USA). Lipid emulsions: Lipidem® and Omegaven®, were from B. Braun Melsungen AG (Germany) and Fresenius Kabi Deutschland GmbH (Germany), respectively. The internal standard of C23:0-M (tricosanoate-methyl ester) was dissolved in the hexane solution at a concentration of 0.982 mg/ml, and the internal standard of C23:0-acid (C23:0-A) was dissolved in the methanol-benzene (4:1, v/v) solution at a concentration of 0.989 mg/ml. All fatty acid standards were flushed with N_2 and stored at −20 °C.

Instrumentation

GC chromatography was performed with a Shimadzu GC2010 chromatography system (Shimadzu Scientific Instruments, Columbia, MA, USA) equipped with an auto sampler and a flame ionization detector. Helium was used as carrier and make-up gas. The injection volume was 1 μl, which was used with a split ratio of 1:50, or alternative ratios as reported elsewhere in the text. The injection port and detector temperatures were 240 and 250 °C, respectively. The column temperature program was as follows: temperature was held at 30 °C for 2 min, increased to 180 °C at 20 °C/min, held at 180 °C for 2 min, increased to 207 °C at 4 °C/min, held at 207 °C for 3 min, increased to 220 °C at 2 °C/min, held at 220 °C for 2 min, and then increased to 240 °C at 2 °C/min before finally being held at 240 °C for 2 min.

Optimization of the One-Step Extraction Transesterification Process

Method A

A 50-μl lipid sample was placed in 10 × 130 mm Pyrex tubes (10 ml) which had Teflon-lined screw caps, and then mixed with 40 μl of the internal standard and 2 ml of methanol-benzene (4:1, v/v). A small magnetic stirring bar

was placed in each tube and, while stirring, 200 µl of acetyl chloride was slowly added over a period of 1 min. The tubes were tightly closed and subjected to transesterification at 100 °C for 1 h. The tubes were allowed to cool in an ice bath, and then 5 ml of 6% K_2CO_3 solution was added slowly to stop the reaction and neutralize the mixture. The tubes were briefly vortexed and then centrifuged at 900×*g* for 10 min (at 25 °C). The top layer was collected and transferred to a sample vial for GC analysis.

Table 1 Fatty acid standard mixture

FA	(mg/ml)	FA	(mg/ml)
C6:0	1.67	C16:1n-7	2.38
C8:0	1.77	C18:1n-9	2.38
C9:0	0.71	C18:2n-6	1.50
C10:0	1.18	C18:3n-6	2.17
C12:0	0.96	C18:3n-3	2.49
C14:0	1.15	C22:6n-3	2.30
C16:0	1.04		

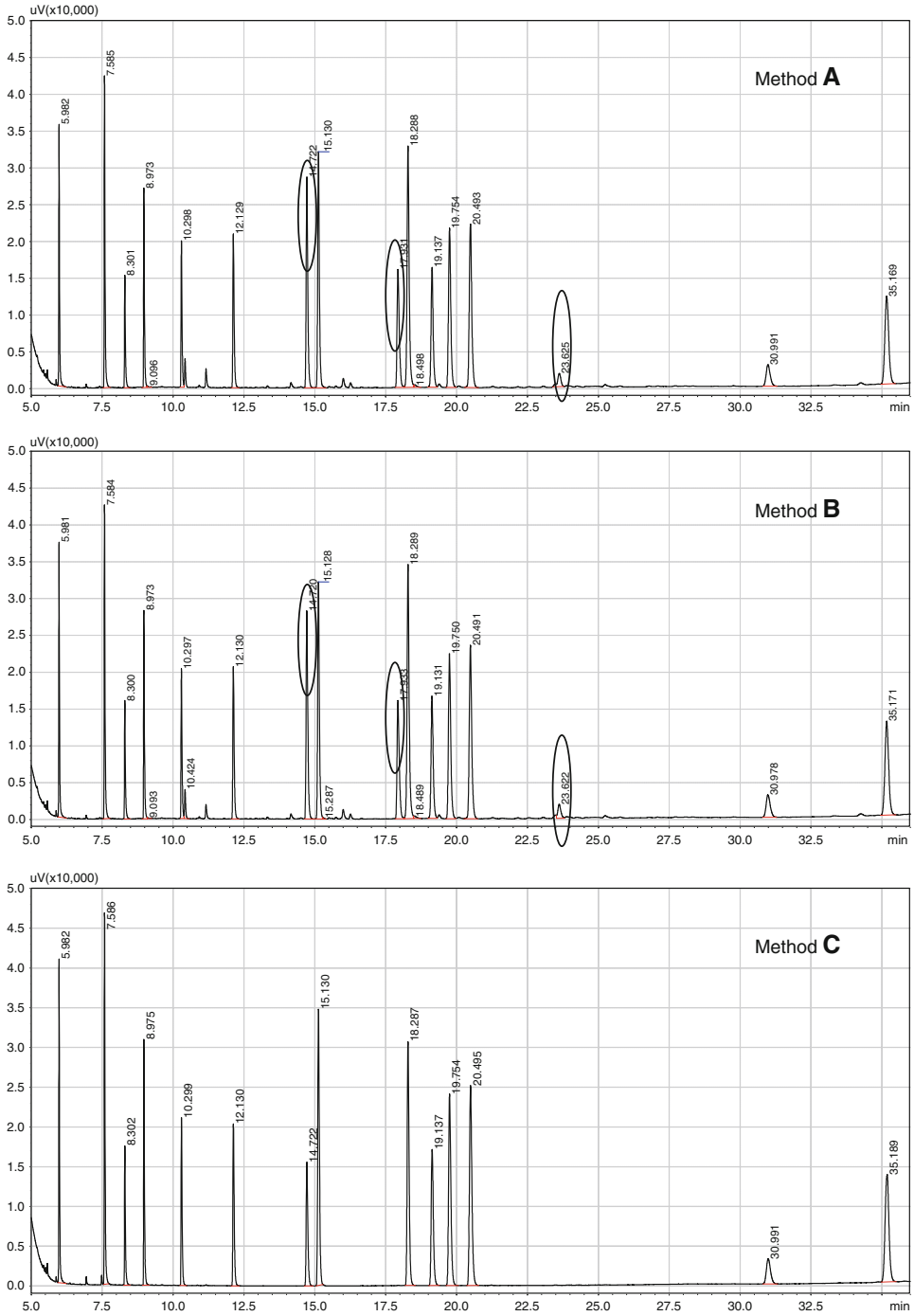

Fig. 1 Comparison of transesterification methods. Standard mixture (listed in Table 1) is used to prepare FAMEs using transesterification Methods A, B or C, as described in the text. The major extra peaks are marked by *black circles*. The GC chromatogram is a representative of three experiments performed in triplicate ($n = 9$)

Method B

A 50-µl sample of the lipid mixture was placed in 10 × 130 mm Pyrex tubes (10 ml) which had Teflon-lined screw caps, and then mixed with 40 µl of the internal standard and 2 ml of methanol-benzene (4:1, v/v). The tubes were gently vortexed, and then placed in a dry ice bath for 10 min. Then 200 µl of acetyl chloride was added to the tubes quickly; the tubes were flushed with N_2, tightly closed, and subjected to transesterification at 100 °C for 1 h. The samples were further processed as described in "Method A".

Method C

The samples were prepared and acetyl chloride was added to each tube as described in "Method B". The tubes were then kept in the dark at room temperature for 24 h. The samples were further processed as described in "Method A".

Data Quantification

The concentration of individual fatty acids ($C_{(GC)}$) were calculated using the expression $C_{(GC)} = A_{(FA)}/A_{(IS)} \times C_{(IS)}$, where $A_{(FA)}$ is the GC peak area of the fatty acid whose concentration is to be determined, $A_{(IS)}$ is the GC peak area of the internal standard, and $C_{(IS)}$ is the concentration (mg/ml) of the internal standard.

Determination of the Relative Response Factor

Theoretical Relative Response Factor

Theoretical relative response factor for each fatty acid (C6–C24) relative to the C23:0 internal standard was calculated according to the active carbon theory [12].

Experimental Relative Response Factor

For determining the $RRF_{(Exp)}$, 130 µl of the GLC-461A reference standard in hexane was mixed with 20 µl of internal standard (C23:0-M; 0.982 mg/ml in hexane) and subjected to the GC analysis. The ratio of the fatty acid to the internal standard, and the instrument parameters, were as indicated elsewhere in the text. Each experiment was done in triplicate. The relative response factor was calculated based on the equation: $RF = C_{(Theo)}/C_{(GC)}$, where $C_{(Theo)}$ is the concentration of the fatty acid based on its weighed amount, and $C_{(GC)}$ is the concentration of the fatty acid calculated based on the GC peak area and internal standard (C23:0) concentration.

Results and Discussion

Optimization of GC Parameters

Based on the recommendations proposed in the official method of the association of analytical chemists (AOAC) [21], we employed C23:0-M as the internal standard, and a wax-type capillary gas chromatograph column to perform the fatty acid analysis. We initially compared the GC analysis of fatty acids with the splitless and split injection modes, using different inlet liners (including no wool, wool-packed, gooseneck and FocusLiner). Our results (not shown) demonstrated that GC analysis with split injection at 250 °C using a FocusLiner inlet yields optimal fatty acid resolution. Most of the analyses were performed using a 1:50 split ratio based on optimization described below.

Optimization of a One-Step Transesterification

In order to develop a safe, simple and highly reproducible transesterification method for accurately determining FA concentrations for routine analysis, we modified and optimized the original Lepage and Roy one-step transesterification method [8, 9]. A standard mixture containing C6 to C22 fatty acids, as shown in Table 1, was used to optimize the transesterification using three different approaches, referred to as Methods A, B and C. "Method A" is the original Lepage and Roy method wherein the addition of acetyl chloride for transesterification is usually done very

Table 2 Recovery of fatty acids using different transesterification methods

FA	$RRF_{(Exp)}$	Method A %, mean ± SD	Method B %, mean ± SD	Method C %, mean ± SD
C6:0	1.44	94.1 ± 1.4	92.2 ± 2.7	100.4 ± 2.3
C8:0	1.20	91.6 ± 2.0	90.1 ± 2.9	97.4 ± 2.4
C9:0	1.19	93.4 ± 1.8	92.3 ± 2.6	97.7 ± 2.2
C10:0	1.16	93.1 ± 1.9	92.0 ± 2.8	98.5 ± 2.2
C12:0	1.15	94.8 ± 1.6	93.9 ± 3.6	99.8 ± 2.1
C14:0	1.14	104.4 ± 3.9	105.4 ± 4.3	104.2 ± 2.5
C16:0	1.12	151.1 ± 38.8	168.8 ± 19.6	105.3 ± 3.6
C16:1n-7	1.12	99.1 ± 0.7	98.1 ± 2.3	103.1 ± 2.4
C18:1n-9	1.07	110.3 ± 14.8	114.6 ± 8.4	101.2 ± 2.8
C18:2n-6	1.07	97.9 ± 0.6	97.5 ± 2.5	102.0 ± 2.2
C18:3n-6	1.07	97.3 ± 1.7	96.5 ± 2.3	102.2 ± 2.2
C18:3n-3	1.08	95.9 ± 1.5	95.3 ± 2.4	100.8 ± 2.2
C22:6n-3	1.16	94.1 ± 2.5	93.0 ± 2.4	100.1 ± 2.1

The concentration of the fatty acid was calculated based on the internal standard peak area and corrected with $RRF_{(Exp)}$, as describe in the text. The recovery was calculated by formula $[C_{(Exp)}/C_{(Theo)} \times 100]$

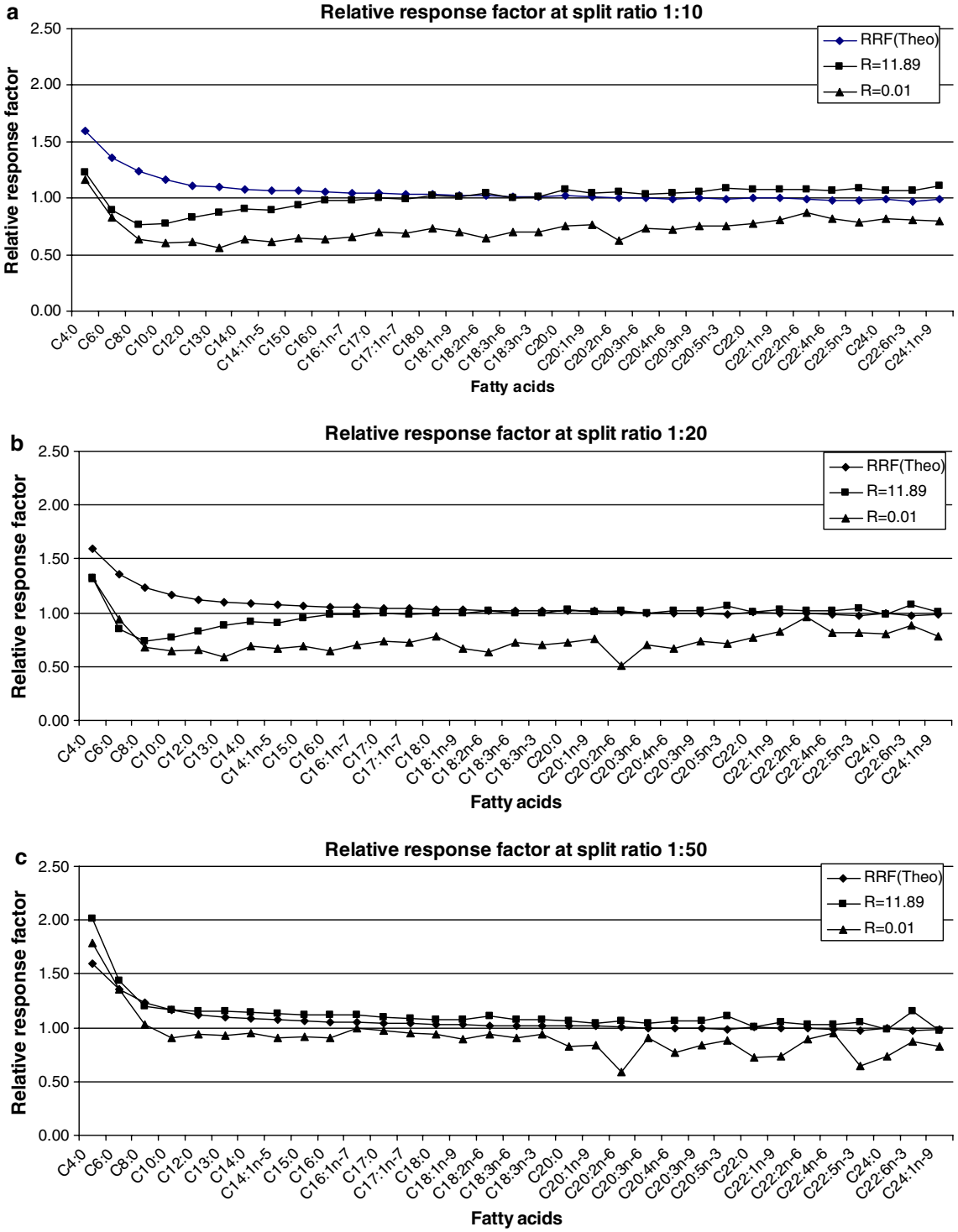

Fig. 2 Effect of injector split ratio on the relative response factor in the presence of variable fatty acid-to-internal standard ($FA_{(Sample)}/FA_{(IS)}$) ratio. Fatty acid-methyl esters from GLC-461A standard mixture (FA_{sample}) and C23:0-M (FA_{IS}) internal standard (0.982 mg/ml) was prepared in hexane to obtained variable (0.01–11.86) $FA_{(Sample)}/FA_{(IS)}$ ratios (*R*) as shown in Table 3. Each mixture ($FA_{(Sample)}/FA_{(IS)}$) was applied for GC analysis using an injector split ratio of **a** 1:10, **b** 1:20, or **c** 1:50, while keeping all other GC run parameters conditions constant. The curves representing the lowest (0.01) and the highest (11.89) *R* are shown for simplicity. All other curves (data not shown) fall within the lowest and the highest *R* curves. Each *point* represents a mean of three experiments

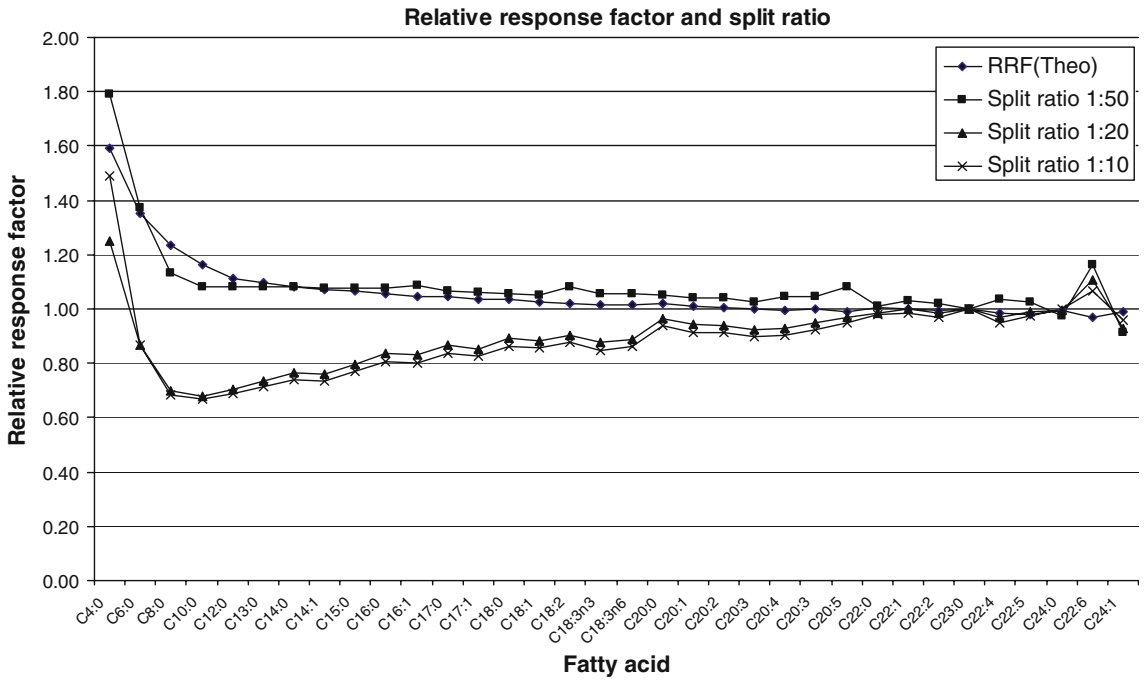

Fig. 3 Effect of injector split ratio on the relative response factor in the presence of a fixed fatty acid-to-internal standard ($FA_{(Sample)}$/$FA_{(IS)}$) ratio. The GLC-461A standard mixture and internal standard (C23:0-M, 0.982 mg/ml) was prepared in hexane to obtained a fixed (0.44) $FA_{(Sample)}/FA_{(IS)}$ ratio. Samples were run using a split ratio of 1:5, 1:10, 1:20, or 1:50, while keeping all other GC run parameters constant. Each *point* represents a mean of three experiments

carefully and slowly to avoid an exothermic reaction. This is usually done while the reaction contents are kept stirring, which takes approximately 1 min to complete. The exothermic nature of the reaction sometimes results in loss of sample because of the splatter, and may also pose a threat of possible injury to the analyst. This procedure is not only cumbersome when a large number of samples are to be analyzed, but transesterification using "Method A" also resulted in the formation of extra peaks, as shown in Fig. 1a. We therefore modified the method and incubated the tubes for transesterification on a dry ice bath for 10 min prior to adding acetyl chloride ("Method B"). The results shown in Fig. 1b also resulted in the formation of extra peaks, as in "Method A". We further modified the procedure, and in "Method C", after adding acetyl chloride in the reaction mixture on a dry bath, the transesterification was performed at room temperature for 24 h. Results shown in Fig. 1c clearly indicate that the extra peaks were no longer present on the chromatogram. These results suggest that the extra peaks may have resulted from side reactions at an elevated temperature. The recoveries of the individual fatty acids using Methods A, B, or C are shown in Table 2. The data demonstrate that the presence of extra peaks induced by transmethylation at 100 °C (Methods A and B) interfere with the estimation of fatty acids, and resulted in overestimation of particularly C16:0 and C18:1n-9. Comparing the data from Methods A and B, it appears that there are no significant differences between acetyl chloride added at room temperature or at low temperature; however, addition of acetyl chloride at low temperature avoids the need of its dropwise addition and constant stirring. We also evaluated the effect of the amount of water present (1–5%) in the transesterification reaction using "Method C". Our results demonstrate that the water content (up to 5% in the transesterification) does not significantly affect fatty acid analysis of the standard mixture or biological samples (data not shown).

Relative Response Factor

Accurate determination of fatty acid concentration by GC using FID not only depends on the optimized extraction/transesterification and instrument parameters, but is also contingent on the signal response of the FID detector to FAMEs of different composition. The early pioneer work by Ackman and Sipos [12], and Bannon [13], proposed using a theoretical relative response factor ($RRF_{(Theo)}$), based on the ionized carbon atoms, to correct the FID response to FAMEs of different composition. We realized from the previously published results [16–20], and also from our preliminary analysis, that the RRF for different FAMEs can be varied depending upon the GC run conditions, and therefore may cause an error in the determination of fatty acid concentrations in a given sample. The data shown in Fig. 2 indicates that when the $FA_{(Sample)}$:$FA_{(IS)}$ is varied, there was a variation in $RRF_{(Exp)}$, and this variation

Table 3 Relative response factor ($RRF_{(Exp)}$) with variable $FA_{(Sample)}/FA_{(IS)}$ ratios at a split ratio 1:50

FA	$RRF_{(Theo)}$	$FA_{(Sample)}/FA_{(IS)}$										
		11.89	5.95	2.97	1.49	0.74	0.37	0.19	0.09	0.05	0.02	0.01
		$RRF_{(Exp)}$										
C4:0	1.59	2.01	2.02	2.04	2.09	2.03	2.03	2.10	1.99	1.92	1.73	1.79
C6:0	1.35	1.44	1.43	1.44	1.43	1.40	1.40	1.40	1.35	1.34	1.23	1.36
C8:0	1.23	1.20	1.19	1.20	1.17	1.12	1.10	1.07	1.05	1.02	0.93	1.03
C10:0	1.16	1.16	1.15	1.16	1.15	1.11	1.03	0.99	0.98	0.96	0.90	0.91
C12:0	1.11	1.15	1.14	1.15	1.16	1.13	1.05	0.99	0.96	0.95	0.89	0.94
C13:0	1.10	1.15	1.15	1.16	1.17	1.14	1.05	0.99	0.94	0.90	0.80	0.93
C14:0	1.08	1.14	1.13	1.14	1.16	1.14	1.06	1.01	0.99	0.96	0.91	0.95
C14:1n-5	1.07	1.13	1.13	1.14	1.15	1.14	1.06	1.02	0.97	0.95	0.90	0.91
C15:0	1.07	1.12	1.12	1.13	1.15	1.14	1.06	1.02	0.98	0.95	0.91	0.92
C16:0	1.05	1.12	1.11	1.12	1.14	1.14	1.06	1.02	0.96	0.93	0.88	0.90
C16:1n-7	1.05	1.12	1.12	1.13	1.15	1.15	1.07	1.03	0.98	0.96	0.86	1.00
C17:0	1.04	1.10	1.09	1.10	1.12	1.12	1.06	1.02	0.98	0.94	0.89	0.97
C17:1n-7	1.04	1.09	1.08	1.09	1.11	1.12	1.05	1.01	0.96	0.96	0.89	0.95
C18:0	1.03	1.07	1.07	1.08	1.09	1.10	1.04	1.00	0.97	0.96	0.90	0.94
C18:1n-9	1.03	1.07	1.07	1.08	1.09	1.10	1.03	1.00	0.94	0.90	0.81	0.89
C18:2n-6	1.02	1.11	1.10	1.11	1.12	1.13	1.06	1.00	0.95	0.94	0.79	0.94
C18:3n-6	1.01	1.08	1.07	1.08	1.09	1.10	1.03	1.00	0.94	0.93	0.90	0.91
C18:3n-3	1.01	1.08	1.07	1.08	1.09	1.10	1.04	1.00	0.96	0.94	0.87	0.94
C20:0	1.02	1.06	1.06	1.07	1.06	1.05	1.02	0.99	0.93	0.90	0.84	0.83
C20:1n-9	1.01	1.04	1.04	1.05	1.06	1.07	1.02	0.99	0.94	0.90	0.90	0.84
C20:2n-6	1.01	1.06	1.05	1.06	1.05	1.07	0.99	0.95	0.87	0.80	0.74	0.59
C20:3n-6	1.00	1.04	1.03	1.04	1.04	1.06	1.01	0.98	0.94	0.89	0.86	0.90
C20:4n-6	0.99	1.06	1.05	1.06	1.06	1.08	1.01	0.99	0.93	0.89	0.80	0.77
C20:3n-9	1.00	1.06	1.05	1.06	1.06	1.08	1.03	0.98	0.93	0.91	0.80	0.84
C20:5n-3	0.99	1.11	1.10	1.11	1.11	1.12	1.06	1.01	0.96	0.94	0.83	0.88
C22:0	1.01	1.01	1.01	1.02	1.02	0.99	0.97	0.93	0.90	0.85	0.82	0.72
C22:1n-9	1.00	1.05	1.04	1.05	1.04	1.05	0.99	0.96	0.90	0.86	0.84	0.74
C22:2n-6	0.99	1.03	1.02	1.03	1.03	1.05	1.00	0.97	0.93	0.90	0.89	0.89
C23:0	1.00	1.00	1.00	1.00	1.00	1.00	1.00	1.00	1.00	1.00	1.00	1.00
C22:4n-6	0.98	1.03	1.02	1.03	1.04	1.06	1.00	1.00	0.98	0.95	0.95	0.95
C22:5n-6	0.98	1.05	1.04	1.05	1.05	1.06	1.00	0.95	0.90	0.85	0.79	0.64
C24:0	0.99	0.98	0.97	0.98	0.98	0.96	0.95	0.91	0.89	0.86	0.83	0.73
C22:6n-3	0.97	1.15	1.15	1.16	1.15	1.18	1.07	1.02	0.97	0.89	0.88	0.87
C24:1n-9	0.99	0.97	0.94	0.95	0.96	0.95	0.91	0.88	0.83	0.82	0.79	0.83

in $RRF_{(Exp)}$ was also influenced by the split ratio used for injection (Fig. 2a–c). It is obvious from these results that there are differences between $RRF_{(Exp)}$ and $RRF_{(Theo)}$ values, which are more pronounced for medium-chain FAs, and become smaller as the carbon-chain length increases. The effect of injection split ratios on $RRF_{(Exp)}$ was also determined using a fixed (0.44) fatty acid to internal standard ($FA_{(Sample)}/FA_{(IS)}$) ratio. The data reported in Fig. 3 indicate that as the split ratio increases, the $RRF_{(Exp)}$ value becomes closer to that of $RRF_{(Theo)}$. Data from Figs. 2 and 3 demonstrated that the optimal $RRF_{(Exp)}$ could be obtained when a split ratio of 1:50 was used; however, the $RRF_{(Exp)}$ was still influenced by the $FA_{(Sample)}$:$FA_{(IS)}$ ratio. We therefore determined $RRF_{(Exp)}$ over a wide range of $FA_{(Sample)}$:$FA_{(IS)}$ ratios for each fatty acid. The data presented in Table 3 indicate that as the $FA_{(Sample)}$:$FA_{(IS)}$ ratio varied, the RRF is also varied. Short- to medium-chain fatty acids (C4–C10), in particular, have much variation between $RRF_{(Theo)}$ and $RRF_{(Exp)}$, and may have potential for underestimation when only the $RRF_{(Theo)}$ is used to calculate their concentration. Based on these results, we suggest the GC analyst should first determine the $RRF_{(Exp)}$

value under optimum GC run conditions for each fatty acid, and should use the $RRF_{(Exp)}$ closest to the $FA_{(Sample)}$:$FA_{(IS)}$ ratio for accurately computing each FA concentration.

Comparison of Methods for Data Calculation

Different approaches are used to quantify fatty acid compositions from the GC chromatograph. The concentration calculation based on the internal standard concentration and peak area offers reasonably accurate values, particularly for long-chain saturated and unsaturated fatty acids; but, this method would not give an accurate concentration for medium-chain fatty acids. One way to overcome this problem is to use multiple internal standards for FAs of different carbon chain lengths [6, 22, 23]. These data can be further corrected using a $RRF_{(Theo)}$ to get an estimation of fatty acid concentrations, including those of the medium-chain fatty acids. However, we realized that if an accurate estimation of short- to long-chain fatty acids is desired in a given sample, and accuracy is the ultimate priority, then concentrations corrected with a $RRF_{(Exp)}$ and/or calculated with an external standard curve combined with the using of internal standard would be superior to calculating FA concentrations, as described above. We, therefore, compared FA data analysis methods inclusive of: Calc. I Fatty acid concentration calculated based on internal standard and peak area; Calc. II Fatty acid concentration calculated with Calc. I and corrected with the theoretical RRF; Calc. III Fatty acid concentration calculated with Calc. I and corrected with the experimental RRF; and Calc. IV Fatty acid concentration calculated based on the internal standard and external standard curves. Data representing fatty acid recovery were calculated with the four data calculation methods (shown in Table 4). The data indicate that Calc. III and IV calculations produced similar results, which are the most consistent relative to the theoretical concentration of fatty acids.

Total Fatty Acid Analysis of Two Lipid Emulsions

Based on our current data, we suggest that our modification of a one-step transesterification process ("Method C") and use of Calc. III ($RRF_{(Exp)}$ instead of $RRF_{(Theo)}$) would yield a superior analysis of FAs. In order to confirm our data, we used two known lipid emulsions. Omegaven® contains 10% lipids as triglycerides enriched in n-3 PUFAs, whereas Lipidem® contains 20% lipids as triglycerides enriched in medium-chain fatty acids. Using these emulsion we further evaluated Methods A, B and C for transesterification. Fatty acid concentrations were calculated based on Calc. III, using $RRF_{(Exp)}$ obtained from Table 3 according to the $FA_{(Sample)}$:$FA_{(IS)}$ ratio of the samples. From the data presented in Table 5, we found that transesterification using Methods A and B resulted in a higher C16:0, C18:0 and C18:1n-9 concentration than that using "Method C". The "Method C" also produced a better recovery of n-3 PUFA. These results further confirmed that transesterification at 100 °C produces extra peaks that interfere with the estimation of some fatty acids. Furthermore, heating during transesterification also resulted in loss of the PUFAs, particularly C20:5n-3 and C22:6n-3.

In conclusion, an improved protocol collectively using "Method C" for a one-step transesterification and $RRF_{(Exp)}$ for data analysis accurately determined both medium- and long-chain fatty acids in commercial lipid emulsion

Table 4 Comparison of calculation methods for fatty acid recovery

FA	Calc. I	Calc. II		Calc. III		Calc. IV
	%, mean ± SD	$RRF_{(Theo)}$	%, mean ± SD	$RRF_{(Exp)}$	%, mean ± SD	%, mean ± SD
C6:0	69.7 ± 2.3	1.35	94.4 ± 2.3	1.44	100.4 ± 2.3	99.6 ± 2.8
C8:0	81.2 ± 2.4	1.23	100.2 ± 2.4	1.20	97.4 ± 2.4	97.3 ± 3.2
C9:0	82.1 ± 2.2	1.19	97.5 ± 2.2	1.19	97.7 ± 2.2	98.7 ± 2.3
C10:0	84.9 ± 2.2	1.16	98.8 ± 2.2	1.16	98.5 ± 2.2	98.3 ± 3.3
C12:0	86.7 ± 2.1	1.12	96.7 ± 2.1	1.15	99.8 ± 2.1	98.9 ± 3.2
C14:0	91.4 ± 2.5	1.08	98.7 ± 2.5	1.14	104.2 ± 2.5	103.0 ± 3.4
C16:0	94.0 ± 3.6	1.06	99.2 ± 3.6	1.12	105.3 ± 3.6	104.2 ± 3.7
C16:1n-7	92.1 ± 2.4	1.05	96.4 ± 2.4	1.12	103.1 ± 2.4	105.2 ± 3.3
C18:1n-9	94.6 ± 2.8	1.03	97.2 ± 2.8	1.07	101.2 ± 2.8	100.9 ± 3.2
C18:2n-6	95.4 ± 2.2	1.02	97.4 ± 2.2	1.07	102.0 ± 2.2	101.2 ± 3.1
C18:3n-6	95.6 ± 2.2	1.01	96.9 ± 2.2	1.07	102.2 ± 2.2	102.7 ± 3.2
C18:3n-3	93.3 ± 2.2	1.01	94.6 ± 2.2	1.08	100.8 ± 2.2	102.1 ± 3.0
C22:6n-3	86.3 ± 2.1	0.97	83.9 ± 2.1	1.16	100.1 ± 2.1	101.2 ± 2.9

Fatty acid mixture was transesterified using "Method C", and run at a split ratio of 1:50

Table 5 Total fatty acid analysis of Omegaven and Lipidem

Emulsion	Omegaven			Lipidem		
Method (mg/ml)	A Mean ± SD	B Mean ± SD	C Mean ± SD	A Mean ± SD	B Mean ± SD	C Mean ± SD
C6:0	0.22 ± 0.01	0.23 ± 0.01	0.16 ± 0.01	0.32 ± 0.00	0.34 ± 0.03	0.27 ± 0.00
C8:0	–	–	–	49.75 ± 1.25	49.55 ± 2.74	50.45 ± 0.36
C10:0	–	–	–	34.98 ± 0.84	34.87 ± 1.83	35.25 ± 0.31
C12:0	0.09 ± 0.01	0.10 ± 0.01	0.08 ± 0.00	0.28 ± 0.01	0.28 ± 0.02	0.25 ± 0.02
C14:0	4.48 ± 0.39	4.56 ± 0.29	4.25 ± 0.01	0.76 ± 0.03	0.53 ± 0.29	0.18 ± 0.01
C15:0	0.36 ± 0.05	0.36 ± 0.04	0.32 ± 0.00	–	–	–
C16:0	14.41 ± 3.64	14.69 ± 3.23	10.95 ± 0.09	17.85 ± 0.55	15.33 ± 2.91	11.04 ± 0.13
C16:1n-7	7.00 ± 0.11	7.19 ± 0.14	7.08 ± 0.01	0.54 ± 0.00	0.45 ± 0.08	0.34 ± 0.01
C16:2n-4	1.48 ± 0.38	1.47 ± 0.34	0.92 ± 0.02	0.71 ± 0.02	0.40 ± 0.31	0.06 ± 0.02
C17:0	0.42 ± 0.17	0.43 ± 0.15	0.27 ± 0.01	0.37 ± 0.02	0.28 ± 0.14	0.10 ± 0.00
C16:3n-4	0.85 ± 0.19	0.86 ± 0.21	0.81 ± 0.02	0.03 ± 0.00	0.03 ± 0.00	0.03 ± 0.00
C17:1n-7	0.22 ± 0.12	0.25 ± 0.13	0.28 ± 0.01	0.08 ± 0.00	0.07 ± 0.01	0.05 ± 0.00
C16:4n-1	1.70 ± 0.01	0.65 ± 0.92	1.80 ± 0.01	–	–	–
C18:0	8.33 ± 5.46	8.31 ± 5.05	2.58 ± 0.16	14.68 ± 0.50	10.97 ± 5.07	4.57 ± 0.17
C18:1n-9	11.08 ± 2.12	11.35 ± 1.88	9.46 ± 0.10	21.57 ± 0.68	20.29 ± 0.97	18.34 ± 0.14
C18:1n-7	3.03 ± 0.32	2.98 ± 0.23	2.75 ± 0.05	2.48 ± 0.56	2.24 ± 0.21	1.72 ± 0.04
C18:2n-6	2.73 ± 0.11	2.81 ± 0.06	2.75 ± 0.01	41.34 ± 0.96	41.40 ± 2.04	41.76 ± 0.32
C18:3n-3	1.18 ± 0.06	1.18 ± 0.03	1.15 ± 0.06	4.85 ± 0.08	4.84 ± 0.21	4.84 ± 0.05
C18:4n-3	4.34 ± 0.07	4.40 ± 0.04	4.50 ± 0.02	0.39 ± 0.01	0.36 ± 0.02	0.32 ± 0.01
C20:0	–	–	–	0.36 ± 0.02	0.32 ± 0.03	0.26 ± 0.01
C20:1n-11	0.26 ± 0.06	0.26 ± 0.04	0.22 ± 0.01	0.14 ± 0.02	0.11 ± 0.03	0.05 ± 0.00
C20:1n-9	1.09 ± 0.03	1.11 ± 0.01	1.10 ± 0.01	0.41 ± 0.04	0.41 ± 0.03	0.38 ± 0.01
C20:1n-7	0.18 ± 0.07	0.17 ± 0.05	0.11 ± 0.00	–	–	–
C20:4n-6	1.66 ± 0.16	1.67 ± 0.11	1.60 ± 0.05	0.90 ± 0.04	0.79 ± 0.07	0.66 ± 0.00
C20:4n-3	0.91 ± 0.04	0.91 ± 0.06	0.99 ± 0.02	0.20 ± 0.01	0.21 ± 0.03	0.24 ± 0.01
C20:5n-3	18.85 ± 0.08	19.23 ± 0.38	19.94 ± 0.10	5.59 ± 0.13	5.63 ± 0.30	5.50 ± 0.06
C22:0	–	–	–	0.36 ± 0.01	0.35 ± 0.01	0.29 ± 0.00
C22:1n-11	1.01 ± 0.09	0.99 ± 0.02	0.97 ± 0.02	0.28 ± 0.02	0.30 ± 0.02	0.28 ± 0.02
C22:1n-9	0.18 ± 0.03	0.17 ± 0.02	0.17 ± 0.02	0.07 ± 0.01	0.06 ± 0.02	0.05 ± 0.01
C21:5n-3	0.65 ± 0.01	0.65 ± 0.02	0.67 ± 0.00	0.25 ± 0.02	0.27 ± 0.02	0.26 ± 0.00
C22:4n-6	0.14 ± 0.02	0.17 ± 0.00	0.17 ± 0.01	0.05 ± 0.01	0.06 ± 0.02	0.08 ± 0.00
C22:5n-6	0.39 ± 0.02	0.42 ± 0.00	0.40 ± 0.00	0.17 ± 0.02	0.18 ± 0.01	0.18 ± 0.00
C22:5n-3	2.09 ± 0.18	2.13 ± 0.14	2.02 ± 0.01	1.10 ± 0.06	0.98 ± 0.10	0.83 ± 0.01
C24:0	–	–	–	0.09 ± 0.00	0.09 ± 0.01	0.08 ± 0.01
C22:6n-3	18.38 ± 0.15	18.69 ± 0.39	19.52 ± 0.12	4.22 ± 0.11	4.26 ± 0.28	4.39 ± 0.02
Total	110.16 ± 14.15	110.83 ± 14.00	100.47 ± 0.96	207.63 ± 6.03	198.69 ± 17.86	185.58 ± 1.75

The lipid emulsions were analyzed at a split ratio of 1:50. The concentration of the fatty acid was calculated based on the internal standard peak area, and subsequently corrected with the $RRF_{(Exp)}$

samples. Transesterification with Methods A and B resulted in higher C16:0 and C18:1n-9 concentrations than using "Method C", due to side reactions. Furthermore, "Method C" also produced a better recovery of n-3 polyunsaturated fatty acids (EPA and DHA). This procedure can be easily adopted for analyzing large quantities of lipid samples for routine analysis in less time and without any threat of hazards imparted to the analyst.

Acknowledgments The work presented in this manuscript is supported by a grant from Baxter Healthcare Corporation. Deerfield, IL 60015, USA.

References

1. Lagerstedt SA, Hinrichs DR, Batt SM, Magera MJ, Rinaldo P, McConnell JP (2001) Quantitative determination of plasma

C8–C26 total fatty acids for the biochemical diagnosis of nutritional and metabolic disorders. Mol Genet Metab 73:38–45
2. Eder K (1995) Gas chromatographic analysis of fatty acid methyl esters. J Chromatogr B Biomed Appl 671:113–131
3. Shantha NC, Napolitano GE (1992) Gas chromatography of fatty acids. J Chromatogr 624:37–51
4. Nota G, Naviglio D, Romano R, Sabia V, Musso S (1998) Evaluation and improvement of transesterification methods of triglycerides. Anal Lett 31:2499–2512
5. Holman RT, Johnson SB, Mercuri O, Itarte HJ, Rodrigo MA, De Tomas ME (1981) Essential fatty acid deficiency in malnourished children. Am J Clin Nutr 34:1534–1539
6. Schreiner M (2005) Quantification of long chain polyunsaturated fatty acids by gas chromatography. Evaluation of factors affecting accuracy. J Chromatogr A 1095:126–130
7. Masood A, Stark KD, Salem N Jr (2005) A simplified and efficient method for the analysis of fatty acid methyl esters suitable for large clinical studies. J Lipid Res 46:2299–2305
8. Lepage G, Roy CC (1984) Improved recovery of fatty acid through direct transesterification without prior extraction or purification. J Lipid Res 25:1391–1396
9. Lepage G, Roy CC (1986) Direct transesterification of all classes of lipids in a one-step reaction. J Lipid Res 27:114–120
10. Fournier V, Destaillats F, Juaneda P, Dionisis F, Lambelet P, Sebedio JL et al (2006) Thermal degradation of long-chain polyunsaturated fatty acids during deodorization of fish oil. Eur J Lipid Sci Technol 108:33–42
11. Ulberth F, Gabernig RG, Schrammel F (1999) Flame-ionization detector response to methyl, ethyl, propyl, and butyl esters of fatty acids. J Am Oil Chem Soc 76:263–266
12. Ackman RG, Sipos JC (1964) Application of specific response factors in the gas-chromatographic analysis of methyl esters of fatty acids with flame ionization detectors. J Am Oil Chem Soc 41:377–380
13. Bannon CD, Craske JD, Hilliker AE (1986) Analysis of fatty acid methyl esters with high accuracy and reliability. V. Validation of theoretical relative response factors of unsaturated esters in the flame ionization detector. J Am Chem Soc 63:105–110
14. Ulberth F, Schrammel F (1995) Accurate quantitation of short-, medium-, and long-chain fatty acid methyl esters by split-injection capillary gas-liquid chromatography. J Chromatogr A 704:455–463
15. Olsson U, Kaufman P, Herslof BG (1990) Multivariate optimization of a gas–liquid chromatographic analysis of fatty acid methyl esters of blackcurrant seed oil. J Chromatogr 505:385–394
16. Eder K, Reichlmayr-Lais AM, Kirchgessner M (1991) Gas chromatographic analysis of fatty acid methyl esters: avoiding discrimination by programmed temperature vaporizing injection. J Chromatogr 588:265–272
17. Albertyn DE, Bannon CD, Craske JD, Hai NT, O'Rourke KL, Szonyi C (1982) Analysis of fatty acid methyl esters with high accuracy and reliability. I. Optimization of flame-ionization detectors with respect to linearity. J Chromatogr 247:47–61
18. Bannon CD, Craske JD, Felder DL, Garland IJ, Norman LM (1987) Analysis of fatty acid methyl esters with high accuracy and reliability. VI. Rapid analysis by split injection capillary gas–liquid chromatography. J Chromatogr 407:231–241
19. Schreiner M, Hulan HW (2004) Determination of the carbon deficiency in the flame ionization detector response of long-chain fatty acid methyl esters and dicarboxylic acid dimethyl esters. J Chromatogr A 1045:197–202
20. Slemr J, Slemr F, D'Souza H, Partridge R (2004) Study of the relative response factors of various gas chromatograph-flame ionisation detector systems for measurement of C2–C9 hydrocarbons in air. J Chromatogr A 1061:75–84
21. Cunniff P (1995) AOAC official method 991.04 DDT in technical products and pesticide formulations. AOAC International, Gaithersburg
22. Armenta RE, Scott SD, Burga AM, Radianingtyas H, Barrow CJ (2009) Optimization of fatty acid determination in selected fish and microalgal oils. Chromatographia 70:629–636
23. Sonnichsen M, Muller BW (1999) A rapid and quantitative method for total fatty acid analysis of fungi and other biological samples. Lipids 34:1347–1349

Lipids (2010) 45:209–224
DOI 10.1007/s11745-010-3391-6

REVIEW

Elevated Production of Docosahexaenoic Acid in Females: Potential Molecular Mechanisms

Alex P. Kitson · Chad K. Stroud · Ken D. Stark

Received: 8 September 2009 / Accepted: 15 January 2010 / Published online: 12 February 2010

Abstract Observational evidence suggests that in populations consuming low levels of n-3 highly unsaturated fatty acids, women have higher blood levels of docosahexaenoic acid (DHA; 22:3n-6) as compared with men. Increased conversion of alpha-linolenic acid (ALA; 18:3n-3) to DHA by females has been confirmed in fatty acid stable isotope studies. This difference in conversion appears to be associated with estrogen and some evidence indicates that the expression of enzymes involved in synthesis of DHA from ALA, including desaturases and elongases, is elevated in females. An estrogen-associated effect may be mediated by peroxisome proliferator activated receptor-α (PPARα), as activation of this nuclear receptor increases the expression of these enzymes. However, because estrogens are weak ligands for PPARα, estrogen-mediated increases in PPARα activity likely occur through an indirect mechanism involving membrane-bound estrogen receptors and estrogen-sensitive G-proteins. The protein kinases activated by these receptors phosphorylate and increase the activity of PPARα, as well as phospholipase A_2 and cyclooxygenase 2 that increase the intracellular concentration of PPARα ligands. This review will outline current knowledge regarding elevated DHA production in females, as well as highlight interactions between estrogen signaling and PPARα activity that may mediate this effect.

A. P. Kitson · C. K. Stroud · K. D. Stark (✉)
Laboratory of Nutritional and Nutraceutical Research, Department of Kinesiology, University of Waterloo, Waterloo, ON N2L 3G1, Canada
e-mail: kstark@uwaterloo.ca

Keywords Estrogen · Sex · Eicosapentaenoic acid · Alpha-linolenic acid · Conversion · PPARα · Phosphorylation · Nuclear receptors · Ligand · Transcription

Abbreviations

ALA	Alpha-linoleic acid
AMPK	AMP-activated protein kinase
Ca^{2+}-PLA_2	Calcium-dependent phospholipase A_2
CE	Cholesteryl esters
COX	Cyclooxygenase
CREB	cAMP response element binding
D5D	Delta-5 desaturase
D6D	Delta-6 desaturase
DHA	Docosahexaenoic acid
DPAn-3	Docosapentaenoic acid, n-3
ELOVL	Elongase of very long chain fatty acids
EPA	Eicosapentaenoic acid
ER	Estrogen receptor
ERK-MAPK	Extracellular receptor kinase-mitogen activated protein kinase
FABP	Fatty acid binding proteins
GPR30	G-protein receptor 30
HUFA	Highly unsaturated fatty acids
LNA	Linoleic acid
MAPK	Mitogen-activated protein kinase
PC	Phosphatidyl choline
PE	Phosphatidyl ethanolamine
PL	Phospholipids
PLA_2	Phospholipase A_2
PPAR	Peroxisome proliferator activated receptor
PPRE	Peroxisome proliferator response element
PS	Phosphatidyl serine
PUFA	Polyunsaturated fatty acids

Introduction

The dietary intake and blood content of omega-3 polyunsaturated fatty acids (n-3 PUFA, ≥18 carbons, ≥2 double bonds), particularly the highly unsaturated fatty acids (HUFA, ≥20 carbons, ≥3 carbon–carbon, double bonds) eicosapentaenoic acid (EPA, 20:5n-3) and docosahexaenoic acid (DHA, 22:3n-3), are associated with a reduced risk of sudden cardiac death when incorporated into cardiac membranes as phospholipids or free fatty acids [1–4]. Also, the incorporation of DHA into brain phospholipids is associated with improved neurological development [5] and performance on spatial tasks [6]. EPA and DHA can either be obtained directly from the diet or produced within the body from dietary precursors such as alpha-linolenic acid (ALA, 18:3n-3). As reviewed recently, it appears that in humans, increasing ALA intakes can significantly increase levels of EPA and n-3 docosapentaenoic acid (DPAn-3), but not DHA in various blood measures [7]. However, even limited production of EPA, DPAn-3 and DHA from dietary ALA may be clinically relevant. The anti-arrhythmic benefit of EPA and DHA is estimated to have a very steep dose–response curve that plateaus at an EPA + DHA consumption of 750 mg/day [8], much higher than the estimated North American intakes of EPA + DHA of approximately 100 mg/day [9–12]. It has recently been suggested that 250–500 mg/day of EPA + DHA should be established as a dietary reference intake [13]. Therefore, even a small contribution to tissue EPA and DHA through ALA conversion could have a significant impact on sudden cardiac death risk reduction.

Dietary ALA intakes are inversely associated with sudden cardiac death in women [14] but not in men [15] in North American populations. North American intakes of ALA are approximately 1,500 mg/day [9–12]. Increased ALA conversion to EPA and DHA has been observed in women consuming <200 mg EPA + DHA/day as compared with men and women consuming >500 mg EPA + DHA/day [16, 17] and may partially explain the inverse association with sudden cardiac death. Increased conversion of ALA to DHA [16, 18, 19] and higher levels of DHA in various lipid fractions of liver, erythrocytes, plasma and whole blood [16, 20–24] have been observed in females consuming typical Western diets as compared with males.

An increased capacity to biosynthesize DHA in women is possibly an evolutionary adaptation to attempt to provide a supply of DHA for maternal–fetal transport during the fetal brain growth spurt [7, 12, 25]. Observational results suggest that pregnant women undergo metabolic adaptations to maintain DHA in blood for placental transport [12, 26–28]. Changes in n-3 HUFA have also been associated with both endogenous and exogenous changes in circulating estrogen [21, 29–32], however, the potential mechanisms for this enhanced biosynthesis has not been elucidated.

The biosynthesis of DHA is mediated by elongases and desaturases in the endoplasmic reticulum and acyl-CoA oxidase and multifunctional protein 2 in the peroxisome. Estrogen-response elements have not been associated with the genes of any of these enzymes to date despite our efforts (unpublished observations). This is despite the fact that estrogen response elements are well characterized [33] and can be identified using a variety of tools. Peroxisome-proliferator receptor α (PPARα), a nuclear receptor that increases the expression of desaturases [34, 35] is a potential target for an estrogen mediated effect, but it also lacks an estrogen response element [36]. However, PPARα activity may be increased by indirect estrogen mediated phosphorylation. Several of the protein kinase systems activated by membrane-bound estrogen receptors, including mitogen-activated protein kinase (MAPK) and protein kinase A, phosphorylate and increase the activity of PPARα [37–39]. We presently review evidence supporting sex differences in the conversion of ALA to DHA and suggest a potential mechanism involving interaction between PPARα and estrogen signaling.

Dietary Sources of DHA

Preformed DHA

Blood levels of DHA are strongly correlated with the dietary intake of DHA [40]. In North America, salmon is a dominant source of dietary EPA and DHA due to its high popularity (ranked 4th in consumption frequency among marine foods after shrimp, tuna and breaded fish, respectively), and a high content of EPA and DHA [8, 9, 41]. Salmon provides 1,100–2,100 mg EPA + DHA/100 g as compared with 130–860 mg from tuna, 320–550 mg from shrimp, and 0–210 mg from breaded fish (per 100 g cooked) [42]. Alternative sources that can provide significant amounts of dietary n-3 HUFA include fish oil capsules and novel EPA and DHA enriched functional foods [43, 44]. All these strategies are largely dependent on fish stocks and fish-farming practices that may not be sustainable [45]. Non-fish sources of preformed dietary DHA include fat extraction from species of microalgae such as *Crypthecodinium cohnii* and *Schizochytrium* [46, 47]. The production of DHA by microalgae varies with some species relying on alternating desaturases and elongases while others utilize polyketide synthase systems [48, 49]. There are ongoing efforts to develop genetically modified organisms capable of producing n-3 HUFA [50, 51].

Dietary Precursors of DHA

The primary dietary precursor of long chain n-3 PUFA that is consumed in North America is ALA, which is found in a variety of plant foods and oils, particularly in flaxseed oil. Canola and soybean oil also contain significant amounts of ALA, but also typically contain relatively higher amounts of linoleic acid (LNA, 18:2n-6). Supplementing with relatively low levels of dietary ALA (2.4 g ALA/day in flaxseed oil) can increase erythrocyte EPA [52] with higher doses of ALA resulting in further increases in blood levels of EPA and DPAn-3, but often not DHA as reviewed extensively [7]. There is no evidence that ALA interventions result in increased DHA in blood, however these studies have been done predominantly with males only [52–55] or with mixed sex groups without specific sex group analyses [56–59]. Recently, we demonstrated that DHA levels in free living females was significantly higher than free living males, and that increases in DHA status is much slower than changes in EPA with fish oil supplementation [24]. Therefore, acute intervention studies may not be appropriate to detect DHA biosynthesis and accumulation in human blood. There are some longer ALA intervention studies that suggest DHA blood measures may possibly increase (for example, 52 weeks) [60]. It is also important to note that blood measures of EPA, DPAn-3, and DHA may only reflect hepatic ALA conversion, while there is evidence suggesting tissue specific ALA conversion with brain capable of synthesizing DHA from ALA, while the heart appears to only convert ALA to EPA and DPAn-3 [61].

Mammalian DHA Biosynthesis

The discovery that dietary ALA was the precursor of DHA was made in 1950 by Widmer and Holman [62] by feeding fat-deficient rats isolated ALA and observing the tissue deposition of DHA. Klenk and Mohrhauer [63] later elucidated the pathway of DHA formation from ALA to be: 18:3n-3 → 18:4n-3 → 20:4n-3 → 20:5n-3 → 22:5n-3 → 22:6n-3. It was then determined that the pathway took place in the endoplasmic reticulum [64]. Testing of the assumption that a delta-4 desaturase was responsible for the conversion of 22:5n-3 into 22:6n-3 revealed no microsomal formation of 22:6n-3, but rather two novel fatty acids were microsomally produced: 24:5n-3 and 24:6n-3 [65]. It was later determined that 22:6n-3 was formed by peroxisomal β-oxidation of the microsomally produced 24:6n-3 (Fig. 1) [66].

The first enzyme in the conversion of ALA to longer chain n-3 HUFA is delta-6 desaturase (D6D) [67]. D6D catalyzes the desaturation of both n-6 and n-3 PUFA, and also appears to act on both 18- and 24-carbon PUFA, representing a significant metabolic "bottle-neck" [68]. A D6D knockout mouse has been demonstrated to lack the ability to make arachidonic acid (20:4n-6) from LNA and to lack the ability to make docosapentaenoic acid (22:5n-6) from dietary arachidonic acid [69]. In addition, the competition between ALA and 24:5n-3 for D6D results in EPA accumulation and limited synthesis and accumulation of DHA in Hep-G2 phospholipids [70]. As a result, the expression and activity of D6D, and substrate competition are considered primary determinants of DHA production rate. However, the large induction of both D6D and delta-5 desaturase (D5D), but not elongases, observed in HepG2 cells in response to essential fatty acid deficiency suggests that HUFA production is dependent on the concentration of both of these enzymes [71]. Additionally, these two genes are located only 11 kb apart on chromosome 11 in humans (chromosome 19 in mice) in a head-to-head orientation, suggesting that the transcription of these two genes may be regulated similarly [67]. A thorough review of the desaturases is available [67].

Sex Differences in DHA Status and Metabolism

Several studies have observed sex differences in blood and tissue DHA content in humans and rats (summarized in Table 1). While consuming a habitual diet, women possess significantly higher levels of DHA in total plasma lipids, as well as plasma non-esterified fatty acids, triacylglycerols, and phosphatidyl choline [23]. Sex specific responses to fish-oil supplementation have been observed including higher levels of DHA in erythrocytes and whole blood at baseline and after 8 weeks washout post-supplementation in women as compared with men [24]. Also, female sex has been significantly associated with increased DHA in studies examining various lifestyle and physiological parameters on fingertip prick whole blood in Italians [72] and serum phospholipids and cholesteryl esters in New Zealanders [22]. Higher levels of DHA in the blood of women as compared with men could be the result of differences in DHA mobilization and partitioning, dietary intake and male–female differences in body mass rather than differences in biosynthesis. However, increased ALA to DHA conversion rates in women relative to men have been determined using fatty acid stable isotope tracer studies [16, 18, 19].

The net fractional conversion of an orally ingested bolus of $U^{13}C$-ALA into EPA and DHA in women capable of bearing children has been observed to be approximately 21 and 9.1%, respectively [18] as compared with conversion rates in men of 7.9% for EPA and DHA production that was undetectable by the investigators means [19]. In these

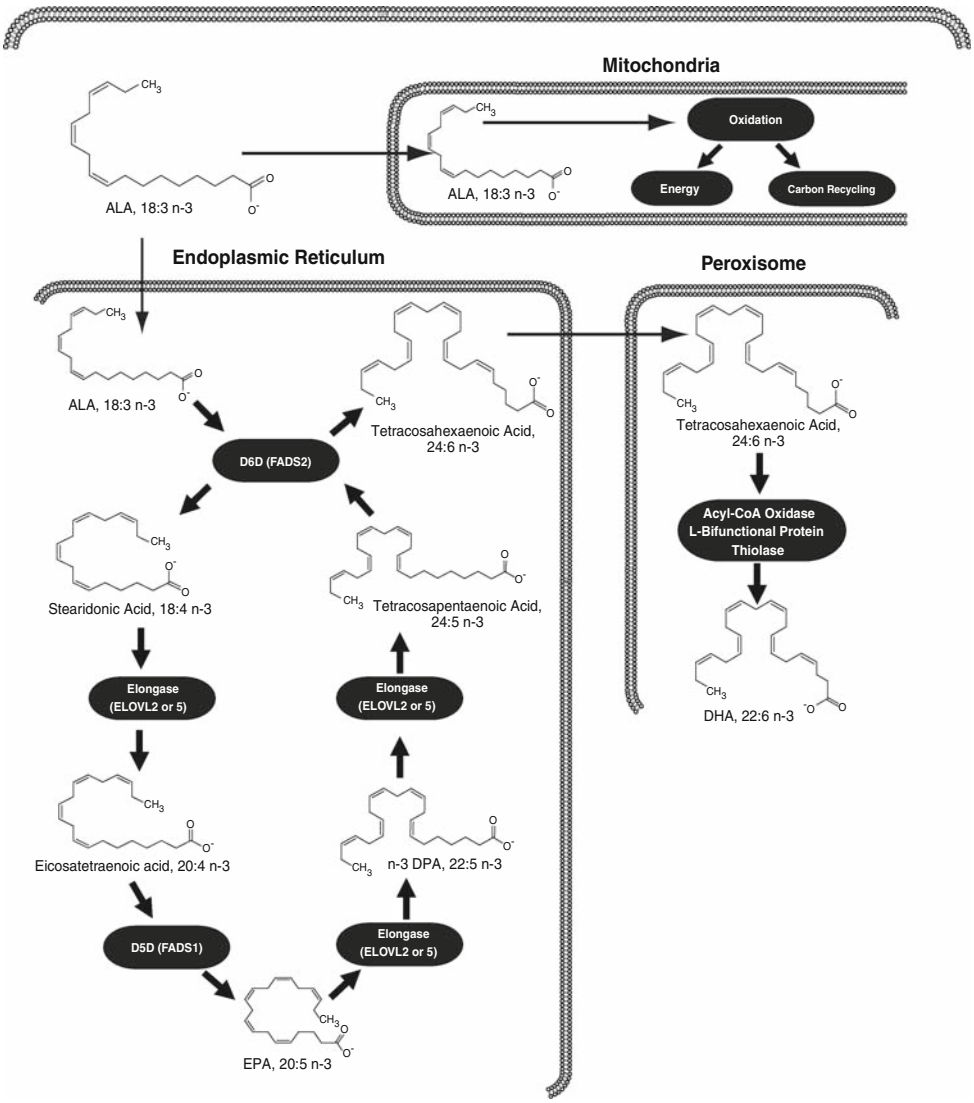

Fig. 1 Two main metabolic fates of alpha-linolenic acid: conversion to longer-chain n-3 polyunsaturated fatty acids in the endoplasmic reticulum and peroxisomes, and mitochondrial oxidation. *ALA* alpha-linolenic acid, *D6D* delta-6 desaturase, *FADS* fatty acid desaturase, *ELOVL* elongase of very long chain fatty acids, *EPA* eicosapentaenoic acid, *D5D* delta-5 desaturase, *DPA* docosapentaenoic acid, *DHA* docosahexaenoic acid

studies, ^{13}C-EPA and DHA primarily appeared in plasma phosphatidyl choline. Labelled U^{13}C-DHA has also been detected in plasma triacylglycerol and phospholipid fractions in women (no men comparison group) after treatment with dietary U^{13}C-ALA [73]. Compartmentalized modeling of ^{2}H-ALA metabolism through examining ^{2}H-HUFA appearance in plasma total lipids has isolated the sex difference to the conversion of labeled 22:5n-3 to labeled 22:6n-3, and that this sex difference was present only when participants consumed a beef-based diet low in n-3 HUFA and not a fish-based diet [16, 17]. Additionally, there may be increased partitioning of ALA towards DHA synthesis in women, as oxidation and carbon-recycling of ALA into saturated and monounsaturated fatty acids are much lower as compared with men [18, 19, 74]. In animal models, elevated DHA has also been observed in the liver phosphatidyl choline and phosphatidyl ethanolamine of mature female relative to male rats [20] and feeding male rats a high-ALA diet containing no EPA or DHA results in elevated liver and heart phospholipid EPA and DPAn-3, but not DHA [75].

In a model of dietary n-3 repletion, increased hepatic expression of D5D and D6D was observed in female rats as compared with male rats that corresponded to higher D5D protein content [76]. An increased expression of D5D only [20] and no differences in D5D and D6D [77] have also been reported. We have observed increased D5D and D6D mRNA expression in females as compared with males at 14 week of age on a standard chow diet (Kitson and Stark, unpublished observations). These results tend to suggest a greater capacity for DHA biosynthesis in females as compared with males. Sexual maturity may contribute to some of the disparity in these studies but this has not been elucidated.

Age may influence DHA accumulation [78]. There are reports of an association between age and DHA levels in

Table 1 Summary of studies investigating sex differences in DHA content or metabolism

Author [references]	Number of subjects	Dietary fatty acid treatment	Results
Rat studies			
Burdge et al. [20]	Wistar, male and female ($n = 24$ for each)	Maternal = 5.9 g ALA/kg diet	Increased DHA in PC and PE (% total fatty acids) in females
		Lactation/weaning = 0.7 g ALA/kg diet	Increased hepatic D5D expression in females.
Extier et al. [76]	Wistar male and female ($n = 6$ for each sex/time point)	Maternal = 0.05 g ALA/kg diet.	Increased DHA in plasma PC and liver PC, PS, and PE in females
		Weanling = 0.2 mg ALA/kg diet.	Increased D5D and D6D and lower PPARα and FABP7 hepatic expression in females
			Increased hepatic D5D protein content in females
			No DHA or gene expression differences in cerebral cortex
Childs et al. [77]	Wistar male and female ($n = 6$ for each sex/diet group)	Low soybean = 1.6 g ALA/kg diet	Increased DHA in plasma PC, liver PC and PE in females in all diets
		High fat soybean = 9.1 g ALA/kg diet	No differences in gene expression
		High fat linseed = 50.2 g ALA/kg diet	
Human studies			
Burdge and Wooton [18]	Women ($n = 6$)	Habitual	Fractional appearance of ^{13}C-labelled fatty acids in plasma was ALA: 63.7%, EPA: 21.1%, n-3 DPA: 5.9%, DHA: 9.2%.
		700 mg of [U-^{13}C] ALA administered	^{13}C recovered in breath was 22.2% of dose.
Burdge et al. [19]	Men ($n = 6$)	Habitual	Fractional appearance of ^{13}C-labelled fatty acids in plasma was ALA: 84%, EPA: 7.9%, n-3 DPA: 8.1%, DHA: n.d.
		700 mg of [U-^{13}C] ALA administered	^{13}C recovered in breath was 33.2% of dose
Pawlosky et al. [16, 17]	Men ($n = 5$)	Ad libitum	Increased conversion of 22:5n-3 to DHA in females within beef-based diet
	Women ($n = 5$)	Fish-based	
		Beef-based	
Giltay et al. [21]	Men ($n = 72$)	Controlled diet, free from fish	Increased DHA in serum CE in females
	Women ($n = 103$)		
Bakewell et al. [23]	Men ($n = 13$)	Habitual intakes	Increased DHA in plasma TG, NEFA, PC, and total lipids in females
	Women ($n = 23$)		
Crowe et al. [22]	Men ($n = 1,246$)	Habitual intakes	Increased DHA in serum PL and CE in females
	Women ($n = 1,547$)		Increased EPA in PL and CE and increased n-3 DPA in PL in men
Marangoni et al. [72]	Men ($n = 47$)	Habitual intakes	Increased n-3 DPA in whole blood in males
	Women ($n = 61$)		
Metherel et al. [24]	Men ($n = 10$)	Baseline habitual diet	Increased DHA and decreased n-3 DPA in whole blood and erythrocytes of females at baseline.
	Women ($n = 10$)	4 week supplementation of 4.8 g/day of EPA + DHA,	Increased DHA:EPA ratio in women in various blood fractions disappeared with supplementation
		8-week washout on habitual diet	

ALA alpha-linolenic acid, *PC* phosphatidyl choline, *PE* phosphatidyl ethanolamine, *D5D* delta-5 desaturase, *D6D* delta-6 desaturase, *DHA* docosahexaenoic acid, *CE* cholesteryl esters, *PL* phospholipids, *EPA* eicosapentaenoic acid, *DPA* docosapentaenoic acid, *PS* phosphatidyl serine, *FABP* fatty acid binding protein, *PPAR* peroxisome proliferators activated receptor, *n.d.* not detected

adult human blood. Although dietary intake of DHA is a potential confounder, age was positively associated with DHA in plasma phospholipids [79, 80], serum phospholipids and cholesteryl esters [22], plasma total lipids [40] and erythrocytes [40, 81] after controlling for DHA intakes. However, no differences in DHA content between subjects over 75 years of age and control subjects between 20 and 48 years of age were observed in plasma phospholipids,

non-esterified fatty acids, triacylglycerides, cholesteryl esters, and erythrocytes [82]. To our knowledge, a direct examination of the effect of age and sex on biosynthesis and accumulation of DHA has not been completed.

Role of Estrogen in DHA Biosynthesis

Sex differences in DHA levels appear to be mediated by circulating sex hormones, particularly estrogen (studies investigating hormone status or hormone manipulations, and DHA are summarized in Table 2). Elevated DHA content of female blood is possibly an evolutionary adaptation meant to provide fetal tissues with sufficient DHA for neural development. During pregnancy, the concentration of DHA in maternal blood is significantly elevated in the third trimester, when circulating levels of estrogen are highest [12, 26, 83]. Presumably, this increase in maternal DHA supports the fetal brain growth spurt in the third trimester, as the fetus' capacity to produce DHA from ALA may be insufficient to meet the extreme demand [25, 84]. With postpartum, maternal estrogen and circulating maternal DHA levels decrease [12, 26].

Blood levels of DHA have been associated with exogenous sex hormone interventions. Postmenopausal women have been observed to have decreased DHA in erythrocyte phospholipids [85], and postmenopausal women undergoing hormone replacement strategies including both direct hormone replacement and selective estrogen-receptor modulators have increased circulating DHA relative to postmenopausal women not using hormone therapies [86, 87]. Women taking an estradiol-based contraceptive pill also have elevated blood and erythrocyte DHA levels as compared to women not taking oral contraceptives [21, 88]. Similarly, DHA increased in the plasma cholesteryl esters of male-to-female transsexuals receiving oral ethinyl estradiol, while plasma cholesteryl ester DHA decreased in the blood of female-to-male transsexuals receiving testosterone treatment [21].

In rats, EPA and DHA in plasma phosphatidyl choline correlate strongly with female sex hormones (estrogen and progesterone), and plasma, liver, and adipose EPA and DHA content vary inversely with testosterone [89]. DHA in liver phospholipids and plasma phosphatidyl choline have been observed to be higher in females as compared with males after n-3 deficiency/repletion [76]. Higher DHA has also been seen in female rat plasma and liver phospholipids in different diets containing varying levels of total fat and ALA [77]. Decreased erythrocyte DHA has been observed after ovariectomization as compared with sham-operated controls [90]. In addition, neuroblastoma cells incubated with ALA and estradiol exhibit higher EPA and DPAn-3 in phosphatidyl ethanolamine and increased expression of D5D as compared with cells incubated with ALA alone [91, 92]. Interestingly, treating neuroblastoma cells with dehydrotestosterone decreases EPA and DHA in phosphatidyl ethanolamine, and decreases D5D expression [91].

Based on current evidence, it appears that sex influences the concentration of circulating DHA, resulting in higher levels in females. This difference is associated with estrogen, and appears to involve increased conversion of ALA to DHA, in particular the conversion of 22:5n-3–22:6n-3, and only during low dietary intake of n-3 HUFA. It is possible that estrogen may increase the concentration or activity of DHA synthesis enzymes, including desaturases, elongases, and peroxisomal β-oxidation enzymes resulting in enhanced DHA biosynthesis.

Estrogen Signalling Mechanisms

Estrogen exerts many effects on a variety of different tissue types, and its actions are mediated by both direct interaction with the genome and nongenomic mechanisms [93]. The effects of estrogen are mediated primarily by estrogen receptors (ERα and ERβ in mammals) which exhibit a variety of subcellular localizations depending on tissue type [94, 95]. For example, in endometrial cells, ERα is primarily found at the cell membrane, whereas in breast cancer cells it is in the nucleus [95].

In direct genomic estrogen signaling, the binding of estrogen to estrogen receptors results in dimerization with another estrogen receptor (ERα or ERβ) followed by binding to an estrogen response element in the promoter of a target gene, causing altered transcription of that gene. In "nongenomic" estrogen signaling, estrogen binds to and activates estrogen receptors anchored to the plasma membrane [96], or a G-protein known as G-protein receptor 30 (GPR30) [97]. Dimerization to another estrogen receptor can also occur with this mechanism [98], however the signal transduction that results from the activation of these membrane bound receptors involves a number of second messenger protein kinases and calcium signaling mechanisms, rather then direct genomic interaction (some are presented below, and are extensively reviewed in [93]).

The observational link between circulating estrogen and DHA production suggests that estrogen increases the expression of the enzymes involved in DHA production from shorter-chain n-3 PUFA. However, to our knowledge, no estrogen response elements have been identified to date that influence the expression of any of the genes involved in DHA synthesis (D6D, D5D, acyl-CoA oxidase), suggesting that the estrogen dependent induction of these genes occurs through indirect mechanisms. Several reliable techniques exist for determining the presence of estrogen

Table 2 Summary of studies investigating effects of exogenous estrogen and menopause on DHA content or metabolism

Author [reference]	Cell/subjects	Treatment	Effects of gender or steroids on measurements
Cell culture			
Alessandri et al. [92]	SH-SY5Y neuroblastoma ($n = 3$ for each condition)	10 nM 17β-estradiol 30 μM of ALA alone 10 nM 17β-estradiol with 30 μM of ALA	Increased EPA and n-3 DPA in PE with 17β-estradiol treatment
Extier et al. [91]	SH-SY5Y neuroblastoma (n = 4 for each condition)	7 μM ALA, LA, or ALA/LA, 10 nM 17β-estradiol, dehydrotestosterone, progesterone or control.	Increased EPA and n-3 DPA and increased D5D expression with ALA, and 17β-estradiol treatment Decreased EPA and DHA and decreased PPARα and D5D expression with ALA and dehydrotestosterone treatment Decreased D6D expression with progesterone treatment
Human			
Stark et al. [29]	Females (43–69 years)	Premenopausal ($n = 19$) Postmenopausal taking hormone therapy ($n = 40$) Postmenopausal not taking hormone therapy ($n = 34$)	Increased DHA and n-3 DPA in plasma PL in postmenopausal women not taking hormone therapy
Sumino et al. [87]	Postmenopausal women (43-63 years)	Taking conjugated equine estrogen and medroxyprogesterone acetate ($n = 59$) Not taking hormone therapy ($n = 45$)	Increased plasma DHA and EPA total lipids in women taking hormones
Giltay et al. [21]	Male-to-female transsexuals (eugonadal)	Cyproterone acetate alone ($n = 16$) Cyproterone acetate with oral ethinyl estradiol ($n = 15$) Transdermal 17β-estradiol ($n = 15$)	Increased DHA in serum CE with cyproterone acetate with oral ethinyl estradiol
	Female-to-male transsexuals (ovariectomized)	Testosterone esters plus anastrozole ($n = 16$) Placebo ($n = 14$) Testosterone esters alone ($n = 17$)	Decreased DHA in serum CE with testosterone esters alone
	Females	Using oral contraceptives ($n = 32$) No oral contraceptive use ($n = 71$) Controlled diet, free from fish	Non-significant increase in DHA in serum CE with oral contraceptive use ($P = 0.08$)
Giltay et al. [86]	Postmenopausal females (47–59 years) Males (60–70 years)	Females 60 mg raloxifene/day ($n = 23$) Females 150 mg raloxifene/day ($n = 20$) Females conjugated equine estrogen with medroxyprogesterone acetate ($n = 17$) Females placebo ($n = 23$). Males 120 mg raloxifene/day ($n = 15$) Males placebo ($n = 15$)	Increased DHA in plasma CE in post-menopausal women taking 150 mg/day raloxifene and in women taking equine estrogens with medroxyprogesterone acetate at 24 months compared to baseline
Stark and Holub [30]	Postmenopausal females (45–70 years)	Postmenopausal taking hormone therapy ($n = 18$) Postmenopausal not taking hormone therapy ($n = 14$) 2.8 g algal DHA vs. placebo in crossover design	Increased estimates of retroconversion of DHA to EPA in plasma phospholipids of women not taking hormone therapy

PLs phospholipids, *DHA* docosahexaenoic acid, *DPA* docosapentaenoic acid, *CE* cholesteryl esters, *ALA* alpha-linolenic acid, *LA* linoleic acid, *D5D* delta-5 desaturase, *D6D* delta-6 desaturase, *PPAR* peroxisome proliferators activated receptor, *EPA* eicosapentaenoic acid, *PE* phosphatidyl ethanolamine

response elements on any gene on a genome-wide basis [99, 100], however genome-wide screening for these elements in DHA-producing genes has not been reported.

Peroxisome Proliferator-Activated Receptor α (PPARα)

The structure, ligand-binding, DNA-binding and metabolic actions of PPARs have been reviewed [101, 102]. PPARs are ligand-activated transcription factors belonging to the nuclear steroid receptor superfamily. Inactive PPARs are bound to corepressor proteins which are released upon ligand binding to the PPAR through a conformational change to the PPAR. This conformational change allows the PPAR to bind to the retinoid-x-receptor and co-activator proteins that facilitate binding of the complex to DNA through a number of different mechanisms including histone acetylase activity [103]. This activated complex then interacts with peroxisome proliferator response elements (PPRE; nucleotide regions with an imperfect direct repeat-1 motif) in the promoter region of target genes, and gene transcription is modulated.

Three distinct PPARs have been discovered with varying tissue expression, genomic targets, and ligands: PPARα, PPARγ (PPARγ$_1$ and PPARγ$_2$ are produced from the same gene by different promoters), and PPARβ/δ. All three subtypes bind to the direct repeat-1 motif, however, each PPAR subtype distinguishes its targets by differences in the region directly upstream of this motif [101].

PPARα is expressed in metabolically active tissues such as liver, heart, kidney, skeletal muscle and brown adipose tissue [104, 105] and is known to regulate the expression of genes involved in PUFA desaturation (D6D, D5D) [35, 106], peroxisomal β-oxidation (acyl-CoA oxidase, D-bifunctional protein) [107, 108], and fatty acid transport (cytosolic fatty acid binding protein, fatty acid transport protein, acyl-CoA binding protein) [109, 110], all of which are involved in DHA formation (a review of PPARα responsive genes is available [111]). PPARα plays a large role in lipid homeostasis by increasing peroxisomal and mitochondrial β-oxidation rates, and producing energy and acetyl units for ketone body formation in periods of fasting and/or low carbohydrate intake [112].

Natural ligands for PPARα include PUFA (n-3 and n-6), monounsaturated fatty acids, and eicosanoids such as leukotriene B4 and hydroxyeicosatetraenoic acids [36]. Fibrates such as clofibrate, fenofibrate, and bezafibrate are synthetic ligands for PPARα and are effective lipid-lowering agents in humans, while in rodents fibrates cause increased hepatic peroxisome number, hepatomegaly, and carcinogenesis at higher doses [111].

PPARα can be phosphorylated at multiple sites, resulting in increased activity (reviewed in [113]). The mechanism by which phosphorylation increases PPARα activity has not been elucidated, however, some evidence suggests that phosphorylation of PPARα results in a decreased affinity for corepressor proteins [114]. This finding is significant, as it suggests that phosphorylated PPARα is more likely to be activated at a biological concentration of PPARα ligands, such as PUFA.

Estrogen and PPARα

There is strong evidence that estrogen signaling interacts with PPARα-dependent gene transcription particularly with regards to lipid metabolism. For example, mice deficient in aromatase, and therefore unable to synthesize estrogen, succumb to hepatic steatosis resulting from elevated hepatic lipid accumulation and deficient β-oxidation [115]. However, estrogen supplementation prevents this effect by increasing mitochondrial and peroxisomal β-oxidation rates via increased expression of mitochondrial and peroxisomal β-oxidation enzymes (acyl-CoA oxidase, medium chain acyl-CoA dehydrogenase) [115, 116], similar to the effect of PPARα activation. Additionally, the expression of stearoyl-CoA desaturase 1, a PPARα-induced gene, is significantly increased in female mouse livers and results in elevated hepatic oleate production [117]. Also, mitochondrial β-oxidation is increased in women but not in men fed a high oleate diet (31.4% of energy), indicating a sex difference in the metabolic response to oleate, a weak PPARα ligand [118]. Treating ovariectomized rats with 17β-estradiol increases PPARα content and expression of PPARα-dependent lipid oxidation genes in red gastrocnemius muscle [119]. Significant increases in the expression and transcriptional activity of PPARβ/δ, and an increase in the expression of lipid oxidation genes under transcriptional control of PPARα, independent of an increase in PPARα expression in liver, muscle, and adipose tissue has been demonstrated using a similar approach [120]. Reduced fat accumulation in female but not male mice has also been observed after treatment with phytol, a peroxisome proliferator [121].

The expression of fatty acid binding proteins (FABP), which is increased following PPARα activation [122], is also much higher in females than in males [123, 124]. FABP transports fatty acids to the nucleus and has been observed to co-localize with and possibly increasing the activity of PPARα in fibroblasts and primary mouse hepatocytes [125–127]. However, transient transfection of fibroblasts with FABPs decreased tetradecylthioacetic acid stimulated PPAR activity [128].

Similarly, estrogen administration causes peroxisome proliferation in the uropygial glands of male and female mallard ducks, accompanied by an increase in the peroxisome-dependent production of 3-hydroxy fatty acid

diesters [129]. In humans, the rate of DHA retroconversion to EPA, a process dependent on peroxisomal activity, is increased in postmenopausal women receiving hormone replacement therapy as compared with postmenopausal women not receiving this treatment [30]. Additionally, phospholipids and long chain PUFA in the brain are increased in female but not male PPARβ knockout mice suggesting sexual dimorphisms and a role of PPARβ in paroxysmal acyl-CoA use in the brain [130]. Considerable differences exist in the response of PPARα and PPARβ/δ to some natural ligands (particularly 8(*S*)-HETE) [131], and that generalizing in vivo results between different PPARs should be done with caution. Nonetheless, it seems that sex differences exist in other PPARs, as well as PPARα.

In a transgenic luciferase-$^{5\times}$PPRE mouse, it was shown that liver exhibited significantly lower PPARα transcriptional activity in females as compared with males in response to oral fibrate administration, food withdrawal, and reversal of feeding schedule [132]. These sexual dimorphisms remained despite ovariectomization and castration that suggests gonadal hormones are not involved. These observations may also be a dependent on the presence of the 5 PPREs in this model as similar observations have not been confirmed in mice with intact genomes. However, this transgenic model does support the notion that sex differences exist in PPARα-dependent gene transcription. Similarly, male as compared with female mice express more PPARα-dependent genes in response to 2 weeks of daily oral trichloroethylene treatment, suggesting a sex specific response to exogenous activators of PPARα [133].

Observations in PPARα-null mice strongly illustrate the interaction between estrogen and PPARα. Normally, ovariectomization results in significant gains in adipose tissue mass, while subsequent treatment with exogenous estradiol relieves this effect. However, in PPARα-null mice, no significant changes in adipose tissue are observed upon ovariectomization and subsequent estradiol administration, suggesting that the effect estrogen has on fat oxidation is dependent on the presence of PPARα [134]. Circulating leptin concentrations decrease in PPARα-null mice as compared with control mice, with a sex-specific effect in the leptin response to feeding as leptin was increased in female PPARα-null mice as compared with male PPARα-null mice [135].

The evidence presented above infers that a significant biological interaction exists between estrogen signaling and PPARα activity, and is present in several animal models. Accordingly, understanding the mechanism by which estrogen regulates PPARα may provide a better understanding of observations of sexual dimorphisms in n-3 PUFA metabolism. Interestingly, in vitro ligand binding analysis has shown that 17-β estradiol is a weak direct activator of PPARα, suggesting that it is not a PPARα ligand [36]. However, many interactions exist between estrogen signaling and PPARα, including protein kinases and other mechanisms, which suggest that estrogen acts on PPARα indirectly.

Estrogen Increases PPARα Activity by Phosphorylation

It is known that the phosphorylation (and corresponding activity) of PPARα is enhanced by several of the protein kinase systems activated by membrane bound estrogen receptors. By phosphorylating PPARα, estrogen will enhance DHA formation by increasing the transcription of enzymes involved in this pathway (Fig. 2).

Estrogen binding to membrane bound estrogen receptors activates extracellular receptor kinase-mitogen activated protein kinase (ERK-MAPK) in a variety of tissue types/cell lines. Injection of 17-β-estradiol increases ERK-MAPK activity in several rat brain structures [38] and the addition of estrogen to male derived hypothalamic nuclei in vitro results in significant elevations in the activity of MAPK [39]. Furthermore, the addition of estrogen to cultured muscle cells [136] and breast cancer cells [137] also results in elevated ERK-MAPK activity, illustrating that this effect is shared by a variety of tissues.

Phosphorylation and increased activity of PPARα resulting from MAPK-mediated signal transduction has been well documented in a variety of cellular processes. Hepatic PPARα is known to be phosphorylated at two serine residues in response to insulin signaling via the ERK-MAPK system, resulting in increased PPARα-dependent gene transcription [114, 138]. The incubation of cultured myotubes with adiponectin results in elevated activity of ERK-MAPK and corresponding phosphorylation of PPARα, resulting in increased target gene expression and lipid catabolism [139]. Similarly, phosphatidyl inositol supplementation also increases PPARα activity via ERK-MAPK-dependent phosphorylation in human hepatocyte cell lines [140], resulting in PPARα-dependent production and secretion of apolipoprotein A-1.

Estrogen also activates protein kinase A phosphorylation systems. In vitro research with hippocampal neurons indicates that estrogen causes significant protein kinase A activation that is dependent on the presence of membrane-bound estrogen receptors [37]. Estrogen has been observed to cause protein kinase A dependent phosphorylation of *N*-methyl-D-aspartic acid receptors in rat spinal neurons, lessening the perception of pain by the animal [141]. In rat liver tissue, estrogen interaction with GPR30 results in activated protein kinase A signal transduction and prevention of apoptosis following organ injury [142]. Activation of protein kinase A signaling by cholera toxin has also been shown to increase the phosphorylation and transcriptional

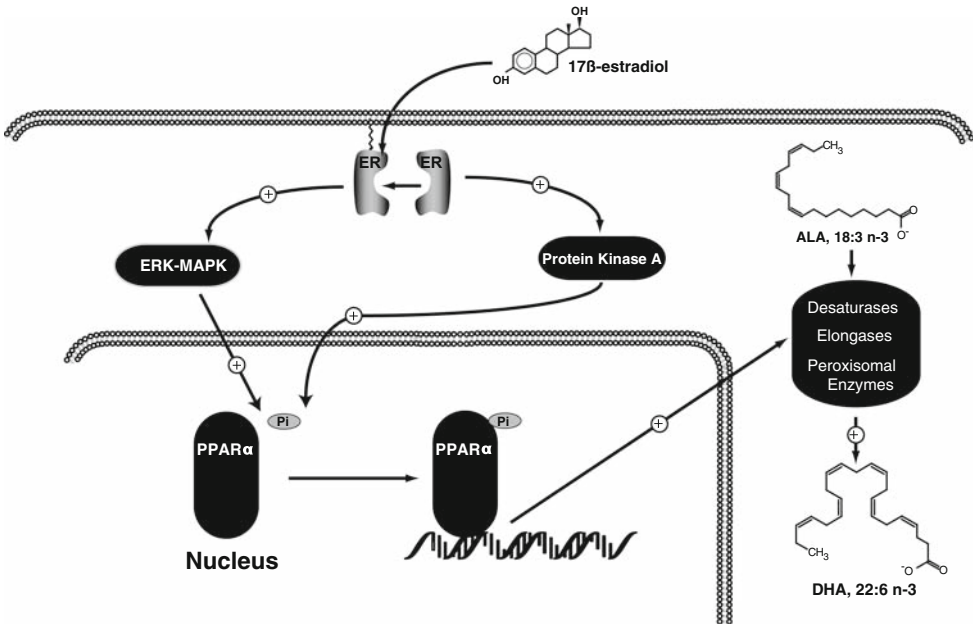

Fig. 2 Proposed mechanism of increased peroxisome-proliferator activated receptor α phosphorylation by estrogen. *ER* estrogen receptor, *ERK-MAPK* extracellular receptor kinase-mitogen activated protein kinase, *Pi* inorganic phosphate, *PPARα* peroxisome-proliferator activated receptor α, *ALA* alpha-linolenic acid, *DHA* docosahexaenoic acid

activity of PPARα [143]. Protein kinase A phosphorylates several enzymes in lipid-utilization systems and metabolism, including diacylglycerol lipase in the brain [144].

Phosphorylation of 5′AMP-activated protein kinase has also been observed in response to 17β-estradiol supplementation in the skeletal muscle of ovariectomized rats. Lipid oxidation in white adipose tissue [145] and skeletal muscle [146] is increased during AMP-activated protein kinase (AMPK) activation, and it has been found that siRNA inhibition of PPARα prevents this response [146].

Phosphorylation of PPARα via activation of membrane bound estrogen receptors is likely similar to the estrogen mediated phosphorylation and increased activity of cAMP response element binding (CREB) protein. Activation of CREB protein results in the increased expression of anti-apoptotic proteins, including the Bcl-2 family [147]. It has been well established that estrogen binding to membrane bound estrogen receptors results in the phosphorylation and increased activity of CREB protein. The precise protein kinase that mediates this phosphorylation varies by tissue, as protein kinase A is responsible in ZR-75 breast cancer cells [148], and protein kinase B/Akt and ERK-MAPK mediate this response in neuronal cells [149]. The increased CREB protein activity that results from phosphorylation has anti-apoptotic effects in all cell types, indicating increased CREB protein-dependent transcription.

Increased Concentration of Intracellular PPARα Ligands

Despite not being a PPARα ligand, estrogen may increase the intracellular concentrations of effective PPARα ligands, particularly PUFA and eicosanoids (Fig. 3). PUFA are most often found in the inner membrane leaflet of cells, in the *sn-2* position of phosphatidyl ethanolamine [150]. Hydrolytic release of PUFA from this position for cell signaling or eicosanoid synthesis is catalyzed by phospholipase A_2 (PLA_2). Upon phosphorylation, the activity and a calcium-dependent isoform of PLA_2 (Ca^{2+}-PLA_2) is increased, and the enzyme becomes localized in the cell membrane and nuclear envelope regions. By localizing in these regions, Ca^{2+}-PLA_2 functions to release PUFA from biological membranes for cell signaling and eicosanoid synthesis.

Similarly to PPARα, activation of the ERK-MAPK signaling cascade has been observed to phosphorylate Ca^{2+}-PLA_2 in HeLa cells [151, 152]. Because estrogen has been observed to activate the ERK-MAPK system [38], as well as IP_3-dependent calcium signaling cascades [153–155], estrogen would be expected to increase the activity of Ca^{2+}-PLA_2. Indeed, in pregnant rats uterine Ca^{2+}-PLA_2 activity is elevated near gestation in response to increased estradiol concentrations [156]. Estradiol-administration also enhanced the activity of Ca^{2+}-PLA_2 of mussel (*Mytilus galloprovincialis*) blood cells [157].

Eicosanoids are known to be involved in atherosclerosis, bronchial asthma, and many other inflammatory conditions [158]. Prostaglandins are produced in most tissue types, and are known to activate PPARα [36]. These cytokines are produced by enzymes known as cyclooxygenases (COX) of which there are two types: COX-1, which is constitutively expressed in most tissue types, and COX-2, the expression of which is induced during periods of inflammation. With regards to estrogen, increased COX-2 expression has been observed in response to elevated estrogen in human

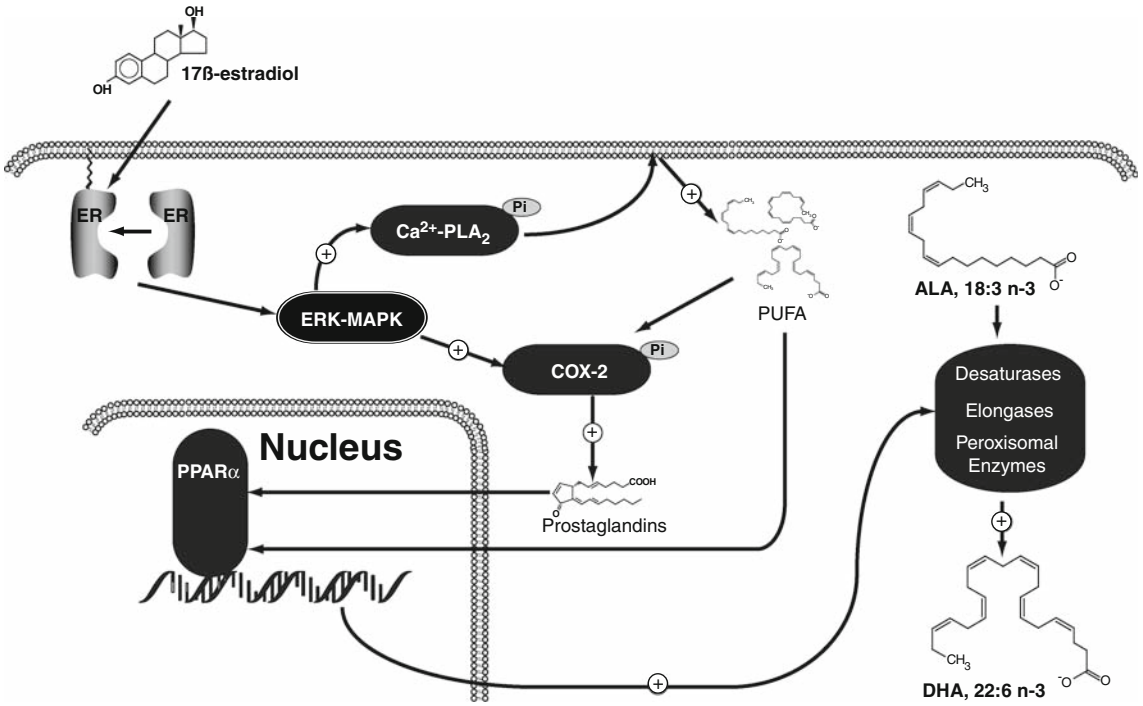

Fig. 3 Proposed mechanism by which estrogen increases intracellular concentration of ligands for peroxisome-proliferator activated receptor α. *ER* estrogen receptor, *ERK-MAPK* extracellular receptor kinase-mitogen activated protein kinase, *Ca^{2+}-PLA_2* calcium-dependent phospholipase A_2, *COX-2* cyclooxygenase-2, *Pi* inorganic phosphate, *PUFA* polyunsaturated fatty acids, *PPARα* peroxisome-proliferator activated receptor α, *ALA* alpha-linolenic acid, *DHA* docosahexaenoic acid

amnion, resulting in elevated prostaglandin E_2 production [159].

Conclusions

The current knowledge of sex differences in n-3 PUFA metabolism is presently outlined and various likely mechanisms mediating the elevated n-3 HUFA synthesis observed in females have been indicated. Women have higher circulating concentrations of DHA as compared with men that is associated with estrogen, and is a result of increased conversion of ALA into DHA. This increased conversion likely involves the increased expression/activity of DHA synthesis enzymes, highlighting possible interaction between estrogen signaling mechanisms and the expression of enzymes responsible for the synthesis of DHA. Two likely mechanisms by which estrogen increases PPARα activity and subsequent DHA formation are presented: (1) estrogen increases the activity of ERK-MAPK and protein kinase A, which phosphorylate and increase the activity of PPARα, and/or (2) estrogen increases the intracellular concentration of both PUFA and eicosanoids, PPARα ligands, via elevated Ca^{2+}-PLA_2 and COX-2 activities, resulting in activation of PPARα. By increasing the activity of PPARα, estrogen likely causes elevated transcription of the enzymes involved in DHA synthesis, including desaturases, elongases, and peroxisomal β-oxidation enzymes. The increased activity of these enzymes results in the increased production of DHA, contributing to the elevated tissue DHA content observed in females.

A more complete understanding of these interactions is required to understand the health benefits of individual n-3 PUFA and to assist in the determination of dietary recommendations for ALA, EPA, DPAn-3 and DHA. The impact of hormonal status on n-3 PUFA metabolism may be important for DHA availability for maternal–fetal transport during pregnancy. In addition, subtle differences in DHA production may be contributing to observed sexual dimorphisms in sudden cardiac death. The interaction between estrogen and fatty acid metabolism requires further research including an examination of the effects of various gonadal hormones, the impact of fluctuations in hormones throughout the life cycle including physiological challenges such as pregnancy, and the impact of the dietary intake of specific fatty acids. In addition, an enhanced understanding of the regulation and control of DHA biosynthesis may assist in efforts to produce alternative food sources of DHA and aid in the challenge of meeting the potential global demand for EPA and DHA.

References

1. Xiao YF, Sigg DC, Leaf A (2005) The antiarrhythmic effect of n-3 polyunsaturated fatty acids: modulation of cardiac ion channels as a potential mechanism. J Membr Biol 206:141–154
2. GISSI-Prevenzione Investigators (1999) Dietary supplementation with n-3 polyunsaturated fatty acids and vitamin E after myocardial infarction: results of the GISSI-Prevenzione trial Gruppo Italiano per lo Studio della Sopravvivenza nell'Infarto miocardico. Lancet 354:447–455
3. Leaf A, Albert CM, Josephson M, Steinhaus D, Kluger J, Kang JX, Cox B, Zhang H, Schoenfeld D (2005) Prevention of fatal arrhythmias in high-risk subjects by fish oil n-3 fatty acid intake. Circulation 112:2762–2768
4. Leaf A, Xiao YF, Kang JX, Billman GE (2005) Membrane effects of the n-3 fish oil fatty acids, which prevent fatal ventricular arrhythmias. J Membr Biol 206:129–139
5. McCann JC, Ames BN (2005) Is docosahexaenoic acid, an n-3 long-chain polyunsaturated fatty acid, required for development of normal brain function? An overview of evidence from cognitive and behavioral tests in humans and animals. Am J Clin Nutr 82:281–295
6. Lim SY, Hoshiba J, Salem N Jr (2005) An extraordinary degree of structural specificity is required in neural phospholipids for optimal brain function: n-6 docosapentaenoic acid substitution for docosahexaenoic acid leads to a loss in spatial task performance. J Neurochem 95:848–857
7. Burdge GC, Calder PC (2005) Conversion of alpha-linolenic acid to longer-chain polyunsaturated fatty acids in human adults. Reprod Nutr Dev 45:581–597
8. Mozaffarian D, Rimm EB (2006) Fish intake, contaminants, and human health: evaluating the risks and the benefits. JAMA 296:1885–1899
9. Gebauer SK, Psota TL, Harris WS, Kris-Etherton PM (2006) n-3 Fatty acid dietary recommendations and food sources to achieve essentiality and cardiovascular benefits. Am J Clin Nutr 83:1526S–1535S
10. Denomme J, Stark KD, Holub BJ (2005) Directly quantitated dietary (n-3) fatty acid intakes of pregnant Canadian women are lower than current dietary recommendations. J Nutr 135:206–211
11. Fratesi JA, Hogg RC, Young-Newton GS, Patterson AC, Charkhzarin P, Block TK, Sharratt MT, Stark KD (2009) Direct quantitation of omega-3 fatty acid intake of Canadian residents of a long-term care facility. Appl Physiol Nutr Metab 34:1–9
12. Stark KD, Beblo S, Murthy M, Buda-Abela M, Janisse J, Rockett H, Whitty JE, Martier SS, Sokol RJ, Hannigan JH, Salem N Jr (2005) Comparison of bloodstream fatty acid composition from African-American women at gestation, delivery, and postpartum. J Lipid Res 46:516–525
13. Harris WS, Mozaffarian D, Lefevre M, Toner CD, Colombo J, Cunnane SC, Holden JM, Klurfeld DM, Morris MC, Whelan J (2009) Towards establishing dietary reference intakes for eicosapentaenoic and docosahexaenoic acids. J Nutr 139:804S–819S
14. Albert CM, Oh K, Whang W, Manson JE, Chae CU, Stampfer MJ, Willett WC, Hu FB (2005) Dietary alpha-linolenic acid intake and risk of sudden cardiac death and coronary heart disease. Circulation 112:3232–3238
15. Mozaffarian D, Ascherio A, Hu FB, Stampfer MJ, Willett WC, Siscovick DS, Rimm EB (2005) Interplay between different polyunsaturated fatty acids and risk of coronary heart disease in men. Circulation 111:157–164
16. Pawlosky R, Hibbeln J, Lin Y, Salem N Jr (2003) n-3 Fatty acid metabolism in women. Br J Nutr 90:993–994
17. Pawlosky RJ, Hibbeln JR, Lin Y, Goodson S, Riggs P, Sebring N, Brown GL, Salem N Jr (2003) Effects of beef- and fish-based diets on the kinetics of n-3 fatty acid metabolism in human subjects. Am J Clin Nutr 77:565–572
18. Burdge GC, Wootton SA (2002) Conversion of alpha-linolenic acid to eicosapentaenoic, docosapentaenoic and docosahexaenoic acids in young women. Br J Nutr 88:411–420
19. Burdge GC, Jones AE, Wootton SA (2002) Eicosapentaenoic and docosapentaenoic acids are the principal products of alpha-linolenic acid metabolism in young men. Br J Nutr 88:355–363
20. Burdge GC, Slater-Jefferies JL, Grant RA, Chung WS, West AL, Lillycrop KA, Hanson MA, Calder PC (2008) Sex, but not maternal protein or folic acid intake, determines the fatty acid composition of hepatic phospholipids, but not of triacylglycerol, in adult rats. Prostaglandins Leukot Essent Fatty Acids 78:73–79
21. Giltay EJ, Gooren LJ, Toorians AW, Katan MB, Zock PL (2004) Docosahexaenoic acid concentrations are higher in women than in men because of estrogenic effects. Am J Clin Nutr 80:1167–1174
22. Crowe FL, Skeaff CM, Green TJ, Gray AR (2008) Serum n-3 long-chain PUFA differ by sex and age in a population-based survey of New Zealand adolescents and adults. Br J Nutr 99:168–174
23. Bakewell L, Burdge GC, Calder PC (2006) Polyunsaturated fatty acid concentrations in young men and women consuming their habitual diets. Br J Nutr 96:93–99
24. Metherel AH, Armstrong JM, Patterson AC, Stark KD (2009) Assessment of blood measures of n-3 polyunsaturated fatty acids with acute fish oil supplementation and washout in men and women. Prostaglandins Leukot Essent Fatty Acids 81:23–29
25. Innis SM (2005) Essential fatty acid transfer and fetal development. Placenta 26 Suppl A:S70–S75
26. Stewart F, Rodie VA, Ramsay JE, Greer IA, Freeman DJ, Meyer BJ (2007) Longitudinal assessment of erythrocyte fatty acid composition throughout pregnancy and post partum. Lipids 42:335–344
27. Otto SJ, van Houwelingen AC, Badart-Smook A, Hornstra G (2001) Comparison of the peripartum and postpartum phospholipid polyunsaturated fatty acid profiles of lactating and nonlactating women. Am J Clin Nutr 73:1074–1079
28. Postle AD, Al MD, Burdge GC, Hornstra G (1995) The composition of individual molecular species of plasma phosphatidylcholine in human pregnancy. Early Hum Dev 43:47–58
29. Stark KD, Park EJ, Holub BJ (2003) Fatty acid composition of serum phospholipid of premenopausal women and postmenopausal women receiving and not receiving hormone replacement therapy. Menopause 10:448–455
30. Stark KD, Holub BJ (2004) Differential eicosapentaenoic acid elevations and altered cardiovascular disease risk factor responses after supplementation with docosahexaenoic acid in postmenopausal women receiving and not receiving hormone replacement therapy. Am J Clin Nutr 79:765–773
31. Oscarsson J, Eden S (1988) Sex differences in fatty acid composition of rat liver phosphatidylcholine are regulated by the plasma pattern of growth hormone. Biochim Biophys Acta 959:280–287
32. Burdge GC, Hunt AN, Postle AD (1994) Mechanisms of hepatic phosphatidylcholine synthesis in adult rat: effects of pregnancy. Biochem J 303(Pt 3):941–947
33. O'Lone R, Frith MC, Karlsson EK, Hansen U (2004) Genomic targets of nuclear estrogen receptors. Mol Endocrinol 18:1859–1875
34. Tang C, Cho HP, Nakamura MT, Clarke SD (2003) Regulation of human delta-6 desaturase gene transcription: identification of a functional direct repeat-1 element. J Lipid Res 44:686–695
35. Guillou H, Martin P, Jan S, D'Andrea S, Roulet A, Catheline D, Rioux V, Pineau T, Legrand P (2002) Comparative effect of fenofibrate on hepatic desaturases in wild-type and peroxisome

proliferator-activated receptor alpha-deficient mice. Lipids 37:981–989
36. Krey G, Braissant O, L'Horset F, Kalkhoven E, Perroud M, Parker MG, Wahli W (1997) Fatty acids, eicosanoids, and hypolipidemic agents identified as ligands of peroxisome proliferator-activated receptors by coactivator-dependent receptor ligand assay. Mol Endocrinol 11:779–791
37. Shingo AS, Kito S (2005) Estradiol induces PKA activation through the putative membrane receptor in the living hippocampal neuron. J Neural Transm 112:1469–1473
38. Bryant DN, Bosch MA, Ronnekleiv OK, Dorsa DM (2005) 17-Beta estradiol rapidly enhances extracellular signal-regulated kinase 2 phosphorylation in the rat brain. Neuroscience 133:343–352
39. Gorosito SV, Cambiasso MJ (2008) Axogenic effect of estrogen in male rat hypothalamic neurons involves Ca(2+), protein kinase C, and extracellular signal-regulated kinase signaling. J Neurosci Res 86:145–157
40. Stark KD, Beblo S, Murthy M, Whitty JE, Buda-Abela M, Janisse J, Rockett H, Martier SS, Sokol RJ, Hannigan JH, Salem N Jr (2005) Alcohol consumption in pregnant, black women is associated with decreased plasma and erythrocyte docosahexaenoic acid. Alcohol Clin Exp Res 29:130–140
41. Mahaffey KR, Clickner RP, Jeffries RA (2008) Methylmercury and omega-3 fatty acids: co-occurrence of dietary sources with emphasis on fish and shellfish. Environ Res 107:20–29
42. Health Canada (2010) Canadian Nutrient File. http://webprod.hc-sc.gc.ca/cnf-fce/index-eng.jsp. Accessed Jan 2010
43. Patterson AC, Stark KD (2008) Direct determinations of the fatty acid composition of daily dietary intakes incorporating nutraceuticals and functional food strategies to increase n-3 highly unsaturated fatty acids. J Am Coll Nutr 27:538–546
44. Kitson AP, Patterson AC, Izadi H, Stark KD (2009) Pan-frying Salmon in an eicosapentaenoic acid (EPA) and docosahexaenoic acid (DHA) enriched margarine prevents EPA and DHA loss. Food Chem 114:927–932
45. Jenkins DJ, Sievenpiper JL, Pauly D, Sumaila UR, Kendall CW, Mowat FM (2009) Are dietary recommendations for the use of fish oils sustainable? CMAJ 180:633–637
46. Hauvermale A, Kuner J, Rosenzweig B, Guerra D, Diltz S, Metz JG (2006) Fatty acid production in *Schizochytrium* sp.: involvement of a polyunsaturated fatty acid synthase and a type I fatty acid synthase. Lipids 41:739–747
47. Spolaore P, Joannis-Cassan C, Duran E, Isambert A (2006) Commercial applications of microalgae. J Biosci Bioeng 101:87–96
48. Chi X, Zhang X, Guan X, Ding L, Li Y, Wang M, Lin H, Qin S (2008) Fatty acid biosynthesis in eukaryotic photosynthetic microalgae: identification of a microsomal delta 12 desaturase in *Chlamydomonas reinhardtii*. J Microbiol 46:189–201
49. Meyer A, Cirpus P, Ott C, Schlecker R, Zahringer U, Heinz E (2003) Biosynthesis of docosahexaenoic acid in *Euglena gracilis*: biochemical and molecular evidence for the involvement of a delta4-fatty acyl group desaturase. Biochemistry 42:9779–9788
50. Damude HG, Kinney AJ (2007) Engineering oilseed plants for a sustainable, land-based source of long chain polyunsaturated fatty acids. Lipids 42:179–185
51. Damude HG, Zhang H, Farrall L, Ripp KG, Tomb JF, Hollerbach D, Yadav NS (2006) Identification of bifunctional delta12/omega3 fatty acid desaturases for improving the ratio of omega3 to omega6 fatty acids in microbes and plants. Proc Natl Acad Sci USA 103:9446–9451
52. Barcelo-Coblijn G, Murphy EJ, Othman R, Moghadasian MH, Kashour T, Friel JK (2008) Flaxseed oil and fish-oil capsule consumption alters human red blood cell n-3 fatty acid composition: a multiple-dosing trial comparing 2 sources of n-3 fatty acid. Am J Clin Nutr 88:801–809
53. Mantzioris E, James MJ, Gibson RA, Cleland LG (1994) Dietary substitution with an alpha-linolenic acid-rich vegetable oil increases eicosapentaenoic acid concentrations in tissues. Am J Clin Nutr 59:1304–1309
54. Li D, Sinclair A, Wilson A, Nakkote S, Kelly F, Abedin L, Mann N, Turner A (1999) Effect of dietary alpha-linolenic acid on thrombotic risk factors in vegetarian men. Am J Clin Nutr 69:872–882
55. Wallace FA, Miles EA, Calder PC (2003) Comparison of the effects of linseed oil and different doses of fish oil on mononuclear cell function in healthy human subjects. Br J Nutr 89:679–689
56. Sanders TA, Younger KM (1981) The effect of dietary supplements of omega 3 polyunsaturated fatty acids on the fatty acid composition of platelets and plasma choline phosphoglycerides. Br J Nutr 45:613–616
57. Cunnane SC, Hamadeh MJ, Liede AC, Thompson LU, Wolever TM, Jenkins DJ (1995) Nutritional attributes of traditional flaxseed in healthy young adults. Am J Clin Nutr 61:62–68
58. Finnegan YE, Minihane AM, Leigh-Firbank EC, Kew S, Meijer GW, Muggli R, Calder PC, Williams CM (2003) Plant- and marine-derived n-3 polyunsaturated fatty acids have differential effects on fasting and postprandial blood lipid concentrations and on the susceptibility of LDL to oxidative modification in moderately hyperlipidemic subjects. Am J Clin Nutr 77:783–795
59. Harper CR, Edwards MJ, DeFilippis AP, Jacobson TA (2006) Flaxseed oil increases the plasma concentrations of cardioprotective (n-3) fatty acids in humans. J Nutr 136:83–87
60. Bemelmans WJ, Broer J, Feskens EJ, Smit AJ, Muskiet FA, Lefrandt JD, Bom VJ, May JF, Meyboom-de JB (2002) Effect of an increased intake of alpha-linolenic acid and group nutritional education on cardiovascular risk factors: the Mediterranean Alpha-linolenic Enriched Groningen Dietary Intervention (MARGARIN) study. Am J Clin Nutr 75:221–227
61. Barcelo-Coblijn G, Murphy EJ (2009) Alpha-linolenic acid and its conversion to longer chain n-3 fatty acids: benefits for human health and a role in maintaining tissue n-3 fatty acid levels. Prog Lipid Res 48:355–374
62. Widmer C Jr, Holman RT (1950) Polyethenoid fatty acid metabolism; deposition of polyunsaturated fatty acids in fat-deficient rats upon single fatty acid supplementation. Arch Biochem 25:1–12
63. Klenk E, Mohrhauer H (1960) Studies on the metabolism of polyenoic fatty acids in the rat. Hoppe Seylers Z Physiol Chem 320:218–232
64. Nugteren DH (1965) The enzymic chain elongation of fatty acids by rat-liver microsomes. Biochim Biophys Acta 106:280–290
65. Voss A, Reinhart M, Sankarappa S, Sprecher H (1991) The metabolism of 7, 10, 13, 16, 19-docosapentaenoic acid to 4, 7, 10, 13, 16, 19-docosahexaenoic acid in rat liver is independent of a 4-desaturase. J Biol Chem 266:19995–20000
66. Luthria DL, Mohammed BS, Sprecher H (1996) Regulation of the biosynthesis of 4, 7, 10, 13, 16, 19-docosahexaenoic acid. J Biol Chem 271:16020–16025
67. Nakamura MT, Nara TY (2004) Structure, function, and dietary regulation of delta6, delta5, and delta9 desaturases. Annu Rev Nutr 24:345–376
68. Goyens PL, Spilker ME, Zock PL, Katan MB, Mensink RP (2006) Conversion of alpha-linolenic acid in humans is influenced by the absolute amounts of alpha-linolenic acid and linoleic acid in the diet and not by their ratio. Am J Clin Nutr 84:44–53

69. Stroud CK, Nara TY, Roqueta-Rivera M, Radlowski EC, Lawrence P, Zhang Y, Cho BH, Segre M, Hess RA, Brenna JT, Haschek WM, Nakamura MT (2009) Disruption of FADS2 gene in mice impairs male reproduction and causes dermal and intestinal ulceration. J Lipid Res 50:1870–1880
70. Portolesi R, Powell BC, Gibson RA (2007) Competition between 24:5n-3 and ALA for Delta 6 desaturase may limit the accumulation of DHA in HepG2 cell membranes. J Lipid Res 48:1592–1598
71. Melin T, Nilsson A (1997) Delta-6-desaturase and delta-5-desaturase in human Hep G2 cells are both fatty acid interconversion rate limiting and are upregulated under essential fatty acid deficient conditions. Prostaglandins Leukot Essent Fatty Acids 56:437–442
72. Marangoni F, Colombo C, Martiello A, Negri E, Galli C (2007) The fatty acid profiles in a drop of blood from a fingertip correlate with physiological, dietary and lifestyle parameters in volunteers. Prostaglandins Leukot Essent Fatty Acids 76:87–92
73. McCloy U, Ryan MA, Pencharz PB, Ross RJ, Cunnane SC (2004) A comparison of the metabolism of eighteen-carbon 13C-unsaturated fatty acids in healthy women. J Lipid Res 45:474–485
74. Burdge GC, Wootton SA (2003) Conversion of alpha-linolenic acid to palmitic, palmitoleic, stearic and oleic acids in men and women. Prostaglandins Leukot Essent Fatty Acids 69:283–290
75. Barcelo-Coblijn G, Collison LW, Jolly CA, Murphy EJ (2005) Dietary alpha-linolenic acid increases brain but not heart and liver docosahexaenoic acid levels. Lipids 40:787–798
76. Extier A, Langelier B, Perruchot MH, Guesnet P, Van Veldhoven PP, Lavialle M, Alessandri JM (2009) Gender affects liver desaturase expression in a rat model of n-3 fatty acid repletion. J Nutr Biochem. doi:10.1016/j.jnutbio.2008.10.008
77. Childs CE, Romeu-Nadal M, Burdge GC, Calder PC (2010) The polyunsaturated fatty acid composition of hepatic and plasma lipids differ by both sex and dietary fat intake in rats. J Nutr 140:245–250
78. Vandal M, Freemantle E, Tremblay-Mercier J, Plourde M, Fortier M, Bruneau J, Gagnon J, Begin M, Cunnane SC (2008) Plasma omega-3 fatty acid response to a fish oil supplement in the healthy elderly. Lipids 43:1085–1089
79. Dewailly EE, Blanchet C, Gingras S, Lemieux S, Sauve L, Bergeron J, Holub BJ (2001) Relations between n-3 fatty acid status and cardiovascular disease risk factors among Quebecers. Am J Clin Nutr 74:603–611
80. de Groot RH, van Boxtel MP, Schiepers OJ, Hornstra G, Jolles J (2009) Age dependence of plasma phospholipid fatty acid levels: potential role of linoleic acid in the age-associated increase in docosahexaenoic acid and eicosapentaenoic acid concentrations. Br J Nutr 102:1058–1064
81. Sands SA, Reid KJ, Windsor SL, Harris WS (2005) The impact of age, body mass index, and fish intake on the EPA and DHA content of human erythrocytes. Lipids 40:343–347
82. Babin F, Abderrazik M, Favier F, Cristol JP, Leger CL, Papoz L, Descomps B (1999) Differences between polyunsaturated fatty acid status of non-institutionalised elderly women and younger controls: a bioconversion defect can be suspected. Eur J Clin Nutr 53:591–596
83. Rump P, Otto SJ, Hornstra G (2001) Leptin and phospholipid-esterified docosahexaenoic acid concentrations in plasma of women: observations during pregnancy and lactation. Eur J Clin Nutr 55:244–251
84. Su HM, Huang MC, Saad NM, Nathanielsz PW, Brenna JT (2001) Fetal baboons convert 18:3n-3 to 22:6n-3 in vivo. A stable isotope tracer study. J Lipid Res 42:581–586
85. Tworek C, Muti P, Micheli A, Krogh V, Riboli E, Berrino F (2000) Fatty acid composition of the red blood cell membrane in relation to menopausal status. Ann Epidemiol 10:477
86. Giltay EJ, Duschek EJ, Katan MB, Zock PL, Neele SJ, Netelenbos JC (2004) Raloxifene and hormone replacement therapy increase arachidonic acid and docosahexaenoic acid levels in postmenopausal women. J Endocrinol 182:399–408
87. Sumino H, Ichikawa S, Murakami M, Nakamura T, Kanda T, Sakamaki T, Mizunuma H, Kurabayashi M (2003) Effects of hormone replacement therapy on circulating docosahexaenoic acid and eicosapentaenoic acid levels in postmenopausal women. Endocr J 50:51–59
88. Magnusardottir AR, Steingrimsdottir L, Thorgeirsdottir H, Gunnlaugsson G, Skuladottir GV (2009) Docosahexaenoic acid in red blood cells of women of reproductive age is positively associated with oral contraceptive use and physical activity. Prostaglandins Leukot Essent Fatty Acids 80:27–32
89. Childs CE, Romeu-Nadal M, Burdge GC, Calder PC (2008) Gender differences in the n-3 fatty acid content of tissues. Proc Nutr Soc 67:19–27
90. McNamara RK, Able J, Jandacek R, Rider T, Tso P (2009) Gender differences in rat erythrocyte and brain docosahexaenoic acid composition: role of ovarian hormones and dietary omega-3 fatty acid composition. Psychoneuroendocrinology 34:532–539
91. Extier A, Perruchot MH, Baudry C, Guesnet P, Lavialle M, Alessandri JM (2009) Differential effects of steroids on the synthesis of polyunsaturated fatty acids by human neuroblastoma cells. Neurochem Int 55:295–301
92. Alessandri JM, Extier A, Langelier B, Perruchot MH, Heberden C, Guesnet P, Lavialle M (2008) Estradiol favors the formation of eicosapentaenoic acid (20:5n-3) and n-3 docosapentaenoic acid (22:5n-3) from alpha-linolenic acid (18:3n-3) in SH-SY5Y neuroblastoma cells. Lipids 43:19–28
93. Bjornstrom L, Sjoberg M (2005) Mechanisms of estrogen receptor signaling: convergence of genomic and nongenomic actions on target genes. Mol Endocrinol 19:833–842
94. Ropero AB, Eghbali M, Minosyan TY, Tang G, Toro L, Stefani E (2006) Heart estrogen receptor alpha: distinct membrane and nuclear distribution patterns and regulation by estrogen. J Mol Cell Cardiol 41:496–510
95. Monje P, Zanello S, Holick M, Boland R (2001) Differential cellular localization of estrogen receptor alpha in uterine and mammary cells. Mol Cell Endocrinol 181:117–129
96. Acconcia F, Ascenzi P, Fabozzi G, Visca P, Marino M (2004) S-palmitoylation modulates human estrogen receptor-alpha functions. Biochem Biophys Res Commun 316:878–883
97. Filardo EJ, Quinn JA, Bland KI, Frackelton AR Jr (2000) Estrogen-induced activation of Erk-1 and Erk-2 requires the G protein-coupled receptor homolog, GPR30, and occurs via trans-activation of the epidermal growth factor receptor through release of HB-EGF. Mol Endocrinol 14:1649–1660
98. Razandi M, Pedram A, Merchenthaler I, Greene GL, Levin ER (2004) Plasma membrane estrogen receptors exist and functions as dimers. Mol Endocrinol 18:2854–2865
99. Kamalakaran S, Radhakrishnan SK, Beck WT (2005) Identification of estrogen-responsive genes using a genome-wide analysis of promoter elements for transcription factor binding sites. J Biol Chem 280:21491–21497
100. Sharov AA, Dudekula DB, Ko MS (2006) CisView: a browser and database of cis-regulatory modules predicted in the mouse genome. DNA Res 13:123–134
101. Berger J, Moller DE (2002) The mechanisms of action of PPARs. Annu Rev Med 53:409–435
102. Fruchart JC, Duriez P, Staels B (1999) Peroxisome proliferator-activated receptor-alpha activators regulate genes governing

lipoprotein metabolism, vascular inflammation and atherosclerosis. Curr Opin Lipidol 10:245–257
103. Zhu Y, Qi C, Calandra C, Rao MS, Reddy JK (1996) Cloning and identification of mouse steroid receptor coactivator-1 (mSRC-1), as a coactivator of peroxisome proliferator-activated receptor gamma. Gene Expr 6:185–195
104. Braissant O, Foufelle F, Scotto C, Dauca M, Wahli W (1996) Differential expression of peroxisome proliferator-activated receptors (PPARs): tissue distribution of PPAR-alpha, -beta, and -gamma in the adult rat. Endocrinology 137:354–366
105. Palmer CN, Hsu MH, Griffin KJ, Raucy JL, Johnson EF (1998) Peroxisome proliferator activated receptor-alpha expression in human liver. Mol Pharmacol 53:14–22
106. Jump DB, Thelen A, Mater M (1999) Dietary polyunsaturated fatty acids and hepatic gene expression. Lipids 34 Suppl:S209–S212
107. Corton JC, Bocos C, Moreno ES, Merritt A, Cattley RC, Gustafsson JA (1997) Peroxisome proliferators alter the expression of estrogen-metabolizing enzymes. Biochimie 79:151–162
108. Chu R, Madison LD, Lin Y, Kopp P, Rao MS, Jameson JL, Reddy JK (1995) Thyroid hormone (T3) inhibits ciprofibrate-induced transcription of genes encoding beta-oxidation enzymes: cross talk between peroxisome proliferator and T3 signaling pathways. Proc Natl Acad Sci USA 92:11593–11597
109. Sandberg MB, Bloksgaard M, Duran-Sandoval D, Duval C, Staels B, Mandrup S (2005) The gene encoding acyl-CoA-binding protein is subject to metabolic regulation by both sterol regulatory element-binding protein and peroxisome proliferator-activated receptor alpha in hepatocytes. J Biol Chem 280:5258–5266
110. Martin G, Schoonjans K, Lefebvre AM, Staels B, Auwerx J (1997) Coordinate regulation of the expression of the fatty acid transport protein and acyl-CoA synthetase genes by PPARalpha and PPARgamma activators. J Biol Chem 272:28210–28217
111. Mandard S, Muller M, Kersten S (2004) Peroxisome proliferator-activated receptor alpha target genes. Cell Mol Life Sci 61:393–416
112. Nakamura MT, Cheon Y, Li Y, Nara TY (2004) Mechanisms of regulation of gene expression by fatty acids. Lipids 39:1077–1083
113. Burns KA, Vanden Heuvel JP (2007) Modulation of PPAR activity via phosphorylation. Biochim Biophys Acta 1771:952–960
114. Juge-Aubry CE, Hammar E, Siegrist-Kaiser C, Pernin A, Takeshita A, Chin WW, Burger AG, Meier CA (1999) Regulation of the transcriptional activity of the peroxisome proliferator-activated receptor alpha by phosphorylation of a ligand-independent trans-activating domain. J Biol Chem 274:10505–10510
115. Nemoto Y, Toda K, Ono M, Fujikawa-Adachi K, Saibara T, Onishi S, Enzan H, Okada T, Shizuta Y (2000) Altered expression of fatty acid-metabolizing enzymes in aromatase-deficient mice. J Clin Invest 105:1819–1825
116. Yoshikawa T, Toda K, Nemoto Y, Ono M, Iwasaki S, Maeda T, Saibara T, Hayashi Y, Miyazaki E, Hiroi M, Enzan H, Shizuta Y, Onishi S (2002) Aromatase-deficient (ArKO) mice are retrieved from severe hepatic steatosis by peroxisome proliferator administration. Hepatol Res 22:278–287
117. Lee KN, Pariza MW, Ntambi JM (1996) Differential expression of hepatic stearoyl-CoA desaturase gene 1 in male and female mice. Biochim Biophys Acta 1304:85–88
118. Kien CL, Bunn JY (2008) Gender alters the effects of palmitate and oleate on fat oxidation and energy expenditure. Obesity (Silver Spring) 16:29–33
119. Campbell SE, Mehan KA, Tunstall RJ, Febbraio MA, Cameron-Smith D (2003) 17beta-estradiol upregulates the expression of peroxisome proliferator-activated receptor alpha and lipid oxidative genes in skeletal muscle. J Mol Endocrinol 31:37–45
120. D'Eon TM, Souza SC, Aronovitz M, Obin MS, Fried SK, Greenberg AS (2005) Estrogen regulation of adiposity and fuel partitioning. Evidence of genomic and non-genomic regulation of lipogenic and oxidative pathways. J Biol Chem 280:35983–35991
121. Atshaves BP, Payne HR, McIntosh AL, Tichy SE, Russell D, Kier AB, Schroeder F (2004) Sexually dimorphic metabolism of branched-chain lipids in C57BL/6 J mice. J Lipid Res 45:812–830
122. Brandes R, Kaikaus RM, Lysenko N, Ockner RK, Bass NM (1990) Induction of fatty acid binding protein by peroxisome proliferators in primary hepatocyte cultures and its relationship to the induction of peroxisomal beta-oxidation. Biochim Biophys Acta 1034:53–61
123. Bass NM, Barker ME, Manning JA, Jones AL, Ockner RK (1989) Acinar heterogeneity of fatty acid binding protein expression in the livers of male, female and clofibrate-treated rats. Hepatology 9:12–21
124. Gorski J, Zendzian-Piotrowska M, Wolfrum C, Nawrocki A, Spener F (2000) Effect of sex and bezafibrate on incorporation of blood borne palmitate into lipids of rat liver nuclei. Mol Cell Biochem 214:57–62
125. Huang H, Starodub O, McIntosh A, Atshaves BP, Woldegiorgis G, Kier AB, Schroeder F (2004) Liver fatty acid-binding protein colocalizes with peroxisome proliferator activated receptor alpha and enhances ligand distribution to nuclei of living cells. Biochemistry 43:2484–2500
126. Hostetler HA, McIntosh AL, Atshaves BP, Storey SM, Payne HR, Kier AB, Schroeder F (2009) L-FABP directly interacts with PPARalpha in cultured primary hepatocytes. J Lipid Res 50:1663–1675
127. McIntosh AL, Atshaves BP, Hostetler HA, Huang H, Davis J, Lyuksyutova OI, Landrock D, Kier AB, Schroeder F (2009) Liver type fatty acid binding protein (L-FABP) gene ablation reduces nuclear ligand distribution and peroxisome proliferator-activated receptor-alpha activity in cultured primary hepatocytes. Arch Biochem Biophys 485:160–173
128. Helledie T, Antonius M, Sorensen RV, Hertzel AV, Bernlohr DA, Kolvraa S, Kristiansen K, Mandrup S (2000) Lipid-binding proteins modulate ligand-dependent trans-activation by peroxisome proliferator-activated receptors and localize to the nucleus as well as the cytoplasm. J Lipid Res 41:1740–1751
129. Bohnet S, Rogers L, Sasaki G, Kolattukudy PE (1991) Estradiol induces proliferation of peroxisome-like microbodies and the production of 3-hydroxy fatty acid diesters, the female pheromones, in the uropygial glands of male and female mallards. J Biol Chem 266:9795–9804
130. Rosenberger TA, Hovda JT, Peters JM (2002) Targeted disruption of peroxisomal proliferator-activated receptor beta (delta) results in distinct gender differences in mouse brain phospholipid and esterified FA levels. Lipids 37:495–500
131. Yu K, Bayona W, Kallen CB, Harding HP, Ravera CP, McMahon G, Brown M, Lazar MA (1995) Differential activation of peroxisome proliferator-activated receptors by eicosanoids. J Biol Chem 270:23975–23983
132. Ciana P, Biserni A, Tatangelo L, Tiveron C, Sciarroni AF, Ottobrini L, Maggi A (2007) A novel peroxisome proliferator-activated receptor responsive element-luciferase reporter mouse reveals gender specificity of peroxisome proliferator-activated receptor activity in liver. Mol Endocrinol 21:388–400
133. Nakajima T, Kamijo Y, Usuda N, Liang Y, Fukushima Y, Kametani K, Gonzalez FJ, Aoyama T (2000) Sex-dependent regulation of hepatic peroxisome proliferation in mice by trichloroethylene via peroxisome proliferator-activated receptor alpha (PPARalpha). Carcinogenesis 21:677–682

134. Kim BH, Won YS, Kim DY, Kim B, Kim EY, Yoon M, Oh GT (2009) Signal crosstalk between estrogen and peroxisome proliferator-activated receptor alpha on adiposity. BMB Rep 42:91–95
135. Lewitt MS, Brismar K (2002) Gender difference in the leptin response to feeding in peroxisome-proliferator-activated receptor-alpha knockout mice. Int J Obes Relat Metab Disord 26:1296–1300
136. Ronda AC, Buitrago C, Colicheo A, de Boland AR, Roldan E, Boland R (2007) Activation of MAPKs by 1alpha, 25(OH)2-vitamin D3 and 17beta-estradiol in skeletal muscle cells leads to phosphorylation of Elk-1 and CREB transcription factors. J Steroid Biochem Mol Biol 103:462–466
137. Migliaccio A, Di DM, Castoria G, de FA, Bontempo P, Nola E, Auricchio F (1996) Tyrosine kinase/p21ras/MAP-kinase pathway activation by estradiol-receptor complex in MCF-7 cells. EMBO J 15:1292–1300
138. Shalev A, Siegrist-Kaiser CA, Yen PM, Wahli W, Burger AG, Chin WW, Meier CA (1996) The peroxisome proliferator-activated receptor alpha is a phosphoprotein: regulation by insulin. Endocrinology 137:4499–4502
139. Yoon MJ, Lee GY, Chung JJ, Ahn YH, Hong SH, Kim JB (2006) Adiponectin increases fatty acid oxidation in skeletal muscle cells by sequential activation of AMP-activated protein kinase, p38 mitogen-activated protein kinase, and peroxisome proliferator-activated receptor alpha. Diabetes 55:2562–2570
140. Pandey NR, Renwick J, Misquith A, Sokoll K, Sparks DL (2008) Linoleic acid-enriched phospholipids act through peroxisome proliferator-activated receptors alpha to stimulate hepatic apolipoprotein A-I secretion. Biochemistry 47:1579–1587
141. Tang B, Ji Y, Traub RJ (2008) Estrogen alters spinal NMDA receptor activity via a PKA signaling pathway in a visceral pain model in the rat. Pain 137:540–549
142. Hsieh YC, Yu HP, Frink M, Suzuki T, Choudhry MA, Schwacha MG, Chaudry IH (2007) G protein-coupled receptor 30-dependent protein kinase A pathway is critical in nongenomic effects of estrogen in attenuating liver injury after trauma-hemorrhage. Am J Pathol 170:1210–1218
143. Lazennec G, Canaple L, Saugy D, Wahli W (2000) Activation of peroxisome proliferator-activated receptors (PPARs) by their ligands and protein kinase A activators. Mol Endocrinol 14:1962–1975
144. Rosenberger TA, Farooqui AA, Horrocks LA (2007) Bovine brain diacylglycerol lipase: substrate specificity and activation by cyclic AMP-dependent protein kinase. Lipids 42:187–195
145. Gaidhu MP, Fediuc S, Anthony NM, So M, Mirpourian M, Perry RL, Ceddia RB (2009) Prolonged AICAR-induced AMP-kinase activation promotes energy dissipation in white adipocytes: novel mechanisms integrating HSL and ATGL. J Lipid Res 50:704–715
146. Lee WJ, Kim M, Park HS, Kim HS, Jeon MJ, Oh KS, Koh EH, Won JC, Kim MS, Oh GT, Yoon M, Lee KU, Park JY (2006) AMPK activation increases fatty acid oxidation in skeletal muscle by activating PPARalpha and PGC-1. Biochem Biophys Res Commun 340:291–295
147. Wilson BE, Mochon E, Boxer LM (1996) Induction of bcl-2 expression by phosphorylated CREB proteins during B-cell activation and rescue from apoptosis. Mol Cell Biol 16:5546–5556
148. Castro-Rivera E, Samudio I, Safe S (2001) Estrogen regulation of cyclin D1 gene expression in ZR-75 breast cancer cells involves multiple enhancer elements. J Biol Chem 276:30853–30861
149. Alexaki VI, Charalampopoulos I, Kampa M, Nifli AP, Hatzoglou A, Gravanis A, Castanas E (2006) Activation of membrane estrogen receptors induce pro-survival kinases. J Steroid Biochem Mol Biol 98:97–110
150. Boon JM, Smith BD (2002) Chemical control of phospholipid distribution across bilayer membranes. Med Res Rev 22:251–281
151. Jupp OJ, Vandenabeele P, MacEwan DJ (2003) Distinct regulation of cytosolic phospholipase A2 phosphorylation, translocation, proteolysis and activation by tumour necrosis factor-receptor subtypes. Biochem J 374:453–461
152. Grewal S, Morrison EE, Ponnambalam S, Walker JH (2002) Nuclear localisation of cytosolic phospholipase A2-alpha in the EA.hy.926 human endothelial cell line is proliferation dependent and modulated by phosphorylation. J Cell Sci 115:4533–4543
153. Improta-Brears T, Whorton AR, Codazzi F, York JD, Meyer T, McDonnell DP (1999) Estrogen-induced activation of mitogen-activated protein kinase requires mobilization of intracellular calcium. Proc Natl Acad Sci USA 96:4686–4691
154. Chen Z, Yuhanna IS, Galcheva-Gargova Z, Karas RH, Mendelsohn ME, Shaul PW (1999) Estrogen receptor alpha mediates the nongenomic activation of endothelial nitric oxide synthase by estrogen. J Clin Invest 103:401–406
155. Marino M, Acconcia F, Bresciani F, Weisz A, Trentalance A (2002) Distinct nongenomic signal transduction pathways controlled by 17beta-estradiol regulate DNA synthesis and cyclin D(1) gene transcription in HepG2 cells. Mol Biol Cell 13:3720–3729
156. Farina MG, Billi S, Leguizamon G, Weissmann C, Guadagnoli T, Ribeiro ML, Franchi AM (2007) Secretory and cytosolic phospholipase A2 activities and expression are regulated by oxytocin and estradiol during labor. Reproduction 134:355–364
157. Burlando B, Marchi B, Panfoli I, Viarengo A (2002) Essential role of Ca^{2+}-dependent phospholipase A2 in estradiol-induced lysosome activation. Am J Physiol Cell Physiol 283:C1461–C1468
158. Das UN (2007) A defect in the activity of Delta6 and Delta5 desaturases may be a factor in the initiation and progression of atherosclerosis. Prostaglandins Leukot Essent Fatty Acids 76:251–268
159. Spaziani EP, Lantz ME, Benoit RR, O'Brien WF (1996) The induction of cyclooxygenase-2 (COX-2) in intact human amnion tissue by interleukin-4. Prostaglandins 51:215–223

Lipids (2010) 45:225–236
DOI 10.1007/s11745-010-3392-5

ORIGINAL ARTICLE

Lysophosphatidylcholine Containing Docosahexaenoic Acid at the *sn*-1 Position is Anti-inflammatory

Long Shuang Huang · Nguyen Dang Hung · Dai-Eun Sok · Mee Ree Kim

Received: 20 October 2009 / Accepted: 26 January 2010 / Published online: 18 February 2010

Abstract Lysophosphatidylcholine is known to be a lipid mediator in various cellular responses. In this study, we examined the anti-inflammatory actions of lysophosphatidylcholine containing docosahexaenoic acid esterified at the *sn*-1 position. First, in RAW 264.7 cells, DHA-lysoPtdCho suppressed the LPS-induced formation of NO concentration-dependently. However, ARA-lysoPtdCho showed a partial suppression, and LNA-lysoPtdCho had no significant effect. Additionally, DHA-lysoPtdCho also reduced the level of TNF-α or IL-6, but not PGE_2. In animal experiments, the i.v. administration of ARA-lysoPtdCho (150 or 500 μg/kg) prevented zymosan A-induced plasma leakage remarkably with a maximal efficacy (Emax) of 50%, in contrast to no effect with LNA-lysoPtdCho. Remarkably, DHA-lysoPtdCho suppressed zymosan A-induced plasma leakage with an ED_{50} value of 46 μg/kg and an Emax value of around 95%. Additionally, mechanistic studies indicated that the anti-inflammatory action of DHA-lysoPtdCho was partially related to the reduced formation of LTC_4, TNF-α, and IL-6. When the interval time between lysoPtdCho administration and zymosan A challenge was extended up to 2 h, such a suppressive action of DHA-lysoPtdCho was augmented, suggesting that a DHA-lysoPtdCho metabolite is important for anti-inflammatory action. In support of this, 17-HPDHA-lysoPtdCho showed a greater anti-inflammatory action than DHA-lysoPtdCho. Furthermore, a similar anti-inflammatory action was also observed with i.p. administration of DHA-lysoPtdCho or a 17(*S*)-hydroperoxy derivative. Additionally, oral administration of DHA-lysoPtdCho also expressed a significant anti-inflammatory action. Taken together, it is proposed that DHA-lysoPtdCho and its metabolites may be anti-inflammatory lipids in vivo systems.

Keywords Anti-inflammatory · Nitric oxide · DHA-lysoPtdCho · 17-HPDHA- lysoPtdCho · Docosahexaenoic · LPS · Zymosan A · RAW 264.7 cell

Abbreviations

lysoPtdCho	Lysophosphatidylcholine
LNA	Linoleic acid
ARA	Arachidonic acid
DHA	Docosahexaenoic acid
LNA-lysoPtdCho	1-Linoleoyl-2-lyso-*sn*-glycerol-3-phosphocholine
ARA-lysoPtdCho	1-Arachidonyl-2-lyso-*sn*-glycerol-3-phosphocholine
DHA-lysoPtdCho	1-Docosahexaenoyl-2-lyso-*sn*-glycerol-3-phosphocholine
14-HPDHA-lysoPtdCho	1-14(*S*)-hydroperoxy-4,7,10,13,15,19-docosahexaenoyl-2-lyso-*sn*-glycerol-3-phosphocholine
17-HPDHA-lysoPtdCho	1-17(*S*)-hydroperoxy-4,7,10,13,15,19-docosahexaenoyl-2-lyso-*sn*-glycerol-3 phosphocholine

L. S. Huang and N. D. Hung contributed equally.

L. S. Huang · N. D. Hung · D.-E. Sok
College of Pharmacy, Chungnam National University, Gung-Dong 220, Yuseong-Gu, Taejon 305-764, Korea

M. R. Kim (✉)
Department of Food and Nutrition, Chungnam National University, Gung-Dong 220, Yuseong-Gu, Taejon 305-764, Korea
e-mail: mrkim@cnu.ac.kr

LOX	Lipoxygenase
ED_{50}	50% effective dose
IC_{50}	50% inhibitory concentration
PLA_2	Phospholipase A_2
LTC_4	Leukotriene C_4
PGE_2	Prostaglandin E_2
IL-6	Interleukin-6
TNF-α	Tumor necrosis factor alpha
NO	Nitric oxide

Introduction

Previously, certain families of lipid-derived mediators were reported to be implicated in inflammatory diseases such as asthma, rheumatoid arthritis, or inflammatory bowel disease [1–6]. Although much is known about the molecular basis of initiating signals and pro-inflammatory chemical mediators in inflammation, it has recently become apparent that endogenous lipid mediators participate in events of inflammatory or anti-inflammatory events [7, 8]. Arachidonic acid (ARA), released from PLA_2-catalyzed hydrolysis of phosphatidylcholine, is converted to leukotrienes or lipoxins via the lipoxygenase enzymatic pathway, and to prostaglandins via the cyclooxygenase enzymatic pathway. Especially, prostaglandin E_2 (PGE_2) and leukotriene B_4 (LTB_4) are well known to be representative pro-inflammatory lipid mediators [9], whereas lipoxins have recently been reported to show an anti-inflammatory action [7]. Remarkably, arachidonate-derived eicosanoids in inflammatory exudates include lipoxins in addition to prostaglandins and leukotrienes. 5-Lipoxygenase (5-LOX) is crucial for the formation of leukotrienes and lipoxins, while 12/15-lipoxygenase is important for the formation of lipoxin [7, 9–12]. Furthermore, resolvins, which are generated from the oxygenation of eicosapentenoic acid at C-15, and protectins, derived from oxygenation of docosahexaenoic acid (DHA) at C-17 have also been reported to be potent anti-inflammatory lipid molecules.

Meanwhile, lysophosphatidylcholine (lysoPtdCho), another product from PLA_2-catalyzed hydrolysis of phosphatidylcholine, has been reported to be pro-inflammatory [1–3, 6, 13]. The pro-inflammatory action of lysoPtdChos, saturated or monounsaturated, may be due to the generation of reactive oxygen species or nitric oxide in various types of cells [14–17]. Additionally, our recent study also indicated that LNA-lysoPtdCho showed a cytotoxic effect, accompanied by ROS formation [18]. Previous studies reported that lysoPtdChos with a polyunsaturated acyl group were present in animal sources. In plasma, LNA-lysoPtdCho, ARA-lysoPtdCho, and DHA-lysoPtdCho existed at a substantial level in plasma [19–21]. In addition, DHA-lysoPtdCho was one of the major lipid components in shark liver extract [22]. Noteworthy, our recent studies demonstrated that polyunsaturated-lysoPtdChos containing linoleoyl, arachidonoyl, or docosahexaenoyl group was efficiently oxygenated by reticulocyte 15-LOX or leukocyte 12/15-LOX [23–25]. Therefore, it was supposed that lysoPtdChos with polyunsaturated acyl groups could affect the formation of lipid mediators such as lipoxin [7]. Separately, in our study, ARA-lysoPtdCho and DHA-lysoPtdCho were found to strongly inhibit mammalian 5-LOX activity [26], responsible for the generation of pro-inflammatory leukotrienes [9]. Meanwhile, DHA, a hydrolysis product of DHA-lysoPtdCho, is known to show anti-inflammatory action [27] while ARA, the hydrolysis product of ARA-lysoPtdCho, is converted to lipid metabolites, pro-inflammatory or anti-inflammatory. Nonetheless, there has been no knowledge about the effect of polyunsaturated-lysoPCs on inflammation in vivo system. In this regard, we examined anti-inflammatory effects of lysoPtdChos containing polyunsaturated acyl group in vitro as well as in vivo system.

Materials and Methods

Materials

Dilinoleoyl phosphatidylcholine, diarachidonoyl phosphatidylcholine, and didocosahexaenoyl phosphatidylcholine (purity, 99%) were from Avanti Polar Lipid (Alabaster, AL, USA). 3-(4,5-dimethylthiazol-2-yl)-2,5-diphenyl-tetrazolium bromide (MTT), soybean lipoxygenase-1 (Type I-B), phospholipase A_2 (PLA_2) (honey bee venom), lipopolysaccharide (LPS) (from *Escherichia coli* serotype 0111:B4; purity >99%) and zymosan A (from *Saccharomyces cerevisiae*) were purchased from Sigma-Aldrich Corp (St. Louis, MO, USA). PGE_2 and LTC_4 EIA kit were procured from Cayman Chemical (Ann Arbor, MI, USA). TNF-α ELISA kit was from Invitrogen Corp (Camarillo, CA, USA) and IL-6 ELISA kit was obtained from Ebioscience Inc Co (California, USA). LNA-lysoPtdCho, ARA-lysoPtdCho, DHA-lysoPtdCho were prepared from PLA_2-catalyzed hydrolysis of the corresponding phosphatidylcholines as described previously with a slight modification [23–26]. In brief, didocosahexaeonyl-phosphatidylcholine (2.5 mg), dissolved in chloroform, was dried under N_2, and then rapidly dispersed in 10 ml of 50 mM borax buffer (pH 9.0) containing 10 mM $CaCl_2$. The hydrolysis was started by adding PLA_2 (100 units), and allowed to continue under N_2 with constant stirring for 2 h at 25 °C. The reaction mixture was partially purified by a Sep-pack column (2 × 1 cm) and the lysophospholipid

product was further purified by silica gel TLC in the solvent system (chloroform: methanol: water: 65:25:4). Finally, the spot containing DHA-lysoPtdCho was scraped off, extracted with methanol, dried under nitrogen and kept at −80 °C until use and 17-HPDHA-lysoPtdCho was prepared as described previously [26]; briefly, soybean LOX-1 (200 units/ml) was incubated with DHA-lysoPtdCho (200 μM) in borax buffer (50 mM, pH 9.0) for 30 min. Subsequently, the mixture was passed through a C_{18} column (2 × 1 cm), and the products were eluted with methanol and concentrated under N_2 gas.

Measurement of Polyunsaturated LysoPtdCho Induced Cytotoxicity in RAW 264.7 cells

RAW 264.7 cells were cultured in DMEM supplemented with penicillin (100 units/ml), streptomycin (100 μg/ml) and heat-inactivated FBS (10% v/v) at 37 °C in 5% CO_2 (19). Cells with passages from 6 to 13 were harvested, and seeded in 96-well plate (5×10^4 cells/well), followed by 24 h incubation. Then, cells were pre-incubated with each polyunsaturated lysoPtdCho (0–60 μM) in the medium for 2 h, and then incubated in the presence or absence of LPS (1 μg/ml) at 37 °C for 20 h. Cell viability was examined by the assay using MTT [18]; briefly, RAW cells (5×10^4 cells/well) were exposed to MTT reagent (500 μg/ml) at 37 °C for 4 h. After the removal of the medium, the formazan was extracted from cells by disrupting the cell membranes with dimethylsulfoxide. The cell viability was measured by determining the absorbance at 570 nm with a reference at 690 nm.

Preventive Effect of LysoPtdCho on LPS-Induced NO Production in RAW 264.7 Cells

RAW 264.7 cells (5×10^4 cells/well) were preincubated with polyunsaturated lysoPtdCho (0–60 μM) at 37 °C for 2 h, and then the production of NO (nitric oxide) was stimulated with LPS (1 μg/ml) during further incubation for 20 h. The production of NO was determined by using the Griess reagent consisting of 1% sulfanilamide and 0.1% *N*-(1-naphthyl) ethylenediamine dihydrochloride in 2.5% H_3PO_4 [18].

Effect of DHA-lysoPtdCho on LPS-Induced TNF-α, IL-6, and PGE_2 Formation in RAW 264.7 Cells

To investigate the effect of DHA-lysoPtdCho on TNF-α, IL-6, and PGE_2 formation in LPS-treated cells, RAW 264.7 cells (5×10^4), seeded on 96-well plate, were pre-incubated with DHA-lysoPtdCho (0–40 μM) 2 h prior to treatment with LPS (1 μg/ml) for 20 h at 37 °C, in a 5% CO_2 incubator. The cell-free supernatants were collected for the determination of TNF-α, and IL-6 by ELISA kit and PGE_2 by EIA kit according to the manufacturers' manuals.

Effect of Polyunsaturated LysoPtdCho on Zymosan A-Induced Peritonitis in Mice

ICR mice (male, 6 weeks) were housed under a 12 h: 12 h light–dark cycle and fed with unlimited commercial food and water. Peritoneal inflammation was induced in ICR mice according to a previously reported method [28, 29] with some modifications. For the measurement of plasma leakage, polyunsaturated PtdChos, polyunsaturated lysoPtdChos (0–500 μg/kg) or their derivatives were administrated intravenously, intraperitoneally or orally 30–60 min prior to intravenous injection of 0.5% Evans blue dye (200 μl), dissolved in PBS, and intraperitoneal injection of zymosan A (100 mg/kg), prepared freshly in PBS. Then 30 min later, mice lightly anesthetized were decapitated and blood was collected to obtain serum as described previously [30]. Meanwhile, peritoneal lavages were performed with 4 ml of ice cold PBS followed by the brief centrifugation to get supernatant. Subsequently, the concentration of Evans blue dye in peritoneal lavage fluid and in serum was determined by measuring absorbance at 620 nm, and calculating the amount to (μg/μl) using an Evan Blue standard curve. The volume of plasma leakage (μl) for 30 min after zymosan A i.p. injection was calculated by dividing the amount of Evans blue dye in the peritoneal lavage fluid (μg) by the concentration of Evans blue dye in the serum (μg/μl) [31].

For the measurement of leukocyte infiltration, lysoPtdChos and their derivatives were administered i.v. 30 min prior to i.p. administration of zymosan A as described above. Total cell counting were performed for lavage fluid collected at the 90 min time point using light microscopy together with trypan blue staining [31, 32].

Determination of LTC_4, TNF-α, and IL-6 Levels in Peritoneal Lavage Fluid

In order to determine the level of LTC_4, TNF-α, and IL-6 in exudates, 1 ml of peritoneal lavage fluid was transferred to microcentrifuge tubes, and centrifuged (15,000 rpm, 5 min). The supernatant was used directly for the analysis of TNF-α and IL-6 by ELISA kit, and analysis of LTC_4 by enzyme immunoassay (EIA) kit according to the manufacture's instructions [31–33].

Effect of DHA-LysoPtdCho on Leukotriene C_4-Induced Plasma Leakage

DHA-lysoPtdCho (0–150 μg/kg) was injected into the tail vein of mice, and 60 min later, 0.2 ml of 0.5% Evans blue

dye dissolved in saline was intravenously injected just before intraperitoneal (i.p.) administration of LTC_4 (100 μg/kg). Samples of blood and peritoneal fluid were collected as described above [34].

Statistical Analysis

Results were expressed as means ± SD. Statistical significance was evaluated using ANOVA and Student's *t* test, and $P < 0.05$ was considered statistically significant.

Results

Our previous study indicated that polyunsaturated lysoPtdChos strongly inhibited mammalian 5-LOX activity [9], an initial enzyme in the biosynthesis of inflammatory LTC_4 [26]. In the present study, we evaluated the anti-inflammatory actions of polyunsaturated lysoPtdChos by determining the effect of lysoPtdChos on LPS-induced formation of inflammatory mediators such as NO, PGE_2, TNF-α, or IL-6.

Effects of Polyunsaturated LysoPtdChos on LPS-Induced Production of Mediators in RAW 264.7 Cells

It is well known that the stimulation of macrophages by LPS results in high-level production of nitric oxide [35] through the expression of inducible nitric oxide synthase (iNOS) in some cells such as macrophages [36]. First, to see the effect of lysoPtdCho on LPS-induced NO formation, each lysoPtdCho (3–60 μM) was pre-incubated with RAW 264.7 cells for 2 h, and then LPS (1 μg/ml) was included in the same incubation. As shown in Fig. 1b, LNA-lysoPtdCho had no significant suppressive effect on LPS-induced NO formation up to 60 μM. Additionally, ARA-lysoPtdCho also showed no significant inhibition of LPS-induced NO formation at lower concentrations (1–20 μM), although it had some suppressive effect at 60 μM. In contrast, DHA-lysoPtdCho diminished the production of NO in a concentration-dependent manner (12–200 μM), and the 50% effective concentration (EC_{50}) of DHA-lysoPtdCho was estimated to be 18.2 ± 2.1 μM (Fig. 1b). Meanwhile, DHA at 20 μM suppressed LPS-induced NO production by approximately 18% (data not shown), much smaller than the suppression (~50%) achieved with DHA-lysoPtdCho at 20 μM. In a separate experiment to see whether the suppressive effect of DHA-lysoPtdCho on LPS-induced NO production was related to its cytotoxic action, the effect of DHA-lysoPtdCho on the viability of RAW 264.7 cells was measured, based on the MTT assay. Figure 1a indicates that DHA-lysoPtdCho and DHA-lysoPtdCho had no remarkable cytotoxic effect within the concentrations used, whereas linoleoyl-lysoPC showed a significant reduction of viability at 6 μM or higher concentrations. Thus, the suppressive effect of DHA-lysoPtdCho on LPS-induced NO production was expressed at non-cytotoxic concentrations. Subsequently, we turned to the effect of DHA-lysoPtdCho on the level of TNF-α or IL-6 in RAW 264.7 cells stimulated with LPS. Again, DHA-lysoPtdCho expressed a dose-dependent suppression of TNF-α or IL-6 formation (Fig. 2). Next, we examined the effect of DHA-lysoPtdCho on PGE_2 formation in RAW 264.7 cells stimulated with LPS. However, DHA-lysoPtdCho up to 200 μM failed to diminish the level of PGE_2 (779 pg/ml) in RAW 264.7 cells stimulated with LPS (1 μg/ml) only (data not shown).

Effects of Polyunsaturated LysoPtdChos on Zymosan A-Induced Plasma Leakage

Since DHA-lysoPtdCho exhibited a remarkable anti-inflammatory action in vitro models, we examined whether

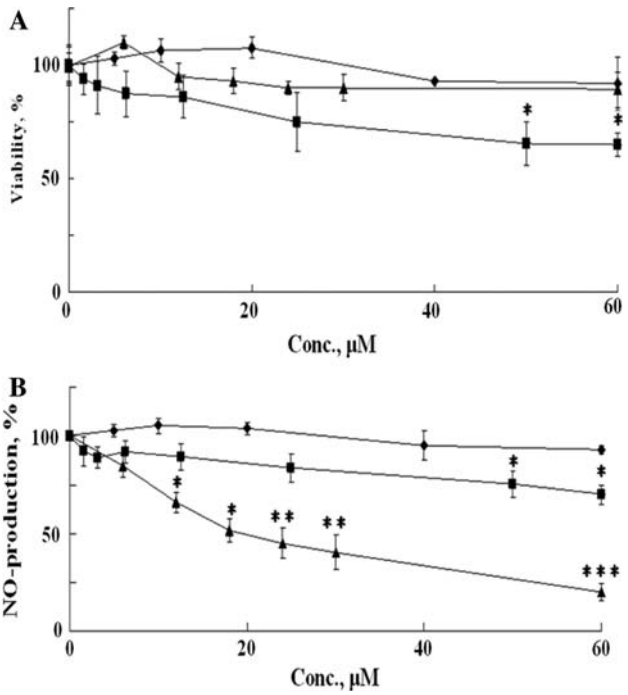

Fig. 1 Effect of polyunsaturated lysoPtdChos on cell viability or LPS-induced NO production. RAW 264.7 cells were preincubated with each polyunsaturated lysoPtdCho (LNA-lysoPtdCho, *filled squares*; ARA-lysoPtdCho, *filled diamonds*; DHA-lysoPtdCho, *filled triangles*) at various concentration (0–60 μM) for 2 h, and then stimulated with LPS (1 μg/ml) for another 20 h. Cell viability (**a**) and LPS-induced NO production (**b**) were determined as described in "Materials and Methods". Data were expressed as a percentile value (%) of the LPS-treated group, which were pre-incubated with LPS (1 μg/ml) in the absence of polyunsaturated-lysoPCs, and were displayed as mean ± SE values of triplicate determinations. *$P < 0.05$ and **$P < 0.01$ versus LPS-treated group

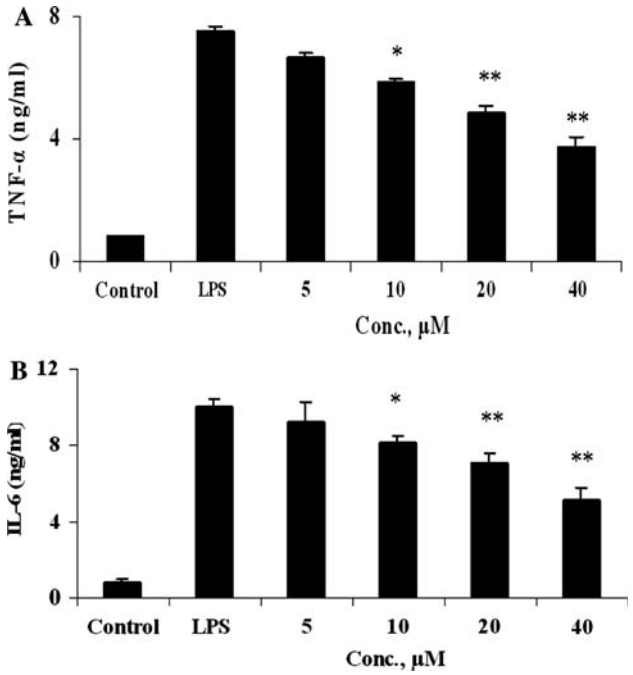

Fig. 2 Effects of DHA-lysoPtdCho on LPS -induced TNF-α (**a**) and IL-6 (**b**) production in RAW 264.7 cells. RAW 264.7 cells (5×10^4 cells/well) were incubated with DHA-lysoPtdCho (5–40 μM) for 2 h and then LPS (1 μg/ml) was treated for another 20 h. TNF-α and IL-6 in the cell-free cultured supernatant were measured by an ELISA kit. Data were expressed as mean ± SEM values of triplicate determinations. $*P < 0.05$ and $**P < 0.01$ versus LPS-treated group

polyunsaturated lysoPtdChos might attenuate zymosan A-induced peritonitis in an animal model. In this study, each lysoPtdCho was tested for the suppression of zymosan A-induced plasma leakage into the peritoneum in mice, based on extravasation of Evans blue dye indicative of vascular permeability. As shown in Fig. 3a, the i.v. administration of LNA-lysoPtdCho up to 500 μg/kg did not reduce the level of exudate infiltration induced by zymosan A, when it was administered 30 min before i.p. administration of zymosan A (100 mg/kg). Meanwhile, ARA-lysoPtdCho (150 μg/kg) was observed to decrease the level of exudate infiltration induced by zymosan A, but the elevation of ARA-lysoPtdCho dose to 500 μg/kg failed to further enhance the suppressive effect (Fig. 3b). Furthermore (Fig. 3c), DHA-lysoPtdCho expressed a remarkable suppression of zymosan A-induced plasma leakage in a dose-dependent way up to 500 μg/kg; a significant decline of zymosan A-induced plasma leakage into the peritoneum was observed with DHA-lysoPtdCho at a dose as small as 15 μg/kg ($P < 0.05$). Further, the administration of DHA-lysoPtdCho at a higher dose (500 μg/kg) almost completely suppressed the zymosan A-induced plasma leakage into the peritoneum, and the ED_{50} value was estimated to be approximately 46 μg/kg. However, zymosan A-induced plasma leakage was not suppressed significantly or remarkably (<10%) by didocosahexaenoyl-phosphatidylcholine (15–50 μg/kg) (data not shown). From these data, it was found that DHA-lysoPtdCho was the most efficient among phospholipids tested in preventing zymosan A-induced plasma leakage. To prove the anti-inflammatory action of DHA-lysoPtdCho in vivo, we examined the effect of DHA-lysoPtdCho on inflammatory mediators such as interleukin-6 or TNF-α in peritoneal exudates. As indicated in Fig. 4, DHA-lysoPtdCho, administered i.v. significantly inhibited zymosan A-induced formation of IL-6 and TNF-α in dose-dependent manner, supporting anti-inflammatory role of DHA-lysoPtdCho. In further study, the effect of DHA-lysoPtdCho on infiltration of leukocytes into the peritoneum was evaluated. Figure 5 showed that DHA-lysoPtdCho prohibited the infiltration of leukocytes into the peritoneum, providing further support for the anti-inflammatory action of DHA-lysoPtdCho.

In the subsequent study, a time-dependent effect of DHA-lysoPtdCho on zymosan A-induced plasma leakage was examined. For this study, DHA-lysoPtdCho (50 μg/kg) was administered 10, 30, 60, or 120 min before i.p. administration of zymosan A, and a time-dependent suppression of plasma leakage was evaluated. As exhibited in Fig. 6, the 10-min interval between administration of DHA-lysoPtdCho and zymosan A challenge was not sufficient to express a remarkable suppression of plasma leakage. Meanwhile, both the 30-min interval and the 60-min interval were sufficient to inhibit zymosan A-induced plasma leakage, although there was no significant difference between two experimental conditions. This may suggest that the same mechanism may apply for anti-inflammatory action of DHA-lysoPtdCho between 30- and 60-min intervals. Meanwhile, the extension of interval time to 120 min augmented the inhibitory effect to some extent. Taken together, it is supposed that anti-inflammatory action of DHA-lysoPtdCho may involve multiple mechanisms. Previously, DHA-lysoPtdCho was observed to inhibit 5-lipoxygenase, an initial enzyme in the biosynthetic pathway responsible for the formation of LTC_4 [9]. Therefore, the accumulation of DHA-lysoPtdCho in the peritoneum may lead to the reduction of LTC_4 formation in the peritoneum. To test this possibility, the effect of DHA-lysoPtdCho administration on the formation of LTC_4 in the peritoneum was investigated [34]. As indicated in Fig. 7, the formation of LTC_4 in peritoneal exudates was suppressed by DHA-lysoPtdCho, i.v. administered in a dose-dependent manner. However, the suppression of leukotriene C_4 formation by DHA-lysoPtdCho at 150 μg/kg was approximately 50%. From this, it is suggested that anti-inflammatory action of DHA-lysoPtdCho may be ascribed at least partially to the inhibition of 5-lipoxygenase. However, the suppressive effect of DHA-lysoPtdCho on

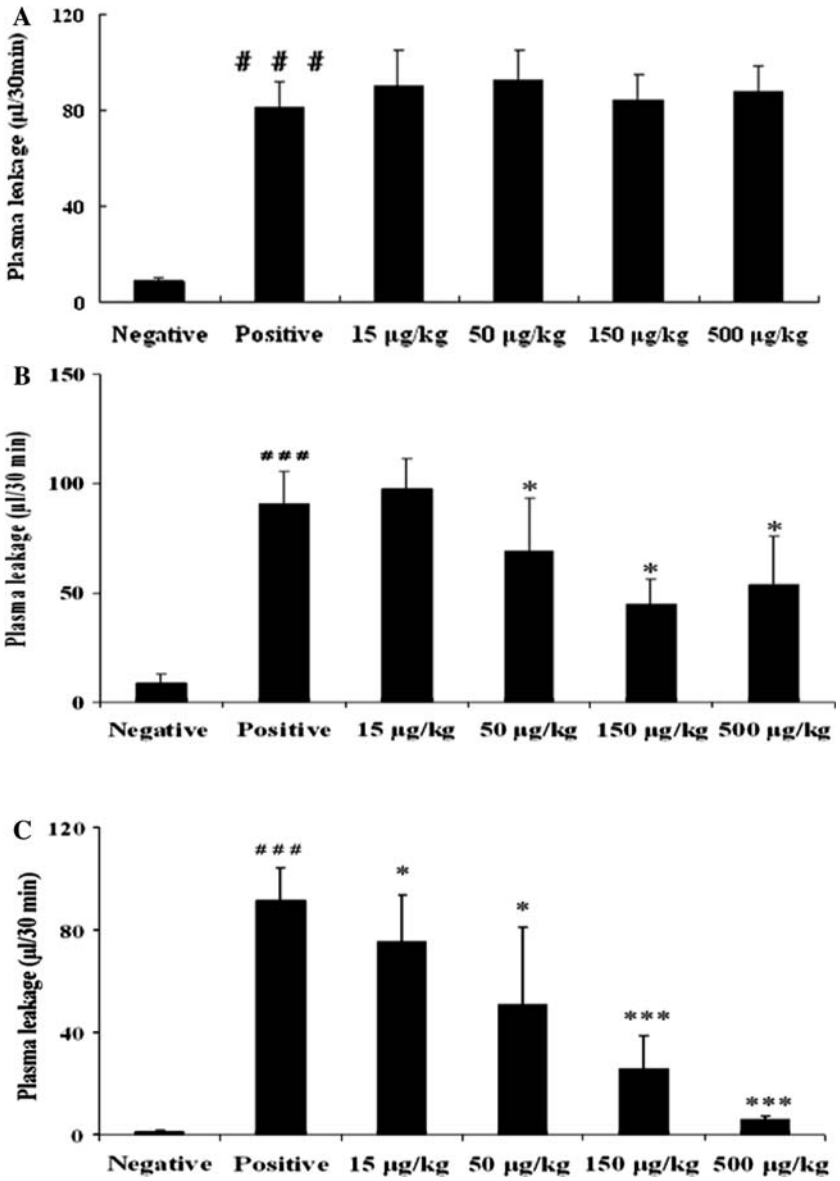

Fig. 3 Effects of polyunsaturated lysoPtdCho, administered i.v. on Zymosan A-induced plasma leakage in mice. LNA-lysoPtdCho (**a**), ARA-lysoPtdCho (**b**) DHA-lysoPtdCho (**c**) was administered i.v. to mice (0–500 μg/kg) 30 min prior to i.p. administration of zymosan A (100 mg/kg), and the plasma leakage was determined as described in Materials and Methods. The *column* and *bar* represent the means ± SEM of results from each group of >10 mice. $^{*}P < 0.05$, $^{**}P < 0.01$, $^{***}P < 0.001$ versus positive group (zymosan A); $^{\#\#\#}P < 0.001$ versus negative group (PBS)

zymosan A-induced LTC_4 formation was smaller than zymosan A-induced plasma leakage (Fig. 3c). This led to the assumption that a process responsible for the change of vascular permeability might be directly affected by DHA-lysoPtdCho or its metabolites. To test this possibility, we examined the effect of DHA-lysoPtdCho on plasma leakage caused by LTC_4, an inflammatory mediator. Figure 8 demonstrates that LTC_4-induced inflammation was suppressed remarkably by DHA-lysoPtdCho. This may support a notion that a mechanism other than the inhibition of LTC_4 formation may also be responsible for the anti-inflammatory action of DHA-lysoPtdCho. In support of this, a time-dependent action of DHA-lysoPtdCho indicates that the metabolism of DHA-lysoPtdCho may be crucial for its anti-inflammatory action. One metabolic pathway is the hydrolysis of DHA-lysoPtdCho to produce DHA. And the other may be a lipoxygenation process to give rise to HPDHA-lysoPtdCho. With this in mind, DHA and 17-HPDHA-lysoPtdCho were examined for their anti-inflammatory action. As demonstrated in Fig. 9, 17-HPDHA-lysoPC, a product from the oxygenation of DHA-lysoPtdCho by 15-lipoxygenase, showed a remarkable anti-inflammatory effect, greater than that of DHA-lysoPtdCho. From this, it is suggested that the anti-inflammatory action of DHA-lysoPtdCho may involve the formation of 17-HPDHA-lysoPtdCho as an intermediate in the metabolic activation of DHA-lysoPtdCho. Meanwhile, the treatment with DHA or 17(*S*)-hydroperoxy-4,7,10,13,15,19-DHA at 50 μg/kg did not show any significant anti-inflammatory action (Fig. 9).

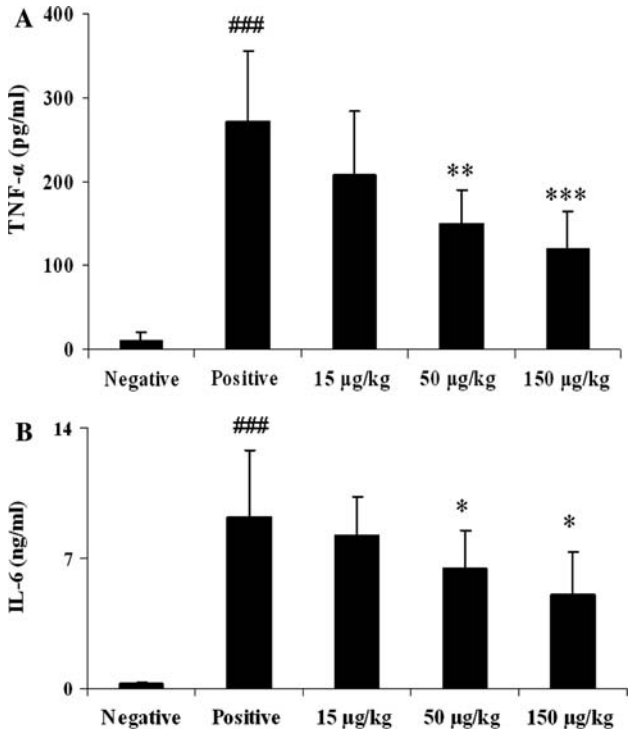

Fig. 4 Effect of DHA-lysoPtdCho, administered i.v. on zymosan A-induced TNF-α and IL-6 formation in mice. DHA-lysoPtdCho was administered i.v. to mice (0–150 μg/kg) 30 min prior to i.p. administration of zymosan A (100 mg/kg). Plasma lavage was performed with 4 ml PBS followed by brief centrifugation (15,000 rpm, 5 min), and cell-free lavage supernatant was used directly for determination of TNF-α and IL-6 levels by ELISA kit. The *column* and *bar* represent the means ± SEM of results from each group of ten mice. $^{*}P < 0.05$, $^{**}P < 0.01$, $^{***}P < 0.001$ versus positive group (zymosan A); $^{\#\#\#}P < 0.001$ versus negative group (PBS)

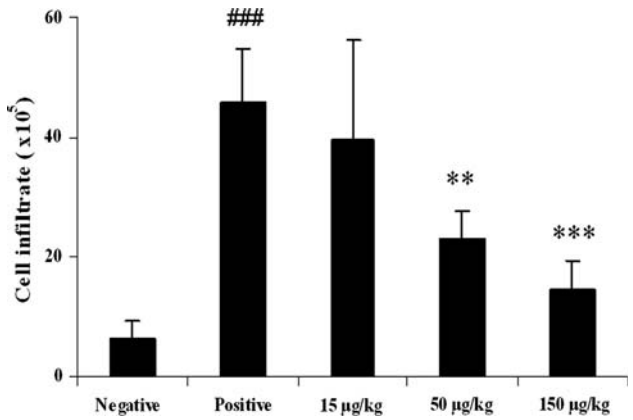

Fig. 5 Effect of DHA-lysoPtdCho, administered i.v. on zymosan A-induced leukocyte infiltration in mice. DHA-lysoPtdCho was administered i.v. 30 min prior to i.p. administration of zymosan A (100 mg/kg). Total cell counts were performed for the lavage fluid collected at the 90-min time point using light microscopy together with trypan blue staining

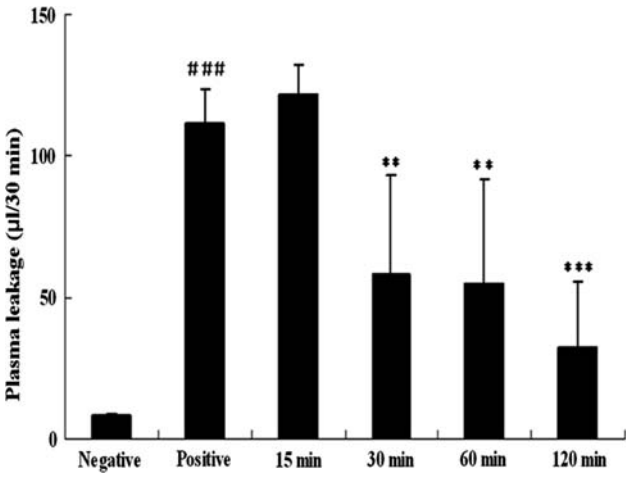

Fig. 6 Time-dependent suppressive effect of DHA-lysoPtdCho, administered i.v. on Zymosan A-induced plasma leakage in mice. DHA-lysoPtdCho was administered i.v. to mice (50 μg/kg) 15 min, 30 min, 60 min or 120 min prior to i.p. administration of zymosan A (100 mg/kg), and the plasma leakage was determined as described in "Materials and Methods". The *column* and *bar* represent the means ± SEM of results from each group of >10 mice. $^{*}P < 0.05$, $^{**}P < 0.01$, $^{***}P < 0.001$ versus positive group (zymosan A); $^{\#\#\#}P < 0.001$ versus negative group (PBS)

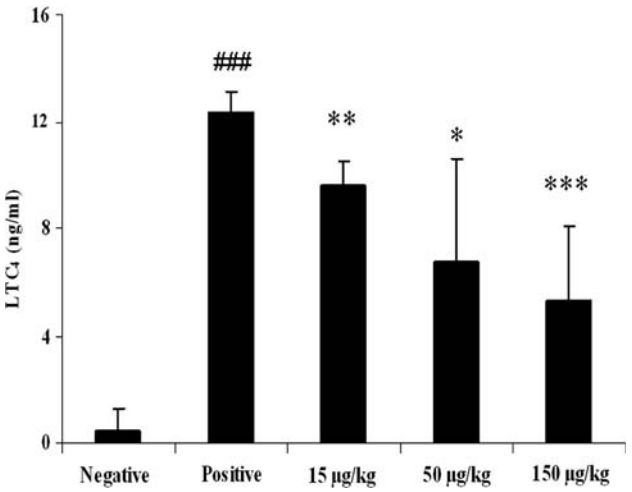

Fig. 7 Effect of DHA-lysoPtdCho, administered i.v. on zymosan A-induced LTC_4 formation in mice. DHA-lysoPtdCho was administered i.v. to mice (0–150 μg/kg) 30 min prior to i.p. administration of zymosan A (100 mg/kg). Plasma lavage was performed with 4 ml PBS followed by brief centrifugation (15,000 rpm, 5 min), and the cell-free lavage supernatant was used directly for determination of LTC_4 level by EIA kit. The *column* and *bar* represent the mean ± SEM of results from each group of 10 mice. $^{*}P < 0.05$, $^{**}P < 0.01$, $^{***}P < 0.001$ versus positive group (zymosan A); $^{\#\#\#}P < 0.001$ versus negative group (PBS)

Effect of DHA-LysoPtdCho, Administered i.p. on Zymosan A-Induced Plasma Leakage

In a separate experiment to see anti-inflammatory action of lysoPtdCho administered by other administration routes,

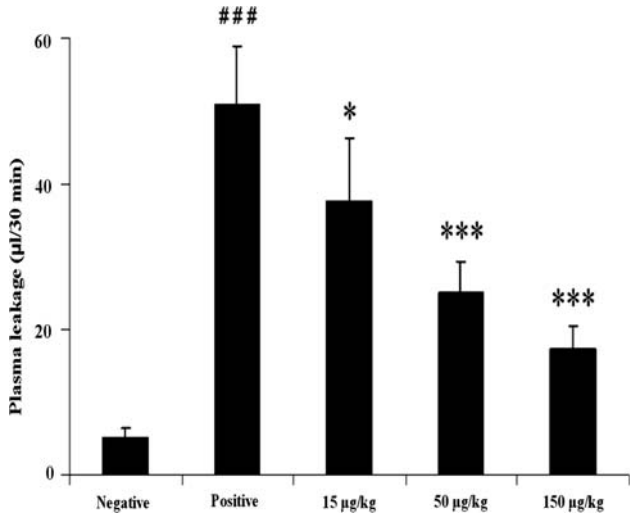

Fig. 8 Effect of DHA-lysoPtdCho, administered i.v. on LTC_4-induced plasma leakage in mice. DHA-lysoPtdCho (0–150 µg/kg) was administered i.v. into tail vein of mice 60 min before i.p. administration injection of LTC_4 (100 µg/kg), and the plasma leakage was determined as described in "Materials and methods". The *column* and *bar* represent the mean ± SEM of results from each group of 10 mice. $^{*}P < 0.05$, $^{**}P < 0.01$, $^{***}P < 0.001$ versus positive group (LTC_4); $^{\#\#\#}P < 0.001$ versus negative group (PBS)

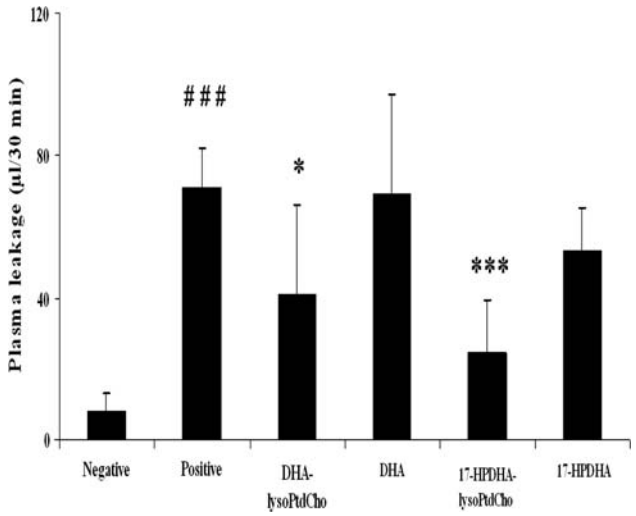

Fig. 9 Effects of DHA, 17-HPDHA, DHA-lysoPtdCho or 17-HPDHA-lysoPtdCho, administered i.v. on zymosan A-induced plasma leakage in mice. Lipids were administered i.v. to mice (50 µg/kg) 30 min before i.p. administration injection of zymosan A (100 mg/kg), and the plasma leakage was determined as described in "Materials and Methods". The *column* and *bar* represent the mean ± SEM of results from each group of >10 mice. $^{*}P < 0.05$, $^{**}P < 0.01$ versus positive group (zymosan A); $^{\#\#\#}P < 0.001$ versus negative group (PBS)

DHA-lysoPtdCho, and 17-HPDHA-lysoPtdCho were administered i.p. 60 min prior to zymosan A challenge, and its suppressive effect was evaluated. As demonstrated in Fig. 10, the i.p. administration of DHA-lysoPtdCho or

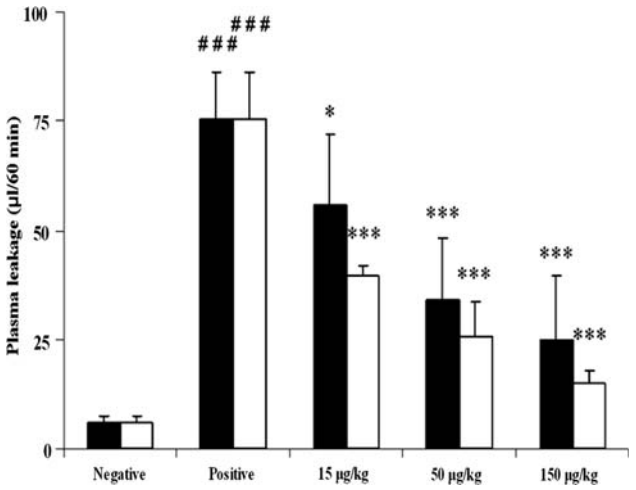

Fig. 10 Effect of DHA-lysoPtdCho or 17-HPDHA-lysoPtdCho, administered i.p. on zymosan A-induced plasma leakage in mice. DHA-lysoPtdCho (*filled bars*) or 17-HPDHA-lysoPtdCho (*open bars*) was administered i.p. (50 µg/kg) to mice 60 min before an i.p. injection of Zymosan A (100 mg/kg), and the plasma leakage was determined as described in "Materials and Methods". The *column* and *bar* represent the mean ± SEM of results from each group of >10 mice. $^{*}P < 0.05$, $^{**}P < 0.01$, $^{***}P < 0.001$ versus positive group (zymosan A); $^{\#\#\#}P < 0.001$ versus negative group (PBS)

17-HPDHA-lysoPtdCho produced a dose-dependent anti-inflammatory action. In comparison, 17-HPDHA-lysoPtdCho was more efficacious than DHA-lysoPtdCho, similar to the finding with the i.v. administration (Fig. 9). Thus, DHA-lysoPtdCho was suggested to be transformed to 17-HPDHA-lysoPtdCho, more bioactive.

Effect of DHA-LysoPtdCho, Administered Orally on Zymosan A-Induced Plasma Leakage

In a further experiment, the anti-inflammatory effect of DHA or DHA-lysoPtdCho, orally administered, was examined. As shown in Fig. 11, oral administration of DHA-lysoPtdCho showed an apparent suppressive effect on zymosan A-induced plasma leakage, although oral administration was less effective than i.p. or i.v. administration. In contrast, the anti-inflammatory action of docosahexaenoic acid, orally administered, was not significant up to 150 µg/kg. Thus, the structure of DHA-lysoPtdCho is suggested to be important for anti-inflammatory action in vivo.

Discussion

Although there have been reports on the anti-inflammatory actions of DHA metabolites in vitro and in vivo [37–39], there has been no report on the anti-inflammatory action of DHA-lysophospholipids. Recently, our previous study

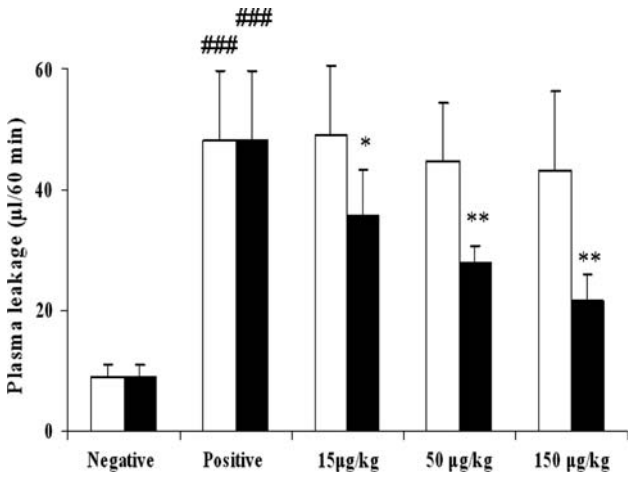

Fig. 11 Effect of DHA-lysoPtdCho or DHA, administered orally, on zymosan A-induced plasma leakage in mice. DHA (*open bars*) or 17-HPDHA-lysoPtdCho (*filled bars*) was administered orally (50 µg/kg) to mice 60 min before i.p. injection of zymosan A (100 mg/kg), and the plasma leakage was determined as described in "Materials and Methods". The *column* and *bar* represent the mean ± SEM of results from each group of >10 mice. $^{*}P < 0.05$, $^{**}P < 0.01$, $^{***}P < 0.001$ versus positive group (zymosan A); $^{\#\#\#}P < 0.001$ versus negative group (PBS)

showed that DHA-lysoPtdCho and its oxygenation products strongly inhibited mammalian 5-LOX activity [26], responsible for the generation of inflammatory lipid mediators such as leukotriene B or cysteinyl-leukotrienes. Very recently, we observed that ARA-lysoPtdCho and its 15-hydroperoxy derivative expressed an anti-inflammatory action in zymosan A-induced peritonitis [40]. Present studies indicate that DHA-lysoPtdCho is more efficient than ARA-lysoPtdCho in LPS-induced production of NO in RAW cells. Moreover, the effective concentrations (5–10 µM) of DHA-lysoPtdCho in inhibiting 5-LOX activity [26] as well as LPS-induced NO production are relatively low. Noteworthy, such an action seems to be peculiar to DHA-lysoPtdCho, since other lysoPtdCho species such as ARA-lysoPtdCho or LNA-lysoPtdCho had no remarkable reduction of NO level. Furthermore, DHA-lysoPtdCho also decreased the level of inflammatory mediators such as TNF-α or IL-6 induced by LPS, supporting the anti-inflammatory action of docosahexaenoyl-lysoPC.

Consistent with its anti-inflammatory action in vitro, DHA-lysoPtdCho, i.v. administered, suppressed zymosan A-induced peritonitis in mice at relatively low doses (15–50 µg/kg). In comparison, DHA-lysoPtdCho, i.v. or i.p. administered, was much more effective than ARA-lysoPtdCho in suppressing zymosan A-induced peritonitis. Even oral administration of DHA-lysoPtdCho exhibited some suppressive effect on zymosan A-induced peritonitis, although it was less efficient than i.v. or i.p. administration. Thus, DHA-lysoPtdCho is supposed to be one of endogenous anti-inflammatory lipids. In support of this, DHA-lysoPtdCho was observed to reduce the levels of TNF-α or IL-6 as well as infiltrated leukocytes in vivo system. In the time course of anti-inflammatory action, a prior administration of DHA-lysoPtdCho seemed to be important for a maximal anti-inflammatory action; the administration of DHA-lysoPtdCho at least 30 min before the zymosan A challenge expressed a remarkable inhibition, but the administration 10 min before the zymosan A challenge did not succeed in showing a noticeable inhibition. From this, it is suggested that the anti-inflammatory action of DHA-lysoPtdCho in the peritoneum may require some delay process. Thus, the appearance of DHA-lysoPtdCho or its metabolites in peritoneal cells, where the mediators responsible for plasma leakage could be generated, may require a transport process. This might be consistent with the previous observation [41] that the appearance of labeled DHA, administered i.v. in peritoneal exudates required approximately a 1-h to 2-h delay for a maximal level. Earlier it had been reported that early vascular permeability, followed by subsequent infiltration of neutrophils into the peritoneum, depended largely on cysteinyl-leukotrienes, derived from 5-lipoxygenation of ARA, released by resident peritoneal macrophages, and to a lesser extent, on mast cell histamine and prostaglandin E_2 of multiple cellular origins [42, 43]. In this respect, the suppressive effect of DHA-lysoPtdCho on zymosan A-induced peritonitis might be partially related to the direct inhibition of 5-LOX [26], an initial enzyme implicated in the biosynthetic pathway of cysteinyl-leukotrienes responsible for vascular permeability [43]. Support for this comes from the finding that the i.v. administration of DHA-lysoPtdCho partially reduced the formation of LTC_4 in peritoneal exudates, reaffirming the notion that one mechanism, responsible for the anti-inflammatory effect of DHA-lysoPtdCho on zymosan A-induced peritonitis, may be related to the reduction of LTC_4 through the inhibition of 5-lipoxygenase. However, a complete inhibition of LTC_4 formation was not achieved using DHA-lysoPtdCho under the conditions used. This led us to the assumption that a process responsible for the change of vascular permeability might be directly affected by DHA-lysoPtdCho or its metabolites. In support of this assumption, the plasma leakage caused by LTC_4 was successfully prevented by DHA-lysoPtdCho administration, confirming that DHA-lysoPtdCho or its metabolites may exert an anti-inflammatory action. Concerned with this, the requirement of the time interval between lysoPC administration and zymosan A challenge may suggest that a metabolism of DHA-lysoPtdCho may be crucial for the maximal expression of anti-inflammatory action at the inflammation site, i.e. the peritoneum. There may be two possible metabolic pathways of DHA-lysoPtdCho; one is the formation of DHA,

and the other, the formation of HPDHA-lysoPtdCho [24]. In the former process, DHA is released from the enzymatic hydrolysis of DHA-lysoPtdCho in vivo. However, this hydrolytic metabolic process may not be directly related to the anti-inflammatory action of DHA-lysoPtdCho in peritoneal cells as suggested from no remarkable effect of DHA administered in this experiment. Rather, HPDHA-lysoPtdCho may more likely be a metabolic intermediate accountable for anti-inflammatory action. In support of this, 17-HPDHA-lysoPtdCho showed greater anti-inflammatory effect than DHA-lysoPtdCho in i.v. administration as well as i.p. injection. The similarity of DHA-lysoPtdCho action between two administration routes may support the idea that the metabolic activation of DHA-lysoPtdCho may occur commonly in vivo. This could be explained by the notion that DHA-lysoPtdCho might be primarily subjected to lipoxygenation by 15-lipoxygenase to generate 17-HPDHA-lysoPtdCho, which could be further utilized for the formation of potent anti-inflammatory mediators such as protectin D type derivative [38]. Alternatively, secondary metabolites such as maresin type derivative [37], derived from 14-HPDHA-lysoPtdCho, may be implicated in the anti-inflammatory action. Taken together, it is likely that the primary metabolites such as 17-HPDHA-lysoPtdCho or 14-HPDHA-lysoPtdCho may be finally converted to bioactive products directly responsible for anti-inflammatory action. This might be well supported by the previous finding [24] that DHA-lysoPtdCho was enzymatically converted to 14-HPDHA-lysoPtdCho derivative or 17-HPDHA-lysoPtdCho derivative. In turn, 14-hydroperoxydocosahexaenoyl derivative and 17-hydroperoxydocosahexaenoyl derivative could be transformed finally to maresin [37] or protectin D [38]. Thus, it is supposed that another mechanism for anti-inflammatory action of DHA-lysoPtdCho may involve a series of metabolic activation pathways. Previous studies showed that in zymosan A-induced peritonitis, protectin D significantly reduced PMN infiltration at very low doses, showing an apparent maximal response approximately in the 50% range [9]. In our present study, meanwhile, an almost complete inhibition of zymosan A peritonitis was achieved with DHA-lysoPtdCho at a dose of 500 μg/kg, indicating that DHA-lysoPtdCho might be more efficient in showing a maximal efficacy. This could be explained by the assumption that DHA-lysoPtdCho might express anti-inflammatory activity through multiple actions, such as suppression of the formation of nitric oxide or TNF-α, inhibition of 5-lipoxygenase activity as well as formation of maresin or protectin D.

Once the *sn*-2 position of phosphatidylcholine is hydrolyzed by PLA_2, unsaturated fatty acids are released, and then metabolized to form bioactive lipid mediators, inflammatory or anti-inflammatory [44]. Meanwhile, the remaining lysoPtdChos with saturated acyl chains or oleoyl group have been found to have cytotoxic effects on various cell systems [14–18]. As a part of the inflammatory actions of lysoPtdChos, lysoPtdChos brought about the superoxide production in neutrophils [17] and nonphagocytic cells [16, 17], and LNA-lysoPtdCho caused oxidative stress in RAW 264.7 cells [18]. In addition, lysoPtdChos elicited the production of pro-inflammatory cytokines in human monocytes and rat aortic smooth muscle cells [45], and played a role as a chemotactic factor for monocytes and T cells [3, 46]. The diverse properties of lysoPtdChos suggest that the functions of this class of lipids are highly dependent on the type of lysoPtdChos. A recent report showed that transcellular secretion of group V phospholipase A_2 from the epithelium induced the synthesis of leukotriene C_4 through the generation of lysoPtdChos in eosinophils [47]. In this regard, it will be of great interest whether or how DHA-lysoPtdCho affects the secretory group V PLA_2-induced formation of LTC_4 in eosinophils.

An apparent advantage with DHA-lysoPtdCho, compared to other types of lysoPtdCho, is that it exhibits anti-inflammatory actions at non-cytotoxic concentrations. Moreover, DHA-lysoPtdCho still exhibits a significant anti-inflammatory action after oral administration. In this respect, it is conceivable that administration of DHA-lysoPtdCho will help ameliorate the pro-inflammatory state, caused by various inflammatory agents including pro-inflammatory lysoPtdChos.

In this respect, DHA-lysoPtdCho therapy is possible if these lipids are introduced through appropriate administration routes in the inflammation progress. For this purpose, the upper limit of DHA-lysoPtdCho dosage, showing anti-inflammatory action selectively, is to be established in further studies.

Acknowledgments This research was supported by Basic Science Research Program through the National Research Foundation of Korea (NRF) funded by the Ministry of Education, Science and Technology (NRF 2009-0069242).

References

1. Daleau P (1999) Lysophosphatidylcholine, a metabolite which accumulates early in myocardium during ischemia, reduces gap junctional coupling in cardiac cells. J Mol Cell Cardiol 31:1391–1401
2. Fuchs B, Schiller J, Wagner U, Häntzschel H, Arnold K (2005) The phosphatidylcholine/lysophosphatidylcholine ratio in human plasma is an indicator of the severity of rheumatoid arthritis: investigations by 31P NMR and MALDI-TOF MS. Clin Biochem 38:925–933
3. Muralikrishna Adibhatla R, Hatcher JF (2006) Phospholipase A2, reactive oxygen species, and lipid peroxidation in cerebral ischemia. Free Radic Biol Med 40:376–387

4. Triggiani M, Granata F, Frattini A, Marone G (2006) Activation of human inflammatory cells by secreted phospholipases A2. Biochim Biophys Acta 1761:1289–1300
5. Matsumoto T, Kobayashi T, Kamata K (2007) Role of lysophosphatidylcholine (LPC) in atherosclerosis. Curr Med Chem 14:3209–3220
6. Shi Y, Zhang P, Zhang L, Osman H, Mohler ER 3rd, Macphee C, Zalewski A, Postle A, Wilensky RL (2007) Role of lipoprotein-associated phospholipase A2 in leukocyte activation and inflammatory responses. Atherosclerosis 191:54–62
7. Serhan CN, Savill J (2005) Resolution of inflammation: the beginning programs the end. Nat Immunol 6:1191–1197
8. Farooqui AA, Horrocks LA, Farooqui T (2007) Modulation of inflammation in brain: a matter of fat. J Neurochem 101:577–599
9. Funk CD (2001) Prostaglandins and leukotrienes: advances in eicosanoid biology. Science 294:1871–1875
10. O'Meara SJ, Rodgers K, Godson C (2008) Lipoxins: update and impact of endogenous pro-resolution lipid mediators. Rev Physiol Biochem Pharmacol 160:47–70
11. Schwab JM, Serhan CN (2006) Lipoxins and new lipid mediators in the resolution of inflammation. Curr Opin Pharmacol 6:414–420
12. Kühn H, O'Donnell VB (2006) Inflammation and immune regulation by 12/15-lipoxygenases. Prog Lipid Res 45:334–356
13. Fuentes L, Hernández M, Fernández-Avilés FJ, Crespo MS, Nieto ML (2002) Cooperation between secretory phospholipase A2 and TNF-receptor superfamily signaling: implications for the inflammatory response in atherogenesis. Circ Res 91:681–688
14. Colles SM, Chisolm GM (2000) Lysophosphatidylcholine-induced cellular injury in cultured fibroblasts involves oxidative events. J Lipid Res 41:1188–1198
15. Matsubara M, Hasegawa K (2005) Benidipine, a dihydropyridine-calcium channel blocker, prevents lysophosphatidylcholine-induced injury and reactive oxygen species production in human aortic endothelial cells. Atherosclerosis 178:57–66
16. Takeshita S, Inoue N, Gao D, Rikitake Y, Kawashima S, Tawa R, Sakurai H, Yokoyama M (2000) Lysophosphatidylcholine enhances superoxide anions production via endothelial NADH/NADPH oxidase. J Atheroscler Thromb 7:238–246
17. Silliman CC, Elzi DJ, Ambruso DR, Musters RJ, Hamiel C, Harbeck RJ, Paterson AJ, Bjornsen AJ, Wyman TH, Kelher M, England KM, McLaughlin-Malaxecheberria N, Barnett CC, Aiboshi J, Bannerjee A (2003) Lysophosphatidylcholines prime the NADPH oxidase and stimulate multiple neutrophil functions through changes in cytosolic calcium. J Leukoc Biol 73:511–524
18. Park CH, Kim MR, Han JM, Jeong TS, Sok DE (2009) Lysophosphatidylcholine exhibits a selective cytotoxicity, accompanied by ROS formation, in RAW 264.7 macrophages. Lipids 44:425–435
19. Okita M, Gaudette DC, Mills GB, Holub BJ (1997) Elevated levels and altered fatty acid composition of plasma lysophosphatidylcholine (lysoPC) in ovarian cancer patients. Int J Cancer 71:31–34
20. Croset M, Brossard N, Polette A, Lagarde M (2000) Characterization of plasma unsaturated lysophosphatidylcholines in human and rat. Biochem J 345:61–67
21. Adachi J, Asano M, Yoshioka N, Nushida H, Ueno Y (2006) Analysis of phosphatidylcholine oxidation products in human plasma using quadrupole time-of-flight mass spectrometry. Kobe J Med Sci 52:127–140
22. Chen S, Li KW (2007) Mass spectrometric identification of molecular species of phosphatidylcholine and lysophosphatidylcholine extracted from shark liver. J Agric Food Chem 55:9670–9677
23. Huang LS, Kim MR, Sok DE (2006) Linoleoyl lysophosphatidylcholine is an efficient substrate for soybean lipoxygenase-1. Arch Biochem Biophys 455:119–126
24. Huang LS, Kim MR, Sok DE (2007) Oxygenation of 1-docosahexaenoyl lysophosphatidylcholine by lipoxygenases; conjugated hydroperoxydiene and dihydroxytriene derivatives. Lipids 42:981–990
25. Huang LS, Kim MR, Sok DE (2008) Oxygenation of arachidonoyl lysophospholipids by lipoxygenases from soybean, porcine leukocyte, or rabbit reticulocyte. J Agric Food Chem 56:1224–1232
26. Huang LS, Kim MR, Sok DE (2008) Regulation of lipoxygenase activity by polyunsaturated lysophosphatidylcholines or their oxygenation derivatives. J Agric Food Chem 56:7808–7814
27. Dimitrow PP, Jawien M (2009) Pleiotropic, cardioprotective effects of omega-3 polyunsaturated fatty acids. Mini Rev Med Chem 9(9):1030–1039
28. Doherty NS, Poubelle P, Borgeat P, Beaver TH, Westrich GL, Schrader NL (1985) Intraperitoneal injection of zymosan in mice induces pain, inflammation and the synthesis of peptidoleukotrienes and prostaglandin E_2. Prostaglandins 30:769–789
29. Rao TS, Currie JL, Shaffer AF, Isakson PC (1994) In vivo characterization of zymosan-induced mouse peritoneal inflammation. J Pharmacol Exp Ther 269:917–925
30. Arita M, Bianchini F, Aliberti J, Sher A, Chiang N, Hong S, Yang RM, Petasis NA, Serhan CN (2005) Stereochemical assignment, anti-inflammatory properties, and receptor for the omega-3 lipid mediator resolvin E1. J Exp Med 20:713–722
31. Leite DF, Echevarria-Lima J, Ferreira SC, Calixto JB, Rumjanek VM (2007) ABCC transporter inhibition reduces zymosan-induced peritonitis. J Leukoc Biol 82(3):630–637
32. Rao NL, Dunford PJ, Xue X (2007) Anti-Inflammatory activity of a potent, selective leukotriene A4 hydrolase inhibitor in comparison with the 5-Lipoxygenase inhibitor zileuton. J Pharmacol Exp Ther 321:1154–1160
33. Dimitrova P, Ivanovska N (2008) Tyrphostin AG-490 inhibited the acute phase of zymosan-induced inflammation. Int Immuno pharmacol 8(11):1567–1577
34. Griswold DE, Webb EF, Hillegass LM (1991) Induction of plasma exudation and inflammatory cell infiltration by leukotriene C4 and leukotriene B4 in mouse peritonitis. Inflammation 15:251–258
35. Xie QW, Whisnant R, Nathan C (1993) Promoter of the mouse gene encoding calcium-independent nitric oxide synthase confers inducibility by interferon gamma and bacterial lipopolysaccharide. J Exp Med 177:1779–1784
36. Petros A, Bennett D, Vallance P (1991) Effect of nitric oxide synthase inhibitors on hypotension in patients with septic shock. Lancet 338:1557–1558
37. Serhan CN, Yang R, Martinod K, Kasuga K, Pillai PS, Porter TF, Oh SF, Spite M (2009) Maresins: novel macrophage mediators with potent antiinflammatory and proresolving actions. J Exp Med 206:15–23
38. Serhan CN, Hong S, Gronert K, Colgan SP, Devchand PR, Mirick G, Moussignac RL (2002) Resolvins: a family of bioactive products of omega-3 fatty acid transformation circuits initiated by aspirin treatment that counter proinflammation signals. J Exp Med 196:1025–1037
39. Hassan IR, Gronert K (2009) Acute changes in dietary {omega}-3 and {omega}-6 polyunsaturated fatty acids have a pronounced impact on survival following ischemic renal injury and formation of renoprotective docosahexaenoic acid-derived protectin D1. J Immunol 182:3223–3232
40. Hung ND, Kim MR, Sok DE (2009) Anti-inflammatory action of arachidonoyl lysophosphatidylcholine or 15-hydroperoxy

derivative in zymosan A-induced peritonitis. Prostaglandins Other Lipid Mediat 90(3–4):105–111
41. Lundy SR, Dowling RL, Stevens TM, Kerr JS, Mackin WM, Gans KR (1990) Kinetics of phospholipase A2, arachidonic acid, and eicosanoid appearance in mouse zymosan peritonitis. J Immunol 144:2671–2677
42. Kolaczkowska E, Arnold B, Opdenakker G (2008) Gelatinase B/MMP-9 as an inflammatory marker enzyme in mouse zymosan peritonitis: comparison of phase -specific production by mast cells, macrophages, and neutrophils. Immunobiology 213:109–124
43. Kolaczkowska E, Shahzidi S, Seljelid R, Van Rooijen N, Plytycz B (2002) Early vascular permeability in murine experimental peritonitis is comediated by residential macrophages and mast cells: crucial involvement of macrophage-derived cysteinyl-leukotrienes. Inflammation 26:61–71
44. Huwiler A, Pfeilschifter J (2009) Lipids as targets for novel anti-inflammatory therapies. Pharmacol Ther 124(1):96–112
45. Roberts JR, Shaw CF 3rd (1998) Inhibition of erythrocyte selenium-glutathione peroxidase by auranofin analogues and metabolites. Biochem Pharmacol 55:1291–1299
46. Maddipati KR, Marnett LJ (1987) Characterization of the major hydroperoxide-reducing activity of human plasma. Purification and properties of a selenium-dependent glutathione peroxidase. J Biol Chem 262:17398–17403
47. Muñoz NM, Meliton AY, Lambertino A, Boetticher E, Learoyd J, Sultan F, Zhu X, Cho W, Leff AR (2006) Transcellular secretion of group V phospholipase A2 from epithelium induces beta 2-integrin-mediated adhesion and synthesis of leukotriene C4 in eosinophils. J Immunol 177(1):574–582

Lipids (2010) 45:237–244
DOI 10.1007/s11745-010-3394-3

ORIGINAL ARTICLE

Protein Tyrosine Phosphatase-1B (PTP-1B) Knockdown Improves Palmitate-Induced Insulin Resistance in C2C12 Skeletal Muscle Cells

Salar Bakhtiyari · Reza Meshkani · Mohammad Taghikhani · Bagher Larijani · Khosrow Adeli

Received: 21 November 2009 / Accepted: 26 January 2010 / Published online: 23 February 2010

Abstract Insulin resistance is the central defect in type 2 diabetes and obesity. During the development of insulin resistance a lipid accumulation is accompanied by increased PTP-1B expression in the muscle. The aim of this study was to examine the effects of PTP-1B knockdown on insulin signaling and insulin resistance in the presence or absence of palmitate in C2C12 skeletal muscle cells. A stable C2C12 cell line was established using short hairpin RNA (shRNA) to knockdown protein expression of PTP1B. Analysis of PTP-1B protein expression and phosphorylation and protein levels of IRS-1 and Akt were detected by western blot. The effects of PTP-1B knockdown on the glucose uptake was also measured in C2C12 cells. The stable C2C12 cell line harboring the PTP-1B shRNA showed 62% decrease in the PTP-1B protein levels. 0.5 mM palmitate significantly induced insulin resistance in both control (26%) and PTP-1B knockdown cells (16.5%) compared to the untreated cells. Under treatment with palmitate, insulin stimulated phosphorylation of IRS-1 (Tyr632) and Akt (Ser473) in knockdown cells was significantly 1.55- and 1.86-fold, respectively, greater than the controls. In the presence of palmitate, insulin dependent glucose uptake was significantly about 3-fold higher in PTP-1B knockdown stable C2C12 cells compared to the control cells. Our data showed that decreasing the PTP-1B protein level by shRNA can enhance the activity of important elements of insulin signaling. The improvement in insulin action persisted even in palmitate treated insulin resistant myotubes.

Keywords Protein tyrosine phosphatase-1B · Short hairpin RNA interference · Insulin resistance · Knockdown · Glucose uptake · Palmitate

Abbreviations

BSA	Bovine serum albumin
2-DOG	2-Deoxyglucose
IR	Insulin receptor
IRS-1	Insulin receptor substrate-1
LAR	Leukocyte antigen related phosphatase
PTP-1B	Protein tyrosine phosphatase-1B
ShRNA	Small hairpin RNA

Introduction

Insulin resistance precedes the diagnosis of type 2 diabetes [1]. It appears that the plasma free fatty acid (FFA) levels contribute to impaired insulin signaling leading to reduced

S. Bakhtiyari · M. Taghikhani
Department of Clinical Biochemistry, Faculty of Medical Sciences, Tarbiat Modares University, Tehran, I.R. Iran

R. Meshkani (✉)
Department of Biochemistry, Faculty of Medicine, Tehran University of Medical Sciences, Tehran, I.R. Iran
e-mail: rmeshkani@tums.ac.ir

B. Larijani
Endocrinology and Metabolism Research Centre, Shariati Hospital, Tehran University of Medical Sciences, Tehran, I.R. Iran

K. Adeli
Division of Clinical Biochemistry, Department of Pediatric Laboratory Medicine, Hospital for Sick Children, University of Toronto, Ontario, Canada

insulin sensitivity and glucose uptake [2, 3] in insulin responsive tissues. Among FFAs, palmitate is the most predominant FFA in the circulation [3]. In vivo and in vitro studies have shown that palmitate causes insulin resistance in insulin target tissues [4–6]. Skeletal muscle is the most important tissue for insulin action [7, 8], where almost 80% of insulin dependent glucose uptake occurs in this tissue. However, the connection between high concentration of plasma FFA and the development of insulin resistance in skeletal muscle is not clearly known. The first theory was glucose-fatty acid cycle, suggested by Randle et al. [9, 10]. Other mechanisms underlying fatty acid-induced insulin resistance have also been proposed. Accordingly, the elevation of plasma FFA inhibits insulin stimulated glucose transport activity, associated with reduced insulin receptor (IR) and insulin receptor substrate-1 (IRS-1) tyrosine phosphorylation [11, 12]. Furthermore, several different phosphatases as inhibitors of insulin action have been suggested to have a role in the development of insulin resistance in the muscle.

PTPases are a large family of enzymes that have a major role in many cellular functions. Enhanced activity of one or more PTPases has been reported in several insulin resistance states, such as obesity and some models of diabetes [13–15]. Specifically, some PTPases such as protein tyrosine phosphatase-1B (PTP-1B), leukocyte antigen related phosphatase (LAR) [16], and SH2-containing protein-tyrosine phosphatase-2 (SHP2) have been implicated in the regulation of normal IR signaling and/or in insulin resistance [17, 18]. Among them, PTP-1B is the main negative regulator of insulin signaling pathway that has received significant attention during the recent years [19, 20]. This enzyme is widely expressed in insulin-sensitive tissues [21]. PTP-1B binds to the IR and efficiently dephosphorylates it in vitro. Early studies have shown that PTP-1B overexpression inhibits phosphorylation of IR and IRS-1 leading to insulin resistance [16, 17, 22–25]. Conversely, deletion of PTP-1B in fat, liver, and muscle tissues increases insulin sensitivity [26–28]. Human and animal studies have also demonstrated that insulin resistance is accompanied by an abnormal increase in PTP-1B activity and protein levels in skeletal muscle [29, 30]. Particularly, animals on a high fat diet showed an enhancement of the expression of PTP-1B in the muscle [31]. However, little is known regarding the role of PTP-1B in palmitate-induced insulin resistance in the muscle. Therefore, in the present study we aimed to investigate the effects of PTP-1B knockdown on the key molecules of insulin signaling in the presence or absence of palmitate in C2C12 skeletal muscle cells. To this end, we assessed glucose uptake and some critical elements of the insulin signaling pathway in PTP-1B knockdown and control C2C12 cells.

Materials and Methods

Plasmid Preparation

shRNA constructs against Mus musculus *Ptpn1* (four *ptpn1*-specific shRNA expression pRS vectors) and one pRS vector (pRS-5) without shRNA cassette sequence (as a negative control) were purchased from OriGene (Rockville, MD, USA). The pRS vectors were transformed into the competent *E. coli* DH5α bacteria. After ampicillin selection, the purified plasmid DNAs (Miniprep Kit, QIAGEN, Hilden, Germany) were tested for identification of the vectors by bidigestion of the clones with *Eco*RI and *Hin*dIII (Fermentas, St. Leon-Rot, Germany) restriction enzymes. Once the requirement was met, the mid-scale preparations of the plasmids were performed.

Cell Culture

C2C12 myoblast (ATCC Number CRL 1772) was purchased from the Pasteur Institute of Iran. Myoblasts were maintained at 37 °C (in an atmosphere of 5% CO_2) in Dulbecco's modified Eagle's Medium (DMEM) (Gibco, Berlin, Germany) containing 10% fetal bovine serum (FBS), 2 mM glutamine, 100 unit/ml penicillin, and 100 μg/ml streptomycin. Differentiation of myoblasts into myotubes was induced when the cells had achieved 70–90% confluence by replacing the media with DMEM containing 2% horse serum, 2 mM glutamine, 100 unit/ml penicillin, and 100 μg/ml streptomycin. Four days after fusion, the differentiated myotubes were used for the experiments.

Myoblast Transient Transfection

C2C12 myoblasts were transiently transfected with shRNA and control plasmids using the calcium phosphate precipitation technique [32] modified by Okayama [33]. In brief, a day prior to transfection, 5×10^5 cells per well were seeded in 0.1% gelatin-coated six-well cluster plates. Six-well plates were transfected with 15 μg of shRNA plasmids (pRS-1–pRS-4), pRS-5 vector without shRNA cassette sequence (negative control) and pEGFP-C1 plasmid (as a control for transfection efficiency).

Stable Transfection

After selecting the pRS-1 (AATTGCACCAGGAAGAT AATGACTATATC) as the best vector silencing the *ptpn1* gene and pRS-5 as negative control, stable transfection was performed. Forty-eight hours after transfection, myoblasts were trypsinized and were divided into a fresh medium containing 4 μg/ml puromycin (Sigma-Aldrich, Munich,

Germany). Cells were divided such that they are no more than 25% confluent, and were nourished with a selective medium every 3–4 days. In the next step, the puromycin-resistant colonies were picked up and expanded in 96-well plates and were nourished with the selection medium for 2 weeks. Stable myoblasts were harvested and assessed for the PTP-1B protein level using western blot. To demonstrate the fact that pRS-1 vector specifically targeted for PTP-1B gene, and does not affect the expression of a similar PTPase, the lysates were also immunoblotted for the expression of leukocyte antigen-related (LAR) gene.

Western Blot Analysis

C2C12 cell lysate was prepared by homogenization in modified RIPA buffer (50 mM Tris–HCl pH 7.4, 1% Triton X-100, 0.2% sodium deoxycholate, 0.2% SDS, 1 mM Na-EDTA, 1 mM PMSF) supplemented with protease inhibitor cocktail (Roche, Mannheim, Germany). For detection of phospho protein, a buffer consisting of 50 mM HEPES pH 7.5, 150 mM NaCl, 100 mM NaF, 10 mM EDTA, 10 mM $Na_4P_2O_7$, 2 mM $NaVO_4$, and protease inhibitor cocktail was used. Protein concentration was determined using Bradford's method [34]. 20–30 μg of total protein was fractionated by SDS-PAGE according to Laemmli method [35]. The gel was transferred onto a PVDF membrane (Millipore, Schwalbach, Germany). The membrane was blocked overnight in blocking buffer (5% skimmed milk in TBST buffer) and then incubated for 1 h with primary antibodies diluted in TBST containing 1% BSA. Primary antibodies used were as follows: PTP-1B, LAR, p-IRS-1 (Tyr632), and IRS-1 (Santa Cruz Biotechnology, Santa Cruz, USA), Akt, and phospho-Akt (Ser473) (Cell Signaling Technology, Beverly, MA, USA), β-actin (Abcam, Cambridge, MA, USA). The membrane was then incubated with secondary antibody conjugated to HRP (Santa Cruz Biotechnology, Santa Cruz, USA) for 1 h and detection was performed using ECL reagents (Amersham Pharmacia Corp, Piscataway, NJ, USA). Films were scanned and protein bands were quantified using Scion Image software. Each experiment was performed at least three times.

Muscle Creatine Kinase (MCK) Assay

MCK activity, which indicates myogenic differentiation over the culture period, was determined using the NADPH-coupled assay following the protocol supplied by the manufacturer (Biomerieux SA, Lyon, France). Briefly, the cells were washed twice with cold calcium–magnesium free PBS, and homogenized in 0.5 ml of cell lysis buffer (1 M NaCl, 1 mM EGTA, 1% Triton X-100, 10 mM Tris–HCl, pH 7.2). The lysate was centrifuged for 10 min at 15,000 rpm and the supernatant was applied to the assay. Creatine kinase levels were normalized to milligram of total protein.

Palmitate Treatment

Palmitate was administered to cells as a conjugate with fatty acid free-BSA. Briefly, sodium palmitate was dissolved in 50% (v/v) ethanol, diluted in DMEM containing 1% (w/v) fatty acid-free BSA to final concentration and was incubated in 37 °C for 2 h while being shaken. Two hours before the experiments, the experiments, myotubes were placed in serum free-DMEM containing 1% BSA and then the cells were incubated in the presence or absence of 0.5 mM palmitate for 16 h.

Glucose Uptake Assay

Glucose uptake was assayed using [^{3}H]2-DOG ([^{3}H]2-deoxyglucose) (Amersham Pharmacia Corp, Piscataway, NJ, USA). Glucose uptake measurements were performed in triplicate and in three independent experiments. In brief, C2C12 cells were seeded on plates. After 4 days of differentiation, myotubes were treated with 0.5 mM palmitate for 16 h followed by a serum starvation of 2–3 h in DMEM plus 0.1% BSA. Myotubes were then treated with or without 100 nM insulin for 30 min and washed two times with wash buffer [20 mM HEPES (pH 7.4), 140 mM NaCl, 5 mM KCl, 2.5 mM $MgSO_4$, and 1 mM $CaCl_2$]. Myotubes were then incubated in the transport buffer (wash buffer containing 0.5 mCi [^{3}H]2-DOG/ml and 10 μM 2-DOG) for 10 min. Cells were lysed in 0.05 M NaOH and [^{3}H]2-DOG levels were counted in the cell lysate using a scintillation counter. Nonspecific uptake was determined by incubating the cells in the presence or absence of 10 μM cytochalasin B.

Statistical Analysis

All statistical analyses were performed using SPSS 13.0. (SPSS, Chicago, IL). Comparisons among all groups were performed with the one-way analysis of variance (ANOVA) test. If statistical significance was found, the Tukey post hoc test was performed. Values of $p < 0.05$ were considered statistically significant.

Results

Confirming Silencing of the PTP-1B in C2C12 Cells

We were able to successfully deliver pRS and pEGFP-C1 plasmids to myoblasts with high efficiency using calcium

phosphate precipitation method. Western blot results showed that the pRS-1 vector caused the highest *ptpn1* gene silencing in transient transfection experiments (Fig. 1). Thus, pRS-1 and pRS-5 vectors (negative control) were selected for stable transfection of C2C12 cells. Our results demonstrated a 62% decrease of PTP-1B protein levels in the C2C12 stable cell line harboring PTP-1B shRNA (Fig. 2a). Figure 2b shows that pRS-1 transfection into C2C12 myoblasts does not affect the expression of LAR suggesting that the pRS-1 vector specifically silence the expression of PTP1B gene.

No Difference in Muscle Creatine Kinase Activity in PTP-1B Knockdown Stable and Control Cell Lines

In order to assess the role of PTP-1B in C2C12 differentiation, muscle creatine kinase (MCK) activity assay was performed. According to our findings, while the MCK activity was undetectable in myoblasts, it was measurable after 24 h of differentiation and gradually increased until 96 h. In the present study, we did not observe any meaningful differences in the activity of MCK in PTP-1B knockdown stable and control C2C12 cells during the differentiation period (Fig. 3).

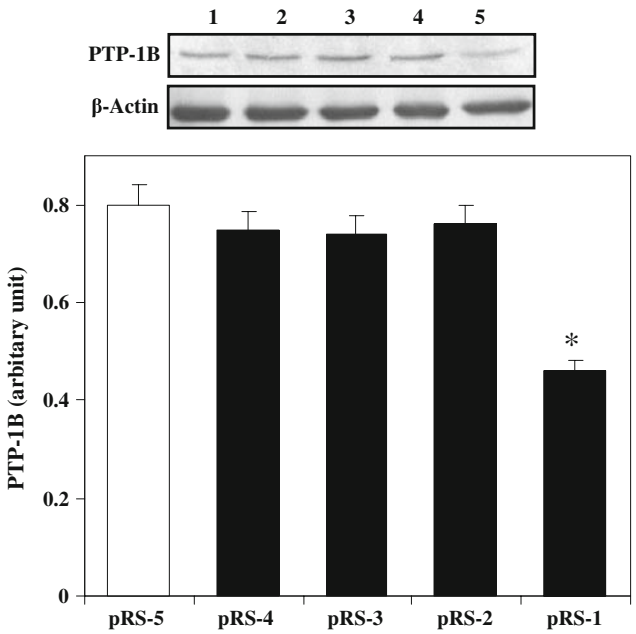

Fig. 1 Knockdown of PTP-1B in C2C12 cells following transient transfection with shRNA expression pRS vectors. C2C12 cells were transfected with 20 μg of pRS-1 to pRS-4 (1–4) and pRS-5 (5) as negative control. Forty-eight hours post-transfection, western blot was performed using antibodies against PTP-1B and β-actin as internal control. Protein level of PTP-1B was normalized to the level of β-actin protein. The figure shows representative data gained from mean ± SD of three independent experiments, $^{*}p < 0.01$

Enhancement of Insulin Signaling by PTP-1B Knockdown in the Presence of Palmitate

The results showed that the insulin-induced phosphorylation of IRS-1 was reduced by palmitate in both control and knockdown cell lines by 22.8% ($p = 0.01$) and 28.3% ($p = 0.008$), respectively. While PTP-1B knockdown stable cells in the basal state had slightly higher IRS-1 (Tyr632) phosphorylation with respect to the control, the presence of insulin caused a greater difference in IRS-1 phosphorylation in PTP-1B knockdown stable cells compared to the controls (1.8-fold, $p = 0.001$) (Fig. 4). 0.5 mM palmitate reduced IRS-1 phosphorylation in both cells, whereas the PTP-1B knockdown cells still had 1.55 fold ($p = 0.01$) higher IRS-1 phosphorylation level than the controls.

We also assessed the effects of palmitate on Akt phosphorylation in both PTP-1B knockdown stable and control cells (Fig. 5). The phosphorylation of Akt in the presence of insulin was decreased by palmitate in both control and knockdown cell lines by 29.2% ($p = 0.009$) and 33.2% ($p = 0.005$), respectively. In the presence of insulin, Akt phosphorylation (Ser473) in PTP-1B knockdown cells was significantly greater than the control cells (2.42-fold, $p < 0.001$). Insulin induced Akt phosphorylation was reduced by palmitate in both cell lines, whereas the knockdown cells still significantly had a higher Akt phosphorylation (1.86-fold, $p = 0.004$) than the control cells. Taken together, these findings suggest that PTP-1B downregulation enhances the activity of key elements of insulin signaling. Increased the activity of insulin signaling pathway remained significant even when palmitate is present in the media. There was no significant difference in the IRS-1 and Akt protein levels of the PTP-1B knockdown stable cells in comparison with the control cells in the presence or absence of palmitate and insulin.

Enhancement of Glucose Uptake in the PTP-1B Knockdown Cells Treated With Palmitate

To determine whether PTP-1B is functional in glucose uptake process,[^{3}H]2-DOG uptake was measured. In the basal condition, PTP-1B knockdown stable and control cells did not show a significant difference in the uptake of glucose (Fig. 6). Insulin stimulation led to a significantly increase in glucose uptake in both cell lines, whereas the PTP-1B knockdown cells showed much higher sensitivity to insulin than the control cells (3.3-fold vs. 1.75-fold, $p = 0.001$). Insulin-stimulated glucose uptake was decreased by palmitate in both control and knockdown cell lines by 26% ($p = 0.01$) and 16.5% ($p = 0.01$), respectively. In the simultaneous presence of insulin and palmitate, PTP-1B knockdown cells remained sensitive to insulin

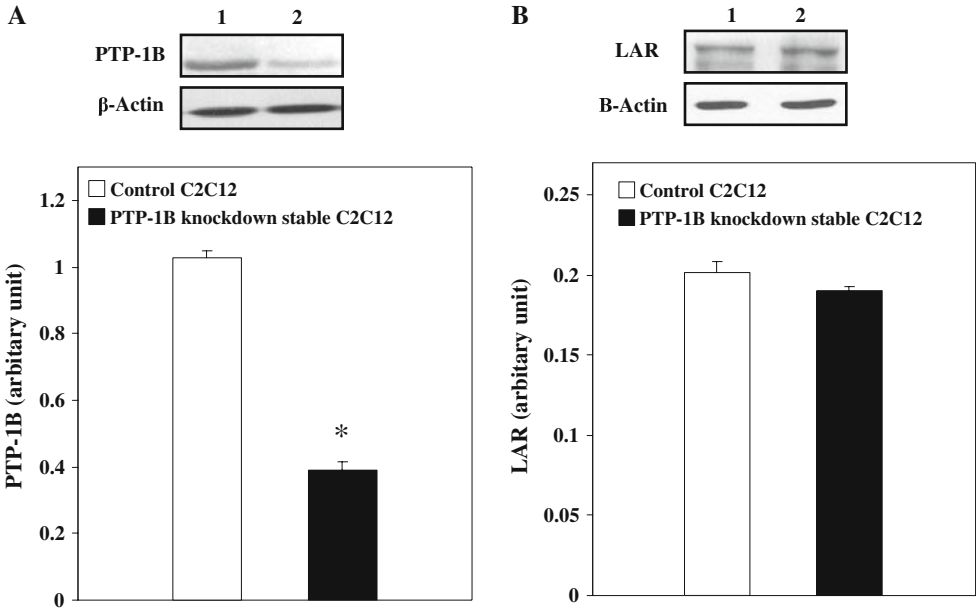

Fig. 2 Knockdown of PTP-1B in C2C12 cells following stable transfection with shRNA expression pRS-1 plasmid. After selection of stable clone. **a** Western blot was performed with antibodies against PTP-1B and β-actin. **b** Western blot was performed with antibodies against LAR and β-actin. Protein levels of PTP-1B and LAR were normalized by protein level of β-actin. The figure shows representative data obtained from mean ± SD of three independent experiments, $^*p < 0.01$. 1 = Control C2C12 cells; 2 = PTP-1B knockdown stable C2C12 cells

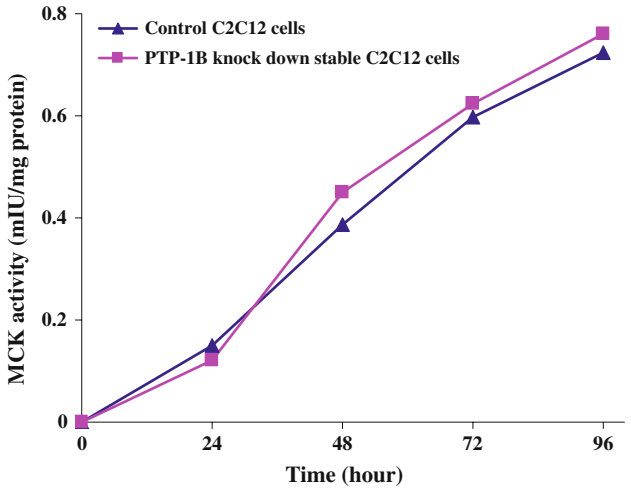

Fig. 3 Muscle creatine kinase (MCK) activity assay for PTP-1B knockdown stable and control C2C12 cells. MCK activity is depicted versus time (h) of differentiation. The figure shows representative data gained from mean ± SD of three independent experiments

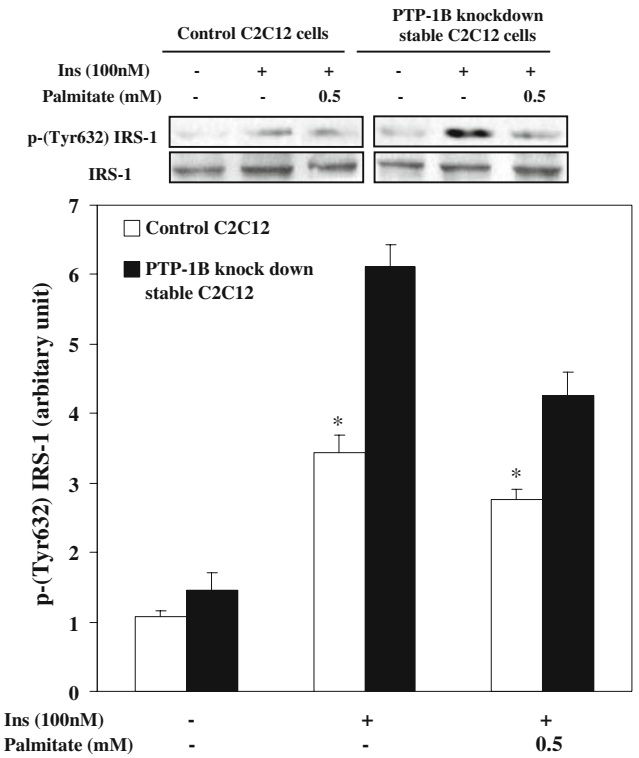

Fig. 4 The effect of palmitate on tyrosine 632 phosphorylation status of IRS-1 in PTP-1B knockdown stable and control C2C12 cells. Palmitate treatment was performed as described in the "Materials and Methods". Before harvesting, the cells were incubated in the presence or absence of 100 nM insulin (INS) for 15 min. Cell lysates were prepared and subjected to western blot using specific antibodies. The figure shows representative data gained from the means ± SD of three independent experiments, $^*p < 0.01$

with about 2.8-fold ($p < 0.001$) increase in glucose uptake in comparison with the control cells. These results indicate that knockdown of PTP-1B improves glucose uptake in C2C12 cells even in the presence of palmitate.

Discussion

Protein Tyrosine Phosphatase-1B is thought to be a negative regulator of insulin signaling through dephosphorylating the activated IR and/or IRSs. Animal with the disrupted PTP-1B gene exhibit enhanced insulin sensitivity [26, 36, 37]. Increased tyrosine phosphorylation of IR in homozygous null mice is detected in muscle and liver but not in adipose tissue [26]. Moreover, the PTP-1B deficient mice show resistance to weight gain on a high fat diet

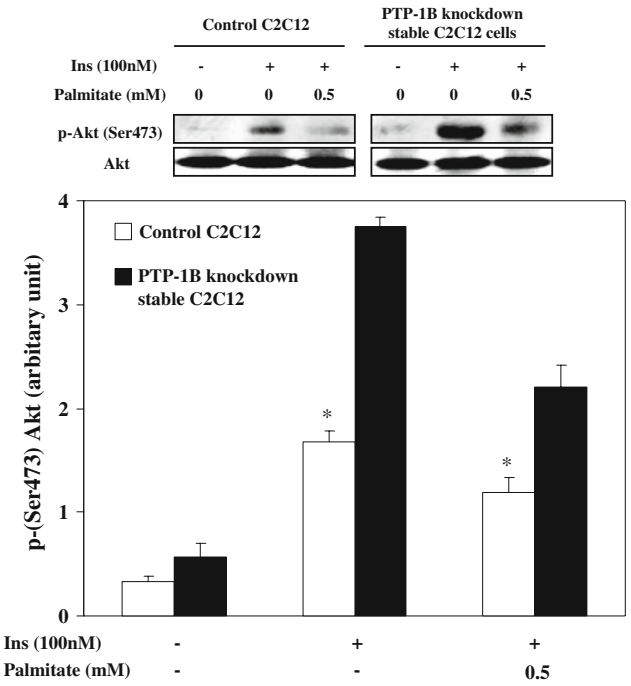

Fig. 5 The effect of palmitate on serine 473 phosphorylation status of Akt in PTP-1B knockdown stable and control C2C12 cells. Palmitate treatment was performed as described in the "Materials and Methods". Before harvesting, the cells were incubated in the presence or absence of 100 nM insulin (INS) for 15 min. Cell lysates were subjected to western blot using specific antibodies. The figure shows representative data gained from means ± SD of three independent experiments, $*p < 0.01$

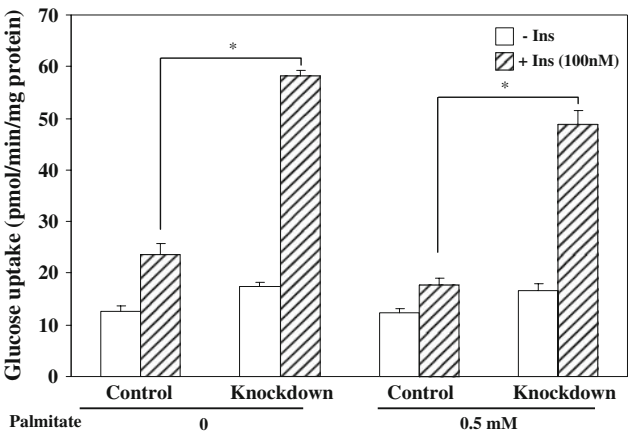

Fig. 6 The effect of 0.5 mM palmitate on glucose uptake in PTP-1B knockdown stable and control C2C12 cells. Myotubes were grown in the absence and presence of 0.5 mM palmitate for 16 h, followed by serum starvation for 2 h in 1% FBS–DMEM. Then, glucose uptake was measured in the presence or absence of insulin (INS) and cytochalasin B, as described in "Materials and Methods". The figure shows representative data gained from mean ± SD of three independent experiments, $*p < 0.01$

[26, 27]. Furthermore, human and animal studies have manifested an abnormal increase in PTP-1B activity and protein levels in skeletal muscle of insulin resistant individuals [29, 30]. Animals on a high fat diet also showed an enhancement in PTP-1B levels in the muscle [31]. Considering the importance of palmitate in inducing insulin resistance and the role of PTP-1B in negatively regulating insulin signaling pathway, we aimed to investigate the effects of PTP1B inhibition on insulin signaling in the presence and absence of palmitate in C2C12 cell line.

Several in vivo studies have been conducted to show the improving effect of PTP-1B deletion on insulin signaling and insulin resistance induced by high fat diet, however, little is known about the direct role of PTP-1B downregulation on the insulin signaling pathway when a fatty acid is present. One recent study by Liu et al. noted that knockdown of PTP-1B in 293HEK cells significantly increased GLUT4 translocation in the presence of palmitate. However, the study findings resulted from a cell line that does not normally exhibit insulin-mediated glucose uptake [38]. The results of our study on a relevant cell line provide more evidence of the effect of PTP1B knockdown on palmitate-induced muscle insulin resistance. In the present study we hypothesized that the knocking down of PTP-1B using shRNA could enhance insulin signaling through benefitting phosphorylation of key signaling molecules, and finally could increase glucose uptake even in the presence of palmitate. In order to be able to study the significance of PTP-1B knockdown on palmitate induced insulin resistance in the muscle, we generated a stable knockdown of PTP-1B gene in C2C12 cells with the protein level 38% of the control C2C12 cell line.

Several PTPases such as PTP-1B and LAR have been implicated in negatively regulating insulin signal transduction [16]. Both LAR and PTP-1B are expressed in insulin-responsive tissues such as muscle, liver, brain and adipose [18, 39–41]. LAR and PTP-1B are both involved as IR and IRS phosphatases [23, 39, 42]. To ensure that silencing was specific for PTP-1B and does not lead to change the expression of LAR, western blot was performed. We did not observe a significant change in LAR protein levels in PTP-1B knockdown stable cells suggesting a specifically downregulation of PTP-1B in our model.

Some studies have shown a role of PTP-1B and other PTPases such as SHP-2 in cellular differentiation in non-muscle tissues [43–45]. To the best of our knowledge, there is no study on the importance of PTP-1B in muscle differentiation. To ensure that PTP-1B knockdown does not interfere with C2C12 differentiation, creatine kinase activity a metabolic marker characteristic of differentiated myotubes was measured. Our data showed no change in MCK activity in PTP-1B knockdown stable cells during the C2C12 differentiation.

To investigate the influence of PTP-1B on the insulin signaling pathway, two key molecules of this pathway were targeted. As expected, insulin stimulated the phosphorylation

of Akt and IRS-1 in the knockdown and control cells. IRS-1 phosphorylation indirectly leads to activation of Akt by activating PI 3-kinase [46]. Phosphorylation of Akt is an important factor in insulin-induced glucose metabolism in the muscle and liver [47]. Our results demonstrating the inhibitory effect of palmitate on insulin signaling molecules are in concordance with the previous studies showing that palmitate induces insulin resistance in skeletal muscle by inhibiting the phosphorlyation of Akt and IRS-1 [4, 48]. Study on downregulating the PTP-1B led to enhanced sensitivity to insulin action even in the insulin resistant myotubes. Several studies have shown that palmitate inhibits insulin-mediated glucose transport mainly in skeletal muscle [49, 50]. Our data showed that PTP-1B knockdown improves glucose uptake in the presence of palmitate. This finding is in the line with the other in vivo studies demonstrating an improvement in the glycemic state in PTP-1B null mice [26, 27].

Conclusion

In the present study we have provided the evidence showing that PTP-1B downregulation may have an insulin sensitizing effect in both the presence and absence of palmitate. Activation of important elements of insulin signaling accompanied by increased glucose uptake in PTP-1B knockdown cells would favor this important enzyme as a therapeutic target for treatment of patients with insulin resistance, dyslipidemia and metabolic syndrome.

Acknowledgments This work was supported by a Grant from the Iran National Science Foundation (INSF) (grant no. 86062/23).

References

1. Czech MP (2002) Fat targets for insulin signaling. Mol Cell 9:695–696
2. McGarry JD (1992) What if Minkowski had been ageusic? An alternative angle on diabetes. Science 258:766–770
3. Paolisso G, Tataranni PA, Foley JE, Bogardus C, Howard BV, Ravussin E (1995) A high concentration of fasting plasma non-esterified fatty acids is a risk factor for the development of NIDDM. Diabetologia 38:1213–1217
4. Chavez JA, Summers SA (2003) Characterizing the effects of saturated fatty acids on insulin signaling and ceramide and diacylglycerol accumulation in 3T3-L1 adipocytes and C2C12 myotubes. Arch Biochem Biophys 419:101–109
5. Reynoso R, Salgado LM, Calderon V (2003) High levels of palmitic acid lead to insulin resistance due to changes in the level of phosphorylation of the insulin receptor and insulin receptor substrate-1. Mol Cell Biochem 246:155–162
6. Schmitz-Peiffer C, Craig DL, Biden TJ (1999) Ceramide generation is sufficient to account for the inhibition of the insulin-stimulated PKB pathway in C2C12 skeletal muscle cells pretreated with palmitate. J Biol Chem 274:24202–24210
7. Pessin JE, Saltiel AR (2000) Signaling pathways in insulin action: molecular targets of insulin resistance. J Clin Invest 106:165–169
8. Vanhaesebroeck B, Alessi DR (2000) The PI3 K-PDK1 connection: more than just a road to PKB. Biochem J 346:561–576
9. Randle PJ, Garland PB, Hales CN, Newsholme EA (1963) The glucose fatty-acid cycle. Its role in insulin sensitivity and the metabolic disturbances of diabetes mellitus. Lancet 1:785–789
10. Randle PJ, Newsholme EA, Garland PB (1964) Regulation of glucose uptake by muscle. 8. Effects of fatty acids, ketone bodies and pyruvate, and of alloxan-diabetes and starvation, on the uptake and metabolic fate of glucose in rat heart and diaphragm muscles. Biochem J 93:652–665
11. Dresner A, Laurent D, Marcucci M, Griffin ME, Dufour S, Cline GW, Slezak LA, Andersen DK, Hundal RS, Rothman DL, Petersen KF, Shulman GI (1999) Effects of free fatty acids on glucose transport and IRS-1-associated phosphatidylinositol 3-kinase activity. J Clin Invest 103:253–259
12. Griffin ME, Marcucci MJ, Cline GW, Bell K, Barucci N, Lee D, Goodyear LJ, Kraegen EW, White MF, Shulman GI (1999) Free fatty acid-induced insulin resistance is associated with activation of protein kinase C theta and alterations in the insulin signaling cascade. Diabetes 48:1270–1274
13. Ahmad F, Considine RV, Bauer TL, Ohannesian JP, Marco CC, Goldstein BJ (1997) Improved sensitivity to insulin in obese subjects following weight loss is accompanied by reduced protein-tyrosine phosphatases in adipose tissue. Metabolism 46:1140–1145
14. Ahmad F, Goldstein BJ (1995) Alterations in specific protein-tyrosine phosphatases accompany insulin resistance of streptozotocin diabetes. Am J Physiol 268:932–940
15. Ahmad F, Goldstein BJ (1995) Increased abundance of specific skeletal muscle protein-tyrosine phosphatases in a genetic model of insulin-resistant obesity and diabetes mellitus. Metabolism 44:1175–1184
16. Seely BL, Staubs PA, Reichart DR, Berhanu P, Milarski KL, Saltiel AR, Kusari J, Olefsky JM (1996) Protein tyrosine phosphatase 1B interacts with the activated insulin receptor. Diabetes 45:1379–1385
17. Byon JC, Kusari AB, Kusari J (1998) Protein-tyrosine phosphatase-1B acts as a negative regulator of insulin signal transduction. Mol Cell Biochem 182:101–108
18. Goldstein BJ, Ahmad F, Ding W, Li PM, Zhang WR (1998) Regulation of the insulin signalling pathway by cellular protein-tyrosine phosphatases. Mol Cell Biochem 182:91–99
19. Simoncic PD, McGlade CJ, Tremblay ML (2006) PTP1B and TC-PTP: novel roles in immune-cell signaling. Can J Physiol Pharmacol 84:667–675
20. Tonks NK (2003) PTP1B: from the sidelines to the front lines! FEBS Lett 546:140–148
21. Goldstein BJ (1993) Regulation of insulin receptor signaling by protein-tyrosine dephosphorylation. Receptor 3:1–15
22. Byon JC, Kenner KA, Kusari AB, Kusari J (1997) Regulation of growth factor-induced signaling by protein-tyrosine-phosphatases. Proc Soc Exp Biol Med 216:1–20
23. Goldstein BJ, Bittner-Kowalczyk A, White MF, Harbeck M (2000) Tyrosine dephosphorylation and deactivation of insulin receptor substrate-1 by protein-tyrosine phosphatase 1B. Possible facilitation by the formation of a ternary complex with the Grb2 adaptor protein. J Biol Chem 275:4283–4289
24. Kenner KA, Anyanwu E, Olefsky JM, Kusari J (1996) Protein-tyrosine phosphatase 1B is a negative regulator of insulin- and insulin-like growth factor-I-stimulated signaling. J Biol Chem 271:19810–19816
25. Zabolotny JM, Haj FG, Kim YB, Kim HJ, Shulman GI, Kim JK, Neel BG, Kahn BB (2004) Transgenic overexpression of protein-tyrosine phosphatase 1B in muscle causes insulin resistance, but

overexpression with leukocyte antigen-related phosphatase does not additively impair insulin action. J Biol Chem 279:24844–24851
26. Elchebly M, Payette P, Michaliszyn E, Cromlish W, Collins S, Loy AL, Normandin D, Cheng A, Himms-Hagen J, Chan CC, Ramachandran C, Gresser MJ, Tremblay ML, Kennedy BP (1999) Increased insulin sensitivity and obesity resistance in mice lacking the protein tyrosine phosphatase-1B gene. Science 283:1544–1548
27. Klaman LD, Boss O, Peroni OD, Kim JK, Martino JL, Zabolotny JM, Moghal N, Lubkin M, Kim YB, Sharpe AH, Stricker-Krongrad A, Shulman GI, Neel BG, Kahn BB (2000) Increased energy expenditure, decreased adiposity, and tissue-specific insulin sensitivity in protein-tyrosine phosphatase 1B-deficient mice. Mol Cell Biol 20:5479–5489
28. Nieto-Vazquez I, Fernandez-Veledo S, de Alvaro C, Rondinone CM, Valverde AM, Lorenzo M (2007) Protein-tyrosine phosphatase 1B-deficient myocytes show increased insulin sensitivity and protection against tumor necrosis factor-alpha-induced insulin resistance. Diabetes 56:404–413
29. Dadke SS, Li HC, Kusari AB, Begum N, Kusari J (2000) Elevated expression and activity of protein-tyrosine phosphatase 1B in skeletal muscle of insulin-resistant type II diabetic Goto-Kakizaki rats. Biochem Biophys Res Commun 274:583–589
30. Ahmad F, Azevedo JL, Cortright R, Dohm GL, Goldstein BJ (1997) Alterations in skeletal muscle protein-tyrosine phosphatase activity and expression in insulin-resistant human obesity and diabetes. J Clin Invest 100:449–458
31. Zabolotny JM, Kim YB, Welsh LA, Kershaw EE, Neel BG, Kahn BB (2008) Protein-tyrosine phosphatase 1B expression is induced by inflammation in vivo. J Biol Chem 283:14230–14241
32. Graham FL, van der Eb AJ (1973) A new technique for the assay of infectivity of human adenovirus 5 DNA. Virology 52:456–467
33. Chen C, Okayama H (1987) High-efficiency transformation of mammalian cells by plasmid DNA. Mol Cell Biol 7:2745–2752
34. Bradford MM (1976) A rapid and sensitive method for the quantitation of microgram quantities of protein utilizing the principle of protein-dye binding. Anal Biochem 72:248–254
35. Laemmli UK (1970) Cleavage of structural proteins during the assembly of the head of bacteriophage T4. Nature 227:680–685
36. Swarbrick MM, Havel PJ, Levin AA, Bremer AA, Stanhope KL, Butler M, Booten SL, Graham JL, McKay RA, Murray SF, Watts LM, Monia BP, Bhanot S (2009) Inhibition of protein tyrosine phosphatase-1B with antisense oligonucleotides improves insulin sensitivity and increases adiponectin concentrations in monkeys. Endocrinology 150:1670–1679
37. Kasibhatla B, Wos J, Peters KG (2007) Targeting protein tyrosine phosphatase to enhance insulin action for the potential treatment of diabetes. Curr Opin Investig Drugs 8:805–813
38. Liu F, Dallas-Yang Q, Castriota G, Fischer P, Santini F, Ferrer M, Li J, Akiyama TE, Berger JP, Zhang BB, Jiang G (2009) Development of a novel GLUT4 translocation assay for identifying potential novel therapeutic targets for insulin sensitization. Biochem J 418:413–420
39. Cheng A, Dube N, Gu F, Tremblay ML (2002) Coordinated action of protein tyrosine phosphatases in insulin signal transduction. Eur J Biochem 269:1050–1059
40. Goldstein BJ, Li PM, Ding W, Ahmad F, Zhang WR (1998) Regulation of insulin action by protein tyrosine phosphatases. Vitam Horm 54:67–96
41. Yeo TT, Yang T, Massa SM, Zhang JS, Honkaniemi J, Butcher LL, Longo FM (1997) Deficient LAR expression decreases basal forebrain cholinergic neuronal size and hippocampal cholinergic innervation. J Neurosci Res 47:348–360
42. Calera MR, Vallega G, Pilch PF (2000) Dynamics of protein-tyrosine phosphatases in rat adipocytes. J Biol Chem 275:6308–6312
43. Sorenson CM, Sheibani N (2002) Altered regulation of SHP-2 and PTP 1B tyrosine phosphatases in cystic kidneys from bcl-2 −/− mice. Am J Physiol Renal Physiol 282:442–450
44. Miranda S, Gonzalez-Rodriguez A, Revuelta-Cervantes J, Rondinone CM, Valverde AM (2010) Beneficial effects of PTP1B deficiency on brown adipocyte differentiation and protection against apoptosis induced by pro- and anti-inflammatory stimuli. Cell Signal 22(4):645–659
45. Wu C, Zhang L, Bourne PA, Reeder JE, di Sant'Agnese PA, Yao JL, Na Y, Huang J (2006) Protein tyrosine phosphatase PTP1B is involved in neuroendocrine differentiation of prostate cancer. Prostate 66:1125–1135
46. Esposito DL, Li Y, Cama A, Quon MJ (2001) Tyr(612) and Tyr(632) in human insulin receptor substrate-1 are important for full activation of insulin-stimulated phosphatidylinositol 3-kinase activity and translocation of GLUT4 in adipose cells. Endocrinology 142:2833–2840
47. Hirata AE, Alvarez-Rojas F, Campello Carvalheira JB, de Oliveira Carvalho CR, Dolnikoff MS, Abdalla Saad MJ (2003) Modulation of IR/PTP1B interaction and downstream signaling in insulin sensitive tissues of MSG-rats. Life Sci 73:1369–1381
48. Storz P, Doppler H, Wernig A, Pfizenmaier K, Muller G (1999) Cross-talk mechanisms in the development of insulin resistance of skeletal muscle cells palmitate rather than tumour necrosis factor inhibits insulin-dependent protein kinase B (PKB)/Akt stimulation and glucose uptake. Eur J Biochem 266:17–25
49. Jove M, Planavila A, Sanchez RM, Merlos M, Laguna JC, Vazquez-Carrera M (2006) Palmitate induces tumor necrosis factor-alpha expression in C2C12 skeletal muscle cells by a mechanism involving protein kinase C and nuclear factor-kappaB activation. Endocrinology 147:552–561
50. Sun C, Zhang F, Ge X, Yan T, Chen X, Shi X, Zhai Q (2007) SIRT1 improves insulin sensitivity under insulin-resistant conditions by repressing PTP1B. Cell Metab 6:307–319

Lipids (2010) 45:245–251
DOI 10.1007/s11745-010-3390-7

ORIGINAL ARTICLE

Trans Fatty Acids in Human Milk are an Indicator of Different Maternal Dietary Sources Containing *Trans* Fatty Acids

A. Mueller · C. Thijs · L. Rist · A. P. Simões-Wüst · M. Huber · H. Steinhart

Received: 28 August 2009 / Accepted: 30 December 2009 / Published online: 11 February 2010

Abstract The *trans* fatty acid (TFA) patterns in the fats of ruminant meat and dairy products differ from those found in other (processed) fats. We have evaluated different TFA isomers in human breast milk as an indicator of dietary intake of ruminant and dairy fats of different origins. Breast milk samples were collected 1 month postpartum from 310 mothers participating in the KOALA Birth Cohort Study (The Netherlands). The study participants had different lifestyles and consumed different amounts of dairy products. Fatty acid methyl esters were determined by GC-FID and the data were evaluated by principal component analysis (PCA), ANOVA/Post Hoc test and linear regression analysis. The two major principal components were (1) 18:1 *trans*-isomers and (2) markers of dairy fat including 15:0, 17:0, 11(*trans*)18:1 and 9(*cis*),11(*trans*)18:2 (CLA). Despite similar total TFA values, the 9(*trans*)18:1/11(*trans*)18:1-ratio and the 10(*trans*)18:1/11(*trans*)18:1-ratio were significantly lower in milk from mothers with high dairy fat intake (40–76 g/day: 0.91 ± 0.48, $P < 0.05$) compared to low dairy fat intake (0–10 g/day: 1.59 ± 0.48), and lower with strict organic meat and dairy use (>90% organic: 0.92 ± 0.46, $P < 0.05$) compared to conventional origin of meat and dairy (1.40 ± 0.61). Similar results were obtained for the 10(*trans*)18:1/11(*trans*)18:1-ratio. We conclude that both ratios are indicators of different intake of TFA from ruminant and dairy origin relative to other (including industrial) sources.

Keywords *Trans* fatty acids · Vaccenic acid · Conjugated linoleic acid · Human milk · Partially hydrogenated fats

Abbreviations

TFA	*trans* fatty acids
EFA	Essential fatty acids
PHVO	Partially hydrogenated vegetable oils
LCPUFA	Long-chain polyunsaturated fatty acids
FFQ	Food frequency questionnaire
MDOO	Meat and/or dairy of organic origin
PCA	Principal component analysis
SAT	Saturated fatty acids
MUFA	Monounsaturated fatty acids
CLA	Conjugated linoleic acid isomer

Introduction

Changes in the Western diet have led to increased values of *trans* fatty acids (TFA, mainly 18:1 isomers with a double bond located between positions 4 and 16 but also minor amounts of 16:1, 18:2, and 18:3 isomers) in human milk

A. Mueller (✉) · H. Steinhart
Department of Food Chemistry, Institute of Biochemistry and Food Chemistry, University of Hamburg, Grindelallee 117, 20146 Hamburg, Germany
e-mail: andrerh.mueller@arcor.de

C. Thijs
Department of Epidemiology, Maastricht University, NUTRIM School for Nutrition, Toxicology and Metabolism, CAPHRI School for Public Health and Primary Care, P.O. Box 616, 6200 MD Maastricht, The Netherlands

L. Rist · A. P. Simões-Wüst
Research Department, Paracelsus Hospital Richterswil, Bergstrasse 16, 8805 Richterswil, Switzerland

M. Huber
Louis Bolk Institute, Hoofdstraat 24, 3972 LA Driebergen, The Netherlands

[1, 2]. In humans, TFA have been associated with adverse effects on essential fatty acids (EFA) and long-chain polyunsaturated fatty acids (LCPUFA) metabolism [3], oxidative stress [4], infant development [5] as well as low density lipoprotein cholesterol levels [6]. These negative effects of TFA are mainly associated with isomers from partially hydrogenated vegetable oils (PHVO), such as 6/7/8(*trans*)18:1, 9(*trans*)18:1, 10(*trans*)18:1 [7], and only weakly with TFA of natural sources like ruminant fats such as 11(*trans*)18:1 [8]. The industry reacted to these observations by optimizing the processes for fat production and fat hardening, which led to a significant reduction in the TFA content in food [9, 10]. The discussion about adverse effects of TFA led to the labeling of total TFA content in food in the USA, Canada and Denmark. In contrast, the European Food Safety Agency decided against a general labeling of TFA in Europe due to inconsistent epidemiologic data [11].

In the randomized, double-blind, controlled, cross-over design TRANSFACT study, a consumption of 11–12 g/day of TFA (5% of energy intake) of either natural or PHVO source led to a significant reduction in HDL-cholesterol only in women [12]. It is also known that a high TFA diet leads to increased TFA amounts in human milk [10]. We evaluated the TFA composition of human milk samples from 310 women participating in the Dutch KOALA study, a prospective birth cohort study, which analyses the effect of diet and life-style (i.e. consumption of organic vs. conventional food) on the occurrence of atopic diseases in children [13]. We were able to show that the 11(*trans*)18:1 (vaccenic acid) and its metabolite 9(*cis*),11(*trans*)18:2 (a conjugated linoleic acid isomer, CLA) significantly increased in human breast milk following a diet of >90% meat and/or dairy products of organic origin, even after correcting for the amount of daily ruminant fat intake, suggesting that organic food provides lower TFA and higher CLA intakes [14].

At the moment, it is not possible to quantitatively estimate the TFA intake of natural and industrial sources (e.g. PHVO) from analytical data. Additionally, comparable data on the TFA isomer distributions in various food matrices are not available. In this study, we have searched for the full spectrum of TFA present in the human mother milk and evaluated whether certain TFA patterns can be used as indicator(s) for the mother's intake of TFA from ruminant products and other sources.

Experimental Procedures

Subjects and Collection of Breast Milk

Breast milk samples were donated by breastfeeding participants of the KOALA study, a prospective birth cohort study described elsewhere [15]. Briefly, we recruited pregnant women with varying lifestyles (conventional and alternative). Pregnant women with a conventional lifestyle ($n = 2{,}343$) were recruited from an ongoing prospective cohort study on pregnancy-related pelvic girdle pain in the Netherlands. During the same recruitment period (December 2002–August 2003) pregnant women with an alternative lifestyle, which often includes the use of organic food, were recruited through several channels, such as organic food shops, anthroposophic doctors and midwives, Rudolf Steiner schools, and relevant magazines. A total of 312 mothers agreed to donate milk samples which were collected 1 month post partum (146 from the conventional and 166 from the alternative lifestyle group without further preselection criteria [16], both groups were recruited from December 2002 to August 2003). The study was approved by the Medical Ethical Committee of Maastricht University/Academic Hospital Maastricht, Maastricht, The Netherlands.

Breast Milk Sampling and Fatty Acids Analysis

Collection and processing of the breast milk samples occurred on the same day. Fractions used for fatty acids analysis were preserved by mixing approximately 2 ml of milk with 2 µl methanol containing 500 mg butylated hydroxytoluene (BHT) per liter. The samples were stored at −80 °C in plastic storage vials (Sarstedt, Nümbrecht, Germany) at the European Biobank in Maastricht (the Netherlands), until analysis. Analyses of the fatty acids composition were completed in milk samples from 310 of 312 subjects. Lipids were extracted from the milk samples with chloroform/methanol (2/1, v/v + 0.001% BHT) in duplicate and fatty acid methyl esters were prepared for GC-FID analysis (Agilent 6890, Agilent, Waldbronn, Germany) on a 100 m × 0.25 mm 0.2 µm CP Sil 88 column (Varian, Darmstadt, Germany). The derivatisation procedure included a saponification step with 0.5 M potassium hydroxide solution in methanol with subsequent acidic esterification with 1 M sulphuric acid in methanol. Standard components for identification and calculation of response factors were obtained as fatty acid methyl esters from Sigma (Munich, Germany). TFA were identified on the basis of the elution order given in [17]. In total, 36 fatty acids were used in the final data analysis. The chosen methodology gives a reasonable separation of the major 18:1-TFA. Co-elutions are indicated in the tables (e.g. co-eluting 6(*trans*), 7(*trans*)- and 8(*trans*)18:1 are labelled as 6/7/8(*trans*)18:1. 16:1 *trans* and *cis* isomers were less well resolved (also due to chromatographically interfering 17:0 isomers) and are presented as total (*trans*)16:1 and total (*cis*)16:1 the elution order of other fatty acids methyl esters was confirmed by their retention times and positive

electron impact ionization GC–MS (Trace GC coupled to a PolarisQ ion trap mass spectrometer, both Thermo Electron, Dreieich, Germany) as described elsewhere [18].

Food Frequency Questionnaire

The food frequency questionnaire (FFQ) was included in a self-administered questionnaire in week 34 of pregnancy. The questionnaire was based on an existing validated FFQ [19], which was extended and modified to meet the specific aims of this study, including products frequently used by people with alternative life styles. The FFQ consisted of approximately 160 food items, for which the frequency of consumption in the last month and portion size were to be estimated by the participants. In addition, the participants were asked to approximate the amounts of consumed food of conventional, organic and biodynamic origin, representing three different types of food production. Biodynamic food is a special type of organic food which is produced according to anthroposophic guidelines. Based on the consumption of organic food, subjects were classified into three groups. The conventional group ($n = 185$) consisted of persons who claimed to consume less than 50% "meat and dairy products of organic origin" (MDOO), whereas people in the other two groups consumed substantial amounts of organic products: Thirty-three persons used 50–90% MDOO and 37 used >90% MDOO; 55 women reported other combinations of meat and dairy products from different categories of organic origin (e.g. conventional dairy and >90% organic meat) [14]. The study participants were also grouped according to the amount of the daily intake of dairy fat, as calculated from the FFQ: 55 women consumed 0–10 g/day, 106 10–20 g/day, 117 20–40 g/day and finally 32 women consumed 40–76 g/day of dairy products. The characteristics of the study participants in these groups have been described in detail elsewhere [14, 16]. The fat intake in these groups was calculated using the data from the FFQ and the Dutch Food Composition Table [20].

Statistical Methods

Duplicate values of fatty acids (expressed as weight percentage (wt%) of total fatty acids in breast milk fat) were averaged for each subject, and the resulting mean values were used for further calculations. Principal component analysis (PCA) was performed to evaluate correlations between groups of fatty acids using breast milk levels. In the PCA a varimax rotation was used in order to maximize the intersubject variance, and the limit of the eigenvalue for meaningful components was set at 1.5. In a first PCA, all measured fatty acids were included, and in a second PCA only compounds known to be enriched in dairy fat and PHVO: 18:1 and 18:2 isomers, and 15:0, 17:0 and 18:0 as markers for ruminant fat intake [7, 14, 21–23]. Both PCAs yielded 2 first components with similar factor loadings and therefore we only present the second PCA. For comparisons between groups, mean wt% of breast milk fatty acid levels and TFA markers were computed for groups of subjects classified by dairy fat intake, and by MDOO intake, using the Tukey–Kramer test for multiple comparisons between groups of unequal size. Linear regression analysis was used to test whether TFA concentrations increased or decreased over the categories of dairy fat intake (categories 0–10, 10–20, 20–40 and 40–76 g/day, respectively) and of MDOO intake (conventional, 50–90% MDOO and >90% MDOO, respectively). All statistical analyses were done in SPSS 12.0 for Windows [24].

Results and Discussion

Our results show that the total TFA content of mothers' milk in the compared groups ranged between 3 and 3.3% of total fatty acids (Table 1), which is lower than the values previously measured in the human milk of German mothers in 1992 (4.4% [25]) and in 1999 (3.8% [26]). The total TFA content in milk from American and Canadian woman has declined since obligatory TFA labeling was introduced in these countries and recent studies [10, 27] revealed a total TFA amount of 7.0% in the United States of America and 4.6% in Canada. Since no significant differences in the total TFA content between groups of organic intake and dairy fat intake could be observed in the present study, we have concluded that the total TFA content is not suitable as a "quality" descriptor for human milk.

Alternatively, the data on the fatty acids composition of the various samples were evaluated by PCA, to detect groups (components) of fatty acids with high correlations within each component and low (or negative) correlations between the components (Table 2). Three components were found, that together explain 61% of the variance of fatty acids included in this analysis. Component 1 represents 18:1 *trans*-isomers with double bonds between positions 6 and 14, with highest factor loadings (>0.80) for 6/7/8(*trans*), 9(*trans*), 10(*trans*), 12(*trans*) and 13/14(*trans*)18:1. Component 2 shows the highest factor loadings for 15:0, 16:0, 17:0, 9(*cis*),11(*trans*)CLA (rumenic acid) and 11(*trans*)18:1. Whereas there is a considerable clustering of TFA known to be typical for PHVO in component 1, component 2 comprises fatty acids typically found in ruminant fats (C15:0 and C17:0) as well as 11(*trans*)18:1 and rumenic acid. This interpretation of the PCA loadings table is further corroborated by the component plot in Fig. 1. PHVO fatty acids form one distinct cluster whereas fatty acid associated with dairy fat such as

Table 1 Most abundant TFA in breast milk (as wt% of total milk fat) by daily dairy fat intake and origin of meat and dairy

	Dairy fat intake						Origin of meat and dairy				
	0–10 g/d ($n = 55$)	10–20 g/d ($n = 106$)	20–40 g/d ($n = 117$)	40–76 g/d ($n = 32$)	Trend	P*	Conventional ($n = 185$)	50–90% organic ($n = 33$)	>90% organic ($n = 37$)	Trend	P*
Total (*trans*)16:1	0.55 ± 0.12	0.50 ± 0.11	0.55 ± 0.14	0.49 ± 0.11		0.3	0.55 ± 0.13	0.55 ± 0.12	0.51 ± 0.11		0.11
6/7/8(*trans*)18:1	0.24 ± 0.21[a]	0.21 ± 0.21	0.18 ± 0.14	0.15 ± 0.15[a]	↓	0.002	0.22 ± 0.18	0.16 ± 0.18	0.17 ± 0.13		0.042
9(*trans*)18:1	0.64 ± 0.31[a b]	0.61 ± 0.26	0.52 ± 0.20[a]	0.49 ± 0.22[b]	↓	<0.001	0.61 ± 0.27[a]	0.47 ± 0.20[a]	0.51 ± 0.24		0.003
10(*trans*)C18:1	0.41 ± 0.27[a b]	0.37 ± 0.23	0.31 ± 0.17[a]	0.26 ± 0.13[b]	↓	<0.001	0.38 ± 0.24[a]	0.29 ± 0.22	0.28 ± 0.16[a]	↓	0.003
11(*trans*)18:1	0.43 ± 0.22[a b]	0.51 ± 0.21	0.52 ± 0.18[a]	0.59 ± 0.19[b]	↑	<0.001	0.48 ± 0.21[a]	0.54 ± 0.26	0.59 ± 0.16[a]	↑	0.001
12(*trans*)18:1	0.18 ± 0.12	0.18 ± 0.09	0.18 ± 0.09	0.17 ± 0.05		NS	0.18 ± 0.10	0.18 ± 0.10	0.18 ± 0.06		NS
13/14(*trans*)18:1[c]	0.29 ± 0.19	0.30 ± 0.15	0.30 ± 0.12	0.31 ± 0.09		NS	0.30 ± 0.15	0.30 ± 0.15	0.30 ± 0.09		NS
Total (*trans*)18:2	0.51 ± 0.08[a]	0.53 ± 0.09[b]	0.55 ± 0.10	0.59 ± 0.08[a b]	↑	<0.001	0.52 ± 0.09[a]	0.56 ± 0.11	0.60 ± 0.07[a]	↑	<0.001
9(*cis*),11(*trans*)CLA	0.21 ± 0.07[a b]	0.26 ± 0.08[a]	0.29 ± 0.08[b]	0.34 ± 0.10[a b]	↑	<0.001	0.25 ± 0.07[a b]	0.29 ± 0.10[a]	0.34 ± 0.10[b]	↑	<0.001
9(*trans*),11(*trans*)CLA	0.04 ± 0.01	0.04 ± 0.01	0.04 ± 0.01	0.03 ± 0.01		NS	0.04 ± 0.01	0.04 ± 0.01	0.04 ± 0.01		NS
Total TFA	3.27 ± 1.28	3.25 ± 0.98	3.11 ± 0.81	3.06 ± 0.63		NS	3.26 ± 1.06	3.05 ± 1.03	3.14 ± 0.66		NS
9(*trans*)18:1/ 11(*trans*)18:1	1.59 ± 0.48[a b]	1.29 ± 0.57[a b]	1.08 ± 0.56[a]	0.91 ± 0.48[b]	↓	<0.001	1.40 ± 0.61[a b]	0.96 ± 0.40[a]	0.92 ± 0.46[b]	↓	<0.001
10(*trans*)18:1/ 11(*trans*)18:1	1.01 ± 0.47[a b]	0.77 ± 0.34[a]	0.63 ± 0.37[a b]	0.47 ± 0.25[b]	↓	<0.001	0.84 ± 0.42[a b]	0.59 ± 0.33[a]	0.49 ± 0.27[b]	↓	<0.001

↑ Increase, ↓ decrease, *NS* not significant

*P-values from linear regression analysis using dairy fat intake or origin of meat as an interval variable

[a,b] Groups sharing the same letter for the respective fatty acids are significantly different (Tukey–Kramer test for multiple comparisons between groups of unequal size, $P < 0.05$). Only fatty acids present in amounts higher than 0.04% of total milk fat are shown. Data are shown as average ± SD. Total TFA include: (*trans*)16:1, 6/7/8(*trans*)18:1, 9(*trans*)18:1, 10(*trans*)18:1, 11(*trans*)18:1, 12(*trans*)18:1, 13/14(*trans*)18:1 and (*trans,trans*)18:2

[c] May include 6/7/8(*cis*)18:1

Table 2 Principal component analysis of marker fatty acids in human milk ($n = 310$)

	Component		
	1	2	3
15:0		0.91	
16:0		0.66	
(*trans*)16:1			0.76
(*cis*)16:1		0.35	0.72
17:0		0.61	
18:0			−0.39
6/7/8(*trans*)18:1	0.93		
9(*trans*)18:1	0.85		
10(*trans*)18:1	0.92		
11(*trans*)18:1	0.62	0.58	
12(*trans*)18:1	0.90		
13/14(*trans*)18:1[a]	0.84	0.29	
9(*cis*)18:1[b]		−0.35	0.38
11(*cis*)18:1			0.84
12(*cis*)18:1	0.74		
13/14(*cis*)18:1	0.53	0.42	
9(*trans*),11(*trans*)CLA			−0.35
9(*cis*),11(*trans*)CLA		0.87	
9(*trans*),12(*trans*)18:2		0.37	
Variance (%)	28	19	14

The table shows factor loadings (values below 0.25 are not shown). Rotation method: Varimax with Kaiser Normalization

[a] May include 6/7/8(*cis*)18:1

[b] May include 15(*trans*)18:1 and 10(*cis*)18:1

11(*trans*)18:1, C15:0 and rumenic acid form a second cluster. Possible markers for TFA from PHVO would be therefore 6/7/8(*trans*)-, 9(*trans*)-, 10(*trans*)- and 13/14(*trans*)18:1 (or the sum of them). The fact that 11(*trans*)18:1 is associated with component 1 as well as with component 2 probably reflects its presence in both natural fat of ruminant origin and in PHVO [28, 29]. Component 3 includes *cis* and *trans* 16:1 fatty acids, as well as 9(*cis*)18:1 (oleic acid) and 11(*cis*)18:1, which are mainly of dietary origin, but can also be synthesized by the stearoyl-desaturase from 16:0 and 18:0. Note that 11*(cis)*18:1 fatty acids can as well derive from the elongation of 7*(cis)*16:1 by means of fatty acid elongation. The PCA suggests that the major variation between the study participants was caused by differences in the intake of ruminant fats and probably other (including industrial) sources of TFA. Therefore, we analyzed our data depending on the intake of MDOO and dairy fat. Unfortunately, it was not possible to assess the intake of PHVO with our FFQ mainly because of the lack of available data on the TFA isomer composition of different food.

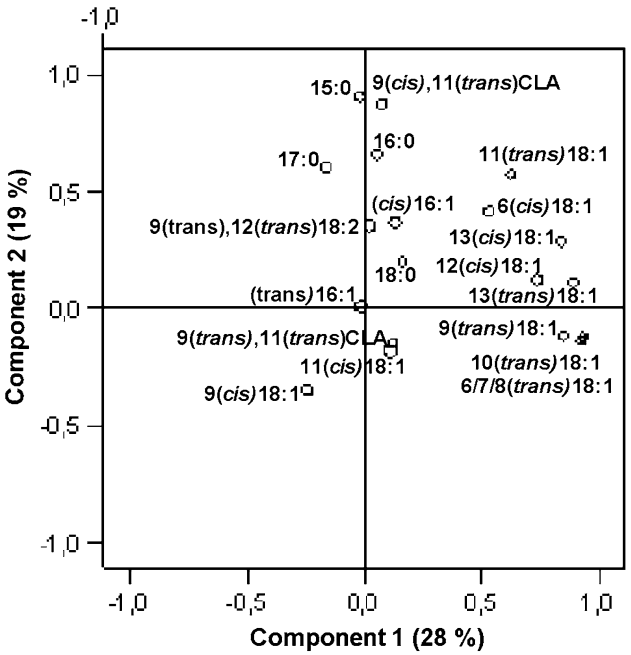

Fig. 1 PCA component plot for marker fatty acids in human milk ($n = 310$)

The amounts of 6/7/8(*trans*)18:1, 9(*trans*)18:1 and 10(*trans*)18:1 in human milk decrease with the dairy fat intake calculated from the FFQ. The amounts of these PHVO-characteristic TFA are the highest in the group with the lowest dairy intake of 0–10 g/day and decrease with increasing amounts of dairy fat intake. The opposite is true for fatty acids known to be present in relatively high amounts in dairy products such as 11(*trans*)18:1 and 9(*cis*),11(*trans*)CLA (Table 1). When the levels of the various TFA-isomers were compared between groups of different MDOO intake, a similar pattern emerged, as can also be seen in Table 1. The PHVO-characteristic 9(*trans*)18:1 and 10(*trans*)18:1 are highest in the conventional group and are significantly lower in the group of >90% MDOO. By contrast, the levels of the dairy products characteristic TFA—11(*trans*)18:1 and 9(*cis*),11(*trans*)CLA—increased with the amount of consumed MDOO. Interestingly, no significant differences of total TFA have been observed among groups of increasing intake of MDOO or among the groups with increasing dairy intake (Table 1), although the isomer distribution differed significantly. Not only were several single TFA considered possible markers either for dairy- or for PHVO-intake, also two ratios between these fatty acids were considered in our work: 10(*trans*)18:1/11(*trans*)18:1 and 9(*trans*)18:1/11(*trans*)18:1 (Table 1). The 9(*trans*)18:1/11(*trans*)18:1 ratio shows a significantly lower value in the groups with either higher dairy fat or higher MDOO intake (Table 1). The same ratios were calculated for the subjects groups consuming different amounts of MDOO: 9(*trans*)

18:1/11(*trans*)18:1 ratio was significantly lower in the group with 50-90% MDOO (0.96 ± 0.40, $P < 0.05$) and >90% MDOO (0.92 ± 0.46, $P < 0.05$) compared to the conventional group (1.40 ± 0.61). Comparable trends were observed for the ratios including 10(*trans*)18:1, which seems to be the most abundant isomer in PHVO in the US [27], relative to 11(*trans*)18:1 (Table 1). These ratios were calculated alternatively for further comparisons.

The observed changes in the TFA patterns and the calculated TFA ratios suggest major differences between TFA intakes of food with different TFA isomer compositions, e.g. TFA from ruminant/dairy fat versus TFA from industrial sources. A previous biomarker study has shown that 6/7/8/9(*trans*)18:1 and 10(*trans*)18:1, but not 11(*trans*)18:1, from PHVO were increased in plasma phospholipids of high margarine consumers compared to groups with high butter intake [7]. Our results from the PCA corroborate that these fatty acids are suitable indicators for TFA intake from PHVO. In order to find a single descriptor of TFA intake, the 9(*trans*)18:1/11(*trans*)18:1-ratio was evaluated as a alternative descriptor for TFA composition in human milk samples in comparison to the total TFA value. This value was significantly lower in both groups with organic meat and dairy intake. Previous work revealed that 11(*trans*)18:1 was the predominant 18:1 isomer in human milk from German women (with a 9(*trans*)18:1/11(*trans*)18:1-ratio of 0.54 and a 10(*trans*)18:1/11(*trans*)18:1-ratio of 0.47) [26]. By contrast, the main isomer in the milk of American mothers was 10(*trans*)18:1, with a 10(*trans*)18:1/11(*trans*)18:1-ratio of 1.36. [27]. The 9(*trans*)18:1/11(*trans*)18:1-ratio was calculated from Mosley's data to be 0.59, revealing the differences in TFA isomer distribution in milk samples from the US and from Europe. Note that the corresponding values in our conventional- and low dairy intake-group were 0.84 (9(*trans*)18:1/11(*trans*)18:1-ratio) and 1.01 (10(*trans*)18:1/11(*trans*)18:1-ratio), respectively. This suggests that milk from American women not only contained higher amounts of total TFA but also that these TFA are derived to a great extent from industrial sources. To estimate the amount of dairy intake, the amounts of other markers of ruminant fat such as 15:0, 17:0 and 9(*cis*), 11(*trans*)CLA could in principle be used as well, but they are only partially correlated to total TFA. The 9(*cis*),11(*trans*)CLA would have the disadvantages of showing seasonal variation [21] and being a metabolite of 11(*trans*)18:1 [30].

We can conclude from our data that a diet rich in dairy products and/or MDOO is strongly associated with a lower 9(*trans*)18:1/11(*trans*)18:1-ratio in human milk, whereas a diet low in dairy products and/or MDOO (and probably higher in TFA of PHVO origin) leads to a high ratio. This isomer ratio is therefore worthy of being taken into account when studying the health-related impact of TFA levels in food [31, 32]. Since it allows the qualitative discrimination between TFA from natural (ruminant) and industrial (partially hydrogenated) origin, it can be used as a tool to relate these two types of product-groups in the diet of the mothers to different health-outcomes in their children.

Acknowledgments This study was financially supported by the Netherlands Organisation for Health Research and Development (ZonMw, the Netherlands), Royal Friesland Foods (the Netherlands), Triodos Foundation (the Netherlands), UDEA organic retail (the Netherlands), Biologica organisation for organic farming and food (The Netherlands), the Consumer Association for Bio-Dynamic Agriculture Zurich (Switzerland), and Johannes Keyenbühl Academy (Switzerland).

References

1. Craig-Schmidt MC (2006) World-wide consumption of *trans* fatty acids. Atheroscler Suppl 7:1–4
2. Innis SM (2006) *Trans* fatty intakes during pregnancy, infancy and early childhood. Atheroscler Suppl 7:17–20
3. Hornstra G (2000) Essential fatty acids in mothers and their neonates. Am J Clin Nutr 71:1262S–1269S
4. Kuhnt K, Wagner A, Kraft J, Basu S, Jahreis G (2006) Dietary supplementation with 11*trans*- and 12*trans*-18:1 and oxidative stress in humans. Am J Clin Nutr 84:981–988
5. Hornstra G, van Eijsden M, Dirix C, Bonsel G (2006) *Trans* fatty acids and birth outcome: some first results of the MEFAB and ABCD cohorts. Atheroscler Suppl 7:21–23
6. Willett WC, Stampfer MJ, Manson JE, Colditz GA, Speizer FE, Rosner BA, Sampson LA, Hennekens CH (1993) Intake of *trans* fatty acids and risk of coronary heart disease among women. Lancet 341:581–585
7. Skeaff CM, Gowans S (2006) Home use of margarine is an important determinant of plasma *trans* fatty acid status: a biomarker study. Br J Nutr 96:377–383
8. Ascherio A, Katan MB, Zock PL, Stampfer MJ, Willett WC (1999) Trans fatty acids and coronary heart disease. N Engl J Med 340:1994–1998
9. Stender S, Dyerberg J, Astrup A (2006) Consumer protection through a legislative ban on industrially produced *trans* fatty acids in foods in Denmark. Scan J Food Nutr 50:155–160
10. Friesen R, Innis SM (2006) *Trans* fatty acids in human milk in Canada declined with the introduction of *trans* fat food labeling. J Nutr 136:2558–2561
11. European Food Safety Authority (2004) Opinion of the Scientific Panel on Dietetic Products, Nutrition, Allergy on a request from the Commission related to the presence of *trans* fatty acids in foods, the effect on human health of the consumption of *trans* fatty acids. EFSA J 81:1–49
12. Chardigny JM, Destaillats F, Malpuech-Brugere C, Moulin J, Bauman DE, Lock AL, Barbano DM, Mensink RP, Bezelgues JB, Chaumont P (2008) Do *trans* fatty acids from industrially produced sources and from natural sources have the same effect on cardiovascular disease risk factors in healthy subjects? Results of the *trans* Fatty Acids Collaboration (TRANSFACT) study. Am J Clin Nutr 87:558–566
13. Kummeling I, Thijs C, Huber M, van de Vijver LP, Snijders BE, Penders J, Stelma F, van Ree R, van den Brandt PA, Dagnelie PC (2008) Consumption of organic foods and risk of atopic disease during the first 2 years of life in the Netherlands. Br J Nutr 99:598–605

14. Rist L, Mueller A, Barthel C, Snijders B, Jansen M, Simoes-Wust AP, Huber M, Kummeling I, von Mandach U, Steinhart H, Thijs C (2007) Influence of organic diet on the amount of conjugated linoleic acids in breast milk of lactating women in the Netherlands. Br J Nutr 97:735–743
15. Kummeling I, Thijs C, Penders J, Snijders BE, Stelma F, Reimerink J, Koopmans M, Dagnelie PC, Huber M, Jansen MC (2005) Etiology of atopy in infancy: the KOALA Birth Cohort Study. Pediatr Allergy Immunol 16:679–684
16. Snijders BEP, Damoiseaux JGMC, Penders J, Kummeling I, Stelma FF, van Ree R, van den Brandt PA, Thijs C (2006) Cytokines and soluble CD14 in breast milk in relation with atopic manifestations in mother and infant (KOALA Study). Clin Exp Allergy 36:1609–1615
17. Cruz-Hernandez C, Deng Z, Zhou J, Hill AR, Yurawecz MP, Delmonte P, Mossoba MM, Dugan ME, Kramer JK (2004) Methods for analysis of conjugated linoleic acids and *trans*-18:1 isomers in dairy fats by using a combination of gas chromatography, silver-ion thin-layer chromatography/gas chromatography, and silver-ion liquid chromatography. J AOAC Int 87:545–562
18. Mueller A, Ringseis R, Duesterloh K, Gahler S, Eder K, Steinhart H (2005) Detection of conjugated dienoic fatty acids in human vascular smooth muscle cells treated with conjugated linoleic acid. Biochim Biophys Acta 1737:145–151
19. Grootenhuis PA, Westenbrink S, Sie CM, de Neeling JN, Kok FJ, Bouter LM (1995) A semiquantitative food frequency questionnaire for use in epidemiologic research among the elderly: validation by comparison with dietary history. J Clin Epidemiol 48:859–868
20. NEVO: Foundation Zeist. NEVO-table 2001, Dutch Food Composition Table 2001. The Hague, The Netherlands Nutrition Centre
21. Kraft J, Collomb M, Moeckel P, Sieber R, Jahreis G (2003) Differences in CLA isomer distribution of cow's milk lipids. Lipids 38:657–664
22. Smedman AE, Gustafsson IB, Berglund LG, Vessby BO (1999) Pentadecanoic acid in serum as a marker for intake of milk fat: relations between intake of milk fat and metabolic risk factors. Am J Clin Nutr 69:22–29
23. Brevik A, Veierod MB, Drevon CA, Andersen LF (2005) Evaluation of the odd fatty acids 15:0 and 17:0 in serum and adipose tissue as markers of intake of milk and dairy fat. Eur J Clin Nutr 59:1417–1422
24. SPSS for Windows (2003) Rel. 12.0. SPSS Inc, Chicago
25. Koletzko B, Thiel I, Abiodun PO (1992) The fatty acid composition of human milk in Europe and Africa. J Pediatr 120:62–70
26. Precht D, Molkentin J (1999) C18:1, C18:2 and C18:3 *trans* and *cis* fatty acid isomers including conjugated *cis* delta 9, *trans* delta 11 linoleic acid (CLA) as well as total fat composition of German human milk lipids. Nahrung 43:233–244
27. Mosley EE, Wright AL, McGuire MK, McGuire MA (2005) *trans* fatty acids in milk produced by women in the United States. Am J Clin Nutr 82:1292–1297
28. Precht D, Molkentin J (2000) Recent trends in the fatty acid composition of German sunflower margarines, shortenings and cooking fats with emphasis on individual C18:1, C18:1, C18:2, C18:3 and C20:1 *trans* isomers. Nahrung 44:222–228
29. Ratnayake WMN, Gagnon C, Dumais L, Lillycrop W, Wong L, Meleta M, Calway P (2007) Trans fatty acid content of Canadian margarines prior to mandatory trans fat labelling. J Am Oil Chem Soc 84:817–825
30. Kuhnt K, Kraft J, Moeckel P, Jahreis G (2006) Trans-11–18:1 is effectively Delta9-desaturated compared with trans-12–18:1 in humans. Br J Nutr 95:752–761
31. Jahreis G (2002) *cis* und *trans*: Ungesättigte Fettsäuren in der Ernährung: Die Aufnahme von *trans*-Fettsäuren hat sich in Deutschland erheblich reduziert. Hamburg, ALLEMAGNE Nahrungs- und Genussmittel-Fachverlag Gordian
32. Leth T, Bysted A, Hansen K, Ovesen L (2003) *Trans* FA content in Danish Margarines and shortenings. JAOCS 80:475–478

Lipids (2010) 45:253–261
DOI 10.1007/s11745-010-3389-0

ORIGINAL ARTICLE

Phospholipid Distribution and Phospholipid Fatty Acids of the Tropical Tunicates *Eudistoma* sp. and *Leptoclinides uniorbis*

Flore Dagorn · Justine Dumay · Gaëtane Wielgosz-Collin · Vony Rabesaotra · Michèle Viau · Claude Monniot · Jean-François Biard · Gilles Barnathan

Received: 6 July 2009 / Accepted: 19 January 2010 / Published online: 21 February 2010

Abstract Two tunicates, *Eudistoma* sp. and *Leptoclinides uniorbis*, collected from the tropical waters off Djibouti were investigated for lipids and phospholipid (PL) fatty acids. PL accounted for 38.2% of the total lipids in *Eudistoma* sp. and for 30.2% in *L. uniorbis.* PL classes were quantified by normal-phase high-performance liquid chromatography using an evaporative light-scattering detector and revealed essential differences. *Eudistoma* sp. contained mainly phosphatidylcholine (PC, 70.3% of total PL) and lysophosphatidylcholine (LPC, 11.9%) and was devoid of phosphatidylserine (PS), whereas the major PL of *L. uniorbis* was PS (59.1%) followed by PC (22.5%) and LPC (8.8%). Gas chromatography–mass spectrometry analyses of fatty acid (FA) derivatives revealed 38 FA in *Eudistoma* sp., and 35 FA in *L. uniorbis*, ranged from C_{12} to C_{24} chain lengths. Polyunsaturated FA accounted for 25.9% in *Eudistoma* sp. and for 32.3% in *L. uniorbis*. Interestingly, *L. uniorbis* contained a high percentage (16.7%) of the 20:5n-3 acid (8.9% in *Eudistoma* sp.) and the 18:4n-3 acid (4.1%). Significant levels of the 20:4n-6 acid were observed in both organisms (7.8 and 6.0% respectively). *Eudistoma* sp. contained the rare 20:3n-7 acid (2.3%) only recorded to date in hydrothermal vent animals. The cyclopropane dihydrosterculic acid was identified in both tunicates (0.7 and 0.5% respectively). These latter FA, together with some unusual branched saturated and monounsaturated FA, revealed the occurrence of associated bacteria in the tunicates. Another noticeable feature was a series of eight C_{16} to C_{18} aldehyde dimethylacetals revealing the presence of plasmalogens at 5.0% in *Eudistoma* sp. and 14.2% in *L. uniorbis*. The results of this study were compared with those previously published for other tunicates regarding mainly PL content and FA composition.

Keywords Ascidians · Dimethylacetals · *Eudistoma* · Fatty acids · *Leptoclinides* · Lipid classes · Phospholipids · Plasmalogens · Tunicates

Abbreviations

amu	Atomic mass unit
CL	Cardiolipin
DMA	Aldehyde dimethylacetals
FA	Fatty acid(s)
DHA	Docosahexaenoic acid (22:6n-3)
ELSD	Evaporative light scattering detector
EPA	Icosapentaenoic acid (20:5n-3)
FAME	Fatty acid methyl ester(s)
GC–MS	Gas chromatography–mass spectrometry
HPLC	High performance liquid chromatography
LPC	Lysophosphatidylcholine
MUFA	Monounsaturated fatty acid(s)
NAP	*N*-acyl pyrrolidide(s)
PL	Phospholipid(s)
PC	Phosphatidylcholine
PE	Phosphatidylethanolamine

This work is dedicated to Claude Monniot, Professor at the Muséum National d'Histoire Naturelle, Paris, France, who died in 2008.

F. Dagorn · J. Dumay · G. Wielgosz-Collin · V. Rabesaotra · J.-F. Biard · G. Barnathan (✉)
Groupe MMS, EA 2160, Equipe Lipides marins à activité biologique, Université de Nantes, Faculté de pharmacie, 1 rue G. Veil, BP 53508, 44035 Nantes Cedex 1, France
e-mail: gilles.barnathan@univ-nantes.fr

M. Viau
UR 1268, Biopolymères Interactions Assemblages, Institut National de la Recherche Agronomique INRA, 44300 Nantes, France

PG	Phosphatidylglycerol
PI	Phosphatidylinositol
PS	Phosphatidylserine
PUFA	Polyunsaturated fatty acid(s)
SPH	Sphingomyelin
SFA	Saturated fatty acid(s)

Introduction

Tunicates are marine invertebrates present in almost every marine community and particularly abundant in coastal regions [1–4]. Tunicates and Ascidians (class Ascidiacea) are now well-known to be rich sources of unique and biologically active metabolites including lipids and lipophilic compounds [5, 6], in particular those from the *Eudistoma* genus (family Polycitoridae) [7, 8], and those from the apparently less documented genus *Leptoclinides* (family Didemnidae) [9, 10]. New amino acid derivatives have been isolated from a polar cytotoxic extract (P-388 cells) of the ascidian *Leptoclinides dubius* [11]. A series of halogenated pyridoacridine alkaloids was isolated from ascidians including a *Leptoclinides* species [12].

In spite of this interesting ascidian chemistry, only a few studies have been directed towards the ascidian lipids and fatty acids (FA). Seasonal changes in the FA composition of the ascidian *Halocynthia roretzi* were reported a long time ago [13]. Other pioneering studies described the phospholipid (PL) FA composition of several ascidian and pelagic tunicate species [14, 15]. A new phytosphingosine type cerebroside and two new carotenoids were isolated from Mediterranean tunicates [16]. New glucosphingolipids were obtained and characterized from the Ascidian *Phallusia fumigata* [17]. Lipid and FA compositions of the pelagic tunicate *Doioloetta gegenbauri* were determined [18]. The lipophilic extract of a tunicate from the Indian Ocean, *Aplidium savignyi*, contained unusual antioxidant isoprenoid hydroquinones [19]. The FA composition of polar lipids from benthic ascidians was reported [20, 21]. The FA composition of the tunicate *Botryllus schlosseri* was compared with those of two associated bacterial strains [22]. High levels of EPA (up to 25% of total FA mixture) and DHA (up to 20%) were reported from total lipids, neutral lipids and polar lipids of the edible tunicate *H. roretzi* [23]. Seasonal changes in thermotropic behavior of particular PL classes, and their fatty acyl chain compositions, were studied in different organs of the ascidian *Halocynthia aurantium* revealing high levels of 20:5n-3 (EPA) and 22:6n-3 (DHA) in almost all samples [24]. New lipids from a *Cystodytes* tunicate were recorded including sphingosines as phospholipase PLA2 inhibitors and inactive ceramides [25]. Interestingly, high levels of DHA were observed in glycolipids (up to 12% of the FA mixture) and especially in PL (38.2%) from the pelagic colonial tunicate *Pyrosoma atlanticum* [26]. Ether-linked glycerophospholipids in muscle and viscera, a major PL subclass of *H. roretzi*, were investigated [27]. Interestingly, the *sn*-2 glycerol positions of these ether lipids contained high levels polyunsaturated FA (PUFA) including EPA and DHA as major components. Several new glycosphingolipids were isolated from the marine ascidian *Microcosmus sulcatus* [28, 29]. Several fractions of a dichloromethane extract obtained from an *Eudistoma* ascidian displayed a cytotoxic activity attributed to heterocyclic aromatic amines [30]. Unprecedented serinolipids were identified from the tunicate *Didemnum* sp. [31]. Recently, some known lipid molecules have been identified in the methanolic extract of the ascidian *Didemnum psammatodes* including sterols, FA, methyl esters and glyceryl ethers [32]. The mixture of three methyl esters from the latter organism showed antiproliferative and cytotoxic effects against human leukemia cell lines. Lipids of Antarctic zooplankton including tunicates were investigated [33]. The lipid contents of the pelagic tunicate *Oikopleura vanhoeffeni* were reported showing PL as the major lipid class [34].

As part of our ongoing studies of lipids from marine invertebrates, tunicates [21], sponges [35–39], and gorgonians [40], we investigated two tropical ascidian species for lipids and PL FA. This work aims at extending knowledge on ascidian lipids and PL FA in comparison with data published for other species living at different places.

Materials and Methods

Animals

Both tunicates studied are classified as Tunicates, Ascidians, order Aplousobranchia. *Eudistoma* sp. belongs to the Polycitoridae family, while *Leptoclinides uniorbis* to the Didemnidae family. Specimens were collected during a scuba diving campaign in October 1998 (Ardoukoba scientific expedition) in the Ghoubbet Bay (Ghoubbet al-Kharab, Djibouti) at approximately 10–20 m depth.

Animals were then kept in sea water and frozen (−20 °C). They were stored at this temperature since the harvesting site up to the laboratory with the technical support of the French army. Voucher specimens were deposited at the Muséum National d'Histoire Naturelle, Paris, France (*L. uniorbis* Monniot C. & F., 1996, registration number n° A2 LEP 111—*Eudistoma* sp., number of collected specimen: D33).

Extraction, Isolation and Analysis of PL

The tunicates were extracted with CH_2Cl_2/CH_3OH (1/1, v/v) at room temperature for 2–3 days in closed bottles. The combined extracts yielded the crude total lipids. PL were separated from other lipids by column chromatography on silica gel (70–230 mesh) using dichloromethane (neutral lipids), acetone (glycolipids) and methanol (PL) as successive eluents. The general methods used for isolation and analysis of lipid mixtures have been described previously [35, 38–40].

Standards of PL [phosphatidylcholine (PC), phosphatidylethanolamine (PE), phosphatidylserine (PS), phosphatidylglycerol (PG), phosphatidylinositol (PI), lysophosphatidylcholine (LPC), sphingomyelin (SPH)] were purchased from Sigma-Aldrich Co. (Saint-Quentin Fallavier, France). PL separations were performed on a modular UltiMate® 3000 RS HPLC System (Dionex, France) coupled to an evaporative light scattering detector Sedex 85 (Sedere S.A., Alfortville, France). Chromeleon® Chromatography Management Software (Dionex) was used for system control and data processing.

Chromatographic analysis of PL was carried out according to the method of Stolyhwo et al. [41]. The nebulizer gas pressure (dried and filtered air) was maintained at 3.5 bar and the drift tube temperature was set at 50 °C. The analytical column (150 mm × 4.6 mm, i.d. 3 µm) was packed with a silica normal-phase Previal (Alltech Associates Inc., Lokeren, Belgium). A precolumn with the same packing and internal diameter was used.

The chromatographic separation was carried out using a binary gradient according to the following scheme: t_0 min: 0% B, t_3 min: 20% B, t_{12} min: 100% B, and finally isocratic conditions (100% B) for 3 min. Eluent A consisted of chloroform and eluent B of methanol/28% ammonia in water/chloroform (92:7:1, v/v/v). The mobile phase was brought back to the initial conditions and the column was allowed to equilibrate until the next injection. The total chromatographic run time was 20 min per sample. The flow rate was maintained at 1.5 mL/min. Samples were dissolved in chloroform (2 mg/mL) and the injection volume was 10 µL per sample. The samples and the column were thermostatized at 10 and 25 °C, respectively. The lipids extracted were injected three times.

The PL identification was carried out by comparison with the retention time of pure standards. To obtain a quantitative evaluation of the PL, calibration curves were determined from the area values obtained by injecting 10 µL of chloroform serial diluted solutions of PE, PC, SPH, LPC (1–10 µg) and PI, PS (0.5–5 µg). Calibration curves were calculated by applying the equations of the power model to the area and concentration values. The sum of the PL concentrations was regarded as total PL concentration. PL species were expressed as % of the total PL.

Preparation and GC–MS Analyses of FA Methyl Esters and *N*-Acyl Pyrrolidides

The PL fatty acids were converted to methyl esters by the reaction (30 min under reflux) with methanolic hydrogen chloride. *N*-Acyl pyrrolidides (NAP) were prepared by direct treatment of methyl esters with pyrrolidine/acetic acid (10/1, v/v) under reflux (2 h) [42].

Fatty acid methyl esters (FAME) and NAP were analyzed using a Agilent model 689 series II gas chromatograph linked to an Agilent 5973 series network mass selective detector (e.i. at 70 eV) equipped with an Agilent model 5973N selective quadrupole mass detector. Separation was achieved with a CP-Sil 5 CB low bleed MS capillary column (60 m × 0.25 mm i.d., 0.25 µm phase thickness; Chrompack, Middelburg, The Netherlands). The temperatures of injector and interface were maintained at 250 °C and helium was used as the carrier gas under a constant flow rate (1 mL/min). For FAME and NAP analyses, the oven temperature was programmed from 200 to 340 °C at a rate of 8 °C/min. The temperature was maintained for 15 min then allowed to drop immediately to 285 °C.

Mass spectral data for the rare icosatrienoic acid pyrrolidide are presented below.

7,10,13-icosatrienoic acid pyrrolidide. MS *m/z* (rel. intensity): 359 (M^+, 29.4), 344 (1.6), 330 (2.4), 316 (2.4), 302 (3.2), 288 (4.5), 274 (7.1), 260 (4.8), 248 (6.3), 234 (5.6), 220 (4.8), 208 (15.9), 194 (5.6), 180 (8.8), 168 (15.9), 154 (8.7), 140 (10.3), 126 (85.7), 113 (100), 98 (42.9), 85 (26.3) 72 (59.4), 70 (61.1), 55 (48.4).

Results

Lipid Content and Lipid Class Composition

The tunicates *Eudistoma* sp. and *L. uniorbis* were composed of respectively 0.86 and 0.82% of lipids (related to dry matter). Neutral lipids (40.20%) and PL (38.17%) were predominant lipid classes for *Eudistoma* sp., while *L. uniorbis* possessed almost similar proportions of neutral lipids, glycolipids and PL (35.78, 33.97 and 30.25%, respectively) (Fig. 1).

Furthermore, the separation and quantification of PL classes were carried out by high-performance liquid chromatography using an evaporative light-scattering detector [41, 43], and showed that the main PL class in *Eudistoma*

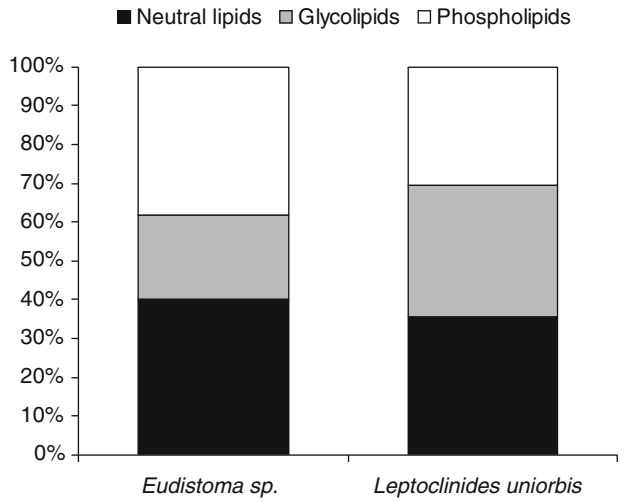

Fig. 1 Lipid class composition of *Eudistoma* sp. and *Leptoclinides uniorbis*

Table 1 Phospholipid class composition of *Eudistoma* sp. and *Leptoclinides uniorbis*

Phospholipid class	*Eudistoma* sp.	*L. uniorbis*
Phosphatidylglycerol	9.4 ± 3.1	4.0 ± 0.9
Cardiolipin	7.8 ± 1.9	3.0 ± 0.8
Phosphatidylinositol	–	2.6 ± 0.2
Phosphatidylserine	–	59.1 ± 2.2
Phosphatidylethanolamine	0.6 ± 0.0	–
Phosphatidylcholine	70.3 ± 3.9	22.5 ± 1.9
Lysophosphatidylcholine	11.9 ± 2.8	8.8 ± 1.0

Traces (<0.5%) of sphingomeylin were observed in *L. uniorbis*

Values expressed as mean ($n = 3$) ± standard deviation

sp. was PC at 70.3%, whereas it was PS at 59.1% in *L. uniorbis*. All PL components are shown in Table 1.

Eudistoma sp. was devoid of PS and contained 11.9% of LPC, and relatively noticeable amounts of PG and cardiolipin (CL). *L. uniorbis* contained 22.5% of PC and lower amounts of LPC (8.8%), PG, CL and PI. *Eudistoma* sp. contained only 0.6% of PE, and *L. uniorbis* contained trace amounts of SPH.

PL Fatty Acid Composition

Thirty-eight FA in PL of *Eudistoma* sp., and 35 FA in PL of *L. uniorbis*, were identified by gas chromatography–mass spectrometry (GC–MS) analyses as methyl esters (FAME) and NAP derivatives. Most of the FA listed in Table 2 were identified as FAME by comparing their equivalent chain length (ECL) values with those previously described or using commercial mixture.

For many compounds, GC–MS data of the NAP derivatives allowed to confirm their structures and to determine the double bond and branching positions [42].

Saturated FA

The PL of *Eudistoma* sp. contained 42.9% of saturated fatty acids (SFA) whereas those of *L. uniorbis* contained only 29.2% of SFA. The SFA were ranged from C_{14} to C_{22} for both organisms. Major SFA were palmitic (15.9%), stearic (8.2%) and myristic (6.5%) acids for *Eudistoma* sp., and myristic (8.2%), palmitic (4.9%) and stearic (3.7%) acids for *L. uniorbis*. A C_{20} isoprenoid FA, phytanic acid, occurred at 2.1% in *Eudistoma* sp. and at 0.8% in *L. uniorbis*.

Monounsaturated FA

Monounsaturated FA (MUFA) of PL from *Eudistoma* sp. represented 31.2% of the total FA identified, with the predominant part consisting of palmitoleic (9.7%), oleic (9.4%) and vaccenic (6.4%) acids. MUFA accounted for 38.5% of the total FA in PL of *L. uniorbis*, with a wide part of vaccenic (15.6%), palmitoleic (12.0%) and oleic (5.8%) acids. The 7-methyl-6-hexadecenoic acid, often found in marine organisms, accounted for 0.8% in *Eudistoma* sp. and 0.4% in *L. uniorbis*. The rare 15-methyl-6-hexadecenoic and 15-methyl-9-hexadecenoic acids occurred as traces only in PL of *Eudistoma* sp. Another interesting MUFA was detected by GC–MS as methyl ester only in *Eudistoma* sp. It was eluted just after the 9–19:1 methyl ester (ECL value of 18.92), and its mass spectrum, showing a molecular ion at *m/z* 310 corresponding to a 19:1 acid structure, was identical to those previously presented [42, 44, 45]. Other diagnostic peaks were the relatively intense peak at *m/z* 278 ($[M-32]^+$, loss of methanol), and peaks at *m/z* 236 ($[M-74]^+$ and *m/z* 194 ($[M-116]^+$, loss of COOMe plus 4 CH_2 from the chain) [45]. This cyclopropane FA, namely 9,10-methyleneoctadecanoic acid, has been recorded for the first time in tunicates to the best of our knowledge.

Polyunsaturated FA

Polyunsaturated FA accounted for 25.9% of total PL FA mixture in *Eudistoma* sp., while they were the most part of PL FA (32.3%) from *L. uniorbis*. The predominant PUFA were 20:5n-3 (EPA, 8.9%), 20:4n-6 (arachidonic, 7.8%) acids in *Eudistoma* sp., and EPA (16.7%), 20:4n-6 (6.0%) and 18:4n-3 (stearidonic, 4.1%) acids in *L. uniorbis*. Thus, arachidonic acid occurred at significant levels in both organisms. The 22:6n-3 acid (DHA) was found at low levels in both organisms (3.0 and 2.5% respectively).

Table 2 Phospholipid fatty acids and dimethylacetals from the tunicates *Eudistoma* sp. and *Leptoclinides uniorbis*

Fatty acids[b]	ECL[a]	Abundance (wt%)	
		Eudistoma sp.[b]	*L. uniorbis*
Saturated fatty acids (SFA)			
Dodecanoic (12:0)	12.00	–	1.2 ± 0.3
Tridecanoic (13:0)	13.00	–	0.8 ± 0.2
Tetradecanoic (14:0)	14.00	6.5 ± 0.1	8.2 ± 0.5
13-Methyltetradecanoic (*i*-15:0)	14.64	0.6 ± 0.1	1.2 ± 0.3
Pentadecanoic (15:0)	15.00	1.1 ± 0.5	1.1 ± 0.2
14-Methylpentadecanoic (*i*-16:0)	15.61	0.7 ± 0.1	0.2 ± 0.0
Hexadecanoic (16:0)	16.00	15.9 ± 1.7	4.9 ± 0.6
15-Methylhexadecanoic (*i*-17:0)	16.61	1.8 ± 0.3	0.7 ± 0.1
14-Methylhexadecanoic (*ai*-17:0)	16.70	0.9 ± 0.2	0.4 ± 0.0
Heptadecanoic (17:0)	17.00	1.8 ± 0.1	0.4 ± 0.1
3,7,11,15-Tetramethylhexadecanoic (br-20:0)	17.69	2.1 ± 0.5	0.8 ± 0.1
Octadecanoic (18:0)	18.00	8.2 ± 0.5	3.7 ± 0.2
17-Methyloctadecanoic (*i*-19:0)	18.63	0.4 ± 0.1	–
Nonadecanoic (19:0)	19.00	1.4 ± 0.1	1.3 ± 0.7
Icosanoic (20:0)	20.00	0.6 ± 0.1	2.3 ± 0.4
Heneicosanoic (21:0)	21.00	0.4 ± 0.0	1.2 ± 0.3
Docosanoic (22:0)	22.00	0.5 ± 0.1	0.8 ± 0.1
Total SFA		42.9 ± 2.9	29.2 ± 1.9
Monounsaturated fatty acids (MUFA)			
9-Hexadecenoic (16:1)	15.76	9.7 ± 0.8	12.0 ± 0.2
11-Hexadecenoic (16:1)	15.82	0.8 ± 0.1	0.7 ± 0.1
7-Methyl-6-hexadecenoic (br-17:1)	16.48	0.8 ± 0.1	0.4 ± 0.1
11-Heptadecenoic (17:1)	16.75	0.8 ± 0.1	0.6 ± 0.3
9-Octadecenoic (18:1)	17.77	9.4 ± 1.1	5.8 ± 0.4
11-Octadecenoic (18:1)	17.83	6.4 ± 1.1	15.6 ± 1.2
9-Nonadecenoic (19:1)	18.75	0.7 ± 0.2	0.4 ± 0.0
9,10-Methyleneoctadecanoic (19:1)	18.91	0.7 ± 0.0	0.5 ± 0.2
12-Icosenoic (20:1)	19.73	0.9 ± 0.3	1.8 ± 0.6
13-Icosenoic (20:1)	19.82	1.0 ± 0.3	0.7 ± 0.1
Total MUFA		31.2 ± 0.3	38.5 ± 0.7
Polyunsaturated fatty acids (PUFA)			
6,9,12-Octadecatrienoic (18:3)	17.46	1.0 ± 0.0	0.8 ± 0.2
6,9,12,15-Octadecatetraenoic (18:4)	17.56	–	4.1 ± 0.4
9,12-Octadecadienoic (18:2)	17.65	2.9 ± 0.5	2.2 ± 0.4
5,8,11,14-Icosatetraenoic (20:4)	19.27	7.8 ± 0.7	6.0 ± 0.4
5,8,11,14,17-Icosapentaenoic (20:5)	19.36	8.9 ± 1.0	16.7 ± 0.6
7,10,13-Icosatrienoic (20:3)	19.50	2.3 ± 0.7	–
4,7,10,13,16,19-Docosahexaenoic (22:6)	21.30	3.0 ± 0.9	2.5 ± 0.4
Total PUFA		25.9 ± 0.4	32.3 ± 0.7
Fatty aldehyde dimethylacetals (DMA)[c]			
br-16:0	16.10	22.3 ± 1.3	1.9 ± 0.3
16:0	16.46	17.1 ± 0.4	35.8 ± 0.6
br-17:0	17.10	13.5 ± 0.9	23.3 ± 0.2
br-17:0	17.20	5.5 ± 0.1	12.6 ± 0.2
17:0	17.46	9.8 ± 0.2	8.2 ± 0.6
br-18:0	18.10	4.2 ± 0.2	3.3 ± 0.1

Table 2 continued

Fatty acids[b]	ECL[a]	Abundance (wt%)	
		Eudistoma sp.[b]	*L. uniorbis*
br-18:0	18.20	4.4 ± 0.4	2.1 ± 0.1
18:0	18.48	23.2 ± 0.3	12.8 ± 0.2
Total DMA		100.0	100.0

Mean ± SD, $n = 3$

i iso, *ai* anteiso, *br* branched

[a] ECL were determined using column CP-Sil 5 CB (Chrompack)

[b] Minor FA identified in *Eudistoma* sp. (<0.3%): 12-methyltetradecanoic (14.72), 15-methyl-6-hexadecenoic (16.30), 15-methyl-9-hexadecenoic (16.53), 9-heptadecenoic (16.76), 2-hydroxy-octadecanoic (19.12), tricosanoic (23.00) and tetracosanoic (24.00); and in *L. uniorbis*: tricosanoic (23.00), 2-hydroxydocosanoic (23.10) and tetracosanoic (24.00)

[c] Total DMA accounted for 5.0% of the FA mixture in *Eudistoma* sp. and for 14.2% in *L. uniorbis*

Interestingly, the quite rare 7,10,13-icosatrienoic acid was readily identified as NAP (see "Materials and Methods"). The mass spectrum of its methyl ester (ECL 19.50) had a molecular ion peak at *m/z* 320, suggesting a 20:3 acid structure. Other major fragment ions were at *m/z* 289 (loss of MeO), 222, 150, 136, 122, 107, 93, 79 (base peak), 67 and 55 (peaks at *m/z* 74 and 87 of low intensity). The NAP showed an intense molecular ion at *m/z* 359 (20:3 acid structure) and the Δ7, Δ10 and Δ13 unsaturations were proved by a difference of 12 amu (instead of the expected gap of 14 amu) between homologous fragment ions at *m/z* 168 and 180, at *m/z* 208 and 220, and at *m/z* 248 and 260, respectively. This rare PUFA has been found for the first time in a shallow-water organism to the best of our knowledge.

Fatty Aldehydes (Dimethylacetals)

Eight fatty aldehydes, characterized as their resulting dimethylacetals, were also present in small amounts in the FA mixture from both ascidians (Table 2). All mass spectra of dimethylacetals displayed a typical base peak at *m/z* 75 $[C_3H_7O_2]^+$ and an appreciable fragment ion $[M\text{-}MeO]^+$. Thus, *Eudistoma* sp. and *L. uniorbis* contained dimethylacetals displaying, in addition to the *m/z* 75, several characteristic fragment ions at respectively *m/z* 255, 269 and 283 ($[M\text{-}MeO]^+$) corresponding to $C_{16:0}$, $C_{17:0}$ and $C_{18:0}$ aldehydes [44]. Such compounds are known to arise from methanolysis of particular PL named plasmalogens containing a vinyl–ether bond at the *sn*-1 position of the glycerol backbone (1-*O*-alk-1-enyl-2-acyl phospholipids) whose biological interest was recently reviewed [46–48].

Discussion

Tunicates seem to be among the least investigated invertebrates for lipids. The lipid content and lipid class distribution of our ascidian species can be compared to those previously published. A recent study showed that *Cystodytes violatinctus* possessed quite similar amount of lipids (1.00%) to those found in the present work (around 0.8%), while another *Eudistoma* species, *E. bituminis*, possessed 4.22% of them [21]. The lipid content of the edible parts of *H. roretzi* was studied monthly and found to be between 0.78 and 2.67% [16]. Other results were obtained using a similar extraction procedure for ascidians such as *H. roretzi* (0.3% of lipids [27]), *A. savignyi* (0.6% of lipids [19]), *Styela* sp. (1.0% of lipids [20]), *P. atlanticum* (5.0–7.0% of lipids [26]). The ascidian *Vanadis antarctica* was characterized by a relatively high lipid content (1.2%) in contrast with the other gelatinous zooplanktonic species (less than 0.1%) [33]. The mean lipid content of *O. vanhoeffeni* was around 5% before the bloom and 7.5% after the bloom (dry weight) [34]. Thus, the lipid contents found in the present work are generally comparable to those published, excepted for a few cases given above.

It was reported that the predominant lipid class in ascidians is mostly PL, which are well-known to be major constituents of the cell membrane. Hence, PL in ascidians ranged from 30 to 90% of the total lipids [21, 25–27, 33, 34]. Nevertheless, knowledge of the PL distribution in tunicates is still limited. In a recent report, the PL contents of *C. violatinctus* and *E. bituminis* accounted for 14.3 and 20.7% of the total lipids [21]. The PL of *P. atlanticum* accounted for 73.7% of the total lipids, and the major PL class was PC (62% of PL), PS being a minor component with PG not reported [26]. Several gelatinous zooplanktonic species also had high PL contents between 40 and 98%, while the non-gelatinous benthic *Distaplia cylindrinca* had 75% of PL [33]. The muscle and viscera of *H. roretzi* contained 39.9 and 28.0% of polar lipids respectively, mainly PL [27]. In this report, the most abundant PL was PC at around 49% followed by PE and SPH. The data obtained in the present work (38.2% of PL

in *Eudistoma* sp. and 30.2% in *L. uniorbis*) are in relatively good agreement with those on other tunicates and ascidians regarding PL contents.

The possible factors determining the PL class distribution in marine organisms were early reviewed [48]. It seemed that the PL pattern of a marine organism is mainly determined by taxonomic position but other factors have to be into account such as the environmental conditions [48]. PL composition has been considered to be an indicator of evolutionary level [14, 15]. PC is the major PL class in a lot of marine organisms including tunicates [26], sponges [37, 38, 48], mollusks and echinoderms [48] and *Eudistoma* sp. in the present study. The second most abundant PL class is often PE, while the acid PS has not been found as the major PL class in any marine organisms to the best of our knowledge.

It is rather surprising to find such a weak content of palmitic acid in *L. uniorbis*, in comparison with other tunicates for which it was found to be 13–40%, including those from the Indian Ocean (40.0% for *E. bituminis* and 21.2% for *C. violatinctus*) [21]. The occurrence of *iso*-branched odd SFA, such as *i*-15:0, *i*-17:0 and *i*-19:0 acids seems to indicate a possible presence of associated bacteria [49] as previously observed in marine sponges [50]. Phytanic acid was reported in *E. bituminis* with a high proportion (16.5%) [21]. It was previously identified as NAP in low amounts in African gorgonians [40]. It is generally assumed to originate from the phytol moiety of chlorophyll, and probably exogenous owing to the ubiquity of photosynthetic organisms in oceans [36].

As reported previously, the predominant MUFA were palmitoleic, oleic and vaccenic acids in both tunicates. They are commonly observed as being abundant in tunicates (13–25% of PL FA), for example, those from the Indian Ocean [21]. The methyl-branched Δ6 MUFA such as 7-methyl-6-hexadecenoic acid are often found in marine organisms. The presence of this FA in tunicates was reported for the first time and these Δ6 unsaturated FA were linked to bacterial origin [21]. This compound was identified in gorgonians [40, 51] and in sponges [52]. Branched short-chain MUFA such as the rare 15-methyl-6-hexadecenoic and 15-methyl-9-hexadecenoic acids were found in gorgonians [40] and in the sponge *Dysidea fragilis* [53], and probably also originated from associated bacteria [54]. The 9,10-methyleneoctadecanoic acid was observed in both tunicates. It has not yet been recorded from tunicates. Cyclopropane FA were observed in marine invertebrates such as sponges [50, 55], and it is known that they are widely distributed among both Gram-positive and Gram-negative bacteria [56].

Interesting results were the occurrence of EPA at the high proportion in *L. uniorbis* (16.7%), and the presence of the 18:4n-3 acid (4.1%). Surprisingly, the 22:6n-3 acid (DHA) was found at low levels in this study and not recorded in *C. violatinctus* and *E. bituminis* [21], whereas it was found in high levels in other tunicates, such as *B. schlosseri* (15.5%, [22], *H. aurantium* (up to 32%, [24]) and *H. roretzi* (13–20%, [23]. Striking results of this study were the unexpected proportion of the 20:5n-3 acid (EPA) in *L. uniorbis* (16.7%) and the occurrence of the 18:4n-3 acid (4.1%) inducing interesting potentialities for this species. These n-3 PUFA are generally attributed to marine photosynthetic phytoplankton. Intense research effort on the role of n-3 long-chain FA in human health and nutrition has continuously increased as shown by a number of recent works [6, 57, 58]. Another result of interest was the identification of the rare 20:3n-7 acid. This FA was quite recently identified (as dimethyloxazoline derivative) in deep-sea cold-seep mussels among several unusual n-4 and n-7 methylene interrupted PUFA but not in shallow-water mussels [59]. Such unusual FA probably originate from chemosynthetic bacteria. Thus, it had been previously found in hydrothermal vent mussels [60] and in vent worms [61], and clearly attributed to thiotrophic symbiotic bacteria.

As revealed by identification of dimethylacetals, both organisms contained plasmalogens. Biological activities of plasmalogens were recently reviewed including their roles in the structure and function of biological membranes [46, 47]. These compounds may protect cells against oxidative stress, since their vinyl–ether bond is preferentially oxidized which protects PUFA at the *sn*-2 position from oxidation. Such compounds have also been described i.e. in sponges [35, 39], gastropods [44], and hydrothermal vent worms [60].

As concluding remarks, the lipid and PL contents of *Eudistoma* sp. and *L. uniorbis* were relatively similar to those published for other tunicates. But the PL class distribution and the PL FA composition of our species were quite different than those reported for other tunicates. The most striking result seems to be the PL class distribution that revealed PC as the major PL in *Eudistoma* sp. whereas it was PS in *L. uniorbis*. Such a strong proportion of PS was not found in any marine invertebrate to date to the best of our knowledge. PL FA composition was different than those previously reported, even for the tunicates of the same genus such as *Eudistoma* sp. (the present study) and *E. bituminis* [21]. Regarding the PL FA, interesting findings of this work seem to be the high content of EPA, the occurrence of the 18:4n-3 acid in *L. uniorbis*, and the identification of the rare 20:3n-7 acid in *Eudistoma* sp. Several FA, such as *iso*-branched odd chain saturated FA, branched MUFA, cyclopropane FA and the 20:3n-7 itself can originate from different types of associated bacteria. Interestingly was the occurrence of plasmalogens among PL of both organisms.

Acknowledgments Organisms were caught during the European Programme "Marine Science and Technology" MAST III, PL950054, 1996–1999, *Bioactive Marine Natural Products in the field of Anti-tumoral, Antiviral and Immunomodulant Activity*. We thank the Ardoukoba association for the assistance during the harvesting of the tunicates. We are indebted to Drs Jean-Pascal Bergé and Jean-Paul Gouygou, the Ifremer Research Center, Nantes, France, where GC-MS analyses were carried out.

References

1. Schmidt GH, Warner GF (1986) Spatial competition between colonial ascidians: the importance of stand-off. Mar Ecol Prog Ser 31:101–104
2. Todd CD, Turner SJ (1988) Ecology of intertidal and sublittoral cryptic epifaunal assemblages. II. Non-lethal overgrowth of encrusting bryozoans by colonial ascidians. J Exp Mar Biol Ecol 115:113–126
3. Monniot F, Monniot C (1996) New collections of Ascidians from the Western Pacific and Southeastern Asia. Micronesica 29:133–279
4. Monniot F, Monniot C (2001) Ascidians from the tropical western Pacific. Zoosystema 23:201–383
5. Kornprobst JM (2005) Substances Naturelles d'Origine Marine. Tec&Doc-Lavoisier, Paris, Tome 2, pp 1589–1729
6. Bergé JP, Barnathan G (2005) Recent advances in fatty acids from lipids of marine organisms: molecular biodiversity, roles as biomarkers, biologically-active compounds and economical aspects. In: Le Gal Y, Uber R (eds) Marine biotechnology. Adv Biochem Eng Biotechnol 96:49–125, Springer, Heidelberg
7. Kobayashi J, Cheng JF, Otha T, Nozoe S, Ohizumi Y, Sasaki T (1990) Eudistomidins B, C and D: novel antileukemic alkaloids from the Okinawan marine tunicate *Eudistoma glaucus*. J Org Chem 55:3666–3670
8. Makarieva TN, Ilyin SG, Stonik VA, Lyssenko KA, Denisenko VA (1999) Pibocin, the first ergoline marine alkaloid from the far-Eastern Ascidian *Eudistoma* sp. Tetrahedron Lett 40:1591–1594
9. De Guzman FS, Schmitz FJ (1989) Chemistry of 2-bromoleptoclinidinone, structure revision. Tetrahedron Lett 30:1069–1070
10. Carroll AR, Avery VM (2009) Leptoclinidamines A-C, indole alkaloids from the Australian ascidian *Leptoclinides durus*. J Nat Prod 72:696–699
11. García A, Vázquez MJ, Quiñoá E, Riguera R, Debitus C (1996) New amino acid derivatives from the marine ascidian *Leptoclinides dubius*. J Nat Prod 59:782–785
12. Dembitsky VM, Tolstikov GA (2003) Natural halogenated alkaloids. Chem Sustain Dev 11:451–466
13. Kuzaka H, Kaga Y, Saiki Y, Ohta S (1985) Seasonal changes in the fatty acid composition of Ascidian lipids. Yukagaku 34:262–270 (Jap.)
14. Kostetsky EY, Naumenko NV, Gerasimenko NI (1983) Phospholipid composition of 13 species of tunicates. Biol Morya 2:51–56
15. Kostetsky E, Naumenko N (1984) Comparative study on fatty acid composition of phospholipids in marine invertebrates. Khim Prir Soed 24–29 (Russ)
16. Aiello A, Fattorusso E, Menna M (1996) Low molecular weight metabolites of three species of ascidians collected in the lagoon of Venice. Biochem Syst Ecol 24:521–529
17. Durán R, Zubia E, Ortega MJ, Naranjo S, Salvá J (1998) Phallusides, new glucosphingolipids from the Ascidian *Phallusia fumigata*. Tetrahedron 54:14597–14602
18. Pond DW, Sargent JR (1998) Lipid composition of the pelagic tunicate *Doiloletta gegenbauri* (Tunicata, Thaliacea). J Plankton Res 20:169–174
19. Aknin M, Lev-Avi Dayan T, Rudi A, Kashman Y, Gaydou EM (1999) Hydroquinone antioxidants from the Indian Ocean Tunicate *Aplidium savignyi*. J Agric Food Chem 47:4175–4177
20. Slantchev K, Yalçin F, Ersöz T, Nechev J, Cahs I, Stefanov K, Popov F (2002) Composition of lipophilic extracts of the two tunicates *Styela* sp. and *Phallusia* sp. from the eastern Mediterranean. Z Naturforsch 57:534–540
21. Viracaoundin I, Barnathan G, Gaydou EM, Aknin M (2003) Phospholipid fatty acids from Indian Ocean Tunicates *Eudistoma bituminis* and *Cystodytes violatinctus*. Lipids 38:85–88
22. Carballeira NM, Shalabi F, Stefanov K, Dimittrov K, Popov S, Kujumgiev A, Andreev S (1995) Comparison of the fatty acids of the tunicate *Botryllus schlosseri* from the black sea with two associated bacterial strains. Lipids 30:677–679
23. Vysotskii MV, Ota T, Takagi T (1992) n-3 Polyunsaturated fatty acids in lipids of ascidian *Halocynthia roretzi*. Nippon Suisan Gakkaishi 58:953–958
24. Sanina NM, Kostetsky EY (2001) Seasonal changes in thermotropic behavior of phosphatidylcholine and phosphatidylethanolamine in different organs of the ascidian *Halocynthia aurantium*. Comp Biochem Physiol B 128:295–305
25. Loukaci A, Bultel-Poncé V, Longeon A, Guyot M (2000) New lipids from the Tunicate *Cystodytes* cf. *dellechiajei*, as PLA2 inhibitors. J Nat Prod 63:799–802
26. Mayzaud P, Boutoute M, Perissinotto R, Nichols P (2007) Polar and neutral lipid composition in the pelagic Tunicate *Pyrosoma atlanticum*. Lipids 42:647–657
27. Jeong BY, Ohshima T, Koizumi C (1996) Hydrocarbon chain distribution of ether phospholipids of the Ascidian *Halocynthia roretzi* and the sea urchin *Strongylocentrotus intermedius*. Lipids 31:9–18
28. Aiello A, Fattorusso E, Mangoni A, Menna M (2002) Sulcaceramide, a novel triglycosylceramide from the marine Ascidian *Microcosmus sulcatus*. Eur J Org Chem 1047–1050
29. Aiello A, Fattorusso E, Mangoni A, Menna M (2003) Three new 2,3-dihydroxy fatty acids glycosphingolipids from the Mediterranean Tunicate *Microcosmus sulcatus*. Eur J Org Chem 734–739
30. Jimenez PC, Wilke DV, Takeara R, Lotufo TMC, Pessoa C, Moraes MO, Lopes NP, Costa-Lotufo LV (2008) Cytotoxic activity of a dichloromethane extract and fractions obtained from *Eudistoma vannamei* (Tunicata:Ascidiacea). Comp Biochem Physiol A 151:391–398
31. Gonzàlez N, Rodríguez J, Jiménez C (1999) Didemniserinolipids A-C, unprecedented serinolipids from the Tunicate *Didemnum* sp. J Org Chem 64:5705–5707
32. Takeara R, Jimenez PC, Wilke DV, Moraes MO, Pessoa C, Lopes NP, Callegari Lopes JL, Lotufo TMC, Costa-Lotufo LV (2008) Antileukemic effects of *Didemnum psammatodes* (Tunicata: Ascidiacea) constituents. Comp Biochem Physiol A 151:363–369
33. Phleger CF, Nichols PD, Virtue P (1998) Lipids and trophodynamics of Antarctic zooplankton. Comp Biochem Physiol B 120:311–323
34. Deibel D, Cavaletto JF, Riehl M, Gardner WS (1992) Lipid and lipid class content of the pelagic tunicate *Oikopleura vanhoeffeni*. Mar Ecol Prog Ser 88:297–302
35. Barnathan G, Kornprobst JM (1993) Sponge fatty acids, 5. Characterization of complete series of 2-hydroxy long-chain fatty acids in phospholipids of two Senegalese marine sponges from the family Suberitidae: *Pseudosuberites* sp. and *Suberites massa*. J Nat Prod 56:2104–2113
36. Barnathan G, Kornprobst JM (1998) Isoprenoid fatty acids in sponge phospholipids. Recent Res Dev Lipids Res 2:235–248

37. Barnathan G, Genin E, Velosaotsy NE, Kornprobst JM, Al-Lihaibi S, Al-Sofyani A, Nongonierma R (2003) Phospholipid fatty acids and sterols of two *Cinachyrella* sponges from the Saudi Arabian Red Sea: comparison with *Cinachyrella* species from other origins. Comp Biochem Physiol B 135:297–308
38. Genin E, Wielgosz-Collin G, Njinkoué JM, Velosaotsy N, Kornprobst JM, Gouygou JP, Vacelet J, Barnathan G (2008) New trends of phospholipid class composition of marine sponges. Comp Biochem Physiol B 150:427–431
39. Denis C, Wielgosz-Collin G, Bretéché A, Ruiz N, Rabesaotra V, Boury-Esnault N, Kornprobst JM, Barnathan G (2009) New 17-methyl-13-octadecenoic and 3, 16-docosadienoic acids from the sponge *Polymastia penicillus*. Lipids 44:655–663
40. Mirallès J, Barnathan G, Galonnier R, Sall T, Samb A, Gaydou EM, Kornprobst JM (1995) New branched-chain fatty acids from the Senegalese Gorgonian *Leptogorgia piccola* (white and yellow morphs). Lipids 30:459–466
41. Stolyhwo A, Martin M, Guiochon G (1987) Analysis of lipid classes by HPLC with the evaporative light scattering detector. J Liq Chromatogr 10:1237–1253
42. Andersson BA (1978) Mass spectrometry of fatty acid pyrrolidides. Prog Chem Fats other Lipids 16:279–308
43. Descalzo AM, Insani EM, Pensel NA (2003) Light-scattering detection of phospholipids resolved by HPLC. Lipids 38:999–1003
44. Misra KK, Shkrob I, Rakshit S, Dembitsky VM (2002) Variability in fatty acids and fatty aldehydes in different organs of two prosobranch gastropod mollusks. Biochem Syst Ecol 30:749–761
45. Christie WW. The lipid library. http://www.lipidlibrary.co.uk, section updated 13.06.09
46. Nagan N, Zoeller RA (2001) Plasmalogens: biosynthesis and functions. Prog Lipid Res 40:199–229
47. Brites P, Waterham HR, Wanders RJA (2004) Functions and biosynthesis of plasmalogens in health and disease. Biochim Biophys Acta 1636:219–231
48. Vaskovky VE (1989) Phospholipids. In: Ackman RG (ed) Biogenic lipids, fats, and oils, vol 1. CRC Press, Boca Raton, pp 199–242
49. Kaneda T (1991) *Iso*- and *anteiso*-fatty acids in bacteria; biosynthesis, function, and taxonomic significance. Microbiol Rev 55:288–302
50. Gillan FT, Stoilov IL, Thompson JE, Hogg RW, Wilkinson CR, Djerassi C (1988) Fatty acids as biological markers for bacterial symbionts in sponges. Lipids 23:1139–1145
51. Carballeira NM, Miranda C, Rodríguez AD (2002) Phospholipid fatty acid composition of *Gorgonia mariae* and *Gorgonia entalina*. Comp Biochem Physiol B 131:83–87
52. Carballeira NM, Shalabi F (1994) Unusual fatty acids in the Caribbean sponges *Amphimedon viridis* and *Desmapsamma anchorata*. J Nat Prod 57:1152–1159
53. Christie WW, Brechany EY, Stefanov K, Popov S (1992) The fatty acids of the sponge *Dysidea fragilis* from the Black Sea. Lipids 27:640–644
54. Suutari M, Laasko S (1993) Signature GLC-MS ions in identification of Δ5- and Δ9-unsaturated *iso*- and *anteiso*-branched fatty acids. J Microbiol Methods 17:39–48
55. Carballeira NM, Montano N, Vicente J, Rodriguez AD (2007) Novel cyclopropane fatty acids from the phospholipids of the Caribbean sponge *Pseudospongorites suberitoides*. Lipids 42:519–524
56. Grogan DW, Cronan JE (1997) Cyclopropane ring formation in membrane lipids of bacteria. Microbiol Mol Biol Rev 61:429–441
57. Riediger ND, Othman RA, Suh M, Moghadasian MH (2009) A systemic review of the roles of n-3 fatty acids in health and disease. J Am Dietetic Assoc 109:668–679
58. Gorjão R, Azevedo-Martins AK, Gomes Rodrigues H, Abdulkader F, Arcisio-Miranda M, Procopio J, Curi R (2009) Comparative effects of DHA and EPA on cell function. Pharmacol Ther 122:56–64
59. Saito H (2008) Unusual novel *n*-4 polyunsaturated fatty acids in cold-seep mussels (*Bathymodiolus japonicus* and *Bathymodiolus platifrons*), originating from symbiotic methanotrophic bacteria. J Chromatogr A 1200:242–254
60. Pond DW, Bell MV, Dixon DR, Fallick AE, Segonzac M, Sargent JR (1998) Stable-carbon-isotope composition of fatty acids in hydrothermal vent mussels containing methanotrophic and thiotrophic bacterial endosymbionts. Appl Environ Microbiol 64:370–375
61. Pond DW, Allen CE, Bell MV, Van Dover CL, Fallick AE, Dixon DR, Sargent JR (2002) Origins of long-chain polyunsaturated fatty acids in the hydrothermal vent worms *Ridgea piscesae* and *Protis hydrothermica*. Mar Ecol Prog Ser 225:219–226

Lipids (2010) 45:263–273
DOI 10.1007/s11745-010-3395-2

ORIGINAL ARTICLE

Fatty Acyl-CoA Reductase and Wax Synthase from *Euglena gracilis* in the Biosynthesis of Medium-Chain Wax Esters

Prapapan Teerawanichpan · Xiao Qiu

Received: 6 November 2009 / Accepted: 2 February 2010 / Published online: 2 March 2010

Abstract *Euglena gracilis*, a unicellular phytoflagellate, can accumulate a large amount of medium-chain wax esters under anaerobic growth conditions. Here we report the identification and characterization of two genes involved in the biosynthesis of wax esters in *E. gracilis*. The first gene encodes a fatty acyl-CoA reductase (*EgFAR*) involved in the conversion of fatty acyl-CoAs to fatty alcohols and the second gene codes for a wax synthase (*EgWS*) catalyzing esterification of fatty acyl-CoAs and fatty alcohols, yielding wax esters. When expressed in yeast (*Saccharomyces cerevisiae*), EgFAR converted myristic acid (14:0) and palmitic acid (16:0) to their corresponding alcohols (14:0Alc and 16:0Alc) with myristic acid as the preferred substrate. EgWS utilized a broad range of fatty acyl-CoAs and fatty alcohols as substrates with the preference towards myristic acid and palmitoleyl alcohol. The wax biosynthetic pathway was reconstituted by co-expressing *EgFAR* and *EgWS* in yeast. When myristic acid was fed to the yeast, myristyl myristate (14:0–14:0), myristyl palmitoleate (14:0–16:1), myristyl palmitate (14:0–16:0) and palmityl myristate (16:0–14:0) were produced. These results indicate EgFAR and EgWS are likely the two enzymes involved in the biosynthesis of medium-chain wax esters in *E. gracilis*.

Keywords *Euglena* · Fatty acyl-CoA reductase · Fatty alcohol · Wax ester · Wax synthase

P. Teerawanichpan · X. Qiu (✉)
Department of Food and Bioproduct Sciences, College of Agriculture and Bioresources, University of Saskatchewan, 51 Campus Drive, Saskatoon, SK S7N 5A8, Canada
e-mail: xiao.qiu@usask.ca

Abbreviations

CoA	Coenzyme A
FAMEs	Fatty acid methyl esters
FAR	Fatty acyl-CoA reductase
RACE	Rapid amplification of cDNA ends
WS	Wax synthase

Introduction

Euglena gracilis is a unicellular phytoflagellate protist that can grow photoautotrophically in a minimal medium as well as heterotrophically in an organic carbon-rich medium. Under light or aerobic conditions, *Euglena* accumulates polysaccharides (mainly β-1,3 glucan, known as paramylon) and wax esters as energy reserves [1, 2]. Once the cell culture is switched from light to dark or from aerobic to anaerobic conditions, the polysaccharide reserve is converted to wax esters in the cytosol and the accumulated wax esters can reach up to 62% of the total lipid content [3]. Wax esters produced in *Euglena* are in a range of the 20- to 36-carbon chains comprised of saturated fatty acids and alcohols of 12–18 carbon chains with myristyl myristate (14:0–14:0) as the major species [4]. Under aerobic growth, *Euglena* mainly accumulates even-numbered wax esters, however an anaerobic growth condition promotes the accumulation of odd-numbered wax esters in some *Euglena* strains [3–6]. In addition to light and oxygen, other environmental factors, such as nutrients and temperature can also affect the production and composition of storage wax esters in *Euglena* cells. The production of wax esters is more efficient when the culture medium contains organic carbon source [7] or when the culture is shifted from low to high temperature (15 °C to 33 °C) [8]. Supplementation of

the medium with unsaturated fatty acids (oleic acid, linoleic acid, linolenic acid) and unusual fatty acid (ricinoleic acid) leads to the accumulation of these fatty acids in both acyl and alcohol moieties of wax esters [6].

The wax ester biosynthetic pathway consists of two successive steps: conversion of fatty acyl-CoA to fatty alcohol and esterification of fatty acyl-CoA and fatty alcohol [9]. The enzymes responsible for these reactions are fatty acyl-CoA reductase (FAR) and acyl-CoA:fatty alcohol acyltransferase or wax synthase (WS), respectively. The genes encoding FARs have been identified from a variety of living organisms, including mouse [10], human [10], silkmoth [11], bean borer moth [12], jojoba [13], *Arabidopsis* [14, 15] and wheat [16]. BmFAR, a fatty acyl-CoA reductase from silkmoth (*Bombyx mori*), is responsible for production of sex pheromone bombykol, (*E,Z*)-10,12–hexadecadien-1-ol [11], whereas OsFARXIII, another fatty acyl-CoA reductase from bean borer moth (*Ostrinia scapulalis*), catalyzes the production of (*Z*)-11-tetradecenol, which can be further converted to acetate or aldehyde pheromones [12]. ScFAR, a fatty acyl-CoA reductase from jojoba (*Simmondsia chinensis*), is responsible for producing storage wax esters in developing seeds [13]. *Arabidopsis* fatty acyl-CoA reductase AtCER4 (At4g33790) is involved in the synthesis of cuticular wax lipids [15]. *TaTAA1a*, *TaTAA1b* and *TaTAA1c*, three orthologs of the jojoba *ScFAR*, were isolated from wheat [16]; they are involved in producing the lipid component in the outer pollen wall.

Wax synthases have also been isolated and characterized from a wide range of living organisms. Some show only wax synthase activity such as mouse WS, human WS [17], jojoba ScWS [18] and petunia PhWS1 [19], while the other exhibit both wax synthase and acyl-CoA:diacylglycerol acyltransferase (DGAT) activities, including *Acinetobacter* WS/DGAT [20] and *Arabidopsis* WSD1 [21]. Mouse and human *WSs* (*MmWS* and *HsWS*) are highly expressed in sebaceous-rich tissues, such as preputial glands and eyelids [17]. Jojoba *ScWS* was isolated from developing seeds and is involved in the synthesis of liquid waxes that accumulate in seeds [18]. *Arabidopsis AtWSD1* (*At5g37300*) is involved in synthesis of stem epicuticular wax esters as shown by a severe reduction of the wax ester content (44 and 46 carbons) in *Arabidopsis wsd1* mutants [21]. Petunia *PhWS1* is highly expressed in petals and involved in the production of very long chain fatty acid esters of methyl, isoamyl and short to medium straight chain alcohols (4–12 carbons) [19].

In *E. gracilis*, the activities of both FAR and WS were found in the microsomal fraction of cultures grown in the dark [22]. The biochemical assays showed that FAR used 14:0, 16:0 and 18:0 as substrates and required NADH as a cofactor [22, 23]. Although the biosynthesis of wax esters in *Euglena* has been extensively studied, the genes encoding these enzymes have not been described. Here we report the identification and characterization of two genes, *EgFAR* and *EgWS*, involved in the biosynthesis of wax esters in *E. gracilis*. Heterologous expression of these genes in yeast revealed the unique properties of the enzymes—preferential utilization of medium chain fatty acyl and alcohol as substrates for synthesis of wax esters.

Experimental Procedures

Isolation of Putative *Euglena Fatty Acyl-CoA Reductase* (*EgFAR*) and *Euglena Wax Synthase* (*EgWS*)

Euglena gracilis was grown aerobically in a TSY medium (0.1 g/l sodium acetate, 0.1 g/l beef extract, 0.2 g/l peptotryptone, 0.2 g/l yeast extract, 0.2 μg vitamin B12, 1 μg/l biotin, 100 μg/l thiamine-HCl, 0.1 μg/l niacinamide, pH 7.0 [24]) at 25 °C for 16 h (120 μE m^{-2} s^{-1})/8 h (light/dark) regime. The *Euglena* cells can accumulate up to 28% wax ester under these conditions. Total RNA was extracted from the *E. gracilis* culture using TRIZOL® reagent (Invitrogen). The full length cDNAs of *EgFAR* and *EgWS* were obtained using Marathon™ cDNA Amplifcation kit under conditions detailed by the supplier (Clontech). The gene-specific primers used for 5′- and 3′-RACE of *EgFAR* are ACR1 (5′-GGCTGGTTGGAGTTGACGTAGCA-3′) and ACF1 (5′-GCCATGAACGATTTCTACGCGGG-3′) primers, respectively. The gene-specific primers used for 5′- and 3′-RACE of EgWS are WSR2 (5′-CTCCGGGTG ACCTTTCGGC-3′) and WSF2 primers (5′-CCAGCCC TACTTTTCCACATCTCTGAG-3′), respectively.

DNA Sequencing and Analysis

All synthesis and sequencing work was performed by the DNA Technologies Unit at the Plant Biotechnology Institute, National Research Council of Canada. Nucleotide sequence and amino acid sequence comparisons were conducted using Lasergene7 (DNASTAR).

Amino Acid Sequence Alignment and Phylogenetic Analysis

Phylogenetic analysis of functionally characterized FARs and WSs were performed as previously described [25].

Construction of Yeast Expression Vectors Harboring *EgFAR*, *EgWS* and *EgFAR-EgWS*

The *EgWS* open reading frame (ORF) was amplified using primers WSFLF (5′-TTCGCGATGGATTTTTTGGGG-3′) and WSFLR (5′-GCCACCCAAGGCACTTGGCCT-3′)

and cloned into pYES2.1/V5-His/lacZ vector (Invitrogen), yielding plasmid pPT504. The *EgFAR* ORF was amplified using primers PT0037 (5′-GATCGGATCCATGAACGAT TTCTACGCG-3′)-PT0041 (5′-ATCAGCTAGCCTATCA CAGCATGGCCCGC-3′) and digested with *Bam*HI and *Nhe*I. The amplified fragment was subsequently cloned into the corresponding restriction sites of a yeast expression vector pESC-URA (Stratagene), yielding pPT515. The amplification was performed using 2.5 units of Platinum® *Pfx* DNA polymerase (Invitrogen) in the presence of 5% (v/v) DMSO. PCR conditions for *EgFAR* were 35 cycles of 94 °C for 15 s, 55 °C for 30 s, 68 °C for 1 min with the final extension at 68 °C for 5 min. PCR conditions for *EgWS* were identical to *EgFAR*, except that the extension time was 30 s instead of 1 min. For the co-expression study, the *EgWS* ORF was amplified from pPT504 using primers PT0049 (5′-GATCATCGATATGGATTTCTTAG GTTTTCCTGAC-3′)-PT0050 (5′-CTGTAGATCTCTAT CAGACAGACAGACCTAGC-3′). The amplified fragment was digested with *Cla*I and *Bam*HI and subsequently cloned into the corresponding sites of pPT515, yielding pPT516.

Functional Analysis of *EgFAR* and *EgWS* in Yeast

pPT515 (*EgFAR*) and pPT504 (*EgWS*) plasmids were transformed into yeast (*Saccharomyces cerevisiae*) strain H1246 (*MATα*; *are1*-Δ::*HIS3 are2*-Δ::*LEU2 dga1*-Δ::*KanMX4 lro1*-Δ::*TRP1 ADE2*) [26] using S.c. Easy-Comp™ transformation kit (Invitrogen). Yeast strains transformed with pPT515 (*EgFAR*), pPT504 (*EgWS*), pPT516 (*EgFAR* + *EgWS*), pESC-URA or pYES2.1 plasmids were grown at 30 °C for 2 days in 10 ml of the synthetic dropout medium containing 0.17% (w/v) yeast nitrogen base, 0.5% (w/v) ammonium sulfate, 2% (w/v) glucose and 0.06% (w/v) dropout supplement lacking uracil (DOB + GLU-URA). After two washes with 10 ml of sterile distilled water, the expression of transgene in yeast were induced by culturing the yeast at 20 °C for 4 days for pPT515 (*EgFAR*) and 30 °C for 2 days for pPT504 (*EgWS*) in 10 ml of the synthetic dropout medium containing 2% (w/v) galactose (DOB + GAL-URA) with or without substrate supplementation in the presence of 0.1% (v/v) tergitol (Nonidet P-40). Two-hundred fifty micromolar of fatty acid was used as a substrate for the pPT515 (*EgFAR*) expression, whereas 250 μM of fatty acid and 250 μM of fatty alcohol were used as substrates for the pPT504 (*EgWS*) expression. After induction, the cultures were washed once with 10 ml of 1% (v/v) tergitol and once with 10 ml of distilled water, and then subjected to fatty acid analysis. For the yeast feeding experiment, fatty acid and fatty alcohol substrates were initially prepared as stock solutions in ethanol at the concentration of 500 mM and the appropriate amount of the stock was then diluted in 10% tergitol at the final concentration of 50 mM used for feeding the yeast.

In Vitro Assays of *EgFAR* and *EgWS*

To investigate substrate specificity of EgFAR and EgWS in vitro, the microsomal fractions of yeast expressing *EgFAR* and *EgWS* were prepared as previously described [27, 28]. For the EgFAR assay, the enzyme reaction (500 μl) contained 200 μg of microsomal proteins, 0.3 M sucrose, 0.1 M MOPS (pH 6.5) or 0.1 M Tris–HCl, (pH 7.4), 1 mM EDTA, 2.5 mM DTT, 5 mM $MgCl_2$, 1 mM PMSF, 100 μM acyl-CoA, 2.5 mM NADH, 2.5 mM NADPH. The reaction was carried out at 30 °C with gentle shaking for 30 min to 2 h. For the EgWS assay, the same amount of protein and the reaction buffer (pH 7.4) were used. One-hundred micromolar of acyl-CoA and 100 μM fatty alcohol were added as substrates. The reaction was carried out at 30 °C with gentle shaking for 2 h. The enzyme reactions were terminated by addition of 100 μl of 6 M HCl. After adding 1 ml of phosphate buffered saline and 1 ml of 0.9% (w/v) NaCl solution, lipids were extracted twice with 2 ml hexane. The known amount of methyl eicosanoate (20:0-ME) was added as the internal standard. The solvent was subsequently removed under a nitrogen stream and the lipid samples were resuspended in 20 μl of hexane, which was derivatized with bis(trimethylsilyl)-acetamide (TMS) and analyzed by GC for the EgFAR assay or was directly analyzed by GC for the EgWS assay (see below). Acyl-CoA stock solutions were prepared in 10 mM sodium acetate buffer (pH5.2)/ethanol (1:1, v/v) at a concentration of 50 mM.

Co-Expression of *EgFAR* and *EgWS* in Yeast

To reconstitute the *Euglena* wax biosynthesis pathway in yeast, the plasmid pPT516 harboring the two-gene cassette (*EgFAR* and *EgWS*) was transformed into the yeast strain H1246. The transformants were grown in the DOB + GLU-URA medium at 30 °C for 2 days and the expression of *EgFAR* and *EgWS* was induced in the DOB + GAL-URA medium supplemented with 500 μM 14:0 in the presence of 0.1% (v/v) tergitol at 20 °C for 4 days. The yeast cells were harvested and analyzed for fatty alcohol and wax monoester production as described above.

Analysis of Fatty Acids, Fatty Alcohols and Wax Esters of Yeast Transformants

Fatty acids of yeast cells were transmethylated with 2 ml of methanol/HCl (3 M) at 80 °C for 2 h and the reaction was terminated by adding 1 ml of 0.9% NaCl solution. Total fatty acid methyl esters (FAMEs) and fatty alcohols were

then extracted twice with 2 ml of hexane and the hexane phase was transferred to a new tube, evaporated under a nitrogen stream and resuspended in 200 μl of hexane. Fifty microliters of samples were derivatized with 50 μl of TMS/pyridine (1:1, v/v) at 80 °C for 30 min and the derivative was analyzed by gas chromatography (GC). For wax ester analysis, the total lipid was extracted by homogenizing yeast cells in the presence of 6 ml of chloroform/methanol (2:1, v/v). The organic phase was dried under a stream of nitrogen gas, resuspended in 50 μl of hexane and analyzed by GC, GC–mass spectrophotometry (MS) and thin layer chromatography (TLC).

GC, GC–MS and TLC Analysis

Fatty acids (10:0, 12:0, 14:0, 16:0, 16:1n-9, 18:0, and 18:1n-9), fatty alcohols (10:0Alc, 12:0Alc, 14:0Alc, 16:0Alc, 16:1n-9Alc, 18:0Alc and 18:1n-9Alc), wax esters (14:0–12:0, 14:0–14:0, 14:0–16:0, 14:0–16:1n-9, 14:0–18:0, 14:0–18:1n-9, 12:0–14:0, 16:0–14:0, 16:1n-9–14:0, 18:0–14:0, 18:1n-9–14:0) and TLC reference standard (cholesterol, cholesteryl oleate, triolein, oleic acid, methyl oleate) with 99% purity were purchased from Nuchek-Prep, Inc. For GC analysis, one-microliter samples were analyzed on an Agilent 6890 N GC equipped with a DB-5 column (10 m × 0.25 mm) (J&W Scientific). The following temperature programs were employed: 70 °C for 1 min, then 10 °C/min to 300 °C, and 300 °C for 10 min with H_2 as the carrier gas. For MS analysis, the mass selective detector was run under standard electron impact conditions (70 eV), scanning an effective *m/z* range of 40–700 at 2.26 scans/s. Identities of FAMEs, fatty alcohols-TMS derivatives and wax esters were identified by comparing their retention times with those of the standards and confirmed by GC–MS on the basis of their fragmentation patterns. For TLC analysis, total lipid samples and standards were spotted on 60-Å silica gel SIL G-25 plates (Macherey–Nagel) and resolved in hexane/diethylether/acetic acid (90:7.5:1, v/v/v) [21]. The plate was air-dried and the lipid metabolites were detected by primuline spraying (0.05% w/v; Sigma) and the pictures were taken under UV light at 254 nm.

Results

Isolation of Two cDNAs Encoding Putative Fatty acyl-CoA Reductase and Wax Synthase from *E. gracilis*

The partial cDNA sequences of *Euglena* putative fatty acyl-CoA reductase *EgFAR* and wax synthase *EgWS* were obtained by a homology search of the *Euglena* EST database using jojoba ScFAR and ScWS as query sequences and the full-length putative *EgFAR* and *EgWS* cDNAs were obtained by 5′- and 3′-RACE using *Euglena* cDNAs as the template. Sequence analysis indicated putative *EgFAR* encodes a polypeptide of 514 amino acids in length with the predicted molecular mass of 56.5 kDa. The deduced protein EgFAR contains a Rossmann-fold NAD/NADP binding domain (NABD; 289 amino acids) [29] linked with a Male Sterile 2 domain (MS2, 97 amino acids) [30] at the carboxyl end (Fig. 1a). A conserved motif (I/V/F)-X-(I/L/V)-T-G-X-T-G-F-L-(G/A), found in other fatty acyl-CoA reductases, was also observed in the NABD domain of EgFAR (Fig. 1b). The hydropathy analysis indicated that the putative EgFAR contains five high hydrophobic regions; one located at the N-terminus and the rest present in the central portion of the protein. Phylogenetic analysis of the putative EgFAR and related sequences reveals that EgFAR is more closely related to plant fatty acyl-CoA reductases, including *Arabidopsis* AtCER4 [15], wheat TaTAA1 [16] and jojoba ScFAR [31], whereas the insect and mammalian fatty acyl-CoA reductases [10] form a distant group (Fig. 2a). Sequence analysis of the putative *EgWS* indicated that it encodes a polypeptide of 368 amino acids with the predicted molecular mass of 41.2 kDa. The deduced protein EgWS contains six distinct hydrophobic regions. Phylogenetic analysis of EgWS and related sequences reveals that *Euglena* EgWS clusters with jojoba ScWS [18], which is distantly related to the rest members of wax synthases, including the mammalian WSs [17], *Acinetobacter* AcWS/DGAT [20], *Arabidopsis* AtWSD1 [21] and petunia PhWS1 [19] (Fig. 2b).

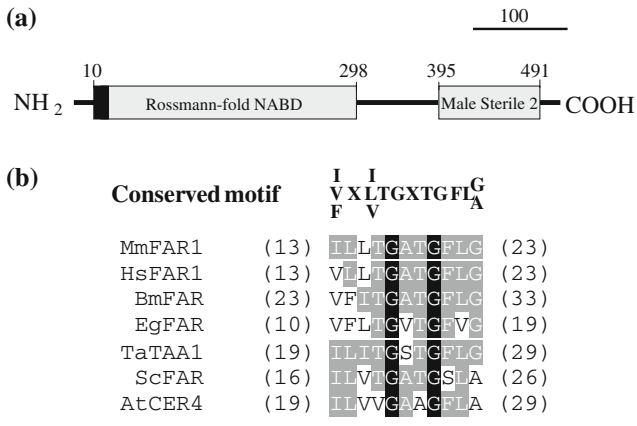

Fig. 1 A schematic diagram illustrating the functional domains (**a**) and a conserved motif (**b**) of EgFAR and other related sequences. The *numbers* indicate amino acid positions. The accession numbers of these sequences are indicated in Fig. 2

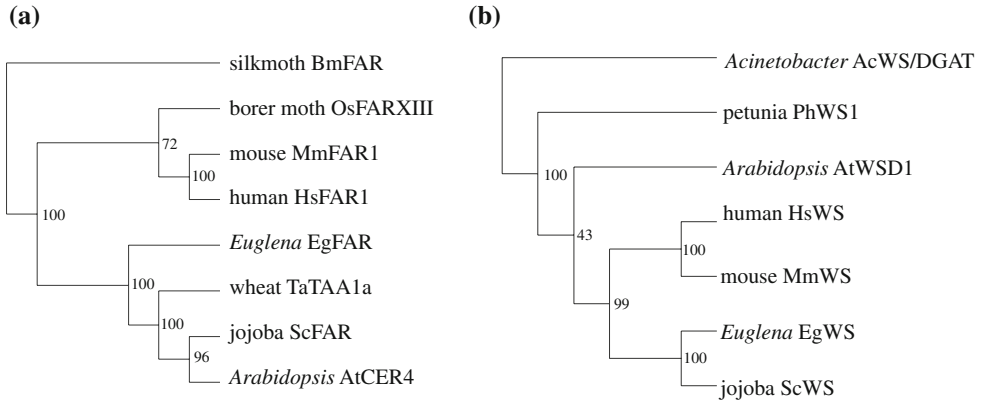

Fig. 2 Phylogenetic analysis of EgFAR (**a**) and EgWS (**b**) and their related sequences. The GenBank accession numbers of the sequences are as follows: mouse MmFAR1, BC007178; mouse MmFAR2, BC055759; human HsFAR1, AY600449; human HsFAR2, BC022267; silkmoth BmFAR, AB104896; borer moth OsFARXIII, EU817405; wheat FAR (TaTAA1a), AJ459249; jojoba ScFAR, AF149917; *Arabidopsis* AtCER4, AY070065-At4g33790; mouse MmWS, AY611032; human HsWS, AY605053; *Arabidopsis* AtWSD1, NM_123089-AT5G37300; *Acinetobacter* AcWS/DGAT, AF529086; jojoba ScWS, AF149919; petunia PhWS1, DQ093641

Functional Analysis of *EgFAR* and *EgWS* in Yeast

To determine the function of putative *EgFAR* and *EgWS*, the full-length cDNAs were cloned into the yeast expression vectors separately and the recombinant plasmids were transformed into the *Saccharomyces cerevisiae* quadruple mutant strain H1246 [26], in which four acyltransferase genes involved in the triacylglycerol (TAG) and sterol ester biosynthesis were disrupted. This strain appeared to have diminished capacity for wax ester biosynthesis (Fig. 3b), thus can serve as a good host system to examine the function of genes involved in the biosynthesis of wax esters.

The activity of the putative *Euglena* fatty acyl-CoA reductase was investigated by feeding the yeast strain carrying *EgFAR* with a variety of probable fatty acid substrates. Analysis of total fatty alcohols in the cells indicated that the transformant expressing *EgFAR* produced new peaks only when myristic acid (14:0) and palmitic acid (16:0) were used as substrates, compared with the vector control (Fig. 3a). The chemical structures of these new peaks were determined as myristyl alcohol (14:0Alc) and palmityl alcohol (16:0Alc) by GC–MS. The conversion efficiencies of the two alcohols were 34 ± 4 and 24 ± 3%, respectively. No other alcohol products were detected when the yeast strain was fed with other saturated fatty acids (10:0, 12:0 and 18:0) or unsaturated fatty acids (16:1n-9, 18:1n-9 and 18:2n-6). A similar result was obtained when *EgFAR* was expressed in yeast strain INVSc.

The activity of the putative EgWS was investigated by feeding the yeast strain expressing *EgWS* with 14:0 and 14:0Alc substrates. The total neutral lipids including triacylglycerols and wax esters in the transformant were first analyzed by TLC. In contrast to the vector control, the yeast expressing *EgWS* produced wax esters in presence of 14:0 and 14:0Alc that were detected on the TLC plate (Fig. 3b). Like the control, the transformant expressing *EgWS* did not produce any triacylglycerols, indicating EgWS possess wax synthase activity, but not diacylglycerol acyltransferase activity as seen in bacterial WS/DGAT [32]. Wax composition analysis by GC and GC–MS indicated that the major components of wax esters produced in the transformant were myristyl myristate (14:0–14:0), myristyl palmitate (14:0–16:0) and myristyl pamitoleate (14:0–16:1) (Fig. 3c). It was also noted that the vector control could produce a trace amount of myristyl myristate (14:0–14:0) when the yeast was fed with substrates (Fig. 3b, c).

To examine the fatty acid substrate specificity of EgWS, the yeast strain was fed with 14:0Alc in combination with a range of fatty acids including 10:0, 12:0, 14:0, 16:0, 16:1n-9,18:0, and 18:1n-9. The wax analysis showed that EgWS could incorporate 12:0, 14:0, 16:0 and 16:1–9 fatty acids into wax esters, but it could not use 10:0, 18:0 or 18:1n-9 as the substrate. Quantitative analysis of the ratio of products versus substrates indicated that the highest conversion efficiency of fatty acids was observed on 14:0, which was followed by 12:0, 16:0 and 16:1n-9 (Table 1). In order to examine fatty alcohol substrate specificity, the yeast strain was fed with 14:0, the most preferred acyl-CoA substrate for EgWS in combination with a range of fatty alcohols including 10:0Alc, 12:0Alc, 14:0Alc, 16:0Alc, 16:1n-9Alc, 18:0Alc and 18:1n-9Alc. Wax analysis indicated that EgWS could utilize 12:0Alc, 14:0Alc, 16:0Alc and 16:1n-9Alc fatty alcohols, but not 10:0Alc, 18:0Alc and 18:1n-9Alc as the substrates. The preferred fatty alcohol was 16:1n-9Alc, which was followed by 14:0Alc, 12:0Alc and 16:0Alc (Table 1).

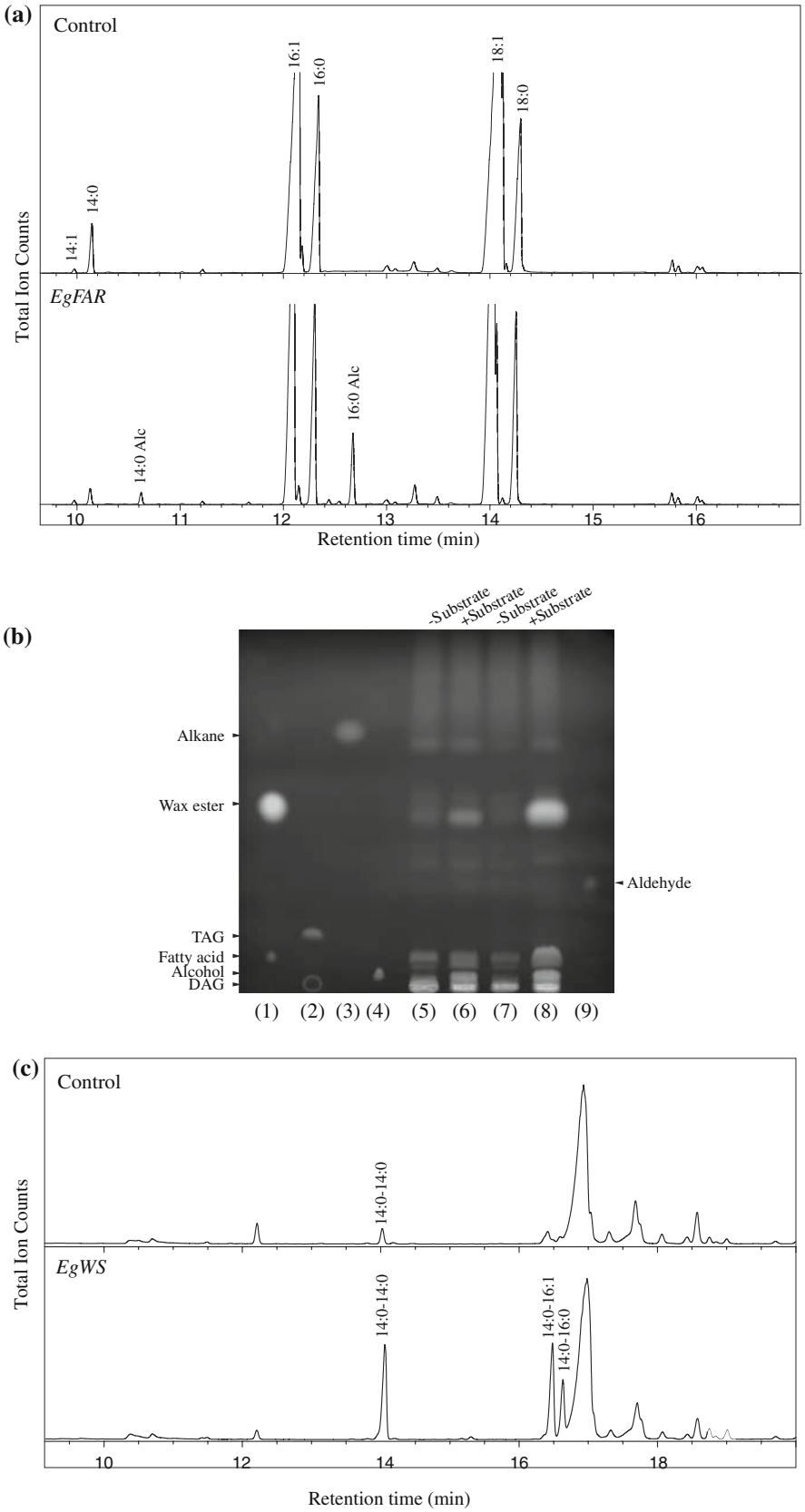

Fig. 3 Activity of EgFAR (**a**) and EgWS (**b**, **c**) in yeast. **a** GC analysis of fatty acid methyl esters and fatty alcohol TMS ethers prepared from the yeast transformed with the pESC-URA vector control or *EgFAR*. **b** TLC analysis of the total lipid of the yeast transformed with the pYES2.1 vector control (*lanes 5* and *6*) or *EgWS* (*lanes 7* and *8*) in the absence (*lanes 5* and *7*) and presence (*lane 6* and *8*) of substrates (14:0 and 14:0Alc). *Lane 1–4*, *9* are standards: *DAG* diacylglycerol, *TAG* triacylglycerol (**c**) GC analysis of the total lipid prepared from yeast transformed with *EgWS* or the pYES2.1 vector control and fed with 14:0 and 14:0Alc substrates

Table 1 Substrate specificity of EgWS for fatty acids and fatty alcohols

Substrate	Conversion efficiency (%)	
	Fatty acid	Fatty alcohol
12:0	37 ± 8	21 ± 2
14:0	47 ± 4	47 ± 6
16:0	31 ± 1	25 ± 2
16:1n-9	33 ± 3	68 ± 5
18:0	n.d.	n.d.
18:1n-9	n.d.	n.d.

The transformant yeast was fed with 14:0Alc in combination with different fatty acids to examine the fatty acid specificity and fed with 14:0 in combination with different fatty alcohols to examine the fatty alcohol specificity. The conversion efficiencies (%) of wax esters were calculated as [(product)/(substrate + product)] × 100 using the values corresponding to the weight percent of fatty alcohol substrates and the wax ester products inside the yeast cells. The values are the average derived from triplicates ± standard deviation (SD)

n.d. not detected

To study the substrate specificity of EgFAR and EgWS in vitro, the microsomal fractions of yeast expressing *EgFAR* or *EgWS* were incubated with a series of fatty acids or fatty acid and alcohol combinations. However, only small activity of wax ester synthesis was detected in the in vitro assay of EgWS, which was basically in agreement with the result from the in vivo experiment. Furthermore, we could not detect any fatty acyl-CoA reductase activity in the in vitro assay of EgFAR with all possible substrates. The reason why the in vitro EgWS and EgFAR activities in yeast were low is unknown. It is noteworthy that so far only three reports have described the in vitro fatty acyl-CoA reductase and wax synthase activities in heterologous systems, including mammalian FARs and WSs in the HEK293 human cell line [10, 17] and *Acinetobacter* WS/DGAT in *E. coli* [20]. The difficulty in the yeast in vitro assays of EgFARs and EgWSs might be related to the nature of this type of enzymes or simply the low activities of the two enzymes in yeast.

Reconstitution of the *Euglena* Wax Biosynthetic Pathway in Yeast

To reconstitute the *Euglena* wax biosynthetic pathway in yeast, *EgFAR* and *EgWS* were cloned into a yeast expression vector, pESC-URA, in which the expression of *EgFAR* and *EgWS* were driven by *GAL1* and *GAL10* inducible promoters, respectively. The recombinant plasmid was then transformed into the yeast strain H1246 and the transformants were grown in the selective medium supplemented with 14:0, a common preferred substrate for both EgFAR and EgWS. Wax ester analysis indicated that the co-expressing yeast, like the *EgFAR*-expressing yeast, could convert 14:0 and 16:0 to 14:0Alc and 16:0Alc, respectively (Fig. 4). In addition, the co-expressing yeast produced three new wax ester peaks which were not detected in either *EgFAR*-expressing yeast or vector control yeast. Identities of these peaks were determined by comparing their retention times and mass spectra to those of standards. Peak 1 had the identical retention time and mass spectrum to

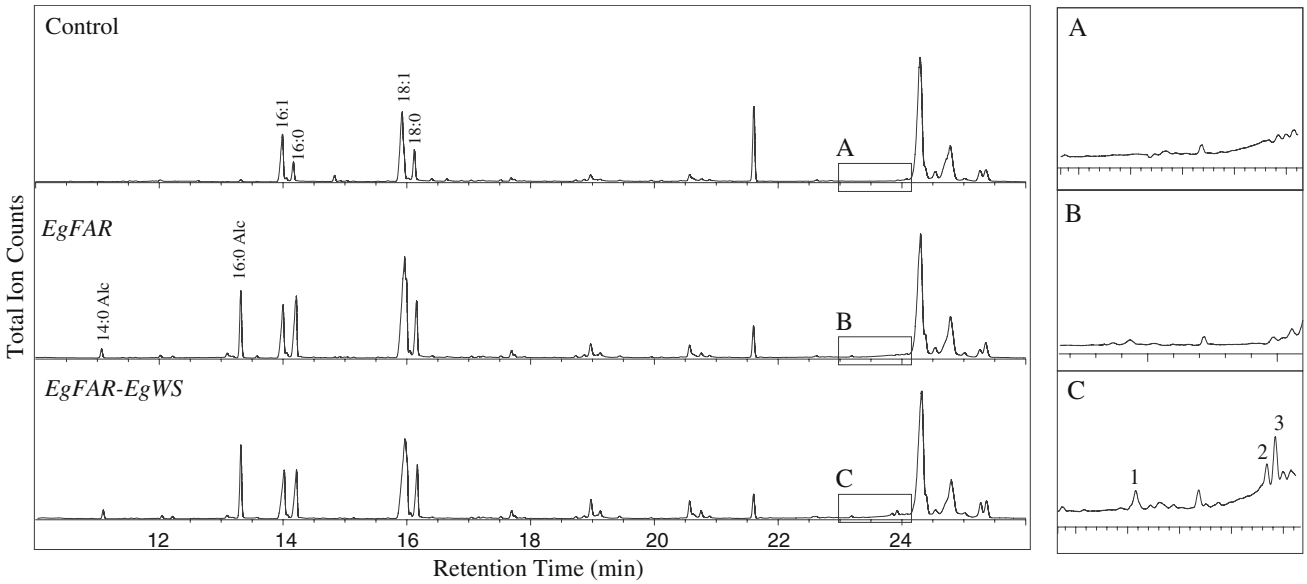

Fig. 4 Co-expression of *EgFAR* and *EgWS* in yeast. GC analysis of the total lipid showing wax ester production prepared from yeast transformed with pESC-URA (empty vector), *EgFAR* and *EgFAR-EgWS* and fed with 14:0 substrate. *Peak 1* myristyl-myristate (14:0–14:0), *Peak 2* myristyl-palmitoleate (14:0–16:1), *Peak 3* myristyl palmitate (14:0–16:0) and palmityl myristate (16:0–14:0). Selected regions of the chromatograms of control, *EgFAR* and *EgFAR-EgWS* expressing yeast are magnified in boxes *A*, *B* and *C*, respectively

myristyl myristate (14:0–14:0) which accounted for ~23% of total wax esters (Fig. 5a) while peak 2 had the identical retention time and mass spectrum to myristyl palmitoleate (14:0–16:1) (Fig. 5b) which accounted for ~22% of total wax esters. Peak 3 appeared to contain two wax ester products, myristyl palmitate (14:0–16:0) and palmityl myristate (16:0–14:0) together they accounted for ~55% of total wax esters. GC and GC–MS analysis showed that it had the same retention time as myristyl palmitate (14:0–16:0) and palmityl myristate (16:0–14:0) and possessed the mass spectrum (Fig. 5c) with diagnostic ions representing the mass spectra of both myristyl palmitate (14:0–16:0) (Fig. 5d) and palmityl myristate (16:0–14:0) (Fig. 5e). Based on the abundance of the diagnostic fragments and the relative response factors of 14:0–16:0 (*m/z* 257) and 16:0–14:0 (*m/z* 229), peak 3 contained ~58% of 14:0–16:0 and ~41% of 16:0–14:0. Collectively, these results indicated that EgWS in the co-expressing yeast could esterify 14:0Alc and 16:0Alc produced by EgFAR with 14:0, 16:0 and 16:1n-9 fatty acids, producing medium chain wax esters, myristyl myristate (14:0–14:0), myristyl palmitate (14:0–16:0), myristyl palmitoleate (14:0–16:1) and palmityl myristate (16:0–14:0).

Discussion

The biosynthesis of wax esters comprises two consecutive catalytic steps, reduction of fatty acyl-CoA to fatty alcohol and subsequent esterification of fatty acyl-CoA and fatty

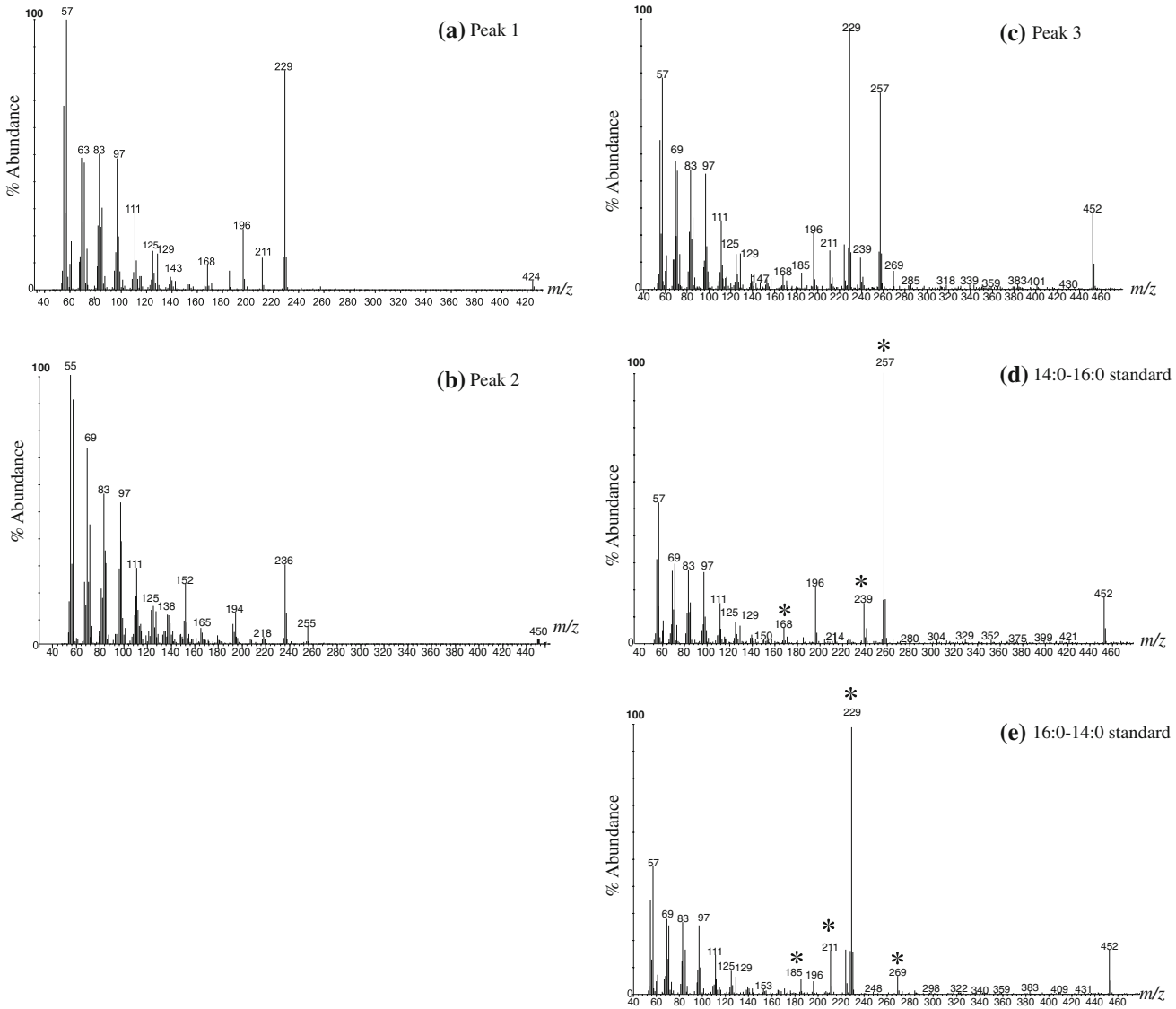

Fig. 5 GC/MS analysis of wax ester peak 1 **a**, peak 2 **b** and peak 3 **c** in Fig. 4, myristyl palmitate (14:0–16:0) standard (**d**) and palmityl myristate (16:0–14:0) standard **e**. *Asterisks* indicate diagnostic ions of the wax esters

alcohol. The reduction of fatty acid to fatty alcohol occurs through aldehyde intermediate and is catalyzed by either one or two enzyme reactions. In the two-enzyme reaction, acyl-CoA reductase first converts the fatty acyl-CoA to aldehyde and then the aldehyde reductase catalyzes the reduction of the aldehyde to alcohol. Evidence supporting the two-step reaction came from the early identification of aldehyde reductase from *Brassica oleracea* [33] and the recent isolation of the *acyl-CoA reductase* gene from *Acinetobacter*, catalyzing the production of fatty aldehyde [34]. However, support for the existence of the two-enzyme reduction is scarce in eukaryotes. In fact, a single enzyme reaction for the fatty acid reduction appears to occur widely in nature where the FAR catalyzes reduction of fatty acyl-CoA to fatty alcohol directly, although aldehyde intermediates could be detected by indirect trapping assays [23]. This type of fatty acyl-CoA reductases has been identified from jojoba cotyledon, pea leaves [23, 35, 36] and many others [37–39], including the one we describe here from *Euglena*.

Although *E. gracilis* has long been known to accumulate a large amount of medium-chain wax esters under dark and anaerobic growth conditions, the genes involved in the biosynthesis of these wax esters have yet to be identified. In this study, we report the isolation and characterization of two cDNAs, *EgFAR* and *EgWS*, from *E. gracilis* encoding two enzymes involved in the biosynthesis of medium chain wax esters. The pairwise sequence comparison of EgFAR and previously identified FARs revealed that EgFAR shares low amino acid identity with other FARs (23–27.4%). Functional analysis of EgFAR in yeast indicated that it could effectively convert 14:0 and 16:0 fatty acids to their corresponding alcohols. Compared with other biochemically characterized FARs, EgFAR possesses a narrower substrate range, only using saturated fatty acids with 14 and 16 carbon chains as substrates with the preferred fatty acid being 14:0 when expressed in yeast.

The pairwise sequence comparison of EgWS and related wax synthases revealed that EgWS also shares low amino acid identity to its related enzymes (in the range of 13–27%). It was noted that EgWS does not contain an *N*-terminal domain with the proposed active site (HHXXXD) found in *Acinetobacter* AcWS/DGAT [20], *Arabidopsis* AtWSD1 [21] and petunia PhWS1 [19]. This domain was believed to be essential for their acyl-CoA acyltransferase activities for the synthesis of wax esters and TAGs [20]. It will be interesting to know how EgWS functions without this domain. To date, three wax synthases including EgWS we report here have been functionally characterized in yeast. AtWSD1 mainly synthesizes wax esters with 16:0 fatty acid and 18:0Alc, 24:0Alc and 28:0Alc alcohols, and PhWS1 produces wax esters with very long chain fatty acids and methyl, isoamyl short to medium chain alcohols (4–12 carbons), whereas EgWS prefers 14 carbon chain fatty acid as the substrate.

Wax esters consisting of medium chain saturated fatty alcohols are sporadically found in animals and microorganisms [40–43]. *E. gracilis* can accumulate up to 28 or 62% of the total lipid as wax esters when grown in aerobic or anaerobic conditions [3] and the major molecular species of the wax esters accumulated is myristyl myristate [4, 6]. Functional expression of *EgFAR* and *EgWS* separately in yeast revealed that both enzymes could use 14 and 16 fatty acid substrates and the co-expression of *EgFAR* and *EgWS* in yeast resulted in production of medium-chain wax esters. These results are consistent with the composition of wax esters naturally present in *Euglena*, suggesting an important role of EgFAR and EgWS in synthesizing the wax esters in *Euglena*. *EgFAR* and *EgWS* were identified by the homology search of an EST database using jojoba *ScFAR* and *ScWS* as query sequences and only one EST of each EgFAR and EgWS was found in the database. However, it could not be excluded that there are additional genes involved in the biosynthesis of medium-chain wax esters in *Euglena* that were not present in the EST database. It should also be noted that *Euglena* can accumulate unsaturated fatty acid (e.g. 18:1n-9) wax esters when the culture medium is supplemented with such fatty acid [6]. Although we have not observed any activity of EgFAR and EgWS towards 18:1n-9 when they were expressed in yeast, this should not exclude the possibility that the difference of the cellular microenvironment between the native host and yeast could have effect on the substrate specificity of the enzymes. Alternatively, there might be additional FARs and WSs present in *Euglena* that can utilize unsaturated fatty acids as substrates.

Medium- and long-chain wax esters have been widely used in food, pharmaceuticals, textiles, perfumes and flavoring. They can also be used in the production of fatty sulfate salts and alcohol ethoxylates in the detergent industry. The current supply of wax from natural sources is limited due to the high production cost and cannot meet the growing demand for its widespread uses. Metabolic engineering of oilseed plants to produce wax esters has been viewed as an attractive alternative to provide cost-effective sources for biological wax. The first attempt of wax metabolic engineering in plants was undertaken by expressing jojoba *ScFAR* and *ScWS*, along with *Lunaria annua β-ketoacyl-CoA synthase* (a component of fatty acid elongase) resulting in the production of very long chain wax esters in *Brassica napus* seeds [18]. Here, we describe two genes *EgFAR* and *EgWS* from *Euglena* encoding fatty acyl-CoA reductase and wax synthase that have a substrate preference towards medium chain substrates. It will be interesting to see how these genes perform in the production of industrially important medium-chain wax esters in oil seed crops.

Acknowledgments We are very grateful to Patricia Vrinten for technical assistance in gene isolation. We thank Devin Polichuk, Darwin Reed and Valerie Catinot for technical help and discussions. This work is part of ICON, a European Community Seventh Framework Programme.

References

1. Inui H, Miyatake K, Nakano Y, Kitaoka S (1982) Wax ester fermentation in *Euglena gracilis*. FEBS Lett 150:89–93
2. Rosenberg A (1963) A comparison of lipid patterns in photosynthesizing and non-photosynthesizing cells of *Euglena gracilis*. Biochemistry 2:1148–1154
3. Tucci S, Vacula R, Krajcovic J, Proksch P, Martin W (2009) Variability of wax ester fermentation in natural and bleached *Euglena gracilis* strains in response to oxygen and the elongase Inhibitor Flufenacet. J Eukaryot Microbiol 57:63–69
4. Koritala S (1989) Microbiological synthesis of wax esters by *Euglena gracilis*. J Am Oil Chem Soc 66:133–134
5. Schneider T, Betz A (1985) Waxmonoester fermentation in *Euglena gracilis* T. Factors favouring the synthesis of odd-numbered fatty acids and alcohols. Planta 166:67–73
6. Tani Y, Okumura M, Li S (1987) Liquid wax ester production by *Euglena gracilis*. Agric Biol Chem 51:225–230
7. Regnault A, Chervin D, Chammai A, Pitona F, Calvayraca R, Mazliakb P (1995) Lipid composition of *Euglena gracilis* in relation to carbon–nitrogen balance. Phytochemistry 40:725–733
8. Kawabata A, Inui H, Miyatake K, Nakano Y, Kitaoka S (1990) Production and composition of *Euglena* wax esters at high temperature. Agric Biol Chem 54:811–812
9. Samuels L, Kunst L, Jetter R (2008) Sealing plant surfaces: cuticular wax formation by epidermal cells. Annu Rev Plant Biol 59:683–707
10. Cheng JB, Russell DW (2004) Mammalian wax biosynthesis. I. Identification of two fatty acyl-coenzyme A reductases with different substrate specificities and tissue distributions. J Biol Chem 279:37789–37797
11. Moto K, Yoshiga T, Yamamoto M, Takahashi S, Okano K, Ando T, Nakata T, Matsumoto S (2003) Pheromone gland-specific fatty-acyl reductase of the silkmoth, *Bombyx mori*. Proc Natl Acad Sci USA 100:9156–9161
12. Antony B, Fujii T, Moto K, Matsumoto S, Fukuzawa M, Nakano R, Tatsuki S, Ishikawa Y (2009) Pheromone-gland-specific fatty-acyl reductase in the adzuki bean borer, *Ostrinia scapulalis* (Lepidoptera: Crambidae). Insect Biochem Mol Biol 39:90–95
13. Miwa T (1971) Jojoba oil wax esters and derived fatty acids and alcohols: gas chromatographic analyses. J Am Oil Chem Soc 48:259–264
14. Doan TT, Carlsson AS, Hamberg M, Bulow L, Stymne S, Olsson P (2008) Functional expression of five *Arabidopsis fatty acyl-CoA reductase* genes in *Escherichia coli*. J Plant Physiol 166:787–796
15. Rowland O, Zheng H, Hepworth SR, Lam P, Jetter R, Kunst L (2006) *CER4* encodes an alcohol-forming fatty acyl-coenzyme A reductase involved in cuticular wax production in Arabidopsis. Plant Physiol 142:866–877
16. Wang A, Xia Q, Xie W, Dumonceaux T, Zou J, Datla R, Selvaraj G (2002) Male gametophyte development in bread wheat (*Triticum aestivum* L.): molecular, cellular, and biochemical analyses of a sporophytic contribution to pollen wall ontogeny. Plant J 30:613–623
17. Cheng JB, Russell DW (2004) Mammalian wax biosynthesis. II. Expression cloning of wax synthase cDNAs encoding a member of the acyltransferase enzyme family. J Biol Chem 279:37798–37807
18. Lardizabal KD, Metz JG, Sakamoto T, Hutton WC, Pollard MR, Lassner MW (2000) Purification of a jojoba embryo wax synthase, cloning of its cDNA, and production of high levels of wax in seeds of transgenic Arabidopsis. Plant Physiol 122:645–655
19. King A, Nam JW, Han J, Hilliard J, Jaworski JG (2007) Cuticular wax biosynthesis in petunia petals: cloning and characterization of an alcohol-acyltransferase that synthesizes wax-esters. Planta 226:381–394
20. Kalscheuer R, Steinbuchel A (2003) A novel bifunctional wax ester synthase/acyl-CoA: diacylglycerol acyltransferase mediates wax ester and triacylglycerol biosynthesis in *Acinetobacter calcoaceticus* ADP1. J Biol Chem 278:8075–8082
21. Li F, Wu X, Lam P, Bird D, Zheng H, Samuels L, Jetter R, Kunst L (2008) Identification of the wax ester synthase/acyl-coenzyme A: diacylglycerol acyltransferase WSD1 required for stem wax ester biosynthesis in Arabidopsis. Plant Physiol 148:97–107
22. Khan AA, Kolattukudy PE (1973) Control of synthesis and distribution of acyl moieties in etiolated *Euglena gracilis*. Biochemistry 12:1939–1948
23. Kolattukudy PE (1970) Reduction of fatty acids to alcohols by cell-free preparations of *Euglena gracilis*. Biochemistry 9:1095–1102
24. Schlösser UG (1994) SAG—Sammlung von Algenkulturen at the University of Göttingen, catalogue of strains. Bot Acta 107:113–186
25. Meesapyodsuk D, Reed DW, Covello PS, Qiu X (2007) Primary structure, regioselectivity, and evolution of the membrane-bound fatty acid desaturases of *Claviceps purpurea*. J Biol Chem 282:20191–20199
26. Sandager L, Gustavsson MH, Stahl U, Dahlqvist A, Wiberg E, Banas A, Lenman M, Ronne H, Stymne S (2002) Storage lipid synthesis is non-essential in yeast. J Biol Chem 277:6478–6482
27. Katavic V, Mietkiewska E, Barton DL, Giblin EM, Reed DW, Taylor DC (2002) Restoring enzyme activity in nonfunctional low erucic acid *Brassica napus* fatty acid elongase 1 by a single amino acid substitution. Eur J Biochem 269:5625–5631
28. Li R, Reed DW, Liu E, Nowak J, Pelcher LE, Page JE, Covello PS (2006) Functional genomic analysis of alkaloid biosynthesis in *Hyoscyamus niger* reveals a cytochrome P450 involved in littorine rearrangement. Chem Biol 13:513–520
29. Rossmann MG, Moras D, Olsen KW (1974) Chemical and biological evolution of nucleotide-binding protein. Nature 250:194–199
30. Aarts MG, Hodge R, Kalantidis K, Florack D, Wilson ZA, Mulligan BJ, Stiekema WJ, Scott R, Pereira A (1997) The Arabidopsis *MALE STERILITY 2* protein shares similarity with reductases in elongation/condensation complexes. Plant J 12:615–623
31. Metz JG, Pollard MR, Anderson L, Hayes TR, Lassner MW (2000) Purification of a jojoba embryo fatty acyl-coenzyme A reductase and expression of its cDNA in high erucic acid rapeseed. Plant Physiol 122:635–644
32. Kalscheuer R, Luftmann H, Steinbuchel A (2004) Synthesis of novel lipids in *Saccharomyces cerevisiae* by heterologous expression of an unspecific bacterial acyltransferase. Appl Environ Microbiol 70:7119–7125
33. Kolattukudy PE (1971) Enzymatic synthesis of fatty alcohols in *Brassica oleracea*. Arch Biochem Biophys 142:701–709
34. Reiser S, Somerville C (1997) Isolation of mutants of *Acinetobacter calcoaceticus* deficient in wax ester synthesis and complementation of one mutation with a gene encoding a fatty acyl coenzyme A reductase. J Bacteriol 179:2969–2975
35. Vioque J, Kolattukudy PE (1997) Resolution and purification of an aldehyde-generating and an alcohol-generating fatty acyl-CoA reductase from pea leaves (*Pisum sativum* L.). Arch Biochem Biophys 340:64–72

36. Pollard MR, McKeon T, Gupta LM, Stumpf PK (1979) Studies on biosynthesis of waxes by developing jojoba seed. II. The demonstration of wax biosynthesis by cell-free homogenates. Lipids 14:651–662
37. Moore C, Snyder F (1982) Properties of microsomal acyl coenzyme A reductase in mouse preputial glands. Arch Biochem Biophys 214:489–499
38. Wang X, Kolattukudy PE (1995) Solubilization, purification and characterization of fatty acyl-CoA reductase from duck uropygial gland. Biochem Biophys Res Commun 208:210–215
39. Johnson RC, Gilbertson JR (1972) Isolation, characterization, and partial purification of a fatty acyl coenzyme A reductase from bovine cardiac muscle. J Biol Chem 247:6991–6998
40. Falk-Petersen S, Hagen W, Kattner G, Clarke A, Sargent JR (2000) Lipids, trophic relationships, and biodiversity in Arctic and Antarctic krill. Can J Fish Aquat Sci 57:178–191
41. Kattner G, Hagen W (1998) Lipid metabolism of the Antarctic euphausid *Euphausia crystallorophias* and its ecological implications. Mar Ecol Prog Ser 170:203–213
42. Kolattukudy PE, Bohnet S, Rogers L (1987) Diesters of 3-hydroxy fatty acids produced by the uropygial glands of female mallards uniquely during the mating season. J Lipid Res 28:582–588
43. Rijpstra WI, Reneerkens J, Piersma T, Damste JS (2007) Structural identification of the β-hydroxy fatty acid-based diester preen gland waxes of shorebirds. J Nat Prod 70:1804–1807

Lipids (2010) 45:275–283
DOI 10.1007/s11745-010-3387-2

ORIGINAL ARTICLE

Fetal Bovine Serum Concentration Affects Δ^9 Desaturase Activity of *Trypanosoma cruzi*

Ana L. Villasuso · Patricio Romero · Mariela Woelke · Patricia Moyano · Estela Machado · Mirta García de Lema

Received: 13 October 2009 / Accepted: 11 January 2010 / Published online: 4 February 2010

Abstract Fetal bovine serum (FBS) is an important factor in the culture of *Trypanosoma cruzi*, since this parasite obtains and metabolizes fatty acids (FAs) from the culture medium, and changes in FBS concentration reduce the degree of unsaturation of FAs in phosphoinositides. When *T. cruzi* epimastigotes were cultured with 5% instead of 10% FBS, and stearic acid was used as the substrate, Δ^9 desaturase activity decreased by 50%. Apparent K_m and V_m values for stearic acid, determined from Lineaweaver–Burk plots, were 2 μM and 219 pmol/min/mg of protein, respectively. In studies of the requirement for reduced pyridine nucleotide, Δ^9 desaturase activity reached a maximum with 8 μM NADH and then remained constant; the apparent K_m and V_m were 4.3 μM and 46.8 pmol/min/mg of protein, respectively. The effect of FBS was observed only for Δ^9 desaturase activity; Δ^{12} desaturase activity was not affected. The results suggest that decreased FBS in culture medium is a signal that modulates Δ^9 desaturase activity in *T. cruzi* epimastigotes.

Keywords *Trypanosoma cruzi* · Δ^9 Desaturase · Δ^{12} Desaturase · Fetal bovine serum

Abbreviations

ATP	Adenosine triphosphate
FBS	Fetal bovine serum
EDTA	Ethylenediaminetetraacetic acid
FAME	Fatty acid methyl esters
FFA	Free fatty acid
FAs	Fatty acids
HPLC	High performance liquid chromatography
HEPES	(4-(2-Hydroxyethyl)-1-piperazineethanesulfonic acid
NADH	Nicotinamide adenine dinucleotide
NADPH	Nicotinamide adenine dinucleotide phosphate
NL	Neutral lipid
PL	Phospholipid
PMSF	Phenylmethylsulphonyl fluoride
PUFAs	Polyunsaturated fatty acids
PC	Phosphatidylcholine
SEM	Standard error of the mean
TLC	Thin layer chromatography

A. L. Villasuso · P. Romero · M. Woelke · P. Moyano · E. Machado · M. García de Lema (✉)
Departamento de Biología Molecular, Facultad de Ciencias Exactas, Físico-Químicas y Naturales, Universidad Nacional de Río Cuarto, CPX5804BYA Río Cuarto, Córdoba, Argentina
e-mail: mgarcia@exa.unrc.edu.ar

Introduction

Protozoan parasites often encounter unpredictable changes in their environment. Modification of their membrane lipid composition helps maintain the biophysical properties for optimal membrane function, allowing them to cope with environmental changes [1, 2]. *Trypanosoma cruzi*, the etiological agent of Chagas' disease, is an intracellular protozoan that undergoes a complex life cycle between a hematophagous insect vector, *Triatoma infestans*, and a mammalian host. In the intestinal tract of the vector, the replicative non-infectious epimastigotes differentiate to the infectious non-dividing metacyclic forms, a process denominated metacyclogenesis.

It is well known that differentiation of these parasites involves changes in the shape of the cell; consequently the membrane fluidity might be essential for trypanosome

transmission. In *T. cruzi*, it has been demonstrated that the oleic acid present in the intestinal extracts of *T. infestans* induce cell differentiation of *T. cruzi* epimastigotes into the infective metacyclic form [3]. As part of a strategy for surviving in these different environmental conditions, *T. cruzi* adjusts the balance between saturated and unsaturated fatty acids (FAs) in certain membrane lipids [4, 5]. Desaturases are key enzymes in FA metabolism required to regulate physical and biochemical properties of membranes [6]. Desaturases are present in most living cells, and play critical roles in the biosynthesis of polyunsaturated fatty acids (PUFAs). PUFAs serve as precursors of biologically active molecules involved in the activation of a variety of signalling mechanisms that affect cellular functions [7].

The endoplasmic reticulum contains membrane-bound enzymes that remove two hydrogen atoms from the aliphatic chain of a FA to produce a *cis* double bond [8]. Δ^9 Desaturase is of particular interest since FAs that contain a double bond at the central C9–C10 position have a maximal disordering effect on membrane physical properties [9]. Since FAs are the main constituents of membrane glycerolipids, modulation of the number and position of double bonds in acyl chains by individual FA desaturases helps maintain the proper dynamic state of the membrane bilayer during environmental impacts [10]. Temperature changes have been shown to modulate the ratio of saturated to unsaturated FAs in *T. cruzi* [5]. The concentration of fetal bovine serum (FBS) in the culture medium also affects the degree of unsaturation. When the FBS concentration in the culture medium is reduced from 10 to 5%, the proportion of linoleic acid in phosphoinositides decreases [4], suggesting that desaturase activity may be modulated by FBS concentration.

We showed previously that the ratio of unsaturated to saturated FAs increases with growth in culture, as indicated by an increased percentage of linoleic acid (18:2), and that carbamoylcholine increases [^{14}C] labelling of triacylglycerols and diacylglycerols [11]. These findings indicate that unsaturated FAs are important factors during parasite aging and response to environmental stimuli. Initial studies from our laboratory demonstrated de novo biosynthesis of palmitic acid in *T. cruzi* [12], and we showed later that epimastigotes of *T. cruzi* are able to incorporate and metabolize exogenous FAs; palmitic acid is elongated to stearic acid and then desaturated to oleic acid and linoleic acid. These data support the existence of Δ^9 and Δ^{12} desaturases [12, 13]. Molecular characterization of oleate desaturase was conducted in *T. brucei* by Petrini et al. [14], using heterologous expression, and in *T. cruzi* by Maldonado et al. [15].

Genomic analysis of trypanosomatids revealed the presence of front-end desaturase genes, tentatively designated as $\Delta^8\Delta^5\Delta^6$ desaturases for *Leishmania major* and Δ^6 for *T. brucei and T. cruzi*, on the basis of sequence similarity. The desaturases were later characterized as $\Delta^6\Delta^5\Delta^4$ for *L. major,* while only Δ^4 is present in *Trypanosoma*. Functional predictions are never conclusive for desaturases; i.e., biochemical characterization is essential for correct assignment of enzyme regioselectivities [16]. Study of biochemical properties of a parasite's desaturases helps provide insight into their role in parasite response to environmental conditions. Since *T. cruzi* is able to sense changes in FBS concentration, and consequently modulate the degree of unsaturation of phosphoinositide FAs, we used FBS concentration change as a tool to elucidate Δ^9 and Δ^{12} desaturase activities. Reduction of FBS concentration in the parasite culture medium decreased Δ^9 desaturase activity by 50%. Therefore we suggest that the Δ^9 desaturase activity would play a possible role as a regulator of oleic acid level and could be implied in the regulation of membrane fluidity necessary for parasite transmission. Partial biochemical characterization of *T. cruzi* Δ^9 and Δ^{12} desaturases using subcellular fractions and radioactive FAs is also described.

Experimental Procedure

Materials

Solvents were either analytical or HPLC grade. Lipid standards were from Sigma Chemical Co. (St Louis, MO, USA). Culture media were from Merck (Germany) or Difco (USA). FBS was from Natocor (Argentina).

Parasite Strain and Growth Conditions

The Tulahuen strain of *T. cruzi* was used. Epimastigote forms were grown at 28 °C in modified Warren's medium [17] as described by Racagni et al. [18]. The medium was supplemented with 5 or 10% FBS and 1,000,000 U penicillin per 4×10^7 parasites. Cells in the logarithmic growth phase (5 days old) were harvested by centrifugation at 4,500*g* for 10 min. The weight of harvested cells and the number of mobile cells per mL culture medium was measured.

Enzyme Extraction

Cells were weighed, frozen at −180 °C and thawed three times. Broken cells were homogenized 1:5 (w/v) in 50 mM 4-(2-hydroxyethyl)-1-piperazineethanesulfonic acid (HEPES), pH 7.4 containing 0.25 M sucrose, 5 mM KCl, 1 mM ethylenediaminetetraacetic acid (EDTA), and protease inhibitors (1 μg/mL leupeptin, 1 mM phenylmethylsulphonyl fluoride (PMSF), 1 μg/mL aprotinin). The

homogenate was centrifuged using three sedimentation steps: 1,000*g* for 10 min, 25,000*g* for 12 min, and 105,000*g* for 60 min. Supernatants of 25,000*g*, and 105,000*g*, and the pellet of the 105,000*g* centrifugation, were used for determination of desaturase activity.

Enzymatic Assays

Δ^9 desaturation of [1-^{14}C]palmitic acid or [1-^{14}C]stearic acid was estimated in subcellular fractions of *T. cruzi* by measuring the formation of [1-^{14}C]palmitoleic acid or [1-^{14}C]oleic acid, respectively. The reaction mixture consisted of 41.7 mM potassium phosphate buffer (pH 7.4), 0.25 M sucrose, 0.15 M KCl, 41.7 mM NaF, 5 mM $MgCl_2$, 1.6 mM *N*-acetyl-cysteine, 60 μM CoA (sodium salt), 1.3 mM adenosine triphosphate (ATP), 0.87 mM nicotinamide adenine dinucleotide (NADH), 3.1 μM of [1-^{14}C] palmitic or stearic acid, and 0.2 mg microsomal protein, in a total volume of 750 μL [19]. For determination of Δ^{12} desaturase activity, [1-^{14}C]oleic acid as substrate and 0.8 mg protein were used. After 1 min preincubation at 37 °C, the reaction was initiated by addition of microsomal protein, and mixtures were incubated in open tubes for 15, 5, or 25 min, respectively, for stearic, palmitic, or oleic acid as substrate. The desaturation reaction was stopped by:

(a) 10% KOH in ethanol, followed by saponification at 80 °C for 45 min under N_2 atmosphere. The unsaponified fraction was extracted twice with 2 mL petroleum hydrocarbon (b.p. 30–60 °C), and discarded. After acidification with HCl, FAs were extracted three times with petroleum hydrocarbon, solvent was evaporated under N_2, and FAs were dissolved in 50 μL petroleum hydrocarbon. Finally, FAs were separated on thin layer chromatography (TLC) plates of silica gel G impregnated with 4% $AgNO_3$ (w/v), using toluene as solvent.

(b) Alternatively, the enzyme reaction was stopped by the addition of an appropriate volume of chloroform/methanol (2:1, by vol) [20] if phospholipids (PL) were to be isolated. The lower phase was dried down under stream of nitrogen and PL were isolated from this total lipid extract by TLC.

Lipid Extraction

Total lipids were extracted from washed parasites by the acidified extraction procedure of Bligh and Dyer [20], and 0.1 M KCl in 50% methanol was added to obtain a lower chloroform phase and an upper phase. The lower phase, containing lipids, was washed once with KCl solution, dried under N_2, and dissolved in an appropriate volume of chloroform/methanol (2:1, by vol).

Processing of Radioactive Samples

Separation and Analysis of PL and Neutral Lipids

Aliquots of the total lipid extracts were subjected to TLC to separate the total PL fraction from the neutral lipid (NL), using hexane/ethyl ether/acetic acid (80:20:1, by vol) as solvent. Following TLC, lipids were located by exposing the plates either to iodine vapour (for radioactivity analysis), or to UV light after spraying with 2,7′dichlorofluorescein in methanol (for further analysis of FAs).

Separation and Analysis of Labelled Fatty Acids from Lipids

Fatty acid methyl esters (FAME) were prepared from the lipid fractions separated by TLC with 10% BF_3 in methanol [21], or from FAs saponified with 10% KOH in ethanol. Labelled FAME were resolved according to their degree of unsaturation on TLC plates of silica gel G impregnated with 4% $AgNO_3$ (w/v), using toluene as solvent. FAME bands were located under UV light after spraying the plates with dichlorofluorescein, eluted [22], and evaporated to dryness at 35 °C, in counting vials. Then, 3 mL of Optiphase Hisafe 2 (PerkinElmer, USA), liquid scintillant was added to each vial, and the radioactivity was measured using a liquid scintillation counter (Beckman LS 60001 C, USA) [23].

Analysis of FBS Fatty Acids

Aliquots of FBS total lipids were subjected to methanolysis as described for labelled samples, in order to prepare FAME from FAs. BF_3 in methanol was added to lipids previously evaporated to dryness in screw-cap tubes. Tubes were added with N_2, sealed, and kept overnight at 45 °C. The resulting FAME were purified by TLC using hexane/diethyl ether (95:5, by vol), on plates of silica gel G pre-washed with methanol/diethyl ether (75:25, by vol). FAME were recovered from the silica support by agitation with water/methanol/hexane (1:1:1, by vol), followed by centrifugation, hexane extraction was repeated three times. FA analysis was performed using a Varian 3700 gas chromatograph equipped with two glass columns (2 m × 2 mm) packed with 15% SP 2330 on Chromosorb WAW 100/120 (Supelco Inc., Bellefonte, PA) and two flame ionization detectors. The column oven temperature was programmed from 155 to 230 °C at a rate of 5 °C/min. Injector and detector temperatures were 220

and 230 °C, respectively; the carrier gas was N_2 with a flow rate 30 mL/min.

Statistical Analysis

Results are shown as the means ± SEM for at least three independent experiments. Statistical analysis of data was carried out using Origin Pro 8 Copyright © 1991–2008.

Results

Effect of FBS on Δ^9 and Δ^{12} Desaturase Activities

FBS is essential for culturing *T. cruzi* epimastigote forms. The parasite obtains and metabolizes FAs from the culture medium, and a decrease in FBS concentration alters the degree of FA unsaturation of the signalling lipid [4]. In order to test the hypothesis that FBS concentration modulates desaturase activities, we first determined the FA composition of FBS. The major FAs were palmitic acid (16:0; 23.56%), stearic acid (18:0; 12.33%), and oleic acid (18:1n-9; 23.92%). Arachidonic acid (20:4n-6) and other long-chain FAs were detected in small amounts. To assess the effect of FBS concentration on desaturase activities, parasites were cultured with 5 or 10% FBS (control). 5% FBS decreased Δ^9 desaturase activity by 50% when stearic acid was used as the substrate. The FBS concentration had no effect on activities of Δ^9 with palmitic acid or Δ^{12} with oleic acid as substrates (Fig. 1). Specific activity of Δ^9 desaturase with 5% FBS and stearic acid as substrate was lower than that with 10% FBS, and was higher in the 105,000*g* pellet than in the supernatant (Table 1). The

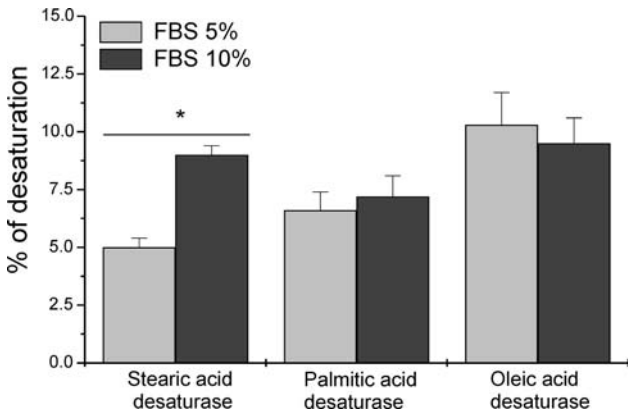

Fig. 1 Effect of fetal bovine serum (FBS) concentration on *T. cruzi* desaturase activities. Parasites were grown with 5 or 10% FBS and harvested at the logarithmic phase of growth (5 days). Δ^9 Desaturase was determined using [1-^{14}C]palmitic acid or [1-^{14}C]stearic as substrate. Δ^{12} Desaturase was assayed using [1-^{14}C]oleic acid as substrate. Results are expressed as percent of desaturation ± SEM, $n = 4$, * $P < 0.05$, *t* test

number of parasites decreased by 30% when they were cultured with 5% instead of 10% FBS (data not shown).

Kinetic Parameters of Desaturases

Δ^9 Desaturase

In view of our previous finding that palmitic acid is elongated to stearic acid and then desaturated to oleic acid and linoleic acid when these substrates are added to culture medium [13], we tested the possibility that both palmitic and stearic acids are substrates of Δ^9 desaturase. Δ^9 Desaturase activity increased up to 140 pmol/min/mg of protein within a stearic acid concentration range of 2.5–3.0 μM (Fig. 2). Apparent K_m and V_m values, determined from a Lineaweaver–Burk plot, corresponded to 2 μM and 219 pmol/min/mg of protein, respectively (Fig. 2, inset). In a study of requirement for reduced pyridine nucleotide, Δ^9 desaturase activity reached a maximum value with 8 μM NADH, and then remained constant (Fig. 3). Apparent K_m and V_m were 4.3 μM and 46.8 pmol/min/mg of protein (Fig. 3, inset). Reduced coenzyme nicotinamide adenine dinucleotide phosphate (NADPH) had the same effect as NADH; both formed 38% of oleic acid. Δ^9 Desaturase required a shorter incubation time when the substrate was palmitic acid; desaturase activity increased until 5 min, and decreased at longer times (data not shown). For palmitic acid, apparent K_m and V_m were 1.33 μM and 58.8 pmol/min/mg of protein (data not shown).

Δ^{12} Desaturase

In view of our finding that the level of diunsaturated FAs was altered by 5% FBS in phosphoinositides, we examined the possibility that Δ^{12} desaturase could be responsible for these changes and be affected by FBS. Δ^{12} Desaturase activity as a function of substrate concentration is shown in Fig. 4. Enzyme activity deviated from Michaelis–Menten kinetics at oleic acid concentrations above 10 μM; however, such an effect is unlikely to occur in vivo since the endogenous substrate concentration is much lower. Apparent K_m and V_m values determined from a Lineweaver–Burk plot were 1.03 μM and 2.8 pmol/min/mg of protein (Fig. 4, inset). There was no difference between NADPH and NADH requirements (data not shown).

Effects of Protein Concentration and Preincubation Time on Desaturase Specific Activities

The effects of the variation in microsomal protein concentration on enzyme activity were tested at 3.02 μM for stearic acid and at 2.6 μM for oleic acid. When the

Table 1 Effect of fetal bovine serum concentration on *T. cruzi* desaturase activities in different fractions

Fatty acids transformation	Specific activity (pmol/min/mg of protein)					
Cell fractions	Stearic acid		Palmitic acid		Oleic acid	
	5% FBS	10%	5% FBS	10%	5% FBS	10%
Supernatant 25,000*g*	65 ± 11	222 ± 37	ND	ND	ND	ND
Supernatant 105,000*g*	34.8 ± 2.2	123.0 ± 7.6	ND	ND	ND	ND
Pellet 105,000*g*	206 ± 10	538 ± 27	141 ± 15	155.9 ± 4.5	7.84 ± 0.94	8.82 ± 0.88

Cell fractions were obtained by differential centrifugation from *T. cruzi* epimastigotes grown with either 5 or 10% of FBS. Values are means ± SEM of three separate experiments

ND not determined

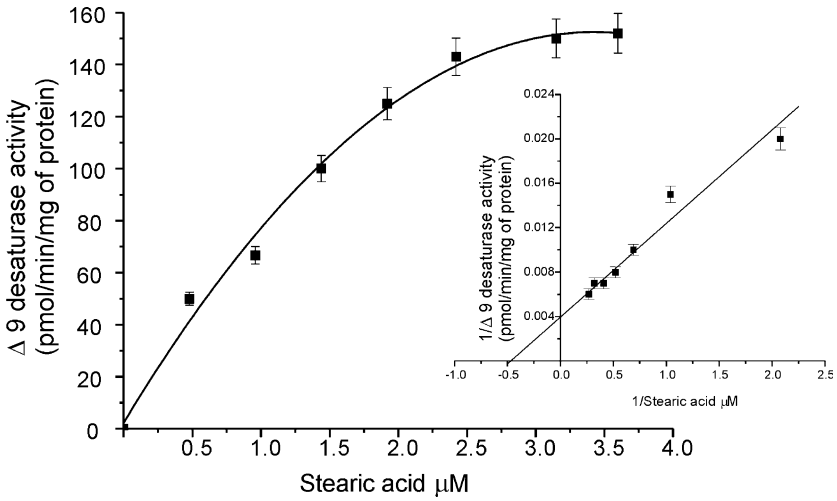

Fig. 2 Effect of concentration of substrate [1-^{14}C]stearic acid on *T. cruzi* Δ^9 desaturase activity. Incubation was performed at 37 °C for 15 min. The assay mixture is described in "Experimental Procedure". A double reciprocal plot was constructed to obtain apparent K_m and V_m (*inset*). Values are means ± SEM from three separate experiments

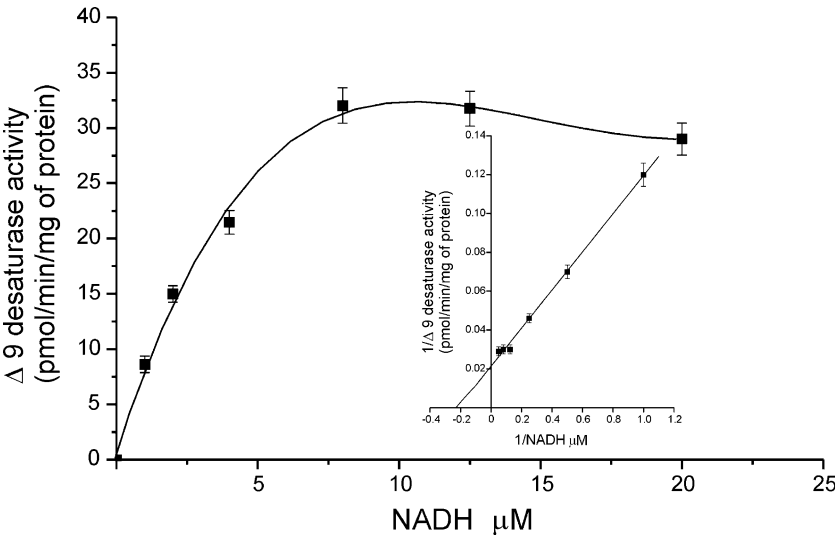

Fig. 3 Δ^9 Desaturase activity as a function of NADH concentration. Incubation was performed at 37 °C for 15 min. The assay mixture is described in "Experimental Procedure". A double reciprocal plot was constructed to obtain apparent K_m and V_m (*inset*). Values are means ± SEM from three separate experiments

microsomal protein concentration increased, Δ^9 desaturase activity increased linearly up to 0.2 mg, and Δ^{12} desaturase activity increased up to 0.8 mg, beyond these protein concentrations, a linear relationship was no longer observed (Fig. 5a, b).

Activity of Δ^9 desaturase required a shorter preincubation time than that of Δ^{12} desaturase. Δ^9 desaturase activity increased up to 15 min, and decreased thereafter (Fig. 6). For Δ^{12} desaturase, maximum activity was observed at 35 min (data not shown). However, it is possible that

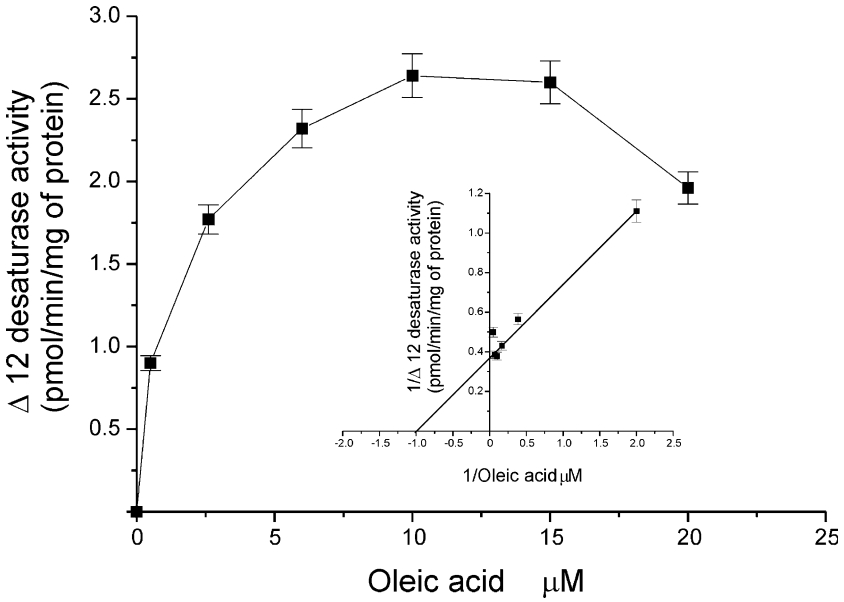

Fig. 4 Effect of [1-^{14}C]oleic acid concentration on *T. cruzi* Δ^{12} desaturase activity. Incubation was performed at 37 °C for 25 min, under the conditions described in "Experimental Procedure". A double reciprocal plot was constructed to obtain the apparent K_m and V_m (*inset*). Values are mean ± SEM obtained from three separate experiments

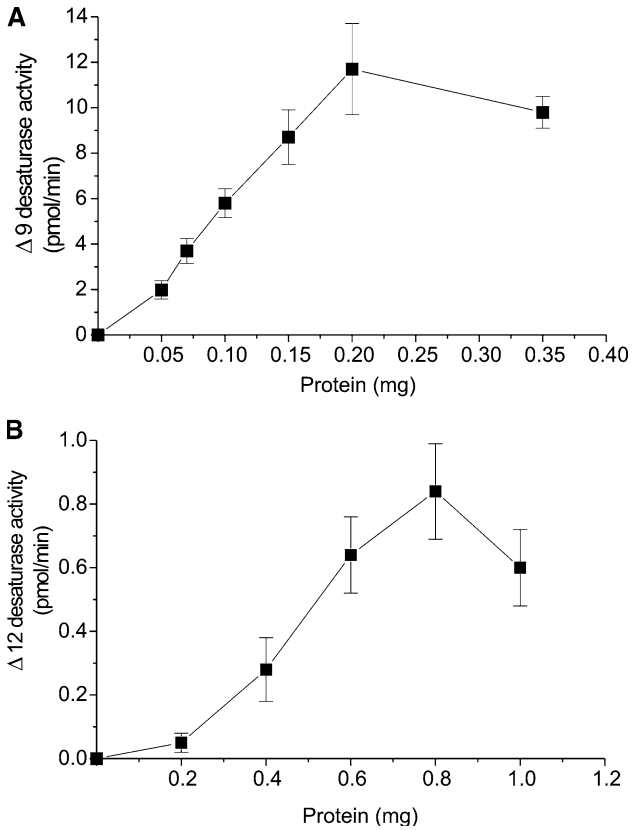

Fig. 5 Effects of 105,000*g* pellet protein concentration on *T. cruzi* Δ^9 (**a**) and Δ^{12} (**b**) desaturase activities. Protein concentration varied from 0.05 to 0.4 mg for Δ^9 desaturase activity, and from 0.2 to 1 mg for Δ^{12} desaturase activity. Incubation was performed at 37 °C for 15 min and 25 min, for Δ^9 and Δ^{12} desaturase, respectively. Reaction conditions are described in "Experimental Procedure". Values are means ± SEM of three separate experiments

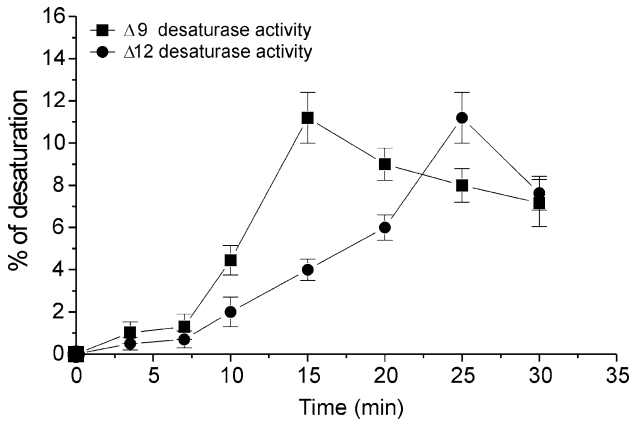

Fig. 6 Effect of incubation time on desaturase activities, determined as described in "Experimental Procedure". 18:0 and 18:1n-9 were used as substrates to test Δ^9 and Δ^{12} desaturase activity, respectively. Values are means ± SEM of three separate experiments

products of non-specific elongation of oleate, linoleate, or FA with the double bond in different positions were formed at this time, giving rise to other desaturase activities. For this reason, Δ^{12} desaturase activity was assayed at 25 min in subsequent experiments.

Other Biochemical Properties of Δ^9 Desaturase

In view of our previous finding that palmitic acid added to the culture medium is metabolized and incorporated into complex lipids by *T. cruzi* epimastigotes [13], we tested the behavior of palmitic acid with the microsomal fraction enzyme source.

Table 2 Effect of time on incorporation of [1-^{14}C] palmitic acid in lipids

Time (min)	Incorporation of radioactive substrate (%)		
	2	5	10
Lipid fractions			
FFA	63.0 ± 1.5	55.6 ± 1.1	45.5 ± 1.7
NL	21.5 ± 1.9	24.8 ± 1.5	24.6 ± 0.1
PL	15.5 ± 1.1	19.5 ± 0.4	29.8 ± 1.8

Incorporation of [1-^{14}C] palmitic acid in neutral lipids (NL) and phospholipids (PL) was followed for 2, 5, and 10 min. Lipids were extracted as described by Bligh and Dyer [20], and different fractions were obtained by TLC. Values represent means ± SEM of three independent experiments

Incorporation of [1-C^{14}]palmitic acid in lipids was dependent on incubation time. We observed different effects on the radioactivity detected in free fatty acid (FFA), NL and PL fractions, especially at 2 vs. 10 min incubation time (Table 2). The greatest radioactivity increase in PL (from 15.5 ± 1.1 to 29.8 ± 1.8%, $n = 3$, $P < 0.05$) and the greatest decrease in FFA (from 63.0 ± 1.5 to 45.5 ± 1.7%, $n = 3$, $P < 0.05$) were found at 10 min. In the presence of reduced coenzymes, a 26% increase in radioactivity incorporation in PL was observed at 10 min (data not shown). FFA showed the highest radioactivity at all times tested. Since [1-^{14}C]palmitic acid was incorporated in PL, the function of phosphatidylcholine (PC) as substrate of *T. cruzi* desaturases was confirmed using 1,2 di [1-^{14}C] palmitoylphosphatidylcholine.

Since it is possible that 1,2 di [1-^{14}C] palmitoylphosphatidylcholine is hydrolyzed before serving as a substrate of desaturases, levels of radioactivity on complex lipids and FFA were tested at various incubation times. Over 93% (93.6 ± 2.2, $n = 12$) of total radioactivity was recovered in PL at 30 min, indicating that hydrolysis did not occur. After testing desaturase activity using 1,2 di [1-^{14}C] palmitoylphosphatidylcholine as substrate, FAs were saponified, FAME were obtained, and analyzed by $AgNO_3$ TLC. When the reaction time was 5 min, 17% of the radioactivity was observed in monounsaturated FAs, and the amount of label increased by 29.1% at 10 min. As a consequence, radioactivity in saturated FAs decreased from 64 to 51% between 5 and 10 min. About 19% of radioactivity was found in the diunsaturated FA fraction, suggesting that 1,2 di [1-^{14}C] palmitoylphosphatidylcholine may also be a desaturase substrate in *T. cruzi*.

Discussion

Our previous biochemical studies showed that the FA composition of *T. cruzi* phosphoinositides is significantly altered by decreased FBS concentrations in culture medium [4], and that the FBS concentration is a key factor for growth of *T. cruzi* epimastigote forms in culture. In the present study, we examined the effect of FBS concentration on Δ^9 and Δ^{12} desaturase activities in *T. cruzi* epimastigotes, in relation to our previous findings. When stearic acid was the substrate and the FBS concentration was lowered from 10 to 5%, epimastigotes were able to modify Δ^9 desaturase; consequently, oleic acid levels were also lower than at 10% FBS. Thus, a smaller amount of substrate was available for Δ^{12} desaturase. This could explain the decreased level of linoleic acid in phosphoinositides we had observed previously [4]. Modulation of desaturase activity occurs only in the presence of FAs that serve as substrates of the enzyme. In *T. cruzi*, a decrease in FBS leads to a reduction in Δ^9 desaturase activity, since a decrease in the stearic acid level from FBS occurred when the concentration was 5%. In contrast, when palmitic acid was the substrate, FBS was not able to modify Δ^9 desaturase activity. Since the palmitic acid level is twice that of stearic acid in FBS, its variation in the culture medium may affect Δ^9 desaturase activity for palmitic acid to a lesser extent. The low susceptibility of Δ^{12} desaturase to FBS concentration suggests a significant role of this enzyme in the synthesis of linoleic acid. Availability of oleic acid may be responsible for the decrease in diunsaturated FAs when parasites are cultured with 5% FBS [4].

Furthermore, since the decrease in FBS concentration also implicates a decrease in the oleic acid level, we alternatively considered that the oleic acid level produce by Δ^9 desaturase activity could also be a signal for triggering the differentiation in the parasite [3].

Modification in the degree of unsaturation of FAs in *T. cruzi* was also observed by Florin-Christensen et al. [5] when epimastigotes were transferred from 28 to 37 °C, reflecting a response to environmental conditions. In the present study, desaturase activity was detected in all fractions studied, indicating a complex distribution pattern as shown for *Tetrahymena pyriformis* [24]. In *T. cruzi* epimastigotes, Δ^9 desaturase showed highest specific activity in the 105,000*g* pellet, similarly observed in mammals and yeast [25–27]. K_m values obtained for *T. cruzi* desaturases show that the same amounts of palmitic, stearic, and oleic acids are required for both desaturases to reach 50% of the maximum velocity. However, once K_m is reached, desaturation of stearic acid by Δ^9 desaturase occurs 3.7 times faster than for palmitic and 78 times faster than for oleic acid by Δ^{12} desaturase. Thus, Δ^9 desaturase is capable of using palmitic acid CoA and stearic acid CoA in spite of the differences in the V_m value. This is consistent with results in mice, where four Δ^9 desaturase isoforms capable of using palmitic acid and stearic acid CoA were reported [28]. Palmitic acid desaturation increased up till 5 min,

whereas enzyme activity increased until 15 min when stearic acid was the substrate. These findings suggest that desaturases use palmitic acid first, the product of de novo synthesis in *T. cruzi,* and then stearic acid. These time courses are consistent with a normal precursor–product metabolic relationship, implying sequential synthesis.

In addition to acyl-CoA desaturases as found in animals and fungi, FAs in plants and cyanobacteria are desaturated by acyl-lipid desaturases [29].

The phylogenetic relationships among Δ^4/Δ^5 desaturases in lower eukaryotes and Δ^6 desaturase from cyanobacteria were analyzed by Tripodi et al. [16]. Our results suggest that *T. cruzi* can desaturate FAs esterified to a phosphoglycerolipid, similarly to *Synechococcus*. In this algal genus, the acyl-lipid Δ^9 desaturase also uses palmitic acid esterified to phosphoglycerides [30]. In contrast, in *Synechocystis*, acyl-lipid Δ^9 desaturases are specific to stearic acid esterified at the C-1 position of a glycerolipid [29].

Both mono and diunsaturated FAs were produced when 1,2 di [1-^{14}C] palmitoylphosphatidylcholine was used as substrate. Desaturation by *T. cruzi* is comparable to the oleic acid desaturation systems in yeast [31] and in *Tetrahymena pyriformis* [32], in that one substrate may be a phospholipid. The *Acanthamoeba castellanii* desaturase, on the other hand, uses only FAs linked to phospholipids [33]. FAD2 microsomal Δ^{12} desaturases in higher plants use FAs esterified to a phosphoglycerolipid backbone, although the FAD2 enzyme does not display a preference for either *sn*-1 or *sn*-2 position [25]. Biochemical characterization of Δ^{12} desaturases from insects indicates that they use acyl-CoA substrates [34]. In *T. cruzi*, desaturation of stearic acid increased up to 15 min and formation of linoleic acid from oleic acid increased up to 35 min, at a much slower rate, suggesting that the activities of the two enzymes are coupled. Gabrielides et al. [35] obtained similar results for *Neurospora.*

T. cruzi desaturases appear to be related to other microsomal Δ^9 and Δ^{12} desaturases, since they show substrate requirements similar to those of microsomal desaturases in higher plants and fungi [36, 37]. Regarding the influence of microsomal protein concentration, the activities of both enzymes showed the same behavior: a breakdown in the linearity in the same concentration range. Since either stearic acid or oleic acid was rapidly incorporated into phospholipids, less substrate may be available for Δ^9 or Δ^{12} desaturation. This could explain the observation that an increase in microsomal protein above 0.2 mg for Δ^9 desaturase, or 0.8 mg for Δ^{12} desaturase, produces a decrease in conversion of stearic acid to oleic acid, or oleic acid to linoleic acid. It is possible that incorporation of the FA substrate in microsomal lipids competes with the desaturation reaction, as suggested by Irazú et al. [38]. Reduced coenzymes NADH and NADPH showed similar effects on desaturation, indicating that they both yield electrons in similar amounts for the enzymatic system. Similar requirements have been reported by Fukushima et al. [39] for *T. pyriformis* MT-1, and by Shipiro and Prescott [24] for *T. pyriformis* W. In *T. pyriformis* W, NADH is three times more efficient than NADPH as an electron donor for this reaction.

We observed that the decreased percentage of radioactivity in free palmitic acid was due to its incorporation into complex lipids, which depended on incubation time (Table 2). These results are consistent with those for *T. cruzi* by Florin-Christensen et al. [5]. These authors explained the process as part of a mechanism for adaptation to different temperatures, and proposed a role of triacylglycerides and sterol esters for storage of FAs in membrane lipids. In our study, incorporation of radioactivity from [1-^{14}C]palmitic acid into PL was at a maximum at 10 min, and was enhanced in the presence of reduced coenzymes. This increase could have resulted from an increase in (1) desaturase activities that form unsaturated FAs efficiently; those would then be incorporated into PL by specific acyl transferases; (2) activity of elongases, which also require an electron donor, and whose products (FAs with a chain length greater than that of palmitic acid) would be incorporated by specific acyl transferases; (3) acyl transferase activities resulting from an increased concentration of FA substrates formed during NADH-dependent reactions. In view of previous and present findings, possibility (1) seems most likely.

In summary, the present results demonstrate the participation of *T. cruzi* Δ^9 desaturase in responses to environmental changes, which enhance our understanding of lipid metabolism in this parasite. Since 18:1n-9 induces cell differentiation to infective forms in *T. cruzi* [3], Δ^9 desaturase can be a potential target to attack parasite transmission and consequently, the determination of Δ^9 desaturase activity provides information that may also lead to improved design of chemotherapy drugs against Chagas' disease.

Acknowledgments The authors thank Dr. Marta Aveldaño and Dr. Carlos Marra for determination of FBS FA composition, and FA analysis, respectively. This work was supported by FONCyT, Argentina and SECyT, UNRC, Río Cuarto, Córdoba, Argentina. A.L.V. is a research career scientist of CONICET, Argentina.

References

1. Fish WR (1995) Lipid and membrane metabolism of the malaria parasite and the African trypanosome. In: Müller M, Marr JJ (eds) Biochemistry and molecular biology of parasites. Academic Press, New York
2. Kasai T, Watanabe T, Fucuchima H, Lida H, Nozawa Y (1981) Adaptative modification of membrane lipids in *Tetrahymena pyriformis* during starvation. Biochim Biophys Acta 666:36–46

3. Wainszelbaum MJ, Belaunzarán ML, Lammel EM, Florin-Christensen M, Florin-Christensen J, Isola EL (2003) Free fatty acids induce cell differentiation to infective forms in *Trypanosoma cruzi*. Biochem J 375:705–712
4. Racagni G, de Lema MG, Hernández G, Machado-Domenech EE (1995) Fetal bovine serum induces changes in fatty acid composition of *Trypanosoma cruzi* phosphoinositides. Can J Microbiol 41:951–954
5. Florin-Christensen MJ, Florin-Christensen E, Isola E, Lammel E, Meinardi R, Brenner RR, Rasmussen L (1997) Temperature acclimation of *Trypanosoma cruzi* epimastigote and metacyclic trypomastigote lipids. Mol Biochem Parasitol 88:25–33
6. Brenner RR (1989) Factors influencing fatty acid long elongation and desaturation. In: Vergrosen AJ, Crawford M (eds) The role of fats in human nutrition. Academic Press, London
7. Pereira SL, Leonard AE, Mukerji P (2003) Recent advances in the study of fatty acid desaturases from animals and lower eukaryotes. Prostag Leukot Ess 86:97–106
8. Su HM, Brenna T (1998) Simultaneous measurement of desaturase activities using stable isotope tracers or a nontracer method. Anal Biochem 261:43–50
9. Barton PG, Gunstone FD (1975) Hydrocarbon chain packing and molecular motion in phospholipid bilayers formed from unsaturated lecithins. J Biol Chem 250:4470–4476
10. Sajbidor J (1997) Effect of some environmental factors on the content and composition of microbial membrane lipids. Crit Rev Biotechnol 17:87–103
11. Villasuso AL, Aveldaño M, Vicario A, Machado-Domenech EE, García de Lema M (2005) Culture age and carbamoylcholine increase the incorporation of endogenously synthesized linoleic acid in lipids of *Trypanosoma cruzi* epimastigotes. Biochim Biophys Acta 1735:185–191
12. Aeberhard EE, de Lema MBG, Bronia DH (1981) Biosynthesis of fatty acids by *Trypanosoma cruzi*. Lipids 16:623–625
13. de Lema MG, Aeberhard EE (1986) Desaturation of fatty acids in *Trypanosoma cruzi*. Lipids 21:718–720
14. Petrini GA, Altabe SG, Uttaro AD (2004) *Trypanosoma brucei* oleate desaturase may use a cytochrome b5-like domain in another desaturase as an electron donor. Eur J Biochem 271:1079–1086
15. Maldonado RA, Kuniyoshi RK, Linss JG, Almeida IC (2006) *Trypanosoma cruzi* oleate desaturase: molecular characterization and comparative analysis in other trypanosomatids. J Parasitol 92:1064–1074
16. Tripodi KE, Buttigliero LV, Altabe SG, Uttaro AD (2005) Functional characterization of front-end desaturases from trypanosomatids depicts the first polyunsaturated fatty acid biosynthetic pathway from a parasitic protozoan. FEBS J 273:271–280
17. Warren LG (1960) Metabolism of *Schizotripanum cruzi* Chagas I. Effect of culture age and substrate concentration on respiration rate. J Parasitol 46:529–539
18. Racagni G, García de Lema M, Domenech CE, Machado de Domenech EE (1992) Phospholipids in *Trypanosoma cruzi*: phophoinositide composition and turnover. Lipids 27:275–278
19. Marra CA, Alaniz MJ, Brenner RR (1988) A dexamethasone-induced protein stimulates Δ^9-desaturase activity in rat liver microsomes. Biochim Biophys Acta 958:93–98
20. Bligh E, Dyer W (1959) A rapid method of total lipid extraction and purification. Can J Biochem Physiol 37:911–917
21. Morrison WR, Smith LM (1964) Preparation of fatty acid methyl esters and dimethylacetals from lipids with boron fluoride-methanol. J Lipid Res 5:600–608
22. Henderson R, Tocher D (1992) Thin Layer Chromatography. In: Hamilton R, Hamilton S (eds) Lipid Analysis a practical approach. Oxford University Press, Oxford
23. Kates M (1972) Radioisotopic techniques in lipidology. In: Work TS, Work E (eds) Techniques in lipidology. North Holland/Elsevier, Amsterdam/New York
24. Shipiro H, Prescott D (1978) Preliminary characterization of the delta-9 desaturase of *Tetrahymena pyriformis* W. Comp Biochem Physiol Part B Biochem 61:513–520
25. Shanklin J, Cahoon EB (1998) Desaturation and related modifications of fatty acids. Annu Rev Plant Physiol Plant Mol Biol 49:611–641
26. Fujimori K, Anamnart S, Nakagawa Y, Sugioka S, Ohta D, Oshima Y, Yamada Y, Harashima S (1997) Isolation and characterization of mutations affecting expression of the delta9- fatty acid desaturase gene, OLE1, in *Saccharomyces cerevisiae*. FEBS Lett 413:226–230
27. Peluffo RO, Brenner RR (1974) Influence of dietary protein on Δ^6 and Δ^9 desaturation of fatty acids in rats of different ages in different seasons. J Nutr 104:894–900
28. Miyazaki M, Bruggink S, Ntambi J (2006) Identification of mouse palimitoyl-CoA Δ^9 desaturase. J Lipid Res 47:700–704
29. Sakamoto T, Wada H, Nishida I, Ohmori M, Murata N (1994) Δ^9 Acyl-lipid desaturases of Cyanobacteria. J Biol Chem 269:25576–25580
30. Los DA, Murata N (2004) Membrane fluidity and its roles in the perception of environmental signals. Biochim Biophys Acta 1666:142–157
31. Pugh EL, Kates M (1975) Characterization of a membrane-bound phospholipid desaturase system of *Candida lipolytica*. Biochim Biophys Acta 380:442–453
32. Koudelka AP, Bradley DK, Kambadur N, Freguson KA (1983) Oleic acid desaturation in *Tetrahymena pyriformis*. Biochim Biophys Acta 751:129–137
33. Sayanova O, Haslam R, Guschina I, Lloyd D, Christie WW, Harwood JL, Napier JA (2006) A bifunctional Δ^{12}, Δ^{15}-desaturase from *Acanthamoeba castellanii* directs the synthesis of highly unusual n-1 series unsaturated fatty acids. J Biol Chem 281:36533–36541
34. Gurr MI, Harwood JL, Frayn KN (2002) Lipid biochemistry, 5th edn. Blackwell Science, Oxford
35. Gabrielides C, Hamill A, Scott W (1982) Requirements of Δ^9 and Δ^{12} fatty acid desaturation in *Neurospora*. Biochim Biophys Acta 712:505–514
36. Domergue F, Abbadi A, Ott C, Zank TK, Zahringer U, Heinz E (2003) Acyl carriers used as substrates by the desaturases and elongases involved in very long chain polyunsaturated fatty acids biosynthesis reconstituted in Yeast. J Biol Chem 278:35115–35126
37. Domergue F, Abbadi A, Zahringer U, Moreau H, Heinz E (2005) In vivo characterization of the first acyl CoA Δ^6 desaturase from a member of the plant kingdom, the microalga *Ostreococcus tauri*. Biochem J 389:483–490
38. Irazú CE, González-Rodríguez S, Brenner RR (1993) Δ^5 Desaturase activity in rat kidney microsomes. Mol Cell Biochem 129:31–37
39. Fukushima H, Nagao S, Okano Y, Nozawa Y (1977) Studies on *Tetrahymena* membranes. Palmitoyl-coenzymeA desaturase, a possible key enzyme for temperature adaptation in *Tetrahymena* microsomes. Biochim Biophys Acta 488:442–453

Lipids (2010) 45:285–290
DOI 10.1007/s11745-010-3388-1

COMMUNICATION

Trans Fatty Acid-Induced NF-κB Activation Does Not Induce Insulin Resistance in Cultured Murine Skeletal Muscle Cells

Pascal P. H. Hommelberg · Ramon C. J. Langen · Annemie M. W. J. Schols · Anon L. M. van Essen · Frank J. M. Snepvangers · Ronald P. Mensink · Jogchum Plat

Received: 21 June 2009 / Accepted: 15 January 2010 / Published online: 9 February 2010

Abstract Long-chain saturated fatty acids such as palmitic acid induce insulin resistance and NF-κB activation in skeletal muscle cells. Here we investigated the effects of long-chain fatty acid (FA) saturation and configuration on NF-κB activity and insulin sensitivity in cultured skeletal muscle cells. Of all tested unsaturated FAs, only elaidic acid (3-fold), *cis*9,*trans*11-CLA (3-fold) and *trans*10,*cis*12-CLA (13-fold) increased NF-κB transactivation in myotubes. This was not accompanied by decreased insulin sensitivity (measured as insulin-induced glucose uptake and GLUT4 translocation). We therefore conclude that FA-induced NF-κB activation is not sufficient for the induction of insulin resistance in skeletal muscle cells.

Keywords Insulin resistance · NF-κB · Skeletal muscle · Saturated fatty acids · Unsaturated fatty acids · C2C12 cells · L6 cells

P. P. H. Hommelberg · R. P. Mensink · J. Plat
Department of Human Biology, Nutrim School for Nutrition, Toxicology and Metabolism, Maastricht University Medical Centre, P.O. Box 616, 6200 MD Maastricht, The Netherlands
e-mail: pascal_hommelberg@yahoo.com

J. Plat
e-mail: j.plat@hb.unimaas.nl

R. C. J. Langen (✉) · A. M. W. J. Schols · A. L. M. van Essen · F. J. M. Snepvangers
Department of Respiratory Medicine, Nutrim School for Nutrition, Toxicology and Metabolism, Maastricht University Medical Centre, Maastricht, The Netherlands
e-mail: r.langen@pul.unimaas.nl

P. P. H. Hommelberg · R. P. Mensink
Top Institute Food and Nutrition, Wageningen, The Netherlands

Abbreviations

AA	Arachidonic acid
BSA	Bovine serum albumin
CLA	Conjugated linoleic acid
DAG	Diacylglycerol
DHA	Docosahexaenoic acid
EPA	Eicosapentaenoic acid
IL-6	Interleukin-6
MUFA	Monounsaturated fatty acids
NF-κB	Nuclear factor kappa B
PUFA	Polyunsaturated fatty acids
SFA	Saturated fatty acids
TNF-α	Tumor necrosis factor-alpha

Introduction

Although the molecular mechanisms underlying the pathogenesis of insulin resistance are still not fully understood, different lines of evidence support the notion that elevated concentrations of plasma free fatty acids (FA) play an important role [1–3]. A relation between the activation of the transcription factor-κB (NF-κB) and FA-induced insulin resistance in skeletal muscle in humans has been proposed [1]. In addition, studies in cultured skeletal muscle cells have shown that the saturated FA palmitate (C16:0) not only induces insulin resistance [4–7] but also activates the NF-κB pathway, which results in the production of pro-inflammatory cytokines such as interleukin-6 (IL-6) and tumor necrosis factor (TNF)-α [8–10]. Still, a causal relationship between NF-κB activation and FA-induced skeletal muscle insulin resistance is disputable [11–15]. Recently, we reported that the differential effects of SFAs on NF-κB activation and insulin resistance in

skeletal muscle cells depend on FA chain length [16]. Incubation with palmitic acid (C16:0) and stearic acid (C18:0) resulted in insulin resistant skeletal muscle cells showing increased NF-κB activation, while incubation with the shorter saturated FAs caprylic acid (C8:0) and lauric acid (C12:0) did not trigger these effects. Effects of individual FAs with the same long-chain length, but with differences in the degree of saturation or in *cis–trans* configuration have not yet been systematically evaluated. To investigate if the association between long-chain SFA-induced NF-κB activation and insulin resistance in skeletal muscle cells can be generalized to all long-chain FAs (≥16 carbon atoms), we investigated the effect of saturation and configuration on long chain FA-induced NF-κB activity in relation to insulin sensitivity in cultured skeletal muscle cells.

Materials and Methods

Cell Culture

The C2C12 murine skeletal muscle cell line (ATCC CRL1772; Manassas, VA), stably transfected with the 6κB-TK-luciferase, was used for the assessment of NF-κB transcriptional activity as described previously [16–18].

The L6 rat skeletal muscle cell line, stably transfected with a construct encoding GLUT4 with an exofacial *myc* epitope (L6-GLUT4*myc*) was kindly provided by Dr. Amira Klip from the Hospital for Sick Children, Toronto, ON, Canada. Cells were cultured and [^{3}H]-deoxyglucose uptake, GLUT4 translocation and NF-κB DNA binding by electrophoretic mobility shift analysis (EMSA) was determined as described previously [16]. All experiments for both cell lines were performed in 5-day differentiated myotubes.

Fatty Acid Incubations

Stock solutions of 40 mmol/l were made in ethanol for all FAs (palmitic, palmitoleic, stearic, oleic, elaidic, vaccenic, linoleic, α-linolenic, arachidonic acid, EPA, DHA (all from Sigma, St. Louis, MO) and *cis*-9, *trans*-11 CLA and *trans*-10, *cis*-12 CLA (Bio-connect, The Netherlands). FAs were conjugated to bovine serum albumin (BSA) [16] prior to addition to the cells. For every type of measurement, the experimental set-up was chosen to include all comparisons between saturated and unsaturated FA as reported.

Statistical Analysis

SPSS (version 16.0) was used for statistical analysis. Values for NF-κB transcriptional activity and [^{3}H]-deoxyglucose uptake measurements were analyzed by one-way ANOVA, and the various treatment groups ($N = 3$) were compared post hoc with Bonferroni correction, in which a p value of ≤0.05 was considered significant.

Results and Discussion

To test whether the previously reported effects of long-chain SFAs on NF-κB activation in skeletal muscle [9, 11, 16] are also present after incubation with monounsaturated (MUFAs) and polyunsaturated FAs (PUFAs), we incubated C2C12 myotubes, stably transfected with an NF-κB sensitive reporter construct, with a variety of FAs. The concentrations FA used in this study are within the range of those found in the plasma of healthy and diabetic subjects [19–21].

The incubation time and FA concentration were optimized for palmitic acid [16] and used for all other FAs tested. In contrast to palmitic acid (C16:0) and stearic acid (C18:0), their mono-unsaturated counterparts [palmitoleic (C16:1) and oleic (C18:1) acid] did not induce NF-κB transactivation in C2C12 skeletal muscle cells (Fig. 1a). Also poly-unsaturated FAs with the same chain length as stearic acid [linoleic (C18:2) and α-linolenic (C18:3) acid] did not show these effects. The absence of activation of NF-κB for these FAs was confirmed in another skeletal muscle cell line, by performing an EMSA for the assessment of RelA DNA binding in L6 myotubes (Fig. 1b).

Deoxyglucose uptake increased ∼4-fold following insulin stimulation of vehicle treated myotubes (Fig. 1c). Pretreatment with the different mono- and polyunsaturated FAs resulted in a similar increase in insulin-induced deoxyglucose uptake (between 3.5- and 4-fold increase compared to their respective vehicle controls), while C16:0 and C18:0 decreased insulin-stimulated deoxyglucose uptake by ∼60 and ∼80%, respectively, compared with vehicle control. These results were confirmed by GLUT4 translocation measurements (Fig. 1d) and are in line with the notion that NF-κB activation and the occurrence of insulin resistance occur simultaneously, suggesting that NF-κB activation may be causally related to long-chain SFA induced insulin resistance.

These results are supported by several in vitro studies in L6 cells, C2C12 cells or primary myotubes, where no insulin desensitizing and NF-κB activating effects were found for C16:1, C18:1 and C18:2 [4–6, 10, 22]. However, Sinha et al. [11] reported an increased NF-κB DNA binding and insulin resistance in L6 myotubes after incubating with C16:0 or C18:2, whereas no effects were found for C18:3 incubation. A possible explanation for this discrepancy may lie in the fact that the experiments by Sinha and co-workers were performed for 6 h, while the other studies

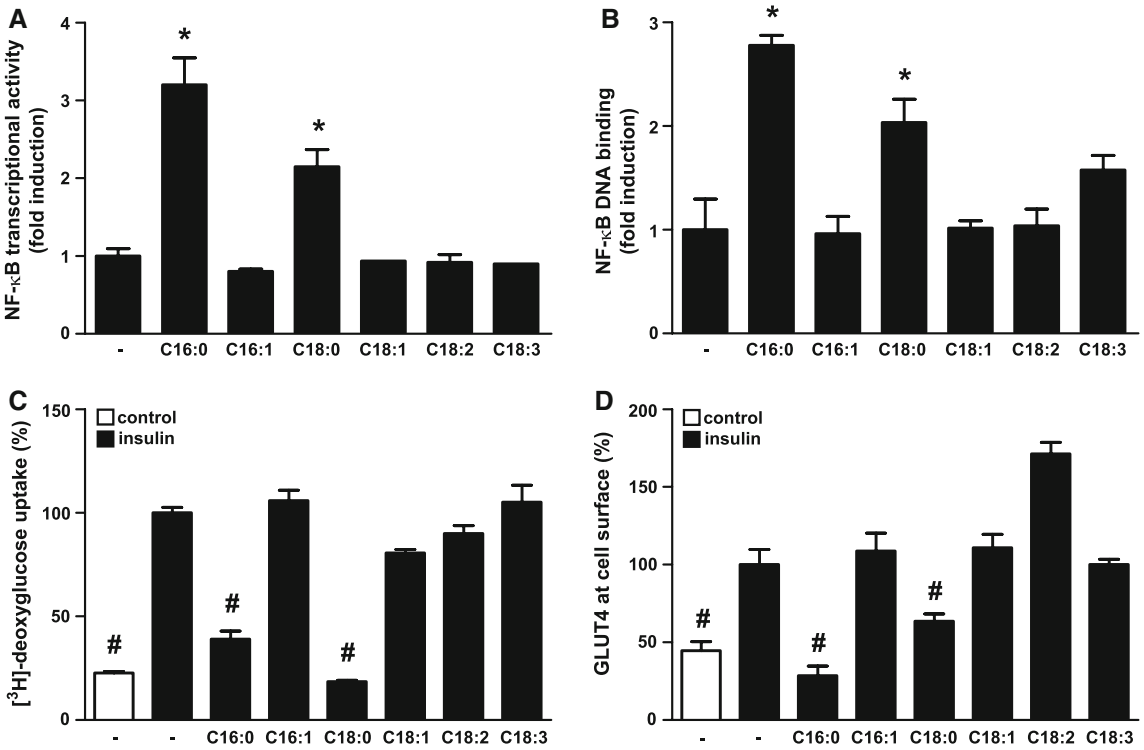

Fig. 1 NF-κB transcriptional activity and insulin sensitivity in skeletal muscle cells after incubation with C16 or C18 FAs differing in degree of saturation. C2C12 myoblasts stably transfected with the 6κB-TK-luciferase construct were differentiated for 5 days and incubated with 400 μmol/l of the indicated FAs for 24 h (**a**). Lysates were prepared for assessment of luciferase activity. Values were corrected for protein content and expressed as fold-induction over control. Alternatively, 5 days differentiated L6-GLUT4myc myotubes were incubated with and without the indicated fatty acids (200 μmol/l, 16 h). Nuclear extracts were prepared and assessed for RelA DNA binding activity to a consensus NF-κB oligonucleotide by EMSA (**b**). Relative DNA binding activity was determined by phosphor-imager analysis and expressed as fold induction. Furthermore, 2-deoxyglucose uptake (**c**) and GLUT4 translocation (**d**) were measured after stimulation with 25 nmol/l insulin for 15 min in 5 days differentiated L6-GLUT4myc myotubes. Data are expressed as percentage of insulin-stimulated glucose uptake or GLUT4 translocation in absence of FA. Basal and insulin-stimulated conditions are represented by the *white* and *black bars*, respectively. $^{*}p < 0.05$ versus control. $^{\#}p < 0.05$ versus insulin-stimulated control. Data shown are representative examples of three independent experiments

mentioned, including ours, evaluated effects after longer exposure time points.

Besides the *cis*-unsaturated FA described so far, unsaturated FA in our diet can have a *trans* configuration. The main sources of dietary *trans*-MUFA include industrially hydrogenated oils, and dairy products and meat containing ruminant fat. The most abundant MUFA *trans*-FAs found in these groups are elaidic acid (*trans*-9 C18:1) and vaccenic acid (*trans*-11 C18:1), respectively [23]. Of these two tested *trans* isomers of oleic acid, only the incubation of myotubes with elaidic acid resulted in an increased (∼3-fold) NF-κB transactivation compared with vehicle-treated myotubes (Fig. 2a). This might suggest that the position of the *trans* double bound determines the potential of a specific FA to activate NF-κB.

Well-known isomers of linoleic acid are the geometric and positional isomers *cis*-9, *trans*-11 conjugated linoleic acid (CLA) and *trans*-10, *cis*-12 CLA. We found an increased NF-κB transactivation (∼3-fold) after culturing the cells with *cis*-9, *trans*-11 CLA, which was comparable with the magnitude of the effects of C16:0 and C18:0. Since a single double bound at the *cis*-9 (oleic acid) or *trans*-11 (vaccenic acid) position of the C18-backbone did not result in an increased NF-κB transactivation, it is remarkable that the combination of these two double bounds in *cis*-9, *trans*-11 CLA caused an increased NF-κB transactivation. Strikingly, *trans*-10, *cis*-12 CLA provoked a ∼13-fold increase in NF-κB transcriptional activity, which is even higher than could maximally be achieved with the pro-inflammatory cytokine TNF-α (10 ng/ml), the prototypical inducer of NF-κB (routinely 5 to 10-fold induction after 4 h incubation, data not shown). In addition, activation of NF-κB after incubation with *trans*-10, *cis*-12 CLA was confirmed by performing an EMSA for the assessment of RelA DNA binding in L6 myotubes (Fig. 2b).

The fact that elaidic acid and *cis*-9, *trans*-11 CLA did not reveal increased DNA binding might be due to transient

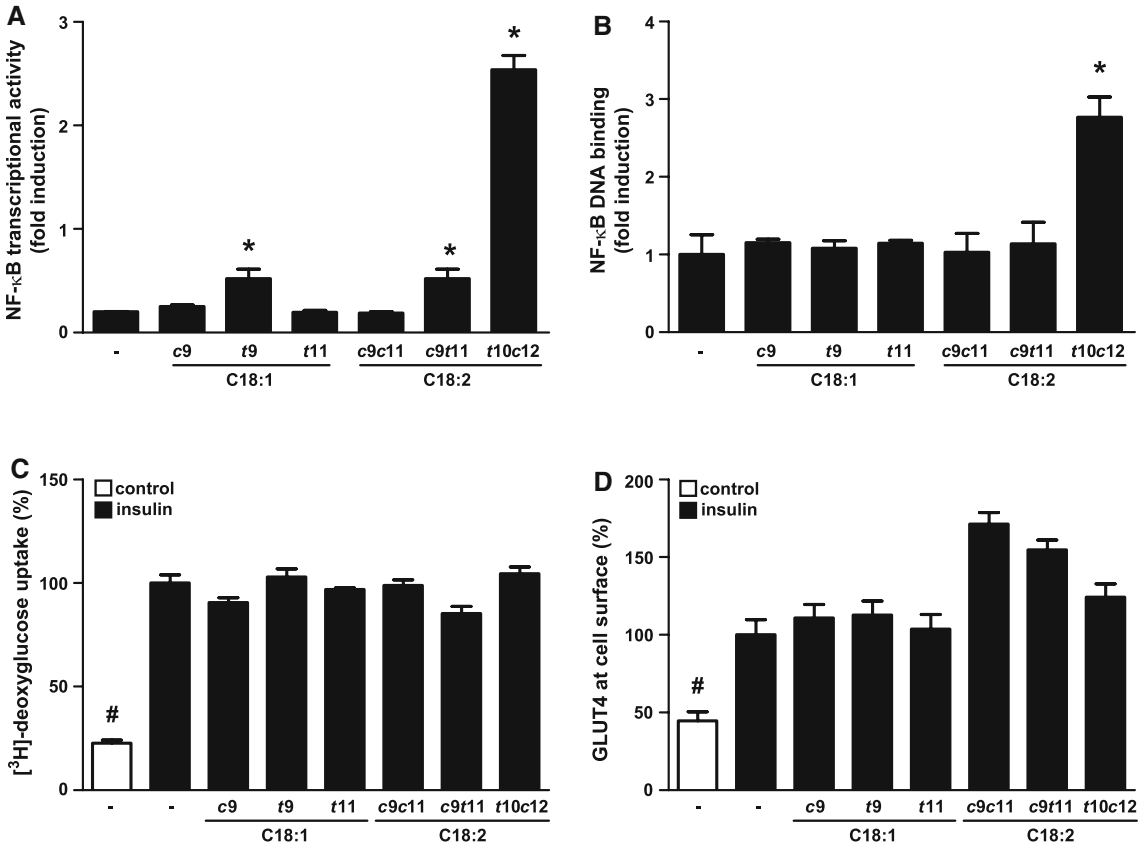

Fig. 2 NF-κB transcriptional activity and insulin sensitivity in skeletal muscle cells after incubation with geometric and positional C18:1 or C18:2 isomers. C2C12 myoblasts stably transfected with the 6κB-TK-luciferase construct were differentiated for 5 days and incubated with 400 μmol/l of the indicated FAs for 24 h (**a**). Lysates were prepared for assessment of luciferase activity. Values were corrected for protein content and expressed as fold-induction over control. Alternatively, 5 days differentiated L6-GLUT4myc myotubes were incubated with and without the indicated fatty acids (200 μmol/l, 16 h). Nuclear extracts were prepared and assessed for RelA DNA binding activity to a consensus NF-κB oligonucleotide by EMSA (**b**). Relative DNA binding activity was determined by phosphor-imager analysis and expressed as fold induction. Furthermore, 2-deoxyglucose uptake (**c**) and GLUT4 translocation (**d**) were measured after stimulation with 25 nmol/l insulin for 15 min in 5 days differentiated L6-GLUT4myc myotubes. Data are expressed as percentage of insulin-stimulated glucose uptake or GLUT4 translocation in absence of FA. Basal and insulin-stimulated conditions are represented by the *white* and *black bars*, respectively. $^{*}p < 0.05$ versus control. $^{\#}p < 0.05$ versus insulin-stimulated control. Data shown are representative examples of three independent experiments

DNA binding, as bi-phasic NF-κB activation in skeletal muscle has been reported, and the use of a reporter construct is less sensitive to transient changes in NF-κB transactivation [24]. Another explanation could be that the demonstrated increase in NF-κB transactivation is based on a mechanism independent from increased DNA binding, for example protein kinase A induced phosphorylation of NF-κB [25].

In spite of the considerable differences in NF-κB activity between the tested C18 *cis* and *trans*-FAs, and in particular between *cis*-C18:2 and C18:2 *trans*-10, *cis*-12 CLA, differential effects were not observed on insulin-stimulated glucose uptake (Fig. 2c) or GLUT4 translocation (Fig. 2d), which were not affected by any of these isomers.

Altogether, our results are in agreement with recent in vitro data, showing no effects on insulin signaling at the level of p-Akt, after incubation of C2C12 myotubes with elaidic and vaccenic acid [26]. The same authors showed that diets enriched in *trans* MUFAs of dairy or industrial origin did not impair muscle insulin sensitivity in Wistar rats. Nevertheless, opposing effects of CLA on insulin sensitivity have been described in rodents: many studies in the obese Zucker rat model describe positive effects on insulin sensitivity [27–29], while studies in mice showed that CLA, and in particular the *trans*-10, *cis*-12 isomer, induces insulin resistance [30–33]. Little is known on the effects of CLA on insulin sensitivity and inflammation in humans. In healthy young men, a diet rich in CLA (5.5 g/day, 5 weeks) did not affect inflammatory and diabetic risk markers [34]. In obese men with metabolic syndrome, supplementation with (3.4 g/day) *trans*-10, *cis*-12 CLA or *cis*-9, *trans*-11 CLA for 12 weeks resulted in an increased insulin resistance [35, 36] and supplementation with

trans-10, *cis*-12 CLA also resulted in increased levels of inflammatory biomarkers in serum [37]. Considering the latter observation and the striking induction of NF-κB by *trans*-10, *cis*-12 CLA in the cultured muscle cells in our study, it appears that *trans*-10, *cis*-12 CLA may initiate systematic inflammatory signaling in multiple tissues, and it remains to be determined if this does have pathological consequences. Finally, we also evaluated the effects of the n-3 FAs eicosapentaenoic acid, docosahexaenoic acid and the n-6 FA arachidonic acid, but none of these FAs affected NF-κB activity or insulin sensitivity (data not shown).

Our results show that the apparent association between SFA-induced NF-κB activation and insulin resistance in skeletal muscle cells cannot be generalized to all long chain FAs. Therefore, the proposed causal role of NF-κB activation in the induction of SFA-induced insulin resistance requires further investigation. It has been proposed that intramuscular accumulation of FA metabolites like diacylglycerol (DAG) [2, 4, 38–40] plays a role in inducing insulin resistance. Increased FA oxidation results in a decreased accumulation of FA metabolites like DAG and a protection against palmitate-induced insulin resistance in skeletal muscle cells [41]. Furthermore, it has been shown that the oxidation rate of FAs in muscle increases proportionally with the number of double bonds [42, 43]. This may explain why C16:0 and C18:0 did [16], but the C16-MUFA and C18-MUFA/PUFAs did not induce insulin resistance.

In conclusion, the results reported here reveal that FA-induced NF-κB activation is not sufficient for the induction of insulin resistance in skeletal muscle cells.

References

1. Itani SI, Ruderman NB, Schmieder F, Boden G (2002) Lipid-induced insulin resistance in human muscle is associated with changes in diacylglycerol, protein kinase C, and IkappaB-alpha. Diabetes 51:2005–2011
2. Boden G, Lebed B, Schatz M, Homko C, Lemieux S (2001) Effects of acute changes of plasma free fatty acids on intramyocellular fat content and insulin resistance in healthy subjects. Diabetes 50:1612–1617
3. Griffin ME, Marcucci MJ, Cline GW, Bell K, Barucci N, Lee D, Goodyear LJ, Kraegen EW, White MF, Shulman GI (1999) Free fatty acid-induced insulin resistance is associated with activation of protein kinase C theta and alterations in the insulin signaling cascade. Diabetes 48:1270–1274
4. Chavez JA, Summers SA (2003) Characterizing the effects of saturated fatty acids on insulin signaling and ceramide and diacylglycerol accumulation in 3T3-L1 adipocytes and C2C12 myotubes. Arch Biochem Biophys 419:101–109
5. Schmitz-Peiffer C, Craig DL, Biden TJ (1999) Ceramide generation is sufficient to account for the inhibition of the insulin-stimulated PKB pathway in C2C12 skeletal muscle cells pretreated with palmitate. J Biol Chem 274:24202–24210
6. Sabin MA, Stewart CE, Crowne EC, Turner SJ, Hunt LP, Welsh GI, Grohmann MJ, Holly JM, Shield JP (2007) Fatty acid-induced defects in insulin signalling, in myotubes derived from children, are related to ceramide production from palmitate rather than the accumulation of intramyocellular lipid. J Cell Physiol 211:244–252
7. Powell DJ, Turban S, Gray A, Hajduch E, Hundal HS (2004) Intracellular ceramide synthesis and protein kinase Czeta activation play an essential role in palmitate-induced insulin resistance in rat L6 skeletal muscle cells. Biochem J 382:619–629
8. Jove M, Planavila A, Laguna JC, Vazquez-Carrera M (2005) Palmitate-induced interleukin 6 production is mediated by protein kinase C and nuclear-factor kappaB activation and leads to glucose transporter 4 down-regulation in skeletal muscle cells. Endocrinology 146:3087–3095
9. Jove M, Planavila A, Sanchez RM, Merlos M, Laguna JC, Vazquez-Carrera M (2006) Palmitate induces tumor necrosis factor-alpha expression in C2C12 skeletal muscle cells by a mechanism involving protein kinase C and nuclear factor-kappaB activation. Endocrinology 147:552–561
10. Weigert C, Brodbeck K, Staiger H, Kausch C, Machicao F, Haring HU, Schleicher ED (2004) Palmitate, but not unsaturated fatty acids, induces the expression of interleukin-6 in human myotubes through proteasome-dependent activation of nuclear factor-kappaB. J Biol Chem 279:23942–23952
11. Sinha S, Perdomo G, Brown NF, O'Doherty RM (2004) Fatty acid-induced insulin resistance in L6 myotubes is prevented by inhibition of activation and nuclear localization of nuclear factor kB. J Biol Chem 279:41294–41301
12. Cai D, Frantz JD, Tawa NE Jr, Melendez PA, Oh BC, Lidov HG, Hasselgren PO, Frontera WR, Lee J, Glass DJ et al (2004) IKKbeta/NF-kappaB activation causes severe muscle wasting in mice. Cell 119:285–298
13. Sriwijitkamol A, Christ-Roberts C, Berria R, Eagan P, Pratipanawatr T, DeFronzo RA, Mandarino LJ, Musi N (2006) Reduced skeletal muscle inhibitor of kappaB beta content is associated with insulin resistance in subjects with type 2 diabetes: reversal by exercise training. Diabetes 55:760–767
14. Ropelle ER, Pauli JR, Prada PO, de Souza CT, Picardi PK, Faria MC, Cintra DE, Fernandes MF, Flores MB, Velloso LA et al (2006) Reversal of diet-induced insulin resistance with a single bout of exercise in the rat: the role of PTP1B and IRS-1 serine phosphorylation. J Physiol 577:997–1007
15. Rohl M, Pasparakis M, Baudler S, Baumgartl J, Gautam D, Huth M, De Lorenzi R, Krone W, Rajewsky K, Bruning JC (2004) Conditional disruption of IkappaB kinase 2 fails to prevent obesity-induced insulin resistance. J Clin Invest 113:474–481
16. Hommelberg PP, Plat J, Langen RC, Schols AM, Mensink RP (2009) Fatty acid-induced NF-{kappa}B activation and insulin resistance in skeletal muscle are chain length dependent. Am J Physiol Endocrinol Metab 296:E114–E120
17. Langen RC, Schols AM, Kelders MC, Wouters EF, Janssen-Heininger YM (2001) Inflammatory cytokines inhibit myogenic differentiation through activation of nuclear factor-kappaB. Faseb J 15:1169–1180
18. Langen RC, Schols AM, Kelders MC, Wouters EF, Janssen-Heininger YM (2003) Enhanced myogenic differentiation by extracellular matrix is regulated at the early stages of myogenesis. In Vitro Cell Dev Biol Anim 39:163–169
19. Bragt MC, Plat J, Mensink M, Schrauwen P, Mensink RP (2009) Anti-inflammatory effect of rosiglitazone is not reflected in expression of NFkappaB-related genes in peripheral blood mononuclear cells of patients with type 2 diabetes mellitus. BMC Endocr Disord 9:8
20. Rijkelijkhuizen JM, Doesburg T, Girman CJ, Mari A, Rhodes T, Gastaldelli A, Nijpels G, Dekker JM (2009) Hepatic fat is not

associated with beta-cell function or postprandial free fatty acid response. Metabolism 58:196–203
21. Mai K, Andres J, Biedasek K, Weicht J, Bobbert T, Sabath M, Meinus S, Reinecke F, Mohlig M, Weickert MO et al (2009) Free fatty acids link metabolism and regulation of the insulin-sensitizing fibroblast growth factor-21. Diabetes 58:1532–1538
22. Dimopoulos N, Watson M, Sakamoto K, Hundal HS (2006) Differential effects of palmitate and palmitoleate on insulin action and glucose utilisation in rat L6 skeletal muscle cells. Biochem J 399:473–481
23. Bauman DE, Mather IH, Wall RJ, Lock AL (2006) Major advances associated with the biosynthesis of milk. J Dairy Sci 89:1235–1243
24. Ladner KJ, Caligiuri MA, Guttridge DC (2003) Tumor necrosis factor-regulated biphasic activation of NF-kappa B is required for cytokine-induced loss of skeletal muscle gene products. J Biol Chem 278:2294–2303
25. Zhong H, Voll RE, Ghosh S (1998) Phosphorylation of NF-kappa B p65 by PKA stimulates transcriptional activity by promoting a novel bivalent interaction with the coactivator CBP/p300. Mol Cell 1:661–671
26. Tardy AL, Giraudet C, Rousset P, Rigaudiere JP, Laillet B, Chalancon S, Salles J, Loreau O, Chardigny JM, Morio B (2008) Effects of *trans* MUFA from dairy and industrial sources on muscle mitochondrial function and insulin sensitivity. J Lipid Res 49:1445–1455
27. Houseknecht KL, Vanden Heuvel JP, Moya-Camarena SY, Portocarrero CP, Peck LW, Nickel KP, Belury MA (1998) Dietary conjugated linoleic acid normalizes impaired glucose tolerance in the Zucker diabetic fatty fa/fa rat. Biochem Biophys Res Commun 244:678–682
28. Ryder JW, Portocarrero CP, Song XM, Cui L, Yu M, Combatsiaris T, Galuska D, Bauman DE, Barbano DM, Charron MJ et al (2001) Isomer-specific antidiabetic properties of conjugated linoleic acid. Improved glucose tolerance, skeletal muscle insulin action, and UCP-2 gene expression. Diabetes 50:1149–1157
29. Henriksen EJ, Teachey MK, Taylor ZC, Jacob S, Ptock A, Kramer K, Hasselwander O (2003) Isomer-specific actions of conjugated linoleic acid on muscle glucose transport in the obese Zucker rat. Am J Physiol Endocrinol Metab 285:E98–E105
30. Tsuboyama-Kasaoka N, Takahashi M, Tanemura K, Kim HJ, Tange T, Okuyama H, Kasai M, Ikemoto S, Ezaki O (2000) Conjugated linoleic acid supplementation reduces adipose tissue by apoptosis and develops lipodystrophy in mice. Diabetes 49:1534–1542
31. Clement L, Poirier H, Niot I, Bocher V, Guerre-Millo M, Krief S, Staels B, Besnard P (2002) Dietary trans-10, cis-12 conjugated linoleic acid induces hyperinsulinemia and fatty liver in the mouse. J Lipid Res 43:1400–1409
32. Kelley DS, Vemuri M, Adkins Y, Gill SH, Fedor D, Mackey BE (2009) Flaxseed oil prevents trans-10, cis-12-conjugated linoleic acid-induced insulin resistance in mice. Br J Nutr 101:701–708
33. Vemuri M, Kelley DS, Mackey BE, Rasooly R, Bartolini G (2007) Docosahexaenoic acid (DHA) but not eicosapentaenoic acid (EPA) prevents trans-10, cis-12 conjugated linoleic acid (CLA)-induced insulin resistance in mice. Metab Syndr Relat Disord 5:315–322
34. Raff M, Tholstrup T, Basu S, Nonboe P, Sorensen MT, Straarup EM (2008) A diet rich in conjugated linoleic acid and butter increases lipid peroxidation but does not affect atherosclerotic, inflammatory, or diabetic risk markers in healthy young men. J Nutr 138:509–514
35. Riserus U, Arner P, Brismar K, Vessby B (2002) Treatment with dietary trans10cis12 conjugated linoleic acid causes isomer-specific insulin resistance in obese men with the metabolic syndrome. Diabetes Care 25:1516–1521
36. Riserus U, Vessby B, Arnlov J, Basu S (2004) Effects of *cis*-9, *trans*-11 conjugated linoleic acid supplementation on insulin sensitivity, lipid peroxidation, and proinflammatory markers in obese men. Am J Clin Nutr 80:279–283
37. Riserus U, Basu S, Jovinge S, Fredrikson GN, Arnlov J, Vessby B (2002) Supplementation with conjugated linoleic acid causes isomer-dependent oxidative stress and elevated C-reactive protein: a potential link to fatty acid-induced insulin resistance. Circulation 106:1925–1929
38. Itani SI, Zhou Q, Pories WJ, MacDonald KG, Dohm GL (2000) Involvement of protein kinase C in human skeletal muscle insulin resistance and obesity. Diabetes 49:1353–1358
39. Perseghin G, Scifo P, De Cobelli F, Pagliato E, Battezzati A, Arcelloni C, Vanzulli A, Testolin G, Pozza G, Del Maschio A et al (1999) Intramyocellular triglyceride content is a determinant of in vivo insulin resistance in humans: a 1H–13C nuclear magnetic resonance spectroscopy assessment in offspring of type 2 diabetic parents. Diabetes 48:1600–1606
40. Schmitz-Peiffer C (2000) Signalling aspects of insulin resistance in skeletal muscle: mechanisms induced by lipid oversupply. Cell Signal 12:583–594
41. Sebastian D, Herrero L, Serra D, Asins G, Hegardt FG (2007) CPT I overexpression protects L6E9 muscle cells from fatty acid-induced insulin resistance. Am J Physiol Endocrinol Metab 292:E677–E686
42. Reubsaet FA, Veerkamp JH, Trijbels JM, Monnens LA (1989) Total and peroxisomal oxidation of various saturated and unsaturated fatty acids in rat liver, heart and m. quadriceps. Lipids 24:945–950
43. DeLany JP, Windhauser MM, Champagne CM, Bray GA (2000) Differential oxidation of individual dietary fatty acids in humans. Am J Clin Nutr 72:905–911

Lipids (2010) 45:291–299
DOI 10.1007/s11745-010-3398-z

ORIGINAL ARTICLE

Genetic Ablation of CD36 Does not Alter Mouse Brain Polyunsaturated Fatty Acid Concentrations

Byung Jun Song · Adrienne Elbert · Tupur Rahman · Sarah K. Orr · Chuck T. Chen · Maria Febbraio · Richard P. Bazinet

Received: 29 October 2009 / Accepted: 8 February 2010 / Published online: 20 March 2010

Abstract In the brain, polyunsaturated fatty acids (PUFA), especially arachidonic acid and docosahexaenoic acid (DHA), are required for regulating membrane fluidity, neuronal survival and signal transduction. Since the brain cannot synthesize n-6 and n-3 PUFA de novo, they must be supplied from the blood. However, the methods of PUFA entry into the brain are not agreed upon. This study tested the necessity of CD36, a candidate transporter of unesterified fatty acids, for maintaining brain PUFA concentrations by comparing brain PUFA concentrations in $CD36^{-/-}$ mice to their wild-type littermates. Because $CD36^{-/-}$ mice have been reported to have impaired learning ability, the PUFA concentrations in different brain regions (cortex, hippocampus, cerebellum and the remainder of brain) were investigated. At 9 weeks of age, the brain was separated into the four regions and fatty acid concentrations in total and phospholipid classes of these brain regions were analyzed using thin layer and gas chromatography. There were no statistical differences in arachidonic acid or DHA concentrations in the different brain regions between wild-type and $CD36^{-/-}$ mice, in total or phospholipid fractions. Concentrations of monounsaturated fatty acids were decreased in several phospholipid fractions in $CD36^{-/-}$ mice. These findings suggest that CD36 is not necessary for maintaining brain PUFA concentrations and that other mechanisms must exist.

Keywords CD36 · Fatty acid translocase · Transporter · Brain · Mouse · Knockout · Arachidonic acid · Docosahexaenoic acid · Polyunsaturated fatty acid

Abbreviations

BBB	Blood brain barrier
CD36	Clusters of differentiation 36
DHA	Docosahexaenoic acid
PUFA	Polyunsaturated fatty acid

Introduction

The brain is enriched with long chain polyunsaturated fatty acids (PUFA) especially arachidonic acid (20:4n-6) and docosahexaenoic acid (DHA; 22:6n-3) [1]. These PUFA are considered essential for normal development and function of the brain as they regulate membrane fluidity, neuronal survival [2–4], and neurotransmission [5]. In addition to these functions, altered brain PUFA metabolism has been associated with psychiatric disorders including schizophrenia [6], bipolar disorder [7], and depression [8]. Whereas dietary PUFA deprivation leads to an upregulation of liver arachidonic acid and DHA synthesis via desaturation/elongation of their 18 carbon precursors, linoleic (18:2n-6) and α-linolenic acid (18:3n-3), respectively, synthesis rates within the brain remain low and unchanged [9–11]. As a result, it is important that PUFA are

B. J. Song and A. Elbert contributed equally to this work.

B. J. Song · A. Elbert · T. Rahman · S. K. Orr · C. T. Chen · R. P. Bazinet (✉)
Department of Nutritional Sciences, Faculty of Medicine, University of Toronto, FitzGerald Building, 150 College St., Room 306, Toronto, ON M5S 3E2, Canada
e-mail: richard.bazinet@utoronto.ca

M. Febbraio
Department of Cell Biology, Cleveland Clinic, Cleveland, OH, USA

transported to the brain from the plasma where they are found as unesterified fatty acids, or esterified fatty acids in lipoproteins derived from the liver or diet [12–14].

While the mechanisms of PUFA uptake in the brain have not been fully characterized [15, 16], two models for PUFA entry into the brain through endothelial cells of the blood–brain barrier (BBB) have been proposed: (1) passive diffusion or transporter-mediated uptake of unesterified fatty acids [17–20], and (2) lipoprotein receptor-mediated endocytosis of lipoprotein particles [20, 21]. It has been shown that the low density and very low density lipoprotein receptors are not necessary for maintaining brain PUFA levels, suggesting that other mechanisms exist and are sufficient [22, 23]. Recently the rates of uptake of DHA and arachidonic acid into brain phospholipids from the plasma unesterified pool have been shown to approximate their respective rate of consumption by the brain, suggesting that plasma unesterified fatty acids are a major pool for brain fatty acid uptake [24–26].

Despite evidence for the uptake of plasma unesterified fatty acids into the brain, whether unesterified fatty acids cross the BBB via passive diffusion or via an active transporter is not agreed upon [18, 19]. Consistent with the Hamilton Model [27–29], Ouellet et al. [30] demonstrated that the brain transport coefficient (Clup, $\mu l\ g^{-1}\ s^{-1}$) of [^{14}C]-DHA and [^{14}C]-eicosapentaenoic acid (EPA) was not saturable at super-physiological concentrations, up to 100 μM, suggesting that DHA and EPA cross the BBB by simple diffusion. It was also reported that, upon crossing the BBB, EPA is rapidly β-oxidized possibly explaining its low concentration within the brain [31].

Several proteins facilitate fatty acid transport in various cell types [32–35]; however, the relevance of these proteins to brain PUFA uptake has yet to be explored. CD36 is an integral membrane glycoprotein expressed on the surface of a wide variety of cells including platelets, monocytes, adipocytes, myocytes, hepatocytes, enterocytes, retinal and mammary epithelial cells, microvasculature endothelial cells, and microglia and microvascular endothelial cells of the brain [36, 37]. CD36 is a 'pattern recognition' receptor, dependent on the intracellular concentrations of its ligands [38–40]. Based on its role in fatty acid binding and uptake in other types of cells, BBB endothelial cell CD36 [41–43] is a putative fatty brain acid transporter [12]. In 1999, Febbraio et al. [44] created a CD36 null mutation in mice by targeted homologous recombination. In 2005, Abumrad et al. [12] found that CD36$^{-/-}$ mice have normal activity, anxiety and exploration of novel environments, but have impaired learning ability, which they hypothesized may occur due to an impaired supply of essential PUFA to the brain. This hypothesis is supported by several studies demonstrating that rodents deprived of n-3 PUFA have impaired learning [45–50]. The purpose of this study was therefore to explore the involvement of CD36 in maintaining brain fatty acid concentrations. To do this, total phospholipid fatty acid concentrations of CD36$^{-/-}$ and wild-type mice within specific brain regions were compared. We hypothesized that if CD36 is necessary for maintaining brain PUFA concentrations, then CD36$^{-/-}$ mice will have decreased brain PUFA concentrations. After not finding a difference in total phospholipid fatty acid concentrations, we examined phospholipid classes to assess if specific pools may have been altered.

Materials and Methods

Animals and Treatments

All procedures were carried out in accordance with the policies set by the Canadian Council on Animal Care, and were approved by the Animal Ethics Committee at the University of Toronto (protocol #2000721) and the Cleveland Clinic IACUC. The brain samples of ten male wild-type and ten male CD36$^{-/-}$ mice were provided by the Cleveland clinic (Cleveland, OH). All mice were ten generations backcrossed to C57Bl/6 and littermate derived wild-type mice were used as controls and genotyped as previously described [51]. The mice were raised until 9 weeks of age in the Cleveland clinic in which temperature, humidity, and light cycle were controlled; the animals had ad libitum access to water and food (Teklad 2018S 18% Rodent Diet with Fenbendazole, Madison, WI). The fatty acid percentage compositions of the mouse diet, as measured by gas chromatography, were as follows: 16:0, 15.2%; 18:0, 3.5%; 18:1n-9, 19.6%; 18:2n-6, 51.8%; 18:3n-3, 5.6%; and fatty acids longer than 20 carbons accounted for less than 1% of total fatty acids. By 9 weeks of age, mice have an intact BBB [52], an adult size brain [21], and plateaued brain PUFA concentrations [53, 54]. Hence, mice were euthanized at 9 weeks of age with carbon dioxide and the cortex, cerebellum, hippocampus, and remainder of the brain were extracted. Brain regions were then frozen in liquid nitrogen prior to storage at −80 °C until further analysis.

Brain Lipid Extraction and Gas Chromatography/Flame Ionization Detection

Total lipids were extracted from the brain regions according to the method of Folch, Lees, and Sloane Stanley [55]. Thin layer chromatography (TLC) plates were activated by heating at 100 °C for 1 h. Total lipids were then loaded on a TLC plate and the plate was placed in a tank with solvents. Total phospholipid was separated along with authentic standards in heptane/diethyl ether/glacial acetic

acid (60:40:2, v/v). Phospholipid fractions were separated along with authentic standards in chloroform/methanol/2-propanol/KCl (0.25%, w/v)/triethylamine (30:9:25:6:18, v/v). Bands corresponding to total phospholipid, choline glycerophospholipid (ChoGpl), ethanolamine glycerophospholipid (EtnGpl), phosphatidylserine (PtdSer), phosphatidylinositol (PtdIns), and ceramide phosphocholine (CerPCho) were visualized under ultraviolet light, after lightly spraying with 8-anilino-1-naphthalene sulfonic acid (0.1%, w/v). Bands were scraped into a test tube containing a known amount of unesterified heptadecanoic acid (Nu-Chek Prep, Elysian, MN, USA), and converted to fatty acid methyl esters with 14% boron trifluoride/methanol at 100 °C for 1 or 1.5 h for CerPCho. Fatty acid methyl esters were quantified on a Varian-430 gas chromatograph (Varian, Lake Forest, CA, USA) equipped with a Varian Factor Four capillary column (VF-23 ms; 30 m × 0.25 mm i.d. × 0.25 μm film thickness), and a flame ionization detector (FID). Samples were injected in splitless mode. The injector and detector ports were set at 250 °C. Fatty acid methyl esters were eluted using a temperature program set initially at 50 °C and held for 2 min, increased at 20 °C/min and held at 170 °C for 1 min, then increased at 3 °C/min and held at 212 °C for 10 min to complete the run. The carrier gas was helium, set to a 0.7 ml/min constant flow rate. Peaks were identified by retention times of fatty acid methyl ester standards (Nu-Chek-Prep, Elysian, MN). Fatty acid concentrations (nmol/g brain) were calculated by proportional comparisons of the gas chromatography peak areas with that of the heptadecanoic acid internal standard. The 2018 Teklad Global 18% Protein Rodent Diet was measured in quadruplicate according to the method described above.

Brain Cholesterol Analysis by Gas Chromatography/Mass Spectrometry

A portion of the total lipid stock solution containing total lipids of cortex, cerebellum, hippocampus, or rest of brain, along with 5-α-cholestane as an internal standard were dried down under nitrogen and saponified in 1 M methanolic NaOH at 90 °C for 1 h. The non-saponifiable material containing sterols and glycerol was separated from saponifiable materials by adding saline and hexane, centrifuging (275 g) for 4 min and removing the upper hexane phase containing sterols. The hexane extraction process

Table 1 Fatty acid concentrations of total phospholipid in cortex, hippocampus, and cerebellum from wild-type and CD36$^{-/-}$ mice

Fatty acid	Cortex		Hippocampus		Cerebellum		Remainder of brain	
	WT ($n = 9$)	CD36$^{-/-}$ ($n = 7$)	WT ($n = 8$)	CD36$^{-/-}$ ($n = 7$)	WT ($n = 6$)	CD36$^{-/-}$ ($n = 5$)	WT ($n = 10$)	CD36$^{-/-}$ ($n = 10$)
14:0	559 ± 141	495 ± 90	760 ± 264	853 ± 189	192 ± 35	118 ± 50	252 ± 57	227 ± 68
14:1n-5	355 ± 124	259 ± 23	110 ± 48	137 ± 142	56 ± 64	66 ± 108	ND	2 ± 6
16:0	27,862 ± 1,311	27,550 ± 1,261	24,389 ± 2,040	25,596 ± 1,061	22,131 ± 713	21,096 ± 1,602	25,257 ± 2,225	25,918 ± 1,304
16:1n-7	663 ± 63	628 ± 62	593 ± 95	659 ± 148	459 ± 22	395 ± 47*	560 ± 54	571 ± 80
18:0	24,959 ± 1,077	23,741 ± 1,093	21,750 ± 1,436	22,160 ± 1,603	23,239 ± 1,175	23,452 ± 965	22,308 ± 2,032	22,382 ± 1,604
18:1n-9	14,251 ± 918	13,910 ± 621	14,707 ± 763	15,751 ± 1,233	18,033 ± 1,106	19,068 ± 1,054	17,311 ± 1,683	17,669 ± 1,647
18:1n-7	3,363 ± 160	3,203 ± 118*	3,125 ± 86	3,148 ± 319	5,138 ± 507	4,337 ± 1,798	4,790 ± 616	4,919 ± 617
18:2n-6	786 ± 67	777 ± 56	683 ± 68	765 ± 82	951 ± 53	982 ± 64	730 ± 91	786 ± 89
20:0	ND	ND	ND	ND	ND	ND	ND	ND
20:1n-9	720 ± 151	676 ± 109	891 ± 109	1,003 ± 183	2,249 ± 280	2,582 ± 292	1,757 ± 267	1,792 ± 356
20:3n-3	96 ± 59	126 ± 17	82 ± 38	59 ± 56	297 ± 11	341 ± 30*	218 ± 59	223 ± 33
22:0	192 ± 50	168 ± 41	ND	ND	ND	ND	ND	ND
20:4n-6	7,934 ± 302	7,915 ± 202	8,139 ± 706	8,271 ± 1,183	6,253 ± 351	6,730 ± 405	7,311 ± 702	7,368 ± 578
22:1n-9	38 ± 48	91 ± 98	62 ± 28	68 ± 56	200 ± 50	212 ± 36	147 ± 27	147 ± 30
20:5n-3	ND	ND	15 ± 29	8 ± 21	112 ± 59	141 ± 26	7 ± 23	34 ± 31
22:4n-6	1,539 ± 107	1,514 ± 74	1,597 ± 133	1,601 ± 206	1,191 ± 153	1,330 ± 195	1,795 ± 203	1,787 ± 227
24:0	ND	ND	ND	ND	ND	ND	ND	ND
24:1n-9	413 ± 108	417 ± 123	1,473 ± 551	1,943 ± 758	ND	ND	ND	ND
22:5n-6	140 ± 137	224 ± 106	775 ± 67	808 ± 126	1,495 ± 235	1,775 ± 297	743 ± 348	709 ± 417
22:5n-3	ND	ND	68 ± 31	35 ± 34	102 ± 6	78 ± 47	97 ± 15	83 ± 9*
22:6n-3	12,531 ± 492	12,492 ± 721	8,768 ± 790	8,818 ± 1,603	9,533 ± 817	9,825 ± 822	8,767 ± 935	8,972 ± 654

Data are nmol/g and are means ± SD

ND not detected (<1 nmol/g), *WT* wild-type

* Statistically significant from wild-type (WT) represents $P < 0.05$

Table 2 Cortex fatty acid concentrations of major phospholipid classes from wild-type and CD36$^{-/-}$ mice

Fatty acid	ChoGpl		EtnGpl		PtdSer		PtdIns	
	WT ($n = 9$)	CD36$^{-/-}$ ($n = 7$)	WT ($n = 9$)	CD36$^{-/-}$ ($n = 7$)	WT ($n = 7$)	CD36$^{-/-}$ ($n = 7$)	WT ($n = 9$)	CD36$^{-/-}$ ($n = 7$)
14:0	185 ± 37	171 ± 57	299 ± 244	268 ± 217	48 ± 18	54 ± 24	48 ± 23	47 ± 23
14:1n-5	41 ± 15	55 ± 51	44 ± 16	33 ± 9	40 ± 13	31 ± 8	35 ± 11	36 ± 17
16:0	21,353 ± 1,277	21,101 ± 1,891	3,295 ± 582	3,604 ± 1,621	480 ± 85	496 ± 110	697 ± 179	611 ± 80
16:1n-7	341 ± 21	351 ± 69	139 ± 28	123 ± 34	59 ± 11	47 ± 23	50 ± 16	67 ± 46
18:0	5,307 ± 859	4,828 ± 320	8,006 ± 901	8,072 ± 921	4,522 ± 169	4,571 ± 290	1,647 ± 436	1,474 ± 194
18:1n-9	7,860 ± 378	7,912 ± 645	2,700 ± 199	2,724 ± 369	1,138 ± 85	1,146 ± 154	439 ± 137	430 ± 73
18:1n-7	2,230 ± 104	2,092 ± 218	433 ± 32	435 ± 66	79 ± 9	81 ± 11	76 ± 8	70 ± 8
18:2n-6	334 ± 41	356 ± 58	124 ± 20	147 ± 62	20 ± 22	36 ± 20	37 ± 19	40 ± 21
20:0	ND	ND	ND	ND	ND	ND	ND	ND
20:1n-9	212 ± 18	207 ± 25	298 ± 79	286 ± 61	47 ± 24	49 ± 14	ND	ND
20:3n-3	73 ± 10	74 ± 15	47 ± 29	33 ± 24	52 ± 47	31 ± 14	71 ± 21	42 ± 17*
22:0	ND	ND	ND	ND	4 ± 10	10 ± 12	ND	ND
20:4n-6	1,875 ± 120	1,931 ± 187	3,145 ± 200	3,221 ± 367	211 ± 29	243 ± 65	993 ± 88	967 ± 142
22:1n-9	ND	ND	ND	ND	ND	ND	ND	ND
20:5n-3	ND	ND	ND	ND	ND	ND	ND	ND
22:4n-6	125 ± 11	135 ± 19	848 ± 64	839 ± 79	189 ± 16	181 ± 26	1,346 ± 249	1,267 ± 162
24:0	ND	ND	ND	ND	ND	ND	ND	ND
22:5n-6	ND	ND	100 ± 21	108 ± 38	ND	ND	ND	ND
22:5n-3	ND	ND	25 ± 20	26 ± 13	ND	ND	ND	ND
22:6n-3	1,109 ± 112	1,174 ± 159	5,814 ± 498	5,874 ± 825	2,495 ± 191	2,423 ± 382	142 ± 25	156 ± 64

Data are nmol/g and are means ± SD

ChoGpl choline glycerophospholipid, *EtnGpl* ethanolamine glycerophospholipid, *PtdIns* phosphatidylinositol, *PtdSer* phosphatidylserine, *ND* not detected (<1 nmol/g), *WT* wild-type

* Statistically significant from wild-type (WT) represents $P < 0.05$

and centrifugation was repeated one more time, in order to maximize the cholesterol yield. The sterol fraction containing cholesterol was dried under nitrogen and subsequently derivatized in trimethylsilyl chloride (Pierce, Rockford, IL, USA) at 60 °C for 30 min. The trimethylsilyl chloride was completely evaporated under nitrogen and the remaining derivatized cholesterol fraction was reconstituted with 150–300 µl of hexane for analysis by gas chromatography/mass spectrometry (GC/MS).

Cholesterol was determined by GC/MS using a HP-5 ms capillary column (30 m 9 0.25 mm i.d. 9 0.25 lm film thickness; Agilent Technologies) in an Agilent 6890 series Gas Chromatograph system equipped with an Agilent 5973 Network Mass Selective Detector (Agilent Technologies, Wilmington, DE, USA). The flow rate of helium carrier gas was 1 ml/min. The oven temperature was programmed as follows: 100 °C held initially for 1 min, increased at 15 °C/min to 280 °C and held for 17 min at 280 °C (total run time 30 min). The temperature of the injection port, ion source, and interface were 250, 230, and 280 °C, respectively. The injection volume was 1 µl and a splitless insert was adapted. A mass range from 50 to 700 amu was scanned using an electron ionization energy of 70 eV. Cholesterol trimethylsilyl ester and 5-α-cholestane (internal standard) were quantified on the basis of selected mass fragments.

Statistics

Results are expressed as means ± SD. Means were compared by unpaired, two-tailed *t* tests, with statistical significance set at $P < 0.05$.

Results

Cortex, Hippocampus, Cerebellum and Remainder of Brain Esterified Fatty Acid Concentrations

With the exception of 22:5n-3 in remainder of brain total phospholipids (Table 1) and 20:3n-3 in cortical PdtIns (Table 2) which were statistically lower in CD36$^{-/-}$ mice as compared to controls, no other significant differences in PUFA concentrations were detected (Tables 1, 2, 3, 4, 5). Total phospholipid 18:1n-7 was lower in the cortex of

Table 3 Hippocampus fatty acid concentrations of major phospholipid classes from wild-type and CD36$^{-/-}$ mice

Fatty acid	ChoGpl		EtnGpl		PtdSer		PtdIns	
	WT ($n = 8$)	CD36$^{-/-}$ ($n = 7$)	WT ($n = 8$)	CD36$^{-/-}$ ($n = 7$)	WT ($n = 8$)	CD36$^{-/-}$ ($n = 7$)	WT ($n = 8$)	CD36$^{-/-}$ ($n = 7$)
14:0	57 ± 19	48 ± 23	42 ± 20	28 ± 16	3 ± 3	2 ± 4	1 ± 3	4 ± 7
14:1n-5	9 ± 15	6 ± 10	3 ± 6	3 ± 9	7 ± 5	9 ± 7	9 ± 8	11 ± 13
16:0	17,839 ± 972	17,375 ± 932	3,367 ± 156	3,154 ± 183*	269 ± 40	257 ± 24	198 ± 159	238 ± 100
16:1n-7	232 ± 61	218 ± 41	79 ± 7	85 ± 17	15 ± 5	15 ± 4	30 ± 7	31 ± 18
18:0	4,912 ± 178	5,347 ± 634	8,793 ± 334	9,233 ± 600	5,006 ± 429	4,968 ± 399	3,055 ± 816	3,314 ± 607
18:1n-9	7,836 ± 235	8,220 ± 474	2,929 ± 268	3,221 ± 411	1,625 ± 193	1,704 ± 212	790 ± 203	1,035 ± 264
18:1n-7	2,047 ± 32	2,005 ± 166	460 ± 36	489 ± 76	107 ± 12	110 ± 17	129 ± 18	142 ± 20
18:2n-6	307 ± 26	364 ± 73	119 ± 16	143 ± 32	38 ± 11	45 ± 17	42 ± 8	65 ± 22
20:0	ND	ND	ND	ND	ND	ND	ND	ND
20:1n-9	224 ± 14	241 ± 24	370 ± 68	423 ± 77	91 ± 19	100 ± 18	67 ± 27	80 ± 18
20:3n-3	43 ± 19	34 ± 23	17 ± 15	9 ± 16	ND	ND	ND	ND
22:0	ND	ND	ND	ND	ND	ND	ND	ND
20:4n-6	2,386 ± 265	2,408 ± 175	3,885 ± 228	4,089 ± 342	384 ± 47	409 ± 51	2,695 ± 953	2,674 ± 699
22:1n-9	8 ± 11	9 ± 12	10 ± 11	7 ± 12	38 ± 14	45 ± 10	37 ± 33	48 ± 18
20:5n-3	ND	ND	ND	ND	ND	ND	ND	ND
22:4n-6	126 ± 13	126 ± 11	1,099 ± 92	1,156 ± 69	270 ± 33	275 ± 17	139 ± 67	162 ± 51
24:0	ND	ND	ND	ND	ND	ND	ND	ND
22:5n-6	ND	ND	113 ± 10	123 ± 36	79 ± 11	81 ± 19	ND	ND
22:5n-3	ND	ND	51 ± 6	32 ± 22	ND	ND	ND	ND
22:6n-3	930 ± 78	948 ± 79	5,358 ± 527	5,627 ± 513	2,573 ± 285	2,520 ± 225	810 ± 422	972 ± 310

Data are nmol/g and are means ± SD

ChoGpl choline glycerophospholipid, *EtnGpl* ethanolamine glycerophospholipid, *PtdIns* phosphatidylinositol, *PtdSer* phosphatidylserine, *ND* not detected (<1 nmol/g), *WT* wild-type

* Statistically significant from wild-type (WT) represents $P < 0.05$

CD36$^{-/-}$ mice as compared to controls (Table 1), whereas hippocampal EtnGpl 16:0 (Table 3) was significantly lower in CD36$^{-/-}$ mice as compared to controls. In the cerebellum, 16:1n-7 was significantly lower in total phospholipids of CD36$^{-/-}$ mice as compared to wild-type controls (Table 1). 16:1n-7 was also significantly lower in the remainder of brain PtdSer in CD36$^{-/-}$ compared to wild-type (Table 5).

Cortex, Hippocampus, Cerebellum and Remainder of Brain Cholesterol Concentrations

There were no statistically significant differences ($P > 0.05$) in cholesterol concentrations between CD36$^{-/-}$ mice as compared to wild-type controls in the four brain regions measured (Fig. 1).

Discussion

The cortical, cerebellar, hippocampal, and remainder of brain total phospholipid and phospholipid fraction esterified fatty acid as well as cholesterol concentrations from wild-type mice in this study are consistent with other reports [22, 23, 53, 56] and slight discrepancies may be due to differences in diet and brain region analysis [1, 57]. Although the majority of fatty acids were not statistically different, small decreases in monounsaturated fatty acids were detected in total phospholipids and the major phospholipid classes of CD36$^{-/-}$ mice. Although we cannot rule out that these minor differences in monounsaturated fatty acids could have been caused by random chance most of the observed changes were a decrease in the fatty acid concentration within CD36$^{-/-}$ mice, suggesting that the results maybe due to genetic ablation of CD36.

In 2009, Mitchell et al. [43] examined the permeability of oleate (18:1n-9) across primary human brain microvessel endothelial cells (HBMEC) using confluent cells grown on Transwell inserts. The necessity of CD36 in transporting oleate across the HBMEC monolayer was tested by knocking-down CD36 with siRNA. After transfecting with CD36 siRNA for 48 h (the expression of CD36 mRNA on HBMEC was reduced by 52%), the radioactivity of [^{14}C]-18:1n-9 transported into the basolateral medium was

Table 4 Cerebellum fatty acid concentrations of major phospholipid classes from wild-type and CD36$^{-/-}$ mice

Fatty acid	ChoGpl		EtnGpl		PtdSer		PtdIns	
	WT ($n = 6$)	CD36$^{-/-}$ ($n = 5$)	WT ($n = 6$)	CD36$^{-/-}$ ($n = 5$)	WT ($n = 6$)	CD36$^{-/-}$ ($n = 5$)	WT ($n = 6$)	CD36$^{-/-}$ ($n = 5$)
14:0	68 ± 21	61 ± 22	43 ± 33	26 ± 13	8 ± 4	20 ± 28	9 ± 17	7 ± 13
14:1n-5	ND	ND	ND	ND	ND	3 ± 8	ND	ND
16:0	14,361 ± 2,412	15,067 ± 1,907	3,484 ± 811	3,444 ± 492	414 ± 76	438 ± 119	314 ± 65	357 ± 181
16:1n-7	168 ± 33	166 ± 32	124 ± 36	107 ± 7	16 ± 2	19 ± 6	4 ± 4	8 ± 13
18:0	5,448 ± 551	5,468 ± 371	8,761 ± 1,015	8,837 ± 520	4,461 ± 674	4,368 ± 437	2,247 ± 322	2,081 ± 404
18:1n-9	7,217 ± 1,203	7,502 ± 709	5,240 ± 905	5,101 ± 428	3,026 ± 444	3,020 ± 393	712 ± 128	707 ± 34
18:1n-7	2,445 ± 387	2,375 ± 263	951 ± 284	894 ± 158	196 ± 55	179 ± 28	134 ± 24	144 ± 20
18:2n-6	374 ± 57	380 ± 29	194 ± 76	167 ± 11	42 ± 12	42 ± 10	35 ± 7	36 ± 6
20:0	ND	ND	ND	ND	ND	ND	ND	ND
20:1n-9	578 ± 95	606 ± 44	1,182 ± 230	1,275 ± 136	293 ± 66	311 ± 40	123 ± 40	135 ± 39
20:3n-3	109 ± 18	111 ± 12	120 ± 27	129 ± 9	8 ± 10	13 ± 8	ND	ND
22:0	ND	ND	ND	ND	ND	ND	ND	ND
20:4n-6	1,160 ± 145	1,197 ± 68	2,919 ± 489	2,816 ± 297	480 ± 380	334 ± 55	1,638 ± 435	1,566 ± 404
22:1n-9	21 ± 18	30 ± 18	74 ± 15	73 ± 18	27 ± 15	30 ± 17	ND	ND
20:5n-3	ND	ND	10 ± 21	ND	2 ± 4	ND	ND	ND
22:4n-6	83 ± 16	83 ± 17	844 ± 177	879 ± 160	176 ± 35	175 ± 27	60 ± 31	49 ± 8
24:0	ND	ND	ND	ND	ND	ND	ND	ND
22:5n-6	4 ± 11	15 ± 20	ND	ND	1 ± 3	2 ± 3	ND	ND
22:5n-3	10 ± 12	14 ± 8	63 ± 13	43 ± 25	5 ± 8	11 ± 6	ND	ND
22:6n-3	1,874 ± 219	1,865 ± 117	5,298 ± 753	4,989 ± 594	1,802 ± 235	1,697 ± 208	465 ± 250	306 ± 62

Data are nmol/g and are means ± SD

ChoGpl choline glycerophospholipid, *EtnGpl* ethanolamine glycerophospholipid, *PtdIns* phosphatidylinositol, *PtdSer* phosphatidylserine, *ND* not detected (<1 nmol/g), *WT* wild-type

* Statistically significant from wild-type (WT) represents $P < 0.05$

significantly reduced by 42% in 20 min, suggesting that CD36 is involved in the movement of oleate across the HBMEC. Interestingly in our study, although the level of 18:1n-9 was not decreased in CD36$^{-/-}$ mice, levels of 16:1n-7 were decreased in several phospholipid fractions within several regions. The lack of change in 18:1n-9 concentrations in our study is difficult to interpret as the brain is capable of synthesizing 18:1n-9 de novo which may be upregulated to compensate for a decrease in plasma 18:1n-9 uptake in CD36$^{-/-}$ mice. It would be of interest to directly test the uptake rate of plasma unesterified mono- and polyunsaturated fatty acids in CD36$^{-/-}$ and wild-type controls [56, 58–60].

In 2005, Abumrad et al. [61] examined the learning ability of CD36$^{-/-}$ mice using the eight radial arm maze. The maze consisted of multiple arms at the end of which contained a sweetened milk reward. Revisiting an arm where the reward was already obtained was considered an error. Unlike their wild-type littermates, CD36$^{-/-}$ mice showed substantially more errors, indicating a deficit in learning [12]. Since n-3 PUFA deprivation is associated with impaired learning in rodents [45–50] we examined PUFA concentrations in 4 major brain regions of CD36$^{-/-}$ and wild-type mice. There were no significant differences in brain DHA concentrations between wild-type and CD36$^{-/-}$ mice. Therefore, it is not clear if a change in brain DHA concentration may be related to the behavioral deficits in CD36$^{-/-}$ mice.

The lack of a significant difference in brain arachidonic acid or DHA concentrations between CD36$^{-/-}$ and wild-type mice suggests that CD36 is not necessary for maintaining brain PUFA concentrations. Since the brain cannot synthesize n-3 or n-6 PUFA de novo, PUFA likely enter the brain through CD36-independent mechanisms such as passive diffusion [18, 30], lipoprotein receptors including the high density lipoprotein receptor [62], or other fatty acid transporters that have not yet been characterized in the brain endothelium. From our study, it is not possible to conclude that CD36 does not play a role in fatty acid transport. It is possible that CD36 is normally involved in fatty acid transport, but previously mentioned

Table 5 Remainder of brain fatty acid concentrations of major phospholipid classes from wild-type and CD36$^{-/-}$ mice

Fatty acid	ChoGpl		EtnGpl		PtdSer		PtdIns	
	WT ($n = 9$)	CD36$^{-/-}$ ($n = 10$)	WT ($n = 7$)	CD36$^{-/-}$ ($n = 9$)	WT ($n = 9$)	CD36$^{-/-}$ ($n = 8$)	WT ($n = 9$)	CD36$^{-/-}$ ($n = 10$)
14:0	104 ± 18	87 ± 17*	460 ± 271	232 ± 213	26 ± 42	8 ± 2	2 ± 5	4 ± 4
14:1n-5	ND	ND	23 ± 22	12 ± 17	4 ± 11	ND	ND	ND
16:0	18,540 ± 1,610	19,051 ± 800	4,479 ± 374	4,590 ± 427	445 ± 98	369 ± 101	265 ± 93	280 ± 87
16:1n-7	283 ± 86	260 ± 36	147 ± 15	138 ± 34	22 ± 8	15 ± 5*	7 ± 7	5 ± 4
18:0	5,533 ± 473	5,584 ± 319	8,770 ± 1,057	9,265 ± 1,056	5,118 ± 606	4,844 ± 857	1,402 ± 337	1,333 ± 197
18:1n-9	9,004 ± 801	9,181 ± 486	5,172 ± 481	5,098 ± 709	2,327 ± 370	2,128 ± 565	418 ± 111	355 ± 60
18:1n-7	2,562 ± 228	2,518 ± 195	1,045 ± 166	990 ± 190	186 ± 28	170 ± 51	69 ± 18	61 ± 13
18:2n-6	345 ± 29	376 ± 47	172 ± 40	170 ± 42	40 ± 8	33 ± 12	23 ± 10	24 ± 7
20:0	ND	ND	ND	ND	ND	ND	ND	ND
20:1n-9	450 ± 55	447 ± 64	1,015 ± 147	1,046 ± 203	206 ± 43	191 ± 66	40 ± 19	41 ± 11
20:3n-3	72 ± 8	76 ± 9	104 ± 35	109 ± 29	17 ± 14	8 ± 6	ND	ND
22:0	ND	ND	ND	ND	ND	ND	ND	ND
20:4n-6	1,958 ± 159	2,013 ± 151	4,263 ± 430	4,127 ± 508	736 ± 162	661 ± 215	891 ± 260	860 ± 165
22:1n-9	22 ± 19	20 ± 18	59 ± 11	58 ± 12	31 ± 8	29 ± 8	ND	ND
20:5n-3	ND	ND	8 ± 14	12 ± 18	ND	6 ± 8	ND	ND
22:4n-6	144 ± 12	142 ± 14	1,367 ± 141	1,323 ± 182	269 ± 49	260 ± 44	48 ± 22	52 ± 15
24:0	ND	ND	ND	ND	ND	ND	ND	ND
22:5n-6	ND	ND	245 ± 305	297 ± 347	42 ± 9	43 ± 7	ND	ND
22:5n-3	2 ± 6	1 ± 4	66 ± 10	55 ± 9	12 ± 4	10 ± 6	ND	ND
22:6n-3	1,362 ± 117	1,419 ± 110	5,863 ± 715	5,821 ± 499	2,278 ± 299	2,298 ± 371	306 ± 72	288 ± 85

Data are nmol/g and are means ± SD

ChoGpl choline glycerophospholipid, *EtnGpl* ethanolamine glycerophospholipid, *PtdIns* phosphatidylinositol, *PtdSer* phosphatidylserine, *ND* not detected (<1 nmol/g), *WT* wild-type

* Statistically significant from wild-type (WT) represents $P < 0.05$

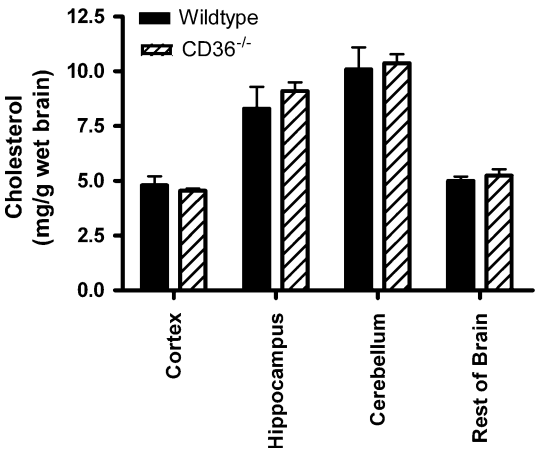

Fig. 1 Cortex, hippocampus, cerebellum and reminder of brain cholesterol concentrations (mg/g wet weight) in wildtype and CD36$^{-/-}$ mice ($n = 5$–10 per group). No statistically significant differences were detected ($P > 0.05$)

mechanisms, including changes respective plasma pools or kinetics, or other compensatory mechanism including a decrease in brain PUFA catabolism compensated for a lack of CD36-mediated transport. Cardiomyocytes from CD36$^{-/-}$ have a one-fold increase in fatty acid transport protein 1 (FATP1) which could be a compensatory mechanism in the absence of CD36 [63]. In addition, esterified PUFA might be cleaved from lipoproteins at the BBB by enzymes such as lipoprotein lipase [20] or endothelial lipase [64–66], thus providing another pool from which PUFA can enter the brain.

In conclusion, CD36 has been implicated as a candidate fatty acid transport protein in several tissues. CD36$^{-/-}$ mice have decreased levels of monounsaturated fatty acids in several brain phospholipid pools, but it is not clear if these changes are related to the altered behavior previously reported in these mice. By examining CD36$^{-/-}$ mice, we have demonstrated that brain PUFA levels, especially arachidonic acid and DHA, are not altered, suggesting that other mechanisms to transport PUFA into the brain must exist and are sufficient.

Acknowledgments This work was funded by a grant from the Natural Sciences and Engineering Research Council of Canada (NSERC) to RPB.

References

1. Diau GY, Hsieh AT, Sarkadi-Nagy EA, Wijendran V, Nathanielsz PW, Brenna JT (2005) The influence of long chain polyunsaturate supplementation on docosahexaenoic acid and arachidonic acid in baboon neonate central nervous system. BMC Med 3:11
2. Akbar M, Calderon F, Wen Z, Kim HY (2005) Docosahexaenoic acid: a positive modulator of Akt signaling in neuronal survival. Proc Natl Acad Sci USA 102:10858–10863
3. Bazan NG (2005) Synaptic signaling by lipids in the life and death of neurons. Mol Neurobiol 31:219–230
4. Rao JS, Ertley RN, Lee HJ, DeMar JC Jr, Arnold JT, Rapoport SI, Bazinet RP (2007) n-3 polyunsaturated fatty acid deprivation in rats decreases frontal cortex BDNF via a p38 MAPK-dependent mechanism. Mol Psychiatry 12:36–46
5. Chalon S, Vancassel S, Zimmer L, Guilloteau D, Durand G (2001) Polyunsaturated fatty acids and cerebral function: focus on monoaminergic neurotransmission. Lipids 36:937–944
6. Skosnik PD, Yao JK (2003) From membrane phospholipid defects to altered neurotransmission: is arachidonic acid a nexus in the pathophysiology of schizophrenia? Prostaglandins Leukot Essent Fatty Acids 69:367–384
7. Rao JS, Lee HJ, Rapoport SI, Bazinet RP (2008) Mode of action of mood stabilizers: is the arachidonic acid cascade a common target? Mol Psychiatry 13:585–596
8. Stahl LA, Begg DP, Weisinger RS, Sinclair AJ (2008) The role of omega-3 fatty acids in mood disorders. Curr Opin Investig Drugs 9:57–64
9. Igarashi M, DeMar JC Jr, Ma K, Chang L, Bell JM, Rapoport SI (2007) Docosahexaenoic acid synthesis from alpha-linolenic acid by rat brain is unaffected by dietary n-3 PUFA deprivation. J Lipid Res 48:1150–1158
10. Igarashi M, DeMar JC Jr, Ma K, Chang L, Bell JM, Rapoport SI (2007) Upregulated liver conversion of alpha-linolenic acid to docosahexaenoic acid in rats on a 15 week n-3 PUFA-deficient diet. J Lipid Res 48:152–164
11. Igarashi M, Ma K, Chang L, Bell JM, Rapoport SI (2007) Dietary n-3 PUFA deprivation for 15 weeks upregulates elongase and desaturase expression in rat liver but not brain. J Lipid Res 48:2463–2470
12. Abumrad NA, Ajmal M, Pothakos K, Robinson JK (2005) CD36 expression and brain function: does CD36 deficiency impact learning ability? Prostaglandins Other Lipid Mediat 77:77–83
13. DeMar JC Jr, Lee HJ, Ma K, Chang L, Bell JM, Rapoport SI, Bazinet RP (2006) Brain elongation of linoleic acid is a negligible source of the arachidonate in brain phospholipids of adult rats. Biochim Biophys Acta 1761:1050–1059
14. Demar JC Jr, Ma K, Chang L, Bell JM, Rapoport SI (2005) alpha-Linolenic acid does not contribute appreciably to docosahexaenoic acid within brain phospholipids of adult rats fed a diet enriched in docosahexaenoic acid. J Neurochem 94:1063–1076
15. (2001) Brain uptake and utilization of fatty acids: applications to peroxisomal biogenesis disorders. Proceedings and abstracts of an international workshop. Bethesda, Maryland, USA. March 2–4, 2000. J Mol Neurosci 16:87–342
16. Qi K, Hall M, Deckelbaum RJ (2002) Long-chain polyunsaturated fatty acid accretion in brain. Curr Opin Clin Nutr Metab Care 5:133–138
17. Rapoport SI, Chang MC, Spector AA (2001) Delivery and turnover of plasma-derived essential PUFAs in mammalian brain. J Lipid Res 42:678–685
18. Hamilton JA, Brunaldi K (2007) A model for fatty acid transport into the brain. J Mol Neurosci 33:12–17
19. Hamilton JA, Johnson RA, Corkey B, Kamp F (2001) Fatty acid transport: the diffusion mechanism in model and biological membranes. J Mol Neurosci 16:99–108 (discussion 151–157)
20. Spector AA (2001) Plasma free fatty acid and lipoproteins as sources of polyunsaturated fatty acid for the brain. J Mol Neurosci 16:159–165 (discussion 215–221)
21. Dobbing J, Sands J (1979) Comparative aspects of the brain growth spurt. Early Hum Dev 3:79–83
22. Chen CT, Ma DW, Kim JH, Mount HT, Bazinet RP (2008) The low density lipoprotein receptor is not necessary for maintaining mouse brain polyunsaturated fatty acid concentrations. J Lipid Res 49:147–152
23. Rahman T, Taha AY, Jun Song B, Orr SK, Liu Z, Chen CT, Bazinet RP (2010) The very low density lipoprotein receptor is not necessary for maintaining brain polyunsaturated fatty acid concentrations. Prostaglandins Leukot Essent Fatty Acids 82:141–145
24. DeMar JC Jr, Ma K, Bell JM, Rapoport SI (2004) Half-lives of docosahexaenoic acid in rat brain phospholipids are prolonged by 15 weeks of nutritional deprivation of n-3 polyunsaturated fatty acids. J Neurochem 91:1125–1137
25. Green JT, Liu Z, Bazinet RP (2010) Brain phospholipid arachidonic acid half lives are not altered following 15 weeks of n-3 polyunsaturated fatty acid adequate or deprived diet. J Lipid Res 51:535–543
26. Rapoport SI, Rao JS, Igarashi M (2007) Brain metabolism of nutritionally essential polyunsaturated fatty acids depends on both the diet and the liver. Prostaglandins Leukot Essent Fatty Acids 77:251–261
27. Brunaldi K, Huang N, Hamilton JA (2010) Fatty acids are rapidly delivered to and extracted from membranes by methyl-beta-cyclodextrin. J Lipid Res 51:120–131
28. Katz R, Hamilton JA, Spector AA, Moore SA, Moser HW, Noetzel MJ, Watkins PA (2001) Brain uptake and utilization of fatty acids: recommendations for future research. J Mol Neurosci 16:333–335
29. Hamilton JA (1998) Fatty acid transport: difficult or easy? J Lipid Res 39:467–481
30. Ouellet M, Emond V, Chen CT, Julien C, Bourasset F, Oddo S, Laferla F, Bazinet RP, Calon F (2009) Diffusion of docosahexaenoic and eicosapentaenoic acids through the blood-brain barrier: an in situ cerebral perfusion study. Neurochem Int 55:476–482
31. Chen CT, Liu Z, Ouellet M, Calon F, Bazinet RP (2009) Rapid beta-oxidation of eicosapentaenoic acid in mouse brain: an in situ study. Prostaglandins Leukot Essent Fatty Acids 80:157–163
32. Abumrad NA, el-Maghrabi MR, Amri EZ, Lopez E, Grimaldi PA (1993) Cloning of a rat adipocyte membrane protein implicated in binding or transport of long-chain fatty acids that is induced during preadipocyte differentiation. Homology with human CD36. J Biol Chem 268:17665–17668
33. Hajri T, Abumrad NA (2002) Fatty acid transport across membranes: relevance to nutrition and metabolic pathology. Annu Rev Nutr 22:383–415
34. Schaffer JE, Lodish HF (1994) Expression cloning and characterization of a novel adipocyte long chain fatty acid transport protein. Cell 79:427–436
35. Stremmel W, Lotz G, Strohmeyer G, Berk PD (1985) Identification, isolation, and partial characterization of a fatty acid binding protein from rat jejunal microvillous membranes. J Clin Invest 75:1068–1076
36. Febbraio M, Guy E, Coburn C, Knapp FF Jr, Beets AL, Abumrad NA, Silverstein RL (2002) The impact of overexpression and deficiency of fatty acid translocase (FAT)/CD36. Mol Cell Biochem 239:193–197

37. Husemann J, Loike JD, Anankov R, Febbraio M, Silverstein SC (2002) Scavenger receptors in neurobiology and neuropathology: their role on microglia and other cells of the nervous system. Glia 40:195–205
38. Cecil DL, Appleton CT, Polewski MD, Mort JS, Schmidt AM, Bendele A, Beier F, Terkeltaub R (2009) The pattern recognition receptor CD36 is a chondrocyte hypertrophy marker associated with suppression of catabolic responses and promotion of repair responses to inflammatory stimuli. J Immunol 182:5024–5031
39. Febbraio M, Hajjar DP, Silverstein RL (2001) CD36: a class B scavenger receptor involved in angiogenesis, atherosclerosis, inflammation, and lipid metabolism. J Clin Invest 108:785–791
40. Oz HS, Zhong J, de Villiers WJ (2009) Pattern recognition scavenger receptors, SR-A and CD36, have an additive role in the development of colitis in mice. Dig Dis Sci
41. Coraci IS, Husemann J, Berman JW, Hulette C, Dufour JH, Campanella GK, Luster AD, Silverstein SC, El-Khoury JB (2002) CD36, a class B scavenger receptor, is expressed on microglia in Alzheimer's disease brains and can mediate production of reactive oxygen species in response to beta-amyloid fibrils. Am J Pathol 160:101–112
42. Cho S, Park EM, Febbraio M, Anrather J, Park L, Racchumi G, Silverstein RL, Iadecola C (2005) The class B scavenger receptor CD36 mediates free radical production and tissue injury in cerebral ischemia. J Neurosci 25:2504–2512
43. Mitchell RW, Edmundson CL, Miller DW, Hatch GM (2009) On the mechanism of oleate transport across human brain microvessel endothelial cells. J Neurochem 110:1049–1057
44. Febbraio M, Abumrad NA, Hajjar DP, Sharma K, Cheng W, Pearce SF, Silverstein RL (1999) A null mutation in murine CD36 reveals an important role in fatty acid and lipoprotein metabolism. J Biol Chem 274:19055–19062
45. Calon F, Lim GP, Yang F, Morihara T, Teter B, Ubeda O, Rostaing P, Triller A, Salem N Jr, Ashe KH, Frautschy SA, Cole GM (2004) Docosahexaenoic acid protects from dendritic pathology in an Alzheimer's disease mouse model. Neuron 43:633–645
46. Catalan J, Moriguchi T, Slotnick B, Murthy M, Greiner RS, Salem N Jr (2002) Cognitive deficits in docosahexaenoic acid-deficient rats. Behav Neurosci 116:1022–1031
47. Hiratsuka S, Koizumi K, Ooba T, Yokogoshi H (2009) Effects of dietary docosahexaenoic acid connecting phospholipids on the learning ability and fatty acid composition of the brain. J Nutr Sci Vitaminol 55:374–380
48. Holguin S, Martinez J, Chow C, Wurtman R (2008) Dietary uridine enhances the improvement in learning and memory produced by administering DHA to gerbils. Faseb J 22:3938–3946
49. Petursdottir AL, Farr SA, Morley JE, Banks WA, Skuladottir GV (2008) Effect of dietary n-3 polyunsaturated fatty acids on brain lipid fatty acid composition, learning ability, and memory of senescence-accelerated mouse. J Gerontol 63:1153–1160
50. Wu A, Ying Z, Gomez-Pinilla F (2008) Docosahexaenoic acid dietary supplementation enhances the effects of exercise on synaptic plasticity and cognition. Neuroscience 155:751–759
51. Okamura DM, Pennathur S, Pasichnyk K, Lopez-Guisa JM, Collins S, Febbraio M, Heinecke J, Eddy AA (2009) CD36 regulates oxidative stress and inflammation in hypercholesterolemic CKD. J Am Soc Nephrol 20:495–505
52. Rapoport SI (1976) Blood–brain barrier in physiology and medicine. Raven Press, New York
53. Ma K, Langenbach R, Rapoport SI, Basselin M (2007) Altered brain lipid composition in cyclooxygenase-2 knockout mouse. J Lipid Res 48:848–854
54. Ward G, Woods J, Reyzer M, Salem N Jr (1996) Artificial rearing of infant rats on milk formula deficient in n-3 essential fatty acids: a rapid method for the production of experimental n-3 deficiency. Lipids 31:71–77
55. Folch J, Lees M, Sloane Stanley GH (1957) A simple method for the isolation and purification of total lipides from animal tissues. J Biol Chem 226:497–509
56. Bazinet RP, Rao JS, Chang L, Rapoport SI, Lee HJ (2006) Chronic carbamazepine decreases the incorporation rate and turnover of arachidonic acid but not docosahexaenoic acid in brain phospholipids of the unanesthetized rat: relevance to bipolar disorder. Biol Psychiatry 59:401–407
57. Levant B, Ozias MK, Carlson SE (2007) Specific brain regions of female rats are differentially depleted of docosahexaenoic acid by reproductive activity and an (n-3) fatty acid-deficient diet. J Nutr 137:130–134
58. Robinson PJ, Noronha J, DeGeorge JJ, Freed LM, Nariai T, Rapoport SI (1992) A quantitative method for measuring regional in vivo fatty-acid incorporation into and turnover within brain phospholipids: review and critical analysis. Brain Res 17:187–214
59. Golovko MY, Murphy EJ (2006) Uptake and metabolism of plasma-derived erucic acid by rat brain. J Lipid Res 47:1289–1297
60. Lee HJ, Rao JS, Chang L, Rapoport SI, Bazinet RP (2008) Chronic *N*-methyl-D-aspartate administration increases the turnover of arachidonic acid within brain phospholipids of the unanesthetized rat. J Lipid Res 49:162–168
61. Crusio WE, Schwegler H, Lipp HP (1987) Radial-maze performance and structural variation of the hippocampus in mice: a correlation with mossy fibre distribution. Brain Res 425:182–185
62. Kozarsky KF, Donahee MH, Rigotti A, Iqbal SN, Edelman ER, Krieger M (1997) Overexpression of the HDL receptor SR-BI alters plasma HDL and bile cholesterol levels. Nature 387:414–417
63. Habets DD, Coumans WA, Voshol PJ, den Boer MA, Febbraio M, Bonen A, Glatz JF, Luiken JJ (2007) AMPK-mediated increase in myocardial long-chain fatty acid uptake critically depends on sarcolemmal CD36. Biochem Biophys Res Commun 355:204–210
64. Chen S, Subbaiah PV (2007) Phospholipid and fatty acid specificity of endothelial lipase: potential role of the enzyme in the delivery of docosahexaenoic acid (DHA) to tissues. Biochim Biophys Acta 1771:1319–1328
65. Jaye M, Lynch KJ, Krawiec J, Marchadier D, Maugeais C, Doan K, South V, Amin D, Perrone M, Rader DJ (1999) A novel endothelial-derived lipase that modulates HDL metabolism. Nat Genet 21:424–428
66. Sovic A, Panzenboeck U, Wintersperger A, Kratzer I, Hammer A, Levak-Frank S, Frank S, Rader DJ, Malle E, Sattler W (2005) Regulated expression of endothelial lipase by porcine brain capillary endothelial cells constituting the blood–brain barrier. J Neurochem 94:109–119

Lipids (2010) 45:301–311
DOI 10.1007/s11745-010-3396-1

ORIGINAL ARTICLE

Trans-Membrane Uptake and Intracellular Metabolism of Fatty Acids in Atlantic Salmon (*Salmo salar* L.) Hepatocytes

Jishu Zhou · Ingunn Stubhaug · Bente E. Torstensen

Received: 14 September 2009 / Accepted: 3 February 2010 / Published online: 27 February 2010

Abstract To elucidate if the trans-membrane uptake of fatty acids is protein-mediated, the uptake of oleic acid (18:1n-9), linoleic acid (18:2n-6), alpha-linolenic acid (18:3n-3), eicosapentaenoic acid (20:5n-3) and docosahexaenoic acid (22:6n-3) was investigated in vitro in Atlantic salmon (*Salmo salar* L.) primary hepatocytes. Firstly, optimal fatty acid incubation time and concentration were established for trans-membrane 18:n-9 uptake. Based on saturation kinetics, a 2-h incubation time and 37.5 μM were used for the following experiments. Secondly, in order to identify whether trans-membrane fatty acid uptake in hepatocytes was mainly passive or protein mediated, hepatocytes were pre-incubated with membrane protein inhibitors followed by 2 h of incubation with [1-^{14}C] labelled 18:1n-9, 18:2n-6, 18:3n-3, 20:5n-3 and 22:6n-3. Fatty acid uptake into hepatocytes was highest with 20:5n-3 and 22:6n-3 and lowest with 18:1n-9. Phloretin was the most potent fatty acid uptake inhibitor, inhibiting uptake in the following order: 20:5n-3 > 18:3n-3 = 22:6n-3 > 18:2n-6 > 18:1n-9. The uptake of FA in Atlantic salmon hepatocytes seem to be due to both saturable and inhibitable protein mediated uptake, as well as passive uptake processes with more unsaturated and long fatty acids (20:n-3 > 22:6n-3 = 18:3n-3 > 18:2n-6) being more dependent on membrane protein mediated uptake compared to 18:1n-9.

Keywords Fatty acid · Trans-membrane uptake · Fatty acid transport protein (FATP) · Fatty acid translocase (FAT/CD36) · Fatty acid binding protein in plasma membrane (FABPpm) · Transport · Passive diffusion · Atlantic salmon · Hepatocytes · Inhibitors

Abbreviations

DAG	Diacylglycerol
DIDS	Diisothiocyanodisulfonic acid
FABPpm	Fatty acid binding protein in plasma membrane
FATP	Fatty acid transport protein
FAT/CD36	Fatty acid translocase
FFA	Free fatty acid
HEPES	4-(2-Hydroxyethyl)-1-piperazineethane-sulfonic acid
OA	Oleic acid
LCFA	Long-chain fatty acid
MAG	Monoacylglycerol
PBS	Phosphate buffered saline
PL	Phospholipids
SSO	Sulfo-*N*-succinimidyl 4-maleimido-oleic acid ester
SSMB	Sulfo-*N*-succinimidyl 4-maleimido-butyric acid ester
TAG	Triacylglycerol

J. Zhou
College of Animal Science and Technology,
Northwest A&F University, Yangling 712100,
Shaanxi, China

J. Zhou · I. Stubhaug · B. E. Torstensen (✉)
National Institute of Nutrition and Seafood Research (NIFES),
P.O. Box 2029, Nordnes 5817 Bergen, Norway
e-mail: bente.torstensen@nifes.no

I. Stubhaug
Pôle d'Hydrobiologie, INRA,
64310 Saint-Pee-Sur-Nivelle, France

Introduction

Fatty acids are key nutrients associated with energy production- and storage, gene regulation [1] and essential components in cell membrane phospholipids [2]. With their hydrophobic nature, LCFAs have long been thought to transverse the lipid bilayer of the cell membrane by simple, non-facilitated diffusion [3–8] then by "flip–flop" in the phospholipid bilayer [9, 10]. However, there are several indications of active protein mediated fatty acid (FA) uptake being present in cells. Energy dependency and an ATP-driven pump have been reported to be involved in FA transport across 3T3F4424 adipocytes [11] and rat hepatocyte membranes [12]. Furthermore, there are a number of FA transport proteins identified in the cell membrane of a variety of tissues, such as fatty acid transport proteins 1 to 6 (FATP1–FATP6) [13–15], plasma membrane associated fatty acid binding protein (FABPpm) [16, 17] and fatty acid translocase (FAT/CD36) [18], which are all thought to function as trans-membrane FA uptake proteins.

Protein modifying agents or membrane protein inhibitors has been found to inhibit cellular LCFAs uptake suggesting the existence of membrane protein dependent transport. Examples of such membrane protein modifying agents are phloretin and sulfo-*N*-succinimidyl oleate (SSO) which have been found to inhibit the LCFAs uptake [19, 20]. Both SSO and phloretin have been reported to decrease 18:1n-9 uptake in rat heart and skeletal muscle [21, 22] and SSO has been found to decrease 18:1n-9 uptake in rat adipocytes [23]. Diisothiocyanodisulfonic acid (DIDS), being a non-permeable anion exchange inhibitor [24], and SSO have been reported to decrease palmitate uptake in rainbow trout (*Oncorhynchus mykiss*) red and white muscle vesicles [25]. Furthermore, methyl-β-cyclodextrin is reported to decrease fatty acid uptake by >50% in COS cells through depletion of cholesterol [26].

In Atlantic salmon hepatocytes, FA uptake has been found to significantly decrease when fish were fed dietary vegetable oil based diets compared with fish oil [27], indicating an effect of dietary fatty acids on the expression or activity of fatty acid uptake associated membrane proteins. Furthermore, the mRNA expression of FAT/CD36 and FATP in Atlantic salmon liver, muscle and adipose tissues have been identified and reported to be significantly affected by dietary fatty acid composition in white muscle but not in liver [28]. However, the mechanism of fatty acid uptake in Atlantic salmon tissues and the relative importance among these membrane proteins have not previously been investigated. The aim of the present study was to elucidate the uptake mechanisms and the following intracellular metabolic fate in Atlantic salmon hepatocytes of18:1n-9, and compared to other long chain fatty acids typical for vegetable- and fish oils; i.e. 18:2n-6, 18:3n-3, 20:5n-3 and 22:6n-3 to give indications of the possible relationship between fatty acid uptake rate and metabolism as a driving force for uptake.

Materials

Atlantic salmon were obtained from the Institute of Marine Research (IMR) and fed a commercial diet containing about 48% crude protein, 25% lipid, 13% nitrogen-free extracts (Skretting, Spirit HH200-75A, Stavanger, Norway). Fetal bovine serum (FBS) and GlutaMax were bought from Gibco-brl/Life Technologies (Gaithersburg, MD, USA). Leibovitz L-15, antibiotics (mixture of penicillin, streptomycin and amphotericin B), metacain (MS222), unradiolabelled fatty acids, laminin, butylated hydroxytoluene (BHT), collagenase (Type VIII), fatty acids free bovine serum albumin (BSA) and 4-(2-hydroxyethyl)-1-piperazineethane-sulfonic acid (HEPES), perchloric acid, diethylether, methyl acetate, isopropanol, isohexane, acetic acid, chloroform, methanol, sodium chloride (NaCl), potassium chloride (KCl), ethylenediaminetetraacetic acid (EDTA), were all obtained from Sigma Chemical Co. (Poole, UK). Nylon gauze (100 μm) and chamber slides were bought from BD Bioscience (Erembodegem, Belgium). Phosphate buffered saline solution (PBS) and trypan blue were supplied by Bio-Whittaker (MD, USA). High-performance thin layer chromatography (HPTLC, silica gel 60) plates were obtained from Merck (Darmstadt, Germany). Radiolabelled [1-^{14}C] fatty acids (50 μCi/mmol) was purchased from American Radiolabelled Chemicals Inc. (Laborel, Oslo, Norway). Scintillation fluid and a TRI-CARB 2000CA scintillation counter were bought from Ecoscint A, National Diagnostics (Atlanta, GA, USA) and United Technologies Packard (UK) respectively. Complete L-15 medium was composed of Leibovitz L-15 supplemented with 10% FBS, 2 mM GlutaMax, 100 U penicillin mL^{-1}, 100 μg streptomycin mL^{-1} and 0.25 μg amphotericin B mL^{-1}. Semi-complete L-15 medium was composed of complete L-15 medium without FBS.

Cyclodextrin, phloretin, diisothiocyanodisulfonic acid (DIDS) and sulfo-*N*-succinimidyl 4-maleimido-butyric acid ester (SSMB) were purchased from Fluka Chemicals (Sigma–Aldrich, Oslo, Norway). Sulfo-*N*-succinimidyl 4-maleimido-oleic acid ester (SSO) was synthetized according to a modified procedure [29] originally described by Staro [30]. Briefly, oleic acid (0.25 mmol), HOSu (SO_3)Na (0.25 mmol), and dicyclohexylcarbodiimide (DCC) (0.275 mmol) were dissolved in 0.5 mL of dry *N,N*-dimethylformamide (DMF) and stirred at room temperature overnight. The precipitated dicyclohexylurea was removed by filtration (Whatman No. 1). The filtrate was

kept at 3 °C for 4 h. Eight volumes of ethyl acetate were added and the precipitated product was collected by filtration (Ultipor Nylon 66, 45-μm pore size) under nitrogen and then stored in a vacuumed desiccator over phosphorus pentoxide. The chemicals and materials for synthesizing SSO were all purchased from Fluka Chemicals (Sigma–Aldrich, Oslo, Norway).

Methods

Preparation of Hepatocytes

Atlantic salmon (500 ± 143 g) were randomly selected and placed in a 50-L bucket with oxygenated seawater. After the fish were sedated with 0.1 g L^{-1} MS222 in water, hepatocytes were isolated by a two-step perfusion essentially as described by Dannevig and Berg [31]. Through the hepatic vein, the liver was first cleared of blood by perfusion with HEPES buffer (NaCl 8.4 g L^{-1}, KCl 0.5 g L^{-1}, EDTA 0.0074 mg L^{-1}) then digested with HEPES-buffer containing collagenase (0.1 mg mL^{-1}). The digested liver was then removed gently put into a sterile Petri-dish on ice, filled with PBS and the hepatocytes were dispersed by using two tweezers. The tissue suspension was subsequently filtered through 100 μm nylon gauze. The cells were collected by centrifugation at 50*g* for 5 min at 4 °C and washed twice more with PBS followed by the same centrifugation. Finally, the cells were resuspended in 20 mL complete L-15 medium. The cell viability was routinely measured by the trypan blue excluded method and >85% of unstained cells was the criterion for further use of the cells. Cells were plated onto 25-cm^2 cell culture flasks (TPP, Trasadingen Switzerland), pre-coated with 2 μg cm^{-2} laminin, at a density of 2 million cells mL^{-1} (5-mL cell suspension $flask^{-1}$) and cultured at 12 °C overnight. Duplicate flasks were cultured from each fish and three fish per treatment were used if not otherwise stated (total $n = 6$).

18:1n-9 Uptake Depending on Time and Concentration

All experiments performed to measure 18:1n-9 uptake were done 12 h after seeding the cells when the hepatocytes were attached. In the first experiment, 5 mL semi-complete L-15 medium was added 60 μM 18:1n-9 together with 1 μM [1-^{14}C] 18:1n-9, and this was incubated with the hepatocytes (0.2 μCi $flask^{-1}$) for 0, 0.5, 1, 2, 4, 6, 12, 24 h. 18:1n-9 bound to BSA with a molar ratio of 2.5:1 were prepared as previously described by Ghioni et al. [32]. In the second experiment, 5 mL of semi-complete L-15 medium was added 0, 37.5, 75, 150, 300, 600 μM 18:1n-9 and [1-^{14}C] 18:1n-9 with the unradiolabelled and radiolabelled 18:1n-9 M ratio of 30:1 were incubated with the cell for 2 h (0, 0.13, 0.24, 0.49, 0.98, 1.98 μCi $flask^{-1}$, respectively). The FA uptake was terminated by removing the medium. The medium was centrifuged at 500*g* for 5 min, 4°C and the supernatant was collected. The cell layer was collected by using a cell scrape and PBS. The cells pellets were washed twice with PBS and centrifuged at 500*g* for 5 min, 4°C before the cells were re-suspended in 0.5 mL 0.88% KCl solution. 50 μL of cell suspension and 500 μL of the medium were mixed with 8 mL scintillation fluid in scintillation vials to count the radioactivity in the scintillation counter. Lipids were extracted from the cell and medium samples as described below.

Inhibition of Fatty Acid Uptake

Hepatocytes were pre-incubated with inhibitors, 10 mM cyclodextrin, 250 μM phloretin, 250 μM DIDS, 200 μM SSO or 200 μM SSMB, in 0.05% DMSO-semi-complete L-15 medium respectively for 0.5 h. Then the medium was removed and the fatty acid uptake study was carried out by adding semi-complete L-15 medium containing 37.5 μM 18:1n-9 and 1.25 μM [1-^{14}C] 18:1n-9 (0.3 μCi $flask^{-1}$) for 2 h including various inhibitors mentioned above. For studying the inhibition of phloretin on the uptake of 18:1n-9, 18:2n-6), 18:3n-3, 20:5n-3 and 22:6n-3, 250 μM phloretin was added to the hepatocytes for 0.5 h. Then the medium was removed and the fatty acid uptake was carried out by adding semi-complete L-15 medium containing 37.5 μM of the different fatty acids and 1.25 μM [1-^{14}C] fatty acid (0.3 μCi $flask^{-1}$) for 2 h including 250 μM phloretin. In addition, hepatocytes (controls) with 0.05% DMSO and (cold and radiolabelled) fatty acids but without inhibitors were run concurrently with experimental treatments. Cell and incubation medium samples were harvested and radioactivity was measured as described above. For fatty acid uptake and metabolism data after 2 h of incubation this was corrected for with a time-zero sample with radiolabelled fatty acids added to correct for background radioactivity.

Incorporation of Fatty Acids into Lipid Classes

Recovery of [1-^{14}C] fatty acids in lipid classes was analyzed by thin-layer chromatography (HPTLC). Lipids were extracted from cells and the medium by adding four to five volumes of chloroform:methanol (2:1) described by Folch et al. [33] with 0.05% BHT in it. After mixing well and centrifugation at 450*g* for 5 min, the lower chloroform phase was transferred carefully and totally into another glass tube and dried under a stream of nitrogen. The lipid was re-suspended in 50 μL of chloroform and applied as a 1-cm line on HPTLC plates alongside 5 μL of a mixed

lipid standard (5 mg mL^{-1}). Lipid classes were separated by an isohexane:diethyl ether:acetic acid (80:25:1.5 v/v/v) solvent system and visualized by exposure to iodine vapor. The plate was marked and the iodine was removed under vacuum. The individual lipid class, total phospholipids (PLs), neutral lipids (NLs including monoacylglycerol, MAG; diacylglycerol, DAG; triacylglycerols, TAG; cholesterol and sterol ester) and free fatty acids (FFA) was scraped into scintillation vials and 8 mL of scintillation fluid was added respectively before radioactivity was measured by the scintillation counter.

Assay of Hepatocytes β-Oxidation Activity

The analysis of ^{14}C-acid soluble fatty acid oxidation products (ASPs) and $^{14}CO_2$ in the hepatocytes and medium samples were determined as described previously by Tocher et al. [34] and Stubhaug et al. [27]. A 100-μL quantity of the sample was transferred into a 2-mL centrifuge tube then 50 μL of BSA solution (6 g mL^{-1}) was added to bind the remaining fatty acids. After the mixture was mixed well, 500 μL of ice-cold perchloric acid (4 M) was added to precipitate the protein-bound un-oxidized FAs. After further mixing well, the mixture was centrifuged at 3,500*g* for 10 min. Then 250 μL of the supernatant was taken to mix with 8 mL scintillation fluid to determine the radioactivity using the scintillation counter.

Apoptosis Test: MTT Test and Hoechst Staining Test

The potential toxicity of the fatty acid uptake inhibitors was investigated either by staining the nucleus using the DNA specific dye Hoechst 33342 (Sigma–Aldrich, Oslo, Norway) or by the MTT based in vitro toxicology assay kit according to the manufacturers protocol (Sigma–Aldrich, Oslo, Norway). Hepatocytes isolated from Atlantic salmon was cultured overnight in 96-well plates (0.4 million cells cm^{-2}) (MTT) and chamber slides (Hoechst), followed by incubation with inhibitors for 2.5 h as described above. For the visualization of the nucleus, hepatocytes were fixed in 4% buffered paraformaldehyde (pH 7.4) for 15 min after 24 or 48 h exposure. Subsequently, the cells were incubated for 3 × 5 min with PBS/1 mM glycine, 1 min in PBS/0.1% Triton X-100 and washed for 3 × 5 min with PBS prior to staining with 1 μg mL^{-1} of the DNA specific dye Hoechst 22242 for 15 min. Apoptosis was scored by assessing the nuclear status of at least 200 cells in each exposure group using a Bx51 Olympus Fluorescence microscope (Olympus Europa GmbH, Hamburg, Germany). The resulting data from the MTT-test on the primary culture used in the experiments presented here are not shown since they revealed no differences; rather they were used to verify the findings from the nucleus staining.

Statistical Analysis

All data are presented as means ± SD. A nonlinear regression model was used to describe the effect of changes in 18:1n-9 concentration on 18:1n-9 uptake by the hepatocytes and to determine the K_m and V_{max} constants of fatty acid membrane transport (Excel, version 2007). Significant differences between treatments and controls were determined using one way ANOVA, followed by the Turkey post-hoc test. All statistical analyses were performed using the STATISTICA 6.1 software (StatSoft Inc., Tulsa, USA). Result were considered significant at $P < 0.05$.

Results

Fatty acids taken up by hepatocytes can either be esterified into cellular lipids, β-oxidized for energy production or further secreted as esterified lipids incorporated into lipoproteins, as very low density lipoprotein (VLDL). Theoretically, uptake should be calculated by the sum of total radioactivity recovered in the cells and radioactivity of esterified lipids and β-oxidation products recovered in the incubation medium. However, neither radioactive esterified lipids nor radioactive β-oxidation products was found accumulated in the incubation medium compared to 0 h control hepatocytes. Therefore 18:1n-9 uptake was first calculated by the radioactivity recovered in the cell (dpm) and then it was transferred into the value of nmol by the specific activity of radiolabelled 18:1n-9 (μCi $mmol^{-1}$). Finally the net total uptake of 18:1n-9 including radiolabelled and unlabelled 18:1n-9 was calculated by the molar ratio of radiolabelled and unlabelled 18:1n-9.

18:1n-9 Uptake-Time Course Study

Incubation of 61 μM 18:1n-9 with 1×10^7 hepatocytes at 12 °C revealed that the uptake was fast and linear over the first 6 h (Fig. 1a). It gradually reached a saturated state after 12 h with no difference in uptake between 12 and 24 h. During the 24 h incubation study the uptake rate was the highest around 2 h (2 nmol h^{-1} million $cells^{-1}$). Therefore this incubation time was chosen for the following experiments.

18:1n-9 Uptake-Concentration Study

Uptake of 18:1n-9 by hepatocytes increased linearly with increasing 18:1n-9 concentration up to 150 μM followed by a saturated state (Fig. 1b) according to the Michaelis–Menten equation (Fig. 2). K_m for this process as a function of the total 18:1n-9 concentration was calculated to be 46.4 ± 0.6 μM, while the V_{max} amounted to 2.25 ± 0.03 nmol h^{-1}

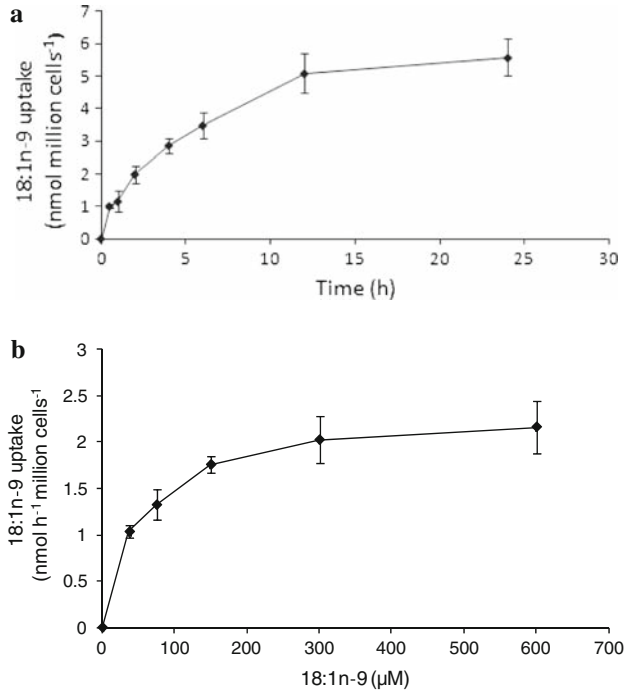

Fig. 1 **a** Uptake of 18:1n-9 from 0 to 24 h in Atlantic salmon hepatocytes during incubation of 61 μM 18:n-9 with the radiolabelled:nonlabelled 18:1n-9 M ratio of 1:60, bound to BSA (18:1n-9: BSA; 2.5:1). Data are presented as means ± SD ($n = 3$). **b** Atlantic salmon hepatocyte 18:1n-9 uptake with increasing 18:1n-9 concentration. Hepatocytes were incubated with 18:1n-9, where the radiolabelled:unradiolabelled 18:1n-9 M ratio was 1:30. The uptake was measured 2 h after addition of the 18:1n-9 substrate. Data are presented as means ± SD ($n = 6$)

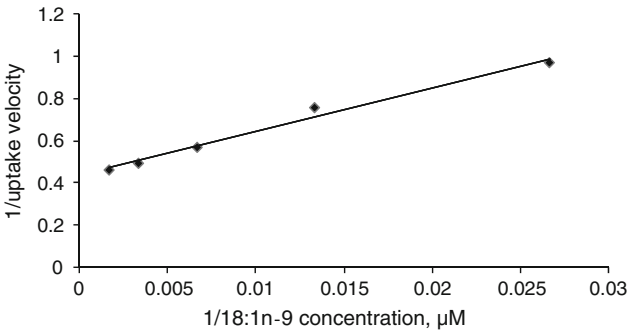

Fig. 2 Lineweaver–Burk plot of rate of 18:1n-9 uptake versus 18:1n-9 concentration. The kinetic parameter was generated from a weighted least-squares fit of the individual data points from each experiment to a rectangular hyperbola (K_m 46.37 ± 0.58 μM; V_{max} 2.25 ± 0.03 nmol h^{-1}million cells^{-1}, $n = 6$). The regression equation and correlation coefficient was $y = 20.61x + 0.437$; $R^2 = 0.985$, $P < 0.05$

million cells^{-1}. Of the concentrations tested, 37.5 μM 18:1n-9 was closest to the K_m value and this concentration was chosen for the following experiments.

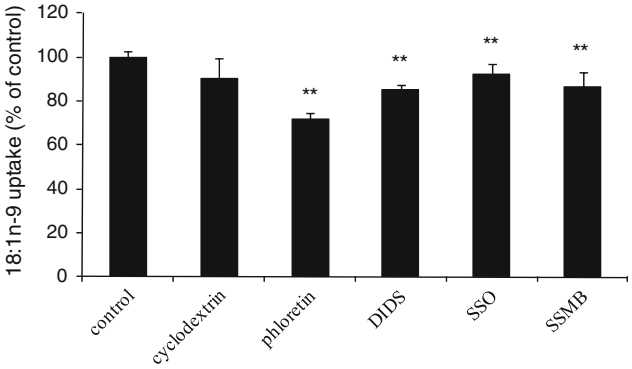

Fig. 3 Inhibition of 18:1n-9 uptake by inhibitors in Atlantic salmon hepatocytes. Data are presented as means ± SD ($n = 6$) and are expressed relative to untreated control (100%). *Asterisks* denote very significant difference compared to control ($P < 0.01$). *DIDS* diisothiocyanodisulfonic acid, *SSO* sulfo-*N*-succinimidyl 4-maleimido-oleic acid ester, *SSMB* sulfo-*N*-succinimidyl 4-maleimido-butyric acid ester

Effects of Different Membrane Protein Inhibitors on 18:1n-9 Uptake

To further clarify whether 18:1n-9 uptake into hepatocytes of Atlantic salmon was mediated by membrane proteins, the effects on fatty acid uptake of membrane protein inhibitors were studied (Fig. 3). Treatment of hepatocytes with phloretin resulted in the highest inhibition of 18:1n-9 uptake by 28.2 ± 2.6% of control. DIDS and SSMB revealed lower inhibition by 14.5 ± 1.7 and 13.4 ± 6.6%, respectively. The lowest inhibition was found in the presence of SSO, inhibiting the uptake by 7.8 ± 4.7%.

Uptake of Vegetable- and Fish Oil Fatty Acids into Hepatocytes

The uptake of FAs was measured respectively as total radioactivity recovered in hepatocytes and further expressed as % of the initially added FAs. Uptake of different FAs ranged between 9.5 and 15% (Fig. 4) with 20:5n-3 being most efficiently taken up (15%), followed by 22:6n-3 (13%), 18:1n-9, 18:2n-6 and 18:3n-3. The most potent membrane protein inhibitor, phloretin, revealed in the first 18:1n-9 study (Fig. 3) inhibited the fatty acid uptake in the following order; 20:5n-3 > 18:3n-3 = 22:6n-3 > 18:2n-6 > 18:1n-9 with the 20:5n-3 uptake being lowered by 67%. This was in contrast to 18:1n-9 revealing the lowest inhibition of phloretin compared to all the other fatty acids tested (Fig. 5).

Incorporation of Fatty Acids into Hepatocyte Lipids

The cellular lipid distribution of fatty acids was calculated by the radioactivity recovered in cellular PLs, NLs and free FAs (% of cellular lipid; Fig. 6). Fatty acids were mainly

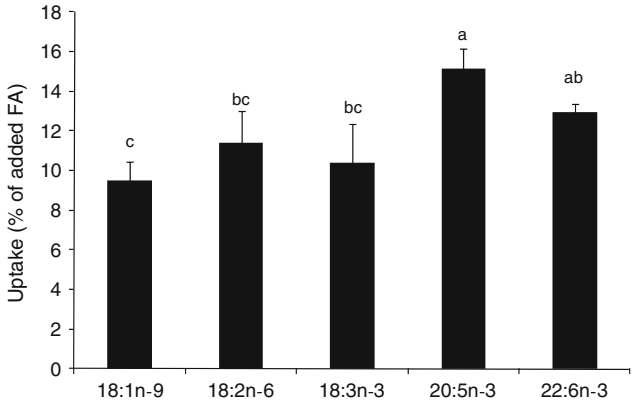

Fig. 4 Trans-membrane uptake of 18:1n-9, 18:2n-6, 18:3n-3, 20:5n-3 and 22:6n-3 by hepatocytes of Atlantic salmon given as % fatty acid taken up of the total fatty acid added. Cells were incubated for 2 h with 37.5 μM radiolabelled and unlabelled fatty acids respectively with molar ratio of 1:30. Data are presented as means ± SD, $n = 10$ for 18:1n-9, $n = 6$ for 18:3n-3 and 18:2n-6, and $n = 4$ for 20:5n-3 and 22:6n-3. Statistical differences analyzed by one-way ANOVA are denoted by *different letters*

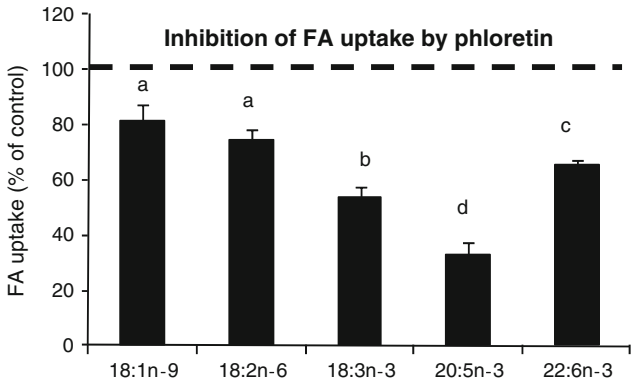

Fig. 5 Inhibition of trans-membrane fatty acid uptake by phloretin in Atlantic salmon hepatocytes given as % of control (no inhibitor added). Data are presented as means ± SD, $n = 6$. Statistical differences between the control and inhibitors are denoted by an *asterisk*

recovered as FFAs (50–70% of cellular lipid), whereas ~30% was recovered esterified into cellular PL and ~6% esterified into NLs. The 22:6n-3 was mainly incorporated into cellular PLs (38% of cellular lipid), followed by 20:5n-3 (27%), and 18:1n-9, 18:2n-6, 18:3n-3 with approximately 20% being recovered in PLs. The incorporation into NLs was not significantly different between the fatty acids, ranging from 5 to 7% of the cellular lipids. The recovery of 18:1n-9, 18:2n-6, 18:3n-3 and 20:5n-3 into cellular FFA was not significantly different, varying from 61 to 68% of the cellular lipids, which was significantly higher than the recovery of 22:6n-3 in cellular FFA, being 50% of the cellular lipids.

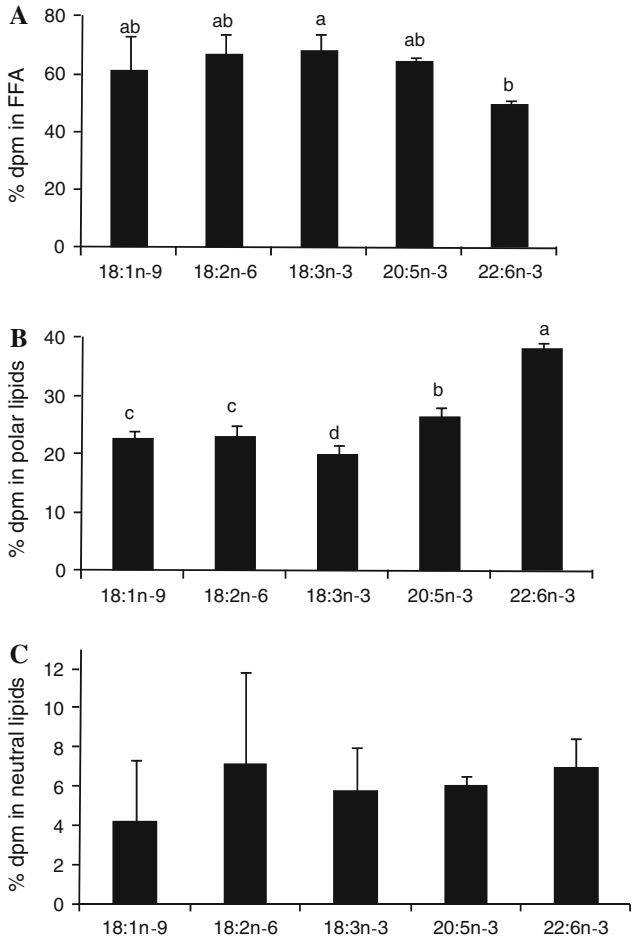

Fig. 6 Recovery of [1-^{14}C] 18:1n-9, 18:2n-6, 18:3n-3, 20:5n-3 and 22:6n-3 in cellular lipid classes given as % dmp in FFA (**a**), polar (**b**) or neutral (**c**) lipids of the total cellular lipids dpm. Neutral lipids includes monoacylglyceride, diacylglyceride, triacylglyceride and sterol ester. Data are presented as means ± SD, $n = 12$ for 18:1n-9 and $n = 6$ for 18:2n-6 and 18:3n-3; $n = 4$ for 20:5n-3 and 22:6n-3. Statistical differences between fatty acids are denoted by *different letters*

Fatty Acid Catabolism

The β-oxidation of fatty acids by the hepatocytes is presented relative to the total radiolabelled fatty acids taken up. The β-oxidation of 18:3n-3 was significantly higher (7%) compared to all the other fatty acids analysed. The β-oxidation of 18:1n-9 was the lowest (<1% of total 18:1n-9 taken up) followed by 18:2n-6 < 20:5n-3 < 22:6n-3 being increasingly more β-oxidation (Fig. 7).

Cell Viability

In order to evaluate if the addition of inhibitors affected the hepatocytes viability or stress resulting in apoptosis of the cells, a chemical (MTT) and morphological (Hoechst staining) test were applied. The cell viability ranged from

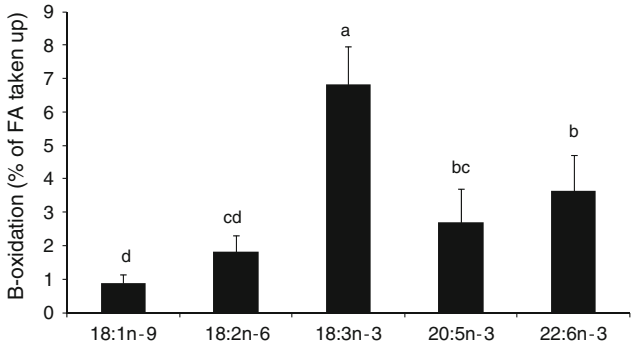

Fig. 7 β-Oxidation of fatty acids given as % dpm recovered in acid soluble products relative to the total fatty acids (dpm) taken up into the cells. Data are presented as means ± SD, $n = 12$ for 18:1-9, $n = 6$ for the other fatty acids. Statistical differences between different fatty acids are denoted by *different letters*

90 to 113% in the presence of inhibitors and no significant difference was found compared with the control by MTT-test (data not shown) and this was further documented by the Hoechst staining test (data not shown), pointing to the fact that neither the cell integrity nor the physiologic state was affected by treating hepatocytes with inhibitors for 2.5 h.

Discussion

Atlantic salmon hepatocytes is an established in vitro system and has been used in a range of lipid metabolic studies [27, 34–38]. The present report is the first to study the fatty acid uptake mechanisms across hepatocyte membranes of Atlantic salmon over a time span relevant to metabolic studies. A previous study by Richards et al. [25] measured fatty acid uptake within seconds, whereas in the present study, the uptake of fatty acids was measured for several hours. The 18:1n-9 uptake occurred through a saturable, transport mechanism, which is in line with Richards and co-workers [25], with uptake being the highest during the first 2 h of incubation. It has been suggested that intracellular metabolism is the driving force and regulator of fatty acid uptake over the cell membranes [39]. Hence, the current results of fatty acid uptake represent not only an isolated uptake across the membrane (s), but the fatty acid uptake over the membrane within a time span which may be more relevant for metabolic studies (h). In line with the present results, previous studies using hepatocytes as well as adipocytes and cardiac myocytes isolated from rat, have shown that 18:1n-9 uptake followed saturation kinetics indicating protein mediated uptake when measured over a longer time span [40]. Saturation kinetics has also been reported to be valid for uptake of the saturated fatty acid palmitate (16:0) into skeletal muscle [41], and for 18:1n-9 uptake into mammalian adipocytes [16, 42], cardiac myocytes [43], and hepatocytes [44]. The ratio of fatty acid:albumin was maintained at 2.5:1 being similar to what was used in previous metabolic and fatty acid uptake studies in Atlantic salmon hepatocytes [38, 45] and rainbow trout muscle membrane [25] where the ratio varied was reported to vary from 8–11:1, 2.5:1 to 0.2–5:1.

Previously, the molar ratio between fatty acid and albumin in the medium has been found to affect the uptake kinetics of fatty acids in rat hepatocytes [40]. Lower FA:albumin ratio than 2.0:1 has been found to decrease the uptake of FA [40], and with a high uptake rate of FA this situation may theoretically occur since the concentration of albumin in the medium would increase relative to the fatty acid concentration as the fatty acids were taken up by the hepatocytes. However, in the current experiments the total fatty acids uptake found never exceeded 15% of the amount of fatty acids added and consequently the molar ratio of FA:BSA was never lower than 2.2:1. The molar ratio of FA:albumin initially being 2.5:1 was safely above the highest ratio used by Sorrentino et al. [40] who tested FA:BSA ratios from 0.1:1 to 2:1. Hence, based on previous 18:1n-9:BSA ratio data, the observed saturation kinetics was unlikely to be due to a sub-optimal 18:1n-9:albumin ratio.

Increasing the concentration of 18:1n-9 adds complexity to the interpretation for the 18:1n-9 uptake and saturation due to the fact that net accumulation of fatty acids within the cells can be a result of changes in fatty acid metabolism and cellular influx. Metabolic demand for fatty acids has been suggested to be the driving force for fatty acid uptake through conversion of fatty acids to acyl-CoA by the action of acyl-CoA synthetases and the regulation of the membrane-bound transport proteins [39]. This has also been exemplified by the finding that with stable over-expression of the initial and rate limiting enzyme in glycerolipid synthesis, glycerol-3-phosphate acyl transferase in CHO cells, the fatty acid uptake increased [46]. Hence, if the intracellular fatty acid metabolism was lower than any other fatty acid transport pathways, especially the transmembrane process, the saturation of fatty acid uptake could also be apparent and firm conclusions on a passive diffusion or a protein mediated uptake mechanism could not be made [47–49]. In the present study of 18:1n-9, low levels of β-oxidation products (>1%) were found when corrected for background activity, using a time-zero sample and approximately 20% of 18:1n-9 taken up was incorporated into PL. This indicates that intracellular metabolism of 18:1n-9 was low compared to especially 18:3n-3, selectively being β-oxidized and 22:6n-3 being esterified into PL approximately twofold higher than 18:1n-9. Therefore the present 18:1n-9 uptake with a saturation curve could also be explained as passive diffusion in combination with

a rate limitation in the subsequent intracellular fatty acid metabolism. Overall, the relative levels of secreted fatty acids (esterified lipids in medium) and ß-oxidation products was lower compared to previously published papers on Atlantic salmon hepatocyte metabolism [27, 34, 38]. This is, however, the first time the results are being corrected for background activity using a time-zero sample in the experimental design. This resulted in lower actual activity data compared to without a zero-sample correction. Furthermore, results expressed as relative amount of radioactivity of the total added or taken up is highly dependent on the total concentration of fatty acids added to the cells. When lower concentrations are used, the relative amount is higher whereas the absolute amount of fatty acids taken up was actually lower in the results of Stubhaug et al. [27] study compared to ours as outlined below. Another important factor influencing metabolic rate is temperature. The lower incubation temperature (12 °C) used in the current study will slow down the overall metabolism compared to incubation at 20 °C used in previous studies [27, 34, 37]. The incubation time used in the current study was identical (2 h) to most previously published studies [27, 34]. Decreased incubation time will naturally result in less total metabolism. Furthermore, the cell viability measurements (by MTT and Hoechst) showing overall no indications of decreased viability further supports the fact that the lower relative metabolism was due to the inclusion of time zero-sample correction and higher fatty acid concentrations, rather than decreased viability and cell integrity.

The efficiency of uptake and the metabolic fate of 18:1n-9, 18:2n-6, 18:3n-3, 20:5n-3 and 22:6n-3 was demonstrated to be significantly different in Atlantic salmon hepatocytes supporting previous studies performed with hepatocyte suspensions [27]. Especially 18:1n-9 and 20:5n-3 seemed to represent the opposites with regards to uptake and degree of inhibition. 18:1n-9 was the least efficiently taken up with the uptake inhibited by phloretin the least, whereas 20:5n-3 was the most efficiently taken up and inhibition by phloretin was the highest of the fatty acids studied. Previously, 20:5n-3 was reported to be the most efficiently taken up fatty acid in hepatocytes from FO fed Atlantic salmon [27] with as much as 90% of added fatty acids being taken up. In the current study 9–15% of the fatty acids added were taken up. However, Stubhaug et al. [27] added 2 μM fatty acids in contrast to 37.5 μM in the current study. When calculating the total amount of fatty acids taken up, actually 3.75 μM fatty acids in the current study was taken up by the cells compared to 1.8 μM reported by Stubhaug et al. [27].

Intracellular metabolism has been suggested to be the driving force and regulator of fatty acid uptake over the cell membranes [39, 50]. However, our results indicate that metabolism alone is not the determining factor. The metabolism of 18:3n-3 and 20:5n-3 was comparable when combining the relative amount being β-oxidized and incorporated into polar lipids. However, 20:5n-3 was significantly more efficiently taken up compared to 18:3n-3. Furthermore, a major proportion of all fatty acids tested were recovered in cellular FFA (50–70% of lipids), suggesting that the amount of fatty acids taken up was sufficient for subsequent intracellular metabolism, esterification or β-oxidation, and that trans-membrane uptake was the primary regulating step of fatty acids uptake in the current study. Furthermore, the metabolic fate of 22:6n-3 differed slightly from the other fatty acids, with more 22:6n-3 being recovered in the polar lipids (mainly phospholipids) and less in FFA and β-oxidation products. Supporting previously published data [27] this confirms that 22:6n-3 has an important role in structural lipids as part of the cell membranes.

It is generally considered that the membrane proteins, FABPpm, FAT/CD36 and FATP, are responsible of the uptake of long and very long chain fatty acids [Reviewed by Frohnert and Bernlohr; 51]. The FA uptake inhibitors used in the current study either inhibits one specifically (e.g. SSO) or all of these membrane bound proteins (phloretin). The 18:1n-9 uptake was differently inhibited by the five inhibitors used with the maximal degree of inhibition by phloretin being 28%, which was lower than earlier studies using rat cardiac myocytes [49, 50, 52], rat adipocytes [24, 29] (varying from 60 to 90%) and trout muscle sarcolemma (about 40%) [25], indicating that salmon hepatocytes are less dependent on protein mediated 18:1n-9 uptake compared to mammalian and trout cells. In line with these previous results, the present study was not able to inhibit fatty acid uptake completely. Considering that phloretin was reported to be a potent non-specific inhibitor of membrane transport proteins [53, 54] and phloretin-containing buffer has also been used as a "stop solution" to suppress the efflux or influx of FAs rapidly and completely [42], the maximal degree of inhibition by phloretin, about 30%, was postulated as the contribution of these FA uptake associated membrane proteins, FABPpm, FAT/CD36 and FATPs. The present remaining 18:1n-9 uptake not being inhibited accounted for about 70% and it can be assumed to be attributed to passive diffusion. In contrast to 18:1n-9, the uptake of 20:5n-3 was inhibited by 70% followed by 18:3n-3 and 22:6n-3 at approximately 50% inhibition. This suggests that FA uptake by Atlantic salmon hepatocytes is accomplished by both passive and carrier-mediated trans-membrane transport, and that the omega-3 fatty acids are more dependent on membrane bound protein mediated uptake than 18:1n-9 and 18:2n-6. When Atlantic salmon are fed diets increasingly replacing fish oil with vegetable oils their dietary fatty acid

composition will be dominated by 18:1n-9 and 18:2n-6 fatty acids [55]. These differences in the mechanisms for fatty acid uptake may have implications when dietary fatty acid compositions are changed in such a manner.

Compared to previous published reports on rainbow trout muscle sarcolemma, the magnitude of inhibition by phloretin of 18:1n-9 uptake was approximately 10% lower compared to the present study. On the other hand, the pattern was similar with phloretin being the most potent inhibitor and SSO being the least [25] indicating the uptake mechanisms being similar between trout muscle sarcolemma and Atlantic salmon hepatocytes. SSO was reported to have the specificity towards FAT/CD36 by specifically inhibiting FAT/CD36 without indicating an effect on FATP or FABPpm [20], hence inhibition of 7.8% 18:1n-9 uptake by SSO can be attributed to the function of FAT/CD36. FABPpm has also been reported to function in conjunction with FAT/CD36 [reviewed by Bonen et al. 56] therefore the two proteins might collaborate to increase the rates of fatty acid transport across membrane [57] and accounted for 8% in the present 18:1n-9 uptake. Considering that 18:1n-9 uptake mediated by total membrane proteins was 28%, 18:1n-9 uptake mediated by another assumed membrane transport protein, FATP, would account for 20%. Cyclodextrin did not significantly lower the 18:1n-9 uptake compared to the control. However, cyclodextrin has previously been reported to disrupt the lipid raft by lowering the cholesterol levels in the lipid raft [reviewed by Ikonen et al. 58], and the 10% of the 18:1n-9 uptake inhibition by cyclodextrin suggested that lipid raft was also included in Atlantic salmon hepatocytes fatty acid uptake and its attribution to fatty acid uptake would be 10%. SSMB is an analogue of SSO, and is an agent with protein modifying properties. SSMB showed higher inhibition on 18:1n-9 uptake compared to SSO suggesting that SSMB can function as a more potent inhibitor than SSO of fatty acid uptake associated membrane proteins.

When the fatty acids are taken up by cells, they may be bound to intracellular fatty acid-binding proteins (FABPs) and transported from the cell surface to the various sites of metabolism or storage [Stoch and Thumser 59]. The main proportion of fatty acids taken up was recovered in FFA probably bound to intracellular FABPs, whereas less than 10% was recovered in TAG. This was in contrast to Stubhaug et al. [27] who reported that the main proportion of fatty acids was recovered in TAG and less than 5% was recovered as FFA. This may likely be due to differences in incubation temperature with decreased temperature (12 °C) in the current study resulting in slower metabolism and incorporation of fatty acids into TAG compared to hepatocytes cultured at 20 °C in the study of Stubhaug et al. [27].

In conclusion, the uptake of fatty acids by Atlantic salmon hepatocytes was shown to be time- and concentration dependent, and to be partly inhibited by membrane protein inhibitors. 20:5n-3, 18:3n-3 and 22:6n-3 seems to be more dependent on membrane bound proteins compared to 18:1n-9 and 18:2n-6, and intracellular metabolism did not seem to be a main regulating factor or driving force for fatty acid uptake in cultured Atlantic salmon primary hepatocytes.

Acknowledgments Thanks are due to Mrs. Betty Irgens and Ms Thu Thao Nguyen for technical assistance. The study was financed by the Norwegian Research Council (158930/I10) and the China Scholarship Council. J. Zhou was the recipient of grant from the China Scholarship Council and the National Institute of Nutrition and Seafood Research (NIFES).

References

1. Jump DB (2004) Fatty acid regulation of gene transcription. Crit Rev Clin Lab Sci 41:41–78
2. Van der Vusse GJ, Glatz JFC, Stam HCG, Reneman RS (1992) Fatty acid nomeostasis in the normoxic and ischemic heart. Physiol Rev 72:881–940
3. Degrella RD, Light RJ (1980) Uptake and metabolism of fatty acids by dispersed adult rat heart myocytes. J Biol Chem 255:9739–9745
4. Hamilton JA (1998) Fatty acid transport: difficult or easy? J Lipid Res 39:467–481
5. Hamilton JA, Kamp F (1999) How are free fatty acids transported in membranes? Diabetes 48:2255–2269
6. Hamilton JA, Johnson RA, Corkey B, Kamp F (2001) Fatty acid transport: the diffusion mechanism in model and biological membranes. J Mol Neurosci 16:99–108
7. Hamilton JA, Guo W, Kamp F (2002) Mechanisms of cellular uptake of long-chain fatty acids: do we need cellular proteins? Mol Cell Biochem 239:17–23
8. Pownall HJ, Hamilton JA (2003) Energy translocation across cell membranes and membrane models. Acta Physiol Scand 178:357–365
9. Kamp F, Guo W, Souto R, Pilch PF, Corkey BE, Hamilton JA (2003) Rapid flip–flop of oleic acid across the plasma membrane of adipocytes. J Biol Chem 278:7988–7995
10. Hamilton JA, Brunaldi K (2007) A model for fatty acid transport into the brain. J Mol Neurosci 33:12–17
11. Kampf JP, Kleinfeld AM (2004) Fatty acid transport in adipocytes monitored by imaging intracellular free fatty acid levels. J Biol Chem 279:35775–35780
12. Stremmel W, Strohmeyer G, Berk PD (1986) Hepatocellular uptake of oleate is energy dependent, sodium linked, and inhibited by an antibody to hepatocyte plasma membrane fatty acid binding protein. Proc Natl Acad Sci USA 83:3584–3588
13. Gimeno RE, Ortegon AM, Patel S, Punreddy S, Ge P, Sun Y, Lodish HF, Stahl A (2003) Characterization of a heart-specific fatty acid transport protein. J Biol Chem 278:16039–16044
14. Hirsch D, Stahl A, Lodish HF (1998) A family of fatty acid transporters conserved from Mycobacterium to man. Proc Natl Acad Sci USA 95:8625–8629
15. Schaffer JE, Lodish HF (1994) Expression cloning and characterization of a novel adipocyte long chain fatty acid transport protein. Cell 79:427–436
16. Schwieterman W, Sorrentino D, Potter BJ, Rand J, Kiang CL, Stump D, Berk PD (1988) Uptake of oleate by isolated rat

adipocytes is mediated by a 40-kDa plasma membrane fatty acid binding protein closely related to that in liver and gut. Proc Natl Acad Sci USA 85:359–363
17. Stremmel W, Strohmeyer G, Borchard F, Kochwa S, Berk PD (1985) Isolation and partial characterization of a fatty acid binding protein in rat liver plasma membranes. Proc Natl Acad Sci USA 82:4–8
18. Abumrad NA, El-Maghrabi MR, Amri EZ, Lopez E, Grimaldi P (1993) Cloning of a rat adipocyte membrane protein implicated in binding or transport of long chain fatty acids that is induced during preadipocyte differentiation. Homology with human CD36. J Biol Chem 268:17665–17668
19. Jennings ML, Solomon AK (1976) Interaction between phloretin and the red blood cell membrane. J Gen Physiol 67:381–397
20. Coort SLM, Willems J, Coumans WA, van der Vusse GJ, Bonen A, Glatz JFC, Luiken JJFP (2002) Sulfo-*N*-succinimidyl esters of long chain fatty acids specifically inhibit fatty acid translocase (FAT/CD36)-mediated cellular fatty acid uptake. Mol Cell Biochem 239:213–219
21. Bonen A, Luiden JJFP, Liu S, Dyck DJ, Kiens B, Kristiansen S, Turcotte LP, Van der Vusse GJ, Glatz JFC (1998) Palmitate transport and fatty acid transporters in red and white muscles. Am J Physiol 275:E471–E478
22. Luiken JJFP, Turcotte LP, Bonen A (1999) Protein-mediated palmitate uptake and expression of fatty acid transport proteins in heart giant vesicles. J Lipid Res 40:1007–1016
23. Pohl J, Ring A, Korkmaz U, Ehehalt R, Stremmel W (2005) FAT/CD36-mediated long-chain fatty acid uptake in adipocytes requires plasma membrane rafts. Mol Biol Cell 16:24–31
24. Abumrad NA, Park JH, Park CR (1984) Permeation of long-chain fatty acid into adipocytes. J Biol Chem 259:8945–8953
25. Richards JG, Bonen A, Heigenhauser GJF, Wood CM (2004) Palmitate movement across red and white muscle membranes of rainbow trout. Am J Physiol Regul Integr Comp Physiol 286:R46–R53
26. Ehehalt R, Sparla R, Kulaksiz H, Herrmann T, Fullekrug J, Stremmel W (2008) Uptake of long chain fatty acids is regulated by dynamic interaction of FAT/CD36 with cholesterol/sphingolipid enriched microdomains (lipid raft). BMC Cell Biol 9:45. doi:10.1186/1471-2121-9-45
27. Stubhaug I, Tocher DR, Bell JG, Dick JR, Torstensen BE (2005) Fatty acid metabolism in Atlantic salmon (*Salmo salar* L.) hepatocytes and influence of dietary vegetable oil. Biochim Biophys Acta 1734:277–288
28. Torstensen BE, Nanton DA, Olsvik PA, Sundvold H, Stubhaug I (2009) Gene expression of fatty acid-binding proteins, fatty acid transport proteins (cd36 and FATP) and β-oxidation-related genes in (*Salmo salar* L.) fed fish oil or vegetable oil. Aquac Nutr 15:440–451
29. Harmon CM, Luce P, Beth AH, Abumrad NA (1991) Labeling of adipocyte membranes by sulfo-*N*-succinimidyl derivatives of long-chain fatty acids: inhibition of fatty acid transport. J Membr Biol 121:261–268
30. Staros JV (1982) *N*-Hydroxysulfosuccinimide active esters: bis (*N*-hydroxysulfosuccinimide) esters of two dicarboxylic acids are hydrophilic, membrane-impermeant, protein cross-linkers. J Biochem 21:3950–3955
31. Dannevig BH, Berg T (1985) Endocytosis of galactose-terminated glycoproteins by isolated liver cells of the rainbow trout (*Salmo gairdneri*). Comp Biochem Physiol B 82:683–688
32. Ghioni C, Taher DR, Sargent JR (1997) The effect of culture on morphology, lipid and fatty acid composition, and polyunsaturated fatty acid metabolism of rainbow trout (*Oncorhynchus mykiss*) skin cells. Fish Physiol Biochem 16:499–513
33. Folch J, Lees M, Sloane-Stanley GH (1957) A simple method for the isolation and purification of total lipids from animal tissues. J Biol Chem 226:497–509
34. Tocher DR, Fonseca-Madrigal J, Bell JG, Dick JR, Henderson RJ, Sargent JR (2002) Effects of diets containing linseed oil on fatty acid desaturation and oxidation in hepatocytes and intestinal enterocytes in Atlantic salmon (*Salmo salar*). Fish Physiol Biochem 26:157–170
35. Ruyter B, Roesjoe C, Maesoeval K, Einen O, Thomassen MS (2000) Influence of dietary n-3 fatty acids on the desaturation and elongation of [1-super(14)C] 18:2 n-6 and [1-super(14)C] 18:3 n-3 in Atlantic salmon hepatocytes. Fish Physiol Biochem 23:151–158
36. Tocher DR, Bell JG, Dick JR, Crampton VO (2003) Effects of dietary vegetable oil on Atlantic salmon hepatocyte fatty acid desaturation and liver fatty acid compositions. Lipids 38:723–732
37. Torstensen BE, Stubhaug I (2004) Beta-oxidation of 18:3n-3 in Atlantic salmon (*Salmo salar* L.) hepatocytes treated with different fatty acids. Lipids 39:1–8
38. Vegusdal A, Gjøen T, Berge RK, Thomassen MS, Ruyter B (2005) Effect of 18:1n–9, 20:5n–3 and 22:6n–3 on lipid accumulation and secretion by Atlantic salmon hepatocytes. Lipids 40:477–486
39. Mashek DG, Coleman RA (2006) Cellular fatty acid uptake: the contribution of metabolism. Curr Opin Lipidol 17:274–278
40. Sorrentino D, Robinson RB, Kiang CL, Berk PD (1989) At physiological albumin/oleate concentrations oleate uptake by isolated hepatocytes, cardiac myocytes and adipocytes is a saturable function of the unbound oleate concentration. Uptake kinetics are consistent with the conventional theory. J Clin Invest 84:1325–1333
41. Turcotte LP, Kiens B, Richter EA (1991) Saturation kinetics of palmitate uptake in perfused skeletal muscle. FEBS Lett 279:327–329
42. Abumrad NA, Perkins RC, Park JH, Park CR (1981) Mechanism of long chain fatty acid permeation in the isolated adipocyte. J Biol Chem 256:9183–9191
43. Sorrentino D, Stump D, Potter BJ, Robinson RB, White R, Kiang CL, Berk PD (1988) Oleate uptake by cardiac myocytes is carrier mediated and involves a 40-Kd plasma membrane fatty acid binding protein similar to that in liver, adipose tissue, and gut. J Clin Invest 82:928–935
44. Stremmel W, Berk PD (1986) Hepatocellular influx of [^{14}C] oleat reflects membrane transport rather than intracellular metabolism or binding. Proc Natl Acad Sci USA 83:3086–3090
45. Tocher DR, Carr J, Sargent JR (1989) Polyunsaturated fatty acid metabolism in fish cells: differential metabolism of (n-3) and (n-6) series acids by cultured cells originating from a freshwater teleost fish and from a marine teleost fish. Comp Biochem Physiol 94B:367–374
46. Igal RA, Wang S, Gonzalez-Baro M, Coleman RA (2001) Mitochondrial glycerol phosphate acyltransferase directs incorporation of exogenous fatty acids into triacylglycerol. J Biol Chem 276:42205–42212
47. Rose H, Hennecke T, Kammermeier H (1990) Sarcolemmal fatty acid transfer in isolated cardiomyocytes governed by albumin/membrane-lipid partition. J Mol Cell Cardiol 22:883–892
48. Zakim D (1996) Fatty acids enter cells by simple diffusion. Proc Soc Exp Biol Med 212:5–14
49. DeGrella RF, Light RJ (1980) Uptake and metabolism of fatty acids by dispersed adult rat heart myocytes. I. Kinetics of homologous fatty acids. J Biol Chem 255:9731–9738
50. Luiken JJFP, van Nieuwenhoven FA, America G, van der Vusse GJ, Glatz JFC (1997) Uptake and metabolism of palmitate by isolated cardiac myocytes from adult rats: involvement of sarcolemmal proteins. J Lipid Res 38:745–758
51. Frohnert BI, Bernlohr DA (2000) Regulation of fatty acid transporters in mammalian cells. Prog Lipid Res 39:83–107

52. Stremmel W (1988) Fatty acid uptake by isolated rat heart myocytes represents a carrier mediated transport process. J Clin Invest 81:844–852
53. Lefevre PG (1975) The present state of the carrier hypothesis. Curr Top Membr Transp 7:109–215
54. Andersen BL, Tarpley HL, Regen DM (1978) Characterization of β-hydroxybutyrate transport in rat erythrocytes and thymocytes. Biochim Biophys Acta 508:525–538
55. Torstensen BE, Bell JG, Rosenlund G, Henderson RJ, Graff JE, Tocher DR, Lie O, Sargent JR (2005) Tailoring of Atlantic salmon (*Salmo salar* L.) flesh lipid composition and sensory quality by replacing fish oil with a vegetable oil blend. J Agric Food Chem 53:10166–10178
56. Bonen A, Chabowski A, Luiken JJFP, Glatz JFC (2007) Mechanisms and regulation of protein-mediated cellular fatty acid uptake: molecular, biochemical, and physiological evidence. Physiol 22:15–28
57. Chabowski A, Gorski J, Luiken JJP, Glatz JFC, Bonen A (2007) Evidence for concerted action of FAT/CD36 and FABPpm to increase fatty acid transport across the plasma membrane. Prostagland Leukot Essent Fatty acids 77:345–353
58. Ikonen E (2001) Roles of lipid rafts in membrane transport. Cell Biol 13:470–477
59. Storch J, Thumser AEA (2000) The fatty acid transport function of fatty acid-binding proteins. Biochim Biophys Acta 1486:28–44

Lipids (2010) 45:313–320
DOI 10.1007/s11745-010-3403-6

ORIGINAL ARTICLE

The Influence of n-3 PUFA Supplements and n-3 PUFA Enriched Foods on the n-3 LC PUFA Intake of Flemish Women

Isabelle Sioen · Jolien Devroe · David Inghels · Ruth Terwecoren · Stefaan De Henauw

Received: 9 November 2009 / Accepted: 1 March 2010 / Published online: 18 March 2010

Abstract Food consumption data of Flemish women of reproductive age collected in 2002 showed a large deficit for ALA and n-3 LC PUFA compared to the recommendations (mean ALA and EPA + DHA intake 1.4 g/day and 209 mg/day, respectively) and indicated a need to tackle the problem of low n-3 PUFA intake. Another recent Belgian study demonstrated that enrichment of commonly eaten food items with n-3 PUFA provides the opportunity to increase the n-3 PUFA intake up to 6.5 g/day and decrease the n-6/n-3 ratio. Since a large supply of n-3 PUFA supplements and n-3 PUFA enriched foods exists on the Belgian market, this study aimed at assessing the influence of these products on the n-3 LC PUFA intake for Flemish women of reproductive age. It was found that n-3 supplements are consumed by 5% of the Flemish women. Of all the n-3 PUFA enriched foods on the Flemish market, margarines and cooking fat are most frequently consumed by young women. The results indicated that a big gap remains between the EPA&DHA intake (mean = 276 mg/day) and the recommendation. Seafood remains the most important source of EPA&DHA. Only 11.6% of the population sample reached an intake level of 500 mg EPA&DHA per day. The study showed that other strategies will be needed to increase the EPA&DHA intake in the long term.

I. Sioen (✉) · S. De Henauw
Department of Public Health, Faculty of Medicine and Health Sciences, Ghent University, UZ-2 Blok A, De Pintelaan 185, 9000 Ghent, Belgium
e-mail: Isabelle.Sioen@UGent.be

J. Devroe · D. Inghels · R. Terwecoren · S. De Henauw
Department of Nutrition and Dietetics, Faculty of Health Care, University College Ghent, Keramiekstraat 80, 9000 Ghent, Belgium

Keywords EPA&DHA · Omega-3 supplements · Omega-3 enrichment · Dietary intake · Women · Belgium · PUFA

Abbreviations

ALA	Alpha-linolenic acid
BMI	Body mass index
CVD	Cardiovascular diseases
DHA	Docosahexaenoic acid
EPA	Eicosapentaenoic acid
FFQ	Food frequency questionnaire
ISSFAL	International society for the study of fatty acids and lipids
LA	Linoleic acid
LC	Long-chain
PUFA	Polyunsaturated fatty acids

Introduction

An adequate intake of n-3 long chain (LC) polyunsaturated fatty acids (PUFA), in particular of docosahexaenoic acid (DHA) during pregnancy and lactation is important to support optimal visual and cognitive development in the foetus and the neonate [1, 2]. Furthermore, consumption of eicosapentaenoic acid (EPA) and DHA, the most important n-3 LC PUFA, during pregnancy reduces the risk of early premature birth [1–3]. In addition, epidemiological studies have clearly shown that n-3 LC PUFA lower the risk of cardiovascular diseases (CVD) in adults [1–4].

To achieve an adequate n-3 LC PUFA intake, appropriate dietary habits are needed. The food source naturally richest in n-3 LC PUFA is fish and other seafood,

particularly oily fish [4]. However, in most European countries, the estimated intake of fish is too low to meet the recommendation for n-3 LC PUFA [4–9]. Moreover, due to negatively perceived messages in the media about contaminants in seafood, people tend to decrease their fish consumption and possibly look for alternatives. In addition, since it is not clear whether the world's oceans could meet the seafood demand, alternatives will be of even bigger interest in the future in view of a sustainable food supply. These alternatives can be found in n-3 PUFA enriched foods as well as in n-3 PUFA supplements based on sustainable sources e.g. algae. The market of foods and supplements containing n-3 PUFA is rapidly growing [10].

Data on food consumption of women of reproductive age living in Flanders (the northern, Dutch speaking part of Belgium) collected in 2002 showed a large deficit for alpha-linolenic acid (ALA) and n-3 LC PUFA compared to the recommendations and indicated a need to tackle the problem of low n-3 PUFA intake [5]. Another recent Belgian study demonstrated that enrichment of commonly eaten food items with n-3 PUFA provides the opportunity to increase the n-3 PUFA intake and to decrease the n-6/n-3 ratio in the diet to around 3.3 [11]. These facts together with the increasing supply of n-3 FA supplements and n-3 FA enriched foods, created the interest to investigate the consumption level of these foods and supplements as well as their effect on the n-3 LC intake of Flemish women of reproductive age. A good reason to focus on this subgroup of the population lies in the importance of n-3 LC PUFA during pregnancy and lactation. Moreover, the development of appropriate dietary habits of this subgroup of the population will (1) influence the dietary habits of their children and (2) influence the dietary habits of themselves and their partners in the future, which can help to prevent both for CVD during later life.

So, the two specific objectives of this study were (1) to collect data on the consumption of n-3 PUFA supplements, n-3 PUFA enriched foods and foods naturally rich in n-3 LC PUFA for Flemish women of reproductive age and (2) to calculate and evaluate the overall intake of n-3 LC PUFA, i.e. the sum of EPA and DHA, and assess the influence of the supplements and enriched foods on the overall EPA&DHA intake for Flemish women of reproductive age.

Materials and Methods

Very few dietary assessment methods are available to adequately assess the intake of n-3 LC PUFA [12, 13]. Since fish is the most important source of n-3 LC PUFA and fish is episodically consumed, a long term dietary assessment method is needed. In Australia, a 28-item semi-quantitative food frequency questionnaire (FFQ) has recently been developed and compared with a 3 day dietary record as well as with the n-3 LC PUFA content of red blood cells and plasma [12, 14]. This FFQ was found to be a valid and reproducible method that can be used to estimate the n-3 LC PUFA intake of healthy adults and is available online. However, since the food items of this FFQ are not representative of the Flemish and Belgian market and the Belgian food habits, it was not useful for this study. Therefore, a new FFQ was developed.

Market Study

In order to include all relevant supplements and food items in the FFQ, a market study was made to list all n-3 PUFA food supplements and all food products containing a labelling on the package indicating the presence of and/or enrichment with n-3 PUFA. During the months August, September, and October 2008, all important supermarket chains in two provinces of Flanders were visited and the relevant food items for this study were listed together with their n-3 PUFA content. In addition, different pharmacies, drugstores and bio-shops were visited as well. At the same time, photos of the relevant products were made for use in the FFQ.

Food Frequency Questionnaire

Based on the knowledge of the market study, a semi-quantitative FFQ was developed with the objective of collecting data on the consumption of n-3 PUFA supplements, food items enriched with n-3 PUFA, and food items naturally rich in n-3 LC PUFA (seafood and seaweed). This type of FFQ assesses the type of product consumed as well as the amount by asking the respondent to indicate the portion they regularly consume in a list of portion size options.

The FFQ started with questions on some socio-demographic and personal characteristics: year and country of birth, number of family members, weight, height, highest level of education, smoking behavior, presence of some diseases (high cholesterol, cardiovascular diseases, cancer, high blood pressure, food allergies, obesity, diabetes) for themselves or family members, pregnancy and/or lactation, taking part in sports regularly, paying attention to what they eat, and following a diet. In a second part of the FFQ, the use of n-3 PUFA supplements during the last 2 months was probed, including the amount and frequency, as well as the person who advised them to take n-3 PUFA supplements. Next, the habitual consumption of foods naturally rich in n-3 LC PUFA and foods enriched with n-3 PUFA was probed, divided in eight different categories: (1) seafood and seaweed, (2) eggs, (3) bread, (4) meat, meat

products and vegetarian substitutes, (5) margarines, (6) cooking/frying fat, (7) mayonnaise and dressings, (8) dairy and soy products. Before finalizing the FFQ, a pre-test was performed with 40 participants, of whom 37 completed and returned the questionnaire, to test the comprehensiveness of the questionnaire.

It was decided to work with an FFQ in paper version (not online). The FFQ was developed with Teleform Designer version 10.1 for an automatic scanning. The FFQ was distributed together with a letter explaining the purpose of the study, instructions on how to complete the FFQ and some photos to illustrate the products about which questions were asked. The FFQ was self-administered by the subjects.

Population Sample

Study volunteers were recruited in February 2009 via a convenience sample strategy, using relatives, colleagues and friends. There were no exclusion criteria, other than the fact that the participants needed to be women between 18 and 39 years old living in Flanders. After the first week of data collection, extra efforts were made to make sure that all age categories were equally divided in the study sample group. In total, 500 FFQs were distributed and needed to be returned within a period of 2.5 weeks.

The questionnaire and the study protocol were approved by the Ethical Committee of the Ghent University Hospital. All participants signed an informed consent form before completing the questionnaire.

Fatty Acid Composition

The second objective of this study was to calculate the intake of LC n-3 PUFA. For this, only EPA and DHA were considered (not DPA, since there is a lack of composition data for this fatty acid). In order to achieve this objective, concentrations of EPA and DHA for the different food items in the FFQ were needed. For the first food group in the FFQ, i.e. fish and other seafood, EPA&DHA concentrations for four different subgroups were determined: (1) lean fish (<2% fat), (2) half-fatty fish (2–10% fat), (3) fatty fish (>10% fat), and (4) crustaceans and mollusks. For each subgroup, mean EPA&DHA concentrations were calculated according to the concentration in the Dutch food composition database as well as data provided by the Belgian Health Council and using a weighting factor to represent the relative frequency of consumption of each fish species by the Belgian population, determined through the pan-European SEAFOODplus consumer survey and by the Belgian Health Council [15–17]. The EPA&DHA concentrations of two types of seaweed (wakame and kelp) were found in the American food composition database [18], for a third type (nori) data were received from the Japanese scientist Dr. Onishi (personal communication). For margarines and eggs, the only available n-3 enriched foods containing EPA&DHA, the EPA&DHA concentrations indicated on the package were used.

To calculate the contribution of the n-3 PUFA supplements to the EPA&DHA intake, the concentrations indicated on the packages were used for those women who indicated the brand name of the supplement they used. For those women who did not give these details, a mean EPA&DHA concentration of all the available supplements was used.

Evaluating the EPA&DHA Intake

Different recommendations exist for evaluating the intake of EPA&DHA. The International Society for the Study of Fatty Acids and Lipids (ISSFAL) recommends a minimum intake of EPA&DHA of 500 mg/day in view of cardiovascular health [19]. For recommendations to pregnant and lactating women, ISSFAL refers to the work recently done by the Perinatal Lipid Intake Working Group (PeriLip), that recommends a dietary intake of n-3 LC PUFA that supplies a DHA intake of at least 200 mg/day [3]. The Belgian Health Council recommends for adults an EPA&DHA intake equal to 0.3% of the total energy intake [20]. It is, however, hard to translate this recommendation for the current study since we have no information on the energy intake of the respondents. Therefore, the ISSFAL and PeriLip recommendations are used for the evaluation.

Statistics

The normality of the continuous variables was tested using a Kolmogorov–Smirnov test (P value <0.01). To investigate correlations between two continuous variables, of which at least one was not normally distributed, Spearman's correlations were used (P value <0.05). To look for significant differences between two groups for a non-normal, continuous variable, a Mann–Whitney U test was used (P value <0.05). To test for significant differences between more than two groups, a Kruskal–Wallis test (P value <0.05) was used. To study associations between two discontinuous variables, a Pearson χ^2- test was used (P value < 0.05).

Results

Market Study

In total, 202 food items were found on the Belgian market carrying on the package an indication that they contained

n-3 PUFA. Of these, 50 (23%) were fish and other seafood, 25 (11%) were ALA-containing oils. The others were margarines ($n = 35$; 16%), vegetarian substitutes ($n = 18$; 8%), soy drinks and soy desserts ($n = 17$; 8%), mayonnaise and dressings ($n = 14$; 6%), yoghurts ($n = 13$; 6%), meat products ($n = 11$; 5%), butter ($n = 3$; 1%), eggs ($n = 5$; 2%), milk ($n = 2$; 1%), cream ($n = 2$; 1%), cheese ($n = 2$; 1%), and five others (e.g. including biscuits and chocolate spread). Of these food items, only one brand of eggs and four brands of margarine contained EPA&DHA, besides ALA.

In addition, 139 different n-3 PUFA supplements were found, produced by 46 different producers. These supplements were found in the form of oils, capsules and tablets. Several brands had also a special supplement for children.

Participation Rate and Sample Characteristics

Of the 500 distributed FFQs, 421 were returned after completion, leading to a response-rate of 84.2%. However, seven of them were excluded since (1) they were completed by men, (2) they were completed by women younger than 18 or older than 39, (3) they did not complete the question about the n-3 PUFA supplement use, or (4) they did not complete the question about the fish and other seafood consumption. This led to a total study population of 414 women, of which 18 were pregnant and five were breastfeeding.

The sample characteristics are shown in Table 1. This table shows that the younger age category (<25 years old) is oversampled, as well as the part of the population following or have followed higher education. As a consequence, 62% of the population is still studying.

Table 1 Sample characteristics ($n = 414$)

Age (years, mean ± standard deviation)	27.7 ± 6.1
Age categories (%)	
18–19 years	5.1
20–24 years	33.8
25–29 years	22.9
30–34 years	20.8
35–39 years	17.4
BMI (kg/m^2: mean ± standard deviation)	22.4 ± 3.3
BMI categories (%)	
≤18.5 kg/m^2	6.5
18.5–25 kg/m^2	74.2
25–30 kg/m^2	15.5
≥30 kg/m^2	3.5
Born in Belgium (%)	
Yes	95.7
Smoking (%)	
Yes	22.0
Family size (%)	
1 or 2 persons	33.2
3 or 4 persons	49.4
5 or more	17.4
Working status (%)	
Student	61.8
Working	35.0
Unemployed or housewife	3.2
Education (%)*	
≤18 years	47.1
>18 years	52.9

* Refers to the age up to which the respondents went to school

Consumption of n-3 PUFA Supplements, n-3 PUFA Enriched Foods and Foods Naturally Rich in n-3 LC PUFA

The first objective of this study was to collect data on the consumption of n-3 PUFA supplements, n-3 PUFA enriched foods (eggs, bread, meat (products) and vegetarian substitutes, margarines, cooking/frying fat, mayonnaise and dressings and dairy and soy products) and foods naturally rich in n-3 LC PUFA (fish, other seafood and seaweed) by Flemish women of reproductive age. Figure 1 shows the percentage of users within the study population for these supplements and food items. The results indicate that fish and other seafood are consumed by the majority of the study population, whereas seaweed is only consumed by 7% of the participating women. Of the total population, only 12 women (3%) never consumed any fish or seafood. Concerning the n-3 PUFA enriched foods, margarine and cooking/frying fat are the most frequently used products, while n-3 PUFA enriched eggs are the least popular. n-3 PUFA containing supplements are only consumed by 5% of the participating women ($n = 21$). Of these 21 women, 12 used it on own initiative, 6 on medical advice, and 3 for other reasons (e.g. advice of parents or pharmacist). Within this group of supplements users, four women were pregnant (i.e. 22% of the pregnant women in this population sample) and one woman was breastfeeding. The Pearson χ^2- test found significant associations between n-3 PUFA supplement usage and (1) being pregnant (P value = 0.001), (2) being on a diet (p-value = 0.022), (3) having a food allergy (P value = 0.028), and (4) paying attention to what they eat (P value = 0.022). Only 4.6% (19 women) never used any n-3 PUFA enriched food or n-3 PUFA containing supplement.

The Intake of EPA&DHA

The second objective of this study was to calculate the intake of EPA&DHA, two n-3 LC PUFAs, via foods

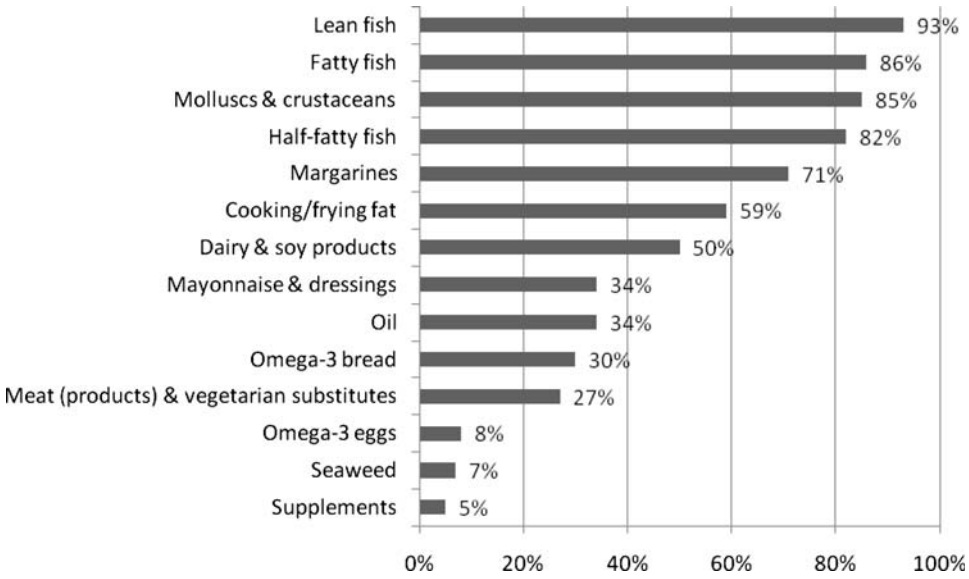

Fig. 1 The percentage of users of foods naturally rich in n-3 LC PUFA, n-3 PUFA enriched foods and n-3 PUFA supplements

naturally rich in these fatty acids (fish, other seafood and seaweed), via n-3 enriched foods containing EPA&DHA (margarines and eggs), and via n-3 PUFA supplements. The results are shown in Table 2. The contribution of each EPA&DHA source is shown in Table 3, in absolute values (mg/day) and percentage, together with the mean and median consumption level of each EPA&DHA source. The EPA&DHA intake was found to be non-normally distributed (P value <0.001), which is also illustrated by the difference between the mean and median intake (276 vs. 199 mg/day). A significant and positive correlation was found between the EPA&DHA intake and the age (correlation coefficient = 0.181, P value <0.001). No correlation was found with BMI. The Mann–Whitney U test found a

Table 2 The EPA&DHA intake (mg/day) for the overall study population (414 women) as well as for subgroups of the population

	EPA&DHA intake (mg/day)			
	Mean ± SD	Minimum	Median	Maximum
Total population (n = 414)	276 ± 362	0	199	4642
Consumers of n-3 foods (n = 395)	281 ± 368	0	209	4642
Supplement users (n = 19)	1067 ± 997	26	998	4642
Pregnant women (n = 18)	328 ± 323	0	232	1331
Breastfeeding women (n = 5)	299 ± 241	80	205	676
Non-consumers of n-3 foods and supplements (n = 19)	181 ± 209	0	118	871

SD standard deviation

Table 3 Mean and median consumption level of the different EPA&DHA sources as well as their absolute and relative contribution to the overall EPA&DHA intake (average data for the whole population, n = 414, including non-consumers per EPA&DHA source)

	Mean consumption (g/week)	Median consumption (g/week)	EPA&DHA intake (mg/day)	Contribution to total EPA&DHA intake (%)
Fatty fish	43.4	25.0	130.7	47.5
Half-fatty fish	38.3	12.5	10.9	4.0
Lean fish	94.6	62.5	54.3	19.7
Molluscs & crustaceans	45.1	17.5	39.1	14.2
Seaweed	0.5	0.0	0.1	0.0
n-3 eggs	0.1	0.0	0.4	0.1
n-3 margarines	38.0	7.5	8.0	2.9
n-3 supplements	0.1	0.0	31.5	11.4

significant difference in the EPA&DHA intake for (1) the supplement users (P value <0.001), (2) the consumers of fish and other seafood (P value <0.001), (3) those paying attention to what they eat (P value = 0.014), (4) those doing sports regularly (P value = 0.017), (5) those having a high cholesterol (P value = 0.018) and (6) those who are currently suffering from cancer or had done so in the past (P value = 0.046). No significant difference in EPA&DHA intake were found according to BMI category, being a student versus working, education level, number of family members, smoking, and certain diseases within the family.

The intake of EPA&DHA was compared to the ISSFAL recommendation of 500 mg/day [19]. The ISSFAL recommendation was only achieved by 48 of the 414 women (11.6%) participating in this study. Another 11.6% had an intake between 375 and 500 mg/day, whereas, respectively, 18.6, 22.9, and 35.3% had an intake between 250 and 375 mg/day, 125 and 250 mg/day and 0 and 125 mg/day.

Discussion

This study investigated the consumption level of n-3 PUFA supplements, n-3 PUFA enriched foods and foods naturally rich in n-3 LC PUFA of Flemish women of reproductive age (18–39 years old). With the collected consumption data, the intake of n-3 LC PUFA, EPA&DHA, was calculated and evaluated against the ISSFAL recommendation. Two important limitations of the study are (1) that due to time and budget constraints, it was impossible to work with a random sample and (2) there was no validated FFQ available that was applicable for the Belgian population. As alternative, a convenience sample strategy and a newly developed FFQ was used. This FFQ was pretested before to ensure the comprehensiveness and the quality of the collected data. It is, however, difficult to generalize the results based on a convenience sample to the overall population of Flemish women of reproductive age. Nevertheless, we tried to collect a large sample of women (n = 414) from different age categories and with a different working status and education level (see Table 1).

During the start of this study, an important problem was encountered, i.e. identifying the n-3 enriched foods. The market study had as objective to list all available n-3 PUFA supplements as well as all n-3 PUFA enriched foods. For the latter, the criterion was that the package of the food items contained a label indicating the presence of and/or enrichment with n-3 PUFA. When considering n-3 PUFA enriched food, it is good to differentiate food items enriched in a direct and in an indirect way. In direct enriched food items, an extra nutrient, e.g. ALA or EPA&DHA, is added to the product at the end of the production process. Examples are bread and mayonnaise enriched with ALA by using ALA-rich oils in the production process, or margarines enriched with EPA&DHA. Direct enrichment with EPA&DHA became possible as technology made it achievable to produce high quality, deodorized, and stabilized oils enriched with LC n-3 PUFAs [21]. Indirect enrichment is performed via modification of animals' diet. In this respect, research efforts to increase the n-3 (LC) PUFA content of terrestrial animal products by enriching the animals' feed contributed to improving the overall intake of n-3 (LC) PUFAs [22]. Examples are chickens partially fed with fish meal that produce eggs containing EPA&DHA, cows fed with linseed enriched feed producing ALA-rich milk and meat. Producers of these directly and indirectly enriched foods indicate the presence of these n-3 PUFA on the packages of their food items. However, during the market study we experienced that also food items naturally rich in n-3 PUFA, e.g. ALA-rich oils and soy based desserts—thus, foods that did not undergo a modification—contained a label indicating the presence of n-3 PUFA. This made it difficult to really separate the enriched ones from the others.

In addition, it was found that most of the n-3 PUFA enriched foods available on the Belgian market are enriched with ALA and not with EPA&DHA. Eggs and margarines were the only available directly enriched food items containing EPA&DHA, so the only food items that could contribute to the n-3 LC PUFA intake of the studied women.

Another problem encountered was to find data on the EPA&DHA content of seaweed. Food composition tables as well as the scientific literature lack data on this issue. If these kinds of alternative EPA&DHA sources were to become more important in the future, these data would be very relevant. Moreover, for enriched margarines and eggs, EPA&DHA contents as reported on the packages were used. However, since inaccurate reporting on some labels exists, these data include a factor of uncertainty.

The results of this study showed that n-3 PUFA supplements are used by 5% of the Flemish women of reproductive age. A significant association was found between those who are pregnant, those who follow a diet, those who have a food allergy and those who report that they pay conscious attention to what they eat. This can be linked with the conclusion of Reinert et al. [23] that using dietary supplements is in general related to a healthier lifestyle.

This study also indicated that, although the supply of n-3 PUFA enriched foods is increasing, there still remains a big gap between the actual EPA&DHA intake and the one recommended. Of the women of reproductive age, 58.2% do not even reach 50% of the recommended intake. Although the mean and median EPA&DHA intake of the

pregnant and breastfeeding women is a bit higher than the overall mean and median intake, their intake is still far removed from the ISSFAL recommendation as well as from the advice of the PeriLip working group who recommended an intake of DHA only equal to at least 200 mg/day. When comparing the calculated EPA&DHA intake of this study to the calculated EPA&DHA intake of Flemish women in 2002, a slight increase is found over the 7 years, from 209 to 276 mg/day, which can be explained by an increased fish and seafood consumption as well as by the use of n-3 PUFA supplements and eggs and margarines enriched with EPA&DHA. Moreover, the results can also be influenced due to an oversampling of more highly educated women.

EPA&DHA intake was positively correlated with age, which means that older women (within the groups of women between 18 and 39 years old) tend to have a higher EPA&DHA intake. In addition, a significant association was found between the EPA&DHA intake on the one hand and suffering from high blood cholesterol, using supplements, doing sports regularly and reportedly paying conscious attention to what they eat on the other hand. These findings show that, in the future, efforts aiming to increase the EPA&DHA intake should focus on those people who do not tend to change their dietary habits on their own initiative and need extra support and information to convince them to change their diet.

Finally, it was also found that fish and other seafood remain the most important source of EPA&DHA intake. Accordingly, appropriate fish and other seafood consumption is the most probable solution to attaining a diet that would meet the recommendations for EPA&DHA. Within fish and seafood, small fatty fish species (e.g. herring, anchovy, sardine, sprat) are most likely to increase the intake of EPA&DHA in a safe way, due to their high LC n-3 PUFA and low contamination load. In the light of the depletion of fish stocks, other (sustainable) strategies are needed to help increase the EPA&DHA intake without creating an ecological problem. In this study, it was found that n-3 PUFA enriched foods do not really help to fill the gap between EPA&DHA intake and recommendation because (1) most of the n-3 PUFA enriched foods contain solely ALA and (2) those that contain EPA&DHA (eggs and margarine) only contribute very marginally to the overall intake. Enriching more foods with EPA&DHA would be an option, with the condition that sustainable sources of EPA&DHA are used, e.g. algae. In contrast, this study indicated that the use of n-3 PUFA supplements in general leads to a much higher EPA&DHA intake and helps to reach a an intake higher than the one recommended. However, these supplements are quite expensive, most of them rely on fish oil (and are therefore not a sustainable source) and as most nutritionists think, they should not be considered as magic bullets to convert an unhealthy diet into a healthy one. Therefore, diet-based approaches increasing the supply of n-3 LC PUFA in the food chain are preferable to the use of supplements. However, supplements based on sustainable sources can be a solution for specific subgroups with an increased need e.g. vegetarian women, pregnant women or patients with cardiovascular diseases.

A first promising and more sustainable solution to increase EPA&DHA supply and intake is to cultivate algae for supplements and direct and indirect enrichment. Algae are the original source of n-3 LC PUFA in fish and, as stated by Winkler [24], the option exists to use them directly for human consumption. Another option is the production of microbial oils, otherwise referred to as single cell oils (SCO), based on a DHA-producing organism that can grow in large-scale industrial fermenters. For example, *Crypthecodinium cohnii* produces a triacylglycerol oil in which DHA can reach levels between 40 and 50% of the total fatty acids and, moreover, occurs as the sole PUFA. Currently, the major application of these SCOs is in the form of a supplement for infant nutrition [25]. A third alternative way to increase the supply of n-3 LC PUFAs is through metabolic engineering in plants which manipulates the lipid metabolism and leads to the production of novel plant oils [26, 27]. It is also worth mentioning that recent studies report on the development of transgenic pigs able to convert n-6 PUFAs to n-3 PUFAs [28, 29]. However, long period of research and a long regulatory path will be needed before they will be able to enter the food chain, that is if ever they do, because a lot of controversy still exists with regard to the presence of transgenic foods on the market.

Conclusion

Although a variety of n-3 PUFA supplements and n-3 PUFA enriched foods are on the market and although a lot of media attention is paid to these n-3 PUFA, this study illustrated that an important gap remains between the actual EPA&DHA intake and that recommended within the group of Flemish women of reproductive age. However, these women are responsible for the health of the next generation, partly during the pregnancy and lactation period and partly during the first decades of their children's lives when they highly influence the dietary habits of their offspring. New and sustainable strategies will be needed to help all people (including the less health-consciousness) to increase their EPA&DHA intake in a sustainable way and to improve public health during the next decades.

Acknowledgments The dietician Mrs. M. Bellemans (Department of Public Health, Ghent University) is thanked for her contribution during the creation of the food frequency questionnaire and during the evaluation of the results. All participants who completed the questionnaire are gratefully acknowledged for their participation in this study.

References

1. Koletzko B, Lien E, Agostoni C, Bohles H, Campoy C, Cetin I, Decsi T, Dudenhausen JW, Dupont C, Forsyth S, Hoesli I, Holzgreve W, Lapillonne A, Putet G, Secher NJ, Symonds M, Szajewska H, Willatts P, Uauy R (2008) The roles of long-chain polyunsaturated fatty acids in pregnancy, lactation and infancy: review of current knowledge and consensus recommendations. J Perinat Med 36(1):5–14
2. Ruxton CHS, Calder PC, Reed SC, Simpson MJA (2005) The impact of long-chain n-3 polyunsaturated fatty acids on human health. Nutr Res Rev 18(1):113–129
3. Koletzko B, Cetin I, Brenna JT (2007) Dietary fat intakes for pregnant and lactating women. Br J Nutr 98(5):873–877
4. Ruxton CHS, Derbyshire E (2009) Latest evidence on omega-3 fatty acids and health. Nutr Food Sci 39:423–438
5. Sioen IA, Pynaert I, Matthys C, De Backer G, Van Camp J, De Henauw S (2006) Dietary intakes and food sources of fatty acids for Belgian women, focused on n-6 and n-3 polyunsaturated fatty acids. Lipids 41(5):415–422
6. Astorg P, Arnault N, Czernichow S, Noisette N, Galan P, Hercberg S (2004) Dietary intakes and food sources of n-6 and n-3 PUFA in French adult men and women. Lipids 39(6):527–535
7. Linseisen J, Schulze MB, Saadatian-Elahi M, Kroke A, Miller AB, Boeing H (2003) Quantity and quality of dietary fat, carbohydrate, and fiber intake in the German EPIC cohorts. Ann Nutr Metab 47(1):37–46
8. Johansson LRK, Solvoll K, Bjorneboe GEA, Drevon CA (1998) Intake of very-long-chain n-3 fatty acids related to social status and lifestyle. Eur J Clin Nutr 52(10):716–721
9. Otto SJ, van Houwelingen AC, Badart-Smook A, Hornstra G (2001) Changes in the maternal essential fatty acid profile during early pregnancy and the relation of the profile to diet. Am J Clin Nutr 73(2):302–307
10. Bailey N (2009) Current choices in omega 3 supplementation. Nutr Bull 34:85–91
11. Sioen I, Hacquebard M, Hick G, Maindiaux V, Larondelle Y, Carpentier YA, De Henauw S (2009) Effect of ALA-enriched food supply on cardiovascular risk factors in males. Lipids 44(7):603–611
12. Sullivan BL, Brown J, Williams PG, Meyer BJ (2008) Dietary validation of a new Australian food-frequency questionnaire that estimates long-chain n-3 polyunsaturated fatty acids. Br J Nutr 99(3):660–666
13. Campbell CG, Wiessinger LE, Filipowicz R, Gelfer GD, Syndergaard S, Bell K (2009) Validation of a food frequency questionnaire to assess docosahexanoic acid (DHA) intake in pregnant women living in a non-coastal community. Poster at the 7th ICDAM conference, Washington, DC
14. Sullivan BL, Williams PG, Meyer BJ (2006) Biomarker validation of a long-chain omega-3 polyunsaturated fatty acid food frequency questionnaire. Lipids 41(9):845–850
15. Belgian Health Council (2004) Aanbevelingen en beweringen betreffende omega-3 vetzuren (Recommendations and allegations concerning omega-3 fatty acids), D/2005/7795/1-http://www.health.fgov.be/CSH_HGR, 2004
16. Honkanen P, Brunsø K (2007) On the average European fish consumption is below recommended levels. Deliverable 4, Project 2.1, SEAFOODplus, http://www.seafoodplus.org/Europen_fish_consumption.411.0.html
17. NEVO Foundation (2006) Nederlands Voedingsstoffenbestand 2006 (Dutch Food Composition Table 2006), Nederlands Voedingscentrum, Den Haag
18. US Department of Agriculture and Agricultural Research Service (2009) USDA National Nutrient Database for Standard Reference. Release 21, http://www.nal.usda.gov/fnic/foodcomp/search/
19. ISSFAL (2004) Report of the sub-committee on the recommendations of polyunsaturated fatty acids in healthy adults. http://www.issfal.org
20. Belgian Health Council (2009) Voedingsaanbevelingen voor België. Herziene versie 2009 (Nutritional recommendations for Belgium. Revised version 2009), https://portal.health.fgov.be/pls/portal/.
21. Harris WS (2007) n-3 Fatty acid fortification: opportunities and obstacles. Br J Nutr 97:593–595
22. Sontrop J, Campbell MK (2006) omega-3 polyunsaturated fatty acids and depression: A review of the evidence and a methodological critique. Prev Med 42(1):4–13
23. Reinert A, Rohrmann S, Becker N, Linseisen J (2007) Lifestyle and diet in people using dietary supplements : a German cohort study. Eur J Nutr 46(3):165–173
24. Winkler JT (2007) Action options on omega-3-recommendations, sources, policies. Nutr Health 18:343–353
25. Ratledge C (2004) Fatty acid biosynthesis in microorganisms being used for Single Cell Oil production. Biochimie 86(11):807–815
26. Kinney AJ (2006) Metabolic engineering in plants for human health and nutrition. Curr Opin Biotechnol 17(2):130–138
27. Voelker T, Kinney AT (2001) Variations in the biosynthesis of seed-storage lipids. Annu Rev Plant Physiol Plant Molec Biol 52:335–361
28. Prather RS (2006) Cloned transgenic heart-healthy pork? Transgenic Res 15(4):405–407
29. Moghadasian MH (2008) Advances in dietary enrichment with n-3 fatty acids. Crit Rev Food Sci Nutr 48:402–410

Lipids (2010) 45:321–327
DOI 10.1007/s11745-010-3401-8

ORIGINAL ARTICLE

Serum Oxidized-LDL is Associated with Diabetes Duration Independent of Maintaining Optimized Levels of LDL-Cholesterol

Manouchehr Nakhjavani · Omid Khalilzadeh · Leila Khajeali · Alireza Esteghamati · Afsaneh Morteza · Arsia Jamali · Sheida Dadkhahipour

Received: 24 November 2009 / Accepted: 23 February 2010 / Published online: 12 March 2010

Abstract Oxidized low-density lipoprotein (ox-LDL) plays a key role in the progression of atherosclerosis and diabetes complications. The aim of this study was first, to evaluate the association between ox-LDL and diabetes duration, and second, to examine serum level of ox-LDL in patients with prolonged diabetes and a desirable LDL-cholesterol level. A total of 36 type-2 diabetic patients with a diabetes duration of more than 5 years, 36 newly diagnosed diabetic patients, and 36 age-, sex- and BMI-matched healthy participants were recruited. Healthy participants and newly diagnosed patients were not receiving any treatment. All patients with prolonged diabetes had desirable LDL-cholesterol levels (<100 mg/dL), according to the adult treatment panel-III guidelines. While LDL-cholesterol was significantly lower in patients with diabetes duration >5 years, in comparison to newly diagnosed patients ($P < 0.01$), ox-LDL was significantly higher in patients with prolonged diabetes ($P < 0.001$). The ox-LDL-to-LDL ratio was dramatically higher in patients with diabetes duration >5 years in comparison to newly diagnosed patients and healthy participants ($P < 0.001$). Ox-LDL was significantly associated with diabetes duration ($r = 0.519, P = 0.001$). In multivariate analysis, this association remained significant ($\beta = 0.501$, $P = 0.003$) after adjustment for potential confounders. In conclusion, this study showed that the serum ox-LDL level increases with the length of diabetes, even though the patients' LDL-cholesterol level is maintained at a desirable level. Our findings highlight that possibly more attention should be focused on markers of oxidative stress in the management of lipids in diabetic patients.

Keywords Diabetes mellitus · Duration · Ox-LDL

M. Nakhjavani (✉) · O. Khalilzadeh · L. Khajeali · A. Esteghamati · A. Morteza · A. Jamali · S. Dadkhahipour
Endocrinology and Metabolism Research Center (EMRC), Vali-Asr Hospital, Tehran University of Medical Sciences, P.O. Box 13145-784, Tehran, Iran
e-mail: nakhjavanim@tums.ac.ir

O. Khalilzadeh
e-mail: khalilzadeh@razi.tums.ac.ir

L. Khajeali
e-mail: leila_khajehali@yahoo.com

A. Esteghamati
e-mail: esteghamati@tums.ac.ir

A. Morteza
e-mail: aafsaneh03@gmail.com

A. Jamali
e-mail: arsia_jamali@yahoo.com

S. Dadkhahipour
e-mail: sdadkhahipour@calpharm.org

Abbreviations

ANOVA	Analysis of variance
AGE	Advanced glycosylated end-products
ATP III	Adult treatment panel III
BMI	Body mass index
CV	Coefficient of variant
ELISA	Enzyme-linked immunosorbent assay
GFR	Glomerular filtration rate
HDL-cholesterol	High density lipoprotein-cholesterol
HPLC	High-pressure liquid chromatography
LDL-cholesterol	Low density lipoprotein-cholesterol
OR	Odds ratio
Ox-LDL	Oxidized LDL
SEM	Standard error of mean
TG	Triglycerides

Introduction

Oxidation of low density lipoprotein (LDL) is a key process in the early progression of atherosclerotic diseases and diabetes complications [1–3]. Oxidized LDL (ox-LDL), derived from LDL-cholesterol under oxidative stress, encompass many atherogenic properties. Several studies have reported the strong association of increased serum ox-LDL level, high serum malondialdehyde and presence of auto-antibodies against ox-LDL, with atherosclerosis, diabetes and its complications [4–7]. Ox-LDL is an independent predictor of endothelial dysfunction [8], with pro-inflammatory, prothrombotic, and pro-apoptotic properties in individuals suffering from oxidative stress, such as diabetic patients [9].

It is widely encouraged to maintain serum LDL-cholesterol below certain levels in diabetic patients [10]. It has been demonstrated that statins can have an influence on the ox-LDL level [11]. However, the efficacy of this function is not well documented in vivo [12]. It is yet to be examined whether maintaining serum LDL-cholesterol at a desirable level is sufficient to reduce the most atherogenic derivates of LDL-cholesterol, i.e. ox-LDL.

Guidelines for the management of the lipid profile in diabetic patients are mainly focused on controlling LDL-cholesterol, triglycerides (TG), high density lipoprotein-cholesterol (HDL) and total cholesterol [10]. Yet, no account is taken of some other important atherogenic lipids such as ox-LDL. It was decided that it would be interesting to evaluate how the ox-LDL level changes in our routine practice for lipid control in diabetic patients. In this study, we decided to evaluate two important subjects: first, to evaluate the association between ox-LDL and diabetes duration, and second, to examine serum level of ox-LDL in patients with prolonged diabetes and a desirable LDL-cholesterol level.

Methods

Participants

This cross-sectional hospital-based study was conducted from February 2008 to April 2009 in the outpatient diabetes clinic of a university general hospital. A total of 36 type-2 diabetic patients with a diabetes duration of more than 5 years, 36 newly diagnosed type-2 diabetic patients, and 36 age-, sex- and BMI-matched healthy participants were recruited. Diabetes mellitus was diagnosed according to the criteria of the American Diabetes Association [13]. Newly diagnosed diabetic patients were not taking oral hypoglycemic agents, aspirin, insulin, statin, and anti hypertensive medications. All patients with diabetes duration >5 years had a desirable LDL-cholesterol level (<100 mg/dL), according to the adult treatment panel (ATP) III guideline [10]. Smokers, patients with proteinuria or renal involvement (creatinine > 1.5 mg/dL or GFR < 70 cc/min), patients receiving anti-oxidants and those with evidence of glomerulonephritis, congestive heart failure, hypo and hyperthyroidism were not included. Demographic and anthropometric data including age, sex, duration of diabetes, height, weight in light clothing and blood pressure (in sitting position after 10 min rest) were recorded. Blood pressure was re-measured twice after 5 min and averaged. The body mass index (BMI; kg/m^2) was calculated according to the Quetelet formula.

The research was carried out according to the principles of the Declaration of Helsinki. The local ethics review committee of Tehran University of Medical Sciences approved the study protocol. All participants gave written informed consent before participation.

Blood Samples

Blood samples were collected after almost 12 h of fasting and, serum creatinine, fasting plasma glucose, total cholesterol, TG, HDL-cholesterol, LDL-cholesterol and HbA1C were measured. Glucose measurements [intra-assay coefficient of variants (CV) 2.1%, inter-assay CV 2.6%] were carried out using the glucose oxidase method. Cholesterol, HDL-cholesterol, LDL-cholesterol and TG were determined using direct enzymatic methods (Parsazmun, Karaj, Iran). HbA1C was estimated by High-Pressure Liquid Chromatography (HPLC) Method. Ox-LDL was measured using a commercially available sandwich enzyme-linked immunosorbent assay (ELISA, Mercodia, Uppsala, Sweden). The intra- and inter-assay coefficient of variation for the assay ranged between 4.5 and 7%. The detection limit was ≤0.03 U/L.

Statistical Analysis

Data were analyzed using SPSS software (version 16.0; SPSS Inc., Chicago, USA). Continuous variables are expressed as means ± standard errors of mean (SEM). Comparison between the three groups was performed using analysis of variance (ANOVA) with Scheffé post hoc. Adjusted partial correlation coefficients were calculated among variables. Multivariate regression analysis, with ox-LDL as the outcome, was used to evaluate the independent association between ox-LDL and the duration of diabetes. $P < 0.05$ was considered statistically significant.

Results

Characteristics of the study participants are presented in Table 1. There were no significant differences between

Table 1 Characteristics of participants in the three groups

	Healthy participants ($n = 36$)	Diabetic patients		P[a]
		New cases ($n = 36$)	Duration > 5 years ($n = 36$)	
Gender (females)	18 (50.0%)	18 (50.0%)	18 (50.0%)	NS[b]
Age (year)	48.92 ± 1.33	49.17 ± 1.58	49.51 ± 1.59	NS
Body mass index (kg/m^2)	27.40 ± 0.53	28.34 ± 0.74	28.81 ± 0.86	NS
Duration of diabetes (months)	–	–	8.22 ± 0.86	–
Systolic blood pressure (mmHg)	120.14 ± 1.94	125.25 ± 2.75	127.03 ± 3.61	0.215
Diastolic blood pressure (mmHg)	78.75 ± 1.22	80.00 ± 1.79	78.38 ± 1.83	0.766
Fasting plasma glucose (mg/dL)	90.61 ± 1.21	187.22 ± 7.57***	208.38 ± 13.06	<0.001
HbA1c (%)	–	8.18 ± 0.33	8.40 ± 0.33	0.634
Treatment with statins (n, %)	–	–	12 (33.3)	–
Anti diabetic drugs (n, %)				
Oral agent	–	–	29 (80.6)	–
Insulin	–	–	8 (22.2)	–
Anti hypertensive drugs (n, %)	–	–	14 (38.9)	–
Creatinine (mg/dL)	0.89 ± 0.03	0.91 ± 0.03	0.96 ± 0.03	0.856
Triglyceride (mg/dL)	145.64 ± 9.83	213.75 ± 24.11	230.35 ± 21.47	0.007
Cholesterol (mg/dL)	200.36 ± 7.44	201.72 ± 6.47	192.43 ± 7.75	0.679
HDL-cholesterol (mg/dL)	45.78 ± 2.01	42.56 ± 1.61	42.46 ± 1.95	0.365
LDL-cholesterol (mg/dL)	106.14 ± 4.21	116.63 ± 4.32	89.95 ± 4.47‡	0.006

Variables are expressed as means ± standard errors of mean (SEM)

[a] The P values are derived from analysis of variances (ANOVA) among the 3 groups

[b] Groups are matched for age, sex and BMI

* $P < 0.05$, ** $P < 0.01$, *** $P < 0.001$ when comparing new cases of diabetes and healthy participants

† $P < 0.05$, $^{\ddagger}P < 0.01$, $^{\dagger\ddagger}P < 0.001$ when comparing new cases and patients with a diabetes duration of more than 5 years

groups with respect to systolic and diastolic blood pressure, HbA1C, creatinine, cholesterol and HDL-cholesterol. Serum TG level was significantly higher in diabetic patients. In patients with a diabetes duration of more than 5 years, 4 patients were not receiving anti-diabetic treatments, 29 patients were using oral hypoglycemic agents (Metformin and/or Glibenclamide), and 8 were on insulin treatment. Fourteen patients (38.9%) with diabetes duration more than 5 years were on antihypertensive treatment (angiotensin converting enzymes inhibitors, angiotensin receptor blockers and/or beta blockers) and 12 patients (33.3%) were using statin. While LDL-cholesterol was significantly ($P < 0.01$) lower in patients with diabetes duration of more than 5 years (89.95 ± 4.47) in comparison to newly diagnosed (116.63 ± 4.32) patients, ox-LDL was significantly higher in patients with prolonged diabetes versus newly diagnosed patients (81.43 ± 1.65 vs. 45.50 ± 1.49; $P < 0.001$). The ox-LDL-to-LDL ratio was significantly ($P < 0.001$) higher in patients with a diabetes duration >5 years (0.94 ± 0.05) in comparison to newly diagnosed (0.42 ± 0.02) patients and healthy (0.42 ± 0.02) participants (Fig. 1). There were no significant differences in ox-LDL in patients receiving statins or not.

After adjustment for age, sex and BMI, ox-LDL was significantly ($P < 0.05$) associated with fasting plasma glucose ($r = 0.337$) and TG ($r = 0.312$) in healthy participants. In diabetic patients, ox-LDL was significantly associated ($r = 0.519$, $P = 0.001$) with diabetes duration (Fig. 2). In multivariate regression analysis, the association between diabetes duration and ox-LDL remained significant ($\beta = 0.536$, $P < 0.001$) after adjustment for age, sex, BMI, cholesterol, LDL-cholesterol, systolic and diastolic blood pressure, HbA1c, creatinine and fasting plasma glucose. In all the three groups, there was no significant association between ox-LDL and LDL-cholesterol.

Discussion

In this study, we showed that ox-LDL is significantly associated with the duration of diabetes. Multivariate regression analysis revealed that the association between

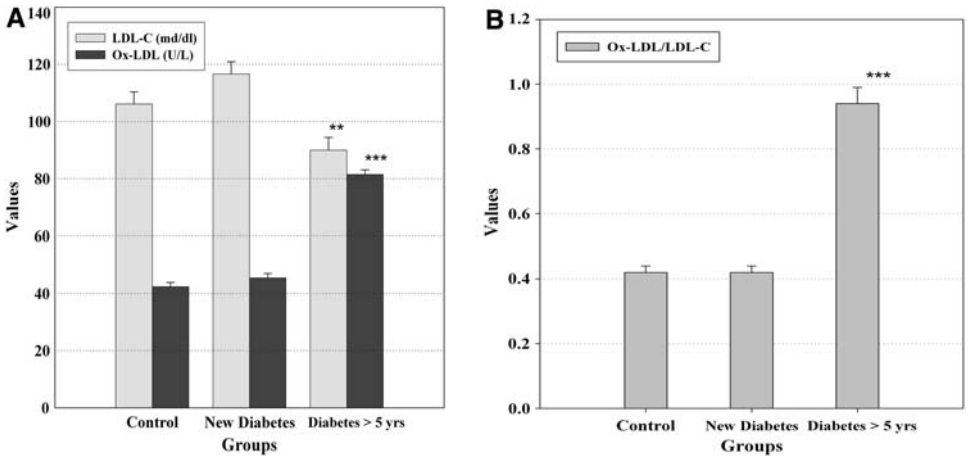

Fig. 1 Mean values of ox-LDL (U/L), LDL-cholesterol (mg/dL), and ox-LDL to LDL-cholesterol ratio (ox-LDL/LDL-C) in the three groups. Although LDL-cholesterol was kept in the desirable range (<100 mg/dL) in patients with diabetes duration of more than 5 years, the serum level of ox-LDL was still escalating (**a**). The contribution of the oxidized form of LDL to the total LDL-cholesterol was significantly higher in patients with prolonged diabetes (**b**). Groups were matched for age, sex and BMI. $*P < 0.05$, $**P < 0.01$, $***P < 0.001$ when comparing patients with prolonged diabetes versus newly diagnosed patients. *Handles* represent standard error of mean

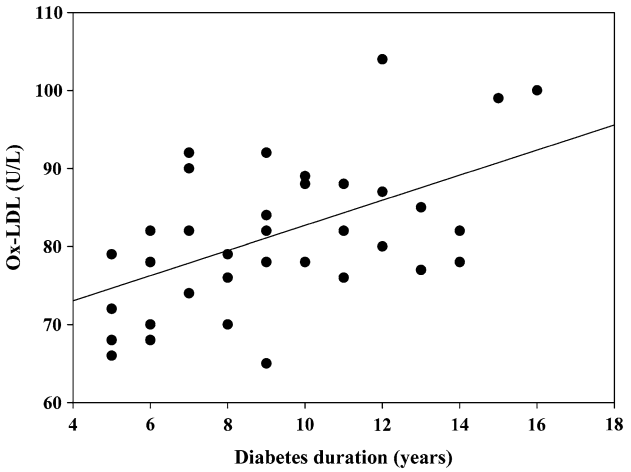

Fig. 2 Scatter plot demonstrating the significant correlation ($r = 0.519$, $P = 0.001$) between diabetes duration and ox-LDL

ox-LDL and diabetes duration was independent of age, sex, BMI, serum lipids, glycemic control and creatinine. Interestingly, our results suggested that maintaining an optimized level of LDL-cholesterol, according to guidelines for management of lipids in diabetic patients [10], does not sufficiently influence the ox-LDL level. Furthermore, we showed that ox-LDL levels corrected for LDL-cholesterol concentrations (ox-LDL/LDL-cholesterol: the proportion of oxidatively modified LDL to total LDL-cholesterol particles) significantly correlates to the diabetes duration.

In agreement with our findings, it has been shown that ox-LDL is associated with fasting plasma glucose [14, 15]. It was reported that serum ox-LDL levels are significantly higher in diabetic patients than healthy individuals [8, 16, 17]. In a study by Gokulakrishnan et al. [18] the mean level of ox-LDL in diabetic patients was higher than subjects with impaired glucose tolerance. Our results showed the association in patients with different durations of diabetes. Ox-LDL (or oxidation ratio of LDL-cholesterol) is reported to have a significant association with diabetes macro- and microvascular complications [6, 19–22]. Our findings, alongside with the results of the previous studies showing that high plasma ox-LDL levels are predictors of subclinical and clinical atherosclerosis [23–25], indicating that controlling ox-LDL level, may prevent the progression of atherosclerotic complications at an early stage.

The origin of ox-LDL is not completely understood. It has been suggested that ox-LDL could be formed enzymatically and/or by metal ion-catalyzed reactions within the circulation [26]. Nevertheless, relative importance of enzyme-mediated and non-enzyme-mediated LDL-cholesterol oxidation remains unclear [27]. These mechanisms are enhanced in diabetic status and progress with diabetes elongation. Increased sensitivity of LDL-cholesterol to oxidation in diabetic patients has been shown in several studies [28, 29]. LDL-cholesterol glycation may represent a predisposing event that facilitates subsequent oxidative modification [28, 29]. Advanced glycosylated end-products (AGEs) may induce the production of ox-LDL from macrophages, even though they do not directly cause oxidation of LDL-cholesterol [30]. Our results support the mechanisms for enhancement of oxidative stress in parallel with an increase in diabetes duration.

Diabetes is a progressive inflammatory condition. As the disease becomes prolonged, elevated free radical formation, elevated inflammatory cytokines and an overwhelming

endogenous anti-inflammatory response, propagate the oxidative stress in diabetic patients [31, 32]. It can be hypothesized that, alongside with the progression of the inflammatory status, ox-LDL increases with the chronicity of diabetes [33]. It was shown that ox-LDL is associated with hypercholesterolemia and high serum LDL-cholesterol [34, 35]. Surprisingly, in our results, we found a significant increase in the ox-LDL level in parallel with a decrease in the LDL-cholesterol level in patients with prolonged diabetes. Our findings can suggest that possibly the chronicity of diabetes is a potential mechanism that can independently increase the level of ox-LDL in diabetic patients. It has already been shown that a change in the ox-LDL level certainly does not occur in parallel with a change in the LDL-cholesterol level. As described by Holvoet [36], impaired glycemic control is associated with an in vivo increase in LDL-cholesterol oxidation irrespective of decreased or stable LDL-cholesterol levels. It has also been reported that a reduction in LDL-cholesterol can occur along with an unchanged ox-LDL level [37].

Maintaining LDL-cholesterol at less than 100 mg/dL is widely encouraged in patients with diabetes [10]; however, our results showed that keeping LDL-cholesterol in the aforementioned range does not guarantee a safe level of ox-LDL in diabetic patients as the disease becomes prolonged. As ox-LDL possesses its own consequences on the progression of diabetic complications [6, 7], it would be wise to try to reduce ox-LDL, alongside with controlling the plasma lipid profile in a healthy state.

Many studies have shown the effects of statins, 3-hydroxy-3-methylglutaryl coenzyme A reductase inhibitors, in lowering LDL-cholesterol and oxidative stress [11]. Of note, it has been demonstrated that statins reduce ox-LDL production [38, 39], and decrease total body fat oxidation [40]. A study by Van Tits et al. [41] reported a decrease of 35–43% in ox-LDL by therapeutic intervention with statins in patients with familial hypercholesterolemia. Statins posses well-documented beneficial effects on vascular redox state [42] and exert anti-inflammatory effects [38, 43–45]. Nevertheless, it should be taken into account that most of the studies on effects of statins on oxidative stress are confined to in vitro researches and there are still doubts about the in vivo effects of these agents. For example, Bredie et al. [12] reported no changes in the oxidative susceptibility of LDL-cholesterol after Simvastatin therapy. In our study, approximately one-third of patients with prolonged diabetes were receiving statins for optimizing their serum LDL-cholesterol levels. There were no significant differences in ox-LDL in patients receiving statins or not. Regardless of statin treatment, patients with prolonged diabetes had dramatically higher ox-LDL in comparison to newly diagnosed patients. Here lies an interesting finding of this study. It can be inferred from our results that independent of the effect of keeping LDL-cholesterol below 100 mg/dL, or using statins, there are other more-influential mechanisms (possibly the chronicity of diabetes) which increase ox-LDL on prolongation of diabetes.

In reviewing this study, one should pay attention to the limitations regarding using cross-sectional data, which precludes a determination of the direction of causality. Using the same ELISA kit as our study, it has been reported that ox-LDL significantly correlates with LDL-cholesterol [34, 41]. In our study, we were unable to show this association in any of our three groups. It should be noted that because of the limited statistical power, this non-significant association should be interpreted with caution. Further prospective studies are paramount to evaluate the effects of lipid lowering agents and/or anti-oxidants in lowering ox-LDL in patients with different durations of diabetes.

In conclusion, this study showed that the serum ox-LDL levels increase with the length of diabetes, even though the patients' lipid profiles are maintained at a desirable level. Our findings highlight that possibly more attention should be focused on markers of oxidative stress in the management of lipids in diabetic patients.

Conflict of interest statement The authors declare that they have no conflict of interests.

References

1. Renie G, Maingrette F, Li L (2007) Diabetic vasculopathy and the lectin-like oxidized low-density lipoprotein receptor-1 (LOX-1). Curr Diabetes Rev 3:103–110
2. Brownlee M (2005) The pathobiology of diabetic complications: a unifying mechanism. Diabetes 54:1615–1625
3. Wei W, Liu Q, Tan Y, Liu L, Li X, Cai L (2009) Oxidative stress, diabetes, and diabetic complications. Hemoglobin 33:370–377
4. Piarulli F, Lapolla A, Sartore G, Rossetti C, Bax G, Noale M, Minicuci N, Fiore C, Marchioro L, Manzato E, Fedele D (2005) Autoantibodies against oxidized LDLs and atherosclerosis in type 2 diabetes. Diabetes Care 28:653–657
5. Rashidi A, Nakhjavani M, Esteghamati A, Asgarani F, Khalilzadeh O, Abbasi M, Safari R (2009) Association between oxidant/antioxidant markers and proteinuria in type 2 diabetes: results in 142 patients. J Nephrol 22(6):733–738
6. Nakhjavani M, Esteghamati A, Khalilzadeh O, Asgarani F, Mansournia N, Abbasi M (2009) Association of macroalbuminuria with oxidized LDL and TGF-beta in type 2 diabetic patients: a case-control study. Int Urol Nephrol [Epub ahead of print]
7. Veiraiah A (2005) Hyperglycemia, lipoprotein glycation, and vascular disease. Angiology 56:431–438
8. Woodman RJ, Watts GF, Playford DA, Best JD, Chan DC (2005) Oxidized LDL and small LDL particle size are independently predictive of a selective defect in microcirculatory endothelial function in type 2 diabetes. Diabetes Obes Metab 7:612–617
9. Silverstein RL (2009) Inflammation, atherosclerosis, and arterial thrombosis: role of the scavenger receptor CD36. Cleve Clin J Med 76(Suppl 2):S27–S30

10. Silverstein RL (2001) Executive summary of the third report of The National Cholesterol Education Program (NCEP) expert panel on detection, evaluation, and treatment of high blood cholesterol in adults (Adult Treatment Panel III). JAMA 285:2486–2497
11. Rosenson RS (2004) Statins in atherosclerosis: lipid-lowering agents with antioxidant capabilities. Atherosclerosis 173:1–12
12. Bredie SJ, de Bruin TW, Demacker PN, Kastelein JJ, Stalenhoef AF (1995) Comparison of gemfibrozil versus simvastatin in familial combined hyperlipidemia and effects on apolipoprotein-B-containing lipoproteins, low-density lipoprotein subfraction profile, and low-density lipoprotein oxidizability. Am J Cardiol 75:348–353
13. American Diabetes Association (2008) Diagnosis and classification of diabetes mellitus. Diabetes Care 31(Suppl 1):S55–S60
14. Lapointe A, Couillard C, Piche ME, Weisnagel SJ, Bergeron J, Nadeau A, Lemieux S (2007) Circulating oxidized LDL is associated with parameters of the metabolic syndrome in postmenopausal women. Atherosclerosis 191:362–368
15. Holvoet P, Lee DH, Steffes M, Gross M, Jacobs DR Jr (2008) Association between circulating oxidized low-density lipoprotein and incidence of the metabolic syndrome. JAMA 299:2287–2293
16. Nakhjavani M, Esteghamati A, Asgarani F, Khalilzadeh O, Nikzamir A, Safari R (2009) Association of oxidized low-density lipoprotein and transforming growth factor-beta in type 2 diabetic patients: a cross-sectional study. Transl Res 153:86–90
17. Njajou OT, Kanaya AM, Holvoet P, Connelly S, Strotmeyer ES, Harris TB, Cummings SR, Hsueh WC (2009) Association between oxidized LDL, obesity and type 2 diabetes in a population-based cohort, the Health, Aging and Body Composition Study. Diabetes Metab Res Rev 25:733–739
18. Gokulakrishnan K, Deepa R, Velmurugan K, Ravikumar R, Karkuzhali K, Mohan V (2007) Oxidized low-density lipoprotein and intimal medial thickness in subjects with glucose intolerance: the Chennai Urban Rural Epidemiology Study-25. Metabolism 56:245–250
19. Girona J, Manzanares JM, Marimon F, Cabre A, Heras M, Guardiola M, Ribalta J, Masana L (2008) Oxidized to non-oxidized lipoprotein ratios are associated with arteriosclerosis and the metabolic syndrome in diabetic patients. Nutr Metab Cardiovasc Dis 18:380–387
20. Huang H, Mai W, Liu D, Hao Y, Tao J, Dong Y (2008) The oxidation ratio of LDL: a predictor for coronary artery disease. Dis Markers 24:341–349
21. Tsuzura S, Ikeda Y, Suehiro T, Ota K, Osaki F, Arii K, Kumon Y, Hashimoto K (2004) Correlation of plasma oxidized low-density lipoprotein levels to vascular complications and human serum paraoxonase in patients with type 2 diabetes. Metabolism 53:297–302
22. El-Bassiouni EA, Helmy MH, El-Zoghby SM, El-Nabi Kamel MA, Hosny RM (2007) Relationship between level of circulating modified LDL and the extent of coronary artery disease in type 2 diabetic patients. Br J Biomed Sci 64:109–116
23. Meisinger C, Baumert J, Khuseyinova N, Loewel H, Koenig W (2005) Plasma oxidized low-density lipoprotein, a strong predictor for acute coronary heart disease events in apparently healthy, middle-aged men from the general population. Circulation 112:651–657
24. Hulthe J, Fagerberg B (2002) Circulating oxidized LDL is associated with subclinical atherosclerosis development and inflammatory cytokines (AIR study). Arterioscler Thromb Vasc Biol 22:1162–1167
25. Ishigaki Y, Katagiri H, Gao J, Yamada T, Imai J, Uno K, Hasegawa Y, Kaneko K, Ogihara T, Ishihara H, Sato Y, Takikawa K, Nishimichi N, Matsuda H, Sawamura T, Oka Y (2008) Impact of plasma oxidized low-density lipoprotein removal on atherosclerosis. Circulation 118:75–83
26. Steinberg D (1997) Low density lipoprotein oxidation and its pathobiological significance. J Biol Chem 272:20963–20966
27. Young IS, McEneny J (2001) Lipoprotein oxidation and atherosclerosis. Biochem Soc Trans 29:358–362
28. Rahimi R, Nikfar S, Larijani B, Abdollahi M (2005) A review on the role of antioxidants in the management of diabetes and its complications. Biomed Pharmacother 59:365–373
29. Scheffer PG, Teerlink T, Heine RJ (2005) Clinical significance of the physicochemical properties of LDL in type 2 diabetes. Diabetologia 48:808–816
30. Matsui J, Onuma T, Tamasawa N, Suda T (1997) Effects of advanced glycation endproducts on the generation of macrophage-mediated oxidized low-density lipoprotein. J Diabetes Complicat 11:338–342
31. Scott JA, King GL (2004) Oxidative stress and antioxidant treatment in diabetes. Ann N Y Acad Sci 1031:204–213
32. Lipinski B (2001) Pathophysiology of oxidative stress in diabetes mellitus. J Diabetes Complicat 15:203–210
33. Chen X, Zhang T, Du G (2008) Advanced glycation end products serve as ligands for lectin-like oxidized low-density lipoprotein receptor-1(LOX-1): biochemical and binding characterizations assay. Cell Biochem Funct 26:760–770
34. van der Zwan LP, Teerlink T, Dekker JM, Henry RM, Stehouwer CD, Jakobs C, Heine RJ, Scheffer PG (2009) Circulating oxidized LDL: determinants and association with brachial flow-mediated dilation. J Lipid Res 50:342–349
35. Duarte MM, Rocha JB, Moresco RN, Duarte T, Da Cruz IB, Loro VL, Schetinger MR (2009) Association between ischemia-modified albumin, lipids and inflammation biomarkers in patients with hypercholesterolemia. Clin Biochem 42:666–671
36. Holvoet P (2008) Relations between metabolic syndrome, oxidative stress and inflammation and cardiovascular disease. Verh K Acad Geneeskd Belg 70:193–219
37. Lee IT, Chan YC, Lin CW, Lee WJ, Sheu WH (2008) Effect of cranberry extracts on lipid profiles in subjects with type 2 diabetes. Diabet Med 25:1473–1477
38. Oka H, Ikeda S, Koga S, Miyahara Y, Kohno S (2008) Atorvastatin induces associated reductions in platelet P-selectin, oxidized low-density lipoprotein, and interleukin-6 in patients with coronary artery diseases. Heart Vessels 23:249–256
39. Obata T, Yonemoti H, Aomine M (2009) The protective effect of fluvastatin on hydroxyl radical generation by inhibiting low-density lipoprotein (LDL) oxidation in the rat myocardium. Microvasc Res 77:163–165
40. Fisher NM, Meksawan K, Limprasertkul A, Isackson PJ, Pendergast DR, Vladutiu GD (2007) Statin therapy depresses total body fat oxidation in the absence of genetic limitations to fat oxidation. J Inherit Metab Dis 30:388–399
41. van Tits LJ, van Himbergen TM, Lemmers HL, de Graaf J, Stalenhoef AF (2006) Proportion of oxidized LDL relative to plasma apolipoprotein B does not change during statin therapy in patients with heterozygous familial hypercholesterolemia. Atherosclerosis 185:307–312
42. Antonopoulos AS, Antoniades C, Tousoulis D, Bakogiannis C, Demosthenous M, Psarros C, Stefanadis C (2009) Novel therapeutic strategies targeting vascular redox in human atherosclerosis. Recent Pat Cardiovasc Drug Discov 4:76–87
43. Okopien B, Krysiak R, Kowalski J, Madej A, Belowski D, Zielinski M, Labuzek K, Herman ZS (2004) The effect of statins and fibrates on interferon-gamma and interleukin-2 release in patients with primary type II dyslipidemia. Atherosclerosis 176:327–335
44. Ferro D, Parrotto S, Basili S, Alessandri C, Violi F (2000) Simvastatin inhibits the monocyte expression of proinflammatory

cytokines in patients with hypercholesterolemia. J Am Coll Cardiol 36:427–431
45. Rosenson RS, Tangney CC, Parker TS, Levine DM, Gordon BR (2002) Statin therapy reduces oxidative stress and inhibits monocyte chemoattractant protein-1 (MCP-1) production in healthy adults with moderate hypercholesterolemia. Circulation 106(Suppl II):A3669

Lipids (2010) 45:329–335
DOI 10.1007/s11745-010-3402-7

ORIGINAL ARTICLE

Pitavastatin Reduces Lectin-Like Oxidized Low-Density Lipoprotein Receptor-1 Ligands in Hypercholesterolemic Humans

Tetsuya Matsumoto · Masatoshi Fujita · Tatsuya Sawamura · Akemi Kakino · Yuko Sato · Yoshiko Fujita · Haruo Matsuda · Mamoru Nakanishi · Kagehiro Uchida · Izuru Nakae · Hiroshi Kanda · Akira Yoshida · Kunihisa Miwa · Hideki Hayashi · Kenichi Mitsunami · Minoru Horie

Received: 30 November 2009 / Accepted: 23 February 2010 / Published online: 13 March 2010

Abstract The aim of this study was to determine the impact of pitavastatin on low-density lipoprotein cholesterol (LDL-C) and lectin-like oxidized LDL receptor-1 (LOX-1) in patients with hypercholesterolemia. Twenty-five hypercholesterolemic patients (8 male, 17 female; age 66 ± 13, 21–80 years) who had not received anti-dyslipidemic agents and had LDL-C levels of more than 160 mg/dL were examined. Biochemical factors were measured at baseline and after treatment with pitavastatin (2 mg/day) for 6 months. Serum levels of LOX-1 with apolipoprotein B-100 particle ligand and a soluble form of LOX-1 (sLOX-1) were measured by ELISA. All subjects completed the study with no adverse side effects. Total-C (268 ± 26 vs. 176 ± 17 mg/dL), LDL-C (182 ± 21 vs. 96 ± 14 mg/dL), and LOX-1 ligand (867 ± 452 vs. 435 ± 262 ng/mL) were reduced with pitavastatin treatment ($P < 0.0001$ for each). Significant decreases in triacylglycerols were noted ($P < 0.0001$), but there were no changes in high-density lipoprotein cholesterol. After 6 months, there were no significant changes in high-sensitivity CRP or soluble LOX-1. At baseline, there were no significant correlations between LOX-1 ligand and either LDL-C or sLOX-1. The decrease in LOX-1 ligand was not correlated with the decrease in LDL-C, but was correlated with the decrease in sLOX-1 ($r = 0.47$, $P < 0.05$). In conclusion, pitavastatin therapy had beneficial effects on markers of oxidative stress in hypercholesterolemic subjects. Serum

T. Matsumoto (✉) · H. Hayashi · M. Horie
Department of Cardiovascular and Respiratory Medicine, Shiga University of Medical Science, Seta Tsukinowa, Otsu, Shiga 520-2192, Japan
e-mail: tetsuyam@belle.shiga-med.ac.jp

M. Fujita
Human Health Sciences, Graduate School of Medicine, Kyoto University, Kyoto, Japan

T. Sawamura · A. Kakino · Y. Sato · Y. Fujita
Department of Vascular Physiology, National Cardiovascular Center Research Institute, Suita, Japan

H. Matsuda
Laboratory of Immunology, Department of Molecular and Applied Biology, Graduate School of Biosphere Science, Hiroshima University, Hiroshima, Japan

M. Nakanishi · K. Uchida
Biomarker Science Co., Ltd., Osaka, Japan

I. Nakae
Department of Internal Medicine, Jyohoku Hospital, Kyoto, Japan

H. Kanda
Division of Internal Medicine, Hamamatsu Rosai Hospital, Hamamatsu, Japan

A. Yoshida
Department of Internal Medicine, Mitsubishi Kyoto Hospital, Kyoto, Japan

K. Miwa
Department of Internal Medicine, Nanto Family and Community Medical Center, Toyama, Japan

K. Mitsunami
Department of Family Medicine, Shiga University of Medical Science, Otsu, Japan

levels of LOX-1 ligand may be a useful biomarker of the pleiotropic effects of statins.

Keywords Pitavastatin · Lectin-like oxidized low-density lipoprotein receptor-1 (LOX-1) · Pleiotropic effects

Abbreviations

LOX-1	Lectin-like oxidized LDL receptor-1
sLOX-1	Soluble LOX-1
LDL-C	Low-density lipoprotein cholesterol
HDL-C	High-density lipoprotein cholesterol
OxLDL	Oxidized low-density lipoprotein
CRP	C-reactive protein
ELISA	Enzyme-linked immunosorbent assay
TAG	Triacylglycerol
TC	Total cholesterol

Introduction

Numerous clinical studies on statin therapy have demonstrated that a reduction in plasma levels of low-density lipoprotein cholesterol (LDL-C) prevents atherosclerotic progression and decreases cardiovascular risk [1–3]. There is a growing body of evidence that the oxidative modification of LDL is involved in the progression of atherosclerosis. It has been reported that plasma levels of oxidized LDL (OxLDL) were elevated in patients with coronary artery disease, and were associated with plaque instability in coronary artery disease [4, 5]. However, the clinical study of LDL oxidation has been hampered by the difficulty of a specific assay for plasma levels of OxLDL. It has been shown that statins reduce the production of reactive oxygen species through pleiotropic effects independent of cholesterol reduction [6–8]. The effects of statins on various circulating biomarkers of oxidative stress have been reported in clinical studies.

Lectin-like OxLDL receptor-1 (LOX-1) is a receptor for OxLDL that is mainly expressed in vascular endothelial cells, and OxLDL uptake through this receptor may be involved in endothelial dysfunction in atherogenesis [9, 10]. More recently, a novel sandwich enzyme immunoassay for LOX-1-ligand, which uses a recombinant soluble form of LOX-1 and anti-apoB antibody, has been developed to detect circulating modified LDL via specific binding to LOX-1 [11].

Pitavastatin is a strong statin similar to atorvastatin and rosuvastatin [12–14], and has been shown to have pleiotropic effects in vitro. To date, there have been no reports on the relations between the effects of pitavastatin on LDL levels and LDL oxidation in humans. Thus, we examined the effects of pitavastatin on serum levels of LOX-1 ligand activity and soluble LOX-1 (sLOX-1), and their relationships in patients with hypercholesterolemia.

Methods

Study Patients

Twenty-five subjects, between the ages of 21 and 80 years, with a baseline LDL-C between 160 and 220 mg/dL who were not receiving lipid-lowering therapy were recruited. Exclusion criteria included exposure to cholesterol-reducing drugs within the previous 6 weeks, coronary artery disease, congestive heart failure, significant renal or hepatic disease, familial hypercholesterolemia, and pregnant or lactating women.

Protocol

After informed consent was obtained from all participants before the study, pitavastatin was administered at a dose of 2 mg/day for 6 months. Data obtained before and after 6 months of treatment with pitavastatin included fasting blood work, adverse events, and the results of a physical examination. Laboratory analyses of blood work included lipid analyses and the assessment of other biomarkers. All assays were carried out by personnel who did not know the clinical characteristics of the patients.

Measurement of Biomarkers

Blood samples for measuring the plasma or serum concentrations of parameters were collected from the peripheral vein at the time of the patient visit. The blood samples were immediately placed on ice and centrifuged at −30 °C until assay.

Lipid parameters [total cholesterol (TC), LDL-C, high-density lipoprotein cholesterol (HDL-C), and triacylglycerol (TAG)] were analyzed from ethylenediaminetetraacetic acid-treated plasma, and determined by commercially available enzymatic-colorimetric methods. Serum levels of high-sensitivity CRP were determined by a sensitive nephelometric assay (Dade, Behring, Japan). Fasting blood sugar, hemoglobin A1c, creatinine, uric acid, and creatine kinase, and a liver function test were measured by standard techniques.

Measurement of sLOX-1

According to a previous report [15], serum sLOX-1 levels were determined by a sandwich ELISA. Forty microliter of

standard recombinant human LOX-1 (61-273) or fourfold-diluted sera were applied to 384-well plates immobilizing anti-human LOX-1 antibody (TS92, 0.25 μg/well) [9]. Bound sLOX-1 was detected by the combination of another anti-human LOX-1 antibody (HUC5-40) and a peroxidase-conjugated donkey anti-chicken IgY (AP194P, Chemicon, MA) with TMB solution.

Measurement of LOX-1 Ligand Activity

LOX-1 ligand activities in plasma were determined according to a previous report [11]. Recombinant LOX-1 (0.4 μg/well) was immobilized on 96-well plates (Maxisorp, Nunc) by incubating overnight at 4 °C in 50 μL of PBS. After being washed twice with PBS, the plates were blocked with 0.3 mL of 20% (v/v) ImmunoBlock (DS Pharma) for 8 h at 4 °C. After being washed three times with PBS, the plates were incubated with 0.1 mL of the standard OxLDL or plasma diluted 40-fold with EDTA–HEPES buffer [10 mM HEPES (pH 7.0), 150 mM NaCl, 2 mM EDTA]. The plates were then washed three times with PBS, and incubated for 1 h at room temperature with 0.5 μg/mL HUC20, a chicken monoclonal antibody that recognizes mouse and human ApoB, in PBS containing 1% (w/v) BSA. After being washed three times with PBS, the plates were incubated for 1 h at room temperature with peroxidase-conjugated goat anti-chicken IgG (H + L) (KPL, Gaithersburg, MD) diluted 2,000-fold with PBS containing 1% (w/v) BSA. After being washed five times with PBS, a substrate solution containing 3,3′, 5,5′-tetramethylbenzidine (TMB solution, Bio-Rad Laboratories, Hercules, CA) was added to the plates and incubated at room temperature for 30 min. The reaction was terminated by the addition of 50 μL of 2 M sulfuric acid. Peroxidase activity was determined by the measurement of absorbance at 450 nm.

Statistical Analysis

Data are expressed as the mean values ± SD. To analyze the effects of treatment with pitavastatin for 6 months, the paired Student's *t* test was applied to paired data. Linear regression analyses were carried out to detect correlations between continuous valuables. A value of $P < 0.05$ was considered statistically significant.

Results

Subject Characteristics

The characteristics of the study population are shown in Table 1. The mean age of the study population was 63 ± 13 years and most of the subjects were female (68%). The subjects enrolled in this study had hypertension ($n = 16$, 64%) and diabetes mellitus ($n = 1$, 4%). Similar medical treatments were continued throughout the study period. Systolic and diastolic arterial pressures and pulse rate did not change during the study period (Table 1). All subjects completed the 6-month study protocol without any adverse side effects, and no clinical disorder developed during the study period.

Effects of Pitavastatin on Biochemical Profiles

Table 1 shows the lipid parameters before and after pitavastatin treatment. Before pitavastatin treatment, TC and LDL-C levels were abnormally high (268 ± 26 and 182 ± 21 mg/dL, respectively). TC (268 ± 26 vs. 176 ± 17 mg/dL) and LDL-C (182 ± 21 vs. 96 ± 14 mg/dL) significantly decreased after pitavastatin treatment ($P < 0.0001$ for each) (Table 1; Fig. 1a). Although pitavastatin treatment significantly decreased TAG from 145 ± 65 to 104 ± 40 mg/dL ($P < 0.0001$), it did not significantly change HDL-C (before, 57 ± 14 mg/dL; after, 58 ± 15 mg/dL; P = ns) (Table 1). Fasting blood sugar, hemoglobin A1c, uric acid, and creatinine phosphokinase were unchanged during the study period (Table 1). Other biochemical markers including liver function were unchanged (data not shown).

Measurement of LDL Ligands, sLOX-1, and High-Sensitivity CRP

LOX-1 ligands remarkably decreased with pitavastatin treatment (867 ± 452 vs. 435 ± 262 ng/mL, $P < 0.0001$)

Table 1 Hemodynamic and biochemical parameters before and after pitavastatin treatment

	Before	After	
Systolic BP (mmHg)	136 ± 20	123 ± 16	ns
Diastolic BP (mmHg)	78 ± 15	69 ± 9	ns
Pulse rate (/min)	71 ± 11	72 ± 12	ns
Total cholesterol (mg/dL)	268 ± 26	176 ± 17	$P < 0.0001$
LDL-cholesterol (mg/dL)	182 ± 21	96 ± 14	$P < 0.0001$
HDL-cholesterol (mg/dL)	57 ± 14	58 ± 15	ns
Triglyceride (mg/dL)	145 ± 65	104 ± 40	$P < 0.0001$
FBS (mg/dL)	108 ± 30	104 ± 20	ns
Hemoglobin A1c (%)	5.6 ± 0.4	5.6 ± 0.5	ns
CK (IU/L)	117 ± 57	162 ± 99	ns
Uric acid (mg/dL)	5.9 ± 2.0	5.6 ± 1.5	ns
Creatinine (mg/dL)	0.8 ± 0.2	0.8 ± 0.2	ns

Values are means ± SD

BP blood pressure, *FBS* fasting blood sugar, *CK* creatine kinase

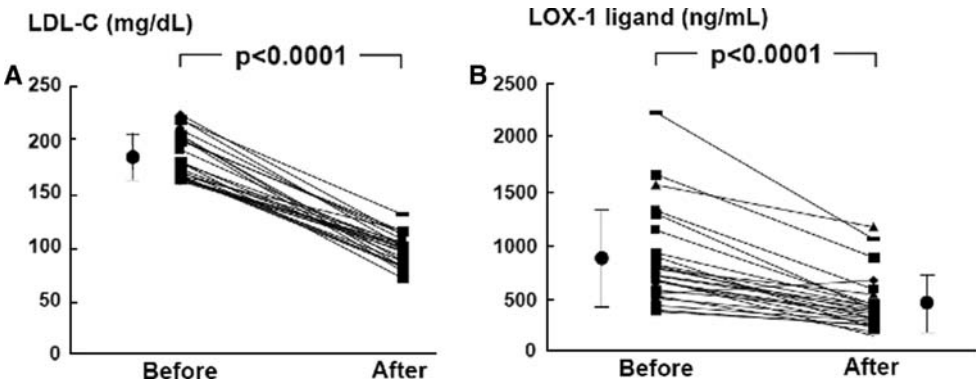

Fig. 1 Levels of low-density lipoprotein cholesterol (LDL-C) (**a**) and lectin-like oxidized LDL receptor-1 (LOX-1) ligand (**b**) before and after 6 months of treatment with pitavastatin

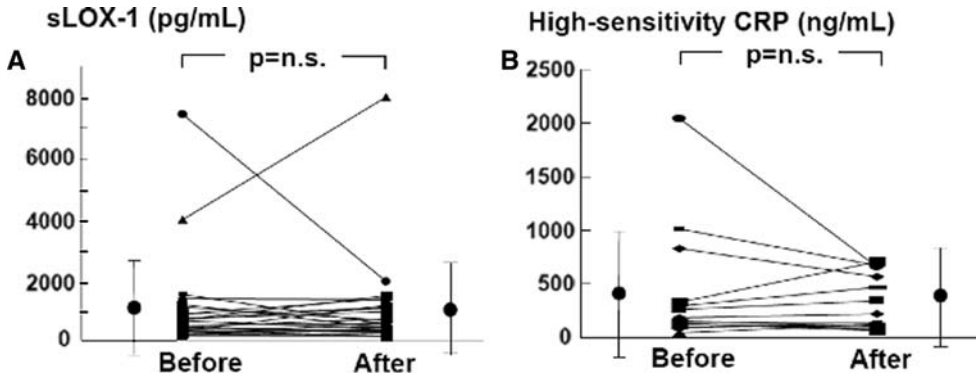

Fig. 2 Levels of soluble LOX-1 (sLOX-1) (**a**) and high-sensitivity CRP (**b**) before and after 6 months of treatment with pitavastatin

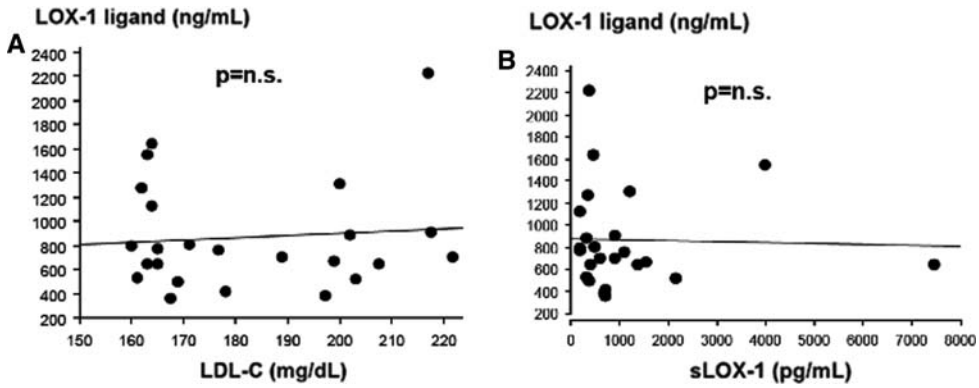

Fig. 3 Relationship between LOX-1 ligands and LDL-C before pitavastatin treatment (**a**). Relationship between LOX-1 ligands and sLOX-1 before pitavastatin treatment (**b**)

(Fig. 1b). Meanwhile, soluble LOX-1 (1,059 ± 1,530 vs. 1,022 ± 1,526 pg/mL) (Fig. 2a) and high-sensitivity CRP (0.42 ± 0.59 vs. 0.39 ± 0.45 mg/L) (Fig. 2b) did not change with pitavastatin treatment. In a 73-year-old woman with hypertension and stable angina pectoris, a marked increase in soluble LOX-1 levels was observed after treatment with pitavastatin (3,980–8,010 pg/mL). Her clinical characteristics and medical treatments did not change during the study period.

Before pitavastatin treatment, there was no significant linear correlation between LOX-1 ligands and LDL-C (Fig. 3a), or between LOX-1 ligands and sLOX-1 (Fig. 3b). In two subjects, basal sLOX-1 levels were far higher (>3,000 pg/mL) than those in the other 22 subjects. In the remaining 22 subjects, the degree of the reduction in LOX-1 ligands correlated with that in sLOX-1 (Fig. 4a), but not that in LOX-1 ligands (Fig. 4b).

Discussion

We first demonstrated that treatment with pitavastatin reduced LOX-1 ligands as well as TC, LDL-C, and TAG in hypercholesterolemic patients. The measurement of LOX-1 ligands may be useful as a tool for estimating pleiotropic effects of statins.

Statin therapy can ameliorate future cardiovascular events, and this improvement has been ascribed not only to

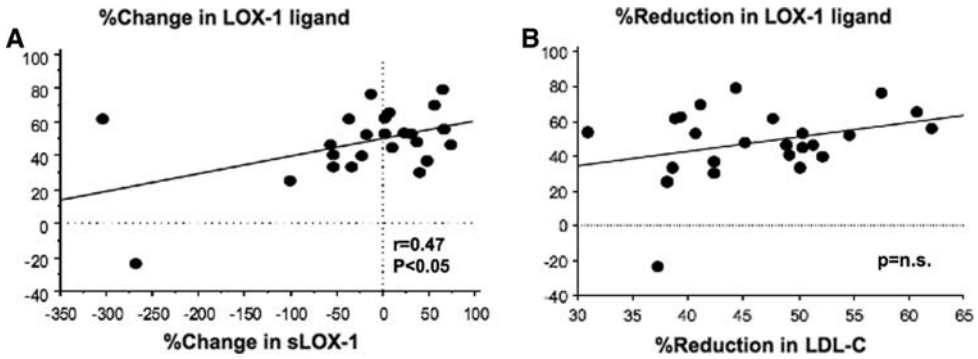

Fig. 4 Relationship between the degree of reduction in LOX-1 ligands and that in sLOX-1 (**a**). Relationship between the degree of reduction in LOX-1 ligands and that in LDL-C (**b**)

reductions in LDL cholesterol but also to the antioxidant properties of statins [6, 8, 16]. Different statins have different antioxidative capacities for LDL oxidation, and it is speculated that pitavastatin hinders the development of atherosclerosis by reducing the oxidative modification of LDL.

OxLDL is implicated in endothelial dysfunction as well as the formation and progression of atherosclerosis [10, 17]. It has been shown that plasma levels of OxLDL were elevated in patients with coronary artery disease, and were associated with the severity of acute coronary syndrome and coronary artery disease [4, 5]. We previously reported that plasma levels of OxLDL were a useful measure of coronary endothelial dysfunction [18]. However, the clinical importance of circulating OxLDL has not yet been fully elucidated.

Several receptors for OxLDL have been identified over the past few years [19–21]. LOX-1 is one such receptor for OxLDL and is expressed in atherosclerotic lesions, including endothelial cells, macrophages, and smooth muscle cells [9, 22]. OxLDL binds to LOX-1, resulting in NADPH oxidase activation and eNOS downregulation, and the atherogenic properties induced by OxLDL are mainly mediated via LOX-1 [10]. LOX-1 can be cleaved at its membrane proximal extracellular domain and released as soluble forms of LOX-1 [23]. It has been reported that serum levels of sLOX-1 are elevated in coronary artery disease [24, 25]. In the present study, soluble LOX-1 did not change after pitavastatin treatment. The expression of LOX-1 could be enhanced by risk factors for atherosclerosis such as hyperlipidemia, hypertension, and diabetes mellitus [22]. In the present study, arterial pressures and biochemical profiles other than lipid levels remained unchanged during the study.

LOX-1 recognizes multiple ligands such as OxLDL, apoptotic cells, bacteria, and platelets [10, 22]. The precise OxLDL epitope recognized by LOX-1 is not known. OxLDL is not one homogeneous entity, but rather represents multiple chemical and immunogenic modifications of the lipid and apoB-100 on LDL. ApoB-containing lipoproteins and their oxidized form play an important role in the pathogenesis of atherosclerosis. We previously demonstrated that plasma levels of LOX-1 ligands were increased in ApoE-deficient mice fed a high-fat diet and there was a link between the level of LOX-1 ligands and the progression of atherosclerosis in mice [11]. Recently, LOX ligands have been shown to be associated with the incidence of cardiovascular disease [15].

In the present study, we showed that pitavastatin can reduce LOX-1 ligands but not sLOX-1. Circulating levels of sLOX-1 may not change after pitavastatin treatment, although the vascular expression of LOX-1 was decreased with pitavastatin treatment. As for pitavastatin, the reduction in LOX-1 ligand levels was similar to that in LDL-cholesterol levels. The changes in LOX-1 ligands were correlated with those in sLOX-1, suggesting a potent link between sLOX-1 and LOX-1 ligands. Before pitavastatin treatment, LOX-1 ligands showed no significant correlation with plasma LDL-C levels. In addition, the degree of the reduction in LOX-1 ligands was not significantly correlated with that in LDL-C levels. Numerous trials have shown that statins can lower LDL-C levels. In addition, LOX-1 ligand levels may be a suitable biomarker for estimating the pleiotropic effects independent of the cholesterol-lowering effects of statins. In previous studies using WHHL rabbits, fluvastatin significantly reduced plasma levels of both LOX-1 ligands and TC, as well as the atherosclerotic lesion area and the cholesterol content of aortic arches [26].

In the present study, treatment with pitavastatin did not change plasma levels of CRP. CRP is produced predominantly in the liver as part of the acute-phase response, and is also expressed in smooth muscle cells within diseased atherosclerotic arteries [27]. CRP and LOX-1 share a range of biological functions. CRP can induce LOX-1 expression [28], and the binding of CRP to LOX-1 enhances the binding affinity of OxLDL to LOX-1 [29]. Statin therapy reduces high-sensitivity CRP by a mechanism beyond LDL reduction [14]. Koshiyama et al. [30] reported that pitavastatin lowered high-sensitivity CRP in patients with hypercholesterolemia. Our modest sample size might have limited the observed effects of pitavastatin on serum high-sensitivity CRP levels. Further studies are needed to

address whether serum levels of LOX-1 ligands are associated with anti-inflammatory, anti-thrombotic, and vascular endothelial effects.

In conclusion, pitavastatin therapy reduces both LDL-C and LOX-1 ligands in hypercholesterolemic subjects. Serum levels of LOX-1 ligands may be a useful biomarker for monitoring the pleiotropic effects of statins, and the reduction of LOX-1 ligands by statins, other antioxidants, or lifestyle modifications may be a promising therapeutic strategy against atherosclerosis and future cardiovascular events.

Study Limitations

Several important questions remain regarding the impact of pitavastatin on LOX-1 in hypercholesterolemic subjects. For example, our findings are limited by the fact that this was an uncontrolled study with a modest number of subjects. Furthermore, we did not address the question of the dose–response effects of pitavastatin on LOX-1. We must validate our findings in randomized, well-controlled and larger human studies. In addition, further analyses must be performed to examine whether patients with risk factors for atherosclerosis have higher levels of LOX-1 ligand activity than healthy subjects.

Acknowledgments We thank Akiko Ikai, Human Health Sciences, Graduate School of Medicine, Kyoto University, for providing technical assistance.

Conflict of interest statement We have no any commercial associations that might pose a conflict of interest in connection with this article.

References

1. Scandinavian Simvastatin Survival Study (4S) Group (1994) Randomized trial of cholesterol lowering in 4444 patients with coronary heart disease. Lancet 344(8934):1383–1389
2. Sacks FM, Pfeffer MA, Moye LA, Rouleau JL, Rutherford JD, Cole TG, Brown L, Warnica JW, Arnold JM, Wun CC, Davis BR, Braunwald E (1996) The effect of pravastatin on coronary events after myocardial infarction in patients with average cholesterol levels. Cholesterol and Recurrent Events Trial investigators. N Engl J Med 335(14):1001–1009
3. Heart Protection Study Collaborative Group (2002) MRC/BHF heart protection study of cholesterol lowering with simvastatin in 20, 536 high-risk individuals: a randomised placebo-controlled trial. Lancet 360(9326):7–22
4. Holvoet P, Vanhaecke J, Janssens S, Van de Werf F, Collen D (1998) Oxidized LDL and malondialdehyde-modified LDL in patients with acute coronary syndromes and stable coronary artery disease. Circulation 98:1487–1494
5. Ehara S, Ueda M, Naruko T, Haze K, Itoh A, Otsuka M, Komatsu R, Matsuo T, Itabe H, Takano T, Tsukamoto Y, Yoshiyama M, Takeuchi K, Yoshikawa J, Becker AE (2001) Elevated levels of oxidized low density lipoprotein show a positive relationship with the severity of acute coronary syndrome. Circulation 103:1955–1960
6. Rikitake Y, Kawashima S, Takeshita S, Yamashita T, Azumi H, Yasuhara M, Nishi H, Inoue N, Yokoyama M (2001) Antioxidative properties of fluvastatin, an HMG-CoA reductase inhibitor, contribute to prevention of atherosclerosis in cholesterol-fed rabbits. Atherosclerosis 154:87–96
7. Wilson SH, Simari RD, Best PJ, Peterson TE, Lerman LO, Aviram M, Nath KA, Holmes DR Jr, Lerman A (2001) Simvastatin preserves coronary endothelial function in hypercholesterolemia in the absence of lipid lowering. Arterioscler Thromb Vasc Biol 21:122–128
8. Sumi D, Hayashi T, Thakur NK, Jayachandran M, Asai Y, Kano H, Matsui H, Iguchi A (2001) A HMG-CoA reductase inhibitor possesses a potent anti-atherosclerotic effect other than serum lipid lowering effects—the relevance of endothelial nitric oxide synthase and superoxide anion scavenging action. Atherosclerosis 155:347–357
9. Sawamura T, Kume N, Aoyama T, Moriwaki H, Hoshikawa H, Aiba Y, Tanaka T, Miwa S, Katsura Y, Kita T, Masaki T (1997) An endothelial receptor for oxidized low-density lipoprotein. Nature 386:73–77
10. Ogura S, Kakino A, Sato Y, Fujita Y, Iwamoto S, Otsui K, Yoshimoto R, Sawamura T (2009) LOX-1: the multifunctional receptor underlying cardiovascular dysfunction. Circ J 73(11):1993–1999
11. Sato Y, Nishimichi N, Nakano A, Takikawa K, Inoue N, Matsuda H, Sawamura T (2008) Determination of LOX-1-ligand activity in mouse plasma with a chicken monoclonal antibody for ApoB. Atherosclerosis 200(2):303–309
12. Hiro T, Kimura T, Morimoto T, Miyauchi K, Nakagawa Y, Yamagishi M, Ozaki Y, Kimura K, Saito S, Yamaguchi T, Daida H, Matsuzaki M, JAPAN-ACS Investigators (2009) Effect of intensive statin therapy on regression of coronary atherosclerosis in patients with acute coronary syndrome: a multicenter randomized trial evaluated by volumetric intravascular ultrasound using pitavastatin versus atorvastatin (JAPAN-ACS [Japan assessment of pitavastatin and atorvastatin in acute coronary syndrome] study). J Am Coll Cardiol 54(4):293–302
13. Yokote K, Bujo H, Hanaoka H, Shinomiya M, Mikami K, Miyashita Y, Nishikawa T, Kodama T, Tada N, Saito Y (2008) Multicenter collaborative randomized parallel group comparative study of pitavastatin and atorvastatin in Japanese hypercholesterolemic patients: collaborative study on hypercholesterolemia drug intervention and their benefits for atherosclerosis prevention (CHIBA study). Atherosclerosis 201(2):345–352
14. Ridker PM, Danielson E, Fonseca FA, Genest J, Gotto AM Jr, Kastelein JJ, Koenig W, Libby P, Lorenzatti AJ, Macfadyen JG, Nordestgaard BG, Shepherd J, Willerson JT, Glynn RJ, JUPITER Trial Study Group (2009) Reduction in C-reactive protein and LDL cholesterol and cardiovascular event rates after initiation of rosuvastatin: a prospective study of the JUPITER trial. Lancet 373(9670):1175–1182
15. Inoue N, Okamura T, Kokubo Y, Fujita Y, Sato Y, Nakanishi M, Yanagida K, Kaikino A, Iwamoto S, Watanabe M, Ogura S, Otsui K, Matsuda H, Uchida K, Yoshimoto R, Sawamura T (2010) LOX index, a novel predictive biochemical marker for coronary heart disease and stroke. Clinical Chemistry (in press)
16. Liao JK (2005) Effects of statins on 3-hydroxy-3-methylglutaryl coenzyme A reductase inhibition beyond low-density lipoprotein cholesterol. Am J Cardiol 96(5A):24F–33F
17. Kugiyama K, Kerns SA, Morrisett JD, Roberts R, Henry PD (1990) Impairment of endothelium-dependent arterial relaxation by lysolecithin in modified low-density lipoproteins. Nature 344:160–162

18. Matsumoto T, Takashima H, Ohira N, Tarutani Y, Yasuda Y, Yamane T, Matsuo S, Horie M (2004) Plasma level of oxidized low-density lipoprotein is an independent determinant of coronary macrovasomotor and microvasomotor responses induced by bradykinin. J Am Coll Cardiol 44(2):451–457
19. Kodama T, Freeman M, Rohrer L, Zabrecky J, Matsudaira P, Krieger M (1990) Type I macrophage scavenger receptor contains alpha-helical and collagen-like coiled coils. Nature 343:531–535
20. Endemann G, Stanton LW, Madden KS, Bryant CM, White RT, Protter AA (1993) CD36 is a receptor for oxidized low density lipoprotein. J Biol Chem 268:11811–11816
21. Ramprasad MP, Terpstra V, Kondratenko N, Quehenberger O, Steinberg D (1996) Cell surface expression of mouse macrosialin and human CD68 and their role as macrophage receptors for oxidized low density lipoprotein. Proc Natl Acad Sci USA 93:14833–14838
22. Chen M, Masaki T, Sawamura T (2002) LOX-1, the receptor for oxidized low-density lipoprotein identified from endothelial cells: implications in endothelial dysfunction and atherosclerosis. Pharmacol Ther 95(1):89–100
23. Murase T, Kume N, Kataoka H, Minami M, Sawamura T, Masaki T, Kita T (2000) Identification of soluble forms of lectin-like oxidized LDL receptor-1. Arterioscler Thromb Vasc Biol 20(3):715–720
24. Hayashida K, Kume N, Murase T, Minami M, Nakagawa D, Inada T, Tanaka M, Ueda A, Kominami G, Kambara H, Kimura T, Kita T (2005) Serum soluble lectin-like oxidized low-density lipoprotein receptor-1 levels are elevated in acute coronary syndrome: a novel marker for early diagnosis. Circulation 112(6):812–818
25. Lubrano V, Del Turco S, Nicolini G, Di Cecco P, Basta G (2008) Circulating levels of lectin-like oxidized low-density lipoprotein receptor-1 are associated with inflammatory markers. Lipids 43(10):945–950
26. Oka K, Yasuhara M, Suzumura K, Tanaka K, Sawamura T (2006) Antioxidants suppress plasma levels of lectin like oxidized low-density lipoprotein receptor-ligands and reduce atherosclerosis in Watanabe heritable hyperlipidemic rabbits. J Cardiovasc Pharmacol 48(4):177–183
27. Calabro P, Willerson JT, Yeh ET (2003) Inflammatory cytokines stimulated C-reactive protein production by human coronary artery smooth muscle cells. Circulation 108:1930–1932
28. Li L, Roumeliotis N, Sawamura T, Renier G (2004) C-reactive protein enhances LOX-1 expression in human aortic endothelial cells: relevance of LOX-1 to C-reactive protein-induced endothelial dysfunction. Circ Res 95(9):877–883
29. Fujita Y, Kakino A, Nishimichi N, Yamaguchi S, Sato Y, Machida S, Cominacini L, Delneste Y, Matsuda H, Sawamura T (2009) Oxidized LDL receptor LOX-1 binds to C-reactive protein and mediates its vascular effects. Clin Chem 55(2):285–294
30. Kansai Investigation of Statin for Hyperlipidemic Intervention in Metabolism and Endocrinology (KISHIMEN) investigators, Koshiyama H, Taniguchi A, Tanaka K, Kagimoto S, Fujioka Y, Hirata K, Nakamura Y, Iwakura A, Hara K, Yamamoto T, Kuroe A, Ohya M, Fujimoto S, Hamamoto Y, Honjo S, Ikeda H, Nabe K, Tsuda K, Inagaki N, Seino Y, Kume N (2008) Effects of pitavastatin on lipid profiles and high-sensitivity CRP in Japanese subjects with hypercholesterolemia. J Atheroscler Thromb 15(6):345–350

Lipids (2010) 45:337–344
DOI 10.1007/s11745-010-3399-y

ORIGINAL ARTICLE

Exercise and Zoledronic Acid on Lipid Profile and Bone Remodeling in Ovariectomized Rats: a Paradoxical Negative Association?

E. Lespessailles · C. Jaffré · G. Y. Rochefort · E. Dolléans · C. L. Benhamou · D. Courteix

Received: 3 August 2009 / Accepted: 11 February 2010 / Published online: 13 March 2010

Abstract Exercise (EXE) and amino-bisphosphonates (BP) are both considered as useful strategies in the prevention of post-menopausal bone loss. Exercise reduces lipid levels, and BP may induce increase in high-density lipoprotein cholesterol (HDL-C). We hypothesized that combined effects of BP and exercise would produce a better improvement of lipid profile. We studied the specific and combined effects of zoledronic acid (Z) and EXE on lipid profile and bone remodeling in mature ovariectomized (OVX) rats. Six-month old female rats were randomly assigned to either a sham-ovx group ($n = 12$) or one of four OVX groups ($n = 12$): vehicle-treated sedentary (OVX); OVX + EXE (OVX-E, running on a treadmill for 12 weeks); OVX + Z (20 μg/kg, i.v.), (OVX-Z); OVX + Z+EXE (OVX-ZE). Total cholesterol (TC), HDL-C and bone remodeling markers were measured at baseline and at the end of the study. We demonstrated that both Z and EXE prevented the increase in bone resorption resulting from OVX, and individually improved the atherosclerotic risk index. Therapy with Z resulted in significant increase (39.00 ± 0.03 vs. 53.6 ± 0.01 mg/dl; +37.4%, $P < 0.05$) in serum concentration of HDL-C and a non significant decrease in TC (135.30 ± 0.03 vs. 144.80 ± 0.05 mg/dl; −5.8%) in the OVX-Z group compared to the OVX group. Post-menopausal women have elevated risk of CVD and bone resorption, hence, these data ultimately demonstrate (except for the elevated ratio in the combined group) that exercise and zoledronic acid are useful in minimizing the impact of these two processes in women and the combination of the two may be clinically relevant.

Keywords Lipid metabolism · Atherosclerosis

Abbreviations

BP	Amino-bisphosphonates
BW	Body weight
CTx	C terminal collagen cross-links
EXE	Exercise
FM	Fat mass
FPPS	Farnesyl pyrophosphate synthetase
HDL-C	High-density lipoprotein cholesterol
HRT	Hormonal-replacement therapy
LBM	Lean body mass
LDL-C	Low-density lipoprotein cholesterol
OC	Osteocalcin
OVX	Ovariectomy/ovariectomized
OVX-E	Ovariectomized + Exercise trained animal
OVX-Z	Ovariectomized + Zoledronic acid treated animal
OVX-ZE	Ovariectomized + Zoledronic acid treated + Exercise trained animal
PTH	Parathyroid hormone
SH	Sham-operated animal
TC	Total cholesterol
TC	Total serum cholesterol
TNF-α	Tumor necrosis factor alpha
UI	Uncoupling index
WB	Whole body
WBBMC	Whole body bone mineral content
WBBMD	Whole body bone mineral density
Z	Zoledronic acid

E. Lespessailles and C. Jaffré contributed equally to this work.

E. Lespessailles · C. Jaffré · G. Y. Rochefort (✉) · E. Dolléans · C. L. Benhamou · D. Courteix
UMR-S658 INSERM, CHR ORLEANS Porte Madeleine, BP 2439, 45032 Orleans Cedex 1, France
e-mail: gael.rochefort@gmail.com

Introduction

In post-menopausal women, amino-bisphosphonates represent one of the pharmacologic options for the prevention and treatment of osteoporosis [1]. Among bisphosphonates one can distinguish medication by their molecular mechanisms of action. Etidronate, clodronate, tiludronate inhibit osteoclast function and induce osteoclast apoptosis by incorporation into intracellular analogs. These compounds do not interfere with intracellular sterol biosynthesis [2]. Amino-bisphosphonates inhibit the prenylation and function of GTP-binding proteins required for osteoclast function [3]. These last compounds inhibit squalene synthase and hence may be cholesterol lowering agents in animal [4]. Recently, it has been shown that high doses of zoledronic acid given in patients with smoldering myeloma may modify their lipid profile [5]. There was an improvement in the atherosclerotic risk index with an increase in the HDL-C/LDL-C ratio (high-density lipoprotein cholesterol/low density lipoprotein cholesterol ratio) and a decrease in the TC/HDL-C ratio (Total cholesterol/high-density lipoprotein cholesterol ratio).

Non pharmacological prevention of osteoporosis fracture by physical activity and particularly regular exercises (EXE) characterized by impact or loading is currently recommended [6]. The effect of regular exercise on the lipid profile has been developed in a lot of studies [7–9]. It has been recently demonstrated that increasing steps walked may have beneficial effects on serum lipids and thus may decrease the cardio vascular disease risks [10].

There is a large body of evidence that bisphosphonates reduce the bone turnover and particularly inhibit bone resorption [11, 12], the target cell being the osteoclast. Conversely, physical activity, and more specifically mechanical stress, has been shown to induce an osteogenic effect mediated by osteocytes and osteoblasts [13–15]. Based on these assumptions, the present study aims at investigating both specific and combined effects of zoledronic acid and treadmill exercise on bone turnover and the lipid profile in mature ovariectomized (OVX) rats.

Materials and Methods

Rat Groups and Treatment

Sixty 6-month old Wistar female rats (Animal Production Center, Olivet, France) were maintained and acclimatized for 2 weeks on a 12-h light/12 h dark cycle at 22 ± 2 °C during the experiment. Rats were housed in standard cages (two animals to a cage) with ad libitum access to food [a commercial standard diet (A04, SAFE, France)] and water. Rats were randomized to either sham-operated (sham; $n = 12$) or bilateral OVX ($n = 48$). We did not ration OVX rats in order to mimic real life conditions in postmenopausal women, knowing that this is usually recommended as obesity induced by OVX may protect against osteopenia [16].

Among the rats randomly selected in the the OVX group, a second randomization procedure was done leading to four groups of 12 animals each in addition to the sham-operated group (SH): OVX sedentary controls (OVX); OVX-exercise (OVX-E); OVX-zoledronic acid (OVX-Z); OVX- zoledronic acid exercise- (OVX-ZE).

Based on a previous dose-ranging study, we selected a single i.v. dose of 20 μg/kg zoledronic acid, as it has been demonstrated, it is the minimum dose required to provide long-term bone protection against the effects of OVX [17]. We injected the drug or a physiological saline solution 2 days before the OVX surgery. Sham operations were performed by exteriorizing the ovaries. Bilateral ovariectomies were performed under ketamine-xylazine anesthesia. This experiment was conducted in conformity with the Public Health Service Policy on Human Care and Use of Laboratory Animals. The procedure for the care and killing of the animals was in accordance with the European Community Standards on the care and use of the laboratory animals (Ministère de l'Agriculture, France, Authorization Inserm 45-001).

Exercise Regimen

The exercise regimen (EXE) consisted of running in an especially home made motor-driven treadmill, which allowed eight rats to exercise together. The running program was initiated gradually. The exercise regimen consisted of daily training. During the first 4 weeks, the speed of the treadmill and the duration of each running were gradually increased from 8 m/min for 3–30 min to 12 m/min for the first 2 weeks. In the two following weeks, the speed and duration of the running session were gradually increased to 15 m/min for 60 min. This speed and duration were maintained for 5 days per week for the rest of the experiment (8 weeks more).

Lipids and Bone Turnover Biomarkers

At baseline and at the end of the study, blood was obtained by venous puncture at the tail. Blood samples were allowed to clot at 4 °C for 20 min before centrifugation at 3,000 rpm for 10 min. Sera were stored at −20 °C for 24 h and then stored at −80 °C until analysis. Analyses of total serum cholesterol (TC), high-density lipoprotein cholesterol (HDL-C), and low density lipoprotein cholesterol (LDL-C) were determined using a high performance

cholesterol colorimetric assay (Hitachi). The inter and intra-assays were in our laboratory <10%.

Osteocalcin (OC) and C terminal collagen cross-links (CTx) which are respectively biomarkers of bone formation and resorption were assayed in duplicate by ELISA (Nordic Bioscience Diagnostics, Herlev Hoved-Gade, Denmark). The within-assay and between assay CVs were <10% in our laboratory. The intra-assay CVs were 5.5 and 5.6% respectively for OC and CTx. The inter-essays CV were 5.0 and 5.6% respectively for OC and CTx.

An uncoupling index (UI) was calculated to assess the relative balance of the formation and resorption processes of bone remodeling, as previously described [18]. First, the means ± SE of the baseline CTx and OC values were determined in each rat. Using the values of the SHAM group, OC and CTx Z-score [(rat value − mean baseline)/SD baseline] were calculated by subtracting the Z-score of the resorption marker from the Z-score of the formation marker. A positive UI indicates bone remodeling unbalanced in favor of bone formation, whereas a negative UI reflects an unbalanced favoring bone resorption.

Plasma Cytokine TNF-α

In order to assess the expression of proinflammatory cytokines potentially induced by the zoledronic acid or the exercise regimen, cytokine TNF-α was measured using an immuno assay ELISA (IBL Hamburg, Deutschland). The intra-essays CV and inter-essays were respectively <5% and <10%.

Body Weight, Fat Mass, Lean Mass and Bone Mineral Content (BMC) Measurements

All analyzes were conducted with the Discovery A densitometer (Hologic, Inc., Bedford, MA) calibrated daily in accordance with the manufacturer's recommendations. The rat whole body (WB) module was used to provide WB fat mass and WB lean mass. At baseline and at 12 weeks (4 weeks of gradually increased exercise and 8 weeks at full regimen, i.e. paragraph exercise regimen described above) lean and fat masses were measured by DXA. The root-mean square CV of in vivo WBBMC, WBBMD and WB fat mass were respectively 1.2, 0.87, and 3.8%. These CVs were determined from two repeated measures with repositioning on 30 animals.

Statistical Analysis

Data are presented as means ± standard deviations (SD) for body weight and body mass; they are presented as mean ± standard error of the mean (SEM) for serum chemistry. Normal distributions (Gaussian) of the data were assessed by a Kolmogorov–Smirnov test. The effect of ovariectomy was determined by comparing the sham-OVX and OVX groups using *t* test. To compare the main and combined effects of exercise and zoledronate between the OVX groups for longitudinal data, a two-way ANOVA with repeated measures was performed. In the event of a significant interaction, exercise and zoledronate effects were considered synergistic. A one-way ANOVA with post hoc, pair-wise comparisons using Fisher's protected least-significant difference [19] was used in case of significant interactions. In the event of a non-significant interaction, the main effect for each intervention (zoledronate, EXE) was explored by Newman–Keuls test and intervention effects were considered additive. The level of significance was set at $P \leq 0.05$. All statistical analyses were performed with software PCSM (OPTIMA-Deltasoft, France).

Results

All the data followed a normal distribution. Significant interaction were found in lipid parameters, serum CTX and uncoupling index between exercise and zoledronic acid.

Anthropometrics and Densitometry Parameters

Body weight in the OVX group was significantly greater than in sham operated rats 12 weeks post-surgery 386 ± 33 versus 333 ± 22 g; $P = 0.002$. There was a significant difference in body weight between the OVX-Z group and the two exercised groups (Table 1). Percentage of fat mass was found significantly higher in the OVX-Z group compared to all the OVX groups (Table 1). There was a higher percentage of fat mass in the OVX group (27.7%) as compared to the one in the SH group (19%), $P < 0.005$. There were no significant differences observed between the groups for WB lean mass. We have found a significant difference for whole body BMC between the OVX-Z group and the OVX, OVX-E and OVX-ZE groups (Table 1).

Lipid Profile

The OVX group had a higher serum total cholesterol and LDC-C levels compared with the SH group (Table 2). The OVX-E group displayed a significantly lower TC (127.2 mg/dl) than in the OVX group (144.8 mg/dl) ($P < 0.05$). We observed a 37.4% higher HDL-C level in the OVX-Z group (53.6 mg/dl) than in the OVX group (33 mg/dl) ($P < 0.05$). Exercise also markedly increased the HDL-C (+25.4%) in the OVX-E group as compared to the OVX group ($P < 0.05$). However, the OVX-ZE group

Table 1 Changes in anthropometric and bone parameters in WBBMC in sham-operated (SH) or ovariectomized (OVX) mature rats treated or not by zoledronic acid (Z) (a single injection 20 μg/kg), exercising on a treadmill or not (E) for 12 weeks

Anthropometric and densitometric parameters	Groups									
	SH		OVX		OVX-Z		OVX-E		OVX-ZE	
	Pre	Post	Pre	Post	Pre	Post	Pre	Post	Pre	Post
BW (g)	300.3 ± 27.3	333.1 ± 21.7	310.5 ± 20.7	386.4 ± 32.6[a]	320.8 ± 23.9	416.5 ± 40.7	319.9 ± 25.7	370.1 ± 35.5[b]	327.9 ± 30.2	370.8 ± 34.4[b]
LBM (g)	242.0 ± 13.5	241.1 ± 13.7	245.0 ± 16.6	259.2 ± 10.7[a]	255.1 ± 16.9	260.7 ± 17.2	245.8 ± 16.9	260.6 ± 21.4	248.7 ± 21.1	270.7 ± 25.0
FM (%)	17.8 ± 3.5	19.0 ± 4.1	17.3 ± 3.6	27.8 ± 7.3[a,b]	16.6 ± 3.5	28.9 ± 3.8	19.5 ± 4.4	24.0 ± 7.4[b]	20.3 ± 5.2	23.0 ± 6.0[b]
WBBMC (g)	11.4 ± 0.7	12.4 ± 0.8	11.7 ± 0.8	12.9 ± 0.7[b]	12.1 ± 0.5	13.9 ± 0.9	11.8 ± 0.8	12.2 ± 1.0[b]	11.9 ± 0.7	13.0 ± 0.8[b,c]

Data are means ± SDs

BW body weight, *LBM* lean body mass, *% FM* % fat mass, *WBBMC* whole body bone mineral content

[a] OVX differences versus SH

[b] Differences versus OVX-Z

[c] Interactions between treatment and exercise

Table 2 Changes in TC, HDL-C, LDL-C, TC/HDL-C and HDL-C/LDL-C ratios and TNF α in shame-operated (SH) or ovariectomized (OVX) mature rats treated or not by zoledronic acid (Z) (a single injection 20 μg/kg), exercising on a treadmill or not (E) for 12 weeks

Lipid profile and TNF α concentration	Groups									
	SH		OVX		OVX-Z		OVX-E		OVX-ZE	
	Pre	Post	Pre	Post	Pre	Post	Pre	Post	Pre	Post
TC (mg/dl)	118.00 ± 0.09	128.40 ± 0.04	104.50 ± 0.07	144.80 ± 0.05[a]	104.52 ± 0.08	135.30 ± 0.03	116.10 ± 0.07	127.20 ± 0.04[b]	105.60 ± 0.05	134.00 ± 0.04
HDL-C (mg/dl)	43.40 ± 0.02	43.50 ± 0.04	43.30 ± 0.01	39.00 ± 0.03	41.80 ± 0.03	53.60 ± 0.01[b]	42.10 ± 0.01	52.30 ± 0.03[b,c]	45.20 ± 0.01	39.20 ± 0.02[c,d]
LDL-C (mg/dl)	77.20 ± 0.03	81.80 ± 0.04	74.20 ± 0.04	99.90 ± 0.06[a]	74.90 ± 0.07	96.40 ± 0.04	74.30 ± 0.05	89.50 ± 0.08	76.80 ± 0.04	103.10 ± 0.05
TC/HDL-C	2.77 ± 0.2	3.14 ± 0.2	2.54 ± 0.1	3.82 ± 0.38	2.57 ± 0.2	2.52 ± 0.02[b]	2.77 ± 0.2	2.54 ± 0.20[b]	2.40 ± 0.1	3.54 ± 0.30[c,d]
HDL-C/LDL-C	0.70 ± 0.03	0.55 ± 0.05	0.77 ± 0.05	0.42 ± 0.05	0.69 ± 0.04	0.55 ± 0.03[b]	0.74 ± 0.05	0.64 ± 0.07[b]	0.73 ± 0.05	0.38 ± 0.02[c,d]
TNF α (pg/ml)	515.29 ± 5.20	523.17 ± 4.91	534.78 ± 14.10	670.90 ± 8.96[a]	515.08 ± 5.52	713.05 ± 6.05[a,b]	521.51 ± 6.05	696.98 ± 7.01[a,b]	516.48 ± 7.00	721.49 ± 12.47[a,b,d,e]

Data are means ± SDs

[a] OVX differences versus SH

[b] Differences versus OVX

[c] Differences versus OVX-Z

[d] Differences versus OVX-E

[e] Interactions between treatment and exercise

LDL-C low-density lipoprotein cholesterol, *HDL-C* high-density lipoprotein cholesterol, *TC* total cholesterol, *TNF α* tumor necrosis factor alpha

displayed lower levels of HDL-C than in the OVX-E and OVX-Z groups (Table 2). There was a trend to a higher TC/HDL-C ratio between baseline and the end of the study in the OVX-group $P = 0.06$. However, this ratio was significantly lower in the OVX-Z and the OVX-E groups respectively 2.53 and 2.54 than in the OVX group ($P < 0.05$). Conversely, the TC/HDL-C ratio in the OVX-ZE group was not significantly different from in the OVX-group and was higher (3.54) than in the OVX-Z and the OVX-E groups (Table 2). Likewise, the HDL-C/LDL-C ratio decreased significantly in the OVX groups between baseline and the end of the study (0.774 vs. 0.416; $P < 0.01$). This latter ratio significantly increased the OVX-Z and OVX-E versus the OVX group and there was a trend to a higher HDL-C/LDL-C ratio in the OVX-Z group than in the OVX group ($P = 0.058$) (Table 2).

Plasma Cytokine TNF-α

Ovariectomy was characterized by an increase in TFN-α between the baseline and at the end of the study (534.8 ± 14 vs. 678.9 ± 9 pg/ml; $P < 0.001$). There was an interaction between exercise and zoledronic acid concerning the levels of plasma TFN-α. As indicated in Table 2 we have found higher values of TNF-α at the end of the study in the OVX-Z, OVX-E and OVX-ZE groups than in the OVX group ones. The highest level of the TNF-α was found in the OVX-ZE group and it was significantly higher than in the OVX-E group, respectively 721.5 ± 12.5 versus 697 ± 7 pg/ml; $P < 0.01$.

Bone Turnover

The CTx level was 27.7% higher in the OVX group (23.8 ng/ml) than in the SH group (18.6 ng/ml), $P < 0.0005$. The CTx levels were significantly lower in OVX-Z and OVX-E groups as compared to the OVX group ($P < 0.05$). However, the CTx levels in the OVX-ZE were not statistically different from those in the OVX group but were significantly higher than in the OVX-Z and OVX-E groups (Table 3). In contrast, at the end of the study, serum osteocalcin levels were not significantly different between the SH group and the OVX group. The OVX-ZE group displayed higher osteocalcin level than in the OVX, the OVX-Z and the OVX-E groups. The osteocalcin level was significantly higher in the OVX-E group (178.27 ng/ml) versus the OVX and OVX-Z groups (respectively, 117.83 and 139.32 ng/ml) (Table 3). As expected the uncoupling index moved from −0.26 at baseline to −4.43 at the end of the study in the OVX group. In the OVX-E group the UI increased from −0.22 at baseline to +3.42 at the end of the study. Results of the UI in the OVX-Z groups are indicated in Table 3.

Table 3 Changes in OC, CTX and uncoupling index (UI) in sham-operated (SH) or ovariectomized (OVX) mature rats treated or not by zoledronic acid (Z) (a single injection 20 μg/kg), exercising on a treadmill or not (E) for 12 weeks

Bone turnover parameters	Groups									
	SH		OVX		OVX-Z		OVX-E		OVX-ZE	
	Pre	Post	Pre	Post	Pre	Post	Pre	Post	Pre	Post
CTx (ng/ml)	19.39 ± 0.53	18.60 ± 0.43	19.08 ± 0.48	23.76 ± 0.65[a]	18.66 ± 0.4	19.21 ± 0.66[b]	18.70 ± 0.41	19.28 ± 0.34[b]	18.78 ± 0.34	22.43 ± 0.63[c,d,e]
OC (ng/ml)	13.34 ± 0.34	12.79 ± 0.39	12.80 ± 0.41	11.78 ± 0.46	12.45 ± 0.3	13.93 ± 0.36[a,b]	12.60 ± 0.22	17.82 ± 0.86[a,b,c]	12.90 ± 0.21	12.90 ± 0.21[a,b,c,d]
UI			−0.27	−4.43	−0.31	0.45[b]	−0.22	3.42[b,c]	-0.015	2.71[b,c,e]

Data are means ± SDs

[a] OVX differences versus SH

[b] Differences versus OVX

[c] Differences versus OVX-Z

[d] Differences versus OVX-E

[e] Interactions between treatment and exercise

OC osteocalcin, *CTx* C-terminal collagen cross-links, *UI* uncoupling index (a positive UI indicates bone remodeling unbalanced in favor of bone formation, whereas a negative UI reflects an unbalanced favoring bone resorption)

Discussion

The main findings of the present study were that the therapy with zoledronic acid (a single injection) resulted in a significant increase (+37.4%) in serum concentration of HDL-C and a trend toward lower TC (−5.8%) as compared to the vehicle-treated ovariectomized mature rats. Moreover, these changes were associated with a significant decrease in the TC/HDL-C ratio and a trend toward an increase in the HDL-C/LDL-C ratio. Such parameters are recognized indicators of atherosclerosis risk. These last results on the lipid profile might have a positive effect on cardiovascular risk if one considers their extrapolation to human.

However, it is noteworthy that, if specific effects of exercise and zoledronic acid were beneficial for atherosclerotic risk, the additive effects of these two interventions had produced a paradoxically negative impact.

To our knowledge, there is only one study in rats with such a consideration, i.e. assessment of blood lipids rodent treated with bisphosphonates [20]. In the latter study, female Sprague–Dawley rats ovariectomized at 11 weeks were treated by alendronate and the authors did not observed any effect on the serum cholesterol levels after 3 weeks of treatment. At the same time, there was a 1.2–1.5 fold higher serum cholesterol level in the OVX group as compared with the sham group. It has been demonstrated that the rat model would be useful for studying the pharmacological effects of estrogen on total serum cholesterol [21]. Differences might be observed concerning the mechanisms for the hypocholesterolemic effect of estrogen between rats and humans. Estrogen lowers cholesterol by up-regulation of the hepatic LDL receptor [22]. In addition, in the rat, both HDL-C and LDL-C may be reduced because rat HDL-C contains apoprotein E (which is not found in human HDL-C) [23]. Hence, the amazing results displayed in the OVX-ZE group might be explained by differences between lipid metabolism in humans and rats (our rat model might not be the more appropriate).

In early postmenopausal women, exercise programs may reduce lipid levels [24]. In addition, it has been noticed that IV amino-bisphosphonates induced, in post-menopausal women with moderate to severe osteoporosis, a significant increase in HDL-C [25]. In our study in mature ovariectomized rats, we investigated the separate and combined effects of treadmill running exercise and zoledronic acid on the lipid profiles. Papers aiming to describe the lipid profile when using bisphosphonates for metabolic bone disorders are scarce and sometimes conflicting. In human it has been recently reported that in smoldering multiple myeloma patients zoledronic acid may have an effect on lipid metabolism with a decrease in both TC and LDL-C [16]. Guney et al. [26] have also recently reported data suggesting in 49 patients treated for osteoporosis with alendronate a beneficial effect on lipid metabolism. Two other studies have shown respectively in patients treated by IV pamidronate for Paget's bone disease [27] and in postmenopausal women with osteoporosis treated by IV neridronate [25] a reduction in LDL-C and an increase in HDL-C. Specific mechanisms leading to the effects of bisphosphonates on lipid metabolism are still unknown. However some bisphosphonates inhibit the squalene synthase enzyme and cholesterol biosynthesis [4] as it has been demonstrated for the first time in vivo by Amin et al. [28]. Indeed squalene synthase is one of the key enzyme in cholesterol biosynthetic pathway but reduction of plasma cholesterol can also be achieved by inhibiting hydroxymethyl-glutaryl-coenzyme A reductase (HMG-CoAR); which is also a key rate-limiting enzyme involved in the cholesterol biosynthesis and the development of such inhibitors of the HMG-CoAR has led to the family of statins [29]. Recent studies have highlighted the role of the farnesyl pyrophosphate synthetase (FPPS) as the molecular target of nitrogen-containing bisphosphonates [11, 12]. The FPPS is a distal enzyme of the mevalonate–squalene pathway and the ability of aminobisphosphonates to inhibit this enzyme is also a possible mechanism in lowering cholesterol.

Physical exercise was also able in our study to significantly decrease TC (−12%) and increase HDL-C (+34%) in trained rats as compared to the ovariectomized sedentary rats. Consequently, the TC/HDL-C and HDL-C/LDL-C ratios were respectively lower and higher in EXEd rats than in sedentary rats as expected [21, 26].

Because exercise and zoledronic acid may have different ways of producing an action on lipid metabolism (i.e. increase in aerobic metabolism, oxygen uptake and fatty acid use for muscular energy supply during exercise [30] and actions on cholesterol biosynthesis with zoledronic acid), we hypothesized in this study that, it was possible to observe additive effects of exercise and zoledronic acid on the lipid profile. This was not the case in our study as we noticed both for TC and HDL-C no statistical differences between ovariectomized rats treated with vehicle and ovariectomized rats practicing exercise treated with zoledronic acid. We cannot explain this effect, it is possible that the expression of certain antioxidant enzyme stimulated by the treadmill running exercise may have been counteracted by the inflammatory effects induced by the injection of zoledronic acid [31]. Indeed it has been shown that bisphosphonates may have pro inflammatory effects and clinicians do know the acute-phase response following the first injection of IV aminobisphosphonates in human. We do not assess in this study the oxidative stress indicators and oxidant status resulting of the exercise regimen

and the bisphosphonate therapy. Furthermore, we only assess the plasma inflammatory cytokine TNF-α. In the present study, the highest value of TNF-α at the end of the study was found in the OVX-ZE group. The TNF-α results found in this group (exercise training is supposed to reduce inflammation by decreasing TNF-α [32]) might be a possible explanation of our paradoxical lipid profile results in this group. Conversely, bisphosphonates are also described to have anti-inflammatory effects [33] and clodronate has been shown to inhibit the in vitro production of super oxide free radicals by polynuclear cells [33]. In turn these last effects may have been counterbalanced by some characteristics of the exercise regimen applied to the animals. Exercise training may rather reduce TNF-α but it has been shown sometimes that TNF-α level was not altered by exercise [10]. We have found a mild but significant increase in the TNF-α level at the end of the study in the OVX-E group as compared to the OVX group ($P = 0.04$).

At the end of the experiment the CTx levels were respectively 18.8 and 19.1% lower in the OVX-E and OVX-Z groups as compared to the OVX group. However, we can easily distinguish the effects of EXE and zoledronic acid on the bone turnover as there was a strong negative UI indicating an imbalance favoring resorption in the OVX group, a strong positive UI in the OVX-E group indicating that bone remodeling was unbalanced in favor of formation and a mild positive UI in the OVX-Z group indicating that zoledronic acid effects in this ovariectomized mature rats study prevented the deleterious effects of OVX, i.e. (increase in bone resorption parameters). Theoretically, it is an attractive hypothesis that a concurrent combination of exercise and zoledronic acid would be superior to either intervention alone as they act on different target sales. In the present study, the lack of additive effect of the combination exercise and zoledronic acid on the bone turnover might be explained by the potency of the antiresorptive effect of the zoledronic acid. The response to the osteogenic effects of exercise might be blunted by the powerful effect of zoledronic acid. Such a hypothesis has been mentioned to explain the lack of efficacy in combining parathyroid hormone with alendronate, the capacity of the antiresorptive drug being superior to a capacity of formation associated with the PTH treatment [34]. To our knowledge there have been two studies aiming at combining a bisphosphonate therapy with exercise in rats [35, 36]. Unfortunately none of them have investigated the effects on bone turnover markers.

We observed an increase in weight in the OVX-Z group as compared to the OVX-E and OVX-ZE groups. However it has been demonstrated that although differences in body weight are often cited as the reason for a better lipid profile between active and inactive persons, some data support an influence of physical activity on lipid profiles independently of the metabolic effect of weight variations [30] and this may be also the case with the action of zoledronic acid on lipid metabolism.

In this study, we aimed to analyze the individual and combined effects of zoledronic acid and treadmill exercise on lipid profile and bone remodeling ovariectomized rats. The present results confirmed that both zoledronic acid and physical exercise prevent the increase in bone resorption resulting from the ovariectomy. However we did not find any positive additive effect when combining these two interventions despite the different mechanisms and action pathways involved.

Both exercise and zoledronic acid were shown to individually improve the atherosclerotic risk index.

Our finding that zoledronic acid given in OVX-rats may interfere with lipid metabolism (mild reduction in TC and a large increase HDL-C) has not yet been reported in animal studies. Several studies [5, 25–27] in humans show that some amino bisphosphonates including zoledronic acid [5] seem to be able to induce effects on lipid metabolism with a profile that might be clinically relevant as amino bisphosphonates are largely used for the treatment of several bone disorders. Our results are hypothesis generating and further studies are needed to corroborate our findings.

Acknowledgments E. Lespessailles was the recipient of a fellowship research grant from Novartis.

Conflict of interest statement The authors declare that there is no conflict of interest that could be perceived as prejudicing the impartiality of the research reported.

References

1. Delmas PD (2002) Treatment of postmenopausal osteoporosis. Lancet 359:2018–2026
2. Fleisch H (1998) Bisphosphonates: mechanisms of action. Endocr Rev 19:80–100
3. Buhaescu I, Izzedine H (2007) Mevalonate pathway: a review of clinical and therapeutical implications. Clin Biochem 40:575–584
4. Ciosek CP Jr, Magnin DR, Harrity TW, Logan JV, Dickson JK Jr, Gordon EM, Hamilton KA, Jolibois KG, Kunselman LK, Lawrence RM et al (1993) Lipophilic 1, 1-bisphosphonates are potent squalene synthase inhibitors and orally active cholesterol lowering agents in vivo. J Biol Chem 268:24832–24837
5. Gozzetti A, Gennari L, Merlotti D, Salvadori S, De Paola V, Avanzati A, Franci B, Marchini E, Tozzi M, Campagna MS, Nuti R, Lauria F, Martini G (2008) The effects of zoledronic acid on serum lipids in multiple myeloma patients. Calcif Tissue Int 82:258–262
6. Bonaiuti D, Shea B, Iovine R, Negrini S, Robinson V, Kemper HC, Wells G, Tugwell P, Cranney A (2002) Exercise for preventing and treating osteoporosis in postmenopausal women. Cochrane Database Syst Rev CD000333
7. Kelley GA, Kelley KS (2008) Efficacy of aerobic exercise on coronary heart disease risk factors. Prev Cardiol 11:71–75

8. Kelley GA, Kelley KS, Tran ZV (2005) Walking and non-HDL-C in adults: a meta-analysis of randomized controlled trials. Prev Cardiol 8:102–107
9. Vasankari TJ, Kujala UM, Vasankari TM, Ahotupa M (1998) Reduced oxidized LDL levels after a 10-month EX program. Med Sci Sports Exerc 30:1496–1501
10. Puglisi MJ, Vaishnav U, Shrestha S, Torres-Gonzalez M, Wood RJ, Volek JS, Fernandez ML (2008) Raisins and additional walking have distinct effects on plasma lipids and inflammatory cytokines. Lipids Health Dis 7:14
11. Benford HL, McGowan NW, Helfrich MH, Nuttall ME, Rogers MJ (2001) Visualization of bisphosphonate-induced caspase-3 activity in apoptotic osteoclasts in vitro. Bone 28:465–473
12. Coxon FP, Helfrich MH, Van't Hof R, Sebti S, Ralston SH, Hamilton A, Rogers MJ (2000) Protein geranylgeranylation is required for osteoclast formation, function, and survival: inhibition by bisphosphonates and GGTI-298. J Bone Miner Res 15:1467–1476
13. Boppart MD, Kimmel DB, Yee JA, Cullen DM (1998) Time course of osteoblast appearance after in vivo mechanical loading. Bone 23:409–415
14. Pead MJ, Skerry TM, Lanyon LE (1988) Direct transformation from quiescence to bone formation in the adult periosteum following a single brief period of bone loading. J Bone Miner Res 3:647–656
15. Skerry TM, Bitensky L, Chayen J, Lanyon LE (1989) Early strain-related changes in enzyme activity in osteocytes following bone loading in vivo. J Bone Miner Res 4:783–788
16. Wronski TJ, Schenck PA, Cintron M, Walsh CC (1987) Effect of body weight on osteopenia in ovariectomized rats. Calcif Tissue Int 40:155–159
17. Gasser JA, Green JR, Novartis Pharma AG (2002) Long-term protective effect of a single IV injection of zoledronic acid on cancellous bone structure and cortical bone in ovariectomized rats. Bone 30:41S
18. Eastell R, Robins SP, Colwell T, Assiri AM, Riggs BL, Russell RG (1993) Evaluation of bone turnover in type I osteoporosis using biochemical markers specific for both bone formation and bone resorption. Osteoporos Int 3:255–260
19. Neter J, Wasserman W, Ahitmore GA (1982) Applied statistics, 4 sub edn. Allyn & Bacon, Boston
20. Frolik CA, Bryant HU, Black EC, Magee DE, Chandrasekhar S (1996) Time-dependent changes in biochemical bone markers and serum cholesterol in ovariectomized rats: effects of raloxifene HCl, tamoxifen, estrogen, and alendronate. Bone 18:621–627
21. Ferreri LF, Naito HK (1978) Effect of estrogens on rat serum cholesterol concentration: consideration of dose, type of estrogens and treatment duration. Endocrinology 102:1621–1627
22. Brown MS, Glodstein JL (1980) The estradiol stimulated lipoprotein receptor of rat liver. J Biol Chem 254:10454–10471
23. Chao Y, Windler EE, Chen GC, Havel RJ (1979) Hepatic catabolism of rat and human lipoproteins in rats treated with 17 alpha-ethinyl-estradiol. J Biol Chem 254:11360–11366
24. Kemmler W, Lauber D, Weineck J, Hensen J, Kalender W, Engelke K (2004) Benefits of 2 years of intense EX on bone density, physical fitness, and blood lipids in early postmenopausal osteopenic women: results of the Erlangen Fitness Osteoporosis Prevention Study (EFOPS). Arch Intern Med 164:1084–1091
25. Adami S, Braga V, Guidi G, Gatti D, Gerardi D, Fracassi E (2000) Chronic intravenous aminobisphosphonate therapy increases high-density lipoprotein cholesterol and decreases low-density lipoprotein cholesterol. J Bone Miner Res 15:599–604
26. Guney E, Kisakol G, Ozgen AG, Yilmaz C, Kabalak T (2008) Effects of bisphosphonates on lipid metabolism. Neuro Endocrinol Lett 29:252–255
27. Montagnani A, Gonnelli S, Cepollaro C, Campagna MS, Franci MB, Pacini S, Gennari C (2003) Changes in serum HDL and LDL cholesterol in patients with Paget's bone disease treated with pamidronate. Bone 32:15–19
28. Amin D, Cornell SA, Gustafson SK, Needle SJ, Ullrich JW, Bilder GE, Perrone MH (1992) Bisphosphonates used for the treatment of bone disorders inhibit squalene synthase and cholesterol biosynthesis. J Lipid Res 33:1657–1663
29. Tobert JA (1987) New developments in lipid-lowering therapy: the role of inhibitors of hydroxymethylglutaryl-coenzyme A reductase. Circulation 76:534–538
30. Thune I, Njolstad I, Lochen ML, Forde OH (1998) Physical activity improves the metabolic risk profiles in men and women: the Tromso Study. Arch Intern Med 158:1633–1640
31. Thiebaud D, Sauty A, Burckhardt P, Leuenberger P, Sitzler L, Green JR, Kandra A, Zieschang J, Ibarra de Palacios P (1997) An in vitro and in vivo study of cytokines in the acute-phase response associated with bisphosphonates. Calcif Tissue Int 61:386–392
32. Pedersen DK (2006) The anti-inflammatory effect of exercise: its role in diabetes and cardio-vascular disease control. Essays Biochem 42:105–117
33. Corrado A, Santoro N, Cantatore FP (2007) Extra-skeletal effects of bisphosphonates. Joint Bone Spine 74:32–38
34. Makkonen N, Salminen A, Rogers MJ, Frith JC, Urtti A, Azhayeva E, Monkkonen J (1999) Contrasting effects of alendronate and clodronate on RAW 264 macrophages: the role of a bisphosphonate metabolite. Eur J Pharm Sci 8:109–118
35. Black DM, Greenspan SL, Ensrud KE, Palermo L, McGowan JA, Lang TF, Garnero P, Bouxsein ML, Bilezikian JP, Rosen CJ (2003) The effects of parathyroid hormone and alendronate alone or in combination in postmenopausal osteoporosis. N Engl J Med 349:1207–1215
36. Fuchs RK, Shea M, Durski SL, Winters-Stone KM, Widrick J, Snow CM (2007) Individual and combined effects of exercise and alendronate on bone mass and strength in ovariectomized rats. Bone 41:290–296

Lipids (2010) 45:345–355
DOI 10.1007/s11745-010-3397-0

ORIGINAL ARTICLE

Expression of Genes Associated with Bone Resorption is Increased and Bone Formation is Decreased in Mice Fed a High-Fat Diet

Ying Xiao · Jue Cui · Ya-Xin Li · Yong-Hui Shi · Guo-Wei Le

Received: 10 September 2009 / Accepted: 11 February 2010 / Published online: 7 March 2010

Abstract A high-fat diet (HFD) leads to an increased risk of osteoporosis-related fractures, but the molecular mechanisms for its effects on bone metabolism have rarely been addressed. The present study investigated the possible molecular mechanisms for the dyslipidemic HFD-induced bone loss through comparing femoral gene expression profiles in HFD-fed mice versus the normal diet-fed mice during the growth stage. We used Affymetrix 430A Gene Chips to identify the significant changes in expression of the genes involved in bone metabolism, lipid metabolism, and the related signal transduction pathways. Quantitative RT-PCR was carried out on some significant genes for corroboration of the microarray results. At the conclusion of the 12-week feeding, the down-regulation of most of the genes related to bone formation and the up-regulation of most of the genes related to bone resorption were observed in the HFD-fed mice, consistent with the changes in plasma bone metabolic biomarkers. Together, the HFD induced a decrease in the majority of the adipogenesis-, lipid biosynthesis-, and fatty acid oxidation-related gene expression, such as PPARg and APOE. Furthermore, some genes engaged in the related signal transduction pathway were strongly regulated at the transcript level, including IGFBP4, TGFbR1, IL-17a, IL-4, and P53. These results indicate that an HFD may induce inhibitory bone formation and enhanced bone resorption, thus causing adverse bone status.

Y. Xiao · J. Cui · Y.-X. Li · Y.-H. Shi · G.-W. Le (✉)
State Key Laboratory of Food Science and Technology, School of Food Science and Technology, BOX 118, Jiangnan University, 1800 Lihu Road, Wuxi 214122, Jiangsu, China
e-mail: lgw@jiangnan.edu.cn

Y. Xiao
e-mail: yxiaonutrition@hotmail.com

Keywords Bone mass · High-fat diet · Hyperlipidemia · Gene expression profiles · Bone metabolism

Abbreviations

BMD	Bone mineral density
HFD	High-fat diet
RT-PCR	Reverse transcription-polymerase chain reaction
P1CP	Propeptide of I collagen C-propeptide
NTx	Cross-linked N-telopeptides of bone type I collagen
ROS	Reactive oxygen species

Introduction

A high-fat diet (HFD) has been recognized as a risk factor for a person's health being involved in conditions such as dyslipidemia, atherosclerosis, obesity, and osteoporosis [1–5]. The intake of lard rich in highly saturated fat is pervasive and consequently results in the increasing prevalence of dyslipidemia in China [5]. Dietary saturated fat intake has been recognized as contributing to the likelihood of osteoporosis-related fractures [4, 6]. Moreover, children treated with a high-fat low-carbohydrate diet could have a worse bone mineral status [7]. In growing animal models, an HFD or high-energy diet could deleteriously affect bone mineral content, structure, and mechanical properties [8–10]. Lac et al. [11] found that significant correlations were noted between body composition, adiponectin, and bone parameters in growing rats fed an HFD. Parhami et al. [12] have pointed out that an atherogenic diet inhibits bone formation by blocking differentiation of osteoblast in growing mice, possibly resulting from lipid oxidation

products. In addition, a recent study has suggested that an HFD may induce an increase in bone resorption in mice [13]. However, none of these studies addressed the effects of HFD on global gene expression profiles of bone.

A gene microarray can provide a broad view of gene expression. Thus, for the first time, we used an Affymetrix GeneChip 430A, which contains over 22,000 probe sets for 12,960 different genes, to study the changes in mRNA expression of the proximal femur of growing C57BL/6 mice fed a dyslipidemic HFD. Genes were categorized as related to lipid metabolism, bone metabolism, and the related signal transduction mainly with the aid of Gene Ontology analysis. The analysis on femoral gene expression profiles will help to elucidate more completely the possible molecular basis for the HFD-induced low bone mass.

Materials and Methods

Animals

The experiment was conducted with male C57BL/6 mice (4 weeks old) from Shanghai Slac Laboratory Animal Co. Ltd. (Shanghai, China). The animals were housed under conditions of controlled temperature (23 ± 2 °C) and humidity (60%) with natural light. The experimental protocol was developed according to the institution's guideline for the care and use of laboratory animals.

Experimental Design and Samples Preparation

Test animals were initially fed standard diets for 3 days for adaptation after arrival. Mice were randomly assigned to two groups ($n = 8$ for each group). Group control received only a normal diet containing 4.8% (w/w) fat. Group HFD received an HFD containing 21.2% fat (additional 17.5% lard and 0.5% cholesterol). This HFD has been found to cause significant dyslipidemia in C57BL/6 mice [5]. All mice were allowed free access to the test diets and deionized water throughout the 12-week test period.

At the end of the experimental periods, mice were deprived of food for 12 h. After mice were anesthetized with aether, blood was collected by removing eyeball, and then mice were sacrificed immediately by cervical vertebra dislocation. The visceral fat pads (perirenal and abdominal) and subcutaneous fat pads (subscapular) were immediately excised and weighed. Plasma was obtained from blood samples after centrifugation (500*g* for 10 min at 4 °C), and then the plasma samples were frozen and stored at −20 °C until analysis. The proximal femur (right) of four mice per group was dissected out immediately and stored in RNA-later solution at −20 °C until used for RNA extraction, and other femur bones (left) were dissected for measurement of bone mineral density and mechanical testing and then stored at −20 °C.

Bone Metabolic Biomarkers in Plasma

The plasma levels of propeptide of I collagen C-propeptide (P1CP) and cross-linked N-telopeptides of bone type I collagen (NTx) were determined by a mouse-P1CP Elisa Kit and a mouse-NTx Elisa kit (USCN Life Science & Technology Company, Missouri City, TX, USA), respectively.

Bone Mineral Density and Mechanical Testing

On the day of testing, femur bones were thawed (20–25 °C). The bone mineral density (BMD) in the left femur was measured by dual-energy X-ray absorptiometry (GE Healthcare, Milwaukee, WI, USA) in animal mode and was analyzed in accordance with the manufacturer's manual.

The maximum load in the central left femur was testing in three-point bending by Texture Analyzer XT (Stable Micro Systems, Haslemere, Surrey, UK). Bones were temperature equilibrated (37 °C) in a physiological buffer solution (PBS, pH 7.4) for at least 1 h prior to testing. A testing systems loaded each bone in three-point bending (10 mm min^{-1}) until failure. The three-point intersupport distance for the femurs was 6 mm, and they were loaded anterior to posterior. For three-point bending, we calculated a maximal load of the bone at the center.

DNA Microarray Procedure

The RNA was prepared from the proximal one-third of the whole right femur including bone marrow using Trizol (P/N 15596-018; Invitrogen Life Technologies, Carlsbad, CA, USA). Subsequently, four samples at each group were pooled. RNA was further purified using Qiagen RNeasy (P/N 74104; RNeasy Mini Kit, Qiagen) columns and the quality verified by the laboratory by a chip analysis (Bioanalyzer 2100; Agilent, Amstelveen, The Netherlands). Ten micrograms of RNA was used for one-cycle cRNA synthesis (Affymetrix, Santa Clara, CA, USA). Hybridization, washing, and scanning of Affymetrix GeneChip mouse genome 430A arrays, which consist of more than 22,000 probe sets for 12,960 different genes, was done according to standard Affymetrix protocols.

DNA Microarray Data Analysis

The GeneArray™ scanner 3000 (Affymetrix) was used to scan and quantitatively analyze the scanned image, and the

data were globally scaled to all the probe sets with an identical target intensity value. Once the probe array had been scanned, GeneChip software automatically calculated intensity values for each probe cell and ascribed a presence or absence call for each mRNA. Algorithms in the software used probe cell intensities to calculate an average intensity for each set of probe pairs representing a gene that directly correlated with the amount of mRNA. The statistical algorithms were implemented in Affymetrix Microarray Suite 5.0. Expression patterns for the HFD group were compared with those of the control group. When the difference between two different RNA samples was assessed, the fold changes from side-by-side comparisons on the same lot of microarrays were compared directly. We set up cut-off values to 1.5 ($P > 0.05$) for the fold change in ratio. These genes were classified into different groups according to their biological functions and analyzed mainly by GenMAPP2 as an assistant analysis tool.

Quantitative Real-Time Reverse Transcription-Polymerase Chain Reaction

Quantitative real-time reverse transcription-polymerase chain reaction (RT-PCR) was carried out to validate our microarray results ($n = 4$ for each group). Total RNA was reverse-transcribed to cDNA according to the manufacturer's instructions (MultiScribe Reverse Transcriptase, Applied Biosystems, Foster City, CA, USA). We used Platinum *Taq* polymerase (Invitrogen Life Technologies) and EvaGreen dye (Biotium, Hayward, CA, USA) to employ real-time quantitative PCR. In this system, the increase in the concentration of EvaGreen dye fluorescent is proportional to the increase in PCR products; the reaction product can be accurately measured in the exponential phase of amplification by the ABI prism 7000 Sequence Detection System. The sequences of the primers are listed in Table 1. The relative expression levels of the target genes were calculated as a ratio to the housekeeping gene β-actin. Melting curve analysis was performed to assess the specificity of the amplified PCR products.

Statistical Analysis

Data of physiological and biochemical markers were reported as means ± standard deviations. Comparisons across groups were performed by analysis of the two sided Student t Test. $P < 0.05$ was considered statistically significant. Analysis was done with SPSS 15 (SPSS, Inc., Chicago, IL, USA).

Results

Food Intake, Body Weight, and Fat Mass

The food intake, body weight change, and fat mass at each group are shown in Table 2. The HFD group exhibited significantly lower food intake but higher energy intake than the control group ($P < 0.05$). A significant increase in body weight gain and fat mass was observed in the HFD group ($P < 0.01$).

Table 1 Sequences of primers used in quantitative real-time reverse transcription polymerase chain reaction

Gene symbol	Gene (full name)	Forward primer (5′–3′)	Reverse primer (5′–3′)
β-actin	Beta-actin	GGGTCAGAAGGACTCCTATG	GTAACAATGCCATGTTCAAT
NOX2	NADPH oxidase2	TGTGGTTGGGGCTGAATGTC	CTGAGAAAGGAGAGCAGATTTCG
BGLAP2	Bone gamma-carboxyglutamate protein 2/ osteocalcin	CTGACCTCACAGATCCCAAGC	TGGTCTGATAGCTCGTCACAAG
COL1a1	Collagen type I alpha 1	GCTCCTCTTAGGGGCCACT	CCACGTCTCACCATTGGGG
RANK	Receptor activator of nuclear factor-κB	GGACGGTGTTGCAGCAGAT	GCAGTCTGAGTTCCAGTGGTA
MMP9	Matrix metallopeptidase 9	CTGGACAGCCAGACACTAAAG	CTCGCGGCAAGTCTTCAGAG
MMP1a	Matrix metallopeptidase 1a	AACTACATTTAGGGGAGAGGTGT	GCAGCGTCAAGTTTAACTGGAA
IGFBP4	Insulin-like growth factor binding protein 4	AGAAGCCCCTGCGTACATTG	TGTCCCCACGATCTTCATCTT
TGFbR1	Transforming growth factor beta receptor I	CAGCTCCTCATCGTGTTGGTG	GCACATACAAATGGCCTGTCTC
PPARg	Peroxisome proliferator activated receptor gamma	TCGCTGATGCACTGCCTATG	GAGAGGTCCACAGAGCTGATT
IL17a	Interleukin 17A	TTTAACTCCCTTGGCGCAAAA	CTTTCCCTCCGCATTGACAC
IL4	Interleukin 4	GGTCTCAACCCCCAGCTAGT	GCCGATGATCTCTCTCAAGTGAT
P53	Transformation related protein 53	GTCACAGCACATGACGGAGG	TCTTCCAGATGCTCGGGATAC

Table 2 Food intake, body weight, and fat mass

Group	Food intake (g/day)	Energy intake (g/day)	Initial body weight (g)	Final body weight (g)	Fat mass (g/g body weight)
Control	3.01 ± 0.16	11.82 ± 0.52	14.98 ± 0.97	23.56 ± 1.53	0.085 ± 0.010
HFD	2.74 ± 0.13*	13.43 ± 0.55*	14.81 ± 0.99	26.44 ± 1.67**	0.117 ± 0.012**

Values are expressed as means ± SDs for eight animals

* $P < 0.05$, ** $P < 0.01$ versus control

Table 3 BMD and bone mechanical testing

Group	Femur BMD (mg/cm^2)	Femur maximum load (N)
Control	75.3 ± 1.3	27.9 ± 3.1
HFD	71.6 ± 2.1*	24.1 ± 2.6*

Values are expressed as means ± SDs for eight animals

* $P < 0.05$ versus control

BMD and Mechanical Testing

As shown in Table 3, the HFD caused a moderate decrease in both BMD and maximum load of femur ($P < 0.05$). Feeding of the HFD for 12 weeks resulted in the development of osteoporosis in the HFD-fed mice.

Bone Metabolism and Related Gene Expression Profiles

The transcript levels of the femora genes related to bone metabolism in the HFD group compared with the control group are presented in Table 4. It is evident that the magnitude of osteoblast-specific genes except Osteopontin (SPP1) were down-regulated in femora of HFD-fed mice and that the majority of osteoclast-specific genes were up-regulated, such as cathepsin K (CTSK), integrin beta 3 (ITGB3) and calcitonin receptor (CALCR). Collagens are the major components of the bone matrix and the extracellular matrix, and matrix metalloproteinases (MMPs) play a role in bone formation and in bone resorption by degrading the bone matrix [14, 15]. The expression levels of the listed genes encoding collagens (type I, II, V, IX and XI) were diminished in femur of HFD-fed mice. The transcription levels of some genes encoding MMP2, MMP9, and MMP13 were slightly increased in the HFD-fed mice, but MMP1a and MMP14 were 9.2- and 1.6-fold down-regulated in the HFD group, respectively. The listed genes engaged in the related regulation factors of bone metabolism were found to be differentially regulated, indicating that the HFD can induce increased bone resorption and decreased bone formation. Moreover, bone metabolic biomarkers were assayed and are shown in Fig. 1. As expected, the HFD significantly reduced plasma levels of P1CP ($P < 0.01$) as a biomarker of bone formation and increased plasma levels of NTx ($P < 0.05$) as a biomarker of bone resorption, supporting the evidence of gene expression profiles.

Lipid Metabolism- and Antioxidant System-Related Gene Expression Profiles in Femur

As presented in Table 4, the majority of the genes engaged in adipogenesis and lipid biosynthesis, such as peroxisome proliferator activated receptor gamma (PPARg), CCAAT/enhancer binding protein beta (CEBPb), twist gene homolog 1 (TWIST1), and stearoyl-coenzyme A desaturase 2 (SCD2), were down-regulated in the HFD group compared with the control group. Also, HFD caused a decrease in most of the gene expression of those engaged in fatty acid oxidation, such as PPARg, apolipoprotein E (APOE), acetyl-Coenzyme A acetyltransferase 1 (ACAT1), and lipase (LIPE). In addition, the transcription levels of genes encoding antioxidant enzymes superoxide dismutase 2 (SOD2), glutathione peroxidase 3 (GPx3), and thioredoxin reductase 1 (TXNRD1) in the HFD group were lower than those in the control group.

Signal Transduction-Related Gene Expression Profiles in Femur

Signal transduction pathway plays a key role in differentiation, proliferation, and the function of bone cells. The changes in the expression of the selected genes involved in signal transduction are listed in Table 4. The genes encoding insulin-like growth factor 1 (IGF1), IGF1 receptor, and some insulin-like growth factor binding proteins (IGFBPs) were down-regulated in the HFD group versus the control group. An increase in the majority of cases of gene expression related to p53 signal pathway associated with osteoblast apoptotic [16] was found in the HFD mice. In addition, the magnitude of genes encoding transforming growth factors, interleukins, and their receptors were up-regulated, especially those transforming growth factor, beta receptor I (TGFbR1, 13.9 folds) and IL-17a (9.8 folds). In contrast, IL-4, a proinflammatory cytokine, was found to be down-regulated by 2.5 fold.

Table 4 Changes in gene expression in the HFD group compared with the control group

Probe set ID	Gene name	Gene symbol	Fold change (HFD vs. Control)[a]
Osteoblast specific			
1449880_s_at	Bone gamma-carboxyglutamate protein 2/ osteocalcin	BGLAP2	−1.6
1423611_at	Alkaline phosphatase 1	ALPl	−1.6
1423669_at	Collagen type I, alpha 1	COL1a1	−1.7
1422176_at	Fibroblast growth factor 23	FGF23	−2.8
1449254_at	Secreted phosphoprotein 1/osteopontin	SPP1	1.5
Osteoclast specific			
1450652_at	Cathepsin K	CTSK	1.7
1451944_a_at	Receptor activator of nuclear factor-kB ligand	RANKL/TNFSF11	1.5
1430259_at	Receptor activator of nuclear factor-κB	RANK	2.1
1422978_at	NADPH oxidase 2	NOX2	2.6
1450413_at	Platelet derived growth factor, B polypeptide	PDGFB	6.1
1421511_at	Integrin beta 3	ITGb3	2.0
1418688_at	Calcitonin receptor	CALCR	6.9
Collagens			
1423669_at	Collagen, type I, alpha 1	COL1a1	−1.7
1450857_a_at	Collagen, type I, alpha 2	COL1a2	−1.5
1450567_a_at	Collagen, type II, alpha 1	COL2a1	−2.0
1416741_at	Collagen, type V, alpha 1	COL5a1	−1.6
1460734_at	Collagen, type IX, alpha 3	COL9a3	−2.5
1423578_at	Collagen, type XI, alpha 2	COL11a2	−2.6
1418599_at	Collagen, type XI, alpha 1	COL11a1	−1.6
Matrix Metalloproteinases			
1422175_at	Matrix metallopeptidase 1a	MMP1a	−9.2
1439364_a_at	Matrix metallopeptidase 2	MMP2	1.5
1416298_at	Matrix metallopeptidase 9	MMP9	1.5
1417256_at	Matrix metallopeptidase 13	MMP13	1.6
1448383_at	Matrix metallopeptidase 14	MMP14	−1.6
1433662_s_at	Tissue inhibitor of metalloproteinase 2	TIMP2	−1.7
1450974_at	Tissue inhibitor of metalloproteinase 4	TIMP4	−1.7
1421910_at	Transcription factor 20	TCF20	1.5
Regulation factors of bone metabolism			
1422912_at	Bone morphogenetic protein 4 (positive regulation of bone mineralization)	BMP4	−2.0
1423635_at	Trans-acting transcription factor 7/Osterix (positive regulation of osteoblast differentiation)	SP7/OSX	−1.5
1449864_at	FBJ osteosarcoma oncogene (positive regulation osteoblast differentiation)	FOS	−1.7
1419762_at	Ubiquitin D (positive regulation osteoblast differentiation)	UBD	−1.6
1417599_at	CD276 antigen (positive regulation of bone mineralization)	CD276	−2.3
1427994_at	CD300 antigen like family member F (positive regulation of osteoclast differentiation)	CD300lf	1.7
1418110_a_at	Inositol polyphosphate-5-phosphatase D (negative regulation of bone resorption)	INPP5D	−1.6

Table 4 continued

Probe set ID	Gene name	Gene symbol	Fold change (HFD vs. Control)[a]
Lipid metabolism: adipogenesis and lipid biosynthesis			
1420715_a_at	Peroxisome proliferator activated receptor gamma	PPARg	−2.1
1449945_at	Peroxisome proliferative activated receptor, gamma, coactivator 1 beta	PPARgC1b	−1.6
1427844_a_at	CCAAT/enhancer binding protein (C/EBP), beta	CEBPb	−4.6
1423402_at	cAMP responsive element binding protein 1	CREB1	1.8
1450403_at	Signal transducer and activator of transcription 2	STAT2	2.3
1426587_a_at	Signal transducer and activator of transcription 3	STAT3	−1.6
1433508_at	Kruppel-like factor 6	KLF6	−1.9
1426065_a_at	Tribbles homolog 3 (Drosophila)	TRIB3	−1.5
1448816_at	Prostaglandin I2 (prostacyclin) synthase	PTGIS	−1.5
1418733_at	Twist gene homolog 1 (Drosophila)	TWIST1	−24.5
1433612_at	Adaptor-related protein complex 2, sigma 1 subunit	AP2s1	−1.6
1448368_at	Dynactin 6	DCTN6	−1.5
1451308_at	Elongation of very long chain fatty acids -like 4	ELOVL4	−1.5
1415824_at	Stearoyl-Coenzyme A desaturase 2	SCD2	−1.8
1435659_a_at	Triose-phosphate isomerase 1	TPI1	−1.5
1438919_x_at	Farnesyl diphosphate farnesyl transferase 1	FDFT1	−3.7
1423832_at	Protein kinase, AMP-activated, gamma 2 non-catalytic subunit	PRKAG2	1.8
1416383_a_at	Pyruvate carboxylase	PCX	1.7
Lipid metabolism: fatty acid Oxidation			
1420715_a_at	Peroxisome proliferator activated receptor gamma	PPARg	−2.1
1432466_a_at	Apolipoprotein E	APOE	−1.5
1455972_x_at	Hydroxyacyl-Coenzyme A dehydrogenase	HADH	−1.6
1435659_a_at	Triose-phosphate isomerase 1	TPI1	−1.5
1451271_a_at	Acetyl-Coenzyme A acetyltransferase 1	ACAT1	−1.5
1417008_at	Carnitine acetyltransferase	CRAT	−1.5
1438156_x_at	Carnitine palmitoyltransferase 1a	CPT1a	−1.7
1422820_at	Lipase, hormone sensitive	LIPE	−1.5
1429581_at	Acyl-Coenzyme A dehydrogenase family, member 9	ACAD9	−1.7
1419031_at	Fatty acid desaturase 2	FADS2	−1.9
1423883_at	Acyl-CoA synthetase long-chain family member 1	ACSL1	1.5
1422703_at	Glycerol kinase	GYK	1.6
Antioxidant system			
1448610_a_at	Superoxide dismutase 2	SOD 2	−1.5
1449106_at	Glutathione peroxidase 3	GPx3	−1.7
1421529_x_at	Thioredoxin reductase 1	TXNRD1	−6.5
Insulin-like growth factor signaling			
1419519_at	Insulin-like growth factor 1	IGF1	−1.5
1426565_at	Insulin-like growth factor I receptor	IGF1R	−1.6
1423062_at	Insulin-like growth factor binding protein 3	IGFBP3	−2.5
1423756_s_at	Insulin-like growth factor binding protein 4	IGFBP4	−2.1

Table 4 continued

Probe set ID	Gene name	Gene symbol	Fold change (HFD vs. Control)[a]
1452114_s_at	Insulin-like growth factor binding protein 5	IGFBP 5	−1.5
1423584_at	Insulin-like growth factor binding protein 6	IGFBP 6	−1.7
1416953_at	Connective tissue growth factor	CTGF	−2.1
1448594_at	WNT1 inducible signaling pathway protein 1	WISP1	−1.5
P53 dependent apoptotic pathway			
1427739_a_at	Transformation related protein 53	TRP53/P53	2.5
1424638_at	Cyclin-dependent kinase inhibitor 1A (P21)	CDKN1a	−1.6
1450223_at	Apoptotic peptidase activating factor 1	APAF1	1.5
1419513_a_at	Ect2 oncogene	ECT2	1.6
1456005_a_at	BCL2-like 11 (apoptosis facilitator)	BCL2L11	1.5
1426165_a_at	Caspase 3	CASP3	1.5
Cytokine factors and related receptors			
1417455_at	Transforming growth factor, beta 3	TGFb3	2.0
1420653_at	Transforming growth factor, beta 1	TGFb1	−1.6
1420893_a_at	Transforming growth factor, beta receptor I	TGFbR1	13.9
1421672_at	Interleukin 17A	IL17a	9.8
1426507_at	Interleukin 1 family, member 5 (delta)	IL1F5	3.2
1422177_at	Interleukin 13 receptor, alpha 2	IL13Ra2	1.6
1449864_at	Interleukin 4	IL4	−2.5
1422397_a_at	Interleukin 15 receptor, alpha chain	IL15Ra	−2.8

[a] The mRNA levels in the HFD group were compared with the control group. Fold-change calculations are based on means of signal values in each group of four mice after background subtraction ($P < 0.05$), with a negative fold change representing down-regulated expression

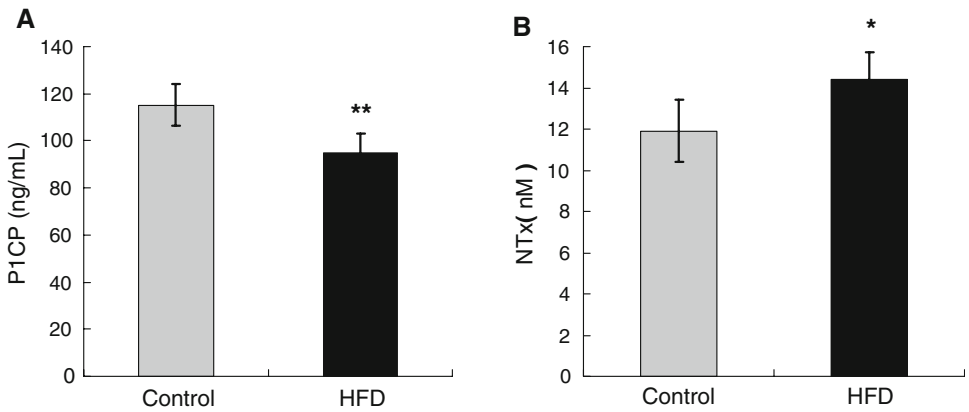

Fig. 1 Comparison of bone metabolic markers including plasma P1CP (**a**) and plasma NTx (**b**) in mice fed a normal diet and an HFD. Values are expressed as means ± SDs ($n = 8$ for each group). *$P < 0.05$, **$P < 0.01$ versus control

Confirmation of Differential Expression of Selected Genes by Real-Time RT-PCR Analysis

We validated our microarray findings by conducting real-time PCR assays on the selected genes. When gene expression profiles obtained by microarray analysis and quantitative RT-PCR were compared, their patterns were very similar with regard to the direction (up- or down-regulation), despite some slight variations (Fig. 2). Collectively, the quantitative PCR results demonstrated the reliability of the microarray analysis.

Discussion

The present study provides gene transcript profiles of the femur bone of growing C57BL/6 mice fed a dyslipidemic HFD for 12 weeks to help to reveal further the molecular mechanisms underlying the HFD-induced bone loss. Our emphasis was primarily on genes engaged in lipid metabolism, bone metabolism, and the related signal transduction pathway mainly through Gene Ontology analysis. Furthermore, the validity of our microarray findings was confirmed by conducting real-time RT-PCR assays on the selected genes.

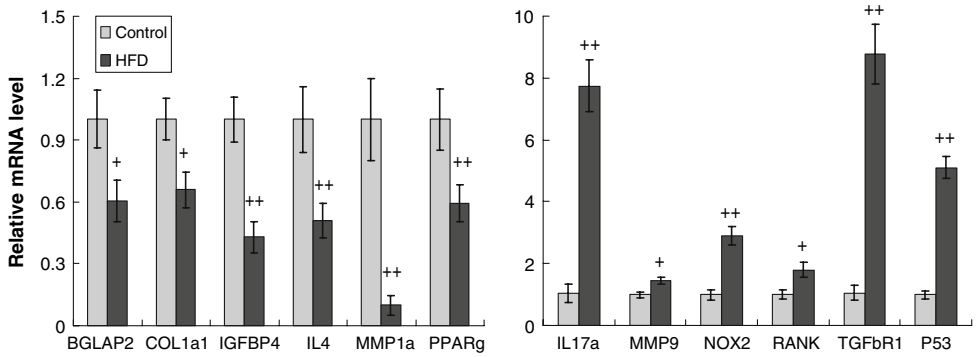

Fig. 2 Verification of the expression changes of BGLAP2 (osteocalcin), COL1a1, IGFBP4, IL4, MMP1a, PPARg, IL17a, MMP9, NOX2, RANK, TGFbR1, and P53 using quantitative RT-PCR. The relative expression level of each sample was calibrated by the comparative threshold cycle method, using β-actin as an endogenous control. Data are expressed as fold changes (means $\pm$ SDs, $n = 4$ for each group), normalized to β-actin mRNA expression, where the values for the control mice were set at 1.0. $^{+}P < 0.01$ and $^{++}P < 0.001$ compared with the control mice

C57BL/6 mice were used as a model for HFD-induced low BMD in our study since the lipid metabolism and bone metabolism changes in these animals are similar to those that occur in humans [17, 18]. Lac et al. [11] have demonstrated that fat mass is negatively correlated with bone mineral density. As expected, the dyslipidemic HFD induced significantly more body weight gain and fat mass but significantly lower femoral BMD and maximum mechanical load. Bone is primarily comprised of collagen and mineral, which together provides its mechanical properties [19]. Accordingly, this finding suggests that both the matrix and mineral content of femurs were affected by the HFD. In addition, the HFD-induced poor mechanical properties suggest that cortical bone was influenced since the three-point bending test evaluates changes in a substantial quantity of cortical bone. This finding is similar to others reports for bone status influenced by other high-fat diets [8, 9, 11].

In the terms of bone formation, the HFD down-regulated most genes engaged in bone mineralization, corresponding to decreased levels of plasma P1CP, a bone formation biomarker. Runx2 and Osterix (OSX), a series of transcriptional activation events, are essential for osteoblast differentiation [20]. Runx2 knockout or OSX knockout mice show the complete lack of both intramembranous and endochondral ossification due to the absence of osteoblast differentiation [20]. In our microarray data, the HFD brought about a 1.5-fold decreased regulation of OSX but no significant change in Runx2 expression. In addition, FOS and other regulators were down-regulated in the HFD group, suggesting that the HFD could depress osteoblastic differentiation and bone formation [20, 21]. Conversely, the HFD up-regulated the majority of genes engaged in osteoclast activity, corresponding to the increased plasma levels of NTx, a bone resorption biomarker. In addition, expression levels of most of the collagens and tissue inhibitors of metalloproteinase were decreased, but some genes encoding matrix metalloproteinase (MMPs) were up-regulated in the HFD-fed mice, such as MMP9 which plays an important role in bone matrix degradation [15, 22]. Interestingly, MMP1a mRNA was strongly decreased by 9.2 folds in the HFD-fed mice. MMP1 is known as a collagenase predominantly expressed in osteoblasts, and it can play a role in bone formation by cleaving the native triple helix of type I collagen [23, 24]. Therefore, the strong down-regulation of MMP1 may reflect the diminished osteoblastic activity in the HFD-fed mice. Overall, the above-mentioned results indicate that the HFD can not only inhibit bone formation but also enhance bone resorption in growing mice.

In some previous studies, HFD was shown to cause inhibitory bone formation and osteoblastic differentiation in mice and in vitro evidence [12, 25–27], but its effects on bone resorption and on osteoclastic proliferation and differentiate had never been observed. However, a new study from Cao et al. [13] has indicated that an HFD may bring about increased bone resorption and osteoclast activity in mice without effects on bone formation. These differences between the previous study results and our results may be attributed to the variations in physiological stages, dietary compositions, feeding periods, and experimental method. In our study, the microarray approach provides an opportunity to examine the effects of HFD on bone metabolism in a global manner, but further studies will be necessary to validate this speculation.

Lipid metabolism is closely associated with bone metabolism, since osteoblasts and adipocytes appear to be derived from a common mesenchymal stem cell pool [28, 29]. HFD-induced LDL oxidation products promote osteoporotic loss of bone by directing progenitor marrow stromal cells to undergo adipogenic instead of osteogenic differentiation through activating PPARg [25]. Indeed, it has been

reported that PPARg plays an important role in lipid metabolism and bone development. PPARg activation has been demonstrated to decrease osteoblastic and osteoclastic formation [30, 31] and to increase adipogenesis and lipid catabolism [31–33]. However, the majority of the examples of gene expression involved in adipogenesis, lipid biosynthesis, and fatty acid oxidation were down-regulated by the HFD in our data, such as PPARg, CEBPb which cooperates with PPARs to induce adipogenesis [34], lipase, and APOE. This gene expression profile is not consistent with the previous reports that HFD could promote lipogenesis and inhibit osteogenesis via PPARg activation [25–27]. This discrepancy may result from differences in pathologic processes or fatty acid compositions of diets. Indeed, HFD provides a higher dietary energy density and consequently can induce obesity [35], several unsaturated fats have been demonstrated to activate PPARs to regulate adipogenesis [36], and high ratios of omega3/omega6 polyunsaturated fatty acids can decrease PPARg mRNA levels [37, 38]. Moreover, a decrease in lipid anabolism profile may be a response to excessive adipogenesis to resist obesity in the present study. On the other hand, the present data indicate that the HFD may cause enhanced osteoclastic function and depressed lipid catabolism through decreased PPARg activation. Some previous similar observations in rodents have also shown that a diet rich in saturated fats brought about high plasma levels of triglyceride and cholesterol together with a small decrease in apolipoproteins [39, 40]. Furthermore, the $APOE^{-/-}$ mice fed an HFD have been demonstrated to enhance reduction of bone formation and vascular atherosclerotic lesions [41]. Accordingly, we presume that the dyslipidemic HFD-induced bone loss may be partially attributed to the impaired lipid catabolism capacity.

Another notable gene engaged in bone resorption was 2.6-fold up-regulated NADPH oxidase 2 (NOX2). NOX has been known to generate large quantities of mitochondrial reactive oxygen species (ROS) during bone resorption [42]. ROS, which specifically regulates signaling pathways by reversible oxidation of proteins [43], not only augments osteoclastic differentiation and function, but also is essential for osteoclastic differentiation [42, 44]. Moreover, in the present data, the genes encoding antioxidant enzymes including SOD2, GPx3, and TXNRD1 were down-regulated in the HFD group, indicating that the HFD could result in bone oxidative stress, an imbalance between free radicals and antioxidant system. Other studies have shown that lipid oxidation caused by excessive levels of ROS may have opposite effects on bone formation [12, 25]. Furthermore, an increasing number of studies have provided evidence for a strong relationship between oxidative injury and osteoporosis in diabetes mellitus and at postmenopause [45–47]. Thus, the HFD-induced bone loss may also be associated with oxidative stress.

Besides changes in bone metabolism- and lipid metabolism-related gene expression, the differential alternations in transcript levels of many genes related to signal transduction in the HFD-fed mice compared with the control were found in our microarray data. There were the down-regulated genes encoding IGF1, IGF1 receptor and some IGFBPs in the HFD group. Previous studies suggested that IGF1 can stimulate osteoblastic proliferation and bone formation [48] and that decreased IGF1 predisposes to osteoporosis [49]. Bielohuby et al. [50] also reported that low-carbohydrate/high-fat diets impaired longitudinal growth, possibly mediated by reductions in IGF-1 in rats. IGFBPs play modifying roles in IGF action by regulating both IGF half-life and access to IGF receptors [51]. IGFBP4 has been shown to increase bone formation in mice upon systemic administration [52]. The decreased IGFBP4 mRNA expression in the HFD mice may therefore have inhibited bone formation in this study.

Hirasawa et al. [41] suggested that APOE gene deficiency enhances the reduction of bone formation induced by an HFD through the stimulation of transformation related protein 53 (P53)-mediated apoptosis in osteoblasts. It is well known that P53 negatively regulates osteoblastic differentiation and bone formation [16, 53]. The strong up-regulation of the gene encoding P53 was observed in the HFD group, indicating that P53 dependent osteoblastic apoptotic may be one of causative factors for the HFD-induced inhibitory bone formation.

On the other hand, there is an increase in mRNA levels of receptor activator of nuclear factor-kB (RANK) and receptor activator of nuclear factor-kB ligand (RANKL) in our data without changes in osteoprotegerin (OPG) expression. Growth transforming factors [54] and cytokines [55–57] have been known to stimulate osteoclastogenesis and bone resorption by RANK/RANKL pathway, such as IL-1, IL-6, IL-17, and TNF-a. In fact, some studies have shown that HFD-induced hypolipidemia and/or obesity is often associated with elevated levels of inflammatory markers [58, 59]. Our microarray data show a large up-regulation of TGFbR1 and IL-17a expressed primarily in T cells[60] in the HFD-fed mice, which can contribute to enhanced bone resorption, despite a small decrease in TGFb1 expression and no significant changes in TNF-a, IL-1, and IL-6 expression.

Another notable observation was the decreased IL-4 mRNA expression in HFD mice, which is secreted by activated Th2 cells [61]. IL-4 has been shown to inhibit bone resorption through inhibiting NF-κB and Ca^{2+} signaling [62] or through a direct action on osteoclast precursors via PPARg [61] in an in vitro model. In atherosclerotic lesions of $Apoe^{-/-}$ mice, Th1 cells are dominant, as the cytokines IFN-γ, IL-2, and TNF-a are highly expressed, whereas low amounts of the Th2

cytokines IL-4, IL-5, and IL-10 can be detected [63]. Indeed, there is a decrease in IL-4, PPARg and APOE expression in the HFD-fed mice in the present data, although the undeterminable changes in expression levels of other cytokines were found, such as IFN-γ and IL-10. Therefore, the HFD-induced decreased IL-4 transcript in bone may have adverse effects on preventing bone loss.

In summary, the present results from various bone parameters indicate that the HFD induces alterations to skeletal growth and consequently causes an adverse bone status in C57BL/6 mice. The changes in global gene expression profiles of proximal femur suggest that the HFD may cause negative effects on bone formation and promotive effects on bone resorption, together with abnormal lipid metabolism as reflected by the decreased transcript levels of most of the genes engaged in adipogenesis and fatty acid oxidation. Furthermore, the HFD-induced inhibitory bone formation maybe due to the changes in gene expression involved in the IGF-1 signaling pathway and P53 apoptotic pathway. The great up-regulation of TGFbR1 and IL-17a and the down-regulation of IL-4 in bone of mice fed HFD may lead to a stimulation of bone resorption through the RANK/RANKL pathway associated with low PPARg expression.

Our study is the first time microarray data has been provided for an opportunity to gain a better understanding of the basis for the impacts of HFD on bone physiological function and to identify the related signal transduction pathway. However, it is necessary to obtain further confirmation at the protein level and with functional analysis.

Acknowledgments The authors thank Mr. Xiao-Jia Pu (Nuclear Medicine Section, Wuxi People's Hospital) for the technical support on BMD measurement and for providing the technical equipment. This work was supported by 111 Project-B07029 and the National Natural Science of Foundation of China (grant 30571347).

References

1. Steinberg D (1991) Antioxidants and atherosclerosis. A current assessment. Circulation 84:1420–1425
2. Kopelman PG (2000) Obesity as a medical problem. Nature 404:635–643
3. Parhami F, Garfinkel A, Demer LL (2000) Role of lipids in osteoporosis. Arterioscler Thromb Vasc Biol 20(11):2346–2348
4. Hou JC-H, Zernicke RF, Barnard RJ (1990) High-fat sucrose diet effects on femoral neck geometry and biomechanics. Clin Biomech 5:162–168
5. Yang RL, Li W, Shi YH, Le GW (2008) Lipoic acid prevents high-fat diet-induced dyslipidemia and oxidative stress: a microarray analysis. Nutrition 24:582–588
6. Salem GJ, Zernicke RF, Barnard RJ (1992) Diet-related changes in mechanical properties of rat vertebrae. Am J Physiol 262:R318–R321
7. Bertoli S, Striul L, Testolin G, Cardinali S, Veggiotti P, Salvatori GC, Tagliabue A (2002) Nutritional status and bone mineral mass in children treated with ketogenic diet. Recenti Prog Med 93:671–675
8. Zernicke RF, Salem GJ, Barnard RJ, Schramm E (1995) Long-term, high-fat-sucrose diet alters rat femoral neck and vertebral morphology, bone mineral content, and mechanical properties. Bone 16:25–31
9. Ward WE, Kim S, Robert Bruce W (2003) A western-style diet reduces bone mass and biomechanical bone strength to a greater extent in male compared with female rats during development. Br J Nutr 90:589–595
10. Li KC, Zernicke RF, Barnard RJ, Li AF (1990) Effects of a high fat-sucrose diet on cortical bone morphology and biomechanics. Calcif Tissue Int 47:308–313
11. Lac G, Gavalie H, Ebal E, Michaux O (2008) Effects of a high fat diet on bone of growing rat. Correlations between visceral fat, adiponectin and bone mass density. Lipids Health Dis 7:16
12. Parhami F, Tintut Y, Beamer WG, Gharavi N, Goodman W, Demer LL (2001) Atherogenic high-fat diet reduces bone mineralization in mice. J Bone Miner Res 16:182–188
13. Cao JJ, Gregoire BR, Gao H (2009) High-fat diet decrease cancellous bone mas but has no effect on cortical bone mass in the tibia in mice. Bone 44:1097–1104
14. Meikle MC, Bord S, Hembry RM, Compston J, Croucher PI, Reynold JJ (1992) Human osteoblasts in culture synthesize collagenase and other matrix metalloproteinases in response to osteotropic hormones and cytokines. J Cell Sci 103:1093–1099
15. Delaisses JM, Engsing MT, Everts V, del Carmen M, Ovejero M et al (2000) Proteinases in bone resorption: obvious and less obvious and less obvious roles. Clin Chim Acta 291:223–234
16. Wang X, Kua HY, Hu Y, Guo K, Zeng Q, Wu Q, Ng HH, Karsenty G, de Crombrugghe B, Yeh J, Li B (2006) P53 functions as a negative regulator of osteoblastogenesis, osteoblast-dependent osteoclastogenesis, and bone remodeling. J Cell Biol 172:115–125
17. Paigen B, Morrow A, Brandon C, Mitchell D, Holmes P (1985) Variation in susceptibility to atherosclerosis among inbred strains of mice. Atherosclerosis 57:65–73
18. Halloran BP, Ferguson VL, Simske SJ, Burghardt A, Venton LL, Majumdar S (2002) Changes in bone structure and mass with advancing age in the male C57BL/6 J mouse. J Bone Miner Res 17:1044–1050
19. Burr DB (2002) The contribution of the organic matrix to bone's material properties. Bone 31:8–11
20. Komori T (2006) Regulation of osteoblast differentiation by transcription factors. J Cell Biochem 99(5):1233–1239
21. Morsczeck C (2006) Gene expression of runx2, Osterix, c-fos, DLX-3, DLX-5, and MSX-2 in dental follicle cells during osteogenic differentiation in vitro. Calcif Tissue Int 78:98–102
22. Wittrant Y, Couillaud S, Theoleyre S, Dunstan C, Heymann D, Redini F (2002) Osteoprotegerin differentially regulates protease expression in osteoclast cultures. Biochem Biophys Res Commun 293:38–44
23. Hayami T, Kapila YL, Kapila S (2008) MMP-1 (collagenase-1) and MMP-13 (collagenase-3) differentially regulate markers of osteoblastic differentiation in osteogenic cells. Matrix Biol 27:682–692
24. Westermarck J, Kahari V (1999) Regulation of matrix metalloproteinase expression in tumor invasion. FASEB J 13:781–792
25. Parhami F, Jackson SM, Tintut Y, Le V, Balucan JP, Territo MC, Demer LL (1999) Atherogenic diet and minimally oxidized low density lipoprotein inhibit osteogenic and promote adipogenic differentiation of marrow stromal cells. J Bone Miner Res 14:2067–2078
26. Parhami F, Morrow AD, Balucan J, Leitinger N, Watson AD, Tintut Y, Berliner JA, Demer LL (1997) Lipid oxidation products have opposite effects on calcifying vascular cell and bone cell differentiation. A possible explanation for the paradox of arterial calcification in osteoporotic patients. Arterioscler Thromb Vasc Biol 17:680–687

27. Takada I, Suzawa M, Matsumoto K, Kato S (2007) Suppression of PPAR transactivation switches cell fate of bone marrow stem cells from adipocytes into osteoblasts. Ann N Y Acad Sci 1116:182–195
28. Bianco P, Riminucci M, Gronthos S, Robey PG (2001) Bone marrow stromal stem cells: nature, biology, and potential applications. Stem Cells 19:180–192
29. Beresford JN, Bennett JH, Devlin C, Leboy PS, Owen ME (1992) Evidence for an inverse relationship between the differentiation of adipocytic and osteogenic cells in rat marrow stromal cell cultures. J Cell Sci 102:341–351
30. Okamoto H, Iwamoto T, Kotake S, Momohara S, Yamanaka H, Kamatani N (2005) Inhibition of NF-kappaB signaling by fenofibrate, a peroxisome proliferator-activated receptor-alpha ligand, presents a therapeutic strategy for rheumatoid arthritis. Clin Exp Rheumatol 23:323–330
31. Spiegelman BM (1998) PPAR-gamma: adipogenic regulator and thiazolidinedione receptor. Diabetes 47:507–514
32. Braissant O, Foufelle F, Scotto C, Dauça M, Wahli W (1996) Differential expression of peroxisome proliferator-activated receptors (PPARs): tissue distribution of PPAR-alpha, -beta, and -gamma in the adult rat. Endocrinology 137(1):354–366
33. Chawla A, Boisvert WA, Lee CH, Laffitte BA, Barak Y, Joseph SB, Liao D, Nagy L, Edwards PA, Curtiss LK, Evans RM, Tontonoz P (2001) A PPAR-LXR-ABCA1 pathway in macrophages is involved in cholesterol efflux and atherogenesis. Mol Cell 7:161–171
34. Brun RP, Tontonoz P, Forman BM, Ellis R, Chen J, Evans RM, Spiegelman BM (1996) Differential activation of adipogenesis by multiple PPAR isoforms. Genes Dev 10(8):974–984
35. Bray GA, Popkin BM (1998) Dietary fat intake does affect obesity!. Am J Clin Nutr 68:1157–1173
36. Fernandez ML, West KL (2005) Mechanisms by which dietary fatty acids modulate plasma lipids. J Nutr 135:2075–2078
37. Bassaganya-Riera J, Hontecillas R, Beitz DC (2002) Colonic anti-inflammatory mechanisms of conjugated linoleic acid. Clin Nutr 21:451–459
38. Zhang L, Geng Y, Yin M, Mao L, Zhang S, Pan J (2010) Low ω-6/ω-3 polyunsaturated fatty acid ratios reduce hepatic C-reactive protein expression in apolipoprotein E–null mice. doi: 10.1016/j.nut.2009.08.018
39. Doolittle MH, LeBoeuf RC, Warden CH, Bee LM, Lusis AJ (1990) A polymorphism affecting apolipoprotein A-II translational efficiency determines high density lipoprotein size, and composition. J Biol Chem 265:16380–16388
40. Smith D, Ahn YS, Pedro-Botet J, Osada J, Mata P, Schaefer EJ (2001) Dietary fat saturation distinctly affects apolipoprotein gene expression and high density lipoprotein size distribution in two strains of Golden Syrian hamsters. Nutr Res 21:215–228
41. Hirasawa H, Tanaka S, Sakai A, Tsutsui M, Shimokawa H, Miyata H, Moriwaki S, Niida S, Ito M, Nakamura T (2007) ApoE gene deficiency enhances the reduction of bone formation induced by a high-fat diet through the stimulation of p53-mediated apoptosis in osteoblastic cells. J Bone Miner Res 22(7):1020–1030
42. Steinbeck MJ, Appel WH Jr, Verhoeven AJ, Karnovsky MJ (1994) NADPH-oxidase expression and in situ production of superoxide by osteoclasts actively resorbing bone. J Cell Biol 126:765–772
43. Poli G, Leonarduzzi G, Biasi F, Chiarpotto E (2004) Oxidative stress and cell signalling. Curr Med Chem 11:1163–1182
44. Garrett IR, Boyce BF, Oretto RO, Bonewald L, Poser J, Mundy GR (1990) Oxygen derived free radicals stimulate osteoclastic bone resorption in rodent bone in vitro and in vivo. J Clin Invest 85:632–639
45. Muthusami S, Ramachandran I, Muthusamy B, Vasudevan G, Prabhu V, Subramaniam V, Jagadeesan A, Narasimhan S (2005) Ovariectomy induces oxidative stress and impairs bone antioxidant. Clin Chim Acta 360:81–86
46. D'Amelio P, Cristofaro MA, Tamone C, Morra E, Di Bella S, Isaia G et al (2008) Role of iron metabolism and oxidative damage in postmenopausal bone loss. Bone 43(6):1010–1015
47. Hamada Y, Fujii H, Kitazawa R, Yodoi J, Kitazawa S, Fukagawa M (2009) Thioredoxin-1 overexpression in transgenic mice attenuates streptozotocin-induced diabetic osteopenia: a novel role of oxidative stress and therapeutic implications. Bone 44(5):936–941
48. Mochizuki H, Hakeda Y, Wakatsuki N, Usui N, Akashi S, Sato T, Tanaka K, Kumegawa M (1992) Insulin-like growth factor-1 supports formation and activation of osteoclasts. Endocrinology 131:1075–1080
49. Niu T, Xu X (2001) Candidate genes for osteoporosis. Therapeutic implications. Am J Pharmacogenomics 1:11–19
50. Bielohuby M, Matsuura M, Herbach N, Kienzle E, Slawik M, Hoeflich A, Bidlingmaier M (2009) Short term exposure to low-carbohydrate/high fat diets induces low bone mineral density and reduces bone formation in rats. J Bone Miner Res. doi: 10.1359/jbmr.090813
51. Mohan S, Baylink DJ (2002) IGF-binding proteins are multifunctional and act via IGF-dependent and–independent mechanisms. J Endocrinol 175:19–31
52. Miyakoshi N, Richman C, Qin X, Baylink DJ, Mohan S (1999) Effects of recombinant insulin-like growth factor-binding protein-4 on bone formation parameters in mice. Endocrinology 140:5719–5728
53. Boast S, de los Santos K, Schieren I, Quiroz M, Teitelbaum SL, Tondravi MM, Goff SP (2000) Mice deficient in Abl are osteoporotic and have defects in osteoblast maturation. Nat Genet 24:304–308
54. Fuller K, Lean JM, Bayley KE, Wani MR, Chambers TJ (2000) A role of TGF_B in osteoclast differentiation and survival. J Cell Sci 113:2445–2453
55. Kwan Tat S, Padrines M, Théoleyre S, Heymann D, Fortun Y (2004) IL-6, RANKL, TNF-alpha/IL-1: interrelations in bone resorption pathophysiology. Cytokine Growth Factor Rev 15:49–60
56. Jagger CJ, Lean JM, Davies JT, Chambers TJ (2005) Tumor necrosis factor—mediates osteopenia caused by depletion of antioxidants. Endocrinology 146:113–118
57. Dj Miljkovic, Cvetkovic I, Vuckovic O, Stosic-Grujicic S, Mostarica Stojkovic M, Trajkovic V (2003) The role of interleukin-17 in inducible nitric oxide synthase-mediated nitric oxide production in endothelial cells. Cell Mol Life Sci 60:518–525
58. Das UN (2001) Is obesity an inflammatory condition? Nutrition 17:953–966
59. Zhang R, Flier EM, Flier JS (2009) Reduced adiposity and high-fat diet-induced adipose inflammation in mice deficient for phosphodiesterase 4B. Endocrinology 150:3076–3082
60. Yao Z, Painter SL, Fanslow WC, Ulrich D, Macduff BM, Spriggs MK, Armitage RJ (1995) Human IL-17: a novel cytokine derived from T cells. J Immunol 155(12):5483–5486
61. Bendixen AC, Shevde NK, Dienger KM, Willson TM, Funk CD, Pike JW (2001) IL-4 inhibits osteoclast formation through a direct action on osteoclast precursors via peroxisome proliferator-activated receptor gamma 1. Proc Natl Acad Sci USA 98(5):2443–2448
62. Mangashetti LS, Khapli SM, Wani MR (2005) IL-4 inhibits bone-resorbing activity of mature osteoclasts by affecting NF-kappa B and Ca^{2+} signaling. J Immunol 175(2):917–925
63. Binder CJ, Chang MK, Shaw PX, Miller YI, Hartvigsen K, Dewan A, Witztum JL (2002) Innate and acquired immunity in atherogenesis. Nat Med 8(11):1218–1226

Lipids (2010) 45:357–365
DOI 10.1007/s11745-010-3400-9

ORIGINAL ARTICLE

Enantioselective Analysis of Chiral Anteiso Fatty Acids in the Polar and Neutral Lipids of Food

Simone Hauff · Georg Hottinger · Walter Vetter

Received: 13 January 2010 / Accepted: 18 February 2010 / Published online: 12 March 2010

Abstract Anteiso fatty acids (*a*FA) are substituted with a methyl group on the antepenultimate carbon of the straight acyl chain. This feature leads to a stereogenic center. The 12-methyltetradecanoic acid (*a*15:0) and the 14-methylhexadecanoic acid (*a*17:0) are the most common *a*FA found in food, although they occur only in very small quantities. In this study we used gas chromatography in combination with a chiral stationary phase to determine the enantiomeric distribution of both *a*15:0 and *a*17:0 in the neutral and polar lipids of aquatic food samples and cheese. The best suited column was selected out of four custom-made combinations of heptakis(6-*O*-*tert*-butyldimethylsilyl-2,3-di-*O*-methyl)-*β*-cyclodextrin (*β*-TBDM) with different amount and polarity of an achiral polysiloxane. After separation of polar and neutral lipids of the food samples by solid phase extraction, fatty acid methyl esters were prepared and the fatty acid methyl esters were fractionated by reversed phase high performance liquid chromatography. Measurements of fractions high in *a*FA by enantioselective GC/MS in the selected ion monitoring mode verified the dominance of the (*S*)-enantiomers of *a*15:0 and *a*17:0 in both lipid fractions. However (*R*)-enantiomers were detectable in all samples. The relative proportion of the (*R*)-enantiomers was up to fivefold higher in the polar lipids than in the neutral lipids. The higher proportions in the polar lipids indicate that microorganisms might be involved in the formation of (*R*)-*a*FA.

Keywords Methyl branched fatty acids · Anteiso fatty acids · Chirality · Enantiomer separation · Dairy products · Fish

Abbreviations

β-TBDM	Heptakis(6-*O*-*tert*-Butyldimethylsilyl-2, 3-di-*O*-methyl)-*β*-cyclodextrin
*a*FA	Anteiso fatty acids
*a*15:0	12-Methyltetradecanoic acid
*a*16:0	13-Methylpentadecanoic acid
*a*17:0	14-Methylhexadecanoic acid
CSP	Chiral stationary phase
ee	Enantiomeric excess
ELSD	Evaporative light scattering detector
FAME	Fatty acid methyl ester
FID	Flame ionization detection
GC	Gas chromatography
GC/EI-MS	Gas chromatography electron ionization mass spectrometry
HPLC	High performance liquid chromatography
NL	Neutral lipids
PL	Polar lipids
RP-HPLC	Reversed phase high performance liquid chromatography
SIM	Selected ion monitoring mode
SPE	Solid phase extraction

Introduction

Anteiso fatty acids (*a*FA) bear a methyl substituent on the antepenultimate carbon of the acyl chain. Consequently, the carbon bearing the methyl branch is stereogenic. The

S. Hauff · W. Vetter (✉)
Institute of Food Chemistry, University of Hohenheim, Garbenstraße 28, 70599 Stuttgart, Germany
e-mail: walter.vetter@uni-hohenheim.de

G. Hottinger
BGB Analytik, Lettenstrasse 97, 8134 Adliswil, Switzerland

12-methyltetradecanoic acid (*a*15:0) and the 14-methylhexadecanoic acid (*a*17:0) are the most prominent *a*FA in food. In marine biota and dairy products they contribute with ~1% to the fatty acid patterns [1, 2]. In contrast, these *a*FA are dominant in the lipid bilayer (phospholipids) of several *gram*-positive bacteria [3, 4], where they are involved in keeping the membrane fluid when these organisms are exposed to cold temperatures [5–7]. Additionally, *a*FA have even been reported to suppress the proliferation of human cancer cells [8, 9].

Chirality is a specific feature of biomolecules which impinges on the biological properties. Biochemical processes are prevalently enantioselective and usually only one enantiomer exhibits full biological activity. Hence, knowledge of the absolute stereo-configuration of chiral biomolecules—including the *a*FA—is essential for the proper assessment of their bioactivity. However, the chromatographic enantioseparation of the long-chain *a*FA is a challenge, because it becomes the more difficult the larger the distance is between the stereogenic center and the functional group [10–12].

So far, an indirect enantiomer separation of long chain *a*FA has been achieved by high performance liquid chromatography (HPLC) [10, 12, 13]. In addition, gas chromatography (GC) in combination with modified cyclodextrins as the chiral stationary phase (CSP) was used for the enantioseparation of food-relevant *a*FA [14]. Several capillary columns coated with different CSP dissolved in diverse polysiloxanes were tested, and *β*-TBDM was the only CSP which allowed for the partial resolution of these *a*FA [14]. Using a capillary column coated with 50% heptakis(2,3-di-*O*-methyl-6-*O*-*tert*-butyldimethylsilyl)-*β*-cyclodextrin (*β*-TBDM) in OV-1701, it was shown that *a*15:0 and *a*17:0 were virtually (*S*)-enantiopure in dairy products although the presence of traces of the respective (*R*)-enantiomers could not be excluded [14]. In fact, small amounts of (*R*)-enantiomers were detected in marine oils [14]. It is noteworthy that *a*FA were higher concentrated in the polar lipids of fish than in its neutral lipids, while no significant differences were found in the lipids of dairy products [15].

Here, we wished to explore whether there are differences in the enantiomeric distribution of *a*FA in neutral and polar lipids of cheese and fish. With this goal in mind, we first attempted to improve the enantioresolution of *a*FA by variations in the ratio between the CSP and the achiral polysiloxane of *β*-TBDM columns. The effect of different ratios of CSP and polysiloxanes on the stereoselectivity has been shown for flavor compounds by Mosandl and coworkers [16]. Nevertheless, further chiral capillary columns varying in terms of the amount of chiral selector, the polarity of the polysiloxane as well as the film thickness of the stationary phase were tested. The best column was finally applied to the enantioselective determination of *a*FA in food. For this purpose, polar (PL) and neutral lipids (NL) were fractionated by solid phase extraction (SPE) [17]. After conversion of the lipid fatty acids into methyl esters (FAME), *a*FA were enriched by means of reversed phase HPLC [18].

Materials and Methods

Chemicals and Standards

Ethyl acetate (purest, Acros Organics, Geel, Belgium) and cyclohexane (purest, VWR, Darmstadt, Germany) were combined (1:1, v/v) and distilled to gain the azeotropic mixture (54:46, v/v). Methanol, *n*-hexane (both HPLC gradient grade), silica gel 60 (particle size 0.063–0.2 mm, 70–230 mesh) and methanolic BF_3 (~10%) were from Fluka (Taufkirchen, Germany). Individual racemic *a*FA were from Larodan (Malmö, Sweden), whereas (*S*)-enantiomers of *a*FA were synthesized by Thurnhofer and Vetter [19].

Food Samples

The following six food samples were selected because they were known to contain *a*FA both in PL and NL [14, 15]: gilthead seabream (*Sparus aurata*) fillet, brown trout (*Salmo trutta fario*) fillet, see bass (*Dicentrarchus labrax*) fillet (all from local supermarkets) and seal oil (*Pusa sibirica*; from a local market on the Lake Baikal), as well as cow mozzarella (made from pasteurized milk, Italy) and camembert (made from raw milk, Germany) cheeses.

Extraction of Food Samples

Lipids of food samples were gained by means of accelerated solvent extraction (ASE 200, Dionex, Idstein, Germany) as recently described [17, 20]. Briefly, ~1 g of the homogenized freeze dried sample was loaded into 11-mL stainless steel cells, and the extraction was performed with three portions of 40 mL of ethyl acetate/cyclohexane (54:46, v/v) followed by two portions of 40 mL of methanol/ethyl acetate (1:1, v/v) [17]. Extracts were combined, concentrated by rotary evaporation (180 mbar, 30 °C water bath temperature) and were then adjusted to a defined volume (10–25 mL).

Solid Phase Extraction

Lipid fractionation was performed as recently described [19]. In summary, approximately 5 mg of food lipids diluted in 100 µL ethyl acetate/cyclohexane/methanol

(45:45:10 by volume) were loaded onto a SPE column containing 350 mg of deactivated silica (20%). NL were eluted with 23 mL cyclohexane/ethyl acetate (1:1, v/v) whereas PL were eluted with ethyl acetate/methanol (1:1, v/v), methanol and methanol/water (98:2, v/v) into another flask [17]. The two lipid fractions were rotary evaporated to about 1 mL, transferred into derivatization tubes, and were finally evaporated to dryness under a gentle stream of N_2 (35 °C). Fatty acids in the dry lipid fractions were transformed into the corresponding FAME using the boron trifluoride method [1].

Enrichment of Anteiso FAME by Reversed Phase High Performance Liquid Chromatography (RP-HPLC)

RP-HPLC analyses of FAME were carried out with a Varian solvent pump and a Varian ProStar 325 UV-vis detector (dual wavelength mode using 206 and 234 nm) serially connected with a PL-ELS 2100 evaporative light scattering detector (ELSD, Polymer Laboratories) (all Varian, Darmstadt, Germany). The N_2 nebulizer temperature was set at 40 °C and the ELSD drift tube flow was set at 1.2 mL/min.

One milligram of FAME diluted in 50 µL methanol was injected via a Rheodyne 7010 injector equipped with a 100-µL sample-loop.

Three serially connected 250 mm × 4.6 mm C_{18} columns (ET 250/8/4 Nucleosil 7 C_{18}; (7 µm particle size), Supelcosil LC-18-DB (5 µm particle size), and ET 250/8/4 Nucleosil 5 C_{18}-AB (5 µm particle size)) served as stationary phase while pure methanol was used as the mobile phase (flow rate 0.9 mL/min) [18]. For the isolation of *a*FA, the ELSD was disconnected and the fractions were manually collected for 30 min, at time intervals of 0.5 min. All HPLC fractions containing the individual *a*FA in highest purity (*a*15:0 ~15 min; *a*16:0 ~17 min; *a*17:0 ~19 min) were combined and concentrated to ~10–150 µL for subsequent GC/EI-MS analysis. Purity of the respective fractions was determined by achiral GC/EI-MS (see below).

Gas Chromatography in Combination with Electron Ionization Mass Spectrometry (GC/EI-MS)

An HP GCD Plus system (Hewlett-Packard, Waldbronn, Germany) was used to perform enantioselective GC/EI-MS analyses. One microliter of standard or sample solution was splitless injected (split opened after 2 min) at 250 °C via an HP 6890 autosampler (Hewlett-Packard). Helium (purity 5.0, Sauerstoffwerke, Friedrichshafen, Germany) was used as the carrier gas at a constant flow rate of 1.0 mL/min. The transfer line temperature and ion source temperatures were set at 280 and 165 °C, respectively. Enantioselective determinations of *a*FA in food samples were performed by GC/EI-MS in the selected ion monitoring (SIM) mode. The six fragment ions *m/z* 74, *m/z* 87 [17, 21], *m/z* 256 (M^+ of 15:0 ME isomers), *m/z* 270 (M^+ of 16:0 ME isomers), *m/z* 284 (M^+ of 17:0 ME isomers), and *m/z* 282 (M^+ of 17:1 ME isomers) were recorded throughout the run.

Frequently, the required low isothermal elution temperatures of *a*15:0, *a*16:0 and *a*17:0 resulted in retention times longer than the maximum run time on our GC/MS system (i.e. 650 min). Thus, a second run was immediately started at the end of the first run (the column equilibration time was set to 0 s, air was injected, the new run started isothermal with the final temperature of the first run). The GC oven program of the first run started at 60 °C, which was held for 1 min; then the temperature was ramped with 20 °C/min to 112 °C (held 455 min) and thereafter with 1 °C/min to 132 °C (held for further 171 min). The GC oven program of the second run started at 132 °C for 115 min, and then the temperature was raised with 30 °C/min to 200 °C (held 15 min). The total run time was 782 min. In this way, *a*17:0 eluted after ~730 min (650 min first run plus ~80 min in the second run).

Achiral GC/EI-MS measurements of HPLC fractions were performed with an HP 5971/5890 combo previously described [21, 22] except for the following modifications: A 60 m × 0.25 mm × 0.20 µm film thickness (d_f) SP 2331 column (Supelco, Bellefonte, PA, USA) was installed in the GC oven and the temperature program started at 60 °C (held 1 min), was then ramped with 7 °C/min to 180 °C (hold time 2 min), afterwards with 3 °C/min to 200 °C (hold time 2 min), and finally at 3 °C/min to 220 °C (held for 10 min). The total run time was 45.5 min.

Heptakis(2,3-di-*O*-methyl-6-*O*-*tert*-butyldimethylsilyl)-*β*-cyclodextrin (*β*-TBDM) Columns Tested

The chiral stationary phase was synthesized as previously described [14]. The following combinations of the CSP with 14% cyanopropylphenyl, 86% dimethyl polysiloxane (OV-1701) or 5% phenyl, 95% methyl polysiloxane (DB-5) were prepared according to Blum and Aichholz [23]: (1) 50% *β*-TBDM in OV-1701 (2) 66% *β*-TBDM in OV-1701 (3) 50% *β*-TBDM in DB-5 (all 30 m long, 0.25 mm i.d., 0.2 µm d_f), as well as (iv) 66% *β*-TBDM in OV-1701 (30 m, 0.25 mm i.d., 0.18 µm d_f).

Initial tests of the *β*-TBDM columns were performed by flame ionization detection (FID) as described elsewhere [14]. For each column, isothermal temperatures (108–125 °C) were stepwise lowered (1 °C steps), until the best resolution was obtained for racemic *a*15:0 and *a*17:0 standards. Temperature changes showed the same effects for both *a*FA (and also *a*16:0), so that final column optimization was carried out with only the *a*15:0. The best

suited column was then transferred to the GC/EI-MS system, making sure that the linear velocity of the carrier gas was equal on both the GC/FID and the GC/EI-MS system. In this way, retention time shifts were marginal (<10 min).

Method Validation and Mode of Evaluation

The enantiomeric distributions of *a*FA in food samples were expressed by the enantiomeric excess (*ee*), which was calculated with formula 1:

$$ee\% = \frac{(S)\text{-}a\text{FA} - (R)\text{-}a\text{FA}}{(S)\text{-}a\text{FA} + (R)\text{-}a\text{FA}} \times 100 \quad (1)$$

with (*S*)-*a*FA and (*R*)-*a*FA being the peak area and (*S*)-*a*FA being the major enantiomer.

Determination of small amounts of (*R*)-*a*FA was carried out as follows. Gas chromatograms from pure (*S*)-*a*FA were superimposed with those containing small amounts of (*R*)-*a*FA and the excess of peak area from the latter was calculated. Repeated integration (n=3) resulted in an accuracy of the *ee*% determination of ±0.5%. Final verification was obtained by weighing the cut chromatograms from prints on 80-g paper. The gravimetric results were generally within the ±0.5% frame assessed by integration. To ensure the absence of potential memory peak from previous runs which could falsify the enantioselective measurements, three runs with fast temperature programs (started at 60 °C (held 1 min) and ramped with 10 °C/min to 200 °C (held 15 min)) were carried out before the analysis of the next sample. The characteristic GC/EI-MS-SIM ions traces (see "Material and Methods") *m/z* 74, *m/z* 87 as well as M^+ were normalized to the same peak high [14]. While the ion traces of the two anteiso enantiomers showed exactly the same peak shape, this feature was not observed for other fatty acids including *i*FA. Additionally, random samples were spiked with racemic standards, which again confirmed the presence of both enantiomers. The GC/EI-MS-SIM method enabled the non-interfered enantioselective analysis of the *a*FA obtained from the NL and PL fractions. Chromatograms with low abundant/noisy peaks were smoothed by using the method of Savitzki and Golay [24].

Results and Discussion

Analysis of Racemic *a*FA as Methyl Esters on Different Chiral Capillary Columns

The enantioselectivity of a CSP is affected by both the type and amount of the CSP and the achiral polysiloxane [16, 25]. Previously, several β-TBDM columns were tested, and columns containing 50% β-TBDM in OV-1701 gave better results than those with lower amounts of the CSP [14]. Starting from the 50% β-TBDM column used in our previous studies [14, 26] two new β-TBDM columns were produced by (a) decreasing the polarity of the polysiloxane from OV-1701 to DB 5 or (b) increasing the amount of the CSP from 50 to 66%. Results from columns with such high amounts of β-TBDM (i.e. 66%) in a polysiloxane have not been published before. The columns were initially installed in a GC/FID system and tested by isothermal elution of *a*15:0-*a*17:0. The temperature was subsequently lowered by 1 °C until the best resolution (i.e. the deepest valley between the two enantiomers) was obtained (see Materials and Methods). Retention times of analytes are known to increase with increasing amounts of the CSP [16, 27], and this was also observed for the racemic *a*FA. At similar retention times, the elution temperature for *a*15:0 was 3 °C lower on the 50% β-TBDM than on the 66% β-TBDM. Nevertheless, the resolution was much better for the 66% β-TBDM column (33 vs. 16% valley between both enantiomers on 50% β-TBDM, Table 1).

On the 50% β-TBDM in DB-5, the elution temperatures even increased by ~8 °C at a given temperature and the resolution was worse than on the 50% β-TBDM in OV-1701 (12 vs. 16%) (Table 1). This is in contrast with chiral flavor compounds where the best enantioresolution

Table 1 Elution temperature and retention time regimes of the enantioseparation of racemic *a*15:0 methyl ester on different heptakis(2,3-di-*O*-methyl-6-*O*-*tert*-butyldimethylsilyl)-β-cyclodextrin (β-TBDM) columns and corresponding resolution expressed in form of the valleys between the two isomers (c ≈ 10 ng/μL)

Column parameters	Isothermal temperature (°C)	Retention time t_{R1}/t_{R2} [min]	Valley (%)[a]
50% β-TBDM in DB-5 (0.2 μm d_f)	117	536.5/541.3	12
50% β-TBDM in OV-1701 (0.2 μm d_f)	109	550/555.5	16
66% β-TBDM in OV-1701 (0.2 μm d_f)	112	526.5/532.5	33
66% β-TBDM in OV-1701 (0.18 μm d_f)	112	430.5/435	35
66% β-TBDM in OV-1701 (0.2 μm d_f)	110	604/611	30
66% β-TBDM in OV-1701 (0.18 μm d_f)	110	491.5/497.5	30

[a] Ratio between the (mean of the) peak maxima of the two enantiomers and the minimum between them

on β-TBDM was obtained in combination with less polar polysiloxanes [16]. The better resolution of *a*FA on the more polar polysiloxane could be due to the fact that OV-1701 provides the best mixing properties with cyclodextrins [16], which is the more difficult the higher the amount of the cyclodextrin (here: 66%), and the lower the operating temperature is [20].

The best results were obtained with 66% β-TBDM in OV-1701 but the retention times of the *a*FA on this column were rather long. We thus attempted to reduce the retention of *a*FA at a given elution temperature by a new column with lower film thickness (0.18 µm instead of 0.2 µm). The thinner film of the 66% β-TBDM in OV-1701 decreased the retention times at a given temperature (e.g. 110 °C) by more than 100 min without loss of enantiomeric resolution (see Table 1). As expected, the enantiomeric resolution waned with increasing chain length of the *a*FA. For *a*15:0 and *a*17:0 the maximum enantiomeric excess that could be established was $ee > 97.5\%$ and $ee = 95\%$, respectively (see below). This resolution was sufficient for the determination in samples with non-racemic composition of the analytes (Fig. 1). Consequently, this column (66% β-TBDM in OV-1701, 30 m, 0.25 mm i.d., 0.18 µm d_f) was used for the analysis of *a*FA in food samples by GC/EI-MS-SIM.

Enrichment of Anteiso Fatty Acids from Food Samples

*a*FA are minor fatty acids in food (<0.6% of total lipids [15]) which need to be enriched before the enantioselective GC analysis can be commenced [14]. Thurnhofer et al. [14] used urea complexation in combination with silver ion liquid chromatography for this purpose. However, these procedures are time consuming and accompanied with significant loss of the analytes (especially during urea complexation). Therefore, we chose to perform the sample fractionation by RP-HPLC (see "Materials and Methods"). In RP-HPLC, retention times of saturated FAME increased with the chain length while the retention decreased the more double bonds were present at a given chain length (e.g. 18:3 < 18:2 < 18:1 < 18:0) [22]. Methyl branches had only a small effect on the retention, so that *a*15:0 and *i*15:0 (longest chain C_{14}, respectively) eluted into the same RP-HPLC fractions as 14:0 (and *a*17:0/*i*17:0 as 16:0) [18]. In dependence of the concentration in the sample, FAME were distributed over 2–5 HPLC fractions with *a*FA mainly targeted in two fractions. Fractions with *a*FA (see "Materials and Methods") contained no further relevant fatty acids than those mentioned and could be subjected to enantioselective analysis by GC/EI-MS on the 66% β-TBDM column. The RP-HPLC enrichment was suited for *a*15:0 and *a*17:0 in NL and PL. Moreover, *a*16:0 was detected in the PL of sea bass and could be studied as well

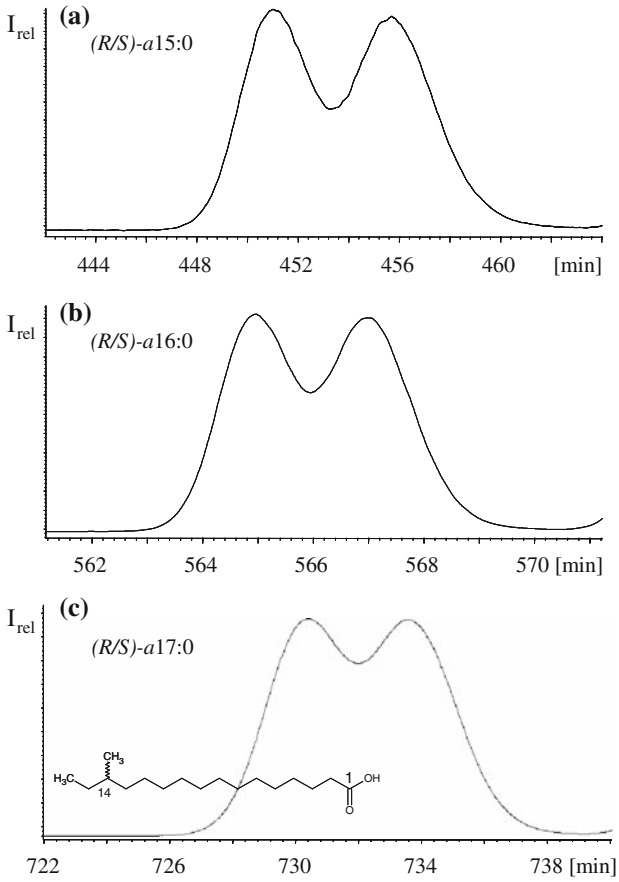

Fig. 1 Gas chromatographic enantioseparation (66% β-TBDM in OV-1701, 30 m, 0.25 mm i.d., 0.18 μm d_f) of racemic standards of methyl esters of *a*15:0, *a*16:0 and *a*17:0 (c $\approx$ 10 ng/µL)

(see below). Before, this even-numbered *a*FA has only been detected after selective enrichment by urea complexation [14]. In the sea bass, the concentration of *a*16:0 was ~0.9% of 15:0 (84 mg/100 g PL [15]) and thus in the 0.8 mg/100 g range. Obviously, the RP-HPLC fractionation provided a similar enrichment effect for branched chain fatty acids as urea complexation.

Enantioselective GC/EI-MS-SIM Analysis of *a*FA in Food Samples after Conversion into Methyl Esters and Enrichment by RP-HPLC

Injections of enantiopure *a*FA standards [19], verified that the (*R*)-enantiomer eluted prior to the (*S*)-enantiomer [14]. We also checked the retention times of other compounds in the HPLC fractions and observed no co-elutions with *a*FA on the 66% β-TBDM in OV-1701 column. However, the elution order of anteiso and iso isomers on β-TBDM was reversed in comparison with achiral stationary phases (e.g. OV-1701, DB-5 or the polar 100% cyanopropyl polysiloxane [15]). Thus, the effect must originate from the interaction of the branched chain fatty acid isomers with

Table 2 Enantiomeric distribution of anteiso fatty acids (*a*FA) in the neutral and polar lipids of food samples, expressed as the enantiomeric excess %(*ee*) and the proportion of the (*R*)-enantiomers

	Sample name	Sea bass	Trout	Gilthead seabream	Seal oil	Camembert	Mozzarella
*a*FA	Lipid class	Enantiomeric excess (%*ee*); proportion of (*R*)-enantiomer					
*a*15:0	NL	>90[a]; <5	93; 3.3	92; 4.1	87; 6.6	96; 2.2	97.5; 1.2
	PL	88; 6.0	88; 5.6	87; 6.5	68; 15.9	75; 12.3	77; 11.4
*a*16:0	NL	n.d.[b]	n.d.	n.d.	n.d.	n.d.	n.d.
	PL	84; 8.2	n.d.	n.d.	n.d.	n.d.	n.d.
*a*17:0	NL	>95[c]; <2.5	>95; <2.5	95; 2.5	89; 5.7	>95; <2.5	>95; <2.5
	PL	86; 7.1	>95; <2.5	95; 2.5	71; 14.5	88; 6.0	>95; <2.5

[a] *ee* could not be determined exactly, due to low signal-to-noise ratio

[b] n.d. = not detected: <0.8 mg/100 g

[c] Detection limit of the (*R*)-enantiomer of *a*17:0 was 2.5% (*ee* > 95%)

the CSP, most likely due to the three-dimensional geometry of the *β*-TBDM.

Fish und Seal Oil

In the sea bass sample, *a*15:0 and *a*17:0 were detected in both the neutral and the polar lipids. In all occasions the (*S*)-enantiomers were predominant. However, low amounts of the (*R*)-enantiomers were detected as well (Table 2).

Interestingly, the (*R*)-*a*17:0 was much more abundant in the PL (*ee* = 86%, 7.1% (*R*)-*a*17:0) than in the NL (*ee* > 95%, <2.5% (*R*)-*a*17:0). This result was observed for *a*15:0 (*ee* = 88% in PL vs. >90% in the NL) as well (see Table 2). As mentioned previously, traces of *a*16:0 were detected in the PL (but not in the NL) of the sea bass sample. The (*S*)-enantiomer dominated over the (*R*)-16:0 (*ee* = 84%) similarly to (*S*)-*a*17:0 in the PL of sea bass (Table 1 and Fig. 2a). One presumed biosynthesis pathway of *a*FA involves isoleucine-derived 2-methyl-butanoyl-CoA as primer instead of acetyl-CoA [28]. While this pathway can explain the formation of odd numbered *a*FA (i.e. *a*15:0 and *a*17:0), it does not fit for *a*16:0. Hence, there must be either a different biosynthesis pathway for even-numbered *a*FA, or the low amounts of *a*16:0 may originate from α-oxidation of *a*17:0. For instance, myxobacteria are able to convert odd-numbered iso-FA (e.g. *i*17:0) into even-numbered iso-FA (e.g. *i*16:0) by α-oxidation [29]. Since *a*16:0 and *a*17:0 (but also *a*15:0) showed almost the same enantiomeric excess of the (*S*)-enantiomer in the PL (Fig. 2b, c; Table 1), *a*16:0 might indeed be formed by oxidative degradation of *a*17:0.

Higher proportions of (*R*)-*a*15:0 in PL than in NL were also measured in trout and gilthead sea bream (Fig. 3) while (*R*)-*a*17:0 was absent or found in traces only in both the PL and the NL (*ee* ≥ 95%) (Table 2). However, the highest relative amounts of (*R*)-*a*FA were determined in the seal oil with 15.9% (*R*)-*a*15:0 (*ee* = 67%) and 14.5% (*R*)-*a*17:0 (*ee* = 71%).

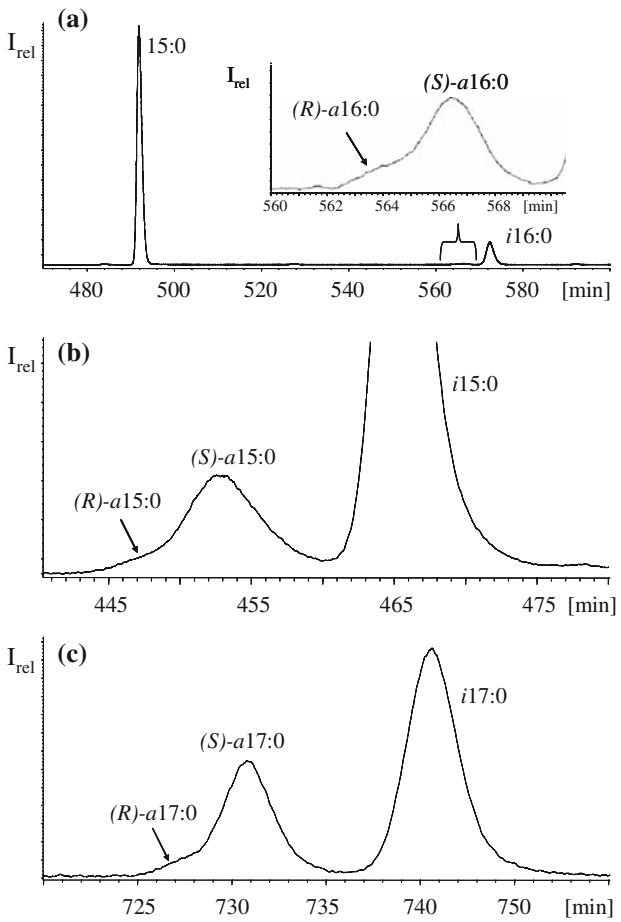

Fig. 2 GC/EI-MS chromatograms (66% *β*-TBDM in OV-1701) of the enantioselective determination of the methyl esters of **a** *a*16:0, **b** *a*15:0 and **c** *a*17:0 in the polar lipids of a sea bass sample. The concentration of *a*16:0 was approximately <0.9% of the 15:0 (84 mg/100 g lipids) and was thus estimated in the 0.8 mg/100 g lipids range

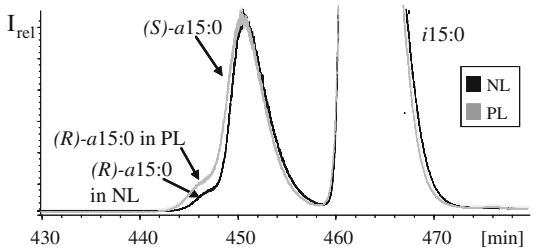

Fig. 3 GC/EI-MS chromatograms (66% β-TBDM in OV-1701) of the enantioselective determination of *a*15:0 methyl ester in the polar and neutral lipids of a gilthead sea bream sample

The relative amounts of the (*R*)-*a*FA were >2.5 times higher in the PL than in the NL (with (*R*)-*a*15:0 = 6.6%, *ee* = 87%, and (*R*)-*a*17:0 = 5.7%, *ee* = 89%). Marine mammals, such as seals are top predators of aquatic food webs and mainly feed on larger fish. The relative high proportions of (*R*)-*a*FA in the seal oil compared with the fish samples analyzed might thus suggest an enantioselective discrimination of *a*FA along the food chain. It is noteworthy in this context that all phospholipids substituted with either (*S*)-*a*FA or (*R*)-*a*FA are diastereomers which have different physicochemical properties. The same is true for triacylglycerides with $R_1 \neq R_3$. This could eventually lead to the preferred accumulation of the (*R*)-enantiomer. Furthermore, it is possible that microorganisms are involved in this process due to the higher relative abundance of (*R*)-*a*FA in the phospholipids.

Cheese Samples

Previously, only the (*S*)-enantiomers of *a*FA had been detected in the lipids of dairy products [14, 30]. Results from the marine samples indicated that (*R*)-*a*FA were more relevant in the PL. However, the PL content of cheese is very low (~1%) and the fatty acid (including the *a*FA) content of total lipids is virtually characterized by the NL. Thus, even large proportions of (*R*)-*a*FA in PL would be overlooked as long as total lipids are analyzed (and for NL mainly containing (*S*)-*a*FA). In this context it was interesting to check this assumption by the separate determination of *a*FA in the NL and PL of cheese samples. In addition, the enantiomeric resolution of *a*FA was significantly improved in this study compared to Thurnhofer et al. [14] which could only verify *ee* < 96% for *a*15:0 due to the worse gas chromatographic enantioresolution on the 50% β-TBDM phase compared to this study. With the novel 66% β-TBDM column we were able to determine lower relative amounts of (*R*)-*a*FA in dairy products (Table 1). In the NL, 1.2% and 2% of (*R*)-*a*15:0 were detected in camembert and mozzarella (see embedded chromatogram in Fig. 4a). The small amounts of (*R*)-*a*15:0 detected in the cheeses clearly demonstrated the improved performance of the new column, since higher enantiomeric excesses (*ee* > 97.5% for *a*15:0) could be verified. However, much higher proportions of (*R*)-*a*15:0 were detected in the PL of camembert (12%, *ee* = 75%, Fig. 4b) and mozzarella (12.3%, *ee* = 75%). (*R*)-*a*17:0 was neither detected in the NL nor in the PL of mozzarella but the PL of camembert also contained 6% of (*R*)-*a*17:0 (*ee* = 88%) while (*R*)-*a*17:0 was not detected in the NL (Fig. 4c, d).

To our knowledge, these results mark the first detection of (*R*)-*a*FA in the lipids of dairy products. These results contradict those of the Shorland group, who found *a*FA to be (*S*)-enantiopure in the lipids of food samples [30, 31]. However, these authors used fractional distillation and

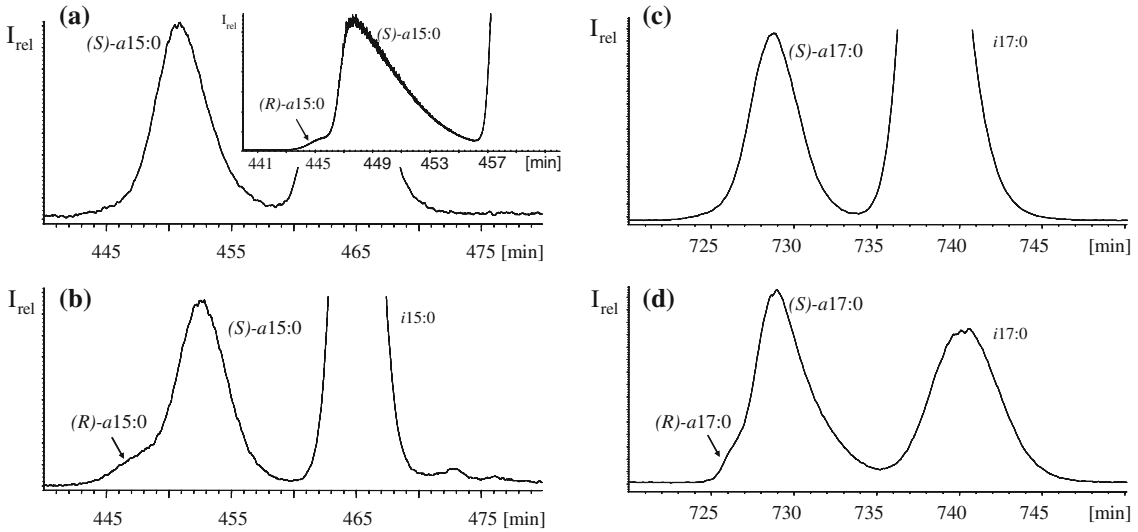

Fig. 4 GC/EI-MS chromatograms (66% β-TBDM in OV-1701) of the enantioselective determination of *a*15:0 methyl ester in **a** the NL and **b** the PL of camembert as well as *a*17:0 methyl ester in **c** the NL and **d** the PL of camembert. The embedded chromatogram in **a** shows a 20-fold higher concentrated fraction with small amounts of (*R*)-*a*15:0 (2%, *ee* = 96%)

crystallization for the isolation of *a*FA from food samples [32]. It could be possible that these procedures are accompanied with enantiomeric fractionation (i.e. the loss of the small amounts of the (*R*)-enantiomers). Alternatively, it could be possible that small amounts of (*R*)-enantiomers were overlooked.

The origin of the (*R*)-*a*FA in the food samples remains largely unexplained. The stronger occurrence of the (*R*)-enantiomer in PL compared to NL (which was up to 5 times higher for (*R*)-*a*15:0) could indicate that microorganisms (e.g. rumen bacteria, marine microorganisms or pathogenic bacteria in the case of the perishable fish) are responsible for this event. Moreover, it is unclear whether the (*R*)-*a*FA are formed in de novo syntheses or if they are the product of (partial) enantiomerization or racemization. These questions and the underlying biochemical mechanisms are interesting topics to be clarified in future.

Acknowledgements We acknowledge financial support of this work by the German Research Foundation (DFG).

References

1. Thurnhofer S, Lehnert K, Vetter W (2008) Exclusive quantification of methyl-branched fatty acids and minor 18:1-isomers in foodstuff by GC/MS in the SIM mode using 10, 11-dichloroundecanoic acid and fatty acid ethyl esters as internal standards. Eur Food Res Technol 226:975–983
2. Vlaeminck B, Lourenco M, Bruinenberg M, Demeyer D, Fievez V (2004) Odd and branched chain fatty acids in rumen contents and milk of dairy cows fed forages from semi-natural grasslands. Commun Agric Appl Biol Sci 69:337–340
3. Singh VK, Hattangady DS, Giotis ES, Singh AK, Chamberlain NR, Stuart MK, Wilkinson BJ (2008) Insertional inactivation of branched-chain alpha-keto acid dehydrogenase in *Staphylococcus aureus* leads to decreased branched-chain membrane fatty acid content and increased susceptibility to certain stresses. Appl Environ Microbiol 74:5882–5890
4. Zhu K, Bayles DO, Xiong A, Jayaswal RK, Wilkinson BJ (2005) Precursor and temperature modulation of fatty acid composition and growth of *Listeria monocytogenes* cold-sensitive mutants with transposon-interrupted branched-chain alpha-keto acid dehydrogenase. Microbiol 151:615–623
5. Beranova J, Jemiola-Rzeminska M, Elhottova D, Strzalka K, Konopasek I (2008) Metabolic control of the membrane fluidity in *Bacillus subtilis* during cold adaptation. Biochim Biophys Acta 1778:445–453
6. Rilfors L (1985) Difference in packing properties between iso and anteiso methyl-branched fatty acids as revealed by incorporation into the membrane lipids of *Acholeplasma laidlawii* strain A. Biochim Biophys Acta 813:151–160
7. Suutari M, Laakso S (1992) Unsaturated and branched chain-fatty acids in temperature adaptation of *Bacillus subtilis* and *Bacillus megaterium*. Biochim Biophys Acta 1126:119–124
8. Wright KC, Yang P, Van Pelt CS, Hicks ME, Collin P, Newman RA (2005) Evaluation of targeted arterial delivery of the branched chain fatty acid 12-methyltetradecanoic acid as a novel therapy for solid tumors. J Exp Ther Oncol 5:55–68
9. Yang P, Collin P, Madden T, Chan D, Sweeney-Gotsch B, McConkey D, Newman RA (2003) Inhibition of proliferation of PC3 cells by the branched-chain fatty acid, 12-methyltetradecanoic acid, is associated with inhibition of 5-lipoxygenase. Prostate 55:281–291
10. Akasaka K, Ohrui H (2004) Chiral discrimination of branched-chain fatty acids by reversed-phase HPLC after labeling with a chiral fluorescent conversion reagent. Biosci Biotechnol Biochem 68:153–158
11. Karl V, Gutser J, Dietrich A, Maas B, Mosandl A (1994) Stereoisomeric flavor compounds. LXVIII. 2-, 3-, and 4-alkyl-branched acids, part 2: chirospecific analysis and sensory evaluation. Chirality 6:427–434
12. Akasaka K, Meguro H, Ohrui H (1997) Enantiomeric separation of carboxylic acids having chiral centers remote from the carboxyl group by labeling with a chiral fluorescent derivatization reagent. Tetrahedron Lett 38:6853–6856
13. Akasaka K, Shichijyukari S, Meguro H, Ohrui H (2002) Determination of the absolute configurations of the anteiso acid moieties of glycoglycerolipid S365A isolated from *Corynebacterium aquaticum*. Biosci Biotechnol Biochem 66:1719–1722
14. Thurnhofer S, Hottinger G, Vetter W (2007) Enantioselective determination of anteiso fatty acids in food samples. Anal Chem 79:4696–4701
15. Hauff S, Vetter W (2010) Quantification of branched chain fatty acids in polar and neutral lipids of cheese and fish samples. J Agric Food Chem 58:707–712
16. Dietrich A, Maas B, Mosandl A (1994) Diluted modified cyclodextrins as chiral capillary gas chromatographic stationary phases: Influence of the polysiloxane solvents on enantioselectivity and column efficiency. J Microcolumn Sep 6:33–42
17. Hauff S, Vetter W (2009) Quantification of fatty acids as methyl esters and phospholipids in cheese samples after separation of triacylglycerides and phospholipids. Anal Chim Acta 636:229–235
18. Hauff S, Vetter W (2010) Creation and evaluation of a two dimensional contour plot of fatty acids methyl esters after offline coupling of revered phase HPLC and GC/EI-MS. Anal Bioanal Chem. doi:10.1007/s00216-010-3502-5, published online February 2010
19. Thurnhofer S, Vetter W (2007) Synthesis of (S)-(+)-enantiomers of food-relevant (*n-5*)-monoenoic and saturated anteiso-fatty acids by a Wittig reaction. Tetrahedron 63:1140–1145
20. Weichbrodt M, Vetter W, Luckas B (2000) Microwave-assisted extraction and accelerated solvent extraction with ethyl acetate-cyclohexane before determination of organochlorines in fish tissue by gas chromatography with electron-capture detection. J AOAC Int 83:1334–1343
21. Thurnhofer S, Vetter W (2005) A gas chromatography/electron ionization-mass spectrometry-selected ion monitoring method for determining the fatty acid pattern in food after formation of fatty acid methyl esters. J Agric Food Chem 53:8896–8903
22. Hauff S, Vetter W (2009) Quantitation of *cis*- and *trans*-monounsaturated fatty acids in dairy products and cod liver oil by mass spectrometry in the selected ion monitoring mode. J Agric Food Chem 57:3423–3430
23. Blum W, Aichholz R (1990) Gas chromatographic enantiomer separation on *tert*-butyldimethylsilylated β-cyclodextrin diluted in PS-086. A simple method to prepare enantioselective glass capillary columns. J High Resolut Chromatogr 13:515–518
24. Savitzky A, Golay MJE (1964) Smoothing and differentiation of data by simplified least squares procedures. Anal Chem 36:1627–1639
25. Dietrich A, Maas B, Messer W, Bruche G, Karl V, Kaunzinger A, Mosandl A (1992) Stereoisomeric flavor compounds, Part LVIII: the use of heptakis(2,3-di-*O*-methyl-6-*O*-*tert*-butyldimethylsilyl)-β-cyclodextrin as a chiral stationary phase in flavor analysis. J High Resolut Chromatogr 15:590–593

26. Hauff S, Rilfors L, Hottinger G, Vetter W (2010) Structure and chirality of an unsaturated anteiso fatty acid from *Bacillus megaterium*. J Chromatogr A 1217:1683–1687
27. Jung M, Schmalzing D, Schurig V (1991) Theoretical approach to the gas chromatographic separation of enantiomers on dissolved cyclodextrin derivatives. J Chromatogr 552:43–57
28. Vlaeminck B, Fievez V, Cabrita ARJ, Fonseca AJM, Dewhurst RJ (2006) Factors affecting odd- and branched-chain fatty acids in milk: a review. Anim Feed Sci Technol 131:389–417
29. Bode HB, Dickschat JS, Kroppenstedt RM, Schulz S, Mueller R (2005) Biosynthesis of iso-fatty acids in myxobacteria: iso-even fatty acids are derived by α-oxidation from iso-odd fatty acids. J Am Chem Soc 127:532–533
30. Hansen RP, Shorland FB, Cooke NJ (1952) Branched-chain fatty acids of mutton fat. I. Isolation of (+)-14-methylhexadecanoic acid. Biochem J 52:203–207
31. Morice IM, Shorland FB (1956) The isolation of iso- and (+)-anteiso-fatty acids of the C15 and C17 series from shark (*Galeorhinus australis*) liver oil. Biochem J 64:461–464
32. Morice IM, Shorland FB (1955) Isolation of *n*-pentadecanoic and *n*-heptadecanoic acids from shark (*Galeorhinus australis*) liver oil. Biochem J 61:453–456

Lipids (2010) 45:367–374
DOI 10.1007/s11745-010-3404-5

METHODS

Preparation of Fatty Acid Methyl Esters by Selective Methanolysis of Polar Glycerolipids

Ken'ichi Ichihara · Chiaki Yamaguchi · Yumiko Araya · Asami Sakamoto · Kumiko Yoneda

Received: 18 September 2009 / Accepted: 1 March 2010 / Published online: 21 March 2010

Abstract KOH in aqueous methanol catalyzes selective methanolysis of polar glycerolipids with *O*-ester-linked acyl residues, while triacylglycerols and sterol esters are inert in the solution. Based on these findings, a convenient and reliable method was developed for the preparation of fatty acid methyl esters (FAMEs) from polar glycerolipids in lipid mixtures without prior isolation. Methanolysis of polar glycerolipids was completed within 2.5 min by vortexing or 20 min by shaking with 0.7 M KOH/70% (v/v) methanol in the presence of hexane at 30 °C. The yields of FAMEs obtained by the present method were greater than 95%. The method was applied successfully to gas chromatographic analysis of the fatty acid compositions of polar glycerolipids in seed oil and blood. No obvious differences were found between the fatty acid compositions determined by the present method and those determined by conventional methods, including lipid extraction with chloroform/methanol followed by isolation of polar lipids by chromatography. The fatty acid composition of polar glycerolipids, including phospholipids, can be determined readily in many crude samples.

Keywords Fatty acid methyl ester · Selective methanolysis · Transesterification · Cholesterol ester · Phospholipid · Polar glycerolipids · Triacylglycerol · Blood lipids · Seed oil

K. Ichihara (✉) · C. Yamaguchi · Y. Araya · A. Sakamoto · K. Yoneda
Department of Biological Chemistry, Graduate School of Agricultural Science, Kyoto Prefectural University, Shimogamo, Kyoto 606-8522, Japan
e-mail: ichihara@kpu.ac.jp

Abbreviations

CE	Cholesterol ester
CEase	Cholesterol esterase
FAME	Fatty acid methyl ester
GC	Gas–liquid chromatography
PC	Phosphatidylcholine
PE	Phosphatidylethanolamine
PL	Phospholipid
TG	Triacylglycerol

Introduction

Phospholipids (PLs) are the major constituents of biological membranes, and the fatty acid composition of PLs affects the physical and chemical properties of the membrane. Some of fatty acids found in PLs are also substrates of physiologically active substances. The fatty acid composition and the n-3/n-6 polyunsaturated fatty acid balance of blood and other organs are suggested to be related to human health [1–4], while the fatty acid composition of blood glyceroPLs reflects medium-term dietary intake from weeks to months and hence also the nutritional and health status of each individual [5–7]. The fatty acid composition of glyceroPLs is determined by gas–liquid chromatography (GC). In conventional analytical procedures [1, 3, 8–13], total lipids are extracted from various biological materials with a mixed solution of chloroform and methanol. After phase separation, the chloroform layer is washed with water, and concentrated to dryness. Total PLs are isolated as polar lipids from total lipids by thin-layer chromatography (TLC) or column chromatography [14–16]. Total PLs are scraped off the TLC plates or total PLs eluted

through a column are concentrated to dryness. GlyceroPLs in total PLs thus isolated are converted to fatty acid methyl esters (FAMEs) by acid- or base-catalyzed methanolysis or by saponification followed by methylation. These steps are laborious and time-consuming, and it is difficult to treat many samples simultaneously by these methods. Our research has been made to prepare FAMEs selectively from polar glycerolipids in lipid mixtures.

Polar glycerolipids are composed of glyceroPLs and glyceroglycolipids in higher plants, while the polar glycerolipids in mammals are exclusively glyceroPLs. In the course of investigating base-catalyzed methanolysis, we found that KOH in 70% methanol efficiently catalyzes methanolysis of polar glycerolipids in the presence of sterol esters and triacylglycerols (TGs) to produce FAMEs derived from polar glycerolipids. Here, we describe a convenient reagent and simplified procedures to prepare FAMEs from polar glycerolipids in crude biological samples including seed oil and blood for GC analysis.

Materials and Methods

Reagents

PLs, TGs, cholesterol esters (CEs), fatty acids, and FAMEs were purchased from Avanti Polar Lipids (Alabaster, AL, USA), Cayman Chemical (Ann Arbor, MI, USA), Doosan Serdary Research Laboratories (Toronto, Canada), Nu-Chek-Prep (Elysian, MN, USA), Sigma-Aldrich (St. Louis, MO, USA), and Wako Pure Chemical Industries (Osaka, Japan). Dioleoyl phosphatidylcholine (PC) was synthesized from *sn*-glycero-3-phosphocholine and oleic acid [17]. Acetone, hexane, and methanol were purchased from Wako Pure Chemical Industries as glass-distilled solvents for analysis of residual pesticides. HPLC grade glass-distilled chloroform was obtained from Sigma-Aldrich. KOH, 50% BF_3 in methanol, *tert*-butyl methyl ether, methyl acetate, and heparin sodium salt were of reagent grade. Cartridge columns packed with 50 and 200 mg of silica gel were Bond Elut (No.12102068; Varian, Palo Alto, CA, USA) and LiChrolut (No.102021; Merck, Darmstadt, Germany), respectively. Microbial cholesterol esterases (CEases, EC3.1.1.13) were purchased from Calbiochem/Merck (Darmstadt, Germany) and from Oriental Yeast (Tokyo, Japan).

TLC and GC

Reaction products of methanolysis were analyzed by TLC on silica gel. Lipids separated were visualized by spraying 50% (w/w) sulfuric acid and then heating at 135 °C. PLs were also detected with the Dittmer and Lester reagent [18]. Plasmalogen was detected by spraying 0.5% 2,4-dinitrophenylhydrazine in 2 M HCl. FAMEs were analyzed with a Shimadzu 2014 gas chromatograph equipped with columns of DB-23 (0.25 mm × 30 m) and SUPELCOWAX 10 (0.53 mm × 30 m) at a column temperature of 215 or 225 °C (isothermal). Prior to GC, FAMEs prepared from biological materials were purified through cartridge columns packed with 200 mg of silica gel. Silica gel cartridges that had been conditioned with 3 mL of hexane were charged with FAMEs dissolved in hexane, and washed with 3 mL of hexane. FAMEs were then eluted with 3 mL of 1.2% (v/v) methyl acetate in hexane.

Conventional Preparation of FAMEs

Lipids were extracted from biological materials, including oil seed and blood, with chloroform/methanol by a modification of the Bligh and Dyer method [19], and the chloroform solution obtained was evaporated to dryness. Polar lipids of oil seeds were isolated from total lipids by column chromatography. Total lipids were dissolved in chloroform and applied to silica gel cartridge columns. Neutral lipids were eluted from the columns with chloroform, and polar lipids were then eluted with methanol. Blood PLs were isolated by TLC. Total lipids extracted from blood were developed on silica gel plates with acetone, and then PLs located at the origin of plate were scraped off together with silica gel. FAMEs were prepared by KOH-catalyzed methanolysis [20] from the polar lipids and PLs thus isolated.

Selective Methanolysis of Polar Glycerolipids

Hexane (2 mL) was added to lipid samples of mg order or less in a glass test tube (16.5 mm × 105 mm) and the resulting solutions were warmed for a few minutes in a water bath at 30 °C. To the hexane solution was added 0.4 mL of 0.7 M KOH in 70% (v/v) methanol, and the tubes were vortexed for 2.5 min or shaken at 200 rpm in a reciprocal shaker at 30 °C for 20 min. The reaction was stopped by addition of 0.03 mL of acetic acid and 1 mL of water. FAMEs in the hexane layer were analyzed by GC. To follow the progress of methanolysis, reaction products were extracted with chloroform and analyzed by TLC.

For lipid samples containing water, 1 M KOH in methanol was added to make 0.7 M KOH/70% methanol. For lipid samples of blood containing large amounts of CEs, the CEs were enzymatically hydrolyzed before methanolysis. The products of hydrolysis, cholesterol and fatty acids, had no effect on methanolysis and could be removed by passing through a silica gel cartridge before GC.

Preparation of FAMEs from Polar Glycerolipids in Blood

To 0.02 mL of CEase solution (500 U/mL of 0.15 M phosphate buffer, pH 7.0) in glass test tubes was added 0.14 mL of blood containing 0.7 U heparin, and the contents were mixed by pipetting several times. The mixtures were incubated for 30 min at 37 °C for hydrolysis of CEs, and then 2 mL of hexane (30 °C) and 0.28 mL of 1 M KOH in methanol (30 °C) were added. Methanolysis of PLs was carried out for 2.5 min with a vortex mixer. The reaction was terminated by addition of 0.03 mL of acetic acid, but no water was added to prevent gelation. FAMEs in the hexane layer were purified with a silica gel column. Alternatively, after treatment with CEase, methanolysis was carried out for 20 min in a reciprocal shaker at 180–200 rpm at a temperature of 30 °C. In this procedure, 3 mL of hexane was added.

For limited volumes of blood samples, 28 μL of blood containing 0.14 U of heparin was added to 4 μL of 2 U CEase solution in 1.5-mL plastic microcentrifuge tubes. The blood and CEase were mixed by pipetting several times, and the mixtures were incubated for 30 min at 37 °C. After addition of 0.5 mL of hexane and 56 μL of 1 M KOH in methanol, the tubes were vortexed at 30 °C for 2.5 min or vigorously mixed with a microcentrifuge tube shaker for 4 min at room temperature. To the reaction mixture was added 6 μL of acetic acid. The hexane layer was applied to a small cartridge column packed with 50 mg of silica gel. The gel was washed with 0.75 mL of hexane, and the FAMEs were eluted with 0.75 mL of 1.2% methyl acetate in hexane. The eluate was concentrated in vacuo and FAMEs obtained were analyzed by GC.

Results

Effects of KOH Concentration, Water Content, and Reaction Time on Methanolysis of PLs

PL mixtures composed of dioleoyl PC and dioleoyl phosphatidylethanolamine (PE) were shaken at 200 rpm in methanolic KOH solutions containing water at 30 °C for 20 min. The PLs were converted into methyl oleate at KOH concentrations of 0.7 M and above, and the reaction was accompanied by formation of small amounts of free oleic acid (Fig. 1a). The presence of water at 30% or less in methanol did not significantly affect methanolysis of PLs, but 40% water markedly inhibited the reaction (Fig. 1b). Although water in methanol caused hydrolysis of PLs, the amounts of free oleic acid released were estimated to be a small percentage of methyl oleate formed as described below. In a separate experiment, there were no differences between the fatty acid composition of FFAs released and that of FAMEs formed. The reaction time required for methanolysis of PLs by shaking was 15–20 min (Fig. 1c), while the reaction was completed within 2–2.5 min by vortexing (Fig. 1d).

Table 1 shows that the yields of methyl eicosenoate formed from dieicosenoyl PC were greater than 95% when determined by GC using an internal standard. Amounts of free eicosenoic acid released from the PL during methanolysis were 2.6–3.1% of the FAMEs formed. In a different experiment with dioleoyl PC, the ratio of methyl oleate and oleic acid formed by vortexing was 97.3 ± 0.1:2.7 ± 0.1 ($n = 3$). In addition, FFAs detected at the end of the reaction were derived from PLs but not from FAMEs formed. Saponification of FAMEs once formed was slow in the solution of 0.7 M KOH/70% methanol/hexane and the FAMEs formed underwent little hydrolysis. With respect to the mixing method, vortexing was better than shaking in terms of FFA formation and reaction time (Table 1; Figs. 1c, d), but the shaking method still has the advantage that it allows simultaneous treatment of more samples at a time.

Contamination with FAMEs Derived from TGs

Products of methanolysis of dioleoyl PC in the presence of trieicosenoyl TG were analyzed to assess the degree of contamination with FAMEs derived from TGs. Table 2 shows that methanolysis of TG proceeded much more slowly than that of PC, and consequently methyl oleate formed from PC was negligibly contaminated with methyl eicosenoate from TG. Even when a mixture of 58.5% PLs (PC and PE) and 41.5% TG was incubated for a long reaction time of 1 h in a reciprocal shaker at 30 °C, 99.0% of the FAMEs produced were derived from PLs.

Methanolysis of a mixture of dipalmitoyl PC and dioleoyl PE with 0.7 M KOH/70% methanol gave FAMEs with a similar fatty acid composition to that of the substrate PLs (Table 3). These observations suggested that methanolysis for PLs was not selective for specific molecular species of fatty acid.

Determination of the Fatty Acid Compositions of Polar Glycerolipids in Seed Oils and Leaf Lipids

TGs are the major components of vegetable oils, while PLs are a minor constituent whose content is a very small percentage of the oil. Seeds of Brassicaceae plants accumulate erucic acid, 13-docosenoic acid, in TGs, but only a small amount of this very long chain fatty acid is present in PLs. Total lipids were extracted from the seeds of *Brassica*

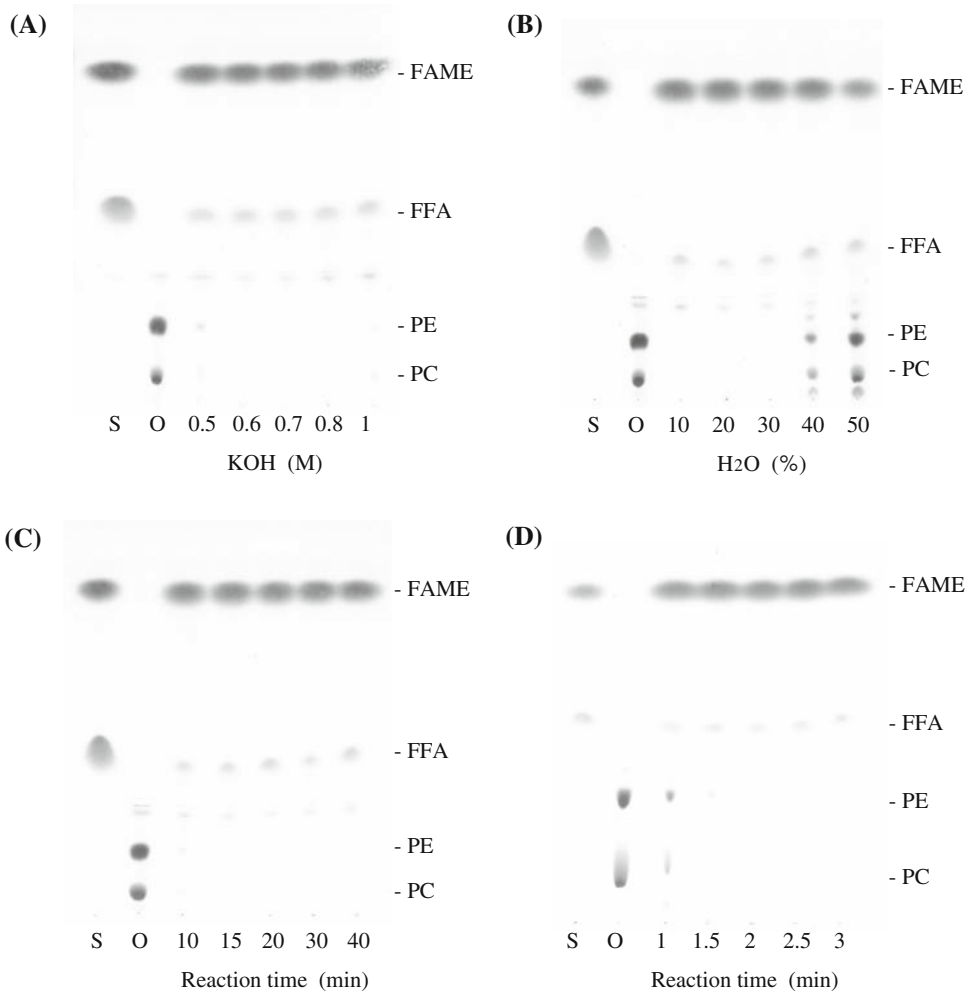

Fig. 1 Effects of (**a**) KOH concentration, (**b**) water content, (**c**) reaction time of shaking, and (**d**) reaction time of vortexing on methanolysis of PLs. PL mixtures composed of 1 mg of dioleoyl PE and 1 mg of dioleoyl PC were incubated with 0.5–1 M KOH (**a**) in 50–90% methanol (**b**) for 10–40 min (**c**) at 30 °C in a reciprocal shaker at 200 rpm. In the experiment for (**d**), PL mixtures were vortexed for 1–3 min at 30 °C. Reaction products were extracted with hexane and chloroform, and these extracts were combined and concentrated in vacuo for analysis by TLC. Silica gel plates spotted with the concentrates were developed to 3 cm from the origin with chloroform/methanol/water/acetic acid (65:35:4:1, v/v/v/v), dried in vacuo, and redeveloped to 8 cm from the origin with hexane/*tert*-butyl methyl ether/acetic acid (85:15:0.5, v/v/v). *S* standards of FAME and FFA, *O* time zero

Table 1 Yields of FAME and FFA formed from PC

Method of mixing	Yield (wt%)	
	Methyl eicosenoate	Eicosenoic acid
Vortexing	96.0 ± 1.2	2.6 ± 0.2
Reciprocal shaking	95.5 ± 0.9	3.1 ± 0.0

Dieicosenoyl PC was incubated with 2 mL of hexane and 0.4 mL of 0.7 M KOH/70% methanol at 30 °C. After methanolysis, methyl heptadecanoate and heptadecanoic acid were added to the reaction mixture as internal standards. Products were extracted three times with hexane, and FAME and FFA were isolated by TLC. FFA was methylated with 10% BF_3 at 45 °C for 20 min. Data are shown as averages of three determinations

oleracea var. *italica* with chloroform/methanol, and polar lipids, including PLs, were isolated from the total lipids by passage through a silica gel column. Nonpolar lipids were removed by elution with chloroform, and polar lipids were then eluted with methanol. The polar lipid fraction contained PE, PC, and phosphatidylinositol as PLs, and also phosphorus-negative compounds. The *Brassica* seeds contained 30% (w/w) oil, most of which was comprised of TGs. Total lipids were treated with 0.7 M KOH/70% methanol/hexane or 2 M KOH/methanol/hexane [20], which was also used for methanolysis of the isolated polar lipids. The fatty acid composition of polar glycerolipids was almost the same as that of the isolated polar lipid fraction (Table 4).

Photosynthetic tissues of plants contain PLs and glycolipids. TGs are a minor constituent, although they accumulate in leaves under ozone fumigation [21]. The major lipid classes of PLs are PC, PE, phosphatidylglycerol, and phosphatidylinositol, while those of glycolipids are monogalactosyldiacylglycerol, digalactosyldiacylglycerol, and sulfoquinovosyldiacylglycerol. Fatty acyl residues of these glyceroglycolipids are also converted to FAMEs by the reaction of leaf total lipids from *Phaseolus vulgaris* with 0.7 M KOH/70% methanol (data not shown).

Table 2 Contamination with FAME derived from TG

Substrate PC:TG (wt%)	FAME formed (wt%)	
	Methyl oleate (FAME from PC)	Methyl eicosenoate (FAME from TG)
50:50	99.7 ± 0.0	0.3 ± 0.0
10:90	97.4 ± 0.1	2.6 ± 0.1

Mixtures of dioleoyl PC and trieicosenoyl TG were vortexed with 2 mL of hexane and 0.4 mL of 0.7 M KOH/70% methanol. Data are shown as averages of two determinations

Table 3 Effects of fatty acyl molecular species on selective methanolysis

FAME formed	Methanolysis with	
	2 M KOH/methanol (wt%)	0.7 M KOH/70% methanol (wt%)
16:0 (from PC)	47.3 ± 0.3	46.7 ± 0.2
18:1 (from PE)	52.7 ± 0.1	53.3 ± 0.1

A mixture of dipalmitoyl PC and dioleoyl PE was incubated with 0.7 M KOH/70% methanol/hexane or with 2 M KOH/methanol/hexane as control at 30 °C in a reciprocal shaker. Data are shown as averages of three determinations

Determination of the Fatty Acid Composition of Polar Glycerolipids in Blood

Removal of CEs from Blood Prior to Methanolysis

To synthesize FAMEs from polar glycerolipids of blood in which polar glycerolipids are glyceroPLs, blood was directly incubated with KOH/methanol taking into account the fact that the water content of blood is about 73%. Polar glycerolipids in blood were converted into FAMEs, while CEs, TGs, and FFAs remained unchanged as expected. The FAME preparations were passed through silica gel cartridge columns, which are more convenient than TLC, but CEs could not be separated completely from FAMEs because they have similar polarities. As the presence of CEs in GC samples of FAMEs probably degrades GC columns and shortens their lifespan, CEs were enzymatically split into cholesterol and fatty acids prior to methanolysis of PLs. As shown in Fig. 2, CEs in blood were hydrolyzed to cholesterol and fatty acids within 30 min, although a trace amount of CEs remained unchanged. As CEase also catalyzed hydrolysis of TGs, the incubation of blood with CEase resulted in the disappearance of both CEs and TGs. CEs and TGs may not be completely decomposed by CEase in blood samples containing high concentrations of these lipids, and this may be the case in the blood of hyperlipidemic patients. However, even if CEs and TGs are not completely hydrolyzed by the esterase, it is expected that the FAME compositions of these nonpolar lipids are not reflected in that of polar glycerolipids due to selective methanolysis.

Preparation of FAMEs from Polar Glycerolipids in Blood

Based on the above observations, a convenient method that requires neither lipid extraction from blood nor isolation of PLs was developed for preparation of FAMEs of blood polar glycerolipids. The products from each reaction step were analyzed by TLC (Fig. 3). The two major blood glyceroPLs, i.e., PE and PC, disappeared after 20 min of reaction, and this demonstrated that these diacyl PLs underwent methanolysis. Small, weak spots that were found at the same position as PC in lanes 2–6 were the lyso form of ethanolamine plasmalogen, which has an *O*-ether linkage. Sphingomyelin, which has no ester bond, remained unchanged. The results shown in Fig. 3 again confirmed that CEs and TGs were both stable in methanolic alkali containing water under the conditions employed and that FAMEs were formed from glyceroPLs. FAMEs in the hexane layer of the reaction (lane 6) were purified through a silica gel cartridge to a single spot on the TLC plate (lane 7).

The fatty acid compositions determined by this method were compared with those determined by a conventional method, including extraction of total lipids, isolation of polar lipids by TLC, and methanolysis (Table 5). There were no significant differences between the fatty acid compositions determined by this method and by the conventional method except for oleic acid (18:1) and docosatetraenoic acid (22:4 n-6).

Discussion

On the selective methanolysis for glyceroPLs in the presence of 90% or less TGs, only limited contamination with FAMEs derived from TGs can occur under the conditions employed (Table 2). As CEs are less reactive than TGs [22, 23], it is reasonable to expect that no FAMEs would be produced from CEs with KOH in aqueous methanol. The accuracy and usefulness of selective methanolysis were confirmed with seed oil and blood lipids by comparison of the fatty acid composition of polar glycerolipids obtained by selective methanolysis without isolation from total lipids with that of polar lipids obtained by conventional methods. The erucic acid content of polar glycerolipids was much lower than that of total lipids and was very similar to that of polar lipids, indicating that almost all the FAMEs produced were derived from polar glycerolipids, and TGs did not act as the substrate of methanolysis (Table 4). The data demonstrated the validity of selective methanolysis for determination of the fatty acid composition of polar glycerolipids in lipid samples in which TGs were predominant. The present method thus does not require the isolation of polar glycerolipids from total lipids prior to preparation of FAMEs.

GlyceroPLs in blood could be directly converted corresponding FAMEs. With small volumes of blood samples, the fatty acid composition of total glycerolipids (TGs and glyceroPLs) can be readily determined by KOH-catalyzed methanolysis of blood loaded on filter paper followed by GC [24], and that of total lipids can be analyzed by finger stick assays [25, 26] where HCl and BF_3 have been used as acid catalysts. FAMEs derived from ester lipids (CEs, TGs, and glyceroPLs) and FFAs can also be prepared from a drop of blood on a small piece of filter paper at 45 °C by methanolysis/methylation with aqueous concentrated HCl/methanol/toluene [27]. Ohta et al. [28] reported a method for determination of the fatty acid compositions of individual lipid classes in small volumes of blood samples, but the method included procedures for separation of individual lipid classes by TLC. The present method using selective methanolysis has enabled us to determine the fatty acid composition of blood glyceroPLs without extraction or isolation of the polar lipids. Although samples of 0.14 mL of blood were treated in this method, the scale could be reduced to at

Table 4 Fatty acid compositions of total lipids, polar lipids, and polar glycerolipids of *Brassica oleracea* seeds

Fatty acid	2 M KOH/methanol (wt%)		0.7 M KOH/70% methanol
	Total lipids	Polar lipids	Polar glycerolipids (wt%)
16:0	4.2 ± 0.0	15.6 ± 0.5	14.9 ± 0.1
16:1	0.3 ± 0.0	1.5 ± 0.0	1.8 ± 0.1
16:2	0.1 ± 0.0	1.1 ± 0.0	1.1 ± 0.0
16:3	ND	0.4 ± 0.0	0.3 ± 0.0
18:0	0.6 ± 0.0	1.8 ± 0.1	0.8 ± 0.0
18:1	10.2 ± 0.0	21.3 ± 0.1	21.4 ± 0.0
18:2	13.5 ± 0.0	35.1 ± 0.4	36.0 ± 0.2
18:3	11.3 ± 0.1	13.5 ± 0.2	13.8 ± 0.0
20:0	0.4 ± 0.0	0.1 ± 0.0	0.1 ± 0.0
20:1	5.1 ± 0.0	2.5 ± 0.0	2.6 ± 0.0
20:2	0.4 ± 0.0	0.4 ± 0.0	0.4 ± 0.1
22:0	0.5 ± 0.0	0.1 ± 0.0	0.1 ± 0.0
22:1	52.6 ± 0.1	6.5 ± 0.0	6.6 ± 0.1
22:2	1.0 ± 0.0	0.2 ± 0.0	0.2 ± 0.0

Polar lipids were isolated from total lipids by silica gel column chromatography. The fatty acid composition of polar glycerolipids was determined by selective methanolysis of the total lipids with 0.7 M KOH/70% methanol/hexane. Data are shown as averages of three determinations

ND not detected

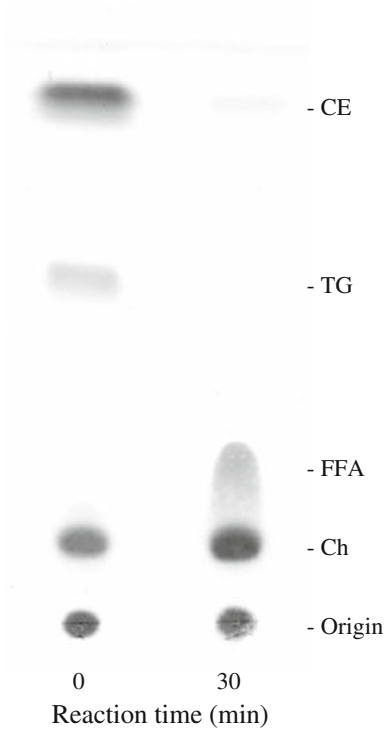

Fig. 2 Hydrolysis of CEs in blood by CEase. A 0.14 mL blood sample was mixed with a 10 U CEase solution (0.02 mL) and incubated at 37 °C for 30 min. Products were extracted with chloroform/methanol, and analyzed by TLC. The silica gel plate was first developed to 5 cm from the origin with hexane/*tert*-butyl methyl ether (75:25, v/v), and then it was developed to 8 cm from the origin with hexane/*tert*-butyl methyl ether (95:5, v/v). *Ch* cholesterol

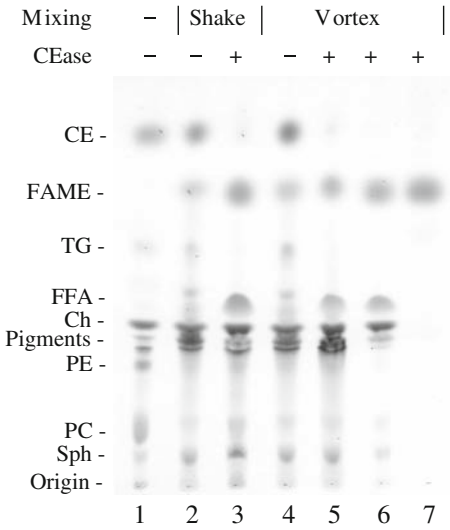

Fig. 3 Reaction products of methanolysis for blood glyceroPLs. Lane 1 shows the profile of total lipids extracted with chloroform/methanol from blood, and lanes 2–7 show the products of methanolysis of blood glyceroPLs. Blood samples (0.14 mL) were incubated with 0.02 mL of 0.15 M phosphate buffer (*lanes 2* and *4*) or CEase solution (*lanes 3* and *5–7*) at 37 °C for 30 min, and then mixed with 2 mL of hexane and 0.28 mL of 1 M KOH/methanol at 30 °C by shaking at 180 rpm for 20 min (*lanes 2* and *3*) or vortexing for 2.5 min (*lanes 4–7*). Methanolysis was stopped by the addition of 0.03 mL of acetic acid, and then the hexane layer was separated. The residual methanol/water layer was extracted with chloroform/methanol to confirm the disappearance of PE and PC. The chloroform extract was combined with the hexane layer, and then the mixed solution was evaporated in vacuo for TLC (*lanes 2–5*). For GC analysis, the hexane layer was concentrated and checked by TLC (*lane 6*), while FAMEs in the hexane layer were purified through a silica gel cartridge column (*lane 7*). *Ch* cholesterol; *Sph* sphingomyelin

least one-fifth as described in Materials and Methods. The procedure could also effectively function on the microscale.

In conclusion, the methanolic KOH solution containing water can catalyze selective methanolysis of polar glycerolipids irrespective of the presence or absence of sterol esters or TGs. The present method for preparation of FAMEs was successfully applied to analysis of seed and blood polar glycerolipids. The methanolysis proceeds under mild conditions, produces no artifacts, and is safe for researchers. The procedure does not include use of chloroform, which is toxic to humans and may contaminate the environment. Fatty acid compositions and yields obtained were almost the same as those obtained with conventional time-consuming methods. The procedure is simple and no sophisticated apparatus is required, and large numbers of crude samples can be treated simultaneously.

Table 5 GlyceroPL fatty acid compositions obtained from blood by different methods

Fatty acid	Conventional method (wt%)	Selective methanolysis (wt%)	
		Vortexing	Shaking
16:0	25.3 ± 0.8	26.4 ± 0.5	24.5 ± 0.6
18:0	13.9 ± 0.1	13.6 ± 0.9	13.7 ± 0.2
18:1	15.0 ± 0.1	13.8 ± 0.2	13.7 ± 0.1
18:2	19.9 ± 0.6	20.8 ± 0.4	20.1 ± 0.2
20:3 n-6	1.5 ± 0.1	1.5 ± 0.0	1.4 ± 0.1
20:4 n-6	11.9 ± 0.7	12.2 ± 0.2	13.1 ± 0.3
20:5 n-3	2.1 ± 0.1	1.8 ± 0.1	2.2 ± 0.0
22:4 n-6	1.3 ± 0.1	0.9 ± 0.1	1.1 ± 0.0
22:5 n-3	1.5 ± 0.1	1.3 ± 0.1	1.7 ± 0.0
22:6 n-3	7.7 ± 0.3	7.7 ± 0.2	8.4 ± 0.1

The conventional method included extraction of total lipids from blood, isolation of PLs, and methanolysis. Data obtained by two different procedures are described for selective methanolysis. Minor components are omitted. Data are shown as averages of three determinations

Acknowledgments We thank Dr. Kouhei Yamamoto (Osaka Prefecture University) for his advice on GC analysis.

References

1. Yu G, Björksten B (1998) Serum levels of phospholipid fatty acids in mothers and their babies in relation to allergic disease. Eur J Pediatr 157:298–303
2. Conquer JA, Tierney MC, Zecevic J, Bettger WJ, Fisher RH (2000) Fatty acid analysis of blood plasma of patients with Alzheimer's disease, other types of dementia, and cognitive impairment. Lipids 35:1305–1312
3. Guerra A, Demmelmair H, Toschke AM, Koletzko B (2007) Three-year tracking of fatty acid composition of plasma phospholipids in healthy children. Ann Nutr Metab 51:433–438
4. Okuyama H, Ichikawa Y, Sun Y, Hamazaki T, Lands WEM (2007) Prevention of coronary heart disease. From the cholesterol hypothesis to $\omega 6/\omega 3$ balance. Karger, Basel, Switzerland, pp 83–157
5. Riboli E, Rönnholm H, Saracci R (1987) Biological markers of diet. Cancer Surv 6:685–718
6. Lands WEM, Libelt B, Morris A, Kramer NC, Prewitt TE, Bowen P, Schmeisser D, Davidson MH, Burns JH (1992) Maintenance of lower proportions of (n-6) eicosanoid precursors in phospholipids of human plasma in response to added dietary (n-3) fatty acids. Biochim Biophys Acta 1180:147–162
7. Chan JK, McDonald BE, Gerrard JM, Bruce VM, Weaver BJ, Holub BJ (1993) Effect of dietary α-linolenic acid and its ratio to linoleic acid on platelet and plasma fatty acids and thrombogenesis. Lipids 28:811–817
8. Ma J, Folsom AR, Shahar E, Eckfeldt JH (1995) Plasma fatty acid composition as an indicator of habitual dietary fat intake in middle-aged adults. Am J Clin Nutr 62:564–571
9. Dewailly E, Blanchet C, Lemieux S, Sauve L, Gingras S, Ayotte P, Holub BJ (2001) n-3 Fatty acids and cardiovascular disease risk factors among the Inuit of Nunavik. Am J Clin Nutr 74:464–473

10. Di Stasi D, Bernasconi R, Marchioli R, Marfisi RM, Rossi G, Tognoni G, Tacconi MT (2004) Early modifications of fatty acid composition in plasma phospholipids, platelets and mononucleates of healthy volunteers after low doses of n-3 polyunsaturated fatty acids. Eur J Clin Pharmacol 60:183–190
11. Levant B, Ozias MK, Carlson SE (2007) Diet (n-3) polyunsaturated fatty acid content and parity affect liver and erythrocyte phospholipid fatty acid composition in female rats. J Nutr 137:2425–2430
12. Rühl R, Koch C, Marosvölgyi T, Mihaly J, Schweigert FJ, Worm M, Decsi T (2008) Fatty acid composition of serum lipid classes in mice following allergic sensitisation with or without dietary docosahexaenoic acid-enriched fish oil substitution. Br J Nutr 99:1239–1246
13. Steffen LM, Vessby B, Jacobs DR Jr, Steinberger J, Moran A, Hong C-P, Sinaiko AR (2008) Serum phospholipid and cholesteryl ester fatty acid and estimated desaturase activities are related to overweight and cardiovascular risk factors in adolescents. Int J Obesity 32:1297–1304
14. Kaluzny MA, Duncan LA, Merritt MV, Epps DE (1985) Rapid separation of lipid classes in high yield and purity using bonded phase columns. J Lipid Res 26:135–140
15. Ågren JJ, Julkunen A, Penttilä I (1992) Rapid separation of serum lipids for fatty acid analysis by a single aminopropyl column. J Lipid Res 33:1871–1876
16. Burdge GC, Wright P, Jones AE, Wootton SA (2000) A method for separation of phosphatidylcholine, triacylglycerol, non-esterified fatty acids and cholesterol esters from plasma by solid-phase extraction. Br J Nutr 84:781–787
17. Ichihara K, Iwasaki H, Ueda K, Takizawa R, Naito H, Tomosugi M (2005) Synthesis of phosphatidylcholine: an improved method without using the cadmium chloride complex of *sn*-glycero-3-phosphocholine. Chem Phys Lipids 137:94–99
18. Dittmer JC, Lester RL (1964) A simple, specific spray for the detection of phospholipids on thin-layer chromatograms. J Lipid Res 5:126–127
19. Bligh EG, Dyer WJ (1959) A rapid method of total lipid extraction and purification. Can J Biochem Physiol 37:911–917
20. Ichihara K, Shibahara A, Yamamoto K, Nakayama T (1996) An improved method for rapid analysis of the fatty acids of glycerolipids. Lipids 31:535–539 31:889 (Erratum)
21. Sakaki T, Kondo N, Yamada M (1990) Pathway for the synthesis of triacylglycerols from monogalactosyldiacylglycerols in ozone-fumigated spinach leaves. Plant Physiol 94:773–780
22. Christie WW (1992) Preparation of fatty acid methyl esters. Inform 3:1031–1034
23. Ichihara K, Yamaguchi C, Nishijima H, Saito K (2003) Preparation of FAME from sterol esters. J Am Oil Chem Soc 80:833–834
24. Ichihara K, Waku K, Yamaguchi C, Saito K, Shibahara A, Miyatani S, Yamamoto K (2002) A convenient method for determination of the $C_{20–22}$ PUFA composition of glycerolipids in blood and breast milk. Lipids 37:523–526
25. Marangoni F, Colombo C, Galli C (2004) A method for the direct evaluation of the fatty acid status in a drop of blood from a fingertip in humans: applicability to nutritional and epidemiological studies. Anal Biochem 326:267–272
26. Bailey-Hall E, Nelson EB, Ryan AS (2008) Validation of a rapid measure of blood PUFA levels in humans. Lipids 43:181–186
27. Ichihara K, Fukubayashi Y (2010) Preparation of fatty acid methyl esters for gas-liquid chromatography. J Lipid Res 51:635–640
28. Ohta A, Mayo MC, Kramer N, Lands WEM (1990) Rapid analysis of fatty acids in plasma lipids. Lipids 25:742–747

Lipids (2010) 45:375–384
DOI 10.1007/s11745-010-3406-3

ORIGINAL ARTICLE

Docosahexaenoic Acid (DHA) and Docosapentaenoic Acid (DPAn-6) Algal Oils Reduce Inflammatory Mediators in Human Peripheral Mononuclear Cells In Vitro and Paw Edema In Vivo

Julie M. Nauroth · Ying Chun Liu · Mary Van Elswyk · Rebecca Bell · Eileen Bailey Hall · Gloria Chung · Linda M. Arterburn

Received: 30 September 2009 / Accepted: 5 March 2010 / Published online: 4 April 2010

Abstract The anti-inflammatory activity associated with fish oil has been ascribed to the long-chain polyunsaturated fatty acids (LC-PUFA), predominantly eicosapentaenoic acid (EPA) and docosahexaenoic acid (DHA). Here we examined the anti-inflammatory effects of two DHA-rich algal oils, which contain little EPA, and determined the contribution of the constituent fatty acids, particularly DHA and docosapentaenoic acid (DPAn-6). In vitro, lipopolysaccharide (LPS)-stimulated Interleukin-1 beta (IL-1β) and Tumor Necrosis Factor-alpha (TNF-α) secretion in human peripheral blood mononuclear cells (PBMC) was inhibited with apparent relative potencies of DPAn-6 (most potent) > DHA > EPA. In addition, DPAn-6 decreased intracellular levels of cyclooxygenase-2 (COX-2) and was a potent inhibitor of pro-inflammatory prostaglandin E2 (PGE2) production. DHA/DPAn-6-rich DHA-S^{TM} (DHA-S) algal oil was more effective at reducing edema in rats than DHA-rich DHA-T^{TM} (DHA-T), suggesting that DPAn-6 has anti-inflammatory properties. Further in vivo analyses demonstrated that feeding DPAn-6 alone, provided as an ethyl ester, reduced paw edema to an extent approaching that of indomethacin and enhanced the anti-inflammatory activity of DHA when given in combination. Together, these results demonstrate that DPAn-6 has anti-inflammatory activity and enhances the effect of DHA in vitro and in vivo. Thus, DHA-S algal oil may have potential for use in anti-inflammatory applications.

Keywords Inflammation · DHA · DPAn-6 · Long-chain polyunsaturated fatty acids

Abbreviations

ARA	Arachidonic acid
COX	Cyclooxygenase
DHA	Docosahexaenoic acid
DPAn-6	Docosapentaenoic acid
EPA	Eicosapentaenoic acid
GRAS	Generally recognized as safe
IL-1β	Interleukin-1 beta
LPS	Lipopolysaccharide
LC-PUFA	Long chain-polyunsaturated fatty acids
OLA	Oleic acid
PBMC	Peripheral blood mononuclear cells
PGE2	Prostaglandin E2
TNF-α	Tumor Necrosis Factor-alpha

Introduction

Chronic or uncontrolled inflammation can lead to tissue damage and is an underlying factor in atherosclerosis, rheumatoid arthritis, diabetes (type 1), asthma, inflammatory bowel disease, and Alzheimer's disease [1–7]. Inflammation results from the release of chemical mediators from activated leukocytes that have migrated to target areas as a consequence of tissue injury or invading pathogens. These inflammatory mediators include IL-1β,

J. M. Nauroth (✉) · Y. C. Liu · M. Van Elswyk · R. Bell · E. B. Hall · G. Chung
Martek Biosciences Corporation, 6480 Dobbin Road, Columbia, MD 21045, USA
e-mail: jnauroth@martek.com

L. M. Arterburn
Alba Therapeutics Corporation, 800 West Baltimore Street, Baltimore, MD 21201, USA

TNF-α, and PGE2. EPA (20:5n-3) and DHA (22:6n-3), LC-PUFA found in fish oil, have anti-inflammatory activity and affect inflammatory mediator production [8–12], lymphocyte proliferation [13, 14], monocyte and neutrophil migration [15], and natural killer (NK) cell activity in vitro [16].

The consumption of fish oil results in the replacement of arachidonic acid (ARA; 20:4n-6) in cell membranes by DHA and EPA [17, 18]. This leads to alterations in the eicosanoids produced and contributes towards a less inflammatory environment [17–20]. EPA and DHA can also be converted into resolvins, which are bioactive molecules that play an important role in the resolution of inflammation [4, 21, 22]. Further, LC-PUFA modulate the expression and activity of genes involved in the inflammatory response. In vitro, EPA or DHA reduced the production of proinflammatory cytokines, including IL-1β and TNF-α [8–12, 20] and cell migration [23–26]. DHA and EPA may have differing mechanisms of action [27]. PBMC derived from humans supplemented with DHA had a decreased ex vivo T cell activation whereas EPA supplementation had no significant effect [28]. DHA was also more efficacious at reducing pro-inflammatory cytokines than EPA, particularly IL-1β and IL-6 in vitro [8, 12].

While many studies to date have examined the anti-inflammatory effects of DHA and EPA from fish oil, this study focused on DHA and DPAn-6 (docosapentaenoic acid; 22:5n-6) derived from algal sources which contain little EPA. We assessed the anti-inflammatory activity of DHA/DPAn-6-rich DHA-S^{TM} (DHA-S) and DHA-rich DHA- T^{TM} (DHA-T) algal oils[1] and their individual constituent LC-PUFA. To our knowledge, this is the first study to show that DPAn-6 has potent anti-inflammatory activity and enhances the effects of DHA.

Materials and Methods

Fatty Acid Sodium Salts for In Vitro Experiments

All in vitro assays used sodium salts of EPA, ARA, DPAn-6, and Oleic acid (OLA) that were purchased from NuChek Prep (Elysian, MN) and were greater than 99% pure. DHA-sodium salt (greater than 98% pure) was purchased from Sigma-Aldrich (St. Louis, MO). Fatty acid sodium salts were prepared by resuspending in distilled water and warming for 1.5 h at 37 °C to ensure solubility before storing at −80 °C. Before use, fatty acids were again warmed to 37 °C for 10 min to ensure homogeneity. The fatty acids were used at the concentrations described in the specific in vitro assays below. Since potencies of the fatty acids were being directly compared in experiments, the concentrations of the fatty acid stock solutions were confirmed by gas-liquid chromatography, accuracy ±5%, both prior to and after the freeze/thaw process.

Human Cell Culture

PBMC were isolated by Ficoll-Hypaque (Amersham, Uppsala, Sweden) density gradient from the peripheral blood of healthy humans per the manufacturer's instructions. Human blood obtained from healthy individuals (negative for HIV and Hepatitis-B and-C) was purchased from All Cells, Emeryville, CA. Isolated PBMC were frozen in heat inactivated fetal calf serum (FCS)/10% dimethylsulfoxide (DMSO) until use when they were thawed, placed in supplemented RPMI 1640 containing 10% FCS (heat inactivated), 1% L-glutamine (200 mM), 100 unit/ml penicillin, and 100 μg/ml streptomycin (all reagents Sigma-Aldrich, St. Louis, MO). PBMC were thawed, washed in supplemented RPMI, and cell viability was assessed by trypan blue exclusion immediately before use in vitro.

In Vitro LPS Stimulation of PBMC

Human PBMC were stimulated with LPS (derived from *E. coli*, Sigma-Aldrich, St. Louis, MO) using a modification of the method originally described [29]. Briefly, PBMC were resuspended in supplemented RPMI 1640, seeded at 2×10^5 cells/200 μl/well of a 96-well flat-bottom plate. PBMC were pretreated for 2 h at 37 °C with 2 μl of the individual fatty acid sodium salts or an equivalent volume of water (negative control); five replicate wells per treatment. Fatty acid concentrations were used at 100 μM or 10–100 μM (dose response). PBMC were then stimulated with 20 μl LPS (0.1 ng/ml final concentration) for 18 h at 37 °C. Following stimulation, cells were pelleted by centrifugation and supernatants were collected and stored at −20 °C for cytokine measurement by ELISA. Cell viability after LPS incubation was monitored by trypan blue exclusion before and after centrifugation and no significant differences in viability were noted between control and fatty acid-treated groups at the doses used in this study.

IL-1β and TNF-α ELISA

Cell supernatants were tested for IL-1β and TNF-α (Research Diagnostics, Minneapolis, MN) following the manufacturer's instructions.

[1] DHA-T oil is also known as DHASCO or DHASCO-T oil; DHA-S was formerly known as DHASCO-S oil. Both are manufactured by Martek Biosciences Corporation.

Determination of COX-1, COX-2, and PGE2 Levels

Human PBMC were seeded at 1×10^6 cells/ml in a 24-well plate with 1 ml supplemented RPMI 1640 per well. Cells were pretreated with 10 μl of the individual fatty acid sodium salts (100 μM) or a combination of two fatty acids (50 μM each for 100 μM total) for 2 h prior to stimulation with 10 μl LPS (0.1 ng/ml); replicates of 6 wells per treatment. Cell viability after LPS incubation was monitored by trypan blue exclusion before and after centrifugation and no significant differences in viability were noted between control and fatty acid-treated groups at the doses used in this study. IL-4 (10 ng/ml (10 μl); BD Biosciences, San Jose, CA) was used as a positive control. After approximately 18 h, PGE2 levels in the supernatants were assayed using an EIA kit (Cayman Chemical, Ann Arbor, MI). For the detection of intracellular COX-1 and COX-2, PBMC were stained for 15 min with PerCP-conjugated CD14 (BD Biosciences, San Jose, CA) to identify the monocytes. After washing, cells were fixed and permeabilized using the BD Cytofix/Cytoperm kit (BD Biosciences, San Jose, CA) following the manufacturer's instructions. Cells were then stained with COX-1-FITC/COX-2-PE antibody combination or the isotype-matched controls (BD Biosciences, San Jose, CA). CD14 + gated cells, 5,000–10,000 per sample, were analyzed on a Coulter Epics Altra flow cytometer using EXPO32 Multi-COMP software (Beckman Coulter, Fullerton, CA).

Animals and Diets

Male Sprague-Dawley rats (100–150 g) from Harlan (Indianapolis, IN) and/or Charles River Laboratories (Wilmington, MA) were quarantined for at least 3 days prior to study initiation. Food and water were provided ad libitum. AIN-76A Diet (Research Diets, New Brunswick, NJ) was used as the base diet and for all diet formulations used in the animal studies as it does not contain any LC-PUFA. Study protocols were approved by the animal facility's Institutional Animal Care and Use Committee and followed the Animal Care and Use Guidelines established by the Office for Laboratory Animal Welfare (OLAW)/NIH. Food consumption, animal body weights, and general health were monitored throughout the studies.

DHA-S, DHA-T, ARASCO™

DHA-S, DHA-T, ARASCO oils, derived from *Schizochytrium* sp., *Crypthecodinium cohnii*, and *Mortierella alpine*, respectively, were manufactured by Martek Biosciences Corporation (Columbia, MD) and their fatty acid compositions are described in Table 1. Both DHA oils are used in food and dietary supplements [30] and are Generally Recognized as Safe (GRAS) for food. DHA-T oil in combination with ARASCO oil, an oil rich in ARA, is GRAS for the fortification of infant formula. DHA-S oil has been used in a number of clinical studies [31–33], as has the DHA-T oil [30, 34]. LC-PUFA are present as triglycerides within these oils.

Table 1 Fatty acid profiles of oils

	% Total fatty acids		
	DHA-S	DHA-T	ARASCO
14:0	8.55	14.69	0.67
16:0	22.79	12.97	13.74
18:0	0.63	0.69	8.72
18:2 (n-6)	0.32	1.21	7.32
20:4 (n-6) ARA	0.80	<0.1	43.61
20:5 (n-3) EPA	2.11	0.25	0.15
22:5 (n-6) DPA	16.26	0	0
22:6 (n-3) DHA	40.39	41.9	0
Others	<8.15	<30	<25

Evaluation of the Algal Oils in a Rodent Model of Carrageenan Paw Edema (CPE)

Rats ($n = 10$ per group) were fed modified AIN-76A rodent diets that were formulated by Research Diets (New Brunswick, NJ) to contain one or more of the following test oils: DHA-S, DHA-T, ARASCO oil and equivalent levels of total fat (5% by weight). The non-test article fat in the experimental diets and the total fat in the placebo diet consisted of a blend of 30% corn, 54% soybean, and 16% coconut oils. Oils were provided by Research Diets (New Brunswick, NJ). The fatty acid content of the formulated diets was confirmed by gas chromatography (GC). In brief, fats in the diet were transesterified in situ with 1.5 N HCl in methanol (Sigma-Aldrich, St. Louis, MO), in the presence of toluene (Sigma-Aldrich, St. Louis, MO) and an internal standard. The resultant fatty acid methyl esters (FAME) were extracted with toluene. The FAME were separated, identified, and quantitated by gas-liquid chromatography with flame ionization detection (GLC-FID) and internal standard calibration.

Experimental diets each provided 1.2% DHA, which is equivalent to approximately 800 mg DHA/kg per day. The ARASCO and DHA-S-containing diets provided approximately 300 mg of ARA or DPAn-6/kg per day (approximately 0.45% of each PUFA), respectively. After 28 days of ad libitum feeding, rats were injected with 0.1 ml of a 10-mg/ml carrageenan solution in water (Sigma-Aldrich, St. Louis MO) in the subplantar right hind foot. Paw volumes were measured by water displacement and differences between the initial and the resultant paw volumes

were determined at 3 h post-carrageenan injection. Animals were euthanized by carbon dioxide (CO_2) asphyxiation after final paw measurements were made.

To determine the minimum efficacious concentration in vivo, DHA-S oil was diluted with corn oil to achieve required doses ranging from 100 mg/kg per day PUFA (DHA + DPAn6 combined) to 1,500 mg/kg per day. In this experiment and those following, rats ($n = 8$ per group) were fed the AIN-76A diet for 7–10 days before administration of test compounds to allow for a wash-out of the LC-PUFA that can be found in typical rodent chows. DHA-S oil was administered by oral gavage (to ensure accuracy of dosing) daily for 14 days to allow plasma levels of LC-PUFA to equilibrate [35]. Doses less than 1,500 mg/kg PUFA per day were equilibrated to 1,500 mg/kg total fat with corn oil. Control and indomethacin treated animals received corn oil by gavage. All test materials contained equivalent levels of antioxidants: ascorbyl palmitate (Tap1010, Vitablend, The Netherlands), mixed tocopherols (Tocoblend L70 IP, Vitablend, The Netherlands), as well as rosemary extract (Herbalox, Kalamazoo, MI). Indomethacin (Sigma-Aldrich, St. Louis, MO) was administered by intraperitoneal injection (i.p.) at 5 mg/kg 30 min prior to carrageenan challenge. The hind paw assay was performed as described above with paw measurements at 2, 4, and 6 h. Immediately following final paw measurements, animals were anesthetized with isoflurane (NLS Animal Health, Owings Mills, MD), 3–5 ml of blood was collected into EDTA-treated tubes by exsanguination via cardiac puncture, and animals were euthanized. Blood was separated by centrifugation, 1,800 rpm for 20 min, and plasma was stored at −80 °C for fatty acid analyses.

Dose-Response Evaluation of DPAn-6 in a Rodent CPE Model

To test the dose-response effect, DPAn-6 was administered at 300, 700 or 1,000 mg/kg per day and compared to DHA doses of 700 or 1,000 mg/kg as well as a DHA/DPAn-6 combo (2.5:1 ratio similar to DHA-S) at 1,000 mg/kg. This LC-PUFA mg/kg dose is equivalent to the dietary dose administered as DHA-S in the previous studies. Doses less than 1,000 mg/kg per day were equilibrated to 1,000 mg/kg total fat with a blend of control fatty acid ethyl esters that mimicked the fatty acid blend found in the base AIN-76A diet: 25% oleate, 13% palmitate, 60% linoleate, 2% alpha-linolenate. Control and indomethacin-treated animals received the control blend of ethyl esters as well. The PUFA, provided as ethyl esters (DHA, DPAn-6, OLA, palmitic acid, linoleic acid, and alpha-linolenic acid) that were used in the animal dosing experiments were purchased from NuChek Prep (Elysian, MN). These fatty acid ethyl esters were greater than 90% pure as confirmed by gas liquid chromatographic techniques. Total fat in the animal diets was 6.25% (by weight) including the 5% in the base diet and the addition of the fatty acid ethyl esters received by gavage. Indomethacin was dosed as previously described. Hind paw measurements and plasma collection were performed as previously described.

Fatty Acid Methyl Ester (FAME) Analysis

Plasma lipids were extracted and phospholipids were isolated by thin-layer chromatography as previously described [36]. In brief, fatty acids from plasma phospholipids were saponified with sodium hydroxide and methanol and then methylated with boron trifluoride (all reagents from Sigma-Aldrich, St. Louis, MO). The resulting methyl esters were identified and quantified by gas–liquid chromatography and flame ionization detection as described [36].

Statistical Analyses

Data were analyzed and compared by one-way ANOVA using the Bonferroni test to compare groups (GraphPad, Prism, Version 4.0). Effects were considered to be statistically significant at $p < 0.05$.

Results

DPAn-6 Has Potent Anti-Inflammatory Activity In Vitro

The effect of the fatty acids on IL-1β and TNF-α secretion was examined. Both DHA and DPAn-6 markedly reduced IL-1β levels in LPS-stimulated PBMC, by approximately 80 and 90% respectively ($p < 0.01$) (Fig. 1a). TNF-α levels were reduced approximately 80% upon treatment with either DHA or DPAn-6 (not significant) (Fig. 1b). EPA reduced the expression of these cytokines to a lesser degree, approximately 60% for IL-1β (not significant) and 40% for TNF-α (not significant) (Fig. 1a, b). Overall, the relative effectiveness of the fatty acids appeared to be DPAn-6 (most potent) > DHA > EPA with respect to reducing both IL-1β and TNF-α. Neither OLA nor AA significantly affected IL-1β or TNF-α secretion. We focused our subsequent studies on the fatty acid effects on IL-1β, as the effect was more striking.

Effects of the Individual and Combinations of Fatty Acids on IL-1β Secretion In Vitro

We compared the potency of the individual fatty acids in a dose response assay. Treatment of human PBMC with each of the LC-PUFA resulted in a dose-dependent reduction in

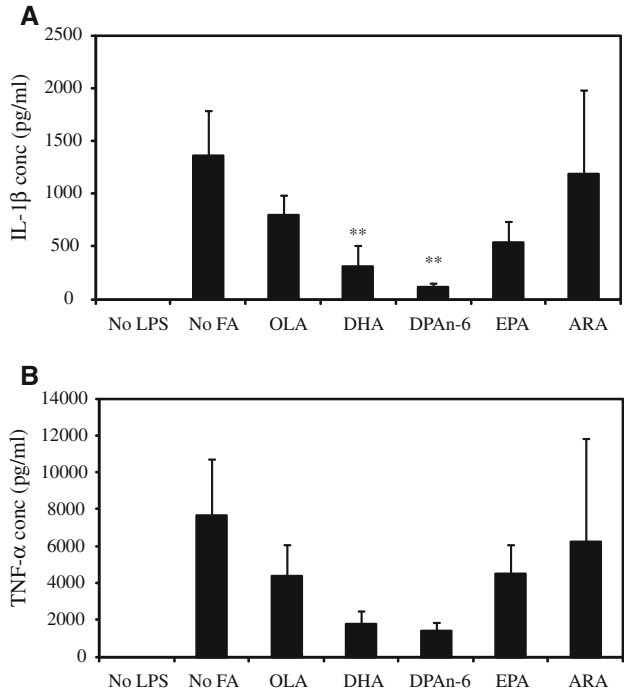

Fig. 1 DPAn-6 has potent anti-inflammatory activity in vitro. Human PBMC were pretreated with individual fatty acids (100 μM final concentration) for 2 h prior to stimulation with LPS. Supernatants were harvested and IL-1β (**a**) and TNF-α (**b**) levels in the culture medium were measured by ELISA following 18 h of culture. Means (5 wells/treatment) +/− SD. $^{**}p < 0.01$ compared to control. Results are representative of at least three independent experiments

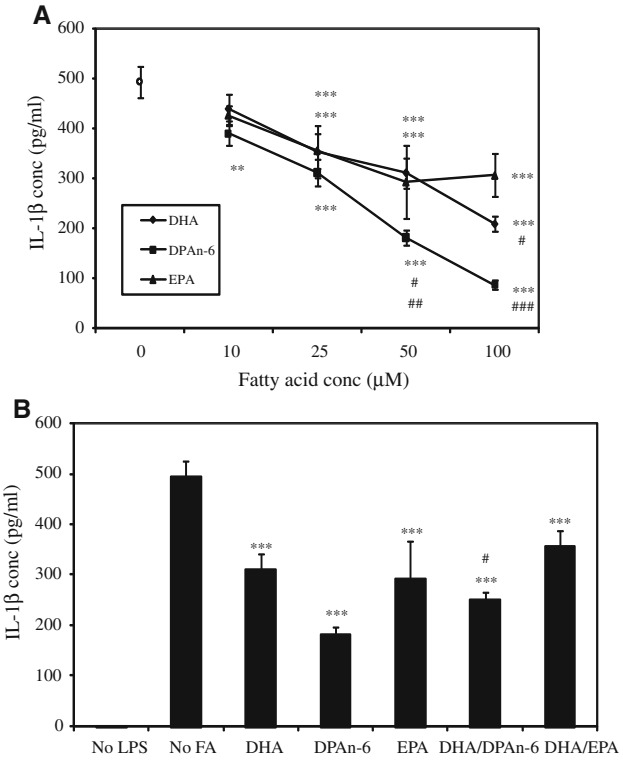

Fig. 2 Effects of the individual and combinations of fatty acids on IL-1β secretion in vitro. **a** Human PBMC were pretreated with the fatty acids at various concentrations 2 h prior to stimulation with LPS. IL-1β levels in the culture supernatants were assessed by ELISA. Means (5 wells/treatment) +/− SD. $^{**}p < 0.01$ and $^{***}p < 0.001$ compared to control. $^{\#}p < 0.01$ compared with an equivalent concentration of EPA. $^{\#\#}p < 0.001$ compared with an equivalent concentration of DHA. $^{\#\#\#}p < 0.001$ compared with an equivalent concentration of DHA or EPA. Results are representative of at least three independent experiments. **b** Human PBMC were incubated with 50 μM of the individual fatty acids or a combination of 25 μM of each fatty acid (50 μM total) prior to stimulation with LPS. Means (5 wells/treatment) +/− SD. $^{***}p < 0.001$ compared to control. $^{\#}p < 0.01$ compared with DHA/EPA. Results are representative of at least three independent experiments

IL-1β (Fig. 2a). DPAn-6 significantly reduced IL-1β with as little as 10 μM ($p < 0.01$). Overall, DPAn-6 was the most effective with maximum inhibition at 100 μM reaching approximately 80% ($p < 0.001$) versus approximately 60% for DHA ($p < 0.001$) and 40% for EPA ($p < 0.001$). Further, at a concentration of 50 μM, DPAn-6 reduced IL-1β levels more effectively than DHA ($p < 0.001$) or EPA ($p < 0.01$). Similar results were seen with 100 μM where DPAn-6 was more effective than DHA ($p < 0.001$) or EPA ($p < 0.001$). DHA was more effective than EPA at 100 μM ($p < 0.01$).

Human PBMC were next incubated with 50 μM of the individual fatty acids or a combination of 25 μM of two fatty acids (50 μM total) prior to stimulation with LPS (Fig. 2b). In PBMC, the DHA/DPAn-6 (50 μM total LC-PUFA) combination reduced IL-1β levels approximately 50% ($p < 0.001$), whereas the DHA/EPA combination reduced levels approximately 30% ($p < 0.001$). The DHA/DPAn-6 combination was more effective than the DHA/EPA combination in reducing IL-1β production ($p < 0.01$).

DPAn-6 Reduces COX-2 and PGE2 Production In Vitro

In LPS-stimulated PBMC, DPAn-6 (100 μM) inhibited levels of intracellular COX-2 approximately 50% ($p < 0.001$) (Fig. 3a). DHA did not affect COX-2 levels in these cells whereas EPA and the DHA/EPA combination increased COX-2 levels approximately 25–30% ($p < 0.01$ and $p < 0.05$, respectively). None of the fatty acids affected COX-1 levels: COX-1 mean fluorescence intensity (MFI) was 81 (control) and ranged from 81 to 90 upon treatment with the various fatty acids (data not shown). As expected, the IL-4 control decreased COX-2 levels ($p < 0.001$) without affecting COX-1 levels [37]. The DHA/DPAn6 combination was more effective than the DHA/EPA combination ($p < 0.001$). As seen in Fig. 3b, DPAn-6 also reduced the levels of PGE2 by approximately 90% ($p < 0.001$). DPAn-6 was similar in efficacy to the positive control IL-4, which is known to decrease PGE2 levels [37, 38]. Interestingly, while COX-2 levels were not affected by DHA, PGE2 levels were decreased approximately 70% ($p < 0.001$) by DHA and the

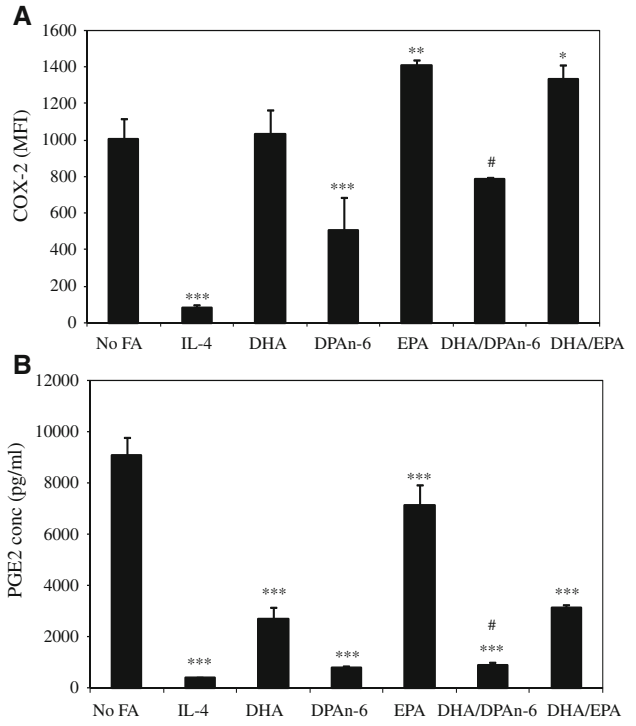

Fig. 3 DPAn-6 reduces COX-2-mediated inflammation in vitro. **a** Intracellular levels of COX-2 in LPS-stimulated cells were determined using flow cytometry following treatment with the individual fatty acids (100 μM) and the fatty acid combinations for a total of 100 μM. Data indicate mean +/− SD of three independent experiments. *$p < 0.05$, **$p < 0.01$, ***$p < 0.001$ compared to the control. #$p < 0.001$ compared to DHA/EPA. **b** PGE2 levels in the culture supernatants were assessed by EIA after treatment with the individual fatty acids or combinations thereof (100 μM total). Means (6 wells/treatment) +/− SD. ***$p < 0.001$ compared to the control. #$p < 0.001$ compared to DHA/EPA. Results are representative of three independent experiments

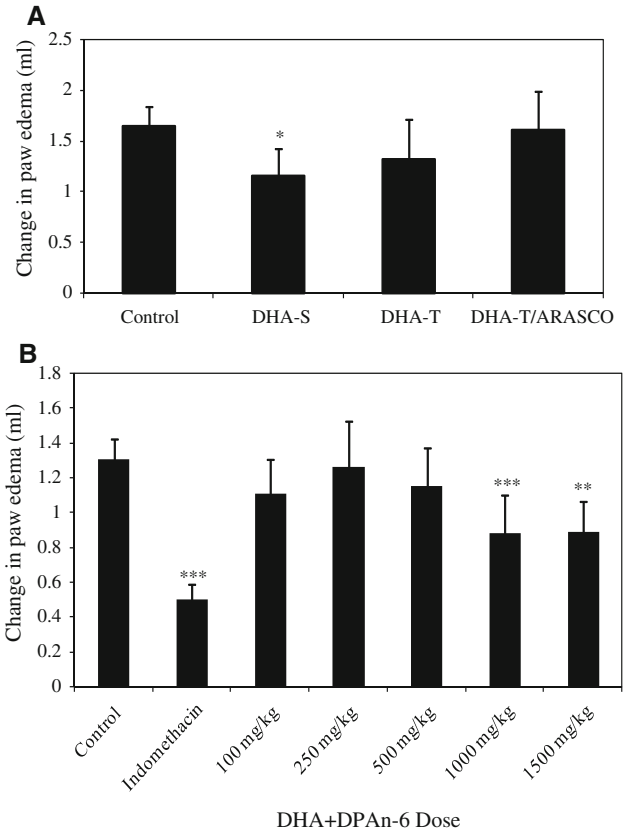

Fig. 4 DHA/DPAn-6-rich DHA-S oil significantly reduced inflammation in a rodent paw edema model. **a** DHA-S, DHA-T, DHA-T/ARASCO oils were administered in the feed for 28 days prior to carrageenan challenge. The experimental diets provided equivalent amounts of DHA (approximately 800 mg/kg) with an additional 300 mg of DPAn-6 or ARA/kg per day for the DHA-S and ARASCO diets, respectively. Paw edema was measured by water displacement 3 h post-challenge with carrageenan stimulation. Means ($n = 10$) +/− SD. *$p < 0.05$ compared to control. **b** DHA-S oil was diluted with corn oil to achieve required doses ranging from 100 mg/kg PUFA (DHA + DPAn6 combined) to 1,500 mg/kg per day. DHA-S oil was administered by oral gavage for 14 days. Doses less than 1,500 mg/kg PUFA per day were equilibrated to 1,500 mg/kg total fat with corn oil. Control and indomethacin treated animals received corn oil by gavage. Indomethacin was administered at 5 mg/kg i.p. 30 min prior to carrageenan challenge. Paw edema was measured at 2 h post carrageenan treatment. Means ($n = 8$) +/− SD. **$p < 0.01$ and ***$p < 0.001$ compared to control

addition of DPAn-6 reduced levels further. In comparison, EPA reduced PGE2 levels approximately 20% ($p < 0.001$), and when EPA was provided in combination with DHA, PGE2 was decreased to levels comparable to those with DHA alone ($p < 0.001$). Further, the DHA/DPAn-6 combination was a more potent inhibitor of PGE2 production than the DHA/EPA combination ($p < 0.001$).

DHA/DPAn-6-rich DHA-S Oil Significantly Reduces Inflammation in a Rodent Paw Edema Model

The anti-inflammatory activity of the DHA-rich algal oils was evaluated in a rodent model of acute inflammation. No significant differences in food intake, weight, or locomotor activity were observed between any of the treatment groups. DHA-S-fed animals had a 30% reduction in mean paw edema ($p < 0.05$), while treatment with DHA-T also tended to reduce paw edema with an approximately 20% reduction (not significant) (Fig. 4a). The animals fed the DHA-T/ARASCO diet had no reduction in paw edema.

Animals were treated with increasing doses of DHA-S oil to determine the minimum efficacious concentration in vivo. Indomethacin reduced paw edema 62% ($p < 0.001$) (Fig. 4b). Maximal inhibition of paw edema, a reduction of 33%, was visible at 1,000 mg/kg DHA + DPAn-6 ($p < 0.001$). As expected, treatment with increasing doses of DHA-S oil resulted in increases in plasma phospholipid levels of both DHA and DPAn-6 (Table 2).

DPAn-6 Reduces Inflammatory Edema in a Dose-Response Rodent Model of Hind Paw Edema

A study was performed to assess the effects of various doses of DPAn-6 on paw edema in this model (Fig. 5). Fatty acids were provided as ethyl esters. Indomethacin reduced paw edema 62% ($p < 0.001$). The 700 mg/kg dose of DPAn-6 reduced paw edema maximally, a 56% reduction ($p < 0.001$). In addition, we confirmed our original findings that the DHA/DPAn-6 combination, as found in the DHA-S oil, reduced edema more than DHA alone (DHA-T oil) ($p < 0.05$). The 700 mg/kg DPAn-6 was as efficacious as the combination of 700 mg/kg DHA + 300 mg/kg DPAn-6. At 2 h post-challenge, treatment with 700 and 1,000 mg/kg DHA reduced paw edema approximately 20% (not significant). However, inhibition seen with 700 mg/kg DHA was increased further by the addition of 300 mg/kg DPAn-6, the PUFA combination found in the DHA-S oil. By 4 h post-challenge, both doses of DHA significantly reduced paw edema ($p < 0.01$, data not shown). DHA and DPAn-6 (1,000 mg/kg doses) elevated plasma levels approximately 4 and 6.5-fold, respectively (Table 3). Higher doses of pure DPAn-6 (700 and 1,000 mg/kg) led to increased plasma ARA levels.

Discussion

The immunomodulatory effects of fish oil and its constituent omega-3 LC-PUFA have been examined in numerous

Table 2 Plasma phospholipid fatty acid levels in rats treated with DHA-S oil

Fatty acid	Treatment groups (Total PUFA dose)						
	Control	100 mg/kg	250 mg/kg	500 mg/kg	1,000 mg/kg	1,500 mg/kg	Indomethacin
n-3							
20:5n-3 EPA	0 (0)	0.12 (0.03)	0.34 (0.03)*	0.77 (0.09)*	1.03 (0)*	1.56 (0.26)*	0 (0)
22:6n-3 DHA	1.59 (0.12)	3.42 (0.32)*	4.52 (0.39)*	5.1 (0.38)*	6.73 (0.32)*	8.13 (0.83)*	1.56 (0.16)
n-6							
20:4n-6 ARA	21.96 (0.55)	19.79 (0.78)*	20.13 (1.25)*	18.18 (0.56)*	19.34 (1.11)*	19.69 (1.48)*	20.66 (0.76)
22:5n-6 DPAn6	1.13 (0.25)	0.57 (0.07)*	0.59 (0.03)*	0.82 (0.05)*	1.40 (0.13)	2.08 (0.43)*	1.02 (0.18)

Mean fatty acid levels (g/100 g fatty acids) ± SD, $n = 8$/group Means and standard deviations were calculated by One-way ANOVA followed by Bonferroni's post test (Graph Pad, Prism, Version 4.0) as compared to the Control group

*$p < 0.05$ compared to control

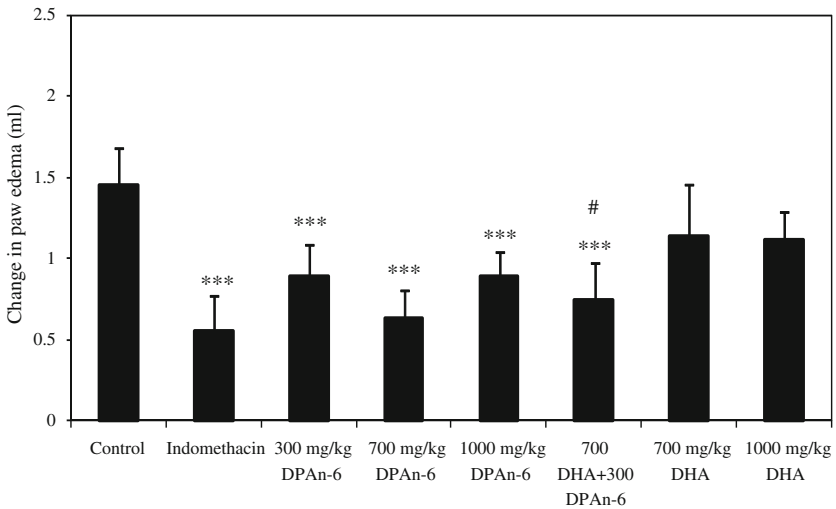

Fig. 5 DHA/DPAn-6 combination reduces inflammatory edema in a rodent model of hind paw edema. A dose response study was performed to assess the effects of various dose levels of DPAn-6 on paw edema in this model. All groups of animals received an equivalent amount of fat which consisted of 300–1,000 mg/kg DHA or DPAn-6 per day, as indicated, with an appropriate amount of control oil to bring the total gavaged fat content to 1,000 mg/kg per day. Indomethacin was administered at 5 mg/kg i.p. 30 min prior to carrageenan challenge. Fatty acids were administered daily for 14 days prior to conducting the paw edema assay at 2 h post-carrageenan challenge. Means ($n = 8$) +/− SD. ***$p < 0.001$ compared to control. #$p < 0.05$ compared to 700 or 1,000 mg/kg DHA group

Table 3 Plasma phospholipid fatty acid levels in DPAn-6 dose response study

Fatty acid	Treatment groups (Total PUFA dose)							
	Control	DPAn-6			DHA/DPAn-6	DHA		Indomethacin
		300 mg/kg	700 mg/kg	1,000 mg/kg	1,000 mg/kg	700 mg/kg	1,000 mg/kg	
n-3								
20:5n-3 EPA	0.04 (0.06)	0.14 (0.25)	0.07 (0.07)	0 (0)	0.78 (0.17)*	1.12 (0.18)*	1.02 (0.14)*	0 (0)
22:6n-3 DHA	1.74 (0.15)	1.72 (0.07)	1.6 (0.07)	1.47 (0.15)	5.85 (0.58)*	6.16 (0.11)*	6.48 (0.56)*	1.65 (0.03)
n-6								
20:4n-6 ARA	21.25 (0.76)	23.03 (1.27)	24.37 (0.62)*	24.4 (0.40)*	18.37 (0.37)	15.99 (1.01)*	15.94 (2.04)*	22.32 (0.53)
22:5n-6 DPAn6	0.98 (0.12)	3.28 (0.61)*	4.95 (0.26)*	6.33 (0.91)*	0.8 (0.14)	0.04 (0.04)	0 (0)	1.15 (0.07)

Mean fatty acid levels (g/100 g fatty acids) +/− SD ($n = 3$ pooled samples/group). Means and standard deviations were calculated by One-way ANOVA followed by Bonferroni's post test (Graph Pad, Prism, Version 4.0)

*$p < 0.05$ as compared to the Control group

studies to date. Here, we demonstrate the anti-inflammatory activity of DHA-rich algal oils in vivo, particularly DHA-S oil, and provide the first evidence of the potent anti-inflammatory activity of the constituent omega-6 LC-PUFA, DPAn-6.

As an omega-6 fatty acid and as a product of ARA, it was unexpected to find anti-inflammatory activity associated with DPAn-6. However, another omega-6 PUFA, gamma linolenic acid (GLA; 18:3n-6) has been shown to have anti-inflammatory activity in vitro and in vivo [39]. GLA decreases levels of IL-1β and TNF-α in LPS-stimulated PBMC and IL-1β in LPS-stimulated human monocytes in vitro [40].

In vitro analyses showed that all three LC-PUFA (DHA, DPAn-6, and EPA) reduced the production of the pro-inflammatory cytokines IL-1β and TNF-α in human PBMC, at concentrations as low as 10 μM (IL-1β). However, DPAn-6 appeared to be the most effective inhibitor in vitro, reducing levels of these pro-inflammatory cytokines, with observed relative potencies of DPAn-6 (most potent) > DHA > EPA. This finding correlates with another recent study that demonstrated the enhanced efficacy of DHA, as compared to EPA, in decreasing IL-1β, IL-6 and TNF-α production in LPS-stimulated THP-1 cells [8].

The consumption of dietary LC-PUFA can alter membrane phospholipids and the production of eicosanoids [11, 17–20]. Our studies show that in addition to decreasing levels of pro-inflammatory cytokines in vitro, DPAn-6 also decreased intracellular COX-2 levels by approximately 50% with a concomitant reduction in PGE2 production. PGE2 mediates acute inflammation, as it is a potent vasodilator and increases vascular permeability and edema [41, 42]. DHA had no effect on COX-2 expression, but PGE2 levels were reduced by DHA, suggesting that DHA may affect COX-2 enzyme activity or PGE synthase, which is also involved in the regulation of PGE2. Both COX-2 and PGE synthase are increased in cells in response to an inflammatory stimulus and the production of PGE2 may require both enzymes [43, 44]. In support of this hypothesis, Roman et al [45] showed a reduction in microsomal PGE synthase RNA in the presence of DHA in vitro, whereas EPA had no effect. Alternatively, DHA treatment may reduce PGE2 production as a result of reduced availability of the PGE2 precursor ARA.

In contrast, EPA and the DHA/EPA combination increased levels of COX-2 and PGE2 in PBMC in vitro. An upregulation of COX-2 has been previously described for EPA in human keratinocytes [46]. It is important to note, however, that the effects of DHA and EPA may be cell-specific and/or dependent on the type of inflammatory stimulus used, as others have described differential COX-2 modulation with these LC-PUFA [46–49].

The rat carrageenan paw edema model is a well-characterized acute model of innate immunity that is commonly used to evaluate anti-inflammatory activity of compounds [50–53]. The DHA-S oil was more effective than DHA-T oil when tested in this in vivo model and the major difference between the two algal oils is the presence of DPAn-6 (DHA-S oil). DPAn-6 treatment resulted in the largest reduction in edema volume, reaching 40–55% inhibition at lower doses. Maximal effects of DPAn-6 were also visible as early as 2 h post-carrageenan challenge, as compared to 4 h with DHA.

Interestingly, the DPAn-6 in vivo dose response resulted in a non-monotonic curve with the maximum effect observed with the 700 mg/kg dose. Lower and higher doses of DPAn-6 reduced inflammation to a lesser degree and their effects were limited to 2–4 h following the inflammatory stimulus. The lack of a standard dose response effect suggests that DPAn-6 might be converted to other fats in vivo, such as ARA. Tam et al [54] showed the retroconversion of DPAn-6 to ARA occurred when ARA levels were decreased by the presence of DHA. In further support of this, humans supplemented with the DHA-T oil

had a dose-dependent decrease in plasma ARA whereas higher doses of the DHA-S oil resulted in relatively higher levels of ARA [30].

Treatment with 1,000 mg/kg DHA ethyl ester resulted in three to fourfold increase in plasma DHA, as compared to control levels. Humans would require a dose of approximately 1.5–2 g DHA per day to achieve a similar increase in plasma DHA [30]. Analysis of plasma phospholipid levels clearly showed that a reduction of ARA levels did not correlate with anti-inflammatory activity, as plasma ARA levels remained high or are increased upon treatment with DPAn-6. We speculate that the ability of DPAn-6 to reduce both COX-2 and PGE2 levels, as seen in vitro, may contribute to the decreased inflammation seen in this COX-2-driven rat paw edema model. Our laboratory has also recently shown that DPAn-6 can be converted into oxylipins, resolvin-like molecules, with potent anti-inflammatory activity which could contribute to the observed reduction in inflammatory response in vivo following dosing with DPAn-6 [55]. Supplementation with DHA-S oil, containing DHA/DPAn-6 may reduce inflammation, raising levels of DHA, while maintaining ARA levels. Taken together, these results suggest that the DHA-S algal oil may be a novel anti-inflammatory supplement.

Acknowledgments The authors would like to thank Valerie Lowe (Washington Biotechnology, Inc., Columbia, MD.) and Dr. Sandy Diltz for technical assistance and Drs. Bindi Dangi, J. Paul Zimmer, Melissa Olson, and Norman Salem for helpful discussions.

Conflict of interest statement This research was solely funded by Martek Biosciences Corporation where all the authors are currently or were employed. Authors may hold patents and/or stock as well.

References

1. Levy BD, De Sanctis GT, Devchand PR, Kim E, Ackerman K, Schmidt BA, Szczeklik W, Drazen JM, Serhan CN (2002) Multi-pronged inhibition of airway hyper-responsiveness and inflammation by lipoxin A(4). Nat Med 8:1018–1023
2. Hansson GK, Libby P (2006) The immune response in atherosclerosis: a double-edged sword. Nat Rev Immunol 6:508–519
3. Haffner SM, Ruilope L, Dahlof B, Abadie E, Kupfer S, Zannad F (2006) Metabolic syndrome, new onset diabetes, and new end points in cardiovascular trials. J Cardiovasc Pharmacol 47:469–475
4. Serhan CN (2005) Novel ω-3 derived local mediators in anti-inflammation and resolution. Pharmacol Ther 105:7–21
5. Kojima FK M, Kawai S, Crofford L (2006) New insights into eicosanoid biosynthetic pathways: implications for arthritis. Clin Immunol 2:277–291
6. Kollias G, Douni E, Kassiotis G, Kontoyiannis D (1999) The function of tumour necrosis factor and receptors in models of multi-organ inflammation, rheumatoid arthritis, multiple sclerosis and inflammatory bowel disease. Ann Rheum Dis 58(Suppl 1):I32–I39
7. Eikelenboom P, Veerhuis R, Scheper W, Rozemuller AJ, van Gool WA, Hoozemans JJ (2006) The significance of neuroinflammation in understanding Alzheimer's disease. J Neural Transm 113:1685–1695
8. Weldon SM, Mullen AC, Loscher CE, Hurley LA, Roche HM (2007) Docosahexaenoic acid induces an anti-inflammatory profile in lipopolysaccharide-stimulated human THP-1 macrophages more effectively than eicosapentaenoic acid. J Nutr Biochem 18:250–258
9. Zhao Y, Joshi-Barve S, Barve S, Chen LH (2004) Eicosapentaenoic acid prevents LPS-induced TNF-alpha expression by preventing NF-kappaB activation. J Am Coll Nutr 23:71–78
10. Zhao G, Etherton TD, Martin KR, Heuvel JPV (2005) Anti-inflammatory effects of polyunsaturated fatty acids in THP-1 cells. Biochem Biophys Res Commun 336:909–917
11. Endres S, Ghorbani R, Kelley VE, Georgilis K, Lonnemann G, van der Meer JW, Cannon JG, Rogers TS, Klempner MS, Weber PC et al (1989) The effect of dietary supplementation with n-3 polyunsaturated fatty acids on the synthesis of interleukin-1 and tumor necrosis factor by mononuclear cells. N Engl J Med 320:265–271
12. Mullen A, Loscher CE, Roche HM (2009) Anti-inflammatory effects of EPA and DHA are dependent upon time and dose-response elements associated with LPS stimulation in THP-1-derived macrophages. J Nutr Biochem [Epub ahead of print]
13. Endres S, Meydani SN, Ghorbani R, Schindler R, Dinarello CA (1993) Dietary supplementation with n-3 fatty acids suppresses interleukin-2 production and mononuclear cell proliferation. J Leukoc Biol 54:599–603
14. Thies F, Nebe-von-Caron G, Powell JR, Yaqoob P, Newsholme EA, Calder PC (2001) Dietary supplementation with gamma-linolenic acid or fish oil decreases T lymphocyte proliferation in healthy older humans. J Nutr 131:1918–1927
15. Gorjao R, Verlengia R, Lima TM, Soriano FG, Boaventura MF, Kanunfre CC, Peres CM, Sampaio SC, Otton R, Folador A et al (2006) Effect of docosahexaenoic acid-rich fish oil supplementation on human leukocyte function. Clin Nutr 25:923–938
16. Thies F, Nebe-von-Caron G, Powell JR, Yaqoob P, Newsholme EA, Calder PC (2001) Dietary supplementation with eicosapentaenoic acid, but not with other long-chain n-3 or n-6 polyunsaturated fatty acids, decreases natural killer cell activity in healthy subjects aged > 55 y. Am J Clin Nutr 73:539–548
17. Gibney MJ, Hunter B (1993) The effects of short- and long-term supplementation with fish oil on the incorporation of n-3 polyunsaturated fatty acids into cells of the immune system in healthy volunteers. Eur J Clin Nutr 47:255–259
18. Sperling RI, Weinblatt M, Robin JL, Ravalese J 3rd, Hoover RL, House F, Coblyn JS, Fraser PA, Spur BW, Robinson DR et al (1987) Effects of dietary supplementation with marine fish oil on leukocyte lipid mediator generation and function in rheumatoid arthritis. Arthritis Rheum 30:988–997
19. Lee TH, Hoover RL, Williams JD, Sperling RI, Ravalese J 3rd, Spur BW, Robinson DR, Corey EJ, Lewis RA, Austen KF (1985) Effect of dietary enrichment with eicosapentaenoic and docosahexaenoic acids on in vitro neutrophil and monocyte leukotriene generation and neutrophil function. N Engl J Med 312:1217–1224
20. Zhao Y, Chen LH (2003) n-3 Polyunsaturated fatty acids/eicosanoids and inflammatory responses. In: Huang Y-S, Li S-J, Huang P-C (eds) Essential fatty acids and eicosanoids: invited papers from the fifth international congress. AOCS Press, Champaign, 219–226
21. Gilroy DW, Lawrence T, Perretti M, Rossi AG (2004) Inflammatory resolution: new opportunities for drug discovery. Nat Rev 3:401–416
22. Serhan CN, Savill J (2005) Resolution of inflammation: the beginning programs the end. Nat Immunol 6:1191–1197
23. Hughes DA, Southon S, Pinder AC (1996) (n-3) Polyunsaturated fatty acids modulate the expression of functionally associated molecules on human monocytes in vitro. J Nutr 126:603–610

24. Ferrante A, Goh D, Harvey D, Robinson B, Hii C, Bates E, Hardy S, Johnson D, Poulos A (1994) Neutrophil migration inhibitory properties of polyunsaturated fatty acids. The role of fatty acid structure, metabolism, and possible second messenger systems. J Clin Invest 93:1063–1070
25. De Caterina R, Cybulsky MI, Clinton SK, Gimbrone MA Jr, Libby P (1994) The omega-3 fatty acid docosahexaenoate reduces cytokine-induced expression of proatherogenic and proinflammatory proteins in human endothelial cells. Arterioscler Thromb 14:1829–1836
26. De Caterina R, Cybulsky MA, Clinton SK, Gimbrone MA Jr, Libby P (1995) Omega-3 fatty acids and endothelial leukocyte adhesion molecules. Prostaglandins Leukot Essent Fatty Acids 52:191–195
27. Gorjao R, Azevedo-Martins AK, Rodrigues HG, Abdulkader F, Arcisio-Miranda M, Procopio J, Curi R (2009) Comparative effects of DHA and EPA on cell function. Pharmacol Ther 122:56–64
28. Kew S, Mesa MD, Tricon S, Buckley R, Minihane AM, Yaqoob P (2004) Effects of oils rich in eicosapentaenoic and docosahexaenoic acids on immune cell composition and function in healthy humans. Am J Clin Nutr 79:674–681
29. Singh U, Tabibian J, Venugopal SK, Devaraj S, Jialal I (2005) Development of an in vitro screening assay to test the antiinflammatory properties of dietary supplements and pharmacologic agents. Clin Chem 51:2252–2256
30. Arterburn LM, Oken HA, Hoffman JP, Bailey-Hall E, Chung G, Rom D, Hamersley J, McCarthy D (2007) Bioequivalence of docosahexaenoic acid from different algal oils in capsules and in a DHA-fortified food. Lipids 42:1011–1024
31. Sanders T, Gleason K, Griffin B, Miller G (2006) Influence of an algal triacylglycerol containing docosahexaenoic acid (22:6n–3) and docosapentaenoic acid (22:5n–6) on cardiovascular risk factors in healthy men and women. Br J Nutr 95(3):525–531
32. Maki KC, Van Elswyk ME, McCarthy D, Hess SP, Veith PE, Bell M, Subbaiah P, Davidson MH (2005) Lipid responses to a dietary docosahexaenoic acid supplement in men and women with below average levels of high density lipoprotein cholesterol. J Am Coll Nutr 24:189–199
33. Green KN, Martinez-Coria H, Khashwji H, Hall EB, Yurko-Mauro KA, Ellis L, LaFerla FM (2007) Dietary docosahexaenoic acid and docosapentaenoic acid ameliorate amyloid-beta and tau pathology via a mechanism involving presenilin 1 levels. J Neurosci 27:4385–4395
34. Clandinin MT, Van Aerde JE, Merkel KL, Harris CL, Springer MA, Hansen JW, Diersen-Schade DA (2005) Growth and development of preterm infants fed infant formulas containing docosahexaenoic acid and arachidonic acid. J Pediatr 146:461–468
35. Arterburn L, Hall E, Oken H (2006) Distribution, interconversion, and dose response of n-3 fatty acids in humans. Am J Clin Nutr 83:1467S–1476S
36. Engler MM, Engler MB, Malloy M, Chiu E, Besio D, Paul S, Stuehlinger M, Morrow J, Ridker P, Rifai N et al (2004) Docosahexaenoic acid restores endothelial function in children with hyperlipidemia: results from the EARLY study. Int J Clin Pharmacol Ther 42:672–679
37. Endo T, Ogushi F, Kawano T, Sone S (1998) Comparison of the regulations by Th2-type cytokines of the arachidonic-acid metabolic pathway in human alveolar macrophages and monocytes. Am J Respir Cell Mol Biol 19:300–307
38. Hart PH, Cooper RL, Finlay-Jones JJ (1991) IL-4 suppresses IL-1 beta, TNF-alpha and PGE2 production by human peritoneal macrophages. Immunology 72:344–349
39. Kapoor R, Huang YS (2006) Gamma linolenic acid: an antiinflammatory omega-6 fatty acid. Curr Pharm Biotechnol 7:531–534
40. Furse RK, Rossetti RG, Zurier RB (2001) Gammalinolenic acid, an unsaturated fatty acid with anti-inflammatory properties, blocks amplification of IL-1 beta production by human monocytes. J Immunol 167:490–496
41. Davies P, Bailey PJ, Goldenberg MM, Ford-Hutchinson AW (1984) The role of arachidonic acid oxygenation products in pain and inflammation. Annu Rev Immunol 2:335–357
42. Dinarello CA, Gatti S, Bartfai T (1999) Fever: links with an ancient receptor. Curr Biol 9:R147–R150
43. Cipollone F, Prontera C, Pini B, Marini M, Fazia M, De Cesare D, Iezzi A, Ucchino S, Boccoli G, Saba V et al (2001) Overexpression of functionally coupled cyclooxygenase-2 and prostaglandin E synthase in symptomatic atherosclerotic plaques as a basis of prostaglandin E(2)-dependent plaque instability. Circulation 104:921–927
44. Jakobsson PJ, Thoren S, Morgenstern R, Samuelsson B (1999) Identification of human prostaglandin E synthase: a microsomal, glutathione-dependent, inducible enzyme, constituting a potential novel drug target. Proc Natl Acad Sci USA 96:7220–7225
45. Roman AS, Schreher J, Mackenzie AP, Nathanielsz PW (2006) Omega-3 fatty acids and decidual cell prostaglandin production in response to the inflammatory cytokine IL-1beta. Am J Obstet Gynecol 195:1693–1699
46. Chene G, Dubourdeau M, Balard P, Escoubet-Lozach L, Orfila C, Berry A, Bernad J, Aries MF, Charveron M, Pipy B (2007) n-3 and n-6 polyunsaturated fatty acids induce the expression of COX-2 via PPARgamma activation in human keratinocyte HaCaT cells. Biochim Biophys Acta 1771:576–589
47. Lo CJ, Chiu KC, Fu M, Lo R, Helton S (1999) Fish oil augments macrophage cyclooxygenase II (COX-2) gene expression induced by endotoxin. J Surg Res 86:103–107
48. Denkins Y, Kempf D, Ferniz M, Nileshwar S, Marchetti D (2005) Role of omega-3 polyunsaturated fatty acids on cyclooxygenase-2 metabolism in brain-metastatic melanoma. J Lipid Res 46:1278–1284
49. Massaro M, Habib A, Lubrano L, Del Turco S, Lazzerini G, Bourcier T, Weksler BB, De Caterina R (2006) The omega-3 fatty acid docosahexaenoate attenuates endothelial cyclooxygenase-2 induction through both NADP(H) oxidase and PKC epsilon inhibition. Proc Natl Acad Sci USA 103:15184–15189
50. Di Rosa M, Giroud JP, Willoughby DA (1971) Studies on the mediators of the acute inflammatory response induced in rats in different sites by carrageenan and turpentine. J Pathol 104:15–29
51. Vinegar R, Schreiber W, Hugo R (1969) Biphasic development of carrageenin edema in rats. J Pharmacol Exp Ther 166:96–103
52. Nantel F, Denis D, Gordon R, Northey A, Cirino M, Metters KM, Chan CC (1999) Distribution and regulation of cyclooxygenase-2 in carrageenan-induced inflammation. Br J Pharmacol 128:853–859
53. Seibert K, Zhang Y, Leahy K, Hauser S, Masferrer J, Perkins W, Lee L, Isakson P (1994) Pharmacological and biochemical demonstration of the role of cyclooxygenase 2 in inflammation and pain. Proc Natl Acad Sci USA 91:12013–12017
54. Tam PS, Umeda-Sawada R, Yaguchi T, Akimoto K, Kiso Y, Igarashi O (2000) The metabolism and distribution of docosapentaenoic acid (n-6) in rats and rat hepatocytes. Lipids 35:71–75
55. Dangi B, Obeng M, Nauroth JM, Teymourlouei M, Needham M, Raman K, Arterburn LM (2009) Biogenic synthesis, purification, and chemical characterization of anti-inflammatory resolvins derived from docosapentaenoic acid (DPAn-6). J Biol Chem 284:14744–14759

Lipids (2010) 45:385–392
DOI 10.1007/s11745-010-3416-1

ORIGINAL ARTICLE

Effects of Partially Hydrogenated, Semi-Saturated, and High Oleate Vegetable Oils on Inflammatory Markers and Lipids

Kim-Tiu Teng · Phooi-Tee Voon · Hwee-Ming Cheng · Kalanithi Nesaretnam

Received: 19 January 2010 / Accepted: 12 April 2010 / Published online: 1 May 2010

Abstract Knowledge about the effects of dietary fats on subclinical inflammation and cardiovascular disease risk are mainly derived from studies conducted in Western populations. Little information is available on South East Asian countries. This current study investigated the chronic effects on serum inflammatory markers, lipids, and lipoproteins of three vegetable oils. Healthy, normolipidemic subjects ($n = 41$; 33 females, 8 males) completed a randomized, single-blind, crossover study. The subjects consumed high oleic palm olein (HOPO diet: 15% of energy 18:1n-9, 9% of energy 16:0), partially hydrogenated soybean oil (PHSO diet: 7% of energy 18:1n-9, 10% of energy 18:1 *trans*) and an unhydrogenated palm stearin (PST diet: 11% of energy 18:1n-9, 14% of energy 16:0). Each dietary period lasted 5 weeks with a 7 days washout period. The PHSO diet significantly increased serum concentrations of high sensitivity C-reactive protein compared to HOPO and PST diets (by 26, 23%, respectively; $P < 0.05$ for both) and significantly decreased interleukin-8 (IL-8) compared to PST diet (by 12%; $P < 0.05$). In particular PHSO diet, and also PST diet, significantly increased total:HDL cholesterol ratio compared to HOPO diet (by 23, 13%, respectively; $P < 0.05$), with the PST diet having a lesser effect than the PHSO diet (by 8%; $P < 0.05$). The use of vegetable oils in their natural state might be preferred over one that undergoes the process of hydrogenation in modulating blood lipids and inflammation.

Keywords Inflammation · C-reactive protein · Lipids · Fatty acids · Cytokines

Abbreviations

HOPO	High oleic palm olein
PHSO	Partially hydrogenated soybean oil
PST	Palm stearin
Lp(a)	Lipoprotein(a)
LSmeans	Least squares means
hsCRP	High-sensitivity C-reactive protein
IL-6	Interleukin-6
IL-1β	Interleukin-1β
IFN-γ	Interferon-γ
TNF-α	Tumor necrosis factor-α
IL-8	Interleukin-8
BP	Blood pressure

Introduction

In the past six decades, a number of epidemiological studies have shown a clear association between certain dietary fatty acids and cardiovascular disease risk [1–3]. A 2% increase in energy intake from partially hydrogenated fats or *trans* fatty acids was associated with a 23% increase in the incidence of cardiovascular heart disease [4]. Replacement of saturated or *cis* unsaturated fatty

K.-T. Teng and P.-T. Voon contributed equally to the study.

K.-T. Teng · P.-T. Voon · K. Nesaretnam (✉)
Food Technology and Nutrition Unit, Malaysian Palm Oil Board (MPOB), 6 Persiaran Institusi, Bandar Baru Bangi, 43000 Kajang, Selangor, Malaysia
e-mail: sarnesar@mpob.gov.my

K.-T. Teng · H.-M. Cheng
Department of Physiology, Faculty of Medicine, University of Malaya, 50603 Kuala Lumpur, Malaysia

acids with *trans* fatty acids has been shown to raise low-density lipoprotein (LDL) cholesterol concentrations, reduce high-density lipoprotein (HDL) cholesterol concentrations, and increase the total:HDL cholesterol ratio [4]. High blood levels of *trans* fatty acids have also been shown to have a more pronounced adverse effect on the lipid profile and other cardiovascular disease risk markers, and are more strongly associated with the incidence of cardiovascular heart disease than saturated fatty acids (SFAs) [5].

At this time, there was emerging evidence that suggested that certain dietary fatty acids could have a direct role in the modulation of cardiovascular disease risk above and beyond that associated with changes in blood lipids [3, 4]. A number of inflammatory markers, such as interleukin-6 (IL-6), interleukin-1β (IL-1β), tumor necrosis factor-α (TNF-α), and interleukin-8 (IL-8) were found to be present in the atherosclerotic plaque, and these can predict cardiovascular heart disease risk [6, 7]. A few human intervention studies demonstrated that *trans* fatty acids increased circulating inflammatory markers, such as IL-6, E-selectin, and hsCRP, compared to other fatty acids [8, 9]. These fatty acids were thought to alter the expression and adherence of the circulating inflammatory markers to endothelium [10]. However, the underlying mechanisms involved are not yet fully understood. It is possible that susceptibility to oxidation could play a role [11]. Inflammation accelerates the atherogenic effects of oxidized lipoproteins, but the mechanisms involved are not clearly defined.

The increasing use of artificially produced *trans* fats in foods drew grave concern from the public, and led to stricter regulatory measures globally. Consequently, the US Food and Drug Administration put out a mandatory '*trans* fatty acids' labeling on packaged food products, effective from 1 January 2006, and this prompted food manufacturers to find alternatives to the use of commercially-hydrogenated vegetable oils in formulating bakery products, and in margarines and fried foods. In South East Asian countries, partially hydrogenated vegetable oils are widely used in the preparation of vanaspati or vegetable ghee, which has up to 40% of *trans* fatty acids [12]. Palm oil, which is widely used in South East Asian countries, is a natural replacement for commercially-produced hydrogenated vegetable oils.

There is no conclusive information concerning the interplay of fats on a wide array of inflammatory markers, and the interaction of inflammatory markers with blood lipids. Thus, the current study was carried out to compare the effects of a high oleic vegetable oil with that of a partially hydrogenated, and an unhydrogenated and more saturated, vegetable oil on serum inflammatory markers and blood lipids.

Methods

Subjects

Subjects were recruited via advertisement posted at the research facilities of the Malaysian Palm Oil Board. Baseline characteristics of the 41 subjects who completed the study are presented in Table 1. All subjects were apparently healthy as indicated by a medical and lifestyle questionnaire and biochemical tests. Exclusion criteria were: BMI $\geq$ 30 kg/m^2, waist hip ratio $>$ 0.9 for men and $>$ 0.8 for women, total cholesterol $>$ 5.2 mmol/L, triacylglycerol (TAG) $>$ 2.2 mmol/L, LDL cholesterol $>$ 3.3 mmol/L, hypertension $>$ 150 mmHg/95 mmHg, chronic diseases and medication. The subjects' habitual diet was assessed by a 3 days dietary record on two weekdays and 1 day weekend day. Calorie intake was assessed by using a nutrition database (NutritionistPro^{TM} Version 2.0.90, Fist Data Bank Inc., 2008). All subjects were instructed to maintain a consistent low or moderate physical activity throughout the study period. The weight of the subjects was monitored on a weekly basis in a fasting state. Throughout the study period subjects recorded food consumed on a weekly basis to ensure that the diet intake did not change during the intervention. To ensure dietary compliance, identical food samples were collected, as consumed on each study day, for analysis.

Study Design

The study was a single-blind, randomized, crossover design dietary intervention study. The study included three dietary intervention periods of 5 weeks each, separated by a 7 days

Table 1 Subject characteristics

Variable	(n = 41)
Age (years)	28.8 ± 9.1
Sex	
Male (n)	8
Female (n)	33
Weight (kg)	55.0 ± 11.3
BMI (kg/m^2)	21.9 ± 3.9
Waist (cm)	76.0 ± 9.4
Systolic BP (mmHg)	116.4 ± 17.4
Diastolic BP (mmHg)	74.1 ± 10.4
Total cholesterol (mmol/L)	4.6 ± 0.6
TAG (mmol/L)	0.8 ± 0.2
LDL cholesterol (mmol/L)	2.8 ± 0.5
HDL cholesterol (mmol/L)	1.6 ± 0.3

Values are means with SD

BP blood pressure

washout period. A total of 43 subjects were recruited, allocated randomly to one of three treatment sequences, using a randomized orthogonal design. Subjects were instructed to maintain their habitual food intake throughout the study. All outcome variables were measured at the start and end of the study.

Diets and Test Fats

During the intervention period, the participants consumed approximately 54 g of test fats incorporated into a cooked meal per day. The test fats used were: high oleic palm olein (HOPO: 54% 18:1n-9, 20% 16:0), partially hydrogenated soybean oil (PHSO: 21% 18:1n-9, 47% 18:1 *trans*) and palm stearin (PST: 25% 18:1n-9, 62% 16:0). The HOPO diet was a high oleic palm olein supplied by Malaysian Palm Oil Board (MPOB), Malaysia. Partially hydrogenated soybean oil (forming the PHSO diet) and palm stearin (forming the PST diet) were supplied by Nisshin-Oillio, Japan. The diets provided approximately 9.2 MJ/day, of which 30–35% of energy fat (test fats accounted for ~20–25% of energy fat), 15% of energy protein and 50–55% of energy carbohydrate. All subjects consumed breakfast and lunch at the dining hall of the research institute, and they were provided a packed dinner for home consumption. Subjects consumed a 5 days rotational meal plan. Breakfast was served with a rice or noodle dish together with a cup of tea or juice. Lunch and dinner consisted of a fish or chicken meal, and two servings of vegetables served with rice along with fruits. The amount and types of food served were the same for the three diets. Subjects were provided guidelines, and test fats to incorporate into their home meal preparation during weekends.

Blood Sampling

Venous blood samples were collected after a 12-h overnight fast before, and at the end of the study at week 4 and week 5. Blood samples, collected at week 4 and week 5, were used to observe the stability of markers tested. The means of week 4 and week 5 were presented in results. Blood samples, for analyses of inflammatory markers, lipids, and lipoproteins, were collected in serum tubes and centrifuged at 2,200×*g* for 15 min at 4 °C, within 1 h of collection. Aliquots of samples were stored at −80 °C for further analyses.

Fatty Acid Analysis

Fatty acid compositions of the test oils were determined in the form of methyl ester by gas–liquid chromatography-flame ionization detector (GC-FID) (Autosystem, Perkin Elmer). Fatty acid methylation was carried out as described in [13]. Samples (2 μL) were injected into the GC fitted with an SP-2560 column (length 100 m, diameter 0.23 mm, and film thickness 0.2 mm). The carrier gas (helium) pressure and injector temperature were set to 40 psi and 250 °C, respectively. The oven temperature was set isothermal at 240 °C for 58 min. Hydrogen and oxygen were used for ignition. A fatty acid methyl esters (FAMEs) mixture (Sigma-Aldrich, Australia) was used as the external standard. Results were expressed in % of energy (Table 2).

Inflammatory Markers

Serum inflammatory markers were measured using ELISA according to protocols described by the manufacturers. All inflammatory markers were measured using the R&D System, USA. In brief, murine monoclonal antibodies against specific human inflammatory markers were precoated onto a 96-well microplate. Then, 100 μL of standard or test samples were added and incubated for 2 h. Diluted conjugates were put into each well and incubated for 1 h. Each of the previous steps was followed with a washing step to remove unbound substances. Stabilized substrate solution (tetramethylbenzidine) was added to each well and color development was stopped using a stop solution. The optical density of each well was read at 450 nm, and corrected for 620 nm.

Table 2 Nutrient composition of test diets

	HOPO diet	PHSO diet	PST diet
Energy, MJ	9.3 ± 1.2	8.9 ± 0.5	9.6 ± 1.1
% of energy			
Carbohydrate	47.2 ± 1.3	48.5 ± 1.3	49.0 ± 1.6
Protein	19.7 ± 0.6	19.3 ± 0.3	19.2 ± 0.4
Total fat	33.5 ± 1.2	32.3 ± 1.2	31.7 ± 1.7
SFAs	10.8 ± 0.1	10.4 ± 0.8	16.4 ± 0.1
12:0 + 14:0	0.7 ± 0.0	0.7 ± 0.1	0.7 ± 0.1
16:0	8.7 ± 0.1	8.1 ± 3.1	13.9 ± 0.3
18:0	1.4 ± 0.0	1.6 ± 1.8	1.8 ± 0.2
MUFAs	15.3 ± 0.1	17.1 ± 1.4	10.7 ± 0.2
18:1	15.3 ± 0.1	7.2 ± 0.2	10.7 ± 0.2
18:1*t*	nd	9.9 ± 1.2	nd
PUFAs	8.6 ± 0.0	4.2 ± 0.6	3.8 ± 0.1
18:2	5.8 ± 0.0	3.9 ± 0.5	3.6 ± 0.1
18:3	2.6 ± 0.0	0.3 ± 0.0	0.2 ± 0.0

All values were derived from identical food samples collected as consumed by subjects on each study day. Values are an average of two determinations

HOPO high oleic palm olein, *PHSO* partially hydrogenated soybean oil, *PST* palm stearin. *nd* not detectable

Lipid, Lipoproteins and hsCRP

Serum total cholesterol and TAG (Cholesterol CHOD-PAP and triglycerides GPO-PAP kits) were measured using enzymatic assays. HDL cholesterol and LDL cholesterol were assessed by enzymatic colorimetric assays (HDL-C plus 3rd generation, and LDL-C plus 2nd generation, respectively). Serum apolipoprotein A-I (apo A-I), apolipoprotein B-100 (apo B-100) and lipoprotein(a) (Lp(a)) were analyzed using immunoturbidimetric procedures (Tina-quant® apolipoprotein A-I ver.2, Tina-quant® apolipoprotein B ver.2 and Tina-quant® lipoprotein (a), respectively). Serum hsCRP was determined using particle-enhanced Tina-quant® CRP (Latex) high sensitive immunoturbidimetric assay (Tina-quant® C-reactive protein (Latex) HS). All kits were purchased from ROCHE and all assays were analyzed using the Hitachi 902 analyzer (Roche Diagnostics GmbH, Germany).

Ethical Considerations

This study was conducted according to the guidelines laid down in the Declaration of Helsinki and all procedures involving human subjects were approved by The University of Malaya Medical Ethics Committee who approved the research protocol (667.14). The study was registered at ClinicalTrial.gov (NCT00715312). Written informed consent was obtained from all subjects.

Statistics

The statistical power to detect a true difference in serum LDL cholesterol concentration between diets if the estimated effect is 10% with an α of 0.05 was 80%. Mixed model ANCOVA was used to compare the effects of dietary fats on all outcome variables. Baseline values for each parameter were included as covariates, and the analyses were adjusted for the baseline values of each variable. Age, BMI, sex and the order in which the participants received the test meals were tested as covariates for influence on the results but none was observed. Fixed effect to dietary treatment and random factor to subject ID number were set. When a significant effect of treatment was detected, we used the Tukey–Kramer test for post hoc analysis. All duplicate data were averaged and tested for normality. Data for TAG, HDL cholesterol, LDL cholesterol, apo B-100, and all serum inflammatory markers were log-transformed. Fasting serum concentrations of all parameters in week 4 and week 5 were tested for any time trend. No time trend was seen, thus an average of the two values was used for further analysis. A two tailed P value of less than 0.05 was considered statistically significant. We presented baseline characteristics of subjects as means ± SD, and all outcome variables as least squares means (LSmeans; adjusted for baseline values) with SEM. All calculations were done by using SAS statistical software (version 9.0; SAS institute Inc, Cary, NC, USA).

Results

Compliance and Dietary Intake

Forty-three subjects entered the study, but two left the study due to medical problems. A total of 41 (33 females, 8 males) subjects completed the study. Two subjects dropped out due to medical problems not related to the study (Fig. 1). Mean energy intake (MJ/day) did not differ between the diet groups. The distribution (% of energy) of fat, protein and carbohydrate showed no significant difference between the diet groups ($P > 0.05$; Table 2). Energy intake was self-controlled by the subjects to achieve energy balance. Initial body weight (56.9 ± 12.4 kg) did not change during the intervention and the weight difference was negligible (<0.5 kg weight gained, $P = 0.871$) [data not shown]. All subjects fully complied with the study protocol throughout the study period shown by >90% attendance to the dinner hall at the research institute.

Serum Inflammatory Markers

The PHSO diet increased hsCRP significantly when compared with HOPO and PST diets (by 32% and 23%, respectively; $P < 0.05$). The PHSO diet, however, significantly decreased IL-8 compared with the PST diet (by 12%; $P < 0.05$) (Table 3). No significant differences in IL-6, IL-1β, and TNF-α were observed between diets after the 5 weeks intervention.

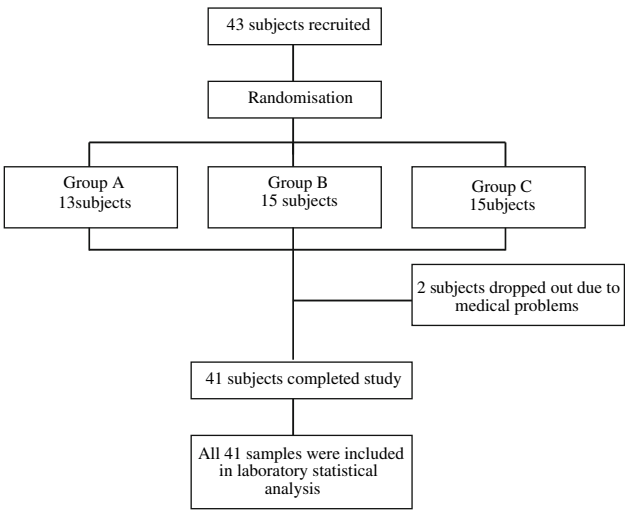

Fig. 1 Consort diagram of 5 weeks dietary intervention

Table 3 Effects of the three diets on serum inflammatory markers in healthy subjects ($n = 41$) participating in the 5 weeks intervention study

Variables	HOPO diet	PHSO diet	PST diet
hsCRP (mg/L)	0.47 ± 0.02[a]	0.59 ± 0.02[b]	0.48 ± 0.02[a]
IL-6 (ng/L)	1.11 ± 0.07	1.05 ± 0.08	0.94 ± 0.08
IL-1β (ng/L)	10.51 ± 3.57	9.56 ± 3.58	9.87 ± 3.57
TNF-α (ng/L)	23.92 ± 0.79	23.18 ± 0.78	22.39 ± 0.80
IL-8 (ng/L)	21.44 ± 1.05[a]	19.64 ± 1.08[a]	24.30 ± 1.23[b]

Values are LSmeans with SEM. All data were analyzed by mixed model ANCOVA with baseline values as covariates. Values within a row with unlike superscript letters (a, b) were significantly different from each other, $P < 0.05$

HOPO high oleic palm olein, *PHSO* partially hydrogenated soybean oil, *PST* palm stearin, *hsCRP* high sensitivity C-reactive protein, *IL-6* interleukin-6, *IL-1β* interleukin-1β, *TNF-α* tumor necrosis factor-α, *IL-8* interleukin-8

Serum Lipids and Lipoproteins

Compared with the HOPO diet, both PHSO and PST diets significantly increased total cholesterol, TAG, LDL cholesterol, apo B-100, total:HDL cholesterol ratio, whereas they significantly decreased apo A-I ($P < 0.05$) (Table 4). The PHSO diet significantly decreased HDL cholesterol when compared with the other two diets ($P < 0.05$); in addition, the PST diet significantly decreased HDL cholesterol when compared with the HOPO diet ($P < 0.05$) (Table 4). In particular, the PHSO diet, and also the PST diet, significantly increased total:HDL cholesterol ratio compared to the HOPO diet (by 23, 13%, respectively; $P < 0.05$). No significant difference was observed for Lp(a) between the three diets.

Table 4 Effects of the three diets on serum lipids and lipoproteins in healthy subjects ($n = 41$) participating in the 5 weeks intervention study

Variables	HOPO diet	PHSO diet	PST diet
Total cholesterol (mmol/L)	4.48 ± 0.04[a]	4.72 ± 0.04[b]	4.66 ± 0.04[b]
TAG (mmol/L)	0.83 ± 0.01[a]	0.89 ± 0.01[b]	0.88 ± 0.01[b]
LDL cholesterol (mmol/L)	2.69 ± 0.05[a]	3.11 ± 0.05[b]	2.95 ± 0.05[b]
HDL cholesterol (mmol/L)	1.63 ± 0.03[a]	1.42 ± 0.03[b]	1.55 ± 0.03[c]
Apo A-I (mmol/L)	3.80 ± 0.03[a]	3.55 ± 0.03[b]	3.57 ± 0.03[b]
Apo B-100 (mmol/L)	2.48 ± 0.03[a]	2.65 ± 0.03[b]	2.68 ± 0.03[b]
Total:HDL cholesterol	2.84 ± 0.06[a]	3.50 ± 0.06[b]	3.22 ± 0.06[c]

Values are LSmeans with SEM. All data were analyzed by mixed model ANCOVA with baseline values as covariates. Values within a row with unlike superscript letters (a, b, c) were significantly different from each other, $P < 0.05$

HOPO high oleic palm olein, *PHSO* partially hydrogenated soybean oil, *PST* palm stearin, *Lp(a)* lipoprotein(a)

Discussion

A significant finding in the present study was that the PHSO (a *trans* fatty acid rich) diet increased hsCRP and total:HDL cholesterol ratio when compared with the PST (a unhydrogenated saturated fat), and the HOPO (high oleic palm olein) enriched diets.

Although the intake and potential adverse health effects of *trans* fatty acids in Western countries have received considerable attention, little is known about intake of partially hydrogenated vegetable oils, a rich source of *trans* fatty acids, in Asian countries. To our knowledge, this study is one of the first to investigate the consumption of partially hydrogenated vegetable oil and its relation to low grade inflammation in an Asian population. Particular interest may exist for developing countries, especially South East Asian countries in which partially hydrogenated vegetable oils are commonly used as cooking oil and represent an inexpensive source of dietary fats. Asian countries such as Iran have also reported a high consumption of partially hydrogenated vegetable oils (>75%). The *trans* fatty acids content of partially hydrogenated vegetable oils used in Iranian households is 25–35%, and up to 50% in food industries [3, 14].

The acute phase reactant, hsCRP, and pro-inflammatory cytokines, IL-6, IL-1β, and TNF-γ, are central mediators of the inflammatory process. These pro-inflammatory cytokines are important in modulating hsCRP secretion and expression of cell adhesion molecules [15]. Epidemiological and clinical studies indicate that *trans* fatty acids are associated with an increase in hsCRP, IL-6, and TNF-α, in both healthy and hypercholesterolemic subjects [9, 16]. Studies have reported that a high *trans* fatty acid diet increased hsCRP, IL-6 and E-selectin, but an oleic acid enriched diet decreased hsCRP and IL-6 [8, 17]. Consistent with these findings are those of our present study which showed that a diet high in *trans* fatty acids (i.e., the partially hydrogenated soybean oil) increases hsCRP concentrations more than one with a semi-saturated fat (i.e., the palm stearin), or one with a high oleic palm olein. Thus, in addition to the hypercholesterolemic effect, *trans* fatty acids might trigger a pro-inflammatory cascade.

In addition, we found higher serum IL-8 concentrations in the semi-saturated fat diet compared with the *trans* fatty acid and high oleic palm olein diets. hsCRP has been shown to trigger the expression of chemokines such as IL-8 and cell adhesion molecules in vitro [18–20]. IL-8 was shown to inhibit neutrophil adhesion to cytokine-activated endothelial cells and protect these cells from neutrophil-mediated

damage [20]. Except for IL-8 and hsCRP, we did not observe any significant differences in the concentrations of serum IL-6, IL-1β, and TNF-α, after consumption of all the three diets. Although hsCRP is primarily secreted in response to IL-6, a regulation of hsCRP that is IL-6-independent has been reported [21]. Our finding is in agreement with that of Han et al. [9], but not with those from other studies [8]. The lack of a significant change in serum inflammatory markers could be explained, in part, by the marked variability in these endpoints as the magnitude of response will vary between subjects. Cytokines produced by adipocytes such as IL-6, IL-1β, and TNF-α have been reported to be associated with increased body weight as a result of the expansion of adipose tissue [22, 23]. Obesity is often accompanied by elevated levels of free fatty acids and hence induces changes in adipose tissue, skeletal muscle, and liver and further lead to systemic inflammation and insulin resistance [23]. In addition, the risks of cardiovascular disease are age-dependent, it has been well established that inflammation increases with age. This might also explain why older subjects possess higher circulating inflammatory levels compared to younger subjects [24]. The present study recruited relatively young healthy subjects (28.8 ± 9.1 year) which may result in lower inflammatory response in IL-6 and TNF-α as contributed by moderate elevation of hsCRP in the serum. Further studies on an older population are warranted.

In addition, the discrepancy in the results may also be due to the study design and the percentage of energy fat incorporated [7]. Baer et al. [8] employed a high fat diet (38% of energy) which might provoke the inflammatory effect of *trans* fatty acids. We hypothesize that the inflammatory pathways will only be stimulated by a longer and increased dietary fat incorporation in the diets. The present amount of fat ($\approx$32% of energy) and 5 weeks feeding duration might not be sufficient to induce a significant change in all inflammatory markers in healthy subjects fed varied dietary fats. In addition, a recent study showed that saturated fats, compared to olive oil, triggered a higher expression of TNF-α from a peripheral mononuclear cell culture but not in serum [25]. This finding suggests that the synthesis and secretion of these cytokines may not happen simultaneously.

The mechanisms by which dietary fatty acids modulate inflammatory markers are not clearly understood. Most of the evidence reported inverse relationship between dietary long chain polyunsaturated fatty acids (PUFAs) and inflammation [26]. Clinical studies reported anti-inflammatory effects of long chain n-3 PUFAs by suppressing pro-inflammatory cytokines and cell adhesion molecules [27–29]. Studies showed that high fat meals enriched with oleic acid reduced postprandial levels of sICAMs and sVCAMs compared to palmitic acid [30]. However, there is insufficient evidence showing the involvement of monounsaturated fatty acids (MUFAs) and SFAs in inflammatory processes. There are several possible mechanisms by which specific fatty acids could regulate inflammatory response. Numerous dietary studies indicate that *trans* fatty acids but not SFAs and MUFAs cause insulin resistance but other studies reported that increasing dietary saturated fats induces insulin resistance whereas PUFAs have a less pronounced effect or even improve insulin sensitivity [31]. We argue that the decrease in insulin levels may contribute to an increase in free fatty acid levels which may further lead to inflammatory process. Elevated levels of CRP, IL-6, TNF-α, and IL-8 have also been reported in diabetic and insulin resistance state [32, 33]. In addition, the induction of gene expression of the inflammatory markers is known to be regulated by the activation of nuclear factor-kappa B (NF-κB) [34]. SFAs, but not monounsaturated fatty acids, were shown to inhibit NF-κB activation and induce the expression of cyclooxygenase-2 (Cox-2) mediated through Toll-like receptor 4 (Tlr 4) [35]. In contrast with this finding, Milanski et al. [36] reported that SFAs, modulate toll-like receptor 4, and trigger the intracellular signaling network that induce an inflammatory response which may explain, in part, the present finding which showed that the PST diet increased IL-8 expression in serum. *Trans* fatty acids, on the other hand, exacerbate a pro-inflammatory milieu through its effect on lipid raft assembly and function [37]. *Trans* fatty acids have been reported to be incorporated into cell membrane by affecting the membrane signaling pathway and modulating the ligand-dependent effects on PPARγ relating to inflammation [38].

The consumption of partially hydrogenated fat has been reported to impair the catabolic pathway of cholesterol-rich lipoproteins by lowering the rate of cholesterol synthesis when compared with soybean oil [39]. This, in fact, could explain the findings in the present study, where partially hydrogenated soybean oil, and palm stearin to a lesser extent, significantly increased serum total cholesterol, TAG, LDL cholesterol, apo B-100 concentrations, and the total: HDL cholesterol ratio (which is a good predictor of CVD risk), compared to the high oleic palm olein diet. Our findings are in agreement with several previous studies [40, 41]. We also observed a decrease in HDL cholesterol and apo A-I levels in the *trans* fat (PHSO) diet group in comparison with the semi-saturated fat (PST) and high oleic palm olein (HOPO) groups, as was also found by other researchers [42].

Studies have reported hypercholesterolemic effects of SFAs in palm oil, compared with oils rich in MUFAs and polyunsaturated fatty acids (PUFAs) [17, 43], though findings from a few studies have questioned these observations [44, 45]. In studies that investigated specific fatty acids, palmitic acid showed fewer hypercholesterolemic

effects than lauric and myristic acids [46]. Human clinical studies have shown that *trans* fatty acids exerted a more atherogenic effect compared with palmitic acid as measured by lipid profiles [41, 42]. There is no uniform agreement on the absolute or relative cholesterol-raising potential of palmitic acid [47]. Stereospecific distribution of specific fatty acids might play a role in explaining the underlying mechanism involved in lipid metabolism [48]. The relatively lower risk of palmitic acid compared to *trans* fatty acids may be related to the combination of less readily absorbed palmitic acids in the *sn*-1, 3 positions and enhanced removal of palmitic acids from the circulation [48, 49]. This observation may, in part, explain the less atherogenic effect of palmitic acid.

Our study has some limitations. One concern is that the sample size was calculated based on the true difference of LDL cholesterol on dietary treatments. We did not include the inflammatory markers as a consideration in the power calculation. However, our study with 41 subjects compared to that of Han et al. [9] with 19 subjects, should allow for the detection of a difference in specific inflammatory markers among the different diets.

Another consideration is that the differences in lipoprotein, lipid and inflammatory marker levels in the present study could not be attributed to the effect of a single fatty acid. This study was designed to assess the effect of commercial fats, with distinct fatty acid profiles, when they are consumed in their normal way, as a cooking oil and in foods, in a South East Asian population. Our investigation was not designed to distinguish the effects of individual fatty acids.

The use of vegetable oils in their natural state might be preferred over one that has undergone the process of hydrogenation. Hence, high oleic palm olein may serve as a suitable cooking oil due to its beneficial effect on blood lipids and inflammatory markers.

Acknowledgments We thank Professor Tom Sanders, Dr Marianne Raff and Professor Geh Sooi Lin for the review of this paper. Our thanks also go to Siew Wai Lin, for her contribution in supplying the high oleic palm olein. There are no conflicts of interest. The study was funded by the Malaysian Palm Oil Board (PD103/07).

References

1. Jakobsen MU, O'Reilly EJ, Heitmann BL, Pereira MA, Bälter K, Fraser GE et al (2009) Major types of dietary fat and risk of coronary heart disease: a pooled analysis of 11 cohort studies. Am J Clin Nutr 89:1425–1432
2. Oh K, Hu FB, Manson JE, Stampfer MJ, Willet WC (2005) Dietary fat intake and risk of coronary heart disease in women: 20 years of follow-up of the nurses' health study. Am J Epidemiol 161:672–679
3. Mozaffarian D, Clarke R (2009) Quantitative effects on cardiovascular risk factors and coronary heart disease risk of replacing partially hydrogenated vegetable oils with other fats and oils. Eur J Clin Nutr 63(Suppl 2):S22–S33
4. Mozaffarian D, Katan M, Ascherio A, Stampfer MJ, Willet WC (2006) *Trans* fatty acids and cardiovascular disease. N Engl J Med 354:1601–1613
5. Willett WC (2006) *Trans* fatty acids and cardiovascular disease–epidemiological data. Atheroscler Suppl 7:5–8
6. Kleemann R, Zadelaar S, Kooistra T (2008) Cytokines and atherosclerosis: a comprehensive review of studies in mice. Cardiovasc Res 79:360–376
7. Ridker PM (2001) Role of inflammatory biomarkers in prediction of coronary heart disease. Lancet 358:946–948
8. Baer DJ, Judd JT, Clevidence BA, Tracy RP (2004) Dietary fatty acids affect plasma markers of inflammation in healthy men fed controlled diets: a randomized crossover study. Am J Clin Nutr 79:969–973
9. Han SL, Leka LS, Lichtenstein AH, Ausman LM, Schaefer EJ, Meydania SM (2002) Effect of hydrogenated and saturated, relative to polyunsaturated, fat on immune and inflammatory responses of adults with moderate hypercholesterolemia. J Lipid Res 43:445–452
10. Giugliano D, Ceriello A, Esposito K (2006) The effects of diet on inflammation: emphasis on the metabolic syndrome. J Am Coll Cardiol 48:677–685
11. Bowen PE, Bortakhur G (2004) Postprandial lipid oxidation and cardiovascular disease risk. Curr Atheroscler Rep 6:477–484
12. Ghafoorunissa G (2008) Role of *trans* fatty acids in health and challenges to their reduction in Indian foods. Asia Pac J Clin Nutr 17(Suppl 1):212–215
13. Morrison WR, Smith LM (1964) Preparation of fatty acid methyl esters and dimethylacetals from lipids with boron fluoride–methanol. J Lipid Res 5:600–608
14. Mozaffarian D, Abdollahi M, Campos H, Houshiarrad A, Willett WC (2007) Consumption of *trans* fats and estimated effects on coronary heart disease in Iran. Eur J Clin Nutr 61:1004–1010
15. Verma S, Szmitko PE, Ridker PM (2005) C-reactive protein comes of age. Nat Clin Pract Cardiovasc Med 2:29–36
16. Mozaffarian D, Pischon T, Hankinson SE, Rifai N, Joshipura K, Willett WC et al (2004) Dietary intake of *trans* fatty acids and systemic inflammation in women1. Am J Clin Nutr 79:606–612
17. Mensink RP (2008) Effects of products made from a high-palmitic acid, trans-free semiliquid fat or a high-oleic acid, low-*trans* semiliquid fat on the serum lipoprotein profile and on C-reactive protein concentrations in humans. Eur J Clin Nutr 62:617–624
18. Galkina E, Ley K (2007) Vascular adhesion molecules in atherosclerosis. Arterioscler Thromb Vasc Biol 27:2292–2301
19. Pasceri V, Chang J, Willerson JT, Yeh ETH (2001) Modulation of C-reactive protein–mediated monocyte chemoattractant protein-1 induction in human endothelial cells by anti-atherosclerosis drugs. Circulation 10:2531–2534
20. Tedgui A, Maliat Z (2006) Cytokines in atherosclerosis: pathogenic and regulatory pathways. Physiol Rev 86:515–581
21. Weinhold B, Rüther U (1997) Interleukin-6-dependent and -independent regulation of the human C-reactive protein gene. Biochem J 327:425–429
22. Corcoran MP, Lamon-Fava S, Fielding RA (2007) Skeletal muscle lipid deposition and insulin resistance: effect of dietary fatty acids and exercise. Am J Clin Nutr 85:662–677
23. De Luca C, Olefsky JM (2008) Inflammation and insulin resistance. FEBS Lett 582:97–105
24. Kritchevsky SB, Cesari M, Pahor M (2005) Inflammatory markers and cardiovascular health in older adults. Cardiovasc Res 66:265–275
25. Jiménez-Gómez Y, López-Miranda J, Blanco-Colio LM, Marín C, Pérez-Martínez P, Ruano J et al (2009) Olive oil and walnut

breakfasts reduce the postprandial inflammatory response in mononuclear cells compared with a butter breakfast in healthy men. Atherosclerosis 204:e70–e76
26. Galli C, Calder PC (2009) Effects of fat and fatty acid intake on inflammatory and immune response: a critical review. Ann Nutr Metab 55:123–139
27. Zhao G, Etherton TD, Martin KR, West SG, Gillies PJ, Kris-Etherton PM (2004) Dietary α-linolenic acid reduces inflammatory and lipid cardiovascular risk factors in hypercholesterolemic men and women. J Nutr 134:2991–2997
28. Calder PC (2003) n-3 polyunsaturated fatty acids and inflammation: from molecular biology to the clinics. Lipids 38:343–352
29. Zhao G, Etherton TD, Martin KR, Gillies PJ, West SG, Kris-Etherton PM (2007) Dietary α-linolenic acid inhibits proinflammatory cytokine production by peripheral blood mononuclear cells in hypercholesterolemic subjects. Am J Clin Nutr 85:385–391
30. Pacheco YM, López S, Bermúdez B, Abia R, Villar J, Muriana FJ (2008) A meal rich in oleic acid beneficially modulates post prandial sICAM-1 in and sVCAM-1 in normotensive and hypertensive hypertriglyceridemic subjects. J Nutr Biochem 19:200–205
31. Lee JS, Pinnamaneni SK, Eo SJ, Cho IH, Pyo JH, Kim CK, Sinclair AJ, Febbraio MA, Watt MJ (2006) Saturated, but not n-6 polyunsaturated, fatty acids induce insulin resistance: role of intramuscular accumulation of lipid metabolites. J Appl Physiol 100:1467–1474
32. Roytblat L, Rachinsky M, Fisher A, Greemberg L, Shapira Y, Douvdevani A, Gelmans S (2000) Raised interleukin-6 levels in obese patients. Obes Res 8:673–675
33. Straczkowski M, Dzienis-Straczkowska S, Stepien A, Kowalska I, Szelachowska M, Kinalska I (2002) Plasma interleukin-8 concentrations are increased in obese subjects and related to fat mass and tumour necrosis factor-alpha system. J Clin Endocrinol Metab 87:4602–4606
34. Lee J-I, Burckart GJ (1998) Nuclear factor kappa B: important transcription factor and therapeutic target. J Clin Pharmacol 38:981–993
35. Lee JY, Sohn KH, Rhee SH, Hwang D (2001) Saturated fatty acids, but not unsaturated fatty acids, induce the expression of cyclooxygenase-2 mediated through Toll-like receptor 4. J Biol Chem 276:16683–16689
36. Milanski M, Degasperi G, Coope A, Morari J, Denis R, Cintra DE et al (2008) Saturated fatty acids produce an inflammatory response predominantly through the activation of TLR4 signaling in hypothalamus: implications for the pathogenesis of obesity. J Neurosci 29(2):359–370
37. Harvey KA, Arnold T, Rasool T, Antalis C, Miller SJ, Siddiqui RA (2008) *Trans*-fatty acids induce pro-inflammatory responses and endothelial cell dysfunction. Br J Nutr 99:723–731
38. Kennedy A, Chung S, LaPoint K, Fabiyi O, McIntosh MK (2008) *Trans*-10, *cis*-12 conjugated linoleic acid antagonizes ligand-dependent PPARγ activity in primary cultures of human adipocytes. J Nutr 138:455–461
39. Matthan NR, Ausman LM, Lichtenstein AH, Jones PJH (2000) Hydrogenated fat consumption affects cholesterol synthesis in moderately hypercholesterolemic women. J Lipid Res 41:834–839
40. Lichtenstein AH, Matthan NR, Jalbert SM, Resteghini NA, Schaefer EJ, Ausman LM (2006) Novel soybean oils with different fatty acid profiles alter cardiovascular disease risk factors in moderately hyperlipidemic subjects. Am J Clin Nutr 84:497–504
41. Sundram K, French MA, Clandinin MT (2003) Exchanging partially hydrogenated fat for palmitic acid in the diet increases LDL-cholesterol and endogenous cholesterol synthesis in normocholesterolemic women. Eur J Nutr 42:188–194
42. de Roos NM, Bots ML, Katan MB (2001) Replacement of dietary saturated fatty acids by *trans* fatty acids lowers serum HDL cholesterol and impairs endothelial function in healthy men and women. Arterioscler Thromb Vasc Biol 21:1233–1237
43. Vega-López S, Ausman LM, Jalbert SM, Erkkilä AT, Lichenstein AH (2006) Palm and partially hydrogenated soybean oils adversely alter lipoprotein profiles compared with soybean and canola oils in moderately hyperlipidemic subjects. Am J Clin Nutr 84:54–62
44. Ng TKW, Hassan K, Lim JB, Lye MS, Ishak R (1991) Nonhypercholesterolemic effects of a palm-oil diet in Malaysian volunteers. Am J Clin Nut 53:1015S–1020S
45. Choudhury N, Tan L, Truswell AS (1995) Comparison of palm olein and olive oil: effects on plasma lipids and vitamin E in young adults. Am J Clin Nutr 61:1043–1051
46. Hayes KC, Pronczuk A, Lindsey S, Diershen-Schade D (1991) Dietary saturated fatty acids (12:0, 14:0, 16:0) differ in their impact on plasma cholesterol and lipoproteins in nonhuman primates. Am J Clin Nutr 53:491–498
47. Mensink RP, Zock PL, Kester DM, Katan MB (2003) Effects of dietary fatty acids and carbohydrates on the ratio of serum total to HDL cholesterol and on serum lipids and apolipoproteins: a meta-analysis of 60 controlled trials. Am J Clin Nutr 77:1146–1155
48. Berry SE (2009) Triacylglycerol structure and interesterification of palmitic and stearic acid-rich fats: an overview and implications for cardiovascular disease. Nutr Res Rev 22:3–17
49. Renaud SC, Ruf JC, Petithory D (1995) The positional distribution of fatty acids in palm oil and lard influences their biologic effects in rats. J Nutr 125:229–237

Lipids (2010) 45:393–400
DOI 10.1007/s11745-010-3411-6

ORIGINAL ARTICLE

Modulation of Platelet Aggregation, Haematological and Histological Parameters by Structured Lipids on Hypercholesterolaemic Rats

Avery Sengupta · Mahua Ghosh

Received: 13 January 2010 / Accepted: 24 March 2010 / Published online: 17 April 2010

Abstract The effect of the consumption of medium-chain fatty acid (MCFA)-rich and polyunsaturated fatty acid (PUFA)-rich mustard oil on platelet aggregation, haematological parameters and the liver was studied in male albino rats. The rats were fed on standard stock diet with control (mustard oil) and experimental oils for 28 days. Haematological examinations in the normal condition showed that there was no significant variation in the platelet count, total white blood cell (WBC) and red blood cell (RBC) counts, haematocrit value and mean cell haemoglobin concentration (MCHC) percentage in the rats fed with control and experimental oils. Haematological examinations in the hypercholesterolaemic condition revealed that there was a significant increase in the platelet count by 39.38% in hypercholesterolaemia, which was decreased by 27.29 and 42.71% by the administration of the experimental oils, respectively. The haemoglobin level was decreased by 5.3%, whereas the haematocrit value was increased by 12.52% in hypercholesterolaemia, which were normalised by treatment with the experimental oils. The platelet aggregation study indicated that the adenosine diphosphate (ADP)-induced platelet aggregation increased by 71.67% in hypercholesterolaemia, but the experimental oils beneficially reduced platelet aggregation by 26.33 and 68.33%, respectively. There was increased total cholesterol, non-high-density lipoprotein (non-HDL) cholesterol and triglyceride levels in liver in hypercholesterolaemia, which was also recovered by the administration of experimental oils. Organopathological examination showed that there was deposition of cholesterol in the liver in the hypercholesterolaemic condition, which was also reduced by treatment with the two experimental oils.

Keywords Medium-chain triglycerides (MCT) · Medium-chain fatty acid (MCFA) · Polyunsaturated fatty acid (PUFA) · Hypercholesterolaemia · Platelet aggregation · Histopathology · Haematology

Abbreviations

ADP	Adenosine diphosphate
AMRD	Age-related macular degeneration
DHA	Docosahexaenoic acid
EPA	Eicosapentaenoic acid
EPA–LA	Eicosapentaenoate–lipoate
HDL	High-density lipoprotein
LCT	Long-chain triglyceride
MCT	Medium-chain triglyceride
MCHC	Mean cell haemoglobin concentration
MCV	Mean corpuscular volume
PRP	Platelet-rich plasma
TAG	Triacylglycerol
PUFA	Polyunsaturated fatty acid
ROS	Reactive oxygen species
5-HT	5-Hydroxytryptamine

Introduction

Hypercholesterolaemia is a major risk factor of cardiovascular diseases, predominantly coronary artery disease [1]. High plasma levels of cholesterol induce vascular

A. Sengupta · M. Ghosh (✉)
Department of Chemical Technology, University College of Science and Technology, University of Calcutta, 92, A.P.C. Road, Kolkata 700009, India
e-mail: mahuag@gmail.com; mgchemtech@caluniv.ac.in

oxidative stress and profoundly change the reactivity of both blood vessels and platelets [2, 3]. In large arteries of the coronary and the systemic circulation, hypercholesterolaemia induces and promotes the development of atherosclerotic lesions and endothelial dysfunction, which is significantly contributed by oxygen-deriving radicals and oxidised low-density protein [4–6]. In platelets, hypercholesterolaemia induces a hyperactive state, which is characterised by increased serotonin release and enhanced responses to platelet aggregators, such as collagen, adenosine diphosphate (ADP) and thromboxane, while the aggregatory activity of prostacyclin is reduced [7].

The major physiological function of platelets is to mediate the haemostatic response. When a blocked blood vessel is damaged, platelets adhere to the exposed subendothelium, where they become activated and aggregate to form a haemostatic plug, in order to arrest the flow of blood and seal off the damaged vessel wall. Platelet activation is controlled by several substances endogenous to the vasculature, such as thrombin, collagen, ADP, adrenaline and 5-hydroxytryptamine (5-HT). These antagonists act through specific receptors expressed on the platelet surface membrane and initiate signal transduction pathways that lead to platelet activation. However, in pathological conditions, platelets form thrombi at the site of vascular lesions and these are associated with ischaemic events and the progression of atherosclerosis. Furthermore, there is evidence of platelet hypersensitivity to aggregating agents in patients with risk factors for coronary heart disease, such as hypertension and hypercholesterolaemia [8].

Feeding a high-cholesterol diet has often been used to elevate serum or tissue cholesterol levels to study the aetiology of hypercholesterolaemia-related lipaemic-oxidative disturbances. In diet-induced hypercholesterolaemia, the liver is the primary organ to metabolise the excessively ingested cholesterol and become affected by subsequent oxidative stress. Endogenous pro-oxidant conditions in liver cells produce effects that influence the development of atherosclerosis [9]. Increased oxidative stress, resulting from both increased oxygen-free radical production and decreased nitric oxide generation, appears to play an important role in the chronic inflammatory responses to hypercholesterolaemia and atherosclerosis [10]. The literature suggests that structured lipids eicosapentaenoate–lipoate (EPA–LA) attenuate hypercholesterolaemia-related disturbances, mainly because of their ability to reduce reactive oxygen species (ROS) production and cholesterol, respectively [11].

The consumption of dietary fats have been long associated to chronic diseases such as obesity, diabetes, cancer, arthritis, asthma and cardiovascular disease. Although some controversy still exists in the role of dietary fats in human health, certain fats have demonstrated their positive effect in the modulation of abnormal fatty acid and eicosanoid metabolism, both of them associated to chronic diseases. Among the different fats, some fatty acids can be used as functional ingredients such as medium-chain fatty acids (MCFA) and polyunsaturated fatty acids (PUFA), such as eicosapentaenoic acid (EPA) and docosahexaenoic acid (DHA).

MCFA (6–10 carbon atoms) containing triglycerides are popularly known as medium-chain triglycerides (MCTs). MCTs are a special-purpose food for use as supportive nutritional therapy. It may be used to increase the calorie value and to improve the palatability, digestibility and absorption. MCTs have a number of properties that may be beneficial in preventing atherosclerosis; among these are that MCTs have anti-coagulating effects and have been shown to lower serum cholesterol. In addition, MCTs reduce levels of cholesterol in the liver and other tissues [12].

PUFAs are remarkably important molecules, both structurally and functionally, and fatty acids with n-3 configuration are predominant class of PUFA. EPA (20:5n-3) and DHA (22:6n-3) are the important n-3 PUFAs. EPA and DHA are important in the treatment of atherosclerosis, cancer, rheumatoid arthritis, psoriasis and diseases of old age, such as Alzheimer's and age-related macular degeneration (AMRD) [13, 14]. A beneficial effect of n-3 PUFA present in marine fishes on atherogenesis is supported from the majority of animal studies showing that feeding with fish oil decreases atherosclerotic lesions [15]. n-3 PUFA may also reduce thrombogenesis and, thereby, decrease the risk of thrombotic complications of plaque rupture/fissure.

A vast population of East Asia use mustard oil as the primary cooking oil. Mustard oil (*Brassica juncea*) contains 8–9% of saturated fatty acid and 88–91% of unsaturated fatty acid, in which 48–50% is erucic acid (22:1) and erucic acid takes time to digest in the human digestive system, which leads to less deposition of lipids in different organs [16]. Moreover, mustard oil contains two essential fatty acids (EFA) in appreciable amounts. There are some opportunities to increase the beneficial effects of mustard oil by incorporating MCFA or PUFA in its glyceride backbone, resulting in the formation of MCT-containing mustard oil (MCTM) and PUFA-containing mustard oil (PUFAM). The aim of this study was to investigate the effects of these two modified forms of mustard oil on different haematological and histological parameters, and also on platelet aggregation.

Materials and Methods

Materials

Mustard oil was extracted from brown mustard seed by the solvent extraction method and physically refined and

bleached in the laboratory. Capric acid (C10:0) was obtained from Sigma Chemical Company. Fish oil containing 32% EPA and 22% DHA was used as the source of PUFA. Lipase TLIM was a gift from Novozymes India Pvt. Ltd. All other reagents used were of analytical grade and procured from Merck India Ltd., Mumbai, India.

Preparation of Oils

Two types of procedures were adopted for the preparation of experimental oil. Capric acid was reacted with mustard oil to obtain MCTM, and EPA- and DHA-containing fish oil was blended with mustard oil to obtain PUFAM. The reaction between capric acid and mustard oil was carried out in a packed-bed bioreactor. The reactor consisted of a tubular glass column of 10 mm ID and was 50 cm long. It was also provided with a water jacket for temperature control. The immobilised enzyme packed into the reactor was retained in place by means of a sintered plate. The substrates were fed from the top and the products were collected at the bottom. The substrates were previously blended and well mixed at the reaction temperature before conducting the packed-bed reaction and were poured into the enzyme bed, maintaining a fixed sample head. Water from a constant temperature bath was circulated through the jacket by a peristaltic pump. A partial suction was given to maintain the constant flow rate (0.4 mL/min; optimised in the previous study); 20 g of enzyme was closely packed into the column by repeated tapping to avoid any air gaps. Transesterification reactions were then carried out by passing the substrate through the column. The temperature was maintained at the desired value of 60°C by passing water through the column jacket. The product mixture was collected at the outlet and the fatty acid composition of the oils was determined by gas chromatography (GC). The fish oil was blended with mustard oil in the mole ratio of 1:2 (fish oil:mustard oil) to obtain PUFA-rich mustard oil (PUFAM). The total amounts of MCFA and PUFA in the modified mustard oils were kept almost equal. Some amount of synthetic antioxidant (TBHQ) was added to both of the oil formulations.

Chromatographic Analysis of Oils

Fatty acid composition of MCTM and PUFAM oils were analysed by GC. Fatty acid ethyl esters (FAME) were prepared by the method described by Metcalfe et al. [17] and the compositions were determined by GC analysis using an analytical gas chromatograph (Agilent 6890 Series gas chromatograph) equipped with a flame ionisation detector (FID) and an HP-Wax capillary column (J & W Scientific Columns from Agilent Technologies) of 30 m length with 0.25 mm ID and 0.25 mm film thickness. The GC inlet temperature and FID detector temperature was maintained at 250°C and the oven temperature was maintained at 250°C for 2 min. Then, the temperature was increased at a rate of 10°C/min, up to 280°C, then a 20-min hold at 280°C. The gas flow was 30, 300 and 29 mL/min for hydrogen, air and nitrogen, respectively.

Experimental Animals

Male Charles Foster rats weighing 80–100 g were grouped into four groups (six rats in each group) by random distribution and housed in individual cages, under a 12-h light/dark cycle. The animals were given a fresh diet daily and the left over food was weighed and discarded. The gain in body weight of animals was monitored at regular intervals. The animals had free access to food and water throughout the study. Each group of rats was fed for a total of 30 days. In the control group, the rats were fed with normal stock diet containing mustard oil and case groups were fed with 20% MCTM and 20% PUFAM, respectively. The protein content of the food was analysed using the Kjeldahl method, fat by the Soxhlet method, and ash and moisture content by oven assay. Samples of the rat faecal matter were collected and analysed once per day. At the end of the experiment, the feeding of rats was stopped and, after 12 h fasting, the rats were anaesthetised by chloroform and 5 ml of blood was taken from the heart. The liver was removed, rinsed with ice-cold saline, blotted, weighed and stored at −20°C until it was analysed. The experimental protocol was approved by the Animal Ethical Committee.

Collection of Blood Samples and Measurement of Haematological Parameters

Blood samples taken from the abdominal aorta were collected in sample bottles containing heparin as the anticoagulant. Total white blood cell (WBC) counts, number of platelets, haemoglobin concentration, mean cell haemoglobin concentration (MCHC), mean corpuscular volume (MCV) and haematocrit value were analysed.

Platelet Preparation

Blood (4.5 mL) was collected from the abdominal aorta of urethane-anaesthetised animals and poured into 0.5 mL trisodium citrate (3.8% w/v) and centrifuged (250 g, 15 min, at room temperature) to obtain platelet-rich plasma (PRP).

Platelet Aggregation Study

PRP was taken and washed platelets were prepared as described by Brunauer and Huestis [18] and suspended in

Tyrode buffer. Platelets were incubated for 15 min at 37°C prior to use. Platelet aggregation measurements were performed using a Chrono-Log dual-channel aggregometer. The aggregometer was calibrated using the light transmission of PRP/platelet suspension and PPP/Tyrode buffer to represent 0 and 100% aggregation, respectively. Platelet suspension of 450 μL was stirred at 1,000 rpm at 37°C and 10 μL of ADP (25 m) was added and aggregation followed for at least 5 min. The reading was recorded until a plateau was reached.

Analysis of Liver Lipids

Liver lipid was extracted by the method of Folch et al. [19]. One gram of tissue was homogenised with 1 mL of 0.74% potassium chloride and 2 mL of different proportions of chloroform and methanol for 2 min and then centrifuged. The mixture was left overnight and the chloroform layer was filtered through a Whatman filter paper (No. 1). The chloroform layer was dried, the tissue lipid contents were measured and the lipid was used for lipid analysis. The liver lipid was used for the estimation of total cholesterol, high-density lipoprotein (HDL) cholesterol, non-HDL cholesterol, triacylglycerol (TAG) and phospholipid estimation by using standard kits.

Histopathology

Permanent preparations were made using routine methods [20]. The livers were fixed in 10% buffered formalin. The tissues were subsequently dehydrated in upgraded concentrations of alcohol, cleansed in xylene, impregnated and embedded in paraffin wax. Several sections of 3–6 μm were cut using a microtome. The sections were stained with haematoxylin and eosin.

Data Analysis and Statistical Procedures

All of the data are presented as mean ± standard deviation (SD). Significance was calculated using one-way analysis of variance (ANOVA).

Results

Composition of Oils

Analysis of the lipids in the diet showed that MCTM contained 19.87% capric acid (C_{10}) and PUFAM contained 18.83% EPA and DHA. The fatty acid compositions of the control oil (mustard oil) and experimental oils, MCTM and PUFAM, are given in Table 1.

Nutritional Performance of Rats Fed with Experimental Oils

The fat level was kept constant at 20% in all of the dietary groups. The amount of diet consumed by the different groups was comparable. The feeding effect of dietary lipids on the body weight gain of normal and hypercholesterolaemic rats is presented in Table 2. There was no significant difference in the food intake of the different groups of

Table 1 Fatty acid composition of control and experimental oils

Fatty acid	Fatty acid (% w/w)													
	$C_{10:0}$	$C_{16:0}$	$C_{18:0}$	$C_{18:1}$	$C_{18:2}$	$C_{18:3}$	$C_{20:0}$	$C_{20:1}$	$C_{20:4}$	$C_{20:5}$	$C_{22:0}$	$C_{22:1}$	$C_{24:0}$	$C_{22:6}$
Mustard oil (control)	–	2.24	1.15	9.42	17.94	10.75	0.80	5.15	–	–	2.00	**48.55**	1.30	–
MCTM	**19.87**	1.75	1.02	11.06	10.55	7.22	0.60	3.57	–	–	1.92	**40.35**	2.09	–
PUFAM	–	1.33	2.33	9.31	17.52	8.18	0.20	4.87	1.68	**10.35**	1.59	**33.00**	1.19	**8.48**

Table 2 Effect of feeding dietary lipids on body weight gain of normal and hypercholesterolaemic rats

Parameters	Control oil		MCTM oil		PUFAM oil	
	Normal condition	Hypercholesterolaemic condition	Normal condition	Hypercholesterolaemic condition	Normal condition	Hypercholesterolaemic condition
Food intake (g/day/rat)	7.94 ± 0.87^{a}	8.05 ± 1.32^{a}	8.44 ± 0.07^{a}	8.27 ± 0.98^{a}	8.04 ± 0.12^{a}	7.91 ± 0.25^{a}
Body weight gain (g)	34.17 ± 0.99^{a}	42.51 ± 0.46^{b}	34.09 ± 0.45^{a}	40.34 ± 0.99^{c}	39.66 ± 0.67^{d}	43.83 ± 1.21^{e}
Food efficiency ratio	0.14 ± 0.01^{a}	0.17 ± 0.01^{a}	0.13 ± 0.02^{a}	0.16 ± 0.01^{a}	0.16 ± 0.01^{a}	0.18 ± 0.03^{a}

Values are mean ± SEM ($n = 6$ rats)

Values not sharing a common superscript within a row are statistically significant ($P < 0.01$)

normal and hypercholesterolaemic rats. However, there was a significant difference between the body weight gain of the normal and hypercholesterolaemic groups ($P < 0.01$). There was no significant difference between the body weight gain of the group fed with mustard oil and the group fed with MCTM oil in the normal case. On the other hand, the body weight gain decreased on feeding the rats with MCTM oil in the hypercholesterolaemic condition. The body weight gain was increased significantly by feeding the rats with PUFAM oil both in the normal and hypercholesterolaemic groups. The food efficiency ratios (FER) of the normal rats fed with three different oils were almost equal and there was no significant difference also between the food efficiency ratios of the hypercholesterolaemic rats fed with the three oils, but the FER value was slightly greater in the case of hypercholesterolaemic groups than that of normal groups.

Haematological Parameters

The blood haematological parameters of the normal and hypercholesterolaemic groups are shown in Table 3. The results show that there were no significant variations in the platelet count, total WBC counts, total red blood cell (RBC) counts, haematocrit value and MCHC percentage in the normal rats fed with control and experimental oils. But there was a significant increase in the platelet counts from 5.82×10^9/L in the normal case to 9.60×10^9/L in the hypercholesterolaemic case, and the count was lowered with the administration of both of the experimental oils. The haemoglobin level of the normal rats fed with control oil was lower in comparison with its level in rats fed with experimental oils and there was further lowering of the haemoglobin level in hypercholesterolaemia, which was raised by feeding the rats with MCTM and PUFAM oils. The results also show that the MCV percentage was raised with the administration of PUFAM oil in the case of normal rats. Similarly the haematocrit and MCHC values were increased with the induction of hypercholesterolaemic condition in rats and the percentages were lowered by treatment with the experimental oils. Among the two experimental oils, the effect of PUFAM was better than MCTM oil.

In Vitro Platelet Aggregation

Table 4 depicts the changes in platelet aggregation by treatment of the normal and hypercholesterolaemic rats with MCTM and PUFAM oils. MCTM and PUFAM oil-fed rats showed a significant decrease ($P < 0.05$) in the percentage aggregation of platelets. The decrease in percentage aggregation was much more pronounced in the case of PUFAM oil than in the case of MCTM oil, both in normal and hypercholesterolaemic subjects. The percentage of ADP-induced platelet aggregation was increased to a very high degree in the case of hypercholesterolaemia, which was decreased significantly ($P < 0.05$) by 26.33 and 68.33% by feeding the rats with MCTM and PUFAM oils, respectively.

Liver Lipid Analysis

The liver is an important site for lipid metabolism. The liver lipid profiles of normal and hypercholesterolaemic rats fed with dietary lipids are shown in Table 5. The total cholesterol of the liver of rats fed with control oil was 14.74 mg/dL in the case of normal rats and 18.72 mg/dL in the case of hypercholesterolaemic rats. These levels of total cholesterol were decreased significantly by treating the rats with MCTM oil and PUFAM oil, both in the normal and hypercholesterolaemic groups. The liver triglyceride concentration was also altered by the type of fat given to the

Table 3 Comparison between the haematological parameters of rats fed with control oil and experimental oils in normal and hypercholesterolaemic condition

Parameters	Control oil		MCTM oil		PUFAM oil	
	Normal condition	Hypercholesterolaemic condition	Normal condition	Hypercholesterolaemic condition	Normal condition	Hypercholesterolaemic condition
Platelets ($\times 10^9$/L)	5.82 ± 0.88^a	9.60 ± 0.22^b	5.35 ± 0.25^a	6.98 ± 0.18^c	5.02 ± 0.39^a	5.50 ± 0.50^a
Haemoglobin (g/dl)	13.20 ± 0.12^a	12.50 ± 0.09^b	14.00 ± 0.29^c	13.28 ± 0.02^d	15.60 ± 0.08^e	14.53 ± 0.20^f
Total WBC ($\times 10^9$/L)	5.12 ± 0.17^a	8.77 ± 0.20^b	4.98 ± 0.12^a	7.47 ± 0.12^c	4.29 ± 0.88^a	5.99 ± 0.06^d
Total RBC ($\times 10^9$/L)	8.50 ± 0.22^a	7.50 ± 0.56^a	8.71 ± 0.18^a	7.89 ± 0.28^a	8.94 ± 0.28^a	8.24 ± 1.20^a
MCV (%)	47.50 ± 1.20^a	45.76 ± 0.20^a	48.30 ± 1.29^a	46.30 ± 0.78^a	53.00 ± 0.29^b	50.89 ± 0.21^c
Haematocrit (%)	40.33 ± 1.02^a	46.10 ± 0.99^a	39.65 ± 0.76^a	44.23 ± 0.17^b	39.53 ± 0.18^a	40.21 ± 0.10^c
MCHC (%)	32.70 ± 0.21^a	30.10 ± 0.31^a	33.21 ± 0.56^a	32.18 ± 0.09^b	32.20 ± 1.34^a	32.68 ± 0.54^b

Values are mean ± SEM ($n = 6$ rats)

Values not sharing a common superscript within a row are statistically significant ($P < 0.01$)

Table 4 Platelet aggregation in rats fed with MCTM and PUFAM oils in comparison with the rats fed with control mustard oil

ADP-induced platelet aggregation (%)	Control oil	MCTM oil	PUFAM oil
Normal case (%)	21.25 ± 0.98^{a}	18.75 ± 1.05^{b}	15.00 ± 0.45^{c}
Hypercholesterolaemic case (%)	75.00 ± 3.67^{a}	55.25 ± 1.88^{b}	23.75 ± 2.76^{c}

Values are mean ± SEM ($n = 6$ rats)

Values not sharing a common superscript within a row are statistically significant ($P < 0.05$)

Table 5 Liver lipid profile (mg/g tissue) of normal and hypercholesterolaemic rats fed with dietary lipids

Parameters	Control oil		MCTM oil		PUFAM oil	
	Normal condition	Hypercholesterolaemic condition	Normal condition	Hypercholesterolaemic condition	Normal condition	Hypercholesterolaemic condition
Total cholesterol	14.74 ± 0.11^{a}	18.72 ± 0.09^{b}	9.94 ± 0.18^{c}	13.53 ± 1.56^{d}	8.63 ± 1.22^{e}	10.27 ± 0.48^{f}
HDL cholesterol	4.47 ± 0.21^{a}	2.11 ± 0.98^{b}	5.54 ± 0.04^{c}	4.13 ± 0.16^{d}	5.72 ± 0.17^{c}	5.32 ± 0.34^{e}
Non-HDL cholesterol	7.49 ± 0.22^{a}	13.14 ± 0.33^{b}	2.27 ± 0.07^{c}	6.71 ± 0.18^{d}	1.47 ± 0.18^{e}	2.85 ± 0.28^{f}
Triacylglycerol	13.88 ± 0.99^{a}	17.33 ± 0.11^{b}	10.66 ± 0.45^{c}	13.47 ± 0.32^{d}	7.22 ± 0.34^{e}	10.49 ± 0.18^{f}
Phospholipids	2.42 ± 0.01^{a}	1.89 ± 0.05^{b}	2.99 ± 0.24^{c}	2.88 ± 0.06^{c}	3.14 ± 0.04^{c}	2.93 ± 0.10^{c}

Values are mean ± SEM ($n = 6$ rats)

Values not sharing a common superscript within a row are statistically significant ($P < 0.05$)

rats. There was a decrease in the triglyceride concentration by 23.2 and 47.9% in normal rats fed with MCTM oil and PUFAM oil, respectively, and by 22.3 and 39.5% in hypercholesterolaemic rats fed with MCTM oil and PUFAM oil, respectively. There was a decrease in the non-HDL levels and an increase in the phospholipid concentrations by treating the rats with the two experimental oils both in the normal and hypercholesterolaemic cases. There was an increase in the level of HDL cholesterol by treating the rats with the experimental oils. The changes were more pronounced in the case of PUFAM oil.

Histopathology of the Liver

Microscopic examination of the liver cells of the six groups was performed and the histopathological slides are shown in Fig. 1. Figure 1a, d highlighted the abnormal fatty changes in hepatic histology of the control rats. The changes are very much pronounced in the case of hypercholesterolaemic control rats. Figure 1b, e highlighted the treatment of the livers with MCTM oil. Figure 1c, f highlighted the treatment of the livers with PUFAM oil. The effect of treatment of the rats with PUFAM oil was much greater in comparison with MCTM oil.

Discussion

The data on the total body weight indicated a decrease in body weight gain in case of administration of MCTM oil, and the reverse occurs in the case of PUFAM oil. This is due to the reason that MCTs have lower calorie content in comparison to long-chain triglycerides (LCT). MCTs are also not stored in fat deposits in the body as much as LCTs [21]. MCTs also contribute to enhanced metabolism to burn even more calories [22].

Hypercholesterolaemia increases markedly the platelet count, haematocrit value and MCHC percentage. Their increase in the blood serves as important markers of vascular disease, such as microangiopathy and macroangiopathy. The treatment of the hypercholesterolaemic rats with MCTM and PUFAM oils decreases the platelet count, haematocrit value and MCHC percentage and, thus, decreases the chances of vascular disease as well.

The actual physiology of the hypercholesterolaemic subjects could be understood by its liver lipid profile, as the liver is the main site for lipid metabolism. The results of the present study indicates that the administration of two structured lipids, MCTM and PUFAM, increases HDL and decreases non-HDL cholesterol, along with a reduction of TAG and increment in phospholipids. Our results also show that the platelets of hypercholesterolaemic rats are significantly more responsive to ADP-induced aggregation in vitro than normal rats in terms of peak height. As cholesterol is responsible for the observed changes in platelet reactivity, an acute elevation in the cholesterol level had a significant effect on ADP-induced platelet aggregation. In the present work, we have only studied aggregation responses to ADP, which is considered to be an important physiological mediator of platelet aggregation. The in vitro

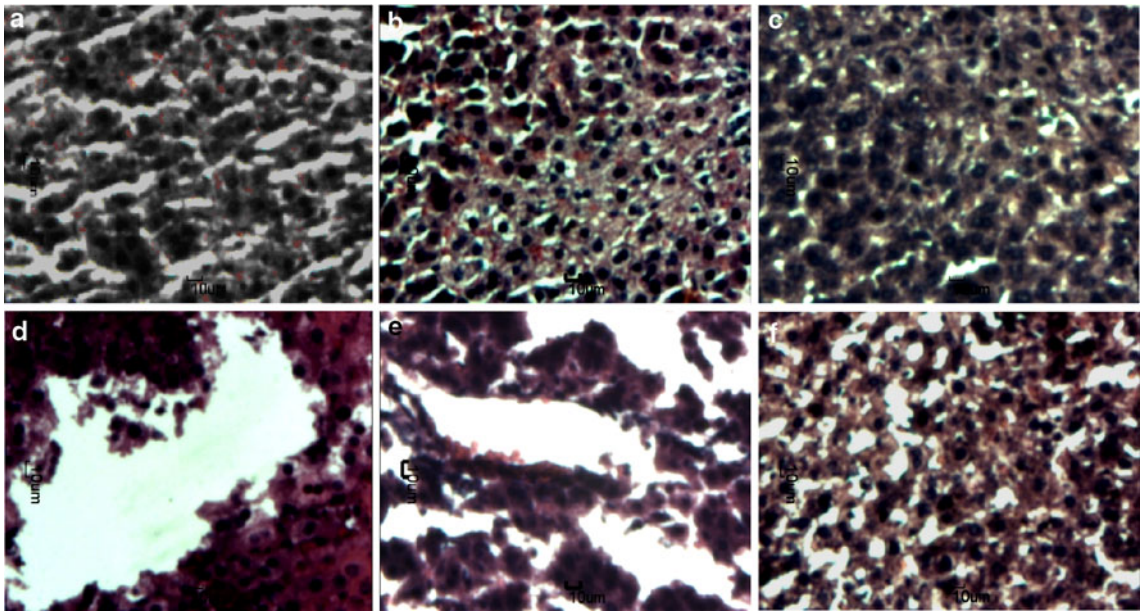

Fig. 1 Pictomicrographs of liver tissues of: **a** normal rats fed with control mustard oil; **b** normal rats fed with MCTM oil; **c** normal rats fed with PUFAM oil; **d** hypercholesterolaemic rats fed with control mustard oil; **e** hypercholesterolaemic rats fed with MCTM oil; **f** hypercholesterolaemic rats fed with PUFAM oil

model of platelet accumulation used in this study has previously been validated and provides a reliable and reproducible method of assessing platelet aggregation responses. It reflects the true accumulation of platelets in the pulmonary vasculature that is not simply a consequence of changes in blood flow or distribution. It is released from dense granules of platelets and acts principally through the platelet $P2Y_{12}$ receptor to induce platelet activation and subsequent aggregation. Clinically, the $P2Y_{12}$ receptor antagonist clopidogrel is widely used for the prevention of arterial thrombotic disease. This may be possibly related to an increase in the ADP sensitivity of platelets. This confirms the importance of ADP as a stimulus for thrombotic disease, especially in hypercholesterolaemic patients. The results of this study show that, in an animal model of hypercholesterolaemia, platelet aggregation was increased in vitro, as determined by the accumulation of platelets in response to ADP. This may contribute to the increase in arterial thrombotic events seen in this condition, so that an increased ability of platelets to aggregate coupled with endothelial dysfunction and vascular damage, which combine to give rise to both macrovascular and microvascular disease. Treatment of the rats with MCTM and PUFAM oils seems to produce an inhibitory effect on platelet aggregation, thus, reducing the chances of vascular diseases and, finally, atherosclerosis by reducing the interaction between platelets and the vessel wall. The effect of PUFAM oil seems to be higher than MCTM oil. Various laboratories have investigated the metabolic mechanisms by which polyunsaturated fatty acids may decrease platelet activation after exposure to several agonists. When EPA is consumed, it is selectively incorporated into various phospholipid components of the platelet membrane. A result of EPA's accumulation in membrane phospholipids is the partial replacement of endogenous arachidonic acid (AA) available for the release and formation of thromboxane A, which is a potent inducer of platelet aggregation and a vasoconstrictor. EPA not only decreases the amount of AA available in tissue phospholipids for conversion into eicosanoids (including prostaglandins and leukotrienes), but it also competitively inhibits the conversion of AA into endoperoxides at the level of cyclo-oxygenase.

The hallmark of atherosclerosis was the accumulation of cells containing excessive lipids, and this was notable in the histopathological observation of the present study, where there was an increased lipid infiltration in hepatocytes of the control rats, especially in the hypercholesterolaemic control rats. Furthermore, the cholesterol levels in the liver of the control rats were also increased. It was reported that the supplementation of n-3 PUFA results in increased cholesterol excretion from the animals, by increasing the transfer of cholesterol into bile [23]. HMG CoA reductase inhibitory property of n-3 PUFA [24] and MCT reduces hepatic endogenous production of cholesterol, thereby, preventing excessive accumulation of lipids in the hepatocytes. It has been demonstrated from the study that the incorporation of MCFA and PUFA in mustard oil in the diet of rats appears to be hypolipidaemic by efficiently reducing the increased lipid infiltration and cholesterol level in hepatic tissues.

Thus, in conclusion, we can say that the consumption of MCTM and PUFAM oils can improve the haematological and histological conditions which were disturbed by hypercholesterolaemia.

Acknowledgements The work was funded by the University of Calcutta under the scheme "University with Potential for Excellence" funded by Government of India. Sincere thanks are also due for Dr. Biswajit Bhattacharya, Medical Officer, Blood Bank, R. G. Kar Medical College and Hospital, Kolkata, and Dr. (Ms.) Maitreyee Bhattacharya and Dr. Sanjoy Misra, Department of Haematology, N.R.S. Medical College and Hospital, Kolkata, for their help in finding out the haematological and platelet aggregation parameters, respectively, performed in the above study. We are very thankful to Prof. D. K. Bhattacharyya, Ex-Professor Emeritus, Department of Chemical Technology, University of Calcutta, for his wonderful mentorship.

References

1. Ross R (1999) Mechanisms of disease: atherosclerosis—an inflammatory disease. N Eng J Med 340:115–126
2. Kojda G, Harrison DG (1999) Interactions between NO and reactive oxygen species: pathophysiological importance in atherosclerosis, hypertension, diabetes and heart failure. Cardiovasc Res 43:562–571
3. Aviram M, Brook JG (1987) Platelet activation by plasma lipoproteins. Prog Cardiovasc Dis 30:61–72
4. Harrison DG (1997) Cellular and molecular mechanisms of endothelial cell dysfunction. J Clin Invest 100(9):2153–2157
5. Kugiyama K, Kerns SA, Morrisett JD, Roberts R, Henry PD (1990) Impairment of endothelium-dependent arterial relaxation by lysolecithin in modified low-density lipoproteins. Nature 344:160–162
6. Steinberg D (1997) Lewis A. Conner memorial lecture. Oxidative modification of LDL and atherogenesis. Circulation 95:1062–1071
7. Tremoli E, Colli S, Maderna P, Baldassarre D, Di Minno G (1993) Hypercholesterolemia and platelets. Semin Thromb Hemost 19:115–121
8. Willoughby S, Holmes A, Loscalzo J (2002) Platelets and cardiovascular disease. Eur J Cardiovasc Nurs 1:273–288
9. Napolitano M, Rivabene R, Avella M, Amicone L, Tripodi M, Botham KM, Bravo E (2001) Oxidation affects the regulation of hepatic lipid synthesis by chylomicron remnants. Free Radic Biol Med 30(5):506–515
10. Napoli C, Lerman LO (2001) Involvement of oxidation-sensitive mechanisms in the cardiovascular effects of hypercholesterolemia. Mayo Clin Proc 76:619–631
11. Kumar SA, Sudhahar V, Varalakshmi P (2006) Protective role of eicosapentaenoate–lipoate (EPA–LA) derivative in combating oxidative hepatocellular injury in hypercholesterolemic atherogenesis. Atherosclerosis 189:115–122
12. Bach AC, Babayan VK (1982) Medium-chain triglycerides: an update. Am J Clin Nutr 36:950–962
13. Drevon CA, Baksaas I, Krokan HE (eds) (1993) Omega-3 fatty acids: metabolism and biological effects. Birkhauser Verlag, Basel, Switzerland, 389 pp
14. Simopoulos AP, Leaf A, Salem N Jr (1999) Essentiality of and recommended dietary intakes for omega-6 and omega-3 fatty acids. Ann Nutr Meta 43:127–130
15. Soei LK, Lamers JMJ, Sassen LMA, van Tol A, Scheek LM, Dekkers DHW, van Meegen J, Verdouw P (1995) Fish oil: a modulator of experimental atherosclerosis in animals. In: Kristensen SD, Schmidt EB, De Caterina R, Endres S (eds) n-3 fattyacids: prevention and treatment of vascular disease. Bi & Gi Publishers, Verona, pp 55–75
16. Bailey AE (1951) Industrial oil and fat products. Interscience Publishers, New York
17. Metcalfe LD, Schmitz AA, Pelka JR (1966) Rapid preparation of fatty acid esters from lipids for gas chromatographic analysis. Anal Chem 38:514–515
18. Paul W, Queen LR, Page CP, Ferro A (2007) Increased platelet aggregation in vivo in the Zucker Diabetic Fatty rat: differences from the streptozotocin diabetic rat. Br J of Pharmacol 150:105–111
19. Folch J, Ascoli I, Lees M, Meath JA, LeBaron N (1951) Preparation of lipid extracts from brain tissue. J Biol Chem 191:833–841
20. Edem DO (2009) Haematological and histological alterations induced in rats by palm oil-containing diets. Eur J Sci Res 32(3):405–418
21. Babayan VK (1981) Medium chain length fatty acid esters and their medical and nutritional applications. J Am Oil Chem Soc 58:49A–51A
22. Fushiki T, Matsumoto K, Inoue K, Kawada T, Sugimoto E (1995) Swimming endurance capacity of mice is increased by chronic consumption of medium-chain triglycerides. J Nutr 125(3):531–539
23. Balasubramaniam S, Simons LA, Chang S, Hickie JB (1985) Reduction in plasma cholesterol and increase in biliary cholesterol by a diet rich in n-3 fatty acids in the rat. J Lipid Res 26(6):684–689
24. Hromadová M, Seböková E, Klimeš I (1994) HMG-CoA reductase activity in the liver of rats with hereditary hypertriglyceridemia: effect of dietary fish oil. Endocr Regul 28:211–214

Lipids (2010) 45:401–407
DOI 10.1007/s11745-010-3405-4

ORIGINAL ARTICLE

Saponified Evening Primrose Oil Reduces Melanogenesis in B16 Melanoma Cells and Reduces UV-Induced Skin Pigmentation in Humans

Jeung-Hyun Koo · Ikjae Lee · Seok-Kweon Yun · Han-Uk Kim · Byung-Hyun Park · Jin-Woo Park

Received: 10 November 2009 / Accepted: 5 March 2010 / Published online: 30 March 2010

Abstract This study was conducted to determine whether saponified evening primrose oil (sap-EPO) has the potential for use as a whitening agent and to investigate its underlying mechanisms of action. In B16 melanoma cells, sap-EPO dose-dependently inhibited isobutylmethylxanthine-induced melanogenesis with no cytotoxicity. This decrease in melanin production was correlated with reduced enzyme activity and decreased mRNA and protein levels of tyrosinase. The mRNA levels of tyrosinase-related proteins 1 and 2 decreased in response to treatment with sap-EPO, indicating that it regulated tyrosinase at the transcriptional level. Expression of microphthalmia-associated transcription factor was also decreased by sap-EPO as evidenced by decreased mRNA and protein levels. Additionally, topical application of sap-EPO resulted in efficient whitening of UVB-induced hyperpigmentation of human skin. Taken together, these results suggest that sap-EPO has the potential for use as a cosmetic whitening agent.

Keywords Saponification · Evening primrose oil · Melanogenesis · B16 melanoma cells · Skin · UV

J.-H. Koo · I. Lee · B.-H. Park (✉) · J.-W. Park (✉)
Department of Biochemistry, Medical School and Diabetes Research Center, Chonbuk National University, Jeonju, Jeonbuk 561-756, Korea
e-mail: bhpark@chonbuk.ac.kr

J.-W. Park
e-mail: jinwoo@chonbuk.ac.kr

S.-K. Yun · H.-U. Kim
Department of Dermatology, Medical School and Diabetes Research Center, Chonbuk National University, Jeonju, Jeonbuk 561-756, Korea

Abbreviations

DHICA	5,6-Dihydroxyindole-2-carboxylic acid
EPO	Evening primrose oil
IBMX	Isobutylmethylxanthine
MITF	Microphthalmia-associated transcription factor
sap-EPO	Saponified evening primrose oil
TRP	Tyrosinase-related protein

Introduction

Melanin is a unique, pigmented biopolymer synthesized by melanocytes that exist in the dermal-epidermal border of the skin. Melanin production is an important defense mechanism against sunlight; however, excessive melanin production due to exposure to UV irradiation or chronic inflammation causes hyperpigmentation of the skin, which can result in melasma, lentigines, nevus, ephelis, freckles or age spots [1]. Accordingly, it is of great interest to develop an effective melanogenesis inhibitor for both pharmaceutical and cosmetic purposes.

The tyrosinase gene family plays a pivotal role in the regulation of melanogenesis [2]. This family consists of tyrosinase, tyrosinase-related protein 1 (TRP-1) and tyrosinase-related protein 2 (TRP-2) [1]. Tyrosinase is a bifunctional enzyme that modulates melanin production by catalyzing the hydroxylation of tyrosine to DOPA and then catalyzing the oxidation of DOPA to DOPAquinone [3]. TRP-2, which functions as a DOPAchrome tautomerase, catalyzes the rearrangement of DOPAchrome to 5,6-dihydroxyindole-2-carboxylic acid [4], while TRP-1 oxidizes dihydroxyindole-2-carboxylic acid to a carboxylated indole-quinone [5].

A number of skin whitening agents have been developed, but these often produce unwanted side effects such as local irritation, contact dermatitis, ochronosis, atrophy and skin cancer [6]. Therefore, it is necessary to find safer therapeutic agents that are still effective. The use of natural products for this purpose has recently been the focus of much attention. For example, arbutin, which is obtained from the leaves of the bearberry plant, is known to inhibit tyrosinase activity [7]. Additionally, kojic acid, which is a hydrophilic fungal derivative obtained from *Aspergillus* and *Penicillium* species, is the most popular agent employed in Asia for the treatment of melasma [6, 8]. Moreover, aleosin, licorice extract, ascorbic acid and soy proteins have been used to interrupt the process of melanogenesis [6]. We also recently reported that xanthohumol, scoparone and *Angelica gigas* extract exerted a potent inhibitory effect against melanogenesis in B16 melanoma cells [9–11]. During screening for new skin-whitening agents from natural sources, we found that the saponification product of evening primrose oil (sap-EPO) effectively whitened skin that had been subjected to UV-induced hyperpigmentation. Therefore, in this study, we investigated the inhibitory mechanism of sap-EPO against isobutylmethylxanthine (IBMX)-induced melanogenesis in B16 melanoma cells.

Experimental Procedures

Cells and Materials

The B16/F10 murine melanoma cell line was obtained from the Korean Cell Line Bank (Seoul, Korea). Cells were cultured in DMEM containing 10% fetal bovine serum, 100 U/ml penicillin, 0.1 mg/ml streptomycin and 0.25 μg/ml amphotericin B at 37 °C in a humidified atmosphere composed of 95% air and 5% CO_2. Drug treatment began 24 h after seeding, and the cells were harvested after 2 days of incubation. IBMX was obtained from Sigma (St. Louis, MO, USA) and evening primrose oil (EPO) was obtained from Dalim Biotech (Evoprim®, Seoul, Korea).

Saponification of Evening Primrose Oil

One gram of EPO was mixed with 0.5 ml of 2.5 N KOH in ethanol, after which saponification was conducted at 80 °C for 30 min. After saponification, the pH of the solution was adjusted to 7.4.

MTT Assay

The viability of cultured cells was determined by reduction of MTT to formazan. Cells were seeded in 96-well plates and cultured for 24 h. After drug treatment, MTT (5 mg/ml in PBS, 100 μl) was added to each well. Cells were incubated at 37 °C for 30 min and dimethyl sulfoxide (100 μl) was added to dissolve the formazan crystals. The absorbance was measured at 570 nm with a spectrophotometer (Spectra MAX PLUS; Molecular Devices, Sunnyvale, CA, USA).

Melanin Content Measurement

The melanin content of the cultured B16 cells was measured as previously described [11]. Briefly, the cells were washed twice with PBS and lysed with 20 mM Tris-0.1% Triton X-100 (pH 7.5). Cell lysates were precipitated with the same amount of 20% trichloroacetic acid. After washing twice with 10% trichloroacetic acid, the pellets were treated with ethyl alcohol:diethyl ether (3:1) and diethyl ether successively. Samples were air-dried, dissolved in 1 ml 0.85 M KOH, and boiled for 15 min. After cooling, the absorbance was measured with a spectrophotometer at 440 nm. The amount of cellular melanin was corrected according to the protein content of the samples. The protein content was determined using Bradford's assay [12].

Tyrosinase Activity Assay

Tyrosinase activity was assayed based on the DOPA oxidase activity using the method described by Lerch [13], with some modification. Briefly, the cell lysate was obtained after washing the cells twice with PBS. The tyrosinase activity was analyzed spectrophotometrically following the oxidation of DOPA to DOPAchrome at 475 nm. A reaction mixture containing 100 μl of freshly prepared substrate solution (0.1% L-DOPA in 0.1 M sodium phosphate, pH 6.0) and 50 μl of enzyme solution was incubated at 37 °C. The change in absorbance was measured during the first ten minutes of the reaction, while the increase in the absorbance was linear, during which time corrections for the auto-oxidation of L-DOPA in the controls were made. The tyrosinase activity was corrected according to the protein content of the samples and is presented as a percentage relative to the IBMX-treated control cells.

Western Blotting

Cells were homogenized in ice-cold lysis buffer. Homogenates containing 10 μg of protein were separated by SDS-PAGE with a 10% resolving and 3% acrylamide stacking gel and transferred to a nitrocellulose membrane in a Western blot apparatus run at 100 V for 1.5 h. The nitrocellulose membrane was blocked with 2% bovine serum

albumin and then incubated overnight with 1 μg/ml goat anti-murine tyrosinase or anti-N-terminus of microphthalmia-associated transcription factor (MITF) IgG (Santa-Cruz Biochemicals, Santa-Cruz, CA, USA). The binding of antibody was detected with anti-goat IgG conjugated to horseradish peroxidase (Sigma). Immunoblots were developed using an Enhanced Chemiluminescence Plus kit (Amersham Biosciences, Buckinghamshire, UK).

RNA Isolation and Real-Time RT-PCR

Total cellular RNA was prepared using Trizol solution (Invitrogen, Paisley, UK) according to the manufacturer's instructions. RNA was then precipitated with isopropanol and dissolved in diethylpyrocarbonate-treated distilled water. First-strand cDNA was generated with the oligo dT-adaptor primers by reverse transcriptase (TaKaRa, Japan). Specific primers (Table 1) were designed using primer express software (Applied Biosynthesis, Foster City, CA, USA). GAPDH was used as the invariant control. The real-time PCR reaction (10 μl) contained 10 ng of reverse transcribed RNA, 200 nM each of forward and reverse primers, and a PCR master mixture. The reaction was performed in 384-well plates using the ABI Prism 7900HT sequence detection system (Applied Biosystems). All reactions were conducted in triplicate.

UVB-Induced Hyperpigmentation

UVB-induced hyperpigmentation was elicited on the skin of the upper arm of three healthy men in their 40s or 50s. Three separate areas (2 cm × 2 cm) on the inside skin of each upper arm were exposed to 400 mJ/cm^2 UVB radiation (Aurora UV-Light, Choyang Medics, Seongnam, Korea) five times a week for one week, which was sufficient for substantial hyperpigmentation to be achieved in each individual. Sap-EPO application was started 14 days after the initial UVB exposure. The sample was topically applied daily to the three hyperpigmented areas on the same arm twice a day for two successive months. The hyperpigmented areas on the other arm were left untreated as a control. The degree of pigmentation and erythema was assessed once every other week from the beginning of sample application using a Mexameter (CK, Mexameter, MPA 9, Courage, Khazaka, Germany). The whitening effect was presented as the difference in the melanogenic index (MI) from the initial sample application day. Informed written consents were obtained from all participants, and the measurements were performed in accordance to the Declaration of Helsinki.

Statistical Analysis

Data were analyzed using ANOVA and the Newman-Keuls test. A $p < 0.05$ was considered to indicate statistical significance.

Results

Inhibition of Melanin Synthesis by sap-EPO

To clarify the whitening mechanism of sap-EPO, we examined its effect on IBMX-induced melanogenesis in B16 melanoma cells. When B16 cells were incubated with IBMX, the cell suspension turned black, indicating increased cellular melanogenesis. EPO itself did not affect melanin production by B16 cells, while sap-EPO led to a dose-dependent decrease in the IBMX-induced black color (Fig. 1a). The cell viability determined by the MTT assay was not affected by EPO or sap-EPO at any of the concentrations tested (data not shown). We quantified the melanin content and observed that even 12.5 μg/ml of sap-EPO inhibited melanin production significantly (Fig. 1b). At concentrations of 100 μg/ml, cells were still viable and the cellular melanin content decreased to 12.8 ± 1.8% of the control.

Table 1 Gene accession numbers and primer sequences used in real-time RT-PCR

Gene	Sequences for primers	Accession No.
Tyrosinase	FOR: TTGCCACTTCATGTCATCATAGAATATT	NM011661
	REV: TTTATCAAAGGTGTGACTGCTATACAAAT	
TRP-1	FOR: ATGCGGTCTTTGACGAATGG	NM031202
	REV: CGTTTTCCAACGGGAAGGT	
TRP-2	FOR: CTCAGAGCTCGGGCTCAGTT	X63349
	REV: TGTTCAGCACGCCATCCA	
MITF	FOR: CGCCTGATCTGGTGAATCG	NM008601
	REV: CCTGGCTGCAGTTCTCAAGAA	
GAPDH	FOR: CGTCCCGTAGACAAAATGGT	NM008084
	REV: TTGATGGCAACAATCTCCAC	

FOR forward, *REV* reverse

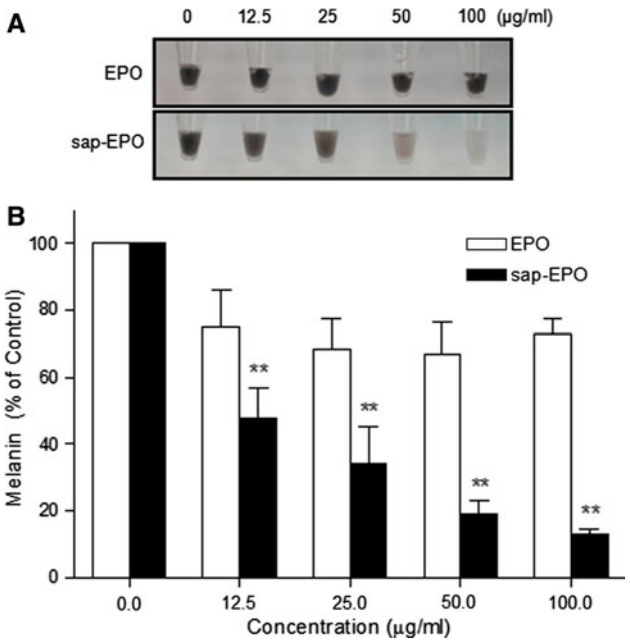

Fig. 1 Effect of EPO or sap-EPO on the melanin content of B16 melanoma cells. B16 cells (5×10^6 cells/well) were incubated with the indicated concentrations of EPO or sap-EPO in the presence of 0.1 mM IBMX for 2 days. A representative photograph is shown (**a**). Melanin contents were determined as described in the "Experimental Procedures" (**b**). Data are expressed as a percentage of the IBMX-treated controls and are presented as the mean ± SEM of three separate experiments. $^{**}p < 0.01$ versus the IBMX-treated control

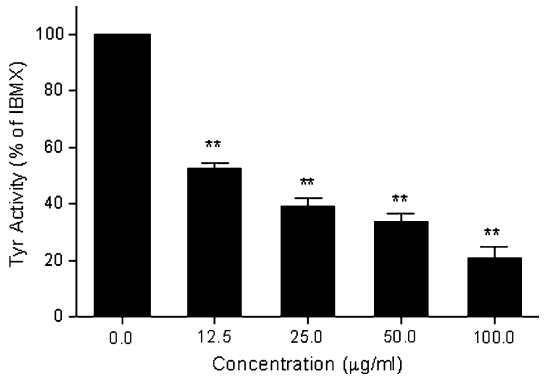

Fig. 2 Effect of saponified oils on cellular tyrosinase activity. B16 cells (5×10^6 cells) were treated with the indicated concentrations of sap-EPO in the presence of 0.1 mM IBMX for 2 days. Tyrosinase activity in the cellular lysates was determined as described in the "Experimental Procedures". Data are expressed as a percentage of the IBMX-treated controls and are presented as the mean ± SEM of three separate experiments. $^{**}p < 0.01$ versus the IBMX-treated control

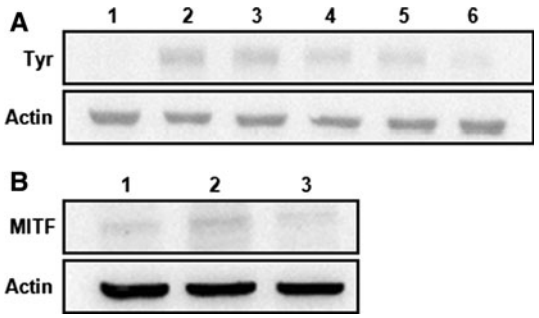

Fig. 3 Effect of saponified oils on tyrosinase and MITF protein expression. B16 cells (5×10^6 cells) were treated with the indicated concentrations of sap-EPO in the presence or absence of 0.1 mM IBMX for 2 days. Tyrosinase (**a**) and MITF (**b**) proteins were then analyzed by Western blotting. Experiments were conducted three times with similar results, and a typical trial is presented. **a** *Lane 1*, control; *lane 2*, 0.1 mM IBMX; *lane 3–5*, 0.1 mM IBMX with 12.5 (*lane 3*), 25 (*lane 4*) 50 (*lane 5*) and 100 μg/ml (*lane 6*) sap-EPO. **b** *Lane 1*, control; *lane 2*, IBMX; *lane 3*, IBMX with 50 μg/ml sap-EPO

Inhibition of Tyrosinase Activity by sap-EPO

Saponified EPO led to a dose-dependent decrease in cellular tyrosinase activity (Fig. 2), which is the rate-limiting step in melanin biosynthesis, and this decrease occurred in parallel to the decrease in melanin content (Fig. 1). However, the direct addition of sap-EPO to the reaction mixture did not impact the tyrosinase activity (data not shown), indicating that the decrease in tyrosinase activity by sap-EPO is not due to inhibition of the tyrosinase activity.

Downregulation of the Expressions of Tyrosinase and Related Genes by sap-EPO

To determine the tyrosinase expression levels of cells treated with sap-EPO, we conducted Western blot and real-time PCR analysis. IBMX treatment increased the expression of tyrosinase protein, and this induction was inhibited by sap-EPO in a dose-dependent manner (Fig. 3a). Sap-EPO also decreased the IBMX-induced tyrosinase mRNA levels (Fig. 4). These findings indicate that sap-EPO inhibits tyrosinase at the transcriptional level. Furthermore, saponified EPO decreased the IBMX-induced mRNA expression of TRP-1, TRP-2 and MITF (Fig. 4). Decreased protein level of MITF was confirmed by Western blotting (Fig. 3b).

Whitening Effect of sap-EPO on UVB-Induced Hyperpigmentation of Human Skin

The whitening effect of sap-EPO was evaluated on UVB-induced hyperpigmented human skin. At two weeks after the initial UVB irradiation of the inside skin of the upper arm, substantial hyperpigmentation and resolving of erythema was observed at the UVB irradiated sites, and topical application of sap-EPO was started. Sap-EPO was topically applied to the hyperpigmented areas two times a day for 2 months. A visible reduction in skin pigmentation

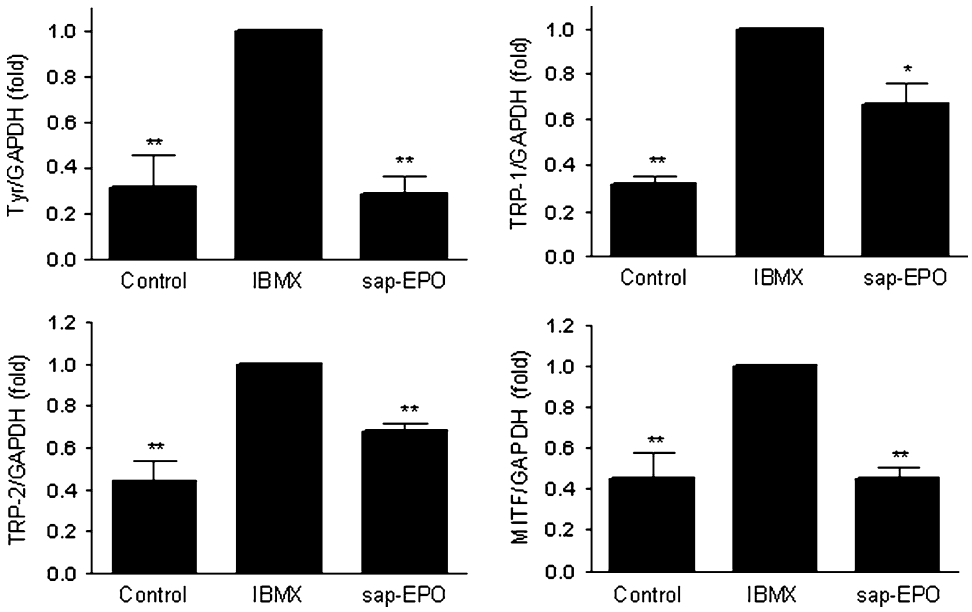

Fig. 4 Effect of saponified oils on the mRNA expressions of melanogenesis-related genes. B16 cells (5×10^6 cells) were treated with 0.1 mM IBMX for 2 days in the presence or absence of 50 μg/ml sap-EPO. Total RNA was extracted and the mRNA expression was analyzed by real-time RT-PCR. Data are expressed as the mean ± SEM of three separate experiments. *$p < 0.05$, **$p < 0.01$ versus IBMX

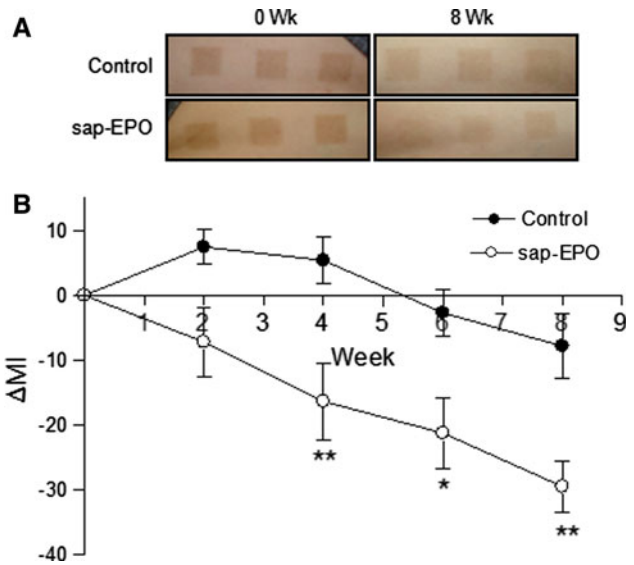

Fig. 5 Effect of sap-EPO on UVB-induced skin hyperpigmentation. UVB-induced hyperpigmentation was elicited on three separate areas on the inside skin of both upper arms. Two weeks after initial UV exposure, sap-EPO was topically applied to the hyperpigmented skin two times a day for eight weeks. Representative photographs are shown (**a**). The degree of pigmentation was assessed and the whitening effect of sap-EPO was presented as the difference in melanogenic index (*MI*) from that of the day of the initial sample application (**b**). *$p < 0.05$, **$p < 0.01$ versus the vehicle-treated control

was observed at eight weeks after the sap-EPO treatment was started when compared to control sites on the other arm of the same person (Fig. 5a). Additionally, the degree of skin pigmentation was measured using a Mexameter before the start and throughout the treatment period to allow objective determination of the treatment effects. Significant differences in the melanogenic index were observed from four weeks after the initial UVB exposure through the end of the experiment (Fig. 5b). No erythema was observed during the sap-EPO treatment.

Discussion

We conducted this study to determine if the saponified product of EPO can be used as a whitening cosmetic agent. To accomplish this, we evaluated the whitening effect of sap-EPO on UVB-induced hyperpigmented skin and IBMX-treated B16 melanoma cells.

Skin whitening compounds suppress melanogenesis in B16 melanoma cells in various ways including through cytotoxic effects on melanocytes, direct tyrosinase inhibition, and melanin biosynthesis inhibition. No cytotoxicity was observed in response to treatment with sap-EPO at the effective concentrations. Arbutin and kojic acid are known to inhibit melanogenesis by directly inhibiting tyrosinase, which is the first and rate-limiting enzyme involved in the production of melanin from tyrosine [6, 7]. We incubated sap-EPO with cellular tyrosinase and found that sap-EPO did not inhibit tyrosinase activity directly. Therefore, we focused on the effect of sap-EPO on the melanin biosynthetic pathway in melanocytes.

IBMX increases cellular cAMP by inhibiting the cAMP-degrading enzyme, phosphodiesterase [14]. Protein kinase A (PKA) phosphorylates and activates the cAMP response element binding protein that binds to the cAMP response element in the M promoter of the MITF gene [15, 16]. In humans, mutations affecting the MITF pathway lead to pigmentary and auditory defects that are known collectively

as Waardenburg syndrome [17]. The increase in MITF-M expression induces the upregulation of members of the tyrosinase gene family, resulting in increased melanin synthesis [17, 18]. In this study, we showed that sap-EPO blocked the IBMX-induced increase in melanogenesis and significantly decreased the expression of MITF mRNA and protein. This decrease was mirrored by reductions in the expression levels of tyrosinase, TRP-1 and TRP-2 mRNAs. Taken together, these results suggest that sap-EPO inhibits the melanogenic process at the transcriptional level. However, Ando et al. [22] reported that unsaturated fatty acid increased the proteolytic degradation of tyrosinase without altering the mRNA level. This discrepancy might be accounted for by the distinct cell state: we here used IBMX-stimulated melanoma cells, whereas they used the unstimulated melanocytes. A similar inhibitory effect of sap-EPO was observed when B16 cells were treated with α-melanocyte stimulating hormone or forskolin, an activator of adenylate cyclase [18] (data not shown), suggesting that sap-EPO inhibits the melanogenesis by affecting the cAMP-dependent pathway, at least in the stimulated state.

The topical application of sap-EPO effectively whitened the UV-induced hyperpigmented skin. Skin color is determined by melanin biosynthesis in melanocytes and the subsequent transfer of melanin to neighboring keratinocytes [19]. Therefore, whitening of the skin color can be achieved by inhibiting either the pathway by which melanin is synthesized in the melanocytes or the pathway responsible for the transfer of melanin to the surrounding keratinocytes. Even though we did not investigate the interaction between keratinocytes and melanocytes with regard to melanogenesis, our in vitro data suggest that the skin-whitening effect of sap-EPO was due to the suppression of melanin biosynthesis in the melanocytes.

EPO is the oil from the seed of the evening primrose (*Oenothera biennis*) plant and is one of the most commonly used herbal medications. The primary uses of evening primrose oil are for atopic dermatitis, mastalgia and lactation. Other potential uses include diabetic neuropathy, premenstrual syndrome, rheumatoid arthritis, seborrhea and fortification of infant formula [20]. Evening primrose seeds contain about 14% fixed oil, the fatty acid of which is composed of approximately 65–75% linoleic acid, 7–10% γ-linolenic acid, 9% oleic acid and some palmitic and stearic acids [20, 21]. It has been reported that linoleic and linolenic acid decrease melanin synthesis and tyrosinase activity, while saturated fatty acids increase melanogenesis [22, 23]. Linoleic acid has also been shown to increase the turnover of the stratum corneum [23]. Thus, the high proportions of unsaturated fatty acids in EPO may underlie the anti-melanogenic effect. Saponification is the hydrolysis of an ester under basic conditions to form an alcohol and the salt of a carboxylic acid. When the oil was reacted with metallic alkali, free fatty acid was released and forms soap. The effectiveness of only the saponified form of EPO indicates that the release of free form fatty acids is a prerequisite for its inhibitory action. Even though our skin experiment on the whitening effect of sap-EPO is preliminary and should be repeated using a larger number of participants, the results presented here combined with those of previous human studies conducted using purified linoleic acid [24, 25] are promising.

Sap-EPO effectively reduced melanogenesis in B16 melanoma cells and decreased pigmentation of UV exposed skin. Our findings are of great interest because EPO is already a component of the human diet and therefore likely to be relatively safe when used over long periods of time. Indeed, EPO and sap-EPO never induced erythema during this experiment. In conclusion, we demonstrated that sap-EPO exerts a pigment-whitening effect by inhibiting the expression of tyrosinase and related enzymes; therefore, we suggest that this effect may be related to the high proportions of linoleic acid released by saponification from EPO.

Acknowledgments This work was supported by a grant from the Ministry of Science & Technology (MoST)/Korea Science & Engineering Foundation (KOSEF) through the Diabetes Research Center at Chonbuk National University (R13-2008-005-0000-0).

References

1. Hearing VJ (1998) Regulation of melanin formation. In: Nordlund JJ, Boissy RE, Hearing VJ, King RA, Ortonne J-P (eds) The pigmentary system: physiology and pathophysiology. Oxford University Press, pp 423–438
2. Pawelek JM, Chakraborty AK (1998) The enzymology of melanogenesis. In: Nordlund JJ, Boissy RE, Hearing VJ, King RA, Ortonne J-P (eds) The pigmentary system: physiology and pathophysiology. Oxford University Press, pp 391–400
3. Hearing VJ, Jimenez M (1987) Mammalian tyrosinase–the critical regulatory control point in melanocyte pigmentation. Int J Biochem 19:1141–1147
4. Yokoyama K, Yasumoto K, Suzuki H, Shibahara S (1994) Cloning of the human DOPAchrome tautomerase/tyrosinase-related protein 2 gene and identification of two regulatory regions required for its pigment cell-specific expression. J Biol Chem 269:27080–27087
5. Kobayashi T, Urabe K, Winder A, Jimenez-Cervantes C, Imokawa G, Brewington T, Solano F, Garcia-Borron JC, Hearing VJ (1994) Tyrosinase related protein 1 (TRP1) functions as a DHICA oxidase in melanin biosynthesis. EMBO J 13:5818–5825
6. Draelos ZD (2007) Skin lightening preparations and the hydroquinone controversy. Dermatol Ther 20:308–313
7. Maeda K, Fukuda M (1996) Arbutin: mechanism of its depigmenting action in human melanocyte culture. J Pharmacol Exp Ther 276:765–769
8. Lim JT (1999) Treatment of melasma using kojic acid in a gel containing hydroquinone and glycolic acid. Dermatol Surg 25:282–284
9. Koo JH, Kim HT, Yoon HY, Kwon KB, Choi IW, Jung SH, Kim HU, Park BH, Park JW (2008) Effect of xanthohumol on melanogenesis in B16 melanoma cells. Exp Mol Med 40:313–319

10. Lv N, Koo JH, Yoon HY, Yu J, Kim KA, Choi IW, Kwon KB, Kwon KS, Kim HU, Park JW, Park BH (2007) Effect of *Angelica gigas* extract on melanogenesis in B16 melanoma cells. Int J Mol Med 20:763–767
11. Yang JY, Koo JH, Song YG, Kwon KB, Lee JH, Sohn HS, Park BH, Jhee EC, Park JW (2006) Stimulation of melanogenesis by scoparone in B16 melanoma cells. Acta Pharmacol Sin 27:1467–1473
12. Bradford MM (1976) A rapid and sensitive method for the quantitation of microgram quantities of protein utilizing the principle of protein-dye binding. Anal Biochem 72:248–254
13. Lerch K (1987) Monophenol monooxygenase from *Neurospora crassa*. Methods Enzymol 142:165–169
14. Beavo JA, Rogers NL, Crofford OB, Hardman JG, Sutherland EW, Newman EV (1970) Effects of xanthine derivatives on lipolysis and on adenosine 3′, 5′-monophosphate phosphodiesterase activity. Mol Pharmacol 6:597–603
15. Levy C, Khaled M, Fisher DE (2006) MITF: master regulator of melanocyte development and melanoma oncogene. Trends Mol Med 12:406–414
16. Tachibana M (2000) MITF: a stream flowing for pigment cells. Pigment Cell Res 13:230–240
17. Lin JY, Fisher DE (2007) Melanocyte biology and skin pigmentation. Nature 445:843–850
18. Busca R, Ballotti R (2000) Cyclic AMP a key messenger in the regulation of skin pigmentation. Pigment Cell Res 13:60–69
19. Imokawa G (2004) Autocrine and paracrine regulation of melanocytes in human skin and in pigmentary disorders. Pigment Cell Res 17:96–110
20. Stonemetz D (2008) A review of the clinical efficacy of evening primrose. Holist Nurs Pract 22:171–174
21. Chapkin RS, Ziboh VA, McCullough JL (1987) Dietary influences of evening primrose and fish oil on the skin of essential fatty acid-deficient guinea pigs. J Nutr 117:1360–1370
22. Ando H, Funasaka Y, Oka M, Ohashi A, Furumura M, Matsunaga J, Matsunaga N, Hearing VJ, Ichihashi M (1999) Possible involvement of proteolytic degradation of tyrosinase in the regulatory effect of fatty acids on melanogenesis. J Lipid Res 40:1312–1316
23. Ando H, Ryu A, Hashimoto A, Oka M, Ichihashi M (1998) Linoleic acid and α-linolenic acid lightens ultraviolet-induced hyperpigmentation of the skin. Arch Dermatol Res 290:375–381
24. Lee MH, Kim HJ, Ha DJ, Paik JH, Kim HY (2002) Therapeutic effect of topical application of linoleic acid and lincomycin in combination with betamethasone valerate in melasma patients. J Korean Med Sci 17:518–523
25. Shigeta Y, Imanaka H, Ando H, Ryu A, Oku N, Baba N, Makino T (2004) Skin whitening effect of linoleic acid is enhanced by liposomal formulations. Biol Pharm Bull 27:591–594

Lipids (2010) 45:409–418
DOI 10.1007/s11745-010-3415-2

ORIGINAL ARTICLE

Fatty Acid Composition of the Maternal Diet During the First or the Second Half of Gestation Influences the Fatty Acid Composition of Sows' Milk and Plasma, and Plasma of Their Piglets

Encarnación Amusquivar · John Laws · Lynne Clarke · Emilio Herrera

Received: 21 November 2009 / Accepted: 7 April 2010 / Published online: 27 April 2010

Abstract Dietary supplements of olive oil (OO) or fish oil (FO) during the first (G1: day 1–60) or second half of gestation (G2: day 60 to term, day 115) were offered to pregnant sows. The proportion of fatty acids in milk and plasma were determined by gas chromatography. When supplements were given during G1, the proportions of oleic acid (OA) and arachidonic acid (AA) in the plasma were higher in the OO group than in the FO group, whereas docosahexaenoic acid (DHA) was higher in the latter group at day 56 of gestation. These differences in plasma DHA were still apparent at day 7 of lactation. Similarly, DHA was also higher in the colostrum and milk on days 3 and 21 of lactation and in the plasma of piglets from FO dams compared to the OO group, whereas AA was lower. When the FO supplement was given during G2, AA was lower and DHA higher in the plasma at day 105 of gestation and at day 7 of lactation compared with the OO group. Likewise, DHA was greater in FO than in OO animals during lactation in colostrum and in milk on days 3 and 21 of lactation, and in 3-day old suckling piglets plasma, whereas AA was lower in these animals. Thus, maternal adipose tissue plays an important role in the storage of dietary long-chain polyunsaturated fatty acids (LCPUFA) during G1. They are mobilized around parturition for milk synthesis, and an excess of dietary n-3 LCPUFA decreases the availability of AA in suckling newborns.

Keywords Pregnancy · Lactation · Pigs · Diet · Fatty acids · Adipose tissue

Abbreviations

OO	Olive oil
FO	Fish oil
G1 and G2	First and second half of gestation, respectively, used for the experimental diets
DHA	Docosahexaenoic acid
AA	Arachidonic acid
EFA	Essential fatty acids
LCPUFA	Long-chain polyunsaturated fatty acids
LA	Linoleic acid
ALA	α-linolenic acid
LPL	Lipoprotein lipase
VLDL	Very low density lipoproteins

Introduction

The dietary essential fatty acids (EFA), linoleic acid (LA, 18:2 n-6) and α-linolenic acid (ALA, 18:3 n-3) and their long-chain polyunsaturated derivatives (LCPUFA) are essential for the formation of new tissues during fetal and postnatal development. The presence of high proportions of certain LCPUFA in vital organs such as the central nervous system of the developing neonate emphasizes their importance [1]. In addition, AA and eicosapentaenoic acid (EPA, 20:5 n-3) are precursors of eicosanoids affecting a variety of biological functions, including immunity [2, 3].

E. Amusquivar · E. Herrera (✉)
Faculties of Pharmacy and Medicine, Universidad CEU San Pablo, Ctra. Boadilla del Monte km 5.3, 28668 Boadilla del Monte (Madrid), Spain
e-mail: eherrera@ceu.es

J. Laws · L. Clarke
Department of Agricultural Sciences, Faculty of Natural Sciences, Imperial College London, Wye, Ashford, Kent TN25 5AH, UK

In humans, the conversion of EFA into LCPUFA is relatively slow [1], and this is especially so in the fetus and neonate in as much as the rate of conversion is unable to support optimal growth and development if LCPUFA deficiency occurs [4–6]. During intrauterine life the fetal supply of both EFA and LCPUFA depends on their concentration in maternal circulation as well as on their placental transfer. In suckling newborns the availability of fatty acids depends on their profile in milk, which is influenced by those ingested by their lactating mother [7]. Moreover, the fatty acids profile of newborn piglets has been shown to be affected by the fatty acids ingested by the mother at different times during pregnancy and lactation [8–10].

During the first half of gestation enhanced lipoprotein lipase (LPL) activity in adipose tissue [11, 12] contribute to the accumulation of fat depots in the mother. Through such augmented LPL activity in adipose tissue, dietary derived LCPUFA transported as triacylglycerols in chylomicrons and very low density lipoproteins (VLDL) are hydrolyzed and the released fatty acids are taken up for storage in the subjacent tissue. During the last third of pregnancy the situation drastically changes; LPL activity in adipose tissue decreases [13, 14], which together with an enhanced lipolytic activity [15, 16] results in the net accelerated breakdown of fat depots. Conversely, the reverse situation occurs in the mammary gland [13] with an increase in LPL activity around parturition, which remains during lactation [17, 18]. Thus, throughout this process, dietary fatty acids in plasma triacylglycerols, mainly carried in chylomicrons and VLDL, can be transported to the mammary gland where they can be used for milk synthesis. Moreover, studies using stable isotopes in lactating women have shown that diet-derived LCPUFA account for about 30% of fat milk [19] and in the late pregnant rat receiving orally labelled triacylglycerols, it has been found that dietary lipids actively contribute to lipid uptake by the mammary gland [20].

On the basis of these antecedents, we hypothesize that diet-derived LCPUFA during early pregnancy are stored in maternal adipose tissue and released into the circulation around parturition. Once converted into their esterified form by the liver and returned to blood, they are taken up by the mammary gland for milk synthesis, thus becoming available to the suckling newborn. The role of dietary fatty acids during either early pregnancy or late pregnancy on milk composition has not yet been fully established. Due to the similarities in the fatty acid metabolism in human and pigs [21] and in order to test our hypothesis, this study aimed to determine the consequences of modifying the fatty acid composition of sows' diets, using dietary supplements with olive oil (OO) or fish oil (FO), during the first or the second half of gestation on the fatty acid profiles of maternal plasma and milk during lactation and in plasma of suckling neonates. The present study is a continuation of previous ones using the same treatment protocol in pregnant sows where it was found that with the exception of a slightly improved growth performance in offspring of FO fed sows, no difference was found in reproductive performance between the two groups [22–25].

Methods

Animals and Diets

All animals used in this study were maintained at the Pig Research and Development Unit, Imperial College, London. Experimental procedures were carried out according to the regulations of the Animals (Scientific Procedures) Act, 1986 and were licensed by the Home Office (UK). At all stages of life, animals were kept according to the guidelines set out by the Department for Environment Food and Rural Affairs (DEFRA 2003).

Multiparous sows of the same commercial genotype (25% Meishan; 12.5% Duroc; 62.5% Large White × Landrace) were selected for study after the previous litter had been weaned and prior to insemination. All sows were artificially inseminated with pooled Large White semen (P17 2006, JSR Genetics). Sows were categorized by parity before being randomly assigned to one of four dietary treatment groups, to ensure that parity was balanced across treatments. Pregnant sows were offered 3 kg/day of the standard diet (ABN HE sow pellets; 13.1 MJ/kg ME; 12.7% protein; 4.5% fat; ABN, Peterborough, Cambridgeshire, UK) plus 10% extra energy derived from either OO ($n = 8$) or FO ($n = 8$) offered during either the first half of gestation (G1: i.e. day 1 of gestation, assuming day of service to be day 0) and continued until day 60 of gestation or the second half of gestation (G2: i.e. day 60 of gestation) and continued until term ($\approx$day 115). The fatty acid profiles of the different diets can be seen in Table 1. After parturition sows were offered 6–9 kg of a lactation diet (ABN supreme lactation pellets; 14.1 MJ/kg ME; 18% protein; 7.2% oil; ABN, Peterborough, Cambridgeshire, UK: Table 1).

Sample Collection

Sow blood samples were collected from the jugular vein on days −5, 56, 105, 115 of gestation and day 7 postpartum and piglet blood samples were collected from the external jugular vein at days 3 and 21 of lactation. Blood was always collected in Na_2-EDTA blood tubes (Teklab, UK) and after centrifugation for 15 min at 1,600×g, plasma aliquots were stored at −20 °C until analysis.

Table 1 Fatty acid composition of the diets

	Olive oil (OO) diet	Fish oil (FO) diet	Standard diet	Lactation diet
Fatty acids (g/100 g fatty acids)				
14:0	0.43	2.35	0.53	0.85
16:0	16.37	16.33	18.24	20.42
18:0	3.11	2.79	3.14	5.23
16:1 (n-7)	0.77	3.28	0.32	0.25
18:1 (n-9)	46.59	19.50	20.00	32.78
18:2 (n-6)	27.17	32.24	50.2	34.84
18:3 (n-6)	0.01	0.03	n.d.	n.d.
18:3 (n-3)	2.3	3.48	4.75	3.97
20:1 (n-9)	0.67	4.12	0.66	0.36
20:4 (n-6)	0.02	0.25	n.d.	0.01
20:5 (n-3)	1.00	4.34	0.35	0.31
22:1 (n-9)	0.25	4.16	0.38	n.d.
22:5 (n-3)	0.14	1.22	n.d.	n.d.
22:6 (n-3)	0.35	4.73	0.21	0.08

Values correspond to the mean of three separate samples processed independently

n.d. Not detected

Colostrum samples were collected on the day of parturition, within 4 h of the first piglet being born. Milk samples were collected on days 3, 7 and 21 of lactation following intra-muscular administration of 2 mL oxytocin (10 i.u./mL; NVS, UK). Immediately after its collection, aliquots of milk were frozen at −80 °C until analysis.

Sample Analyses

Lipids were extracted and purified in chloroform:methanol (2:1) [26] in the diets, plasma, colostrum and milk samples. Total lipid extracts were saponified and the fatty acids methylated following the method of Lepage and Roy [27, 28]. Fatty acid methyl esters were separated on a 30 m × 0.25 mm Omegawax capillary column (Supelco, Bellefonte, PA, USA) and quantified using a PerkinElmer gas chromatograph (Autosystem; Norwalk, CT, USA) with a hydrogen flame ionization detector. Nitrogen was used as a carrier gas, and the fatty acid methyl esters were compared with purified standards (Sigma Chemical Co., St. Louis, MO, USA).

Statistical Analyses

Data are expressed as means ± SE. Statistical differences between groups were determined by ANOVA, and Tukey's test was used when differences were statistically significant ($p < 0.05$) by using SPSS 15.0 for Windows, Differences between two groups were analyzed by Student's *t* test.

Results

G1 sows were in positive energy balance during the first half of gestation as their backfat thickness increased over this period (OO 4 ± 1: FO 5 ± 1 mm). However, they were in negative energy balance during the last half of gestation because despite a significant increase in body weight (OO 30 ± 3: FO 29 ± 3 kg) there was little change in their backfat thickness (1 ± 1 mm). G2 sows were not in negative energy balance at any time throughout the study, as shown by their body weight and backfat thickness increase during the first (OO 21 ± 4, FO 24 ± 3 kg and OO 1 ± 1, FO 3 ± 1 mm, respectively), and the second half of gestation (OO 36 ± 3, FO 36 ± 3 kg an OO 4 ± 1, FO 5 ± 1 mm, respectively). This is what it was expected since during the second half of gestation the dietary intake of the G2 sows was above their energy requirements for this stage of pregnancy.

Basal values of plasma fatty acid profiles 5 days before pregnancy or just at the time of starting the corresponding dietary treatments did not differ between the groups (data not shown). When sows received the OO or FO dietary supplements during G1, neither the sum of total saturated fatty acids (12:0, 14:0, 16:0 plus 18:0) nor the sum of n-6 PUFAs (18:2 and 20:4) in maternal plasma differed between the two groups, at either day 56 of gestation or at day 7 of lactation (Table 2). However, the sum of the plasma monounsaturated fatty acids (16:1 n-7 and 18:1 n-9) at day 56 of gestation was higher in G1 OO sows compared to G1 FO mothers with this difference disappearing by day 7 of lactation. The sum of the n-3 PUFAs (18:3 n-3, 20:5 n-3 and 22:6 n-3) appeared higher in G1 FO, particularly at day 56 of pregnancy. When considering the longitudinal changes of the most characteristic fatty acids in plasma of the G1 sows (Fig. 1a), it is seen that oleic acid (OA) increased during the phase that sows were receiving the OO supplement (day 56 of gestation) whereas it decreased in those supplemented with FO, although this

Table 2 Fatty acid composition of maternal plasma in sows receiving the olive oil or fish oil supplemented diet during the first or the second half of pregnancy (g/100 g fatty acids)

	Olive oil diet	Fish oil diet	Olive oil diet	Fish oil (FO) diet
Maternal sows receiving a supplemented diet during the first half of gestation (G1)				
	Day 56 of gestation		*Day 7 of lactation*	
Saturated FA	25.2 ± 2.8	27.8 ± 1.7	35.1 ± 1.3	30.7 ± 1.6
Monounsaturated FA	31.5 ± 2.1	20.6 ± 0.4***	22.8 ± 1.3	21.8 ± 1.5
n-6 PUFA	39.1 ± 0.8	37.5 ± 1.9	37.5 ± 0.3	39.7 ± 1.2
n-3 PUFA	3.9 ± 0.4	15.8 ± 1.7***	4.4 ± 0.7	7.8 ± 0.6**
Maternal sows receiving a supplemented diet during the second half of gestation (G2)				
	Day 105 of gestation		*Day 7 of lactation*	
Saturated FA	28.6 ± 0.8	30.2 ± 1.5	30.1 ± 1.2	35.8 ± 1.7*
Monounsaturated FA	29.5 ± 1.3	20.9 ± 0.5***	23.5 ± 1.1	20.7 ± 0.2*
n-6 PUFA	38.4 ± 1.2	31.6 ± 0.7**	41.9 ± 1.7	35.5 ± 1.3*
n-3 PUFA	3.4 ± 0.3	17.2 ± 1.4***	4.4 ± 0.7	7.8 ± 0.8*

Values correspond to means ± SE of five dams per group

Student's *t* test comparisons between the two groups within the same day are shown by *asterisks*: * $p < 0.05$, ** $p < 0.01$, *** $p < 0.001$

difference was no longer apparent on day 7 of lactation (Fig. 1a). As expected, the proportion of AA in plasma was similar between the two groups in basal samples (day 0), but concentrations declined by day 56 in the G1 FO sows and only returned to values that did not differ from basal levels by day 7 of lactation (Fig. 1a). The proportion of DHA in plasma increased from basal levels at day 56 in the sows fed the FO supplemented diet and remained elevated at day 7 of lactation (Fig. 1a), despite these animals not received FO supplement from day 60 of gestation onwards.

The proportion of saturated fatty acids in colostrum and milk did not differ between the two G1 groups at any of the time points studied (Table 3). In contrast, monounsaturated fatty acids were higher in both colostrum and milk at day 3 of lactation in G1 OO compared to G1 FO sows, whereas the proportion of n-6 PUFA in colostrum and of n-3 PUFA in milk of day 3 were lower in the former group, with no other differences observed between the two groups in these variables (Table 3). On further examination of these aforementioned differences, OA appeared higher in both colostrum and milk of 3 days in G1 OO sows than in G1 FO, whereas no differences were found in AA but DHA was higher in either colostrum or milk in the sows that received the FO supplement as compared to the G1 OO group (Fig. 1b).

As expected, plasma obtained from suckling piglets also reflected those changes observed in FA milk composition (Table 4); at day 3 of lactation, piglets from G1 OO dams exhibited a higher proportion of monounsaturated fatty acids and a lower proportion of n-3 PUFAs than those of the FO group, whereas these differences disappeared at day 21 of lactation. These changes in piglets born to G1 sows corresponded to a lower proportion of OA in their plasma at day 3 of lactation, a significant decrease in AA at both day 3 and 21 of lactation, and an increase in DHA at day 3 (Fig. 1c).

Differences were also shown when pregnant sows received the supplements during G2. Amounts of saturated fatty acids in sow plasma at day 105 of gestation were similar between the G2 OO and G2 FO groups, whereas both monounsaturated and n-6 PUFAs were higher and n-3 PUFA were lower in the former group (Table 2). At day 7 of lactation, the proportion of saturated fatty acids and of n-3 PUFAs in plasma were lower in the G2 OO group than in G2 FO, whereas the proportions of monounsaturated fatty acids and n-6 PUFA were higher. In the case of the G2 OO sows such differences corresponded to an increase in plasma OA at day 105 of pregnancy and day 7 of lactation (Fig. 2a). Whereas in G2 FO mothers there was a decline in the proportion of AA at day 105 of gestation, values had recovered by day 7 of lactation; there was also an increase in the proportion of DHA at both day 105 of gestation and 7 of lactation.

Despite these changes observed in maternal plasma, with the exception of a higher proportion of n-3 PUFA in G2 FO compared to G2 OO sows, corresponding to an increase in DHA at day 3 and day 21 of lactation (Fig. 2b), and an increase in EPA in colostrum and milk at 3 days of lactation (data not shown), neither of the other studied fatty acids differed between G2 FO and G2 OO in colostrum or mature milk (Table 3).

In the plasma of piglets born to G2 OO sows as compared to G2 FO sows the proportion of monounsaturated fatty acids was higher, whilst n-3 PUFAs were lower at day

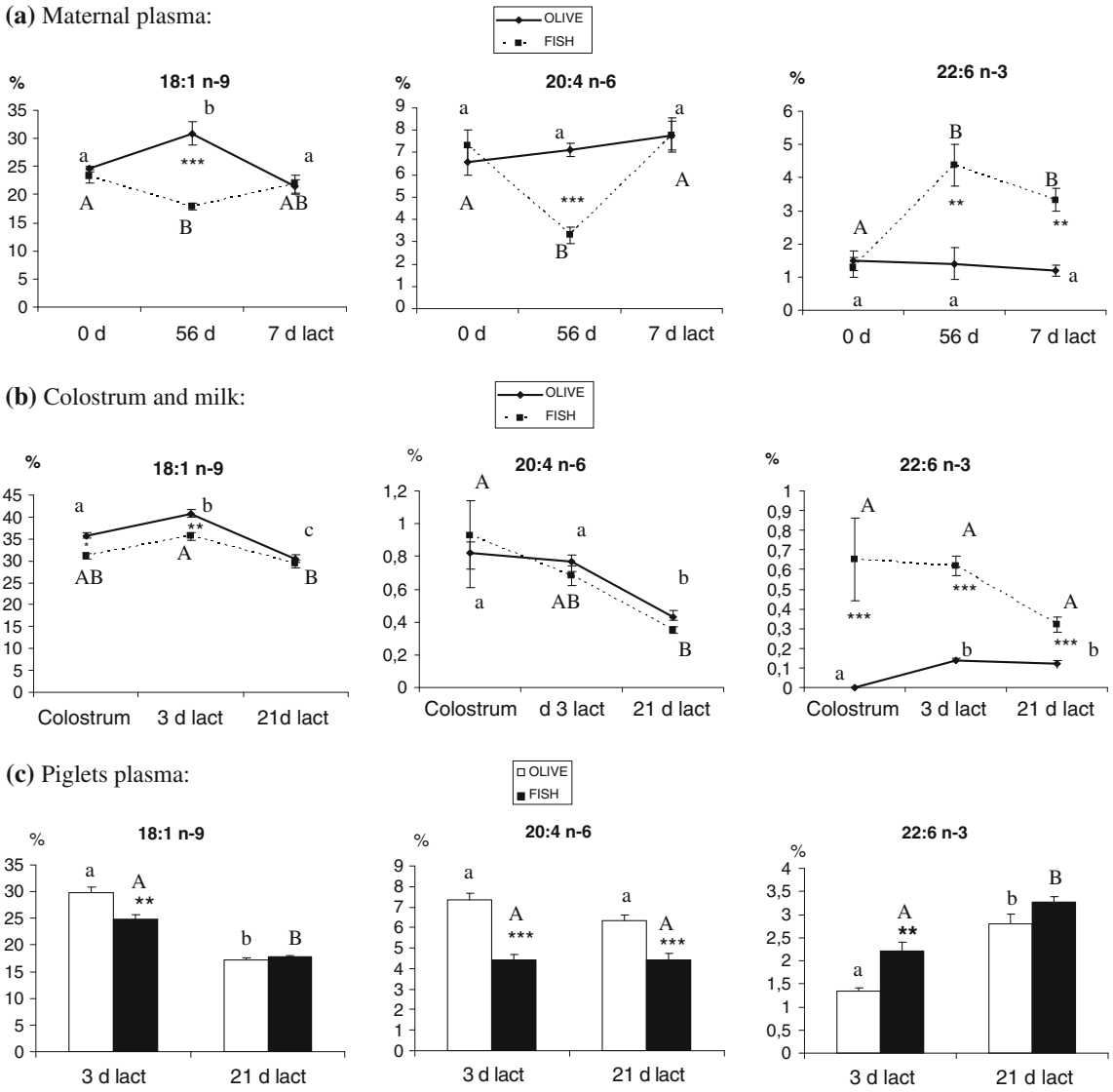

Fig. 1 Proportions of oleic, arachidonic and docosahexaenoic acids in maternal plasma, colostrum and milk and piglets plasma from sows fed either olive oil supplemented diet or fish oil supplemented diet during the first half of gestation. (% = g/100 g fatty acid). Student's *t* test was used to compare values between olive oil and fish oil groups within the same day and are shown by *asterisks*: $*p < 0.05$, $**p < 0.01$, $***p < 0.001$. Tukey's test was used to determine differences between different time points after one-way ANOVA and shown by *small letters* in the olive oil group and by *capital letters* in the fish oil group (*different letters* indicating statistically significant differences, $p < 0.05$)

3 of lactation, with these differences disappearing by day 21 of lactation (Table 4). In the case of the G2 OO piglets the difference in the monounsaturated fatty acids seen at day 3 corresponded to higher OA (Fig. 2c), whereas the differences in n-3 PUFA corresponded to a higher proportion of DHA in those of the FO group. Additionally, these same animals exhibited a lower proportion of AA in plasma at day 3, but at day 21 of lactation plasma AA did not differ between the two groups (Fig. 2c). This finding differs from that commented above for the maintenance of decreased plasma AA values up to 21 days of age in G1 FO piglets when compared to those of G1 OO.

Discussion

These results in pregnant and lactating sows show for the first time that fatty acid composition during either the first half or the second half of gestation greatly influence the fatty acid profile of maternal plasma during lactation, of colostrum and mature milk and even of suckling piglets' plasma. Furthermore, they show that suckling piglets of mothers receiving a FO supplement compared to those receiving an OO supplement have a decreased proportion of AA in the plasma, with the effect being more pronounced and lasting longer (until day 21 of lactation) in

Table 3 Fatty acid composition of colostrum and milk of lactating sows that received dietary olive oil or fish oil supplements during the first or the second half of gestation (g/100 g fatty acids)

	Colostrum		Milk, 3 days of lactation		Milk, 21 days o f lactation	
	Olive oil diet	Fish oil diet	Olive oil diet	Fish oil diet	Olive oil diet	Fish oil diet
Sows receiving a supplemented diet during the first half of gestation (G1)						
Saturated FA	29.9 ± 1.0	29.3 ± 0.9	30.9 ± 0.9	33.7 ± 1.0	39.1 ± 1.1	40.1 ± 1.3
Monounsaturated FA	39.4 ± 1.8	33.7 ± 0.8*	47.0 ± 0.8	42.6 ± 0.9**	40.0 ± 1.0	38.7 ± 0.8
n-6 PUFA	27.1 ± 1.6	32.7 ± 0.5*	18.9 ± 0.9	19.0 ± 1.0	17.7 ± 0.7	17.7 ± 0.6
n-3 PUFA	3.4 ± 0.6	3.9 ± 0.5	2.4 ± 0.2	4.0 ± 0.4**	2.7 ± 0.1	3.0 ± 0.2
Sows receiving a supplemented diet during the second half of gestation (G2)						
Saturated FA	29.5 ± 1.0	29.0 ± 0.8	33.4 ± 1.4	32.0 ± 1.2	40.8 ± 1.1	38.7 ± 1.6
Monounsaturated FA	37.2 ± 3.0	38.9 ± 0.9	45.2 ± 1.3	43.1 ± 1.6	37.8 ± 1.2	38.9 ± 1.2
n-6 PUFA	29.0 ± 2.2	28.3 ± 1.2	18.1 ± 0.9	17.9 ± 2.0	17.4 ± 0.5	18.6 ± 0.6
n-3 PUFA	2.8 ± 0.3	3.4 ± 0.1	2.5 ± 0.2	4.3 ± 0.4***	3.1 ± 0.4	3.3 ± 0.3

Values correspond to means ± SE of (5–8) dams per group

Student's *t* test comparisons between the two groups within the same day are shown by *asterisks*: * $p < 0.05$, ** $p < 0.01$, *** $p < 0.001$

Table 4 Fatty acid composition of plasma of piglets from sows receiving either a dietary olive oil or a fish oil supplement during the first or the second half of pregnancy (g/100 g fatty acids)

	Day 3 lactation		Day 21 lactation	
	Olive oil diet	Fish oil diet	Olive oil diet	Fish oil diet
Sows receiving a supplemented diet during the first half of gestation (G1)				
Saturated FA	36.3 ± 0.9	38.6 ± 1.3	39.7 ± 1.0	42.4 ± 1.2
Monounsaturated FA	33.0 ± 1.0	29.2 ± 0.8*	21.2 ± 0.6	21.8 ± 0.4
n-6 PUFA	28.9 ± 1.0	29.7 ± 1.7	35.7 ± 1.2	32.2 ± 1.3
n-3 PUFA	1.8 ± 0.1	2.5 ± 0.2**	3.3 ± 0.3	3.7 ± 0.1
Sows receiving a supplemented diet during the second half of gestation (G2)				
Saturated FA	37.9 ± 1.0	38.0 ± 0.8	41.4 ± 1.1	40.8 ± 1.8
Monounsaturated FA	32.6 ± 1.7	27.7 ± 0.7*	25.0 ± 0.9	24.2 ± 1.2
n-6 PUFA	27.4 ± 2.2	29.6 ± 0.6	28.7 ± 1.3	31.4 ± 1.2
n-3 PUFA	2.1 ± 0.3	4.7 ± 0.4***	2.6 ± 0.43	3.5 ± 0.3

Values correspond to means ± SE of 6–7 dams per group

Student's *t* test comparisons between the two groups within the same day are shown by *asterisks*: * $p < 0.05$, ** $p < 0.01$, *** $p < 0.001$

those piglets of sows receiving the supplemented diet during G1 compared to G2. Since AA was practically absent in the maternal diet, these findings may be due to altered endogenous synthesis of this fatty acid. Although it is well established that the essential fatty acid composition of human colostrum and milk is dependent on adipose tissue stores during lactation [29, 30] present findings support the notion that fat depots normally accumulated during pregnancy, and more specifically during its anabolic stage (i.e., its first half) [31, 32] constitute an important source of LCPUFA for milk synthesis during lactation. These results agree with the known effective influence of dietary PUFA enhancing the proportion of n-3 fatty acids of fat tissue in pigs [33, 34].

Dietary Supplement During the First Half of Gestation

Present findings clearly show that diet supplement with either OO or FO during G1 modify the fatty acid profile of plasma not only at the end of the dietary treatment period but during lactation, as well as the FA composition of both the colostrum and mature milk. This is especially highlighted by the increase of DHA found in G1 FO sows; it is speculated that such changes must be originally caused by its high presence in this oil. In fact, although α-linolenic acid (ALA) can be converted into DHA, from studies in humans it is known that the conversion is low, especially when the absolute amount of ALA in the diet is low [35], as it was the case in our animals, which ALA in the diet

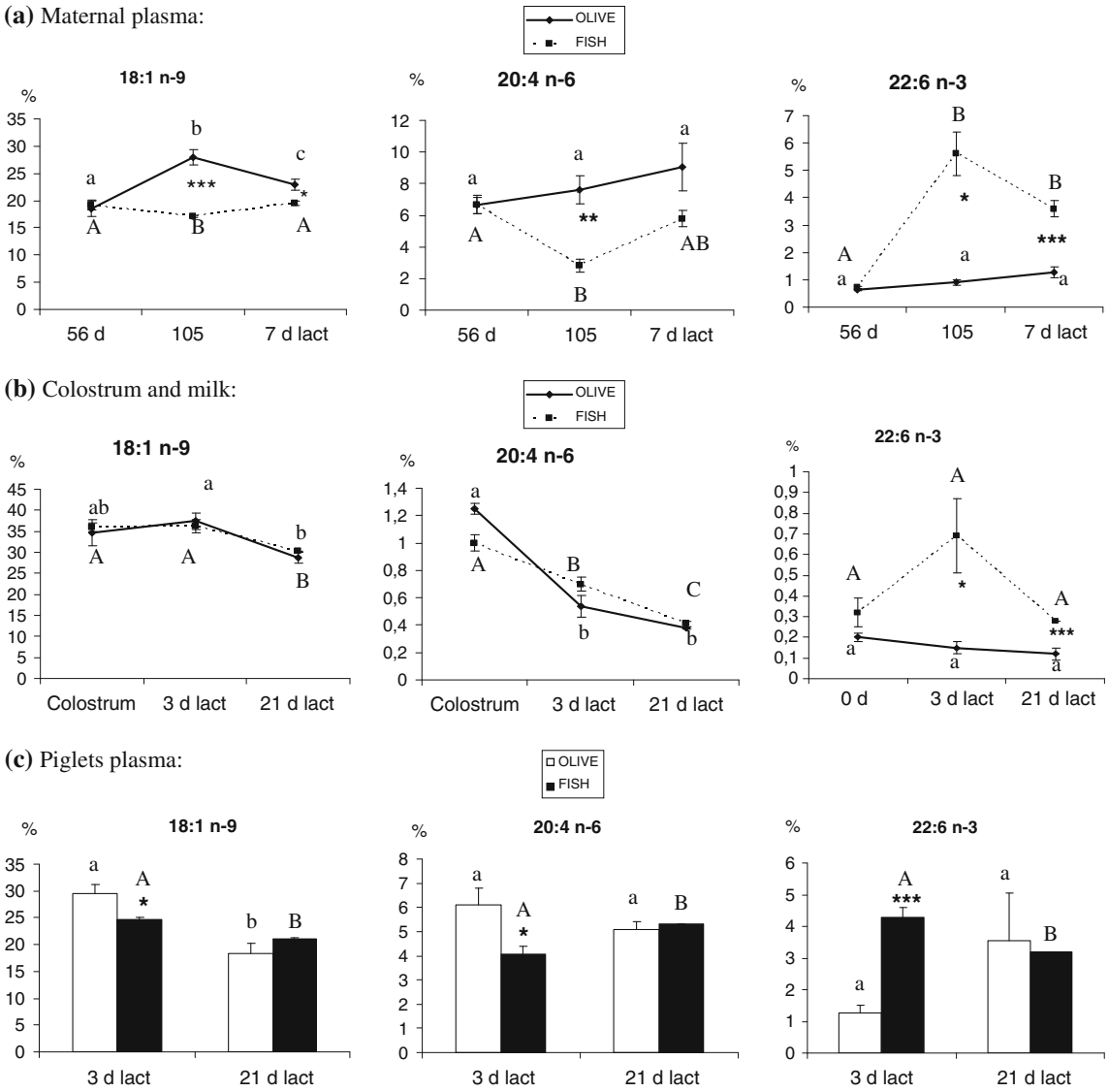

Fig. 2 Proportions of oleic, arachidonic and docosahexaenoic acids in maternal plasma, colostrum and milk and piglets plasma from sows fed either an olive oil supplemented diet or a fish oil supplemented diet during the second half of gestation. (% = g/100 g fatty acid). Student's *t* test was used to compare values between olive oil and fish oil groups within the same day and are shown by *asterisks*: $*p < 0.05$, $**p < 0.01$, $***p < 0.001$. Tukey's test was used to determine differences between different time points after one-way ANOVA and shown by *small letters* in the olive oil group and by *capital letters* in the fish oil group (*different letters* indicating statistically significant differences, $p < 0.05$)

was practically absent. Our explanation for this increase in DHA in both lactating sow plasma and in milk, more than 50 days after dietary supplementation had ceased, is that DHA was accumulated in adipose tissue during the first half of gestation, when the animals were receiving the fish oil supplement, and subsequently released around parturition.

In sows, when energy intake is adequate, during gestation there is an increase in body fatness [36], the effect being particularly striking during the first half of gestation [37]. Besides, studies in humans and in rats, have revealed that the mother is in an anabolic condition during the first half of pregnancy as result of enhanced plasma insulin levels [38, 39] and insulin sensitivity [32, 40, 41], and this justifies the augmented LPL activity found in adipose tissue in the rat at mid pregnancy [12, 42]. Thus, circulating LCPUFA transported in their esterified form associated to triacylglycerol-rich lipoproteins [11, 31, 43] are hydrolyzed by the LPL activity present in capillary endothelium of adipose tissue and released fatty acids are taken up by the subjacent tissue to be reesterified for storage. Indeed, under non-pregnant conditions it has been shown that in human adipose tissue the relative mobilization rate of DHA is lower than of other LCPUFA [44], and in the rat fed FO

diet it has been demonstrated that this fatty acid is retained in adipose tissue during late pregnancy at a higher proportion that any other LCPUFA [45]. It is, therefore, proposed that DHA after being taken up and stored in adipose tissue during the first half of pregnancy is mobilized during late pregnancy and the first days of lactation, when lipolytic activity is highly enhanced [17, 46, 47], becoming available to the mammary gland for milk synthesis. This proposal fits with the high proportion of DHA seen in the plasma at day 7 of lactation and in colostrum and milk at days 3 and 21 of lactation in sows on the diet supplemented with FO during G1.

The highest proportion of DHA in plasma seen in G1 FO sows during the last days of their treatment was associated with a decreased proportion of AA. As AA was practically absent in the diet, plasma AA must come from endogenous synthesis, and such a decline in AA could be therefore interpreted as an inhibition of this pathway as a result of the well-known inhibitory effect of DHA on the Δ6 desaturase [48, 49], which is a key enzyme for AA synthesis from its essential fatty acid precursor, linoleic acid. Since AA does not differ in colostrum or milk of sows that received the FO or OO supplement, probably due to the fact that mammary gland AA synthesis from linoleic acid is low [50], a similar reasoning could be applied to the decreased proportion of AA consistently seen in the plasma of piglets of sows receiving a FO-supplemented diet during G1. The augmented proportion of DHA present in colostrum and mature milk would allow a higher availability of this fatty acid to the suckling piglets' liver, where the most active synthesis of AA takes place, thereby inhibiting this pathway. Moreover, AA synthesis has been shown to be effective in term and preterm infants [4, 51–53] and fetal baboons [54], and we propose that it is also active in our suckling piglets, with this pathway being inhibited at early lactation in those animals born to G1 FO sows as a consequence of their enhanced availability of DHA.

Dietary Treatment During the Second Half of Gestation

The effects of fatty acid dietary supplementation during the second half of gestation found here agree with and amplify those previously reported. The influence of dietary fatty acids during lactation on milk fatty acid composition has been well recognized in humans [19, 55, 56] and has been associated to the fatty acid composition in maternal adipose tissue [29, 30]. Dietary fatty acids during pregnancy in rats have been shown to determine their proportion in maternal adipose tissue [45, 57, 58], and feeding tuna oil in sows during late pregnancy is known to affect fatty acid composition in newborn piglet tissues and plasma [8, 59].

During the last third of gestation the mother is in a net catabolic condition, where breakdown of fat depots is increased and maternal hyperlipidemia develops [32]; circulating PUFAs coming from either the diet or released from adipose tissue are mainly transported in their esterified form associated to different lipoproteins [31, 43]. Around parturition there is an induction of LPL activity in the mammary gland [13], which drive circulating triglyceride-rich lipoproteins to mammary gland [20] for their hydrolysis and tissue uptake of the hydrolytic products, actively contributing to the disappearance of such maternal hyperlipidemia and to the onset of milk synthesis. Since both mammary gland LPL and adipose tissue lipolytic activity remain augmented during lactation, it is not surprising that LCPUFA present in maternal adipose tissue could affect maternal plasma and milk fatty acid composition for a certain period of time, independently of the diet composition at that particular time. This was seen in the current study as the proportion of n-3 fatty acids, and more specifically of DHA in plasma and milk at 7 and 21 days after parturition, respectively, were higher in lactating sows that were fed the FO supplemented diet during G2 compared to those receiving an OO supplemented diet.

It is worth commenting that the OO supplemented diet only increased the proportion of OA in maternal plasma during the experimental period. This is probably a consequence of the active Δ9 desaturase normally present in the adult liver and in the mammary gland during lactation [60, 61], which facilitates an active OA synthesis. Its proportion in lactating sows plasma and in colostrum or mature milk becomes independent of what the sows were fed during the G2. Here again, special attention should be paid to the AA values. The absence of this fatty acid in any of the diets forces the endogenous synthesis from its main source linoleic acid. As commented above, the inhibitory action of DHA and EPA on the Δ6 desaturase seems to be responsible for the low proportion of AA shown in maternal plasma of sows fed with a diet supplemented with FO as well as in plasma of their piglets at day 3 of suckling.

Conclusion

Although further studies are needed to establish the efficacy of the various feeding strategies to provide n-3 LCPUFA for foetal and infant development and growth, the present findings allow us to reach the following conclusions.

The maternal dietary fatty acid composition, specifically during the first half of gestation, influences the fatty acid composition in the milk of lactating sows and in the plasma of newborn piglets in a manner similar to the influence of maternal dietary fatty acid composition during the second half of gestation. This indicates an important role of maternal adipose tissue as a store of dietary LCPUFA,

especially DHA, during the anabolic stage of gestation, which are mobilized around parturition and early lactation to be used for milk synthesis, making them available to the suckling newborn. Also, an excess of dietary n-3 LCPUFA, like DHA and EPA caused by a FO supplement during pregnancy, decreases the availability of AA in suckling newborns.

Acknowledgments We thank Milagros Morante, Kate Perkins, Anne Corson and Jennie Litten, for their excellent technical assistance and the staff at Imperial College London's pig unit for the maintenance and supply of animals used in this study. Supported by grants from the European Community (specific RTD programme "Quality of Life and Management of Living Resources", QLK1-2001—00138, PeriLip) and Ministerio de Educación y Ciencia (SAF2008-04518) of Spain.

References

1. Hornstra G (2000) Essential fatty acids in mothers and their neonates. Am J Clin Nutr 71(suppl):1262S–1269S
2. Calder PC (1998) Dietary fatty acids and the immune system. Nutr Rev 56:570–583
3. Calder PC, Krauss-Etschmann S, de Jong EC, Dupont C, Frick JS, Forkiaer H, Heinrich J, Garn H, Koletzko S, Lack G, Mattelio G, Renz H, Sngild PT, Schrezenmeir J, Stulnig TM, Thymann T, Wold AE, Koletzko B (2006) Early nutrition and immunity-progress and perspectives. Br J Nutr 96:774–790. doi:10.1079/BJN20061881
4. Demmelmair H, Schenk U, Behrendt E, Sauerwald T, Koletzko B (1995) Estimation of arachidonic acid synthesis in full term neonates using natural variation of ^{13}C content. J Pediatr Gastroenterol Nutr 21:31–36
5. Makrides M, Neumann MA, Byard RW, Simmer K (1994) Fatty acid composition of brain, retina and erythrocytes in breast- and formula-fed infants. Am J Clin Nutr 60:189–194
6. Van Aerde JE, Wilke MS, Feldman M, Clandinin MT (2004) Accretion of lipid in the fetus and newborn. In: Fox WW, Abman SH, Polin RA (eds) Fetal and neonatal physiology. W.B. Saunders, Philadelphia
7. Arbuckle LD, Innis SM (1993) Docosahexaenoic acid is transferred through maternal diet to milk and to tissues of natural milk-fed piglets. J Nutr 123:1668–1675
8. Rooke JA, Sinclair AG, Edwards SA (2001) Feeding tuna oil to the sow at different times during pregnancy has different effects on piglet long-chain polyunsaturated fatty acid composition at birth and subsequent growth. Br J Nutr 86:21–30. doi:10.1079/BJN2001363
9. Rooke JA, Shanks M, Edwards SA (2000) Effect of offering maize, linseed or tuna oils throughout pregnancy and lactation on sow and piglet tissue composition and piglet performance. Anim Sci 71:289–299
10. Fritsche KL, Huang SC, Cassity NA (1993) Enrichment of omega-3 fatty acids in suckling pigs by maternal dietary fish oil supplementation. J Anim Sci 71:1841–1847
11. Herrera E (2002) Lipid metabolism in pregnancy and its consequences in the fetus and newborn. Endocrine 19:43–55. doi:10.1385/ENDO:19:1:43
12. Herrera E, Lasunción MA, Martín A, Zorzano A (1992) Carbohydrate–lipid interactions in pregnancy. In: Herrera E, Knopp RH (eds) Perinatal biochemistry. CRC Press, Boca Raton
13. Ramírez I, Llobera M, Herrera E (1983) Circulating triacylglycerols, lipoproteins, and tissue lipoprotein lipase activities in rat mothers and offspring during the perinatal period: effect of postmaturity. Metabolism 32:333–341. doi:10.1016/0026-1495(83)90040-9
14. Alvarez JJ, Montelongo A, Iglesias A, Lasunción MA, Herrera E (1996) Longitudinal study on lipoprotein profile, high density lipoprotein subclass, and postheparin lipases during gestation in women. J Lipid Res 37:299–308
15. Elliott JA (1975) The effect of pregnancy on the control of lipolysis in fat cells isolated from human adipose tissue. Eur J Clin Invest 5:159–163. doi:10.111/j.1365-2362.1975.tb00442.x
16. Knopp RH, Herrera E, Freinkel N (1970) Carbohydrate metabolism in pregnancy. VIII. Metabolism of adipose tissue isolated from fed and fasted pregnant rats during late gestation. J Clin Invest 49:1438–1446. doi:10.1172/JCI106361
17. Martín-Hidalgo A, Holm C, Belfrage P, Schotz MC, Herrera E (1994) Lipoprotein lipase and hormone-sensitive lipase activity and mRNA in adipose tissue during pregnancy. Am J Physiol 266:E930–E935
18. Ramos P, Martín-Hidalgo A, Herrera E (1999) Insulin-induced up-regulation of lipoprotein lipase messenger ribonucleic acid and activity in mammary gland. Endocrinology 140:1089–1093. doi:10.1210/en.140.3.1089
19. Hachey DL, Thomas MR, Emken EA, Garza C, Brown-Booth L, Adlof RO, Klein PD (1987) Human lactation: maternal transfer of dietary triglycerides labeled with stable isotopes. J Lipid Res 28:1185–1192
20. Argilés J, Herrera E (1989) Appearance of circulating and tissue ^{14}C-lipids after oral ^{14}C-tripalmitate administration in the late pregnant rat. Metabolism 32:333–341. doi:10.1016/0026-0495(89)90247-3
21. Innis SM (1993) The colostrum-deprived piglet as a model for study of infant lipid nutrition. J Nutr 123:386–390
22. Laws J, Amusquivar E, Laws A, Herrera E, Dodds PF, Clarke L (2009) Supplementation of sows diets with oil during gestation: sow body condition, milk yield and milk composition. Livest Sci 123:88–96. doi:10.1016/j.livsci.2008.10.012
23. Laws J, Laws A, Lean IJ, Dodds PF, Clarke L (2008) Supplementation of sow diets with oil during early-to-mid gestation: growth of offspring. Animal 10:1482–1489. doi:10.1017/S1751731107000705
24. Laws J, Laws A, Lean IJ, Dodds PF, Clarke L (2008) Supplementation of sow diets with oil during mid-to-late gestation: growth of offspring. Animal 10:1490–1496. doi:10.1017/S1751731107000699
25. Laws J, Litten JC, Laws A, Lean IJ, Dodds PF, Clarke L (2009) Effect of type and timing of oil supplements to sows during pregnancy on the growth performance and endocrine profile of low and normal weight offspring. Br J Nutr 101:240–249. doi:10.1017/S0007114508998469
26. Folch J, Lees M, Sloane-Stanley GH (1957) A simple method for the isolation and purification of total lipids from animal tissues. J Biol Chem 226:497–509
27. Lepage G, Roy CC (1984) Improved recovery of fatty acid through direct transesterification without prior extraction and purification. J Lipid Res 25:1391–1396
28. Lepage G, Roy CC (1986) Direct transesterification of all classes of lipids in a one-step reaction. J Lipid Res 27:114–120
29. Martin JC, Bougnoux P, Fignon A, Theret V, Antoine JM, Lamisse F, Couet C (1993) Dependence of human milk essential fatty acids on adipose stores during lactation. Am J Clin Nutr 58:653–659
30. Martin JC, Niyongabo T, Moreau L, Antoine JM, Lanson M, Berger C, Lamisse F, Bougnoux P, Couet C (1991) Essential fatty

acid composition of human colostrum triglycerides: its relationship with adipose tissue composition. Am J Clin Nutr 54:829–835
31. Herrera E, Amusquivar E, López-Soldado I, Ortega H (2006) Maternal lipid metabolism and placental lipid transfer. Horm Res 65(suppl 3):59–64
32. Herrera E, Ortega H (2008) Metabolism in normal pregnancy. In: Hod M, Jovanovic L, Di Renzo GC, De Leiva A, Langer O (eds) Textbook of diabetes and pregnancy. Informa Healthcare, London
33. Warnants N, Van Oeckel MJ, Boucqué CV (1999) Incorporation of dietary polyunsaturated fatty acids into pork fatty tissues. J Anim Sci 77:2478–2490
34. Jaturasitha S, Khiaosa-ard R, Pongpiachan P, Kreuzer M (2009) Early deposition of n-3 fatty acids from tuna oil in lean and adipose tissue of fattening pigs is mainly permanent. J Anim Sci 87:693–703. doi:10.2527/jas.2008-0863
35. Goyens PL, Spilker ME, Zock PL, Katan MB, Mensink RP (2006) Conversion of α-linolenic acid in humans is influenced by the absolute amounts of α-linolenic acid and linoleic acid in the diet and not by their ratio. Am J Clin Nutr 84:44–53
36. Dourmad JY, Etienne M, Noblet J (1996) Reconstitution of body reserves in multiparous sows during pregnancy: effect of energy intake during pregnancy and mobilization during the previous lactation. J Anim Sci 74:2211–2219
37. Shields RG Jr, Mahan DC, Maxson PF (1985) Effect of dietary gestation and lactation protein levels on reproductive performance and body composition of first-litter female swine. J Anim Sci 60:179–189
38. Kühl C (1975) Glucose metabolism during and after pregnancy in normal and gestational diabetic women. 1. Influence of normal pregnancy on serum glucose and insulin concentration during basal fasting conditions and after a challenge with glucose. Acta Endocrinol (Kbh) 79:709–719
39. Muñoz C, López-Luna P, Herrera E (1995) Glucose and insulin tolerance tests in the rat in different days of gestation. Biol Neonate 68:282–291
40. Crombech G, Siebolds M, Mies R (1993) Insulin use in pregnancy. Clinical pharmacokinetic considerations. Clin Pharmacokinet 24:89–100. doi:10.2165/00003088-199324040-0001
41. Ramos P, Crespo-Solans MD, Del Campo S, Cacho J, Herrera E (2003) Fat accumulation in the rat during early pregnancy is modulated by enhanced insulin responsiveness. Am J Physiol Endocrinol Metab 285:E318–E328. doi:10.1152/ajpendo.00283.2003
42. Knopp RH, Sandek CD, Arky RA, O'Sullivan JB (1973) Two phases of adipose tissue metabolism in pregnancy. Maternal adaptations for fetal growth. Endocrinology 92:984–988. doi:10.1210/endo-92-4-984
43. Herrera E (2002) Implications of dietary fatty acids during pregnancy on placental, fetal and postnatal development. A review. Placenta 23:9–19. doi:10.1053/plac.2002.0771
44. Raclot T, Langin D, Lafontan M, Groscolas R (1997) Selective release of human adipocyte fatty acids according to molecular structure. Biochem J 324:911–915
45. Amusquivar E, Herrera E (2003) Influence of changes in dietary fatty acids during pregnancy on placental and fetal fatty acid profile in the rat. Biol Neonate 83:136–145. doi:10.1159/000067963
46. Parmley KLS, Machado CR, McNamara JP (1996) Rates of lipid metabolism in adipose tissue of pigs adapt to lactational state and dietary energy restriction. J Nutr 126:1644–1656
47. McNamara JP (1995) Role and regulation of metabolism in adipose tissue during lactation. J Nutr Biochem 6:120–129. doi:10.1016/0955-2863(95)00017-T
48. Garg ML, Thomson ABR, Clandinin MT (1990) Interactions of saturated, n-6 and n-3 polyunsaturated fatty acids to modulate arachidonic acid metabolism. J Lipid Res 6:51–62
49. Raz A, Kamin-Belsky N, Przedecki F, Obukowicz MG (1998) Dietary fish oil inhibits Δ6-desaturase activity in vivo. J Am Oil Chem Soc 75:241–245. doi:10.1007/S11746-998-0037-4
50. Del Prado M, Villalpando S, Elizondo A, Rodríguez M, Demmelmair H, Koletzko B (2001) Contribution of dietary and newly formed arachidonic acid to human milk lipids in women eating a low-fat diet. Am J Clin Nutr 74:242–247
51. Salem N, Wegher B, Mena P, Uauy R (1996) Arachidonic and docosahexaenoic acids are biosynthesized from their 18-carbon precursors in human infants. Proc Natl Acad Sci USA 93:49–54. doi:10.1073/pnas.93.1.49
52. Sauerwald TU, Hachey DL, Jensen CL, Chen H, Anderson RE, Heird WC (1997) Intermediates in endogenous synthesis of C22:6ω3 and C20:4ω6 by term and preterm infants. Pediatr Res 41:183–187. doi:10.1203/00006450-199702000-00005
53. Uauy R, Mena P, Wegher B, Nieto S, Salem N (2000) Long chain polyunsaturated fatty acid formation in neonates: effect of gestational age and intrauterine growth. Pediatr Res 47:127–135. doi:10.1203/00006450-200001000-00022
54. Su H, Corso TN, Nathanielsz PW, Brenna JT (1999) Linoleic acid kinetics and conversion to arachidonic acid in the pregnant and fetal baboon. J Lipid Res 47:1304–1311
55. Scopesi F, Ciangherotti S, Lantieri PB, Risso D, Bertini I, Campone F, Pedrotti A, Bonacci W, Serra G (2001) Maternal dietary PUFAs intake and human milk content relationships during the first month of lactation. Clin Nutr 20:393–397. doi:10.1054/clnu.2001.0464
56. Chappell JE, Clandinin MT, Kearney-Volpe C (1985) Trans fatty acids in human milk lipids: influence of maternal diet and weight loss. Am J Clin Nutr 42:49–56
57. Buison A, Lu HQ, Guo F, Jen KL (1997) High-fat feeding of different fats during pregnancy and lactation in rats: effects on maternal metabolism, pregnancy outcome, milk and tissue fatty acid profiles. Nutr Res 17:1541–1554. doi:10.1016/S0271-5317(97)00150-4
58. Valenzuela A, Von Bernhardi R, Valenzuela A, Ramírez G, Alarcón R, Sanhueza J, Nieto S (2004) Supplementation of female rats with α-linolenic acid or docosahexaenoic acid leads to the same omega-6/omega-3 LC-PUFA accretion in mother tissues and in fetal and newborn brains. Ann Nutr Metab 48:28–35. doi:10.1159/000075082
59. Rooke JA, Bland IM, Edwards SA (1999) Relationships between fatty acid status of sow plasma and that of umbilical cord, and tissues of newborn piglets when sows were fed on diets containing tuna oil or soyabean oil in late pregnancy. Br J Nutr 82:213–221
60. Kouba M, Mourot J, Peiniau P (1997) Stearoyl-CoA desaturase activity in adipose tissues and liver of growing Large White and Meishan pigs. Comp Biochem Physiol B 118B:509–514. doi:10.1016/S0305-0491(97)00173-9
61. Singh K, Hartley DG, McFadden TB, Mackenzie DDS (2004) Dietary fat regulates mammary stearoyl CoA desaturase expression and activity in lactating mice. J Dairy Res 71:1–6. doi:10.1017/S0022029903006502

Lipids (2010) 45:419–427
DOI 10.1007/s11745-010-3407-2

ORIGINAL ARTICLE

Molecular Dynamics and Partitioning of Di-*tert*-butyl Nitroxide in Stratum Corneum Membranes: Effect of Terpenes

Heverton Silva Camargos · Adolfo Henrique Moraes Silva · Jorge Luiz Vieira Anjos · Antonio Alonso

Received: 26 October 2009 / Accepted: 8 March 2010 / Published online: 2 April 2010

Abstract In this work, we have used electron paramagnetic resonance (EPR) spectroscopy of the small spin label di-*tert*-butyl nitroxide (DTBN), which partitions the aqueous and hydrocarbon phases, to study the interaction of the terpenes α-terpineol, 1,8-cineole, L(−)-carvone and (+)-limonene with the uppermost skin layer, the stratum corneum, and the membrane models of 1,2-dipalmitoyl-*sn*-glycero-3-phosphatidylcholine (DPPC) and 1,2-dimyristoyl-*sn*-glycero-3-phosphocholine (DMPC). The EPR spectra indicated that the terpenes increase both the partition coefficient and the rotational correlation time of the spin labels in the stratum corneum membranes, whereas similar effects were observed in the DMPC and DPPC bilayers only at temperatures below the liquid-crystalline phase. The EPR parameter associated to probe polarity inside the membranes showed thermotropically induced changes, suggesting relocations of spin probe, which were dependent on the membrane phases. While the DMPC and DPPC bilayers showed abrupt changes in the partitioning and rotational correlation time parameters in the phase transitions, the SC membranes were characterized by slight changes in the total range of measured temperatures, presenting the greatest changes or membranes reorganizations in the temperature range of ∼50 to ∼74 °C. The results suggest that terpenes act as spacers, weakening the hydrogen-bonded network at the polar interface and thus fluidizing the stratum corneum lipids.

H. S. Camargos · A. H. M. Silva · J. L. V. Anjos · A. Alonso (✉)
Instituto de Física, Universidade Federal de Goiás, Goiânia, GO 74001-970, Brazil
e-mail: alonso@if.ufg.br

Keywords Stratum corneum · EPR · Spin label · Lipid dynamics · Terpene

Abbreviations

SC	Stratum corneum
DMPC	1,2-Dimyristoyl-*sn*-glycero-3-phosphocholine
DPPC	1,2-Dipalmitoyl-*sn*-glycero-3-phosphatidylcholine
DTBN	Di-*tert*-butyl nitroxide
EPR	Electron paramagnetic resonance

Introduction

The major limitation of implementing transdermal drug delivery systems is the generally low permeability of the drug across the skin. Several approaches have been implemented to facilitate drug transport through the skin. One important approach is the use of chemical penetration enhancers, which ideally reduce the resistance of the physical barrier of the SC safely and reversibly to enhance the drug's delivery through the skin. In particular, terpenes have been reported as permeation enhancers of several polar and non-polar drugs and many terpenes, including 1,8-cineole, menthol and α-terpineol, are claimed to be generally recognized as safe (GRAS) materials. The interactions of terpenes with the SC are of interest to understand how small amphiphilic molecules may enhance skin permeability. It is generally accepted that penetration enhancers may increase the permeability of a drug mainly by affecting the intercellular lipids of the SC via extraction or fluidization [1] and/or by increasing the partitioning of the drug in the SC

membranes [2]. However, very few studies have focused on mechanisms of permeation enhancement by terpenes in SC. The most commonly used techniques are Fourier transform infrared spectrophotometry (FTIR) and differential scanning calorimetry (DSC) [3–5] and small-angle X-ray diffraction [5].

Electron paramagnetic resonance (EPR) of spin labels has been employed to obtain information on the molecular dynamics of SC membranes [6–12] and SC proteins [13–16] in the intact tissue. The EPR spectra of spin-labeled stearic acids in SC membranes were able to distinguish two main environments for the probe distribution into the membranes. In a previous study [9], the origin of these two spectral components was interpreted based on the ability of spin labels to participate in intermolecular hydrogen bonding within the membrane. The more motionally restricted component was assigned to a class of spin probe hydrogen bonded to the polar head groups (more rigid structure) and the more mobilized component was attributed to the spin labels temporarily non-hydrogen-bonded to the polar interface and more deeply inserted in the hydrophobic core. Recently, the effect of the terpenes L-menthol and 1,8-cineole on the SC lipid dynamics was examined in detail [10, 11]. The presence of 1% terpenes (w/w) in the solvent drastically increased the lipid fluidity, especially by transferring the spin probes from a more to a less motionally restricted spectral component into the membranes. Furthermore, these two terpenes increased the rotational diffusion rates only of spin probes from the more mobilized component.

In a more recent work, we used the small water-soluble spin label TEMPO, which partitions between the bilayer and aqueous phase, to examine the interactions of terpenes with the SC membranes [12]. Since the partitioning of a substance in a membrane correlates with the drug's absorption [17] and is an essential step in diffusion [18], this spin probe may be used to mimic drugs and thus to investigate the mechanisms of terpenes as accelerants of permeation in the SC. This spin probe was sensitive to the phase transitions of SC membranes and showed that, in essence, terpenes increase the molecular mobility and partitioning in SC membranes at much lower concentrations than those generally used for these terpenes as skin penetration enhancers. In the present study, the spin label DTBN, also of low molecular weight (145 g) but with higher molecular dynamics and considerably better EPR spectral resolution than that of TEMPO, was used seeking to obtain more detailed information about the influence of terpenes on SC membranes and bilayer models of DMPC and DPPC, particularly on the major probe's localization within these membranes.

Materials and Methods

Preparation of SC Membranes

SC membranes of neonatal Wistar rats less than 24 h old were prepared as described previously [10–12]. After the animal was killed, its skin was excised and fat removed by rubbing in distilled water. The skin was allowed to stand for 5 min in a desiccator containing 0.5 L of anhydrous ammonium hydroxide, after which it was floated in distilled water for 2 h with the internal side in contact with the water. The external side was placed in contact with a filter paper and the SC sheet was carefully separated from the remaining epidermis. Subsequently, the SC was transferred to a Teflon-coated screen, washed with distilled water and allowed to dry at room temperature. The membranes were stored with 1 L of silica gel in a desiccator under a moderate vacuum.

Spin Labeling and Treatment of SC

In order to prevent nitroxide reductions, the sulfhydryl groups of the SC tissue were blocked by incubating the SC membranes in a solution of 50 mM *N*-ethyl maleimide (Sigma Chem. Co., St. Louis, MO, USA) for about 15 h. The SC membranes were dried again and an intact portion of SC (3 mg) was then rehydrated and incubated for 90 min in 45 μL of acetate-buffered saline (10 mM acetate, 150 mM NaCl and 1 mM EDTA, pH 5.5) plus 5 μL of ethanol containing the corresponding terpene concentration (Acros Organics, Geel, Belgium). After this incubation, 0.2 mM spin label DTBN (Fig. 1) purchased from Sigma Chem. Co. (St. Louis, MO, USA) was added and the intact SC membrane was then introduced into a 1-mm ID capillary for EPR measurements. The excess solvent was removed and the capillary was flame-sealed. The molecular structures of spin label DTBN and of terpenes used in this work are shown in Fig. 1.

Preparation of Lipid Dispersions

DPPC or DMPC, purchased from Avanti (Alabaster, AL), was dissolved in a mixture of chloroform:methanol (2:1) and dried under a nitrogen stream. The residual solvent was removed by vacuum-drying the tube overnight. In the hydration step to form multilamellar vesicles, the samples were incubated in PBS (10 mM phosphate, 150 mM NaCl and 1 mM EDTA, pH 7.2) for about 5 min at 50 °C and subsequently vortexed several times. 2 μL of 10 mM DTBN and 1.5 μL terpene in ethanol solution (about 33%, v/v, depending on the density of the terpene) were added to each sample containing 3 mg DPPC or DMPC membranes

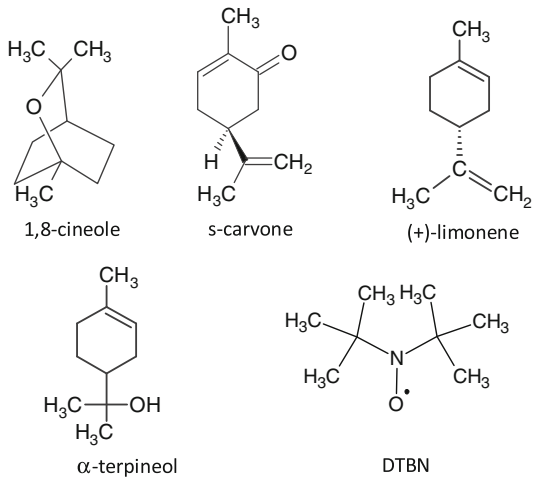

Fig. 1 Chemical structures of terpenes and spin label DTBN used in this work

in 40 μL PBS. The suspension was vortexed again and transferred to a capillary, which was then flame-sealed.

EPR Spectroscopy

EPR spectroscopy was carried out with a Bruker ESP 300 spectrometer (Bruker, Rheinstetten, Germany) equipped with an ER 4102 ST resonator and a Bruker temperature controller. The instrumental settings were: microwave power of 2 mW; modulation frequency of 100 kHz; modulation amplitude of 0.25 G; magnetic field scan of 100 G; sweep time of 168 s; and detector time constant of 41 ms. The capillary containing the sample was introduced into a 3-mm ID quartz tube together with a fine-wire thermocouple to monitor the sample's temperature. EPR spectra simulations were performed using the software EPRSIM (version 4.99) [19, 20]. This program allows a single spectrum to be fitted with two components having different mobility and magnetic tensor parameters. For each spectral component, the program provides the relative population and the associated rotational motion of the probe, through the parameter rotational correlation time, τ_c. The magnetic tensor values used for the simulation were $g_{xx} = 2.0099$, $g_{yy} = 2.0061$, and $g_{zz} = 2.0024$ for the g-tensor, and $A_{xx} = 5.3$ G, $A_{yy} = 7.0$ G, and $A_{zz} = 35.0$ G for the A-tensor [21]. In the limit of fast motion, where the motional narrowing approximation is valid, the τ_c is described as follows [22]:

$$\tau_c = \frac{\sqrt{3} g_{iso} \beta \, \Delta H(0)}{2h \quad (C - B)} \left[1 - \sqrt{\frac{1(0)}{1(-1)}} \right] \tag{1}$$

where $g_{iso} = 1/3(g_{xx} + g_{yy} + g_{zz})$ is the isotropic g-factor, β is the Bohr magneton, h is Planck's constant, H is the external magnetic field, $\Delta H(0)$ is the central line peak-to-peak linewidth, and $I(0)$ and $I(-1)$ are the intensities of central and high field resonance lines, respectively. Parameters B and C are derived in terms of the g- and A-tensor anisotropies through the following expressions:

$$B = \frac{-16\beta H}{45h}(A_{zz} - A_{xx}) \left[g_{zz} - \frac{1}{2}(g_{xx} + g_{yy}) \right], \tag{2}$$

and

$$C = \frac{2\pi^2}{9}(A_{zz} - A_{xx})^2. \tag{3}$$

These magnetic interaction tensors A and g were linearly corrected using the fitting program with polarity correction factors on the trace of hyperfine coupling tensor A and the spin-magnetic field coupling tensor g, denoted by parameters p_A and p_g, respectively. The EPR signal corresponding to the interaction electron-spin nuclear C-13 spin coupling is present in the EPR spectra of DTBN (satellite lines); in the program, a magnitude of 5.6 G with abundance of 0.0115% was assumed for this interaction.

Results

Analysis of EPR Spectra

The typical EPR spectrum of spin probe DTBN (Fig. 1) in membrane is shown in Fig. 2. The spectrum is composed of two spectral components, H (Fig. 2c) and P (Fig. 2d), which are provided by the spin-label fractions dissolved in the hydrophobic and polar environments, respectively. Figure 2b shows the same experimental EPR spectrum (line) and its best-fit spectrum (open circles), which is the sum of the components H (spectrum c) and P (spectrum d). The fitting program was able to simulate the lateral satellite lines originating from the electron-spin nuclear C-13 spin coupling. The experimental (line) and best-fit (open circles) EPR spectra of DTBN in DMPC, DPPC and SC membranes are shown in Fig. 3 for three temperatures, where is possible to observe that the relative population of component H increased by raising the temperature.

Partition Coefficient of DTBN between the Hydrocarbon and Polar Phases

According to the solubility-diffusion mechanism, the permeability coefficient, P, of a molecule crossing a bilayer membrane is generally related to the partition coefficient in the bilayer, K, the diffusion constant across it, D, and the bilayer thickness, Δx, by the following equation [23]:

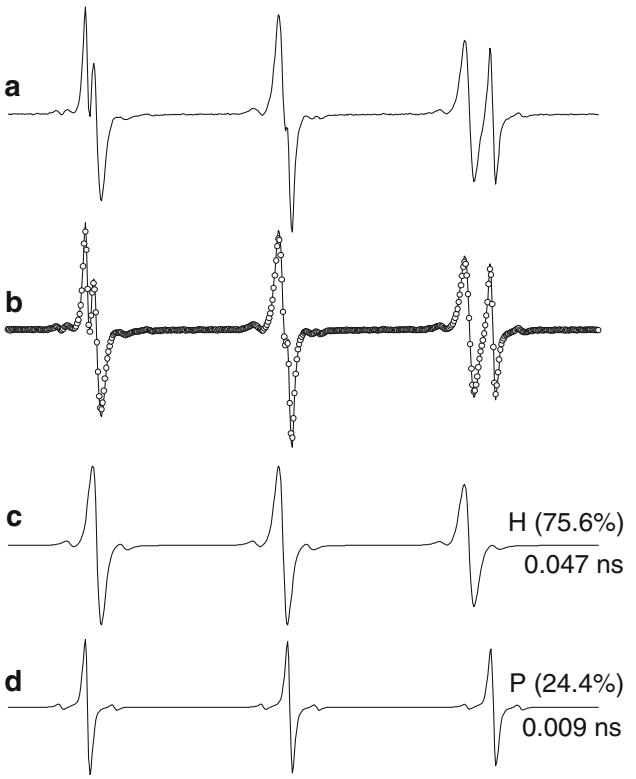

Fig. 2 **a** EPR spectrum of DTBN in stratum corneum (pH 5.1, 50 °C); **b** the same spectrum (*line*) superimposed with its best-fit EPR spectrum (*open circles*). The best-fit spectra were obtained with the fitting program EPRSIM, using a simulation model of two spectral components. The theoretical component H (spectrum c) refers to the spin label fraction in the hydrophobic environment and the component P (spectrum d) is generated by the spin probes in solvent. The figure also indicates the fitting results: the percentage of spin label in each component, N_H and N_P, and its respective rotational correlation time, τ_c, in ns. The total scan range of the magnetic field was 50 G

$$P = KD/\Delta x. \tag{4}$$

The diffusion coefficient is defined as:

$$D = k_B T/6\pi\eta r, \tag{5}$$

where $k_B T$ is the thermal energy, η is the membrane viscosity, and r is the molecular radius. The partition coefficient is the equilibrium ratio of the solute concentration in the bilayer, c_H, and in aqueous concentration, c_P. K can be determined if the relative volumes of membrane and solvent in the sample are known.

$$K = c_H/c_p. \tag{6}$$

or

$$K = (N_H/V_{membrane})/(N_p/V_{solvent}), \tag{7}$$

where N_H and N_P are the relative spin-label populations in the hydrophobic and polar environments, respectively, that are provided by the fitting program. The relative membrane-solvent volumes for the two systems were estimated taking into account the volume of sample in the capillary tube (about 20 μL) and the weight before and after drying the sample; the water content in the samples (w/w) was on average 22% for DPPC or DMPC and 65% for SC. It was considered that the SC has 16% lipids (w/w) relative to dry tissue [24].

The standard Gibbs free energy change required to transfer a molecule from an aqueous to a hydrocarbon phase, ΔG°, can be calculated based on the partition coefficient, as follows [25, 26]:

$$\Delta G^\circ = -RT \ln K, \tag{8}$$

or

$$\ln K = -\Delta H^\circ/RT + \Delta S^\circ/R, \tag{9}$$

where R is the gas constant, T is the absolute temperature, ΔH° is the standard enthalpy change for transferring the permeating molecules from solvent to the interior of the membrane, and ΔS° is the associated entropic change.

The thermodynamic parameters can be obtained from a van't Hoff plot of ln K versus $1/T$, as shown in Fig. 4. This type of plot is suitable for analyzing phase transitions, since the slope coefficient of each curve yields $\Delta H^\circ/R$. The phase transitions observed for DPPC bilayers are well known [27, 28]: the transition at ~34 °C corresponds to the gel structure ($L_{\beta'}$)-ripple structure ($P_{\beta'}$) phase transition, called pre-transition, and the transition at ~42 °C corresponds to a ripple structure ($P_{\beta'}$)-fluid bilayer structure (L_α) phase transition. In DMPC, these phase transitions occur at ~13 °C ($L_{\beta'}$–$P_{\beta'}$) and 23 °C ($P_{\beta'}$–L_α) [27]. In the presence of terpenes, it appears that only the phase transition ($P_{\beta'}$–L_α) is still present and that the transition temperatures are about 8 °C lower. Compared to phospholipid bilayers, SC membranes are characterized by phase transitions with minor changes within a temperature range whose highest slope lies between ~50 and ~74 °C. DMPC and DPPC membranes were not affected by terpenes in the liquid-crystalline phase but showed pronounced effects below the $P_{\beta'}$–L_α phase transition. In contrast, the SC samples presented increases of DTBN partitioning caused by terpenes in the entire temperature interval.

Molecular Dynamics of DTBN into Hydrocarbon and Aqueous Phases

Figure 5 shows the rotational correlation time parameter, τ_c, of DTBN in DMPC, DPPC and SC plotted on a logarithmic scale as a function of the reciprocal absolute temperature. Panels A and B refer to spin labels in the membrane and solvent, respectively. These well-known Arrhenius plots allow us to calculate the apparent

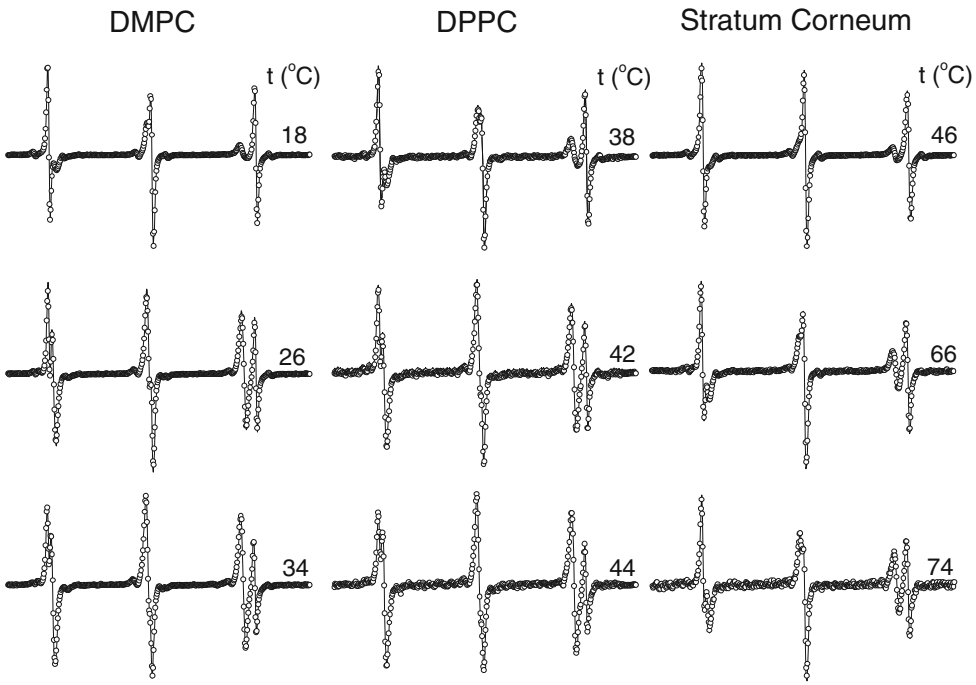

Fig. 3 Experimental (*line*) and best-fit (*open circles*) EPR spectra of DTBN in DMPC, DPPC, and stratum corneum membranes at several temperatures. The total scan range of the magnetic field was 50 G

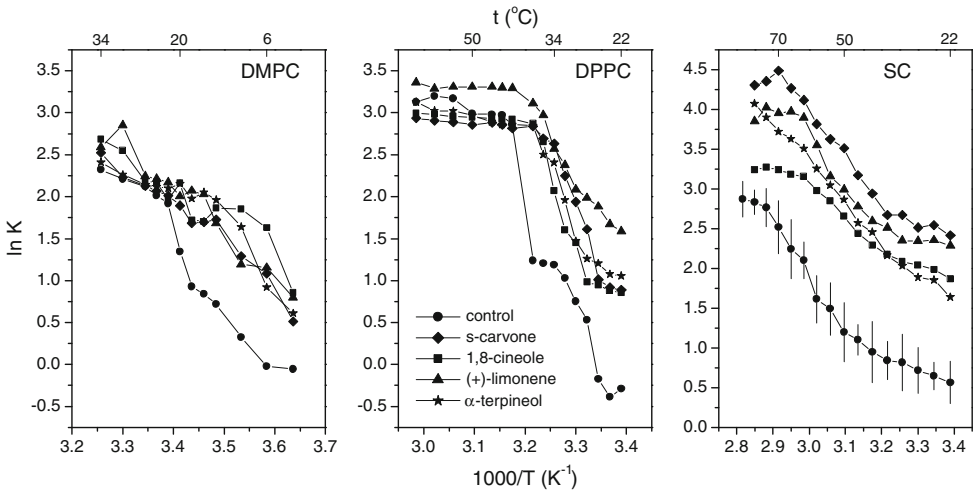

Fig. 4 Natural logarithm of the partition coefficient, ln *K*, of DTBN in multilamellar vesicles of DMPC, DPPC and stratum corneum (SC) membranes versus the reciprocal absolute temperature. Terpenes were added at a terpene:lipid molar ratio of 0.75:1 for DMPC and DPPC and at 1% terpene (w/v) in stratum corneum

activation energy, E_a, of rotational motion in the regions of linear dependence, using the following equation:

$$1/\tau_c = A\exp(-E_a/RT), \tag{10}$$

where A is a pre-exponential factor and E_a is the energy barrier that the spin probe must overcome to achieve higher states of motion. The greater the slope in these plots the higher the E_a values and the breaks in slopes indicate possible phase transitions. The terpenes did not increase the rotational motion of the spin probe in the fluid phase of DMPC and DPPC bilayers, where the partition coefficients were higher. Figure 5b shows that the τ_c parameter of spin labels in SC aqueous phase increased with temperature, suggesting that spin probes from the polar phase may penetrate the region of the polar head groups.

Polarity Environments of DTBN into Hydrocarbon and Aqueous Phases

The EPR parameter isotropic hyperfine coupling constant, a_0, is associated with the polarity of the solvent in which the nitroxide radical is dissolved. To examine the predominant location of DTBN in the membranes and ascertain if terpenes can alter this location, the parameter a_0 of the three systems under study was measured in the presence and absence of terpenes (Fig. 6). Polarity profiles through membrane were determined in spin-labeled glycerophospholipids with the DOXYL-nitroxide group at position n in the *sn*-2 chain (n-PCSL) in DPPC membranes, whose a_0 values were 15.1 G for $n = 4$ and 14.5 G for $n = 16$ [29]. The a_0 values observed for DTBN in DMPC,

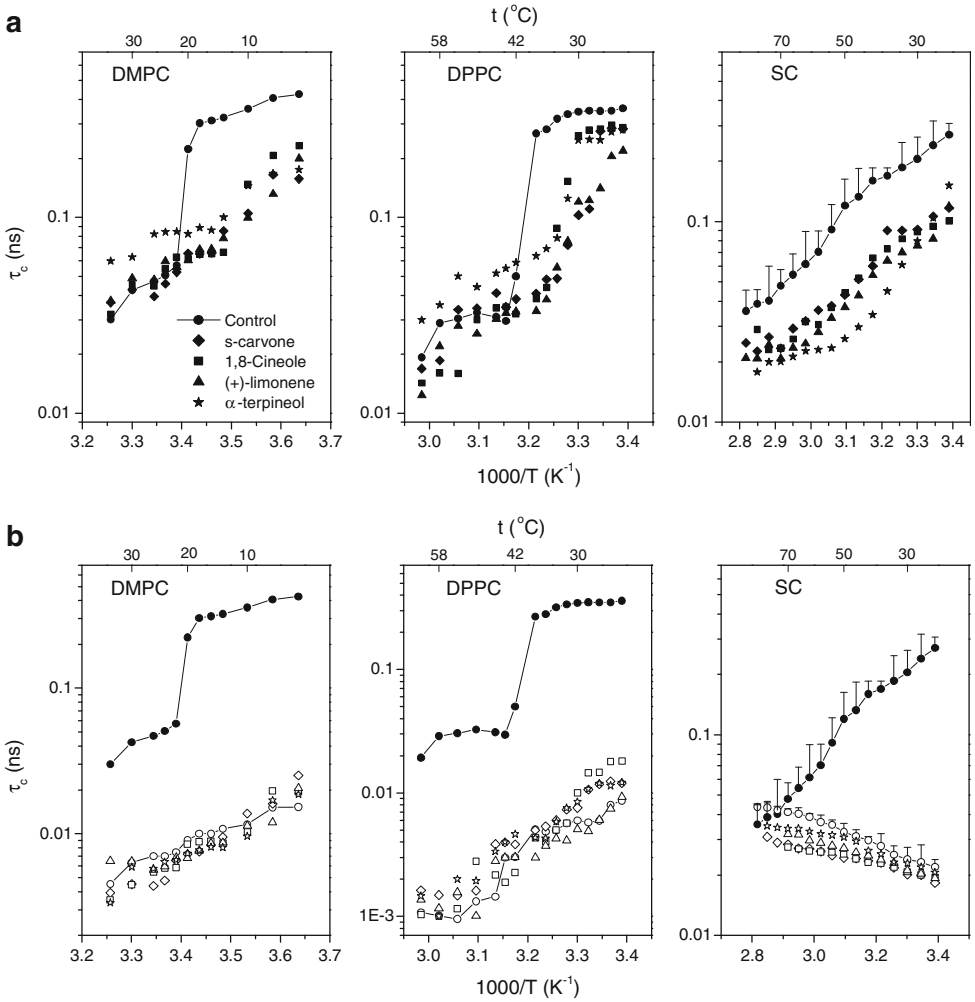

Fig. 5 Rotation correlation time, τ_c, of DTBN in DMPC, DPPC and stratum corneum (SC) membranes versus the reciprocal absolute temperature. **a**, **b** refer to DTBN in hydrocarbon and aqueous phases, respectively. Terpenes were added at a terpene:lipid molar ratio of 0.75:1 for DMPC and DPPC and at 1% terpene (w/v) in stratum corneum

DPPC and SC membranes were in the range of 15.55–15.85 G (Fig. 6). The a_0 parameters were measured at 25 °C for the spin labels DTBN and DOXYL (5-DOXYL stearic acid) in terpenes and other solvents, with varying dielectric constants (data not shown) and the a_0 values found for DTBN were on average 1.0 higher than DOXYL. Similar results were reported recently in a study comparing the a_0 values of several spin labels with those of DOXYL class [30]. Thus, with the subtraction of 1.0 G from the a_0 values presented in Fig. 6, the maximum value reached would be 14.85 G, which corresponds to the mean value between 14.5 ($n = 16$) and 15.1 ($n = 4$) observed for DOXYL in the bilayers. Therefore, the a_0 values of about 15.85 G observed above the main phase transition of DMPC and DPPC (Fig. 6) is consistent with the DTBN distributed throughout the membrane, while the value of about 15.6 G found in the gel phases is compatible with the probes located predominantly in the center of bilayer.

DMPC and DPPC in the presence of α-terpineol and (+)-limonene presented polarity levels similar to those above the main phase transition, whereas in the case of L(−)-carvone and 1,8-cineole, such levels were only observed above 6 °C for DMPC and above 26 °C for DPPC. In contrast, in the SC samples, only α-terpineol maintained the probe's polarity at the highest level observed and the other terpenes did not significantly change the probe's polarity. A particular characteristic of α-terpineol is that it contains a hydrogen-bonding donor group to form hydrogen-bonded nitroxide.

As can be observed in Fig. 6a, the polarity detected by the spin labels in SC aqueous phase decreased with increasing temperature, suggesting that the probes outside the membrane may enter the membrane in the vicinities of the polar groups and that the probability of this occurrence increases with temperature. This behavior is also apparent for DPPC and, in this case, seems to reflect the main bilayer phase transition. The terpenes did not alter the solvent's polarity.

Discussion

In the current study, the better EPR spectral resolution of DTBN relative to that of TEMPO, used in previous work [12], was explored to obtain additional information about

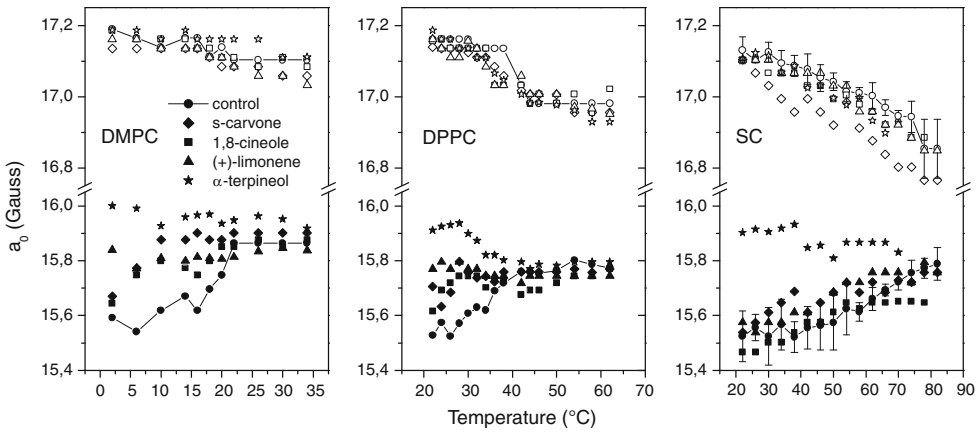

Fig. 6 The EPR parameter isotropic ^{14}N-hyperfine splitting constant, a_0, of DTBN in DMPC, DPPC and stratum corneum (SC) membranes as a function of temperature

the probe's polarity. The EPR parameter a_0, which is sensitive to the environmental polarity of nitroxyl spin labels, indicated that DTBN is distributed throughout the membranes of DMPC and DPPC in the liquid-crystalline phase and this also occurs in SC at higher temperatures (~60–80 °C). At lower temperatures, however, the spin label tends to concentrate in the central region of the membranes. Interestingly, in the case of DMPC and DPPC bilayers, the thermally induced relocation of DTBN into the bilayer reflected their main phase transitions (Fig. 6). Furthermore, the DTBN from aqueous phase should penetrate the region of the polar head groups, as deduced from the temperature-induced reduction of its environmental polarity (Fig. 6), and the concomitant reduction of rotational motion (Fig. 5b). The thermotropic behavior of the partitioning and rotational motion of DTBN in SC membranes presented here is in close agreement with the data obtained by Fourier transform infrared spectroscopy (FTIR) in a study of the thermotropic phase behaviors in porcine SC and its extracted lipids. That study found a more pronounced increase of νsCH_2 in the temperature range of ~60 to ~80 °C, which was associated with alkyl chain melting [31].

In this work, the EPR spectra were simulated using the fitting program EPRSIM instead of the NLLS, which was less suitable in the specific case of DTBN, especially due to the presence of satellite lines in the spectra and the faster rotational motion of this probe. Whereas the program NLLS generates the parameter Log Rbar, whose value for TEMPO in SC samples at 70 °C was 9.1 [12], the EPRSIM generates τ_c, whose corresponding value for DTBN was 0.035 ns (Fig. 5a). Because the transformation is given by $\text{Rbar} = 1/6\tau_c$, the corresponding Log Rbar for DTBN will be 9.7, which represents a greater rate of rotational diffusion. Efforts were made to describe the phase transitions in SC membranes through these probes. The increases in the slopes observed in the curves of control samples plotted in Figs. 4 and 5a, which were apparent in the temperature range of ~50 to ~74 °C, were analyzed exhaustively. At ~50 °C, the change in slope was clear in all the experiments, while the decrease in slope at ~70 °C was the result of an average, but was not clearly visible in all the experiments. It is interesting to note that the rotational correlation times of spin probe in the membranes (Fig. 5a) also reflected their phase transitions and the terpenes' effects further support the results observed for the partition coefficient in Fig. 4. DSC experiments have identified four phase transitions in neonatal rat SC (used in this work) at about at 42 °C (T_1), 55 °C (T_x), 70 °C (T_2) and 78 °C (T_3), which have been attributed to lipid melting [4]. The two major phase transitions in human SC occur at 72 °C (T_2) and 83 °C (T_3), and the terpenes D-limonene and 1,8-cineole have been found to reduce the temperatures of these two transitions by about 20 °C [5]. Here, the phase transitions were not clearly defined in the presence of terpenes, but in general, a reduction of at least 8 °C in the temperatures of the main phase transitions may be observed for DMPC, DPPC and SC.

Attenuated total reflectance Fourier transform infrared spectroscopy (ATR-FTIR) has been used to study the molecular organization of a model SC lipid system and, in the presence of the terpenes 1,8-cineole and L-menthol, alterations were detected in the amide-I frequencies, suggesting that they disrupt the hydrogen-bonding network at the membrane interface [32]. These results are in agreement with those obtained by EPR spectroscopy of spin-labeled analogs of stearic acid incorporated in SC membranes, where 1% L-menthol or 1,8-cineole (w/v) caused a dramatic increase in the membrane fluidity [10, 11]. The authors' interpretation of this finding was that terpenes weaken the hydrogen-bonded network of the polar head groups. In the present work, we studied one terpene containing a hydrogen-bonding donor group (the alcohol α-terpineol), two with hydrogen-bonding acceptor groups (the ether 1,8-cineole and the ketone L(−)-carvone), and one that does not have polar groups [the hydrocarbon

(+)-limonene]. Although terpenes can, in principle, weaken the hydrogen-bonding interactions at the membrane–water interface, the results of the present work suggest that the effects of terpenes on membranes do not necessarily depend on direct competition for H-bonds with the polar head groups, since the effects of (+)-limonene, which does not form H-bonds, did not differ significantly from that of the other terpenes.

In conclusion, using a small spin label to mimic a drug, this study shows that, at a concentration of 1% (w/v) in SC membranes, terpenes increase the partitioning and rotational motion of the spin probe throughout the temperature range measured. The action of terpenes on ordered membranes is stronger, as in the case of SC, and diminishes when the membrane is already disordered, like DMPC and DPPC bilayers in the liquid-crystalline phase. In comparison with the other two membrane systems, the thermotropic behavior of SC membranes was characterized by phase transitions with minor changes, showing the greatest thermally induced changes in the temperature range of $\sim$50 to $\sim$74. Polarity measurements indicated a throughout distribution of DTBN in the membranes at higher temperatures and a major location in the center of the membranes at lower temperatures (in the physiological range of SC). In addition, the polarity measurements also showed that a fraction of the spin probes outside the membrane may penetrate the polar interface of the membranes and that this fraction of probes gradually increases with rising temperature. Terpenes are small molecules that are able to penetrate the membrane and, at higher concentrations, may effectively act as spacers, increasing the membrane's fluidity and weakening the hydrogen-bonded network of the polar interface. This process may facilitate the partition of small polar molecules and, hence, their permeation through membranes. Since the effects of different types of terpenes on the membranes did not differ significantly, this work also shows that, in practice, terpenes or combinations of terpenes may be chosen in order to achieve permeation enhancement effects at physiological temperatures with minimal toxicity to the skin.

Acknowledgments The authors are indebted to the Brazilian research funding agencies CNPq and FUNAPE. Adolfo H. M. Silva, Heverton S. Camargos and Jorge L. V. Anjos were recipients of studentships from CNPq, CAPES and UFG, respectively. A. Alonso is grateful to CNPq for a research grant.

References

1. Yamane MA, Williams AC, Barry BW (1995) Effects of terpenes and oleic acid as skin penetration enhancers towards 5-fluorouracil as assessed with time, permeation, partitioning and differential scanning calorimetry. Int J Pharm 116:237–251
2. Gao S, Singh J (1998) In vitro percutaneous absorption enhancement of a lipophilic drug tamoxifen by terpenes. J Control Release 51:193–199
3. Vaddi HK, Ho PC, Chan SY (2002) Terpenes in propylene glycol as skin-penetration enhancers: permeation and partition of haloperidol, Fourier transform infrared spectroscopy, and differential scanning calorimetry. J Pharm Sci 91:1639–1651
4. Al-Saidan SM (2004) Transdermal self-permeation enhancement of ibuprofen. J Control Release 100:199–209
5. Cornwell PA, Barry BW, Bouwstra JA, Gooris GS (1996) Modes of action of terpene penetration enhancers in human skin; differential scanning calorimetry, small-angle X-ray diffraction and enhancer uptake studies. Int J Pharm 127:9–26
6. Alonso A, Meirelles NC, Tabak M (1995) Effect of hydration upon the fluidity of intercellular membranes of stratum corneum: an EPR study. Biochim Biophys Acta 1237:6–15
7. Alonso A, Meirelles NC, Yushmanov VE, Tabak M (1996) Water increases the fluidity of intercellular membranes of stratum corneum: correlation with water permeability, elastic, and electrical properties. J Invest Dermatol 106:1058–1063
8. Alonso A, Meirelles NC, Tabak M (2000) Lipid chain dynamics in stratum corneum studied by spin label electron paramagnetic resonance. Chem Phys Lipids 104:101–111
9. De Queiros WP, Neto DD, Alonso A (2005) Dynamics and partitioning of spin-labeled stearates into the lipid domain of stratum corneum. J Control Release 106:374–385
10. Dos Anjos JLV, Neto DD, Alonso A (2007) Effects of ethanol/L-menthol on the dynamics and partitioning of spin-labeled lipids in the stratum corneum. Eur J Pharm Biopharm 67:406–412
11. Dos Anjos JLV, Neto DD, Alonso A (2007) Effects of 1,8-cineole on the dynamics of lipids and proteins of stratum corneum. Int J Pharm 345:81–87
12. Dos Anjos JLV, Alonso A (2008) Terpenes increase the partitioning and molecular dynamics of an amphipathic spin label in stratum corneum membranes. Int J Pharm 350:103–112
13. Alonso A, Dos Santos JG, Tabak M (2000) Stratum corneum protein mobility as evaluated by a spin label maleimide derivative. Biochim Biophys Acta 1478:89–101
14. Alonso A, Dos Santos WP, Leonor SJ, Tabak M (2001) Stratum corneum protein dynamics as evaluated by a spin-label maleimide derivative: effect of urea. Biophys J 81:3566–3576
15. Alonso A, Da Silva JV, Tabak M (2003) Hydration effects on the protein dynamics in stratum corneum as evaluated by EPR spectroscopy. Biochim et Biophys Acta 1646:32–41
16. Do Couto SG, Oliveira MD, Alonso A (2005) Dynamics of proteins and lipids in the stratum corneum: effects of percutaneous permeation enhancers. Biophys Chem 116:23–31
17. Liu XY, Nakamura C, Yang Q, Kamo N, Miyake J (2002) Immobilized liposome chromatography to study drug-membrane interactions. J Chromatogr A 961:113–118
18. Tammela P, Laitinen L, Galkin A, Wennberg T, Heczko R, Vuorela H, Slotte JP, Vuorela P (2004) Permeability characteristics and membrane 52 affinity of flavonoids and alkyl gallates in Caco-2 cells and in phospholipids vesicles. Arch Biochem Biophys 425:193–199
19. Arsov Z, Schara M, Strancar J (2002) Quantifying the lateral lipid domain properties in erythrocyte ghost membranes using EPR-spectra decomposition. J Magn Reson 157:52–60
20. Stopar D, Strancar J, Spruijt RB, Hemminga MA (2006) Motional restrictions of membrane proteins: a site-directed spin labeling study. Biophys J 91:3341–3348
21. Nordio PL (1976) General magnetic resonance theory. In: Berliner LJ (ed) Spin labeling, theory and application. Academic Press, New York, pp 5–51
22. Tabak M, Alonso A, Nascimento OR (1983) Single-crystal electron-spin-resonance studies of a nitroxide spin label. 1.

Determination of the g and A tensors. J Chem Phys 79:1176–1184
23. Finkelstein A (1976) Water and nonelectrolyte permeability of lipid bilayer membranes. J Gen Physiol 68:127–135
24. Wertz PW, Downing DT (1987) Covalently bound v-hydroxy-acylsphingosine in the stratum corneum. Biochim Biophys Acta 917:108–111
25. Rogers JA, Wong A (1980) The temperature dependence and thermodynamics of partitioning of phenols in the *n*-octanol-water system. Int J Pharm 6:339–348
26. Da Y-Z, Ito K, Fujiwara H (1992) Energy aspects of oil/water partition leading to the novel hydrophobic parameters for the analysis of quantitative structure activity relationships. J Med Chem 35:3382–3387
27. Shimshick EJ, McConnell HM (1973) Lateral phase separation in phospholipid membranes. Biochemistry 12:2351–2360
28. Wang D-C, Taraschi TF, Rubin E, Janes N (1993) Configuration entropy is the driving force of ethanol action on membrane architecture. Biochim Biophys Acta 1145:141–148
29. Kurad D, Jeschke G, Marsh D (2003) Lipid membrane polarity profiles by high-field EPR. Biophys J 85:1025–1033
30. Marsh D, Toniolo C (2008) Polarity dependence of EPR parameters for TOAC and MTSSL spin labels: correlation with DOXYL spin labels for membrane studies. J Magn Reson 190:211–221
31. Ongpipattanakul B, Francoeur ML, Potts RO (1994) Polymorphism in stratum corneum lipids. Biochim Biophys Acta 1190:115–122
32. Narishetty STK, Panchagnula R (2005) Effect of l-menthol and 1,8-cineole on phase behavior and molecular organization of SC lipids and skin permeation of zidovudine. J Control Release 102:59–70

Lipids (2010) 45:429–436
DOI 10.1007/s11745-010-3410-7

ORIGINAL ARTICLE

Impact of Administered *Bifidobacterium* on Murine Host Fatty Acid Composition

Rebecca Wall · R. Paul Ross · Fergus Shanahan · Liam O'Mahony · Barry Kiely · Eamonn Quigley · Timothy G. Dinan · Gerald Fitzgerald · Catherine Stanton

Received: 14 December 2009 / Accepted: 25 March 2010 / Published online: 20 April 2010

Abstract Recently, we reported that administration of *Bifidobacteria* resulted in increased concentrations of eicosapentaenoic acid (EPA) and docosahexaenoic acid (DHA) in murine adipose tissue [1]. The objective of this study was to assess the impact of co-administration of *Bifidobacterium breve* NCIMB 702258 and the substrate for EPA, α-linolenic acid, on host fatty acid composition. α-Linolenic acid-supplemented diets (1%, wt/wt) were fed to mice ($n = 8$), with or without *B. breve* NCIMB 702258 (daily dose of 10^9 microorganisms) for 8 weeks. Two further groups received either supplement of *B. breve* alone or unsupplemented diet. Tissue fatty acid composition was assessed by gas liquid chromatography. Dietary supplementation of α-linolenic acid resulted in higher ($P < 0.05$) α-linolenic acid and EPA concentrations in liver and adipose tissue and lower ($P < 0.05$) arachidonic acid in liver, adipose tissue and brain compared with mice that did not receive α-linolenic acid. Supplementation with *B. breve* NCIMB 702258 in combination with α-linolenic acid resulted in elevated ($P < 0.05$) liver EPA concentrations compared with α-linolenic acid supplementation alone. Furthermore, the former group had higher ($P < 0.05$) DHA in brain compared with the latter group. These results suggest a role for interactions between fatty acids and commensals in the gastrointestinal tract. This interaction between administered microbes and fatty acids could result in a highly effective nutritional approach to the therapy of a variety of inflammatory and neurodegenerative conditions.

Keywords Omega-3 fatty acids · Eicosapentaenoic acid · Docosahexaenoic acid · *Bifidobacteria* · Microbiota · Probiotics

R. Wall · R. P. Ross · F. Shanahan · L. O'Mahony · E. Quigley · T. G. Dinan · G. Fitzgerald · C. Stanton
Alimentary Pharmabiotic Centre (APC), Co. Cork, Ireland

R. P. Ross · C. Stanton (✉)
Teagasc, Moorepark Food Research Centre, Fermoy, Co. Cork, Ireland
e-mail: catherine.stanton@teagasc.ie

G. Fitzgerald
University College Cork, National University of Ireland, Cork, Ireland

B. Kiely
Alimentary Health (AH), Co. Cork, Ireland

Abbreviations

ANOVA	Analysis of variance
CFU	Colony forming units
CLA	Conjugated linoleic acid
DHA	Docosahexaenoic acid
EPA	Eicosapentaenoic acid
FAME	Fatty acid methyl esters
IBD	Inflammatory bowel disease
IFN-γ	Interferon-γ
MTP	Microsomal triglyceride transfer protein
MRS	de Man, Rogosa and Sharpe
PBS	Phosphate buffered saline
PUFA	Polyunsaturated fatty acids
PFGE	Pulse-field gel electrophoresis
SDS	Special diets services
SEM	Standard error mean
TNF-α	Tumor necrosis factor-α

Introduction

Mammals can produce all but two of the fatty acids they require; thus linoleic acid (C18:2n-6, precursor of n-6

series of fatty acids) and α-linolenic acid (C18:3n-3, precursor of n-3 series of fatty acids) are essential dietary fatty acids. Although mammalian cells cannot synthesize these fatty acids, they can metabolize them into more physiologically active compounds through a series of elongation and desaturation reactions, in which linoleic acid is converted to arachidonic acid (C20:4n-6) and α-linolenic acid is metabolized to eicosapentaenoic acid (EPA) (C20:5n-3) via the action of the enzymes Δ^6 desaturase, Δ^5 desaturase and elongase [2]. The resulting highly unsaturated fatty acid metabolites play essential roles in cell membrane function, brain and nervous system development and function, and through the production of eicosanoids (thromboxanes, leukotrienes and prostaglandins) in the inflammatory process [2]. Eicosanoids derived from arachidonic acid, such as the 2-series prostaglandins and the 4-series leukotrienes are in general, regarded as being proinflammatory in nature [3, 4], whereas the eicosanoids derived from EPA, such as the 3-series prostaglandins and the 5-series leukotrienes are considered less inflammatory or even anti-inflammatory in nature [3–5]. Thus, by increasing the ratio of n-3 to n-6 fatty acids in the diet, and consequently favouring the production of EPA, the balance of eicosanoids can be shifted in a less inflammatory direction. EPA can be further metabolized to docosahexaenoic acid (DHA, C22:6n-3), which is one of the major n-3 polyunsaturated fatty acids (PUFA) in the brain. DHA is required for fetal brain development and is held to be critical in the newborn for appropriate development and intelligence [6]. Studies have also shown that DHA provides support to learning and memory events in animal models of Alzheimer's disease [7] and brain injury [8].

The human gut is a diverse microbial ecosystem containing about 100 trillion microorganisms, comprised of more than 1,000 different species, whose collective genome, the microbiome, contains ~100-fold more genes than the entire human genome [9]. It has been well documented that the enteric microbiota play an important role in the health and well-being of the host, exerting effects on host lipid metabolism and acting as an environmental factor that contributes to development of obesity [10, 11]. In this respect, recent studies suggest that symbiosis between the microbiome and the host influences energy extraction from the diet. In addition, the promotion of fat deposition and influence on systemic inflammation have been proposed as mechanisms by which the microbiome contribute to obesity [12].

Little is known regarding the interplay between members of the enteric microbiota and fatty acids. However, some interactions between PUFAs and components of the indigenous gut microbiota and some probiotics have been reported, which might affect the biological roles of both. Recent studies by our group and others have reported that intestinal bacteria of human origin can convert linoleic and linolenic acids to bioactive isomers of conjugated linoleic acid (CLA) and conjugated α-linolenic acid, respectively [13–15]. Some bacteria of marine origin are also known to synthesise EPA and DHA de novo through the actions of polyunsaturated fatty acid synthase genes, which results in EPA and DHA being abundantly present in fish and fish oil [16–19]. Furthermore, it has been shown that administration of probiotics (*Lactobacillus rhamnosus* GG and *Bifidobacterium animalis* subsp. *lactis* Bb12) to pregnant women had an affect on placental fatty acid composition [20]. It has also been demonstrated that administration of formula supplemented with different probiotics (*B. animalis* subsp. *lactis* Bb12 and *L. rhamnosus* GG) to infants resulted in changes in serum fatty acid composition [21].

We have recently shown that feeding different animal species a CLA-producing *Bifidobacterium* of human origin (*B. breve* NCIMB 702258), in combination with linoleic acid as substrate, resulted in modulation of the fatty acid composition of the host, including significantly elevated concentrations of *c*9, *t*11 CLA in the liver. This study also demonstrated that oral administration of *B. breve* NCIMB 702258 to mice resulted in significantly higher concentrations of EPA and DHA in adipose tissue, coupled with reductions in the proinflammatory cytokines tumor necrosis factor-α (TNF-α) and interferon-γ (IFN-γ) [1]. The objective of this study was, therefore, to investigate the effects of co-administration of *B. breve* NCIMB 702258 and the substrate for EPA, α-linolenic acid, on fatty acid composition of different host tissues in mice.

Experimental Procedure

Preparation and Administration of *B. breve* NCIMB 702258

Rifampicin resistant variants of *B. breve* NCIMB 702258 were isolated by spread-plating ~10^9 colony forming units (CFU) from an overnight culture onto MRS agar (de Man, Rogosa & Sharpe; Difco Laboratories, Detroit, MI, USA) supplemented with 0.05% (wt/v) L-cysteine hydrochloride (98% pure; Sigma Chemical Co., St. Louis, MO, USA) (mMRS) containing 500 μg/ml rifampicin (Sigma Chemical Co., Poole, Dorset, UK). Following anaerobic incubation at 37 °C for 3 days, colonies were stocked in mMRS broth containing 40% (v/v) glycerol and stored at −80 °C. To confirm that the rifampicin resistant variant was identical to the parent strain, molecular fingerprinting using pulse-field gel electrophoresis (PFGE) was employed.

Prior to freeze drying, *B. breve* NCIMB 702258 was grown in mMRS by incubating overnight at 37 °C under anaerobic conditions. The culture was washed twice in

phosphate buffered saline (PBS) and then resuspended at a concentration of $\sim 1 \times 10^{10}$ cells/ml in 15% (wt/v) trehalose (Sigma) in dH_2O. One millilitre aliquots were freeze-dried using a 24 h programme (freeze temp. −40 °C, condenser set point −60, vacuum set point 600 mTorr). Each mouse that received *B. breve* consumed approximately 1×10^9 live microorganisms per day. This was achieved by resuspending appropriate quantities of freeze-dried powder in water which mice consumed ad libitum. Mice that did not receive the bacterial strain received placebo freeze-dried powder (15% wt/v trehalose in dH_2O).

Animals and Treatment

Female BALB/c mice were purchased from Harlan Ltd. (Briester, Oxon, UK) at 8 weeks of age and were fed ad libitum with standard non-purified CRM(P) diet (Special Diets Services (SDS), Witham, Essex, UK) with free access to water at all times. The diet contained the following nutrient composition (wt/wt): nitrogen free extract (57.39%), crude protein (18.35%), moisture (10%), ash (6.27%), crude fibre (4.23%) and crude oil (3.36%), which consisted of saturated fatty acids: lauric acid (C12:0, 0.03%), myristic acid (C14:0, 0.14%), palmitic acid (C16:0, 0.33%) and stearic acid (C18:0, 0.06%), monounsaturated fatty acids: myristoleic acid (C14:1, 0.02%), palmitoleic acid (C16:1, 10%) and oleic acid (C18:1, 0.87%), polyunsaturated fatty acids: linoleic acid (C18:2n-6, 0.96%), linolenic acid (C18:3n-3, 0.11%) and arachidonic acid (C20:4n-6, 0.11%). Mice were maintained at four per cage and kept in a controlled environment at 25 °C under a 12-h-light/12-h-dark cycle. All laboratory animal experiments were performed according to the guidelines for the care and use of laboratory animals approved by the Department of Health and Children of the Irish Government.

One week after arrival, the mice were divided into four groups (A–D, $n = 8$) and subjected to the following dietary treatments daily: Group A received standard nonpurified CRM(P) diet supplemented with 1% α-linolenic acid (C18:3n-3, wt/wt, triglyceride bound form, Larodan Fine Chemicals AB, Malmo, Sweden) in combination with approximately 1×10^9 live *B. breve* NCIMB 702258 per mouse, Group B received standard non-purified CRM(P) diet supplemented with 1% α-linolenic acid and placebo freeze-dried powder, Group C received standard nonpurified CRM(P) diet and $\sim 1 \times 10^9$ live *B. breve* NCIMB 702258, Group D received standard nonpurified CRM(P) diet and placebo freeze-dried powder. For α-linolenic acid treatment, a powdered diet (milled standard non-purified CRM(P) pellets) was blended with the α-linolenic acid to yield a concentration of approximately 90 mg α-linolenic acid per mouse per day (based on studies by Bassaganya-Riera et al. [22] who reported an optimal intake of fatty acids of 1 g/100 g per day). All prepared diets were stored at −20 °C and fresh diets were provided twice weekly. Following 8 weeks on experimental diets, the animals were sacrificed by cervical dislocation. Liver, adipose tissue and brain were removed from the carcasses, blotted dry on filter paper, weighed and frozen in liquid nitrogen. All samples were stored at −80 °C until processed.

Microbial Analysis

Fresh faecal samples were taken directly from the anus of each mouse every second week for microbial analysis. Large intestinal contents were also sampled at sacrifice for enumeration of the administered *B. breve* strain. Microbial analysis of *B. breve* NCIMB 702258 was performed by pour plating onto mMRS agar supplemented with 100 μg of mupirocin (Oxoid)/ml and 100 μg rifampicin (Sigma)/ml. Agar plates were incubated anaerobically at 37 °C for 72 h. Anaerobic environments were created using CO_2 generating kits (Anaerocult A; Merck, Darmstadt, Germany) in sealed gas jars.

Lipid Extraction and Fatty Acid Analysis

Lipids were extracted according to the method of O'Fallon et al. [23]. Briefly, tissue samples were cut into 1.5-mm rectangular strips and placed into a screw-cap Pyrex culture tube together with 0.7 ml of 10 mol/l KOH in dH_2O and 5.3 ml of MeOH. The tubes were incubated in a water bath at 55 °C for 1.5 h with vigorous hand-shaking every 20 min. After cooling below room temperature, 0.58 ml of 12 mol/l of H_2SO_4 in dH_2O was added. The tubes were mixed by inversion and with precipitated K_2SO_4 present incubated again at 55 °C for 1.5 h with hand-shaking every 20 min. Fatty acid methyl esters (FAME) were recovered by addition of 3 ml hexane and vortex mixed and separated by gas liquid chromatography (Varian 3400, Varian, Walnut Creek, CA, USA fitted with a flame ionisation detector) using a Chrompack CP Sil 88 column (Chrompack, Middleton, The Netherlands, 100 m × 0.25 mm i.d., 0.20 μm film thickness) and He as the carrier gas. The column oven was initially programmed at 80 °C for 8 min, and increased at 8.5 °C/min to a final column temperature of 200 °C. The injection volume was 0.6 μl, with automatic sample injection on a SPI 1093 splitless on-column temperature programmable injector. Data were recorded and analysed on a Minichrom PC system (VG Data System, Manchester, UK). Peaks were identified with reference to retention times of fatty acids in a standard mixture. All fatty acid results are shown as means ± standard error means (SEM) g/100 g FAME.

Statistical Analysis

Results in the text, tables and figures are presented as means per group ± SEM. Data were analysed using analysis of variance (ANOVA) followed by Tukey's post hoc test using GraphPad InStat for Windows (GraphPad Software, La Jolla, CA, USA) in order to assess if differences between treatment groups (A–D) were significant. Probability values of $P < 0.05$ were set as a threshold for statistical significance.

Results

Microbial Analysis

The administered *B. breve* NCIMB 702258 was recovered in faeces from all mice that received the strain, within 2 weeks of feeding, confirming gastrointestinal transit and survival of the strain. Stool recovery of *B. breve* NCIMB 702258 was approximately 4×10^5 CFU/g faeces by week 8 of the trial in mice that received *B. breve* in combination with α-linolenic acid (group A) and approximately 2.2×10^6 CFU/g faeces in mice that received *B. breve* without α-linolenic acid (group C) (data not shown). The *B. breve* strain was detected in large intestinal contents at $\sim 4.6 \times 10^5$ CFU/g in mice that received *B. breve* and α-linolenic acid (group A) and $\sim 1.4 \times 10^6$ CFU/g in mice that received *B. breve* alone (group C). *B. breve* NCIMB 702258 was not isolated from any of the mice within group B (administered α-linolenic acid alone) or group D (unsupplemented).

Tissue Fatty Acid Composition

Oral administration of *B. breve* NCIMB 702258 and/or α-linolenic acid (C18:3n-3) did not significantly influence body weight throughout the trial period. Supplementation of α-linolenic acid, either in combination with *B. breve* or in the absence of the *B. breve* strain (group A and group B) resulted in tenfold higher concentrations of α-linolenic acid and EPA (C20:5n-3) in liver ($P < 0.05$; Table 1) and adipose tissue ($P < 0.05$; Table 2) compared with groups that did not receive the fatty acid supplement (group C and group D). In addition, the α-linolenic acid supplemented groups exhibited significantly higher concentrations of docosapentaenoic acid (DPA, C22:5n-3) in liver ($P < 0.05$; Table 1) and adipose tissue ($P < 0.05$; Table 2), significantly higher concentrations of DHA (C22:6n-3) in liver ($P < 0.05$; Fig. 2) and significantly lower concentrations of arachidonic acid (C20:4n-6) in liver ($P < 0.05$; Table 1), adipose tissue ($P < 0.05$, Table 2) and brain ($P < 0.05$, Table 3) compared with groups that did not receive fatty acid supplementation (group C and group D). The arachidonic acid/EPA ratios in liver and adipose tissue were approximately 30-fold and 20-fold lower, respectively, in the α-linolenic acid supplemented groups (group A and B) compared with unsupplemented controls (group D) ($P < 0.05$). In addition, the n-6/n-3 ratio was significantly lower in all tissues except the brain of animals supplemented with α-linolenic acid (group A and B) ($P < 0.05$; Table 1 and 2).

Administration of *B. breve* in combination with α-linolenic acid resulted in significant changes in the fatty acid composition of host liver and brain in comparison to animals that were administered α-linolenic acid alone. Mice that received *B. breve* in combination with α-linolenic acid (group A) exhibited on average, 23% more EPA (C20:5n-3) and 20% more dihomo-γ-linolenic acid (C20:3n-6) in the liver compared with the group that was administered α-linolenic acid alone (group B) ($P < 0.05$; Fig. 1; Table 1). Group A also exhibited a 12% higher concentration of DHA (C22:6n-3) in brain ($P < 0.05$; Fig. 2), as well as numerically, though not significantly, higher concentrations of DHA (C22:6n-3) in adipose tissue and liver (27 and 16%, respectively) compared with group B (Fig. 2). In addition, mice that received *B. breve* without α-linolenic acid (group C), exhibited numerically, though not significantly, higher concentrations of DHA (C22:6n-3) in brain tissue in comparison to unsupplemented controls (group D) (Fig. 2).

Oral administration of *B. breve*, both in combination with α-linolenic acid and without α-linolenic acid supplementation (group A and C), also resulted in significantly higher concentrations of arachidonic acid (C20:4n-6) and stearic acid (C18:0) incorporated in the liver compared to mice that did not receive *B. breve* (group B and group D) ($P < 0.05$; Table 1).

Discussion

The influence of dietary PUFA on phospholipids, their eicosanoid derivatives and the transmembrane-signalling lipid rafts into which they are arranged provide multiple targets for the dietary modulation of the balance of inflammatory mediators in the human gut. In addition, gut mucosal inflammation is now recognised as being heavily influenced by the gastrointestinal microbiota [24, 25]. The delicate balance of inflammatory mediators derived from PUFA may be readjusted by members of the indigenous gut microbiota. In this study, we investigated how co-administration of *B. breve* NCIMB 702258 and the substrate for EPA, α-linolenic acid affected the EPA and DHA concentrations of different host tissues. We found that dietary supplementation of *B. breve* NCIMB 702258 in combination with α-linolenic

Table 1 Fatty acid composition (%) of liver from BALB/c mice

FAME	Liver			
	A	B	C	D
C16:0	23.11 ± 0.99^{c,d}	23.89 ± 0.71^{c,d}	27.78 ± 0.64^{a,b}	27.64 ± 0.42^{a,b}
C16:1c9	1.56 ± 0.10^{b,c,d}	2.07 ± 0.18^{a,d}	2.32 ± 0.18^{a}	2.73 ± 0.27^{a,b}
C18:0	13.83 ± 0.42^{b,c,d}	12.36 ± 0.44^{a,d}	11.50 ± 0.35^{a,d}	10.40 ± 0.35^{a,b,c}
C18:1c9	9.16 ± 0.36^{c,d}	10.16 ± 0.62^{c,d}	13.75 ± 0.57^{a,b}	15.16 ± 0.75^{a,b}
C18:2n-6	18.70 ± 0.35	18.32 ± 0.21^{d}	18.21 ± 0.32^{d}	19.38 ± 0.42^{b,c}
C18:3n-3	8.37 ± 0.91^{c,d}	9.47 ± 0.64^{c,d}	0.50 ± 0.03^{a,b}	0.58 ± 0.04^{a,b}
C18:3n-6	0.20 ± 0.02^{c,d}	0.17 ± 0.01^{c,d}	0.30 ± 0.03^{a,b}	0.32 ± 0.01^{a,b}
C18:4n-3	0.14 ± 0.01^{c,d}	0.16 ± 0.01^{c,d}	0.23 ± 0.03^{a,b}	0.22 ± 0.02^{a,b}
C20:3n-6	0.73 ± 0.05^{b}	0.61 ± 0.02^{a}	0.69 ± 0.04	0.63 ± 0.03
C20:4n-6	6.71 ± 0.29^{b,c,d}	5.57 ± 0.14^{a,c,d}	11.45 ± 0.58^{a,c,d}	9.78 ± 0.53^{a,b,c}
C22:5n-3	1.02 ± 0.06^{c,d}	0.94 ± 0.05^{c,d}	0.23 ± 0.02^{a,b}	0.26 ± 0.02^{a,b}
n-6/n-3	1.36 ± 0.10^{c,d}	1.30 ± 0.07^{c,d}	4.70 ± 0.23^{a,b}	5.07 ± 0.16^{a,b}

Results are expressed as means ± SEM g/100 g FAME ($n = 8$). Different superscript letters within a column indicate significant difference ($n = 8$, $P < 0.05$). *FAME* fatty acid methyl esters. Group A = 1% α-linolenic acid in combination with 1×10^9 live *B. breve* NCIMB 702258 per day, Group B = 1% α-linolenic acid, Group C = standard diet in combination with 1×10^9 live *B. breve* NCIMB 702258, and Group D = unsupplemented mice (standard diet). *ND* not detected

Table 2 Fatty acid composition (%) of adipose tissue from BALB/c mice

FAME	Adipose tissue			
	A	B	C	D
C16:0	28.84 ± 2.83^{c}	28.73 ± 2.16^{c}	30.92 ± 0.82^{a,b,d}	29.87 ± 0.83^{c}
C16:1c9	5.39 ± 0.73	6.07 ± 2.01	6.69 ± 1.95	6.54 ± 2.31
C18:0	8.76 ± 1.00	8.00 ± 2.33	7.71 ± 1.99	7.31 ± 2.87
C18:1c9	14.41 ± 1.29	14.83 ± 3.01	16.92 ± 3.07	18.35 ± 4.84
C18:2n-6	18.22 ± 0.25^{c}	18.80 ± 0.81^{c}	16.56 ± 0.77^{a,b}	17.96 ± 3.39
C18:3n-3	6.56 ± 1.00^{c,d}	7.35 ± 2.15^{c,d}	0.66 ± 0.10^{a,b}	0.79 ± 0.28^{a,b}
C18:3n-6	0.15 ± 0.02	0.13 ± 0.03	0.15 ± 0.03	0.14 ± 0.04
C18:4n-3	0.16 ± 0.02	0.12 ± 0.03	0.14 ± 0.04	0.14 ± 0.03
C20:3n-6	0.37 ± 0.04	0.30 ± 0.09	0.32 ± 0.09	0.29 ± 0.16
C20:4n-6	6.20 ± 0.97^{c}	5.27 ± 2.04^{c,d}	10.57 ± 3.45^{a,b}	9.29 ± 5.27^{b}
C22:5n-3	0.67 ± 0.06^{c,d}	0.55 ± 0.14^{c,d}	0.27 ± 0.03^{a,b}	0.27 ± 0.16^{a,b}
n-6/n-3	2.20 ± 0.21^{c,d}	2.15 ± 0.15^{c,d}	10.80 ± 0.28^{a,b}	11.56 ± 0.92^{a,b}

Results are expressed as means ± SEM g/100 g FAME ($n = 8$). Different superscript letters within a column indicate significant difference ($n = 8$, $P < 0.05$). *FAME* fatty acid methyl esters. Group A = 1% α-linolenic acid in combination with 1×10^9 live *B. breve* NCIMB 702258 per day, Group B = 1% α-linolenic acid, Group C = standard diet in combination with 1×10^9 live *B. breve* NCIMB 702258, and Group D = unsupplemented mice (standard diet). *ND* not detected

acid resulted in the modulation of host fatty acid composition, and, specifically, resulted in significantly higher EPA and dihomo-γ-linolenic acid concentrations in liver and higher DHA in brain compared to mice that received α-linolenic acid without microbial supplementation. Some recent studies have shown that the gut microbiota modifies a number of lipid species in serum, adipose tissue and liver [26] as well as the eye lipidome of mice [27] when compared to germ-free mice, suggesting that interactions between intestinal bacteria and fatty acids occur.

Supplementation of α-linolenic acid, both in combination with *B. breve* and in the absence of the *B. breve* strain, resulted in significant increases in EPA and DHA in the liver and adipose tissue, at the expense of arachidonic acid. Since EPA replaces arachidonic acid as an eicosanoid

Table 3 Fatty acid composition (%) of brain from BALB/c mice

FAME	Brain			
	A	B	C	D
C16:0	30.69 ± 0.65	32.38 ± 0.44^{c}	28.88 ± 0.90^{b,d}	31.47 ± 0.51^{c}
C16:1c9	0.81 ± 0.02^{b,c}	0.94 ± 0.03^{a,c,d}	0.73 ± 0.03^{a,d}	0.84 ± 0.03^{b,c}
C18:0	20.22 ± 0.07^{b}	19.87 ± 0.14^{a}	20.11 ± 0.20	19.85 ± 0.28
C18:1c9	17.58 ± 0.19	17.61 ± 0.24	17.14 ± 0.29	17.23 ± 0.33
C18:2n-6	1.18 ± 0.04^{b,c}	1.54 ± 0.10^{a,c,d}	1.00 ± 0.05^{a,b}	1.14 ± 0.03^{b}
C18:3n-3	0.10 ± 0.01^{b,c,d}	0.18 ± 0.02^{a,c,d}	ND	ND
C18:3n-6	ND	ND	ND	ND
C18:4n-3	ND	ND	ND	ND
C20:3n-6	ND	ND	ND	ND
C20:4n-6	7.06 ± 0.07^{c}	6.88 ± 0.12^{c,d}	7.84 ± 0.23^{a,b}	7.37 ± 0.17^{b}
C22:5n-3	0.25 ± 0.01^{c,d}	0.24 ± 0.01^{c}	0.11 ± 0.01^{a,b}	0.17 ± 0.04^{a}
n-6/n-3	0.79 ± 0.03^{b,d}	0.89 ± 0.03^{a}	0.87 ± 0.04	0.97 ± 0.04^{a}

Results are expressed as means ± SEM g/100 g FAME ($n = 8$). Different superscript letters within a column indicate significant difference ($n = 8$, $P < 0.05$). *FAME* fatty acid methyl esters. Group A = 1% α-linolenic acid in combination with 1×10^9 live *B. breve* NCIMB 702258 per day, Group B = 1% α-linolenic acid, Group C = standard diet in combination with 1×10^9 live *B. breve* NCIMB 702258, and Group D = unsupplemented mice (standard diet). *ND* not detected

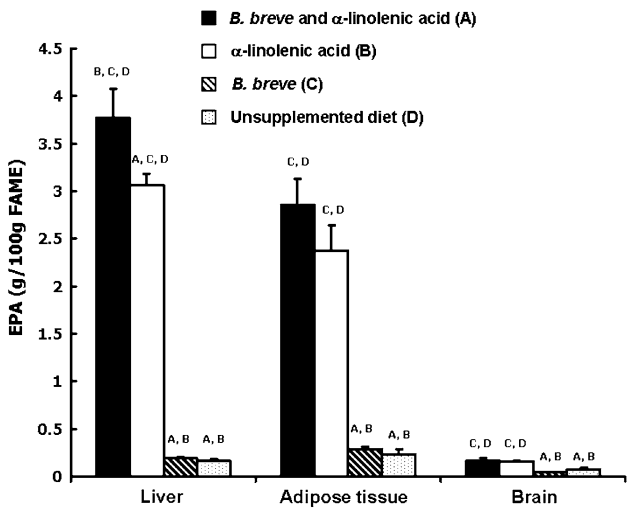

Fig. 1 Eicosapentaenoic acid (EPA) concentrations in murine liver, adipose tissue and brain. Different superscript letters within a column indicate significant differences ($n = 8$, $P < 0.05$). EPA is expressed as Mean ± SEM g/100 g fatty acid methyl esters (FAME)

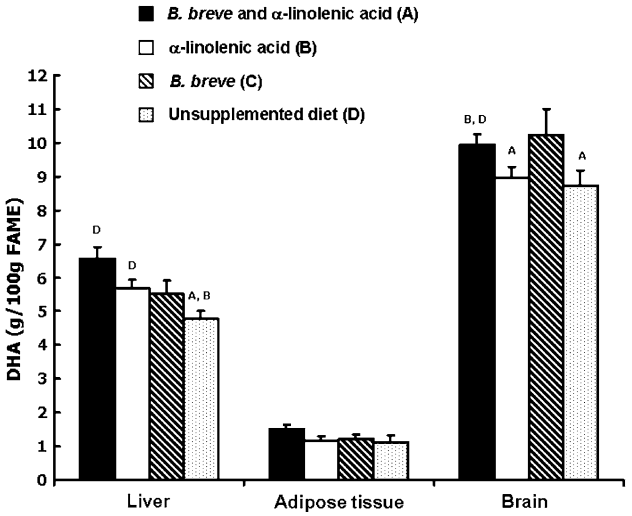

Fig. 2 Docosahexaenoic acid (DHA) concentrations in murine liver, adipose tissue and brain. Different superscript letters within a column indicate significant differences ($n = 8$, $P < 0.05$). DHA is expressed as mean ± SEM g/100 g fatty acid methyl esters (FAME)

precursor in cell membranes of platelets, erythrocytes, neutrophils, monocytes and hepatocytes [28], this results in a reduced synthesis of inflammatory eicosanoids from arachidonic acid and, subsequently, elevated production of anti-inflammatory eicosanoids from EPA. This alteration towards a more anti-inflammatory profile could be of importance in a variety of chronic inflammatory settings that are of high prevalence in Western societies such as inflammatory bowel disease (IBD), rheumatoid arthritis, cardiovascular disease, obesity, Alzheimer's disease and certain psychiatric diseases such as depression, which are characterised by an excessive production of arachidonic acid-derived eicosanoids [29–33]. Moreover, since excessive intake of n-6 PUFA, characteristic of modern Western diets, could potentiate inflammatory processes and so could predispose to, or exacerbate associated diseases, increasing the intake of α-linolenic acid and/or EPA may have a protective effect. A recent study using IL-10 knock-out mice (mice that spontaneously develop colitis) demonstrated significantly reduced colonic inflammation of mice that were fed fish oil (enriched in EPA and DHA) compared with mice that were fed n-6 PUFA-rich corn oil [34].

Oral administration of *B. breve*, both in combination with α-linolenic acid and without α-linolenic acid supplementation, resulted in significantly higher amounts of arachidonic acid incorporated in liver compared to mice that did not receive *B. breve*. Given that the administration of *B. breve* resulted in significantly higher concentrations of long-chain PUFA such as EPA, DHA and arachidonic acid, administration of this strain resulted in an increase in the levels of unsaturation within fatty acids. Interestingly, it was previously shown that a mixture of probiotics (*Bacillus subtilis, B. natto, B. megaterium, B. thermophilus, Lactobacillus acidophilus, L. plantarum, L. brevis, L. casei, Streptococcus faecalis, S. lactis, S. thermophilus, Clostridium butyricum, Saccharomyces cerevisiae* and *Candida utilis*) increased the activity of liver Δ6-desaturase in rats, which resulted in increased amounts of arachidonic acid derived from linoleic acid [35]. Consequently, in our study, the increased levels of long-chain PUFA in *B. breve* supplemented groups may have arisen from the reported properties of probiotics in regulating desaturase activity involved in the metabolism of fatty acids to their longer-chain unsaturated derivatives. *B. breve* NCIMB 702258 may also have influenced the mechanisms of PUFA uptake to the intestinal epithelium in the present study. It was recently demonstrated that exposure of *L. plantarum* WCFSI to human intestinal mucosa induced an upregulation of genes involved in fatty acid uptake, i.e. CD36 and microsomal triglyceride transfer protein (MTP) [36].

Quantification of the numbers of bacteria of the *B. breve* strain monitored in the feces of individual mice confirmed gastrointestinal transit and survival of *B. breve* NCIMB 702258. Faecal recovery was approximately 2×10^6 CFU/g feces in mice that received *B. breve* without α-linolenic acid and approximately 4×10^5 CFU/g feces in mice that received *B. breve* in combination with α-linolenic acid. The fecal recovery of *B. breve* NCIMB 702258 in mice that received *B. breve* without α-linolenic acid is consistent with our previous study [1], however the fecal recovery of *B. breve* was reduced in the presence of α-linolenic acid. Since free PUFA have been shown to be antibacterial and to inhibit the growth of bacteria [37–39] and adhesion of bacteria to intestinal surfaces [40], this might explain the lower numbers of *B. breve* obtained from mice that received supplementation of α-linolenic acid compared to mice that did not receive fatty acid supplementation.

Since the effect of the combined *B. breve* and α-linolenic acid intervention on EPA- and DHA concentrations was greater than that of α-linolenic acid intervention alone, this effect could be attributed to *B. breve* NCIMB 702258 and suggests that feeding a metabolically active strain can influence the fatty acid composition of host tissues. In conclusion, the present study shows that the administration of *B. breve* NCIMB 702258 is associated with alterations in the fatty acid composition of host liver and brain, including elevated concentrations of EPA and DHA. This interaction between administered microbes and n-3 fatty acids could result in more efficient probiotic preparations, which may be beneficial for a range of immunoinflammatory disorders as well as having significance for the promotion of neurological development in infants.

Acknowledgments The authors acknowledge the technical assistance of Seamus Aherne for fatty acid analysis, Frances O'Brien and Grainne Hurley for assistance with the murine trial. The authors are supported, in part, by Science Foundation Ireland (SFI), the Irish Ministry for Food and Agriculture, the Higher Education Authority and the Health Research Board of Ireland and the Irish Government under the National Development Plan 2000–2006.

References

1. Wall R, Ross RP, Shanahan F, O'Mahony L, O'Mahony C, Coakley M, Hart O, Lawlor P, Quigley EM, Kiely B, Fitzgerald GF, Stanton C (2009) The metabolic activity of the enteric microbiota influences the fatty acid composition of murine and porcine liver and adipose tissues. Am J Clin Nutr 89:1393–1401
2. Simopoulos AP (2002) The importance of the ratio of omega-6/omega-3 essential fatty acids. Biomed Pharmacother 56:365–379
3. Calder PC (2008) Polyunsaturated fatty acids, inflammatory processes and inflammatory bowel diseases. Mol Nutr Food Res 52:885–897
4. Bagga D, Wang L, Farias-Eisner R, Glaspy JA, Reddy ST (2003) Differential effects of prostaglandin derived from omega-6 and omega-3 polyunsaturated fatty acids on COX-2 expression and IL-6 secretion. Proc Natl Acad Sci USA 100:1751–1756
5. Robinson JG, Stone NJ (2006) Antiatherosclerotic and antithrombotic effects of omega-3 fatty acids. Am J Cardiol 98:39–49
6. Salem N, Wegher B, Mena P, Uauy R (1996) Arachidonic and docosahexaenoic acids are biosynthesized from their 18-carbon precursors in human infants. Proc Natl Acad Sci USA 93:49–54
7. Hashimoto M, Hossain S, Shimada T, Sugioka K, Yamasaki H, Fujii Y, Ishibashi Y, Oka J, Shido O (2002) Docosahexaenoic acid provides protection from impairment of learning ability in Alzheimer's disease model rats. J Neurochem 81:1084–1091
8. Wu A, Ying Z, Gomez-Pinilla F (2004) The interplay between oxidative stress and brain-derived neurotrophic factor modulates the outcome of saturated fat diet on synaptic plasticity and cognition. Eur J Neurosci 19:1699–1707
9. O'Hara AM, Shanahan F (2006) The gut as a forgotten organ. EMBO Rep 7:688–693
10. Bäckhed F, Ding H, Wang T, Hooper LV, Koh GY, Nagy A, Semenkovich CF, Gordon JI (2004) The gut microbiota as an environmental factor that regulates fat storage. Proc Natl Acad Sci USA 101:15718–15723
11. Marchesi J, Shanahan F (2007) The normal intestinal microbiota. Curr Opin Infect Dis 20:508–513
12. Tsai F, Coyle WJ (2009) The microbiome and obesity: is obesity linked to our gut flora? Curr Gastroenterol Rep 11:307–313
13. Barrett E, Ross RP, Fitzgerald GF, Stanton C (2007) Rapid screening method for analyzing the conjugated linoleic acid production capabilities of bacterial cultures. Appl Environ Microbiol 73:2333–2337
14. Lee K, Paek K, Lee HY, Park JH, Lee Y (2007) Antiobestity effect of *trans*-10, *cis*-12-conjugated linoleic acid-producing

Lactobacillus plantarum PL62 on diet-induced obese mice. J Appl Microbiol 103:1140–1146
15. Coakley M, Ross RP, Nordgren M, Fitzgerald G, Devery R, Stanton C (2003) Conjugated linoleic acid biosynthesis by human-derived *Bifidobacterium* species. J Appl Microbiol 94:138–145
16. Orikasa Y, Yamada A, Yu R, Ito Y, Nishida T, Yumoto I (2004) Characterization of the eicosapentaenoic acid biosynthesis gene cluster from *Shewanella* sp. strain SCRC-2738. Cell Mol Biol 50:625–630
17. Metz JG, Roessler P, Facciotti D, Levering C, Dittrich F, Lassner M (2001) Production of polyunsaturated fatty acids by polyketide synthases in both prokaryotes and eukaryotes. Science 293:290–293
18. Russell NJ, Nichols DS (1999) Polyunsaturated fatty acids in marine bacteria—a dogma rewritten. Microbiology 145:767–779
19. Yano Y, Nakayama A, Saito H, Ishihara K (1994) Production of docosahexaenoic acid by marine bacteria isolated from deep sea fish. Lipids 29:527–528
20. Kaplas N, Isolauri E, Lampi AM, Ojala T, Laitinen K (2007) Dietary counselling and probiotic supplementation during pregnancy modify placental phospholipid fatty acids. Lipids 45:865–870
21. Kankaanpää PE, Yang B, Kallio HP, Isolauri E, Salminen SJ (2002) Influence of probiotic supplemented infant formula on composition of plasma lipids in atopic infants. J Nutr Biochem 13:364–369
22. Bassaganya-Riera J, Reynolds K, Martino-Catt S, Cui Y, Hennighausen L, Gonzalez F, Rohrer J, Benninghoff U, Hontecillas R (2004) Activation of PPARγ and δ by conjugated linoleic acid mediates protection from experimental inflammatory bowel disease. Gastroenterology 127:777–791
23. O'Fallon JV, Busboom JR, Nelson ML, Gaskins CT (2007) A direct method for fatty acid methyl ester synthesis: application to wet meat tissues, oils, and feedstuffs. J Anim Sci 85:1511–1521
24. Swidsinski A, Ladhoff A, Pernthaler A, Swidsinski S, Loening-Baucke V, Ortner M, Weber J, Hoffmann U, Schreiber S, Dietel M, Lochs H (2002) Mucosal flora in inflammatory bowel disease. Gastroenterology 122:44–54
25. Favier C, Neut C, Mizon C, Cortot A, Colombel JF, Mizon J (1997) Fecal beta-D-galactosidase production and *Bifidobacteria* are decreased in Crohn's disease. Dig Dis Sci 42:817–822
26. Velagapudi VR, Hezaveh R, Reigstad CS, Gopalacharyulu PV, Yetukuri L, Islam S, Felin J, Perkins R, Boren J, Oresic M, Bäckhed F (2009) The gut microbiota modulates host energy and lipid metabolism in mice. J Lipid Res doi:10.1194/jlr.M002774
27. Oresic M, Seppänen-Laakso T, Yetukuri L, Bäckhed F, Hänninen V (2009) Gut microbiota affects lens and retinal lipid composition. Exp Eye Res 89(5):604–607
28. Simopoulos AP (2003) Importance of the ratio of omega-6/omega-3 essential fatty acids: evolutionary aspects. World Rev Nutr Diet 92:1–22
29. Dinan T, Siggins L, Scully P, O'Brien S, Ross P, Stanton C (2008) Investigating the inflammatory phenotype of major depression: focus on cytokines and polyunsaturated fatty acids. J Psychiatr Res 43:471–476
30. Jupp J, Hillier K, Elliott DH, Fine DR, Bateman AC, Johnson PA, Cazaly AM, Penrose JF, Sampson AP (2007) Colonic expression of leukotriene-pathway enzymes in inflammatory bowel diseases. Inflamm Bowel Dis 13:537–546
31. Wallace JL (2001) Prostaglandin biology in inflammatory bowel disease. Gastroenterol Clin North Am 30:971–980
32. James MJ, Gibson RA, Cleland LG (2000) Dietary polyunsaturated fatty acids and inflammatory mediator production. Am J Clin Nutr 71:343S–438S
33. Simopoulos AP, Leaf A, Salem N (2000) Workshop statement on the essentiality of and recommended dietary intakes for omega-6 and omega-3 fatty acids. Prostaglandins Leukot Essent Fatty Acids 63:119–121
34. Chapkin RS, Davidson LA, Ly L, Weeks BR, Lupton JR, McMurray DN (2007) Immunomodulatory effects of (n-3) fatty acids: putative link to inflammation and colon cancer. J Nutr 137:200–204
35. Fukushima M, Yamada A, Endo T, Nakano M (1999) Effects of a mixture of organisms, Lactobacillus acidophilus or Streptococcus faecalis on delta-6 desaturase activity in the livers of rats fed a fat and cholesterol-enriched diet. Nutrition 15:373–378
36. Troost FJ, van Baarlen P, Lindsey P, Kodde A, de Vos WM, Kleerebezem M, Brummer RJ (2008) Identification of the transcriptional response of human intestinal mucosa to Lactobacillus plantarum WCFSI in vivo. BMC Genomics 9:374–388
37. Nieman C (1954) Influence of trace amounts of fatty acids on the growth of microorganisms. Bacteriol Rev 18(2):147–163
38. Laser H (1951) Adaptation of *Bacillus subtilis* to fatty acids. Biochem J 49(5):lxvi–lxvii
39. Kelsey JA, Bayles KW, Shafii B, McGuire MA (2006) Fatty acids and monoacylglycerols inhibit growth of *Staphylococcus aureus*. Lipids 41(10):951–961
40. Kankanpää PE, Salminen SJ, Isolauri E, Lee YK (2001) The influence of polyunsaturated fatty acids on probiotic growth and adhesion. FEMS Microbiol Lett 194:149–153

Lipids (2010) 45:437–444
DOI 10.1007/s11745-010-3414-3

ORIGINAL ARTICLE

Occurrence of the *cis*-4,7,10, *trans*-13-22:4 Fatty Acid in the Family Pectinidae (Mollusca: Bivalvia)

Edouard Kraffe · Jacques Grall · Elena Palacios · Citlali Guerra · Philippe Soudant · Yanic Marty

Received: 18 September 2009 / Accepted: 7 April 2010 / Published online: 29 April 2010

Abstract The present study aimed to elucidate the effective phylogenetic specificity of distribution of a *cis*-4,7,10, *trans*-13-22:4 (22:4(n-9)Δ13*trans*) among pectinids. For this purpose, we extended the analysis of membrane glycerophospholipids FA composition to 13 species of scallops, covering 11 genera and 7 tribes representatives of the three subfamilies Chlamydinae, Palliolinae and Pectininae and the subgroup Aequipecten. In species belonging to the subfamily Pectininae and the Aequipecten subgroup, 22:4(n-9)Δ13*trans* was found in substantial amounts, but it was absent in other species belonging to the subfamilies Chlamydinae and Palliolinae. Homologous non-methylene-interrupted (NMI) FA, also hypothesized to differ along phylogenetic lines in bivalves, were totally absent or present only in trace amounts in representatives of the Aequipecten subgroup but ranged from 0.3 to 4.5% of the total FA in Pectinidae, Chlamydinae, and Palliolinae subfamilies. The species-specific occurrence of NMI and 22:4(n-9)Δ13*trans* FA in membrane lipids of pectinids agrees with the most recent phylogenies based on shell morphology and molecular characteristics. We examined the potential timing of the appearance of 22:4(n-9)Δ13*trans* in pectinids on a geologic time scale.

Keywords *cis*-4,7,10, *trans*-13-22:4 fatty acid · Fatty acid composition · Bivalve · Scallops · Pectinidae · Phylogeny

Abbreviations

NMI	Non-methylene-interrupted fatty acids
NMID	Dienoic non-methylene-interrupted fatty acids
NMIT	Trienoic non-methylene-interrupted fatty acids
SerGpl	Phosphatidylserine
PlsSer	Phosphatidylserine plasmalogen

Introduction

To date, 4,7,10,13*trans*-22:4 FA (22:4(n-9)Δ13*trans*) has been reported and characterized in significant amounts in glycerophospholipids of three species of the family Pectinidae, the scallops *Pecten maximus*, *Argopecten purpuratus*, and *Aequipecten opercularis* [1, 2]. This 22:4(n-9)Δ13*trans* is particularly concentrated in the plasmalogen and diacyl forms of serine glycerophospholipids (SerGpl) [2]. This association was in evidence in all tissues analyzed, but the proportions of the 22:4(n-9)Δ13*trans* in these subclasses were highest in the gills and lowest in the adductor muscle.

The presence of 22:4(n-9)Δ13*trans* FA in the scallop species investigated was combined with very low levels of

E. Kraffe (✉) · Y. Marty
Unité Mixte CNRS 6521, Université de Bretagne Occidentale, CS 93837, 29238 Brest Cedex 3, France
e-mail: Edouard.Kraffe@univ-brest.fr

J. Grall · P. Soudant
Unité Mixte CNRS 6539, Institut Universitaire Européen de la Mer, Université de Bretagne Occidentale, 29280 Plouzané, France

E. Palacios
Centro de Investigaciones Biologicas del Noroeste (CIBNOR), Mar Bermejo 195, Col. Playa Palo de Santa Rita, 23090 La Paz, BCS, Mexico

C. Guerra
Alfred-Wegener Institute for Polar and Marine Research (AWI), 27515 Bremerhaven, Germany

C_{20} and C_{22} non-methylene-interrupted dienoic (NMID) and trienoic (NMIT) FA. Earlier reports on scallop FA compositions also indicated that the levels of these unusual NMI FA are generally very low in pectinids [3, 4], while they are seemingly ubiquitous components in other members of the class Bivalvia, occurring in concentrations up to 20% of the total FA [3, 5–9]. Interestingly, the specific association of the plasmalogen form of SerGpl (PlsSer) with the 22:4(n-9)Δ13*trans* for pectinids parallels the specific association found for PlsSer with NMI FA in non pectinid species [10]. Although these peculiar FA are structurally different, this led us to argue that these two types of FA could play similar roles in membrane functions [1]. First proposed by Ackman and Hooper [11], and demonstrated later by Zhukova [6, 8], NMI FA are considered to be the only polyunsaturated fatty acids (PUFA) synthesized de novo by bivalve mollusks. We thus hypothesized that 22:4(n-9)Δ13*trans* could be of endogenous origin, representing a specific attribute of Pectinidae [2]. Nevertheless, in the work of Napolitano and Ackman on the scallop *Placopecten magellanicus*, no peak (gas chromatogram) or unknown FA that could be interpreted as the 22:4(n-9)Δ13*trans* was described [4, 12, 13]. The fact that this FA is not found in *P. magellanicus* was recently confirmed [14]. Such observations raised the question whether 22:4(n-9)Δ13*trans* systematically occurs throughout the Pectinidae family.

This study investigated the occurrence of the 22:4 (n-9)Δ13*trans* and NMI FA in an expanded range of species of Pectinidae. The FA composition of membrane phospholipids was characterized in 13 different species of scallops that span 11 of the 56 genera, representing 7 tribes and belonging to 3 of the 4 most important subfamilies in term of number of extant species. We examined the chemotaxonomic relationships revealed by the distribution of 22:4(n-9)Δ13*trans* and NMI FA, and compared them with existing morphological and molecular classifications for the Pectinidae family.

Materials and Methods

Scallop Species Collection

The locations and time of collection of the pectinid species studied are presented in Table 1. Collected species are classified according to genera described by Waller [15].

Sample Preparation and Lipid Extraction

For all species analyzed, the digestive tract was first removed to limit contamination by ingested algae. Then gills and muscle tissues were excised, weighed and homogenized with a Dangoumeau homogenizer at −180 °C. One species was analyzed as a whole animal (i.e. *Euvola ziczac*). Lipids were extracted from an aliquot of approximately 100 mg of tissue homogenates according to the method described by Folch et al. [16]. To ensure complete extraction of the lipids, a solvent to tissue ratio of 70:1 was used as described by Nelson [17]. After removing the organic phase, the residue was washed with a mixture of $CHCl_3$/MeOH (2:1, vol/vol) to avoid any solvent

Table 1 Sampling location and time of collection of scallop species used in the analysis (following current classifications [15] and [32])

Subfamily	Tribe	Species	Origin	Time of collection
Chlamydinae	Chlamydini	*Zygochlamys patagonica* (2)	Argentina	June 05
		Mizuhopecten yessoensis (3)	Japan	July 05
		Chlamys distorta (5)	France (B[a])	April 05
		Chlamys islandica (4)	Norway	November 04
	Mimachlamydini	*Mimachlamys varia* (4)	France (B)	July 04
Palliolinae	Palliolini	*Placopecten magellanicus* (3)	Canada (MI[b])	September 06
	Adamussiini	*Adamusium colbecki* (5)		December 07
Pectininae	Pectinini	*Pecten maximus* (3)	France (B), Norway	July 07
		Nodipecten subnodosus (3)	Mexico (BCS[c])	June 06
	Amusiini	*Euvola ziczac* (4)	Bermuda	December 05
Aequipecten subgroup	Aequipectinini	*Aequipecten opercularis* (3)	France (B)	June 05
		Argopecten purpuratus (3)	Chile	July 05
		Argopecten ventricosus (3 for each month)	Mexico (BCS[c])	January, May, July 08

The number of individuals for analysis is indicated in brackets

[a] Brittany/Bay of Brest

[b] Madeleine Islands

[c] Baja California Sur

retention. The final extract was stored at −20 °C under a nitrogen atmosphere after adding 0.01% wt/vol butylated hydroxytoluene (BHT, antioxidant).

Separation of Polar Lipids by Silica Gel Micro-column and FA Analysis

An aliquot of the lipid extracts (approximately 100 μg of total lipids) was evaporated to dryness and the lipids were recovered with three washings of 500 μl of $CHCl_3$/MeOH (98/2, vol/vol) and deposited at the top of a silica gel micro-column (30 × 5 mm I.D., packed with Kieselgel 60 70–230 mesh previously heated at 450 °C and deactivated with 5 wt% H_2O) [18]. Neutral lipids were eluted with 10 ml of $CHCl_3$/MeOH (98/2 vol/vol). The polar lipid fraction was recovered with 20 ml of MeOH and stored at −20 °C before FA composition analysis by gas chromatography (GC).

The polar lipid fraction was used for the direct determination of the total glycerophospholipid (GPL) FA composition after transesterification (MeOH/BF_3). Fatty acid methyl esters (FAME) obtained were identified and quantified by GC using C23:0 FA as an internal standard [18]. FAME were analyzed in a Varian CP 8400 gas chromatograph equipped with an on-column injector and a flame ionization detector. FA were identified by comparing their retention times using both polar (CPWAX 52 CB—30 m × 0.25 mm, 0.25 μm film thickness) and non-polar (CP-Sil 8 CB—30 m × 0.25 mm, 0.25 μm film thickness) capillary columns by means of a standard mixture containing 37 FAME (SUPELCO/Sigma–Aldrich, St-Quentin Fallavier, France), and other known standard mixtures from marine bivalves [1, 10]. A total of 40 FA were quantified and expressed as the molar percentage of the total FA content.

Results

Scallop species analyzed in this study are distributed among three of the four proposed subfamilies, including the Chlamydinae, Palliolinae, and Pectininae (Table 1). The subfamily not analyzed was the Camptonectinae, hypothesized as the sister group of all other existent Pectinidae.

Along with NMI FA and 22:4(n-9)Δ13*trans*, glycerophospholipids of the 13 pectinid species were dominated by five major FA (16:0, 18:0, 20:4n-6, 20:5n-3, and 22:6n-3). Table 2 reports the proportions of the total NMI FA, 22:4(n-9)Δ13*trans*, 20:4n-6, 20:5n-3, and 22:6n-3. In 11 of the 13 species investigated, gills and muscle glycerophospholipids FA compositions were analyzed separately. Long-chain PUFA 20:4n-6, 20:5n-3, and 22:6n-3 varied markedly among species and both organs analyzed. There was no relationship with taxonomic affiliation.

Two main clusters among the suprageneric groups of Pectinidae can be formed when considering the presence or absence of the 22:4(n-9)Δ13*trans*. This FA was found in substantial amounts in all species belonging to the Aequipecten group (*A. opercularis, A. purpuratus*, and *A. ventricosus*) and the subfamily Pectininae (*P. maximus, N. subnodosus*, and *E. ziczac*), but was absent in species belonging to Chlamydinae (*Z. patagonica*, *M. yessoensis*, *C. islandica*, and *M. varia*) and Palliolinae subfamilies (*P. magellanicus*, *A. colbecki*) (Table 2). One exception was observed for *C. distorta* (tribe Chlamydini), for which the presence of 22:4(n-9)Δ13*trans* was clearly established, even if it was found in low amounts in comparison to species of the Pectininae subfamily and Aequipecten group.

Except for the three species belonging to the Aequipecten group, for which NMI FA were not detectable (or only found in trace amounts in the case of *A. opercularis*), the other pectinid species contained minor but noticeable amounts of NMI FA, ranging from 0.3 to 4.5% according to species and organs. In the 11 species where gills and muscle were analyzed separately, NMI FA and/or 22:4(n-9)Δ13*trans* content in the membrane glycerophospholipids were found higher in the gills than in muscle. Predominant NMI FA were 22:2 NMID (7,15–22:2 and 7,13–22:2), while 20:2 NMID (5,11–20:2 and 5,13–20:2) and NMIT (5,11,14–20:3 and 7,13,16–22:3) were only detectable in trace amounts. Among 22:2 NMID FA, no characteristic predominance of one of the two isomers was found according to species and phylogenetic groups.

To evaluate intra-specific variability of NMI FA and 22:4(n-9)Δ13*trans*, FA compositions of *P. maximus* specimens sampled in the bay of Brest (French coast) and in the Norwegian coastal waters were compared. Despite some differences in proportions of the long-chain PUFA 20:4n-6, 20:5n-3 and 22:6n-3 (mainly in gills), 22:4(n-9)Δ13*trans* and NMI FA in gills and muscle were found in similar amounts in both populations. We also examined whether levels of NMI FA and 22:4(n-9)Δ13*trans* vary within a species according to the period of the year, by sampling *A. ventricosus* from the same location (Baja California Sur, Mexico) at 3 months within a year. Despite some variability in the proportions of 20:4n-6, 20:5n-3 and 22:6n-3, levels of 22:4(n-9)Δ13*trans* varied less within this species than between the different species.

Discussion

Previous studies on glycerophospholipids FA composition in non-pectinid bivalves species *Glycymeris glycymeris*, *Mytilus edulis*, *Ostrea edulis*, *Crassostrea gigas*, *Ruditapes decussatus*, and *Cerastroderma edule* did not reveal the

Table 2 FA composition of glycerophospholipids in the scallop species investigated

Subfamilies and species	20:4n-6	20:5n-3	22:6n-3	Total NMI[a]	22:4(n-9)Δ13*trans*
Chlamydinae					
Zygochlamys patagonica					
Muscle	1.8 ± 0.1	14.1 ± 0.2	30.7 ± 0.8	2.6 ± 0.2	–
Mizuhopecten yessoensis					
Gills	8.5 ± 0.2	11.7 ± 0.3	26.0 ± 0.6	2.1 ± 0.2	–
Muscle	9.0 ± 0.3	13.4 ± 0.4	23.5 ± 0.4	1.2 ± 0.0	–
Chlamys distorta					
Gills	3.3 ± 0.1	15.3 ± 0.4	27.3 ± 0.5	1.4 ± 0.1	0.5 ± 0.1
Muscle	2.8 ± 0.1	16.9 ± 0.2	29.8 ± 0.7	0.3 ± 0.0	Trace
Chlamys islandica					
Gills	6.3 ± 0.2	11.8 ± 0.5	36.0 ± 1.0	4.5 ± 0.5	–
Muscle	2.2 ± 0.5	22.1 ± 0.5	25.2 ± 0.7	0.4 ± 0.1	–
Mimachlamys varia					
Gills	6.3 ± 0.5	14.0 ± 0.3	26.9 ± 0.7	4.5 ± 0.1	–
Muscle	4.1 ± 0.1	21.8 ± 0.6	23.2 ± 0.9	0.8 ± 0.1	–
Palliolinae					
Placopecten magellanicus					
Gills	5.6 ± 0.5	15.7 ± 0.3	39.9 ± 1.0	1.7 ± 0.2	–
Muscle	1.5 ± 0.1	21.7 ± 1.2	25.0 ± 0.5	0.3 ± 0.1	–
Adamusium colbecki					
Gills	2.6 ± 0.2	18.4 ± 0.4	18.6 ± 0.4	1.4 ± 0.1	
Muscle	1.9 ± 0.1	23.8 ± 0.8	18.5 ± 0.3	0.3 ± 0.2	–
Pectininae					
Pecten maximus—Brest, France					
Gills	10.1 ± 0.4	10.7 ± 0.2	23.0 ± 0.6	2.0 ± 0.2	9.4 ± 0.1
Muscle	4.5 ± 0.2	17.1 ± 0.3	25.2 ± 0.5	0.4 ± 0.1	1.9 ± 0.3
Pecten maximus—Norway					
Gills	8.2 ± 0.3	10.1 ± 0.1	30.2 ± 0.4	2.8 ± 0.1	10.2 ± 0.1
Muscle	2.3 ± 0.1	16.5 ± 0.2	27.6 ± 0.7	0.6 ± 0.1	1.2 ± 0.1
Nodipecten subnodosus					
Gills	6.8 ± 0.2	7.2 ± 0.1	25.7 ± 0.7	4.5 ± 0.3	7.7 ± 0.1
Muscle	3.2 ± 0.2	25.9 ± 1.1	27.8 ± 0.9	0.4 ± 0.2	1.7 ± 0.1
Euvola ziczac					
Whole animal	11.8 ± 0.5	5.9 ± 0.1	25.6 ± 1.0	0.5 ± 0.1	5.9 ± 0.1
Aequipecten group					
Aequipecten opercularis					
Gills	10.6 ± 0.3	12.9 ± 0.3	22.9 ± 0.5	0.2 ± 0.1	10.0 ± 1.8
Muscle	6.2 ± 0.1	20.9 ± 0.3	22.9 ± 0.4	0.1 ± 0.0	1.3 ± 0.5
Argopecten purpuratus					
Gills	2.8 ± 0.1	9.9 ± 0.1	29.2 ± 0.8	–	9.3 ± 0.1
Argopecten ventricosus					
Gills (January)	6.0 ± 0.2	6.0 ± 0.1	26.4 ± 0.8	–	12.7 ± 0.1
Gills (May)	3.1 ± 0.2	9.7 ± 0.2	21.3 ± 1.1	–	12.0 ± 0.1
Gills (July)	6.1 ± 0.3	9.2 ± 0.1	26.7 ± 0.6	–	12.5 ± 0.1

For the purpose of the study, only predominant PUFA are depicted in addition to total NMI and 22:4(n-9)Δ13*trans* FA. Results are expressed in mol% of the total FA of glycerophospholipids. Values are means ± SD

[a] Total NMI is the sum of 20 and 22 NMID isomers (5,11–20:2NMI, 5,13–20:2NMI, 7,13–22:2NMI, 7,15–20:2NMI), and 22 NMIT (7,13,16–22:3NMI). 5,11,14–20:3 NMIT was only detectable in trace amounts

presence of 22:4(n-9)Δ13*trans,* suggesting that this peculiar FA is only present in bivalves of the Pectinidae family [1, 10]. However, our characterization of the FA composition of phospholipids in a greater number of scallop species showed that 22:4(n-9)Δ13*trans* only occurred in some of the 13 species studied.

Our present results confirmed that pectinids contain lower levels of NMI FA than other bivalve mollusks [3, 4]. Actually, Pectinidae seem to represent an exception since NMI FA are seemingly ubiquitous mollusk components with non-negligible proportions and a definite regularity in their distribution in bivalves (up to 20%) [3, 7]. These NMI FA are considered to be the only PUFA synthesized de novo in bivalves. While NMID FA (namely 5,11–20:2, 5,13–20:2, 7,13–22:2, 7,15–22:2) were demonstrated to be de novo synthesized in bivalve mollusks by active FA elongation and desaturation of 18:1n-9 and 16:1n-7 [6, 8], NMIT (5,11,14–20:3 and 7,13,16–22:3) FA were suggested to be synthesized from 20:2n-6 [9]. The occurrence of NMI FA in mollusks was originally thought to represent a phylogenetic characteristic of mollusks [11]. Later, based on a study on five bivalves and two gastropods species from the Sea of Japan, it was proposed that NMI FA have some evolutionary significances in bivalves, with the oldest families of Bivalvia having the highest NMI FA contents, while in evolutionary "advanced" species, these FA are either found in lower amounts or absent [7]. However, authors pointed out the exception of Pectinidae since NMI FA were almost absent or in trace amounts in this ancient family. Rabinovich and Ripatti [19] suggested that the higher content of FA acyl chains with non-methylene-interrupted double bonds in the oldest families of Bivalvia appeared as a result of primitive disorganizations in the reaction sequence of the normal system of desaturases and elongases.

The desaturase and elongase intermediates in the synthesis of 22:4(n-9)Δ13*trans* have still not been elucidated in pectinids. However, as it is absent from the diet, this 22:4(n-9)Δ13*trans* should be, as NMI FA, of endogenous origin [1]. In addition, 22:4(n-9)Δ13*trans* and NMI FA shared some interesting characteristics in bivalve tissues. Both are found in higher proportions in gills than in muscle glycerophospholipids and both are specifically associated to the plasmalogen form of glycerophospholipids [2, 10]. Considering this, the phylogenetic significance of 22:4(n-9)Δ13*trans* occurrence was assessed using the recently updated phylogeny of scallops by Waller [15], based on shared derived morphological characters and molecular genetic characteristics, and scaled against geologic time (Fig. 1). According to the presence or absence of the 22:4(n-9)Δ13*trans* in gills glycerophospholipids, two groups of pectinids were apparent. One group of species belonging to the Aequipecten group and Pectininae subfamily was characterized by substantial amounts of 22:4(n-9)Δ13*trans* in gills, whereas the second group including representatives of the Chlamydinae and Palliolinae

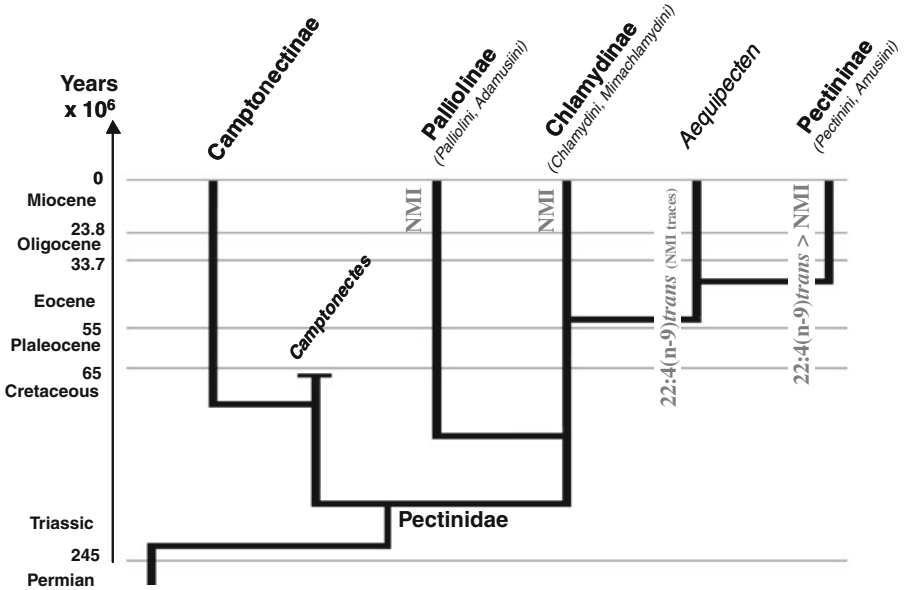

Fig. 1 Phylogeny of subfamilies of Pectinidae plotted against time in million of years and compartmentalized into standard European stages. This representation was reconstructed from the publication of Waller [15, Figs. 1.1 and 1.3] who postulated new evolutionary relationships among scallops on the basis of shared morphological characters and findings of molecular genetic studies. Also indicated is the "Aequipecten group" now considered to be at the base of the lineage conducing to the subfamily Pectininae. The different tribes analyzed in the present study are indicated for each subfamily. Indications on lineages refer to the characteristic distribution of 22:4(n-9)Δ13*trans* and NMI FA within pectinid clades

subfamilies contained no or only trace amounts of this FA. According to Waller's phylogenetic tree, 22:4(n-9)Δ13*trans* is then only present in the most evolutionary advanced species. This observation suggests that members of the Pectininae subfamily and the Aequipecten group have originated from a common ancestor that belonged to a common lineage that gave rise to the 22:4(n-9)Δ13*trans* in Pectinidae.

At this stage, distribution of 22:4(n-9)Δ13*trans* and NMI FA within pectinid clades supports the idea that the capacity to synthesize these peculiar fatty acids is genetically controlled and has phylogenetic and evolutionary significance. However, it is important in comparative studies of this type to separate adaptive properties from characters that exist in species for reasons of phylogenetic lineage. Because of their possible importance in membrane structure and function, the proportions of these FA can be expected to be modulated by extrinsic (i.e., temperature, diet, salinity, depth) and/or intrinsic factors (i.e. age, reproductive cycle). However, while studies on scallops and other bivalve species show a dependence of 20:4n-6, 20:5n-3, and 22:6n-3 compositions of membrane phospholipids on dietary composition [20–23], NMI FA and 22:4(n-9)Δ13*trans* in phospholipids seemed less sensitive to dietary changes in PUFA contents [20, 22–25]. Only small modifications of NMI FA contents were observed according to temporal and geographical changes [4, 12, 13, 25–27]. NMI and/or 22:4(n-9)Δ13*trans* FA also appear to be less sensitive to reproductive stages than 20:4n-6, 20:5n-3, and 22:6n-3 [12, 14, 26, 28]. In the present study, species sampled in the Bay of Brest (France) for which 22:4(n-9)Δ13*trans* was present in substantial proportions (i.e. *P. maximus, A. opercularis*) or was not detected or only in trace amounts (i.e. *C. distorta*, *M. varia*), were species growing in similar habitats and sampled at the same periods of the year. This observation suggests that the occurrence of this peculiar FA in scallops is not linked to adaptive responses in their environment. Analysis of *P. maximus* originating from France or Norway (south of Bergen) revealed that the proportions of 22:4(n-9)Δ13*trans* in phospholipids are not markedly influenced by rearing site conditions and/or latitudes. As well, despite modifications in 20:4n-6, 20:5n-3, and 22:6n-3 and other FA levels in gills membranes of *A. ventricosus* originating from a same location and sampled at three different months ($P < 0.05$), the differences in 22:4(n-9)Δ13*trans* proportions over the sampling period were not significant. These modifications being probably associated with multiple factors such as diet, temperature, or reproductive stages and age, the stability of 22:4(n-9)Δ13*trans* levels compared to those of 20:4n-6, 20:5n-3, and 22:6n-3 suggest a regulation of this FA in the membrane lipids. These results corroborate the constant proportions of 22:4(n-9)Δ13*trans* and NMI FA found during a seasonal survey (including a reproductive cycle) of fatty acid compositions in the mantle tissues of a 1-year-old population of giant lion's-paw scallop *N. subnodosus* [28].

All these considerations support the idea that these membrane fatty acids could have a phylogenetic significance rather than being due to environmental conditions. The present data support some of the new assignments of bivalves of the Pectinidae family that have recently emerged [15, 29–32]. The occurrence of 22:4(n-9)Δ13*trans* in two clades, the "Aequipecten group" and the subfamily Pectininae, supports the close relationship between them [15, 30] (Fig. 1), while a previous phylogeny placed Pectininae and Aequipecten in well separated positions [33]. Nevertheless, these two clades seemed to be distinguishable according to their NMI FA contents. Indeed, NMI FA were in very low amounts or absent in species of the Aequipecten group while they were found in significant amounts in the Pectininae subfamily when compared to other pectinids. Furthermore, an interesting point is the almost lack of 20:1n-11 in glycerophospholipids of the Aequipecten group species (data not shown). As previously suggested, 20:1n-11 is probably biosynthesized in bivalves by a Δ9 desaturase acting on 20:0 [10] in the same way as a Δ9 desaturation and elongation of 16:0 and 18:0, produces the two NMI FA precursors 20:1n-7 and 20:1n-9 [8]. This observation would corroborate a loss of NMI FA biosynthesis pathways in species belonging to the Aequipecten group, suggesting an independent evolution in species of the Aequipecten group after the split with the subfamily Pectininae.

The presence of both NMI FA and 22:4(n-9)Δ13*trans* in *N. subnodosus* is in good agreement with two recent molecular phylogenetic studies that established a closer relationship between *Nodipecten* and the Pectininae subfamily [31, 32]. Placement of *M. yessoensis* (synonym. *Patinopecten*) close to the Chlamys group [15, 29], in contrast to its previous position close to Pecten [34], is also corroborated by the absence of 22:4(n-9)Δ13*trans* in *M. yessoensis* glycerophospholipids.

In contrast, the presence of 22:4(n-9)Δ13*trans* in *C. distorta* (tribe Chlamydini), raises a question of whether this species belongs to the Chlamydinae subfamily. Unfortunately, none of the recent molecular studies addressed phylogenetic relationships of this species in Pectinidae families.

A discussion on the functional, physiological and/or evolutionary significance of the specificity of distribution of 22:4(n-9)Δ13*trans* among pectinids can only be speculative and has yet to be addressed. For NMI FA, due to their large quantities reported in membrane lipids of marine organisms, some authors assume that they play an important role in biomembrane functioning such as fluidity, and

control of negative influence of thermal changes on enzyme activity. They have also been related to the low oxidizability of membrane lipids and high resistance to hemolytic agents [19, 35, 36]. Although 22:4(n-9)Δ13*trans* and NMI FA appears structurally very different, their specific association with the plasmalogen form of SerGpl (PlsSer) and their uneven distribution among organs argue for similar targeted roles in membrane functions [2].

In conclusion, representatives of the Pectinidae family are unique in terms of the de novo biosynthesized NMI FA proportions and the existence of the 22:4(n-9)Δ13*trans* FA in their membrane lipids. A striking relationship between the occurrence of NMI FA and 22:4(n-9)Δ13*trans* and the recent phylogenies of the Pectinidae family suggests that an event(s) in pectinids evolution occurred in the root for the Aequipecten and Pectininae allowing scallops to develop the enzyme machinery for 22:4(n-9)Δ13*trans* biosynthesis. Any consequences for membrane functions that underlie these specificities in membrane lipid composition remain to be explained, but the present data could help us to gain further knowledge on these questions.

Acknowledgments We would like to thank A. Lorrain, A. Druinker, L. Chauvaud, and Y-M. Paulet for supply of some of the species we characterized. This work was supported by a grant from "Ministère de l'Education Nationale de la Recherche et de la Technologie" (M.E.N.R.T., France). We also would like to thank Prof. H. Guderley for her English revision and comments, and also anonymous reviewers for their helpful comments.

References

1. Marty Y, Soudant P, Perrotte S, Moal J, Dussauze J, Samain JF (1999) Identification and occurrence of a novel *cis*-4,7,10,*trans*-13-docosatetraenoic fatty acid in the scallop *Pecten maximus* (L.). J Chromatogr A 839:119–127
2. Kraffe E, Soudant P, Marty Y (2006) cis-4,7,10,*trans*-13-22:4 Fatty acid distribution in phospholipids of pectinid species *Aequipecten opercularis* and *Pecten maximus*. Lipids 41:491–497
3. Joseph JD (1982) Lipid composition of marine and estuarine invertebrates. Part II: Mollusca. Prog Lipid Res 21:10–153
4. Napolitano GE, Ackman RG (1992) Anatomical distributions and temporal variations of lipid classes in sea scallops *Placopecten magellanicus* (Gmelin) from Georges bank (Nova Scotia). Comp Biochem Phys 103:645–650
5. Paradis M, Ackman RG (1975) Occurrence and chemical structure of non-methylene-interrupted dienoic fatty acids in American oyster *Crassostrea virginica*. Lipids 10:12–16
6. Zhukova NV (1986) Biosynthesis of non-methylene-interrupted fatty acids from [^{14}C] acetate in molluscs. Biochim Biophys Acta 878:131–133
7. Zhukova NV, Svetashev VI (1986) Non-methylene-interrupted dienoic fatty acids in molluscs from the Sea of japan. Comp Biochem Phys 83B:643–646
8. Zhukova NV (1991) The pathway of the biosynthesis of non-methylene-interrupted dienoic fatty acids in molluscs. Comp Biochem Phys 100B:801–804
9. Dunstan GA, Volkman JK, Barett SM (1993) The effect of lyophilization on the solvent extraction of lipid classes, fatty acids and sterols from the oyster *Crassostrea gigas*. Lipids 28:937–944
10. Kraffe E, Soudant P, Marty Y (2004) Fatty acids of serine, ethanolamine and choline plasmalogens in some marine bivalves. Lipids 39:59–66
11. Ackman RG, Hooper SN (1973) Non-methylene-interrupted fatty acids in lipids of shallow-water marine invertebrates: a comparison of two molluscs (*Littorina littorea* and *Lunatia triserita*) with the sand shrimp (*Crangon septumspinosus*). Comp Biochem Phys 46B:153–165
12. Napolitano GE, Ackman RG (1993) Fatty acid dynamics in sea scallops *Placopecten magellanicus* (Gmelin, 1791) from Georges bank, Nova Scotia. J Shell Res 12:267–277
13. Napolitano GE, MacDonald BA, Thompson RJ, Ackman RG (1992) Lipid composition of eggs and adductor muscle in giant scallops (*Placopecten magellanicus*) from different habitats. Mar Biol 113:71–76
14. Kraffe E, Tremblay R, Belvin S, Le Coz JR, Marty Y, Guderley H (2008) Effect of reproduction on escape responses, metabolic rates and muscle mitochondrial properties in the scallop *Placopecten magellanicus*. Mar Biol 156:25–38
15. Waller TR (2006) New phylogenies of the Pectinidae (Mollusca: Bivalvia): reconciling morphological and molecular approaches. In: Shumway SE, Parsons GJ (eds) Scallops: biology, ecology and aquaculture. Elsevier, pp 1–44
16. Folch J, Lees M, Sloane-Stanley GH (1957) A simple method for the isolation and purification of total lipides from animal tissues. J Biol Chem 226:497–509
17. Nelson GJ (1993) Isolation and purification of lipids from biological matrices. In: Perkins EG (ed) Analyses of fats, oils and derivatives. AOCS Press, Champaign, pp 20–89
18. Marty Y, Delaunay F, Moal J, Samain JF (1992) Changes in the fatty acid composition of the scallop *Pecten maximus* (L.) during larval development. J Exp Mar Biol Ecol 163:221–234
19. Rabinovich AL, Ripatti PO (1991) The flexibility of natural hydrocarbon chains with non-methylene-interrupted double bonds. Chem Phys Lipids 58:185–192
20. Soudant P, Marty Y, Moal J, Robert R, Quéré C, Le Coz JR, Samain JF (1996) Effect of food fatty acids and sterol quality on *Pecten maximus* gonad composition and reproduction process. Aquaculture 143:361–378
21. Pernet F, Tremblay R, Bourget E (2003) Biochemical indicator of sea scallop (*Placopecten magellanicus*) quality based on lipid class composition. Part I: Broodstock conditioning and young larvae performance. J Shell Res 22:365–376
22. Delaporte M, Soudant P, Moal J, Kraffe E, Marty Y, Samain JF (2005) Impact and modification of dietary fatty acids in gill polar lipids by two bivalve species *Crassostrea gigas* and *Ruditapes philippinarum*. Comp Biochem Phys Part A 140:460–470
23. Pirini M, Manuzzi MP, Pagliarani A, Trombetti F, Borgatti AR, Ventrella V (2007) Changes in fatty acid composition of *Mytilus galloprovincialis* (Lamarck) fed on microalgal and wheat germ diets. Comp Biochem Phys 147:616–626
24. Soudant P, Marty Y, Moal J, Masski H, Samain JF (1998) Fatty acid composition of polar lipid classes during larval development of scallop *Pecten maximus* (L.). Comp Biochem Phys A 121:279–288
25. Ventrella V, Pirini M, Pagliarani A, Trombetti F, Pia Manuzzi M, Borgatti AR (2008) Effect of temporal and geographical factors on fatty acid composition of *M. galloprovincialis* from the Adriatic sea. Comp Biochem Phys 149:241–250
26. Soudant P, Van Ryckeghem K, Marty Y, Moal J, Samain JF, Sorgeloos P (1999) Comparison of the lipid class and fatty acid composition between a reproductive cycle in nature and a standard hatchery conditioning of the Pacific Oyster *Crassostrea gigas*. Comp Biochem Phys 123:209–222

27. Pernet F, Tremblay R, Comeau L, Guderley H (2007) Temperature adaptation in two bivalve species from different thermal habitats: energetic and remodeling of membrane lipids. J Exp Biol 210:2999–3014
28. Palacios E, Racotta IS, Kraffe E, Marty Y, Moal J, Samain JF (2005) Lipid composition of the giant lion's-paw scallop (*Nodipecten subnodosus*) in relation to gametogenesis I. Fatty acids. Aquaculture 250:270–282
29. Matsumoto M, Hayami I (2000) Phylogenetic analysis of the family Pectinidae (Bivalvia) based on mitochondrial cytochrome c oxidase subunit I. J Mollus Stud 66:477–488
30. Barucca M, Olmo E, Schiaparelli S, Canapa A (2004) Molecular phylogeny of the family Pectinidae (Mollusca: Bivalvia) based on mitochondrial 16S and 12S rRNA genes. Mol Phylogenet Evol 31:89–95
31. Saavedra C, Peña JB (2006) Phylogenetics of American scallops (Bivalvia: Pectinidae) based on partial 16S and 12S ribosomal RNA gene sequences. Mar Biol 150:111–119
32. Puslednik L, Serb JM (2008) Molecular phylogenetics of the Pectinidae (Mollusca: Bivalvia) and effect of increased taxon sampling and outgroup selection on tree topology. Mol Phylogenet Evol 48:1178–1188
33. Waller TR (1991) Evolutionary relationship among commercial scallops (Mollusca: Bivalvia: Pectinidae). In: Shumway SE (ed) Scallops: biology, ecology and aquaculture. Elsevier, pp 1–73
34. Waller TR (1993) The evolution of "Chlamys" (Mollusca: Bivalvia: Pectinidae) in the tropical western Atlantic and eastern Pacific. Am Malacol Bull 10:195–249
35. Chelomin VP, Zhukova NV (1981) Lipid composition and some aspects of aminophospholipid organization in erythrocyte membrane of the marine bivalve mollusc *Scapharca broughtoni* (Schrenck). Comp Biochem Phys 69B:599–604
36. Zakhartsev MV, Naumenko NV, Chelomin VP (1998) Non-methylene-interrupted fatty acids in phospholipids of the membranes of the mussel *Crenomytilus grayanus*. Russ J Mar Biol 24:183–186

Lipids (2010) 45:445–450
DOI 10.1007/s11745-010-3409-0

COMMUNICATION

The Effects of Ezetimibe and/or Orlistat on Triglyceride-Rich Lipoprotein Metabolism in Obese Hypercholesterolemic Patients

E. S. Nakou · T. D. Filippatos · A. P. Agouridis · C. Kostara · E. T. Bairaktari · M. S. Elisaf

Received: 11 February 2010 / Accepted: 15 March 2010 / Published online: 9 April 2010

Abstract We investigated the factors influencing triglycerides (TG) reduction during ezetimibe, alone or combined with orlistat, administration. Eighty-six obese hypercholesterolemic subjects were prescribed a low-fat diet and were randomized to ezetimibe (E group), orlistat (O group), or both (OE group) for 6 months. Plasma TG and apolipoprotein (apo) C-III reduction was significantly greater in the combination group compared with monotherapy. Multivariate analysis showed that in E group apoC-III reduction and baseline TG levels were independently positively correlated, whereas baseline apoC-II levels were negatively correlated, with TG lowering. In OE group apoC-III reduction was the only independent contributor to TG reduction.

Keywords Ezetimibe · Orlistat · Triglycerides · Apolipoprotein C-II · Apolipoprotein C-III · Cholesterol

Abbreviations

apo	Apolipoprotein
apoA-I	Apolipoprotein A-I
apoB	Apolipoprotein B
apoC-II	Apolipoprotein C-II
apoC-III	Apolipoprotein C-III
apoE	Apolipoprotein E
BMI	Body mass index
CVD	Cardiovascular disease
Group O	Orlistat group
Group E	Ezetimibe group
Group OE	Orlistat plus ezetimibe group
HDL	High density lipoproteins
HDL-C	High density lipoprotein cholesterol
HL	Hepatic lipase
HOMA	Homeostasis model assessment
LDL-C	Low density lipoprotein cholesterol
LPL	Lipoprotein lipase
MetS	Metabolic syndrome
TG	Triglycerides
TC	Total cholesterol
VLDL	Very low density lipoproteins

E. S. Nakou · T. D. Filippatos · A. P. Agouridis · M. S. Elisaf (✉)
Department of Internal Medicine, School of Medicine, University of Ioannina, 45 110 Ioannina, Greece
e-mail: egepi@cc.uoi.gr

C. Kostara · E. T. Bairaktari
Laboratory of Clinical Chemistry, School of Medicine, University of Ioannina, Ioannina, Greece

Introduction

The human apolipoproteins (apo) Cs are constituents of chylomicrons, very low density lipoproteins (VLDL) and high density lipoproteins (HDL) [1]. ApoC-II in normal ranges is an activator of lipoprotein lipase (LPL) [1, 2]. In contrast, excess apoC-II inhibits LPL-mediated hydrolysis of triglycerides (TGs) [1]. ApoC-III is a powerful inhibitor of LPL activity [1, 3].

Ezetimibe selectively inhibits intestinal cholesterol absorption [4, 5]. This effect leads to decreased cholesterol delivery to the liver and subsequent increased cholesterol clearance from the blood [4].

Orlistat is an inhibitor of intestinal lipases that are responsible for the breakdown of dietary TG into fatty acids and monoglycerides [6–8]. Orlistat-induced weight loss improves CVD risk factors, including serum TG levels [9–11].

Our group showed that ezetimibe, alone or in combination with orlistat, significantly reduced serum TG concentration in obese patients with hypercholesterolemia [12, 13]. In this study we show the effect of ezetimibe administration, alone or combined with orlistat, on apoC-II and apoC-III levels and we investigate the factors influencing TG reduction during these treatments.

Patients and Methods

Participants

Consecutive patients attending the Outpatient Obesity and Lipid Clinic of the University Hospital of Ioannina (Ioannina, Greece) were recruited [12]. The study protocol has been described in detail elsewhere [12, 13]. Briefly, eligible patients were those with body mass index (BMI) >28 kg/m^2 and hypercholesterolemia [total cholesterol (TC) >200 mg/dl, 5.2 mmol/l]. Patients with symptomatic ischemic heart disease or any other clinically evident vascular disease, impaired renal, liver or thyroid function, diabetes mellitus or receiving lipid-lowering therapy were excluded from the study.

An individualized low-fat diet, promoting a 500–1,000 kcal reduction in daily energy intake, was given to all patients [12]. Patients were randomized to receive for 6 months: orlistat, *Group O* (120 mg, three times a day) or ezetimibe, *Group E* (10 mg/day) or a combined treatment with orlistat plus ezetimibe, *Group OE*.

All participants gave their informed consent and the study protocol was approved by the institutional ethics committee.

Laboratory Measurements

Lipid and carbohydrate metabolism parameters were determined as previously described [12]. All laboratory determinations were carried out after an overnight fast. Serum concentrations of fasting glucose, TC and TGs were determined enzymatically on an Olympus AU600 clinical chemistry analyzer (Olympus Diagnostica, Hamburg, Germany). High density lipoprotein cholesterol (HDL-C) was determined in the supernatant, after precipitation of the apoB-containing lipoproteins with dextran sulfate-Mg^{2+} (Sigma Diagnostics, St. Louis, MO, USA). Low density lipoprotein cholesterol (LDL-C) was calculated using the Friedewald formula (provided that triglycerides were <3.9 mmol/l, 350 mg/dl). Fasting serum insulin levels were measured by an AxSYM insulin assay microparticle enzyme immunoassay on an AzSYM analyzer (Abbott Diagnostics, IL, USA). Finally, homeostasis model assessment (HOMA) index was calculated as follows: fasting insulin (mU/l) × fasting glucose (mg/dl)/405.

ApoC-II and apoC-III were determined by an immunoturbidimetric assay provided by Kamiya Biomedical Company (Seattle, USA) [14].

For all measurements in our laboratory, the coefficients of inter-assay and intra-assay variation were less than 5.0%, and blinded quality-control specimens were included in each assay. Analyses were conducted at the Laboratory of Clinical Chemistry of the University Hospital of Ioannina, under regular quality control procedures including the use of reference pools and blinded duplicate samples.

The Laboratory of the University Hospital of Ioannina is currently participating in external quality assurance services (EQAS) programme provided by Bio-Rad Laboratories, Inc.

Statistical Analysis

Each value is given as mean ± standard deviation (SD) and median (range) for parametric and non parametric data, respectively. Analysis of covariance (ANCOVA), adjusted for baseline values, was used for comparisons between treatment groups. Spearman's correlation coefficients were used to describe the relationship of TG reduction with age, waist circumference, BMI, HOMA index, lipid and apolipoprotein levels (univariate analysis). Stepwise multivariate linear regression analyses were performed to assess in each treatment group the independent contribution of the variables that significantly associated with TG reduction in univariate analysis.

The results were analyzed after excluding the eight patients who dropped out during the study. Significance was defined as $p < 0.05$. All analyses were carried out with SPSS 15.0 (SPSS Inc., Chicago, IL, USA).

Results

We enrolled 94 patients (70 females and 24 males, mean age 55 ± 10 years). Of these, 8 (8.5%) did not complete the study. Baseline characteristics did not differ between the three groups [12].

As previously shown [12], significant in-group changes were observed for BMI and waist circumference at 6 months [12]. There were significant in-group reductions in plasma levels of TC, LDL-C, TG and apoB. Levels of HDL-C and apoA-I were not significantly changed at 6 months in any group [12].

In E and OE groups plasma apoC-II (E group: from 4.6 to 4.1 mg/dl, $p < 0.05$; OE group from 4.8 to 4.2 mg/dl; $p < 0.05$) and apoC-III (E group: from 11.4 to 9.9 mg/dl, $p < 0.05$; OE group from 11.7 to 9.8 mg/dl; $p < 0.05$)

levels were significantly reduced. In O group a significant reduction of plasma apoC-III concentrations was observed (from 11.9 to 10.7 mg/dl, $p = 0.01$). In this group plasma apoC-II levels were not significantly changed (from 4.9 to 4.8 mg/dl, $p =$ NS). The reduction of apoC-II levels in E and OE groups was significantly greater compared with O group. The reduction of apoC-III levels was significantly greater in OE group compared with O group.

There were significant in-group reductions in serum TG levels in all treatment groups. We observed a significantly greater TG reduction in the combination group compared with each monotherapy [12]. Stepwise multiple linear regression analysis revealed that in E group, apoC-III reduction and baseline TG levels were significantly and independently positively correlated, while baseline apoC-II levels were negatively correlated, with TG reduction. In O group, the alterations in apoC-III levels and the baseline TG concentration were independently positively correlated, while the baseline apoC-II levels were negatively correlated with TG lowering (Table 1). In OE group alterations in apoC-III levels were independently and significantly positively correlated with TG lowering (Table 1).

Discussion

Multivariate analysis showed that the TG lowering during ezetimibe treatment is independently positively associated with the apoC-III reduction and the baseline TG levels, while it is negatively associated with the baseline apoC-II concentration in obese hypercholesterolemic patients. ApoC-III is an 8.8 kDa glycoprotein secreted mostly by the liver and, to a lesser extent, by the intestine [15]. ApoC-III is a major component of TG-rich lipoproteins (chylomicrons and VLDL) and HDL. ApoC-III is considered a regulator of lipolysis through non-competitive inhibition of endothelial-bound lipoprotein lipase (LPL) [16, 17]. This enzyme hydrolyses triacylglycerols in TG-rich lipoproteins [3, 15]. Individuals lacking apoC-III have low TG levels [17–20]. ApoC-III at high concentrations may also inhibit hepatic lipase (HL), an effect that reduces further the lipolysis and uptake of TG-rich lipoproteins by the liver [15]. Therefore, apoC-III plays a key role in TG-rich lipoprotein metabolism and, consistent with the multivariate analysis, is a major factor responsible for TG alterations during ezetimibe treatment.

Table 1 Multivariate regression analysis for the prediction of TG reduction

Parameter	Group O		Group E		Group OE	
	Beta	*p*	Beta	*p*	Beta	*p*
Changes in apoC-III	0.45	0.02	1.21	<0.001	0.59	0.01
Baseline TG	0.29	0.03	0.44	<0.01	0.33	0.14
Baseline apoC-II	−0.18	0.04	−0.41	0.02	−0.47	0.17

Only significant correlations are shown. Variables included in the model are those which were significantly correlated with triglyceride reduction in univariate analysis

E ezetimibe, *O* orlistat, *OE* ezetimibe + orlistat, *TG* triglycerides, *apo* apolipoprotein

Baseline TG levels were an independent contributor to TG alterations during ezetimibe treatment. It has been shown that ezetimibe induces greater TG reductions in patients with higher baseline TG levels [12, 21, 22]. Generally, baseline TG levels are associated with TG reduction during treatment with drugs which exhibit hypolipidemic activity. For example, our study group showed that baseline TG levels were the most important contributor to TG reduction during rosuvastatin administration [23]. Various mechanisms have been proposed to support these observations. Specifically, the conformation of apoE contained on VLDL in hypertriglyceridemic states is different than that of VLDL in normotriglyceridemic conditions and seems to have greater affinity to the LDL-receptor [24, 25]. Additionally, in normotriglyceridemic individuals there is a shorter resident time of VLDL, which results in VLDL particles to acquire less apoE from HDL by transfer [26]. These apoE-depleted VLDL particles exhibit less affinity to the LDL receptor [26, 27]. Ezetimibe localizes at the brush border of the small intestine and selectively inhibits cholesterol absorption from the intestinal lumen into enterocytes [4]. Kinetic studies suggested that in subjects with primary hypercholesterolemia, ezetimibe-induced inhibition of intestinal cholesterol absorption led to decreased chylomicron formation and delivery to the liver and subsequent upregulation of hepatic LDL receptor activity [28, 29]. Thus, during ezetimibe treatment (and subsequent upregulation of hepatic LDL receptor activity) individuals with normal TG levels may exhibit less apoE-mediated clearance of the VLDL compared with patients with high TG levels.

Multivariate analysis also showed that baseline apoC-II concentration was negatively associated with TG alterations during ezetimibe treatment. ApoC-II is considered an important activator of LPL [30–32]. Patients with genetic defects in the structure or production of apoC-II exhibit a high plasma TG concentration and are phenotypically indistinguishable from patients with LPL deficiency [33, 34]. Plasma apoC-II is present in human plasma at a physiological concentration of approximately 4 mg/dl [1]. However, at high protein concentrations (>4 mg/dl), such as those observed in our study, apoC-II was demonstrated to inhibit LPL activity rather than stimulate it [35]. Additionally, apoC-II at high concentration has been reported to inhibit the apoE- and apoB-mediated clearance of the TG-rich lipoproteins via the LDL-receptor [1, 36, 37].

Therefore, we assume that the increased concentration of apoC-II in our subjects minimized the ezetimibe-induced (due to up-regulation of LDL receptors) apoE- and apoB-mediated clearance of the TG-rich lipoproteins.

Orlistat is a potent and specific inhibitor of intestinal lipases that are responsible for the breakdown of dietary TG into fatty acids and monoglycerides, which are then absorbed [6]. Several studies showed that orlistat administration improves the lipid profile in patients with hypercholesterolemia [6, 38]. This drug mainly improves postprandial lipoprotein metabolism (reduces the concentration of chylomicrons and VLDL), which in turn decreases the delivery of dietary lipid and fatty acids to the liver and subsequently upregulates the hepatic LDL receptors [39, 40]. Our study group has investigated the factors contributing to TG reduction during orlistat treatment in obese subjects with MetS [41]. In accordance with the present results, we showed that baseline TG levels consist an independent positive contributor and baseline apoC-II concentration is an independent negative contributor to TG reduction during orlistat treatment. However, multivariate analysis in the present study revealed that apoC-III alterations consist the major contributing factor to TG reduction. This effect was not observed when orlistat was given to obese patients with MetS. In the present study, TG levels were lower than the previous study (151 vs. 216 mg/dl at baseline). Hence, the finding of the present study that apoC-III is an independent contributor to TG reduction during orlistat treatment may be attributed to the different baseline TG concentration compared with the previous study.

The results of multivariate analysis showed that in ezetimibe and orlistat combination group TG lowering was significantly and independently associated with apoC-III alterations. It seems that the additive effect of these drugs on TG concentration is only dependent on the greater reduction in apoC-III levels compared with each monotherapy.

In the present study we show that ezetimibe administration, alone or combined with orlistat, decreases plasma apoC-II and apoC-III in obese patients with hypercholesterolemia. Apolipoproteins C-II and C-III are secreted mostly by the liver and, to a lesser extent, by the intestine. The mechanism of action of ezetimibe, that is inhibition of intestinal cholesterol absorption, leads to a reduction in chylomicron formation [29]. We speculate that this reduction is accompanied by a decrease in the synthesis of apoC-II and apoC-III (which are constituents of chylomicrons) by the intestine. Orlistat also acts via improvement of postprandial lipoprotein metabolism and may reduce apoC-III plasma levels with a similar mechanism. The dual inhibition of intestinal lipid and cholesterol absorption by the combination of orlistat and ezetimibe may further improve TG-rich lipoproteins metabolism, a fact that may explain the greater impact of this combined treatment on apoC-II and apoC-III reduction. However, the improvement of postprandial metabolism by both drugs leads to alterations of hepatic lipoprotein production (for example of VLDL) and, consequently, changes in the production of apoCs by the liver cannot be excluded. Additionally, the weight loss observed in all three groups taking part in the present study may play a significant role, since weight reduction results in a significant decrease in apoC-III levels [42].

The reduction of apoC-II and apoC-III plasma concentrations may be of clinical significance, since it has been shown that the levels of these apolipoproteins were a potent predictor of cardiovascular disease (CVD) risk in patients with type 2 diabetes mellitus [43, 44] and patients with coronary heart disease [45, 46]. Furthermore, increased plasma levels of apoC-III lead to delayed catabolism of TG-rich lipoproteins and hypertriglyceridemia, which contribute to elevated CVD risk. In the Monitored Atherosclerosis Regression study, in which 220 subjects with angiographically proven coronary heart disease received lovastatin or placebo treatment, the on-trial level of non-HDL-apoC-III in lovastatin group was the only independent of plasma TG concentration risk factor associated with progression of mild/moderate lesions [47]. Moreover, in a case–control analysis of 418 patients from the Cholesterol and Recurrent Events (CARE) trial who had a myocardial infarction or coronary death and 370 control subjects without a CVD event, non-HDL-apoC-III and TG levels were predictors of subsequent coronary events [48]. Furthermore, there is evidence that apoC-III exerts a direct effect on vascular and inflammatory functions, such as induction of adhesion molecules in vascular endothelial cells and activation of nuclear factor-kB [15]. Based on this evidence, the greater impact of ezetimibe plus orlistat administration on apoC-III compared with orlistat monotherapy should be taken into account when assessing the probable clinical benefit of this combination treatment.

In the present study we did not measure LPL activity or mass. We also did not measure apoB-48 levels as an index of chylomicron formation. Kinetic studies looking at both synthesis and catabolism of the apoCs are needed to examine the effects of ezetimibe and orlistat on apoCs and TG metabolism.

Conflict of interest statement None.

References

1. Jong MC, Hofker MH, Havekes LM (1999) Role of ApoCs in lipoprotein metabolism: functional differences between ApoC1, ApoC2, and ApoC3. Arterioscler Thromb Vasc Biol 19:472–484

2. Wang CS (1991) Structure and functional properties of apolipoprotein C-II. Prog Lipid Res 30:253–258
3. Chan DC, Chen MM, Ooi EM, Watts GF (2008) An ABC of apolipoprotein C-III: a clinically useful new cardiovascular risk factor? Int J Clin Pract 62:799–809
4. Filippatos TD, Mikhailidis DP (2009) Lipid-lowering drugs acting at the level of the gastrointestinal tract. Curr Pharm Des 15:490–516
5. Garcia-Calvo M, Lisnock J, Bull HG, Hawes BE, Burnett DA, Braun MP, Crona JH, Davis HR Jr, Dean DC, Detmers PA, Graziano MP, Hughes M, Macintyre DE, Ogawa A, O'Neill KA, Iyer SP, Shevell DE, Smith MM, Tang YS, Makarewicz AM, Ujjainwalla F, Altmann SW, Chapman KT, Thornberry NA (2005) The target of ezetimibe is Niemann-Pick C1-Like 1 (NPC1L1). Proc Natl Acad Sci USA 102:8132–8137
6. Kiortsis DN, Filippatos TD, Elisaf MS (2005) The effects of orlistat on metabolic parameters and other cardiovascular risk factors. Diabetes Metab 31:15–22
7. Filippatos TD, Derdemezis CS, Gazi IF, Nakou ES, Mikhailidis DP, Elisaf MS (2008) Orlistat-associated adverse effects and drug interactions: a critical review. Drug Saf 31:53–65
8. Filippatos T, Derdemezis C, Elisaf M (2009) Effects of orlistat, alone or combined with hypolipidemic drugs, on cardiovascular risk factors. Clin Lipidol 4:331–341
9. Filippatos TD, Gazi IF, Liberopoulos EN, Athyros VG, Elisaf MS, Tselepis AD, Kiortsis DN (2007) The effect of orlistat and fenofibrate, alone or in combination, on small dense LDL and lipoprotein-associated phospholipase A2 in obese patients with metabolic syndrome. Atherosclerosis 193:428–437
10. Filippatos TD, Kiortsis DN, Liberopoulos EN, Georgoula M, Mikhailidis DP, Elisaf MS (2005) Effect of orlistat, micronised fenofibrate and their combination on metabolic parameters in overweight and obese patients with the metabolic syndrome: the FenOrli study. Curr Med Res Opin 21:1997–2006
11. Filippatos TD, Liberopoulos EN, Kostapanos M, Gazi IF, Papavasiliou EC, Kiortsis DN, Tselepis AD, Elisaf MS (2008) The effects of orlistat and fenofibrate, alone or in combination, on high-density lipoprotein subfractions and pre-beta1-HDL levels in obese patients with metabolic syndrome. Diabetes Obes Metab 10:476–483
12. Nakou ES, Filippatos TD, Georgoula M, Kiortsis DN, Tselepis AD, Mikhailidis DP, Elisaf MS (2008) The effect of orlistat and ezetimibe, alone or in combination, on serum LDL and small dense LDL cholesterol levels in overweight and obese patients with hypercholesterolaemia. Curr Med Res Opin 24:1919–1929
13. Nakou ES, Filippatos TD, Kiortsis DN, Derdemezis CS, Tselepis AD, Mikhailidis DP, Elisaf MS (2008) The effects of ezetimibe and orlistat, alone or in combination, on high-density lipoprotein (HDL) subclasses and HDL-associated enzyme activities in overweight and obese patients with hyperlipidaemia. Expert Opin Pharmacother 9:3151–3158
14. Sakurabayashi I, Saito Y, Kita T, Matsuzawa Y, Goto Y (2001) Reference intervals for serum apolipoproteins A-I, A-II, B, C-II, C-III, and E in healthy Japanese determined with a commercial immunoturbidimetric assay and effects of sex, age, smoking, drinking, and Lp(a) level. Clin Chim Acta 312:87–95
15. Ooi EM, Barrett PH, Chan DC, Watts GF (2008) Apolipoprotein C-III: understanding an emerging cardiovascular risk factor. Clin Sci (Lond) 114:611–624
16. Yamamoto M, Morita SY, Kumon M, Kawabe M, Nishitsuji K, Saito H, Vertut-Doi A, Nakano M, Handa T (2003) Effects of plasma apolipoproteins on lipoprotein lipase-mediated lipolysis of small and large lipid emulsions. Biochim Biophys Acta 1632:31–39
17. Wang CS, McConathy WJ, Kloer HU, Alaupovic P (1985) Modulation of lipoprotein lipase activity by apolipoproteins: effect of apolipoprotein C-III. J Clin Invest 75:384–390
18. Ginsberg HN, Le NA, Goldberg IJ, Gibson JC, Rubinstein A, Wang-Iverson P, Norum R, Brown WV (1986) Apolipoprotein B metabolism in subjects with deficiency of apolipoproteins CIII and AI Evidence that apolipoprotein CIII inhibits catabolism of triglyceride-rich lipoproteins by lipoprotein lipase in vivo. J Clin Invest 78:1287–1295
19. Jong MC, Rensen PC, Dahlmans VE, van der Boom H, van Berkel TJ, Havekes LM (2001) Apolipoprotein C-III deficiency accelerates triglyceride hydrolysis by lipoprotein lipase in wild-type and apoE knockout mice. J Lipid Res 42:1578–1585
20. McConathy WJ, Gesquiere JC, Bass H, Tartar A, Fruchart JC, Wang CS (1992) Inhibition of lipoprotein lipase activity by synthetic peptides of apolipoprotein C-III. J Lipid Res 33:995–1003
21. Kalogirou M, Tsimihodimos V, Gazi I, Filippatos T, Saougos V, Tselepis AD, Mikhailidis DP, Elisaf M (2007) Effect of ezetimibe monotherapy on the concentration of lipoprotein subfractions in patients with primary dyslipidaemia. Curr Med Res Opin 23:1169–1176
22. Derdemezis C, Filippatos T, Tselepis A, Mikhailidis D, Elisaf M (2008) Effects of ezetimibe, either alone or in combination with atorvastatin, on serum visfatin levels: a pilot study. Expert Opin Pharmacother 9:1829–1837
23. Kostapanos MS, Milionis HJ, Filippatos TD, Nakou ES, Bairaktari ET, Tselepis AD, Elisaf MS (2007) A 12-week, prospective, open-label analysis of the effect of rosuvastatin on triglyceride-rich lipoprotein metabolism in patients with primary dyslipidemia. Clin Ther 29:1403–1414
24. Bradley WA, Hwang SL, Karlin JB, Lin AH, Prasad SC, Gotto AM Jr, Gianturco SH (1984) Low-density lipoprotein receptor binding determinants switch from apolipoprotein E to apolipoprotein B during conversion of hypertriglyceridemic very-low-density lipoprotein to low-density lipoproteins. J Biol Chem 259:14728–14735
25. Brown SA, Via DP, Gotto AM Jr, Bradley WA, Gianturco SH (1986) Apolipoprotein E-mediated binding of hypertriglyceridemic very low density lipoproteins to isolated low density lipoprotein receptors detected by ligand blotting. Biochem Biophys Res Commun 139:333–340
26. Packard CJ, Demant T, Stewart JP, Bedford D, Caslake MJ, Schwertfeger G, Bedynek A, Shepherd J, Seidel D (2000) Apolipoprotein B metabolism and the distribution of VLDL and LDL subfractions. J Lipid Res 41:305–318
27. Caslake MJ, Packard CJ (2004) Phenotypes, genotypes and response to statin therapy. Curr Opin Lipidol 15:387–392
28. Tremblay AJ, Lamarche B, Cohn JS, Hogue JC, Couture P (2006) Effect of ezetimibe on the in vivo kinetics of apoB-48 and apoB-100 in men with primary hypercholesterolemia. Arterioscler Thromb Vasc Biol 26:1101–1106
29. Masuda D, Nakagawa-Toyama Y, Nakatani K, Inagaki M, Tsubakio-Yamamoto K, Sandoval JC, Ohama T, Nishida M, Ishigami M, Yamashita S (2009) Ezetimibe improves postprandial hyperlipidaemia in patients with type IIb hyperlipidaemia. Eur J Clin Invest 39:689–698
30. Wang CS, Downs D, Dashti A, Jackson KW (1996) Isolation and characterization of recombinant human apolipoprotein C-II expressed in *Escherichia coli*. Biochim Biophys Acta 1302:224–230
31. Fojo SS, Brewer HB (1992) Hypertriglyceridaemia due to genetic defects in lipoprotein lipase and apolipoprotein C-II. J Intern Med 231:669–677

32. Jong MC, Havekes LM (2000) Insights into apolipoprotein C metabolism from transgenic and gene-targeted mice. Int J Tissue React 22:59–66
33. Baggio G, Manzato E, Gabelli C, Fellin R, Martini S, Enzi GB, Verlato F, Baiocchi MR, Sprecher DL, Kashyap ML et al (1986) Apolipoprotein C-II deficiency syndrome clinical features, lipoprotein characterization, lipase activity, and correction of hypertriglyceridemia after apolipoprotein C-II administration in two affected patients. J Clin Invest 77:520–527
34. Reina M, Brunzell JD, Deeb SS (1992) Molecular basis of familial chylomicronemia: mutations in the lipoprotein lipase and apolipoprotein C-II genes. J Lipid Res 33:1823–1832
35. Shachter NS, Hayek T, Leff T, Smith JD, Rosenberg DW, Walsh A, Ramakrishnan R, Goldberg IJ, Ginsberg HN, Breslow JL (1994) Overexpression of apolipoprotein CII causes hypertriglyceridemia in transgenic mice. J Clin Invest 93:1683–1690
36. Kowal RC, Herz J, Weisgraber KH, Mahley RW, Brown MS, Goldstein JL (1990) Opposing effects of apolipoproteins E and C on lipoprotein binding to low density lipoprotein receptor-related protein. J Biol Chem 265:10771–10779
37. Clavey V, Lestavel-Delattre S, Copin C, Bard JM, Fruchart JC (1995) Modulation of lipoprotein B binding to the LDL receptor by exogenous lipids and apolipoproteins CI, CII, CIII, and E. Arterioscler Thromb Vasc Biol 15:963–971
38. Lucas CP, Boldrin MN, Reaven GM (2003) Effect of orlistat added to diet (30% of calories from fat) on plasma lipids, glucose, and insulin in obese patients with hypercholesterolemia. Am J Cardiol 91:961–964
39. Reitsma JB, Castro Cabezas M, de Bruin TW, Erkelens DW (1994) Relationship between improved postprandial lipemia and low-density lipoprotein metabolism during treatment with tetrahydrolipstatin, a pancreatic lipase inhibitor. Metabolism 43:293–298
40. Tan KC, Tso AW, Tam SC, Pang RW, Lam KS (2002) Acute effect of orlistat on post-prandial lipaemia and free fatty acids in overweight patients with Type 2 diabetes mellitus. Diabet Med 19:944–948
41. Filippatos T, Tsimihodimos V, Kostapanos M, Kostara C, Bairaktari E, Kiortsis D, Elisaf M (2008) Analysis of the 6-month effect of orlistat, alone or in combination with fenofibrate, administration on triglyceride-rich lipoprotein metabolism in overweight and obese patients with metabolic syndrome. J Clin Lipidol 2:279–284
42. Fernandez ML, Metghalchi S, Vega-Lopez S, Conde-Knape K, Lohman TG, Cordero-Macintyre ZR (2004) Beneficial effects of weight loss on plasma apolipoproteins in postmenopausal women. J Nutr Biochem 15:717–721
43. Gervaise N, Garrigue MA, Lasfargues G, Lecomte P (2000) Triglycerides, apo C3 and Lp B:C3 and cardiovascular risk in type II diabetes. Diabetologia 43:703–708
44. Lee SJ, Campos H, Moye LA, Sacks FM (2003) LDL containing apolipoprotein CIII is an independent risk factor for coronary events in diabetic patients. Arterioscler Thromb Vasc Biol 23:853–858
45. Gerber Y, Goldbourt U, Segev S, Harats D (2003) Indices related to apo CII and CIII serum concentrations and coronary heart disease: a case-control study. Prev Med 37:18–22
46. Luc G, Fievet C, Arveiler D, Evans AE, Bard JM, Cambien F, Fruchart JC, Ducimetiere P (1996) Apolipoproteins C-III and E in apoB- and non-apoB-containing lipoproteins in two populations at contrasting risk for myocardial infarction: the ECTIM study. Etude Cas Temoins sur 'Infarctus du Myocarde. J Lipid Res 37:508–517
47. Hodis HN, Mack WJ, Azen SP, Alaupovic P, Pogoda JM, LaBree L, Hemphill LC, Kramsch DM, Blankenhorn DH (1994) Triglyceride- and cholesterol-rich lipoproteins have a differential effect on mild/moderate and severe lesion progression as assessed by quantitative coronary angiography in a controlled trial of lovastatin. Circulation 90:42–49
48. Sacks FM, Alaupovic P, Moye LA, Cole TG, Sussex B, Stampfer MJ, Pfeffer MA, Braunwald E (2000) VLDL, apolipoproteins B, CIII, and E, and risk of recurrent coronary events in the cholesterol and recurrent events (CARE) trial. Circulation 102:1886–1892

Lipids (2010) 45:451–455
DOI 10.1007/s11745-010-3417-0

COMMUNICATION

Identification of Glucosylceramides Containing Sphingatrienine in Maize and Rice Using Ion Trap Mass Spectrometry

Tatsuya Sugawara · Jingjing Duan · Kazuhiko Aida · Tsuyoshi Tsuduki · Takashi Hirata

Received: 10 March 2010 / Accepted: 12 April 2010 / Published online: 30 April 2010

Abstract We characterized the glucosylceramide moieties from maize and rice using liquid chromatography-ion trap mass spectrometry. Glucosylceramides containing 4,8-sphingadienine (d18:2) acylated to hydroxy-fatty acids were detected as the predominant molecules both in maize and in rice. In addition, 4-hydroxy-8-sphingenine (t18:1) and sphingatrienine (d18:3) were found in maize and rice glucosylceramides, and in the case of rice, sphingenine (d18:1) was also detected. Glucosylceramides containing d18:3 were acylated to hydroxyl fatty acids (16–24 carbon atoms). Our results indicate the presence of the triene type of sphingoid base in higher plants.

Keywords HPLC (High performance liquid chromatography) · Mass spectrometry (MS) · Plant lipids · Glycosphingolipids · Sphingoid bases

Abbreviations

d18:0	Sphinganine
d18:1	Sphingenine
d18:2	Sphingadienine
d18:3	Sphingatrienine
t18:0	Phytosphingosine
t18:1	Hydroxysphingenine
HPLC	High-performance liquid chromatography
MS	Mass spectrometry

T. Sugawara (✉) · J. Duan · T. Hirata
Division of Applied Biosciences,
Graduate School of Agriculture,
Kyoto University, Kyoto 606-8502, Japan
e-mail: sugawara@kais.kyoto-u.ac.jp

K. Aida
Central Laboratory, Nippon Flour Mills Co., Ltd.,
Kanagawa 243-0041, Japan

T. Tsuduki
Laboratory of Food and Biomolecular Science,
Graduate School of Life Science and Agriculture,
Tohoku University, Sendai 981-8555, Japan

Introduction

Sphingolipids are found in a wide variety of organisms, and constitute a family of compounds that have a sphingoid base (long-chain base) with an amide-linked fatty acid and a polar head group. The hydrolyzed products of sphingolipids (ceramides and sphingoid bases) are highly bioactive compounds that play roles as second messengers that are known to be involved in many aspects of cell regulation, such as cell growth, cell differentiation and apoptosis [1–3]. Recently, dietary sphingolipids have gained attention for their potential to protect the intestine from inflammation and cancer [4–9]. In addition, other physiological functions of sphingolipids, such as improving the barrier function of skin, lowering plasma lipids and prevention of melanin formation, have also been reported [10–12].

Diverse structures of the sphingoid base occur in nature. The most common sphingoid base of mammalian sphingolipids is sphingosine (*trans*-4-sphingenine, d18:1^4). Smaller amounts of other sphingoid bases, such as sphinganine (dihydrosphingosine, d18:0) and phytosphingosine (4-hydroxysphinganine, t18:0) are frequently encountered. The structures of sphingoid bases in higher plants are more complicated than in mammals [13]. Plants primarily contain *cis*- and *trans*-isomers of Δ8-unsaturated sphingoid bases, such as 8-sphingenine (d18:1^8), 4,8-sphingadienine

(d18:$2^{4,8}$) and 4-hydroxy-8-sphingenine (t18:1). Determination of those diverse structures including variations of the sphingoid backbone is important to understand the functional and nutritional significance of dietary sphingolipids.

Mass spectrometry is one of the most powerful methods for detecting and identifying the chemical structures of lipids including sphingolipids [14–16]. In this study, we characterized the structures of glucosylceramide, one of the predominant glycosphingolipids in plants, from rice and from maize using liquid chromatography-ion trap mass spectrometry. Our results demonstrate the presence of sphingatrienine (d18:3) in higher plants, which has been described previously in marine invertebrates [17–19] and has been found in tobacco leaf [20].

Experimental Procedures

Materials

Glucosylceramides were prepared from maize grain and from rice grain using a silica gel column after lipid extraction and saponification as described previously [21]. All other chemicals and solvents were of reagent grade.

LC–MS/MS Analyses

An HPLC system coupled to an LCMS-IT-TOF spectrometer equipped with an electrospray ionization interface (Shimadzu, Kyoto, Japan) was used. A TSK gel ODS-100Z column (2.0 × 50 mm, 3 μm, Tosoh, Tokyo, Japan) was eluted with acetonitrile/water (93:7, v/v) at a flow rate of 0.2 mL/min. The MS was operated with the following conditions: probe voltage of 4.50 kV, CDL temperature of 200°C, block heater temperature of 200°C, nebulizer gas flow of 1.5 L/min, ion accumulation time of 100 ms, MS range of *m/z* 650–900, MS^2 range of *m/z* 200–300, and CID parameters as follows: energy, 60%; collision gas 60%. For the structural analysis of glucosylceramide, $[M + H - 18]^+$ (loss of water) in the positive scan mode was used for MS/MS analysis to obtain the product ions. The typical signals which are characteristic for the sphingoid base moieties were observed as the product ions using the auto MS/MS detection mode. In this system, product ions corresponding to d18:1, d18:2 and d18:3 were *m/z* 264.3, 262.3 and 260.2, respectively [14–16]. In the case of glucosylceramide molecules consisting of t18:1, the loss of glucose $[M + H - 162]^+$ was used as the precursor ion and the product ions corresponding to t18:1 were *m/z* 280.3 and 262.3 [16]. Pairs of the structurally specific product ions of sphingoid bases and their precursor ions were used for the identification of glucosylceramide molecules.

Results and Discussion

In the positive full scan mode, $[M + Na]^+$, $[M + H]^+$ and $[M + H - H_2O]^+$ were the predominant signals in each peak. It is well known that the sugar moiety of glycosylceramides in plants is mostly glucose [22]. In the case of molecules consisting of t18:1, the loss of glucose $[M + H - 162]^+$ was also clearly detected. Glucosylceramide molecules containing d18:2 and t18:1 were determined both in maize and in rice as described previously (Figs. 1a, 2a) [16]. In the case of rice glucosylceramide, molecules consisting of d18:1 were also identified. Detection of glucosylceramide consisting of d18:2 and t18:1 was separated into two peaks, *cis*- and *trans*-isomers of Δ8-unsaturated sphingoid bases. *Cis*-isomer was detected earlier than *trans*-isomer by separation of the reverse phase [20]. Predominantly hydroxy fatty acids containing 16–26 carbon atoms were detected both in maize and in rice glucosylceramides.

We verified that the characteristic product ion at *m/z* 260.2 corresponding to d18:3 was detected in maize glucosylceramide using the auto MS/MS detection mode (Fig. 1a). Five peaks in the total ion chromatogram of maize glucosylceramide showed the product ion at *m/z* 260.2 (peak 1–5 in Fig. 1a). The MS spectra of those 5 peaks are shown in Fig. 1b–f. As the precursor ion of *m/z* 260.2, $[M + H - 18]^+$ ions at *m/z* 694.5, 722.5, 750.6, 778.6 and 806.6 were detected. The identification of each peak component is summarized in Table 1. The acylated fatty acid moieties were hydroxy fatty acids with 16–24 carbon atoms. In the case of rice, glucosylceramide consisted of d18:3-C18:0h and d18:3-C20:0h (Fig. 2; Table 1).

It has been reported that the sphingoid bases in marine invertebrates are quite different from those in mammals and in plants [13]. Triene bases with conjugated diene, such as 2-amino-4,8,10-octatriene-1,3-diol (d18:3) and 2-amino-9-methyl-4,8,10-octatriene-1,3-diol (d19:3), were identified in marine invertebrates including ascidians [17], starfish [18, 19] and squid [23] and also some fungi [24]. We have also reported that sea cucumber glucosylceramide has sphingoid bases with three double bonds [25]. Sperling et al. [20] described the presence of sphingatrienine in tobacco leaf by HPLC analysis of a sphingoid base derivatized with dinitrophenyl. In this study, we identified several molecular species of sphingatrienine-containing glucosylceramides in maize and rice by LC–MS/MS system. However, the locations of double bonds in sphingatrienine structure have not been identified. Sphingolipids of plant organisms contain primarily d18:1^8, d18:$2^{4,8}$ and t18:1^8 as sphingoid bases and sphingolipid Δ4-desaturase and sphingolipid Δ8-desaturase have been identified in plants [22]. It has been reported that the composition of sphingoid bases differs between chilling sensitive and

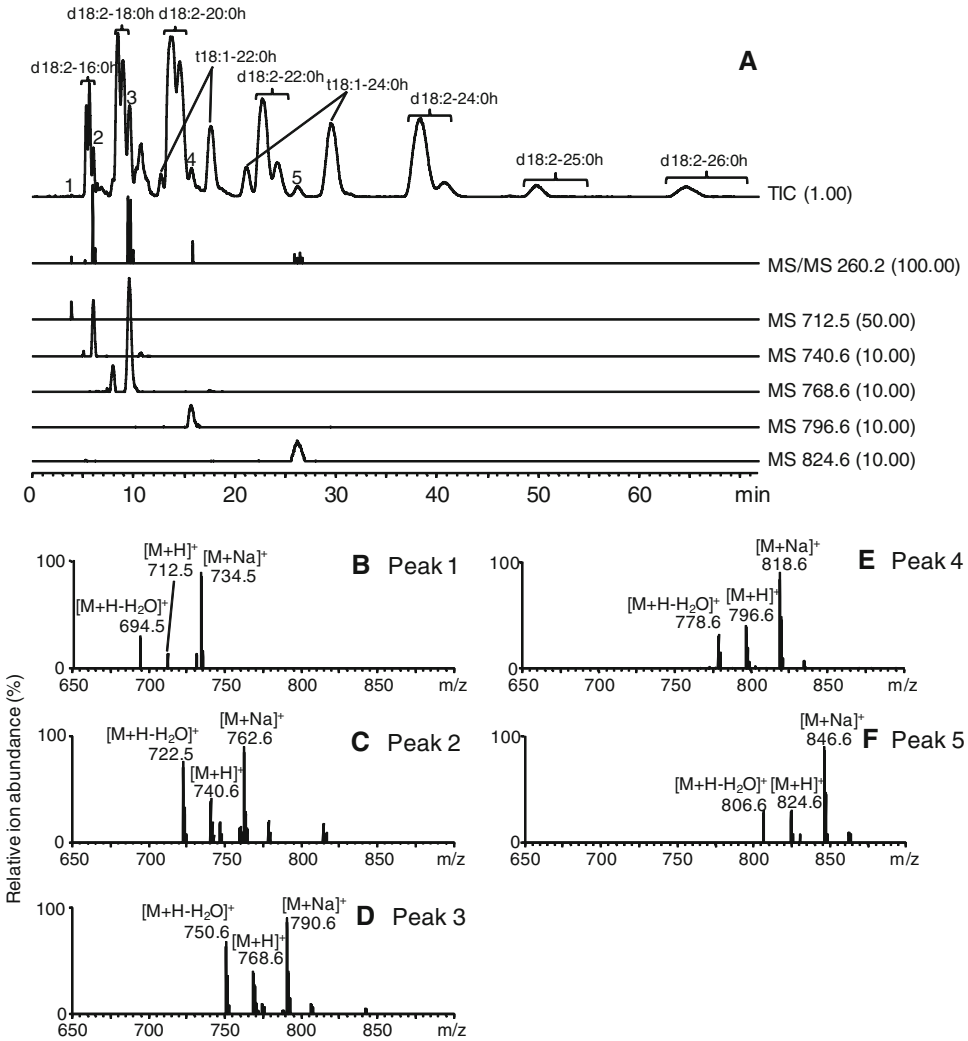

Fig. 1 Total ion and selected ion chromatograms of maize glucosylceramide (**a**) and mass spectra of peak components (**b**–**f**)

Table 1 Glucosylceramides containing sphingatrienine (d18:3) from maize and from rice identified by HPLC–MS/MS analysis

Peak no. in Figs. 1 and 2	Precursor ion *m/z*		Product ion *m/z*	Molecule	Source
	$[M + H]^+$	$[M + H - 18]^+$			
1	712.5	694.5	260.2	d18:3-C16:0h	Maize
2	740.5	722.5	260.2	d18:3-C18:0h	Maize, rice
3	768.6	750.6	260.2	d18:3-C20:0h	Maize, rice
4	796.6	778.6	260.2	d18:3-C22:0h	Maize
5	824.6	806.6	260.2	d18:3-C24:0h	Maize

tolerant plants [26]. Details of tissue distribution, synthetic pathways and functions of plant sphingatrienines remain to be elucidated.

Recently, dietary sphingolipids have gained attention for their potential to protect the intestine from inflammation and cancer [4–9]. We reported that the daily intake of plant-origin glucosylceramides in Japan is estimated to be 50 mg due to their presence in foodstuffs [27] and we investigated the digestion and absorption of plant-derived sphingolipids [21]. Our findings indicate that the metabolic fate of plant-derived sphingoid bases, such as 4,8-sphingadienine, within enterocytes differs from that of sphingosine. Sphingoid bases, except for sphingosine, appear to be transported out of cells across the apical membranes of enterocytes by P-glycoprotein after absorption and consequently the intestinal uptake is quite poor [28, 29]. Thus, the determination of sphingolipid structures, including variation of the sphingoid backbone, from dietary sources

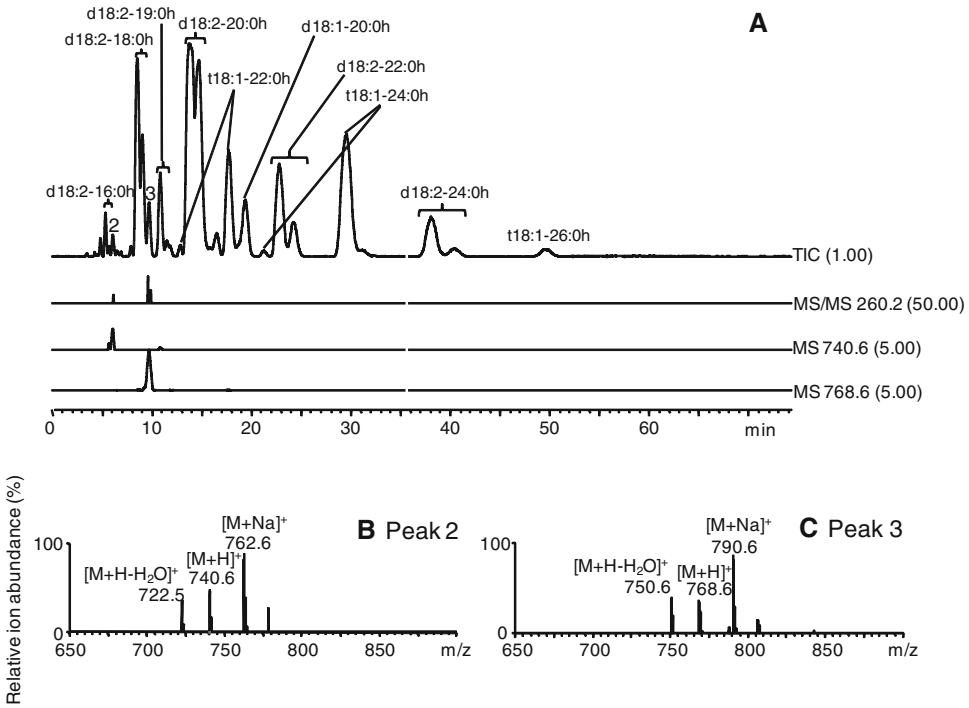

Fig. 2 Total ion and selected ion chromatograms of rice glucosylceramide (**a**) and mass spectra of peak components (**b**, **c**)

is important to understand their functional and nutritional significance.

In this study, we analyzed the chemical structures of glucosylceramides from maize and from rice using liquid chromatography-ion trap mass spectrometry. Our results indicate the presence of sphingatrienine (d18:3) in higher plant sphingolipids. MS/MS analysis is a powerful method for identifying the molecular structures of sphingolipids from biological sources.

Acknowledgments This work was supported by the Program for Promotion and Applied Researches for Innovations in Bio-oriented Industry (BRAIN).

References

1. Spiegel S, Merrill AH Jr (1996) Sphingolipid metabolism and cell growth regulation. FASEB J 10:1388–1397
2. Cuvillier O (2002) Sphingosine in apoptosis signaling. Biochim Biophys Acta 1585:153–162
3. Hannun YA, Obeid LM (2008) Principles of bioactive lipid signaling: lessons from sphingolipids. Nat Rev Mol Cell Biol 9:139–150
4. Duan RD, Nilsson Å (2009) Metabolism of sphingolipids in the gut and its relation to inflammation and cancer development. Prog Lipid Res 4:62–72
5. Schmelz EM (2004) Sphingolipids in the chemoprevention of colon cancer. Front Biosci 9:2632–2639
6. Schmelz EM, Sullards MC, Dillehay DL, Merrill AH Jr (2000) Colonic cell proliferation and aberrant crypt formation are inhibited by dietary glycosphingolipids in 1,2-dimethylhydrazine-treated CF1 mice. J Nutr 130:522–527
7. Schmelz EM, Roberts PC, Kustin EM, Lemonnier LA, Sullards MC, Dillehay DL, Merrill AH Jr (2001) Modulation of intracellular β-catenin localization and intestinal tumorigenesis in vivo and in vitro by sphingolipids. Cancer Res 61:6723–6729
8. Aida K, Kinoshita M, Tanji M, Sugawara T, Tamura M, Ono J, Ueno N, Ohnishi M (2005) Prevention of aberrant crypt foci formation by dietary maize and yeast cerebrosides in 1,2-dimethylhydrazine-treated mice. J Oleo Sci 54:45–49
9. Kinoshita M, Aida K, Tokuji Y, Sugawara T, Ohnishi M (2009) Effects of dietary plant cerebroside on gene expression in the large intestine of 1, 2-dimethylhydrazine (DMH)-treated mice determined by DNA microarray analysis. J Food Lipids 16:200–208
10. Tsuji K, Mitsutake S, Ishikawa J, Takagi Y, Akiyama M, Shimizu H, Tomiyama T, Igarashi Y (2006) Dietary glucosylceramide improves skin barrier function in hairless mice. J Dermatol Sci 44:101–107
11. Duivenvoorden I, Voshol PJ, Rensen PC, van Duyvenvoorde W, Romijn JA, Emeis JJ, Havekes LM, Nieuwenhuizen WF (2006) Dietary sphingolipids lower plasma cholesterol and triacylglycerol and prevent liver steatosis in APOE*3Leiden mice. Am J Clin Nutr 84:312–321
12. Kinoshita M, Hori N, Aida K, Sugawara T, Ohnishi M (2007) Prevention of melanin formation by yeast cerebroside in B16 mouse melanoma cells. J Oleo Sci 56:645–648
13. Sperling P, Heinz E (2003) Plant sphingolipids: structural diversity, biosynthesis, first gene and functions. Biochim Biophys Acta 1632:1–15
14. Bartke N, Fischbeck A, Humpf HU (2006) Analysis of sphingolipids in potatoes (*Solanum tuberosum* L.) and sweet potatoes (*Ipomoea batatas* (L.) Lam.) by reversed phase high-performance liquid chromatography electrospray ionization tandem mass spectrometry (HPLC-ESI-MS/MS). Mol Nutr Food Res 50:1201–1211
15. Shaner RL, Allegood JC, Park H, Wang E, Kelly S, Haynes CA, Sullards MC, Merrill AH Jr (2009) Quantitative analysis of sphingolipids for lipidomics using triple quadrupole and quadrupole linear ion trap mass spectrometers. J Lipid Res 50:1692–1707
16. Sugawara T, Aida K, Duan J, Hirata T (2010) Analysis of glucosylceramides from various sources by liquid chromatography-ion trap mass spectrometry. J Oleo Sci 59:387–394

17. Duran R, Zubia E, Ortega MJ, Naranjo S, Salva J (1998) Phallusides, new glucosphingolipids from the ascidian *Phallusia fumigate*. Tetrahedron 54:14597–14602
18. Jin W, Rinehart KL, Jares-Erijman EA (1994) Ophidiacerebrosides: cytotoxic glycosphingolipids containing a novel sphingosine from a sea star. J Org Chem 59:144–147
19. Diaz de Vivar ME, Seldes AM, Maier MS (2002) Two novel glucosylceramides from gonads and body walls of the Patagonian starfish *Allostichaster inaequalis*. Lipids 37:597–603
20. Sperling P, Franke S, Lüthje S, Heinz E (2005) Are glucocerebrosides the predominant sphingolipids in plant plasma membranes? Plant Physiol Biochem 43:1031–1038
21. Sugawara T, Kinoshita M, Ohnishi M, Nagata J, Saito M (2003) Digestion of maize sphingolipids in rats and uptake of sphingadienine by Caco-2 cells. J Nutr 133:2777–2782
22. Warnecke D, Heinz E (2003) Recently discovered function of glucosylceramides in plants and fungi. Cell Mol Life Sci 60:919–941
23. Ohashi Y, Tanaka T, Akashi S, Morimoto S, Kishimoto Y, Nagai Y (2000) Squid nerve sphingomyelin containing an unusual sphingoid base. J Lipid Res 41:1118–1124
24. Shu RG, Wang FW, Yang YM, Liu YX, Tan RX (2004) Antibacterial and xanthine oxidase inhibitory cerebrosides from *Fusarium* sp. IFB-121, an endophytic fungus in *Quercus variabilis*. Lipids 39:667–673
25. Sugawara T, Zaima N, Yamamoto A, Sakai S, Noguchi R, Hirata T (2006) Isolation of sphingoid bases of sea cucumber cerebrosides and their cytotoxicity against human colon cancer cells. Biosci Biotechnol Biochem 70:2906–2912
26. Imai H, Ohnishi M, Hotsubo K, Kojima M, Ito S (1997) Sphingoid base composition of cerebrosides from plant leaves. Biosci Biotechnol Biochem 61:351–353
27. Sugawara T, Miyazawa T (1999) Separation and determination of glycolipids from edible plant sources by high-performance liquid chromatography and evaporative light-scattering detection. Lipids 34:1231–1237
28. Sugawara T, Kinoshita M, Ohnishi M, Tsuzuki T, Miyazawa T, Nagata J, Hirata T, Saito M (2004) Efflux of sphingoid bases by P-glycoprotein in human intestinal Caco-2 cells. Biosci Biotechnol Biochem 68:2541–2546
29. Sugawara T, Tsuduki T, Yano S, Hirose M, Duan J, Aida K, Ikeda I, Hirata T (2010) Intestinal absorption of dietary maize glucosylceramide in lymphatic duct cannulated rats. J Lipid Res (in press)

Lipids (2010) 45:457–461
DOI 10.1007/s11745-010-3413-4

COMMUNICATION

Pecipamide, a New Sphingosine Derivative from the Cultures of *Polyporus picipes* (Basidiomycetes)

Yong Li · Ya-Tuan Ma · Yi Kuang · Jin-Ming Gao · Jian-Chun Qin

Received: 13 December 2009 / Accepted: 31 March 2010 / Published online: 27 April 2010

Abstract A new C_{18}-ceramide congener named pecipamide (**1**), together with the known ergosta-4,6,8(14),22-tetraen-3-one (**2**), was isolated from the solid fermentations of the basidiomycetous fungus *Polyporus picipes*. The structure of the new metabolite was established as (2′*R*,2*S*,3*R*)-*N*-2′-hydroxyheptadecanoyl-2-amino-octadecane-1,3-diol on the basis of spectroscopic data, including 1D- and 2D- nuclear magnetic resonance spectroscopy (NMR) experiments, as well as by means of mass spectrometric measurements (MS).

Keywords Sphingosine · Pecipamide · Ceramide · Fungal metabolites · *Polyporus picipes* · Basidiomycetes

Abbreviations

CC	Column chromatography
COSY	Correlation spectroscopy
DEPT	Distortionless enhancement by polarization transfer
ESI-MS	Electrospray ionization-mass spectroscopy
FAB-MS	Fast atom bombardment-mass spectrometry
HMBC	Heteronuclear multiple bond correlation
HMQC	Heteronuclear multiple quantum correlation
HR	High resolution
MS	Mass spectrometric measurements
*m*NBA	*meta*-Nitrobenzyl alcohol
NMR	Nuclear magnetic resonance spectroscopy
PDA	Potato dextrose agar
TLC	Thin layer chromatography

Y. Li · Y.-T. Ma · Y. Kuang · J.-M. Gao (✉)
Natural Medicinal Chemistry Research Centre, College of Science, Northwest A&F University, Yangling 712100, Shaanxi, China
e-mail: jinminggao@nwsuaf.edu.cn

J.-M. Gao
National Engineering Research Center for Phytochemistry in West China, Yangling 712100, Shaanxi, China

J.-C. Qin
College of Plant Science, Jilin University, Changchun 130062, China

Introduction

Sphingolipids constitute a biologically important class of compounds [1, 2]. These lipids have been reported from all groups of organisms thus far analyzed, including marine organisms [3–8], plants [9–11], and fungi [12–16]. Sphingolipids, e.g., ceramides, sphingomyelin, cerebrosides and gangliosides, are important building blocks of the plasma membrane of eukaryotic cells. Their function is to anchor lipid-bound carbohydrates to cell surfaces and to create an epidermal water permeability barrier, as well as to participate in antigen–antibody reactions and transmission of biological information [1]. Some of these metabolites have been reported to display a wide range of biological activities, such as antihepatotoxic [9], cytotoxic [5–7], antitumor [7], immunostimulatory [8], antifungal [7], antimicrobial [6, 17], antiviral or Ca^{2+} ATPase [18], and anti-inflammatory effects [19].

In recent years, renewed attention has been paid to the constituents of higher basidiomycetes because of their possible medical usage [2, 20]. For examples, antiviral, antibiotic, antiinflammatory, hypoglycemic, hypocholesterolemic, and hypotensive properties were ascribed to ingredients of such mushrooms [2, 21, 22]. The mushroom *Polyporus picipes* (family Polyporaceae) has some

activities, including inhibiting cancer, enhancing immunity, softening blood vessels, preventing aging of the heart, as well as improving brain memory function. No phytochemical study of this fungus has previously been carried out.

In a continuation of our investigation into bioactive fungal metabolites, especially lipids from higher fungi (macrofungi) [12–16], a new ceramide, (2′*R*,2*S*,3*R*)-*N*-2′-hydroxyhepta-decanoyl-2-amino-octadecane-1,3-diol (**1**), was isolated from the solid fermented cultures of *P. picipes*, along with a sterone, ergosta-4,6,8(14),22-tetraen-3-one (**2**) [23]. Herein, we report the isolation and structural elucidation of the new ceramide.

Results and Discussion

The AcOEt-soluble fraction of AcOEt-MeOH-HAc extract from the solid cultures of *P. picipes* was subjected to repeated CC to yield compounds **1** and **2**. The structure of new compound **1** was elucidated as follows (Fig. 1).

Compound **1** was isolated as white needle crystals. It gave pseudo-molecular ion peaks $[M–1]^-$ at *m/z* 568 and $[M–1 + MNBA$ (*m*-nitrobenzyl alcohol, $M_r = 153$) as matrix$]^-$ at 721 in the negative ion FAB-MS spectrum and $[M + Na]^+$ at *m/z* 592 in the positive ion ESI-TOF-MS spectrum, indicating a molecular weight of 569. It has a molecular formula $C_{35}H_{71}NO_4$, established by a quasi-molecular ion peak $[M + Cl–2H]^-$ at *m/z* 602.4904 (calc. 602.4915 for $C_{35}H_{69}NO_4Cl$) in the HR-FAB-MS (negative-ion mode), combined with ^{13}C- and ^{1}H-NMR data. The IR spectrum showed absorption bands for a secondary amide (1,625, 1,545 cm^{-1}) and hydroxyl (3,434 cm^{-1}) functionalities. The ^{1}H- and ^{13}C-NMR spectral data of **1** indicated the presence of an amide linkage and two long chain aliphatic moieties, suggesting the sphingolipid nature of the molecule (Table 1).

The overlapped signals of aliphatic methylenes at δ 1.18–1.34 in the ^{1}H-NMR spectrum and at δ 29.67–30.21 in the ^{13}C-NMR spectrum were observed. Moreover, the ^{1}H-NMR spectrum presented signals attributable to two terminal methyl groups at δ 0.81 (6H, *brt*, $J = 6.64$ Hz), one methylene group at δ 3.94 (1H, *dd*, $J = 10.9$, 4.3 Hz, H-1) and 3.70 (1H, *dd*, $J = 10.9$, 5.3 Hz, H-1), and three methines at δ 3.74 (1H, m, H-3), 4.06 (2H, m, H-2 and H-2′), indicating the presence of two long aliphatic chains instead of the branched chain [16]. A downfield doublet appearing at δ 7.25 (1H, *d*, $J = 7.84$ Hz) was assigned to an amide NH. In addition, the ^{13} C-NMR and DEPT spectra showed the existence of characteristic signals, an amide carbonyl group [δ 174.56 (CONH, C-1′)], three methine groups [δ 53.71(CHNH, C-2), 73.88 (CHOH, C-3), 72.34 (CHOH, C-2′)], and one hydroxymethyl group [δ 62.31(CH_2OH, C-1)] in this molecule (Table 1). The aforementioned data implied that compound **1** is a ceramide derivative [12–15]. Detailed analysis of the ^{1}H-^{1}H COSY spectrum (in pyridine-d_5) of compound **1** indicated connectivities for the H_2-1 was found to be coupled with H-2, which in turn was coupled with H-3, H-4, and an amide proton, and for the H-2′ was found to be coupled with H-3′. Interpretation of HMBC spectrum revealed correlations from an amide proton (CONH) to C-1′; and H-2′ to C-1′ (Fig. 2).

Table 1 ^{1}H- (400 MHz) and ^{13}C-NMR (100 MHz) data of **1** in $CDCl_3$

Position	^{13}C (DEPT)	^{1}H (J in Hz)
1	62.31 (CH_2)	3.70 (*dd*, $J = 10.9$, 5.3)
		3.94 (*dd*, $J = 10.9$, 4.3)
2	53.71 (CH)	4.06 (m)
3	73.88 (CH)	3.74 (m)
4	31.90 (CH_2)	1.71 (m)
5	25.99 (CH_2)	1.45 (m)
6–15	29.67–30.21 (CH_2)	1.18–1.34 (brs)
16	31.93 (CH_2)	
17	22.67 (CH_2)	
18	14.11 (CH_3)	0.81(t, $J = 6.64$)
CONH		7.25 (*d*, $J = 7.84$)
1′	174.56 (C)	
2′	72.34 (CH)	4.06 (m) (overlapping)
3′	34.77 (CH_2)	1.32 (m)
4′–14′	29.67–30.21 (CH_2)	1.18–1.34 (brs)
15′	31.93 (CH_2)	
16′	22.67 (CH_2)	
17′	14.11 (CH_3)	0.81 (t, 6.64)

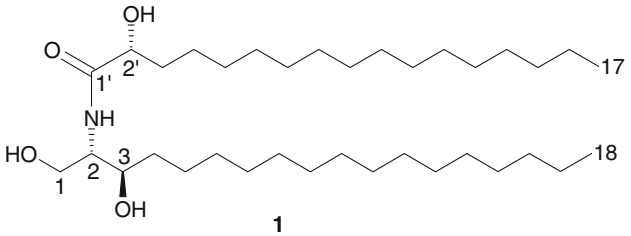

Fig. 1 Structure of compound **1**

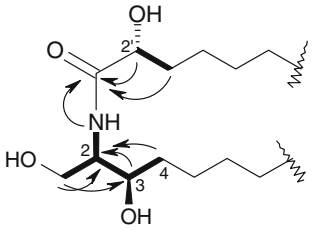

Fig. 2 Key COSY and HMBC interactions in compound **1**

The lengths of the long chain base and the fatty acid were determined by FAB-MS. The negative FAB-MS presented the characteristic fragments at *m/z* 269$[C_{15}H_{30}CH(OH)CO]^-$ and 284 $[C_{15}H_{30}CH(OH)$-$CONH + H]^-$ in this molecule (Fig. 3), suggesting that the long chain base and fatty acid of **1** should be 2-amino-octadecane-1,3-diol and 2-hydroxyheptadecanoic acid, respectively. Methanolysis of compound **1** afforded the fatty acid methyl ester, which exhibited a base peak at *m/z* 300 $[M^+]$ and an ion at *m/z* 241 $[M–COOCH_3]^+$ in the EIMS. This established the molecular weight of the fatty acid fragment to be 286. The structure of the acyl moiety was determined to be 2-hydroxyheptadecanoic acid.

The relative stereochemistry at C-2, C-3 and C-2′ were deduced to be 2*S*,3*R* and 2′*R*, respectively, identical to that of *D*-sphingosine on the basis of ^{13}C-NMR spectral data, since the chemical shifts of C-2 (δ 53.71), C-3 (δ 73.88), and C-2′ (δ 72.34) were in agreement with those of the previously reported natural product, (2′*R*,2*S*,3*R*)-*N*-2′-hydroxyoctadecanoyl-2-amino-9-methyl-heptadecadiene-1,3-diol (δ 54.4, 74.4, and 72.4), a ceramide that was isolated from the mushroom *Ramaria botrytis* [24], and with those of other related compounds [25, 26], in connection with their optical rotations of **1** ($[\alpha]_D$ + 2.3) and the natural relative ($[\alpha]_D$ + 7.4) [24]. On the other hand, biogenetically, in higher mushrooms, these ceramides all have common biosynthetic pathways [15]. So, this new compound in the current study has a relative configuration of 2'*R*,2*S*,3*R* tentatively determined. In view of these evidence, thus, the structure of **1**, which we named as pecipamide, was elucidated as (2′*R*,2*S*,3*R*)-*N*-2′-hydroxyheptadecanoyl-2-amino-octadecane-1,3-diol.

Sphingolipids are ubiquitous membrane constituents of animals, plants, and also lower forms of life, the principal component of which is the long chain base or sphingoid base. In nature, the most widely occurring sphingoid bases are D-*erythro*-4*E*-sphingenine, 4-hydroxysphinganine (phytosphingosine), and 9-methyl-4*E*,8*E*-sphingadienine [12–16], whereas in higher mushrooms and other basidiomycetes, D-*erythro*-sphinganine is an uncommon minor sphingoid base. Fungal sphingolipids consist of phytosphingosine in the ceramide moiety instead of sphingosine, which is mainly present in mammals [27].

The present investigation demonstrated the presence in *Polyporus picipes* of a previously unrecognized sphingolipid, consisting of D-*erythro*-sphinganine in an amide linkage with a hydroxyl C_{17}-fatty acid. To our knowledge, this seems to be the first time that a D-*erythro*-sphinganine-type ceramide has been identified from the higher fungi.

Experimental Section

General Experimental Procedures

Optical rotations were measured on a PerkinElmer Model 341 polarimeter. NMR experiments were performed on a Bruker AM-400 or Bruker Avance-500 spectrometer with TMS as the internal standard, in $CDCl_3$, δ in ppm, *J* in Hz. Mass spectra were recorded on a VG Auto Spec-3000 (VG, Manchester, UK) or an API QSTAR Pulsar 1 spectrometer. IR spectra were recorded on a Bruker Tensor 27 spectrometer with KBr pellets. GC–MS with a Finnigan 4510 GC–MS system, at 70 eV for EI, a capillary column (30 m × 0.25 mm) packed with 5% phenyl and 95% methyl silicone on HP-5, Carrier gas: He, Column temperature: 160–240 °C, at 5 °C/min).

Column chromatography (CC) was performed on silica gel (200–300 mesh; Qingdao Marine Chemical Ltd., Qingdao, People's Republic of China) and Sephadex LH-20 (Amersham Biosciences, Sweden). TLC analysis was carried out on silica gel GF254 precoated plates (0.20–0.25 mm; Qingdao) with detection by heating silica gel plates sprayed with 10% H_2SO_4 in EtOH.

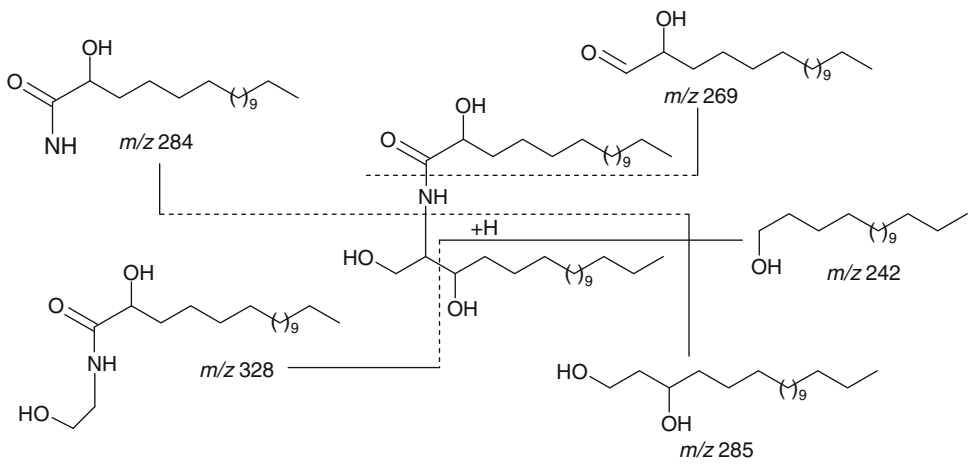

Fig. 3 Proposed FAB-MS (negative ion mode) fragmentation pattern in compound **1**

Producing Fungus

The mushroom strain of a basidiomycete *Polyporus picipes* (S 0318) was isolated from a tissue culture of the fruiting bodies of wild mushrooms collected at Laojunshan, Yunnan Province, P. R. China, in July 2003 and identified by Prof. Da-Gan Ji, Kunming Institute of Botany, Chinese Academy of Sciences. A voucher specimen was deposited at the herbarium of Kunming Institute of Botany, Chinese Academy of Sciences.

Fermentation

The *P. picipes* strain was maintained on a potato dextrose agar slant (PDA) at 4 °C. The activated strain was inoculated into 500-mL flasks containing 100 mL of a sterilized solid medium consisting of glucose (20 g/L), peptone (3 g/L), $MgSO_4{\cdot}7H_2O$ 0.5 (g/L), and KH_2PO_4 (1 g/L), and potato extract prepared by extracting from 100 g of peeled potato with 1 L of water boiled for 20 min. Stationary fermentation was carried out at 28 °C under a humidity of 50–70%. After 38 days of fermentation, the cultures were harvested.

Extraction and Isolation

The solid cultures were ultrasonically extracted five times with a mixture of AcOEt-MeOH-HAc (80:15:5). After evaporation of the solvent, the resultant extract was partitioned between water and EtOAc. The organic layers were combined and concentrated in vacuo. The EtOAc residue (4 g) obtained was subjected to a CC over silica gel and eluted with $CHCl_3$–MeOH (100:0 → 70:30) in a gradient elution manner to provide ten fractions (Fr1.–Fr10.) Fr5. (167 mg) was passed through a Sephadex LH-20 column (methanol) to obtain subfr.1–40. Subfr. 9–13 was subjected to a CC on silica gel using $CHCl_3$–MeOH (96:4), and a Sephadex LH-20 column with $CHCl_3$–MeOH (1:1), and further purified by a CC over silica gel with $CHCl_3$–acetone (85:15) to furnish compound **1** (7 mg). Subfr. 34 was subjected to a CC over silica gel with $CHCl_3$-MeOH (95:5) to yield ergosta-4,6,8(14),22-tetraen-3-one (**2**) (2 mg).

Methanolysis of Compound **1**

Compound **1** (2 mg) was treated with 2.5 mL of 1 N HCl in 82% MeOH and refluxed for 12 h. The reaction mixture was extracted with hexane, and the hexane layer was washed with water, dried, and evaporated to give methyl 2-hydroxyheptadecanoate, whose retention time (t_R) was 18.9 min; EI-MS (70 eV) *m/z* (rel. int. %) 300 $[M]^+$, 241 $[M–COOMe]^+$. The data were identical to those published earlier [13].

(2′*R*,2*S*,3*R*)-*N*-2′-hydroxyheptadecanoyl-2-amino-octadecane-1,3-diol (**1**). Amorphous white solid (chloroform). $[\alpha]_D^{20}$ + 2.3 (c = 0.1, acetone); ^{1}H- and ^{13}C-NMR data: see Table. IR (KBr): ν_{max} 3,434, 2,923, 2,850, 1,625, 1,545, 1,470, 1,070, 980, 714 cm^{-1}. ESI-MS (positive ion mode) *m/z*: 592.4 $[M + Na]^+$; FAB-MS (negative ion mode; matrix: *meta*-nitrobenzyl alcohol, mNBA) *m/z* (%): 567 $[M–2]^-$ (100), 568$[M–1]^-$ (40), 721 $[M–1 + 153]^-$, 328 $[M–C_{16}H_{33}O]^-$ (2.7), 285 $[C_{15}H_{33}CH(OH)CH\text{-}CH_2OH]^-$(5), 284 $[C_{15}H_{30}CH(OH)\ CONH + H]^-$ (22.5), 269$[C_{15}H_{30}CH(OH)CO]^-$(4), 242$[C_{15}H_{31}CH(OH) +H]^-$(9), 197 $[C_{14}H_{29}]^-$ (12); HR-FAB-MS *m/z*: 602.4904 $[(M + Cl–2H)^-$, calc. for $C_{35}H_{69}NO_4Cl$: 602.4915].

Acknowledgments We would like to thank funding support from the National Natural Science Foundation of China (Grant No. 30370019, 30670221), the Program for Changjiang Scholars and the Innovative Research Team in University (IRT0749). The authors also thank the Project Sponsored by the Scientific Research Foundation for the Returned Overseas Chinese Scholars, State Education Ministry (to J.-M.G.).

References

1. Hannun YA, Bell RM (1989) Functions of sphingolipids and sphingolipid breakdown products in cellular regulation. Science 243:500–507
2. Gao JM (2006) New biologically active metabolites from Chinese higher fungi. Curr Org Chem 10:849–871
3. Chebaane K, Guyot M (1986) Occurrence of *erythro*-docosasphinga-4, 8-dienine, as an ester, in *Anemonia sulcata*. Tetrahedron Lett 27:1495–1496
4. Chakrabarty M, Batabyal A, Barua AK, Patra A (1994) New ceramides from the hypotensive extract of a sea anemone, *Paracondylactis indicus*. J Nat Prod 57:393–395
5. Jin W, Rinehart KL, Jares-Erijman EA (1994) Ophidiacerebrosides: cytotoxic glycosphingolipids containing a novel sphingosine from a sea star. J Org Chem 59:144–147
6. Shin J, Seo Y (1995) Isolation of new ceramides from the Gorgonian *Acabaria undulata*. J Nat Prod 58:948–953
7. Li HY, Matsunaga S, Fusetani N (1995) Halicylindrosides, antifungal and cytotoxic cerebrosides from the marine sponge *Halichondria cylindrata*. Tetrahedron 51:2273–2280
8. Natori T, Morita M, Akimoto K, Koezuka Y (1994) Agelaspins, novel antitumor and immunostimulatory cerebrosides from the marine sponge *Agelas mauritianus*. Tetrahedron 50:2771–2784
9. Kim SY, Choi YH, Huh H, Kim JW, Kim YC, Lee HS (1997) New antihepatotoxic cerebroside from *Lycium chinense* fruits. J Nat Prod 60:274–276
10. Shibuya H, Kawashima K, Sakagami M, Kawanishi H, Shimomura M, Ohashi K, Kitagawa I (1990) Sphingolipids and glycerolipids I. Chemical structures and ionophoretic activities of soyacerebrosides I and II from soybean. Chem Pharm Bull 38:2933–2938
11. Liu HW, He LY, Gao JM, Ma YB, Zhang XM, Peng H, Chen JJ (2008) Chemical constituents from the aquatic weed *Pistia stratiotes*. Chem Nat Compd 44:236–238
12. Gao JM, Yang X, Wang CY, Liu JK (2001) Armillaramide, a new sphingolipid from the fungus *Armillaria mellea*. Fitoterapia 72:858–864

13. Gao JM, Hu L, Dong ZJ, Liu JK (2001) New glycosphingolipid containing an unusual sphingoid base from the basidiomycete *Polyporus ellisii*. Lipids 36:521–527
14. Gao JM, Zhu WM, Zhang SQ, Zhang X, Chen H, Zhang AL, Sun YY, Tang M (2004) Sphingolipids from the edible fungus *Tuber indicum*. Eur J Lipid Sci Technol 106:815–821
15. Gao JM, Zhang AL, Chen H, Liu JK (2004) Molecular species of ceramides from the ascomycete truffle *Tuber indicum*. Chem Phys Lipids 131:205–213
16. Gao JM, Zhang AL, Zhang CL, Liu JK (2004) Paxillamide, a novel phytosphingosine derivative from the fruiting bodies of *Paxillus panuoides*. Helv Chim Acta 87:1483–1487
17. Carter GT, Rinehart KL Jr (1978) Aplidiasphingosine, an antimicrobial and antitumor terpenoid from an *Aplidium* species (marine tunicate). J Am Chem Soc 100:7441–7442
18. Kobayashi J, Ishibashi M, Nakagawa H, Hirata Y, Yamasu T, Sasaki T, Ohizumi Y (1988) Symbioramide, a novel calcium ATPase activator from the cultured dinoflagellate *Symbiodinium* sp. Experientia 44:800–802
19. Cheng SY, Wen ZH, Chiou SF, Tsai CW, Wang SK, Hsu CH, Dai CF, Chiang MY, Wang WH, Duh CY (2009) Ceramide and cerebrosides from the octocoral *Sarcophyton ehrenbergi*. J Nat Prod 72:465–468
20. Wasser SP, Weis AL (1999) Therapeutic effects of substances occurring in higher basidiomycetes mushrooms: a modern perspective. Crit Rev Immunol 19:65–96
21. Borthers AT, Stern JS, Hackman RM, Keen CL, Gershwin ME (1999) Mushrooms, tumors, and immunity. Proc Soc Exp Biol Med 221:281–293
22. Moradali M-F, Mostafavi H, Ghods S, Hedjaroude G-A (2007) Immunomodulating and anticancer agents in the realm of macromycetes fungi (macrofungi). Int Immunopharmacol 7:701–724
23. Gao JM, Hu L, Liu JK (2001) A novel sterol from Chinese truffles *Tuber indicum*. Steroids 66:771–775
24. Yaoita Y, Satoh Y, Kikuchi M (2007) A new ceramide from *Ramaria botrytis* (Pers.) Ricken. J Nat Med 61:205–207
25. Xu SH, Zeng LM (2001) Study on the chemical constituents of marine sponge *Polymastia sobustia*. Chin J Org Chem 21:45–48
26. Cafieri F, Fattorusso E (1990) Variceramides, three new sphingolipids from the marine sponge *Ircinia variabilis.* Liebigs Ann Chem (11):1141–1142
27. Aoki K, Uchiyama R, Itonori S, Sugita M, Che F-S, Isogai A et al (2004) Structural elucidation of novel phosphocholine-containing glycosylinositol-phosphoceramides in filamentous fungi and their induction of cell death of cultured rice cells. Biochem J 378:461–472

Lipids (2010) 45:463–464
DOI 10.1007/s11745-010-3419-y

ERRATUM

Erratum to: *Trans* Fatty Acid-Induced NF-κB Activation Does Not Induce Insulin Resistance in Cultured Murine Skeletal Muscle Cells

Pascal P. H. Hommelberg · Ramon C. J. Langen · Annemie M. W. J. Schols · Anon L. M. van Essen · Frank J. M. Snepvangers · Ronald P. Mensink · Jogchum Plat

Published online: 30 April 2010

Erratum to: Lipids (2010) 45:285–290
DOI 10.1007/s11745-010-3388-1

In error, an incorrect version of Fig. 2a was published. The *y*-axis of Fig. 2a was erroneously labeled, whereas the description in the text contained the correct data. The correct version of Fig. 2a is displayed below. These changes do not impact the interpretation of the data.

The online version of the original article can be found under doi:10.1007/s11745-010-3388-1.

P. P. H. Hommelberg · R. P. Mensink · J. Plat
Department of Human Biology, Nutrim School for Nutrition, Toxicology and Metabolism, Maastricht University Medical Centre, P.O. Box 616, 6200 MD Maastricht, The Netherlands
e-mail: pascal_hommelberg@yahoo.com

J. Plat
e-mail: j.plat@hb.unimaas.nl

R. C. J. Langen (✉) · A. M. W. J. Schols · A. L. M. van Essen · F. J. M. Snepvangers
Department of Respiratory Medicine, Nutrim School for Nutrition, Toxicology and Metabolism, Maastricht University Medical Centre, Maastricht, The Netherlands
e-mail: r.langen@pul.unimaas.nl

P. P. H. Hommelberg · R. P. Mensink
Top Institute Food and Nutrition, Wageningen, The Netherlands

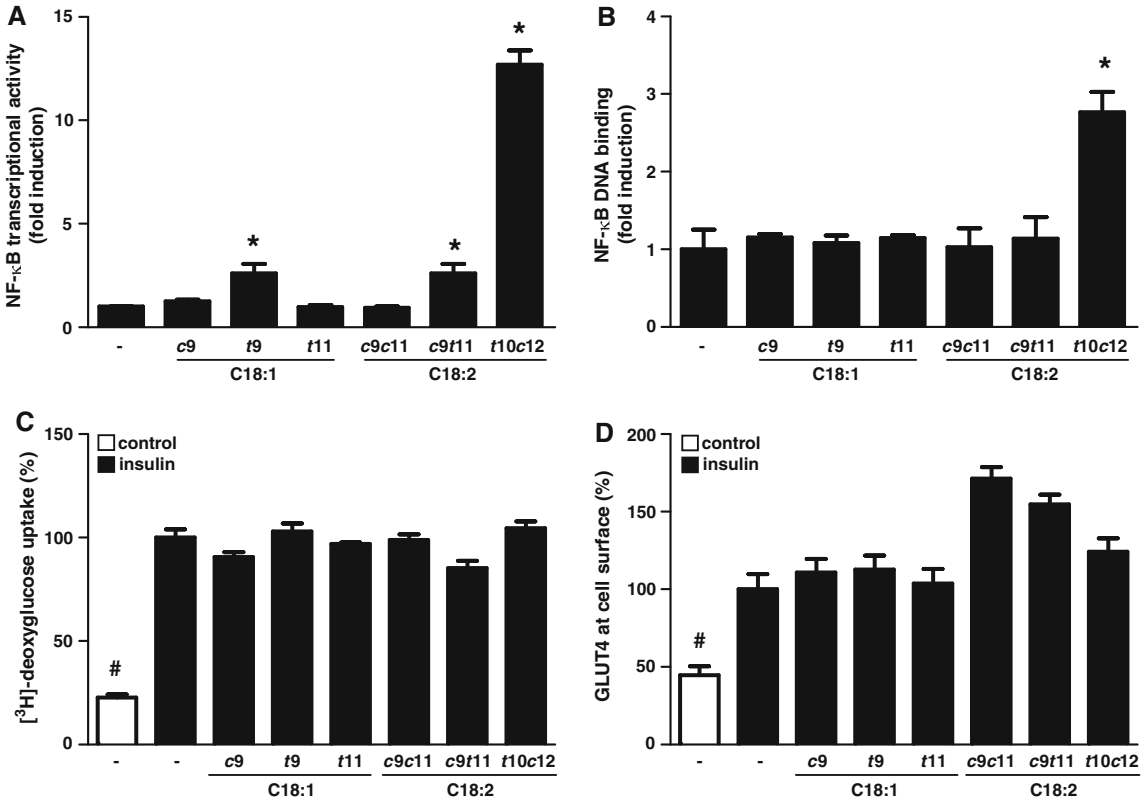

Fig. 2 NF-κB transcriptional activity and insulin sensitivity in skeletal muscle cells after incubation with geometric and positional C18:1 or C18:2 isomers. C2C12 myoblasts stably transfected with the 6κB-TK-luciferase construct were differentiated for 5 days and incubated with 400 μmol/l of the indicated FAs for 24 h (**a**). Lysates were prepared for assessment of luciferase activity. Values were corrected for protein content and expressed as fold-induction over control. Alternatively, 5 days differentiated L6-GLUT4myc myotubes were incubated with and without the indicated fatty acids (200 μmol/l, 16 h). Nuclear extracts were prepared and assessed for RelA DNA binding activity to a consensus NF-κB oligonucleotide by EMSA (**b**). Relative DNA binding activity was determined by phosphor-imager analysis and expressed as fold induction. Furthermore, 2-deoxyglucose uptake (**c**) and GLUT4 translocation (**d**) were measured after stimulation with 25 nmol/l insulin for 15 min in 5 days differentiated L6-GLUT4myc myotubes. Data are expressed as percentage of insulin-stimulated glucose uptake or GLUT4 translocation in absence of FA. Basal and insulin-stimulated conditions are represented by the *white* and *black bars*, respectively. $^{*}p < 0.05$ versus control. $^{\#}p < 0.05$ versus insulin-stimulated control. Data shown are representative examples of three independent experiments

Lipids (2010) 45:465–477
DOI 10.1007/s11745-010-3424-1

ORIGINAL ARTICLE

Intracellular Lipid Droplets Contain Dynamic Pools of Sphingomyelin: ADRP Binds Phospholipids with High Affinity

Avery L. McIntosh · Stephen M. Storey · Barbara P. Atshaves

Received: 11 November 2009 / Accepted: 23 April 2010 / Published online: 15 May 2010

Abstract During the last several years, intracellular lipid droplets have become the focus of intense study. No longer an inert bystander, the lipid droplet is now known as a dynamic organelle contributing lipids to many cellular events. However, while the dynamics of cholesterol efflux from both the plasma membrane and lipid droplets have been studied, less is known regarding the efflux of sphingomyelin from these membranes. In order to address this issue, sphingomyelin efflux kinetics and binding affinities from different intracellular pools were examined. When compared to the plasma membrane, lipid droplets had a smaller exchangeable sphingomyelin efflux pool and the time required to efflux that pool was significantly shorter. Fluorescence binding assays revealed that proteins in the plasma membrane and lipid droplet pool bound sphingomyelin with high affinity. Further characterization identified adipose differentiation-related protein (ADRP) as one of the sphingomyelin binding proteins in the lipid droplet fraction and revealed that ADRP demonstrated saturable binding to 6-((*N*-(7-nitrobenz-2-oxa-1,3-diazol-4-yl) amino)-hexanoyl)sphingosyl-phosphocholine (NBD-sphingomyelin) and also 2-(6-(7-nitrobenz-2-oxa-1, 3-diazol-4-yl)amino)hexanoyl-1-hexadecanoyl-*sn*-glycero-3-phosphocholine (NBD-phosphatidylcholine) with binding affinities in the nanomolar range. Taken together, these results suggest that lipid droplet associated proteins such as ADRP may play a significant role in regulating the intracellular distribution of phospholipids and lipids in general. Overall, insights from the present work suggest new and important roles for lipid droplets and ADRP in phospholipid metabolism.

Keywords Lipid droplets · Sphingomyelin · Efflux · ADRP

Abbreviations

ADRP	Adipose differentiation-related protein
ACBP	Acyl-CoA binding protein
NBD-sphingomyelin	6-((*N*-(7-nitrobenz-2-oxa-1, 3-diazol-4-yl)amino)-hexanoyl)sphingosyl-phosphocholine
NBD-phosphatidylcholine	2-(6-(7-nitrobenz-2-oxa-1, 3-diazol-4-yl)amino)hexanoyl-1-hexadecanoyl-*sn*-glycero-3-phosphocholine
Chol	Cholesterol
SM	Sphingomyelin
PL	Phospholipid
TG	Triacylglycerides
CE	Cholesteryl ester
FFA	Free fatty acid
PE	Ethanolamine glycerophospholipid
PI	Phosphatidylinositol
PS	Phosphatidylserine

A. L. McIntosh · S. M. Storey
Department of Physiology and Pharmacology, Texas A&M University, TVMC, College Station, TX 77843, USA

B. P. Atshaves (✉)
Department of Biochemistry and Molecular Biology, Michigan State University, East Lansing, MI 48824, USA
e-mail: atshaves@msu.edu

PC	Choline glycerophospholipid or phosphatidylcholine
PA	Phosphatidic acid

Introduction

As defined by the body mass index, greater than one-third of the American adult population is considered to be obese, with a greater risk of developing cardiovascular disease and diabetes [1–3]. When chronic over-nutrition leading to obesity occurs, excess lipids are stored in intracellular organelles called lipid droplets. Once thought to be simple storage vesicles for neutral lipids, it is now clear that lipid droplets serve as reservoirs for lipids and proteins involved in many cellular processes. However, despite growing awareness of the health problems associated with excessive lipids in tissues and cells, details on the molecular mechanism of intracellular lipid storage remain unclear.

Lipid droplets have been the focus of increasing scrutiny in the last decade and the subject of several reviews [4–6]. Lipid droplets are composed of a neutral lipid core surrounded by a phospholipid monolayer, within which proteins reside [7, 8]. Initially, the only known proteins were the perilipins [7], adipose differentiation-related protein (ADRP) [9, 10], P_{200} capsule protein [11, 12], and vimentin [11]. Proteomic analysis later revealed associations with proteins involved in cell signaling, cholesterol/fatty acid metabolism, and membrane trafficking [13–15]. Caveolin proteins, normally found in flask-like invaginations of the plasma membrane called caveolae, were also present. However, while the function of plasma membrane caveolins in binding and facilitating the transport of cholesterol and fatty acids is well-documented [16–19], it remains unclear what role these proteins play in lipid droplet function.

In cells, the bulk of cholesterol and sphingolipids such as sphingomyelin are in the plasma membrane, a lipid bilayer where the deposition of cholesterol is defined by its high affinity for the saturated acyl chains of sphingolipids. Cholesterol and sphingomyelin are essential membrane components, yet, excess levels are toxic and increase the risk for arteriosclerosis. Therefore, the levels are strictly regulated through several processes, including efflux, to remove excess lipids from the cell and the body. As lipid reservoirs, the regulation of cholesterol and sphingolipid levels within lipid droplets is important to maintain lipid homeostasis. However, while the dynamics of cholesterol efflux from the plasma membrane and lipid droplets have been studied [20], less is known regarding the efflux of sphingomyelin from membranes. The present work was undertaken to examine the efflux kinetics and binding affinity of different intracellular sphingomyelin pools. The results presented herein establish, for the first time, ADRP as a phospholipid (sphingomyelin, phosphatidylcholine) binding protein and define the affinity and capacity of NBD-sphingomyelin for lipid droplet and plasma membrane proteins.

Materials and Methods

Materials

Silica Gel G and Silica Gel 60 thin layer chromatography (TLC) plates were from Analtech (Newark, DE) and EM Industries, Inc. (Darmstadt, Germany), respectively. Neutral lipid standards were purchased from Nu-Chek Prep, Inc. (Elysian, MN), while phospholipid standards were obtained from Avanti (Alabaster, AL). Rabbit polyclonal antiserum to mouse ADRP was prepared as described [21]. Rabbit anti-human caveolin-1 (cat. no. 610059) was purchased from BD Transduction Laboratories (Palo Alto, CA). Rabbit anti-human caveolin-2 (cat. no. NB100-79911) and rabbit anti-human Na^+ K^+-ATPase (cat. no. NB100-80005) were purchased from Novus Biologicals (Littleton, CO). Mouse anti-human cytochrome c oxidase (clone AS70, cat. no. C9229) was purchased from Sigma (St. Louis, MO). Mouse anti-human transferrin receptor (CD71, clone H68.4, cat. no. 13-6800), NBD-sphingomyelin, Nile red, and NBD-phosphatidylcholine were purchased from Invitrogen (Camarillo, CA). Primary antibodies were diluted 1:1,000 for Western blot analysis. Human high-density lipoprotein (HDL) was from Calbiochem (San Diego, CA). All reagents and solvents used were of the highest grade available and were cell culture tested.

L-Cell Culture

Murine L-cells (L $arpt^-tk^-$) were grown to confluency in Higuchi medium [22] supplemented with 10% fetal bovine serum (Hyclone, Logan, UT), as described in [23]. For fluorescence imaging and efflux experiments, cells were seeded at a density of 50,000 cells/chamber onto Lab-Tek Chamber Coverglass slides (Nunc, Naperville, IL). To ensure a monolayer, samples were examined within 20 h of seeding. Lipid droplets were isolated from L-cells grown to confluency on culture trays (245 × 245 × 25 mm, Nunc, Naperville, IL), as described previously [8].

Laser Scanning Confocal Microscopy

Confocal and co-localized images were acquired on a Bio-Rad (Hercules, CA) MRC-1024 Laser Scanning Confocal Imaging System using multiple photomultiplier tubes

under the control of LaserSharp v.3.2 software (Bio-Rad). For probe excitation, the MRC-1024 system utilized a 15-mW krypton-argon laser (American Laser Corp., Salt Lake City, UT) with a 5-mW output. Cells cultured on Lab-Tek Chamber Coverglass slides were placed on the stage of a Zeiss Axiovert 135 inverted epifluorescence microscope (Zeiss, Thornwood, NY) and examined with a 63× oil-immersion, infinity objective (numerical aperture 1.4). For co-localization experiments, cells were incubated with NBD-sphingomyelin (0.2 μM) and Nile red (0.1 μM) for 10 min in a 37°C, 5% CO_2 incubator. After incubation, cells were washed with phosphate-buffered saline (PBS) buffer and then sequentially imaged for NBD-sphingomyelin (488 nm excitation, 540/30 emission, green channel) and Nile red (568 nm excitation, HQ598/40 emission, red channel). The confocal images from the green and red channels were merged and appeared yellow where superimposition occurred (red and green are additive and yield yellow to orange in the RGB color space). NBD-sphingomyelin was mainly localized to lipid droplets and the plasma membrane, with other internal staining evident after 20–30 min of incubation. Pixel fluorograms were constructed and correlation coefficients used to estimate the extent of probe overlap were determined from the fluorograms as described previously [20]. Samples were exposed to the light source for minimal time periods to minimize photobleaching effects. The gain and black levels of each photomultiplier tube were optimized to minimize the levels of the autofluorescence signal and to increase the dynamic range. Residual auto fluorescence remaining was subtracted from the data. Image files were analyzed using either Metamorph software (West Chester, PA) or NIH Image, a program written by W. Rasband and available by anonymous FTP from http://zippy.nimh.nih.gov.

NBD-Sphingomyelin Stability

In experiments performed to assess the stability of the NBD-sphingomyelin probe, L-cells were grown to confluency on 35-mm tissue culture dishes as described above. Cells were incubated with NBD-sphingomyelin (0.5 μM) in PBS for 3 min at 37°C, after which the buffer was removed and the cells washed with PBS to remove unincorporated NBD-labeled probe. Thereafter, the cells were incubated in PBS at 37°C for various timed intervals (0–60 min). At the indicated time, the buffer was removed, the cells were washed once with PBS before freezing, and then scraped into *n*-hexane-2-propanol extraction solvent 3:2 (v/v) [24]. Polar lipids (including NBD-sphingomyelin) were separated from neutral lipids using silicic acid columns washed with chloroform–methanol 59:1 (v/v), followed by methanol. The polar lipids were resolved on Silica Gel 60 TLC plates using chloroform:methanol:water:acetic acid (150:112.5:6:10.5, v/v/v/v). NBD-labeled lipids were visualized on the TLC plates under UV light at 360 nm using an Alpha Innotech FluorChem Imager (San Leandro, CA). Levels of NBD-sphingomyelin remaining at each time point were compared to NBD-sphingomyelin at time zero (initial concentration) to obtain the percentage of NBD-sphingomyelin remaining in the cells.

NBD-Sphingomyelin Efflux

In order to perform the HDL-mediated NBD-sphingomyelin efflux experiments, cells were loaded with NBD-sphingomyelin (0.2 μM) and Nile red (0.1 μM) in PBS buffer for 10 min in a 37°C, 5% CO_2 incubator. After incubation, the cells were washed with PBS buffer and then imaged sequentially for NBD-sphingomyelin (488 nm excitation, 540/30 emission) and Nile red (568 nm excitation, HQ598/40 emission). Lipid droplets were identified by morphology and confirmed by Nile red and NBD-sphingomyelin co-localization data. Once a suitable field of cells was chosen, a medial section passing through 5–10 cells was selected, and the section was scanned for the initial fluorescence intensity of NBD-sphingomyelin. HDL (10 μg HDL/mL) was added to start the efflux experiment. Since stability studies indicated that greater than 85% of the NBD-sphingomyelin probe remained intact after 40 min incubation, all experiments were completed within 40 min. Fluorescence intensity in the total area of lipid droplet and plasma membrane was measured over time and was used to gauge the extent of NBD-sphingomyelin efflux from each cell compartment. Cells were imaged and analyzed by Metamorph software to graphically determine the separate contributions of the efflux process. Data points were fitted ($R^2 = 0.996$) to the following three-parameter, sigmoidal equation: $y = A/(1 - e^{-((t - t0)/b)})$, where y is the percentage of HDL-mediated NBD-sphingomyelin efflux at time t, A indicates the percentage of sphingolipid pool available for efflux, $1/b$ is an apparent rate constant (k), and t_0 is the time required to reach 50% of the maximal efflux, representing the half-time ($t_{1/2}$) of the exchangeable pool. Half-time and k values were apparent values due to dependence on HDL acceptor concentrations. Using a nonlinear least squares routine, all parameters were obtained simultaneously from the fitted data. Unique fittings were obtained individually for each time course involving individual cells. Statistical methods involving the paired *t*-test (GraphPad Prism, San Diego, CA) were used to compare the parameters derived from lipid droplet and plasma membrane efflux curves. Experiments were performed in triplicate with $n = 50$–60 lipid droplets from $n = 25$ cells. Values with $P < 0.05$ were considered to be statistically significant.

Western Blot Analysis

Expression levels of lipid droplet (ADRP, caveolin-1, caveolin-2), plasma membrane (Na^+, K^+-ATPase, transferrin), and mitochondrial (cytochrome c oxidase) protein markers in homogenate and lipid droplet fractions isolated from L-cells [8] were determined by Western blot analysis. In brief, cell homogenate (5 μg/lane) and lipid droplet (10 μg protein/lane) proteins were subjected to SDS-PAGE using 12% tricine gels before transferring to 0.45-μm nitrocellulose paper (Sigma Chemical Co., St. Louis, MO) by electroblotting in a continuous buffer system at 0.8 mA/cm^2 for 2 h. After transfer, blots were blocked in 3% gelatin in TBST (10 mM Tris–HCL, pH 8, 100 mM NaCl, 0.05% Tween-20) before incubation with the primary antibodies. Alkaline-phosphatase conjugates of goat anti-rabbit IgG and Sigma Fast 5-bromo-4-chloro-3-indolyl phosphate/nitro blue tetrazolim tablets (Sigma, St. Louis, MO) were used to visualize bands of interest. Proteins were quantitated by densitometric analysis after image acquisition using a single-chip CCD (charge-coupled device) video camera and a computer workstation (IS-500 system from Alpha Innotech, San Leandro, CA). Image files were analyzed (mean 8-bit grayscale density) using NIH Image, available by anonymous FTP from http://zippy.nimh.nih.gov.

Lipid Analyses

Lipid droplets were isolated from L-cell fibroblasts as described in [8]. Lipids from lipid droplets were extracted with *n*-hexane-2-propanol 3:2 (v/v) and resolved into individual lipid classes using Silica Gel G TLC plates developed in petroleum ether:diethyl ether:methanol:acetic acid 90:7:2:0.5 [8]. Total cholesterol, free fatty acid, triacylglyceride, cholesteryl ester, and phospholipid content were determined by the method of Marzo et al. [25]. Individual phospholipids, including phosphatidic acid (PA), ethanolamine glycerophospholipid (PE), phosphatidylinositol (PI), phosphatidylserine (PS), choline glycerophospholipid (PC), and sphingomyelin (SM), were resolved from total phospholipid (PL) samples in the following manner: PL were eluted from the Silica Gel G TLC plates using chloroform:methanol:HCL (100:50:0.375, v/v/v) and applied to Silica Gel 60 TLC plates, where individual phospholipids were resolved using chloroform:methanol:water:acetic acid (150:112.5:6:10.5, v/v/v/v). Individual phospholipids were quantitated densiometrically as described previously [26, 27]. Protein concentration was determined by the method of Bradford from the dried protein extract residue digested overnight in 0.2 M KOH [28]. All glassware was washed with sulfuric acid-chromate before use.

NBD-Sphingomyelin Binding Affinity

Lipid droplet and plasma membrane fractions were isolated as described previously [8, 26]. To measure the sphingomyelin and choline glycerophospholipid (phosphatidylcholine) binding affinities of membranes (lipid droplet and plasma membrane) and lipid binding proteins (ADRP, ACBP), a fluorescent ligand, saturation binding assay was performed with NBD-sphingomyelin and NBD-phosphatidylcholine using a steady-state photon-counting fluorimeter [29]. Briefly, the NBD-labeled lipid (in 100 μM stock) was added incrementally (0.2–4.0 μL) to membrane (50 μg), ADRP (180 nM), or ACBP (180 nM) protein aliquots equilibrated in phosphate buffer (10 mM, pH 7.4). After each addition, the samples were allowed to mix at 25°C for 3–4 min before exciting the NBD-labeled probe at 480 nM. Fluorescence emission spectra was recorded from 490 to 600 nm and integrated after each aliquot addition. Corrections were made for blank (without lipid droplet or plasma membrane present) and background emission. The data were fitted using a simple, single binding site model as in [30] to determine binding capacities (B_{max}) and binding affinities from the K_d values. Since B_{max} was protein-mass-dependant, values were normalized by the protein mass for each sample.

Results

Intracellular Localization of NBD-Sphingomyelin

While it has been shown that NBD-labeled cholesterol and filipin (a cholesterol analog) localize to lipid droplets in living cells [8, 31], it was not known whether NBD-labeled sphingomyelin targeted to the lipid droplet phospholipid monolayer. Therefore, a series of experiments was performed with NBD-sphingomyelin and Nile red, a lipid droplet marker, to establish the intracellular localization of sphingomyelin in living cells. The NBD-sphingomyelin probe was initially observed in the plasma membrane, followed by lipid droplets after 5–10 min (Fig. 1a). After 20 min, the presence of NBD-sphingomyelin was observed in areas resembling the endoplasmic reticulum (ER) and Golgi apparatus. Nile red co-staining confirmed NBD-sphingomyelin targeted to lipid droplets (Fig. 1b). Overlap of Nile red with NBD-sphingomyelin was observed as yellow to red pixels, indicating the co-localization of probes (Fig. 1c). The extent of co-localization was quantified in pixel fluorograms where coefficients of overlap indicated that 28% of the NBD-label co-localized with the lipid stain (Nile red), while 64% of the Nile red was co-localized with NBD-sphingomyelin (Fig. 1d). These results were in agreement with NBD-sphingomyelin

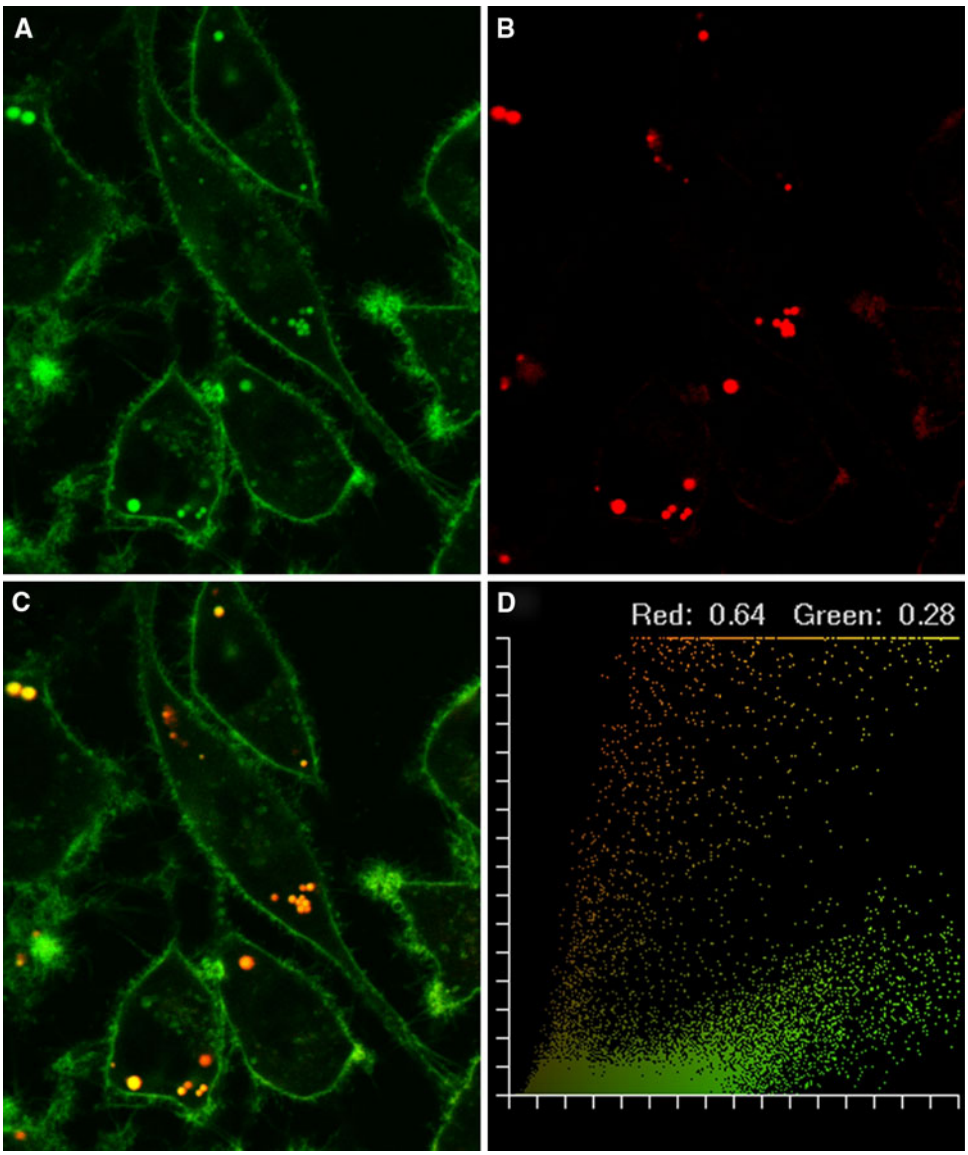

Fig. 1 Intracellular distribution of NBD-sphingomyelin and Nile red in L-cell fibroblasts. Co-localization patterns of NBD-sphingomyelin and Nile red were shown using pseudo-coloring derived from confocal image acquisition from red- and green-specific PMT channels. A 24-bit RGB image was created from the red plus green plus blue (null) channels. Red and green are additive in the RGB color space, yielding yellow-orange. L-cell fibroblasts stained with NBD-sphingomyelin (**a**) and Nile red (**b**) were combined to yield yellow-orange (**c**) where co-localization occurred. Superimposition of the probes was graphically demonstrated in a pixel fluorogram (**d**). The correlation coefficients corresponding to red and green were proportional to the degree of fluorescence probe co-localizing in each component of the image relative to the total fluorescence and indicated the extent of probe overlap. The cells were examined using the Bio-Rad MRC-1024 confocal system. Objective, 63×

targeting to both the lipid droplet and plasma membrane compartments.

HDL-Mediated NBD-Sphingomyelin Efflux from Lipid Droplets and the Plasma Membrane

Since there are at least three different metabolic pathways for sphingomyelin catabolism in cultured fibroblasts, including: (1) degradation by sphingomyelinase in the lysosome; (2) hydrolysis by cellular sphingomyelinase in the plasma membrane to form ceramide and phosphoryl-choline; or (3) hydrolysis of sphingomyelin to form lecithin (review in [32]), it was necessary to determine the stability of the NBD-labeled probe in culture. Stability studies were performed as described in the "Materials and Methods" to ensure that the NBD-labeled probe was intact during the time frame of the efflux experiments. After 40 min incubation of NBD-sphingomyelin in culture, more than 85% of the probe remained (data not shown). Therefore, all experiments were kept under 40 min to ensure minimal probe degradation.

HDL-mediated NBD-sphingomyelin efflux from lipid droplets and the plasma membrane was next examined. The existence of mobile pools of cholesterol in lipid droplets was previously reported in [20], where the analysis of data from HDL-mediated NBD-cholesterol efflux curves revealed that lipid droplets contained two kinetic sterol domains, one with $t_{1/2}$ = 10–20 min and the other with $t_{1/2}$ near 1 min, suggesting vesicular- and protein-mediated sterol transfer, respectively [20]. However, examining sterol domains within the plasma membrane was not possible with NBD-cholesterol since the probe was not observed in the plasma membrane [20]. In contrast, NBD-sphingomyelin exhibited a high fluorescence intensity in both plasma membrane and

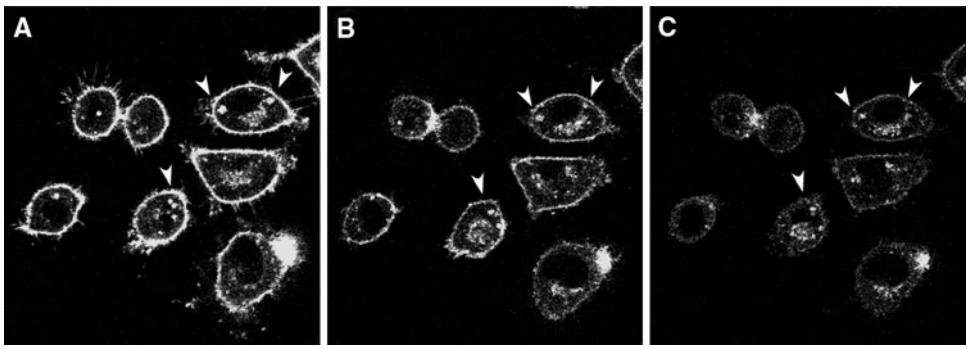

Fig. 2 HDL-mediated NBD-sphingomyelin efflux in L-cell fibroblasts. Cells were labeled with NBD-sphingomyelin (0.2 μM) and incubated with HDL (10 μg HDL/mL) to begin the efflux process. **a** 0 min, **b** 20 min, and **c** 30 min after the addition of HDL. The *arrows* indicate high-retention lipid droplets during the time course. Cells were examined with the Bio-Rad MRC-1024 confocal imaging system. Objective, 63×

lipid droplets (Figs. 1 and 2). Therefore, the relative distribution of fluorescence in lipid droplets and the plasma membrane during HDL-mediated sphingomyelin efflux could be observed as in Fig. 2 at: 0 min (Fig. 2a), 20 min (Fig. 2b), and 30 min (Fig. 2c) from the point of HDL addition.

Next, cells were imaged and graphically partitioned to separate the lipid droplet contribution from the plasma membrane component of the cell as described in the "Materials and Methods" section. Kinetic analysis of NBD-sphingomyelin fluorescence revealed that efflux from the lipid droplet (Fig. 3, open circles) and the plasma membrane (Fig. 3, closed circles) best fit to a multiparameter, sigmoidal equation ($R^2 = 0.996$). Further examination revealed that the maximal HDL-mediated efflux from lipid droplets was less than that from the plasma membrane, suggesting that lipid droplets contained a smaller exchangeable sphingomyelin efflux pool. Parameters derived from the lipid droplet and plasma membrane efflux curves included the available NBD-sphingomyelin pool size (A), rate constant (k), and time required to reach 50% of maximal efflux (T_0). A comparison of the available sphingomyelin pool size (Table 1) between lipid droplets and plasma membrane revealed not only that lipid droplets had a smaller exchangeable pool size (42.6 ± 1.1 vs. 81.9 ± 1.2), but also that the time required to efflux that pool was 22% less in lipid droplets, in keeping with a significantly faster lipid droplet versus plasma membrane efflux rate constant (0.3 ± 0.03 vs. 0.18 ± 0.06, $P < 0.04$).

The slower plasma membrane efflux parameters may also, in part, be attributed to the efflux of NBD-sphingomyelin from lipid droplets and other compartments cycling through the plasma membrane [33]. These contributions were included in the efflux measurements to ensure that the natural dynamics of the cell were represented. Thus, the kinetic domains of NBD-labeled sphingomyelin within lipid droplets versus the plasma membrane exhibited significant differences.

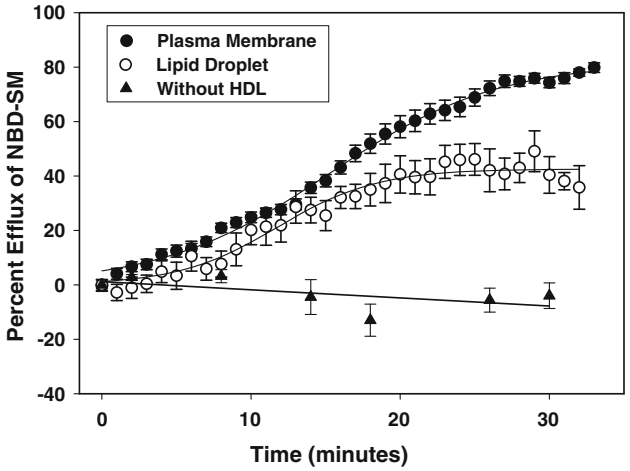

Fig. 3 Percent efflux of NBD-sphingomyelin. The percentage of HDL-mediated NBD-sphingomyelin efflux from the plasma membrane and lipid droplet compartments of living cells was determined as described in the "Materials and Methods" section. Data analysis of NBD-sphingomyelin fluorescence showed that efflux from the lipid droplet (*open circles*) and the plasma membrane (*closed circles*) best fit the following sigmoidal equation: $y = A/(1 - e^{-((t- -t0)/b)})$, where y is the percentage of HDL-mediated NBD-sphingomyelin efflux at time t, A indicates the percentage of sphingolipid pool available for efflux, $1/b$ is an apparent rate constant (k), and t_0 is the time required to reach 50% of the maximal efflux, representing the half-time ($t_{1/2}$) of the exchangeable pool. Percentage efflux in the presence of medium without HDL present is indicated by *closed triangles*

NBD-Sphingomyelin Binding Affinity for Proteins in Isolated Membrane Fractions

In order to determine the affinity of proteins associated with lipid droplets and the plasma membrane for sphingomyelin, fluorescence binding assays were performed. First, the purity and enrichment of isolated lipid droplets and plasma membranes were determined by Western blot

analysis as described in [8, 26]. Protein expression of the lipid droplet marker proteins ADRP (Fig. 4a), caveolin-1 (Fig. 4b), and caveolin-2 (Fig. 4c) was detected in L-cell homogenates (lane 1) and purified lipid droplets (lane 2). The plasma membrane protein markers Na^+, K^+-ATPase (Fig. 4d), and transferrin (Fig. 4e), while present in the L-cell homogenate (lane 1), were not detected in the lipid droplet enriched fraction (lane 2), indicating that there was little to no plasma membrane present in the purified lipid droplet fractions. Similarly, the mitochondrial protein marker, cytochrome c oxidase (Fig. 4f), while observed in the homogenate (Fig. 4, lane 1), was not present in the lipid droplet (Fig. 4, lane 2) fraction.

Table 1 Kinetic parameters of HDL-mediated NBD-sphingomyelin efflux from lipid droplets and plasma membrane

Cell compartment	A	k (min^{-1})	T_0 (min)
Lipid droplet	42.6 ± 1.1	0.3 ± 0.03	11.8 ± 0.4
Plasma membrane	81.9 ± 1.2*	0.18 ± 0.06*	15.2 ± 0.3*

The percentage of exchangeable sphingolipid pool size (A), rate constant (k), and time required to reach 50% of the maximal efflux (T_0) was determined for lipid droplet and plasma membrane cell compartments within living cells as described in the "Materials and Methods" section. Values represent the mean ± SEM, with $n = 25$ cells, 50–60 lipid droplets

* Indicates significance, $P < 0.003$ as compared to lipid droplets

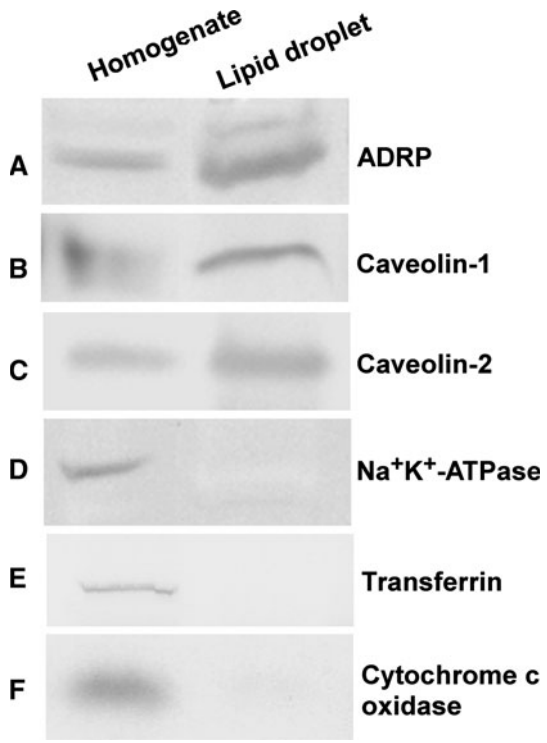

Fig. 4 Western blot analysis of lipid droplet proteins isolated from L-cell fibroblasts. Western blots on cell homogenate (*lane 1*) and lipid droplets (*lane 2*) were probed with the following affinity-purified antibodies as described in the "Materials and Methods" section: **a** anti-ADRP, **b** anti-caveolin-1, **c** anti-caveolin-2, **d** anti-Na^+, K^+-ATPase, **e** transferrin, and **f** anti-cytochrome c oxidase

Second, the enrichment of neutral lipids and the presence of sphingomyelin in the isolated lipid droplet fraction were verified by lipid analysis. There has been some conjecture as to whether lipid droplets contain sphingomyelin in the phospholipid monolayer [34]. However, numerous studies on lipid droplets isolated from different cell types, including those from alveolar macrophages [35], Niemann–Pick cells [36], mammary tissue [37], and HepG2 cells [38], record the presence of sphingomyelin in lipid droplet preparations. It should be noted that the lack of sphingomyelin, PS, and PA observed in the former study [34] may be based on the specific cell type or from the isolation and extraction procedure. In the present work, lipid droplet lipids were extracted and the lipid profile resolved as described in the "Materials and Methods" section. The lipid droplet fraction showed an almost exclusive presence of core lipids (cholesteryl ester and triacylglyceride) over surface lipids (sphingomyelin, cholesterol, phospholipids, and fatty acids), with the core lipids present at almost equal levels in L-cell lipid droplets (Fig. 5), further confirming the purity and enrichment of the lipid droplet preparation since lipid droplets are the only organelle composed mostly of cholesteryl esters and triglycerides. Analysis of the individual phospholipid classes revealed the following lipid profile (nmol/mg protein): sphingomyelin, 1.8 ± 0.3; PC, 2.1 ± 0.3; PS/PI, 0.7 ± 0.1; and PE, 0.35 ± 0.2. PA was below the level of detection. These results confirmed the enrichment of neutral lipids and the presence of sphingomyelin (among other lipids) in the isolated lipid droplet fraction.

Third, the ability of proteins associated with the plasma membrane and lipid droplets to bind NBD-labeled sphingomyelin and phosphatidylcholine was established through a fluorescent ligand, saturation binding assay using a steady-state photon-counting fluorimeter [29]. The interaction of plasma membrane and lipid droplet associated proteins with NBD-labeled lipids was monitored as increased fluorescence intensity at 530 nm, consistent with localization of the ligand in a more hydrophobic environment. Plasma membrane (Fig. 6a) and lipid droplet (Fig. 6b) fractions exhibited saturation binding for NBD-sphingomyelin. From the saturation curves, fitted to a simple, single binding site model as in [29], binding affinities (K_d) and binding capacities (B_{max}) were determined (Table 2). Analysis of the binding data revealed that the association of NBD-sphingomyelin for proteins in the lipid droplet fraction was 3.8-fold greater ($P < 0.05$, $n = 3$) than that for plasma membrane proteins (K_d 201 ± 19 nM vs. K_d 758 ± 118 nM). When NBD-sphingomyelin binding studies were performed with recombinant ADRP (Fig. 7a), it was shown that

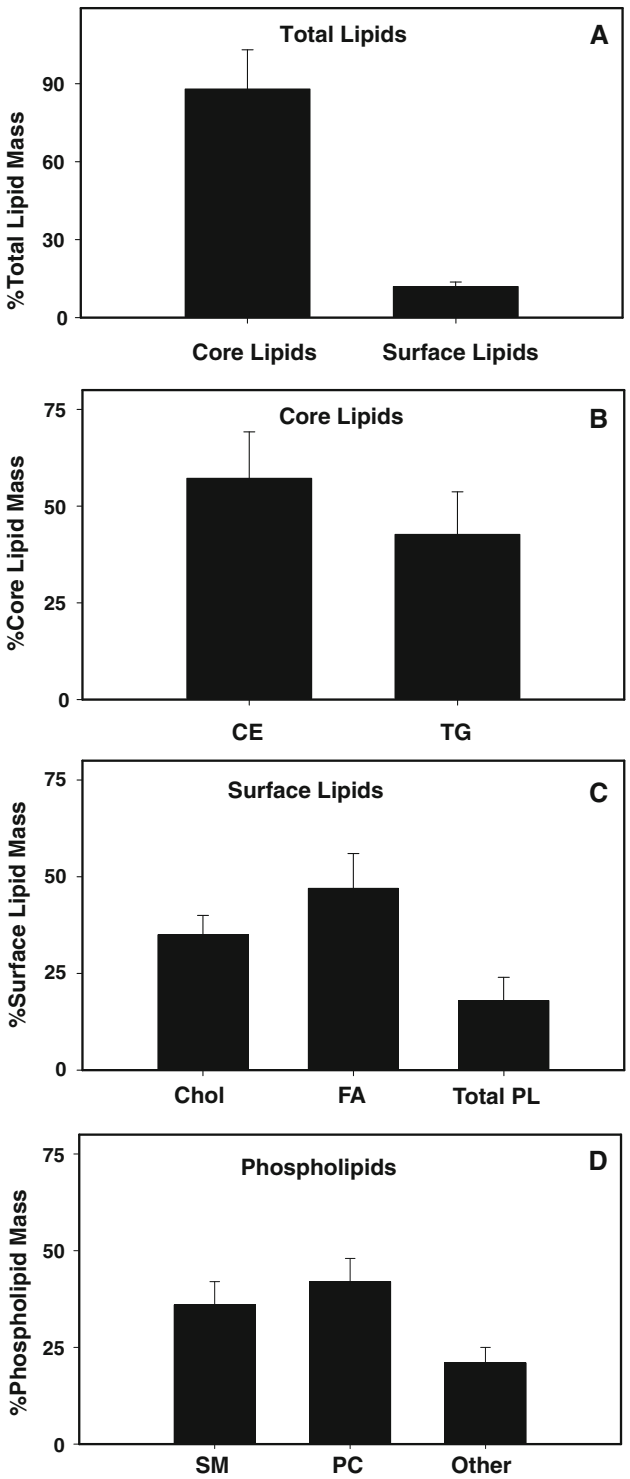

Fig. 5 Percentage lipid mass of lipid droplets isolated from L-cell fibroblasts. Percentage lipid mass of total lipids (**a**), core lipids (**b**), surface lipids (**c**), and phospholipids (**d**) were determined from lipid droplets isolated from L-cells. Core lipids include triacylglycerol (*TG*) and cholesteryl esters (*CE*). Surface lipids include cholesterol (*Chol*), phospholipids (*PL*), and free fatty acids (*FA*). Phospholipids include sphingomyelin (*SM*), choline glycerophospholipid (*PC*), phosphatidylserine (*PS*), phosphatidylinositol (*PI*), ethanolamine glycerophospholipid (*PE*), and phosphatidic acid (*PA*)

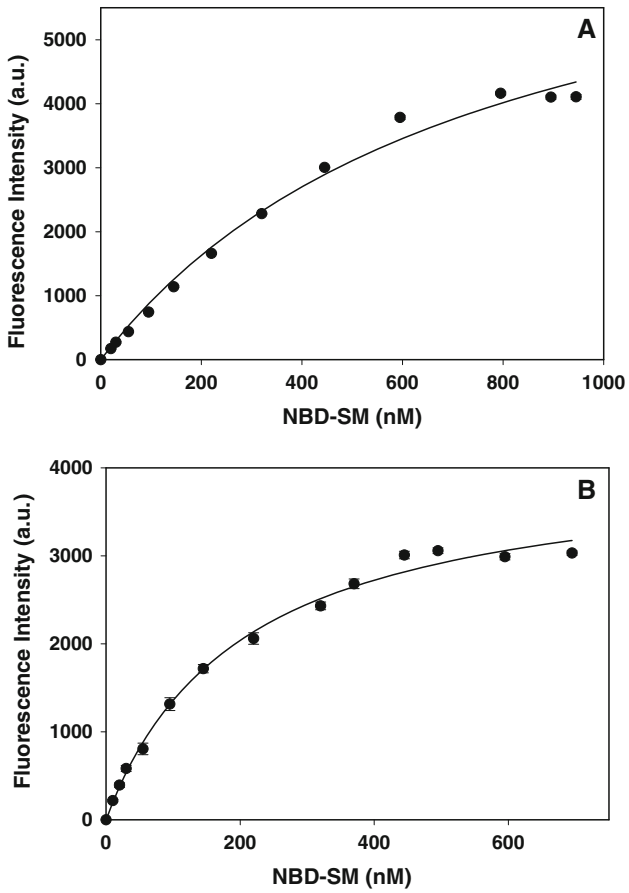

Fig. 6 Titration of plasma membrane and lipid droplet fractions with NBD-sphingomyelin. The titration of plasma membranes (**a**) and lipid droplet (**b**) fractions with NBD-sphingomyelin was followed by an increase in fluorescence intensity as described in the "Materials and Methods" section. The fluorescent intensity data, representing the mean ± SE of three independent measurements, were analyzed to determine the dissociation constant K_d and binding capacity B_{max}

ADRP exhibited similar binding affinities to that of the purified lipid droplet fraction (K_d 201 ± 19 nM vs. K_d 257 ± 64 nM). Differences were also observed in the NBD-sphingomyelin binding capacities (B_{max}). Under the experimental conditions presented herein, differences in B_{max} indicated differences in the number of lipid binding proteins and lipid binding sites. The NBD-sphingomyelin binding capacity of lipid droplet proteins was 1.9-fold lower ($P < 0.005$, $n = 3$) than that observed with plasma membranes (Table 2), suggesting that the plasma membrane contained more sphingomyelin binding proteins. However, there was no significant difference between the NBD-sphingomyelin binding capacity of the lipid droplet protein fraction and ADRP. Thus, fluorescence binding assays revealed the presence of sphingomyelin binding proteins in the purified lipid droplet fraction. Further characterization identified ADRP as one of the sphingomyelin binding proteins in the lipid droplet fraction.

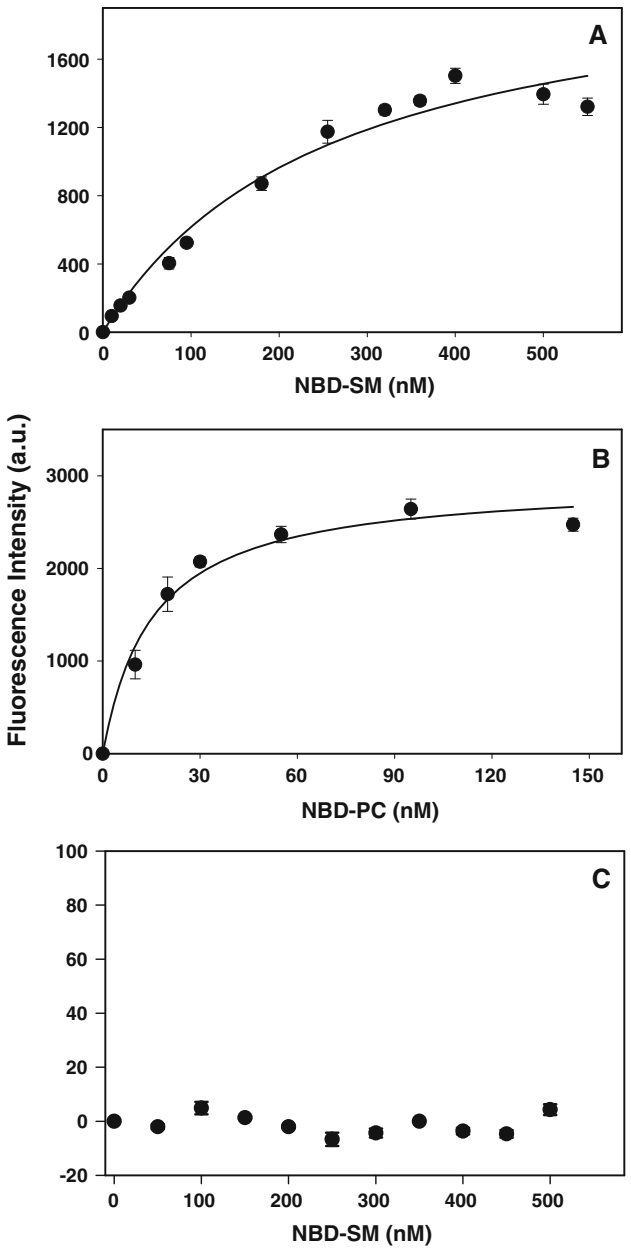

Fig. 7 Titration of ADRP and ACBP with NBD-labeled lipids. The titration of ADRP (**a**, **b**) or ACBP (**c**) with NBD-sphingomyelin (**a**, **c**) or NBD-phosphatidylcholine (**b**) was followed by an increase in fluorescence intensity as described in the "Materials and Methods" section. The fluorescent intensity data, representing the mean ± SE of three independent measurements, were analyzed to determine the dissociation constant K_d and binding capacity B_{max}

The ability of ADRP to interact with another NBD-labeled phospholipid (NBD-phosphatidylcholine) was also examined. Upon titration of ADRP with increasing concentrations of NBD-phosphatidylcholine, an increase in fluorescence intensity was observed as before with NBD-sphingomyelin, indicating binding (Fig. 7b). Analysis

Table 2 Binding affinity and capacity of plasma membrane and lipid droplet proteins, ADRP, and ACBP for NBD-labeled sphingomyelin and phosphatidylcholine

Protein	NBD label	K_d (nM)	B_{max}/μg protein
PM	NBD-SM	758 ± 119	156 ± 13
LD	NBD-SM	201 ± 19[a]	82 ± 3[a]
ADRP	NBD-SM	257 ± 64[a]	111 ± 12
ADRP	NBD-PC	15 ± 3[a,b,c]	148 ± 8
ACBP	NBD-SM	ND[a,b,c]	ND[a,b,c]

The binding affinity and capacity of plasma membrane (PM) and lipid droplet (LD) proteins and ADRP and ACBP for NBD-labeled sphingomyelin (SM) and phosphatidylcholine (PC) was measured by a fluorescent lipid binding assay as described in the "Materials and Methods" section. Values represent the mean ± SEM, $n = 3$

[a] Indicates significance, $P < 0.02$ as compared to PM binding of NBD-SM

[b] Indicates significance, $P < 0.0001$ as compared to LD binding of NBD-SM

[c] Indicates significance, $P < 0.02$ as compared to ADRP binding of NBD-SM

ND indicates not detected

of the data revealed that ADRP bound NBD-phosphatidylcholine with high affinity ($K_d = 15 \pm 3$ nM), 17.1-fold greater than that observed for NBD-sphingomyelin (Table 2). Despite this, there were no significant differences between the B_{max} of NBD-labeled sphingomyelin and phosphatidylcholine indicating that, regardless of the stronger binding affinity of ADRP for NBD-phosphatidylcholine, ADRP contained the same number of sphingomyelin and phosphatidylcholine binding sites.

The specificity of ADRP binding sphingomyelin was examined next. The NBD-sphingomyelin fluorescence binding assay was performed with an unrelated protein, acyl-CoA binding protein (ACBP), a cytosolic lipid binding protein that exclusively binds long-chain fatty acyl-CoA [39]. Increased fluorescence was not observed when ACBP was titered with increasing concentrations of NBD-sphingomyelin (Fig. 7c). A plot of the maximal intensity of NBD-sphingomyelin emission at 530 nm versus increasing NBD-sphingomyelin concentration yielded a line with scattered points, not the saturation curve observed previously with ADRP binding of sphingomyelin and phosphatidylcholine. These results suggested that NBD-sphingomyelin did not enter the ACBP binding pocket and indicated that ACBP had little to no sphingomyelin binding affinity in this assay.

In summary, fluorescence binding assays indicated that the purified lipid droplet and plasma membrane protein fractions contained sphingomyelin binding proteins. The lipid droplet associated protein ADRP was identified as a phospholipid binding protein with nanomolar affinity for sphingomyelin and phosphatidylcholine.

Discussion

Although there is growing interest in the role that lipid droplets play in lipid transport, cell signaling, immune function, and membrane trafficking (review in [40, 41]), questions remain regarding the means by which lipid droplet proteins and lipids interact to regulate cellular dynamics. Cholesterol and sphingomyelin are essential membrane components, and when levels are high, the ability to remove excess lipids through storage or efflux remains an effective method for cells to regulate otherwise harmful lipids. Therefore, the regulation of cholesterol and sphingomyelin within lipid reservoirs such as lipid droplets is important to maintain lipid homeostasis. However, while the dynamics of cholesterol efflux from lipid droplets and the plasma membrane has been studied [20], less is known regarding the efflux of sphingomyelin from these membranes. The present work was undertaken to examine the efflux kinetics and binding affinities of different intracellular sphingomyelin pools in lipid droplets versus the plasma membrane.

In preparation for efflux studies, NBD-sphingomyelin targeting to lipid droplets in living cells was established. It should be noted that, while there are some reports that NBD-labeled lipids do not distribute to the same organelles as the natural lipids [42], it has been shown in other work that NBD-labeled probes are metabolized similarly [29] and traffic by similar uptake, intracellular, and secretory pathways [29, 43]. In CHO-K1 cells, NBD-sphingomyelin internalized from the plasma membrane to vesicles and other internal sites, and then transported back to the plasma membrane [33, 44]. In a similar fashion, NBD-sphingomyelin in primary cultures of rat astrocytes [45] and in L-cells (present work) were endocytosed and sorted to several intracellular sites, including lipid droplets (results herein). Furthermore, with other NBD-labeled probes such as NBD-cholesterol, there is substantial evidence to suggest that NBD-cholesterol undergoes metabolism and utilizes the same intracellular trafficking pathways as the endogenous lipid [20, 29]. For example, in hamster intestinal enterocytes, $CaCO_2$ cells, and L-cells [29, 43, 46], NBD-cholesterol was esterified similarly to cholesterol and dehydroergosterol, a natural cholesterol analog [47], while in $CaCO_2$ cells and L-cells, NBD-cholesterol was shown to traffic by similar pathways [29, 43, 46]. Taken together, these studies suggest that, while the behaviors of NBD-labeled probes are not identical to their natural lipid counterparts, they can be useful to examine lipid trafficking and metabolism in living cells. Therefore, NBD-sphingomyelin was used to show sphingomyelin targeting to lipid droplets in living cells. Next, NBD-sphingomyelin was used to perform efflux studies where HDL-mediated NBD-sphingomyelin efflux from lipid droplets and the plasma membrane was graphically delineated. Kinetic analysis of the NBD-sphingomyelin efflux curves from lipid droplets revealed the presence of resolvable sphingolipid pools that exhibited properties which were different from those found in the plasma membrane (Table 1). The exchangeable sphingomyelin pool (A) in lipid droplets (42.6 ± 1.1) was smaller than the sphingomyelin pool associated with plasma membranes (81.9 ± 1.2). Despite this, the rate of sphingomyelin efflux was faster in lipid droplets and the half-time was significantly less. Sphingomyelin in lipid droplets is constrained to the surface, bound and unbound to resident proteins. Consistent with the data in the present work, at least two sphingomyelin pools were observed with lipid droplets, one smaller, dynamic pool with a half-time of 11.8 min, and another larger, relatively inert pool with a half-time on the order of hours to days. It should be noted that HDL-mediated NBD-cholesterol [20] and NBD-sphingomyelin efflux rates are comparable, yet faster and reach equilibrium quicker (minutes) than that observed in similar studies with [^{3}H]-labeled lipids (hours) [20]. These results may be due to the higher aqueous solubility of NBD-labeled lipids versus the natural lipid counterparts [48]. Nevertheless, the rapid turnover of NBD-sphingomyelin in the current study is in keeping with the fact that L-cells endocytose the equivalent of their entire cell surface membrane within about 2 h [49], similar to the activity of macrophages [50].

In contrast to lipid droplets, sphingomyelin in the plasma membrane exhibited a small, inert pool (18% of total sphingolipid) and a large, exchangeable pool comprising 82% of the available sphingomyelin (half-time of 15.2 min) was observed. Sphingomyelin from this large, dynamic plasma membrane pool is readily available for participation in at least three different sphingomyelin metabolic pathways, including the degradation of sphingomyelin by sphingomyelinases in the lysosome, hydrolysis of sphingomyelin to form lecithin, and the sphingomyelin cycle [32, 51]. In cells, most of the sphingomyelin is located in the outer leaflet of the plasma membrane (review in [52]). The sphingomyelin cycle begins with the activation of sphingomyelinases located in the plasma membrane which hydrolyze sphingomyelin to form phosphorylcholine and ceramide. Ceramide acts as a second messenger with effects in multiple cellular processes, including the activation of specific kinases and phosphatases, cell cycle arrest, induction of cell differentiation, and apoptosis [53]. The presence of ceramide generated from activated sphingomyelinases also leads to the clustering of CD95 and CD40 receptors [54] and the activation of a number of signaling agents, including tumor necrosis factor α, γ-interferon, and arachidonate [55–57]. Sphingomyelin is resynthesized by the addition of a phosphorylcholine headgroup from phosphatidylcholine

through the action of sphingomyelin synthase to complete the sphingomyelin cycle. However, while evidence for the above events occurring in lipid droplets is minimal, the presence of a small dynamic sphingomyelin pool in the lipid droplet monolayer is evocative of new roles for the storage organelle in lipid signaling.

The extent of specific organelle protein–lipid interactions in lipid droplets was next examined using a NBD-sphingomyelin fluorescence binding assay as described in the "Materials and Methods" section. While both lipid droplet and plasma membrane proteins exhibited saturable binding to NBD-labeled sphingomyelin, binding affinities of NBD-sphingomyelin for lipid droplet proteins (K_d 201 ± 19 nM) were higher than for plasma membrane proteins (K_d 758 ± 119 nM). In agreement with the binding studies, lipid droplets exhibited a larger inert sphingomyelin pool with strong binding affinity for sphingomyelin in comparison to the plasma membrane, which had a small inert sphingomyelin pool with weak sphingomyelin binding affinity. Thus, not only did the kinetic domains of NBD-labeled sphingomyelin within lipid droplets and the plasma membrane exhibit significant differences, the results presented herein show, for the first time, that collective proteins associated with lipid droplets versus plasma membrane show differential binding affinity to NBD-sphingomyelin.

While little is known regarding the identity or binding affinities of sphingomyelin-binding proteins within lipid droplets, the surface coat protein ADRP [10, 20, 29] was a likely choice based on its ability to bind other lipid molecules. ADRP was shown to bind hydrophobic lipids such as NBD-stearic acid (K_d 145 nM) and NBD-cholesterol (K_d 2.0 nM) in a 1:1 stoichiometry with high affinity [20, 29], and to also increase fatty acid uptake [9]. As shown in the present work, ADRP demonstrated saturable binding to NBD-sphingomyelin and also NBD-phosphatidylcholine with binding affinities in the nanomolar range. However, there was no significant difference in NBD-sphingomyelin binding capacity between the lipid droplet protein fraction and ADRP. Thus, fluorescence binding assays revealed the presence of sphingomyelin binding proteins in the purified lipid droplet fraction. Further examination confirmed that ADRP contributed to this pool and bound sphingomyelin and phosphatidylcholine with high affinity. The specificity of ADRP binding of sphingomyelin was also examined by determining whether an unrelated protein, ACBP, would bind sphingomyelin. A plot of the maximal intensity of NBD-sphingomyelin emission versus increasing NBD-sphingomyelin concentration yielded a line with scattered points, indicating that ACBP had little to no sphingomyelin binding affinity in this assay. Thus, while ADRP exhibited high affinity for sphingomyelin and phosphatidylcholine, performing the same assay with ACBP revealed little to no binding of sphingomyelin.

While this work presents the first evidence of a lipid droplet associated protein exhibiting phospholipid binding ability, there are other phospholipid binding proteins with similar binding affinities. Sterol carrier protein-2 (SCP-2) bound sphingomyelin with affinity near 173 nM [58], an affinity slightly higher than that observed with ADRP (K_d = 257 nM). Moreover, SCP-2 exhibited high binding affinities for other sphingolipids, including ceramides, GM1, and globosides [58]. In addition, surface plasmon resonance measurements of lysenin, a 41-kDa protein that causes contraction of the rat vascular smooth muscle, bound to sphingomyelin membranes with K_d = 5.3 nM [59]. However, while there are other proteins that bind sphingomyelin with similar affinity, it is ADRP's position on the surface of the lipid droplet that makes it uniquely qualified to provide phospholipids to meet the needs of the cell during membrane synthesis, signaling, and cellular metabolism. Indeed, the ability of ADRP to bind with high affinity the two major phospholipids in cell membranes (sphingomyelin, phosphatidylcholine) suggests that ADRP may play an important role in intracellular phospholipid trafficking and lipid metabolism in general.

In summary, the results presented herein confirmed, through confocal fluorescence imaging and fluorescence binding studies, the existence of exchangeable sphingolipid domains in lipid droplets. In addition, the present investigation shows, for the first time, that ADRP binds phospholipids with high affinity. More importantly, ADRP exhibited similar binding affinities to other known phospholipid binding proteins. These results suggest that ADRP may play a significant role in regulating the intracellular distribution of phospholipids and lipids in general. Overall, insights from the present work suggest new and important roles for lipid droplets in phospholipid and lipid metabolism.

Acknowledgments The helpful technical assistance of Bonnie M. McCann, Jessica Z. Howsley, Meredith Dixon, and Anas M. Fathalla was much appreciated. This work was supported in part by the USPHS National Institutes of Health grant DK70965 (BPA).

References

1. Rexrode KM, Manson JE, Hennekens CH (1996) Obesity and cardiovascular disease. Curr Opin Cardiol 11:490–495
2. Schwartz MW, Brunzell JD (1997) Regulation of body adiposity and the problem of obesity. Arterioscler Thromb Vasc Biol 17:223–238
3. Ogden CL, Carroll MD, Flegal KM (2003) Epidemiologic trends in overweight and obesity. Endocrinol Metab Clin North Am 32:741–760
4. Bickel PE, Tansey JT, Welte MA (2009) PAT proteins, an ancient family of lipid droplet proteins that regulate cellular lipid stores. Biochim Biophys Acta 1791:419–440

5. Fujimoto T, Ohsaki Y, Cheng J, Suzuki M, Shinohara Y (2008) Lipid droplets: a classic organelle with new outfits. Histochem Cell Biol 130:263–279
6. Martin S, Parton RG (2006) Lipid droplets: a unified view of a dynamic organelle. Nat Rev Mol Cell Biol 7:373–378
7. Londos C, Brasaemle DL, Schultz CJ, Segrest JP, Kimmel AR (1999) Perilipins, ADRP, and other proteins that associate with intracellular neutral lipid droplets in animal cells. Semin Cell Dev Biol 10:51–58
8. Atshaves BP, Storey SM, McIntosh AL, Petrescu AD, Lyuksyutova OI, Greenberg AS, Schroeder F (2001) Sterol carrier protein-2 expression modulates protein and lipid composition of lipid droplets. J Biol Chem 276:25324–25335
9. Gao J, Serrero G (1999) Adipose differentiation related protein (ADRP) expressed in transfected COS-7 cells selectively stimulates long chain fatty acid uptake. J Biol Chem 274:16825–16830
10. Brasaemle DL, Barber T, Wolins NE, Serrero G, Blanchette-Mackie EJ, Londos C (1997) Adipose differentiation-related protein is an ubiquitously expressed lipid storage droplet-associated protein. J Lipid Res 38:2249–2263
11. Wang SM, Fong TH, Hsu SY, Chien CL, Wu JC (1997) Reorganization of a novel vimentin-associated protein in 3T3-L1 cells during adipose conversion. J Cell Biochem 67:84–91
12. Fong TH, Wang SM, Lin HS (1996) Immunocytochemical demonstration of a lipid droplet-specific capsule in cultured Leydig cells of the golden hamsters. J Cell Biochem 63:366–373
13. Liu P, Ying Y, Zhao Y, Mundy DI, Zhu M, Anderson RGW (2004) Chinese hamster ovary K2 cell lipid droplets appear to be metabolic organelles involved in membrane traffic. J Biol Chem 279:3787–3792
14. Brasaemle DL, Dolios G, Shapiro L, Wang R (2004) Proteomic analysis of proteins associated with lipid droplets of basal and lipolytically stimulated 3T3-L1 adipocytes. J Biol Chem 279:46835–46842
15. Fujimoto Y, Itabe H, Sakai J, Makita M, Noda J, Mori M, Higashi Y, Kojima S, Takano T (2004) Identification of major proteins in the lipid droplet-enriched fraction isolated from the human hepatocyte cell line HuH7. Biochim Biophys Acta 1644:47–59
16. Trigatti BL, Anderson RGW, Gerber GE (1999) Identification of caveolin-1 as a fatty acid binding protein. Biochem Biophys Res Commun 255:34–39
17. Uittenbogaard A, Ying YS, Smart EJ (1998) Characterization of a cytosolic heat-shock protein-caveolin chaperone complex. Involvement in cholesterol trafficking. J Biol Chem 273:6525–6532
18. Uittenbogaard A, Everson WV, Matveev SV, Smart EJ (2002) Cholesteryl ester is transported from caveolae to internal membranes as part of a caveolin-annexin II lipid–protein complex. J Biol Chem 277:4925–4931
19. Murata M, Peränen J, Schreiner R, Wieland F, Kurzchalia TV, Simons K (1995) VIP21/caveolin is a cholesterol-binding protein. Proc Natl Acad Sci USA 92:10339–10343
20. Atshaves BP, Starodub O, McIntosh AL, Petrescu A, Roths JB, Kier AB, Schroeder F (2000) Sterol carrier protein-2 alters high density lipoprotein-mediated cholesterol efflux. J Biol Chem 275:36852–36861
21. Atshaves BP, Petrescu AD, Starodub O, Roths JB, Kier AB, Schroeder F (1999) Expression and intracellular processing of the 58 kDa sterol carrier protein-2/3-oxoacyl-CoA thiolase in transfected mouse L-cell fibroblasts. J Lipid Res 40:610–622
22. Higuchi K (1970) An improved chemically defined culture medium for strain L mouse cells based on growth responses to graded levels of nutrients including iron and zinc ions. J Cell Physiol 75:65–72
23. Atshaves BP, Storey SM, Petrescu AD, Greenberg CC, Lyuksyutova OI, Smith RI 3rd, Schroeder F (2002) Expression of fatty acid binding proteins inhibits lipid accumulation and alters toxicity in L cell fibroblasts. Am J Physiol Cell Physiol 283:C688–C703
24. Hara A, Radin NS (1978) Lipid extraction of tissues with a low-toxicity solvent. Anal Biochem 90:420–426
25. Marzo A, Ghirardi P, Sardini D, Meroni G (1971) Simplified measurement of monoglycerides, diglycerides, triglycerides, and free fatty acids in biological samples. Clin Chem 17:145–147
26. Atshaves BP, Gallegos AM, McIntosh AL, Kier AB, Schroeder F (2003) Sterol carrier protein-2 selectively alters lipid composition and cholesterol dynamics of caveolae/lipid raft vs nonraft domains in L-cell fibroblast plasma membranes. Biochemistry 42:14583–14598
27. Eckert GP, Igbavboa U, Müller WE, Wood WG (2003) Lipid rafts of purified mouse brain synaptosomes prepared with or without detergent reveal different lipid and protein domains. Brain Res 962:144–150
28. Bradford MM (1976) A rapid and sensitive method for the quantitation of microgram quantities of protein utilizing the principle of protein-dye binding. Anal Biochem 72:248–254
29. Frolov A, Petrescu A, Atshaves BP, So PTC, Gratton E, Serrero G, Schroeder F (2000) High density lipoprotein-mediated cholesterol uptake and targeting to lipid droplets in intact L-cell fibroblasts. A single- and multiphoton fluorescence approach. J Biol Chem 275:12769–12780
30. Schroeder F, Myers-Payne SC, Billheimer JT, Wood WG (1995) Probing the ligand binding sites of fatty acid and sterol carrier proteins: effects of ethanol. Biochemistry 34:11919–11927
31. Prattes S, Hörl G, Hammer A, Blaschitz A, Graier WF, Sattler W, Zechner R, Steyrer E (2000) Intracellular distribution and mobilization of unesterified cholesterol in adipocytes: triglyceride droplets are surrounded by cholesterol-rich ER-like surface layer structures. J Cell Sci 113:2977–2989
32. Spence MW, Clarke JTR, Cook HW (1983) Pathways of sphingomyelin metabolism in cultured fibroblasts from normal and sphingomyelin lipidosis subjects. J Biol Chem 258:8595–8600
33. Lipsky NG, Pagano RE (1985) Intracellular translocation of fluorescent sphingolipids in cultured fibroblasts: endogenously synthesized sphingomyelin and glucocerebroside analogues pass through the Golgi apparatus en route to the plasma membrane. J Cell Biol 100:27–34
34. Bartz R, Li WH, Venables B, Zehmer JK, Roth MR, Welti R, Anderson RGW, Liu P, Chapman KD (2007) Lipidomics reveals that adiposomes store ether lipids and mediate phospholipid traffic. J Lipid Res 48:837–847
35. Ishii I, Onozaki R, Takahashi E, Takahashi S, Fujio N, Harada T, Morisaki N, Shirai K, Saito Y, Hirose S (1995) Regulation of neutral cholesterol esterase activity by phospholipids containing negative charges in substrate liposome. J Lipid Res 36:2303–2310
36. Knudson AG Jr (1961) Inborn errors of sphingolipid metabolism. Am J Clin Nutr 9:55–62
37. Hood LF, Patton S (1973) Isolation and characterization of intracellular lipid droplets from bovine mammary tissue. J Dairy Sci 56:858–863
38. Tauchi-Sato K, Ozeki S, Houjou T, Taguchi R, Fujimoto T (2002) The surface of lipid droplets is a phospholipid monolayer with a unique fatty acid composition. J Biol Chem 277:44507–44512
39. Frolov A, Schroeder F (1998) Acyl coenzyme A binding protein. Conformational sensitivity to long chain fatty acyl-CoA. J Biol Chem 273:11049–11055
40. Simons K, Ikonen E (2000) How cells handle cholesterol. Science 290:1721–1726
41. Murphy DJ (2001) The biogenesis and functions of lipid bodies in animals, plants, and microorganisms. Prog Lipid Res 40:325–438

42. Mukherjee S, Zha X, Tabas I, Maxfield FR (1998) Cholesterol distribution in living cells: fluorescence imaging using dehydroergosterol as a fluorescent cholesterol analog. Biophys J 75:1915–1925
43. Sparrow CP, Patel S, Baffic J, Chao Y-S, Hernandez M, Lam M-H, Montenegro J, Wright SD, Detmers PA (1999) A fluorescent cholesterol analog traces cholesterol absorption in hamsters and is esterified in vivo and in vitro. J Lipid Res 40:1747–1757
44. Koval M, Pagano RE (1989) Lipid recycling between the plasma membrane and intracellular compartments: transport and metabolism of fluorescent sphingomyelin analogues in cultured fibroblasts. J Cell Biol 108:2169–2181
45. Tomás M, Durán JM, Lázaro-Diéguez F, Babià T, Renau-Piqueras J, Egea G (2004) Fluorescent analogues of plasma membrane sphingolipids are sorted to different intracellular compartments in astrocytes; Harmful effects of chronic ethanol exposure on sphingolipid trafficking and metabolism. FEBS Lett 563:59–65
46. Reaven E, Tsai L, Azhar S (1996) Intracellular events in the "selective" transport of lipoprotein-derived cholesteryl esters. J Biol Chem 271:16208–16217
47. McIntosh AL, Gallegos AM, Atshaves BP, Storey SM, Kannoju D, Schroeder F (2003) Fluorescence and multiphoton imaging resolve unique structural forms of sterol in membranes of living cells. J Biol Chem 278:6384–6403
48. Avdulov NA, Chochina SV, Igbavboa U, Warden CS, Schroeder F, Wood WG (1999) Lipid binding to sterol carrier protein-2 is inhibited by ethanol. Biochim Biophys Acta 1437:37–45
49. Schroeder F, Kinden DA (1983) Measurement of phagocytosis using fluorescent latex beads. J Biochem Biophys Methods 8:15–27
50. Tangirala RK, Jerome WG, Jones NL, Small DM, Johnson WJ, Glick JM, Mahlberg FH, Rothblat GH (1994) Formation of cholesterol monohydrate crystals in macrophage-derived foam cells. J Lipid Res 35:93–104
51. Perry DK, Hannun YA (1998) The role of ceramide in cell signaling. Biochim Biophys Acta 1436:233–243
52. Schroeder F, Atshaves BP, Gallegos AM, McIntosh AL, Liu JC, Kier AB, Huang H, Ball JM (2004) Lipid rafts and caveolae organization. In: Lisanti MP, Frank PG (eds) Advances in molecular and cell biology. CRC Press, Boca Raton
53. Ghosh S, Strum JC, Bell RM (1997) Lipid biochemistry: functions of glycerolipids and sphingolipids in cellular signaling. FASEB J 11:45–50
54. Grassme H, Jekle A, Riehle A, Schwarz H, Berger J, Sandhoff K, Kolesnick R, Gulbins E (2001) CD95 signaling via ceramide-rich membrane rafts. J Biol Chem 276:20589–20596
55. Okazaki T, Bielawska A, Bell RM, Hannun YA (1990) Role of ceramide as a lipid mediator of 1 alpha,25-dihydroxyvitamin D3-induced HL-60 cell differentiation. J Biol Chem 265:15823–15831
56. Kim MY, Linardic C, Obeid L, Hannun Y (1991) Identification of sphingomyelin turnover as an effector mechanism for the action of tumor necrosis factor alpha and gamma-interferon. Specific role in cell differentiation. J Biol Chem 266:484–489
57. Jayadev S, Linardic CM, Hannun YA (1994) Identification of arachidonic acid as a mediator of sphingomyelin hydrolysis in response to tumor necrosis factor alpha. J Biol Chem 269:5757–5763
58. Atshaves BP, Jefferson JR, McIntosh AL, Gallegos AM, McCann BM, Landrock KK, Kier AB, Schroeder F (2007) Effect of sterol carrier protein-2 expression on sphingolipid distribution in plasma membrane lipid rafts/caveolae. Lipids 42:871–884
59. Yamaji A, Sekizawa Y, Emoto K, Sakuraba H, Inoue K, Kobayashi H, Umeda M (1998) Lysenin, a novel sphingomyelin-specific binding protein. J Biol Chem 273:5300–5306

Lipids (2010) 45:479–489
DOI 10.1007/s11745-010-3422-3

ORIGINAL ARTICLE

β_3-Adrenergic Signaling Acutely Down Regulates Adipose Triglyceride Lipase in Brown Adipocytes

Jeffrey A. Deiuliis · Li-Fen Liu · Martha A. Belury · Jong S. Rim · Sangsu Shin · Kichoon Lee

Received: 5 February 2010 / Accepted: 21 April 2010 / Published online: 28 May 2010

Abstract Mice exposed to cold rely upon brown adipose tissue (BAT)-mediated nonshivering thermogenesis to generate body heat using dietary glucose and lipids from the liver and white adipose tissue. In this report, we investigate how cold exposure affects the PI3 K/Akt signaling cascade and the expression of genes involved in lipid metabolism and trafficking in BAT. Cold exposure at an early time point led to the activation of the PI3 K/Akt, insulin-like signaling cascade followed by a transient decrease in adipose triglyceride lipase (ATGL) gene and protein expression in BAT. To further investigate how cold exposure-induced signaling altered ATGL expression, cultured primary brown adipocytes were treated with the β_3-adrenergic receptor (β_3AR) agonist CL 316,243 (CL) resulting in activation of PI3 K/Akt, ERK 1/2, and p38 signaling pathways and significantly decreased ATGL protein levels. ATGL protein levels decreased significantly 30 min post CL treatment suggesting protein degradation. Inhibition of PKA signaling by H89 rescued ATGL levels. The effects of PKA signaling on ATGL were shown to be independent of relevant pathways downstream of PKA such as PI3 K/Akt, ERK 1/2, and p38. However, CL treatment in 3T3-L1 adipocytes did not decrease ATGL protein and mRNA expression, suggesting a distinct response in WAT to β3-adrenergic agonism. Transitory effects, possibly attributed to acute Akt activation during the early recruitment phase, were noted as well as stable changes in gene expression which may be attributed to β3-adrenergic signaling in BAT.

Keywords Nonshivering thermogenesis · Brown adipose tissue · Akt signaling · CL 316,243 · β_3-adrenergic receptor signaling

J. A. Deiuliis · S. Shin · K. Lee (✉)
Department of Animal Sciences, The Ohio State University, 2029 Fyffe Rd., Columbus, OH 43210, USA
e-mail: lee.2626@osu.edu

J. A. Deiuliis · L.-F. Liu · M. A. Belury · K. Lee
The Ohio State University Interdisciplinary Human Nutrition Program, The Ohio State University, Columbus, OH 43210, USA

L.-F. Liu · M. A. Belury
The Department of Human Nutrition, The Ohio State University, Columbus, OH 43210, USA

J. S. Rim
Pennington Biomedical Research Center, Louisiana State University System, Baton Rouge, LA 70808, USA

Present Address:
J. S. Rim
NuPotential, Inc., Louisiana Emerging Technology Center, Baton Rouge, LA 70808, USA

Abbreviations

AC	Adenylyl cyclase
A-FABP	Adipocyte-type fatty acid-binding protein
ATCC	American type culture collection
ATGL	Adipose triglyceride lipase
BAT	Brown adipose tissue
BCA	Bicinchoninic acid
β_3AR	β_3-adrenergic receptor
Carb3	Carboxylesterase 3
CL	CL 316,243
CPT1	Carnitine palmitoyltransferase I
DMEM	Dulbecco's modified Eagle's medium
FABP5	Fatty acid binding protein 5
FAT/CD36	Fatty acid transporter/Cluster of Differentiation 36
FBS	Fetal bovine serum

GLUT	Glucose transporter
GPCR	G-protein coupled receptors
GSK-3β	Glycogen synthase kinase 3β
H 89	cAMP-dependent protein kinase inhibitor
H-FABP	Heart-type fatty acid binding protein
HRP	Horseradish peroxidase
HSL	Hormone sensitive lipase
IRS	Insulin receptor substrate
LPL	Lipoprotein lipase
LY 294002	PI3 K gamma inhibitor
NE	Norepinephrine
PI3 K	Phosphoinositide-3 kinase
PKA	Protein kinase A
PTEN	Phosphatase and tensin homolog
SB 203580	p38 inhibitor
TBST	Tris-buffered saline with Tween 20
TAG	Triacylglycerol
UCP1	Uncoupling protein 1
WAT	White adipose tissue

Introduction

Brown adipose tissue (BAT) in mammals is the site of nonshivering thermogenesis, which creates heat by actively oxidizing substrate via mitochondrial uncoupling protein (UCP1) without ATP production. Nonshivering thermogenesis, controlled by sympathetic neural-derived norepinephrine (NE) release [1], lowers metabolic efficiency while greatly increasing the thermogenic capacity of the animal. Application of our knowledge of BAT metabolism in mice to obesity-related health problems in humans is quite promising. β-adrenergic agonists, as well as cold exposure, have been shown to induce a brown fat phenotype in the white adipose tissue (WAT) of mice, resulting in metabolic inefficiency and prevention of diet and genetically induced obesity [1–3]. In addition, Tiraby et al. demonstrated that human white adipocytes can acquire [1, 2, 4] features of brown adipocytes [5]. Others have shown that β-adrenergic agonists and cold exposure results in the remodeling of some white fat depots with an induction of brown fat-like characteristics in a variety of mammals [4, 6–9]. The expression of UCP1 in WAT depots of adult humans has been shown to be variable [10]; a group of morbidly obese subjects were reported to have significantly lower UCP1 expression in the intraperitoneal adipose when compared to lean controls [11]. Cinti reported brown adipocytes were found dispersed among the WAT in 24% of individuals with the percentage increasing to 50% in adults under 50 years of age in 100 perirenal biopsies (32–87 years of age, $\bar{x} = 65$) [12]. Exposure to cool or cold ambient temperatures in humans may lead to increased BAT [13]. Adult humans with endocrine and non-endocrine pathologies have been shown to possess detectible UCP1 expression within periadrenal WAT depots. Presence of UCP1, a marker of brown adipose tissue, suggests certain hormonal signals may induce islets of brown adipocytes within WAT [3, 11]. For example, adult humans producing abnormally high amounts of adrenal catecholamines have been shown to regain BAT [3, 14, 15].

The process of BAT recruitment during chronic cold exposure occurs over weeks and requires major changes to cellular contents at a structural and enzymatic level in order to allow for maximal nonshivering thermogenesis. Much of this process is mediated by NE. Each brown adipocyte is innervated by the ortho-sympathetic nervous system, which releases NE when stimulated [16]. NE binds to β_3, α_1, and α_2-adrenergic receptors, thus affecting signaling events which effect lipolysis, thermogenesis, and apoptosis. Of the three β-adrenergic receptors, β_3 is the most common in rodents [17]. There is evidence that β_3-adrenergic receptor (β_3AR) couple to the G_s subtype of G proteins [18, 19]. This pathway has been suggested to be responsible for crosstalk between the β_3AR and MAPK signaling pathways [20, 21]. The binding of NE or CL 316,243 (CL) to the β_3AR results in the activation of adenylyl cyclase (AC), increased levels of cyclic AMP, and activated protein kinase A (PKA). In general, activated PKA phosphorylates many cellular protein substrates including signaling molecules (Src, ERK1/2, p38, and JNK). PKA activation leads to NE-induced lipolysis in brown adipocytes as demonstrated by the attenuation of lipolysis by H89, a PKA inhibitor [22]. Prolonged β-adrenergic stimulation and PKA activation in BAT leads to the processes necessary for sustained thermogenic activity. It is well known that transcription of lipoprotein lipase (LPL) is increased in BAT to mobilize fatty acid from the circulation during adaptation to chronic cold exposure. However, the roles of newly discovered lipolytic genes such as adipose triglyceride lipase (ATGL) and carboxylesterase 3 (Carb3) in BAT have not been studied.

Adipose triglyceride lipase (ATGL), a recently discovered triglyceride lipase that hydrolyzes the first ester bond of stored triacylglycerol (TAG) in adipocytes releasing non-esterified free fatty acids [23], has been shown to be the rate-limiting lipase in hormone-stimulated TAG hydrolysis [24]. ATGL and its homologues are associated with lipid droplets in eukaryotic cells and is highly upregulated in adipose tissue [25]. The product of ATGL TAG lipase activity, diacylglycerol, is hydrolyzed by activated hormone sensitive lipase (HSL). Thus, ATGL and HSL work in concert to mobilize free fatty acid stores from lipid storing tissues [23]. ATGL expression has been shown to be induced in mice by fasting over 12, 24, and 48 h with refeeding reducing ATGL expression [26]. Importantly, Smas and colleagues have

shown that insulin activation of the PI3 K pathway leads to the down-regulation of ATGL gene expression with PI3 K inhibitors rescuing expression [27]. Dexamethasone upregulates ATGL gene expression; whereas, insulin, tumor necrosis factor alpha, and isoproterenol, downregulate ATGL gene expression in 3T3-L1 preadipocytes [26, 28]. Phosphorylation of ATGL has been demonstrated; however, it is not believed to be a substrate for phosphorylation by PKA [23, 29], leaving the mechanism by which ATGL is regulated undefined. The biochemical significance of the phosphorylation of ATGL remains to be shown. In this report, we investigate how cold stress and CL-mediated signaling affects ATGL and other lipolytic genes in BAT and primary brown adipocytes, respectively.

Materials and Methods

Animals and Cold Exposure

C57BL/6J mice (four males, 2 months old) were kept on a 12-h light/dark cycle and provided with food and water ad libitum. During cold exposure, 2–3 mice per pen were placed at 4 °C for 0.125, 0.25, 1, and 5–7 days. At the indicated time points, interscapular brown adipose tissue (four mice for each time point) was harvested. Animal experiments were approved by the Pennington Biomedical Research Center Animal Care and Use Committee.

In Vitro and Ex Vivo Experiments

Interscapular brown fat was dissected from weanling mice. Primary cell culture was performed by mincing the pooled tissue of two mice, followed by digestion with 3 mg/mL type II collagenase (Sigma–Aldrich, St. Louis, MO) in DMEM media (10% FBS) with shaking (140 rpm) at 37 °C. Digesta was strained with a 100 μM cell strainer and spun at 400 × g for 5 min. The pellet (stromal vascular fraction—SVF) was re-suspended in growth media [Dulbecco's modified Eagle's medium (DMEM), 15% fetal bovine serum (FBS), antibiotics (50 units/mL penicillin, 50 μg/mL streptomycin)], seeded in a 12-well plate, and cultured in a humidified 5% CO_2 incubator. If greater numbers of wells were needed to accomplish an experiment more mice were pooled proportional to the additional wells needed to assure consistency of cells within an independent experiment. Cells were grown to 2 days post-confluence at which time growth media was replaced with differentiation media (DMEM, 15% FBS, antibiotics, insulin 5 μg/mL, dexamethasone 0.4 μg/mL, 0.5 mM 3-isobutyl-1-methyl-xanthine, and 500 nM rosiglitazone) for 3 days. The cells were maintained in growth media (lacking differentiation factors) for another 4 days. At this point, the average well was 70–80% differentiated and showed obvious and abundant lipid accumulation. The adipose cell line, 3T3-L1, was purchased from American type culture collection (ATCC). Low passage number cells were grown to confluence in DMEM 10% FBS and differentiated 2 days post confluence with the same cocktail as the primary brown adipocytes. Primary and 3T3-L1 cells were treated on the same day of differentiation after 3 h of serum starvation. CL 316,243 (Sigma–Aldrich) was used at 1 μM for all experiments according to a dose response curve and the concentrations used in the literature. Inhibitors [H 89 (cAMP-dependent protein kinase inhibitor—Sigma–Aldrich), LY 294002 (PI3 K gamma inhibitor—Cell Signaling technology, Denver, MA), PD 98059 (MEK inhibitor—Cell Signaling Technology), SB 203580 (p38 inhibitor—Santa Cruz Biotechnology, Santa Cruz, CA)] were added 45 min before CL treatments at the concentration indicated in the figure legends.

Brown adipose tissue and white adipose tissue for ex vivo experiments was minced in the same manner as for digestion. The minced tissue was suspended in DMEM and aliquoted at equal volumes into 12-well plates. CL (1 μM) was added and the tissue was collected at the time points indicated, spun down, media removed, and frozen for analysis.

Quantitative-Real-Time PCR Detection of Total Gene Expression

RNA was isolated from BAT of mice using Trizol™ (Invitrogen, Carlsbad, CA) according to the manufacturer's instructions. RNA quality was assessed by agarose gel electrophoresis. cDNA was reverse transcribed using approximately 1 μg of total RNA according the manufacturer's instructions (Invitrogen Life Technologies—M-MLV reverse transcriptase). Real-time PCR was performed using SYBR green I nucleic acid dye (Molecular Probes Invitrogen detection technologies) on an ABI 7300. AmpliTaq Gold™ (Applied Biosystems, Foster City, CA) was used in all real-time reactions as was the following thermal profile: 95 °C 10 m, 40 cycles of 94 °C 30 s, 60 °C 60 s, 82 °C 30 s. The C_T values for the internal control (cyclophilin) and target genes as determined by the ABI software were used to calculate gene expression. All target genes were normalized to cyclophilin and displayed as a fold increase in proportion to the zero hour time points. Randomly selected samples from all real-time runs were resolved by agarose gel electrophoresis to ensure the production of one product. In addition, dissociation curves were performed. Real time primers were designed to span genomic introns, thus avoiding amplification of genomic DNA possibly present in the RNA samples. Primer sequences can be provided upon request. "No template" negative controls were included in all PCR reactions to detect possible contamination.

Protein Isolation and Immunoblotting

Approximately 80 mg of BAT was cut to weight and homogenized in 800 μL of lysis buffer (1% Triton X-100, 150 mM NaCl, 20 mM HEPES pH 7.5, 10% glycerol, 1 mM EDTA, 100 mM NaF, 100 μM sodium orthovanadate, 1 mM PMSF, and 10 μL/mL commercial protease inhibitor cocktail). The protein content of cell lysate was determined using the bicinchoninic acid (BCA) protein assay kit (Pierce Chemical, Rockford, IL). Samples were separated by SDS–PAGE using the mini-Protean system (Bio-Rad, Hercules, CA). The protein was wet-transferred to a PVDF membrane (Amersham Biosciences, Uppsala, Sweden) and blocked in 5% nonfat dry milk (NFDM) in 1x-TBST (0.1% Tween 20) and incubated with primary antibody (5% NFDM) overnight at 4 °C specific to ATGL, P-Akt, P-ERK1/2, total ERK1/2, P-p38 (Cell Signaling Technologies, 1:1,000); β-actin (Santa Cruz Biotechnology, 1:2,000); A-FABP (R&D systems, Minneapolis, MN, 1:2,000); and H-FABP (Abcam, Cambridge, MA, 1:1,000). After washing in 1×-TBST, blots were incubated with the appropriated HRP-conjugated secondary antibody for 1 h at room temperature. Blots were washed before addition of ECL plus™ (Amersham Biosciences) and detection of bands with Kodak Biomax™ film. Some immunoblotting used a fluorescent luminescence detection system. After washing in 1×-TBST, blots were incubated with fluorescence-labeled secondary antibodies (Irdye800 anti-rabbit IgG and Alexa680 anti-mouse IgG). Bands were visualized using the Odyssey imaging system (LI-COR Bioscience, Lincoln, NE).

Glycerol Release Assay

Differentiated primary mouse brown adipocytes were serum starved for 3 h in phenol red-free, serum-free DMEM. Those cells receiving PD 98059 (50 μM) and CL (1 μM) were pretreated with the inhibitor 45 min before stimulation. The media was collected after 3 h and centrifuged to remove cells and cellular debris. Glycerol content of conditioned medium was determined using the "free glycerol reagent" kit (Sigma–Aldrich). The final concentration of free glycerol was determined according to the kit instructions using a free glycerol standard and normalized to the protein content of cell lysates.

Statistical Analysis

All statistical analysis was performed using SAS™. Gene expression was analyzed using one-way ANOVA analysis followed by Fisher's Protected LSD. Densitometry for immunoblotting was analyzed as a randomized complete block design in order to measure how dependent the effect of CL was on the presence of the inhibitor. Treatments were compared via Fisher's Protected LSD. The minimum level of significance was set at $P < 0.05$. All statistical values using primary cultured brown adipoctyes are derived from three or greater independent experiments cultured from separate isolations/differentiations of primary mouse preadipocytes isolated from interscapular brown adipose (2 mice per 12 well dish—see "Materials and Methods") unless otherwise specified.

Results

Cold Stress Modulates Fatty Acid Binding Protein and Fatty Acid Transport Expression Levels in BAT

Fatty acids are the main substrate oxidized during BAT-mediated nonshivering thermogenesis. Among several fatty acid binding proteins, A-FABP, H-FABP and mal1 (FABP5) have been shown to be expressed in BAT tissue of mice [30]. The increased expression levels of specific FABPs are putatively explained by a greater need for fatty acid metabolism and trafficking in BAT than other bodily tissues. We tested the response of these genes within BAT to cold exposure. The level of FABP5 was not significantly changed during 1 week of cold exposure (data not shown). The levels of A-FABP gene expression decreased gradually, reaching a significantly lower level (60% reduction) at day 1 and returned to pre-cold exposure control levels (Fig. 1c). In contrast, the levels of H-FABP gene expression linearly increased with increasing time achieving statistical significance in 6 h and a fivefold induction at day 5–7 in BAT of mice (Fig. 1a). It has been shown that FABP concentrations are largely controlled at the transcriptional level [31]. In order to confirm the upregulation, we performed immunoblotting demonstrating H-FABP gene expression corresponded with an increase in protein levels in vivo and decreases in A-FABP gene expression corresponded with decreases in protein levels (Fig. 1b). Since transmembrane transport of free fatty acids is actively facilitated by transporter proteins, we assayed the gene expression of the fatty acid transporter, FAT/CD36. FAT/CD36 gene expression increased dramatically at 6 h, returning to normal by 5–7 days (Fig. 1d). The opposing trends in A- and H-FABP expression during cold exposure suggest they play different roles in fatty acid mobilization during cold stress.

Cold Induces Down-Regulation of Lipolytic Genes in BAT

In addition to fatty acid transport, lipolysis plays an important role in the utilization of fatty acid in BAT. In

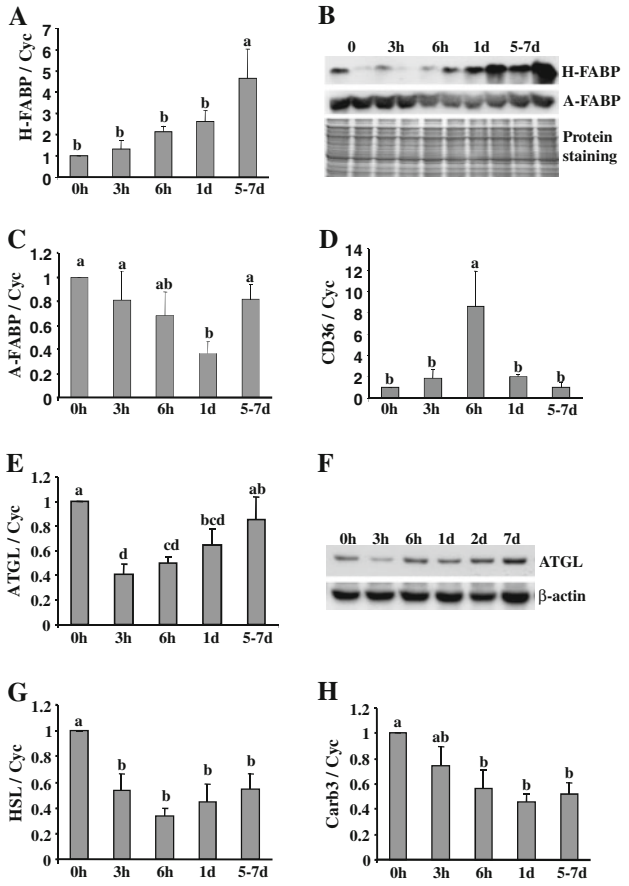

Fig. 1 Lipase expression in BAT of mice with cold exposure. All graphs represent real-time PCR analysis ($n = 4$). Target genes as a ratio to the housekeeping gene cyclophilin are expressed in fold difference to control. **a** Gene expression levels of H-FABP increased in a linear fashion with time of exposure. **b** The corresponding protein levels of H-FABP and A-FABP were measured by immunoblotting, confirming the gene expression pattern. **c** Real time PCR analysis of A-FABP gene expression decreased with cold exposure and was significantly ($P < 0.05$) lower at day 1 when compared to control mice (0 h). **d** FAT/CD36 fatty acid transporter gene expression increased acutely (6 h) in the BAT during cold exposure only to return to control levels by 5–7 days. **e** ATGL gene expression in the brown adipose of mice dropped significantly after 3, 6, and 24 h of cold exposure. However, expression rebounded reaching near normal levels after 7 days. **f** The corresponding protein levels of ATGL were measured by immunoblotting, confirming an initial decrease followed by normalization and an increase in ATGL protein levels as shown in this representative blot from three independent experiments ($n = 3$). **g** HSL gene expression was significantly decreased at all times during cold exposure. **h** Carboxylesterase 3.0 gene expression was significantly decreased at 6 h, 1 day, and 5–7 days when compared to 0 h control as measured by real-time PCR. The letters (*a*, *b*, *c*, *d*) represent a significant difference among groups at various time points by using one-way ANOVA at $P < 0.05$

order to better understand lipolysis in BAT during cold exposure, we analyzed the expression of the major lipolytic genes. Real-time gene expression analysis of three lipolytic enzymes, i.e., ATGL, carboxylesterase 3, and HSL, revealed ATGL levels decreased initially and gradually

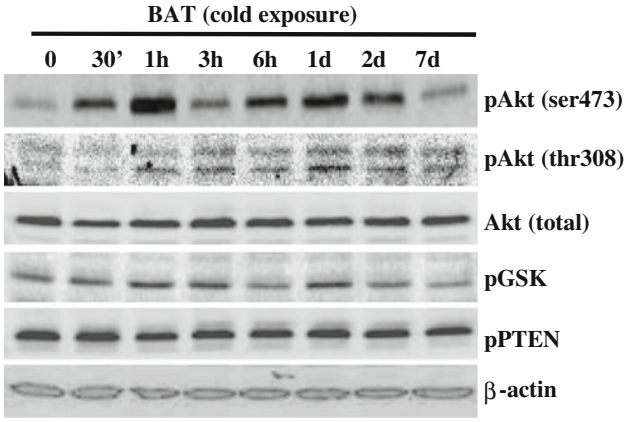

Fig. 2 Akt and related signaling in the BAT of cold exposed-mice. Phosphorylation and total proteins in BAT of mice during cold exposure are presented by immunoblotting. Phosphorylation of Akt, GSK, PTEN are reported as well as the loading control, β-actin. Data represent three independent experiments ($n = 3$)

increased; whereas, carboxylesterase 3 (EC 3.1.1.1) and HSL expression levels were consistently depressed in BAT of mice during cold exposure (Fig. 1e, g, h). In addition, ATGL protein levels were transiently decreased during the early period of cold exposure but returned to normal (Fig. 1f). The rapid changes in gene and protein levels in BAT in vivo indicated there was an acute response to cold exposure.

Cold Exposure Affects BAT Intracellular Signaling Events

To better understand the acute response to cold exposure, we focused on the main intracellular signaling pathway controlling insulin and fatty acid utilization, PI3 K/Akt. We found cold exposure increased phosphorylation of Akt at serine 473 with an increase obvious at 30 min and maximal induction at 1 h (Fig. 2). Activated Akt was maintained through day 2 and returned to control levels by day 7. Detection of Akt phosphorylation at threonine 308 was increased steadily with maximal phosphorylation on day 1. Phosphorylated GSK-3β levels, a downstream target of pAkt, increased in parallel with Akt signaling as expected. Antagonists of Akt signaling, such as pPTEN, lipid phosphatase and tensin homologue slightly decreased during cold exposure when Akt activation was maximal. Total Akt, as well as β-actin, remained consistent during treatment. ATGL levels were decreased due to cold exposure. Previous reports demonstrated that insulin treatment/insulin receptor substrate signaling (IRS) decreased ATGL expression and that LY294002 rescued the down-regulation of ATGL by blocking PI3 K [27, 28, 32]. Analyzing our findings in the context of the literature on ATGL and lipolysis, we hypothesized that PI3 K/Akt

signaling antagonized the lipolytic system by downregulating ATGL levels. In order to test this hypothesis mechanistically, we used ex vivo mouse brown adipose, primary mouse brown pre-adipocytes grown and differentiated in culture and a mouse adipocyte cell line.

The β_3AR Agonist, CL 316,243, Down-Regulates ATGL Protein and Gene Transcript Levels in Mouse Brown Adipocytes, but not White

It is well documented that NE signaling via the β_3-adrenergic receptor controls the thermogenic process; thus, we utilized a β_3AR agonist in ex vivo and in vitro analysis of brown adipose/adipocyte signaling. Treatment of small segments of BAT ex vivo with CL showed activation of Akt at 3 and 6 h and a decrease of ATGL protein (Fig. 3a). We continued this line of investigation in primary mouse brown adipocytes that were differentiated in vitro. In order to validate the system, we tested the effects of CL (1 μM) on UCP1 gene expression in differentiated brown adipocytes. CL administration resulted in a ~20 fold increase ($P < 0.01$) in UCP1 gene expression in 3 h (Fig. 3b). In addition, CL (1 μM) treatment of primary brown adipocytes induced lipolysis as indicated by an approximate three-fold increase in glycerol release ($P < 0.01$). In order to determine the most effective dose of CL on ATGL expression in our in vitro system, we performed a dose response curve, measuring ATGL protein levels at 3 h post treatment (Fig. 3c). The levels of ATGL protein were decreased by CL in a dose-dependent manner. One μM showed consistent efficacy in reducing ATGL protein levels and was the dose used in the majority of the literature on β_3-adrenergic signaling. WAT, like brown, expresses the β_3AR and is sensitive to CL-activated PKA signaling. We show, however, that CL administration did not result in a significant change in ATGL protein levels in 3T3-L1 cells and WAT ex vivo (Fig. 3d, e).

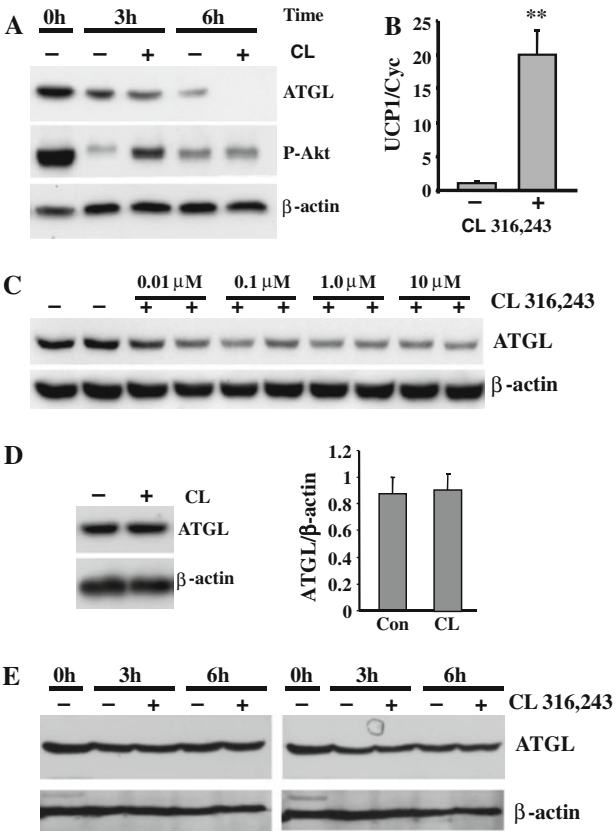

Fig. 3 ATGL and phosphorylated Akt in BAT ex vivo and in differentiated primary brown adipocytes. **a** CL (1 μM) decreases ATGL protein levels after 3 h in BAT ex vivo at 3 and 6 h. CL activated Akt in BAT ex vivo similar to the results obtained from in vivo cold exposure. **b** CL increased UCP1 gene expression in primary mouse brown adipocytes and significantly (**, $P < 0.01$) induced lipolysis as measured by glycerol release ($n = 3$). **c** CL treatment lowered ATGL protein levels in this representative immunoblot after 3 h at even nanomolar concentrations with maximal effects being observed at 1 μM. **d**, **e** Immunoblotting results ($n = 3$) show that β_3AR signaling in 3T3-L1 adipocytes ($n = 3$) and WAT ex vivo (two independent experiments with pooled adipose tissues from two mice per experiment) does not result in the same decrease in ATGL as observed in brown adipocytes. Both BAT and WAT express the β_3AR, however, β_3AR agonism results in depot-specific regulation of ATGL expression levels

CL 316,243 Activates Akt, However, Blockade of PI3 K Does not Rescue ATGL Protein Levels

CL 316,243 (1 μM) administration down-regulated ATGL protein and potently activated Akt ex vivo and in vitro. Activation of Akt by the β_3AR signaling is non-classical and involves crosstalk between G-protein coupled receptors (GPCR) and the PI3 K signaling pathway. In order to determine if PI3 K signaling caused the decrease in ATGL protein levels, we blocked Akt activation with the PI3 K inhibitor LY294002. However, blocking Akt activation did not prevent ATGL down-regulation in vitro (Fig. 4b, c). In addition, insulin treatment potently activated PI3 K but did not result in decreased ATGL protein levels in differentiated primary brown adipocytes (Fig. 4b). These findings led us to conclude that the PI3 K/Akt signaling pathway does not antagonize PKA signaling as it does in other tissues. From this point, we focused on classical β_3AR-signaling as a putative ATGL regulatory mechanism in BAT.

β_3AR Signaling-Mediated Degradation of ATGL is PKA Dependent in Brown but not White Adipocytes

We show that inhibition of PKA signaling by H89 rescues the down-regulation of ATGL (Fig. 4a, b). An H89 dose curve with CL (1 μM) shows that 10 μM H89 was most effective at rescuing ATGL (Fig. 4a). This is also a commonly used dose in the literature for inhibition of PKA

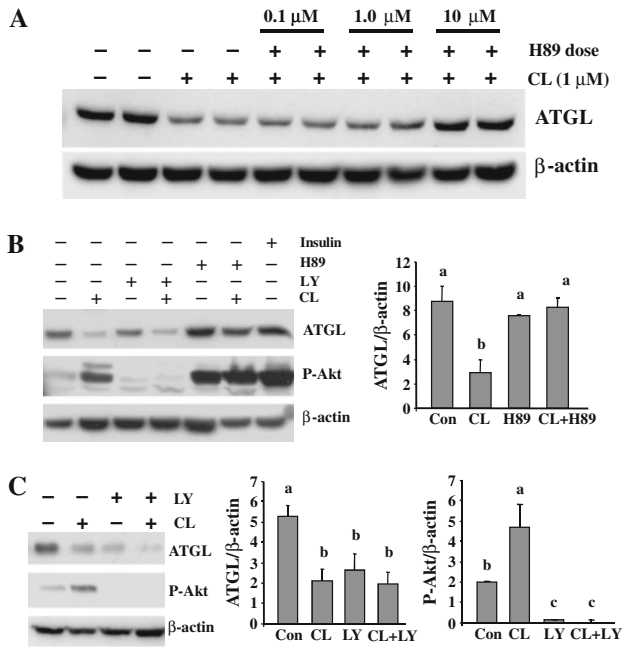

Fig. 4 Inhibition of PKA signaling, not Akt signaling, rescues ATGL protein levels in a dose-dependent manner. **a** The PKA inhibitor, H89, rescues the CL-mediated decrease in ATGL protein in a dose-dependent manner at 3 h in primary brown adipocytes as shown in this immunoblot. **b**, **c** CL as well as 100 nM insulin potently activated Akt, however, blockage of Akt signaling did not rescue ATGL protein levels. The letters (*a, b*) represent a significant difference among groups by using one-way ANOVA at $P < 0.05$. Statistical values are derived from three independent experiments ($n = 3$) using primary brown adipoctyes cultured from separate isolations/differentiations of primary mouse preadipocytes isolated from interscapular brown adipose (2 mice per 12 well dish—see "Materials and Methods")

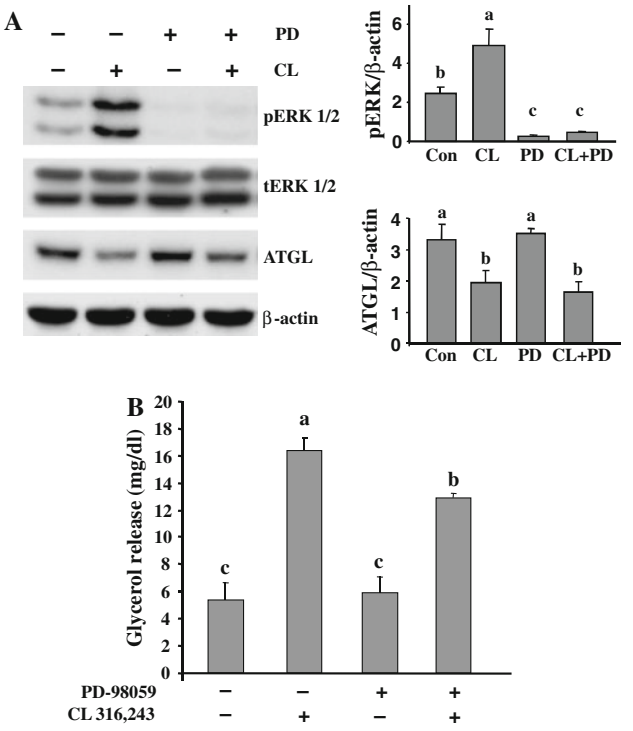

Fig. 5 Activation of ERK 1/2 in brown adipocytes by CL; ERK 1/2 are not downstream of CL-PKA-mediated ATGL downregulation. **a** CL potently activated ERK 1/2, which correlates with a decrease in ATGL protein levels; however, blocking ERK 1/2 with PD 98059 (50 μM) does not rescue ATGL expression ($n = 3$). **b** CL potently induces lipolysis in brown adipocytes as measured by glycerol release. ERK 1/2 inhibition resulting in a significant ($P < 0.01$) decrease, approximately 20%, in β_3AR-stimulated lipolysis ($n = 3$). The letters (*a*, *b*, *c*) represent a significant difference among groups by using one-way ANOVA at $P < 0.05$

signaling. Interestingly, CL and H89 treatment did not modulate ATGL protein levels in differentiated 3T3-L1 adipocytes at 3 h (data not shown).

Adipose triglyceride lipase can exist as a phosphoprotein, although it has been reported that ATGL is *not* a direct substrate of PKA [23, 29]. Due to the rapid decrease in ATGL levels after β_3AR agonism, we hypothesized that ATGL phosphorylation leads to degradation via an intermediate downstream of PKA. In order to identify this intermediate, we focused on known signaling pathways downstream of β_3AR-mediated lipolysis, including ERK 1/2 and p38 signaling [33]. CL administration potently activated ERK1/2 (Fig. 5a). The inhibition of ERK 1/2 by PD 98059, however, did not rescue ATGL protein levels. We do show that inhibition of ERK 1/2 by PD 98059 led to a significant inhibition of CL-mediated lipolysis. This shows that ERK1/2 signaling is important in β_3AR-mediated BAT lipolysis. Also, brown adipocytes are capable of increased lipolysis concurrent with significant decreases in ATGL protein levels. H89 attenuated CL-mediated upregulation of UCP1 gene expression by blocking PKA-mediated phosphorylation of p38 [34]. Therefore, we assessed the role of p38 signaling on ATGL expression. CL treatment results in p38 activation; however, the p38 blockade by 10 and 25 μM of SB 203580 did not rescue ATGL protein expression in cultured primary brown adipocytes (data not shown).

Adipose triglyceride lipase protein levels decreased significantly after only 30 min of CL treatment and reached maximal downregulation by 1 h which was maintained to the 3 h time point (Fig. 6a). H89 pretreatment rescued ATGL protein levels 1 and 3 h after CL treatment. In order to determine if the decrease in ATGL protein was due to decreased transcription of ATGL gene expression, we treated the primary mouse brown adipocytes with 1 μM of CL over a time course. ATGL gene expression showed a downward trend which became significant after 3 h as in the in vivo study (Fig. 6b). CL administration results in decreased ATGL transcription, however, ATGL protein levels decrease at a greater rate than can be attributed to transcriptional effects. Our data suggest that the decrease in ATGL protein is partially due to the protein degradation via PKA signaling. Thus, we hypothesized that ATGL was

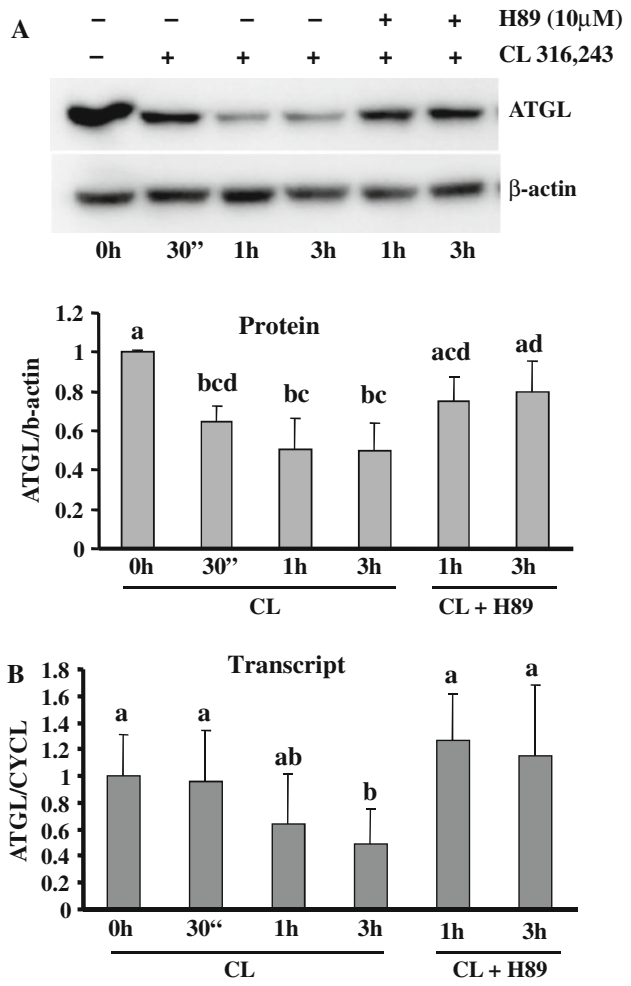

Fig. 6 CL-PKA-mediated ATGL protein degradation occurs rapidly while effects on transcript lag. **a** Immunoblotting ($n = 3$) shows that CL administration results in a significant decrease in ATGL protein levels in as little as 30 min ($P < 0.05$). H89 pretreatment rescues ATGL protein. **b** ATGL gene expression is significantly reduced only at 3 h post CL administration and is rescued by H89 at 1 and 3 h ($n = 3$). The letters (*a*, *b*, *c*, *d*) represent a significant difference among groups at various time points by using one-way ANOVA at $P < 0.05$

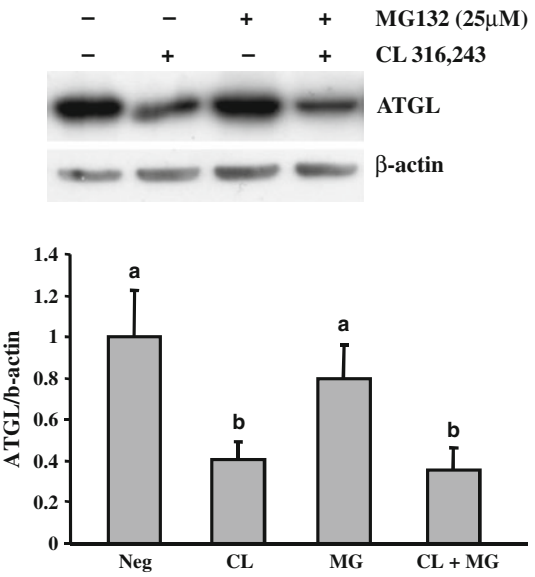

Fig. 7 ATGL protein level decrease in CL 316,243-treated cells is not due to 26S proteasomal degradation. **a** Inhibition of the proteasome by MG 132 (25 μM) does not rescue CL-mediated ATGL protein degradation at 3 h as shown in this representative immunoblot ($n = 3$). The letters (*a, b*) represent a significant difference among groups by using one-way ANOVA at $P < 0.05$

being degraded by 26S proteasome hydrolysis. In order to test this hypothesis, we pretreated primary brown adipocytes with the proteasome inhibitor MG 132 (25 μM) for 1 h then stimulated the cells with CL. The cells were collected at 3 h. However, blockade of the proteasome did not prevent ATGL degradation (Fig. 7), suggesting degradation by an alternative pathway.

Discussion

The nine currently identified cytoplasmic fatty acid binding proteins ($FABP_C$) belong to the superfamily of lipid binding proteins. $FABP_C$ all possess similar protein structures but show tissue specific expression [35]. This tissue specific expression pattern suggests unique or specialized functions for the various $FABP_C$. H- and A-FABP proteins are $FABP_C$ that function to increase cytoplasmic diffusion and transport of FFA from the plasma membrane [36, 37]. A-FABP is exclusively expressed in adipose tissue where it has been shown to be involved in increasing the solubility and aiding in trafficking of free fatty acids between cellular compartments. Whereas, H-FABP is mainly expressed in cardiac and skeletal muscles where fatty acid oxidization is a major source of energy. For example, H-FABP increased in rat heart and skeletal muscle tissues in conditions of increased fatty acid oxidation, such as diabetes and fasting, respectively [38, 39]. In humans, increased H-FABP expression is correlated to increased fatty acid oxidation in type two diabetic individuals undergoing dietary and exercise interventions [40]. In the current studies, the dramatic increase in H-FABP transcription contrasted by the decrease in A-FABP transcription suggests that cold shock alters the fatty acid trafficking within the brown adipocytes. We propose that the FFA flux into the BAT has a direct or indirect affect upon the transcription of A- and H-FABP. While H-FABP's precise role in intracellular trafficking and fat metabolism is undefined, our study suggests that H-FABP may function to transport/direct the influx of intracellular FFAs to the mitochondrial FFA transport system (CPT1) for oxidation thus fueling non-shivering thermogenesis. Finally, the FFA influx and

trafficking in BAT has a direct/indirect affect upon the transcription of A- and H-FABP.

Nonshivering thermogenesis requires the up-regulation of β-oxidation and uncoupled oxidative phosphorylation in BAT. Cold stress-induced NE release stimulates the β_3 and α_2-adrenergic receptors and has profound effects on BAT including upregulation of lipolysis and UCP1 expression, promotion of proliferation and differentiation, and inhibition of apoptosis [17]. It has been shown recently that in vitro stimulation of the β_3-adrenergic receptor by NE, isoprenaline, and CL induced glucose uptake in brown adipocytes in culture by increasing GLUT1 gene expression with decreasing GLUT4 expression [41]. Adams and colleagues showed that cold exposure from 1 to 48 h increased glucose uptake and de novo lipogenesis while increasing β-oxidation [42]. Our in vivo cold exposure data show phosphorylation of GSK-3β, suggesting an increase in glycogen synthesis in BAT during cold exposure. This finding complements the work of others [41, 42] showing increased glucose uptake in brown adipocytes upon NE or cold exposure. PI3 K/Akt signaling is the main regulator of GLUT4 translocation to the plasma membrane due to the effects of insulin [43]. Thus, β_3AR mediated activation of PI3 k/Akt may function to increase glucose uptake in the tissue as well as increase sensitivity to circulating insulin levels. This response appears to be specific to BAT, as PI3 K/Akt signaling normally antagonizes the lipolytic pathway. In addition, muscle and WAT exhibit reduced sensitivity of PI3 K/Akt signaling to insulin in the rat during cold exposure [44].

Current studies show in cold exposure that ATGL is transiently down-regulated with a corresponding increase in Akt signaling in vivo. During cold exposure, changes in ATGL expression were more sensitive and occurred before the decrease in the other lipases, HSL and Carb3. Also, supporting the sensitivity of ATGL to metabolic stress are data from mouse fasting and refeeding studies where ATGL expression changes in the WAT according to positive or negative energy balances [26]. A recently published article shows that noradrenaline-induced lipolysis was positively correlated with HSL protein levels, but not with ATGL protein levels in the WAT of women [45]. In agreement with this, CL treatment did not affect ATGL protein levels in 3T3-L1 adipocytes or in WAT treated ex vivo. However, defective cold adaptation of ATGL knockout mice clearly indicates an important role of ATGL-mediated lipolysis in WAT to supply BAT with free fatty acids. Considering no change in expression of ATGL protein in response to CL, ATGL activity can be regulated by other interacting proteins. The recent discovery of two proteins, comparative gene identification-58 (CGI-58) and the G0/G1 switch gene 2 (G0S2) that physically interact with ATGL protein, increases the complexity of ATGL regulation. CGI-58 functions as an activator of ATGL without affecting HSL activity, increasing lipolysis [46]. In contrast to CGI-58, interaction of G0S2 with ATGL decreased ATGL-mediated lipolysis, acting as a negative regulator of ATGL [47]. Up-regulation of G0S2 by anti-lipolytic hormone insulin and drastic down-regulation by β-adrenergic agonist isoproterenol or another lipolysis-inducing hormone, tumor necrosis factor α, demonstrated the importance of G0S2 as a regulator of ATGL activity in response to metabolic hormones [47]. This implicates possible mechanisms by which alteration of G0S2 amounts affect ATGL activity without changing ATGL protein levels in WAT in response to CL.

It has been reported that the ATGL gene is a target for PPARγ transactivation [27]. Decreases in PPARγ levels have been shown in primary brown adipocytes treated with NE as well as in white adipocytes treated with β_3AR agonists, leading to its degradation and lowered transcription of PPARγ mediated genes [48, 49]. Thus, the decreases in ATGL levels during cold-stress in vivo may be due to decreases in PPARγ levels. ATGL gene expression has been shown to be down-regulated in 3T3-L1 cells, a mouse adipocyte cell line, by insulin and isoproterenol administration [27, 28]. Smas et al. [27] went onto show that insulin activation of the PI3 K pathway leads to the down-regulation of ATGL with PI3 K inhibitors rescuing transcript levels. Rapid down-regulation of ATGL by both anabolic and catabolic hormones is intriguing and is as of yet unexplained. Hormones that increase lipolysis such as CL and isoproterenol paradoxically decrease ATGL gene and protein levels. This would suggest that catecholamine-induced lipolysis is partially independent of ATGL protein levels and most probably relies on regulation of ATGL activation. Zimmerman et al. [23] showed that ATGL is a phosphoprotein. Phosphorylation is a key signal for ubiquitination and 26S proteasomal catabolism of proteins [50]. However, ATGL was demonstrated *not* to be a substrate for PKA [23]; however, our data suggests ATGL is an indirect target of PKA signaling in brown adipocytes. In addition, our data show the proteasome inhibitor MG 132 does not rescue ATGL protein levels indicating β_3AR signaling causes ATGL protein level decreases due to non-proteasomal degradation. ERK 1/2 plays a role in MAPK signaling mediated lipolysis and can be activated by PKA. However, while blocking ERK 1/2 decreases lipolysis in primary brown adipocytes by $\sim$20%, it does not rescue ATGL protein levels. Similarly, the p38 signaling pathway does not mediate PKA-dependent ATGL degradation. Importantly, current studies show that CL activates Akt in primary mouse brown adipocytes and decreases ATGL protein levels via a PKA dependent, ERK 1/2, p38, and Akt-independent mechanism.

The current study showed that cold exposure at early time points elicits β_3AR and insulin-like signaling in BAT and primary brown adipocytes, including transient decreases in ATGL gene and protein levels. In this situation, fatty acids from the diet and mobilization of fatty acids from WAT can be a primary source for nonshivering thermogenesis in BAT rather than the break down of TAG stored in BAT. Also, appetite and glucose uptake in BAT increases during the early stage of cold exposure [42] providing metabolic substrates for nonshivering thermogenesis. Under conditions of long-term cold exposure with limited dietary glucose and circulating fatty acids, the TAG in BAT will most likely be hydrolyzed by ATGL to produce an energy substrate for nonshivering thermogenesis. H-FABP expression increases purportedly to shuttle fatty acids within the cell to the mitochondria as an oxidative substrate for nonshivering thermogenesis. Further investigation into the crosstalk between the PI3 K/Akt and the β_3-adrenergic pathway and how they affect lipid storage, fatty acid mobilization, transport, and utilization within BAT is warranted. A better understanding of the distinct differences between PI3 K and β_3AR crosstalk in WAT and BAT is important to endocrinology, adipose physiology, and metabolism. Finally, β_3AR agonists are exciting potential targets for pharmaceutical therapy of obesity; however, a better understanding of the mechanisms underlying this process is needed and will advance clinical management of obesity.

Acknowledgments This work was supported by the Ohio Agricultural Research and Development Center (K. Lee), and partially supported by the National Research Foundation of Korea Grant funded by the Korean Government [NRF-2009-352-F00029]. We would like to thank Bethany (Elizabeth) Larue for her assistance with the preparation of this manuscript and Michelle Milligan for formatting the manuscript.

References

1. Collins S, Daniel KW, Petro AE, Surwit RS (1997) Strain-specific response to beta 3-adrenergic receptor agonist treatment of diet-induced obesity in mice. Endocrinology 138:405–413
2. Ghorbani M, Himms-Hagen J (1997) Appearance of brown adipocytes in white adipose tissue during CL 316,243-induced reversal of obesity and diabetes in Zucker fa/fa rats. Int J Obes Relat Metab Disord 21:465–475
3. Garruti G, Ricquier D (1992) Analysis of uncoupling protein and its mRNA in adipose tissue deposits of adult humans. Int J Obes Relat Metab Disord 16:383–390
4. Guerra C, Koza RA, Yamashita H, Walsh K, Kozak LP (1998) Emergence of brown adipocytes in white fat in mice is under genetic control. Effects on body weight and adiposity. J Clin Invest 102:412–420
5. Tiraby C, Tavernier G, Lefort C, Larrouy D, Bouillaud F, Ricquier D, Langin D (2003) Acquirement of brown fat cell features by human white adipocytes. J Biol Chem 278:33370–33376
6. Ashwell M, Stirling D, Freeman S, Holloway BR (1987) Immunological, histological and biochemical assessment of brown adipose tissue activity in neonatal, control and beta-stimulant-treated adult dogs. Int J Obes (Lond) 11:357–365
7. Cousin B, Cinti S, Morroni M, Raimbault S, Ricquier D, Penicaud L, Casteilla L (1992) Occurrence of brown adipocytes in rat white adipose tissue: molecular and morphological characterization. J Cell Sci 103(Pt 4):931–942
8. Loncar D, Bedrica L, Mayer J, Cannon B, Nedergaard J, Afzelius BA, Svajger A (1986) The effect of intermittent cold treatment on the adipose tissue of the cat. Apparent transformation from white to brown adipose tissue. J Ultrastruct Mol Struct Res 97:119–129
9. Lowell BB, Susulic V, Hamann A, Lawitts JA, Himms-Hagen J, Boyer BB, Kozak LP, Flier JS (1993) Development of obesity in transgenic mice after genetic ablation of brown adipose tissue. Nature 366:740–742
10. Kortelainen ML, Pelletier G, Ricquier D, Bukowiecki LJ (1993) Immunohistochemical detection of human brown adipose tissue uncoupling protein in an autopsy series. J Histochem Cytochem 41:759–764
11. Oberkofler H, Dallinger G, Liu YM, Hell E, Krempler F, Patsch W (1997) Uncoupling protein gene: quantification of expression levels in adipose tissues of obese and non-obese humans. J Lipid Res 38:2125–2133
12. Cinti S (2006) The role of brown adipose tissue in human obesity. Nutr Metab Cardiovasc Dis 16:569–574
13. Huttunen P, Hirvonen J, Kinnula V (1981) The occurrence of brown adipose tissue in outdoor workers. Eur J Appl Physiol Occup Physiol 46:339–345
14. English JT, Patel SK, Flanagan MJ (1973) Association of pheochromocytomas with brown fat tumors. Radiology 107:279–281
15. Ricquier D, Nechad M, Mory G (1982) Ultrastructural and biochemical characterization of human brown adipose tissue in pheochromocytoma. J Clin Endocrinol Metab 54:803–807
16. Nicholls DG, Locke RM (1984) Thermogenic mechanisms in brown fat. Physiol Rev 64:1–64
17. Cannon B, Nedergaard J (2004) Brown adipose tissue: function and physiological significance. Physiol Rev 84:277–359
18. Granneman JG (1988) Norepinephrine infusions increase adenylate cyclase responsiveness in brown adipose tissue. J Pharmacol Exp Ther 245:1075–1080
19. Marette A, Bukowiecki LJ (1991) Noradrenaline stimulates glucose transport in rat brown adipocytes by activating thermogenesis. Evidence that fatty acid activation of mitochondrial respiration enhances glucose transport. Biochem J 277:119–124
20. Gerhardt CC, Gros J, Strosberg AD, Issad T (1999) Stimulation of the extracellular signal-regulated kinase 1/2 pathway by human beta-3 adrenergic receptor: new pharmacological profile and mechanism of activation. Mol Pharmacol 55:255–262
21. Soeder KJ, Snedden SK, Cao W, Della Rocca GJ, Daniel KW, Luttrell LM, Collins S (1999) The beta3-adrenergic receptor activates mitogen-activated protein kinase in adipocytes through a Gi-dependent mechanism. J Biol Chem 274:12017–12022
22. Fredriksson JM, Thonberg H, Ohlson KB, Ohba K, Cannon B, Nedergaard J (2001) Analysis of inhibition by H89 of UCP1 gene expression and thermogenesis indicates protein kinase A mediation of beta(3)-adrenergic signalling rather than beta(3)-adrenoceptor antagonism by H89. Biochim Biophys Acta 1538:206–217
23. Zimmermann R, Strauss JG, Haemmerle G, Schoiswohl G, Birner-Gruenberger R, Riederer M, Lass A, Neuberger G, Eisenhaber F, Hermetter A, Zechner R (2004) Fat mobilization in adipose tissue is promoted by adipose triglyceride lipase. Science 306:1383–1386
24. Haemmerle G, Zimmermann R, Strauss JG, Kratky D, Riederer M, Knipping G, Zechner R (2002) Hormone-sensitive lipase deficiency in mice changes the plasma lipid profile by affecting the tissue-specific expression pattern of lipoprotein lipase in adipose tissue and muscle. J Biol Chem 277:12946–12952

25. Smirnova E, Goldberg EB, Makarova KS, Lin L, Brown WJ, Jackson CL (2006) ATGL has a key role in lipid droplet/adiposome degradation in mammalian cells. EMBO Rep 7:106–113
26. Villena JA, Roy S, Sarkadi-Nagy E, Kim KH, Sul HS (2004) Desnutrin, an adipocyte gene encoding a novel patatin domain-containing protein, is induced by fasting and glucocorticoids: ectopic expression of desnutrin increases triglyceride hydrolysis. J Biol Chem 279:47066–47075
27. Kim JY, Tillison K, Lee JH, Rearick DA, Smas CM (2006) The adipose tissue triglyceride lipase ATGL/PNPLA2 is downregulated by insulin and TNF-alpha in 3T3–L1 adipocytes and is a target for transactivation by PPARgamma. Am J Physiol Endocrinol Metab 291:E115–E127
28. Kralisch S, Klein J, Lossner U, Bluher M, Paschke R, Stumvoll M, Fasshauer M (2005) Isoproterenol, TNFalpha, and insulin downregulate adipose triglyceride lipase in 3T3–L1 adipocytes. Mol Cell Endocrinol 240:43–49
29. Jenkins CM, Mancuso DJ, Yan W, Sims HF, Gibson B, Gross RW (2004) Identification, cloning, expression, and purification of three novel human calcium-independent phospholipase A2 family members possessing triacylglycerol lipase and acylglycerol transacylase activities. J Biol Chem 279:48968–48975
30. Maeda K, Uysal KT, Makowski L, Görgün CZ, Atsumi G, Parker RA, Brüning J, Hertzel AV, Bernlohr DA, Hotamisligil GS (2003) Role of the fatty acid binding protein mal1 in obesity and insulin resistance. Diabetes 52:300–307
31. Glatz JF, van der Vusse GJ (1996) Cellular fatty acid-binding proteins: their function and physiological significance. Prog Lipid Res 35:243–282
32. Kershaw EE, Hamm JK, Verhagen LA, Peroni O, Katic M, Flier JS (2006) Adipose triglyceride lipase: function, regulation by insulin, and comparison with adiponutrin. Diabetes 55:148–157
33. Robidoux J, Kumar N, Daniel KW, Moukdar F, Cyr M, Medvedev AV, Collins S (2006) Maximal beta3-adrenergic regulation of lipolysis involves Src and epidermal growth factor receptor-dependent ERK1/2 activation. J Biol Chem 81:37794–37802
34. Cao W, Medvedev AV, Daniel KW, Collins S (2001) Beta-Adrenergic activation of p38 MAP kinase in adipocytes: cAMP induction of the uncoupling protein 1 (UCP1) gene requires p38 MAP kinase. J Biol Chem 276:27077–27082
35. Chmurzynska A (2006) The multigene family of fatty acid-binding proteins (FABPs): function, structure and polymorphism. J Appl Genet 47:39–48
36. McArthur MJ, Atshaves BP, Frolov A, Foxworth WD, Kier AB, Schroeder F (1999) Cellular uptake and intracellular trafficking of long chain fatty acids. J Lipid Res 40:1371–1383
37. Thumser AE, Storch J (2000) Liver and intestinal fatty acid-binding proteins obtain fatty acids from phospholipid membranes by different mechanisms. J Lipid Res 41:647–656
38. Carey JO, Neufer PD, Farrar RP, Veerkamp JH, Dohm GL (1994) Transcriptional regulation of muscle fatty acid-binding protein. Biochem J 298:613–617
39. Glatz JF, van Breda E, Keizer HA, de Jong YF, Lakey JR, Rajotte RV, Thompson A, van der Vusse GJ, Lopaschuk GD (1994) Rat heart fatty acid-binding protein content is increased in experimental diabetes. Biochem Biophys Res Commun 199:639–646
40. Blaak EE, Glatz JF, Saris WH (2001) Increase in skeletal muscle fatty acid binding protein (FABPC) content is directly related to weight loss and to changes in fat oxidation following a very low calorie diet. Diabetologia 44:2013–2017
41. Dallner OS, Chernogubova E, Brolinson KA, Bengtsson T (2006) β3-Adrenergic receptors stimulate glucose uptake in brown adipocytes by two mechanisms independently of GLUT4 translocation. Endocrinology 147:5730–5739
42. Yu XX, Lewin DA, Forrest W, Adams SH (2002) Cold elicits the simultaneous induction of fatty acid synthesis and beta-oxidation in murine brown adipose tissue: prediction from differential gene expression and confirmation in vivo. FASEB J 16:155–168
43. Watson RT, Pessin JE (2006) Bridging the GAP between insulin signaling and GLUT4 translocation. Trends Biochem Sci 31:215–222
44. Gasparetti AL, De Souza CT, Pereira-da-Silva M, Oliveira RL, Saad MJ, Carneiro EM, Velloso LA (2003) Cold exposure induces tissue-specific modulation of the insulin-signalling pathway in Rattus norvegicus. J Physiol 552:149–162
45. Ryden M, Jocken J, Van HV, Dicker A, Hoffstedt J, Wiren M, Blomqvist L, Mairal A, Langin D, Blaak E, Arner P (2007) Comparative studies of the role of hormone sensitive lipase and adipose triglyceride lipase in human fat cell lipolysis. Am J Physiol Endocrinol Metab 292:E1847–E1855
46. Lass A, Zimmermann R, Haemmerle G, Riederer M, Schoiswohl G, Schweiger M, Kienesberger P, Strauss JG, Gorkiewicz G, Zechner R (2006) Adipose triglyceride lipase-mediated lipolysis of cellular fat stores is activated by CGI-58 and defective in Chanarin-Dorfman Syndrome. Cell Metab 3:309–319
47. Yang X, Lu X, Lombès M, Rha GB, Chi YI, Guerin TM, Smart EJ, Liu J (2010) The G(0)/G(1) switch gene 2 regulates adipose lipolysis through association with adipose triglyceride lipase. Cell Metab 11:194–205
48. Lindgren EM, Nielsen R, Petrovic N, Jacobsson A, Mandrup S, Cannon B, Nedergaard J (2004) Noradrenaline represses PPAR (peroxisome-proliferator-activated receptor) gamma2 gene expression in brown adipocytes: intracellular signalling and effects on PPARgamma2 and PPARgamma1 protein levels. Biochem J 82:597–606
49. Margareto J, Larrarte E, Marti A, Martinez JA (2001) Up-regulation of a thermogenesis-related gene (UCP1) and down-regulation of PPARgamma and aP2 genes in adipose tissue: possible features of the antiobesity effects of a beta3-adrenergic agonist. Biochem Pharmacol 61:1471–1478
50. Hochstrasser M (1996) Ubiquitin-dependent protein degradation. Annu Rev Genet 30:405–439

Lipids (2010) 45:491–500
DOI 10.1007/s11745-010-3420-5

ORIGINAL ARTICLE

Influence of Simvastatin on apoB-100 Secretion in Non-Obese Subjects with Mild Hypercholesterolemia

Heiner K. Berthold · Jessica Mertens · Julia Birnbaum · Susanne Brämswig · Thomas Sudhop · P. Hugh R. Barrett · Klaus von Bergmann · Ioanna Gouni-Berthold

Received: 25 January 2010 / Accepted: 14 April 2010 / Published online: 12 May 2010

Abstract Statins decrease apoB-100-containing lipoproteins by increasing their fractional catabolic rates through LDL receptor-mediated uptake. Their influence on hepatic secretion of these lipoproteins is controversial. The objective of the study was to examine the influence of simvastatin on the secretion of apoB-100-containing lipoproteins in fasting non-obese subjects. Turnover of apoB-100-containing lipoproteins was investigated using stable isotope-labeled tracers. Multicompartmental modeling was used to derive kinetic parameters. Eight male subjects (BMI 25 ± 3 kg/m^2) with mild hypercholesterolemia (LDL cholesterol 135 ± 30 mg/dL) and normal triglycerides (111 ± 44 mg/dL) were examined under no treatment (A), under chronic treatment with simvastatin 40 mg/day (B) and after an acute-on-chronic dosage of 80 mg simvastatin under chronic simvastatin treatment (C). Lipoprotein concentrations changed as expected under 40 mg/day simvastatin. Fractional catabolic rates increased in IDL and LDL but not in VLDL fractions versus control [VLDL +35% in B (n.s.) and +21% in C (n.s.); IDL +169% in B ($P = 0.08$) and +187% in C ($P = 0.032$); LDL +87% in B ($P = 0.025$) and +133% in C ($P = 0.025$)]. Chronic (B) and acute-on-chronic simvastatin treatment (C) did not affect lipoprotein production rates [VLDL −8 and −13%, IDL +47 and +38%, and LDL +19 and +30% in B and C, respectively (all comparisons n.s.)]. The data indicate that simvastatin does not influence the secretion of apoB-100-containing lipoproteins in non-obese subjects with near-normal LDL cholesterol concentrations.

Keywords Apolipoprotein B-100 · Lipoprotein · Cholesterol · Statin · Simvastatin · Gas chromatography/mass spectrometry · Kinetics · Stable isotopes · Turnover · Multicompartmental modeling

Abbreviations

apoB-100	Apolipoprotein B-100
BMI	Body mass index
CHOD-PAP	Cholesterol oxidase phenol aminoantipyrine peroxidase
EDTA	Ethylene-diamine-tetra-acetic acid
FCR	Fractional catabolic rate
GPO-PAP	Glycerol-3-phosphate oxidase phenol aminoantipyrine peroxidase
HDL	High-density lipoproteins
HMG	4-Hydroxy-3-methylglutaryl
IDL	Intermediate-density lipoproteins
LDL	Low-density lipoproteins

H. K. Berthold and J. Mertens have contributed equally.

H. K. Berthold · J. Mertens · J. Birnbaum · S. Brämswig · T. Sudhop · K. von Bergmann
Department of Clinical Pharmacology, University of Bonn, Bonn, Germany

H. K. Berthold (✉)
Lipid Clinic, Interdisciplinary Metabolism Center, Charité University Medicine Berlin, Campus Virchow Clinic, Augustenburger Platz 1, 13353 Berlin, Germany
e-mail: heiner.berthold@charite.de

P. H. R. Barrett
School of Medicine and Pharmacology, University of Western Australia, Perth, Australia

I. Gouni-Berthold
Department of Internal Medicine II, University of Cologne, Cologne, Germany

PR Production rate
VLDL Very low-density lipoproteins

Introduction

3-Hydroxy-3 methylglutaryl (HMG) coenzyme A-reductase inhibitors (statins) have an established role in the treatment of hypercholesterolemia. Their efficacy in reducing cardiovascular morbidity and mortality in secondary [1, 2] and primary prevention [3] has been demonstrated in large randomized trials. HMG-CoA-reductase inhibitors inhibit competitively the rate-limiting enzyme of endogenous cholesterol biosynthesis. As a consequence, the intracellular pool of free cholesterol decreases and low-density lipoprotein (LDL) receptors are up-regulated, leading to an increased receptor-mediated clearance of LDL from plasma [4]. This mechanism is responsible for a large proportion of their cholesterol-lowering effect. However, a statin-induced decrease in lipoprotein production has also been proposed as a mechanism for their lipid-lowering effects [5]. The underlying mechanisms in vivo, however, that would mediate such an effect, are not fully understood. Except for their pronounced cholesterol-lowering properties, statins have also a modest effect (about 15–20%) in decreasing triglyceride concentrations [6]. In subjects with high intra-abdominal fat stores, an increased flux of free fatty acids to the liver produces an increased rate of hepatic triglyceride synthesis, which in turn leads to increased very low-density lipoprotein (VLDL) production, since the latter is partly determined by the intracellular availability of triglycerides [7–9]. This is also found in subjects with type 2 diabetes mellitus [10, 11] and there are a number of studies showing that, in this pathophysiological state, statins are able to decrease lipoprotein production [12, 13]. Interestingly, in obese individuals it has been shown that statins increase the catabolism of apoB-100-containing lipoproteins but do not alter their rates of production or secretion [14].

In the present study we focused on subjects with near normal body weight (mean body mass index 25 $\pm$ 3 kg/m^2) and normal serum triglyceride concentrations to investigate, in the fasting state, whether statins influence hepatic lipoprotein production. Since recent evidence suggests that the supply of cholesterol available for incorporation into nascent lipoprotein particles also exerts a regulatory influence on apoB secretion by the liver [15, 16], we investigated in addition the acute inhibitory effects of a high bolus dose of simvastatin in order to inhibit cholesterol synthesis and to stimulate LDL receptor expression to a maximum degree.

The main goal of the present study was to determine the influence of simvastatin on apoB-100 appearance rates and lipoprotein kinetics in fasting non-obese subjects with mild hypercholesterolemia. For this purpose, each subject was investigated with three turnover protocols: once without treatment, once during chronic simvastatin treatment at a standard dosage, and once during chronic simvastatin treatment after an additional acute-on-chronic high bolus dose of simvastatin.

Experimental Procedures

Study Design

This was an open label, three-way cross-over trial evaluating lipoprotein turnover under control (no treatment) conditions (phase A), under chronic simvastatin treatment (phase B) and under chronic simvastatin treatment after additional acute-on-chronic dosage (phase C). All subjects provided written informed consent. The study protocol was approved by the Ethics Committee of the Medical Faculty of the University of Bonn, and all procedures were performed in accordance with the Helsinki Declaration and its current revision. The trial was publicly registered (ClinicalTrials.gov Identifier: NCT00905541).

Study Population and Drug Treatment

Eight male healthy volunteers with mild hypercholesterolemia [LDL cholesterol (LDL-C) average 135 mg/dL] and normal triglycerides (average 111 mg/dL) were recruited on campus and in the community (to convert mg/dL into mmol/L multiply with 0.0259 for cholesterol and with 0.0114 for triglycerides). Main exclusion criteria were coronary events during the last year, unstable angina, active liver disease or persistent elevations of liver transaminases, renal insufficiency, diabetes mellitus or impaired glucose tolerance, thyroid dysfunction, alcohol abuse, any other metabolic disease or treatment with drugs affecting lipid metabolism. Subjects were unrelated at the first and second degree.

Each subject was studied three times. Five subjects were studied in the sequence A–B–C and three in the sequence B–C–A. Before phase A there was a wash-out period of at least 8 weeks for all drugs affecting lipid metabolism. Before phase B, subjects were treated with simvastatin 40 mg once daily in the evening for at least 6 weeks. The last dose before the infusion studies was taken at 07:00 PM on the preceding day. Before phase C, subjects took their normal evening dose at 07:00 PM; in addition, they received an oral dose of 80 mg simvastatin in the morning of the turnover protocol 1 h before isotope infusion.

Medication with 40 mg/day was continued through the whole sampling period of the turnover studies (phases B and C).

Experimental Protocol For In Vivo Stable Isotope Kinetics

The subjects were asked to adhere to their usual nutritional habits throughout the entire trial. For 4 days before turnover studies they kept a food diary to document nutrient intake. During the 4 days preceding the second and third turnover study, the subjects were asked to consume an identical diet based on their previously documented food diaries and again kept 4-day food diaries.

The subjects were admitted to the metabolic ward on the day of the infusion study at 07:30 AM. The last meal on the previous day was taken at 07:00 PM. This meal was a standardized meal provided by the investigators. After 07:00 PM neither food nor calorie-containing beverages were allowed until the end of the infusion study on the next day at 07:00 PM in order to prevent nutrient-induced lipoprotein production. Drinking of tap water or mineral water was permitted after 12:00 noon on the study day. Clinical status and vital signs were recorded during the infusion. Measurements of body weight and body composition (including body fat and body lean mass, intra- and extracellular water), performed between 08:00 and 09:00 AM on the study day, were determined by bioelectrical impedance analysis (Multi Frequency Analyzer B.I.A. 2000-M; Data Input, Frankfurt, Germany) in combination with the manufacturer's software Nutri4.

In the morning of the study day the subjects received an indwelling cannula for blood drawing in one forearm and another in the other forearm for isotope infusion. They remained in a recumbent position (45°) from 08:00 AM until the end of the infusion. At 08:00 AM they drank 400 mL of mineral water. At 09:00 AM, tracer administration was started with a bolus injection of [D_3]leucine (1.4 mg/kg body weight) immediately followed by a continuous infusion of [D_3]leucine (1.4 mg kg^{-1} h^{-1}) for a period of 10 h. Tri-deuterated leucine (L-[5,5,5-$^2H_3$]leucine) was obtained from MassTrace (Woburn, MA, USA), was dissolved in saline and was tested sterile and pyrogen-free.

During each turnover study, two baseline samples were drawn immediately before 09:00 AM and further blood samples were obtained for up to 240 h. Isotopic enrichment of free leucine in plasma was determined at 16 time points, in VLDL-apoB-100 at 20 time points, in intermediate-density lipoprotein (IDL)-apoB at 13 time points and in LDL-apoB at 12 time points.

Measurement of Lipoprotein and apoB Concentrations

Lipoprotein concentrations for pool size determinations were measured on the infusion days in eight separate samples. In each sample, cholesterol, triglycerides, and apoB-100 were determined in total blood and in the VLDL, IDL, and LDL fraction. Cholesterol and triglycerides were measured enzymatically according to the CHOD-PAP and the GPO-PAP method (Boehringer Mannheim, Germany), respectively. HDL cholesterol (HDL-C) was determined enzymatically after precipitation of apoB-100-containing lipoproteins [17]. The coefficient of variation for cholesterol measurements was 0.99% for total cholesterol, 2.64% for LDL-C, 2.22% for HDL-C and 1.14% for triglycerides. ApoB-100 concentration in plasma and in lipoprotein fractions was determined with a noncompetitive, enzyme-linked immunoabsorbent assay using immunopurified polyclonal antibodies on the Beckmann Array®-360 System (Beckmann Instruments, Munich, Germany).

Isolation of apoB-100 and Amino Acid Preparation

Lipoprotein Separation

Isolation of the lipoprotein fractions VLDL, IDL and LDL was performed using preparative sequential density ultracentrifugation. A 3.2-mL polycarbonate tube was filled with a 1.5-mL aliquot of plasma and 1.5 mL sodium chloride density solution (0.9%) and centrifuged at 16 °C in a TLA 100.4 rotor for 2.5 h at 100,000×*g* in an Optima TLX centrifuge (Beckmann Instruments, Munich, Germany). All used density solutions contained 1 g/L EDTA. After centrifugation, the supernatant containing VLDL (density $d < 1.006$ g/mL) was removed after tube-slicing with a CentriTube Slicer (Beckmann Instruments, Munich, Germany). To isolate the IDL fraction ($1.006 < d < 1.020$ g/mL), the remaining infranatant was transferred into a new tube adding a second, more dense sodium chloride solution (4.5%) and an analogous centrifugation step was started. After tube-slicing and transfer of the infranatant into a new tube the centrifugation procedure was repeated using an even more dense sodium chloride solution (15%) to separate the LDL lipoprotein fraction ($1.020 < d < 1.063$ g/mL).

ApoB-100 Separation, Isolation of Amino Acids and Amino Acid Derivatization

The apoB-100 of the lipoprotein fractions VLDL, IDL and LDL was isolated and purified using a previously described isopropanol precipitation method [18]. Sample preparation for gas chromatography–mass spectrometry was performed as previously described [19].

Determination of Isotopic Enrichment

Isotopic enrichment determination of leucine was performed on a Fisons GC8060/Trio 1000 quadrupole system (ThermoQuest, Egelsbach, Germany). The samples were injected into a 30 m × 0.32 mm, 0.25 μm DB-5MS capillary column (J & W Scientific, Rancho Cordova, CA, USA). Mass spectrometry was performed by negative-ion chemical ionization with methane as the reagent gas. Selected ion monitoring (SIM) of the leucine peak was performed for [$^2H_3$]-enrichment using the [M−HF] and [M−HF + 3] isotopomers ($m/z = 349$ and 352), respectively. Measurements were done in quadruplicates at baseline and in triplicates in subsequent samples. Because of the non-negligible mass associated with stable isotope tracers, raw enrichment data were transformed to tracer/tracee ratios using predescribed algorithms [20].

Kinetic Analysis

A multicompartmental model (Fig. 1) was used to describe VLDL-, IDL-, and LDL-apoB-100 isotopic enrichment data and to derive kinetic information. Each compartment or pool represents a group of kinetically homogenous particles. In the present study, the SAAM II program (SAAM Institute, Seattle, WA, USA) was used to fit the model to the observed tracer data. Metabolic parameters were subsequently derived from the model parameters giving the best fit. The model assumes that apoB-100 enters plasma through compartments 11, 21, or 31 (Fig. 1). Compartment 11 is used to describe the kinetics of apoB-100 in the VLDL subfraction. The VLDL particles in compartment 11 can be converted to IDL, or can be removed directly from plasma. The IDL section of the model is described by compartment 21. Particles in compartment 21 can be converted to LDL, or can be removed directly from the plasma. LDL-apoB-100 kinetics is described by compartment 31. IDL apoB can be derived from VLDL (compartment 11) or directly from the site of secretion. Similarly, LDL apoB can be derived from the delipidation cascade (IDL, compartment 21), or from the site of secretion.

Compartment apoB masses were included in the fitting procedure. After we fitted the model to the tracer/tracee data, apoB-100 fractional catabolic rates (FCR) and production rates (PR) were determined using the best fit. The FCR for all lipoprotein fractions were calculated by adding the individual rate constants, termed k values, leaving the compartments. For turnover calculation, we used a weighted, related to mass distribution, average of the turnover rates of individual pools. We were able to apply this model to all subjects studied under medication and under control conditions. All parameters were fitted as adjustables.

As indicated by the fractional distribution parameters d (Fig. 1), about 87% of the material was secreted as VLDL,

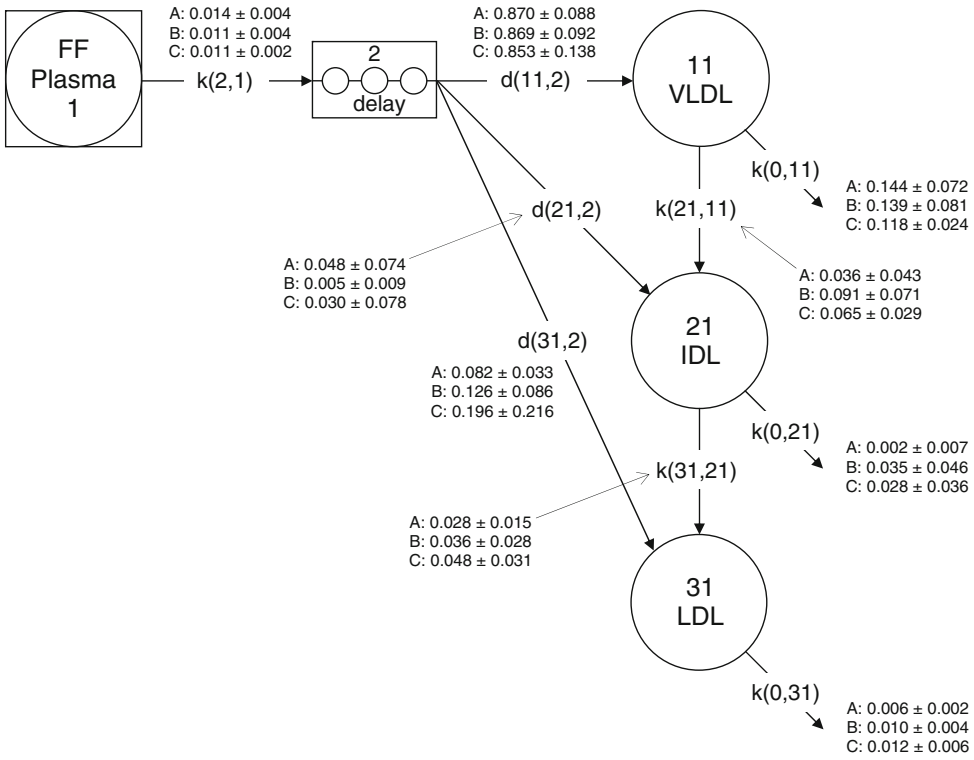

Fig. 1 Rate constants, pool sizes of apoB-100 and fractional distribution parameters out of the delay compartment in eight subjects under no-treatment conditions (phase A), during treatment with 40 mg/day simvastatin (phase B) and during chronic treatment with an additional oral bolus of 80 mg simvastatin (phase C). Unit for delay is given as hours ± SD, unit for rate constants is given as pools/d ± SD. *FF* forcing function

up to 4% as IDL and up to 8% as LDL. Under simvastatin treatment there was a trend towards a decrease in the proportion secreted as VLDL from 87 to 85%. However, these differences were not significant. There were significant differences between the main rate constants of the lipoprotein delipidation cascade between the three treatment phases. The conversion of VLDL to IDL was increased by simvastatin, as were the conversion from IDL to LDL and the final catabolism from the LDL compartment (see legend to Fig. 1).

Statistical Analysis

The primary study outcomes were the main kinetic parameters pool size, FCR, and PR determined by multicompartmental modeling. The null hypothesis was no change in kinetic parameters between treatment phases. Statistical analysis was performed using the non-parametric Friedman test to determine overall differences. Multiple comparisons between groups were performed using Wilcoxon signed rank tests. The trial was powered to achieve statistically significant results in the event of six out of eight cases showing unidirectional changes for one parameter. Statistical analysis was carried out using StatView Version 5.0 (SAS Institute, Inc., Cary, NC, USA). Compartment modeling was performed using SAAM II (Simulation, Analysis, and Modeling Software for Kinetic Analysis), Version 1.1.2 (SAAM Institute, University of Washington, WA, USA). Dietary protocols were evaluated using Prodi Version 4.5 Software (Wissenschaftliche Verlagsgesellschaft, Stuttgart, Germany).

Results

Characteristics of Subjects

Table 1 shows the baseline characteristics of the subjects. Mean age was 43 years and subjects were non-obese with a mean BMI of 25.3 kg/m^2. Lean body mass and fat mass were 76 and 24%, respectively, as measured by bioelectrical impedance analysis. Their apolipoprotein E (apoE) phenotype consisted of E2 and/or E3 alleles. None of the subjects smoked. All had normal fasting plasma glucose and insulin concentrations, and normal thyroid hormone levels. All other blood values were also in the normal range. Their mean ± SD baseline HDL cholesterol concentration was 35 ± 7 mg/dL. All subjects maintained their body weights throughout the study. Analysis of their dietary protocols did not show any differences between the three treatment phases (Table 2). Medication compliance was excellent as documented by pill count.

Table 1 Baseline characteristics of the subjects

Parameter	Mean ± SD	Range
Age (years)	43 ± 15	28–67
Height (cm)	180 ± 6	170–187
Weight (kg)	82 ± 7	74–95
Body mass index (kg/m^2)	25.3 ± 2.7	21.5–29.4
Lean body mass (%)	76 ± 4	69–80
Body fat mass (%)	24 ± 4	20–31
ApoE phenotype	E2/E3 (2 subjects) E3/E3 (6 subjects)	
HDL cholesterol (mg/dL)	35 ± 7	23–44
Plasma glucose (mg/dL)[a]	74 ± 7	67–89
Plasma insulin (mU/L)[a], normal range 3–17 mU/L	5.4 ± 2.1	1.7–9.0
Thyroid stimulating hormone (mU/L)[b]	1.2 ± 0.7	0.3–2.2

[a] All subjects were in the non-insulin resistant state, as analyzed by the homeostasis model assessment [(insulin × glucose)/405 < 1]

[b] All subjects were euthyroid

Lipoprotein Concentrations and Relative Composition

Lipoprotein Concentrations

Table 3 shows the lipoprotein concentrations at baseline (A) and during the two treatment phases (B and C). Between phases A and B total cholesterol, VLDL-C, IDL-C, and LDL-C decreased significantly by 27, 34, 44, and 29%, respectively. Decreases in phase C were significantly more pronounced when compared to phase B. Similarly, total plasma triglycerides, VLDL-, IDL-, and LDL-triglycerides decreased by 19, 13, 27, and 24% with significantly greater effects for plasma and VLDL-triglycerides during phase C. Plasma apoB-100, VLDL-, IDL-, and LDL-apoB-100 decreased significantly by 38, 25, 42, and 37%. There was no significant difference of phase B versus phase C.

Lipoprotein Composition

The ratio of cholesterol to apoB-100 indicates the density of lipoprotein particles, since each lipoprotein particle contains only one apoB-100 molecule. Under baseline conditions, the cholesterol content in relation to the apoB-100 content was highest in VLDL (ratio 2.6), followed by IDL (ratio 2.0) and LDL (ratio 1.7). Simvastatin treatment decreased the ratio in VLDL significantly by 14%, while it was unchanged in IDL and increased significantly in LDL by 13% (Table 3). In phase C, the decrease in VLDL was even more pronounced (−30%) and it reached also statistical significance in IDL (−18%), while the relative composition of LDL was not significantly

Table 2 Dietary protocols

Parameter	Phase A	Phase B	Phase C
Total energy (kcal/day)	2,363 ± 580	2,272 ± 564	2,321 ± 592
Energy per kg body weight (kcal/day)	29 ± 7	27 ± 5	28 ± 6
Proteins (%)	15 ± 2	15 ± 2	15 ± 3
Carbohydrates (%)	48 ± 7	46 ± 7	47 ± 8
Fats (%)	36 ± 6	38 ± 6	38 ± 7
Saturated fats (%)	14 ± 2	15 ± 3	15 ± 3
Monounsaturated fats (%)	12 ± 3	12 ± 2	13 ± 3
Polyunsaturated fats (%)	5.5 ± 1.3	6.1 ± 1.6	5.9 ± 1.7
Cholesterol (mg/day)	365 ± 123	373 ± 123	361 ± 144
Fiber (g/day)	25 ± 9	24 ± 7	24 ± 8
Alcohol (%)	0.1 ± 0.19	0.05 ± 0.09	0.1 ± 0.2

Individual data are mean values of 4-day dietary protocols. There were no statistically significant differences between phases A, B, and C

Table 3 Lipoprotein concentrations at no treatment (Phase A), during treatment with 40 mg/day simvastatin (Phase B) and during treatment with 40 mg/day simvastatin and an additional oral bolus of 80 mg simvastatin (Phase C)

Parameter (mean ± SD)	Phase A	Phase B	Phase C	% change A versus B†	% change A versus C†	% change B versus C†	Overall *P* value‡
Cholesterol (mg/dL)							
Total cholesterol	238 ± 35	172 ± 17	154 ± 17	–27 ± 9.6**	–35 ± 7**	–10 ± 9**	0.0011
VLDL-C	31 ± 24	17 ± 10	13 ± 8	–34 ± 35**	–44 ± 36**	–18 ± 20*	0.0312
IDL-C	29 ± 9	16 ± 6	12 ± 5	–44 ± 13**	–55 ± 13**	–18 ± 23**	0.0008
LDL-C	135 ± 30	94 ± 17	82 ± 15	–29 ± 14**	–38 ± 12**	–12 ± 13**	0.0008
Triglycerides (mg/dL)							
Plasma TG	111 ± 44	87 ± 31	77 ± 28	–19 ± 20**	–28 ± 19**	–11 ± 10**	0.0111
VLDL TG	70 ± 35	58 ± 27	49 ± 25	–13 ± 30*	–24 ± 30**	–12 ± 16*	0.135
IDL TG	9 ± 2	6 ± 2	6 ± 2	–27 ± 16**	–27 ± 20**	+3 ± 27	0.0098
LDL TG	19 ± 4	14 ± 5	13 ± 3	–24 ± 15**	–32 ± 10**	–9 ± 16	0.0046
ApoB-100 (mg/dL)							
Plasma apoB	108 ± 16	66 ± 11	59 ± 12	–38 ± 10**	–46 ± 7**	–11 ± 13*	0.0022
VLDL apoB	11 ± 6	8 ± 4	7 ± 2	–25 ± 29*	–20 ± 32*	+18 ± 69	0.223
IDL apoB	15 ± 5	8 ± 3	8 ± 4	–42 ± 16**	–44 ± 17**	–2 ± 28	0.0022
LDL apoB	80 ± 13	50 ± 10	45 ± 7	–37 ± 12**	–43 ± 8**	–8 ± 13	0.0022
Ratio cholesterol/apoB							
Ratio C/apoB in plasma	2.2 ± 0.2	2.6 ± 0.3	2.7 ± 0.3	+20 ± 12**	+21 ± 12**	+2 ± 9	0.0022
Ratio C/apoB in VLDL	2.6 ± 1.1	2.1 ± 0.4	1.7 ± 0.6	–14 ± 23*	–30 ± 28**	–20 ± 22**	0.0015
Ratio C/apoB in IDL	2.0 ± 0.2	1.9 ± 0.2	1.6 ± 0.2	–2 ± 12	–18 ± 14**	–15 ± 15**	0.0547
Ratio C/apoB in LDL	1.7 ± 0.2	1.9 ± 0.1	1.8 ± 0.1	+13 ± 11**	+8 ± 13	–5 ± 8	0.0847
Ratio triglycerides/apoB							
Ratio TG/apoB in plasma	1.0 ± 0.4	1.3 ± 0.5	1.3 ± 0.4	+39 ± 54*	+35 ± 41*	+1 ± 14	0.216
Ratio TG/apoB in VLDL	6.5 ± 1.4	7.6 ± 1.6	6.4 ± 1.9	+18 ± 18*	+2 ± 34	–15 ± 23**	0.197
Ratio TG/apoB in IDL	0.6 ± 0.1	0.8 ± 0.2	0.9 ± 0.3	+37 ± 53*	+49 ± 67*	+13 ± 41	0.093
Ratio TG/apoB in LDL	0.2 ± 0.1	0.3 ± 0.1	0.3 ± 0.1	+24 ± 32	+21 ± 26*	–2 ± 16	0.43

C cholesterol, *TG* triglyceride and *apoB* apolipoprotein B-100

* $P < 0.1$, ** $P < 0.05$

† Wilcoxon signed rank test

‡ Friedman test

changed. The ratio of triglycerides to apoB-100 showed a large variability. Under baseline conditions, VLDL had the largest triglyceride content (ratio 6.5) while it was lower in IDL (ratio 0.6) and LDL (ratio 0.2). Treatment did not significantly affect the relative composition, but an increase of the ratio of 20 to 50% indicated that treatment decreased apoB-100 to a greater extent than triglyceride content.

Kinetics of apoB-100

Detailed kinetic information obtained by multicompartmental model analysis is summarized in Table 4 and in Fig. 1. Mean VLDL, IDL, and LDL apoB-100 tracer/tracee ratios during phases A, B and C are shown in Fig. 2.

In short, IDL and LDL apo-B-100 pool sizes decreased significantly during phases B and C as compared to phase A [for IDL −42% ($P = 0.012$) and −49% ($P = 0.012$)]; for LDL [−36% ($P = 0.012$) and −42% ($P = 0.012$), for phases B and C respectively]. Pool size tended to decrease in VLDL [−25% in B ($P = 0.069$) and −20% in C ($P = 0.069$)]. There were no significant differences between phase B and C.

Fractional catabolic rates were significantly higher in IDL and LDL during phase B (+169 and +87%). The change in VLDL FCR did not reach statistical significance.

Table 4 Pool sizes, fractional catabolic rates, and production rates of VLDL, IDL, and LDL apoB-100 during phases A, B, and C

Parameter (mean ± SD; range; *P* value)	Phase A	Phase B	Phase C	% change A versus B†	% change A versus C†	% change B versus C†	Overall *P* value‡
VLDL apoB-100							
Pool size (mg)	419 ± 249 (148–856)	293 ± 146 (69–472)	279 ± 99 (135–421)	−25 ± 30 (−62 to +22) $P = 0.069$	−20 ± 32 (−51 to +37) $P = 0.069$	+17 ± 68 (−33 to +177) $P = 0.67$	0.22
FCR (pools/d)	4.3 ± 1.6 (1.6–6.6)	5.5 ± 2.6 (2.9–11.0)	4.4 ± 1.1 (2.3–5.6)	+35 ± 52 (−13 to +130) $P = 0.21$	+21 ± 76 (−50 to +195) $P = 0.89$	−15 ± 50 (−80 to +56) $P = 0.48$	0.61
PR (mg kg^{-1} d^{-1})	18 ± 5 (12–26)	16 ± 6 (9–27)	15 ± 6 (7–23)	−8 ± 26 (−33 to +27) $P = 0.26$	−13 ± 41 (−64 to +47) $P = 0.26$	−13 ± 52 (−76 to +87) $P = 0.78$	0.61
IDL apoB-100							
Pool size (mg)	531 ± 171 (207–713)	297 ± 102 (193–438)	258 ± 82 (145–381)	−42 ± 16 (−60 to −7) $P = 0.0117$	−49 ± 12 (−69 to −30) $P = 0.0117$	−10 ± 19 (−29 to +31) $P = 0.16$	0.0015
FCR (pools/d)	0.73 ± 0.32 (0.41–1.32)	1.71 ± 1.01 (0.89–4.02)	1.82 ± 0.57 (1.0–2.7)	+169 ± 184 (+9 to +559) $P = 0.08$	+187 ± 147 (+27 to +472) $P = 0.032$	+102 ± 125 (−49 to +368) $P = 0.093$	0.0008
PR (mg kg^{-1} d^{-1})	4.3 ± 1.5 (2.9–7.4)	5.6 ± 2.6 (2.0–10)	5.4 ± 1.7 (4.1–9.5)	+47 ± 87 (−48 to +194) $P = 0.26$	+38 ± 65 (−34 to +175) $P = 0.21$	+79 ± 103 (−59 to +270) $P = 0.67$	0.20
LDL apoB-100							
Pool size (mg)	2,932 ± 437 (2,073–3,547)	1,841 ± 305 (1,415–2,410)	1,670 ± 206 (1,387–2,011)	−36 ± 12 (−52 to −22) $P = 0.0117$	−42 ± 8 (−52 to −29) $P = 0.0117$	−8 ± 13 (−23 to +14) $P = 0.124$	0.0022
FCR (pools/d)	0.14 ± 0.04 (0.09–0.20)	0.23 ± 0.10 (0.12–0.40)	0.28 ± 0.14 (0.12–0.57)	+87 ± 115 (−19 to +342) $P = 0.0251$	+133 ± 173 (−17 to +522) $P = 0.0251$	+41 ± 61 (−49 to +148) $P = 0.093$	0.011
PR (mg kg^{-1} d^{-1})	5.1 ± 1.9 (3.3–9.2)	5.2 ± 2.2 (3.0–9.6)	5.6 ± 2.7 (3.1–11.1)	+19 ± 76 (−67 to +162) $P = 0.69$	+30 ± 90 (−62 to +203) $P = 0.67$	+30 ± 61 (−51 to +149) $P = 0.40$	0.69

FCR fractional catabolic rate, *PR* production rate, *apoB-100* apolipoprotein B-100

† Wilcoxon signed-rank test

‡ Friedman test

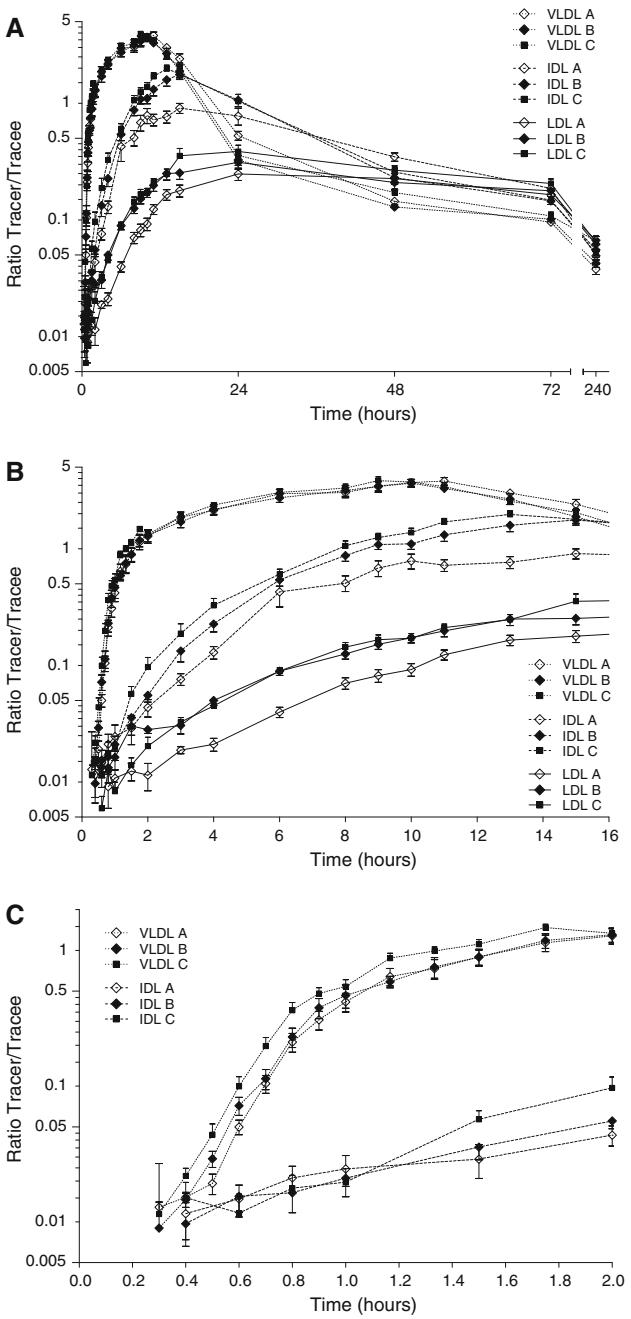

Fig. 2 Leucine tracer/tracee ratios for VLDL apoB-100 under no-treatment conditions (phase A), during treatment with 40 mg/day simvastatin (B), and after an additional bolus of 80 mg simvastatin during chronic treatment with 40 mg/day (C). Results are means ± SEM. To increase readability, *panel A* shows the whole time course of the study until 240 h, *panel B* until 16 h and *panel C* until 2 h (only VLDL and IDL)

During phase C, IDL and LDL FCRs tended to be further significantly increased (+187 and +133%) in comparison to phase B, while there was no difference between phases B and C in the VLDL FCR.

Regarding production rates, mean values were decreased in VLDL and increased in IDL and LDL, however these changes were not statistically significant.

Discussion

There is experimental [21, 22] and clinical [23–27] evidence suggesting that HMG-CoA-reductase inhibitors decrease the hepatic secretion of VLDL apoB-100, the precursor of the major apoB-100-containing lipoproteins. ApoB-100 is synthesized by the liver and secreted primarily with VLDL. Once in plasma, VLDL is subjected to hydrolysis by lipoprotein lipase that converts the triglyceride-rich particles into IDL and LDL. Therefore, the fall in LDL concentrations during statin treatment could also be due to a reduction in the conversion rate of VLDL to LDL, in addition to the enhanced receptor-mediated fractional removal of LDL from the circulation. This has been suggested by early investigations using radioisotope tracers [28]. In the present study we investigated apoB-100 lipoprotein turnover with a special focus on lipoprotein secretion or production.

The influence of simvastatin on apoB-100 kinetics was investigated in fasting non-obese subjects with near normal LDL cholesterol levels and normal triglycerides, to test the hypothesis that simvastatin decreases production of apoB-100-containing lipoproteins. Fasting state was chosen since it has been shown that the major predictor for VLDL apoB-100 production rate is feeding [29]. In our study, inhibition of HMG-CoA reductase (and thus cholesterol synthesis) using a standard dose of the most widely used statin resulted in the following major findings: Pools sizes of all three lipoprotein fractions decreased due to increased FCRs. FCRs were significantly increased in IDL and LDL. In VLDL, mean FCR also increased slightly but the change did not reach statistical significance due to a large variation of the response. Production rates tended to decrease in VLDL and to increase in IDL and LDL lipoprotein fractions, as derived from the multicompartment model.

It is generally assumed that statins lower cholesterol by enhancing lipoprotein catabolism through a statin-induced up-regulation of hepatic LDL receptors. However, additional mechanisms have been postulated, such as the production of an apoB-100-containing lipoprotein particle that is a better ligand for the LDL receptor or a reduced production of LDL apoB-100 due to either a decreased secretion of LDL directly into the plasma, or to a decreased conversion of VLDL to LDL (via IDL) [30]. Decreased conversion may be due to either reduced secretion of hepatic VLDL or increased removal of VLDL (and IDL) from the plasma by up-regulated LDL receptors. The

findings of our study confirm and expand these hypotheses. We found a clearly enhanced catabolic rate of LDL (FCRs increased by 87 and 133%, phases B and C, respectively). It should be pointed out that under our experimental conditions in phase C, acute-on-chronic statin administration, we achieved a situation in vivo where the expression of the LDL receptor can be expected to be maximal. Our data support the assumption that statins induce the production of a lipoprotein particle that is a better ligand for the LDL receptor, since the catabolic rate also of IDL but not of VLDL increased. We found that simvastatin treatment was associated with increased removal rate constants of IDL and LDL ($k(0,21)$ and $k(0,31)$). This finding could be explained by the simvastatin-induced changes in the composition of apoB-100-containing lipoproteins, thus increasing their affinity for the LDL receptor, as previously described [30]. The acute large dose of statin, however, was not reflected in changes to apoB-100 kinetic variables although cholesterol was reduced in lipoprotein fractions. These findings suggest that a further up-regulation of the processes responsible for the metabolism and clearance of apoB-100 from plasma is not possible due to the uncoupling of the statin effect on cholesterol concentrations (and synthesis?) and the impact on apoB-100 kinetics.

Our subjects had baseline VLDL PR and FCR very similar to those previously described in the literature for normolipidemic subjects [31]. Our data show that under simvastatin treatment the VLDL PR was not significantly decreased. Our results are in agreement to those of Lamon-Fava et al. [32] who showed that atorvastatin does not alter the VLDL PR of subjects with apo B-100 PR within the normal range of normolipidemic men and women. The VLDL-lowering effect (decrease in pool size of approximately 25%) is probably due to an increased catabolism of VLDL particles, although the VLDL FCR showed a large variability in the response to statin treatment from a decrease of −13% to an increase of +130%, whereas the variability in PR was not as great.

Regarding the observed increase in the LDL FCR, our results are in agreement to the results of Malmendier et al. [33] who, using radiolabeled isotopes, showed in normocholesterolemic subjects that simvastatin increases LDL FCR, and to those of Parhofer et al. [34] who found that in subjects with combined hyperlipidemia pravastatin had no effect on the kinetics of VLDL but was associated with an increased FCR of LDL. However, in a study in subjects with combined hyperlipidemia, Cuchel et al. [35] showed that lovastatin has no significant influence on the FCR of VLDL, IDL or LDL, but there was a significant decrease by 25 to 35% in the PRs in all three fractions. Differences in the characteristics of the subjects, study design, methodology and kinetic model may account for the differences in results among the studies. In particular, the relatively low baseline FCRs in our study may be explained by these differences.

In summary, it could be postulated that the reduction of LDL by statins through a decreased production of apoB can be assumed mainly in hyperlipidemic, but not in normolipidemic subjects [23–28, 35, 36]. Thus, higher baseline cholesterol and/or high triglyceride concentrations seem to be a prerequisite for this mechanism of action, which supports the hepatic lipid-availability hypothesis [7, 8].

The study has a number of limitations. Multicompartmental analyses usually require steady state conditions, which may not have been perfectly reached in phase C of our study, although mass changes were modeled in parallel. However, in lipoprotein turnover studies samples are usually taken over several days and a strict steady state cannot be assumed, unless subjects are completely fasted or continuously fed, both being unphysiological conditions. Another limitation may be the power of the statistical analyses. It has been shown though, that physiologically meaningful results in paired-design studies can be obtained with approx. eight subjects [37].

In conclusion, our data suggest that simvastatin affects mostly the metabolism of apoB-100-containing lipoproteins through an increase in their catabolic rate, which is further robustly increased after an acute-on-chronic statin administration. The lipid-lowering effect of simvastatin is not mediated through a decrease in apoB-100 lipoprotein production rates.

Acknowledgments The authors wish to thank Mrs. Anja Kerksiek for her excellent technical assistance.

Conflict of interest statement None.

References

1. Sacks FM, Pfeffer MA, Moye LA, Rouleau JL, Rutherford JD, Cole TG, Brown L, Warnica JW, Arnold JM, Wun CC, Davis BR, Braunwald E (1996) The effect of pravastatin on coronary events after myocardial infarction in patients with average cholesterol levels. Cholesterol and recurrent events trial investigators. N Engl J Med 335:1001–1009
2. Scandinavian Simvastatin Survival Study Group (1994) Randomized trial of cholesterol lowering in 4444 patients with coronary heart disease: the Scandinavian Simvastatin Survival Study (4S). Lancet 334:1383–1389
3. Shepherd J, Cobbe SM, Ford I, Isles CG, Lorimer AR, Macfarlane PW, McKillop JH, Packard CJ (1995) Prevention of coronary heart disease with pravastatin in men with hypercholesterolemia. West of Scotland coronary prevention study group. N Engl J Med 333:1301–1307
4. Bilheimer DW, Grundy SM, Brwon MS, Goldstein JL (1983) Mevinolin and colestipol stimulate receptor-mediated clearance of low density lipoproteins from plasma in familial hypercholesterolemia heterozygotes. Proc Natl Acad Sci USA 80:4124–4128

5. Marais AD, Naoumova RP, Firth JC, Penny C, Neuwirth CK, Thompson GR (1997) Decreased production of low density lipoprotein by atorvastatin after apheresis in homozygous familial hypercholesterolemia. J Lipid Res 38:2071–2078
6. Schaefer EJ, McNamara JR, Tayler T, Daly JA, Gleason JL, Seman LJ, Ferrari A, Rubenstein JJ (2004) Comparisons of effects of statins (atorvastatin, fluvastatin, lovastatin, pravastatin, and simvastatin) on fasting and postprandial lipoproteins in patients with coronary heart disease versus control subjects. Am J Cardiol 93:31–39
7. Dixon JL, Ginsberg HN (1993) Regulation of hepatic secretion of apolipoprotein B-containing lipoproteins: information obtained from cultured liver cells. J Lipid Res 34:167–179
8. Sniderman AD, Cianflone K (1993) Substrate delivery as a determinant of hepatic apoB secretion. Arterioscler Thromb 13:629–636
9. Cummings MH, Watts GF, Pal C, Umpleby M, Hennessy TR, Naoumova R, Sonksen PH (1995) Increased hepatic secretion of very-low-density lipoprotein apolipoprotein B-100 in obesity: a stable isotope study. Clin Sci (Lond) 88:225–233
10. Cummings MH, Watts GF, Umpleby AM, Hennessy TR, Naoumova R, Slavin BM, Thompson GR, Sonksen PH (1995) Increased hepatic secretion of very-low-density lipoprotein apolipoprotein B-100 in NIDDM. Diabetologia 38:959–967
11. Duvillard L, Pont F, Florentin E, Galland-Jos C, Gambert P, Verges B (2000) Metabolic abnormalities of apolipoprotein B-containing lipoproteins in non-insulin-dependent diabetes: a stable isotope kinetic study. Eur J Clin Invest 30:685–694
12. Myerson M, Ngai C, Jones J, Holleran S, Ramakrishnan R, Berglund L, Ginsberg HN (2005) Treatment with high-dose simvastatin reduces secretion of apolipoprotein B-lipoproteins in patients with diabetic dyslipidemia. J Lipid Res 46:2735–2744
13. Ouguerram K, Magot T, Zair Y, Marchini JS, Charbonnel B, Laouenan H, Krempf M (2003) Effect of atorvastatin on apolipoprotein B-100 containing lipoprotein metabolism in type-2 diabetes. J Pharmacol Exp Ther 306:332–337
14. Chan DC, Watts GF, Barrett PH, Mori TA, Beilin LJ, Redgrave TG (2002) Mechanism of action of a 3-hydroxy-3-methylglutaryl coenzyme a reductase inhibitor on apolipoprotein B-100 kinetics in visceral obesity. J Clin Endocrinol Metab 87:2283–2289
15. Thompson GR, Naoumova RP, Watts GF (1996) Role of cholesterol in regulating apolipoprotein B secretion by the liver. J Lipid Res 37:439–447
16. Pease RJ, Leiper JM (1996) Regulation of hepatic apolipoprotein-B-containing lipoprotein secretion. Curr Opin Lipidol 7:132–138
17. Burstein M, Scholnick HR, Morfin R (1970) Rapid method for the isolation of lipoproteins from human serum by precipitation with polyanions. J Lipid Res 11:583–595
18. Egusa G, Brady DW, Grundy SM, Howard BV (1983) Isopropanol precipitation method for the determination of apolipoprotein B specific activity and plasma concentrations during metabolic studies of very low density lipoprotein and low density lipoprotein apolipoprotein B. J Lipid Res 24:1261–1267
19. Berthold HK, Reeds PJ, Klein PD (1995) Isotopic evidence for the differential regulation of arginine and proline synthesis in man. Metabolism 44:466–473
20. Berthold HK, Hachey DL, Reeds PJ, Thomas OP, Hoeksema S, Klein PD (1991) Uniformly 13C-labeled algal protein used to determine amino acid essentiality in vivo. Proc Natl Acad Sci USA 88:8091–8095
21. Khan B, Fungwe TV, Wilcox HG, Heimberg M (1990) Cholesterol is required for secretion of very-low-density lipoprotein: In vivo studies. Biochim Biophys Acta 1044:287–304
22. Khan BK, Wilcox HG, Heimberg M (1989) Cholesterol is required for secretion of very-low-density lipoprotein by rat liver. Biochem J 254:807–816
23. Ginsberg HN, Le NA, Short MP, Ramakrishnan R, Desnick RJ (1987) Suppression of apolipoprotein B production during treatment of cholesteryl ester storage disease with lovastatin. J Clin Invest 80:1692–1697
24. Vega GL, East C, Grundy SM (1988) Lovastatin therapy in familial dysbetalipoproteinemia: effects on kinetics of apolipoprotein B. Atherosclerosis 70:131–143
25. Vega GL, Krauss RM, Grundy SM (1990) Pravastatin therapy in primary moderate hypercholesterolemia: changes in metabolism of apolipoprotein B-containing lipoproteins. J Intern Med 227:81–94
26. Watts GF, Cummings MH, Umpleby M, Quiney JR, Naoumova R, Thompson GR, Sönkesen PH (1995) Simvastatin decreases the hepatic secretion of very-low-density lipoprotein apolipoprotein B-100 in heterozygous familial hypercholesterolemia: pathophysiological and therapeutic implications. Eur J Clin Invest 25:559–567
27. Arad Y, Ramakrishnan R, Ginsberg HN (1990) Lovastatin therapy reduces low density lipoprotein apoB levels in subjects with combined hyperlipidemia by reducing the production of apoB-containing lipoproteins: implications for the pathophysiology of apoB production. J Lipid Res 31:567–582
28. Grundy SM, Vega GL (1985) Influence of mevinolin on metabolism of low density lipoproteins in primary moderate hypercholesterolemia. J Lipid Res 26:1464–1475
29. Watts GF, Moroz P, Barrett PH (2000) Kinetics of very-low-density lipoprotein apolipoprotein B-100 in normolipidemic subjects: pooled analysis of stable-isotope studies. Metabolism 49:1204–1210
30. Benitez S, Ordonez-Llanos J, Franco M, Marin C, Paz E, Lopez-Miranda J, Otal C, Perez-Jimenez F, Sanchez-Quesada JL (2004) Effect of simvastatin in familial hypercholesterolemia on the affinity of electronegative low-density lipoprotein subfractions to the low-density lipoprotein receptor. Am J Cardiol 93:414–420
31. Welty FK, Lichtenstein AH, Barrett PH, Dolnikowski GG, Schaefer EJ (1999) Human apolipoprotein (Apo) B-48 and ApoB-100 kinetics with stable isotopes. Arterioscler Thromb Vasc Biol 19:2966–2974
32. Lamon-Fava S, Diffenderfer MR, Barrett PH, Buchsbaum A, Matthan NR, Lichtenstein AH, Dolnikowski GG, Horvath K, Asztalos BF, Zago V, Schaefer EJ (2007) Effects of different doses of atorvastatin on human apolipoprotein B-100, B-48, and A-I metabolism. J Lipid Res 48:1746–1753
33. Malmendier CL, Lontie JF, Delcroix C, Magot T (1989) Effect of simvastatin on receptor-dependent low density lipoprotein catabolism in normocholesterolemic human volunteers. Atherosclerosis 80:101–109
34. Parhofer KG, Barrett PH, Dunn J, Schonfeld G (1993) Effect of pravastatin on metabolic parameters of apolipoprotein B in patients with mixed hyperlipoproteinemia. Clin Investig 71:939–946
35. Cuchel M, Schaefer EJ, Millar JS, Jones PJ, Dolnikowski GG, Vergani C, Lichtenstein AH (1997) Lovastatin decreases de novo cholesterol synthesis and LDL Apo B-100 production rates in combined-hyperlipidemic males. Arterioscler Thromb Vasc Biol 17:1910–1917
36. Gaw A, Packard CJ, Murray EF, Lindsay GM, Griffin BA, Caslake MJ, Vallance BD, Lorimer AR, Shepherd J (1993) Effects of simvastatin on apoB metabolism and LDL subfraction distribution. Arterioscler Thromb 13:170–189
37. Magkos F, Patterson BW, Mittendorfer B (2007) Reproducibility of stable isotope-labeled tracer measures of VLDL-triglyceride and VLDL-apolipoprotein B-100 kinetics. J Lipid Res 48:1204–1211

Lipids (2010) 45:501–510
DOI 10.1007/s11745-010-3418-z

ORIGINAL ARTICLE

Medium- and Long-Chain Triacylglycerols Reduce Body Fat and Blood Triacylglycerols in Hypertriacylglycerolemic, Overweight but not Obese, Chinese Individuals

Yuehong Zhang · Yinghua Liu · Jin Wang · Rongxin Zhang · Hongjiang Jing · Xiaoming Yu · Yong Zhang · Qin Xu · Jieying Zhang · Zixin Zheng · Naohisa Nosaka · Chie Arai · Michio Kasai · Toshiaki Aoyama · Jian Wu · Changyong Xue

Received: 13 August 2009 / Accepted: 7 April 2010 / Published online: 15 May 2010

Abstract In contrast to the consumption of long-chain triacylglycerols (LCT), consumption of medium- and long-chain triacylglycerols (MLCT) reduces the body fat and blood triacylglycerols (TAG) level in hypertriacylglycerolemic Chinese individuals. These responses may be affected by BMI because of obesity-induced insulin resistance. We aimed to compare the effects of consuming MLCT or LCT on reducing body fat and blood TAG level in hypertriacylglycerolemic Chinese subjects with different ranges of BMI. Employing a double-blind, randomized and controlled protocol, 101 hypertriacylglycerolemic subjects (including 67 men and 34 women) were randomly allocated to ingest 25–30 g/day MLCT or LCT oil as the only cooking oil for 8 consecutive weeks. Anthropometric measurements of body weight, BMI, body fat, WC, HC, blood biochemical variables, and subcutaneous fat area and visceral fat area in the abdomen were measured at week 0 and 8. As compared to subjects with BMI 24–28 kg/m^2 in the LCT group, corresponding subjects in the MLCT group showed significantly greater decrease in body weight, BMI, body fat, WC, ratio of WC to HC, total fat area and subcutaneous fat area in the abdomen, as well as blood TAG and LDL-C levels at week 8. Based upon our results, consumption of MLCT oil may reduce body weight, body fat, and blood TAG and LDL-C levels in overweight hypertriacylglycerolemic Chinese subjects but may not induce these changes in normal or obese hypertriacylglycerolemic subjects.

Keywords Medium-and long-chain triacylglycerols · Body fat · Blood triacylglycerols · Hypertriacylglycerolemia · Overweight · Chinese · Long-chain triacylglycerols

Abbreviations

ALT	Alanine aminotransferase
AST	Aspartate aminotransferase
BMI	Body mass index
HC	Hip circumference
HDL-C	High-density lipoprotein-cholesterol
LCT	Long-chain triacylglycerols
LDL-C	Low-density lipoprotein-cholesterol
MLCT	Medium- and long-chain triacylglycerols
SFA	Subcutaneous fat area
TAG	Triacylglycerols
TFA	Total fat area
VFA	Visceral fat area
WC	Waist circumference
WHR	Ratio of waist circumference to hip circumference

Y. Zhang · Y. Liu · J. Wang · R. Zhang · H. Jing · X. Yu · Y. Zhang · Q. Xu · J. Zhang · Z. Zheng · C. Xue (✉)
Department of Nutrition, Chinese People's Liberation Army General Hospital, No 28 Fuxing Road, Beijing 100853, China
e-mail: cnxcy@163.com

N. Nosaka · C. Arai · M. Kasai · T. Aoyama · J. Wu
Central Research Laboratory, Nisshin Oillio Group, Yokosuka, Japan

Introduction

The prevalence of being overweight or obese has increased by 40.7 and 97.2%, respectively, in mainland China since 1992 [1]. This trend will undoubtedly increase the incidence of chronic diseases such as hypertension, diabetes, stroke and coronary heart disease. The total medical cost

that can be attributed to being overweight and obese was estimated at 21.11 billion Chinese Renminbi (RMB) Yuan and accounted for 25.5% of the total medical costs for the four chronic diseases, or 3.7% of the total national medical costs, in 2003 [2]. The high economic burden of being overweight or obese suggests an urgent need to develop effective interventions for preventing and controlling overweightedness and obesity. Hypertriacylglycerolemia is an independent risk factor for cardiovascular disease [3, 4]. There is a suggestion that choosing the right type of dietary fat could be an effective strategy for preventing weight gain or fat deposition and reducing the blood levels of triacylglycerols (TAG) under an appropriate dietary regimen [3, 5].

Ordinary dietary fats are mainly long-chain triacylglycerols (LCT) composed of long-chain fatty acids with carbon numbers ranging from 14 to 18. In contrast, medium-chain triacylglycerols (MCT), composed of fatty acids with carbon numbers of 8–12, are found in palm oil and coconut oil, which are minor components of a normal diet. However, the carbon numbers of MCT used in our study were 8–10. Because MCT are hydrolyzed more rapidly and metabolized more completely than are LCT, rapid oxidation prevents deposition of fat [6]. For these reasons, MCT may be useful in dietary therapy. Animal studies have shown that consumption of MCT decreases body weight and the amount of fat deposited [7]. Dietary MCT also reduce body fat accumulation in healthy men and women [8]. Furthermore, ingestion of 18 g/day MCT has been shown to decrease body weight and waist circumference (WC) in moderately overweight humans with type 2 diabetes mellitus [9].

MCT are difficult to use as cooking oil because of a low smoke point and foam generation on being mixed with other vegetable oils or in frying. A new oil composed of medium- and long-chain triacylglycerols (MLCT) in the same glycerol molecule range produced by a transesterification technique has been developed recently as a cooking oil [10]. Our previous studies indicated that MLCT reduced body fat and blood TAG in Chinese hypertriacylglycerolemic subjects [11]. However, whether body mass index (BMI) affects the response in these hypertriacylglycerolemic Chinese individuals is unknown.

Elevated levels of free fatty acids (FFA) in the blood commonly seen in obese persons are associated with the expansion of adipose mass and insulin resistance. Blood cytokines such as leptin, plasminogen activator inhibitor-1 (PAI-1), tumor necrosis factor-α (TNF-α), and interleukin-6 (IL-6) levels were often increased in obese subjects. These are thought to promote insulin resistance [12]. Insulin resistance might hinder any increase in fat oxidation and induce difficulties in the reduction of body fat and TAG in obese subjects. These observations prompted us to investigate the response to MLCT consumption in subjects with different BMI categories.

The working group on obesity in China suggested that BMI values of 24–28 kg/m^2 and ≥28 kg/m^2 indicated overweight and obesity, respectively, in Chinese individuals [13]. We analyzed our previous data based on the BMI categories to elucidate whether overweight individuals responded differently to MLCT consumption than did obese individuals.

Materials and Methods

Study Design and Subjects

The study was carried out in accordance with the Helsinki Declaration and was approved by the Ethics Committee of the Chinese People's Liberation Army General Hospital. The study procedures were fully explained to all subjects, who gave their informed consent before the start of the study. The study was a double-blind, randomized clinical trial involving 76 men and 36 women with hypertriacylglycerolemia values of 1.7–4.5 mmol/L. All subjects had no history of diabetes, hypertension, renal and hepatic disease, or gastrointestinal disease and were not receiving any medication. The study population was randomly allocated to receive MLCT or LCT oil by random numbers assigned by the providers of the MLCT and LCT oil, who also encoded the oils with matching random numbers. Neither the subjects nor the researchers of this study knew which subject was receiving which oil during the study. Before starting the study, dietary energy intake for each individual was calculated using the Harris–Benedict equation. Food choice and amount for each subject were suggested by experienced dietitians and doctors by face-to-face communication. Recommended daily carbohydrates were about 55–60% of total daily calorie intake, and mainly came from complex carbohydrate of the starch food group, such as cereals and tubers. Ready-to-eat cereal products such as biscuits, crackers, instant noodles, etc. containing higher fat and/or higher refined sugar and alcoholic beverage were not allowed to be eaten during the study period. Recommended daily fats were about 25–30% of total energy intake, MLCT or LCT oil, as the only cooking oil, was to be consumed at a rate of 25–30 g/day, which was about 12–15% of the total daily energy intake, other types oil such as coconut were not allowed to be used during our study. Other fat mainly came from balanced foods such as egg, milk, lean red meat and white meat. These recommended foods provide balanced nutrients. The dietary regimen was maintained at relatively fixed energy and nutrients intake. In addition, both the time and the intensity of physical activity for

each subject were well controlled. A manual on the study was distributed to all subjects, in which all subjects were specifically advised how to maintain healthy bodily activity and to take moderately intensive exercise daily throughout the trial. The recommended activities were walking (4–5 km/h), housework, babysitting, and bicycle-riding (8–10 km/h), etc.

The subjects were instructed to record their physical activity intensity, duration and method for 3 days and the intake of the type and quantity of food for 3 days each week (including one weekend day) at baseline (week 0) and at weeks 2, 4, 6 and 8. The physical activities included walking (4–5 km/h), housework, childcare, and bicycle riding (8–10 km/h). The diaries were collected weekly to confirm that subjects were following the instructions, and if not, the subjects were advised to drop out of the study. Daily intake of energy, fat, protein, and carbohydrates was calculated from the food record on the basis of the China Food Composition Tables published in 2002.

Anthropometric and Biochemical Measurements

Anthropometric variables were measured by trained investigators. Body weight and height were measured to the nearest 0.1 kg and 0.1 cm. WC was measured at the umbilical level. Hip circumference (HC) was measured at the level of the greatest posterior protuberance. Both WC and HC were measured to the nearest 0.1 cm with the subject in a standing position, and the ratio of WC to HC (WHR) was calculated. All measurements were taken at baseline and at week 8.

Blood samples were taken in the morning after 12 h of overnight fasting at baseline and week 8. Levels of aspartate aminotransferase (AST), alanine aminotransferase (ALT), blood glucose, total cholesterol (TC), TAG, high-density lipoprotein cholesterol (HDL-C), and low-density lipoprotein cholesterol (LDL-C) were measured using a 7600-automated system (Hitachi, Tokyo, Japan).

Measurement of Body Fat and Abdominal Fat Area by Computed Tomography (CT)

The measurements were carried out after 12 h overnight fasting at baseline and at week 8. Body fat was measured by use of a BCA-2A body composition analyzer (Tongfang, Qinghua, Beijing, China). Subjects underwent CT [Pro 16 CT (GE, USA)] scanning at the umbilical level at the Chinese People's Liberation Army General Hospital. Visceral fat area (VFA) and subcutaneous fat area (SFA) were obtained from the CT images as described in [14]. Blood sampling, anthropometric measurements and CT scanning were performed on the same day.

Test Oils

The test oils of MLCT and LCT were supplied by The Nisshin Oillio Group (Tokyo). The fatty acids and TAG compositions of MLCT and LCT are listed in Table 1 and the same as those in a previous report [10]. In MLCT, the concentration of medium-chain fatty acids (MCFA), C8:0 and C10:0, was 13% of total MLCT oil weight (Table 1).

Statistical Analysis

Data were expressed as means ±SD. The general linear model (GLM) was used to test almost all data except for a chi-square test for gender distribution. In our GLM analysis, fixed factors were BMI and oil, a random factor was gender, covariate was age. The full factorial model, which included main effects and factors interaction, was used in our study. If a significant difference was detected, comparisons of means were performed by Student's t test between the two groups and by a paired t test between the initial and final values in the same group. All analyses involved use of SPSS v10.0 for Windows (SPSS Inc.,

Table 1 Fatty acid and triacylglycerols compositions of LCT and MLCT oil

Fatty acid	LCT (g/100 g total weight)	MLCT (g/100 g total weight)
8:0	ND	9.7
10:0	ND	3.3
16:0	6.2	3.8
16:1	0.2	0.2
18:0	2.5	1.7
18:1	48.8	51.2
18:2	30.2	18.4
18:3	9.4	9.0
20:0	0.6	0.6
20:1	1.1	1.2
22:0	0.4	0.3
22:1	0.2	0.3
24:0	0.2	0.1
24:1	0.2	0.2
Total	100	100
Triacylglycerols		
L, L, L	100.0	55.1
L, L, M	ND	35.2
L, M, M	ND	9.1
M, M, M	ND	0.6
Total	100.0	100.0

L long-chain fatty acids, *M* medium-chain fatty acids, *LCT* long-chain triacylglycerols, *MLCT* medium- and long-chain triacylglycerols, *ND* not detected

Chicago, IL, USA). The level of significant difference was set at $P < 0.05$.

Results

Subjects

Among the subjects, one had a traffic accident, one had a cerebral infarction, two were not willing to consume the specified oil and seven were unable to consume the oil for consecutive days (three were out of town on business and four were on vacation). Thus these eleven subjects were excluded from our study, and 101 subjects were enrolled finally in the study. There were 34 men and 16 women left in the LCT group, and 33 men and 18 women in the MLCT group at the end of the study. No gender distribution differences were noted between the two groups. The characteristics of the groups at the beginning of the study are shown in Table 2.

Intakes of Energy, Protein, Fat, Carbohydrate and Physical Activity Time and Gender Distribution

GLM analysis revealed that there was no significant difference in daily intake of total energy, protein, fat and carbohydrate or daily physical activity time among all the subgroups at baseline and week 8 ($P > 0.05$). In addition, chi-square analysis showed that there was no significant difference in gender distribution among all subgroups (Table 3).

Table 2 Characteristics of subjects consuming long-chain triacylglycerols (LCT) or medium- and long-chain triacylglycerols (MLCT) oil at baseline

Index	LCT ($n = 50$)	MLCT ($n = 51$)
Age (year)	53.2 ± 13.0	54.2 ± 12.5
Male (%)	34 (68.0%)	33 (64.7%)
Height (cm)	165.9 ± 8.8	166.5 ± 6.7
Body weight (kg)	71.5 ± 9.0	72.0 ± 11.4
BMI (kg/m^2)	25.9 ± 2.4	25.9 ± 3.3
Body fat weight (kg)	17.2 ± 4.4	17.4 ± 5.8
Body fat (%)	24.2 ± 6.2	23.9 ± 5.7
ALT (U/L)	25.5 ± 14.3	25.3 ± 14.9
AST (U/L)	22.1 ± 6.2	23.7 ± 8.9
Glucose (mmol/L)	5.1 ± 0.9	5.4 ± 1.0
TC (mmol/L)	5.2 ± 0.9	5.2 ± 0.8
TAG (mmol/L)	2.6 ± 0.7	2.7 ± 0.8

ALT alanine aminotransferase, *AST* aspartate aminotransferase, *BMI* body mass index, *TC* total cholesterol, *TAG* triacylglycerols

Anthropometric Measurements

GLM analysis showed that the oil had an effect, but the BMI no effect. As compared with their initial levels, body weight, BMI and WC decreased significantly in subjects with different BMI categories in the MLCT group. HC and WHR were lowered significantly in subjects with BMI 24–28 kg/m^2 in the MLCT group. WHR decreased significantly in subjects with BMI ≥28 kg/m^2 in the MLCT group ($P < 0.05$; Table 4). However, no similar changes in these indices were observed in the LCT group.

BMI × oil interaction was found using GLM analysis, further analysis revealed that there were greater decreases in the changes of body weight, BMI, WC and WHR in subjects with a BMI 24–28 kg/m^2 in the MLCT group as compared to their corresponding controls in the LCT group ($P < 0.05$; Table 4 and Fig. 1).

Body Fat Composition

GLM analysis showed that the oil has effects, but the BMI no effect. When compared with their baseline, body fat weight, TFA and SFA decreased significantly in subjects with BMI 24–28 kg/m^2 in MLCT group, but TFA and VFA increased in the same BMI category in the LCT group. Body fat weight and TFA was lowered significantly in subjects with a BMI <24 kg/m^2 in the MLCT group, however, VFA increased in the same BMI category in the LCT group ($P < 0.05$; Table 5).

BMI × oil interaction was found using GLM analysis, further analysis revealed the extent of decreases in changes and change rates of body fat weight, TFA and SFA in subjects with a BMI 24–28 kg/m^2 were greater in the MLCT group than those in corresponding subjects in the LCT group ($P < 0.05$; Table 5).

Blood Biochemical Variables

GLM analysis showed that the oil had effects, but the BMI no effect. When compared to their baseline, a significant decrease in blood TAG and an increase in HDL-C in subjects with a BMI 24–28 kg/m^2 in the MLCT group were observed; however, blood TAG, LDL-C and TC levels were significantly higher in the same BMI category subjects in the LCT group; LDL-C and TC increased significantly in subjects with a BMI <24 kg/m^2 in the LCT group. Blood TAG levels decreased significantly in subjects with a BMI ≥ 28 kg/m^2 in the MLCT group ($P < 0.05$; Table 6).

BMI × oil interaction was found by using GLM analysis, further analysis revealed that the extent of decreases in changes and change rates in blood TAG and LDL-C were greater in subjects with a BMI 24–28 kg/m^2 in the

Table 3 Mean intake of energy, protein, fat, and carbohydrates, mean physical activity time and gender distribution in subjects consuming LCT or MLCT oil

	Time	LCT ($n = 50$)			MLCT ($n = 51$)		
		BMI <24 kg/m^2 $n = 16$	BMI 24–28 kg/m^2 $n = 17$	BMI ≥28 kg/m^2 $n = 17$	BMI <24 kg/m^2 $n = 19$	BMI 24–28 kg/m^2 $n = 20$	BMI ≥28 kg/m^2 $n = 12$
Energy (kcal/day)	Baseline	1803.7 ± 281.3	1773.9 ± 253.7	1762.9 ± 218.9	1746.8 ± 164.2	1811.0 ± 233.8	1843.2 ± 191.6
	1–8 week	1760.0 ± 108.2	1786.2 ± 130.9	1724.4 ± 137.9	1767.5 ± 100.8	1758.0 ± 103.2	1727.1 ± 95.4
Protein (g/day)	Baseline	62.61 ± 14.03	58.84 ± 14.76	59.30 ± 12.28	60.87 ± 10.17	64.11 ± 14.11	59.99 ± 10.00
	1–8 week	60.91 ± 6.80	61.59 ± 4.80	60.32 ± 4.29	62.96 ± 6.92	60.67 ± 8.16	62.00 ± 7.67
Fat (g/day)	Baseline	51.07 ± 8.69	50.37 ± 10.62	51.11 ± 8.59	51.42 ± 7.63	52.31 ± 8.14	51.29 ± 8.72
	1–8 week	51.98 ± 3.86	52.14 ± 3.39	51.45 ± 2.43	51.77 ± 5.74	51.93 ± 5.26	51.06 ± 4.26
Carbohydrates (g/day)	Baseline	263.98 ± 54.42	261.23 ± 42.80	256.60 ± 43.73	251.06 ± 22.09	263.99 ± 32.86	269.20 ± 42.45
	1–8 week	252.40 ± 21.33	257.99 ± 26.18	246.42 ± 33.49	252.16 ± 15.28	251.00 ± 17.39	245.54 ± 11.49
Protein (% of total energy)	Baseline	13.75 ± 2.08	13.09 ± 2.05	13.38 ± 2.20	13.95 ± 1.43	14.11 ± 1.65	13.25 ± 1.72
	1–8 week	13.74 ± 1.17	13.66 ± 0.55	13.90 ± 1.00	14.15 ± 1.04	13.63 ± 1.27	14.20 ± 1.10
Fat (% of total energy)	Baseline	25.51 ± 3.90	25.52 ± 4.06	26.19 ± 3.76	27.39 ± 3.26	25.96 ± 2.96	23.71 ± 3.94
	1–8 week	26.72 ± 1.97	26.30 ± 2.01	27.04 ± 2.60	26.24 ± 2.43	26.67 ± 2.24	26.58 ± 1.67
Carbohydrates (% of total energy)	Baseline	58.61 ± 5.69	59.13 ± 5.80	58.19 ± 5.79	56.72 ± 3.07	58.02 ± 4.09	60.32 ± 4.79
	1–8 week	57.33 ± 2.87	57.86 ± 2.46	57.08 ± 3.44	57.10 ± 2.84	57.58 ± 3.02	57.29 ± 2.47
Physical activity time (min/day)	Baseline	104.90 ± 42.24	122.82 ± 43.72	129.49 ± 49.84	125.26 ± 37.91	116.25 ± 30.55	113.61 ± 41.82
	1–8 week	118.93 ± 25.83	114.07 ± 16.99	130.09 ± 27.75	123.50 ± 19.41	124.80 ± 20.65	119.41 ± 20.97
Gender distribution	Male	11 (68.8%)	12 (70.6%)	11 (64.5%)	13 (68.4%)	13 (65.0%)	7 (58.3%)
	Female	5 (31.2%)	5 (39.4%)	6 (35.5%)	6 (31.6%)	7 (35.0%)	5 (41.7%)

There were no significant differences among all subgroups, $P > 0.05$

Table 4 Changes in anthropometric measurements in the two groups consuming LCT or MLCT oil with different body mass indexes at baseline (week 0) and week 8

	BMI (kg/m^2)	Time (week)	LCT ($n = 50$)			MLCT ($n = 51$)		
			Mean ± SD	Δ	Δ%	Mean ± SD	Δ	Δ%
Body weight (kg)	<24	0	64.53 ± 5.99			62.53 ± 5.37		
		8	63.83 ± 6.20	–0.77 ± 1.45	–1.18 ± 2.20	60.92 ± 5.06*	–1.60 ± 1.71	–2.51 ± 2.73
	24–28	0	71.32 ± 5.71			72.20 ± 8.08		
		8	70.74 ± 5.54	–0.59 ± 1.59	–0.78 ± 2.18	70.15 ± 7.57*	–2.05 ± 1.52#	–2.78 ± 2.03#
	≥28	0	79.38 ± 6.52			86.17 ± 7.56		
		8	79.18 ± 6.51	–0.21 ± 2.22	–0.21 ± 2.78	84.41 ± 8.15*	–1.75 ± 2.57	–2.06 ± 3.06
BMI (kg/m^2)	<24	0	22.24 ± 1.91			22.75 ± 1.06		
		8	22.10 ± 1.88	–0.30 ± 0.58	–1.33 ± 2.47	22.13 ± 0.89*	–0.63 ± 0.66	–2.69 ± 2.85
	24–28	0	26.07 ± 1.28			25.98 ± 1.07		
		8	25.88 ± 1.55	–0.19 ± 0.61	–0.75 ± 2.34	25.25 ± 1.18*	–0.73 ± 0.61#	–2.80 ± 2.36#
	≥28	0	30.28 ± 1.81			30.61 ± 2.08		
		8	30.13 ± 2.11	–0.14 ± 0.95	–0.49 ± 3.19	29.85 ± 2.33*	–0.76 ± 0.88	–2.51 ± 2.95
WC (cm)	<24	0	84.28 ± 6.53			82.89 ± 4.36		
		8	83.78 ± 6.44	–0.5 ± 2.75	–0.53 ± 3.31	81.94 ± 4.54*	–0.95 ± 1.05	–1.15 ± 1.28
	24–28	0	88.32 ± 5.06			90.2 ± 6.13		
		8	88.09 ± 4.86	–0.24 ± 1.13	–0.25 ± 1.29	88.85 ± 6.06*	–1.35 ± 0.86#	–1.49 ± 0.95#
	≥28	0	93.88 ± 6.24			98.25 ± 7.02		
		8	93.82 ± 5.79	–0.06 ± 1.42	–0.02 ± 1.53	97.13 ± 7.53*	–1.13 ± 1.52	–1.17 ± 1.56
HC (cm)	<24	0	94.4 ± 2.61			92.87 ± 2.92		
		8	94.2 ± 2.61	–0.20 ± 1.16	–0.21 ± 1.24	92.45 ± 2.77	–0.42 ± 1.10	–0.44 ± 1.19
	24–28	0	98.85 ± 5.56			99.40 ± 4.69		
		8	98.35 ± 5.43	–0.5 ± 1.13	–0.49 ± 1.12	98.77 ± 4.81*	–0.63 ± 0.84	–0.63 ± 0.86
	≥28	0	102.93 ± 3.81			106.35 ± 4.98		
		8	102.71 ± 4.14	–0.21 ± 0.97	–0.22 ± 0.96	106.10 ± 5.80	–0.25 ± 1.40	–0.26 ± 1.32
WHR	<24	0	0.88 ± 0.06			0.89 ± 0.04		
		8	0.88 ± 0.06	–0.00 ± 0.03	–0.31 ± 2.93	0.89 ± 0.05	–0.01 ± 0.01	–0.70 ± 1.48
	24–28	0	0.90 ± 0.06			0.91 ± 0.06		
		8	0.90 ± 0.06	0.00 ± 0.01	0.26 ± 1.52	0.90 ± 0.06*	–0.01 ± 0.01#	–0.86 ± 1.03#
	≥28	0	0.93 ± 0.06			0.91 ± 0.06		
		8	0.93 ± 0.06	–0.00 ± 0.01	–0.10 ± 1.34	0.90 ± 0.06*	–0.01 ± 0.01	–1.14 ± 1.61

Δ represents week 8 versus week 0, Δ% represents change rate against week 0

BMI body mass index, *HC* hip circumference, *WC* waist circumference, *WHR* ratio of waist circumference to hip circumference

* Different from week 0, $P < 0.05$

\# Different from LCT group, $P < 0.05$

MLCT group than those in corresponding subjects in the LCT group ($P < 0.05$; Table 6).

Discussion

In this study, consumption of MLCT oil induced significant decreases in body weight, body fat, and SFA in hypertriacylglycerolemic and overweight subjects as compared with that of LCT oil. Our results agree with those of St-Onge et al. [15], who found that consumption of a diet rich in MLCT for 28 days resulted in greater loss of adipose tissue in overweight men than did a diet rich in LCT. Our results are similar to those of Tsuji et al. [8], Nosaka et al. [16] and Kasai et al. [17]. Tsuji et al. [8] who found that a 10-g/day MLCT consumption might reduce body weight and fat in individuals with a BMI ≥23 kg/m^2 as compared with LCT consumption. Nosaka [16] found similar effects on the body composition with one-half of the MCT intake than that in the previous study. Kasai et al. [17] reported that subjects consuming the test bread, which had been made with 14 g (about 6% of total energy) of

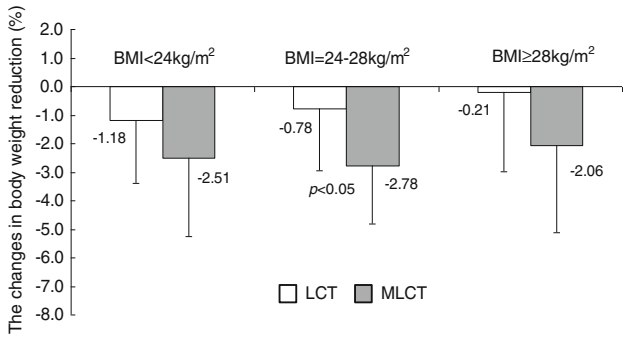

Fig. 1 The effects of LCT and MLCT on the changes in body weight reduction

MLCT containing 1.7 g MCFA had significant reduced body weight and body fat accumulation. From these results, we can suggest that an intake of 10–14 g MLCT can reduce body weight and body fat.

Yost and Eckel [18] conducted a study of the effect of an 800 kcal diet containing MCT. MCT intake did not result in greater weight loss in obese women than an isocaloric diet containing LCT. It is possible that small weight loss of MCT intake may be indistinguishable from the large weight loss effects of very low calorie diets. The study supports our finding that MLCT consumption may not be more effective at reducing fat mass in obese individuals than in overweight individuals.

Our results indicated that overweight subjects responded better to MLCT consumption than did lean or obese subjects. These different effects might be due to the metabolic difference in energy expenditure and fat oxidation in subjects with different body weights. A previous study showed that normal weight and morbidly obese subjects had similar increases in postprandial energy expenditure over resting metabolic rate value [19]; however, fat oxidation was found to be greater in normal weight subjects than in obese

Table 5 Changes in body fat in two groups consuming LCT or MLCT oil with different BMI at baseline (week 0) and week 8

	BMI (kg/m^2)	Time (week)	LCT ($n = 50$)			MLCT ($n = 51$)		
			Mean ± SD	Δ	Δ%	Mean ± SD	Δ	Δ%
Body fat weight (kg)	<24	0	15.13 ± 1.97			14.17 ± 2.32		
		8	14.44 ± 2.21	–0.7 ± 1.19	–4.53 ± 8.79	12.84 ± 1.98*	–1.33 ± 1.22	–8.98 ± 8.07
	24–28	0	18.31 ± 4.59			18.05 ± 3.17		
		8	17.77 ± 4.67	–0.55 ± 1.10	–3.21 ± 6.49	16.46 ± 3.62*	–1.59 ± 1.26#	–9.25 ± 8.34#
	≥28	0	18.31 ± 3.85			24.06 ± 6.81		
		8	18.08 ± 3.75	–0.24 ± 1.93	–0.66 ± 10.37	22.56 ± 6.81*	–1.50 ± 2.07	–6.99 ± 9.60
TFA (cm^2)	<24	0	308.14 ± 96.93			268.98 ± 45.82		
		8	315.34 ± 79.87	7.19 ± 25.02	5.05 ± 12.06	252.30 ± 41.41*	–16.68 ± 24.14#	–5.72 ± 8.44#
	24–28	0	337.55 ± 99.93			349.19 ± 82.60		
		8	359.91 ± 91.54*	22.35 ± 35.10	7.99 ± 10.99	333.73 ± 81.58*	–15.46 ± 25.22#	–4.34 ± 7.50#
	≥28	0	341.15 ± 71.88			426.73 ± 133.60		
		8	354.52 ± 70.70	13.37 ± 40.97	5.38 ± 13.53	420.17 ± 152.51	–6.56 ± 73.99	–1.95 ± 18.61
VFA (cm^2)	<24	0	123.29 ± 45.57			118.83 ± 33.89		
		8	130.67 ± 36.05*	14.73 ± 16.72	20.82 ± 29.53	112.44 ± 25.76	–6.39 ± 15.12#	–3.45 ± 12.00#
	24–28	0	135.09 ± 28.29			151.59 ± 56.08		
		8	151.43 ± 30.79*	17.66 ± 27.88	15.92 ± 24.48	152.40 ± 51.37	0.81 ± 27.51	3.49 ± 22.04
	≥28	0	160.32 ± 46.99			194.43 ± 64.65		
		8	178.28 ± 38.39	17.95 ± 34.62	17.08 ± 28.95	210.73 ± 79.28	16.29 ± 52.83	9.99 ± 29.54
SFA (cm^2)	<24	0	181.53 ± 80.85			150.14 ± 33.02		
		8	173.96 ± 74.39	–7.57 ± 15.04	–2.94 ± 9.74	139.85 ± 37.07	–10.29 ± 23.39	–6.40 ± 15.90
	24–28	0	202.43 ± 96.31			197.60 ± 61.83		
		8	208.49 ± 99.85	4.69 ± 19.06	2.27 ± 11.54	181.31 ± 67.22*	–16.29 ± 19.25#	–9.29 ± 9.77#
	≥28	0	180.81 ± 47.79			232.33 ± 98.58		
		8	176.23 ± 51.89	–4.58 ± 22.10	–2.37 ± 11.22	209.44 ± 91.42	–22.88 ± 46.76	–9.79 ± 18.25

Δ represents 8 week versus week 0, Δ% represents change rate against week 0

TFA total fat area, *VFA* visceral fat area, *SFA* subcutaneous fat area

* Different from week 0, $P < 0.05$

Different from LCT group, $P < 0.05$

Table 6 Changes in levels of triacylglycerols, lipoproteins, hepatic enzymes, blood glucose and total cholesterol in two groups consuming LCT or MLCT oil with different BMI at baseline (week 0) and week 8

Index	BMI kg/m^2	Time (week)	LCT ($n = 50$)			MLCT ($n = 51$)		
			Mean ± SD	Δ	Δ%	Mean ± SD	Δ	Δ%
TAG (mmol/L)	<24	0	2.77 ± 0.67			2.42 ± 0.70		
		8	3.13 ± 1.33	0.36 ± 1.09	12.52 ± 37.39	2.28 ± 1.26	–0.14 ± 0.87	–8.10 ± 31.63
	24–28	0	2.58 ± 0.84			2.75 ± 0.97		
		8	3.23 ± 1.29*	0.65 ± 1.10	27.96 ± 48.08	2.18 ± 0.85*	–0.57 ± 0.86#	–17.00 ± 30.02#
	≥28	0	2.37 ± 0.67			2.90 ± 0.77		
		8	2.62 ± 0.88	0.25 ± 0.92	15.76 ± 45.77	2.13 ± 0.67*	–0.77 ± 1.10	–20.65 ± 34.17
HDL–C (mmol/L)	<24	0	1.42 ± 0.31			1.36 ± 0.22		
		8	1.38 ± 0.29	–0.05 ± 0.14	–2.72 ± 9.10	1.29 ± 0.23	–0.07 ± 0.20	–4.59 ± 15.20
	24–28	0	1.39 ± 0.37			1.26 ± 0.23		
		8	1.35 ± 0.49	–0.03 ± 0.22	–2.91 ± 14.24	1.37 ± 0.28*	0.11 ± 0.23	10.47 ± 19.14#
	≥28	0	1.35 ± 0.24			1.27 ± 0.19		
		8	1.27 ± 0.25	–0.08 ± 0.17	–5.45 ± 11.77	1.30 ± 0.34	0.03 ± 0.23	1.97 ± 16.07
LDL–C (mmol/L)	<24	0	2.78 ± 0.76			2.75 ± 0.59		
		8	3.39 ± 0.60*	0.55 ± 0.59	25.08 ± 33.32	2.86 ± 0.70	0.10 ± 0.44	4.76 ± 16.10
	24–28	0	2.56 ± 0.76			2.88 ± 0.76		
		8	2.93 ± 0.68*	0.38 ± 0.58	19.91 ± 29.46	2.83 ± 0.65	–0.05 ± 0.64#	1.29 ± 22.35#
	≥28	0	2.77 ± 0.63			3.15 ± 0.50		
		8	2.95 ± 0.64	0.18 ± 0.45	8.14 ± 19.59	2.94 ± 0.77	–0.21 ± 0.68	–6.45 ± 20.87
ALT (U/L)	<24	0	24.33 ± 13.05			19.97 ± 4.86		
		8	30.38 ± 18.85	6.06 ± 12.91	26.20 ± 53.37	21.48 ± 7.74	1.51 ± 5.27	7.22 ± 26.18
	24–28	0	22.91 ± 8.22			28.02 ± 18.76		
		8	27.6 ± 13.44	4.69 ± 14.50	28.38 ± 60.86	28.68 ± 18.67	0.87 ± 8.67	11.33 ± 38.07
	≥28	0	29.29 ± 19.38			29.03 ± 16.84		
		8	31.49 ± 18.2	2.20 ± 16.80	18.83 ± 47.22	28.93 ± 13.17	–0.1 ± 20.09	30.05 ± 105.14
AST (U/L)	<24	0	22.04 ± 5.71			21.48 ± 8.47		
		8	24.17 ± 9.54	2.13 ± 8.39	10.89 ± 38.92	19.57 ± 7.36	–1.92 ± 4.14	–7.17 ± 18.00
	24–28	0	21.26 ± 5.77			25.01 ± 9.72		
		8	20.37 ± 4.06	–0.88 ± 6.95	1.69 ± 30.42	25.59 ± 18.30	0.58 ± 17.67	6.02 ± 60.60
	≥28	0	23.02 ± 7.17			25.02 ± 8.36		
		8	23.64 ± 6.32	0.62 ± 6.50	6.91 ± 27.39	25.29 ± 13.7	0.26 ± 16.29	11.19 ± 71.58
Glucose (mmol/L)	<24	0	5.12 ± 0.86			5.01 ± 0.69		
		8	5.53 ± 1.11	0.41 ± 1.07	8.85 ± 18.16	5.18 ± 0.89	0.16 ± 0.43	3.10 ± 8.71
	24–28	0	5.30 ± 1.10			5.48 ± 0.98		
		8	5.45 ± 1.46	0.15 ± 0.76	2.44 ± 15.02	5.65 ± 1.09	0.17 ± 0.55	3.36 ± 10.12
	≥28	0	4.95 ± 0.50			5.69 ± 1.25		
		8	5.19 ± 0.56	0.24 ± 0.64	5.58 ± 13.56	5.98 ± 1.32	0.30 ± 0.60	5.57 ± 10.30
TC (mmol/L)	<24	0	5.36 ± 0.97			5.16 ± 0.80		
		8	6.03 ± 0.75*	0.67 ± 0.73	14.52 ± 18.20	5.16 ± 0.74	0.00 ± 0.40	0.53 ± 7.47
	24–28	0	5.04 ± 0.95			5.11 ± 0.83		
		8	5.50 ± 0.84*	0.45 ± 0.62	10.44 ± 14.17	5.35 ± 0.89	0.24 ± 0.57	5.33 ± 11.75
	≥28	0	5.17 ± 0.70			5.30 ± 0.81		
		8	5.39 ± 0.69	0.22 ± 0.43	4.62 ± 8.23	5.58 ± 0.54	0.29 ± 0.66	6.86 ± 14.06

Δ represents week 8 versus week 0, Δ% represents change rate against week 0

ALT alanine aminotransferase, *AST* aspartate aminotransferase, *HDL-C* high-density lipoprotein-cholesterol, *LDL-C* low-density lipoprotein-cholesterol, *TAG* triacylglycerols, *TC* total cholesterol

* Different from week 0, $P < 0.05$

\# Different from LCT group, $P < 0.05$

subjects with MLCT consumption relative to LCT in another study [20]. Furthermore, in overweight people, those with relatively a lower body weight had the greatest increase in energy expenditure and fat oxidation [21]. Therefore, the intake of MLCT may be effective in reducing body weight and body fat with body weight not yet highly elevated.

Our results might be explained in part by a greater increase in diet-induced thermogenesis after ingesting MLCT than LCT [10, 22]. Ogawa et al. [10] conducted a study of 20 volunteers given a liquid meal containing 14 g of MLCT or LCT; intake of MLCT significantly increased diet-induced thermogenesis. With regard to the mechanism of thermogenesis, several studies have shown that MCT-fed rats had a higher oxygen consumption than LCT-fed rats after administration of norepinephrine or the sympathetic activation of brown adipose tissue [23–25]. Hence, intake of MLCT might not trigger greater diet-induced thermogenesis in obese subjects than in lean and overweight subjects.

Obesity is associated with insulin resistance [12]. Insulin resistance that is characterized by decreasing adipose tissue lipolysis and resisting increases in fat oxidation and increasing hepatic synthesis of triacylglycerols may explain in part that our results showed less response in obese subjects than in overweight subjects in body weight control after intake of MLCT. In other words, intake of MLCT did not induce greater lipolysis and fatty acid oxidation in obese subjects than in overweight subjects.

We also found that consumption of MLCT resulted in a reduced level of fasting blood TAG in hypertriacylglycerolemic and overweight subjects. The mechanism remains unclear. MCT promoting energy expenditure and fat oxidation in both liver and adipose tissue may have contributed to our results [26–29]. In addition to the effect of MCT consumption on fasting blood TAG reduction, MCT intake also induces lower postprandial TAG levels than with consumption of LCT or a soybean oil liquid diet [30, 31].

MLCT consumption did not affect blood cholesterol concentration as compared with LCT consumption; however, MLCT consumption decreased LDL-C concentration and increased HDL-C level. These results suggest that MLCT may have a protective role in the cardiovascular system. Why MLCT consumption does not affect serum cholesterol levels needs to be determined. One possible explanation is that the activity of 3-hydroxy-3-methylglutaryl-CoA, a key enzyme in cholesterol synthesis, is reduced after MLCT administration [32]. In addition, LDL receptor activity in mononuclear cells is higher with MLCT than trilaurin consumption [33].

In contrast to our results, Cater et al. [34] found that natural food supplemented with MLCT increased plasma TC, LDL and TAG levels as compared with a diet supplemented with long-chain fatty acids. The fat accounted for 53% of intake, the mean BMI was 27 ± 5 kg/m^2, and the total amount of fat intake and subject selection, as well as food composition, which may explain their conclusions. In the Temme et al. [35] study, exchanging of oleic acid with MCFA increased serum TC and LDL-C concentrations; however, the response did not differ significantly from the responses to oleic acid and myristic acid, so their conclusions need to be confirmed.

Conclusion

Intake of MLCT might help reduce body fat and levels of fasting blood TAG and LDL-C in hypertriacylglycerolemic and overweight Chinese subjects under an appropriate dietary regimen. MLCT might be useful for control of abnormal TAG metabolism and body fat accumulation in overweight subjects. However, a longer term and larger sample size clinical trial is needed to confirm the substantial effects of MLCT in overweight and hypertriacylglycerolemic individuals.

Acknowledgments This work was supported by the Nisshin Oillio Company. Authors are grateful to Dr. Akira Seto and Ms. Kaori Nakajima for technical support. We also gratefully acknowledge the dedicated volunteers who participated in this project.

Conflict of interest statement None of the authors have any conflicts of interest.

References

1. Chen CM, Zhao W, Yang Z, Zhai Y, Wu Y, Kong L (2008) The role of dietary factors in chronic disease control in China. Obes Rev 9:100–103
2. Zhao W, Zhai Y, Hu J, Wang J, Yang Z, Kong L, Chen C (2008) Economic burden of obesity-related chronic diseases in Mainland China. Obes Rev 9(Suppl 1):62–67
3. Yuan G, Al-Shali KZ, Hegele RA (2007) Hypertriglyceridemia: its etiology, effects and treatment. CMAJ 176:1113–1120
4. Zhou B, Wu Y, Yang J, Li Y, Zhang H, Zhao L (2002) Overweight is an independent risk factor for cardiovascular disease in Chinese populations. Obes Rev 3:147–156
5. Moussavi N, Gavino V, Receveur O (2008) Could the quality of dietary fat, and not just its quantity, be related to risk of obesity? Obes (Silver Spring) 16:7–15
6. Babayan VK (1987) Medium chain triglycerides and structured lipids. Lipids 22:417–420
7. Hashim SA, Tantibhedyangkul P (1987) Medium chain triglyceride in early life: effects on growth of adipose tissue. Lipids 22:429–434
8. Tsuji H, Kasai M, Takeuchi H, Nakamura M, Okazaki M, Kondo K (2001) Dietary medium-chain triacylglycerols suppress accumulation of body fat in a double-blind, controlled trial in healthy men and women. J Nutr 131:2853–2859
9. Han JR, Deng B, Sun J, Chen CG, Corkey BE, Kirkland JL, Ma J, Guo W (2007) Effects of dietary medium-chain triglyceride on

weight loss and insulin sensitivity in a group of moderately overweight free-living type 2 diabetic Chinese subjects. Metabolism 56:985–991
10. Ogawa A, Nosaka N, Kasai M, Aoyama T, Okazaki M, Igarashi O, Kondo K (2007) Dietary medium- and long-chain triacylglycerols accelerate diet-induced thermogenesis in humans. J Oleo Sci 56:283–287
11. Xue C, Liu Y, Wang J, Zhang R, Zhang Y, Zhang J, Zhang Y, Zheng Z, Yu X, Jing H, Nosaka N, Arai C, Kasai M, Aoyama T, Wu J (2009) Consumption of medium- and long-chain triacylglycerols decreases body fat and blood triglyceride in Chinese hypertriglyceridemic subjects. Eur J Clin Nutr 63:879–886
12. Westphal SA (2008) Obesity, abdominal obesity, and insulin resistance. Clin Cornerstone 9:23–31
13. Zhou B, Cooperative Meta-analysis Group of China Obesity Task Force (2002) Predictive values of body mass index and waist circumference to risk factors of related disease in Chinese adult population. Zhonghua Liu Xing Bing Xue Za Zhi 23:5–10
14. Tokunaga K, Matsuzawa Y, Ishikawa K, Tarui S (1983) A novel technique for the determination of body fat by computed tomography. Int J Obes 7:437–445
15. St-Onge MP, Ross R, Parsons WD, Jones PJ (2003) Medium-chain triglycerides increase energy expenditure and decrease adiposity in overweight men. Obes Res 11:395–402
16. Nosaka N, Maki H, Suzuki Y, Haruna H, Ohara A, Kasai M, Tsuji H, Aoyama T, Okazaki M, Igarashi O, Kondo K (2003) Effects of margarine containing medium-chain triacylglycerols on body fat reduction in humans. J Atheroscler Thromb 10:290–298
17. Kasai M, Nosaka N, Maki H, Negishi S, Aoyama T, Nakamura M, Suzuki Y, Tsuji H, Uto H, Okazaki M, Kondo K (2003) Effect of dietary medium- and long-chain triacylglycerols (MLCT) on accumulation of body fat in healthy humans. Asia Pac J Clin Nutr 12:151–160
18. Yost TJ, Eckel RH (1989) Hypocaloric feeding in obese women: metabolic effects of medium-chain triglyceride substitution. Am J Clin Nutr 49:326–330
19. Scalfi L, Coltorti A, Contaldo F (1991) Postprandial thermogenesis in lean and obese subjects after meals supplemented with medium-chain and long-chain triglycerides. Am J Clin Nutr 53:1130–1133
20. Binnert C, Pachiaudi C, Beylot M, Hans D, Vandermander J, Chantre P, Riou JP, Laville M (1998) Influence of human obesity on the metabolic fate of dietary long- and medium-chain triacylglycerols. Am J Clin Nutr 67:595–601
21. St-Onge MP, Jones PJ (2003) Greater rise in fat oxidation with medium-chain triglyceride consumption relative to long-chain triglyceride is associated with lower initial body weight and greater loss of subcutaneous adipose tissue. Int J Obes Relat Metab Disord 27:1565–1571
22. Noguchi O, Takeuchi H, Kubota F, Tsuji H, Aoyama T (2002) Larger diet-induced thermogenesis and less body fat accumulation in rats fed medium-chain triacylglycerols than in those fed long-chain triacylglycerols. J Nutr Sci Vitaminol (Tokyo) 48:524–529
23. Rothwell NJ, Stock MJ (1987) Stimulation of thermogenesis and brown fat activity in rats fed medium chain triglyceride. Metabolism 36:128–130
24. Baba N, Bracco EF, Hashim SA (1987) Role of brown adipose tissue in thermogenesis induced by overfeeding a diet containing medium chain triglyceride. Lipids 22:442–444
25. Young JB, Walgren MC (1994) Differential effects of dietary fats on sympathetic nervous system activity in the rat. Metabolism 43:51–60
26. Hill JO, Peters JC, Swift LL, Yang D, Sharp T, Abumrad N, Greene HL (1990) Changes in blood lipids during six days of overfeeding with medium or long chain triglycerides. J Lipid Res 31:407–416
27. Roynette CE, Rudkowska I, Nakhasi DK, Jones PJ (2007) Structured medium and long chain triglycerides show short-term increases in fat oxidation, but no changes in adiposity in men. Nutr Metab Cardiovasc Dis 18:298–305
28. St-Onge MP, Bourque C, Jones PJ, Ross R, Parsons WE (2003) Medium- versus long-chain triglycerides for 27 days increases fat oxidation and energy expenditure without resulting in changes in body composition in overweight women. Int J Obes Relat Metab Disord 27:95–102
29. Shinohara H, Wu J, Kasai M, Aoyama T (2006) Randomly interesterified triacylglycerol containing medium- and long-chain fatty acids stimulates fatty acid metabolism in white adipose tissue of rats. Biosci Biotechnol Biochem 70:2919–2926
30. Kasai M, Maki H, Nosaka N, Aoyama T, Ooyama K, Uto H, Okazaki M, Igarashi O, Kondo K (2003) Effect of medium-chain triglycerides on the postprandial triglyceride concentration in healthy men. Biosci Biotechnol Biochem 67:46–53
31. Takeuchi H, Kasai M, Taguchi N, Tsuji H, Suzuki M (2002) Effect of triacylglycerols containing medium- and long-chain fatty acids on serum triacylglycerol levels and body fat in college athletes. J Nutr Sci Vitaminol (Tokyo) 48:109–114
32. Takase S, Morimoto A, Nakanishi M, Muto Y (1977) Long-term effect of medium-chain triglyceride on hepatic enzymes catalyzing lipogenesis and cholesterogenesis in rats. J Nutr Sci Vitaminol (Tokyo) 23:43–51
33. Tsai YH, Park S, Kovacic J, Snook JT (1999) Mechanisms mediating lipoprotein responses to diets with medium-chain triglyceride and lauric acid. Lipids 34:895–905
34. Cater NB, Heller HJ, Denke MA (1997) Comparison of the effects of medium-chain triacylglycerols, palm oil, and high oleic acid sunflower oil on plasma triacylglycerol fatty acids and lipid and lipoprotein concentrations in humans. Am J Clin Nutr 65: 41–45
35. Temme EH, Mensink RP, Homstra G (1997) Effects of medium chain fatty acids (MCFA), myristic acid, and oleic acid on serum lipoproteins in healthy subjects. J Lipid Res 38:1746–1754

Lipids (2010) 45:511–517
DOI 10.1007/s11745-010-3426-z

ORIGINAL ARTICLE

APOA1/A5 Variants and Haplotypes as a Risk Factor for Obesity and Better Lipid Profiles in a Brazilian Elderly Cohort

Elizabeth Suchi Chen · Tatiane Katsue Furuya · Diego Robles Mazzotti · Vanessa Kiyomi Ota · Maysa Seabra Cendoroglo · Luiz Roberto Ramos · Lara Quirino Araujo · Rommel Rodriguez Burbano · Marília de Arruda Cardoso Smith

Received: 16 November 2009 / Accepted: 22 April 2010 / Published online: 18 May 2010

Abstract Genetic variations in the *APOA1/C3/A4/A5* gene cluster have been studied and proposed to be the leading key for susceptibility to cardiovascular diseases and age-associated disorders. We aimed to investigate the associations of rs12721026 (*APOA1*) and rs1729408 (*APOA5*) polymorphisms and their haplotypes with some age-related diseases, as well as with lipids and proteins serum levels in a cohort from a Brazilian Elderly Longitudinal Study (EPIDOSO). Genotyping was performed by polymerase chain reaction restriction fragment length polymorphism (PCR-RFLP). Statistical analyses were carried out using logistic regression analysis, Student's *t*-test, and linkage disequilibrium (LD) analysis. Polymorphic allele frequencies were 0.095 and 0.449 for rs12721026 and rs1729408, respectively. The C-allele of rs1729408 was associated with higher high-density lipoprotein (HDL) ($P = 0.022$) and glycated hemoglobin levels ($P = 0.020$). We also showed that rs12721026 and rs1729408 were in LD. The GC haplotype, which is composed of the G-allele of rs12721026 and the C-allele of rs1729408, was significantly associated with obesity ($P = 0.028$), with higher glycated hemoglobin ($P = 0.006$), and fasting glucose ($P = 0.0003$) compared to the TT haplotype, which includes the wild-type alleles of both polymorphisms. Moreover, we found an association between the TC haplotype and higher HDL levels ($P = 0.0039$). This is the first time that haplotypes involving these polymorphisms were evaluated. Our results showed that these polymorphisms were involved in the development of obesity and in alterations of lipids and proteins serum levels in a Brazilian population. The present findings might also clarify the role of these polymorphisms and their haplotypes in lipids and proteins metabolism.

Keywords Obesity · Glycated hemoglobin · Polymorphisms · *APOA1* · *APOA5* · HDL · Haplotype

Abbreviations

BMI	Body mass index
CVD	Cardiovascular disease
HbAc1	Glycated hemoglobin
LD	Linkage disequilibrium
MMSE	Mini-Mental State Examination
SD	Standard deviation
SNP	Single nucleotide polymorphism
TG	Triglyceride
OR	Odds ratio
CI	Confidence interval

Introduction

Increased low-density lipoprotein (LDL) and triglyceride (TG) [1] and decreased high-density lipoprotein (HDL) plasma levels have been shown to be independent risk factors for cardiovascular diseases (CVDs) [2] and

E. S. Chen · T. K. Furuya · D. R. Mazzotti · V. K. Ota · L. Q. Araujo · R. R. Burbano · M. de Arruda Cardoso Smith (✉)
Genetics Division, Department of Morphology and Genetics, Universidade Federal de São Paulo (UNIFESP), Rua Botucatu, 740, Edifício Leitão da Cunha, 1° Andar, São Paulo, SP 04023-900, Brazil
e-mail: betty.morf@epm.br

M. S. Cendoroglo · L. R. Ramos
Department of Medicine, Universidade Federal de São Paulo (UNIFESP), São Paulo, Brazil

important determinants of atherosclerosis susceptibility [3]. In Brazil, the main cause of adult death is CVD (32%), followed by neoplasia [4]. Genetic and environmental factors play a key role in lipoproteins and lipids serum levels [5]. In fact, several genetic variants have been evaluated and associated with lipid profiles [6]. In 2009, three genome-wide association studies described 20 new loci associated with lipid serum levels [1, 7, 8], including the apolipoprotein gene cluster *APOA1/C3/A4/A5*, on 11q23, which has been associated with CVD and alterations on HDL, LDL, and TG serum levels [9].

APOA1 comprises roughly 70% of the HDL protein mass and acts in the transport of cholesterol from the peripheral tissues to the liver [10]. Indeed, several studies have shown a relationship between *APOA1* and protection against atherosclerosis [11]. The rs12721026 polymorphism (also known as *Pst*I), located in the 3′ flanking region of *APOA1*, has been associated with the development of CVD [12, 13] and decreased HDL levels [13].

APOA5 has been involved in TG metabolism [14] and presents lower serum concentration in comparison to other apolipoproteins. *APOA5* knockout mice showed four-fold increased TG compared to wild-type alleles [15]. In the promoter region of *APOA5*, there is a well described polymorphism (rs662799) which has been widely associated with TG levels. Our previous report showed no association of rs662799 with age-related morbidities in the same elderly cohort studied in the present study [16]. rs1729408 (also known as SNP4—single nucleotide polymorphism 4), an *APOA4/A5* intergenic polymorphism, has been associated with systolic blood pressure and measures of obesity in European populations [17] and with higher HDL in the Chinese population [18]. However, rs1729408 was not associated with CVD and lipid plasma levels in the French population [19].

In the current study, we aimed to investigate the association of the rs12721026 and rs1729408 polymorphisms and their haplotypes with morbidities affecting a cohort from a Brazilian Elderly Longitudinal Study (EPIDOSO), as well as with TG, total cholesterol, HDL, very-low-density lipoprotein (VLDL), LDL, creatinine, urea, albumin, glycated hemoglobin (HbAc1), and fasting glucose serum levels.

Experimental Procedure

Studied Population

The studied population was a subsample of 341 subjects (238 females and 103 males) who participated in wave 4 (2000–2001) of the Elderly Longitudinal Study (EPIDOSO) [20]. This population was composed of individuals of European (89.2%), Japanese (3.3%), Middle Eastern (1.8%), mixed, and/or other (5.7%) origins. The mean age of this population was 79.75 ± 5.38 years (range 66–97). All participants were informed about the study protocol and provided information about previous medical conditions. The Institutional Research Ethics Committee approved this study and all subjects or their legal representatives signed an informed consent according to the Declaration of Helsinki.

Clinical inquiries were performed to obtain information about previous diseases, current medication use, lifestyle, anthropometric, and blood pressure measurements. Physicians performed the physical examination and blood samples were collected for laboratory procedures. Table 1 summarizes all of the characteristics of our sample. CVD was considered to be positive when individuals self-reported previous CVD and were taking specific medication prescribed by physicians. Subjects either currently using anti-hypertensive drugs or those with systolic blood pressure above 140 or diastolic blood pressure above 95 mmHg were considered to be positive for hypertension [21]. Those currently taking insulin or oral medication and those with fasting glucose equal to or above 126 mg/dl were considered to be positive for type II diabetes [22]. Subjects with body mass index (BMI) above 27 kg/m^2 were considered to be positive for obesity [23]. Cognitive function was evaluated using the Mini-Mental State Examination (MMSE) screening instrument, validated for

Table 1 Characterization of the sample

Variables	*N*	Number of affected individuals (%)	Mean ± SD
Cardiovascular disease	341	72 (21.1%)	
Type II diabetes	340	216 (63.5%)	
Hypertension	339	289 (85.3%)	
Obesity	278	112 (40.3%)	
Depression	318	62 (19.5%)	
Dementia	335	28 (8.4%)	
Total cholesterol (mg/dl)	223		216.63 ± 41.39
Triglyceride (mg/dl)	223		145.63 ± 65.76
VLDL (mg/dl)	219		28.22 ± 11.04
HDL (mg/dl)	222		54.99 ± 13.94
LDL (mg/dl)	217		132.30 ± 35.36
Urea (mg/dl)	215		40.19 ± 12.64
Creatinine (mg/dl)	214		0.95 ± 0.24
Albumin (g/dl)	214		4.04 ± 0.32
Glycated hemoglobin (%)	304		5.77 ± 1.51
Fasting glucose (mg/dl)	312		98.56 ± 32.78

N number of consulted individuals; *SD* standard deviation

the Brazilian population. A cut-off score for low cognition level (roughly classified as dementia) was 24 (out of 30) and presents 80–90% sensitivity and 80% specificity [24, 25]. Depression was characterized by a score of above 5 using a validated Brazilian version of the Older Americans Resources and Services (OARS) questionnaire [26]. Although some studies have shown that self-reported past history and medical records are usually concordant for selected medical conditions in the elderly [27], past histories were only accepted when there was also evidence in physical examinations, electrocardiograms, computed tomography scans, or physician reports.

Laboratory Examinations

Laboratory examinations were performed as routine examinations using commercial kits. Lipids and lipid fraction measurements were performed using routine enzymatic tests. Urea, creatinine, and albumin serum levels and fasting glucose were investigated routinely by colorimetric, kinetic, and ultraviolet tests. HbAc1 was measured by high-performance liquid chromatography. The coefficients of variation for these measurements ranged from 2 to 3.5%.

DNA Extraction

Genomic DNA from whole blood was isolated using the QIAamp® DNA Blood Midi Kit (Qiagen, Hilden, Germany), according to the manufacturer's instructions.

Polymorphism Detection

For both polymorphisms, polymerase chain reaction (PCR) was carried out in 25 µl containing 100 ng genomic DNA, 0.1 mmol/l dNTPs (LGC, São Paulo, Brazil), 2.0 mmol/l $MgCl_2$, 1 U Taq DNA polymerase (LGC, São Paulo, Brazil), and 0.4 µmol/l of each primer (Biosynthesis Inc., Lewisville, TX) in 10% buffer. The primers used for genotyping were as previously described [28, 29]. For rs1729408, the mixture was denaturated for 5 min at 94°C, passed through 35 cycles of denaturing at 94°C for 30 s, annealing at 60°C for 30 s, and extension at 72°C for 30 s, with a final extension at 72°C for 7 min. Six microliters of PCR product (162 bp) were digested with 2 U of *Hae*III (NEB, Ipswich, MA) at 37°C for 16 h. For amplification of the 740 bp-fragment of rs12721026, the mixture underwent 5 min denaturation at 94°C, 35 cycles of 94°C for 40 s, 66°C for 40 s, and 72°C for 60 s, with a final extension at 72°C for 10 min. Four units of *Pst*I (NEB, Ipswich, MA) were added to 10 µl of PCR product and then incubated for 3 h at 37°C.

Statistical Analyses

Allele frequencies were calculated by allele counting as described by Emery [30]. The Hardy–Weinberg equilibrium was evaluated using the χ^2 test. To assess the association between allele and morbidity, we used logistic regression analysis, which considered morbidity as a dependent variable and allele, age, and sex as covariates in the model. Odds ratios (ORs) with 95% confidence intervals (CIs) were also calculated. The mean serum levels concerning lipids, lipid fractions, urea, albumin, creatinine, HbAc1, and fasting glucose were compared between the two allele groups by Student's *t*-test. The χ^2 test, logistic regression analyses, and Student's *t*-test were performed using SPSS® 16.0. Linkage disequilibrium (LD) and haplotype association analysis with morbidities were performed by a linkage disequilibrium analyzer (LDA) [31] and Haploview software [32]. The expectation–maximization algorithm was used to estimate haplotype frequencies and to verify the association between haplotypes and morbidities. The χ^2 test was used to compare the haplotypes frequencies of cases and controls concerning the morbidities studied. Haplotype association with serum levels was performed using a *F*-test computed from a linear model fitted to the estimated haplotypes by the SNPStats web tool [33]. Statistical significance was accepted at $P < 0.05$.

Results

Polymorphic allele frequencies were 0.095 and 0.449 for the rs12721026 and rs1729408 polymorphisms, respectively. These polymorphisms followed the Hardy–Weinberg equilibrium in the whole population ($\chi^2 = 2.5464$; df = 1; $P = 0.1105$ and $\chi^2 = 1.7059$; df = 1; $P = 0.1915$, respectively).

Our results showed that the C-allele of rs1729408 was associated with higher HDL ($P = 0.022$) and HbAc1 levels ($P = 0.020$; Table 2). Nevertheless, the rs12721026 polymorphism was neither associated with lipids and proteins serum levels nor with the detected morbidities. We found that the rs12721026 and rs1729408 polymorphisms were in LD ($D' = 0.5438$; $r^2 = 0.0366$; $P = 0.0016$). When haplotypes were analyzed, the GC haplotype, which is composed of the minor alleles of rs12721026 and rs1729408 respectively, was associated with obesity (Table 3; $P = 0.028$), higher levels of HbAc1 ($P = 0.006$), and fasting glucose ($P = 0.0003$) compared to the TT haplotype, which includes the wild-type alleles of both polymorphisms (Table 4). In addition, we also found an association of the TC haplotype, composed of the T-allele

Table 2 Student's *t*-test results concerning lipids and proteins serum levels and polymorphisms in the Brazilian elderly cohort

Variables	*N*	rs12721026 polymorphism		*P*-value	*N*	rs1729408 polymorphism		*P*-value
		T-allele Mean ± SD	G-allele Mean ± SD			T-allele Mean ± SD	C-allele Mean ± SD	
Age	592	79.78 ± 5.50	79.21 ± 4.68	0.461	652	79.91 ± 5.38	79.71 ± 5.46	0.641
Total cholesterol	406	217.62 ± 42.64	217.09 ± 35.84	0.893	430	215.06 ± 40.11	217.23 ± 41.65	0.582
Triglycerides	406	146.06 ± 66.73	137.65 ± 53.31	0.306	430	142.14 ± 60.76	146.19 ± 69.07	0.517
VLDL	398	28.11 ± 10.72	27.47 ± 10.75	0.511	422	27.88 ± 10.87	27.83 ± 10.44	0.963
HDL	406	55.28 ± 14.28	56.30 ± 12.84	0.852	428	53.76 ± 13.10	56.84 ± 14.52	0.022*
LDL	396	33.21 ± 36.45	130.20 ± 28.65	0.903	418	132.87 ± 35.05	130.68 ± 34.26	0.519
Urea	396	40.21 ± 12.22	43.50 ± 17.46	0.076	414	40.01 ± 12.50	39.97 ± 12.58	0.975
Creatinine	394	0.95 ± 0.24	0.91 ± 0.23	0.243	412	0.97 ± 0.25	0.93 ± 0.23	0.099
Albumin	394	4.04 ± 0.32	4.07 ± 0.29	0.663	412	4.03 ± 0.31	4.05 ± 0.32	0.581
Glycated hemoglobin	536	5.77 ± 1.47	6.04 ± 1.51	0.398	580	5.62 ± 1.20	5.95 ± 1.69	0.020*
Fasting glucose	548	96.77 ± 26.23	98.66 ± 24.11	0.528	596	97.14 ± 25.78	98.99 ± 38.52	0.484

SD standard deviation; *N* number of alleles with measured lipid serum levels

* $P < 0.05$

Table 3 χ^2 test results comparing the frequency of cases and controls of the rs12721026/rs1729408 haplotypes and obesity

Morbidity	Haplotype	Frequency			χ^2	*P*-value
		Total	Case	Control		
Obesity	TT	0.526	0.494	0.527	0.585	0.4445
	TC	0.38	0.388	0.399	0.064	0.8008
	GC	0.07	0.098	0.050	4.831	0.0279*
	GT	0.024	0.020	0.024	0.123	0.7261

* $P < 0.05$

of rs12721026 and the C-allele of rs1729408, with higher HDL levels ($P = 0.0039$; Table 4).

Discussion

Our results showed that the rs1729408 C-allele frequency was 0.449 in our Brazilian elderly cohort, similar to other European populations (30–41%) [14, 17], such as French (0.39) [19] and British (0.34) [29]. Regarding the rs12721026 polymorphism, the G-allele frequency was 0.095 in our sample, similar to those observed in Australian (0.09) [34] and Mediterranean populations (0.11) [35].

We found a significant association between the rs1729408 C-allele and higher HDL levels ($P = 0.022$). Likewise, the CC genotype presented higher HDL plasma levels in Chinese patients with CVD [18], whereas no association was found with CVD in our sample, confirming previous data in the French population [19].

In addition, our results revealed an association of the rs1729408 C-allele with higher HbAc1 levels ($P = 0.020$). It has recently been shown that D-glucose regulates *APOA5* expression by dephosphorylation [36], suggesting an involvement of *APOA5* in glucose metabolism [17]. Another previous study including four regions of Europe also showed that this variant influenced insulin and glucose levels after an oral glucose tolerance test (OGTT) [17]. Furthermore, it has been reported that there are higher HbAc1 levels in hypertensive patients in relation to controls [37], as well as a correlation of the CC genotype with higher blood pressure [17]. In an European population, CC genotype carriers presented significant association with higher systolic blood pressure and higher waist-to-hip ratio, which is a measure of obesity [17], suggesting that HbAc1 levels may participate in hypertension development. Taken together, these data suggest that the *APOA4* and *APOA5* intergenic region might present binding sites for nuclear factors, which can be inhibited or altered in the presence of the rs1729408 C-allele, leading to alterations in lipid and glucose metabolisms.

Although we did not observe any association between rs12721026 and the studied morbidities, a tendency of association between the G-allele and obesity was shown in our sample ($P = 0.069$) (data not shown). In fact, rs12721026 has not been associated with CVD in Caucasians [34, 38], confirming our results. We have previously described an association of another polymorphism in the first intron of *APOA1*, rs5069, with obesity ($P = 0.04$) in the same cohort [39]. In addition, *APOA1* was correlated to adipokines in Asian Indian and Caucasian populations [40].

Table 4 SNPStats results associating rs12721026/rs1729408 haplotypes with glycated hemoglobin, fasting glucose, and HDL levels compared to the TT haplotype

Serum levels	*N*	Haplotype	Frequency	Difference (95% CI)	*P*-value
Glycated hemoglobin	304	GC	0.0756	0.81 (0.24–1.39)	0.006*
Fasting glucose	312	GC	0.0663	23.12 (10.69–35.55)	0.0003*
HDL	222	TC	0.3871	4.46 (1.46–7.46)	0.0039*

N number of individuals with measured lipid serum levels; 95% *CI* 95% of confidence intervals

* $P < 0.05$

Therefore, *APOA1* might be implicated in the development of obesity.

We did not detect any association between the rs12721026 polymorphism and lipids parameters levels, confirming other studies in European [41], Korean [42], and Swedish [43] populations. Conversely, TG genotype carriers presented higher TG levels than TT in the European population [44] and the G-allele has been associated with lower *APOA1* and HDL levels in several populations [13, 35, 45, 46]. These controversial results indicate that there might be another polymorphism in this cluster influencing the association results which deserves further investigation.

rs1729408 and rs12721026 polymorphisms were in LD ($P = 0.0016$) and their haplotypes were investigated. The GC haplotype was associated with obesity and presented a higher frequency in cases (0.098) than in controls (0.050), suggesting that the GC haplotype might be a risk factor for obesity. In the current study, we did find a tendency of association between the G-allele of the rs12721026 polymorphism and obesity; however, only in the presence of the rs1729408 C-allele did this association become significant. These findings suggest a synergistic effect of these polymorphisms on influencing obesity. Although rs12721026 and rs1729408 are located in a non-coding region, they might have a functional role in the metabolism. Other variants within *APOA5* have been described and associated with changes in BMI, supporting our findings [47].

We also observed higher HbAc1 and fasting glucose levels in GC compared to TT haplotype carriers. In the Indian population, rs12721026 was associated with increased risk for type II diabetes [48]. Our results showed an association of the rs1729408 C-allele and higher HbAc1 levels. Nevertheless, the association of the GC haplotype became stronger ($P = 0.006$), suggesting that the interaction between rs1729408 and rs12721026 polymorphisms might be involved in the development of hypertension.

Furthermore, our data showed that the TC haplotype was associated with higher HDL levels ($P = 0.0039$). *APOA1* and *APOA5* gene expression are modulated by peroxisome proliferator-activated receptor α (*PPARα*). Our group has previously reported an association of the C-allele of rs4253778 (*PPARα*) and higher HDL compared to the G-allele [49], suggesting that *APOA1* and *APOA5* are involved in the regulation of HDL levels, probably via *PPARα*.

In conclusion, rs1729408 was associated with higher HDL and HbAc1 levels. Moreover, the GC haplotype was associated with obesity and higher HbAc1 and fasting glucose levels and TC haplotype was associated with higher HDL levels. To our knowledge, this is the first time that haplotypes involving these polymorphisms have been evaluated. The present findings might clarify the influence of these polymorphisms in lipids and proteins metabolisms and their association with age-related diseases. Therefore, genetic variations in the *APOA1/C3/A4/A5* gene cluster may characterize important risk factors for metabolic homeostasis.

Acknowledgments This research was supported by Conselho Nacional de Desenvolvimento Científico e Tecnológico (CNPq, Brazil), Coordenadoria de Aperfeiçoamento de Pessoal de Ensino Superior (CAPES, Brazil), and Fundação de Amparo à Pesquisa do Estado de São Paulo (FAPESP, Brazil).

References

1. Aulchenko YS, Ripatti S, Lindqvist I, Boomsma D, Heid IM, Pramstaller PP, Penninx BW, Janssens AC, Wilson JF, Spector T, Martin NG, Pedersen NL, Kyvik KO, Kaprio J, Hofman A, Freimer NB, Jarvelin MR, Gyllensten U, Campbell H, Rudan I, Johansson A, Marroni F, Hayward C, Vitart V, Jonasson I, Pattaro C, Wright A, Hastie N, Pichler I, Hicks AA, Falchi M, Willemsen G, Hottenga JJ, de Geus EJ, Montgomery GW, Whitfield J, Magnusson P, Saharinen J, Perola M, Silander K, Isaacs A, Sijbrands EJ, Uitterlinden AG, Witteman JC, Oostra BA, Elliott P, Ruokonen A, Sabatti C, Gieger C, Meitinger T, Kronenberg F, Döring A, Wichmann HE, Smit JH, McCarthy MI, van Duijn CM, Peltonen L (2009) Loci influencing lipid levels and coronary heart disease risk in 16 European population cohorts. Nat Genet 41:47–55
2. Hokanson JE, Austin MA (1996) Plasma triglyceride level is a risk factor for cardiovascular disease independent of high-density lipoprotein cholesterol level: a meta-analysis of population-based prospective studies. J Cardiovasc Risk 3:213–219
3. Steinberg D, Gotto AM Jr (1999) Preventing coronary artery disease by lowering cholesterol levels: fifty years from bench to bedside. JAMA 282:2043–2050
4. DATASUS (2006) MS/SVS/DASIS—Sistema de Informações sobre Mortalidade—SIM [cited 1st June 2009]. Available online

at: http://tabnet.datasus.gov.br/cgi/deftohtm.exe?sim/cnv/obtuf.def
5. Ordovas JM, Lopez-Miranda J, Mata P, Perez-Jimenez F, Lichtenstein AH, Schaefer EJ (1995) Gene-diet interaction in determining plasma lipid response to dietary intervention. Atherosclerosis 118(Suppl):S11–S27
6. Lanktree MB, Anand SS, Yusuf S, Hegele RA (2009) Replication of genetic associations with plasma lipoprotein traits in a multiethnic sample. J Lipid Res 50:1487–1496
7. Kathiresan S, Willer CJ, Peloso GM, Demissie S, Musunuru K, Schadt EE, Kaplan L, Bennett D, Li Y, Tanaka T, Voight BF, Bonnycastle LL, Jackson AU, Crawford G, Surti A, Guiducci C, Burtt NP, Parish S, Clarke R, Zelenika D, Kubalanza KA, Morken MA, Scott LJ, Stringham HM, Galan P, Swift AJ, Kuusisto J, Bergman RN, Sundvall J, Laakso M, Ferrucci L, Scheet P, Sanna S, Uda M, Yang Q, Lunetta KL, Dupuis J, de Bakker PI, O'Donnell CJ, Chambers JC, Kooner JS, Hercberg S, Meneton P, Lakatta EG, Scuteri A, Schlessinger D, Tuomilehto J, Collins FS, Groop L, Altshuler D, Collins R, Lathrop GM, Melander O, Salomaa V, Peltonen L, Orho-Melander M, Ordovas JM, Boehnke M, Abecasis GR, Mohlke KL, Cupples LA (2009) Common variants at 30 loci contribute to polygenic dyslipidemia. Nat Genet 41:56–65
8. Sabatti C, Service SK, Hartikainen AL, Pouta A, Ripatti S, Brodsky J, Jones CG, Zaitlen NA, Varilo T, Kaakinen M, Sovio U, Ruokonen A, Laitinen J, Jakkula E, Coin L, Hoggart C, Collins A, Turunen H, Gabriel S, Elliot P, McCarthy MI, Daly MJ, Järvelin MR, Freimer NB, Peltonen L (2009) Genome-wide association analysis of metabolic traits in a birth cohort from a founder population. Nat Genet 41:35–46
9. Olivier M, Wang X, Cole R, Gau B, Kim J, Rubin EM, Pennacchio LA (2004) Haplotype analysis of the apolipoprotein gene cluster on human chromosome 11. Genomics 83:912–923
10. Kuyl JM, Mendelsohn D (1992) Observed relationship between ratios HDL-cholesterol/total cholesterol and apolipoprotein A1/apolipoprotein B. Clin Biochem 25:313–316
11. Srivastava RA, Srivastava N (2000) High density lipoprotein, apolipoprotein A-I, and coronary artery disease. Mol Cell Biochem 209:131–144
12. Dan Q, Huang Y, Peng Z (1995) DNA polymorphisms of the apolipoprotein AI-CIII-AIV gene cluster in coronary artery disease. Zhonghua Yi Xue Za Zhi 75:584–7, 637
13. Vavatsi NA, Kouidou SA, Geleris PN, Tachmatzidis C, Gikas T, Tsifodimos DK, Trakatellis AC (1995) Increased frequency of the rare PstI allele (P2) in a population of CAD patients in northern Greece. Clin Genet 47:22–26
14. Pennacchio LA, Olivier M, Hubacek JA, Cohen JC, Cox DR, Fruchart JC, Krauss RM, Rubin EM (2001) An apolipoprotein influencing triglycerides in humans and mice revealed by comparative sequencing. Science 294:169–173
15. Pennacchio LA, Rubin EM (2003) Apolipoprotein A5, a newly identified gene that affects plasma triglyceride levels in humans and mice. Arterioscler Thromb Vasc Biol 23:529–534
16. Chen ES, Cendoroglo MS, Ramos LR, Araujo LM, Carvalheira GM, de Lábio RW, Burbano RR, Payão SL, de Arruda Cardoso Smith M (2006) APO A-V-1131T–>C polymorphism frequency and its association with morbidity in a Brazilian elderly population. Clin Chem Lab Med 44:32–36
17. Martin S, Nicaud V, Humphries SE, Talmud PJ (2003) Contribution of APOA5 gene variants to plasma triglyceride determination and to the response to both fat and glucose tolerance challenges. Biochim Biophys Acta 1637:217–225
18. Liu HK, Wang CT, Zhang SZ, Xiao CY, Li XF, Zhang KL, Zhang L, Su ZG, Ma YX, Zhou B, Zheng KQ, Li GX (2004) Association of APOA5 gene single nucleotide polymorphism with levels of lipids and coronary heart disease in Chinese. Zhonghua Yi Xue Yi Chuan Xue Za Zhi 21:335–338
19. Dallongeville J, Cottel D, Montaye M, Codron V, Amouyel P, Helbecque N (2006) Impact of APOA5/A4/C3 genetic polymorphisms on lipid variables and cardiovascular disease risk in French men. Int J Cardiol 106:152–156
20. Ramos LR, Toniolo J, Cendoroglo MS, Garcia JT, Najas MS, Perracini M, Paola CR, Santos FC, Bilton T, Ebel SJ, Macedo MB, Almada CM, Nasri F, Miranda RD, Gonçalves M, Santos AL, Fraietta R, Vivacqua I, Alves ML, Tudisco ES (1998) Two-year follow-up study of elderly residents in S. Paulo, Brazil: methodology and preliminary results. Rev Saude Publica 32:397–407
21. Jones DW, Hall JE (2004) Seventh report of the Joint National Committee on Prevention, Detection, Evaluation, and Treatment of High Blood Pressure and evidence from new hypertension trials. Hypertension 43:1–3
22. [No authors listed] (1999) Is fasting glucose sufficient to define diabetes? Epidemiological data from 20 European studies. The DECODE-study group. European Diabetes Epidemiology Group. Diabetes Epidemiology: Collaborative analysis of Diagnostic Criteria in Europe. Diabetologia 42:647–654
23. Kyle UG, Genton L, Hans D, Karsegard VL, Michel JP, Slosman DO, Pichard C (2001) Total body mass, fat mass, fat-free mass, and skeletal muscle in older people: cross-sectional differences in 60-year-old persons. J Am Geriatr Soc 49:1633–1640
24. Bertolucci PH, Brucki SM, Campacci SR, Juliano Y (1994) The Mini-Mental State Examination in a general population: impact of educational status. Arq Neuropsiquiatr 52:1–7
25. Bertolucci PH, Okamoto IH, Brucki SM, Siviero MO, Toniolo Neto J, Ramos LR (2001) Applicability of the CERAD neuropsychological battery to Brazilian elderly. Arq Neuropsiquiatr 59:532–536
26. Blay SL, Ramos LR, Mari Jde J (1988) Validity of a Brazilian version of the Older Americans Resources and Services (OARS) mental health screening questionnaire. J Am Geriatr Soc 36:687–692
27. Bush TL, Miller SR, Golden AL, Hale WE (1989) Self-report and medical record report agreement of selected medical conditions in the elderly. Am J Public Health 79:1554–1556
28. Juvonen T, Savolainen MJ, Kairaluoma MI, Lajunen LH, Humphries SE, Kesäniemi YA (1995) Polymorphisms at the apoB, apoA-I, and cholesteryl ester transfer protein gene loci in patients with gallbladder disease. J Lipid Res 36:804–812
29. Talmud PJ, Hawe E, Martin S, Olivier M, Miller GJ, Rubin EM, Pennacchio LA, Humphries SE (2002) Relative contribution of variation within the APOC3/A4/A5 gene cluster in determining plasma triglycerides. Hum Mol Genet 11:3039–3046
30. Emery AEH (1986) Methodology in medical genetics—an introduction to statistical methods. Longman Group, Edinburgh
31. Ding K, Zhou K, He F, Shen Y (2003) LDA—a java-based linkage disequilibrium analyzer. Bioinformatics 19:2147–2148
32. Barrett JC, Fry B, Maller J, Daly MJ (2005) Haploview: analysis and visualization of LD and haplotype maps. Bioinformatics 21:263–265
33. Solé X, Guinó E, Valls J, Iniesta R, Moreno V (2006) SNPStats: a web tool for the analysis of association studies. Bioinformatics (Oxford, England) 22:1928–1929
34. Simons LA, Balasubramaniam S, Szanto A, Simons J, Friedlander Y, Hickie JB, Shine J (1991) High density lipoproteins, genetic polymorphism for apo A-I and coronary artery disease. Aust N Z J Med 21:330–334
35. Balanyà J, Marsal S, LaVille A, Margalef J, Turner PR, Masana L (1993) Polymorphism (RFLP-PstI) of the apoprotein A-I gene in a healthy population. Its relation to high-density lipoproteins. Med Clin (Barc) 100:90–93

36. Nowak M, Helleboid-Chapman A, Jakel H, Moitrot E, Rommens C, Pennacchio LA, Fruchart-Najib J, Fruchart JC (2008) Glucose regulates the expression of the apolipoprotein A5 gene. J Mol Biol 380:789–798
37. Sathiyapriya V, Selvaraj N, Nandeesha H, Bobby Z, Agrawal A, Pavithran P (2007) Enhanced glycation of hemoglobin and plasma proteins is associated with increased lipid peroxide levels in non-diabetic hypertensive subjects. Arch Med Res 38:822–826
38. Dorow DS, Burke J, Goding JW (1989) Assessment of a PstI polymorphism of the apolipoprotein-AI gene in Australian patients with coronary artery disease. Aust N Z J Med 19:677–681
39. Chen ES, Mazzotti DR, Furuya TK, Cendoroglo MS, Ramos LR, Araujo LQ, Burbano RR, de Arruda Cardoso Smith M (2009) Apolipoprotein A1 gene polymorphisms as risk factors for hypertension and obesity. Clin Exp Med 9:319–325
40. Smith J, Al-Amri M, Sniderman A, Cianflone K (2006) Leptin and adiponectin in relation to body fat percentage, waist to hip ratio and the apoB/apoA1 ratio in Asian Indian and Caucasian men and women. Nutr Metab (Lond) 3:18
41. Kee F, Amouyel P, Fumeron F, Arveiler D, Cambou JP, Evans A, Cambien F, Fruchart JC, Ducimetière P, Dallongeville J (1999) Lack of association between genetic variations of apo A-I-C-III-A-IV gene cluster and myocardial infarction in a sample of European male: ECTIM study. Atherosclerosis 145:187–195
42. Song J, Park JW, Park H, Kim JQ (1998) Linkage disequilibrium of the Apo AI-CIII-AIV gene cluster and their relationship to plasma triglyceride, apolipoprotein AI and CIII levels in Koreans. Mol Cells 8:12–18
43. Peacock RE, Hamsten A, Johansson J, Nilsson-Ehle P, Humphries SE (1994) Associations of genotypes at the apolipoprotein AI-CIII-AIV, apolipoprotein B and lipoprotein lipase gene loci with coronary atherosclerosis and high density lipoprotein subclasses. Clin Genet 46:273–282
44. Wick U, Witt E, Engel W (1995) Restriction fragment length polymorphisms at the apoprotein genes AI, CIII and B-100 and in the 5′ flanking region of the insulin gene as possible markers of coronary heart disease. Clin Genet 47:184–190
45. Maslennikov AB, Kovalenko SP, Oteva EA, Filimonova TA, Mertvetsov NP (1991) Restriction fragment length polymorphism of the apolipoprotein A-I gene among inhabitants of Novosibirsk. Genetika 27:2152–2156
46. Paulweber B, Friedl W, Krempler F, Humphries SE, Sandhofer F (1988) Genetic variation in the apolipoprotein AI-CIII-AIV gene cluster and coronary heart disease. Atherosclerosis 73:125–133
47. Aberle J, Evans D, Beil FU, Seedorf U (2005) A polymorphism in the apolipoprotein A5 gene is associated with weight loss after short-term diet. Clin Genet 68:152–154
48. Singh P, Singh M, Gaur S, Kaur T (2007) The ApoAI-CIII-AIV gene cluster and its relation to lipid levels in type 2 diabetes mellitus and coronary heart disease: determination of a novel susceptible haplotype. Diab Vasc Dis Res 4:124–129
49. Chen ES, Mazzotti DR, Furuya TK, Cendoroglo MS, Ramos LR, Araujo LQ, Burbano RR, Smith Mde A (2010) Association of PPARalpha gene polymorphisms and lipid serum levels in a Brazilian elderly population. Exp Mol Pathol 88:197–201

Lipids (2010) 45:519–530
DOI 10.1007/s11745-010-3421-4

ORIGINAL ARTICLE

Identification and Characterization of Δ12, Δ6, and Δ5 Desaturases from the Green Microalga *Parietochloris incisa*

Umidjon Iskandarov · Inna Khozin-Goldberg · Zvi Cohen

Received: 3 February 2010 / Accepted: 15 April 2010 / Published online: 14 May 2010

Abstract The freshwater microalga *Parietochloris incisa* accumulates, under nitrogen starvation, large amounts of triacylglycerols containing approximately 60% of the ω6 very long-chain polyunsaturated fatty acid (VLC-PUFA), arachidonic acid. Based on sequence homology, we isolated three cDNA sequences from *P. incisa*, designated *PiDesD12*, *PiDesD6*, *PiDesD5*. The deduced amino acid sequences of the three genes contained three conserved histidine motifs; the front-end desaturases, PiDes6 and PiDes5, contained a fused N-terminal cytochrome *b5* domain. By functional characterization in the yeast *Saccharomyces cerevisiae*, we confirmed that *PiDesD6*, *PiDesD5* cDNA encode membrane bound desaturases with Δ6, and Δ5 activity, respectively. Both PiDes6 and PiDes5 can indiscriminately desaturate both ω6 and ω3 substrates. A phylogenetic analysis showed that the three genes were homologous to the corresponding desaturases from green microalgae and lower plants that were functionally characterized. Quantitative real-time PCR revealed the concerted expression pattern of all three genes in *P. incisa* cells subjected to nitrogen starvation, featuring maximum expression level on day 3 of starvation, corresponding to the sharpest increase in the share of arachidonic acid.

Keywords Arachidonic acid · Δ12-desaturase · Δ5-desaturase · Δ6-desaturase · Microalgae · Expression pattern · Nitrogen starvation · *Parietochloris incisa*

Abbreviations

ARA	Arachidonic acid
DGTS	Diacylglyceroltrimethylhomoserine
DHA	Docosahexaenoic acid
DGLA	Dihomo-γ-linolenic acid
EPA	Eicosapentaenoic acid
GLA	γ-Linolenic acid
LNA	Linoleic acid
PtdCho	Phosphatidylcholine
PtdEtn	Phosphatidylethanolamine
RTQPCR	Real time quantitative polymerase chain reaction
TFA	Total fatty acids
VLC-PUFA	Very long-chain polyunsaturated fatty acids

Introduction

Very long-chain polyunsaturated fatty acids (VLC-PUFA) of 20 or 22 carbon atoms are indispensable components of human nutrition. They are necessary for normal life-long physiology and contribute to the well-being of the human body. Nutritionally important VLC-PUFA include the ω3-fatty acids, eicosapentaenoic acid (EPA, $20{:}5^{\Delta 5,8,11,14,17}$)

GenBank accession numbers for *PiDes12*, *PiDes6* and *PiDes5* and a partial sequence of actin gene of *P. incisa* are GU390531, GU390532, GU390533 and FJ548973.

Electronic supplementary material The online version of this article (doi:10.1007/s11745-010-3421-4) contains supplementary material, which is available to authorized users.

U. Iskandarov · I. Khozin-Goldberg (✉) · Z. Cohen
Microalgal Biotechnology Laboratory,
French Associates Institute for Agriculture
and Biotechnology of Drylands,
Jacob Blaustein Institutes for Desert Research,
Ben-Gurion University of the Negev,
84990 Midreshet Ben-Gurion, Israel
e-mail: khozin@bgu.ac.il

and docosahexaenoic acid (DHA, 22:6$^{\Delta4,7,10,13,16,19}$) and the ω6-fatty acid, arachidonic acid (ARA, 20:4$^{\Delta5,8,11,14}$) which are the major components of membrane phospholipids of the retina, brain and testis. ARA, together with DHA, are the predominant fatty acids in the human brain and breast milk. ARA is necessary for normal fetal growth, and cognitive development in infants [1]. Many studies highly recommended supplementation of infant formula with DHA and ARA [2]. Besides the structural function in membranes, ARA is the primary substrate in eicosanoids biosynthesis which regulates many physiological processes such as homeostasis, reproduction, immune and inflammatory responses.

The green freshwater microalga *Parietochloris incisa* (Trebouxiophyceae) is known to accumulate extraordinarily large amounts of ARA-rich triacylglycerols (TAG) [3, 4]. When *P. incisa* is cultivated under nitrogen starvation, ARA constitutes about 60% of total fatty acids (TFA) and over 95% of cellular ARA is deposited in TAG in cytoplasmic lipid bodies [5].

The biosynthesis of VLC-PUFA in microalgae follows two major pathways, designated as ω6 and ω3. In these pathways, linoleic acid (LNA; 18:2$^{\Delta9,12}$) and α-linolenic acid (ALA; (18:3$^{\Delta9,12,15}$) go through sequential Δ6 desaturation, Δ6 elongation and Δ5 desaturation, yielding ARA and EPA, respectively [6–9]. For example, in the red microalga *Porphyridium cruentum* and the green microalga *P. incisa*, oleic acid (18:1$^{\Delta9}$) is first desaturated to 18:2$^{\Delta9,12}$ and γ-linolenic acid (GLA, 18:3$^{\Delta6,9,12}$) through Δ12 and Δ6 desaturations, followed by elongation to dihomo-γ-linolenic acid (DGLA, 20:3$^{\Delta8,11,14}$) and Δ5 desaturation to yield ARA via the ω6 pathway [9, 10]. In *P. incisa*, the extraplastidial lipids, phosphatidylcholine (PtdCho) and the betaine lipid, diacylglyceroltrimethylhomoserine (DGTS), are involved in the Δ12 and, subsequently, the Δ6 desaturations, whereas phosphatidylethanolamine (PtdEtn) along with PtdCho are the suggested major substrates for the Δ5 desaturation of 20:3$^{\Delta8,11,14}$ to 20:4$^{\Delta5,8,11,14}$ [10]. The same enzymes are involved in the biosynthesis of VLC-PUFA through the ω3 pathway in the green microalga *Ostreococcus tauri* [11]. VLC-PUFAs may also be generated by an alternative Δ8 desaturation pathway. For example, in the marine haptophyte *Isochrysis galbana* and in the fresh water euglenophyte *Euglena gracilis*, where LNA and ALA are first elongated by C18 Δ9-specific fatty acid elongase followed by sequential Δ8 and Δ5 desaturations to ARA or EPA [8, 12, 13]. The extraplastidial Δ12 desaturase is an integral ER-bound protein which is responsible for the desaturation of 18:1$^{\Delta9}$ and production of 18:2$^{\Delta9,12}$, mainly on PtdCho [14–16]. Δ5 and Δ6 desaturases contain a fused cytochrome *b*5 domain in their N-terminus, serving as an electron donor, and introduce a double bond at a site closer to the carboxyl group than any of the pre-existing double bonds in the substrate fatty acid, thereby called 'front-end' desaturases [17–20]. Desaturases with Δ6 or Δ5 activity have been isolated from various organisms [21–26]. In algae, particularly, genes coding for desaturases were cloned from two diatoms *Phaeodactylum tricornutum* [27] and *Thalassiosira pseudonana* [28], and few species of marine picoeukaryotes, belonging to the class Prasinophyceae of Chlorophyta, such as *Ostreococcus tauri* [29], *Mantoniella squamata* [30], and *Micromonas pusilla* [31]. Some of these desaturases have been introduced together with PUFA-specific elongases into constructs for transformation of yeast and oil seed plants to reconstitute VLC-PUFA biosynthesis in the heterologous organisms [13, 29, 31–35].

Coexpression of the Δ5 and Δ6 desaturases from the diatom *P. tricornutum* in yeast in the presence of either ω3 or ω6 C18 substrates yielded ARA and EPA, demonstrating that they can function in both the ω3 and ω6 pathways with similar efficiency [27]. In *Arabidopsis thaliana*, VLC-PUFA biosynthesis was achieved through reconstitution of an alternative pathway by introducing genes encoding Δ9 elongase from *I. galbana*, Δ8 desaturase from *E. gracilis* and Δ5 desaturase from *Mortierella alpina* [13]. Recently, it was shown that some algal front end desaturases can act also on fatty acids esterified to CoA [29–31] similarly to mammalian front-end desaturases. These desaturases attracted much attention since such acyl-CoA-dependent enzymes, originating from photosynthetic organisms and having the correct substrate specificities may eliminate the need for the rate-limiting exchange of substrates between lipid and acyl-CoA in oil seed plants genetically modified to produce VLC-PUFA [29–34].

In the present work, we report the identification of three cDNA putatively encoding for Δ12, Δ6, and Δ5 desaturases, respectively, in *P. incisa.* Functional activities with fatty acid preferences were conferred for Δ6 and Δ5 desaturases by heterologous expression in the yeast *Saccharomyces cerevisiae*. Transcripts for all three desaturases are concertedly up-regulated during nitrogen starvation, that triggers ARA accumulation, and the level of expression is correlated with the increase in the share of ARA.

Materials and Methods

Strains and Growth Conditions

Axenic cultures of *P. incisa* were cultivated on BG-11 nutrient medium [36] in 250-ml Erlenmeyer glass flasks in an incubator shaker at controlled temperature (25°C) and illumination (115 μmol quanta m^{-2} s^{-1}) under an air/CO_2 atmosphere (99:1, v/v) and a speed of 170 rpm [3]. For N-starvation experiments, cells of daily-diluted cultures were collected by centrifugation, washed three times in

sterile double distilled water and resuspended in N-free BG11 medium. To prepare an N-free BG-11 medium, sodium nitrate was omitted and ferric ammonium citrate was substituted with ferric citrate. Biomass was sampled at time 0, and in 1.5, 3, 7 and 14 days from the onset of N-starvation for determination of growth parameters, and was further used for fatty acid analysis and RNA isolation. Duplicate samples were collected from three separate flasks for each time point and measurement. Growth parameters, dry weight and chlorophyll contents were determined as previously described [37].

RNA Isolation

Aliquots of the cultures were filtered through a glass fiber filter (GF-52, Schleicher & Schuell, Germany); cells were collected by scraping and immediately flash-frozen in liquid nitrogen and stored at −80°C for further use. Total RNA was isolated by the procedure described by Bekesiova et al. [38]. Three independent RNA isolations were conducted for each time point. The total RNA samples were treated with RNase-free Baseline-ZERO™ DNase (Epicentre Technologies, Madison, WI, USA) before being used in cDNA synthesis for real-time PCR experiments.

Gene Cloning

Partial sequences of the Δ12, Δ6, Δ5 desaturase and actin genes were obtained by PCR (ReddyMix PCR Master Mix, Thermo Scientific, Surrey, UK) using the degenerated primers listed in the Table 1. To generate the full-length cDNA, 3′-and 5′-rapid amplification of the cDNA ends (RACE) was performed using a BD Smart™ RACE cDNA Amplification Kit (BD Biosciences Clontech, Foster City, CA, USA). Gene specific primers were designed (Table 1) and RACE PCR reactions were conducted using 5′ and 3′-RACE-Ready cDNA made from 1 μg total RNA of N-starved cells with 50× BD Advantage 2 polymerase mix

Table 1 Primers used for obtaining partial, 5′ and 3′ end fragments of actin, Δ12, Δ6 and Δ5 desaturase genes of *P. incisa* followed by full-length assembly

Gene	Forward/reverse primer (sequence 5′–3′)	Source of primers
Primers used for partial sequence		
Des Δ12	CAC MYC VTS THC VWG CTG CTG VWB CCC CAC	This work
	CTG CCC GAA GTT GAC CGC GGC GTG CTG	This work
Des Δ6	TGG TGG AAR CAY AAR CAY AAY	[26]
	GCG AGG GAT CCA AGG RAA NAR RTG RTG YTC	This work
Des Δ5	ATH RAI GRI AAR GTI TAY GAY GT	[26]
	GGI AYI KWI TSD ATR TCI GGR TC	[26]
Actin	AGA TCT GGC ACC ACA CCT TCT TCA	This work
	TGT TGT TGT AGA GGT CCT TGC GGA	This work
Primers used for 5′ and 3′ RACE amplification		
Des Δ12	CCACATAGCGGCACAGGCTGAAATC	This work
	GCTCTGGGAGGATTTCAGCCTGTGC	
Des Δ6	GACACAATCTGGGCCGTCACAAAGTC	This work
	GGACTTTGTGACGGCCCAGATTGTGTC	
Des Δ5	ACTGACCCTCCTCTGTGTCCTCTTCG	This work
	TGTACGCCAAGTCGCTGACCATCC	

Gene	Forward/reverse primer (sequence 5′–3′)	Restriction sites[a]
Primers used for full-length cloning and yeast transformations		
Des Δ12	TGGAATTC**AAA**ATGGGGAAAGGAGGCTG	*Eco*RI
	CTGTCTAGA**TCA**AGCGCGGAACCACAGG	*Xba*I
Des Δ6	TCGAATTC**AAA**ATGTGCCAGGGACAGG	*Eco*RI
	GGCTCTAGA**CTA**GGCCTCAGCTGCCACG	*Xba*I
Des Δ5	CCAAAGCTT**AAA**ATGATGGCTGTAACAGA	*Hind*III
	GCTCTAGA**CTA**TCCCACGGTGGCCA	*Xba*I

N, R, Y, H, K, W, S, D and I designate mixtures of nucleotides, A/G/T/C, A/G, T/C, A/T/C, G/T, A/T, G/C, A/G/T and inosine, respectively

[a] Underlined

(Clontech Laboratories Inc., Mountain View, CA, USA). The PCR products of the expected sizes were excised, purified from the gel (NucleoSpin Extract II purification kit, Machery-Nagel, Duren, Germany) and ligated into a pGEM T-Easy vector (Promega, Madison, WI, USA). The full-length cDNA were assembled based on the sequences of the 5′ and 3′ RACE fragments.

Expression and Functional Characterization in the Yeast *Saccharomyces cerevisiae*

The ORFs encoding for the Δ12, Δ6, and Δ5 desaturases were amplified using *PfuUltra* II fusion HS DNA polymerase (Stratagene, La Jolla, CA, USA) with the respective primer pairs (Table 1). The forward primers contained a restriction site (underlined) and a yeast translation consensus (boldfaced) followed by ATG. The reverse primers contained a restriction site (underlined) and a stop codon (boldfaced). Following restriction and ligation to the pYES2 vector (Invitrogen, Carlsbad, CA, USA), the constructs were used to transform *S. cerevisiae* strain W303 by the PEG/lithium acetate method [39]. The yeast cells harboring the empty pYES2 vector were used as control. Transformants were selected by uracil prototrophy on yeast synthetic medium (YSM) lacking uracil (Invitrogen, Carlsbad, CA, USA). For functional expression, a minimal selection medium containing 2% (w/v) raffinose was inoculated with the pY*PiDesΔ12*, pY*PiDesΔ6* or pY*PiDesΔ5* transformants and grown at 27°C for 24 h in a water bath shaker. Five ml of sterile YSM, containing 1% (w/v) Tergitol-40 and 250 μM of the appropriate fatty acid substrate, were inoculated with raffinose-grown cultures to obtain an OD of 0.2 at 600 nm. Expression was induced by adding galactose to a final concentration of 2% (w/v) and cultures were further grown at 27°C for 48 h. Cells were harvested by centrifugation, washed twice with 0.1% $NaHCO_3$, freeze-dried and used for fatty acid analysis.

Fatty Acid Analysis

Fatty acid methyl esters (FAME) were obtained by transmethylation of the freeze-dried *P. incisa* or yeast biomass, with dry methanol containing 2% H_2SO_4 (v/v) and heating at 80°C for 1.5 h while stirring under an argon atmosphere. Gas chromatographic analysis of FAME was performed on a Thermo Ultra Gas chromatograph (Thermo Scientific, Italy) equipped with PTV injector, FID detector and a fused silica capillary column (30 m × 0.32 mm; ZB WAXplus, Phenomenex). FAME were identified by co-chromatography with authentic standards (Sigma Chemical Co., St. Louis, MO, USA; Larodan Fine Chemicals, Malmö, Sweden) and FAME of fish oil (Larodan Fine Chemicals). Each sample was analyzed in duplicates of three independent experiments. The structures of fatty acids were confirmed by GC-MS of their pyrrolidine derivatives [40] on HP 5890 equipped with a mass selective detector (HP 5971A) utilizing a HP-5 capillary column and a linear temperature gradient from 120 to 300°C.

Lipid Analysis

The biomass of *S. cerevisiae* was heated with isopropanol at 80°C for 10 min and lipids were extracted by the method of Bligh and Dyer [41]. Total lipid extract was separated into neutral and polar lipids by silica Bond-Elute cartridges (Varian, CA, USA) using 1% of ethanol in chloroform (v/v) and methanol to elute neutral and polar lipids, respectively [42].

Polar lipids were separated into individual lipids by two dimensional TLC on Silica Gel 60 glass plates (10 × 10 cm, 0.25 mm thickness (Merck, Darmstadt, Germany) according to Khozin et al. [9]. Neutral lipids were resolved with petroleum ether:diethyl ether:acetic acid (70:30:1, v/v/v). Lipids on TLC plates were visualized by brief exposure to iodine vapors, scraped from the plates and were transmethylated for the fatty acid analysis as previously described.

Real-Time Quantitative PCR

Template cDNA for real-time quantitative PCR (RTQPCR) was synthesized using 1 μg of total RNA in a total volume of 20-μL, using oligo dT primer (Reverse-iT TM 1st Strand Synthesis Kit, ABgene, Surrey, UK). Each 20-μL cDNA reaction was then diluted threefold with PCR grade water.

Primer Design and Validation for Real-Time Quantitative PCR

Real-Time Quantitative PCR (RTQPCR) primer pairs were designed for the *PiDes12*, *PiDes6*, and *PiDes5* genes and the house keeping gene actin, *PiAct* using the PrimerQuest tool (http://test.idtdna.com/Scitools/Applications/Primerquest/). Primer pairs were validated as described by Iskandarov et al. [43]. The nucleotide sequences of primer pairs and the amplicon sizes are presented in Table 2.

Results

Isolation and Identification of cDNA for Δ12, Δ6, and Δ5 Desaturase Genes of *P. incisa*

The partial sequences of the Δ12, Δ6 and Δ5 desaturase gene homologues were isolated using degenerate oligonucleotides (Table 1) targeting conserved amino acid motifs identified in algae, lower plants and fungi [26, 27, 44, 45].

Table 2 Primers used in RTQPCR experiments

Gene	Forward primer/reverse primer	Amplicon size (bp)
PiDes12	5′-GAAGCACCACCAAGGATGAGGT-3′	112
	5′-AGCGAGACGAAGATGACCAGGAA-3′	
PiDes6	5′-ACTTCCTGCACCACCAGGTCTTC-3′	112
	5′-TCGTGCTTGCTCTTCCACCAGT-3′	
PiDes5	5′-TAAGTGCCAGGGCTGTGCTAGA-3′	110
	5′-GAACTGACCCTCCTCTGTGTCCT-3′	
PiAct	5′-CGTCCAGCTCCACGATTGAGAAGA-3′	154
	5′-ATGGAGTTGAAGGCGGTCTCGT-3′	

A partial sequence of the actin gene was amplified based on nucleotide similarity with the actin gene of *Chlamydomonas reinhardtii* [46] to be used as a house keeping gene in RTQPCR experiments.

Partial sequences of 503, 558 and 636 bp, corresponding to the Δ12, Δ6, and Δ5 desaturase genes, respectively, were used for designing gene specific primers that were used to amplify the 5′- and 3′- ends of the expected genes. Assembling the 5′ and 3′ RACE PCR product sequences resulted in the identification of three cDNA clones with sequence homologies to known Δ12, Δ6, and Δ5 desaturase genes. The full-length cDNA corresponding to Δ12, Δ6, and Δ5 desaturase genes were thus designated *PiDes12*, *PiDes6*, and *PiDes5*. The ORFs for *PiDes12*, *PiDes6* and *PiDes5* genes were 1.140, 1.443, and 1.446 bp in length, respectively, coding for the corresponding predicted proteins of 380, 481 and 482 amino acids. The predicted amino acid sequence of *PiDes12* is 64 and 62% identical to that of *Chlorella vulgaris* (BAB78716) and *C. reinhardtii* (XP_001691669), respectively, while it shares more than 50% identity with those of higher plants. It contains three conserved histidine motifs HxxxH, HxxHH and HxxHH. The deduced amino acid sequence of PiDes6 is 52 and 51% identical to those of the Δ6 desaturases from the liverwort *Marchantia polymorpha* (AAT85661) and the moss *Ceratodon purpureus*, respectively (CAB94993). It is also 45% identical to the *M. alpina* Δ6 desaturase (ABN69090). PiDes5 shares 55 and 51% identity with the Δ5 desaturase from the microalgae *M. squamata* (CAQ30478), and *O. tauri* (CAL57370), respectively, and 54% with that from *M. polymorpha* (AAT85663) but is only 36% identical to the *M. alpina* Δ5 desaturase (AAC72755). Both PiDes6 and PiDes5 contain N-terminal fused cytochrome *b5* domain including the HPGG motif and the three histidine boxes found to be conserved in front-end desaturases [19, 27]. The three characteristically conserved histidine-rich motifs with amino acid patterns of $HD_{(E)}$xxH, HxxHH, QxxHH in Δ6 desaturases, and HDxxH, QHxxxHH, QxxHH in Δ5 desaturases are also present in PiDes6 and PiDes5, respectively (Supplementary Fig. 1).

Phylogenetic Analysis

An unrooted phylogenetic tree (Fig. 1) of PiDes12, PiDes6, PiDes5 and several functionally characterized desaturases from all three groups was constructed to identify their functional and phylogenetic relationships by the neighbor-joining program in MEGA4 [47]. The deduced amino acid sequence of PiDes12 is closely related to Δ12 desaturases of green algae and very similar to those of higher plants. The sequences of PiDes6 and PiDes5 cluster with Δ6 and Δ5 desaturases, respectively, from algae, moss and fungi. PiDes6 is very similar to the *M. polymorpha* (MpDEs6) and *P. tricornutum* (PtD6p) Δ6 desaturases, while PiDes5 appears to be closely related to the Δ5 desaturase from the moss *M. polymorpha* and shares more sequence similarity with the Δ5 desaturase from the chlorophytes *M. squamata* and *O. tauri* than with those of fungal origin. However, both Δ6 or Δ5 desaturases from *M. squamata*, Δ6 desaturases of *O. tauri*, *O. lucimarinus,* and *M. pusilla* appear to be structurally more similar to each other than to any of the known desaturases from either group.

Functional Expression of PiDes12, PiDes6, and PiDes5 in *S. cerevisiae*

The functional activities of the proteins encoded by *PiDes12*, *PiDes6* and *PiDes5* were examined by heterologous expression in *S. cerevisiae*. To this aim, the pYES2 constructs pY*PiDes12,* pY*PiDes6* and pY*PiDes5* containing the ORFs for PiDes12, PiDes6, and PiDes5, respectively, were transformed into *S. cerevisiae*. The yeast cells, harboring the empty vector pYES2 (control), did not demonstrate desaturation activity on the exogenously provided fatty acid substrates (Fig. 2). GC analysis of the FAME of the yeast transformed with pY*PiDes12,* did not reveal a significant conversion of endogenous $18{:}1^{\Delta 9}$ since only a small peak corresponding to $18{:}2^{\Delta 9,12}$ appeared on chromatograms (0.3% of TFA; Supplementary Fig. 2). An attempt to increase the activity of the recombinant protein by the optimization of yeast translation consensus was not successful.

PiDes6 and PiDes5 expressions were induced in the presence of the main ω6 substrates for Δ6 or Δ5 fatty acid desaturases, $18{:}2^{\Delta 9,12}$ and $20{:}3^{\Delta 8,11,14}$, respectively. New peaks corresponding to $18{:}3^{\Delta 6,9,12}$ and $20{:}4^{\Delta 5,8,11,14}$, respectively, were detected, confirming the predicted function of PiDes6 and PiDes5. The expression of PiDes6 in the presence of $18{:}3^{\Delta 9,12,15}$ resulted in the appearance of the corresponding Δ6 desaturation product $18{:}4^{\Delta 6,9,12,15}$ (Fig. 2). PiDes6 desaturase was neither active on endogenous yeast fatty acids nor on exogenously-provided $18{:}1^{\Delta 9}$. PiDes6 was not active on $20{:}3^{\Delta 11,14,17}$ either, whereas PiDes5 desaturated it to the non-methylene-interrupted $20{:}4^{\Delta 5,11,14,17}$. PiDes5 converted $20{:}4^{\Delta 8,11,14,17}$ into the

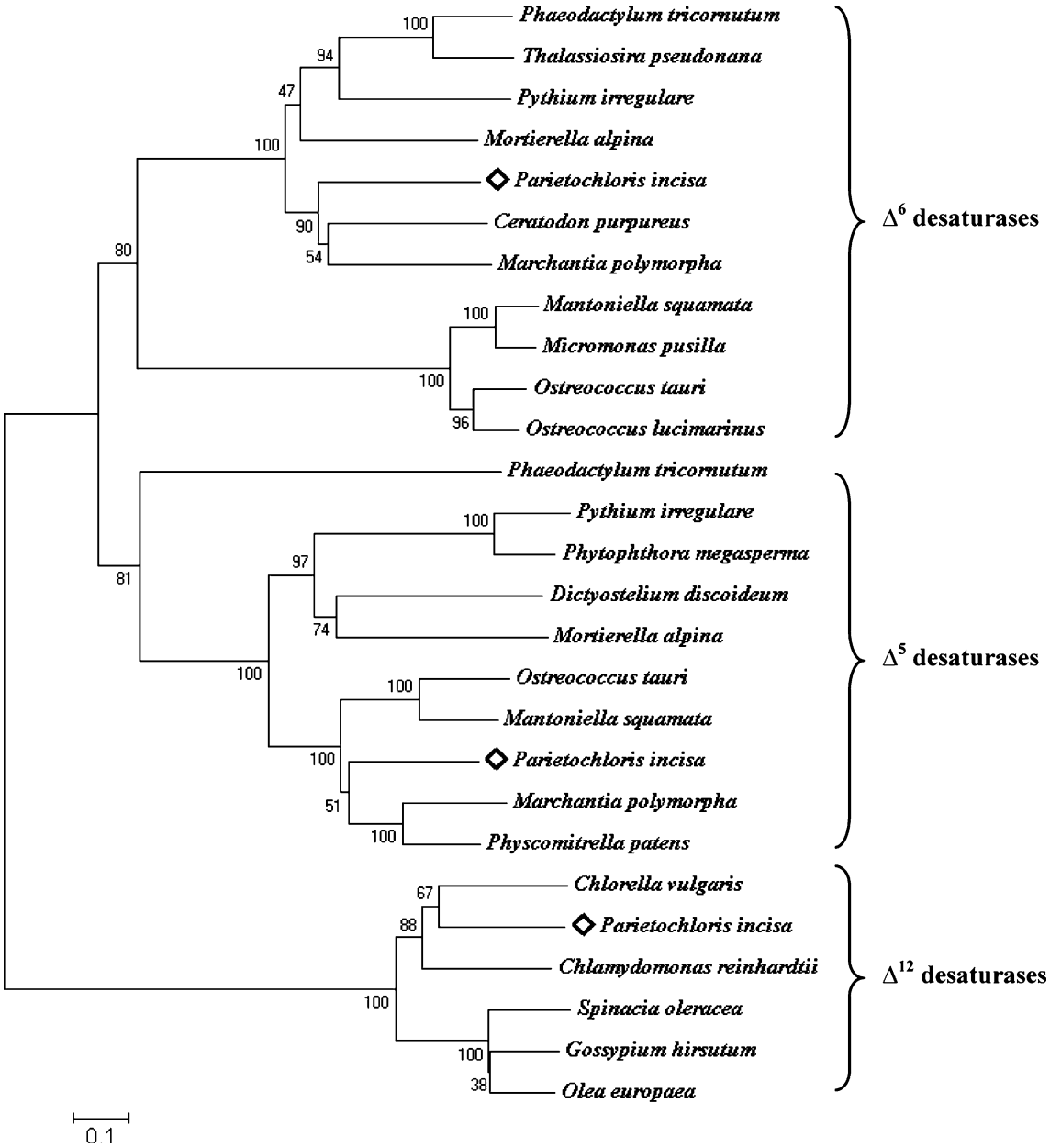

Fig. 1 An unrooted phylogram of PiDes12, PiDes6, PiDes5 and some functionally characterized Δ12, Δ6 and Δ5 desaturases (vertebrate and invertebrate desaturases are not included). The alignment was generated by the CLUSTAL W program and the unrooted phylogram was constructed in the neighbor-joining method using the MEGA4 software [47]. GenBank sources of the sequences are: BAB78716 (Δ12, *Chlorella vulgaris*), XP_001691669 (Δ12, *C. reinhardtii*), BAC22091 (Δ12, *Spinacia oleracea*), AAL37484 (Δ12, *Gossypium hirsutum*), AAW63040 (Δ12, *Olea europaea*), CAB94993 (Δ6, *Ceratodon purpureus*), AAT85661 (Δ6, *M. polymorpha*), BAA85588 (Δ6, *M. alpina*), AAL92563 (Δ6, *P. tricornutum*), AAX14505 (Δ6, *T. pseudonana*), (Δ6, *Pythium irregulare*), CAL57370 (Δ5, *O. tauri*), AAT85663 (Δ5, *M. polymorpha*), AAL13311 (Δ5, *P. irregulare*), CAD53323 (Δ5, *Phytophthora megasperma*), BAA37090 (Δ5, *Dictyostelium discoideum*), AAC72755 (Δ5, *M. alpina*), CAQ30478 (Δ5, *M. squamata*), CAQ30479 (Δ6, *M. squamata*), AAW70159 (Δ6, *O. tauri*), CS020055 (Δ5, *P. patens*)

respective Δ5 product, $20{:}5^{\Delta5,8,11,14,17}$ (EPA) as well as the added $18{:}1^{\Delta9}$ into the non-methylene-interrupted $18{:}2^{\Delta5,9}$ (Fig. 2). The Δ5 position on $18{:}2^{\Delta5,9}$ was determined by a characteristic peak of $m/z = 180$ on the GC-MS spectra of its pyrrolidine derivative (not shown). The presence of $18{:}2^{\Delta5,9}$ was also observed in the chromatograms of the PiDes5 transformant supplied with C20 fatty acids. In addition, a tiny peak, tentatively identified as $18{:}4^{\Delta5,9,12,15}$ was present on the chromatogram of the PiDes5 transformant fed with $18{:}3^{\Delta9,12,15}$ (Table 3).

We also conducted a kinetic analysis of ARA emergence in TFA of the PiDes5 transformant during 24 h following

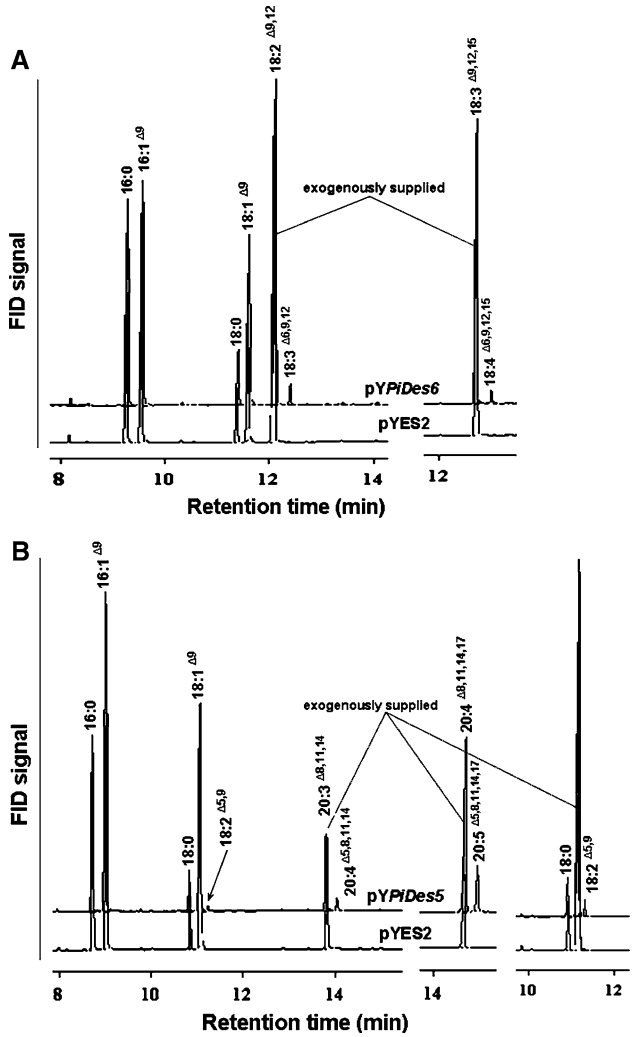

Fig. 2 GC of FAME of recombinant yeast harboring pYES2 (control), pY*PiDes6* (**a**) fed with $18{:}2^{\Delta 9,12}$ or $18{:}3^{\Delta 9,12,15}$, and pY*PiDes5* (**b**) fed with $20{:}3^{\Delta 8,11,14}$, $20{:}^{\Delta 8,11,14,17}$ or $18{:}^{\Delta 9}$

the addition of $20{:}3^{\Delta 8,11,14}$ (DGLA). Results showed that ARA peak was evident already after 3 h (corresponding to 10.9% substrate conversion) with a gradual but slow increase (up to 15.1% conversion) after 24 h. Fatty acid analysis of the major polar and neutral lipids of the yeast transformed with pY*PiDes5* was performed 24 h after feeding with $20{:}3^{\Delta 8,11,14}$ to study the pattern of ARA distribution within individual lipids. In the transformed yeast, ARA appeared in phospholipids with similar conversion rates (Table 4), but with the highest proportion detected in PtdCho. It was also present in the neutral lipids: TAG, free fatty acids (FFA), diacylglycerol (DAG) and sterol esters (SE). Given that TFA content in PtdCho, a major phospholipid of *S. cerevisiae* [48], amounted for about 16% of total lipids in pY*PiDes5* transformant fed with DGLA (Table 4), PtdCho allocated the main part of ARA attached to phospholipids.

Table 3 Conversion percent of the supplied fatty acids by PiDes6 and PiDes5 in *S. cerevisiae*

Fatty acid substrate	Desaturase product and conversion (%)	
	PiDesΔ6	PiDesΔ5
$18{:}1^{\Delta 9}$	–	$18{:}2^{\Delta 5,9}$ (4.2)
$18{:}2^{\Delta 9,12}$	$18{:}2^{\Delta 6,9,12}$ (5.1)	–
$18{:}3^{\Delta 9,12,15}$	$18{:}4^{\Delta 6,9,12,15}$ (4.5)	$18{:}4^{\Delta 5,9,12,15}$ (1.4)[a]
$18{:}3^{\Delta 6,9,12}$		–
$20{:}3^{\Delta 11,14,17}$	–	$20{:}4^{\Delta 5,11,14,17}$ (10.0)
$20{:}3^{\Delta 8,11,14}$	–	$20{:}4^{\Delta 5,8,11,14}$ (16.4)
$20{:}4^{\Delta 8,11,14,17}$		$20{:}5^{\Delta 5,8,11,14,17}$ (17.1)

Yeast strain W303 transformed with pYES2-*PiDES6* and pYES2-*PiDES5* was grown for 48 h at 26°C in the presence or absence of different fatty acid substrates (250 μM). FAME from the whole cells were prepared and analyzed by GC as described in "Materials and Methods". Desaturation (percentage of conversion) was calculated as (product × 100)/(substrate + product)

[a] Tentative identification

Expression Profiles of *PiDes12, PiDes6*, and *PiDes5* Under Nitrogen Starvation

To use actin as a house-keeping gene in quantitative real-time PCR experiments, we amplified a partial fragment (503 bp) of the *P. incisa* actin gene using the primers whose design was based on the *C. reinhardtii* actin cDNA (XM_001699016). Indeed, the expression level of the actin gene did not significantly change throughout the nitrogen starvation. *PiDes12, PiDes6,* and *PiDes5* were upregulated following the transfer to Nitrogen starvation, reaching the highest expression level on day 3 and decreasing thereafter to a level about 15–20 fold higher than that at time 0 (Fig. 3). Both the *PiDes12* and *PiDes5* genes were expressed at levels approximately 65- to 70-fold higher on day 3 than at time 0, while the *PiDes6* transcript was about 45-fold higher (Fig. 3). The expression patterns of *PiDes12, PiDes6,* and *PiDes5* correlated with the enhanced biosynthesis of ARA in *P. incisa* cells (Table 5).

Discussion

The capacity of *P. incisa* to accumulate large quantities of ARA-rich TAG under nitrogen starvation, suggested that it would be of great interest to study its genes and enzymes involved in the accumulation of VLC-PUFA. In the present work, we have thus cloned the *P. incisa* Δ12, Δ6, and Δ5 desaturases which in conjunction with a recently cloned Δ6 specific PUFA elongase [43], represent a set of *P. incisa* genes involved in the biosynthesis of ARA. The deduced amino acid sequences of PiDes12, PiDes6, and PiDes5 contain three histidine rich motifs (his-boxes) that are

Table 4 Fatty acid composition and distribution of individual lipid classes of *S. cerevisiae* expressing the *PiDes5* ORF

Lipid	Fatty acid composition (% of total fatty acids)							Conversion (%)	TL (%)*	ARA (% TL)*
	16:0	16:1	18:0	$18:1^{\Delta 9}$	$18:2^{\Delta 5,9}$	DGLA	ARA			
TAG	17.4	27.6	9.6	23.0	0.4	19.6	2.0	9.3	61.3	55.2
SE	10.5	38.5	7.1	30.4	0.0	12.2	1.1	8.4	3.6	1.8
DAG	27.9	16.3	21.9	24.3	0.1	7.2	2.0	24.0	1.6	1.4
FFA	26.1	20.3	23.5	8.9	0.2	17.2	3.6	17.2	5.5	9.1
PtdCho	19.7	30.1	9.3	24.3	0.7	11.6	3.6	24.2	15.7	25.7
PtdEtn	21.7	34.9	2.8	32.8	0.5	5.0	1.6	24.6	3.2	2.3
PI + PS**	34.0	20.8	12.4	26.5	0.2	4.6	1.1	18.1	9.0	4.4

TL total lipids, *PI* phosphatidylinositol, *PS* phosphatidylserine

characteristic of all membrane bound desaturases [22–29, 49–51]. Both PiDes6 and PiDes5 contain a fused cytochrome *b5* at their N-terminus, supporting their microsomal localization, similar to other functionally characterized front-end desaturases [52, 53].

Heterologous expression of PiDes6 and PiDes5 in yeast cells confirmed their Δ6 and Δ5 activity by conversion of supplemented fatty acids to the corresponding desaturation products. PiDes12, however, demonstrated very low desaturation activity, which we could not improve by the 5′ modification of the inserted sequence. A similar low activity in yeast was also demonstrated in some cases, such as for Δ5 and Δ12 desaturases of *O. tauri* and *Chlorella vulgaris* NJ-7, respectively [30, 54]. There are several possible explanations for the low activity of the recombinant protein in the heterologous expression including mistargeting, posttranslational modifications, etc., although we do not have experimental data to support this assumption.

Functional characterization of PiDes6 and PiDes5 confirmed the previously reported substrate specificities of the Δ5 and Δ6 desaturases which are generally restricted to C18 and C20 substrates, respectively [23, 24, 27]. PiDes6 and PiDes5 desaturated both ω3 and ω6 fatty acids with similar efficiency (Fig. 2; Table 3). Various results concerning ω3/ω6 substrate preference were reported for functionally characterized Δ6 and Δ5 desaturases from different organisms that were expressed in yeast. The ω6 and ω3 substrates were equally used by the Δ6, Δ5 and Δ4 desaturases of *Leishmania major* [55], the Δ6 desaturases of the diatom *P. tricornutum* [27] and the green alga *O. tauri* [29]. The Δ6 desaturase of *T. pseudonana* exhibited a slightly higher preference for the exogenous ω3 fatty acid, ALA [28], whereas the Δ5 desaturase of *T. pseudonana* did not show a preference for either ω6 or ω3 substrates. Recently cloned Δ6 desaturases from the microalgae *M. squamata, M. pussila* and *O. lucimarinus* displayed a strong preference for the ω3 substrate ALA [30, 31, 56]. A preference for ω3 substrates was also reported for the *Primula* Δ6-desaturase [57] and for all fish Δ6 desaturases studied to date [58].

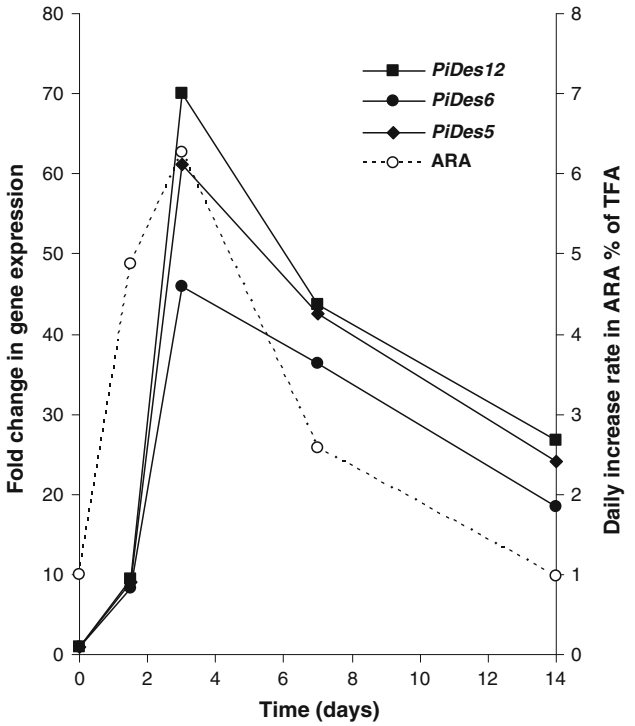

Fig. 3 Changes in expression of the *PiDes12*, *PiDes6*, and *PiDes5* genes under N-starvation and daily increase in ARA percent share in total fatty acids. The transcript abundance of the genes was normalized to that of the actin gene

A front-end PiDes5 desaturated its principal substrate $20:3^{\Delta 8,11,14}$ as well as $20:4^{\Delta 8,11,14,17}$; in addition, non-methylene interrupted fatty acids were also produced as a result of its activity on $20:3^{\Delta 11,14,17}$, and on both endogenous and exogenous $18:1^{\Delta 9}$, but with lower efficiency. The Δ5 desaturases of different origins have been previously shown to be promiscuous in heterologous systems [13, 23, 32, 50], as a result, non-methylene interrupted FA were detected in yeast [23, 27, 28] and in transgenic canola [50]. Exceptionally, the Δ5 desaturase of trypanosome *L. major* utilized $20:3^{\Delta 8,11,14}$ and $20:4^{\Delta 8,11,14,17}$ with a similar efficiency but not $20:3^{\Delta 11,14,17}$ or $20:2^{\Delta 11,14}$ [55]. An unusual

Table 5 Major fatty acid composition and content of *P. incisa* cells grown under N-starvation

Time (days)	Fatty acid composition (% of total fatty acids)												TFA (% DW)
	16:0	16:1	16:2	16:3	18:0	18:1	18:2	18:3 ω6	18:3 ω3	20:3 ω6	20:4 ω6	20:5 ω3	
0	19.1	5.6	4.1	2.9	3.1	9.1	20.1	1.2	6.0	0.5	23.0	0.7	6.4
1.5	15.9	3.1	2.3	2.1	3.8	15.6	15.6	2.1	2.9	1.0	30.3	0.6	8.7
3	12.7	2.3	1.5	1.9	3.8	15.2	13.5	1.6	2.0	0.9	39.7	0.6	11.0
7	10.7	1.0	0.6	1.1	3.5	14.9	10.0	1.1	0.9	1.0	50.0	0.5	21.2
14	9.0	0.2	0.3	0.8	3.1	13.4	8.8	0.9	0.6	0.9	56.9	0.6	29.0

case is the *C. reinhardtii* cytochrome *b5* fusion protein (CrDES) which acts as an ω13 desaturase and inserts Δ5 double bond on both $18{:}1^{\Delta 9}$ and $18{:}2^{\Delta 9,12}$ producing the non-methylene interrupted $18{:}2^{\Delta 5,9}$ and $18{:}3^{\Delta 5,9,12}$, while adding a Δ7 double bond to $20{:}2^{\Delta 11,14}$ and $20{:}3^{\Delta 11,14,17}$ [59]. Apparently, in addition to the fatty acid chain length, the location and number of double bond, and the form of the substrate (lipid- or CoA-bound) are also crucial for Δ5 desaturation.

Differently from PiDes5, PiDes6 desaturated neither the yeast major monounsaturated fatty acids nor the exogenously supplied 18:1. Unlike some reported Δ6 desaturases [27, 28, 60–63], PiDes6 did not act on $20{:}3^{\Delta 11,14,17}$, indicating that it is specific for Δ9 C18 PUFA. It appears that not only the organism being transformed, but also the gene origin, may determine the substrate specificity of the recombinant Δ6 and Δ5 desaturases.

It was shown in the radiolabeling studies with *P. incisa*, that PtdCho and DGTS are used for lipid-linked C18 Δ6 desaturation whereas mostly PtdEtn is used for C20 Δ5 desaturation [3]. In recent years, a few examples of desaturases that act on CoA-activated rather than on lipid-linked fatty acids were reported [29–31, 56]. Sequence similarity analysis of algal and lower plant Δ6 or Δ5 desaturases, revealed that the Δ6 and Δ5 desaturases of *M. squamata* are highly similar to those of *O. tauri* and *O. lucimarinus,* respectively (Fig. 1). One can indeed assume that their structural similarity may indicate to the functionally confirmed acyl-CoA dependency. Unlike Δ5 desaturases of *M. squamata* and *O. tauri*, their Δ6 desaturases appear to be somewhat more similar to their mammalian Δ6 desaturases homologs, e.g., mouse (NR_062673) and human (NP_04256) [64] than to those of lower plants.

PiDes5 featured higher substrate conversion rate in comparison to PiDes6. A relatively fast emergence of substantial percentage of ARA (10.6% conversion after 3 h of feeding) pursued us to study ARA distribution in individual lipid classes of the transformed yeast (24 h of feeding). A uniform distribution of desaturation products in yeast lipids may serve as an indication for acyl-CoA dependency [30, 31]. Interestingly, the *M. polymorpha* Δ6 desaturase was suggested to use acyl substrates in both glycerolipids and the acyl-CoA pool [26]. The expression of the *M. squamata* Δ5 desaturase in the presence of DGLA resulted in the accumulation of nearly similar amounts of ARA in all phospholipid classes and in the neutral lipids [30]. At the same time, the expression acyl-lipid desaturases resulted in a preferential accumulation of the product in PtdCho. In the present work, ARA was detected in all analyzed phospho- and neutral lipid classes of *S. cerevisiae* expressing PiDes5 (Table 4). Similar conversion rates were determined in phospholipids, however, ARA partition showed preference for the major phospholipid PtdCho followed by PtdEtn. Thus, these data and sequence similarity with functionally characterized acyl-lipid desaturases (Fig. 1) confirmed that in *P. incisa*, phospholipids PtdCho and PtdEtn are the main site for lipid-linked Δ5 desaturation [10]. It is necessary to mention that *P. incisa* desaturases produced relatively low activity in heterologous yeast system in comparison with high endogenous activity in the algal cells.

The quantitative RT-PCR results revealed that the gene expression levels of *PiDes12*, *PiDes6*, and *PiDes5* during the course of nitrogen starvation followed a similar pattern. The major transcriptional activation of the all three desaturases occurred on day 3 coinciding with a sharp rise in the percentage of ARA, which almost doubled (Fig. 3, Table 5). The same expression pattern featured the *P. incisa* Δ6 PUFA elongase [43], however, at lower level. The concerted transcriptional activation of the *PiDes12*, *PiDes6*, *PiDes5,* and *PiELO1* genes was accompanied by an increase in the percent share of 18:1, a main chloroplast-derived fatty acid exported to ER and substrate of microsomal Δ12 desaturase. Thus, we assume that despite the lack of significant activity in the yeast expression system, we cloned the Δ12 desaturase of *P. incisa* responsible for 18:2 production in the ER. This gene is highly expressed in the alga under conditions requiring active production of 18:2. Possibly, further optimization of the codon usage could result in higher conversion rates. High expression of ARA biosynthetic genes in *P. incisa* was accompanied by enhanced Δ5 and Δ6 desaturations of precursor fatty acids in the ω6 pathway (Table 5), a major pathway of ARA biosynthesis in *P. incisa* [10, 65].

Understanding the mechanisms underlying gene transcription regulation in metabolic pathways and characteristics of enzymes involved in ARA-rich TAG biosynthesis in *P. incisa* is a prerequisite for manipulating algal species for sustainable production of algal oils of high pharmaceutical and nutraceutical values. There is a significant body of information on the reconstitution of VLC-PUFA biosynthetic pathway in yeast and higher plants using microalgae-derived Δ6 and Δ5 desaturases in different combinations with PUFA elongases [31–35], whereas, so far, there were no attempts in molecular engineering of algal VLC-PUFA biosynthesis. Acyl-CoA algal desaturases, when expressed in higher plants, are often characterized by higher substrate conversion rates than that of the lipid-linked desaturases and convert precursors to VLC-PUFA more efficiently [29, 31, 34]. A most recent example is a metabolic engineering of an EPA biosynthesis pathway in tobacco leaf, consisting of the three algal enzymes, the acyl-CoA dependent Δ6-desaturase of *M. pusilla* with ω3 preference, the Δ6-elongase of the marine microalga *Pyramimonas cordata* and the Δ5-desaturase of *Pavlova salina,* producing 26% EPA in TAG [31]. This was performed employing an elegant and fast leaf assay for the transient expression and identification of the effective gene combination to produce desired VLC-PUFA *in planta*. The metabolic engineering of microalgae for desired fatty acid composition will be facilitated by the further development of genetic transformation tools for the wide range of microalgal species.

Acknowledgments Authors would like to thank Mrs. Shoshana Didi-Cohen for the dedicated technical assistance.

References

1. Horrocks LA, Yeo YK (1999) Health benefits of docosohexaenoic acid (DHA). Pharmacol Res 40:211–225
2. Crawford MA, Costeloe K, Ghebremeskel K, Phylactos A, Skirvin L, Stacey F (1997) Are deficits of arachidonic acid and docosahexaenoic acids responsible for the neural and vascular complications of preterm babies? Am J Clin Nutr 66:1032–1041
3. Bigogno C, Khozin-Goldberg I, Boussiba S, Vonshak A, Cohen Z (2002) Lipid and fatty acid composition of the green oleaginous alga *Parietochloris incisa*, the richest plant source of arachidonic acid. Phytochemistry 60:497–503
4. Cohen Z, Khozin-Goldberg I (2005) Searching for PUFA-rich microalgae. In: Cohen Z, Ratledge C (eds) Single cell oils. Am Oil Chem Soc, Champaign, pp 53–72
5. Khozin-Goldberg I, Bigogno C, Shrestha P, Cohen Z (2002) Nitrogen starvation induces the accumulation of arachidonic acid in the freshwater green alga *Parietochloris incisa* (Trebouxiophyceae). J Phycol 38:991–994
6. Cohen Z, Reungjitchachawali M, Siangdung W, Tanticharoen M, Heimer YM (1993) Herbicide resistant lines of microalgae: growth and fatty acid composition. Phytochemistry 34:973–978
7. Abbadi A, Domergue F, Bauer J, Napier JA, Welti R, Zähringer U, Cirpus P, Heinz E (2004) Biosynthesis of very-long-chain polyunsaturated fatty acids in transgenic oilseeds: constraints on their accumulation. Plant Cell 16:2734–2748
8. Meyer A, Kirsch H, Domergue F, Abbadi A, Sperling P, Bauer J, Cirpus P, Zank TK, Moreau H, Roscoe TJ, Zähringer U, Heinz E (2004) Novel fatty acid elongases and their use for the reconstitution of docosahexaenoic acid biosynthesis. J Lipid Res 45:1899–1909
9. Khozin I, Adlerstein D, Bigogno C, Heimer YM, Cohen Z (1997) Elucidation of the biosynthesis of eicosapentaenoic acid in the microalga *Porphyridium cruentum* (II. Studies with radiolabeled precursors). Plant Physiol 114:223–230
10. Bigogno C, Khozin-Goldberg I, Adlerstein D, Cohen Z (2002) Biosynthesis of arachidonic acid in the oleaginous microalga *Parietochloris incisa* (Chlorophyceae): radiolabeling studies. Lipids 37:209–216
11. Amanda E, Pereira SL, Sprecher H, Huang YS (2004) Elongation of long-chain fatty acids. Prog Lipid Res 43:36–54
12. Nichols BW, Appleby RS (1969) The distribution of arachidonic acid in algae. Phytochemistry 8:1907–1915
13. Qi B, Fraser T, Mugford S, Dobson G, Sayanova O, Butler J, Napier JA, Stobart AK, Lazarus CM (2004) Production of very long chain polyunsaturated omega-3 and omega-6 fatty acids in plants. Nat Biotechnol 22:739–745
14. Serghini HC, Demandre C, Justin AM, Mazliak P (1988) Linolenic acid biosynthesis via glycerolipid molecular species in pea and spinach leaves. Phytochemistry 7:2543–2548
15. Ohlrogge J, Browse J (1995) Lipid biosynthesis. Plant Cell 7:957–970
16. Brown AP, Dann R, Bowra S, Hills MJ (1998) Characterization of expression of a plant oleate desaturase in yeast. J Am Oil Chem Soc 75:77–82
17. Sayanova O, Smith MA, Lapinskas P, Stobart AK, Dobson G, Christie WW, Shewry PR, Napier JA (1997) Expression of a borage desaturase cDNA containing an N-terminal cytochrome *b5* domain results in the accumulation of high levels of Δ6-desaturated fatty acids in transgenic tobacco. Proc Natl Acad Sci USA 94:4211–4216
18. Sperling P, Heinz E (2001) Desaturases fused to their electron donor. Eur J Lipid Sci Technol 103:158–180
19. Napier JA, Michaelson LV, Sayanova O (2003) The role of cytochrome b_5 fusion desaturases in the synthesis of polyunsaturated fatty acids. Prostaglandins Leukot Essent Fatty Acids 68:135–143
20. Sperling P, Ternes P, Zank TK, Heinz E (2003) The evolution of desaturases. Prostaglandins Leukot Essent Fatty Acids 68:73–95
21. Napier JA, Hey SJ, Lacey DJ, Shewry PR (1998) Identification of a *Caenorhabditis elegans* Δ6-fatty-acid-desaturase by heterologous expression in *Saccharomyces cerevisiae*. Biochem J 330:611–614
22. Michaelson LV, Napier JA, Lewis M, Griffiths G, Lazarus CM, Stobart AK (1998) Functional identification of a fatty acid Δ^5 desaturase gene from *Caenorhabditis elegans*. FEBS Lett 439:215–218
23. Watts JL, Browse J (1999) Isolation and characterization of a Δ5-fatty acid desaturase from *Caenorhabditis elegans*. Arch Biochem Biophys 362:175–182
24. Michaelson LV, Lazarus CM, Griffiths G, Napier JA, Stobart AK (1998) Isolation of a Δ5-fatty acid desaturase gene from *Mortierella alpina*. J Biol Chem 273:19055–19059
25. Kaewsuwan S, Cahoon EB, Perroud P, Wiwat C, Panvisavas N, Quatrano RS, Cove DJ, Bunyapraphatsara N (2006) Identification and functional characterization of the moss *Physcomitrella patens* Δ5 desaturase gene involved in arachidonic and eicosapentaenoic acids biosynthesis. J Biol Chem 281:21988–21997

26. Kajikawa M, Yamato KT, Kohzu Y, Nojiri M, Sakuradani E, Shimizu S, Sakai Y, Fukuzawa H, Ohyama K (2004) Isolation and characterization of Δ6-desaturase, an ELO-like enzyme and Δ5-desaturase from the liverwort *Marchantia polymorpha* and production of arachidonic and eicosapentaenoic acids in the methylotrophic yeast *Pichia pastoris*. Plant Mol Biol 54:335–352
27. Domergue F, Lerchl J, Zähringer U, Heinz E (2002) Cloning and functional characterization of *Phaeodactylum tricornutum* front-end desaturases involved in eicosapentaenoic acid biosynthesis. Eur J Biochem 269:4105–4113
28. Tonon T, Sayanova O, Michaelson LV, Qing R, Harvey D, Larson TR, Li Y, Napier JA, Graham IA (2005) Fatty acid desaturases from the microalga *Thalassiosira pseudonana*. FEBS J 272:3401–3412
29. Domergue F, Abbadi A, Zähringer U, Moreau H, Heinz E (2005) In vivo characterization of the first acyl-CoA Delta6-desaturase from a member of the plant kingdom, the microalga *Ostreococcus tauri*. Biochem J 389:483–490
30. Hoffmann M, Wagner M, Abbadi A, Fulda M, Feussner I (2008) Metabolic engineering of ω3-very long chain polyunsaturated fatty acid production by an exclusively acyl-CoA-dependent pathway. J Biol Chem 283:22352–22362
31. Petrie JR, Shrestha P, Mansour MP, Nichols PD, Liu Q, Singh SP (2010) Metabolic engineering of omega-3 long-chain polyunsaturated fatty acids in plants using an acyl-CoA Δ6-desaturase with ω3-preference from the marine microalga Micromonas pusilla. Met Eng 12:233–240. doi:10.1016/j.ymben.2009.12.001
32. Abbadi A, Domergue F, Bauer J, Napier JA, Welti R, Zähringer U, Cirpus P, Heinz E (2004) Biosynthesis of very-long-chain polyunsaturated fatty acids in transgenic oilseeds: constraints on their accumulation. Plant Cell 16:2734–2748
33. Kinney AJ, Cahoon EB, Damude HG, Hitz WD, Kolar CW, Zhan-Bin L (2004) Production of very long chain polyunsaturated fatty acids in oilseeds. Patent WO 2004/071467 A2
34. Wu G, Truksa M, Datla N, Vrinten P, Bauer J, Zank T, Cirpus P, Heinz E, Qiu X (2005) Stepwise engineering to produce high yields of very long-chain polyunsaturated fatty acids in plants. Nat Biotechnol 23:1013–1017
35. Chen R, Matsui K, Ogawa M, Oe M, Ochiai M, Kawashima H, Sakuradani E, Shimizu S, Ishimoto M, Hayashi M, Murooka Y, Tanaka Y (2006) Expression of Δ6, Δ5 desaturase and GLELO elongase genes from *Mortierella alpina* for production of arachidonic acid in soybean [*Glycine max* (L.) Merrill] seeds. Plant Sci 170:399–406
36. Stanier RY, Kunisawa R, Mandel M, Cohen-Bazire G (1971) Purification and properties of unicellular blue-green algae (order Chroococcales). Bacteriol Rev 35:171–205
37. Solovchenko AE, Khozin-Goldberg I, Cohen Z, Merzlyak MN (2008) Carotenoid-to-chlorophyll ratio as a proxy for assay of total fatty acids and arachidonic acid content in the green microalga *Parietochloris incisa*. J Appl Phycol 21:361–366
38. Bekesiova I, Nap JP, Mlynarova L (1999) Isolation of high quality DNA and RNA from leaves of the carnivorous plant *Drosera rotundifolia*. Plant Mol Biol Rep 17:269–277
39. Gietz RD, Schiestl RH, Willems AR, Woods RA (1995) Studies on the transformation of intact yeast cells by the LiAc/SS-DNA/PEG procedure. Yeast 11:355–360
40. Christie WW (2003) The analysis of fatty acids. In: Christie WW (ed) Lipid analysis. Isolation, separation, identification and structural analysis of lipids, vol. 15, 3rd edn. The Oily Press, Bridgewater, pp 205–225
41. Bligh EG, Dyer WJ (1959) A rapid method of total lipid extraction and purification. Can J Biochem Physiol 37:911–917
42. Cohen Z, Didi S, Heimer YM (1992) Overproduction of γ-linolenic and eicosapentaenoic acids by algae. Plant Physiol 98:569–572
43. Iskandarov U, Khozin-Goldberg I, Ofir R, Cohen Z (2009) Cloning and characterization of the Δ6 polyunsaturated fatty acid elongase from the green microalga *Parietochloris incisa*. Lipids 44:545–554
44. Los DA, Murata N (1998) Structure and expression of fatty acid desaturases. Biochim Biophys Acta 1394:3–15
45. Sakuradani E, Kobayashi M, Ashikari T, Shimizu S (1999) Identification of delta12-fatty acid desaturase from arachidonic acid-producing *Mortierella* fungus by heterologous expression in the yeast *Saccharomyces cerevisiae* and the fungus *Aspergillus oryzae*. Eur J Biochem 261:812–820
46. Sugase Y, Hirono M, Kindle KL, Kamiya R (1996) Cloning and characterization of the actin-encoding gene of *Chlamydomonas reinhardtii*. Gene 168:117–121
47. Tamura K, Dudley J, Nei M, Kumar S (2007) MEGA4: Molecular evolutionary genetics analysis (MEGA) software version 4.0. Mol Biol Evol 24:1596–1599
48. Schneiter R, Daum G (2008) Analysis of yeast lipids. In: Wei X (ed) Yeast protocols, methods in molecular biology, vol 313. Humana Press, Totowa, pp 75–84
49. Shanklin J, Cahoon EB (1998) Desaturation and related modifications of fatty acids. Annu Rev Plant Physiol Plant Mol Biol 49:611–641
50. Knutzon DS, Thurmond JM, Huang YS, Chaudhary S, Bobik EG Jr, Chan GM, Kirchner SJ, Mukerji P (1998) Identification of Δ5-desaturase from *Mortierella alpina* by heterologous expression in bakers' yeast and canola. J Biol Chem 273:29360–29366
51. Suga K, Honjoh K, Furuya N, Shimizu H, Nishi K, Shinohara F, Hirabaru Y, Maruyama I, Miyamoto T, Hatano S, Iio M (2002) Two low-temperature-inducible *Chlorella* genes for Δ12 and ω-3 Fatty Acid Desaturase (FAD): isolation of Δ12 and ω-3 *fad* cDNA clones, expression of Δ12 *fad* in *Saccharomyces cerevisiae*, and expression of ω-3 fad in *Nicotiana tabacum*. Biosci Biotechnol Biochem 66:1314–1327
52. Sayanova O, Shewry PR, Napier JA (1999) Histidine-41 of the cytochrome *b5* domain of the borage Δ6 fatty acid desaturase is essential for enzyme activity. Plant Physiol 121:641–646
53. Guillou H, D'Andrea S, Rioux V, Barnouin R, Dalaine S, Pedrono F, Jan S, Legrand P (2004) Distinct roles of endoplasmic reticulum cytochrome *b5* and fused cytochrome b5-like domain for rat Δ6-desaturase activity. J Lipid Res 45:32–40
54. Lu Y, Chi X, Yang Q, Li Z, Liu S, Gan Q, Qin S (2009) Molecular cloning and stress-dependent expression of a gene encoding *D*12-fatty acid desaturase in the Antarctic microalga *Chlorella vulgaris* NJ-7. Extremophiles 13:875–884
55. Tripodi KEJ, Buttigliero LV, Altabe SG, Uttaro AD (2006) Functional characterization of front-end desaturases from trypanosomatids depicts the first polyunsaturated fatty acid biosynthetic pathway from a parasitic protozoan. FEBS J 273:271–280
56. Petrie JR, Liu Q, Mackenzie AM, Shrestha P, Mansour MP, Robert SS, Frampton DF, Blackburn SI, Nichols PD, Singh SP (2009) Isolation and characterisation of a high-efficiency desaturase and elongases from microalgae for transgenic LC-PUFA production. Mar Biotechnol. doi:10.1007/s10126-009-9230-1
57. Sayanova O, Beaudoin F, Michaelson VL, Shewry RP, Napier JA (2003) Identification of *Primula* fatty acid Δ6-desaturases with *n*-3 substrate preference. FEBS Lett 542:100–104
58. Zheng XZ, Ding ZK, Xu YQ, Monroig O, Morais S, Tocher DR (2009) Physiological roles of fatty acyl desaturases and elongases in marine fish: Characterisation of cDNA of fatty acyl Δ6 desaturase and elovl5 elongase of cobia (*Rachycentron canadum*). Aquaculture 290:122–131
59. Kajikawa M, Yamato KT, Kohzu Y, Shoji S, Matsui K, Tanaka Y, Sakai Y, Fukuzawa H (2006) A front-end desaturase from *Chlamydomonas reinhardtii* produces pinolenic and coniferonic

acids by omega13 desaturation in methylotrophic yeast and tobacco. Plant Cell Physiol 47:64–73
60. Girke T, Schimdt H, Zähringer U, Reski R, Heinz E (1998) Identification of a novel Δ6-acyl-group desaturase by targeted gene disruption in *Physcomitrella patens*. Plant J 15:39–48
61. Hong H, Dalta N, Reed DW, Covello PS, MacKenzie SL, Qiu X (2002) High-level production of γ-linolenic acid in *Brassica juncea* using a Δ6 desaturase from *Pythium irregulare*. Plant Physiol 129:354–362
62. Sayanova O, Davies GM, Smith MA, Griffiths G, Stobart AK, Shewry PR, Napier JA (1999) Accumulation of Δ6-unsaturated fatty acids in transgenic tobacco plants expressing a Δ6-desaturase from *Borago officinalis*. J Exp Bot 50:1647–1652
63. Domergue F, Abbadi A, Ott C, Zank TK, Zähringer U, Heinz E (2003) Acyl carriers used as substrates by the desaturases and elongases involved in very long-chain polyunsaturated fatty acids biosynthesis reconstituted in yeast. J Biol Chem 278:35115–35126
64. Cho HP, Nakamura M, Clarke SD (1999) Cloning, expression, and fatty acid regulation of the human Δ5 desaturase. J Biol Chem 274:37335–37339
65. Bigogno C, Khozin-Goldberg I, Cohen Z (2002) Accumulation of arachidonic acid-rich triacylglycerols in the microalga *Parietochloris incisa* (Trebouxiophyceae, Chlorophyta). Phytochemistry 60:135–143

Lipids (2010) 45:531–536
DOI 10.1007/s11745-010-3425-0

ORIGINAL ARTICLE

Effect of Conjugated Linoleic Acid on *Cyprinus carpio* var. Jian Regarding Growth, Immunity, and Disease Resistance to *Aeromonas hydrophila*

Jun Jiang · Ming-jiang Zhao · Feng Lin · Liu Yang · Xiao-qiu Zhou

Received: 20 December 2009 / Accepted: 23 April 2010 / Published online: 16 May 2010

Abstract The present study was performed to investigate the effect of dietary conjugated linoleic acid (CLA) on the growth performance, immune parameters and disease resistance to *Aeromonas hydrophila* of juvenile Jian carp. A total of 900 juvenile Jian carp (10.71 ± 0.02 g) were randomly allocated into six groups of each three replicates, feeding isonitrogenous (35% crude protein) and isolipidic (7.8% crude fat) diets containing graded amounts of CLA (0, 0.5, 0.8, 1.4, 1.7, and 2.0%) for 60 days. After a 60-day growth test, a challenge trial was conducted by intraperitoneal injection of *Aeromonas hydrophila* to determine the effect of CLA on disease resistance of juvenile Jian carp. The results showed that diets incorporated with a proportion of up to 2.0% CLA without effect on weight gain, feed intake, and feed conversion ratio, but improved immune parameters and disease resistance of juvenile Jian carp. The dietary CLA level of optimal disease resistance to *Aeromonas hydrophila* was estimated to be 1.7% in juvenile Jian carp using broken-line analysis.

Keywords Conjugated linoleic acid · Growth · Immunity · Disease resistance · Juvenile Jian carp

Abbreviations

CLA	Conjugated linoleic acid
LD_{50}	50% lethal dose
CFU	Clonal formation unit
SD	Standard deviation
FI	Feed intake
WG	Weight gain
FCR	Feed conversion ratio
RBC	Red blood cell count
WBC	White blood cell count
SRF	Survival rate during growth trail
SRV	Survival rate after challenge
LA	Lysozyme activity
TIBC	Total iron-binding capacity

J. Jiang · M. Zhao · F. Lin · L. Yang · X. Zhou (✉)
Institute of Animal Nutrition, Sichuan Agricultural University, Yaan 625014, Sichuan, China
e-mail: zhouxq@sicau.edu.cn

J. Jiang · X. Zhou
Aquaculture Department, Sichuan Agricultural University, Yaan, Sichuan, China

Introduction

Conjugated linoleic acid (CLA) is a mixture of positional (9, 11; 10, 12; or 11, 13) and geometric (*cis* or *trans*) isomers of linoleic acid (18:2n-6). The two main naturally occurring isomers being *cis*-9, *trans*-11 and *trans*-10, *cis*-12, are known to possess biological activity [1]. Schwarz et al. [2] found the amounts of monounsaturated and polyunsaturated fatty acids are reduced, and the amounts of saturated fatty acids are increased in carp after being given a diet containing CLA. Choi et al. [3] carried out a study showing that carp fed with the CLA supplemented diets with the c9, t11- and tl0, c12-CLA isomers as the major components and the c9, c11-, cl0, cl2-, t9, t11-, and tl0, t12-CLA as the minor ones incorporated into the phospholipids and neutral lipid fractions. The CLA content in the muscle hepatopancreas, testes, and ovaries of carp fed with a CLA supplemented diet for 8 weeks was positively related to the CLA content of the diets [3]. The effects of dietary CLA supplements on growth performance have

been studied in a number of fish species. In common carp *Cyprinus carpio* [2], Atlantic salmon *Salmo salar* [4, 5], yellow perch *Perca flavescens* [6], tilapia *Oreochromis niloticus* [7], rainbow trout *Oncorhynchus mykiss* [8–10], channel catfish *Ictalurus punctatus* [11], a dietary CLA supplement did not affect their weight gain, feed intake, and feed conversion ratio. However, some studies found that weight gains and specific growth rates were improved in channel catfish [12] and common carp [13] fed with the diets containing CLA. Therefore, the effects of CLA on fish growth performance remain uncertain.

Recently it has been reported that CLA has immunomodulatory properties and enhances terrestrial animal immune function [14–16] when the animals have been fed with a CLA supplemented diet. To our knowledge, there is a lack of information about the relationship between CLA and the immune response in fish. Only recently, has one study showed that inclusion of CLA up to 1% increased sea bass juveniles *Dicentrarchus labrax* plasma lysozyme activity and was positively correlated with an alternative complement pathway [17].

The present study aim was to determine the effects of a dietary CLA supplement on growth performance, immune parameters, and disease resistance to *Aeromonas hydrophila* of juvenile Jian carp *Cyprinus carpio* var. Jian.

Materials and Methods

Diet Preparation

The formulation of the basal diet is shown in Table 1. Fish meal, soybean meal and rice gluten meal were used as protein sources. The CLA was added to the diets at the expense of the fish oil so that all the diets remained isolipidic. The CLA (containing 87.6% CLA methyl esters as a 50:50 mixture of c9, t11 and t10, c12 isomers) was obtained from the Xin Jiang Technical Institute of Physics and Chemistry, Chinese Academy of Sciences. Six experimental diets were formulated to supplement with 0, 0.5, 0.8, 1.4, 1.7 and 2.0% CLA. Table 2 shows the fatty acid profiles of the diets. Crude protein and lipid content values were the measured according to AOAC [18]. Available phosphorus, lysine, methionine and cystine content values were calculated according to feed ingredients composition values [19].

Fish Feeding and Challenge

A total of 900 juvenile Jian carp (10.71 ± 0.02 g) were randomly allocated into each of 18 glass aquaria (90 × 30 × 40 cm^3). Each aquarium was randomly assigned to one of three replicates of six groups. Fish were acclimatized to the experimental conditions with their respective diet for 1 week prior to starting the growth trial. Fish were fed daily with the respective diet 8 times per day at 0700, 0900, 1100, 1300, 1500, 1700, 1900, and 2100 hours, and were carefully observed to ensure satiation without overfeeding for 60 days. A closed system with continuous aeration and daily replacement of water in the

Table 1 Ingredients and approximate composition of the basal diet

Ingredients	Dry diet (g kg^{-1})	Chemical composition	Dry diet (g kg^{-1})
Fish meal	217.0	Crude protein	350.0
Soybean meal	195.8	Crude fat	78.0
Rice gluten meal	165.0	Available phosphorus	6.0
α-Starch	338.1	Lysine	21.0
Fish oil	47.3	Methionine + cystine	11.0
Ca $(H_2PO_4)_2$	22.6		
DL-Methionine	4.2		
Mineral mixture[a]	5.0		
Vitamin mixture[b]	3.0		
Choline chloride	1.3		
Ethoxyquin	0.7		

[a] Per kg of mineral mix: $FeSO_4 \cdot 7H_2O$, 152.00 g; $CuSO_4 \cdot 5H_2O$, 2.40 g; $ZnSO_4 \cdot 7H_2O$, 31.20 g; $MnSO_4 \cdot H_2O$, 8.20 g; $Na_2SeO_3 \cdot 5H_2O$, 0.18 g; KI, 0.16 g; $CaCO_3$, 805.86 g

[b] Per kg of vitamin mix: retinyl acetate (500,000 IU g^{-1}), 2.667 g; cholecalciferol (500,000 IU g^{-1}), 1.666 g; DL-α-tocopherol acetate (50%), 66.667 g; menadione (50%), 0.667 g; thiamin nitrate (98%), 0.170 g; riboflavin (80%), 2.917 g; pyridoxine·HCl (98%), 2.040 g; cyanocobalamin (1%), 0.333 g; ascorbyl acetate (35%), 66.667 g; D-calcium pantothenate (98%), 10.204 g; niacin (99%), 10.101 g; biotin (2%), 16.670 g; myo-inositol (98%), 149.663 g; folic acid (96%), 0.347 g

Table 2 Fatty acids compositions of the diets, % of total fatty acids

Fatty acids	0	0.5	0.8	1.4	1.7	2.0
14:0	7.3	6.4	5.9	5.4	4.8	4.3
16:0	13.8	12.5	11.8	11.0	10.3	9.8
16:1	5.3	4.6	4.2	3.9	3.8	3.1
18:0	1.6	1.5	1.5	1.5	1.5	1.5
18:1	13.6	12.6	12.0	11.5	10.9	10.3
18:2n6	3.5	3.2	3.0	2.7	2.5	2.3
CLA	0	8.9	14.4	21.9	27.3	32.7
18:3n3	1.3	1.1	1.0	0.9	0.8	0.7
18:4n3	2.4	2.1	2.0	1.8	1.6	1.4
20:1	12.0	10.5	9.6	8.8	7.9	7.0
20:4n6	0.5	0.4	0.4	0.4	0.3	0.3
20:5n3	6.6	5.8	5.3	4.9	4.4	3.9
22:1	18.1	15.9	14.6	13.3	12.0	10.6
22:5n3	0.7	0.6	0.6	0.5	0.5	0.4
22:6n3	7.1	6.2	5.7	5.2	4.7	4.2

CLA: sum of c9, t11 and t10, c12 isomers

aquarium was used. The aquaria system, operation of the culture system, and water quality were as previously described in [20].The experimental units were under a natural light and dark cycle (approximately 13 h L:11 h D). The water temperature was maintained at 21 ± 1 °C.

After the growth trial, five fish with a similar body weight were removed from each aquarium and moved to a tank with the same conditions, allowed to adapt to the culture conditions for 5 days, and then kept for another 17 days in a challenge trial. Fish were challenged by intraperitoneal injection with *Aeromonas hydrophila* (10^{10} cfu mL^{-1}, LD_{50}) at a dose of 0.5 mL $fish^{-1}$ by the method reported in [21]. The experiment conditions were the same as in the growth trial.

Sample Collection and Analysis

Fish were weighed at the beginning and end of the growth trial. At the end of the growth trial, five fish were taken from each aquarium, the blood was collected from the caudal vein using a syringe with heparin to prevent coagulation. The red blood cells and the white blood cells were counted by the method in [21]. At the end of the challenge trial, five fish per aquarium were anesthetized with MS-222 (Sigma Chemical) 12 h after their last feeding. Blood was collected from the caudal vein, stored at 4 °C overnight, and centrifuged at 3,000*g* for 10 min, the supernatant was stored at −20 °C for analysis. The serum agglutination activity was determined using a hemagglutination assay [22]. The activity was expressed as the titer, i.e., the reciprocal of the highest dilution showing complete agglutination. The lysozyme activity of the serum was measured using a method based on the ability of lysozyme to lyse the bacterium *Micrococcus lysodeikticus* described in [21]. The total iron-binding capacity was determined according to [23].

Calculations and Statistical Analyses

All data are presented as means ± SD and subjected to one-way analysis of variance followed by Tukey's test to determine significant differences among treatments, and probability values $P < 0.05$ indicates a significant difference. The broken-line model was used to calculate the optimal dietary CLA supplement in juvenile Jian carp for the maximal survival rate after challenge [24].

Table 4 Effect of dietary CLA supplementation on red blood cell count (RBC, 10^8 cell mL^{-1}) and white blood cell count (WBC, 10^6 cell mL^{-1}) in juvenile Jian carp

CLA (%)	RBC	WBC
0	11.60 ± 0.18^{a}	1.80 ± 0.14^{a}
0.5	12.37 ± 0.17^{b}	2.67 ± 0.29^{b}
0.8	12.75 ± 0.06^{c}	3.33 ± 0.16^{c}
1.4	13.80 ± 0.13^{d}	3.60 ± 0.24^{cd}
1.7	13.78 ± 0.07^{d}	3.72 ± 0.20^{d}
2.0	13.78 ± 0.13^{d}	3.61 ± 0.28^{d}

Mean ± SD ($n = 3$).Values sharing the same superscripts are not significantly different ($P < 0.05$)

Results

Table 3 shows growth and feed utilization parameters of fish fed the basal diet or diets with varying levels of CLA. Growth of the Jian carp was unaffected by CLA, neither having any significant effect on final weight, weight gain, and feed intake, nor feed conversion ratio ($P > 0.05$). Red blood cell count and white blood cell count were significantly increased in response to the CLA increasing up to 1.4%, and remaining nearly constant thereafter ($P < 0.05$, Table 4). There was no difference in survival rate among all dietary treatments in growth trail ($P > 0.05$, Table 5). However, with the increasing of dietary CLA levels, survival rate after challenge with *Aeromonas hydrophila* was increased with CLA increasing gradually up to 1.4%, and then remaining nearly constant ($P < 0.05$, Table 5). Lysozyme activity, hemagglutination titer, total iron-binding capacity, and blood cell counts showed the same change, increased significantly with the CLA increasing up

Table 3 Effects of dietary CLA supplementation on final weight and feed intake (FI, g $fish^{-1}$), weight gain (WG), and feed conversion ratio (FCR) of juvenile Jian carp

CLA (%)	Initial weight	Final weight	WG	FI	FCR
0.0	10.73 ± 0.02	33.55 ± 1.96	212.64 ± 18.12	32.59 ± 1.85	1.43 ± 0.04
0.5	10.70 ± 0.03	33.39 ± 0.82	212.05 ± 7.04	32.81 ± 0.89	1.45 ± 0.01
0.8	10.70 ± 0.01	34.45 ± 1.26	221.99 ± 11.78	32.54 ± 0.86	1.37 ± 0.04
1.4	10.71 ± 0.01	34.74 ± 1.37	224.47 ± 12.63	33.45 ± 0.43	1.39 ± 0.08
1.7	10.72 ± 0.02	33.97 ± 0.77	216.78 ± 6.70	32.64 ± 0.38	1.40 ± 0.06
2.0	10.71 ± 0.03	34.54 ± 1.00	222.42 ± 8.63	33.32 ± 0.28	1.40 ± 0.06

Mean ± SD ($n = 3$). There were no significant differences between dietary groups ($P > 0.05$)

WG = 100 × (final weight − initial weight)/initial weight. FCR = feed intake/weight gain

Table 5 Effect of dietary CLA supplementation on survival rate during growth trail (SRF) and survival rate after challenge (SRV) with *Aeromonas hydrophila* of juvenile Jian carp

CLA (%)	SRF	SRV
0	99.33 ± 0.67[a]	33.33 ± 5.77[a]
0.5	100.00 ± 0.00[a]	40.00 ± 0.00[a]
0.8	99.33 ± 0.67[a]	43.33 ± 5.77[ab]
1.4	100.00 ± 0.00[a]	53.33 ± 5.77[bc]
1.7	100.00 ± 0.00[a]	60.00 ± 10.00[c]
2.0	100.00 ± 0.00[a]	56.67 ± 5.77[c]

Mean ± SD ($n = 3$).Values sharing the same superscripts are not significantly different ($P < 0.05$)

Survival rate = 100 × N_t/N_0, N_t and N_0 were final and initial numbers of fish in each replicate, respectively

Table 6 Effect of dietary CLA supplementation on lysozyme activity (LA, μg ml^{-1}), hemagglutination titer (log_2HA), total iron-binding capacity (TIBC, μg ml^{-1}) of juvenile Jian carp after challenge with *Aeromonas hydrophila*

CLA (%)	LA	log_2HA	TIBC
0	9.38 ± 0.75[a]	6.33 ± 0.58[a]	7.47 ± 0.61[a]
0.5	12.09 ± 0.84[b]	6.67 ± 0.58[ab]	8.40 ± 0.40[b]
0.8	13.64 ± 0.97[b]	7.00 ± 0.00[b]	9.73 ± 0.61[c]
1.4	15.74 ± 0.82[c]	7.67 ± 0.58[c]	10.00 ± 0.40[c]
1.7	16.36 ± 0.97[c]	8.00 ± 1.00[c]	10.40 ± 0.40[c]
2.0	15.58 ± 0.84[c]	7.67 ± 0.58[c]	10.40 ± 0.40[c]

Mean ± SD. ($n = 3$).Values sharing the same superscripts are not significantly different ($P < 0.05$)

to 1.4%, thereafter kept nearly constant ($P < 0.05$, Table 6). According to the broken-line analysis, the values of the parameters of dietary CLA level were: for SRV, 1.7 ± 0.1%, $Y = 57.7 - 14.7x$ (R-X_{LR}); for RBC, 1.4 ± 0.1%, $Y = 13.8 - 1.6x$ (R-X_{LR}); for WBC, 1.0 ± 0.1%, $Y = 3.6 - 1.9x$ (R-X_{LR}); for LA, 1.2 ± 0.1%, $Y = 15.9 - 5.3x$ (R-X_{LR}); for log_2HA, 1.6 ± 0.2%, $Y = 7.8 - 1.0x$ (R-X_{LR}); for TIBC, 1.1 ± 0.2%, $Y = 10.3 - 2.7x$ (R-X_{LR}). ($P < 0.05$, $R^2 = 0.99$). The nutrient response curve generated by the broken-line equation is given in Fig. 1.

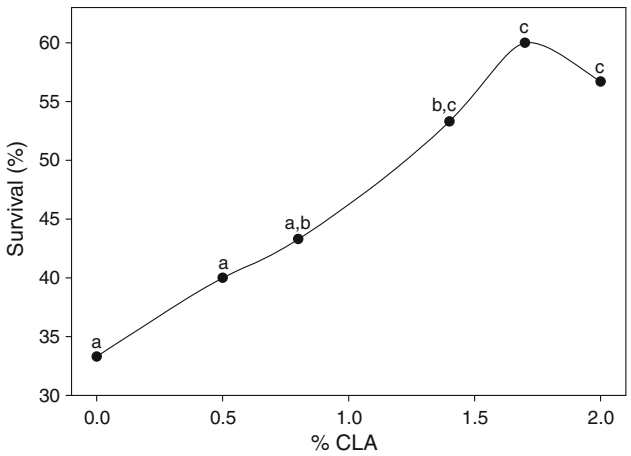

Fig. 1 Broken line analysis of the survival rate after *Aeromonas hydrophila* challenge in Jian carp fed the diets containing different CLA levels for 60 days (values sharing the same superscripts are not significantly different, $P < 0.05$)

Discussion

The results show that juvenile Jian carp weight gain, feed intake and feed conversion ratio were not influenced significantly by a 0.5–2.0% CLA supplement. Similar results have been reported for common carp weight gain, feed conversion ratio, and daily growth rate [3]. Some reports showed that 1.0% CLA in the diet improved the specific daily growth rate and feed conversion ratio in common carp, but 5.0 and 10.0% CLA decreased growth performance [13]. These different results may possibly be attributed to the total dietary lipid level different, 15% [13] and 10% [3].

The survival rate in the challenge trial is usually used to reflect fish disease resistance [25–28]. The present study firstly indicated dietary supplement CLA could improve the survival rate of juvenile Jian carp after being challenged with *Aeromonas hydrophila*. To our knowledge, there is no available information on CLA increasing fish disease resistance. The dietary CLA supplement in juvenile Jian carp to optimal disease resistance was 1.7% using broken-line regression with the survival rate after challenge with *Aeromonas hydrophila*.

The positive effect of CLA on disease resistance of juvenile Jian carp may be attributed to the improved immunity parameters. Fish possess non-specific defense mechanisms, such as the phagocytic mechanisms developed by macrophages and granular leukocytes, and are also the first animals to have developed both cellular and humoral immune responses mediated by lymphocytes [29]. The non-specific immune system is started up immediately and a series of immune responses are activated, including recognition, adhesive and opsonization, and bacterial growth inhibition and lysis [30]. As a variety of germ line-encoded pattern recognition receptors, lectins show binding specificity for different carbohydrates such as mannose, *N*-acetyl glucosamine or fucose, this leads to opsonization, phagocytosis and activation of the complement system [31]. The hemagglutination titer was improved by CLA in the present study. There is no information about the relationship between CLA and the serum hemagglutination titer of fish or animal. A recent study has shown that CLA was positively correlated with an alternative complement

pathway in sea bass juveniles [17]. Transferrins reduce infection by binding iron, thereby reducing iron availability to invading organisms, which restrict bacterial or fungal multiplication until the immune system can respond [29]. The total iron-binding capacity reflects serum transferrins' iron-binding properties [32]. The present result showed CLA could enhance total iron-binding capacity of juvenile Jian carp serum. There is no available information about CLA increasing fish total iron-binding capacity. Lysozyme, an important factor in the immune defense of both invertebrates and vertebrates, is found in the serum, mucus, and other tissues of fish [29]. Gram-positive bacteria can be directly damaged by lysozyme [29]. The present results indicated that CLA could improve serum lysozyme activity of juvenile Jian carp. A recent study has shown that CLA increased sea bass juveniles plasma lysozyme activity [17].

In conclusion, the present results showed that diets a supplement of up to 2.0% CLA did not alter weight gain, feed intake, and feed conversion ratio, but promoted immune parameters and disease resistance of juvenile Jian carp. The dietary CLA supplement was estimated to be 1.7% for optimal disease resistance to *Aeromonas hydrophila* in juvenile Jian carp.

Acknowledgments The National Science Foundation of China (30771671, 30871926) financially supported this research. The authors wish to thank the personnel of these teams for their kind assistance.

References

1. Pariza MW, Park Y, Cook ME (2001) The biologically active isomers of conjugated linoleic acid. Prog Lipid Res 40:283–298
2. Schwarz F, Maass D, Schabbel W, Steinhart H (2002). Dietary conjugated linoleic acid supplementation and the effects on performance, body composition, fatty acid pattern and sensory quality of carp (*Cyprinus carpio*), 2–7 June 2002; Rhodes pp 79
3. Choi BD, Kang SJ, Ha YL, Park GB, Ackman RG (2002) Conjugated linoleic acid as a supplemental nutrient for common carp (*Cyprinus carpio*). Food Sci Biotechnol 11:457–461
4. Berge GM, Ruyter B, Åsgård T (2004) Conjugated linoleic acid in diets for juvenile Atlantic salmon (*Salmo salar*); effects on fish performance, proximate composition, fatty acid and mineral content. Aquaculture 237:365–380
5. Leaver MJ, Tocher DR, Obach A, Jensen L, Henderson RJ, Porter AR, Krey G (2006) Effect of dietary conjugated linoleic acid (CLA) on lipid composition, metabolism and gene expression in Atlantic salmon (*Salmo salar*) tissues. Comp Biochem Physiol A Mol Integr Physiol 145:258–267
6. Twibell RG, Watkins BA, Brown PB (2001) Dietary conjugated linoleic acids and lipid source alter fatty acid composition of juvenile yellow perch, *Perca flavescens*. J Nutr 131:2322–2328
7. Yasmin A, Takeuchi T, Hayashi M, Hirota T, Ishizuka W, Ishida S (2004) Effect of conjugated linoleic and docosahexaenoic acids on growth of juvenile tilapia *Oreochromis niloticus*. Fish Sci 70:473–481
8. Yasmin A, Takeuchi T, Hirota T, Ishida S (2004) Effect of conjugated linolenic acid (*cis*-9, *trans*-11, *cis*-13–18:3) on growth performance and lipid composition of fingerling rainbow trout *Oncorhynchus mykiss*. Fish Sci 70:1009–1018
9. Figueiredo-Silva AC, Rema P, Bandarra NM, Nunes ML, Valente LMP (2005) Effects of dietary conjugated linoleic acid on growth, nutrient utilization, body composition, and hepatic lipogenesis in rainbow trout juveniles (*Oncorhynchus mykiss*). Aquaculture 248:163–172
10. Bandarra NM, Nunes ML, Andrade AM, Prates JAM, Pereira S, Monteiro M, Rema P, Valente LMP (2006) Effect of dietary conjugated linoleic acid on muscle, liver and visceral lipid deposition in rainbow trout juveniles (*Oncorhynchus mykiss*). Aquaculture 254:496–505
11. Twibell RG, Wilson RP (2003) Effects of dietary conjugated linoleic acids and total dietary lipid concentrations on growth responses of juvenile channel catfish, *Ictalurus punctatus*. Aquaculture 221:621–628
12. Manning BB, Li MH, Robinson EH, Peterson BC (2006) Enrichment of channel catfish (*Ictalurus punctatus*) fillets with conjugated linoleic acid and omega-3 fatty acids by dietary manipulation. Aquaculture 261:337–342
13. Choi BD, Kang SJ, Ha YL, Ackman RG (1999) Accumulation of conjugated linoleic acid (CLA) in tissues of fish fed diets containing various levels of CLA. In: Xiong YL, Ho CT, Shahidi F (eds) Quality attributes of muscle foods. Kluwer Academic Plenum Publishers, New York, pp 61–71
14. Kang JH, Lee GS, Jeung EB, Yang MP (2007) *Trans*-10, *cis*-12-conjugated linoleic acid increases phagocytosis of porcine peripheral blood polymorphonuclear cells in vitro. Br J Nutr 97:117–125
15. Nunes EA, Bonatto SJ, de Oliveira HH, Rivera NL, Maiorka A, Krabbe EL, Tanhoffer RA, Fernandes LC (2008) The effect of dietary supplementation with 9-*cis*:12-*trans* and 10-*trans*:12-*cis* conjugated linoleic acid (CLA) for nine months on serum cholesterol, lymphocyte proliferation and polymorphonuclear cells function in Beagle dogs. Res Vet Sci 84:62–67
16. Ramirez-Santana C, Perez-Cano FJ, Castell M, Castellote C, Franch A (2008) Potentiation of systemic humoral immune response in suckling rats by conjugated linoleic acid (CLA). Proc Nutr Soc 67:E22
17. Makol A, Torrecillas S, Fernández-Vaquero A, Robaina L, Montero D, Caballero MJ, Tort L, Izquierdo M (2009) Effect of conjugated linoleic acid on dietary lipids utilization, liver morphology and selected immune parameters in sea bass juveniles (*Dicentrarchus labrax*). Comp Biochem Physiol B Biochem Mol Biol 154:179–187
18. Cunniff P (1997) Official methods of analysis of AOAC international, 16th edn, 3rd Rev. Association of Official Analytical Chemists, Gaithersburg, MD, USA
19. NRC (1993) In: Council NR (ed) Nutrient requirement of fish. National Academy Press, Washington DC
20. Jiang W-D, Feng L, Liu Y, Jiang J, Zhou X-Q (2009) Growth, digestive capacity and intestinal microflora of juvenile Jian carp (*Cyprinus carpio* var. Jian) fed graded levels of dietary inositol. Aquac Res 40:955–962
21. Yang Q-H, Zhou X-Q, Jiang J, Liu Y (2008) Effect of dietary vitamin A deficiency on growth performance, feed utilization and immune responses of juvenile Jian carp (*Cyprinus carpio* var. Jian). Aquac Res 39:902–906
22. Wen Z-P, Zhou X-Q, Feng L, Jiang J, Liu Y (2009) Effect of dietary pantothenic acid supplement on growth, body composition and intestinal enzyme activities of juvenile Jian carp (*Cyprinus carpio* var. Jian). Aquac Nutr 15:470–476
23. Welker TL, Lim C, Yildirim-Aksoy M, Klesius PH (2007) Growth, immune function, and disease and stress resistance of juvenile Nile tilapia (*Oreochromis niloticus*) fed graded levels of bovine lactoferrin. Aquaculture 262:156–162

24. Robbins KR, Saxton AM, Southern LL (2006) Estimation of nutrient requirements using broken-line regression analysis. J Anim Sci 84(Suppl):155–165
25. Lin M-F, Shiau S-Y (2005) Dietary L-ascorbic acid affects growth, nonspecific immune responses and disease resistance in juvenile grouper, *Epinephelus malabaricus*. Aquaculture 244:215–221
26. Kumari J, Sahoo PK (2005) High dietary vitamin C affects growth, non-specific immune responses and disease resistance in Asian catfish, *Clarias batrachus*. Mol Cell Biochem 280:25–33
27. Ai Q, Mai K, Tan B, Xu W, Zhang W, Ma H, Liufu Z (2006) Effects of dietary vitamin C on survival, growth, and immunity of large yellow croaker, *Pseudosciaena crocea*. Aquaculture 261:327–336
28. Chiu S-T, Tsai R-T, Hsu J-P, Liu C-H, Cheng W (2008) Dietary sodium alginate administration to enhance the non-specific immune responses, and disease resistance of the juvenile grouper *Epinephelus fuscoguttatus*. Aquaculture 277:66–72
29. Moore MM, Hawke JP (2004) Immunology. In: Craig ST, John AH (eds) Developments in aquaculture and fisheries science. Elsevier, Amsterdam, pp 349–386
30. Shoemaker C, Klesius P, Lim C (2001) Immunity and disease resistance in fish. In: Lim C, Webster CD (eds) Nutrition and fish health. Haworth Press, New York, pp 149–162
31. Arason GJ (1996) Lectins as defence molecules in vertebrates and invertebrates. Fish Shellfish Immunol 6:277–289
32. Ramsay WNM (1997) The determination of the total iron-binding capacity of serum. Clin Chim Acta 259:25–30

Lipids (2010) 45:537–548
DOI 10.1007/s11745-010-3436-x

ORIGINAL ARTICLE

Characteristics of the Fatty Acid Composition of a Deep-Sea Vent Gastropod, *Ifremeria nautilei*

Hiroaki Saito · Jun Hashimoto

Received: 16 November 2009 / Accepted: 23 April 2010 / Published online: 12 June 2010

Abstract Neutral and polar lipids in the soft parts of a gastropod species, *Ifremeria nautilei*, collected from deep-sea hydrothermal vents, were examined to assess the trophic relationships in hydrothermal vents. The vent gastropod obtains many of its lipids from symbiotic chemosynthetic microorganisms. The major polyunsaturated fatty acids (PUFA) both in the triacylglycerols and phospholipids of the gastropod consist of a limited number of n-3 and n-6 PUFA: arachidonic acid (20:4n-6), icosapentaenoic acid (20:5n-3), and docosapentaenoic acid (22:5n-3), without docosahexaenoic acid (DHA, 22:6n-3). Noticeable levels of various n-6 PUFA, such as 18:2n-6,9, 20:2n-6,9, 20:3n-6,9,12, and 20:3n-6,9,15 with significant levels of 16:1n-6 and 18:1n-6 indicate the biosynthetic characteristic of the endosymbionts. The lack of DHA in all specimens suggests a limitation of its lipid biosynthesis ability with its symbionts. This finding with regard to the lipids is unusual for a marine animal in the grazing or detrital food chain because many marine animal lipids evidently contain high levels of DHA with low levels of n-6 fatty acids. Such contradictory findings lead to some new insights into the absence of a biosynthetic pathway for DHA in *I. nautilei*, and provide evidence that DHA in this species is dispensable. Similar to herbivorous gastropods, the lack of DHA with significant levels of n-6 PUFA in this species also indicates its selective assimilation of specific microorganisms, such as chemosynthetic bacteria in hydrothermal vents, because significant levels of DHA were found in carnivorous mollusk lipids.

Keywords Chemoecology · Gastropod · Docosapentaenoic acid · Geothermal energy · Hydrothermal vents · Marine-grazing food chain · Polyunsaturated fatty acids · Symbiotic microorganisms

Abbreviations

ARA	Arachidonic acid
DMA	Dimethylacetals
DMOX	4,4-Dimethyloxazoline
DHA	Docosahexaenoic acid
DPA	Docosapentaenoic acid
EPA (IPA)	Icosapentaenoic acid
GC–MS	Gas chromatography–mass spectroscopy
MUFA	Monounsaturated fatty acids
NMID	Non-methylene interrupted dienes
NMR	Nuclear magnetic resonance
PtdCho	Phosphatidylcholine
PtdEtn	Phosphatidylethanolamine
PUFA	Polyunsaturated fatty acids
TAG	Triacylglycerols
TFA	Total fatty acids

H. Saito (✉) · J. Hashimoto
National Research Institute of Fisheries Science,
Fisheries Research Agency, 2-12-4 Fuku-ura, Kanazawa-ku,
Yokohama 236-8648, Japan
e-mail: hiroakis@affrc.go.jp

Present Address:
J. Hashimoto
Faculty of Fisheries, Nagasaki University, Nagasaki, Japan

Introduction

It is generally known that all marine animals, not only marine fishes but also invertebrates, characteristically accumulate various sorts of n-3 polyunsaturated fatty acids (PUFA) in their cell membranes; in particular, docosahexaenoic acid

(DHA, 22:6 n-3) and icosapentaenoic acid (EPA, 20:5 n-3) are the major PUFA in their tissues [1–3]. These n-3 PUFA are considered to originate from phytoplankton, which depend on solar energy, and from unique deep-sea barophilic bacteria [1, 4, 5]. It is also well-known that many marine animals in higher trophic levels through the food web, accumulate these long-chain PUFA [1, 6, 7]. As for the fatty acid determination of mollusk lipids, some bivalve species (Bivalvia), such as oysters and mussels, have been investigated in detail (for oysters, Ostreidae: [8–11]; for pearl oysters, Pteriidae: [12]; for scallops, Pectinidae: [13, 14]; for clams, Veneridae: [15]; and for mussels, Mytilidae: [16–18]). Nevertheless, there is relatively little information available on the biochemical components of other mollusk species; there are only a few reports on both lipids and the fatty acid compositions of Gastropoda (for limpets: [19], for abalones Haliotidae: [20]).

The deep-sea gastropod, *Ifremeria nautilei* (black snail), occurs in the hydrothermal vents of the Manus Basin in the Western Pacific Ocean [21]. Although adequate attention has been paid to the clarification of this species' ecological function [22–24], the chemical components in its glycerolipids have yet to be rigorously elucidated [25]; in particular, a detailed analysis of its PUFA. Although the isolation from their hosts and cultivation of symbiotic marine microorganisms is very difficult, in particular vent organisms, we are able to know their lipid physiology by investigation of the host lipids, which reflect those of the symbionts. Information on the symbionts' lipids may be obtained by comparative analysis of the lipid and fatty acids in its muscles and gills, in which they specifically have bacteriocytes. Moreover, the nutrition of the snail mainly depends on the products of the symbionts, because of the hosts' reduced stomach [23–25]. To assess the trophic relationships in hydrothermal vents, the lipid and fatty acid compositions of the lipids in its various organs were analyzed in the present study.

Materials and Methods

Materials

The samples of *I. nautilei* are listed in Table 1. They were collected in the Manus Basin of the Western Pacific Ocean at a depth of 1,668 m at 03°43′S and 151°41′E on 07 November 1999 (dive No. 1150 of the submersible "*Shinkai 2000*," which belongs to the Japan Marine Science and Technology Center). In total, ten *I. nautilei* samples were obtained (Table 1; Fig. 1). In the Manus Basin, research of the JAMSTEC has systematically been performed for more than 10 years, and much data has been collected on vent and seep animals. We also had a chance

Table 1 Biological data of the *Ifremeria nautilei*

Scientific name	Date	Locality	Depth (m)	Temperature (°C)	Replicate animals (n)	Height (mm)	Width (mm)	Weight (g)
Ifremeria nautilei	November 7, 1999	Manus Basin Pacific Ocean 03°43.27′S 151°41.48′E	1,668	4.6	10	58.7 ± 1.2	47.9 ± 0.7	48.3 ± 1.4

Results are expressed as means ± standard error ($n = 10$). *I. nautilei* were collected by dive #1150 of *Shinkai 2000*

Fig. 1 Photograph of the vent gastropod *Ifremeria nautilei* Bouchet & Warén. Samples were collected by the submersible *Shinkai 2000*. The vent snail was caught at a depth of 1,668 m at 03°43′S and 151°41′E in the Manus Basin of the Southwestern Pacific Ocean on 07 November 1999 (dive No. 1150 of the submersible "*Shinkai 2000*," which belongs to the Japan Marine Science and Technology Center). *Scale* shown in "cm"

to get some specimens of black snails at the Basin. The snails were considered to be in the growing stage, because we could not find any signs of maturation.

Lipid Extraction and Analysis of Lipid Classes

After 4 months of storage at −40 °C in the laboratory, all samples of *I. nautilei* were dissected into three groups of organs (gill, foot and viscera) after taking measurements, the organs were individually immersed in a mixture of chloroform and methanol (2:1, vol/vol) at −25 °C for 2 days prior to lipid extraction (Table 1). Each sample was homogenized in the same solvent and a portion of the homogenized sample was extracted according to the Folch procedure [26]. The crude lipids of the organs of *I. nautilei* were separated into classes on silicic acid columns (Merck and Co. Ltd., Kieselgel 60, 70–230 mesh), and a quantitative analysis of the lipid constituents was performed using gravimetric analysis of fractions collected from column chromatography [27]. The first eluate (dichloromethane/*n*-hexane, 2:3, v/v) was collected as steryl esters, wax esters, and diacyl glyceryl ethers fractions. This was followed by eluting triacylglycerols (TAG) with dichloromethane and eluting the sterols with dichloromethane/ether (35:1, v/v); eluting the diacylglycerols with dichloromethane/ether (9:1, v/v); eluting the free fatty acids with dichloromethane/methanol (9:1, v/v); eluting the phosphatidylethanolamine (PtdEtn) with dichloromethane/methanol (1:5, v/v); eluting ceramide aminoethyl phosphonate and other minor phospholipids with dichloromethane/methanol (1:20,v/v); and eluting phosphatidylcholine (PtdCho) with dichloromethane/methanol (1:50, v/v). The lipid classes from each lipid fraction were identified by comparison of the retention factor (Rf) values of standards using plate thin-layer chromatography (Merck and Co. Ltd., Kieselgel 60, with a thickness of 0.25 mm for analysis), and by the characteristic peaks observed in nuclear magnetic resonance (NMR) [27]. All sample lipids were dried under argon at room temperature and stored at −40 °C (Table 2).

NMR Spectrometry and the Determination of Lipid Classes

Spectra were recorded on a GSX-270 NMR spectrometer (JEOL Co. Ltd., Tokyo, Japan) in a pulsed Fourier transform mode at 270 MHz in a deuterochloroform solution using tetramethylsilane as the internal standard [27].

Preparation of Methyl Esters and Gas–Liquid Chromatography Analysis

The compositions of the fatty acid methyl esters were determined by gas–liquid chromatography. Analysis was performed on a Shimadzu GC-8A (Shimadzu Seisakusho Co. Ltd., Kyoto, Japan) and an HP-5890 (Hewlett Packard Co., Yokogawa Electric Corporation, Tokyo, Japan) and both gas chromatographs were equipped with an Omegawax-250 fused silica capillary column (30 m × 0.25 mm i.d.; 0.25 μm film, Supelco Japan Co. Ltd., Tokyo, Japan). The temperatures of the injector and the column were held at 230 and 215 °C, respectively, and the split ratio was 1:76 (FID detector at 240 °C). Helium was used as the carrier gas at a constant inlet rate of 0.7 mL/min. In the fatty acid compositions of PtdEtn, low levels of dimethylacetals (DMA), such as DMA 18:0 and DMA 20:1, were included (Table 3). The theoretical values of the fatty acid compositions were obtained by subtracting the DMA from the total fatty acids (TFA) of PtdEtn [12].

Quantitation of individual components was performed by means of a Shimadzu Model C-R3A (Shimadzu Seisakusho Co. Ltd.) and an HP ChemStation System (A. 06 revision, Yokogawa HP Co. Ltd.) electronic integrators.

Preparation of 4,4-Dimethyloxazoline Derivatives (DMOX) and Its Analysis by Gas Chromatography–Mass Spectrometry (GC–MS)

DMOX derivatives were prepared by adding an excess amount of 2-amino-2-methyl- propanol to a small amount of the fatty acid methyl esters (for example, 30 mg of the acid methyl esters with 1 mL of 2-amino-2-methylpropanol) in a test tube under an argon atmosphere. The mixture was heated at 180 °C for 18 h. The reaction mixture was cooled and poured into saturated brine and extracted with

Table 2 The lipid classes of *Ifremeria nautilei*

Scientific name	Organs	Replication for lipid extractions	Lipid content[a]	Replications for separation	WE[b]	SE[b]	DAGE[b]	TAG[b]	ST[b]	DG[b]	FFA[b]	PtdEtn[b]	CAEP[b]	PtdCho[b]
Ifremeria nautilei	Gill	10	2.2 ± 0.2	10	0.8 ± 0.2	4.6 ± 0.8	3.1 ± 0.8	29.3 ± 3.3	10.5 ± 0.8	2 ± 0.1	14 ± 0.6	24.9 ± 1.9	2.1 ± 0.3	8.6 ± 0.5
	Viscera	10	6 ± 0.9	10	0.1 ± 0.1	0.8 ± 0.2	1.9 ± 0.9	65.1 ± 8.1	3.8 ± 1	1.6 ± 0.3	9.9 ± 2.5	9.5 ± 2.2	1.8 ± 0.6	5.4 ± 1.1
	Foot	10	0.9 ± 0.1	10	0.2 ± 0.2	1.4 ± 0.2	3.1 ± 0.9	37.6 ± 6.5	17.5 ± 2.2	0.5 ± 0	7.8 ± 0.9	19.2 ± 2.2	2.3 ± 0.7	10.4 ± 1.1

Data are means ± standard errors ($n = 10$)

WE wax esters, *SE* steryl esters, *DAGE* glyceryl ethers, *TAG* triacylglycerols, *ST* sterols, *DG* diacylglycerols, *FFA* free fatty acids, *PtdEtn* phosphatidylethanolamine, *CAEP* ceramide aminoethylphosphonate with other phospholipids, *PtdCho* phosphatidylcholine

[a] Results are expressed as weight per cent of wet tissues

[b] Results are expressed as weight per cent of total lipids

n-hexane. Triplicate extractions with *n*-hexane were carried out, and the extract was washed with saturated brine, then dried over anhydrous sodium sulfate. The solvent was removed under reduced pressure, and the samples were again dissolved in *n*-hexane for analysis by GC–MS [27].

Analysis of the DMOX derivatives and the methyl esters was performed on an HP G1800C GCD Series II GC–MS (Hewlett Packard Co., Yokogawa Electric Corporation) instrument equipped with the same capillary column for determining the fatty acids with an HP WS (HP Kayak XA, G1701BA version, PC workstations). The temperatures of the injector and the column were held at 230 and 215 °C, respectively. The split ratio was 1:75, and the ionization voltage was 70 eV. Helium was used as the carrier gas at a constant inlet rate of 0.7 mL/min.

The fatty acid methyl esters and DMOX derivatives were identified by comparison of the mass spectral data obtained by GC–MS (Table 4; Figs. 2, 3, 4). For example, the representative chromatograms of the DMOX derivatives (visceral and foot TAG of specimen No. 8) are shown in Figs. 2 and 3 plus Table 4. The MS-spectra of its DMOX derivatives representing several major PUFA, such as two n-3 PUFA 20:5n-3 and 22:5n-3, are displayed in Figs. 3 and 4. As presented in Fig. 3 (a representative spectrum of 20:5n-3 at 15.526 min in one peak from 15.2 to 15.7 min in the chromatogram of visceral TAG DMOX in Fig. 2), the MS peaks of its DMOX derivative are M^+-355 and 126 (base peak), with four pairs of peaks (M-312/300, M-272/260, M-232/220, and M-192/180) reflected by four double bonds as Δ-17 (n-3), Δ-14 (n-6), Δ-11 (n-9), and Δ-8 (n-12), and two peaks (M-153/136) reflected by a Δ-5 (n-15) double bond. Similarly, for 22:5n-3 at 27.274 min in one peak from 27.0 to 27.6 min in the chromatogram in Fig. 2, the MS peaks of its DMOX derivative in Fig. 4 are M^+-383 and 126 (base peak), with five pairs of peaks (M-340/328, M-300/288, M-260/248, M-220/208, and M-180/168) reflected by five double bonds as Δ-19 (n-3), Δ-16 (n-6), Δ-13 (n-9), Δ-10 (n-12), and Δ-7 (n-15).

Statistical Analyses

Ten experimental replications were completed for each lipid class. For all samples of fatty acids analyzed by GLC, 11 to 22 replications were completed. Significant differences of the means were determined using Student's *t* test at a significance level of $P < 0.05$.

Results and Discussion

Lipid Content and Lipid Classes of *I. nautilei*

The lipid content data of the *I. nautilei* samples are shown in Table 2, together with the lipid classes. The lipid

Table 3 Fatty acid composition of visceral lipids of the *Ifremeria nautilei* examined

	Gill			Viscera			Foot		
	TAG Mean ± SE	PtdEtn Mean ± SE	PtdCho Mean ± SE	TAG Mean ± SE	PtdEtn Mean ± SE	PtdCho Mean ± SE	TAG Mean ± SE	PtdEtn Mean ± SE	PtdCho Mean ± SE
Total saturated	**14.9 ± 0.4**	**12.5 ± 0.3**	**8.7 ± 0.2**	**18.5 ± 0.8**	**12.7 ± 0.4**	**11.3 ± 0.5**	**19.6 ± 0.6**	**9.49 ± 0.2**	**9.1 ± 0.2**
14:0	1.2 ± 0.1	0.3 ± 0.0	0.7 ± 0.1	0.8 ± 0.1	0.2 ± 0.0	1.5 ± 0.2	0.6 ± 0.0	0.1 ± 0.0	1.3 ± 0.1
16:0	9.5 ± 0.3	6.2 ± 0.2	6.3 ± 0.2	14.3 ± 0.9	4.0 ± 0.4	7.9 ± 0.3	15.4 ± 0.6	2.0 ± 0.1	6.3 ± 0.1
17:0	0.3 ± 0.0	0.2 ± 0.0	0.5 ± 0.0	0.3 ± 0.0	0.3 ± 0.0	0.4 ± 0.0	0.3 ± 0.0	0.2 ± 0.0	0.3 ± 0.0
18:0	3.7 ± 0.1	5.8 ± 0.1	1.0 ± 0.0	2.8 ± 0.1	7.9 ± 0.2	1.4 ± 0.0	3.1 ± 0.1	7.2 ± 0.1	1.0 ± 0.0
Total monoenoic	**76.6 ± 0.9**	**37.7 ± 0.8**	**42.0 ± 0.8**	**63.6 ± 1.6**	**31.8 ± 1.2**	**52.2 ± 0.9**	**60.8 ± 1.3**	**18.1 ± 0.3**	**39.5 ± 0.5**
14:1n-9	0.7 ± 0.1	0.5 ± 0.0	0.2 ± 0.0	0.4 ± 0.0	0.1 ± 0.0	0.3 ± 0.0	0.3 ± 0.0	0.0 ± 0.0	0.2 ± 0.0
16:1n-11	0.0 ± 0.0	0.0 ± 0.0	0.0 ± 0.0	0.3 ± 0.0	0.0 ± 0.0	0.0 ± 0.0	0.2 ± 0.0	0.0 ± 0.0	0.0 ± 0.0
16:1n-7(6)[a]	38.7 ± 1.5	17.5 ± 0.6	14.7 ± 0.5	19.9 ± 0.6	7.1 ± 0.5	14.0 ± 0.4	19.7 ± 1.5	1.9 ± 0.2	12.3 ± 0.2
16:1n-5	0.0 ± 0.0	0.1 ± 0.0	0.1 ± 0.1	0.3 ± 0.1	0.0 ± 0.0	0.3 ± 0.1	0.2 ± 0.1	0.1 ± 0.0	0.1 ± 0.1
17:1n-6	0.3 ± 0.0	0.2 ± 0.0	0.2 ± 0.0	0.2 ± 0.0	0.1 ± 0.0	0.2 ± 0.0	0.2 ± 0.0	0.0 ± 0.0	0.1 ± 0.0
18:1n-9	0.7 ± 0.0	0.5 ± 0.0	1.6 ± 0.1	1.4 ± 0.0	0.9 ± 0.0	2.2 ± 0.1	1.2 ± 0.1	0.6 ± 0.0	1.7 ± 0.2
18:1n-7	24.9 ± 0.5	14.0 ± 0.4	19.4 ± 0.7	23.7 ± 1.3	12.5 ± 0.8	24.7 ± 0.9	21.4 ± 0.6	7.7 ± 0.2	18.5 ± 0.4
18:1n-6	6.0 ± 0.3	0.2 ± 0.1	1.0 ± 0.3	5.2 ± 0.2	1.6 ± 0.2	1.6 ± 0.4	4.9 ± 0.2	0.5 ± 0.1	0.4 ± 0.2
18:1n-5	0.2 ± 0.1	0.0 ± 0.0	0.3 ± 0.1	0.7 ± 0.1	0.2 ± 0.0	0.2 ± 0.1	0.6 ± 0.1	0.0 ± 0.0	0.1 ± 0.0
20:1n-13	2.2 ± 0.3	2.6 ± 0.1	2.7 ± 0.1	7.3 ± 0.4	4.7 ± 0.1	5.5 ± 0.4	8.3 ± 0.6	4.1 ± 0.1	3.3 ± 0.1
20:1n-7	2.5 ± 0.1	1.6 ± 0.0	1.6 ± 0.1	3.6 ± 0.3	4.2 ± 0.1	2.7 ± 0.0	3.4 ± 0.1	2.7 ± 0.1	2.2 ± 0.1
Total NMID	**3.3 ± 0.3**	**18.9 ± 0.3**	**13.2 ± 0.3**	**9.8 ± 0.4**	**18.8 ± 0.3**	**14.3 ± 0.9**	**9.9 ± 0.6**	**24.5 ± 0.4**	**14.8 ± 0.2**
18:2n-8,13	0.8 ± 0.1	0.8 ± 0.1	1.5 ± 0.1	1.2 ± 0.1	1.2 ± 0.0	1.9 ± 0.1	1.0 ± 0.1	0.6 ± 0.1	1.7 ± 0.0
20:2n-9,15	0.2 ± 0.0	1.4 ± 0.3	0.0 ± 0.0	0.3 ± 0.1	1.0 ± 0.2	0.0 ± 0.0	0.4 ± 0.1	0.4 ± 0.2	0.0 ± 0.0
20:2n-7,15	1.5 ± 0.1	16.4 ± 0.3	10.7 ± 0.4	4.9 ± 0.2	15.9 ± 0.3	9.2 ± 0.6	4.8 ± 0.3	22.9 ± 0.4	11.9 ± 0.3
20:2n-6,13	0.7 ± 0.1	0.1 ± 0.0	0.6 ± 0.2	2.5 ± 0.1	0.3 ± 0.1	2.7 ± 0.2	2.5 ± 0.2	0.2 ± 0.1	0.8 ± 0.2
22:2n-7,15	0.2 ± 0.0	0.2 ± 0.0	0.3 ± 0.0	0.7 ± 0.1	0.3 ± 0.0	0.5 ± 0.0	1.1 ± 0.1	0.3 ± 0.0	0.3 ± 0.0
Total polyenoic	**4.2 ± 0.4**	**22.7 ± 0.8**	**28.6 ± 0.8**	**6.9 ± 0.6**	**21.9 ± 1.5**	**18.2 ± 1.2**	**8.0 ± 0.4**	**28.3 ± 0.3**	**30.1 ± 0.4**
Total n-4 polyenoic	**0.2 ± 0.0**	**0.1 ± 0.0**	**0.3 ± 0.0**	**0.4 ± 0.0**	**0.2 ± 0.0**	**0.3 ± 0.0**	**0.4 ± 0.0**	**0.2 ± 0.0**	**0.3 ± 0.0**
18:2n-4,7	0.2 ± 0.0	0.1 ± 0.0	0.3 ± 0.0	0.4 ± 0.0	0.2 ± 0.0	0.3 ± 0.0	0.3 ± 0.0	0.2 ± 0.0	0.3 ± 0.0
Total n-6 polyenoic	**3.1 ± 0.2**	**17.1 ± 0.5**	**19.2 ± 0.6**	**3.1 ± 0.2**	**9.5 ± 0.6**	**8.7 ± 0.5**	**3.5 ± 0.1**	**12.4 ± 0.2**	**14.2 ± 0.1**
18:2n-6,9	0.3 ± 0.0	2.7 ± 0.1	3.7 ± 0.1	0.4 ± 0.0	1.5 ± 0.1	2.2 ± 0.1	0.4 ± 0.0	2.4 ± 0.1	4.1 ± 0.1
20:2n-6,9	0.8 ± 0.0	1.9 ± 0.1	3.4 ± 0.1	0.7 ± 0.0	1.5 ± 0.2	1.6 ± 0.2	0.8 ± 0.0	1.3 ± 0.0	2.3 ± 0.1
20:3n-6,9,15	0.4 ± 0.0	2.6 ± 0.1	2.0 ± 0.1	0.7 ± 0.1	1.4 ± 0.1	1.4 ± 0.1	0.7 ± 0.0	2.2 ± 0.1	1.9 ± 0.1
20:3n-6,9,12	0.8 ± 0.0	1.5 ± 0.0	2.8 ± 0.2	0.4 ± 0.1	0.7 ± 0.1	0.8 ± 0.1	0.3 ± 0.1	0.8 ± 0.0	1.2 ± 0.0
20:4n-6,9,12,15	0.7 ± 0.1	7.8 ± 0.3	5.0 ± 0.2	0.7 ± 0.1	3.8 ± 0.3	1.9 ± 0.1	0.9 ± 0.0	4.8 ± 0.1	3.5 ± 0.1
22:4n-6,9,12,15	0.2 ± 0.0	0.5 ± 0.0	2.1 ± 0.1	0.1 ± 0.0	0.4 ± 0.0	0.6 ± 0.0	0.2 ± 0.0	0.8 ± 0.0	0.9 ± 0.1
Total n-3 polyenoic	**0.9 ± 0.2**	**5.5 ± 0.3**	**9.2 ± 0.3**	**3.4 ± 0.5**	**12.3 ± 0.9**	**9.2 ± 0.7**	**4.2 ± 0.3**	**15.6 ± 0.3**	**15.6 ± 0.3**
20:4n-3,6,9,15	0.1 ± 0.0	0.8 ± 0.1	0.8 ± 0.0	0.2 ± 0.0	0.6 ± 0.0	0.5 ± 0.0	0.3 ± 0.0	0.8 ± 0.0	0.7 ± 0.0
20:5n-3,6,9,12,15	0.5 ± 0.1	3.4 ± 0.2	5.8 ± 0.2	2.2 ± 0.3	9.4 ± 0.8	5.1 ± 0.3	2.6 ± 0.2	10.2 ± 0.2	8.7 ± 0.2
22:4n-3,6,9,15	0.1 ± 0.0	0.0 ± 0.0	0.2 ± 0.0	0.2 ± 0.0	0.0 ± 0.0	0.1 ± 0.0	0.3 ± 0.0	0.0 ± 0.0	0.1 ± 0.0

Table 3 continued

	Gill			Viscera			Foot		
	TAG Mean ± SE	PtdEtn Mean ± SE	PtdCho Mean ± SE	TAG Mean ± SE	PtdEtn Mean ± SE	PtdCho Mean ± SE	TAG Mean ± SE	PtdEtn Mean ± SE	PtdCho Mean ± SE
22:5n-3,6,9,12,15	0.2 ± 0.0	1.3 ± 0.1	2.4 ± 0.1	0.8 ± 0.1	2.3 ± 0.2	3.4 ± 0.4	1.0 ± 0.1	4.6 ± 0.1	6.1 ± 0.1
Total fatty acids	**99.1 ± 0.2**	**91.8 ± 0.7**	**92.5 ± 0.5**	**98.9 ± 0.1**	**85.2 ± 0.6**	**96.1 ± 0.5**	**98.4 ± 0.2**	**80.4 ± 0.8**	**93.5 ± 0.5**
DMA 15:0		**0.0 ± 0.0**			**0.0 ± 0.0**			**0.0 ± 0.0**	
DMA 16:0		0.2 ± 0.0			0.6 ± 0.0			0.8 ± 0.1	
DMA 18:0		0.8 ± 0.1			2.0 ± 0.1			1.3 ± 0.2	
DMA 18:1		0.6 ± 0.1			1.1 ± 0.1			1.3 ± 0.1	
DMA 20:1		3.8 ± 0.5			9.0 ± 0.4			13.0 ± 0.7	
Total DMA		**5.4 ± 0.8**			**12.1 ± 0.9**			**17.1 ± 0.9**	

Data are mean ± SE (replications, $n = 11$–22). The major fatty acids were selected if at least one mean datum was detected at a level of 0.3% or more of the total fatty acids

[a] 16:1n-7 contained significant levels of 16:1n-6

content in the foot was 0.9% of the wet weight in all samples. The mean lipid content in the foot samples was low, while that of the others (2.2% of wet weight for the gills and 6.0% for the viscera) was high, suggesting that *I. nautilei* accumulates lipids mostly in the viscera. As shown in Table 2, triacylglycerols (TAG, 29.3–65.1%) was the major component in all organ lipids, with low levels of other neutral lipids, such as wax esters, steryl esters, diacylglyceryl ethers, diacylglycerols, and free fatty acids. The gastropod contained medium levels of sterols (3.8–17.5%) and phospholipids (PtdEtn at 9.5–24.9% of TFA and PtdCho at 5.4–10.4% of total lipids), with small levels of ceramide aminoethyl phosphonate (1.8–2.3% of total lipids). Comparatively high levels of lipid content and TAG in all organs suggests a high nutritional condition in the hydrothermal vents and high ability of the endosymbionts to produce autotrophically because the gastropod wholly depends on thiotrophic chemoautotrophic bacteria [23, 24]. All *I. nautilei* lipids mainly contained glycerol derivatives (TAG, diacylglycerols, free fatty acids, PtdEtn, and PtdCho) and the total proportion of these derivatives reached about 75.5–91.5%, with low levels of other lipids (wax esters and diacylglyceryl ethers). The lipid class of vent gastropod *I. nautilei*, which contained TAG as the major component in all organs (Table 1), differed from those of normal gastropod species (*Haliotis fulgens*: [20]), whose neutral lipid levels were very low. The foot of normal shallow-water snails generally contains phospholipids as the major components [28].

Fatty Acid Composition and Its Similarity to Depot TAG Lipids Among All Organs of *I. nautilei*

The fatty acids of TAG (more than 0.3% of TFA) in all organs (gill, viscera, and foot) are shown in Table 3. Although the fatty acid composition of TAG slightly varied among the three organs, the kinds of major fatty acids were almost the same in all organs. Five dominant fatty acids (more than about 3% of TFA) in gill TAG were found in the samples: 16:0 and 18:0 as saturated fatty acids, 16:1n-7(6), 18:1n-6, and 18:1n-7 as monounsaturated fatty acids (MUFA), with significant levels (more than about 1% of TFA) of four fatty acids: 14:0, 20:1n-7, 20:1n-13, and 22:2n-7,15. Similarly, eight dominant fatty acids in tissue (viscera and foot) TAG were also found in all samples: 16:0 and 18:0 as saturated fatty acids, 16:1n-7(6), 18:1n-6, 18:1n-7, 20:1n-7, and 20:1n-13 as MUFA, and 20:2n-7,15 as non-methylene interrupted dienoic acid (NMID), with significant levels of five other fatty acids: 18:1n-9, 18:2n-8,13, 20:2n-6,13, 20:5n-3 (icosapentaenoic acid; EPA), and 22:5n-3 (docosapentaenoic acid; DPA). In the neutral lipids, both in the gill and tissues (foot and viscera), unusually high levels of total n-7 MUFA were found and this suggests

Table 4 Composition of DMOX and fatty acid methyl esters of *I. nautilei*

	DMOX (Fig. 2) Visceral TAG R. time[a, b] (min)
14:0	2.75
14:1n-9	2.85
15:0	3.24
15:1n-8(10)	3.36
16:0	3.95
16:1n-11	4.00
16:1n-7	4.15
16:1n-6	4.19
16:1n-5	4.24
16:2n-4	4.62
17:0	4.82
17:1n-8	5.05
17:1n-6	5.17
18:0	6.09
18:1n-13	6.20
18:1n-9	6.38
18:1n-7	6.58
18:1n-6	6.64
18:2n-5(8),13	6.68
18:2n-6	7.02
18:2n-4,8	
18:2n-4,7	7.42
19:1n-12	
19:1n-7	8.27
20:0	
20:1n-13	10.37
20:1n-10	
20:1n-9	10.55
20:1n-7	10.90
20:2n-7,15	11.08
20:2n-6,13	11.17
20:2n-6	11.86
20:3n-6,9,15	12.16
20:3n-6	
20:4n-6	13.09
20:4n-3	
20:5n-3	15.53
22:2n-9,15	
22:2n-7,15	18.97
22:3n-6,9,15	21.11
22:4n-Δ	22.80
22:4n-3,6,9,15	25.20
22:5n-3	27.27

All the retention times of DMOX derivatives in I. nautilei accord with Fig. 2

a "R. time" means "retention time."

bacterial contributions [22–24, 29] because high levels of n-7 MUFA, such as vaccenic acid, 18:1n-7, were found in sulfur-oxidizing bacteria [30, 31]. Vaccenic acid is considered to be derived from Δ9-desaturation before C_2 elongation of 16:0, and 20:1n-13 may also be derived from 18:0 by Δ5-desaturation and C_2 elongation, similar to the findings previously reported [32].

Despite similar fatty acids found both in gill (bacterial) and tissue TAG, some of the fatty acid levels in the tissue TAG differed from those in gill TAG. In the tissue TAG, two NMID (18:2n-8,13 and 20:2n-7,15) occurred and higher levels of relatively longer-chain and higher-unsaturated acids (18:2n-8,13, 20:1n-7, 20:1n-13, 20:2n-6,13, 20:2n-7,15, and 22:2n-7,15) with lower levels of the shorter-chain ones (14:0, 16:1n-7, 18:1n-6, and 18:1n-7) were found, compared with those in the gill TAG. In consideration of the first absorption of assimilated lipids in the gill, where the symbionts specifically inhabit, these findings suggest lipid conveyance from the gill to the tissues, and enzymatic biosynthesis in *I. nautilei* tissues. Such a phenomenon is probably caused by the active function of Δ-5 desaturase and C_2 elongase at the tissue levels [33]. Furthermore, significant levels of n-3 PUFA (2.2–2.6% for EPA and 0.8–1.0% for n-3 DPA) were characteristically found only in tissue TAG. The EPA and n-3 DPA in the tissue TAG suggest that these long-chain n-3 PUFA were concentrated or biosynthesized in the tissue TAG, similar to other normal shallow-water gastropod tissues (*Haliotis laevigata* and *Haliotis rubra*: [34]). At least, the mollusks have Δ-5 desaturase [18, 33] and are able to synthesis a double bond at the n-15 position in C_{20} fatty acids; for example, 20:3n-6,9,15, ARA, 20:4n-3,6,9,15, EPA, and 22:4n-3,6,9,15 were considered to be derived by Δ-5 desaturase [33].

In the present study, the detailed fatty acid composition of the gastropod was determined; in particular, all n-3 and n-6 PUFA were determined [25]. The thiotrophic symbionts, which mainly produced n-3 and n-6 PUFA, markedly differed from some vent-bivalve symbionts, which biosynthesize only n-4 non-methylene interrupted (NMI) PUFA [27].

Fatty Acid Composition in Tissue Phospholipids of *I. nautilei*

The major fatty acid compositions in the gill, viscera, and foot phospholipids of *I. nautilei* are also presented in Table 3. The fatty acid composition in the tissue PtdEtn included medium levels of DMA, such as DMA 18:0 and DMA 20:1 and this finding suggests that plasmalogens-type PtdEtn are biosynthesized in the gastropod tissue.

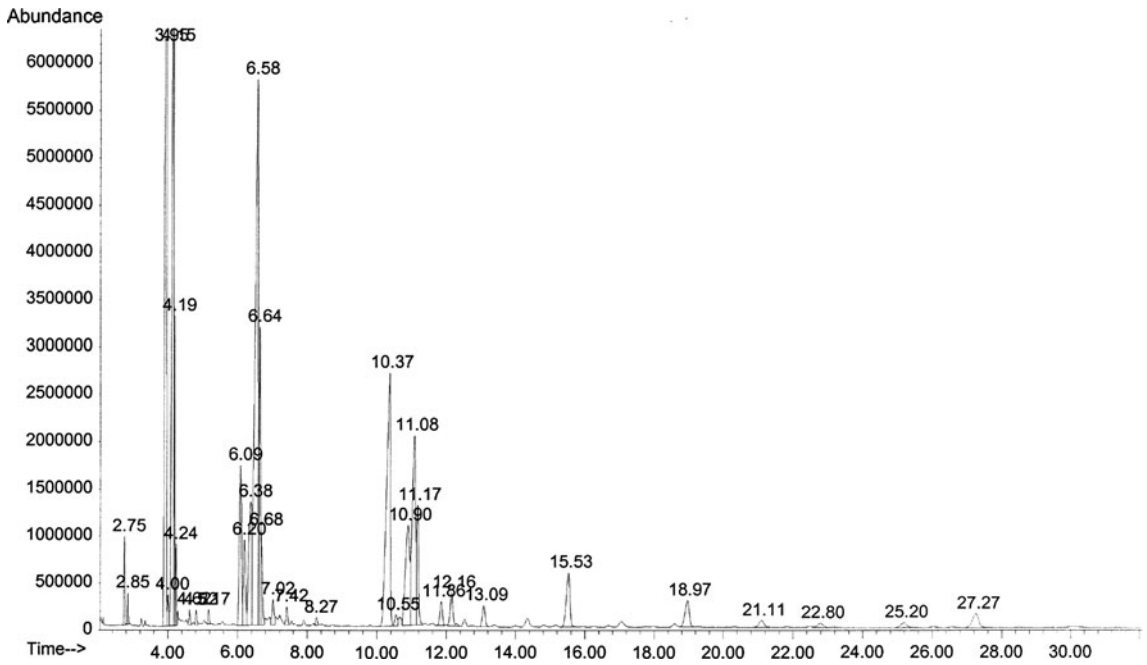

Fig. 2 The chromatogram of the DMOX derivatives of the fatty acids in *I. nautilei* visceral TAG (measured on 20 February 2001). Analysis of the DMOX derivatives was performed on a HP G1800C GCD Series II gas chromatograph mass spectrometer equipped with an Omegawax-250 fused silica capillary column with the HP WS (HP Kayak XA, G1701BA version, personal computer workstations). The temperatures of the injector and the column were held at 230 and 210 °C, respectively. The split ratio was 1:75, and the ionization voltage was 70 eV, respectively. Helium was used as the carrier gas at a constant inlet rate of 0.7 mL/min. Each MS spectrum was obtained by every 0.009 min; for example, a spectrum at 15.526 min (Scan No. 1505 in Fig. 3) is one of the representative spectra of EPA, because the EPA was detected from 15.2 to 15.7 min as one peak in the chromatogram of DMOX derivative of the *I. nautilei* visceral TAG and more than 50 spectra of EPA were obtained by scanning of the peak. Simiarly, a spectrum at 27.274 min (Scan No. 2816 in Fig. 4) is one of the representative spectra of n-3 DPA, because the n-3 DPA was detected from 26.9 to 27.5 min as one peak in the chromatogram of DMOX derivative of the *I. nautilei* visceral TAG and more than 50 spectra of EPA were obtained by scanning of the peak

Although the fatty acid composition of phospholipids differed from that in TAG, the kinds of all fatty acids were the same in all organs. In addition, significant levels of 18:2n-6 (linoleic acid) and 20:2n-6 were observed only in the polar lipids, compared with low levels of those in TAG. Linoleic acid was probably derived from 18:1n-6 by using Δ-9 desaturase, and noticeable levels of 18:1n-6 were found only in TAG.

Ten major fatty acids were found in all organ PtdEtn: 16:0 and 18:0 as saturated fatty acids, 16:1n-7(6), 18:1n-7, 20:1n-7, and 20:1n-13 as MUFA, 20:2n-7,15 as NMID, 20:4n-6 (arachidonic acid; ARA) as n-6 PUFA, and EPA and n-3 DPA as n-3 PUFA, with significant levels of six n-6 fatty acids: 18:1n-6, 18:2n-6, 20:2n-6, 20:3n-6,9,12, 20:3n-6,9,15, and 22:2n-6,9,12,15. Nine similar fatty acids were the major components in PtdCho: 16:0 as saturated acid, 16:1n-7(6), 18:1n-7, and 20:1n-13 as MUFA, 20:2n-7,15 as NMID, 18:2n-6 and ARA as n-6 PUFA, and EPA and n-3 DPA as n-3 PUFA, with significant levels of 18:0, 18:1n-6, 20:1n-7, 20:2n-6, 20:3n-6,9,12, and 20:3n-6,9,15. Although the saturated fatty acid and MUFA levels in PtdEtn differed from those in PtdCho, the major kinds of PUFA in PtdEtn were the same as those in PtdCho. As for PUFA in the gastropod, three PUFA (ARA, EPA, and n-3 DPA) were the major PUFA both in PtdEtn and PtdCho, and this phenomenon differed from that in TAG, which contained low levels of these PUFA. In the present study, it has been confirmed that all *I. nautilei* polar lipids contained medium levels of total PUFA (21.9–28.3% for PtdEtn and 18.2–30.1% for PtdCho), which were probably concentrated of the tissue level. The significant PUFA levels in the *I. nautilei* lipids may be influenced by the high pressures in the deep sea, similar to those in barophilic bacteria [35, 36]. Compared with the fatty acid compositions of shallow-water carnivorous mollusks [19, 28], high levels of 18:1n-7 and 20:1n-13 and significant levels of long-chain n-6 PUFA, such as ARA and 22:4n-6, without shorter-chain n-3 PUFA (18:3n-3 and 18:4n-3) and DHA were only observed in the *I. nautilei* lipids. In particular, the polar lipids of *I. nautilei* gills contained high levels of n-6 PUFA, while high n-3 PUFA levels were found in those of its viscera and foot. The levels of long-chain PUFA in the *I. nautilei* lipids are similar to those of some herbivorous gastropod lipids [20, 34] because significant levels of long-chain PUFA, such as ARA, 22:4n-6, and n-3 DPA, without DHA, were found in both species.

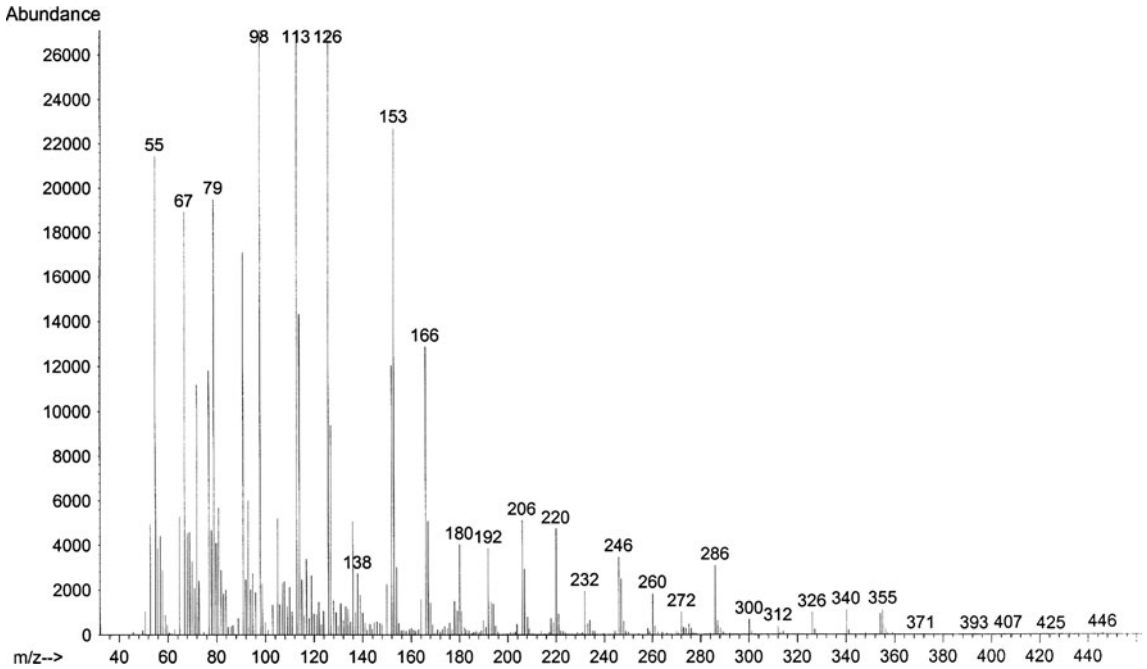

Fig. 3 The MS peaks of the DMOX derivative of EPA are M^+-355, 340, 326, 312, 300, 286, 272, 260, 246, 232, 220, 206, 192, 180, 166, 153, 136, 126, 113 (base peak), and four pairs of the peaks M-312 and M-300, M-272 and M-260, M-232 and M-220, and M-192 and M-180 is, respectively, reflected by Δ-17 (n-3), Δ-14 (n-6), Δ-11 (n-9), and Δ-8 (n-12) double bonds, and a pair of the M-153 and M-136 shows a Δ-5 (n-15) double bond

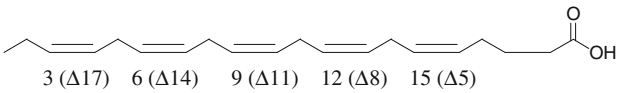

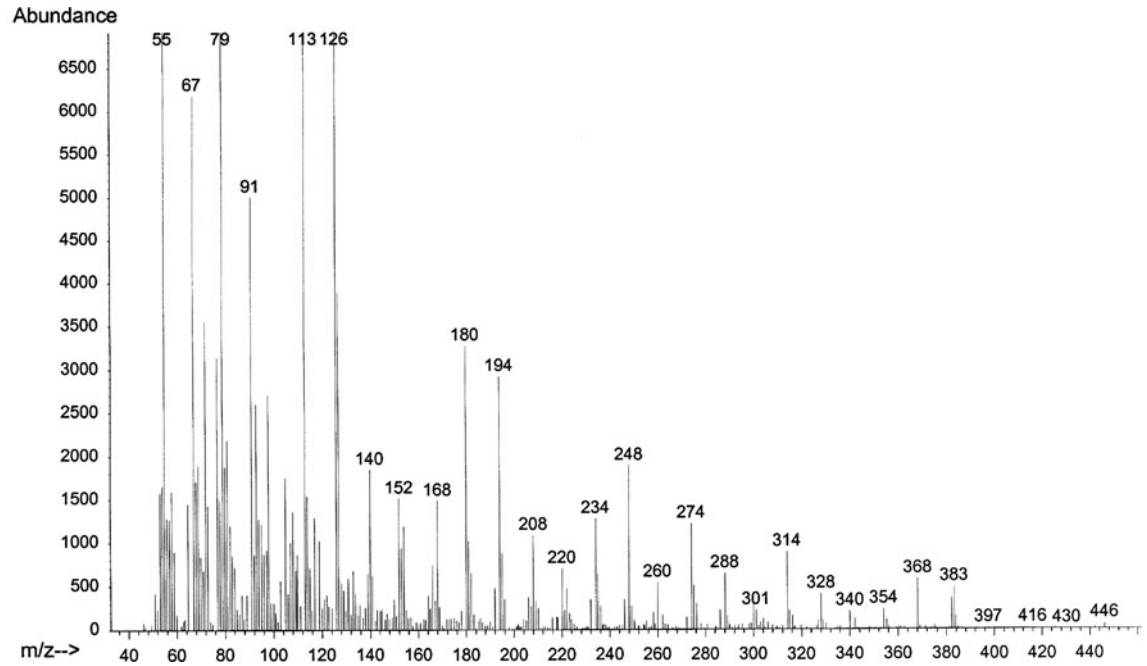

Fig. 4 The MS peaks of the DMOX derivative of n-3 DPA are M^+-383, 368, 354, 340, 328, 314, 300, 288, 274, 260, 248, 234, 220, 208, 194, 180, 166, 152, 140, 126, 113 (base peak), and four pairs of the peaks M-340 and M-328, M-300 and M-288, M-260 and M-248, M-220 and M-208, is, respectively, reflected by Δ-19 (n-3), Δ-16 (n-6), Δ-13 (n-9), and Δ-10 (n-12) double bonds and three peaks of M-166, M-168, and M-180 shows a Δ-7 (n-15) double bond

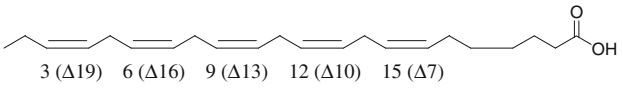

The profile of PUFA in all the polar lipids of *I. nautilei* differed from those in other marine carnivorous gastropods [19, 25, 28], which have high levels of n-3 PUFA (from 18 to 20 carbons) with low or trace levels of n-6 PUFA. For example, 18:2n-6 and its various derivatives (20:2n-6, 20:3n-6, 20:3n-6,9,15, ARA and 22:4n-6) were the characteristic fatty acids in all organ PtdEtn and PtdCho of *I. nautilei*, similar to those in herbivorous gastropod lipids [20, 34]. This implies a specific trophic relationship with the symbiotic bacteria because there are no macroalga species in the deep sea. In particular, the high levels of total n-6 PUFA in the gill phospholipids (17.1% for PtdEtn and 19.2% for PtdCho), which may be directly influenced by the bacterial lipids [22–25], were *I. nautilei*'s unusual characteristic. The levels of total n-6 PUFA in the gill phospholipids were significantly higher than those of total n-3 PUFA. On the contrary, in the gastropod tissues (foot and viscera), the levels of total n-3 PUFA (n-3 PUFA: 12.3–15.6% for PtdEtn and 9.2–15.6% for PtdCho) were higher than those of total n-6 PUFA (n-6 PUFA: 9.5–12.4% for PtdEtn and 8.7–14.2% for PtdCho), and this indicates the requirement of n-3 PUFA in *I. nautilei*, similar to normal gastropods and fishes. Based on the present facts, the existence of medium levels of n-3 PUFA in the phospholipids differed from those in TAG, demonstrating a high accumulation mechanism of all PUFA in the gastropod tissues [1, 12, 33]. Furthermore, in spite of the accumulation of n-3 PUFA in the tissue polar lipids, the lack of DHA in all tissues is unusual for marine animals, and such a phenomenon points to the regulation of lipids assimilated from the symbiotic bacteria, because it is thought that the products of the symbionts are a major component of *I. nautilei*'s diet [22–24]. The lack of DHA in all organs of *I. nautilei* tissues also indicates its specific nutritional source as being only the symbionts [23] and its incapability to biosynthesize DHA. This speculatory remark is well supported by some reports, in which extremely low levels of DHA are said to be exhibited in the tissue lipids of some herbivorous marine gastropods (DHA: 0.21% for periwinkle *Littorina littorea*, [28]; non-detectable and 0.4% for the limpets *Patella peroni* and *Cellana tramoserica*, and 0.2–0.9% for the chiton *Ponerplax costata*, [19]; 0.2–0.3% for wild green lip abalone *Haliotis laevigata* and black lip abalone *Haliotis rubra*, [34]; non-detectable for *Haliotis fulgens*, [20]), which also feed on specific macroalgae. These findings suggest the non-essentiality of DHA for these mollusks [32, 37]. These herbivorous marine mollusks also have limited kinds of n-6 PUFA (only 18:2n-6 and ARA) as the major acids (ARA levels: 10.6–38.8% for the limpets *Patella peroni* and *Cellana tramoserica*, and 12.6–30.9% for the chiton *Ponerplax costata*, [19]; 10.7–14.3% for wild green lip abalone *Haliotis laevigata* and black lip abalone *Haliotis rubra*, [34]; 10.0–14.2% for *Haliotis fulgens*, [20], which originate from their dietary algae, while the symbionts may biosynthesize significant levels of various n-6 PUFA, such as 18:2n-6, 20:2n-6, 20:3n-6, 20:3n-6,9,15, and ARA. Furthermore, the similarity of the fatty acid compositions of the same snail, which were collected from different areas, indicates its species' characteristic [25].

Non-essentiality of DHA in the Lipids of *I. nautilei*

Differing from the essentiality of n-3 PUFA for marine fishes and shallow-water bivalves [38], *I. nautilei* may accumulate n-6 PUFA as a possible substitute for n-3 PUFA in order to maintain cell membrane fluidity. It is noteworthy that all marine animals show a tendency to accumulate PUFA in their tissues, but differences in the degree of accumulation of n-6 and n-3 PUFA among mollusks species might be regulated by their food web [12]. In connection with the role of the food web, many pelagic fishes accumulate n-3 PUFA, such as DHA, through the marine-grazing food chain originating from phytoplankton having an elongation of shorter n-3 PUFA. In general, DHA is the dominant PUFA in both the PtdEtn and PtdCho of almost all higher trophic marine animals and they maintain consistently high DHA levels by continuous exploitation and its subsequent accumulation in vivo [7]. In addition, all marine fishes require DHA as the most important fatty acid, because it is an essential fatty acid that they are unable to biosynthesize in vivo, which differs from the ability of freshwater fishes [39, 40].

On the contrary, similar to the fluctuation of DHA levels in the polar tissue lipids of *P. fucata* (PtdEtn; 18.4–33.2% and PtdCho; 23.2–40.9%, [12]), the lack of DHA in the fatty acid composition of vent bivalves [18, 27] and the vent gastropod, *I. nautilei*, suggests that DHA is not indispensable as the most important essential fatty acid for mollusks, and they possibly contain these higher PUFA for the maintenance of the fluidity of their cell membranes. Thus, our findings encapsulate some typical features of the regulation of the lipid physiology of *I. nautilei*, and the lack of DHA content implies a limitation on the part of the symbiotic organisms and the absence of a biosynthetic pathway for DHA in this species. The lack of DHA with significant levels of other various PUFA in *I. nautilei* lipids suggests that it is unable to biosynthesize DHA, similar to the incapability of marine fishes. With respect to the level of PUFA, almost all marine animals mainly have n-3 PUFA as the major PUFA, while ARA is generally undetectable or negligible in their lipids [1, 6, 7]. On the contrary, phytoplankton are often rich in both n-3 PUFA and n-6 PUFA, therefore, significant levels of n-6 PUFA are found in the phospholipids of their primary consumers (e.g., sweet smelt *Plecoglossus altivelis*, [41]). This

characteristic indicates that its symbionts produce various n-6 PUFA and simultaneously have a limit for lipid biosynthesis of n-3 PUFA.

Biosynthesis of NMID in *I. nautilei*

The noticeable levels of 22:4n-6 and DPA in both tissue lipids suggest that this snail may have the enzymes for biosynthetic C_2 elongation in its tissues, similar to the synthetic pathway of other bivalves [15, 18, 33]. For example, 22:4n-6, which is considered to be derived from C_2 elongation of ARA, indicates the contribution of elongase. Furthermore, the levels of 20:2n-7,15, which is a long-chain NMID, in the phospholipids were markedly higher than those in TAG, with lower levels of 14:0, 16:1n-7, and 18:1n-7 in the phospholipids, compared with the high levels of shorter MUFA in TAG. These points imply that bacterial 16:1n-7 and 18:1n-7 are precursors for 20:2n-7,15, which is considered to be derived from Δ-5 desaturation and the second C_2 elongation of 18:1n-7 after the C_2 elongation of 16:1n-7 also suggests the contribution of desaturase, similar to other NMID derivatives [33]. *I. nautilei* may be able to biosynthetically transform shorter MUFA to longer NMID, localizing mainly close to the polar phospholipids [12], because specific high levels of NMID were observed only in the polar lipids. In light of the above discussion, it is inferred that the same physiological elongation and desaturation mechanisms exist as in other mollusks, such as *Pinctada fucata* [12]. Consequently, the high levels of NMID in the phospholipids suggest that this snail is able to biosynthesize only lowly unsaturated PUFA, such as NMID at the tissue level using Δ5- and Δ9-desaturases, similar to other mollusk species [18, 33].

Acknowledgments The authors thank Prof. Mutsumi Sugita, Shiga University, for kindly donating the authentic ceramide aminoethyl phosphonate which originated from the freshwater clam *Corbicula sandai* and for his valuable discussion of the bivalve lipids. The authors also thank Ms. Sumiko Terada, Ms. Mikiko Tanaka, and Mr. Akihito Takashima for their skilled technical assistance. This work was supported in part by a research project, "Development of New Technology for Treatment and Local Recycling of Biomass, D-2100" from the Ministry of Agriculture, Forestry, and Fisheries of Japan.

References

1. Ackman RG (1989) Fatty Acids. In: Ackman RG (ed) Marine biogenic lipids, fats and oils, vol I. CRC Press, Boca Raton, pp 103–137
2. Joseph JD (1989) Distribution and composition of lipids in marine invertebrates. In: Ackman RG (ed) Marine Biogenic Lipids, Fats and Oils, vol II. CRC Press, Boca Raton, pp 49–143
3. Morris RJ, Culkin F (1989) Fish. In: Ackman RG (ed) Marine biogenic lipids, fats, and oils, vol II. CRC Press, Boca Raton, pp 145–178
4. DeLong EF, Yayanos AA (1986) Biochemical function and ecological significance of novel bacterial lipids in deep-sea prokaryotes. Appl Environ Microbiol 51:730–737
5. Yano Y, Nakayama A, Saito H, Ishihara K (1994) Production of docosahexaenoic acid by marine bacteria isolated from deep-sea fish. Lipids 29:527–528
6. Saito H, Yamashiro R, Ishihara K, Xue C (1999) The lipids of three highly migratory fishes: *Euthynnus affinis*, *Sarda orientalis*, and *Elagatis bipinnulata*. Biosci Biotech Biochem 63:2028–2030
7. Saito H, Seike Y, Ioka H, Osako K, Tanaka M, Takashima A, Keriko JM, Kose S, Souza JCR (2005) High docosahexaenoic acid levels in both neutral and polar lipids of a highly migratory fish: *Thunnus tonggol* Bleeker. Lipids 40:941–953
8. Koizumi C, Jeong BY, Ohshima T (1990) Fatty chain composition of ether and ester glycerophospholipids in the Japanese oyster *Crassostrea gigas* (Thunberg). Lipids 25:363–370
9. Thompson PA, Harrison PJ (1992) Effects of monospecific algal diets of varying biochemical composition on the growth and survival of Pacific oyster (*Crassostrea gigas*) larvae. Mar Biol 113:645–654
10. Dunstan GA, Volkman JK, Barrett SM (1993) The effect of lyophilization on the solvent extraction of lipid classes, fatty acids and sterols from the oyster *Crassostrea gigas*. Lipids 28:937–944
11. Soudant P, Ryckeghem KV, Marty Y, Moal J, Samain JF, Sorgeloos P (1999) Comparison of the lipid class and fatty acid composition between a reproductive cycle in nature and a standard hatchery conditioning of the Pacific oyster *Crassostrea gigas*. Comp Biochem Physiol 123B:209–222
12. Saito H (2004) Lipid and FA composition of the pearl oyster *Pinctada fucata martensii*: influence of season and maturation. Lipids 39:997–1005
13. Napolitano GE, MacDonald BA, Thompson RJ, Ackman RG (1992) Lipid composition of eggs and adductor muscle in giant scallops (*Placopecten magellanicus*) from different habitats. Mar Biol 113:71–76
14. Pazos AJ, Sánchez JL, Román G, Pérez-Parallé ML, Abad M (2003) Lipid class fatty acid composition in the female gonad of *Pecten maxima* in relation to reproductive cycle and environmental variables. Comp Biochem Physiol 134B:367–380
15. Kraffe E, Soudant P, Marty Y, Kervarec N (2005) Docosahexaenoic acid- and eicosapentaenoic acid-enriched cardiolipin in the Manila clam *Ruditapes philippinarum*. Lipids 40:619–625
16. Kluytmans JH, Boot JH, Oudejand RCHM, Zandee DI (1985) Fatty acid synthesis in relation to gametogenesis in the mussel *Mytilus edulis* L. Comp Biochem Physiol 81B:959–963
17. Freites L, Fernandez-Reiriz MJ, Labarta U (2002) Fatty acid profiles of *Mytilus galloprovincialis* (Lmk) mussel of subtidal and rocky shore origin. Comp Biochem Physiol 132B:453–461
18. Saito H (2008) Unusual novel n-4 polyunsaturated fatty acids in cold-seep mussels (*Bathymodiolus japonicus* and *Bathymodiolus platifrons*), originating from symbiotic methanotrophic bacteria. J Chromatgr A 1200:242–254
19. Johns RB, Nichols PD, Perry GJ (1980) Fatty acid components of nine species of molluscs of the littoral zone from Australian waters. Comp Biochem Physiol 65B:207–214
20. Nelson MM, Leighton DL, Phleger CF, Nichols PD (2002) Comparison of growth and lipid composition in the green abalone, *Haliotis fulgens*, provided specific macroalgal diets. Comp Biochem Physiol 131B:695–712
21. Bouchet P, Waren A (1991) *Ifremeria nautilei*, nouveau gastéropode d'évents hydrothermaux, probablment associe à des bactéries symbiothique. C R Acad Sci Paris, Ser III 312:495–501
22. Galkin SV (1992) The benthic fauna of hydrothermal vents in the Manus Basin. Oceanology 32:768–774

23. Windoffer R, Giere O (1992) Symbiosis of the hydrothermal vent gastropod *Ifremeria nautilei* (Provannidae) with endobacteria—structural analyses and ecological considerations. Biol Bull 193:381–392
24. Erickson KL, Macko SA, Van Dover CL (2009) Evidence for a chemoautotrophically based food web at inactive hydrothermal vents (Manus Basin). Deep Sea Res II 456:1577–1585
25. Pranal V, Fiala-Médioni A, Guezennec J (1996) Fatty acid characteristics in two symbiotic gastropods from a deep hydrothermal vent of the West Pacific. Mar Ecol Prog Ser 142:175–184
26. Folch J, Lees M, Stanley GH (1957) A simple method for the isolation and purification of total lipids from animal tissues. J Biol Chem 226:497–509
27. Saito H (2007) Identification of novel n-4 series polyunsaturated fatty acids in a deep-sea clam, *Calyptogena phaseoliformis*. J Chromatogr A 1163:247–259
28. Ackman RG, Hooper SN (1973) Non-methylene-interrupted fatty acids in lipids of shallow-water marine invertebrates: a comparison of two molluscs (*Littorina littorea* and *Lunatia triseriata*) with the sand shrimp (*Crangon septemspinosus*). Comp Biochem Physiol 46B:153–165
29. Fulco AJ (1983) Fatty acid metabolism in bacteria. Prog Lipid Res 22:133–160
30. Thiele OW, Oulevey J, Hunneman DH (1984) Ornithine-containing lipids in Thiobacillus A2 and Achromobacter sp. Eur J Biochem 139:131–135
31. Knief C, Altendorf K, Lipski A (2003) Linking autotrophic activity in environmental samples with specific bacterial taxa by detection of 13C-labelled fatty acids. Environ Microbiol 5:1155–1167
32. Saito H, Osako K (2007) Confirmation of a new food chain utilizing geothermal energy: unusual fatty acids of a deep-sea bivalve, *Calyptogena phaseoliformis*. Limnol Oceanogr 52:1910–1918
33. Zhukova NV (1991) The pathway of the biosynthesis of non-methylene-interrupted dienoic fatty acids in molluscs. Comp Biochem Physiol 100B:801–804
34. Dunstan GA, Baillie HJ, Barrett SM, Volkman JK (1996) Effect of diet on the lipid composition of wild and cultured abalone. Aquaculture 40:115–127
35. DeLong EF, Yayanos AA (1985) Adaptation of the membrane lipids of a deep-sea bacterium to changes in hydrostatic pressure. Science 228:1101–1103
36. Yano Y, Nakayama A, Ishihara K, Saito H (1998) Adaptive changes in membrane lipids of barophilic bacteria in response to changes in growth pressure. Appl Environ Microbiol 64:479–485
37. Pond DW, Bell MV, Dixon DR, Fallick AE, Segonzac M, Sargent JR (1998) Stable carbon-isotope composition of fatty acids in hydrothermal vent mussels containing methanotrophic and thiotrophic bacterial endosymbionts. Appl Environ Microbiol 64:370–375
38. Budge SM, Parrish CC, Mckenzie CH (2001) Fatty acid composition of phytoplankton, settling particulate matter and sediments at a sheltered bivalve aquaculture site. Mar Chem 76:285–303
39. Owen JM, Adron JW, Middleton C, Cowey CB (1975) Elongation and desaturation of dietary fatty acids in turbot *Scophthalmus maximus* L., and rainbow trout *Salmo gairdneri* Rich. Lipids 10:528–531
40. Yamada K, Kobayashi K, Yone Y (1980) Conversion of linolenic acid to $\omega 3$ highly unsaturated fatty acids in marine fishes and rainbow trout. Bull Jap Soc Sci Fish 46:1231–1233
41. Ohshima T, Widjaja HD, Wada S, Koizumi C (1982) A comparison between cultured and wild Ayu lipids. Bull Jap Soc Fish 48:1795–1801

Lipids (2010) 45:549–558
DOI 10.1007/s11745-010-3433-0

ORIGINAL ARTICLE

Sitosterol Thermo-oxidative Degradation Leads to the Formation of Dimers, Trimers and Oligomers: A Study Using Combined Size Exclusion Chromatography/Mass Spectrometry

Magdalena Rudzinska · Roman Przybylski · Yuan Yuan Zhao · Jonathan M. Curtis

Received: 30 October 2009 / Accepted: 21 April 2010 / Published online: 29 May 2010

Abstract Phytosterols are recognized as functional food components with cholesterol reducing properties in humans. The formation of phytosterol oligomers as a result of the thermo-oxidative degradation of sitosterol is shown to occur. The existence of oligomers is demonstrated by size exclusion chromatography (SEC) and confirmed by combined SEC-atmospheric pressure chemical ionization mass spectrometry (SEC/APCI-MS). A speculative structure for the sitosterol dimer with 3,7′ linkage is proposed consistent with data from tandem mass spectrometry and exact mass measurements. Higher molecular weight species arising from the formation of trimers or higher oligomers are seen in the mass spectra. Fragments of sitosterol formed by thermo-oxidative processes are also shown to oligomerize and their common structural characteristics are demonstrated by tandem mass spectrometry. The results presented provide evidence for the possible formation of oligomeric species involving sterols in addition to those known for acylglycerides in vegetable oils subjected to extreme oxidative stress such as in frying.

M. Rudzinska
Faculty of Food Science and Nutrition, Poznan University of Life Sciences, Poznan, Poland

Y. Y. Zhao · J. M. Curtis
Department of Agricultural, Food and Nutritional Science, University of Alberta, Edmonton, Canada

R. Przybylski (✉)
Department of Chemistry and Biochemistry, University of Lethbridge, Lethbridge, AB T1K 3M4, Canada
e-mail: roman.przybylski@uleth.ca

Keywords Sitosterol · Oxyphytosterols · Thermo-oxidative degradation · Oligomers · LC/MS · SEC · HPLC-APCI/MSMS

Abbreviations

APCI	Atmospheric pressure chemical ionization
ELSD	Evaporative light scattering detector
ESI	Electrospray ionization
HPLC	High pressure liquid chromatography
LC/MS	Liquid chromatography–mass spectrometry
SEC	Size exclusion chromatography

Introduction

Sterols comprise a major portion of the unsaponifiable matter of most vegetable oils and are mainly present as free, esterified with fatty and phenolic acids, and as glucosides. Phytosterols similar in chemical structure to cholesterol, are prone to oxidation particularly at elevated temperatures as used during frying [1, 2]. Oxidative degradation of phytosterols leads to the formation of oxidized sterol derivatives, volatile flavor components and oligomers [3–6]. Dutta et al. [7] studied the formation of phytosterol oxides during potato chips and French fries frying in different oils. Lampi et al. [8] and Soupas et al. [9] established that the sterol structure and oil matrix are the main factors affecting the formation of oxidative derivatives.

The mechanism of sterol oxidation is similar to free radical oxidation of fatty acids [10]. The initial step involves the formation of a C-7 carbon centered radical adjacent to the double bond at C-5 and C-6 in ring B of the

sterol. As a result, 7-hydroperoxide epimers are formed and due to their instability decompose to corresponding hydroxyl derivatives [11]. Interaction of hydroperoxy radicals with another sterol molecule leads to the formation of epoxy derivatives [11]. When sterols and their oxidized derivatives are subjected to elevated temperatures, a variety of low and high molecular weight components are formed indicating that oxidized derivatives are precursors and initiators [3, 11]. In sterol oligomers, monomers are connected by bridges formed by carbon–carbon, ether, and peroxy types of bonds [11, 12]. Dimers of steroids are formed during metabolism and are a physiologically important form of molecules involved in regulation and for these compounds a variety of bonding between monomers has been established [13]. Interest in oligomer formation in oils has been mainly aimed at triacylglycerol polymerization. Oligomers formed during frying in soybean oil have been shown to contain carbon–carbon and ether type bonds between triacylglyceride molecules [12, 14]. Triacylglyceride oligomers negatively affect digestion of lipids in experimental animals often leading to the initiation of negative changes during the development of large intestine cells [15].

Soupas et al. [16] demonstrated the formation of oxyphytosterols and oligomers of triacylglycerols during short time pan-frying using canola oil and margarine enriched in phytosterols and phytostanols. Even though only small amounts of these components were formed, the data indicates the formation of free radicals and the free radical mechanism of degradation which may initiate degradation of other lipids and the formation of detrimental compounds [16, 17]. Rudzinska et al. [3] showed that temperature and time are the main factors affecting the type and the amounts of degradation products formed. At frying temperatures, predominantly oligomers were formed with limited amounts of oxidized phytosterols; this indicates that the latter were the main precursors of all components formed during thermo-oxidative degradation of phytosterols [3].

Recently it has been established that phytosterols can be effective in impeding atherosclerosis and hypercholesterolemia mainly by lowering the cholesterol level in the blood [18–20]. Oxidative instability of phytosterols, similar to cholesterol, and formation of oxysterols may negatively affect health due to already proven negative effects of oxyphytosterols on some metabolic processes [21].

This study is a part of a larger program aimed at increasing our understanding of phytosterol oxidation chemistry. Here, we focus on the identification of oligomers formed during heating of sitosterol in the presence of sufficient amounts of oxygen. Although the literature contains many studies showing the formation of oligomers in oils, most rely on the use of size exclusion chromatography with non-specific detectors such as refractive index or evaporative light scattering detectors and hence give little information on the molecular structures of the oligomeric products. In contrast, recent studies have combined reversed phase chromatography to mass spectrometry using atmospheric pressure chemical ionization (APCI) or electrospray ionization (ESI) to study triacylglyceride oligomers [22, 23]. In this way, oligomers up to tetramers of triolein with and without additional oxygen atoms were observed. A similar technique was applied for the separation and identification of cholesterol and phytosterol oxides [24, 25]. In this paper we present for the first time to our knowledge, the mass spectra of phytosterol oligomers and proposing fragmentation of these molecules. The data presented underline the complexity of oligomeric products formed during degradation of sterols. Although the assignment of chemical structure remains somewhat speculative, the level of detail provided by LC/MS experiments still represents a significant advance.

Materials and Methods

Materials

β-Sitosterol was purchased from Calbiochem Brand (San Diego, CA, USA). The supplier declared 95% purity for the β-sitosterol, however when analyzed its composition was as follows: 71% β-sitosterol, 19% sitostanol, 8% campesterol and 2% campestanol. Solvent, tetrahydrofuran (THF) with HPLC purity was obtained from VWR (Mississauga, ON, Canada).

Sample Preparation

The sitosterol standard (500 mg) was put into glass tubes with a 200 mL capacity. To the tubes, 100 mL of pure oxygen was added to prevent oxygen starvation conditions, which usually change the mechanism of oxidation. Samples were heated at 180 °C for 24 h.

Separation of Oligomers

Oligomers were analyzed by size exclusion chromatography (SEC) according to ISO Method 16931-2009 [26]. Separation was performed on a Finnigan Surveyor HPLC (Thermo Electron Corporation, Waltham, MA, USA). Components were separated on three size exclusion columns coupled in series (Phenogel 500A, 100A and 50A; 5μ, 300 × 4.60 mm; Phenomenex, Torrance, CA, USA). THF was used as the mobile phase at a flow rate of 0.3 mL/min, and column temperature of 30 °C. Sample solution in THF of 10 µL was injected onto the columns and

components detected with an evaporative light scattering detector (ELSD, Sedex 75, Sedere, Alfortville, France) operated at 30 °C with an air pressure of 2.5 bar. Fractions of tetramers, trimers, dimers, monomer and fragmented sterol were collected, however oligomer and fragmented sterol fractions were contaminated because baseline separation was impossible to achieve (Fig 1a). Collected oligomer fractions were stored at −18 °C prior to LC/MS analysis.

Identification of Polymers

All LC/MS analyses were conducted on an Agilent 1200 HPLC (Agilent Technologies; Palo Alto, CA, USA) coupled to a QSTAR Elite mass spectrometer (Applied Biosystems/MDS Sciex; Concord, ON, Canada) using an atmospheric pressure chemical ionization (APCI) in positive ion mode. Analyst QS 2.0 software was employed for data acquisition and analysis. Two size exclusion columns (Phenogel 100Å, 5 μm, 4.6 mm × 250 mm, Phenomenex, Torrance, CA, USA) connected in series were used with THF as mobile phase in isocratic mode with a flow rate of 0.2 mL/min.

The mass spectra were acquired over the mass range of *m/z* 100–2,000. The APCI probe was kept at 370 °C. The other instrumental conditions were as follows (nitrogen gas flow rates are given in arbitrary units assigned by the Analyst QS2.0 software) curtain gas 30; auxiliary gas 6; nebulizing gas 75; discharge needle current 2 μA. The declustering potential (DP), focus potential (FP), and DP2 were 30 V, 120 V and 5 V, respectively. All mass spectra were recorded using the high resolution time-of-flight mass analyzer providing mass accuracies below 5 mDa over the range of *m/z* reported here. In the interests of clarity, all *m/z* values in the figures are reported as nominal values or rounded to one decimal place. All elemental compositions reported in the text and schemes are the most probable matches within the expected *m/z* range and wherever possible are confirmed by multiple experiments.

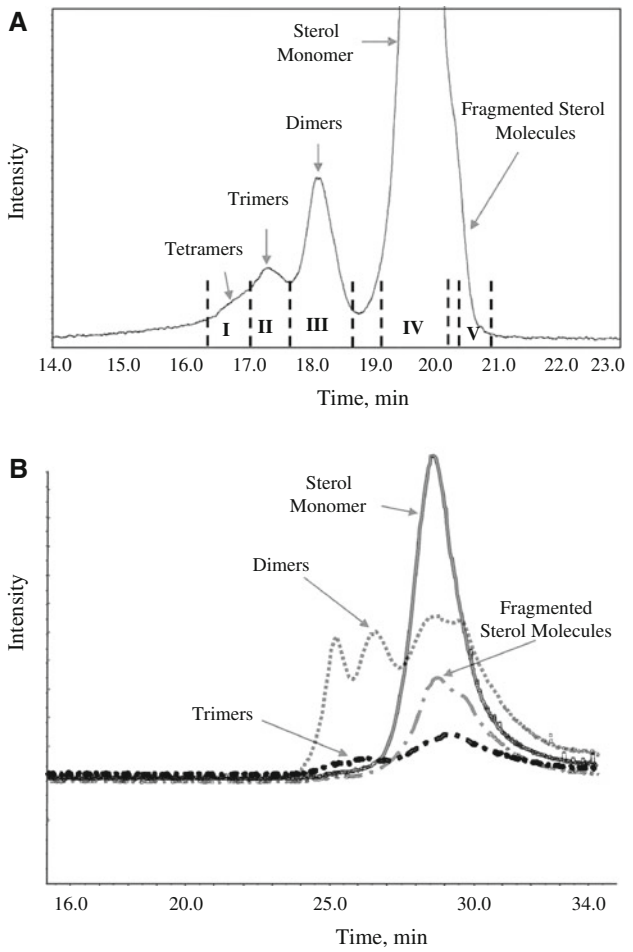

Fig. 1 **a** SEC-ELSD chromatogram of sitosterol thermo-oxidative degradation products formed during heating at 180 °C for 24 h showing times for collected fractions I to V; **b** SEC-APCI/MS total ion current (*TIC*) chromatograms of the five fractions collected in the SEC separation shown in **a**. For details see "Methods"

Results and Discussion

The sitosterol standard was heated at 180 °C for 24 h and Fig. 1a shows the SEC chromatogram of the products formed using ELSD (3). We were able to separate five groups of components differentiated by molecular size, where the monomer dominated. Dimers, trimers and tetramers were separated from monomer, however, these groups overlap. The amount of oligomers increased as time increased during heating at 180 °C (3). We reported earlier that oligomers were formed at 120 °C in a similar way to those formed at 180 °C but with lower abundance and largely without the formation of fragmented sterols (FSs). In contrast, at 60 °C there was little or no oligomer formation (3).

The five fractions identified in Fig. 1a were collected from SEC runs in a semi-preparative mode and components were identified by combined SEC/APCI-MS. In Fig. 1b the combined total ion chromatograms of these fractions are presented. It should be noted that the ELSD detects all non-volatile compounds that are nebulized to aerosol particles, whereas LC/MS requires molecules to be first converted to ions in the gas phase. For APCI, this results in considerable discrimination against molecules due to high molecular weight, volatility, thermal stability, polarity etc. Hence, for example, the distinct trimer peak seen in the SEC/ELSD trace (Fig. 1a) is not seen in the corresponding trimer fraction by SEC/APCI-MS (Fig. 1b) due to the low response to this high molecular weight compound. Nonetheless, qualitatively at least, it can be

seen that the dimer and trimer fractions do show earlier eluting peaks in the SEC traces (Fig. 1b) compared to the monomer.

Sterol Monomer Fraction

The monomer peak collected after heating at 180 °C for 24 h was analysed by combined SEC-APCI/MS as shown in Fig. 2. Surprisingly, the expected MH^+ at *m/z* 415 for the sitosterol was not observed in this fraction. As we have established already, under the conditions applied all sterols present in the standard mixture were oxidized and transformed into variety of the degradation products (3). An extracted total ion chromatogram (TIC) of low abundance ion at *m/z* 415 is shown in Fig. 2a but from the exact mass it was clear that this has elemental composition of $C_{28}H_{47}O_2$ rather than $C_{29}H_{51}O$ as expected for the MH^+ ion of sitosterol. This was consistent with the MSMS spectrum of *m/z* 415 which showed losses of two water molecules, confirming the presence of two oxygen atoms in the structure. Furthermore, the APCI spectrum of sitosterol gave a base peak at *m/z* 397 (i.e. $[M + H\text{-}H_{20}]^+$, $C_{29}H_{49}$) not observed in Fig. 2. Thus, the monomer fraction likely contains largely oxidized sterols. This can be seen in Fig. 2b where the major species at *m/z* 429 was found to have an elemental composition of $C_{29}H_{49}O_2$ and the presence of two oxygen atoms is also confirmed by losses of the two water molecules observed in the MSMS spectrum (not shown) giving fragment ions at *m/z* 411 and 393. In addition, in the MSMS spectrum of *m/z* 429 a fragment ion at *m/z* 175, confirmed as $C_{12}H_{15}O$ was observed, consistent with fragmentation across the C ring of the mono-oxygenated form of the basic sitosterol structure (Scheme 1). A further fragment in the MSMS spectrum at *m/z* 253 has an elemental composition of $C_{19}H_{25}$ which is due to loss of two water molecules and the side chain (Scheme 1). Thus, the major component of the monomer fraction is confirmed to be a mono-oxygenated sitosterol;

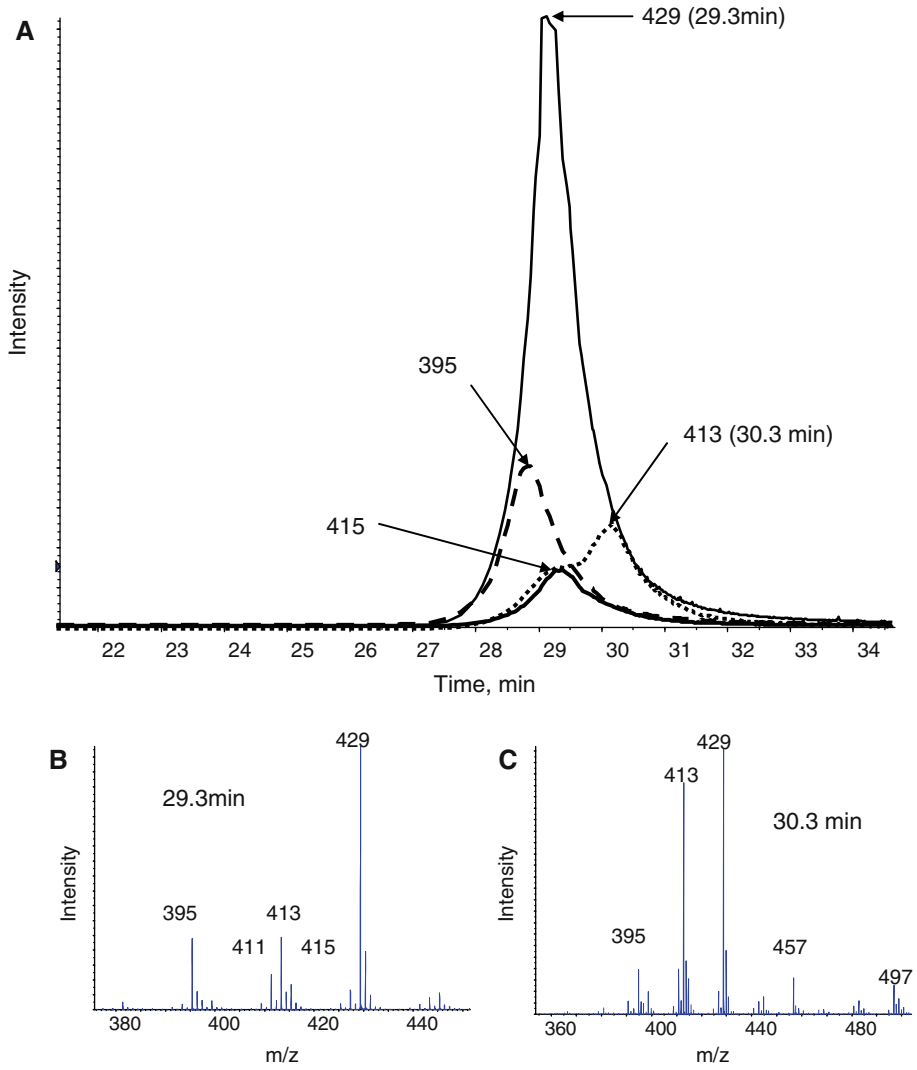

Fig. 2 SEC-APCI/MS extracted ion chromatograms **a** and mass spectra **b**, **c** of the monomer fraction. For details see text

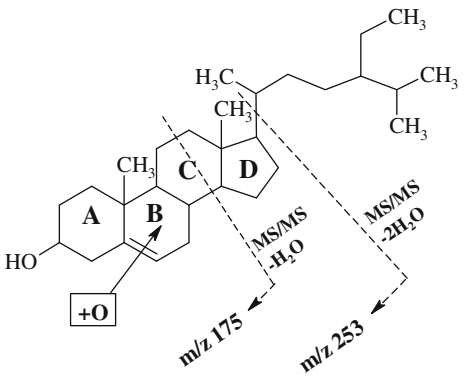

Scheme 1 The proposed MS/MS fragmentation for oxidized sterol molecule at *m/z* 429 ($C_{29}H_{49}O_2$)

whether this additional oxygen is added to the ring structure or side chain or exists as hydroperoxide cannot be determined from this experiment.

Figure 2c also indicates the presence of a compound at *m/z* 413 with elemental composition $C_{29}H_{49}O$ eluting at 30.3 min. This compound has a molecular formula consistent with an additional double bond compared to sitosterol. The MS/MS spectrum of this compound shows a fragment ion at *m/z* 255 with an elemental composition of $C_{19}H_{27}$ which is an unsaturated steroid ring system. Also seen in Fig. 2c is a lower intensity ion at *m/z* 411 whose MSMS spectrum shows a fragment ion at *m/z* 253 indicating further ring unsaturation.

Note that the sterol standard used in these experiments contained 71% *β*-sitosterol, 19% sitostanol, 8% campesterol and 2% campestanol which further complicates interpretation of the mass spectra of monomers. Overall, fragmentation of monomer ions indicates the presence of two oxygen molecules, indicative of sterol oxides. Kemmo et al. [24, 25] also established similar fragmentation and type of ions during the analysis of different types of sterol oxides.

Fragmented Sterol Fraction

It is clear that the component of the thermo-oxidative degradation that represents FSs cannot be fully resolved from the monomers (Fig. 1). Thus, as expected the fragmented monomer fraction obtained still contains a large amount of monomers as seen by the SEC-APCI/MS trace (Fig. 3). In Fig. 3, the two mass spectra presented are the background subtracted spectra averaged across the two marked retention time periods **1** and **2**. In period **1**, a large number of species are seen not only in the mass region of *m/z* 390–420 expected for altered and unaltered sterol monomers. In fact, compounds with *m/z* range extending to ~700 are evident as well as the expected lower molecular weight fragments. It is difficult to interpret all of these

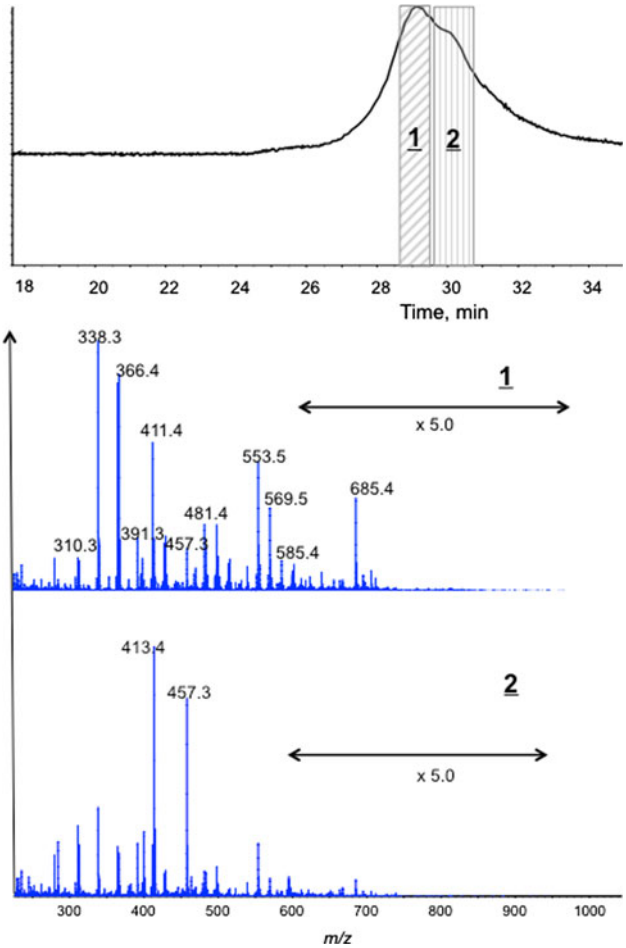

Fig. 3 SEC-APCI/MS total ion current chromatogram and background subtracted mass spectra of components present in portion 1 and 2 of the "fragmented" monomer fraction. For details see text

species, but an illustration of the chemistry occurring is found in period **2**, whose components actually overlap period **1** and beyond. Two major ions are seen in period **2**, namely *m/z* 413 and 457. The former ion has been described above as the dominant species in the monomer fraction. An extracted total ion chromatogram of ions with *m/z* 457 is seen in Fig. 4a. Surprisingly, this ion was found to have likely elemental composition of $C_{24}H_{41}O_8$ containing an apparently disproportionate number of oxygen atoms. The MSMS spectrum of these species is shown in Fig. 4c which suggests that *m/z* 457 might be the protonated dimer of *m/z* 228 since the latter ion has an elemental composition of $C_{12}H_{21}O_4$. Further investigation of the FS fraction for higher oligomers revealed the presence of these FS trimer and tetramer ions at *m/z* 685 and 913, respectively. It should be pointed out that these ions are not cluster ions formed in the ion source of the mass spectrometer since they are separated chromatographically as the distinct compounds in the mass chromatograms shown in Fig. 4a. The FS monomers (not shown) were present at

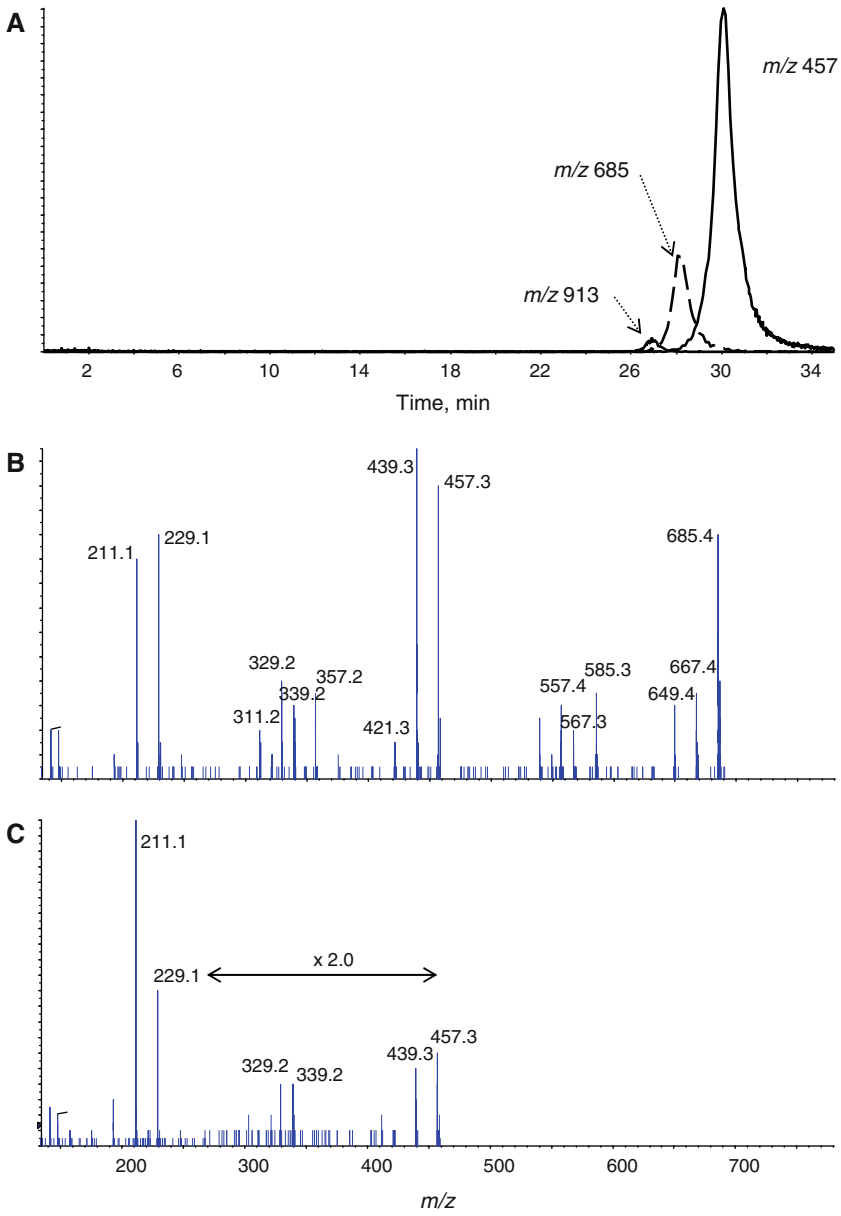

Fig. 4 **a** SEC-APCI/MS extracted ion chromatograms and **b**, **c** MS/MS spectra of the components present in the fragmented monomer fraction. For details see text

very low intensity which could be due to their reactivity, the fractionation procedure, or both.

The MSMS spectrum of the FS trimer with elemental composition of $C_{36}H_{61}O_{12}$ is given in Fig. 4b. The protonated FS monomer and FS dimer peaks can be seen at *m/z* 229 and 457, respectively and the similarities between the MSMS spectra of FS dimer and FS trimer are clearly seen (Fig. 4b and c). Scheme 2 gives a possible rationalization of the formation of these FS oligomeric compounds based on the sitosterol structure. The nature of the oxygenated FS monomer must at this point remain highly speculative. It is believed that sterol oxidation is initiated by abstraction of a hydrogen atom to generate a free radical, which in turn reacts with oxygen forming next generation of radicals and sterol 7-hydroperoxides [11, 24]. It seems likely that the A/B sterol rings are involved in forming the monomer and that reactive hydroperoxy radicals would be involved in further reactions to give oligomers and other products. The position(s) of oxygen atoms cannot be determined from the MSMS spectra and hence are not located in Scheme 2. However, common neutral losses of 100, 118, 128 and 146 fragments are seen from each FS oligomer and additionally the protonated forms of these neutrals (i.e *m/z* 101,119, 129 and 147) were seen in MSMS spectra (not shown in Fig. 4). The elemental compositions indicate that the fragment ions due to loss of 100 Da retain three of the four oxygen atoms present in the monomer and this is indicated by their location on ring B in Scheme 2 whilst the original sitosterol hydroxyl group is left unchanged. However, many other arrangements are possible.

Scheme 2 Formation of sterol oxides, oligomers, sterol fragments and oligomers of sterol fragments. A speculative structure of an observed fragmented sterol monomer and MS/MS data is included. The elemental compositions are based on measured exact masses but the location of the oxygen atoms cannot be determined

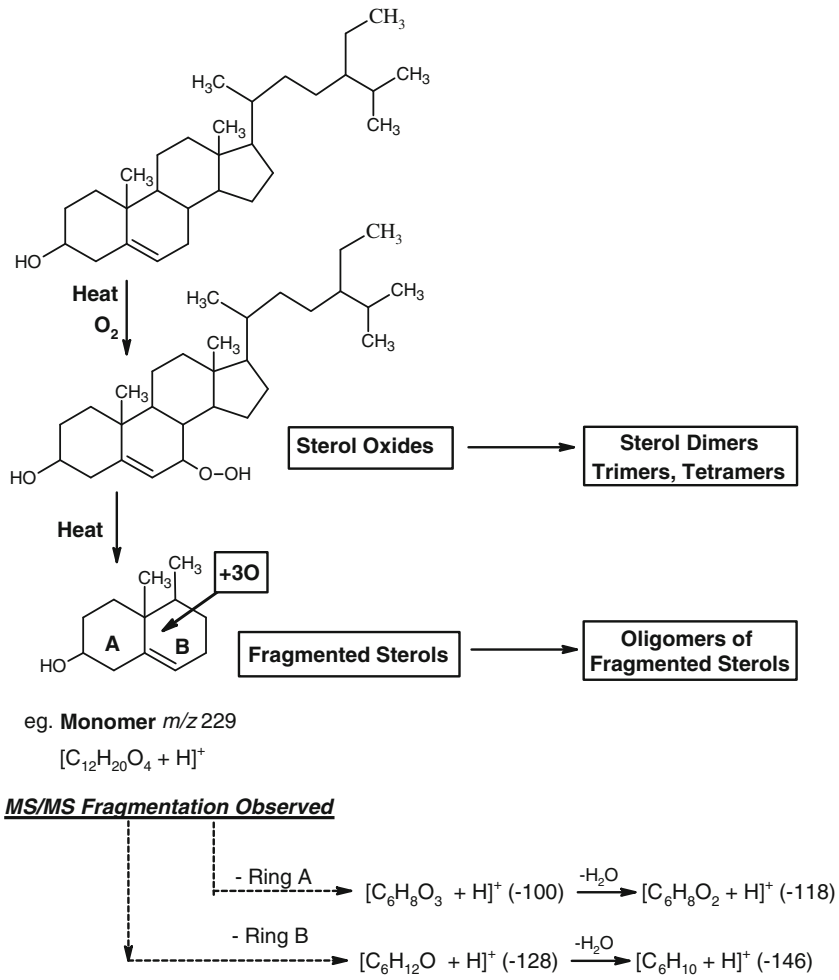

Sterol Dimer Fraction

It can be seen from Fig. 1a that the intact sterol dimer fraction is relatively small compared to the sterol monomer fraction. Furthermore, the dimer peak is not completely separated from either monomer or trimer peaks. Thus, it is not surprising that the SEC-APCI/MS total ion chromatogram of the sterol dimer fraction shows presence of other components. These peaks can be further resolved by considering extracted ion chromatograms based on the following *m/z* ranges 350–450, 450–900 and 950–1,500 corresponding to sterol monomers, dimers and trimers (Fig. 5). The extracted ion chromatogram for the monomer *m/z* range is comprised of two major peaks; the one at longer retention time (~29 min) corresponds to the major monomer component, as seen in Figs. 1 and 2, whilst the peak at shorter retention time (~27 min) is also seen in the sterol dimer *m/z* range trace below it in Fig. 5. The extracted ion chromatogram for the sterol trimer *m/z* range shows a single major component at the expected high molecular size end of the chromatogram (i.e shorter retention time on SEC). The corresponding peak seen in

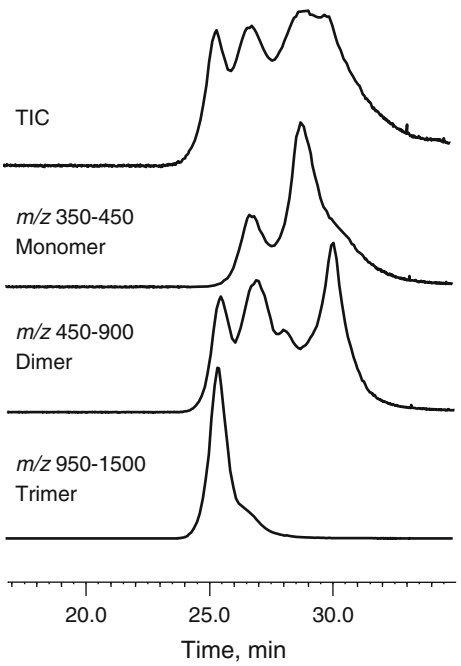

Fig. 5 SEC-APCI/MS total ion current (*TIC*) and extracted ion chromatograms of the sterol dimer fraction formed during heating sitosterol at 180 °C for 24 h. See text for details

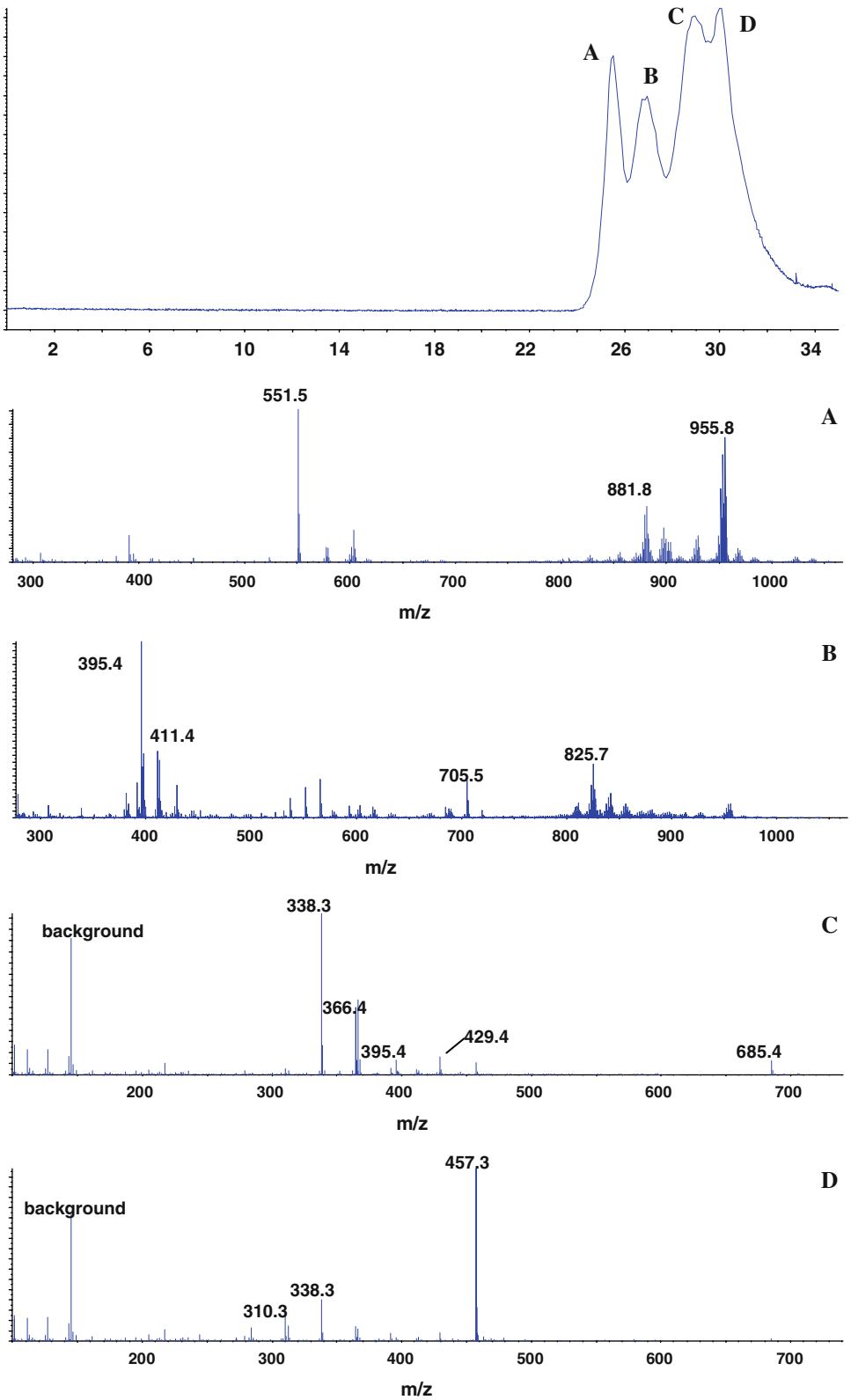

Fig. 6 SEC-APCI/MS TIC and spectra of the four peaks detected in the sterol dimer fraction formed during heating sitosterol at 180 °C for 24 h. For details see text

the sterol dimer *m/z* range trace above it in Fig. 5 is most likely due to ion source fragmentation of sterol trimer ions under APCI conditions, although the presence of molecular species in this *m/z* range cannot be ruled out.

In Fig. 6, mass spectra are presented which were obtained by averaging across each of the four partially resolved peaks (labelled **A** to **D**) in the total ion chromatogram of the sterol dimer fraction. The mass spectrum of peak **D** is dominated by *m/z* 457 which is formed as a result of thermo-oxidative fragmentation followed by dimerization as described above for the FS fraction; in peak **C** *m/z* 685 is the FS trimer. Peak **B** contains a wide range of species in the *m/z* 800–900 which correspond to oxidized sterol dimers. The dominant fragment ion at *m/z* 395 ($C_{29}H_{47}$) is characteristic of the dehydrated form of the sitosterol monomer and the most abundant dimer ion at *m/z* 825 ($C_{58}H_{97}O_2$) could be a dimer of two sterol molecules. Scheme 3 shows a putative structure where a 3-, 7′- ether bridge links an oxidized sitosterol monomer to a second sitosterol molecule in its dehydrated form. Clear evidence exists for preferential oxidation of sterols at the 7 position [8, 24, 25]. The MSMS spectrum of this sterol dimer shows the major loss of a water molecule (minor loss of two waters) and an abundant fragment ion at *m/z* 395, as also seen in the mass spectrum. Minor peaks at *m/z* 411 and 413, also significant fragment ions in the mass spectrum, may reflect fragmentation across the bridging ether group as suggested in Scheme 3.

In addition to the most abundant ion at *m/z* 825, many other dimeric species are present in peak **B** within *m/z* 800 and 960 (Fig. 6b) mainly containing either two or four oxygen atoms. Thus, although the present data is inadequate to deduce definitive structures, it nonetheless provides clear proof for the formation of sterol dimers under thermo-oxidative conditions, consistent with the prediction from the SEC chromatograms (Fig. 1a). Furthermore, the data confirms that oxidized derivatives are the main precursor in oligomer formation. The spectrum of peak **A** is dominated by an oligomer of *m/z* 955 of unknown structure and an ion at *m/z* 551 ($C_{35}H_{67}O_4$) (Fig. 6a). Ions of *m/z* intermediate between those expected for sterol dimers and trimers including the dominant ion of *m/z* 955 may be formed by reactions between oxidized fragments and sterol monomers and dimers. In fact, many dimers might be formed considering the many possibilities for connecting bridges, particularly among phytosterols where there are additional tertiary and quaternary carbons in the side chain structure. However, it is also possible that ions such as *m/z* 955 are actually fragment ions of sterol trimers formed in the mass spectrometer ion-source.

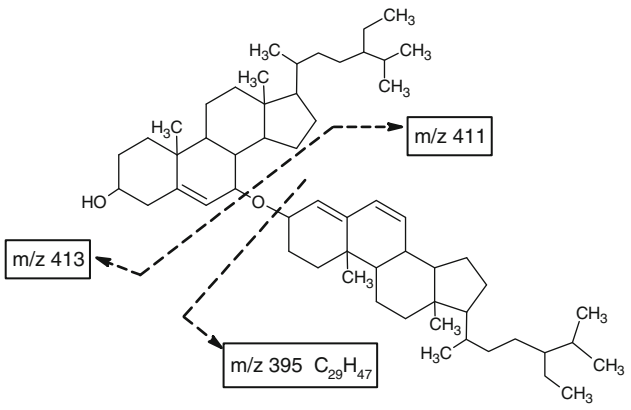

Scheme 3 The proposed structure and potential MS/MS fragmentation of the sterol dimer with *m/z* 825

Sterol Trimer Fraction

The SEC-APCI/MS extracted ion chromatograms for the trimer fraction is shown in Fig. 7 using the same *m/z* ranges as used in Fig. 5. Despite the fact that total ion trace shows little response at the retention times corresponding to trimers (earlier than about 26.5 min), compounds with *m/z* > 950 were detected, thus demonstrating the existence of trimers. The low signal-to-noise that is evident in the chromatogram makes it apparent that APCI is not ideal for the analysis of these compounds. However, the ions with *m/z* above those expected for dimers can be observed, as in Fig. 6 peak A, and can be tentatively interpreted as ions formed from the fragmentation of trimer ions. The oligomers with the highest molecular weight, tetramers, were

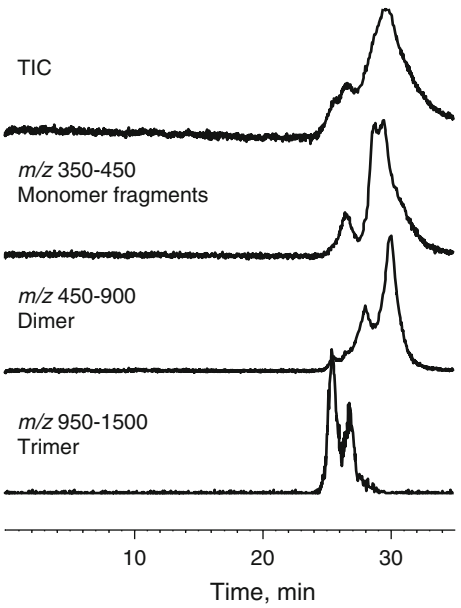

Fig. 7 SEC-APCI/MS TIC and extracted ion chromatograms of the sterol trimer fraction formed during heating sitosterol at 180 °C for 24 h. For details see text

detected using an ELSD (Fig. 1a) but intact tetramers could not be detected by APCI/MS. Future work will therefore look at alternative ionization methods more suitable for the study of labile high molecular weight species.

In conclusion, the above work demonstrates the ability of phytosterols to form oligomeric structures when heated in the presence of oxygen for prolonged time, as occurs during frying. Further work is required to understand the mechanism of oligomer formation and the effect of oil matrixes. The formation of oxidative derivatives of sterols and their subsequent interactions with sterols and triacylglycerides is clearly of importance in food processing. Assessment of any biological activity of phytosterol oligomers and oxidized derivatives needs to be considered especially due to the recent trend of enriching foods with phytosterols.

Acknowledgments This work was financed by the State Committee for Scientific Research, grant # N312 071 32/3209, by the Alberta Value Added Corporation, the Agriculture Funding Consortium project #2006F018R; project #2009FO32R supported by the Agriculture and Food Council of Canada and the Alberta Agricultural Research Institute, and by an NSERC Discovery Grant (to J.M. Curtis).

References

1. Przybylski R, Zambiazi R, Li W (1999) Kinetics of sterols changes during storage and frying of canola oils. In: Proceedings of the 10th international rapeseed congress, 26–29 September, Canberra, Australia
2. Rudzińska M, Korczak J, Wąsowicz E (2005) Changes in phytosterols and their oxidation products during frying of French fries in rapeseed oil. Pol J Food Nutr Sci 14:381–387
3. Rudzinska M, Przybylski R, Wasowicz E (2009) Products formed during thermo-oxidative degradation of phytosterols. JAOCS 86:651–662
4. Kim SK, Nawar WW (1993) Parameters influencing cholesterol oxidation. Lipids 28:917–922
5. Oehrl LL, Hansen AP, Rohrer CA, Fenner GP, Boyd LC (2001) Oxidation of phytosterols in a test food system. JAOCS 78:1073–1078
6. Dutta PC (2004) Chemistry, analysis, and occurrence of phytosterol oxidation products in foods. In: Dutta PC (ed) Phytosterols as functional food components and nutraceuticals. Marcel Dekker Inc, New York, pp 397–417
7. Dutta PC, Appelqvist LÅ (1997) Studies on phytosterol oxides I: effect of storage on the content in potato chips prepared in different vegetable oils. JAOCS 74:647–657
8. Lampi AM, Juntunen L, Toivo J, Piironen V (2002) Determination of thermo-oxidation products of plant sterols. J Chrom B 777:83–92
9. Soupas L, Juntunen L, Lampi A-M, Piironen V (2004) Effects of sterol structure, temperature, and lipid medium on phytosterol oxidation. J Agric Food Chem 52:6485–6491
10. Lercker G, Rodriguez-Estrada MT (2002) Cholesterol oxidation mechanisms. In: Guardiola F, Dutta PC, Codony R, Savage GP (eds) Cholesterol and phytosterol oxidation products. AOCS, Champaign, pp 1–25
11. Smith LL (1981) Cholesterol autoxidation. Plenum, New York, pp 125–458
12. Christopoulou CN, Perkins EG (1989) Isolation and characterization of dimmers formed in used soybean oil. JAOCS 66:1360–1370
13. Li T, Dias JR (1997) Dimeric and oligomeric steroids. Chem Rev 97:283–304
14. Choe E, Min DB (2007) Chemistry of deep-fat frying oils. J Food Sci 72:77–86
15. Billek G (2000) Health aspects of thermoxidized oils and fats. Eur J Lipid Sci Technol 102:587–593
16. Soupas L, Huikko L, Lampi AM, Piironen V (2007) Pan-frying may induce phytosterol oxidation. Food Chem 101:286–297
17. Lampi AM, Kemmo S, Makela A, Heikkinen S, Piironen V (2009) Distribution of monomeric, dimeric and polymeric products of stigmasterol during thermo-oxidation. Eur J Lipid Sci Technol 111:1027–1034
18. Clifton P (2002) Plant sterol and stanols—comparison and contrasts: sterols versus stanols in cholesterol-lowering: is there a difference? Atherosclerosis Suppl 3:5–9
19. Moreau RA, Norton RA, Hicks KB (1999) Phytosterols and phytostanols lower cholesterol. Inform 10:572–577
20. Hicks KB, Moreau RA (2001) Phytosterol and phytostanols: functional food cholesterol busters. Food Technol 55:63–67
21. Oehrl DL, Boyd LC (2004) Biological effects and safety aspects of phytosterol oxides. In: Dutta PC (ed) Phytosterols as functional food components and nutraceuticals. Marcel Dekker Inc, New York, pp 419–430
22. Neff WE, Byrdwell WC (1998) Characterization of model triacylglycerol (triolein, trilinolein and trilinolenin) autoxidation products via high-performance liquid chromatography coupled with atmospheric pressure chemical ionization mass spectrometry. J Chrom A 818:169–186
23. Byrdwell WC, Neff WE (2004) Electrospray ionization MS of high M.W TAG oligomers. JAOCS 81:13–26
24. Kemmo S, Ollilainen V, Lampi AM, Piironen V (2007) Determination of stigmasterol and cholesterol oxides using atmospheric pressure chemical ionization liquid chromatography/mass spectrometry. Food Chem 101:1438–1445
25. Kemmo S, Ollilainen V, Lampi AM, Piironen V (2008) Liquid chromatography mass spectrometry for plant sterol oxide determination in complex mixture. Eur Food Res Technol 226:1325–1334
26. ISO/FDIS 16931-2009, Animal and vegetable fats and oils: determination of polymerized triglycerides content by high-performance size-exclusion chromatography (HPSEC)

Lipids (2010) 45:559–565
DOI 10.1007/s11745-010-3423-2

ORIGINAL ARTICLE

Near-Infrared Spectroscopy and Partial Least-Squares Regression for Determination of Arachidonic Acid in Powdered Oil

Meiyan Yang · Shaoping Nie · Jing Li · Mingyong Xie · Hua Xiong · Zeyuan Deng · Weiwan Zheng · Lin Li · Xiaoming Zhang

Received: 18 March 2010 / Accepted: 21 April 2010 / Published online: 14 May 2010

Abstract Near-infrared (NIR) spectroscopy was evaluated as a rapid method of predicting arachidonic acid content in powdered oil without the need for oil extraction. NIR spectra of powdered oil samples were obtained with an NIR spectrometer and correlated with arachidonic acid content determined by a modification of the AOCS Method. Partial Least-Squares regression was applied to calculate models for the prediction of arachidonic acid. The model developed with the raw spectra had the best performance in cross-validation ($n = 72$) and validation ($n = 21$) with a correlation coefficient of 0.965, and the root mean square error of cross-validation and prediction were both 0.50. The results show that NIR, a well-established and widely applied technique, can be applied to determine the arachidonic acid content in powdered oil.

Keywords Arachidonic acid · Near-infrared spectroscopy · Partial least-squares regression

M. Yang · S. Nie · J. Li · M. Xie (✉) · H. Xiong · Z. Deng · W. Zheng
State Key Laboratory of Food Science and Technology, Nanchang University, Nanchang 330047, China
e-mail: myxie@ncu.edu.cn

L. Li
College of Light Industry and Food Sciences, South China University of Technology, Guangzhou 510640, China

X. Zhang
State Key Laboratory of Food Science and Technology, Jiangnan University, Wuxi 214122, China

Abbreviations

NIR	Near-infrared
ARA	Arachidonic acid
PUFA	Polyunsaturated fatty acids
FAMEs	Fatty acid methyl esters
FID	Flame ionization detector
SNV	Standard normal variate
MSC	Multiplicative scatter correction
WT	Wavelet transforms
OSC	Orthogonal signal correction
PLS	Partial Least-Squares
RMSEC	Root mean square error of calibration
RMSECV	Root mean square error of cross-validation
RMSEP	Root mean square error of prediction

Introduction

Arachidonic acid (ARA, C20:4, n-6), one of the members of the n-6 fatty acid family, is an important structural component of the central nervous system. The content of ARA present in brain and nerve tissue is 40–50% of the polyunsaturated fatty acids (PUFA), and it even reaches 70% in nerve endings. Many studies have shown the prenatal and postnatal importance of ARA in early human (brain) development [1–3]. Though ARA can be synthesized by linoleic acid in vivo through chain elongation and desaturation, the process is quite complicated, which not only needs sufficient substrate and positive equilibrium energy condition but also enough activity of fatty acid desaturases. Early studies have shown that the ARA status of bottle-feeding infants is lower than that of breast-feeding infants [4–6]. So the addition of ARA in the form of powdered oil to infant formula milk powder is widely accepted nowadays.

An adequate amount of ARA in newborn nutrition is important, as the investigation results indicated that the average content of ARA in human milk is 0.5–0.7% in different places across the world [7]. Determination of ARA is usually carried out according to the official method by gas chromatography with a flame ionization detector, which is time-consuming, expensive and labor-intensive when used to monitor industrial processes. Therefore, a rapid, simple and accurate method is in great demand to evaluate the ARA content in powdered oil.

Near-infrared (NIR) spectroscopy has proved to be a valid analytical tool for food products [8]. Several references of the use of NIR spectroscopy to construct models evaluating components content were found in the literature. For example, it has been employed to analyze fat content in milk powder [9], to estimate fatty acid content in intact seeds of oilseed [10], to evaluate carotenoids content in maize [11], and α-tocopherol in vegetable oils [12]. However, none of these was related to new technique products, such as powdered oil.

The main objective of this work was to construct a model based on FT-NIR spectroscopy, in combination with multivariate calibration methodologies to predict the ARA content in powdered oil.

Materials and Methods

Reagents

All reagents were of analytical grade and absolute *n*-hexane was of chromatographic grade. Standard methyl arachidonate was purchased from Sigma-Aldrich Co. (St. Louis, MO). Standard solutions of methyl arachidonate were prepared in absolute *n*-hexane and stored at 4 °C before analysis.

Samples Preparation

ARA oil was used to prepare unknown samples with different ARA concentrations as weight percentages. By a spray drying process, one hundred ($n = 100$) powdered oil samples were manufactured with ARA oil concentrations ranging from 10 to 34% to represent the diversity of commercially available powdered oils. All the samples were stored at room temperature (20 °C) in the dark.

Reference Methods

Total fat and fatty acid methyl esters content were measured using Rose-Gottlieb and AOCS Method with a modification [13]. The modification was a change in GC temperature programming (described later). Briefly, 1.0 g of sample was weighed into a Mojonnier tube, and 0.1 g Taka amylase and 10 mL distilled water at about 50 °C were added. The sample was treated with ammonia–alcohol in a water bath (65 °C) for 15 min, and subsequently extracted with diethyl and petroleum ethers. The diethyl and petroleum ethers were evaporated over a steam bath, and the extracts were the total fat. The method [14] for the preparation of fatty acid methyl esters (FAMEs) was as follows: 10 mg extracted oil (accurate to 0.1 mg) was accurately weighed into a stoppered-glass tube, 2 mL of hexane added, followed by adding 1 mL of 2 mol/L potassium hydroxide in methanol, and then, the tube was closed and shaken well for 2 min. After 30 min, the upper layer was transferred to a test tube, followed by adding a small amount of anhydrous sodium sulfate to remove excessive moisture, and then the dry hexane solution was transferred to a 1.5-mL glass vial for the following analysis.

FAMEs analysis was performed on an Agilent 6890N gas chromatograph equipped with a flame ionization detector (FID) and an Agilent autosampler 7683-B injector (Agilent Technologies, Little Fall, NY, USA). A fused-silica capillary column CP Sil-88 (100 m × 0.25 mm id., 0.20 μm film thickness, Varian Inc.) was used for the separation of fatty acid methyl esters. Hydrogen was the carrier gas with a flow rate of 1.8 mL/min. The temperature of the injector and detector was set at 250 °C with an injection volume of 1.0 μL by using the splitless mode. The analysis was carried out using a temperature programming consisting of an initial temperature 45 °C (held 4 min), ramp 13 °C/min to 175 °C (held 27 min), ramp 4 °C/min to 215 °C final temperature (held 25 min). A standard curve was calibrated by a series of methyl arachidonate samples with the concentrations of 0.5, 1.0, 1.5, 2.0, 2.5, 3.0 and 4.0 mg/mL, respectively. The ARA in the analyzed oil samples was identified by comparing the retention times with the standard. Quantification of ARA was performed using the external calibration curve.

FT-NIR Instrumentation and Spectral Collection

The NIR spectra were measured on a Nicolet 5700 spectrometer using a Baseline™ Diffuse Reflectance Accessory and an InGaAs detector (Madison, USA).

NIR absorbance spectra were registered in the range of 4,000–10,000 cm^{-1} with a 16 cm^{-1} resolution and 64 scans. Gain was selected automatically. Happ–Genzel apodization was applied, mode zero filling was disabled, and the interferometer mirror speed was set at 1.5798 cm/s. About 1 g of the sample in powder form was densely packed in a glass sample vial (2 cm in diameter and

1.2 mm in wall thickness). The background spectrum was recorded every 4 h while each sample underwent four replications and the spectra were averaged before they were subjected to multivariate analysis. All spectra were collected by OMNIC 7.0 software and recorded as log $(1/R)$, where R is the relative reflectance.

Data Processing and Development of the Calibration Model

The data acquired from the NIR spectrometer contain noises in addition to sample information. In order to obtain reliable, accurate and stable calibration models, it is necessary to pre-process spectral data before modeling. At present, there are many pre-processing methods, such as smoothing, derivative, standard normal variate (SNV), multiplicative scatter correction (MSC) and some new methods including wavelet transforms (WT) and orthogonal signal correction (OSC) [15, 16]. Smoothing that includes Savitzky–Golay smoothing is one of the methods often used to eliminate noises [17]; the first and second derivatives are used to remove background and increase spectral resolution. SNV removes the multiplicative interferences of scatter, particle size, and the change of light distance as well as MSC [18, 19]. It corrects both multiplicative and additive scatter effects. In this study, five data pre-processing methods were applied comparatively, which were SNV, MSC, first derivative, second derivative and Savitzky–Golay smoothing.

Calibration models between chemical data (data from gas chromatography) and NIR spectra were developed using Partial Least-Squares (PLS) regression with cross-validation in the TQ analyst 7.1.0 software package (Thermo-Nicolet). The data set was split randomly into a training ($n = 75$) and a validation set ($n = 25$). The optimum number of PLS factors in the calibration models was determined by cross-validation and defined by the PRESS function (predicted residual error sum of squares) in order to avoid overfitting of the models [20]. The relative performance of the established model was assessed by the required number of factors while the root mean square error of calibration (RMSEC), the root mean square error of cross-validation (RMSECV), and its predictive ability were evaluated from the root mean square error of prediction (RMSEP). The spectral regions used for PLS models were selected automatically.

In addition to these statistics, the importance of calibration outliers must be considered. The spectrum outlier diagnostic finds the spectra of the standards which are most unlike the others, and the Chauvenet test was used to decide whether the difference is significant. If the standard fails the test, it is considered an outlier.

Results and Discussion

Reference Method Measurement of ARA

Figure 1 shows the GC chromatograms of the standard and a sample, which were used to identify and quantify the contents of ARA in our samples. The standard curve is shown in Fig. 2 with the equation $Y = 6978.8X + 320.71$ ($R^2 = 0.9997$). The accuracy, precision and detection limit of the laboratory using the modified AOCS Method is 90.2–101.4%, 0.8% and 0.25 mg/L, respectively.

Range, mean value, and standard deviation for ARA content in the samples are given in Table 1 for the calibration and validation data sets.

Spectral Characteristics

Representative NIR spectra of powdered oil samples are shown in Fig. 3 as raw spectra (Fig. 3a) and spectra treated with first derivative processing (Fig. 3b). As shown in Fig. 3, the main absorption peaks of the samples were observed in the range of 4,000–6,000 cm^{-1} instead of the whole NIR region. The regions we chose to develop models were suggested by the software automatically, which are 4,250–4,358 cm^{-1} (A), 5,723–5,881 cm^{-1} (B), respectively. Region A is characteristic of the combination of C–H stretching vibration with bending vibration mode of $-CH_3$ and $-CH_2$. The spectrum of region B is characteristic of the first overtone of the C–H stretching vibration of $-CH_3$ and $-CH = CH-$ groups [21].

NIR Models

The outliers should be eliminated as an essential step in the optimization procedure of the models already developed. During the calibration development, seven spectral outliers were detected. Table 2 shows the statistics of the NIR spectral data for predicting ARA in powdered oil samples after the outlier samples elimination. The data confirm that the spectral allows the creation of a calibration set which represents the usual variability encountered by powdered oil.

PLS models were developed using five spectral pretreatments based on the selected 93 NIR spectra of the powdered oil samples. The prediction capability was evaluated by correlation coefficient (r), RMSEC and RMSECV. It is expected to have ideal models with the lower RMSEC and RMSECV as well as the higher correlation coefficient r. Different latent variables were applied to build the calibration models and the optimum number of factors was selected by the PRESS diagnostic shown in Fig. 4. The results of different spectral pretreatment models are shown in Table 3.

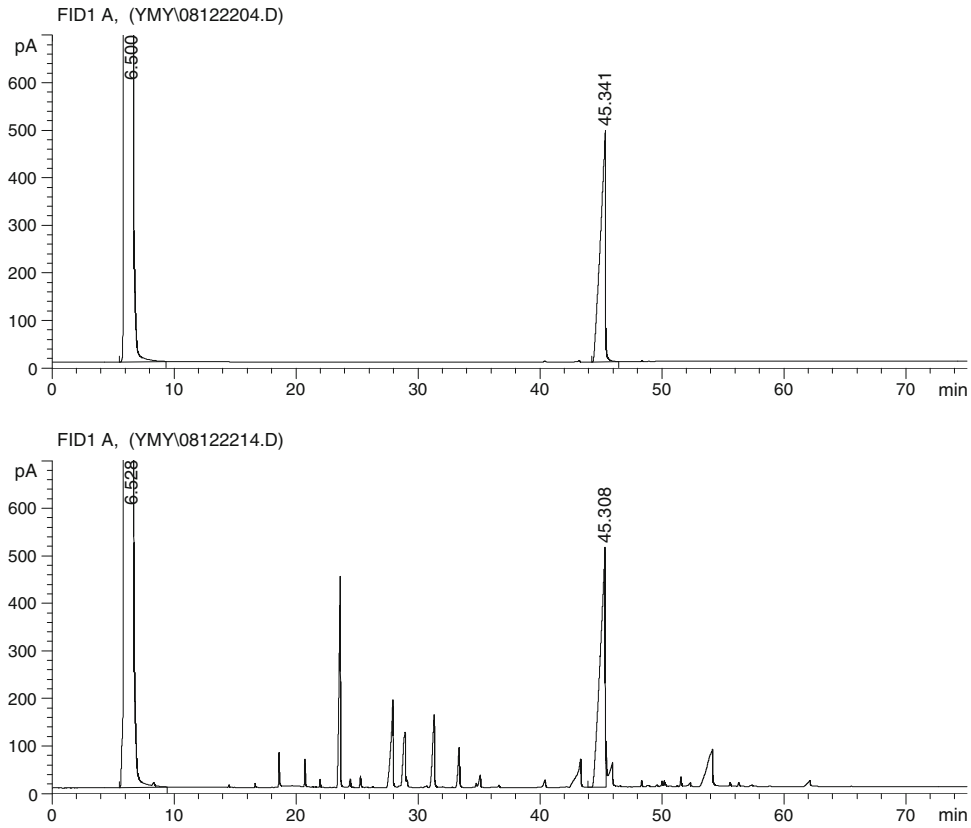

Fig. 1 GC chromatograms of the standard and a sample

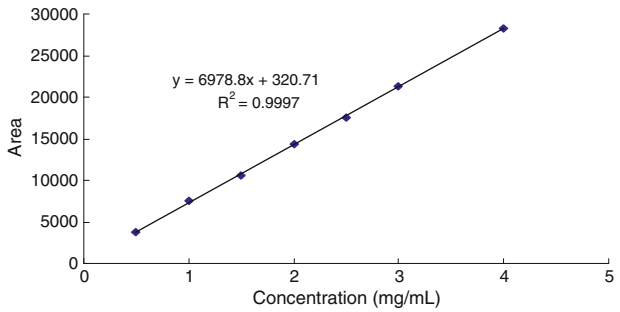

Fig. 2 The standard curve of methyl arachidonate

Table 1 Range, mean value and standard deviation of reference method measured AA content for powdered oil samples in the PLS calibration and validation data sets

Calibration				Validation			
n	Range (%)	Mean (%)	SD (%)	*n*	Range (%)	Mean (%)	SD (%)
75	3.88–11.05	7.91	1.90	25	5.15–11.09	8.07	2.02

n number of samples, *SD* standard deviation

Figure 4 shows that the RMSECV decreases sharply with the first two factors and gradually decreases as the third variable is incorporated into the calibration model. As the number of factors increases further, RMSECV begins to increase at 4 PLS factors. An increase in the RMSECV indicates that the data have been overfitted by incorporating spectral information into the model that is not related to ARA. In this case, 3 PLS factors were chosen as the optimum.

The model developed with the raw spectra had the best performance in cross-validation ($n = 72$) and validation ($n = 21$) with RMSECV of 0.50, correlation coefficient of 0.965, RMSEP of 0.50 (Table 3 and Fig. 5). The models developed with various pretreatments such as derivative, smoothing, SNV, MSC and the combination of these pretreatments decrease the modeling effect, and it may be because of the useless information they introduced due to their own characteristics. Just as the first and second derivatives are used to remove background and increase spectral resolution, the drawback of derivative is that it would bring noises [22]. Or some useful information was smoothed out when use Savitzky–Golay smoothing to eliminate noises, which might cause distortion of spectral signals. Another possible explanation for this can be that pretreatments affect the information distribution, while the spectral regions used to build models with different pretreatments were the regions chose by original spectra, which lead to unsatisfactory treatment effects. Thus, it is necessary to choose appropriate data pretreatment to build

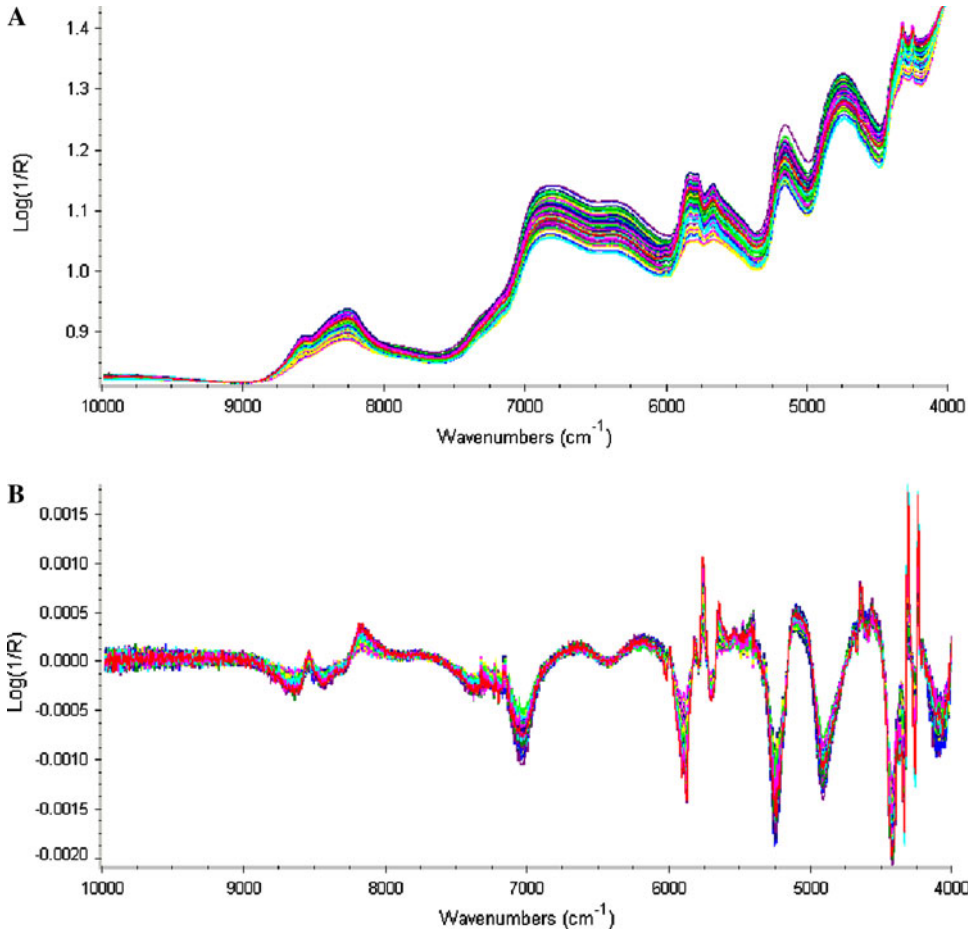

Fig. 3 NIR spectra of 100 representative powdered oil samples showing **a** raw spectra and **b** spectra after first-derivative processing

Table 2 The statistics of the samples in the PLS calibration and validation data sets after the outlier samples elimination

Calibration				Validation			
n	Range (%)	Mean (%)	SD (%)	*n*	Range (%)	Mean (%)	SD (%)
72	4.01–11.05	7.80	1.95	21	5.15–11.09	8.11	2.0

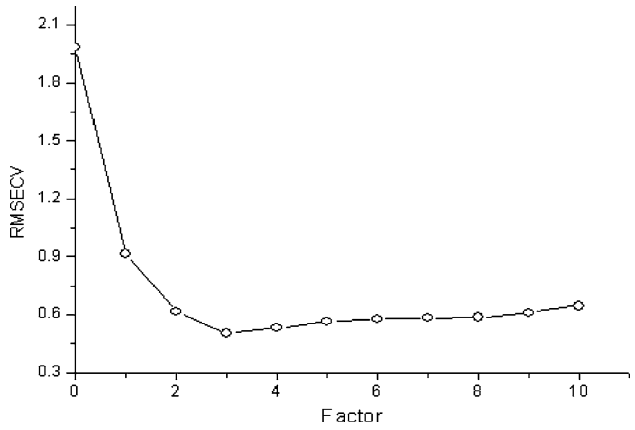

Fig. 4 The PRESS diagnostic results for PLS calibration model

the calibration model based on the detection objective and instrument function.

The satisfied calibration and prediction result of the PLS model show the feasibility for the measurement of ARA content in powdered oil using NIR spectra. Moreover, the algorithm used for developing calibration equations (PLS) allows one to optimize the number of factors to avoid overfitting.

The present study has provided a rapid determination method for ARA content in powdered oil. The results indicate that the determination of ARA content in powdered oil could be successfully performed through NIR spectroscopy combined with chemometrics methods of the PLS model. Five spectral pretreatments methods, SNV, MSC, first derivative, second derivative and Savitzky–Golay smoothing were used. The spectral regions used for ARA analysis in powdered oil were selected by software automatically. The model using raw spectra achieve higher accuracy compared to other pretreatments. This nondestructive method could greatly simplify the analysis of such compounds, because no extraction step with organic solvents is required and samples are readily analyzed in minutes. Further selection of valuable information of

Table 3 The results for AA content determination based on different numbers of factors with different spectral pretreatments

No.	Factor	Pretreatment	*r*	RMSEC	RMSECV	RMSEP
1	3	Raw	0.965	0.48	0.50	0.50
2	3	1st-Der	0.962	0.47	0.53	0.49
3	2	2nd-Der	0.905	0.66	0.83	0.79
4	3	SNV	0.960	0.49	0.54	0.51
5	2	1st-Der + SNV	0.961	0.51	0.53	0.51
6	3	MSC	0.960	0.49	0.54	0.51
7	2	1st-Der + MSC	0.961	0.51	0.53	0.51
8	2	1st-Der + SNV + SG(9,3)	0.961	0.51	0.53	0.51
9	2	1st-Der + MSC + SG(9,3)	0.961	0.51	0.53	0.51

1st-Der first derivative, *2nd-Der* second derivative, *SNV* standard normal variate, *MSC* multiplicative scatter correction, *SG* Savitzky–Golay smoothing, *r* correlation coefficient of cross-validation, *RMSEC* root mean square error of calibration, *RMSECV* root mean square error of cross-validation, *RMSEP* root mean square error of prediction

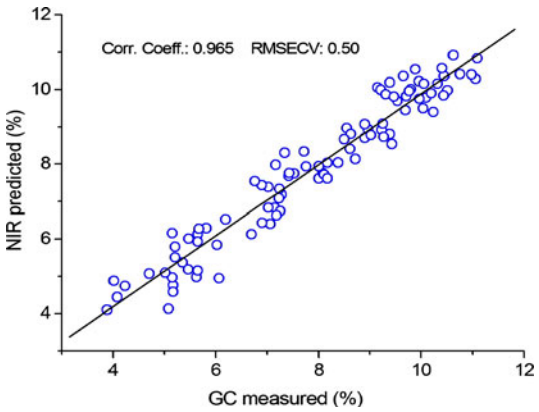

Fig. 5 Correlation between GC measured and NIR predicted values in cross-validation set for AA content of PLS model with raw spectral

spectral data and an explanation of the result would be needed to improve the model generalization and stability.

Acknowledgments The authors gratefully acknowledge the financial support provided by National Key Technology R&D Program (No. 2006BAD27B04), Changjiang Scholars and Innovative Research Team in the University (No: IRT0540), and Nanchang University Testing Fund (No.2008034).

References

1. Bouwstra H, Dijck-Brouwer DA, Wildeman JAL, Tjoonk HM, van der Heide JC, Boersma ER, Muskiet FAJ, Hadders-Algra M (2003) Long-chain polyunsaturated fatty acids have a positive effect on the quality of general movements of healthy term infants. Am J Clin Nutr 78:313
2. Larque E, Demmelmair H, Koletzko B (2002) Perinatal supply and metabolism of long-chain polyunsaturated fatty acids. Ann NY Acad Sci 967:299–310
3. Uauy R, Hoffman DR, Mena P, Llanos A, Birch EE (2003) Term infant studies of DHA and ARA supplementation on neurodevelopment: results of randomized controlled trials. J Pediatr 143:17–25
4. Carlson SE (2001) Docosahexaenoic acid and arachidonic acid in infant development. Semin Neonatol 6:437–449
5. Putnam JC, Carlson SE, DeVoe PW, Barness LA (1982) The effect of variations in dietary fatty acids on the fatty acid composition of erythrocyte phosphatidylcholine and phosphatidylethanolamine in human infants. Am J Clin Nutr 36:106
6. Sanders TAB, Naismith DJ (2007) A comparison of the influence of breast-feeding and bottle-feeding on the fatty acid composition of the erythrocytes. Brit J Nutr 41:619–623
7. FAO (1994) Fats and oils in human nutrition: report of a joint expert consultation. FAO Food Nutr Pap 57:1–147
8. Blanco M, Villarroya I (2002) NIR spectroscopy: a rapid-response analytical tool. Trends Analyt Chem 21:240–250
9. Wu D, Feng S, He Y (2007) Infrared spectroscopy technique for the nondestructive measurement of fat content in milk powder. J Dairy Sci 90:3613
10. Koprna R, Nerusil P, Kolovrat O, Kucera V, Kohoutek A (2006) Estimation of fatty acid content in intact seeds of oilseed rape (*Brassica napus* L.) lines using near-infrared spectroscopy. Czech J Genet Plant Breed 42:132
11. Brenna OV, Berardos N (2004) Application of near-infrared reflectance spectroscopy (NIRS) to the evaluation of carotenoids content in maize. J Agric Food Chem 52:5577–5582
12. Szlyk E, Szydlwska-Czerniak A, Kowalczyk-Marzec A (2005) NIR spectroscopy and partial least-squares regression for determination of natural alpha-tocopherol in vegetable oils. J Agric Food Chem 53:6980–6987
13. AOCS (2007) Determination of *cis*-, *trans*-, saturated, monounsaturated, and poly unsaturated fatty acids in dairy and ruminant fats by capillary GLC. AOCS Press Champaign
14. AOCS (1997) Preparation of methyl ester of fatty acids. AOCS Press Champaign
15. Helland IS, Naes T, Isaksson T (1995) Related versions of the multiplicative scatter correction method for preprocessing spectroscopic data. Chemo Intell Lab Syst 29:233–241
16. Luypaert J, Heuerding S, Heyden YV, Massart DL (2004) The effect of preprocessing methods in reducing interfering variability from near-infrared measurements of creams. J Pharm Biomed 36:495–503
17. Gorry PA (1990) General least-squares smoothing and differentiation by the convolution (Savitzky–Golay) method. Anal Chem 62:570–573
18. Barnes RJ, Dhanoa MS, Lister SJ (1989) Standard normal variate transformation and de-trending of near-infrared diffuse reflectance spectra. Appl Spectrosc 43:772–777

19. Isaksson T, Naes T (1988) The effect of multiplicative scatter correction (MSC) and linearity improvement in NIR spectroscopy. Appl Spectrosc 42:1273–1284
20. Fearn T, Naes T, Isaksson T, Davies T (2002) A user-friendly guide to multivariate calibration and classification. In: NIR publications, Chichester, UK
21. Hourant P, Baeten V, Morales MT, Meurens M, Aparicio R (2000) Oil and fat classification by selected bands of near-infrared spectroscopy. Appl Spectrosc 54:1168–1174
22. Cen H, He Y (2007) Theory and application of near infrared reflectance spectroscopy in determination of food quality. Trends Food Sci Technol 18:72–83

Lipids (2010) 45:567–580
DOI 10.1007/s11745-010-3437-9

ORIGINAL ARTICLE

Acyl-CoA Binding Protein Gene Ablation Induces Pre-implantation Embryonic Lethality in Mice

Danilo Landrock · Barbara P. Atshaves · Avery L. McIntosh · Kerstin K. Landrock · Friedhelm Schroeder · Ann B. Kier

Received: 1 April 2010 / Accepted: 29 May 2010 / Published online: 18 June 2010

Abstract Unique among the intracellular lipid binding proteins, acyl-CoA binding protein (ACBP) exclusively binds long-chain fatty acyl-CoAs (LCFA-CoAs). To test if ACBP is an essential protein in mammals, the ACBP gene was ablated by homologous recombination in mice. While ACBP heterozygotes appeared phenotypically normal, intercrossing of the heterozygotes did not produce any live homozygous deficient (null) $ACBP^{(-/-)}$ pups. Heterozygous and wild type embryos were detected at all post-implantation stages, but no homozygous ACBP-null embryos were obtained—suggesting that an embryonic lethality occurred at a pre-implantation stage of development, or that embryos never formed. While ACBP-null embryos were not detected at any blastocyst stage, ACBP-null embryos were detected at the morula (8-cell), cleavage (2-cell), and zygote (1-cell) pre-implantation stages. Two other LCFA-CoA binding proteins, sterol carrier protein-2 (SCP-2) and sterol carrier protein-x (SCP-x) were significantly upregulated at these stages. These findings demonstrate for the first time that ACBP is an essential protein required for embryonic development and its loss of function may be initially compensated by concomitant upregulation of two other LCFA-CoA binding proteins, but only at the earliest pre-implantation stages. The fact that ACBP is the first known intracellular lipid binding protein whose deletion results in embryonic lethality suggests its vital importance in mammals.

Keywords ACBP · DBI · Gene targeting · Pre-implantation embryonic lethality

Abbreviations

ACAC	Acetyl CoA carboxylase
ACBP	Acyl-CoA binding protein
CAPN2	m-calpain
CoA	Coenzyme A
DBI	Diazepam binding inhibitor protein
FASN	Fatty acid synthase
L-FABP	Liver fatty acid binding protein
LCFA-CoA	Long-chain fatty acyl-CoA
PCR	Polymerase chain reaction
PPARα	Peroxisome proliferator-activated receptor-α
PPARγ	Peroxisome proliferator-activated receptor-γ
SCP-2	Sterol carrier protein-2
SCP-x	Sterol carrier protein-x
SREBP	Sterol regulatory element binding protein

Introduction

Acyl-CoA binding protein (ACBP), also known as diazepam-binding inhibitor (DBI), is a soluble 10-kDa lipid-binding protein ubiquitously expressed in all tissues of eukaryotic species examined [1, 2]. ACBP expression differs significantly among cell types and is highly regulated by hormones (insulin, androgens). Via the ACBP

Electronic Supplementary Material The online version of this article (doi:10.1007/s11745-010-3437-9) contains supplementary material, which is available to authorized users.

D. Landrock · A. B. Kier (✉)
Department of Pathobiology, Texas A&M University, TAMU 4467, College Station, TX 77843-4467, USA
e-mail: akier@cvm.tamu.edu

B. P. Atshaves · A. L. McIntosh · K. K. Landrock · F. Schroeder
Department of Physiology and Pharmacology, Texas A&M University, TAMU 4466, College Station, TX 77843-4466, USA

promoter, ACBP expression is also determined by several nuclear transcription factors important in lipid and glucose metabolism: peroxisome proliferator-activated receptors (PPARs) -α and -γ as well as sterol regulatory element binding protein (SREBP) [3–7]. Unique among the intracellular lipid protein families, ACBP exhibits very high affinity (<10 nM K_ds) and specificity exclusively for long-chain fatty acyl-CoAs (LCFA-CoAs) [8, 9]. LCFA-CoAs are potent regulators of a wide variety of enzymes, signaling receptors, and nuclear regulatory proteins involved in fatty acid and glucose metabolism [1, 10, 11]. In vivo, pancreatic insulin secretion is affected by LCFA-CoA and ACBP levels as well as by glucose [12–14]. Most important, the key enzymes in de novo fatty acid synthesis (ACAC, acetyl CoA carboxylase; FASN, fatty acid synthase) are inhibited by the LCFA-CoA end product ($K_i < 50$ nM) [10, 15]. By binding LCFA-CoA, ACBP removes this end-product inhibition to stimulate ACAC and FAS [10, 15]. Likewise, by binding and reducing the unbound levels of LCFA-CoAs, ACBP plays important roles not only in normal regulation of LCFA-CoA transport, metabolism, signaling, vesicular trafficking, and nuclear regulation, but also in opposing the deleterious effects of elevated intracellular LCFA-CoA levels associated with diabetes and obesity [10, 13]. The physiological relevance of ACBP is supported mainly by studies of ACBP overexpression in yeast, mice, rats, and plants (*Arabidopsis*) [16–18]. ACBP-overexpressing mice fed control chow exhibit altered hepatic lipid metabolism [9]. ACBP-overexpressing rats fed a medium-chain fatty acid-rich diet have improved glucose tolerance and lower serum insulin levels [18]. Finally, a single nucleotide polymorphism in the human ACBP gene promoter is associated with reduced risk of type 2 diabetes in two German study populations—probably due to increased transcriptional activity of ACBP [19].

While the above findings suggest that loss of ACBP could result in major disruptions of normal phenotype and possible lethality, the available evidence to date is unclear. Depletion of the ACBP protein in the wild-type DTY10A yeast strain results in a slower growing phenotype, which subsequently adapts to a faster growing phenotype (frequency > $1{:}10^5$), while other ACBP-null yeast strains rapidly adapt, such that growth rate is unaffected [20, 21]. A conditional ACBP knock-down in yeast alters lipids, membranes, and vesicle accumulation, but is not lethal [20]. Although disruption of the 10-kDa ACBP gene in the plant *Arabidopsis* is not lethal, *Arabidopsis* expresses at least five additional ACBP genes that also bind LCFA-CoAs—probably compensating for the loss of the 10-kDa ACBP [22, 23]. Multiple independent genes encode different functional paralogues of ACBP even within a single species [2, 24]. In mammals, these include: (1) 10-kDa ACBP [also called liver ACBP (L-ACBP)] and its two distinct homologues (testes, T-ACBP; brain, B-ACBP); (2) ACBP-like domains in several large, multifunctional proteins; and (3) multiple inactive pseudogenes [2, 24]. Several studies with transformed mouse and human cell lines suggest that knock-down of ACBP (ACBP antisense RNA or siRNA) is very deleterious—inhibiting differentiation or resulting in lethality [25, 26]. However, because transformed cells are often deficient in the other LCFA-CoA-binding proteins [1, 11, 27, 28], it is difficult on this basis alone to predict if ACBP is an essential protein in mammals. While recent studies with mice carrying the spontaneous nm1054 mutation suggest that deletion of ACBP is not an embryonic lethality, this conclusion is complicated by the nature of the nm1054 mutation, which arose in CBA/J mice as a result of a large genomic deletion (about 400 kb) that contains all or part of at least six genes, only one of which encodes ACBP [29–31]. On a homozygous C57BL/6J mouse background, the nm1054 mutation results in significant prenatal lethality, and the very few live-born homozygotes almost all die before weaning [31]. However, on a mixed background comprised of at least two different mouse strains, the nm1054 mutation is not embryonically lethal, but instead the mice live to adulthood and exhibit a phenotype characterized by sparse hair, skin lipid metabolic abnormalities, male infertility (uniformly infertile on all genetic backgrounds), failure to thrive, hydrocephaly, and anemia [29–31]. Consequently, the complexity of the nm1054 mutation makes it difficult to assign the individual contribution(s) of ACBP to the phenotype independent of the other five concomitantly deleted genes, and/or downstream effects of deleting the promoter and intronic regions of all six genes.

The purpose of the present investigation was to resolve whether ACBP is an essential protein in a mammalian system by ablating only the ACBP gene function by homologous recombination in mice. The data show that loss of ACBP resulted in early pre-implantation embryonic lethality by the 8-cell stage. The fact that ACBP is the first known intracellular lipid binding protein whose single gene deletion results in embryonic lethality suggests its vital importance in mammals.

Materials and Methods

Materials

Construct Preparation

A BAC clone containing the known expressed ACBP sequence was obtained from the BACPAC Resource Center (Oakland, CA). This clone was fully sequenced to

confirm the presence of the full-length expressed mouse ACBP gene rather than one of many inactive mouse pseudogenes (DNA Technologies Core Laboratory, Texas A&M University). Restriction enzymes were from Invitrogen (Carlsbad, CA) while DNA purification kits (Miniprep, Maxiprep, Agarose Gel Extraction kits, PCR purification kits) were from Qiagen (Valencia, CA). Prime-A-Gene labeling was from Promega (Madison, WI), and oligonucleotides from Integrated DNA Technologies (Coralville, IA)

Embryonic Stem Cells

The 129S6-derived embryonic stem (ES) cell line W4 was from Taconic Inc. (Hudson, NY) while primary mouse embryonic fibroblasts (PMEF) were from Specialty Media (Phillipsburg, NJ). Fetal bovine serum was from Summit Biotechnology (Fort Collins, CO) while cell culture media and components (non-essential amino acids, penicillin, streptomycin, L-glutamine, G418, sodium pyruvate) were from Invitrogen (Carlsbad, CA). Leukemia inhibitory factor (LIF, ESGRO®) was from Chemicon (Temecula, CA).

Embryo Isolations

M2 and M16 media, Pregnant Mare Serum Gonadotropin (PMSG), human chorionic gonadotropin (hCG), mineral oil and hyaluronidase were from Sigma-Aldrich (St. Louis, MO), Potasium Simplex Optimized Medium (KSOM) was from Millipore (Billerica, MA), and ES cell injection needles and blastocyst holding capillaries were from Eppendorf (Hamburg, Germany).

Animals

All animal protocols were approved by the Institutional Animal Care and Use Committee (IACUC) at Texas A&M University. Male and female inbred C57BL/6NCr mice were from the National Cancer Institute (Frederick Cancer Research and Developmental Center, Maryland). ACBP genetically-engineered mice were generated as described in the section below. All mice were maintained in microisolators, with a 12 h light/dark cycle in a temperature-controlled facility (25 °C), access to standard commercial rodent chow (Teklad®, Harlan, Indianapolis, IN, USA) and water ad libitum. Mice were monitored by the presence of sentinels quarterly and found negative for all known mouse pathogens.

Generation of ACBP Gene-Ablated Mice

The ACBP-null targeting construct was designed to replace the N-terminal promoter region (including the known SREBP and PPARγ response elements), exon 1, intron 1, exon 2, and part of intron 2 of the ACBP gene with a neomycin cassette. The following two overlapping genomic DNA fragments from mouse clone RP23-430P22 (BACPAC Resources Center, BPRC, Oakland, CA, USA) were used to form the backbone of the ACBP gene targeting construct: a 7 kbp *Xho*I clone containing the promoter region, exon 1, exon 2, and the surrounding intronic sequences of the ACBP gene, and a 7 kbp *Hin*dIII clone containing exons 1 through 3 and surrounding intronic sequences. ACBP genomic sequences were confirmed by extensive restriction mapping and DNA sequencing (DNA Technologies Core Laboratory, Texas A&M University). The 5′ arm of homology was generated by ligating a 4.2 kbp *Xho*I/*Sma*I fragment from the 7 kbp *Xho*I clone into pBlueScript-SK (pBS-SK; Stratagene, La Jolla, CA, USA). An intermediate targeting construct consisting of the neomycin resistance marker and a 3.9 kbp *Xho*I/*Hin*dIII fragment from the 7 kbp *Hin*dIII clone was generated by ligating the neo cassette from a pPGK-Neo vector to the 3.9 kbp *Xho*I/*Hin*dIII fragment. Ligating the 5′ homology arm with the intermediate targeting construct pre-digested with *Sma*I completed the targeting construct. Once complete, the targeting construct was linearized with *Not*I and electroporated into the W4 ES cell line maintained on a PMEF feeder layer. Disruption of the ACBP gene was generated through homologous recombination. After selection with G418, DNA was isolated from surviving clones, digested with *Hin*dIII, and screened by Southern blotting analysis following standard protocols. Using a 760-bp 3′ probe, targeted clones were identified by Southern blotting with the presence of a 4.5-kbp band while absence of the targeting construct was indicated by a 7-kbp band. Southern blotting used a 3′ probe constructed from sequence immediately after the disrupted locus (between *Bam*/*Sma* and *Hin*dIII). Four positive clones were expanded and injected into C57BL/6NCr blastocysts to create chimeric mice following standard procedures. Four male chimeras from two separate ES cell clones were identified by coat color and bred to C57BL/6NCr females to determine germ-line transmission of the targeted allele. Tail DNA from the chimera/wild-type backcross F1 offspring were initially screened with Southern blotting by standard procedures to verify germline transmission. Subsequent generations of heterozygote/heterozygote and wild-type crosses (for PCR controls) were genotyped by PCR, with the following primer sets: forward primer (ACBP-anchor, 5′-CAA CCT CTG CCA TCA CCT ATT C-3′); reverse primer wild type (ACBP-wt, 5′-TTC TCT GTA TAG CTC TGG CTG G-3′) and reverse primer gene ablation (ACBP-ko, 5′-GGT GGC TAC CCG TGA TAT TG-3′), for 35 cycles with an annealing temperature set at 58 °C. The ACBP-null mice described herein were

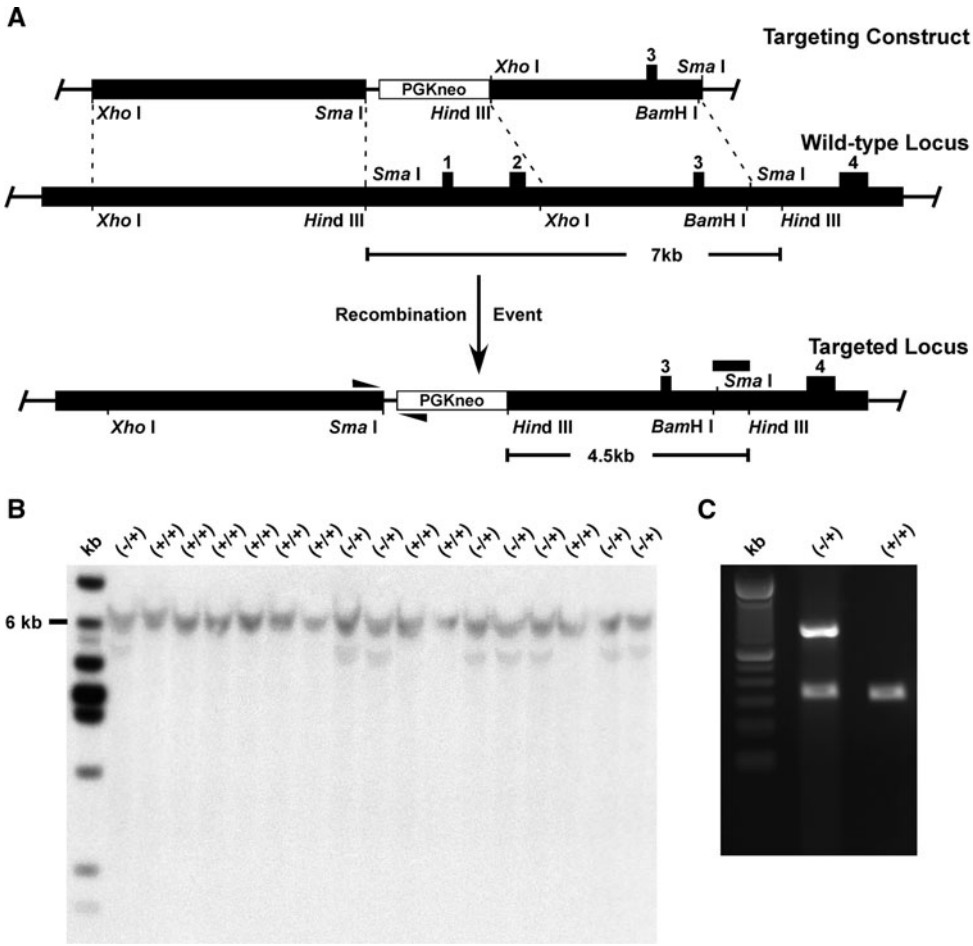

Fig. 1 Construct design and screening of ACBP gene-ablated mice. **a** The targeting construct, wild-type ACBP locus and targeted locus after homologous recombination. Two lower diagrams show the wild-type locus and targeted ACBP locus with expected *Hin*dIII fragment sizes with the indicated probe (*solid bar* after exon 3). **b** Southern blotting analysis of genomic DNA from F1 offspring of chimera/wild-type backcrosses using the 3′ probe just outside of the disrupted ACBP locus. **c** PCR analysis of genomic DNA from offspring of heterozygote/heterozygote intercrosses using 2 primer sets. (−/+) ACBP heterozygotes; (+/+) wild-type counterparts

backcrossed to C57BL/6NCr mice for at least six generations.

Isolation of Pre- and Post-Implantation Stage Embryos

ACBP heterozygous or wild-type (control) females were paired overnight with ACBP heterozygous or wild-type males, respectively and checked for the presence of a copulation plug the next morning. The day of the copulation plug was designated 0.5 post coitum (dpc). Females were humanely euthanized by cervical dislocation immediately prior to embryo isolation. Post-implantation embryos were obtained by dissecting the uterus at 9.5, 11.5, 14.5 and 17.5 dpc. These embryos were freed of any extra-embryonic tissue and then prepared for PCR analysis. Pre-implantation embryos were obtained by flushing the oviducts or uterus, depending upon the time point. One-cell and two-cell (cleavage) oocytes were isolated from the oviducts the same morning of the copulation plug (0.5 dpc) and the following morning (1.5 dpc), respectively. Eight-cell (morula) stage embryos were isolated from the oviduct on the third day (2.5 dpc) and blastocysts were obtained by flushing the uterus on the fourth day (3.5 dpc). Hepes-buffered M2 medium was used to flush and handle all embryos, and KSOM under mineral oil was used for up to 6 days for in vitro culture of all pre-implantation embryos at 37 °C, 5% CO_2. One-cell stage embryos were treated with 1 mg/ml of hyaluronidase and subsequently rinsed 5–10 times in sterile M2 medium to remove cumulus cells. The development and morphology of pre-implantation stages were monitored by visualizing the embryos with an inverted phase contrast microscope (Nikon Diaphoto 300, Nikon, Tokyo, Japan) at 12-h intervals after oocyte collection.

Genotyping of Pre- and Post-Implantation Embryos

Genotyping of individual pre-implantation embryos was performed using the REDExtract-N-Amp Tissue PCR kit (Sigma-Aldrich, St. Louis, MO) according to the manufacturer's protocol. Genomic DNA from post-implantation embryos was obtained by digesting a small section of tail in 500 μl of lysis buffer (10 mM Tris–HCl, 1 mM EDTA, 300 mM Na acetate, 1% SDS, 0.2 mg/ml proteinase K) for 6 h at 55 °C, followed by 20 min at 95 °C to inactivate the proteinase K. The lysate was used directly for PCR

genotyping. The same PCR primer sets to genotype embryos were used as with the live offspring. Initial embryo genotyping was performed on embryos isolated from the F2 intercross heterozygote generation. All embryos genotyped for real-time reverse transcriptase polymerase chain reaction (Q-rtPCR) were from the N6 heterozygote intercross generation or greater.

Quantitative (Real-Time) Reverse Transcriptase PCR

Q-rtPCR was performed on total RNA from 2.5-dpc embryos isolated and purified using RNeasy Micro kit (Qiagen,Valencia, CA, USA) according to manufacturer's protocol. Expression patterns were analyzed with an ABI PRISM 7000 Sequence Detection System (Applied Biosystems, Foster City, CA, USA) using TaqMan® One Step PCR Master Mix Reagent kit, gene specific TaqMan® PCR probes and primers, and the following thermal cycler protocol: 48 °C for 30 min for reverse transcription prior to amplification, 95 °C for 10 min before the first cycle, 95 °C for 15 s, and 60 °C for 1 min, repeated 60 times. For other specific probes and primers, TaqMan® Gene Expression Assay products for mouse peroxisome proliferator-activated receptor-α (Pparα, Mm00440939_m1); sterol carrier protein 2 (Scp-2, Mm01257982_m1); m-calpain (Capn2, Mm00486669_m1), and Custom-TaqMan®-Assay products sterol carrier protein-x (Scp-x, SEQ_SCPX-EX23); acyl-CoA binding protein (Acbp, SEQ_ACBP). Measurements were performed in duplicate and analyzed with ABI PRISM 7000 SDS software to determine the threshold cycle (C_T) from each well. Primer concentrations and cycle number were optimized to ensure that reactions were analyzed in the linear phase of amplification. To analyze the Q-rtPCR data, mRNA expression of Pparα, Scp-2, Scp-x, and Capn2 in homozygous null pre-implantation embryos were normalized to a housekeeping gene (18S rRNA); made relative to the control wild-type pre-implantation embryos, and calculated using the comparative $2^{-\Delta\Delta C_T}$ method [32], where $\Delta\Delta C_T = [C_T$ of target gene $- C_T$ of 18 s$]_{\text{ACBP-nullembryos}} - [C_T$ of target gene $- C_T$ of 18 s$]_{\text{wild typeembryos}}$ as described in User Bulletin 2, ABI PRISM 7000 SDS.

Results

Generation of ACBP Gene-Ablated Mice

The strategy for generation of a mouse ACBP-null targeting construct was dictated by the biological activity of ACBP proteolytic fragments as well as the unique nature of the ACBP gene itself. For example, the N-terminal region of ACBP is the precursor of two major biologically active peptides active in lipid metabolism, signaling, and insulin secretion [14, 33, 34]. In addition, alternative splicing in the mouse ACBP gene results in transcription of two mRNA transcripts encoding proteins of 86 and 135 amino acids, respectively [7]. Although western blotting of mouse liver homogenates with several different polyclonal anti-ACBP antisera detected the 10-kDa ACBP coded by the transcript for 86 amino acids, these antisera did not detect a 15.9-kDa ACBP coded by the alternate transcript for 135 amino acids (not shown). Nevertheless, the mouse ACBP-null targeting construct was designed to replace the N-terminal promoter region (including the known SREBP and PPARγ response elements), exon 1, intron 1, exon 2, and part of intron 2 of the ACBP gene with a neomycin cassette (Fig. 1a). Chimeric ACBP gene ablated mice were developed using this construct as described in Methods. The offspring from chimera/wild-type backcrosses were genotyped by Southern blotting using a 3′ probe constructed from sequence almost completely after the disrupted locus (horizontal solid bar after exon 3 and *Bam*/*Sma*). Southern blotting of *Hind*III-digested DNA revealed wild-type (7 kB) and targeted heterozygous (4.5 kB) DNA (Fig. 1b). A PCR screen from tail clips was then developed (Fig. 1c), using the two primer sets as described in Methods, for genotyping all other offspring.

ACBP Heterozygous Mice Are Phenotypically Normal

Wild-type and heterozygous mice were indistinguishable with respect to visual appearance, post-implantation embryonic weight (Fig. 2a), body weight at weaning (not shown), adult body weight (Fig. 2b), and fertility (not shown). Since only one of the two ACBP alleles was deleted in the heterozygous mice, rtPCR and Western blotting detected only the expected 10-kDa ACBP in livers of both wild-type and heterozygous mice (not shown).

The ACBP-Null Mutation is Embryonically Lethal

The F1 ACBP heterozygotes were intercrossed to produce ACBP-null offspring. Instead of the expected Mendelian 1:2:1 ratio of 25% wild-type, 50% heterozygous, and 25% null ACBP mice, examination of 171 total F2 offspring from 21 litters yielded no homozygous null ACBP pups (Fig. 3). The remaining greater than 2:1 ratio of heterozygous to wild-type mice was consistent with the absence of adverse effects of the mutant allele in the heterozygotes (Fig. 3), and average litter size was within the normal range of a hybrid B6:129 strain (D. Landrock, unpublished data). Pregnant females were carefully monitored until the day of parturition. No evidence for increased neonatal lethality or cannibalization was noted. Taken together, these data indicated a potential embryonic lethality.

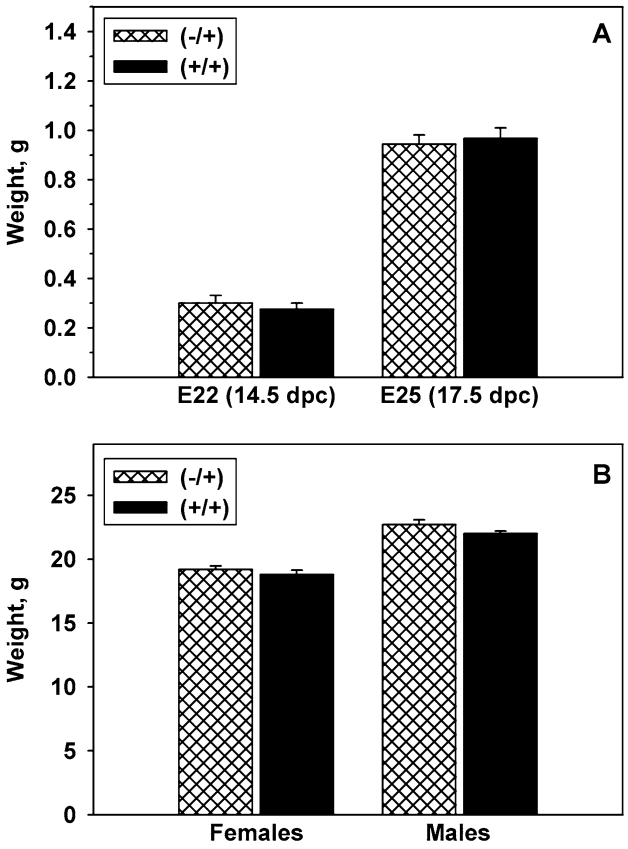

Fig. 2 Body weights of heterozygous (−/+) and wild-type (+/+) post-implantation embryo littermates and adult counterparts. Full body weights of wild-type (**a**, *solid bars*) and ACBP heterozygous (**a**, *cross-hatched bars*) post-implantation embryos are indicated at the E22 (14.5 dpc) and E25 (17.5 dpc) stages. Body weights of adult wild-type (**b**, *solid bars*) and ACBP heterozygous ACBP (**b**, *cross-hatched bars*) male and female counterparts. There were no significant differences in any of the groups

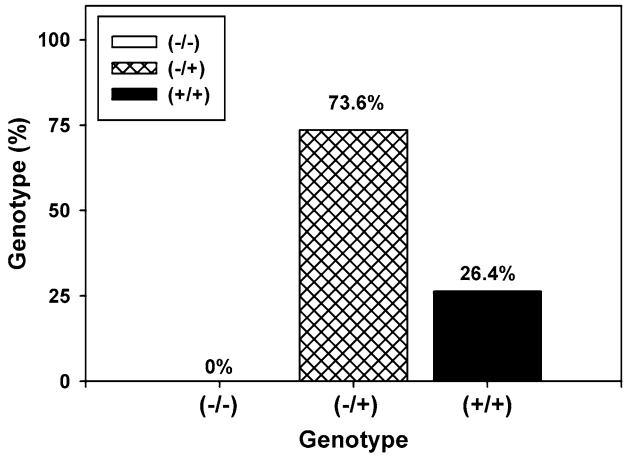

Fig. 3 Genotypes of live F2 offspring from ACBP heterozygote male and female F1 intercrosses. From 21 intercross litters of mice, no homozygous ACBP-null offspring were detected. ACBP heterozygotes constituted 73.6% (126) of offspring (*cross-hatched bar*). Wild-type mice represented 26.4% [45] of offspring (*solid bar*). (−/−) homozygous ACBP-null; (−/+) ACBP heterozygotes; (+/+) wild-type mice from the same litters

Genotypes of Post-implantation Embryos

To determine if ACBP gene ablation resulted from a post-implantation embryonic lethality, the genotypes of post-implantation F2 embryos from F1 ACBP heterozygote/heterozygote intercrosses were determined. Of the 35 post-implantation embryos isolated, no ACBP homozygous null embryos were recovered 9.5 dpc (E15, 9 total, Fig. 4a), 11.5 dpc (E19, 8 total, Fig. 4b), 14.5 dpc (E22, 9 total, Fig. 4c), and 17.5 dpc (E25, 9 total embryos, Fig. 4d). No evident indicators of resorbed embryos were found during dissection. Thus, ACBP-null embryos never formed, or died prior to or very shortly after implantation.

Genotypes of Pre-implantation Embryos

To determine if ACBP-null mice resulted in a pre-implantation embryonic lethality, the genotypes of 310 of 510 pre-implantation F2 embryos from F1 ACBP heterozygote intercrosses were determined at the 2-cell (oocyte), ~8-cell (morula), and ~32-cell (blastocyst) stages. At the oocyte stage, the amount of DNA recovered for PCR was minimal; thus it was not possible to identify the genotype of all oocytes at this stage. Of over 200 oocytes recovered, 36 were clearly identified as to genotype, of which 4 were the homozygous null ACBP genotype (Table 1). As shown by representative light microscopic images, the null ACBP oocytes (Fig. 5a) did not differ in appearance from wild-type oocytes (Fig. 5e). Of 146 morulae recovered, 17 were the ACBP homozygous null genotype (Table 1). Similarly, light microscopy showed that the ACBP-null morulae (Fig. 5b) did not differ significantly in appearance from wild-type (Fig. 5f). In contrast, while 128 blastocysts were recovered and genotyped, none were the ACBP-null genotype (Table 1). Furthermore, light microscopy showed that some blastocysts appeared to be undergoing degeneration (Fig. 5d), while the majority appeared normal (Fig. 5h). Due to DNA degradation, it was not possible to definitively genotype the degenerating blastocysts. These dead/dying blastocysts most probably represented ACBP homozygous null embryos. Thus, ACBP gene ablation resulted in early pre-implantation embryonic lethality beginning by the 2.5-dpc morula (8-cell) stage, and none were viable by the 3.5-dpc blastocyst (~32-cell) stage.

Q-rtPCR of ACBP in Pre-implantation Embryos

To determine if the lethality was associated with total absence of ACBP transcription, 2.5 and 3.0-dpc embryos

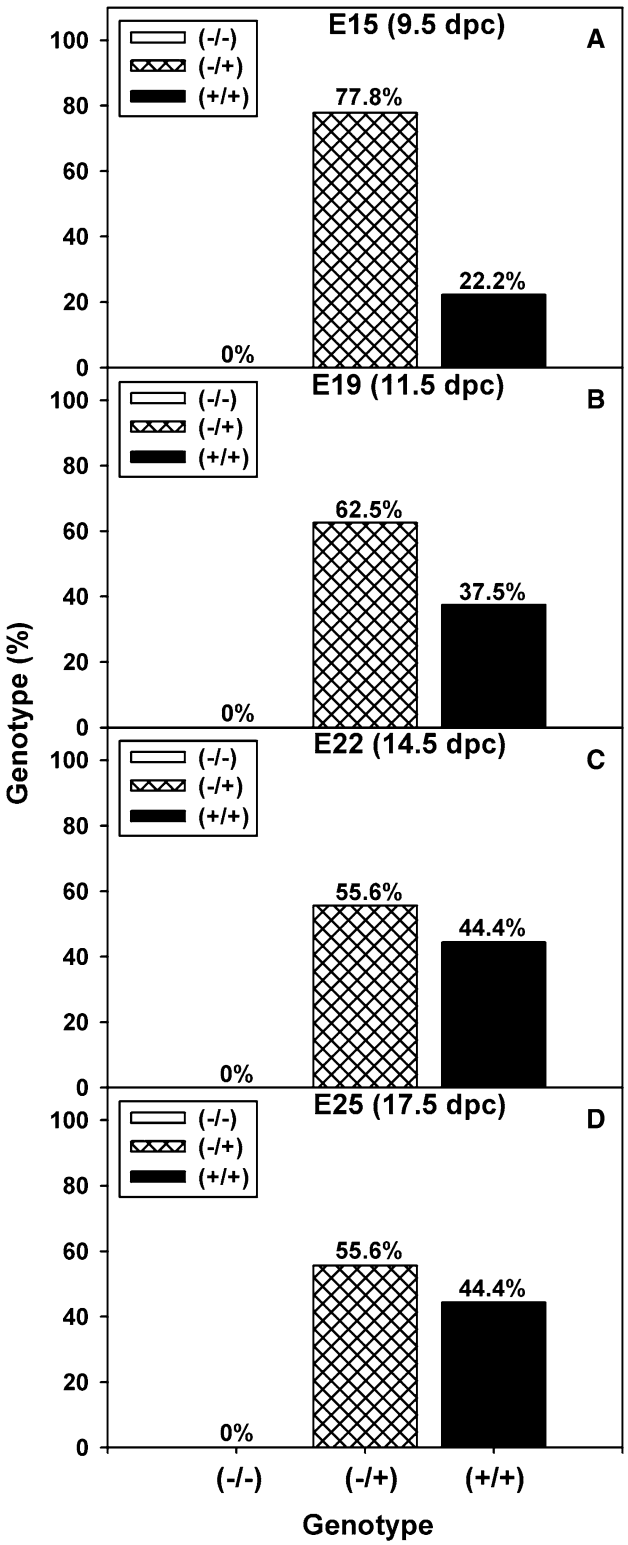

Fig. 4 Genotypes of post-implantation embryos from ACBP heterozygote intercrosses. Embryos were examined at four stages of development: **a** E15 (9.5 dpc, 9 total embryos); **b** E19 (11.5 dpc, 8 total embryos); **c** E22 (14.5 dpc, 9 total embryos); and **d** E25 (17.5 dpc, 9 total embryos). (−/−) homozygous ACBP null (*open bars*); (−/+) ACBP heterozygotes (*cross-hatched bar*); (+/+) wild-type mice from the same litters (*black bar*). Values represent percent of total embryos for each genotype obtained at the indicated developmental stages

Table 1 Genotype distribution among pre-implantation embryos from heterozygote F1 intercrosses

Embryo		Genotype					
Stage	Age (dpc)	(−/−)		(−/+)		(+/+)	
		Total	%	Total	%	Total	%
Blastocyst (∼32-cell)	3.5	0	0	81	63.3	47	36.7
Morula (∼8-cell)	2.5	17	11.6	99	67.8	30	20.6
Oocyte (2-cell)	1.5	4	11.1	22	61.1	10	27.8

Genotyping was performed by PCR (*dpc* days post coitum)

from ACBP heterozygote intercrosses were examined by Q-rtPCR. The ACBP transcript was detected in wild-type and heterozygous embryos at the 2.5-dpc morula (Fig. 6a, b) and 3.0-dpc stage (Fig. 6b) just prior to blastocyst formation. In contrast, no Acbp gene transcript or alternate spliced longer transcript was detected in the morula 2.5-dpc stage of ACBP-null embryos (Fig. 6a, b). The absence of Acbp transcript in the 2.5-dpc null embryos was consistent with correct insertion of the construct into the Acbp gene. Detection of Acbp transcript in 3-dpc ACBP-null embryos was not possible because no ACBP-null embryos were found by this late morula/early blastocyst stage (Fig. 6b, ∞). Thus, the Acbp transcript was absent in the ACBP homozygous null 2.5-dpc stage morula, preceding the embryonic lethality by the blastocyst 3–3.5-dpc stage (Figs. 5d, 6b). Western blotting to determine presence of the ACBP protein in the null morulae was not possible due to the limited amount of material present at this early stage of development.

Concomitant Upregulation Of Other Long-Chain Fatty Acyl-CoA Binding Proteins

Since ACBP gene ablation was not lethal at the morula 2.5-dpc stage, the possibility that loss of ACBP was temporarily compensated for at least in part by upregulation of another cytosolic LCFA-CoA binding protein was examined. Sterol carrier protein-2 (SCP-2) and sterol carrier protein-x (SCP-x) bind LCFA-CoAs with similar affinities as ACBP [8, 35]; their ablation is not lethal [36–38]; and they are expressed as early as the zygote 1-cell stage, slightly earlier than ACBP at the 2-cell stage (Supplemental Fig. S1A). Scp-2 expression in ACBP-null 2.5-dpc morulae was upregulated tenfold (Fig. 6a). Likewise, expression of Scp-x in ACBP-null morulas (2.5 dpc) was upregulated over 50-fold (Fig. 6a). These data suggest that significant upregulation of SCP-2 and SCP-x may indicate an attempt to compensate for the loss of ACBP to maintain viability.

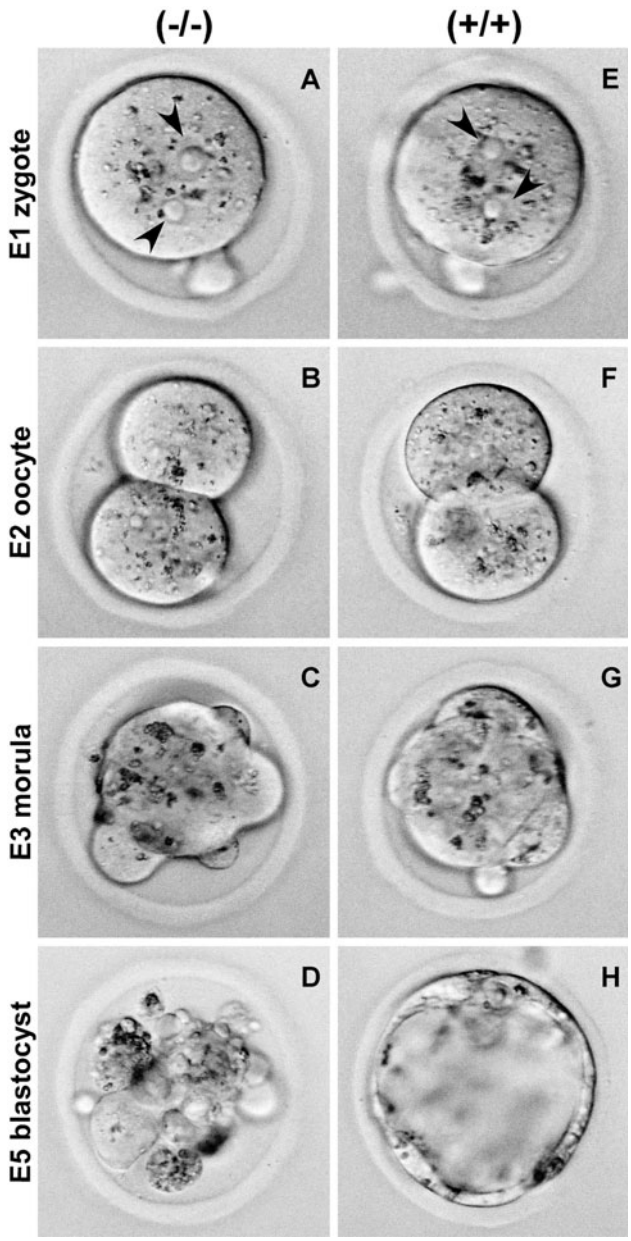

Fig. 5 Pre-implantation development of homozygous ACBP-null and wild-type embryos. E1 (0.5-dpc) oocytes from ACBP heterozygote intercrosses were isolated, cultured in KSOM medium, and photographed every 12 h to monitor their development. At the indicated times, each embryo was genotyped by PCR. **a**–**d** show representative homozygous null ACBP pre-implantation embryos, while **e**–**h** show representative wild-type embryos at the same stages. Pre-implantation embryos at the E1 early oocyte stage (0.5 dpc, **a**, **e**) have *arrows* pointing to the two pronuclei, indicating fertilization; **b**, **f** indicate the E2 oocyte cleavage stage (1.5 dpc); **c**, **g**, the E3 morula stage (2.5 dpc); and **d**, **h** the E5 blastocyst stage (3.5 dpc). Degeneration of several embryos at the blastocyst stage probably represent dead/dying ACBP homozygous null embryos (**d**); DNA isolation was attempted numerous times but was too degenerated for definitive genotyping. (−/−) homozygous ACBP null; (−/+) ACBP heterozygotes; (+/+) wild-type mice

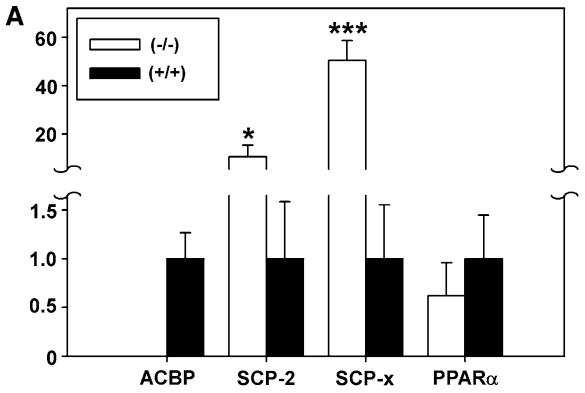

B

Genotypes	ACBP		m-calpain	
	2.5 dpc	3.0 dpc	2.5 dpc	3.0 dpc
(-/-)	-	∞	-	∞
(-/+)	+	+	-	+
(+/+)	+	+	-	+

Fig. 6 Expression of ACBP and other key long-chain fatty acyl-CoA binding proteins in pre-implantation embryos. Embryos were isolated from ACBP heterozygote intercross mice, and levels of ACBP, sterol carrier protein-2 (SCP-2), sterol carrier protein-x (SCP-x), peroxisome proliferator-activated receptor-α (PPARα), and m-calpain were determined by Q-rtPCR as described in "Methods". **a** Acbp, Scp-2, Scp-x, and Pparα expression was determined in homozygous ACBP-null embryos (*open bars*) and wild-type embryos (*solid bars*) at the 2.5-dpc morula stage (E3). Values represent means ± SEM; $*p < 0.05$ between ACBP-null and wild-type embryo; $***p < 0.0001$ between ACBP-null and wild-type embryo. **b** Acbp and m-calpain expression was determined in homozygous null ACBP, heterozygous ACBP, and wild-type ACBP embryos at the morula (E3, 2.5 dpc) and early blastocyst (E4, 3.0 dpc) stages. (∞) indicates no live embryos found. (−/−) homozygous ACBP null; (−/+) ACBP heterozygous; (+/+) wild-type embryos

The possibility that ACBP gene ablation may result in compensatory upregulation of the nuclear peroxisome proliferator-activated receptor-α (PPARα) was also investigated. PPARα exhibits high affinity for LCFA-CoAs [39, 40] and PPARα coactivator recruitment and transcriptional activity are regulated by both LCFA-CoAs and ACBP [39–42]. Furthermore, expression of the PPARα transcript occurred by the zygote (1-cell) stage, thereby preceding the appearance of ACBP, which normally occurs at the oocyte cleavage (2-cell) stage (Supplemental Fig. S1A). However, ACBP gene ablation did not significantly alter the expression of Pparα transcript at the morula (2.5-dpc) stage. Thus, viability of very early pre-implantation ACBP-null embryos was not associated with concomitant upregulation of PPARα.

Since ACBP is a potent activator of m-calpain, a protease involved in apoptosis [43], the possibility that

m-calpain transcript (Capn2) is expressed at an early pre-implantation embryonic stage was investigated. Capn2 was not expressed in the morula (2.5 dpc) embryonic stage of ACBP-null, heterozygote, or wild-type embryos (Fig. 6b). Since Capn2 was not detected until 3.0 dpc and no ACBP-null pre-implantation embryos were detected by that stage, embryonic lethality at >2.5 dpc was not associated with ACBP activation of m-calpain.

Effect on Unbound Free Long-Chain Fatty Acyl-CoA (LCFA-CoA) Concentration

LCFA-CoAs are potent regulators (K_is as low as 50 nM) of many enzymes, transporters, and receptors involved in lipid and glucose metabolism (Supplemental Table S1). Since determination of LCFA-CoA and ACBP protein concentrations would require more material than is present in these early stage embryos to be detectable, the effect of ACBP on the free unbound LCFA-CoA concentration was modeled over the known physiological range of LCFA-CoAs and ACBP concentrations in mammalian tissues (see Supplementary Materials, Methods). At the upper range of physiological ACBP concentration (50 μM), ACBP very effectively buffered the unbound LCFA-CoA concentrations over a relatively broad range (Supplemental Fig. S2A). The unbound LCFA-CoA concentration was <50 nM up to 40 μM total LCFA-CoA (Supplemental Fig. S2B). In contrast, estimated lower physiological ACBP concentration (6 μM) was relatively ineffective in buffering the unbound LCFA-CoA level (Supplemental Fig. S2A), which was >50 nM even at 10 μM total LCFA-CoA (Supplemental Fig. S2B). Taken together, these data suggest that the loss of ACBP would probably result in significantly increased free unbound LCFA-CoA levels within the null embryo cells, which in turn would adversely affect many proteins, enzymes, and receptors involved in both lipid and glucose metabolism.

Discussion

Although long-chain fatty acyl CoAs (LCFA-CoAs) are well known intermediates in fatty acid metabolism, they are also potent metabolic regulators of multiple enzymes/proteins involved in fatty acid and glucose metabolism [1, 10, 13]. While physiologic tissue total LCFA-CoA levels are in the 5–150 μM range [1, 10, 13], even surprisingly low levels (50–500 nM) of free unbound LCFA-CoAs inhibit a broad variety of enzymes, transporters, signaling receptors, and nuclear receptors involved in key cellular processes such as fatty acid and cholesterol synthesis, transcription of genes in lipid metabolism, mitochondrial fatty acid oxidation, and glucose metabolism (Supplemental Table S1). The respective K_is by LCFA-CoA for many of these proteins are as much as 3,000-fold lower than the range of total LCFA-CoA levels in tissues [1, 10, 13]. Since these proteins are known to be active in tissues, the actual unbound free LCFA-CoA levels are much lower (10–20 nM) due to buffering by intracellular LCFA-CoA binding proteins–especially by ACBP (rev. in [1, 10, 13]. The present investigation determining the effect of ACBP gene ablation on the phenotype of mice yielded the following insights.

First, the phenotype of ACBP gene-ablated mice on a C57BL/6NCr background was more severe than that of the more complex nm1054 spontaneous mouse mutation on a C57BL/6J or mixed strain background. Loss of only the ACBP gene function was embryonically lethal at the pre-implantation stage in ACBP-null mice on a C57BL/6NCr background. While spontaneous loss of ACBP together with at least five other genes (an earlier study indicated as many as 200 genes) also resulted in significant prenatal lethality in homozygous nm1054 null mice on a C57BL/6J background, almost all of the few live-born pups die before weaning and few have been weaned successfully [30, 31]. In contrast, loss of ACBP (along with 5 other genes) elicited a somewhat milder phenotype (sparse hair, skin lipid metabolic abnormalities, male infertility, failure to thrive, hydrocephaly, anemia) in homozygous nm1054 mice on a mixed (two different strains) mouse background [29–31]. It is yet to be determined why the nm1054 mutation resulting in loss of ACBP as well as five other genes is less 'lethal' than deletion of the ACBP gene alone. While it cannot be ruled out that loss of the promoter sequences in our construct may have also affected the expression of other genes and thereby contributed to pre-implantation embryonic lethality, it is unclear why the loss of even more promoter sequences due to deletion of six genes in the nm1054 mutation resulted in a less severe phenotype. One possibility is that the loss of one or more of the five additional genes (i.e. loss of exons as well as intronic sequences, and N-terminal promoter sequences) may have contributed in an as yet not understood manner to compensate for the loss of the ACBP. The different mouse strain backgrounds of the ACBP-null mice (C57BL/6NCr) and nm1054 mice (C57BL/6J or mixed CBA, 129) may also have played a role, since phenotype versus strain differences have also been noted in ACBP gene deletions in different yeast strains [20, 21] as well as deletions of other gene-ablated mouse models [44, 45]. The importance of genetic background is emphasized by a recent report comparing two yeast strains (Σ1278b and S288c) wherein about 5,100 genes were systematically deleted [46]. While 894 genes were essential in both strains, 44 genes were essential only in Σ1278b and 13 genes were essential only

in S288c. Examination of hybrid strain crosses of 18 mutants that were lethal in Σ1278b, but not in S288c, yielded viable progeny in all cases and their conditional phenotype was associated with numerous modifier genes that differ between the strains [46]. On the basis of this and previous work, it was concluded that "conditional essentiality is almost always a consequence of complex genetic interactions involving multiple modifiers associated with strain specific genetic variation rather than classical digenic synthetic lethality" [46]. As has been seen in many other cases, genetic background can profoundly affect the phenotypes manifest upon gene ablation. While such 'discrepancies' often cause controversy, they also identify potentially important areas of future research.

Second, deletion of the 10-kDa ACBP encoding gene in the mouse is the first known embryonically lethal mutation in any of the intracellular LCFA-CoA binding protein families. At least three families of soluble lipid binding proteins appear to buffer cytoplasmic LCFA-CoA levels by binding LCFA-CoAs with high affinity, in the order: acyl-CoA binding protein (ACBP) [1, 10, 13] >sterol carrier proteins (SCP-2, SCP-x) [47] >select fatty acid binding proteins [FABP1 (L-FABP) >>FABP7, FABP2, FABP3 (B-FABP, I-FABP, H-FABP)] [48–50]. Of these LCFA-CoA binding proteins, only ACBP, SCP-2/SCP-x, and FABP3 are expressed in pre-implantation embryos (Supplementary Figure S1). However, FABP3 (H-FABP) binds LCFA-CoA even more weakly than FABP1 (L-FABP)—a protein not expressed in pre-implantation embryos (Supplementary Figure S1) [48, 49]. Thus, redundancy in LCFA-CoA binding proteins is much more limited in pre-implantation embryos than in more mature tissues. These data would suggest that loss of one of the lower affinity LCFA-CoA binding proteins would not probably be lethal, and to date lethality has not been observed upon gene ablation of several members of the large FABP protein family, including: Fabp1 (liver L-FABP), Fabp2 (intestinal I-FABP), Fabp3 (heart H-FABP), Fabp4 (adipocyte A-FABP), Fabp5 (keratinocyte K-FABP), and Fapb7 (brain B-FABP) [44, 51, 52]. Likewise, ablation of SCP-2 and SCP-x is not lethal [37, 38, 53]. Even loss of both L-FABP and SCP-2/SCPx (intercross of L-FABP null mice and SCP-2/SCP-x null mice) does not result in lethality [54]. Thus, embryonic lethality in mice ablating the gene encoding the 10-kDa ACBP is unique among the multiple LCFA-CoA binding proteins known to exist in the cytoplasm of mammalian tissues.

Third, the ACBP gene ablation-induced embryonic lethality at very early pre-implantation stages where the embryo is not well differentiated was consistent with studies showing that ACBP-specific siRNA treatment of highly undifferentiated mouse and human tumor cells is lethal [26]. The observed lethality of ACBP-specific siRNA treatment was probably due to loss of LCFA-CoA buffering capacity concomitant with loss of ACBP in the context of the already markedly reduced levels of other LCFA-CoA binding proteins (e.g. FABPs, SCP-2/SCPx) in transformed cells (rev. in [1, 11, 27, 28]. The fact that some apparently normal ACBP-null embryos, albeit reduced in expected numbers, were still alive at the 1–8 cell pre-implantation stages, but not at later embryonic stages, was most probably due to the presence of residual maternal ACBP protein. Consistent with the fact that almost all maternal mRNA is degraded by the end of the 2-cell stage [55, 56], the ACBP mRNA was not longer detected in the 8-cell stage pre-implantation embryos. However, since the ACBP protein has a relatively long half life (i.e. $t_{1/2}$ of 25–53 h) [55–57], some maternal ACBP protein was probably present in the 4-cell, but not in the 8-cell pre-implantation stage. Concomitant upregulation of two less prevalent LCFA-CoA binding proteins (SCP-2 and SCP-x, primarily in peroxisomes) shown herein may have also facilitated survival at the morula (8 cell) stage, but was insufficient to assure survival by the blastocyst (~32 cell, 3.5-dpc) stage.

Fourth, the early pre-implantation embryonic lethality in ACBP-null mice was consistent with the importance of ACBP in preventing deleterious effects of LCFA-CoAs on sensitive enzymes involved in energy production and fatty acid biosynthesis. While fatty acids (primarily derived from endogenous triglycerides) are the major energy source in unfertilized oocytes, thereafter very little energy is derived from fatty acids and intracellular triglyceride is maintained relatively constant [58]. Since there is too little glycogen to sustain the pre-implantation embryo, especially that of the mouse, the pre-implantation embryo is heavily dependent on an exogenous energy supply for synthesizing fatty acids [58]. Pyruvate and lactic acid in oviductal fluid represent the major carbon sources of mouse pre-implantation embryos up to the 4-cell stage, while glucose serves this purpose thereafter [58–60]. Acetyl CoA derived from these nutrients is oxidized to produce energy or is used as a substrate for fatty acid synthesis required for formation of membranes and longer-term energy storage than can be accomplished by energy storage as glycogen. The two key enzymes in fatty acid synthesis [acetyl CoA carboxylase (ACAC, rate limiting); fatty acid synthase (FASN)] are both end-product inhibited by fatty acyl-CoA [10, 15]. Acetyl CoA carboxylase is especially sensitive (K_i 50 nM) to the presence of even very low levels of LCFA-CoA [10]. By binding LCFA-CoAs, ACBP very effectively removes the LCFA-CoA end-product inhibition of ACC and FASN [10, 15]. The importance of these fatty acid synthetic enzymes in early embryogenesis is underscored by the fact that ablation of ACC or FASN results in an early embryonic and

pre-implantation embryonic lethality [61, 62]. As shown herein, loss of ACBP (the major high-affinity LCFA-CoA binding protein) is expected to eliminate most of the LCFA-CoA buffering capacity. The other major LCFA-CoA binding protein (FABP1, i.e. L-FABP) is not induced until much later in development. While two other LCFA-CoA binding proteins (SCP-2, SCP-x) are present and concomitantly upregulated in ACBP-null pre-implantation embryos, these proteins are largely compartmentalized in peroxisomes and are present at much lower level (rev. in [47]. Since ACBP is thought to be the most effective of the LCFA-CoA binding proteins in buffering the unbound free LCFA-CoA concentration [1, 10, 63], complete loss of ACBP would thus be expected to greatly increase unbound free LCFA-CoAs over that normally present in cells and tissues—thereby inhibiting ACC and FASN enzymes essential for de novo fatty acid synthesis.

Fifth, ACBP exhibits a unique role in early pre-implantation embryonic development as compared to the other intracellular LCFA-CoA binding proteins. Several other cytoplasmic LCFA-CoA binding proteins (FABPs 5, 4, and 3; SCP-2, SCP-x) are expressed already by the zygote 1-cell to morula 8-cell stages (Supplemental Fig. S1), but gene ablation of many of these proteins is not lethal [37, 38, 44, 51–53]. ACBP is also known to enter the nucleus, bind nuclear receptors (PPARα, PPARγ) involved in lipid and glucose metabolism, and regulate transcriptional activity of these receptors [11, 64–66]. PPARα itself exhibits high affinity for and is regulated by LCFA-CoAs transported by ACBP [11, 39, 40]. While PPARs α and γ are both present at the zygote one-cell stage (Supplemental Fig. S1), ablation of PPARα is not lethal, and ablation of PPARγ is lethal but not until much later, i.e. the post-implantation E10 stage [67, 68]. Thus, it is unlikely that dysregulation of PPARs in response to ACBP deletion accounts for the observed very early pre-implantation lethality.

Finally, the 10-kDa ACBP does not appear to be an essential protein in other eukaryotes, since its deletion results in the appearance of revertants (yeast) and probably compensated by distinct other ACBP genes in the nematode (*C. elegans*), insect (*D. melanogaster*), and plants (*Arabidopsis*) [20, 22, 23, 69–71]. It is also important to note that in mammals the gene encoding the 10-kDa ACBP also expresses two additional transcripts (due to alternate transcription initiation) encoding distinct ACBP homologues (testes T-ACBP; brain B-ACBP) [2, 24]. In silico analyses of several databases (NCBI UniGene, http://www.ncbi.nlm.nih.gov/unigene; European Bioinformatics Institute, http://www.ebi.ac.uk) indicates the presence of expressed sequence tags (ESTs) for all three mRNAs derived from the human ACBP gene (only two have active promoters), for only the mRNA encoding the rat 10-kDa ACBP, and for two mRNAs encoding the mouse 10-kDa ACBP (87 amino acid) and a mouse 15.9 kDa (135 amino acid) ACBP-related protein [7]. While two additional mouse ESTs [one from brain (BE652768) and one from testis (AA4927130)] have been reported [7], a search of several databases attributed both of these ESTs to the known gene encoding the 10-kDa ACBP protein (Mouse Genome Informatics Database, Jackson Labs, Bar Harbor, ME; NCBI UniGene database, October 2009, http://www.ncbi.nlm.nih.gov/unigene). Mammals (mouse, rat, human) also process multiple inactive pseudogenes [NCBI UniGene database, October 2009, http://www.ncbi.nlm.nih.gov/unigene); [2, 24]]. While the physiological relevance of potentially two mRNA transcripts of the mouse ACBP gene in early pre-implantation embryonic development is not clear, the mRNA encoding ACBP was present in all wild-type mouse embryos examined but not in homozygous ACBP-null 8-cell stage pre-implantation embryos or thereafter.

In summary, the studies presented herein addressed for the first time the role of ACBP single gene ablation on development in mice. ACBP gene ablation resulted in pre-implantation embryonic lethality between the morula (8 cell) and blastocyst (32 cell) stages. In contrast to ACBP-null mouse, gene ablation of several other cytosolic LCFA-CoA binding proteins also expressed at these early pre-implantation embryonic stages is not lethal. Thus, ACBP represents the first discovered LCFA-CoA binding protein whose ablation results in lethality. While the exact role of ACBP in normal pre-implantation embryonic development remains to be identified, at least two general possibilities may be considered: (1) Since the high affinity of ACBP for LCFA-CoAs results in highly effective buffering of total LCFA-CoAs to maintain unbound free LCFA-CoAs at low levels, loss of ACBP probably results in a significant increase of unbound free LCFA-CoA levels. The elevated unbound free LCFA-CoA levels would consequently inhibit highly LCFA-CoA sensitive enzymes (e.g. acetyl CoA carboxylase, fatty acid synthase) required for normal glucose metabolism and fatty acid synthesis in these rapidly growing pre-implantation embryos; and (2) Since ACBP normally interacts with and regulates several nuclear receptors (e.g. PPARs) present in early pre-implantation embryos, loss of such interactions may result in abnormal transcriptional regulation of genes involved not only in lipid and glucose metabolism but also development. Both factors could contribute to the lethality observed in these early pre-implantation ACBP-null embryos. Future studies using an inducible construct or a conditional knockout approach (e.g. as applied to acetyl-CoA carboxylase and fatty acid synthase [72, 73]) should allow further discrimination of the physiological functions of ACBP.

Acknowledgments This work was supported in part by the USPHS, National Institutes of Health grants, DK41402 (FS and ABK), GM31651 (FS and ABK), and DK70965 (BPA). The helpful professional assistance of Dr. Danna Zimmer and technical assistance of Amy L. Boedeker is very much appreciated.

References

1. Gossett RE, Frolov AA, Roths JB, Behnke WD, Kier AB, Schroeder F (1996) Acyl-CoA binding proteins: multiplicity and function. Lipids 31:895–918
2. Faergeman NJ, Wadum MCT, Feddersen S, Burton BB, Knudsen J (2007) Acyl-CoA binding proteins: structural and functional conservation over 2000 MYA. Mol Cell Biochem 299:55–65
3. Mandrup S, Hummel R, Ravn S, Jensen G, Andreasen PH, Gregersen N, Knudsen J, Kristiansen K (1992) Acyl-CoA binding protein/diazepam-binding inhibitor gene and pseudogenes. A typical housekeeping gene family. J Mol Biol 228:1011–1022
4. Helledie T, Grontved L, Jensen SS, Kiilerich P, Rietveld L, Albrektsen T, Boysen MS, Nohr J, Larsen LK, Fleckner J, Stunnenberg HG, Kristiansen K, Mandrup S (2002) The gene encoding the acyl-CoA binding protein is activated by peroxisome proliferator-activated receptor gamma through an intronic response element functionally conserved between humans and rodents. J Biol Chem 277:26821–26830
5. Neess D, Kiilerich P, Sandberg MB, Helledie T, Nielsen R, Mandrup S (2006) ACBP-, a PPAR and SREBP modulated housekeeping gene. Mol Cell Biochem 284:149–157
6. Sandberg MB, Bloksgaard M, Duran-Sandoval D, Duval C, Staels B, Mandrup S (2005) The gene encoding for ACBP is subject to metabolic regulation by both SREBP and PPAR-alpha in hepatocytes. J Biol Chem 280:5258–5266
7. Nitz I, Doring F, Schrezenmeir J, Burwinkel B (2005) Identification of new acyl-CoA binding protein transcripts in human and mouse. Int J Biochem Cell Biol 37:2395–2405
8. Frolov AA, Schroeder F (1998) Acyl-coenzyme A binding protein: conformational sensitivity to long-chain fatty acyl-CoA. J Biol Chem 273:11049–11055
9. Huang H, Atshaves BP, Frolov A, Kier AB, Schroeder F (2005) Acyl-coenzyme A binding protein expression alters liver fatty acyl-coenzyme A metabolism. Biochemistry 44:10282–10297
10. Faergeman NJ, Knudsen J (1997) Role of long-chain fatty acyl-CoA esters in the regulation of metabolism and in cell signalling. Biochem J 323:1–12
11. Schroeder F, Petrescu AD, Huang H, Atshaves BP, McIntosh AL, Martin GG, Hostetler HA, Vespa A, Landrock K, Landrock D, Payne HR, Kier AB (2008) Role of fatty acid binding proteins and long-chain fatty acids in modulating nuclear receptors and gene transcription. Lipids 43:1–17
12. Gribble FM, Proks P, Corkey BE, Ashcroft FM (1998) Mechanism of cloned ATP-sensitive potassium channel activation by oleoyl CoA. J Biol Chem 273:26383–26387
13. Corkey BE, Deeney JT, Yaney GC, Tornheim K (2000) The role of long-chain fatty acyl-CoA esters in beta-cell signal transduction. J Nutr 130:299S–304S
14. Ostenson C-G, Ahren B, Karlsson S, Knudsen J, Efendic S (1994) Inhibition by rat diazepam-binding inhibitor/acyl-CoA binding protein of glucose-induced insulin secretion in the rat. Eur J Endocrinol 131:201–204
15. Rasmussen JT, Rosendal J, Knudsen J (1993) Interaction of acyl-CoA binding protein (ACBP) on processes for which acyl-CoA is a substrate, product or inhibitor. Biochem J 292:907–913
16. Knudsen J, Faergeman NJ, Skott H, Hummel R, Borsting C, Rose TM, Andersen JS, Hojrup P, Roepstorff P, Kristiansen K (1994) Yeast acyl-CoA binding protein: acyl-CoA binding affinity and effect on intracellular acyl-CoA pool size. Biochem J 302: 479–485
17. Mandrup S, Jepsen R, Skott H, Rosendal J, Hojrup P, Kristiansen K, Knudsen J (1993) Effect of heterologous expression of acyl-CoA binding protein on acyl-CoA level and composition in yeast. Biochem J 290:369–374
18. Oikari S, Ahtialansaari T, Huotari A, Kiehne K, Folsch UR, Wolffram S, Janne J, Alhonen L, Herzig K-H (2008) Effect of medium and long-chain fatty acid diets on PPAR and SREBP-1 expression and glucose homeostasis in ACBP overexpressing transgenic rats. Acta Physiol 194:57–65
19. Fisher E, Nitz I, Gieger C, Grallert H, Gohlke H, Lindner I, Dahm S, Boeing H, Burwinkel B, Rathmann W, Wichmann H-E, Schrezenmeier J, Illig T, Doring F (2007) Association of acyl-CoA binding protein (ACBP) single nucleotide polymorphisms and type 2 diabetes in two German study populations. Mol Nutr Food Res 51:178–184
20. Gaigg B, Neergard TB, Schneiter R, Hansen JK, Faergeman NJ, Jensen NA, Andersen JR, Friis J, Sandhoff K, Knudsen J (2001) Depletion of acyl-CoA binding protein affects sphingolipid synthesis and causes vesicle accumulation and membrane defects in *S. cerevisiae*. Mol Biol Cell 12:1147–1160
21. Schjerling CK, Hummel R, Hansen JK, Borsting C, Mikkelsen J, Kristiansen K, Knudsen J (1996) Disruption of the gene encoding the acyl-CoA binding protein (ACB1) perturbs acyl-CoA metabolism in *Saccharomyces cerevisiae*. J Biol Chem 271: 22514–22521
22. Chen Q-F, Xiao S, Chye M-L (2008) Overexpression of the Arabidopsis 10-kiloDalton acyl-CoA binding protein ACBP6 enhances freezing tolerance. Plant Physiol 148:304–315
23. Leung K-C, Li H-Y, Xiao S, Tse M-H, Chye M-L (2006) Arabidopsis ACBP3 is an extracellularly targeted acyl-CoA binding protein. Planta 223:871–881
24. Burton M, Rose TM, Faergeman NJ, Knudsen J (2005) Evolution of the acyl-CoA binding protein (ACBP). Biochem J 392:299–307
25. Mandrup S, Sorensen RV, Helledie T, Nohr J, Baldursson T, Gram C, Knudsen J, Kristiansen K (1998) Inhibition of 3T3-L1 adipocyte differentiation by expression of acyl-CoA binding protein antisense RNA. J Biol Chem 273:23897–23903
26. Faergeman NJ, Knudsen J (2002) Acyl-CoA binding protein is an essential protein in mammalian cell lines. Biochem J 368:679–682
27. Chapkin RS, Clark AE, Davidson LA, Schroeder F, Zoran DL, Lupton JR (1998) Dietary fiber differentially alters cellular fatty acid binding protein expression in exfoliated colonocytes during tumor development. Nutr Cancer 32:107–122
28. Petrescu AD, Payne HR, Boedeker AL, Chao H, Hertz R, Bar-Tana J, Schroeder F, Kier AB (2003) Physical and functional interaction of acyl-CoA binding protein (ACBP) with hepatocyte nuclear factor-4alpha (HNF4alpha). J Biol Chem 278:51813–51824
29. Lee L, DeBono CA, Campagna DR, Young DC, Moody DB, Fleming MD (2007) Loss of acyl-CoA binding protein (ACBP) results in fatty acid metabolism abnormalities in mouse hair and skin. J Invest Dermatol 127:16–23
30. Ohgami RS, Campagna DR, Greer EL, Antiochos B, McDonald A, Chen J, Sharp JJ, Fujiwara Y, Barker JE, Fleming MD (2005) Identification of a ferrireductase required for efficient transferrin-dependent iron uptake in erythroid cells. Nat Genet 37:1264–1269
31. Ohgami RS, Campagna DR, Antiochos B, Wood EB, Sharp JJ, Barker JE, Fleming MD (2005) nm1054: a spontaneous, recessive, hypochromic, microcytic anemia mutation in the mouse. Blood 106:3625–3631

32. Livak KJ, Schmittgen TD (2001) Analysis of relative gene expression data using real-time quantitative PCR and the $2^{-\Delta\Delta CT}$ method. Methods 25:402–408
33. Chen Z-W, Bergman T, Jornvall H, Bonetto V, Norberg A, Mutt V, Longone P, Costa E, Efendic S, Ostenson C-G (1997) Full-length and N-terminally truncated diazepam-binding inhibitor: purification, structural characterization, and influence on insulin release. Regul Pept 69:63–68
34. Borboni P, Magnaterra R, Porzio O, Fusco A, Sesti G, Bertoli A, Lauro R, Marlier LNJL (1995) DBI mRNA is expressed in endocrine pancreas and its post-translational product DBI33–50 inhibits insulin release. Endocr J UK 3:267–271
35. Frolov A, Cho TH, Billheimer JT, Schroeder F (1996) Sterol carrier protein-2, a new fatty acyl-coenzyme A-binding protein. J Biol Chem 271:31878–31884
36. Seedorf U, Raabe M, Ellinghaus P, Kannenberg F, Fobker M, Engel T, Denis S, Wouters F, Wirtz KWA, Wanders RJA, Maeda N, Assmann G (1998) Defective peroxisomal catabolism of branched fatty acyl-coenzyme A in mice lacking the sterol carrier protein-2/sterol carrier protein-x gene function. Genes Dev 12:1189–1201
37. Atshaves BP, McIntosh AL, Payne HR, Gallegos AM, Landrock K, Maeda N, Kier AB, Schroeder F (2007) Sterol carrier protein-2/sterol carrier protein-x gene ablation alters lipid raft domains in primary cultured mouse hepatocytes. J Lipid Res 48:2193–2211
38. Atshaves BP, McIntosh AL, Landrock D, Payne HR, Mackie J, Maeda N, Ball JM, Schroeder F, Kier AB (2007) Effect of SCP-x gene ablation on branched-chain fatty acid metabolism. Am J Physiol 292:939–951
39. Hostetler HA, Petrescu AD, Kier AB, Schroeder F (2005) Peroxisome proliferator-activated receptor alpha (PPARalpha) interacts with high affinity and is conformationally responsive to endogenous ligands. J Biol Chem 280:18667–18682
40. Hostetler HA, Kier AB, Schroeder F (2006) Very-long-chain and branched-chain fatty acyl-CoAs are high affinity ligands for the peroxisome proliferator-activated receptor alpha (PPARalpha). Biochemistry 45:7669–7681
41. Elholm M, Dam I, Jorgenesen C, Krogsdam A-M, Holst D, Kratchamarova I, Gottlicher M, Gustafsson JA, Berge RK, Flatmark T, Knudsen J, Mandrup S, Kristiansen K (2001) Acyl-CoA esters antagonize the effects of ligands on peroxisome proliferator-activated receptor α conformation, DNA binding, and interaction with cofactors. J Biol Chem 276:21410–21416
42. Helledie T, Antonius M, Sorensen RV, Hertzel AV, Bernlohr DA, Kolvraa S, Kristiansen K, Mandrup S (2000) Lipid binding proteins modulate ligand-dependent trans-activation by peroxisome proliferator-activated receptors and localize to the nucleus as well as the cytoplasm. J Lipid Res 41:1740–1751
43. Melloni E, Averna M, Salamino F, Sparatore B, Minafra R (2000) Acyl-CoA binding protein is a potent m-calpain activator. J Biol Chem 275:82–86
44. Atshaves BP, Martin GG, Hostetler HA, McIntosh AL, Kier AB, Schroeder F (2010) Liver fatty acid binding protein (L-FABP) and Dietary Obesity. J Nutr Biochem. doi:10.1016/j.nutbio.2010.01.005
45. Akiyama TE, Nicol CJ, Fievet C, Staels B, Ward JM, Auwerx J, Lee SST, Gonzalez FJ, Peters JM (2001) Peroxisome proliferator-activated receptor-α regulates lipid homeostasis, but is not associated with obesity. J Biol Chem 276:39088–39093
46. Dowell RD, Ryan O, Jansen A, Cheung D, Agarwala S, Danford T, Bernstein DA, Rolfe PA, Heisler LE, Chin B, Nislow C, Giaever G, Phillips PC, Fink GR, Gifford DK, Boone C (2010) Genotype to phenotype: a complex problem. Science 328:469
47. Gallegos AM, Atshaves BP, Storey SM, Starodub O, Petrescu AD, Huang H, McIntosh A, Martin G, Chao H, Kier AB, Schroeder F (2001) Gene structure, intracellular localization, and functional roles of sterol carrier protein-2. Prog Lipid Res 40:498–563
48. Frolov A, Cho TH, Murphy EJ, Schroeder F (1997) Isoforms of rat liver fatty acid binding protein differ in structure and affinity for fatty acids and fatty acyl-CoAs. Biochemistry 36:6545–6555
49. Myers-Payne SC, Hubbell T, Pu L, Schnutgen F, Borchers T, Wood WG, Spener F, Schroeder F (1996) Isolation and characterization of two fatty acid binding proteins from mouse brain. J Neurochem 66:1648–1656
50. McArthur MJ, Atshaves BP, Frolov A, Foxworth WD, Kier AB, Schroeder F (1999) Cellular uptake and intracellular trafficking of long-chain fatty acids. J Lipid Res 40:1371–1383
51. Haunerland NH, Spener F (2004) Fatty acid binding proteins–insights from genetic manipulations. Prog Lipid Res 43:328–349
52. Storch J, Corsico B (2008) The emerging functions and mechanisms of mammalian fatty acid binding proteins. Annu Rev Nutr 28:18.1–18.23
53. Raabe M, Seedorf U, Hameister H, Ellinghaus P, Assmann G (1996) Structure and chromosomal assignment of the murine sterol carrier protein-2 gene (SCP-2) and two related pseudogenes by in situ hybridization. Cytogenet Cell Genet 73:279–281
54. Storey SM, Atshaves BP, McIntosh AL, Landrock KK, Martin GG, Huang H, Johnson JD, MacFarlane RD, Kier AB, Schroeder F (2010) Effect of sterol carrier protein-2 gene ablation on HDL-mediated cholesterol efflux from primary cultured mouse hepatocytes. Am J Physiol (in press)
55. Giebelhaus DH, Heikkila JJ, Schultz GA (1983) Changes in the quantity of histone and actin messenger RNA during the development of preimplantation mouse embryos. Dev Biol 98:148–154
56. Clegg KB, Piko L (1983) Poly(A) length, cytoplasmic adenylation and synthesis of Poly(A)+ RNA in early mouse embryos. Dev Biol 95:331–341
57. Buus CL, Kristiansen K, Knudsen J (1994) Turnover of acyl-CoA binding protein in four different cell lines measured by using two-dimensional polyacrylamide-gel electrophoresis. Biochem J 297:555–560
58. Ferguson E, Leese HJ (2006) A potential role for triglyceride as an energy source during bovine oocyte maturation and early embryonic development. Mol Reprod Dev 73:1195–1201
59. Kane MT, Carney EW, Ellington JE (1992) The role of nutrients, peptide growth factors, and co-culture cells in development of preimplantation embryos in vitro. Theriogenology 38:297–313
60. Kane MT, Foote RH (1971) Factors affecting blastocyst expansion of rabbit zygotes and young embryos in defined media. Biol Reprod 4:41–47
61. Abu-Elheiga L, Matzuk MM, Kordari P, Oh WK, Shaikenov T, Gu Z, Wakil SJ (2005) Mutant mice lacking acetyl-CoA carboxylase 1 are embryonically lethal. Proc Natl Acad Sci USA 102:12011–12016
62. Chirala SS, Chang H, Matzuk M, Abu-Elheiga L, Mao J, Mahon K, Finegold M, Wakil SJ (2010) Fatty acid synthesis is essential in embryonic development: fatty acid synthase null mutants and most of the heterozygotes die in utero. Proc Natl Acad Sci USA 100:6358–6363
63. Knudsen J, Jensen MV, Hansen JK, Faergeman NJ, Neergard T, Gaigg B (1999) Role of acyl-CoA binding protein in acyl-CoA transport, metabolism, and cell signaling. Mol Cell Biochem 192:95–103
64. Helledie T, Grontved L, Jensen SS, Kiilerich P, Rietveld L, Albrektsen T, Boysen MS, Nohr J, Larsen LK, Fleckner J, Stunnenberg HG, Kristiansen K, Mandrup S (2002) The gene encoding the acyl-CoA binding protein is activated by peroxisome proliferator-activated receptor gamma through an intronic response element functionally conserved between humans and rodents. J Biol Chem 277:26821–26830
65. Elholm M, Garras A, Neve S, Tarnehave D, Lund TB, Skorve J, Flatmark T, Kristiansen K, Berge RK (2000) Long-chain

acyl-CoA esters and acyl-CoA binding protein are present in the nucleus of rat liver cells. J Lipid Res 41:538–545
66. Helledie T, Jorgenesen C, Antonius M, Krogsdam A-M, Kratchmarova I, Kristiansen K, Mandrup S (2002) Role of adipocyte lipid binding protein (ALBP) and acyl-CoA binding protein (ACBP) in PPAR-mediated transactivation. Mol Cell Biochem 239:157–164
67. Aoyama T, Peters JM, Iritani N, Nakajima T, Furihata K, Hashimoto T, Gonzalez FJ (1998) Altered constitutive expression of fatty acid metabolizing enzymes in mice lacking PPARalpha. J Biol Chem 273:5678–5684
68. Barak Y, Nelson MC, Ong ES, Jones YZ, Ruiz-Lozano P, Chien KR, Koder A, Evans RM (1999) PPARg is required for placental, cardiac, and adipose tissue development. Mol Cell 4:585–595
69. Elle IC, Simonsen KT, Olsen L, Sorensen P, Fredens J, Tuck S, Faergeman NJ (2008) Functional analysis of acyl-CoA binding proteins in Caenorhabditis elegans. Chem Phys Lipids 154S:S39
70. Wadum M, Faergeman NJ, Knudsen J (2007) Differential function of acyl-CoA binding protein isoforms in Drosophila melanogaster and yeast *Saccharomyces cerevisiae*. Chem Phys Lipids 149S:S9
71. Chye M-L, Li H-Y, Yung MH (2000) Single amino acid substitutions in the acyl-CoA binding domain interrupt 14[C]palmitoyl CoA binding of ACBP2, an Arabidopsis acyl-CoA binding protein with ankyrin repeats. Plant Mol Biol 44:711–721
72. Harada N, Oda Z, Fujinami K, Okawa M, Ohbuchi K, Yonemoto M, Ikeda Y, Ohwaki K, Aragane K, Tamai Y, Kusunoki J (2007) Hepatic de novo lipogenesis is present in liver specific ACC1-deficient mice. Mol Cell Biol 27:1881–1888
73. Chakravarthy MV, Pan Z, Zhu Y, Tordjman K, Schneider JG, Coleman T, Turk J, Semenkovich CF (2005) "New" hepatic fat activates PPARalpha to maintain glucose, lipid, and cholesterol homeostasis. Cell Metab 1:309–322

Lipids (2010) 45:581–591
DOI 10.1007/s11745-010-3428-x

ORIGINAL ARTICLE

Dissimilar Properties of Vaccenic Versus Elaidic Acid in β-Oxidation Activities and Gene Regulation in Rat Liver Cells

Zhen-Yu Du · Pascal Degrace · Joseph Gresti · Olivier Loreau · Pierre Clouet

Received: 9 September 2009 / Accepted: 6 May 2010 / Published online: 28 May 2010

Abstract Vaccenic acid (*trans*-11-$C_{18:1}$) chemically resembles elaidic acid (*trans*-9-$C_{18:1}$) which is assumed to increase the risk of cardiovascular diseases, and thus could exert similar effects. Possible different oxidation rates of vaccenic versus elaidic acid were checked in muscles and liver, and through related gene expression in normal rat liver cells. In hepatic mitochondria, carnitine palmitoyltransferase (CPT) I exhibited comparable activity rates with both *trans*-isomers. CPT II activity was 30% greater ($P < 0.05$) with vaccenic than with elaidic acid as nonesterified fatty acids (NEFAs) or acyl-CoAs. Activity of the first β-oxidation step was similar between the isomers in all the tissue slices and liver extracts assayed. Respiration rates were comparable with both *trans*-isomers as NEFAs in various liver extracts, but were 30% greater ($P < 0.05$) with vaccenoyl-CoA than with elaidoyl-CoA in liver mitochondria. Vaccenic acid was oxidised 25% more ($P < 0.05$) by liver peroxisomes than elaidic acid. In hepatocytes cultured with *trans*- and corresponding *cis*-$C_{18:1}$ isomers, gene expression of CPT I, hydroxyacyl-CoA dehydrogenase and hydroxymethylglutaryl-CoA synthase was at least 100% increased ($P < 0.05$), but was unchanged with vaccenic acid, relative to controls. In conclusion, the position and geometry of the double bonds in acyl chains are suggested to confer on vaccenic and elaidic acid specific biochemical properties that might differently affect their fates in tissues.

Keywords Vaccenic and elaidic acid · β-Oxidation · Mitochondria · Carnitine palmitoyltransferase · Peroxisomes · Gene expression

Abbreviations

ACO	Acyl-CoA oxidase
ACS	Acyl-CoA synthetase
BSA	Bovine serum albumin
CPT	Carnitine palmitoyltransferase
FA	Fatty acid
HAD	Hydroxyacyl-CoA dehydrogenase
HMG	Hydroxymethylglutaryl (in HMG-CoA synthase)
NEFA	Nonesterified FA
PFAOS	Peroxisomal FA-oxidising system
PPAR	Peroxisome proliferator-activated receptor

Introduction

Coronary artery disease has been correlated with increased plasma LDL/HDL cholesterol ratios and apolipoprotein B levels [1, 2]. These atherosclerosis risk factors have allowed to assess the potential atherogenicity of dietary fats, particularly of partially hydrogenated vegetable oils (PHVO) processed for margarine production [3–5].

Z.-Y. Du · P. Degrace · J. Gresti · P. Clouet (✉)
Faculté des Sciences Gabriel, UMR 866, INSERM-UB,
Equipe Physiopathologie des dyslipidémies,
Université de Bourgogne, 21000 Dijon, France
e-mail: pclouet@u-bourgogne.fr

Z.-Y. Du
National Institute of Nutrition and Seafood Research,
5817 Bergen, Norway

O. Loreau
CEA, iBiTecS, Service Chimie Bioorganique et Marquage,
91191 Gif sur Yvette, France

Increasing the intensity of the hydrogenation process gave rise to the formation of *trans*-FAs whose levels ranged from 1 to 60% of total FAs [6]. Elaidic acid (*trans*-9-$C_{18:1}$) may reach 30–40% and vaccenic acid (*trans*-11-$C_{18:1}$) 10% of total *trans*-FAs [7, 8]. Elaidic acid was suspected to exert atherogenic effects because the consumption of margarines rich in this isomer was associated with increased LDL cholesterol and apolipoprotein B in humans [9–11]. *Trans*-FAs are also synthesised in ruminants by biohydrogenation of ingested fats and are recovered in meat and milk fats, as well as dairy derivatives [12]. Of all the *trans*-$C_{18:1}$ isomers identified in dairy fats, vaccenic acid is the most abundant (>80%) [7, 13, 14]. Epidemiological surveys have shown that there is an increased risk of developing coronary heart disease with diets enriched in PHVO, compared to fats of ruminant milk, meat and derivatives [15–17]. However in hamsters fed triglycerides containing *trans*-FAs, plasma LDL/HDL cholesterol ratios increased more with vaccenic than with elaidic acid [18]. Yet with the same animal model, the hypercholesterolemic effect of PHVO was recently demonstrated not to directly depend on the presence of elaidic or vaccenic acid [19].

To date, studies aimed at examining atherogenic fats have failed to directly ascribe to *trans*-FAs negative effects on lipoprotein composition and/or vessel wall structure. Indeed, the fates and properties of elaidic or vaccenic acid may be greatly altered, for instance, by the beneficial presence of FAs contained in the associated fats of diets, as n-3 polyunsaturated FAs or conjugated linoleic acid derived from vaccenic acid [20, 21]. The fact that versatile experimental models, atherosclerosis markers and dietary fat blends provide inconsistent results, prompted us to use ex vivo experimental models exposed to pure *trans*-FAs. In these assays performed in rats with different cell extracts, our goal was to determine whether vaccenic acid exhibits the same biochemical fates and properties as elaidic acid. If these *trans*-FAs exert singular biological effects, a necessity was that they are weakly, and possibly differentially, *β*-oxidised by cells. The present study was then devoted to reactions promoting complete or partial degradation of $C_{18:1}$ isomers in whole cells, mitochondria and peroxisomes. The effects of both *trans*-FAs on the gene expression of FA-oxidation-related proteins were also investigated in cultured hepatocytes. Elaidic and vaccenic acids were compared in parallel with oleic acid (*cis*-9 isomer) and *cis*-11-$C_{18:1}$, respectively. The study was mainly focussed on cell activities of liver whose pivotal role in the re-distribution of ingested lipids to the other organs is achieved via lipoprotein secretion. Rats received a common standard diet, instead of diets enriched in the mentioned isomers, to prevent specific effects on enzyme activities through selective incorporation in membranes [22, 23].

Experimental Procedure

Chemicals

Oleic (*cis*-9-$C_{18:1}$), elaidic (*trans*-9-$C_{18:1}$), *cis*-11-octadecenoic (*cis*-11-$C_{18:1}$) and vaccenic (*trans*-11-$C_{18:1}$) acids were purchased from Sigma Chemical Co. (St. Louis, MO). [1-^{14}C]oleic acid was obtained from Amersham Biosciences Europe (Saclay, France). The other [1-^{14}C]isomers were specifically prepared by CEA (Gif sur Yvette, France) from commercial unlabelled FAs and $^{14}CO_2$ using procedures described in [24]. Radiochemical purity (>98%) of [1-^{14}C]labelled compounds was determined by RP-HPLC (Zorbax SB C18; acetone/(methanol/water/acetic acid, 50:50:1, by vol), 60:40, by vol) and TLC (Silicagel Merck 60F254, pentane/diethylether/acetic acid, 80:20:0.1, by vol). They were all stored in chloroform/ethyl alcohol (50:50, by vol) at −30 °C. Evaporation of solvents under nitrogen was followed by the saponification of FA with NaOH or KOH for assays with whole cells or intracellular organelles, respectively, and their binding to essentially FA-free bovine serum albumin (BSA). These preparations were added to the other components of media immediately prior to incubation. L-[*methyl*-^{3}H]carnitine was from Amersham. BSA, collagenase (type I) and other biochemicals were from Sigma. Methylene chloride, 2,4,6-collidine, ethyl chloroformate and tetrahydrofuran, supplied by Aldrich Chemical Co. (Milwaukee, WI), were used for acyl-CoA synthesis [25]. Concentrations of synthesised acyl-CoAs were determined through their respective molar extinction coefficients at 260 nm and correction based on their 232/260 nm ratios, relative to those with pure products [26–28].

Animals

Official French regulations (N° 87848) for the use and care of laboratory animals were followed throughout and the experimental protocol was approved by the local ethic committee for animal experimentation (N° BL0612). Male Wistar rats were purchased from Janvier (Le Genest St Isle, France). They were kept at 23 °C in a light-controlled room (light period fixed between 08:00 am and 08:00 pm). They had free access to tap water and were fed a standard laboratory chow (ref AO4 from UAR, Epinay-sur-Orge, France) containing 58.7% carbohydrate, 17% protein, and 3% fat (palmitic, stearic, oleic and linoleic acids representing 8.7, 1.7, 26.7 and 48.3%, respectively, of the total FA mass). When rats were 7–8-week-old (250–300 g), they

were fasted for ~18 h, anaesthesised with isoflurane and killed by exsanguination at 08:00 am.

Activity Rate Measurements

All the biochemical activity measurements were previously carried out with increasing substrate concentrations, but the concentration adopted for each experimental procedure was selected among those giving rise to the increasing part of activity curves.

FA Oxidation by Tissue Slices

Gastrocnemius muscle, heart and liver tissues were cut with a scalpel blade on an ice-cooled glass plate in slices of ~0.5 mm in thickness, divided into strips of ~2 × 1 mm (1 to 1.5 mm^3 volume) in Krebs-Henseleit buffer consisting of 118 mM NaCl, 4.7 mM KCl, 1 mM KH_2PO_4, 1.2 mM $MgSO_4$, 0.5 mM $CaCl_2$, and 25 mM $NaHCO_3$, pH 7.4, rinsed five times in the same medium and blotted on absorbent paper. Tissue strips (0.2 g each) were placed on a circular glass filter (16 mm diameter) with 0.4–0.6 mm diameter pores, limited in periphery by a glass ring (2 mm in height). This assembly was supported by 10-mm high glass legs that allowed the incubation medium to be conveniently stirred with a magnetic bar. The device was inserted in a 30-mm high beaker containing 2.5 mL of Krebs-Henseleit buffer with 1 mM L-carnitine. The reaction was started by the injection of 1 mL of [1-^{14}C]FA (84 GBq/mol) with BSA (0.4 mM and 50 μM of final concentration, respectively) between the device and the beaker, which allowed the total medium to nearly cover the tissue strips. The whole system was placed into a 50-mL plastic bottle under 95% O_2, 5% CO_2 atmosphere. After 1 h of incubation at 37 °C, the reaction was stopped by addition of 1.5 mL of 25% (w/v) perchloric acid, which precipitated proteins, FAs still unesterified, acyl-CoAs and acylcarnitines. A small glass ladle (10 mm diameter) containing 0.4 mL of Hyamine (Packard, Meriden, CT) and fitted to a rubber cork was immediately introduced into the plastic bottle to trap the $^{14}CO_2$ released from the acidified medium. After 2 h, the media were filtered using Millipore filters (0.45 μm pore size) under very low pressure and 1 mL of each filtrate containing the acid-soluble products (ASP; short metabolites issued from FA oxidation) was added to 3.5 mL of Ultima Gold XR (Packard) for radioactivity measurements. The radioactivity of $^{14}CO_2$ trapped into Hyamine was counted in the same scintillation mixture. The radioactivity of ASP + CO_2 allowed to determine the number of FA molecules whose β-oxidation reactions affected at least the labelled carboxylic end of each $C_{18:1}$ isomer studied.

FA Oxidation by Liver Cells

Hepatocytes were isolated through a two-step collagenase perfusion as in [29]. Cell viability was assessed by trypan blue exclusion and suspensions with viability lower than 85% were discarded. FA oxidation was performed in 1 mL of Krebs-Henseleit buffer containing 1 mM L-carnitine, 0.4 mM [1-^{14}C]FA (16 GBq/mol) and 0.2 mM BSA. The reaction was initiated by the addition of 0.8 million cells (about 1.76 mg protein) per assay and was stopped after 30 min with 3 mL of 10% (w/v) perchloric acid. Radioactivity of CO_2 and ASP was measured as indicated for liver slices. Oxygen consumption with FAs was measured polarographically at 30 °C using a Clark-type oxygen-electrode (Yellow Springs Instruments, Yellow Springs, OH) in 1.6 mL Krebs-Henseleit buffer with 2 mM malate. After addition of 0.8 million cells, 1 mM L-carnitine was first injected to consume endogenous FAs. After 3 min, a volume of 50 μL of a mixture containing each $C_{18:1}$ isomer and BSA was added both at 0.2 mM of final concentration. Respiration rates were corrected from control values obtained in the absence of exogenous FA.

FA Oxidation by Liver Homogenates

Liver pieces were homogenised by manual rotation of a Teflon pestle in an ice-cooled Potter–Elvehjem apparatus [30] and diluted (1:40, w/v) in a chilled mixture of 0.25 M sucrose, 2 mM EGTA and 10 mM Tris/HCl, pH 7.4. Mitochondrial and peroxisomal β-oxidation of labelled FAs was performed in two specific media as indicated in [30, 31]. Liver homogenate (2.5 mg of wet tissue) was added to each vial containing 1 mL of either medium. The reaction was initiated by the addition of 50 μM [1-^{14}C]FA (55 GBq/mol) with 35 μM BSA. After 30 min, CO_2 and ASP were collected after addition of 3 mL of 10% (w/v) perchloric acid and their radioactivity was measured as described above for liver slices. For respiration measurements, a volume of freshly prepared homogenate corresponding to 2.5 mg of fresh liver was injected in 1.6 mL of medium containing 130 mM KCl, 25 mM HEPES, 0.1 mM EGTA, 3 mM $MgCl_2$, 10 mM KP_i, 1 mM ATP, 50 μM CoA, 0.5 mM DTT, 2 mM malate. L-carnitine and ADP (1 and 2 mM, respectively) were then added. Control oxygen consumption was recorded for 3 min, then a 50 μL-volume of a mixture containing each $C_{18:1}$ isomer with BSA (both at 0.2 mM of final concentration) was added. Final respiration rates were corrected from control values, as for hepatocytes.

FA Oxidation by Mitochondrial Fractions

The procedure of mitochondrial isolation is reported in [30] using a medium containing 1% FA-free BSA to bind free

FAs released during the cell disruption. The protein content of mitochondrial fractions cleared from BSA was performed using the bicinchoninic acid procedure [32]. The purity of these fractions was checked through activity of enzymes specific to mitochondria, peroxisomes and microsomes, as detailed in [33]. Oxidation of labelled FAs was determined in the presence of 0.3 mg of mitochondrial protein as in [34] with 50 μM [1-^{14}C]FA (66 GBq/mol) and 35 μM BSA. The reaction was stopped after 8 min by addition of 4 mL of 10% (w/v) perchloric acid and the radioactivity of CO_2 and ASP was measured as above. Oxygen consumption was recorded in the presence of 1.2 mg of mitochondrial protein with 10 μM $C_{18:1}$ isomers as NEFAs in the medium used for liver homogenates, or as acyl-CoAs in a similar medium devoid of $MgCl_2$, ATP and CoA. Respiration rates were corrected from control values obtained in the presence of carnitine before the injection of NEFAs or acyl-CoAs.

FA Oxidation-Related Enzyme Activities

Acyl-CoA synthetase (ACS) activity was measured in 0.5 mL of medium containing 0.35 M Tris (pH 7.4), 8 mM $MgCl_2$, 5 mM DTT, 10 mM ATP, 0.1 mM CoA, Triton WR 1339 (1 mg/mL), 10 μM [1-^{14}C]FA (1 TBq/mol) at 25 °C, in the presence of 40 μg mitochondrial or 8 μg microsomal (prepared as in [33]) protein. The reaction was stopped after 1 min with 1.5 mL of 10% perchloric acid (w/v). Unreactive NEFAs were removed by three extractions with 2 mL of diethylether. The aqueous medium was then neutralised with 25% Tris (w/v) to solubilise acyl-CoAs, and the associated radioactivity was measured in Ultima Gold XR. The transfer of isomers onto carnitine *via* carnitine palmitoyltransferase (CPT) I and II activities was studied using NEFAs (that require to be previously esterified to CoA through mitochondrial ACS activity) or directly using acyl-CoAs. CPT I activity was measured with 80 μM NEFAs or acyl-CoAs in the presence of 25 or 50 μM BSA, respectively, and CPT II with 50 μM NEFAs or acyl-CoAs, both in the absence of BSA. The common point of these assays carried out in 1 mL of medium in the presence of ~0.3 mg of mitochondrial protein was the preincubation time of 2 min before addition of 0.4 mM L-[methyl-^{3}H]carnitine (92.5 GBq/mol). The complete procedure with extraction of acylcarnitines has been detailed in [30].

Peroxisomal FA Oxidation-Related Activities

To complement the peroxisomal FA oxidation measurements obtained above with whole liver homogenates, the activity of the peroxisomal FA oxidising system (PFAOS), that is a key-sequence of the peroxisomal FA oxidation pathway, was achieved through the CN^--insensitive acyl-CoA-dependent NAD^+ reduction in the presence of 20 μM $C_{18:1}$-CoA isomers as in [35]. Peroxisome-enriched fractions used for greater accuracy were prepared from liver homogenised in a sucrose medium with 1% BSA, centrifuged between 12,000 and 18,000*g* for 10 min, and rinsed two times in the absence of BSA.

Gene Expression

Hepatocytes isolated as above were preincubated in William Medium E (PAN-Biotech GmbH, Aidenbach, Germany) containing 10% (v/v) fetal bovine serum and 1% (v/v) antibiotic antimycotic solution (Sigma Chemical, Co.) in water-saturated atmosphere (5% CO_2, 95% air) for ~3 h at 37 °C, in dishes of 60 mm in diameter (~3×10^6 cells per dish). The attached cell monolayer was gently washed with 3 mL of fresh William Medium E medium without fetal bovine serum to remove the unattached and non-viable cells. The incubation was started with the addition of 4 mL of William Medium E containing 100 μM $C_{18:1}$ isomer bound to 50 μM BSA and 1% antibiotic antimycotic solution, in a water-saturated atmosphere (5% CO_2, 95% air) at 37 °C. After 24 h of incubation, total mRNA of the hepatocyte monolayers from three distinct dishes were extracted using Tri-Reagent (Euromedex, Souffelweyersheim, France) as in [36] and were reverse-transcripted using an Iscript cDNA kit (Bio-Rad, Marnes-la-Coquette, France). Real-time PCR was performed as already described [37] in a 96-well plate using an iCycler iQ (Bio-Rad) from 2.5 ng cDNA for samples or 25, 2.5, 0.25 and 0.025 ng for standards). Primer pairs were designed using 'Primers!' software and were synthesised by MWG-Biotech AG (Ebersberg, Germany). Table 1 details the sequences of the forward and reverse primers, the melting temperatures of these primers and the length of PCR products. Data were analysed using the Bio-Rad and Microsoft Excel software. The relative gene expression was calculated from standard curves for each gene after normalisation with β-actin.

Statistics

Differences between groups were determined performing repeated measures of ANOVA followed by the Tukey–Kramer multiple comparison post-hoc test using GraphPad Instat 3.1 software. Differences were considered significant at $P < 0.05$.

Results

Entry of Isomer $C_{18:1}$ Chains into Mitochondria

This entry of FAs into mitochondria is mediated by CPT I whose activity depends on acyl-CoA formation by ACS.

Table 1 Primers for real-time PCR

Gene	5′-sense primer-3′ 5′-antisense primer-3′	Melting temperature (°C)	Length of PCR products (bp)
ACO	aggtggctgttaagaagagtgc	60.3	62
	ccgagatgccatattccctc	59.4	
CPT-I	atcggagcagggatacagag	59.4	94
	accacctgtcaaagcatcttc	57.9	
CPT-II	gcccctggttcgatatgtatt	57.9	91
	agactttgggtccggatt	56.7	
HAD	aggagcgtcttggaaaacag	57.3	104
	actctcgcaaaagaaatggc	55.3	
HMG-CoA synthase	ggcatagataccaccaacgc	59.4	95
	atagcgaccatcccagtagc	59.4	
PPARα	accctctctccagcttcca	59.9	113
	gtccccacatattcgacactc	59.3	
β-actin	cgtgaaaagatgacccaggt	57.3	71
	gtgctgagaagttgacccaata	58.4	

ACO acyl-CoA oxidase, *CPT* (carnitine palmitoyltransferase) I and II, *HAD* hydroxyacyl-CoA dehydrogenase, *HMG* (hydroxymethylglutaryl)-CoA synthase, *PPARα* peroxisome proliferator-activated receptor α

Activity rates of ACS in microsomes and mitochondria towards oleic acid were found to be 23.0 ± 3.5 and 5.1 ± 1.2 nmol/min per mg protein, respectively, and these values did not exhibit, in either cellular fraction, statistical differences towards the other $C_{18:1}$ isomers assayed (unpublished data). Figure 1a shows that activity rates of the ACS-CPT I sequence with NEFAs were comparable with all $C_{18:1}$ isomers. Strict CPT I activity with vaccenoyl-CoA was 45% lower than with elaidoyl-CoA or oleoyl-CoA (Fig. 1b). CPT II activity measured with NEFAs (Fig. 1c) or acyl-CoAs (Fig. 1d) was ~28% greater with vaccenic acid than with elaidic acid. CPT II exhibited opposite effects between both *cis*-isomers when they were used as NEFAs (*cis*-9 > *cis*-11) or acyl-CoA (*cis*-11 > *cis*-9) (Fig. 1c vs. 1d).

Oxidation Related to the Carboxylic End of $C_{18:1}$ Isomers

Slices of skeletal muscle and heart, both energy-demanding organs, exhibited equivalent capacities to oxidise the four $C_{18:1}$ isomers, as assessed by the release onto CO_2 + acid-soluble products (ASP) of the radioactivity initially hold by

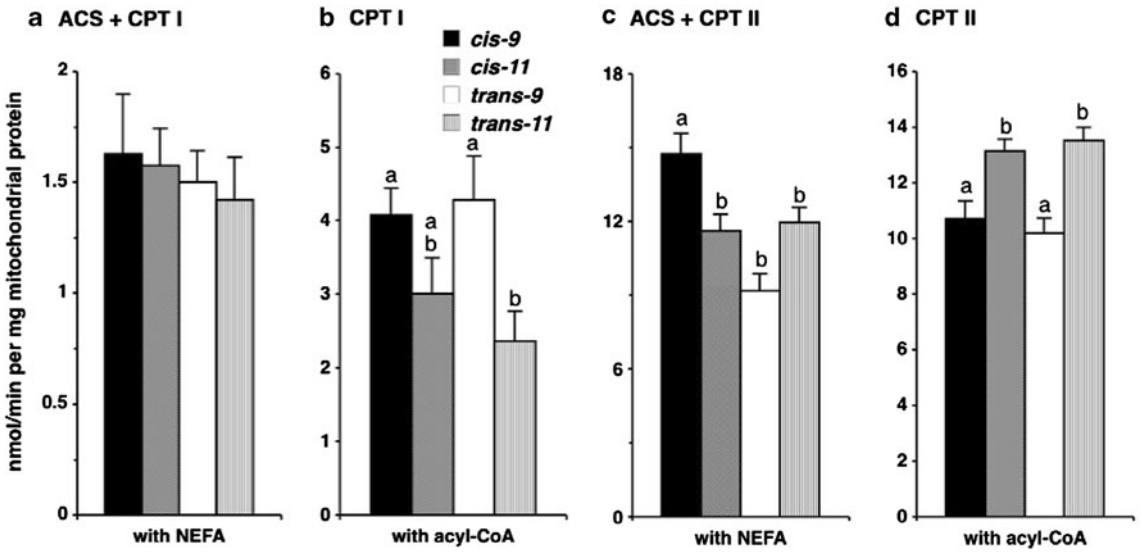

Fig. 1 Carnitine palmitoyltransferase (CPT) I and II activities in liver mitochondria with $C_{18:1}$ isomers used as nonesterified fatty acids (NEFA) requiring the previous action of acyl-CoA synthetase (ACS), or directly as acyl-CoAs. Concentrations of either substrate in the final media were 80 and 50 μM for CPT I and CPT II, respectively. All results are expressed as nmol of $C_{18:1}$ isomers in either form bound to carnitine/min per mg of mitochondrial protein. *T-bars* show SEM ($n = 4$). For each series of incubation, values with different *letters* on columns statistically differ at $P < 0.05$

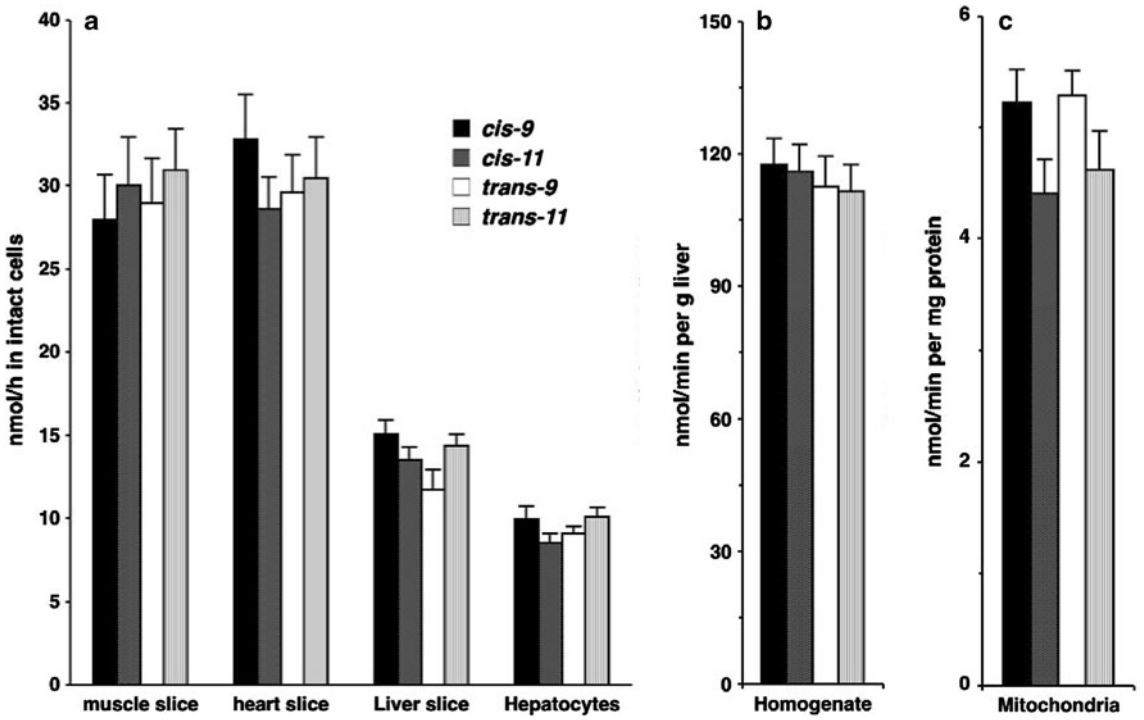

Fig. 2 Carboxylic end β-oxidation of $C_{18:1}$ isomers. The number of molecules involved was expressed per g of gastrocnemius muscle, heart and liver slices, or per mg of hepatocyte protein after 1 h of incubation in the presence of 0.4 mM [1-^{14}C]$C_{18:1}$ isomers. The results with liver homogenates and mitochondrial fractions were expressed per min per g liver and mg mitochondrial protein, respectively, after incubation in the presence of 50 μM [1-^{14}C]$C_{18:1}$ isomers. *T-bars* show SEM ($n = 4$). For each series of experiments performed with a same tissue or tissue extract, values found between the isomers tested did not differ ($P > 0.05$) as the statistic test used

the carboxylic end of FAs (Fig. 2a). This denotes that a same number of FA molecules entered into mitochondria have at least undergone the first β-oxidation cycle. This is qualitatively worth for liver slices and hepatocytes, but at 55 and 70% lower amplitudes, respectively, than for muscle slices (Fig. 2a). As regards the activity exerted by FA oxidation-related organelles in liver homogenates, i.e. after cell disruption, or in liver mitochondria, no statistical difference in FA oxidation rates was observed between the four isomers (Fig. 2b, c). Figure 3 shows that vaccenic acid was ~25% more oxidised by liver peroxisomes than the other $C_{18:1}$ isomers on the basis of the radioactivity released from labelled carboxylic end by liver homogenates (carnitine-independent FA oxidation). In partially purified peroxisomal fractions, PFAOS activity rates were 25% greater with vaccenic and elaidic acid than with their *cis*-isomers.

Oxidation Related to the Whole Isomer $C_{18:1}$ Molecules

Mitochondrial oxygen consumption was stimulated with FA substrates when the respiratory chain was activated through dehydrogenation of metabolites originating from β-oxidation reactions (as acetyl moieties) and concomitant ADP phosphorylation. As the number of acyl chains entering the β-oxidation process was the same in each tissue for all the isomers assayed (Fig. 2a) and slightly different in liver mitochondria (Fig. 2c), respiration rates on the isomers could provide further information about the amount of acetyl moieties successively released from each FA chain by β-oxidation. Figure 4 shows that oxygen consumption rates by hepatocytes, liver homogenates and isolated mitochondria were at least 50% lower with *trans*- than with *cis*-$C_{18:1}$ isomers used as NEFAs (panels a, b, c). With liver mitochondria and acyl-CoAs that are direct substrates for CPT I, respiration rates were comparable with vaccenoyl, oleoyl and *cis*-11-octadecenoyl chains, but 33% lower with elaidoyl chain (Fig. 4d).

Hepatocyte FA Oxidation-Related Gene Expression

Long- and very-long chain FAs are known to exert regulatory effects on FA metabolism-related pathways. Here we studied the effects of the four $C_{18:1}$ isomers on the expression levels of FA oxidation-related proteins in cultured hepatocytes (already depleted from carnitine during the isolation procedure). When hepatocytes were incubated in the absence of carnitine, gene expression of CPT I, HAD and hydroxymethylglutaryl-CoA (HMG-CoA) synthase was statistically increased with *cis*-9, *cis*-11 and *trans*-9-$C_{18:1}$

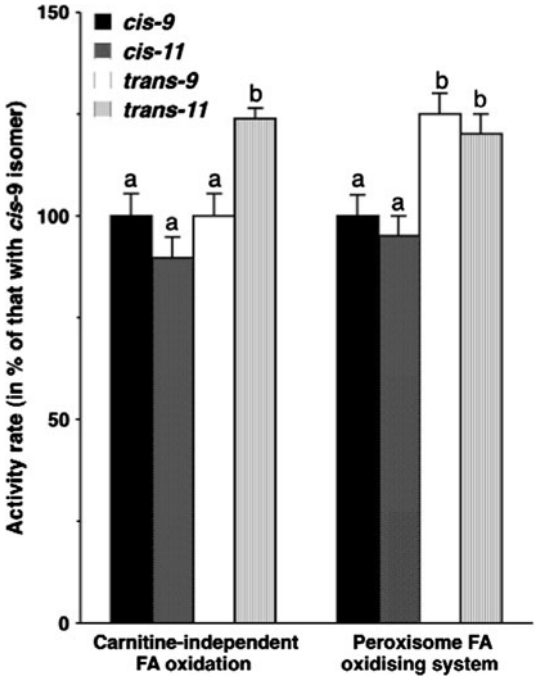

Fig. 3 Peroxisomal activities with $C_{18:1}$ isomers as substrates in rat liver. Results are expressed as percentages ± SEM ($n = 3$) by reference to values obtained with *cis*-9 isomer (oleic acid). The carnitine-independent FA oxidation rate was measured in liver homogenates with unesterified [1-^{14}C]$C_{18:1}$ isomers and was 38 ± 2 nmol/min per g wet liver with oleic acid. The NADH production by the peroxisomal FA oxidising system (PFAOS) was recorded in partially purified peroxisomal fractions with CoA-esterified $C_{18:1}$ isomers and was 0.20 ± 0.01 μmol/min per g wet liver with oleoyl-CoA. For each activity, values with different *letters* on columns statistically differ at $P < 0.05$

isomers, but not with vaccenic acid (Fig. 5a, c, d). In the presence of carnitine, increased expression levels were still observed for CPT I, particularly with oleic and elaidic acids (Fig. 5a), but were absent for HAD or of very low amplitude for HMG-CoA synthase with the effective isomers (Fig. 5c, d).

Discussion

Most of our observations related to β-oxidation and obtained with cell extracts in the presence of pure isomers reflect only part of the biochemical cell actuality. The studied reactions should be also considered in the context of other FA-related metabolic pathways. Under these ex vivo conditions, the slightly shifted location of the *trans*-double bond in vaccenic versus elaidic acid appeared to have unequal consequences for both mitochondrial and peroxisomal FA oxidation activities and FA oxidation-related gene expression.

Entry of FA Chains into Mitochondria

Activation of NEFAs by CoA is a prerequisite before the carnitine-dependent activities allow acyl chains to cross the mitochondrial inner membranes. Comparable acyl-CoA synthetase activities with the four isomers in the presence of responsible organelles fully support previous results obtained with *cis*- [38] and *trans*- [39] isomers under other experimental conditions. This suggests that CPT I was

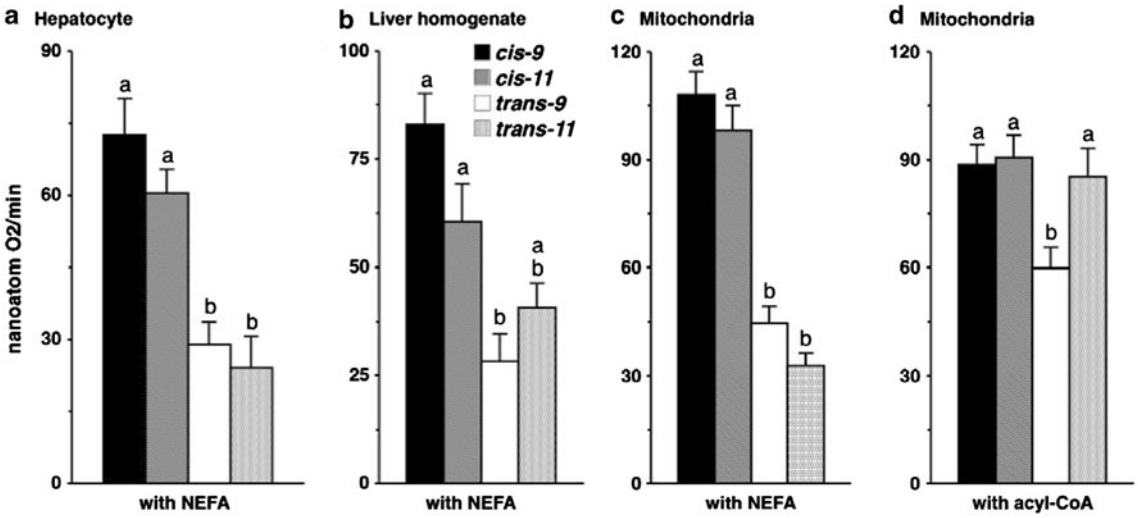

Fig. 4 Respiration on $C_{18:1}$ isomers in hepatocytes, liver homogenates and mitochondria. The isomers were used as nonesterified fatty acids (NEFA) at 0.2 mM, 20 and 10 μM concentrations with hepatocytes, liver homogenates and mitochondria, respectively, and as acyl-CoA at 10 μM concentration with mitochondria. The results are expressed as nanoatom O_2/min per mg hepatocyte protein, per g homogenised liver and per mg mitochondrial protein. *T-bars* show SEM ($n = 4$). For each series of incubation, values with different *letters* on columns statistically differ at $P < 0.05$

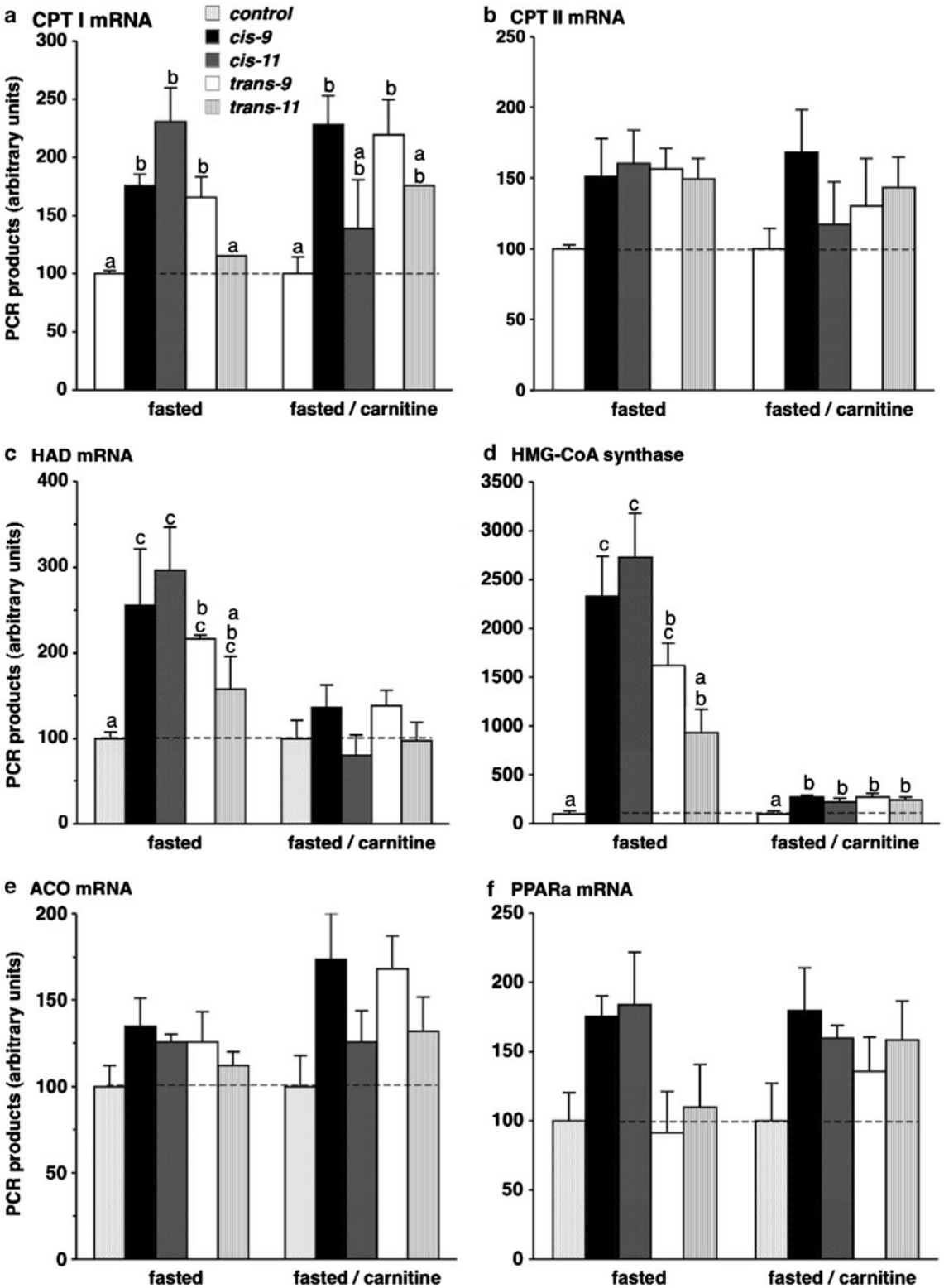

Fig. 5 mRNA levels of β-oxidation-related proteins after incubation of fasted rat hepatocytes with $C_{18:1}$ isomers in the absence or presence of carnitine. Arbitrary units $\pm$ SEM with $n = 3$ (different hepatocyte culture dishes) are percentages expressed by reference to control assays (*dotted lines*) performed in the absence of any $C_{18:1}$ isomer (=100 for each series of experiments). Different *letters* on columns denote statistically different results at $P < 0.05$

provided, through our experimental procedures, with equal amounts of $C_{18:1}$-CoA isomers. However in whole cells, NEFAs and acyl-CoAs are very largely bound to specific FA- and acyl-CoA binding proteins, respectively, while unbound forms remain in the nanomolar range concentrations [40, 41]. At lowest concentrations assayed, ACS/CPT I sequence, strict CPT I and CPT II were found to exhibit comparable activities with any of isomers (unpublished data). This would allow an identical number of acyl chains, bound to carnitine, to cross the mitochondrial inner membranes and to equally provide, bound to CoA, the actual β-oxidation reactions. Nevertheless, the requirement of other cell metabolic pathways for acyl-CoAs could limit the availability of these substrates for the CPT I reaction. Indeed, CPT I activity rates were comparable with elaidoyl- and oleoyl-CoA in isolated mitochondria (Fig. 1b), but the data obtained with permeabilised hepatocytes [42] showed that elaidic acid was transferred less to carnitine that oleic acid. This suggests that, in whole cells, other metabolic pathways could have differential affinities for elaidic and vaccenic isomers, with direct consequences on the respective in situ CPT I action. However the data obtained with isolated mitochondria show that elaidic and vaccenic acids exhibit clear different specificities for either CPT I or II activity (Fig. 1b, d).

β-Oxidation Reaction

In muscle, heart and liver cells, the same number of $C_{18:1}$ isomer molecules losing their first carbon pair by β-oxidation totally agrees with other data obtained only with [1-^{14}C] labelled oleic and elaidic acid in vivo [43–45] and in vitro [46]. In our study, the four isomers having crossed mitochondrial membranes, through comparable carnitine-dependent activity rates, were then equivalent substrates for long-chain acyl-CoA dehydrogenase (LCAD) both in whole cells and liver extracts. With equal numbers of $C_{18:1}$ chains entering the mitochondrial β-oxidation reactions, oxygen consumption rates due to dehydrogenations connected to the respiratory chain informed about the extent to which each fatty chain was β-oxidised. This technique shows that respiration in liver cells, homogenates and mitochondria was always lower with *trans*-isomers (elaidic acid > vaccenic acid) than with *cis*-isomers, all used as NEFAs. It was, however, unexpected that mitochondrial respiration rates with vaccenoyl-CoA and both *cis*-acyl-CoAs were to the same extent and ~30% lower with elaidoyl-CoA. Such a difference has been previously observed, but only between oleoyl- and elaidoyl-CoA, by Yu et al. [45]. These authors showed that the major β-oxidation intermediate of elaidic acid, 5-*trans*-tetradecanoyl-CoA, reduces the β-oxidation progress because of its low-affinity for LCAD. Under comparable experimental conditions, our results suggest that the formation of *trans*-intermediates occurring during the β-oxidation of vaccenoyl-CoA has no negative effect on the mitochondrial β-oxidation activity. On the whole, our data show that vaccenoyl-CoA is a worthy β-oxidation substrate in isolated mitochondria and peroxisomes. This conclusion does not exclude that, in intact cells, acyl-CoAs can be diverted towards other metabolic pathways.

Effect of $C_{18:1}$ Isomers on β-Oxidation-Related Gene Regulation

In hepatocytes cultured in the absence of carnitine, it is worth underlining the increased expression of CPT I and more particularly of HAD and HMG-CoA synthase, with the $C_{18:1}$ isomers in the order *cis*-11 ≥ *cis*-9 ≥ *trans*-9, relative to controls, but also the lack of effect with vaccenic acid. In the media devoid of carnitine, very few intermediates of mitochondrial β-oxidation were produced, which limits to acyl chains and derivatives outside mitochondria a role in the transcription mechanisms. Under these conditions, the respective capacity of isomers to bind transcription factors, such as CoA-derivatives [47], appears to differ according to the position and geometry of the double bond, with weak or null efficiency for the *trans* isomers whose the double bond was in 9 or 11 position, respectively. Because PPARα expression was unaffected by any of isomers, the up-regulation of CPT I, HAD and HMG-CoA synthase might be due to the ability of acyl-CoAs to bind PPARα at basal level in cells [47, 48]. However in the presence of NEFAs, CPT I was also demonstrated to be up-regulated through a PPARα-independent mechanism [49]. Such mechanisms could also apply to our culture assays, in which the isomers transferred into cells were still under free form and also partially esterified to CoA. In hepatocytes cultured in the presence of carnitine, isomers were further esterified as acylcarnitines [50], which allowed part of them to enter the β-oxidation pathway. The weak levels of HAD and HMG-CoA synthase expression with *cis*-9, *cis*-11 and *trans*-9 isomers could be then due to the loss of induction capacities of active isomers when their concentrations decreased under limit values. Under the artificial conditions of culture hepatocytes, vaccenic acid did not appear to exert the same induction effect on FA oxidation-related genes as elaidic acid.

On the whole, a number of FA oxidation related-parameters with vaccenic versus elaidic acid did not match each other both in whole cells and isolated organelles. The data suggest that vaccenic acid is a better oxidation substrate than elaidic acid with subcellular organelles related to FA β-oxidation, and it does not affect FA oxidation-related gene expression. Within cells, vaccenic and elaidic acid could also enter other metabolic pathways and could

be, for example, esterified into membranes or desaturated as conjugated *cis*-9, *trans*-11 linoleic acid [20, 21].

Acknowledgments We thank Mr Jean-Michel Chardigny DR INRA, Mr Koenraad Duhem, Mrs Corinne Marmonier for helpful discussions, and Mrs Monique Baudoin for figure construction and typing of the manuscript. This work was supported by grants from the CNIEL (Paris) and the Region Bourgogne (Dijon), France.

References

1. Noma A, Yokosuka T, Kitamura K (1983) Plasma lipids and apolipoproteins as discriminators for presence and severity of angiographically defined coronary artery disease. Atherosclerosis 49:1–7
2. Whayne TF, Alaupovic P, Curry MD, Lee ET, Anderson PS, Schechter E (1981) Plasma apolipoprotein B and VLDL-, LDL-, and HDL-cholesterol as risk factors in the development of coronary artery disease in male patients examined by angiography. Atherosclerosis 39:411–424
3. Constant J (2004) The role of eggs, margarines and fish oils in the nutritional management of coronary artery disease and strokes. Keio J Med 53:131–136
4. Han SN, Leka LS, Lichtenstein AH, Ausman LM, Schaefer EJ, Meydani SN (2002) Effect of hydrogenated and saturated, relative to polyunsaturated, fat on immune and inflammatory responses of adults with moderate hypercholesterolemia. J Lipid Res 43:445–452
5. Schwandt P (1995) *Trans*-fatty acids and atherosclerosis. Med Monatsschr Pharm 18:78–79
6. Ackman RG, Mag TK (1998) *Trans* fatty acids and the potential for less in technical products. In: Sébédio JL, Christie WW (eds) *Trans* fatty acids in human nutrition, The Oily Press, Dundee
7. Chardigny JM, Destaillats F, Malpuech-Brugere C, Moulin J, Bauman DE, Lock AL, Barbano DM, Mensink RP, Bezelgues JB, Chaumont P, Combe N, Cristiani I, Joffre F, German JB, Dionisi F, Boirie Y, Sebedio JL (2008) Do *trans* fatty acids from industrially produced sources and from natural sources have the same effect on cardiovascular disease risk factors in healthy subjects? Results of the *trans* fatty acids collaboration (transfact) study. Am J Clin Nutr 87:558–566
8. Wolff RL, Combe NA, Destaillats F, Boue C, Precht D, Molkentin J, Entressangles B (2000) Follow-up of the Delta4 to Delta16 *trans*-18:1 isomer profile and content in French processed foods containing partially hydrogenated vegetable oils during the period 1995–1999. Analytical and nutritional implications. Lipids 35:815–825
9. Katan MB, Zock PL, Mensink RP (1995) *Trans* fatty acids and their effects on lipoproteins in humans. Ann Rev Nutr 15:473–493
10. Mensink RP, Katan MB (1993) *Trans* monounsaturated fatty acids in nutrition and their impact on serum lipoprotein levels in man. Prog Lipid Res 32:111–122
11. Zock PL, Katan MB (1992) Hydrogenation alternatives: effects of *trans* fatty acids and stearic acid versus linoleic acid on serum lipids and lipoproteins in humans. J Lipid Res 33:399–410
12. Griinari JM, Bauman DEP (1999) Biosynthesis of conjugated linoleic acid and its incorporation into meat and milk in ruminants. In: Yurawecz MP, Mossoba MM, Kramer JKG, Pariza MW, Nelson GJ (eds) Advances in conjugated linoleic acid research. AOCS Press, Champaign, Urbana
13. Ledoux M, Rouzeau A, Bas P, Sauvant D (2002) Occurrence of *trans*-C18:1 fatty acid isomers in goat milk: effect of two dietary regimens. J Dairy Sci 85:190–197
14. Precht D, Molkentin J (1997) Effect of feeding on *trans* positional isomers of octadecenoic acid in milk fats. Milchwissenschaft 52:564–568
15. Ascherio A, Hennekens CH, Buring JE, Master C, Stampfer MJ, Willett WC (1994) *Trans*-fatty acids intake and risk of myocardial infarction. Circulation 89:94–101
16. Bolton-Smith C, Woodward M, Fenton S, Brown CA (1996) Does dietary *trans* fatty acid intake relate to the prevalence of coronary heart disease in Scotland? Eur Heart J 17:837–845
17. Willett WC, Stampfer MJ, Manson JE, Colditz GA, Speizer FE, Rosner BA, Sampson LA, Hennekens CH (1993) Intake of *trans* fatty acids and risk of coronary heart disease among women. Lancet 341:581–585
18. Meijer GW, van Tol A, van Berkel TJ, Weststrate JA (2001) Effect of dietary elaidic versus vaccenic acid on blood and liver lipids in the hamster. Atherosclerosis 157:31–40
19. Tyburczy C, Major C, Lock AL, Destaillats F, Lawrence P, Brenna JT, Salter AM, Bauman DE (2009) Individual *trans* octadecenoic acids and partially hydrogenated vegetable oil differentially affect hepatic lipid and lipoprotein metabolism in golden Syrian hamsters. J Nutr 139:257–263
20. Kelley DS, Erickson KL (2003) Modulation of body composition and immune cell functions by conjugated linoleic acid in humans and animal models: benefits vs. risks. Lipids 38:377–386
21. Pariza MW, Park Y, Cook ME (2001) The biologically active isomers of conjugated linoleic acid. Prog Lipid Res 40:283–298
22. Høy CE, Hølmer G (1979) Incorporation of *cis*- and *trans*-octadecenoic acids into the membranes of rat liver mitochondria. Lipids 14:727–733
23. Zevenbergen JL, Houtsmuller UM, Gottenbos JJ (1988) Linoleic acid requirement of rats fed *trans* fatty acids. Lipids 23:178–186
24. Channing MA, Simpson N (1993) Radiosynthesis of [1–11C] polyhomoallylic fatty acids. J Label Compd Radiopharm 33:541–546
25. Goldman P, Vagelos PR (1961) The specificity of triglyceride synthesis from diglycerides in chicken adipose tissue. J Biol Chem 236:2620–2623
26. Korsrud GO, Conacher HB, Jarvis GA, Beare-Rogers JL (1977) Studies on long chain *cis*- and *trans*-acyl-CoA esters and acyl-CoA dehydrogenase from rat heart mitochondria. Lipids 12:177–181
27. Lawson LD, Kummerow FA (1979) Beta-oxidation of the coenzyme A esters of elaidic, oleic, and stearic acids and their full-cycle intermediates by rat heart mitochondria. Biochim Biophys Acta 573:245–254
28. Lawson LD, Kummerow FA (1979) Beta-oxidation of the coenzyme A esters of vaccenic, elaidic, and petroselaidic acids by rat heart mitochondria. Lipids 14:501–503
29. Seglen PO (1973) Preparation of rat liver cells. 3. Enzymatic requirements for tissue dispersion. Exp Cell Res 82:391–398
30. Demizieux L, Degrace P, Gresti J, Loreau O, Noel JP, Chardigny JM, Sebedio JL, Clouet P (2002) Conjugated linoleic acid isomers in mitochondria: evidence for an alteration of fatty acid oxidation. J Lipid Res 43:2112–2122
31. Veerkamp JH, van Moerkerk TB, Glatz JF, Zuurveld JG, Jacobs AE, Wagenmakers AJ (1986) $^{14}CO_2$ production is no adequate measure of [^{14}C]fatty acid oxidation. Biochem Med Metab Biol 35:248–259
32. Smith PK, Krohn RI, Hermanson GT, Mallia AK, Gartner FH, Provenzano MD, Fujimoto EK, Goeke NM, Olson BJ, Klenk DC (1985) Measurement of protein using bicinchoninic acid. Anal Biochem 150:76–85
33. Niot I, Pacot F, Bouchard P, Gresti J, Bernard A, Bézard J, Clouet P (1994) Involvement of microsomal vesicles in part of the sensitivity of carnitine palmitoyltransferase I to malonyl-CoA

inhibition in mitochondrial fractions of rat liver. Biochem J 304:577–584
34. Degrace P, Demizieux L, Gresti J, Chardigny JM, Sebedio JL, Clouet P (2004) Hepatic steatosis is not due to impaired fatty acid oxidation capacities in C57bl/6j mice fed the conjugated *trans*-10, *cis*-12-isomer of linoleic acid. J Nutr 134:861–867
35. Bronfman M, Inestrosa NC, Leighton F (1979) Fatty acid oxidation by human liver peroxisomes. Biochem Biophys Res Commun 88:1030–1036
36. Chomczynski P, Sacchi N (1987) Single-step method of RNA isolation by acid guanidinium thiocyanate-phenol-chloroform extraction. Anal Biochem 162:156–159
37. Degrace P, Moindrot B, Mohamed I, Gresti J, Du ZY, Chardigny JM, Sebedio JL, Clouet P (2006) Upregulation of liver VLDL receptor and FAT/CD36 expression in LDLR−/− ApoB100/100 mice fed *trans*-10, *cis*-12 conjugated linoleic acid. J Lipid Res 47:2647–2655
38. Lippel K, Carpenter D, Gunstone FD, Ismail IA (1973) Activation of long chain fatty acids by subcellular fractions of rat liver. 3. Effect of ethylenic bond position on acyl-CoA formation of *cis*-octadecenoates. Lipids 8:124–128
39. Lippel K, Gunstone FD, Barve JA (1973) Activation of long chain fatty acids by subcellular fractions of rat liver. II. Effect of ethylenic bond position on acyl-CoA formation of *trans*-octadecenoates. Lipids 8:119–123
40. Faergeman NJ, Knudsen J (1997) Role of long-chain fatty acyl-CoA esters in the regulation of metabolism and in cell signalling. Biochem J 323:1–12
41. Richieri GV, Ogata RT, Kleinfeld AM (1999) Fatty acid interactions with native and mutant fatty acid binding proteins. Mol Cell Biochem 192:77–85
42. Guzman M, Klein W, del Pulgar TG, Geelen MJ (1999) Metabolism of *trans* fatty acids by hepatocytes. Lipids 34:381–386
43. Coots RH (1964) A comparison of the metabolism of elaidic, oleic, palmitic, and stearic acids in the rat. J Lipid Res 5:468–472
44. Ono K, Fredrickson DS (1964) The metabolism of ^{14}C-labeled *cis* and *trans* isomers of octadecenoic and octadecadienoic acids. J Biol Chem 239:2482–2488
45. Yu W, Liang X, Ensenauer RE, Vockley J, Sweetman L, Schulz H (2004) Leaky beta-oxidation of a *trans*-fatty Acid: incomplete beta-oxidation of elaidic acid is due to the accumulation of 5-*trans*-tetradecanoyl-CoA and its hydrolysis and conversion to 5-*trans*-tetradecanoylcarnitine in the matrix of rat mitochondria. J Biol Chem 279:52160–52167
46. Tardy AL, Giraudet C, Rousset P, Rigaudiere JP, Laillet B, Chalancon S, Salles J, Loreau O, Chardigny JM, Morio B (2008) Effects of *trans* MUFA from dairy and industrial sources on muscle mitochondrial function and insulin sensitivity. J Lipid Res 49:1445–1455
47. Berge RK, Aarsland A (1985) Correlation between the cellular level of long-chain acyl-CoA, peroxisomal beta-oxidation, and palmitoyl-CoA hydrolase activity in rat liver. are the two enzyme systems regulated by a substrate-induced mechanism? Biochim Biophys Acta 837:141–151
48. Nakamura MT, Cheon Y, Li Y, Nara TY (2004) Mechanisms of regulation of gene expression by fatty acids. Lipids 39:1077–1083
49. Louet JF, Chatelain F, Decaux JF, Park EA, Kohl C, Pineau T, Girard J, Pegorier JP (2001) Long-chain fatty acids regulate liver carnitine palmitoyltransferase I gene (L-CPT I) expression through a peroxisome-proliferator-activated receptor alpha (PPARalpha)-independent pathway. Biochem J 354:189–197
50. McGarry JD, Brown NF (1997) The mitochondrial carnitine palmitoyltransferase system. From concept to molecular analysis. Eur J Biochem 244:1–14

Lipids (2010) 45:593–602
DOI 10.1007/s11745-010-3432-1

ORIGINAL ARTICLE

Lipidomic Analysis of Porcine Olfactory Epithelial Membranes and Cilia

Simona Lobasso · Patrizia Lopalco · Roberto Angelini · Maristella Baronio · Francesco P. Fanizzi · Francesco Babudri · Angela Corcelli

Received: 7 April 2010 / Accepted: 6 May 2010 / Published online: 29 May 2010

Abstract The use of the matrix 9-aminoacridine has been recently introduced in matrix-assisted laser desorption/ionization time-of-flight (MALDI-TOF) mass spectrometry analysis of both anionic and cationic phospholipids. In the present study, we take advantage of this technique to analyze the lipids of porcine olfactory mucosa and a membrane fraction enriched in cilia. Thin-layer chromatography (TLC) and ^{31}P-NMR analyses of the lipid extracts were also performed in parallel. MALDI-TOF-MS allowed the identification of lipid classes in the total lipid extract and individual lipids present in the main TLC bands. The comparison between the composition of the two lipid extracts showed that: (1) cardiolipin, present in small amount in the whole olfactory mucosa lipid extract, was absent in the extract of membranes enriched in olfactory cilia, (2) phosphatidylethanolamine species were less abundant in ciliary than in whole epithelial membranes, (3) sulfoglycosphingolipids were detected in the lipid extract of ciliary membranes, but not in that of epithelial membranes. Our results indicate that the lipid pattern of ciliary membranes is different from that of whole-tissue membranes and suggest that olfactory receptors require a specific lipid environment for their functioning.

Keywords Olfactory epithelium · Pig · Lipids · MALDI-TOF-MS · TLC · ^{31}P-NMR

Abbreviations

AC3	Adenylcyclase III
cAMP	Cyclic-adenosine-monophosphate
Cer	Ceramides
CHOL	Cholesterol
CM	Ciliary membranes
DMSO	Dimethylsulfoxide
DTT	Dithiothreitol
Gb5	Globopentaosylceramides
IBMX	Isobutylmethylxanthine
MALDI-TOF-MS	Matrix-assisted laser desorption/ionization time-of-flight mass spectrometry
OR	Olfactory receptor
OSN	Olfactory sensory neuron
PtdOH	Phosphatidic acid
PtdCho	Phosphatidylcholine
PtdEtn	Phosphatidylethanolamine
p-PtdEtn	Plasmenyl-Phosphatidylethanolamine
PtdIns	Phosphatidylinositol
PMSF	Phenylmethanesulfonyl fluoride
PtdSer	Phosphatidylserine
Ptd_2Gro	Cardiolipin
S-GalCer	Sulfoglycosphingolipids

S. Lobasso · R. Angelini · M. Baronio · A. Corcelli (✉)
Department of Medical Biochemistry Medical Biology and Medical Physics, University Aldo Moro, Pl. G. Cesare, 70124 Bari, Italy
e-mail: a.corcelli@biologia.uniba.it

P. Lopalco
Institute for Microelectronics and Microsystems (IMM), National Research Council (CNR), Lecce, Italy

F. P. Fanizzi
Department of Biological and Environmental Sciences and Technologies, University of Salento, Lecce, Italy

F. Babudri
Department of Chemistry, University Aldo Moro, Bari, Italy

A. Corcelli
Institute for Chemical-Physical Processes, National Research Council (IPCF-CNR), Bari, Italy

CerPCho	Sphingomyelin
WM	Whole-tissue membranes

Introduction

Inhalation of odors across the surface of the olfactory epithelium of the animal nose activates the olfactory signaling cascade, which involves the binding of ligands to receptors localized on primary sensory cells, the olfactory sensory neurons (OSN). The OSN are bipolar neurons of the pseudostratified olfactory epithelium, having a thin sensory axon extending to higher brain regions and a single dendrite that ends with a knob, from which long fine cilia protrude, directly projected into the mucous of the olfactory epithelium.

Olfactory cilia are the sites of the sensory transduction apparatus. The binding of odorants to G-protein-coupled seven-transmembrane olfactory receptors (OR) activates the $G\alpha_{olf}$ subunit of a specific heterotrimeric G-protein complex, which stimulates the enzyme adenylcyclase III (AC3) to synthesize the second messenger molecule cyclic-adenosine-monophosphate (cAMP). cAMP in turn activates the opening of cyclic-nucleotide-gated ion channels present on the plasma membrane, generating electrical signals in the primary sensory axons [1, 2].

Each OSN expresses only one type of OR out of a repertoire of about 1,000 [3]. Numerous OSN expressing the same OR are dispersed in the olfactory mucosa, while their axons converge to form glomeruli in the olfactory bulb, where a precise distribution or map of odors exists.

It is known that several proteins involved in the sensory signaling cascade are compartmentalized in specialized membrane subdomains, called lipid rafts, which are expected to be spread in the olfactory ciliary membranes [4, 5].

In the lipidomics era it is surprising to find out that only a few analyses of the lipids of olfactory mucosa have been reported in the literature. Old reports described the lipid composition of plasma membranes isolated from bovine [6] and rat [7] olfactory mucosa, while no data are available either on pig olfactory mucosa in toto, or on isolated olfactory cilia.

It would be helpful to have an overview of the specific set of lipids in the sensory cilia in order to investigate the possible functions of lipids in signal transduction, adaptation, xenobiotic metabolism and OSN maturation.

The present study provides the first general characterization of the membrane lipids of the neuroepithelial olfactory mucosa covering pig turbinates and information on lipids associated with the specialized membrane domain of pig olfactory cilia.

Materials

The nasal cornets of pig were kindly provided immediately after sacrifice by the slaughterhouse in Ruvo di Puglia (Bari, Italy). The Cyclic AMP [^{3}H] assay system was purchased from Amersham (Freiburg, Germany). Odorants (Sigma–Aldrich, St. Louis, MO) were usually prepared as stock solutions in ethanol or DMSO. All organic solvents used were commercially distilled and of the highest available purity (Sigma–Aldrich). Plates for TLC (Silica gel 60A, 10 × 20 cm, 0.25 mm thick layer), obtained from Merck (Darmstadt, Germany), were washed twice with chloroform/methanol (1:1, by vol) and activated at 120 °C before use. The following lipid standards were obtained from Avanti Polar Lipids, Inc. (Alabaster, AL): 1,2-dimyristoyl-*sn*-glycero-3-phosphate (sodium salt) (14:0 PtdOH), 1,2-dimyristoyl-*sn*-glycero-3-phospho-L-serine (sodium salt) (14:0 PtdSer), 1,2-dipalmitoleoyl-*sn*-glycero-3-phosphoethanolamine (16:1 PtdEtn), 1,2-dioleoyl-*sn*-glycero-3-phospho-(1′-myo-inositol) (ammonium salt) (18:1 PtdIns), 1′,3′-bis [1,2-dimyristoyl-*sn*-glycero-3-phospho]-*sn*-glycerol (sodium salt) (14:0 Ptd_2Gro), 1,2-dimyristoleoyl-*sn*-glycero-3-phosphocholine (14:1 (Δ9-Cis) PtdCho), 1,2-distearoyl-*sn*-glycero-3-phosphocholine (18:0 PtdCho), 1,2-di-*O*-phytanyl-*sn*-glycero-3-phosphocholine (4ME 16:0 diether PtdCho), *N*-palmitoyl-D-*erythro*-sphingosylphosphorylcholine 16:0 CerPCho (d18:1/16:0). The matrix for MALDI-TOF–MS (9-aminoacridine hemihydrate) was purchased from Acros Organics (Morris Plains, MJ).

Methods

Isolation of Membranes Enriched in Olfactory Cilia

Ciliary membranes were detached and isolated from pig olfactory epithelia as previously described [8, 9]. The pig olfactory epithelia, situated on both left and right ethmoturbinates, were carefully stripped from the underlying bone and washed in ice-cold Ringer solution (120 mM NaCl, 5 mM KCl, 1.6 mM K_2HPO_4, 1.2 mM $MgS0_4$, 25 mM $NaHCO_3$, 7.5 mM glucose, pH 7.4) plus 1 mM PMSF within 10–20 min of slaughter. All operations were carried at 0–4 °C. The olfactory cilia were detached using a calcium shock procedure, raising the calcium concentration in the Ringer solution up to 10 mM. After gently shaking (20 min at 4 °C), the deciliated epithelia were removed by centrifugation (7,000*g* for 5 min). The supernatant was collected and the pellet incubated again with the solution containing 10 mM calcium ion for 20 min. After removing the deciliated epithelia by centrifugation, the supernatants containing the detached cilia were combined. Membranes enriched in olfactory cilia were collected by centrifuging at

27,000*g* for 15 min, and resuspended in Buffer A (3 mM $MgCl_2$, 2 mM EDTA, 10 mM Tris/HCl, 1 mM PMSF, pH 7.4) with 5% glycerol. Ciliary membranes were apportioned into small volumes and saved at −80 °C. The protein concentration was determined by the Bradford method [10], with bovine serum albumin as standard.

Whole-Tissue Membrane Isolation

Pig olfactory epithelia, carefully dissected as described in the previous paragraph, were suspended in 5–7 volumes of hypotonic Ringer solution (Ringer without NaCl) and homogenized on ice with a Potter homogenizer. Cartilage fragments and large epithelia pieces were removed by low speed centrifugation followed by filtration. The filtrate was then centrifuged twice at 1,500*g* for 10 min and the pigmented pellet removed. The final supernatant was centrifuged at 27,000*g* for 20 min to generate a light yellow pellet. This pellet was suspended in 5% glycerol-containing Buffer A and stored at −80 °C.

Adenylcyclase Assay

Adenylcyclase activity was assayed according to a modified version of the method described previously [11, 12]. All assays were carried out at 37 °C. Briefly 70 µl of cilia suspension (50–100 µg protein/ml) was mixed with 360 µl of stimulating buffer containing 200 mM NaCl, 10 mM EGTA, 50 mM MOPS, 2.5 mM $MgCl_2$, 1 mM DTT, 0.05% sodium cholate, 1 mM ATP, 20 µM GTP, 1 mM IBMX buffered at pH 7.4, with or without a stimulant (200 µM odorants or 5 µM forskolin). The incubation of cilia with the stimulating buffer (15 min at 37 °C) was stopped by adding 350 µl of ice cold 10% perchloric acid. Then samples were centrifuged at 2,500*g* for 5 min at 4 °C; 400 µl of the supernatant was added to 100 µl of 10 mM EDTA pH 7.0. The samples were then neutralized by adding 500 µl of a mixture containing 1,1,2-trichlorotrifluoroethane and tri-*n*-octylamine, mixed and then three phases were obtained by centrifugation; the upper phase contained the water soluble components and was used to estimate the amount of cAMP produced during the incubation of cilia with substrates. The cAMP was determined by radioimmunoassay using an Amersham kit.

Lipid Extraction

Total lipids were extracted from membranes using the Bligh and Dyer method [13] in the presence of 0.01% DTT as antioxidant. 6 ml of methanol/chloroform (2:1, by vol) was added to a 1.6 ml membrane suspension (about 6 mg proteins). The mixture was gently shaken for 15 min and then centrifuged to collect the supernatant. The residue pellet was re-extracted by adding 7.6 ml of methanol/chloroform/water (2:1:0.8, by vol). The mixture was again shaken for 15 min and centrifuged. Then 4 ml each of chloroform and 0.2 M KCl were added to the combined supernatant extracts to obtain a two-phase system, chloroform and methanol/water (1:0.9, by vol). After complete phase separation, the lipid-containing chloroform phase was brought to dryness under argon; dried lipids were weighed, suspended in a small chloroform volume and saved at −20 °C.

Thin-Layer Chromatography

Total lipid extracts were analyzed by TLC on silica gel plates and lipids were eluted with Solvent A, chloroform/methanol/acetic acid/water (85:15:10:3.5, by vol). For 2D-analysis, the plates were developed using Solvent B, chloroform/methanol/ammonium hydroxide (65:25:5, by vol), in the first dimension, and Solvent A in the second dimension. The solvent used for separation of neutral lipids on 1D-TLC was Solvent C, hexane/ethyl ether/acetic acid (70:30:1, by vol). Individual phospholipids were identified by reference to authentic lipid standards (Sigma–Aldrich). Lipids were detected by spraying plates with 5% sulfuric acid, followed by charring at 120 °C. Additional confirmation of the identity of lipids was obtained using (a) molybdenum blue reagent (Sigma–Aldrich), specific for phospholipids, (b) 0.5% α-naphthol in methanol/water (1:1, by vol), specific for glycolipids, (c) ninhydrine 0.25% in acetone/lutidine (9:1, by vol), for free amino groups [14]. To analyze in detail the various lipid components of the extracts, bands present on 1D-TLC, developed in Solvent A, were scraped and lipids extracted from silica, as previously described [14]; then lipid bands were analyzed by mass spectrometry.

MALDI-TOF Mass Spectrometry

Lipid analysis was performed as previously described [15]. Briefly total lipid extracts (10 mg/ml; dissolved in chloroform/methanol (1:1, by vol)) were diluted from 20 to 200 µl with isopropanol/acetonitrile (60:40, by vol). After mixing 10 µl of diluted sample with 10 µl of 9-aminoacridine (10 mg/ml; dissolved in isopropanol/acetonitrile (60:40, by vol)), 0.3 µl of the mixture was spotted on the instrument plate. The same procedure was followed to analyze the lipid standards (1 mg/ml). MS analysis was performed on a Bruker Microflex spectrometer (Bruker Daltonics, Bremen, Germany). Mass spectra were acquired in the positive and negative mode by averaging 600 consecutive laser shots (50 shots per subspectra). Synthetic lipid standards (Avanti Polar Lipids) were used as external standards for calibration.

NMR Spectroscopy

^{31}P-NMR analysis of phospholipids present in the total lipid extract was performed by following the previously described method [16, 17]. The method is based on the use of a methanol reagent containing D_2O and a dissolved EDTA salt, prepared as follows. The cesium salt of EDTA was prepared by titrating a 0.2 M suspension of EDTA free acid with CsOH to a pH of 6.0, at which point free EDTA was in solution; EDTA salt solutions were evaporated to dryness on a freeze-dry apparatus, dissolved in a minimum volume of D_2O to exchange labile ^{1}H for ^{2}D, dried a second time and dissolved in D_2O to a concentration of 0.2 M. The final methanol reagent was prepared by dissolving 1 ml of D_2O-EDTA solution in 4 ml of methanol. The use of D_2O is solely in order to provide a deuterium reference signal for magnetic resonance field-frequency stabilization; it is not essential for signal narrowing. Between 1 and 5 mg of phospholipid standards and 12 mg of total lipid extract were dissolved in 0.8 ml of deuterated chloroform. To this solution 0.4 ml of methanol reagent (containing Cs/EDTA) was added, and the mixture stirred gently. Two liquid phases were obtained, a larger chloroform phase and a smaller water phase. By using a Pasteur pipette, the sample was placed in an NMR test tube, where it separated within 1 min. The sample tube turbine was adjusted so that only the chloroform phase was detected by the NMR spectrometer's receiver coil. Magnetic field stabilization was obtained through the deuterium resonance of deuterated chloroform. Unless otherwise specified, samples were analyzed with proton broad-band decoupling to eliminate ^{1}H-^{31}P multiplets. Under these conditions each spectral resonance corresponded to single phosphorus. ^{31}P chemical shifts were relative to 85% H_3PO_4 as an external standard. Samples were analyzed using a Bruker DRX500 Avance instrument (Bruker Daltonics, Bremen, Germany).

Results

Whole-tissue membranes (WM) of neuroepithelial cells were isolated from pig olfactory epithelium and total lipids were extracted to be analyzed; in addition to the WM, a membrane fraction enriched in olfactory cilia (CM) was isolated by following the so-called calcium-shock method [8, 9], briefly described in Fig. 1.

Ciliary membrane enrichment was estimated by assay of odor-stimulated AC3 activity (i.e. an activity marker for olfactory cilia); Table 1 reports the specific AC3 activity both in membranes enriched in olfactory cilia and in the whole-tissue membranes, in the absence and in the presence of stimulants. Basal, forskolin-stimulated and odor-stimulated AC3 activity was observed in both the

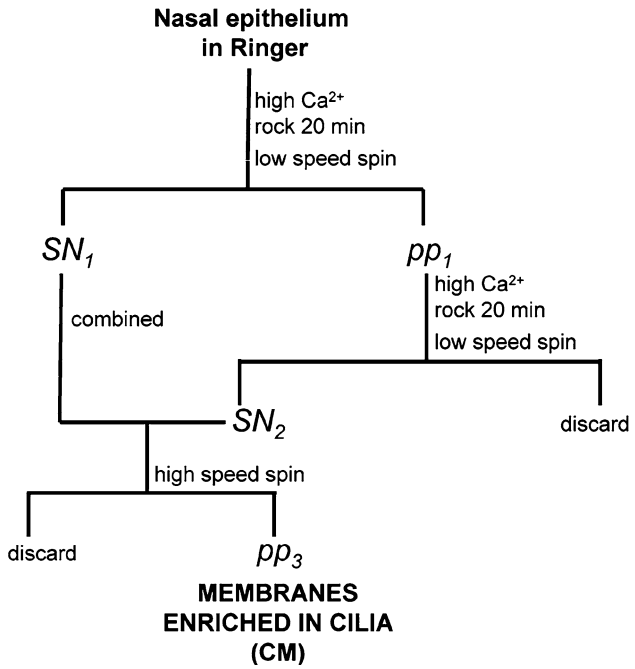

Fig. 1 Calcium-shock scheme for isolating membranes enriched in olfactory cilia. The pig olfactory epithelia were suspended in ice-cold Ringer solution containing 10 mM $CaCl_2$ (twice). To separate tissue fragments, fractions were centrifuged at low speed (7,000*g* for 5 min). To collect membranes enriched in olfactory cilia, the combined supernatants were centrifuged at high speed (27,000*g* for 15 min). The final membrane pellet was resuspended in Buffer A/5% glycerol and stored at −80 °C

membrane preparations, but it is evident that forskolin- and odor-stimulated activities were higher in the membrane fraction enriched in cilia.

Total lipids were extracted from the two different membrane preparations isolated from epithelial cells of pig nose; the lipid/protein ratio was about 1.2 in both membrane fractions. Figure 2 shows the two-dimensional TLC analyses of the total lipid extracts of CM (a) and WM (b). Lipid band identification was performed by comparison with authentic standards (St, in Fig. 2c). The two lipid profiles were similar; five main bands arose from the separation of polar lipid components during the chromatographic run, while neutral lipid bands could be seen close to the solvent front. Polar lipid bands corresponded to the following lipid classes (in R_f order): sphingomyelin (CerPCho) (as a doublet), phosphatidylinositol (PtdIns), phosphatidylcholine (PtdCho), phosphatidylserine (PtdSer), and phosphatidylethanolamine (PtdEtn); cardiolipin (Ptd_2Gro) was a minor lipid component present in the lipid extract of WM, while it was absent in the lipid extract of CM. Another difference between the two TLC plates in Fig. 2a, b was in the intensity of PtdEtn spot, which was more intense in whole than ciliary membranes. Glycosphingolipids (cerebrosides, gangliosides, sulfatides), relatively abundant components of nervous tissue cells, could

Table 1 Adenylcyclase activity in isolated membranes

	Basal activity ± SEM	Forskolin-stimulated activity ± SEM	Odor-stimulated activity ± SEM
Membranes enriched in cilia	197.7 ± 25.3	850.5 ± 39.4	480.1 ± 26.6
Whole-tissue membranes	60.9 ± 18.6	280.3 ± 13.2	150.5 ± 10.2

Cyclase assay was carried out with 5 μM forskolin or with an odor mixture containing 100 μM each of eugenol and citralva, as described in "Methods". The specific activity is reported as pmol cAMP/mg/min. The values are averages of three separate experiments. SEM refers to standard error of the mean

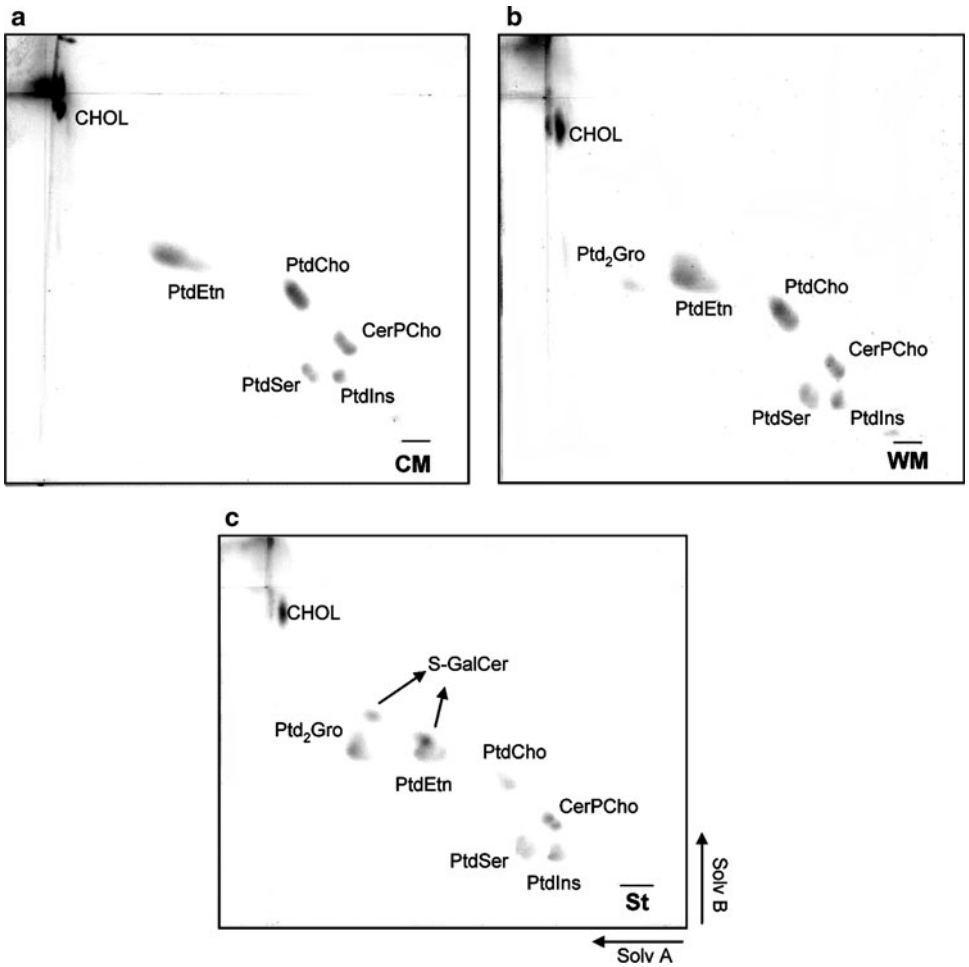

Fig. 2 2D-TLC of the lipid extracts of membranes isolated from pig olfactory epithelium. Total lipids were extracted from the membrane preparations isolated from epithelial cells of pig nose and from membranes enriched in olfactory cilia, as described in "Methods". Eighty micrograms of the lipid extract of whole-tissue (WM) and enriched in olfactory cilia (CM) membranes were loaded in the TLC plates (**a**) and (**b**), respectively. The following pair of solvents was used: Solvent B chloroform/methanol/ ammonium hydroxide (65:25:5, by vol), and then Solvent A chloroform/methanol/acetic acid/water (85:15:10:3.5, by vol). Total lipids were detected by spraying with 5% sulfuric acid and charring at 120 °C. On the TLC plate in (**c**) eight micrograms of each lipid standard were loaded. S-GalCer, galactocerebroside sulfate; Ptd_2Gro, cardiolipin; CHOL, cholesterol; PtdCho, phosphatidylcholine; PtdEtn, phosphatidylethanolamine; PtdIns, phosphatidylinositol; PtdSer, phosphatidylserine; CerPCho, sphingomyelin

be not detected by this technique either in whole or in ciliary membranes. Finally it was difficult to compare the cholesterol (CHOL) spots in WM and CM, because they were too close to the solvent front overlapping with other neutral lipid components, such as fatty acids and diacylglycerols. All together the TLC data in Fig. 2 document that our preparation of ciliary membranes was devoid of mitochondrial membranes and is characterized by a lower PtdEtn content than the whole membranes.

The difference in the PtdEtn content was also evident in the 1D-TLC lipid profiles (Fig. 3). To further investigate on the CHOL content of WM and CM, we analyzed their lipid extracts by 1D-TLC using a solvent for neutral lipids (as described in "Methods"). The results revealed that cholesterol percentage did not differ between the two lipid extracts and amounted to about 10% (Fig. 4).

To gain detailed information on the lipid classes present in pig olfactory mucosal cells, the total lipid extract of whole-tissue membranes was analyzed by MALDI-TOF-MS, using the novel matrix 9-aminoacridine allowing a fast reliable analysis of both zwitterionic and anionic lipid species [15]. Main lipid bands isolated from preparative 1D-TLC were also analyzed by MALDI-MS. Furthermore ESI-MS analysis of the lipid extract was performed to support the identification of lipid classes by MALDI-TOF-MS (not shown).

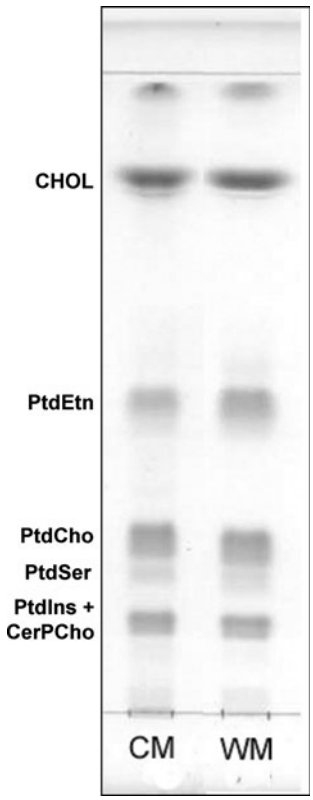

Fig. 3 1D-TLC lipid profiles of whole-tissue (WM) and enriched in olfactory cilia (CM) membranes. Total lipids (60 micrograms) were detected by charring. Solvent A was used

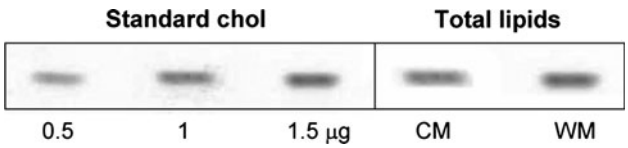

Fig. 4 Cholesterol content of whole-tissue (WM) and enriched in olfactory cilia (CM) membranes. Ten micrograms of each lipid extract was loaded on the TLC plate. The following solvent was used: Solvent C, hexane/ethyl ether/acetic acid (70:30:1, by vol). Only the CHOL bands are shown (note that with Solvent C polar lipids do not separate and are all together at the sample deposition line). The quantitative analysis of CHOL content was performed by video-densitometry (ImageJ software), using standard CHOL loaded on the same plate to construct the calibration curve

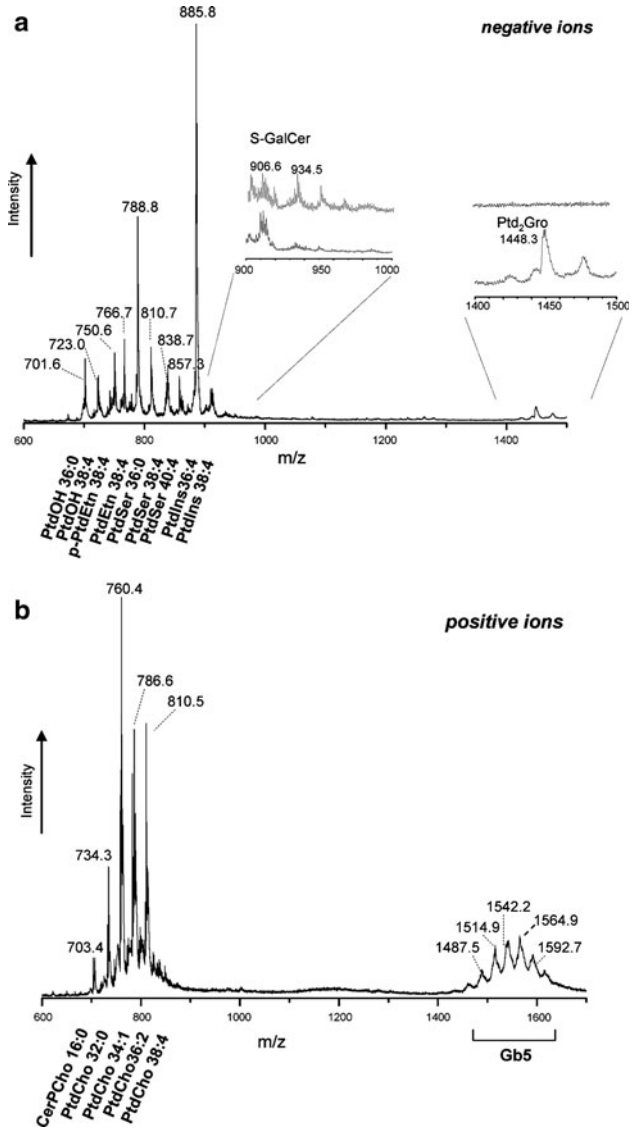

Fig. 5 MALDI-TOF mass spectrum profiles of the lipid extract of pig epithelial membranes in the negative (**a**) and positive (**b**) mode. The insets enlarge the two regions *m/z* 900–1,000 and 1,400–1,500 and show the comparison of the lipid profile of membranes isolated from the whole epithelium (*lower line*) with that of membranes enriched in olfactory cilia (*upper line*). PtdOh, phosphatidic acid; p-PtdEtn, plasmenyl-phosphatidylethanolamine; S-GalCer, galactosylceramide sulfated; Gb5, globopentaosylceramides

The mass spectrum acquired in the negative mode (Fig. 5a) showed two main peaks at *m/z* 885.8 and 788.8, corresponding to the molecular ions $[M - H]^-$of PtdIns 38:4 and PtdSer 36:2, respectively. The minor peaks at *m/z* 750.6, 766.7 and 810.7 corresponded to the molecular ions $[M - H]^-$ of plasmenyl-PtdEtn, PtdEtn and PtdSer (all 38:4 species), respectively. Furthermore the peaks at *m/z* 838.7 and 857.3 were attributed to a PtdSer 40:4 and PtdIns 36:4. Two small peaks were present in the high *m/z* range; the peak at *m/z* 1448.3 was attributed to the molecular ions $[M - H]^-$ of a cardiolipin, having four linoleic acid (18:2) chains, while the peak at *m/z* 1475.8 was not assigned. Of course the apparent amounts of the various lipids in the MALDI profiles depend on the lipid individual tendency to ionization together with its abundance in the extracts.

MALDI-TOF-MS analysis also allowed the direct identification of minor lipid components of olfactory neuroepithelial cells, such as sulfoglycosphingolipids (i.e. sulfatides). A detailed description of the advantages of MALDI-TOF in the analysis of sulfatides has been recently reported [18].

The peak at *m/z* 906.6 in the inset of the mass spectrum of Fig. 5a can be attributed to a sulfoglycosphingolipid, precisely to the sulfated galactosylceramide (S-GalCer), consisting of a C24:0 hydroxy-fatty acid plus the sphingoid 4-sphingenine (d18:1).

The mass spectrum acquired in the positive mode (Fig. 5b) was dominated by PtdCho species: the peaks at *m/z* 734.3, 760.4, 786.6 and 810.5 corresponded to the molecular ions $[M + H]^+$ of PtdCho 32:0, 34:1, 36:2 and 38:4, respectively; the minor peak at *m/z* 703.4 can be attributed to the molecular ion $[M + H]^+$ of the sphingolipid CerPCho 16:0.

Furthermore the peaks at higher *m/z* suggested the presence of other complex glycosphingolipids, such as gangliosides. The peaks between *m/z* 1,400 and 1,600 were attributed to globopentaosylceramides (Gb5), which give strong $[M + Na]^+$ ions, corresponding to glycosphingolipids all containing a C_{18}-sphingosine base and various fatty acids. The oligosaccharide chain of these glycosphingolipids consists of two *N*-acetylgalactosamine, two galactose and one glucose residue. In particular the major peaks at *m/z* 1,564.9 and 1,542.2 appear to correspond to the $[M + Na]^+$ and $[M + H]^+$ ions of species containing saturated fatty acids with 24 carbon atoms respectively, while that at *m/z* 1,514.9 to the $[M + H]^+$ ion of a specie having C22:0. The minor peaks at *m/z* 1,487.5 and 1,592.7 can be attributed to the $[M + H]^+$ ion of Gb5 with C20:0 and to the $[M + Na]^+$ ion of Gb5 with C26:0, respectively. Galactocerebrosides, giving signals in the range *m/z* 800–850, were not well distinct from the background.

The lipid extract obtained from the membrane fraction enriched in cilia was also analyzed by MALDI-TOF-MS; the mass spectra obtained (negative and positive mode) were similar to those of whole-tissue membranes. Some differences were found in the spectrum acquired in the negative mode, in the intervals of *m/z* values 900–1,000 and 1,200–1,600. These regions of the MALDI-TOF mass spectrum are reported in the insets of Fig. 5a, in order to allow direct comparison of MALDI-TOF-MS lipid profiles of the two different lipid extracts. It can be seen that in the mass spectrum of CM lipid extract: (a) cardiolipin was absent, in agreement with previous TLC data (see Fig. 2a); (b) additional peaks were present between *m/z* 930–960 suggesting that the ciliary membranes contained other sulfoglycosphingolipids, besides the S-GalCer at *m/z* 906 (see inset in Fig. 5a).

This last finding arises from the particularly high sensitivity of MALDI-MS in the detection of sulfoglycosphingolipids in the tissue lipid extracts; the cluster centered at *m/z* 934 indicates, on qualitative basis, the presence of an enrichment of long-chain sulfoglycosphingolipids (S-GalCer 26:0) in the specialized membrane of cilia.

Tables 2 and 3 report the main phospholipid and glycolipid classes, resulting from the MALDI-TOF-MS analysis of the total lipid extracts and individual TLC bands. Like lipids of nervous tissue, polar lipids of the olfactory mucosa contain mainly arachidonic (20:4) and stearic (18:0) fatty acids.

Finally, in order to check for quantitative differences in lipid composition between the whole-tissue and ciliary membranes, the total lipid extracts of both the membrane preparations were analyzed by ^{31}P-NMR spectroscopy. In order to assign NMR peaks to the lipid components in the extracts, authentic standard phospholipids were analyzed under the same experimental conditions and their chemical shifts are reported in Table 4.

Table 2 MALDI-TOF signals of phospholipids of pig olfactory epithelium

Class of phospholipid	Ion	Total fatty acid carbon n:n of double bonds													
		(32:0)	(32:1)	(34:1)	(34:2)	(36:0)	(36:2)	(36:4)	(38:4)	(40:4)	(16:0)	(18:0)	(22:0)	(24:0)	(36:4) (36:4)
Ptd_2Gro	$[M - H]^-$	–	–	–	–	–	–	–	–	–	–	–	–	–	1,448
PtdOH	$[M - H]^-$	–	–	–	–	701	–	–	723	–	–	–	–	–	–
PtdEtn	$[M - H]^-$	–	–	–	–	–	742	–	766	–	–	–	–	–	–
p-PtdEtn	$[M - H]^-$	–	–	–	–	–	–	–	750	–	–	–	–	–	–
PtdCho	$[M + H]^+$	734	–	760	–	–	786	–	810	–	–	–	–	–	–
PtdSer	$[M + H]^+$	–	734	–	–	–	–	–	–	–	–	–	–	–	–
PtdSer	$[M - H]^-$	–	–	–	760	788	–	–	810	838	–	–	–	–	–
PtdIns	$[M - H]^-$	–	–	–	–	–	–	857	885	–	–	–	–	–	–
CerPCho	$[M - H]^+$	–	–	–	–	–	–	–	–	–	703	731	787	815	–

Data reported are obtained from the analysis of total lipid extracts and bands isolated from preparative TLC. The *m/z* values are reported. The numbers (*x*:*y*) denote the total length and number of double bonds of both acyl chains, respectively, except for PtdEtn plasmalogen species (denoted with p-PtdEtn), in which the acyl chain at the *sn*-1 position is replaced with an alkenyl. For CerPCho species, the numbers in brackets correspond to the length and number of double bonds of the acyl chain, attached to the sphingosine base. For Ptd_2Gro species, the numbers refer to the two pairs of acyl chains

Table 3 MALDI-TOF signals of glycolipids of pig olfactory epithelium

Class of glycolipid	Ion	*m/z*	No. of sulfated residue	Chain length (carbon n:n of double bonds)		Oligosaccharides (no. of residues)		
				Sphingoid	Acyl	Glc	Gal	GalNAc
S-GalCer 24:0	$[M - H]^-$	906.6	1	18:1	24:0h	–	1	–
S-GalCer 26:0	$[M - H]^-$	934.5	1	18:1	26:0h	–	1	–
Gb5 26:0	$[M + Na]^+$	1,592.7	–	18:0	26:0	1	2	2
Gb5 24:0	$[M + Na]^+$	1,564.9	–	18:0	24:0	1	2	2
Gb5 24:0	$[M + H]^+$	1,542.2	–	18:0	24:0	1	2	2
Gb5 22:0	$[M + H]^+$	1,514.9	–	18:0	22:0	1	2	2
Gb5 20:0	$[M + H]^+$	1,487.5	–	18:0	20:0	1	2	2

S-GalCer, galactosylceramide sulfate; Gb5, globopentaosylceramide; Sphingoid, amino-alcohol chain; Acyl, fatty acid; h, hydroxylated fatty acid; Glc, glucose; Gal, galactose; GalNAc *N*-acetylglucosamine

Table 4 ^{31}P-chemical shifts of standard phospholipids

Lipid	ppm
PtdCho	0.115
PtdIns	0.621
CerPCho	0.911
PtdSer	0.894
PtdEtn	1.066
Ptd_2Gro	1.148

Chemical shifts are referenced to 85% H_3PO_4 as an external standard. The samples were prepared in the Cs/EDTA analytical reagent, as described in "Methods"

By comparing the two NMR spectra illustrated in Fig. 6 it can be seen that PtdCho, PtdIns, PtdSer, PtdEtn and CerPCho species were present in both the lipid extracts of WM (a) and CM (b); PtdSer and CerPCho peaks (at about 0.9 ppm) were very close to each other and not well resolved in the case of spectrum in panel a, because WM possibly contain more PtdSer and CerPCho species than CM.

The sums of the peak areas in the two spectra were 13.87 and 15.39 in CM and WM, respectively; this indicates that the total lipid phosphorus per mg of total lipid extract in CM was slightly lower than in WM and represents an indirect indication of the presence of an higher proportion of glycosphingolipids in cilia, compared to whole membranes. The last main peak at 1.05 ppm was assigned to a plasmenyl-PtdEtn lipid, in agreement with a previous literature report [19]; also the small, but clearly visible peak at 0.18 ppm can be attributed to plasmalogen PtdCho species, as well [19]. The Ptd_2Gro peak in the NMR profile of whole membranes was absent because its relative proportion in the lipid extract was below the sensitivity limit of NMR analysis.

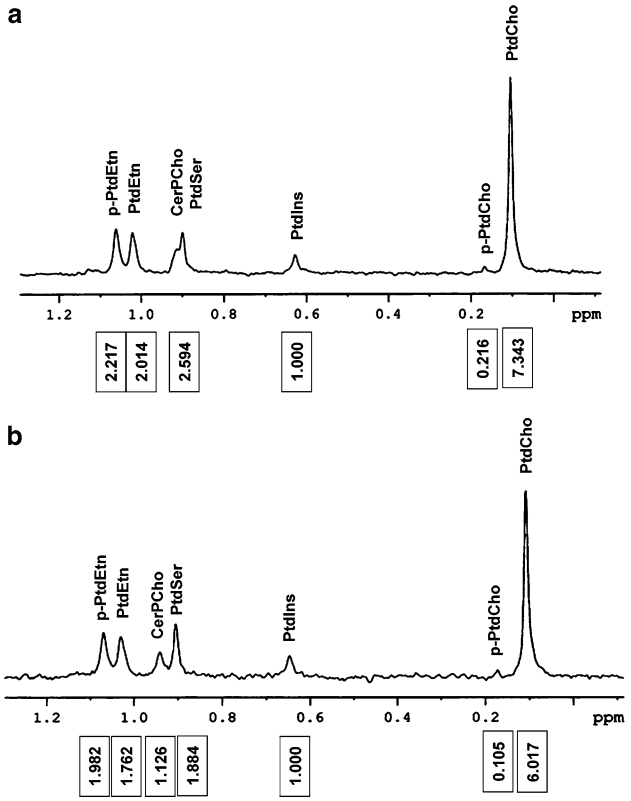

Fig. 6 ^{31}P-NMR spectra of the lipid extract of whole-tissue (**a**) and enriched in olfactory cilia (**b**) membranes. The areas of peaks are reported below the *x*-axis

The differences in the area peaks of the two NMR spectra indicate that the proportions of various lipid classes in the two lipid extracts were different. The area ratios PtdEtn species/(PtdSer + CerPCho) in CM and WM were 1.23 and 1.62 respectively, indicating that the proportion of PtdEtn species (as the sum of diacyl- and acyl-alkyl forms) was lower in CM extract in agreement with results from TLC analyses (Figs. 2, 3).

Discussion

Lipid research can offer important elements to complete our understanding of the genesis of sensory perception pathologies. For example anosmia, i.e. the inability to perceive odors, can arise from loss of olfactory cilia or impairment in the olfactory signaling cascade [20]. The complete comprehension of the mechanisms of ciliogenesis and assembly of membrane signaling molecules requires an integration of lipid and protein studies.

The present paper describes the results of a study on cellular lipids of porcine olfactory mucosa, previously selected to investigate the response of olfactory cilia to explosives, in the frame of an investigation to understand the molecular basis of the ability of an animal nose to detect buried landmines [21]. In the pig nose the olfactory mucosa is well distinct from the respiratory mucosa, while in other mammals technical difficulties are often involved in obtaining olfactory tissue from ethmoids without concomitant excision of non-olfactory tissue [7].

As the olfactory mucosa consists of three cell types (olfactory sensory neurons, supporting and basal cells), results of whole membrane lipid analyses refer to the average lipid composition of membranes arising from the different cell types in the epithelium.

A combination of a number of different analytical techniques was used to analyze in detail the lipids of olfactory neuroepithelium together with the novel MALDI-TOF-MS approach based on the use of the versatile matrix 9-aminoacridine [15].

The results shown here indicate that the lipid composition of olfactory mucosa in pig is similar to that of bovine and rat [6, 7]. Phospholipids account for about 85–90% (by weight) of the total lipid of mucosa, with zwitterionic lipids (PtdEtn, PtdCho and CerPCho) being more abundant (about 70%) than anionic species (PtdSer, PtdIns, Ptd_2Gro, PtdOH). Most phospholipids show a polyunsaturated fatty acid content with the arachidonic acid (20:4) residue predominating. The fatty acids in sphingomyelin, however, are totally saturated and include C16:0, C18:0, C22:0, and C24:0 chains.

Although separation of acyl-acyl from alkyl-acyl forms of phospholipids cannot be easily achieved by TLC, NMR analyses reveal that peak areas of alkyl-acyl PtdEtn almost equal the diacyl-PtdEtn species, as previously reported for mammalian brain tissue [22]. MALDI-TOF-MS analyses indicate that the main PtdEtn species contain C18 and C20 chains.

As regards glycosphingolipids, sulfoglycosphingolipids having C24:0 hydroxy-fatty acid and the sphingoid 4-sphingenine (d18:1), and pentaosylceramides containing a C_{18}-sphingosine base and various fatty acids, were only detected by MALDI-TOF analysis.

Here information on the lipid composition of a membrane fraction enriched in olfactory cilia is also reported. In the past biochemical exploration of the olfactory cilia was mostly based on a membrane preparation protocol established by Chen and Lancet [9]. Thus, the examination of the cilia preparations yields many of the molecular details, which support the current concept for olfactory signal transduction. In the present study we isolated a membrane fraction enriched in ciliary membranes of about the same quality as the analogous preparation obtained by other authors from rat tissue [23]. The lack of cardiolipin in the lipid extract of cilia represents a good internal index of the absence of mitochondrial and possibly other intracellular membranes in our preparation. However, we cannot exclude the presence of microvillar fragments of support cells in our ciliary membrane preparation.

In summary, the present analysis of the lipid extracts of whole-tissue membranes and enriched ciliary membranes shows that: (1) PtdEtn species are less abundant in ciliary membranes than in total epithelial membranes (TLC and NMR findings), and (2) long-chain sulfoglycosylsphingolipids (S-GalCer 26:0) are enriched in ciliary membranes compared to the crude olfactory membranes. The roles of sulfoglycosylsphingolipids in metabolism and functions of nervous tissue have been recently reviewed [24]. In principle, given the importance of lipids in signaling, any difference in the lipid bilayer composition might be considered a factor that can affect the membrane transduction properties. A decrease of membrane PtdEtn content was previously described in brain pathologies [22]. In olfactory cilia a decrease of PtdEtn level implies an increase in other membrane lipids, such as CerPCho, PtdSer and PtdIns, having a well known role in the assembly of lipid rafts (CerPCho, PtdSer) and signal transduction (PtdIns).

On the other hand, PtdEtn is preferentially located in the inner membrane leaflet, where it is associated with acidic phospholipids such as PtdIns [25]. Being cone-shaped phospholipid, PtdEtn can influence the determination of membrane curvature; it has been reported that intracellular tubular membranes of Golgi apparatus have a minor amount of PtdEtn compared to plasma membrane [25]. The possibility of a correlation between the low PtdEtn content and the high curvature in cross section of tubules of olfactory cilia remains to be investigated.

Although the presence of cholesterol-rich rafts in the olfactory cilia has been indirectly suggested by some biochemical studies [4, 5], here no cholesterol enrichment was found in the lipid extract of the ciliary membranes. However it should be considered that the analysis of the CM lipid extract gives information on the average lipid composition of the membrane lining the long (up to 100 μm) tubular structure of cilia, which presumably consist of different biochemical and functional domains.

In particular as it has been shown that cholesterol is absent at the necklace (or base) of the ciliary structure [26,

27], cholesterol in the CM lipid extract might represent the average of cholesterol in the proximal and distal tubular membranes. In conclusion, we cannot exclude the presence of cholesterol-rich domains (i.e., rafts) in ciliary membranes on the basis of the lack of cholesterol enrichment in the lipid extract of ciliary membranes.

Another element of complexity in the interpretation of lipid data arises from the recent finding that the chemosensory apparatus of cilia is also present at the level of the emergency cone of the sensory olfactory axon [28].

Here besides reporting the first lipidomic data on olfactory mucosa in toto, we show for the first time the presence of different lipid domains in the membranes of neuroepithelial olfactory cells. Our study complements recent proteomic studies, in which many ciliary proteins, that mediate chemo-electrical transduction, amplification and adaptation of the primary sensory signal, have been identified [29–32].

Acknowledgments We thank F. Naso of the University of Bari for the use of the MALDI-TOF instrument. This work was supported by the Italian Ministry of Defence (Contract n. 685/18.12.2003), by Regione Puglia (Grant code 15, Sens&MicroLab) and by Fondazione Cassa di Risparmio di Puglia, Bari, Italy.

References

1. Firestein S (2001) How the olfactory system makes sense of scents. Nature 413:211–217
2. Munger SD, Leinders-Zufall T, Zufall Z (2009) Subsystem organization of the mammalian sense of smell. Annu Rev Physiol 71:115–140
3. Buck L, Axel R (1991) A novel multigene family may encode odorant receptors: a molecular basis for odor recognition. Cell 65:175–187
4. Schreiber S, Fleischer J, Breer H, Boekhoff I (2000) A possible role for caveolin as a signaling organizer in olfactory sensory membranes. J Biol Chem 275:24115–24123
5. Brady JD, Rich TC, Le X, Stafford K, Fowler CJ, Lynch L, Karpen JW, Brown LR, Martens JR (2004) Functional role of lipid raft microdomains in cyclic nucleotide-gated channel activation. Mol Pharmacol 65:503–511
6. Koyama N, Sawada K, Kurihra K (1971) Isolation and some properties of plasma membranes from bovine olfactory epithelium. Biochim Biophys Acta 241:42–48
7. Russel Y, Evans P, Dodd GH (1989) Characterization of the total lipid and fatty acid composition of rat olfactory mucosa. J Lipid Res 30:877–883
8. Anholt RR, Aebi U, Snyder H (1986) A partially purified preparation of isolated chemosensory cilia from the olfactory epithelium of the Bullfrog, *Rana catesbeiana*. J Neurosci 6:1962–1969
9. Chen Z, Pace U, Heldman J, Shapira A, Lancet D (1986) Isolated frog olfactory cilia: a preparation of dendritic membranes from chemosensory neurons. J Neurosci 6:2146–2154
10. Bradford MM (1976) A rapid and sensitive method for the quantitation of microgram quantities of protein utilizing the principle of protein-dye binding. Anal Biochem 72:248–254
11. Schandar M, Laugwitz K, Boekhoff I, Kroner C, Gudermann T, Schultz G, Breer H (1998) Odorants selectively activate distinct G protein subtypes in olfactory cilia. J Biol Chem 273:16669–16677
12. Boekhoff I, Tareilus E, Strotmann J, Breer H (1990) Rapid activation of alternative second messenger pathways in olfactory cilia from rats by different odorants. EMBO J 9:2453–2458
13. Bligh EG, Dyer WJ (1959) A rapid method of total lipid extraction and purification. Can J Biochem Physiol 37:911–917
14. Kates M (1986) Techniques of lipidology laboratory techniques in biochemistry and molecular biology, vol 3. Elsevier, Amsterdam
15. Sun G, Yang K, Zhao Z, Guan S, Han X, Gross RW (2008) Matrix-assisted laser desorption/ionization time-of-flight mass spectrometric analysis of cellular glycerophospholipids enabled by multiplexed solvent dependent analyte-matrix interactions. Anal Chem 80:7576–7585
16. Meneses P, Glonek T (1988) High resolution ^{31}P NMR of extracted phospholipids. J Lipid Res 29:679–689
17. Corcelli A, Lattanzio VMT, Mascolo G, Papadia P, Fanizzi FP (2002) Lipid-protein stoichiometries in a crystalline biological membrane: NMR quantitative analysis of the lipid extract of the purple membrane. J Lipid Res 43:132–140
18. Cheng H, Sun G, Yang K, Gross RW, Han X (2010) Selective desorption/ionization of sulphatides by MALDI-MS facilitated using 9-aminoacridine as matrix. J Lipid Res. doi:101194/jlrD004077
19. Pearce JM, Komoroski RA, Mrak RE (2009) Phospholipid composition of postmortem schizophrenic brain by ^{31}P NMR spectroscopy. Magn Reson Med 61:28–34
20. Jenkins PM, McEwen DP, Martens JR (2009) Olfactory cilia: linking sensory cilia function and human disease. Chem Senses 34:451–464
21. Corcelli A, Lobasso S, Lopalco P, Dibattista M, Araneda R, Peterlin Z, Firestein S (2010) Detection of explosives by olfactory sensory neurons. J Hazard Mater 175:1096–1100
22. Käkelä R, Somerharju P, Tyynelä J (2003) Analysis of phospholipid molecular species in brains from patients with infantile and juvenile neuronal-ceroid lipofuscinosis using liquid chromatography-electrospray ionization mass spectrometry. J Neurochem 84:1051–1065
23. Washburn KB, Turner TJ, Talamo BR (2002) Comparison of a mechanical agitation and calcium shock methods for preparation of a membrane fraction enriched in olfactory cilia. Chem Senses 27:635–642
24. Eckhardt M (2008) The role and metabolism of sulfatides in the nervous system. Mol Neurobiol 37:93–103
25. Van Meer G, Voelker DR, Feigenson GW (2008) Membrane lipids: where they are and how they behave. Nat Rev Mol Cell Biol 9:112–124
26. Cuevas P, Gutierrez Diaz JA (1985) Absence of filipin-sterol complexes from the ciliary necklace of ependymal cells. Anat Embryol (Berl) 172:97–99
27. Satir P, Christensen ST (2007) Overview of structure and function of mammalian cilia. Annu Rev Physiol 69:377–400
28. Maritan M, Monaco G, Zamparo I, Zaccolo M, Pozzan T, Lodovichi C (2009) Odorant receptors at the growth cone are coupled to localized cAMP and Ca^{2+} increases. Proc Natl Acad Sci USA 106:3537–3542
29. Klimmeck D, Mayer U, Ungerer N, Warnken U, Schnölzer M, Frings S, Möhrlen F (2008) Calcium-signaling networks in olfactory receptor neurons. Neuroscience 151:901–912
30. Mayer U, Ungerer N, Klimmeck D, Warnken U, Schnölzer M, Frings S, Möhrlen F (2008) Proteomic analysis of a membrane preparation from rat olfactory sensory cilia. Chem Senses 33:145–162
31. Mayer U, Kuller A, Daiber FC, Neudorf I, Warnken U, Schnolzer M, Frings S, Mohrlen F (2009) The proteome of rat olfactory sensory cilia. Proteomics 9:322–334
32. Saavedra MV, Smalla KH, Thomas U, Sandoval S, Olavarria K, Castillo K, Delgado MG, Delgado R, Gundelfinger ED, Bacigalupo J, Wyneken U (2008) Scaffolding proteins in highly purified rat olfactory cilia membranes. Chem Senses 19:1123–1126

Lipids (2010) 45:603–612
DOI 10.1007/s11745-010-3434-z

ORIGINAL ARTICLE

Reversible Inhibitory Effects of Saturated and Unsaturated Alkyl Esters on the Carboxylesterases Activity in Rat Intestine

Ping Li · Chun-liu Zhu · Xin-xin Zhang · Li Gan · Hong-zhen Yu · Yong Gan

Received: 3 March 2010 / Accepted: 19 May 2010 / Published online: 8 June 2010

Abstract This study was conducted to investigate the relationship between the carbon chain length/double bonds of alkyl esters and their inhibitory potency/mechanism on carboxylesterases (CESs). CESs activity was evaluated by inhibition of adefovir dipivoxil (ADV) metabolism in rat intestinal homogenates. Furthermore, the inhibitory effect of BNPP and ethyl (*E*)-hex-2-enoate (C8:1) on drug absorption was evaluated in situ intestinal perfusion model. The results showed that the rank order of the inhibitory potency on CESs was C10:0 > C8:0 > C6:0 > C4:0 > C12:0, C8:1 > C8:0, C6:1 > C6:0, while the esters (C14:0, C13:1, C16:0, C18:0, C17:1, C20:0) were found to have no inhibitory effect at investigated concentrations. However, the unsaturated esters (C20:1, C20:2, C20:3) displayed the inhibitory effect on CESs. Moreover, the double reciprocal plots indicated that alky esters inhibited the CESs in competitive and mixed competitive ways which were reversible. In addition, the result of most effective CESs inhibitor C8:1 from in situ experiment showed that C8:1 can inhibit the CESs-mediated intestinal metabolism and improve the drug absorption. And the inhibition had no time-dependent effect, compared with that of BNPP groups. The study suggested that alkyl esters can be served as effective and reversible CESs inhibitors, besides that their inhibitory potency/mechanism can be affected by their carbon chain length/double bonds.

Keywords Carboxylesterases · Metabolism · Enzyme inhibitor · Ethyl esters · Methyl esters · Inhibitory mechanism · In situ intestine · Adefovir dipivoxil

P. Li · C. Zhu · X. Zhang · L. Gan · H. Yu · Y. Gan (✉)
Shanghai Institute of Materia Medica,
Chinese Academy of Sciences,
555 Zuchongzhi Road, Shanghai 201203, China
e-mail: simm2122@vip.sina.com

Abbreviations

ADF	Adefovir
ADV	Adefovir dipivoxil
BNPP	Bis-*p*-nitrophenylphosphate
CESs	Carboxylesterases
EE	Ethyl (*E*)-hex-2-enoate
LDH	Lactate dehydrogenase
Mono-ADV	Mono-(POM) PMEA

Introduction

The mammalian carboxylesterases (CESs; EC.3.1.1.1) belong to the α/β hydrolase-fold family of enzymes which are highly expressed in liver, intestine and kidney [1–3]. These enzymes are responsible for activation of ester prodrugs such as antitumor drugs (CPT-11 and capecitabin), antiviral drugs (tenofovir disoproxil and bis(POC)-PMPA) and narcotics (cocaine, heroin, and meperidine) [4–7]. They also play an important role in detoxification of many insecticides [8] and pharmaceuticals [9]. Because CESs metabolize a range of pharmaceuticals, the use of its inhibitors could potentially be valuable in modulating the efficacy of these therapeutics. Thus, studies concerned about inhibitors of CESs have attracted increased interest recently.

A number of different structural motifs have been developed for the inhibition of CESs, for example, organophosphates, trifluoromethyl ketones and aromatic ethane-1, 2-diones [10–12]. However, none of these inhibitors has been used in laboratory animals as oral administration, due to the unclear biocompatibility. While

some of the fruit extracts like edible strawberry juice [5, 13] and grapefruit juice [14, 15] are reported as relative safe CESs inhibitors, which can also be also used orally. The fruit extracts can inhibit the CESs because they contain various flavoring esters which have the ability to inhibit the CESs. In previous studies, several kinds of alkyl esters were described as inhibitors, such as: ethyl butyrate, ethyl caproate and so on [6, 13]. However, the relationship between the carbon chain length/double bonds of alkyl esters and the potency of CESs inhibition has not been described. Therefore, in our paper, we compared with each other various alkyl esters' inhibitory potency on CESs. Then we determined the relationship between the carbon chain length/double bonds of the alkyl esters and their inhibitory potency on CESs. Furthermore, we characterized the type of inhibitory mechanism of the selected ethyl esters and evaluated the inhibitory effect on drug absorption by the in situ perfusion experiment of rat.

Experimental Procedure

Materials

ADV and ADF were bought from the Sunheat Chemical Co. (Purity >96%). (Shanghai, China). Mono-ADV (Purity >98%) was a gift from Taizhou Shanhyu Chemical Import and Export Co. (Hangzhou, China). Ethyl acetate (>99%), ethyl caproate (99%), ethyl oleate (98%) were all purchased from the Sinopharm Chemical Reagent Co. (Shanghai, China). Ethyl butyrate (99%), ethyl caprylate (98%), capric acid ethyl ester (98%), ethyl laurate (98%), and ethyl myristate (98%), ethyl palmitate (98%) were purchased from the Shenbao Flavors and Fragrances Co. (Shanghai, China). Ethyl stearate (99%) was from the QianWei Oil Science & Technology Co. (Shanghai, China). Ethyl linoleate (99%) was a gift from the JinBan Food Co. (Shanghai, China). Ethyl γ-linolenate (99%) was purchased from the Energy Chemical Co. (Shanghai, China). Ethyl (*E*)-hex-2-enoate (98%) was from the Apple Flavors and Fragrances Co. (Shanghai, China). Crotonic acid ethyl ester (98%) was purchased from TCI Co. (Shanghai, China). 11-Dodecenoic methyl (>99%) and palmitelaidic acid methyl ester (>99%) were purchased from the Shanghai Zhongyitai International Trading Co. (Shanghai, China). BNPP (Purity >98%) was purchased from Sigma (Shanghai, China). Hanks' balanced salt solution (HBSS) was composed of 0.40 g/l KCl, 0.06 g/l KH_2PO_4, 8.00 g/l NaCl, 0.05 g/l Na_2HPO_4 (anhydrous), 1.00 g/l D-glucose, 0.35 g/l $NaHCO_3$, and was adjusted to pH 7.4. Krebs–Ringer Buffer (K–R) composition: 7.80 g/l NaCl, 0.35 g/l KCl, 0.37 g/l $CaCl_2$, 1.37 g/l $NaHCO_3$, 0.02 g/l NaH_2PO_4, 0.02 g/l $MgCl_2$, 1.48 g/l D-glucose (pH 6.8). Double distilled water was used. All other chemicals were of reagent grade.

Animals

Male Sprague–Dawley (SD) rats (body weight 280 ± 20 g) were obtained from the Medical Animal Test Center of the Shanghai Institute of Materia Medica (Shanghai, China). All experiments were performed according to the Shanghai Institute of Materia Medica guidelines for experimental animal care. The rats were fasted for 12 h prior to the experiment and had free access to water.

Preparation of Homogenates from Rat Intestinal Mucosa

The intestinal homogenates were prepared following the method used by Van Gelder et al. [16]. Briefly, the rat jejunum excised within 30 min after anesthetizing the animals, subsequently, a 20 cm segment was cut along the longitudinal axis and washed with ice-cold HBSS (pH 7.4) to remove the intestinal contents. Mucosa was removed by scraping with a glass microscope slide. The scrapings were homogenized at 0 °C in 10 ml of cold HBSS for 5 min using Ultra Turrax (IKA, Type T 10B, Guangzhou, China) at 6,000 rpm. After centrifugation at 10,000 rpm for 10 min at 4 °C, the supernatants were harvested and kept at −20 °C. The protein content was prepared to 0.1 mg/ml as an enzymatic preparation according to the Bradford method [17] using BSA as the standard when being used.

IC_{50} Determination

To determine the IC_{50} (concentration of inhibitors that results in 50% inhibition of original esterase ability) value [18]: the enzymatic preparations (0.1 mg/ml) were preincubated for 5 min; then the ADV solutions (10 mM DMSO stock solution) together with various concentrations of the inhibitors were added and incubated for 15 min at 37 °C. The same system without inhibitors served as the control group. The final drug concentration was always 100 μM and the final DMSO concentration was 1% which had no effect on esterase activity. By taking 100 μl of the incubation solution into 200 μl of ice-cold methanol, the reactions were stopped. The concentration range of each inhibitor was as follows: C4:0 ethyl acetate (6.38–102.15 mM); C6:0 ethyl butyrate (3.12–49.93 mM); C8:0 ethyl caproate (2.57–41.14 mM); C10:0 ethyl caprylate (2.10–33.67 mM); C12:0 capric acid ethyl ester (11.11–177.72 mM); C6:1 crotonic acid ethyl ester (3.36–53.74 mM); C8:1 ethyl (*E*)-hex-2-enoate (2.78–44.54 mM); C14:0 ethyl laurate (37.79–151.16 mM); C16:0 ethyl myristate (33.54–134.15 mM); C18:0 ethyl palmitate (30.13–120.50 mM);

C20:0 ethyl stearate (33.82–135.28 mM); C13:1 11-Dodecenoic methyl ester (38.14–152.54 mM); C17:1 palmitelaidic acid methyl ester (32.60–130.39 mM); C20:1 ethyl oleate (1.17–18.68 mM); C20:2 ethyl linoleate (1.18–18.80 mM); C20:3 ethyl γ-linolenate (1.24–19.87 mM). All the alkyl esters were expressed according to the literatures [19, 20] and their structures are described in Fig. 1. By taking 100 μl of the incubation solution into 200 μl of ice-cold methanol, the reactions were stopped. The samples were vortexed for 20 s and centrifuged at 8,000 rpm for 5 min at 4 °C, then the supernatant was taken and analyzed by HPLC as described below.

Inhibitory Mechanism of Ethyl Caproate, Ethyl (*E*)-hex-2-enoate and Ethyl Oleate

Three esters (C8:0, C8:1 and C20:1) were chosen and represented the saturated short-chain esters, the unsaturated short-chain esters and the unsaturated long-chain esters respectively. To characterize the inhibitory models of the representative esters, the enzymatic preparations (0.1 mg/ml) were preincubated for 5 min; then the ADV solution (10 mM DMSO stock solution) was added and incubated in the presence of various concentrations of the inhibitors for 5 min at 37 °C. The final drug concentration ranges from 25 to 100 μM. The concentration range of each inhibitor was as follows: ethyl caproate (0–41.14 mM); ethyl (*E*)-hex-2-enoate (0–44.54 mM); ethyl oleate (0–18.68 mM). All samples were processed and analyzed as described in section "IC_{50} determination".

The enzyme kinetics equations were as follows:

$$V = \frac{V_{\max}[S]}{K_m\left(1+\frac{[I]}{K_i}\right)+[S]}$$
$$\frac{1}{[V]} = \frac{K_m}{V_{\max}}\left(1+\frac{[I]}{K_i}\right)\cdot\frac{1}{[S]}+\frac{1}{V_{\max}} \quad (1)$$

where $[S]$ is the concentration of the substrate (μM), $[I]$ is the concentration of the inhibitor (mM).

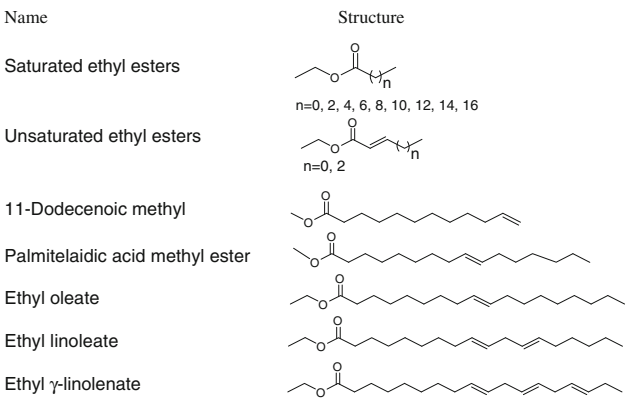

Fig. 1 The chemical structures of the alkyl esters

In Situ Perfusion Experiments with Superior Mesenteric Vein Blood Sampling

In situ perfusion experiments were performed primarily based on a previously described method [13, 21, 22] with modifications. Briefly, Male Sprague–Dawley (SD) rats were used. The terminal 10–20 cm of the ileum was cannulated. Blood from the superior mesenteric vein was collected in heparinized tubes at 27.5 min. In addition, 100 μl samples were taken from the perfusion medium after 2.5, 7.5, 12.5, 17.5, 22.5, and 27.5 min respectively. Then each of the sample was added to 400 μl of ice-cold methanol to stop the reaction and processed as in the section "IC_{50} determination" before being analyzed by HPLC. ADV absorption was evaluated in the absence (control group) of two CESs inhibitors ethyl (*E*)-hex-2-enoate (EE) and BNPP. In the control group, the investigated intestine was pre-exposed for 40 min to a K–R (pH 6.8) solution. Posteriorly, an isotonic solution of ADV (200 μM) was perfused. In additional experimental groups, we analyzed the effect of previous exposure (40 min) to the BNPP (400 μM)/EE (63.3 mM) upon ADV intestinal absorption and the absorption assay was performed as previously described. In BNPP/EE group I, after being pre-exposed identically as the control group, in the absorption experiment, a solution containing ADV (200 μM) plus BNPP (400 μM)/EE (63.3 mM) was perfused. In BNPP/EE group II, the investigated intestine was pre-exposed to an isotonic and buffered solution of BNPP (400 μM)/EE (63.3 mM) for 40 min, the absorption experiment was carried out as in BNPP/EE group I. Perfusate samples were tested for lactate dehydrogenase (LDH) release to measure cellular membrane damage using the LDH kit (Nan Jing Jian Cheng Shen Wu Yan Jiu Suo, 50T, Shanghai, China) [6].

HPLC Analysis for Drug Concentration In Vitro

ADV and its metabolite Mono-ADV were analyzed using a validated HPLC method with some modifications [23]. The HPLC system (Model SIL-20A, Shamadzu, Japan) was composed of an autosampler (SIL-20A), a pump (LC-20AT), a diode array detector (SPD-M20A) and a work station (Shimadzu liquid chromatography). The column used was Intersil $ODSC_{18}$ (4.6 mm×150 mm, 5 μm). The inject volume was 20 μl and the flow rate was 1 ml/min, mobile phase B consisted of 50 mM ammonium acetate buffer solution, 2 mM tetrabutylammonium hydrogen sulfate (pH 4.0); while A consisted of total methanol. Separation was carried out with 95% mobile phase B over 5 min, followed by a linear gradient from 95% to 30% mobile phase B over 5 min and with an isocratic stage of 5 min, then return to the initial condition (95% phase B) for 5 min. The retention time for ADV,

mono-ADV was 17.2, 14.6 min respectively. The intra-day and inter-day RSD were all below 5% for ADV concentration ranging from 0.625 to 40 μg/ml and mono-ADV concentration ranging from 0.625 to 40 μg/ml.

LC/MS/MS Analysis for Plasma Drug Concentration

The concentration of Mono-ADV and ADF in plasma was determined by a validated LC–MS/MS method [24], wherein, 9-(3-phosphonylmethoxypropyl) adenine was selected as the internal standard. The serum sample (0.2 ml) was pretreated by precipitating protein with methanol (0.4 ml) and the supernatant was injected for analysis. The analyte was separated on a Diamonsil C_{18} column (250×4.6 mm i.d., 5 μm; Beijing Dikma Co., Beijing, China) by isocratic elution with methanol: water: formic acid (20: 80: 1 v/v/v) at a flow rate of 0.5 ml/min and analyzed by an API 4000 triple-quadrupole mass spectrometric instrument (Applied Biosystems, Foster City, CA, USA) in multiple reaction monitoring mode. An electrospray ionization (ESI) source was applied and operated in the positive ion mode. Selected reaction monitoring (SRM) mode with the transitions of m/z 274 → m/z 162, m/z 388 → m/z 256/358 and m/z 288 → m/z 176 were used to quantify ADF, mono-ADV and the internal standard, respectively. The linear calibration curve was obtained in the concentration range of 0.02–4.0 μg/ml for ADF and 0.001–1.0 μg/ml for mono-ADV. The lower limit of quantitation of ADF/mono-ADV was 0.02/0.001 μg/ml.

Data Analysis

For the determination of the IC_{50}/K_i values, all analyses were performed using the mean values obtained from two independent experiments. The esterase activities in the presence of the inhibitors were expressed as percentages of the corresponding control values. The IC_{50} value was determined graphically. Moreover, the ClogP was calculated at http://www.organic-chemistry.org/prog/peol. The inhibition model was evaluated by graphical analysis with Lineweaver–Burk double reciprocal plots (1/[velocity] versus 1/[substrate]). Fits to competitive, noncompetitive, or mixed type inhibition models were evaluated according to the method described by Tseng SJ [25]. The K_i/K_i' values were calculated according to the following ways. Slopes of the inhibition lines were determined from linear regression analysis and converted to apparent K_m/V_m (K_m/V_m, app) values. Apparent K_m/V_m values were then plotted versus the concentration of inhibitors to generate K_i values (the x-intercepts of the linear regression line). Likewise, the y-intercepts were determined from linear regression analysis and converted to apparent $1/V_m$ ($1/V_m$, app) values. Apparent $1/V_m$ values were then plotted versus the concentration of inhibitors to generate K_i' values (the x-intercepts of the linear regression line).

For the perfusion experiments, on the one hand, due to slight variations in perfusate concentrations, the calculated steady-state perfusate concentration of ADV in each experiment was normalized to a target concentration of 200 μM, and the steady-state perfusate concentration of mono-ADV in each experiment was calculated as increased mono-ADV; on the other hand, results of the perfusion experiments with ADV absorption were expressed as ADV metabolites (ADF plus mono-ADV) appearing in the mesenteric plasma.

Statistical Analysis

All values were expressed as means ± standard deviation (SD). Statistically difference were determined by ANOVA followed by Tukey's test for multiple comparisons at a significance level of $P = 0.01$ or 0.05. All statistical analysis was performed using the GraphPad Instat for windows version 3.05 (GraphPad Software, Inc., CA, USA).

Results

IC_{50} Determination

Table 1 summarizes the comparative inhibitory effects of saturated alkyl esters and unsaturated alkyl esters on the metabolite formation in rat intestinal homogenates. The ADV was chosen as a probe and the CESs activity was evaluated by measuring metabolite formation in intestinal homogenates. The IC_{50} value was determined by plotting the log concentration versus relative remaining esterase activity of each test sample using software Origin 8.0, as shown in Figs. 2 and 3. The results showed that inhibitory potency of alkyl esters was based on their carbon chain length and the number of double bounds in the esters. The rank order of the inhibitory potency on CESs was C10:0 > C8:0 > C6:0 > C4:0, with a chain length of the esters less than or equal to 10. As the chain length of esters increases to 12, the inhibitory potency decreased acutely; and when the chain length of esters exceeded 12, both the saturated esters (C14:0, C16:0, etc.) and unsaturated esters (C13:1, C17:1) were found to have no inhibitory effect at investigated concentrations. However, the inhibitory effect emerged as the double bonds appear in the long-chain alkyl esters, like the C20:1, C20:2, etc. In addition, we compared the inhibitory potency between the saturated ethyl esters and unsaturated ethyl esters with the same carbon chain length. We found that unsaturated ethyl esters demonstrated even stronger inhibitory potency compared with

Table 1 IC_{50} values of alkyl esters on inhibiting the metabolism of ADV mediated by CESs

Alkyl esters	IC_{50} (mM)	ClogP	Alkyl esters/reference inhibitor	IC_{50} (mM)	ClogP
C4:0 ethyl acetate	124.1 ± 43.5	0.91	Reference inhibitor	$(3.3 \pm 1.2) \times 10^{-4}$	
C6:0 ethyl butyrate	70.2 ± 26.8	1.84	C6:1 crotonic acid ethyl ester	9.5 ± 3.6	1.48
C8:0 ethyl caproate	26.4 ± 4.3	2.77	C8:1 ethyl (*E*)-hex-2-enoate	5.6 ± 0.8	2.41
C10:0 ethyl caprylate	9.2 ± 1.0	3.7	C13:1 11-Dodecenoic methyl	NI	4.82
C12:0 capric acid ethyl ester	865.7 ± 515.6	4.63	C17:1 palmitelaidic acid methyl ester	NI	6.62
C14:0 ethyl laurate	NI	5.55	C20:1 ethyl oleate	7.5 ± 2.4	7.98
C16:0 ethyl myristate	NI	6.48	C20:2 ethyl linoleate	31.6 ± 1.0	7.62
C18:0 ethyl palmitate	NI	7.41	C20:3 ethyl γ-linolenic	21.0 ± 8.3	7.26
C20:0 ethyl stearate	NI	8.34			

NI Non-inhibited

Reference inhibitor BNPP was used as the specific inhibitor of CESs

the saturated ethyl esters, for instance: C8:1 > C8:0, C6:1 > C6:0.

Inhibitory Mechanism Determination

Type of inhibition of each inhibitor on CESs is shown in Fig. 5 and the K_i/K_i' values of them are also presented in Table 2. The Lineweaver–Burk plots below proved that all three investigated alkyl esters were reversible inhibitors, with different plots indicating different mechanisms. The inhibition lines of ethyl caproate intersect on the *y*-axis, illustrating that such inhibitors do not affect V_{max}, showing a competitive inhibitory mechanism. Similarly, the inhibition lines of ethyl (*E*)-hex-2-enoate intersect on the second quadrant, displaying a mixed competitive inhibitory mechanism. The results showed that ethyl oleate with long carbon chain also inhibit CESs in a mixed competitive way, with the inhibition lines intersect on the second quadrant.

In Situ Perfusion Experiments with Superior Mesenteric Vein Blood Sampling

Figure 6a shows the disappearance of ADV equivalents (ADV plus mono-ADV) and the appearance of a mono-ADV metabolite in the lumen during perfusion of the rat intestinal segment with ADV in the pre-exposed or co-perfused of BNPP (400 μM). A significant ($P < 0.05$)

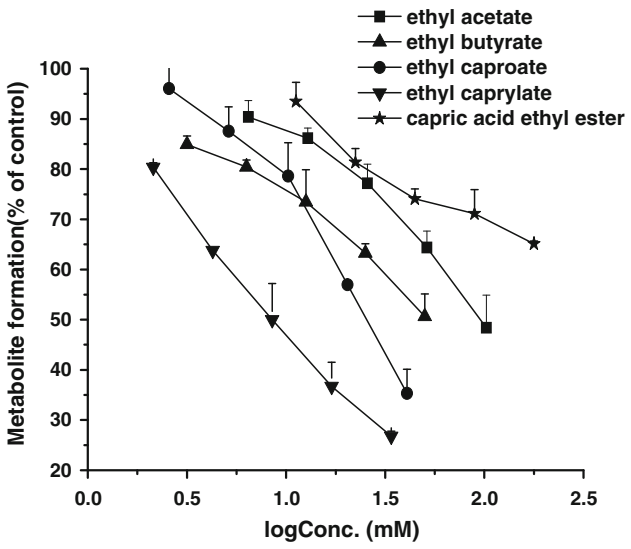

Fig. 2 The IC_{50} determination of saturated ethyl esters in intestinal homogenates of rat. Activities were expressed as a percentage of metabolite formation compared with the control group. Results were means ± SD error bar of duplicate determinations

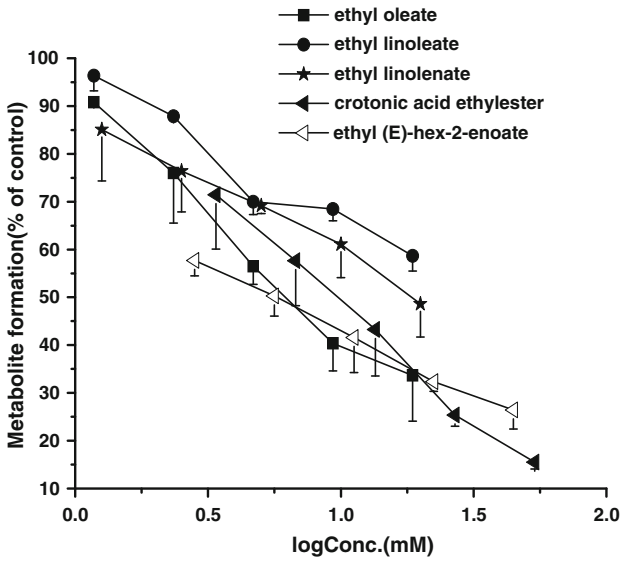

Fig. 3 The IC_{50} determination of unsaturated ethyl esters in intestinal homogenates of rat. Activities were expressed as a percentage of metabolite formation compared with the control group. Results were means ± SD error bar of duplicate determinations

Table 2 K_i/K_i' values and inhibitory models of alkyl esters on inhibiting the metabolism of ADV mediated by CESs

Alkyl esters	C8:0 ethyl caproate	C8:1 ethyl (*E*)-hex-2-enoate	C20:1 ethyl oleate
K_i/K_i' (mM)	18.3	11.8/9.3	5.6/21.7
Models	Competitive	Mixed competitive	Mixed competitive

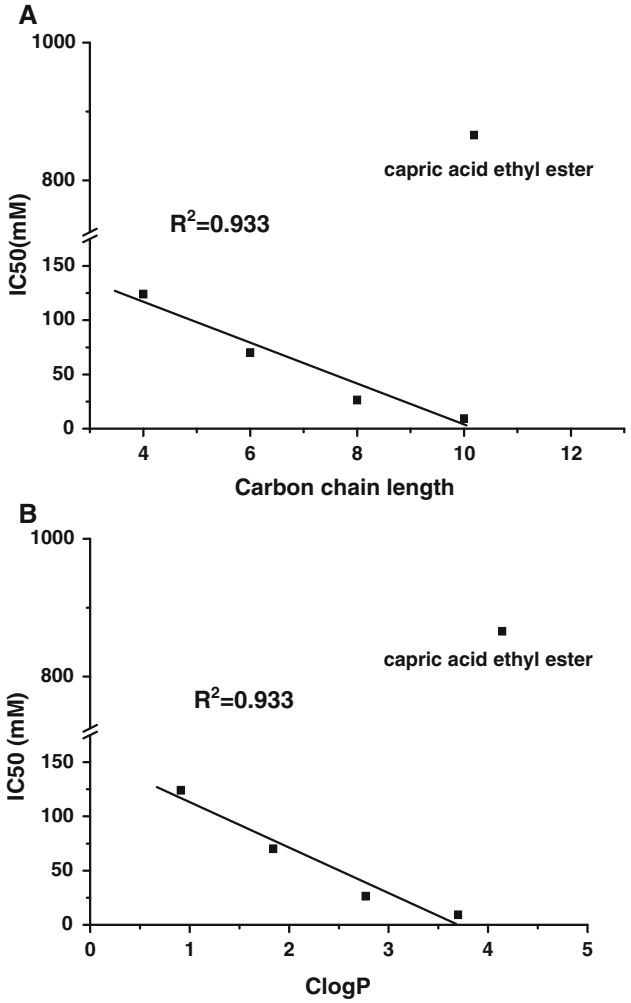

Fig. 4 The relationship between carbon chain length/ClogP of ethyl esters and inhibitory potency

decrease of ADV equivalents was observed in BNPP group I and II at 27.5 min, compared with that of control group; meanwhile, there was a very significant ($P < 0.01$) increase in mono-ADV metabolite in the lumen at 27.5 min in the control group, compared with that of both BNPP groups; simultaneously, a 4.4/2.2-fold increase in ADV metabolites appearing in the plasma was observed at 27.5 min in BNPP groups II/I respectively, as compared with the control group (Fig. 7). On the other hand, the effect of prior 40 min exposure of the rat intestine to BNPP in BNPP group II increased the drug disappearance at 27.5 min significantly with respect to the BNPP group I ($P < 0.05$) (Fig. 6a); in addition, a significant ($P < 0.05$) appearance of mono-ADV metabolite was observed at 27.5 min in BNPP group I, compared with that of BNPP group II; meanwhile, a 0.8-fold increase in ADV metabolites appearing in the plasma was observed in BNPP group II, compared with BNPP group I (Fig. 7).

Figure 6b shows the disappearance of ADV equivalents and the appearance of mono-ADV metabolite in the lumen during perfusion of the rat intestinal segment with ADV in the pre-exposed or co-perfused of EE (63.3 mM). A significant ($P < 0.01$) decrease of ADV equivalents was observed in both two EE groups at 27.5 min, compared with that of the control group; in addition, a significant ($P < 0.01$) appearance of mono-ADV metabolite was observed in control group, compared with that of two EE groups; simultaneously, a similar increase (1.0/1.2-fold) of ADV metabolites absorbing in the plasma was observed at 27.5 min in EE group II/I respectively, as compared with the control group (Fig. 7). On the other hand, the effect of prior 40 min exposure of the rat intestine to EE in EE group II did nöt increase the drug disappearance or decrease the metabolite formation with respect to the EE group I ($P = 0.1/0.8$) (Fig. 6b); meanwhile, no more ADV metabolites appearing in the plasma was observed in EE group II, compared with EE group I (Fig. 7).

Discussion

Previous studies have demonstrated that alkyl esters could be one kind of safe and effective CESs inhibitor, however, no other studies concerning the relationship between the alkyl esters' structure and inhibitory potency have been reported [6, 13]. It is necessary to provide structure-related insights into the interaction between CESs and alkyl esters. Thus, the development of alkyl esters for use in modulating CESs-mediated metabolism in vivo would be easier.

The present study investigated the influence of carbon chain length and level of unsaturation on the inhibitory potency of a homologous series of esters (Figs. 2, 3, 4). As we can see, there are four kinds of alkyl esters in this homologous series of esters. They are saturated short-chain esters (C4–C12), unsaturated short-chain esters (C4–C12), saturated long-chain esters (C14–C20), unsaturated long-chain esters (C14–C20). The result of saturated short-chain esters was inconsistent with previous studies, as shown in Fig. 4a, there is linear correlation between carbon chain length and IC_{50} values with $R^2 = 0.933$ [6]; besides, we found that IC_{50} values were also dependent on ClogP values of the saturated short-chain esters, which was in line with the CESs inhibitors isatins [12]. Meanwhile,

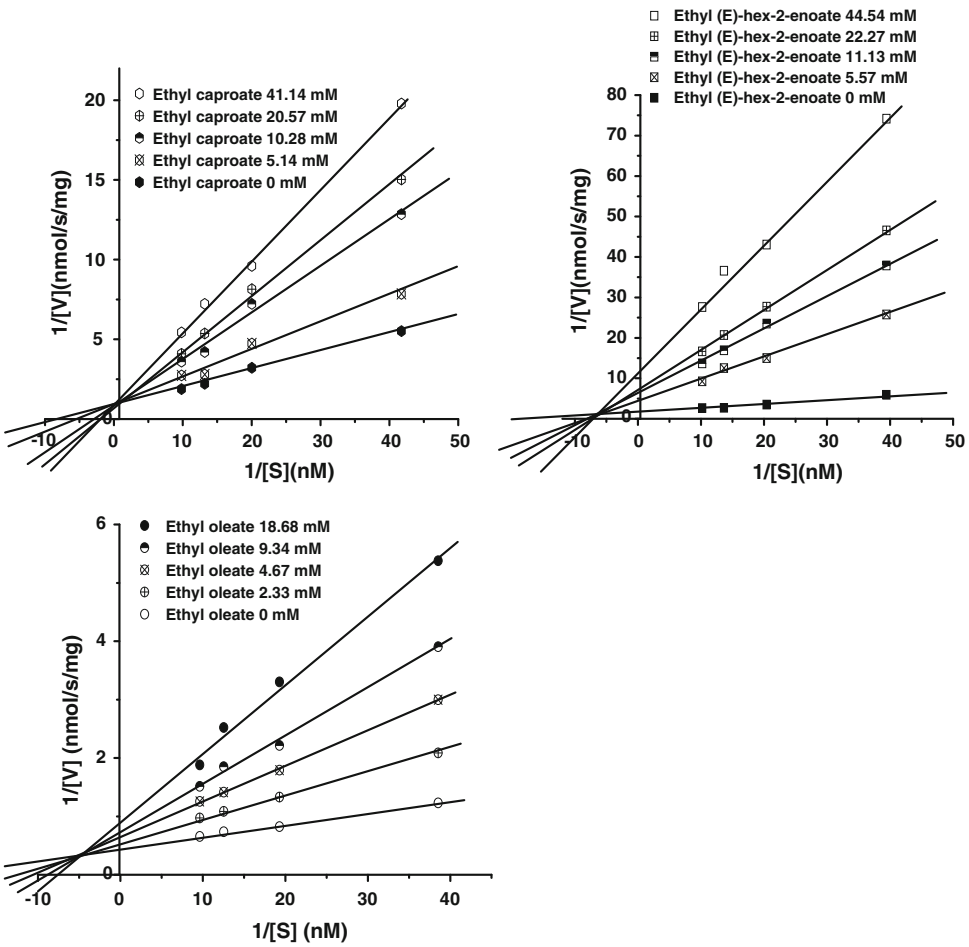

Fig. 5 Lineweaver–Burk plots of the effect of ethyl esters on formation of mono-ADV in rat intestinal homogenates. Each result represents the mean of duplicate determinations. *Lines* represented results of linear regression of transformed data

unsaturated short-chain esters demonstrated even stronger inhibitory potency compared with the saturated short-chain esters, which has not been reported before. Furthermore, both the saturated long-chain esters (C14:0, C16:0, C18:0, C20:0) and unsaturated long-chain esters (C13:1, C17:1) showed no inhibitory effect on CESs. But the unsaturated long-chain esters (C20:1, 2, 3) demonstrated a similar inhibitory potency as the saturated short-chain esters did, which has not been reported before. According to the literature [26], fatty acid esters like C20:1 may be hydrolyzed by CESs in vivo, which indicates that fatty acid esters can interact with the enzyme. It then explains why the (C20:1, 2, 3) demonstrated an inhibitory potency similar to that of the saturated short-chain esters. Moreover, the fatty acid esters are often employed as an excipient in lipid formulation as the oil phase or cosurfactant [27], which makes it possible to incorporate the fatty acid esters as CESs inhibitors into the formulations, thus improving the absorption of ester prodrugs. In addition, the above-mentioned different inhibitory potencies of these esters may be due to various affinities of esters for the active pocket of CESs [28, 29]. As reported [6], there are all kinds of physiochemical characteristics that can affect the inhibitor's affinity to the active site of the enzyme, including the size, steric hindrance and hydrogen bonding potential. In our study, we chose a homologous series of esters with different carbon chain length and level of unsaturation of carboxylic acids, which would lead to different steric hindrances and hydrogen bonding potentials respectively, thus finally influence the inhibitors' affinity to the active site of the enzyme, resulting in different inhibitory potency.

Our result also showed that the structure of the inhibitors can also affect the inhibitory mechanism. According to the Lineweaver–Burk plots (Fig. 5), all investigated ethyl esters demonstrated reversible inhibitory mechanism but with different specific ones. The ethyl caproate (C8:0) can inhibit the CESs in a competitive mechanism, which may be owing to its similar structure to the real substrate of the CESs [30]. Because ADV is the substrate of CESs [22], the C8:0 and ADV compete for access to the active pocket of CESs. However, the ethyl (*E*)-hex-2-enoate (C8:1) and ethyl oleate (C20:1) indicated the different inhibitory mechanisms of CESs. The exact reason for the observations was unknown, but one possible explanation is that the CESs utilizes a two-step serine hydrolase mechanism

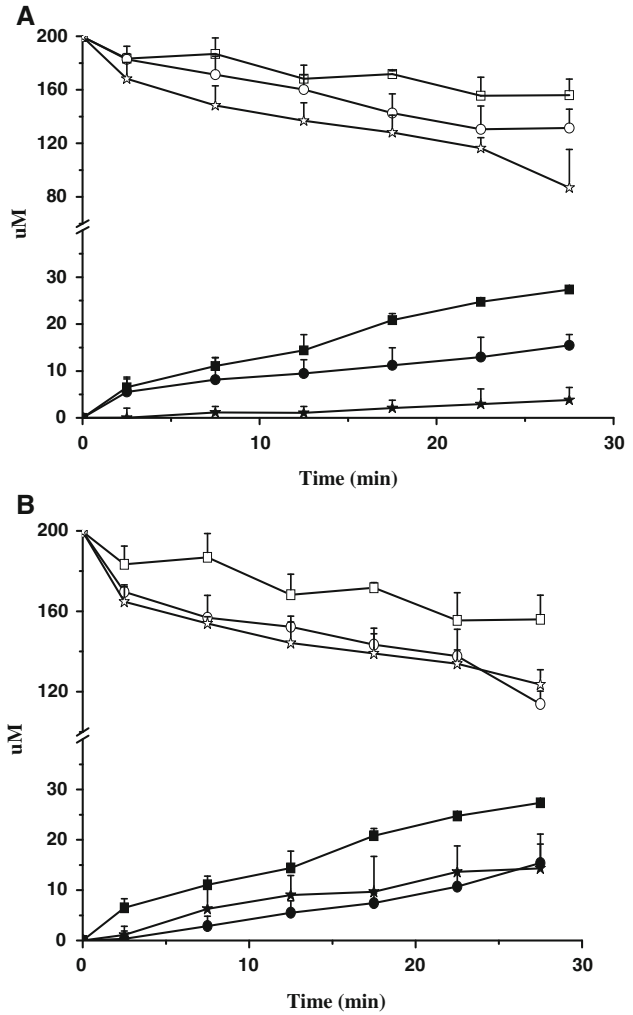

Fig. 6 Disappearance of perfusate concentrations of ADV equivalents (*open signs*) and appearance of its mono-ADV metabolite (*full signs*) in perfusate during in situ perfusion experiments. Results were expressed as means ± SD error bar ($n = 4$). **a** Control group (*squares*), BNPP group I (*circles*), BNPP group II (*stars*). **b** Control group (*squares*), EE group I (*circles*), EE group II (*stars*)

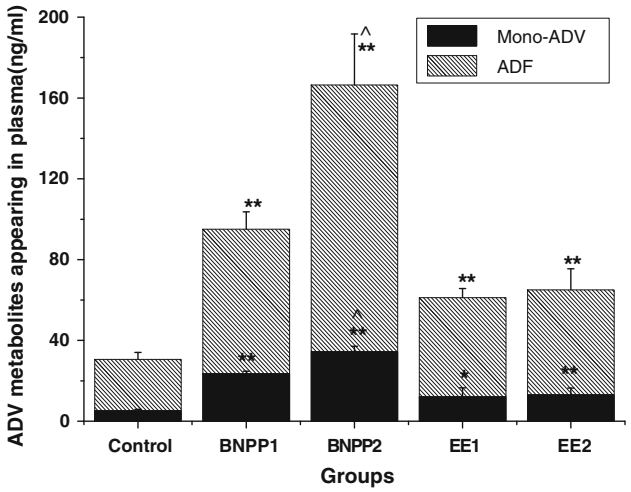

Fig. 7 ADV metabolites appearing in plasma during in situ perfusion experiments in different groups. *Black bars*, appearance of the mono-ADV concentration in plasma; *gray bars*, appearance of the ADF concentration in plasma. No intact ADV could be detected. Results were expressed as means ± SD error bar ($n = 4$). **, very significantly different from the appearance of total ADV metabolites or mono-ADV in the control group ($P < 0.01$). *, significantly different from the appearance of mono-ADV in the control group ($P < 0.05$). ^, very significantly different from the appearance of total ADV metabolites or mono-ADV in the BNPP group I ($P < 0.01$)

involving the formation of a covalent acyl-intermediate on the active site serine residue, enabling larger and more varied substrate molecules access to the buried catalytic residues [31]. As reported, unsaturated fatty acids could bind to CYP enzymes to form a type I spectral change and inhibit the metabolism of some drugs, but saturated fatty acids, were not capable of producing the type I spectral change when binding to CYP enzymes [32]. Thus, we hypothesized that the unsaturated alkyl esters might bind to the CESs-substrate complexes, which would cause the enzymes' conformation change, reducing the enzyme activity and showing a mixed inhibitory mechanism [33].

Rat ileum perfusion was used to study the effect of CESs inhibitors on the intestinal absorption of the prodrug ADV, because of the similar degradation rate of its homologue prodrug tenofovir disoproxil in homogenates from rat ileum compared with homogenates from human ileum [17]. EE (C8:1) was chosen to be studied in the intestinal perfusion experiment, owing to its strongest inhibitory effect on CESs (Table 1). The result of the perfusion study showed that a significant decrease in mono-ADV metabolite formation during perfusion in the presence of BNPP/EE (Fig. 6), indicated that ADV was protected against CESs-mediated metabolism by BNPP/EE. In addition, there was increased absorption of ADV in BNPP/EE groups (Fig. 7), which was in accordance with the drug disappearance in perfusate. This is because BNPP/EE can prevent ADV from degrading into its metabolites and more prodrug ADV remained (Fig. 6). Since the prodrug ADV is more permeable than its metabolites [23], the absorption could be enhanced in the presence of BNPP/EE. Moreover, according to our results, 40 min of intestine pre-exposure to BNPP decreased the mono-ADV metabolite formation and increased ADV absorption versus the BNPP group I (Figs. 6a, 7), which suggested that BNPP inhibition has time-dependent effect. This can be attributed to BNPP's covalent binding to the CESs, which is irreversible. Consequently, a CES-inhibited condition might be obtained by 40 min preperfusion with BNPP at 400 μM [34–36]. However, 40 min of intestine pre-exposure to EE didn't show any difference with the EE group I which had no pre-exposure to EE (Figs. 6b, 7). The result demonstrated that the EE inhibition has no time-dependent effect. Because EE may bind to enzymes with non-covalent interactions

such as hydrogen bonds, hydrophobic interactions and ionic bonds, which are reversible and can be easily removed by dilution or dialysis. Therefore, EE could be a transitory and safe CESs inhibitor, compared with the irreversible inhibitor BNPP that was also proved to have a toxic effect (e.g. $LD_{50} = 410$ mg/kg i.p. in mice) [37].

The increase absorption of ADV by the CESs inhibitors was not due to any considerable mucosa damage. This was shown by measuring the effect of CESs inhibitors on the release of LDH in the perfusate as an indication of cell membrane disruption [38]. No significant increase in LDH activity was observed when it was in the presence of CESs inhibitors such as: BNPP and EE ($22.0 \pm 1.9/19.0 \pm 2.1$ U/l cm in BNPP group II/EE II, compared with 19.9 ± 1.4 U/l cm in control group). Therefore, it can be concluded that BNPP and EE at the investigated concentration, did not affect the intestinal cell membranes.

In conclusion, the present study indicates that alkyl esters showed variable inhibitory effects on CESs-mediated ADV metabolism and that the number of double bonds, as well as the carbon chain lengths in the esters, may therefore play an important role in the inhibition of CESs. Furthermore, the alkyl eaters, especially the aliphatic esters, are biocompatible and can be used as a functional excipient in formulations to increase the ester prodrug absorption.

Acknowledgments We thank Mrs Dan Li for help on calculating K_i/K_i' values by offering the GraphPad Prism 4.00 (GraphPad Software, San Diego California, USA). This work was supported by the National Natural Sciences Foundation of China (No. 30701054) and National Science & Technology Major Project "Key New Drug Creation and Manufacturing Program" (No. 2009ZX09301-001). This work was also supported in part by the National Basic Research Program of China (No. 2009CB930300).

References

1. Bianca ML, Ronald TB (2006) Enzymes involved in the bioconversion of ester-based prodrugs. J Pharm Sci 95:1177–1195
2. Heikinheimo P, Goldman A, Jeffries C, Ollis D (1999) Of barn owls and bankers: a lush variety of alpha/beta hydrolases. Struct Fold Des 7:R141–R146
3. Tetsuo S, Masakiyo H (1998) The mammalian carboxylesterase: from molecules to functions. Annu Rev Pharmacol Toxicol 38:257–288
4. Hyatt JL, Tsurkan L, Wierdl M, Edwards CC, Danks MK, Potter PM (2006) Intracellular inhibition of carboxylesterases by benzil: modulation of CPT-11 cytotoxicity. Mol Cancer Ther 5(9):2281–2288
5. Naesens L (1999) Inhibition of intestinal metabolism of the antiviral ester prodrug Bis(POC)-PMPA by nature identical fruit extracts as a strategy to enhance its oral absorption: in vitro study. Pharm Res 16(7):1035–1040
6. Van Gelder J, Deferme S, Naesens L, De Clercq E, van den Mooter G, Kinget R, Augustijns P (2002) Intestinal absorption enhancement of the ester prodrug tenofovir disoproxil fumarate through modulation of the biochemical barrier by defined ester mixtures. Drug Metab Dispos 30(8):924–930
7. Zhang J, Burnell JC, Dumaual N, Bosron WF (1999) Binding and hydrolysis of meperidine by human liver carboxylesterase hCE-1. J Pharmacol Exp Ther 290:314–318
8. Wheelock CE, Shan G, Ottea J (2005) Overview of carboxylesterases and their role in the metabolism of insecticides. J Pestic Sci 30:75–83
9. Redinbo MR, Potter PM (2005) Mammalian carboxylesterases: from drug targets to protein therapeutics. Drug Discov Today 10:313–325
10. Brandt E, Heymann E, Mentlein R (1980) Selective inhibition of rat liver carboxylesterases by various organophosphorus diesters in vivo and in vitro. Biochem Pharmacol 29:1927–1931
11. Harada T, Nakagawa Y, Wadkins RM, Potter PM, Wheelock CE (2009) Comparison of benzil and trifluoromethyl ketone (TFK)-mediated carboxylesterase inhibition using classical and 3D-quantitative structure–activity relationship analysis. Bioorg Med Chem 17:149–164
12. Hyatt JL, Moak T, Hatfield MJ, Tsurkan L, Edwards CC, Wierdl M, Danks MK, Wadkins RM, Potter PM (2007) Selective inhibition of carboxylesterases by isatins, indole-2, 3-diones. J Med Chem 50:1876–1885
13. Van Gelder J, Deferme S, Naesens L, De Clercq E, Van den Mooter G, Kinget R, Augustijns P (2000) Increased absorption of the antiviral ester prodrug tenofovir disoproxil in rat ileum by inhibiting its intestinal metabolism. Drug Metab Dispos 28:1394–1396
14. Ping L, Patrick SC, Liang-Shang G, Suresh KB (2007) Esterase inhibition attribute of grapefruit juice leading to a new drug interaction. Drug Metab Dispos 35:1023–1031
15. Ping L, Patrick SC, Liang-Shang G, Suresh KB (2007) Esterase inhibition by grapefruit juice flavonoids leading to a new drug interaction. Drug Metab Dispos 35:1203–1208
16. Van Gelder J, Shafiee M, De Clercq E, Penninckx F, Van den Mooter G, Kinget R, Augustijns P (2000) Species-dependent and site-specific intestinal metabolism of ester prodrugs. Int J Pharm 205:93–100
17. Bradford MM (1976) A rapid and sensitive method for the quantitation of microgram quantities of protein utilizing the principle of protein-dye binding. Anal Biochem 72:248–254
18. Xiuhua R, Xinliang M, Lei C, Kewen X, Luqin S, Jun Q, Aaron DS, Gao L (2009) Nonionic surfactants are strong inhibitors of cytochrome P4503A biotransformation activity in vitro and in vivo. Eur J Pharm Sci 36:401–411
19. Kelsey JA, Bayles KW, Shafii B, McGuire MA (2006) Fatty acids and monoacylglycerols inhibit growth of *Staphylococcus aureus*. Lipids 41:951–961
20. Du ZY, Demizieux L, Degrace P, Gresti J, Mointrot B, Liu YJ, Tian LX, Cao JM, Clouet P (2004) Alteration of 20:5n-3 and 22:6n-3 fat contents and liver peroxisomal activities in fenofibrate-treated rainbow trout. Lipids 39:849–855
21. Molina AJ, Prieto JG, Merino G, Mendoza G, Real R, Pulido MM, Alvarez AI (2007) Effects of ischemia–reperfusion on the absorption and esterase metabolism of diltiazem in rat intestine. Life Sci 80:397–407
22. Annaert P, Tukker JT, Van Gelder J, Naesens L, De Clercq E, Van den Mooter G, Kinget R, Augustijns P (2000) In vitro, ex vivo and in situ intestinal absorption characteristics of the antiviral ester prodrug adefovir dipivoxil. J Pharm Sci 89:1054–1062
23. Annaert P, Kinget R, Naesens L, De Clercq E, Augustijns P (1997) Transport, uptake, and metabolism of the bis(pivaloyloxymethyl)-ester prodrug of 9-(2-phosphonylmethoxyethyl)adenine in an in vitro cell culture system of the intestinal mucosa (Caco-2). Pharm Res 14:492–496
24. Li yan Z, Xiao yan C, Yong Z, Han yu Y, Da fang Z (2003) Determination of adefovir in monkey plasma by liquid chromatography-tandem mass spectrometry. Acta Pharm Sin 38:120–123

25. Tseng SJ, Hsu JP (1990) A comparison of the parameter estimating procedures for the Michaelis–Menten model. J Theor Biol 145(4):457–464
26. Michael L (1999) Fatty acid ethyl esters: nonoxidative ethanol metabolites with emerging biological and clinical significance. Lipids 34:281–285
27. Porter CJH, Pouton CW (2008) Formulation of lipid-based delivery systems for oral administration: materials, methods and strategies. Adv Drug Delivery Rev 60:625–637
28. Durrer A, Wernly-Chung GN, Boss G, Testa B (1992) Enzymic hydrolysis of nicotinate esters: comparison between plasma and liver catalysis. Xenobiotica 22:273–282
29. Foroutan SM, Watson DG (1999) The in vitro evaluation of polyethylene glycol esters of hydrocortisone 21-succinate as ocular prodrugs. Int J Pharm (Amst) 182:79–92
30. Teruko I, Megumi T, Mayumi S, Masakiyo H, Kan C (2006) Substrate specificity of carboxylesterase isozymes and their contribution to hydrolase activity in human liver and small intestine. Drug Metab Dispos 34:1734–1741
31. Fleming CD, Bencharit S, Edwards CC, Hyatt JL, Tsurkan L, Bai F, Fraga C, Morton CL, Howard-Williams EL, Potter PM, Redinbo MR (2005) Structural insights into drug processing by human carboxylesterase 1: tamoxifen, mevastatin, and inhibition by benzil. J Mol Biol 352:165–177
32. Gibson GG, Cinti DL, Sligar SG, Schenkman JB (1980) The effect of microsomal fatty acids and other lipids on the spin state of partially purified cytochrome P-450. J Biol Chem 255(5):1867–1873
33. Berg J, Tymoczko JL, Stryer L (2002) Biochemistry. W.H. Freeman & Co., New York
34. White KN, Eggermont J, Hope DB (1987) Effect of the carboxylesterase inhibitor bis-(4-nitrophenyl)phosphate in vivo on aspirin hydrolase and carboxylesterase activities at first-pass sites of metabolism in the guinea pig. Biochem Pharmacol 36:2687–2688
35. Mentlein R, Rix-Matzen H, Heymann E (1988) Subcellular localization of non-specific carboxylesterases, acylcarnitine hydrolase, monoacylglycerol lipase and palmitoyl-CoA hydrolase in rat liver. Biochim Biophys Acta 964:319–328
36. Masaki K, Hashimoto M, Imai T (2007) Intestinal first-pass metabolism via carboxylesterase in rat jejunum and ileum. Drug Metab Dispos 35:1089–1095
37. Krisch K (1971) Carboxylic ester hydrolases. In: Boyer PD (ed) The enzymes. Academic Press, New York
38. Wu SJ, Robinson JR (1999) Transcellular and lipophilic complex-enhanced intestinal absorption of human growth hormone. Pharm Res 16:1266–1272

Lipids (2010) 45:613–618
DOI 10.1007/s11745-010-3441-0

ORIGINAL ARTICLE

Anti-scratching Behavioral Effects of *N*-Stearoyl-phytosphingosine and 4-Hydroxysphinganine in Mice

Kwon-Ryeol Ryu · Bomi Lee · In-Ah Lee · Sekwan Oh · Dong-Hyun Kim

Received: 2 February 2010 / Accepted: 3 June 2010 / Published online: 29 June 2010

Abstract *N*-Stearoyl-phytosphingosine (SPS) and 4-hydroxysphinganine (phytosphingosine, PS), which are sphingolipids frequently found in mammalian skin, plants, and yeast, have been used as ingredients in cosmetics. In mice, treatment with SPS and PS inhibited histamine-induced scratching behavior and vascular permeability. These agents inhibited the expression of the allergic cytokines, IL-4 and TNF-α, and the activation of the transcription factors, NF-κB and c-jun, in histamine-stimulated skin tissues. These agents also showed potent anti-histamine effects in the Magnus test using guinea pig ileum. Based on these results, SPS and PS may improve scratching behavioral reactions in skin by regulating the action of histamine and the activation of the transcription factors NF-κB and c-jun.

Keywords Scratching behavior · Phytosphingosine · Histamine · IL-4

Abbreviations

IL	Interleukin
NF-κB	Nuclear factor kappaB
PS	Phytosphingosine
SPS	*N*-Stearoyl-phytosphingosine

K.-R. Ryu · B. Lee · I.-A. Lee · D.-H. Kim (✉)
Department of Life and Nanopharmaceutical Sciences, Department of Pharmaceutical Science, College of Pharmacy, Kyung Hee University, 1, Hoegi, Dongdaemun-ku, Seoul 130-701, Korea
e-mail: dhkim@khu.ac.kr

S. Oh
Department of Neuroscience and Medical Research Institute, School of Medicine, Ewha Womans University, Seoul 158-710, Korea

Introduction

Pruritus, an unpleasant cutaneous sensation that provokes the desire to scratch, can be local or widespread and is associated with atopic dermatitis, urticaria, cholestasis, and uremia. Many endogenous amines, proteases, growth factors, neuropeptides, opioids, eicosanoids and cytokines can act as pruritogens [1–3]. Pruritus can cause skin lesions and contribute to severe psychological disturbances [4]. Thus, inhibition of this response can improve the quality of life. To evaluate the effect of scratching-inhibitory agents, mouse models of histamine, substance P- or compound 48/80-induced scratching behavior have been used [2, 5]. However, there is no specific remedy available for this common symptom.

Ceramides play an important role as intracellular lipid second messengers and as components of the outer layer of the skin [6–8]. Indeed, the outer layer of mammalian skin is abnormally rich in long chain ceramides [9, 10]. These ceramides are located in the lipid phase between the corneocytes of the skin; this lipid phase is composed of ceramides, free fatty acids and cholesterol. The ceramides of the skin are composed of long chain fatty acids with lengths between C16 and C34 and are bound to a long chain di- or tri-hydroxy base through an amide linkage. The most common ceramides are sphingosine, 6-hydroxysphingosine and phytosphingosine. The lipid phase regulates skin water homeostasis and protects the body from bacterial, enzymatic or chemical assaults [10–12]. Therefore, the amounts and the ratios of different ceramide molecules in the skin are crucial for the barrier properties of the skin. The lack or reduction of a ceramide fraction in the skin directly impacts physiological function, leading to the appearance of a number of skin diseases and/or skin irritations [13, 14].

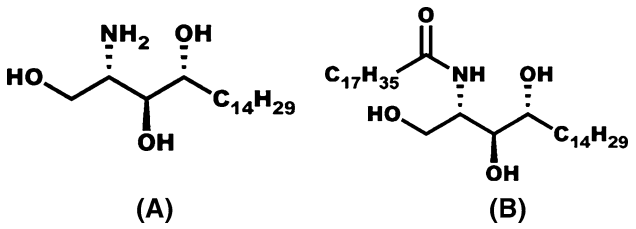

Fig. 1 Structures of phytosphingosine (**a**) and *N*-stearoyl-phytosphingosine (**b**)

Sphinganine (dihydrosphingosine) and 4-hydroxysphinganine (phytosphingosine) are the predominant free long-chain bases in lipid extracts of plant tissues, although they are typically minor components of complex plant sphingolipids [15, 16]. Sphinganine, 4-hydroxysphinganine and their C18 and C20 analogs are the major long-chain bases in yeast. These analogues have been used as cosmetic ingredients due to their pharmacological activities in dermal inflammatory disorders [17]. In particular, *N*-stearoyl-phytosphingosine (SPS) and 4-hydroxysphinganine (PS) (Fig. 1) are widely used as cosmetics ingredients. However, their anti-scratching effects have not been studied thoroughly. Therefore, in the present study, we investigated their anti-scratching behavioral effects in mice.

Experimental Procedure

Materials and Reagents

Histamine and Evans blue dye were purchased from Sigma Co. (St. Louis, MO, U.S.A.). Azelastine was donated by Dr. Nam-Jae Kim, an adjunct professor at Kyung Hee University. Antibodies were purchased from Santa Cruz Biotechnology (Santa Cruz, CA, USA). Enzyme-linked immunosorbent assay (ELISA) kits were from Pierce Biotechnology (Rockford, IL, USA). Optimal Cutting Temperature (OCT) compound was purchased from Sakura Finetek (Torrance, CA, USA).

Animals

Male ICR mice (20–22 g, 5 weeks old) were obtained from the Charles River Orient Experimental Animal Breeding Center (Seoul, Korea). All animals were housed in wire cages at 20–22 °C, relative humidity of 50 ± 10%, air ventilation frequency of 15–20 times/h and 12-h illumination (07:00–19:00; intensity, 150–300 Lux), fed standard laboratory chow (Charles River Orient Experimental Animal Breeding Center, Seoul, Korea), and allowed water ad libitum. All procedures related to the animals and their care conformed to international guidelines, 'Principles of Laboratory Animal Care' (NIH publication no. 85-23, revised 1985 and Kyung Hee University 2008).

Assay of Scratching Behavior Frequency

The behavioral experiments were performed as previously described [18]. Before the experiments, male ICR mice were acclimated in acrylic cages (22 × 22 × 24 cm) for about 10 min and divided into groups of six. The rostral part of the skin on the back was clipped, and 300 μg/50 μL of histamine dissolved in saline was injected intradermally using a 29-gauge needle. The control mice received a saline injection instead of histamine. Immediately after the intradermal injection, the mice (one animal/cage) were put back into the same cages and their scratching behavior was recorded using an 8-mm video camera (SV-K80, Samsung, Seoul, Korea) under automated conditions. The number of times the mouse scratched the injection site using the hind paws was counted and compared with the scratching of other sites, such as the ears. Each mouse was used for only one experiment. The mice generally scratched several times during 1 s, thus each series of such behavior over 60 min was counted as one incident of scratching.

Measurement of Vascular Permeability

The increase in vascular permeability caused by scratching agents was assessed as reported by Choo et al. [18]. After the intradermal injection of 300 μg/50 μl of histamine into the rostral part of the back of each mouse, 0.2 ml of 1% saline solution of Evans blue dye was injected intravenously. Test samples were orally administered 1 h before the scratching agents. Mice were sacrificed 60 min later by cervical dislocation and the scratching agent-injection site was excised. The skin specimen was dissolved in 1 ml of 1 M KOH solution by overnight incubation, and 4 ml of 0.2 M phosphoric acid solution-acetone (5:13) mixture was added. After shaking, the precipitates were filtered off and the amount of dye was measured colorimetrically at 620 nm.

Histopathological Study

For histopathological analysis, 300 μg of histamine was injected intradermally into the back skin of mice and a skin specimen was excised 60 min later. The skin specimen was fixed in 4% paraformaldehyde, embedded in OCT compound, sectioned (5 μm), stained with hematoxylin and eosin, and examined at ×40–100 magnification.

Analysis of IL-4 and TNF-α by Enzyme-Linked Immunosorbent Assay (ELISA) and Immunoblot

Histamine-induced skin tissue specimens were homogenized in ice-cold lysis buffer (10 mM Tris, pH 7.5, 10 mM NaCl, 3 mM $MgCl_2$, 0.05% Nonidet P-40, 1 mM EGTA,

1:100 protease inhibitor cocktail, and 1:100 phosphatase inhibitor cocktail). Lysed specimens were centrifuged at 2700×*g* for 10 min at 4 °C. The supernatant containing the cytosol was further centrifuged at 20,800×*g* for 15 min at 4°C to obtain the cytosolic fraction. The nuclei in the pellet were washed 3 times by gentle resuspension in wash buffer (10 mM PIPES, pH 6.8, 300 mM sucrose, 3 mM $MgCl_2$, 1 mM EGTA, 25 mM NaCl, 1:100 protease inhibitor cocktail and 1:100 phosphatase inhibitor cocktail) and centrifugation at 2700×*g* for 5 min at 4 °C [19, 20]. The supernatants (50 µl) were transferred to 96-well ELISA plates, and the concentrations of IL-4 and TNF-α were then determined using commercial ELISA kits (Pierce Biotechnology, Inc., Rockford, IL, USA)

Immunoblot analyses of phospho-p65 and phospho-c-Jun in the nuclear fraction and p65 NF-κB and c-jun in the cytosolic fraction were performed as previously reported [20]. The protein fractions of the skin tissue specimens were subjected to electrophoresis on 10% sodium dodecyl sulfate–polyacrylamide gel and then transferred to a nitrocellulose membrane. Phospho-p65, phospho-c-Jun, p65 NF-κB and c-jun were assayed with the corresponding antibodies. Immunodetection was carried out using an enhanced chemiluminescence detection kit (Thermo Fisher Scientific Inc., Rockford, IL, USA).

Anti-histamine Action Assay

Male Hartley guinea pigs (300 ± 30 g) were sacrificed by exsanguination and the ilea were prepared in cold Tyrode solution. The prepared ileal strip was then suspended in a 10-ml Magnus tube (32°C, 95% O_2 + 5% CO_2) containing Tyrode solution. Each test agent was added to the preparation 30 s before treatment with histamine (1×10^{-6} M). The percentage contraction is shown as a percentage of the maximal response to histamine.

Statistics

All data are expressed as the means ± standard deviation, and statistical significance was analyzed by one-way ANOVA followed by a Student Newman–Keuls test.

Results

Inhibitory Effects of SPS and PS on Histamine-Induced Scratching Behavior in Mice

To evaluate the anti-scratching behavioral effects of SPS and PS, we first measured the inhibition of histamine-induced scratching behavior frequency in mice (Fig. 2a). SPS and PS inhibited the scratching behaviors induced by histamine. At 50 mg/kg, orally administered SPS and PS reduced the scratching behavior frequency by 67 and 59% in histamine-stimulated mouse skin. We also investigated their effects in histological exams (Fig. 2b). Compared to the normal group, the histamine-treated control group exhibited severe inflammation, manifested as remarkable epidermal hyperplasia and the infiltration of inflammatory cells, such as dendritic cells, into the dermis. SPS and PS inhibited these inflammatory symptoms.

Inhibitory Effects of SPS and PS on IL-4 and TNF-α Protein Expression Induced by Histamine in Mice

The inhibitory effects of SPS and PS against IL-4 and TNF-α protein expression in mouse skin stimulated with histamine were measured by ELISA (Fig. 3a, b). Histamine increased IL-4 and TNF-α protein expression by 2.5- and 2.3-fold, respectively. SPS and PS potently inhibited histamine-induced cytokine production. At 50 mg/kg, SPS and PS inhibited IL-4 expression by 75 and 37%, respectively, and TNF-α expression by 88 and 70%, respectively.

SPS and PS also inhibited the histamine-induced activation of the transcription factors, NF-κB and c-jun, which regulate TNF-α and IL-4 expression, respectively (Fig. 3c).

Inhibitory Effects of SPS and PS on Histamine-Increased Vascular Permeability and Ileal Contraction

We also measured the inhibitory effects of SPS and PS on the histamine-induced vascular permeability in mice (Fig. 4). Orally administered SPS and PS potently inhibited the histamine-induced vascular permeability. At 50 mg/kg, SPS and PS inhibited the vascular permeability by 51 and 50%, respectively.

We also investigated the inhibitory effect of SPS and PS on the histamine-induced small intestine muscle contraction involving the H1-receptor in guinea pig ilea (Fig. 5). At 10 µM, SPS and PS inhibited histamine-induced ileal contraction by 55 and 51%, respectively.

Discussion

Mast cells and basophils are critical components in various biological processes of allergic diseases [21, 22]. These cells express surface membrane receptors with high affinity and specificity for IgE. The interaction of antigen-bound IgE and surface membrane receptors releases histamine, prostaglandins, leukotrienes and cytokines. These endogenous amines and cytokines can act as pruritogens [22, 23]. The cytokines also activate chemotaxis and phagocytosis of neutrophils and

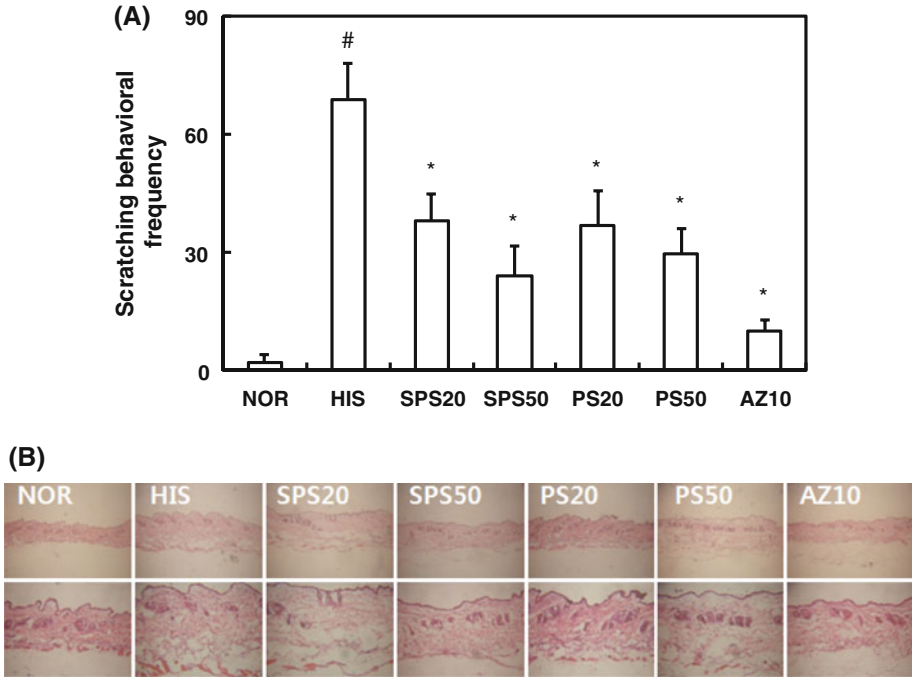

Fig. 2 Inhibitory effects of SPS and PS on histamine-induced scratching behavior in mice. **a** Effect on scratching behavior. The scratching behaviors in the normal control group treated with saline alone and in the histamine-treated groups with and without test agents were counted for 1 h. Test agents were orally administered 1 h before histamine administration. **b** Histological exam. The skins of mice stimulated with histamine with and without test agents were stained by hematoxylin–eosin. NOR, normal group; HIS, control treated with histamine alone; SPS20, 20 mg/kg SPS with histamine; SPS50, 50 mg/kg SPS with histamine; PS20, 20 mg/kg PS with histamine; PS50, 50 mg/kg SPS with histamine; AZ10, 10 mg/kg azelastine with histamine. Mean ± SD ($n = 5$). $^{\#}p < 0.05$ versus normal control group. $^{*}p < 0.05$ versus histamine-treated group

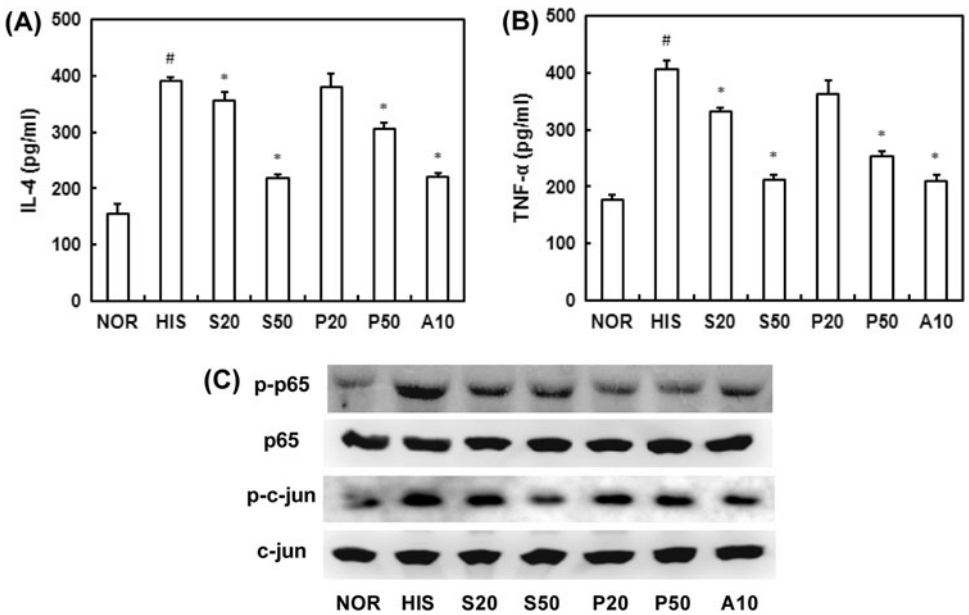

Fig. 3 Inhibitory effects of SPS and PS on the protein expressions of TNF-α (**a**) and IL-4 (**b**) and the activation of their transcription factors NF-κB and c-jun (**c**) in histamine-induced mouse skin tissues. TNF-α and IL-4 were assayed by ELISA, and NF-κB and c-jun by immunoblot analysis. SPS, PS and azelastine were orally administered to mice: NOR, normal group; HIS, control treated with histamine alone; S20, 20 mg/kg SPS with histamine; S50, 50 mg/kg SPS with histamine; P20, 20 mg/kg PS with histamine; P50, 50 mg/kg SPS with histamine; A10, 10 mg/kg azelastine with histamine. Mean ± SD ($n = 5$). $^{\#}p < 0.05$ versus normal control group. $^{*}p < 0.05$ versus histamine-treated group

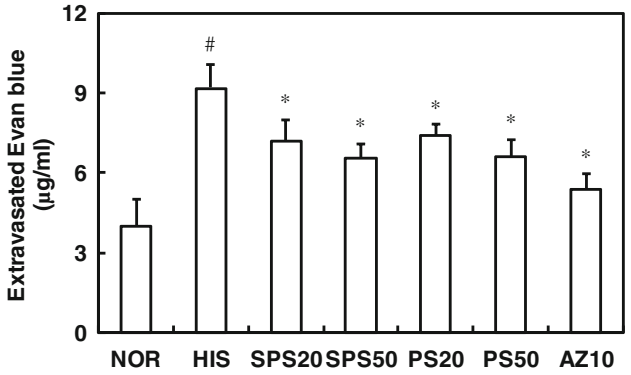

Fig. 4 Inhibitory effect of SPS, PS and azelastine on histamine-induced vascular permeability in mice. The vascular permeability was increased by histamine in ICR mice. Mice were treated with or without oral administration of test agents (NOR, normal group; HIS, control treated with histamine alone; S20, 20 mg/kg SPS with histamine; S50, 50 mg/kg SPS with histamine; P20, 20 mg/kg PS with histamine; P50, 50 mg/kg SPS with histamine; A10, 10 mg/kg azelastine with histamine) 1 h before the intradermal injection of 300 μg/50 μl of histamine into the shaved back skin. The amounts of Evans blue dye extravasated from the dorsal skin (1 × 1 cm) were determined. The values indicate means ± SD ($n = 5$). $^{\#}p < 0.05$ versus normal control group. $^{*}p < 0.05$ versus histamine-treated group

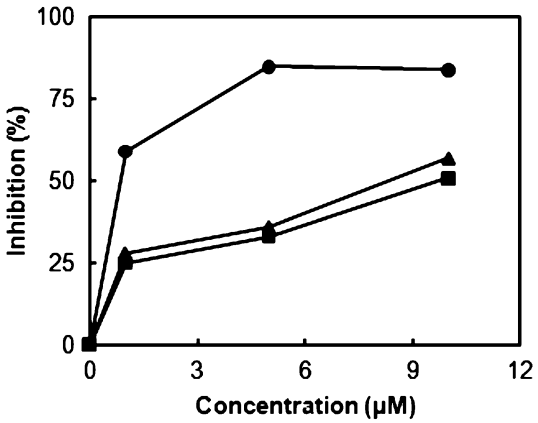

Fig. 5 Anti-histamine effect of SPS, PS and azelastine in Magnus test using guinea pig ileum. The ileal strip was set in a 10-ml Magnus tube (32 °C, 95% O_2 + 5% CO_2) containing Tyrode solution. Each test agent (dissolved in 2% Triton X-100) was added to the preparation 30 s before treatment with histamine (1×10^{-6} M): *closed triangles*, SPS; *closed squares*, PS; *closed circles*, azelastine. Each experiment was performed in duplicate

macrophages. Finally, cytokine-induced reactions cause tissue inflammation. Exogenous pruritogens, such as compound 48/80, also increase the permeability of the lipid bilayer membrane by causing membrane instability. The increase of lipid bilayer membrane permeability may be essential for the release of mediators from mast cells [24]. Therefore, antiallergic agents, such as anti-histamines, steroids and immunosuppressants, have been used to treat allergic and pruritic diseases [25–27]. Even though antiallergic agents are widely used, many of these agents have limited effects in terms of improving these diseases.

In this study, SPS and PS inhibited the scratching behaviors and vascular permeability induced by histamine. The anti-scratching behavioral effects of SPS and PS were proportional to their inhibitory effects against vascular permeability. SPS and PS also inhibited the scratching behavior induced by compound 48/80, an exogenous pruritogen (data not shown). Moreover, SPS and PS showed antihistamine activity in the guinea pig ileum. These results suggest that SPS and PS may repress vascular permeability by inhibiting histamine action and thus inhibit scratching behavior. In a study of their inhibitory mechanism, SPS and PS inhibited TNF-α and IL-4 expression as well as activation of the transcription factors, NF-κB and c-jun, in skin tissues stimulated with histamine. NF-κB is an important signal in immune responses of allergic diseases [28]. Histamine activates NF-κB in skin tissues. In the present study, SPS and PS inhibited histamine-induced activation of NF-κB. Furthermore, SPS and PS inhibited c-jun activation. c-Jun regulates expression of IL-4, which is an IgE-switching cytokine [29]. These results suggest that SPS and PS may inhibit TNF-α and IL-4 expression by regulating the activation of their transcription factors, NF-κB and c-jun.

Ceramides are major lipid second messengers that inhibit cell proliferation and induce apoptosis via dephosphorylation and inactivation of several proliferative and anti-apoptotic molecules [30–32]. In addition, various studies have reported the beneficial role of ceramide molecules in the renewal of the skin's intrinsic protective layer, especially to increase the effective barrier function with respect to water loss, thus reducing skin irritation and inflammation [21, 22]. These results suggest that SPS and PS may regulate skin water homeostasis and protect the body against bacterial, enzymatic or chemical impacts.

Based on these findings, SPS and PS may improve pruritic reactions in skin by regulating the action of histamine, the activation of the transcription factors NF-κB and c-jun, and skin water homeostasis.

References

1. Maintz L, Novak N (2007) Histamine and histamine intolerance. Am J Clin Nutr 85:1185–1196
2. Reich A, Szepietowski JC (2007) Mediators of pruritus in psoriasis. Mediators Inflamm 2007:647270
3. Schmeiz M, Schmidt R, Bickel A, Handerker HO, Torebjork HE (1977) Specific C-receptors for itch in human skin. J Neurosci 17:8003–8008

4. Raiford DS (1995) Pruritus of chronic cholestasis. QJM 88:603–607
5. Kuraishi Y, Nagasawa T, Hayashi K, Satoh M (1995) Scratching behavior induced by pruritogenic but not algesiogenic agents in mice. Eur J Pharmacol 275:229–233
6. Kim MY, Linardic C, Obeid L, Hannun Y (1991) Identification of sphingomyelin turnover as an effector mechanism for the action of tumor necrosis factor a and r-interferon. Specific role in cell proliferation. J Biol Chem 266:484–489
7. Huang HW, Goldberg EM, Zidovetzki R (1999) Ceramides modulate protein kinase C activity and perturb the structure of phosphatidylcholine/phosphatidylserine bilayers. Biophys J 77:1489–1497
8. Sawei H, Hannun YA (1999) Ceramide and sphingomyelinase in the regulation of stress responses. Chem Phys Lipids 102:141–147
9. Stewart ME, Downing DT (1999) A new 6-hydroxy-4-sphingenine-containing ceramide in human skin. J Lipid Res 40:1434–1439
10. Garidel P (2006) Structural characterization and phase behavior of a stratum corneum lipid analogue: ceramide 3A. Phys Chem Chem Phys 8:2265–2275
11. De Paepe K, Derde MP, Roseeuw D, Rogiers V (2000) Incorporation of ceramide 3B in dermatocosmetic emulsions: effect on the transepidermal water loss of sodium lauryl sulphate damaged skin. J Eur Acad Dermatol Venereolz 14:272–279
12. Lampe MA, Burlingame AL, Whitney J, Williams MI, Brown BE, Roitman E, Elias PM (1983) Human stratum corneum lipids: characterization and regional variations. J Lipid Res 24:120–130
13. Motta S, Sesana S, Ghidonin R, Monti M (1995) Content of the different lipid classes in psoriatic scale. Arch Dermatol Res 287:691–694
14. Olaniran AK, Baker BS, Paige DG, Garioch JJ, Powles AV, Fry L (1996) Cytokine expression in psoriatic skin lesions during PUVA therapy. Arch Dermatol Res 288:421–425
15. Wright BS, Snow JW, O'Brien TC, Lynch DV (2004) Synthesis of 4-hydroxysphinganine and characterization of sphinganine hydroxylase activity in corn. Arch Biochem Biophys 415:184–192
16. Imai H, Morimoto Y, Tamura K (2000) Sphingoid base composition of monoglucosylceramide in Brassicaceae. J Plant Physiol 157:453–456
17. Bizot-Foulon V, Godeau G, Guessous F, Lati E, Rousset G, Roch-Arveillier M, Hornebeck W (1995) Inhibition of human neutrophil elastase by wheat ceramides. Int J Cosmet Sci 17:255–264
18. Choo MK, Park EK, Han MJ, Kim DH (2003) Antiallergic activity of ginseng and its ginsenosides. Planta Med 69:518–522
19. Matsuda H, Tewtrakul S, Morikawa T, Nakamura A, Yoshikawa M (2004) Anti-allergic principles from Thai zedoary: structural requirements of curcuminoids for inhibition of degranulation and effect on the release of TNF-alpha and IL-4 in RBL-2H3 cells. Bioorg Med Chem 12:5891–5898
20. Han SJ, Ryu SN, Trinh HT, Joh EH, Jang SY, Han MJ, Kim DH (2009) Metabolism of cyanidin-3-O-beta-D-glucoside isolated from black colored rice and its antiscratching behavioral effect in mice. J Food Sci 74:H253–H258
21. Stevens RL, Austen KF (1989) Recent advances in the cellular and molecular biology of mast cells. Immunol Today 10:381–386
22. Plaut M, Pierce JH, Whatson C, Hanley-Hyde J, Nordan RP, Paul WE (1989) Mast cell lines produce lymphokines in response to cross-linkage of Fc epsilon RI or to calcium ionophore. Nature 339:64–67
23. Mitre E, Nutman TB (2006) Basophils, basophilia and helminth infections. Chem Immunol Allergy 90:141–156
24. Tasaka K, Mio M, Okamoto M (1986) Intracellular calcium release induced by histamine releasers and its inhibition by some antiallergic drugs. Ann Allergy 56:464–469
25. Sakuma S, Higashi Y, Sato N, Sasakawa T, Sengoku T, Ohkubo Y (2001) Tacrolimus suppressed the production of cytokines involved in atopic dermatitis by direct stimulation of human PBMC system (Comparison with steroids). Int Immunopharmacol 1:1219–1226
26. Schafer-Korting M, Schmid MH, Korting HC (1996) Topical glucocorticoids with improved risk-benefit ratio. Drug Safety 14:375–385
27. Simons FER (1992) The antiallergic effects of antihistamines (H1-receptor antagonists). J Allergy Clin Immunol 90:705–715
28. Zhao W, Oskeritzian CA, Pozez AL, Schwartz LB (2005) Cytokine production by skin-derived mast cells: endogenous proteases are responsible for degradation of cytokines. J Immunol 175:2635–2642
29. Hirano T, Higa S, Arimitsu J, Naka T, Ogata A, Shima Y, Fujimoto M, Yamadori T, Ohkawara T, Kuwabara Y, Kawai M, Matsuda H, Yoshikawa M, Maezaki N, Tanaka T, Kawase I, Tanaka T (2006) Luteolin, a flavonoid, inhibits AP-1 activation by basophils. Biochem Biophys Res Commun 340:1–7
30. Hannun YA, Obeid LM (2002) The ceramide-centric universe of lipid-mediated cell regulation: stress encounters of the lipid kind. J Biol Chem 277:25847–25850
31. Pettus BJ, Chalfant CE, Hannun YA (2006) Ceramide in apoptosis: An overview and current perspectives. Biochim Biophys Acta 1761:281–291
32. Duan RD, Nilsson A (2009) Metabolism of sphingolipids in the gut and its relation to inflammation and cancer development. Prog Lipid Res 48:62–72

Lipids (2010) 45:619–625
DOI 10.1007/s11745-010-3439-7

ORIGINAL ARTICLE

Electronegative Low-Density Lipoprotein is Associated with Dense Low-Density Lipoprotein in Subjects with Different Levels of Cardiovascular Risk

Ana Paula de Queiroz Mello · Isis Tande da Silva · Aline Silva Oliveira · Valéria Sutti Nunes · Dulcineia Saes Parra Abdalla · Magnus Gidlund · Nágila Raquel Teixeira Damasceno

Received: 26 January 2010 / Accepted: 26 May 2010 / Published online: 24 June 2010

Abstract Dyslipidemias and physicochemical changes in low-density lipoprotein (LDL) are very important factors for the development of coronary artery disease (CAD). However, pathophysiological properties of electronegative low-density lipoprotein [LDL(−)] remain a controversial issue. Our objective was to investigate LDL(−) content in LDL and its subfractions (phenotypes A and B) of subjects with different cardiovascular risk. Seventy-three subjects were randomized into three groups: normolipidemic (N; $n = 30$) and hypercholesterolemic (HC; $n = 33$) subjects and patients with CAD ($n = 10$). After fasting, blood samples were collected and total, dense and light LDL were isolated. LDL(−) content in total LDL and its subfractions was determined by ELISA. LDL(−) content in total LDL was lower in the N group as compared to the HC ($P < 0.001$) and CAD ($P = 0.006$) groups. In the total sample and in those of the N, HC, and CAD groups, LDL(−) content in dense LDL was higher than in light LDL ($P = 0.001$, 0.001, 0.001, and 0.033, respectively) The impact of LDL(−) on cardiovascular risk was reinforced when LDL(−) content in LDL showed itself to have a positive association with total cholesterol ($\beta = 0.003$; $P < 0.001$), LDL-C ($\beta = 0.003$; $p < 0.001$), and non-HDL-C ($\beta = 0.003$; $P < 0.001$) and a negative association with HDL-C ($\beta = -0.32$; $P = 0.04$). Therefore, LDL(−) is an important biomarker that showed association with the lipid profile and the level of cardiovascular risk.

Keywords Oxidation · Electronegative low-density lipoprotein · LDL phenotype B · Atherosclerosis

Abbreviations

BMI	Body mass index
CAD	Coronary artery disease
CHD	Cardiovascular heart diseases
ELISA	Enzyme-linked immunosorbent assay
HC	Hypercholesterolemic
HDL-C	High-density lipoprotein cholesterol
LDL	Low-density lipoprotein
LDL(−)	Electronegative low-density lipoprotein
LDL-C	Low-density lipoprotein cholesterol
PAF-AH	Platelet-activating factor acetylhydrolase
TC	Total cholesterol
TAG	Triglycerides

Introduction

Cardiovascular heart diseases (CHD) are among the non-transmissible diseases that are a major cause of death. They are responsible for 30% of all deaths (about 17.5 million

A. P. de Queiroz Mello · I. T. da Silva · A. S. Oliveira · N. R. T. Damasceno (✉)
Department of Nutrition, School of Public Health, Faculdade de Saúde Pública, University of Sao Paulo, Av Dr Arnaldo, 715, São Paulo, SP 01246-904, Brazil
e-mail: nagila@usp.br

V. S. Nunes
Lipids Laboratory (LIM 10), School of Medicine, University of Sao Paulo, São Paulo, SP, Brazil

D. S. P. Abdalla
Department of Clinical and Toxicological Analyses, School of Pharmaceutical Sciences, University of Sao Paulo, São Paulo, SP, Brazil

M. Gidlund
Department of Immunology, Institute of Biomedical Sciences, University of Sao Paulo, São Paulo, SP, Brazil

people) in the world, followed by cancer (7.6 million deaths) and chronic respiratory diseases (4.1 million deaths) [1].

The "traditional" risk factors for CHD, as identified in the Framingham study, include high levels of total cholesterol (TC) and low-density lipoprotein cholesterol (LDL-C), low levels of high-density lipoprotein cholesterol (HDL-C), as well as elevated blood pressure, tabagism, and age [2]. In addition, obesity, familial history of premature CHD, and physical inactivity contribute to other classical risk factors being now considered important associated factors [3].

Despite the environmental risk factors and LDL-C blood levels, evaluation of low-density lipoprotein (LDL) subfractions according to the phenotype is a more specific marker. LDL can be separated into two subclasses: Phenotype A (predominance of large and light LDL particles) and Phenotype B (small and dense LDL particles), which have been considered predictors of cardiovascular risk [4].

Beyond the phenotypic differences, growing evidence suggests that qualitative changes in LDL are related to the development of atherosclerosis [5–7]. Electronegative particles generated by oxidative modification appear to play a key role in the atherogenicity of LDL. However, non-enzymatic glycosylation, enrichment of non-esterified fatty acids, enzymatic modification by phospholipase A_2 or platelet-activating factor acetylhydrolase (PAF-AH), hemoglobin cross-linking, and possibly other mechanisms not yet identified could contribute to increasing the proportion of electronegative low-density lipoprotein [LDL(−)] in plasma [8].

LDL(−) is a minimally modified form of LDL that can both be identified as an initiating factor of atherosclerosis and contribute to the atherogenic potential of LDL, thus increasing cardiovascular risk [7, 9]. LDL(−) is enriched with lipid peroxides and is associated with small and dense LDL [10, 11]. Apo E, apo C-III [12], hemoglobin [13], and PAF-AH [14] have been reported to be associated with LDL(−). Presence of these proteins would increase LDL(−) density, which has been observed in normocholesterolemic subjects [8]. Moreover, Chappey et al. [12] showed a bimodal distribution of LDL(−) between the light and dense LDL subfractions. Nevertheless, the pathophysiological action of LDL(−) is yet unclear.

In this context, the aim of our study was to evaluate LDL(−) distribution between LDL subfractions (phenotypes A and B) in subjects with different levels of cardiovascular risk.

Materials and Methods

Study Population

Seventy-three outpatients of both sexes, aged 25–65 years, and with different levels of cardiovascular risk were recruited in the Heart Institute and the Clinical Hospital (School of Medicine, University of Sao Paulo), SP, Brazil. The subjects were randomly distributed into the normolipidemic (N; LDL-C <160.0 mg/dL, with no clinical cardiovascular events, $n = 30$), hypercholesterolemic (HC; LDL-C ≥160.0 mg/dL, with no clinical cardiovascular events, $n = 33$), and coronary artery disease (CAD; LDL-C ≥160.0 mg/dL, with clinical diagnosis of atherosclerosis, $n = 10$) groups. The atherosclerotic coronary disease was diagnosed by clinical evaluation, electrocardiogram with ischemia, and positive ergometric test and/or positive myocardial scintigraphy and/or coronarography with obstruction of at least 50% in one of the arteries. Subjects with diabetes, renal disease, obesity (BMI ≥35.0 kg/m^2), smokers and alcoholics were excluded from the trial. A 2-month period was observed for washout of hypocholesterolemic drugs, hormone therapy, and antioxidant supplements. The present study was approved by the Ethics Committee of both the Heart Institute (InCor) (#2585/05/005) and Clinical Hospital (#562/05) of the Medical School, University of Sao Paulo (Brazil).

Sample Characteristics

Information on the subject's race, risk factor for CAD [2], and daily metabolic energy consumption were obtained by direct interview. BMI was determined as weight (kg) divided by standing height (m) squared [15], and waist circumference (WC) was measured midway between the lowest rib margin and the iliac crest [16].

Blood Samples

After a fasting period of 12–15 h, aliquots of venous blood (20.0 mL) were collected into Vacutainer® tubes with ethylenediamine tetraacetic acid (EDTA; 1.0 mg/mL). Plasma was immediately separated and aliquoted into tubes containing butylhydroxytoluene (BHT; 100.0 μM), aprotinin (10.0 μg/mL), benzamidine (10.0 μM), and phenylmethylsulphonyl fluoride (PMSF; 5.0 μM) and stored at −70 °C until analysis. Very low-density lipoprotein (VLDL), LDL, and HDL were isolated from the plasma by preparative sequential ultracentrifugation (18 h, 105,000×g, 4 °C) using a Sorvall ultracentrifuge (Sorvall Ultra Pro80, Sorvall Products, Newtown, CT, USA) equipped with a fixed-angle rotor (T-1270) [17]. Subfractions were separated from LDL by ultracentrifugation (18 h, 105,000×g, 4 °C), using a density cut-off point of 1.043 g/mL to separate low- and high-density LDL particles. The denser LDL subfraction (phenotype B) contained particles with $1.043 \leq d < 1.063$ g/mL and the most buoyant LDL subfraction (phenotype A) contained particles with $1.019 < d < 1.043$ g/mL. These LDL subfractions were dialyzed

against 150.0 mM sodium chloride, 1.0 mM EDTA and 10.0 mM trizma base (pH 7.2, 4 °C, 12 h). All reagents were purchased from Sigma Chemical (St. Louis, MO, USA).

Lipid and Protein Analyses

Cholesterol and triglyceride concentrations were determined from plasma and lipoprotein fraction by using colorimetric enzymatic commercial kits (Labtest®, MG, Brazil). Non-HDL cholesterol levels and the TC/HDL-C and LDL-C/HDL-C ratios were calculated for all samples. Protein concentration in plasma and lipoproteins were determined by using the Lowry method [18].

LDL(−) Analyses

LDL, and the dense and light LDL subfractions were diluted (1:800, 1:10, and 1:10, respectively) in 0.01 M carbonate–bicarbonate buffer (pH 9.6) and were used to coat (overnight, 4 °C) the microtiter plates (Costar®, model 3690, Cambridge, MA, USA). Non-adsorbed material was washed and discarded; then the plates were blocked with 5% skimmed milk in phosphate-buffered saline (PBS) and incubated (2 h, 37 °C). The plates were washed with PBS-Tween (0.05%, 4 times) and, after addition of anti-LDL(−) monoclonal antibody (MAb; INPI #2637/2002; 9.2 μg/mL; 50 μL/well), they were again incubated (2 h, 37 °C). After a new wash with PBS-Tween, horseradish peroxidase-conjugated polyclonal goat anti-mouse IgG antibody (Rockland Immunochemicals for Research, Gilbertsville, PA, USA; 50 μL/well) diluted 1:5,000 (v/v) in skimmed milk (1% in PBS) was added to the wells and incubated (2 h, 37 °C). After the plates were washed, a solution containing the substrate 3,3′,5,5′-tetramethylbenzidine (TMB; 250.0 μL), phosphate–citrate buffer (12.0 mL; pH 4.2), and hydrogen peroxide (10.0 μL) was added (50.0 μL/well). All samples were analyzed in triplicate. After a 30-min delay for color development, the colored product concentration was evaluated by light absorption (Bio-Tek® Instruments, Winooski, VT, USA; $\lambda = 450$ nm); the concentrations were calculated as a function of optical density (OD) readings: $(OD_{sample} - OD_{background}) \times$ title.

Statistical Analyses

Differences between the values for the N, HC, and CAD groups were evaluated by one-way analysis of variance (ANOVA) and the Kruskal–Wallis test. Differences between the LDL subfractions were evaluated by the Student's *t* test for independent samples and the Mann–Whitney test. Univariate linear regression analysis was used to evaluate the association between LDL(−) levels (dependent variable) and the lipid profile (independent variable). Data were expressed as means ± standard deviation (SD). The SPSS Statistical Package (version 15.0) was used for all analyses. A cut-off level of $P < 0.05$ was adopted to infer statistical significance.

Results

The characteristics of the subjects included in this study are shown in Table 1. Groups N (40.0 ± 9.9 years), HC (45.0 ± 10.0 years), and CAD (54.0 ± 7.7 years) consisted of male ($n = 7$, 11, and 5, respectively) and female ($n = 23$, 22, and 5, respectively) subjects. The subjects in the CAD group were older than those in the N and HC groups ($P = 0.001$ and 0.03, respectively). No statistical differences were found between sexes and races in the groups. Therefore, all results were analyzed using age as a covariate. No significant differences were found between groups for BMI and WC. None of the subjects were smokers or consumed alcohol. The risk factors for hypertension and age were different in the CAD group as compared to the N ($P < 0.001$ and =0.01, respectively) and HC ($P < 0.001$ and =0.02, respectively) groups. The percentage of subjects with low HDL-C in the N group was lower than that in the CAD group ($P = 0.04$). The values for energy consumption were similar among the three groups. As expected, the subjects in the N group showed lower values for TC and LDL-C than those in the HC ($P < 0.001$ and 0.001, respectively) and CAD ($P < 0.001$ and 0.001, respectively) groups. The values for HDL-C in the CAD group were lower than those in the N group ($P = 0.02$). However, no significant differences in TAG concentration were found among the three groups. In addition, the values for non-HDL-C and the TC/HDL-C and LDL-C/HDL-C ratios in the N group were lower than in the HC ($P < 0.001$, 0.001, and 0.001, respectively) and the CAD ($P < 0.001$, 0.001, and 0.001, respectively) groups.

The levels (OD in Log) for LDL(−) in LDL in the HC (7.1 ± 0.4) and CAD (7.1 ± 0.2) groups were higher than in the N (6.7 ± 0.5) ($P < 0.001$ and =0.006, respectively) group (Fig. 1). The levels (OD in Log) for LDL(−) in dense LDL were higher than in light LDL in the total sample (2.7 ± 0.8 vs. 2.1 ± 0.5, $P = 0.001$) in the N (2.7 ± 0.8 vs. 2.1 ± 0.4, $P = 0.001$), HC (2.7 ± 0.8 vs. 2.0 ± 0.6, $P = 0.001$), and CAD (2.7 ± 0.8 vs. 2.2 ± 0.4, $P = 0.033$) groups (Fig. 2). Therefore, LDL(−) content in LDL varied according to the cardiovascular risk and, independently of this characteristic, LDL(−) content showed a higher association with dense LDL when LDL(−) was analyzed in subfractions of LDL from the N (55.6 vs. 44.4%), HC (57.1 vs. 42.9%), and CAD (55.7 vs. 44.3%) groups. The intra- and inter-assay coefficients for total

Table 1 Characteristics of subjects

	N ($n = 30$)	HC ($n = 33$)	CAD ($n = 10$)
Age (years)	40.0 ± 9.9	45.0 ± 10.0	54.0 ± 7.7*,§
Men [*n* (%)]	7 (23)	11 (33)	5 (50)
Women [*n* (%)]	23 (77)	22 (67)	5 (50)
Race [*n* (%)]			
White	19 (63)	21 (64)	3 (30)
Black	5 (17)	6 (18)	1 (10)
Others	6 (20)	6 (18)	6 (60)
BMI (kg/m^2)	25.9 ± 4.3	25.9 ± 4.1	27.8 ± 3.5
Waist circumference (cm)			
Male	98.3 ± 6.6	87.6 ± 12.6	96.6 ± 17.2
Female	82.2 ± 9.7	86.3 ± 10.3	89.6 ± 2.2
Tabagism [*n* (%)]	0 (0)	0 (0)	0 (0)
Ethilism [*n* (%)]	0 (0)	0 (0)	0 (0)
Risk factors for CAD [*n* (%)]			
Low HDL-C	16 (53)	19 (58)	9 (90)*
Hypertension	0 (0)	0 (0)	8 (80)*,§
Age	4 (13)	6 (18)	6 (60)*,§
Familiar history	7 (23)	7 (21)	3 (30)
Framingham risk score	3.70 ± 5.93	9.24 ± 5.12*	13.90 ± 3.38*,§
Energy (kcal/day)	1,904.9 ± 602.0	1,935.2 ± 537.4	2,300.5 ± 799.4
Cholesterol (mg/dL)			
Total	180.5 ± 19.6	243.5 ± 29.7*	221.0 ± 19.6*,§
LDL	117.4 ± 15.9	178.5 ± 26.9*	170.3 ± 15.9*
HDL	42.9 ± 13.8	31.1 ± 13.8	31.2 ± 8.3*
Triglycerides (mg/dL)	101.6 ± 41.6	134.5 ± 68.8	97.8 ± 28.3
Non-HDL-C (mg/dL)	137.7 ± 21.2	205.4 ± 31.2*	189.9 ± 17.4*,§
TC/HDL-C	4.5 ± 1.2	7.2 ± 2.8*	7.6 ± 2.3*,§
LDL-C/HDL-C	3.0 ± 0.9	5.4 ± 2.4*	5.9 ± 2.0*,§

Values are means ± SD

* $P < 0.05$ versus N group

§ $P < 0.05$ versus HC group

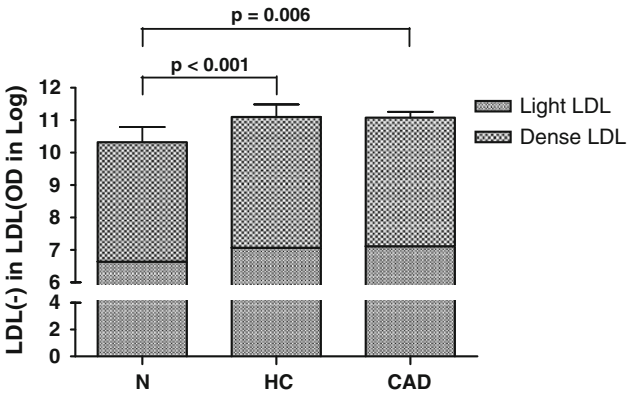

Fig. 1 LDL(−) concentration in LDL among the three groups. Normolipidemic (*N*; $n = 30$), hypercholesterolemic (*HC*; $n = 33$) and coronary artery disease (*CAD*; $n = 10$) groups

LDL (intra = 1.8 ± 1.9; inter = 3.8 ± 2.7), dense LDL (intra = 3.5 ± 4.1; inter = 2.6 ± 1.2), and light LDL (intra = 4.5 ± 4.6; inter = 2.9 ± 1.9) showed that ELISA, as used in the present study, was a valid method for assessing LDL(−) content.

In addition, when univariate linear regression analysis was used, the content of LDL(−) in total LDL showed a positive association with TC ($\beta = 0.003$; $P < 0.001$), LDL-C ($\beta = 0.003$; $P < 0.001$), and non-HDL-C ($\beta = 0.003$; $P < 0.001$). However, a negative association with HDL-C was obtained for LDL(−) content in total LDL ($\beta = -0.32$; $P = 0.04$) and dense LDL ($\beta = -0.66$; $P = 0.02$) when all samples ($n = 73$) were analyzed (Table 2).

Discussion

The purpose of this study was to evaluate LDL(−) content in subjects with different levels of cardiovascular risk and to determine the association between their cardiovascular risk and lipid profile. CHD are complex and multifactorial, and dyslipidemia is present in most subjects with clinical events. Other factors were recently investigated and LDL(−) was associated with increased cardiovascular risk [8, 19].

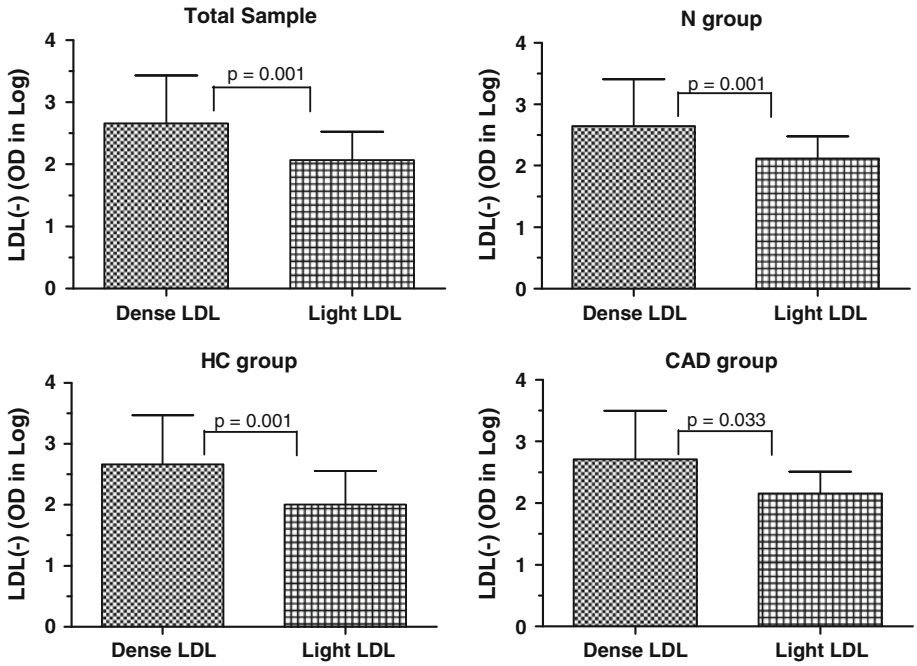

Fig. 2 LDL(−) concentration in dense and light LDL in total sample and groups isolated. Normolipidemic (*N*; $n = 30$), hypercholesterolemic (*HC*; $n = 33$) and coronary artery disease (*CAD*; $n = 10$) groups

Table 2 Linear regression analysis of LDL(−) content in LDL and dense LDL

	β	R^2 (%)	*P*
LDL(−) in LDL			
Total cholesterol	0.003	0.24	<0.001
LDL-C	0.003	0.30	<0.001
HDL-C	−0.321	0.06	0.043
Non-HDL-C	0.003	0.28	<0.001
LDL(−) in dense LDL			
HDL-C	−0.661	0.08	0.022

However, a number of technical limitations have made LDL(−) detection difficult [19]. Some studies evaluated LDL(−) by semi-quantitative methods [9, 11, 20]. Sensitive and specific anti-LDL(−) MAb-based ELISA evaluations were developed allowing the role of LDL(−) to be investigated [19, 21, 22].

Oliveira et al. [7], proposed that LDL(−) levels may be a biochemical marker for cardiovascular disease risk. Furthermore, Hulthe and Fagerberg [6] concluded that subjects with at least one plaque in the carotid or femoral arteries have oxLDL levels significantly higher than those found in subjects without plaques. These observations reinforce the notion that oxidized LDL and possibly LDL(−) have a potential role in atherosclerosis. LDL(−) was found to be elevated in animals and humans with hypercholesterolemia and atherosclerosis [19, 23, 24]. In the present study, as in the studies mentioned above, the values for LDL(−) content in subjects with dyslipidemia and atherosclerosis were shown to be higher than those in the N group. Such profiles could be observed only when LDL(−) content was analyzed in LDL.

In fact, LDL(−) content in LDL from subjects in the HC and CAD groups was shown to be higher than in the N group. Moreover, LDL(−) content in dense LDL was higher than in light LDL, irrespective of the clinical status of the subjects evaluated. Such a profile had previously been observed by Sevanian et al. [10, 11], who showed that LDL(−) has a higher association with small and dense LDL. However, Sánchez-Quesada et al. [25] observed that LDL(−) was equally distributed between light (1.022–1.027 g/L) and dense (1.047–1.056 g/L) LDL from hypertriglyceridemic subjects. LDL(−) was relatively frequent in dense LDL subfractions (1.039–1.056 g/L) from normolipidemic subjects. Finally, LDL(−) proportion was relatively high in all LDL subfractions, mainly in the two lightest (1.022–1.027 g/L) ones from patients with familial hyperlipidemia [25]. According to these authors, distribution of LDL(−) in these subjects depends on their lipid profile. We propose that LDL(−) content was influenced by the lipid profile being more frequent in dense LDL particles (phenotype B), although independently of the subjects' clinical status. In addition, the subjects included in this study did not show hypertriglyceridemia or familial hyperlipidemia, suggesting that LDL(−) has different physicochemical characteristics and origin as previously observed by Sánchez-Quesada et al. [25].

It should be emphasized that both different density cut off values and different (quantitative or qualitative) methods were used to determine LDL(−) content in the LDL

subfractions in those studies. To our knowledge, the present study is the first one in which LDL(−) content in LDL subfractions was determined by ELISA. Thus, our results should be confirmed with a larger sample.

Regarding the oxidative origin of LDL(−), our results confirm those reported in the study of Dejager et al. [26]. These authors observed that the lag phase in dense LDL was shorter than in light LDL after copper-induced oxidation. Thereafter, La Belle et al. [27] verified that dense LDL was more electronegative than light LDL. Therefore, among light and dense LDL particles, the dense ones showed themselves to have the highest oxidative susceptibility [10].

It is well established that the proportion of small and dense LDL particles in patients with CAD is higher than in healthy subjects [28, 29]. Although the size of LDL particles was not evaluated in the present study, detection of LDL(−) in dense LDL contributed to better understand the atherogenic role of the particles present in phenotype B. The impact of these results was reinforced by regression analysis, which revealed that LDL(−) content has a positive association with classical markers of cardiovascular risk (TC, LDL-C, and non-HDL-C), but a negative association with HDL-C.

In conclusion, we report herein that LDL(−) content in HC and atherosclerotic subjects was higher than in normolipidemic individuals. The atherogenic role of LDL(−) was evidenced by both association of this subfraction with the patients' lipid profile and a higher proportion of dense LDL in phenotype B. Regarding the clinical importance of our findings, we suggest that evaluation of LDL(−) content should be included in future epidemiological studies to better assess the risk of individuals with cardiovascular disease.

Acknowledgments The present study was financially supported by grants from FAPESP (#04/11792-6). The authors acknowledge Dr Paulo Boschcov, former professor at UNIFESP, for his revision of the final version of the manuscript.

References

1. World Health Organization (2006) World Health Statistics. Report. Geneva
2. Expert Panel on Detection, Evaluation, Treatment of High Blood Cholesterol in Adults (2001) Summary of the third report of the National Cholesterol Education Program (NCEP) Expert Panel on Detection, Evaluation, and Treatment of High Blood Cholesterol in Adults (Adult Treatment Panel III). JAMA 285:2486–2497
3. Sociedade Brasileira de Cardiologia (2007) IV Diretriz Brasileira sobre Dislipidemias e Prevenção da Aterosclerose; Departamento de Aterosclerose da Sociedade Brasileira de Cardiologia. Arquivos Brasileiros de Cardiologia S88:2–19
4. Berneis KK, Krauss RM (2002) Metabolic origins and clinical significance of LDL heterogeneity. J Lipid Res 43:1363–1379
5. Toshima S, Hasegawa A, Kurabayashi M et al (2000) Circulating oxidized low density lipoprotein levels. A biochemical risk marker for coronary heart disease. Arterioscler Thromb Vasc Biol 20(10):2243–2247
6. Hulthe J, Fagerberg B (2002) Circulating oxidized LDL is associated with subclinical atherosclerosis development and inflammatory cytokines (AIR Study). Arterioscler Thromb Vasc Biol 22:1162–1167
7. Oliveira JA, Sevanian A, Rodrigues RJ, Apolinário E, Abdalla DSP (2006) Minimally modified electronegative LDL and its autoantibodies in acute and chronic coronary syndromes. Clin Biochem 39:708–714
8. Sánchez-Quesada JL, Benítez S, Ordóñez-Llanos J (2004) Electronegative low-density lipoprotein. Curr Opin Lipidol 15:329–335
9. Chen HH, Hosken BD, Huang M, Gaubatz JW et al (2007) Electronegative LDL from familial hypercholesterolemic patients are physico-chemically heterogeneous but uniformly proapoptotic. J Lipid Res 48:177–184
10. Sevanian A, Hwang J, Hodis H, Cazzolato G, Avogaro P, Bittolo-Bon G (1996) Contribution of an in vivo oxidized LDL to LDL oxidation and its association with dense LDL subpopulations. Arterioscl Thromb Vasc Biol 16:784–793
11. Sevanian A, Bittolo-Bon G, Cazzolato G et al (1997) LDL$^-$ is a lipid hydroperoxide-enriched circulating lipoprotein. J Lipid Res 38:419–428
12. Chappey B, Myara I, Benoit MO, Mazière C, Mazière JC, Moatti N (1995) Characteristics of ten charge-differing subfractions isolated from human native low-density lipoproteins (LDL). No evidence of peroxidative modifications. Biochim Biophys Acta 1259(3):261–270
13. Ziouzenkova O, Asatryan L, Akmal M et al (1999) Oxidative cross-linking of ApoB100 and hemoglobin results in low density lipoprotein modification in blood. J Biol Chem 274(27):18916–18924
14. Gaubatz JW, Gillard BK, Massey JB, Hoogeveen RC, Huang M, Lloyd EE, Raya JL, Yang CY, Pownall HJ (2007) Dynamics of dense electronegative low density lipoproteins and their preferential association with lipoprotein phospholipase A_2. J Lipid Res 48(2):348–357
15. World Health Organization (WHO) (2000) Obesity. Preventing and managing the global epidemic. Report. Geneva (WHO—Technical Report Series, 894)
16. IDF Clinical Guidelines Task Force (2006) Global guideline for type 2 diabetes: recommendations for standard, comprehensive, and minimal care. Diabet Med 23(6):579–593
17. Havel RJ, Eder HA, Bragdon JH (1955) The distribution and chemical composition of ultracentrifugally separated lipoprotein in human serum. J Clin Invest 34(9):1345–1353
18. Lowry OH, Rosebrough NJ, Farr AL, Randall RJ (1951) Protein measurement with the Folin-phenol reagent. J Biol Chem 193(1):265–275
19. Damasceno NRT, Sevanian A, Apolinário E, Oliveira JMA, Fernandes I, Abdalla DSP (2006) Detection of electronegative low density lipoprotein (LDL$^-$) in plasma and atherosclerotic lesions by monoclonal antibody-based immunoassays. Clin Biochem 39:28–38
20. Sánchez-Quesada JL, Camacho M, Antón R, Benítez S, Vila L, Ordóñez-Llanos J (2003) Electronegative LDL of FH subjects: chemical characterization and induction of chemokine release from human endothelial cells. Atherosclerosis 166:261–270
21. Araújo DB, Bertolami MC, Ferreira WP et al (2007) Simvastatin 80 mg and coadministration of simvastatin 10 mg and Ezetimibe 10 mg: effects on LDL(−) and anti-LDL(−) antibodies. Int J Atheroscler 2:272–278

22. Faulin TES, Sena KCM, Telles AER, Grosso DM, Faulin EJB, Abdalla DSP (2008) Validation of a novel ELISA for measurement of electronegative low density lipoprotein. Clin Chem Lab Med 46:1769–1775
23. Hodis HN, Kramsch DM, Avogaro P et al (1994) Biochemical and cytotoxic characteristic of an in vivo circulating oxidized low density lipoprotein (LDL^{-}). J Lipid Res 35:669–677
24. Siqueira AF, Abdalla DS, Ferreira SR (2006) LDL: from metabolic syndrome to instability of the atherosclerotic plaque. Arq Bras Endocrinol Metabol 50(2):334–343
25. Sánchez-Quesada JL, Benítez S, Otal C, Franco M, Blanco-Vaca F, Ordóñez-Llanos J (2002) Density distribution of electronegative LDL in normolipemic and hyperlipemic subjects. J Lipid Res 43:699–705
26. Dejager S, Bruckert E, Chapman MJ (1993) Dense low density lipoprotein subspecies with diminished oxidative resistance predominate in combined hyperlipidemia. J Lipid Res 34:295–308
27. La Belle M, Blanche PJ, Krauss RM (1997) Charge properties of low density lipoprotein subclasses. J Lipid Res 38(4):690–700
28. Akanji AO, Suresh CG, Fatania HR, Al-Radwan R, Zubaid M (2007) Associations of apolipoprotein E polymorphism with low-density lipoprotein size and subfraction profiles in Arab patients with coronary heart disease. Metabolism 56(4):484–490
29. Rizzo M, Pernice V, Frasheri A, Berneis K (2008) Atherogenic lipoprotein phenotype and LDL size and subclasses in patients with peripheral arterial disease. Atherosclerosis 197(1):237–241

Lipids (2010) 45:627–633
DOI 10.1007/s11745-010-3435-y

ORIGINAL ARTICLE

Oxidative Modification and Poor Protective Activity of HDL on LDL Oxidation in Thalassemia

Supeenun Unchern · Narumon Laohareungpanya · Yupin Sanvarinda · Kovit Pattanapanyasat · Pansakorn Tanratana · Udom Chantharaksri · Nathawut Sibmooh

Received: 24 March 2010 / Accepted: 15 May 2010 / Published online: 9 June 2010

Abstract Oxidative modification of low-density lipoprotein (LDL) has been reported in thalassemia, which is a consequence of oxidative stress. However, the levels of oxidized high-density lipoprotein (HDL) in thalassemia have not been evaluated and it is unclear whether HDL oxidation may be linked to LDL oxidation. In this study, the levels of total cholesterol, iron, protein, conjugated diene (CD), lipid hydroperoxide (LOOH), and thiobarbituric acid reactive substances (TBARs) were determined in HDL from healthy volunteers and patients with β-thalassemia intermedia with hemoglobin E (β-thal/Hb E). The protective activity of thalassemic HDL on LDL oxidation was also investigated. The iron content of HDL_2 and HDL_3 from β-thal/HbE patients was higher while the cholesterol content was lower than those in healthy volunteers. Thalassemic HDL_2 and HDL_3 had increased levels of lipid peroxidation markers i.e., conjugated diene, LOOH, and TBARs. Thalassemic HDL had lower peroxidase activity than control HDL and was unable to protect LDL from oxidation induced by $CuSO_4$. Our findings highlight the oxidative modification and poor protective activity of thalassemic HDL on LDL oxidation which may contribute to cardiovascular complications in thalassemia.

Keywords Thalassemia · HDL · LDL oxidation · Oxidative stress · Oxidized HDL

Abbreviations

CD	Conjugated diene
HDL	High-density lipoprotein
LDL	Low-density lipoprotein
LOOH	Lipid hydroperoxide
OD	Optical density
TBARs	Thiobarbituric acid reactive substances
β-thal/Hb E	β-Thalassemia with hemoglobin E

Introduction

β-Thalassemia/hemoglobin E (β-thal/Hb E) is a syndrome caused by mutation on β-globin gene (from β-26 glutamine to lysine) that is prevalent in the southeast Asia. The abnormal globin complex is unstable and leads to hemolytic anemia and hemosiderosis [1]. The iron-bound molecules such as hemichrome and hemin may undergo a chain of oxidative reactions with biomolecules and cause dysfunctions of platelets and vascular endothelial cells [2–5]. Dyslipoproteinemia in thalassemia [6–9] is a consequence of lipid peroxidation associated with iron overload [10, 11]. The low cholesterol levels were related to depletion of vitamin E and severity of thalassemia [2, 12].

S. Unchern · Y. Sanvarinda · P. Tanratana · N. Sibmooh (✉)
Department of Pharmacology, Faculty of Science,
Mahidol University, Rama 6 Rd, Bangkok 10400, Thailand
e-mail: scnsm@mahidol.ac.th

N. Laohareungpanya
Laboratory of Immunology, Chulabhorn Research Institute,
Vibhavadee-Rangsit Highway, Laksi, Bangkok 10210, Thailand

K. Pattanapanyasat
Office for Research and Development, Faculty of Medicine
Siriraj Hospital, Mahidol University, Bangkok, Thailand

U. Chantharaksri
Faculty of Chinese Medicine, Huachiewchalermprakiet
University, 18/18, Bangna-Trad Road, k.m. 18, Bangplee,
Samut Prakarn 10540, Thailand

Oxidative modification of thalassemic LDL had been reported [7–11, 13, 14] which was related to the increased protein and triglyceride content but decreased cholesterol and vitamin E content [9]. The presence of oxidized LDL in thalassemia was evidenced by high levels of CD and TBARs in LDL [10, 11], and the elevated levels of oxidized LDL antibody in plasma [13]. The high levels of circulating oxidized LDL in thalassemia were demonstrated to associate with the early atherosclerosis and endothelial dysfunction responsible for cardiovascular complications of the disease [14, 15].

HDL particles exert anti-atherogenic activities by three major mechanisms: reverse cholesterol transport, carrying oxidized lipids from tissues and LDL back to liver, and protection of LDL from oxidation [16–20]. The protective activity of HDL on LDL oxidation involves enzymatic and non-enzymatic mechanisms. Enzymes located in HDL such as paraoxonase-1, platelet-activating factor acetylhydrolase, and lecithin-cholesterol acyltransferase have been shown to hydrolyze oxidized lipids and thus inhibit LDL oxidation [17, 21, 22]. For example, HDL-associated paraoxonase-1 was shown to possess peroxidase activity because of its ability to hydrolyze LOOH and hydrogen peroxide [23]. This enzyme was believed to protect HDL and LDL from oxidation. By non-enzymatic mechanisms, HDL could inhibit LDL oxidation by chelation of metal ions by apolipoprotein A-I [24] and by action of antioxidants such as vitamin E and carotenoids [25]. These findings indicate that several antioxidant mechanisms exist in HDL.

Thalassemic HDL was shown to have low cholesterol content, high triglyceride content, abnormal apo A-I [7, 8], and impairment of paraoxonase activity [26, 27]. Although the increased levels of oxidized LDL in thalassemia have been reported, the levels of oxidized HDL and its association with LDL oxidation have not been defined. We hypothesize that thalassemic HDL is oxidatively modified and has impaired activity to protect LDL from oxidation.

Methods

Subjects

This study was approved by the Committee on Ethical Practice and the Ethical and Scientific Review Subcommittee of Mahidol University. Informed consent was obtained from 27 healthy volunteers at the blood bank, Ramathibodi hospital and 22 patients with thalassemia intermedia (β-thalassemia/Hb E) at the Hematology Unit, Faculty of Medicine Siriraj Hospital, Mahidol University. The healthy volunteers (11 males and 16 females) were 24–52 years of age (mean ± SD = 32 ± 10.3 years). The thalassemic patients (10 males and 12 females), aged 17–50 years (mean ± SD = 32 ± 11.6 years), were clinically in a steady state with no iron chelation therapy and blood transfusion for at least 1 month before the study. The serum ferritin levels of patients ranged from 322 to 5,602 ng/mL. The patients and healthy volunteers who had history of supplemental vitamin intake within a month or cigarette smoking were excluded from the study.

Blood Collection and Plasma Preparation

Blood was collected in glass tubes using EDTA (1.5 mg/mL) as anticoagulant after 8 h of fasting. Plasma was separated by centrifugation at 2500*g* for 10 min at 4 °C and kept at −70 °C within a week before use. For assay of the peroxidase activity of HDL, heparinized blood (1 unit/mL) was used.

Lipoprotein Separation

Lipoproteins were separated by sequential density gradient ultracentrifugation using a Beckman Optima LE-80K centrifuge and a Ti 90 rotor at 548,000*g* at 4 °C. The plasma was adjusted to desired density by addition of a mixture of Mork's salt solution and concentrated KBr solution. LDL was obtained at density between 1.019–1.063 g/mL, HDL_2 at density between 1.063 and 1.125 g/mL, and HDL_3 at density between 1.125 and 1.210 g/mL [28]. These lipoproteins were stored at −70 °C until analysis within 1 week.

HDL Composition

The composition of HDL_2 and HDL_3 was determined by the following methods: levels of protein content by modified Lowry's method [29], total cholesterol by an enzymatic test kit (Bio-medical Laboratory, Thailand) to yield quinoneimide dye with maximum absorption at 550 nm, and total iron content by measuring the ferrozine-ferrous ion complex at the optical density (OD) 562 nm [30].

Lipid Peroxidation

Measurement of conjugated diene (CD, an initial lipid peroxidation marker): 100 μg protein/mL of lipoprotein suspension was diluted with 2 mL of 10 mM PBS. The OD at 234 nm was measured immediately to avoid autoxidation in room air [31]. The amount of CD was calculated with the use of the molar extinction coefficient (ε_{234} = 29,500 M^{-1} cm^{-1}) [32].

Measurement of lipid hydroperoxide (LOOH, a marker of lipid peroxidation produced in the propagation phase): 100 μg protein/mL of lipoprotein suspension was added to 3 mL of 4.5 mM $FeSO_4$ dissolved in 0.2 M HCl with 3%

deaerated methanolic solution of KSCN. The mixture was incubated at room temperature for 30 min, then the OD at 500 nm was measured [33].

Measurement of thiobarbituric acid reactive substances (TBARs, a final lipid peroxidation marker): 500 μL of lipoprotein suspension (100 μg protein/mL) was used to determine the levels of TBARs with spectrofluorometer (Jasco FP 770, Japan Spectroscopic Co. Ltd. Tokyo, Japan) at 515 nm excitation and 553 nm emission wavelength [34].

Protective Activity of HDL on LDL Oxidation

LDL oxidation was determined as LOOH levels. LDL and HDL were dialyzed in 10 mM PBS (pH 7.4) for 24 h at 4 °C. LDL oxidation was conducted in the absence or presence of HDL. LDL/HDL mixture (ratio 1:1) containing 200 μg protein/mL in 2 mL of 10 mM PBS buffer (pH = 7.4) was incubated with 30 μM $CuSO_4$ at 37 °C for 90 min.

Peroxidase Activity of HDL

Hydrogen peroxide (H_2O_2, 2.5 μg/mL) was added to the HDL suspension (100 μg protein/mL). The levels of peroxide in HDL were determined by the KSCN-method [33] at the times 0, 15, 30, 60, and 90 min, comparing them with the levels of peroxide in PBS.

Statistical Analysis

All data are presented as means ± SD. Data processing and statistical analysis were done by Prism, version 4.0 (GraphPad Software Inc., San Diego, CA). Analysis of variance (ANOVA) with Tukey's multiple comparison test or Student's *t* test were used to compare with acceptable *P* value less than 0.05.

Results

Composition and Oxidation of Thalassemic HDL

The cholesterol content in HDL_2 and HDL_3 of β-thal/Hb E patients was significantly lower in β-thal/Hb E than those of control ($P < 0.01$) (Fig. 1a). Total iron content of thalassemic HDL_2 and HDL_3 (6.80 ± 3.38 and 6.94 ± 3.38 mM, respectively) was higher than the levels found in healthy volunteers (1.03 ± 0.40 and 0.57 ± 0.34 mM) ($P < 0.01$) (Fig. 1b), but no difference in protein content was noted between the two groups (Fig. 1c).

HDL_3 of β-thal/Hb E, however, showed increased levels of CD (Fig. 2a). The HDL_2 and HDL_3 of β-thal/Hb E had increased levels of LOOH (HDL_2, 1.14 ± 0.34 versus 0.48 ± 0.42 μM; HDL_3, 1.23 ± 0.38 vs 0.70 ± 0.39 μM) ($P < 0.05$) (Fig. 2b). Levels of the final lipid peroxidation product (TBARs) in thalassemic HDL_3 were higher than those of control HDL_3 (0.41 ± 0.08 versus 0.22 ± 0.08 μM) ($P < 0.05$) (Fig. 2c). Although the levels of CD and TBARs in HDL_2 were not different from control, the ratio of CD, LOOH, and TBARs to cholesterol in HDL_2 and HDL_3 appeared to be higher in thalassemia than in control (Fig. 2d–f).

Protective Effect of HDL on LDL Oxidation

The peroxidase activity of HDL from healthy volunteers and of β-thal/Hb E patients was monitored by measuring a

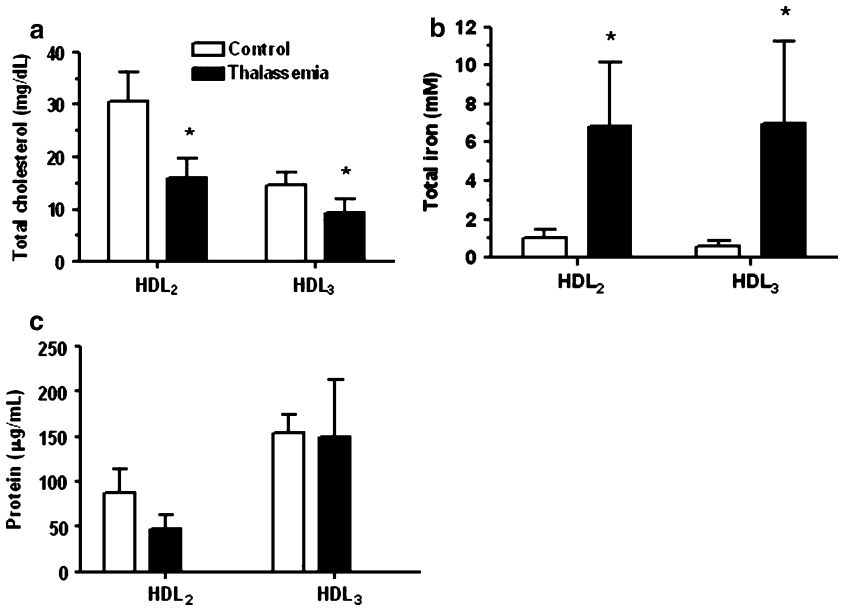

Fig. 1 Biochemical composition of HDL_2 and HDL_3 obtained from control healthy volunteers ($n = 12$) and thalassemia patients ($n = 10$). **a** Total cholesterol (mg/dL). **b** Total iron content (mM). **c** Protein content (μg/mL). Data are means ± SD. *$P < 0.05$ with the unpaired *t*-test compared with control

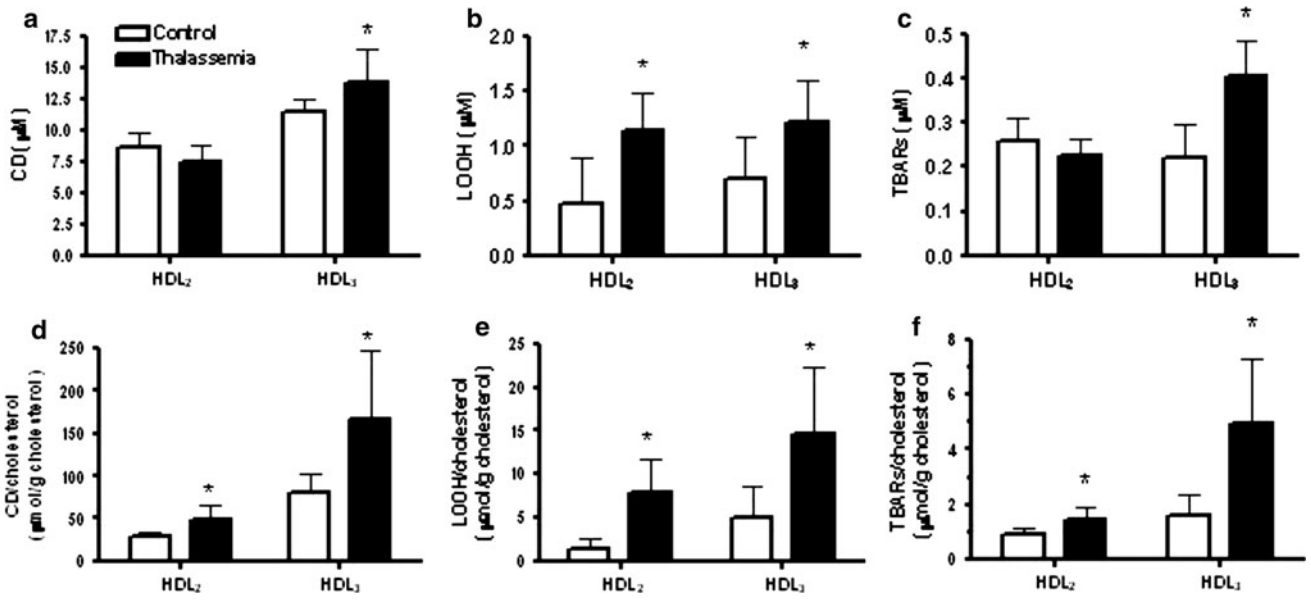

Fig. 2 Lipid peroxidation markers of HDL_2 and HDL_3 from control healthy volunteers ($n = 12$) and thalassemic patients ($n = 10$). **a** Conjugated diene (CD, μM). **b** Lipid hydroperoxide (LOOH, μM). **c** Thiobarbituric acid reactive substances (TBARs, μM). **d–f** Ratio of CD, LOOH, and TBARs to cholesterol (μmol/g cholesterol). Data are means ± SD. $^*P < 0.05$ with the unpaired *t* test compared with control

decrease of peroxide levels after addition of 2.5 μg/mL H_2O_2 to the HDL mixture for 90 min (Fig. 3a). In PBS, without addition of HDL, there was no change in peroxide levels after 90 min. Control HDL from healthy volunteers decreased peroxide levels to 47% of the initial values after 90 min of incubation. Thalassemic HDL showed the slower rate of peroxide decrease and after 90 min of incubation the levels decreased to 72% of the initial levels.

To test whether thalassemic HDL has the ability to prevent LDL oxidation, oxidation of LDL (200 μg protein/mL) obtained from healthy volunteers was induced by 30 μM $CuSO_4$ in the presence and absence of HDL. The maximal LOOH levels (6.23 ± 1.43 μM) were obtained at 90 min following incubation of LDL and $CuSO_4$ at 37 °C and then the levels decreased gradually. Thus, the effect of HDL on LDL oxidation induced by $CuSO_4$ was examined by measuring LOOH levels at this time point. Control and thalassemic HDL was also oxidized by the same concentration of $CuSO_4$ and the LOOH levels at 90 min were 4.81 ± 0.97 and 4.75 ± 0.63 μM, respectively (Fig. 3b). When the control HDL from healthy volunteers was added into the LDL/$CuSO_4$ mixture, LDL oxidation was decreased significantly by 44% (LOOH content = 3.46 ± 0.57 μM, $P < 0.05$ compared with the mixture without HDL). However, the thalassemic HDL was unable to prevent LDL oxidation (23% decrease, LOOH content = 4.82 ± 0.83 μM).

Discussion

HDL is known to regulate lipoprotein metabolism and reverse cholesterol transport which contributes to the anti-atherogenic property. The anti-atherogenic activity of HDL is related to their cholesterol levels, especially when those levels are higher than 60 mg/dL [35]. In addition, HDL possesses the protective activities that prevent lipoprotein oxidation by carrying oxidized lipids from peripheral tissues and LDL to liver. HDL also contains enzymes including paraoxonase-1 [23, 36], lecithin/cholesterol acyltransferase [19, 22], and platelet-activating factor acetylhydrolase [17] that are believed to be responsible for the protective antioxidant activity on LDL oxidation.

Our study demonstrates that thalassemic HDL is oxidatively modified, probably because of oxidative stress, high iron content, and impaired peroxidase activity to protect HDL itself. The oxidative changes of thalassemic HDL are also related to the low cholesterol content in HDL. Thalassemic HDL contains high concentrations of lipid peroxidation products (CD, LOOH and TBARs), but low cholesterol content. HDL_3 had significantly higher levels of lipid peroxidation markers than HDL_2. HDL_2 had no difference in the levels of CD and TBARS compared to control, however, the ratio of these markers to cholesterol content was increased. These suggest that the oxidative modification of thalassemic HDL has association with the

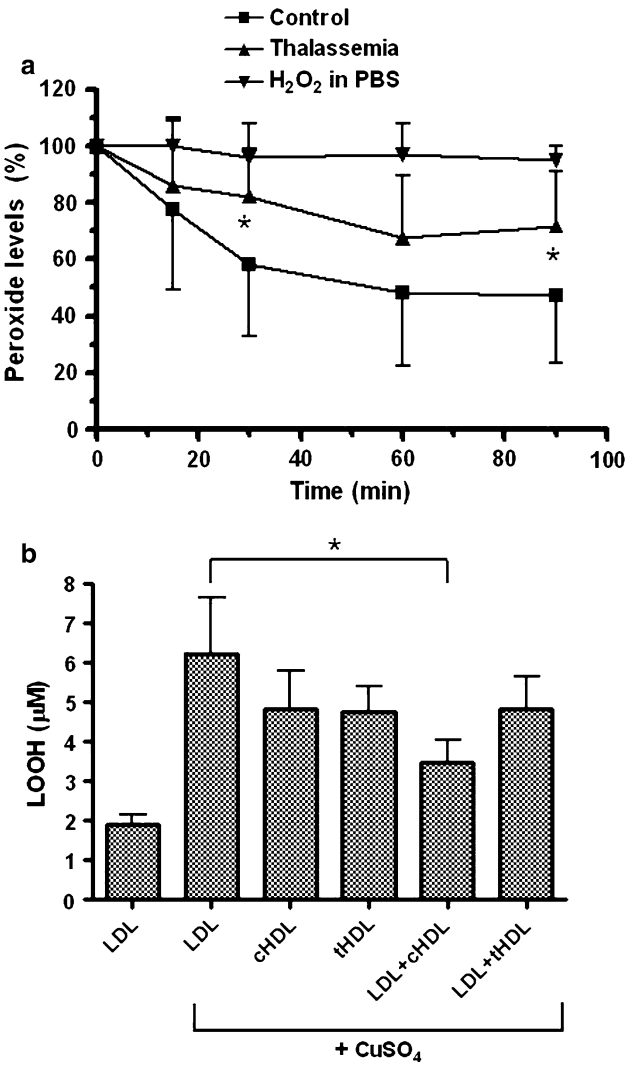

Fig. 3 Peroxidase activity and protective effect of HDL on LDL oxidation. **a** Peroxidase activity of HDL from healthy volunteers ($n = 10$) and β-thal/HbE patients ($n = 10$). Levels of peroxide were measured at different time after addition of 2.5 μg/mL H_2O_2 into HDL mixture (100 μg protein/mL) at 37 °C. *$P < 0.05$ compared between control and thalassemia. **b** Lipid hydroperoxide (LOOH) levels in LDL obtained from healthy volunteers ($n = 5$) were measured before and after incubation with 30 μM $CuSO_4$ for 90 min at 37 °C. LOOH levels were also determined in control HDL (cHDL) and thalassemic HDL (tHDL) ($n = 5$ each) in the presence of $CuSO_4$. All reaction mixtures contained final protein concentration of 200 μg/mL. The ratio of LDL:HDL was 1:1. Data are mean ± SD. * $P < 0.05$ as analyzed by one-way ANOVA with Tukey's multiple comparison test

increased oxidative stress in thalassemia [2, 4]. Our data that HDL_3 (an innate HDL which is important in reverse cholesterol transport) has higher lipid peroxidation markers than HDL_2 (a form of HDL after accepting cholesterol) corresponds to the functions of HDL_3 that serves to accept oxidized lipids from other lipoproteins and tissues [18, 37–39]. Thus, the antioxidant mechanisms within HDL_3 act to remove oxidized intermediates and lessen accumulation of LOOH and TBARs in HDL_2.

In addition to accepting oxidized lipids from tissues and lipoproteins and carrying them back to liver [18], HDL_3 contains paraoxonase-1 which possesses peroxidase activity [40]. This enzyme located on HDL_3 is believed to involve in the enzymatic protection against lipoprotein oxidation [23]. Decreased activity of plasma and HDL-associated paraoxonase-1 was reported in thalassemia [26, 27]. The impaired peroxidase (or paraoxonase-1) activity of thalassemic HDL could be secondary to an increase of circulating proinflammatory oxidized lipids that negatively regulate paraoxonase-1 functions [41]. In other words, the oxidative stress and iron overload in thalassemia could lead to inhibition of HDL-associated paraoxonase-1 that protects both HDL and LDL from oxidation. Consequently, both HDL and LDL are oxidatively modified in thalassemia, causing an accumulation of oxidized lipids as indicated by elevated levels of oxidative markers in thalassemic HDL. Apart from the low peroxidase activity of HDL, increased oxidative stress in thalassemia would result in elevated oxidized lipids in blood and tissues, which are transferred to HDL. Thus, the low peroxidase activity within HDL and increased transfer of oxidized lipids to HDL would cause accumulation of lipid peroxidation markers in thalassemic HDL.

LOOH is an important intermediate of lipid peroxidation. Lipid peroxidation is triggered by free radical species such as hydroxyl radical derived from iron-mediated reduction of hydrogen peroxide (H_2O_2) and by non-radical species including LOOH. The process is generally described as three phases: initiation, propagation, and termination. In initiation phase, for example, hydroxyl radical ($^{\cdot}OH$) can abstract hydrogen from polyunsaturated fatty acids at the Sn-2 position of phospholipids of LDL. The process proceeds via the formation of conjugated diene and peroxyl radical ($LOO^{\cdot}$) which either forms LOOH or degrades to release aldehydes [17]. In propagation phase, LOOH undergoes Fenton-like reaction in the presence of metal ions, producing lipid alkoxyl ($LO^{\cdot}$) and peroxyl radicals that cause chain of reactions. Finally, the bi-molecular reactions of alkyl ($L^{\cdot}$) or peroxyl radicals produce non-radical products in termination phase. The peroxidase activity of HDL is thus important in terminating the propagation of lipid peroxidation by removal of LOOH and H_2O_2. Poor peroxidase activity of thalassemic HDL-associated paraoxonase-1 would result in retention of LOOH in HDL and increased susceptibility of LDL to oxidation in the presence of high iron content.

In conclusion, our study demonstrates the existence of oxidized HDL in thalassemia, which has low peroxidase activity and poor ability to protect LDL from oxidation. The poor protective activity of thalassemic HDL is

consistent with the compositional changes and high levels of oxidative markers. This impaired function of HDL would promote generation of pathogenic oxidized LDL that could be responsible for cardiovascular complications in thalassemia.

Acknowledgments The authors would like to thank Prof. Dr. Suthat Fucharoen, Prof. Dr. Pensri Pootrakul from Thalassemia Research Center, Institute of Science and Technology for Research and Development, Mahidol University; Dr. Wanchai Wanachivanawin from Department of Medicine, Faculty of Medicine Siriraj Hospital, Mahidol University for screening and care of thalassemic patients. We also thank to all staffs and blood donors of Blood Bank Ramathibodi Hospital.

References

1. Sorensen S, Rubin E, Polster H, Mohandas N, Schrier S (1990) The role of membrane skeletal-associated alpha-globin in the pathophysiology of beta-thalassemia. Blood 75:1333–1336
2. Unchern S, Laoharuangpanya N, Phumala N, Sipankapracha P, Pootrakul P, Fucharoen S, Wanachivanawin W, Chantharaksri U (2003) The effects of vitamin E on platelet activity in beta-thalassaemia patients. Br J Haematol 123:738–744
3. Sutipornpalangkul W, Unchern S, Sanvarinda Y, Chantharaksri U, Fucharoen S (2009) Modification of platelet shape change parameter by oxidized lipoprotein from beta-thalassemia/Hemoglobin E. J Med Assoc Thai 92:504–509
4. Kukongviriyapan V, Somparn N, Senggunprai L, Prawan A, Kukongviriyapan U, Jetsrisuparb A (2008) Endothelial dysfunction and oxidant status in pediatric patients with hemoglobin E-beta thalassemia. Pediatr Cardiol 29:130–135
5. Butthep P, Nuchprayoon I, Futrakul N (2004) Endothelial injury and altered hemodynamics in thalassemia. Clin Hemorheol Microcirc 31:287–293
6. Papanastasiou DA, Siorokou T, Haliotis FA (1996) beta-Thalassaemia and factors affecting the metabolism of lipids and lipoproteins. Haematologia (Budap) 27:143–153
7. Maioli M, Cuccuru GB, Pranzetti P, Pacifico A, Cherchi GM (1984) Plasma lipids and lipoproteins pattern in beta-thalassemia major. Acta Haematol 71:106–110
8. Maioli M, Vigna GB, Tonolo G, Brizzi P, Ciccarese M, Donega P, Maioli M, Fellin R (1997) Plasma lipoprotein composition, apolipoprotein(a) concentration and isoforms in beta-thalassemia. Atherosclerosis 131:127–133
9. Goldfarb AW, Rachmilewitz EA, Eisenberg S (1991) Abnormal low and high density lipoproteins in homozygous beta-thalassaemia. Br J Haematol 79:481–486
10. Altamentova SM, Marva E, Shaklai N (1997) Oxidative interaction of unpaired hemoglobin chains with lipids and proteins: a key for modified serum lipoproteins in thalassemia. Arch Biochem Biophys 345:39–46
11. Livrea MA, Tesoriere L, Maggio A, D'Arpa D, Pintaudi AM, Pedone E (1998) Oxidative modification of low-density lipoprotein and atherogenetic risk in beta-thalassemia. Blood 92:3936–3942
12. Tesoriere L, D'Arpa D, Maggio A, Giaccone V, Pedone E, Livrea MA (1998) Oxidation resistance of LDL is correlated with vitamin E status in beta-thalassemia intermedia. Atherosclerosis 137:429–435
13. Brizzi P, Isaja T, D'Agata A, Malaguarnera L, Malaguarnera M, Musumeci S (2002) Oxidized LDL antibodies (OLAB) in patients with beta-thalassemia major. J Atheroscler Thromb 9:139–144
14. Stakos DA, Tavridou A, Margaritis D, Tziakas DN, Kotsianidis I, Chalikias GK, Tsatalas K, Bourikas G, Manolopoulos VG, Boudoulas H (2009) Oxidised low-density lipoprotein and arterial function in beta-thalassemia major. Eur J Haematol 82:477–483
15. Hahalis G, Kremastinos DT, Terzis G, Kalogeropoulos AP, Chrysanthopoulou A, Karakantza M, Kourakli A, Adamopoulos S, Tselepis AD, Grapsas N et al (2008) Global vasomotor dysfunction and accelerated vascular aging in beta-thalassemia major. Atherosclerosis 198:448–457
16. Mackness MI, Abbott C, Arrol S, Durrington PN (1993) The role of high-density lipoprotein and lipid-soluble antioxidant vitamins in inhibiting low-density lipoprotein oxidation. Biochem J 294(Pt 3):829–834
17. Mackness MI, Durrington PN (1995) HDL, its enzymes and its potential to influence lipid peroxidation. Atherosclerosis 115:243–253
18. Christison J, Karjalainen A, Brauman J, Bygrave F, Stocker R (1996) Rapid reduction and removal of HDL- but not LDL-associated cholesteryl ester hydroperoxides by rat liver perfused in situ. Biochem J 314(Pt 3):739–742
19. Christison JK, Rye KA, Stocker R (1995) Exchange of oxidized cholesteryl linoleate between LDL and HDL mediated by cholesteryl ester transfer protein. J Lipid Res 36:2017–2026
20. Parthasarathy S, Barnett J, Fong LG (1990) High-density lipoprotein inhibits the oxidative modification of low-density lipoprotein. Biochim Biophys Acta 1044:275–283
21. Klimov AN, Nikiforova AA, Pleskov VM, Kuz'min AA, Kalashnikova NN (1989) Protective effect of high density lipoproteins, their subfractions and lecithin-cholesterol-acyltransferases on the peroxidation modification of low density lipoproteins. Biokhimiia 54:118–123
22. Watson AD, Navab M, Hama SY, Sevanian A, Prescott SM, Stafforini DM, McIntyre TM, Du BN, Fogelman AM, Berliner JA (1995) Effect of platelet activating factor-acetylhydrolase on the formation and action of minimally oxidized low density lipoprotein. J Clin Invest 95:774–782
23. Aviram M, Rosenblat M, Bisgaier CL, Newton RS, Primo-Parmo SL, La Du BN (1998) Paraoxonase inhibits high-density lipoprotein oxidation and preserves its functions. A possible peroxidative role for paraoxonase. J Clin Invest 101:1581–1590
24. Kunitake ST, Jarvis MR, Hamilton RL, Kane JP (1992) Binding of transition metals by apolipoprotein A-I-containing plasma lipoproteins: inhibition of oxidation of low density lipoproteins. Proc Natl Acad Sci USA 89:6993–6997
25. Goulinet S, Chapman MJ (1997) Plasma LDL and HDL subspecies are heterogenous in particle content of tocopherols and oxygenated and hydrocarbon carotenoids. Relevance to oxidative resistance and atherogenesis. Arterioscler Thromb Vasc Biol 17:786–796
26. Selek S, Aslan M, Horoz M, Gur M, Erel O (2007) Oxidative status and serum PON1 activity in beta-thalassemia minor. Clin Biochem 40:287–291
27. Phumala Morales N, Cherlermchoung C, Fucharoen S, Chantharaksri U (2007) Paraoxonase and platelet-activating factor acetylhydrolase activities in lipoproteins of beta-thalassemia/hemoglobin E patients. Clin Chem Lab Med 45:884–889
28. Havel RJ, Eder HA, Bragdon JH (1955) The distribution and chemical composition of ultracentrifugally separated lipoproteins in human serum. J Clin Invest 34:1345–1353
29. Markwell MA, Haas SM, Bieber LL, Tolbert NE (1978) A modification of the Lowry procedure to simplify protein determination in membrane and lipoprotein samples. Anal Biochem 87:206–210
30. White JM, Flashka HA (1973) An automated procedure, with use of ferrozine, for assay of serum iron and total iron-binding capacity. Clin Chem 19:526–528

31. Esterbauer H, Striegl G, Puhl H, Rotheneder M (1989) Continuous monitoring of in vitro oxidation of human low density lipoprotein. Free Radic Res Commun 6:67–75
32. Kleinveld HA, Hak-Lemmers HL, Stalenhoef AF, Demacker PN (1992) Improved measurement of low-density-lipoprotein susceptibility to copper-induced oxidation: application of a short procedure for isolating low-density lipoprotein. Clin Chem 38:2066–2072
33. Mihaljevic B, Katusin-Razem B, Razem D (1996) The reevaluation of the ferric thiocyanate assay for lipid hydroperoxides with special considerations of the mechanistic aspects of the response. Free Radic Biol Med 21:53–63
34. Kovachich GB, Mishra OP (1980) Lipid peroxidation in rat brain cortical slices as measured by the thiobarbituric acid test. J Neurochem 35:1449–1452
35. Ohta T, Takata K, Horiuchi S, Morino Y, Matsuda I (1989) Protective effect of lipoproteins containing apoprotein A-I on Cu^{2+}-catalyzed oxidation of human low density lipoprotein. FEBS Lett 257:435–438
36. Watson AD, Berliner JA, Hama SY, La Du BN, Faull KF, Fogelman AM, Navab M (1995) Protective effect of high density lipoprotein associated paraoxonase. Inhibition of the biological activity of minimally oxidized low density lipoprotein. J Clin Invest 96:2882–2891
37. Hahn M, Subbiah MT (1994) Significant association of lipid peroxidation products with high density lipoproteins. Biochem Mol Biol Int 33:699–704
38. Sakuma N, Saeki T, Yajima K, Hibino T, Yoshida T, Mizuno H, Mukai S, Sakata S, Kunimatsu M, Kimura G (2005) Both HDL3 and HDL2 exert a powerful anti-oxidative and protective effect against acceleration of oxidative modification of LDL by ascorbic acid. J Nutr Sci Vitaminol (Tokyo) 51:75–79
39. Singh K, Chander R, Kapoor NK (1997) High density lipoprotein subclasses inhibit low density lipoprotein oxidation. Indian J Biochem Biophys 34:313–318
40. Bergmeier C, Siekmeier R, Gross W (2004) Distribution spectrum of paraoxonase activity in HDL fractions. Clin Chem 50:2309–2315
41. Vakili L, Hama S, Kim JB, Tien D, Safarpoor S, Ly N, Vakili G, Hough G, Navab M (2010) The effect of HDL mimetic peptide 4F on PON1. Adv Exp Med Biol 660:167–172

Lipids (2010) 45:635–643
DOI 10.1007/s11745-010-3438-8

ORIGINAL ARTICLE

Biochemical Studies on Sphingolipid of *Artemia franciscana* (I) Isolation and Characterization of Sphingomyelin

Hisao Kojima · Takashi Inoue · Mutsumi Sugita · Saki Itonori · Masahiro Ito

Received: 19 November 2009 / Accepted: 27 January 2010 / Published online: 24 June 2010

Abstract Sphingomyelin was isolated from cysts of the brine shrimp *Artemia franciscana* using QAE-Sephadex A25, Florisil and Iatrobeads column chromatographies. The chemical structure was identified using thin-layer chromatography, gas–liquid chromatography, infrared spectroscopy and matrix-assisted laser desorption ionization time-of-flight mass spectrometry. The ceramide moiety of sphingomyelin consisted of stearic, arachidic, and behenic acids as fatty acids, and hexadeca-4- and heptadeca-4-sphingenines as sphingoids. By comparative analysis, the ceramide component of *Artemia* sphingomyelin appears unique in invertebrates and vertebrates. Biological functions of sphingomyelin have largely been investigated using mammalian-derived sphingomyelin. In mammals, a wide variety of molecular species of sphingomyelins have been reported, especially derived from nerve tissue, while the lower animal *Artemia* contains this unusual sphingomyelin perhaps because of having a much simpler nervous system. The purified unusual sphingomyelin derived from *Artemia franciscana* might be a very useful tool in elucidating the functions and mechanisms of action of this mediator.

Keywords Sphingomyelin · Chemical characterization · Comparative analysis of ceramide composition

H. Kojima · T. Inoue · M. Ito (✉)
Department of Bioinformatics,
Institute of Science and Engineering, Ritsumeikan University,
1-1-1 Nojihigashi, Kusatsu, Shiga 525-8577, Japan
e-mail: maito@sk.ritsumei.ac.jp

H. Kojima · M. Sugita · S. Itonori
Department of Chemistry, Faculty of Liberal Arts
and Education, Shiga University, 2-5-1 Hiratsu, Otsu,
Shiga 520-0862, Japan

Abbreviations

SM	Sphingomyelin
GC	Gas chromatography
GC-MS	Gas chromatography-mass spectrometry
IR	Infrared spectroscopy
MALDI-TOF MS	Matrix-assisted laser desorption ionization time-of-flight mass spectrometry
PSD	Post-source decay
TLC	Thin-layer chromatography

Introduction

Sphingomyelin (SM), or ceramide phosphocholine, consists of ceramide and phosphorylcholine moieties. It is the sphingolipid analogue of phosphatidylcholine, which is important as a precursor of intracellular mediators [1, 2]. SM is a component of microdomains and lipid rafts, which play the foundational role in several immune responses and intercellular signaling [3, 4].

The study of SM began in the late nineteenth century, and SM was first isolated from brain tissue in the 1880s [5] and its structure characterized as *N*-acyl-sphingosine-1-phosphorylcholine in 1927 [6]. Later, SM was isolated and characterized from many vertebrate organisms such as humans, bovines, rats, mice, and frogs [7–10], but was not isolated from invertebrates until later. SM was reported as a major phosphosphingolipid in vertebrates and a minor phosphosphingolipid in invertebrates using thin-layer chromatography (TLC) [11]. In the last few decades, SMs have been isolated and characterized from several

invertebrate organisms, i.e. the octopus *Octopus vulgaris* [12], the crawfish *Cambarus claki* [13], the pearl oyster *Pinctada martensii* [14, 15], the squid *Loligo paelei* [16, 17], the parasitic nematode *Ascaris suum* [18], the crab *Erimacrus isenbeckii* [19], the honey bee *Apis melliferea* [20], the moth *Manduca sexta* [21], and the ascidians *Ciona intestinalis*, *Halocynthia roretzi*, *Halocynthia aurantium* and *Styela clava* [22]. An SM-recognizing toxin, lysenin, was extracted from the earthworm *Eisenia foetida* [23]. The phylogenetic distribution of SM on invertebrate and vertebrate spermatozoa was screened using lysenin binding as an SM-specific probe, and was shown to be different from the previously-accepted distribution. In other words, SM was widely distributed in invertebrates except for Echinodermata and Lophotrochozoa [24–26]. SM should be identified from such organisms to better understand its phylogenetic distribution and fundamental role.

In this paper, we report the isolation and characterization of SM from cysts of the brine shrimp *Artemia franciscana*, and compare the ceramide composition of SM in known invertebrate and vertebrate organisms.

Experimental Procedure

Isolation of Sphingomyelin

The cysts (diapausing eggs) of brine shrimp (2.5 kg) purchased from A & A Marine LLC (Salt Lake City, Utah, USA) were ground to powder in a mortar. Lipids were extracted once with 4.5 l of chloroform/methanol (2:1, by vol) for 3 h, once with 4.5 l of the same solvent mixture over night and once with 4 l of chloroform/methanol (1:1, by vol) over night at room temperature. The combined chloroform–methanol extracts were concentrated by a rotary evaporator at 40 °C, and subjected to mild alkaline hydrolysis in 700 ml of 0.5 M KOH in methanol to eliminate acyl- and alkenyl-glycerolipids. The hydrolyzate was acidified with several drops of conc. HCl (pH 1), kept for 1 h at room temperature, and dialyzed against tap-water for 2 days. The inner fluid was concentrated to near dryness in vacuo at 40 °C, and dissolved in 120 ml of chloroform/methanol (2:1, by vol). The solution was divided into 8 centrifugal tubes, precipitated with 150 ml of cold acetone per tube, centrifuged at 3,000 rpm at 4 °C for 15 min, and the resulting supernatant was removed by decantation. The remaining precipitate was re-suspended with cold acetone, and centrifuged. This step was repeated once more, and the resulting precipitate was dried (yield: 4.4 g). The alkaline-stable product was dissolved in 90 ml of chloroform/methanol (2:1, by vol), and to this was added 90 ml of methanol and 16 ml of water to obtain a volume ratio of chloroform/methanol/water of 30:60:8. This was mixed with 20 g of QAE-Sephadex A-25, OH^- form (GE Healthcare Co.). The resulting slurry was applied to a column (3.4 × 32 cm) packed with 40 g of QAE-Sephadex A-25 equilibrated with chloroform/methanol/water (30:60:8, by vol). The column was chromatographed successively with chloroform/methanol/water (30:60:8, by vol; 1.5 l), pure methanol (300 ml), and 0.45 M ammonium acetate in methanol (1.5 l). The separation of sphingolipids was monitored by TLC. The neutral and zwitterionic sphingolipid fraction obtained from the pass-through eluate was acetylated in 40 ml of pyridine/acetic anhydride (3:2, by vol) for 18 h, and evaporated to dryness. The acetylated fraction was then chromatographed on a column (2.0 × 90 cm) packed with 120 g of Florisil, 60–100 mesh (Nacalai Tesque, Inc.) using the slightly modified method of Saito and Hakomori [27]. The column was eluted successively with 840 ml of hexane/dichloroethane (1:4, by vol), 840 ml of pure dichloroethane, 840 ml of dichloroethane/acetone (1:1, by vol), 1.68 l of dichloroethane/methanol (9:1, by vol), 1.4 l of dichloroethane/methanol (3:1, by vol), 843 ml of dichloroethane/methanol/water (2:8:1, by vol), 1.1 l of chloroform/methanol/water (6:4:1, by vol), and 843 ml of chloroform/methanol/water (2:8:1, by vol). The eluate obtained using chloroform/methanol/water (6:4:1, by vol) was evaporated to dryness, deacetylated with 40 ml of 0.5 M KOH in methanol at 37 °C for 6 h, neutralized with conc. HCl, and dialyzed against tap-water for 2 days. The inner fluid was concentrated to near dryness in vacuo at 40 °C.

Thin-Layer Chromatography

The solvents used for TLC were as follows; *n*-butanol/acetic acid/water (12:3:5, by vol), chloroform/methanol (92:8, by vol), chloroform/methanol/water (6:4:1, by vol), and chloroform/methanol/acetic acid/water (6:4:1:1, by vol). The zwitterionic sphingolipid on thin layer plates of silica gel 60 (Merck KGaA) was visualized by spraying with Dittmer-Lester reagent [28]. The hydrophilic material obtained from the zwitterionic sphingolipid was developed on a cellulose plate, Avicel SF (Funakoshi Chemicals Co.) and visualized with Hanes-Isherwood reagent [29].

Fatty Acid Analysis

For determination of fatty acid composition, 0.1 mg of sample was methanolyzed with 0.2 ml of 1 M anhydrous methanolic HCl at 100 °C for 3 h. The fatty acid methyl esters produced were extracted with *n*-hexane and analyzed by GC and GC–MS.

Sphingoid Analysis

Sphingoid composition was determined by the method of Gaver and Sweeley [30]. In brief, about 0.2–0.3 mg of sample was methanolyzed in 0.2 ml of aqueous HCl-methanol reagent (methanolic reagent containing 8.6% conc. HCl and 9.4% water) at 70 °C in the oven for 18 h. The hydrolyzate was extracted with *n*-hexane to remove fatty acids, and the residual methanolic phase was dried under nitrogen gas and made alkaline with 0.6 ml of methanol/1 M sodium hydroxide (4:3, by vol). Sphingoids were extracted into a lower phase by adding 0.72 ml of chloroform, which was then washed twice with 0.4 ml of methanol/water (1:1, by vol), trimethylsilylated, and analyzed by GC and GC–MS.

Gas Chromatography and Gas Chromatography-Mass Spectrometry

Compositional analyses of fatty acids and sphingoids were carried out using a Shimadzu GC-18A gas chromatograph with a capillary column of Shimadzu HiCap-CBP 5 (0.22 mm × 25 m). The temperature increase was programmed at 4 °C/min from 170 to 230 °C for fatty acid analysis and 2 °C/min from 210 to 230 °C for sphingoid analysis. Electron impact ionization mass spectra were taken using a Shimadzu GCMS-QP5050 gas chromatograph-mass spectrometer with the same capillary column under the following conditions; interface temperature, 250 °C, injection port temperature, 240 °C, helium gas pressure, 100 kPa, and ionizing voltage, 70 eV. The oven temperatures for GC–MS analysis were 80 °C (2 min) → 170 °C (20 °C/min) → 240 °C (4 °C/min) for fatty acids, and 80 °C (2 min) → 210 °C (20 °C/min) → 230 °C (4 °C/min) for sphingoids, respectively.

Infrared Spectroscopy

Infrared spectroscopy (IR) was performed using a Shimadzu FTIR-8400S spectrophotometer with a MIRacle A single reflection horizontal ATR using a ZnSe prism (PIKE Technologies, Inc). *Artemia* SM was dissolved in chloroform/methanol (2:1, by vol) and 50 μg of SM was put on the sampling area of the ATR and air-dried, and was scanned by 45 times accumulation.

Hydrolysis with Butanolic HCl

About 5 mg of SM was hydrolyzed with 1 ml of *n*-butanol/6 M HCl (1:1, by vol) in boiled water for 60 min. The reaction mixture was partitioned by adding 1 ml of water. The butanolic phase was dried by a rotary evaporator and the residue was washed with acetone. The acetone insoluble material was dissolved in chloroform/methanol (9:1, by vol) and fractionated on a column (0.6 × 10 cm) packed with Iatrobeads (6RS-8060, Mitsubishi Kagaku Iatron Inc., Tokyo). The column was eluted successively stepwise with 10 ml of chloroform/methanol at ratios of 8:2, 7:3, 6:4, and 5:5 (by vol). The eluates obtained from this column using chloroform/methanol 6:4 were pooled and analyzed by TLC and IR for identification of sphingosylphosphocholine.

Hydrolysis with Hydrofluoric Acid

About 5 mg of SM dissolved in 0.5 ml of dimethylsulfoxide was hydrolyzed in 3.5 ml of hydrofluoric acid at room temperature for 20 h. The reaction mixture was dialyzed against tap-water for 2 days and the inner fluid concentrated to near dryness in vacuo at 40 °C. The product was dissolved in chloroform and fractionated on a column (1.4 × 6 cm) packed with Iatrobeads. The column was eluted successively with 10 ml of chloroform/methanol 98:2 (by vol), 95:5, 9:1 and 8:2. The eluates obtained from this column using chloroform/methanol 9:1 were pooled and analyzed by TLC and IR for identification of the ceramide moiety.

Hydrolysis with Phospholipase C

About 2 mg of SM was suspended in 0.2 ml of 50 mM Tris–HCl buffer (pH7.5), containing 0.1 ml of 20 mM calcium chloride and 0.2 ml of diethyl ether, and hydrolyzed with 500 μg of phospholipase C derived from *Clostridium perfringens* (Sigma–Aldrich Co.) at 37 °C for 24 h. The reacted mixture was heated in boiled water for a few seconds to evaporate diethyl ether. The residual fluid was partitioned by adding 2 ml of chloroform/methanol (2:1, by vol) and the upper phase was analyzed by TLC for identification of phosphocholine. The lower phase was applied to a column (1.4 × 6 cm) packed with Iatrobeads and eluted successively with 10 ml of chloroform/methanol 98:2 (by vol), 95:5, 9:1, and 8:2. The eluates obtained using chloroform/methanol 9:1 were pooled and analyzed by TLC and IR for ceramide identification.

MALDI-TOF MS

MALDI-TOF MS analysis was performed using an Applied Biosystems/Voyager-DE STR Biospectrometer with a nitrogen laser (337 nm) and an acceleration voltage of 20 kV, operating in the reflector positive-ion mode and the post-source decay (PSD) mode. The matrix used was α-cyano-4-hydroxycinnamic acid (α-CHCA; Proteomics Grade, Wako Chemical Co.). External mass calibration was provided by the $[M + Na]^+$ ions of angiotensin I (1296.69

mass units; Sigma–Aldrich Co.) in the reflector and PSD modes and Bradykinin Fragment I–V (573.31 mass units; Sigma–Aldrich Co.) in the reflector mode.

Results and Discussion

Isolation of Sphingomyelin

Crude sphingolipids (4.4 g) were obtained from 2.5 kg of cysts of the brine shrimp *Artemia franciscana* after alkaline and acid treatment of chloroform/methanol extracts (398 g). In TLC analysis of the crude sphingolipids, a single positive band was detected using Dittmer-Lester reagent (Fig. 1). This band was assumed to be sphingomyelin from its R_f value. There was no double positive band to either Dittmer-Lester or ninhydrin reagents, as would have been seen if ceramide aminoethylphosphonate (CAEPn) and ceramide phosphoethanolamine (CPEA) were present (data not shown). The crude sphingolipids were chromatographed on a QAE-Sephadex column and the lipid fraction obtained was purified by Florisil column chromatography after acetylation. SM was deacetylated and returned to its original state (634 mg).

Infrared Spectroscopy Analysis

Artemia SM was analyzed by infrared spectroscopy (Fig. 2). Absorption peaks corresponding to the amide bond, the hydroxyl group of phosphoric acid, and choline were observed at about 1,550, 1,650, 1,220, and 960 cm^{-1} from *Artemia* SM and standard SM of bovine brain, respectively.

Gas Chromatography Analysis

Gas chromatography was carried out to determine the fatty acid and sphingoid composition of the ceramide portion of *Artemia* SM (Table 1). In the analysis of fatty acids, behenic acid was a dominant component (85.4%), with stearic acid (11.6%) and arachidic acid (3.0%) also being present (Fig. 3a). In the sphingoid analysis, only two sphingenines, hexadeca-4-sphingenine (67.9%) and heptadeca-4-sphingenine (32.1%), were detected (Fig. 3b, c).

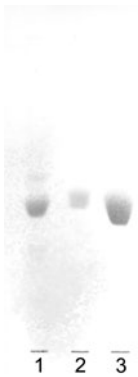

Fig. 1 Thin layer chromatogram of the zwitterionic sphingolipids isolated from cysts of the brine shrimp *Artemia franciscana*. *Lane 1* crude sphingolipids obtained from *Artemia franciscana* (Alkaline stable lipids); *lane 2* sphingomyelin of bovine brain; *lane 3* Zwitterionic brine shrimp sphingolipid fraction obtained by Florisil column chromatography with chloroform/methanol/water (60:40:10, by vol)

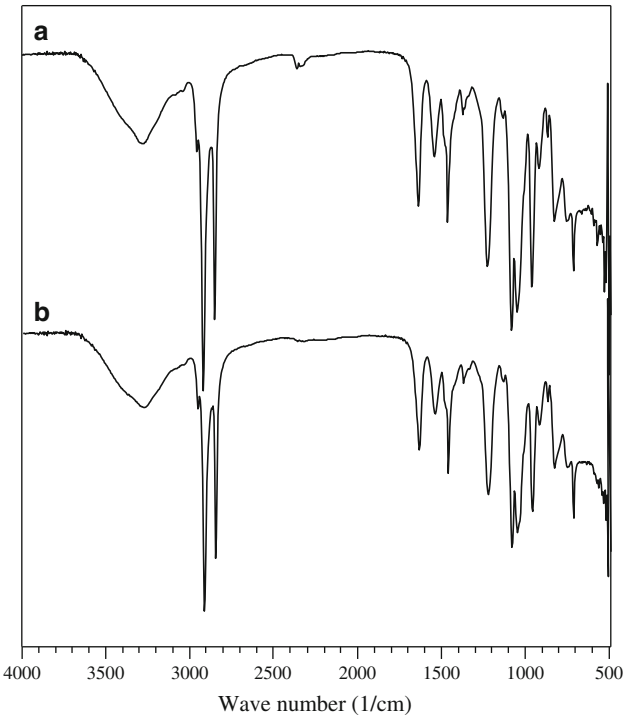

Fig. 2 Infrared spectrum of the isolated zwitterionic brine shrimp sphingolipid. **a** Material isolated from cysts of the brine shrimp *Artemia franciscana* after Florisil chromatography with chloroform/methanol/water (60:40:10, by vol); **b** bovine brain sphingomyelin

Table 1 Ceramide composition of *Artemia* sphingomyelin

Fatty acid (%)		Sphingoid (%)	
18:0	11.6	d16:1	67.9
20:0	3.0	d17:1	32.1
22:0	85.4		

Confirmation of Sphingomyelin

To confirm the existence of the *N*-acylamide bond, SM from both *Artemia* and bovine brain was hydrolyzed with *n*-butanol and HCl. Following butanolysis, the product from both types of SM was positive to ninhydrin reagent and shifted to a lower R_f value (Fig. 4a). Another IR analysis was performed after this butanolysis. Compared with the spectra of intact SM, absorption by the reaction product showed loss of both the amide bond at about 1,550 and 1,650 cm^{-1} and the methylene group at about 2,800 and 2,900 cm^{-1} (Fig. 5b). This shows the loss of the fatty

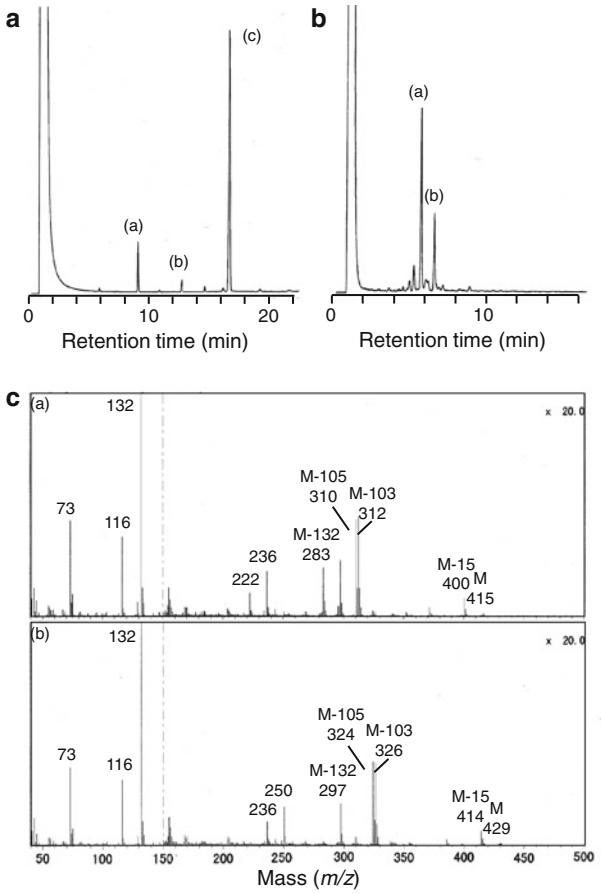

Fig. 3 Gas chromatograms and mass spectra of ceramide constituents from *Artemia* sphingomyelin. **a** Fatty acid methyl esters of (*a*) stearic, (*b*) arachidic, and (*c*) behenic acid. **b** Sphingoids of *N*-free trimethylsilyl derivative of (*a*) hexadeca-4-sphingenine, (*b*) heptadeca-4-sphingenine. **c** Mass spectra of trimethylsilylated sphingoids, (*a*) and (*b*), correspond to peaks (*a*) and (*b*) in **b**

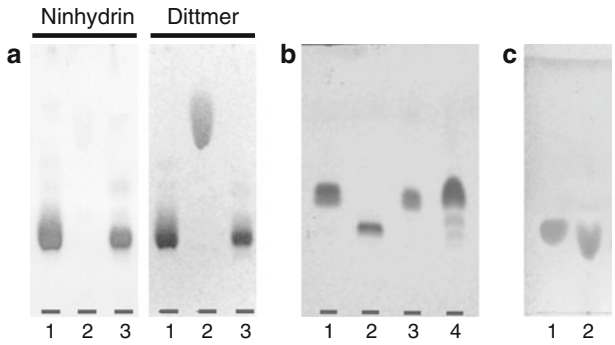

Fig. 4 Thin layer chromatograms of products of degradation analysis of *Artemia* sphingomyelin. **a** Thin layer chromatogram of butanolysate of sphingomyelins, *lane 1* sphingosylphosphocholine obtained by acid butanolysis of bovine brain sphingomyelin; *lane 2* intact sphingomyelin of *Artemia franciscana*; *lane 3* Butanolysate of sphingomyelin of *Artemia franciscana*. **b** Thin layer chromatogram of the hydrophobic hydrolyzate obtained after hydrofluoric acid treatment of sphingomyelins. *Lane 1* non-hydroxy ceramide of bovine brain; *lane 2* hydroxy ceramide of bovine brain; *lane 3* hydrolyzate of bovine brain sphingomyelin using hydrofluoric acid; *lane 4* hydrolyzate of *Artemia* sphingomyelin using hydrofluoric acid. **c** Thin layer chromatogram of the hydrophilic hydrolyzate of sphingomyelin after phospholipase C treatment. *Lane 1* Authentic phosphocholine; *lane 2* Hydrolyzate of *Artemia* sphingomyelin by phospholipase C. Lipids on TLC plates were developed by **a**, chloroform/methanol/acetic acid/water (60:40:10:10, by vol) and visualized by ninhydrin or Dittmer-Lester reagent; **b** chloroform/methanol (98:2, by vol) and visualized by sulfuric acid reagent. **c** Materials on TLC plate precoated with cellulose were developed by *n*-butanol/acetic acid/water (12:3:5, by vol) and visualized by Hanes-Isherwood reagent

acid portion by butanolysis and the existence of sphingosylphosphocholine in *Artemia* SM.

Furthermore, *Artemia* SM was hydrolyzed with hydrofluoric acid to dissociate the ester bond. After hydrolysis, the R_f value of hydrophobic material from *Artemia* SM corresponded on TLC to that of non-hydroxy ceramide of bovine brain (Fig. 4b). IR analysis was also performed on this hydrophobic material. Compared to the spectra of intact *Artemia* SM, absorption of the hydrolyzate disappeared both for the hydroxyl group of phosphoric acid at about 1,220 cm^{-1} and for choline at about 960 cm^{-1} (Fig. 5c). This shows the removal of phosphocholine by the hydrofluoric acid treatment and the existence of non-hydroxy ceramide in *Artemia* SM.

Artemia SM was also hydrolyzed with phospholipase C to dissociate the phosphoric diester bond. After hydrolysis, the R_f value of hydrophilic material derived from *Artemia* SM corresponded to that of authentic phosphocholine on cellulose TLC (Fig. 4c). On the other hand, the IR spectrum of the phospholipase C hydrolyzate's hydrophobic component showed the disappearance of both the hydroxyl group of phosphoric acid at about 1,220 cm^{-1} and choline at about 960 cm^{-1} (Fig. 5d). This indicates both the existence of phosphocholine in *Artemia* SM, and its removal by phospholipase C treatment. The analytic methods employed here (gas chromatography, and TLC and IR analysis before and after various hydrolytic treatments) have thus demonstrated that *Artemia* SM consists of fatty acid, sphingoid, sphingosylphosphocholine, ceramide and phosphocholine. Consequently, this SM is confirmed to be ceramide phosphorylcholine.

MALDI-TOF MS Analysis

The putative structures of *Artemia* SM were confirmed by positive-ion mode MALDI-TOF MS analysis as shown in Fig. 6a and summarized in Table 2. Mass spectra were observed corresponding to the combination of fatty acids and sphingoids detected in gas chromatographic analyses. Several different pseudomolecular ions were observed because of different ceramide species, which were in agreement with the mass values calculated from the proposed structures, e.g.: the $[M + H]^+$ ions at *m/z* 759.61 and

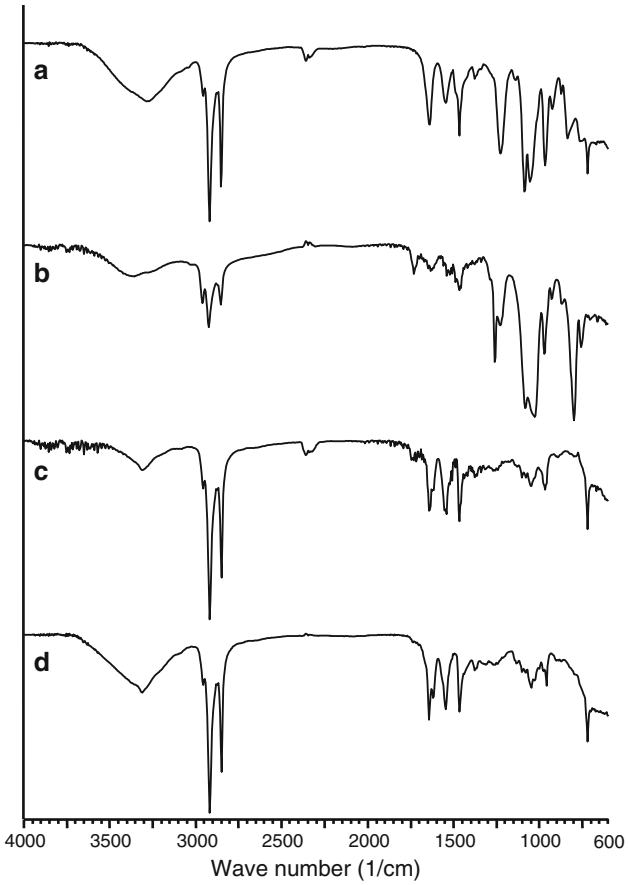

Fig. 5 Infrared spectra of *Artemia* sphingomyelin and its hydrolyzate. **a** Sphingomyelin, **b** sphingosylphosphocholine obtained by acid butanolysis, **c** ceramide obtained by hydrofluoric acid hydrolysis, and **d** ceramide obtained by phospholipase C hydrolysis

773.62 coincided with the mass value of 1 mol each of phosphocholine, fatty acid (22:0) and sphingoid (d16:1 and d17:1; see Table 2); and the $[M + Na]^+$ ion at *m/z* 781.60 and 795.62 coincided with the mass value of the same combination. The sodiated peaks were of stronger intensity than the protonated ones.

To confirm the assignment of SM species, MALDI-TOF MS analysis in the PSD mode was carried out (Fig. 6b). The three major fragments in this mass spectrum correspond to the sodiated product less the trimethylamine ($[M–N(CH3)3 + Na]^+$ ion at *m/z* 722.5) or less the phosphocholine head group ($[M–N(CH3)3C2H5O4P + Na]^+$ ion at *m/z* 598.3), as well as protonated phosphocholine ($[N(CH3)3C2H6O4P]^+$ ion at *m/z* 183.7). The theoretical mass of protonated phosphocholine is *m/z* 184.1. The difference between measured mass and theoretical mass was 0.4 Da, which is within measurement error of PSD mode on Voyager spectrometer. Consequently, we assigned the fragment *m/z* 183.7 as protonated phosphocholine. From spectrometric data and degradation analyses, we identified the chemical structure of *Artemia* SM (Fig. 6c).

Ceramide Components of Sphingomyelin in Vertebrate and Invertebrate

In vertebrates, SMs have been detected in mammals and frogs [9], but their structures have only been characterized in mammals [32–43]. Fatty acids of SM in several tissues from various mammals are predominantly composed of palmitic and lignoceric acids, and there has been no report showing arachidic acid as the major component. In studies of SM sphingoids in mammals, octadecasphingenine is dominant while hexadeca-, heptadeca- and cosadecasphingenine are reported as minor components. Structural analyses of SM in invertebrates have been reported from *Pinctada martensii* [15] and *Loligo paelei* [16, 17] (Mollusca), *Ascaris suum* (Nematoda) [18], *Cambarus clarki*, *Erimacrus isenbeckii*, *Apis melliferea* and *Manduca sexta* (Arthropoda) [13, 19–21], and the ascidians *Ciona intestinalis*, *Halocynthia roretzi*, *Halocynthia aurantium* and *Styela clava* (Urochordata) [22]. The major fatty acids are palmitic and stearic acid in Mollusca, lignoceric and hydroxylignoceric acid in *Ascaris suum*, unsaturated docosanoic and behenic acid in Arthropoda, and stearic, palmitic and behenic acid in Urochordata. Dihydroxy sphingoids with a polyunsaturated base are common in SMs from Mollusca. Tetradecasphingenine is common in SMs from Arthropoda. In Urochordata the main sphingoids are octadecasphingadienine and hexadecasphingenine.

This study presents the isolation and characterization of *Artemia* SM as the 8th report in protostomes. The major components of SM from the brine shrimp are, unusually, behenic acid-hexadecasphingenine and behenic acid-heptadecasphingenine, although these components are found as minor components in SM of bovine milk [34, 35, 43], rennet stomach [36] and *Halocynthia aurantium* and *Styela clava* [22]. All of these are deuterostomes. In all phosphosphingolipids except for SM, the ceramide components of *Artemia* SM are present in millipede CPEA, although only as minor components [31]. In other words, it is characteristic of the ceramide composition of SM from the brine shrimp that behenic acid-hexadecasphingenine and behenic acid-heptadecasphingenine are present in unusually high proportions, namely about 60 and 30%, respectively.

Sphingomyelin plays an important role in several immune responses and intercellular signaling. Ceramide and sphingosylphosphocholine have been reported to act as lipid mediators, ceramide in apoptosis [44] and cell cycle arrest [45], and sphingosylphosphocholine in Ca^{2+} influx inhibition [46], stimulation of inositol phosphate production [47] and induction of superoxide anion formation [48]. Most of these investigations utilized commercially supplied lipids composed of octadecasphingenine. Furthermore, there is an interesting report that relates function and acyl-group components [49]. That report indicates that SM

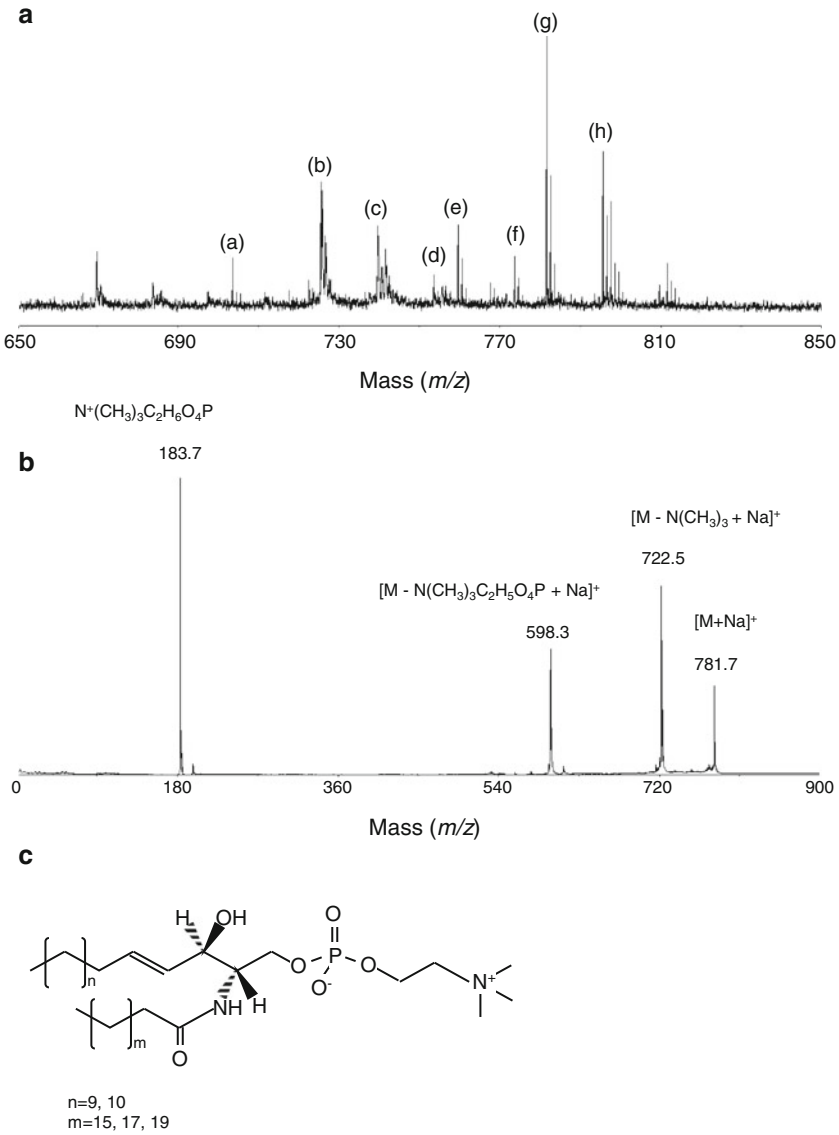

Fig. 6 MALDI-TOF MS analyses of *Artemia* sphingomyelin. **a** MALDI-TOF MS spectra of *Artemia* sphingomyelin in the positive ion reflector mode. **b** PSD spectra of *m/z* 781.6 species corresponding to spectrum (g) in **a**. **c** Chemical structure of *Artemia* sphingomyelin

Table 2 Summary of MALDI-TOF MS analysis of *Artemia* sphingomyelin

	Fatty acid—Sphingoid	Found (*m/z*)	Calculated (*m/z*)	Ionization
(a)	C18:0—d16:1	703.55	703.58	$[M + H]^+$
(b)	C18:0—d16:1	725.54	725.56	$[M + Na]^+$
(c)	C18:0—d17:1	739.56	739.57	$[M + Na]^+$
(d)	C20:0—d16:1	753.57	753.59	$[M + Na]^+$
(e)	C22:0—d16:1	759.61	759.64	$[M + H]^+$
(f)	C22:0—d17:1	773.62	773.65	$[M + H]^+$
(g)	C22:0—d16:1	781.60	781.62	$[M + Na]^+$
(h)	C22:0—d17:1	795.62	795.64	$[M + Na]^+$

is specifically required for expression of glucuronyltransferase activity and that difference in enzyme activity is affected by the degree of saturation in the fatty acid portion. Thus, acyl-chain differences in the aliphatic component may affect function. Fortunately, *Artemia* SM could supply unusual ceramides and sphingosylphosphocholine for research purposes, after hydrolytic removal of its phosphoric acid group and after butanolysis, respectively. The unusual SM derived from *Artemia franciscana* might be very useful in elucidating functions and mechanisms of action of the mediators.

Acknowledgments The authors thank Dr. Fujita for his valuable comments. The authors also thank Dr. John T. Dulaney who kindly read this manuscript while it was in preparation and for providing helpful comments.

References

1. Hannun YA (1994) The sphingomyelin cycle and the second messenger function of ceramide. J Biol Chem 269:3125–3128

2. Meyer zu Heringdorf D, Himmei HM, Jakobs KH (2002) Sphingosylphosphorylcholine biological functions and mechanisms of action. Biochim Biophys Acta 1582:178–189
3. Hancock JF (2006) Lipid rafts: contentious only from simplistic standpoints. Nat Rev Mol Cell Biol 7:456–462
4. Rietveld A, Simons K (1998) The differential miscibility of lipids as the basis for the formation of functional membrane rafts. Biochim Biophys Acta 1376:467–479
5. Thudicum JLW (1884) A treatise on the chemical constitution of brain. Bailliere, Tindall and Cox, London
6. Pick L, Bielschowsky M (1927) Über lipoidzellige splenomegalie (Typus Niemann-Pick) und amaurotishe Idiotie. Klin Wschr 6:1631–1632
7. Rouser G, Kritchevsky G, Heller D, Lieber E (1963) Lipid composition of beef brain, beef liver, and the sea anemone: two approaches to quantitative fractionation of complex lipid mixtures. J Am Oil Chem Soc 40:425–454
8. Byrdwell WC, Perry RH (2006) Liquid chromatography with dual parallel mass spectrometry and 31P nuclear magnetic resonance spectroscopy for analysis of sphingomyelin and dihydrosphingomyelin I. Bovine brain and chicken egg yolk. J Chromatogr A 1133:149–171
9. Rouser G, Simon G, Kritchevsky G (1969) Species variations in phospholipid class distribution of organs: I. kidney, liver and spleen. Lipids 4:599–606
10. Bettger WJ, Blackadar CB, McCorquodale ML, Ewing R (1998) The occurrence of iso 24:0 (22-methyltricosanoic acid) fatty acid in sphingomyelin of rat tissues. Comp Biochem Physiol 119B:299–304
11. Hori T, Itasaka O, Sugita M, Arakawa I (1967) Distribution of ceramide 2-aminoethylphosphonate in nature and its quantitative correlation to sphingomyelin. Mem Fac Ed Shiga Univ 17:23–26
12. Koning AJ (1972) Phospholipids of marine origin VI. The octopus (*Octopus vulgaris*). J Sci Fd Agric 23:1471–1475
13. Komai Y, Matsukawa S, Satake M (1973) Lipid composition of the nervous tissue of the invertebrates *Aplysia kurodai* (Gastropod) and *Cambarus clarki* (Arthropod). Biochim Biophys Acta 316:271–281
14. Sugita M, Arakawa I, Itasaka O, Hori T (1968) Biochemistry of shellfish lipids (XI) Isolation of sphingomyelin and fatty acid composition. Seikagaku 40:254–256 (in Japanese)
15. Itonori S, Kitamura T, Tanaka R, Saito H, Sugita M (2004) Long chain base in sphingomyelin of the pearl oyster, *Pinctada martensii*. Mem Fac Ed Shiga Univ 54:41–48 (in Japanese)
16. Yamaguchi H, Tanaka T, Ichioka T, Stoskopf M, Kishimoto Y, Gould R (1987) Characterization and comparison of lipids in different squid nervous tissues. Biochim Biophys Acta 922:78–84
17. Ohashi Y, Tanaka T, Akashi S, Morimoto S, Kishimoto Y, Nagai Y (2000) Squid nerve sphingomyelin containing an unusual sphingoid base. J Lipid Res 41:1118–1124
18. Sugita M, Kurimoto A, Dulaney JT, Suzuki A, Ota S (1996) Sphingomyelin in the parasitic nematode, *Ascaris suum*. J Jpn Oil Chem Soc 45:1261–1266 (in Japanese)
19. Itonori S, Kimura K, Kitamura T, Kitamura T, Sugita M (2002) Occurrence of sphingomyelin in the marine crab, *Erimacrus isenbeckii*. Mem Fac Ed Shiga Univ 52:9–16 (in Japanese)
20. Karlander SG, Karlsson KA, Leffler H, Lilja A, Samuelsson BE, Steen GO (1972) The structure of sphingomyelin of the honey bee (*Apis melliferea*). Biochim Biophys Acta 270:117–131
21. Abeytunga DTU, Glick JJ, Gibson NJ, Oland LA, Somogyi A, Wysocki VH, Polt R (2004) Presence of unsaturated sphingomyelins and changes in their composition during the life cycle of the moth *Manduca sexta*. J Lipid Res 45:1221–1231
22. Ito M, Yokoi K, Inoue T, Asano S, Hatano R, Shinohara R, Itonori S, Sugita M (2009) Sphingomyelins in four ascidians, *Ciona intestinalis*, *Halocynthia roretzi*, *Halocynthia aurantium*, and *Styela clava*. J Oleo Sci 58:473–480
23. Yamaji A, Sekizawa Y, Emoto K, Sakuraba H, Inoue K, Kobayashi H, Umeda M (1998) Lysenin, a novel sphingomyelin-specific binding protein. J Biol Chem 273:5300–5306
24. Kobayashi H, Sekizawa Y, Aizu M, Umeda M (2000) Lethal and non-lethal responses of spermatozoa from a wide variety of vertebrates and invertebrates to lysenin, a protein from the coelomic fluid of the earthworm *Eisenia foetida*. J Exp Zool 286:538–549
25. Aizu M, Kobayashi E, Omura A, Umeda M (2001) Phylogenetic distribution of sphingomyelin: analysis with the sphingomyelin-binding protein, lysenin. Proc Jpn Conf Biochem Lipids 43:217–219
26. Aizu M, Kita N, Ogawa K, Kobayashi H, Kobayashi T (2006) Phylogenetic distribution of sphingomyelin and its analogs in Mollusca. In 20th IUBMB international congress of biochemistry and molecular biology and 11th FAOBMB congress, Kyoto, Abstracts 499
27. Saito T, Hakomori S (1971) Quantitative isolation of total glycosphingolipids from animal cells. J Lipid Res 12:257–259
28. Dittmer JC, Lester RL (1964) A simple, specific spray for the detection of phospholipids of thin-layer chromatograms. J Lipid Res 5:126–127
29. Hanes CS, Isherwood FA (1949) Separation of the phosphoric esters on the filter paper chromatogram. Nature 164:1107–1112
30. Gaver RC, Sweeley CC (1965) Methods for methanolysis of sphingolipids and direct determination of long-chain bases by gas chromatography. J Am Oil Chem Soc 42:294–298
31. Hori T, Hayata C, Nakatani F, Yoshida T, Sugita M (1993) Occurrence of sphingoethanolamine in millipede *Parafontaria laminata armigera*. Bull Shiga Bunka Coll 3:71–78 (in Japanese)
32. Svennerholm E, Stenhagen SS, Svennerholm L (1966) Fatty acid composition of sphingomyelin in blood, spleen, placenta, liver, lung and kidney. Biochim Biophys Acta 125:60–69
33. Pfleger RC, Anderson NG, Snyder F (1968) Lipid class and fatty acid composition of rat liver plasma membranes isolated by zonal centrifugation. Biochemistry 7:2826–2833
34. Morrison WR (1969) Polar lipids in bovine milk I. Long chain bases in sphingomyelin. Biochim Biophys Acta 176:537–546
35. Byrdwell WC, Perry RH (2007) Liquid chromatography with dual parallel mass spectrometry and 31P nuclear magnetic resonance spectroscopy for analysis of sphingomyelin and dihydrosphingomyelin II. Bovine milk sphingolipids. J Chromatogr A 1146:164–185
36. Karlsson KA, Nilsson K, Samuelsson BE, Steen GO (1969) The presence of hydroxyl fatty acids in sphingomyelins of bovine rennet stomach. Biochim Biophys Acta 176:660–663
37. Slomiany BL, Horowitz MI (1970) Long chain bases in the sphingomyelins of bovine serum. Biochim Biophys Acta 210:493–495
38. Kinsella JE (1971) The lipid composition of microsomal preparation from lactating bovine mammary tissue. Lipids 7:165–170
39. White DA (1973) The phospholipid composition of mammalian tissues. In: Ansell GB, Hawthorne JN, Dawson RMC (eds) Form and function of phospholipids, Elsevier Scientific
40. Breimer ME, Karlsson KA, Samuelsson BE (1975) Presence of phytosphingosine combined with 2-hydroxy fatty acids in sphingomyelins of bovine kidney and intestinal mucosa. Lipids 10:17–19
41. Breimer ME (1975) Distribution of molecular species of sphingomyelins in different parts of bovine digestive tract. J Lipid Res 16:189–194
42. Bouhours JF, Bouhours D (1981) Ceramide structure of sphingomyelin from human milk fat globule membrane. Lipids 16:726–731

43. Ramstedt B, Leppimäki P, Axberg M, Slotte JP (1999) Analysis of natural and synthetic sphingomyelins using high-performance thin-layer chromatography. Eur J Biochem 266:997–1002
44. Jarvis WD, Kolesnick RN, Fornari FA, Traylor RS, Gewirts DA, Grant S (1994) Induction of apoptotic DNA damage and cell death by activation of the sphingomyelin pathway. Proc Natl Acad Sci USA 91:73–77
45. Jayadev S, Liu B, Bielawska AE, Lee JY, Nazaire F, Pushkareva MY, Obeid LM, Hannum YA (1995) Role for ceramide in cell cycle arrest. J Biol Chem 270:2047–2052
46. Törnquist K, Pasternack M, Kaila K (1995) Sphingosine derivatives inhibit depolarization-evoked calcium entry in rat GH4C1 cells. Endocrinol 136:4894–4902
47. Orlati S, Porcelli AM, Hrelia S, Rugolo M (1998) Sphingosylphosphorylcholine and sphingosine-1-phosphate mobilize cytosolic calcium through different mechanisms in human airway epithelial cells. Cell Calcium 23:387–394
48. van Koppen CJ, zu Heringdorf DM, Zhang C, Laser KT, Jakobs KH (1996) A distinct Gi protein-coupled receptor for sphingosylphosphorylcholine in human leukemia HL-60 cells and human neutrophils. Mol Pharmacol 49:956–961
49. Terayama K, Seiki T, Nakamura A, Matsumori K, Ohta S, Oka S, Sugita M, Kawasaki T (1998) Purification and characterization of a glucuronyltransferase involved in the biosynthesis of the HNK-1 epitope on glycoproteins from rat brain. J Biol Chem 273:30295–30300

Lipids (2010) 45:645–649
DOI 10.1007/s11745-010-3427-y

COMMUNICATION

Enhanced Bioavailability of Eicosapentaenoic Acid from Fish Oil After Encapsulation Within Plant Spore Exines as Microcapsules

Ammar Wakil · Grahame Mackenzie · Alberto Diego-Taboada · J. Gordon Bell · Stephen L. Atkin

Received: 12 March 2010 / Accepted: 30 April 2010 / Published online: 22 May 2010

Abstract Benefits of eicosapentaenoic acid (EPA) can be enhanced by raising their bioavailability through microencapsulation. Pollen can be emptied to form hollow shells, known as exines, and then used to encapsulate material, such as oils in a dry powder form. Six healthy volunteers ingested 4.6 g of fish oil containing 20% EPA in the form of ethyl ester first alone and then as 1:1 microencapsulated powder of exines and fish oil. Serum bioavailability of EPA was measured by area under curve ($AUC_{0–24}$). The mean $AUC_{0–24}$ of EPA from ethyl ester with exine ($M = 19.7$, $SD = 4.3$) was significantly higher than ethyl ester without exines ($M = 2$, $SD = 1.4$, $p < 0.01$).The bioavailability of EPA is enhanced by encapsulation by pollen exines.

Keywords Exines · Microencapsulation · Eicosapentaenoic acid · Bioavailability

Abbreviations

Ar	Argon laser
$AUC_{(0–24)}$	Area under the curve between time 0–24 h
BHT	Butylated hydroxytoluene
C/M	Chloroform methanol
EPA	Eicosapentaeoic acid
FAME	Fatty acid methyl esters
GLC	Gas liquid chromatography
HeNe	Helium neon
LCPUFA	Long chain poly unsaturated fatty acids
M	Mean
SD	Standard Deviation
SEM	Scanning electron microscopy
SPSS	Statistical Package for the Social Sciences

A. Wakil (✉) · S. L. Atkin
Hull Royal Infirmary, Michael White Diabetes Centre, 220-236 Anlaby Road, HU3 2RW Hull, UK
e-mail: ammar.wakil@gmail.com

G. Mackenzie · A. Diego-Taboada
Department of Chemistry, University of Hull, Cottingham Road, Hull HU6 7RX, UK

J. G. Bell
Nutrition Group, Institute of Aquaculture, University of Stirling, Stirling FK9 4LA, UK

Introduction

Eicosapentaenoic acid (EPA) and docosahexaenoic acid, the main long chain polyunsaturated fatty acids (LCPUFA), can only be obtained from a fish and shellfish rich diet. Recent trials have shown that EPA in the form of ethyl ester added to statins in hypercholesterolaemic Japanese resulted in 19% relative risk reduction in major cardiovascular events [1]. Instead of being taken to prevent nutritional deficiency they are now being taken to prevent diseases with an inflammatory pathology, including cardiovascular diseases [2]. One strategy to raise plasma concentration of LCPUFA is to optimise their absorption and bioavailability.

Microencapsulation has been used to mask unpleasant taste in food sciences as well as to protect against light and airborne oxidation [3, 4]. Pollen and plant spores, from mosses and ferns have an outer layer skeleton known as the exine that is composed of sporopollenin [5, 6]. Exine microencapsulation technology has been shown to provide excellent taste masking for fish oils [7], they have been investigated for use as a contrast agent [8] and attempts have been made to introduce them as a novel method of

oral delivery of substances into the blood stream as opposed to the parenteral route [9].

In this study we have investigated whether encapsulating the ethyl ester form of fish oil with exine microcapsules extracted from readily available and renewable *Lycopodium clavatum* spores, can enhance the bioavailability, measured by area under the curve, of EPA delivered as ethyl ester alone.

Experimental Procedure

This was an open-labelled study. Six healthy volunteers without concomitant illnesses or medications were recruited from an advertisement for healthy volunteers in Hull University and Hull Royal Infirmary. The study protocol was approved by the Hull and East Riding Research Ethics Committee. All subjects received dietary counselling by an academic dietician to avoid fish or omega-3 fatty acid intake in their diet 2 weeks before and during the course of the trial. Coffee, flax seed and alcohol were avoided a day prior, during and a day after each visit. A run in period of 1 week was followed by two visits with a 3-week between-visits wash-out period. Each subject ingested 4.6 g of fish oil containing 20% of EPA in the form of the ethyl ester at each visit. In the first visit the fish oil was given in the form of a liquid immediately after defrosting. In the second visit the fish oil was encapsulated into exines and the subsequent powder was ingested. Blood samples were taken at baseline (prior to ingesting the fish oil preparations) for fatty acids and lipid analysis and again at 2, 4, 6, 8 and 24 h from ingesting the fish oil for fatty acids analysis. Serum was instantly separated by centrifugation at 2,000*g*, and stored at −80 °C before batch analysis of total serum fatty acid compositions by the Nutrition Group, Institute of Aquaculture, University of Stirling, Stirling UK, as described before [10]. 0.5 mL serum was extracted by the Folch et al. method [11], using chloroform/methanol (C/M; 2:1 vol/vol). The extracted lipid was dissolved in 0.8 mL of C/M, 2:1 vol/vol and dried under nitrogen in a pre-weighed glass vial, and desiccated for 16 h. Final lipid extracts were re-suspended in C/M (2:1 vol/vol) + 0.01% (wt/vol) butylated hydroxytoluene (BHT), at a concentration of 10 mg/mL and stored at −70 °C.

Fatty acid methyl esters (FAME) were prepared by acid-catalysed transesterification of 0.5 mg of total lipid and 50 μg of 17:0 internal standard in 2 mL of 1% (vol/vol) H_2SO_4 in methanol at 50 °C overnight [12]. Samples were neutralised with 2% $KHCO_3$ and extracted twice with 5 mL isohexane/diethyl ether (1:1 vol/vol) + BHT and finally dissolved in 0.3 mL of isohexane prior to FAME analysis.

Measurement of Serum Fatty Acids

FAME were separated and quantified by GLC (Fisons 8160, Carlo Erba, Milan, Italy) using a 60 m × 0.32 mm × 0.25 μm film thickness capillary column (ZB Wax, Phenomenex, Macclesfield, England). Hydrogen was used as carrier gas (flow rate of 4.0 mL/min) and the temperature programme was from 50 to 150 °C at 40 °C/min then to 195 °C at 2 °C/min and finally to 215 °C at 0.5 °C/min. FAME were identified using well characterised in house standards and commercial FAME mixtures (Supelco™ 37 FAME mix, Sigma-Aldrich Ltd., Gillingham, England). Blood was withdrawn after 30 min and examined under a confocal microscope to investigate for the presence of exines, which are naturally fluorescent.

Fish oil supplements were provided by Croda Europe, Goole, UK. Each vial had 4.6 g of fish oil containing 20% EPA in the form of its ethyl ester. They were shipped in dark containers and kept in a −20 °C freezer until ready for defrosting at visit 1. At visit 2, the defrosted oil was encapsulated with 4.6 g of exines no more than 24 h prior to ingestion and the dark container was filled with nitrogen to prevent oxidation. Exines extracted from *Lycopodium clavatum* spores were supplied by Sporomex Ltd, UK, and were prepared as detailed previously [7]. Microencapsulation was performed by mixing exines with oil (1:1 weight for weight) by gently stirring to form a homogeneous paste that was then subjected to a vacuum (ca. 10 hPa) for 2 h to facilitate passive loading of oil into the particles through the nano-porous sporopollenin walls.

Area under the curve ($AUC_{0-24\ h}$) was used to determine the bioavailability of EPA from the different supplements. The mean $AUC_{0-24\ h}$ for EPA was calculated using the linear trapezoid method and baseline levels were normalised to zero. We also observed visually the time of the maximum concentration (T_{max}). Comparisons of mean AUCs and T_{max} with and without exines were made using paired sample *t* test via SPSS version 15.

Results

The two male and four females' demographics are summarised in Table 1. The mean baseline of EPA percentage to total fatty acids in the six subjects was comparable to that reported in another study with healthy volunteers; $M = 0.69$, SEM = 0.04% versus $M = 0.64$, SEM = 0.08%, respectively [13]. There was no significant difference between the baseline concentration of EPA (mg/100 mL) in the first visit ($M = 2.15$, SD = 0.6) and the second visit ($M = 2.0$, SD = 0.6, $p = 0.49$). The mean AUC of EPA from ethyl ester with exine ($M = 19.7$, SD = 4.3) was significantly higher than that obtained from ethyl ester

Table 1 Subjects' demographics

Demographics	Mean (SD)
Systolic blood pressure (mm Hg)	131 (7)
Diastolic blood pressure (mm Hg)	78 (4)
Total cholesterol (mmol/L)	4.7 (0.45)
Triglyceride (mmol/L)	1.06 (0.24)
High density lipoprotein (mmol/L)	1.25 (0.35)
Low density lipoprotein (mmol/L)	2.7 (0.84)
Total cholesterol/high density lipoprotein	4 (1.21)
Body mass index (Kg/m^2)	23.5 (2.2)

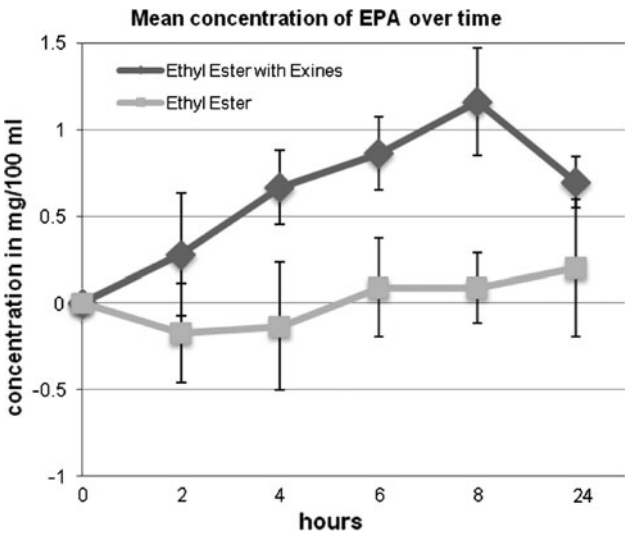

Fig. 1 The change in mean EPA serum level over time obtained from the ethyl ester of EPA with and without exines

without exines ($M = 2$, SD $= 1.4$, $p < 0.01$). When the mean concentration of EPA in serum over time was plotted, after subtracting the mean sera concentrations of the respective time from the mean baseline concentration, it was evident that microencapsulation in exines had significantly enhanced the EPA absorption as reflected by the serum concentration (Fig. 1). The mean time of maximum (T_{max}) concentration for EPA when fish oil was encapsulated with exines ($M = 7.6$ h) was not different from the maximum concentration without exines ($M = 6.8, p = 0.4$), results not shown. Confocal microscopy (Bio-Rad Radiance 2100 laser scanning microscope equipped with Ar (488 nm), Green HeNe (563 nm) and Red diode (637 nm) laser lines connected to a Nikon TE-2000E inverted microscope) showing an empty fluorescent exine before ingestion and an apparently intact exine in blood plasma after ingestion (Fig. 2). Micrographs of oil filled exines before ingestion and those recovered from blood, following ingestion, were also obtained using a Leica Cambridge Stereoscan 360 scanning electron microscope (SEM) operated by Tony Sinclair, Institute of Chemistry for Industry, University of Hull (Fig. 3).

Discussion

In this study, there was a significant rise in the bioavailability of EPA as measured by $AUC_{0–24\ h}$ when the ethyl ester form of fish oil was encapsulated into the novel exine microcapsules, which has not been reported before. Previous studies have focussed on the encapsulation of fish oil to preserve its qualities and prevent oxidation [4], rather than to enhance bioavailability. Although there are no previous studies on the effect of the bioavailability of EPA encapsulated into exines, encapsulation technology is commonly used in pharmaceutical preparations to improve bioavailability. For example, the use of a mixture of wax and fat has been used to achieve controlled drug release in the circulation [14] while the use of microspheres to produce mucoadhesive polymers can help maintain intimate contact with the mucosa of the gastrointestinal tract thereby achieving improved bioavailability [15]. Exines have been used as a natural substance to mask-taste but this is the first pilot study to investigate its potential use to improve bioavailability of orally ingested fish oil in the ethyl ester form

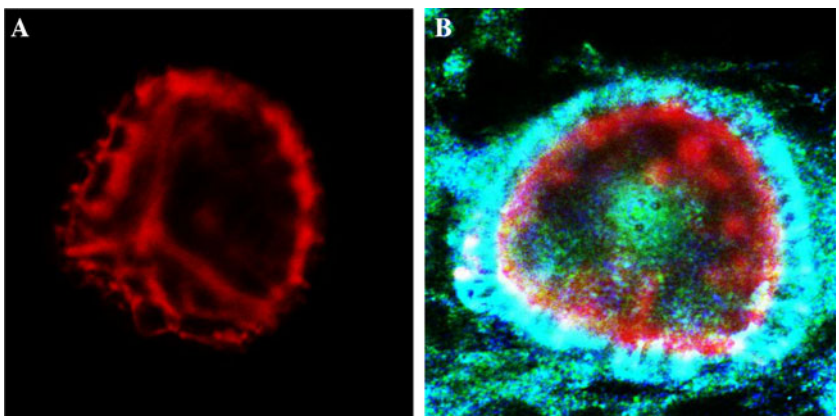

Fig. 2 **a** Confocal microscopy (×60) of an empty sporopollenin exine (*red*) showing its architecture and fluorescence. **b** An exine (*red*) previously filled with fish oil, found in the blood, 30 min after ingestion showing accumulation of material on the outside (*blue*)

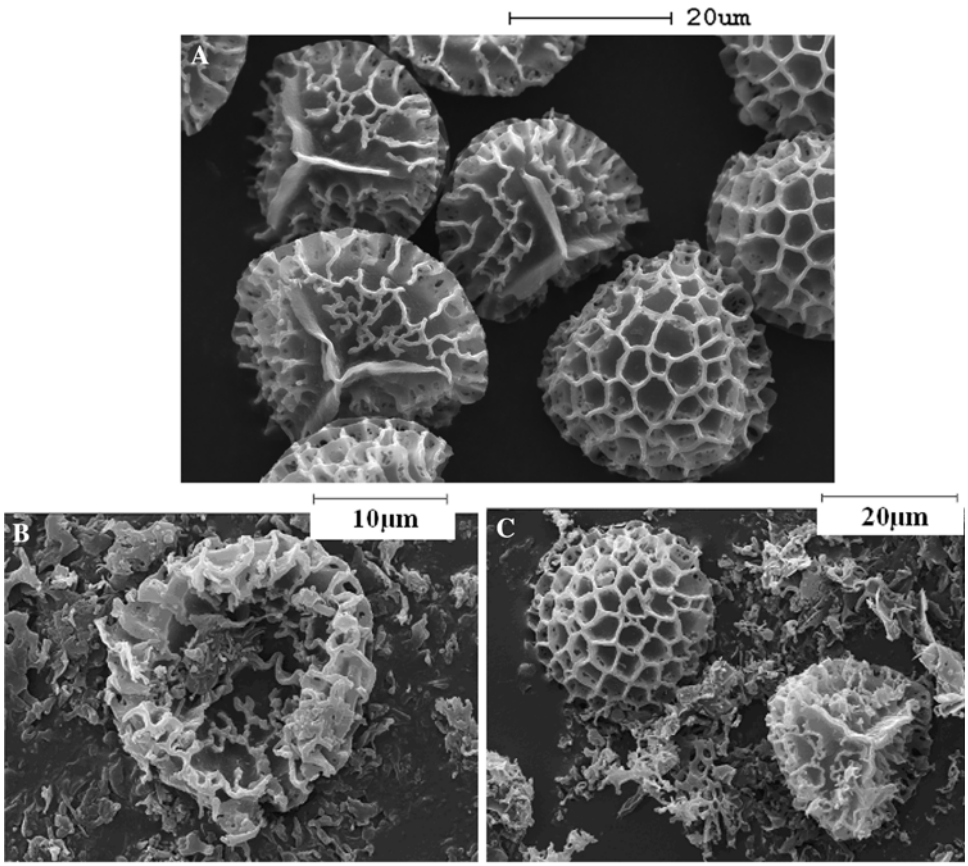

Fig. 3 SEM images of exines (25 µm) from *L. clavatum* spores prior to ingestion, filled with oil (**a**) and those recovered in vivo 30 min after ingestion (**b**, **c**)

[7]. The mechanism by which exine microencapsulation can enhance oil absorption is unclear, but might be due to the protective structure of fish oil-enriched exines whereby the whole unit could travel unhindered through the mucosal lining without releasing its inner core until it has entered into the circulation. This increase in bioavailability was independent of the T_{max} that is a measure of the time to achieve the maximum concentration, suggesting that exines may enhance the absorption at the early stages and continue to do so throughout the 24 h period, in contrast to a natural slower pace of absorption of EPA in the early period of supplementation.

Whilst it is difficult to cost this method, it is expected there would be no significant extra cost compared with other microencapsulation processes; however, no other technique has the advantage of anti-oxidant properties giving a long shelf-life, or has been shown to taste mask and also to have a relatively high loading level. The preparation of the exines is simple and inexpensive with the total cost of the microencapsulation within the exines being less with readily available pollens such as that for rye or maize.

The major limitation to this pilot study is the small number of participants. However, as a proof of the hypothesis, our results were highly significant and further in vitro and in vivo studies are warranted to explain this phenomenon.

In summary, this study showed that exines obtained from *Lycopodium clavatum* spores encapsulating fish oil in the ethyl ester are associated with an improvement in LCPUFA bioavailability as measured by the $AUC_{0-24\ h}$, that may be due to the oil being transported into the blood stream more efficiently by the intact exines.

Conflict of interest statement None.

References

1. Yokoyama M, Origasa H, Matsuzaki M, Matsuzawa Y, Saito Y, Ishikawa Y, Oikawa S, Sasaki J, Hishida H, Itakura H, Kita T, Kitabatake A, Nakaya N, Sakata T, Shimada K, Shirato K (2007) Effects of eicosapentaenoic acid on major coronary events in hypercholesterolaemic patients (JELIS): a randomised open-label, blinded endpoint analysis. Lancet 369:1090–1098
2. Gebauer SK, Psota TL, Harris WS, Kris-Etherton PM (2006) n-3 Fatty acid dietary recommendations and food sources to achieve essentiality and cardiovascular benefits. Am J Clin Nutr 83:S1526–S1535

3. Gibbs BF, Kermasha S, Alli I, Mulligan CN (1999) Encapsulation in the food industry: a review. Int J Food Sci Nutr 50:213–224
4. Kolanowski W, Laufenberg G, Kunz B (2004) Fish oil stabilisation by microencapsulation with modified cellulose. Int J Food Sci Nutr 55:333–343
5. Shaw G (1997) Sporopollenin in Phytochemical Phylogeny. Academic Press, London
6. Barrier S, Löbbert A, Boasman AJ, Boa AN, Lorch M, Atkin SL, Mackenzie G (2010) Access to a primary aminosporopollenin solid support from plant spores. Green Chem 12:234–240
7. Barrier S, Rigby AS, Diego-Taboada A, Thomasson MJ, Mackenzie G, Atkin SL (2010) Sporopollenin exines: a novel natural taste masking material. LWT Food Sci Technol 43:73–76
8. Lorch M, Thomasson MJ, Diego-Taboada A, Barrier S, Atkin SL, Mackenzie G, Archibald SJ (2009) MRI contrast agent delivery using spore capsules: controlled release in blood plasma. Chem Commun (Camb) 6442–6444
9. Paunov VN, Mackenzie G, Stoyanov SD (2007) Sporopollenin micro-reactors for in situ preparation, encapsulation and targeted delivery of active components. Mater Chem 17:609–612
10. Gordon Bell J, Miller D, MacDonald DJ, MacKinlay EE, Dick JR, Cheseldine S, Boyle RM, Graham C, O'Hare AE (2009) The fatty acid compositions of erythrocyte and plasma polar lipids in children with autism, developmental delay or typically developing controls and the effect of fish oil intake. Br J Nutr 103:1160–1167
11. Folch J, Lees M, Sloane Stanley GH (1957) A simple method for the isolation and purification of total lipides from animal tissues. J Biol Chem 226:497–509
12. Christie W (2003) Lipid analysis. The Oily Press, Bridgewater
13. Tremoli E, Eligini S, Colli S, Maderna P, Rise P, Pazzucconi F, Marangoni F, Sirtori CR, Galli C (1994) n-3 Fatty acid ethyl ester administration to healthy subjects and to hypertriglyceridemic patients reduces tissue factor activity in adherent monocytes. Arterioscler Thromb 14:1600–1608
14. Gowda D, Ravi V, Shivakumar H, Hatna S (2009) Preparation, evaluation and bioavailability studies of indomethacin-bees wax microspheres. J Mater Sci Mater Med 20:1447–1456
15. Tao Y, Lu Y, Sun Y, Gu B, Lu W, Pan J (2009) Development of mucoadhesive microspheres of acyclovir with enhanced bioavailability. Int J Pharm 378:30–36

Lipids (2010) 45:651–657
DOI 10.1007/s11745-010-3440-1

METHODS

Methods of Emulsifying Linoleic Acid in Biohydrogenation Studies In Vitro May Bias the Resulting Fatty Acid Profiles

Ratchaneewan Khiaosa-ard · Florian Leiber · Carla R. Soliva

Received: 28 August 2009 / Accepted: 9 June 2010 / Published online: 27 June 2010

Abstract The effects of three emulsifying methods on ruminal fatty acid biohydrogenation (BH) in vitro were compared. Using a static in-vitro gas test system, four replicates of each treatment were incubated in buffered ruminal fluid. Hemicellulose (300 mg dry matter) was supplemented either with or without linoleic acid (9*c*12*c*-18:2, 5% in diet dry matter) and incubated for 4 and 24 h. Three methods of emulsifying 9*c*12*c*-18:2 were tested: (1) ethanol, (2) Tween® 80, and (3) sonication. The products were then compared to non-emulsified 9*c*12*c*-18:2. Out of the three emulsifying methods tested, ethanol and sonication resulted in stable 9*c*12*c*-18:2 emulsions, indicating good 9*c*12*c*-18:2 distribution, while the Tween® 80 emulsion was less stable. BH was strongly inhibited by treating 9*c*12*c*-18:2 with ethanol and sonication at different steps of the BH-pathway, resulting in changed concentrations of certain BH intermediates. The fatty acid profile generated from the major BH-pathways of 9*c*12*c*-18:2 with Tween® 80 was comparable to that without emulsification after 24 h of incubation. We conclude that it is not recommended to emulsify lipids before incubating them in vitro when investigating fatty acid BH. If emulsification of 9*c*12*c*-18:2 is necessary, Tween® 80 seems to be the method that interferes least with BH.

Keywords Emulsion · Ruminal biohydrogenation · Ethanol · Tween® 80 · Sonication · Linoleic acid · C18-fatty acids

R. Khiaosa-ard · F. Leiber · C. R. Soliva (✉)
Institute of Plant, Animal and Agroecosystem Sciences, ETH Zurich, Universitätstrasse 2, 8092 Zurich, Switzerland
e-mail: carla.soliva@inw.agrl.ethz.ch

Abbreviations

BH	Biohydrogenation
FAME	Fatty acid methyl esters
LNA	Linoleic acid
PUFA	Polyunsaturated fatty acids

Introduction

Investigations on the ruminal biohydrogenation (BH) of polyunsaturated fatty acids (PUFA) are commonly conducted using in-vitro techniques, as well as other methods, due to the lack of rumen-fistulated animals. Often, PUFA are emulsified before being administered to the various types of fermenters. The most common emulsifying methods applied in such studies so far are ethanol [1], Tween® 80 (commercial non-ionic surfactant) [2], and sonication [3]. The emulsification of fatty acids is used to promote fatty acid distribution in the incubation liquid; in addition, this technique allows for a more precise dosage of the lipids when using micropipettes. However, fatty acid emulsification methods might have additional side effects such as affecting the microbial metabolism. Therefore, they could alter the extent and kinetics of ruminal lipolysis and BH [4]. Such side effects are unwanted, as in-vitro studies aim to simulate in-vivo conditions as well as possible. Furthermore, in trials using ruminants, the emulsification of dietary fatty acids is only very rarely required.

There are indications of side effects on some ruminal microbes due to certain fatty acid emulsification methods but, to the authors' knowledge, no investigation has been carried out so far to investigate their actions on microbial BH-pathways or their implications for the interpretation of

the fatty acid results obtained. It has been shown that concentrations of linoleic acid (9*c*12*c*-18:2) up to 0.8 mg ml^{-1} were appropriate, i.e., they revealed no inhibitory effect on ruminal microbial BH, for in-vitro BH studies investigating either non-emulsified 9*c*12*c*-18:2 [5] or 9*c*12*c*-18:2 emulsified with Tween® 80 [6]. In addition, about the same dosage of non-emulsified 9*c*12*c*-18:2 showed no effects on microbial fermentation patterns [7]. In contrast, sonicated 9*c*12*c*-18:2 at a concentration of 50 μg ml^{-1} of incubation liquid revealed an inhibitory action on the growth of *Clostridium proteoclasticum*, a ruminal stearate producer [8]. The third emulsifying method, ethanol, was shown to affect the mixed ruminal microbes at a dosage of 34 ml l^{-1} by increasing total short-chain fatty acid and acetate formation, as well as methane production, in vitro [9]. These results emphasize the importance of not only choosing suitable emulsifying methods when investigating specific fatty acid–related aspects of BH in vitro, but also considering possible systematic artifacts induced by the emulsifying method chosen, as these might affect the ruminal microbes.

The aim of this in-vitro study was to investigate and compare the three emulsifying methods, each of which has been used individually for emulsification in previous fatty acid-related in-vitro studies. In this way, the study assessed their possible side effects on fatty acid BH profiles when they have been incubated with mixed ruminal microbes. The emulsification methods chosen for testing in the present study were sonication, Tween® 80, and the most frequently used emulsifier, ethanol. The present study should give enough information for determining the most suitable emulsification method when carrying out ruminal BH studies in vitro.

Experimental Procedure

In-Vitro System and Experimental Design

Two experimental runs were carried out using the static in-vitro gas test system (Hohenheim gas test, [10]). As a carbohydrate source for the ruminal microbes, hemicellulose (xylan from oat spelt containing ≥70% xylose, ≤10% arabinose, and ≤15% glucose after hydrolysis; Sigma-Aldrich, MO, USA) was incubated as a single feed source in the amount of 300 mg dry matter (DM) without or with 15 mg (50 g kg^{-1} of feed DM) of 9*c*12*c*-18:2 (non-esterified, ≥99% purity, Sigma-Aldrich GmbH, Buchs, Switzerland). The fatty acid 9*c*12*c*-18:2 was either directly added into the incubation liquid serving as control or pretreated with one of the three different emulsifying methods. The three emulsifying methods for distributing 9*c*12*c*-18:2 in incubation liquid were applied as follows: (1) Tween® 80 (polyoxyethylene sorbitan mono-oleate, containing 10% total fatty acids consisting of 71.8% 9*c*-18:1, 0.17% 9*c*12*c*-18:2 in the fatty acid composition; Sigma-Aldrich, Saint Louis, MO, USA) was used as an aqueous Tween® 80 solution (1% Tween® 80, v/v) and 9*c*12*c*-18:2 was added at an amount of 50 mg ml^{-1} Tween® 80 solution following [2]; (2) an ethanol-9*c*12*c*-18:2 emulsion was prepared by dissolving 50 mg of 9*c*12*c*-18:2 in 1 ml of 96% ethanol, as described in [1]; (3) finally, 50 mg of 9*c*12*c*-18:2 was dispersed with 10 ml of deionized water in an ultrasonic bath (TEC-25, Telsonic AG, Bronschhofen, Switzerland) for 3 min, applying a method slightly modified from Fellner et al. [11] and Wallace et al. [3]. Further treatments consisted of incubations where the emulsifying methods were applied without 9*c*12*c*-18:2 (the same amounts of Tween® 80, ethanol, and deionized water added to the incubation liquid already containing hemicellulose). Another treatment containing neither 9*c*12*c*-18:2 nor any emulsifying agent was also included. The four treatments containing no 9*c*12*c*-18:2 were subsequently used only as functional treatments for the calculation of result for the 9c12c-18:2-containing experimental treatments.

Incubations were carried out for 4 and 24 h, with each treatment being incubated in four replicates at an incubation temperature of 39 °C following the protocol outlined in Soliva and Hess [10]. Briefly, ruminal fluid was collected before morning feeding from a non-lactating Brown-Swiss cow receiving hay ad libitum and 1 kg of concentrate per day. The cow was handled according to the Swiss guidelines for animal welfare. Ruminal fluid was then filtered through four layers of medicinal gauze (1,000 μm pore size, Type 17; MedPro Novamed AG, Flawil, Switzerland) and mixed with pre-warmed buffer solution (1:2; v/v). Then, 30 ml of the ruminal fluid/buffer mixture (hence "incubation liquid") was dispensed anaerobically into the incubation units already containing the feed substrate hemicellulose. Once they were filled with incubation liquid, 15 mg of non-emulsified or emulsified 9*c*12*c*-18:2, or only the emulsifier itself, was introduced into the incubation units and the liquid volume was recorded. When the incubation was halted after 4 or 24 h, the incubation liquid was stored at −20 °C until being analyzed for its fatty acids profiles and recovery. Incubation liquid samples of the treatments with and without 9*c*12*c*-18:2 at 0 h (not incubated) were also collected for analysis.

Fatty Acid Analysis

The incubation liquid samples were thawed at refrigerator temperature overnight. Then, 0.3 ml of an internal standard, 19:0 (Sigma-Aldrich GmbH, Buchs, Switzerland, prepared as 1 mg ml^{-1} in dichloromethane), was added to 10 ml of the incubation liquid samples. The lipids were

extracted from the samples using a non-chlorinated extraction technique [12], i.e., by adding 8 parts of propan-2-ol and 10 parts of cyclohexane to 11 parts of incubation liquid (v/v/v). For the second extraction step, a propan-2-ol to cyclohexane mixture of 1.3:10 (v/v) was used. The organic phase was collected and the solvents were evaporated using a Rota-Vap (Heidolph VV2000, Heidolph Elektro & Co., KG, Kelheim, Germany). The lipids were dissolved with 2 ml of chloroform that was later evaporated under a nitrogen gas stream. Subsequently, the free fatty acids were methylated by adding 1 ml of a toluene: methanol mixture (1:2; v/v) and 0.1 ml of trimethylsilyl-diazomethane (2 M in hexane), as recommended for samples containing conjugated fatty acids [13]. The methylation process, which was carried out at 40 °C for 10 min, was terminated by adding a drop of glacial acetic acid. Spare solvent and trimethylsilyl-diazomethane were removed by flushing with nitrogen gas. Lipid residues, including the fatty acid methyl esters (FAME), were then resolved with 200 µl of hexane and subsequently cleaned using thin layer chromatography [14]. The identification of the individual FAME was accomplished by carrying out two separate runs on a gas chromatograph (model HP 6890, Agilent Technologies Inc., Wilmington, DE, USA) equipped with a flame ionization detector. For the first run, a 30 m × 0.32 mm Supelcowax-10^{TM} capillary column (Supelco Inc., Bellefonte, PA, USA) was applied. A mixed FAME standard (Supelco 37 Component, Bellefonte, PA, USA) was used for the identification of the individual fatty acids. For detailed *cis*- and *trans*-18:1 isomer identification, a second run using a 200 m × 0.25 mm CP7421 capillary column (Varian Inc., Lake Forest, CA, USA) was performed. The identification of 18:1 isomers was achieved using reference *cis*- and *trans*-18:1 fatty acids (Sigma-Aldrich GmbH, Buchs, Switzerland) and the guidance provided by Kramer et al. [15]. Details of the conditions of both gas chromatograph procedures are described in Khiaosa-Ard et al. [16].

Calculations and Statistical Analysis

The fatty acid content in the incubation liquid was calculated from the known amount of the internal standard. The fatty acid recovery was calculated from the amount of fatty acid recovered after 4 or 24 h of incubation, compared to 0 h using the values of the functional treatments without 9*c*12*c*-18:2 as covariance. For the calculation of the results of the fatty acid profile, and prior to the calculation of the extent of BH, the respective amounts of fatty acids found in the incubation liquid for the functional treatments containing no 9*c*12*c*-18:2 were subtracted from the respective experimental treatments containing 9*c*12*c*-18:2. Thus, in the results, only fatty acids derived from the BH-pathway of 9*c*12*c*-18:2 were considered. The proportion of 9*c*12*c*-18:2 that was apparently biohydrogenated (%; 9*c*12*c*-18:2-BH) was quantified using an equation adapted from Li and Meng [17]: 100× (proportionate 9*c*12*c*-18:2 in total C18 FAME at 0 h—proportionate 9*c*12*c*-18:2 in total C18 FAME after 4 or 24 h of incubation)/proportionate 9*c*12*c*-18:2 in total C18 FAME at 0 h. This was done under the assumption, substantiated by findings of Moate et al. [6], that the concentration of 9*c*12*c*-18:2 (0.5 mg ml^{-1}) used had no inhibitory influence on the BH of the fatty acids. Total C18 unsaturated fatty acids were used to calculate the overall apparent extent of BH extent (%) in the same manner as for 9*c*12*c*-18:2.

Means of all results obtained were subjected to analysis of variance applying the GLM procedure of SAS (version 9.1, SAS Institute Inc., Cary, NC, USA), with emulsifying treatment and incubation time considered fixed effects, and the experimental run considered a blocking factor. Multiple comparisons among means were performed for all statistical evaluations using Tukey's method.

Results

The Emulsifying Methods' Distribution Quality and Effects on Fatty Acid Profile and Recovery

By visual observation, it was found that distribution of 9*c*12*c*-18:2 in the emulsion was better when ethanol (clear solution) was used in comparison to sonication (milky suspension) or Tween® 80 (some droplets aggregated on the surface). All emulsifying methods tested showed a better visual distribution in the emulsion and in the incubation liquid compared to non-emulsified 9*c*12*c*-18:2, where all of the 9*c*12*c*-18:2 aggregated on the liquid's surface.

The C18 fatty acid fraction of the 9*c*12*c*-18:2-supplemented incubation liquid made up 95.6% of total FAME prior to incubation (0 h). Related to total FAME, the C18 fraction consisted mainly of 9*c*12*c*-18:2 (89.9%), while 2.3% were made up of 9*c*11*t*-18:2 and 18:0, and 1.1% consisted of various C18 fatty acid isomers.

Recovery of total, as well as C18, fatty acids after 4 h of incubation was generally low, but clearly higher ($P < 0.001$) with the sonication and ethanol treatments compared to Tween® 80 and non-emulsified 9*c*12*c*-18:2 (control; Table 1). The extent of apparent 9*c*12*c*-18:2-BH was higher ($P < 0.001$) with Tween® 80 and sonication compared to the control and ethanol. By contrast, the extent of apparent overall BH was smaller ($P < 0.001$) with the sonication and ethanol method compared to the Tween® 80 method and the control. The emulsifying methods generally influenced most of the individual C18

Table 1 C18 fatty acid isomer profile and recovery in incubation liquid (g/100 g C18 fatty acids) after 4 and 24 h of ruminal linoleic acid (LNA, 9*c*12*c*-18:2) biohydrogenation in vitro ($n = 4$)

Emulsifying method	4 h of incubation				*P* level	24 h of incubation				*P* level	Time effect (*P*)
	None	Tween® 80	Sonication	Ethanol		None	Tween® 80	Sonication	Ethanol		
C18 FA in total FAME (%)	90.6	89.8	92.6	90.8	0.145	91.3	93.3	91.3	90.3	0.286	0.363
C18 FA recovery[A] (%)	33.0^{b}	39.8^{b}	57.9^{a}	65.2^{a}	0.001	59.4^{ab}	49.7^{b}	51.3^{b}	65.0^{a}	0.009	0.264
FAME recovery[A] (%)	29.3^{b}	38.6^{ab}	56.0^{a}	68.7^{a}	<0.001	65.0	53.0	54.6	65.2	0.060	0.915
LNA biohydrogenated, %[B]	47.5^{b}	81.2^{a}	85.4^{a}	62.2^{b}	<0.001	92.9^{ab}	97.0^{ab}	99.0^{a}	90.6^{b}	0.041	<0.001
Over all BH extent, %[C]	23.12^{a}	31.11^{a}	4.55^{b}	2.13^{b}	<0.001	55.0^{a}	52.5^{a}	18.8^{b}	14.4^{b}	<0.001	<0.001
18:0	24.80^{a}	32.60^{a}	6.64^{b}	4.13^{b}	<0.001	56.0^{a}	53.5^{a}	20.6^{b}	16.3^{b}	<0.001	<0.001
4*t*-18:1	0.06^{b}	0.22^{a}	0.02^{b}	0.01^{b}	<0.001	0.19^{ab}	0.28^{a}	0.10^{b}	0.07^{b}	0.001	<0.001
5*t*-18:1	0.06^{b}	0.22^{a}	0.02^{b}	0.01^{c}	<0.001	0.13^{b}	0.21^{a}	0.07^{b}	0.07^{b}	0.009	0.003
6*t*-8-18:1	0.75^{b}	2.84^{a}	0.21^{c}	0.15^{c}	<0.001	1.39^{b}	2.48^{a}	0.71^{b}	0.69^{b}	<0.001	0.014
9*t*-18:1	0.52^{b}	1.92^{a}	0.18^{bc}	0.09^{c}	<0.001	0.70^{b}	1.42^{a}	0.45^{bc}	0.30^{c}	<0.001	0.556
10*t*-18:1	2.40^{b}	9.49^{a}	1.75^{b}	1.53^{b}	<0.001	3.15^{b}	7.78^{a}	3.61^{b}	1.54^{b}	<0.001	0.565
11*t*-18:1	8.64	11.4	30.8	22.9	0.053	20.5^{b}	15.2^{b}	63.1^{a}	34.2^{b}	0.001	0.010
12*t*-18:1	0.89^{b}	3.28^{a}	0.34^{b}	0.23^{b}	<0.001	1.52^{b}	2.71^{a}	1.06^{bc}	0.79^{b}	<0.001	0.040
13/14*t*-, 6-8*c*-18:1	1.40^{b}	4.91^{a}	0.45^{bc}	0.28^{c}	<0.001	2.44^{b}	4.26^{a}	1.18^{c}	1.03^{c}	<0.001	0.063
16*t*-18:1	0.56^{b}	1.54^{a}	0.15^{c}	0.24^{bc}	<0.001	1.25^{b}	1.90^{a}	0.56^{c}	0.71^{c}	<0.001	<0.001
9*c*/15*t*-18:1	1.14^{b}	3.01^{a}	1.00^{b}	0.96^{b}	<0.001	1.17^{b}	2.07^{a}	0.77^{c}	1.00^{bc}	<0.001	0.008
10*c*-18:1	0.05^{ab}	0.16^{b}	0.06^{ab}	0.03^{b}	0.028	0.10	0.11	0.31	0.14	0.152	0.028
11*c*-18:1	0.22^{b}	0.44^{a}	0.27^{b}	0.27^{b}	0.005	0.24	0.29	1.07	0.61	0.090	0.053
12*c*-18:1	1.15^{b}	3.98^{a}	1.32^{b}	1.23^{b}	<0.001	0.77^{b}	2.14^{a}	0.95^{b}	0.73^{b}	<0.001	0.002
13*c*-18:1	0.06^{b}	0.19^{a}	0.02^{b}	0.04^{b}	<0.001	0.06^{b}	0.13^{a}	0.03^{b}	0.07^{ab}	0.007	0.641
15*c*-18:1	0.10^{b}	0.31^{a}	0.06^{b}	0.08^{b}	<0.001	0.11^{b}	0.21^{a}	0.07^{b}	0.07^{b}	<0.001	0.147
16*c*-18:1	0.05^{b}	0.23^{a}	0.06^{b}	0.05^{b}	<0.001	0.01^{b}	0.06^{a}	0.04^{ab}	0.03^{ab}	0.017	<0.001
9*c*12*c*-18:2	49.4^{a}	17.7^{b}	13.8^{b}	35.5^{a}	0.018	6.68^{ab}	2.85^{ab}	0.99^{b}	8.83^{a}	0.041	<0.001
Other non-conjugated 18:2	0.55^{b}	0.70^{a}	0.37^{c}	0.45^{bc}	0.001	0.12	0.17	0.18	0.26	0.080	<0.001
9*c*11*t*-18:2	5.91^{b}	3.16^{b}	37.63^{a}	27.41^{a}	<0.001	2.44^{b}	1.31^{b}	3.14^{b}	24.74^{a}	0.035	0.011
Other conjugated 18:2	1.24^{b}	1.59^{b}	4.80^{a}	4.27^{a}	<0.001	0.99^{b}	0.87^{b}	1.05^{b}	7.54^{a}	0.037	0.731

LNA added to the incubation liquid accounted for 94% of LNA in the total C18 fatty acid profile of the incubation liquid at 0 h incubation time

Within each subclass (i.e. row for 4 and 24 h of incubation), mean values followed by different letters are significantly different at $P < 0.05$

[A] Statistically analyzed using the positive controls as covariance

[B] Percentage of LNA apparently hydrogenated during 4 and 24 h of incubation, respectively, compared to LNA at 0 h incubation

[C] Referring to apparent completeness of biohydrogenation

fatty acid isomers differently ($P < 0.05$), except for 11*t*-18:1. The ethanol and sonication treatments had higher concentrations of 9*c*11*t*-18:2 by 4.64 and 6.37 times ($P < 0.001$), as well as higher 11*t*-18:1 by 2.65 and 3.56 times ($P = 0.053$), compared to non-emulsified 9*c*12*c*-18:2, respectively. Regarding these isomers, as well as 18:0, Tween® 80 was found to be in the same range as non-emulsified 9*c*12*c*-18:2. Both fatty acids, 9*c*11*t*-18:2 and 11*t*-18:1, were the most prevalent BH intermediate isomers in the profile in all treatments except for Tween® 80, which showed a higher 10*t*-18:1 proportion ($P < 0.05$) after 4 h of incubation compared to the other three treatments.

Total fatty acid recovery of the control was markedly higher after 24 h than after 4 h of incubation, and numerical treatment differences were not significant ($P > 0.05$). In contrast, the C18 fatty acid recovery showed a clear treatment effect ($P < 0.01$) and was highest for the ethanol treatment and lowest for the Tween® 80 method, with the other treatments being intermediate. The extent of overall apparent BH after 24 h of incubation was generally higher ($P < 0.001$), but showed the same trend as after 4 h of

incubation, with the sonication and ethanol treatments having lower BH than the other two treatments ($P < 0.001$). There was a significant incubation time effect regarding apparent 9*c*12*c*-18:2-BH ($P < 0.001$) as, after 24 h of incubation, 9*c*12*c*-18:2 (90–99%) had been biohydrogenated to a greater extent. The proportions of most C18 isomers, including 11*t*-18:1, 9*c*11*t*-18:1, and 9*c*12*c*-18:2 and 18:0, increased after 24 h compared to 4 h of incubation. The proportion of 9*c*11*t*-18:2 after 24 h was less in all treatments except ethanol. Compared to the other treatments, the proportion of conjugated linoleic acids, other than 9*c*11*t*-18:2, was higher ($P < 0.05$), with the ethanol method exhibiting about 7.5 times the initial amount. The BH intermediate 11*t*-18:1 and the BH end product 18:0 were more abundant in the incubation liquid after 24 h compared to after 4 h of incubation. Regarding 11*t*-18:1, higher ($P < 0.05$) proportions were found with the sonication method compared to the other treatments. The highest proportions of 18:0 in total C18 fatty acid occurred with non-emulsified 9*c*12*c*-18:2 and the Tween® 80 method ($P < 0.001$). There was a clear incubation time effect on almost all fatty acid parameters, except for the fatty acid isomers 9*t*-18:1, 10*t*-18:1, 13*c*-18:1, 15*c*-18:1, and conjugated 18:2 (9*c*11*t*-18:2 excluded).

Discussion

In the present in-vitro study, three common emulsifying methods were investigated and compared with each other and with non-emulsification with the aim of identifying possible side effects of this processes on ruminal lipid BH. This is important research because such effects would appear as artifacts and therefore bias the results in fatty acid-related ruminal in-vitro studies. Therefore, when planning an in-vitro experiment where lipid administration is required that necessitates the help of emulsification, these aspects are of high relevance.

Effects of the Emulsification Methods on Fatty Acid Recovery and BH of Linoleic Acid

The recovery of fatty acids was generally low in the present study, even with the stable emulsion treatments ethanol and sonication, which had been expected to improve fatty acid recovery. However, any system, either in vitro or in vivo, results in a basic loss of fatty acids to some extent [11, 18, 19]. During in-vitro incubation, lipids may be lost in several ways. For example, some lipids may attach to the incubation devices and, as a result, will not be retrieved in the sampling procedure. In the context of the present study, this might be due to the rather large glass surface of the incubation vessels and small amounts of incubation liquid. As expected, there was a higher fatty acid loss in the non-emulsified 9*c*12*c*-18:2, as well as in the emulsion prepared with the Tween® 80 method; this was more particularly the case at the short incubation time (4 h). Thus, for short-term in-vitro studies, to improve the recovery of added fatty acids, only sonication or the use of ethanol can be recommended. However, the clear time effect on the fatty acid profile and the terminal BH product, 18:0, found in general, as well as the different responses with time when using different emulsification methods, showed that results obtained after short-time incubation are not reliable unless they are used for kinetic evaluations in the context of repeated measurements [6]. The increase of fatty acid recovery found in the non-emulsified 9*c*12*c*-18:2 group with a time restriction of 4 h cannot be explained; however, it occurred repeatedly in each of the two experimental runs ($n = 4$).

Adhesion properties are a function of the chemical and physical nature of the fats, and therefore the possibility that the various BH products adsorbed onto the incubation vessels to different degrees cannot be excluded. However, when comparing the BH profile of the non-emulsified 9*c*12*c*-18:2 with profiles obtained in previous in-vitro studies [4, 6], as well as in an in-vivo trial [20], the pattern is comparable, i.e. the transient production of 9*c*11*t*-18:2 followed by a large accumulation of 11*t*-18:1. This supports the assumption that although the fatty acid recovery was limited in the present study, the actual fat recovered was of the same composition as the fat not recovered, and therefore the validity of the fatty acid profile was ensured.

The emulsifier Tween® 80 apparently induced alternative BH-pathways, which differed from the main cascade [21]. Thus, Tween® 80 produced artifacts in the BH-pathway of 9*c*12*c*-18:2 that have to be considered when comparing the results with those found in other studies. However, the main fatty acids, indicative of the extent of ruminal BH, did not substantially differ between non-emulsified 9*c*12*c*-18:2 and the Tween® 80–treated 9*c*12*c*-18:2 in the present study. Thus, provided the proportions of 18:1 isomers are interpreted with caution, Tween® 80 appears to be a suitable emulsification method in cases where the ruminal BH is to be tested in vitro.

In contrast, sonication and the addition of ethanol resulted in severe biases in the BH-pathway, rendering them unsuitable for appropriately simulating ruminal BH processes in vivo. It has been shown that the presence of feed particles promotes lipid BH by providing a site for lipids to adsorb and allowing exposure to BH processes [22]. Interestingly, a study by Harfoot et al. [23] found that low lipolysis and BH of trilinolein (0.3 mg ml^{-1} rumen content) occurred when only small amounts of the lipids were adsorbed to the plant particles. In contrast, in a second experiment in the same study, when a high proportion of

trilinolein was associated with the feed particle fraction, lipolysis and BH were high; this resulted in large amounts of free 18:0 in the feed particle fraction. Related to the results of the present study, this would mean that the small 9*c*12*c*-18:2 droplets formed in the stable 9*c*12*c*-18:2 emulsions with ethanol and sonication tended to stay in the liquid phase rather than being attached to feed particles. The unstable 9*c*12*c*-18:2 emulsion with Tween® 80 and no emulsification, however, might have attached to the feed particles to a greater extent, which would explain their higher apparent BH.

Using different emulsification methods to enhance the distribution quality of 9*c*12*c*-18:2 in the incubation liquid might cause toxicity of the fatty acid due to different bacterial species responsible for BH. This could result in different BH fatty acid profiles. The fact that the final step of the BH-pathway appeared to be specifically and severely impaired by sonicated 9*c*12*c*-18:2, resulting in an accumulation of 11*t*-18:1 and correspondingly lower concentrations of 18:0, is consistent with Maia et al. [8]. They showed that sonicated 9*c*12*c*-18:2 particularly inhibited some rumen bacterial species, including stearate-producing bacteria such as *C. proteoclasticum*. A significant increase in the 9*c*11*t*-18:2 and 11*t*-18:1 proportion observed with ethanol treatment indicates that there are inhibitory effects being generated in the second-last and last step of 9*c*12*c*-18:2 BH, which signified the inhibition of the double-bond hydrogenating steps, including *cis*-9 double-bond BH. This is a step that many bacterial species are capable of performing [21]. In the incubation study of Caldwell and Murray [24], which used higher ethanol concentrations than were employed in the present study, a general toxicity to ruminal bacteria was found. This was not the case in the present experiment, where no changes in total bacterial count (data not shown) were observed with the ethanol treatment. However, this does not exclude the possibility that specific rumen bacterial species and their activity were affected by the ethanol treatment.

Conclusion

The present study demonstrated that using emulsification methods to improve lipid distribution in incubation liquid in investigations of ruminal BH in vitro may bias the resulting fatty acid profile. Thus, when carrying out such studies, pretreatment of the lipids with any of the emulsification methods tested cannot be recommended. For cases when the emulsification of lipids seems necessary, Tween® 80 was the emulsification method that exhibited the least interference with the treatment effects, but the results might still be biased by some minor 18:1 isomers in this method. Sonication and ethanol were shown to severely inhibit ruminal BH when used as the administration method for 9*c*12*c*-18:2.

Acknowledgments We owe our thanks to Prof. M. Kreuzer for his support in the planning of this experiment.

References

1. AbuGhazaleh AA, Riley MB, Thies EE, Jenkins TC (2005) Dilution rate and pH effects on the conversion of oleic acid to *trans* C18:1 positional isomers in continuous culture. J Dairy Sci 88:4334–4341
2. Harfoot CG, Noble RC, Moore JH (1973) Factors influencing the extent of biohydrogenation of linoleic acid by rumen microorganisms in vitro. J Sci Food Agric 24:961–970
3. Wallace RJ, McKain N, Shingfield KJ, Devillard E (2007) Isomers of conjugated linoleic acids are synthesized via different mechanisms in ruminal digesta and bacteria. J Lipid Res 48:2247–2254
4. Fievez V, Vlaeminck B, Jenkins T, Enjalbert F, Doreau M (2007) Assessing rumen biohydrogenation and its manipulation in vivo, in vitro and in situ. Eur J Lipid Sci Technol 109:740–756
5. Beam TM, Jenkins TC, Moate PJ, Kohn RA, Palmquist DL (2000) Effect of amount and source of fat on the rates of lipolysis and biohydrogenation of fatty acids in ruminal contents. J Dairy Sci 83:2564–2573
6. Moate PJ, Boston RC, Jenkins TC, Lean IJ (2008) Kinetics of ruminal lipolysis of triacyglycerol and biohydrogenation of long-chain fatty acids: new insights from old data. J Dairy Sci 91:731–742
7. Dohme F, Machmüller A, Wasserfallen A, Kreuzer M (2001) Ruminal methanogenesis as influenced by individual fatty acids supplemented to complete ruminant diets. Lett Appl Microbiol 32:47–51
8. Maia MRG, Chaudhary LC, Figueres L, Wallace RJ (2007) Metabolism of polyunsaturated fatty acids and their toxicity to the microflora of the rumen. Antonie Van Leeuwenhoek 91:303–314
9. Yoshii T, Asanuma N, Hino T (2005) Effect of ethanol on nitrate and nitrite reduction and methanogenesis in the ruminal microbiota. Anim Sci J 76:37–42
10. Soliva CR, Hess HD (2007) Measuring methane emission of ruminants by in vitro and in vivo techniques. In: Makkar HPS, Vercoe PE (eds) Measuring methane production from ruminants. Springer, Dordrecht
11. Fellner V, Sauer FD, Kramer JKG (1995) Steady-state rates of linoleic acid biohydrogenation by ruminal bacteria in continuous culture. J Dairy Sci 78:1815–1823
12. Smedes F (1999) Determination of total lipid using non-chlorinated solvents. Analyst 124:1711–1718
13. Aldai N, Murray BE, Nájera AI, Troy DJ, Osoro K (2005) Derivatization of fatty acids and its application for conjugated linoleic acid studies in ruminant meat lipids. J Sci Food Agric 85:1073–1083
14. Kramer JKG, Zhou J (2001) Conjugated linoleic acid and octadecanoic acids: extraction and isolation of lipids. Eur J Lipid Sci Technol 103:594–600
15. Kramer JKG, Blackadar CB, Zhou J (2002) Evaluation of two GC columns (60-m SUPELCOWAX 10 and 100-m CP Sil 88) for analysis of milkfat with emphasis on CLA, 18:1, 18:2 and 18:3 isomers, and short- and long-chain FA. Lipids 37:823–835
16. Khiaosa-Ard R, Bryner SF, Scheeder MRL, Wettstein H-R, Leiber F, Kreuzer M, Soliva CR (2009) Evidence for the inhibition

of the terminal step of ruminal α-linolenic acid biohydrogenation by condensed tannins. J Dairy Sci 92:177–188
17. Li Y, Meng Q (2006) Effect of different types of fibre supplemented with sunflower oil on ruminal fermentation and production of conjugated linoleic acids in vitro. Arch Anim Nutr 60:402–411
18. Czerkawski JW (1967) Incubation inside the bovine rumen. Br J Nutr 21:865–878
19. Wu Z, Ohajuruka OA, Palmquist DL (1991) Ruminal synthesis, biohydrogenation, and digestibility of fatty acids by dairy cows. J Dairy Sci 74:3025–3034
20. Scollan ND, Dhanoa MS, Choi NJ, Maeng WJ, Enser M, Wood JD (2001) Biohydrogenation and digestion of long chain fatty acids in steers fed on different sources of lipid. J Agric Sci 136:345–355
21. Harfoot CG, Hazlewood GP (1997) Lipid metabolism in the rumen. In: Hobson PN, Stewart CS (eds) The rumen microbial ecosystem. 2nd edn. Blackie Academic & Professional, London
22. Harfoot CG, Noble RC, Morre JH (1973) Food particles as a site for biohydrogenation of unsaturated fatty acids in the rumen. Biochem J 132:829–832
23. Harfoot CG, Noble RC, Moore JH (1975) The role of plant particles, bacteria and cell-free supernatant fractions of rumen contents in the hydrolysis of trilinolein and the subsequent hydrogenation of linoleic acid. Antonie Van Leeuwenhoek 41:533–542
24. Caldwell DR, Murray K (1986) Some effects of ethyl alcohol on the growth of rumen bacteria. Curr Microbiol 14:193–197

Lipids (2010) 45:659–668
DOI 10.1007/s11745-010-3443-y

ORIGINAL ARTICLE

Repletion of n-3 Fatty Acid Deficient Dams with α-Linolenic Acid: Effects on Fetal Brain and Liver Fatty Acid Composition

Akiko Harauma · Norman Salem Jr. · Toru Moriguchi

Received: 10 November 2009 / Accepted: 9 June 2010 / Published online: 13 July 2010

Abstract Docosahexaenoic acid (DHA) supply to the fetal brain depends upon the dam's dietary intake of n-3 fats. In this study, we measured the incorporation of DHA into the fetal brain and liver in n-3 fatty acid deficient (0.1% alpha-linolenate) mice upon switching to an n-3 fatty acid adequate (2.1% alpha-linolenate) diet. Second generation mice raised and maintained on an n-3 deficient diet during mating were switched to an n-3 adequate diet on embryonic day 1 (ED 1) or ED 13. Fatty acid analysis was performed on fetal brains and livers and on maternal serum on ED 13, 15, 17, and 19. Although fetal brain and liver DHA began at a very low level (both exhibited an 85% decline), recovery was nearly complete by ED 15 in the group switched near conception but thereafter diverged. The maternal serum and fetal liver were very similar in their DHA and docosapentaenoic acid time courses. However, when repletion began on ED 13, brain DHA recovery was only about 44%. These results suggest that a nutritional intervention with alpha-linolenic acid can nearly but incompletely rescue the mouse fetal DHA deficiency if began at the time of conception but that the third trimester is too late, thus leaving a large DHA gap.

Keywords Docosahexaenoic acid · Docosapentaenoic acid · Fetal brain · Infant nutrition · n-3 fatty acid deficiency

Abbreviations

DHA	Docosahexaenoic acid, 22:6n-3
DPAn-6	Docosapentaenoic acid, 22:5n-6
DTA	Docosatetraenoic acid, 22:4n-6
ALA	Alpha-linolenic acid, 18:3n-3
ARA	Arachidonic acid, 20:4n-6

Introduction

During prenatal development, polyunsaturated fatty acids, and docosahexaenoic acid (DHA, 22:6n-3), in particular, must be supplied by the mother via the utero-placental circulation. DHA may be synthesized from the precursor alpha-linolenic acid (ALA) by the maternal, placental and fetal tissues and long chain polyunsaturated fatty acids (LC-PUFAs) such as DHA may become concentrated in the fetal tissues and fetal brain, a phenomenon termed "biomagnification" by Crawford et al. [1]. The LC-PUFAs are also concentrated on the fetal side of the placental circulation [2, 3]. There has recently been a renewed interest in fetal accumulation of essential fatty acids, particularly with regard to DHA in the nervous system, as studies have explored the benefit for neurodevelopment of maternal supplementation with DHA [4]. Such studies are

A. Harauma · T. Moriguchi
Healthcare Research Institute,
Wakunaga Pharmaceutical Co. Ltd, Hiroshima, Japan

Present Address:
A. Harauma · T. Moriguchi
Department of Food and Life Science, Azabu University,
1-17-71 Fuchinobe, Chuou, Sagamihara,
Kanagawa 252-5201, Japan

N. Salem Jr.
Laboratory of Membrane Biochemistry and Biophysics,
National Institutes on Alcohol Abuse and Alcoholism,
National Institutes of Health, Rockville, USA

N. Salem Jr. (✉)
6480 Dobbin Road, Columbia, MD 21045, USA
e-mail: nsalem@martek.com

often done against a background of the low n-3 fatty acid intake that is common in the US and many Western countries [5].

In the past, several studies have begun to establish the normal developmental pattern for fetal accumulation of organ DHA and its relationship to the maternal circulation and diet. An early study by Cunnane and Chen described the time courses of the major fatty acid concentrations in phospholipids and triglycerides in the developing rat brain, liver and carcass including an embryonic day (ED) 21 [6]. Green et al. [7] studied the phospholipid distribution and LC-PUFA concentration including that of DHA in rat brain over the last 10 days of prenatal development. Tam and Innis [8] recently presented the phospholipid and cholesterol distributions and the major brain phospholipid fatty acyl compositions in rat cortex on ED 19 and in postnatal development.

There have also been several investigations of dietary modulation of fatty acids on fetal brain and other organ composition. Yonekubo et al. [9] studied the effects of a maternal fish oil diet on brain and liver phospholipid DHA and arachidonic acid (ARA, 20:4n-6) content on ED 17, 19 and 21. Schiefermeier and Yavin [10] presented a detailed investigation of rats fed a control and an n-3 deficient diet that included maternal liver, and fetal brain and liver phospholipid fatty acyl compositions between ED 15 and 20. Innis and coworkers studied the effects of diets with a high and very low ALA content on brain cortex phospholipid fatty acyl compositions on ED 19 [8, 11].

The present work extends these studies by establishing a second generation n-3 fatty acid deficient female such that repletion with the n-3 fatty acid, ALA could be studied from the day of conception. This was compared to repletion with ALA on ED 13, i.e., the beginning of the third trimester of mouse gestation. Two reference groups were also maintained throughout the study, those with high (2.1% of total fatty acids) and very low ALA. The maternal serum was monitored for the expected effects of the dietary interventions and the fetal liver and fetal brain DHA and docosapentaenoic acid (DPAn-6, 22:5n-6) served as principal endpoints.

Materials and Methods

Animals and Study Design

The experimental protocol was approved by the Animal Care and Use Committee of the Wakunaga Pharmaceutical Co. in Japan. Female CD-1 (ICR) mice (F1) were obtained at 3 weeks of age from Charles River Japan, Inc. (Yokohama, Japan) and fed an n-3 fatty acid deficient (n-3 Def) diet or an n-3 fatty acid adequate (n-3 Adq) diet (see below for descriptions). They were maintained within our animal facility under conventional conditions, with controlled temperature (23 ± 3 °C), humidity (55 ± 10%), and illumination (12 h, 0700–1900 hours). At 7 weeks of age, they were mated with 8-week-old males of the same strain. Their litters were culled to 10 pups and the pups were weaned onto the same diet as their mothers. When the n-3-Def offspring females (F2) were 7 weeks old, they were mated with 8-week-old males of the same strain. The 60 pregnant n-3 Def mice thus obtained were divided into three dietary groups such that each dam within a group was from a different litter, thus the *n* number was based on the use of independent litters. There were 20 n-3 Adq dams to serve as an additional reference point.

One group of 20 dams was switched to an n-3 Adq diet at the time of mating (vaginal plug verified) and this group was termed the "ED1 Switch" group (Fig. 1). A second group of 20 pregnant dams was switched to the n-3 Adq diet at ED 13 and this group was termed the "ED13 Switch" group. The third group was maintained on the n-3 Def diet throughout pregnancy and was termed the "n-3 Def" group. In addition, the fourth group was maintained on the n-3 Adq diet throughout the F1 and F2 generations and was termed the "n-3 Adq" group. At days 13, 15, 17 and 19 of pregnancy, the dams were killed by decapitation, and brain and truncal blood was collected from the dams and the latter spun in a plastic centrifuge tube at 2300×*g* for 15 min at 4 °C. An aliquot of the upper phase (serum) was transferred to another tube. The liver and brains from each fetus were dissected out and all of the samples were then frozen at −80 °C prior to lipid extraction. The males were identified by a PCR method with Zfy gene primer (Proligo-Japan Co., Kyoto, Japan) to identify the Y gene in a liver DNA extract and using this criteria [12], the samples from one male fetus from each dam was selected for lipid analysis.

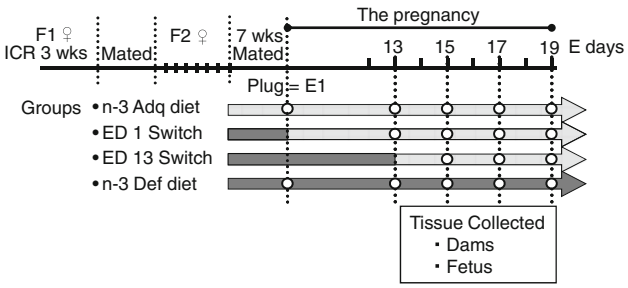

Fig. 1 Flow diagram illustrates study design. The n-3 Def diet was switched to the n-3 Adq diet at the time of mating (ED1 Switch) or on embryonic day 13, (ED13 Switch). The dams were killed by decapitation and tissues of dams and fetus collected at days 13, 15, 17 and 19 of pregnancy and analyzed for fatty acid composition by gas chromatography

Table 1 Composition of experimental diets

Ingredient	Amount (g/100 g diet)	
	n-3 Def.	n-3 Adq.
Casein, vitamin free	20	20
Carbohydrate:	60	60
Cornstarch	15	15
Sucrose	10	10
Dextrose	19.9	19.9
Maltose-dextrin	15	15
Cellulose	5	5
Mineral-salt mix	3.5	3.5
Vitamin mix	1	1
L-Cystine	0.3	0.3
Choline bitartrate	0.25	0.25
TBHQ	0.002	0.002
Fat	10	10
Hydrogenated coconut oil	8.1	7.75
Safflower oil	1.9	1.77
Flaxseed oil	None	0.48
Fatty acid composition[a]		
Saturates	83.8	80.2
Monounsaturates	2.9	4.0
18:2n-6	12.1	12.2
18:3n-3	0.10	2.1
20:4n-6	nd	nd
22:6n-3	nd	nd
n-6/n-3	101	5.7
18:2n-6/18:3n-3	121	5.7

The two experimental diets, an n-3 fatty acid adequate diet (n-3 Adq) and an n-3 fatty acid deficient diet (n-3 Def), were based on the AIN-93 [13] formulation with several modifications to obtain the extremely low basal level of n-3 fatty acid required in this study

[a] The 20:5n-3 and 22:5n-3 fatty acids were less than 0.01%, i.e., not detected (*nd*)

Experimental Diets

The diets used were modeled after the AIN-93G diet recommendations for rodents [13] (Table 1). However, the fat sources were altered to provide for the low n-3 fatty acid content required as a basal composition and balanced at 10 wt% fat content. The basal fat ingredients used were hydrogenated coconut and safflower oils for the n-3 Def diet and with flaxseed oil added to the n-3 Adq diet (Table 1). This diet was custom prepared and pelleted using low heat conditions (about 55 °C), then stored at 4 °C to prevent lipid oxidation (Oriental Yeast Co, Chiba, Japan) and the fatty acid distributions of the entire diets were quality assured within our own laboratory. The content of the key variable, alpha-linolenic acid (ALA) was 0.10 and 2.1% in the n-3-Def and n-3 Adq diets, respectively, while DHA was not detectable in either (Table 1). Diet and water were provided ad libitum.

Lipid Extraction, Transmethylation, and Gas Chromatography

Tissue samples were thawed, weighed, and homogenized in methanol-hexane and transmethylated in acetyl chloride according to the method of Lepage and Roy [14]. Varying amounts of the internal standards methyl docosatrienoate (22:3n-3) for brain and liver, and methyl tricosanoate (23:0) for serum, were added to each sample to compensate for differences in tissue weight and lipid concentration (70 μg/250 mg brain, 100 μg/250 mg liver, 20 μg/100 μl serum). As an aid in preventing lipid oxidation during the procedures, 50 μg/ml of butylated hydroxytoluene was added in methanol. The hexane extracts were concentrated in microvials for gas chromatographic (GC) injection.

GC Analyses

Fatty acid methyl esters were analyzed with an Agilent 6890N Network Gas Chromatograph (Agilent Technologies; Palo Alto, CA) equipped with a split injector, an 7683 automatic liquid sampler, an FID and a 208 V power supply to enable fast temperature ramping. The instrument was controlled and data was collected with GC Chemstation Rev.A.09.03 (Agilent Technologies). The column used was a DB-FFAP (15 m × 0.1 mm I.D. × 0.1 μM film thickness, J&W Scientific, Agilent Technologies). The detector and injector temperatures were set to 250 °C. The oven temperature program began at 150 °C with 0.25 min hold, ramp 35 °C/min to 200 °C, then 8 °C/min to 225 °C with 3.2 min hold and 80 °C/min to 245 °C with 2.75 min hold. Hydrogen was used as carrier gas at a linear velocity of 56 cm/s [15]. A custom-mixed, 28 component, quantitative methyl ester standard containing 10–24 carbons and 0–6 double bonds was used for assignment of retention times and to ensure accurate quantification (NuChek Prep 462, Elysian, MN). Fatty acid data were expressed as % of total peak area, which corresponded to weight% to within 5%, as demonstrated by quantitative standard mixtures. Internal standards were used to calculate tissue fatty acid concentrations.

Statistical Analysis

Data are expressed as the mean ± the standard error of the mean (SEM). All data were analyzed by two-way ANOVA using Statistica (Statsoft, Tulsa, OK, USA). These analyses of group, time and interaction for dam serum and fetal liver and brain all showed a highly significant result with $p < 0.0001$.

Results

Male offspring were compared to female offspring with respect to their liver and brain fatty acid composition, however, no changes were detected (data not shown). Therefore, only the male data are presented here.

In order to demonstrate the effects of the dietary fatty acid variation on the dam, an analysis of maternal brain (Table 3) and serum (Table 2; Fig. 2) was performed between 13 and 19 days gestation (ED 13 to ED 19). Analysis of the dam serum in the n-3 Def group indicated a much lower level of DHA (0.67 ± 0.04% of total fatty acids) relative to the n-3 Adq group (7.50 ± 0.54%, Fig. 2a). The ED1 Switch group, which had been switched to the n-3 Adq diet on the day of conception, displayed considerable recovery of DHA as it reached a level of 5.63 ± 0.28% on ED 13. By ED 15, the ED13 Switch group had increased to 2.56 ± 0.30% and thereafter gradually increased to 2.96 ± 0.21% by ED 19. It was of interest to note that in both the n-3 Adq and ED1 Switch groups, there was a decrease in serum DHA between days ED 15 and ED 19. This may possibly be due to the increased demand for DHA by the growing fetus. This decline was somewhat greater in the ED1 Switch group that the n-3 Adq group leading to a greater difference between these two groups in DHA content at ED 19 than was evident at ED 13.

Maternal serum DPAn-6 content (Table 2; Fig. 2b) was considerably greater in the n-3 Def group (3.82 ± 0.26%) relative to the n-3 Adq reference point (0.35 ± 0.03%) at ED 13. DPAn-6 appeared to increase in the n-3 Def and ED13 Switch group by ED 15 and decrease thereafter. Thus, it did not simply behave in an inverse manner to the DHA but was somewhat delayed in decreasing when DHA was increasing. The ED1 Switch group and the n-3 Adq group DPAn-6 levels remained fairly constant throughout the period of ED 13 thru ED 19. Although the ED1 Switch group had a content of DPAn-6 that had already declined by 73% (considering the starting point as n-3 Def at ED 1 and relative to the n-3 Adq level at ED 13), during the subsequent 6 days there was only a marginal further decline.

Of great importance with respect to maternal nutrition is the support of fetal brain DHA content. On ED 13, the brain DHA content in the n-3 Adq group was 4.95 ± 0.27% but only 0.72 ± 0.02% in the n-3 Def group (Fig. 3a) indicating an 85% decrease in the n-3 Def group. The ED1 Switch group had gained substantial DHA as it had 3.91 ± 0.26% DHA. The ED1 Switch group had nearly "caught up" to the n-3 Adq group by ED 15 as it attained a level of DHA that was about 98% of that the n-3 Adq animals. However, in subsequent time points it appeared not able to match the increases in brain DHA content found in the n-3 Adq group as they had very substantially grown to 12.62 ± 0.26% by ED 19 while the ED1 Switch group increased to 10.40 ± 0.10% at this time. The ED13 Switch group exhibited a slightly increased DHA content at ED 15 but a substantially greater amount relative to the n-3 Def on ED 17, rising to 4.38 ± 0.40%. By ED 19, this group had increased brain DHA content to 6.49 ± 0.49%, a level that was about half that of the n-3 Adq animals. The n-3 Def group increased brain DHA content only marginally between ED 13 (0.72 ± 0.02%) and 19 (1.66 ± 0.08%).

In the n-3 Def animals, the increase in brain LC-PUFAs that accompanied growth from ED 13 to ED 19 was largely composed of DPAn-6 (Fig. 3B) as it rose from 3.34 ± 0.16% to 9.12 ± 0.07% over this period. The ED13 Switch group exhibited a greater brain DPAn-6 at ED 15 (5.65 ± 0.17%) but remained constant at that level up until ED 19. This period of ED 15 to ED 19 corresponded to the rather rapid increase in DHA in this group. The ED1 Switch group had a brain DPAn-6 content (1.26 ± 0.11%) only marginally greater than the n-3 Adq group (0.84 ± 0.09%) at ED 13. The ED1 Switch group exhibited a gradually rising content of brain DPAn-6 ending up at 2.22 ± 0.10% by ED 19.

A more complete brain fatty acid profile is presented in Table 4 with the behavior of many other fatty acids during the ED 13 to ED 19 time period. There was a greater PUFA content at ED 19 relative to ED 13 in all groups. In the n-3 Def groups, there was generally greater n-6 PUFA content at ED 19 relative to ED 13, including 20:4n-6 and 22:4n-6, and principally DPAn-6. This was compensated for largely by a decreased content in monounsaturates, principally 18:1n-9. This pattern of increased brain n-6 PUFA and lower monounsaturate content associated with development was observed in all groups. There was a small increment in saturated fatty acid content in the ED 19 groups relative to the ED 13 groups.

The fetal liver DHA patterns for the four dietary groups were quite similar to the patterns described above for fetal brain. The n-3 Def group had very low liver DHA at ED 13 (0.90 ± 0.05%) while the n-3 Adq group contained 6.09 ± 0.32% (Fig. 4a) indicating an 85% decrease in the n-3 Def group. The ED1 Switch group contained 4.74 ± 0.13% DHA at ED 13 and this increased rapidly by ED 15 reaching 7.81 ± 0.17%, a value equal to that of the n-3 Adq group. However, it was of interest that the ED1 Switch group diverged from the n-3 Adq thereafter and ended the experiment at ED 19 at a value of 7.88 ± 0.48% DHA whereas the n-3 Adq group contained 9.46 ± 1.1% DHA. The ED13 Switch group increased in liver DHA continuously and gradually, reaching a final value of 4.25 ± 0.35% at ED 19. The n-3 Def group declined slightly in liver DHA over the course of the experiment, falling to 0.66 ± 0.11% on ED 19.

The fetal liver DPAn-6 profile for the four dietary groups bore a striking resemblance to the maternal serum. The n-3

Table 2 Maternal serum fatty acid composition

Fatty acid	n-3 Def		ED13 Switch	ED1 Switch		n-3 Adq		Non pregnant	
	ED 13	ED 19	ED 19	ED 13	ED 19	ED 13	ED 19	Def	Adq
12:0	1.30 ± 0.37	1.49 ± 0.53	1.37 ± 0.28	0.89 ± 0.13	2.35 ± 0.27	1.37 ± 0.81	0.75 ± 0.09	1.21 ± 0.22	1.27 ± 0.18
14:0	1.43 ± 0.20	1.89 ± 0.39	1.91 ± 0.33$^{w, y}$	1.31 ± 0.11	2.79 ± 0.15^{e}	1.34 ± 0.40	1.16 ± 0.10	1.26 ± 0.16	1.19 ± 0.10
16:0 DMA	0.14 ± 0.01	0.14 ± 0.02	0.14 ± 0.02	0.13 ± 0.01	0.13 ± 0.01	0.16 ± 0.02	0.20 ± 0.03	0.18 ± 0.01	0.17 ± 0.01
16:0	18.33 ± 0.39	21.22 ± 0.35$^{w, y}$	21.55 ± 0.31$^{w, y}$	18.52 ± 0.52	21.19 ± 0.25$^{w, y}$	17.53 ± 0.55	20.59 ± 0.82$^{w, y}$	15.56 ± 0.64	15.58 ± 0.82
18:0	14.60 ± 0.31	10.01 ± 0.59$^{e, w, y}$	9.14 ± 0.66$^{e, w, y}$	14.20 ± 0.26	9.00 ± 0.35$^{e, w, y}$	14.80 ± 0.24	11.02 ± 0.56^{e}	13.48 ± 0.52	13.08 ± 0.41
20:0	0.11 ± 0.01	0.11 ± 0.01	0.07 ± 0.01	0.11 ± 0.01	0.11 ± 0.01	0.11 ± 0.01	0.07 ± 0.01	0.11 ± 0.01	0.11 ± 0.01
22:0	0.22 ± 0.01	0.15 ± 0.004^{x}	0.14 ± 0.01^{x}	0.28 ± 0.02	0.19 ± 0.02	0.26 ± 0.02	0.18 ± 0.02	0.24 ± 0.02	0.22 ± 0.01
24:0	0.13 ± 0.01	0.13 ± 0.01	0.13 ± 0.02	0.17 ± 0.01	0.13 ± 0.01	0.15 ± 0.01	0.16 ± 0.01	0.16 ± 0.02	0.14 ± 0.01
Total saturates	36.26 ± 0.70$^{x, y}$	35.14 ± 0.36	34.46 ± 0.48	35.61 ± 0.45^{z}	35.90 ± 0.62$^{x, z}$	35.72 ± 1.67^{z}	34.13 ± 0.67	32.20 ± 0.52	31.75 ± 0.64
16:1n-7	2.41 ± 0.20	4.47 ± 0.42$^{e, x, y}$	4.43 ± 0.63$^{e, x, y}$	2.73 ± 0.25	4.88 ± 0.23$^{e, w, y}$	2.36 ± 0.23	3.52 ± 0.36	2.78 ± 0.16	2.62 ± 0.15
18:1n-9	13.44 ± 0.79	17.60 ± 1.09$^{w, z}$	18.12 ± 1.53$^{f, d, w}$	11.69 ± 0.32	17.11 ± 1.21$^{e, x}$	11.52 ± 0.59	12.76 ± 1.54^{b}	11.89 ± 0.54	12.86 ± 0.57
18:1n-7	2.10 ± 0.14	2.51 ± 0.15	2.64 ± 0.30	1.71 ± 0.18	2.11 ± 0.15	1.52 ± 0.10	1.93 ± 0.25	2.38 ± 0.20	2.54 ± 0.13
20:1n-9	0.14 ± 0.01$^{x, y}$	0.39 ± 0.07^{e}	0.22 ± 0.02b	0.14 ± 0.01$^{x, y}$	0.31 ± 0.04$^{b, f}$	0.11 ± 0.01$^{w, y}$	0.16 ± 0.02$^{a, z}$	0.30 ± 0.03	0.34 ± 0.02
22:1n-9	0.04 ± 0.003^{z}	0.05 ± 0.01	0.04 ± 0.002	0.04 ± 0.002	0.05 ± 0.01	0.04 ± 0.01^{z}	0.04 ± 0.01^{z}	0.06 ± 0.003	0.06 ± 0.003
24:1n-9	0.63 ± 0.03	0.39 ± 0.03$^{f, w, y}$	0.37 ± 0.03$^{f, w, y}$	0.74 ± 0.06	0.43 ± 0.03$^{e, w, z}$	0.76 ± 0.06	0.49 ± 0.06$^{e, x}$	0.73 ± 0.03	0.69 ± 0.05
Total monounsat.	18.76 ± 0.97	25.42 ± 1.40$^{f, w, z}$	25.81 ± 2.11$^{d, f, w, z}$	17.05 ± 0.61	24.89 ± 1.48$^{e, x}$	16.30 ± 0.88	18.90 ± 2.06^{b}	18.14 ± 0.75	19.10 ± 0.64
18:2n-6	11.02 ± 0.64^{y}	12.17 ± 0.80	12.56 ± 0.74	11.13 ± 0.49^{y}	13.32 ± 0.66	11.93 ± 1.34^{z}	16.37 ± 1.30	14.71 ± 1.14	16.99 ± 0.50
18:3n-6	0.31 ± 0.02	0.39 ± 0.06$^{x, y}$	0.45 ± 0.06$^{w, y}$	0.48 ± 0.01$^{w, y}$	0.51 ± 0.06$^{w, y}$	0.34 ± 0.01^{z}	0.37 ± 0.07$^{x, y}$	0.17 ± 0.02	0.15 ± 0.01
20:2n-6	0.04 ± 0.002$^{w, y}$	0.09 ± 0.01$^{f, z}$	0.07 ± 0.01^{y}	0.04 ± 0.002$^{w, y}$	0.06 ± 0.004$^{x, y}$	0.04 ± 0.003$^{w, y}$	0.09 ± 0.01$^{f, z}$	0.11 ± 0.01	0.13 ± 0.01
20:3n-6	0.40 ± 0.04$^{w, y}$	0.45 ± 0.08$^{w, y}$	0.42 ± 0.11$^{d, w, y}$	0.37 ± 0.05$^{w, y}$	0.33 ± 0.04$^{e, w, y}$	0.51 ± 0.05$^{w, y}$	0.75 ± 0.05$^{x, y}$	1.11 ± 0.05	1.69 ± 0.08
20:4n-6	22.26 ± 1.00	15.00 ± 1.57^{x}	14.31 ± 1.79$^{f, w}$	21.53 ± 0.62	11.44 ± 0.51$^{e, w}$	20.68 ± 2.12	16.11 ± 1.23^{x}	23.70 ± 1.81	17.89 ± 0.54
22:4n-6	0.30 ± 0.02^{y}	0.52 ± 0.05$^{e, w, y}$	0.38 ± 0.03$^{a, c, x, y}$	0.23 ± 0.02^{z}	0.27 ± 0.01$^{a, y}$	0.13 ± 0.01$^{a, x}$	0.19 ± 0.02^{a}	0.25 ± 0.02^{y}	0.10 ± 0.01
22:5n-6	3.82 ± 0.26^{y}	4.28 ± 0.15^{y}	2.30 ± 0.18	1.17 ± 0.19$^{a, c, e, x, y}$	1.17 ± 0.11$^{a, w}$	0.35 ± 0.03$^{a, w}$	0.65 ± 0.06$^{a, w}$	3.41 ± 0.26^{y}	0.22 ± 0.01
Total n-6 PUFAs	38.14 ± 1.08	32.91 ± 1.63^{w}	30.50 ± 2.55$^{f, w, z}$	34.94 ± 0.53^{w}	27.09 ± 0.85$^{d, f, w, y}$	33.97 ± 1.18^{w}	34.53 ± 2.12^{w}	43.45 ± 0.92^{y}	37.17 ± 0.78
18:3n-3	0.02 ± 0.003^{y}	0.03 ± 0.005^{y}	0.25 ± 0.04$^{a, e, w}$	0.21 ± 0.03$^{b, x}$	0.51 ± 0.04$^{a, e, w, y}$	0.29 ± 0.09$^{a, w}$	0.36 ± 0.06$^{a, w}$	0.02 ± 0.002^{y}	0.27 ± 0.03
20:5n-3	0.05 ± 0.002^{y}	0.06 ± 0.003^{y}	0.16 ± 0.01^{y}	0.33 ± 0.07$^{b, x, y}$	0.26 ± 0.02^{y}	0.60 ± 0.05$^{a, w}$	0.41 ± 0.03$^{a, w, y}$	0.06 ± 0.005^{y}	0.79 ± 0.10
22:5n-3	0.03 ± 0.01	0.04 ± 0.004	0.39 ± 0.04$^{a, c, e, w, y}$	0.36 ± 0.05$^{a, w, y}$	0.48 ± 0.04$^{a, d, w, y}$	0.32 ± 0.06$^{a, w, z}$	0.65 ± 0.08$^{a, e, w, y}$	0.03 ± 0.01	0.13 ± 0.01
22:6n-3	0.67 ± 0.04^{y}	0.51 ± 0.03^{y}	2.96 ± 0.21$^{a, c, e, w, y}$	5.63 ± 0.28$^{a, c, w}$	3.91 ± 0.22$^{a, c, e, w, y}$	7.50 ± 0.54$^{a, w, y}$	6.25 ± 0.52$^{a, w}$	0.91 ± 0.08^{y}	5.90 ± 0.20
Total n-3 PUFAs	0.77 ± 0.04^{y}	0.64 ± 0.03^{y}	3.77 ± 0.23$^{a, c, e, w, y}$	6.53 ± 0.22$^{a, w}$	5.16 ± 0.26$^{a, c, e, w, y}$	8.71 ± 0.50$^{a, w, y}$	7.67 ± 0.43$^{a, w}$	1.01 ± 0.07^{y}	7.08 ± 0.19
Total PUFAs	38.91 ± 1.11	33.55 ± 1.65$^{w, y}$	34.26 ± 2.71$^{d, w, y}$	41.47 ± 0.59	32.25 ± 1.10$^{d, e, w, y}$	42.68 ± 1.28	42.20 ± 2.26^{a}	44.47 ± 0.98	44.25 ± 0.81
Total fatty acid (μg/μl)	2.82 ± 0.11	2.26 ± 0.22	2.27 ± 0.22	2.51 ± 0.13	2.21 ± 0.25	2.51 ± 0.16	2.86 ± 0.23	2.48 ± 0.14	3.05 ± 0.12
DHA (mg/100 μl)	1.88 ± 0.13^{y}	1.14 ± 0.08^{y}	6.71 ± 0.83$^{a, e, x, y}$	14.05 ± 0.51$^{a, d, w, z}$	8.54 ± 0.84$^{a, c, e, w, y}$	18.56 ± 1.20$^{a, w}$	17.63 ± 1.22$^{a, w}$	2.30 ± 0.26^{y}	18.05 ± 0.99

Fatty acid methyl esters from 12:0 to 24:1n-9 were analyzed. Each parameter is presented as the mean ± SEM, ($n = 5$). *DMA* indicates a dimethylacetal derivative of a plasmalogenic phospholipid

Statistically significant changes are represented as follow: $^{a}P < 0.01$, $^{b}P < 0.05$ compared with ED 13 or ED 19 in n-3 Def group, $^{c}P < 0.01$, $^{d}P < 0.05$ compared with ED 13 or ED 19 in n-3 Adq group, $^{e}P < 0.01$, $^{f}P < 0.05$ compared between ED 13 and ED 19 in each group, $^{w}P < 0.01$, $^{x}P < 0.05$ compared with non-pregnant n-3 Def mice, $^{y}P < 0.01$, $^{z}P < 0.05$ compared with non-pregnant n-3 Adq mice (one-way ANOVA followed by Tukey's HSD multiple range test)

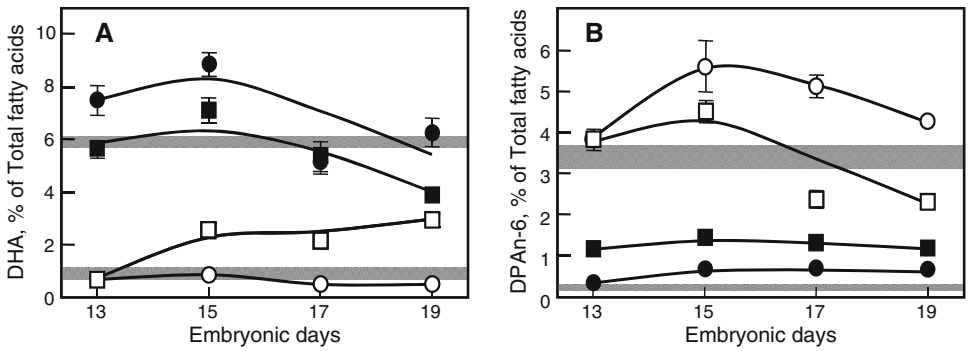

Fig. 2 Variation in docosahexaenoic acid (DHA) (**a**) and docosapentaenoic acid (DPAn-6) (**b**) in maternal serum during the period of the third trimester. The *hatched bars* indicate the level of the DHA or DPA in non-pregnant female mice bred by n-3 Def or n-3 Adq diet, respectively (DHA, n-3 Def, 0.91 ± 0.08; n-3 Adq, 5.90 ± 0.20; DPAn-6, n-3 Def, 3.41 ± 0.26; n-3 Adq, 0.22 ± 0.01%). The *closed circles* represent the n-3 Adq group, the *closed squares* are ED1 Switch group, the *open squares* are ED13 Switch group, and the *open circles* the n-3 Def group. Data at various time points are given as mean percent ± SEM ($n = 5$ mice per time point). The differences were statistically significant in a two-way ANOVA (DHA, $F(3, 63) = 293.0$, $P < 0.001$; n-3 Def, $P < 0.001$; ED13 switch, $P < 0.001$; ED1 switch, $P < 0.001$ compared with n-3 Adq group and ED13 switch, $P < 0.001$; ED1 switch, $P < 0.001$ compared with n-3 Def group, $P < 0.001$ between ED13 and ED1 switch groups by Tukey's HSD multiple range test, a group by embryonic day interaction $F(9, 63) = 9.187$; $P < 0.001$: DPAn-6, $F(3, 63) = 257.9$, $P < 0.001$; n-3 Def, $P < 0.001$; ED13 switch, $P < 0.001$; ED1 switch, $P < 0.001$ compared with n-3 Adq group and ED13 switch, $P < 0.001$; ED1 switch, $P < 0.001$ compared with n-3 Def group, $P < 0.001$ between ED13 and ED1 switch groups by Tukey's HSD multiple range test, a group by embryonic day interaction $F(9, 63) = 7.126$; $P < 0.001$)

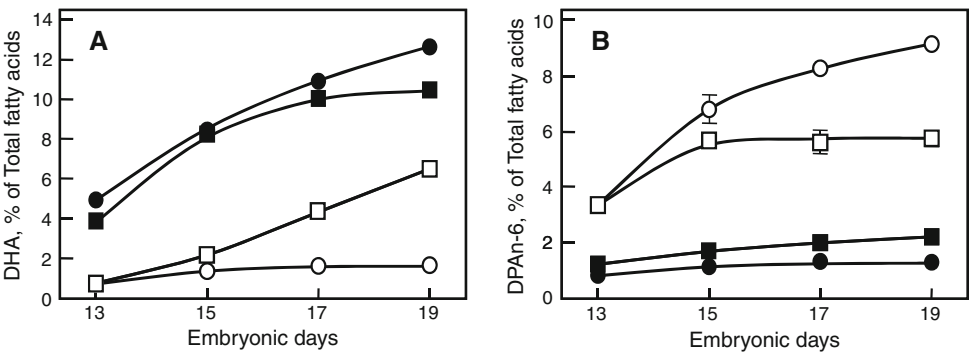

Fig. 3 Alteration of DHA (**a**) and DPAn-6 (**b**) in fetal brains during the period of the third trimester. *Symbols* same as in Fig. 2. The differences were statistically significant in a two-way ANOVA (DHA, $F(3, 63) = 427.8$, $P < 0.001$; n-3 Def, $P < 0.001$; ED13 switch, $P < 0.001$; ED1 switch, $P < 0.001$ compared with n-3 Adq group and ED13 switch, $P < 0.001$; ED1 switch, $P < 0.001$ compared with n-3 Def group, $P < 0.001$ between ED13 and ED1 switch groups by Tukey's HSD multiple range test, a group by embryonic day interaction $F(9, 63) = 15.04$; $P < 0.001$: DPAn-6, $F(3, 63) = 655.4$, $P < 0.001$; n-3 Def, $P < 0.001$; ED13 switch, $P < 0.001$; ED1 switch, $P < 0.001$ compared with n-3 Adq group and ED13 switch, $P < 0.001$; ED1 switch, $P < 0.001$ compared with n-3 Def group, $P < 0.001$ between ED13 and ED1 switch groups by Tukey's HSD multiple range test, a group by embryonic day interaction $F(9, 63) = 25.96$; $P < 0.001$)

Def group exhibited the properties of a high initial value for DPAn-6 (3.66 ± 0.10%) and a sizeable increase by ED 15 (to 5.56 ± 0.32%) and declining values thereafter, ending on ED 19 at 3.46 ± 0.45% (Fig. 4b). The ED13 Switch group responded to the increasing n-3 intake by decreasing DPAn-6 only after the ED 15 time point. The ED1 Switch group initially contained a rather low level of DPAn-6 (0.99 ± 0.07%) but gradually increased over the course of the experiment, ending at ED 19 at a value of 1.32 ± 0.09%. The n-3 Adq group remained constant over the course of the experiment at a liver DPAn-6 content of 0.50 ± 0.03%.

Discussion

This study established a very marked deficiency in brain DHA in the dams whose fetuses were studied; at the time of birth, the dams had a 62% lower brain DHA (n-3 Def, 4.92 ± 0.19%; n-3 Adq, 13.04 ± 0.20%) with compensation by a 30-fold greater content of DPAn-6 (n-3 Def, 9.89 ± 0.15%; n-3 Adq, 0.33 ± 0.01%). The effects of immediate repletion of the diet with ALA on the day of conception and also at the beginning of the third trimester were then evaluated with fetal brain and liver DHA and

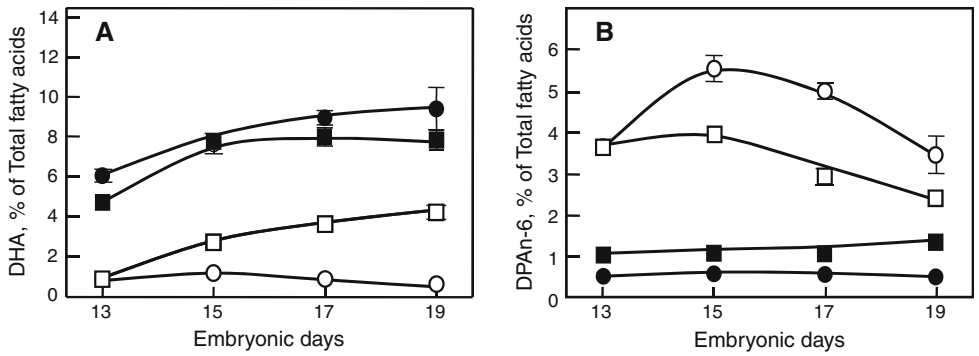

Fig. 4 Alteration of DHA (**a**) and DPAn-6 (**b**) in fetal livers during the period of the third trimester. *Symbols* are the same as in Fig. 2. The differences were statistically significant in a two-way ANOVA (DHA, $F(3, 63) = 311.2$, $P < 0.001$; n-3 Def, $P < 0.001$; ED13 switch, $P < 0.001$; ED1 switch, $P < 0.001$ compared with n-3 Adq group and ED13 switch, $P < 0.001$; ED1 switch, $P < 0.001$ compared with n-3 Def group, $P < 0.001$ between ED13 and ED1 switch groups by Tukey's HSD multiple range test, a group by embryonic day interaction $F(9, 63) = 4.841$; $P < 0.001$: DPAn-6, $F(3, 63) = 468.2$, $P < 0.001$; n-3 Def, $P < 0.001$; ED13 switch, $P < 0.001$; ED1 switch, $P < 0.001$ compared with n-3 Adq group and ED13 switch, $P < 0.001$; ED1 switch, $P < 0.001$ compared with n-3 Def group, $P < 0.001$ between ED13 and ED1 switch groups by Tukey's HSD multiple range test, a group by embryonic day interaction $F(9, 63) = 12.50$; $P < 0.001$

DPAn-6 as key endpoints. Our key findings are that repletion of fetal brain DHA when ALA is repleted on ED 1 is nearly complete at ED 13 and 15 and DPAn-6 has declined to values near those of the n-3 Adq group. This recovery in the fetal brain tracks closely with DHA recovery in the maternal serum and the fetal liver; there is a striking similarity of the maternal serum DPAn-6 time course and that of the fetal liver. Repletion with dietary ALA on ED 13 leads to a slow and continuous replacement of fetal brain and liver DPAn-6 with DHA, a process that is about halfway completed by ED 19. Overall, the time courses of DHA content appeared to be very similar in fetal brain and fetal liver.

Only one other study exists in the literature, to our knowledge, where dietary n-3 fatty acid repletion was carried out during gestation and the fetal fatty acid composition studied, that of Schiefermeier and Yavin [10]. This detailed and pioneering study showed that there was an approximately 33% decline in DHA in the brain aminophospholipids, phosphatidylserine (PS) and phosphatidylethanolamine (PE), and in phosphatidylcholine (PC) when dams were fed an n-3 deficient diet (sunflower oil containing 0.26% ALA) relative to their control diet (soybean oil containing 6.7% ALA). Some of the dams were then subjected on ED 15 to a repletion diet containing over 21 wt% DHA and recovery of DHA was studied over the period of ED 15 to 20. These authors reported no significant changes in phospholipid distributions either as a result of the deficiency or of the repletion diet. However, a most notable result was that the high level infusion of dietary DHA beginning at ED 15 was capable of completely restoring fetal rat brain and liver DHA to the level of the soybean plus DHA diet by ED 18 in the brain and even more rapidly (ED 16.5) in the liver. It is also of significance that the levels of PE DHA were considerably higher in both the maternal and fetal tissues than the level found in the soybean diet, even though it contained a very high level of ALA (6.7 wt%). This study contrasts with ours in that the degree of DHA recovery was much faster and more complete. Of course, the rate and extent of tissue DHA recovery will be related to the fatty acid used (ALA vs. DHA) and the level of the fatty acid in the repletion diet. The 21 wt% level of DHA in the lipids of the Schiefermeier and Yavin study contrasts with 2.1% ALA used in our study for repletion. The 21% DHA dose may be considered as a therapeutic rescue whereas our approach would be considered the effects of a nutritional intervention. The degree of recovery must also be related to the degree of initial deficiency which in the present study was considerably greater as the deficiency was carried through two generations as opposed to starting at conception. Thus, these two papers together are complimentary in outlining the degree of maternal and fetal recovery of tissue DHA as it relates to several factors including the degree of initial deficiency, the particular n-3 fatty acid used for repletion and the level of that fatty acid as well as the length of time required for recovery. These studies show that a nutritional intervention with 2 wt% ALA in the third trimester or even on the day of conception is too late to normalize DHA and DPAn-6 content of fetal brain and liver in n-3 deficient rodents, but as demonstrated by Schiefermeier and Yavin, a large dose of preformed DHA is capable of restoring fetal DHA in the third trimester. It may be possible to normalize fetal brain DHA content with a somewhat lower dose of DHA so as to not antagonize the ARA levels.

In the Schiefermeier and Yavin study, it was demonstrated that the loss of DHA in the n-3 deficient diet group occurred within the aminophospholipids, PE and PS [10]. This was confirmed for rat brain PE and PS in ED 19

Table 3 Maternal brain fatty acid composition

Fatty acid	n-3 Def		ED13 Switch	ED1 Switch		n-3 Adq		Non pregnant	
	ED 13	ED 19	ED 19	ED 13	ED 19	ED 13	ED 19	Def	Adq
14:0	0.16 ± 0.01	0.20 ± 0.01^{z}	0.19 ± 0.003	0.17 ± 0.004	0.20 ± 0.01$^{x, z}$	0.15 ± 0.01	0.19 ± 0.02	0.16 ± 0.01	0.15 ± 0.01
16:0 DMA	2.11 ± 0.03	2.04 ± 0.02	2.19 ± 0.10	2.20 ± 0.08	2.08 ± 0.04	2.13 ± 0.03	2.14 ± 0.06	2.08 ± 0.04	2.03 ± 0.01
16:0	17.61 ± 0.06^{y}	17.35 ± 0.12	17.26 ± 0.26	17.50 ± 0.36^{z}	17.24 ± 0.08^{f}	16.88 ± 0.09^{b}	16.49 ± 0.06^{b}	17.12 ± 0.11	16.66 ± 0.07
18:0 DMA	3.57 ± 0.04	3.47 ± 0.04	3.34 ± 0.24	3.43 ± 0.18	3.53 ± 0.04	3.78 ± 0.05^{x}	3.79 ± 0.04^{x}	3.31 ± 0.09^{y}	3.77 ± 0.04
18:0	19.35 ± 0.14	19.49 ± 0.11	18.81 ± 0.28	19.46 ± 0.37	19.30 ± 0.12	19.10 ± 0.08	19.06 ± 0.07	19.23 ± 0.14	19.21 ± 0.04
20:0	0.52 ± 0.02	0.49 ± 0.02^{z}	0.55 ± 0.02	0.55 ± 0.02	0.52 ± 0.02	0.57 ± 0.01	0.56 ± 0.01	0.53 ± 0.01	0.56 ± 0.005
22:0	0.58 ± 0.02	0.57 ± 0.02^{z}	0.64 ± 0.02	0.64 ± 0.02	0.61 ± 0.02	0.64 ± 0.03	0.67 ± 0.02^{b}	0.64 ± 0.01	0.66 ± 0.01
24:0	0.96 ± 0.04^{y}	1.00 ± 0.07^{y}	1.10 ± 0.08$^{c, y}$	1.50 ± 0.09^{y}	1.04 ± 0.02$^{c, y}$	1.50 ± 0.19^{y}	2.22 ± 0.24$^{a, f, w}$	1.00 ± 0.03^{y}	2.61 ± 0.19
Total saturates	44.86 ± 0.13	44.61 ± 0.17$^{f, y}$	44.08 ± 0.23$^{c, y}$	45.46 ± 0.11^{w}	44.52 ± 0.05^{y}	44.73 ± 0.09^{z}	45.11 ± 0.27^{w}	44.074 ± 0.14^{y}	45.65 ± 0.18
16:1n-7	0.47 ± 0.004	0.49 ± 0.02	0.52 ± 0.03^{x}	0.47 ± 0.03	0.51 ± 0.02	0.50 ± 0.02	0.54 ± 0.02$^{x, z}$	0.43 ± 0.01	0.44 ± 0.01
18:1 DMA	1.21 ± 0.01	1.21 ± 0.05	1.26 ± 0.08	1.24 ± 0.06	1.16 ± 0.02^{d}	1.29 ± 0.01	1.37 ± 0.03^{x}	1.18 ± 0.03	1.32 ± 0.02
18:1n-9	14.08 ± 1.32	13.03 ± 0.20	13.13 ± 0.13	13.04 ± 0.10	13.08 ± 0.07	14.62 ± 0.47	14.56 ± 0.26	13.23 ± 0.07	14.36 ± 0.12
18:1n-7	3.62 ± 0.04^{z}	3.54 ± 0.06	3.66 ± 0.15^{z}	3.55 ± 0.10	3.55 ± 0.02	3.31 ± 0.02^{x}	3.30 ± 0.07^{x}	3.66 ± 0.05^{y}	3.28 ± 0.03
20:1n-9	1.79 ± 0.04^{y}	1.80 ± 0.09^{y}	1.91 ± 0.10	1.90 ± 0.10	1.87 ± 0.07$^{d, z}$	2.11 ± 0.07^{f}	2.20 ± 0.03^{a}	1.98 ± 0.03	2.19 ± 0.02
22:1n-9	0.26 ± 0.004	0.23 ± 0.01	0.22 ± 0.03	0.24 ± 0.02	0.24 ± 0.01	0.28 ± 0.002	0.26 ± 0.01	0.29 ± 0.03	0.27 ± 0.004
24:1n-9	2.46 ± 0.02^{w,y}	2.63 ± 0.09	2.75 ± 0.11	2.65 ± 0.07	2.67 ± 0.06	2.65 ± 0.03	2.93 ± 0.05	2.88 ± 0.06	2.91 ± 0.05
Total monounsat.	23.88 ± 1.34	22.93 ± 0.38	23.46 ± 0.25	23.09 ± 0.21	23.07 ± 0.19	24.75 ± 0.49	25.16 ± 0.27^{b}	23.64 ± 0.10	24.76 ± 0.14
18:2n-6	0.34 ± 0.01	0.36 ± 0.01	0.37 ± 0.01	0.36 ± 0.01	0.38 ± 0.01	0.39 ± 0.02	0.46 ± 0.01^{b}	0.37 ± 0.02	0.41 ± 0.01
20:2n-6	0.13 ± 0.01	0.11 ± 0.004	0.12 ± 0.004	0.14 ± 0.004	0.12 ± 0.004	0.14 ± 0.005	0.12 ± 0.01	0.15 ± 0.02	0.15 ± 0.01
20:3n-6	0.23 ± 0.01^{y}	0.20 ± 0.01^{y}	0.23 ± 0.01$^{c, y}$	0.25 ± 0.01^{y}	0.23 ± 0.02$^{c, y}$	0.43 ± 0.03^{w}	0.39 ± 0.02$^{a, x}$	0.28 ± 0.02^{y}	0.47 ± 0.02
20:4n-6	8.85 ± 0.09^{y}	8.78 ± 0.09^{y}	8.51 ± 0.16$^{d, y}$	8.34 ± 0.09$^{d, z}$	8.45 ± 0.09$^{d, y}$	7.72 ± 0.13$^{a, w}$	7.83 ± 0.07$^{a, w}$	8.60 ± 0.11^{y}	7.78 ± 0.11
22:4n-6	3.41 ± 0.06^{y}	3.27 ± 0.08^{y}	3.23 ± 0.05$^{c, y}$	3.14 ± 0.09$^{b, c, x, y}$	3.00 ± 0.04$^{b, c, w, y}$	2.47 ± 0.04$^{a, w}$	2.41 ± 0.05$^{a, w}$	3.40 ± 0.04^{y}	2.50 ± 0.03
22:5n-6	10.13 ± 0.12^{y}	10.34 ± 0.17^{y}	9.31 ± 0.25$^{a, c, e, y}$	7.85 ± 0.21$^{a, c, w, y}$	6.58 ± 0.15$^{a, c, e, w, y}$	0.41 ± 0.01$^{a, w}$	0.37 ± 0.02$^{a, w}$	9.89 ± 0.15^{y}	0.33 ± 0.01
Total n-6 PUFAs	23.09 ± 0.06^{y}	23.06 ± 0.24^{y}	21.76 ± 0.36$^{a, c, e, x, y}$	20.07 ± 0.23$^{a, c, w,y}$	18.75 ± 0.20$^{a, c, e, w, y}$	11.56 ± 0.13$^{a, w}$	11.58 ± 0.08$^{a, w}$	22.69 ± 0.24^{y}	11.64 ± 0.10
20:5n-3	0.07 ± 0.01^{y}	0.08 ± 0.004	0.09 ± 0.004^{d}	0.06 ± 0.01$^{c, y}$	0.08 ± 0.004^{c}	0.12 ± 0.01$^{a, w}$	0.13 ± 0.01$^{a, w}$	0.08 ± 0.002^{y}	0.11 ± 0.003
22:5n-3	0.06 ± 0.01^{y}	0.06 ± 0.001^{y}	0.15 ± 0.01$^{a, c, e, w}$	0.14 ± 0.01$^{a, c, w}$	0.15 ± 0.01$^{a, c, w}$	0.18 ± 0.01$^{a, w}$	0.20 ± 0.004$^{a, w, y}$	0.05 ± 0.004^{y}	0.16 ± 0.002
22:6n-3	4.63 ± 0.08^{y}	5.04 ± 0.14^{y}	5.67 ± 0.30$^{c, f, y}$	6.68 ± 0.28$^{a, c, w}$	8.99 ± 0.13$^{a, c, e, w, y}$	14.02 ± 0.18$^{a, w}$	13.36 ± 0.31$^{a, w}$	4.92 ± 0.19^{y}	13.04 ± 0.20
Total n-3 PUFAs	4.75 ± 0.08^{y}	5.18 ± 0.13^{y}	5.91 ± 0.30$^{c, f, y}$	6.89 ± 0.28$^{a, c, w, y}$	9.23 ± 0.12$^{a, c, e, w, y}$	14.32 ± 0.16$^{a, w}$	13.69 ± 0.32$^{a, w}$	5.06 ± 0.19^{y}	13.31 ± 0.20
Total PUFAs	27.84 ± 0.10^{y}	28.23 ± 0.34^{y}	27.67 ± 0.20$^{c, y}$	26.96 ± 0.12$^{d, y}$	27.98 ± 0.20$^{c, y}$	25.88 ± 0.25$^{a, w}$	25.28 ± 0.27$^{a, w}$	27.74 ± 0.09^{y}	24.95 ± 0.27
Total fatty acid (μg/mg wet wt)	44.00 ± 0.54	41.91 ± 0.33	43.22 ± 0.75	44.22 ± 0.62	43.30 ± 0.51	42.82 ± 1.51	45.49 ± 1.40^{b}	42.59 ± 0.27	42.14 ± 0.32
Brain weight (mg)	532.4 ± 9.2	541.8 ± 5.8	541.0 ± 9.3	546.2 ± 8.1	548.4 ± 15.0	534.2 ± 5.2	510.0 ± 8.3	542.3 ± 9.4	541.1 ± 6.4
DHA (mg/brain)	1.1 ± 0.03^{y}	1.1 ± 0.02^{y}	1.3 ± 0.1$^{c, y}$	1.6 ± 0.1$^{a, c, w, y}$	2.1 ± 0.1$^{a, c, e, w, y}$	3.2 ± 0.1$^{a, w}$	3.1 ± 0.1$^{a, w}$	1.1 ± 0.1^{y}	3.0 ± 0.04

Fatty acid methyl esters from 12:0 to 24:1n-9 were analyzed and 12:0 and 18:3n-3, 18:3n-6 were not detected (i.e. <0.001%). Each parameter is presented as the mean ± SEM, ($n = 5$). *DMA* indicates a dimethylacetal derivative of a plasmalogenic phospholipid

Statistically significant changes are represented as follow: $^{a}P < 0.01$, $^{b}P < 0.05$ compared with ED 13 or ED 19 in n-3 Def group, $^{c}P < 0.01$, $^{d}P < 0.05$ compared with ED 13 or ED 19 in n-3 Adq group, $^{e}P < 0.01$, $^{f}P < 0.05$ compared between ED 13 and ED 19 in each group, $^{w}P < 0.01$, $^{x}P < 0.05$ compared with non-pregnant n-3 Def mice, $^{y}P < 0.01$, $^{z}P < 0.05$ compared with non-pregnant n-3 Adq mice (one-way ANOVA followed by Tukey's HSD multiple range test)

Table 4 Fetal brain fatty acid composition

Fatty acid	n-3 Def		ED13 Switch	ED1 Switch		n-3 Adq	
	ED 13	ED 19	ED 19	ED 13	ED 19	ED 13	ED 19
14:0	2.03 ± 0.05	2.06 ± 0.06	2.05 ± 0.07	2.11 ± 0.07	2.12 ± 0.03	1.92 ± 0.11	2.26 ± 0.09
16:0 DMA	2.07 ± 0.04	2.17 ± 0.02	2.23 ± 0.08	1.93 ± 0.11	2.03 ± 0.01	1.97 ± 0.09	2.01 ± 0.04
16:0	25.85 ± 0.35	26.14 ± 0.21	26.41 ± 0.57	25.60 ± 0.41	26.60 ± 0.18	24.75 ± 0.68	25.03 ± 0.14
18:0 DMA	0.97 ± 0.02	1.32 ± 0.02[e]	1.23 ± 0.10[e]	0.89 ± 0.04	1.32 ± 0.02[e]	0.99 ± 0.03	1.40 ± 0.04[e]
18:0	14.08 ± 0.38	14.54 ± 0.95	15.44 ± 0.37	13.85 ± 0.33	15.57 ± 0.11	13.95 ± 0.38	15.36 ± 0.17
20:0	0.11 ± 0.01	0.08 ± 0.003[f]	0.08 ± 0.003[e]	0.11 ± 0.01	0.08 ± 0.001[f]	0.12 ± 0.01	0.08 ± 0.001[e]
22:0	0.13 ± 0.01	0.08 ± 0.004[f]	0.08 ± 0.002[f]	0.10 ± 0.01	0.08 ± 0.01	0.15 ± 0.02	0.07 ± 0.003[e]
24:0	0.12 ± 0.01	0.10 ± 0.02	0.12 ± 0.01	0.09 ± 0.01	0.12 ± 0.004	0.14 ± 0.03	0.10 ± 0.01
Total saturates	45.37 ± 0.41	46.50 ± 0.84	47.63 ± 0.39[f]	44.67 ± 0.22	47.93 ± 0.14[e]	43.98 ± 0.64	46.31 ± 0.19[f]
16:1n-7	3.48 ± 0.14	2.73 ± 0.03[e]	2.74 ± 0.16[e]	3.49 ± 0.09	2.52 ± 0.05[e]	3.33 ± 0.17	2.70 ± 0.02[e]
18:1 DMA	0.81 ± 0.02	0.35 ± 0.01[e]	0.32 ± 0.02[e]	0.75 ± 0.05	0.32 ± 0.01[e]	0.82 ± 0.03	0.32 ± 0.005[e]
18:1n-9	14.11 ± 0.42	12.32 ± 0.16[e]	11.43 ± 0.29[e]	14.95 ± 0.24	12.16 ± 0.16[e]	14.96 ± 0.31	12.02 ± 0.04[e]
18:1n-7	4.10 ± 0.12	3.52 ± 0.01	3.55 ± 0.23	4.27 ± 0.23	3.37 ± 0.05[e]	4.17 ± 0.08	3.25 ± 0.04[e]
20:1n-9	0.59 ± 0.05	0.30 ± 0.01[e]	0.27 ± 0.01[e]	0.62 ± 0.08	0.32 ± 0.02[e]	0.59 ± 0.07	0.26 ± 0.05[e]
22:1n-9	0.03 ± 0.01	0.02 ± 0.004	0.02 ± 0.001	0.07 ± 0.01	0.03 ± 0.01[f]	0.07 ± 0.01	0.03 ± 0.01[f]
24:1n-9	0.27 ± 0.02	0.20 ± 0.003	0.18 ± 0.01	0.35 ± 0.07	0.18 ± 0.02	0.48 ± 0.08[b]	0.13 ± 0.01[e]
Total monounsat.	23.39 ± 0.59	19.44 ± 0.18[e]	18.49 ± 0.26[e]	24.49 ± 0.46	18.90 ± 0.20[e]	24.41 ± 0.42	18.70 ± 0.06[e]
18:2n-6	1.38 ± 0.14	0.46 ± 0.02[e]	0.45 ± 0.04[e]	1.26 ± 0.10	0.50 ± 0.08[e]	1.68 ± 0.24	0.60 ± 0.05[e]
18:3n-6	0.11 ± 0.03	0.05 ± 0.004	0.05 ± 0.01	0.07 ± 0.003	0.04 ± 0.002	0.08 ± 0.003	0.07 ± 0.01
20:2n-6	0.07 ± 0.01	0.04 ± 0.002	0.04 ± 0.002	0.07 ± 0.01	0.05 ± 0.004	0.09 ± 0.01	0.05 ± 0.004
20:3n-6	0.29 ± 0.02	0.21 ± 0.02	0.20 ± 0.02[f]	0.28 ± 0.03	0.20 ± 0.01	0.36 ± 0.03	0.31 ± 0.02
20:4n-6	10.21 ± 0.18	11.72 ± 0.11[e]	11.38 ± 0.21	8.80 ± 0.60[b]	10.46 ± 0.11[b, e]	9.29 ± 0.08	10.73 ± 0.17[e]
22:4n-6	2.78 ± 0.15	3.12 ± 0.06	3.02 ± 0.07	2.02 ± 0.16[a]	2.76 ± 0.05[d, e]	2.17 ± 0.08[a]	2.57 ± 0.07[a]
22:5n-6	3.34 ± 0.16	9.12 ± 0.07[e]	5.77 ± 0.28[a, c, e]	1.26 ± 0.11[a]	2.22 ± 0.10[a, c, e]	0.84 ± 0.09[a]	1.28 ± 0.06[a]
Total n-6 PUFAs	18.18 ± 0.47	24.73 ± 0.08[e]	20.91 ± 0.45[a, c, e]	13.76 ± 0.92[a]	16.23 ± 0.11[a, e]	14.51 ± 0.15[a]	15.62 ± 0.21[a]
20:5n-3	0.08 ± 0.005	0.08 ± 0.004	0.08 ± 0.01[e]	0.10 ± 0.003	0.09 ± 0.001[c]	0.11 ± 0.01	0.16 ± 0.01[a, e]
22:5n-3	0.02 ± 0.002	0.04 ± 0.002	0.25 ± 0.03[a, c, e]	0.17 ± 0.01[a]	0.24 ± 0.01[a, c]	0.24 ± 0.03[a]	0.39 ± 0.01[a, e]
22:6n-3	0.72 ± 0.02	1.66 ± 0.08	6.49 ± 0.49[a, c, e]	3.91 ± 0.26[a]	10.40 ± 0.10[a, c, e]	4.95 ± 0.27[a]	12.62 ± 0.26[a, e]
Total n-3 PUFAs	0.83 ± 0.02	1.78 ± 0.08	6.81 ± 0.49[a, c, e]	4.18 ± 0.26[a]	10.72 ± 0.11[a, c, e]	5.29 ± 0.24	13.18 ± 0.26[a, e]
Total PUFAs	19.0 ± 0.47	26.5 ± 0.15	27.7 ± 0.33[e]	17.9 ± 1.16	27.0 ± 0.14[e]	19.8 ± 0.14	28.8 ± 0.33[e]
Total fatty acid (μg/mg wet wt)	12.21 ± 1.02	18.73 ± 0.32[e]	18.50 ± 0.45[e]	13.95 ± 1.16	19.68 ± 0.09[e]	13.03 ± 2.06	19.96 ± 0.38[e]
Brain weight (mg)	11.8 ± 0.7	78.2 ± 3.5	71.4 ± 2.7[e]	9.6 ± 3.2	61.8 ± 4.0[b, e]	10.8 ± 1.7	67.6 ± 4.1[e]
DHA (μg/brain)	1.1 ± 0.1	24.4 ± 1.9	86.9 ± 10.5[a, c, e]	4.9 ± 1.3	126.4 ± 7.7[a, c, e]	6.6 ± 1.0	170.7 ± 12.6[a, e]

Fatty acid methyl esters from 12:0 to 24:1n-9 were analyzed and 12:0 and 18:3n-3 were not detected (i.e. <0.001%). Each parameter is presented as the mean ± SEM, ($n = 5$). *DMA* indicates a dimethylacetal derivative of a plasmalogenic phospholipid

Statistically significant changes are represented as follow: [a]$P < 0.01$, [b]$P < 0.05$ compared with ED 13 or ED 19 in n-3 Def group, [c]$P < 0.01$, [d]$P < 0.05$ compared with ED 13 or ED 19 in n-3 Adq group, [e]$P < 0.01$, [f]$P < 0.05$ compared between ED 13 and ED 19 in each group (one-way ANOVA followed by Tukey's HSD multiple range test)

embryos in a study of n-3 deficient (fed safflower oil) versus n-3 adequate (fed soybean oil) by Bertrand et al. [11] and for newborn brain cortex PE by Tam and Innis [8]. This is the expected result as it has long been appreciated that the main repository for brain DHA is within the aminophospholipids with PE being the largest component [16, 17] as has also been observed in rat liver [6, 9]. Therefore, it may be surmised that, although our study did not explicitly delineate the fatty acyl composition of various phospholipid pools, the loss and repletion of DHA as well as its replacement by DPAn-6 likely occurred in these aminophospholipids pools. Previous work has also shown that a low brain DHA status leads to a selective loss of brain PS [18] whereas an intra-amniotic administration of DHA leads to increased brain and liver PS [19].

Although the ED1 Switch group had "caught up" with respect to the brain and liver DHA level in the n-3 Adq reference group by ED 15, subsequent to that, the DHA level began to fall off with increasing divergence from ED 17 to ED 19. By ED 19, the DHA level in the ED1 Switch group was lower than that of the n-3 Adq group in the maternal serum and the fetal liver and brain. It is, however, of significance that the ARA level in the ED1 Switch group by ED19 had normalized relative to the n-3 Adq level.

It is noted that the maternal serum DHA level also declined in the n-3 Adq group, however, this group maintained a level similar to that of non-pregnant females (Table 2). This raises the question as to whether the rapid growth of the fetus at this end stage of development is placing too great a demand on the maternal ability to supply DHA due to her low body stores of DHA. The maternal serum DHA in the ED1 Switch group does in fact fall off after ED 15 and is only about 55% of what it was on ED 15 (see Fig. 2a). Analysis of the dam brain indicated that DHA in the n-3 Def group began at conception at $4.92 \pm 0.19\%$, rises to $6.68 \pm 0.28\%$ by ED 13 and to $8.99 \pm 0.13\%$ by ED 19 in the ED1 Switch group, while the n-3 Adq reference level is $13.36 \pm 0.31\%$ at ED 19. These data indicate that the dam brain is rapidly incorporating a large amount of DHA during gestation when she is switched to an n-3 Adq diet. We surmise that the origin of this DHA is from maternal liver and/or brain in vivo metabolism of the ALA being consumed in the diet.

At the same time, the total fatty acid of brain (μg/mg wet wt) is increasing from 13.95 ± 1.16 to 19.68 ± 0.09 between ED 13 and 19 in the ED1 Switch group. The total amount of DHA per brain in the ED1 Switch group over this 6 day time period rises in a rather spectacular fashion from 4.9 ± 1.3 to 126.4 ± 7.7 μg/brain (Table 4). This dramatic increase between ED 13 and 19 is associated with several factors including an increased total fatty acid concentration (41%), an over sixfold increase in brain weight and a selective increase in DHA content (rising over 25-fold). Similar observations were made in both the n-3 Def and the n-3 Adq groups during this period of development, with the latter group increasing DHA content the most. This rather extreme demand for fetal DHA coupled with the falling maternal serum percentage of DHA and the continuous uptake into maternal organs suggests that the ED1 Switch dams have a limited capacity to supply DHA. It is thus likely that the maternal dietary history with respect to n-3 fatty acid intake and tissue DHA accretion is an important factor for optimal maternal and infant nutrition. Low n-3 fatty acid intake clearly can lead to deficiencies in both fetal and maternal tissues and organs including the brain. An adequate source of preformed DHA is likely to prevent such deficiencies during fetal development.

Acknowledgment We would like to thank Ms. Yasuda of Wakunaga Pharmaceutical Co., for identification of fetus sex by PCR.

References

1. Kuhn DC, Crawford MA (1986) Placental essential fatty acid transport and prostaglandin synthesis. Prog Lipid Res 25:345–353
2. Ruyla M, Connor WE, Anderson GJ, Lowensohn RI (1990) Placental transfer of essential fatty acids in humans: venous-arterial difference for docosahexaenoic acid in fetal umbilical erythrocytes. Proc Natl Acad Sci USA 87:7902–7906
3. Haggarty P, Page K, Abramovich DR, Ashton J, Brown D (1997) Long-chain polyunsaturated fatty acid transport across the perfused human placenta. Placenta 18:635–642
4. Jensen CL (2006) Effects of n-3 fatty acids during pregnancy and lactation. Am J Clin Nutr 83:1452S–1457S
5. Hibbeln JR, Nieminen LRG, Blasbalg TL, Riggs JA, Lands WEM (2006) Healthy intakes of n-3 and n-6 fatty acids: estimations considering worldwide diversity. Am J Clin Nutr 83:1483S–1493S
6. Cunnane SC, Chen Z-Y (1992) Quantitative changes in long-chain fatty acids during fetal and early postnatal development in rats. Am J Physiol 262:R14–R19
7. Green P, Glozman S, Kamensky B, Yavin E (1999) Developmental changes in rat brain membrane lipids and fatty acids: the preferential prenatal accumulation of docosahexaenoic acid. J Lipid Res 40:960–966
8. Tam O, Innis SM (2006) Dietary polyunsaturated fatty acids in gestation alter fetal cortical phospholipids, fatty acids and phosphatidylserine synthesis. Dev Neurosci 28:222–229
9. Yonekubo A, Honda S, Okano M, Takahashi K, Yamamoto Y (1993) Dietary fish oil alters rat milk composition and liver and brain fatty acid composition of fetal and neonatal rats. J Nutr B123:1703–1708
10. Schiefermeier M, Yavin E (2002) n-3 Deficient and docosahexaenoic acid-enriched diets during critical periods of the developing prenatal rat brain. J Lipid Res 43:124–131
11. Bertrand PC, O'Kusky JR, Innis M (2006) Maternal dietary (n-3) fatty acid deficiency alters neurogenesis in the embryonic rat brain. J Nutr 136:1570–1575
12. Kunieda T, Xian M, Kobayashi E, Imamichi T, Moriwaki K, Toyoda Y (1992) Sexing of mouse preimplantation embryos by detection of Y chromosome-specific sequences using polymerase chain reaction. Biol Reprod 46:692–697
13. Reeves PG, Nielsen FH, Fahey GC (1993) Committee report on the AIN-93 purified rodent diet. J Nutr 123:1939–1951
14. Lepage G, Roy CC (1986) Direct transesterification of all classes of lipids in a one-step reaction. J Lipid Res 27:114–120
15. Masood A, Stark KD, Salem N Jr (2005) A simplified and efficient method for the analysis of fatty acid methyl esters suitable for large clinical studies. J Lipid Res 46:2299–2305
16. O'Brien JS, Sampson EL (1965) Fatty acid and aldehyde composition of the major brain lipids in normal gray matter, white matter and myelin. J Lipid Res 6:545–551
17. Salem N Jr (1989) Omega-3 fatty acids: molecular and biochemical aspects. In: Spiller G, Scala J (eds) New protective roles of selected nutrients in human nutrition. Alan R. Liss, New York, pp 109–228
18. Hamilton L, Greiner R, Salem N Jr, Kim HY (2000) n-3 Fatty acid deficiency decreases phosphatidylserine accumulation selectively in neonatal tissue. Lipids 35:863–869
19. Green P, Yavin E (1995) Modulation of fetal rat brain and liver phospholipids content by intraamniotic ethyl-docosahexaenoate administration. J Neurochem 65:2555–2560

Lipids (2010) 45:669–681
DOI 10.1007/s11745-010-3450-z

ORIGINAL ARTICLE

Effects of Seal Oil and Tuna-Fish Oil on Platelet Parameters and Plasma Lipid Levels in Healthy Subjects

Neil J. Mann · Stella L. O'Connell · Kylie M. Baldwin · Indu Singh · Barbara J. Meyer

Received: 3 May 2010 / Accepted: 29 June 2010 / Published online: 23 July 2010

Abstract Fish are a rich source of eicosapentaenoic acid (EPA) and docosahexaenoic acid (DHA), two long-chain polyunsaturated n-3 fatty acids (LC n-3 PUFA) with cardiovascular benefits. A related but less-investigated LC n-3 PUFA, docosapentaenoic acid (DPA), is more common in seal oil and pasture-fed red meats. This study compared indicators of platelet function and plasma lipids in healthy volunteers given supplements containing these different fatty acids (FA) for 14 days. Subjects, randomised into three groups of ten, consumed capsules of tuna oil (210 mg EPA, 30 mg DPA, 810 mg DHA), seal oil (340 mg EPA, 230 mg DPA, 450 mg DHA) or placebo (sunola) oil. Supplementary LC n-3 PUFA levels were approximately 1 g/day in both fish and seal oil groups. Baseline dietary FA and other nutrient intakes were similar in all groups. Both fish and seal oil elevated platelet DHA levels ($P < 0.01$). Seal oil also raised platelet DPA and EPA levels ($P < 0.01$), and decreased p-selectin ($P = 0.01$), a platelet activation marker negatively associated with DPA ($P = 0.03$) and EPA ($P < 0.01$) but not DHA. Plasma triacylglycerol decreased ($P = 0.03$) and HDL-cholesterol levels increased ($P = 0.01$) with seal oil only. Hence, seal oil may be more efficient than fish oil at promoting healthy plasma lipid profiles and lowering thrombotic risk, possibly due to its high DPA as well as EPA content.

Keywords Docosapentaenoic acid · Omega-3 polyunsaturated fatty acids · Cardiovascular disease · Triacylglycerols · Platelet activation · P-selectin

Abbreviations

AA	Arachidonic acid
ADP	Adenosine diphosphate
ANOVA	Analysis of variance
ATP	Adenosine triphosphate
BMI	Body mass index
cAMP	Cyclic adenosine monophosphate
CRP	C-reactive protein
CVD	Cardiovascular disease
DHA	Docosahexaenoic acid
DPA	Docosapentaenoic acid
EPA	Eicosapentaenoic acid
FA	Fatty acid(s)
HDL	High density lipoprotein
LC n-3 PUFA	Long-chain omega-3 polyunsaturated fatty acids
LDL	Low density lipoprotein
MPV	Mean platelet volume
MUFA	Monounsaturated fatty acids
SD	Standard deviation

This study was supported by a grant from Meat and Livestock Australia (MLA).

N. J. Mann (✉) · S. L. O'Connell
School of Applied Sciences, RMIT University,
GPO Box 2476V, Melbourne, VIC 3001, Australia
e-mail: neil.mann@rmit.edu.au

S. L. O'Connell
e-mail: staroc@gotalk.net.au

K. M. Baldwin · I. Singh
School of Medical Sciences, RMIT University,
PO Box 71, Bundoora, VIC 3083, Australia
e-mail: kandh@netspace.net.au

I. Singh
e-mail: indu.singh@rmit.edu.au

B. J. Meyer
School of Health Sciences, University of Wollongong,
Wollongong, NSW 2522, Australia
e-mail: bmeyer@uow.edu.au

Greek Symbols

Ω Ohm (electrical resistance)

Introduction

Cardiovascular diseases (CVD) are the leading causes of death in most westernised countries [1], the primary cause being atherosclerosis [2], a multi-factorial condition which becomes critical when it affects the supply of blood to the heart or brain [3]. One critical indicator of CVD risk appears to be the ratio between low-density lipoprotein (LDL)-cholesterol and high-density lipoprotein (HDL)-cholesterol [4], as atherosclerosis develops when distinct morphological forms of LDL invade the inner cellular lining of arteries and become oxidised [5, 6], promoting endothelial cell dysfunction. Subsequently, trapped monocytes and necrotic debris can rupture and trigger platelet activation and aggregation to induce an occlusive thrombus [6].

In general, if circulating platelets encounter endothelial damage, agonists such as collagen, adenosine triphosphate (ATP), adenosine diphosphate (ADP) and thrombin promote the activation of platelets and their adherence to exposed subendothelium, leading to thrombus formation [7]. Once activated, the platelets undergo shape change, exposing the cell adhesion molecule (CAM) p-selectin on their surface, initiating aggregation and releasing procoagulants. Mechanisms for controlling platelet activation are poorly understood, but there are indications that this may be linked to prostacyclin and nitrous oxide increasing intracellular levels of cyclic adenosine monophosphate (cAMP) [8, 9], as cAMP controls intracellular levels of calcium ions important for aggregation and adhesion; if levels of cAMP are increased, platelet activation and aggregation are reduced [9].

Epidemiological studies indicate that high intakes of long chain (>18 carbons) omega-3 polyunsaturated fatty acids (LC n-3 PUFA) are associated with decreased morbidity and mortality from CVD [10]. These LC n-3 PUFA at doses of around 3 g/day or more become incorporated in cell membrane phospholipids and then act to reduce inflammatory factors [10] and decrease hepatic triacylglycerols [11]. However, free LC n-3 PUFA in extracellular fluids appear to affect cardiac arrhythmias at doses of only 1 g/day [10]. In general intake of fish or use of fish oil supplement lowers CVD risk factors [12–14], apparently through the actions of eicosapentaenoic acid, C20:5n-3 (EPA), and docosahexaenoic acid, C22:6n-3 (DHA).

Both EPA and DHA have been shown to lower plasma triacylglycerol levels, an independent risk factor for CVD [15], as well as increase levels of HDL-cholesterol [16]. Supplementary EPA has successfully suppressed the expression of platelet activation markers and the release of platelet-derived microparticles capable of generating thrombin (a potent platelet aggregator), thereby retarding further platelet activation [17, 18]. There is evidence that EPA and DHA also reduce platelet aggregation [19].

Red meat contains relatively small amounts of EPA and DHA, but is rich in another LC n-3 PUFA: docosapentaenoic acid, C22:5n-3 (DPA), which is only present in small amounts in a few oily fish [20]. Reported intakes of DPA in countries such as France [21], Japan [22] and Denmark [23] are generally similar to Australian values [24]. Since Australians consume around six times as much meat as fish and seafood [25], this food contributes significantly (up to 43%) to the total LC n-3 PUFA intake of many Australians, and DPA may make up almost one-third of the LC n-3 PUFA in the average adult Australian diet [24]. As such, further investigation of its effects on cardiovascular and general health is required.

The similarity in molecular structure of DPA to EPA and DHA makes it feasible that DPA has similar beneficial effects to DHA and EPA on cardiovascular parameters. All three of these LC n-3 PUFA are significantly and inversely related to carotid intimal-medial thickness [22], and DPA, like EPA and DHA, has been shown to have an anti-aggregatory effect on platelets [26, 27]. A large prospective study in healthy males found that serum levels of EPA were not associated with reduced risk of acute coronary events, whereas subjects with the highest levels of combined DHA and DPA were at reduced risk compared to those with the lowest levels [28]. Supplementary seal oil, relatively rich (compared with fish oil) in DPA, has been found to induce an increase in the LC n-3 PUFA status of serum phospholipids in normal men, with the suggestion of a favourable shift in the balance of plasma pro-coagulant and anticoagulant activity [29]. LC n-3 PUFA have also shown anti-inflammatory effects in many experimental models as well as in clinical conditions of inflammation [10], and evidence for the specific benefits of seal oil in such cases has been mainly positive [30, 31], although not always significant [32].

Commercial quantities of pure food-grade DPA are not currently available for use in a clinical trial. Seal oil (which also contains EPA and some DHA) is the richest commercially-available source of DPA but, to our knowledge, no report of its effect on platelet activation has previously been published. This study examined the effects of seal oil on blood lipids and platelet factors compared to those of tuna-fish oil (which contains minimal DPA, 40% less EPA and double the DHA of seal oil) in healthy volunteers. A placebo oil containing no LC n-3 PUFA provided a control in this randomised double-blind parallel intervention study.

Experimental Procedures

Ethics Approval

The study protocol was approved by the RMIT University Human Research Ethics Committee and notification forwarded to the Australian Therapeutics Goods Administration.

Recruitment and Study Population

Thirty healthy volunteers (19 female and 11 male), aged from 20 to 50 years, were recruited for this pilot clinical trial after advertisement of the study and screening for suitability. Subjects had no known metabolic, endocrine or haematological diseases, were not smokers nor on any form of medication, and had moderate physical activity levels. Signed informed consent was obtained from all volunteers prior to randomisation. Study participants were required to complete a 7-day weighed food record before commencing the dietary fatty acid supplementation, to confirm that they were not consuming antioxidant or other nutrient supplements and to compare the general nutrient and fatty acid intakes in the different groups. The volunteers were requested not to modify their diet whilst participating in this study, and also asked to refrain from consuming aspirin-type products and fish oil supplements for 2 weeks prior to and during the study.

Experimental Design

The study was a randomised parallel double-blind placebo-controlled clinical trial conducted over 14 days (sufficient for complete platelet turnover). After an initial 14-day wash-out period (on a common diet very low in LC n-3 PUFA), subjects were randomly assigned to one of three groups: a placebo oil (Sunola—high oleic acid sunflower oil), tuna-fish oil or seal oil group. Each group consumed their combination of supplementary fatty acids in the form of 10 soft-gel capsules per day over the trial period. Subjects were instructed to consume their daily supplementary capsules with or after breakfast.

The placebo group received ten 500 mg capsules/day of sunola oil (85% 18:1n9, 5% 18:2n6, 5% 16:0) (Nu-Mega Ingredients Pty. Ltd., Australia), which is devoid of EPA, DPA, DHA and other LC PUFA, but provided approximately 4 g monounsaturated oil per day (Table 1). The fish oil subjects received four of the placebo capsules/day plus six 500 mg capsules/day of tuna-fish oil, which is rich in DHA and also contains EPA and a small amount of DPA (Nu-Mega Ingredients Pty. Ltd., Australia). The third group received ten 500 mg seal oil capsules/day (BGI Atlantic Marine Product Inc., Canada), containing EPA, DHA and significant amounts of DPA (over seven times that in the fish oil). The tuna-fish and the seal oil groups both received a total of just over 1 g/day of supplementary LC n-3 PUFA (Table 2).

Table 1 The principal fatty acid composition of supplementary oils used in this study (mg FA/500 mg oil)

Fatty acid	Placebo (sunola) oil	Fish oil	Seal oil
C18:1n-9	425	61	142
C20:5n-3 (EPA)	0	35	34
C22:5n-3 (DPA)	0	5	23
C22:6n-3 (DHA)	0	135	45
Total LC n-3 PUFA per 500 mg capsule	0	175	102

Subjects received 10 sunola oil capsules or six fish oil plus four sunola oil capsules or ten seal oil capsules, per day

Table 2 Total amount of supplementary oleic acid and principal long-chain n-3 PUFA (mg/day) supplied to subjects in each test group (through consumption of 10 soft-gel capsules per day)

Fatty acid	Placebo (Sunola) oil group	Fish oil group	Seal oil group
C18:1n-9	4,250	1,944	1,420
C20:5n-3 (EPA)	0	210	340
C22:5n-3 (DPA)	0	30	230
C22:6n-3 (DHA)	0	810	450
Total LC n-3 PUFA	0	1,050	1,020

Since only the seal oil contained squalene (12.5 mg/500 mg seal oil capsule), the fish oil and placebo group participants were given one 875 mg squalene capsule per week (equivalent to the seal group intake of 125 mg/day), to equalise squalene intakes within the groups.

It should be noted that seal oil also contains 0.3 mg/100 g vitamin A and 4.5 mg/100 g alpha-tocopherol [32], whereas tuna-fish oil contains less than 10 International Units of vitamin A and 0.21% of mixed natural tocopherols (NuMega Ingredients Ltd., Sydney).

All subjects initially completed a 7-day weighed food record to provide baseline nutrient values. Fasting blood was collected from each subject at day 0 and day 14 of the trial. Samples were analysed for whole blood platelet aggregation and adenosine triphosphate (ATP) release from platelet-dense granules. A full blood examination provided a platelet count and mean platelet volume (MPV). Platelet activation markers were measured using flow cytometry, and inflammation assessed via plasma C-reactive protein (CRP). A full blood lipid profile provided plasma total cholesterol, HDL-cholesterol, LDL-cholesterol and triacylglycerol levels, and platelet fatty acid content was assessed.

Dietary Analyses

The baseline nutrient intakes were determined using the software package FoodWorks (Xyris Software, Australia). Baseline fatty acid intakes were assessed using the RMIT University Fatty Acid Database available on FoodWorks.

Blood Collection

Subjects were requested to fast overnight (12–14 h), then blood was taken in the laboratory between 0700–0800 hours on days 0 and 14 of supplementation. To reduce platelet activation from venipuncture, subjects were carefully bled without a tourniquet. A 21-gauge needle was employed to collect blood into Greiner Bio-one Vacutainers (Interpath Services, Victoria, Australia) in the following sequence: one 2-mL tri-potassium ethylene-diamine-tetra acetic acid (EDTA) (1.8 mg/mL) tube, two 5-mL tri-sodium citrate (3.8%) tubes, and one 10-mL serum separator tube. Handling and agitation of specimens were kept to a minimum.

Platelet Function Tests

Mean platelet volume (MPV) and platelet count were measured by using whole blood collected in EDTA-containing tubes with the use of a Beckman Coulter $A^c.T^{TM}$ 5diff analyser (Coulter Corporation, Miami, FL, USA), within 20 min of venipuncture**.** The performance of the analyser was validated daily, prior to full blood examination (FBE), using Coulter Calibrator and Controls Plus.

Blood collected in citrate-containing tubes was used to determine the extent of platelet aggregation and to measure the release of ATP from platelets. Whole blood platelet aggregation was measured within 1 h of venipuncture with an impedance aggregometer (Chrono-Log Corp, Philadelphia) equipped with MacLab software (ADInstruments Pty, Ltd, Castle Hill, Australia) for data quantisation and analysis. This method has been previously described by Murphy et al. [33]. Calibrations for impedance and ATP release were performed daily before analysing blood samples. Briefly, citrated whole blood was diluted with saline (1:1), 100 μL Chrono-lume® reagent (Chrono-Log Corp, Philadelphia) was added, the sample was then incubated, and mixed with agonists, either 2 μg collagen/mL [Chrono-Log Corp] or 1 mmol arachidonic acid/L (which was used to stimulate platelets for repeating the aggregation as a check for anti-inflammatory intake). Aggregation was recorded for 6 min. ATP released from the platelets reacted with luciferin-luciferase in the Chrono-Lume reagent and luminescence was measured at 650 nm by a photomultiplier tube (PMT) within the aggregometer, simultaneously with platelet aggregation.

Additional aliquots of citrated whole blood were used for measuring platelet activation. Whole blood was diluted with modified Tyrode's buffer and incubated for 5 min in the presence of 2 μg collagen/mL. Subsequently, aliquots of activated blood were incubated in the dark with monoclonal antibodies: phycoerythrin-conjugated CD41 (Immunotech, Marseille; which was used to identify platelets because it has specificity for the glycoprotein IIb portion of the glycoprotein IIb-IIIa antigen present on resting and activated platelets); fluorescein isothiocyanate-conjugated CD62P (Immunotech, Marseille; an activation-dependent antibody directed against P-selectin, a component of the α-granule membrane of resting platelets that becomes expressed on the platelet surface membrane upon activation); or one of the isotype controls, immunoglobulin G_1 (IgG_1). Samples were fixed with paraformaldehyde and incubated to prevent further artifactual in vitro platelet activation. Modified Tyrode's buffer was added to terminate the fixation, and samples were analysed on an EPICS Elite flow cytometer (Coulter Electronics) equipped with a 15-mW argon laser, with excitation at 488 nm. The fluorescence of fluorescein isothiocyanate and phycoerythrin was detected using 525 and 575 nm band pass filters, respectively. Single platelets were identified by gating on both phycoerythrin positivity (CD41 binding) and characteristic light scatter. (Because single platelets are smaller and less complex than other blood cells, including aggregated platelets, their forward scatter and side scatter are lower in comparison with other cells.) Once identified, the expression of P-selectin was determined by analysing 20,000 free platelets, collected at a rate of between 1,300 and 1,600 events/s. Activated platelets were defined as CD41-positive events that expressed P-selectin. The data are reported as a proportion of maximum CD62P expression.

C-Reactive Protein and Lipid Profile

Serum was separated from blood collected in a serum separator tube and analysed at the St. Xavier Francis Cabrini Hospital (Malvern, Victoria, Australia) using an automated biochemical analyser (Olympus AU2700). Calibrators and controls (Biorad Liquichek™ human chemistry controls) were run routinely to validate the performance of this instrument.

Anti-CRP antibodies (goat) were employed to aggregate with CRP in serum. The immuno-turbidimetric method (polyethylene glycol with tris-aminomethane buffer) was utilized for analysing the absorbance of the aggregates that were proportional to the CRP concentration within the sample.

Total cholesterol was measured using an enzymatic assay system (Integrated Sciences Ltd., Sydney, Australia) which produced a chromophore (quinoneimine dye)

quantified at 520/600 nm. Triacyglycerols were measured using a multi-step enzymatic assay (Integrated Sciences Ltd, Sydney, Australia) that resulted in production and measurement of the same quinoneimine dye. Similarly, HDL-cholesterol was determined using an enzymatic colorimetry kit (Thermo Trace Ltd, Melbourne, Australia), with the product detected at 340 nm. LDL-cholesterol was calculated using the Freidewald calculation [34].

Platelet Fatty Acid Content

Platelet-rich plasma was obtained by centrifugation at 1,950 rpm for 5 min and then the supernatant spun again at 1,000 rpm for 20 min. The platelet fatty acids were determined at Flinders Medical Centre (Bedford Park, Adelaide, Australia), following trans-esterification, separation and quantification as fatty acid methyl esters using a Hewlett-Packard 6890 gas chromatograph equipped with a 50 m BPX-70 capillary column (0.32 mm ID, 0.25 μm film thickness) (SGE Pty Ltd Victoria, Australia) [35].

Statistics

Statistical analyses were performed using the statistical package SPSS, version 13.0 (SPSS Inc., USA). Student's paired t tests were used to test significance between baseline and post-trial samples within groups, and one-way analysis of variance (ANOVA) used to determine significance between groups. Regression analysis was performed using Microsoft Excel 2002 (Microsoft Corporation) to examine associations between selected parameters. A statistical significance of $P < 0.05$ was applied to all data.

Results

Subjects

Three of the original 30 subjects withdrew from the study due to time constraints or difficulty with phlebotomy, all coincidently members of the placebo group. Remaining subjects were reasonably well matched for age and weight (Table 3). Subjects' compliance was verified through capsule count. No side effects were recorded other than 'fishy burps' experienced by a few subjects from the fish and seal oil groups during supplementation. No subject reported ingestion of aspirin during the study and this was confirmed by normal platelet aggregation curves obtained using (AA) as an agonist.

Table 3 Descriptive characteristics of study participants in the three test groups at baseline ($n = 27$)

Demographic parameters	Placebo ($n = 7$)	Fish oil ($n = 10$)	Seal oil ($n = 10$)
Gender: female/male	5/2	5/5	8/2
Age (years)	29 ± 5 (23–36)	30 ± 8 (21–43)	31 ± 6 (23–41)
Weight (kg)	68 ± 17 (50–98)	72 ± 14 (48–88)	78 ± 14 (60–99)

Values are means ± SD (range). n is number of participants

Baseline Nutrient and Fatty Acid Intakes

Incomplete food intake data were obtained from three subjects (one placebo and two seal oil volunteers), so that these final values were provided by 6 subjects (5 female, 1 male) in the placebo group, 10 (5 male, 5 female) in the fish oil and 8 (7 female, 1 male) in the seal oil group.

The baseline dietary data for all three study groups were generally similar, with no significant differences except for alcohol consumption, which was high in the seal oil group due to the atypical intake of one subject (Table 4). Total fat consumption was of the order of 70–80 g/day for all groups.

Baseline fatty acid intakes, including background levels of intake of EPA, DPA and DHA, and of total LC n-3 PUFA (of the order of 0.10 g/day), were also similar in all treatment groups (Table 5).

Fatty Acid Incorporation into Platelet Phospholipids

Table 6 shows that while most mean platelet fatty acid concentrations did not change in the placebo group, there were unexpected increases of almost 10% in DHA and 7% in total LC n-3 PUFA ($P = 0.04$ for both) at day 14. Subjects in the fish oil group had decreased platelet levels of total saturated fatty acids (−5%, $P = 0.03$), and highly significant increases in DHA (+78%, $P \leq 0.001$) and total LC n-3 PUFA levels (+40%) ($P \leq 0.01$). An increase in platelet EPA (41%) approached significance ($P = 0.06$) in the fish oil group. Platelet arachidonic acid (AA) levels did not change in any group. In subjects who received the seal oil supplement, levels of several fatty acids changed significantly. A decrease in 16:0 (−4%) was observed ($P = 0.02$), as was a decrease in total monounsaturated fatty acids (−6%, $P = 0.01$). Total n-9 and total n-7 contents both decreased ($P = 0.04$ and $P = 0.01$, respectively). Platelet concentrations of EPA increased considerably with seal oil (+204%, $P = 0.000$), as did those of DPA (+49%, $P = 0.01$) and DHA (+51%, $P < 0.01$). Total LC n-3 PUFA increased by 63% ($P < 0.01$). Analysis by ANOVA showed that the change in total n-9 was unique to the seal

Table 4 Average baseline daily nutrient intakes of the study participants who then received supplementary placebo (sunola oil), tuna-fish oil or seal oil capsules

Nutrient (day^{-1})	Placebo ($n = 6$)[a]	Fish oil ($n = 10$)	Seal oil ($n = 8$)[a]
Energy (E) (kJ)	8,939 ± 2,675	8,452 ± 3,628	9,522 ± 2,475
Protein (g)	89.92 ± 25.92	81.17 ± 37.48	93.23 ± 29.12
Total fat (g)	82.23 ± 38.35	69.31 ± 34.68	80.40 ± 36.24
Saturated fatty acids (g)	35.88 ± 23.63	28.93 ± 14.77	30.65 ± 14.51
Monounsaturated fatty acids (g)	28.14 ± 11.31	24.03 ± 11.82	30.40 ± 13.54
Polyunsaturated fatty acids (g)	10.54 ± 2.74	10.31 ± 5.87	11.99 ± 5.68
Cholesterol (mg)	410.51 ± 296.08	244.32 ± 168.54	236.12 ± 77.60
Carbohydrate (g)	245.90 ± 58.12	246.35 ± 97.55	267.82 ± 55.80
Alcohol (g)	2.77 ± 3.79	7.41 ± 6.03	11.32 ± 5.59
Dietary fibre (g)	23.43 ± 5.21	22.01 ± 11.23	21.05 ± 5.80
Thiamin, B1 (mg)	1.54 ± 0.32	1.39 ± 0.62	1.43 ± 0.27
Riboflavin, B2 (mg)	2.34 ± 0.83	2.09 ± 1.03	1.98 ± 0.43
Niacin, B3 (mg)	18.30 ± 3.27	17.90 ± 7.51	19.81 ± 6.22
Vitamin C (mg)	152.92 ± 35.84	143.89 ± 107.41	126.64 ± 53.89
Folate (μg)	350.32 ± 70.43	303.64 ± 143.10	267.37 ± 58.75
Vitamin A (μg)	889.17 ± 314.94	840.03 ± 344.34	794.20 ± 304.18
Sodium (mg)	2,533.77 ± 621.64	2,501.37 ± 1124.27	2,778.42 ± 948.78
Potassium (mg)	3,346.85 ± 800.34	3,089.29 ± 1549.37	3,045.19 ± 707.63
Magnesium (mg)	321.72 ± 77.07	295.27 ± 144.15	294.68 ± 69.18
Calcium (mg)	1,083.68 ± 331.42	992.45 ± 508.74	945.07 ± 269.24
Phosphorus (mg)	1,582.82 ± 433.49	1,458.65 ± 729.69	1,514.06 ± 369.51
Iron (mg)	13.01 ± 2.25	11.44 ± 5.17	12.29 ± 3.47
Zinc (mg)	12.15 ± 4.03	11.13 ± 5.83	11.76 ± 3.06
Protein (%E)	17.55 ± 3.07	16.50 ± 1.76	16.79 ± 2.12
Fat (%E)	33.34 ± 5.03	30.16 ± 3.00	30.61 ± 6.75
Carbohydrate (%E)	48.10 ± 4.56	50.64 ± 5.49	49.01 ± 6.47
Alcohol (%E)	1.01 ± 1.48	2.71 ± 2.51	3.59 ± 1.93

Values are means ± SD

[a] Subject numbers were reduced because of incomplete dietary data (see text). Values were obtained from the following gender mix of subjects in the placebo, fish oil and seal oil groups: 5 female/1 male, 5 female/5 male, 7 female/1 male, respectively

group ($P = 0.04$). The unexpected increases in platelet DHA and total LC n-3 PUFA measured for the placebo group were significantly less than those observed for the fish and seal oil groups ($P < 0.01$). The increases in platelet EPA, DPA, DHA and total LC n-3 PUFA concentrations measured for the seal oil group were not matched by any other group (ANOVA: $P < 0.01$), except for DHA in the fish oil group.

Platelet Parameters

At baseline, there were no significant differences between groups for any platelet parameters, including LC n-3 PUFA levels. After 14 days' supplementation with placebo oil, fish oil or seal oil, no significant changes were observed in platelet volume (Table 7). An unexplained increase in platelet count was noted in the placebo (sunola) group, but fish oil and seal oil groups were unchanged. Platelet activation, determined by P-selectin (CD62p %) expression, decreased significantly after seal oil supplementation ($P = 0.01$), with no significant change in either the fish oil or placebo groups. ANOVA analysis confirmed a highly significant difference ($P < 0.01$) in effect on platelet activation between the seal oil group and the other two groups. Platelet aggregation was not significantly changed by supplementation in any of the three groups. An unexplained increase in platelet ATP release was induced by fish oil supplementation ($P = 0.02$), where the day 0–day 14 difference was approximately twice that observed in placebo and seal groups.

Because of the large effect of seal oil on platelet activation, platelet DPA, EPA and DHA levels were correlated with P-selectin expression. When the data pairs for all treatment groups at Day 0 and Day 14 of supplementation were pooled, there was no significant correlation between P-selectin and DPA ($P = 0.12$) or DHA ($P = 0.16$), but EPA and P-selectin were significantly negatively correlated ($P = 0.02$). When these Day 0 and Day 14 data were analysed separately, the baseline levels of EPA, DHA and DPA were not significantly associated with p-selectin levels. However, at Day 14 of supplementary treatment, a significant negative correlation was found between platelet p-selectin and both DPA ($P = 0.03$) and EPA levels ($P < 0.01$), but not DHA levels ($P = 0.13$) (Fig. 1).

Table 5 Average baseline daily fatty acid intakes (grams per day) for subjects who then consumed supplementary placebo (sunola oil), tuna-fish oil or seal oil capsules

Fatty acid	Placebo ($n = 6$)[a]	Fish oil ($n = 10$)	Seal oil ($n = 8$)[a]
C4:0	0.83 ± 0.69	0.62 ± 0.53	0.42 ± 0.24
C6:0	0.59 ± 0.50	0.45 ± 0.38	0.28 ± 0.17
C8:0	0.38 ± 0.28	0.35 ± 0.22	0.29 ± 0.18
C10:0	0.78 ± 0.61	0.64 ± 0.46	0.48 ± 0.28
C12:0	1.15 ± 0.63	1.35 ± 0.74	1.51 ± 0.96
C14:0	3.64 ± 2.43	3.09 ± 1.96	2.63 ± 1.26
C15:0	0.41 ± 0.28	0.32 ± 0.22	0.24 ± 0.13
C16:0	17.24 ± 9.14	13.68 ± 7.62	14.65 ± 5.61
C17:0	0.29 ± 0.16	0.26 ± 0.16	0.19 ± 0.11
C18:0	8.84 ± 6.43	6.63 ± 3.49	6.74 ± 2.70
C20:0	0.32 ± 0.25	0.22 ± 0.14	0.20 ± 0.10
C22:0	0.06 ± 0.07	0.04 ± 0.03	0.08 ± 0.05
C24:0	0.02 ± 0.03	0.02 ± 0.02	0.03 ± 0.02
C14:1	0.36 ± 0.22	0.33 ± 0.24	0.25 ± 0.11
C16:1n-7	1.45 ± 0.53	1.12 ± 0.69	1.27 ± 0.64
C17:1	0.04 ± 0.02	0.03 ± 0.03	0.03 ± 0.03
C18:1n-9	22.69 ± 8.71	18.89 ± 10.21	21.80 ± 6.81
C18:1t	0.03 ± 0.07	0.09 ± 0.24	0.10 ± 0.22
C20:1	0.11 ± 0.06	0.08 ± 0.05	0.14 ± 0.07
C18:2n-6	7.34 ± 2.37	6.87 ± 3.68	8.20 ± 2.15
C18:3n-3	0.84 ± 0.22	0.69 ± 0.36	0.96 ± 0.50
C20:4n-6 (AA)	0.10 ± 0.10	0.05 ± 0.04	0.07 ± 0.05
C20:5n-3 (EPA)	0.03 ± 0.04	0.03 ± 0.03	0.03 ± 0.01
C22:5n-3 (DPA)	0.02 ± 0.02	0.01 ± 0.01	0.01 ± 0.01
C22:6n-3 (DHA)	0.06 ± 0.07	0.06 ± 0.06	0.07 ± 0.02
Total n-6	7.46 ± 2.36	6.93 ± 3.71	8.27 ± 2.16
Total n-3	0.94 ± 0.26	0.79 ± 0.43	1.06 ± 0.51
Total LC[b] n-3 PUFA	0.11 ± 0.12	0.10 ± 0.09	0.10 ± 0.04

Values are means ± SD

[a] Subject numbers were reduced because of incomplete dietary data (see text). The gender mix for placebo, fish oil and seal oil groups was 5 female/1 male, 5 female/5 male, 7 female/1 male, respectively

[b] *LC* Long chain polyunsaturated fatty acids, >18 carbons

Blood Lipid Profile and C-Reactive Protein

Baseline blood lipid profile parameters (total cholesterol, HDL- and LDL-cholesterol, and triacylgylcerols) and C-reactive protein (CRP) levels did not differ significantly between groups (Table 7). At day 14 of supplementation, total cholesterol and LDL-cholesterol were unchanged compared to baseline in all treatment groups. HDL-cholesterol increased significantly ($P = 0.01$) after 14 days' of seal oil intake, and approached significance in the fish oil group ($P = 0.06$). This pattern was maintained in the triacylglycerol results, where a significant decrease was induced by seal oil supplementation ($P = 0.03$) but only a tendency to decrease was observed in the fish oil group ($P = 0.06$). CRP did not change significantly within any group.

Discussion

This study compared the effects of a 14-day supplementation with seal oil, tuna-fish oil or a monounsaturated vegetable (sunola) oil in healthy volunteers. The results indicated that relatively small supplements of approximately 5 g/day of seal oil and 3 g/day of tuna-fish oil (each containing approximately 1 g LC n-3 PUFA) were sufficient to induce significant increases in the total LC n-3 PUFA content of platelets. Both seal and fish oil induced highly significant increases in platelet DHA, even though the supplementary intake of this fatty acid was almost twice as great in the fish oil group. The pattern of increase in platelet EPA levels roughly followed the relative amounts of EPA supplied by the supplements: EPA increase with fish oil was almost significant ($P = 0.06$), whereas the seal oil supplement, which provided approximately 60% more EPA, induced a highly significant increase in platelet EPA ($P < 0.01$), possibly involving some retroconversion of DPA to EPA as observed by Kaur et al. [36] in a rat model. In addition, the higher levels of DPA present in the seal oil supplement were reflected in a significant rise in platelet DPA ($P < 0.01$), while the very small DPA content of the fish oil induced no change. An unexpected increase in platelet DHA and in total LC n-3

Table 6 Platelet fatty acid profiles (% of total fatty acids) of subjects on day 0 and day 14 of supplementary placebo (sunola oil), tuna-fish oil or seal oil capsule consumption

Fatty acid (FA)	Placebo ($n = 7$)			Fish Oil ($n = 10$)			Seal Oil ($n = 10$)			ANOVA[b]
	Day 0	Day 14	Diff[a]	Day 0	Day 14	Diff[a]	Day 0	Day 14	Diff[a]	*P* value
16:0	21.44 ± 1.40	20.84 ± 1.24	−0.60	22.37 ± 1.71	21.16 ± 1.13	−1.22	23.88 ± 1.68	22.99 ± 1.37	−0.90*	0.696
18:0	8.11 ± 0.93	7.97 ± 0.91	−0.14	8.42 ± 1.67	7.76 ± 0.89	−0.66	7.32 ± 0.96	7.62 ± 0.65	0.30	0.346
Total saturated FA	33.15 ± 1.57	32.67 ± 1.32	−0.49	34.90 ± 2.93	33.14 ± 1.88	−1.75*	35.04 ± 2.50	34.62 ± 1.45	−0.43	0.317
16:1n-7	1.85 ± 0.61	1.68 ± 0.58	−0.17	1.87 ± 0.50	1.68 ± 0.48	−0.20	3.01 ± 0.81	2.60 ± 0.68	−0.41*	0.549
18:1n-9	18.19 ± 1.60	19.06 ± 2.01	0.87	17.51 ± 1.84	16.76 ± 1.55	−0.75	18.69 ± 2.03	17.70 ± 1.68	−0.99*	0.056
Total MUFA[c]	22.61 ± 1.99	23.35 ± 2.33	0.75	22.04 ± 2.12	20.89 ± 1.90	−1.15	24.66 ± 2.63	23.26 ± 1.89	−1.40*	0.079
Total n-9	19.29 ± 1.59	20.27 ± 2.02	0.98	18.66 ± 1.76	17.94 ± 1.53	−0.72	19.90 ± 2.07	19.00 ± 1.65	−0.90*	0.043
Total n-7	3.31 ± 0.69	3.13 ± 0.62	−0.18	3.33 ± 0.52	3.02 ± 0.51	−0.32	4.80 ± 0.96	4.27 ± 0.77	−0.53*	0.415
18:2n-6	29.92 ± 3.77	29.17 ± 3.43	−0.74	27.24 ± 4.29	28.78 ± 4.10	1.54	24.92 ± 4.01	24.48 ± 2.05	−0.43	0.298
18:3n-3	0.64 ± 0.20	0.67 ± 0.14	0.02	0.58 ± 0.22	0.51 ± 0.18	−0.07	0.47 ± 0.17	0.46 ± 0.14	−0.01	0.702
20:4n-6 (AA)	7.02 ± 1.71	7.22 ± 0.41	0.20	7.89 ± 2.14	7.84 ± 1.82	−0.05	7.78 ± 1.39	8.18 ± 1.27	0.39	0.391
Total n-6	39.48 ± 3.02	38.99 ± 3.10	−0.48	37.67 ± 3.86	38.99 ± 3.03	1.33	35.71 ± 3.48	35.26 ± 2.23	−0.45	0.383
20:5n-3 (EPA)	0.67 ± 0.19	0.69 ± 0.23	0.02	0.92 ± 0.35	1.30 ± 0.43	0.38	0.54 ± 0.26	1.64 ± 0.47	1.10****	0.000
22:5n-3 (DPA)	0.56 ± 0.12	0.58 ± 0.12	0.02	0.70 ± 0.21	0.61 ± 0.11	−0.09	0.47 ± 0.15	0.70 ± 0.19	0.24**	0.001
22:6n-3 (DHA)	1.74 ± 0.38	1.91 ± 0.53	0.17*	1.87 ± 0.45	3.32 ± 0.58	1.45***	1.92 ± 0.46	2.89 ± 0.55	0.96****	0.001
Total LC n-3 PUFA	3.84 ± 0.53	4.10 ± 0.76	0.27*	4.31 ± 0.85	6.04 ± 1.03	1.73**	3.65 ± 0.49	5.95 ± 0.90	2.30****	0.002

Values are means ± SD. * $P < 0.05$, ** $P < 0.01$, *** $P < 0.005$, **** $P < 0.0001$ for differences between 0 and 14 days, within-group analysis, paired two-tail *t* test

n number of participants in groups

[a] Mean difference between day 0 and day 14 values

[b] Between-group ANOVA of changes in platelet fatty acid concentrations

[c] Monounsaturated Fatty acids

Table 7 Platelet and serum parameters in subjects on day 0 and day 14 of consumption of supplementary placebo (sunola oil), tuna-fish oil or seal oil capsules

Fatty acid (FA)	Placebo ($n = 7$)			Fish Oil ($n = 10$)			Seal Oil ($n = 10$)			ANOVA[b]
	Day 0	Day 14	Diff[a]	Day 0	Day 14	Diff[a]	Day 0	Day 14	Diff[a]	*P* value
Platelet volume (MPV, fL)	7.90 ± 0.47	8.07 ± 0.65	0.17	8.50 ± 0.70	8.53 ± 0.65	0.03	8.10 ± 0.79	8.25 ± 0.75	0.15	0.647
Platelet count ($\times 10^9$ L^{-1})	243.3 ± 48.9	266.0 ± 56.8	22.7*	202.2 ± 65.9	211.2 ± 73.7	9.0	232.1 ± 42.7	236.4 ± 48.9	4.3	0.308
Platelet activation (P selectin expression, %)	7.80 ± 9.78	16.36 ± 8.52	9.24	10.75 ± 5.38	13.13 ± 7.59	2.38	5.90 ± 5.83	0.24 ± 0.45	−5.66*	0.008
Platelet aggregation (s)	25.27 ± 3.03	22.87 ± 4.47	−2.39	24.54 ± 5.49	27.50 ± 4.80	2.97	25.61 ± 4.79	23.71 ± 5.51	1.90	0.094
Slope (Ω/s)	0.184 ± 0.034	0.213 ± 0.067	0.028	0.174 ± 0.059	0.184 ± 0.049	0.010	0.189 ± 0.036	0.181 ± 0.042	−0.008	0.139
Platelet ATP release (μM)	2.06 ± 1.53	3.05 ± 1.69	0.99	0.85 ± 0.70	2.61 ± 1.77	1.77*	2.09 ± 2.46	3.08 ± 1.14	0.99	0.658
Cholesterol (mmol/L)	5.01 ± 1.22	4.87 ± 0.98	−0.14	5.15 ± 0.91	5.18 ± 0.89	0.03	5.01 ± 0.52	5.06 ± 0.65	0.05	0.597
LDL-cholesterol (mmol/L)	2.84 ± 1.03	2.67 ± 0.89	−0.18	3.07 ± 0.78	3.17 ± 0.82	0.09	2.87 ± 0.53	2.96 ± 0.62	0.09	0.316
HDL-cholesterol (mmol/L)	1.61 ± 0.41	1.63 ± 0.34	0.02	1.51 ± 0.25	1.56 ± 0.26	0.06	1.42 ± 0.19	1.56 ± 0.17	0.14*	0.179
Triacylglycerol (mmol/L)	1.23 ± 0.50	1.26 ± 0.54	0.03	1.25 ± 0.65	0.99 ± 0.45	−0.26	1.58 ± 0.52	1.18 ± 0.37	−0.40*	0.096
C-reactive protein (CRP) (mg/dL)	0.71 ± 0.76	1.00 ± 1.00	0.29	1.70 ± 1.70	1.50 ± 1.51	−0.20	6.80 ± 7.89	5.10 ± 5.67	−1.70	0.078

Values are means ± SD. * $P < 0.05$ for differences between 0 and 14 days, within-group analysis, paired two-tail *t* test

n number of participants in groups

[a] Mean difference between day 0 and day 14 values

[b] Between-group ANOVA of changes in platelet and serum parameters

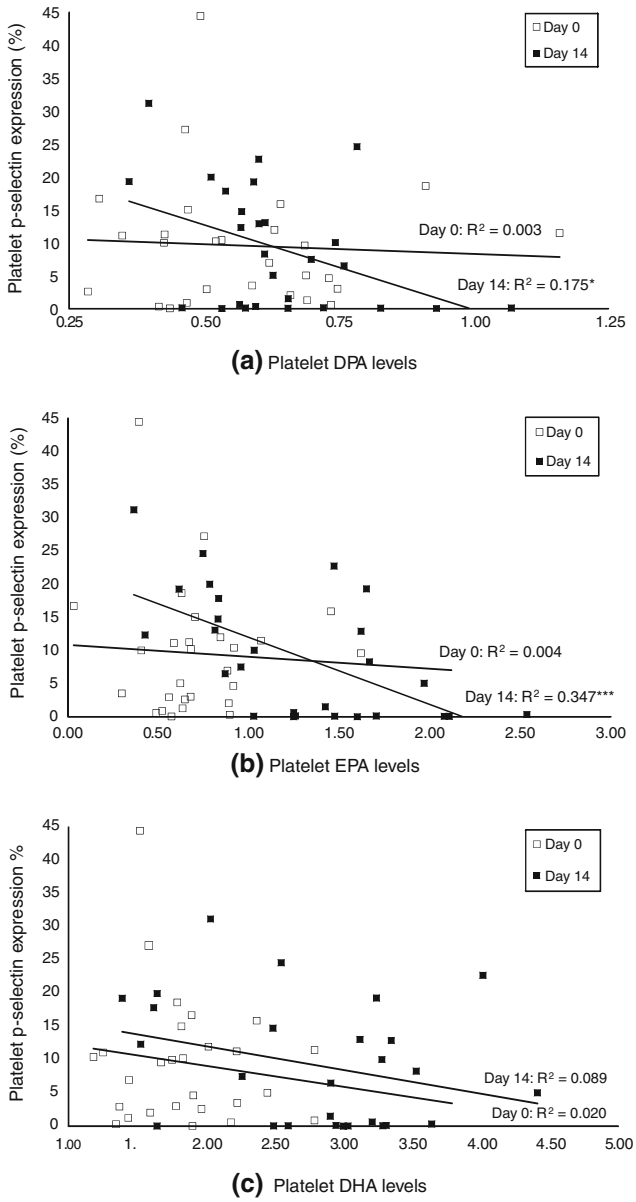

Fig. 1 Correlations between platelet levels of **a** DPA, **b** EPA, and **c** DHA (% of total FA) and platelet activation (P-selectin expression, %) for the pooled treatment groups (placebo/sunola oil, fish oil and seal oil) at day 0 and day 14 of supplementation. (*$P < 0.05$, ***$P < 0.005$ for Pearson's product moment)

PUFA was recorded for the placebo group, despite no DHA or alpha-linolenic (18:3n-3) acid being present in the placebo (sunola) oil. Similarly, there was a significant rise in platelet DHA levels in the seal oil group, despite the low concentration of DHA in the seal oil, most likely due to further desaturation of the DPA as seen in other studies [36].

Although both EPA and DHA have been shown to competitively displace AA from platelet phospholipids [11], AA levels did not change in this study with either seal or fish oil supplement, perhaps because of the relatively low dosages consumed. However, significant decreases in the cumulative content of platelet n-7 and n-9 fatty acids, as well as total MUFA, following seal oil intake were very likely due to displacement by the supplementary LC n-3 PUFA in the platelets. Interestingly, such changes were not seen with the tuna-fish oil, which contained the same total amount of LC n-3 PUFA but twice the DHA content and 60% of the EPA content of seal oil. Instead, fish oil induced a significant decrease in total saturated FA that was not observed with seal oil, suggestive of a preferential displacement of saturated FA in the platelets by DHA. As the overall total amount of n-6 fatty acids did not change significantly with fish or seal oil supplementation whilst total LC n-3 PUFA increased, both the fish oil and seal oil intakes induced a decrease in the n-6/n-3 ratio, also observed following 20 g/day seal oil treatment [29]. Such a reduction in platelet n-6/n-3 (LC PUFA) ratio is generally considered beneficial for the prevention of CVD [37], although a large study indicated that having a higher intake of n-3 PUFA is more critical for the prevention of coronary heart disease than the relative level of n-6 intake [38].

The most important finding in response to seal oil supplementation in this study was a significant reduction in platelet activation, as determined by platelet p-selectin expression. In contrast, fish oil supplementation did not affect this factor, although EPA has previously been shown to decrease platelet activation [17]. Rather, an unexpected increase in platelet ATP release, a promoter of platelet activation, was observed with fish oil consumption ($P = 0.02$). Although the dose of EPA in the fish oil (0.21 g/day) was less than that in the seal oil (0.34 g/day) the strength of the response to seal oil suggests that DPA along with EPA may be having a potent suppressive effect upon platelet activation, or the retroconversion of DPA to EPA is resulting in sufficient EPA to affect platelet surface activity. The finding of an inverse correlation between platelet activation and platelet DPA levels agrees well with the inhibitory effect on platelet reactivity previously observed with DPA treatment in vitro [26]. A lack of change in platelet activation with the fish oil treatment is consistent with its high DHA content (77%) and lesser EPA and DPA content compared to seal oil (Table 2), since DHA seems to have no association with p-selectin. At higher dosages of fish oil, the larger quantities of EPA might eventually result in depressed platelet activation, since we also found a negative correlation between platelet EPA levels and platelet P-selectin expression. Others have previously concluded that EPA but not DHA reduces platelet activation [39].

The lack of significant change in platelet aggregation with either seal oil or fish oil is not unexpected given the low doses used in this study; it echoes one result found with a 20-g dose of seal oil given to healthy males [29], but

not a later study which did find that 15 mL seal oil suppressed platelet aggregation in mixed gender subjects with mild hypercholesterolemia [40]. In the present study, as the DPA/EPA-rich seal oil supplementation was shown to decrease one aspect of platelet activation, we might have expected it to decrease platelet aggregation in turn, but this process may have required longer than 14 days or a higher dose of LC n-3 PUFA to reach significance. Others have reported that EPA and DHA appeared to have anti-platelet aggregation effects in vitro through differing actions on thromboxane production in platelets [11, 41]. However, thromboxane-induced aggregation was more potently blocked by DHA than EPA [41]. In vitro studies testing each of these LC n-3 PUFA individually demonstrated that DPA had a potent dose-dependant effect on collagen or AA-stimulated aggregation superior to that of DHA or EPA, which were very similar in effect [27]. The authors speculated that DPA has a potent effect which results in interference with the cyclooxygenase pathway and acceleration of the lipoxygenase pathway to inhibit aggregation [27]. Inhibition of collagen-induced aggregation and preservation of platelet morphology by DPA appears to be surface-mediated, as with DHA [26]. Evidence also exists for gender differences in in vitro platelet aggregation responses to LC n-3 PUFA [42], with EPA effectively decreasing platelet aggregation in blood from healthy males and females, while both DPA and DHA were significantly less effective in males compared with females.

In this study, the seal oil supplement also produced another outcome protective of CVD: a significant increase in HDL-cholesterol that was not observed with the fish oil. When Buckley et al. [43] compared the effects of 4.8 g/day EPA or DHA in normal adults, they found no effects on HDL-cholesterol. In contrast, supplementation with 2.4 g/day of EPA plus 1.6 g/day DHA (a combined total of 4 g/day, with exercise) induced increases in HDL-cholesterol [44] in a dose-dependent manner resembling the effects of fish consumption [16]. In our study, lack of significant change in HDL-cholesterol with the fish oil may reflect the considerably lower content of EPA (210 mg/day) plus DHA (810 mg/day) (i.e. 1.02 g/day combined) provided in this supplement. However, the combined dose of these FAs in the seal oil was even lower at 0.790 g/day (EPA 340 mg/day, DHA 450 mg/day), suggesting that it may be the 230 mg/day DPA that positively affected HDL-cholesterol in our participants, even at this low supplementary dose. In view of this result, it is difficult to explain why HDL-cholesterol did not change in two previous investigations with seal oil [29, 45], one involving a very large (20 g/day) oil supplement [29]. Confusingly, subjects given pure seal oil and those who received cod liver oil (rich in EPA and DHA) did not show a change in HDL-cholesterol, yet this factor increased significantly after supplementation with the same volume of a combination of seal oil and cod liver oil [45]. This almost suggests a synergistic effect of DPA and EPA, or else that the amount of EPA present in the combination oil dose reached a level which effected a detectable change.

Modest decreases in serum total cholesterol have been described after seal oil supplementation [12], but we observed no changes in either total cholesterol or LDL-cholesterol, in line with some other studies [29, 45]. Supplementary fish oil has previously been shown to decrease both total and LDL-cholesterol in patients at risk of CVD [13, 46], but this was not the case in our study of healthy volunteers taking relatively small dosages of tuna-fish oil. Larger doses or longer periods of supplementation may be necessary to see beneficial changes in lipid profile in healthy subjects. However, the ratio of HDL-cholesterol: LDL-cholesterol is generally considered more indicative of risk of CVD than total cholesterol levels, with a higher ratio reducing the risk of atherosclerotic heart disease [4]. As HDL-cholesterol increased significantly in our subjects receiving seal oil supplement, their corresponding HDL-cholesterol: LDL-cholesterol ratios must have shifted favourably.

Elevated triacylglycerols are a risk factor for CVD, and the seal oil supplementation induced a significant reduction in triacylglycerols. This agrees with some other findings in healthy subjects investigating seal oil [12, 47], but not all [29]. Intriguingly, combined seal oil/cod liver oil treatment reportedly decreased subject triacylglycerol levels where pure seal oil or cod liver oil did not [45], even at almost three times the dose of this study. The same modest seal oil dose as we have described, given over 6 weeks, also resulted in a significant decrease in plasma triacylglycerols as well as a significant improvement in blood pressure in hypertriglyceridaemic subjects, without a change in HDL-cholesterol [48]. In the present work, tuna-fish oil supplementation caused a non-significant ($P = 0.06$) decrease in triacylglycerols. The seal oil and fish oil both supplied approximately 1 g/day LC n-3 PUFA to the healthy volunteers, so the higher levels of DPA and/or of EPA in seal oil may be responsible for its greater effect on HDL-cholesterol and triacylglycerol levels. Buckley et al. [43] found a decrease in triacylglycerols in healthy subjects with DHA-rich but not EPA-rich oil supplementation. The DHA-rich oil they used contained six times the amount of DPA as the EPA-rich oil, which adds support to our speculation that DPA rather than EPA is the component in the (low-DHA) seal oil active in reducing triacylglycerol levels. Proposed mechanisms for decreases in triacylglycerol with LC n-3 PUFA involve chylomicron triacylglycerol clearance [49] and reduced absorption and synthesis of hepatic triacylglycerols and their increased catabolism [50]. Animal studies have specifically indicated that DPA may decrease triacylglycerols through a decrease in fatty acid synthesis [51].

Levels of inflammation, as indicated by CRP in this healthy volunteer population, were not significantly changed by any of the supplementary oils, an outcome shared by other studies [52]. However, recent work with high sensitivity-CRP showed a negative correlation between this surrogate marker of CVD risk and plasma total n-3 FA levels, as well as plasma EPA and DPA levels, in a larger subject population [53].

In conclusion, DPA in a low-dose seal oil supplement appeared to induce changes protective of cardiovascular health in healthy subjects. This relatively little-investigated LC n-3 PUFA appears to have acted (alone or with EPA) to depress platelet activation at the same time as it increased serum HDL-cholesterol and decreased triacylglycerol levels. The beneficial effects of the seal oil supplementation were greater than those of tuna-fish oil, which contained a similar amount of total LC n-3 PUFA but much more DHA, less EPA, and minimal DPA. Our results suggest that DPA, either directly or through retroconversion to EPA, may be more efficient at reducing some CVD risk factors than DHA. Larger and perhaps longer controlled studies, ideally using purified EPA, DPA and DHA in isolation, are needed to determine the mechanisms of DPA effects on platelet function particularly at different dosages in comparison with those of EPA and DHA. In the interim, this study suggests that seal oil may already be of use in modified foods, as a prophylactic for healthy individuals or as an aid to treatment for those with CVD or thrombosis. The current findings also have implications for consumers favouring meat over fish meals, as it appears that lean red meat, cooked appropriately using unsaturated fats, could provide beneficial amounts of DPA and EPA, without compromising cardiovascular health.

Acknowledgments We gratefully acknowledge the time and effort contributed by the study volunteers. This study was funded through a research grant from Meat & Livestock Australia (MLA).

References

1. Australian Bureau of Statistics (2008) Causes of Death 2006. Publication No. 3303.0. Australian Bureau of Statistics, Government Publisher, Canberra, Australia
2. De Lorgeril M (2007) Essential polyunsaturated fatty acids, inflammation, atherosclerosis and cardiovascular diseases. Subcell Biochem 42:283–297
3. Australian Institute of Health, Welfare (AIHW) (2004) Heart, stroke and vascular diseases: Australian facts 2004 (Cardiovascular Disease Series No. 22). Australian Institute of Health and Welfare and National Heart Foundation of Australia, Canberra
4. Wierzbicki AS (2005) Have we forgotten the pivotal role of high-density lipoprotein cholesterol in atherosclerosis prevention? Curr Med Res Opin 21:299–306
5. Pentikainen MO, Oorni K, Ala-Korpela M, Kovanen PT (2000) Modified LDL—trigger of atherosclerosis and inflammation in the arterial intima. J Intern Med 247:359–370
6. Colwell J (2000) Pathogenesis of vascular disease. Diabetes Obes Metab 2(Suppl 2):S19–S24
7. Rivera J, Lozano ML, Navarro-Nūňez L, Vicente V (2009) Platelet receptors and signalling in the dynamics of thrombus formation. Haematologica. (in press)
8. Ruggeri ZM (2002) Platelets in atherothrombosis. Nat Med 8:1227–1234
9. Fabre JE, Nguyen M, Athirakul K, Coggins K, McNeish JD, Austin S, Parise LK, FitzGerald GA, Coffman TM, Koller BH (2001) Activation of the murine EP3 receptor for PGE2 inhibits cAMP production and promotes platelet aggregation. J Clin Invest 107:603–610
10. Massaro M, Scoditti E, Carluccio MA, De Caterina R (2008) Basic mechanisms behind the effects of n-3 fatty acids on cardiovascular disease. Prostaglandins Leukot Essent Fatty Acids 79:109–115
11. Kinsella JE, Lokesh B, Stone RA (1991) Dietary n-3 polyunsaturated fatty acids and amelioration of cardiovascular disease: possible mechanisms. Am J Clin Nutr 53:177–178
12. Deutch B, Jørgensen E, Hansen J (2000) N-3 PUFA from fish or seal oil reduce atherogenic risk indicators in Danish women. Nutr Res 20:1065–1077
13. Pirich C, Gaszo A, Granegger S, Sinzinger H (1999) Effects of fish oil supplementation on platelet survival and ex vivo platelet function in hypercholesterolemic patients. Thromb Res 96:219–227
14. Albert CM, Hennekens CH, O'Donnell CJ, Ajani UA, Carey VJ, Willett WC, Ruskin JN, Manson JE (1998) Fish consumption and risk of sudden cardiac death. JAMA 279:23–28
15. Weber P, Raederstorff D (2000) Triglyceride-lowering effect of omega-3 LC–polyunsaturated fatty acids: a review. Nutr Metab Cardiovasc Dis 10:28–37
16. Dewailly E, Blanchet C, Gingras S, Lemieux S, Holub BJ (2003) Fish consumption and blood lipids in three ethnic groups in Québec (Canada). Lipids 38:359–365
17. Nomura S, Kanazawa S, Fukuhara S (2003) Effects of eicosapentaenoic acid on platelet activation markers and cell adhesion molecules in hyperlipidemic patients with Type 2 diabetes mellitus. J Diabetes Complicat 17:153–159
18. Nomura S, Inami N, Shouzu A, Omoto S, Kimura Y, Takahashi N et al (2009) The effects of pitavastatin, eicosapentaenoic acid and combined therapy on platelet-derived microparticles and adiponectin in hyperlipidemic, diabetic patients. Platelets 20:16–22
19. Harris WS, Miller M, Tighe AP, Davidson MH, Schaefer EJ (2008) Omega-3 fatty acids and coronary heart disease risk: clinical and mechanistic perspectives. Atherosclerosis 197:12–24
20. Howe PRC, Meyer BJ, Record S, Baghurst K (2003) Contribution of red meat to dietary intakes of polyunsaturated fatty acids. Confidential Report to meat and livestock Australia
21. Astorg P, Arnault N, Czernichow S, Noisette N, Galan P, Hercberg S (2004) Dietary intakes and food sources of n-6 and n-3 PUFA in French adult men and women. Lipids 39:527–535
22. Hino A, Adachi H, Toyomasu K, Yoshida N, Enomoto M, Hiratsuka A, Hirai Y, Satoh A, Imaizumi T (2004) Very long chain n-3 fatty acid intake and carotid atherosclerosis: an epidemiological study evaluated by ultrasonography. Atherosclerosis 176:145–149
23. Joensen AM, Schmidt EB, Dethlefsen C, Johnsen SP, Tjønneland A, Rasmussen LH, Overvad K (2010) Dietary intake of total marine n-3 polyunsaturated fatty acids, eicospentaenoic acid, docosahexaenoic acid and docosapentaenoic acid and the risk of acute coronary syndrome—a cohort study. Br J Nutr 103:602–607
24. Howe P, Meyer B, Record S, Baghurst K (2006) Dietary intake of long-chain omega-3 polyunsaturated fatty acids: contribution of meat sources. Nutrition 22:47–53

25. McLennan W, Podger A (1997) National Nutrition Survey, Selected Highlights, Australia. Australian Government Publishing Service, Canberra
26. Cheryk LA, Conquer JA, Holub PA, Gentry PA (1999) Docosahexaenoic acid and docosapentaenoic acid incorporation into human platelets after 24 and 72 hours: Inhibitory effects on platelet reactivity. Platelets 10:203–211
27. Akiba S, Murata T, Kitatani K, Sato T (2000) Involvement of lipoxygenase pathway in docosapentaenoic acid-induced inhibition of platelet aggregation. Biol Pharm Bull 23:1293–1297
28. Rissanen T, Voutilainen S, Nyyssönen K, Lakka TA, Salonen JT (2000) Fish oil-derived fatty acids, docosahexaenoic acid and docosapentaenoic acid, and the risk of acute coronary events: the Kuopio Ischaemic Heart Disease Risk Factor Study. Circulation 102:2677–2679
29. Conquer JA, Cheryk LA, Chan E, Gentry PA, Holub BJ (1999) Effect of supplementation with dietary seal oil on selected cardiovascular risk factors and hemostatic variables in healthy male subjects. Thromb Res 96:239–250
30. Bjørkkjaer T, Brunborg LA, Arslan G, Lind RA, Brun JG, Valen M, Klementsen B, Berstad A, Frøyland L (2004) Reduced joint pain after short-term duodenal administration of seal oil in patients with inflammatory bowel disease: comparison with soy. Scand J Gastroenterol 39:1088–1094
31. Arslan G, Brunborg LA, Frøyland L, Brun JG, Valen M, Berstad A (2002) Effects of duodenal seal oil administration in patients with inflammatory bowel disease. Lipids 37:935–940
32. Brunborg LA, Madland TM, Lind RA, Arslan G, Berstad A, Frøyland L (2008) Effects of short-term oral administration of dietary marine oils in patients with inflammatory bowel disease and joint pain: a pilot study comparing seal oil with cod liver oil. Clin Nutr 27:614–622
33. Murphy KJ, Chronopoulos AK, Singh I, Francis MA, Moriarty H, Pike MJ, Turner AH, Mann NJ, Sinclair AJ (2003) Dietary flavanols and procyanidin oligomers from cocoa (*Theobroma cacao*) inhibit platelet function. Am J Clin Nutr 77:1466–1473
34. Freidewald WT, Levy RI, Fredrickson DS (1972) Estimation of the concentration of LDL-cholesterol in plasma without the use of the preparative ultracentrifuge. Clin Chem 18:499–502
35. Blank C, Neumann MA, Makrides M, Gibson RA (2002) Optimizing DHA levels in piglets by lowering the linoleic acid to alpha-linolenic acid ratio. J Lipid Res 43:1537–1543
36. Kaur G, Begg D, Barr D, Garg M, Cameron-Smith D, Sinclair A (2010) Short-term docosapentaenoic acid (22:5 n-3) supplementation increases tissue docosapentaenoic acid, DHA and EPA concentrations in rats. Br J Nutr 103(1):32–37
37. Russo GL (2009) Dietary n-6 and n-3 polyunsaturated fatty acids: from biochemistry to clinical implications in cardiovascular prevention. Biochem Pharmacol 77:937–946
38. Mozaffarian D, Ascherio A, Hu FB, Stampfer MJ, Willet WC, Siscovick DS, Rimm EB (2005) Interplay between different polyunsaturated fatty acids and risk of coronary heart disease in men. Circulation 111:157–164
39. Park Y, Harris W (2002) EPA, but not DHA, decreases mean platelet volume in normal subjects. Lipids 37:941–946
40. Brox J, Olaussen K, Osterud B, Elvevoll EO, Bjørnstad E, Brattebøg G, Iversen H (2001) A long-term seal- and cod-liver-oil supplementation in hypercholesterolemic subjects. Lipids 36:7–13
41. Swann PG, Venton DL, Le Breton GC (1989) Eicosapentaenoic acid and docosahexaenoic acid are antagonists at the thromboxane A2/prostaglandin H2 receptor in human platelets. FEBS Lett 243:244–246
42. Phang M, Garg ML, Sinclair AJ (2009) Inhibition of platelet aggregation by omega-3 polyunsaturated fatty acids is gender-specific—redefining platelet response to fish oils. Prostaglandins Leukot Essent Fatty Acids 81:35–40
43. Buckley R, Shewring B, Turner R, Yaqoob P, Minihane AM (2004) Circulating triacylglycerol and apoE levels in response to EPA and docosahexaenoic acid supplementation in adult human subjects. Br J Nutr 92:477–483
44. Thomas TR, Smith BK, Donahue OM, Altena TS, James-Kracke M, Sun GY (2004) Effects of omega-3 fatty acid supplementation and exercise on low-density lipoprotein and high-density lipoprotein subfractions. Metabolism 53:749–754
45. Osterud B, Elvevoli E, Barstad H, Brox J, Halvorsen H, Lia K et al (1995) Effect of marine oils supplementation on coagulation and cellular activation in whole blood. Lipids 30:1111–1118
46. Wilkinson P, Leach C, Ah-Sing EE, Hussain N, Miller GJ, Millward DJ, Griffin BA (2005) Influence of [alpha]-linolenic acid and fish-oil on markers of cardiovascular risk in subjects with an atherogenic lipoprotein phenotype. Atherosclerosis 181:115–124
47. Bonefeld-Jorgensen EC, Moller SM, Hansen JC (2001) Modulation of atherosclerotic risk factors by seal oil: a preliminary assessment. Int J Circumpolar Health 60:25–33
48. Myer BJ, Lane AE, Mann NJ (2009) Comparison of seal oil to tuna oil on plasma lipid levels and blood pressure in hypertriglyceridaemic subjects. Lipids 44:827–835
49. Park Y, Harris WS (2003) Omega-3 fatty acid supplementation accelerates chylomicron triglyceride clearance. J Lipid Res 44:455–463
50. Malle E, Kostner G (1993) Effects of fish oil on lipid variables and platelet function indices. Prostaglandins Leuko Essent Fatty Acids 49:645–663
51. Yoshida H, Mawatari M, Ikeda I, Imaizumi K, Seto A, Tsuji H (1999) Effect of dietary seal and fish oils on triacylglycerol metabolism in rats. J Nutr Sci Vitaminol (Tokyo) 45:411–421
52. Balk EM, Lichstenstein AH, Chung M, Kupelnick B, Chew P, Lau J (2006) Effects of omega-3 fatty acids on serum markers of cardiovascular disease risk: a systematic review. Atherosclerosis 189:19–30
53. Micallef MA, Munro IA, Garg ML (2009) An inverse relationship between plasma n-3 fatty acids and C-reactive protein in healthy individuals. Eur J Clin Nutr 63:1154–1156

Lipids (2010) 45:683–692
DOI 10.1007/s11745-010-3430-3

ORIGINAL ARTICLE

Decreasing the Linoleic Acid to α-Linolenic Acid Diet Ratio Increases Eicosapentaenoic Acid in Erythrocytes in Adults

Michelle Wien · Sujatha Rajaram · Keiji Oda · Joan Sabaté

Received: 3 February 2010 / Accepted: 6 May 2010 / Published online: 22 May 2010

Abstract The n-6/n-3 fatty acid (FA) ratio has increased in the Western-style diet to ~10–15:1 during the last century, which may have contributed to the rise in cardiovascular disease (CVD). Prior studies have evaluated the effects on CVD risk factors of manipulating the levels of n-6 and n-3 FA using food and supplements or investigated the metabolic fate of linoleic acid (LNA) and α-linolenic acid (ALA) by varying the n-6/n-3 ratios. However, no previous studies have investigated the potential interaction between diet ratios and supplementation with eicosapentaenoic acid (EPA, 20:5n-3) and docosahexaenoic acid (DHA, 22:6n-3). We used a factorial design approach with adults ($n = 24$) in a controlled feeding trial to compare the accretion of EPA and DHA into red blood cell membranes (RBC) by adding a direct source (algal oil supplement) of EPA and DHA in a diet with a 10:1 versus 2:1 ratio of n-6/n-3 FA. Subjects were randomized into 8-week crossover diet sequences and each subject consumed three of four diets [10:1, 10:1 plus supplement (10:1 + S), 2:1 and 2:1 + S]. LNA and ALA intakes were 9.4 and 7.7%, and 1.0 and 3.0% during the low and high ALA diets, respectively. Compared to the Western-style 10:1 diet, the 2:1 diet increased EPA by 60% ($P < 0.0001$) in RBC membranes without the direct EPA source and a 34% increase ($P = 0.027$) was observed with the 10:1 + S diet; however, DHA levels increased in both diet ratios only with a direct DHA source. Shifting towards a 2:1 diet is a valid alternative to taking EPA-containing supplements.

Keywords n-3 Fatty acids · n-6 Fatty acids · Docosahexaenoic acid · Fish oil · Fatty acid modifications · Algal lipids · Adult · Human

Abbreviations

ANOVA	Analysis of variance
ALA	Alpha-linolenic acid
ARA	Arachidonic acid
BMI	Body mass index
DGLA	Dihomo-gamma-linolenic acid
DHA	Docosahexaenoic acid
DPA	Docosapentaenoic acid
EPA	Eicosapentaenoic acid
FA	Fatty acid(s)
HDL	High density lipoproteins
HSD	Honestly significant difference
LSM	Least squares mean
LNA	Linoleic acid
LDL	Low density lipoprotein
MUFA	Monounsaturated fatty acid
PEG	Polyethylene glycol
PUFA	Polyunsaturated fatty acids
SFA	Saturated fatty acids
SD	Standard deviation
SE	Standard error
SAS	Statistical analysis system
TG	Triglyceride(s)

M. Wien (✉) · S. Rajaram · J. Sabaté
Department of Nutrition, School of Public Health, Loma Linda University, Nichol Hall 1102, Loma Linda, CA 92350, USA
e-mail: mwien@llu.edu

K. Oda · J. Sabaté
Department of Epidemiology and Biostatistics, Loma Linda University, Loma Linda, CA, USA

Introduction

The intake of n-3 fatty acids (FA) is associated with beneficial effects in the context of brain and visual development [1, 2], carcinogenesis [3], and modification of cardiovascular disease (CVD) risk [4–7]. More specifically, daily consumption of n-3 FA produces favorable effects on plasma lipids, eicosanoid metabolism, inflammatory markers, platelet aggregability, hemostasis, and, myocardial function [8].

The n-3 FA, eicosapentaenoic acid (EPA; 20:5n-3), docosahexaenoic acid (DHA; 22:6n-3) and α-linolenic acid (ALA; 18:3n-3) contribute only a small fraction of the total daily intake of FA in Western societies [9, 10]. Oily fish and fish-oil supplements are rich sources of EPA and DHA, the latter typically containing 30–50% n-3 FA by weight [11]. EPA and DHA are also naturally found in disproportionately low levels compared to saturated fat in animal tissue lipids (e.g. beef, pork, poultry, etc.), however they contribute to the overall intake because of the large amounts consumed by omnivores in Western societies [11]. Specific vegetable oils such as flax seed, canola and soybean oil and walnuts are rich sources of the essential n-3 FA ALA in contrast to n-6 rich oils such as corn, safflower and sunflower that contain only trace levels of ALA [12]. The typical Western-style diet has a n-6/n-3 ratio of approximately 10–15:1 as it features foods rich in corn, safflower and sunflower oil, and, contains scant sources of n-3 FA. Alternatively, the Mediterranean-style diet has a n-6/n-3 ratio of 2:1 as the main fats are monounsaturated n-9 FA coming from the ubiquitous olive oil [13].

Numerous studies have evaluated the effects of manipulating the absolute levels of n-6 and n-3 FA using fish, fish oil capsules, walnuts, algal oil capsules and flax seed oil [14–18]. Others have investigated the metabolic fate of LNA and ALA in the context of varying the n-6/n-3 ratios [19]. It is interesting that it is still unclear whether the addition of direct sources of EPA and DHA in the context of a diet with a high (10:1) versus low (2:1) ratio of n-6/n-3 FA yields increased levels of EPA and DHA in red blood cell (RBC) membranes. For example, if an individual consumes a 2:1 diet, does adding a supplement (fish or algal oil) containing EPA and DHA increase these FA in RBC membranes? Or, if an individual follows a Western style 10:1 diet, will they accrue EPA and DHA in RBC membranes while taking a supplement containing EPA and DHA? When evaluating the biological equivalency of ALA with that of EPA and DHA, it appears that the limiting factor may be the membrane saturation with these long chain n-3 FA. Increasing the absolute amount of ALA or decreasing the n-6/n-3 ratio to 4:1 appears to be inadequate for reaching desirable DHA levels that are achieved when a direct source of DHA is consumed. However, several practical issues remain unresolved and our present study revisits the two aforementioned questions using a novel approach. More specifically, would RBC membrane levels of EPA and DHA increase when the n-6/n-3 ratio is further reduced to 2:1, or does an individual still need to add a direct source of these FA to a Mediterranean-type diet? Additionally, would consuming a Western-style 10:1 diet ensure increased levels of EPA and DHA in RBC membranes as long as a direct source of these FA is included?

To address these two specific questions, we designed a trial using a factorial design approach in healthy adults to evaluate RBC membrane changes due to the consumption of a 10:1 versus 2:1 diet alone, and, changes resulting from consumption of a 10:1 versus 2:1 diet plus EPA/DHA supplement. This trial allows for the further evaluation of a potential interaction between the diet ratio and supplement.

Materials and Methods

Volunteers

Eligibility criteria included nonsmoking men and women, 20–70 years of age, body mass index (BMI) below 34.9 kg/m^2, and not known to have food allergies, hyperlipidemia, glucose intolerance, diabetes or any chronic disease likely to affect lipid metabolism, or to consume any fish, FA supplement or medications that would interfere with the study outcomes. A multi-stage participant screening process was employed that included a web-based screening questionnaire, informational group meeting, personal interview with two senior investigators and a preliminary blood test to rule out severe hyperlipidemia. Fasting blood lipid tests were performed spectrophotometrically by the Loma Linda University Medical Center clinical laboratory on a Roche Modular Analytics analyzer using a P800 module. Total cholesterol and triglyceride (TG) assays were evaluated using standard enzymatic methods. High density lipoprotein (HDL) cholesterol was evaluated using polyethylene (PEG) modified enzymes and dextran sulfate to provide selective catalytic activity toward the lipoprotein fractions. Low density lipoprotein (LDL) cholesterol was evaluated using a nonionic detergent combined with a sugar compound to selectively solubilize the lipid micelles to react with the enzymatic cholesterol reagents. Potential subjects were excluded if their plasma total cholesterol was >7.76 mmol/l and plasma TG was >3.33 mmol/l. Twenty-eight subjects were enrolled and 24 completed the study. The study was approved by the Loma Linda University Institutional Review Board. Informed written consent was obtained from all subjects.

Study Design

This was a controlled, factorial design, single blind, randomized, 4 × 3 incomplete cross-over study to evaluate the incorporation of EPA and DHA into RBC membranes from consumption of diets enriched with two different sources of n-3 FA in the background of two n-6/n-3 diet ratios. Subjects consumed a diet containing 30–35% energy from fat during a 1-week pre-study phase. Baseline data was collected at the end of this phase and subjects were then randomized to one of the multiple crossover diet sequences in which each subject consumed three of four study diets [10:1, 10:1 plus supplement (10:1 + S), 2:1 and 2:1 plus supplement (2:1 + S)] (Fig. 1). The 3 8-week study periods and 4 diets yielded 24 treatment sequences. All 24 subjects completed one sequence to achieve a balance for carry-over and period effect, which resulted in 18 subjects per group. There was a 4 to 6-week wash-out period between the dietary intervention periods.

The four study diets were defined by their EPA/DHA content and n-6/n-3 ratios (10:1 and 2:1; Table 1). The 10:1 "control" diet was low in both ALA and EPA/DHA and had a ratio approaching that of the American diet. The 2:1 diet was high in ALA-containing plant sources (~8 g ALA/2,400 kcal/day) and low in EPA/DHA. The 10:1 + S diet was high in EPA/DHA (0.20/0.72 g EPA/DHA per 2,400 kcal/day) and low in ALA-containing plant sources. Globally declining fish stocks and post-Kyoto awareness of the size of the human footprint have placed interest in finding alternative sources of n-3 FA that are readily available in large quantities and are renewable [20]. Thus, the high content of EPA/DHA was achieved by supplementing the diet with algal oil capsules (V-Pure®, Water 4 Investments, United Kingdom), which were administered proportional to a subject's isocaloric requirements (1 capsule per 300 kcal; 1 capsule contains 25 mg EPA and 90 mg DHA). The dose was selected based upon the American Heart Association's recommendation that persons consume between 650 and 1,000 mg of EPA + DHA daily [21]. The FA concentrations in the V-Pure® capsules were verified by ©Lipomics Technologies, Inc. using TrueMass® Total Lipid Analysis procedures that have been previously described [22]. The 2:1 + S diet was high in both ALA and EPA/DHA and was achieved by incorporating ALA-containing plant sources and the algal oil capsules.

Menus were designed for seven levels of energy intake, ranging from 1,500 to 3,300 kcal/day to accommodate the eucaloric requirements of the subjects. Daily energy intake was adjusted when necessary to maintain a stable body weight. The diets were in accordance with the "Acceptable Macronutrient Distribution Ranges" of the Dietary Reference Intakes for adults [23] and the recommendations of the 2005 Dietary Guidelines for Americans [24]. The target macronutrient distribution as percent energy was approximately 55–60% carbohydrate, 10–15% protein, 30–35% total fat, <10% saturated FA (SFA), 7–10% polyunsaturated FA (PUFA), 10–15% monounsaturated FA (MUFA), and, dietary cholesterol was less than 300 mg/day. Total trans FA content of the diet was <1% due to their known interference with the desaturation and elongation of both LNA and ALA.

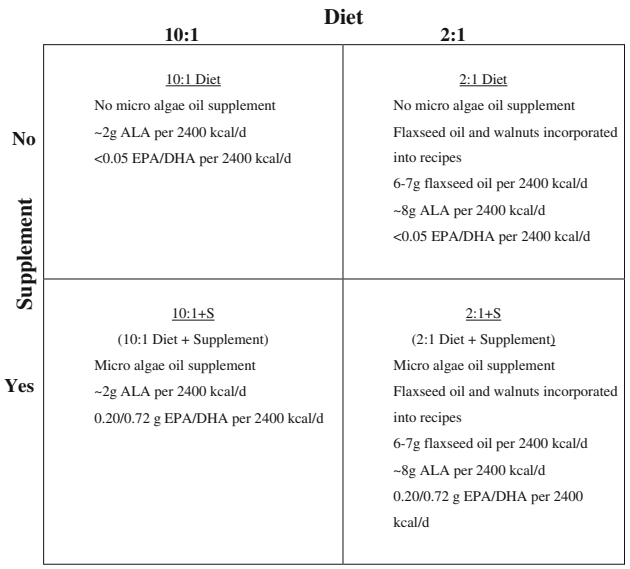

Fig. 1 Experimental dietary interventions for the 2 × 2 factorial design

Table 1 Planned nutrient analysis (Nutrition Data System for Research software version 2006, Nutrition Coordinating Center, University of Minnesota, Minneapolis, MN) and actual nutrient composition (Analyzed at Covance Laboratories, Madison, WI) of the 10:1 and 2:1 diets for the 2400 kcal (1 kilocalorie = 4.184 kJ) menu

Nutrient	10:1 diets		2:1 diets	
	Planned	Actual	Planned	Actual
Energy, kcal	2,372	2,556	2,384	2,568
Carbohydrate, % energy[a]	61	60	61	60
Protein, % energy	11	12	11	12
Fat, % energy	31	28	30	28
SFA, % energy	9	8	8	7
MUFA, % energy	10	8	10	9
PUFA, % energy	10	10	10	10
Trans FA, % energy	<1	<1	<1	<1
18:2n-6, g	22.9	26.6	17.2	21.9
18:3n-3, g	2.2	2.9	8.2	8.6
n-6/n-3 diet ratio	10.2	9.3	2.1	2.5

[a] Carbohydrate is calculated by subtracting the values for fat and protein intake from total energy intake

Participants were requested to maintain their usual lifestyle activities and to record in diaries provided to them any signs of illness, medications used, and any deviation from their current assigned diet.

Food Development and Preparation

Using commonly available food items, the research dietitian developed 11 meatless daily menus (including 2 weekends) using Nutrition Data System for Research software version 2006, developed by the Nutrition Coordinating Center, University of Minnesota, Minneapolis, MN. The 10:1 and 2:1 diets differed in the proportion and type of oils that were added to dinner entrees or that were constituents of salad dressings, baked goods, margarine and fried snacks (e.g. chips). More specifically, the 10:1 diets included a high proportion of corn oil and a lesser amount of soybean oil in contrast to the 2:1 diets that incorporated clear flax seed (Barlean's Organic Oils, Edmonds, WA), canola and soybean oil. Also, the 10:1 diets included peanut butter whereas the 2:1 diets featured walnuts.

Sunday through Friday, all foods were prepared in the University Metabolic Kitchen and individually weighed or apportioned for each subject, and, dinner was consumed in a private dining area. Breakfast, lunch and snacks for the following day were provided to the subjects after consumption of the dinner meal, which were consumed by the subjects on the following day. On Fridays, foods were provided for all Saturday meals and Sunday breakfast and lunch.

Quality Control and Dietary Compliance

Menu quality control was assessed by collecting duplicate food samples of the 11 menus on randomly selected days during each study period. The samples were homogenized and a 2% aliquot from each menu was kept frozen at −80 °C until chemically analyzed (Covance Laboratories, Madison, WI) for comparison with the computer analysis.

Subject deviations from the study protocol were not tolerated. Monitoring of dietary compliance was achieved by direct observation during the dinner meal by a senior investigator and by periodic examination of the subject's diaries.

Biological Data Collection and Assays

Venous blood was collected after an overnight 12-h fast at the start of each study period and on two non-consecutive days during week 8 for each study period. Plasma and serum were separated by centrifugation at 4 °C at 1,300×*g* for 10 min and made into aliquots and frozen at −80 °C until analyzed. FA composition of the RBC membrane was determined (Lipomics Inc., Sacramento, CA) at the end of each treatment using methods previously described [22]. Briefly, individual lipid classes were separated by preparative thin-layer chromatography and each lipid fraction was trans-esterified in 3 N methanolic HCL in a sealed vial under a nitrogen atmosphere at 100 °C for 45 min. The resulting FA methyl esters were extracted from the mixture with hexane containing 0.05% butylated hydroxytoluene and analyzed using a gas chromatograph (Hewlett-Packard model 6890, Wilmington, DE) equipped with a 30 m DB-225MS capillary column (J&W Scientific, Folsom, CA) and a flame-ionization detector as described previously [22]. All samples were analyzed in duplicate.

Statistical Analyses

A mixed model was used to compare effects of diet on the FA. The model included experimental diet (10:1, 10:1 + S, 2:1, 2:1 + S) and study period (1, 2, 3) as factors, and, controlled for baseline measurements, age and gender. Blocks of sequence, subjects nested within blocks, and study period × subject nested within blocks were also added into the model as random effects. The Kenward-Roger method was employed to estimate denominator degrees of freedom for tests of fixed effects. Tukey–Kramer Honestly Significantly Different (HSD) tests were performed to detect significant pair-wise differences among the four diets. A factorial design approach was also used to test the effect of the diet ratio, the supplement and for potential interaction between the diet ratio and supplement. All statistical analyses were performed using Statistical Analysis System software (version 9.1, SAS Institute Inc., Cary, NC). Significance was determined at $P < 0.05$.

Results

Characteristics of Study Subjects

Demographic and biological characteristics at baseline are shown in Table 2.

Dietary FA Intakes

During the three study periods, the mean fat intake from all food sources in both the 10:1 and 2:1 diets was 28% of total energy (Table 1). Mean carbohydrate and protein intake were equivalent, as well as SFA, MUFA, PUFA and trans FA. Flax seed oil and walnuts were substituted for high LNA oil in food preparation of the low LNA diets, which yielded a three to fourfold greater level of ALA and resulting n-6/n-3 ratio of 2.5:1 in contrast to a 9.3:1 ratio for the high LNA diets.

Table 2 Characteristics of study subjects at baseline

Characteristic	$n = 24$
Age (years)	42 ± 3
Gender	
Female	15 (62)
Male	9 (38)
Race	
Caucasian	16 (67)
Hispanic	4 (17)
African American	1 (4)
Asian	3 (12)
Weight (kg)	75.6 ± 14.5
BMI (kg/m^2)	25.4 ± 4.3
Plasma lipids, mg/dl[a]	
Total cholesterol	165 ± 48
LDL cholesterol	102 ± 41
HDL cholesterol	47 ± 14
TG	102 ± 56
Systolic blood pressure (mm Hg)	123 ± 16
Diastolic blood pressure (mm Hg)	74 ± 11

Data are means ± SD or *n* (%)

[a] To obtain mmol/l values for LDL cholesterol and HDL cholesterol, multiply values by 0.0259; and for TG, multiply values by 0.0113

Change in Participants' RBC Membrane FA Composition

The RBC membrane levels (mol%) of total SFA, MUFA, PUFA and specific n-6 and n-3 FA, and the ratios of arachidonic acid (20:4n-6) to dihomogamma linolenic acid (20:3n-6) (ARA:DGLA), ARA:EPA and DHA to docosapentaenoic acid DPA(n-3) after consuming the high and low n-6/n-3 diets with and without the algal oil supplement for 8 weeks were measured (Table 3). Neither the n-6/n-3 ratio of the diets nor the intake of the algal oil supplement affected the total levels of SFA, MUFA and PUFA after 8 weeks. The absolute levels of ALA, EPA, DHA and DPA(n-3) are shown in Fig. 2. LNA levels did not differ after the 8 week diet interventions, in contrast to the levels of ALA (Fig. 2a) that showed an expected increase in the 2:1 (0.52 ± 0.02) and 2:1 + S (0.44 ± 0.02) diets as compared to the 10:1 and 10:1 + S diets ($P < 0.0001$). All of the subjects showed an increase in ALA levels after consuming the 2:1 and 2:1 + S diets, hence reflecting the diet composition and serving as a biological marker of each subject's compliance. Compared to the 10:1 diet, the EPA (Fig. 2b) level after consumption of the 10:1 + S, 2:1 and 2:1 + S diets increased and were 0.60 ± 0.04 ($P = 0.02$), 0.71 ± 0.04 and 0.86 ± 0.04 ($P < 0.0001$), respectively. Notably, DHA (Fig. 2c) levels increased for the 10:1 + S ($P < 0.001$) and 2:1 + S ($P < 0.01$) diets while the DHA levels in the 10:1 and 2:1 diets were equivalently lower.

DPA(n-6) and ARA levels did not differ for the 4 dietary interventions. An increase in DPA(n-3; Fig. 2d) was found for the 2:1 diet (2.77 ± 0.12, $P = 0.019$) compared to the 10:1, 10:1 + S and 2:1 + S diets. In contrast to the 10:1 diet, DGLA levels decreased for the 10:1 + S and 2:1 + S diets, 1.43 ± 0.07 ($P = 0.04$) and 1.34 ± 0.07 ($P < 0.01$) respectively, however the ARA:DGLA ratio was equivalent for all 4 diets. The ARA:EPA ratio was lower in the 10:1 diet compared to the 10:1 + S, 2:1 and 2:1 + S diets, 22.00 ± 1.93 ($P = 0.002$), 18.25 ± 1.93 ($P < 0.0001$) and 15.59 ± 1.93 ($P < 0.0001$), respectively. Lastly, the EPA:ALA and the DHA:DPA(n-3) ratios were higher in the 10:1 + S diet, 3.52 ± 0.21 ($P < 0.001$) and 2.66 ± 0.16 ($P = 0.001$) respectively, in contrast to similar levels for the 10:1, 2:1 and 2:1 + S diets.

The factorial analysis for the diet effect (10:1 diet versus 2:1 diet) showed that the ARA level ($P = 0.037$) and the ratios for ARA:EPA ($P < 0.001$), EPA:ALA ($P < 0.001$) and DHA:DPA(n-3) ($P = 0.019$) were lower in contrast to the ALA ($P < 0.001$), EPA ($P < 0.001$), DPA(n-3) ($P = 0.003$) levels that were higher in the 2:1 diet (Table 4). The factorial analysis for the supplement effect (10:1 diet versus 10:1 + S diet) showed that the DGLA ($P < 0.001$), ALA ($P = 0.046$) and DPA(n-3) ($P = 0.007$) levels and the ARA:EPA ratio ($P = 0.001$) decreased in the 10:1 + S diet, and, the EPA and DHA levels and the ratios for EPA:ALA and DHA:DPA(n-3) increased (all $P < 0.001$). A negative interaction was found for the ARA:EPA ($P = 0.048$) and EPA:ALA ($P = 0.026$) ratios, which indicates that the combined effect was less than the sum of the separate diet effect and supplement effect.

Discussion

This controlled feeding study demonstrates that using flax seed oil and walnuts in the diets of healthy adult men and women to achieve a n-6/n-3 ratio of ~2:1 yields increased levels of EPA in RBC membranes without the use of a direct EPA source; however, DHA levels do not increase. Also, adding an algal oil capsule containing EPA and DHA to a n-6/n-3 ratio of 10:1 increases the levels of both EPA and DHA in RBC membranes. This study was also designed to test the interaction between an algal oil supplement in the context of an n-6/n-3 ratio of 10:1 that is found in Western societies versus a 2:1 ratio that approaches the traditional Mediterranean-style diet. To prepare the 2:1 and 2:1 + S diets, we incorporated flax seed oil and walnuts into the recipes and provided 3.0% in contrast to 1.0% dietary energy from ALA in the 10:1 and 10:1 + S diets. An intake of 3% energy from ALA is approximately

Table 3 Red blood cell membrane fatty acid composition at the end of each diet intervention

Fatty acid, mol%	10:1 diet (LSM ± SE)	2:1 diet (LSM ± SE)	10:1 + S diet (LSM ± SE)	2:1 + S diet (LSM ± SE)
ΣSFA	45.66 ± 0.24	45.31 ± 0.24	45.86 ± 0.24	45.50 ± 0.24
ΣMUFA	16.62 ± 0.28	16.62 ± 0.28	16.21 ± 0.28	16.62 ± 0.28
ΣPUFA	37.72 ± 0.34	38.13 ± 0.33	37.85 ± 0.34	37.91 ± 0.34
18:2n-6, LNA	12.40 ± 0.20	12.23 ± 0.20	11.80 ± 0.20	12.15 ± 0.20
20:3n-6, DGLA	1.66 ± 0.07^{c,d}	1.54 ± 0.07	1.43 ± 0.07^{a}	1.34 ± 0.07^{a}
20:4n-6, ARA	12.84 ± 0.26	12.22 ± 0.26	12.38 ± 0.26	11.89 ± 0.26
22:5n-6, DPA(n-6)	0.47 ± 0.02	0.43 ± 0.02	0.45 ± 0.02	0.43 ± 0.02
18:3n-3, ALA	0.22 ± 0.02^{b,d}	0.52 ± 0.02^{a,c}	0.19 ± 0.02^{b,d}	0.44 ± 0.02^{a,b,c}
20:5n-3, EPA	0.44 ± 0.04^{b,d}	0.71 ± 0.04^{a,d}	0.60 ± 0.04^{d}	0.86 ± 0.04^{a,c}
22:5n-3, DPA(n-3)	2.35 ± 0.12^{b}	2.77 ± 0.12^{a,b,d}	2.19 ± 0.12^{c}	2.38 ± 0.12^{b}
22:6n-3, DHA	3.92 ± 0.26^{c,d}	3.85 ± 0.26^{c,d}	5.54 ± 0.26^{a,b}	5.15 ± 0.26^{a,b}

Values within a row with different superscript letters are significantly different from 10:1 (^{a}), 2:1 (^{b}), 10:1 + S (^{c}) or 2:1 + S (^{d}), $P < 0.05$ (ANOVA, with Tukey–Kramer HSD adjustments)

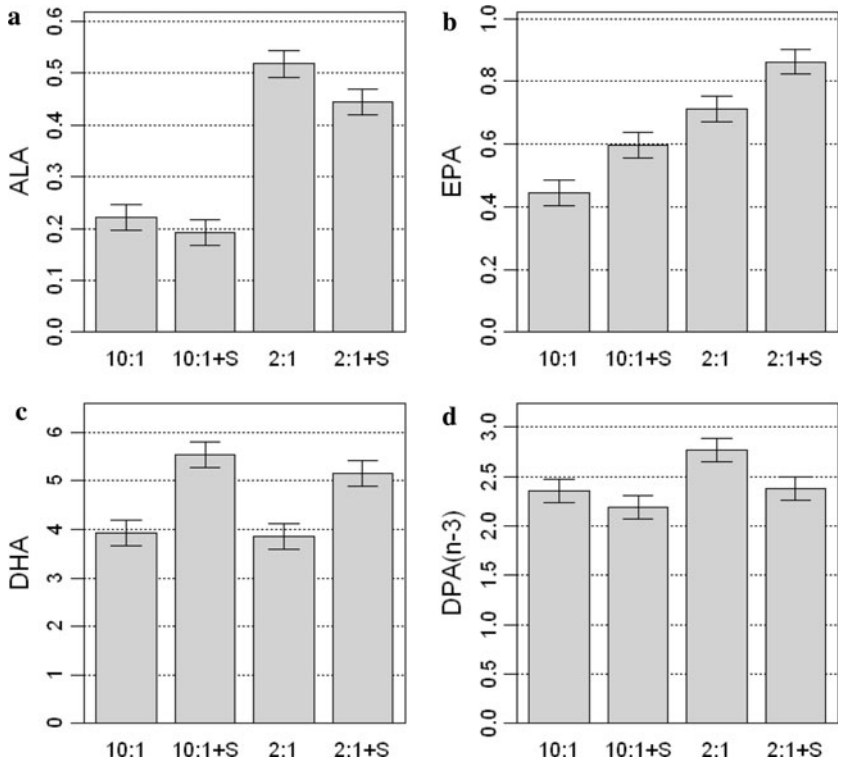

Fig. 2 Levels of fatty acids in red blood cell membranes

6 times the current mean ALA intake in the US diet [23]. In the context of the background diets, we provided LNA intakes of 9.4 and 7.7% total energy for the 10:1 and 2:1 diets, respectively, and did not induce higher levels of ARA. Liou et al. [19] have similarly reported that an intake of 10.5% energy from LNA with a n-6/n-3 ratio of 10:1 resulted in lower plasma phospholipids levels of EPA but did not induce higher levels of ARA when compared to an intake of 3.8% from LNA with a n-6/n-3 ratio of 4:1 in the context of an omnivorous diet. The 8 weeks of algal oil supplementation in this current study yielded a range of 575–1,265 mg/day of EPA plus DHA across the 1,500–3,300 kcal/day menus, yet the ARA levels in the RBC membranes were not changed. Alternatively, Arterburn et al. [25] compared the effects of supplementation with EPA and DHA on plasma FA and found a reduction in ARA levels. A possible explanation for our unexpected findings is that the V-Pure® supplement that we used contained 2.3 mol% of ARA, which may have masked a reduction in ARA levels.

Both n-6 and n-3 FA are known to compete for common enzymes in the synthesis of FA [26]. Ratios of substrates

Table 4 Factorial analysis for red blood cell membrane fatty acid composition at the end of each diet intervention

Fatty acid	Diet effect (10:1 diet vs. 2:1 diet)	Supplement effect	Interaction
18:2n-6, LNA	−0.17 (0.25)	−0.60 (0.25)	None
22:5n-6, DPA(n-6)	−0.04 (0.03)	−0.02 (0.03)	None
20:4n-6, ARA	−0.62 (0.37)*	−0.46 (0.37)	None
20:3n-6, DGLA	−0.12 (0.08)	−0.23 (0.08)***	None
18:3n-3, ALA	+0.30 (0.04)***	−0.03 (0.04)*	None
20:5n-3, EPA	+0.27 (0.05)***	+0.15 (0.05)***	None
22:6n-3, DHA	−0.06 (0.37)	+1.62 (0.37)***	None
22:5n-3, DPA(n-3)	+0.42 (0.14)**	−0.16 (0.14)**	None
ARA:DGLA	+0.22 (0.70)	+0.92 (0.70)	None
ARA:EPA	−13.89 (2.61)***	−10.14 (2.61)**	Negative
EPA:ALA	−0.61 (0.28)***	+1.35 (0.28)***	Negative
DHA:DPA(n-3)	−0.33 (0.22)*	+0.87 (0.22)***	None

Values are LSM (SE)

* $P < 0.05$; ** $P < 0.01$; *** $P < 0.001$

and products are somewhat useful in evaluating potential major points of regulation in the stepwise conversion of LNA to both ARA and DPA(n-6), and, conversion of ALA to both EPA and DHA. LNA and ALA are both substrates for microsomal Δ6 desaturase (D6D); however there is an approximately two- to three-fold affinity of D6D for ALA [27]. Synthesis of DHA and 22:5n-6 from the 24 carbon FA (24:5n-3 and 24:4n-6) is also dependent on D6D, which provides a second opportunity for competition between substrates and the preferential entry of FA into cell membranes [28]. The resulting cell membrane composition from this competition has profound effects on eicosanoid metabolism, inflammatory markers, platelet aggregability, hemostasis, and, myocardial function [29–31].

The highest increase in EPA (94%) in RBC membranes was found after consumption of the 2:1 + S diet, which was expected as a result of providing both a direct source of EPA from the algal oil supplement and the metabolic conversion of ALA to EPA. Notably, the 60% increase in EPA levels after consumption of the 2:1 diet using flax seed oil and walnuts was not significantly different to the 34% increase found after consumption of the 10:1 + S diet, which implies that an adequate conversion from ALA to EPA occurs when a n-6/n-3 ratio of 2:1 exists. The ARA:DGLA ratio in the RBC membranes was not different between the 4 diets indicating that the step catalyzed by Δ5 desaturase (D5D) in the LNA pathway is not a limiting factor in the context of converting ALA to EPA providing that adequate ALA substrate is available.

Cell culture studies [28] support the hypothesis that high dietary consumption of LNA interferes with the desaturation of ALA due to competition for D6D between LNA and ALA, thus yielding increased levels of ARA and reduced levels of EPA and DHA. Our findings are consistent with this hypothesis as we demonstrated that the ARA:EPA ratio in the RBC membranes was lower for the 10:1 + S, 2:1 and 2:1 + S diets compared to the 10:1 diet in the context of similar ARA levels among the four dietary treatments. Consistent with the results of our study, Liou et al. [19] found that manipulating LNA-containing vegetable oils and keeping ALA constant to produce a 8.2:1 diet ratio decreased plasma phospholipid EPA levels, increased the ARA:EPA ratio, and, did not favor higher ARA levels after 4 weeks in healthy adult male omnivores as compared to a 2.1:1 diet ratio. When the conversion from ALA to EPA occurs, the conversion of DGLA to ARA is competitively inhibited and yields reduced amounts of ARA. Thus, the high ARA:EPA ratio observed in our 10:1 diet was due to the lack of a direct source of EPA and minimal availability of ALA for conversion to EPA.

Docosahexaenoic acid levels significantly increased by 41% in the RBC membranes after consumption of the 10:1 + S diet and 31% in the 2:1 + S diet as compared to the non supplemented 10:1 and 2:1 diets. Cell culture studies have shown that the accretion of DHA in cells supplemented with DHA is a result of incorporation of the direct DHA source as compared to the net effect of DHA synthesis via metabolic pathways and incorporation into cells supplemented with ALA [28]. The limited accretion of DHA derived from ALA in our study suggests that DHA synthesis from ALA is tightly regulated and relies upon the second D6D step, which is also used to convert ALA to 18:4n-3. Hence, there is the potential competition for D6D between ALA and 24:5n-3, and, ALA is the preferred substrate that saturates D6D leaving the conversion of 24:5n-3 to DHA compromised. It has also been shown that the elongase-2 (*Elo-2*) which converts 22:5n-3 to 24:5n-3 may be the limiting step in the synthesis of DHA from ALA [32]. The enzyme *Elo-2* is subject to genetic control [33] and exhibits tissue specific expression [34]. Thus, the

incorporation of DHA into the RBC membrane, although a good marker for dietary compliance, may not fully reflect the conversion of ALA to DHA in different tissues.

Consistent with our findings, Arterman et al. [16] demonstrated significant and equivalent increases in DHA in plasma phospholipids and erythrocytes from salmon intake or algal oil capsules in healthy adults. Also, Innis et al. [18] found a 50% increase in plasma DHA levels in healthy adults consuming an ARA (0.8 g/day) enriched fungal oil and a microalgal oil containing DHA (0.6 g/day) using a ARA:DHA diet ratio of 1.25:1 after 14 days. We found that when the n-6/n-3 ratio was altered to 2:1, or if we increased the absolute amount of ALA, this conversion was inefficient. In contrast, Goyens et al. [35] provided a 7:1 ratio omnivorous diet (7% energy from LNA and 1.1% energy from ALA) to 30 Dutch adults and found an increase in the absolute amount of DHA synthesized from ALA compared to a control diet [19:1 diet ratio; 7% energy from LNA and 0.4% energy from ALA] or low LNA diet [7:1 diet ratio; 3% energy from LNA and 0.4% energy from ALA]. However, there were no differences in percent DHA incorporated in the plasma phospholipids among the different diets in this study.

Investigating the ratio of DHA:DPA(n-3) may further an explanation of our study's DHA findings. There is no known physiological function for DPA(n-3), which is the intermediate FA produced by elongation of EPA prior to desaturation by the Δ4 desaturase (D4D) enzyme. The DHA:DPA(n-3) ratio was found to be similarly low after consumption of the 10:1 and 2:1 diets compared to the algal oil supplemented 10:1 + S and 2:1 + S diets. The lower ratios noted in the 10:1 and 2:1 diets are due to the high DPA(n-3) and low DHA levels in these diets. The significantly higher ratios found in the 10:1 + S and 2:1 + S diets suggests that providing a direct source of DHA is more influential than the n-6/n-3 ratio for successful accretion of DHA into RBC membranes.

Barcelo et al. [16] found that an intake of 2.4 g flax seed oil/day produced significant increases in ALA, EPA and DPA(n-3) compared to fish oil which produced only significant increases in EPA and DHA. Consistent to these findings, we demonstrated the highest increase in DPA (n-3) in the RBC membrane after consumption of the 2:1 diet indicating adequate conversion from EPA. The DPA(n-3) in the RBC membranes after consumption of the 10:1 + S diet and the 2:1 + S diet was similar to that of the 10:1 diet and significantly lower than the 2:1 diet. These findings suggest that DPA(n-3) levels may increase only as a means to produce DHA, and when a direct DHA source is provided DPA(n-3) may not be required. Also, Arterman et al. [15] found that levels of EPA and DPA(n-3) increased in plasma phospholipids and erythrocytes in a group of subjects consuming salmon (which contains EPA) versus a group of subjects consuming an algal oil supplement as the sole source of DHA. An additional explanation for these aforementioned findings may be that a retro-inhibition by DHA and/or EPA of desaturase activities occurs in the pathway leading to the synthesis of ARA from LNA, which has been consistently shown in cell culture studies using rats fed fish oil containing EPA and DHA [36, 37].

Our crossover feeding study had several strengths. The 8 week study periods and 4–6 week washout periods were of sufficient duration to assess changes in RBC membranes resulting from dietary manipulation of the n-6/n-3 ratio and/or absolute amount of EPA/DHA. By varying the type of oils, we achieved a greater extreme of ratios compared to prior investigations. Others have tested the effects of ratios further from these extremes or have kept only LNA or ALA constant. Our factorial design approach allowed us to test for interactions between the diet ratios and algal oil supplement. Additionally, the increase in ALA level observed in all of the subjects consuming the 2:1 and 2:1 + S diets served as a biomarker of excellent dietary compliance. Lastly, the background diet was meatless, which allowed us to evaluate the substrate and product ratios of solely plant-derived sources of ALA.

In conclusion, our study indicates that providing a diet with 3% energy from ALA and a n-6/n-3 diet ratio of 2:1 yields significantly higher EPA levels in RBC membranes and a 43% lower ARA:EPA ratio compared to a 10:1 diet. Use of a direct algal oil source of EPA/DHA yields significantly higher levels of EPA and DHA in persons consuming a Western-style 10:1 diet as well as a Mediterranean-style 2:1 diet. Many Western-style diets contain n-6/n-3 ratios in excess of 10:1, however a ratio of 4:1 or lower has been recommended for optimal health-promoting effects [38–40]. In practice, a 4:1 ratio is difficult to achieve as most people are reluctant to include several servings of oily fish in their diets weekly or take multiple fish oil capsules daily [12]. We showed that reducing LNA-rich oils and incorporating ALA-rich plant sources (flaxseed oil and walnuts) in recipes achieved an n-6/n-3 ratio potentially conducive to improved health outcomes and is sufficient to meet the EPA needs of individuals adhering to a vegetarian or meatless diet. The requirement for D6D by both ALA and 24:5n-3 and differences in tissue specific expression of *Elo-2* may influence the ability of RBC membranes to accumulate significant levels of DHA, which has implications for vegetarians, vegans, and persons unable or unwilling to include oily fish or fish oil capsules into their dietary regimens. Thus, inclusion of plant sources of ALA within a 2:1 diet negates the need to use a supplement containing EPA, but a DHA-rich source (i.e. algal oil supplement, DHA-enriched eggs) may be warranted for the aforementioned populations. At the population level, a

decreased intake of LNA with a concurrent increased intake of ALA-containing plant sources to achieve a ~2:1 diet ratio, plus a marine derived algal oil supplement containing EPA and DHA, is a sustainable alternative to ongoing public health recommendations supporting the intake of fish for the primary prevention of CVD.

Acknowledgments We would like to thank Water 4 Investment for supplying the V-Pure® Omega-3 EPA & DHA supplement, the California Walnut Commission for supplying the walnuts, and Barlean's Organic Oils for supplying the clear flax seed oil. We would like to express our gratitude to our Research Dietitian, Jennifer Fix, MPH, RD, and to the study participants without whom this investigation would not have been possible. M.W., S.R. and J.S. designed research; M.W. and J.S. conducted research; K.O. analyzed data; M.W., S.R. and J.S. wrote the paper. M.W. had primary responsibility for the final content. All authors have read and approved the final manuscript. This study was supported by the Center for Health and Nutrition Research at University of California, Davis.

Conflict of interest statement None of the authors disclose any conflicts of interest.

References

1. Fleith M, Clandinin MT (2005) Dietary PUFA for preterm and term infants: review of clinical studies. Crit Rev Food Sci Nutr 45:205–229
2. Morale SE, Hoffman DR, Castaneda YS, Wheaton DH, Burns RA, Birch EE (2005) Duration of long-chain polyunsaturated fatty acids availability in the diet and visual acuity. Early Hum Dev 81:197–203
3. Tsubura A, Yuri T, Yoshizawa K, Uehara N, Takada H (2009) Role of fatty acids in malignancy and visual impairment: epidemiological evidence and experimental studies. Histol Histopathol 24:223–234
4. Albert CM, Oh K, Whang W, Manson JE, Chae CU, Stampfer MJ et al (2005) Dietary alpha-linolenic acid intake and risk of sudden cardiac death and coronary heart disease. Circulation 112:3232–3238
5. Connor WE (2000) Importance of n-3 fatty acids in health and disease. Am J Clin Nutr 71:171S–175S
6. Djousse L, Pankow JS, Eckfeldt JH, Folsom AR, Hopkins PN, Province MA et al (2001) Relation between dietary linolenic acid and coronary artery disease in the national heart, lung, and blood institute family heart study. Am J Clin Nutr 74:612–619
7. Lemaitre RN, King IB, Mozaffarian D, Kuller LH, Tracy RP, Siscovick DS (2003) n-3 Polyunsaturated fatty acids, fatal ischemic heart disease, and nonfatal myocardial infarction in older adults: the cardiovascular health study. Am J Clin Nutr 77:319–325
8. Saremi A, Arora R (2008) The utility of omega-3 fatty acids in cardiovascular disease. Am J Ther 16:421–436
9. Innis SM, Elias SL (2003) Intakes of essential n-6 and n-3 polyunsaturated fatty acids among pregnant Canadian women. Am J Clin Nutr 77:473–478
10. Stephen AM, Wald NJ (1990) Trends in individual consumption of dietary fat in the United States, 1920–1984. Am J Clin Nutr 52:457–469
11. Surette ME (2008) The science behind dietary omega-3 fatty acids. CMAJ 178:177–180
12. Gebauer SK, Psota TL, Harris WS, Kris-Etherton PM (2006) n-3 fatty acid dietary recommendations and food sources to achieve essentiality and cardiovascular benefits. Am J Clin Nutr 83:1526S–1535S
13. Saura-Calixto F, Goni I (2009) Definition of the Mediterranean diet based on bioactive compounds. Crit Rev Food Sci Nutr 49:145–152
14. Agren JJ, Hanninen O, Julkunen A, Fogelholm L, Vidgren H, Schwab U et al (1996) Fish diet, fish oil and docosahexaenoic acid rich oil lower fasting and postprandial plasma lipid levels. Eur J Clin Nutr 50:765–771
15. Arterburn LM, Oken HA, Bailey Hall E, Hamersley J, Kuratko CN, Hoffman JP (2008) Algal-oil capsules and cooked salmon: nutritionally equivalent sources of docosahexaenoic acid. J Am Diet Assoc 108:1204–1209
16. Barcelo-Coblijn G, Murphy EJ, Othman R, Moghadasian MH, Kashour T, Friel JK (2008) Flaxseed oil and fish-oil capsule consumption alters human red blood cell n-3 fatty acid composition: a multiple-dosing trial comparing 2 sources of n-3 fatty acid. Am J Clin Nutr 88:801–809
17. Innis SM, Hansen JW (1996) Plasma fatty acid responses, metabolic effects, and safety of microalgal and fungal oils rich in arachidonic and docosahexaenoic acids in healthy adults. Am J Clin Nutr 64:159–167
18. Rajaram S, Haddad EH, Mejia A, Sabate J (2009) Walnuts and fatty fish influence different serum lipid fractions in normal to mildly hyperlipidemic individuals: a randomized controlled study. Am J Clin Nutr 89:1657S–1663S
19. Liou YA, King DJ, Zibrik D, Innis SM (2007) Decreasing linoleic acid with constant alpha-linolenic acid in dietary fats increases (n-3) eicosapentaenoic acid in plasma phospholipids in healthy men. J Nutr 137:945–952
20. Jenkins DJ, Sievenpiper JL, Sumaila UR, Kendall CW, Mowat FM (2009) Are dietary recommendations for the use of fish oils sustainable? CMAJ 180:633–637
21. Kris-Etherton PM, Harris WS, Appel LJ (2002) Fish consumption, fish oil, omega-3 fatty acids, and cardiovascular disease. Circulation 106:2747–2757
22. Watkins SM, Reifsnyder PR, Pan HJ, German JB, Leiter EH (2002) Lipid metabolome-wide effects of the PPARgamma agonist rosiglitazone. J Lipid Res 43:1809–1817
23. Panel on Macronutrients, Panel on the Definition of Dietary Fiber, Subcommittee on Upper Reference Levels of Nutrients, Subcommittee on Interpretation and Uses of Dietary Reference Intakes, Standing Committee on the Scientific Evaluation of Dietary Reference Intakes (2002) Dietary reference intakes for energy, carbohydrate, fiber, fat, fatty acids, cholesterol, protein, and amino acids. Washington, DC
24. US Department of Health and Human Services and US Department of Agriculture. Dietary Guidelines for Americans, 2005, 6th edn. Government Printing Office
25. Arterburn LM, Hall EB, Oken H (2006) Distribution, interconversion, and dose response of n-3 fatty acids in humans. Am J Clin Nutr 83:1467S–1476S
26. Kris-Etherton PM, Hill AM (2008) N-3 fatty acids: food or supplements? J Am Diet Assoc 108:1125–1130
27. Rodriguez A, Sarda P, Nessmann C, Boulot P, Leger CL, Descomps B (1998) Delta 6- and delta 5-desaturase activities in the human fetal liver: kinetic aspects. J Lipid Res 39:1825–1832
28. Portolesi R, Powell BC, Gibson RA (2007) Competition between 24:5n-3 and ALA for Delta 6 desaturase may limit the accumulation of DHA in HepG2 cell membranes. J Lipid Res 48:1592–1598
29. Bouwens M, van de Rest O, Dellschaft N, Bromhaar MG, de Groot LC, Geleijnse JM et al (2009) Fish-oil supplementation

induces antiinflammatory gene expression profiles in human blood mononuclear cells. Am J Clin Nutr 90:415–424
30. Calder PC, Yaqoob P (2009) Omega-3 polyunsaturated fatty acids and human health outcomes. Biofactors 35:266–272
31. Leon H, Shibata MC, Sivakumaran S, Dorgan M, Chatterley T, Tsuyuki RT (2008) Effect of fish oil on arrhythmias and mortality: systematic review. BMJ 337:a2931. doi:10.1136/bmj.a2931
32. Barceló-Coblijn G, Murphy EJ (2009) Alpha-linolenic acid and its conversion to longer chain n-3 fatty acids: benefits for human health and a role in maintaining tissue n-3 fatty acid levels. Prog Lipid Res 48:355–374
33. Moon YA, Shah NA, Mohapatra S, Warrington JA, Horton JD (2001) Identification of a mammalian long chain fatty acyl elongase regulated by sterol regulatory element-binding proteins. J Biol Chem 276:45358–45366
34. Wang Y, Botolin D, Christian B, Busik J, Xu J, Jump DB (2005) Tissue-specific, nutritional, and developmental regulation of rat fatty acid elongases. J Lipid Res 46:706–715
35. Goyens PL, Spilker ME, Zock PL, Katan MB, Mensink RP (2006) Conversion of alpha- linolenic acid in humans is influenced by the absolute amounts of alpha-linolenic acid and linoleic acid in the diet and not by their ratio. Am J Clin Nutr 84:44–53
36. Garg ML, Sebokova E, Thomson AB, Clandinin MT (1988) Delta-6-desaturase activity in liver microsomes of rats fed diets enriched with cholesterol and/or omega-3 fatty acids. Biochem J 249:351–356
37. Garg ML, Thomson AB, Clandinin MT (1988) Effect of dietary cholesterol and/or omega-3 fatty acids on lipid composition and delta-5-desaturase activity of rat liver microsomes. J Nutr 118:661–668
38. Harper CR, Edwards MJ, DeFilippis AP, Jacobson TA (2006) Flaxseed oil increases the plasma concentrations of cardioprotective (n-3) fatty acids in humans. J Nutr 136:83–87
39. Mantzioris E, James MJ, Gibson RA, Cleland LG (1994) Dietary substitution with an alpha-linolenic acid-rich vegetable oil increases eicosapentaenoic acid concentrations in tissues. Am J Clin Nutr 59:1304–1309
40. Zhao G, Etherton TD, Martin KR, West SG, Gillies PJ, Kris-Etherton PM (2004) Dietary alpha-linolenic acid reduces inflammatory and lipid cardiovascular risk factors in hypercholesterolemic men and women. J Nutr 134:2991–2997

Lipids (2010) 45:693–700
DOI 10.1007/s11745-010-3442-z

ORIGINAL ARTICLE

trans-Fatty Acid Isomers in Adipose Tissue Have Divergent Associations with Adiposity in Humans

Liesbeth A. Smit · Walter C. Willett · Hannia Campos

Received: 20 January 2010 / Accepted: 14 June 2010 / Published online: 14 July 2010

Abstract The aim of this study was to evaluate the association between adipose tissue *trans*-fatty acid isomers and adiposity. This cross-sectional study included 1,785 subjects from Costa Rica. Fatty acid concentrations (as a percentage of the total fatty acids) in subcutaneous adipose tissue were assessed by gas–liquid chromatography. Dietary intakes were assessed with a food frequency questionnaire. Multivariate linear regression models were used to relate adipose tissue *trans*-fatty acid content to BMI, waist circumference, and skinfold thickness while adjusting for age, sex, and area of residence. To account for variations in lifestyle, we adjusted for smoking, physical activity, income, self-reported history of diabetes and hypertension, and for adipose tissue alpha-linolenic acid and energy intake in a third model. After adjustments, positive associations were found between 18:2*t*-fatty acids (primarily from partially hydrogenated oils) and BMI, waist circumference, and skinfold thickness (P for each association <0.01). Rumenic acid was positively associated with skinfold thickness ($P < 0.0001$), but not with BMI or waist circumference ($P > 0.05$). Inverse associations were found between 16:1n-7*t*-fatty acids and skinfold thickness and between 18:1*t*-fatty acids and BMI and waist circumference ($P < 0.0001$). This study suggests that individual *trans*-fatty acid isomers may have divergent effects on adiposity. 18:2*t*-fatty acids show consistent positive associations with measures of adiposity. These isomer-specific associations are an interesting new finding. Other prospective and intervention studies are necessary to examine these relationships further.

Keywords *trans*-fatty acids · Adipose tissue · Body weight · Obesity · Conjugated linoleic acid · Diet

Abbreviations

BMI	Body mass index
CLA	Conjugated linoleic acid
CVD	Cardiovascular disease
GLC	Gas–liquid chromatography

Introduction

trans-Fatty acids are unsaturated fatty acids characterized by the *trans* configuration of their double bonds. The two main industrially produced *trans*-isomers,18:1*t*-and 18:2*t*-fatty acids are created by partial hydrogenation of unsaturated fats and have well documented adverse effects on health [1, 2]. The health effects of 16:1n-7*t*-fatty acids and 18:2n-7*t* fatty acids collectively known as conjugated linoleic acid (CLA) are less well understood.

The 9c, 11*t* isomer of CLA, also known as rumenic acid, is found in ruminant food products. These natural *trans*-fats originate mainly from biohydrogenation of linoleic acid by fermentive bacteria in ruminants and by endogenous

L. A. Smit · W. C. Willett
Department of Nutrition, Harvard School of Public Health, 665 Huntington Ave, Boston, MA 02115, USA

H. Campos (✉)
Department of Nutrition, Bld1, Room 201, Harvard School of Public Health, 665 Huntington Ave, Boston, MA 02115, USA
e-mail: hcampos@hsph.harvard.edu

H. Campos
Centro Centroamericano de Población, Universidad de Costa Rica, San Pedro, Costa Rica

synthesis from vaccenic acid by delta-9 desaturase [3]. Rumenic acid, represents ~80% of all CLA isomers in the diet [4], and is mainly found in dairy products in this population [5].

In humans and monkeys, high 18:1*t* and 18:2*t*-fatty acid intake appears to predispose to accumulation of body fat, particularly abdominal fat [6, 7]. Among more than 16,000 men who provided two measurements of abdominal circumference at an interval of 9 years, each 2% increase in total energy from *trans*-fatty acids (versus the same percent of energy from *cis*-polyunsaturated fat) was associated with a 2.7-cm increase in abdominal circumference ($P < 0.001$) after adjustment for measurement error and other risk factors [7]. Among more than 41,000 women who provided two measurements of body weight at an interval of 8 years, increases in *trans*-fatty acid intake were robustly associated with increases in body weight in both cross-sectional and longitudinal analyses, whereas intakes of other types of fat were not [8]. In a 6-year randomized controlled trial among 42 male African green monkeys feeding ~8% of energy 18:1*t*- and 18:2*t*-fatty acids resulted in a threefold greater weight gain compared with controls assigned to a diet containing *cis*-monounsaturated fatty acids ($P < 0.05$) [6]. However, evidence from human intervention studies has been inconclusive [9, 10].

The purpose of this study was to evaluate the associations between the most common *trans*-fatty acid isomers (18:1*t*, 18:2*t*, 16:1n-7*t* and rumenic acid) and adiposity in a population of Costa Rican adults. We used adipose tissue levels of *trans*-fatty acids as a marker for intake because the *trans*-fatty acid content of foods has changed considerably and subcutaneous adipose tissue is considered the best choice for the study of long-term fatty acid intake [11, 12].

Methods

Study Population

Subjects were randomly selected population controls from a case–control study on diet and heart disease conducted in Costa Rica as previously described [13]. Participation was 88%. We included a total of 1,334 men and 451 women. Subjects gave informed consent on documents approved by the Human Subjects Committee of the Harvard School of Public Health and the University of Costa Rica.

Data Collection

Data were collected by trained personnel visiting the subjects at their homes. Subjects provided information on socioeconomic, demographic, diet, and medical history during an interview. Anthropometric measures collected were height, weight, waist circumference and skinfold thickness for subscapular, suprailiac and triceps. All anthropometric measurements were taken from subjects wearing light clothing and no shoes, and collected in duplicate and averaged out for analyses. Field workers measured triceps (posterior upper arm, midway between the elbow and acromion), subscapular (1 cm below the lower tip of the scapula), and suprailiac (at the midline and above the iliac crest) using Holtain skinfold calipers. All measurements were taken on the right side of the body. Nonstretching fiberglass or metal tapes were used to measure the waist (smallest horizontal trunk circumference) and hip (largest horizontal circumference around the hip and buttocks) girths. A steel anthropometer and a Detecto bathroom scale or a Seca Alpha Model 770 digital scale accurate to 50 g were used to measure height and weight, respectively. The two scales were calibrated biweekly. Body mass index (BMI) was then calculated as weight (kg) divided by the square of the height (m^2). BMI categories were defined by general accepted cut-off points. Normal weight was determined as a BMI lower than 25 kg/m^2, overweight as a BMI between 25 and 30 kg/m^2 and obesity was defined as a BMI above 30 kg/m^2.

A subcutaneous adipose tissue biopsy was collected from the upper buttock with a 16-gauge needle and disposable syringe following procedures previously described [14]. Samples were stored in a cooler at 4 °C and transported to the fieldwork station where they were stored at −80 °C. Within 6 months, they were shipped on dry ice to the Harvard School of Public Health for long term storage in nitrogen tanks. Energy and nutrient intakes were assessed with a food frequency questionnaire developed and validated specifically for use among Costa Ricans [14, 15]. Dietary information obtained by the food frequency questionnaire was used for validation purposes and to assess confounding by dietary factors that do not have good biomarkers of intake. The fatty acid composition of all foods commonly used in Costa Rica was determined [16] and incorporated into the nutrient calculation.

Fatty Acid Analysis

Fatty acids were extracted from adipose tissue and analyzed by gas–liquid chromatography (GLC) [14]. The fatty acids in the adipose tissue biopsy were extracted using hexane/isopropanol (3:2) mixture and esterified with methanol and acetyl chloride. After esterification, the methanol and acetyl chloride were evaporated and the fatty acid methyl esters were dissolved in isooctane. The methyl esters were quantified by GLC using the following parameters: fused silica capillary *cis*/*trans*-column SP2560, 100 m × 250 mm internal diameters × 0.20 mm film

(Supelco, Belefonte, PA); splitless injection port at 240 °C; hydrogen carrier gas at 1.3 ml/min, constant flow; Hewlett-Packard Model (now Agilent) GC 6890 FID gas chromatograph with 7673 Autosampler injector (Palo Alto, CA); 1 ml of sample injected; temperature program of 90–170 °C at 10 °C/min, 170 °C for 5 min, 170–175 °C at 5 °C/min, 175–185 °C at 2 °C/min, 185–190 °C at 1 °C/min, 190–210 at 5 °C/min, 210 °C for 5 min, 210–250 °C at 5 °C/min, 250 °C for 10 min. Peak retention time and area percentages of total fatty acids were identified by injecting known standards (catalog numbers 47791, GLC-463, GLC-481b, N-16-M, N-21-M, N-23-M, N-24-M, U-45-M, U-46-M, U-59-M, U-71-M and UC-60-M, Nu-Chek_prep, Elysium, MN), and analyzed with the Agilent Technologies ChemStation A.08.03 software (Agilent Technologies, Inc., Palo Alto, CA). Twelve identical samples were analyzed throughout the study. The inter-assay coefficients of variation for 18:1*t*, 18:2*t*, and 18:2n-7*t* (9*c*,11*t*) fatty acids were 15.7, 6.4, and 5.2%, respectively. We previously showed that the *trans*-fatty acid concentration in adipose tissue is a good biomarker of *trans*-fatty acid intake in the Costa Rican population [14].

Statistical Analysis

Data are presented as means ± SD or *n* (%). The *trans*-fatty acids that we used in the analysis were defined as follows: 18:1*t* = 18:1*t* (n-7*t*) + 18:1*t* (n-9*t*) + 18:1*t* (n-11*t*); 18:2*t* = 18:2*t* (n-6*tt*) + 18:2*t* (n-6*ct*) + 18:2*t* (n-6*tc*). Data were analyzed with the SAS software v9.1 (SAS Institute, Cary, NC, USA) with the significance level set at $P < 0.05$. Partial Spearman correlation coefficients were calculated, adjusted for age, sex, and area of residence for the association between adipose tissue fatty acids and several subject characteristics and potential confounders.

Multivariate regression was used to estimate the β coefficients and *P* values of the association between adipose tissue *trans*-fatty acid isomer content and indicators of adiposity. These calculations were adjusted for the matching factors age, sex and area of residence. To account for variation in lifestyle and dietary habits, further models adjusted for smoking status, physical activity and income, and self-reported history of diabetes and hypertension. In a third model we also adjusted for adipose tissue alpha-linolenic acid, which is present in partially hydrogenated soybean oil used for cooking and was the major dietary source of 18:2*t*-fatty acids in this population [13].

Other potential confounders that were examined but not included in the final models were alcohol intake, fruit and vegetable intake, currently on weight loss diet, menopausal status, adipose tissue linoleic acid, arachidonic acid, long chain omega-3 fatty acids, and dietary patterns.

Results

The average BMI of all subjects was 26.4 kg/m^2 (Table 1). Subjects in the obese category were more likely to be female, have a higher income, a history of diabetes and hypertension and less likely to be physically active or smoke. Obese subjects had higher adipose levels of 18:2*t*-fatty acids and arachidonic acid, and lower levels of 18:1*t*-fatty acids, linoleic acid and alpha-linolenic acid.

The mean percentage plus standard deviation (SD) of *trans*-fatty acids in adipose tissue as percentage of total fatty acids was 2.7 ± 0.7 for total *trans*-fatty acids, 1.47 ± 0.53 for 18:1*t*, 1.15 ± 0.35 for 18:2*t,* 0.15 ± 0.06 for 16:1n-7*t* and 0.56 ± 0.18 for rumenic acid (Table 1).

Adipose tissue *trans*-fatty acid content corresponded with their intake from the diet. The average *trans*-fatty acid intake as a percentage of total calories was 0.77 ± 0.30% for 18:1*t*, 0.07 ± 0.07% for 18:2*t*, 0.06 ± 0.03% for 16:1n-7*t* and 0.10 ± 0.05% for rumenic acid.

Adipose tissue 18:1*t*, 18:2*t* and rumenic acid, but not 16:1n-7*t* were inversely associated with physical activity (Table 2). Within adipose tissue, the strongest correlation was between 18:1*t* and 18:2*t*-fatty acids (Spearman $r = 0.51$). Rumenic acid was weakly inversely associated with linoleic acid and alpha-linolenic acid (Spearman $r = -0.17$ and -0.08, respectively) and weakly positively with arachidonic acid (Spearman $r = 0.06$) (data not shown).

Results of the multivariate regression models for associations were reported as one SD unit increase in adipose tissue *trans*-fatty acids and measures of adiposity (Table 3). Increased adipose tissue 16:1n-7*t*- and 18:2*t*-fatty acids were associated with higher BMI and waist circumference, and 18:1*t*-fatty acids were associated with lower BMI and waist circumference. In contrast, 16:1n-7*t*-fatty acids were inversely associated with individual skinfold thicknesses, while rumenic acid was positively associated with each skinfold thickness. Adipose tissue 18:1*t*-fatty acids were not significantly associated with skinfold thickness. Rumenic acid was not significantly associated with BMI or waist circumference, but was positively related to skinfold thicknesses. In additional analyses, alpha-linolenic acid was inversely associated with BMI (model 3, beta −4.2, $p < 0.0001$) and waist circumference (model 3, beta −10.0, $p < 0.0001$).

Discussion

This cross-sectional study in the Costa Rican population evaluated the association between adipose tissue *trans*-fatty acid isomers and adiposity. We included both industrially produced (18:1*t* and 18:2*t*) and naturally occurring (16:1n-7*t* and 18:2n-7, 9*c*, 11*t*) *trans*-fatty acids. The most

Table 1 General characteristics of Costa Rican subjects by BMI category

	All subjects (n = 1,785)	Normal weight BMI < 25 kg/m^2 (n = 688)	Overweight 25 < BMI < 30 kg/m^2 (n = 787)	Obese BMI > 30 kg/m^2 (n = 310)
Age (years)	58 ± 11	58 ± 12	58 ± 11	57 ± 11
Women (%)	25	20	25	38
Area of residence rural (%)	34	35	34	35
Monthly household income, ($US/mo)	583 ± 429	548 ± 417	597 ± 430	631 ± 449
Physical activity (METS/day)	35.3 ± 15.0	36.9 ± 17.2	35.1 ± 13.7	32.3 ± 12.4
Current smokers (%)[a]	22	30	18	13
History of diabetes (%)[b]	14	11	14	21
History of hypertension (%)[b]	29	18	32	48
Measures of adiposity				
BMI (kg/m^2)	26.4 ± 4.2	22.5 ± 1.9	27.2 ± 1.4	33.2 ± 3.0
Waist circumference (cm)	91.0 ± 9.9	83.1 ± 6.7	93.1 ± 6.0	103.2 ± 8.6
Triceps skin fold (mm)	13.8 ± 6.7	11.0 ± 4.9	14.2 ± 6.1	18.8 ± 8.1
Subscapular skin fold (mm)	16.8 ± 7.5	13.0 ± 4.6	17.9 ± 6.8	22.4 ± 9.7
Suprailiac skin fold (mm)	12.5 ± 6.8	9.7 ± 5.1	13.2 ± 6.5	16.9 ± 8.0
Adipose tissue fatty acids (% of total fatty acids)[c]				
Total 18:1*t*[d]	1.47 ± 0.53	1.57 ± 0.56	1.43 ± 0.52	1.35 ± 0.47
18:1 (n-12*t*)	0.61 ± 0.25	0.64 ± 0.26	0.60 ± 0.25	0.57 ± 0.23
18:1 (n-9*t*)	0.50 ± 0.20	0.53 ± 0.22	0.48 ± 0.19	0.46 ± 0.18
18:1 (n-7*t*)	0.36 ± 0.18	0.39 ± 0.20	0.35 ± 0.18	0.32 ± 0.15
Total 18:2*t*	1.15 ± 0.35	1.15 ± 0.38	1.15 ± 0.35	1.13 ± 0.31
18:2 (n-6*tt*)	0.28 ± 0.10	0.28 ± 0.10	0.28 ± 0.10	0.28 ± 0.09
18:2 (n-6c*t*)	0.56 ± 0.18	0.56 ± 0.19	0.56 ± 0.18	0.55 ± 0.16
18:2 (n-6*t*c)	0.31 ± 0.10	0.31 ± 0.11	0.31 ± 0.10	0.30 ± 0.09
16:1 (n-7*t*)	0.15 ± 0.06	0.14 ± 0.06	0.15 ± 0.06	0.15 ± 0.05
Rumenic acid[f]	0.56 ± 0.18	0.56 ± 0.18	0.56 ± 0.17	0.57 ± 0.17
18:2 (n-6)	15.63 ± 3.81	15.68 ± 3.95	15.68 ± 3.85	15.40 ± 3.34
20:4 (n-6)	0.47 ± 0.14	0.41 ± 0.12	0.50 ± 0.14	0.54 ± 0.13
18:3 (n-3)	0.65 ± 0.21	0.68 ± 0.22	0.65 ± 0.21	0.61 ± 0.19
Dietary fatty acids (% fatty acids)				
Total 18:1*t*[d]	2.4 ± 0.9	2.4 ± 1.0	2.4 ± 0.9	2.4 ± 0.9
Total 18:2*t*	1.4 ± 1.0	1.4 ± 1.1	1.4 ± 1.0	1.4 ± 1.0
16:1 (n-7*t*)	0.19 ± 0.08	0.19 ± 0.08	0.19 ± 0.08	0.19 ± 0.08
Rumenic acid[f]	0.32 ± 0.13	0.32 ± 0.14	0.32 ± 0.13	0.33 ± 0.14

Values are means ± SD or n (%)

METS/day metabolic equivalents for 24 h

[a] Smoking ≥1 cigarette/day

[b] Self-reported

[c] As percent of total adipose fatty acids

[d] 18:1*t* is the sum of 18:1n-7*t*, 18:1n-9*t* and 18:1n-11*t*

[e] 18:2*t*-is the sum of 18:2n-6*tt,* 18:2n-6*ct* and 18:2n-6*tc*

[f] Rumenic acid is the 9c, 11*t* isomer of 18:2 (n-7*t*) conjugated linoleic acid

striking result was the apparent heterogeneity in the associations between the different *trans*-fatty acid isomers in adipose tissue and measures of adiposity.

Among the specific *trans*-fatty acids, the most consistent finding was that the industrial 18:2*t*-fatty acids, coming from partially hydrogenated oils used for cooking, were

Table 2 Correlations between adipose fatty acids and general characteristics of all subjects

Adipose tissue fatty acids:	18:1*t*[c]	18:2*t*[d]	16:1n-7*t*	Rumenic acid[e]
General characteristics				
Monthly household income ($US/mo)	0.13***	0.11***	0.15***	0.06**
Physical activity (METS/day)	−0.10***	−0.07**	0.06*	−0.10***
Current smokers (%)[a]	−0.09**	−0.07**	−0.10***	0.06**
History of diabetes (%)[b]	−0.04	−0.05*	0.05*	−0.07**
History of hypertension (%)[b]	0.06**	−0.007	0.04	−0.05*
Adipose tissue fatty acids (% total fatty acids)				
Total 18:1*t*[c]	–	0.51***	0.06**	0.32***
Total 18:2*t*[d]	0.51***	–	0.003	0.37***
16:1n-7*t*	0.06**	0.003	–	0.11***
Rumenic acid[e]	0.32***	0.37***	0.11***	–
18:2 (n-6)	0.08**	0.45***	0.15***	−0.17***
20:4 (n-6)	−0.34***	−0.04	0.07**	0.06*
18:3 (n-3)	0.05*	0.46***	0.14***	−0.08**
Dietary fatty acids (% total fatty acids)				
Total 18:1*t*	0.28***	0.39***	−0.003	0.25***
Total 18:2*t*	0.19***	0.52***	−0.08***	0.05
16:1n-7t	0.05*	−0.03	0.28***	0.21***
Rumenic acid[e]	0.06**	−0.03	0.31***	0.23***

Partial Spearman correlation coefficients between adipose tissue *trans*-fatty acids (% of total fatty acids) and several variables (adjusted for age, sex and area of residence)

METS/day metabolic equivalents for 24 h

* $P < 0.05$; ** $P < 0.01$; *** $P < 0.0001$, $n = 1{,}785$

[a] Smoking $\geq$ 1 cigarette/day

[b] Self-reported

[c] 18:1*t* is the sum of 18:1n-7*t*-, 18:1n-9*t*-, and 18:1n-11*t*-adipose tissue fatty acids

[d] 18:2*t* is the sum of 18:2n-6*tt*-, 18:2n-6*ct*-, and 18:2n-6*tc*-adipose tissue fatty acids

[e] Rumenic acid is the 9*c*,11*t*-isomer of 18:2 (n-7*t*) conjugated linoleic acid

associated with increased visceral and subcutaneous adiposity.

In addition to positive associations with adiposity, 18:2 *trans*-fatty acids have been found to be more adversely related to risk of cardiovascular disease (CVD) than are 18:1 *trans*-fatty acids [17–19]. A possible explanation for these adverse effects on CVD is that 18:2*t*-fatty acids are incorporated in the *sn*-2 position of phospholipids, where polyunsaturated fatty acids are usually found. This substitution might affect membrane properties and have effects on atherosclerotic pathways through increased macrophage adhesion [20].

16:1n-7*t*-fatty acids, from ruminant food sources, have not been widely investigated. In this study 16:1n-7*t*-fatty acids were positively associated with BMI and waist circumference, and inversely with skinfold thickness. This suggests that 16:1n-7*t*-may be associated with increased visceral, rather than subcutaneous fat storage. These findings are in contrast with rumenic acid, also from ruminant food sources, which is associated with increased subcutaneous adiposity. Although differences in fatty acid metabolism between visceral and subcutaneous fat depots have been found [21], we cannot explain the different associations of these natural *trans*-fatty acids with visceral and subcutaneous adiposity.

The finding of an inverse association between adipose tissue 18:1*t*-fatty acids and BMI is unexpected, given the positive associations found in other studies where 18:1*t*-fatty acids were the main *trans*-fatty acids in the diet [6, 8]. However, although the distribution of fat in monkeys fed a *trans*-fat diet favored an intra-abdominal distribution, the increases in body weight, weight circumference, subcutaneous and intra-abdominal fat were not significant, which is in line with our study [6]. We cannot exclude that this redistribution of fat also happened in our subjects. Also, Koh-Banerjee et al. [7] reported an increase in waist gain with higher *trans*-fat intake, but they did not validate the intake of *trans*-fatty acids in their food frequency questionnaire, which could introduce considerable bias since *trans*-fat content of foods has changed over time. In addition, short

Table 3 Multivariate regression coefficients for the association between adipose tissue *trans*-fatty acids (shown as one standard deviation change) and measures of adiposity

	Adipose tissue *trans*-fatty acids			
	18:1*t*[a]	18:2*t*[b]	16:1n-7*t*	Rumenic acid[c]
BMI (kg/m^2)				
Model 1	−0.91 ± 0.12***	0.20 ± 0.12	0.35 ± 0.10**	0.20 ± 0.11
Model 2	−0.92 ± 0.11***	0.12 ± 0.12	0.22 ± 0.10*	0.28 ± 0.11**
Model 3	−1.13 ± 0.11***	0.69 ± 0.13***	0.37 ± 0.10**	0.03 ± 0.11
Waist circumference (cm)				
Model 1	−2.39 ± 0.27***	0.58 ± 0.28*	0.87 ± 0.23**	0.75 ± 0.25**
Model 2	−2.39 ± 0.26***	0.43 ± 0.27	0.60 ± 0.22**	0.92 ± 0.24**
Model 3	−2.88 ± 0.26***	1.78 ± 0.31***	0.95 ± 0.22***	0.34 ± 0.25
Subscapular skinfold (mm)				
Model 1	−0.20 ± 0.19	0.15 ± 0.20	−2.42 ± 0.17***	1.79 ± 0.18***
Model 2	−0.23 ± 0.19	0.05 ± 0.19	−2.61 ± 0.16***	1.91 ± 0.18***
Model 3	−0.69 ± 0.18**	1.33 ± 0.22***	−2.27 ± 0.16***	1.36 ± 0.18***
Triceps skinfold (mm)				
Model 1	0.08 ± 0.15	0.11 ± 0.16	−1.51 ± 0.13***	1.30 ± 0.15***
Model 2	0.05 ± 0.15	0.05 ± 0.16	−1.61 ± 0.13***	1.35 ± 0.14***
Model 3	−0.27 ± 0.15	0.93 ± 0.18***	−1.38 ± 0.13***	0.97 ± 0.15***
Suprailiac skinfold (mm)				
Model 1	−0.23 ± 0.16	−0.07 ± 0.17	−1.78 ± 0.14***	1.35 ± 0.15***
Model 2	−0.25 ± 0.16	−0.14 ± 0.17	−1.89 ± 0.14***	1.41 ± 0.15***
Model 3	−0.55 ± 0.16**	0.70 ± 0.19**	−1.67 ± 0.14***	1.06 ± 0.16***

Associations are β coefficients for 1 standard deviation (SD) difference in percentage of *trans*-fatty acids ± standard error, SD 16:1n-7*t* = 0.06, SD 18:1*t* = 0.53, SD 18:2*t* = 0.35, SD rumenic acid = 0.18

Model 1: Includes all *trans*-fatty acid variables plus age, sex and area of residence

Model 2: Model 1 plus smoking status, physical activity, income, self reported history of diabetes and hypertension

Model 3: Model 2 plus energy intake and adipose tissue 18:3n-3 (alpha-linolenic acid)

* $P < 0.05$; ** $P < 0.01$; *** $P < 0.0001$, $n = 1{,}785$

[a] 18:1*t* is the sum of 18:1n-7*t*-, 18:1n-9*t*-, and 18:1n-11*t*-adipose tissue fatty acids

[b] 18:2*t* is the sum of 18:2n-6*tt*-, 18:2n-6*ct*-, and 18:2n-6*tc*-adipose tissue fatty acids

[c] Rumenic acid is the 9*c*,11*t*-isomer of 18:2 (n-7*t*)-conjugated linoleic acid

term studies conducted in small animals fed 18:1*t*-fatty acids as their main source of *trans*-fatty acids support our findings. These randomized controlled trials with rabbits and mice showed decreases in body weight, and perirenal and epididymal weight when fed diets high in 18:1*t*-fatty acids [22, 23]. The discrepancy between the observations in this study and those in other studies on industrial *trans*-fatty acids and weight might also be explained by the relatively low consumption of 18:1*t*-fatty acids in Costa Rica.

Adipose tissue rumenic acid was not significantly associated with BMI or waist circumference but did relate positively to skinfold thickness. Studies in rodents show associations between CLA and decreases in body fat [24], but in humans the effects of CLA consumption on body weight are inconsistent [9, 10], which is in line with our findings.

Adiposity is primarily caused by an imbalance in energy consumption, leading to deposition of excess calories. However, Flint et al. [25] showed that *trans*-fatty acid consumption had no effect on either appetite or energy expenditure. Food sources of 18:1*t*-fatty acids are mostly processed baked goods, while the main source of 18:2*t*-fatty acids in our population is cooking oil. However, this does not logically explain why 18:1*t*-fatty acids are associated with decreased adiposity, and 18:2*t*-fatty acids with increased adiposity. A clear mechanism for the observed associations cannot be given. Also, biochemical mechanisms to explain these observations such as interference with essential fatty acid desaturation and elongation [26], insulin sensitivity [27] and fat cell size [28] does not explain the inverse associations we see with 18:1*t*-fatty acids and adiposity.

Together with the studies on *trans*-fatty acid isomers and CVD risk, the results from this study suggest that different associations exist between the individual *trans*-

fatty acid isomers and health outcomes. Currently there is a trend among the food industry to reduce *trans*-fatty acids in common foods, which then might be replaced with oils that are less hydrogenated and contain relatively more 18:2*t*-fatty acids. Although the primary goal is to improve public health, this might have more adverse effects because of the adverse associations of 18:2*t*-fatty acids with CVD and adiposity. While a causal effect cannot be determined in this study, extrapolation of our findings suggests that eliminating all industrial 18:2*t*-fatty acids would be associated with a 7.1-cm decrease in waist circumference.

The use of adipose tissue *trans*-fatty acids is both a strength and a limitation of the study. Adipose tissue levels are not dependent on imperfect measures of dietary intake or food composition tables to determine the amount of *trans*-fatty acids in foods, which can pose a problem in dietary analyses since the *trans*-fatty acid content of foods can vary considerably over time. However, the concentration of fatty acids in adipose tissue not only reflects intake, but also metabolism and substitutions between fatty acids.

Reverse causation may influence the associations found in this study; increases in body weight are readily noticed by participants, which can lead to changes in energy intake and the choice of foods or to increased physical activity. Also, residual confounding is possible because of imperfect measurements of physical activity, dietary factors, and health consciousness.

In summary, our study provides evidence that individual *trans*-fatty isomers have divergent effects on adiposity. The main finding is the consistent adverse association between industrial 18:2*t* and all measures of adiposity. Also, 16:1n-7*t* and rumenic acid, both *trans*-isomers mainly found in dairy foods, have divergent effects which has not been reported previously. These isomer-specific associations pose new questions on how *trans*-fatty acids influence metabolism and weight. Other prospective and intervention studies are necessary to examine this further. Regardless of an association with adiposity, elimination of partially hydrogenated oils from the diet is important in efforts to reduce the burden of cardiovascular disease.

Conflict of interest statement None.

References

1. Katan MB, Zock PL, Mensink RP (1995) Dietary oils, serum lipoproteins, and coronary heart disease. Am J Clin Nutr 61:1368S–1373S
2. Mozaffarian D, Katan MB, Ascherio A, Stampfer MJ, Willett WC (2006) *Trans*-fatty acids and cardiovascular disease. N Engl J Med 354:1601–1613
3. Griinari JM, Corl BA, Lacy SH, Chouinard PY, Nurmela KV, Bauman DE (2000) Conjugated linoleic acid is synthesized endogenously in lactating dairy cows by Delta(9)-desaturase. J Nutr 130:2285–2291
4. Kepler CR, Hirons KP, McNeill JJ, Tove SB (1966) Intermediates and products of the biohydrogenation of linoleic acid by Butyrinvibrio fibrisolvens. J Biol Chem 241:1350–1354
5. Smit LA, Baylin A, Campos H (2010) Conjugated linoleic acid in adipose tissue and risk of myocardial infarction. Am J Clin Nutr 92(1):34–40
6. Kavanagh K, Jones KL, Sawyer J, Kelley K, Carr JJ, Wagner JD, Rudel LL (2007) *Trans* fat diet induces abdominal obesity and changes in insulin sensitivity in monkeys. Obesity (Silver Spring) 15:1675–1684
7. Koh-Banerjee P, Chu NF, Spiegelman D, Rosner B, Colditz G, Willett W, Rimm E (2003) Prospective study of the association of changes in dietary intake, physical activity, alcohol consumption, and smoking with 9-year gain in waist circumference among 16,587 US men. Am J Clin Nutr 78:719–727
8. Field AE, Willett WC, Lissner L, Colditz GA (2007) Dietary fat and weight gain among women in the nurses' health study. Obesity (Silver Spring) 15:967–976
9. Salas-Salvado J, Marquez-Sandoval F, Bullo M (2006) Conjugated linoleic acid intake in humans: a systematic review focusing on its effect on body composition, glucose, and lipid metabolism. Crit Rev Food Sci Nutr 46:479–488
10. Li JJ, Huang CJ, Xie D (2008) Anti-obesity effects of conjugated linoleic acid, docosahexaenoic acid, and eicosapentaenoic acid. Mol Nutr Food Res 52:631–645
11. Baylin A, Kim MK, Donovan-Palmer A, Siles X, Dougherty L, Tocco P, Campos H (2005) Fasting whole blood as a biomarker of essential fatty acid intake in epidemiologic studies: comparison with adipose tissue and plasma. Am J Epidemiol 162:373–381
12. London SJ, Sacks FM, Caesar J, Stampfer MJ, Siguel E, Willett WC (1991) Fatty acid composition of subcutaneous adipose tissue and diet in postmenopausal US women. Am J Clin Nutr 54:340–345
13. Kabagambe EK, Baylin A, Ascherio A, Campos H (2005) The type of oil used for cooking is associated with the risk of nonfatal acute myocardial infarction in Costa Rica. J Nutr 135:2674–2679
14. Baylin A, Kabagambe EK, Siles X, Campos H (2002) Adipose tissue biomarkers of fatty acid intake. Am J Clin Nutr 76:750–757
15. Kabagambe EK, Baylin A, Allan DA, Siles X, Spiegelman D, Campos H (2001) Application of the method of triads to evaluate the performance of food frequency questionnaires and biomarkers as indicators of long-term dietary intake. Am J Epidemiol 154:1126–1135
16. Baylin A, Siles X, Donovan-Palmer A, Fernandez X, Campos H (2007) Fatty acid composition of Costa Rican foods including *trans*-fatty acid content. J Food Comp Anal 20:182–192
17. Baylin A, Kabagambe EK, Ascherio A, Spiegelman D, Campos H (2003) High 18:2 *trans*-fatty acids in adipose tissue are associated with increased risk of nonfatal acute myocardial infarction in Costa Rican adults. J Nutr 133:1186–1191
18. Lemaitre RN, King IB, Raghunathan TE, Pearce RM, Weinmann S, Knopp RH, Copass MK, Cobb LA, Siscovick DS (2002) Cell membrane *trans*-fatty acids and the risk of primary cardiac arrest. Circulation 105:697–701
19. Lemaitre RN, King IB, Mozaffarian D, Sotoodehnia N, Rea TD, Kuller LH, Tracy RP, Siscovick DS (2006) Plasma phospholipid *trans*-fatty acids, fatal ischemic heart disease, and sudden cardiac

death in older adults: the cardiovascular health study. Circulation 114:209–215
20. Calder PC, Bond JA, Harvey DJ, Gordon S, Newsholme EA (1990) Uptake and incorporation of saturated and unsaturated fatty acids into macrophage lipids and their effect upon macrophage adhesion and phagocytosis. Biochem J 269:807–814
21. Hannukainen JC, Kalliokoski KK, Borra RJ, Viljanen AP, Janatuinen T, Kujala UM, Kaprio J, Heinonen OJ, Viljanen T, Haaparanta M, Iozzo P, Parkkola R, Nuutila P (2010) Higher free fatty acid uptake in visceral than in abdominal subcutaneous fat tissue in men. Obesity (Silver Spring) 18:261–265
22. Faulconnier Y, Roy A, Ferlay A, Chardigny JM, Durand D, Lorenz S, Gruffat D, Chilliard Y (2006) Effect of dietary supply of butters rich either in *trans*-10–18 : 1 or in *trans*-11–18 : 1 plus *cis*-9, *trans*-11–18 : 2 on rabbit adipose tissue and liver lipogenic activities. Br J Nutr 96:461–468
23. Atal S, Zarnowski MJ, Cushman SW, Sampugna J (1994) Comparison of body weight and adipose tissue in male C57Bl/6 J mice fed diets with and without *trans*-fatty acids. Lipids 29:319–325
24. Park Y, Albright KJ, Liu W, Storkson JM, Cook ME, Pariza MW (1997) Effect of conjugated linoleic acid on body composition in mice. Lipids 32:853–858
25. Flint A, Helt B, Raben A, Toubro S, Astrup A (2003) Effects of different dietary fat types on postprandial appetite and energy expenditure. Obes Res 11:1449–1455
26. Thomassen MS, Rortveit T, Christiansen EN, Norum KR (1984) Changes in the content of n-6 fatty acids in liver phospholipids in rats as a consequence of partially hydrogenated dietary oils. Br J Nutr 51:315–322
27. Ibrahim A, Natrajan S, Ghafoorunissa R (2005) Dietary *trans*-fatty acids alter adipocyte plasma membrane fatty acid composition and insulin sensitivity in rats. Metabolism 54:240–246
28. Ostlund-Lindqvist AM, Albanus L, Croon LB (1985) Effect of dietary *trans*-fatty acids on microsomal enzymes and membranes. Lipids 20:620–624

Lipids (2010) 45:701–711
DOI 10.1007/s11745-010-3454-8

ORIGINAL ARTICLE

Enhanced Aortic Macrophage Lipid Accumulation and Inflammatory Response in LDL Receptor Null Mice Fed an Atherogenic Diet

Shu Wang · Dayong Wu · Nirupa R. Matthan · Stefania Lamon-Fava · Jaime L. Lecker · Alice H. Lichtenstein

Received: 15 March 2010 / Accepted: 8 July 2010 / Published online: 5 August 2010

Abstract The effect of an atherogenic diet on inflammatory response and elicited peritoneal macrophage (Mϕ) cholesterol accumulation in relation to aortic lesion formation was assessed in LDL receptor null (LDLr−/−) mice. Mice were fed an atherogenic or control diet for 32 weeks. The atherogenic relative to control diet resulted in significantly higher plasma monocyte chemoattractant protein-1 (MCP-1), tumor necrosis factor alpha (TNFα) and interleukin-6 (IL-6) concentrations, more aortic wall Mϕ deposition, higher serum non HDL-cholesterol concentrations and total cholesterol to HDL-cholesterol ratios, and greater accumulation of both aortic free and esterified cholesterol. Elicited peritoneal Mϕ selectively accumulated longer chain unsaturated fatty acids in their membrane, independent of the dietary fatty acid profile. Elicited peritoneal Mϕ isolated from mice fed the atherogenic relative to control diet had significantly less arachidonic acid levels, accumulated significantly higher esterified cholesterol, had significantly higher mRNA levels and secretion of MCP-1, and mRNA and protein levels of ATP-binding cassette A1. Diet treatment had no significant effect in elicited peritoneal Mϕ on TNFα and IL-6 mRNA levels and secretion. These data suggest that the atherogenic relative to control diet resulted in higher plasma inflammatory factor concentrations, less favorable lipoprotein profile, higher elicited peritoneal Mϕ cholesterol accumulation and inflammatory factor secretion, and more aortic wall Mϕ deposition, which in turn were associated with greater aortic cholesterol accumulation.

Keywords Atherogenic diet · Atherosclerosis · Cholesterol accumulation · Inflammatory response · Macrophage · LDLr−/− mouse

Abbreviations

Mϕ	Macrophage
LDLr−/−	LDL receptor null
MCP-1	Monocyte chemoattractant protein-1
TNFα	Tumor necrosis factor alpha
IL-6	Interleukin-6
MSR1	Membrane bound Mϕ scavenger receptor 1
CD36	Cluster of differentiation 36
ABCA1	ATP-binding cassette A1
SR-B1	Scavenger receptor B class 1
CCR2	CC chemokine receptor 2
PBS	Phosphate-buffered saline
TC	Total cholesterol
FC	Free cholesterol

Electronic supplementary material The online version of this article (doi:10.1007/s11745-010-3454-8) contains supplementary material, which is available to authorized users.

S. Wang · N. R. Matthan · J. L. Lecker · A. H. Lichtenstein (✉)
Cardiovascular Nutrition Laboratory, JM USDA Human Nutrition Research Center on Aging, Tufts University, 711 Washington Street, Boston, MA 02111, USA
e-mail: alice.lichtenstein@tufts.edu

D. Wu
Nutritional Immunology Laboratory, JM USDA Human Nutrition Research Center on Aging, Tufts University, 711 Washington Street, Boston, MA 02111, USA

S. Lamon-Fava
Lipid Metabolism Laboratory, JM USDA Human Nutrition Research Center on Aging, Tufts University, 711 Washington Street, Boston, MA 02111, USA

Present Address:
S. Wang
Department of Nutrition, Hospitality and Retailing, Texas Tech University, Lubbock, TX 79409, USA

EC	Esterified cholesterol
BCA	Bicinchoninic acid
HDL-C	High density lipoprotein-cholesterol
non HDL-C	Non-high density lipoprotein-cholesterol
LPS	Lipopolysaccharide
SD	Standard deviation
MUFA	Monounsaturated fatty acid
PUFA	Polyunsaturated fatty acid
ALA	Alpha-linolenic acid
EPA	Eicosapentaenoic acid
DHA	Docosahexaenoic acid
LNA	Linoleic acid
ARA	Arachidonic acid
CVD	Cardiovascular disease
TLR4	Toll-like receptor 4
NF-kB	Nuclear factor-kappa B
ox-LDL	Oxidized LDL
LXR	Liver-X-receptors

Introduction

Historically, lipoprotein profiles and lipid accumulation in the blood vessel wall have been the major focus of research related to atherogenesis. More recently, a preponderance of evidence from clinical and experimental studies has suggested that inflammation is an important factor [1]. Macrophages (Mϕ) play a critical role in both intracellular cholesterol accumulation and deposition in the arterial wall. Aortic Mϕs express scavenger receptors that take up modified lipoproteins through membrane-bound Mϕ scavenger receptor 1 (MSR1) and CD36. Increased expression of MSR1 and CD36 facilitates the uptake of modified lipoproteins [2, 3]. Two Mϕ membrane proteins involved in cholesterol efflux are ATP-binding cassette A1 (ABCA1) and scavenger receptor B class 1 (SR-B1) [4]. When the Mϕ cholesterol influx is greater than the efflux, cholesterol homeostasis in Mϕ is disturbed, and cholesterol accumulation is favored. The resulting Mϕ-derived foam cells produce reactive oxygen species, which in turn modify lipoproteins, and secrete pro-inflammatory factors, which amplify the local inflammatory reaction [1].

Exposure of endothelial cells to inflammatory factors results in the expression of monocyte chemoattractant protein-1 (MCP-1) and its receptor, CC chemokine receptor 2 (CCR2), which direct the migration of monocytes into the intimal wall. Subsequent exposure of the monocytes to Mϕ colony-stimulating factor causes differentiation to Mϕ. Overexpression of MCP-1 is positively associated with monocyte accumulation in fatty streaks [5]. Major pro-inflammatory factors include interleukin-6 (IL-6) and tumor necrosis factor alpha (TNFα). They are synthesized by monocytes/Mϕ and several other types of cells, such as T cells, endothelial cells and adipocytes, and in turn stimulate the synthesis of other inflammatory factors [6, 7]. Dietary fatty acids and cholesterol have been shown to alter the concentrations of these biomarkers of inflammation and the atherogenic process [8–10].

We used the LDL receptor null (LDLr−/−) mouse fed diets high in saturated fat and cholesterol (atherogenic diet) or low in those components (control diet) as an animal model to assess the relationship between aortic lesion formation and the inflammatory response. Our hypothesis was that the atherogenic diet would accelerate aortic lipid accumulation due to induction of an atherogenic lipoprotein profile, elevate plasma inflammatory biomarker concentrations, increase cholesterol accumulation in and inflammatory factor secretion from elicited peritoneal Mϕ, and change expression and protein levels of genes associated with these processes.

Experimental Procedures

Animals and Diets

Twenty-two 8-week-old, male LDLr−/− mice (Jackson Laboratory, Bar Harbor, Maine) initially weighing 20.2 ± 2.8 g were placed in individual cages with stainless-steel wire bottoms in a windowless room maintained at 22–24°C, 45% relative humidity and a daily 10/14 light/dark cycle with the light period from 0600 to 1600 hours. After 1 week of acclimation, mice were weighed and randomly assigned to one of two groups. The mice were fed either a control diet low in butterfat (4% fat, w/w, 9% energy) and cholesterol (0.02%, w/w) or an atherogenic diet high in butterfat (20% fat, w/w, 38% energy) and cholesterol (0.2%, w/w) ad libitum. The atherogenic diet was modified from Harlan Teklad atherogenic diet TD.88137. The composition of the diets is provided in Supplementary Table 1, and the fatty acid profile of the diets is provided in Supplementary Table 2. Body weight and food intake were recorded weekly over a 32-week period. In order to ensure adequate quantities of Mϕ for the proposed work, 5 days prior to killing, mice were given an intraperitoneal injection of 1.0 ml Brewer thioglycollate broth (4.05 g/100 ml) to elicit peritoneal Mϕ accumulation [11]. Immediately after a 16–18 h fast, the mice were anesthetized with CO_2 and killed by exsanguination. Blood was collected by retro-orbital bleeding to harvest serum at weeks 0, 12 and 32 and by cardiac puncture to harvest plasma at week 32. Heart, aorta and elicited peritoneal Mϕ were collected and treated as described in the next section. Serum and plasma were obtained by blood centrifugation at

1,100×g at 4°C for 25 min. The animal protocol was approved by the Animal Care and Use Committee of the Jean Mayer USDA Human Nutrition Research Center on Aging, Tufts University, and was in accordance with guidelines provided by the National Institutes of Health Guide for the Care and Use of Laboratory Animals. Data from the mice fed the atherogenic diet were used for comparison purposes to address an unrelated experimental question [12].

Atherosclerosis Lesion Quantitation

The mouse hearts were perfused in situ for 1 min with diethylpyrocarbonate treated-phosphate-buffered saline (PBS) containing 1.5 μmol/l aprotinin and 0.1 mmol/l phenylmethylsulfonyl fluoride through a cannula inserted into the left ventricle. Eight randomly chosen aortas were dissected from the aortic root to the iliac bifurcation using a stereoscopic zoom microscope. As a measure of atherosclerotic lesion, total cholesterol (TC) and free cholesterol (FC) were quantified (8 aortas/group) as previously described [13, 14]. Esterified cholesterol (EC) was calculated as the difference between the two measures. The residual delipidated aortic tissue was digested in 1N NaOH, and total protein was determined using a bicinchoninic acid (BCA) kit (Pierce Ins., Rockford, IL).

Immunohistochemistry

In each group of mice, three randomly chosen aortic arches, from the left aortic valve to the right subclavian artery branch, were embedded in OCT compound (Tissue-Tek 4583; Sakura Finetek), snap-frozen in liquid nitrogen and stored at −80°C until sectioning. The aortic arches were sectioned at a 5-μm thickness and stained in the pathology facility at New England Medical Center. Rat anti-mouse monocyte/Mϕ antibody (MCA519G; Serotec, Raleigh, NC) was used to identify monocyte/Mϕ deposition.

Serum Lipid Profile

Serum TC, HDL-cholesterol (HDL-C) and triglyceride concentrations were measured using an Olympus AU400 analyzer with enzymatic reagents (Olympus America, Melville, NY). Non-HDL-cholesterol (non HDL-C) was calculated as the difference between TC and HDL-C [15].

Plasma Concentrations of Inflammatory Factors

Plasma TNFα, IL-6 and MCP-1 concentrations were measured using Quantikine® ELISA kits (R&D Systems, Minneapolis, MN).

Elicited Peritoneal Mϕ Culture and Stimulation

Immediately after harvesting, elicited peritoneal Mϕ were cultured in RPMI1640 medium (ATCC, Manassas, VA) containing 2% heat-inactivated fetal bovine serum (Invitrogen, Carlsbad, CA) for 2 h (1×10^6 cells per ml). One million cells were stimulated with 1 μg/ml lipopolysaccharide (LPS) for 15 h, and inflammatory factors released into the culture medium were measured. The remaining cells were washed with PBS three times and used for the measurement of cholesterol content, fatty acid profile, mRNA and protein levels of genes involved in inflammation and cholesterol accumulation.

Cholesterol content and fatty acid profile: elicited peritoneal Mϕ TC, FC and protein concentrations were determined as described above for the aorta. Mϕ fatty acid profiles were determined by gas chromatography as previously described [16].

Secretion of inflammatory factors: TNFα, IL-6 and MCP-1 secretion from LPS-stimulated elicited peritoneal Mϕ were measured using DuoSet® ELISA kits (R&D Systems, Minneapolis, MN). Elicited peritoneal Mϕ attached to the culture plates were digested with 0.5N NaOH, and total protein was determined using BCA kits (Pierce Ins., Rockford, IL).

Western blot and real-time PCR: protein was extracted from elicited peritoneal Mϕ using RIPA kit (Santa Cruz, Santa Cruz, CA). Western blotting was performed as previously described [15] with the following primary antibodies: SR-B1 (Novus Biologicals, Littleton, CO), ABCA1 (Novus Biologicals, Littleton, CO), CD36 (Cascade Bioscience, Winchester, MA) and β-actin (Sigma, St. Louis, MO). Signals were visualized by chemiluminescence (Amersham Biosciences, Piscataway, NJ) and quantified using a GS-800 calibrated densitometer (Bio-Rad, Hercules, CA).

RNA was extracted from Mϕ using RNeasy mini kit (Qiagen, Valencia, CA). cDNA was synthesized from RNA using SuperScript™ II reverse transcriptase according to the manufacturer's instruction (Invitrogen, Carlsbad, CA). Primers for peroxisomal proliferator activated receptor (PPAR)β, PPARγ, MSR1, CD36, SR-B1, ABCA1, MCP-1, TNFα and β-actin (Table 1) were designed using Primer Express version 2.0 (Applied Biosystems, Foster City, CA). β-actin was used as an endogenous control. Primer amplification efficiency and specificity were verified for each set of primers. cDNA levels of the genes of interest were measured using power SYBR green master mix on real-time PCR 7300 (Applied Biosystems, Foster City, CA). cDNA levels of IL-6 and PPARα were measured using Taqman® gene expression assays and Taqman® PreAmp master mix kit (Applied Biosystems, Foster City, CA). The reaction condition was 95°C for 10 min, 40 cycles of 95°C for 15 s, 60°C for 1 min and one cycle of

Table 1 Mouse oligonucleotide sequences of primers

Gene name	Accession no.	Forward primer	Reverse primer
ABCA1	NM_013454	CCTGCTAAAATACCGGCAAGG	GTAACCCGTTCCCAACTGGTTT
SR-B1	NM_016741	TGGAACGGACTCAGCAAGATC	AATTCCAGCGAGGA TTCGG
CD36	NM_007643	ATTAATGGCACAGACGCAGC	CCGAACACAGCGTAGATAGACC
MSR1	AF203781	TCTACAGCAAAGCAACAGGAGG	TCCACGTGCGCTTGTTCTT
TNFα	NM_013693	TGTAGCCCACGTCGTAGCAAA	GCTGGCACCACTAGTTGGTTGT
MCP-1	NM_011333	TCTCTCTTCCTCCACCACCATG	GCGTTAACTGCATCTGGCTGA
PPARβ/δ	NM_011145	AGTGCGATCGGATCTGCAAGA	TCCAAAGCGGATAGCGTTGTG
PPARγ	NM_011146	TCTTAACTGCCGGATCCACAAA	CCAAACCTGATGGCATTGTGA
β-Actin	NM_007393	CTTTTCCAGCCTTCCTTCTTGG	CAGCACTGTGTTGGCATAGAGG

dissociation stage. mRNA fold change was calculated using the 2[-Delta Delta C(T)] method [17].

Statistical Methods

Prior to statistical testing, data were checked for normality, and appropriate transformations were made when necessary (PROC UNIVARIATE; SAS version 9.1, SAS Institute Inc, Cary, NC). Unpaired Student's t test (PROC TTEST) was performed to compare group means. Differences were considered significant at $P < 0.05$. Untransformed data are presented in text, figures and tables as mean $\pm$ standard deviation (SD).

Results

Animal Body Weight and Food Intake

With one exception at the 10-week feeding point, there was no significant difference in the body weight between mice fed the two experimental diets during the 32-week feeding period (data not shown). Although the weight of food eaten was higher in the mice fed the control diet, on the basis of energy intake, the two groups were similar.

Aortic Lesion Composition

Shown in Fig. 1a is a representative aorta from each group of mice. Chemical composition of eight aortas per group indicated that mean TC was 5.5-fold ($P < 0.001$) higher in mice fed the atherogenic compared to control diet (Fig. 1b). This was contributed by higher amounts of both FC (4.9-fold, $P < 0.001$) and EC (6.4-fold, $P < 0.001$). There was stronger staining for Mϕ in the cross sections of aortic arch isolated from the atherogenic compared to control diet-fed mice (Fig. 1c).

Serum Lipid Profile

Although similar at baseline, serum non-HDL-C ($P < 0.001$) concentrations and ratios of TC to HDL-C

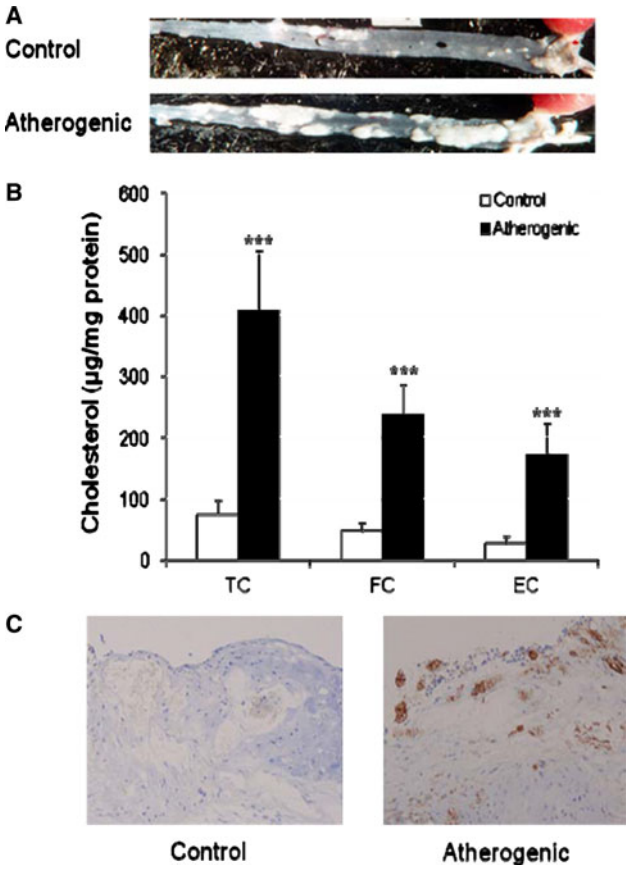

Fig. 1 Representative aortas from each diet group; white areas denote atherosclerotic lesion (**a**); aortic cholesterol content in whole aortas (**b**), and Mϕ immunostaining by an antibody to mouse Mϕ surface marker in the cross-sections of aortic arches (**c**) in LDLr−/− mice. Magnified (×200) images of aortic arch cross sections. The intensity of the *brown color* corresponds to the presence of Mϕ. $n = 11$ in each group. Values are mean $\pm$ SD. Unpaired Student's t test (PROC TTEST) was performed to compare two group values. The difference is expressed as $^{***}P < 0.001$

($P < 0.001$) were significantly higher in the atherogenic relative to control diet-fed mice at the 12-week feeding point, and these differences were maintained throughout the study period (Fig. 2). By the end of the 32-week feeding period, serum HDL-C concentrations declined

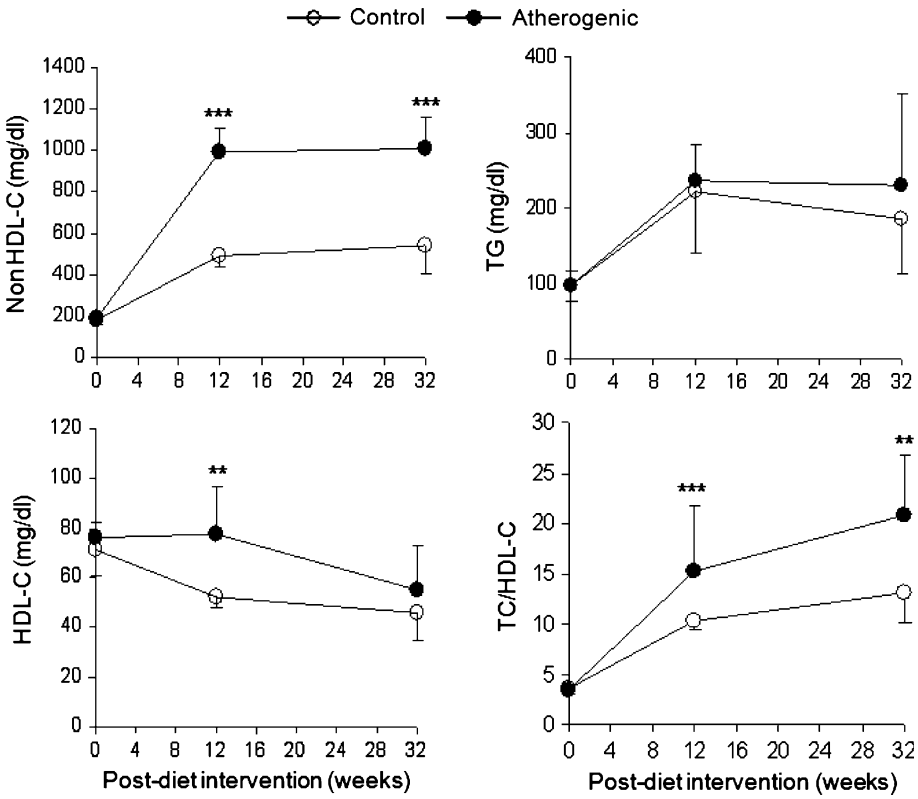

Fig. 2 Serum lipid profiles in LDLr−/− mice. Serum was obtained at 0-, 12- and 32-week post-diet interventions. $n = 11$ in each group. Values are mean ± SD of untransformed data. Prior to the statistical analysis the following transformations were made: TG at 0 week (*inverse*), HDL at 12 week (*square*), non-HDL-C at 12 week (*inverse*), TC/HDL-C at 32 week (*square*). Unpaired Student's *t* test (PROC TTEST) was performed to compare two group values. The difference is expressed as $^{**}P < 0.01$, $^{***}P < 0.001$

similarly between the two groups of mice, 35 and 28% in mice fed the control and atherogenic diets, respectively. During that same time period, triglyceride concentrations increased by 94 and 139% in the mice fed the control and atherogenic diets, respectively.

Plasma Concentrations of Inflammatory Factors

At the end of the 32-week feeding period, the mice fed the atherogenic relative to control diet had significantly higher plasma concentrations of all three of the inflammatory factors assessed: MCP-1 (144%, $P < 0.01$), TNFα (325%, $P < 0.01$) and IL-6 (188%, $P < 0.001$) (Fig. 3).

Elicited Peritoneal Mϕ Fatty Acid Profiles

The total SFA, monounsaturated fatty acid (MUFA) and polyunsaturated fatty acid (PUFA) profile of the elicited peritoneal Mϕ was similar between the two diet groups. With the exception of small differences, the percentage of omega (ω)-6 PUFA ($P < 0.01$) was significantly lower, whereas that of ω-3 PUFA ($P < 0.001$) was significantly higher in the elicited peritoneal Mϕ isolated from the atherogenic relative to control diet-fed mice (Table 2). Although alpha-linolenic acid (ALA, C18:3ω-3) levels were higher than eicosapentaenoic acid (EPA, C20:5ω-3) and docosahexaenoic acid (DHA, C22:6ω-3) in both diets,

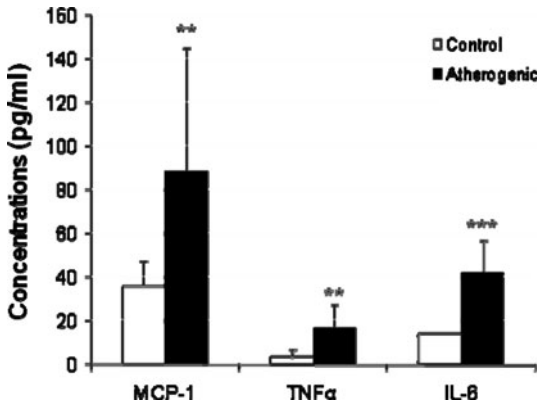

Fig. 3 Plasma concentrations of inflammatory factors in LDLr−/− mice. $n = 11$ in each group. Values are mean ± SD of untransformed data. Prior to the statistical analysis, the following transformations were made: MCP-1 (inverse) and IL-6 (inverse). Unpaired Student's *t* test (PROC TTEST) was performed to compare two group values. The difference is expressed as $^{**}P < 0.01$, $^{***}P < 0.001$

DHA plus EPA levels were 18-fold higher than ALA in elicited peritoneal Mϕ isolated from the two groups of mice. Although linoleic acid (LNA, C18:2ω-6) levels were more than 60-fold higher than arachidonic acid (ARA, C20:4ω-6) in both diets, ARA levels were 1.8-fold and 1.4-fold higher than LNA in elicited peritoneal Mϕ isolated from mice fed the control and atherogenic diet, respectively.

Table 2 Peritoneal Mϕ membrane fatty acid profile (mol %)

Fatty acid	Diet	
	Control[a]	Atherogenic[b]
SFA	37.58 ± 6.43	34.74 ± 6.21
C12:0	0.31 ± 0.15	0.38 ± 0.34
C14:0	1.10 ± 0.10	1.86 ± 0.21***
C16:0	24.33 ± 4.56	21.51 ± 3.38
C18:0	11.48 ± 2.11	10.60 ± 3.09
C20:0	0.15 ± 0.10	0.14 ± 0.07
C22:0	0.10 ± 0.03	0.10 ± 0.07
C24:0	0.12 ± 0.02	0.14 ± 0.04
MUFA	38.38 ± 3.51	42.54 ± 6.01
C16:1ω-9	1.05 ± 0.15	1.30 ± 0.06**
C16:1ω-7	4.17 ± 0.68	4.04 ± 1.27
C18:1ω-9	24.43 ± 2.82	28.69 ± 5.47
C18:1ω-7	6.44 ± 0.59	5.57 ± 1.20
C20:1ω-9	0.88 ± 0.07	1.13 ± 0.19**
C22:1ω-9	0.27 ± 0.08	0.31 ± 0.12
C24:1ω-9	0.62 ± 0.18	0.66 ± 0.28
PUFA	24.04 ± 4.73	22.72 ± 2.49
ω-6	22.20 ± 4.16	16.61 ± 1.91**
C18:2	5.15 ± 0.88	4.68 ± 0.86
C18:3	0.03 ± 0.03	0.02 ± 0.01
C20:2	1.38 ± 0.17	1.03 ± 0.14***
C20:3	1.23 ± 0.30	1.31 ± 0.30
C20:4	9.22 ± 2.17	6.43 ± 1.17**
C22:2	0.96 ± 0.26	1.34 ± 1.42
C22:4	4.18 ± 1.16	1.67 ± 0.43***
C22:5	0.05 ± 0.05	0.15 ± 0.19
ω-3	1.84 ± 0.62	6.11 ± 0.67***
C18:3	0.07 ± 0.02	0.19 ± 0.04***
C20:5	0.21 ± 0.19	1.03 ± 0.73***
C22:5	0.50 ± 0.12	2.45 ± 0.38***
C22:6	1.07 ± 0.40	2.44 ± 0.69***

$n = 11$ in each group. Values are mean ± SD of untransformed data. Prior to the statistical analysis, the following transformations were made: C16:0 (square), C20:1 (inverse), C20:2 (inverse), C20:5ω-3 (square root), C22:2 (1/square root), C22:5ω-6 (square root), PUFA (inverse), ω-6 PUFA (inverse). Unpaired Student's t test (PROC TTEST) was performed to compare two group values. Within a row the difference is expressed as $^{**}P < 0.01$, $^{***}P < 0.001$

[a] Control: low saturated fatty acid and low cholesterol diet

[b] Atherogenic: high saturated fatty acid and high cholesterol diet

Elicited Peritoneal Mϕ Cholesterol Content

To examine the potential relationship between aortic and Mϕ cholesterol accumulation, we measured elicited peritoneal Mϕ cholesterol content. Elicited peritoneal Mϕ TC was 34% ($P < 0.01$) higher in the atherogenic relative to control diet-fed mice (Fig. 4). This was accounted for primarily by the EC fraction, which was 104% ($P < 0.01$) higher in the atherogenic diet-fed mice.

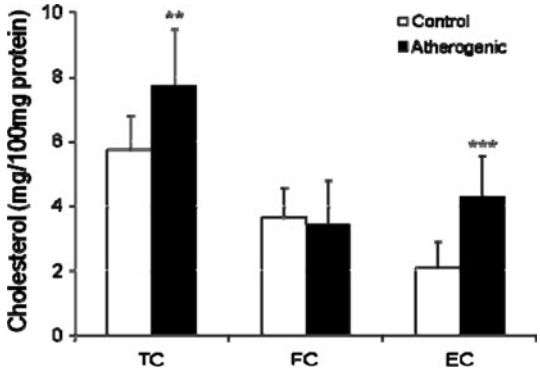

Fig. 4 Elicited peritoneal Mϕ cholesterol content in LDLr−/− mice. $n = 11$ in each group. Values are mean ± SD of untransformed data. Prior to the statistical analysis, FC (inverse) was transformed. Unpaired Student's t test (PROC TTEST) was performed to compare two group values. The difference is expressed as $^{**}P < 0.01$, $^{***}P < 0.001$

mRNA and Protein Levels of Genes Involved in Cholesterol Accumulation in Elicited Peritoneal Mϕ

To investigate the mechanism(s) underlying the higher EC content in the elicited peritoneal Mϕ harvested from the mice fed the atherogenic diet, we measured the protein and mRNA levels of genes involved in cholesterol accumulation. The atherogenic diet resulted in significantly higher ABCA1 mRNA ($P < 0.01$) and protein ($P < 0.01$) levels, albeit a modest difference, whereas SR-B1 and CD36 mRNA and protein levels were similar between two diet groups (Fig. 5a, c). There was no significant effect of diet treatment on mRNA levels of MSR1, PPARα, PPARβ/δ and PPARγ.

mRNA Levels and Secretion of Inflammatory Factors in/From Elicited Peritoneal Mϕ

To explore whether plasma concentrations of inflammatory factors were determined by Mϕ secretion, we measured MCP-1, TNFα and IL-6 mRNA levels and secretion in/from elicited peritoneal Mϕ. MCP-1 secretion was 51% higher ($P < 0.01$) in mice fed the atherogenic relative to control diet (Fig. 5b). This was accompanied by 1.5-fold higher MCP-1 mRNA levels ($P < 0.05$) (Fig. 5c). There was no significant effect of diet treatment on TNFα and IL-6 mRNA levels in and secretion from elicited peritoneal Mϕ—suggesting these cells were not a major determinant of plasma TNFα and IL-6 concentrations.

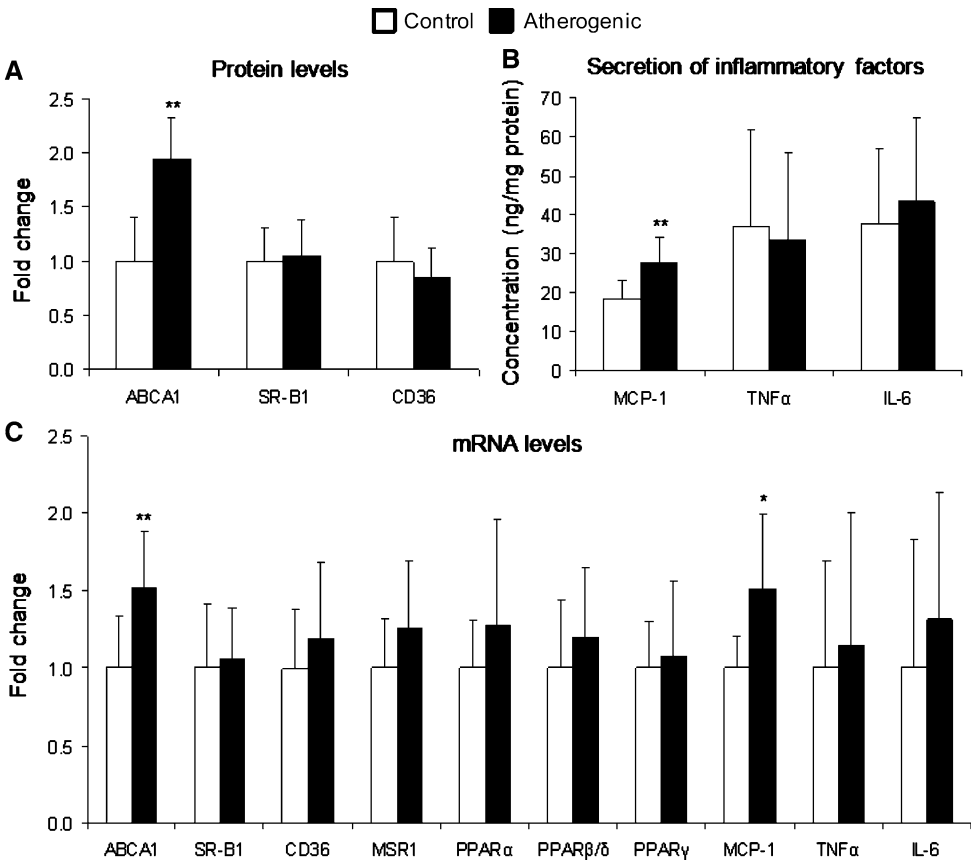

Fig. 5 Protein levels of ABCA1, SR-B1 and CD36 (**a**), secretion of MCP-1, TNFα and IL-6 (**b**), and mRNA levels of genes (**c**) in/from elicited peritoneal Mϕ isolated from LDLr−/− mice at the end of the 32-week feeding period. $n = 11$ in each group. Values are mean ± SD of untransformed data. Prior to the statistical analysis, mRNA levels of TNFα [1/log(TNFα)] were transformed. Unpaired Student's t test (PROC TTEST) was performed to compare two group values. The difference is expressed as $^{*}P < 0.05$, $^{**}P < 0.01$

Discussion

In humans, consumption of high SFA and cholesterol diets is positively associated with cardiovascular disease (CVD) risk [18, 19]. The inflammatory process is a major contributor to the development of atherosclerotic plaque [1, 20]. IL-6, MCP-1 and TNFα are important biomarkers of inflammation [6, 21, 22]. Epidemiological studies have shown a positive association between the Western-type diet and plasma MCP-1, IL-6 and TNFα concentrations [23–25]. The present study is the first to simultaneously assess the effect of an atherogenic diet in the LDLr−/− mouse on atherosclerotic lesion formation, aortic Mϕ accumulation, plasma inflammatory factor concentrations, cholesterol accumulation and inflammatory factor secretion in/from elicited peritoneal Mϕ isolated from these mice, and Mϕ gene expression and protein levels associated with these processes. We demonstrated that diet-induced atherosclerotic lesion formation in LDLr−/− mice was associated with higher inflammatory response. Changes in peritoneal Mϕ isolated from these mice may, in part, have exacerbated the aortic lesion formation.

LNA and ALA were the most abundant ω-6 fatty acids, and accounted for more than 84 and 79% of total ω-6 and ω-3 fatty acids in two diets, respectively. ARA only accounted for 0.2 and 1.4% of total ω-6 fatty acids in the control and atherogenic diet, respectively. However, ARA accounted for about 41.5 and 38.7% of total ω-6 fatty acids in elicited peritoneal Mϕ isolated from the control and atherogenic diet-fed mice, respectively. The percentage of LNA was about one third less than that of ARA in elicited peritoneal Mϕ isolated from two groups of mice. ALA represented about 3% of total ω-3 fatty acids in elicited peritoneal Mϕ. EPA and DHA were the most abundant ω-3 fatty acids and accounted for more than 56% of total ω-3 fatty acids in elicited peritoneal Mϕ. These data suggest that peritoneal Mϕ selectively accumulated longer chain unsaturated fatty acids in their membrane, independent of the fatty acid profile of the diet. Similar data have been reported by others [26]. Whereas the total SFA, MUFA and PUFA prolife of the elicited peritoneal Mϕ was similar between the two groups of mice, the ω-6 PUFAs were significantly higher, and ω-3 PUFAs were significantly lower in elicited peritoneal Mϕ isolated from the control relative to atherogenic diet-fed mice. ARA accounted for about 38.4 and 28.3% of total PUFA in elicited peritoneal Mϕ isolated from the control and atherogenic diet-fed mice, respectively. EPA plus DHA accounted for about 5.3 and 15.3% of total PUFA in elicited peritoneal Mϕ isolated from the control and atherogenic diet-fed mice,

respectively. ARA was significantly lower and EPA plus DHA significantly higher in elicited peritoneal Mϕ isolated from the atherogenic relative to control diet-fed mice. Further studies are required to detect whether these differences are a result of uptake of cholesterol-rich lipoproteins or specific fatty acid synthesis caused by diets or inflammation.

Overexpression of MCP-1 has been positively related to monocyte accumulation in the arterial vessel wall, a major event leading to the development of atherosclerosis [5, 27]. Studies in humans have shown that elevated serum MCP-1 concentrations are an inflammatory biomarker positively associated with CVD [27–29]. In MCP-1 and LDL receptor double null mice, lower monocyte deposition and vessel wall lipid accumulation have been observed compared to LDLr−/− mice [30, 31]. LDLr−/− mice fed a Western diet had elevated plasma MCP-1 concentrations, which were associated with more aortic lesion area compared to the mice fed chow diet [32]. In this study, in elicited peritoneal Mϕ, both MCP-1 mRNA levels and secretion were significantly higher in LDLr−/− mice fed the atherogenic diet compared to those fed the control diet. This is consistent with previous reports that a similar atherogenic diet resulted in higher MCP-1 mRNA levels in and protein secretion from adipocytes in mice [32–34]. Although the atherogenic diet resulted in elevated plasma IL-6 and TNFα concentrations, there was no significant difference in mRNA and secretion of TNFα and IL-6 from elicited peritoneal Mϕ isolated from two groups of mice. TNFα and IL-6 can be produced by liver, endothelial, adipocytes or T cells [35–37]. Preliminary work suggested that liver TNFα and IL-6 production was 1.5-fold ($P < 0.05$) and 2.0-fold higher ($P < 0.05$), respectively, in mice fed the atherogenic relative to control diet despite higher plasma concentrations of these cytokines (unpublished data). These data suggest that elevated plasma IL-6 and TNFα concentrations were mediated, as least in part, by liver cells.

Apolipoprotein E-deficient mice fed a high SFA and cholesterol diet had significantly higher MCP-1 mRNA levels in both liver and aorta compared to mice fed only a high SFA diet [38]. The atherogenic diet might increase the expression of MCP-1 through upregulated Toll-like receptor 4 (TLR4). Stimulation of TLR4 by LPS can induce activation of nuclear factor-kappa B (NF-kB) and expression of cytokines [39]. TLR4 is expressed in murine and human lipid-rich atherosclerotic lesions, and colocalized with Mϕ both in murine atherosclerotic lesion and human shoulder coronary artery plaque [40]. In vitro studies have shown that oxidized LDL (ox-LDL) can upregulate the expression of TLR4 in human monocyte-derived Mϕ [40]. We cannot rule out the possibility that high levels of ox-LDL in the atherogenic diet-fed mice stimulated the expression of TLR4, which increased the binding of LPS, and further upregulated the expression of MCP-1. Due to the limited number of elicited peritoneal Mϕ obtained from each mouse, we could not test the above hypotheses in this study.

In this study, ARA levels were significantly higher than EPA plus DHA in the elicited peritoneal Mϕ isolated from two groups of mice. In addition, the percentage of ARA was significantly higher, whereas that of EPA plus DHA were significantly lower, in the elicited peritoneal Mϕ isolated from the control relative to atherogenic diet-fed mice. Our previous study [41] has shown that ARA significantly lowered MCP-1 mRNA levels and secretion from Mϕ differentiated from THP-1 monocytes. ARA and EPA had a more pronounced effect than DHA. ARA can be metabolized to 15-deoxy-delta^{12,14}-PGJ$_2$ (15dPGJ$_2$), a natural ligand for PPARγ [42]. 15dPGJ$_2$ has been consistently shown to have anti-inflammatory properties by serving as a potent agonist to activate PPARγ [43, 44]. Some studies have shown that activated PPARγ could be a promoter-specific repressor of NF-kB target genes that regulate inflammation in Mϕ [45]. There was not a significant difference in the PPARγ expression in the elicited peritoneal Mϕ isolated from two groups of mice. ARA might lower MCP-1 expression through activating PPARγ instead of changing its expression.

The atherogenic diet resulted in more Mϕ deposition in the aortic wall. In situ, these cells play an important role not only in the inflammatory response, but also in uptake of modified LDL, and accumulation and deposition of cholesterol [46, 47]. Based on the results from previous studies [11, 48, 49], the expression and production of inflammatory factors is comparable between resident and elicited peritoneal Mϕ. In our study, elicited peritoneal Mϕ were used to ensure an adequate number of cells were harvested. Elicited peritoneal Mϕ TC and EC content change was similar to that seen in the aortas of the respective mice. To determine whether the difference in Mϕ cholesterol content resulting from the two different diets was due to an imbalance of influx or efflux, we assessed mRNA and protein levels of two genes involved in cholesterol efflux, SR-B1 and ABCA1, and two genes involved in cholesterol influx, MSR1 (only mRNA levels) and CD36. There was no significant difference in protein levels of CD36 and SR-B1 in elicited peritoneal macrophages isolated from the two groups of mice. An antibody to detect protein levels of MSR1 was not available. The atherogenic diet resulted in higher mRNA and protein levels of ABCA1 in this study, but not the other factors assessed. These data are consistent with other studies showing that Mϕ ABCA1 expression is upregulated in atherosclerotic lesions, as a compensatory mechanism in response to cholesterol enrichment [50, 51]. ABCA1 is a direct transcriptional target of liver-X-receptors (LXR) [52–54]. LXR is activated by cholesterol

metabolites. We speculate that higher circulating lipoprotein concentrations, especially apolipoprotein B-containing lipoproteins, would favor increased Mϕ cholesterol content, which in turn would alter cellular cholesterol homeostasis and trigger an upregulation of ABCA1 expression. The atherogenic diet may have activated LXR through increasing Mϕ production of LXR ligands, such as 22(R)-hydroxycholesterol and 27-hydroxycholesterol. Ligand activated-LXR can upregulate ABCA1 gene expression and enhance ABCA1-mediated cholesterol efflux from elicited peritoneal Mϕ isolated from the atherogenic diet-fed mice. In addition to the cholesterol enrichment-induced regulation, it has been reported that SFA increase and PUFA decrease ABCA1 expression at both transcription and post-translation levels [55, 56]. However, there was no significant difference in SFA and PUFA composition in elicited peritoneal Mϕ isolated from two groups of mice. The higher levels of TC and EC in the peritoneal Mϕ may have resulted from higher circulation oxLDL concentrations, upregluation of genes associated with cholesterol influx or/and downregulation of genes associated with cholesterol efflux, which were not determined due to limited numbers of Mϕ harvested from each mouse.

In summary, these data suggest that LDLr−/− mice fed a diet high in SFA and cholesterol, relative to the control diet, had higher plasma inflammatory factor concentrations, less favorable lipoprotein profiles, higher elicited peritoneal Mϕ cholesterol accumulation and inflammatory factor secretion, and more Mϕ deposition in the aortic wall, which in turn were associated with greater aortic cholesterol accumulation.

Acknowledgments The authors are grateful for the technical expertise provided by Susan Jalbert, and Drs. Donald Smith and Mohsen Meydani, and for the thoughtful manuscript review by Drs. Julian Marsh and Alice Dillard. This project was supported by T32 HL69772-01A1 (S.W., J.L.), RO1 HL 54727 and USDA agreement 588-1950-9-001. Any opinions, findings, conclusions or recommendations expressed in this publication are those of authors, and do not necessarily reflect the view of USDA.

Conflict of interest All authors have no conflict of interest.

References

1. Willerson JT, Ridker PM (2004) Inflammation as a cardiovascular risk factor. Circulation 109:II2–II10
2. Lam MC, Tan KC, Lam KS (2004) Glycoxidized low-density lipoprotein regulates the expression of scavenger receptors in THP-1 macrophages. Atherosclerosis 177:313–320
3. Moore KJ, Freeman MW (2006) Scavenger receptors in atherosclerosis: beyond lipid uptake. Arterioscler Thromb Vasc Biol 26:1702–1711
4. Baranova I, Vishnyakova T, Bocharov A, Chen Z, Remaley AT, Stonik J, Eggerman TL, Patterson AP (2002) Lipopolysaccharide down regulates both scavenger receptor B1 and ATP binding cassette transporter A1 in RAW cells. Infect Immun 70: 2995–3003
5. Vita JA, Keaney JF Jr, Larson MG, Keyes MJ, Massaro JM, Lipinska I, Lehman BT, Fan S, Osypiuk E, Wilson PW, Vasan RS, Mitchell GF, Benjamin EJ (2004) Brachial artery vasodilator function and systemic inflammation in the Framingham Offspring Study. Circulation 110:3604–3609
6. Fiotti N, Giansante C, Ponte E, Delbello C, Calabrese S, Zacchi T, Dobrina A, Guarnieri G (1999) Atherosclerosis and inflammation. Patterns of cytokine regulation in patients with peripheral arterial disease. Atherosclerosis 145:51–60
7. Haddy N, Sass C, Droesch S, Zaiou M, Siest G, Ponthieux A, Lambert D, Visvikis S (2003) IL-6, TNF-alpha and atherosclerosis risk indicators in a healthy family population: the STANISLAS cohort. Atherosclerosis 170:277–283
8. Seierstad SL, Seljeflot I, Johansen O, Hansen R, Haugen M, Rosenlund G, Froyland L, Arnesen H (2005) Dietary intake of differently fed salmon; the influence on markers of human atherosclerosis. Eur J Clin Invest 35:52–59
9. Meydani M (2000) Omega-3 fatty acids alter soluble markers of endothelial function in coronary heart disease patients. Nutr Rev 58:56–59
10. Basu A, Devaraj S, Jialal I (2006) Dietary factors that promote or retard inflammation. Arterioscler Thromb Vasc Biol 26:995–1001
11. Wu D, Marko M, Claycombe K, Paulson KE, Meydani SN (2003) Ceramide-induced and age-associated increase in macrophage COX-2 expression is mediated through up-regulation of NF-kappa B activity. J Biol Chem 278:10983–10992
12. Wang S, Wu D, Matthan NR, Lamon-Fava S, Lecker JL, Lichtenstein AH (2009) Reduction in dietary omega-6 polyunsaturated fatty acids: eicosapentaenoic acid plus docosahexaenoic acid ratio minimizes atherosclerotic lesion formation and inflammatory response in the LDL receptor null mouse. Atherosclerosis 204:147–155
13. Rudel LL, Kelley K, Sawyer JK, Shah R, Wilson MD (1998) Dietary monounsaturated fatty acids promote aortic atherosclerosis in LDL receptor-null, human ApoB100-overexpressing transgenic mice. Arterioscler Thromb Vasc Biol 18: 1818–1827
14. Matthan NR, Giovanni A, Schaefer EJ, Brown BG, Lichtenstein AH (2003) Impact of simvastatin, niacin, and/or antioxidants on cholesterol metabolism in CAD patients with low HDL. J Lipid Res 44:800–806
15. Dorfman SE, Wang S, Vega-Lopez S, Jauhiainen M, Lichtenstein AH (2005) Dietary fatty acids and cholesterol differentially modulate HDL cholesterol metabolism in Golden-Syrian hamsters. J Nutr 135:492–498
16. Lichtenstein AH, Matthan NR, Jalbert SM, Resteghini NA, Schaefer EJ, Ausman LM (2006) Novel soybean oils with different fatty acid profiles alter cardiovascular disease risk factors in moderately hyperlipidemic subjects. Am J Clin Nutr 84: 497–504
17. Livak KJ, Schmittgen TD (2001) Analysis of relative gene expression data using real-time quantitative PCR and the 2(-Delta Delta C(T)) method. Methods 25:402–408
18. Millen BE, Quatromoni PA, Nam BH, O'Horo CE, Polak JF, D'Agostino RB (2002) Dietary patterns and the odds of carotid atherosclerosis in women: the Framingham Nutrition Studies. Prev Med 35:540–547
19. Klor HU, Hauenschild A, Holbach I, Schnell-Kretschmer H, Stroh S (1997) Nutrition and cardiovascular disease. Eur J Med Res 2:243–257

20. Paoletti R, Gotto AM Jr, Hajjar DP (2004) Inflammation in atherosclerosis and implications for therapy. Circulation 109:III20–III26
21. Brueckmann M, Bertsch T, Lang S, Sueselbeck T, Wolpert C, Kaden JJ, Jaramillo C, Huhle G, Borggrefe M, Haase KK (2004) Time course of systemic markers of inflammation in patients presenting with acute coronary syndromes. Clin Chem Lab Med 42:1132–1139
22. Hoogeveen RC, Morrison A, Boerwinkle E, Miles JS, Rhodes CE, Sharrett AR, Ballantyne CM (2005) Plasma MCP-1 level and risk for peripheral arterial disease and incident coronary heart disease: atherosclerosis risk in communities study. Atherosclerosis 183:301–307
23. Pawlak K, Pawlak D, Mysliwiec M (2006) Inflammation but not oxidative stress is associated with beta-chemokine levels and prevalence of cardiovascular disease in uraemic patients. Cytokine 35:258–262
24. Baer DJ, Judd JT, Clevidence BA, Tracy RP (2004) Dietary fatty acids affect plasma markers of inflammation in healthy men fed controlled diets: a randomized crossover study. Am J Clin Nutr 79:969–973
25. Lopez-Garcia E, Schulze MB, Fung TT, Meigs JB, Rifai N, Manson JE, Hu FB (2004) Major dietary patterns are related to plasma concentrations of markers of inflammation and endothelial dysfunction. Am J Clin Nutr 80:1029–1035
26. Miles EA, Wallace FA, Calder PC (2000) Dietary fish oil reduces intercellular adhesion molecule 1 and scavenger receptor expression on murine macrophages. Atherosclerosis 152:43–50
27. Ballantyne CM, Nambi V (2005) Markers of inflammation and their clinical significance. Atheroscler Suppl 6:21–29
28. Martinovic I, Abegunewardene N, Seul M, Vosseler M, Horstick G, Buerke M, Darius H, Lindemann S (2005) Elevated monocyte chemoattractant protein-1 serum levels in patients at risk for coronary artery disease. Circ J 69:1484–1489
29. Charo IF, Taubman MB (2004) Chemokines in the pathogenesis of vascular disease. Circ Res 95:858–866
30. Ishibashi M, Egashira K, Zhao Q, Hiasa K, Ohtani K, Ihara Y, Charo IF, Kura S, Tsuzuki T, Takeshita A, Sunagawa K (2004) Bone marrow-derived monocyte chemoattractant protein-1 receptor CCR2 is critical in angiotensin II-induced acceleration of atherosclerosis and aneurysm formation in hypercholesterolemic mice. Arterioscler Thromb Vasc Biol 24:e174–e178
31. Gu L, Okada Y, Clinton SK, Gerard C, Sukhova GK, Libby P, Rollins BJ (1998) Absence of monocyte chemoattractant protein-1 reduces atherosclerosis in low density lipoprotein receptor-deficient mice. Mol Cell 2:275–281
32. Tian J, Pei H, Sanders JM, Angle JF, Sarembock IJ, Matsumoto AH, Helm GA, Shi W (2006) Hyperlipidemia is a major determinant of neointimal formation in LDL receptor-deficient mice. Biochem Biophys Res Commun 345:1004–1009
33. Chen A, Mumick S, Zhang C, Lamb J, Dai H, Weingarth D, Mudgett J, Chen H, MacNeil DJ, Reitman ML, Qian S (2005) Diet induction of monocyte chemoattractant protein-1 and its impact on obesity. Obes Res 13:1311–1320
34. Kanda H, Tateya S, Tamori Y, Kotani K, Hiasa K, Kitazawa R, Kitazawa S, Miyachi H, Maeda S, Egashira K, Kasuga M (2006) MCP-1 contributes to macrophage infiltration into adipose tissue, insulin resistance, and hepatic steatosis in obesity. J Clin Invest 116:1494–1505
35. Charo IF, Ransohoff RM (2006) The many roles of chemokines and chemokine receptors in inflammation. N Engl J Med 354:610–621
36. Glass CK, Witztum JL (2001) Atherosclerosis the road ahead. Cell 104:503–516
37. Vignali DA, Collison LW, Workman CJ (2008) How regulatory T cells work. Nat Rev Immunol 8:523–532
38. Tous M, Ferre N, Rull A, Marsillach J, Coll B, Alonso-Villaverde C, Camps J, Joven J (2006) Dietary cholesterol and differential monocyte chemoattractant protein-1 gene expression in aorta and liver of apo E-deficient mice. Biochem Biophys Res Commun 340:1078–1084
39. Vink A, Schoneveld AH, van der Meer JJ, van Middelaar BJ, Sluijter JP, Smeets MB, Quax PH, Lim SK, Borst C, Pasterkamp G, de Kleijn DP (2002) In vivo evidence for a role of toll-like receptor 4 in the development of intimal lesions. Circulation 106:1985–1990
40. Xu XH, Shah PK, Faure E, Equils O, Thomas L, Fishbein MC, Luthringer D, Xu XP, Rajavashisth TB, Yano J, Kaul S, Arditi M (2001) Toll-like receptor-4 is expressed by macrophages in murine and human lipid-rich atherosclerotic plaques and upregulated by oxidized LDL. Circulation 104:3103–3108
41. Wang S, Wu D, Lamon-Fava S, Matthan NR, Honda KL, Lichtenstein AH (2009) In vitro fatty acid enrichment of macrophages alters inflammatory response and net cholesterol accumulation. Br J Nutr 102:497–501
42. Scher JU, Pillinger MH (2005) 15d-PGJ2: the anti-inflammatory prostaglandin? Clin Immunol 114:100–109
43. Jiang C, Ting AT, Seed B (1998) PPAR-gamma agonists inhibit production of monocyte inflammatory cytokines. Nature 391:82–86
44. Ricote M, Li AC, Willson TM, Kelly CJ, Glass CK (1998) The peroxisome proliferator-activated receptor-gamma is a negative regulator of macrophage activation. Nature 391:79–82
45. Pascual G, Fong AL, Ogawa S, Gamliel A, Li AC, Perissi V, Rose DW, Willson TM, Rosenfeld MG, Glass CK (2005) A SUMOylation-dependent pathway mediates transrepression of inflammatory response genes by PPAR-gamma. Nature 437:759–763
46. Kunjathoor VV, Febbraio M, Podrez EA, Moore KJ, Andersson L, Koehn S, Rhee JS, Silverstein R, Hoff HF, Freeman MW (2002) Scavenger receptors class A-I/II and CD36 are the principal receptors responsible for the uptake of modified low density lipoprotein leading to lipid loading in macrophages. J Biol Chem 277:49982–49988
47. Ludewig B, Laman JD (2004) The in and out of monocytes in atherosclerotic plaques: Balancing inflammation through migration. Proc Natl Acad Sci USA 101:11529–11530
48. Hayek MG, Mura C, Wu D, Beharka AA, Han SN, Paulson KE, Hwang D, Meydani SN (1997) Enhanced expression of inducible cyclooxygenase with age in murine macrophages. J Immunol 159:2445–2451
49. Wu D, Mura C, Beharka AA, Han SN, Paulson KE, Hwang D, Meydani SN (1998) Age-associated increase in PGE2 synthesis and COX activity in murine macrophages is reversed by vitamin E. Am J Physiol 275:C661–668
50. Langmann T, Klucken J, Reil M, Liebisch G, Luciani MF, Chimini G, Kaminski WE, Schmitz G (1999) Molecular cloning of the human ATP-binding cassette transporter 1 (hABC1): evidence for sterol-dependent regulation in macrophages. Biochem Biophys Res Commun 257:29–33
51. Lawn RM, Wade DP, Garvin MR, Wang X, Schwartz K, Porter JG, Seilhamer JJ, Vaughan AM, Oram JF (1999) The Tangier disease gene product ABC1 controls the cellular apolipoprotein-mediated lipid removal pathway. J Clin Invest 104:R25–31
52. Laffitte BA, Repa JJ, Joseph SB, Wilpitz DC, Kast HR, Mangelsdorf DJ, Tontonoz P (2001) LXRs control lipid-inducible expression of the apolipoprotein E gene in macrophages and adipocytes. Proc Natl Acad Sci USA 98:507–512
53. Fu X, Menke JG, Chen Y, Zhou G, MacNaul KL, Wright SD, Sparrow CP, Lund EG (2001) 27-hydroxycholesterol is an endogenous ligand for liver X receptor in cholesterol-loaded cells. J Biol Chem 276:38378–38387

54. Beyea MM, Heslop CL, Sawyez CG, Edwards JY, Markle JG, Hegele RA, Huff MW (2007) Selective up-regulation of LXR-regulated genes ABCA1, ABCG1, and APOE in macrophages through increased endogenous synthesis of 24(S), 25-epoxycholesterol. J Biol Chem 282:5207–5216
55. Uehara Y, Miura S, von Eckardstein A, Abe S, Fujii A, Matsuo Y, Rust S, Lorkowski S, Assmann G, Yamada T, Saku K (2007) Unsaturated fatty acids suppress the expression of the ATP-binding cassette transporter G1 (ABCG1) and ABCA1 genes via an LXR/RXR responsive element. Atherosclerosis 191:11–21
56. Murthy S, Born E, Mathur SN, Field FJ (2004) Liver-X-receptor-mediated increase in ATP-binding cassette transporter A1 expression is attenuated by fatty acids in CaCo-2 cells: effect on cholesterol efflux to high-density lipoprotein. Biochem J 377:545–552

Lipids (2010) 45:713–721
DOI 10.1007/s11745-010-3449-5

ORIGINAL ARTICLE

Purified Canola Lutein Selectively Inhibits Specific Isoforms of Mammalian DNA Polymerases and Reduces Inflammatory Response

Sho Horie · Chiaki Okuda · Takatoshi Yamashita · Kenichi Watanabe · Kouji Kuramochi · Masashi Hosokawa · Toshifumi Takeuchi · Makiko Kakuda · Kazuo Miyashita · Fumio Sugawara · Hiromi Yoshida · Yoshiyuki Mizushina

Received: 20 March 2010 / Accepted: 1 July 2010 / Published online: 29 July 2010

Abstract In the screening of DNA polymerase (pol) inhibitor, we isolated lutein, a carotenoid, from the crude (unrefined) pressed oil of canola (low erucic acid rapeseed, *Brassica napus* L.). Commercially prepared carotenoids such as lutein (**1**), zeaxanthin (**2**), β-cryptoxanthin (**3**), astaxanthin (**4**), canthaxanthin (**5**), β-carotene (**6**), lycopene (**7**), capsanthin (**8**), fucoxanthin (**9**) and fucoxanthinol (**10**), were investigated for the inhibitory activities of pols. Compounds **1**, **2** and **8** exhibited strong inhibition of the activities of mammalian pols β and λ, which are DNA repair- and/or recombination-related pols. On the other hand, all carotenoids tested had no influence on the activity of a mammalian pol α, which is a DNA replicative pol. Lutein (**1**) was the strongest pol inhibitor of mammalian pols β and λ in the prepared ten carotenoids tested, but did not influence of the activities of mammalian pols α, γ, δ and ε. The tendency for pols β and λ inhibition by these carotenoids showed a positive correlation with the suppression of TPA (12-*O*-tetradecanoylphorbol-13-acetate)-induced inflammation. These results suggest that cold pressed unrefined canola/rapeseed oil, or other oils with high levels of lutein and other carotenoids, may be useful for their anti-inflammatory properties.

Keywords Lutein · Carotenoids · Canola/rapeseed · Industrial waste · DNA polymerase (pol) · Enzyme inhibitor · Anti-inflammation · Structure and bioactivity relationship

S. Horie · C. Okuda · H. Yoshida · Y. Mizushina (✉)
Laboratory of Food and Nutritional Sciences, Department of Nutritional Science, Kobe-Gakuin University, Nishi-ku, Kobe, Hyogo 651-2180, Japan
e-mail: mizushin@nutr.kobegakuin.ac.jp

H. Yoshida · Y. Mizushina
Cooperative Research Center of Life Sciences, Kobe-Gakuin University, Chuo-ku, Kobe, Hyogo 650-8586, Japan

T. Yamashita · K. Watanabe
J-Oil Mills Inc., Tsurumi-ku, Yokohama, Kanagawa 230-0053, Japan

K. Kuramochi
Graduate School of Life and Environmental Science, Kyoto Prefectural University, Sakyo-ku, Kyoto 606-8522, Japan

M. Hosokawa · K. Miyashita
Faculty of Fisheries Sciences, Hokkaido University, Hakodate, Hokkaido 041-8611, Japan

T. Takeuchi · M. Kakuda · F. Sugawara
Department of Applied Biological Science, Tokyo University of Science, Noda, Chiba 278-8510, Japan

Abbreviations

Pol	DNA polymerase (EC 2.7.7.7)
TPA	12-*O*-tetradecanoylphorbol-13-acetate
dsDNA	Double-stranded DNA
dTTP	2′-deoxythymidine 5′-triphosphate
DNase I	Deoxyribonuclease I
HIV-1	Human immunodeficiency virus type-1
DMSO	Dimethyl sulfoxide

Introduction

Our laboratory has long been interested in the integrity of the genome of eukaryotes and its relation to cell differentiation. DNA replication, recombination and repair in eukaryotes are key systems to maintain these processes [1], and DNA polymerases (pols) have important roles. Pol

catalyzes the addition of deoxyribonucleotides to the 3′-hydroxyl terminus of primed double-stranded DNA (dsDNA) molecules [2]. In this regard, we have concentrated our efforts on investigating eukaryotic pols associated with these processes [3].

The human genome encodes at least 14 pols to conduct cellular DNA synthesis [4, 5]. Eukaryotic cells contain three replicative pols (α, δ and ε), mitochondrial pol γ, and at least ten non-replicative pols (β, ζ, η, θ, ι, κ, λ, μ, ν and REV1) [4–6]. Pols have a highly conserved structure, which means that their overall catalytic subunits vary, on the whole, very little among species. Conserved structures usually indicate important, irreplaceable functions of the cell, the maintenance of which provides evolutionary advantages. Because not all functions of eukaryotic pols have been fully elucidated, selective inhibitors of pols are useful tools for distinguishing pols and clarifying their biological functions. Pols are not only essential for DNA replication, repair and recombination, but are also involved in cell division. Selective inhibitors of pol are considered a group of potentially useful anticancer and antiparasitic agents, because some inhibitors suppress human cancer cell proliferation and have cytotoxicity [7].

We have therefore been searching for natural compounds that selectively inhibit each of these eukaryotic pols [7, 8]. In this study, we screened pol inhibitors from Canola/rapeseed (*Brassica napus* L.) crude extract, which is the screw pressed component after canola oil production. We isolated lutein, a carotenoid, as a mammalian pol inhibitor, focused on the anti-inflammatory effect of the carotenoids (i.e., compounds **1** to **10**), and investigated the chemical constituents which inhibited the activities of pols and anti-inflammation.

Experimental Procedures

Materials

The crude (unrefined) oil of canola (low erucic acid rapeseed, *Brassica napus* L.) was pressed by J-Oil Mills Inc. (Yokohama, Japan). Lutein (**1**), zeaxanthin (**2**), β-cryptoxanthin (**3**), astaxanthin (**4**), canthaxanthin (**5**), β-carotene (**6**), lycopene (**7**), capsanthin (**8**) and fucoxanthin (**9**) were purchased from Sigma-Aldrich Japan K.K. (Tokyo, Japan), and the purity of these carotenoids was ~98%. Fucoxanthinol (**10**) was enzymatically converted from fucoxanthin (**9**), as described by Tsukui et al. [9]. The chemically synthesized DNA template and nucleotides, such as poly(dA) and [^{3}H]-deoxythymidine 5′-triphosphate (dTTP) (43 Ci/mmol), were purchased from GE Healthcare Bio-Sciences (Little Chalfont, UK). DNA primer, such as oligo(dT)$_{18}$, was customized by Sigma-Aldrich Japan K.K. (Hokkaido, Japan). All other reagents were of analytical grade and purchased from Nacalai Tesque Inc. (Kyoto, Japan).

Structure Determination

The NMR spectra (^{1}H and ^{13}C) were recorded on a Bruker 400 MHz spectrometer (Avance DRX-400). The IR spectrum was recorded on a Jasco FT/IR-410 spectrometer. The mass spectrum was obtained with an Applied Biosystems mass spectrometer (APIQSTAR pulsar i).

Enzymes

Pol α was purified from calf thymus by immuno-affinity column chromatography, as described by Tamai et al. [10]. Recombinant rat pol β was purified from *E. coli* JMpβ5, as described by Date et al. [11]. The human pol γ catalytic gene was cloned into pFastBac. Histidine-tagged enzyme was expressed using the BAC-TO-BAC HT Baculovirus Expression System according to the supplier's manual (Life Technologies, MD, USA) and purified using Pro-Boundresin (Invitrogen Japan, Tokyo, Japan) [12]. Human pols δ and ε were purified from the nuclear fraction of human peripheral blood cancer cells (Molt-4) using the second subunit of pols δ and ε-conjugated affinity column chromatography, respectively [13]. Recombinant human His-pol λ was overexpressed and purified according to a method described by Shimazaki et al. [14]. Fish pol δ was purified from the testis of cherry salmon (*Oncorhynchus masou*) [15]. Fruit fly pols α, δ and ε were purified from early embryos of *Drosophila melanogaster*, as described by Aoyagi et al. [16, 17]. Pol α from a higher plant, cauliflower inflorescence, was purified according to the methods outlined by Sakaguchi et al. [18]. The Klenow fragment of pol I from *E. coli* and human immunodeficiency virus type-1 (HIV-1) reverse transcriptase (recombinant) were purchased from Worthington Biochemical Corp. (Freehold, NJ, USA). T4 pol, *Taq* pol, T7 RNA polymerase and T4 polynucleotide kinase were purchased from Takara Bio (Tokyo, Japan). Bovine pancreas deoxyribonuclease I (DNase I) was obtained from Stratagene Cloning Systems (La Jolla, CA, USA).

DNA Polymerase Assays

The reaction mixtures for pol α, pol β, plant pol α and prokaryotic pols were described previously [19, 20], and those for pol γ, and pols δ and ε were as described by Umeda et al. [12] and Ogawa et al. [21], respectively. The reaction mixture for pol λ was the same as for pol β. For pols, poly(dA)/oligo(dT)$_{18}$ (A/T = 2/1) and dTTP were used as the DNA template-primer and nucleotide (i.e., dNTP) substrate,

respectively. For HIV-1 reverse transcriptase, poly(rA)/oligo(dT)$_{18}$ (A/T = 2/1) and dTTP were used as the template-primer and nucleotide substrate, respectively.

The compounds were dissolved in distilled dimethyl sulfoxide (DMSO) at various concentrations and sonicated for 30 s. Aliquots of 4 μl sonicated samples were mixed with 16 μl of each enzyme (final amount 0.05 units) in 50 mM Tris–HCl (pH7.5) containing 1 mM dithiothreitol, 50% glycerol and 0.1 mM EDTA, and kept at 0 °C for 10 min. These inhibitor-enzyme mixtures (8 μl) were added to 16 μl of each enzyme standard reaction mixture, and incubation was carried out at 37 °C for 60 min, except for *Taq* pol, which was incubated at 74 °C for 60 min. Activity without the inhibitor was considered 100%, and the remaining activity at each concentration of the inhibitor was determined relative to this value. One unit of pol activity was defined as the amount of enzyme that catalyzed the incorporation of 1 nmol dNTP (i.e., dTTP) into synthetic DNA template-primers in 60 min at 37 °C under the normal reaction conditions for each enzyme [19, 20].

Other DNA Metabolic Enzymes Assays

The activities of calf primase of pol α, T7 RNA polymerase, T4 polynucleotide kinase and bovine DNase I were measured in standard assays according to the manufacturer's specifications, as described by Tamiya-Koizumi et al. [22], Nakayama and Saneyoshi [23], Soltis and Uhlenbeck [24], and Lu and Sakaguchi [25], respectively.

Anti-Inflammatory Assay

The mouse inflammatory test was performed according to Gschwendt's method [26]. This experiment complied with the regulations concerning animal experimentation and the care of experimental animals of Kobe-Gakuin University. Briefly, a solution of the test compound in acetone (250 μg and 500 μg/20 μl) was applied to the inner part of the ear. Thirty minutes after the test compound was applied, a solution of 12-*O*-tetradecanoylphorbol-13-acetate (TPA) (0.5 μg/20 μl of acetone) was applied to the same part of the ear. To the other ear of the same mouse, methanol and a TPA solution were applied as a control. After 7 h, a disk (6 mm in diameter) was obtained from the ear and weighed. The inhibitory effect (IE) of inflammation is presented as the ratio of the increase in weight of the ear disks: IE: {[(TPA only)-(tested compound plus TPA)]/[(TPA only)-(vehicle)] × 100}.

Molecular Simulation

The molecular structure of lutein (**1**) was constructed based on Discovery Studio (DS) 2.1 (Accelrys, Inc., San Diego, CA) on a PC terminal (Express; NEC) linked with Regatta (96 nodes; IBM). Energy minimization was achieved using a solvation model and calculated by the GBSW parameter with Minimization and Dynamics protocols within DS. The calculation used a CHARMm (Chemistry at HARvard Macromolecular Mechanics) force-field.

Results

Isolation of the Mammalian Pol Inhibitor from the Pressed Extract of Canola/Rapeseed (*Brassica napus* L.)

Since the chloroform-soluble phase of the Canola/rapeseed crude pressed extract (1 g extract per 10 ml chloroform) had inhibitory activity against mammalian pols, the chloroform extract (50 g) was subjected to SiO_2 column chromatography and then eluted with $CHCl_3$:MeOH (v/v 50:1). The active fractions were purified by SiO_2 column chromatography using benzene:MeOH (v/v 15:1). The active fractions were subjected to SiO_2 column chromatography and then eluted with *n*-hexane : acetone (v/v 3:1). The active fractions were finally purified by Sephadex LH-20 column chromatography eluted with $CHCl_3$:MeOH (v/v 1:1). Finally, a yellow powder (compound **1**) was obtained (5.8 mg).

Structure Determination of Compound **1**

The molecular formula of compound **1** was determined to be $C_{40}H_{56}O_2$ by the high resolution mass spectrum. The presence of two secondary hydroxyl groups was revealed by two methine signals at δ 4.00 and 4.25 and IR absorption at 3416 cm^{-1}. The ^{1}H- and ^{13}C-NMR spectra showed that compound **1** has a polyene structure and ten methyl groups. From the above data, compound **1** was identified as a carotenoid, lutein. These spectroscopic data were consistent with those reported [27, 28]. The analyzed data of compound **1** are shown below.

Lutein (**1**): ^{1}H NMR (400 MHz, $CDCl_3$) : δ = 0.85 (3H, s), 1.00 (3H, s), 1.07 (6H, s), 1.37 (1H, dd, J = 13.2 Hz, 6.8 Hz), 1.48 (1H, t, J = 12.0 Hz), 1.63 (3H, s), 1.74 (3H, s), 1.77 (1H, m), 1.84 (1H, dd, J = 13.2 Hz, 6.0 Hz), 1.91 (3H, s), 1.97 (3H, s), 1.97 (3H, s), 1.97 (3H, s), 2.04 (1H, dd, J = 16.8 Hz, 9.6 Hz), 2.36-2.42 (2H, m), 4.00 (1H, m), 4.25 (1H, m), 5.43 (1H, dd, J = 15.6 Hz, 10 Hz), 5.55 (1H, s), 6.12 (2H, m), 6.14–6.17 (3H, m), 6.24 (1H, m), 6.26 (1H, m), 6.36 (1H, d, J = 14.8 Hz), 6.36 (1H, d, J = 14.8 Hz), 6.58–6.68 (4H, m). ^{13}C NMR (100 MHz, $CDCl_3$): δ = 12.75, 12.75, 12.81, 13.1, 21.6, 22.9, 24.3, 28.7, 29.5, 30.3, 34.0, 37.1, 42.5, 44.6, 48.4, 55.0, 65.1, 65.9, 124.5, 124.8, 124.9, 125.6, 126.2, 128.7, 130.0, 130.1, 130.8,

131.3, 132.6, 132.6, 135.1, 135.7, 136.4, 136.5, 137.6, 137.6, 137.72, 137.74, 138.0, 138.5. IR (NaCl): 3416, 3018, 2960, 2927, 2867, 1577, 1443, 1368, 1037, 970 cm^{-1}. HRMS (ESI): *m/z* calcd for $C_{40}H_{56}O_2Na$ ($[M + Na]^+$): 591.4172, found: 591.4180.

Effects of Lutein-Related Carotenoids (Compounds **1**–**10**) on Mammalian Pols α, β and λ

First, we investigated the pol inhibitory activity of the purified compound **1** compared with the commercially purchased reagent (specially purified grade of lutein), which showed the same strong inhibitory effect (data not shown); therefore, we used the commercially purified reagent in later parts of this study.

We obtained commercially-available carotenoids, lutein (**1**), zeaxanthin (**2**), β-cryptoxanthin (**3**), astaxanthin (**4**), canthaxanthin (**5**), β-carotene (**6**), lycopene (**7**), capsanthin (**8**) and fucoxanthin (**9**), and fucoxanthinol (**10**) was enzymatically synthesized from fucoxanthin (**9**), as described by Tsukui et al. [9]. The inhibitory activity of calf pol α, rat pol β and human pol λ against 10 and 100 μM of each compound was investigated (Fig. 1). In mammalian pols, pol α and pols β and λ were used as representative replicative pol and repair/recombination-related pols, respectively [5, 29]. All compounds tested had no influenced on pol α activity (Fig. 1a), but lutein (**1**), zeaxanthin (**2**) and capsanthin (**8**) inhibited the activities of pols β and λ (Fig. 1b, c). The inhibitory effect on pol β showed the same tendency as that on pol λ, lutein (**1**) had the strongest inhibitory effect on these pols of the tested compounds, and the effect of the three compounds ranked as follows: lutein (**1**) > zeaxanthin (**2**) > capsanthin (**8**). When activated DNA (i.e., DNA digested by bovine DNase I) was used as the DNA template-primer instead of poly (dA)/oligo$(dT)_{18}$ (A/T = 2/1), the mode of inhibition by these compounds did not change (data not shown).

Effects of Lutein (**1**) on Various Pols and Other DNA Metabolic Enzymes

Since lutein (**1**) was the strongest inhibitor of mammalian pols β and λ in the carotenoids (compounds **1**–**10**) investigated (Fig. 1), we focused on lutein (**1**) in this section. As shown in Table 1, this compound only inhibited pols β and λ activities in mammalian pols, and these pols were dose-dependently suppressed to the same extent, with IC_{50} values of 45.0 and 12.8 μM, respectively. On the other hand, lutein (**1**) had no significant influence on the activities of fish (cherry salmon) pol δ, insect (fruit fly) pols α, δ and ε, pol α from plants (cauliflower) and prokaryotes, such as the Klenow fragment of *E. coli* pol I, T4 pol and *Taq* pol. This compound did not inhibit the activities of the other DNA metabolic enzymes tested, including calf primase of pol α, HIV-1 reverse transcriptase, T7 RNA polymerase, T4 polynucleotide kinase and bovine DNase I.

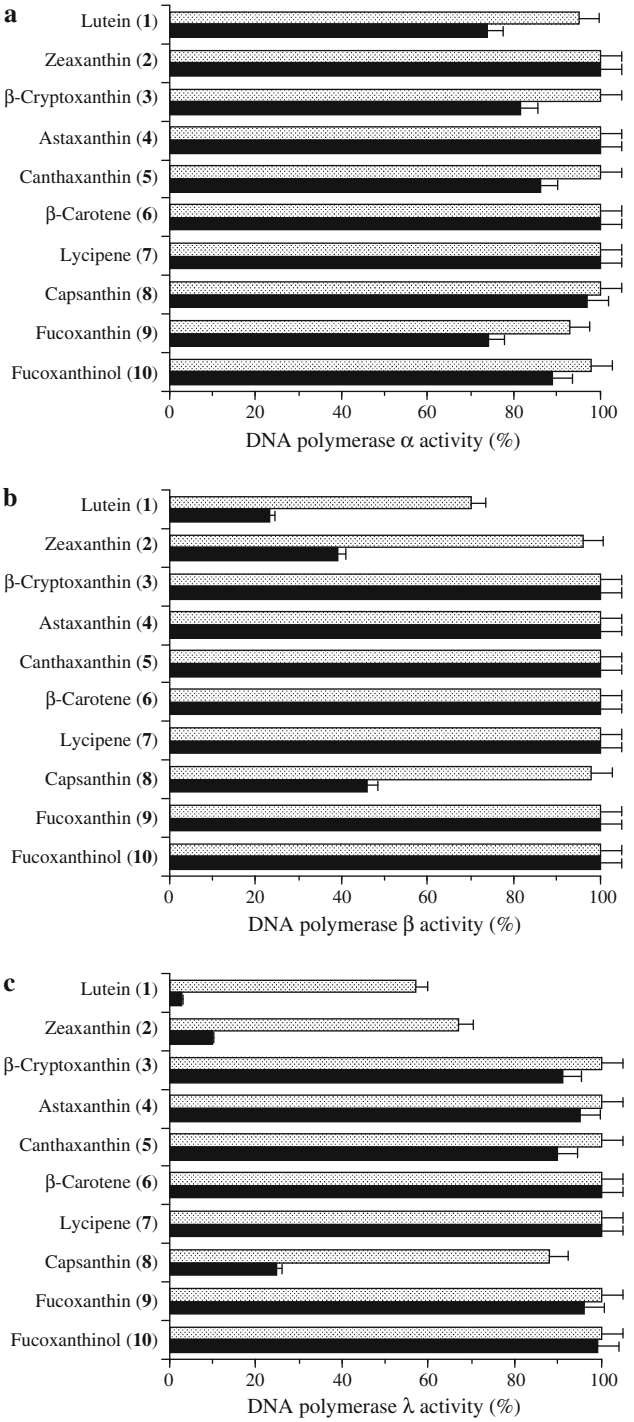

Fig. 1 Inhibitory effect of carotenoids (compounds **1**–**10**) on the activities of mammalian pols. Ten μM (*gray bar*) and 100 μM (*black bar*) of each compound was incubated with calf pol α (**a**), rat pol β (**b**) and human pol λ (**c**) (0.05 units each). Percent relative activity is shown. Pol activity in the absence of the compound was taken as 100%. Data are shown as the means ± SEM of three independent experiments

Table 1 IC_{50} values of lutein (**1**) on the activities of various DNA polymerases and other DNA metabolic enzymes

Enzyme	IC_{50} value (μM)
Mammalian DNA polymerases	
Calf DNA polymerase α	>200
Rat DNA polymerase β	45.0 ± 2.3
Human DNA polymerase γ	>200
Human DNA polymerase δ	>200
Human DNA polymerase ε	>200
Human DNA polymerase λ	12.8 ± 0.7
Fish DNA polymerases	
Cherry salmon DNA polymerase δ	>200
Insect DNA polymerases	
Fruit fly DNA polymerase α	>200
Fruit fly DNA polymerase δ	>200
Fruit fly DNA polymerase ε	>200
Plant DNA polymerases	
Cauliflower DNA polymerase α	>200
Prokaryotic DNA polymerases	
E. coli DNA polymerase I (Klenow fragment)	>200
T4 DNA polymerase	>200
Taq DNA polymerase	>200
Other DNA metabolic enzymes	
Calf primase of DNA polymerase α	>200
HIV-1 Reverse transcriptase	>200
T7 RNA polymerase	>200
T4 polynucleotide kinase	>200
Bovine deoxyribonuclease I	>200

This compound was incubated with each pol (0.05 units) and other DNA metabolic enzymes. One unit of pol activity was defined as the amount of enzyme that catalyzed the incorporation of 1 nmol of dNTP (i.e., dTTP) into the synthetic DNA template-primers (i.e., poly(dA)/oligo$(dT)_{18}$, A/T = 2/1) in 60 min at 37 °C under normal reaction conditions for each enzyme. Enzyme activity in the absence of the compound was taken as 100%. Data are shown as the means ± SEM of four independent experiments

To determine whether the inhibitor resulted in binding to DNA or the enzyme, the interaction of lutein (**1**) with dsDNA was investigated based on the thermal transition of dsDNA with or without the compound. The Tm of dsDNA with an excess amount of lutein (**1**) (100 μM) was measured using a spectrophotometer equipped with a thermoelectric cell holder. In the concentration range used, thermal transition of Tm was not observed, whereas ethidium bromide used as a positive control, a typical intercalating compound, produced a clear thermal transition. We then investigated whether an excessive amount of nucleic acid (i.e., poly(rC)) or protein (i.e., bovine serum albumin (BSA)) could prevent the inhibitory effect of lutein (**1**) to determine whether the effect resulted from their non-specific adhesion to mammalian pols β and λ, or selective binding to specific sites. Poly(rC) and BSA had little or no influence on the pol inhibitory effect of lutein (**1**), suggesting that binding to the pol molecule occurs selectively. These observations indicated that lutein (**1**) did not intercalate to DNA as a template-primer, and the compound could directly bind to the enzyme and inhibit its activity.

These results suggested that lutein (**1**) might be a potent and selective inhibitor of mammalian repair/recombination-related pols, such as pols β and λ.

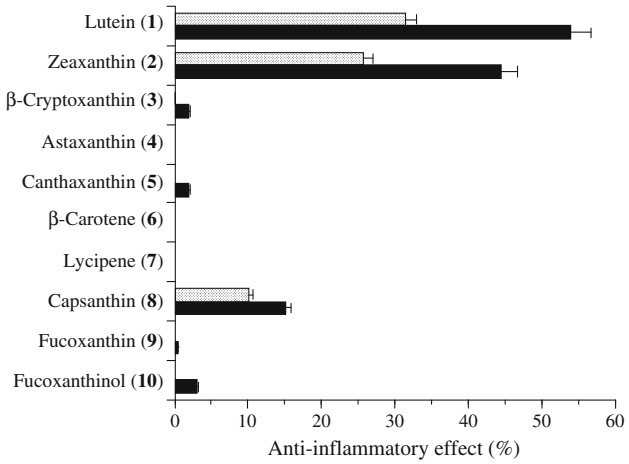

Fig. 2 Anti-inflammatory activity of carotenoids (compounds **1–10**) toward TPA-induced edema on mouse ear. 250 μg (*gray bar*) and 500 μg (*black bar*) of compounds **1–10** were applied individually to one ear of each mouse, and after 30 min TPA (0.5 μg) was applied to both ears. Edema was evaluated after 7 h. The inhibitory effect is expressed as the percentage of edema. Data are shown as the means ± SEM of six independent experiments

Anti-Inflammatory Effects of Lutein-Related Carotenoids (Compounds **1–10**)

We previously reported a relationship between mammalian pol λ inhibitors and anti-inflammatory activity [30–33]. Using the mouse inflammatory test, we examined the anti-inflammatory properties of the carotenoids. An application of TPA (0.5 μg) to the ear induced edema, the weight of an ear disk 7 h after the application having increased 241%. As shown in Fig. 2, lutein (**1**) achieved the strongest reduction in TPA-induced inflammation among the compounds tested, and the inhibitory effect was 31.4 and 54.0% for 250 and 500 μg/ear, respectively. The 2nd and 3rd compounds, zeaxanthin (**2**) and capsanthin (**8**), respectively, showed inhibitory effects, but other compounds had little or no effect on inflammation. The effect of ten carotenoids on anti-inflammation showed almost the same tendency as the inhibitory effect on pols β and λ (Fig. 1).

TPA is a compound that promotes tumorigenesis [34], and is generally used as an artificial inducer of

inflammation [35, 36]. TPA-induced inflammation can be distinguished from acute inflammation, and is accompanied by fibroblastic proliferation and granulation. These results suggested that the molecular basis of the so-called promotion of oncogenesis involves a biochemical process which requires pols, especially repair/recombination-related pol λ; therefore, some carotenoids, such as lutein (**1**), could have anti-inflammatory activity based on its inhibition of mammalian pol λ.

Structure and Bioactivity Relationship of Lutein-Related Carotenoids

Lutein (**1**), a xanthophyll family of carotenoid, consists of chains with 8 conjugated double bonds (polyene chain) containing closed rings at each end of the chain. Zeaxanthin (**2**) is a stereoisomer of lutein (**1**), differing only in the location of a double bond in one of the hydroxyl groups. Figure 3a shows the chemical structures between bioactive

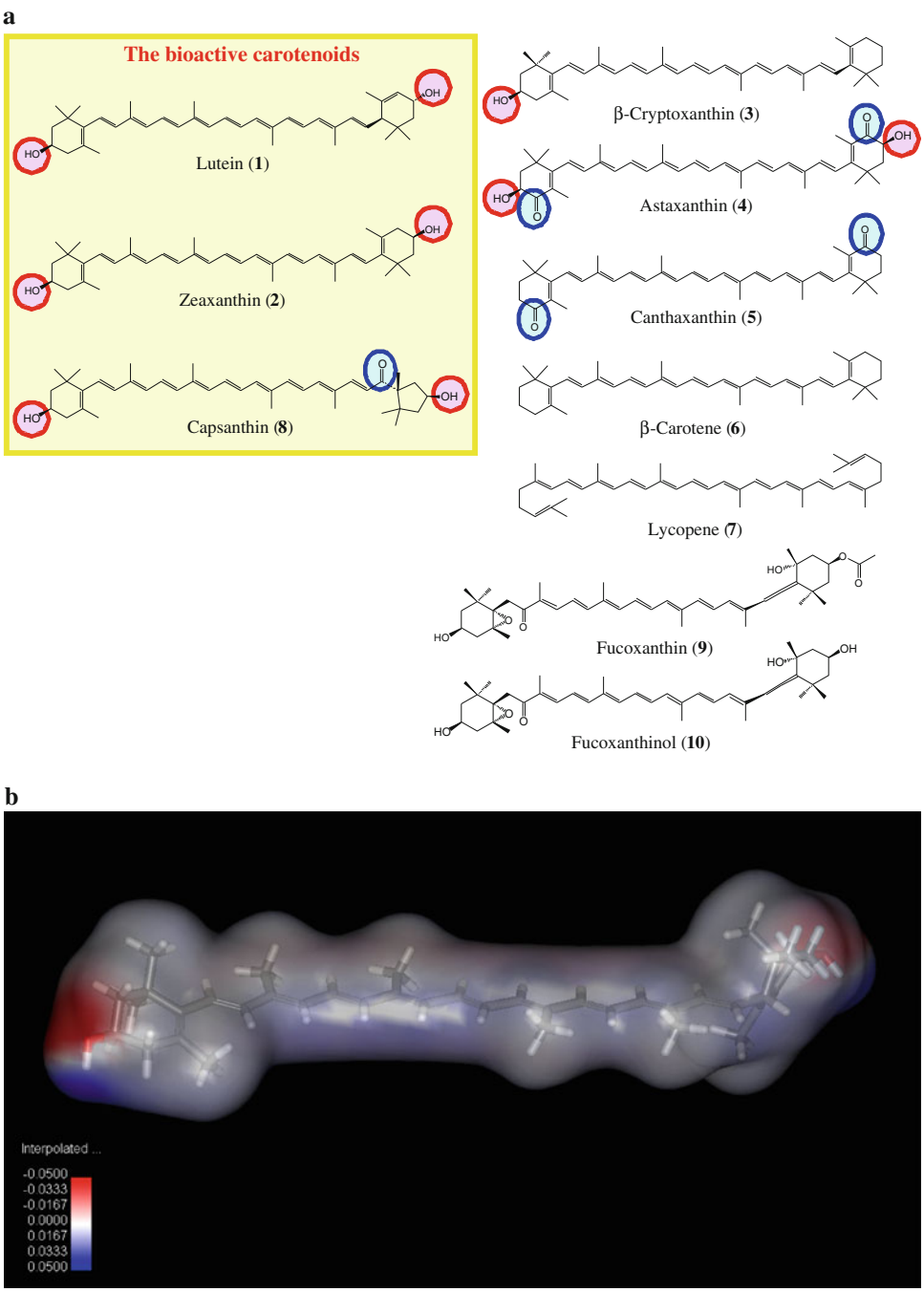

Fig. 3 Chemical structures of bioactive carotenoids. **a** Bioactive carotenoids, which have mammalian pols β and λ inhibitory activity and anti-inflammatory activity, are shown. Lutein (**1**), zeaxanthin (**2**), β-cryptoxanthin (**3**), astaxanthin (**4**), canthaxanthin (**5**), β-carotene (**6**), lycopene (**7**), capsanthin (**8**), fucoxanthin (**9**) and fucoxanthinol (**10**). Hydroxyl and ketone groups are highlighted by *red* and *blue circles*, respectively. **b** Stick model of energy-minimized three-dimensional structure of lutein (**1**) was built using the Discovery Studio (DS) 2.1 modeling software (Accelrys Inc., San Diego, CA, USA). Carbons, oxygens and hydrogens are indicated in *gray*, *red* and *white*, respectively. Electrostatic potential over commonly surfaces was also analyzed using DS. *Blue areas* are positively charged, *red areas* are negatively charged, and white areas are neutral

carotenoids [i.e., lutein (**1**), zeaxanthin (**2**) and capsanthin (**8**)] and other compounds. In the bioactive carotenoids, two hydroxyl groups (i.e., red circles in Fig. 3a) one on each side of the carotenoid molecule must be important for pols β and λ inhibition and anti-inflammation. Although astaxanthin (**4**) has two hydroxyl groups on both side rings, this compound did not show prominent inhibitory activities against these pols and the anti-inflammatory effect; therefore, two ketone groups (i.e., blue circles in Fig. 3a) on both sides of the carotenoid molecule markedly prevented these activities. Since fucoxanthin (**9**) and fucoxanthinol (**10**) had no inhibitory effects on pol activity and inflammation, these frames of the carotenoids must significantly prevent bioactivity.

Lutein (**1**) was the strongest inhibitor of mammalian pols β and λ and had the strongest anti-inflammation activity of the carotenoids tested. To obtain information about the molecular basis of the difference in inhibition between lutein (**1**) and its nine related carotenoids, computational analysis was performed using molecular simulation and surface analysis software. As shown in Fig. 3b, energy-minimized three-dimensional structure of lutein (**1**) is stick shaped, and both sides of the compound consist of a ball-like conformation. The length and width of this molecule were 30 and 5.0 Å, respectively, which might fit the pocket of the active site in mammalian pols β and λ. Lutein (**1**) consists of both hydrophilic ends and a hydrophobic center, and the distribution of positive- and negative-charged regions in the hydrophilic areas of the both sides must be important for bioactivity.

Discussion

Evaluation of the purified carotenoids (compounds **1**–**10**) revealed that the inhibitory activities of pols β and λ had a high correlation with the anti-inflammatory effect (Figs. 1, 2). On the other hand, no compounds affected the activity of replicative pol α. These results led to the speculation that TPA-induced inflammation may involve a process requiring repair/recombination-related pols.

Pols β and λ are in the pol X family [37]. Although the in vivo biochemical function of pol λ is unclear as yet, pol λ appears to work in a similar manner to pol β. Pol β, which is widely known to have roles in the short-patch base excision repair (BER) pathway [38–41], plays an essential role in neural development [42]. Recently, pol λ was found to contain 5′-deoxyribose-5-phosphate (dRP) lyase activity, but no apurinic/apyrimidinic (AP) lyase activity [43] and to be able to substitute pol β in in vitro BER, suggesting that pol λ also participates in BER. Northern blot analysis indicated that transcripts of pol β were abundantly expressed in the testis, thymus, and brain in rats [44], but pol λ was efficiently transcribed mostly in the testis [37]. Bertocci et al. [45] reported that in mutant mice in which pol λ was knocked out were not only viable and fertile, but also displayed a normal hyper-mutation pattern.

TPA not only causes inflammation, but also influences cell proliferation and has physiological effects on cells because it is a tumor promoter [36]; therefore, anti-inflammatory agents are expected to suppress both mammalian cell proliferation and DNA replication/repair in nuclei related to the action of TPA. Since pol λ is a repair-related pol [46], the result that the molecular target of carotenoids was pol λ is well-matched. If so, the pol λ inhibitor might be an inhibitor of chronic inflammation. A positive relationship between anti-inflammatory and pol λ-inhibitory activities was found, and this might be useful as a new and convenient in vitro assay to screen for novel anti-chronic inflammatory compounds.

Lutein (**1**) is one of over 600 known naturally occurring carotenoids. Found in green leafy vegetables such as spinach and kale, this compound is employed by organisms as an antioxidant and for blue light absorption. Lutein is sometimes present in plants as fatty-acid esters, with one or two fatty acids bound to the two hydroxyl groups. Saponification of lutein esters yields lutein in approximately a 1:2 M ratio. This compound is also found in egg yolks, animal fats and the corpus luteum. Lutein is a lipophilic molecule and is generally insoluble in water. The presence of the long chromophore of conjugated double bonds provides the distinctive light-absorbing properties. The polyene chain is susceptible to oxidative degradation by light or heat and is chemically unstable in acids. Lutein is widely known as the primary nutrient for protecting ocular function. No toxicities or adverse reactions have been reported in the scientific literature for lutein at doses of up to 40 mg daily for 2 months [47]. It has long been thought that carotenoid intake also reduces the risk of certain forms of cardiovascular disease [48–50], stroke [51, 52] and cancer [53, 54]. From this study, we could suggest that some carotenoids, such as lutein, have new bioactivity as anti-inflammation.

In conclusion, the inhibitory effects on repair/recombination-related pols had the same tendency as on TPA-induced inflammation, suggesting that the inhibitory activity of pol λ might be important for the anti-inflammatory effect. A biologically active carotenoid, lutein, was isolated from pressed unrefined canola (rapeseed) oil. It is likely that a significant portion of the lutein would be removed during the bleaching step of conventional refining, bleaching and deodorization [55]. A cold pressed unrefined canola oil may have valuable anti-inflammatory properties and inhibit mammalian pol λ. Carotenoids, especially lutein (**1**), may provide valuable structural information that can be used in a drug design strategy for new anti-inflammatory agents.

Acknowledgments This work was supported in part by the "Academic Frontier" Project for Private Universities: matching fund subsidy from the Ministry of Education, Science, Sports, and Culture of Japan (MEXT), 2006–2010, (Y.M. and H.Y.). Y.M. acknowledges a Grant-in-Aid for Young Scientists (A) (No. 19680031) from MEXT.

References

1. DePamphilis ML (1996) DNA replication in eukaryotic cells. Cold Spring Harbor Laboratory Press, Cold Spring Harbor
2. Kornberg K, Baker TA (1992) Eukaryotic DNA polymerase. In: DNA replication, 2nd edn. Freeman WD, New York, vol 6, pp 197–225
3. Seto H, Hatanaka M, Kimura S, Oshige M, Tsuya Y, Mizushina Y, Sawado T, Aoyagi N, Matsumoto T, Hashimoto J, Sakaguchi K (1998) Purification and characterization of a 100 kDa DNA polymerase from cauliflower inflorescence. Biochem J 332: 557–563
4. Hubscher U, Maga G, Spadari S (2002) Eukaryotic DNA polymerases. Ann Rev Biochem 71:133–163
5. Bebenek K, Kunkel TA (2004) DNA repair and replication. In: Yang W (ed) Advances in protein chemistry. Elsevier, San Diego, vol 69, pp 137–165
6. Takata K, Shimizu T, Iwai S, Wood RD (2006) Human DNA polymerase N (POLN) is a low fidelity enzyme capable of error-free bypass of 5S-thymine glycol. J Biol Chem 281:23445–23455
7. Sakaguchi K, Sugawara F, Mizushina Y (2002) Inhibitors of eukaryotic DNA polymerases. Seikagaku 73:244–251
8. Mizushina Y (2009) Specific inhibitors of mammalian DNA polymerase species. Biosci Biotechnol Biochem 73:1239–1251
9. Tsukui T, Konno K, Hosokawa M, Maeda H, Sashima T, Miyashita K (2007) Fucoxanthin and fucoxanthinol enhance the amount of docosahexaenoic acid in the liver of KKAy obese/diabetic mice. J Agric Food Chem 55:5025–5029
10. Tamai K, Kojima K, Hanaichi T, Masaki S, Suzuki M, Umekawa S, Yoshida S (1988) Structural study of immunoaffinity-purified DNA polymerase α-DNA primase complex from calf thymus. Biochim Biophys Acta 950:263–273
11. Date T, Yamaguchi M, Hirose F, Nishimoto Y, Tanihara K, Matsukage A (1988) Expression of active rat DNA polymerase β in *Escherichia coli*. Biochemistry 27:2983–2990
12. Umeda S, Muta T, Ohsato T, Takamatsu C, Hamasaki N, Kang D (2000) The D-loop structure of human mtDNA is destabilized directly by 1-methyl-4-phenylpyridinium ion (MPP+), a parkinsonism-causing toxin. Eur J Biochem 267:200–208
13. Oshige M, Takeuchi R, Ruike R, Kuroda K, Sakaguchi K (2004) Subunit protein-affinity isolation of Drosophila DNA polymerase catalytic subunit. Protein Expr Purif 35:248–256
14. Shimazaki N, Yoshida K, Kobayashi T, Toji S, Tamai T, Koiwai O (2002) Over-expression of human DNA polymerase λ in *E. coli* and characterization of the recombinant enzyme. Genes Cells 7:639–651
15. Yamaguchi T, Saneyoshi M, Takahashi H, Hirokawa S, Amano R, Liu X, Inomata M, Maruyama T (2006) Synthetic Nucleoside and Nucleotides. 43. Inhibition of vertebrate telomerases by carbocyclic oxetanocin G (C.OXT-G) triphosphate analogues and influence of C.OXT-G treatment on telomere length in human HL60 cells. Nucleosides Nucleotides Nucleic Acids 25:539–551
16. Aoyagi N, Matsuoka S, Furunobu A, Matsukage A, Sakaguchi K (1994) Drosophila DNA polymerase δ: purification and characterization. J Biol Chem 269:6045–6050
17. Aoyagi N, Oshige M, Hirose F, Kuroda K, Matsukage A, Sakaguchi K (1997) DNA polymerase ε from *Drosophila melanogaster*. Biochem Biophys Res Commun 230:297–301
18. Sakaguchi K, Hotta Y, Stern H (1980) Chromatin-associated DNA polymerase activity in meiotic cells of lily and mouse. Cell Struct Funct 5:323–334
19. Mizushina Y, Tanaka N, Yagi H, Kurosawa T, Onoue M, Seto H, Horie T, Aoyagi N, Yamaoka M, Matsukage A, Yoshida S, Sakaguchi K (1996) Fatty acids selectively inhibit eukaryotic DNA polymerase activities in vitro. Biochim Biophys Acta 1308:256–262
20. Mizushina Y, Yoshida S, Matsukage A, Sakaguchi K (1997) The inhibitory action of fatty acids on DNA polymerase β. Biochim Biophys Acta 1336:509–521
21. Ogawa A, Murate T, Suzuki M, Nimura Y, Yoshida S (1998) Lithocholic acid, a putative tumor promoter, inhibits mammalian DNA polymerase β. Jpn J Cancer Res 89:1154–1159
22. Tamiya-Koizumi K, Murate T, Suzuki M, Simbulan CG, Nakagawa M, Takemura M, Furuta K, Izuta S, Yoshida S (1997) Inhibition of DNA primase by sphingosine and its analogues parallels with their growth suppression of cultured human leukemic cells. Biochem Mol Biol Int 41:1179–1189
23. Nakayama C, Saneyoshi M (1985) Inhibitory effects of 9-β-D-xylofuranosyladenine 5′-triphosphate on DNA-dependent RNA polymerase I and II from cherry salmon (*Oncorhynchus masou*). J Biochem (Tokyo) 97:1385–1389
24. Soltis DA, Uhlenbeck OC (1982) Isolation and characterization of two mutant forms of T4 polynucleotide kinase. J Biol Chem 257:11332–11339
25. Lu BC, Sakaguchi K (1991) An endo-exonuclease from meiotic tissues of the basidiomycete *Coprinus cinereus*: its purification and characterization. J Biol Chem 266:21060–21066
26. Gschwendt M, Kittstein W, Furstenberger G, Marks F (1984) The mouse ear edema: a quantitatively evaluable assay for tumor promoting compounds and for inhibitors of tumor promotion. Cancer Lett 25:177–185
27. Eichenberger W, Grob EC (1963) Beiträge zur Chemie der pflanzlichen Plastiden. 3. Mitteilung. Über das Vorkommen von Lutein-3-linolenat in gelben Herbstblättern von *Acer platanoides* (L.). Helvetica Chimica Acta 46:2411–2417
28. Molnár P, Deli J, Ösz E, Zsila F, Simonyi M, Tóth G (2004) Confirmation of the absolute (3*R*, 3′*S*, 6′*R*)-configuration of (all-*E*)-3′-epilutein. Helvetica Chim Acta 87:2159–2168
29. Friedberg EC, Feaver WJ, Gerlach VL (2000) The many faces of DNA polymerases: strategies for mutagenesis and for mutational avoidance. Proc Natl Acad Sci USA 97:5681–5683
30. Mizushina Y, Hirota M, Murakami C, Ishidoh T, Kamisuki S, Shimazaki N, Takemura M, Perpelescu M, Suzuki M, Yoshida H, Sugawara F, Koiwai O, Sakaguchi K (2003) Some anti-chronic inflammatory compounds are DNA polymerase lambda-specific inhibitors. Biochem Pharmacol 66:1935–1944
31. Mizushina Y, Kuramochi K, Ikawa H, Kuriyama I, Shimazaki N, Takemura M, Oshige M, Yoshida H, Koiwai O, Sugawara F, Kobayashi S, Sakaguchi K (2005) Structural analysis of epolactaene derivatives as DNA polymerase inhibitors and anti-inflammatory compounds. Int J Mol Med 15:785–793
32. Mizushina Y, Saito A, Tanaka A, Nakajima N, Kuriyama I, Takemura M, Takeuchi T, Sugawara F, Yoshida H (2005) Structural analysis of catechin derivatives as mammalian DNA polymerase inhibitors. Biochem Biophy Res Commun 333: 101–109
33. Mizushina Y, Akihisa T, Ukiya M, Hamasaki Y, Murakami-Nakai C, Kuriyama I, Takeuchi T, Sugawara F, Yoshida H (2005) Structural analysis of isosteviol and related compounds as DNA polymerase and DNA topoisomerase inhibitors. Life Sci 77:2127–2140
34. Hecker E (1978) Carcinogenesis, vol 2. Raben Press, NY, pp 11–48

35. Fujiki H, Sugimura T (1987) Advances in cancer research, vol 49. Academic Press, London, pp 223–264
36. Nakamura Y, Murakami A, Ohto Y, Torikai K, Tanaka T, Ohigashi H (1998) Suppression of tumor promoter-induced oxidative stress and inflammatory responses in mouse skin by a superoxide generation inhibitor 1′-acetoxychavicol acetate. Cancer Res 58:4832–4839
37. Garcia-Diaz M, Dominguez O, Lopez-Fernandez LA, de Lera LT, Saniger ML, Ruiz JF, Parraga M, Garcia-Ortiz MJ, Kirchhoff T, del Mazo J, Bernad A, Blanco L (2000) DNA polymerase λ (Pol λ), a novel eukaryotic DNA polymerase with a potential role in meiosis. J Mol Biol 301:851–867
38. Singhal RK, Wilson SH (1993) Short gap-filling synthesis by DNA polymerase β is processive. J Biol Chem 268:15906–15911
39. Matsumoto Y, Kim K (1995) Excision of deoxyribose phosphate residues by DNA polymerase β during DNA repair. Science 269:699–702
40. Sobol RW, Horton JK, Kuhn R, Gu H, Singhal RK, Prasad R, Rajewsky K, Wilson SH (1996) Requirement of mammalian DNA polymerase-β in base-excision repair. Nature 379:183–186
41. Ramadan K, Shevelev IV, Maga G, Hubscher U (2002) DNA polymerase λ from calf thymus preferentially replicates damaged DNA. J Biol Chem 277:18454–18458
42. Sugo N, Aratani Y, Nagashima Y, Kubota Y, Koyama H (2000) Neonatal lethality with abnormal neurogenesis in mice deficient in DNA polymerase β. EMBO J 19:1397–1404
43. Garcia-Diaz M, Bebenek K, Kunkel TA, Blanco L (2001) Identification of an intrinsic 5'-deoxyribose-5-phosphate lyase activity in human DNA polymerase λ: a possible role in base excision repair. J Biol Chem 276:34659–34663
44. Hirose F, Hotta Y, Yamaguchi M, Matsukage A (1989) Difference in the expression level of DNA polymerase β among mouse tissues: high expression in the pachytene spermatocyte. Exp Cell Res 181:169–180
45. Bertocci B, De Smet A, Flatter E, Dahan A, Bories JC, Landreau C, Weill JC, Reynaud CA (2002) Cutting edge: DNA polymerases μ and λ are dispensable for Ig gene hypermutation. J Immunol 168:3702–3706
46. Garcia-Diaz M, Bebenek K, Sabariegos R, Dominguez O, Rodriguez J, Kirchhoff T, Garcia-Palomero E, Picher AJ, Juarez R, Ruiz JF, Kunkel TA, Blanco L (2002) DNA polymerase λ, a novel DNA repair enzyme in human cells. J Biol Chem 277:13184–13191
47. Kritchevsky SB (1999) Beta-carotene, carotenoids and the prevention of coronary heart disease. J Nutr 129:5–8
48. Dagnelie G, Zorge IS, McDonald TM (2000) Lutein improves visual function in some patients with retinal degeneration: a pilot study via the Internet. Optometry 71:147–164
49. Street DA, Comstock GW, Salkeld RM, Schüep W, Klag MJ (1994) Serum antioxidants and myocardial infarction. Are low levels of carotenoids and alpha-tocopherol risk factors for myocardial infarction? Circulation 90:1154–1161
50. Connor SL, Ojeda LS, Sexton G, Weidner G, Connor WE (2004) Diets lower in folic acid and carotenoids are associated with the coronary disease epidemic in Central and Eastern Europe. J Am Diet Assoc 104:1793–1799
51. Ascherio A, Rimm EB, Hernan MA, Giovannucci E, Kawachi I, Stampfer MJ, Willett WC (1999) Relation of consumption of vitamin E, vitamin C, and carotenoids to risk for stroke among men in the United States. Ann Int Med 130:963–970
52. Hirvonen T, Virtamo I, Korhonen P, Albanes D, Pietinen P (2000) Intake of flavonoids, carotenoids, vitamin C and E, and risk of stroke in male smokers. Stroke 31:2301–2306
53. Holick CN, Michaud DS, Stolzenberg-Solomon R, Mayne ST, Pietinen P, Taylor PR, Virtamo J, Albanes D (2002) Dietary carotenoids, serum beta-carotene, and retinol and risk of lung cancer in the Alpha-Tocopherol, Beta-Carotene cohort study. Am J Epidemiol 156:536–547
54. Voorrips LE, Goldbohm RA, Brants HA, van Poppel GA, Sturmans F, Hermus RJ, van den Brandt PA (2000) A prospective cohort study on antioxidant and folate intake and male lung cancer risk. Cancer Epidemiol Biomarkers Prev 9:357–365
55. Proctor A, Clark PK, Parker CA (1995) Rice hull ash adsorbent performance under commercial soy oil bleaching conditions. J Am Oil Chem Soc 72:459–462

Lipids (2010) 45:723–731
DOI 10.1007/s11745-010-3453-9

ORIGINAL ARTICLE

Increased Lipid Peroxidation in LDL from Type-2 Diabetic Patients

Romain Colas · Valérie Pruneta-Deloche · Michel Guichardant · Céline Luquain-Costaz · Christine Cugnet-Anceau · Myriam Moret · Hubert Vidal · Philippe Moulin · Michel Lagarde · Catherine Calzada

Received: 22 June 2010 / Accepted: 16 July 2010 / Published online: 12 August 2010

Abstract Increased oxidative stress is associated with type-2 diabetes and related cardiovascular diseases, but oxidative modification of LDL has been partially characterized. Our aim was to compare the lipid and fatty acid composition as well as the redox status of LDL from diabetic patients and healthy subjects. First, to ensure that isolation of LDL by sequential ultracentrifugation did not result in lipid modifications, lipid composition and peroxide content were determined in LDL isolated either by ultracentrifugation or fast-protein liquid chromatography. Both methods resulted in similar concentrations of lipids, fatty acids, hydroxy-octadecadienoic acid (HODE) and malondialdehyde (MDA). Then, LDLs were isolated by ultracentrifugation from eight type-2 diabetic patients and eight control subjects. Compared to control LDL, diabetic LDL contained decreased cholesteryl esters and increased triglyceride concentrations. Ethanolamine plasmalogens decreased by 49%. Proportions of linoleic acid decreased in all lipid classes, while proportions of arachidonic acid increased in cholesteryl esters. Total HODE concentrations increased by 56%, 12- and 15-hydroxy-eicosatetraenoic acid by 161 and 86%, respectively, and MDA levels increased by twofold. α-Tocopherol concentrations, expressed relative to triglycerides, were lower in LDL from patients compared to controls, while γ-tocopherol did not differ. Overall, LDL from type-2 diabetic patients displayed increased oxidative stress. Determination of hydroxylated fatty acids and ethanolamine plasmalogen depletion could be especially relevant in diabetes.

Keywords Diabetes · Fatty acids · Peroxidation · Plasmalogens · Ultracentrifugation · Fast-protein liquid chromatography

R. Colas · V. Pruneta-Deloche · M. Guichardant · C. Luquain-Costaz · H. Vidal · P. Moulin · M. Lagarde · C. Calzada
Université de Lyon, 69622 Lyon, France

R. Colas · V. Pruneta-Deloche · M. Guichardant · C. Luquain-Costaz · H. Vidal · P. Moulin · M. Lagarde · C. Calzada
INSA-Lyon, RMND, 69621 Villeurbanne, France

R. Colas · V. Pruneta-Deloche · M. Guichardant · C. Luquain-Costaz · H. Vidal · P. Moulin · M. Lagarde · C. Calzada (✉)
INSERM U870, INSA-Lyon, Régulations métaboliques, Nutrition et Diabètes, Bât Louis Pasteur, INSA-Lyon, IMBL, 20 avenue Albert Einstein, 69621 Villeurbanne, France
e-mail: Catherine.Calzada@insa-lyon.fr

R. Colas · V. Pruneta-Deloche · M. Guichardant · C. Luquain-Costaz · H. Vidal · P. Moulin · M. Lagarde · C. Calzada
INRA U1235, 69921 Oullins, France

R. Colas · V. Pruneta-Deloche · M. Guichardant · C. Luquain-Costaz · C. Cugnet-Anceau · M. Moret · H. Vidal · P. Moulin · M. Lagarde · C. Calzada
Hospices Civils de Lyon, 69003 Lyon, France

Abbreviations

BHT	Butylhydroxytoluene
CE	Cholesteryl ester
DMA	Dimethylacetal
ELSD	Evaporative light-scattering detector
Etn-PL	Ethanolamine phospholipids
FPLC	Fast-protein liquid chromatography
GPE	Glycerophosphoethanolamine
HETE	Hydroxy-eicosatetraenoic acid
HODE	Hydroxy-octadecadienoic acid
MDA	Malondialdehyde

MUFA	Monounsaturated fatty acids
PC	Phosphatidylcholine
PL	Phospholipid
PUFA	Polyunsaturated fatty acids
SFA	Saturated fatty acids
SM	Sphingomyelin
TBA	Thiobarbituric acid
TBARS	Thiobarbituric acid reactive species
TG	Triacylglycerols
UC	Ultracentrifugation

Introduction

Type-2 diabetes is associated with an increased risk for atherosclerosis. There is strong evidence that oxidative stress plays a key role in the onset of diabetes [1] and in the development of vascular complications of the disease [2]. Low-density lipoproteins (LDL) are important targets of oxidation, and oxidative modification of LDL is involved in the pathogenesis of atherosclerosis [3]. Oxidative stress has been mostly assessed in plasma from diabetic patients, which showed increased concentrations of thiobarbituric acid-reactive species (TBARS) [4] and isoprostanes [5], both end-products of lipid peroxidation. Evidence for increased oxidative stress in LDL from type-2 diabetic patients is indirect, mostly based on increased plasma levels of autoantibodies against oxidatively modified LDL [6]. More data on specific parameters of LDL oxidation are therefore needed and could be useful to define predictive biomarkers for cardiovascular risk.

The aim of this study was to assess oxidative stress specifically in LDL from type-2 diabetic patients compared to LDL from healthy subjects. First, we compared the lipid composition and redox status of LDL isolated by the conventional sequential flotation ultracentrifugation (UC) to that of LDL separated by fast-protein liquid chromatography (FPLC) in order to check if isolation of LDL by UC did not lead to artifactual oxidation of the particles, as previously suggested [7]. Then, we performed detailed analysis of lipid classes including fatty acids and different complementary markers of lipid peroxidation in diabetic and control LDL.

Materials and Methods

Blood Collection

Regarding the comparative study of LDL separated by UC or FPLC, venous blood from three healthy blood donors (33 ± 13 years) was collected on citrate phosphate dextrose (citrate 15.6 mM, sodium citrate 89.4 mM, monosodic phosphate 16.1 mM, dextrose 128.7 mM, pH 5.6, one volume for seven volumes of blood) as an anticoagulant. Plasma was immediately separated by centrifugation at 1,500*g* for 10 min and spiked with 1 mM EDTA and 10 μM butylhydroxytoluene (BHT).

Regarding the clinical study, type-2 diabetic patients (8 men, aged 59 ± 2 years) recruited in the Department of Endocrinology and Metabolic Diseases (HCL Lyon) were matched for sex and age to healthy subjects (8 men, aged 51 ± 4 years). Exclusion criteria were smoking, antioxidant/vitamin supplementation, anti-aggregatory drugs and insulin treatment. Hypolipidemic drug (statins and fibrates) treatment was suspended for 7 days before venipuncture. Control subjects were in good health as assessed by medical history, and exclusion criteria were any pathology including diabetes. Written informed consent was obtained from all participants, and the study was approved by the local ethics committee (CCP Sud Est IV). Plasma was separated by centrifugation at 1,500*g* for 10 min of blood collected on EDTA; 10 μM BHT was added to plasma, which was immediately frozen at −80°C under nitrogen for further characterizations.

LDL Isolation by Ultracentrifugation

LDLs (density 1.019–1.063) were separated from plasma by potassium bromide stepwise UC. UC was carried out in a TLA 100.3 fixed-angle rotor of a Beckman TL-100 table top UC (Beckman Coulter France, Roissy CDG, France). The LDL fraction was dialyzed extensively against phosphate buffered saline (NaCl 136.8 mM, KCl 2.6 mM, KH_2PO_4 1.71 mM, Na_2HPO_4, $12H_2O$ 8 mM, pH 7.2) containing 1 mM EDTA.

LDL Isolation by FPLC

LDLs were isolated from plasma by gel filtration chromatography at 4°C as previously described [8] and modified as follows [9]. Briefly, a BioRad System FPLC (Bio-Rad Laboratories, Marnes-la-Coquette, France) equipped with a Superose 6 HR 10/30 column (GE Healthcare Europe GmbH, Munich, Germany) was used with 10 mM Tris-HCl, 150 mM NaCl, pH 7.4 buffer containing 2 mM EDTA and 0.02% sodium azide as a running buffer. After loading filtered plasma, chromatography was carried out with a flow rate of 0.3 ml/min under a pressure of 150 psi. Fractions of 0.3 ml were collected, and the concentrations of triglycerides (TG) and total cholesterol in the eluted fractions were measured (BioMérieux, Marcy l'Etoile, France). LDL fractions were concentrated on a Millipore filter of 30,000 MW (10 min at 4,000*g*).

Protein, Total LDL Cholesterol and Triacylglycerol Determinations

Colorimetric determination of protein concentration was processed according to the modified Lowry method [10]. Enzymatic determination of total cholesterol and TG were processed using commercial kits (BioMérieux, Marcy l'Etoile, France).

LDL Cholesterol Determination

Lipid classes were separated by HPLC coupled to an Evaporative Light Scattering Detector (ELSD) according to the modified method of Seppanen-Laakso [11].

Fatty Acid Composition of LDL Lipid Classes

After the addition of appropriate internal standards (1,2-diheptadecanoyl-sn-glycero-3-phosphocholine, 1,2-diheptadecanoyl-sn-glycero-3-phosphoethanolamine, 1,2,3-triheptadecanoyl-sn-glycerol and heptadecanoyl cholesteryl ester), total LDL lipids were extracted twice by the addition of ethanol (3 vol) and chloroform (6 vol) in the presence of BHT (50 μM). Lipid classes were then separated by thin-layer chromatography. The first solvent mixture chloroform/methanol (80:8, v/v) allowed us to separate neutral lipids from phospholipids (PL). The second solvent mixture chloroform/methanol/water (63:27:4, by vol.) separated phosphatidylcholines (PC), ethanolamine phospholipids (Etn-PL) and sphingomyelins (SM). Neutral lipids were separated in TG and cholesteryl esters (CE) by a second thin-layer chromatography using hexane/diethylether/acetic acid (80:20:1, by vol.) as solvent. The different spots were scrapped off, treated with trifluoride boron/methanol (1:1, v/v) for 90 min at 100°C. The derivatized fatty acid methyl esters were then extracted twice with isooctane and separated by GLC, using an HP 6890 gas chromatograph equipped with a SP 2380 capillary column (0.25 μm, 30 m × 0.25 mm, Supelco, Bellefonte, PA).

Quantification of Total LDL Monohydroxylated Fatty Acids

Following the lipid extraction as described above, dried extracts were subjected to ethanolic hydrolysis with 10 M KOH for 20 min at 60°C [12]. No reduction of lipid hydroperoxides was carried out. Non-esterified hydroxylated fatty acids and fatty acids were first separated on an Oasis Sep-Pak cartridge column (Waters, Milford, MA). The column was activated with 6 ml of methanol and 6 ml of water before loading the sample. Then, it was washed with 8 ml of 2% NH_4OH water and 8 ml of methanol. Products were eluted with 8 ml of acetonitrile/2-propanol (60:40, v/v) containing 5% formic acid. Non-esterified hydroxylated fatty acids were secondly separated by thin-layer chromatography with hexane/diethylether/acetic acid (60:40:1, by vol.) as mobile phase and extracted from silica with methanol. Then, hydroxylated fatty acids were separated by reverse phase-HPLC on X Bridge C_{18} column (3.5 μm, 4.6 × 150 mm column, Waters, Milford, MA) using a gradient solvent of acetonitrile and water (pH 3) and detected at 235 nm.

Malondialdehyde Determination in LDL

Malondialdehyde (MDA) concentration was determined by RP-HPLC according to the method of Therasse and Lemonnier [13]. LDL samples, mixed with thiobarbituric acid (TBA) (10 mM), acetic acid and BHT (5 mM), were heated for 60 min at 95°C. The TBA-MDA adducts were then extracted with ethyl acetate and separated onto a Nucleosil C_{18} column (5 μm, 4.6 × 250 mm, Macherey–Nagel, Hoerdt, France) using methanol/water (20:80, v/v) as mobile phase. Detection was performed by fluorimetry (excitation 515 nm, emission 553 nm).

Vitamin E Determination in LDL and Plasma

Tocopherol concentrations were determined by RP-HPLC [14]. Tocopherols were first extracted from LDL and plasma (1 vol) twice with hexane (4 vol) after the addition of ethanol (1 vol). Then, they were separated onto a Nucleosil C_{18} column (5 μm, 4 × 150 mm, Macherey-Nagel, Hoerdt, France) using methanol/water (98:2, v/v) as mobile phase. Detection was performed by fluorimetry (excitation 295 nm, emission 340 nm) and quantification was allowed by the addition of tocol as an internal standard.

Statistical Analysis

Results are expressed as the mean ± SEM. Comparisons between groups were performed using a non-parameter Mann-Whitney test. Statistical significance was established at $p \leq 0.05$. Correlation coefficients were determined using linear regression analysis.

Results

Comparison of LDL Isolated by Ultracentrifugation and Fast-Protein Liquid Chromatography

In order to determine whether isolation of LDL by UC generated LDL with a lipid composition and lipid redox

status comparable to those issued from FPLC separation, fresh plasma samples from healthy volunteers were subjected in parallel to the two procedures. There were no differences between lipid composition in LDL either separated by UC or FPLC. As expected, CE was the major lipid class in LDL (51%) followed by cholesterol (29%) and few TG (3.4%). PCs were the major phospholipids present in LDL (11%) (data not shown).

The GLC analysis of fatty acid methylesters derived from Etn-PL allowed us to determine the fatty dimethylacetals (DMA) representative of alkeny,acyl-GPE (or PE plasmalogens), a subclass particularly sensitive to oxidative stress. No difference in total DMA concentrations was found between both methods of isolation (6.1 ± 1.7 nmol/mg protein in LDL isolated by UC vs. 4.6 ± 2.9 nmol/mg protein in LDL isolated by FPLC) representing 15.8 ± 4.6% vs. 12.5 ± 8% total fatty acids in Etn-PL, respectively.

The concentrations of linoleic acid (18:2n-6), the most abundant polyunsaturated fatty acid (PUFA) and substrate for lipid peroxidation, were similar in LDL either isolated by UC or FPLC (1,638 ± 44 vs. 1,543 ± 17 nmol/mg protein). As shown in Table 1, the stable primary products issued from the peroxidation of 18:2n-6, 9-hydroxy-octadecadienoic acid (HODE) and 13-HODE represented 0.05% of the parent molecule and were present in similar concentrations regardless of the LDL isolation method. The ratio of total HODEs to its parent fatty acid was also similar in LDL isolated by UC or FPLC. One of the aldehydes arising from the decomposition of fatty acid hydroperoxides, MDA, was found to be formed in similar amounts in LDL either separated by UC or FPLC. Concerning the main antioxidants, α- and γ-tocopherol were present in similar concentrations in LDL isolated by either method. Overall, the lipid composition and the redox status were similar whatever the LDL separation method.

Table 1 Redox status of LDL isolated by UC or FPLC

	UC	FPLC
9-HODE (pmol/mg cholesterol)	217 ± 140	196 ± 132
13-HODE (pmol/mg cholesterol)	242 ± 47	228 ± 25
HODE/18:2n-6 (μmol/mol)	519 ± 162	499 ± 151
MDA (pmol/mg cholesterol)	118 ± 9	131 ± 32
α-tocopherol (nmol/mg cholesterol)	3.68 ± 0.58	3.68 ± 0.72
γ-tocopherol (nmol/mg cholesterol)	0.39 ± 0.14	0.31 ± 0.06

Values represent means ± SD of three experiments

UC ultracentrifugation, *FPLC* fast-protein liquid chromatography, *HODE* hydroxy-octadecadienoic acid, *MDA* malondialdehyde

Lipid Composition and Redox Status of LDL from Diabetic Patients Compared to LDL from Healthy Subjects

Clinical Characteristics

Type-2 diabetic patients ($n = 8$) had poorly controlled diabetes as shown by elevated values of glycated hemoglobin HbA_{1c} (10.6 ± 0.9%) and glycemia (9.2 ± 1.3 mM) compared to healthy volunteers (5.4 ± 0.1% and 5.6 ± 0.2 mM, respectively, $n = 8$). They presented a metabolic syndrome as assessed by their large waist circumference of 118.1 ± 8.4 cm, elevated TG of 2.5 ± 0.2 mM and low HDL-cholesterol of 0.9 ± 0.1 mM [15]. Sex- and age-matched healthy volunteers had values of waist circumference (91.3 ± 1.7 cm), TG (1.3 ± 0.1 mM) and HDL-cholesterol (1.4 ± 0.1 mM) in the expected normal range.

Lipid and Fatty Acid Compositions of Diabetic LDL Compared to Control LDL

The concentrations of main lipid classes were determined in LDL from type-2 diabetic patients and healthy subjects (Table 2). In diabetic LDL, the concentration of CE, the main LDL lipid class, decreased by 21%, whereas concentrations of TG increased by 75%. No changes in cholesterol, PC and Etn-PL concentrations were observed between the two groups.

The fatty acid composition of the main LDL lipid classes, namely CE and PC, showed several differences between diabetic patients and control subjects. As shown in Table 3, PUFA represented 62% of the total fatty acids in CE from control LDL, and their proportion significantly decreased in diabetic LDL. In particular, 18:2n-6, the main PUFA, decreased, whether expressed in mole percent (−11%) or in nmol/mg protein (−30%). Arachidonic acid

Table 2 Lipid classes in LDL from healthy subjects and type-2 diabetic patients

Lipid class	Healthy subjects nmol/mg protein	Type-2 diabetic patients nmol/mg protein
Cholesteryl esters	2,472 ± 152	1,949 ± 110**
Cholesterol	1,112 ± 187	1,199 ± 76
Triacylglycerols	154 ± 16	269 ± 49*
Phosphatidylcholine	504 ± 15	473 ± 12
Ethanolamine phospholipids	17 ± 2	19 ± 2

Values represent means ± SEM of at least six determinations per group

* $p \leq 0.05$ and ** $p \leq 0.01$ compared with healthy subjects

Table 3 Fatty acid composition of LDL cholesteryl esters from healthy subjects and type-2 diabetic patients

Fatty acid	Healthy subjects		Type-2 diabetic patients	
	mol%	nmol/mg protein	mol%	nmol/mg protein
16:0	12.3 ± 0.5	325.7 ± 15.7	13.8 ± 0.4	288.4 ± 15.5
16:1n-7	2.5 ± 0.4	63.7 ± 7.8	2.7 ± 0.4	56.2 ± 9.0
16:1n-9	0.3 ± 0.1	7.4 ± 2.1	0.4 ± 0.1	8.7 ± 1.8
18:0	1.0 ± 0.1	23.3 ± 2.2	1.0 ± 0.1	18.9 ± 2.5
18:1n-7	1.1 ± 0.2	26.0 ± 4.8	0.9 ± 0.3	18.2 ± 5.4
18:1n-9	20.7 ± 0.9	500.5 ± 22.1	22.5 ± 0.8	430.5 ± 19.0
18:2n-6	52.4 ± 1.4	1295.5 ± 102.6	46.6 ± 1.4**	909.3 ± 72.0**
18:3n-3	0.4 ± 0.1	11.2 ± 2.0	0.5 ± 0.1	8.8 ± 2.3
18:3n-6	0.7 ± 0.2	18.3 ± 4.8	0.7 ± 0.2	13.4 ± 3.2
20:3n-6	0.7 ± 0.1	16.6 ± 1.7	0.8 ± 0.1	15.2 ± 2.2
20:4n-6	6.0 ± 0.5	140.7 ± 20.6	8.6 ± 0.7**	151.8 ± 9.5
20:5n-3	1.2 ± 0.3	26.9 ± 5.9	0.9 ± 0.2	15.5 ± 2.6
22:6n-3	0.7 ± 0.1	13.6 ± 1.9	0.6 ± 0.1	10.0 ± 1.7
SFA	13.3 ± 0.6	350.5 ± 17.6	14.8 ± 0.3*	308.4 ± 16.6
MUFA	24.5 ± 1.0	598.5 ± 22.0	26.6 ± 0.6	514.2 ± 19.4*
PUFA	62.2 ± 1.4	1523.2 ± 125.4	58.6 ± 0.8*	1124.2 ± 77.0*

Values expressed as mole percent of main fatty acids and nmol/mg protein are means ± SEM of at least six subjects per group

MUFA monounsaturated fatty acids, *PUFA* polyunsaturated fatty acids, *SFA* saturated fatty acids

* $p \leq 0.05$ and ** $p \leq 0.01$ compared with LDL from healthy subjects

(20:4n-6) proportion significantly increased by 43% in diabetic LDL, unlike its concentration. An increase in saturated fatty acid (SFA) proportion was observed, while the monounsaturated fatty acid (MUFA) proportion was unchanged between the two groups (Table 3). Concerning PC, the main PL class, lower proportions and concentrations of the major fatty acid 18:2n-6 (−12 and −17%, respectively) were present in diabetic LDL compared to control LDL, while the proportion of 20:4n-6 tended to increase. No significant changes of SFA and MUFA were observed (Table 4). In Etn-PL including the PE plasmalogen subclass, DMA represented 22.9% of the total fatty chains present in Etn-PL from control LDL and only 11.8% of those in PE from diabetic LDL. The 49% decrease reflected a significant decrease of each DMA species, namely 16:0, 18:0 and 18:1n-9 DMA produced by transmethylation of the sn-1 position of plasmalogens (Fig. 1). The sum of DMA species negatively correlated with HbA_{1c} % ($r^2 = 0.61, p < 0.001$).

Lipid Peroxide and Antioxidant Content of Diabetic LDL Compared To Controls

The concentrations of total (both free and esterified) hydroxylated fatty acids, the stable primary products of non-enzymatic peroxidation of PUFA, were assessed in LDL from patients and control groups. As shown in Table 5, 9-HODE and 13-HODE, derived from 18:2n-6, were detected, and their concentrations significantly increased by 49 and 44%, respectively. In addition, the ratio of total HODE to its parent fatty acid increased by

Table 4 Fatty acid composition of LDL phosphatidylcholine from healthy subjects and type-2 diabetic patients

Fatty acid	Healthy subjects		Type-2 diabetic patients	
	mol%	nmol/mg protein	mol%	nmol/mg
16:0	33.0 ± 0.9	358.7 ± 16.7	34.2 ± 0.4	347.6 ± 9.5
16:1n-7	0.3 ± 0.1	3.7 ± 0.9	0.2 ± 0.1	2.3 ± 0.7
18:0	15.8 ± 0.5	154.8 ± 4.9	15.4 ± 0.8	142.9 ± 9.6
18:1n-7	1.4 ± 0.3	14.0 ± 2.3	1.3 ± 0.3	11.8 ± 2.5
18:1n-9	10.9 ± 0.5	108.4 ± 6.0	11.6 ± 0.4	108.0 ± 5.0
18:2n-6	22.0 ± 0.9	220.0 ± 14.1	19.4 ± 0.7*	181.9 ± 10.3*
18:3n-3	0.2 ± 0.0	1.5 ± 0.2	0.2 ± 0.1	2.0 ± 0.7
18:3n-6	0.1 ± 0.0	0.6 ± 0.2	0.0 ± 0.0	0.3 ± 0.2
20:3n-6	2.9 ± 0.2	26.7 ± 2.2	3.4 ± 0.3	29.3 ± 2.5
20:4n-6	7.8 ± 0.7	71.4 ± 5.6	9.1 ± 1.0	78.0 ± 7.7
20:5n-3	1.2 ± 0.4	10.3 ± 2.8	0.8 ± 0.2	7.0 ± 1.6
22:5n-3	0.3 ± 0.2	2.9 ± 1.4	0.3 ± 0.1	2.7 ± 0.9
22:6n-3	3.3 ± 0.5	27.6 ± 3.3	3.0 ± 0.2	24.3 ± 2.1
SFA	49.1 ± 1.0	516.7 ± 20.1	50.0 ± 0.8	493.7 ± 15.7
MUFA	13.2 ± 0.6	130.4 ± 7.4	13.5 ± 0.4	125.3 ± 4.5
PUFA	37.7 ± 0.8	361.1 ± 11.6	36.4 ± 0.8	326.1 ± 9.7

Values expressed as mole percent of main fatty acids and nmol/mg protein are means ± SEM of at least six subjects per group

* $p \leq 0.05$ compared with LDL from healthy subjects

MUFA monounsaturated fatty acids, *PUFA* polyunsaturated fatty acids, *SFA* saturated fatty acids

58% in diabetic LDL. Among hydroxy-eicosatetraenoic acids (HETE) derived from 20:4n-6, 8-, 11-, 12- and 15-HETE were detected in LDL from each volunteer, but not

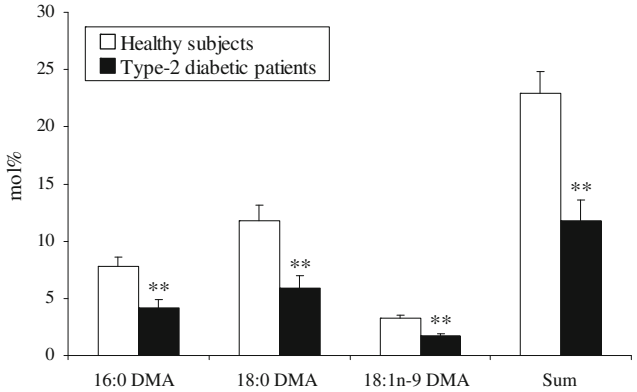

Fig. 1 Plasmalogen alkenyl-chain composition of LDL ethanolamine phospholipids from healthy subjects and type-2 diabetic patients. Values, expressed as mole percent of main fatty acids, are means ± SEM of at least seven subjects per group. ** $p \leq 0.01$ compared with LDL from healthy subjects. *DMA* dimethylacetal

Table 5 Monohydroxylated fatty acids in LDL from healthy subjects and type-2 diabetic patients

Hydroxylated fatty acid	Healthy subjects	Type-2 diabetic patients
9-HODE (pmol/mg cholesterol)	148 ± 17	235 ± 21*
13-HODE (pmol/mg cholesterol)	133 ± 18	205 ± 17*
8-HETE (pmol/mg cholesterol)	26 ± 8	44 ± 8
11-HETE (pmol/mg cholesterol)	23 ± 9	43 ± 11
12-HETE (pmol/mg cholesterol)	13 ± 6	34 ± 7*
15-HETE (pmol/mg cholesterol)	29 ± 5	54 ± 8*
HODEs/18:2n-6 (μmol/mol)	394 ± 39	624 ± 42**
HETEs/20:4n-6 (μmol/mol)	822 ± 188	1222 ± 185

Values are means ± SEM of seven subjects per group

* $p \leq 0.05$ and ** $p \leq 0.01$ compared with LDL from healthy subjects

HETE hydroxy-eicosatetraenoic acid, *HODE* hydroxy-octadecadienoic acid

5- and 9-HETE. The concentrations of 12-HETE and 15-HETE increased by 161 and 86%, respectively, whereas the ratio of HETE to 20:4n-6 did not increase significantly. Concentrations of MDA significantly increased by twofold in diabetic LDL compared to control LDL (102 ± 18 vs. 49 ± 5 pmol/mg cholesterol, respectively, $n = 7$ to 8). They positively correlated with HbA_{1c} % ($r^2 = 0.62$, $p < 0.001$).

α-Tocopherol concentrations in LDL did not differ between patients and controls when expressed per mg cholesterol (3.47 ± 0.43 vs. 2.79 ± 0.24 nmol/mg cholesterol). However, when expressed relative to TG, α-tocopherol levels significantly decreased by 32% in LDL from diabetic patients compared to control subjects (14.3 ± 1.1 vs. 21.2 ± 2.5 nmol/mg TG, $p < 0.05$). γ-Tocopherol did not significantly change in diabetic LDL compared to control LDL when expressed per mg cholesterol (0.46 ± 0.08 vs. 0.29 ± 0.06 nmol/mg cholesterol) or per mg TG (1.8 ± 0.3 vs. 2.3 ± 0.5 nmol/mg TG). In plasma, α-tocopherol concentrations did not differ between diabetic patients and control subjects (12.2 ± 1.2 vs. 11.9 ± 1.2 μmol/l). The concentrations of plasma α-tocopherol in patients (5.4 ± 0.5 mmol/mol TG) were significantly lower than concentrations in controls (9.8 ± 0.7 mmol/mol TG) when expressed relative to TG, but not when expressed relative to cholesterol (2.8 ± 0.5 vs. 2.0 ± 0.2 mmol/mol cholesterol). γ-Tocopherol concentrations were similar in plasma from diabetic patients and controls (1.7 ± 0.3 vs. 1.6 ± 0.4 μmol/l) and whether expressed relative to cholesterol (0.41 ± 0.10 vs. 0.25 ± 0.06 mmol/mol cholesterol) or TG (0.68 ± 0.09 vs. 1.22 ± 0.21 mmol/mol TG).

Discussion

In the present study, we first compared LDL isolated by UC to those isolated by FPLC in order to use a method expected to minimize the artifactual oxidative modification of the particles during processing. It has indeed been suggested that conventional UC may cause structural changes in lipoproteins, whereas FPLC does not affect lipoprotein structure [7]. Our results show that the isolation of lipoproteins by UC or FPLC results in similar concentrations of lipids, fatty acid proportions and lipid peroxide content in LDL. Proportions of lipid classes were equivalent in LDL isolated by either method and close to those reported in the literature [16, 17]. Concentrations of PE plasmalogens particularly prone to oxidation [18] were similar in LDL, whatever the method of isolation, suggesting that the procedure of UC and dialysis was not more damaging than FPLC.

Regarding the substrates for lipid peroxidation in LDL isolated by UC, total concentrations of PUFA were 2,074 nmol/mg protein, including 1,638 nmol/mg protein of 18:2n-6, in good agreement with published data [19, 20]. Similar concentrations were obtained after FPLC isolation of LDL (1,961 nmol/mg protein PUFA including 1,543 nmol/mg protein 18:2n-6), indicating that PUFAs were not more autooxidized in LDL separated by UC and further dialyzed. In accordance with the PUFA composition of LDL, very little peroxidation of PUFA occurred in LDL from healthy volunteers since hydroxylated derivatives of 18:2n-6 (9- and 13-HODE) represented 0.05% of the parent molecule, whatever the method of LDL isolation. Finally, concentrations of MDA, commonly used as an index of overall lipid peroxidation, and of tocopherol isomers, the main LDL antioxidants, were similar in LDL either isolated by UC and FPLC. This rules out a loss of

MDA and vitamin E during the dialysis process following UC, as previously reported [21, 22]. As separation of lipoproteins by UC led to LDL particles with lipid and lipid peroxide contents comparable to those issued from FPLC, UC was used to determine the profile of LDL from type-2 diabetic patients compared to that of LDL from healthy subjects.

Although there is evidence of increased oxidative stress in type-2 diabetes, it has been mainly based to date on the measurement of a single biomarker, not reflecting the overall oxidative damage. In addition, oxidative stress has been mostly assessed in plasma [23] and not in LDL. We provide evidence that LDL from type-2 diabetic patients displayed increased oxidative stress compared to LDL from healthy volunteers. First, diabetic LDL showed increased TG and decreased CE. Such a modified lipid composition may reflect a higher percentage of small dense LDLs, which are known to be more prevalent in type-2 diabetes [24, 25]. It has indeed been shown that small, dense, TG-rich LDL particles are subjected to exchange processes that remove CE from the core and replace it with TG [26, 27], and are more susceptible to oxidation [28]. To identify original markers of oxidative stress in LDL from diabetic patients, different complementary indices representative of different steps in the lipid peroxidation process were assessed. We show that PE plasmalogens decreased by 49% in diabetic LDL compared to control LDL. Plasmalogens were shown to contribute to the oxidation resistance of LDL and can serve as endogenous antioxidants in situ and in vitro [18, 29]. Loss of plasmalogens in LDL could represent a marker of oxidative stress in diabetic patients. In addition, plasmalogens have been involved in many diseases [30], but to our knowledge, this is the first evidence for decreased concentrations of plasmalogens in type 2 diabetes.

Since 18:2n-6 and 20:4n-6 are the main PUFA in LDL, their stable primary products of peroxidation, HODE and HETE, were determined as well as the ratio of oxidation product to parent fatty acids, described as a biomarker of oxidation status of LDL [31]. We show for the first time that both free and esterified HODE, representing 0.04% of the parent molecule in control LDL, increased by 49% in LDL from diabetic patients. This reflects free radical peroxidation of 18:2n-6 and is in line with the decrease of 18:2n-6 in the PUFA-rich, lipid classes, CE and PC. Consequently, the HODE to 18:2n-6 ratio was significantly higher (+58%) in diabetic LDL than in control LDL. Because of the lack of appropriate standards, we could not confirm the presence of trans,trans-HODE stereoisomers as shown in plasma [32, 33], but cannot exclude them. Total HETE represented 0.08% of the parent molecule in control LDL, indicating that 20:4n-6 is more susceptible to oxidation. 12- and 15-HETE increased by 161 and 86% in diabetic LDL, while 8- and 11-HETE tended to increase. However, there was no significant increase of the HETE to 20:4n-6 ratio due in part to the increased proportion of 20:4n-6 in CE. This paradoxical increase of 20:4n-6 cannot be explained from the present investigation, but might result from exacerbation of Δ6 and Δ5 desaturase activities in type-2 diabetes leading to increased production of 20:4n-6 from 18:2n-6. As insulin activates both enzymes [34], this situation may occur in type-2 diabetes, which is associated with chronic hyperinsulinemia periods. Finally, increased lipid peroxidation in LDL from diabetic patients compared to control LDL was confirmed by twofold increased concentrations of MDA. This is in agreement with previously reported increased levels of serum lipid peroxides, measured as thiobarbituric acid-reactive substances, in plasma from patients suffering from diabetes [4, 35]. Regarding the main lipid-soluble antioxidant in LDL, α-tocopherol, its concentration was significantly lower in LDL from diabetic patients compared to control LDL when expressed relative to TG, but not when expressed relative to cholesterol. Similar results were obtained in plasma. While most studies did not show any difference in α-tocopherol between diabetic patients and control subjects [4], a previous study also reported decreased α-tocopherol-to-TG ratios, but unchanged α-tocopherol-to-total cholesterol ratios in LDL [36]. Although these results need to be confirmed in a larger population, the decrease of plasma and LDL α-tocopherol relative to TG in patients could be simply due to increased triglycerides levels in diabetic patients.

Altogether, our results show higher levels of lipid peroxidation markers in LDL from poorly controlled type 2 diabetic patients compared to control LDL. Since significant negative and positive correlations between HbA_{1C}% and plasmalogens and MDA, respectively, were observed, it can be then hypothesized that the increased non-enzymatic glycation of LDL, as assessed by HbA_{1C}, could have contributed to the increased non-enzymatic lipid peroxidation of LDL in patients [37]. The role of these modified parameters in the biological properties of oxidatively modified LDL in atherosclerosis still needs to be elucidated.

In conclusion, we show that isolation of LDL by UC is no more damaging than FPLC separation, as far as oxidative modification of lipids is concerned. We give new information on the baseline values of different and complementary lipid peroxides present in LDL from healthy subjects, which may serve as references to unravel lipid abnormalities in LDL from diabetic patients. We also show that increased lipid peroxidation is present in LDL from type-2 diabetic patients and may be evidenced by the measurement of hydroxylated fatty acids and PE plasmalogens.

Acknowledgments We thank the subject participants for their contribution. We also thank the nursing staff at the Hospices Civils de Lyon for their help with blood sample collection and some analyses. We acknowledge the French Ministry of Education and Research for RC's grant. CC is supported by CNRS.

References

1. Mehta JL, Rasouli N, Sinha AK, Molavi B (2006) Oxidative stress in diabetes: a mechanistic overview of its effects on atherogenesis and myocardial dysfunction. Int J Biochem Cell Biol 38:794–803
2. Baynes JW (1991) Role of oxidative stress in development of complications in diabetes. Diabetes 40:405–412
3. Witztum JL, Steinberg D (1991) Role of oxidized low density lipoprotein in atherogenesis. J Clin Invest 88:1785–1792
4. Griesmacher A, Kindhauser M, Andert SE et al (1995) Enhanced serum levels of thiobarbituric-acid-reactive substances in diabetes mellitus. Am J Med 98:469–475
5. Gopaul NK, Anggard EE, Mallet AI, Betteridge DJ, Wolff SP, Nourooz-Zadeh J (1995) Plasma 8-epi-PGF2 alpha levels are elevated in individuals with non-insulin dependent diabetes mellitus. FEBS Lett 368:225–229
6. Bellomo G, Maggi E, Poli M, Agosta FG, Bollati P, Finardi G (1995) Autoantibodies against oxidatively modified low-density lipoproteins in NIDDM. Diabetes 44:60–66
7. Napoli C, Mancini FP, Corso G et al (1997) A simple and rapid purification procedure minimizes spontaneous oxidative modifications of low density lipoprotein and lipoprotein (a). J Biochem 121:1096–1101
8. Zambon A, Schmidt I, Beisiegel U, Brunzell JD (1996) Dimeric lipoprotein lipase is bound to triglyceride-rich plasma lipoproteins. J Lipid Res 37:2394–2404
9. Pruneta V, Autran D, Ponsin G et al (2001) Ex vivo measurement of lipoprotein lipase-dependent very low density lipoprotein (VLDL)-triglyceride hydrolysis in human VLDL: an alternative to the postheparin assay of lipoprotein lipase activity? J Clin Endocrinol Metab 86:797–803
10. Lowry OH, Rosebrough NJ, Farr AL, Randall RJ (1951) Protein measurement with the Folin phenol reagent. J Biol Chem 193:265–275
11. Seppanen-Laakso T, Laakso I, Vanhanen H, Kiviranta K, Lehtimaki T, Hiltunen R (2001) Major human plasma lipid classes determined by quantitative high-performance liquid chromatography, their variation and associations with phospholipid fatty acids. J Chromatogr B Biomed Sci Appl 754:437–445
12. Browne RW, Armstrong D (2000) HPLC analysis of lipid-derived polyunsaturated fatty acid peroxidation products in oxidatively modified human plasma. Clin Chem 46:829–836
13. Therasse J, Lemonnier F (1987) Determination of plasma lipoperoxides by high-performance liquid chromatography. J Chromatogr 413:237–241
14. Calzada C, Coulon L, Halimi D et al (2007) In vitro glycoxidized low-density lipoproteins and low-density lipoproteins isolated from type 2 diabetic patients activate platelets via p38 mitogen-activated protein kinase. J Clin Endocrinol Metab 92:1961–1964
15. Grundy SM, Cleeman JI, Daniels SR et al (2005) Diagnosis and management of the metabolic syndrome: an American Heart Association/National Heart, Lung, and Blood Institute scientific statement. Circulation 112:2735–2752
16. Wiesner P, Leidl K, Boettcher A, Schmitz G, Liebisch G (2009) Lipid profiling of FPLC-separated lipoprotein fractions by electrospray ionization tandem mass spectrometry. J Lipid Res 50:574–585
17. Kuksis A, Myher JJ, Geher K, Breckenridge WC, Jones GJ, Little JA (1981) Lipid class and molecular species interrelationships among plasma lipoproteins of s subjects. J Chromatogr 224:1–23
18. Engelmann B, Brautigam C, Thiery J (1994) Plasmalogen phospholipids as potential protectors against lipid peroxidation of low density lipoproteins. Biochem Biophys Res Commun 204: 1235–1242
19. Esterbauer H, Gebicki J, Puhl H, Jurgens G (1992) The role of lipid peroxidation and antioxidants in oxidative modification of LDL. Free Radic Biol Med 13:341–390
20. Barre E (2003) A more detailed fatty acid composition of human lipoprotein(a)—a comparison with low density lipoprotein. Chem Phys Lipids 123:99–105
21. Esterbauer H, Jurgens G, Quehenberger O, Koller E (1987) Autoxidation of human low density lipoprotein: loss of polyunsaturated fatty acids and vitamin E and generation of aldehydes. J Lipid Res 28:495–509
22. Scheek LM, Wiseman SA, Tijburg LB, van Tol A (1995) Dialysis of isolated low density lipoprotein induces a loss of lipophilic antioxidants and increases the susceptibility to oxidation in vitro. Atherosclerosis 117:139–144
23. Stephens JW, Khanolkar MP, Bain SC (2009) The biological relevance and measurement of plasma markers of oxidative stress in diabetes and cardiovascular disease. Atherosclerosis 202:321–329
24. Mora S, Otvos JD, Rosenson RS, Pradhan A, Buring JE, Ridker PM (2010) Lipoprotein particle size and concentration by nuclear magnetic resonance and incident type 2 diabetes in women. Diabetes 59:1153–1160
25. Feingold KR, Grunfeld C, Pang M, Doerrler W, Krauss RM (1992) LDL subclass phenotypes and triglyceride metabolism in non-insulin-dependent diabetes. Arterioscler Thromb 12:1496–1502
26. Packard CJ (2003) Triacylglycerol-rich lipoproteins and the generation of small, dense low-density lipoprotein. Biochem Soc Trans 31:1066–1069
27. Verges B (2009) Lipid modification in type 2 diabetes: the role of LDL and HDL. Fundam Clin Pharmacol 23:681–685
28. Tribble DL, Holl LG, Wood PD, Krauss RM (1992) Variations in oxidative susceptibility among six low density lipoprotein subfractions of differing density and particle size. Atherosclerosis 93:189–199
29. Jurgens G, Fell A, Ledinski G, Chen Q, Paltauf F (1995) Delay of copper-catalyzed oxidation of low density lipoprotein by in vitro enrichment with choline or ethanolamine plasmalogens. Chem Phys Lipids 77:25–31
30. Nagan N, Zoeller RA (2001) Plasmalogens: biosynthesis and functions. Prog Lipid Res 40:199–229
31. Niki E (2009) Lipid peroxidation: physiological levels and dual biological effects. Free Radic Biol Med 47:469–484
32. Mashima R, Onodera K, Yamamoto Y (2000) Regioisomeric distribution of cholesteryl linoleate hydroperoxides and hydroxides in plasma from healthy humans provides evidence for free radical-mediated lipid peroxidation in vivo. J Lipid Res 41:109–115
33. Liu W, Yin H, Akazawa YO, Yoshida Y, Niki E, Porter NA (2010) Ex vivo oxidation in tissue and plasma assays of hydroxyoctadecadienoates: Z, E/E, E stereoisomer ratios. Chem Res Toxicol 23:986–995
34. Brenner RR (2003) Hormonal modulation of delta6 and delta5 desaturases: case of diabetes. Prostaglandins Leukot Essent Fatty Acids 68:151–162
35. Kesavulu MM, Giri R, Kameswara Rao B, Apparao C (2000) Lipid peroxidation and antioxidant enzyme levels in type 2 diabetics with microvascular complications. Diabetes Metab 26:387–392

36. Schneider M, Verges B, Klein A et al (2004) Alterations in plasma vitamin E distribution in type 2 diabetic patients with elevated plasma phospholipid transfer protein activity. Diabetes 53:2633–2639

37. Hunt JV, Smith CC, Wolff SP (1990) Autoxidative glycosylation and possible involvement of peroxides and free radicals in LDL modification by glucose. Diabetes 39:1420–1424

Lipids (2010) 45:733–741
DOI 10.1007/s11745-010-3452-x

METHODS

Isomerization of 9c11t/10t12c CLA in Triacylglycerols

Alfred A. Christy

Received: 20 May 2010 / Accepted: 16 July 2010 / Published online: 6 August 2010

Abstract Isomers of conjugated linoleic acid from 7t9c through 12t14t can be induced by thermal treatment of triacylglycerol samples of 9c11t or 10t12c fatty acids in glass tubes. The formation of conjugated linoleic acids (CLAs) has been observed during thermal induction of the above-mentioned triacylglycerols at 250, 280 and 320°C. The concentrations of isomers formed in the mixture varied depending on the temperature and duration of the heating experiments. The objective of this study was to find a suitable thermal induction temperature and time that can produce most of the isomers of CLAs from the above-mentioned triacylglycerols. Such a mixture would give researchers a reference standard that can be used in the identification of CLAs in GC analyses of relevant samples. Fifteen-microlitre portions of the triacylglycerol samples containing 9c11t/10t12c fatty acid were placed in micro-glass ampoules, sealed under nitrogen and then subjected to thermal treatment. The glass ampoules were removed at regular time intervals, cut open, and part of the samples was analysed by infrared spectroscopy using attenuated internal reflectance technique. The remainder of the samples was subjected to derivatisation into their methyl esters. The methyl esters of the isomerised fatty acids were then analysed by gas chromatography after appropriate dilution in heptane. The results show that the thermally induced glyceride samples of 9c11t/10t12c fatty acids gave CLA profiles containing isomers ranging from 7t9c to 12t14t. However, the concentrations of the isomers are different depending on the duration of the thermal induction. It appears that [1,5] sigmatropic rearrangements and positional isomerisations take place in the heated mixtures. The rearrangements and positional isomerisations are accelerated by increasing temperature. The glyceride samples heated to 325°C form isomers within 30 min and provide a mixture of CLA isomers that can be used as reference sample containing the methyl esters of CLAs.

Keywords Thermal induction · Isomerisation · Conjugated linoleic acids · Gas chromatography

Abbreviations

CLA	Conjugated linoleic acids
ATR	Attenuated total internal reflectance
GC	Gas chromatography
FAME	Fatty acid methyl esters

Introduction

Research on conjugated linoleic acids (CLA) has become intense during the past few years because of their effects on carcinosis, atherosclerosis, the immune system, lipid metabolism and body composition. Furthermore, the focus on CLA is also due to their health benefits [1–9].

The conjugated isomers of linoleic acid in milk and fats are generally found in *trans*/*cis*, *cis*/*trans* and *trans*/*trans* forms. There are several conjugated linoleic acids present in milk and fat from the cud-chewing animals. Of these, 9c11t is dominant, with about 80–90% of all the conjugated linoleic acids. The isomer 7t 9c was found in most of the dairy products as the second dominant CLA fatty acid

A. A. Christy (✉)
Department of Science, Faculty of Engineering and Science, University of Agder, Serviceboks 422, Kristiansand, Norway
e-mail: alfred.christy@uia.no

[10]. The isomer 9c11t is also thought to be the most biologically active [1, 2]. There are other isomers of CLAs in small concentrations [11]. These include *cis–cis*; *trans–trans*; *cis–trans* and *trans–cis* isomers of 7,9; 8,10; 9,11; 10,12 and 11,13 CLAs. There are 20 isomers from the above five CLA positional isomers. Several of these isomers have been identified in different food products. The 9c11t and 10c12t isomers are found in hydrogenated vegetable oils [11]. These are also found in equal proportion in the alkali isomerised methyl linoleate [13]. The concentrations of the other isomers are negligible [13].

The identification of different isomers of CLAs in samples of interest, in a chemical reaction aimed at synthesising CLA isomers or to prove or disprove the presence or absence of any CLA in a system of interest needs reference samples of CLAs. The two important CLAs namely 9c11t and 10t12c were prepared in large quantities by alkali isomerisation of 9c12c linoleic acid [14]. Eulitz et al. [14] synthesised eight CLA isomers, 8,10 through 11,13, by isomerising CLA mixtures by p-toluene sulfinic acid or iodine catalyst. Jain and Proctor [15] synthesised 9c11t, 9t11c, 10t12c and 10c12t CLA isomers in large quantities for the first time by UV photoirradiation of soya oil in the presence of iodine catalyst. The photoirradiation was carried out for 144 h to achieve this. Destaillats and Angers [16] were able to prepare 8t10c and 11c13t CLA isomers by heat teatment of 9c11t and 10t12c CLAs. Destaillats and Angers [11] demonstrated that the whole series of CLA isomers could be produced by starting from a mixture of methyl esters of 9c11t and 10t12c fatty acids. A two-step process was necessary in the preparation of these isomers: a heat-induced [1, 5] sigmatropic rearrangement in the first step and catalyst-induced positional isomerisation in the second. The formation of different isomers followed the mechanistic pathways outlined by Destaillats and Angers [11].

The chemistry and mechanistic pathways involved in the formation of CLAs as discussed in the research reports above spurred interest in looking at alternative ways of producing the isomers of CLAs. During preliminary investigations, it came to light that the [1, 5] sigmatropic transformations and positional isomerisations could be achieved by subjecting triacylglycerols of CLAs to a suitable high temperature. It was also clear that the duration of thermal treatment altered the concentrations of different isomers. The procedure adopted for the directed sequential synthesis of conjugated linoleic acids by Destaillats and Angers needed a total of 33 h (13 h for sigmatropic rearrangement reaction and 20 h for subsequent geometrical isomerisation) for the synthesis of CLA isomers ranging from $\Delta^{7,9}$ to $\Delta^{12,14}$. A straight-forward procedure that can reduce the isomerisation time and give a mixture that contains the same isomers should be preferred. The triacyl glycerols of 9c11t and 10t12c were selected because these can be easily prepared through alkali isomerisation, and then this mixture could be thermally induced to produce all the other isomers.

The aim of this paper is to demonstrate for the first time that the formation of CLA isomers ranging from 7,9 to 12,14 can be induced through the thermal induction of the triacylglycerol of 9c11t or 10t12c fatty acid. Furthermore, it is also the intention to look at the mechanistic aspects of the thermal induction for the formation of CLA isomers.

Experimental

Samples and Methods

The triacylglycerols of the 9c11t and 10t12c fatty acids were purchased from Larodan Chemicals, Sweden. The chemicals such as methanol, BF_3/methanol, NaOH, NaCl and $MgSO_4$ needed for derivatisation were purchased from Sigma-Aldrich. Methyl esters of 9c11t and 10t12c were prepared by esterification of the respective triacylglycerols.

The heating experiments were carried out in micro-glass ampoules as described in Ref. [17]. Three sets of glass ampoules containing the triacylglycerol samples were prepared. The first set of samples containing the triacylglycerols of the 9c11t or 10t12c fatty acids were placed in small glass vials and placed in a gas chromatographic oven (Agilent 5890) set at 250°C. Samples were then removed at 24-h intervals until the all the samples were exhausted. The experiment was repeated in the same manner with the second and third set of samples at 280 and 325°C except the samples treated at 325°C were removed at 30-min time intervals.

Infrared Spectroscopic Measurements

The samples from the thermal induction experiments were subjected to infrared measurements. A PerkinElmer Spectrum One FT-IR spectrometer equiped with a Harrick single reflectance ATR accessory and lead glycine sulphate detector was used in measuring the infrared spectra. Each sample was spread on the ATR crystal using a capillary glass tube. A total of 30 scans at a resolution of 4 cm^{-1} were then measured in the range of 4,000 to 600 cm^{-1} with previously scanned ATR crystal spectrum as the background. The ATR crystal was washed with acetone and dichloromethane after each measurement. A new capillary tube was used each time for the application of the sample to avoid cross contamination. All the infrared spectra were saved in absorbance format. Second derivative spectra of the absorption spectra were obtained using the derivative option in the scanning program of the instrument.

Gas Chromatographic Analysis

The glass ampoules containing the rest of the triacylglycerol samples were subjected to derivatisation as described in Ref. [17]. The methyl esters of the products of the thermal induction were extracted in heptane. The GC analysis was carried out by using a PerkinElmer auto XL system gas chromatograph. A 100-m capillary column with 0.25 mm internal diameter coated with 0.20-µm-thick 90%-bis-(cyanopropyl)-methyl polysiloxane stationary phase with a small amount of phenyl groups in the backbone of the polymer (HP 88) was used in the separation of the methyl esters of the fatty acid isomers. A temperature program with initial temperature 150°C with equilibration time of 1 min, then a temperature gradient of 0.5°C/min up to 170°C was used. The temperature was held at 170°C for 40 min. The peak identification was carried out by comparing the reported conjugated linoleic acid profiles in references [10, 11, 13, 14] and methyl esters prepared from the 9c11t and 10t12c triacylglycerols as described in the section "Samples and methods". The peaks in the chromatograms were then integrated, and their relative percentages were calculated using an excel spread sheet.

Results and Discussion

Infrared Spectroscopy

Infrared spectra of the CLA samples from the above experiments were recorded to confirm and complement the gas chromatographic analysis. CLAs with *cis–trans* and *trans–cis* configurations give rise to two specific absorptions at around around 946 and 986 cm^{-1} because of the =CH out-of-plane deformation vibration [18]. The CH out-of-plane deformation vibration of the *trans–trans* isomers absorb around 982–988 cm^{-1}, and *cis–cis* isomers do not absorb in this region. The =CH deformation vibrations of the methylene interupted *cis–trans, trans–cis* and *trans–trans* linoleic acid isomers absorb at approximately 967 at 4 cm^{-1} resolution at room temperature [19–22].

The second derivative profiles of the infrared spectra of the 9c11t/10t12c triaclylglycerol samples thermally induced at 250°C are shown in Fig. 1. The spectra show that the peak at 947 cm^{-1} decreases in intensity. The peak at 985 cm^{-1} also decreases, but because of the contribution of the absorption due to the *trans-trans* isomers of the CLA formed, the decrease is not parallel to the decrease in the intensity of the peak at 947 cm^{-1}. There is also a new peak appearing around 967 cm^{-1} indicating the formation of methylene interupted *cis–trans/trans–cis/trans–trans* isomers in the mixture.

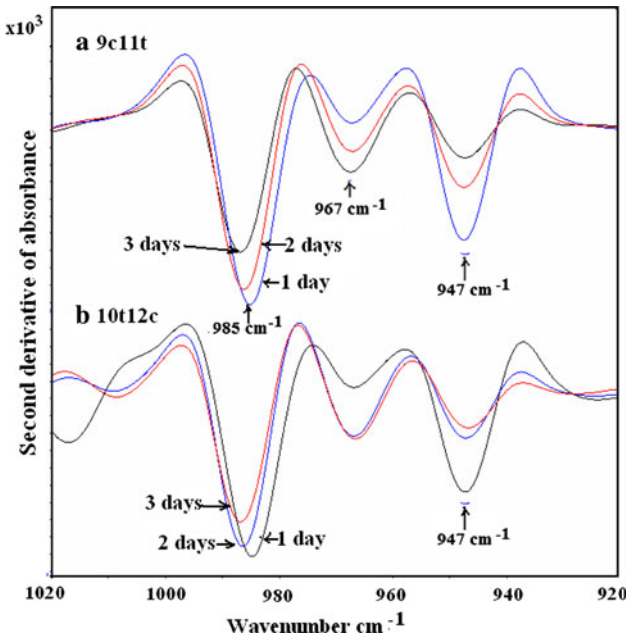

Fig. 1 Second derivative infrared profiles of thermally treated 9c11t and 10t12c triacylglycerol samples at 250°C

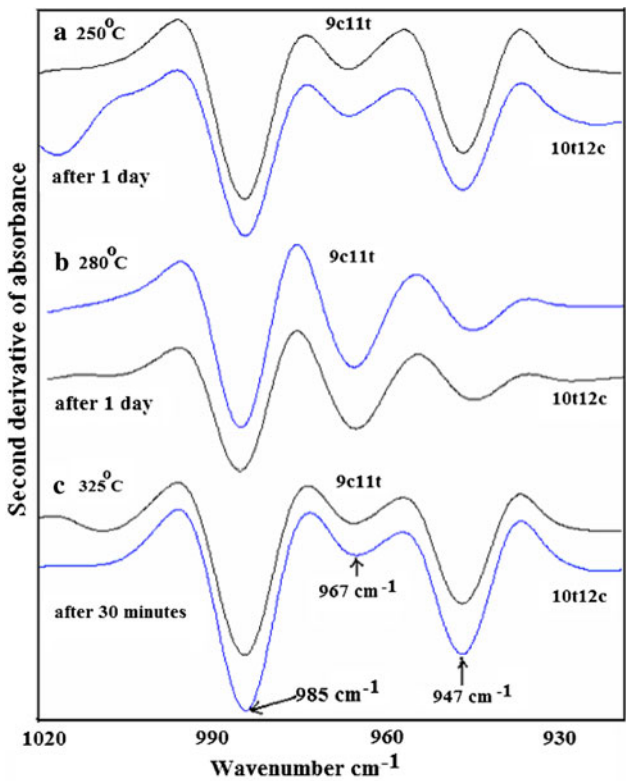

Fig. 2 Second derivative infrared profiles of thermally treated 9c11t and 10t12c triacylglycerol samples at 250, 280 and 325°C

The second derivative profiles of the infrared spectra of the 9c11t/10t12c triacylglycerol samples thermally induced at 250, 280 and 325°C are shown in Fig. 2. The spectra in

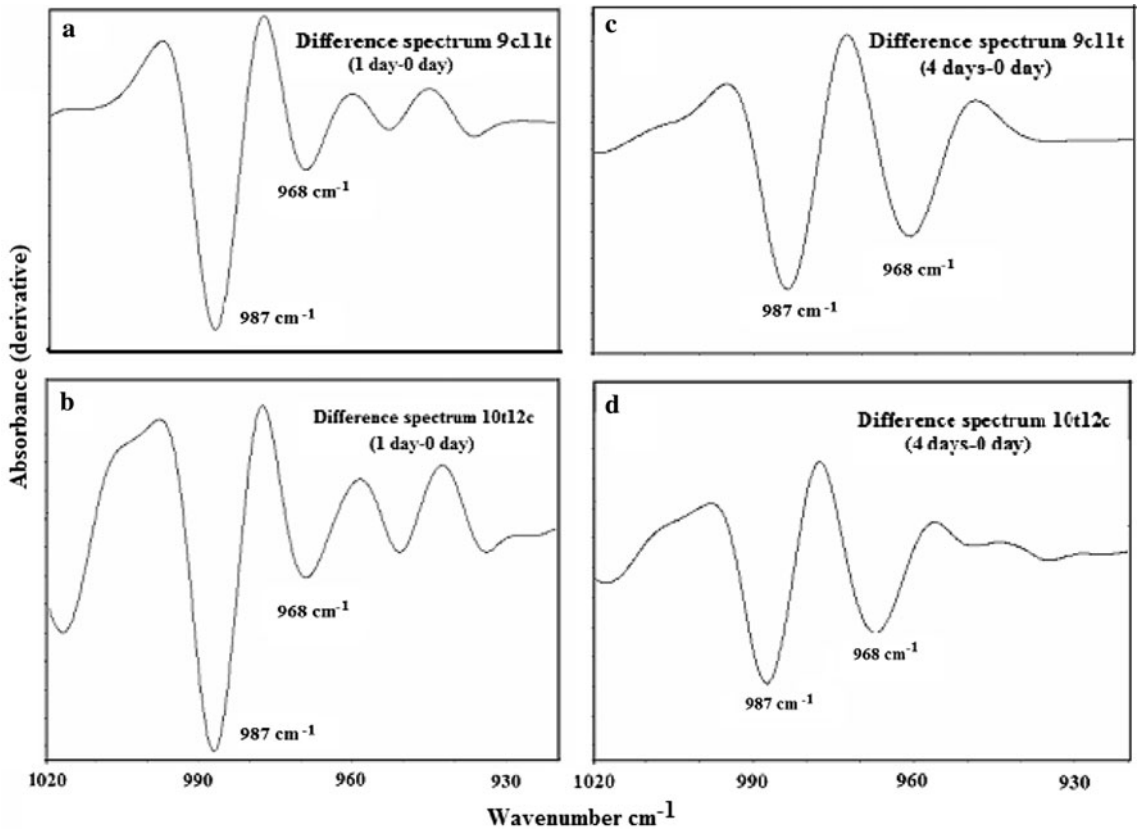

Fig. 3 Interactive substraction of the second derivative infrared spectrum of the starting material from the spectra of samples thermally induced at 250°C

the figure show that the intensity of the second derivative infrared peaks at 985 cm^{-1} of the samples thermally induced for 30 min at 325°C are higher than the peaks of the samples thermally induced for 24 h at 250 or 280°C. This is an indication of the formation of relatively higher concentrations of *trans–trans* CLAs in the thermally induced samples. This can be further confirmed by a proper interactive subtraction of the second derivative spectrum from the spectrum of starting material. The subtraction was carried out using the procedure found in the PerkinElmer instrument software. The results of the substraction are shown in Fig. 3.

Gas Chromatography

The gas chromatograms of the FAME of the thermally induced triacylglycerol samples containing 9c11t and 10t12c fatty acids are shown in Figs. 4 and 5, respectively, CLA profiles are identical to the FAME of most of the CLAs ranging from 7,9 through 12,14, except their relative concentrations. The effect of temperature is clear from the first two samples of the thermal induction. The samples heated at 280°C contain all the isomers of the CLAs, but their relative concentrations are small. The *trans–trans* isomers dominate in the sample. A comparison of the CLA profiles in the heated samples at 250, 280 and 325°C show that there are three pairs of CLA isomers standing out clearly from the rest of the profiles. They are 9c11t, 8t10c; 10c12t, 9t11c and 11c13t, 10t12c. The relationships between the area percentages of the components in the above pairs and thermal induction times are given in Fig. 6. For each starting material, the members in each pair have the similar relative concentrations in all the test samples. When the thermal induction experiments were carried out with 9c11t, the relative concentrations of 9t11c and 10c12t were higher than the concentrations of 10t12c and11c13t (Fig. 6). The thermal induction with triacylglycerol containing 10t12c shows again that the concentrations of 9t11c and 10c12t were higher than the concentrations of the pair 8t10c and 9c11t. It appears that the isomers 10c12t and 9t11c are at the intermediate position of the [1, 5] sigmatropic transformation sequence of the three pairs mentioned above.

Mechanism

A figure depicting the [1, 5] sigmatropic transformations and positional isomerisations in the CLAs from 7,9 through 12,14 is given in Fig. 7. The mechanisms related to the

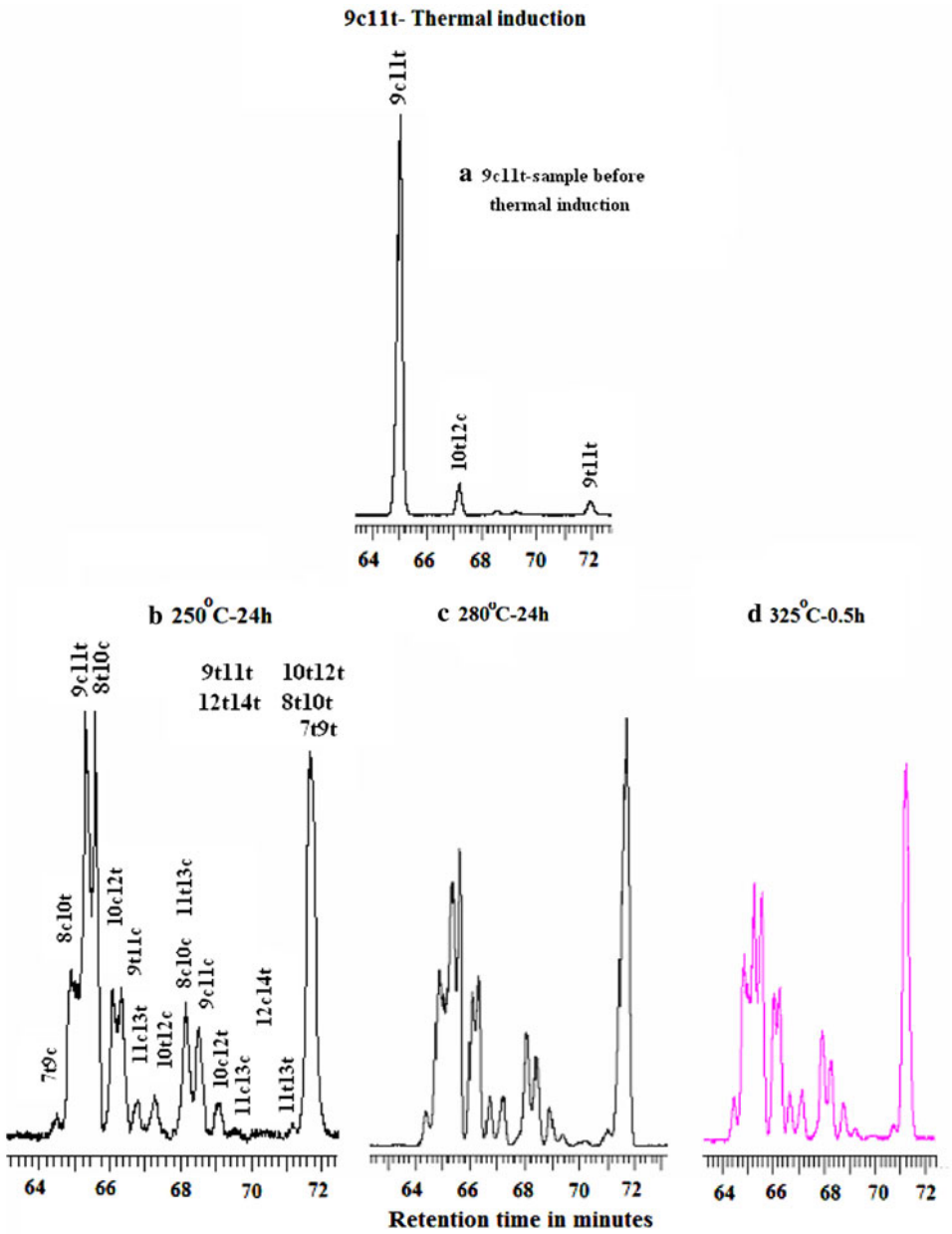

Fig. 4 Gas chromatograms of thermally induced 9c11t triacylglycerol samples

[1, 3] and [1, 5] sigmatropic transformations, and positional isomerizations can be found in Destaillats and Angers [11, 16] and Christy [23]. The figure is similar to the one formulated by Destaillats and Angers [11, 16] and Christy [23], but presented collectively in a manner to explain the appearance of the *cis–trans* and *trans–cis* isomers of CLAs that can be expected in a thermal induction experiment of another *cis–trans* CLA isomer. Thermal induction of 9c11t yields very little or no 11t13c and 12c14t isomers. The 9c11t isomer lies far away from this pair in the sequence. At the same time, the thermal induction of 10t12c, which lies closer to this pair in the sequence than 9c11t, shows the presence of 11t13c and 12c14t. Similarly, the weak appearance of the peaks representing 7t9c and 8c10t isomers during the thermal induction of 10t12c can be explained in the same manner. Furthermore, the 9c11t isomer lies closer to the 7t9c and 8c10t isomers in the sequence, and therefore thermal induction of 9c11t should show peaks representing these CLA isomers. It is interesting to note that the CLA fatty acids 9t11c and 10c12t are in the middle of the sequence of CLAs ranging from 7,9 to 12,14. It appears that a part of CLA isomers with relatively high concentrations compared to the rest of the CLA isomers can be prepared by selecting and thermally inducing a triaclyl glycerol containing a suitable *cis–trans* CLA fatty acid. Accordingly, thermal induction of either 9t11c or 10c12t should give CLA isomers with relatively higher concentrations of most of the isomers.

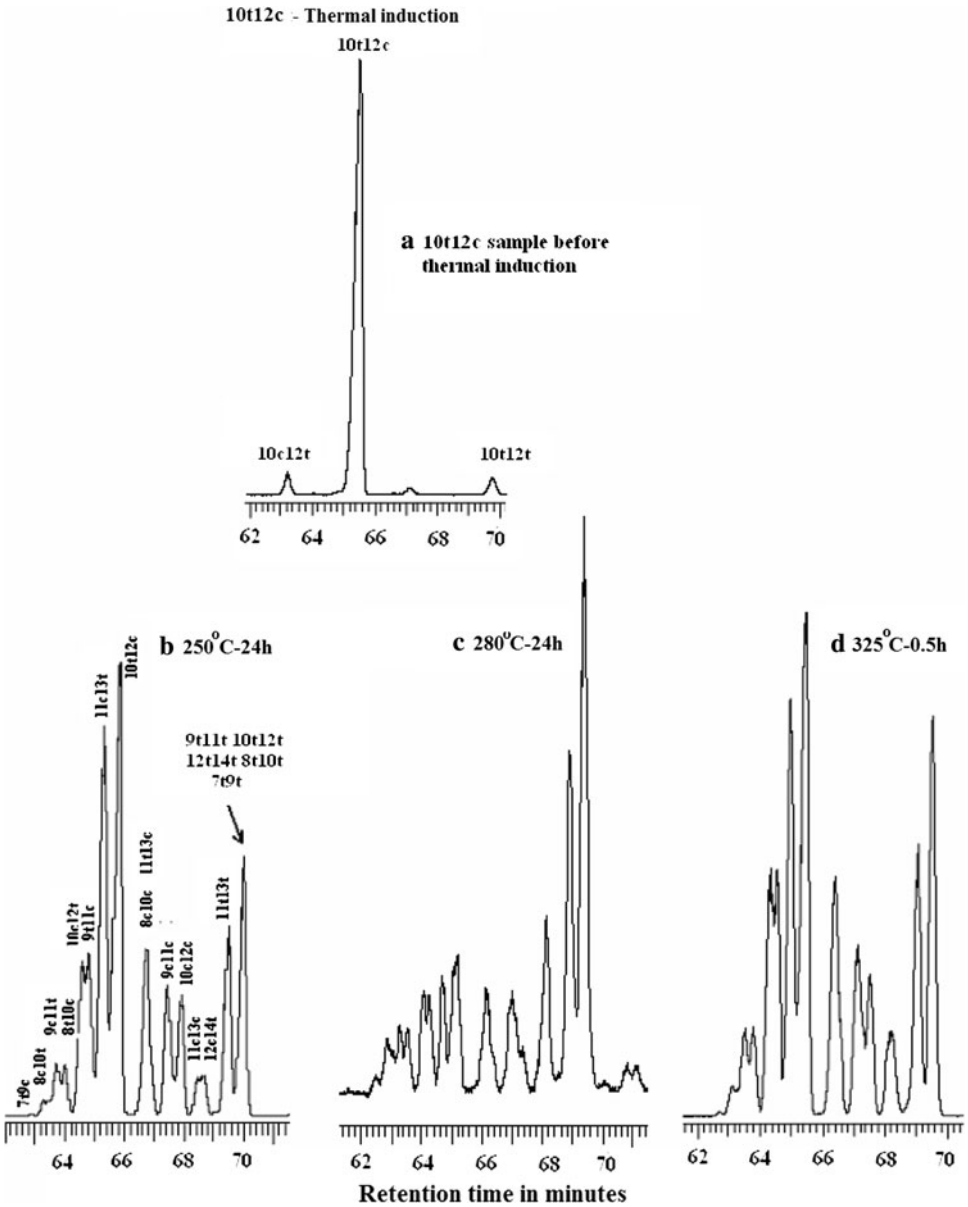

Fig. 5 Gas chromatograms of thermally induced 10t12c triacylglycerol samples

In addition to CLA isomers, the thermally induced mixtures also contain another peak accompanied by other very minor peaks in the chromatograms eluting 15 min earlier than the CLA isomers (Fig. 8). This peak is prominent in the samples thermally induced for 1 day at 250 and 280°C. At the same time, it is very small in the samples thermally induced for 30 min at 325°C. The identity of the relatively large peak in the group was confirmed as methylene interrupted 9t12t (18:2) fatty acid. In an earlier report [23], it was shown that the CLAs can also be formed by thermally inducing a triacylglycerol containing 9t12t fatty acid. Therefore, the formation of 9t12t (18:2) is possible during thermal induction of CLA fatty acids. The reaction takes place through an intramolecular [1, 3], sigmatropic rearrangement or a free radical chain reaction mechanism [16, 23]. The identification of 9t12t led to the inclusion of the [1, 3] sigmatropic transformation part in the mechanism presented in Fig. 7.

The peak in the infrared at 967 cm^{-1} also supports the identity. The absorption can be due to methylene interupted *cis–trans*, *trans–cis* and *trans–trans* isomers of fatty acids. The formation of 18:2 *trans–trans* fatty acid during the induction of either 9c11t or 10t12c fatty acids also stresses one point that the formation is specific of their standards. If the thermal induction of 9t12t can form 9c11t and 10t12c through an intermediate 9t11t, then the other CLA fatty acids can also be formed from *trans–trans* fatty acids such as 7t10t, 8t11t, 10t13t and 12t15t. However, it was not

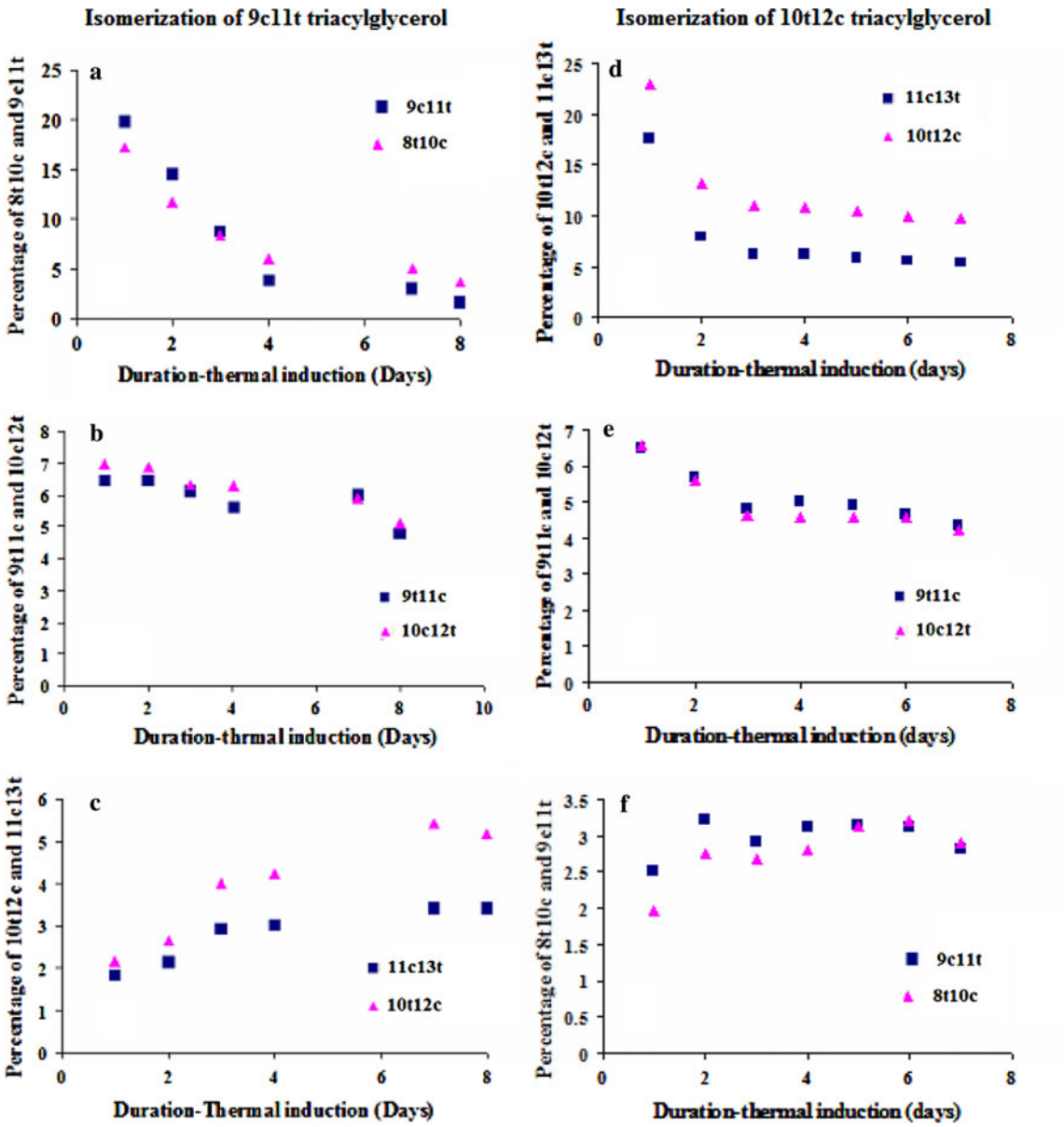

Fig. 6 Plots showing the relationships between relative percentages of the isomers formed in the mixtures during thermal induction of 9c11t and 1oc12t triacyl glycerol samples at 250°C

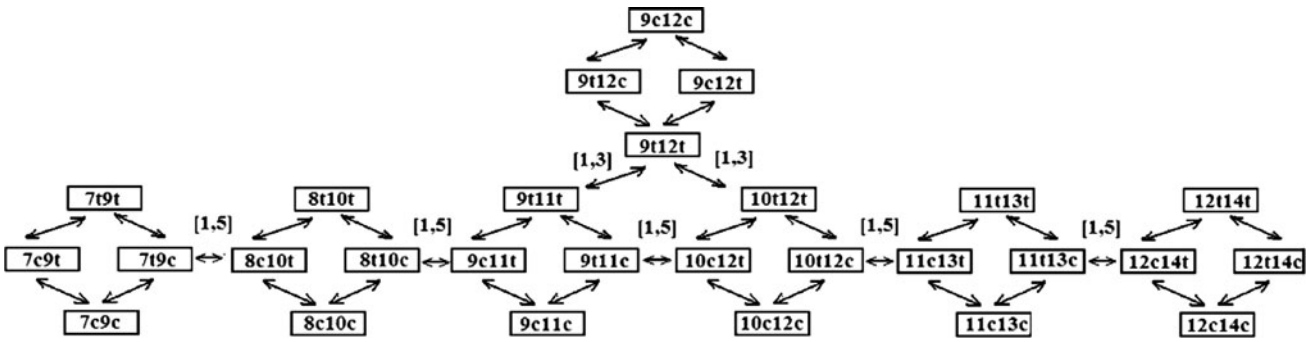

Fig. 7 Isomerisation sequence of conjugated linoleic acids

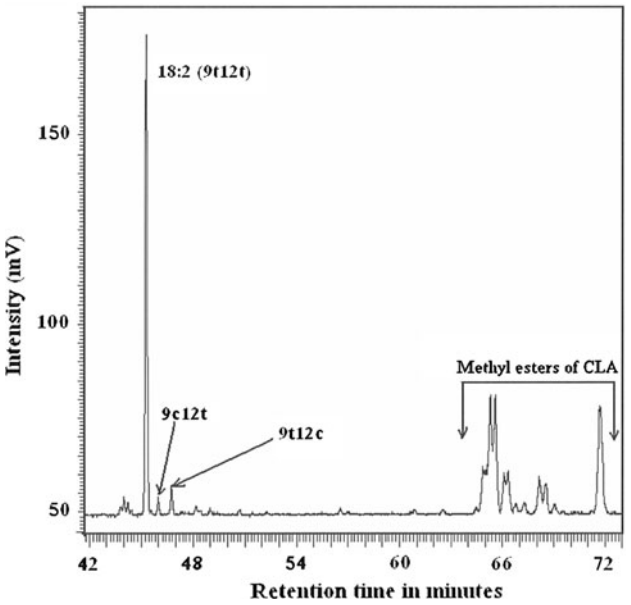

Fig. 8 Gas chromatogram of thermally induced 9c11t triacylglycerol sample

possible to confirm the presence of any of these *trans–trans* fatty acids because of the low concentrations and non-availability of the standards.

In this paper, it has been shown that the CLA isomers ranging from 7,9 through 12,14 can be prepared in one step by thermally inducing either 9c11t or 10t12c CLA. The formation of the isomers is relatively faster in the thermal induction of the samples at 325°C. The thermal induction of 10t12c CLA at 325°C for 30 min yields almost all the CLA isomers in detectable amounts that can be used as a reference sample. Furthermore, the preparation time of the isomers can be shortened from several hours to minutes, and several steps involving wet chemical reactions can be avoided. In addition, the isomerisation time used in the two-step synthesis forms high concentrations of *trans–trans* isomers of the CLAs, which elute together at the end as a very tall and broad peak (as shown in Ref. [11]) and dilute the other CLAs in the sample mixture. The isomerisation sequence presented in Fig. 7 and the experimental evidence provided in Fig. 6 clearly indicate the direction of isomerisation and the products one can expect in an experiment. Thermal induction of a CLA isomer is expected to give isomers that are close to the starting material. However, with the relative ease of obtaining either 9c11t or 10t12c CLA isomers, it is convenient to start with one of these isomers.

To illustrate the formation and the relative concentrations of the CLA isomers in the mixture, a thermal induction sequence diagram is presented utilising the pioneering work of Destaillats and Angers [12]. The figure gives an idea about which CLA isomer to select for the thermal induction to induce and form the CLA isomers one desires to prepare.

With the information presented in this paper, the mechanism involving the formation of CLA isomers has advanced one more step in the forward direction.

References

1. Ip C, Chin SF, Scimeca JA, Pariza MW (1991) Mammary cancer prevention by conjugated dienoic derivatives of linoleic acid. Cancer Res 51:6118–6124
2. Ip C, Chin SF, Scimeca JA, Thompson HJ (1994) Conjugated linoleic acid. A powerful anticarcinogen from animal fat sources. Cancer Suppl 74:1050–1054
3. Nicolosi RJ, Courtemanche KV, Laitinen L, Scimeca JA, Huth PJ (1993) Effect of feeding diets Enriched in conjugated linoleic acid on lipoproteins and aortic atherogenesis in hamsters. Circulation 88(suppl):2458
4. Shanta NC, Decker EA, Ustunol Z (1992) Conjugated Linoleic acids concentration in processed cheese. J Am Oil Chem Soc 69:425–428
5. Voorrips LE, Brants HA, Kardinaal AF, Hiddink GJ, Van den Brandt PA, Goldbohm RA (2002) Intake of conjugated linoleic acid, fat and other fatty acids in relation to postmenopausal breast cancer: the Netherlands Cohort Study on Diet and Cancer. Am J Clin Nutr 76:873–882
6. Belury MA, Vanden Heuvel JP (1997) Protection against cancer and heart disease by the dietary fat, conjugated linoleic acid: potential mechanisms of action. Nutr Dis Update J 1:58–63
7. Schrezenmeir J, Jagia A (2000) Milk and diabetes. J Am Coll Nutr 19(90002):176S–190S
8. Scimeca JA, Miller GD (2000) Potential health benefits of conjugated linoleic acid. J Am Coll Nutr 19:470S–471S
9. Parodi PW (1996) Milk fat components-possible chemopreventive agents for cancer and other diseases. Aust J Dairy Technol 51:24–32
10. Yurawecz MP, Roach JAG, Sehat N, Mossoba MM, Kramer JKG, Fritsche J, Steinhart H, Ku Y (1998) A new conjugated linoleic acid isomer, 7trans, 9 cis octadecanoic acid, in cow-milkcheese, beef and human milk and adipose tissue. Lipids 33:803–809
11. Destaillats F, Angers P (2003) Directed sequential synthesis of conjugated linoleic acid isomers from $\Delta^{7,9}$ to $\Delta^{12,14}$. Eur J Lipid Sci Technol 105:3–8
12. Cawood P, Wickens DG, Iversen SA, Braganza JM, Dormandy TL (1983) The nature of diene conjugation in human serum, bile and duodenal juice. FEBS 162:239–243
13. Berdeaux O, Voinot L, Angioni E, Juaneda P, Sebedio JL (1998) A simple method of preparation of methyl *trans*-10, *cis*-12 and *cis*-9, *trans*-11-Octadecadienoates from methyl linoleate. J Am Oil Chem Soc 75:1749–1755
14. Eulitz K, Yurawecz MP, Sehat N, Fritsche J, Roach JAG, Mossoba MM, Kramer JKG, Adlof RO, Ku Y (1999) Preparation, separation, and confirmation of the eight geometrical cis/trans conjugated linoleic acid isomers 8, 10-through 11, 13–18:2. Lipids 34:873–877
15. Jain VP, Proctor A (2007) Kinetics of photoirradiation-induced synthesis of soy oil-conjugated linoleic acid isomers. J Agric Food Chem 55:889–894
16. Destaillats F, Angers P (2002) Evidence for [1, 5] sigmatropic rearrangements of CLA in heated oils. Lipids 30:435–438

17. Christy AA, Xu Z, Harrington PB (2009) Thermal degradation and isomerisation kinetics of triolein studied by infrared spectrometry and GC–MS combined with chemometrics. Chem Phys Lipids 158:22–31
18. Mossoba MM, McDonald RE, Armstrong DJ, Page SW (1991) Identification of minor C_{18} triene and conjugated diene isomers in hydrogenated soybean oil and margarine by GC-MI-FT-IR spectroscopy. J Chromatogr Sci 29:324–330
19. Mossoba MM, Yurawecz MP, McDonald RE (1996) Rapid determination of total *trans* content of neat hydrogenated oils by attenuated total reflection spectroscopy. JOACS 73:1003–1009
20. Belton PS, Wilson RH, Sadehgi-Jorabegi H, Peers KE (1988) A Rapid Method for the Estimation of Isolated trans double bonds in Oils and fats Using FTIR combined with ATR. Lebensm Wiss Technol 21:153–157
21. Dutten HJ (1974) Analysis and monitoring of *trans*-isomerization by IR ATR spectrometry. J Am Oil Chem Soc 51:406–409
22. Lancer AC, Emkem EA (1988) Comparison of FTIR and capillary GC methods for quantitation of *trans* unsaturation in fatty acids methyl esters. Ibid 65:1483–1487
23. Christy AA (2009) Evidence in the formation of conjugated linoleic acids from thermally induced 9t12t linoleic acid: a study by gas chromatography and infrared spectroscopy. Chem Phys Lipids 161:86–94

Lipids (2010) 45:743–756
DOI 10.1007/s11745-010-3447-7

METHODS

RP-HPLC/MS-APCI Analysis of Branched Chain TAG Prepared by Precursor-Directed Biosynthesis with *Rhodococcus erythropolis*

Olga Schreiberová · Tereza Krulikovská · Karel Sigler · Alena Čejková · Tomáš Řezanka

Received: 26 May 2010 / Accepted: 29 June 2010 / Published online: 16 July 2010

Abstract Reversed phase liquid chromatography–atmospheric pressure chemical ionization mass spectrometry (RP-HPLC/MS-APCI) was used to analyze both synthetic triacylglycerols (TAG) having 1–3 branched fatty acids (FA) in the molecule, and natural TAG prepared by precursor directed biosynthesis from valine, leucine and isoleucine and the corresponding branched short-chain acids in cultivations of *Rhodococcus erythropolis*. The technique made it possible to identify and quantify TAG differing in a single branched-chain FA. Altogether 11 TAG were synthesized, out of which 8 were synthesized stereospecifically. Branched- and straight-chain-TAG were separated and identified while TAG differing only in *iso* or *anteiso* FA could not be separated. The APCI mass spectra of *iso*-, *anteiso*- and straight-chain TAG were completely identical. The natural material was found to contain 19 TAG having at least one branched FA. Cultivation on six different substrates showed, apart from the presumed and common incorporation of precursors to *iso*-even, *iso*-odd and *anteiso* FA, also some unusual features such as an increase in the content of odd-FA after the addition of Val (attributed to catabolism of Val to propionate) or the appearance of branched monounsaturated FA. The two-sample paired *t* test, when applied to the TAG, showed that only the pair Val and isobutyrate differ in incorporation into FA—see, e.g. proportions of M/M/O and brM/brM/O (1.2:1.2 and 1.9:1.2, respectively). Also, incorporation of Val (isobutyrate) yielded only TAG having two branched FA in the molecule, whereas Leu and Ile (isovalerate and 2-methylbutyrate) gave only TAG with a single branched FA in the molecule.

Keywords *Rhodococcus erythropolis* · RP-HPLC/MS-APCI · Branched chain triacylglycerols · Precursor directed biosynthesis

Abbreviations

GC-MS	Gas chromatography–mass spectrometry.
LC-MS	Liquid chromatography–mass spectrometry
RP-HPLC/MS-APCI	Reversed phase liquid chromatography–atmospheric pressure chemical ionization mass spectrometry
FA	Fatty acid(s)
TAG	Triacylglycerol(s)
DAG	Diacylglycerol(s)
MAG	Monoacylglycerol(s)
BrFA	Branched (i or ai) FA
BrTAG	Branched (i or ai) TAG
i-Bu	Isobutyric acid
i-Va	Isovaleric acid
2-MeBu	2-Methylbutyric acid
Val	Valine
Leu	Leucine
Ile	Isoleucine
DMAP	4-Dimethylaminopyridine
DCC	*N*,*N*′-Dicyclohexylcarbodiimide
ACN	Acetonitrile

O. Schreiberová · T. Krulikovská · A. Čejková
Department of Fermentation Chemistry and Bioengineering, Institute of Chemical Technology Prague, Technická 5, 166 28 Prague, Czech Republic

K. Sigler · T. Řezanka (✉)
Institute of Microbiology, Academy of Sciences of the Czech Republic, Vídeňská 1083, 142 20 Prague, Czech Republic
e-mail: rezanka@biomed.cas.cz

iPrOH	2-Propanol
i-14:0 (iM)	12-Methyltridecanoic acid
14:0 (M)	Tetradecanoic acid
i-15:0 (iX)	13-Methyltetradecanoic acid
ai-15:0 (aiX)	12-Methyltetradecanoic acid
15:0 (X)	Pentadecanoic acid
i-16:0 (iP)	14-Methylpentadecanoic acid
16:0 (P)	Hexadecanoic acid
i-16:1 (iPo)	14-Methylpentadecenoic acid
16:1 (Po)	Hexadecenoic acid
i-17:0 (iMa)	15-Methylhexadecanoic acid
ai-17:0 (aiMa)	14-Methylhexadecanoic acid
17:0 (Ma)	Heptadecanoic acid
i-17:1 (iMo)	15-Methylhexadecenoic acid
ai-17:1 (aiMo)	14-Methylhexadecenoic acid
17:1 (Mo)	Heptadecenoic acid
i-18:0 (iS)	16-Methyloctadecanoic acid
18:0 (S)	Octadecanoic acid
i-18:1 (iO)	16-Methyloctadecenoic acid
18:1 (O)	Octadecenoic acid

Introduction

Many prokaryotic microorganisms such as *Mycobacterium* sp., *Nocardia* sp., *Micromonospora* sp., *Dietzia* sp., *Gordonia* sp., *Streptomyces* sp. and *Rhodococcus* sp. accumulate large amounts of lipids in lipid bodies in the cells and mycelia [1, 2]. In the genus *Rhodococcus*, the information about the structure of lipids in the cytoplasmic lipid bodies, in particular triacylglycerols (TAG), is rather scarce [3, 4].

As a carbon source, the genus *Rhodococcus* can utilize very unusual compounds such as hexadecane [5] or phenyldecane that gives rise to triacylglycerol in which one fatty acid was replaced by a phenyldecanoic acid residue [6], or 1-chloro-, l-bromo- and 1-iodohexadecane that ultimately yield ω-halogen fatty acids (FA) [7]. Furthermore, alkanes can be directly oxidized and activated to the respective acyl-CoA thioesters and incorporated into TAG [3, 8]. The composition of the TAG is known to vary strongly when the cells are cultivated on propionic acid, which is activated to propionyl-CoA, resulting in a much higher fraction of odd-numbered FA (over 95% total FA) [8]. With valerate addition the proportions of odd-chain FA can reach nearly 85% total FA.

With other bacteria, the addition of branched amino acids, i.e. Val, Leu or Ile, or their metabolites such as isobutyric (i-Bu), isovaleric (i-Va) or 2-methylbutyric (2-MeBu) acids into the culture medium induces the production of increased amounts of branched FA enriched with the given branched-FA depending on the starter unit (addition of Val produces even-*iso*-FA, addition of Leu odd-*iso*-FA, addition of Ile odd-ai-FA). This fact has been noted many times in myxobacteria [9], in *Nonomuraea* sp. [10], *Propionibacterium freudenreichii* [11], *Staphylococcus xylosus* [12] or *S. carnosus* [13].

Current studies have shown that branched chain FA, predominantly i-15:0 (*iso*-pentadecanoic) and ai-15:0 (*anteiso*-pentadecanoic) inhibit the growth of various cancer cell lines both in vitro and in vivo [14, 15]. Other experiments have documented that their activity decreases with an increase or decrease in chain-length from i-16:0 (isopalmitic) [16]. This effect is explained as being due to cancer cells being more dependent on fatty acid biosynthesis than healthy cells.

As shown in our earlier study of *Rhodococcus* lipids [17], LC–MS analysis of odd-chain TAG is still largely unexplored, mostly due to the scarcity of sources with odd-chain TAG. The situation with branched-chain TAG from natural sources is even worse. To our knowledge only two sources of branched TAG have so far been identified, both of them of bacterial origin. Metz et al. [18] used GC–MS to separate and identify intact TAG from *Streptomyces avermitilis* containing odd- and even-chain FA including *iso*- and *anteiso*-FA. Another source of branched TAG is milk; branched FA contained in it are largely derived from bacteria leaving the rumen [14, 15]. With one exception [19], even here branched TAG have not been separated from straight-chain TAG. All other studies [20, 21] mention only odd-chain TAG, although branched-TAG also have to be present, as seen from the analysis of FA in butter [19, 21]. Figure 1 in the paper by Marai et al. [21] clearly shows the presence, between peaks 48:0 (PPP) and 49:0 (PPMa), of two unidentified peaks that could belong to TAG 49:0 having branched margaric acids (i.e. i-17:0 and/or ai-17:0). Only Myher et al. [19] have given the TCN (theoretical carbon number) for branched TAG 0.38 less than for straight-chain TAG; to our knowledge this is thus the only paper that has explored the LC–MS of branched TAG.

Based on our previous experience with the cultivation of *Rhodococcus* [22] and with LC–MS of lipids [23, 24] we used here precursor directed biosynthesis to prepare branched TAG, which were qualitatively and quantitatively analyzed by using synthetic standards.

Experimental

Microbial Material

Rhodococcus erythropolis CCM 2595 obtained from the Czech Collection of Microorganisms (Masaryk University, Brno, Czech Republic) was subjected to a 6-month

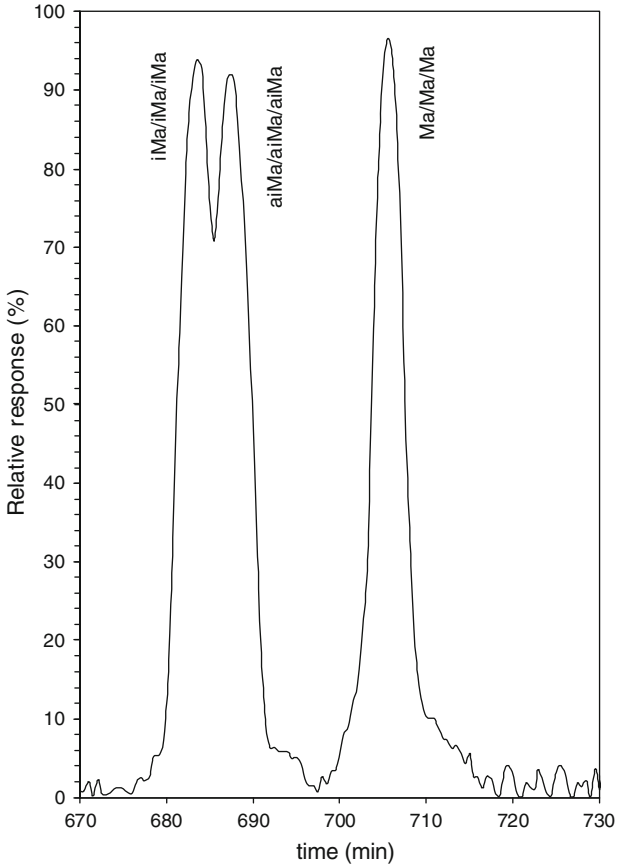

Fig. 1 RP-HPLC/APCI-MS chromatogram of three synthetic TAG (Ma/Ma/Ma, iMa/iMa/iMa, and aiMa/aiMa/aiMa)

physiological adaptation to phenol. The strain reached a high growth rate in the presence of succinate (10 g/L) used as the sole carbon source. Cells were grown in the basic mineral medium (g/L: KH_2PO_4 0.17; $MnCl_2{\cdot}4H_2O$ 0.001; K_2HPO_4 0.13; $CaCl_2{\cdot}2H_2O$ 0.00026; $(NH_4)_2SO_4$ 0.71; $FeSO_4{\cdot}7H_2O$ 0.0006; $MgCl_2{\cdot}6H_2O$ 0.34; $Na_2MoO_4{\cdot}2H_2O$ 0.002; pH was adjusted to 7.0) containing alternatively amino acids or short carboxylic acids (sodium salts) as the carbon source (valine, leucine, isoleucine, isovalerate, isobutyrate, 2-methyl butyrate—each 3 g/L) and 1 g/L of succinate as cosubstrate. The cultivations were performed on a rotary shaker at 100 rpm and 30 °C.

The cells were collected at the end of exponential phase (97 h) by centrifugation (10 min, 9,050*g*), washed twice with physiological solution and lyophilized (dry biomass yield depending on the C-sources: 353 mg/L—valine, 438 mg/L—leucine, 663 mg/L—isoleucine, 690 mg/L—isovalerate, 583 mg/L—isobutyrate, 645 mg/L—2-methyl butyrate, 890 mg/L—succinate).

Standards and Isolation

Acetonitrile, 2-propanol, hexane, dichloromethane, glycerol, 4-dimethylaminopyridine (DMAP), *N*,*N*′-dicyclohexyl-carbodiimide (DCC), and standards of glyceryl tripalmitate and glyceryl triheptadecanoate were purchased from Sigma-Aldrich (Prague, CR). The mono- and diacylglycerols were purchased from Larodan Fine Chemicals, Malmo, Sweden.

Preparation of Mixed FA Composition TAG

The esterification of glycerol with acids has been described previously [25]. Briefly, a rapidly stirred suspension of 1,3-diacylglycerol or 1,2-diacylglycerol (10 μmol), the acid (11 μmol), and a catalytic amount of 4-dimethylamino-pyridine (2 μmol) in anhydrous CH_2Cl_2 (5 mL) was treated with *N*,*N*′-dicyclohexyl-carbodiimide (12 μmol). The resulting mixture was stirred under N_2 for 24 h at room temperature, diluted with CH_2Cl_2, and filtered to remove precipitated 1,3-dicyclohexyl urea. The filtrate was washed with 0.5 N HCl, saturated aqueous $NaHCO_3$, H_2O, and brine and dried ($MgSO_4$). The solvent was removed in vacuo, and the remaining residue was purified by TLC (silica gel H, developed in hexane/diethyl ether/acetic acid (70:30:1, by vol.). The yields of appropriate TAG are in Table 1. The purity (see also Table 1) of individual synthesized TAG was determined by RP-HPLC, for the conditions see below.

Preparation of Single FA Composition TAG

The TAG were prepared as described above, only the ratios of FA and glycerol were different, i.e. for 10 μmol of FA, 3 μmol of glycerol, 4 μmol of 4-dimethylaminopyridine, and 36 μmol of *N*,*N*′-dicyclohexyl-carbodiimide was used. Further separation and purification was identical, see above. The yields are in Table 1.

The lyophilized cells were mixed with 10 mL of hexane and the mixture was stirred for 15 min. The cells were filtered off, hexane was evaporated and the oil samples

Table 1 Synthesis of TAG

Alcohol (1 μmol)	Acid/μmol	TAG	Yield (%)	Purity (%)
Glycerol	Ma/3.15	Ma/Ma/Ma	92	≥99
Glycerol	iMa/3.15	iMa/iMa/iMa	90	≥99
Glycerol	aiMa/3.15	aiMa/aiMa/aiMa	87	≥99
1-Monopalmitin	Ma/2.10	P/Ma/Ma	75	≥99
1-Monopalmitin	iMa/2.10	P/iMa/iMa	73	≥99
1-Monopalmitin	aiMa/2.10	P/aiMa/aiMa	76	≥99
1,2-Dipalmitin	Ma/1.05	P/P/Ma	69	>98
1,2-Dipalmitin	iMa/1.05	P/P/iMa	68	>98
1,2-Dipalmitin	aiMa/1.05	P/P/aiMa	70	>98
1,3-Dipalmitin	Ma/1.05	P/Ma/P	68	>98
1,3-Diheptadecanoin	P/1.05	Ma/P/Ma	64	>97

were dissolved in an acetonitrile-2-propanol-hexane mixture (1:1:1, v/v/v), which was injected on the column.

FAME Analysis

The TAG (10 mg) were saponified overnight in 10% KOH–MeOH at room temperature. A fatty acid fraction obtained from saponification was partitioned between alkali solution (pH 9) and Et_2O to remove basic and neutral components. The aqueous phase, containing FA, was acidified to pH 2 and extracted with hexane. The fatty acid fraction was methylated using CH_2N_2. GC–MS of fatty acid methyl ester (FAME) mixture was done on a Finnigan 1020 B in EI mode. Splitless injection was at 100 °C, and a fused silica capillary column (Supelcowax 10; 60 m × 0.25 mm i.d., 0.25 mm film thickness; Supelco, Prague) was used. The temperature program was as follows: 100 °C for 1 min, subsequently increasing at 20 °C/min to 180 °C and at 2 °C/min to 280 °C, which was maintained for 1 min. The carrier gas was helium at a linear velocity of 60 cm/s. All spectra were scanned within the range of *m/z* 50–500. The structures of FAME were confirmed by comparison of retention times and fragmentation patterns with those of the standard FAME (Supelco, Prague).

RP-HPLC/MS-APCI

The HPLC equipment consisted of a 1090 Win system, PV5 ternary pump and automatic injector (HP 1090 series, Agilent, USA) and two Hichrom columns HIRPB-250AM 250 × 2.1 mm ID, 5-μm particle size, in series. This setup provided us with a high-efficiency column—approximately 26,000 plates/250 mm. A quadrupole mass spectrometer system Navigator (Finnigan MAT, San Jose, CA, USA) was used for analysis. The instrument was fitted with an atmospheric pressure chemical ionization source [vaporizer temperature 390 °C, capillary heater temperature 260 °C, corona current 7 μA, sheath gas—high-purity nitrogen, pressure 0.45 MPa, and auxiliary gas (also nitrogen) flow rate 15 mL/min]. Positively charged ions with *m/z* 200–1,000 were scanned with a scan time of 0.5 s. The whole HPLC flow (0.35 mL/min) was introduced into the APCI source without any splitting. TAG were separated using a gradient solvent program with acetonitrile (ACN) and 2-propanol (iPrOH) as follows: initial ACN/iPrOH (99:1, v/v); linear from 5 to 120 min ACN/iPrOH 30:70, v/v); held until 30 min; the composition was returned to the initial conditions over 10 min. Isocratic separation by the mixture ACN/iPrOH 65:35, v/v) was used for resolution of the regioisomers. A peak threshold of 0.07% intensity was applied to the mass spectra.

The saturated synthesized TAG (Ma/Ma/Ma, iMa/iMa/iMa, and aiMa/aiMa/aiMa) were dissolved in ACN/iPrOH mixture (99:1, v/v) to concentrations of 1, 5, 10, 50, and 100 μg/mL. All calibration curves were measured using a 10 μL injection volume of solutions in three repeated analyses and the average peak areas were used for the construction of calibration curves. For reliable quantitation, concentrations of individual TAG in analyzed samples have to be in a given interval (after a suitable dilution). The limits of detection at S/N = 3 were determined with the injection volume 10 μL and averaged as 1 μg/mL for saturated TAG. RFs are expressed relative to Ma/Ma/Ma, which is set to 1.00. For MS-APCI *a* and *b* values are coefficients of the linear calibration dependence $y = ax + b$ and RFs are calculated as $RF = a_{Ma/Ma/Ma}/a_{TAG}$, because *b* values can be neglected. Here r^2 is the value of coefficient of determination, *y* corresponds to the peak areas and *x* is the concentration in μg/mL.

Data acquisition and analyses were performed using PC with MassLab 2.0 for Windows XP applications/operating software.

Results and Discussion

As seen in Table 2, FA from *Rhodococcus* comprise not only odd-chain FA [17], but also branched-chain FA that

Table 2 Fatty acid compositions (%) of seven cultivations of *R. erythropolis* at 30 °C with different carbon sources [succinate, Val, Leu, Ile, isobutyric (i-Bu), isovaleric (i-Va) and 2-methyl-butyric (2-MeBu) acid] as determined by GC–MS

	Succinate	Val	i-Bu	Leu	i-Va	Ile	2-MeBu
i-14:0 (iM)	–[a]	8.1	6.7	–	–	–	–
14:0 (M)	9.8	6.3	5.9	4.5	5.3	3.8	4.4
i-15:0 (iX)	–	–	–	14.8	14.2	–	–
ai-15:0 (aiX)	–	–	–	–	–	19.1	20.4
15:0 (X)	8.2	13.5	14.2	11.6	10.8	7.6	6.7
i-16:0 (iP)	–	18.2	17.6	–	–	–	–
16:0 (P)	19.3	12.1	13.0	16.3	15.7	11.2	10.8
i-16:1 (iPo)		0.3	0.2	–	–	–	–
16:1 (Po)	18.5	13.1	14.1	13.1	14.5	10.9	11.3
i-17:0 (iMa)	–	–	–	19.5	20.2	–	–
ai-17:0 (aiMa)	–	–	–	–	–	21.3	19.7
17:0 (Ma)	4.9	9.3	8.8	3.4	4.1	4.2	4.6
i-17:1 (iMo)	–	–	–	0.7	0.6	–	–
ai-17:1 (aiMo)	–	–	–	–	–	0.6	0.5
17:1 (Mo)	9.2	6.7	7.1	5.4	4.8	5.7	6.2
i-18:0 (iS)	–	0.6	0.5	–	–	–	–
18:0 (S)	3.1	1.8	1.6	0.9	0.6	2.8	2.9
i-18:1 (iO)	–	0.4	0.5	–	–	–	–
18:1 (O)	27.0	9.6	9.8	9.8	9.2	12.8	12.5

[a] Minority fatty acids up to 0.1% of total fatty acids were omitted

were produced by precursor directed biosynthesis from branched chain precursors. In view of the scarcity of data on branched chain TAG (see above) we decided to synthesize a series of standards (see Table 1) that were used to verify the basic chromatographic and mass spectral characteristics. The standards were synthesized by conventional procedures, as simply as possible and with the highest yield. We followed the procedure described by Lie Ken Jie and Lam [26] who synthesized TAG of AAB, ABA, BBA and BAB types. Commercially available glycerol, monoacyl- and diacylglycerols (1-palmitin, 1,2-dipalmitin, 1,3-dipalmitin and 1,3-diheptadecanoin) yielded a total of 11 TAG by mild organic synthesis performed at 25 °C for 24 h under catalysis with dicyclohexylcarbodiimide (DCC) and 4-dimethylaminopyridine (DMAP) (see "Experimental").

Individual TAG were analyzed by RP-HPLC. Figure 1 shows the chromatographic analysis of three synthetic TAG, Ma/Ma/Ma, iMa/iMa/iMa, and aiMa/aiMa/aiMa. The separation of straight-chain TAG from both branched-chain TAG presented no problems while separation of iMa/iMa/iMa from aiMa/aiMa/aiMa was hours-long—a time span unacceptable in the analysis of a natural sample—and succeeded only under isocratic conditions using the mobile phase ACN-iPrOH (65:35, v/v).

Chromatographic separation of branched TAG having two branched FA in the molecule (two i-17:0 or two ai-17:0) from straight-chain counterparts presents no problems—gradient elution provided a base-line separation of P/Ma/Ma from P/aiMa/aiMa or P/Ma/Ma from P/iMa/iMa, as shown in Figs. 2 and 3. Separation of two branched TAG such as P/iMa/iMa and P/aiMa/aiMa could be accomplished only by isocratic elution and only with synthetic TAG. We ascribe this phenomenon to the much higher complexity of the natural mixture that results in a mutual influencing and overlapping of peaks.

In the case of TAG having a single branched FA we succeeded in separating only those TAG that differed in the site of branching. The separation was successful only in the pairs P/P/Ma and P/P/iMa, and P/P/Ma and P/P/aiMa, in both the synthetic and the natural mixture and with both isocratic and gradient elution. The separation P/P/iMa and P/P/aiMa was unsuccessful.

Positional isomers such as P/P/Ma and P/Ma/P or P/Ma/Ma and Ma/P/Ma were partially separated only with isocratic elution (see [27] for positional isomers, i.e. POP and PPO). These two pairs were much more poorly separated than positional isomers in which individual FA differ in two methylene groups, such as P/P/S and P/S/P [17].

The APCI mass spectra of an AAA type TAG are very simple. For instance, trianteisomargarin (aiMa/aiMa/aiMa), exhibits four clusters of ions, i.e. $[M+H]^+$ ($[TAG]^+$, i.e. $[aiMa/aiMa/aiMa]^+$) at *m/z* 849, $[M\text{-}RCOO]^+$ ion ($[DAG]^+$, i.e. $[aiMa/aiMa]^+$) at *m/z* 579 arising by the loss of margarate $[RCOO+58]^+$ called also ($[MAG]^+$, i.e. $[aiMa]^+$) at *m/z* 327, and $[RCO]^+$ ion (FA^+, i.e. $aiMa^+$) at *m/z* 253, see also Table 3 and Fig. 4.

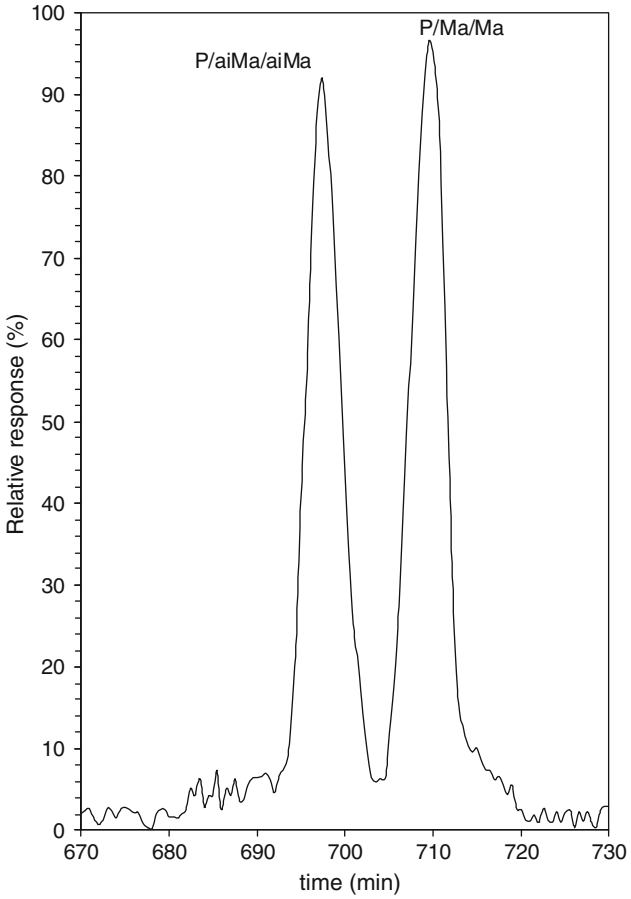

Fig. 2 RP-HPLC/APCI-MS chromatogram of two synthetic TAG (P/Ma/Ma and P/aiMa/aiMa)

APCI mass spectra of all synthetic TAG, i.e. Ma/Ma/Ma, iMa/iMa/iMa, and aiMa/aiMa/aiMa were completely identical. Minute differences in the intensity of ions at *m/z* 41, 43, 55, and 57 can be found only in electron impact mass spectra. These ions arise probably by splitting of the termini of aliphatic chains although Dinh-Nguyen [28] states, based on the comparison with deuterium-labeled compounds, that the situation is more complex. Unfortunately, the HPLC-electron impact connection is not feasible and the determination of all three chain types, i.e. *n-*, *iso-* and *anteiso-* would always require a comparison of natural TAG with a synthetic TAG standard.

The above data clearly show that any combination of branched- and straight-chain acyls in TAG cannot be resolved based on mass spectrum. Even so we performed another experiment with synthetic TAG (P/Ma/Ma and P/aiMa/aiMa, see Figs. 5, 6) that could facilitate the

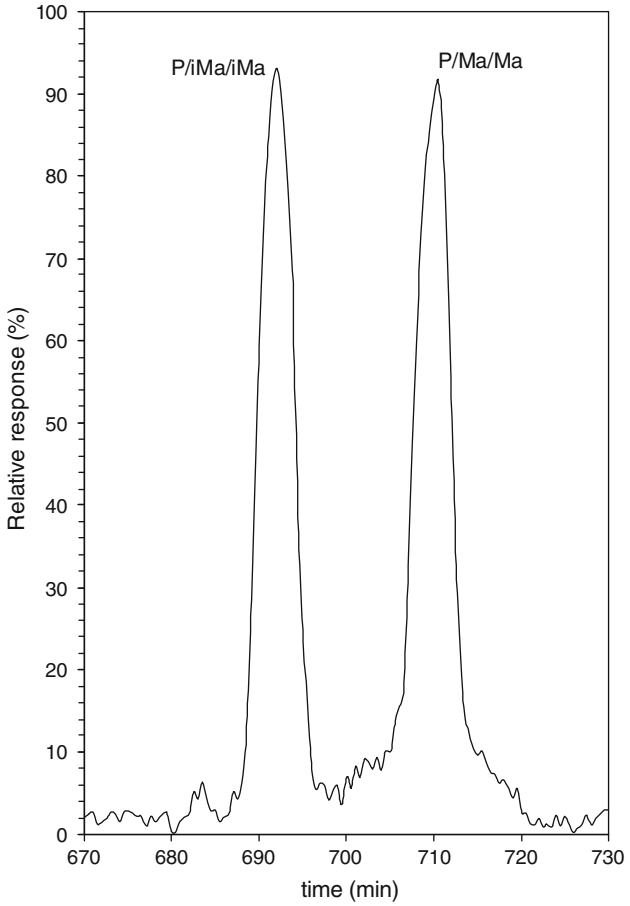

Fig. 3 RP-HPLC/APCI-MS chromatogram of two synthetic TAG (P/Ma/Ma and P/iMa/iMa)

resolution of individual acyls by using MS/MS. However, the MS/MS of the daughter ion at *m/z* 253 ($[RCO]^+$), i.e. ion with the same *m/z* value for all three acyls of all three acids (margaric, *iso*-margaric and *anteiso*-margaric acids) failed to reveal any perceptible change in the intensity of ions in the interval of 35–253 Da (spectrum not shown); this result finally excluded the possibility of distinguishing branched- and straight-chain TAG by MS-APCI.

The mass spectrum of ABB type TAG such as P/aiMa/aiMa (Fig. 6), which contains two FA, exhibits, in addition to $[M+H]^+$ at *m/z* 835, also two acylium ions, with *m/z* at 239 (P^+) and *m/z* 253 ($aiMa^+$), respectively. The spectrum naturally features also ions of the type $[MAG]^+$ at *m/z* 313 ($[P]^+$) and *m/z* 327 ($[aiMa]^+$), respectively. Like with aiMa/aiMa/aiMa, also $[DAG]^+$ ions caused by the loss of margarate at *m/z* 565 and palmitate at *m/z* 579 are present, resulting in ($[P/aiMa]^+$ (type $[AB]^+$) and $[aiMa/aiMa]^+$ (type $[BB]^+$) ions, respectively.

Similarly, the mass spectrum of an ABC type TAG, i.e. TAG containing three different FA, such as P/brMa/S, see Fig. 7, shows three triplets of ions—three $[M\text{-}RCOO]^+$ ions at *m/z* 565, 579, and 593, corresponding to loss of stearate to give $[brMa/P]^+$, loss of margarate to give $[P/S]^+$, and palmitate to give $[brMa/S]^+$, respectively. Another triplet, $[MAG]^+$ at *m/z* 341, 327, and 313 is formed by $[S]^+$, $[brMa]^+$, and $[P]^+$ ions. The last triplet belongs to ions S^+ (*m/z* 267), $brMa^+$ (*m/z* 253), and P^+ (*m/z* 239).

Some authors [17, 29–32] observed that the relative intensities of the $[M\text{-}RCOO]^+$ ions, i.e. $[DAG]^+$, could be used to obtain information on the positions of FA within

Table 3 TAG identified in *R. erythropolis*, their retention times (RT), acyl carbon number (ACN), the masses of protonated molecules, and characteristic fragment ions of TAG

Peak no.	TAG	RT[e]	ACN:n	$[M+H]^+$	$[DAG]^+$	*m/z*	$[DAG]^+$	*m/z*	$[DAG]^+$	*m/z*
1	Po/Po/O	50.7	50:3	829	Po/O	575	Po/Po	547	–	–
2	brX/Po/Po	51.0	47:2	789	brX/Po	535	Po/Po	547	–	–
3	Po/Po/Mo	51.2	49:3	815	Po/Mo	561	Po/Po	547	–	–
4	X/Po/Po	51.6	47:2	789	X/Po	535	Po/Po	547	–	–
5	M/Po/O	53.4	48:2	803	Po/O	575	M/Po	521	M/O	549
6	brM/brM/O	53.5	46:1	777	brM/O	549	brM/brM	495	–	–
7	P/Po/Po	53.8	48:2	803	P/Po	549	Po/Po	547	–	–
8	M/P/Po	54.3	46:1	777	P/Po	549	M/P	523	M/Po	521
9	M/M/O	54.7	46:1	777	M/O	549	M/M	495	–	–
10	brM/brM/P	55.1	44:0	751	brM/P	523	brM/brM	495	–	–
11	M/M/P	56.4	44:0	751	M/P	523	M/M	495	–	–
12	Po/Mo/O	58.2	51:3	843	Mo/O	589	Po/Mo	561	Po/O	575
13	P/Po/Mo	58.4	49:2	817	Mo/P	521	Po/Mo	561	Po/P	549
14	Po/O/O	60.9	52:3	857	O/O	603	Po/O	575	–	–
15	M/O/O	61.3	50:2	831	O/O	603	M/O	549	–	–
16	P/Po/O	61.9	50:2	831	Po/O	575	P/Po	549	P/O	577
17	Po/Po/S	62.6	50:2	831	Po/S	577	Po/Po	547	–	–
18	brP/brP/Po	62.9	48:1	805	brP/Po	549	brP/brP	551	–	–
19	M/brP/brP	63.1	46:0	779	brP/brP	551	M/brP	523	–	–

Table 3 continued

Peak no.	TAG	RT[e]	ACN:n	$[M+H]^+$	$[DAG]^+$	*m/z*	$[DAG]^+$	*m/z*	$[DAG]^+$	*m/z*
20	M/P/O	63.5	48:1	805	P/O	577	M/P	523	M/O	549
21	brM/brM/S	63.9	46:0	779	brM/S	551	brM/brM	495	–	–
22	P/P/Po	64.2	48:1	805	P/Po	549	P/P	551	–	–
23	M/P/P	64.7	46:0	779	P/P	551	M/P	523	–	–
24	Mo/Mo/O	65.1	52:3	857	Mo/O	589	Mo/Mo	575	–	–
25	M/M/S	65.2	46:0	779	M/S	551	M/M	495	–	–
26	M/Po/S	65.5	48:1	805	Po/S	577	M/Po	521	M/S	551
27	brX/O/O	65.6	49:1	819	O/O	603	brX/O	563	–	–
28	MoOO	65.9	53:3	871	O/O	603	Mo/O	589	–	–
29	brX/P/O	66.2	51:2	845	P/O	577	brX/P	537	brX/O	563
30	X/O/O	66.3	49:1	819	O/O	603	X/O	563	–	–
31	P/Mo/O	66.7	51:2	845	Mo/O	589	P/Mo	521	P/O	577
32	X/P/O	67.1	51:2	845	P/O	577	X/P	537	X/O	563
33	O/O/O	69.0	54:3	885	O/O	603	–	603	–	–
34	P/O/O	69.5	52:2	859	O/O	603	P/O	577	–	
35	Po/S/O	70.8	52:2	859	S/O	605	Po/S	577	Po/O	575
36	brP/brP/O	70.9	50:1	833	brP/O	577	brP/brP	551	–	–
37	P/P/O	72.2	50:1	833	P/O	577	P/P	551	–	–
38	Po/P/S	72.6	50:1	833	P/S	579	Po/P	549	Po/S	577
39	M/O/S	73.1	50:1	833	O/S	605	M/O	549	M/S	551
40	brMa/O/O	74.5	53:2	873	O/O	603	brMa/O	591	–	–
41	brX/O/S	74.7	51:1	847	O/S	605	brX/O	563	brX/S	565
42	brP/brP/P	74.9	48:0	807	brP/brP	551	brP/P	551	–	–
43	Ma/O/O	75.3	53:2	873	O/O	603	Ma/O	591	–	–
44	X/O/S	75.6	51:1	847	O/S	605	X/O	563	X/S	565
45	P/P/P	76.2	48:0	807	P/P	551	–	–	–	–
46	brMa/O/P	76.3	51:1	847	O/P	577	brMa/O	591	brMa/P	565
47	M/P/S	76.7	48:0	807	P/S	579	M/P	523	M/S	551
48	P/Mo/S	77.1	51:1	805	Mo/S	591	P/Mo	521	P/S	579
49	Ma/O/P	77.2	51:1	847	O/P	577	Ma/O	591	Ma/P	565
50	P/P/brMa	77.2	49:0	821	brMa/P	565	P/P	551	–	–
51	P/P/Ma	78.1	49:0	821	Ma/P	565	P/P	551	–	–
52	Po/S/S	78.2	52:1	861	S/S	607	Po/S	577	–	–
53	O/O/S	79.4	54:2	887	O/S	605	O/O	603	–	–
54	P/O/S	81.4	52:1	861	O/S	605	P/O	577	P/S	579
55	brP/brP/S	84.2	50:0	835	brP/S	579	brP/brP	551	–	–
56	P/P/S	85.5	50:0	835	P/S	579	P/P	551	–	–
57	iMa/iMa/iMa	86.4	51:0	849	iMa/iMa	579	–	–	–	–
58	P/brMa/brMa	85.6	50:0	835	brMa/brMa	579	brMa/P	565	–	–
58	aiMa/aiMa/aiMa	86.6	51:0	849	aiMa/aiMa	579	–	–	–	–
59	M/S/S	86.7	50:0	835	S/S	607	M/S	551	–	–
60	Ma/Ma/P	86.8	50:0	835	Ma/Ma	579	Ma/P	565	–	–
61	brMa/S/O	87.0	53:1	875	S/O	605	brMa/S	593	brMa/O	591
62	Ma/S/O	87.8	53:1	875	S/O	605	Ma/S	593	Ma/O	591
63	P/brMa/S	88.0	51:0	849	brMa/P	565	brMa/S	593	P/S	579
64	Ma/Ma/Ma	88.2	51:0	849	Ma/Ma	579	–	–	–	–
65	Mo/S/S	88.3	53:1	875	S/S	607	Mo/S	591	–	–
66	P/Ma/S	88.9	51:0	849	Ma/P	565	Ma/S	593	P/S	579
67	O/S/S	89.6	54:1	889	S/O	605	S/S	607	–	–
68	P/S/S	93.6	52:0	863	S/P	579	S/S	607	–	–
69	brMa/S/S	96.2	53:0	877	S/S	607	brMa/S	593	–	–
70	Ma/S/S	97.1	53:0	877	S/S	607	Ma/S	593	–	–

ACN acyl carbon number, *n* number of double bond(s), RT^e experimental retention time (min)

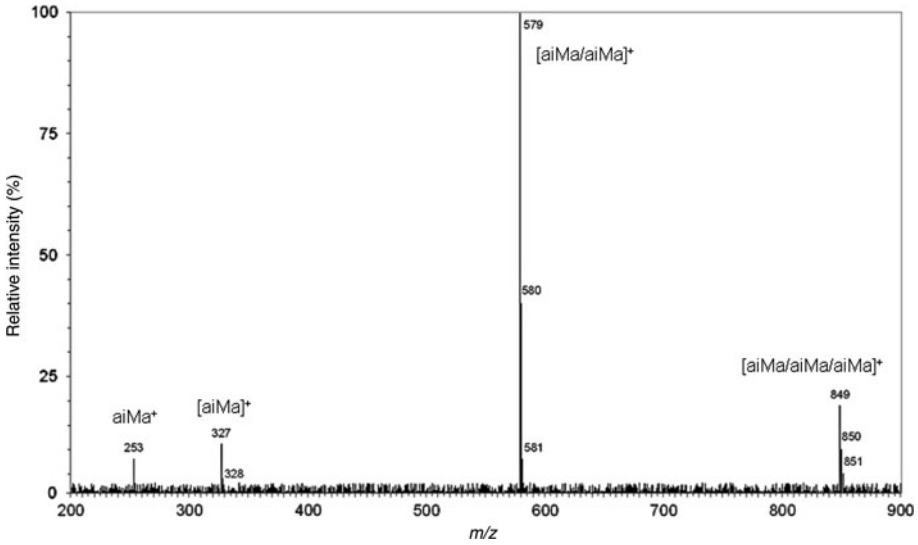

Fig. 4 Mass spectrum (APCI) of aiMa/aiMa/aiMa

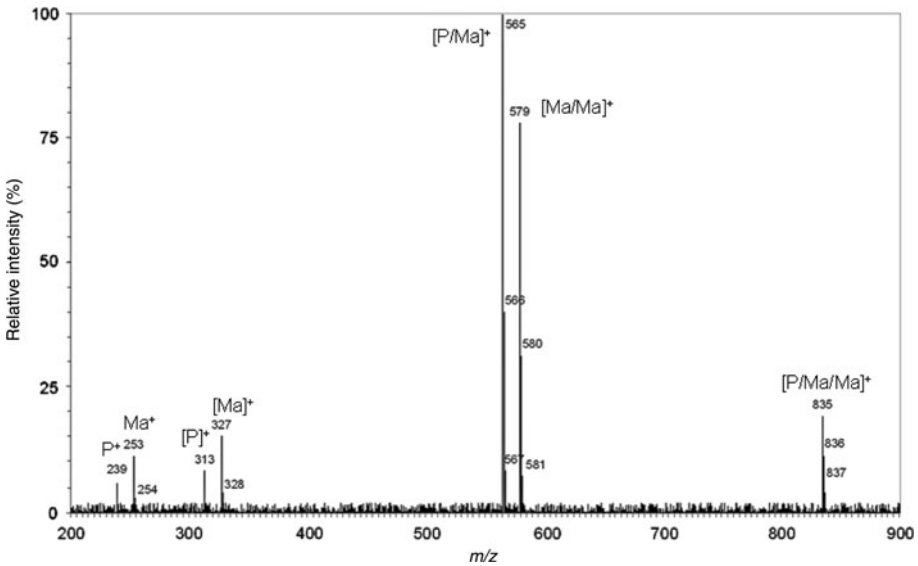

Fig. 5 Mass spectrum (APCI) of molecular species of TAG (i.e. P/Ma/Ma)

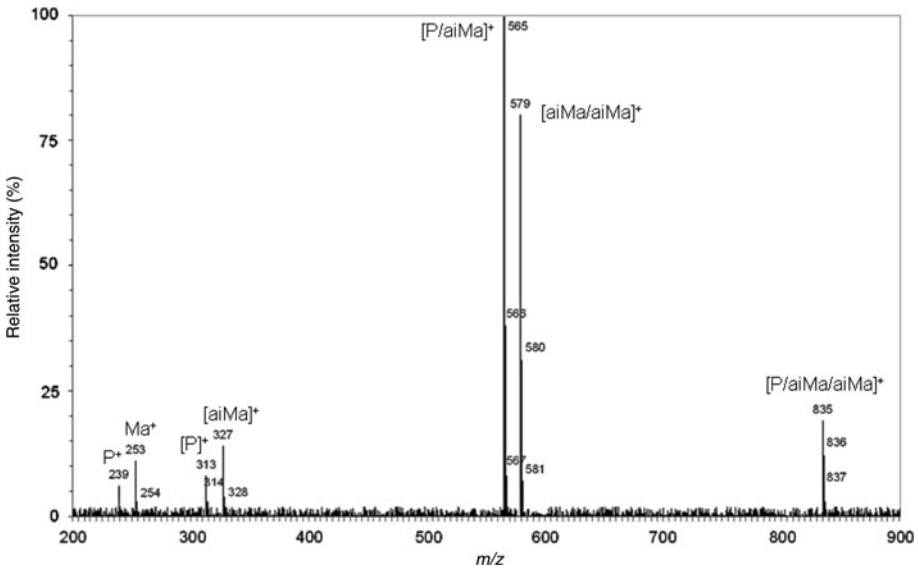

Fig. 6 Mass spectrum (APCI) of molecular species of TAG (i.e. P/aiMa/aiMa)

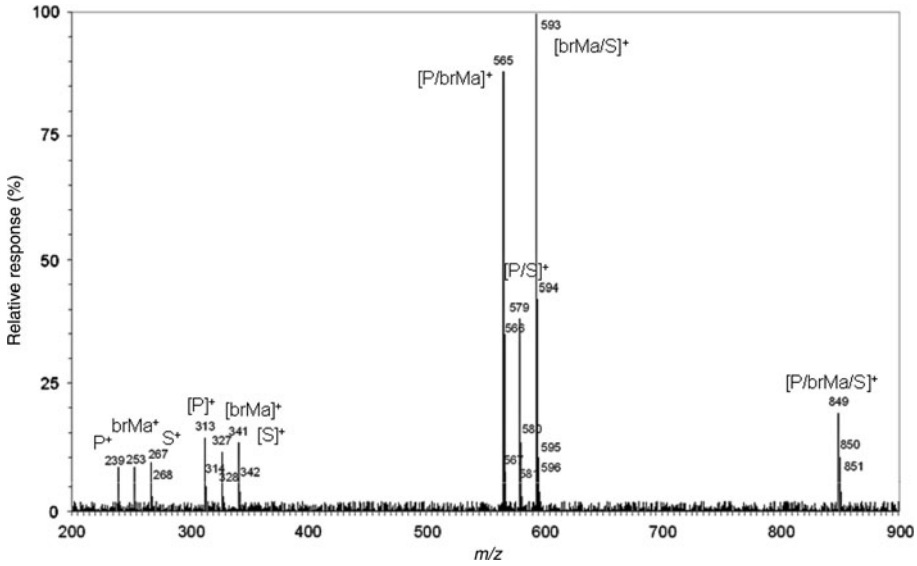

Fig. 7 Mass spectrum (APCI) of P/brMa/S, i.e. molecular species isolated from *Rhodococcus*

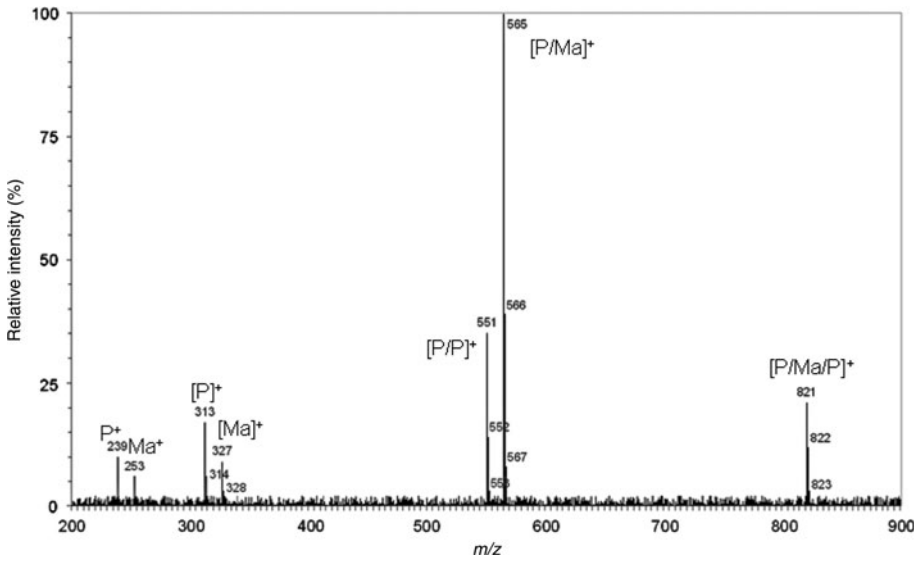

Fig. 8 Mass spectrum (APCI) of molecular species (i.e. P/Ma/P)

the TAG. A rule was formulated about the energetically less favorable loss of FA from position *sn*-2 and formation of $[M\text{-}RCOO]^+$ i.e. 1,3-$[DAG]^+$ ions. The cleavage of these bifunctional TAG gives rise to an isomeric pair of the same $[DAG]^+$ ions, i.e. $[AA]^+$ and $[AB]^+$. The ratio of $[AA]^+$:$[AB]^+$ was found to be lower for the ABA isomer, since formation of the 1,2-isomer of the $[AB]^+$ ion is energetically more favorable than generating the analogous 1,3-$[AB]^+$ ion from the AAB isomer. If these two fragments were energetically equivalent, then the intensity of ions $[AA]^+$ and $[AB]^+$ should be in a 1:2 ratio irrespective of the position of the A or B acyl substitution on the glycerol backbone, which does not occur—see, e.g. Figs. 8 and 9. The positional isomers understandably differed in the intensity of ions types $[P/P]^+$ and $[P/iMa]^+$ since the least abundant $[M\text{-}RCOO]^+$ ion is known to correspond to loss of the FA from the *sn*-2 position.

The $[P/P]^+$:$[P/Ma]^+$ ratio observed for P/Ma/P (Fig. 8) is only 35:100, indicating that the formation of the 1,3-$[PP]^+$ ion is energetically unfavorable. On the other hand, in P/P/iMa (Fig. 9) the $[P/P]^+$:$[P/iMa]^+$ ratio is 80:100 and the rule can thus be used to determine the structure of this positional isomer. This is in agreement with the result of the organic synthesis. Apart from determining the structure of natural compounds the rule can be used for confirming the structure of synthesized standards, since the synthesis may involve racemization or the original diacylglycerols need not contain only pure *sn*-1,2 or *sn*-1,3 positional isomer. Consequently, the two regioisomers show two different spectra.

To show that even a complex biological material such as *R. erythropolis* biomass can yield mass spectra that make it possible to identify TAG, we present in Figs. 10 and 11 the spectra of brM/brM/O and also brX/P/O. Identification of

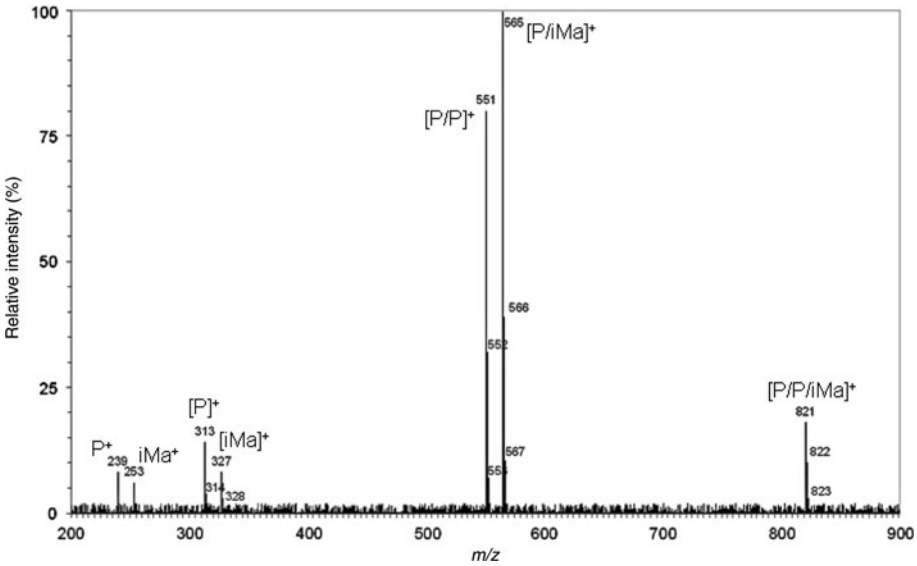

Fig. 9 Mass spectrum (APCI) of molecular species (i.e. P/P/iMa)

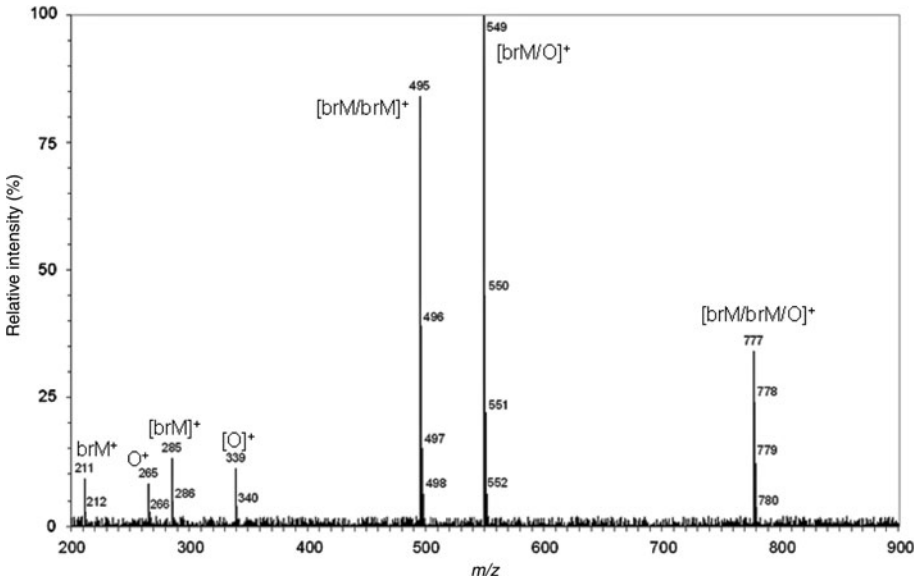

Fig. 10 Mass spectrum (APCI) of brM/brM/O, i.e. molecular species isolated from *Rhodococcus*

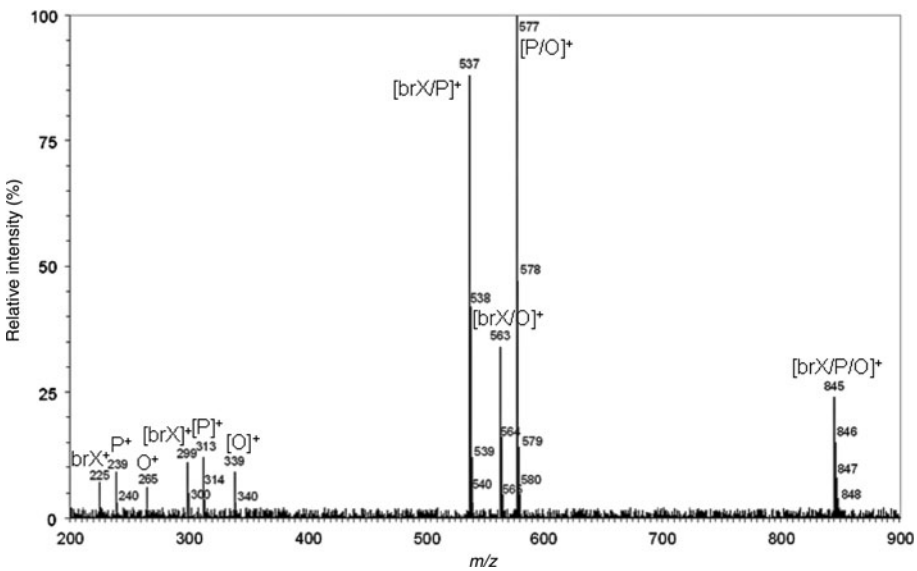

Fig. 11 Mass spectrum (APCI) of brX/P/O, i.e. molecular species isolated from *Rhodococcus*

these and other TAG was performed as described above and given in Table 3.

As expected, and in agreement with literature data, addition of Val and isobutyrate [10, 32] induced the biosynthesis of branched FA. No i- or ai-FA, neither odd- nor even-chain ones, were detected in control cultivation whereas the addition of any of the two precursors caused an increase of i-14:0 from 0 to 8.1% and a rise of i-16:0 from 0 to 18.1% (precursor Val). Precursor directed biosynthesis based on i-Bu showed comparable results, see Table 2. The overall proportion of even-i-FA increased to one quarter of total FA as compared to control (cultivation on succinate as the only carbon and energy source).

Apart from the increase in even-i-FA, an increased content was also noted with odd-straight-chain FA, i.e. 15:0 and 17:0. This is probably due to the fact that one of the possible products of Val (and also isobutyrate) catabolism is propionate, which serves as a starter unit of odd-straight-chain FA. Analogous effect, i.e. increased proportion of odd-straight-chain FA, was found in cultivations of other bacteria [10, 33].

Precursor directed biosynthesis of FA with the use of Leu or i-Va as starter units leads to an increase in odd-i-FA (i-15:0 to 14.8% with Leu and 14.2% with i-Va, i-17:0 to as much as 19.5% with Leu and 20.2% with i-Va). The proportion of these FA rose to 35% of total FA. These results are in agreement with the effect of both starter units described in the literature [12, 34].

The presence of Ile and 2-MeBu in the medium caused an expected increase [11] in ai-FA (ai-15:0 to 19.1% with Ile and 20.4% with 2-MeBu; ai-17:0 to 21.3% with Ile and 19.7% with 2-MeBu). These C-sources had the greatest effect on the FA composition, the content of ai-FA increasing to 40% of total FA.

Following the addition of given precursors, corresponding branched-chain monoenoic FA were identified in amounts of about 0.5% total FA. In contrast to straight-chain monoenoic FA only C17 and C18 branched-chain monoenoic FA were identified. This phenomenon can be explained in two ways. The first possibility is that the appropriate desaturase has a higher affinity for longer chains; this corresponds with the fact that no straight-chain monoenoic C14 and C15 FA were found. The other possibility is that the high melting point of straight-chain FA lowers the membrane fluidity to an extent that forces the bacterium to biosynthesize branched-chain monoenoic FA with a lower melting point in order to enhance membrane fluidity. The melting point of myristic acid je 54 °C, margaric (n-17:0) 61 °C, while that of ai-margaric (ai-17:0) is a mere 37 °C. Hence a change of branching from straight-chain to ai (e.g. C17 fatty acid) the melting point drops by 24 °C, whereas chain shortening of straight-chain from C17 to C14 (i.e. myristic acid) only by 17 °C. Melting point of (*Z*)-15-methyl-hexadec-12-enoic acid (i-17:1) is 21–22 °C. We therefore assume that fluidity change is affected much more by branching than the shortening of FA.

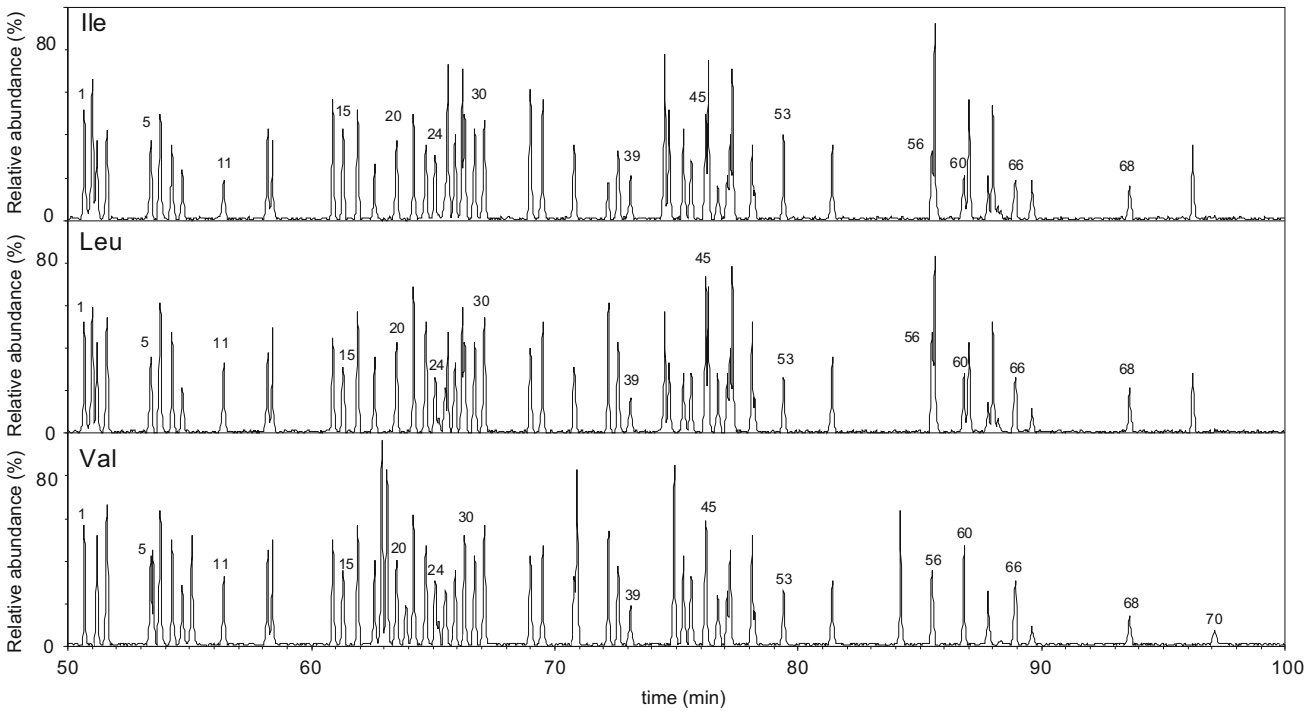

Fig. 12 RP-HPLC/APCI-MS chromatogram of the TAG from *R. erythropolis* cultivations at 30 °C with different carbon sources (Val, Leu, and Ile) as determined by RP-HPLC/MS-APCI

Cultivations in the presence of Leu and Ile and the corresponding short FA (i-Va and 2-MeBu) did not show any catabolism to acetate and propionate. Ile is known to be catabolized to acetate and propionate, Leu to acetoacetate and acetate [35]. In the former case we can assume that the starter units, i.e. acetate and propionate, have the same influence on the biosynthesis of even and odd FA and their contribution is thereby in fact eliminated (1 mol of Leu or i-Va gives rise to 1 mol of acetate and propionate and contributes thereby by the same molar amount to the biosynthesis of even and odd FA).

In the case of Ile (2-MeBu) only acetate and no propionate is formed. Because the proportion of even FA is major (more than 75% of total FA), an increase in the content of the precursor, i.e. acetate, has no further effect on the ratio of even and odd FA arising in the biosynthesis.

The results of the cultivation fully supported our assumption that *Rhodococcus* is eminently suitable for precursor directed biosynthesis of branched FA.

Chromatogram of TAG obtained after cultivation of *Rhodococcus* with three amino acids (Val, Leu and Ile) is shown in Fig. 12. Three pairs of mutually metabolically coupled precursors were used - Val and i-Bu, Leu and i-Va, Ile and 2-MeBu. The given amino acid gives rise to corresponding branched FA, which is then incorporated into the molecule of appropriate FA.

Table 4 gives mean (three independent sequential measurements) relative peak areas of 69 TAG from *Rhodococcus* determined in control cultivation on succinate and in individual cultivations using precursor directed biosynthesis with six starter units. It should be stressed that these values were calculated without using response factors, similarly as in our preceding paper in which we also analyzed unusual plant TAG [36]. None of the standards is commercially available and the 11 TAG that we synthesized represent a small fraction (<1/6) of the total possible TAG. Since the other standards are not available, the values are only semi-quantitative. This however does not prevent comparison of the outcomes of individual cultivations because these comparisons involve structurally similar TAG. An extrapolation of the response factors for TAG differing only in the branched chain (e.g. brMa/S/O and Ma/S/O) is unfortunately not feasible since we do not know the differences between straight- and branched chains. Despite this we attempted to quantify the results for Ma/Ma/Ma, iMa/iMa/iMa, and aiMa/aiMa/aiMa, see "Experimental". If a value of 1.00 is arbitrarily allotted to straight-chain TAG (Ma/Ma/Ma), the correction factor for *iso* TAG is 0.97 and for ai-TAG 0.99. In the case of a real sample, and also of several synthetic standards, we have failed to separate TAG differing only in branching (i.e. *iso* and *anteiso*).

Table 4 Relative quantities (%) of TAG identified in *R. erythropolis* cultivations at 30 °C with different carbon sources [succinate, Val, Leu, Ile, isobutyric (i-Bu), isovaleric (i-Va) and 2-methyl-butyric (2-MeBu) acid] as determined by RP-HPLC/MS-APCI

TAG	Succinate	Val	i-Bu	Leu	i-Va	Ile	2-MeBu
Po/Po/O	2.5	2.4	2.7	2.2	2.1	2.2	2.3
brX/Po/Po	–[a]	–	–	2.5	2.2	2.8	3.0
Po/Po/Mo	0.0	2.2	2.4	1.8	2.8	1.6	1.7
X/Po/Po	1.7	2.8	3.1	2.3	2.2	1.8	1.8
M/Po/O	2.0	1.8	1.9	1.5	2.4	1.6	1.7
brM/brM/O	–	1.9	1.2	–	–	–	–
Po/Po/P	2.1	2.7	3.0	2.6	3.4	2.1	2.1
M/Po/P	1.6	2.1	2.2	2.0	2.9	1.5	1.5
M/M/O	1.5	1.2	1.2	0.9	1.6	1.0	1.0
brM/brM/P	–	2.2	1.5	–	–	–	–
M/M/P	1.1	1.4	1.5	1.4	2.1	0.8	0.9
Po/Mo/O	0.8	1.9	2.0	1.6	2.3	1.8	1.8
Po/P/Mo	0.7	2.1	2.3	2.1	2.9	1.6	1.7
Po/O/O	3.8	2.1	2.3	1.9	2.7	2.4	2.4
M/O/O	3.3	1.5	1.5	1.3	1.9	1.8	1.8
Po/P/O	3.4	2.4	2.6	2.4	3.2	2.2	2.3
Po/Po/S	1.2	1.7	1.9	1.5	0.3	1.1	1.4
Po/brP/brP	–	4.1	2.9	–	–	–	–
M/brP/brP	–	3.5	2.1	–	–	–	–
M/P/O	2.9	1.7	1.8	1.8	2.1	1.6	1.6
brM/brM/S	–	0.8	0.4	–	–	–	–
Po/P/P	3.0	2.6	2.9	2.9	3.7	2.1	2.1
M/P/P	2.5	2.0	2.1	2.2	3.0	1.5	1.5
Mo/Mo/O	1.4	1.3	1.4	1.1	1.5	1.3	1.4
M/M/S	0.1	0.5	0.4	0.3	0.0	0.1	0.2
M/Po/S	0.7	1.1	1.2	0.9	0.0	0.7	0.8
brX/O/O	–	–	–	2.0	2.4	3.1	3.2
MoOO	3.2	1.5	1.6	1.4	1.9	1.7	1.9
brX/P/O	–	–	–	2.5	2.9	3.0	3.1
X/O/O	3.1	2.2	2.3	1.8	2.4	2.1	2.0
P/Mo/O	2.9	1.8	1.9	1.8	2.4	1.8	1.8
X/P/O	2.8	2.4	2.6	2.3	2.9	2.0	1.8
O/O/O	5.1	1.8	1.9	1.7	2.3	2.6	2.5
P/O/O	4.7	2.0	2.2	2.2	2.8	2.4	2.4
Po/S/O	2.5	1.4	1.5	1.3	0.4	1.5	1.5
brP/brP/O	–	3.5	2.5	–	–	–	–
P/P/O	4.3	2.3	2.5	2.6	3.3	2.3	2.2
Po/P/S	2.1	1.6	1.8	1.8	0.8	1.4	1.4
M/O/S	1.9	0.8	0.8	0.7	0.1	0.9	0.9
brMa/O/O	–	–	–	2.4	1.8	3.3	3.2
brX/O/S	–	–	–	1.4	0.0	2.2	2.4
brP/brP/P		3.6	2.8	–	–	–	–
Ma/O/O	3.4	1.8	1.8	1.2	1.1	1.8	1.8
X/O/S	0.0	1.4	1.5	1.2	0.8	1.2	1.1
P/P/P	3.9	2.5	2.8	3.1	3.8	2.1	2.1
P/brMa/O	–	–	–	2.9	2.4	3.2	3.0

Table 4 continued

TAG	Succinate	Val	i-Bu	Leu	i-Va	Ile	2-MeBu
M/P/S	1.6	1.0	1.1	1.2	0.4	0.7	0.7
P/Mo/S	0.0	1.1	1.2	1.2	0.2	0.9	0.9
P/Ma/O	3.0	1.9	2.1	1.7	2.4	1.7	1.6
P/P/brMa	–	–	–	3.3	2.9	3.0	2.9
P/P/Ma	–	2.2	2.4	2.2	2.9	1.5	1.5
Po/S/S	1.1	0.7	0.8	0.7	0.6	0.6	0.7
O/O/S	3.7	1.1	1.1	1.1	0.8	1.7	1.6
P/O/S	3.4	1.3	1.4	1.5	0.5	1.5	1.5
brP/brP/S	–	2.7	1.8	–	0.0	–	0.0
P/P/S	3.0	1.5	1.7	2.0	0.4	1.4	1.3
P/brMa/brMa	–	–	–	3.5	2.0	3.9	3.7
M/S/S	0.6	0.1	0.0	0.1	0.1	0.0	0.0
P/Ma/Ma	0.1	2.0	2.0	1.2	2.0	0.9	0.9
brMa/O/S	–	–	–	1.8	0.5	2.4	2.3
Ma/O/S	2.0	1.1	1.0	0.6	0.4	0.9	0.9
P/brMa/S	–	–	–	2.2	1.2	2.3	2.1
Ma/Ma/Ma	–	–	1.6	0.3	1.2	0.3	0.3
Mo/S/S	0.4	0.1	0.1	0.1	0.1	0.2	0.2
P/Ma/S	0.3	1.3	1.3	1.1	0.6	0.8	0.8
O/S/S	2.4	0.4	0.4	0.5	0.3	0.8	0.8
P/S/S	2.0	0.6	0.7	0.9	0.2	0.7	0.6
brMa/S/S	–	–	–	1.2	0.2	1.5	1.4
Ma/S/S	0.2	0.3	0.3	0.1	0.3	0.1	0.0

[a] Minority TAGs up to 0.1% of total TAGs were omitted

The two-sample paired *t* test revealed that a significant incorporation of precursors into the molecules of TAG appeared only in the pair Val and i-Bu (*P* value is 0.012). This value of the *t* test shows that at 5% significance level we reject the hypothesis of zero differences. The values for the other two pairs, i.e. Leu and i-Va and Ile and 2-MeBu, are different (*P* value is 0.154 and 0.453, respectively). This feature can be demonstrated in the ensuing pair of TAG, i.e. M/M/O and iM/iM/O. Precursors such as Val or i-Bu cannot give rise to ai-FA. Based on the *t* test we can thus infer that more Val was incorporated in branched TAG than i-Bu, because the ratio of Val:i-Bu incorporation in the former species was 1.2:1.2 while in branched TAG it was 1.9:1.2. Further confirmation of this fact is seen in Table 4. Another feature distinguishing the incorporation of Val (i-Bu) from that of the other two pairs (Leu/i-Va and Ile/2-MeBu) into the molecular species of TAG is the presence of only those molecular species that have two branched FA in the molecule, whereas with Leu and Ile (and the corresponding short-branched acids) the only identified molecular species of TAG were those having only one branched FA in the molecule. Based on the chromatographic behavior of the standards we synthesized we can confirm that the separation and identification of the molecular species of TAG potentially produced by *Rhodococcus* and differing in branched chain FA is feasible. The outcome of such analysis depends understandably on the detection limit, which was in our case 0.1% total TAG. We cannot exclude the possibility that under conditions different from those used in this study, e.g. in stress-inducing culture conditions or in biofilm, the proportions of individual TAG will change. The sum of branched TAG after precursor directed biosynthesis ranged from 21% for the compound with the lowest incorporation, i.e. i-Bu, to 33% for Ile. These data strongly imply that *Rhodococcus* is a good producer of branched chain FA and corresponding TAG and can be successfully used as a biotechnologically important microorganism producing these substances that have considerable pharmacological potential.

In conclusion, RP-HPLC/MS-APCI made it possible to identify and quantify TAG differing in a single branched-chain FA. Branched- and straight-chain-TAG were separated and identified while TAG differing only in *iso*- or *anteiso*-FA could not be separated since their APCI mass spectra were completely identical. Branched TAG having two branched FA in the molecule were successfully separated from straight-chain counterparts by gradient elution. TAG having a single branched FA were separated only if they differed in the site of branching. Positional isomers such as P/P/Ma and P/Ma/P or P/Ma/Ma and Ma/P/Ma were partially separated only with isocratic elution.

Acknowledgments This work was supported by the Institutional Research Concepts AV0Z50200510, projects MSM6046137305 and AROMAGEN—2B08062.

References

1. Waltermann M, Steinbuchel A (2005) Neutral lipid bodies in prokaryotes: recent insights into structure, formation, and relationship to eukaryotic lipid depots. J Bacteriol 187:3607–3619
2. Alvarez HM, Steinbuchel A (2002) Triacylglycerols in prokaryotic microorganisms. Appl Microbiol Biotechnol 60:367–376
3. Alvarez HM, Mayer F, Fabritius D, Steinbuchel A (1996) Formation of intracytoplasmic lipid inclusions by *Rhodococcus opacus* strain PD630. Arch Microbiol 165:377–386
4. Waltermann M, Luftmann H, Baumeister D, Kalscheuer R, Steinbuchel A (2000) *Rhodococcus opacus* strain PD630 as a new source of high-value single-cell oil? Isolation and characterization of triacylglycerols and other storage lipids. Microbiology 146:1143–1149
5. Hernandez MA, Mohn WW, Martinez E, Rost E, Alvarez AF, Alvarez HM (2008) Biosynthesis of storage compounds by *Rhodococcus jostii* RHA1 and global identification of genes involved in their metabolism. BMC Genomics 9:600
6. Alvarez HM, Luftmann H, Silva RA, Cesari AC, Viale A, Waltermann M, Steinbüchel A (2002) Identification of phenyldecanoic acid as a constituent of triacylglycerols and wax ester produced by *Rhodococcus opacus* PD630. Microbiology 148:1407–1412

7. Hamilton JTG, McRoberts WC, Larkin MJ, Harper DB (1995) Long-chain haloalkanes are incorporated into fatty acids by *Rhodococcus rhodochrous* NCIMB 13064. Microbiology 141:2611–2617
8. Alvarez HM, Kalscheuer R, Steinbuchel A (1997) Accumulation of storage lipids in species of *Rhodococcus* and *Nocardia* and effect of inhibitors and polyethylene glycol. Fett/Lipid 99:239–246
9. Bode HB, Dickschat JS, Kroppenstedt RM, Schulz S, Muller R (2005) Biosynthesis of *iso*-fatty acids in *Myxobacteria*: *iso*-even fatty acids are derived by alpha-oxidation from *iso*-odd fatty acids. J Am Chem Soc 127:532–533
10. Jovetic S, Feroggio M, Marinelli F, Lancini G (2008) Factors influencing cell fatty acid composition, A40926 antibiotic complex production in *Nonomuraea* sp. ATCC 39727. J Ind Microbiol Biotechnol 35:1131–1138
11. Dherbecourt J, Maillard MB, Catheline D, Thierry A (2008) Production of branched-chain aroma compounds by *Propionibacterium freudenreichii*: links with the biosynthesis of membrane fatty acids. J Appl Microbiol 105:977–985
12. Beck HC (2005) Branched-chain fatty acid biosynthesis in a branched-chain amino acid aminotransferase mutant of *Staphylococcus carnosus*. FEMS Microbiol Lett 243:37–44
13. Beck HC, Hansen AM, Lauritsen FR (2004) Catabolism of leucine to branched-chain fatty acids in *Staphylococcus xylosus*. J Appl Microbiol 96:1185–1193
14. Vlaeminck B, Fievez V, Cabrita ARJ, Fonseca AJM, Dewhurst RJ (2006) Factors affecting odd- and branched-chain fatty acids in milk: a review. Anim Feed Sci Technol 131:389–417
15. Parodi PW (2005) Dairy product consumption and the risk of breast cancer. J Am Coll Nutr 24:556S–568S
16. Wongtangtintharn S, Oku H, Iwasaki H, Toda T (2004) Effect of branched-chain fatty acids on fatty acid biosynthesis of human breast cancer cells. J Nutr Sci Vitaminol 50:137–143
17. Rezanka T, Schreiberova O, Krulikovska T, Masak J, Sigler K (2010) RP-HPLC/MS-APCI analysis of odd-chain TAG from *Rhodococcus erythropolis* including some regioisomers. Chem Phys Lipids 163:373–380
18. Metz PA, Omstead DR, Kaplan L, Liesch JM, Stearns RA, Vandenheuvel WJA (1988) Characterization of a lipid-rich fraction synthesized by *Streptomyces avermitilis*. J Chromatogr A 441:31–44
19. Myher JJ, Kuksis A, Marai L (1993) Identification of the less common isologous short-chain triacylglycerols in the most volatile 2.5% molecular distillate of butter oil. J Am Oil Chem Soc 70:1183–1191
20. Mottram HR, Evershed RP (2001) Elucidation of the composition of bovine milk fat triacylglycerols using high-performance liquid chromatography-atmospheric pressure chemical ionisation mass spectrometry. J Chromatogr A 926:239–253
21. Marai L, Kuksis A, Myher JJ (1994) Reversed-phase liquid chromatography-mass spectrometry of the uncommon triacylglycerol structures generated by randomization of butteroil. J Chromatogr A 672:87–99
22. Cejkova A, Masak J, Jirku V, Vesely M, Patek M, Nesvera J (2005) Potential of *Rhodococcus erythropolis* as a bioremediation organism. World J Microbiol Biotechnol 21:317–321
23. Rezanka T, Mares P (1987) Unusual and very long-chain fatty-acids produced by Basidiomycetes. J Chromatogr 409:390–395
24. Rezanka T (1990) Identification of very long polyenoic acids as picolinyl esters by Ag^{+} ion-exchange high-performance liquid chromatography, reversed-phase high-performance liquid chromatography. J Chromatogr 513:344–348
25. Ziegler FE, Berger GD (1979) A mild method for the esterification of fatty acids. Synth Commun 9:539–543
26. Lie Ken Jie MSF, Lam CC (1995) ^{1}H-Nuclear magnetic resonance spectroscopic studies of saturated, acetylenic and ethylenic triacylglycerols. Chem Phys Lipids 77:155–171
27. Momchilova S, Itabashi Y, Nikolova-Damyanova B, Kuksis A (2006) Regioselective separation of isomeric triacylglycerols by reversed-phase high-performance liquid chromatography: stationary phase and mobile phase effects. J Sep Sci 29:2578–2583
28. Dinh-Nguyen N (1968) Contribution to the study of mass spectrometry m. 3: use of methyl esters of normal long-chain fatty acids labelled with deuterium or C-13. Ark Kemi 28:289–362
29. Mottram HR (2005) Regiospecific analysis of triacylglycerols using high performance liquid chromatography/atmospheric pressure chemical ionization mass spectrometry. In: Byrdwell WC (ed) Modern methods for lipid analysis by liquid chromatography/mass spectrometry and related techniques, AOCS Press, Champaign
30. Byrdwell WC (2005) Qualitative and quantitative analysis of triacylglycerols by atmospheric pressure ionization (APCI & ESI) techniques. In: Byrdwell WC (ed) Modern methods for lipid analysis by liquid chromatography/mass spectrometry and related techniques. AOCS Press, Champaign
31. Fauconnot L, Hau J, Aeschlimann JM, Fay LB, Dionisi F (2004) Quantitative analysis of triacylglycerol regioisomers in fats and oils using reversed-phase high-performance liquid chromatography and atmospheric pressure chemical ionization mass spectrometry. Rapid Commun Mass Spectrom 18:218–224
32. Leskinen H, Suomela JP, Kallio H (2007) Quantification of triacylglycerol regioisomers in oils and fat using different mass spectrometric and liquid chromatographic methods. Rapid Commun Mass Spectrom 21:2361–2373
33. Dickschat JS, Bode HB, Kroppenstedt RM, Muller R, Schulz S (2005) Biosynthesis of *iso*-fatty acids in myxobacteria. Org Biomol Chem 2824–2831
34. Zhu K, Bayles DO, Xiong A, Jayaswal RK, Wilkinson BJ (2005) Precursor and temperature modulation of fatty acid composition and growth of *Listeria monocytogenes* cold-sensitive mutants with transposon-interrupted branched-chain α-keto acid dehydrogenase. Microbiology 151:615–623
35. Massey LK, Sokatch JR, Conrad RS (1976) Branched-chain amino-acid catabolism in bacteria. Bacteriol Rev 40:42–54
36. Lisa M, Holcapek M, Rezanka T, Kabatova N (2007) HPLC/APCI-MS and GC/FID characterization of 5-olefinic fatty acids in triacylglycerols from conifer seed oils. J Chromatogr 1146:67–77

Lipids (2010) 45:757–764
DOI 10.1007/s11745-010-3448-6

METHODS

Development of a Novel Sandwich ELISA for Measuring Cell Lysate ABCA1 Protein Levels

Jason S. Troutt · William E. Alborn · Melissa A. Bellinger · Karen L. Cox · Mariam E. Ehsani · Xiliang Wang · Yue-wei Qian · John H. Sloan · Mark B. Willey · Guoqing Cao · Robert J. Konrad

Received: 2 March 2010 / Accepted: 30 June 2010 / Published online: 17 July 2010

Abstract ATP-binding cassette transporter A-1 (ABCA1) mediates the transfer of cellular cholesterol to lipid-poor apolipoproteins. Liver X receptors (LXRs) are regulators of cholesterol homeostasis that increase transcription of ABCA1. Synthetic LXR agonists developed to date have been shown to induce ABCA1 mRNA expression and increase reverse cholesterol transport. Unfortunately, there have been few options for quantitatively measuring ABCA1 protein levels, including a previously described competitive ELISA standardized to an ABCA1 peptide with a sensitivity of 80 ng/ml. To address this unmet need, we developed a novel sandwich ELISA standardized to full-length human recombinant ABCA1 protein with sensitivity of approximately 0.5 ng/ml. To determine if the sandwich ELISA had adequate sensitivity to detect LXR-induced increases in ABCA1, we utilized it to measure ABCA1 levels in untreated and LXR agonist-treated human (THP-1) macrophage cells and human peripheral blood mononuclear cells (PBMC). Data obtained from the ELISA demonstrated an approximately eightfold increase in ABCA1 levels in both macrophages as well as PBMC in response to LXR agonist treatment, and results were highly correlated with those obtained by immunoprecipitation and western blotting. Together, these results suggest that the sandwich ELISA may be a sensitive and effective method for quantitating ABCA1 protein levels.

J. S. Troutt · W. E. Alborn · M. A. Bellinger · K. L. Cox · M. E. Ehsani · X. Wang · Y. Qian · J. H. Sloan · M. B. Willey · G. Cao · R. J. Konrad (✉)
Lilly Research Laboratories, Eli Lilly and Company, Indianapolis, IN 46285, USA
e-mail: konrad_robert@lilly.com

Keywords ABCA1 · HDL · Cholesterol · Reverse cholesterol transport · Liver X receptor · Macrophages

Abbreviations

ABCA1	ATP-binding cassette transporter A-1
ApoA1	Apolipoprotein A1
CPT	Cell preparation tube
DMSO	Dimethyl sulfoxide
ELISA	Enzyme-linked immunosorbent assay
HDL	High density lipoprotein
HDL-C	High density lipoprotein cholesterol
LXR	Liver X receptor
LDL	Low density lipoprotein
LDL-C	Low density lipoprotein cholesterol
PBMC	Peripheral blood mononuclear cells
PMA	Phorbol 12-myristate 13-acetate
PPAR	Peroxisome proliferator-activated receptor
RCT	Reverse cholesterol transport
TD	Tangier disease

Introduction

ABCA1-mediated active transport of cellular cholesterol and phospholipids to lipid poor apolipoprotein A1 (Apo-A1) produces high-density lipoproteins (HDL) and represents the initial and rate-limiting step in the reverse cholesterol transport (RCT) pathway [1–4]. Cellular cholesterol efflux and the RCT pathway ultimately lead to inhibition of atherosclerotic lesion formation [5]. Moreover, an inverse correlation exists between HDL levels and cardiovascular disease, and several efforts have identified HDL as being an

atheroprotective factor against coronary artery disease [6–9]. In light of these observations, many researchers have investigated ways to up-regulate RCT [10, 11]. As a result, ABCA1 has become a target for up-regulation.

ABCA1 is a 254 kDa integral membrane protein and is a member of a superfamily of ABC transporters that utilize ATP to transport substrates between cellular compartments and across cell membranes [3, 12]. The function of ABCA1 as a key regulator of HDL became apparent in 1999, when loss of ABCA1 gene function was determined to be the cause of Tangier disease (TD). Patients with TD exhibit extremely low levels of HDL, and have increased incidence of premature coronary artery disease [2, 13–15]. In recent years, several novel gene mutations and defects in the ABCA1 transporter have been characterized as resulting in TD [16–18].

ABCA1 expression is modulated by several metabolites including cAMP, sterols, and peroxisome proliferator-activated receptor agonists [4, 19]. Furthermore, the nuclear liver X receptors α and β (LXRs) are oxysterol activated cholesterol sensors that have been shown to play a key role in increasing serum HDL-C concentrations in mice [20–23]. Additionally, synthetic LXR agonists have been described as up-regulating ABCA1 mRNA and stimulating reverse cholesterol efflux [19, 24, 25].

Methods for measuring ABCA1 mRNA levels have thus been critical in understanding RCT [26]; however, the hydrophobic nature of ABCA1, a protein that contains 12 membrane spanning domains, has made it difficult to develop quantitative assays for ABCA1 protein levels. Recently Paul and colleagues described a competitive assay for measuring ABCA1 in cell lysates from human tissues and fibroblasts with a sensitivity of 80 ng/ml [27]. In order to better understand the effects of LXRs and related compounds on ABCA1 protein, an even more sensitive assay that can be used with different cellular matrices would be desirable. Recognizing the advantages that such an assay would provide, we set out to develop a sandwich ELISA to measure ABCA1 protein levels.

Experimental Procedures

Expression and Purification of Human ABCA1 Protein

Human ABCA1 (accession number: NM_005502) cDNA was purchased from Openbiosystem Co. (Cat# EHS1001-99865381, Clone ID: 9056784, accession number: BC146856). The cDNA contains one mutation based on accession number NM_005502 and the human genome sequence database. The mutation was corrected using PCR–based mutagenesis (Current Protocols in Molecular Biology). The corrected nucleotide sequences encoding full-length ABCA1 were inserted into pFastBac1 vector (Invitrogen) with a C-terminal Flag tag. P0 recombinant baculovirus was generated according to the Bac-to-Bac protocol (Invitrogen). P0 virus was amplified by infecting Sf9 cells (Invitrogen) with 0.1% volume of virus and harvesting 5 days post infection to generate P1 virus. For protein production, 500 ml of Sf9 cells per 2-L flask were infected at 1.5×10^6 cells/ml using 5 ml of P1 virus per flask. Infections were carried out at 27 °C and 135 rpm. Cells were spun down, rinsed with PBS and the pellets frozen at −80 °C. Flag-tagged ABCA1 was purified by anti-Flag M2 affinity chromatography from frozen cell pellets according to the manufacturer's instructions (Sigma).

Purified rABCA1-Flag protein was solubilized in buffer (50 mM Tris, pH 7.5, 150 mM NaCl, and 0.1% Triton X-100) and the final protein concentration was determined by Bradford using BSA as a standard. The identity of the purified protein was confirmed by western blotting, and the protein was stored at −80 °C in small aliquots prior to subsequent use. Purity of the recombinant ABCA1 protein was assessed by loading 250 ng of the protein onto a 4–20% tris–glycine polyacrylamide gel (Invitrogen). Molecular weight markers (SeeBlue, Invitrogen) were also loaded onto the gel for size comparison. One-dimensional electrophoresis was performed for 85 min at 175 V in a gel chamber containing tris–glycine SDS running buffer, and the gel was visualized following staining with Coomassie Blue.

ABCA1 Antibodies

Due to the hydrophobic nature of this 12-membrane spanning domain protein, a number of different approaches were taken to raise antibodies against the protein that could recognize both the recombinant and endogenous human ABCA1 protein in native phase. These approaches included attempting to raise rabbit polyclonal antibodies against six independent ABCA1 peptides. These rabbit polyclonal anti-peptide antibodies and a number of other antibodies including commercial antibodies were evaluated for their ability to recognize ABCA1 protein in native phase. To determine which antibodies might be suitable, more than a dozen different antibodies were evaluated for their ability to immunoprecipitate ABCA1 from control or TO901317-stimulated THP-1 cell lysates. Eventually, two antibodies were identified that were capable of immunoprecipitating ABCA1 and were compatible with each other in a sandwich ELISA format. The first was a monoclonal antibody that was raised against a C-terminal portion of the protein corresponding approximately to amino acids 1,800–2,250. The second was a polyclonal antibody raised against a mid-region of the protein corresponding approximately to amino acids 1100–1300. The exact epitopes of these

antibodies are not known at the present time, although the monoclonal antibody likely recognizes a linear epitope as it proved capable of detecting recombinant and endogenous ABCA1 protein via Western blotting as described below.

Macrophage Lysate Preparation

Human (THP-1) monocytes were differentiated with 20 nM PMA for 24 h, trypsinized, and seeded at 1.5×10^6 cells/well in RPMI 1640 (Hyclone) with 10% LPDS and 50 μM 2-mercapthoethanol (Sigma) in 96-well plates and incubated at 37 °C in 95% air:5% CO_2 for 6 h. Following attachment, cells were treated with 1 μM of Tularik LXR agonist TO901317 (purchased from Sigma) or 0.1% DMSO (vehicle) in the same media for 24 h. After treatment, media was removed, and the cells were washed once with PBS. Cells were then lysed with 25 μl/well of ice cold lysis buffer (50 mM HEPES, 150 mM NaCl, 5 mM EDTA, 5 mM EGTA, and 1.0% Triton X-100, pH 7.40 supplemented with Sigma phosphatase inhibitor cocktails I and II and Roche protease inhibitor cocktail). The plate was shaken at 900 rpm for 1 min, frozen at −20 °C, thawed, shaken again and the contents of the wells were collected and stored at −80 °C prior to subsequent analysis.

Peripheral Blood Mononuclear Cell Preparation

Whole blood was collected from four human donors directly into 8-ml sodium heparin cell preparation tubes (CPT). Immediately following collection, tubes were centrifuged for 25 min at 2,200 rpm in a large swinging bucket centrifuge (Jouan CR312). CPT plasma was transferred to fresh, siliconized borosilicate tubes in 5-ml aliquots for treatment. Aliquots from each donor were treated as follows: un-treated, 0.1% DMSO (vehicle), 1 μM LXR agonist TO901317, and 10 μM LXR agonist TO901317. The samples were incubated at 37 °C under an atmosphere of 95% air:5% CO_2 for 24 h. Following incubation, samples were spun 10 min at 1,500 rpm, and the supernatant (plasma) was drawn off. Peripheral blood mononuclear cells (PBMC) were washed three times with 500 μl of PBS. Cells were lysed with 500 μl of lysis buffer at 4 °C for 1 h, and PBMC lysates were transferred to polypropylene microfuge tubes and stored at −80 °C.

Immunoprecipitation of ABCA1

For THP-1 macrophages, immunoprecipitations (IP) were performed on 50 μl of lysate (4×10^6 cells/ml) added to 950 μl of lysis buffer. For PBMC, IP were performed on 400 μl of lysate (3×10^5 cells/ml) added to 1.6 ml of lysis buffer. ABCA1 protein was immunoprecipitated with 5 μg of anti-ABCA1 monoclonal antibody (raised against a C-terminal portion of the protein corresponding approximately to amino acids 1,800–2,250) covalently attached to 20 μl of Seize Primary covalent coupling beads (Pierce) by incubating antibody in phosphate buffer with aminolink resin and coupling beads according to the manufacturer's protocol. Following overnight incubation at 4 °C, beads were washed three times with lysis buffer, and 30 μl of 2X sample buffer (100 mM Tris, pH 6.80, 40 g/l SDS, 200 ml/l glycerol, 20 mg/l bromophenol blue, 0.05% 2-mercaptoethanol) were added to the beads. Samples were vortexed, boiled for 5 min, vortexed again and spun down. Each supernatant was then transferred to a fresh microfuge tube and stored at −20 °C prior to subsequent Western blotting.

Western Blotting

Samples, molecular weight markers (SeeBlue, Invitrogen), and controls were loaded onto a 4–20% tris–glycine polyacrylamide gel (Invitrogen) and electrophoresed for 85 min at 175 V in a gel chamber with tris–glycine SDS running buffer. Contents from the gel were then transferred to nitrocellulose (Amersham) by applying 100 V for 2 h at 4 °C. Blots were blocked with TBS-Casein blocking buffer for 1 h at room temperature. Following blocking, blots were washed three times with Tris buffered saline + Tween (TBST) and probed with monoclonal anti-ABCA1 antibody (1 μg/ml in blocking buffer) for 1 h at room temperature. Blots were washed three times with TBST and probed with an HRP-labeled goat anti-mouse IgG (diluted 1:2,500 in blocking buffer) for 1 h at room temperature. Blots were washed three times with TBST and once with TBS. Afterward, blots were developed with the chemiluminescent reagent Supersignal ECL substrate reagent (Thermo) for approximately 1 min, air-dried, and exposed to Kodak Bio-Max Light film for approximately 1–2 min.

ABCA1 ELISA

The 96-well polystyrene plates were coated overnight at 4 °C with 100 μl of 5 μg/ml polyclonal anti-ABCA1 antibody (diluted in Pierce carbonate-bicarbonate coating buffer, pH 9.0). The following day, wells were washed three times with TBST and blocked for 1 h with TBS-casein (Pierce). After washing again as above, 100 μl of recombinant ABCA1 standard curve aliquots (serial 1:2 dilutions ranging from 250 ng/ml to 0.25 ng/ml in lysis buffer + 1% BSA) and cell lysate samples were added to the appropriate wells. In the case of PBMC lysates, samples were run neat on the ELISA, while THP-1 lysates were run at a 1:10 dilution on the ELISA. The plate was allowed to incubate 2 h at room temperature. Following six washes with TBST, biotinylated monoclonal anti-ABCA1 antibody

(1 μg/ml, prepared using a Pierce EZ-link kit according to the manufacturer's protocol) was added to the plate at 100 μl/well, and allowed to incubate 1 h at room temperature. Following this incubation, the plate was again washed six times with TBST. Afterward, 100 μl of streptavidin-HRP (Jackson Labs) diluted 1:5,000 was added to each well. The plate was again incubated for 1 h, a final series of six washes was performed, and 100 μl of 3,3′, 5,5′-tetramethylbenzidene substrate (TMB, Pierce) was added to the wells and incubated at room temperature for 30 min. The development reaction was stopped with an equal volume addition of 2 N phosphoric acid, and plates were read on a Spectromax plate reader at 450 nm. ELISA dilution curves for the recombinant standards and samples were determined to be parallel, and the ELISA also demonstrated excellent dilutional linearity. The sensitivity of the assay (limit of the blank or mean plus 3 SD of the zero calibrator) was determined to be 0.5 ng/ml.

Data Analysis

SigmaPlot, version 8.0 was used for fitting of the calibration curves for the ABCA1 ELISA. Data were analyzed and plotted using the program FigP (Biosoft, St. Louis, MO). Statistical analysis was performed using the same program. A p value of less than 0.05 was considered to indicate statistical significance.

Results

The first step toward development of our novel sandwich ABCA1 ELISA consisted of production of recombinant full-length ABCA1 protein (rABCA1). The resulting recombinant protein was a C-terminal, flag-tagged, baculovirus-generated full-length rABCA1. Purity of the rABCA1 protein was assessed by one-dimensional gel electrophoresis followed by Coomassie blue staining (Fig. 1a), which indicated that the protein migrated as a predominate 250 kDa band. Based on the results shown in Fig. 1a, the recombinant protein was judged to be approximately 90% pure. The identity of the protein was subsequently confirmed by Western blotting (Fig. 1b).

Following expression and characterization of rABCA1, multiple antibodies were evaluated by immunoprecipitating ABCA1. To determine which antibodies might be suitable, more than a dozen different antibodies were evaluated for their ability to immunoprecipitate ABCA1 from control or TO901317-stimulated THP-1 cell lysates. As Fig. 2a demonstrates, many of these antibodies (including Abcam 7360 and Novus NB 400) failed to efficiently immunoprecipitate ABCA1 in native phase, and this was not unexpected considering the hydrophobic

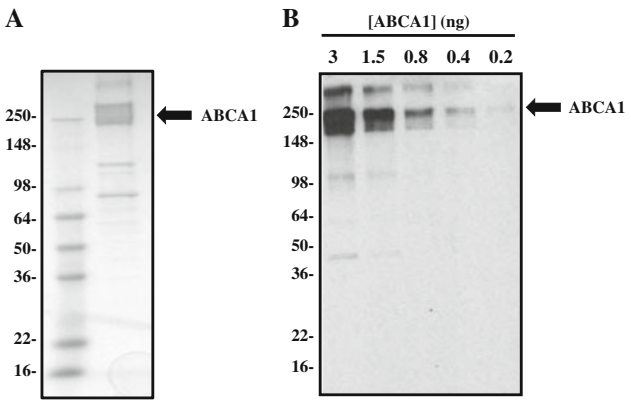

Fig. 1 Characterization of full length human recombinant ABCA1 protein. **a** Recombinant ABCA1 protein (250 ng) prepared as described in the Methods was analyzed by SDS-PAGE followed by Coomassie blue staining to assess purity of the protein. Recombinant ABCA1 protein migrated as a predominate band with a molecular weight of approximately 250 kDa, consistent with both the predicted molecular weight of the protein and the observed size of endogenous ABCA1 from THP-1 cells and PBMC. **b** In order to further confirm the identity of the recombinant ABCA1 protein, multiple dilutions of recombinant ABCA1 protein were analyzed by Western blotting with monoclonal anti-ABCA1 antibody. Western blotting analysis demonstrated an immunoreactive band at 250 kDa, consistent with the migration of the protein as described in **a**

nature of the 12 membrane-spanning domain protein. Two antibodies were eventually identified that were capable of binding the protein in native phase. The two antibodies were tested with each other in a sandwich ELISA format and were found to be compatible with each other with the optimal orientation determined to be polyclonal capture antibody (raised against a mid-region of the protein corresponding approximately to amino acids 1,100–1,300) and monoclonal conjugate antibody (raised against a C-terminal portion of the protein corresponding approximately to amino acids 1,800–2,250).

The resulting ELISA thus incorporated a polyclonal capture antibody that is paired with a biotinylated monoclonal detection antibody, which is subsequently detected with streptavidin-HRP. To prepare a suitable standard curve for the assay, recombinant protein was first diluted to a concentration of 250 ng/ml and then subsequently serially diluted 1:2 to establish a 12-point standard curve. Figure 2b shows a representative standard curve from the final version of the sandwich ELISA.

Once the ABCA1 sandwich ELISA was developed, we examined the effect of a well known LXR agonist (TO901317) on human THP-1 macrophage expression of ABCA1 protein. In order to do this, human-THP-1 macrophages were differentiated and treated with 1 μM LXR agonist TO901317 or 0.1% DMSO (vehicle control), and incubated for 24 or 48 h. Following cell lysis, the resulting lysates were analyzed using the ELISA as well as by

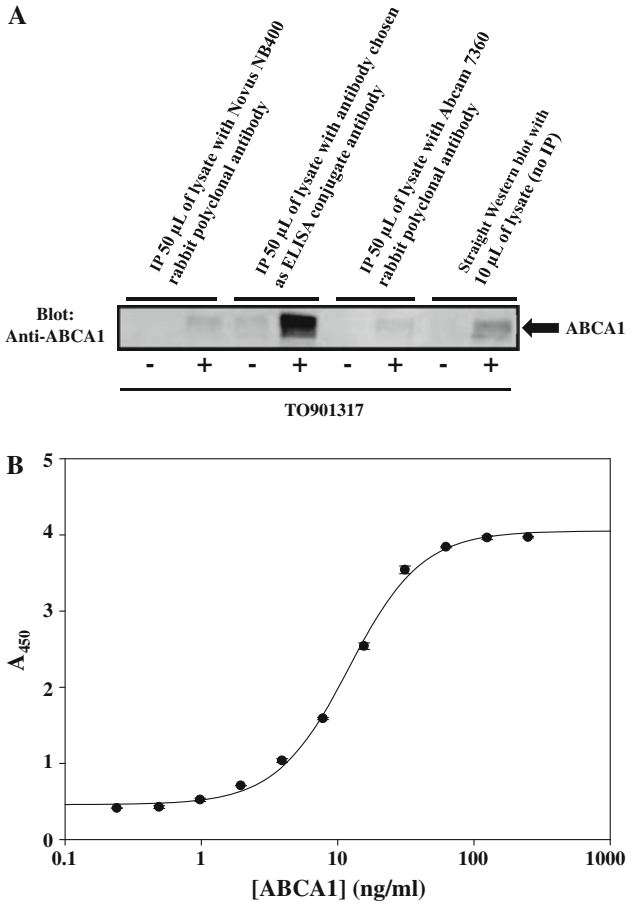

Fig. 2 Development of ABCA1 sandwich ELISA. **a** To determine suitable antibodies for a sandwich ELISA, more than a dozen different antibodies were evaluated for their ability to immunoprecipitate ABCA1 from control or TO901317-stimulated THP1 cell lysates. Most antibodies such as Novus NB400 or Abcam 7360 were not able to efficiently immunoprecipitate ABCA1. In contrast, the antibody eventually chosen as one of the antibodies for the sandwich ELISA very effectively immunoprecipitated ABCA1. Results are representative of those obtained from screening more than a dozen different anti-ABCA1 antibodies. **b** Following screening of antibodies as described in **a**, an ABCA1 sandwich ELISA was developed using a polyclonal capture antibody and monoclonal conjugate antibody. The optimal orientation of antibodies was determined to consist of a polyclonal capture antibody and conjugate, biotinylated monoclonal antibody. A recombinant ABCA1 standard curve was established by starting at a concentration of 250 ng/ml followed by serial 1:2 dilutions down to 0.25 ng/ml. The resulting ELISA standard curve provided a suitable dynamic range for quantitation of ABCA1 protein, with an approximate sensitivity of 0.5 ng/ml

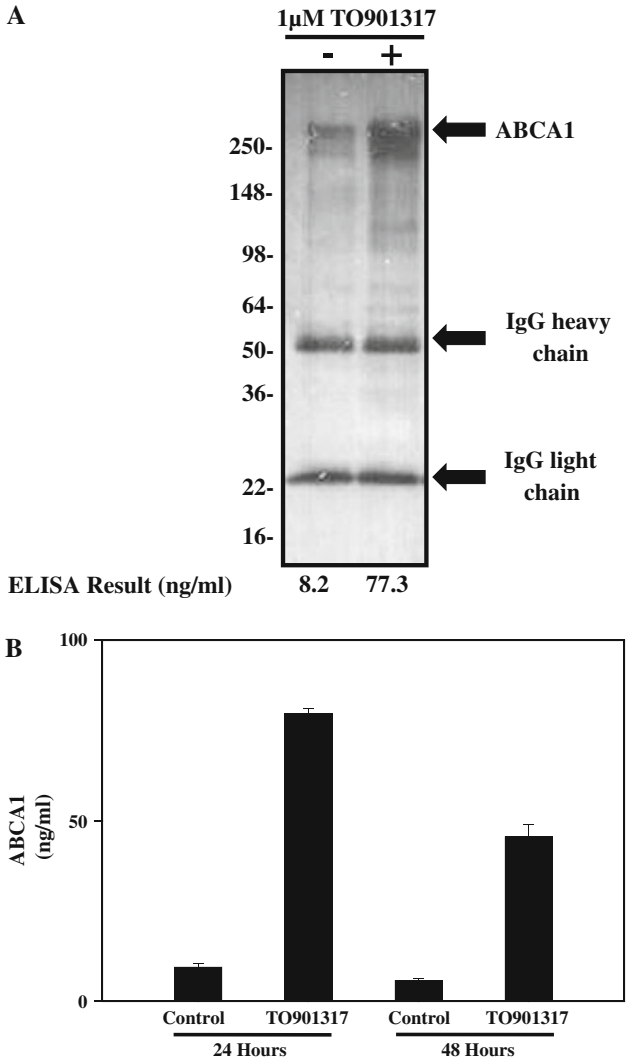

Fig. 3 Liver X receptor (LXR) agonist-induced increases in ABCA1 protein levels in THP-1 human macrophages. **a** Human THP-1 macrophage cells were treated with 1 µM of the LXR agonist TO901317 for 24 h. Following processing, cell lysates were analyzed by immunoprecipitation and Western blotting. Results are representative of two independent experiments. **b** LXR agonist-induced increases in THP-1 macrophage cell ABCA1 protein at 24 and 48 h were quantitated using the ABCA1 sandwich ELISA described in Fig. 2. Results are shown as the mean ± SEM for triplicate determinations

immunoprecipitation and Western blotting. Figure 3 shows the results from these experiments in which TO901317 caused a dramatic increase in ABCA1 protein expression in the THP-1 cells.

THP-1 lysates were analyzed using our novel sandwich ABCA1 ELISA, and the results were compared to those obtained using immunoprecipitation and Western blotting. Figure 3a shows the immunoprecipitation and Western blotting results. Figure 3b shows the ELISA results, which quantitated the LXR agonist up-regulation of ABCA1. As Fig. 3b demonstrates, TO901317 caused a significant increase in THP-1 ABCA1 protein expression at both 24 and 48 h compared to vehicle control. After 24 h, vehicle-treated THP-1 lysates contained 9.6 ± 0.7 ng/ml of ABCA1 protein while TO901317-treated lysates contained 79.7 ± 1.4 ng/ml of ABCA1 protein ($p < 0.001$ vs. control). After 48 h, vehicle-treated THP-1 lysates contained 5.8 ± 0.4 ng/ml of ABCA1 protein while TO901317-treated lysates contained

45.6 ± 3.4 ng/ml of ABCA1 protein ($p = 0.005$ vs. control).

To investigate the possibility that our novel sandwich ABCA1 ELISA might have relevance as a clinical biomarker for LXR agonists, PBMC were harvested from human donors and incubated with 1 or 10 μM TO901317 or 0.1% DMSO (vehicle control) for 24 h. Following cell lysis, the resulting PBMC lysates were analyzed by ELISA as well as by immunoprecipitation and Western blotting. Figure 4a shows the immunoprecipitation and Western blotting results from these experiments in which TO901317 caused a marked increase in ABCA1 protein expression in the human PBMC.

Similar to the THP-1 lysates, PBMC lysates were also analyzed using our novel sandwich ABCA1 ELISA, and the results were compared to those obtained in Fig. 4a using immunoprecipitation and Western blotting. Figure 4b shows the results of this series of experiments, in which the use of the sandwich ELISA quantitated LXR agonist up-regulation of ABCA1 in human PBMC. As Fig. 4b demonstrates, TO901317 caused a significant increase in THP-1 ABCA1 protein expression in human PBMC at 24 h compared to vehicle control. After 24 h, untreated and vehicle-treated human PBMC lysates contained less than 0.5 ng/ml of ABCA1 protein while 1 μM TO901317-treated human PBMC lysates contained 3.2 ± 0.3 ng/ml of ABCA1 protein ($p = 0.002$ vs. control) and 10 μM TO901317-treated human PBMC lysates contained 4.6 ± 0.6 ng/ml of ABCA1 protein ($p = 0.008$ vs. control).

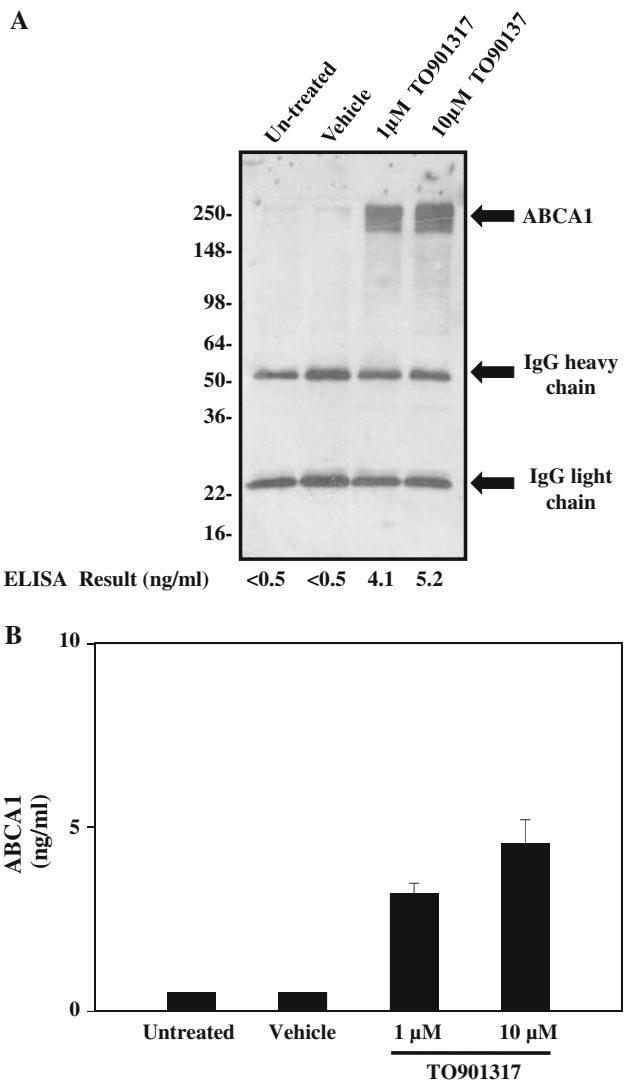

Fig. 4 A Liver X receptor (LXR) agonist increases ABCA1 protein levels in human PBMC. **a** Human PBMC were treated with 1 and 10 μM of the LXR agonist TO901317 for 24 h. Following processing, PBMC lysates were analyzed by immunoprecipitation and Western blotting. Results are representative of those observed from four different human blood donors. **b** LXR agonist-induced increases in human PBMC at 24 h were quantitated using the ABCA1 sandwich ELISA described in Fig. 2. Results are shown as the mean ± SEM for quadruplicate determinations

Discussion

The critical role of ABCA1 in cholesterol efflux and RCT makes it an attractive target for therapeutic development on several fronts. As a result, there has been a need for a sensitive method for quantifying ABCA1 at the protein level. This has been made difficult due to the fact that ABCA1 is a membrane protein containing 12 membrane-spanning domains. Paul and colleagues recently described a competitive ELISA that was standardized to an ABCA1 peptide and had a reported sensitivity of 80 ng/ml [27]. In the current study, we describe a sandwich ELISA standardized to full-length recombinant ABCA1 protein with a sensitivity of approximately 0.5 ng/ml.

This estimation of sensitivity of the ELISA, however, must be interpreted with some caution due to the fact that the recombinant protein used to standardize the assay was not 100% pure, but was only approximately 90% pure as judged by Coomassie blue staining. As a result, the true sensitivity of the assay may not be 0.5 ng/ml. In addition, it is possible that the assay may recognize authentic cellular ABCA1 protein differently than recombinant ABCA1 protein. This too could mean that the actual sensitivity of the assay for endogenous analyte may not be 0.5 ng/ml. It also cannot be ruled out that the assay may have cross-reactivity for other cellular protein components, which could also alter the estimate of true sensitivity of the assay. Nor can it be ruled out that there may be some cellular fraction of ABCA1 protein (perhaps up to 10%) that is not measured by the assay. Therefore, while the ELISA can be used to measure relative changes in ABCA1 protein expression levels such as those that occur in THP-1 cells and PBMC following LXR agonist stimulation, absolute

protein levels measured by the assay must be interpreted in the proper context.

Macrophage LXRs play a major role in the inhibition of atherosclerosis via direct regulation of ABCA1 gene expression [28, 29]. Therefore, THP-1 macrophage cells provide a relevant model for screening LXR agonists, and additional non-LXR compounds that may target up-regulation of RCT by increasing ABCA1. In this study, we used our novel ABCA1 sandwich ELISA to examine the effect of a well-known LXR agonist, TO901317, on THP-1 macrophage ABCA1 protein expression. Our ELISA demonstrated that TO901317 induced an approximate eightfold increase in ABCA1 protein levels. The dramatic increases observed help indicate that the sandwich ELISA may be a reliable method to measure the efficacy of LXR agonists.

We also isolated and treated human PBMC with TO901317 to determine if a similar LXR-induced increase in ABCA1 could be measured. Similar to what was observed for the THP-1 cells, the resulting data again demonstrated an approximate eightfold increase induced by the LXR agonist. Together, these data are consistent with the known up-regulation of ABCA1 mRNA and protein (as assessed by Western blotting) following LXR agonist treatment [24, 30, 31], indicating that our ELISA is capable of quantitating LXR agonist-induced increase in ABCA1 in human PBMC.

While statins are currently the most effective lipid lowering agents for at risk hyperlipidemic patients, there remains a significant portion of affected patients who are either not able to tolerate statins, or for whom statin treatment does not result in a desired reduction of LDL-C levels. Furthermore, there are data that suggest statins actually down-regulate ABCA1 gene expression in macrophages by inhibiting the synthesis of an oxysterol ligand for LXR [32, 33]. Such findings imply that treatments targeting the up-regulation of ABCA1 could be beneficial in enhanced lipid lowering for patients already being treated with statins. As cardiovascular disease remains the leading cause of morbidity and mortality in developed countries, several approaches are being taken to capitalize on the atheroprotective benefits of increasing RCT. Therefore, our novel sandwich ELISA described in this study, which provides a sensitive method to quantitatively measure ABCA1 protein levels, may have utility for the development of compounds designed to increase ABCA1 protein expression and reverse cholesterol transport.

References

1. Attie AD, Kastelein JP, Hayden MR (2001) Pivotal role of ABCA1 in reverse cholesterol transport influencing HDL levels and susceptibility to atherosclerosis. J Lipid Res 42:1717–1726
2. Oram JF (2000) Tangier disease and ABCA1. Biochim Biophys Acta 1529:321–330
3. Oram JF, Lawn RM (2001) ABCA1. The gatekeeper for eliminating excess tissue cholesterol. J Lipid Res 42:1173–1179
4. Santamarina-Fojo S, Remaley AT, Neufeld EB, Brewer HB (2001) Regulation and intracellular trafficking of the ABCA1 transporter. J Lipid Res 42:1339–1345
5. Spady DK (1999) Reverse cholesterol transport and atherosclerosis regression. Circulation 100:576–578
6. Assmann G, Gotto AM (2004) HDL cholesterol and protective factors in atherosclerosis. Circulation 109:III8–III14
7. Gordon T, Castelli WP, Hjortland MC, Kannel WB, Dawber TR (1977) High density lipoprotein as a protective factor against coronary heart disease. The Framingham Study. Am J Med 62:707–714
8. Kwiterovich PO (1998) The antiatherogenic role of high-density lipoprotein cholesterol. Am J Cardiol 82:13Q–21Q
9. Troutt JS, Alborn WE, Mosior MK, Dai J, Murphy AT, Beyer TP, Zhang Y, Cao G, Konrad RJ (2008) An apolipoprotein A-I mimetic dose-dependently increases the formation of prebeta1 HDL in human plasma. J Lipid Res 49:581–587
10. Brewer HB, Remaley AT, Neufeld EB, Basso F, Joyce C (2004) Regulation of plasma high-density lipoprotein levels by the ABCA1 transporter and the emerging role of high-density lipoprotein in the treatment of cardiovascular disease. Arterioscler Thromb Vasc Biol 24:1755–1760
11. Forrester JS, Shah PK (2006) Emerging strategies for increasing high-density lipoprotein. Am J Cardiol 98:1542–1549
12. Dean M, Hamon Y, Chimini G (2001) The human ATP-binding cassette (ABC) transporter superfamily. J Lipid Res 42:1007–1017
13. Bodzioch M, Orso E, Klucken J, Langmann T, Bottcher A, Diederich W, Drobnik W, Barlage S, Buchler C, Porsch-Ozcurumez M, Kaminski WE, Hahmann HW, Oette K, Rothe G, Aslanidis C, Lackner KJ, Schmitz G (1999) The gene encoding ATP-binding cassette transporter 1 is mutated in Tangier disease. Nat Genet 22:347–351
14. Brooks-Wilson A, Marcil M, Clee SM, Zhang LH, Roomp K, van Dam M, Yu L, Brewer C, Collins JA, Molhuizen HO, Loubser O, Ouelette BF, Fichter K, Ashbourne-Excoffon KJ, Sensen CW, Scherer S, Mott S, Denis M, Martindale D, Frohlich J, Morgan K, Koop B, Pimstone S, Kastelein JJ, Genest J, Hayden MR (1999) Mutations in ABC1 in Tangier disease and familial high-density lipoprotein deficiency. Nat Genet 22:336–345
15. Rust S, Rosier M, Funke H, Real J, Amoura Z, Piette JC, Deleuze JF, Brewer HB, Duverger N, Denefle P, Assmann G (1999) Tangier disease is caused by mutations in the gene encoding ATP-binding cassette transporter 1. Nat Genet 22:352–355
16. Maekaw M, Kikuchi J, Kotani K, Nagao K, Odgerel T, Ueda K, Kawano M, Furukawa Y, Sakurabayashi I (2009) A novel missense mutation of ABCA1 in transmembrane alpha-helix in a Japanese patient with Tangier disease. Atherosclerosis 206:216–222
17. Pisciotta L, Bocchi L, Candini C, Sallo R, Zanotti I, Fasano T, Chakrapani A, Bates T, Bonardi R, Cantafora A, Ball S, Watts G, Bernini F, Calandra S, Bertolini S (2009) Severe HDL deficiency due to novel defects in the ABCA1 transporter. J Intern Med 265:359–372
18. Schippling S, Orth M, Beisiegel U, Rosenkranz T, Vogel P, Munchau A, Hagel C, Seedorf U (2008) Severe Tangier disease with a novel ABCA1 gene mutation. Neurology 71:1454–1455
19. Langmann T, Klucken J, Reil M, Liebisch G, Luciani MF, Chimini G, Kaminski WE, Schmitz G (1999) Molecular cloning of the human ATP-binding cassette transporter 1 (hABC1): evidence for sterol-dependent regulation in macrophages. Biochem Biophys Res Commun 257:29–33

20. Schultz JR, Tu H, Luk A, Repa JJ, Medina JC, Li L, Schwendner S, Wang S, Thoolen M, Mangelsdorf DJ, Lustig KD, Shan B (2000) Role of LXRs in control of lipogenesis. Genes Dev 14:2831–2838
21. Schwartz K, Lawn RM, Wade DP (2000) ABC1 gene expression and ApoA-I-mediated cholesterol efflux are regulated by LXR. Biochem Biophys Res Commun 274:794–802
22. Venkateswaran A, Laffitte BA, Joseph SB, Mak PA, Wilpitz DC, Edwards PA, Tontonoz P (2000) Control of cellular cholesterol efflux by the nuclear oxysterol receptor LXR alpha. Proc Natl Acad Sci USA 97:12097–12102
23. Cao G, Beyer TP, Yang XP, Schmidt RJ, Zhang Y, Bensch WR, Kauffman RF, Gao H, Ryan TP, Liang Y, Eacho PI, Jiang XC (2002) Phospholipid transfer protein is regulated by liver X receptors in vivo. J Biol Chem 277:39561–39565
24. Sparrow CP, Baffic J, Lam MH, Lund EG, Adams AD, Fu X, Hayes N, Jones AB, Macnaul KL, Ondeyka J, Singh S, Wang J, Zhou G, Moller DE, Wright SD, Menke JG (2002) A potent synthetic LXR agonist is more effective than cholesterol loading at inducing ABCA1 mRNA and stimulating cholesterol efflux. J Biol Chem 277:10021–10027
25. Hozoji M, Munehira Y, Ikeda Y, Makishima M, Matsuo M, Kioka N, Ueda K (2008) Direct interaction of nuclear liver X receptor-beta with ABCA1 modulates cholesterol efflux. J Biol Chem 283:30057–30063
26. Kielar D, Dietmaier W, Langmann T, Aslanidis C, Probst M, Naruszewicz M, Schmitz G (2001) Rapid quantification of human ABCA1 mRNA in various cell types and tissues by real-time reverse transcription-PCR. Clin Chem 47:2089–2097
27. Paul V, Meyer HH, Leidl K, Soumian S, Albrecht C (2008) A novel enzyme immunoassay specific for ABCA1 protein quantification in human tissues and cells. J Lipid Res 49:2259–2267
28. Larrede S, Quinn CM, Jessup W, Frisdal E, Olivier M, Hsieh V, Kim MJ, Van Eck M, Couvert P, Carrie A, Giral P, Chapman MJ, Guerin M, Le Goff W (2009) Stimulation of cholesterol efflux by LXR agonists in cholesterol-loaded human macrophages is ABCA1-dependent but ABCG1-independent. Arterioscler Thromb Vasc Biol 29:1930–1936
29. Levin N, Bischoff ED, Daige CL, Thomas D, Vu CT, Heyman RA, Tangirala RK, Schulman IG (2005) Macrophage liver X receptor is required for antiatherogenic activity of LXR agonists. Arterioscler Thromb Vasc Biol 25:135–142
30. DiBlasio-Smith EA, Arai M, Quinet EM, Evans MJ, Kornaga T, Basso MD, Chen L, Feingold I, Halpern AR, Liu QY, Nambi P, Savio D, Wang S, Mounts WM, Isler JA, Slager AM, Burczynski ME, Dorner AJ, LaVallie ER (2008) Discovery and implementation of transcriptional biomarkers of synthetic LXR agonists in peripheral blood cells. J Transl Med 6:59
31. Katz A, Udata C, Ott E, Hickey L, Burczynski ME, Burghart P, Vesterqvist O, Meng X (2009) Safety, pharmacokinetics, and pharmacodynamics of single doses of LXR-623, a novel liver X-receptor agonist, in healthy participants. J Clin Pharmacol 49:643–649
32. Sone H, Shimano H, Shu M, Nakakuki M, Takahashi A, Sakai M, Sakamoto Y, Yokoo T, Matsuzaka K, Okazaki H, Nakagawa Y, Iida KT, Suzuki H, Toyoshima H, Horiuchi S, Yamada N (2004) Statins downregulate ATP-binding-cassette transporter A1 gene expression in macrophages. Biochem Biophys Res Commun 316:790–794
33. Wong J, Quinn CM, Brown AJ (2004) Statins inhibit synthesis of an oxysterol ligand for the liver x receptor in human macrophages with consequences for cholesterol flux. Arterioscler Thromb Vasc Biol 24:2365–2371

Lipids (2010) 45:765–775
DOI 10.1007/s11745-010-3463-7

ORIGINAL ARTICLE

A High Legume Low Glycemic Index Diet Improves Serum Lipid Profiles in Men

Zhiying Zhang · Elaine Lanza · Penny M. Kris-Etherton · Nancy H. Colburn · Deborah Bagshaw · Michael J. Rovine · Jan S. Ulbrecht · Gerd Bobe · Robert S. Chapkin · Terryl J. Hartman

Received: 21 May 2010 / Accepted: 5 August 2010 / Published online: 24 August 2010

Abstract Clinical studies have shown that fiber consumption facilitates weight loss and improves lipid profiles; however, the beneficial effects of high fermentable fiber low glycemic index (GI) diets under conditions of weight maintenance are unclear. In the Legume Inflammation Feeding Experiment, a randomized controlled cross-over feeding study, 64 middle-aged men who had undergone colonoscopies within the previous 2 years received both a healthy American (HA) diet (no legume consumption, fiber consumption = 9 g/1,000 kcal, and GI = 69) and a legume enriched (1.5 servings/1,000 kcal), high fiber (21 g/1,000 kcal), low GI (GI = 38) diet (LG) in random order. Diets were isocaloric and controlled for macronutrients including saturated fat; they were consumed each for 4 weeks with a 2–4 week break separating dietary treatments. Compared to the HA diet, the LG diet led to greater declines in both fasting serum total cholesterol (TC) and low density lipoprotein cholesterol (LDL-C) ($P < 0.001$ and $P < 0.01$, respectively). Insulin-resistant (IR) subjects had greater reductions in high density lipoprotein cholesterol (HDL-C; $P < 0.01$), and triglycerides (TAG)/HDL-C ($P = 0.02$) after the LG diet, compared to the HA diet. Insulin-sensitive (IS) subjects had greater reductions in TC ($P < 0.001$), LDL-C ($P < 0.01$), TC/HDL-C ($P < 0.01$), and LDL-C/HDL-C ($P = 0.02$) after the LG diet, compared to the HA diet. In conclusion, a high legume, high fiber, low GI diet improves serum lipid profiles in men, compared to a healthy American diet. However, IR individuals do not achieve the full benefits of the same diet on cardiovascular disease (CVD) lipid risk factors.

Keywords Legume intake · Lipids · Insulin resistance

Abbreviations

ANOVA	Analysis of variance
apo A-I	Apolipoprotein A-I
apo B	Apolipoprotein B
AIC	Akaike Information Criteria
BIC	Bayesian Information Criteria
BMI	Body mass index
CHD	Coronary heart disease
CVD	Cardiovascular disease
CV	Coefficients of variations
DGA	Dietary Guidelines for Americans
GCRC	General clinical research center

Z. Zhang · P. M. Kris-Etherton · D. Bagshaw · T. J. Hartman
Department of Nutritional Sciences, The Pennsylvania State University, University Park, PA, USA

M. J. Rovine
Department of Human Develop and Family Studies, The Pennsylvania State University, University Park, PA, USA

J. S. Ulbrecht
Department of Biobehavioral Health and Medicine, The Pennsylvania State University, University Park, PA, USA

E. Lanza · N. H. Colburn · G. Bobe
Laboratory of Cancer Prevention, Center for Cancer Research, The National Cancer Institute, Bethesda and Frederick, MD, USA

R. S. Chapkin
Program in Integrative Nutrition and Complex Diseases, Texas A&M University, College Station, TX, USA

T. J. Hartman (✉)
110 Chandlee Laboratory, The Department of Nutritional Sciences, The Pennsylvania State University, University Park, PA 16802, USA
e-mail: tjh9@psu.edu

GI	Glycemic index
GL	Glycemic load
HA	Healthy American diet
HDL-C	High density lipoprotein cholesterol
HOMA-IR	Homeostasis model assessment index
IOM	Institute of Medicine
IR	Insulin-resistant
IS	Insulin-sensitive
LDL-C	Low density lipoprotein cholesterol
LDL-C/HDL-C	Low density lipoprotein cholesterol to high density lipoprotein cholesterol ratio
LG	Legume diet
LIFE	Legume inflammation feeding experiment
mRNA	Messenger ribonucleic acid
MUFA	Monounsaturated fatty acid
NDS-R	Nutrition data system for research
PUFA	Polyunsaturated fatty acid
RIA	Radioimmunoassay
SFA	Saturated fatty acid
sd-LDL	Small dense LDL-C particle
TC	Total cholesterol
TC/HDL-C	Total cholesterol to high density lipoprotein cholesterol ratio
TAG	Triglyceride
TAG/HDL-C	Triglyceride to high density lipoprotein cholesterol ratio
VLDL	Very low density lipoprotein

Introduction

Numerous studies have shown an inverse association between intake of dietary fiber and risk for chronic diseases such as cardiovascular disease (CVD) [1, 2] and type 2 diabetes mellitus [3]. The beneficial effects may be partially due to fiber's hypocholesterolemic [4–6] and hypoinsulinemic effects [3]. On the basis of a number of epidemiological studies on coronary heart disease (CHD) [7–9], the Institute of Medicine (IOM) currently recommends a daily consumption of 14 g of fiber per 1,000 kcal for Americans (DGA 2005).

Legumes, such as pinto, navy, kidney, lima, and black beans, are a rich source of dietary fiber but the effects of these types of beans on blood lipid levels are limited. A meta-analysis of 67 controlled trials was conducted to quantify the hypocholesterolemic effects of major dietary fibers [10]. The results demonstrated that daily intake of 2–10 g of soluble fiber was associated with significant decreases in total cholesterol (TC, −1.7 mg/L per gram) and low density lipoprotein cholesterol (LDL-C, −2.2 mg/L per gram). A 12-week randomized dietary intervention with 40 men and women with metabolic syndrome and 40 healthy subjects [11] reported that daily intake of a bean entrée (130 g of cooked dry pinto beans) lowered serum TC by 8% in the healthy population and by 4% in the metabolic syndrome group. A limitation of legume-related studies is that most recent interventions have been conducted with a single test meal [12–15] or fiber supplement [16, 17] and some of these studies were designed to test short-term effects in hours or days [12, 14, 15].

The Legume Inflammation Feeding Experiment (LIFE Study, [18]) was a randomized controlled cross-over feeding study designed to test the effects of a legume-rich, high fermentable fiber, low glycemic index (GI) diet on biomarkers of inflammation and insulin resistance in middle-aged men at high risk for colorectal cancer. An important secondary objective of the LIFE Study was to evaluate the effects of diet on serum lipids. We hypothesized that the high legume low GI diet would significantly improve serum lipid profiles. To our knowledge, this was the first randomized controlled, cross-over feeding study designed to assess the hypocholesterolemic effects of a mixture of the five types of beans under conditions of weight maintenance.

Subjects and Methods

Subjects and Recruitment

All aspects of this study were approved by the Institutional Review Boards of the Pennsylvania State University and the National Cancer Institute. Sixty six non-smoking male subjects age 35–75 who had undergone colonoscopies within the previous 2 years were recruited in Central Pennsylvania. The study was conducted from February 1st, 2006 to August 6th, 2008. History of colorectal adenomas (yes or no) was combined with insulin resistance (yes or no) for group classification. Insulin resistance was defined by a homeostasis model assessment (HOMA-IR) index level. The formula for calculation is as follows: fasting insulin (μU/mL) × fasting glucose (mmol/L)/22.5 [19]. Subjects with a HOMA-IR index level equal or higher than 2.6 were considered insulin resistant [20, 21].

Criteria and Restrictions

All participants were prescreened by telephone interview and a clinical screening test for study eligibility. In addition to the colonoscopy, subjects had to meet the following criteria: (1) weight maintenance or less than 10% body weight loss 6 months prior to the present study, (2) body mass index (BMI) within 20–37 kg/m^2, (3) no history of

colorectal cancer, bowel resection or inflammatory bowel disease, (4) no serious medical conditions, e.g., heart disease, stroke, diabetes, renal or kidney disease, liver disease or cirrhosis, or cancer within the last 10 years, (5) not taking vitamin/mineral, herbal, or other nutritional supplements, and (6) not taking any cholesterol-lowering, glucose-controlling, or non-steroidal anti-inflammatory (e.g. aspirin) medications.

The subjects who met the eligibility criteria were invited to undergo clinical screening tests including a fasting blood draw at the General Clinical Research Center (GCRC) at Penn State University in University Park, PA, USA. Eligible subjects were asked to return to the GCRC to have resting metabolic rate measured and completed three 24-h telephone diet calls (two on weekdays and one on weekend) to estimate daily energy requirements.

Diet and Study Design

A detailed explanation of diet and study design was published previously [18]. In brief, the randomized controlled cross-over feeding study consisted of a first 4-week diet period, a 2–4 week compliance break, and a second 4-week diet period. The time period allowed for the test diet intervention was sufficient to assure that lipids had stabilized [22]. Subjects were first randomly assigned to either a healthy American diet (HA) or an isocaloric legume diet (LG; approximately 250 g of cooked pinto, navy, kidney, lima, and black beans per day), and then were switched to the other diet for the second feeding period. All foods for this study were prepared and distributed by the metabolic diet center at the GCRC. On weekdays, the participants ate breakfast or dinner at the GCRC and on Fridays, all the packed foods for weekends were taken home. The dietitians recorded body weight and food consumption at each visit. Uneaten foods were very little; they were returned to the GCRC and were measured and recorded by study dietitians daily as a measure of compliance. Seven-day cycle menus were created for each test diet and evaluated for percentages of energy contributed by each of the macronutrients using Nutrition Data System for Research (NDS-R, 2006, Minneapolis, MN, USA); GI and GL were calculated using Food Processor (2005). Total energy intake was adjusted by study dietitians in 200 kcal increments to maintain participants' body weights during the diet periods (e.g. 2,000, 2,200, 2,400, 2,600 kcal, etc.). Subjects were allowed up to two alcoholic beverages per week while consuming the study diets. We used the same or similar foods to design our menus. For example, subjects had tuna pasta salad as lunch during the HA menu which was replaced by Italian bean and tuna salad during the LG menu. For dinner, the HA diet provided ginger chicken and rice, while the LG diet provided ginger chicken and beans. The ingredients of the two ginger chicken dishes were the same except that the substitution of beans for rice. The LG diet provided much of the protein from plant sources and the HA diet provided more protein from chicken (skinless) in order to meet the dietary recommendation for cholesterol. Daily compliance questionnaires indicated very good test diet adherence. Table 1 shows the composition of the participants' diets at entry (pre-study) and the two test diets.

Sample Collection and Measurements

Anthropometric measurements were completed using standardized methods by well-trained nurses at the GCRC on Penn State University Park campus. At the beginning and end of each test diet period, a 12-h overnight fasting blood sample was drawn and serum was collected for measurement of TC, LDL-C, HDL-C and TAG. All blood samples were centrifuged at $3{,}200 \times g$ for 15 min at 4°C, the supernatant was separated and aliquoted in cryovials, and stored at −80°C. Serum lipids were measured at Penn State Hershey Medical Center in the laboratory of Dr. Laurence Demers. All samples from each subject were grouped together for analysis in the same batch. Lipids were measured using enzymatic procedures on an automated chemistry analyzer (Roche); the intra- and inter-assay coefficients of variations (CV) for all biomarkers of interest were less than 5%. Fasting plasma insulin was measured using a human-specific insulin RIA (Linco-Millipore, MA, USA, HI-14 K; sensitivity, 2–200 μU/mL; inter-assay CV, 2.9–6.0%; intra-assay CV, 2.4–4.4%). Fasting plasma glucose was measured via an immobilized enzyme biosensor using the YSI 2300 STAT Plus Glucose and Lactate analyzer (Yellow Springs Instruments; inter- and intra-assay CV were less than 5%).

Statistical Analysis

The means for the pre-study diet were calculated by 3-day diet recalls and the means for the two test diets were based on the average of each 7-day menu for a 2,000 kcal diet (Table 1). The experimental diets and participants' pre-study diets were compared using one-way analysis of variance (ANOVA) with the Tukey test to adjust for the multiple comparisons. Baseline characteristics stratified by subjects' insulin resistance status were compared using one-way ANOVA. Log-transformation of HOMA-IR index, TAG, and TAG/HDL-C were performed for the analyses because of skewed distributions. General linear mixed models with repeated measurement (Proc mixed) were used to test for the effects of diet, period, and their interactions with change scores of all outcome variables. Subject was treated as a random and diet treatment as a

Table 1 Nutrient and food profile of the experimental diets (compared to pre-study diet)

Nutrient/food group	Pre-study diet	Healthy American (high GI) diet	Legume (low GI) diet	*P* value[a]
Glycemic index	60 ± 6	69 ± 3[b]	38 ± 2[b,c]	<0.001
Glycemic load	165 ± 77	152 ± 8	84 ± 4[b,c]	<0.001
Total Fat (% kcal)	35 ± 7	34 ± 1	34 ± 1	0.85
SFA (% kcal)	12 ± 3	11 ± 1	12 ± 1	0.71
MUFA (% kcal)	13 ± 3	13 ± 1	13 ± 2	0.87
PUFA (% kcal)	7 ± 2	8 ± 1	7 ± 2	0.41
Protein (% kcal)	16 ± 3	18 ± 1	18 ± 1	0.05
Carbohydrate (% kcal)	48 ± 8	50 ± 2	51 ± 1	0.60
Added sugar (g/1,000 kcal)	31 ± 15	25 ± 15	20 ± 7	0.14
Total fiber (g/1,000 kcal)[d]	9 ± 3	9 ± 1	21 ± 1[b,c]	<0.001
Soluble fiber (g/1,000 kcal)[d]	2 ± 1	2 ± 1	4 ± 1[b,c]	<0.001
Insoluble fiber (g/1,000 kcal)[d]	7 ± 2	7 ± 1	17 ± 1[b,c]	<0.001
Cholesterol (mg/1,000 kcal)[d]	125 ± 52	98 ± 9	70 ± 11[b]	0.001
Fruit (serving/1,000 kcal)[d]	0.7 ± 0.6	0.9 ± 0.4	1.3 ± 0.3[b]	0.02
Vegetable (serving/1,000 kcal)	1.4 ± 0.7	1.8 ± 0.5	2.2 ± 0.6[b]	0.01
Legume (serving/1,000 kcal)[d,e]	0.1 ± 0.2	0.0 ± 0.0	1.5 ± 0.0[b,c]	<0.001

Values are reported as means ± SD. The mean for 3-day diet recalls were used to assess participants' pre-study diets, the means of 7-day menus (on 2,000 kcal level) reflect the two test diets (HA and LG)

[a] *P* values reflect the overall difference across the three diets using one-way ANOVA with Tukey tests to adjust for the multiple comparisons

[b] Different from pre-study diet, $P < 0.1$

[c] Different from Healthy American diet, $P < 0.1$

[d] Data were log-transformed for analysis

[e] Legumes were excluded in the vegetables

fixed effect. Akaike Information Criteria (AIC) and Bayesian Information criteria (BIC) were evaluated to decide model correlation structure; we used unstructured based on these comparisons and because we believed the covariance between diet treatments might be different. Likelihood ratio tests were used to test for treatment effects. Analyses were also completed using paired *t* tests with similar results. Potential confounding by age, BMI, adenoma status (yes/no), insulin resistance status (yes/no) and initial biomarker status at study entry was assessed. We also evaluated potential diet period and diet order effects for their influence on end points of interest and no carry over effect was detected. The results indicated that initial insulin resistance status may be an important modifier for the interpretation of the changes of some biomarkers at study entry; therefore, we conducted analyses stratified by insulin resistance status. There was no evidence that adenoma status was an important effect modifier; therefore, stratified results were not presented. The change scores of outcomes were based on the differences between the beginning and the end of each dietary period for this variable. The percentage changes were calculated based on the change scores and respective biomarker value at study entry. In addition, we evaluated and visualized the association between insulin resistance at study entry and the changes in lipids during dietary intervention using Pearson correlation and linear regression. Analyses were performed using SAS version 9.1 (SAS Institute, Inc, Cary, NC, USA). Significance was set at $P < 0.05$.

Results

Sixty-four subjects finished all test diet periods. Two subjects dropped out in the first week of the first test diet period because of loss of interest (completion rate = 97%). Subjects who were insulin-resistant (IR) had higher BMIs, larger waist circumferences, and higher fasting serum glucose, insulin, and TAG levels than those who were insulin-sensitive (IS) (Table 2). Subjects with a previous history of adenomas were older than those who were adenoma-free; other descriptive variables did not vary significantly by adenoma status (data not shown).

Effects of Experimental Diets on Serum Lipids

Changes in lipids on the two test diets are presented in Table 3. Compared with the HA diet, the LG diet resulted in significantly greater reductions in TC (−11 ± 3 mg/dL, $P < 0.001$) and LDL-C (−9 ± 3 mg/dL, $P < 0.01$) levels.

Table 2 Baseline characteristics of study subjects by insulin resistance status

	Overall mean	Insulin sensitive (IS)	Insulin resistant (IR)	*P* value[a]
N	64	36	28	
Age (years)	54.5 ± 7.8	53.8 ± 7.6	55.5 ± 8.0	0.38
BMI (kg/m^2)	28.7 ± 3.5	27.4 ± 3.2[a]	30.3 ± 3.2[b]	<0.001
Waist circumference (cm)	97.2 ± 9.3	93.2 ± 8.7[a]	102.3 ± 7.5[b]	<0.001
Systolic blood pressure (mmHg)	123 ± 11	121 ± 10	126 ± 12	0.11
Diastolic blood pressure (mmHg)	81 ± 7	79 ± 6[a]	82 ± 7[b]	0.04
TC (mg/dL)	200 ± 37	195 ± 37	207 ± 37	0.19
HDL-C (mg/dL)	45 ± 11	47 ± 12	43 ± 10	0.15
LDL-C (mg/dL)	129 ± 32	127 ± 31	131 ± 35	0.60
TAG (mg/dL)[b]	135 ± 72	108 ± 48[a]	171 ± 83[b]	<0.001
Glucose (mg/dL)	97.3 ± 8.9	93.7 ± 7.9[a]	101.9 ± 7.9[b]	<0.001
Insulin (μU/mL)[b]	11.6 ± 7.6	7.4 ± 2.6[a]	17.0 ± 8.5[b]	<0.001

Values are reported as means ± SD

[a] Baseline characteristics stratified by subject's insulin resistant status were compared using one-way ANOVA. The different letters show statistical differences at $\alpha = 0.05$

[b] Data were log-transformed for the analysis

Table 3 Effects of diets on study endpoints

	Study entry	ΔLG	*P* value[a]	ΔHA	*P* value[b]	ΔLG − ΔHA[c]	*P* value[d]
TC (mg/dL)	200 ± 5	−20 ± 3 (10%)	<0.001	−8 ± 3 (4%)	<0.01	−11 ± 3	<0.001
HDL-C (mg/dL)	45 ± 1	−3 ± 1 (6.7%)	<0.001	−1 ± 1 (2.2%)	0.04	−2 ± 1	0.05
LDL-C (mg/dL)	129 ± 4	−14 ± 2 (10.9%)	<0.001	−4 ± 2 (3.1%)	0.09	−9 ± 3	<0.01
TAG (mg/dL)[e]	135 ± 9	−20 ± 6 (14.8%)	<0.01	−17 ± 5 (12.6%)	<0.01	−3 ± 8	0.93
TC/HDL-C	4.61 ± 0.15	−0.15 ± 0.06 (3%)	0.02	−0.08 ± 0.06 (1.7%)	0.17	−0.07 ± 0.08	0.39
LDL-C/HDL-C	2.97 ± 0.12	−0.12 ± 0.05 (3.5%)	0.02	−0.01 ± 0.05 (0.3%)	0.87	−0.11 ± 0.06	0.09
TAG/HDL-C[e]	3.40 ± 0.31	−0.28 ± 0.18 (9.4%)	0.27	−0.40 ± 0.17 (13.5%)	0.03	0.12 ± 0.27	0.52

Values are reported as means ± SEM (percentage change); $n = 64$. General linear mixed models with repeated measurement (Proc mixed) were used to test for the effects of diet, period, and their interactions with study outcomes

ΔLG = change over the 4-week enriched-legume diet, ΔHA = change over the four-week isocaloric healthy American diet

[a] Statistical significance over the enriched-legume diet

[b] Statistical significance over the healthy American diet

[c] ΔLG − ΔHA = difference in change between the two diets

[d] Statistical significance of the difference in change between the two diets

[e] Data were log-transformed for the analysis

The LG diet reduced TC (10%, $P < 0.001$), LDL-C (10.9%, $P < 0.001$), and TAG (14.8%, $P < 0.01$) over the 4 week feeding period. The HA diet also reduced TC (4%, $P < 0.01$) and TAG (12.6%, $P < 0.01$) but had less effect on LDL-C (3.1%, $P = 0.09$). Both test diets slightly lowered HDL-C concentrations. We also analyzed three ratios (TC/HDL-C, LDL-C/HDL-C, and TAG/HDL-C) that are predictors of CVD risk. The changes between test diets did not differ. The LG diet was associated with significant reductions in TC/HDL-C (3%, $P = 0.02$) and LDL-C/HDL-C (3.5%, $P = 0.02$) over the 4 week feeding period. The HA diet was associated with a significant reduction in TAG/HDL-C (13.5%, $P = 0.03$).

Effects of Experimental Diets on Serum Lipids Stratified by Insulin Resistance Status

We observed effect modification of the diet on biomarkers of interest by IR status (HDL-C, P-interaction = 0.03; TAG, P-interaction = 0.03; TC/HDL-C, P-interaction < 0.001; TAG/HDL-C, P-interaction = 0.01); therefore, we present our results stratified by insulin resistance status (IR or IS, Table 4). Among IS subjects, the LG diet led to greater reductions in TC (−14 ± 4 mg/dL, $P < 0.001$), LDL-C (−10 ± 4 mg/dL, $P < 0.01$), TC/HDL-C (−0.30 ± 0.10, $P < 0.01$), and LDL-C/HDL-C (−0.20 ± 0.08, $P = 0.02$), compared with the HA diet. The 4-week LG diet favorably

Table 4 Effects of diets on study endpoints among subjects stratified by insulin resistance status

	Changes during the LG diet			Changes during the HA diet			Difference between the two diets	
	Baseline	ΔLG	*P* value	Baseline	ΔHA	*P* value	ΔLG − ΔHA[a]	*P* value
IS ($n = 36$)								
TC (mg/dL)	192 ± 6	−22 ± 3 (11.3%)	<0.001	188 ± 5	−7 ± 3 (3.7%)	0.04	−14 ± 4	<0.001
HDL-C (mg/dL)	46 ± 2	−2 ± 1 (4.3%)	0.02	47 ± 2	−2 ± 1 (4.3%)	0.02	0 ± 1	0.97
LDL-C (mg/dL)	124 ± 5	−15 ± 3 (12.1%)	<0.001	121 ± 4	−4 ± 3 (3.3%)	0.17	−10 ± 4	<0.01
TAG (mg/dL)[b]	123 ± 12	−27 ± 8 (22.0%)	<0.01	102 ± 7	−5 ± 6 (4.9%)	0.22	−23 ± 10	0.12
TC/HDL-C	4.34 ± 0.18	−0.30 ± 0.08 (6.9%)	<0.001	4.14 ± 0.15	−0.01 ± 0.07 (0.2%)	0.93	−0.30 ± 0.10	<0.01
LDL-C/HDL-C	2.79 ± 0.14	−0.19 ± 0.06 (6.8%)	<0.01	2.67 ± 0.13	0.001 ± 0.069 (0.04%)	0.98	−0.20 ± 0.08	0.02
TAG/HDL-C[b]	3.03 ± 0.41	−0.67 ± 0.23 (22.1%)	0.05	2.43 ± 0.25	−0.02 ± 0.22 (0.8%)	0.71	−0.65 ± 0.34	0.21
IR ($n = 28$)								
TC (mg/dL)	204 ± 7	−17 ± 3 (8.3%)	<0.001	206 ± 8	−10 ± 4 (4.9%)	0.01	−7 ± 5	0.13
HDL-C (mg/dL)	43 ± 2	−4 ± 1 (9.3%)	<0.001	42 ± 2	−0.4 ± 0.9 (1.0%)	0.69	−4 ± 1	<0.01
LDL-C (mg/dL)	128 ± 6	−12 ± 3 (9.4%)	<0.001	129 ± 7	−4 ± 4 (3.1%)	0.33	−8 ± 4	0.05
TAG (mg/dL)[b]	164 ± 15	−10 ± 9 (6.1%)	0.30	180 ± 17	−33 ± 7 (18.3%)	<0.001	23 ± 12	0.11
TC/HDL-C	4.88 ± 0.24	0.05 ± 0.09 (1.0%)	0.60	5.05 ± 0.26	−0.17 ± 0.09 (3.4%)	0.05	0.22 ± 0.12	0.06
LDL-C/HDL-C	3.07 ± 0.18	−0.01 ± 0.07 (0.3%)	0.84	3.14 ± 0.20	−0.02 ± 0.08 (0.6%)	0.77	0.01 ± 0.09	0.93
TAG/HDL-C[b]	4.12 ± 0.47	0.21 ± 0.26 (5.1%)	0.57	4.79 ± 0.62	−0.90 ± 0.26 (18.8%)	<0.01	1.11 ± 0.39	0.02

Values are reported as means ± SEM (percentage change)

IS insulin-sensitive subjects, Δ*LG* = change over the enriched-legume diet, Δ*HA* = change over the isocaloric healthy American diet, *IR* insulin-resistant subjects

[a] ΔLG − ΔHA = change between the two diets

[b] Data were log-transformed for the analysis

reduced almost all lipid profiles; however, the 4-week HA diet only improved TC concentrations. Both test diets reduced HDL-C concentrations (−2 ± 1 mg/dL, $P = 0.02$, respectively) without between-diet difference.

Among IR subjects, the HA diet tended to have more favorable effects on the TAG/HDL-C ratio ($P = 0.02$), compared with the LG diet. The LG diet significantly decreased fasting serum TC, HDL-C, and LDL-C concentrations ($P < 0.001$ for each) but not in TAG or the HDL-related ratios. The HA diet significantly decreased TC, TAG, and TAG/HDL-C ($P = 0.01$, $P < 0.001$, and $P < 0.01$, respectively).

Effects of Insulin Resistance Status at Study Entry on Lipid R esponses

We calculated the differences between the change scores during the LG diet and those during the HA diet (subtract the change scores over the HA diet from the change scores over the LG diet) and regressed on HOMA-IR values (at study entry). Figure 1 shows an inverse association; subjects with worse insulin resistance at study entry had smaller reductions in TC/HDL-C ratio ($\beta = 0.27, R^2 = 0.11$, $P = 0.03$).

Discussion

In the LIFE study under conditions of weight maintenance, the legume-rich, high fermentable fiber, low GI diet (LG) led to greater reductions in fasting serum TC and LDL-C concentrations. It is possible that the higher fiber and reduced cholesterol consumption acted to decrease fat absorption and lower hepatic synthesis of cholesterol contributing to lower circulating lipids. Another possibility is that the reduced GI and GL of the legume diet played a role in favorably altering lipid concentrations. Low GI and GL diets favor insulin sensitivity. Insulin inhibits the mobilization of free fatty acids from adipose tissue, thus lowering hepatic production of very low density lipoprotein (VLDL) and maintaining low levels of TC and LDL-C. Possibly, these changes accounted for greater reductions in TC and LDL-C concentrations on the LG diet.

Many but not all [23, 24] studies have shown hypocholesterolemic effects of dietary fiber [11, 13, 16, 17, 25–27]; however, studies specifically on legume consumption are still limited. Anderson et al. [4] reported that incorporating 100 g of dried beans into a Western diet for 28 days decreased TC (18.7%) and LDL-C (23.1%) in men ($n = 6$). In a feeding study of 24 hyperlipidemic men who

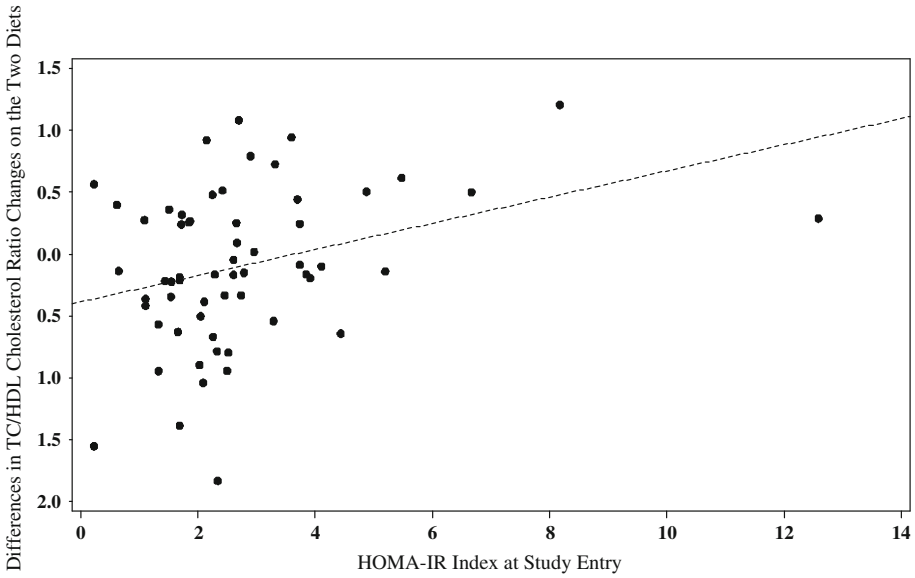

Fig. 1 Relationship between HOMA-IR index at study entry and differences in TC/HDL cholesterol ratio changes (Delta TC/HDL-C ratio) on the two diets. Delta TC/HDL cholesterol was calculated by subtracting the change scores over the HA diet from the change score over the LG diet, thus $\text{change}_{LG} - \text{change}_{HA}$ ($n = 64$; $\beta = 0.266$, $R^2 = 0.11$, $P = 0.025$)

consumed 120 or 162 g beans with tomato sauce for 21 days [28], both serum TC and LDL-C were significantly decreased (10.4 and 8.4%, respectively). Pittaway et al. [29] reported that an addition of 104 g of chickpeas into ad libitum diet for 12 weeks led to improvements in both TC (7.7 mg/dL) and LDL-C (7.3 mg/dL) among 13 pre- and 19 postmenopausal women and 13 men at high risk for CVD. Collectively, these studies demonstrate a hypocholesterolemic effect of legume consumption; yet, they were not designed as controlled feeding experiments. Among these clinical studies, weight changes either were not mentioned [14, 25, 30] or weight slightly decreased [26]. In our study, subject body weights were measured daily and their calorie intake adjusted for weight maintenance; therefore, changes in lipids were independent of weight loss.

The present study showed that both the LG diet and the HA diet significantly lowered fasting TAG concentrations. Our observations supported several [28, 31] but not all [13, 14] earlier feeding studies in terms of TAG-lowering influence. We observed that the HA diet lowered fasting TAG similarly to the LG diet. We compared the total and added sugars of the two experimental diets with that of the subjects' own diet; however, we did not find significant differences. It is possible that the TAG-lowering effects might not result from fiber consumption or GI. The LG diet provided increased plant protein in the diet. To match protein intake and maintain a lower cholesterol intake, we added more chicken, milk, and fish to the HA diet. Differences among both test diets compared to pre-study diets (e.g. protein consumption) may have contributed to the reductions in TAG observed with both diets [32].

Fruit and vegetables are good sources of many vitamins, minerals and bioactive compounds, which have been shown to possess cardioprotective effects. Antioxidants in fruit and vegetables such as vitamin C, carotenoids, vitamin E, and flavonoids may reduce CVD by reducing lipid oxidation and inflammation in the artery wall. The B-complex vitamins such as folate and B_6 may reduce CVD by lowering circulation homocysteine. A number of epidemiological studies demonstrate the inverse association between fruit and vegetable consumption and CVD risk [33–37]. In the National Heart, Lung, and Blood Institute Family Heart Study of 4,466 men and women aged 25 and older followed from 1993 to 1995 [38], persons in the higher range of fruit and vegetable consumption (mean of 5.4 servings/day for men and 5.5 servings/day for women) had lower fasting LDL-C concentrations (P for trend <0.0001 for each), compared to those in the lower range (mean of 1.4 servings for both). In the present study, we observed that both the LG and HA diets provided higher amounts of fruit and vegetables compared with subjects' usual diets, although the differences were only significant between the LG diet and subjects' usual diets.

Several cross-sectional studies have reported that high dietary GI was inversely associated with HDL-C [39–43] and positively associated with LDL-C [43] and TAG concentrations [40, 43]. High dietary GL was inversely associated with HDL-C [39, 40, 43, 44] and was positively associated with TAG concentrations [40, 43, 44]. Ma et al. [41] reported an inverse associations between GL, TC and LDL-C concentrations; however, Du et al. [42] reported non-significant associations between GL and lipid and lipoprotein concentrations. Randomized intervention trials

showed that low GL diets [45, 46] favorably improved HDL-C and/or TAG concentrations. In the present study, we observed that a high legume low GI/GL diet significantly reduced fasting serum TC and LDL-C concentrations; the results are consistent with the previous investigations. We also observed that fasting HDL-C concentrations decreased after the 4-week low GI/GL dietary intervention, which is not consistent with the aforementioned studies. The difference may be due to different study designs and target populations. In addition, unlike these studies, the present study controlled subjects' body weight and overall food intake.

The LIFE study was designed to evaluate the effects of fiber consumption on lipid profiles; however, other components such as phytosterols may also consider a mechanism for lipid reduction. Stanols and sterols, are primarily present in nuts, vegetable oils, seeds, cereals, and legumes [47]. Plant stanols and sterols have similar chemical structures to cholesterol; they may reduce cholesterol absorption by enterocytes [48] and the esterification rate of cholesterol in the enterocytes [49]. Decreased cholesterol absorption stimulates cholesterol synthesis [50] as well as the expression of LDL receptor mRNA [51] increasing LDL clearance and lowering LDL production resulting in lower circulating total cholesterol levels.

Metabolic syndrome causes dyslipidemia partially as the result of insulin resistance [52]. Our results demonstrate that insulin resistance may blunt response to a legume-enriched, high fiber diet. Among IS subjects, the LG diet led to significant reductions of all lipid profiles as well as the three ratios; however, among IR subjects, the same diet only had strong effects on the reductions of TC, LDL-C, and HDL-C. The HA diet led to significant reductions in TC and HDL-C among IS subjects; the same diet also had strong effects on TC, TAG, and TAG/HDL-C among IR subjects. Lefevre et al. [53] reported that subjects who had higher BMIs and waist circumferences, greater percentages of body fat and higher fasting insulin concentrations had smaller reductions in TC, LDL-C, TC/HDL-C after a Step II (low fat, low saturated fat) diet. Our results are consistent with this study. We observed that subjects who had higher HOMA-IR values at study entry had smaller reductions in TAG, TC/HDL-C, LDL-C/HDL-C, and TAG/HDL-C after the LG diet, though the reduction was only statistically significant for TC/HDL-C. Different from Lefevre's report, we found that subjects' BMIs at study entry did not predict changes in any lipid profiles or HDL-C related ratios.

Many human clinical studies have shown that a reduced intake of saturated fat may lower the risk for cardiovascular disease by decreasing TC and LDL-C concentrations [22, 32, 53, 54]. The effects of these types of diets on lowering TAG levels have been variable [22, 32, 54]. In the present study, we observed that moderate total (34%) and saturated fat (12%) with high fermentable fiber consumption also lowered TC and LDL-C concentrations, whereas the HA diet only lowered TC. The differences observed between test diets was significant for TC and LDL-C demonstrating an effect of total and soluble fiber, and possibly GL. Changes of this magnitude suggest that high fermentable fiber consumption may be another approach to lower risk for CVD [55].

There are several strengths of our study. First, we implemented a randomized, cross-over controlled feeding study design. In addition, we matched the two test diets so that they were isocaloric and provided similar percentages of energy from total fat, saturated fat, carbohydrate, and protein under conditions of weight maintenance. Second, though fiber consumption was higher than daily recommendations, the LG diet was well-tolerated.

There are some limitations in the present study. The present study defined insulin resistance by the HOMA-IR index, which has been widely used for clinical evaluation of insulin resistance. The cutoff value used in our study and others is somewhat subjective; however, the decision was based on two recent human clinical trials [20, 21]. Additionally, studies show that the classification of insulin resistance according to the HOMA-IR index is highly correlated to the ones based on the euglycemic insulin clamp technique, the gold standard for evaluation of insulin sensitivity/resistance [56, 57]. The LG diet included less dietary cholesterol than the HA diet; therefore, we are not able to rule out the possibility that dietary cholesterol consumption contributed to the observed effects on serum cholesterol levels. However, our analysis showed that the difference in dietary cholesterol between the LG and HA diet was not statistically significant. In addition, a 20 mg/day increment in dietary cholesterol intake only results in a very small change of serum cholesterol according to a meta-analysis of 27 studies [58]. Next, we only measured the changes in selected lipid/lipoprotein biomarkers. Recent studies indicate that small dense LDL-C particle (sd-LDL) level is a better predictor for CHD [59] than LDL-C. Apolipoprotein B (apoB) is the primary apolipoprotein in LDL-C; measurement of apo B may provide additional information on changes in LDL particle size. Similarly, apo A-I is the primary apolipoprotein in HDL-C; measuring the change in apo A-I may help to track the change in HDL particle size.

In conclusion, this study adds to the growing evidence that incorporating legumes in the moderate-fat diet improves lipid profiles, thus potentially lowering CVD risk. However, a cautionary note must be added since insulin resistance is highly prevalent and increasing, and individuals in this study with insulin resistance responded less favorably to the legume enriched, high fermentable fiber,

low glycemic index diet than those without insulin resistance.

Acknowledgments The present study was supported by the National Cancer Institute (subcontract 25XS101) with partial support provided by the General Clinical Research Center at Penn State University (NIH M01 RR 10732). We would like to thank Amy Ciccarella, Sami Heim, and Mary Lou Kiel for their help with menu and food preparation, Diane Mitchell and Linda Phelps for their assistance with the analysis of 24-h dietary recalls, and Dr. Lawrence Demers at Hershey Medical Center for the measurement of lipid profiles. All of the authors have read and approved the final submitted manuscript and there was no conflict of interest with the present paper. The authors' contributions were as follows: ZZ conducted research with participants, data analysis, and write up of manuscript; EL designed the research, contributed to data interpretation and manuscript preparation; PMKE and NHC contributed to data interpretation and manuscript preparation; DB conducted research with participants and and was involved with the write up of the manuscript; MJR contributed to data analysis and the write up of the manuscript; JSU, GB, and RSC contributed to data interpretation and the write up of the manuscript; and TJH designed research, contributed to data interpretation and manuscript preparation, and study oversight.

References

1. Kushi LH, Meyer KA, Jacobs DR Jr (1999) Cereals, legumes, and chronic disease risk reduction: evidence from epidemiologic studies. Am J Clin Nutr 70:451S–458S
2. Bazzano LA, He J, Ogden LG, Loria C, Vupputuri S, Myers L, Whelton PK (2001) Legume consumption and risk of coronary heart disease in US men and women: NHANES I epidemiologic follow-up study. Arch Intern Med 161:2573–2578
3. Ylonen K, Saloranta C, Kronberg-Kippila C, Groop L, Aro A, Virtanen SM (2003) Associations of dietary fiber with glucose metabolism in nondiabetic relatives of subjects with type 2 diabetes: the Botnia Dietary Study. Diabetes Care 26:1979–1985
4. Anderson JW (1987) Dietary fiber, lipids and atherosclerosis. Am J Cardiol 60:17G–22G
5. Fukagawa NK, Anderson JW, Hageman G, Young VR, Minaker KL (1990) High-carbohydrate, high-fiber diets increase peripheral insulin sensitivity in healthy young and old adults. Am J Clin Nutr 52:524–528
6. Duane WC (1997) Effects of legume consumption on serum cholesterol, biliary lipids, and sterol metabolism in humans. J Lipid Res 38:1120–1128
7. Pietinen P, Rimm EB, Korhonen P, Hartman AM, Willett WC, Albanes D, Virtamo J (1996) Intake of dietary fiber and risk of coronary heart disease in a cohort of Finnish men. The Alpha-Tocopherol, Beta-Carotene Cancer Prevention Study. Circulation 94:2720–2727
8. Rimm EB, Ascherio A, Giovannucci E, Spiegelman D, Stampfer MJ, Willett WC (1996) Vegetable, fruit, and cereal fiber intake and risk of coronary heart disease among men. JAMA 275:447–451
9. Liu S, Buring JE, Sesso HD, Rimm EB, Willett WC, Manson JE (2002) A prospective study of dietary fiber intake and risk of cardiovascular disease among women. J Am Coll Cardiol 39:49–56
10. Brown L, Rosner B, Willett WW, Sacks FM (1999) Cholesterol-lowering effects of dietary fiber: a meta-analysis. Am J Clin Nutr 69:30–42
11. Finley JW, Burrell JB, Reeves PG (2007) Pinto bean consumption changes SCFA profiles in fecal fermentations, bacterial populations of the lower bowel, and lipid profiles in blood of humans. J Nutr 137:2391–2398
12. Weickert MO, Mohlig M, Schofl C, Arafat AM, Otto B, Viehoff H, Koebnick C, Kohl A, Spranger J, Pfeiffer AF (2006) Cereal fiber improves whole-body insulin sensitivity in overweight and obese women. Diabetes Care 29:775–780
13. Keenan JM, Goulson M, Shamliyan T, Knutson N, Kolberg L, Curry L (2007) The effects of concentrated barley beta-glucan on blood lipids in a population of hypercholesterolaemic men and women. Br J Nutr 97:1162–1168
14. Samra RA, Anderson GH (2007) Insoluble cereal fiber reduces appetite and short-term food intake and glycemic response to food consumed 75 min later by healthy men. Am J Clin Nutr 86:972–979
15. Bourdon I, Olson B, Backus R, Richter BD, Davis PA, Schneeman BO (2001) Beans, as a source of dietary fiber, increase cholecystokinin and apolipoprotein b48 response to test meals in men. J Nutr 131:1485–1490
16. Anderson JW, Allgood LD, Lawrence A, Altringer LA, Jerdack GR, Hengehold DA, Morel JG (2000) Cholesterol-lowering effects of psyllium intake adjunctive to diet therapy in men and women with hypercholesterolemia: meta-analysis of 8 controlled trials. Am J Clin Nutr 71:472–479
17. Queenan KM, Stewart ML, Smith KN, Thomas W, Fulcher RG, Slavin JL (2007) Concentrated oat beta-glucan, a fermentable fiber, lowers serum cholesterol in hypercholesterolemic adults in a randomized controlled trial. Nutr J 6:6–13
18. Hartman TJ, Albert PS, Zhang Z, Bagshaw D, Kris-Etherton PM, Ulbrecht J, Miller CK, Bobe G, Colburn NH, Lanza E (2010) Consumption of a legume-enriched, low-glycemic index diet is associated with biomarkers of insulin resistance and inflammation among men at risk for colorectal cancer. J Nutr 140:60–67
19. Matthews DR, Hosker JP, Rudenski AS, Naylor BA, Treacher DF, Turner RC (1985) Homeostasis model assessment: insulin resistance and beta-cell function from fasting plasma glucose and insulin concentrations in man. Diabetologia 28:412–419
20. Ascaso JF, Pardo S, Real JT, Lorente RI, Priego A, Carmena R (2003) Diagnosing insulin resistance by simple quantitative methods in subjects with normal glucose metabolism. Diabetes Care 26:3320–3325
21. Gazzaruso C, Solerte SB, De Amici E, Mancini M, Pujia A, Fratino P, Giustina A, Garzaniti A (2006) Association of the metabolic syndrome and insulin resistance with silent myocardial ischemia in patients with type 2 diabetes mellitus. Am J Cardiol 97:236–239
22. Ginsberg HN, Kris-Etherton P, Dennis B, Elmer PJ, Ershow A, Lefevre M, Pearson T, Roheim P, Ramakrishnan R, Reed R, Stewart K, Stewart P, Phillips K, Anderson N (1998) Effects of reducing dietary saturated fatty acids on plasma lipids and lipoproteins in healthy subjects: the DELTA Study, protocol 1. Arterioscler Thromb Vasc Biol 18:441–449
23. Ullrich IH, Albrink MJ (1982) Lack of effect of dietary fiber on serum lipids, glucose, and insulin in healthy young men fed high starch diets. Am J Clin Nutr 36:1–9
24. Oosthuizen W, Scholtz CS, Vorster HH, Jerling JC, Vermaak WJ (2000) Extruded dry beans and serum lipoprotein and plasma haemostatic factors in hyperlipidaemic men. Eur J Clin Nutr 54:373–379
25. Cara L, Dubois C, Borel P, Armand M, Senft M, Portugal H, Pauli AM, Bernard PM, Lairon D (1992) Effects of oat bran, rice bran, wheat fiber, and wheat germ on postprandial lipemia in healthy adults. Am J Clin Nutr 55:81–88
26. Davy BM, Davy KP, Ho RC, Beske SD, Davrath LR, Melby CL (2002) High-fiber oat cereal compared with wheat cereal consumption favorably alters LDL-cholesterol subclass and particle

numbers in middle-aged and older men. Am J Clin Nutr 76:351–358
27. Katcher HI, Legro RS, Kunselman AR, Gillies PJ, Demers LM, Bagshaw DM, Kris-Etherton PM (2008) The effects of a whole grain-enriched hypocaloric diet on cardiovascular disease risk factors in men and women with metabolic syndrome. Am J Clin Nutr 87:79–90
28. Anderson JW, Gustafson NJ, Spencer DB, Tietyen J, Bryant CA (1990) Serum lipid response of hypercholesterolemic men to single and divided doses of canned beans. Am J Clin Nutr 51:1013–1019
29. Pittaway JK, Robertson IK, Ball MJ (2008) Chickpeas may influence fatty acid and fiber intake in an ad libitum diet, leading to small improvements in serum lipid profile and glycemic control. J Am Diet Assoc 108:1009–1013
30. Lanza E, Hartman TJ, Albert PS, Shields R, Slattery M, Caan B, Paskett E, Iber F, Kikendall JW, Lance P, Daston C, Schatzkin A (2006) High dry bean intake and reduced risk of advanced colorectal adenoma recurrence among participants in the polyp prevention trial. J Nutr 136:1896–1903
31. Jenkins DJ, Kendall CW, Popovich DG, Vidgen E, Mehling CC, Vuksan V, Ransom TP, Rao AV, Rosenberg-Zand R, Tariq N, Corey P, Jones PJ, Raeini M, Story JA, Furumoto EJ, Illingworth DR, Pappu AS, Connelly PW (2001) Effect of a very-high-fiber vegetable, fruit, and nut diet on serum lipids and colonic function. Metabolism 50:494–503
32. Appel LJ, Sacks FM, Carey VJ, Obarzanek E, Swain JF, Miller ER 3rd, Conlin PR, Erlinger TP, Rosner BA, Laranjo NM, Charleston J, McCarron P, Bishop LM (2005) Effects of protein, monounsaturated fat, and carbohydrate intake on blood pressure and serum lipids: results of the OmniHeart randomized trial. JAMA 294:2455–2464
33. Joshipura KJ, Ascherio A, Manson JE, Stampfer MJ, Rimm EB, Speizer FE, Hennekens CH, Spiegelman D, Willett WC (1999) Fruit and vegetable intake in relation to risk of ischemic stroke. JAMA 282:1233–1239
34. Liu S, Manson JE, Lee IM, Cole SR, Hennekens CH, Willett WC, Buring JE (2000) Fruit and vegetable intake and risk of cardiovascular disease: the Women's Health Study. Am J Clin Nutr 72:922–928
35. Bazzano LA, He J, Ogden LG, Loria CM, Vupputuri S, Myers L, Whelton PK (2002) Fruit and vegetable intake and risk of cardiovascular disease in US adults: the first National Health and Nutrition Examination Survey Epidemiologic Follow-up Study. Am J Clin Nutr 76:93–99
36. Steffen LM, Jacobs DR Jr, Stevens J, Shahar E, Carithers T, Folsom AR (2003) Associations of whole-grain, refined-grain, and fruit and vegetable consumption with risks of all-cause mortality and incident coronary artery disease and ischemic stroke: the Atherosclerosis Risk in Communities (ARIC) Study. Am J Clin Nutr 78:383–390
37. Rissanen TH, Voutilainen S, Virtanen JK, Venho B, Vanharanta M, Mursu J, Salonen JT (2003) Low intake of fruits, berries and vegetables is associated with excess mortality in men: the Kuopio Ischaemic Heart Disease Risk Factor (KIHD) Study. J Nutr 133:199–204
38. Djousse L, Arnett DK, Coon H, Province MA, Moore LL, Ellison RC (2004) Fruit and vegetable consumption and LDL cholesterol: the National Heart, Lung, and Blood Institute Family Heart Study. Am J Clin Nutr 79:213–217
39. Ford ES, Liu S (2001) Glycemic index and serum high-density lipoprotein cholesterol concentration among us adults. Arch Intern Med 161:572–576
40. Amano Y, Kawakubo K, Lee JS, Tang AC, Sugiyama M, Mori K (2004) Correlation between dietary glycemic index and cardiovascular disease risk factors among Japanese women. Eur J Clin Nutr 58:1472–1478
41. Ma Y, Li Y, Chiriboga DE, Olendzki BC, Hebert JR, Li W, Leung K, Hafner AR, Ockene IS (2006) Association between carbohydrate intake and serum lipids. J Am Coll Nutr 25:155–163
42. Du H, van der AD, van Bakel MM, van der Kallen CJ, Blaak EE, van Greevenbroek MM, Jansen EH, Nijpels G, Stehouwer CD, Dekker JM, Feskens EJ (2008) Glycemic index and glycemic load in relation to food and nutrient intake and metabolic risk factors in a Dutch population. Am J Clin Nutr 87:655–661
43. Levitan EB, Cook NR, Stampfer MJ, Ridker PM, Rexrode KM, Buring JE, Manson JE, Liu S (2008) Dietary glycemic index, dietary glycemic load, blood lipids, and C-reactive protein. Metabolism 57:437–443
44. Liu S, Manson JE, Stampfer MJ, Holmes MD, Hu FB, Hankinson SE, Willett WC (2001) Dietary glycemic load assessed by food-frequency questionnaire in relation to plasma high-density-lipoprotein cholesterol and fasting plasma triacylglycerols in postmenopausal women. Am J Clin Nutr 73:560–566
45. Ebbeling CB, Leidig MM, Feldman HA, Lovesky MM, Ludwig DS (2007) Effects of a low-glycemic load vs low-fat diet in obese young adults: a randomized trial. JAMA 297:2092–2102
46. Maki KC, Rains TM, Kaden VN, Raneri KR, Davidson MH (2007) Effects of a reduced-glycemic-load diet on body weight, body composition, and cardiovascular disease risk markers in overweight and obese adults. Am J Clin Nutr 85:724–734
47. de Jong A, Plat J, Mensink RP (2003) Metabolic effects of plant sterols and stanols (Review). J Nutr Biochem 14:362–369
48. Child P, Kuksis A (1986) Investigation of the role of micellar phospholipid in the preferential uptake of cholesterol over sitosterol by dispersed rat jejunal villus cells. Biochem Cell Biol 64:847–853
49. Child P, Kuksis A (1983) Critical role of ring structure in the differential uptake of cholesterol and plant sterols by membrane preparations in vitro. J Lipid Res 24:1196–1209
50. Gylling H, Miettinen TA (1994) Serum cholesterol and cholesterol and lipoprotein metabolism in hypercholesterolaemic NIDDM patients before and during sitostanol ester-margarine treatment. Diabetologia 37:773–780
51. Plat J, Mensink RP (2002) Effects of plant stanol esters on LDL receptor protein expression and on LDL receptor and HMG-CoA reductase mRNA expression in mononuclear blood cells of healthy men and women. Faseb J 16:258–260
52. Plat J, Mensink RP (2002) Third Report of the National Cholesterol Education Program (NCEP) Expert Panel on Detection, Evaluation, and Treatment of High Blood Cholesterol in Adults (Adult Treatment Panel III) final report. Circulation 106:3143–3421
53. Lefevre M, Champagne CM, Tulley RT, Rood JC, Most MM (2005) Individual variability in cardiovascular disease risk factor responses to low-fat and low-saturated-fat diets in men: body mass index, adiposity, and insulin resistance predict changes in LDL cholesterol. Am J Clin Nutr 82:957–963
54. Harsha DW, Sacks FM, Obarzanek E, Svetkey LP, Lin PH, Bray GA, Aickin M, Conlin PR, Miller ER 3rd, Appel LJ (2004) Effect of dietary sodium intake on blood lipids: results from the DASH-sodium trial. Hypertension 43:393–398
55. Wilson PW, D'Agostino RB, Levy D, Belanger AM, Silbershatz H, Kannel WB (1998) Prediction of coronary heart disease using risk factor categories. Circulation 97:1837–1847
56. Bonora E, Targher G, Alberiche M, Bonadonna RC, Saggiani F, Zenere MB, Monauni T, Muggeo M (2000) Homeostasis model assessment closely mirrors the glucose clamp technique in the assessment of insulin sensitivity: studies in subjects with various

degrees of glucose tolerance and insulin sensitivity. Diabetes Care 23:57–63
57. Emoto M, Nishizawa Y, Maekawa K, Hiura Y, Kanda H, Kawagishi T, Shoji T, Okuno Y, Morii H (1999) Homeostasis model assessment as a clinical index of insulin resistance in type 2 diabetic patients treated with sulfonylureas. Diabetes Care 22:818–822
58. Hopkins PN (1992) Effects of dietary cholesterol on serum cholesterol: a meta-analysis and review. Am J Clin Nutr 55:1060–1070
59. Koba S, Yokota Y, Hirano T, Ito Y, Ban Y, Tsunoda F, Sato T, Shoji M, Suzuki H, Geshi E, Kobayashi Y, Katagiri T (2008) Small LDL-cholesterol is superior to LDL-cholesterol for determining severe coronary atherosclerosis. J Atheroscler Thromb 15:250–260

Lipids (2010) 45:777–784
DOI 10.1007/s11745-010-3462-8

ORIGINAL ARTICLE

Canola Oil Inhibits Breast Cancer Cell Growth in Cultures and In Vivo and Acts Synergistically with Chemotherapeutic Drugs

Kyongshin Cho · Lawrence Mabasa · Andrea W. Fowler · Dana M. Walsh · Chung S. Park

Received: 11 February 2010 / Accepted: 6 August 2010 / Published online: 22 August 2010

Abstract Certain fatty acids in canola oil (CAN) have been associated with a reduced risk of breast cancer. This study assessed the effects of CAN on proliferation and death of human breast cancer cells in vitro and in vivo in chemically induced mammary carcinogenesis. We hypothesize that CAN reduces breast cancer cell growth by inducing cell death. In a series of in vitro experiments, human breast cancer T47D and MCF-7 cells were cultured and treated with CAN and two chemotherapeutic drugs, tamoxifen and cerulenin. Cell proliferation and caspase-3 and p53 activities were measured. Reduced cancer cell growth and increased expression of caspase-3 and p53 were seen in T47D and MCF-7 cells treated with CAN. Moreover, CAN showed synergistic cancer cell growth inhibition effects with tamoxifen and cerulenin. In a subsequent live animal experiment, 42 female Sprague–Dawley rats were randomly assigned to corn oil (CORN) or CAN diets, and mammary tumors were chemically induced by *N*-nitroso-*N*-methylurea. CAN-dieted rats had reduced tumor volumes and showed an increased survival rate as compared to CORN-dieted rats. We demonstrated that CAN has suppressive effects on cancer growth, and reduces tumor volumes. The results suggest that CAN may have inhibitory effects on breast cancer cell growth, and warrants further investigation of the synergistic effects of CAN with anti-cancer drugs.

K. Cho · L. Mabasa · A. W. Fowler · D. M. Walsh · C. S. Park (✉)
Department of Animal Sciences, North Dakota State University, North University Drive, Fargo, ND 58108, USA
e-mail: c.park@ndsu.edu

Keywords Canola oil · Breast cancer · Tamoxifen · Cerulenin · Caspase-3 · p53 · Sprague–Dawley rat · *N*-nitroso-*N*-methylurea

Abbreviations

ALA	Alpha-linolenic acid
CAN	Canola oil
CORN	Corn oil
ER	Estrogen receptor
FITC	Fluorescein isothiocyanate
MTS	Dimethylthiazol carboxymethoxyphenyl sulfophenyl tetrazolium
NMU	*N*-nitroso-*N*-methylurea
OA	Oleic acid
PI	Propidium iodide

Introduction

Breast cancer is the most common malignancy among women in western countries, where one out of every eight will develop it during her lifetime [1, 2]. More than 180,000 new breast cancer diagnoses are made in the United States each year, and over 40,000 women will die from the disease [3]. This high incidence of breast cancer in the US is associated with diets rich in total and saturated fats, which are typical of western lifestyles [1, 4]. However, many epidemiological studies provide evidence for a close relationship between certain fatty acids, such as omega-3, and reduced cancer risk [5, 6].

Dietary fats have profound effects on cell membrane, metabolism and gene expression. Essential fatty acids, like omega-3 and omega-6, cannot be synthesized by the human

body and must be obtained in the diet [7]. Canola oil (CAN) contains both of these fats, along with low levels of saturated fat, and high levels of monounsaturated (oleic acid, OA) and polyunsaturated (alpha-linolenic acid, ALA) fatty acids [8, 9]. The majority of studies to date have linked ALA and OA with a reduced risk of breast cancer, but omega-6 and saturated fats with an increased risk [6, 10].

A lower ratio between omega-6 and omega-3 fatty acids seems to be helpful in reducing the risk of breast cancer, and CAN has a very favorable 2:1 ratio between omega-6 and omega-3 fatty acids [8]. When this ratio is imbalanced, a variety of health issues may appear, including breast cancer [11, 12]. It has been established that certain fatty acids have inhibitory effects on cancer cells, but the role of omega-6 and omega-3 fatty acids remains controversial [13]. Even so, ensuring that the consumption of omega-6 and omega-3 fatty acids is in the correct ratio could protect against breast cancer [9, 10].

The health benefits of CAN are widely accepted in the field of nutrition, particularly in relation to cardiovascular disease. However, information is limited on its effects on breast cancer. We hypothesize that CAN reduces breast cancer cell growth by inducing cell death. The objectives of this study were to determine if CAN affects the proliferation and death of human breast cancer cells in vitro with chemotherapeutic drugs, and to see if it reduces the susceptibility of cancer cells to chemically induced mammary carcinogenesis in vivo.

Experimental Procedure

Cell Culture

The estrogen receptor (ER) positive human breast cancer T47D (ductal carcinoma) and MCF-7 (adenocarcinoma) cell lines were obtained from the American Type Culture Collection (ATCC, Manassas, VA, USA). They were grown in Roswell Park Memorial Institute 1640 medium (RPMI 1640, Gibco-Invitrogen, Carlsbad, CA, USA) and Dulbecco's modified Eagle's minimum essential medium (DMEM, Gibco-Invitrogen), respectively. Both were supplemented with 10% v/v heat-inactivated fetal bovine serum (Gibco-Invitrogen) and 1% v/v antibiotic–antimycotic solution (Gibco-Invitrogen) and grown at 37 °C in a 5% CO_2-humidified atmosphere.

Materials

CAN was filtered and added aseptically from stock solutions to 100% ethanol and brought to a final ethanol concentration of 0.5% v/v [14]. CAN stock solutions were pre-warmed and vigorously stirred before addition to cell medium. The appropriate or optimal doses of CAN and chemotherapeutic drugs, tamoxifen (10 μM, Sigma-Aldrich, St Louis, MO, USA) and cerulenin (5 mg/l, Sigma-Aldrich), were determined from dose response studies. Controls always included ethanol at the appropriate concentration.

Cell Proliferation Assay

The colorimetric MTS (3-(4,5-dimethylthiazol-2-yl)-5-(3-carboxymethoxyphenyl)-2-(4-sulfophenyl)-2*H*-tetrazolium) assay (CellTiter 96 Aqueous One Solution Reagent, Promega, Madison, WI, USA) was used to measure cell proliferation. Briefly, cells were seeded in 96-well flat-bottomed tissue culture plates (5×10^3 cells/well in 100 μl), and exposed to CAN. After 24–96 h of incubation, they were incubated for 1–4 h with 10% MTS solution. The degree of cell proliferation was evaluated numerically by measuring the absorbance at 490 nm with a SpectraMax Microplate Reader (Molecular Devices, Sunnyvale, CA, USA). The cell proliferation was calculated and expressed based on the following formula: ([treated cell absorbance − initial (seeding) cell absorbance]/initial (seeding) cell absorbance) × 100.

Caspase-3 Assay

The protease activity of caspase-3 was measured using a colorimetric assay with the CaspACE assay system (Promega). Briefly, cells were cultured in 24-well flat-bottomed tissue culture plates (5×10^4 cells/ml) and treated with CAN. Cultured cells were washed twice with phosphate-buffered saline (PBS) and re-suspended in a cell lysis buffer (Promega). Cell lysates were incubated with a colorimetric substrate, *N*-acetyl-Asp-Glu-Val-Asp-amino-*p*-nitroanilide (Ac-DEVD-*p*NA). After an overnight incubation, the release of *p*-nitroaniline from Ac-DEVD-*p*NA was measured at 405 nm.

p53 Assay

The p53 activity was determined by using an enzyme immunometric assay kit (TiterZyme EIA Kit, Assay Designs, Ann Arbor, MI, USA). Cultured cells (5×10^4 cells/ml) were washed twice with PBS and re-suspended in cell lysis buffer (Sigma-Aldrich). The cell lysates were centrifuged. The supernatants were incubated on a plate pre-immobilized with p53 polyclonal antibody and they reacted with the labeled antibody. The absorbance was measured at 450 nm.

Flow Cytometric Analysis

Cell death was determined by double-staining with fluorescein isothiocyanate (FITC)-conjugated annexin V and propidium iodide (PI) (Sigma-Aldrich) as described previously [15]. Cells were harvested and washed with PBS containing 0.5% bovine serum albumin (Sigma-Aldrich) and 0.1% sodium azide (Sigma-Aldrich). They were then incubated with FITC-conjugated annexin V and PI. Cells were washed and then analyzed using an Accuri C6 cytometer and Cflow software (Accuri Cytometers, Ann Arbor, MI, USA).

Chemotherapeutic Drug Treatments

T47D and MCF-7 cells were seeded in 96-well flat-bottomed tissue culture plates (5×10^4 cells/ml). They were cultured simultaneously for 24–96 h with media containing various combinations of CAN and the chemotherapeutic drugs tamoxifen and cerulenin. Afterwards, cell proliferation was measured.

Animals and Diets

Forty-two female Sprague–Dawley rats (3 weeks of age) were purchased from Harlan (Indianapolis, IN, USA) and acclimated to the experimental environment for 1 week with ad libitum access to water and a standard control AIN-76 diet. After acclimation, all rats were randomly assigned to receive modified AIN-76 CORN or CAN diets (Table 1) [16]. All animal procedures and techniques were approved by the Institutional Animal Care and Use Committee of North Dakota State University. The experimental diets were formulated to be both isocaloric and isonitrogenous.

Table 1 Composition of the experimental diets

Ingredients	Diets (per 100 g)	
	Corn oil	Canola oil
Sucrose	50.0	37.8
Casein	20.0	20.0
Corn starch	15.0	15.0
Cellulose	5.0	12.2
Mineral mix	3.5	3.5
Vitamin mix	1.0	1.0
DL-Methionine	0.3	0.3
Ethoxyquin (antioxidant, mg)	10.0	21.0
Corn oil	5.0	–
Canola oil	–	10.0

Tumor Induction and Measurement

All rats were injected subcutaneously with a single dose of *N*-nitroso-*N*-methylurea (NMU, Sigma-Aldrich, 50 mg/kg body weight) dissolved in PBS acidified with acetic acid. The rats were palpated twice weekly to detect the presence of mammary tumors. The time of appearance of the first tumor (latency period) and location of mammary tumors were recorded and tumor sizes were measured. The tumor volume was calculated using the following formula: (length $\times$ width)/2 [17].

Statistical Analysis

Cell culture experiments were conducted at least three times in triplicate or quadruplicate. Results are expressed as means $\pm$ SEM of independent determinations. Statistical analysis was performed using Student's t test and one-way ANOVA followed by Tukey's test (Minitab Release 14.1, Minitab Inc., State College, PA, USA). Differences were considered significant at $P < 0.05$. Animal experiment data were analyzed using the General Linear Models (SAS 9.1, Statistical Analysis System Institute, Cary, NC, USA) with a two sample t test. For comparison of the least square means, values on tumor volumes were log scaled ($\log_{10}$ tumor volume).

Results

T47D and MCF-7 Cancer Cell Growth Response

The cell proliferation of T47D and MCF-7 cells was examined in the presence of 0.001–1 mM of CAN for time- and dose-dependent studies. At 0.001 and 0.01 mM concentrations, CAN did not have any significant inhibitory effect on T47D and MCF-7 cells. However, cell growth was decreased at 0.1 mM (data not shown). As shown in Fig. 1, CAN treatment resulted in a significant growth inhibition of T47D and MCF-7 cells in a time-dependent manner. In T47D cells, a 1 mM dose of CAN caused 31.4% growth inhibition (Fig. 1a) after 96 h of CAN treatment. Similar inhibition was also evident in MCF-7 cells, at 21.8% cell growth inhibition (Fig. 1b) after 96 h of CAN treatment. CAN showed a time- and dose-dependent effect which was detectable during early and late phases of cell growth in T47D and MCF-7 cells.

Caspase-3 and p53 Activities, and Cancer Cell Death

In order to determine if the cell growth inhibition effect of CAN was caused by the induction of apoptosis, caspase-3 and p53 expressions were analyzed by enzyme assays. In

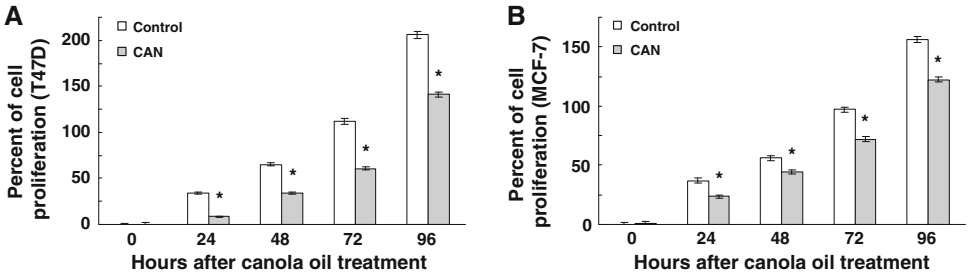

Fig. 1 Effects of CAN on time-dependent cancer cell growth. **a** T47D and **b** MCF-7 cells were treated with 1 mM of CAN. Data in **a** and **b** are means ± SEM ($n = 12$) and expressed as percentages of cell proliferation ([treated cell absorbance − initial (seeding) cell absorbance]/initial (seeding) cell absorbance) × 100. *Different from control, $P < 0.05$

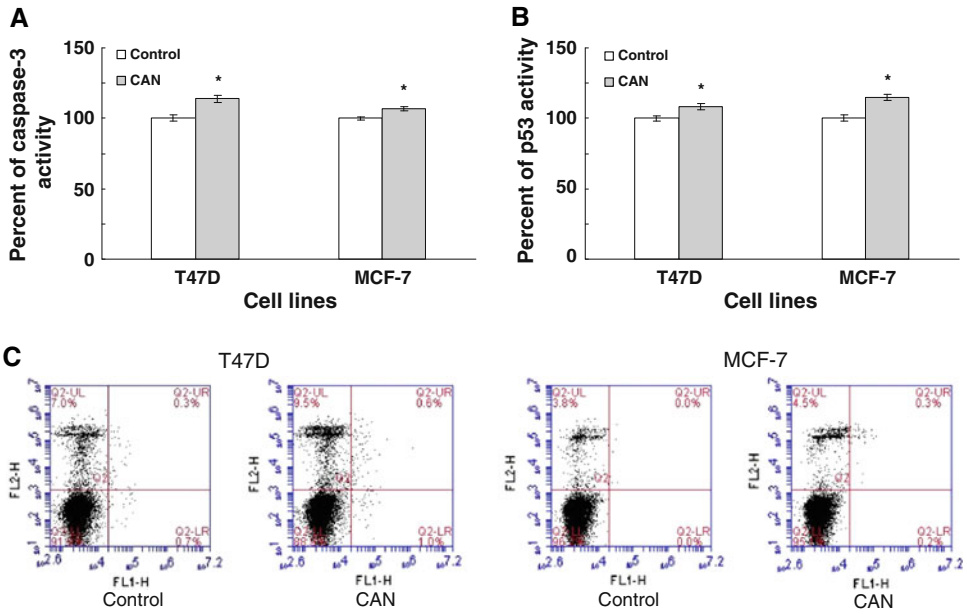

Fig. 2 Caspase-3 and p53 activities of 1 mM CAN-treated T47D and MCF-7 cells. **a** Caspase-3 activity of CAN treatment (1 mM) for 96 h. **b** p53 activity of CAN treatment (1 mM) for 96 h. **c** Cell death and apoptosis of 1 mM CAN-treated T47D and MCF-7 cells for 72 h. Cells were stained with Annexin V-FITC (FL1, *X* axis) and PI (FL2, *Y* axis). Data in **a** and **b** are means ± SEM ($n = 9$) and expressed as percentages of control cell caspase-3 or p53 activities (treated cell absorbance/control cell absorbance) × 100. *Different from control, $P < 0.05$

T47D and MCF-7 cells, 1 mM of CAN significantly increased caspase-3 and p53 activities. At 96 h after CAN treatment, the change in caspase-3 of T47D and MCF-7 cells was 16.2 and 8.2% (Fig. 2a), and the change in p53 was 8.4 and 14.8% (Fig. 2b), respectively. These results suggest significant up-regulation of caspase-3 and p53 activities in both cell lines. Consistent results were also obtained with flow cytometric data on cancer cell death. CAN showed increased cell death in both T47D (7.0 vs. 9.5%) and MCF-7 (3.8 vs. 4.5%) cells (Fig. 2c).

Possible Synergistic Effects of CAN with Chemotherapeutic Drugs on Cancer Cell Growth Inhibition

Based on the data showing cell growth inhibition and apoptosis in T47D and MCF-7, in order to evaluate a possible synergistic or additive effect of CAN, the anti-cancer drugs tamoxifen and cerulenin were assessed in combination with CAN. CAN showed significant synergistic effects with tamoxifen and cerulenin. As shown in Fig. 3, a combination of 1 mM CAN and 10 μM tamoxifen resulted in 49.0 and 5.7% growth inhibition (Fig. 3a, compared to tamoxifen alone) in T47D and MCF-7 cells at 96 h after treatment. Similar to tamoxifen, a combination of 1 mM CAN and 5 mg/l cerulenin resulted in 40.5% and 6.5% growth inhibition (Fig. 3b) at 96 h after treatment, compared to cerulenin alone.

Tumor Volumes and Survival Rate In Vivo

We determined the in vivo effect of CAN using Sprague–Dawley rats. Breast tumors were induced in rats by subcutaneous injection of the alkylating carcinogen NMU. There were no significant differences in initial (85.9–86.5 g) and final (231.3–234.1 g) average body weights between CORN and CAN groups. The latency period was determined to be the days between NMU administration and the first day of tumor detection. The tumor incidence was based on the percentage of rats that developed at least one tumor at

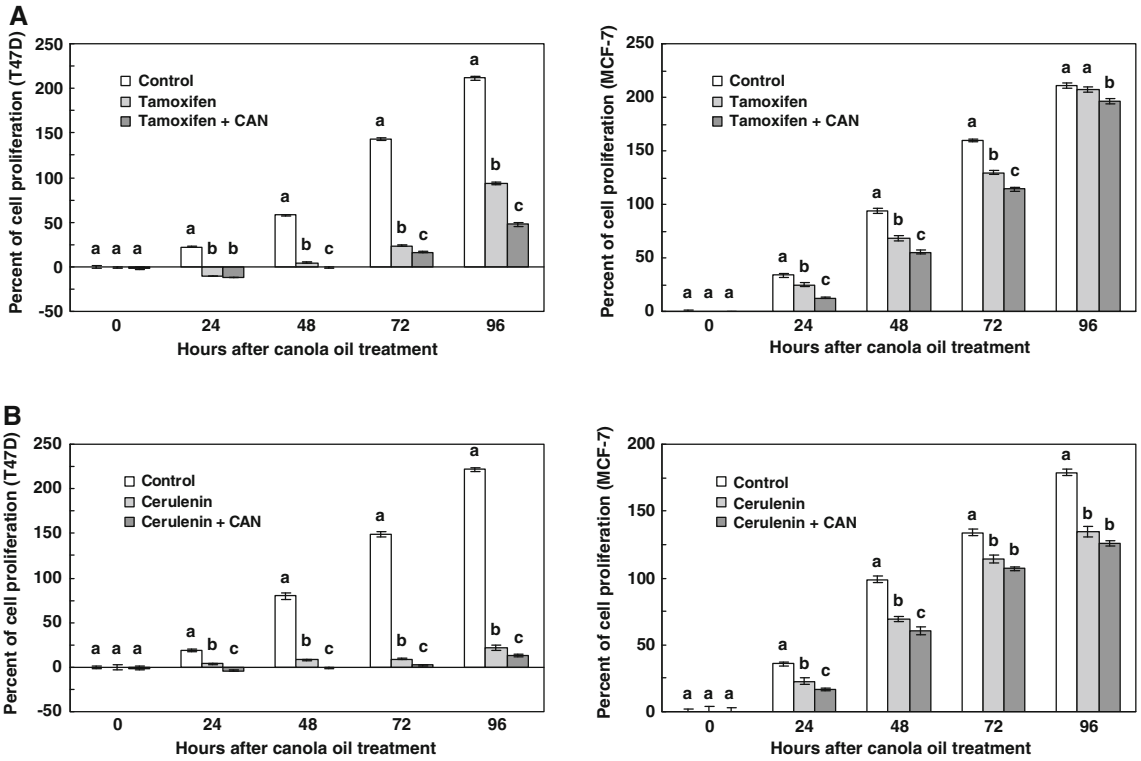

Fig. 3 Effects of CAN with tamoxifen and cerulenin on T47D and MCF-7 cell proliferation. **a** Effect of 1 mM CAN and 10 μM tamoxifen. **b** Effect of 1 mM CAN and 5 mg/l cerulenin. *Bars* represent means ± SEM ($n = 12$) and are expressed as percentages of cell proliferation ([treated cell absorbance − initial (seeding) cell absorbance]/initial (seeding) cell absorbance) × 100. *Bars* within time with *different superscripts* are different ($P < 0.05$)

25 weeks after NMU administration. As shown in Table 2, the latency period was not affected by the CAN diet compared to the CORN diet. However, the CAN diet reduced the tumor incidence (Table 2) and increased the survival rate (Fig. 4a). Moreover, mammary tumor volumes were significantly reduced in the CAN group, compared to the CORN diet (Fig. 4b, Table 2).

Table 2 Comparison of the tumor incidence, latency period, number of tumors, and tumor volumes between CORN and CAN groups

	Corn oil	Canola oil	*P* value
Tumor incidence[a] (%)	71	57	
Latency period[b] (days)	93.00 ± 6.90	103.40 ± 7.70	0.34
Number of tumors[c] (tumors/rat)	1.93 ± 0.30	1.50 ± 0.33	0.33
Tumor volume[d] (mm^3/rat)	2.32 ± 0.06	1.61 ± 0.06	0.01

Values are means ± SEM

[a] Percentage of rats that developed at least one or more tumors at 25 weeks after NMU injection

[b] Determined as the days between NMU injection and the first day of tumor detection

[c] Values were determined at 25 weeks after NMU injection

[d] Values were averaged over the 15-week period of tumor existence and then log scaled, $\log_{10}$ (tumor volume)

Discussion

Dietary fats are important not only as energy sources, but also for their role in metabolism and gene expression [7]. Regulation of genes associated with cell growth and death may reflect an adaptive response to changes in the type of fatty acids ingested and demonstrate that the type of lipid is more closely associated with breast cancer risk than the quantity of lipid [18]. The two major fatty acids in CAN, ALA and OA, have been shown to play important roles in the modulation of cancer cell growth and death [6, 10]. This study investigated the effects of CAN in the well established ER+ breast cancer cells and NMU-induced mammary tumor animal models, particularly those concerning cancer cell growth and synergism of CAN with chemotherapeutic drugs.

CAN was shown to be effective in reducing cancer cell growth and inducing cell death (Figs. 1, 2). Moreover, as shown in Fig. 3, the growth of T47D was completely inhibited by the chemotherapeutic agents, tamoxifen and cerulenin with CAN (1 mM) at 24 h of treatments. However, MCF-7 showed continued growth with tamoxifen and cerulenin, and this may imply that T47D and MCF-7 cells have distinct growth patterns. Although there were similar increases in caspase-3 and p53 activities between T47D

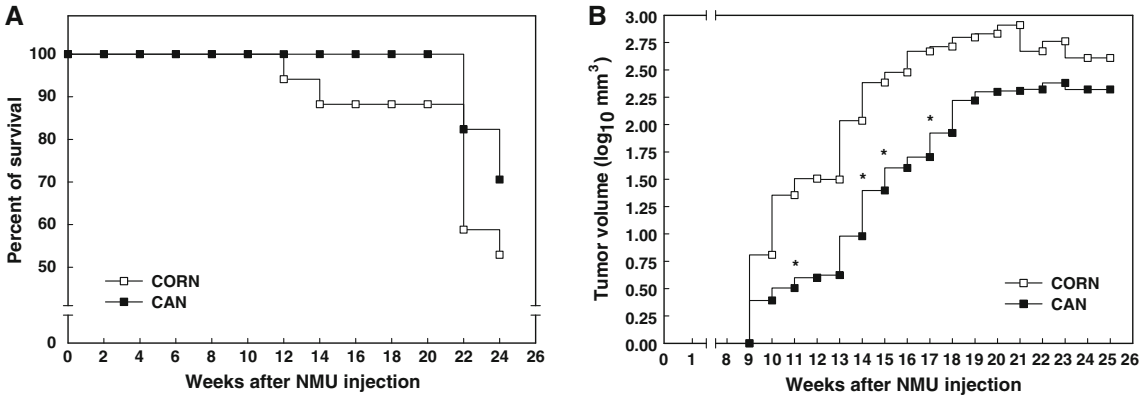

Fig. 4 In vivo effects of CAN in Sprague–Dawley rats. Data represent the average survival rates (**a**) and tumor volumes (**b**) of rats fed CORN and CAN in response to a single dose of NMU carcinogen injection. Data are expressed as percentages of survival and logarithmic average tumor volumes ($n = 21$). *Different from control, $P < 0.05$

and MCF-7 cells in response to CAN, the growth inhibition of T47D was greater than that of MCF-7, suggesting that other mechanisms may also participate in the reduction of cell growth. We have also shown that dietary CAN may reduce tumor volumes in NMU-induced carcinogenesis. Mammary tumor growth was significantly reduced in the CAN fed group (Fig. 4b, $P = 0.01$) and the survival rate of the CAN group increased compared to the CORN group (Fig. 4a). The CAN group also showed a lower number of tumors and longer latency period than the CORN group (Table 2, no statistically significant differences).

The effect of CAN on cell growth and caspase-3 activity was also investigated in the non-cancerous human mammary epithelial MCF-10A (fibrocystic disease) cell line. In contrast to T47D and MCF-7 cancer cell lines, which showed significant reduced cell growth, CAN did not affect the proliferation of non-cancerous mammary cells (MCF-10A) in vitro at concentrations as high as 1 mM (Fig. 5a). The explanation for the differential effect of CAN on cancerous and non-cancerous mammary cells is not known. However, it is interesting to note that caspase-3 activity is similar in CORN and CAN treated MCF-10A cells, suggesting that caspase-3 may play a role in T47D and MCF-7 cancer cell death (Fig. 5b, $P = 0.87$).

ERs play important roles in mammary growth and differentiation [19]. The specific receptors ER alpha and ER beta have distinct roles in mammary development [19]. Some studies indicate that ERs mediate the breast cancer-promoting (ER alpha) or -inhibiting (ER beta) effects of estrogens [20]. However, the exact role of ERs in breast cancer is still not clear. In a study by Hardman [21], 8% of CAN significantly reduced ER negative MDA-MB 231 tumor cell growth and modified cell membrane composition in nude mice. It is not clear how CAN affects both kinds of breast tumors, but CAN seems to reduce cell growth in both ER positive and ER negative breast cancer cells.

Dietary fat intake and breast cancer risk has been a considerable topic of interest in cancer research. Many of the established risk factors are linked with nutrition, suggesting that dietary intervention may be a significant factor in breast cancer prevention and therapy [22]. A recently published population-based, multi-ethnic, case–control study suggests that women cooking with hydrogenated fats or CORN have a higher risk of breast cancer than women cooking with CAN [23]. Flaxseed, a rich source of ALA (with approximately a 1:2 ratio between omega-6 and omega-3 fatty acids), has been shown to decrease breast cancer risk; 10% of dietary flaxseed reduced 50% of MCF-7 cancer cell growth with tamoxifen in nude mice [24].

Several in vivo and in vitro studies have also shown that omega-3 fatty acids have inhibitory effects on the initiation, promotion, and progression stages of breast cancer [6, 25]. Epidemiological studies showed that groups of people who consume diets high in omega-3 and OA could have lower breast cancer incidence rates [6, 11]. Omega-3 and OA have also been found to inhibit mammary tumor cell proliferation and to enhance immune cell function against breast cancer [18, 26].

The anti-estrogen agent, tamoxifen, and fatty acid synthase inhibitor, cerulenin, were used to measure the synergistic effects of CAN in this study. Tamoxifen is used for the treatment and prevention of ER+ breast cancer in high-risk women. The drug competes with estrogen for ER binding and therefore inhibits ER-mediated cancer growth [27]. Cerulenin, a noncompetitive inhibitor of fatty acid synthase, inhibits fatty acid synthesis and thereby induces cell death of breast cancer cells [28]. Increasing the susceptibility of cancer cells to chemotherapeutic agents may have significant implications in cancer therapy, and

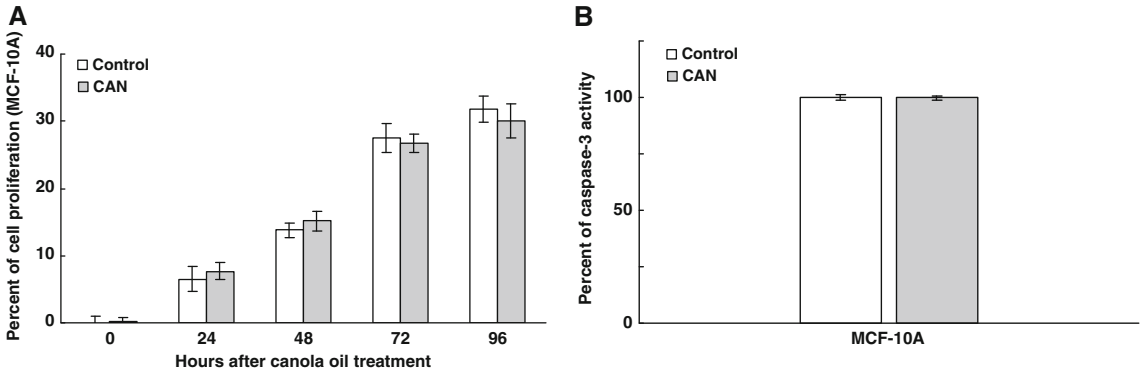

Fig. 5 Cell growth and caspase-3 activities of 1 mM CAN treated MCF-10A cells. Data in **a** are means ± SEM ($n = 12$) and are expressed as percentages of cell proliferation ([treated cell absorbance − initial (seeding) cell absorbance]/initial (seeding) cell absorbance) × 100. Data in **b** are means ± SEM ($n = 9$) and are expressed as percentages of control cell caspase-3 activities (treated cell absorbance/control cell absorbance) × 100. *Different from control, $P < 0.05$

inducing cell death in cancer cells may be an effective strategy to inhibit cancer growth [29].

Our findings suggest that a 2:1 omega-6 to omega-3 fatty acid ratio may be optimal for cancer growth inhibition, while a higher ratio may increase tumor growth. In addition, our work also suggests that OA may reduce tumor growth. The inhibitory effect of CAN may be due to its low omega-6 to omega-3 fatty acid ratio (2:1) and high OA (61%) as compared to the high omega-6 to omega-3 fatty acid ratio (57:1) and low OA content (29%) in CORN [8]. T47D and MCF-7 cells showed significant cell growth inhibition with CAN supplementation to both drug treatments. However, the inhibition of T47D cells was greater than that of MCF-7 cells (Fig. 3a, b). This discrepancy may have been the result of other mechanisms at work in T47D cell proliferation. These mechanisms may have inhibited the growth of T47D cells more than that of MCF-7 cells. Since the mechanisms responsible are not known, further studies need to be conducted, especially in the expression of several key genes involved in tumor growth. This may show differences in expression of tumor growth-related genes in T47D and MCF-7.

In conclusion, our results show that CAN has anti-proliferative and synergistic effects on breast cancer cell growth in vitro with chemotherapeutic drugs, and reduces in vivo mammary tumor cell growth in rats. The synergistic effects of CAN with tamoxifen and cerulenin may be useful in reducing the doses of chemotherapeutic drugs and increasing the chance of long-term survival. In order to validate these findings, a more in-depth investigation into the relationship between CAN and chemotherapeutic drugs is needed. For example, since ER beta induces breast cancer cell death, further studies could determine whether CAN increases ER beta expression, inhibiting breast cancer cell growth and increasing susceptibility of breast cancer cells to chemotherapeutic drug actions. Moreover, how CAN shows synergistic effects with therapeutic drugs may be examined in relation to ER expression, membrane composition and gene expression changes. These results may provide useful data for the development of improved nutritional strategies for reducing breast cancer risk.

Acknowledgments This research was supported by USDA-CSREES grant 2007-38624-18602.

References

1. McPherson K, Steel CM, Dixon JM (2000) ABC of breast diseases. Breast cancer-epidemiology, risk factors, and genetics. BMJ 321:624–628
2. Feuer EJ, Wun LM, Boring CC, Flanders WD, Timmel MJ, Tong T (1993) The lifetime risk of developing breast cancer. J Natl Cancer Inst 85:892–897
3. Jemal A, Siegel R, Ward E, Hao Y, Xu J, Murray T, Thun MJ (2008) Cancer statistics, 2008. CA Cancer J Clin 58:71–96
4. Parkin DM, Bray F, Ferlay J, Pisani P (2005) Global cancer statistics, 2002. CA Cancer J Clin 55:74–108
5. Astorg P (2004) Dietary N-6 and N-3 polyunsaturated fatty acids and prostate cancer risk: a review of epidemiological and experimental evidence. Cancer Causes Control 15:367–386
6. Thiébaut AC, Chajès V, Gerber M, Boutron-Ruault MC, Joulin V, Lenoir G, Berrino F, Riboli E, Bénichou J, Clavel-Chapelon F (2009) Dietary intakes of omega-6 and omega-3 polyunsaturated fatty acids and the risk of breast cancer. Int J Cancer 124:924–931
7. Jiang WG, Bryce RP, Horrobin DF (1998) Essential fatty acids: molecular and cellular basis of their anti-cancer action and clinical implications. Crit Rev Oncol Hematol 27:179–209
8. U.S. Department of Agriculture, Agricultural Research Service (2007). USDA National Nutrient Database for Standard Reference, Release 20. Nutrient Data Laboratory Home Page, Beltsville, MD, USA
9. Hu FB, Stampfer MJ, Manson JE, Rimm E, Colditz GA, Rosner BA, Hennekens CH, Willett WC (1997) Dietary fat intake and the risk of coronary heart disease in women. N Engl J Med 337:1491–1499
10. Escrich E, Moral R, Grau L, Costa I, Solanas M (2007) Molecular mechanisms of the effects of olive oil and other dietary lipids on cancer. Mol Nutr Food Res 51:1279–1292

11. Rose DP, Connolly JM (1999) Omega-3 fatty acids as cancer chemopreventive agents. Pharmacol Ther 83:217–244
12. Simopoulos AP (2002) The importance of the ratio of omega-6/omega-3 essential fatty acids. Biomed Pharmacother 56:365–379
13. MacLean CH, Newberry SJ, Mojica WA, Khanna P, Issa AM, Suttorp MJ, Lim YW, Traina SB, Hilton L, Garland R, Morton SC (2006) Effects of omega-3 fatty acids on cancer risk: a systematic review. JAMA 295:403–415
14. Stulnig TM, Berger M, Sigmund T, Raederstorff D, Stockinger H, Waldhäusl W (1998) Polyunsaturated fatty acids inhibit T cell signal transduction by modification of detergent-insoluble membrane domains. J Cell Biol 143:637–644
15. Nam SY, Cho KS, Heo YM, Ha JC, Kim YH, Yi HK, Hwang PH, Kim HM, Podack ER (2002) Regulation of lymphocyte clustering by CD30-mediated ICAM-1 up-regulation. Cell Immunol 219:38–47
16. Benyon LS, Eisen EJ, Jones EE (1997) Effects of canola oil-based high fat diets on growth, fat deposition and serum triglyceride and cholesterol levels in lines of mice selected for high and low fat percentage. Braz J Genet 20:203–213
17. Corbett T, Valeriote F, LoRusso P, Polin L, Panchapor C, Pugh S, White K, Knight J, Demchik L, Jones J, Jones L, Lisow L (1997) In vivo methods for screening and preclinical testing. In: Teicher BA (ed) Anticancer drug development guide. Humana Press, USA, pp 75–99
18. Jenski LJ, Sturdevant LK, Ehringer WD, Stillwell W (1993) Omega-3 fatty acid modification of membrane structure and function. I. Dietary manipulation of tumor cell susceptibility to cell- and complement-mediated lysis. Nutr Cancer 19:135–146
19. Lewis JS, Jordan VC (2005) Selective estrogen receptor modulators (SERMs): mechanisms of anticarcinogenesis and drug resistance. Mutat Res 591:247–263
20. Paruthiyil S, Parmar H, Kerekatte V, Cunha GR, Firestone GL, Leitman DC (2004) Estrogen receptor beta inhibits human breast cancer cell proliferation and tumor formation by causing a G2 cell cycle arrest. Cancer Res 64:423–428
21. Hardman WE (2007) Dietary canola oil suppressed growth of implanted MDA-MB 231 human breast tumors in nude mice. Nutr Cancer 57:177–183
22. Davis CD (2007) Nutritional interactions: credentialing of molecular targets for cancer prevention. Exp Biol Med 232:176–183
23. Wang J, John EM, Horn-Ross PL, Ingles SA (2008) Dietary fat, cooking fat, and breast cancer risk in a multiethnic population. Nutr Cancer 60:492–504
24. Chen J, Hui E, Ip T, Thompson LU (2004) Dietary flaxseed enhances the inhibitory effect of tamoxifen on the growth of estrogen-dependent human breast cancer (MCF-7) in nude mice. Clin Cancer Res 10:7703–7711
25. Chajès V, Sattler W, Stranzl A, Kostner GM (1995) Influence of n-3 fatty acids on the growth of human breast cancer cells in vitro: relationship to peroxides and vitamin-E. Breast Cancer Res Treat 34:199–212
26. Owen RW, Haubner R, Würtele G, Hull E, Spiegelhalder B, Bartsch H (2004) Olives and olive oil in cancer prevention. Eur J Cancer Prev 13:319–326
27. MacGregor JI, Jordan VC (1998) Basic guide to the mechanisms of antiestrogen action. Pharmacol Rev 50:151–196
28. Pizer ES, Jackisch C, Wood FD, Pasternack GR, Davidson NE, Kuhajda FP (1996) Inhibition of fatty acid synthesis induces programmed cell death in human breast cancer cells. Cancer Res 56:2745–2747
29. Wong ST, Goodin S (2009) Overcoming drug resistance in patients with metastatic breast cancer. Pharmacotherapy 29:954–965

Lipids (2010) 45:785–798
DOI 10.1007/s11745-010-3459-3

ORIGINAL ARTICLE

Chemopreventive Effect of Different Ratios of Fish Oil and Corn Oil in Experimental Colon Carcinogenesis

Pooja Sarotra · Gayatri Sharma · Shevali Kansal · Anjana Kumari Negi · Ritu Aggarwal · Rajat Sandhir · Navneet Agnihotri

Received: 22 April 2010 / Accepted: 29 July 2010 / Published online: 25 August 2010

Abstract n-3 Polyunsaturated fatty acids (PUFA) have a chemopreventive effect while n-6 PUFA promote carcinogenesis. The effect of these essential fatty acids may be related to oxidative stress. Therefore, the study was designed to evaluate the effect of different ratios of fish oil (FO) and corn oil (CO) in the prevention of colon cancer. Male Wistar rats were divided into control, dimethylhydrazine dihydrochloride (DMH) treated, FO + CO (1:1) and FO + CO (2.5:1). All the groups, except the control received a weekly injection of DMH for 4 weeks. The animals were sacrificed either 48 h later (initiation phase) or kept for 16 weeks (post initiation phase). DMH treatment in the initiation phase animals showed mild to moderate inflammation, decreased ROS and TrxR activity, increased antioxidants, apoptosis and ACF multiplicity. The post initiation study showed severe inflammation with hyperplasia, increased ACF multiplicity and ROS levels, a decrease in antioxidants and apoptosis. The FO + CO (1:1) treated animals showed severe inflammation, a decrease in ROS, an increase in antioxidants and apoptosis in the initiation phase. FO + CO (1:1) in the post initiation phase and FO + CO (2.5:1) in the initiation showed mild inflammation, increased ROS, apoptosis and decreased antioxidants. There was a decrease in ACF multiplicity and ROS levels, increased antioxidants and apoptosis in the post initiation phase study. The present study suggests that FO has a dose- and time-dependent chemopreventive effect in colon cancer mediated through oxidative stress and apoptosis.

Keywords Dietary fat · Edible oils · n-3 Fatty acids · Antioxidants · Free radicals · Cancer · Fish oil · n-6 Fatty acids

Abbreviations

CDNB	1-Chloro-2,4-dinitrobenzene
DCFH-DA	2′,7′-Dichlorofluorescein diacetate
DCF	2′,7′-Dichlorofluorescein
DTNB	5,5′-Dithiobis-(2-nitro-benzoic acid)
TNB	5-Thio-2-nitrobenzoic acid
AA	Arachidonic acid
DMH	*N*,*N*′-Dimethylhydrazine dihydrochloride
DTT	Dithiothreitol
DHA	Docosahexaenoic acid
EPA	Eicosapentaenoic acid
FACS	Fluorescence-activated cell sorter
HBSS	Hank's buffered salt solution
MALT	Mucosa associated lymphoid tissue
NBT	Nitro blue tetrazolium
PUFA	Polyunsaturated fatty acids
ROS	Reactive oxygen species
SPSS	Statistical package for social sciences
TrxR	Thioredoxin reductase

Introduction

Colon cancer is the third most common cancer in males and the second most common cancer in females of the

P. Sarotra · G. Sharma · S. Kansal · A. K. Negi · R. Sandhir · N. Agnihotri (✉)
Department of Biochemistry, Panjab University, Chandigarh 160014, India
e-mail: agnihotri.navneet@gmail.com

R. Aggarwal
Department of Immunopathology, Postgraduate Institute of Medical Education and Research, Chandigarh 160012, India

industrialized countries and its incidence is increasing in the developing countries [1]. Cancer is a disease associated with very high mortality. Diagnosis of cancer at the early stages can be made with the estimation of the biomarkers. Aberrant crypt foci (ACF) have been regarded as precancerous lesions and are widely used as a biomarker of colon cancer in a number of studies [2]. ACF are the only endpoints which provides a quantitative approach to assess the disease process and the underlying cellular and molecular events as affected by cancer preventive or promoting agents [3].

Cancer is strongly influenced by various environmental factors, with diet being one of the major modifying agents [4]. Dietary factors have been documented as playing a significant role in the development and progression of the colon cancer [5]. Diets high in fat have been linked with an increased risk of various types of cancers particularly of the breast, colon and prostate gland [6]. Increasing evidence from animal and human studies indicate that not only the amount but in particular the types of dietary fat differing in fatty acid composition are important factors in colon tumor development [7, 8]. It has been reported that, a higher intake of total saturated fat leads to an increased risk of cancer [9]. Out of the essential PUFA, the beneficial effect of marine-derived n-3 polyunsaturated fatty acids on coronary artery disease, hypertension, diabetes, arthritis and other inflammatory and autoimmune disorders and cancer has been convincingly demonstrated by epidemiological and experimental studies [8, 10–12]. On the other hand, n-6 PUFA have been shown to have proinflammatory and procarcinogenic effect [8, 13]. Both of these classes of fatty acids are important components of cell membranes and are substrates for the same enzymes and thus compete with each other [14]. n-3 PUFA have greater affinities for the enzyme, which means that increasing the dietary intake of n-3 PUFA reduces the desaturation of linoleic acid (LA) and consequently increase the production of eicosanoids that are anti-inflammatory and anticarcinogenic in nature [15]. Therefore, it has been suggested that a balanced n-3/n-6 PUFA ratio in diet rather than the absolute intake of either is essential for normal growth and development and may be responsible for a decrease in the incidence of various disorders including cardiovascular diseases and cancer [10, 12, 13]. Moreover, it is believed that therapeutic ratio of n-3 and n-6 is different for different diseases and for colon cancer this ratio has still not been worked out. Hence two different ratios of n-3 and n-6 have been used in the present study to assess the chemopreventive potential in experimental colon carcinogenesis.

There has been a lot of interest in characterizing the mechanism by which these fatty acids exert their effects in carcinogenesis. The possible mechanism includes one or more of the following: oxidative stress, apoptosis, disrupted cell cycle and cell proliferation [14] Oxidative stress is a condition associated with an increased generation of reactive oxygen species (ROS) or impaired cellular antioxidant capacity leading to an imbalance between radical generating and scavenging potential. The unsaturation in the lipids is prone to oxidation and the metabolites of the lipid peroxidation (LPO) generate the promutagenic exocyclic DNA adducts [16, 17]. It was reported that low-levels of PUFA induced oxidative stress which was cytostatic, while higher levels of oxidative stress resulted in apoptosis and still higher levels caused cellular necrosis [18]. Oxidative stress can initiate and/or mediate a number of signalling cascades, including apoptosis due to alterations in the cellular redox balance. Oxidative stress caused by increased free radical generation and/or decreased antioxidant levels in the target cells and tissues has been suggested to play an important role in carcinogenesis [19, 20]. It has been observed that the tumoricidal action of n-3 PUFA is a free radical dependent process [21] and their consumption leads to an increase in lipid peroxidation by reactive oxygen species due to a multiplicity of double bonds [22]. An increase in lipid peroxidation may lead to oxidative stress which is counteracted by various antioxidants including glutathione (GSH), thioredoxin (Trx), catalase (CAT), superoxide dismutase (SOD), glutathione peroxidase (GPx) [23, 24]. Takashi et al. [25] reported that genes for antioxidant enzymes were upregulated in mice fed with fish oil supplemented diets.

It has been reported that higher oxidative stress leads to apoptosis. Programmed cell death plays an essential role in the elimination of mutated cells/transformed cells [26].Thus, in order to survive, cancer cells must develop highly efficient and usually multiple mechanisms which help in averting apoptosis. In fact, evading apoptosis is regarded as one of the hallmarks of cancer cells [27]. A number of workers have shown that the effect of n-3 PUFA on the colon cancer might be mediated through an increase in apoptosis [28–30].

To date the effect of alteration of dietary ratio of n-3 and n-6 PUFA on oxidative stress and apoptosis has not been evaluated. Therefore this study is designed to evaluate the effect of different dietary ratios of fish oil and corn oil on dimethyl hydrazine induced colon cancer and mediation of oxidative stress in this process.

Materials and Methods

Chemicals

N,*N*′-Dimethylhydrazine dihydrochloride (DMH) and a thioredoxin reductase assay kit were obtained from Sigma

Chemical Company, St. Louis, USA. M-30 cytoDEATH monoclonal antibody was purchased from Boehringer Mannheim, Germany. Fluorescein isothiocyanate (FITC)-conjugated goat anti-mouse IgG_1 was purchased from Bangalore Genei, Bangalore, India. Fish oil under the brand name Seven Seas Sea cod was a generous gift from Universal Medicare Pvt. Ltd., Mumbai, India. The fish oil contains 20% of EPA and DHA, 24% of other n-3 Fatty acids, 0.16% of Vitamin A and 0.001% of Vitamin D. Corn oil under the brand name Arawana from Wilmar International Ltd. was obtained from Shanghai, China. It contains 50% of n-6, 1.3% of n-3 and 26.4% of n-9 PUFA. The mineral mixture (Agrimin) was obtained from Virbac Animal health India Pvt. Ltd., Mumbai, India. All other chemicals used in the study were of analytical grade.

Experimental Animals

Male Wistar rats weighing 100–150 g were obtained from and housed in the Central Animal House, Panjab University, Chandigarh. The experimental protocols were approved by the Institutional Ethics Committee and conducted according to Indian National Science Academy Guidelines for the use and care of experimental animals. Rats were housed in polypropylene cages in the animal house and were acclimatized for 7–10 days before being used in the experimental study. Water was given ad libitum.

Diets

To assess food consumption, 20 randomly selected rats were monitored for 10 consecutive days. Food consumption per cage was calculated by subtracting the leftover food from that of the previous day. Spillage was also monitored and was negligible. Finally, the diets were prepared fresh and modified according to the groups as shown in the Table 1. The diets were prepared on the basis of the American Institute of Nutrition standard reference diet AIN-76A [31]. The purified diet was supplemented with 5% soya oil instead of corn oil to meet the essential fatty acid requirement in the diet. The soya oil contained 54.3% of n-6, 6.3% of n-3 and 22.2% of n-9 PUFA [32]. The composition of diet was adjusted so that the animals in all the dietary groups would consume the same amount of calories. The lipid composition in normal diet for the rodents should be up to 30% [33] and for the humans the dietary recommendations of lipids is 20% for adult females and 15% for the adult male [34]. Therefore, to explore the therapeutic potential, it was decided to vary the ratios of n-3 PUFA rich fish oil and n-6 PUFA rich corn oil at 20% which is well within the normal optimal range. In the modified diets PUFA were supplemented with varying ratios of n-6 and n-3 along with 5% soya oil. The lower ratio had 7.5% corn oil and 7.5% fish oil in (1:1) while the higher ratio (2.5:1) had fish oil (10.3%) and corn oil (4.7%). However, the dietary regimens fall in the optimal range of the fat to be given to rodents to meet the better growth. In order to prevent the formation of oxidized lipids, diets were prepared fresh every day. Feeders were removed and washed daily.

Experimental Design

The experimental protocol is clearly represented in Fig. 1. The animals ($n = 112$) were divided into the following experimental groups:

Control group Rats received a purified diet and a weekly sham injection of the 1 mM ethylenediamine tetra-acetic acid (EDTA), pH 6.5, for a period of 4 weeks.

DMH treated Rats received a purified diet and were administered a weekly intraperitoneal injection of DMH (20 mg/kg body weight) for a period of 4 weeks. DMH was dissolved in 1 mM EDTA (pH-6.5). DMH is metabolized in the liver to azoxymethane (a known colon carcinogen), ultimately leading to the generation of methyldiazonium ions and carbonium ions, which are active carcinogenic electrophiles that manifest their action in the colon [35].

FO + CO (1:1) The animals received a modified diet supplemented with an equal ratio of fish oil and corn oil

Table 1 Composition of the experimental diets

Diet content (%)	Control	DMH treated	FO + CO (1:1)	FO + CO (2.5:1)
Casein	20	20	23.5	23.5
Fat	5 (soya oil)	5 (soya oil)	5 (soya oil) + 7.5 corn oil + 7.5 fish oil	5 (soya oil) + 4.3 corn oil + 10.7 fish oil
Sucrose	65	65	44.72	44.72
Fiber (wheat bran)	5	5	5.9	5.9
Mineral mix	3.8	3.8	4.46	4.46
Vitamin mix	1.0	1.0	1.18	1.18
Choline chloride	0.2	0.2	0.24	0.24

Diet was formulated according to the American Institute of Nutrition standard reference diet, with the modification of varying sources of carbohydrate and protein

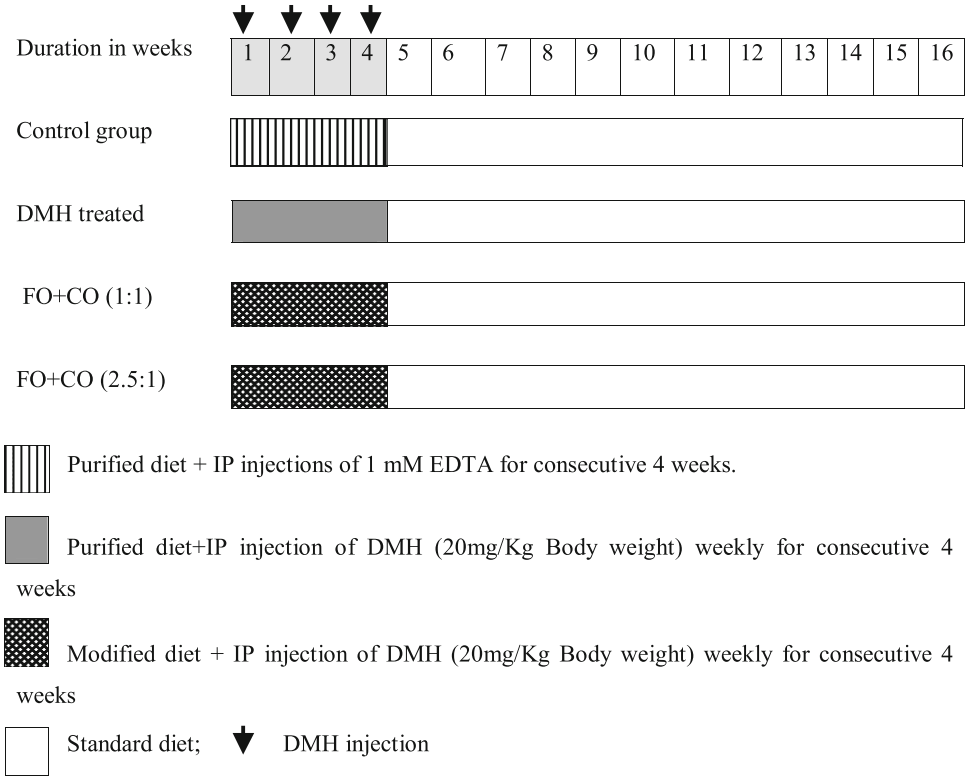

Fig. 1 Experimental design of the study

and were given a weekly intraperitoneal injection of 20 mg/kg body weight DMH for 4 weeks.

FO + CO (2.5:1) The animals were given a modified diet with a varying ratio of fish oil and corn oil and administered a weekly dose of intraperitoneal injection of DMH (20 mg/kg body weight) for 4 weeks.

The initiation phase study comprised of animals sacrificed 48 h after EDTA/DMH injections [36] and the animals kept for 12 weeks after the treatment regimen constituted the post initiation phase study. All the animals were sacrificed by cervical dislocation.

Measurement of ACF Count

The entire colon was processed for the determination of ACF in the following manner [2]. The entire colon (from caecum to anus) was removed and washed thoroughly with PBS, cut longitudinally, laid flat on a wet filter paper, and fixed with 10% buffered formaldehyde solution overnight. The colon was then stained with 0.2% methylene blue prepared in saline for 3–5 min. The ACF formed by one or more aberrant crypts, can be easily visualized on a background of normal crypts since aberrant crypts have larger, often elongated openings and a thicker lining of epithelial cells compared with normal crypts. For topographic assessment of the colon, mucosal ACF was counted using a light microscope (40×). The ACF were classified as small (1–3); medium (4–6); or large (6 and more) by the number of crypts per foci. The total number of ACF/rat was calculated as the sum of the small, medium and large ACF.

Histopathological Examination

The colon was removed and flushed with warm Ca^{2+} and Mg^{2+} free phosphate buffered saline (PBS). For each rat, the 10 cm of the distal colon was taken for histopathology and fixed in the 10% formalin. Sections were prepared and stained with hematoxylin and eosin. The slides were photographed and evaluated by a histopathologist without any prior knowledge of the experimental design.

Isolation of Colonocytes

The colonocytes were isolated by the method of Sanders et al. [37]. The rats were killed by cervical dislocation and the entire colon from the caecum to rectal ampulla was removed and flushed with Ca^{2+} and Mg^{2+} free-PBS. The colon was cut longitudinally to expose the lumen and placed in warm Ca^{2+} and Mg^{2+} free-Hank's buffered salt solution (HBSS), 30 mM EDTA, 5 mM dithiothreitol (DTT), 0.1% bovine serum albumin (BSA). After a 15-min incubation, the mucosal side was gently scraped, to remove intact crypts and surface cells from lamina propria. The isolated cells was then centrifuged at 600×*g* and washed

twice in warm HBSS with Ca^{2+} and Mg^{2+} and 0.1% BSA. The final volume was made up to 2 mL. The cells were counted using a hemocytometer and were adjusted to contain 1×10^5 cells/mL. The cell viability was measured according to the trypan blue exclusion method of Freshney [38] and found to be in the range of 60–90%.

Assay for the Generation of Reactive Oxygen Species

The net intracellular generation of ROS was measured by the method of Rosenkranz et al. [39], using oxidation sensitive fluorescent dye, 2′,7′-dichlorofluorescein diacetate (DCFH-DA). The 2′,7′-dichlorofluorescein is non-permeable and gets trapped in the cells. It gets oxidized to the highly fluorescent compound 2′,7′-dichlorofluorescein by intracellular ROS. Briefly, the isolated colonocytes were incubated with 10 μM DCFH-DA at 37 °C for 30 min, washed with HBSS and finally suspended in 300 μl of HBSS. The intensity of DCF fluorescence was measured in the cells with Fluorescence-activated cell sorter (FACS) Calibur flow cytometer (Becton–Dickinson) equipped with an excitation and emission laser line at 488 and 530 nm, respectively. A total of 10,000 events were counted and the histograms were analyzed using Cell Quest software and compared with histograms of control untreated cells.

Measurement of Antioxidant Enzymes

The cell lysates was prepared by homogenization of cells in 50 mM potassium phosphate buffer containing 250 mM sucrose, 1 mM EDTA, 1 mM DTT, 0.1% Triton X-100 (v/v) followed by centrifugation for 3 min at 10,000×*g*. The supernatant was used for further assays.

SOD (EC 1.15.1.1) activity was assayed by the method of Kono [40] in the cell lysates. One unit of enzyme was defined as the enzyme concentration required for inhibiting the reduction of NBT dye by 50% in 1 min under the assay conditions and expressed as units per milligram protein.

CAT (EC 1.11.1.6) activity was assayed by the method of Luck [41] in the cell lysates. CAT activity was assayed spectrophotometrically following a decrease in absorbance of H_2O_2 at 240 nm. One unit of enzyme activity is defined as amount of enzyme required to degrade 1 micromole of H_2O_2 in 1 min and is expressed as units per milligram protein.

GSH content was estimated in the cell lysates according to the method of Ellman [42]. GSH on reaction with 5,5′-dithiobis-(2-nitro-benzoic acid) [DTNB] gives a yellow colored product with absorption maxima at 412 nm. The standard curve was prepared for GSH with a concentration range of 0.2–1 mM. The results were expressed in micromoles per milligram protein.

Glutathione peroxidase (EC 1.11.1.9) was measured in the cell lysates by the method of Lawrence and Burk [43]. The reaction measured the rate of GSH oxidation by H_2O_2, catalyzed by GPx. GSH was maintained at constant concentration by the addition of exogenous GR and NADPH, which converted the GSSG to GSH. The rate of GSSG formation was then measured by change in the absorbance of NADPH at 340 nm for 3 min at 30 s intervals. One unit of GPx is defined as enzyme concentration required for the formation of 1 μmol of $NADP^+$ per min and results are expressed as Unit/mg protein

Glutathione reductase (EC 1.8.1.7) activity was assayed using the method of Carlberg and Mannervik [44] by measuring GSH formed by NADPH. The values are expressed as micromoles of NADPH oxidised per minute milligram protein.

Glutathione-*S*-transferase (GST) (EC 2.5.1.18) was assayed in cell lysates according to the method of Habig et al. [45]. This assay was based on the rate of increase in conjugate formation between GSH and 1-chloro-2,4-dinitrobenzene (CDNB). The enzyme activity was determined by monitoring the changes in absorbance at 340 nm for 3 min at 30 s interval. The enzymatic activity was expressed as micromoles of CDNB-GSH conjugates formed per minute per milligram protein.

Thioredoxin reductase (TrxR) (EC 1.8.1.9) was estimated by the method of Arner and co-workers [46] using a thioredoxin reductase assay kit obtained from Sigma Chemical Company, St. Louis, USA. The assay is based on the reduction of DTNB with NADPH to 5-thio-2-nitrobenzoic acid (TNB) that produces a strong yellow color that is measured at 412 nm. In crude biological samples, other enzymatic activities, such as GR and GPx also reduce DTNB. Therefore, determination of activity of thioredoxin reductase was done by subtracting the activity of sample with the activity in the presence of thioredoxin reductase inhibitor.

The protein in the cell lysates sample was done by the method of Lowry et al. [47] and the results were expressed in milligram per milliliter.

Apoptosis Measurement Using the M-30 cytoDEATH Antibody

Apoptosis was measured by using M-30 cytoDEATH (Boehringer Mannheim, Germany). M-30 cytoDEATH is the monoclonal antibody that recognizes a specific caspase cleavage site with cytokeratin 18 that is not detectable in native CK 18 of the normal cells as well as in the necrotic cells. It is a unique and specific tool for the easy and reliable determination of early apoptotic events in the cell and is the valid and acceptable method in comparison to the TUNEL [48, 49]. Cells were fixed and permeabilized in methanol by adding the alcohol drop wise with constant shaking to avoid the aggregate formation and kept at

−20 °C overnight. The cells were centrifuged at 5,000 rpm and alcohol was removed. The pellet was again washed twice with PBS/BSA. The final pellet was suspended in the PBS/BSA and incubated with M30 CytoDEATH monoclonal antibody for 30 min, at room temperature. The cells were washed with PBS and counterstained with FITC conjugated anti mouse IgG1 (Bangalore Genei, India) for 1 h at room temperature in the dark. The cells were washed with PBS and finally suspended in PBS. The mean fluorescence intensity, as a measure of apoptosis, was determined with fluorescence-activated cell sorter (FACS) Canto flow cytometer (Becton–Dickinson) equipped with an excitation and emission laser line at 495 and 520 nm, respectively. A total of 10,000 events were counted and the histograms were analyzed using Cell Quest software and compared with the histogram of control untreated cells.

DNA Fragmentation

Genomic DNA was extracted with the help of DNA extraction kit (Chromous Biotech, India). The purified samples were electrophoresed on 1% agarose gel. After electrophoresis, the DNA was visualized for fragmentation by ethidium bromide staining.

Statistical Analysis

The results are expressed as mean ± standard error of mean (SEM). The statistical significance of data was evaluated by one way analysis of variance (ANOVA), using statistical package for social sciences (SPSS) software version 9.0 for windows. The data was analyzed by post-hoc analysis with Least Square Difference to compare means. A value of $P < 0.05$ was considered to indicate a significant difference between groups. Data was analyzed using general factorial analysis of variance after testing for normality and homogeneity of variance.

Results

Effect of Fish Oil and Corn Oil on Oxidative Stress Parameters

Initiation phase study

The results of ROS generation are shown in Table 2. A decrease in ROS levels was observed on treatment with DMH as compared to control animals ($P < 0.001$).The ROS levels were elevated in animals fed a high fat diet with the effect being more pronounced at a higher ratio of fish oil which was not significantly different from the control animals. The results of antioxidants' are tabulated in Table 3. There was a significant elevation in the activities of SOD and CAT in DMH treated animals with respect to control animals ($P < 0.05$).The marked elevation was also observed in the activities of both the enzymes, SOD and CAT in the animals fed with FO + CO (1:1) with respect to controls ($P < 0.001$) and DMH treated animals ($P < 0.01$ and $P < 0.001$), respectively. However, a significant decrease was observed in the activity of both the enzymes in the animals fed on FO + CO (2.5:1).

The glutathione levels in the carcinogen treated animals and in animals fed with FO + CO (1:1) were increased significantly as compared to the normal controls ($P < 0.05$) while a significant decrease in GSH was observed in animals fed with FO + CO (2.5:1) with respect to the carcinogen treated ($P < 0.001$) and animals on the lower ratio of the oils.

DMH treatment did not alter GPx activity, though in rats fed with FO + CO (1:1), GPx activity significantly increased ($P < 0.01$) with respect to control and DMH treated group ($P < 0.05$).

GR activity was increased in all the treated groups as compared to the controls. The activity was elevated most in the DMH treated group ($P < 0.001$).However, FO + CO treatment led to a decrease in the activity of the GR as compared to the DMH treated animals ($P < 0.05$) with the effect being more pronounced at higher ratio.

GST activity was drastically increased in carcinogen treated rats as compared to the controls ($P < 0.001$). On feeding the high fat diets, the activity was still significantly higher as compared to the normal controls ($P < 0.001$).

There was no significant decrease in the activity of TrxR in DMH treated and FO + CO (2.5:1) in comparison to controls but the activity was significantly decreased in animals fed FO + CO (1:1).

Post Initiation Phase Study

The results of ROS generation are shown in Table 2. The ROS levels were found to be significantly higher in the carcinogen treated group ($P < 0.001$) as well as in the group fed FO + CO (1:1) as compared to the control ($P < 0.001$) in the post initiation phase study. However, the animals on FO + CO (2.5:1) showed no significant difference from control animals.

The antioxidants' level in the post initiation study is shown in Table 4. There was a marked decrease in the activities in the CAT and SOD in all the groups ($P < 0.001$) as compared to the control. The activity was elevated in the group treated with FO + CO (2.5:1) as compared to the DMH treated group.

A significant decrease in the GSH levels were observed in all the groups in the post initiation phase as compared to the control animals ($P < 0.01$) with the effect being more pronounced in FO + CO (2.5:1) fed animals ($P < 0.001$).

Table 2 ROS levels in the initiation phase and post initiation phase studies in the colon carcinogenesis

Groups	Initiation phase	Post initiation phase
ROS generation (MFI)		
Control	104.08 ± 5.10	44.30 ± 2.41
DMH treated	32.85 ± 5.55[a]	69.78 ± 3.43[a]
FO + CO (1:1)	53.99 ± 5.27[a,c]	81.33 ± 4.21[a,b]
FO + CO (2.5:1)	107.63 ± 22.4[d,e]	44.98 ± 1.10[d,e]

The results are expressed as mean ± SEM for $n = 8$

[a] $P < 0.001$ with respect to control

[b] $P < 0.01$ with respect to DMH treated

[c] $P < 0.05$ with respect to DMH treated

[d] $P < 0.001$ with respect to DMH treated

[e] $P < 0.001$ with respect to FO + CO (1:1)

There was a significant decrease in the activities of GPx, GR and GST in the DMH treated group and the group fed FO + CO (1:1) in comparison to the control animals ($P < 0.05$, $P < 0.001$ and $P < 0.001$, respectively). However in animals fed FO + CO (2.5:1), there was an elevation in the activities of these enzymes in comparison to the DMH treated group ($P < 0.001$, $P < 0.05$ and $P < 0.05$) respectively.

The Effect of Fish Oil and Corn Oil on M-30 cytoDEATH Levels

The levels of M-30 cytoDEATH on administration of fish oil and corn oil in different ratios are presented in Table 5. A significant increase in apoptosis in DMH treated animals was observed in the initiation phase ($P < 0.001$). The treatment with fish oil and corn oil in both the ratios showed significant decrease in the apoptotic levels as compared to DMH treated group ($P < 0.05$). In the post initiation phase study, there was a significant decrease in apoptosis in DMH treated group ($P < 0.05$). On treatment with the oils, the apoptosis were significantly increased with FO + CO (1:1) ($P < 0.05$) and FO + CO (2.5:1) ($P < 0.001$) respectively. The increase in apoptosis with higher ratio was also significant in comparison to the lower ratio of fish oil and corn oil ($P < 0.001$).

The Effect of Fish Oil and Corn Oil on DNA Fragmentation

The results of the DNA fragmentation are presented in Fig. 2 (initiation phase and post initiation phase). In the initiation phase study, there was an increased DNA fragmentation in the carcinogen treated group as compared to FO + CO treated groups. In the post initiation phase groups, there was maximum fragmentation in the animals treated with FO + CO at a ratio of 2.5:1, followed by FO + CO (1:1) and DMH treated group.

The Effect of Fish Oil and Corn Oil on the ACF Count

The results for the ACF count are documented in Table 6 and were identified as the discrete aggregation of aberrant/abnormal crypts.

In the initiation phase study, ACF multiplicity was significantly increased in DMH treated group as compared to the controls ($P < 0.001$). A major decrease in the ACF

Table 3 Activity of antioxidants in the isolated colonocytes in the initiation phase study

Groups	Control	DMH treated	FO + CO (1:1)	FO + CO (2.5:1)
SOD (U/mg protein)	412.23 ± 41.97	645.19 ± 96.18[c]	974.57 ± 41.67[a,d]	411.45 ± 48.33[e,f]
CAT (U/mg protein)	88.56 ± 8.48	189.66 ± 27.09[c]	349.35 ± 40.46[a,d]	128.98 ± 13.14[f]
GSH (μmol/mg protein)	0.25 ± 0.01	0.32 ± 0.02[c]	0.33 ± 0.03[c]	0.21 ± 0.02[d,f]
GR (μmol of NADPH oxidized/min/mg protein)	47.19 ± 6.08	153.06 ± 38.43[a]	94.41 ± 6.12[e]	69.13 ± 16.62[e]
GPx (U/mg protein)	0.05 ± 0.004	0.07 ± 0.012[b]	0.11 ± 0.022[e]	0.05 ± 0.003[g]
GST (μmol of CDNB-GSH conjugate formed/min/mg protein	7.89 ± 1.41	166.19 ± 15.54[a]	106.62 ± 8.3[a,d]	132.16 ± 6.75[a,e]
TrxR (U/mg protein)	0.64 ± 0.07	0.55 ± 0.02	0.38 ± 0.03[a,e]	0.57 ± 0.09 [h]

Values are mean ± SEM of eight observations in each group

[a] $P < 0.001$ with respect to control

[b] $P < 0.01$ with respect to control

[c] $P < 0.05$ with respect to control

[d] $P < 0.001$ with respect to DMH treated

[e] $P < 0.05$ with respect to DMH treated

[f] $P < 0.001$ with respect to FO + CO (1:1)

[g] $P < 0.01$ with respect to FO + CO (1:1)

[h] $P < 0.05$ with respect to FO + CO (1:1)

Table 4 Activity of antioxidants in the isolated colonocytes in the post initiation phase study

Groups	Control	DMH treated	FO + CO (1:1)	FO + CO (2.5:1)
SOD (U/mg protein)	1,580.01 ± 104.12	361.94 ± 22.46[a]	469.32 ± 41.40[a]	618.29 ± 64.23[a,e]
CAT (U/mg protein)	43.33 ± 4.00	17.17 ± 3.1[a]	21.87 ± 2.3[a]	23.51 ± 3.1[a]
GSH (μmol/mg protein)	0.54 ± 0.06	0.39 ± 0.03[b]	0.37 ± 0.02[a]	0.20 ± 0.01[a,d,g]
GR (μmol of NADPH oxidized/min/mg protein)	48.88 ± 7.71	21.20 ± 2.12[a]	23.57 ± 2.64[a]	68.17 ± 4.28[c,d,g]
GPx (U/mg protein)	32.17 ± 3.15	20.00 ± 4.04[c]	18.72 ± 3.07[c]	45.87 ± 4.34[c,d,g]
GST (μmol of CDNB-GSH conjugate formed/min/mg protein	16.47 ± 1.33	8.32 ± 0.68[a]	10.24 ± 0.72[a]	15.93 ± 1.17[f,g]

Values are mean ± SEM of eight observations in each group

[a] $P < 0.001$ with respect to control

[b] $P < 0.01$ with respect to control

[c] $P < 0.05$ with respect to control

[d] $P < 0.001$ with respect to DMH treated

[e] $P < 0.01$ with respect to DMH treated

[f] $P < 0.05$ with respect to DMH treated

[g] $P < 0.001$ with respect to FO + CO (1:1)

Table 5 Effect of fish oil and corn oil on apoptosis

Groups	Initiation phase	Post initiation phase
Apoptotic levels in colonocytes (MFI)		
Control	39.57 ± 4.73	61.57 ± 9.81
DMH treated	68.57 ± 6.94[b]	42.60 ± 4.06[a]
FO + CO (1:1)	43.67 ± 5.55[c]	62.75 ± 2.74[c]
FO + CO (2.5:1)	53.87 ± 3.27[c]	96.25 ± 4.89[b,d,e]

Values are mean ± SEM of eight observations in each group

[a] $P < 0.05$ with respect to control

[b] $P < 0.001$ with respect to control

[c] $P < 0.05$ with respect to DMH treated

[d] $P < 0.001$ with respect to DMH treated

[e] $P < 0.001$ with respect to group FO + CO (1:1)

count was observed in the animals treated with FO + CO (2.5:1) in comparison to the DMH treated rats ($P < 0.01$) and FO + CO (1:1) ($P < 0.01$).

A similar trend was observed in ACF count in the post initiation phase study.

The Effect of Fish Oil and Corn Oil on Histopathology of the Colon

The normal histological features of the colon are shown in Fig. 3a. In the initiation phase study, the animals in the DMH treated group showed mild to moderate inflammation (Fig. 3b). The inflammation consisted predominantly of lymphocytes and some plasma cells and was chiefly centered in the submucosa. Animals with moderate inflammation showed prominent lymphoid follicles surrounded by lymphocytes and plasma cells. However, in the group supplemented with FO + CO (1:1) (Fig. 3c), the inflammation was dense and infiltrated the mucosa. In addition, Low grade lymphoma of MALT type was found in two animals. The FO + CO (2.5:1) animals showed a normal mucosa or mild inflammation (Fig. 3d) demonstrating the inhibitory effect of the higher ratio of fish oil and corn oil in the experimental colon carcinogenesis.

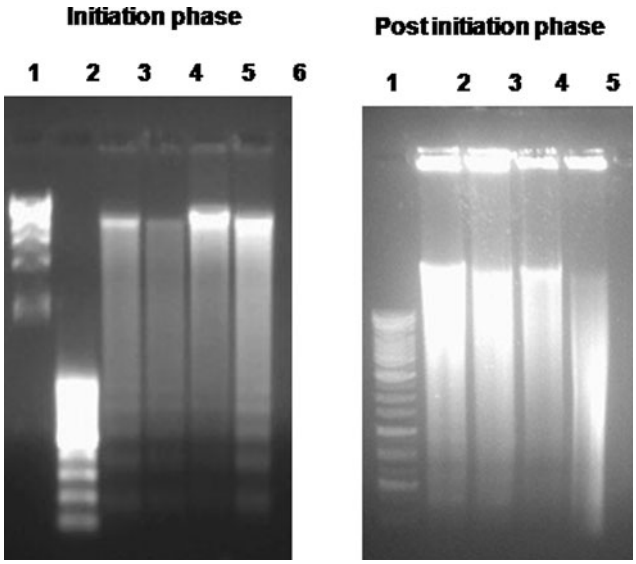

Fig. 2 A representative gel photograph of the DNA fragmentation pattern observed in the animals of various groups in the initiation phase and post initiation phase study. Initiation phase: *lane 1* markers (23–10 kbps), *lane 2* markers (1–0.1 kbps), *lane 3* controls, *lane 4* carcinogen treated, *lane 5* FO + CO (1:1) and *lane 6* FO + CO (2.5:1). Post initiation phase: *lane 1* markers (2–0.1 kbps), *lane 2* control, *lane 3* carcinogen treated, *lane 4* FO + CO (1:1) and *lane 5* FO + CO (2.5:1)

Table 6 Effect of FO + CO on the number of ACF present in the colonic mucosa

Groups	Small	Medium	Large	Total no. of ACF
Initiation phase study (ACF/colon)				
Control	0.25 ± 0.25	1.75 ± 0.85	1.50 ± 0.29	3.50 ± 0.87
DMH treated	4.66 ± 2.67	3.00 ± 0.58	9.30 ± 0.33[a]	17.00 ± 2.52[a]
FO + CO (1:1)	3.5 ± 1.19	2.00 ± 0.58	6.25 ± 0.48[a,d]	11.75 ± 2.06[b]
FO + CO (2.5:1)	3.0 ± 1.00	2.00 ± 0.58	4.00 ± 0.41[a,d]	8.00 ± 1.96[e,g]
Post initiation phase study (ACF/colon)				
Control	1.60 ± 1.03	3.00 ± 0.63	4.80 ± 0.86	9.40 ± 1.54
DMH treated	7.00 ± 1.87[b]	2.60 ± 1.16	20.80 ± 2.42[a]	30.60 ± 420[a]
FO + CO (1:1)	6.00 ± 1.29[b]	4.50 ± 2.50	13.25 ± 3.09[c,f]	23.75 ± 5.94[c]
FO + CO (2.5:1)	2.00 ± 0.91[d]	3.50 ± 0.29	8.50 ± 1.26[d]	13.75 ± 2.10[e]

The results are expressed as mean ± SEM for $n = 6$

[a] $P < 0.001$ with respect to control

[b] $P < 0.01$ with respect to control

[c] $P < 0.05$ with respect to control

[d] $P < 0.001$ with respect to DMH treated

[e] $P < 0.01$ with respect to DMH treated

[f] $P < 0.05$ with respect to DMH treated

[g] $P < 0.01$ with respect to FO + CO (1:1) treated

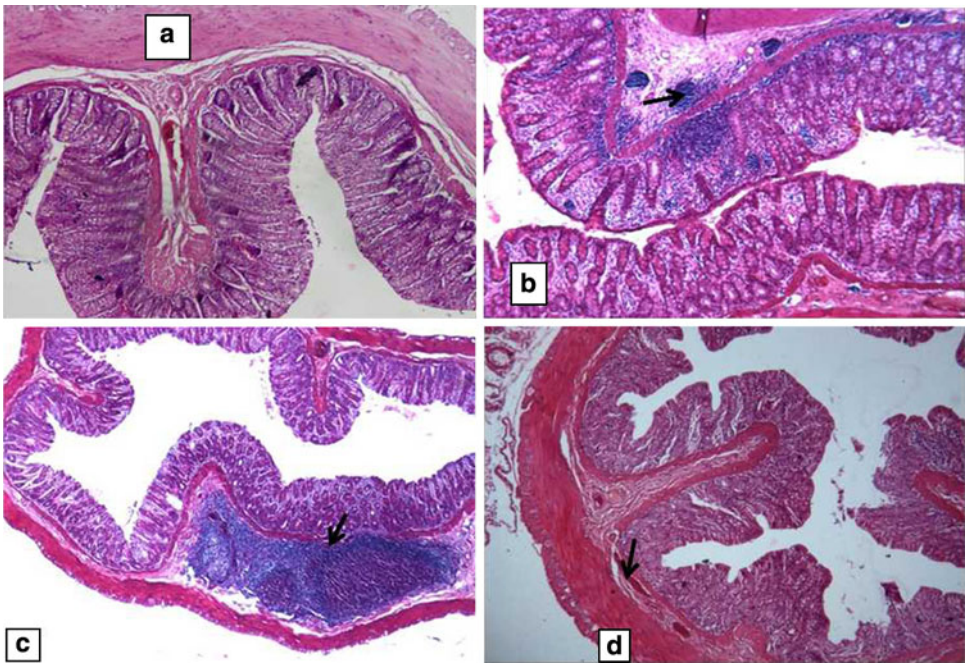

Fig. 3 **a** Light micrograph of the rat colon in the control showing normal mucosa, submucosa and crypt (H&E, ×40). **b** Light micrograph of the rat colon in the DMH treated animals showing mild inflammation (H&E, ×40). **c** Light micrograph of the rat colon in the FO + CO (1:1) showing severe inflammation (H&E, ×40) and low grade lymphoma of mucosa associated lymphoid tissue (MALT) formation (H&E, ×40). **d** Light micrograph of animals in FO + CO (2.5:1) showing normal mucosa

Figure 4a represents the histopathological features of colon in the post initiation phase study. There is severe inflammation with large lymphoid tissue formation and hyperplasia. There was distorted morphology of cells in carcinogenic animals (Fig. 4b). However, in FO + CO treated group in the equal ratio, there is varied gland size with increased intraglandular space and colitis with marked regenerative changes (Fig. 4c). The animals in the group supplemented with FO + CO (2.5:1) showed normal features with increased intra glandular space and regenerative changes (Fig. 4d).

Discussion

The results clearly indicate that administration of the procarcinogen DMH in the presence of fish oil and corn oil brings about profound alterations in the ROS and

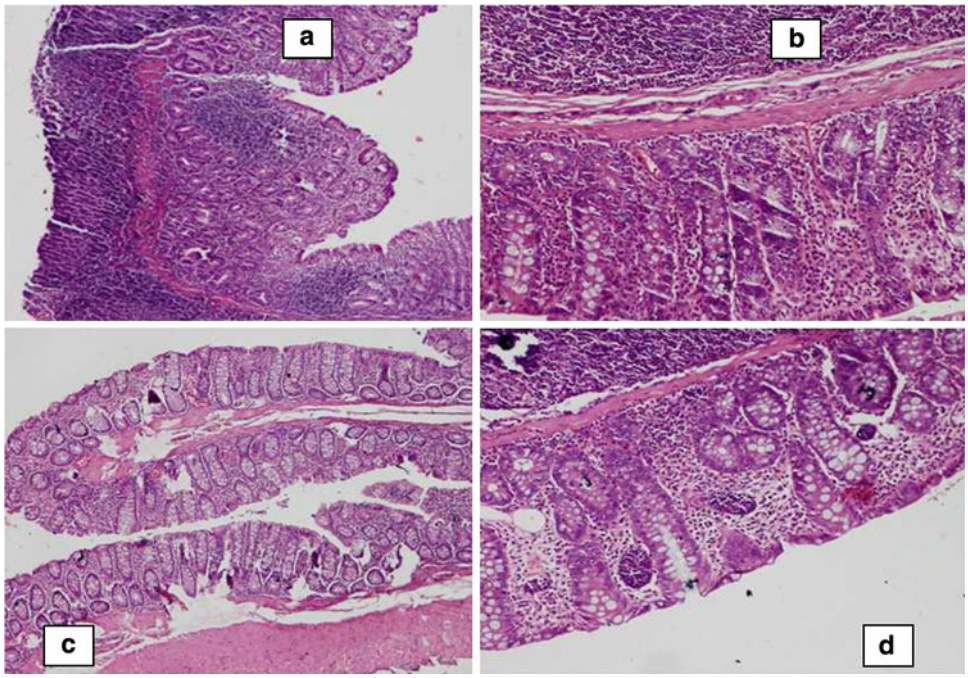

Fig. 4 **a** Light micrograph of rat colon treated with DMH showing severe inflammation with large lymphoid tissue formation and hyperplasia (H&E, ×40). **b** Distorted morphology of cells on treatment with DMH (H&E, ×100). **c** Light micrograph of rat colon treated with FO + CO (1:1) with varied gland size and increased intraglandular space (H&E, ×40). **d** Light micrograph of the rat colon supplemented with FO + CO (2.5:1) showing normal features with increased intra glandular space and regenerative changes (H&E, ×40)

antioxidant status. ROS have multiple functions and are implicated in tumor initiation and progression [20, 50]. While the higher levels of ROS can cause DNA damage and ultimately apoptosis, low levels of ROS in cancer cells has been suggested to promote cell proliferation mediated by redox signalling [51].

In the present investigation, treatment with DMH led to a decrease in the ROS generation with a concomitant increase in SOD and CAT in initiation phase. The level of GSH and GSH dependent enzymes were raised along with the increase in the apoptosis. Increase in the activities of SOD and CAT in the carcinogen treated animals have also been reported by other workers [52, 53]. An increased expression of GSH, GPx and GST in the neoplastic cell confers a selective growth advantage against onslaught of oxidative stress and allows these cells to propagate and proliferate [54]. The TrxR activity was reduced on treatment with DMH. It has been observed that TrxR and GPx expression are regulated in the contrasting manner in colon cancer cell line [55], which indeed was the observation in the present study. The upregulation of the antioxidants with a decrease in ROS levels may be an early cellular adaptive response. Therefore the cells may be able to maintain the ROS levels below the toxic threshold that benefit their proliferation as required in the process of carcinogenesis which is also suggested by other workers [56–58]. The increase in the apoptosis in the initiation phase indicates the enhanced rate of cell death with the carcinogen treatment. Most studies have shown that the proportion of epithelial cells undergoing apoptotic cell death increases in the course of the adenoma–carcinoma sequence [59, 60].

However, in the post initiation phase study, there was an increase in the levels of ROS generation and decreased activities of antioxidants and apoptosis. An increase in ROS generation in the progression phase of carcinogenesis has also been documented earlier [61, 62]. Increased ROS generation may serve as an endogenous source of DNA damaging agents that promote genetic instability and favor the process of carcinogenesis. There was decrease in the apoptosis as indicated by M-30 cytoDEATH levels and DNA fragmentation. Hence, the decreased apoptosis and increased DNA damage will favor the survival of the cancerous cell and promote the process of carcinogenesis as documented by the other studies also [62–64]. The increased damage in the colon was also supported by the increased ACF count and the hyperplastic changes observed in the histopathology in the present study.

On supplementing the fish oil and corn oil at the lower ratio (1:1), there was a decrease in ROS generation, TrxR and apoptosis with a concomitant rise in the antioxidants' activity in the initiation phase study. These results of initiation phase of lower ratio of fish oil and corn oil are in agreement with the study of Wang et al. [65], who reported decreased generation of ROS with increased activities of SOD, CAT and GPx in fish oil fed group in the atherosclerotic rats. A higher SOD activity will lead to an increased generation of H_2O_2 in the animals. H_2O_2 are detoxified by CAT and GPx. Hence, higher antioxidant levels in the treated cells are able to neutralize the free radical generation. TrxR activity is targeted by a number of anti-cancer drugs and potent inhibitors that alter cancer related properties of malignant cells [66]. Thus, its decrease

may be an important defense in the cancer progression which indeed is the result on treatment with the lower ratios of fish oil and corn oil. In addition, n-3 PUFA were able to activate the immune response and cause increased inflammation which indeed was the observation in the present study. In the post initiation phase study, fish oil in the lower ratios could enhance ROS levels and decrease the antioxidants' levels. n-3 PUFA are known to activate the chemoprevention by increasing the ROS levels. It is also known that n-3 PUFA improves the efficacy of chemotherapeutic regimens by increasing the ROS levels and that leads to tumoricidal effect [50].The histopathological observations and the decreased ACF count of the present study also support the preventive effect of fish oil with regenerative changes.

Administration of higher ratio of fish oil and corn oil (2.5:1) in the initiation phase showed a significant increase in the ROS levels as compared to the carcinogen treated animals with increased antioxidant levels. The cancer chemopreventive strategies have been reported to induce ROS levels which lead to DNA damage and ultimately apoptosis [51, 67]. Our findings of supplementation with the higher ratio of fish oil and corn oil are in agreement with the report showing a decrease in the activities of the CAT and GPx in the cancer cells lines on treatment with the DHA [68]. Increased LPO with decreased GPx and GST activities in tumorigenic rats are suggestive of the oxidative stress [69–71].

However, in the post initiation phase there was a decrease in the ROS levels on supplementing the fish oil and corn oil in the (2.5:1) ratio in the present study. CAT, SOD, GSH levels were decreased while there was an increase in the GR and GPx activity and DNA fragmentation. The normal levels of ROS with decrease in SOD and CAT attributes to the fact that GSH/GSSG redox signalling may play a major role. GSH/GSSG ratio is maintained by GR which uses the reducing power of NADPH to convert to GSSG to GSH [72]. Our study has also shown an increase in the GR activity along with the decrease in the GSH levels that may affect the redox potential. Therefore, the redox potential is modulated in the fish oil and corn oil treated animals which in turn have been implicated to modulate cell survival and death signals such as NF-$\kappa\beta$, PKC and caspases leading to apoptosis [72, 73]. Our study had also shown an associated increase in the apoptotic levels. In addition, regenerative changes were also seen in the groups administered with the fish oil and corn oil thereby supporting our hypothesis.

The ambiguity in the levels of ROS in the present study on supplementing different ratio of fish oil and corn oil can be explained by the fact that DHA is known to have a dose- and time-dependent effect on lipid peroxidation [74].It has been reported that low doses of DHA led to a decrease in the lipid peroxidation while an increase in dosage led to an increase in the lipid peroxidation. Lipid peroxidation in turn, is modulated by the cellular antioxidant defense system [74].

Morphological changes along with the ACF with the increased multiplicity serve as the markers of the chemopreventive response in both human and experimental colon cancer [75]. Treatment with the DMH in the rats led to an increase in the incidence and multiplicity of the ACF and inflammation in the colon. Various studies involving DMH induced colon carcinogenesis in rat model indicate that morphological surface alterations such as the proliferative activity and dysplasia in colonic mucosal epithelium start developing during the process of carcinogenesis [76–78]. However, there was a decrease in the ACF incidence and multiplicity with decreased inflammation of colon on treatment with the fish oil and corn oil in different ratios. A reduction in the ACF multiplicity has been reported in connection to the cancer chemoprevention [79, 80]. The protective action of the higher ratio in reducing the multiplicity of ACF are supported by the studies showing dose dependent effect of DHA administration on ACF incidence and multiplicity in colon cancer [81, 82]. The increase in the ACF incidence and multiplicity in the post initiation study may be attributed to the age related changes which has been reported by the previous studies [81, 82]. In the present study, the decreased ACF count with histopathological examination showing a normal mucosa and crypt accompanied by regenerative changes suggest the efficacy of the higher doses of fish oil and corn oil.

To conclude, the present study suggests that administration of fish oil and corn oil has a dose- and time-dependent chemopreventive effect in experimental colon cancer with a better efficacy of FO + CO (2.5:1). The chemoprevention effect may be mediated by modulation of oxidative stress and apoptosis.

Acknowledgments The study would have been incomplete without the invaluable help of Dr. Sharma and Mr. S. Singh, Department of Statistics, Panjab University, Chandigarh who provided the necessary expertise in the statistical analysis. The authors would like to acknowledge funding from the Indian Council of Medical Research as Ms. Pooja Sarotra is SRF-ICMR [Grant No. 3/1/3/JRF/75/MPD/2005 (11143)].

References

1. Boyle P, Langman JS (2000) ABC of colorectal cancer: epidemiology. BMJ 321:805–808. doi:10.1136/bmj.321.7264.805
2. Bird R (1995) Role of aberrant crypt foci in understanding the pathogenesis of colon cancer. Cancer Lett 93:55–71. doi:10.1016/0304-3835(95)03788-X
3. Bird RP, Good CK (2000) The significance of aberrant crypt foci in understanding the pathogenesis of colon cancer. Toxicol Lett 112–113:395–402. doi:10.1016/S0378-4274999)00261-1

4. Vogelstein B, Fearon ER, Hamilton SR, Kern SE, Preisinger AC, Leppert M, Nakamura Y, White R, Smits AM, Bos JL (1988) Genetic alterations during colorectal-tumor development. N Engl J Med 319:525–532
5. Lipkin M, Reddy B, Newmark H, Lamprecht SA (1999) Dietary factors in human colorectal cancer. Annu Rev Nutr 19:545–586. doi:10.1146/annurev.nutr.19.1.545
6. Simopoulos AP (1999) Essential fatty acids in health and chronic disease. Am J Clin Nutr 70:560S–569S
7. Doll R, Peto R (1981) The causes of cancer: quantitative estimates of avoidable risks of cancer in the United States today. J Natl Cancer Inst 66:1191–1308
8. Simopoulos AP (2002) The importance of the ratio of omega-6/omega-3 essential fatty acids. Biomed Pharmacother 56:365–379. doi:10.1016/S0753-3322(02)00253-6
9. Nkondjock A, Krewski D, Johnson KC, Ghadirian P, The Canadian Cancer Registries Epidemiology Research Group (2005) Specific fatty acid intake and the risk of pancreatic cancer in Canada. BJC 92:971–977. doi:10.1038/sj.bjc.6602380
10. Simopoulos AP (2008) The importance of the omega-6/omega-3 fatty acid ratio in cardiovascular disease and other chronic diseases. Exp Biol Med 233:674–688. doi:10.3181/0711-MR-311
11. De Lorgeril M, Renaud S, Mamelle N, Salen P, Martin JL, Monjaud I, Guidollet J, Touboul P, Delaye J (1994) Mediterranean α-linolenic acid-rich diet in secondary prevention of coronary heart disease. Lancet 343:1454–1459. doi:10.1016/S0140-6736(94)92580-1
12. Raheja BS, Sadikot SM, Phatak RB, Rao MB (1993) Significance of the N-6/N-3 ratio for insulin action in diabetes. Ann N Y Acad Sci 683:258–271. doi:10.1111/j.1749-6632.1993.tb35715.x
13. Simopoulos AP (1993) Omega-3 fatty acids in health and disease and in growth and development. Am J Clin Nutr 54:438–463
14. Benatti P, Peluso G, Nicolai R, Calvani M (2004) Polyunsaturated fatty acids: biochemical, nutritional and epigenetic properties. J Am Coll Nutr 23:281–302
15. Rose DP, Connolly JM (1999) Omega-3 fatty acids as cancer chemopreventive agents. Pharmacol Ther 83:217–244. doi:10.1016/S0163-7258(99)00026-1
16. Raharjo S, Sofos JN (1993) Methodology for estimating malonaldehyde as a product of lipid peroxidation in muscle tissue: a review. Meat Sci 35:145–169. doi:10.1016/0309-1740(93)90046-K
17. Sharma RA, Gescher A, Plastaras JP, Leuratti C, Singh R, Gallacher-Horley B, Offord E, Mernett LJ, Stewart WP, Plummer SM (2001) Cyclooxygenase-2, malondialdehyde and pyrimidopurinone adducts of deoxyguanosine in human colon cells. Carcinogenesis 22:1557–1560. doi:10.1093/carcin/22.9.1557
18. Aw TY (1999) Molecular and cellular responses to oxidative stress and changes in oxidation-reduction imbalance in the intestine. Am J Clin Nutr 70:557–565
19. Halliwell B (1987) Oxidants and human disease: some new concepts. FASEB J 1:358–364
20. Valko M, Rhodes CJ, Moncol J, Izakovic M, Mazur M (2006) Free radicals, metals and antioxidants in oxidative stress-induced cancer. Chem Biol Interact 160:1–40. doi:10.1016/j.cbi.2005.12.009
21. Das UN (1991) Tumoricidal action of *cis*-unsaturated fatty acids and their relationship to free radicals and lipid peroxidation. Cancer Lett 56:235–243. doi:10.1016/0304-3835(91)90008-6
22. Okuyama H, Kobayashi T, Watanabe S (1996) Dietary fatty acids—the N-6/N-3 balance and chronic elderly diseases. Excess linoleic acid and relative N-3 deficiency syndrome seen in Japan. Prog Lipid Res 35:409–457. doi:10.1016/SO163-7827(96)00012-4
23. Sies H (1991) Role of reactive oxygen species in biological processes. J Mol Med 69:965–968. doi:10.1007/BF01645140
24. Mustacich D, Powsi G (2000) Thioredoxin reductase. Biochem J 346:1–8
25. Takahashi M, Tsuboyama-Kasaoka N, Nakatani T, Ishii M, Tsutsumi S, Aburatani H, Ezaki O (2002) Fish oil feeding alters liver gene expressions to defend against PPARα activation and ROS production. Am J Physiol GI 282:338–348. doi:10.1152/ajpgi.00376.2001
26. Makin G, Hickman JA (2000) Apoptosis and cancer chemotherapy. Cell Tissue Res 301:143–152. doi:10.1007/s004419900160
27. Hanahan D, Weinberg RA (2000) The hallmark of cancer. Cell 100:57–70. doi:10.1016/S0092-8674(00)81683-9
28. Hong MY, Chapkin RS, Barhoumi R, Burghardt RC, Turner ND, Henderson CE, Sanders LM, Fan Y, Davidson LA, Murphy ME, Spinka CM, Carroll RJ, Lupton JR (2002) Fish oil increases mitochondrial phospholipid unsaturation, upregulating reactive oxygen species and apoptosis in rat colonocytes. Carcinogenesis 23:1919–1926. doi:10.1093/carcin/23.11.1919
29. Hong MY, Lupton JR, Morris JS, Wang N, Carroll RJ, Davidson LA, Elder RH, Chapkin RS (2000) Dietary fish oil reduces O^6-methylguanine DNA adduct levels in rat colon in part by increasing apoptosis during tumor initiation. Cancer Epidemiol Biomarkers Prev 9:819–826
30. Davidson LA, Nguyen DV, Hokanson RM, Callaway ES, Isett RB, Turner ND, Dougherty ER, Wang N, Lupton JR, Carroll RJ, Chapkin RS (2004) Chemopreventive n-3 polyunsaturated fatty acids reprogram genetic signatures during colon cancer initiation and progression in the rat. Cancer Res 64:6797–6804
31. Committee on Laboratory Animal Diets (1978) Control of diets in laboratory animal experimentation. National Academy of Sciences, Washington, DC
32. Johnson S, Saikia N (2009) Fatty acid profile of edible oils and fats in India. CSE, pp 3–31
33. Benevenga NJ, Calvert C, Eckhert CD, Fahey GC, Greger JL, Keen CL, Knapka JJ, Magalhaes H, Oftedal OT (1995) Nutrient requirement for laboratory animals. National Academy Press Washington, DC
34. Mann J, Skeaff M (2007) Lipids. In: Mann J, Truswell AS (eds) Essential of human nutrition. Oxford University Press, Oxford
35. Fiala ES (1977) Investigations into the metabolism and mode of action of the colon carcinogens 1,2-dimethylhydrazine and azoxymethane. Cancer 40:2436–2445. doi:10.1002/1097-0142(197711)40:5+<2436:AID-CNCR2820400908>3.0.CO;2-U
36. Latham P, Lund EK, Johnson IT (1999) Dietary n-3 PUFA increases the apoptotic response to 1,2-dimethylhydrazine, reduces mitosis and suppresses the induction of carcinogenesis in the rat colon. Carcinogenesis 20:645–650. doi:10.1093/carcin/20.4.645
37. Sanders LM, Henderson CE, Hong MY, Barhoumi R, Burghardt RC, Wang N, Spinka CM, Carroll RJ, Turner ND, Chapkin RS, Lupton JR (2004) An increase in reactive oxygen species by dietary fish oil coupled with the attenuation of antioxidant defenses by dietary pectin enhances rat colonocytes apoptosis. J Nutr 134:3233–3238
38. Freshney RI (1994) Culture of animal cells: a manual of basic technique. Wiley, New York, pp 287–307
39. Rosenkranz AR, Schmaldienst S, Stuhlmeier KM, Chen W, Knapp W, Zlabinger GJ (1992) A microplate assay for the detection of oxidative products using 2′,7′-dichlorofluorescin-diacetate. J Immunol Methods 156:39–45. doi:10.1016/0022-1759(92)90008-H
40. Kono Y (1978) Generation of superoxide radicals during autoxidation of hydroxylamine and an assay for superoxide dismutase. Arch Biochem Biophys 186:189–195. doi:10.1016/0003-9861(78)90479-4
41. Luck H (1963) Catalase. In: Bergemeyer HU (ed) Methods of enzymatic analysis. Academic Press, London, pp 885–891

42. Ellman GL (1959) Tissue sulfhydryl groups. Arch Biochem Biophys 82:70–77. doi:10.1016/0003-9861(59)90090-6
43. Lawrence RA, Burk RF (1978) Species, tissue and sub cellular distribution of non selenium glutathione peroxidase activity. J Nutr 108:211–215
44. Carlberg I, Mannervik B (1985) Glutathione reductase. In: Meister A (ed) Methods in enzymology. Academic Press, New York, pp 484–490
45. Habig WH, Pabst MJ, Jakoby WB (1974) Glutathione-*S*-transferase: the first step in enzymatic step in mercapturic acid formation. J Biol Chem 249:7130–7139
46. Arnér ESJ, Zhong L, Holmgren A (1999) Preparation and assay of mammalian thioredoxin and thioredoxin reductase. Methods Enzymol 300:226–239. doi:10.1016/S0076-6879(99)00129-9
47. Lowry OH, Roserbrough NJ, Farr AL, Randall RJ (1951) Protein measurement with folin phenol reagent. J Biol Chem 193:265–275
48. Bao S, Knoell DL (2006) Zinc modulates airway epithelium susceptibility to death receptor-mediated apoptosis. Am J Physiol Lung Cell Mol Physiol 290:L433–L444. doi:10.1152/ajplung.00341.2005
49. Roy HK, DiBaise JK, Black J, Karolski WJ, Ratashak A, Ansari S (2001) Polyethylene glycol induces apoptosis in HT-29 cells: potential mechanism for chemoprevention of colon cancer. FEBS Lett 496:143–146. doi:10/1016/S0014-5793(01)02420-6
50. Nishigori C, Hattori Y, Toyokuni S (2004) Role of reactive oxygen species in skin carcinogenesis. Antioxid Redox Signal 6:561–570
51. Hail N Jr, Cortes M, Drake EN, Spallholz JE (2008) Cancer chemoprevention: a radical perspective. Free Radic Biol Med 45:97–110. doi:10.1016/j.freeradbiomed.2008.04.004
52. Rainis T, Maor I, Lanir A, Shnizer S, Lavy A (2007) Enhanced oxidative stress and leukocyte lipid peroxidation and antioxidant status in colorectal cancer activation in neoplastic tissues of the colon. Dig Dis Sci 52:526–530. doi:10.1007/s10620-006-9177-2
53. Skrzydlewska E, Sulkowski S, Koda M, Zalewski B, Kanczuga-Koda L, Sulkowska M (2005) Lipid peroxidation and antioxidant status in colorectal cancer. World J Gastroenterol 11:403–406
54. Hardman WE, Munoz J Jr, Cameron IL (2002) Role of lipid peroxidation and antioxidant enzymes in omega 3 fatty acids induced suppression of breast cancer xenograft growth in mice. Cancer Cell Int 2:1–10. doi:10.1186/1475-2867-2-10
55. Gladyshev VN, Factor VM, Housseau F, Hatfield DL (1998) Contrasting patterns of regulation of the antioxidant selenoproteins, thioredoxin reductase, and glutathione peroxidase, in cancer cells. Biochem Biophys Res Commun 251:488–493. doi:10.1006/bbrc.1998.9495
56. Trachootham D, Alexandre J, Huang P (2009) Targeting cancer cells by ROS-mediated mechanisms: a radical therapeutic approach? Nat Rev Drug Discov 8:579–591. doi:10.1038/nrd2803
57. Manju V, Balasubramaniyan V, Nalini N (2005) Rat colonic lipid peroxidation and antioxidant status: the effects of dietary luteolin on 1,2-dimethylhydrazine challenge. Cell Mol Bio Lett 10:535–551
58. Nakagami K, Uchida T, Ohwada S, Koibuchi Y, Morishita Y (1999) Increased choline kinase activity in 1,2-dimethylhydrazine-induced rat colon cancer. Jpn J Cancer Res 90:1212–1217. doi:10.1111/j.1349-7006.1999.tb00698.x
59. Koike M (1996) Significance of spontaneous apoptosis during colorectal tumorigenesis. J Surg Oncol 62:97–108. doi:10.1002/(SICI)1096-9098(199606)62:2<97:AID-JSO5>3.0.CO;2-L
60. Takano Y, Saegusa M, Ikenaga M, Mitomi H, Okayasu I (1996) Apoptosis of colon cancer: comparison with Ki-67 proliferative activity and expression of p53. J Cancer Res Clin Oncol 122:166–170. doi:10.1007/BF01366957
61. Szatrowski TP, Nathan CF (1991) Production of large amounts of hydrogen peroxide by human tumor cells. Cancer Res 51:794–798
62. Toyokuni S, Okamoto K, Yodoi J, Hiai H (1995) Persistent oxidative stress in cancer. FEBS Lett 358:1–3. doi:10.1016/0014-5793(94)01368-B
63. Zhivotovsky B, Kroemer G (2004) Apoptosis and genomic instability. Nat Rev Mol Cell Biol 5:752–762. doi:10.1038/nrm1443
64. Liang Q, Benjamin CYW (2009) Targeting apoptosis as an approach for gastrointestinal cancer therapy. Drug Resist Update 12:55–64. doi:10.1016/j.drup.2009.02.002
65. Wang HH, Hung TM, Wei J, Chiang AN (2004) Fish oil increases antioxidant enzyme activities in macrophages and reduces atherosclerotic lesions in apoE-knockout mice. Cardiovasc Res 61:169–176. doi:10.1016/j.cardiores.2003.11.002
66. Hatfield DL, Yoo MH, Carlson BA, Gladyshev VN (2009) Selenoproteins that function in cancer prevention and promotion. Biochim Biophys Acta 1790:1541–1545. doi:10.1016/jbbagen.2009.03.001
67. Salganik RI, Albright CD, Rodgers J, Kim J, Zeisel SH, Sivashinskiy MS, Van-Dyke TA (2000) Dietary antioxidant depletion: enhancement of tumor apoptosis and inhibition of brain tumor growth in transgenic mice. Carcinogenesis 21:909–914. doi:10.1093/carcin/21.5.909
68. Vibet S, Goupille C, Bougnoux P, Steghens JP, Gore J, Maheo K (2008) Sensitization by docosahexaenoic acid (DHA) of breast cancer cells to anthracyclines through loss of glutathione peroxidase (GPx1) response. Free Radic Biol Med 44:1483–1491. doi:10.1016/j.freeradbiomed.2008.01.009
69. Rehman H, Ali M, Atif F, Kaur M, Bhatia K, Raisuddin S (2006) The modulatory effect of deltamethrin on antioxidants in mice. Clin Chim Acta 369:61–65. doi:10.1016/j.cca.2006.01.010
70. Sreedharan V, Venkatachalam KK, Namasivayam N (2009) Effect of morin on tissue lipid peroxidation and antioxidant status in 1,2-dimethylhydrazine induced experimental colon carcinogenesis. Invest New Drugs 27:21–30. doi:10.1016/j.etap.2009.09.006
71. Meister A, Anderson ME (1983) Glutathione. Ann Rev Biochem 52:711–760. doi:10.1146/annurev.bi.52.070183.003431
72. Hampton MB, Orrenius S (1997) Dual regulation of caspase activity by hydrogen peroxide: implications for apoptosis. FEBS Lett 414:552–556. doi:10.1016/S0014-5793(97)01068-5
73. Klatt P, Lamas S (2000) Regulation of protein function by *S*-glutathiolation in response to oxidative and nitrosative stress. Eur J Biochem 267:4928–4944. doi:10.1046/j.1432-1327.2000.01601.x
74. Leonardi F, Attorri L, Benedetto RD, Biase AD, Sanchez M, Tregno FP, Nardini M, Salvati S (2007) Docosahexaenoic acid supplementation induces dose and time dependent oxidative changes in C6 glioma cells. Free Radic Res 41:748–756. doi:10.1080/10715760701324067
75. Shiptz B, Klein E, Bklan G, Neufeld D, Nissan A, Freund HR, Grankin M, Bernheim J (2003) Suppressive effects of aspirin on aberrant crypt foci in patients with colorectal cancer. Gut 52:1598–1601. doi:10.1136/gut.52.11.1598
76. Sharma P, Kaur J, Sanyal SN (2010) Effect of etoricoxib, a cyclooxygenase-2 selective inhibitor on aberrant crypt formation and apoptosis in 1,2-dimethyl hydrazine induced colon carcinogenesis in rat model. Nutr Hosp 25:39–48
77. Kanwar SS, Vaiphei K, Nehru B, Sanyal SN (2007) Chemopreventive effects of non-steroidal anti-inflammatory drugs in the membrane lipid composition and fluidity parameters of the 1,2-dimethyl hydrazine induced colon carcinogenesis in rats. Drug Chem Toxicol 30:293–309. doi:10.1080/01480540701522106
78. Aranganathan S, Nalini N (2009) Efficacy of the potential chemopreventive agent, hesperetin (citrus flavanone), on

1,2-dimethylhydrazine induced colon carcinogenesis. Food Chem Toxicol 47:2594–2600. doi:10.1016/j.fct.2009.07.019
79. Kawamori T, Tanaka T, Hara A, Yamahara J, Mori H (1995) Modifying effects of naturally occurring products on the development of colonic aberrant crypt foci induced by azoxymethane in F344 rats. Cancer Res 55:1277–1282
80. Tanaka T, Kojima T, Suzui M, Mori H (1993) Chemoprevention of colon carcinogenesis by the natural product of a simple phenolic compound protocatechuic acid: Suppressing effects on tumor development and biomarkers expression of colon tumorigenesis. Cancer Res 53:3908–3913
81. Takahashi M, Fukutake M, Isoi T, Fukuda K, Sato H, Yazawa K, Sugimura T, Wakabayashi K (1997) Suppression of azoxymethane-induced rat colon carcinoma development by a fish oil component, docosahexaenoic acid (DHA). Carcinogenesis 18:1337–1342. doi:10.1093/carcin/18.7.1337
82. Takahashi M, Minamoto T, Yamashita N, Kato T, Yazawa K, Esumi H (1994) Effect of docosahexaenoic acid on azoxymethane induced colon carcinogenesis in rats. Cancer Lett 83:177–184. doi:10.1016/0304-3835(94)90316-6

Lipids (2010) 45:799–808
DOI 10.1007/s11745-010-3464-6

ORIGINAL ARTICLE

Lower Efficacy in the Utilization of Dietary ALA as Compared to Preformed EPA + DHA on Long Chain n-3 PUFA Levels in Rats

Ramaprasad R. Talahalli · Baskaran Vallikannan · Kari Sambaiah · Belur R. Lokesh

Received: 17 March 2010 / Accepted: 8 August 2010 / Published online: 24 August 2010

Abstract We made a comparative analysis of the uptake, tissue deposition and conversion of dietary α-linolenic acid (ALA) to its long chain metabolites eicosapentaenoic acid (EPA) and docosahexaenoic acid (DHA) with preformed EPA + DHA. Diets containing linseed oil [with ALA at ~2.5 (4 g/kg diet), 5 (8 g/kg diet), 10 (16 g/kg diet), 25% (40 g/kg diet)] or fish oil [with EPA + DHA at ~1 (1.65 g/kg diet), 2.5 (4.12 g/kg diet), 5% (8.25 g/kg diet)] or groundnut oil without n-3 polyunsaturated fatty acids (n-3 PUFA) were fed to rats for 60 days. ALA and EPA + DHA in serum, liver, heart and brain increased with increments in the dietary ALA level. When preformed EPA + DHA were fed, the tissue EPA + DHA increased significantly compared to those given ALA. Normalized values from dietary n-3 PUFA to tissue EPA + DHA indicated that 100 mg of dietary ALA lead to accumulation of EPA + DHA at 2.04, 0.70, 1.91 and 1.64% of total fatty acids respectively in liver, heart, brain and serum. Similarly 100 mg of preformed dietary EPA + DHA resulted in 25.4, 23.8, 15.9 and 14.9% of total fatty acids in liver, heart, brain and serum respectively. To maintain a given level of EPA + DHA, the dietary ALA required is 12.5, 33.5, 8.3 and 9.1 times higher than the dietary EPA + DHA for liver, heart, brain and serum respectively. Hence the efficacy of precursor ALA is lower compared to preformed EPA + DHA in elevating serum and tissue long chain n-3 PUFA levels.

Keywords α-Linolenic acid · Eicosapentaenoic acid · Docosahexaenoic acid · Serum lipids · Tissue lipids

Abbreviations

ALA	α-Linolenic acid (18:3 n-3)
ANOVA	Analysis of variance
ARA	Arachidonic acid (20:4 n-6)
DHA	Docosahexaenoic acid (22:6 n-3)
DPA	Docosapentaenoic acid (22:5 n-3)
EPA	Eicosapentaenoic acid (20:5 n-3)
FO	Fish oil
GNO	Groundnut oil (peanut oil)
HDL	High density lipoprotein
LDL	Low density lipoprotein
LNA	Linoleic acid (18:2 n-6)
LSO	Linseed oil
ND	Not detected
PUFA	Polyunsaturated fatty acid (s)
SD	Standard deviation
SFA	Saturated fatty acid

Introduction

The principal n-3 polyunsaturated fatty acids (n-3 PUFA) consumed by vegetarian populations are α- linolenic acid (ALA, 18:3n-3) and the dietary intake of eicosapentaenoic acid (EPA, 20:5n-3) and docosahexaenoic acid (DHA, 22:6n-3) in these subjects is negligible. The intake of EPA and DHA is restricted to people who consume fish. However the vegetarians refrain from consuming fish and have to depend on the dietary ALA for EPA and DHA. ALA is elongated and

R. R. Talahalli · B. R. Lokesh (✉)
Department of Lipid Science and Traditional Foods,
Central Food Technological Research Institute,
Mysore 570 020, India
e-mail: lokesh_lipids@yahoo.co.in

B. Vallikannan · K. Sambaiah
Department of Biochemistry and Nutrition,
Central Food Technological Research Institute,
Mysore 570 020, India

desaturated to 24:6 (n-3) by the following steps, 18:3 → 18:4 → 20:4 → 20:5 → 22:5 → 24:5 → 24:6 after which 24:6 (n-3) is shortened to DHA by one step of β-oxidation in peroxisomes [1]. Therefore ALA has to play a major role in vegetarians for the maintenance of EPA and DHA supply to the body.

The bioavailability of an individual fatty acid is influenced by the presence of other fatty acids and, for many years, studies have focused on apparent differences in the deposition of linoleic acid (LNA, 18:2n-6) and ALA in tissue lipids [2]. The ALA did not appear to accumulate to the same extent as that of LNA even under circumstances where equal amounts of LNA and ALA are fed [3]. Bazinet et al. [4] evaluated the utilization of ALA in growing rats consuming a diet deficient in n-6 PUFA. After 90 days, whole-body ALA accumulation was 55% lower, total n-3 PUFA accumulation was 21% lower, and ALA disappearance was 14% higher in n-6 PUFA deficient rats. Part of the reduction of whole-body ALA in n-6 PUFA-deficient rats was due to the 25% increase in net conversion of ALA to long-chain n-3 PUFA. Despite adequate ALA intake, n-6 PUFA deficiency decreased the accumulation of ALA and total n-3 PUFA. Thus n-6 PUFA affected the homeostasis of ALA. Humans show differences in LNA and ALA accumulation. While linear relationships were found between dietary ALA and EPA levels in plasma, LNA in the plasma increases linearly with dietary LNA [5]. The factors controlling the conversion of ALA to EPA and DHA may be an important determinant for maintaining adequate amounts of ALA, EPA and DHA in cells for optimal tissue function. Many researchers have extensively reviewed the essentiality of n-3 PUFA and emphasized on dose response effects of these fatty acids on its incorporation in tissues [6]. The levels of the long chain n-3 PUFA in serum and tissue are dependent on intake of either their precursors or preformed product. If an increased level of ALA is to be promoted for maintaining a given level of long chain n-3 PUFA, it is necessary to consider to what extent dietary ALA is absorbed, stored and converted into long chain metabolites.

In the present investigation, the effect of different levels of ALA or preformed EPA + DHA on the incorporation of long chain n-3 PUFA into serum and tissue lipids were studied. The implications of this uptake of n-3 PUFA on the risk factors that have a bearing on cardiovascular functions were also studied.

Experimental Procedures

Materials

Cholesterol, Dipalmitoyl phosphatidyl choline, triolein, and α-cellulose were purchased from Sigma Chemical Co, (St. Louis, MO, USA). Heparin and MnCl2 were obtained from Sisco Research Laboratory (Mumbai. India). Refined groundnut oil (Peanut oil) was purchased from a local supermarket. Fish oil (FO) (Sea Cod; brand name for cod liver oil by Seven Seas Ltd, Hull UK which is marketed in India by Universal Medicare Pvt. Ltd. Gujarat, India) was purchased from a Government pharmacy. Linseed oil (LSO) was obtained by cold pressing linseed which was double filtered and stored at 4°C after flushing the container with nitrogen gas. All the chemicals and solvents used were of analytical grade and solvents were distilled prior to use.

Animals and Diets

Male Wistar rats (OUTB-Wistar. IND-cft (2c) weighing 50 ± 4 g were grouped by random distribution ($N = 6$ animals per group). They were placed in individual cages with a 12-h light: dark cycle, in an approved animal house facility at the Central Food Technological Research Institute in Mysore, India. Rats were given the diet fresh each day and leftovers from the diets were weighed and discarded. Growth of the rats was monitored by weighing at regular intervals. The rats had free access to food and water throughout the study. The ingredients used in the basal diet were (g/100 g): casein 20; cellulose 5; sucrose 54; AIN-76 mineral mix 3.5; AIN-76 vitamin mix 1; methionine 0.3; choline chloride 0.2; and fat 16 [7]. Diet containing only groundnut oil (GNO) as sole source of fat served as control. Incremental amounts of LSO or FO were added and made isocaloric with GNO. After 60 days of feeding, rats were fasted overnight and sacrificed under ether anesthesia. Blood was drawn by cardiac puncture and serum was separated by centrifugation at 1,100*g* for 30 min. Liver, heart, brain and adipose were removed, rinsed with ice-cold saline, blotted, weighed and stored at −20°C until analyzed. The experimental protocol for these studies was approved by Animal Ethics Committee Nominated by Government of India.

Analysis of Lipids

Lipids were extracted from serum and tissues by the method of Folch et al. [8]. Serum and liver cholesterol levels were quantitated by the method of Searcy and Bergquist [9]. HDL cholesterol was estimated after precipitating LDL with heparin-MnCl2 reagent [10]. Phospholipids were measured by the method of Stewart [11] using dipalmitoylphosphatidyl choline as reference standard. Triacylglycerol were estimated by the method of Fletcher [12]. Fatty acids were analyzed as methyl esters [13] by gas chromatography (Shimadzu 14B fitted with FlD) using fused silica capillary column 25 m × 0.25 mm (Parma bond FFAP-DF-0.25: Machery-Nagel Gm BH Co.

II Duren, Germany). The operating conditions were: initial column temperature 160°C, injector temperature 210°C and detector temperature 250°C; column temperature was programmed to ramp 6°C per min to reach final temperature of 240°C. Nitrogen gas was used as the carrier. Individual fatty acids were identified by comparing retention times of standards (NU-Check prep. Inc., Elysian Minnesota, USA) and were quantitated by online chromatopack CR-6A integrator.

Statistics

The results were analyzed statistically by ANOVA [14]. A p value of <0.001 is considered to be significantly different.

Results

Fatty Acid Composition of Diet

Fatty acid composition of control and experimental diets are given in Table 1. LSO was added to increase the ALA content of the diet to provide ~2.5, 5.0, 10.0 and 25.0% ALA. The LNA/ALA ratios in the LSO containing diets were found to be 9.15, 4.52, 1.96 and 0.69. Similarly addition of FO increased the EPA and DHA level of the diet. The diet with FO provided approximately 1.0, 2.5 and 5.0% EPA + DHA. The LNA/EPA + DHA ratios in the diet were found to be 16.46, 7.62 and 4.18. The LNA content was maintained between 18 and 24% in all the experimental diets. The amounts of diet consumed in different groups were comparable. There was no significant change in the food efficiency ratio and body weight gained by rats fed diet containing different amounts of LSO or FO compared to control groups (Data not shown).

Serum Lipid Profile of Rats Fed Diets Containing Different Levels of LSO or FO

The rats fed ALA containing diets were found to contain 1.0, 1.9, 3.3 and 5.9% of ALA in serum lipids when the diet contained 2.5, 5.0, 10.0 and 25.0% ALA respectively (Table 2). The sum of EPA and DHA content in these animals were found to be 1.0, 1.7, 2.9 and 5.1% respectively. The corresponding ratios of EPA + DHA/ALA in serum lipids were 1.0. 0.89, 0.88 and 0.86 respectively indicating a moderate conversion of ALA to long chain n-3 PUFA. However, the total amount of ALA accumulated in the serum of rats fed LSO containing diets did not exceed 5.9% of total fatty acids even when the diet contained ALA to an extent of 40 g/kg diet. The EPA + DHA levels in the serum of rats fed diet containing 1.0, 2.5 and 5.0% EPA + DHA were found to be 3.4, 6.1, and 9.7% indicating that preformed long chain n-3 PUFA on weight basis compared to ALA was efficiently incorporated in lipoproteins and as shown in following sections was also incorporated in tissue lipids. Thus feeding diets containing LSO or FO at increasing concentrations resulted in accumulation of n-3 PUFA in the serum. The n-3 PUFA was not detected in control rats fed GNO. A dose dependent decrease in the serum total cholesterol level in both LSO and FO fed rats was observed (Table 3). At 2.5, 5.0, 10.0 and 25.0% ALA level in the diet the total cholesterol in serum was decreased by 7, 14, 17 and 26% respectively compared to rats given control diets. Whereas, at 1.0, 2.5 and 5.0%

Table 1 Fatty acid composition (mg%) of diets

Fatty acid	GNO	ALA 2.5%	ALA 5.0%	ALA 10.0%	ALA 25.0%	EPA + DHA 1.0%	EPA + DHA 2.5%	EPA + DHA 5.0%
14:0	ND	ND	ND	ND	ND	1.5	1.8	2.9
16:0	14.47	13.80	13.16	12.69	10.9	12.5	12.72	14.2
16:1 (n-7)	ND	ND	ND	ND	ND	2.60	2.64	3.0
18:0	2.56	2.77	3.30	3.5	4.5	2.36	3.50	3.83
18:1 (n-9)	56.87	56.20	54.78	52.05	40.5	56.8	53.51	46.36
18:2 (n-6)	26.09	24.54	23.54	21.04	18.0	21.9	20.9	21.2
18:3 (n-3)	ND	2.68	5.2	10.71	26.0	ND	ND	ND
20:4 (n-6)	ND	ND	ND	ND	ND	0.9	2.00	3.16
20:5 (n-3)	ND	ND	ND	ND	ND	0.61	1.26	2.43
22:5 (n-3)	ND	ND	ND	ND	ND	0.10	0.18	0.27
22:6 (n-3)	ND	ND	ND	ND	ND	0.72	1.48	2.64
SFA	17.03	16.57	16.46	16.19	15.40	16.36	18.02	20.93
PUFA	26.09	27.22	28.74	31.75	44.00	24.13	25.64	29.43
PUFA/SFA	1.53	1.65	1.74	1.88	2.85	1.48	1.42	1.40
n-6/n-3	–	9.15	4.52	1.96	0.69	16.46	7.62	4.18

Values are means of triplicate samples

ND not detected, *GNO* groundnut oil, *LSO* linseed oil, *FO* fish oil

Table 2 Serum fatty acid profile (%) of rats fed n-3 fatty acids from LSO or FO at incremental levels

Fatty acid	GNO	ALA 2.5%	ALA 5.0%	ALA 10.0%	ALA 25.0%	EPA + DHA 1.0%	EPA + DHA 2.5%	EPA + DHA 5.0%
16:0	21.9 ± 2.0^{b}	24.9 ± 1.9^{b}	25.3 ± 2.0^{b}	25.9 ± 2.3^{b}	24.9 ± 2.3^{b}	24.6 ± 1.5^{b}	24.1 ± 1.8^{b}	24.9 ± 3.0^{b}
16:1 (n-7)	0.6 ± 0.3^{b}	1.0 ± 0.2^{b}	0.9 ± 0.2^{b}	1.0 ± 0.3^{b}	0.9 ± 0.3^{b}	2.0 ± 0.4^{c}	2.6 ± 0.3^{c}	3.4 ± 1.0^{d}
18:0	7.2 ± 1.3^{b}	8.7 ± 1.6^{b}	8.9 ± 0.9^{b}	10.1 ± 2.3^{b}	9.2 ± 3.0^{b}	9.2 ± 0.8^{b}	10.1 ± 2.0^{b}	9.6 ± 2.3^{b}
18:1 (n-9)	40.9 ± 1.3^{b}	38.1 ± 2.9^{b}	37.8 ± 2.3^{b}	36.2 ± 3.0^{b}	35.7 ± 2.7^{b}	39.1 ± 3.6^{b}	38.1 ± 4.8^{b}	37.2 ± 5.3^{b}
18:2 (n-6)	22.6 ± 2.5^{b}	19.6 ± 4.4^{bc}	18.1 ± 2.3^{bc}	16.1 ± 3.9^{c}	14.3 ± 4.0^{cd}	15.0 ± 2.3^{cd}	13.3 ± 2.3^{cd}	10.6 ± 2.9^{d}
18:3 (n-3)	ND	1.0 ± 0.08^{b}	1.9 ± 0.08^{c}	3.3 ± 0.1^{d}	5.9 ± 0.4^{e}	ND	ND	ND
20:4 (n-6)	5.9 ± 0.3^{b}	4.8 ± 0.3^{c}	4.4 ± 0.4^{c}	3.6 ± 0.3^{d}	3.1 ± 0.2^{d}	5.4 ± 0.4^{b}	4.2 ± 1.0^{c}	3.1 ± 0.8^{d}
20:5 (n-3)	ND	0.7 ± 0.2^{b}	1.2 ± 0.3^{c}	1.9 ± 0.3^{d}	3.2 ± 0.9^{e}	1.6 ± 0.3^{cd}	3.1 ± 0.6^{e}	4.8 ± 1.0^{f}
22:5 (n-6)	0.9 ± 0.2^{b}	0.8 ± 0.1^{b}	0.8 ± 0.1^{b}	0.7 ± 0.2^{b}	0.6 ± 0.2^{b}	0.8 ± 0.2^{b}	0.8 ± 0.1^{b}	0.6 ± 0.1^{b}
22:5 (n-3)	ND	ND	0.1 ± 0.05^{b}	0.18 ± 0.05^{b}	0.2 ± 0.05^{b}	0.4 ± 0.1^{c}	0.6 ± 0.1^{cd}	0.8 ± 0.09^{d}
22:6 (n-3)	ND	0.3 ± 0.1^{b}	0.5 ± 0.2^{b}	1.0 ± 0.1^{c}	1.9 ± 0.3^{d}	1.8 ± 0.2^{d}	3.0 ± 0.4^{e}	4.9 ± 0.4^{f}

Values are means ± SD ($n = 6$ rats). Values not sharing a common superscript within a row are statistically significant (0.001). For abbreviations see Table 1

Table 3 Serum lipid profile (mg/dL) of rats fed n-3 fatty acids from LSO or FO at incremental levels

Parameters	GNO	ALA 2.5%	ALA 5.0%	ALA 10.0%	ALA 25.0%	EPA + DHA 1.0%	EPA + DHA 2.5%	EPA + DHA 5.0%
Total cholesterol	93.4 ± 3.8^{b}	86.9 ± 2.6^{c}	80.0 ± 3.1^{de}	77.2 ± 3.2^{efg}	69.2 ± 3.8^{f}	83.7 ± 2.9^{ce}	76.0 ± 4.5^{e}	70.4 ± 4.7^{fg}
HDL cholesterol	48.0 ± 3.0^{b}	44.4 ± 1.9^{b}	38.5 ± 1.5^{cd}	36.0 ± 2.6^{cd}	34.6 ± 2.5^{d}	41.5 ± 2.2^{c}	36.6 ± 0.9^{d}	35.4 ± 1.9^{d}
LDL + VLDL cholesterol	45.4 ± 1.9^{b}	42.4 ± 1.2^{b}	41.0 ± 2.7^{bc}	40.0 ± 3.5^{bc}	34.6 ± 5.5^{c}	42.2 ± 3.8^{b}	39.4 ± 4.0^{b}	37.0 ± 4.1^{bc}
Phospholipids	114.4 ± 10.2^{b}	106.7 ± 8.5^{b}	104.6 ± 8.4^{b}	108.9 ± 5.6^{b}	107.9 ± 7.5^{b}	114.2 ± 7.9^{b}	120.6 ± 7.1^{b}	110.4 ± 5.5^{b}
Triacylglycerol	147.5 ± 6.7^{b}	138.9 ± 3.8^{b}	130.8 ± 6.3^{c}	119.6 ± 8.8^{d}	106.7 ± 10.4^{c}	129.6 ± 4.9^{c}	117.3 ± 8.4^{d}	107.7 ± 9.7^{d}

Values are means ± SD ($n = 6$ rats). Values not sharing a common superscript within a row are statistically significant (0.001). For abbreviations see Table 1

levels of EPA + DHA in the diet, the total cholesterol was decreased by 10, 19 and 25% respectively. Similarly, serum triacylglycerol in rats fed diets with 2.5. 5.0, 10.0 and 25.0% ALA levels decreased by 6, 11, 19 and 28% respectively compared to control animals. In rats fed diets with EPA + DHA at 1.0, 2.5 and 5.0% levels decreased triacylglycerol by 12, 20 and 27% respectively. These studies indicated that both ALA as well as long chain n-3 PUFA in the diet can effectively decrease serum cholesterol and triacylglycerol levels in rats, but higher levels of ALA were required to get comparable effects of EPA + DHA containing diets.

Liver Lipid Profile of Rats Fed Diets Containing Different Levels of LSO or FO

The fatty acid profile in liver lipids of rats fed diet with different amounts of ALA or EPA + DHA are given in Table 4. The ALA levels of liver lipids in rats fed diets containing 2.5. 5.0, 10.0 and 25.0% ALA were found to be 0.8, 1.9, 3.2 and 4.4% respectively. The EPA and DHA level in these rats were found to increase in a dose dependent manner with an increase in the ALA level in the diet. The EPA levels in the liver of rats fed diets with ALA content of 2.5, 5.0, 10.0 and 25.0% were found to be 0.7, 1.2, 3.5 and 3.9% of total fatty acids respectively and the DHA levels in the liver were found to be 0.4, 0.9, 1.6 and 2.7% of total fatty acids respectively. Control rats fed GNO contained neither ALA nor EPA + DHA. These studies indicated that ALA from the diet was taken up and further metabolized to long chain n-3 PUFA to a certain extent. Similarly, the EPA + DHA in the diets significantly increased the EPA and DHA level in the liver lipids. The EPA levels in the liver of rats fed diets containing 1.0, 2.5 and 5.0% EPA + DHA were found to be 2.4, 6.2 and 9.5% respectively and DHA levels were found be 2.6, 5.7 and 8.7% of total fatty acids respectively. These studies indicated that ALA or EPA + DHA from the diet is taken up and incorporated in liver lipids. However, higher levels of preformed long chain n-3 PUFA accumulated in liver even

Table 4 Liver tissue fatty acid profile (%) of rats fed n-3 fatty acids from LSO or FO at incremental levels

Fatty acid	GNO	ALA 2.5%	ALA 5.0%	ALA 10.0%	ALA 25.0%	EPA + DHA 1.0%	EPA + DHA 2.5%	EPA + DHA 5.0%
16:0	18.3 ± 2.1^{b}	17.7 ± 1.2^{b}	17.4 ± 2.0^{b}	16.4 ± 2.0^{b}	17.7 ± 3.0^{b}	16.9 ± 2.3^{b}	18.1 ± 3.0^{b}	17.9 ± 2.9^{b}
16:1 (n-7)	1.1 ± 0.2^{b}	1.0 ± 0.3^{b}	0.8 ± 0.3^{b}	0.9 ± 0.1^{b}	1.2 ± 0.1^{b}	1.9 ± 0.1^{c}	2.8 ± 0.4^{d}	4.8 ± 2.9^{e}
18:0	13.0 ± 1.2^{b}	15.3 ± 1.7^{bd}	20.0 ± 1.1^{c}	21.1 ± 2.3^{c}	23.3 ± 3.1^{c}	17.6 ± 2.3^{cd}	16.1 ± 3.0^{b}	15.2 ± 2.1^{b}
18:1 (n-9)	38.2 ± 3.6^{b}	37.1 ± 4.2^{b}	34.1 ± 3.6^{b}	32.2 ± 4.0^{bc}	$28.3 \pm 3.^{c}$	34.6 ± 2.9^{bc}	30.8 ± 3.9^{c}	28.6 ± 3.4^{c}
18:2 (n-6)	14.3 ± 1.9	13.1 ± 1.3^{bc}	12.0 ± 2.0^{bd}	11.5 ± 1.1^{ce}	9.9 ± 1.3^{e}	11.4 ± 1.9^{cd}	9.6 ± 1.0^{d}	7.1 ± 0.8^{e}
18:3 (n-3)	ND	0.8 ± 0.2^{b}	1.9 ± 0.3^{c}	3.2 ± 0.6^{d}	4.4 ± 0.7^{e}	ND	ND	ND
20:4 (n-6)	13.9 ± 1.3^{b}	13.0 ± 1.8^{b}	10.8 ± 1.0^{bc}	8.8 ± 0.9^{cd}	7.6 ± 0.9^{cd}	11.5 ± 0.9^{b}	9.6 ± 0.8^{c}	6.9 ± 1.0^{d}
20:5 (n-3)	ND	0.7 ± 0.2^{b}	1.2 ± 0.9^{c}	3.5 ± 0.8^{de}	3.9 ± 0.4^{de}	2.4 ± 0.8^{e}	6.2 ± 0.9^{f}	9.5 ± 1.0^{g}
22:5 (n-6)	1.1 ± 0.2^{b}	0.8 ± 0.1^{bc}	0.7 ± 0.2^{bc}	0.6 ± 0.2^{c}	0.6 ± 0.1^{c}	0.8 ± 0.1^{bc}	0.7 ± 0.2^{bc}	0.7 ± 0.1^{c}
22:5 (n-3)	ND	ND	0.17 ± 0.08^{b}	0.2 ± 0.05^{bc}	0.3 ± 0.1^{c}	0.2 ± 0.1^{bc}	0.3 ± 0.05^{bc}	0.5 ± 0.05^{d}
22:6 (n-3)	ND	0.4 ± 0.08^{b}	0.9 ± 0.09^{c}	1.6 ± 0.2^{d}	2.7 ± 0.7^{e}	2.6 ± 1.0^{e}	5.7 ± 0.7^{f}	8.7 ± 1.1^{g}

Values are means ± SD ($n = 6$ rats). Values not sharing a common superscript within a row are statistically significant (0.001). For abbreviations see Table 1

Table 5 Liver lipid profile (mg/g tissue) of rats fed n-3 fatty acids from LSO or FO at incremental levels

Parameter	GNO	ALA 2.5%	ALA 5.0%	ALA 10.0%	ALA 25.0%	EPA + DHA 1.0%	EPA + DHA 2.5%	EPA + DHA 5.0%
Total cholesterol	10.9 ± 0.4^{b}	9.9 ± 0.2^{c}	9.45 ± 0.1^{dg}	8.61 ± 0.1^{e}	8.00 ± 0.2^{f}	10.09 ± 0.1^{c}	9.72 ± 0.1^{cg}	9.2 ± 0.1^{df}
Triacylglycerol	16.9 ± 0.9^{b}	15.5 ± 0.5^{bc}	14.4 ± 0.6^{cd}	13.53 ± 0.6^{de}	12.12 ± 0.5^{e}	15.29 ± 0.5^{c}	13.98 ± 0.5^{de}	12.77 ± 0.9^{e}
Phospholipids	25.2 ± 1.4^{b}	26.0 ± 2.9^{b}	28.2 ± 2.3^{b}	28.2 ± 3.0^{b}	28.77 ± 2.0^{b}	25.14 ± 2.3^{b}	25.14 ± 1.3^{b}	25.36 ± 1.3^{b}

Values are means ± SD ($n = 6$ rats). Values not sharing a common superscript within a row are statistically significant (0.001). For abbreviations see Table 1

though it was provided at a dosage, which is significantly lower than that of ALA. The total cholesterol and triacylglycerol level decreased in a dose dependent manner when rats were fed a diet containing incremental amounts of ALA or EPA + DHA (Table 5). In rats fed diets containing LSO to provide ALA at 2.5, 5.0, 10.0 and 25.0% levels, the total cholesterol levels decreased by 9, 13, 21, and 27% respectively and triacylglycerol levels were lowered by 8, 15, 20 and 28% respectively compared to the control group. In rats fed diets containing FO with EPA + DHA levels of 1.0, 2.5 and 5.0% lowered the total cholesterol level by 7, 11 and 16% respectively and triacylglycerol levels by 10. 17 and 24% respectively compared to the control group.

Heart, Brain and Adipose Tissue Fatty Acid Profile of Rats Fed Diet with Different Levels of LSO or FO

The fatty acid profile of the heart (Table 6), brain (Table 7) and adipose (Table 8) tissues were significantly altered when different levels of ALA or EPA + DHA were fed to rats. EPA was not detected in the heart of control rats as well as in rats fed 2.5% ALA in the diet, but very small amounts of EPA was detected when ALA was fed at levels greater than 5.0% in the diet. The initial level of DHA in the heart tissue of control rats was found to be 3.8% of total fatty acids and was raised to 4.2, 4.8 and 6.0% respectively when ALA levels were maintained at 5.0, 10.0 and 25.0% in the diets. However, feeding FO at incremental levels significantly increased the DHA level in the heart. From the initial 3.8% of total fatty acids, the DHA level was raised to 8.2, 11.2 and 15.1% of total fatty acids in rats fed diet with 1.0, 2.5 and 5.0% EPA + DHA.

Feeding incremental level of ALA to rats resulted in an increase in the levels of DHA by 13–49% in brain tissue. The initial level of DHA in brain tissue of control rats was found to be 8.3% and was raised to 9.4, 10.4, 11.2 and 12.4% respectively when ALA levels were maintained at 2.5, 5.0, 10.0 and 25.0% in the diet. ALA was detected in the brain tissue of rats fed diets containing ALA at 10.0 and 25.0%. Feeding diets containing FO resulted in a 37–104% increase in the DHA level from 8.3 in the control to 11.4, 13.1 and 16.9% of total FAs in rats when EPA + DHA levels in the diet were maintained at 1.0, 2.5 and 5.0% levels respectively.

The level of ALA in the adipose tissue increased when incremental amounts of ALA were given in the diet. The ALA in adipose tissue was found to be 1.9, 3.9, 6.9 and

Table 6 Heart tissue fatty acid profile (%) of rats fed n-3 fatty acids from LSO or FO at incremental levels

Fatty acid	GNO	ALA 2.5%	ALA 5.0%	ALA 10.0%	ALA 25.0%	EPA + DHA 1.0%	EPA + DHA 2.5%	EPA + DHA 5.0%
16:0	14.7 ± 2.1^{b}	14.2 ± 2.3^{b}	14.9 ± 1.9^{b}	15.6 ± 2.0^{b}	17.4 ± 3.3^{b}	14.4 ± 3.1^{b}	14.4 ± 2.3^{b}	14.3 ± 2.0^{b}
16:1 (n-7)	1.5 ± 0.7^{bc}	1.3 ± 0.6^{bc}	0.9 ± 0.2^{b}	1.2 ± 0.4^{bc}	1.3 ± 0.3^{bc}	1.8 ± 0.7^{bc}	2.1 ± 0.9^{c}	2.9 ± 1.0^{c}
18:0	27.3 ± 2.3^{b}	28.0 ± 3.1^{b}	27.9 ± 2.7^{b}	29.5 ± 3.8^{b}	29.2 ± 3.4^{b}	25.1 ± 3.6^{b}	25.8 ± 1.9^{b}	25.5 ± 2.3^{b}
18:1 (n-9)	20.1 ± 2.1^{b}	19.8 ± 3.0^{b}	19.9 ± 2.0^{b}	18.5 ± 3.0^{b}	19.7 ± 2.8^{b}	19.3 ± 3.6^{b}	19.3 ± 1.3^{b}	18.2 ± 2.0^{b}
18:2 (n-6)	14.6 ± 1.9^{b}	14.7 ± 1.2^{b}	14.4 ± 2.0^{b}	13.3 ± 3.1^{bc}	11.9 ± 2.4^{c}	13.0 ± 2.6^{bc}	10.8 ± 1.9^{c}	9.3 ± 2.0^{c}
18:3 (n-3)	ND	ND	ND	0.2 ± 0.05^{c}	0.3 ± 0.1^{d}	ND	ND	ND
20:4 (n-6)	17.0 ± 3.0^{b}	17.1 ± 2.8^{b}	16.7 ± 3.1^{b}	15.8 ± 3.3^{b}	13.0 ± 2.7^{b}	16.1 ± 2.3^{b}	13.9 ± 3.1^{b}	12.0 ± 1.9^{b}
20:5 (n-3)	ND	ND	0.1 ± 0.08^{b}	0.1 ± 0.1^{c}	0.2 ± 0.1^{d}	0.7 ± 0.2^{d}	1.0 ± 0.3^{d}	1.2 ± 0.2^{e}
22:5 (n-6)	0.9 ± 0.1^{b}	0.8 ± 0.2^{b}	0.7 ± 0.2^{bc}	0.7 ± 0.1^{bc}	0.6 ± 0.1^{c}	0.8 ± 0.2^{bc}	0.8 ± 0.1^{bc}	0.7 ± 0.1^{bc}
22:5 (n-3)	ND	0.1 ± 0.07^{b}	0.2 ± 0.08^{b}	0.2 ± 0.07^{b}	0.3 ± 0.1^{b}	0.5 ± 0.09^{c}	0.6 ± 0.1^{c}	0.7 ± 0.1^{c}
22:6 (n-3)	3.8 ± 0.6^{b}	3.9 ± 1.1^{b}	4.2 ± 1.3^{bc}	4.8 ± 1.0^{bc}	6.0 ± 1.6^{c}	8.2 ± 1.3^{d}	11.2 ± 1.8^{e}	15.1 ± 2.1^{f}

Values are means ± SD ($n = 6$ rats). Values not sharing a common superscript within a row are statistically significant (0.001). For abbreviations see Table 1

Table 7 Brain tissue fatty acid profile (%) of rats fed n-3 fatty acids from LSO or FO at incremental levels

Fatty acid	GNO	ALA 2.5%	ALA 5.0%	ALA 10.0%	ALA 25.0%	EPA + DHA 1.0%	EPA + DHA 2.5%	EPA + DHA 5.0%
16:0	20.9 ± 2.1^{b}	21.2 ± 2.0^{b}	20.0 ± 3.1^{b}	20.3 ± 0.9^{b}	19.4 ± 1.3^{b}	22.1 ± 1.9^{b}	22.7 ± 2.7^{b}	21.9 ± 3.0^{b}
16:1 (n-7)	0.3 ± 0.5^{b}	0.2 ± 0.04^{b}	0.3 ± 0.03^{b}	0.3 ± 0.05^{b}	0.2 ± 0.06^{b}	0.4 ± 0.06^{c}	0.7 ± 0.03^{d}	0.9 ± 0.07^{e}
18:0	17.1 ± 1.6^{b}	17.0 ± 2.3^{b}	18.1 ± 2.0^{bc}	20.0 ± 1.9^{bc}	22.0 ± 3.0^{c}	15.6 ± 2.3^{bd}	15.5 ± 2.9^{bd}	13.9 ± 3.0^{d}
18:1 (n-9)	36.7 ± 4.1^{b}	35.6 ± 1.9^{b}	34.8 ± 2.6^{b}	33.0 ± 2.6^{b}	31.5 ± 3.6^{b}	34.3 ± 2.3^{b}	33.3 ± 4.0^{b}	32.2 ± 2.6^{b}
18:2 (n-6)	3.4 ± 1.0^{b}	3.4 ± 1.1^{b}	3.2 ± 0.6^{b}	2.6 ± 1.0^{bc}	2.0 ± 0.8^{cd}	3.0 ± 0.9^{bd}	2.8 ± 1.0^{bd}	2.7 ± 0.6^{bd}
18:3 (n-3)	ND	ND	ND	0.1 ± 0.1^{b}	0.2 ± 0.1^{b}	ND	ND	ND
20:4 (n-6)	12.3 ± 2.1^{b}	12.2 ± 1.9^{b}	12.0 ± 0.9^{b}	11.2. ± 2.0^{bc}	10.7 ± 1.2^{bc}	11.9 ± 1.6^{bc}	10.3 ± 2.0^{bc}	9.6 ± 1.0^{c}
20:5 (n-3)	ND	ND	0.1 ± 0.06^{b}	0.2 ± 0.09^{b}	0.3 ± 0.1^{bc}	0.1 ± 0.05^{b}	0.3 ± 0.08^{bc}	0.4 ± 0.1^{c}
22:5 (n-6)	0.6 ± 0.2^{b}	0.5 ± 0.2^{b}	0.5 ± 0.1^{b}	0.4 ± 0.1^{b}	0.4 ± 0.1^{b}	0.5 ± 0.1^{b}	0.4 ± 0.1^{b}	0.4 ± 0.1^{b}
22:5 (n-3)	0.3 ± 0.09^{b}	0.4 ± 0.1^{b}	0.5 ± 0.08^{bc}	0.6 ± 0.1^{c}	0.8 ± 0.15^{d}	0.6 ± 0.09^{bc}	0.8 ± 0.04^{d}	1.0 ± 0.07^{e}
22:6 (n-3)	8.3 ± 1.0^{b}	9.4 ± 0.9^{bc}	10.4 ± 1.3^{bcd}	11.2 ± 1.6^{cd}	12.4 ± 1.5^{d}	11.4 ± 2.0^{cd}	13.1 ± 1.2^{d}	16.9 ± 1.6^{e}

Values are means ± SD ($n = 6$ rats). Values not sharing a common superscript within a row are statistically significant (0.001). For abbreviations see Table 1

12.1% of total fatty acids respectively when the ALA content in the diets was kept at 2.5, 5.0, 10.0 and 25.0%. EPA and DHA were not detected in the adipose tissue of rats fed diet with different levels of ALA; however, feeding FO resulted in a significant incorporation of EPA and DHA in adipose tissue. The EPA levels were found to be 0.8, 2.6 and 4.9% of total fatty acids respectively when diets containing 1.0, 2.5 and 5.0% were fed to the rats. The corresponding DHA levels observed in the adipose tissue of these rats were 0.9, 2.8 and 5.2% respectively.

Discussion

The primary objective of this investigation was to evaluate the uptake of ALA from a vegetable oil source and its subsequent conversion to long chain n-3 PUFA in different tissues. This is compared with the uptake of preformed long chain n-3 PUFA obtained from FO. These uptakes were monitored at comparable levels of LNA in the diet. The study indicated that with the increase in the dietary ALA levels, there was a corresponding increase in the levels of ALA with a small but significant increase in the accumulation of EPA + DHA in the serum and liver. Though ALA levels in the diet were increased from 4 to 40 g/kg diet, the ALA levels in serum lipids increased from only 1.0–5.9% of total fatty acids. Long chain metabolites of ALA, namely, EPA + DHA also increased from 1 to 5% of total fatty acids in serum lipids. This indicated that though higher amounts of ALA are fed to rats, only a small proportion of ALA and its long chain metabolites are accumulating in serum lipids. Earlier studies have shown that dietary ALA increased the

Table 8 Adipose tissue fatty acid profile (%) of rats fed n-3 fatty acids from LSO or FO at incremental levels

Fatty acid	GNO	ALA 2.5%	ALA 5.0%	ALA 10.0%	ALA 25.0%	EPA + DHA 1.0%	EPA + DHA 2.5%	EPA + DHA 5.0%
14:0	2.6 ± 0.06^{b}	1.4 ± 0.09^{c}	1.3 ± 0.07^{c}	1.4 ± 0.1^{c}	1.0 ± 0.1^{d}	1.9 ± 0.2^{e}	1.5 ± 0.4^{ce}	1.6 ± 0.09^{f}
16:0	17.0 ± 3.6^{b}	16.1 ± 1.0^{b}	16.7 ± 1.1^{b}	15.3 ± 0.9^{b}	17.2 ± 1.0^{b}	18.2 ± 1.9^{b}	16.2 ± 2.1^{b}	17.4 ± 1.3^{b}
16:1 (n-7)	3.6 ± 1.0^{b}	3.7 ± 0.4^{b}	4.0 ± 0.6^{b}	4.2 ± 1.0^{b}	3.7 ± 0.3^{b}	4.4 ± 0.8^{b}	5.6 ± 1.2^{bc}	6.5 ± 0.8^{c}
18:0	1.3 ± 0.08^{b}	2.0 ± 0.2^{c}	1.3 ± 0.1^{b}	0.8 ± 0.1^{d}	0.5 ± 0.06^{e}	1.3 ± 0.2^{b}	1.1 ± 0.03^{b}	0.8 ± 0.04^{c}
18:1 (n-9)	55.1 ± 3.6^{b}	54.0 ± 1.9^{b}	53.7 ± 1.2^{b}	53.2 ± 1.3^{b}	49.5 ± 1.0^{c}	53.9 ± 2.4^{b}	52.6 ± 3.9^{bd}	49.0 ± 1.8^{cd}
18:2 (n-6)	19.5 ± 2.6^{b}	20.0 ± 1.1^{b}	18.1 ± 2.0^{bc}	17.4 ± 0.9^{c}	15.5 ± 0.5^{d}	17.8 ± 3.4^{c}	16.8 ± 2.9^{cd}	13.9 ± 2.9^{e}
18:3 (n-3)	ND	1.9 ± 0.1^{b}	3.9 ± 0.3^{c}	6.9 ± 1.0^{d}	12.1 ± 0.3^{e}	ND	ND	ND
20:4 (n-6)	0.8 ± 0.08^{b}	0.8 ± 0.04^{b}	0.9 ± 0.06^{b}	0.7 ± 0.02^{b}	0.4 ± 0.01^{c}	0.7 ± 0.06^{b}	0.6 ± 0.05^{b}	0.5 ± 0.01^{c}
20:5 (n-3)	ND	ND	ND	ND	ND	0.8 ± 0.01^{b}	2.6 ± 0.2^{c}	4.9 ± 0.4^{d}
22:5 (n-3)	ND	ND	ND	ND	ND	ND	0.1 ± 0.02^{b}	0.1 ± 0.05^{b}
22:6 (n-3)	ND	ND	ND	ND	ND	0.9 ± 0.02^{b}	2.8 ± 0.6^{c}	5.2 ± 0.9^{d}

Values are means ± SD ($n = 6$ rats). Values not sharing a common superscript within a row are statistically significant (0.001). For abbreviations see Table 1

tissue long chain n-3 PUFA level in rats [15, 16] and in suckling piglets [17]. However, preformed EPA + DHA were taken up by the serum and liver much more efficiently than that derived from ALA. Thus at 2.5 and 5.0% ALA in the diet, EPA + DHA was observed to an extent of 1.0 and 1.7% in serum and 1.1 and 2.1% of total fatty acids in liver lipids. Whereas, with similar levels of preformed EPA + DHA in the diet, these long chain n-3 PUFA were found to accumulate to an extent of 6.0 and 9.7% in serum, and 11.9 and 18.2% of total fatty acids in liver lipids respectively. This indicated a more efficient uptake and retention of preformed long chain n-3 PUFA in serum and liver [18].

The lower levels of long chain n-3 PUFA in subjects given ALA rich diets compared to those given preformed EPA + DHA is the subject matter of many recent studies. Most of the investigators are of the opinion that this is due to extensive oxidation of ALA once it is ingested [19–21]. The competition of LNA for delta-6 desaturase may reduce conversion of ALA to long chain n-3 PUFA. The background diet is another factor which can modulate the conversion process. MacDonald and Garg [22] noticed that conversion of ALA to EPA was highest in rats receiving saturated fats but lowest in the PUFA fed rats. In addition, the ability of ALA conversion to long chain n-3 PUFA particularly DHA varied depending on the animal models used. Fu and Sinclair [23] noted that increased ALA intake increases tissue ALA but had very little effect on tissue DHA in guinea pigs. Humans also showed limited capacity to convert ALA to DHA [24]. However, in rats, dietary ALA increased DHA to a small but significant level [22, 25]. The ALA can also undergo metabolism in a recycling pathway [26]. Unlike ALA, long chain fatty acids like DHA seem to undergo less β-oxidation and carbon recycling.

These studies indicate that ALA is subjected to metabolism in different routes and hence the actual amount that is available for its conversion to long chain n-3 PUFA may be limited under most circumstances. On the other hand, preformed long chain n-3 PUFA are more resistant to metabolic changes such as β-oxidation and carbon recycling [26] which may indicate its ready availability for uptake by tissues. This may contribute to an increased uptake of preformed long chain n-3 PUFA in comparison with those derived from ALA.

The ratio of n-6 to n-3 fatty acids is often considered to be crucial for the conversion of ALA to long chain n-3 PUFA as n-6 fatty acid (LNA) can compete with delta-6 desaturase which acts on both n-6 and n-3 fatty acids [27, 28]. It is also shown that in the presence of LNA, the ALA is oxidized to greater extent and hence may not be available as substrate for synthesis of its long chain metabolites [29]. In our studies the ratio of n-6 to n-3 fatty acids were varied from 9.11 to 0.69. In spite of such large range of ratios used for LNA to ALA in the diet, ALA was converted to EPA and DHA in serum and tissues at all the ratios of n-6 to n-3 fatty acids used in the diet. This indicated that LNA did not influence delta-6 desaturase responsible for converting ALA to long chain n-3 PUFA. Further, LNA accumulation and its conversion to arachidonic acid (ARA) were also found to be dependent on the levels LNA available in the diet. ALA even though varied from 2.5 to 25.0% in the diet, did not significantly influence accumulation of LNA and the conversion to ARA again indicating that neither LNA nor the ALA interfered with each other metabolism to long chain PUFA. However, when preformed EPA + DHA were given in the diet, there was a progressive accumulation of these fatty acids in serum and the liver, which took place at the expense of LNA and ARA. This may indicate that n-6 fatty acids are displaced by long chain n-3 PUFA in serum and the liver.

The changes in the n-3 PUFA levels in different tissues in response to dietary lipids were not uniform. The DHA content in heart did not change appreciably up to 10.0% ALA in the diet. Even at a 25.0%, the ALA level in the diet there had only a 54% increase in DHA content above that found in the control group. However, DHA levels increased by 110, 187 and 287% when EPA + DHA was included in the diet at 1.0, 2.5 and 5.0% respectively. The EPA levels were also increased in FO fed animals as compared to those given higher levels of ALA in the diet. The extent of dietary EPA uptake compared to dietary DHA was significantly lower. Studies have shown that the DHA incorporation exceeds that of EPA even if DHA is fed at lower levels [30]. Our results, supports the general view that heart tissue readily takes the n-3 fatty acids, particularly DHA.

The brain is another organ, which is highly enriched in DHA. The high levels of DHA in the brain of a number of mammalian species irrespective of their size led to early speculations that this fatty acid plays a crucial role in the nervous system [31]. Many studies using ALA deficient diets have shown reductions in the level of DHA in brain and loss of many cognitive functions [32, 33]. Feeding incremental amounts of ALA in the diets progressively increased DHA levels by 13-49% when ALA levels were increased from 2.5 to 25% in the diet. Similarly in rats fed 1.0–5.0% EPA + DHA in the diet increased DHA levels in brain by 37–104% over that found in the control animals. A small increase in the EPA and docosapentaenoic acid (DPA) (22:5 n-3) level was also observed in rats fed diets containing ALA or EPA + DHA. Even limited production/accumulation of EPA and DPA from dietary ALA may be physiologically relevant as they may provide a circulating reservoir for DHA synthesis in tissues.

Adipose tissue normally does not contain long chain n-6 or n-3 fatty acids. However, ALA accumulation in the adipose tissue increased linearly in response to an increasing ALA content in the diet. Feeding incremental amounts of ALA from 2.5 to 25.0% in the diet resulted in the accumulation of ALA from 1.9 to 12.1% in the adipose tissue. This is of particular interest, since adipose tissue represents one of the important storage tissues for ALA [34] that can be made available to the body when needed. We, however, did not detect any long chain n-3 PUFA in adipose tissue. Our findings are in agreement with the results of Lin and Connors [34] and also Kajwara et al. [35], which showed that when rats were given perilla oil which contained ALA to an extent of 60% resulted in an accumulation of ALA to an extent of 12% but less than 1% EPA and DHA was detected in adipose tissue. These studies indicated that adipose tissue might not be of major importance in DHA deposition following ALA intake, whereas they represent the main storage compartment for ALA [15].

These studies indicated that significant differences do exist in handling ALA and long chain n-3 PUFA which prompted Abedin et al. [36] to suggest that effect of LNA, ALA, ARA and DHA on tissue fatty acid composition may be an indicator for differential handling of essential fatty acids by the body. They further state that the incorporation of long chain n-3 PUFA in neural tissue which has been most extensively studied are not the same as those observed in other tissues like liver and heart and therefore it is necessary to explore the potential differences in handling of long chain PUFA which may have distinguishable effects on physiological factors [36]. This again underscores the need for caution while recommending dietary ALA as an alternative to long chain n-3 PUFA. The low conversion of ALA to DHA even when used in low and high concentrations in the diet in rat and pig models is shown in Table 9. Based on our results, the amount of dietary n-3 PUFA required to increase EPA + DHA levels in different tissues was calculated. Consumption of 100 mg

Table 9 Studies showing the effect of dietary ALA on tissues DHA level in experimental animals

Reference	Dietary ALA (%)	Plasma DHA (%)	Liver DHA (%)	Brain DHA (%)	Heart DHA (%)	Species
Hwang et al. [41]	Low 0.16	1.26	1.01	NA	NA	Rat
	High 23.46	4.04	6.04	NA	NA	
Bourre et al. [40]	Low 0.1	NA	2.3	9.3	2.1	Rat
	High 4.5	NA	5.0	11.2	8.2	
Igarashi et al. [42]	Low 0.2	0.07	0.017	1.57	NA	Rat
	High 4.6	1.48	0.73	3.52	NA	
Abedin et al. [36]	Low 0.1	NA	0.28	8.63	0.3	Pig
	High 7.1	NA	0.84	11.47	0.75	
Fu and Sinclair [23]	Low 0.3	NA	0.2	6.4	0.4	Pig
	High 17.3	NA	0.4	7.4	0.6	
Bazinet et al. [17]	Low 2.3	1.1	3.7	7.2	NA	Pig
	High 17.9	1.4	5.7	8.9	NA	

NA not analyzed

of ALA will result in the accumulation of EPA + DHA at 2.04, 0.70, 1.91 and 1.64% of total fatty acids respectively in the liver, heart, brain and serum. Similarly consumption of 100 mg of preformed EPA + DHA in the diet resulted in 25.4, 23.8, 15.9 and 14.9% of total fatty acids in liver, heart, brain and serum respectively. This indicated that to maintain a given level of long chain n-3 PUFA the dietary ALA required is 9.1, 12.5, 33.5 and 8.3 times higher than that could be achieved with preformed EPA + DHA in the diet for serum, liver, heart and brain respectively. Earlier studies on weanling rats showed that 0.16% of radio-labeled DHA given orally is recovered in the brain compared with 0.008% recovered when radio-abeled ALA was given which is a difference of 20 fold between ALA and DHA for its incorporation in brain lipids [37]. In guinea pigs, 10 times more dietary ALA compared to DHA was required to maintain a given level of DHA in brain [36]. In baboons preformed dietary DHA was 7 times more effective as a substrate for neural DHA than that derived from dietary ALA [38]. These studies indicated high efficiency of preformed DHA to raise the levels of tissue DHA as compared to that obtained from ALA in the diet. All these observations have prompted Sinclair to suggest that there is a clear need to define a physiological end point while fixing the requirements for ALA rather than the conventional criteria adopted for fixing recommended dietary allowance for essential fatty acids [39]. Our studies do support such a need for fixing the criteria for ALA intake.

In conclusion, the present study indicates that ALA could be an alternative source for long chain n-3 PUFA if taken at higher levels in the diet. This could be elongated and desaturated to long chain n-3 PUFA to a limited extent and it also has beneficial effects in lowering serum lipid levels. However, significantly higher levels of ALA in the diet are required for mimicking the effects of preformed EPA + DHA in the diet. These results, which were observed in rats, however need to be validated in humans using natural sources of n-3 PUFA before recommending ALA as an alternative to EPA + DHA in the diet.

Acknowledgments T.R. Ramaprasad acknowledges a Senior Research Fellowship grant from the Council of Scientific and Industrial Research, New Delhi, India. The authors thank Dr. Visheweshwariah Prakash, Director, CFTRI for his suggestions in the manuscript preparation.

Conflict of interest All authors have no conflict of interest.

References

1. Graham CB, Philip CC (2005) Conversion of α-linolenic acid to longer-chain polyunsaturated fatty acids in human adult. Reprod Nutr Dev 45:581–597
2. Davis BC, Kris-Etherton (2003) Achieving optimal essential fatty acid status in vegetarians: current knowledge and practical implications. Am J Clin Nutr 78(suppl):640S–646S
3. Li D, Sinclair AJ, Wilson A, Nakkote S, Kelly F, Abedin L, Mann NJ, Turner AJ (1999) Effects of dietary alpha linolenic acid on thrombotic risk factors in vegetarian men. Am J Clin Nutr 69:872–882
4. Bazinet RP, Douglas H, Cunnane SC (2003) Whole body utilization of n-3 PUFA deficient rats. Lipids 38:187–189
5. Mantzioris E, James MJ, Gibson RA, Cleland LG (1995) Differences exist in the relationship between dietary linoleic and alpha linolenic acids and their respective long chain metabolites. Am J Clin Nutr 61:320–324
6. Lauritzen L, Hansen HS (2003) Which of the n-3 fatty acids should be called essential? Lipids 38:889–891
7. Anonymous (1977) Report on the American institute of nutrition, Ad-hoc committee on standards for nutritional studies. J Nutr 107:1340–1348
8. Folch J, Lee M, Sloane SGH (1957) A simple method for isolation and purification of total lipids from animal tissues. J Biol Chem 226:497–509
9. Searcy RL, Bergquist LM (1960) A new color reaction for the quantification of cholesterol. Clin Chim Acta 5:192–199
10. Warnick GR, Albers JJ (1978) A comprehensive evaluation of the heparin-manganese chloride precipitation procedure for estimating HDL-cholesterol. J Lipid Res 19:65–76
11. Stewart JCM (1980) Colorimetric estimation of phospholipids with ammonium ferrothiocyanate. Anal Biochem 104:10–14
12. Fletcher MJ (1968) A colorimetric method for estimating serum triacylglycerol. Clin Chim Acta 22:303–307
13. Morrison MR, Smith M (1963) Preparation of fatty acid methyl esters and dimethylacetyls from lipids with boron fluoride methanol. J Lipids Res 5:600–608
14. Fisher RA (1970) Statistical methods for researcher workers, 14th edn. Oliver and Boya, Edinburg
15. Ballihaut CP, Lengelier B, Houlier F, Alessandril JM, Durand G, Latge C, Guesnet P (2001) Comparative bioavailability of dietary alpha-linolenic and docosahexaenoic acids in the growing rat. Lipids 36:793–800
16. Valenzuela A, Bernhardi R, Valenzuela V, Ramirez G, Alarcon R, Sanhueza J, Nieto S (2004) Supplementation of female rats with alpha-linolenic acid or docosahexaenoic acid leads to the same omega-6/omega-3 LC-PUFA accretion in mother tissues and in fetal and newborn brains. Ann Nutr Metab 48: 28–35
17. Bazinet RP, McMillan EG, Cunnane SC (2003) Dietary alpha-linolenic acid increases the n-3 PUFA content of sow's milk and tissues of the suckling piglet. Lipids 38:1045–1049
18. Burdge GC, Jones AE, Wootton SA (2002) Eicosapentaenoic acid and docosahexaenoic acids are the principal products of alpha linolenic acid metabolism in young men. Br J Nutr 88: 355–363
19. Leyton J, Drury P, Crawford M (1987) Differential oxidation of saturated and monounsaturated fatty acids in vivo in rat. Br J Nutr 57:383–393
20. Cunnane SC, Anderson MJ (1997) The majority of dietary linolenate in growing rats is beta-oxidized or stored in visceral fat. J Nutr 127:146–152
21. Bazinet RP, MacMillan EG, Seebaransing R, Hayes AM, Cunnane HC (2003) Whole-body beta oxidation of 18:2 w-2 and 18:3 w-3 in the pig varies markedly with weaning strategies and dietary 18:3 w3. J Lipid Res 44:314–319
22. MacDonald-Wicks LK, Gard ML (2004) Incorporation of n-3 fatty acids into plasma and liver lipids of rats: importance of background dietary fat. Lipids 39:545–551

23. Fu Z, Sinclair AJ (2000) Increased alpha-linolenic acid intake increases the tissue alpha-linolenic acid content and apparent oxidation with little effect on tissue docosahexaenoic acid in the guinea pig. Lipids 35:395–400
24. Pawlosky RJ, Hibbelin JR, Novotny JA, Salem J Jr (2001) Physiological compartmental analysis of alpha-linolenic acid metabolism in adult humans. J Lipid Res 42:1257–1265
25. Sinclair AJ, Crawford MA (1972) The incorporation of linolenic acid and docosahexaenoic acid into liver and brain lipids of developing rats. FEBS Lett 26:127–129
26. Cunnane SC, Ryan MA, Nadeau CR, Bazinet RP, Velso KM, McCloy U (2003) Why is carbon from some polyunsaturates extensively recycled into lipid synthesis? Lipids 38:477–484
27. Christiansen EN, Lund JS, Rortveit T, Rustan AC (1991) Effect of dietary n-3 and n-6 fatty acids on fatty acid desaturation in rat liver. Biochim Biophys Acta 1082:57–62
28. Emken EA, Adolf RO, Duval SM, Nelson GJ (1999) Effect of dietary docosahexaenoic acid on desaturation and uptake in vivo of isotope labeled oleic, linoleic and linolenic acids by male subjects. Lipids 34:785–791
29. Emken EA, Adlot RO, Gulley RM (1994) Dietary linoleic acid influences desaturation, elongation and acylation of deuterium labeled linoleic and linolenic acid in young adult males. Biochim Biophy Acta 1213:277–288
30. Croset M, Black JM, Sawnson JE, Kinsella JE (1989) Effects of dietary n-3 PUFA on phospholipids compositions and calcium transport in mouse cardiac sarcoplasmic reticulum. Lipids 24: 278–285
31. Connor WE, Neuringer M (1988) The effects of n-3 FA deficiency and repletion upon the FA composition and function of the brain and retina. Prog Clin Biol Res 282:275–294
32. Greiner RS, Moriguchi T, Hutton A, Slotnick BM, Salem N Jr (1999) Rats with low levels of brain docosahexaenoic acid show impaired performance in olfactory based and spatial learning task. Lipids 34:S239–S243
33. Ahmed A, Moriguchi T, Salem N Jr (2002) Decrease in neuron size in DHA deficient brain. Pediatr Neurol 26:210–218
34. Lin DS, Connors WE (1990) Are the n-3 FA from dietary fish oil deposited in the triglyceride stores of adipose tissue. Am J Clin Nutr 51:535–539
35. Kajwara MOK, Imai S, Koboyashi T, Honma N, Maki T, Suruga K, Goda T, Takase S, Muto Y, Moriwaki H (1997) Perilla oil prevents excessive growth of visceral adipose tissue in rats by down regulating adipocyte differentiation. J Nutr 127:1752–1757
36. Abedin L, Lien E, Vingnys AJ, Sinclair AJ (1999) The effect of dietary alpha linolenic acid compared with docosahexaenoic acid on brain, retina, liver and heart in guinea pig. Lipids 34:475–482
37. Sinclair AJ (1975) Incorporation of radioactive polyunsaturated fatty acids into liver and brain of the developing rat. Lipids 10:175–184
38. Greiner RC, Winter J, Nathanielsz PV, Brenna JT (1997) Brain docosahexaenoate accretion in fetal baboons: bioequivalence of dietary alpha-linolenic acid and docosahexaenoic acid. Pediatr Res 42:826–834
39. Sinclair AJ, Attar Bash NM, Li D (2002) What is the role of alpha-linolenic acid for mammals. Lipids 37:1113–1123
40. Bourre JM, Dumont O, Pascal G, Durand G (1993) Dietary α-linolenic acid at 1.3 g/kg maintains docosahexaenoic acid concentration in brain, heart and liver of adult rats. J Nutr 123: 1313–1319
41. Hwang DH, Boudreau M, Chanmugam P (1988) Dietary linoleic acid and longer chain n-3 fatty acids: comparison of effects on arachidonic acid metabolism in rats. J Nutr 118:427–437
42. Igarashi M, DeMar JC, Ma K, Chang L, Bell JM, Rapoport S (2007) Up regulated liver conversion of α-linolenic acid to docosahexaenoic acid in rats on a 15 week n-3 PUFA-deficient diet. J Lipid Res 48:152–164

Lipids (2010) 45:809–819
DOI 10.1007/s11745-010-3461-9

ORIGINAL ARTICLE

Dietary Free Oleic and Linoleic Acid Enhances Neutrophil Function and Modulates the Inflammatory Response in Rats

Hosana Gomes Rodrigues · Marco Aurélio Ramirez Vinolo · Juliana Magdalon · Haroldo Fujiwara · Danielle M. H. Cavalcanti · Sandra H. P. Farsky · Philip C. Calder · Elaine Hatanaka · Rui Curi

Received: 10 February 2010 / Accepted: 6 August 2010 / Published online: 22 August 2010

Abstract The high ingestion of oleic (OLA) and linoleic (LNA) acids by Western populations, the presence of inflammatory diseases in these populations, and the importance of neutrophils in the inflammatory process led us to investigate the effects of oral ingestion of unesterified OLA and LNA on rat neutrophil function. Pure OLA and LNA were administered by gavage over 10 days. The doses used (0.11, 0.22 and 0.44 g/kg of body weight) were based on the Western consumption of OLA and LNA. Neither fatty acid affected food, calorie or water intake. The fatty acids were not toxic to neutrophils as evaluated by cytometry using propidium iodide (membrane integrity and DNA fragmentation). Neutrophil migration in response to intraperitoneal injection of glycogen and in the air pouch assay, was elevated after administration of either OLA or LNA. This effect was associated with enhancement of rolling and increased release of the chemokine CINC-2$\alpha\beta$. Both fatty acids elevated L-selectin expression, whereas no effect on β_2-integrin expression was observed, as evaluated by flow cytometry. LNA increased the production of proinflammatory cytokines (IL-1β and CINC-2$\alpha\beta$) by neutrophils after 4 h in culture and both fatty acids decreased the release of the same cytokines after 18 h. In conclusion, OLA and LNA modulate several functions of neutrophils and can influence the inflammatory process.

Keywords Neutrophil migration · Inflammation · Adhesion molecules · Cytokines · Oleic acid and linoleic acid

Abbreviations

ALT	Alanine transaminase
AST	Aspartate transaminase
CINC-2$\alpha\beta$	Cytokine-induced neutrophil chemoattractant-2$\alpha\beta$
ICAM-1	Intercellular adhesion molecule-1
IL-1	Interleukin-1
IL-6	Interleukin-6
LDH	Lactate dehydrogenase
LTB_4	Leukotriene B4
LNA	Linoleic acid
LPS	Lipopolysaccharide
MCP-1	Macrophage chemoattractant protein-1
mRNA	Messenger RNA
fMLP	*N*-formyl-methionyl-leucyl-phenylalanine
NF-κB	Nuclear factor kappa B
OLA	Oleic acid
PUFA	Polyunsaturated fatty acids

Electronic supplementary material The online version of this article (doi:10.1007/s11745-010-3461-9) contains supplementary material, which is available to authorized users.

H. G. Rodrigues (✉) · M. A. R. Vinolo · J. Magdalon · H. Fujiwara · R. Curi
Department of Physiology and Biophysics, Institute of Biomedical Sciences, São Paulo University, Avenida Prof. Lineu Prestes, 1524, Butantã, São Paulo, SP 05508-900, Brazil
e-mail: hosanagr@icb.usp.br

D. M. H. Cavalcanti · S. H. P. Farsky
Department of Clinical and Toxicological Analyses, Faculty of Pharmaceutical Sciences, São Paulo University, São Paulo, Brazil

P. C. Calder
Institute of Human Nutrition, School of Medicine, University of Southampton, Southampton, UK

E. Hatanaka
Institute of Physical Activity and Sport Sciences, Cruzeiro do Sul University, São Paulo, Brazil

PGE_2	Prostaglandin E2
ROS	Reactive oxygen species
TNF-α	Tumor necrosis factor-α
VCAM-1	Vascular cell adhesion molecule-1

Introduction

The interest in studying the effects of fatty acids on aspects of the immune response began in 1970, when Pipette and Saugier [1] demonstrated the effects of an intravenous infusion of lipid emulsion on leukocytes isolated from rabbits. Although the effects of ω-3 [2] and ω-6 [3–6] polyunsaturated fatty acids have been frequently addressed in previous studies, little information is available about the action of oleic acid (OLA), the major ω-9 fatty acid in the human diet, on immune function. Previous in vitro studies have shown that OLA inhibits protein kinase C activity in lymphocytes [7], the release of myeloperoxidase [8] and the chemotaxis of human neutrophils [9], but that it can promote necrosis and apoptosis of human lymphocytes [10]. Increased ingestion of olive oil (a major source of oleic acid) has been associated with a reduction in cardiovascular disease, rheumatoid arthritis and a variety of cancers (reviewed by Waterman et al. [11]). These effects are attributed to OLA and/or the phenols present in this oil. Since oxidative stress and inflammation are important factors involved in the etiology of these diseases and neutrophils are important cells involved in the inflammatory response, it is relevant to study the effects of OLA and other fatty acids on neutrophil functions.

Neutrophils are the first cells that migrate into tissues in response to invading bacteria or other microorganisms, and they act to destroy invading pathogens through an array of microbiocidal mechanisms [12] such as phagocytosis, and production of reactive oxygen species, cytokines and proteolytic enzymes.

Here we investigate the effects of oral administration of unesterified OLA and LNA on neutrophil responses: migration, expression of adhesion molecules, interaction with endothelium and production of proinflammatory cytokines. Changes in neutrophil responses due to fatty acids could delay or accelerate inflammation onset and/or resolution.

Experimental Procedure

Reagents

OLA, LNA, fetal bovine serum (FBS), HEPES, penicillin, streptomycin, sodium bicarbonate, lipopolysaccharide (LPS) (*Escherichia coli* strain 0111:B4), *N*-formyl-methionyl-leucyl-phenylalanine (fMLP), oyster glycogen and RPMI-1640 culture medium supplemented with L-glutamine were from Sigma Chemical Co. (St. Louis, MO, USA). Fluorescein isothiocyanate labeled anti rat-L-Selectin (anti-rat CD62L) and anti rat-b2-integrin (anti-rat CD18) were purchased BD PharMingen Technical (San Diego, CA, USA).

Animals

Male Wistar rats weighing 180 ± 20 g (from the Department of Physiology and Biophysics, Institute of Biomedical Sciences, São Paulo University, Brazil) were maintained at 23°C under a light: dark cycle of 12:12 h. Animals received chow (Nuvital, Curitiba, Brazil—containing 22% protein, 4.5% fat, 40.8% carbohydrate, 8% fiber, reaching 3.0 kcal/g total metabolizable energy) and water ad libitum. The fatty acid composition of the chow is presented in Table 1. Food and water consumption were evaluated after each 48 h.

The Animal Care Committee of the Institute of Biomedical Sciences approved the experimental procedure of this study (Protocol number: 86).

Administration of Oleic and Linoleic Acids

According to the Department of Agriculture of USA [13] the average daily consumption of monounsaturated and polyunsaturated fat by adult men in the USA is 38 and 23 g,

Table 1 Fatty acid composition of the chow

Fatty acids	(%)
Caproic acid (6:0)	–
Caprylic acid (8:0)	0.37
Capric acid (10:0)	0.21
Lauric acid (12:0)	15.35
Myristic acid (14:0)	0.05
Palmitic acid (16:0)	17.06
Margaric acid (17:0)	0.10
Estearic acid (18:0)	2.23
Eicosapentaenoic acid (20:5 ω-3)	1.81
α-Linolenic acid (18:3 ω-3)	3.04
Docosahexaenoic acid (22:6 ω-3)	–
Arachidonic acid (20:4 ω-6)	–
Palmitoleic acid (16:1)	–
Linoleic acid (18:2 ω-6)	42.59
Oleic acid (18:1 ω-9)	17.15
Total	100
Saturated fatty acids	35.39
Unsaturated fatty acids	64.60

respectively. This is mainly in the form of OLA and LNA, respectively [13]. Considering this information, we calculated the equivalent doses to use in rats. The diets were supplemented by the oral route (by gavage) with pure OLA or LNA at doses of 0.11, 0.22 and 0.44 g/kg body weight, daily for 10 days. Control animals received 0.22 g/kg body weight of water by gavage. Other studies have demonstrated that ingestion of fatty acids for short periods is able to change low density lipoprotein fatty acid composition [14], modify plasma concentrations of inflammatory markers [15] and reduce the severity of diabetes mellitus in rats [16].

Nutritional Parameters

Based on food intake and fatty acid supplementation, total caloric intake (kcal/day) was calculated as ((mean food intake × 3.0 kcal) + kcal from fatty acid supplementation)/days of supplementation.

Biochemical Determinations

Blood samples were allowed to clot, and the sera were isolated by centrifugation at 1,000×*g* for 10 min and kept at −20°C before determination. Serum alanine transaminase (ALT), aspartate transaminase (AST), lactate dehydrogenase (LDH) and free fatty acids were determined by routine laboratory methods using BioClin kits (Belo Horizonte, Brazil) and Wako chemicals (Neuss, Germany).

Histological Analysis

Histological evaluation of the small intestine was done by a pathologist who was blinded to the experimental groups, and it was based on the following parameters: villus:crypt ratio, epithelium, reactivity of the crypt, calciform cells number, number of intraepithelium lymphocytes, Peyer plates reactivity, muscle layer, nerve plexuses.

Neutrophil Preparation

Rat neutrophils were obtained by intraperitoneal (i.p.) lavage with 40 mL calcium and magnesium free PBS (pH 7.4), 3 h after i.p. injection of 10 mL 1% (w/v) sterile glycogen solution (Sigma type II, from oyster) in PBS. The cell suspension was centrifuged at 4°C (500*g* for 10 min). The number of viable cells (>95% neutrophils) was determined in a Neubauer chamber under an optical microscope by trypan blue exclusion.

Determination of Neutrophil Fatty Acid Composition

Extraction of total lipids from neutrophils (1×10^6 cells) was performed following the method of Folch et al. [17]. Fatty acid composition of neutrophils was determined by reverse phase high performance liquid chromatography (HPLC). In brief, the samples were saponified and methylated by heating for 2 h with 2 mL of 0.5 mol/L sodium methylate. The fatty acid methyl esters formed were recovered with hexane and analyzed in a Shimadzu HPLC equipped with a fluorescence detector, using a Supelco fused silica column (25 cm × 4.6 mm).

Culture Conditions

Neutrophils obtained as described above were maintained in RPMI-1640 culture medium containing 10% FBS, glutamine (2 mmol/L), Hepes (20 mmol/L), streptomycin (100 μg/mL), penicillin (100 international units/mL) and sodium bicarbonate (24 mmol/L). Cells (2.5×10^6 cells/mL) were incubated in 24-well polystyrene culture plates at 37°C and 5% CO_2 with or without 5 μg/mL LPS for 4 and 18 h. This concentration of LPS is used to stimulate rat neutrophils [18]. At the end of the incubation period, cell supernatant was collected and stored at −80°C until to the measurement of CINC-2$\alpha\beta$ and IL-1β concentrations.

Cell Membrane Integrity Assay

Cells (1×10^6) were centrifuged at 1,000 rpm for 5 min at 4°C and the pellet obtained was resuspended in 500 μL PBS. Thereafter, 50 μL propidium iodide (50 mg/mL in PBS) were added and the cells then were analyzed by flow cytometry (FACSCalibur, Becton–Dickinson, USA). Propidium iodide is a highly water-soluble fluorescent compound that cannot pass through intact membranes and is generally excluded from viable cells. Fluorescence was measured using the FL2 channel (orange-red fluorescence-585/42 nm). Ten thousand events were analyzed per experiment. Cells with propidium iodide fluorescence were then evaluated by using Cell Quest software (Becton–Dickinson).

DNA Fragmentation Assay

Cells were centrifuged as described above. The pellet obtained was resuspended in 300 μL hypotonic solution containing 50 μg/mL propidium iodide, 0.1% sodium citrate, and 0.1% Triton-X-100. This detergent permeabilizes the cells, allowing the dye to be promptly incorporated into DNA. Cells were then incubated for 30 min at room temperature. DNA fragmentation was analyzed by flow cytometry after DNA staining with propidium iodide according to the method described above. Fluorescence was measured and analyzed also as described.

Expression of Adhesion Molecules (L-Selectin and β_2-Integrin) Evaluated by Flow Cytometry

In order to estimate L-selectin or β_2-integrin expression, leukocytes were isolated from abdominal aorta blood and collected with EDTA solution (100 mg/mL). Erythrocytes were lysed using an ammonium chloride solution (0.13 M) and leukocytes were recovered after washing with PBS. Cells (1.0×10^6) were stimulated with *N*-formyl-methionyl-leucyl-phenylalanine (fMLP; 10 nM) for 10 min for L-selectin and 30 min for β_2-integrin measurement. After washing, leukocytes were further incubated for 30 min at 4°C in the dark with 10 µL fluorescently conjugated monoclonal antibody against rat L-selectin or rat β_2-integrin. Immediately after incubation, cells were analyzed in a FACScalibur flow cytometer. Data from 10,000 cells were obtained and only morphologically viable neutrophils were considered for analysis. Leukocytes were separated by size and granularity through flow cytometry. As circulating leukocytes in rats are represented by lymphocytes (about 80–85%), neutrophils (about 10–15%), monocytes (about 4–5%) and eosinophils (about 1%), gates were selected as mononuclear (lymphocytes and monocytes) and polymorphonuclear (neutrophils and eosinophils) leukocytes [19, 20].

Intravital Microscopic Assay

Rats were anesthetized and the mesentery was exteriorized. After surgery, the animals were kept on a special board thermostatically controlled at 37°C that included a transparent platform on which the tissue to be transilluminated was placed. The preparation was kept moist and warmed by irrigating the tissue with a warmed Ringer-Locke solution (pH: 7.2–7.4; NaCl 154 mM; KCl 5.6 mM; $CaCl_2 \cdot 2H_2O$ 2 mM; $NaHCO_3$ 6 mM and glucose 5 mM) containing 1% gelatin. The rate of the solution outflow onto the exposed tissue was controlled to keep the preparation in continuous contact with a film of liquid. Transilluminated images were obtained by optical microscopy (Axioplan II, equipped with ×5.0/0.30 plan-neofluar or ×10.0/0.25 Achroplan longitudinal distance objectives/numeric aperture and ×1.0, 1.25 or 1.60 optovar, Carl Zeiss). The images were captured using a video camera (ZVS, 3C75DE, Carl Zeiss) and were transmitted simultaneously to a TV monitor and a computer. Images obtained in the TV monitor were recorded on video-tape. Digitized images were subsequently analyzed by using an image-analyzing software (KS 300, Kontron).

Leukocyte–Endothelial Interaction

The interaction between leukocytes and vessel walls was evaluated by determining the number of rolling and adherent leukocytes on the post capillary venule wall (20–30 µm diameter, 200 µm length) of the mesentery at 10-min intervals. Three fields were evaluated in each animal. Leukocytes moving in the peripheral of the axial stream, in contact with the endothelium, were considered to be rollers [19]. These leukocytes moved sufficiently slowly to be individually visible and were counted as they rolled past a selected point on one side of the vessel during 10 min. The number of leukocytes adherent to the endothelium (stopped at the vessel wall) was determined in the same vascular segment during 10 min. A positive control (fMLP) was used in this assay. After analysis of rolling and adhered cells, 10 µL fMLP (10^{-8} M) was applied on the mesentery and after 10 min rolling and adherent cells were counted.

Air Pouch Assay and Exudate Preparation

Induction of rat skin air pouches was performed according to the method described by Edwards et al. [21]. Briefly, 20 mL of sterile air (using 0.22 µm Fluoropore filters) was insufflated into the subcutaneous tissue of the back trunk of rats under anaesthesia. Seven days later, an additional 10 mL of sterile air was insufflated. Negative controls received 1 mL of sterile PBS, and positive controls received 1 mL of sterile PBS plus fMLP (10 nM) through the same route. Four hours after the injection of the stimulus, the animals were killed by decapitation and the inflammatory exudate was collected after washing the cavity with 2 mL of sterile PBS. The suspension was centrifuged at 500*g* for 10 min at 4°C. Cells were counted in a Neubauer chamber. The supernatant was assayed for CINC-2$\alpha\beta$ by ELISA (DuoSet; R&D Systems, Minneapolis, MN, USA), according to the supplier's instructions.

Ex Vivo Cytokine Production

Neutrophils (2.5×10^6 cells) were incubated in the presence or absence of LPS (5 µg/mL) in an environment containing 5% CO_2 at 37°C in a humid atmosphere for 4 or 18 h. The concentrations of CINC-2$\alpha\beta$ and IL-1β in the supernatant were determined by using a commercially available enzyme-linked immunosorbent assay kit (R&D Systems, Minneapolis, MN, USA).

Statistical Analysis

Comparisons were performed using one-way ANOVA and Dunnett's multiple comparison post test. The significance was set at $p < 0.05$. Results were expressed as means ± SEM. Pearson's correlation test was used to identify the association between the production of cytokines and the doses of the fatty acids.

Results

Food, calorie and water intake were not modified by administration of OLA or LNA (Table 2). Animals receiving OLA or LNA did not show any clinical sign of toxicity, such as diarrhea or hair loss. The concentrations of free fatty acids in plasma were not changed by administration of either OLA or LNA (data not shown). The highest dose (0.44 g/kg body weight) of OLA or LNA did not induce an alteration in the activity of AST, ALT or LDH (Fig. 1a, b, c).

Furthermore, morphological analysis of the small intestine was performed to investigate if the route of administration, as a single bolus, and the amount of fatty acids given caused changes. There was no change in the following parameters measured: villus:crypt ratio, epithelium, reactivity of the crypt, calciform cells number, Peyer plates reactivity, muscle layer and nerve plexuses (Supplemental Fig. S1).

No alteration in membrane integrity of DNA fragmentation of neutrophils was observed in cells isolated from rats treated with OLA or LNA for 10 days compared to neutrophils isolated from control rats (water) (Fig. 2), indicating that any functional effects observed in this study do not result from increased cell death due to fatty acid administration.

Neutrophils from the OLA and LNA groups (dose 0.22 g/kg body weight) had higher contents of oleic and linoleic acids (increase of fourfold and 14%, respectively) (Fig. 3). No alteration was observed in the content of arachidonic acid between the groups (Fig. 3). The contents of saturated, unsaturated, and ω-3 fatty acids were not affected by OLA or LNA administration (data not shown).

Neutrophil recruitment in response to injection of glycogen solution was increased in the animals that received OLA (0.22 and 0.44 g/kg body weight) or LNA (all doses) (Fig. 4). Considering this result, we evaluated the expression of adhesion molecules on the surface of neutrophils. We chose the dose of 0.22 g/kg body weight because this dose of either OLA or LNA markedly increased the recruitment of neutrophils. Both fatty acids increased L-selectin expression on the membrane surface (Fig. 5a) in

Table 2 Food intake (g/day), caloric intake (kcal/day) and water ingestion (mL/day) by rats supplemented with different doses of oleic or linoleic acid during 10 days

Doses	0	0.11	0.22	0.44
Oleic acid (g/kg body weight)				
Food intake (g/day)	23.00 ± 0.92	20.65 ± 0.38	22.19 ± 0.85	22.59 ± 0.91
Caloric intake (kcal/day)	69.02 ± 2.76	62.19 ± 1.15	67.04 ± 2.56	68.68 ± 1.25
Water ingestion (mL/day)	37.5 ± 1.70	35.5 ± 0.84	41.75 ± 2.72	40.00 ± 1.58
Linoleic acid (g/kg body weight)				
Food intake (g/day)	23.00 ± 0.92	20.53 ± 0.27	20.65 ± 1.69	21.0 ± 0.63
Caloric intake (kcal/day)	69.02 ± 2.76	61.81 ± 0.81	62.40 ± 5.08	63.9 ± 1.91
Water ingestion (mL/day)	37.5 ± 1.70	36.25 ± 0.39	37.40 ± 2.68	35.25 ± 2.03

The values are presented as means ± SEM of ten animals per group

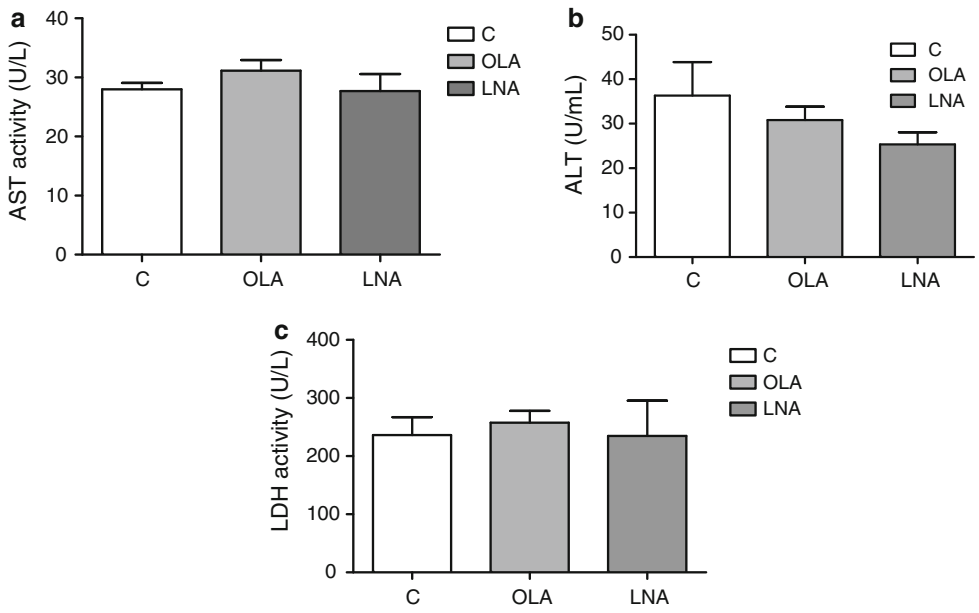

Fig. 1 Activities of aspartate transaminase (AST), alanine transaminase (ALT) and lactate dehydrogenase (LDH) in the serum of rats supplemented with oleic or linoleic acids (dose 0.44 g/kg body weight). The values are presented as means ± SEM of five animals per group

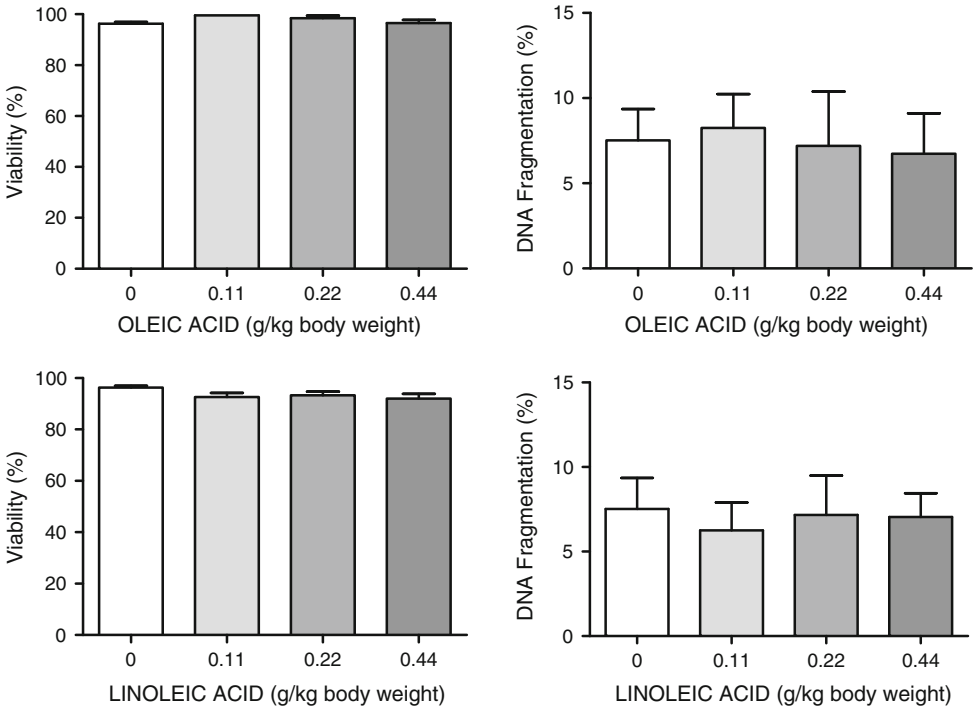

Fig. 2 Cellular viability and DNA fragmentation of neutrophils isolated from rats supplemented with different doses of oleic or linoleic acid. The values are presented as means ± SEM of seven animals per group

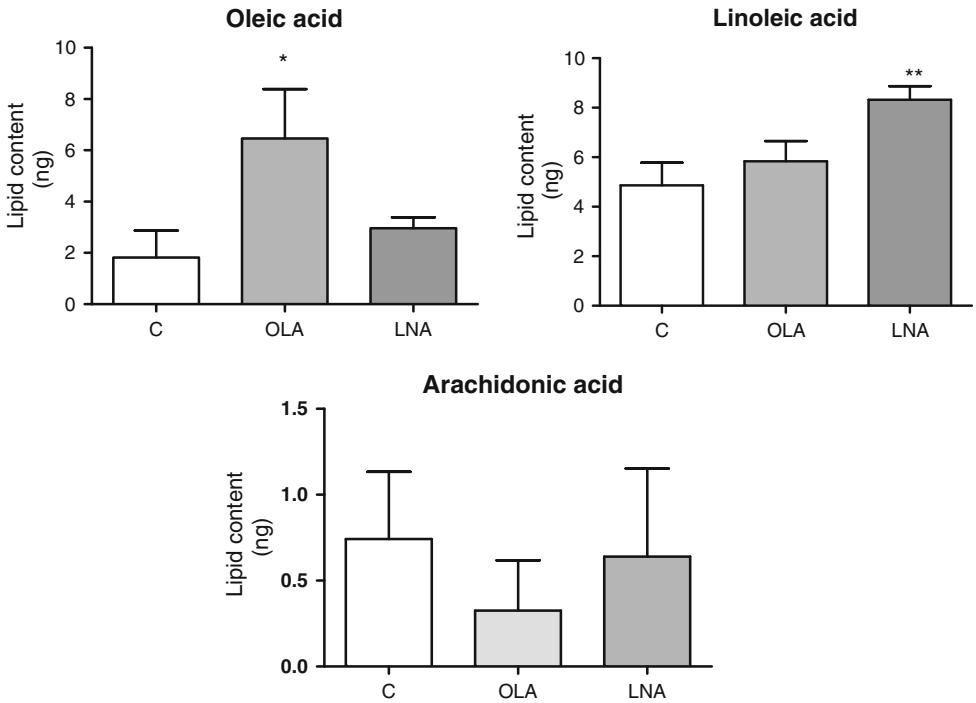

Fig. 3 Content of oleic, linoleic and arachidonic acids in neutrophils isolated from rats supplemented with oleic or linoleic acids (dose 0.22 g/kg body weight). Content is presented as ng in 1×10^6 cells. The values are presented as means ± SEM of seven animals per group. $^*p < 0.05$ and $^{**}p < 0.01$ indicates significant difference in relation to C, as indicated by ANOVA and Dunnett post hoc test

non-stimulated neutrophils, but no alteration was found for β_2-integrin expression (Fig. 5b). Neutrophil stimulation with fMLP increased the expression of both adhesion molecules. However, no effect of OLA or LNA was observed on the expression of adhesion molecules in fMLP stimulated neutrophils (Fig. 5a, b).

In vivo analysis, by intravital microscopy, of neutrophil interaction with the endothelium, showed that both fatty acids increase the rolling of leukocytes, but only LNA augmented the number of adherent leukocytes under basal conditions (Fig. 6a, b). After application of fMLP there was a significant increase in the number of rolling and

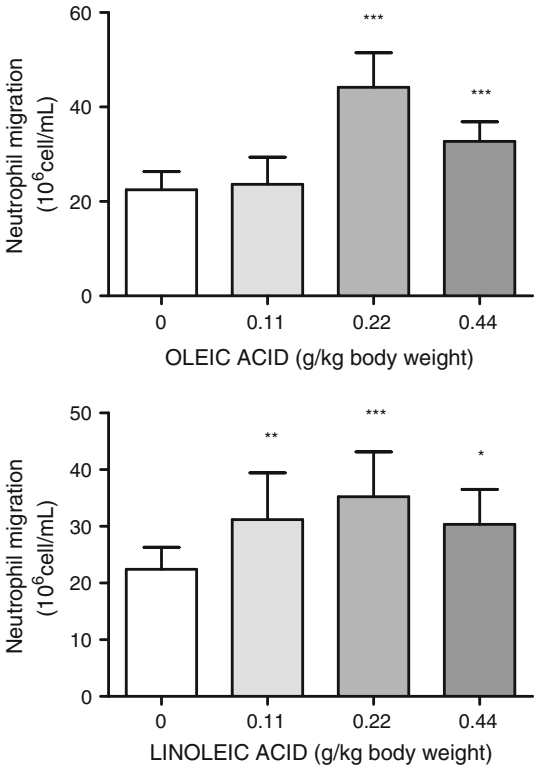

Fig. 4 Neutrophil influx into the peritoneal cavity induced by injection of glycogen solution in rats supplemented with different doses of oleic or linoleic acids. The values are presented as means ± SEM of ten animals per group. $*p < 0.05$, $**p < 0.01$ and $***p < 0.001$ indicates significant difference in relation to C as indicated by ANOVA and Dunnett post hoc test

adherent cells. LNA increased the number of rolling and adherent leukocytes after fMLP stimulus (Fig. 6a, b).

To further investigate the effect of fatty acids on neutrophil migration, the air pouch assay was used. The migratory response of neutrophils in vivo was elevated by both fatty acids in comparison to control (without fMLP). This response was accompanied by a significant increase in the concentration of CINC-2$\alpha\beta$, which plays an important role in neutrophil recruitment in rats (Fig. 7a, b). In a stimulated condition (fMLP), however, no significant alteration was observed with the fatty acid treatments (Fig. 7a, b).

The influence of the ingestion of OLA or LNA on the ex vivo production of proinflammatory cytokines by neutrophils was also evaluated. The concentration of CINC-2$\alpha\beta$ and IL-1β in the supernatants of neutrophils incubated for 4 and 18 h was determined. Despite a positive correlation between the treatment with OLA (doses 0.11, 0.22 and 0.44 g/kg body weight) and the production of CINC-2$\alpha\beta$ ($r^2 = 0.92$ Pearson correlation test; $p = 0.02$) and IL-1β ($r^2 = 0.92$ Pearson correlation test; $p = 0.001$) by neutrophils incubated for 4 h in the absence of LPS, no significant difference was observed compared to the control group (Fig. 8a, c). LNA increased the production of CINC-2$\alpha\beta$ and IL-1β by unstimulated neutrophils in a dose-dependent manner ($r^2 = 0.93$ and 0.98, respectively; $p = 0.01$ and 0.003, respectively). This effect was statistically significant at the dose of 0.44 g/kg body weight (Fig. 8a, d). After LPS-stimulation, OLA had no effects in the production of these cytokines, whereas, LNA (0.44 g/kg body weight) reduced the production of CINC-2$\alpha\beta$ (Fig. 8a, b).

After 18 h of incubation, both fatty acids significantly diminished CINC-2$\alpha\beta$ and IL-1β production by neutrophils in basal condition (PBS). In LPS-stimulated neutrophils, OLA (all doses) reduced the production of IL-1β but did not alter production of CINC-2$\alpha\beta$ (Fig. 9a, c).

Discussion

OLA is a major fatty acid component of meat, animal fat, milk, eggs, and some vegetable oils and is also a major fatty acid component of vegetable oils used in food manufacture [22]. LNA is a major fatty acid component of many vegetable oils, including some used in food manufacture and in animal feeds [22]. Thus, OLA and LNA are the predominant unsaturated fatty acids in the Western diet

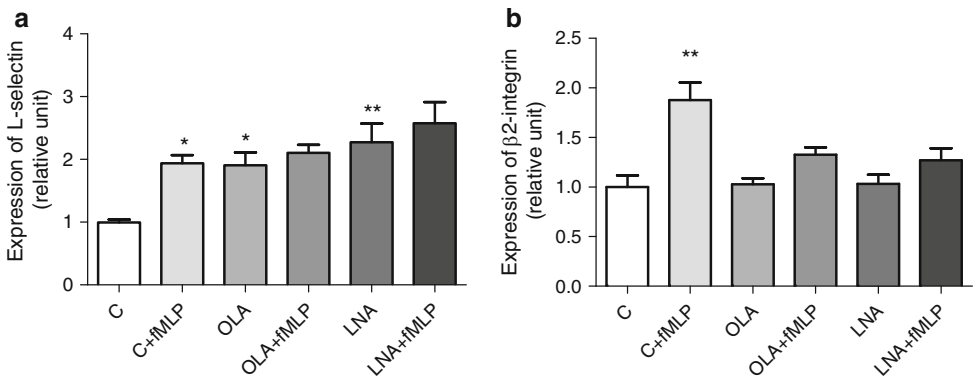

Fig. 5 Expression of L-selectin (**a**) and β2-integrin (**b**) in neutrophils isolated from rats supplemented with 0.22 g/kg body weight of oleic (OLA) or linoleic (LNA) acids. The values are presented as means ± SEM of six animals per group. $*p < 0.05$ and $**p < 0.01$ indicates significant difference in relation to C as indicated by ANOVA and Dunnett post hoc test

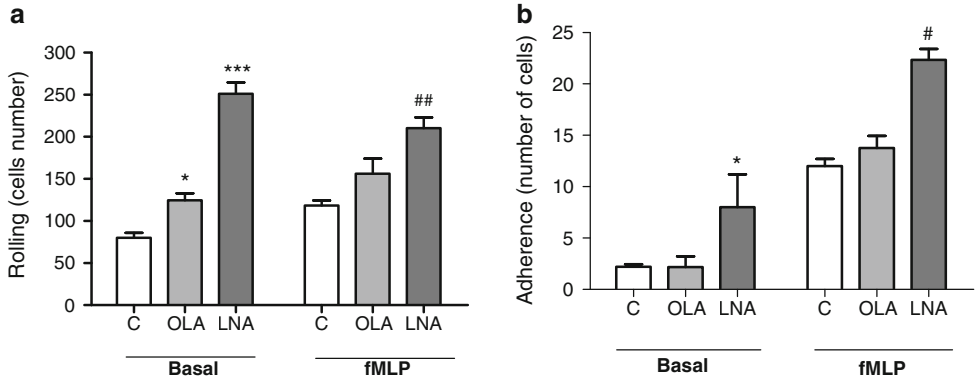

Fig. 6 Rolling (**a**) and adherence (**b**) of neutrophils isolated from rats supplemented with 0.22 g/kg body weight of oleic (OLA) or linoleic (LNA) acids. The values are presented as mean ± SEM of three animals per group. $^{*}p < 0.05$ and $^{***}p < 0.001$ indicate significant difference in relation to C; $^{\#}p < 0.05$ and $^{\#\#}p < 0.01$ indicate significant difference in relation to C + fMLP as indicated by ANOVA and Dunnett post hoc test

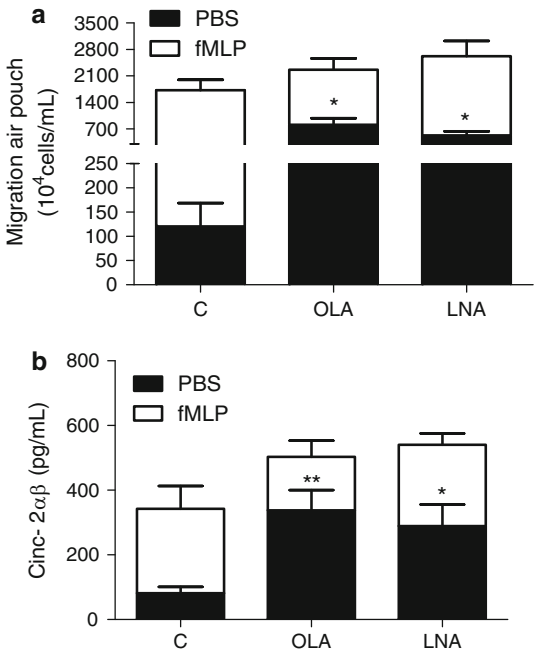

Fig. 7 Influx of neutrophils to the air-pouch (**a**) and CINC-2$\alpha\beta$ (**b**) concentrations in the exudate of the air-pouch induced in control (C), oleic acid (OLA) and linoleic acid (LNA) groups. The dose administrated was 0.22 g/kg body weight. The values are presented as means ± SEM of six animals per group. $^{*}p < 0.05$ and $^{**}p < 0.01$ indicate significant difference in relation to C in PBS condition

[13]. Variation in intake of these two fatty acids may influence chronic disease risk, particularly diseases with an inflammatory component.

The serum activity of AST, ALT and LDH is used as a clinical marker of liver injury [23, 24]. Damaged hepatocytes release these enzymes into the extracellular space from where they enter into the circulation, so augmenting their circulating activity. The finding that the highest dose of OLA or LNA (0.44 g/kg body weight) did not elevate the serum activity of these enzymes, indicates a lack of toxicity when these fatty acids are administered in the free form by gavage as was done here.

The augmentation in neutrophil migration seen is possibly due to an increase in L-selectin expression and in the production of chemoattractant CINC-2$\alpha\beta$. LNA promoted the release of proinflammatory cytokines after a short incubation period (4 h) and both fatty acids inhibited this release after a prolonged incubation (18 h). In the presence of LPS, only LNA reduced CINC-2$\alpha\beta$ production by neutrophils after 4 h. However, OLA inhibited the production of IL-1β but did not affect CINC-2$\alpha\beta$ release by stimulated neutrophils incubated for 18 h. These observations reinforce the idea that OLA modifies neutrophil responses and should not be used as a control in further studies.

Fatty acids can accumulate into droplets in the cytoplasm or be incorporated into the phospholipids in cell membranes. The incorporation of fatty acids in neutrophils (either in the membrane or in droplets) is one, but not the only, possible mechanism involved in the effects seen here [25]. Since the cells continually degrade and replace their lipids [26], the difference in the incorporation of OLA and LNA into neutrophils could be due to the metabolism of LNA, keeping in mind that an inflammatory process was induced in the peritoneum and the cells were collected 3 h after. Another possible explanation is that each of these fatty acids exerts its effect by a different mechanism, which may not necessarily involve incorporation of the fatty acid into the cell membrane. More studies are necessary to clarify which mechanisms are involved in the effects of OLA and LNA seen in the present study.

Neutrophil recruitment requires adhesion and transmigration through blood-vessel walls, a process that involves at least four steps: rolling, activation, adhesion and transmigration. This is a highly regulated process that requires

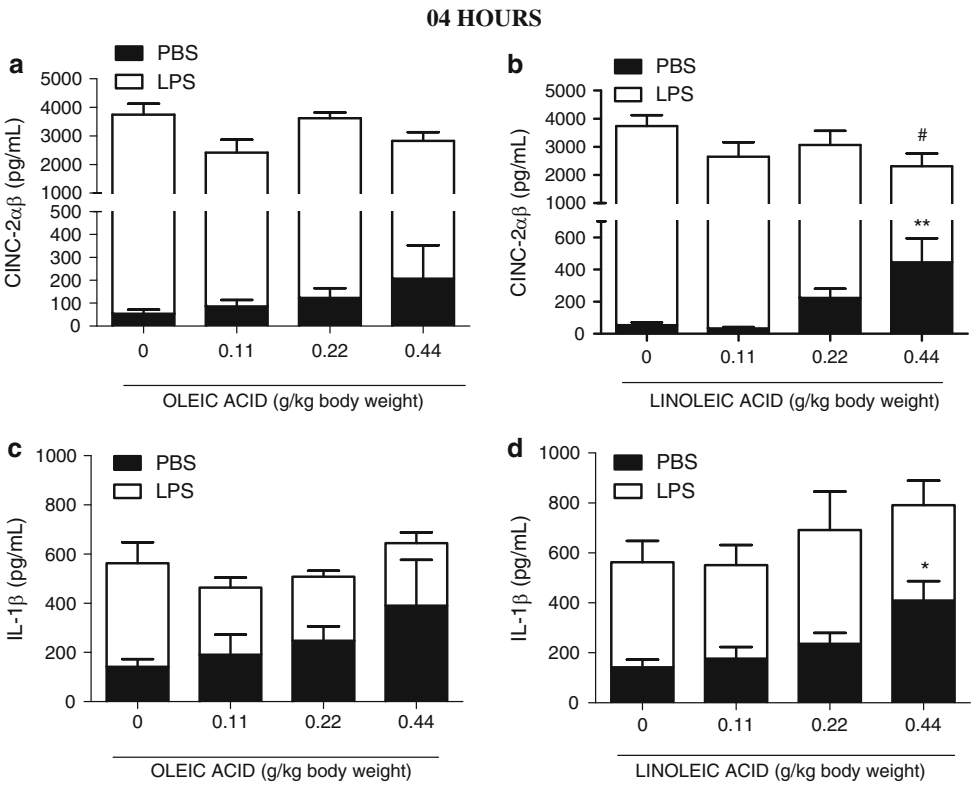

Fig. 8 Concentrations of CINC-2$\alpha\beta$ (**a, b**) and IL-1β (**c**, **d**) in the supernatant of neutrophils isolated from rats supplemented with different doses of oleic and linoleic acids and cultured during 4 h. The values are presented as means ± SEM of six animals per group. *$p < 0.05$ and **$p < 0.01$ indicate significant difference in relation to C in PBS condition; $^{\#}p < 0.05$ indicates significant difference in relation to C in stimulated (LPS) condition as indicated by ANOVA and Dunnett post hoc test

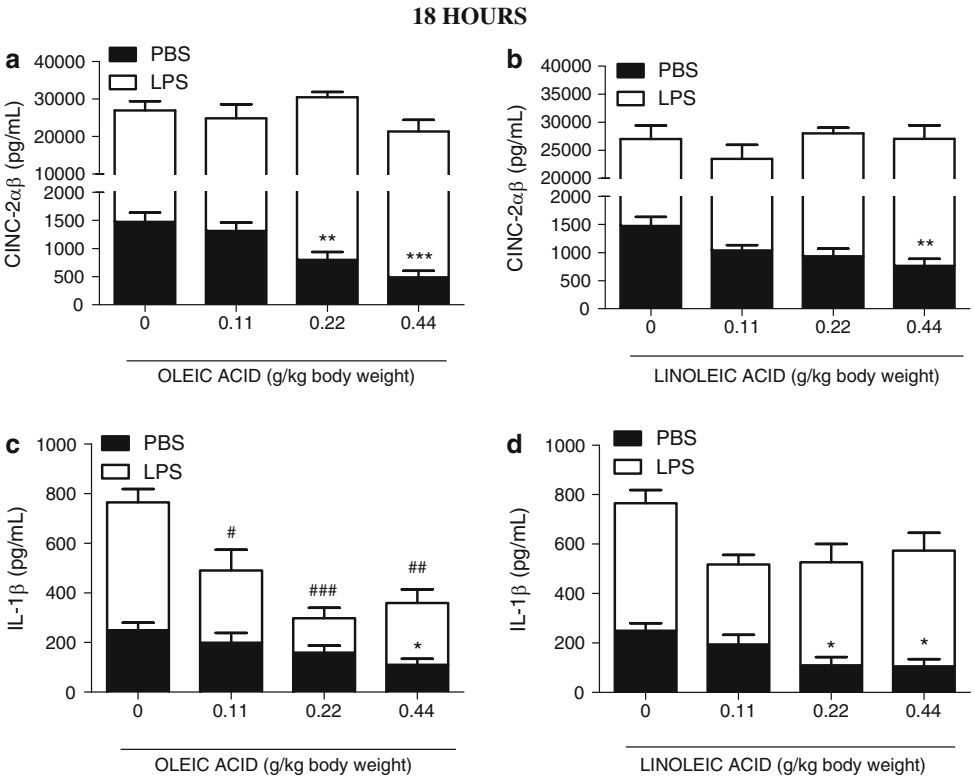

Fig. 9 Concentrations of CINC-2$\alpha\beta$ (**a, b**) and IL-1β (**c, d**) in the supernatant of neutrophils isolated from rats supplemented with different doses of oleic and linoleic acids and cultured during 18 h. The values are presented as means ± SEM of six animals per group. *$p < 0.05$, **$p < 0.01$ and ***$p < 0.001$ indicate significant difference in relation to C in PBS condition; $^{\#}p < 0.05$, $^{\#\#}p < 0.01$ and $^{\#\#\#}p < 0.001$ indicate significant difference in relation to C in stimulated (LPS) condition as indicated by ANOVA and Dunnett post hoc test

coordinated participation of cytokines (including chemokines), and endothelial and leukocyte adhesion molecules (immunoglobulins and selectins) [12]. Selectin–ligand interactions are characterized by rapid bond formation and dissociation, an interaction that mediates the first step of leukocyte adhesion, the rolling [12]. Firm attachment of

leukocytes to the endothelium requires the interaction of integrin ligands on the leukocyte surface through immunoglobulin superfamily members, i.e., ICAM-1, ICAM-2 and VCAM-1, expressed on the endothelium [27]. Effects of OLA and LNA on endothelial cell expression of integrin ligands are conflicting: some authors demonstrated increases [15, 28] and others found decreases in the expression of adhesion molecules [29–31]. These contrasting results possibly occurred due to differences in the experimental conditions such as the cell type, time of incubation and fatty acid concentrations used.

In the present study the administration of either OLA or LNA augmented the rolling of neutrophils and the migration response without affecting the expression of β_2-integrin. Considering that the slowing of neutrophils allows these cells to recognize chemotactic molecules and to elicit a chemoattractant-receptor-mediated event [12], these results can be associated to the increase in L-selectin expression and chemokine production by neutrophils in a β_2-integrin independent-response. Studies with ω-6 fatty acids have shown an increase in the migratory response of neutrophils through the increase in the production of prostaglandin D_2 [32]. According to Tsuzuki et al. [33], olive oil increases the expression of α_4-integrin and L-selectin on lymphocytes and thereby enhances the adherence of these cells. We observed an elevation in the number of adherent neutrophils after administration of LNA, but OLA had no effect. In our study, the use of pure fatty acids ensured that the effects observed are not due to minor constituents present in the parent oils or to the combination of different fatty acids as found in oils.

Another important function of neutrophils is the production of proinflammatory cytokines such as CINC-2$\alpha\beta$ and IL-1β. CINC-2$\alpha\beta$ (also referred as IL-8) is a potent chemoattractant for neutrophils. Blockade of IL-8 receptors inhibits neutrophil influx to inflamed areas [34]. Augmentation in the production of CINC-2$\alpha\beta$ hastens the inflammatory response through an increase of neutrophil influx and activation. IL-1β is produced by leukocytes after infection or injury. This cytokine stimulates cell metabolism and increases the expression of several genes coding for enzymes than increase the production of biologically active molecules such as arachidonic acid metabolites [35].

Previous studies investigated the effect of OLA and LNA ingestion on the production of inflammatory mediators. Baer et al. [36] did not observe significant differences in the concentration of C-reactive protein and IL-6 after ingestion of an OLA-rich diet by humans. Mice supplemented with olive oil exhibited reduced neutrophil production of PGE_2, LTB_4, MCP-1, and TNF-α in endotoxic shock [37]. Ingestion of a diet rich in OLA resulted in a reduction of IL-1β, TNF-α and IL-6 release by murine macrophages cultured for 18 h [38]. On the other hand, consumption of LNA by mice was correlated with an increase in plasma concentration of IL-1β after LPS injection [39].

The production of cytokines is transient and time-dependent [40]. These characteristics are important to avoid the overproduction and, consequently, the deleterious effects of cytokines. In the present study, we observed that LNA increased the production of IL-1β and CINC-2$\alpha\beta$ after 4 h of incubation, but at 18 h, the concentration of these cytokines was lower than in the control group. This effect shows that LNA can accelerate the mechanisms responsible for the production/release of cytokines early in the inflammatory response, perhaps by promoting the transcription of pre-formed RNA [41]. The later decrease in production/release of cytokines could be due to the synthesis of a transcriptional repressor and/or a decrease in mRNA half-life [41]. OLA, at the same doses, did not alter the production of IL-1β and CINC-2$\alpha\beta$ after a short period of incubation (i.e., 4 h). However, OLA also reduced the production of these cytokines after 18 h of incubation in the presence (IL-1β) or absence of LPS (IL-1β and CINC-2$\alpha\beta$). The difference in the concentrations of CINC-2$\alpha\beta$ between 4 and 18 h is small in the OLA group. This suggests that the action of OLA is more pronounced upon the inhibition of the later process. Our results reinforce the point that LNA is more pro-inflammatory than OLA, although both alter cytokine production by neutrophils. The different responses observed between the incubation times can involve a diverse range of mechanisms [42, 43], but further studies are necessary to clarify this point.

In conclusion, we demonstrated that unesterified OLA or LNA given by gavage modify several neutrophil functions, in vivo and ex vivo, and indicate that these fatty acids may affect the course of inflammation.

Acknowledgments This research is supported by the Fundação de Amparo a Pesquisa do Estado de São Paulo (FAPESP), Coordenação de Aperfeiçoamento de Pessoal de Nível Superior (CAPES) and Conselho Nacional de Desenvolvimento Cientifico e Tecnológico. The authors acknowledge the Prof. Patricia Gama and Roberto Cabado Modia Junior for help in the histological pictures.

References

1. Pipette M, Saugier J (1970) Effect of the intravenous infusion of a lipid emulsion on blood leukocytes in the rabbit. Ann Pharm Fr 28:529–534
2. Verlengia R, Gorjao R, Kanunfre CC, Bordin S, Martins de Lima T, Martins EF, Newsholme P, Curi R (2004) Effects of EPA and DHA on proliferation, cytokines production and gene expression in Raji cells. Lipids 39:857–864
3. Barcelo-Coblijn G, Murphy EJ, Othman R, Moghadasian MH, Kashour T, Friel JK (2008) Flaxseed oil and fish-oil capsule consumption alters human red blood cell n–3 fatty acid

composition: a multiple-dosing trial comparing 2 sources of n–3 fatty acid. Am J Clin Nutr 88:801–809
4. Chang HH, Chen CS, Lin JY (2008) Dietary perilla oil inhibits proinflammatory cytokine production in the bronchoalveolar lavage fluid of ovalbumin-challenged mice. Lipids 43:499–506
5. Jeffrey NM, Sanderson P, Sherrington EJ, Newsholme EA, Calder PC (1996) The ratio of n-6 to n-3 polyunsaturated fatty acids in the rat diet alters serum lipid levels and lymphocyte functions. Lipids 31:737–745
6. Verlengia R, Gorjao R, Kanunfre CC, Bordin S, Martins de Lima T, Martins EF, Newsholme P, Curi R (2003) Genes regulated by arachidonic and oleic acids in Raji cells. Lipids 38:1157–1165
7. May CL, Southworth AJ, Calder PC (1993) Inhibition of lymphocyte protein kinase C by unsaturated fatty acids. Biochem and Bio Res Comm 195:823–828
8. Higazi A al-R, Bargouthi II (1994) Regulation of neutrophil activation by oleic acid. Biochim Biophys Acta 1201:442–446
9. Malawista SE, Chevance AB, van Damme J, Serhan CN (2008) Tonic inhibition of chemotaxis in human plasma. PNAS 105:17949–17954
10. Cury-Boaventura MF, Gorjão R, de Lima TM, Newsholme P, Curi R (2006) Comparative toxicity of oleic and linoleic acids on human lymphocytes. Life Sci 78:1448–1456
11. Waterman E, Lockwood B (2007) Active components and clinical applications of olive oil. Altern Med Rev 12:331–342
12. Ley K, Laudanna C, Cybulky MI, Nourshagh S (2007) Getting to the site of inflammation: the leukocyte adhesion cascade updated. Nat Rev Immunol 7:678–689
13. U.S. Department of Agriculture, A.R.S. Nutrient intakes from food: mean amounts consumed per individual, One Day, 2005–2006, 2008. http://www.ars.usda.gov/ba/bhnrc/fsrg. Accessed Nov 2009
14. Cicero AFG, Nascetti F, Lopez-Sabater MC, Elosua R, Salomen JT et al (2008) Changes in LDL fatty acid composition as a response to olive oil treatment are inversely related to lipid oxidative damage: the EUROLIVE Study. J Am Coll Nutr 27:314–320
15. Pacheco YM, Lopez S, Bermudez B, Abia R, Villar J, Muriana FJG (2008) A meal rich in oleic acid beneficially modulates postprandial sICAM-1 and sVCAM-1 in normotensive and hypertensive hypertriglyceridemic subjects. J Nutr Biochem 19:200–205
16. Suresh Y, Das UN (2003) Long-chain polyunsaturated fatty acids and chemically induced diabetes mellitus: effect of ω-6 fatty acids. Nutrition 19:93–114
17. Folch J, Lees M, Sloane Stanley GH (1957) A simple method for the isolation and purification of total lipides from animal tissues. J Biol Chem 226:497–509
18. Hatanaka E, Monteagudo PT, Marrocos MSM, Campa A (2006) Neutrophils and monocytes as potentially important sources of proinflammatory cytokines in diabetes. Clin Exp Immun 146:443–447
19. Farsky SH, Walber J, Costa-Cruz M, Cury Y, Teixeira CF (1997) Leukocyte response induced by *Bothrops jararaca* crude venom: in vivo and in vitro studies. Toxicon 35:185–193
20. Vinolo MA, Rodrigues HG, Hatanaka E, Hebeda CB, Farsky SH, Curi R (2009) Short chain fatty acids stimulate migration of neutrophils to inflammatory site. Clin Sci 117:331–338
21. Edwards JC, Sedgwick AD, Willoughby DA (1981) The formation of a structure with the features of synovial lining by subcutaneous injection of air: an in vivo tissue culture system. J Pathol 134:147–156
22. British Nutrition Foundation (1992) Unsaturated fatty acids: nutritional and physiological significance. Chapman and Hall, London
23. Amacher DE (1998) Serum transaminase elevations as indicators of hepatic injury following the administration of drugs. Regul Toxicol Pharmacol 27:119–130
24. Cho MH, Niles A, Huang R, Inglese J, Austin CP, Riss T, Xia M (2008) A bioluminescence toxicity assay for assessment of membrane integrity using a proteolytic biomarker. Toxicol In Vitro 22:1099–1106
25. Cabral GA (2005) Lipids as bio effectors in the immune system. Life Sciences 77:1699–1710
26. Nelson DL, Cox MM (2000) Lehninger principles of biochemistry, 3rd edn. Worth Publishers, New York
27. Sengelov H, Kjeldseng L, Diamond MS, Springer TA, Borregaard N (1993) Subcellular localization and dynamics of Mac-1 (alpha m beta 2) in human neutrophils. J Clin Invest 92:1467–1476
28. Perez-Martinez P, Lopez-Miranda J, Blanco-Colio L, Bellido C, Jimenez Y, Moreno JA, Delgado-Lista J, Egido J, Perez-Jimenez F (2007) The chronic intake of a Mediterranean diet enriched in virgin olive oil, decreases nuclear transcription factor kappaB activation in peripheral blood mononuclear cells from healthy men. Atherosclerosis 194:e141–e146
29. Massaro M, Carluccio MA, Paolicchi A, Bosetti F, Solaini G, De Caterina R (2002) Mechanisms for reduction of endothelial activation by oleate: inhibition of nuclear factor-kappaB through antioxidant effects. Prostaglandins Leukot Essent Fatty Acids 67:175–181
30. Couloubaly S, Delomenie C, Rousseau D, Paul JL, Grynberg A, Pourci ML (2007) Fatty acid incorporation in endothelial cells and effects on endothelial nitric oxide synthase. Eur J Clin Invest 37:692–699
31. Moussa M, Le Boucher J, Garcia J, Tkaczuk J, Ragab J, Dutot G, Ohayon E, Ghisolfi J, Thouvenot JP (2000) In vivo effects of olive oil-based lipid emulsion on lymphocyte activation in rats. Clin Nutr 19:49–54
32. Tull SP, Yates CM, Maskrey BH, O'Donnell VB, Madden J, Grimble RF, Calder PC, Nash GB, Rainger G (2009) Omega-3 fatty acids and inflammation: novel interactions reveal a new step in neutrophil recruitment. PLOS Biol 7:e1000177
33. Tsuzuki Y, Miura S, Kurose I, Suematsu M, Higuchi H, Shigematsu T et al (1997) Enhanced lymphocyte interaction in postcapillary venules of Peyer's patches during fat absorption in rats. Gastroenterology 112:813–825
34. Walz A, Peveri P, Aschauer H, Baggiolini M (1987) Purification and amino acid sequencing of NAF, a novel neutrophil-activating factor produced by monocytes. Biochem Biophys Res Commun 149:755–761
35. Dinarello CA (2009) Immunological and inflammatory functions of the interleukin-1 family. Annu Rev Immunol 27:519–550
36. Baer DJ, Judd JT, Clevidence BA, Tracy RP (2004) Dietary fatty acids affect plasma markers of inflammation in healthy men fed controlled diet: a randomized crossover study. Am J Clin Nutr 79:969–973
37. Leite MS, Pacheco P, Gomes RN, Guedes AT, Castro-Faria-Neto HC, Bozza PT, Koatz VLG (2005) Mechanisms of increased survival after lipopolysaccharide-induced endotoxic shock in mice consuming olive oil-enriched diet. Shock 23:173–178
38. de la Puerta R, Marquez-Martins A, Fernandez-Arche A, Ruiz-Gutierrez V (2009) Influence of dietary fat on oxidative stress and inflammation in murine macrophages. Nutrition 25:548–554
39. Sadeghi S, Wallace FA, Calder PC (1999) Dietary lipids modify the cytokine response to bacterial lipopolysaccharide in mice. Immunology 96:404–410
40. Thonsom A (1998) The cytokine handbook. 3rd edn
41. Jarrous N, Kaempfer R (1994) Induction of human interleukin-1 gene expression by retinoic acid and its regulation at processing of precursor transcripts. J Biol Chem 269:23141–23149
42. Hirasawa A, Hara T, Katsuma S, Adachi T, Tsujimoto G (2008) Free fatty acid receptors and drug discovery. Biol Pharm Bull 31:1847–1851
43. Serhan CN, Yacoubian S, Yang R (2008) Anti-inflammatory and proresolving lipid mediators. Annu Rev Pathol 3:279–312

Lipids (2010) 45:821–832
DOI 10.1007/s11745-010-3451-y

ORIGINAL ARTICLE

Regulation of Hepatocyte Lipid Metabolism and Inflammatory Response by 25-Hydroxycholesterol and 25-Hydroxycholesterol-3-sulfate

Leyuan Xu · Qianming Bai · Daniel Rodriguez-Agudo · Phillip B. Hylemon · Douglas M. Heuman · William M. Pandak · Shunlin Ren

Received: 19 March 2010 / Accepted: 15 July 2010 / Published online: 11 August 2010

Abstract Dysregulation of lipid metabolism is frequently associated with inflammatory conditions. The mechanism of this association is still not clearly defined. Recently, we identified a nuclear oxysterol, 25-hydroxycholesterol-3-sulfate (25HC3S), as an important regulatory molecule involved in lipid metabolism in hepatocytes. The present study shows that 25HC3S and its precursor, 25-hydroxycholesterol (25HC), diametrically regulate lipid metabolism and inflammatory response via LXR/SREBP-1 and IκBα/NFκB signaling in hepatocytes. Addition of 25HC3S to primary rat hepatocytes decreased nuclear LXR and SREBP-1 protein levels, down-regulated their target genes, acetyl CoA carboxylase 1 (ACC1), fatty acid synthase (FAS), and SREBP-2 target gene HMG reductase, key enzymes involved in fatty acid and cholesterol biosynthesis. 25HC3S reduced TNFα-induced inflammatory response by increasing cytoplasmic IκBα levels, decreasing NFκB nuclear translocation, and consequently repressing expression of NFκB-dependent genes, IL-1β, TNFα, and TRAF1. NFκB-dependent promoter reporter gene assay showed that 25HC3S suppressed luciferase activity in the hepatocytes. In contrast, 25HC elicited opposite effects by increasing nuclear LXR and SREBP-1 protein levels, and by increasing ACC1 and FAS mRNA levels. 25HC also decreased cytoplasmic IκBα levels and further increased TNFα-induced NFκB activation. The current findings suggest that 25HC and 25HC3S serve as potent regulators in cross-talk of lipid metabolism and inflammatory response in the hepatocytes.

Keywords Oxysterol sulfation · Oxysterol metabolism · Lipid metabolism · Inflammatory response · Nuclear orphan receptor · LXR · NFκB · IκBα

Abbreviations

25HC	25-Hydroxycholesterol
25HC3S	25-Hydroxycholesterol-3-sulfate
ABCA1	ATP-binding cassette, sub-family A, member 1
ABCG5	ATP-binding cassette, sub-family G, member 5
ACC1	Acetyl-CoA carboxylase 1
CYP27A1	Mitochondrial cholesterol 27-hydroxylase
FAS	Fatty acid synthase
GAPDH	Glyceraldehyde-3-phosphate dehydrogenase
HepG2	Human hepatocellular carcinoma cell line
HMGR	3-Hydroxy-3-methylglutaryl-coenzyme A reductase
IκBα	Nuclear factor of kappa light polypeptide gene enhancer in B-cells inhibitor, alpha
IL-1β	Interleukin-1, beta
LDLR	Low density lipoprotein receptor
LXR	Liver X receptor
LXRE	LXR responsive elements
NAFLD	Nonalcoholic fatty liver disease
NFκB	Nuclear factor of kappa light polypeptide gene enhancer in B-cells

Electronic supplementary material The online version of this article (doi:10.1007/s11745-010-3451-y) contains supplementary material, which is available to authorized users.

L. Xu · Q. Bai · D. Rodriguez-Agudo · D. M. Heuman · W. M. Pandak · S. Ren (✉)
Department of Medicine, McGuire Veterans Affairs Medical Center, Virginia Commonwealth University, Research 151, 1201 Broad Rock Blvd, Richmond, VA 23249, USA
e-mail: sren@vcu.edu

P. B. Hylemon
Department of Microbiology/Immunology, McGuire Veterans Affairs Medical Center, Virginia Commonwealth University, Richmond, VA 23249, USA

PRH	Primary rat hepatocyte
SREBP	Sterol regulatory element binding protein
StarD1	Steroidogenic acute regulatory protein, D1
SULT2B1b	Sulfotransferase family, cytosolic, 2B, member 1b
TNFα	Tumor necrosis factor, alpha
TRAF1	TNF receptor associated factor 1

Introduction

Lipid metabolic disorders and inflammation are closely associated and contribute to the pathogenesis of many serious diseases including atherosclerosis, diabetes, and nonalcoholic fatty liver disease (NAFLD), which are major causes of morbidity and mortality in the United States. The American Liver Foundation estimated that currently up to 5% of American children over age 5 have NAFLD. A "two-hit" model has been proposed for the development of NAFLD [1]. The "first hit" is the initial excess lipid accumulation in the form of free cholesterol, free fatty acid, and triglycerides, induced by insulin resistance in hepatocytes. In the "second hit," excess lipids in hepatocytes lead to cell injury, setting off a cascade of necro-inflammatory changes that include the accumulation of mixed inflammatory cells and hepatocyte ballooning with Mallory body. A sub-set of NAFLD patients goes on to develop progressive fibrosis. Therefore, decreasing hepatic lipid levels and repressing the inflammatory response are the keys to NAFLD therapy. Understanding the cross-talk between lipid accumulation and inflammation is fundamental for the prevention of NAFLD. However, the cellular mechanisms controlling lipid metabolism and inflammatory response are presently unknown.

Oxysterols can act at multiple points in cholesterol homeostasis and lipid metabolism [2–5]. Recently, we identified a novel oxysterol, 25-hydroxycholesterol-3-sulfate (25HC3S), that accumulates in hepatocyte nuclei following overexpression of the mitochondrial cholesterol delivery protein, StarD1 [6–8]. This oxysterol is synthesized from sulfation of 25-hydroxycholesterol (25HC) by sterol sulfotransferase 2B1 (SULT2B1b) [9]. Sulfation of oxysterol is expected to make an even more polar sterol that should efflux more rapidly from cells. The oxysterol sulfation is believed to be an inactivation process since expression of SULT2B1b attenuated oxysterol-stimulated LXR signaling both in vivo and in vitro cultured mouse cells [10]. However, our recent reports have suggested that 25HC3S has different direct effects on lipid metabolism in HepG2 cells and macrophages compared to its precursor 25HC. 25HC increased SREBP-1c mRNA and protein levels and induced its targeting genes, but 25HC3S had the opposite effects [11, 12]. Because the expression of SREBP-1c is a target gene of LXR [13], the results indicate that 25HC and 25HC3S may diametrically opposite-regulate LXR activation. Several chemically synthesized oxysterol sulfates also display antagonistic activity against LXR [14].

Several reports show that the nuclear oxysterol receptor, LXR, actively participates in the inflammatory response [15–18]. The mechanism is not fully understood. For example, while synthetic LXR agonists could blunt the LPS-induced up-regulation of adhesion molecules (ICAM-1, VCAM-1, E-Selectin), 22-hydroxycholesterol and 24, 25-epoxycholesterol enhanced the response. Microarray profiling further showed that the endothelial gene expression profiles of 22-hydroxycholesterol and the artificial LXR ligand T0901317 largely differed, and unexpectedly shared only a restricted number of genes [19]. Other LXR-activating oxysterols such as 24,25-epoxycholesterol, 25-hydroxycholesterol, and 27-hydroxycholesterol, stimulated the endothelial expression of inflammatory markers [19].

In this study, we further demonstrate that 25HC3S and its precursor 25HC are potent regulators of hepatic lipid metabolism as well as inflammatory response in hepatocytes. We provide the evidence that their effects are mediated via activation/inactivation of the nuclear receptors, SREBP and NFκB signaling pathways, in both HepG2 cells and primary rat hepatocytes.

Materials and Methods

Cell culture reagents and supplies were purchased from GIBCO BRL (Grand Island, NY). Hepatoma cell line (HepG2) cells were obtained from American Type Culture Collection (Rockville, MD). The reagents for real-time RT-PCR were obtained from AB Applied Biosystems (Warrington WA1 4 SR, UK). Antibodies against LXRα/β (sc-13068), SREBP-1 (sc-8984), FAS (sc-55580), ACC1 (sc-30212), IκBα (sc-371), NFκB (sc-372), Lamin B1 (sc-56145), and Lamin AC (sc-20681) were purchased from Santa Cruz Biotechnology (Santa Cruz, CA). Antibodies against ABCA1 (ab18180) were from Abcam (Cambrige, MA). LXR agonist T0901317 was from New Cayman Chemical (Ann Arbor, MI). Assay kits for cholesterol E assay, free cholesterol assay, and Wako NEFA-HR [2] assay kits for free fatty acid were obtained from Wako Bioproducts (Richmond, VA). Infinity triglyceride assay kit was from Thermo Electron (Arlington, TX). FuGENE HD transfection reagent was obtained from Roche Applied Science (Indianapolis, IN). The Dual-Glo Luciferase Assay System and pGL3-NFκB-luc were purchased from Promega (Wisconsin, WI). The chemicals used in this research were obtained from Sigma Chemical (St. Louis, MO) or Bio-Red Laboratories (Hercules, CA). All solvents were obtained from Fisher (Fair Lawn, NJ) unless otherwise indicated.

Cell Culture

HepG2 cells were grown in MEM media containing non-essential amino acids, 30 mM $NaHCO_3$, 10% fetal bovine serum (FBS), 1 mM L-glutamine, 1 mM sodium pyruvate, and 1% Pen/Strep, and incubated at 37°C in 5% CO_2. When cells reached ~80% confluence, the oxysterols in DMSO or in ethanol (the final concentration in media was <0.1%) were added, and the cells were harvested as indicated. Nuclear and cytoplasmic fractions were isolated using NE-PER®, Nuclear and Cytoplasmic Extraction Reagents (Pierce, Rockford, IL).

Primary rat hepatocytes (PRH) were provided by the core facility in Virginia Commonwealth University (Richmond, VA) as described previously [20]. Cells were seeded on 60-mm tissue culture dishes in Williams' E medium containing 10% FBS, thyroxine (0.1 μM), and dexamethasone (0.1 μM). Three hours after plating, culture medium was removed, and fresh medium and the oxysterols in DMSO or in ethanol were added as indicated. Experiments were performed in PRH to corroborate findings in experiments conducted in HepG2 cells.

Cell Proliferation and Cytotoxicity Assay

HepG2 cells were plated in 96-well plates. After treatment with 25HC or 25HC3S for 48 h, 10 μl/well of CellTiter 96Aqueous One Solution Reagent [3-(4,5-dimethyl-2-thiazolyl)-2,5-diphenyl-2H-tetrazolium bromide (MTT) reagent] was added. After incubation at 37°C for 1 h in a humidified 5% CO_2 atmosphere, the absorbance at 490 nm was recorded with an ELISA plate reader. Control refers to incubations in the presence of vehicle only (0.1% of DMSO or ethanol) and was considered as 100% viable cells [20].

Western Blot Analysis of Nuclear LXR, NFκB, SREBP-1, and Intracellular FAS, ACC1, ABCA1, and IκBα Levels

Cytoplasmic protein extracts or nuclear protein extracts, 50 μg, otherwise as indicated, were separated on 7.5 or 10% SDS-PAGE gels and transferred onto a polyvinylidene difluoride (PVDF) membrane using a Bio-Rad Mini-Blot transfer apparatus as described previously [21]. Membranes were blocked in Tris-buffered saline (TBS) containing 5% nonfat dried milk for 1 h. The specific proteins were determined by incubation with specific antibodies against LXR, SREBP-1, NFκB, FAS, ACC1, ABCA1, or IκBα overnight at 4°C with shaking. After washing, the membrane was incubated in a 1:3,000 dilution of a secondary antibody (goat anti-rabbit or anti-mouse IgG-HRP conjugate; Bio-Rad, Hercules, CA) at room temperature for 1 h in the washing buffer (TBS containing 0.5% Tween 20). The protein bands were visualized using SuperSignal West Pico Chemiluminescent Substrate Kit (Pierce, Rockford, IL). Cytoplasmic proteins were normalized to β-actin; nuclear proteins were normalized to Lamin AC.

LXR Transcription Factor Assay

LXR transcription factor activity was measured using an enzyme-linked immunosorbent assay (LXR Transcription Factor Assay kit; Cayman Chemical, Ann Arbor, MI). HepG2 cells were treated with 25HC3S or 25HC for 2 h. The cells were then rinsed, and the nuclear proteins were extracted according to the manufacturer's instructions. Twenty micrograms of the nuclear proteins was added to a 96-well plate that had been immobilized by specific dsDNA sequences containing the LXR responsive elements (LXRE). After incubating for 1 h, the wells were washed and incubated with primary LXR antibody, which recognizes the accessible epitope on LXR protein upon LXRE DNA binding. The HRP conjugated secondary antibody, which provides a sensitive colorimetric readout, was added and incubated for 1 h. The reaction was stopped, and absorbance was read at 450 nm in a spectrophotometer.

Determination of mRNA Levels by Real-Time RT-PCR

Total RNA was isolated from oxysterol- or vehicle-treated HepG2 or PRH using SV Total RNA Isolation Kit (Promega, Wisconsin, WI), which included DNase treatment. Total RNA, 2 μg, was used for the first-strand cDNA synthesis as recommended by the manufacturer (Invitrogen, Carlsbad, CA). Real-time RT-PCR was performed using SYBR Green as indicator on ABI 7500 Fast Real-Time PCR System (Applied Biosystems, Foster City, CA). The final reaction mixture contained 10 ng of cDNA, 100 nM of each primer, 10 μl of 2× SYBR® Green PCR Master Mix (Applied Biosystems, Foster City, CA), and RNase-free water to complete the reaction mixture volume to 20 μl. All reactions were performed in triplicate. PCR was carried out for 40 cycles of 95°C for 15 s and 60°C for 1 min. The intensity of fluorescence was read during the reaction, allowing a continuous monitoring of the amount of PCR product. Each CT value of target gene was normalized to the CT value of internal control GAPDH. The sequences of primers are summarized (Table 1, Supplemental Materials) as previously described at http://www.pga.mgh.harvard.edu/primerbank/.

Oil Red O Staining of Total Intracellular Neutral Lipids

HepG2 or PRH cells were seeded on 22 × 22-mm glass coverslips in six-well plates. After the medium was replaced, cells were cultured in fresh medium with 20%

FBS and treated with different concentrations of 25HC3S or vehicle control for 48 h as indicated. Cells were fixed with 3.7% formaldehyde in phosphate-buffered saline (PBS) for 30 min followed by washing three times with PBS. The cells were stained with 0.2% Oil Red O in 60% isopropanol for 10 min and washed three times with PBS. The images were taken with the use of a microscope (Olympus, Tokyo, Japan) equipped with 40× lenses.

Quantitative Measurements of Total Cholesterol, Free Cholesterol, Free Fatty Acids, and Triglycerides

HepG2 cells were seeded on 60-mm tissue culture dishes and treated with control vehicle and different concentrations of 25HC3S or 25HC for 48 h as indicated. The cells were collected with 0.5 ml of PBS and sonicated. Total lipids were extracted by addition of 10 ml of chloroform–methanol (2:1, vol/vol) mixture. The extract, 0.5 ml, was evaporated to dryness and dissolved in 100 μl of isopropanol containing 10% of triton X-100 for cholesterol assays, isopropanol only for triglyceride assay, or the NEFA solution (0.5 g of EDTA-Na_2, 2 g of Triton X-100, 0.76 ml of 1 N NaOH, and 0.5 g of sodium azide/l, pH 6.5) for free fatty acid assay. The total and free cholesterol, triglyceride, and free fatty acid assays were performed according to the manufacturer's instructions. Each lipid concentration was normalized to protein concentration.

Transfection and Promoter Reporter Gene-Luciferase Assays

HepG2 cells were seeded in 96-well plates. When cell density reached 90–95%, the cells were transfected with an expression plasmid as indicated using a lipid-based FuGENE HD transfection reagent according to the manufacturer (Roche, Indianapolis, IN). A synthetic *renilla* luciferase reporter, phRG-TK (Promega, Wisconsin, WI), was used as a luciferase internal standard. For NFκB reporter gene assay, 50 ng of pGL3-NFκB-luciferase reporter and 50 ng of phRG-TK vector (internal standard) were co-transfected following the manufacturer's instructions. After 24 h following the transfection, HepG2 cells were treated with different concentrations of 25HC3S or 25HC for another 24 h or further stimulated with TNFα for 6 h. Luciferase activities were determined using the Dual-Glo Luciferase Assay System according to the manufacturer's protocol (Promega, Wisconsin, WI). The amount of luciferase activity was measured using a TopCount NXT Microplate Scintillation and Luminescence Counter (Packard, Meriden, CT) and normalized to the amount of phRG-TK luciferase activity. Transfection was carried out in triplicate for each sample, and each experiment was repeated three times.

Examination of Intracellular NFκB Translocation by Confocal Microscopy

HepG2 cells were cultured on coverslips in six-well plates. When cell density reached 20–30%, the cells were treated with 25HC or 25HC3S at different concentrations as indicated for 3 h alone or for 8 h before adding 100 ng/ml of TNFα for 15 min. The cells on coverslips were washed with PBS, fixed with 3.7% formaldehyde for 10 min at 4°C, and then rinsed with PBS three times at room temperature. They were permeabilized with PBS containing 0.1% of Triton X-100 for 3 min and washed with PBS before blocking by incubation with 5% normal goat serum in PBS overnight at 4°C. For interaction with primary antibodies, cells were incubated with 2.5% normal goat serum in PBS containing antibody against NFκB for 1 h at room temperature. Cells were washed in PBS containing 0.05% of Tween 20 for three times, each time for 10 min. The bound primary antibodies were visualized with Alexa Fluor 488 goat anti-mouse IgG. The minor groove of double-stranded DNA as a nuclear marker was stained with DAPI. After washing, coverslips were mounted on slides and viewed with a Zeiss LSM 510 Meta confocal microscope, scale bar = 20 μm.

Statistics

Data are reported as mean ± standard deviation (SD). Where indicated, data were subjected to *t*-test or ANOVA analysis and determined to be significantly different at $P < 0.05$.

Results

Effects of 25HC3S and 25HC on Nuclear LXR Levels

To examine the effect of 25HC3S and its precursor 25HC on LXR activation, total nuclear proteins were extracted, and nuclear LXR protein levels were determined by Western blot analysis. As shown in Fig. 1, addition of 25HC3S to primary rat hepatocytes led to time- (Fig. 1a, upper panels) and concentration- (Fig. 1b, upper panels) dependent decreases in LXR protein levels in the nuclei. When the cells were incubated in the presence of oxysterols for 2 h, 25HC3S decreased while 25HC increased the nuclear LXR levels to the maxima. The changes are concentration dependent at the indicated time. Similar results were observed in HepG2 cells as shown in Fig. 1A in Supplemental Online Materials. To confirm that the increasing band with molecular weight 48 kDa in the nuclei was LXR protein, an artificial LXR ligand, T0901317, was used as positive control. As shown in

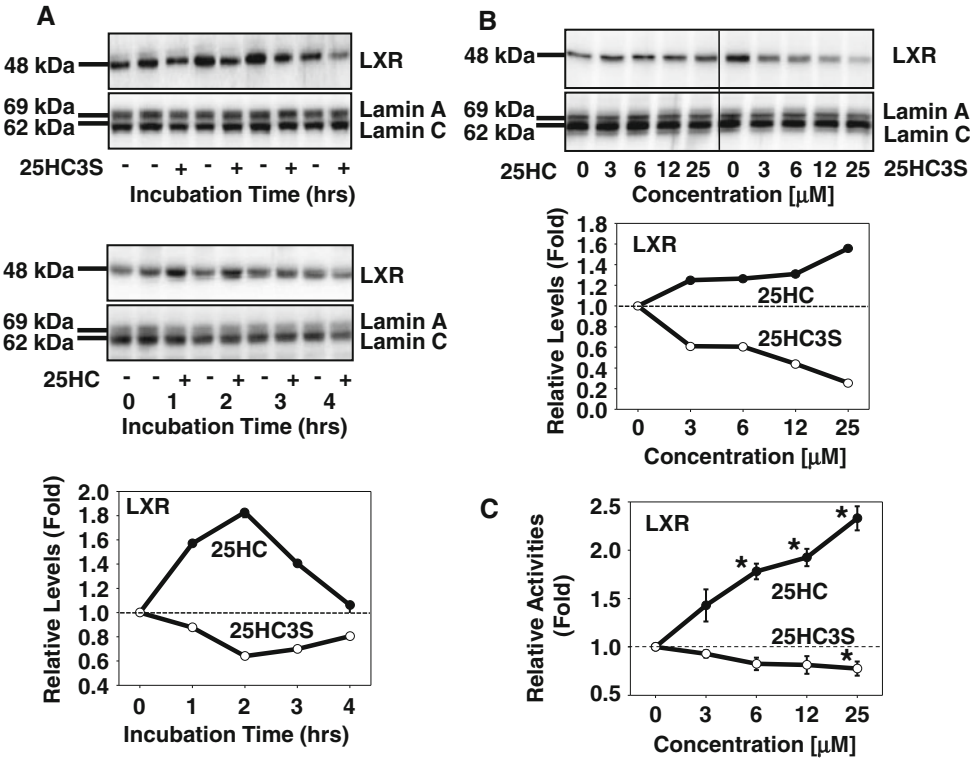

Fig. 1 Effects of 25HC3S and 25HC on nuclear LXR protein levels. The nuclear LXR protein levels in the treated PRH with 25HC or 25HC3S at the different times (**a**) and at different concentration points (**b**). Each positive band was quantified by the Image Data Analyzer and normalized to Lamin AC. The data represent one typical blot of three separate experiments. The LXR transcription factor-binding activities in the treated HepG2 with 25HC3S or 25HC were determined by the ELISA (**c**). Each value represents the mean of triplicate determination ±SD. *Asterisk* represents statistical significance ($P < 0.05$)

Fig. 1B in Supplemental Online Materials, T0091317 showed a time- and concentration-dependent increase in the nuclear LXR levels with the same molecular weight. The results suggest that 25HC3S suppresses LXR activation while 25HC increases activation. To confirm the nuclear LXR levels, LXR responsive element (LXRE)-immobilized ELISA was carried out as shown in Fig. 1c. As expected, the ELISA assay showed that nuclear extracts treated with 25HC3S decreased their LXRE-binding activities, while nuclear extracts treated with 25HC increased their LXRE-binding activities, both in a concentration-dependent manner ($P < 0.01$) (Fig. 1c).

Effects of 25HC3S and 25HC on LXR and SREBP Target Gene Expression

To determine the effects of 25HC3S and 25HC on LXR activities, total RNA was isolated from primary rat hepatocytes treated for 6 h. Real-time RT-PCR was used to determine the mRNA levels of LXR responsive genes, SREBP-1, ABCA1, and ABCG5; SREBP-1 responsive genes, FAS and ACC1; and SREBP-2 responsive genes, HMGR and LDLR. As shown in Fig. 2, there were significant decreases in SREBP-1, ACC1, FAS, SREBP-2, HMGR, and LDLR mRNA levels following 25HC3S treatment and increases in ABCA1, ABCG5, FAS, and ACC1 mRNA levels following 25HC addition to the cells in culture. Interestingly, both 25HC3S and 25HC decreased the levels of SREBP-2 mRNA and its responsive genes, HMGR and LDLR. Western blot densitometry analysis showed that 25HC increased nuclear SREBP-1, cytoplasmic FAS, and ACC1, while 25HC3S decreased nuclear SREBP-1, cytoplasmic FAS, and ACC1 protein levels, as shown in Fig. 3. Similar results were observed in HepG2 cells (data not shown). These results are consistent with the mRNA data in Fig. 2.

Effects of 25HC3S and 25HC on Intracellular and Total Cellular Lipid Levels in Primary Rat Hepatocytes and HepG2 Cells

To examine the intracellular lipid levels, total neutral lipids were examined by Oil Red-O staining. As shown in Fig. 2(A) in Supplemental Online Materials, 25HC3S significantly decreased the intracellular neutral lipid levels in HepG2 and primary rat hepatocytes. Biochemical quantitative analysis showed that addition of 6 μM 25HC3S decreased cellular total cholesterol (48 μg/mg protein) by 40%, free cholesterol (30 μg/mg protein) by 50%, triglyceride (150 μg/mg protein) by 25%, and free fatty acids (4.8 μg/mg protein) by 40%, compared to control cells as shown in Fig. 4. In contrast, 25HC increased free fatty acid levels, slightly decreased total cholesterol and triglycerides, and did not affect free cholesterol levels. These results are consistent with those from mRNA and protein analysis. 25HC3S decreases nuclear LXR and

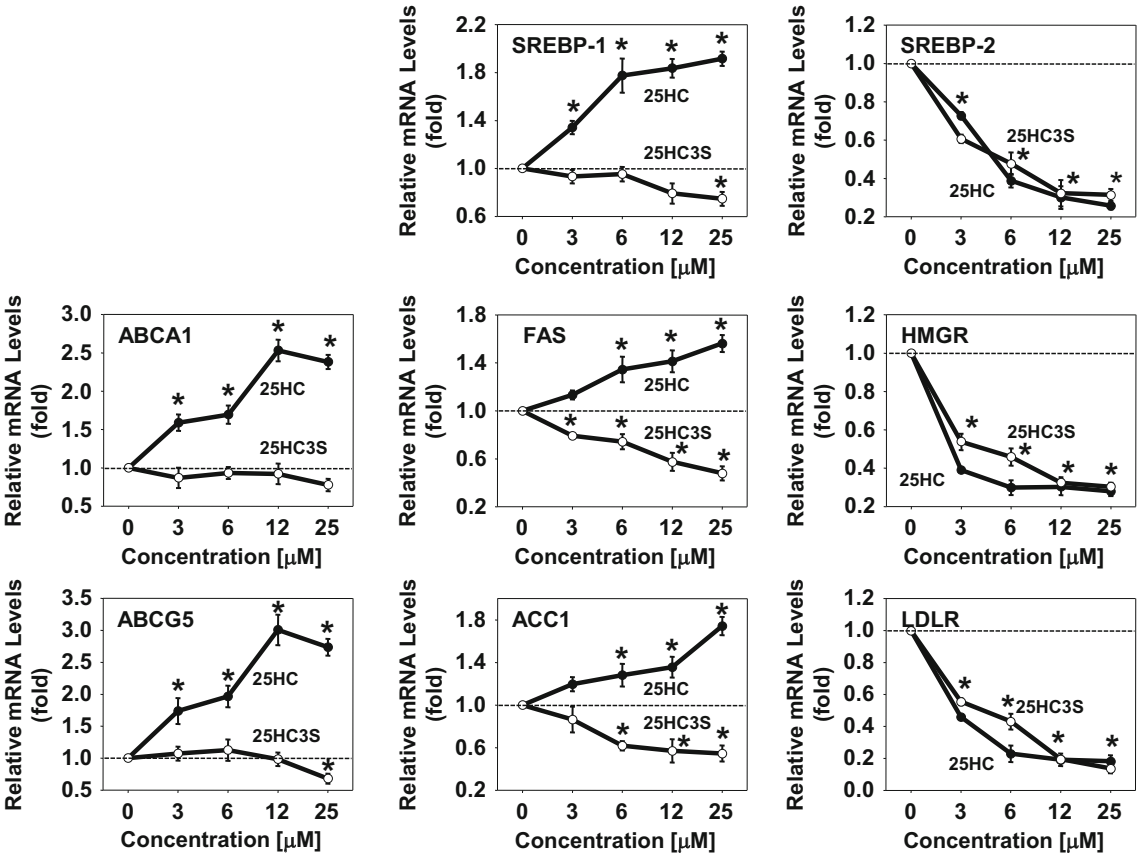

Fig. 2 Effects of 25HC3S and 25HC on the expression of LXR and SREBP target genes at mRNA levels. Following the treatment of PRH cells with 25HC3S or 25HC at the indicated concentrations for 6 h, effects of 25HC3S and 25HC on the expression of LXR target genes (*left*); SREBP-1 target genes (*middle*); SREBP-2 target genes (*right*) were determined by real-time RT-PCR analysis. Each value represents the mean of triplicate determinations ±SD. Symbol *asterisk* represents statistically significance ($P < 0.05$)

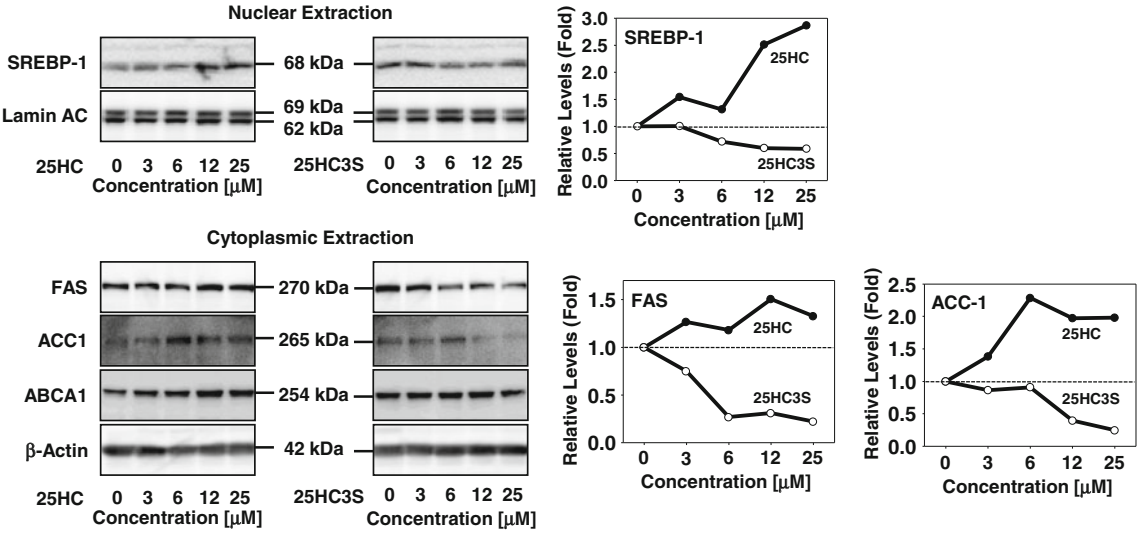

Fig. 3 Effects of 25HC3S and 25HC on the expression of SREBP-1, ABCA1, FAS and ACC1 at protein levels. Following the treatment of PRH cells with 25HC3S or 25HC at the indicated concentrations, nuclear SREBP-1 protein levels after 6 h treatment and cytoplasmic ABCA1, FAS and ACC1 protein levels after 24 h treatment, were determined by Western blot. Each positive band was quantified by the Image Data Analyzer and normalized to Lamin AC or β-actin. *Solid circles* represent 25HC treatments; *open circles* represent 25HC3S treatments

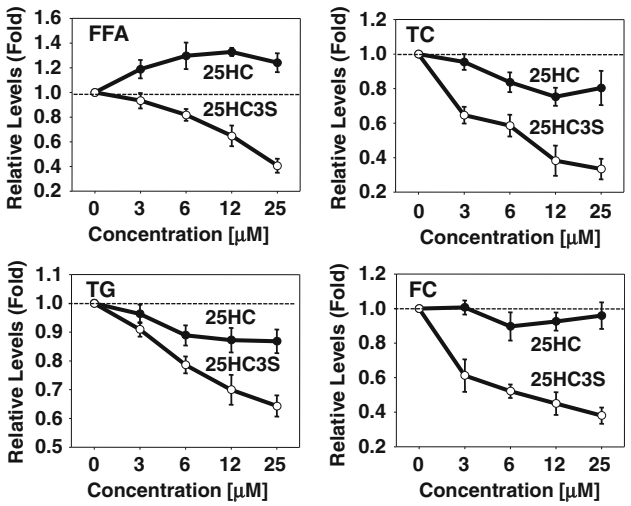

Fig. 4 Effects of 25HC3S and 25HC on total cellular lipid levels in HepG2 cells. HepG2 were treated with 25HC3S or 25HC at the indicated concentrations in the presence of 20% FBS for 48 h, total cellular lipids were extracted, and each individual lipid was chemically analyzed and normalized by protein amount as described in "Materials and Methods." Each value represents the mean of triplicate determination ±SD

subsequently inhibits expression of SREBP-1 and its target genes, while both 25HC3S and 25HC decrease SREBP-2 mRNA levels and its target gene expression (Figs. 2, 3).

Effects of 25HC3S and 25HC on Cell Proliferation in HepG2 Cells

MTT reagent assay was used to study the effect of 25HC and 25HC3S on the cell viability. As shown in Fig. 2(B) in Supplemental Online Materials, the percentages of relative cell number after treatment for 48 h were not affected by 25HC3S and slightly decreased by 25HC. The difference in cell viability between 25HC3S and control vehicle was not significant, as previously reported [11]. These results indicate that 25HC3S does not induce cell death and cytotoxicity.

Effects of 25HC3S and 25HC on Cytoplasmic IκBα and Nuclear NFκB Levels in Primary Rat Hepatocytes and HepG2 Cells

Both IκBα and NFκB play an important role in the inflammatory response pathway [22, 23]. To study the effects of

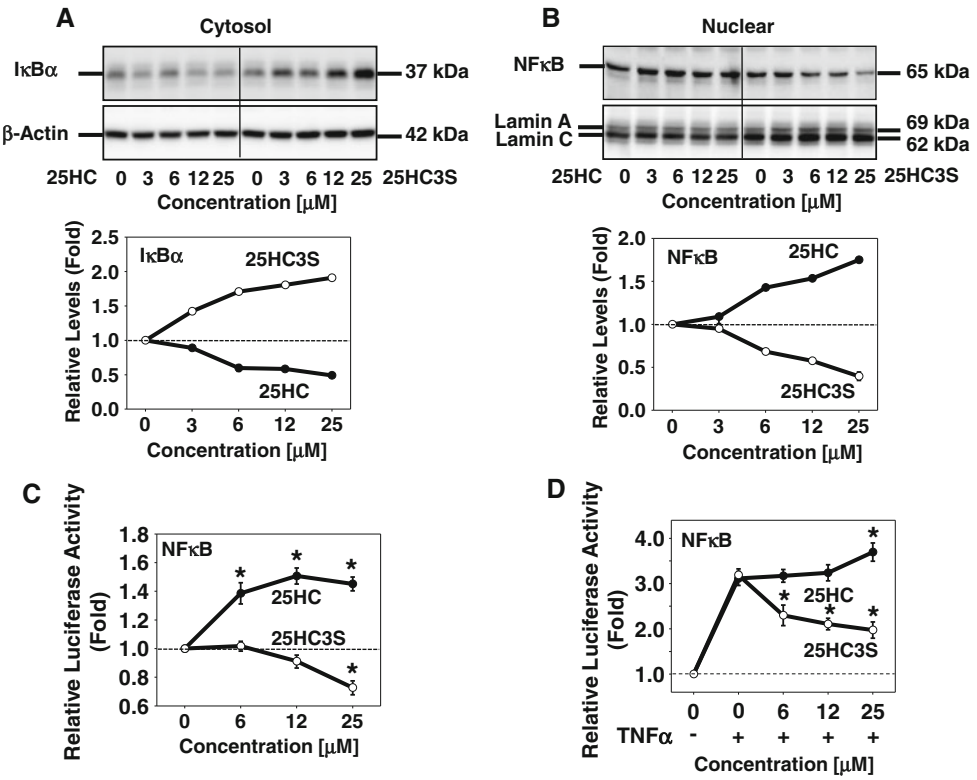

Fig. 5 Effects of 25HC3S and 25HC on expression of IκBα protein levels in cytoplasmic extracts and NFκB protein levels in nuclear extracts in HepG2 cells. Effects of 25HC3S and 25HC on IκBα protein levels (**a**) in cytoplasm and NFκB protein in nuclei (**b**) were analyzed by Western blot. Effects of 25HC3S and 25HC on NFκB promoter reporter gene activities were determined by luciferase activity assay and normalized by the amount of phRG-TK luciferase activity. HepG2 cells were cotransfected with pGL3-NFκB-dependent reporter gene-Luc and phRG-TK vector for 24 h, and treated with the indicated concentrations of 25HC3S or 25HC for another 24 h (**c**), or further stimulated with the 100 ng/ml of human TNFα for 6 h (**d**). The data represent the mean of triplicate determinations ±SD. Symbol *asterisk* represents statistically significance ($P < 0.05$) compared with TNFα treatment

25HC3S and 25HC on the inflammatory response, the cytoplasmic and nuclear proteins were extracted from the treated HepG2 cells (Fig. 5) and primary rat hepatocytes (Fig. 3 in Supplemental Online Material). The protein levels of IκBα in the cytoplasmic fractions and NFκB in the nuclear fractions were determined by Western blot analysis. Addition of 25HC decreased cytoplasmic IκBα and increased nuclear NFκB levels, while 25HC3S increased cytoplasmic IκBα and decreased nuclear NFκB levels in a concentration-dependent manner (Fig. 5a, b).

NFκB-dependent reporter gene assay showed that treatment with 25HC increased luciferase activity while 25HC3S decreased its activity in HepG2 cells (Fig. 5c). As a positive control, treatment with TNFα increased luciferase activity by threefold. Interestingly, pretreatment with 25HC3S inhibited TNFα-induced increase in NFκB reporter activity, while 25HC slightly increased the reporter activity (Fig. 5d). The results indicate 25HC3S not only blocks the NFκB nuclear translocation, but also decreases NFκB promoter-binding activity.

Addition of 25HC3S Represses Inflammatory Response

Addition of TNFα significantly decreased IκBα protein levels in the cytoplasm of HepG2 cells during 15–30-min incubation. The lκBα levels had rebounded by 60 min as shown in Fig. 6a. These results suggest that TNFα rapidly increases IκBα degradation, and the lower levels of IκBα feed back to stimulate its synthesis. The results are consistent with the previously published mechanism [24, 25]. Thus, the 15-min incubation with TNFα was chosen for the study of effects of 25HC3S and 25HC on the inflammatory response. Pretreatment with 25HC3S significantly blocked TNFα induced-decreases in IκBα levels in a concentration-dependent manner in cytoplasmic fractions, while 25HC further lowered IκBα levels as shown in Fig. 6b. Moreover, pretreatment with 25HC further increased TNFα-induced increases in nuclear NFκB levels. In contrast, 25HC3S decreased TNFα-induced nuclear NFκB levels in a concentration-dependent manner as shown in Fig. 6c.

Immunohistochemical study using DAPI nuclear staining together with the NFκB antibody showed that NFκB proteins were widely distributed in the cytoplasm and nuclei of HepG2 cells (Fig. 7). Compared with control cells treated with ethanol, treatment with 25HC increased the nuclear NFκB fluorescence intensity and decreased the intensity in the cytoplasm, which are similar with those treated with TNFα. However, treatment with 25HC3S decreased the nuclear intensity and blunted TNFα stimulation. The results indicate that 25HC3S decreases NFκB

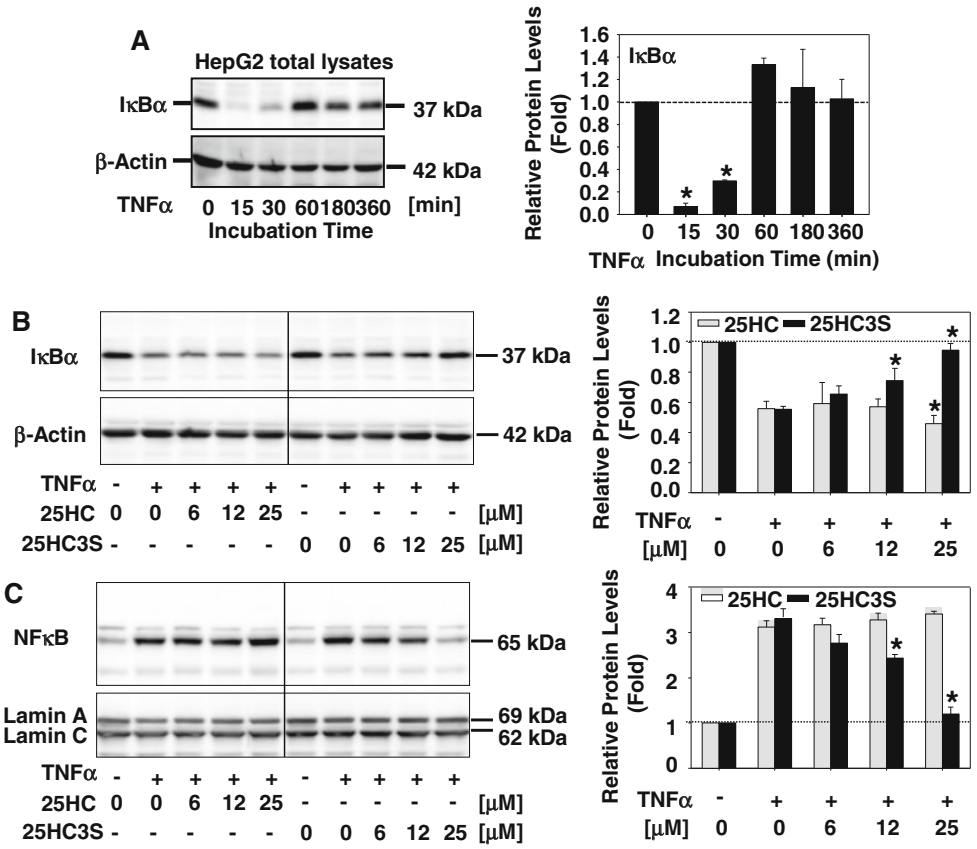

Fig. 6 Effects of 25HC3S and 25HC on IκBα protein levels and translocation of NFκB protein induced by TNFα in HepG2 cells. Cytoplasmic IκBα protein and nuclear NFκB were determined by Western blot after HepG2 cells were treated with 100 ng/ml of human TNFα for different times (**a**) or stimulated with TNFα for 15 min in the pre-treated cells with 25HC3S or 25HC at the indicated concentration for 8 h (**b**, **c**). The data represent the mean ± SD of three repeat experiments. Symbol *asterisk* represents statistical significance ($P < 0.05$)

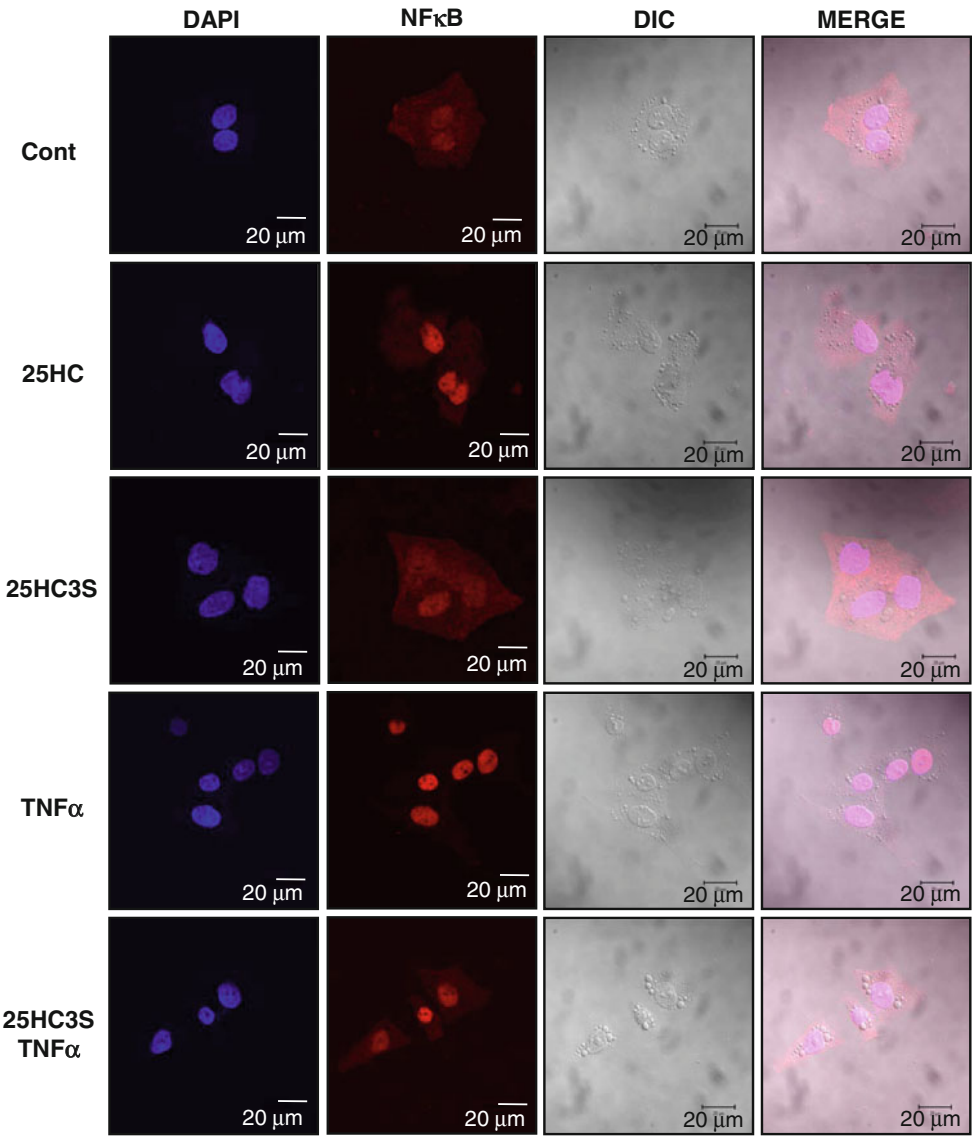

Fig. 7 Effects of 25HC3S and 25HC on NFκB translocation and 25HC3S on the TNFα-stimulated NFκB translocation into the nuclei in HepG2. Intracellular distribution of NFκB protein in HepG2 cells was analyzed by confocal microscopy. The left panel shows nuclear staining (*blue*); the middle left panel shows the localization of NFκB with the monoclonal antibody (*red*); the middle right panel shows a differential interference contrast (DIC) image; the right panel shows the merged image obtained by superimposing the three images mentioned above. The data represent randomly selected pictures as described in "Materials and Methods"

levels in the nuclei by increasing cytoplasmic IκBα levels and decreasing NFκB nuclear translocation.

TNFα increased expression of pro-cytokines including TNFα by 200 fold, IL-8 by 100 fold, NFκB by 4 fold, TRAF1 by 10 fold, IL-1b by 10 fold, and IκBα 9 fold, which are similar with those previously reported [22, 23]. Consistently, pretreatment of 25HC3S repressed the TNF-induced expression of NFκB, IL-8, TRAF1, and TNFα in HepG2 cells as shown in Fig. 8.

Discussion

We previously reported that 25HC and 25HC3S appear to function as agonist and antagonist of nuclear receptor LXR in macrophages [12]. 25HC sulfation links the regulation of cholesterol metabolism with fatty acid biosynthesis via LXR signaling pathway. LXRs present in two forms, LXRα and LXRβ. LXRα is restricted to the liver, adipose tissue, and macrophage, whereas LXRβ is ubiquitously expressed. Hepatic lipogenic activity of LXRs is predominantly under control of LXRα, although the oxysterols can activate both forms of LXRs [26–28]. Based on our results, we are assuming that most of the response LXR protein was LXRα since 25HC3S significantly decreased SREBP-1 and FAS. However, the results from Cayman Chemical LXRβ assay (Fig. 1c) indicate that 25HC3S decreases nuclear LXRβ protein levels, too. We concluded that 25HC3S represses both LXRα and LXRβ activities. When intracellular cholesterol levels increase, cholesterol can be delivered to mitochondria and metabolized to oxysterols, including 25-hydroxycholesterol (25HC) and 27-hydroxycholesterol (27HC) by CYP27A1 [9]. The oxysterols can in turn activate LXRs and subsequently regulate expression of

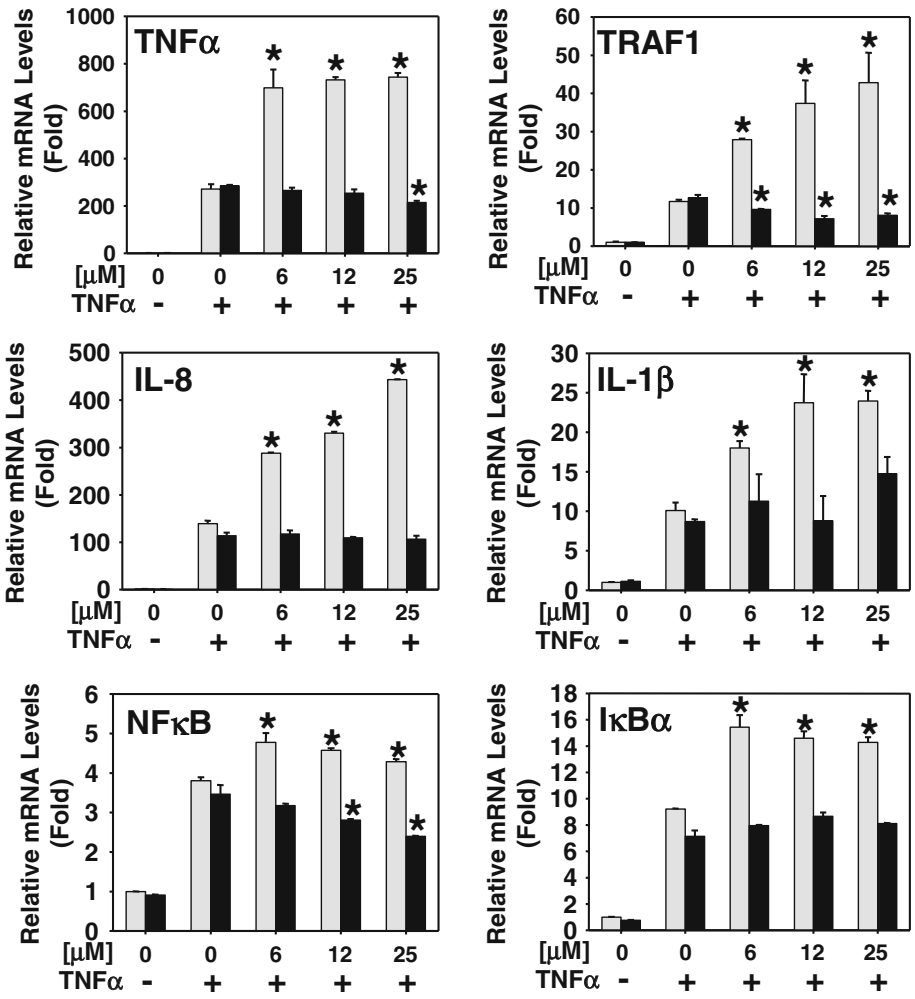

Fig. 8 Effects of 25HC3S and 25HC on NFκB target gene expression stimulated by human TNFα in HepG2. Following the stimulation of HepG2 cells with 100 ng/ml of human TNFα for 6 h in the pre-treatment with 25HC3S (*solid bar*) or 25HC (*open bar*) at the indicated concentration for 8 h, total mRNA was extracted, and NFκB target genes were determined by real-time RT-PCR analysis and were normalized to GAPDH. The graphs represent one of three experiments. Each value represents the mean of triplicate determination ±SD. *Asterisk* represents statistical significance ($P < 0.05$) compared with TNFα treatment

their targeting genes, which are involved in cholesterol metabolism, cholesterol efflux, and cholesterol uptake [2, 4, 29, 30]. On the other hand, we have shown that oxysterols such as 25HC also increase the gene expression involved in fatty acid biosynthesis, which may decrease cholesterol biosynthesis via using acetyl CoA as a common metabolic precursor. When the level of 25HC increases, 25HC can be further sulfated by SULT2B1b to 25HC3S [9]. The present results show that 25HC3S inhibits LXR activation, decreases SREBP-1 expression and activation, and subsequently downregulates lipid biosynthetic pathways. Thus, the present results provide the evidence that 25HC3S and 25HC are potent regulators that link cholesterol metabolism to fatty acid biosynthesis. 27-Hydroxycholesterol 3-sulfate (27HC3S) has never been detected in cells. Thus, whether 27-hydroxycholesterol can be sulfated is unknown.

The role of oxysterols in inflammatory response is controversial: some reports describe that oxysterols suppress the inflammatory response via the LXR signaling pathway [15–18]. Oxysterols can activate LXRs and subsequently repress a set of proinflammatory gene expressions after stimulation with LPS and cytokines [19, 31]. However, many other studies found that oxysterols induce inflammatory response and oxidation [19, 32, 33]. For example, 25HC substantially increased LPS-induced IL-1β mRNA expression and secretion in human monocyte-derived macrophages. 25HC is also a potent inducer of MCP-1, MIP-1β and IL-8 secretion in vitro [31, 34]. 25HC treatment gives rise to a significant increase in NFκB transcriptional activity, not only by affecting the IκB degradation and the translocation of p65/NFκB to the nucleus, but also by regulating the p65/NFκB transactivation [35]. 25HC also induces inflammation and oxidation through inducing slight mitochondrial dysfunctions and increasing reactive oxygen species (ROS) [35]. The present study shows that 25HC decreases cytoplasmic IκBα and increases nuclear NFκB levels following TNFα stimulation in hepatocytes. In contrast, 25HC3S increases the IκBα and decreases the nuclear NFκB levels. The results indicate that 25HC and 25HC3S diametrically regulate the inflammatory response.

Accumulation of fatty acids, free cholesterol, or oxysterols is able to induce inflammatory responses. It is possible that all of these compounds play their roles in pro-inflammatory responses respectively. We cannot rule out specific response by each of the elements at the presence. The important finding in the present study is that 25HC3S is able to suppress TNFα-induced inflammatory response, which is different from free cholesterol, fatty acids, or oxysterols. Oxysterols are reported to play an important role in both the lipid metabolism and inflammatory response [18, 36–38]. However, the mechanism of the cross-talk between lipid metabolism and inflammatory response has not been fully understood. The present results that 25HC (substrate) and 25HC3S (product) diametrically regulate activities of key enzymes, receptors, and transporters by interacting with two or more nuclear receptors implies the physiological role of 25-hydroxycholesterol sulfation. These results suggest that the oxysterol sulfation could be another novel systematic regulatory pathway involved in regulating lipid metabolism and inflammation.

It is noted that the concentrations we used for 25HC3S are relatively high. The levels of endogenous 25HC3S are very low. We barely detected the compound in human liver tissues, 0.1 μg/g of liver tissues, by the LC/MS/MS system [8]. This level can be substantially increased by overexpression of mitochondrial cholesterol delivery protein (StAR), indicating a physiological significance. We have tried to monitor 25HC3S levels following the addition of 25HC3S at the indicated concentrations in the macrophages but failed, indicating only a few of the molecules are able to enter the cells because of its hydrophilic properties. The effective concentration would be much lower than what we added in the experiments. 25HC3S was discovered in hepatocyte nuclei following increasing mitochondrial cholesterol delivery, indicating this compound is initially synthesized in mitochondria and translocated to nuclei. We believe that 25HC3S functions as an intracellular regulatory molecule via nuclear receptor(s) rather than through plasma membrane receptor(s).

Acknowledgments We acknowledge excellent technical help from Dalila Marques, Kaye Redford, and Patricia Bohdan. This work was supported by grants from the National Institutes of Health (R01 HL078898) and Veterans Administration (VA Merit Review).

References

1. James OF, Day CP (1998) Non-alcoholic steatohepatitis (NASH): a disease of emerging identity and importance. J Hepatol 29:495–501
2. Accad M, Farese RV Jr (1998) Cholesterol homeostasis: a role for oxysterols. Curr Biol 8:R601–R604
3. Bjorkhem I, Diczfalusy U (2002) Oxysterols: friends, foes, or just fellow passengers? Arterioscler Thromb Vasc Biol 22:734–742
4. Gill S, Chow R, Brown AJ (2008) Sterol regulators of cholesterol homeostasis and beyond: the oxysterol hypothesis revisited and revised. Prog Lipid Res 47:391–404
5. Javitt NB (2004) Oxysteroids: a new class of steroids with autocrine and paracrine functions. Trends Endocrinol Metab 15:393–397
6. Pandak WM, Ren S, Marques D, Hall E, Redford K, Mallonee D, Bohdan P, Heuman D, Gil G, Hylemon P (2002) Transport of cholesterol into mitochondria is rate-limiting for bile acid synthesis via the alternative pathway in primary rat hepatocytes. J Biol Chem 277:48158–48164
7. Ren S, Hylemon PB, Marques D, Gurley E, Bodhan P, Hall E, Redford K, Gil G, Pandak WM (2004) Overexpression of cholesterol transporter StAR increases in vivo rates of bile acid synthesis in the rat and mouse. Hepatology 40:910–917
8. Ren S, Hylemon P, Zhang ZP, Rodriguez-Agudo D, Marques D, Li X, Zhou H, Gil G, Pandak WM (2006) Identification of a novel sulfonated oxysterol, 5-cholesten-3beta, 25-diol 3-sulfonate, in hepatocyte nuclei and mitochondria. J Lipid Res 47:1081–1090
9. Li X, Pandak WM, Erickson SK, Ma Y, Yin L, Hylemon P, Ren S (2007) Biosynthesis of the regulatory oxysterol, 5-cholesten-3{beta}, 25-diol 3-sulfate, in hepatocytes. J Lipid Res 48:2587–2596
10. Chen W, Chen G, Head DL, Mangelsdorf DJ, Russell DW (2007) Enzymatic reduction of oxysterols impairs LXR signaling in cultured cells and the livers of mice. Cell Metab 5:73–79
11. Ma Y, Xu L, Rodriguez-Agudo D, Li X, Heuman DM, Hylemon PB, Pandak WM, Ren S (2008) 25-Hydroxycholesterol-3-sulfate regulates macrophage lipid metabolism via the LXR/SREBP-1 signaling pathway. Am J Physiol Endocrinol Metab 295:E1369–E1379
12. Ren S, Li X, Rodriguez-Agudo D, Gil G, Hylemon P, Pandak WM (2007) Sulfated oxysterol, 25HC3S, is a potent regulator of lipid metabolism in human hepatocytes. Biochem Biophys Res Commun 360:802–808
13. Schultz JR, Tu H, Luk A, Repa JJ, Medina JC, Li L, Schwendner S, Wang S, Thoolen M, Mangelsdorf DJ, Lustig KD, Shan B (2000) Role of LXRs in control of lipogenesis. Genes Dev 14:2831–2838
14. Song C, Hiipakka RA, Liao S (2001) Auto-oxidized cholesterol sulfates are antagonistic ligands of liver X receptors: implications for the development and treatment of atherosclerosis. Steroids 66:473–479
15. Delvecchio CJ, Bilan P, Radford K, Stephen J, Trigatti BL, Cox G, Parameswaran K, Capone JP (2007) Liver X receptor stimulates cholesterol efflux and inhibits expression of proinflammatory mediators in human airway smooth muscle cells. Mol Endocrinol 21:1324–1334
16. Fowler AJ, Sheu MY, Schmuth M, Kao J, Fluhr JW, Rhein L, Collins JL, Willson TM, Mangelsdorf DJ, Elias PM, Feingold KR (2003) Liver X receptor activators display anti-inflammatory activity in irritant and allergic contact dermatitis models: liver-X-receptor-specific inhibition of inflammation and primary cytokine production. J Invest Dermatol 120:246–255
17. Joseph SB, Bradley MN, Castrillo A, Bruhn KW, Mak PA, Pei L, Hogenesch J, O'connell RM, Cheng G, Saez E, Miller JF, Tontonoz P (2004) LXR-dependent gene expression is important for macrophage survival and the innate immune response. Cell 119:299–309
18. Torocsik D, Szanto A, Nagy L (2009) Oxysterol signaling links cholesterol metabolism and inflammation via the liver X receptor in macrophages. Mol Aspects Med 30:134–152
19. Morello F, Saglio E, Noghero A, Schiavone D, Williams TA, Verhovez A, Bussolino F, Veglio F, Mulatero P (2009) LXR-activating oxysterols induce the expression of inflammatory markers in endothelial cells through LXR-independent mechanisms. Atherosclerosis 207:38–44

20. Gupta S, Todd SR, Pandak WM, Muller M, Reno VZ, Hylemon PB (2000) Regulation of multidrug resistance 2 P-glycoprotein expression by bile salts in rats and in primary cultures of rat hepatocytes. Hepatology 32:341–347
21. Ren S, Hylemon P, Marques D, Hall E, Redford K, Gil G, Pandak WM (2004) Effect of increasing the expression of cholesterol transporters (StAR, MLN64, and SCP-2) on bile acid synthesis. J Lipid Res 45:2123–2131
22. Jin JQ, Li CQ, He LC (2008) Down-regulatory effect of usnic acid on nuclear factor-kappaB-dependent tumor necrosis factor-alpha and inducible nitric oxide synthase expression in lipopolysaccharide-stimulated macrophages RAW 264.7. Phytother Res 22:1605–1609
23. Hwang HJ, Lee HJ, Kim CJ, Shim I, Hahm DH (2008) Inhibitory effect of amygdalin on lipopolysaccharide-inducible TNF-alpha and IL-1beta mRNA expression and carrageenan-induced rat arthritis. J Microbiol Biotechnol 18:1641–1647
24. Solt LA, Madge LA, May MJ (2009) NEMO-binding domains of both IKKalpha and IKKbeta regulate IkappaB kinase complex assembly and classical NF-kappaB activation. J Biol Chem 284:27596–27608
25. Tergaonkar V, Perkins ND (2007) p53 and NF-kappaB crosstalk: IKKalpha tips the balance. Mol Cell 26:158–159
26. Lund EG, Peterson LB, Adams AD, Lam MH, Burton CA, Chin J, Guo Q, Huang S, Latham M, Lopez JC, Menke JG, Milot DP, Mitnaul LJ, Rex-Rabe SE, Rosa RL, Tian JY, Wright SD, Sparrow CP (2006) Different roles of liver X receptor alpha and beta in lipid metabolism: effects of an alpha-selective and a dual agonist in mice deficient in each subtype. Biochem Pharmacol 71:453–463
27. Bensinger SJ, Tontonoz P (2008) Integration of metabolism and inflammation by lipid-activated nuclear receptors. Nature 454:470–477
28. Hong C, Tontonoz P (2008) Coordination of inflammation and metabolism by PPAR and LXR nuclear receptors. Curr Opin Genet Dev 18:461–467
29. Ferber D (2000) Lipid research. Possible new way to lower cholesterol. Science 289:1446–1447
30. Janowski BA, Willy PJ, Devi TR, Falck JR, Mangelsdorf DJ (1996) An oxysterol signalling pathway mediated by the nuclear receptor LXR alpha. Nature 383:728–731
31. Rosklint T, Ohlsson BG, Wiklund O, Noren K, Hulten LM (2002) Oxysterols induce interleukin-1beta production in human macrophages. Eur J Clin Invest 32:35–42
32. Joffre C, Leclere L, Buteau B, Martine L, Cabaret S, Malvitte L, Acar N, Lizard G, Bron A, Creuzot-Garcher C, Bretillon L (2007) Oxysterols induced inflammation and oxidation in primary porcine retinal pigment epithelial cells. Curr Eye Res 32:271–280
33. Vejux A, Malvitte L, Lizard G (2008) Side effects of oxysterols: cytotoxicity, oxidation, inflammation, and phospholipidosis. Braz J Med Biol Res 41:545–556
34. Prunet C, Montange T, Vejux A, Laubriet A, Rohmer JF, Riedinger JM, Athias A, Lemaire-Ewing S, Neel D, Petit JM, Steinmetz E, Brenot R, Gambert P, Lizard G (2006) Multiplexed flow cytometric analyses of pro- and anti-inflammatory cytokines in the culture media of oxysterol-treated human monocytic cells and in the sera of atherosclerotic patients. Cytometry A 69:359–373
35. Calleros L, Lasa M, Toro MJ, Chiloeches A (2006) Low cell cholesterol levels increase NFkappaB activity through a p38 MAPK-dependent mechanism. Cell Signal 18:2292–2301
36. Schroepfer GJ Jr (2000) Oxysterols: modulators of cholesterol metabolism and other processes. Physiol Rev 80:361–554
37. Weinhofer I, Kunze M, Rampler H, Bookout AL, Forss-Petter S, Berger J (2005) Liver X receptor alpha interferes with SREBP1c-mediated Abcd2 expression. Novel cross-talk in gene regulation. J Biol Chem 280:41243–41251
38. Wolf G (1999) The role of oxysterols in cholesterol homeostasis. Nutr Rev 57:196–198

Lipids (2010) 45:833–841
DOI 10.1007/s11745-010-3458-4

ORIGINAL ARTICLE

γ-Tocotrienol Reduces Squalene Hydroperoxide-Induced Inflammatory Responses in HaCaT Keratinocytes

Kiyotaka Nakagawa · Akira Shibata · Toru Maruko · Phumon Sookwong · Tsuyoshi Tsuduki · Kayoko Kawakami · Hiroshi Nishida · Teruo Miyazawa

Received: 25 February 2010 / Accepted: 27 July 2010 / Published online: 17 August 2010

Abstract Squalene hydroperoxide (SQ-OOH), the primary peroxidation product of squalene (SQ), accumulates at the surface of sunlight-exposed human skin. There are however only a few studies on the pathogenic actions (i.e., inflammatory stimuli) of SQ-OOH. Here, we evaluated whether SQ-OOH induced inflammatory responses in immortalized human keratinocytes (HaCaT). We found that SQ-OOH caused an increase in the expression of inflammatory genes such as the interleukins as well as cyclooxygenase-2 (COX-2). In concordance with the upregulation of COX-2 mRNA, SQ-OOH enhanced reactive oxygen species generation, nuclear factor kappa B activation, COX-2 protein expression, and prostaglandin E2 production. Therefore, the pro-inflammatory effects of SQ-OOH may be mediated in part via COX-2. On the other hand, γ-tocotrienol (γ-T3, an unsaturated form of vitamin E) was found to ameliorate the SQ-OOH actions. These results suggest that SQ-OOH induces inflammatory responses in HaCaT, implying that SQ-OOH plays an important role in inflammatory skin disorders. As a preventive strategy, inflammation could be reduced via the use of γ-T3.

K. Nakagawa (✉) · A. Shibata · T. Maruko · P. Sookwong · T. Miyazawa
Food and Biodynamic Chemistry Laboratory,
Graduate School of Agricultural Science,
Tohoku University, Sendai 981-8555, Japan
e-mail: nkgw@biochem.tohoku.ac.jp

T. Tsuduki
Laboratory of Food and Biomolecular Science,
Graduate School of Agricultural Science,
Tohoku University, Sendai 981-8555, Japan

K. Kawakami · H. Nishida
Niigata University of Pharmacy and Applied Life Sciences,
Niigata 956-8603, Japan

Keywords Cyclooxygenase-2 · Inflammatory skin diseases · Squalene hydroperoxide · γ-Tocotrienol

Abbreviations

COX-2	Cyclooxygenase-2
DCDHF	2,7-Dichlorodihydrofluorescein
DMEM	Dulbecco's modified Eagle medium
FBS	Fetal bovine serum
HaCaT	Human keratinocytes
IL	Interleukin
iNOS	Inducible nitric oxide synthase
NF-κB	Nuclear factor kappa B
PGE2	Prostaglandin E2
SQ	Squalene
SQ-OOH	Squalene hydroperoxide
ROS	Reactive oxygen species
T3	Tocotrienol
TNF-α	Tumor necrosis factor-α
UV	Ultraviolet

Introduction

By virtue of covering the entirety of the body, human skin is the largest of the human organs. The skin surface contains secretions from the sebaceous gland, which consist mainly of squalene (SQ; Fig. 1), triacylglycerol, wax esters, and sterols [1]. When skin is exposed to sunlight including ultraviolet (UV) light [2, 3], peroxidation of the skin surface lipids can occur.

Previously, we have established methods for the sensitive and selective determination of lipid hydroperoxides [4–8], and have discovered that SQ hydroperoxide (SQ-OOH;

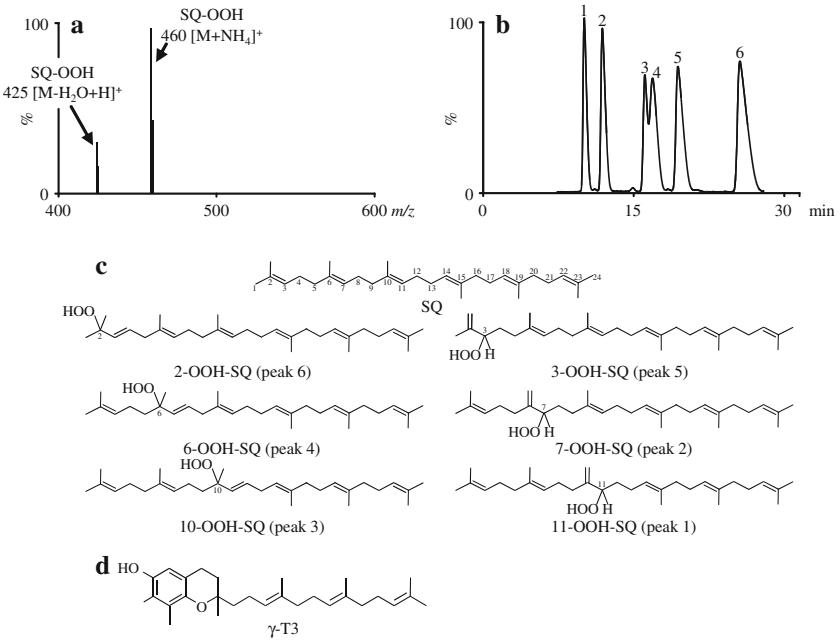

Fig. 1 SQ-OOH and γ-T3. For preparation of SQ-OOH, SQ (100 mg) was dissolved in 50 mL of ethanol (containing 0.01 mg/mL Rose Bengal as a sensitizer), and was photooxidized with a 100 W tungsten lamp at 4 °C for 6 h. From the photooxidation products, SQ-OOH was chromatographically purified. To evaluate purity, the isolated SQ-OOH was subjected to high-performance liquid chromatography coupled to UV, mass spectrometry, or tandem mass spectrometry, and NMR. Analytical conditions were the same as those described in our previous study [14]. From the data [e.g., MS spectrum (**a**) and UV chromatogram (**b**)], the SQ-OOH was considered to be a pure mixture of six isomers (2-OOH-SQ, 3-OOH-SQ, 6-OOH-SQ, 7-OOH-SQ, 10-OOH-SQ, and 11-OOH-SQ) (**c**). Percentages of the SQ-OOH isomers were 19 mol% 2-OOH-SQ, 17 mol% 3-OOH-SQ, 24 mol% 6-OOH-SQ, 10 mol% 7-OOH-SQ, 13 mol% 10-OOH-SQ, and 17 mol% 11-OOH-SQ. The chemical structure of γ-T3 is shown in (**d**)

Fig. 1) is produced in human skin [9, 10], which suggests that skin SQ may be the principal lipid photooxidation target. In support of this supposition, there have been an increasing number of studies concerning skin SQ-OOH production due to sunlight or UV exposure [11–13]. For instance, we recently reported that the concentration of SQ-OOH in normal forehead skin was about 1,000 μg/g skin lipids, which increased to 2,800 μg/g skin lipids after 3 h of sunlight exposure [14].

As increasing evidence of skin SQ-OOH has emerged, it has become implicated in the pathogenesis of skin alterations (e.g., sunburn and acne) [15–20]. A recent cell culture study using keratinocytes [21] suggested possible mechanisms for the pathogenic actions of SQ-OOH, which include the activation of nuclear factor kappa B (NF-κB) and the production of inflammatory interleukin (IL)-6. The study [21] provided some understanding of the role of SQ-OOH in the development of inflammatory skin diseases, although it had some weaknesses due to the lack of data concerning other inflammatory mediators [e.g., cxyclooxygenase-2 (COX-2)] as well as the uncertainty of the crude SQ-OOH used as the test compound. Other possible oxidation products in the crude SQ-OOH could have been responsible for intervention effects during the physiological evaluation of SQ-OOH. Therefore, the inflammatory action of SQ-OOH needs to be further clarified by the use of authentic, pure SQ-OOH.

On the other hand, as a preventive strategy against skin inflammation, compounds that can ameliorate the actions of SQ-OOH might be of therapeutic utility [22]. In the present study, we hypothesized that tocotrienol (T3, unsaturated vitamin E) could be a candidate to inhibit these inflammatory actions because T3 accumulates in the skin of animals fed a diet containing T3 [23, 24], and, besides its physiological activities [25], T3 has been suggested to provide skin protection against UV-induced inflammatory damage in a rat study [26].

In this study, we prepared pure SQ-OOH and evaluated the effect of SQ-OOH, either alone or with γ-T3 (a representative T3 isomer found in natural sources such as rice bran [27]; Fig. 1d), on various inflammatory mediators in a cell culture of human keratinocytes (HaCaT) [28].

Materials and Methods

Materials

SQ-OOH was prepared from SQ by our previously described method [14]. The SQ-OOH had high purity

(>98% by high-performance liquid chromatography to mass spectrometry), but was a mixture of six isomers differing in the position of the hydroperoxide group (Fig. 1). γ-T3 (purity > 92%) was purchased from Chromadex (Santa Ana, CA, USA). WST-1 reagent was obtained from Dojindo Laboratories (Kumamoto, Japan). All other reagents were of the highest grade commercially available.

Cells and Cultures

HaCaT were supplied by Prof. Norimichi Nakahata (Graduate School of Pharmaceutical Sciences, Tohoku University, Japan). The cells were cultured in Dulbecco's modified Eagle medium (DMEM) (Sigma, St. Louis, MO, USA), supplemented with 10% fetal bovine serum (FBS) (Dainippon Pharmaceutical, Osaka, Japan), 100 U/mL penicillin, and 100 μg/mL of streptomycin (GIBCO, Milan, Italy) at 37 °C in a humidified atmosphere of 95% air and 5% CO_2.

Preparation of the Experimental Media

SQ-OOH (or γ-T3) was dissolved in ethanol at a concentration of 50 μM. The solution was diluted with DMEM to prepare the experimental medium. The experimental medium contained 0.1% FBS and 0.5–5.0 μM SQ-OOH, either alone or together with 0.1–1.0 μM γ-T3. The concentration of ethanol in the experimental medium was up to 0.1%, which did not affect cell viability. Similarly, media containing only vehicle (0.1% ethanol) or SQ (0.5–5.0 μM) were prepared.

RNA Extraction

HaCaT (1×10^6 cells/60-mm dish) were preincubated in 0.1% FBS/DMEM for 24 h, and then the medium was changed to the experimental medium. After incubation for 3 h, total RNA was isolated with an RNeasy plus Mini kit (Qiagen, Valencia, CA, USA) for the real-time quantitative reverse transcriptase-PCR (RT-PCR) assay. The amount of total RNA was spectrophotometrically determined at 260 and 280 nm. RNA integrity was confirmed by visualizing intact 28S and 18S ribosomal RNA on formaldehyde denaturing agarose gel.

Real-Time RT-PCR Assay

For the real-time RT-PCR assay using a DNA Engine Opticon 2 System (MJ Research, Waltham, MA, USA), cDNA was synthesized from the total RNA using a Ready-To-Go T-Primed First-Strand Kit (Amersham Pharmacia Biotech, NJ, USA). The cDNA was subjected to PCR amplification using a SYBR Premix Ex Taq (Takara Bio, Shiga, Japan) and gene specific primers for IL-1β, IL-6, IL-8, tumor necrosis factor-α (TNF-α), COX-2, and β-actin. Sequences of the PCR primers for each gene are outlined in Table 1. Melt curve analysis was performed following each PCR reaction to confirm the presence of a single reaction product. In addition, representative PCR products were subjected to electrophoresis on a 2.0% agarose gel to verify that a single band was present. The ratio between the mRNA content of β-actin and each gene was defined as the normalization factor.

Cell Viability

Cell viability was evaluated by WST-1 assay [29]. WST-1 is a tetrazolium salt that is converted into a soluble formazan salt by succinate-tetrazolium reductase in the respiratory chain of active mitochondria in proliferating, viable cells. The amount of formazan produced is directly proportional to the number of viable cells. HaCaT (1×10^4 cells/well) were preincubated in 0.1% FBS/DMEM in 96-well plates for 24 h, and then the medium was changed to

Table 1 Primer sequences for cDNA amplification of selected genes

Gene	GenBank accession number	Sequence
IL-1β	NM_000576	Forward 5′-CCAGGGACAGGATATGGAGCA-3′
		Reverse 5′-TTCAACACGCAGGACAGGTACAG-3′
IL-6	NM_000600	Forward 5′-AAGCCAGAGCTGTGCAGATGAGTA-3′
		Reverse 5′-TGTCCTGCAGCCACTGGTTC-3′
IL-8	NM_000584	Forward 5′-ACACTGCGCCAACACAGAAATTA-3′
		Reverse 5′-TTTGCTTGAAGTTTCACTGGCATC-3′
TNF-α	NM_000594	Forward 5′-GACAAGCCTGTAGCCCATGTTGTA-3′
		Reverse 5′-CAGCCTTGGCCCTTGAAGA-3′
COX-2	NM_000963	Forward 5′-TGAGCATCTACGGTTTGCTG-3′
		Reverse 5′-TGCTTGTCTGGAACAACTGC-3′
β-Actin	NM_001101	Forward 5′-TGGCACCCAGCACAATGAA-3′
		Reverse 5′-CTAAGTCATAGTCCGCCTAGAAGCA-3′

the experimental medium. After incubation for 3 and 24 h, 10 μL of WST-1 solution was added to each well and was incubated at 37 °C for 3 h. Cell viability was estimated by measuring the absorbance (450/655 nm) of the medium using a microplate reader (Model 550, Bio-Rad, Tokyo, Japan).

Evaluation of Reactive Oxygen Species

The generation of intracellular reactive oxygen species (ROS) was evaluated using the fluorescent dye 2, 7-dichlorodihydrofluorescein (DCDHF) diacetate (Cayman Chemicals, Ann Arbor, MI, USA) [30]. ROS in cells cause oxidation of DCDHF diacetate, yielding the fluorescent product 2,7-dichlorofluorescein. HaCaT (1×10^4 cells) were preincubated in 0.1% FBS/DMEM in 96-well plates for 24 h, and then the medium was changed to the experimental medium. After incubation for 3 h, the medium was changed to fresh DMEM containing 10 μM DCDHF diacetate, followed by incubation for 30 min. The cells were washed with HBSS, and fluorescence intensity was determined using a GENios Plus Multi-Detection Microplate Reader with enhanced fluorescence (Tecan Inc., Research Triangle Park, NC, Switzerland) at an excitation wavelength of 485 nm and an emission wavelength of 535 nm.

Electrophoretic Mobility Shift Assays

HaCaT (1×10^6 cells/60 mm dish) were preincubated in 0.1% FBS/DMEM for 24 h, and then the medium was replaced with the experimental medium. After 2 h incubation, the nuclear fraction of HaCaT cells was extracted and then applied to an electrophoretic mobility shift assay as described previously [31]. Briefly, the nuclear fraction was incubated with ^{32}P-end-labeled NF-κB oligonucleotides. The DNA-protein complex was separated from the unbound DNA probe in native 6% polyacrylamide gel at 150 V in 0.5% Tris–Boric acid EDTA (TBE) buffer. After electrophoresis, the gels were dried and visualized by autoradiography.

Western Blot Analysis

HaCaT (2×10^6 cells) were preincubated in 0.1% FBS/DMEM for 24 h, and then the medium was changed to the experimental medium. After incubation for 24 h, cellular proteins were prepared from the cells as previously described [32]. The cellular proteins (60 μg/well) were separated by sodium dodecyl sulphate polyacrylamide gel electrophoresis (SDS-PAGE, 4–20% e-PAGEL, Atto, Tokyo, Japan). The protein bands were then transferred to polyvinylidine fluoride membranes (Amersham Pharmacia Biotech). After blocking nonspecific sites, the membrane was probed with primary antibodies, followed by a horseradish peroxidase-conjugated secondary antibody (Cell signaling Technology, Beverly, MA, USA). The detection of antibody reactions was performed with ECL Plus Western blotting reagents (Amersham Pharmacia Biotech). The antibodies used were anti-COX-2 (IBL, Takasaki, Japan), anti-inducible nitric oxide synthase (iNOS, BD Transduction Laboratories, San Diego, CA, USA), and anti-β-actin (Cell signaling Technology). Band intensities were evaluated by densitometry.

Enzyme-Linked Immunosorbent Assay

HaCaT (1×10^4 cells) were preincubated in 0.1% FBS/DMEM for 24 h, and then the medium was changed to the experimental medium. After incubation for 24 h, the conditioned medium was used to measure the levels of prostaglandin E2 (PGE2) using a commercial enzyme-linked immunosorbent assay (ELISA) kit (R&D Systems, Minneapolis, MN, USA), according to the manufacturer's instructions. The results were normalized to the number of cells per well.

Statistical Analysis

The data are expressed as means ± standard deviation (SD). We performed statistical analysis using ANOVA, followed by the Bonferroni/Dunn test for multiple comparisons among several groups. Differences were considered significant at $P < 0.05$.

Results

SQ-OOH Induces Expression of Inflammatory Mediator Genes in HaCaT Keratinocytes

Using the synthetic, purified SQ-OOH (Fig. 1), we observed upregulation of inflammatory mediator genes (IL-1β, IL-6, IL-8, TNF-α, and COX-2) in HaCaT treated with 5.0 μM SQ-OOH as compared to the gene levels of vehicle control or SQ treatment (Fig. 2). In the dose range employed (0.5–5.0 μM SQ-OOH; a range expected to encompass the physiological concentration encountered in human skin [14]), SQ-OOH did not affect cell viability (Fig. 3). Thus, it is conceivable that SQ-OOH at certain concentrations can lead to changes in the expression of HaCaT inflammatory genes (especially, IL-8 and COX-2) without affecting cell viability. Since the upregulation of COX-2 by SQ-OOH had not been previously reported, this was further evaluated in the following study.

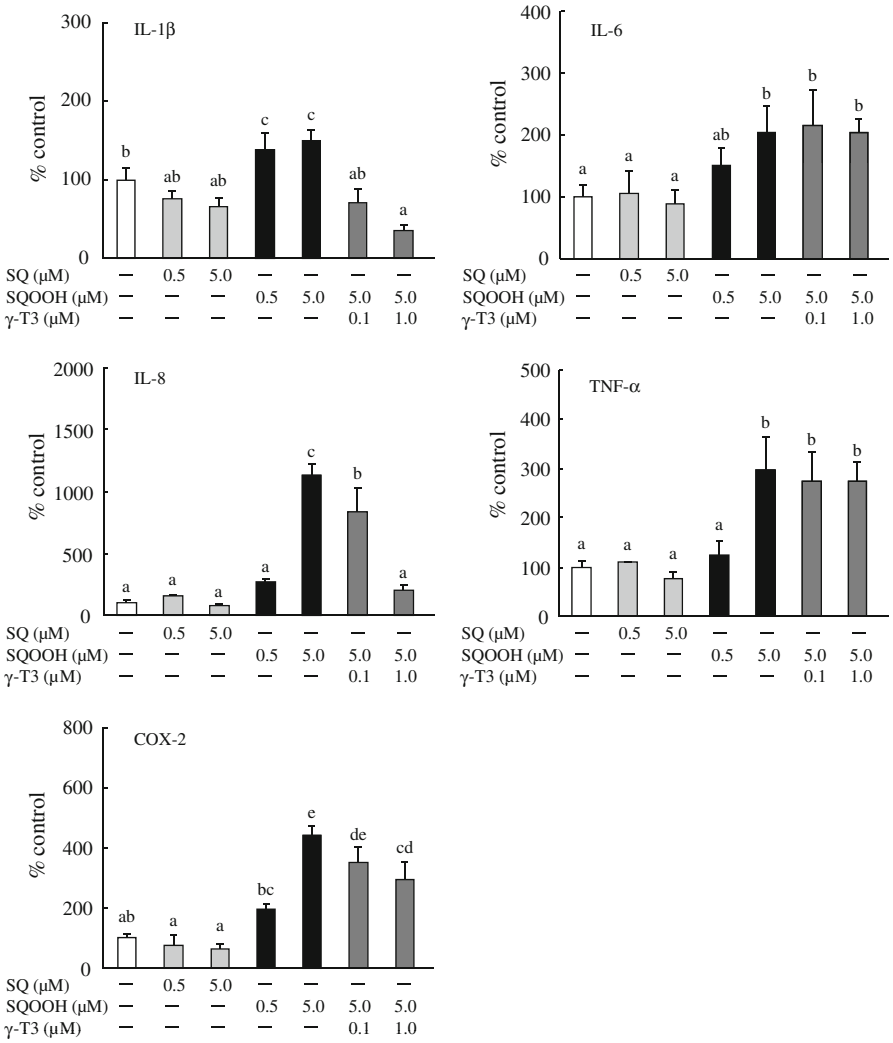

Fig. 2 Effect of SQ-OOH, either alone or with γ-T3, on IL-1β, IL-6, IL-8, TNF-α, and COX-2 mRNA expression in HaCaT cells. Experimental procedures are described in "Materials and methods". Data are expressed as percentages of vehicle (0.1% ethanol) control. Values are means ± SD ($n = 5$–6). Values with different superscripts are significantly different ($P < 0.05$)

COX-2 is Involved in the Inflammatory Effect of SQ-OOH in HaCaT Keratinocytes

In accordance with the upregulation of COX-2 mRNA (Fig. 2), 5.0 μM SQ-OOH enhanced ROS generation, NF-κB activation, COX-2 protein expression, and PGE2 production (Fig. 4). In addition to COX-2, an NF-κB-regulated protein (iNOS) was evaluated, but SQ-OOH had no effect on iNOS (Fig. 4). These results suggest that the pro-inflammatory effect of SQ-OOH is due in part to COX-2 expression through ROS generation and NF-κB activation.

γ-T3 Attenuates Inflammatory Effects of SQ-OOH in HaCaT Keratinocytes

γ-T3 (1.0 μM) attenuated SQ-OOH (5.0 μM) induced ROS generation, NF-κB activation, COX-2 mRNA expression,

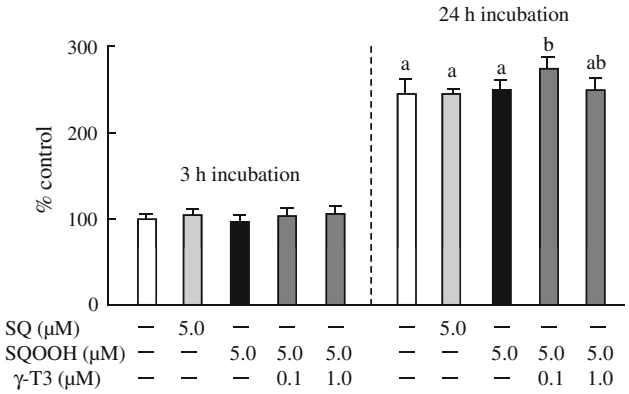

Fig. 3 Effect of SQ-OOH, either alone or with γ-T3, on HaCaT viability. Experimental procedures are described in "Materials and methods". Data are expressed as the percentage of vehicle (0.1% ethanol) control (3 h; 100%). Values are means ± SD ($n = 6$). Values with different superscripts are significantly different ($P < 0.05$)

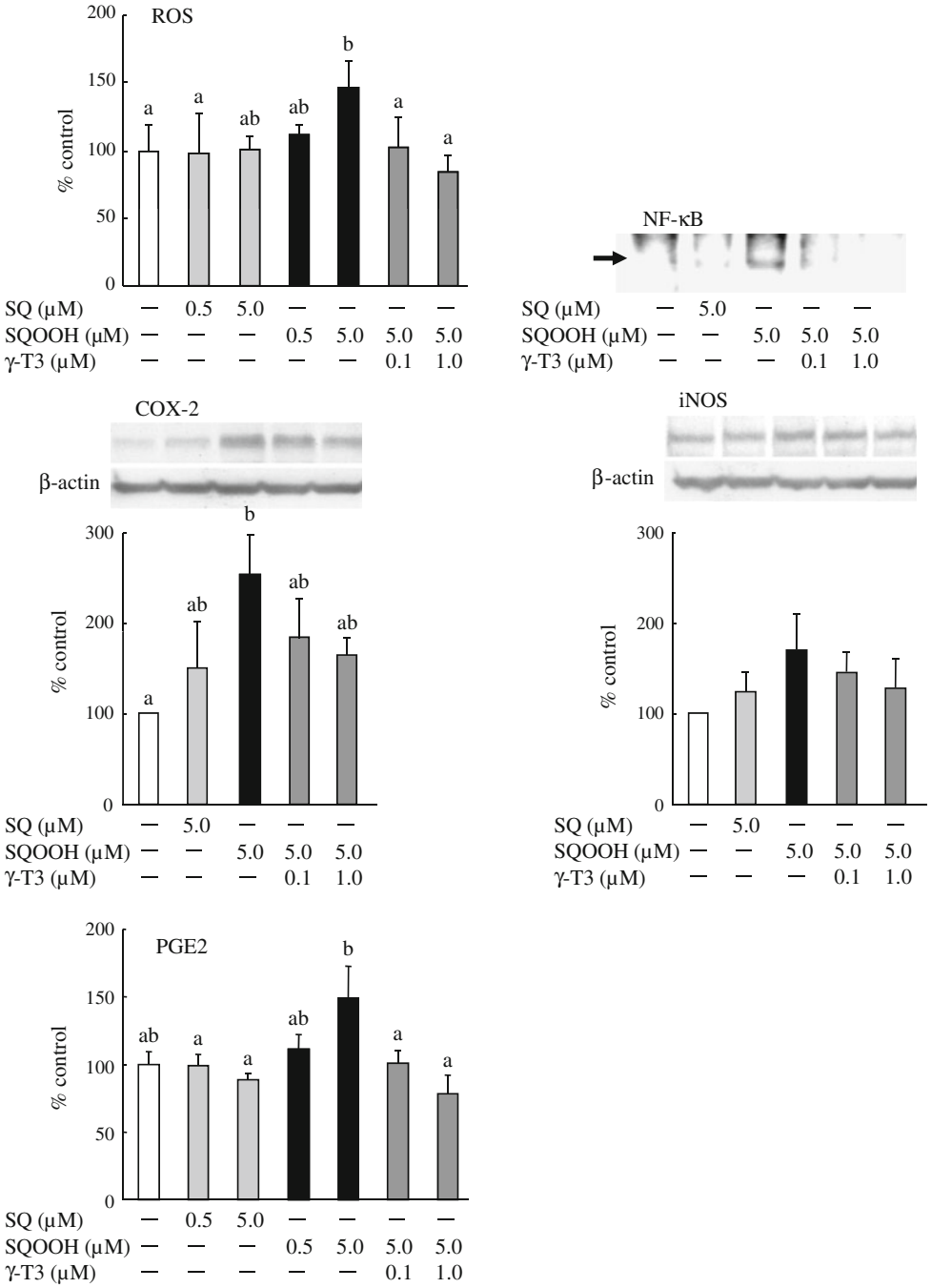

Fig. 4 Effect of SQ-OOH, either alone or with γ-T3, on ROS generation, NF-κB activation, COX-2 and iNOS protein expressions, and PGE2 production in HaCaT cells. Experimental procedures are described in "Materials and methods". Data are expressed as percentage of vehicle (0.1% ethanol) control. Values are means ± SD ($n = 5$–6 for ROS generation, $n = 3$ for NF-κB activation, $n = 3$ for COX-2 and iNOS protein expressions, and $n = 3$–4 for PGE2 secretion). Values with different superscripts are significantly different ($P < 0.05$). Representative examples of data from three replicate experiments are shown for the mobility shift assay and western blot analysis

and PGE2 production nearly to basal levels (Figs. 2, 4). Also, SQ-OOH induced COX-2 protein expression was moderately decreased ($P = 0.09$) by γ-T3 (1.0 μM) treatment. No meaningful differences in cell viability were found between cells treated with SQ-OOH alone or in combination with γ-T3 (Fig. 3). These results suggest a possible anti-inflammatory effect for γ-T3 by its ability to reduce SQ-OOH-induced ROS and inflammatory mediators (i.e., COX-2).

Discussion

Squalene, a component of human sebum normally absent in other primates [33], comprises 11–13% of the total skin surface lipids in human adults, and its highest concentrations are found in the chest and forehead [34, 35]. Because of the high distribution of SQ in skin and its tendency to undergo photooxidation [9–14], there has been interest in possible pathogenic actions of skin SQ-OOH.

In previous studies (mainly in vitro) evaluating potential pathogenic roles for SQ-OOH, researchers prepared SQ-OOH by subjecting SQ to UV exposure or photooxidation [17–21]. Such SQ-OOH preparations often cause excessive SQ peroxidation, yielding unwanted dihydroperoxide, trihydroperoxide, epoxide, ketone, and/or aldehyde products [18]. In many of these cases, the crude (or partly purified) SQ-OOH was subsequently used as a test mixture to evaluate pathogenic actions (e.g., inflammatory effect [21]). Thus, it would be difficult to definitively attribute any observed effects to specifically SQ-OOH. In the present study, SQ was subjected to photooxidation, and the SQ-OOH was chromatographically purified (Fig. 1). The purified SQ-OOH was a mixture of six isomers and did not contain other oxidation products. Since the purified SQ-OOH free from other oxidation products could induce inflammatory responses in HaCaT, SQ-OOH, and not other oxidation products, was deemed to play a principal role in inflammatory skin diseases.

Ottaviani et al. [21] were the first to report IL-6 production in HaCaT treated with SQ-OOH. However, an effect of SQ-OOH on other inflammatory mediators such as COX-2 remained unclear. We therefore aimed to evaluate the effect of SQ-OOH on various inflammatory mediators (IL-1β, IL-6, IL-8, TNF-α, and COX-2). We found that SQ-OOH caused significantly changes in the expression of these inflammatory genes in HaCaT (Fig. 2). Because SQ-OOH appeared to significantly impact the expression of IL-8 and COX-2 (Fig. 2), these two genes may play an important role in keratinocyte inflammation. On the other hand, some studies have shown a toxic effect of SQ-OOH [20, 22], while one study reported a proliferative effect [21]. In this study, no inverse effect of SQ-OOH was observed on cell viability (Fig. 3), which might be a reflection of the relatively low dose of SQ-OOH used (0.5–5.0 μM).

To our knowledge, this is the first report that shows an upregulation of COX-2 mRNA by SQ-OOH. COX-2 is one of the most critical enzymes related to inflammation and is required for the biosynthesis of PGE2 from arachidonic acid [36]. PGE2 induces cutaneous inflammation and modulates cellular immunity, which causes skin diseases such as atopic dermatitis [37]. ROS induce COX-2 expression via activation of the NF-κB signaling pathway [38, 39]. For these reasons, we investigated ROS, NF-κB, COX-2, and PGE2, and found that SQ-OOH induces ROS generation, NF-κB activation, COX-2 protein expression, and PGE2 production (Fig. 4). It is therefore likely that SQ-OOH generates ROS or affects the gene expression concerning ROS production. ROS cause activation of NF-κB, and activated NF-κB induces COX-2 expression, which result in the initiation of inflammatory responses (e.g., PGE2 production) in HaCaT. In summary, the pro-inflammatory effects of SQ-OOH may be due in part to COX-2 expression through ROS generation and NF-κB activation. On the other hand, unlike SQ-OOH, its reduced compound (SQ-OH) as well as other hydroperoxides (e.g., phospholipid hydroperoxides and hydrogen peroxide) (each 5 μM) had little or no effect on COX-2 mRNA expression (data not shown). This data implies that SQ-OOH plays an important role in inflammatory skin conditions.

Our findings (Figs. 2, 4) also suggest SQ-OOH is a potential therapeutic target for inflammatory skin diseases. Because T3 is capable of accumulating in skin and combating oxidative stress from UV or ozone in skin [23, 24, 40], we picked T3 from the array of available anti-oxidant compounds and investigated its possible ameliorative effect on SQ-OOH. T3 has recently received considerable attention for its biological properties [41–44], and we have previously found that T3 suppresses pathological angiogenesis [32, 45], an important stage in the progression of some disorders (i.e., diabetic retinopathy, rheumatoid arthritis, and cancers). In this study, we found that γ-T3 could attenuate SQ-OOH induced ROS generation, NF-κB activation, COX-2 mRNA and protein expressions, and PGE2 production (Figs. 2, 4). These results suggest a possible anti-inflammatory effect for γ-T3 that functions by reducing SQ-OOH-induced ROS and inflammatory mediators (i.e., COX-2). In support of this supposition, a previous study reported the ability of T3 to reduce COX-2 expression [46].

In conclusion, we have shown that SQ-OOH can induce inflammatory responses in HaCaT, which would in part be mediated via COX-2. On the other hand, other studies have mentioned that UV irradiation at the cutaneous surface can be trapped by SQ in the form of peroxidation products [15], and the cutis is not directly damaged by UV irradiation, which suggest that peroxidation of SQ has a functional, protective role against UV irradiation on the cutaneous surface. However, in this study, SQ-OOH acted as an inflammatory stimulus, implying that excessive SQ peroxidation causes inflammatory effects. SQ-OOH could therefore be considered a potential therapeutic target for skin inflammatory disorders. From this perspective, γ-T3 has potential use as a protective agent against skin diseases.

Acknowledgments We thank Prof. Norimichi Nakahata (Graduate School of Pharmaceutical Sciences, Tohoku University, Japan) for the donation of HaCaT, and Dr. Tadashi Uchino (National Institute of Health Sciences, Tokyo, Japan) for excellent technical advice. A part of this study was supported by KAKENHI (20228002 and 22780110) of JSPS, Japan. Financial support was also provided by the Foundation of Oil and Fat Industry Kaikan, Japan.

References

1. Ramasastry P, Downing DT, Pochi PE, Strauss JS (1970) Chemical composition of human skin surface lipids from birth to puberty. J Invest Dermatol 54:139–144

2. Bruls WA, Van Weedlden H, Van der Leun JC (1984) Transmission of UV-radiation through human epidermal layers as a factor influencing the minimal erythema dose. Photochem Photobiol 39:63–67
3. Fujita H, Matsuo I, Okazaki M, Yoshino K, Ohkido M (1986) Chlorpromazine-sensitized photooxidation of squalene. Arch Dermatol Res 278:224–227
4. Miyazawa T, Yasuda K, Fujimoto K, Kaneda T (1988) Presence of phosphatidylcholine hydroperoxide in human plasma. J Biochem 103:744–746
5. Miyazawa T (1989) Determination of phospholipid hydroperoxides in human blood plasma by a chemiluminescence-HPLC assay. Free Radic Biol Med 7:209–217
6. Miyazawa T, Suzuki T, Fujimoto K, Yasuda K (1992) Chemiluminescent simultaneous determination of phosphatidylcholine hydroperoxide and phosphatidylethanolamine hydroperoxide in the liver and brain of the rat. J Lipid Res 33:1051–1059
7. Miyazawa T, Fujimoto K, Suzuki T, Yasuda K (1994) Determination of phospholipid hydroperoxides using luminol chemiluminescence-high-performance liquid chromatography. Methods Enzymol 233:324–332
8. Kinoshita M, Oikawa S, Hayasaka K, Sekikawa A, Nagashima T, Toyota T, Miyazawa T (2000) Age-related increase in plasma phosphatidylcholine hydroperoxide concentrations in normal subjects and patients with hyperlipidemia. Clin Chem 46:822–828
9. Kohno Y, Sakamoto O, Tomita K, Horii I, Miyazawa T (1991) Determination of human skin surface lipid peroxides by chemiluminescence-HPLC. J Jpn Oil Chem Soc 40:715–718
10. Kohno Y, Sakamoto O, Nakamura T, Miyazawa T (1993) Determination of human skin surface lipid peroxides by chemiluminescence-HPLC. II. Detection of squalene hydroperoxide. J Jpn Oil Chem Soc 42:204–209
11. Kohno Y, Takahashi M (1995) Peroxidation in human skin and its prevention. J Jpn Oil Chem Soc 44:10–17
12. Maes D, Mammone T, McKeever MA, Pelle E, Fthenakis C, Declercq L, Giacomoni PU, Marenus K (2000) Noninvasive techniques for measuring oxidation products on the surface of human skin. Methods Enzymol 319:612–622
13. Mudiyanselage SE, Hamburger M, Elsner P, Thiele JJ (2003) Ultraviolet A induces generation of squalene monohydroperoxide isomers in human sebum and skin surface lipids in vitro and in vivo. J Invest Dermatol 120:915–922
14. Nakagawa K, Ibusuki D, Suzuki Y, Yamashita S, Higuchi O, Oikawa S, Miyazawa T (2007) Ion-trap tandem mass spectrometric analysis of squalene monohydroperoxide isomers in sunlight-exposed human skin. J Lipid Res 48:2779–2787
15. Ohsawa K, Watanabe T, Matsukawa R, Yoshimura Y, Imaeda K (1984) The possible role of squalene and its peroxide of the sebum in the occurrence of sunburn and protection from the damage caused by UV irradiation. J Toxicol Sci 9:151–159
16. Saint-Leger D, Baque A, Cohen E, Chivo M (1986) A possible role for squalene in the pathogenesis of acne. II. Br J Derm 114:535–552
17. Picardo M, Zompetta C, De Luca C, Cirone M, Faggioni A, Nazzaro-Porro M, Passi S, Prota G (1991) Role of skin surface lipids in UV-induced epidermal cell changes. Arch Dermatol Res 283:191–197
18. Chiba K, Yoshizawa K, Makino I, Kawakami K, Onoue M (2000) Comedogenicity of squalene monohydroperoxide in the skin after topical application. J Toxicol Sci 25:77–83
19. Chiba K, Yoshizawa K, Makino I, Kawakami K, Onoue M (2001) Changes in the levels of glutathione after cellular and cutaneous damage induced by squalene monohydroperoxide. J Biochem Mol Toxicol 15:150–158
20. Uchino T, Tokunaga H, Onodera H, Ando M (2002) Effect of squalene monohydroperoxide on cytotoxicity and cytokine release in a three-dimensional human skin model and human. Biol Pharm Bull 25:605–610
21. Ottaviani M, Alestas T, Flori E, Mastrofrancesco A, Zouboulis C, Picardo M (2006) Peroxidated squalene induces the production of inflammatory mediators in HaCaT keratinocytes: a possible role in acne vulgaris. J Invest Dermatol 126:2430–2437
22. Uchino T, Kawahara N, Sekita S, Satake M, Saito Y, Tokunaga H, Ando M (2004) Potent protecting effects of Catuaba (*Anemopaegma mirandum*) extracts against hydroperoxide-induced cytotoxicity. Toxicol In Vitro 18:255–263
23. Ikeda S, Niwa T, Yamashita K (2000) Selective uptake of dietary tocotrienols into rat skin. J Nutr Sci Vitaminol (Tokyo) 46:141–143
24. Kawakami Y, Tsuzuki T, Nakagawa K, Miyazawa T (2007) Distribution of tocotrienols in rats fed a rice bran tocotrienol concentrate. Biosci Biotechnol Biochem 71:464–471
25. Miyazawa T, Shibata A, Sookwong P, Kawakami Y, Eitsuka T, Asai A, Oikawa S, Nakagawa K (2009) Antiangiogenic and anticancer potential of unsaturated vitamin E (tocotrienol). J Nutr Biochem 20:79–86
26. Yamada Y, Obayashi M, Ishikawa T, Kiso Y, Ono Y, Yamashita K (2008) Dietary tocotrienol reduces UVB-induced skin damage and sesamin enhances tocotrienol effects in hairless mice. J Nutr Sci Vitaminol (Tokyo) 54:117–123
27. Sookwong P, Nakagawa K, Murata K, Kojima Y, Miyazawa T (2007) Quantitation of tocotrienol and tocopherol in various rice brans. J Agric Food Chem 55:461–466
28. Boukamp P, Petrussevska RT, Breitkreutz D, Hornung J, Markham A, Fusenig NE (1988) Normal keratinization in a spontaneously immortalized aneuploid human keratinocyte cell line. J Cell Biol 106:761–771
29. Ishiyama M, Tominaga H, Shiga M, Sasamoto K, Ohkura Y, Ueno K (1996) A combined assay of cell viability and in vitro cytotoxicity with a highly water-soluble tetrazolium salt, neutral red and crystal violet. Biol Pharm Bull 19:1518–1520
30. Crow JP (1997) Dichlorodihydrofluorescein and dihydrorhodamine 123 are sensitive indicators of peroxynitrite in vivo: implications for intracellular measurement of reactive nitrogen and oxygen species. Nitric Oxide Biol Chem 1:145–157
31. Sung B, Pandey MK, Nakajima Y, Nishida H, Konishi T, Chaturvedi MM, Aggarwal BB (2008) Identification of a novel blocker of IκBα kinase activation that enhances apoptosis and inhibits proliferation and invasion by suppressing nuclear factor-κB. Mol Cancer Ther 7:191–201
32. Nakagawa K, Shibata A, Yamashita S, Tsuzuki T, Kariya J, Oikawa S, Miyazawa T (2007) In vivo angiogenesis is suppressed by unsaturated vitamin E, tocotrienol. J Nutr 137:1938–1943
33. De Luca C, Fanfoni GB, Picardo M, Nazzaro-Porro M, Passi S (1989) The skin surface lipids of man compared with those of other different primates. J Invest Dermatol 92:473
34. Nazzaro-Porro M, Passi S, Boniforti L, Belsito F (1979) Effects of aging on fatty acids in skin surface lipids. J Invest Dermatol 73:112–121
35. Nicolaides N (1976) Skin lipids: the biochemical uniqueness. Science 186:19–23
36. Black AT, Gray JP, Shakarjian MP, Mishin V, Laskin DL, Heck DE, Laskin JD (2008) UVB light upregulates prostaglandin synthases and prostaglandin receptors in mouse keratinocytes. Toxicol Appl Pharmacol 232:14–24
37. Fogh K, Herlin T, Kragballe K (1989) Eicosanoids in skin of patients with atopic dermatitis: prostaglandin E2 and leukotriene B4 are present in biologically active concentrations. J Allergy Clin Immunol 83:450–455
38. Vega A, Chacón P, Alba G, El Bekay R, Martín-Nieto J, Sobrino F (2006) Modulation of IgE-dependent COX-2 gene expression by reactive oxygen species in human neutrophils. J Leukoc Biol 80:152–163

39. Piette J, Piret B, Bonizzi G, Schoonbroodt S, Merville MP, Legrand-Poels S, Bours V (1997) Multiple redox regulation in NF-κB transcription factor activation. Biol Chem 378:1237–1245
40. Packer L, Weber SU, Rimbach G (2001) Molecular aspects of α-tocotrienol antioxidant action and cell signalling. J Nutr 131: 369–373
41. Serbinova E, Kagan V, Han D, Packer L (1991) Free radical recycling and intramembrane mobility in the antioxidant properties of α-tocopherol and α-tocotrienol. Free Radic Biol Med 10:263–275
42. Qureshi AA, Sami SA, Salser WA, Khan FA (2002) Dose-dependent suppression of serum cholesterol by tocotrienol-rich fraction (TRF25) of rice bran in hypercholesterolemic human. Atherosclerosis 161:199–207
43. Hiura Y, Tachibana H, Arakawa R, Aoyama N, Okabe M, Sakai M, Yamada K (2009) Specific accumulation of γ- and δ-tocotrienols in tumor and their antitumor effect in vivo. J Nutr Biochem 20:607–613
44. Khanna S, Roy S, Slivka A, Craft TKS, Chaki S, Rink C, Notestine MA, DeVries AC, Parinandi NL, Sen CK (2005) Neuroprotective properties of the natural vitamin E α-tocotrienol. Stroke 36:2258–2264
45. Shibata A, Nakagawa K, Sookwong P, Tsuzuki T, Oikawa S, Miyazawa T (2008) Tumor anti-angiogenic effect and mechanism of action of δ-tocotrienol. Biochem Pharmacol 76:330–339
46. Wu SJ, Liu PL, Ng LT (2008) Tocotrienol-rich fraction of palm oil exhibits anti-inflammatory property by suppressing the expression of inflammatory mediators in human monocytic cells. Mol Nutr Food Res 52:921–929

Lipids (2010) 45:843–854
DOI 10.1007/s11745-010-3455-7

ORIGINAL ARTICLE

Potential of Magnetic Resonance Spectroscopy in Assessing the Effect of Fatty Acids on Inflammatory Bowel Disease in an Animal Model

Sonal Varma · Michael N. A. Eskin · Ranjana Bird · Brion Dolenko · Jayadev Raju · Omkar B. Ijare · Tedros Bezabeh

Received: 25 January 2010 / Accepted: 29 July 2010 / Published online: 19 August 2010

Abstract People with inflammatory bowel disease (IBD) are at risk for developing colorectal cancer, and this risk increases at a rate of 1% per year after 8–10 years of having the disease. Saturated and ω-6 polyunsaturated fatty acids (PUFAs) have been implicated in its causation. Conversely, ω-3 PUFAs may have the potential to confer therapeutic benefit. Since proton magnetic resonance spectroscopy (^{1}H MRS) combined with pattern recognition methods could be a valuable adjunct to histology, the objective of this study was to analyze the potential of ^{1}H MRS in assessing the effect of dietary fatty acids on colonic inflammation. Forty male Sprague-Dawley rats were administered one of the following dietary regimens for 2 weeks: low-fat corn oil (ω-6), high-fat corn oil (ω-6), high-fat flaxseed oil (ω-3) or high-fat beef tallow (saturated fatty acids). Half of the animals were fed 2% carrageenan to induce colonic inflammation similar to IBD. ^{1}H MRS and histology were performed on ex vivo colonic samples, and the ^{1}H MR spectra were analyzed using a statistical classification strategy (SCS). The histological and/or MRS studies revealed that different dietary fatty acids modulate colonic inflammation differently, with high-fat corn oil being the most inflammatory and high-fat flaxseed oil the least inflammatory. ^{1}H MRS is capable of identifying the biochemical changes in the colonic tissue as a result of inflammation, and when combined with SCS, this technique accurately differentiated the inflamed colonic mucosa based on the severity of the inflammation. This indicates that MRS could serve as a valuable adjunct to histology in accurately assessing colonic inflammation. Our data also suggest that both the type and the amount of fatty acids in the diet are critical in modulating IBD.

Keywords Beef tallow · Corn oil · Flaxseed oil · Inflammatory bowel disease · Proton magnetic resonance spectroscopy · Statistical classification strategy

Abbreviations

FID	Free induction decay
GA_ORS	Genetic-algorithm-based optimal region selection
GC	Gas chromatography
H&E	Hematoxylin and eosin
HFB	High-fat beef tallow
HFC	High-fat corn oil
HFF	High-fat flaxseed oil
HPLC	High-performance liquid chromatography
HR MAS	High-resolution magic angle spinning
IBD	Inflammatory bowel disease
LDA	Linear discriminant analysis
LFC	Low-fat corn oil

S. Varma · B. Dolenko · O. B. Ijare · T. Bezabeh (✉)
National Research Council Institute for Biodiagnostics,
435 Ellice Ave., Winnipeg, MB R3B 1Y6, Canada
e-mail: tedros.bezabeh@nrc-cnrc.gc.ca

S. Varma · M. N. A. Eskin · T. Bezabeh
Department of Human Nutritional Sciences,
University of Manitoba, Winnipeg, MB, Canada

R. Bird
Department of Biological Sciences,
University of Windsor, Windsor, ON, Canada

J. Raju
Department of Biology, University of Waterloo,
Waterloo, ON, Canada

Present Address:
S. Varma
Department of Pathology and Molecular Medicine,
Queen's University, Kingston, ON, Canada

LT	Leukotriene
MRS	Magnetic resonance spectroscopy
PAF	Platelet activating factor
PBS/D_2O	Phosphate-buffered saline in deuterium oxide
PUFA	Polyunsaturated fatty acids
SCS	Statistical classification strategy
TSP	3-Trimethylsilylpropionic acid-d_4 sodium salt

List of symbols

Gamma	γ
Omega	ω
Proton	^{1}H

Introduction

Inflammatory bowel disease (IBD) is a very common condition in industrialized countries, including North America. It is estimated that about 1.4 million people in the US and 2.2 million people in Europe suffer from IBD [1]. The exact cause and pathogenesis of IBD are not known; however, the interplay of genetic, environmental and immune factors is considered to be involved in its causation. Many epidemiological and experimental studies have pointed out that there is a strong connection between diet and IBD. A diet that is particularly rich in ω-6 fatty acids and saturated fats is one of the major environmental factors implicated in the etiology of IBD [2]. Conversely, ω-3 polyunsaturated fatty acids (PUFAs) have been considered to be partially agonistic compared to ω-6 PUFAs and may confer therapeutic benefit in IBD [3, 4]. IBD is not a point event; it is a continuum of a disease process with remitting and relapsing course. People with long-standing IBD have a significant risk of developing colorectal cancer, and this risk increases at the rate of 1% per year after 8–10 years of the disease [5]. As such, early diagnosis and intervention can help prevent the progression of IBD to colon cancer. Currently, the data from experimental or randomized trials on the benefits of pharmacologic or dietary intervention on this window between IBD and colon cancer are very limited.

Presently, colonoscopy with biopsy of grossly inflamed and random parts of the colon is the gold standard for diagnosing IBD. However, it is known that in the diseased state, biochemical and physiological changes precede the histological manifestations of the disease, and as such, the technique exploiting metabolic abnormalities may be suitable to aid in early diagnosis. One such technique that can provide extensive biochemical information from tissue samples is proton magnetic resonance spectroscopy (^{1}H MRS) [6, 7]. MRS makes use of magnetic properties of atomic nuclei and provides information about the molecular structures of biochemicals/biomolecules. It is non-destructive, quantitative and highly reproducible. It has been utilized in lipid analysis of intact tissues and their aqueous/organic extracts as well as dietary fats due to its unique advantage in differentiating various lipid classes without the need for any chemical modification [8–11]. It has been used as an alternative to conventional techniques such as gas chromatography (GC) and/or high-performance liquid chromatography (HPLC) for the analysis of lipids from various biological specimens and dietary fats [8, 11]. It has been shown that the accuracy of MRS-based lipid analysis is comparable to that of GC and/or HPLC [9]. Although recent developments in MRS technology, such as high-resolution magic angle spinning (HR MAS), have greatly simplified the spectral data obtained from tissues/biopsied samples, the spectra are still very complex and require specialized methods for thorough data analysis [12]. The pattern recognition methods have proven to be valuable in the classification of biomedical data. These methods are being used in discriminating data obtained from humans and laboratory animals in pathologic and healthy states and have shown diagnostic value [13, 14]. In this study, we are using a statistical classification strategy (SCS)—a pattern recognition methodology developed in-house—for the data analysis. SCS methodology has been used for the classification of MRS data in biomedical applications [15, 16]. The study is based on the hypothesis that various dietary fatty acids modulate colonic inflammation differently and that ^{1}H MRS combined with SCS methodology has the potential to detect changes in the colonic metabolite profile induced by these dietary fatty acids.

Materials and Methods

Forty 3–4-week-old male Sprague-Dawley rats (Charles River, Canada) were used for this study. The rats were kept on a basic laboratory chow for 2 weeks before starting the study. For the 2-week duration of the study, the animals were divided into two major groups with 20 animals in each group. The animals in both groups were further divided into four subgroups (five animals in each subgroup) depending upon the composition of fatty acids in their diet. Low-fat corn oil (LFC) subgroup animals received an AIN 76A diet containing 5% corn oil; the high-fat corn oil (HFC) subgroup received 23% corn oil; the high-fat flaxseed oil (HFF) subgroup animals received 14% corn oil with 9% flaxseed oil; the high-fat beef tallow (HFB) subgroup received 5% corn oil with 18% beef tallow. The detailed composition of the diet mixture for each subgroup is provided in Table 1. The amount of cellulose (as Cellufil), vitamin mix, mineral mix and casein in the diet was adjusted to ensure that animals were fed isocaloric diets. In addition, all the animals in group 1 were fed with 2%

Table 1 Detailed composition of the diets fed to animals in each group (g/kg of the diet)

Ingredients	LFC	HFC	HFF	HFB
Corn starch	520	337.5	337.5	337.5
Casein	200	230	230	230
Dextrose	130	85.2	85.2	85.2
Cellufil	50	59	59	59
AIN-76 mineral mix	35	41.1	41.1	41.1
AIN-76 vitamin mix	10	11.3	11.3	11.3
Methionine	3	3	3	3
Choline bitartarate	2	2.4	2.4	2.4
Corn oil	50	230	140	50
Flaxseed oil	0	0	90	0
Beef tallow	0	0	0	180

LFC low-fat corn oil, *HFC* high-fat corn oil, *HFF* high-fat flaxseed oil, *HFB* high-fat beef tallow

carrageenan in their diet for the entire 2-week period of the study. Carrageenan is an extract of red seaweed and has been shown to cause colon-specific inflammation. The animals in group 2, however, were not fed with carrageenan. The grouping of animals is schematically depicted in Fig. 1. Table 2 lists the detailed percent fatty acid composition of the different diet groups.

All the animal housing, specialized feeding and sample collection procedures were undertaken at the animal facility in the Department of Biology, University of Waterloo. At the end of 2 weeks, the animals were euthanized using the CO_2 asphyxiation method. This project was approved by the animal care committee at the Institute for Biodiagnostics, National Research Council of Canada and the University of Waterloo. The colon of each animal was excised after euthanizing the animal. The mucosal layer of the colon was scraped off using a glass slide by the method previously described by Briere et al. [17]. The mucosal samples were coded and stored in cryovials containing phosphate-buffered saline in deuterium oxide (PBS/D_2O) medium at −70°C. These coded cryovials were shipped on dry ice to the National Research Council of Canada, Winnipeg, for MRS and histological assessment.

^{1}H MRS Analysis

One-Dimensional Experiments

For ^{1}H MRS experiments, the samples were thawed and cut into 5–7-mm-long pieces along the longitudinal axis of the colon. This yielded 18–20 samples from each animal. ^{1}H MRS was conducted on alternate samples from each animal. Thus, a total of 119 spectra from group 1 and 127 spectra from group 2 were generated for our study. Each piece from the colon was counted as an independent observation for both MR analysis and histology. This was done as it is known that IBD can be very focal and does not involve all the parts of the colon in a consistent manner. This holds true in the clinical setting too as not all of the biopsies taken during a single colonoscopy at a single point of time show IBD-related changes. As we were comparing MR spectra from each piece with the histology of that piece, we found it more appropriate to compare the pieces as separate samples rather than group them together per animal.

The sample preparation technique used for conducting ^{1}H MRS was similar to the technique described by Kuesel et al. [18]. Briefly, the colon sample was placed in a glass

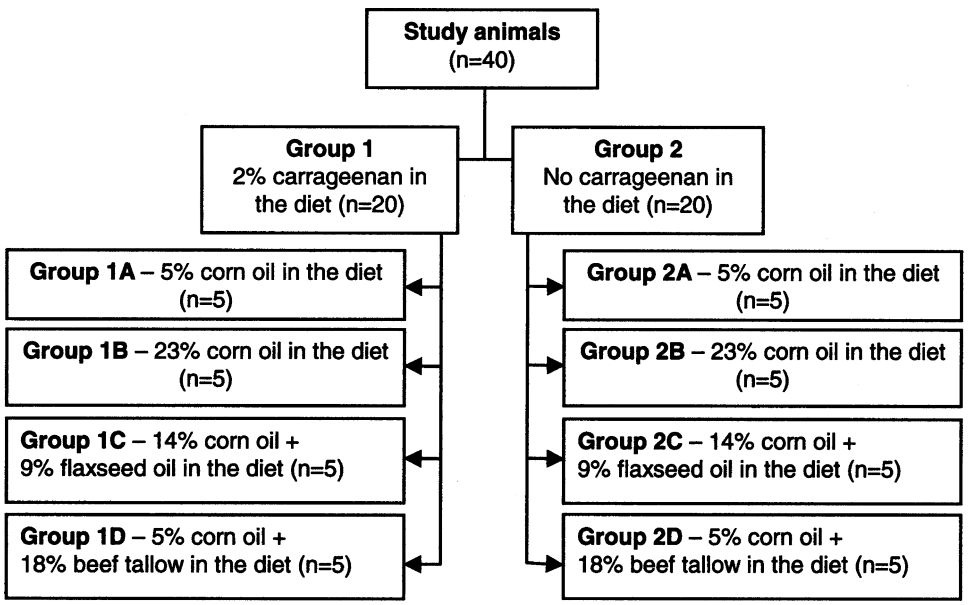

Fig. 1 Schematic diagram showing the grouping of the animals into various study groups

Table 2 Fatty acid composition of low-/high-fat corn oil, high-fat flaxseed oil and high-fat beef tallow diets (expressed as % weight of the total fat content)

Fatty acids	LFC/HFC	HFF	HFB
C 10:0			0.066
C 12:0			0.067
C 14:0	0.041	0.044	1.882
C 14:1			0.268
C 15:0		0.02	0.292
C 16:0	10.817	8.482	21.830
C 16:1	0.111	0.091	1.833
C 17:0	0.084	0.082	0.945
C 18:0	1.872	2.693	16.995
C 18:1ω9	29.131	25.295	34.182
C 18:1ω11	0.584	0.577	1.420
C 18:2ω6	55.282	39.259	18.343
C 18:3ω6			0.029
C 18:3ω3	0.958	22.401	
C 20:0	0.491	0.434	0.336
C 20:1	0.278	0.240	
C 20:2	0.039	0.036	0.177
C 20:3ω4			0.067
C 20:3ω3		0.026	0.028
C 20:4			0.105
C 22:0	0.165	0.152	0.075
C 22:4			0.057
C 22:5			0.050
C 22:6			
C 24:0	0.199	0.163	0.505

Abbreviations are the same as in Table 1

capillary tube filled with PBS/D_2O with one end plugged. This capillary was inserted into the NMR tube containing 300 µl of PBS/D_2O solution along with 5 µl of chemical shift reference, 3-trimethylsilylpropionic acid-d_4 sodium salt (TSP). ^{1}H MRS was conducted on these samples using a Bruker Avance 360 MHz spectrometer at 25°C with presaturation of the water signal. The acquisition parameters included: 90° pulse at 9.30 µs, number of scans = 256, spectral width = 4,990.02 Hz, relaxation delay = 3 s and time domain data points = 8 k. The samples were fixed in 10% neutral buffered formalin immediately after ^{1}H MRS experiments for histological assessment. Since the experimental time was only ~16 min, and the spectra were recorded without sample spinning, any mechanical damage to the tissue should be precluded.

Two-Dimensional MRS Experiments

^{1}H-^{1}H correlated spectroscopy (COSY) experiments using gradient pulses were performed on representative colon mucosal samples to unambiguously identify the metabolites whose signals were overlapping in one-dimensional (1D) spectra or were present at very low concentration. The acquisition parameters used were: spectral width = 4,990.02 Hz in both dimensions; time domain data points = 2,048; number of free induction decays (FIDs) with t_1 increments = 256; relaxation delay = 1 s and number of transients = 128. The resulting data were zero filled to 1,024 points in the t_1 dimension and Fourier transformed along both dimensions after multiplying the data by sine-bell window function shifted by $\pi/_2$.

Gas Chromatography

Fatty acid composition of dietary fats used in this study was analyzed by GC following the method described in AOCS-Official methods and protocols [19]. In brief, samples of all dietary groups underwent fat extraction/evaporation cycles using a mixture (1:1, v/v) of HPLC grade chloroform and methanol (Fisher Scientific Limited, Nepean, ON, Canada). Total amount of fat extracted from each dietary lipid was weighed before GC analysis. To 50 µl of extracted fat, 1 µl isooctane containing an exact amount of internal standard (C17: 1) and 12 ml 2% H_2SO_4 in methanol were added. The resulting mixture was heated with vortex for 2 h at 65–70°C to obtain a monophase system. After cooling to room temperature, 6 ml isooctane and 6 ml distilled water were added, stirred and allowed to stand. One milliliter of the upper clear layer of the esterified sample was subjected to automated GC analysis. In addition to the internal standard, we also ran a mixture of standard fatty acid methyl esters (Sigma Chemicals Co., St. Louis, MO) to ensure that the fatty acids are identified appropriately. The contribution of individual fatty acids to the dietary fat was calculated with reference to the internal standard.

Histology

Histology was performed on representative animals from both groups 1 and 2, using the same tissue used for the MRS experiment. Each sample was coded to avoid analysis bias, fixed in 10% neutral buffered formalin and finally embedded into paraffin blocks. The paraffin blocks were cut into 5-µm-thin sections and collected on coated glass slides. The sections were stained with hematoxylin and eosin (H&E) stain and examined at 60× magnification under a light microscope. Cellularity, crypt architecture and fibrosis were the broad criteria used for grading inflammation in the samples. Predominantly, the density of lymphocytes (represented by an arrow in Fig. 3) within the surface epithelium, lamina propria and invasion within the crypt epithelium were considered when assessing increased

cellularity. Destruction of crypt architecture (represented by a star in Fig. 3) by inflammatory cells and formation of crypt abscess were assessed under architecture. Fibrosis (represented by an arrowhead in Fig. 3) denoting chronicity of the inflammatory process was also assessed. When assessing each sample, these criteria were independently assigned mild, moderate or severe grade, and then a compiled composite score was given to the sample. The degree of inflammation was graded based on the proportion of the total sample inflamed. If 30% or less of the total section was inflamed, it was graded as mild. Sections having 30–60% inflammation were graded as moderate, and those with over 60% inflamed area were graded as having severe inflammation.

Statistical Classification Strategy

The statistical classification strategy (SCS) [16] is comprised of several stages, and depending on the data, some or all of the stages may be invoked. We employed the following stages:

Preprocessing

All spectra were subjected to normalization (scaling to unit area), smoothing and peak alignment (with respect to the external reference, TSP). This step also involves transformations (e.g., forming derivatives or ranking the spectral intensities). Only the subregion 0.5–4.5 ppm (1,184 data points) was used for SCS analysis. This region was selected to avoid artifacts due to the residual water signal at 4.7 ppm and also the external reference (TSP) peak at 0 ppm. Finally, the resultant 1,184-point spectra were rank-ordered to eliminate baseline differences between the spectra (The actual intensity values were replaced by their ranks to eliminate or reduce the influence of excessively large resonance intensities.)

Feature Selection/Extraction

The feature selection/extraction is a genetic-algorithm-based optimal region selection algorithm (GA_ORS) that involves the reduction of feature space dimension but retains the spectral identity [16]. A small number of discriminatory subregions are selected from the spectra in which adjacent spectral intensities are averaged. In an extension of the feature selection method, the data are split randomly into a number (N, e.g., $N = 50$) of training-test set pairs; one half of the split is for the training set, the other half the test set. For each split, a set of features is determined using a simple classifier, in this case linear discriminant analysis (LDA). This process produces N feature sets (generally different), and a histogram is constructed of feature selection frequency. The features most frequently selected are the eventual inputs for the final classifier. This stage is essential for reliable classifier development. Subregions identified in this study have been listed in Tables 3 and 4 for groups 1 and 2 (with and without carrageenan treatment).

Classifier Generation

In this step, the subregions determined by histogramming form the feature set that is submitted to the ultimate classifier, also an LDA classifier. The classifier's coefficients are obtained by our bootstrap-inspired approach. This involves splitting the data randomly 5–10,000 times into training and test sets, determining the individual coefficients for LDA and using these to test the corresponding test sets. A weighted average of the above coefficients is taken, and weights are determined by the classifier's performances on the test sets.

Results

Figure 2 shows the two-dimensional (2D) ^{1}H-^{1}H COSY spectrum of a typical colonic mucosa showing assignments for various metabolites. ^{1}H MR spectrum of the same sample is shown above the 2D plot. These assignments were also compared with those from recent reports [12, 20]. Owing to an extensive broadening of the lipid signals, the chemical shift region 2.70–2.90 ppm representing diallylic methylene protons [–CH=CH–(C**H**$_2$–CH=CH)$_n$–] was not well resolved. This obviates the identification of individual PUFAs present in the colonic mucosa. Similar observations were made in recent studies despite the use of advanced NMR techniques such as HR MAS [12, 20]. In addition to the lipid components, we have also detected choline-containing phospholipids such as phosphatidylcholine and other small molecules such as creatine, leucine, valine, lysine, alanine, threonine, aspartate, glutamine, glutamate, ethanolamine, uracil, tyrosine and phenylalanine.

SCS methodology was applied to the spectra obtained from colonic mucosa in three stages of the study. In the first stage, all the specialized dietary subgroups were compared with the LFC fed subgroup. The results of the first stage of SCS analysis from group 1 (treated with 2% carrageenan) and group 2 (not treated with carrageenan) are shown in Table 3. In group 1, the classifier assigned the spectra to their respective groups with high accuracy ranging from about 91–100%. The lowest accuracy of 91% was seen for the comparison between the LFC- and the HFB-fed subgroups. In this comparison, 4 out of 32 spectra from the LFC subgroup were misclassified, and 2 out of 34

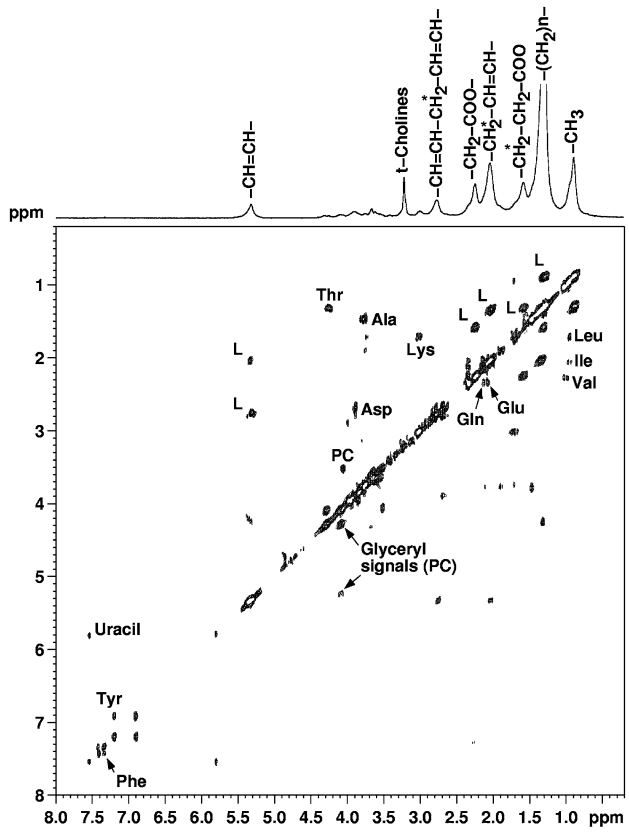

Fig. 2 Two-dimensional ^{1}H-^{1}H COSY spectrum (360 MHz, 25°C) of a typical colonic mucosa with labeling of various fatty acid signals along with other predominant biochemicals. Corresponding 1D ^{1}H spectrum is shown on the top of the 2D spectrum with assignments of lipid signals. Abbreviations: *L* lipid, *Leu* leucine, *Ile* isoleucine, *Val* valine, *Lys* lysine, *Glu* glutamate, *Gln* glutamine, *Ala* alanine, *Asp* aspartate, *Thr* threonine, *Tyr* tyrosine, *Phe* phenylalanine, *PC* phosphatidylcholine

spectra from the HFB subgroup were misclassified. The spectral subregions identified by SCS as being discriminatory are listed in Table 3. These regions could be attributed to the resonances due to the protons of the fatty acyl chain, creatine, leucine/isoleucine, valine and glyceryl protons of phospholipids. Similar observations were made for group 2 (see Table 3). The classification accuracy was very high, ranging from 96 to 100%. A major difference observed between the two groups was that creatine signals were found to be discriminatory in the classification of LFC and HFB in group 2, whereas glyceryl signals of phospholipids were found to be discriminatory in group 1 (for detailed assignments, see Table 3). The first stage of SCS analysis from group 1 and group 2 shows that dietary fat causes enough differences in the metabolite profile of rat colon that it can be discerned by SCS methodology. The results hold true when there is no extrinsic inflammatory agent and even when there is carrageenan-induced colonic inflammation. These differences could be due to difference in the amount of fatty acids, type of fatty acid or extent of inflammation within these groups. Therefore, the first stage of SCS analysis was followed by a second stage to assess if ^{1}H MRS could identify the differences between the effects of various dietary fats containing different fatty acids when keeping the total fat content in each dietary group constant.

In the second stage, the three specialized diet groups were compared against each other. All the animals in these three groups received 23% fat by weight in their diets; however, the type of fatty acid differed. The results of the second stage of SCS analysis of samples from groups 1 and 2 are shown in Table 4. ^{1}H MRS combined with SCS analysis depicted an accuracy of 98–100% in classifying

Table 3 SCS analysis of low-fat corn oil group vs. each dietary subgroup in groups 1 ($N = 127$) and 2 ($N = 119$)

Group 1*					Group 2			
Class	*N*	Accuracy (%)	Regions (ppm)	Metabolites	*N*	Accuracy (%)	Regions (ppm)	Metabolites
LFC	32	100	2.68–2.86	=HC–C**H**$_2$–CH=	24	96.6	2.69–2.79	=HC–C**H**$_2$–CH=
			1.95–2.0	–**H**$_2$C–CH=CH–			2.05–2.11	–**H**$_2$C–CH=CH–
HFC	31		1.59–1.61	–C**H**$_2$–CH$_2$–COO–	35		1.35–1.4	(–C**H**$_2$–) chain
			1.12–1.19	Leucine/isoleucine, valine			1.1–1.22	Leucine/isoleucine, valine
LFC	32	98.4	3.02–3.05	Creatine	24	98.2	3.0–3.08	Creatine
			2.78–2.95	=HC–C**H**$_2$–CH=			2.69–2.83	=HC–C**H**$_2$–CH=
HFF	30		2.66–2.88	=HC–C**H**$_2$–CH=	32		1.15–1.22	Leucine/isoleucine, valine
							0.87–0.94	–C**H**$_3$
LFC	32	90.9	3.75–3.80	Glyceryl moiety	24	100	3.0–3.05	Creatine
			2.66–2.68	=HC–C**H**$_2$–CH=			2.76–2.9	=HC–C**H**$_2$–CH=
HFB	34		2.20–2.27	–CH$_2$–C**H**$_2$–COO–	28		2.04–2.08	–**H**$_2$C–CH=CH–

* In group 1, all animals were treated with 2% carrageenan to induce IBD; abbreviations are the same as in Table 1

Table 4 SCS analysis of different dietary subgroups in groups 1 and 2 to assess the differences between individual dietary subgroups

Group 1*					Group 2			
Class	*N*	Accuracy (%)	Regions (ppm)	Metabolites	*N*	Accuracy (%)	Regions (ppm)	Metabolites
HFC	31	98.4	4.18–4.29	Glyceryl moiety	35	97.0	2.90–3.10	Creatine
			3.20–3.24	Total cholines			2.58–2.78	=HC–**H**$_2$C–HC=
HFF	30		2.75–2.79	=HC–**H**$_2$C–HC=	32		1.95–1.98	–**H**$_2$C–HC=CH–
			1.49–1.54	–**H**$_2$C–H$_2$C–COO–			0.94–0.98	–C**H**$_3$
HFC	31	100	3.73–3.80	Glutamic acid	35	98.4	2.99–3.04	Creatine
			2.58–2.71	=HC–**H**$_2$C–HC=			2.69–2.77	=HC–**H**$_2$C–CH=
HFB	34		1.79-1.82	Unassigned	28		1.94-2.00	–**H**$_2$C–CH=CH–
HFF	30	100	3.28	Glycerophosphoethanolamine	32	100	2.88-3.05	Creatine
			2.79–2.98	=HC–**H**$_2$C–HC=			2.57–2.68	=HC–**H**$_2$C–HC=
HFB	34		2.31–2.35	Glutamic acid	28		1.59–1.61	–**H**$_2$C–H$_2$C–COO–

* In group 1, all animals were treated with 2% carrageenan to induce IBD; abbreviations are the same as in Table 1

the spectra to their respective groups. In addition to the regions identified during comparison of each group to the LFC group, resonances due to glutamic acid, total cholines and glycerophosphoethanolamine were also ascribed to be discriminatory in this analysis. In the second stage of group 2 analysis, ^{1}H MRS with SCS attained an accuracy of 97% in differentiating HFC from HFF, 98.4% between HFC and HFB, and 100% between HFB and HFF subgroups.

These results indicate that ^{1}H MRS can detect subtle differences in the metabolite profile of colon when the animals receive the same amount but different types of fats. The stage 1 analyses showed that MRS combined with SCS can detect differences between the LFC subgroup and HFC, HFF and/or HFB subgroups. The combination of these two results shows that ^{1}H MRS can detect differences in the colon caused not only by different amounts but also different types of fatty acids. The metabolites found to be discriminatory in the SCS analysis included creatine, glyceryl signals of glycerophospholipids, glycerophosphoethanolamine, glutamic acid, total cholines and signals from fatty acyl chains, particularly, the allylic/diallylic methylene protons (–**H**$_2$C–CH=CH–/–CH=HC–C**H**$_2$–CH=CH–) including (–C**H**$_2$–) chain, terminal –C**H**$_3$, and –C**H**$_2$–CH$_2$–COO– groups. It is worthwhile to note that the diallylic methylene protons (–CH=CH–C**H**$_2$-CH=CH–) are the predominant entities responsible for the classification of different dietary PUFAs in both groups 1 and 2. Metabolites resonating in the region 1.10–1.22 ppm could be assigned to the amino acids leucine/isoleucine and valine.

Having established that both the amount and type of dietary fat caused enough differences in the fatty acid profile of the rat colon and that ^{1}H MRS can accurately detect these changes, we proceeded to the third stage of analysis. The goal of this stage of analysis was to assess the accuracy of ^{1}H MRS in detecting changes in the metabolite profiles of the rat colons predominantly due to inflammation. For this, each subgroup in group 1 was compared to the corresponding subgroup in group 2 of our study. As shown in Table 5, the SCS analysis was highly accurate in classifying the spectra from each subgroup in group 1 versus the corresponding subgroup in group 2. SCS identified resonances due to total cholines, creatine, valine, leucine, phosphatidylcholine, and methyl and diallylic methylene protons of the fatty acid chain as discriminatory.

Table 5 Results of comparative SCS analysis between group 1 and group 2

Class	Accuracy (%)	Regions (ppm)	Metabolites
LFC	100	4.18–4.23	Phosphatidylcholine (–O–C**H**$_2$–)
		3.64–3.67	Phosphatidylcholine (–N–C**H**$_2$–)
		0.89–0.93	–C**H**$_3$
HFC	97.0	2.85–2.93	=HC–C**H**$_2$–CH=
		2.63–2.67	=HC–C**H**$_2$–CH=
		1.21–1.25	–Leucine/isoleucine/valine
HFF	100	3.20–3.24	Total cholines
		0.87–0.93	–C**H**$_3$
HFB	100	3.22–3.24	Total cholines
		2.95–3.04	Creatine
		0.85–0.92	–C**H**$_3$

Abbreviations are the same as in Table 1

The representative sections of H&E-stained samples from each group are shown in Fig. 3. Details of the criteria used to grade inflammation have been described in the Methods section. In group 1, sections from 21 out of 23 samples analyzed from the HFF subgroup were either not inflamed or had very mild inflammation. Similarly, out of 21 samples from the LFC subgroup, only 1 sample had

severe inflammation. On the other hand, all of the samples from HFB ($n = 20$) and HFC ($n = 23$) subgroups showed moderate to severe inflammation. Figure 4 shows the corresponding ^{1}H MR spectra of the colon tissue specimens whose histological sections are shown in Fig. 3. Due to extensive broadening of the ^{1}H MRS signals, it was difficult to monitor the modulation in the levels of various dietary fatty acids. However, it is obvious from Fig. 4 that creatine and total-cholines are decreased with the severity of the inflammation. Such metabolic information supplements histological data, which in turn can help in the accurate diagnosis of inflammation. In group 2 animals, very mild or no inflammation was observed in all the sections examined (data not shown).

Discussion

The main objective of this work was to study the effect of various dietary lipids on the modulation of the colonic inflammation in an IBD model. We utilized ^{1}H MRS combined with pattern recognition methods such as SCS to study the above effect. Inflammatory reactions cause biochemical changes, and MRS has the potential to detect these changes before histological manifestations [21]. In our earlier studies, we have confirmed that ^{1}H MRS in combination with pattern recognition methods could be a valuable adjunct to histology for the assessment of tissue whose status is intermediate between normal and malignant [22, 23]. Hence, ^{1}H MRS could be used for indirectly assessing the inflammatory processes.

The data were analyzed in three stages to answer three specific objectives of our study, sequentially. The first step was to identify whether ^{1}H MRS was able to identify differences between a low-fat diet and different types of high-fat diet in inflamed (group 1) and non-inflamed (group 2) colons. Those results showed that MRS was able to categorize the samples in their respective group with high sensitivity. Then the questions arose whether the differences seen were purely because of a difference in the amount of total fat in the diet or whether MRS was sensitive enough to categorize the samples accurately even when the same concentration, but different type of fatty acids was introduced in the diets. This led to stage 2 of the analyses where we compared the MR spectra from different high-fat diet groups against each other in both inflamed (group 1) and non-inflamed (group 2) colons. The results showed that ^{1}H MRS with SCS methodology was able to accurately classify the samples to their respective groups again. At this stage, we had confirmed the basic hypothesis of our overall project that different amounts and types of dietary fats affect the colon differently and that ^{1}H MRS is a sensitive technique to identify these differences. Therefore, we were at a stage where we could proceed to assess whether ^{1}H MRS could still categorize the samples with confidence when comparing the difference in inflammation between 'normal' and 'IBD-like' states of the colon. This was the reasoning for doing stage 3 of the analyses where

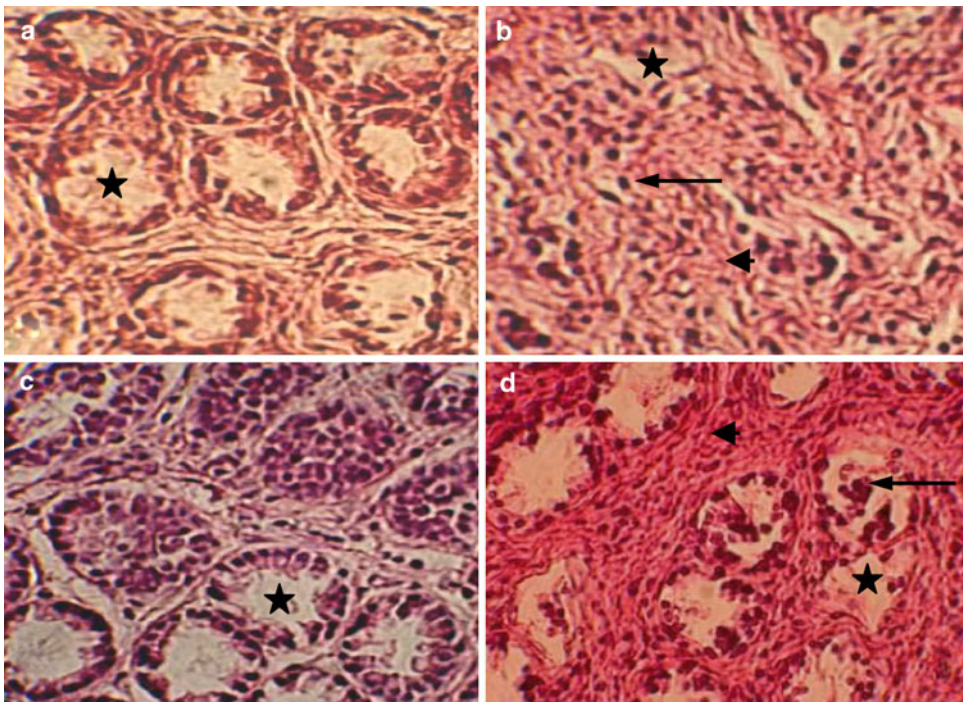

Fig. 3 Representative H&E-stained sections from each dietary group: the low-fat corn oil (LFC) group (**a**) showing normal architecture with uniform, well-spaced crypts (*star*) and no interstitial fibrosis or inflammation, while the section from the high-fat corn oil (HFC) group (**b**) shows moderate inflammation with distorted crypts (*star*), lymphocytic infiltrate (*arrow*) and interstitial fibrosis (*arrow head*). The section from high-fat flaxseed oil (HFF) (**c**) shows unremarkable architecture with uniform crypts (*star*) and no evidence of inflammation; the section from high-fat beef tallow (HFB) group (**d**) shows moderate inflammation with distortion of crypt architecture (*star*), lymphocytic infiltrate (*arrow*) and interstitial fibrosis (*arrowhead*)

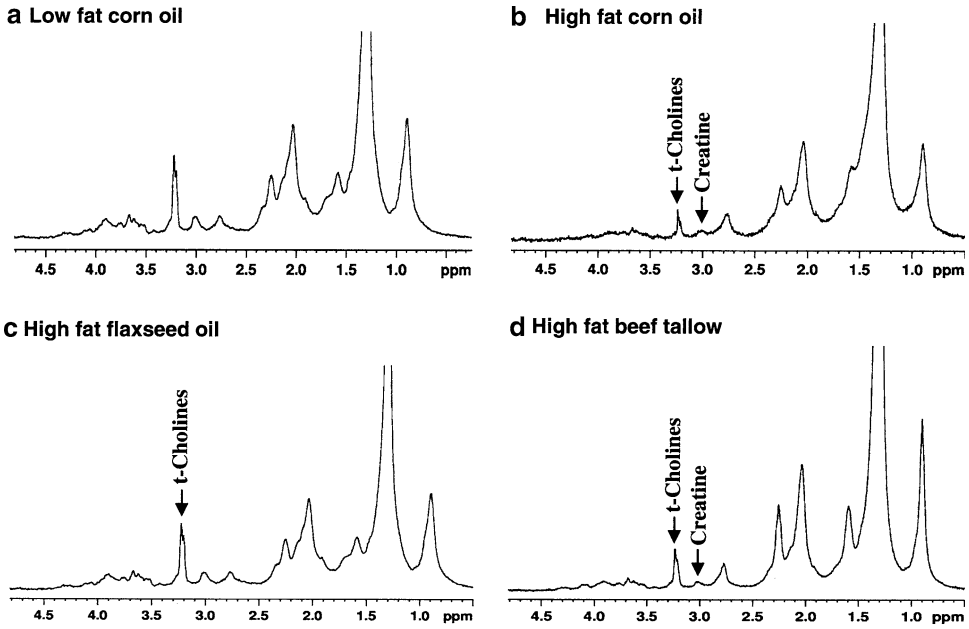

Fig. 4 ^{1}H MR spectra (360 MHz, 25°C) of the corresponding colonic tissue specimens whose histology is shown in Fig. 3 from each dietary group: **a** low-fat corn oil group (LFC), **b** high-fat corn oil (HFC) group, **c** high-fat flaxseed oil (HFF) group and **d** high-fat beef tallow (HFB) group. Some of the *peaks/metabolites* that showed change in their relative levels have been marked in the spectra

we compared each dietary subgroup from the 'carrageenan-treated' (group 1) with the corresponding subgroup from the 'non-carrageenan-treated' (group 2) separately. Since the dietary composition was the same, any differences seen in the MR spectra could be attributed to the difference in inflammation between the two subgroups. As we aim to eventually apply this methodology to assess the effect of different dietary fatty acids on modulation of inflammation in IBD, this was a critical step to confirm that ^{1}H MRS has the capability to categorize samples based on differences in the degree of inflammation.

The ^{1}H MRS signals found to be discriminatory in the SCS analysis included those from creatine, glyceryl signals of glycerophospholipids, glycerophosphoethanolamine, glutamine/glutamic acid, total cholines and parts of the fatty acyl chain, particularly the allylic/diallylic methylene protons. The implications of these metabolites are discussed herewith. Creatine is a metabolite that is found in normal tissues and serves as an energy reservoir. It is converted into phosphocreatine by adding a high energy phosphate bond in the presence of the enzyme creatine kinase. This is a reversible reaction, and whenever energy is needed, phosphocreatine is broken down to creatine while releasing the energy as ATP. Significant concentrations of creatine have previously been detected in human colonic mucosa [24]. The creatine kinase isoenzyme BB has been isolated from normal [25] and infracted colonic mucosa [26]. In an earlier study, the presence of significant amounts of creatine in normal colon tissue was attributed to a more developed muscular morphology of the colon [12]. In this study, we observed relatively high levels of creatine (2.88–3.10 ppm) in the LFC subgroup, whereas creatine was detected in negligible amounts in animals fed with HFC and HFB. However, the creatine levels were intact in the animals fed with HFF (Fig. 4). These observations indicate that muscular morphology was not disturbed in the animals fed with HFF, whereas it was upset in animals fed with HFC/HFB. As colonic inflammation causes cellular damage, demand for the energy would be high, which may result in the depletion of creatine stocks in these cells.

The region around 2.7–2.8 ppm denotes diallylic methylene protons from PUFAs [9]. PUFAs are critical for maintaining the membrane structure and function of various cells in the body [27]. Linoleic acid is an abundant PUFA in the cell membrane and a precursor of arachidonic acid. Arachidonic acid is the precursor in the synthesis of many inflammatory mediators such as the products of lipoxygenase pathway LT B4 and LT C4. These inflammatory markers are increased in many disorders in the human body including IBD [28]. Nishida et al. [29] observed an increase in arachidonic acid concentration in the colonic mucosa of patients with ulcerative colitis. Nieto et al. [30] also observed an increase in linoleic acid concentration in the colonic mucosa of rats 2 weeks after inducing experimental colitis. The linoleic acid incorporated into colonic cells may be used to synthesize arachidonic acid and inflammatory mediators. The GI tract is well known to be affected by dietary lipids. Colonocytes have fatty acid synthase including in colorectal cancer [31]. A high-fat diet does affect eicosanoid production in colonic mucosa. However, we recognize that inflammation is mediated via a complex network of different cell types in the colon, and almost every cell type is affected in the body by dietary lipids [32, 33]. These changes in colonic

mucosal lipid profile are similar in human ulcerative colitis as well as experimental colitis induced in animals. Using a gas chromatography technique, Hawthrone et al. [34] observed that the levels of unsaturated fatty acids, EPA and DHA increased in rectal mucosa after ω-3 PUFA supplementation. A similar effect on the colonic fatty acid profile was seen by Bartoli et al. [35] in Sprague-Dawley rats after ω-3 supplementation for 12 weeks. As mentioned earlier, due to extensive broadening of the ^{1}H MRS signals, we could not determine which specific PUFA contributed to the peak due to protons in the unsaturated region based solely on these spectra. We deduced that the predominant PUFA in a particular dietary group must have been responsible for the selection of the allylic/diallylic methylene protons peak as discriminatory (Tables 3 and 4).

Glutamine is the major fuel for intestinal cells. Significant levels of glutamine were observed both in human colon [36] and rat colonic mucosa [37]. Glutamate acts as an excitatory neurotransmitter in the intestinal neuronal cells. Intense glutamate staining was observed in the neural plexuses of human colon. It is being postulated that glutamate regulates acetylcholine release and motility in the colon [38]. Glutamic acid is converted to γ-aminobutyric acid by glutamic acid decarboxylase enzyme. Recently, it was shown that glutamic acid decarboxylase and γ-aminobutyric acid are present in the lamina propria of colonic mucosa of rats and may be involved in maturation and differentiation of colonic epithelial cells [39]. In the present study, although we detected small amounts of glutamine/glutamate in colonic mucosa using 2D COSY experiments, they were overlapping with those of lipid signals. As a result, we were not able to quantify these metabolites.

The comparison between group 1 and group 2 spectra shows that ^{1}H MRS combined with SCS can differentiate between inflamed and non-inflamed samples from the animals fed the same amount and type of fatty acids. In this comparison, total cholines were found to be discriminatory in addition to the metabolites mentioned above. In this study, total cholines were decreased in HFC/HFB fed animals. Martin et al. [12] observed significant levels of phosphatidylcholine, creatine, glycerol and triglycerides in the normal colon. Phosphatidylcholine is the predominant phospholipid present in the lipid bilayer of cell membranes [40] and in the colonic mucosal lining [41]. It is synthesized via the CDP-choline pathway, and the final step of this de novo synthesis is catalyzed by cholinephosphotransferase [42, 43]. Cholinephosphotransferase has also been implicated in the synthesis of platelet-activating factor (PAF), which is an inflammatory mediator and necessary signal for steps in the inflammatory cascade such as platelet activation and increase in vascular permeability. The active species of PAF have been shown to increase significantly in mucosal biopsies from ulcerative colitis patients [44]. Levels of PAF in stool are even considered to be diagnostic and indicative of severity in patients with ulcerative colitis [45]. The decreased levels of phosphatidylcholine in animals with severe inflammation seen in our study could be due to increased levels of PAF in colonic inflammation. We speculate that the cholinephosphotransferase could be more active towards the synthesis of PAF under inflammatory conditions. As there is increased apoptosis and cell turnover in IBD, there is increased demand for phosphatidylcholine to repair and regenerate the cells in colonic mucosa. This may have also contributed to the decreased levels of phosphatidylcholine/total cholines seen in our spectra, in line with earlier reports [14, 46, 47].

The histological assessment of group 1 (Fig. 3) samples showed that both LFC and HFF may be protective against inflammation. It points to the fact that both the amount and type of fatty acids supplemented may be important in modulating colonic inflammation. HFC and HFB subgroups showed significant inflammation in our study. The HFC diet supplied a high concentration of ω-6 fatty acids, which are pro-inflammatory and may have caused severe inflammation in that subgroup. The same trend holds true for the HFB diet, which supplies high amounts of saturated fats. On the contrary, the LFC diet, although it provides mainly ω-6 PUFAs, did not have a high enough concentration of these PUFAs to manifest severe pro-inflammatory effects. In a randomized control trial on patients with IBD, Bamba et al. [48] observed that a low-fat diet induced remission in 80% patients as compared to only 25% in the high-fat diet group. Interestingly, the fat they supplemented in the diet was soybean oil, which has a significant amount of ω-3 PUFAs. Similar effects were observed by Reddy et al. in a study on colon cancer [49]. They showed that rats fed with 20% corn oil had a significantly higher incidence of colon cancer than rats fed with 5% corn oil for the same duration [49]. More recently, Rao et al. [50] reported that in rats fed with high-fat fish oil (ω-3) and LFC (ω-6), this exerted a similar protective effect on colon tumor development as compared to a high saturated fat diet. Our results are in agreement with all these reports. In addition, the duration for which these PUFAs are administered is also important in regulating the outcome of the therapy. The effects of ω-3 and ω-6 fatty acids on IBD need to be studied in long-term studies. It is necessary to assess whether the effects of these fatty acids on IBD are reversible and the relapse and remission rates for patients who become non-compliant to the dietary modifications. Very mild or no inflammation seen in animals from group 2 could be due to variation in the normal mucosa, as usually some inflammatory cells are always present in the colon.

The results of this study show that ^{1}H MRS combined with SCS methodology can detect differences in the prevalence of inflammation in the colon of animals fed with both low-fat and high-fat diets. It can also differentiate between the subtle changes caused by the different fatty acids on the colon of animals fed with specialized diet. The fact that both LFC and HFF subgroups showed very mild or no inflammation implies that both the amount and the type of fatty acid in the diet are crucial in modulating inflammation. Our approach has the potential to complement histological examination of colon biopsies. The role of ^{1}H MRS as an adjunct to histology for diagnosing and differentiating between Crohn's disease and ulcerative colitis has already gained some footing [6]. The results of the current study will facilitate future endeavors to determine the utility of ^{1}H MRS in assessing inflammation, disease progression and response to dietary modification augmenting the mainstream methods such as histology. In this study, we kept the level of fat the same, but the fatty acid composition was altered in different high-fat diets. One of our future research goals is to conduct a study using different timelines for each dietary group of animals to show the temporal separation between biochemical and histological changes in IBD. Moreover, we will focus our study on the effect of individual fatty acids on colonic inflammation to understand their respective roles. We intend to use a combination of serum markers, ^{1}H MRS and histology at various time points.

Acknowledgements We would like to thank Saro Bascaramurty, who was the key resource for tissue sectioning and staining for histological assessment. We thank the Natural Sciences and Engineering Research Council of Canada (NSERC) for the strategic project grant to R.P. Bird, M. Eskin and T. Bezabeh.

Conflict of interest There are no conflicts of interest to report.

References

1. Loftus EV (2004) Clinical epidemiology of inflammatory bowel disease: incidence, prevalence and environmental influences. Gastroenterology 126:1504–1517
2. Shoda R, Matsueda K, Yamato S, Umeda N (1996) Epidemiologic analysis of Crohn disease in Japan: increased dietary intake of n-6 polyunsaturated fatty acids and animal protein relates to the increased incidence of Crohn disease in Japan. Am J Clin Nutr 63:741–745
3. Stenson WF, Cort D, Rodgers J, Burakoff R, DeSchryver-Kecskemeti K, Gramlich TL, Beeken W (1992) Dietary supplementation with fish oil in ulcerative colitis. Ann Intern Med 116:609–614
4. Lands WE (1992) Biochemistry and physiology of n-3 fatty acids. FASEB J 6:2530–2536
5. Eaden JA, Abrams KR, Mayberry JF (2001) The risk of colorectal cancer in ulcerative colitis: a meta-analysis. Gut 48: 526–535
6. Bezabeh T, Somorjai RL, Smith ICP, Nikulin AE, Dolenko B, Bernstein CN (2001) The use of ^{1}H magnetic resonance spectroscopy in inflammatory bowel diseases: distinguishing ulcerative colitis from Crohn's disease. Am J Gastroenterol 96:442–448
7. Varma S, Bird R, Eskin M, Dolenko B, Raju J, Bezabeh T (2007) Detection of inflammatory bowel disease by proton magnetic resonance spectroscopy (^{1}H MRS) using an animal model. J Inflamm (Lond) 4:24
8. Kriat M, Vion-Dury J, Confort-Gouny S, Favre R, Viout P, Sciaky M, Sari H, Cozzone PJ (1993) Analysis of plasma lipids by NMR spectroscopy: application to modifications induced by malignant tumors. J Lipid Res 34:1009–1019
9. Adosraku RK, Choi GT, Constantinou-Kokotos V, Anderson MM, Gibbons WA (1994) NMR lipid profiles of cells, tissues, and body fluids: proton NMR analysis of human erythrocyte lipids. J Lipid Res 35:1925–1931
10. Singer S, Sivaraja M, Souza K, Millis K, Corson JM (1996) ^{1}H-NMR detectable fatty acyl chain unsaturation in excised leiomyosarcoma correlate with grade and mitotic activity. J Clin Invest 98:244–250
11. Gunstone FD (1994) High resolution ^{13}C NMR. A technique for the study of lipid structure and composition. Prog Lipid Res 33:19–28
12. Martin FP, Wang Y, Sprenger N, Holmes E, Lindon JC, Kochhar S, Nicholson JK (2007) Effects of probiotic Lactobacillus paracasei treatment on the host gut tissue metabolic profiles probed via magic-angle-spinning NMR spectroscopy. J Proteome Res 6:1471–1481
13. Sands CJ, Coen M, Maher AD, Ebbels TM, Holmes E, Lindon JC, Nicholson JK (2009) Statistical total correlation spectroscopy editing of ^{1}H NMR spectra of biofluids: application to drug metabolite profile identification and enhanced information recovery. Anal Chem 81:6458–6466
14. Bjerrum JT, Nielsen OH, Hao F, Tang H, Nicholson JK, Wang Y, Olsen J (2010) Metabonomics in ulcerative colitis: diagnostics, biomarker identification, and insight into the pathophysiology. J Proteome Res 9:954–962
15. Nikulin AE, Dolenko B, Bezabeh T, Somorjai RL (1998) Near-optimal region selection for feature space reduction: novel preprocessing methods for classifying MR spectra. NMR Biomed 11:209–217
16. Somorjai RL, Alexander M, Baumgartner R, Booth S, Bowman C, Demko A, Dolenko B, Mandelzweig M, Nikulin AE, Pizzi N, Pranckeviciene E, Summers R, Zhilkin P (2004) A data-driven, flexible machine learning strategy for the classification of biomedical data. In: Azuaje F, Dubitsky W (eds) Computational biology, vol 5: artificial intelligence methods and tools for systems biology. Kluwer Academic Publishers, Boston, pp 67–85
17. Briere KM, Kuesel AC, Bird RP, Smith ICP (1995) ^{1}H MR visible lipids in colon tissue from normal and carcinogen-treated rats. NMR Biomed 8:33–40
18. Kuesel AC, Kroft T, Saunders JK, Prefontaine M, Mikhael N, Smith ICP (1992) A simple procedure for obtaining high-quality NMR spectra of semiquantitative value from small tissue specimens: cervical biopsies. Magn Reson Med 27:349–355
19. AOCS Official Method Ce 1–62. (1998) Fatty acid composition by packed column gas chromatography, American Oil Chemist's Society—official methods and recommended protocols. AOCS Press, Champaign
20. Righi V, Durante C, Cocchi M, Calabrese C, Di Febo G, Lecce F, Pisi A, Tugnoli V, Mucci A, Schenetti L (2009) Discrimination of healthy and neoplastic human colon tissues by ex vivo HR-MAS NMR spectroscopy and chemometric analyses. J Proteome Res 8:1859–1869
21. Lean CL, Newland RC, Ende DA, Bokey EL, Smith ICP, Mountford CE (1993) Assessment of human colorectal biopsies

by ^{1}H MRS: correlation with histopathology. Magn Reson Med 30:525–533
22. Smith ICP, Blandford DE (1998) Diagnosis of cancer in humans by ^{1}H NMR of tissue biopsies. Biochem Cell Biol 76:472–476
23. Bezabeh T, Smith ICP, Krupnik E, Somorjai RL, Kitchen DG, Bernstein CN, Pettigrew NM, Bird RP, Lewin KJ, Briere KM (1996) Diagnostic potential for cancer via ^{1}H magnetic resonance spectroscopy of colon tissue. Anticancer Res 16:1553–1558
24. Ende D, Rutter A, Russell P, Mountford CE (1996) Chemical shift imaging of human colorectal tissue (ex vivo). NMR Biomed 9:179–183
25. Jockers-Wretou E, Giebel W, Pfleiderer G (1977) Immunohistochemical localization of creatinkinase isoenzymes in human tissue. Histochemistry 54:83–95
26. Graeber GM, Cafferty PJ, Wolf RE, Harmon JW (1984) An analysis of creatine phosphokinase in the mucosa and the muscularis of the gastrointestinal tract. J Surg Res 37:376–382
27. Clandinin MT, Cheema S, Field CJ, Garg ML, Venkatraman J, Clandinin TR (1991) Dietary fat: exogenous determination of membrane structure and cell function. FASEB J 5:2761–2769
28. Simopoulos AP (2002) Omega-3 fatty acids in inflammation and autoimmune diseases. J Am Coll Nutr 21:495–505
29. Nishida T, Miwa H, Shigematsu A, Yamamoto M, Iida M, Fujishima M (1987) Increased arachidonic acid composition of phospholipids in colonic mucosa from patients with active ulcerative colitis. Gut 28:1002–1007
30. Nieto N, Giron MD, Suarez MD, Gil A (1998) Changes in plasma and colonic mucosa fatty acid profiles in rats with ulcerative colitis induced by trinitrobenzene sulfonic acid. Dig Dis Sci 43:2688–2695
31. Rashid A, Pizer ES, Moga M, Milgraum LZ, Zahurak M, Pasternack GR, Kuhajda FP, Hamilton SR (1997) Elevated expression of fatty acid synthase and fatty acid synthetic activity in colorectal neoplasia. Am J Pathol 150:201–208
32. Robblee NM, Farnworth ER, Bird RP (1998) Phospholipid profile and production of prostanoids by murine colonic epithelium: effect of dietary fat. Lipids 23:334–339
33. Robblee NM, Bird RP (1994) Effects of high corn oil diet on preneoplastic murine colons: prostanoid production and lipid composition. Lipids 29:67–71
34. Hawthorne AB, Daneshmend TK, Hawkey CJ, Belluzzi A, Everitt SJ, Holmes GK, Malkinson C, Shaheen MZ, Willars JE (1992) Treatment of ulcerative colitis with fish oil supplementation: a prospective 12 month randomised controlled trial. Gut 33:922–928
35. Bartolí R, Fernández-Bañares F, Navarro E, Castellà E, Mañé J, Alvarez M, Pastor C, Cabré E, Gassull MA (2000) Effect of olive oil on early and late events of colon carcinogenesis in rats: modulation of arachidonic acid metabolism and local prostaglandin E(2) synthesis. Gut 46:191–199
36. James LA, Lunn PG, Elia M (1998) Glutamine metabolism in the gastrointestinal tract of the rat assess by the relative activities of glutaminase (EC 3.5.1.2) and glutamine synthetase (EC 6.3.1.2). Br J Nutr 79:365–372
37. James LA, Lunn PG, Middleton S, Elia M (1998) Distribution of glutaminase and glutamine synthetase activities in the human gastrointestinal tract. Clin Sci 94:313–319
38. Giaroni C, Zanetti E, Chiaravalli AM, Albarello L, Dominioni L, Capella C, Lecchini S, Frigo G (2003) Evidence for a glutamatergic modulation of the cholinergic function in the human enteric nervous system via NMDA receptors. Eur J Pharmacol 476:63–69
39. Wang FY, Zhu RM, Maemura K, Hirata I, Katsu K, Watanabe M (2006) Expression of gamma-aminobutyric acid and glutamic acid decarboxylases in rat descending colon and their relation to epithelial differentiation. Chin J Dig Dis 7:103–108
40. Cullis PR, Hope MJ (1992) Physical properties and functional roles of lipids in membranes. In: Vance DE (ed) Biochemistry of lipids, lipoproteins and membranes. Elsevier Science publishers, Amsterdam, pp 1–41
41. White DA (1973) The phospholipid composition of mammalian tissue. In: Ansell GB, Hawthorne JN, Dawson RMC (eds) Form and function of phospholipids. Elsevier Scienctific publishing Co, Amsterdam, pp 441–482
42. Snyder F (1997) CDP-choline:alkylacetylglycerol cholinephosphotransferase catalyzes the final step in the de novo synthesis of platelet-activating factor. Biochim Biophys Acta 4(1348): 111–116
43. Henneberry AL, Wistow G, McMaster CR (2000) Cloning, genomic organization, and characterization of a human cholinephosphotransferase. J Biol Chem 275:29808–29815
44. Thyssen E, Turk J, Bohrer A, Stenson WF (1996) Quantification of distinct molecular species of platelet activating factor in ulcerative colitis. Lipids 31:255–259
45. Hocke M, Richter L, Bosseckert H, Eitner K (1999) Platelet activating factor in stool from patients with ulcerative colitis and Crohn's disease. Hepatogastroenterology 46:2333–2337
46. Sharma U, Singh RR, Ahuja V, Makharia GK, Jagannathan NR (2010) Similarity in the metabolic profile in macroscopically involved and un-involved colonic mucosa in patients with inflammatory bowel disease: an in vitro proton (^{1}H) MR spectroscopy study. Magn Reson Imaging 28:1022–1029
47. Balasubramanian K, Kumar S, Singh RR, Sharma U, Ahuja V, Makharia GK, Jagannathan NR (2009) Metabolism of the colonic mucosa in patients with inflammatory bowel diseases: an in vitro proton magnetic resonance spectroscopy study. Magn Reson Imaging 27:79–86
48. Bamba T, Shimoyama T, Sasaki M, Tsujikawa T, Fukuda Y, Koganei K, Hibi T, Iwao Y, Munakata A, Fukuda S, Matsumoto T, Oshitani N, Hiwatashi N, Oriuchi T, Kitahora T, Utsunomiya T, Saitoh Y, Suzuki Y, Nakajima M (2003) Dietary fat attenuates the benefits of an elemental diet in active Crohn's disease: a randomized, controlled trial. Eur J Gastroenterol Hepatol 15:151–157
49. Reddy BS, Narisawa T, Vukusich D, Weisburger JH, Wynder EL (1976) Effect of quality and quantity of dietary fat and dimethylhydrazine in colon carcinogenesis in rats. Proc Soc Exp Biol Med 151:237–239
50. Rao CV, Hirose Y, Indranie C, Reddy BS (2001) Modulation of experimental colon tumorigenesis by types and amounts of dietary fatty acids. Cancer Res 61:1927–1933

Lipids (2010) 45:855–862
DOI 10.1007/s11745-010-3456-6

ORIGINAL ARTICLE

Phytosterol Ester Constituents Affect Micellar Cholesterol Solubility in Model Bile

Andrew W. Brown · Jiliang Hang · Patrick H. Dussault · Timothy P. Carr

Received: 14 June 2010 / Accepted: 27 July 2010 / Published online: 13 August 2010

Abstract Plant sterols and stanols (phytosterols) and their esters are nutraceuticals that lower LDL cholesterol, but the mechanisms of action are not fully understood. We hypothesized that intact esters and simulated hydrolysis products of esters (phytosterols and fatty acids in equal ratios) would differentially affect the solubility of cholesterol in model bile mixed micelles in vitro. Sodium salts of glycine- and taurine-conjugated bile acids were sonicated with phosphatidylcholine and either sterol esters or combinations of sterols and fatty acids to determine the amount of cholesterol solubilized into micelles. Intact sterol esters did not solubilize into micelles, nor did they alter cholesterol solubility. However, free sterols and fatty acids altered cholesterol solubility independently (no interaction effect). Equal contents of cholesterol and either campesterol, stigmasterol, sitosterol, or stigmastanol (sitostanol) decreased cholesterol solubility in micelles by approximately 50% compared to no phytosterol present, with stigmasterol performing slightly better than sitosterol. Phytosterols competed with cholesterol in a dose-dependent manner, demonstrating a 1:1 M substitution of phytosterol for cholesterol in micelle preparations. Unsaturated fatty acids increased the micelle solubility of sterols as compared with saturated or no fatty acids. No differences were detected in the size of the model micelles. Together, these data indicate that stigmasterol combined with saturated fatty acids may be more effective at lowering cholesterol micelle solubility in vivo.

Keywords Phytosterols · Phytosterol esters · Cholesterol absorption · Bile · Mixed micelle · Plant sterol · Plant stanol

Abbreviations

DHA	Docosahexaenoic acid
EPA	Eicosapentaenoic acid
GC	Gas chromatography
HDL	High-density lipoprotein
LDL	Low-density lipoprotein
N_2	Molecular nitrogen

Introduction

Supplementation of human diets with plant sterols and stanols (collectively referred to here as phytosterols) and their esters can decrease serum LDL cholesterol concentrations [1], which is regarded as a modifiable risk factor for atherosclerosis. One way phytosterols lower serum LDL cholesterol is by disrupting intestinal cholesterol solubilization into micelles [2–5], which is a necessary step in the efficient absorption of cholesterol from the intestine [6]. However, the exact mechanisms for the actions of phytosterols have not been adequately defined.

Several studies have investigated the effects of individual sterols in simple systems of single bile acids with [2] or without [3–5] oleate or monoolein. However, the most quantitatively important source of cholesterol in the intestinal lumen is secreted from the gall bladder in a

A. W. Brown · T. P. Carr (✉)
Department of Nutrition and Health Sciences,
University of Nebraska-Lincoln, 316 Leverton Hall,
Lincoln, NE 68583-0806, USA
e-mail: tcarr2@unl.edu

J. Hang · P. H. Dussault
Department of Chemistry,
University of Nebraska-Lincoln, Lincoln, NE, USA

complex mixture of bile salts and phospholipids. In spite of the relevance to intestinal uptake of sterols, few studies have compared phytosterol solubilities and their effects on cholesterol solubility in a mixed micelle system similar to bile [7]. In addition, some phytosterol esters, namely sterol stearates [8], are superior to other phytosterols in their ability to lower serum cholesterol, yet the mechanisms by which these esters impart their unique effects is unknown. Thus, the objectives of this study were to examine the effects of (1) sterol esters, (2) simulated hydrolysis products of sterol esters (fatty acids and sterols in equal ratios), and (3) phytosterol concentration on micellar cholesterol solubility in a model bile, mixed-micelle system.

Materials and Methods

Cholesteryl oleate (98%), oleic acid (99%), stearic acid (99%), sodium taurodeoxycholate (>97%), and sodium glycodeoxycholate (>97%) were purchased from Sigma-Aldrich (St. Louis, MO). Sodium glycocholate (98%) and granular phosphatidylcholine were purchased from ACROS Organics (Geel, Belgium). Sodium taurocholate (>97%) was purchased from Alfa Aesar (Ward Hill, MA). 5α-Cholestane was obtained from Steraloids (Newport, RI). Cholesterol (95%) was obtained from Mallinckrodt OR (Paris, KY). Palmitic acid (99+%) was obtained from MP Biomedicals (Irvine, CA). Sodium chloride, sodium azide, chloroform, and hexanes were purchased from Fisher Scientific (Fair Lawn, NJ). Methanol was purchased from VWR (West Chester, PA). Linoleic and α-linolenic acids (99+%) were purchased from Nu-Chek Prep (Elysian, MN). The total cholesterol kit, Chol, was purchased from Roche Diagnostics (Indianapolis, IN). Phospholipids C and Free Cholesterol E colorimetric assay kits, and campesterol (98.7%) were obtained from Wako Chemicals USA, Inc. (Richmond, VA). 24-Ethyl sterols were purchased or synthesized as previously described [9]. Briefly, stigmasterol (95%) was purchased from TCI America (Portland, OR) and partially or completely hydrogenated to make sitosterol or stigmastanol (a.k.a. sitostanol), respectively [10, 11].

Procedures

Model Bile Mixed Micelles

Simplified bile salt solutions modeling biliary bile salt compositions were limited to the glyco- and tauro-conjugates of cholate and deoxycholate in ratios similar to published values [7, 12, 13] for a final concentration of 52.5 mM total sodium salts of bile acids: glycocholate, 29.1 mM; taurocholate, 11.4 mM; glycodeoxycholate, 8.8 mM; and taurodeoxycholate, 3.4 mM. Concentrated stock solutions of phosphatidylcholine, free fatty acids, free sterols, and sterol esters were made in chloroform. Model bile mixed micelles were created by combining stock solutions and evaporating chloroform under a stream of N_2 at 50°C, followed by addition of the 52.5 mM bile salt stock solution to create a 1 ml solution. All solutions had a final concentration of 52.5 mM bile salts and 15 mM phosphatidylcholine, with the concentrations of free sterols, free fatty acids, and sterol esters varying depending on the experiment. Lipids and bile acids were sonicated in an ice bath using a Branson 450 Sonifier (Branson, Danbury, CT) with a probe tip at 30% of maximum output (400 W) for 15 min [7]. Immediately after sonication, micelles were separated by injecting 200 µl of the solution onto a 10/300 Superose 6 column using a Waters 600 Multisolvent Delivery System and eluted at 0.5 ml/min using a 6 mM bile salt eluent. Eluent was made by addition of 3:1 taurocholate/taurodeoxycholate (w/w) dissolved in 0.9% sodium chloride (w/v) with 0.01% sodium azide (w/v), followed by vacuum filtration using Millipore (Bedford, MA) 47 mm, 0.2-µm pore size, and nylon filters. Fractions were collected every minute (0.5 ml) in 12 × 75 mm polystyrene tubes (VWR) using an ISCO Retriever 500 (Lincoln, NE). Individual fractions were analyzed for phosphatidylcholine using Wako's Phospholipids C Kit. Phosphatidylcholine-containing fractions indicated the presence of micelles [7, 14] and were pooled for subsequent analysis of free sterols by GC.

Micelle Sterol Analysis

Free sterols were analyzed by extracting an aliquot of the pooled micelle-containing fractions with 5α-cholestane as an internal standard. The sample was dried under a stream of N_2 at 60°C and was extracted using a modified Folch procedure [15]. Briefly, 2 ml of chloroform/methanol (2:1, v/v) was added to each sample, and samples were vigorously vortexed for 1 min followed by addition of deionized water for a final water content of 20% of the total volume. Samples were centrifuged at 1,000×*g* for 5 min to separate phases; the organic phase was transferred to a new tube, dried under a stream of N_2, and resuspended in hexanes. Sterols were analyzed by GC using an HP (Wilmington, DE) 5890 Series II Plus Gas Chromatograph equipped with an HP 6890 Autosampler, a 30-m DB-5 column (Agilent Technologies, Santa Clara, CA), and a flame-ionizing detector. Peaks were identified by comparing retention times with that of known standards. For the experiments examining the effects of intact sterol esters on micellar cholesterol, total and free sterols were quantified enzymatically.

Statistics

Data were analyzed using the Mixed procedure of SAS software (version 9.2; SAS Institute, Cary, NC). Sterol and fatty acid effects on micelles were analyzed as a split-block design, with stock solutions of sterols or fatty acids as main effects, correcting for cholesterol stock solutions as blocking effects. Pairwise comparisons were made with the 'pdiff' option and corrected for multiple comparisons using the 'simulate' adjustment to account for unequal sample sizes. Significance was set at $P < 0.05$. Functions in the dose dependence study were calculated using Proc Model.

Results

Micellar Incorporation of Free Sterols

Initial tests demonstrated similar elution patterns and volumes to previous work [7]. The elution profile of a model bile mixed micelle containing 3 mM cholesterol, 52.5 mM bile salt, and 15 mM phosphatidylcholine is shown in Fig. 1a.

Sterol Esters and Model Bile Mixed Micelles

Elution profiles of free cholesterol, total sterols (free plus esterified sterols), and phospholipids did not differ when cholesteryl oleate was included in a mixed micelle containing free cholesterol, bile salt, and phosphatidylcholine as compared with a model micelle devoid of sterol ester (Fig. 1a, b). When only cholesteryl oleate was added, with no free cholesterol, neither free nor esterified sterol was detected in the micelle fraction, and the elution pattern of phospholipids was altered (Fig. 1c). The lack of incorporation of sterol esters in micelles was further shown by preparing model micelles with or without stearate esters of stigmasterol, sitosterol, stigmastanol, or cholesterol. Total sterol content (free plus esterified sterols) did not differ from free sterol content (2.22 ± 0.02 vs. 2.19 ± 0.04 mM, respectively, pooled across preparations, $n = 4$), indicating no measurable incorporation of sterol esters in the micelles. Additionally, the presence or absence of sterol esters in the preparation did not affect the free cholesterol content of the micelles.

Micelle Solubility of Individual Sterols

The solubilities of free sterols within micelles prepared from solutions containing 3 mM cholesterol, campesterol, stigmasterol, sitosterol, or stigmastanol were quantified (Fig. 2). Stigmasterol was incorporated into micelles quantitatively and significantly less as compared to cholesterol, sitosterol, and stigmastanol, while cholesterol, campesterol, sitosterol, and stigmastanol were equally incorporated.

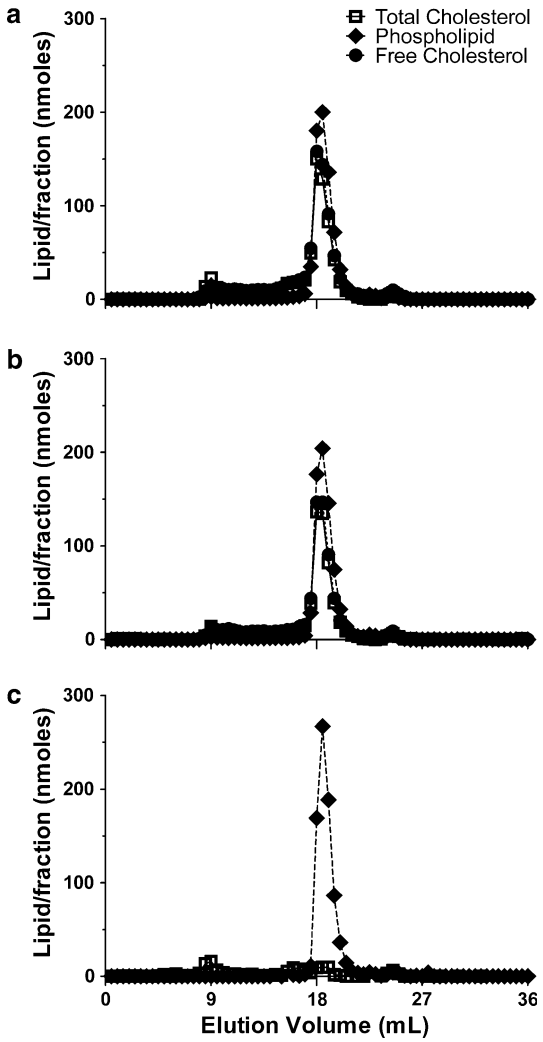

Fig. 1 Elution profiles of micelles separated by size-exclusion chromatography. Model mixed micelles were made by sonicating 3 mM cholesterol (**a**), 3 mM cholesterol and cholesteryl oleate (**b**), or 3 mM cholesteryl oleate (**c**) in the presence of 52.5 mM mixed bile salts and 15 mM phosphatidylcholine, followed by separation on a Superose 6 column at a flow rate of 0.5 ml/min. Fractions (1 min, 0.5 ml) were collected and analyzed for cholesterol, phosphatidylcholine, and total sterol. Each panel represents one preparation

Dose-Dependent Competition Between Sterols for Micellar Incorporation

Competition between stigmasterol and cholesterol for micelle incorporation was determined by adding 0, 1.5, 3, or 6 mM stigmasterol to model bile preparations containing 3 mM cholesterol (Fig. 3). As stigmasterol content increased, cholesterol content in the micelle decreased. Micellar cholesterol and stigmasterol contents were

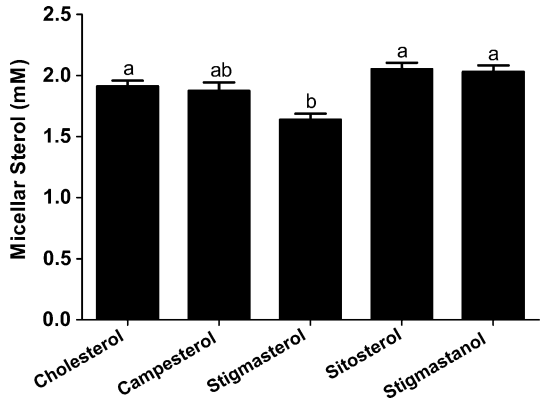

Fig. 2 Sterol solubility in mixed micelles. Mixed micelles were prepared by sonicating 3 mM of each sterol in the presence of 52.5 mM mixed bile salts and 15 mM phosphatidylcholine. Micelles were isolated by size-exclusion chromatography, and sterols were quantified by GC. Data are represented as means ± pooled SEM, $n = 3$; bars with differing letters indicate significantly different means, $P < 0.05$

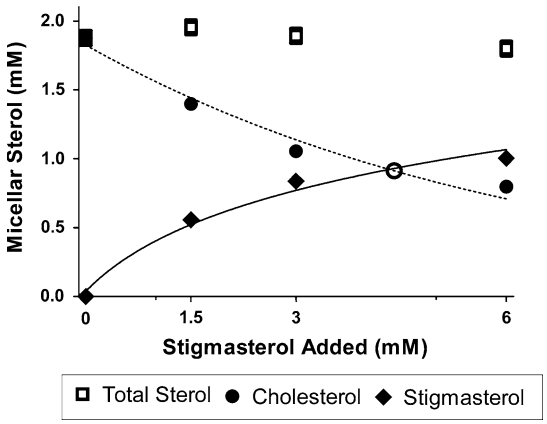

Fig. 3 Competition of stigmasterol and cholesterol for micelle incorporation. Stigmasterol (0, 1.5, 3, or 6 mM) was sonicated in the presence of 3 mM cholesterol, 15 mM phosphatidylcholine, and 52.5 mM mixed bile salts. Micelles were isolated by size-exclusion chromatography, and cholesterol and stigmasterol were quantified by gas chromatography. Micellar cholesterol solubility, modeled as a function of added stigmasterol, is represented by the *dashed line* (Eq. 1). Micellar stigmasterol solubility, modeled as a function of added stigmasterol, is represented by the *solid line* (Eq. 2). The *open circle* indicates the concentration of added stigmasterol at which micellar cholesterol would be expected to be decreased by half, which closely coincides with the intersection of the curves. Data represent means ± pooled SEM, $n = 3$; *error bars* may be eclipsed by the data markers

modeled as logarithmic and exponential functions, respectively. Cholesterol content was modeled as:

$$C = 1.83\exp(-0.158X) \quad (1)$$

and stigmasterol content was modeled as:

$$S = 0.53\ln(1.073(X + 1)) \quad (2)$$

where C is the final micellar cholesterol content in mM, S is the final micellar stigmasterol content in mM, and X is the stigmasterol added to the preparation in mM.

The amount of stigmasterol that would need to be added to decrease the cholesterol content by 50% according to Eq. 1 was 4.40 mM. This value corresponded closely to the solution of the two functions of $X = 4.33$ mM, where the amount of micellar stigmasterol and cholesterol are equal. Together, these values indicate approximately a 1:1 M substitution of micellar cholesterol for stigmasterol. The observation that more stigmasterol needs to be added than cholesterol for a 1:1 competition further demonstrates a lower micellar solubility of stigmasterol. Because stigmasterol had a lower solubility than other sterols (Fig. 2), other phytosterols may compete for micelle incorporation differently.

Free Sterol and Fatty Acid Effects on Micellar Sterol Content

Mixed micelles containing 3 mM free cholesterol were made with or without 3 mM palmitic, stearic, oleic, linoleic, or α-linolenic acids, and with or without 3 mM free campesterol, stigmasterol, sitosterol, stigmastanol, or additional cholesterol. Micellar cholesterol and phytosterol concentrations were measured by GC. No statistical interactions were detected between fatty acids and sterols, so pairwise comparisons were conducted among preparations pooled across fatty acids ('sterol effects,' Table 1, pooled $n = 17$–28) or among preparations pooled across sterols ('fatty acid effects,' Table 2, pooled $n = 15$–19). The fatty acid effects were calculated only on micelles that contained both phytosterols and cholesterol because the preparations that contained only cholesterol skewed the average cholesterol content upward and phytosterol content downward.

Adding an additional 3 mM cholesterol to the micellar mixture (for a total of 6 mM cholesterol) resulted in a significant increase, although not a doubling, in the concentration of cholesterol in the micelles, indicating that the micelles are saturated with cholesterol at a concentration somewhere between 3 and 6 mM.

The presence of phytosterols significantly decreased micellar cholesterol, with the phytosterol-containing preparations solubilizing approximately 50% of the micellar cholesterol of the saturated micelles. Modest differences were observed among the phytosterols tested: a 9% difference in the amount of micellar cholesterol was observed for the most (stigmasterol) and least (sitosterol) effective phytosterols, although neither stigmasterol nor sitosterol differed from stigmastanol and campesterol. However, stigmasterol itself was less well incorporated compared

Table 1 Molar phospholipid and sterol compositions of model bile mixed micelles formed with 3 mM cholesterol and with 0 or 3 mM additional sterol

Additional sterol	None	Cholesterol	Campesterol	Stigmasterol	Sitosterol	Stigmastanol
	mmol/l					
Cholesterol	2.02 ± 0.02[a]	2.33 ± 0.02[b]	1.15 ± 0.03 [cd]	1.09 ± 0.02[c]	1.19 ± 0.02[d]	1.17 ± 0.02 [cd]
Phytosterol[A]	0.00	0.00	1.11 ± 0.02[ab]	0.93 ± 0.02[b]	1.16 ± 0.02[a]	1.16 ± 0.02[ab]
Phospholipid	3.63 ± 0.03[a]	3.20 ± 0.03[b]	3.22 ± 0.04[bc]	3.30 ± 0.03[bc]	3.26 ± 0.03[bc]	3.37 ± 0.03[c]
Total sterol	2.02 ± 0.03[a]	2.33 ± 0.03[b]	2.27 ± 0.04[b]	2.02 ± 0.03[a]	2.36 ± 0.03[b]	2.33 ± 0.03[b]
	mol%					
% Sterol as cholesterol[A]	100.00	100.00	51.22 ± 0.63[a]	53.98 ± 0.43[b]	50.74 ± 0.43[a]	50.12 ± 0.43[a]

Values represent means ± pooled SEM of 17–28 replicates, averaged across experiments that also included 0 or 3 mM fatty acids. Values with different superscripts within a row differ by $P < 0.05$

[A] Phytosterol and mole percent data for the 'none' and 'cholesterol' preparations were not compared to other preparations because neither contained phytosterols

Table 2 Molar phospholipid and sterol compositions of model bile mixed micelles formed with 3 mM phytosterol and with 0 or 3 mM free fatty acid

Fatty acid	None	Palmitic	Stearic	Oleic	Linoleic	Linolenic
	mmol/l					
Cholesterol	1.09 ± 0.02[a]	1.08 ± 0.02[a]	1.07 ± 0.02[a]	1.25 ± 0.02[b]	1.22 ± 0.03[b]	1.22 ± 0.03[b]
Phytosterol	1.03 ± 0.02[a]	1.03 ± 0.02[a]	1.03 ± 0.02[a]	1.17 ± 0.02[b]	1.15 ± 0.03[b]	1.14 ± 0.03[b]
Total sterol	2.12 ± 0.04[a]	2.11 ± 0.04[a]	2.10 ± 0.04[a]	2.42 ± 0.04[b]	2.37 ± 0.05[b]	2.35 ± 0.05[b]
Phospholipid	3.27 ± 0.03	3.25 ± 0.03	3.27 ± 0.03	3.32 ± 0.03	3.31 ± 0.04	3.30 ± 0.04
	mol%					
% Sterol as cholesterol	51.44 ± 0.37	51.08 ± 0.39	51.13 ± 0.37	51.81 ± 0.37	51.73 ± 0.46	51.89 ± 0.46

Values represent means ± pooled SEM of 15–19 replicates, averaged across experiments that also included 3 mM cholesterol and 3 mM additional phytosterol. Values with different superscripts within a row differ by $P < 0.05$

with sitosterol, although again neither stigmasterol nor sitosterol differed from stigmastanol or campesterol. Together, these differences in individual sterol solubilities resulted in stigmasterol-containing preparations having significantly less total sterol than the other preparations except for the preparations that contained only 3 mM instead of 6 mM total sterol. Stigmasterol also differed from the other phytosterol-containing preparations by containing a greater proportion of micellar total sterol that was cholesterol, despite having a lower magnitude of cholesterol incorporated.

The presence or absence of saturated fatty acids (palmitic and stearic) had no effect on the incorporation of cholesterol or phytosterols in micelles. However, the presence of unsaturated fatty acids (oleic, linoleic, and α-linolenic), as compared with the saturated and no fatty acids preparations, increased micellar cholesterol (1.23 vs. 1.08 mM, respectively) and phytosterol (1.03 vs. 1.15 mM, respectively) contents. Total sterol content was similarly affected, but the proportion of micellar total sterol that was cholesterol was unaffected, indicating that incorporation of unsaturated fatty acids increased the sterol capacity of micelle preparations. However, no differences were detected in phospholipid content, indicating an additive rather than substitutive change.

Micelle Size

Elution volume was used as a surrogate marker of micelle size [16]. No differences were seen in elution volumes, indicating no detectable differences in micelle sizes across all sterol and fatty acid combinations (data not shown).

Discussion

Phytosterols and their esters are potent nutraceuticals. Understanding the mechanisms by which phytosterols lower serum LDL cholesterol may be important in optimizing a more potent phytosterol treatment. Variations in the fatty acid [8] and sterol [17] components of phytosterol esters can result in different efficacies with regard to cholesterol lowering. One mechanism by which this difference could occur is through differences in rates of hydrolysis of the esters. However, we previously demonstrated no differences in the hydrolysis of sitosterol and stigmastanol

esters or stearate and palmitate esters by pancreatic cholesterol esterase (EC 3.1.1.13) in vitro, and thus efficiency of hydrolysis likely does not directly determine the unique properties of some phytosterol esters [9]. Another mechanism for decreasing serum cholesterol concentrations could be diminishing cholesterol absorption by decreasing intestinal micellar cholesterol in the presence of mixtures of free fatty acids, free phytosterols, and/or intact phytosterol esters. We therefore examined the effects of sterol esters and their simulated hydrolysis products in a model bile, mixed-micelle system to approximate the effects of dietary sterols on biliary cholesterol, which is quantitatively more important than dietary cholesterol with regards to cholesterol absorption [18].

The model bile, mixed micelle system we used was created by using a combination of bile acids [7, 12, 13], while the ratio of cholesterol to phytosterol approximated the relative amounts of the sterols in the intestinal lumen during phytosterol supplementation. On average, 1,000 mg of cholesterol are secreted into the small intestine from the gall bladder daily [18], and the United States Cholesterol Education Program recommends up to 2,000 mg/day of phytosterols to lower serum cholesterol [19]. We therefore chose equal concentrations of sterols in the model micelle preparations to examine equal competition for micelle solubilization, as well as concentrations up to the 2:1 ratio of phytosterol to cholesterol that is expected in the intestinal lumen when consuming the recommended dose of phytosterols in order to examine dose-dependent effects. By examining equal ratios of phytosterol:cholesterol:free fatty acid, we also modeled the effects of complete hydrolysis of phytosterol esters on biliary cholesterol.

In this study, we demonstrated that intact phytosterol esters do not alter cholesterol micelle solubility, nor do they incorporate at a detectable level into mixed bile-salt/phosphatidylcholine micelles. In vivo models, however, demonstrate that both free and esterified sterols impart cholesterol-lowering effects [1]. This apparent discrepancy reinforces the concept that sterol esters must be first hydrolyzed to impart their cholesterol-lowering properties. The direct influence of phytosterol esters on enterocytes or intestinal phase compositions, however, cannot be precluded. Indeed, Nissinen and colleagues detected esters and free sterols in both the oily and aqueous fractions of jejunal aspirates [20]. The presence of esters in what was labeled the 'micellar phase' in the jejunal contents, combined with the absence of esters in micelles in our model, may indicate that esters are suspended in small lipid droplets [21] or solubilized in an aqueous particle other than mixed bile salt micelles in vivo.

The effects of fatty acids on the micellar solubility of sterols have been little studied. Previous results implicating improved cholesterol-lowering effects of stearic acid-containing phytosterol esters [8] led us to investigate the simulated hydrolysis products of various phytosterol esters, with the hypothesis that the stearic acid-containing micelles would solubilize less cholesterol when compared to micelles prepared with other fatty acids. While our data did indicate a lower cholesterol content in stearic acid-enriched micelles, the effect was not unique to stearic acid, but was also seen in palmitic acid-enriched micelles as well as micelles prepared without fatty acids. In addition, the difference between cholesterol content in micelles that incorporated unsaturated and saturated fatty acids was small (1.23 vs. 1.08 mM, respectively) compared to the 70% decrease in non-HDL cholesterol and the 85% decrease in cholesterol absorption observed in hamsters fed stearic acid esters of phytosterols [8]. Thus, the dietary effects of stearic acid-enriched phytosterol esters are likely not completely explained by decreasing the micellar solubility of cholesterol.

In a study of phytosterol esters derived from three oils used as supplements in humans (olive, sunflower, fish), no differences were observed among the treatment groups with regard to serum cholesterol concentrations [22], consistent with the similar cholesterol solubilization observed in the present study among micelles containing different unsaturated fatty acids. Conversely, another study showed that esterifying phytosterols with long chain omega-3 fatty acids synergistically lowered cholesterol, and the authors surmised that the effect was the result of decreasing micelle solubility [23]. Our data indicate the opposite: unsaturated fatty acids increased micellar cholesterol. Although the only omega-3 fatty acid we investigated was α-linolenic acid, whereas they used eicosapentaenoic (EPA) and docosahexaenoic (DHA) acids, our data suggest that if there is a unique effect of EPA and DHA on micellar cholesterol solubility, it is likely not the result of the degree of unsaturation or the omega-3 positioning of a double bond.

A number of studies have examined the thermodynamics of sterol solubilities in micelles and have demonstrated competition between cholesterol and other sterols for incorporation into micelles [4, 5, 7, 24, 25]. Although we also observed this competition, our results contrast markedly with those from several other studies. For instance, we found that four different phytosterols decreased cholesterol solubility to a very similar extent. Stigmasterol was, by a small margin, the most potent of the four, decreasing the concentration of micellar cholesterol and total solubilized sterols. This result is in contrast to a previous study on the solubility of cholesterol in sodium taurodeoxycholate micelles [4] that found stigmasterol to have the smallest effect among the sterols tested. The same study reported poor relative solubility of individual phytosterols in their system compared to cholesterol, whereas we observed almost equal solubility. The results of that study were

consistent with ours in terms of total sterol solubility: in their binary (two sterol) systems, total sterol content was relatively equal. On the other hand, a third study that used micelles of sodium taurocholate and oleate demonstrated an approximately 50% decrease in total solubilized sterol as the amount of sitosterol was increased [2]. In contrast, our dose-dependence experiment demonstrated no decrease in total solubilized sterol, but instead showed a 1:1 substitution of stigmasterol for cholesterol. The competition model we demonstrated does, however, reinforce the observations of Armstrong and Carey that micelles have a limited number of binding sites [5].

The disparities in results in sterol solubility studies probably reflect the differences in the micellar systems employed. The work reported here is based upon a model bile system, whereas other systems often use a single bile salt with or without another lipid component such as oleate. While these simpler systems do provide insight into the inherent solubility of various sterols in bile salt micelles, they may be less effective as models of intestinal micellar solubilization. Indeed, the lack of difference between individual phytosterols in our studies coincides with observations in clinical and animal trials. For example, similar decreases in serum cholesterol reduction were observed in humans upon administration of different combinations of phytosterols [26]. Analogous outcomes have been observed in rats [27] and hamsters (Ash and Carr, unpublished data) fed phytosterol esters varying only in the sterol component. It is likely that the differences in solubilities arise from the micelle composition, as the bile salt type and concentration both affect the solubility of sterols [5], as well as the presence of lyso- or phospholipids [28], oxidation of fatty acids [29], and amount of fatty acid [2]. The complexity of bile, then, is likely better able to accommodate different sterols than simpler systems. However, the decreased cholesterol solubilities when stigmasterol and saturated fatty acids are present may indicate that the combination of these components is more effective at decreasing cholesterol solubility in micelles than other combinations, though in vivo experiments must be conducted to validate these results on serum cholesterol and cholesterol absorption.

Acknowledgments The authors would like to thank Kate Wolford, Aaron Brandt, and Paige Lundy for help with sample preparation and analysis. A.W.B. and J.H. were supported by National Research Initiative Grant 2007-35200-18298 from the USDA National Institute of Food and Agriculture. The research was also supported in part by the University of Nebraska Agricultural Research Division with funds provided through the Hatch Act. Portions of this work were conducted in facilities remodeled with support from National Institutes of Health (NIH RR016544-01).

Conflict of interest None of the authors have any conflicts of interest to disclose.

References

1. Demonty I, Ras RT, van der Knaap HCM, Duchateau GSMJE, Meijer L, Zock PL, Geleijnse JM, Trautwein EA (2009) Continuous dose-response relationship of the LDL-cholesterol-lowering effect of phytosterol intake. J Nutr 139:271–284. doi:10.3945/jn.108.095125
2. Slota T, Kozlov NA, Ammon HV (1983) Comparison of cholesterol and beta-sitosterol: effects on jejunal fluid secretion induced by oleate, and absorption from mixed micellar solutions. Gut 24:653–658
3. Nagadome S, Okazaki Y, Lee S, Sasaki Y, Sugihara G (2001) Selective solubilization of sterols by bile salt micelles in water: a thermodynamic study. Langmuir 17:4405–4412. doi:10.1021/la010087h
4. Matsuoka K, Kajimoto E, Horiuchi M, Honda C, Endo K (2010) Competitive solubilization of cholesterol and six species of sterol/stanol in bile salt micelles. Chem Phys Lipids 163:397–402. doi:10.1016/j.chemphyslip.2010.03.006
5. Armstrong MJ, Carey MC (1987) Thermodynamic and molecular determinants of sterol solubilities in bile salt micelles. J Lipid Res 28:1144–1155
6. Woollett LA, Wang Y, Buckley DD, Yao L, Chin S, Granholm N, Jones PJH, Setchell KDR, Tso P, Heubi JE (2006) Micellar solubilisation of cholesterol is essential for absorption in humans. Gut 55:197–204. doi:10.1136/gut.2005.069906
7. Jesch ED, Carr TP (2006) Sitosterol reduces micellar cholesterol solubility in model bile. Nutr Res 26:579–584
8. Rasmussen HE, Guderian DMJ, Wray CA, Dussault PH, Schlegel VL, Carr TP (2006) Reduction in cholesterol absorption is enhanced by stearate-enriched plant sterol esters in hamsters. J Nutr 136:2722–2727
9. Brown AW, Hang J, Dussault PH, Carr TP (2009) Plant sterol and stanol substrate specificity of pancreatic cholesterol esterase. J Nutr Biochem. doi:10.1016/j.jnutbio.2009.04.008
10. Xie M, Qiu A, He Y (2004) Catalytic hydrogenation of stigmasterol to sitostanol. Jingxi Huagong 21:735–737
11. Kircher HW, Rosenstein FU (1973) Hydrogenation of stigmasterol. Lipids 8:101–106
12. Cowles RL, Lee J, Gallaher DD, Stuefer-Powell CL, Carr TP (2002) Dietary stearic acid alters gallbladder bile acid composition in hamsters fed cereal-based diets. J Nutr 132:3119–3122
13. Fisher MM, Yousef IM (1973) Sex differences in the bile acid composition of human bile: studies in patients with and without gallstones. Can Med Assoc J 109:190–193
14. Cohen DE, Carey MC (1990) Rapid (1 hour) high performance gel filtration chromatography resolves coexisting simple micelles, mixed micelles, and vesicles in bile. J Lipid Res 31:2103–2112
15. Folch J, Lees M, Sloane Stanley GH (1957) A simple method for the isolation and purification of total lipides from animal tissues. J Biol Chem 226:497–509
16. Nichols JW, Ozarowski J (1990) Sizing of lecithin-bile salt mixed micelles by size-exclusion high-performance liquid chromatography. Biochemistry 29:4600–4606
17. O'Neill FH, Sanders TAB, Thompson GR (2005) Comparison of efficacy of plant stanol ester and sterol ester: short-term and longer-term studies. Am J Cardiol 96:29D–36D. doi:10.1016/j.amjcard.2005.03.017
18. Grundy SM, Metzger AL (1972) A physiological method for estimation of hepatic secretion of biliary lipids in man. Gastroenterology 62:1200–1217
19. National Institutes of Health (2002) Third Report of the National Cholesterol Education Program (NCEP) Expert Panel on Detection, Evaluation, and Treatment of High Blood Cholesterol in

Adults (Adult Treatment Panel III) final report. Circulation 106:3143–3421
20. Nissinen M, Gylling H, Vuoristo M, Miettinen TA (2002) Micellar distribution of cholesterol and phytosterols after duodenal plant stanol ester infusion. Am J Physiol Gastrointest Liver Physiol 282:G1009–G1015. doi:10.1152/ajpgi.00446.2001
21. Armand M, Borel P, Pasquier B, Dubois C, Senft M, Andre M, Peyrot J, Salducci J, Lairon D (1996) Physicochemical characteristics of emulsions during fat digestion in human stomach and duodenum. Am J Physiol 271:G172–G183
22. Jones PJH, Demonty I, Chan Y, Herzog Y, Pelled D (2007) Fish-oil esters of plant sterols differ from vegetable-oil sterol esters in triglycerides lowering, carotenoid bioavailability and impact on plasminogen activator inhibitor-1 (PAI-1) concentrations in hypercholesterolemic subjects. Lipids Health Dis 6:28. doi:10.1186/1476-511X-6-28
23. Micallef MA, Garg ML (2008) The lipid-lowering effects of phytosterols and (n-3) polyunsaturated fatty acids are synergistic and complementary in hyperlipidemic men and women. J Nutr 138:1086–1090
24. Matsuoka K, Nakazawa T, Nakamura A, Honda C, Endo K, Tsukada M (2008) Study of thermodynamic parameters for solubilization of plant sterol and stanol in bile salt micelles. Chem Phys Lipids 154:87–93. doi:10.1016/j.chemphyslip.2008.05.002
25. Matsuoka K, Hirosawa T, Honda C, Endo K, Moroi Y, Shibata O (2007) Thermodynamic study on competitive solubilization of cholesterol and beta-sitosterol in bile salt micelles. Chem Phys Lipids 148:51–60. doi:10.1016/j.chemphyslip.2007.04.007
26. Clifton PM, Mano M, Duchateau GSMJE, van der Knaap HCM, Trautwein EA (2008) Dose-response effects of different plant sterol sources in fat spreads on serum lipids and C-reactive protein and on the kinetic behavior of serum plant sterols. Eur J Clin Nutr 62:968–977. doi:10.1038/sj.ejcn.1602814
27. Mattson FH, Volpenhein RA, Erickson BA (1977) Effect of plant sterol esters on the absorption of dietary cholesterol. J Nutr 107:1139–1146
28. Homan R, Hamelehle KL (1998) Phospholipase A2 relieves phosphatidylcholine inhibition of micellar cholesterol absorption and transport by human intestinal cell line Caco-2. J Lipid Res 39:1197–1209
29. Penumetcha M, Khan-Merchant N, Parthasarathy S (2002) Enhanced solubilization and intestinal absorption of cholesterol by oxidized linoleic acid. J Lipid Res 43:895–903

Lipids (2010) 45:863–875
DOI 10.1007/s11745-010-3457-5

ORIGINAL ARTICLE

Lipid Profiling Reveals Tissue-Specific Differences for Ethanolamide Lipids in Mice Lacking Fatty Acid Amide Hydrolase

Aruna Kilaru · Giorgis Isaac · Pamela Tamura · David Baxter · Scott R. Duncan · Barney J. Venables · Ruth Welti · Peter Koulen · Kent D. Chapman

Received: 16 June 2010 / Accepted: 29 July 2010 / Published online: 17 August 2010

Abstract *N*-Acylethanolamines (NAE) are fatty acid derivatives, some of which function as endocannabinoids in mammals. NAE metabolism involves common (phosphatidylethanolamines, PEs) and uncommon (*N*-acylphosphatidylethanolamines, NAPEs) membrane phospholipids. Here we have identified and quantified more than a hundred metabolites in the NAE/endocannabinoid pathway in mouse brain and heart tissues, including many previously unreported molecular species of NAPE. We found that brain tissue of mice lacking fatty acid amide hydrolase ($FAAH^{-/-}$) had elevated PE and NAPE molecular species in addition to elevated NAEs, suggesting that FAAH activity participates in the overall regulation of this pathway. This perturbation of the NAE pathway in brain was not observed in heart tissue of $FAAH^{-/-}$ mice, indicating that metabolic regulation of the NAE pathway differs in these two organs and the metabolic enzymes that catabolize NAEs are most likely differentially distributed and/or regulated. Targeted lipidomics analysis, like that presented here, will continue to provide important insights into cellular lipid signaling networks.

Keywords FAAH · Endocannabinoids · *N*-Acylethanolamines · Lipid profiling · Lipid signaling · Lipid mediators · Mass spectrometry

A. Kilaru · D. Baxter · B. J. Venables · P. Koulen · K. D. Chapman (✉)
Department of Biological Sciences, Center for Plant Lipid Research, University of North Texas, 1155 Union Circle #305220, Denton, TX 76203-5017, USA
e-mail: chapman@unt.edu

G. Isaac · P. Tamura · R. Welti
Division of Biology, Kansas Lipidomics Research Center, Kansas State University, Ackert Hall, Manhattan, KS 66506-4901, USA

S. R. Duncan · P. Koulen
Departments of Basic Medical Science and Ophthalmology, School of Medicine, University of Missouri-Kansas City, 2411 Holmes Street, Kansas City, MO 64108, USA

Present Address:
A. Kilaru
Department of Plant Biology, Michigan State University, 366 Plant Biology Building, East Lansing, MI 48824, USA

Present Address:
G. Isaac
Pacific Northwest National Laboratory, PO Box 999, MSIN: K8-98, Richland, WA 99352, USA

Abbreviations

AG	Arachidonoylglycerol
ePC	Alk(en)yl,acyl glycerophosphocholine
ePE	Alk(en)yl,acyl glycerophosphoethanolamine
ESI	Electrospray ionization
FAAH	Fatty acid amide hydrolase
FFA	Free fatty acid
FW	Fresh weight
KO	Knockout
LPC	Lysophosphatidylcholine
LPE	Lysophosphatidylethanolamine
NAE	*N*-Acylethanolamine
NAPE	*N*-Acylphosphatidylethanolamine
NL	Neutral loss
PA	Phosphatidic acid
PC	Phosphatidylcholine
PE	Phosphatidylethanolamine
PI	Phosphatidylinositol
PLD	Phospholipase D
Pre	Precursor

PS	Phosphatidylserine
SM	Sphingomyelin
WT	Wild type
X:Y	Designates carbon chain length: total number of carbon–carbon double bonds

Introduction

Endocannabinoids are endogenous lipid mediators that bind to and activate cannabinoid receptors in mammals to regulate a wide range of physiological and behavioral processes [1, 2]. The first endocannabinoid discovered was anandamide [3], or *N*-arachidonylethanolamine (a type of *N*-acylethanolamine, 20:4 NAE). It was promptly revealed that anandamide and other members of its class are generated as part of a metabolic pathway involving the common membrane lipid phosphatidylethanolamine (PE) and an unusual *N*-acylated derivative of PE, *N*-acylphosphatidylethanolamine (NAPE; reviewed in [4]). Although earlier research had established the metabolic relationship between these lipid classes in mammals and characterized the enzyme activities involved [5], molecular identification of fatty acid amide hydrolase (FAAH) was a critical step, leading to the ability to perturb the NAE metabolic pathway in order to further elucidate the pathway's physiological functions [6–8].

The overall pathway, termed the *N*-acylation-phosphodiesterase pathway, has more recently been designated the "endocannabinoid signaling pathway" to reflect its physiological function [9, 10]. However, this designation does not indicate the role of the pathway during response to ischemia; in fact, most of the early metabolic studies of this pathway were related to observations that both NAE and NAPE contents were elevated markedly in ischemic brain and heart tissues [11–14]. The overall endocannabinoid pathway, the structures of representative principal metabolite classes, and key enzymatic steps are summarized in Fig. 1.

Although the function of the endocannabinoid pathway relies mostly on the production and turnover of bioactive NAEs, the precursor pools of NAPEs can determine the prevailing mix of endogenous NAEs [4]. Indeed, a concept called the "entourage effect" has been proposed to explain how abundant NAE molecular species that do not activate cannabinoid receptors can influence the activity of minor components, such as 20:4 NAE, that do activate receptors. To date, the many ethanolamine lipid components of the NAE-metabolic pathway have rarely been profiled comprehensively and concomitantly [15–17]. Here, we employ a targeted lipidomics approach to exhaustively identify and quantify the major and minor PE, NAPE, and NAE species in mouse heart and brain tissues and examine the impact of the loss of FAAH in $FAAH^{-/-}$ mice [18] on the metabolites of the endocannabinoid pathway.

In the current work, *O*-diacyl and *O*-alk(en)yl,*O*-acyl PE and NAPE molecular species were identified directly in lipid extracts by electrospray ionization mass spectrometry (ESI-MS) using neutral loss scans and quantifying in relation to internal standards. NAEs were identified by GC-MS after chromatographic clean-up and quantified by isotope dilution MS, using procedures similar to those developed elsewhere [19]. Our results detail the metabolites of this important lipid signaling pathway. Moreover,

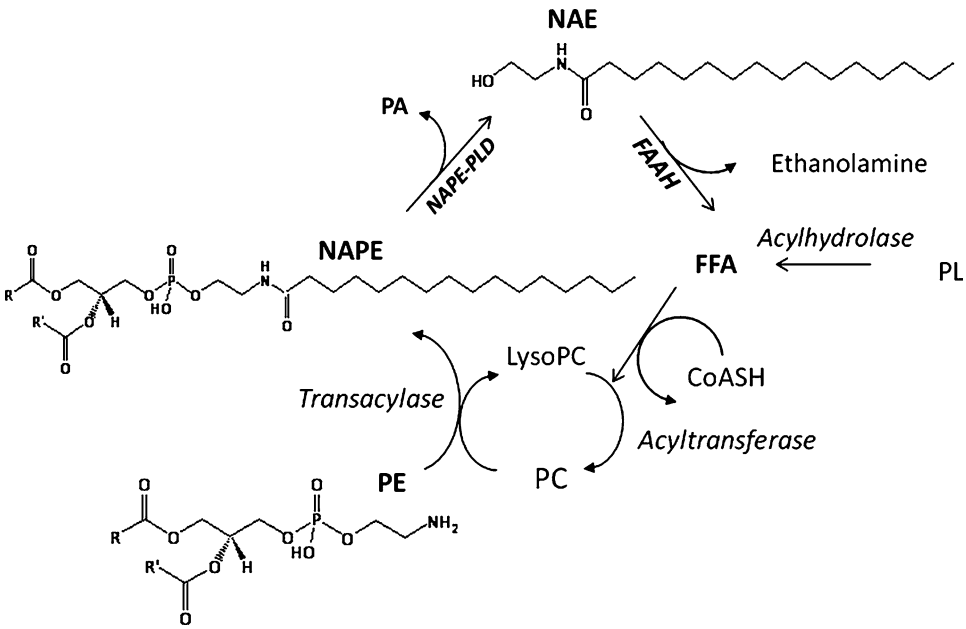

Fig. 1 *N*-acylethanolamine (NAE) metabolism in mammals. NAEs are derived from the hydrolysis of a minor membrane lipid, *N*-acylphosphatidylethanolamine (NAPE), by a phospholipase D (PLD) and are hydrolyzed by a fatty acid amide hydrolase (FAAH) into ethanolamine and free fatty acid (FFA). NAPEs are synthesized from free fatty acid (FFA) via a coordinated acyltransferase-transacylase reaction in which the *sn*-1-*O*-acyl moiety of phosphatidylcholine (PC) generated is transferred to the *N*-atom of phosphatidylethanolamine (PE)

the results suggest that ablation of FAAH in brain tissue results in dysregulation throughout the pathway, not just in anandamide content, as previously reported, while similar effects were not apparent in heart tissue [18, 20]. Comprehensive profiling approaches like those utilized here enable understanding of the metabolic regulation of important signaling pathways.

Experimental Procedures

Animals and Tissue Extracts

FAAH$^{-/-}$ mice were kindly provided by Dr. Benjamin F. Cravatt, The Scripps Research Institute, La Jolla, CA, and were genotyped as described previously [18]. Wild-type littermate control mice were used for comparisons. Animals were kept in a temperature-controlled room with 12-h light/dark cycles and free access to food and water. Animal use and care were reviewed and approved by the Institutional Animal Care and Use Committee. For each treatment, after euthanasia, brains and heart tissue from five animals were removed and flash frozen in liquid nitrogen.

Lipid Extractions

For glycerolipid analyses, tissues were homogenized with hot 2-propanol (70°C) with glass beads by beating for five 30-s bursts and combined with chloroform (0.45 g FW:2 ml 2-propanol:1 ml chloroform), and incubated on ice for 30 min before extracting overnight at 4°C. Monophasic lipid extracts were partitioned with chloroform and 1 M KCl (1:2 v/v). The lower organic phase was collected and washed three additional times with 2 volumes of 1 M KCl. Extracts were stored under nitrogen at −80°C until further analysis.

Phospholipid Analysis and Quantification

An automated electrospray ionization (ESI)-tandem mass spectrometry approach was used, and data acquisition was carried out as described previously [22] with modifications. Dried mouse brain and heart lipid extracts were dissolved in 1 ml chloroform/methanol (9:1). An aliquot of 2–30 µl of extract, equivalent to 0.5–2 mg tissue FW, was used. Precise amounts of internal standards, obtained and quantified as previously described [24], were added in the following quantities (with some small variation in amounts in different batches of internal standards): 0.66 nmoles of di14:0 PC, di24:1 PC, 13:0 lysoPC, and19:0 lysoPC, 0.36 nmoles of di14:0 PE, di24:1 PE, 14:0 lysoPE, 18:0 lysoPE, di14:0 PA, and di20:0 (phytanoyl) PA, 0.24 nmol di14:0 PS and di20:0 (phytanoyl) PS, 0.20 nmoles of 16:0–18:0 PI, and 0.16 nmoles of di18:0 PI. Solvent was added to the sample/standard mixture so that the final ratio of chloroform/methanol/300 mM ammonium acetate in water was approximately 300:665:35, and the final volume was 1.3 ml.

Mass spectra were acquired on a triple quadrupole MS/MS system (API 4000, Applied Biosystems, Foster City, CA). Unfractionated samples were introduced by continuous infusion into the Turbo V ESI source at 30 µl/min using an autosampler (LC Mini PAL, CTC Analytics AG, Zwingen, Switzerland) fitted with the required injection loop for the acquisition time. Sequential precursor and neutral loss scans of the extracts produced a series of spectra, with each spectrum revealing a set of lipid species containing a common head group fragment. Lipid species were detected in positive mode with the following scans: PC and lysoPC, $[M + H]^+$ ions with precursors of 184.1 (Pre 184.1); PE and lysoPE, $[M + H]^+$ ions with neutral loss of 141.0 (NL 141.0); PI, $[M + NH_4]^+$ ions with NL 277.0; PS, $[M + H]^+$ ions with NL 185.0; and PA, $[M + NH_4]^+$ ions with NL 115.0. The ion spray voltage was set at +5.5 kV, the source temperature at 100°C, the curtain gas at 20 (arbitrary units), and the ion source gases at 45 (arbitrary units); the interface heater was on. Declustering potentials were +100 V. Entrance potentials were +15 V for PE and +14 V for PC, PI, PA, and PS. Exit potentials were +11 V for PE and +14 V for PC, PI, PA, and PS. The collision gas, nitrogen, was set at 2 (arbitrary units). The collision energies were +28 V for PE, +40 V for PC, and +25 V for PI, PS and PA. The mass analyzers were adjusted to a resolution of 0.7 u full width at half height. For each spectrum, 8–80 continuum scans were collected in multiple channel analyzer (MCA) mode at a scan speed of 50 or 100 u per s.

The data were smoothed, the background of each spectrum was subtracted, and the peaks were centroided and integrated using custom script and Applied Biosystems Analyst software. Peaks corresponding to the target lipids in these spectra were identified, the data were corrected for isotopic overlap, and molar amounts were calculated in comparison to the internal standards in the same lipid class. A sample containing internal standard mixture only was also run through the same series of scans to correct for chemical or instrumental noise. The molar amounts of each lipid metabolite detected in the "internal standards-only" spectra were subtracted from the molar amounts of each metabolite calculated from the experimental mouse sample spectra. The "internal standards-only" spectra were used to correct the data from the following nine samples run on the instrument. Finally, the data were adjusted to account for the fraction of sample analyzed and normalized to the sample fresh weight. Data were reported as nmol or µmol of each detected lipid metabolite/g tissue FW. Measured

metabolite species include both diacyl and alk(en)yl,acyl glycerophospholipids. Although these two groups may exhibit some differences in mass spectral response, values for the alk(en)yl,acyl (as well as diacyl) species were quantified in relation to the diacyl/monoacyl phospholipid internal standards, and no response correction factors were employed for the alk(en)yl,acyl species.

NAPE Standard Acquisition and Synthesis

C17:0 fatty acid chloride was purchased from Nu-Check Prep (Elysian, MN); 1,2-dihexadecanoyl-*sn*-glycero-3-phosphoethanolamine (di16:0 PE) and 1,2-dioleoyl-*sn*-glycero-3-phospho(*N*-arachidonoyl)ethanolamine (*N*-20:4 di18:1 PE) were from Avanti Polar Lipids (Alabaster, AL); 1-2-dipalmitoyl-*sn*-glycero-3-phospho(*N*-palmitoyl)ethanolamine (*N*-16:0 di16:0 PE) was from Sigma-Aldrich (St. Louis, MO); TLC plates (10 × 20 cm, scored, HPTLC-GHL silica gel, 150 μm) were from Analtech (Newark, DE). Other organic solvents and reagents were of the highest purity commercially available.

The NAPE molecular species *N*-17:0 di16:0 PE was prepared as described previously [23], with modifications. Briefly, C17:0 fatty acid chloride was reacted with a two-fold molar excess of di16:0 PE. The reaction was conducted in dichloromethane at 25°C for 2 h, using triethylamine as a catalyst. The products were washed with water and fractionated by silica gel TLC (chloroform/methanol/ammonia, 65:35:4) to separate the desired product NAPE species from unreacted PE and fatty acid chloride. The calculated retention factors for NAPE and PE were 0.60 and 0.40, respectively. Both the purchased and synthesized NAPE species were quantified by phosphate assay [25].

NAPE Analysis and Quantification

As noted above in the phospholipid analysis section, dried mouse brain and heart lipid extracts were dissolved in chloroform/methanol (9:1). The same sample solutions were used for both phospholipid and NAPE analysis. The synthesized *N*-17:0 di16:0 PE was employed as an internal standard to quantify the NAPE species in the sample extracts. *N*-17:0 di16:0 PE (1.1 nmole) was added to an aliquot of extract equivalent to 6–25 mg tissue FW. Solvent was added to the sample/standard mixture so that the final ratio of chloroform/methanol/300 mM ammonium acetate in water was 300:665:35, and the final volume was 1.3 ml.

Mass spectra were acquired on a triple quadrupole MS/MS system (API 4000 QTrap, Applied Biosystems, Foster City, CA). Unfractionated samples were introduced by continuous infusion into the Turbo V ESI source at 30 μl/min using an autosampler (LC Mini PAL, CTC Analytics AG, Zwingen, Switzerland) fitted with the required injection loop for the acquisition time. Sequential neutral loss scans produced a series of spectra, with each spectrum revealing a set of lipid species containing a common ammoniated *N*-fatty amide head group fragment corresponding to each common fatty acid. Lipids were detected in positive ion mode as $[M + NH_4]^+$ ions with the following scans: *N*-16:0 species with NL 396.3, *N*-18:2 species with NL 420.3, *N*-18:1 species with NL 422.3, *N*-18:0 species with NL 424.3, *N*-20:4 species with NL 444.3, *N*-22:6 species with NL 468.3, and *N*-22:5 species with NL 470.3. A scan for *N*-17:0 species (NL 410.3) was included in order to detect the internal standard. The declustering potential was set at +60 V, the entrance potential at +8 V, and the exit potential at +15 V. The ion spray voltage was set at +5.5 kV. The collision gas, nitrogen, was set at 2 (arbitrary units), and the collision energy was +45 V. The source temperature, curtain gas, ion source gases, interface heater, and mass analyzers were adjusted as for phospholipid analysis. For each spectrum, 100 cumulative scans were collected in multiple channel analyzer (MCA) mode at a scan speed of 50 u per s.

The data were smoothed, the background of each spectrum was subtracted, and the peaks were centroided and integrated using custom script and Applied Biosystems Analyst software. Peaks corresponding to the target lipids in each *N*-acyl class (each spectrum) were identified, the data were corrected for isotopic overlap due to the diacylglycerol portion of NAPE, and molar amounts were quantified relative to the *N*-17:0 di16:0 PE internal standard. A sample containing only the *N*-17:0 di16:0 PE standard was subjected to the same series of scans. The molar amounts of each lipid metabolite detected in the "standard-only" spectra were subtracted from the molar amounts of each metabolite calculated from the experimental mouse sample spectra to correct for chemical or instrumental noise. The "standard-only" spectra were used to correct the data from the following nine samples run on the instrument. Finally, the data were corrected for isotopic overlap between head groups (NL fragments), adjusted to account for the fraction of sample analyzed, and normalized to the sample fresh weight. Due to the presence in the NL 444.3 scan of peaks with *m/z* inconsistent with NAPEs in the *m/z* range of *N*-20:4-e40:7, *N*-20:4-e40:6, *N*-20:4-40:8, and *N*-20:4-40:7 NAPEs, these compounds were not measured in brain tissues. The interfering compounds were not present in the spectra of mouse heart tissue. Data were reported as mass spectral signal normalized to *N*-17:0 di16:0 PE/g tissue FW; the amount of signal produced by 1 pmol of *N*-17:0 di16:0 PE is 1. Data were evaluated for possible outliers using the *Q*-test [26] on NAPE lipid class totals; one *FAAH* ($^{-/-}$) mouse brain replicate (out of 5) was determined to be an outlier and was removed from

calculations. Measured species include both *N*-acylated diacyl and *N*-acylated alk(en)yl,acyl glycerophospholipids. As described for the phospholipid species, no response correction factors were employed for the alk(en)yl,acyl species.

Validation of NAPE Quantitation Method

Three experiments were performed to validate the above sequential NL scanning method for NAPE quantitation. To assess the linearity of the response, varied amounts (10–1,000 pmol) of the purchased *N*-16:0 di16:0 PE and *N*-20:4 di18:1 PE were analyzed in the presence of 200 pmol of the synthesized *N*-17:0 di16:0 PE internal standard. An abbreviated mass spectral analysis with scans for *N*-16:0, *N*-20:4, and *N*-17:0 NAPEs was performed on the API 4000 mass spectrometer. Responses of the *N*-16:0 di16:0 PE and *N*-20:4 di18:1 PE signals relative to the *N*-17:0 standard were measured.

The ability of ESI-MS/MS NAPE profiling to detect small changes in NAPE molecular species levels was also evaluated. Purchased *N*-16:0 di16:0 PE and *N*-20:4 di18:1 PE were utilized. Stepwise-increasing known amounts of these two species (4, 8, 20, and 60 pmol for the *N*-16:0 compound; 5, 10, 25, and 75 pmol for the *N*-20:4 compound) were spiked into samples containing roughly a 10 mg FW equivalent of a mixture of WT and $FAAH^{-/-}$ mouse brain extract. Each sample also contained 100 pmol of the synthesized *N*-17:0 di16:0 PE internal standard. An abbreviated mass spectral analysis with scans for *N*-16:0, *N*-20:4, and *N*-17:0 NAPE was performed on the API 4000 QTrap mass spectrometer. Responses of the targeted *N*-16:0 and *N*-20:4 compounds relative to the *N*-17:0 standard were calculated.

The variation in mass spectral response due to variation in the amount of biological sample analyzed was also examined. Samples were prepared with varying amounts of a mixture of WT and $FAAH^{-/-}$ mouse brain extract, approximately equivalent to 3.5, 7, 14, and 28 mg FW, and 200 pmol of the synthesized *N*-17:0 di16:0 PE internal standard. The full mass spectral analysis, with scans for *N*-16:0, *N*-18:2, *N*-18:1, *N*-18:0, *N*-20:4, *N*-22:6, *N*-22:5, and *N*-17:0, was performed on the API 4000 QTrap mass spectrometer. Data were processed as described above and reported as mass spectral signal of each targeted NAPE species relative to the *N*-17:0 di16:0 PE internal standard.

NAE Analyses

NAE extraction and purification were conducted as described by Muccioli and Stella [29]. Brain and heart tissues (mean fresh weights of 425 mg and 170 mg, respectively) from $FAAH^{-/-}$ and WT animals were removed from −80°C storage and homogenized in ice cold chloroform (1 ml per 100 mg of fresh tissue) using a glass tissue grinder. The homogenate was placed in an ultrasonic bath (60 W) for 2 min to disrupt cells. The extract was combined with 10 ml of ice cold chloroform containing deuterated NAE standards (D4-NAE 16:0 and D4-NAE 20:4, Cayman Chemical Co., Ann Arbor, MI; 50 ng each). Lipids were extracted by extraction (4:2:1 chloroform:methanol:water) by the addition of 5 ml cold methanol and 2.5 ml cold PBS buffer and returned to an ice cold ultrasonic (60 W) water bath for 10 min, followed by centrifugation. The organic phase was collected for further purification by solid phase extraction.

Silica SPE cartridges (100 mg, 1.5 ml; Grace Davison Discovery Sciences, Deerfield, IL) were conditioned with 2 ml methanol followed by 4 ml chloroform and, subsequent to loading the samples, the column was washed with 2 ml chloroform, and NAEs were eluted with 2 ml of 1:1 (v/v) ethyl acetate:acetone. The eluate was collected, evaporated under nitrogen, and derivatized with 50 µl BSTFA (Fisher Scientific, Houston, TX) and 25 µl dichloromethane for 30 min at 55°C. After derivatization, the samples were again evaporated under nitrogen and reconstituted in 50 ul hexane.

NAEs were identified via selective ion monitoring and quantified against the internal deuterated standards (saturated species against deuterated NAE 16:0 and unsaturated species against deuterated NAE 20:4) as TMS-ether derivatives by gas chromatography/mass spectrometry (model 6890 GC coupled with a 5973 mass selective detector; Agilent, Wilmington DE), as described previously [21]. NAE concentration was calculated based on fresh weight.

Results

In previous work, methods for analysis of NAEs by GC-MS [21] and phospholipids by direct infusion electrospray ionization mass spectrometry [27] were developed. Here, in order to comprehensively analyze lipids in the NAE biosynthetic pathway, we developed a method for direct infusion electrospray ionization mass spectrometry analysis of NAPE species. In solvent containing ammonium acetate, NAPE species form positively charged ammonium adducts $[M + NH_4]^+$ by electrospray ionization. By collision-induced dissociation, the ammonium adducts of NAPEs can be fragmented into a neutral head group fragment and a charged diradylglycerol (i.e., diacylglycerol or alk(en)yl, acylglycerol) fragment (Fig. 2). Scanning for neutral loss of an ammoniated *N*-fatty amide head group in a triple quadrupole mass spectrometer produces a spectrum revealing the NAPE molecular species that contain the

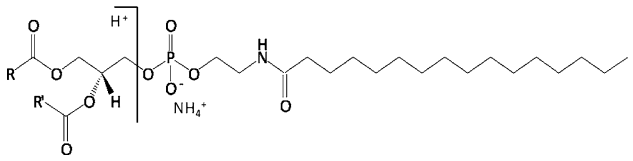

Fig. 2 Collision induced fragmentation of the ammonium adduct of *N*-16:0 PE

fragment, in other words, a spectrum of the NAPE class (Fig. 3). Sequential scanning for neutral loss of ammoniated *N*-fatty amide head groups corresponding to each common fatty acid provides a method to detect the molecular species of NAPE in all *N*-acyl classes (Fig. 3).

To determine whether neutral loss scanning provides an appropriate method for quantification, the linearity of the mass spectral response of the neutral loss scans was investigated (Fig. 4). The signals for two pure NAPEs were determined in relation to the signal from a known quantity of an internal standard, *N*-17:0 di16:0 PE. The response was determined to be linear, but both *N*-16:0 di16:0 PE and *N*-20:4 di18:1PE produced somewhat less signal per mole than *N*-17:0 di16:0 PE. This suggests that different NAPE molecular species vary somewhat in their ability to ionize and/or to undergo fragmentation under particular fixed mass spectral conditions. On the other hand, a spike-in experiment in which pure NAPE species were added to a biological mixture of lipids showed that their mass spectral signals, normalized to the *N*-17:0 di16:0 PE internal standard, were approximately proportional to the amount of each NAPE species added (Fig. 5). Finally, varying amounts of the biological sample while holding the level of internal standard constant resulted in normalized mass spectral responses proportional to the amount of sample added (Fig. 6). Taken together, the data in Fig. 3 through 6 show that, although response factors for individual NAPE molecular species vary (Fig. 3), the NAPE analysis provides a reliable means to compare levels of NAPE species among samples.

Endocannabinoid metabolism is influenced by both phospholipase D (PLD)-mediated hydrolysis of NAPE and FAAH-mediated breakdown of NAEs (Fig. 1). We examined the effect of FAAH disruption on the content and composition of NAE and various phospholipids, including NAPE and PE, in brain and heart tissue of wild-type and $FAAH^{-/-}$ mice. Total levels are summed from the individual molecular species. The data show that lipid content was generally higher in brain than in the heart tissue (Fig. 7). Compared to brain, heart phospholipids had little PS or PA. Both total NAE and PE content were significantly elevated in brain tissue of $FAAH^{-/-}$ mice compared to the wild-type controls. On the other hand, in heart tissue there was a significant increase only in PE, PI, and lysoPC content, while NAE content was the same between $FAAH^{-/-}$ and control mice.

To examine the relationship between NAE composition and the NAPE precursor pool, NAPEs were quantified according to *N*-acyl head group and these NAPE classes

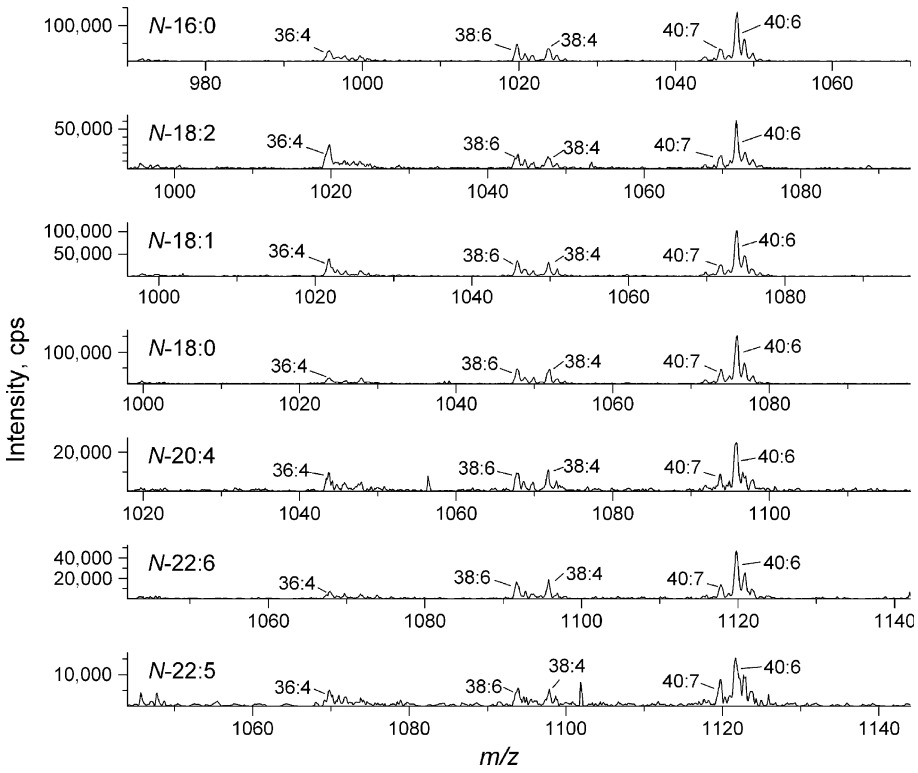

Fig. 3 Neutral loss scans targeting analysis of NAPE species with varying *N*-acyl groups. From top to bottom panels, the scans target *N*-16:0 PE (NL 396.3), *N*-18:2 PE (NL 420.3), *N*-18:1 PE (NL 422.3), *N*-18:0 PE (NL 424.3), *N*-20:4 PE (NL 444.3), *N*-22:6 PE (NL 468.3), and *N*-22:5 PE (NL 470.3) in mouse heart extract corresponding to 6–25 mg FW. The labels indicate the diacyl component (total acyl carbons: total carbon–carbon double bonds) of each detected NAPE

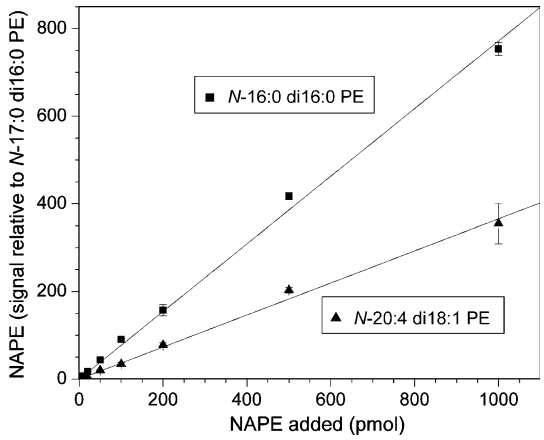

Fig. 4 Linearity of the mass spectral response. Varying amounts of *N*-16:0 di16:0 PE and *N*-20:4 di18:1 PE were combined with 200 pmol of internal standard *N*-17:0 di16:0 PE. Neutral loss signals for each NAPE molecular species are presented in relation to the signal from the internal standard; the amount of signal produced by 1 pmol of *N*-17:0 di16:0 PE is 1. $N = 5 \pm$ SD

were compared to the principal NAE types. Absolute quantities of NAPE and NAE and their composition were quite different between brain and heart tissue of mice (Figs. 8 and 9, respectively). The significantly higher level of NAE in the brain tissue of $FAAH^{-/-}$ mice, as compared to wild-type mice, was attributable mostly to 16:0 NAE (Fig. 8); the level of *N*-16:0 PE was also significantly higher in the brain tissue of $FAAH^{-/-}$ mice, as compared to wild-type mice. The concentration of 18:0 NAE species was higher in brain tissue of $FAAH^{-/-}$ mice as well. In contrast to predominant 16:0 NAEs and *N*-16:0 PEs in brain, heart tissue did not reveal a prevalent NAPE class or NAE type. Murine hearts showed no differences between $FAAH^{-/-}$ and wild-type animals in NAE types or NAPE classes. This suggests that FAAH disruption has a considerably greater effect on steady-state levels of endocannabinoid pathway metabolites in brain tissue than in heart tissue. Major differences in steady-state anandamide levels in brain extracts between $FAAH^{-/-}$ mice and wildtype littermates were not evident in our studies, which was inconsistent with previous reports quantifying 15-fold higher anandamide levels in brain tissues of $FAAH^{-/-}$ mice compared to FAAH+/+ mice [20, 28]. Differences may be due to organ preparation (euthanasia rather than decapitation) and/or tissue extraction procedures since anandamide levels seem to be particularly sensitive to preparation methods [29]. Nonetheless, the principal saturated NAE types (NAE18:0 and NAE16:0) quantified in our samples showed a significant elevation in brain tissues of knockout mice as expected (Fig. 8).

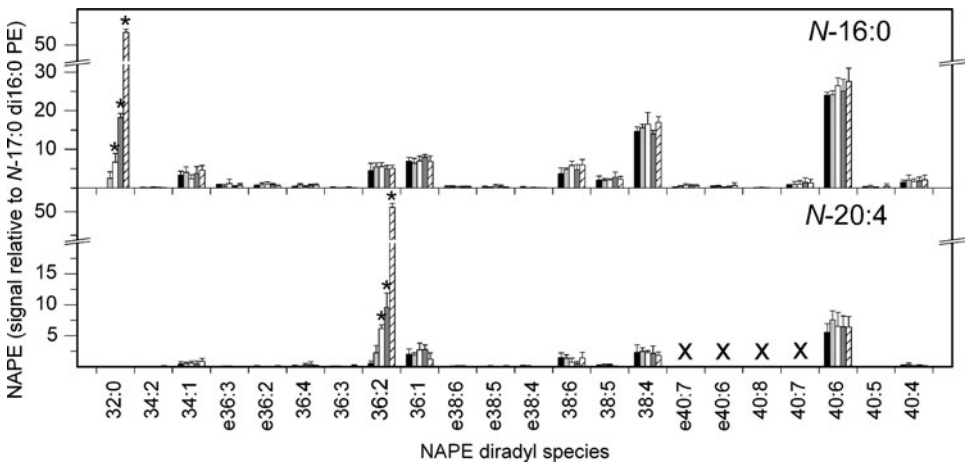

Fig. 5 The ability of ESI-MS/MS lipid profiling to detect small changes in NAPE molecular species. The lipid species in roughly 10 mg FW of mouse brain were analyzed and, to demonstrate the ability of the lipid profiling methodology to detect changes, small, known amounts of specific lipid species were added to the extract. One hundred pmol of internal standard *N*-17:0 di16:0 PE was added to each sample to provide quantitation. Neutral loss scans were performed as described in Experimental Procedures. Signals for each NAPE molecular species are presented in relation to the signal of internal standard *N*-17:0 di16:0 PE; the amount of signal produced by 1 pmol of *N*-17:0 di16:0 PE is 1. The additions of the lipid species indicated by the *asterisks* varied over a 15-fold range (with *bars* for each species representing no addition, 1× addition, 2× addition, 5× addition, and 15× addition). Specifically, the *black bars* (first series) represent the composition of the extract. The light *gray bars* (second series) represent extract with 4 pmol *N*-16:0 di16:0(32:0) PE and 5 pmol *N*-20:4 di18:1(36:2) PE added. The *white bars* (third series) represent extract with 8 pmol *N*-16:0 di16:0(32:0) PE and 10 pmol *N*-20:4 di18:1(36:2) PE added. The *dark gray bars* (fourth series) represent extract with 20 pmol *N*-16:0 di16:0(32:0) PE and 25 pmol *N*-20:4 di18:1(36:2) PE added. The *hatched bars* (fifth series) represent extract with 60 pmol *N*-16:0 di16:0(32:0) PE and 75 pmol *N*-20:4 di18:1(36:2) PE added. Designations for diradyl molecular species are: numbers only represent diacyl species as total acyl carbons: total carbon–carbon double bonds; e before a number indicates an ether-linked (alk(en)yl,acyl) species as total alk(en)yl + acyl carbons: total carbon–carbon double bonds, including any vinyl ether bonds present. "X" indicates molecular species that were not determined (see "Experimental Procedures"). $N = 5 \pm$ SD

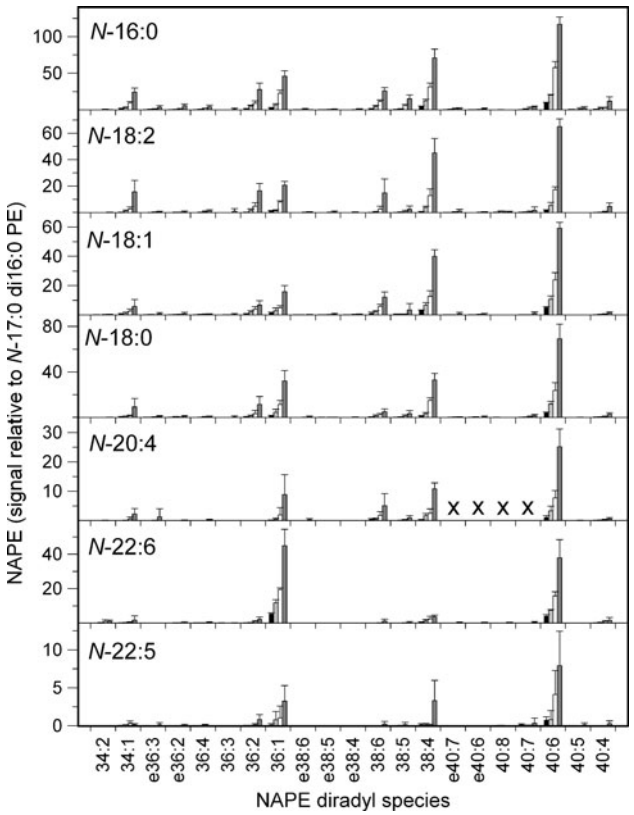

Fig. 6 Variation in mass spectral response with variation in amount of biological sample. Varying amounts of mouse brain extract were combined with 200 pmol of internal standard N-17:0 di16:0 PE. The amounts of mouse brain extract corresponded to approximately 3.5 mg FW (*black bars*, first series), 7 mg FW (*light gray bars*, second series), 14 mg FW (*white bars*, third series), and 28 mg FW (*dark gray bars*, fourth series). Neutral loss signals for each NAPE molecular species are presented in relation to the signal from the internal standard; the amount of signal produced by 1 pmol of *N*-17:0 di16:0 PE is 1. Designations for diradyl molecular species are: numbers only represent diacyl species as total acyl carbons: total carbon–carbon double bonds; e before a number indicates an ether-linked (alk(en)yl,acyl) species as total alk(en)yl + acyl carbons: total carbon–carbon double bonds, including any vinyl ether bonds present. "X" indicates molecular species that were not determined (see "Experimental Procedures"). $N = 5 \pm$ SD

Although useful for visualizing potential NAE precursors, grouping of NAPE species by common *N*-acyl chains (Figs. 8, 9) does not reveal the remarkable complexity of NAPEs. Therefore, a detailed molecular species profile of NAPE was generated for brain and heart tissue of wild-type and $FAAH^{-/-}$ mice (Figs. 10, 11). In brain tissue of mice, the most abundant molecular species with 16:0 at the *N*-position contained PE 36:2, 36:1, 38:6, 38:4, and 40:6, where the species are indicated by total acyl carbons:total carbon–carbon double bonds in the combined acyl chains in the 1 and 2 positions on the glycerol (Fig. 10). Many *N*-16:0-containing species were significantly elevated in knockout mice compared to wild type, suggesting that the elevation of the *N*-16:0 PE molecular species in $FAAH^{-/-}$ mice affected those molecular species already prevalent in wild-type mice. *N*-18:2-containing NAPE molecular species were much less abundant overall; only five molecular species were quantified at more than 0.1 nmol/g FW, and none of these were elevated in $FAAH^{-/-}$ brain tissue (Fig. 10). *N*-18:1 and *N*-18:0 molecular species were somewhat more abundant and distributed among diradyl species in a manner similar to *N*-16:0 PEs; several molecular species were significantly higher in the $FAAH^{-/-}$ knockout tissues (Fig. 10). The anandamide-containing (*N*-20:4) NAPE pool was relatively minor in terms of overall abundance, and this subgroup showed no differences between wild-type and $FAAH^{-/-}$ in terms of quantity or composition. Similarly, the *N*-22:6 PE molecular species were not very abundant, and the *N*-22:5 PE class was very minor in brain tissue, with only a few molecular species identified in this subgroup. There were no significant differences in *N*-22:6 and *N*-22:5 PE species between wild-type and $FAAH^{-/-}$ mice.

Similar to brain tissue, murine heart tissue showed complexity in the molecular species composition of NAPE (Fig. 11). Some differences were immediately evident between heart and brain NAPE molecular species. First, the content of all NAPE molecular species in heart tissue was two- to four-fold less than in the brain tissue (compare NAPE class data in Figs. 8 and 9), and there was no difference in molecular species content of any NAPE type in heart tissue of $FAAH^{-/-}$ mice compared to wild type (Fig. 11).

Comparisons of PC and PE compositions of brain and heart (Figs. 12, 13) show that the diradyl compositions of these two major phospholipid classes are quite different from each other. In brain, 40:6 PE was the most abundant diradyl species for *N*-acylation, with 36:1, 38:6, and 38:4 species also being prominent (Fig. 10). In heart, 40:6 and 38:6 were most prominent with 38:4 and 36:4 also abundant (Fig. 11). These NAPE compositions resemble the PE compositions (Figs. 12, 13), supporting the notion that NAPE is derived from PE (Fig. 1).

Discussion

Considerable prior evidence has established the metabolic relationship of PE, its *N*-acylation to form NAPE, and the hydrolysis of NAPE to form the bioactive NAEs (Fig. 1). Several NAE types have been identified as endogenous ligands for the cannabinoid receptors, while other types act on other cellular targets [30–32]. The hydrolysis of the NAEs (endocannabinoids and others) by FAAH terminates their lipid mediator functions [8, 33]. Given the broad range of activities of the NAEs, the enzymes of this pathway represent important therapeutic targets [34, 35].

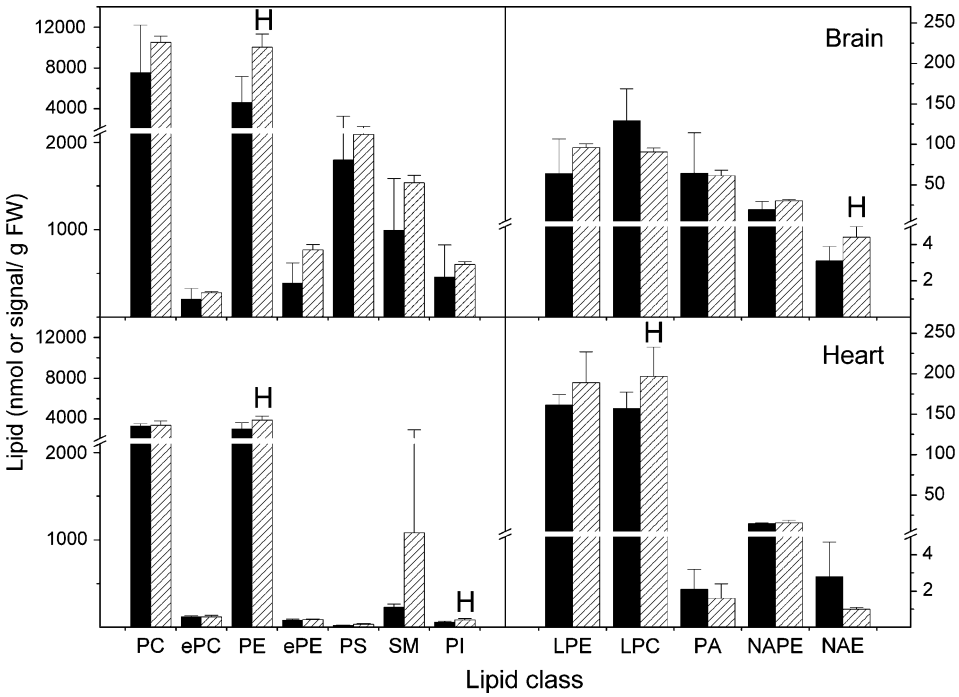

Fig. 7 Endogenous phospholipids and ethanolamine-containing NAE metabolites. Total lipid extracts of brain and heart tissue of wild-type (WT, *black bars*) and $FAAH^{-/-}$ (KO, *hatched bars*) mice were analyzed for phospholipid, including PE and NAPE and NAE content as described in "Experimental Procedures." *Right panels* use right-hand scale and *left panels* use left-hand scale. NAPEs are expressed as normalized signal/g FW; all others are expressed as nmol/g FW. $N = 4$ or 5 ± SD. Significance ($P < 0.05$) was determined by unpaired Student's t test for KO vs. WT. "H" indicates that the KO level is significantly higher than the wild-type value

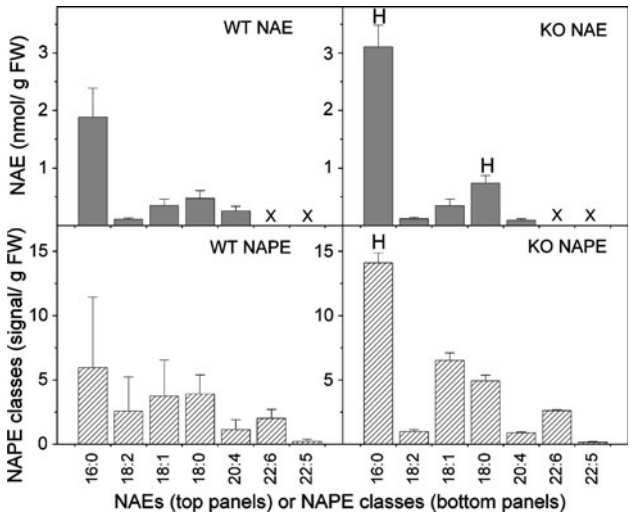

Fig. 8 Brain NAE species (*dark gray bars*) and NAPE classes (*hatched bars*) in wild-type (WT) and $FAAH^{-/-}$ (KO) mice. $N = 4$ or 5 ± SD. "X" indicates species that were not determined. Significance ($P < 0.05$) was determined by unpaired Student's t test for KO vs. WT. "H" indicates that the KO level is significantly higher than the wild-type value

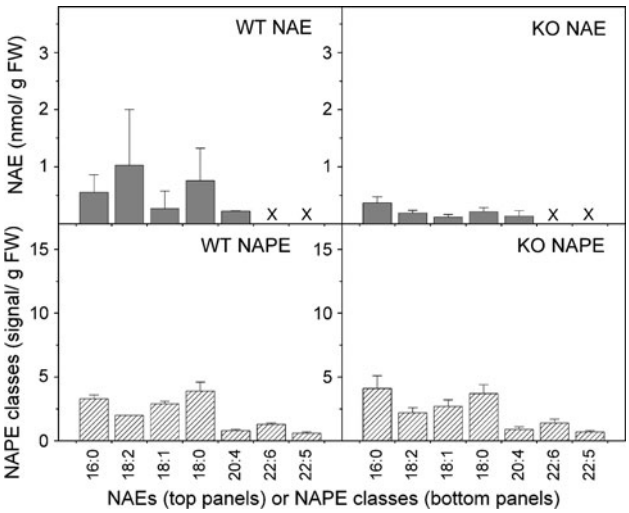

Fig. 9 Heart NAE species (*dark gray bars*) and NAPE classes (*hatched bars*) in wild-type (WT) and $FAAH^{-/-}$ (KO) mice. $N = 4$ or 5 ± SD. "X" indicates species that were not determined. Significance ($P < 0.05$) was determined by unpaired Student's t test for KO vs. WT

Often less appreciated are the large numbers of metabolites that are generated in this overall *N*-acylation-phosphodiesterase-FAAH pathway, many of which are cellular lipids with other functions and only some of which are identified and quantified for their lipid mediator functions.

Targeted lipidomics approaches permit comprehensive analysis of metabolites involved in a specific lipid metabolic pathway. Recently, sensitive and high-throughput analytical tools have been established to unravel the biological significance of individual molecules of the endocannabinoid system in the context of the interconnected network of their precursors and derivatives [36–38]. However, these studies were limited mostly to endocannabinoids that occur in minor quantities relative to the other non-cannabimimetic members of the large *N*-acylethanolamide family. Since we do not fully understand the nature of selective biosynthesis or degradation of a specific NAE type

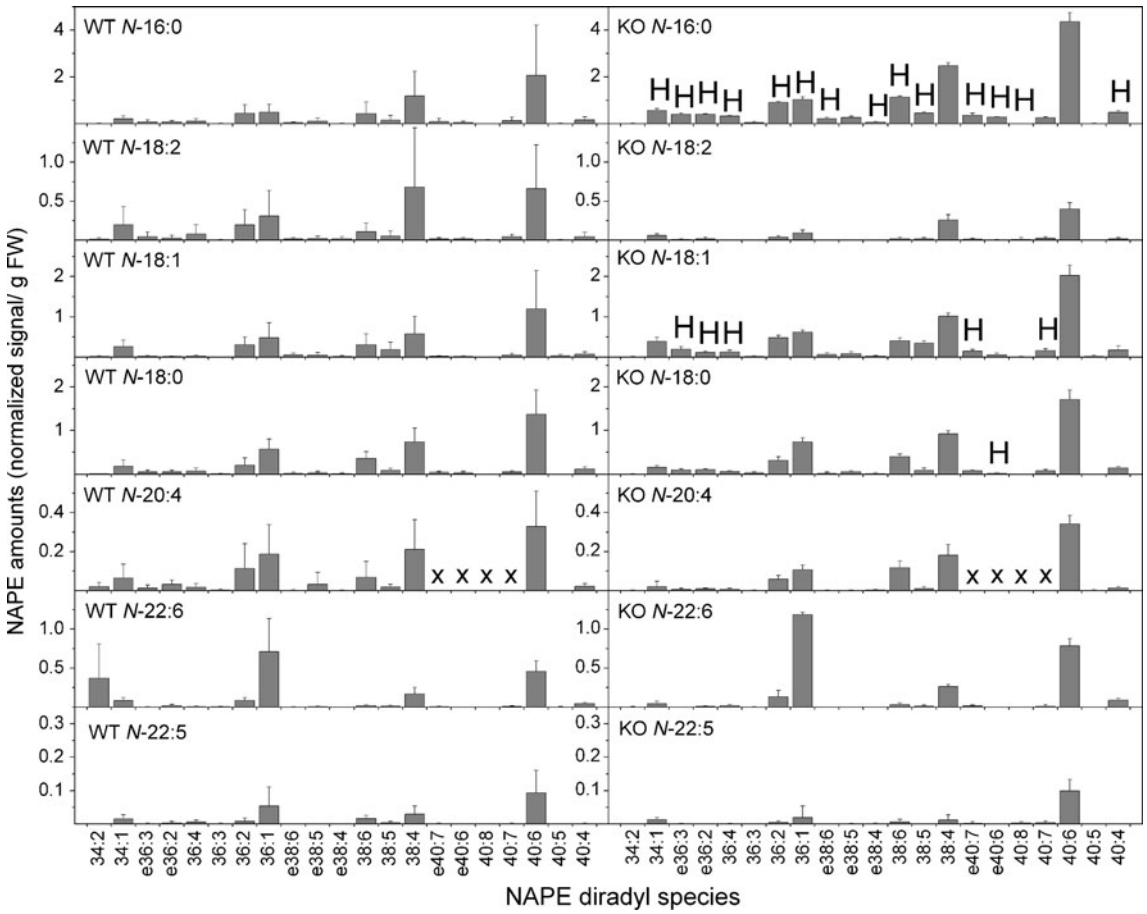

Fig. 10 Detailed profile of NAPE molecular species from brain tissue of wild-type (WT) and $FAAH^{-/-}$ (KO) mice. Designations for diradyl molecular species are: numbers only represent diacyl species as total acyl carbons: total carbon–carbon double bonds; e before a number indicates an ether-linked (alk(en)yl,acyl) species as total alk(en)yl + acyl carbons: total carbon–carbon double bonds, including any vinyl ether bonds present. "X" indicates molecular species that were not determined (see "Experimental Procedures"). $N = 4$ or $5 \pm$ SD. Significance ($P < 0.05$) was determined by unpaired Student's t test for KO vs. WT. "H" indicates that the KO level is significantly higher than the wild-type value

or its precursors (Fig. 1), especially under the influence of genetic perturbations of this regulatory pathway, we used a targeted lipidomics approach to elucidate changes in the profiles of PE, NAPE, and NAE in brain and heart tissue of wild-type and $FAAH^{-/-}$ mice.

Comparison of NAE metabolites and major and minor phospholipids between brain and heart tissue of mice revealed some similarities, but also several tissue-specific differences. The most abundant metabolite of the NAE regulatory pathway in brain and heart tissue was PE (Figs. 1, 7). It appears that the relative abundance of specific PE molecular species in the PE pool determines the molecular composition of NAPE rather than a preferential substrate selectivity of *N*-acyltransferase (Figs. 10 vs. 12 and 11 vs. 13). Furthermore, brain tissue of $FAAH^{-/-}$ mice showed accumulation of already abundant PE and NAPE molecular species rather than synthesis and accumulation of new or less abundant molecular species or remodeling of the amide-linked fatty acids of NAPE. These data suggest that lack of FAAH in brain tissue results in accumulation of NAE species, which may in turn affect the content but not the composition of the NAE precursor pool. Although total PE was significantly higher in the heart tissue of $FAAH^{-/-}$ mice when compared with wild type (Fig. 7), fewer PE molecular species contributed significantly to the overall increase in PE content in heart than in brain (Figs. 12, 13). The lesser FAAH-specific effect on NAE and its metabolites in heart tissue (Figs. 7–13) was not surprising because FAAH activity was reported to be negligible in heart tissue of mice [39].

Although the total NAE content was similar between the two tissue types, it is interesting to note that total PE and NAPE levels are lower in heart tissue (Fig. 7). Furthermore, *N*-16:0 PE and 16:0 NAE were the most predominant species in brain tissue, while heart tissue did not show preference for any specific type (Figs. 8, 9). It is possible that

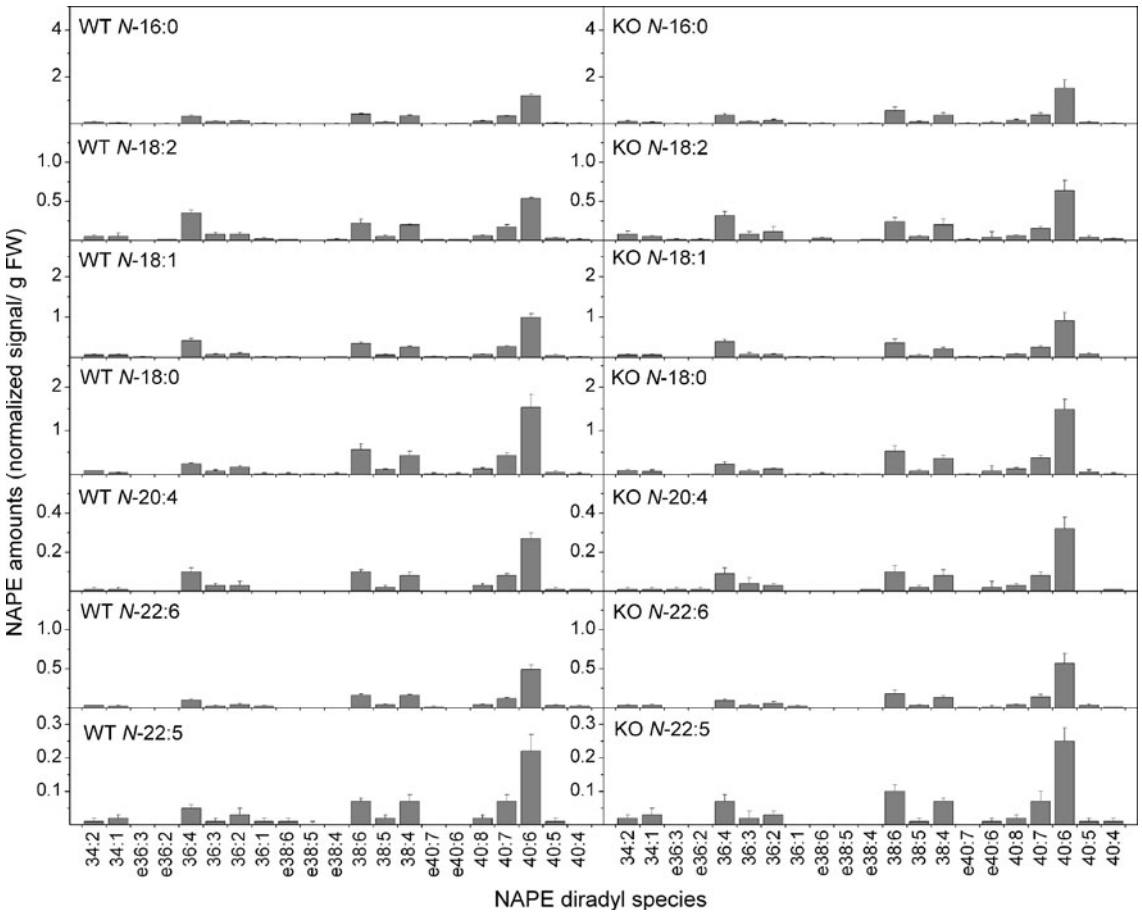

Fig. 11 Detailed profile of NAPE molecular species from heart tissue of wild-type (WT) and $FAAH^{-/-}$ (KO) mice. Designations for diradyl molecular species are: numbers only represent diacyl species as total acyl carbons: total carbon–carbon double bonds; e before a number indicates an ether-linked (alk(en)yl,acyl) species as total alk(en)yl + acyl carbons: total carbon–carbon double bonds, including any vinyl ether bonds present. $N = 4$ or $5 \pm$ SD. Significance ($P < 0.05$) was determined by unpaired Student's t test for KO vs. WT

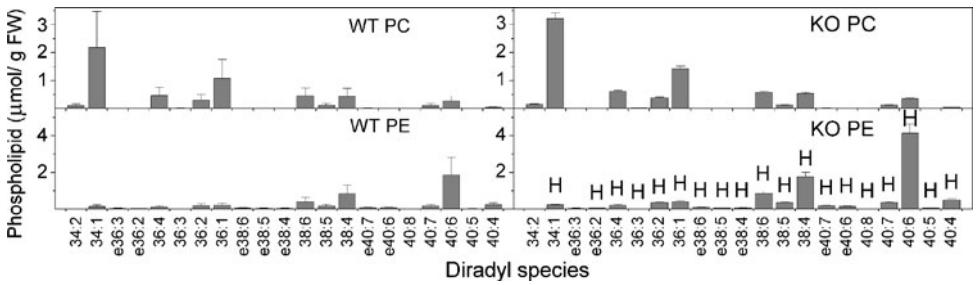

Fig. 12 PC and PE species from brain tissue of wild-type (WT) and $FAAH^{-/-}$ (KO) mice. Designations for diradyl molecular species are: numbers only represent diacyl species as total acyl carbons: total carbon–carbon double bonds; e before a number indicates an ether-linked (alk(en)yl,acyl) species as total alk(en)yl + acyl carbons: total carbon–carbon double bonds, including any vinyl ether bonds present. $N = 4$ or $5 \pm$ SD. Significance ($P < 0.05$) was determined by unpaired Student's t test for KO vs. WT. "H" indicates that the KO level is significantly higher than the wild-type value

N-acylethanolamine-hydrolyzing acid amidase, a second NAE-degrading amidase expressed in the heart and brain [40], may exhibit differential expression and activity in these tissues, potentially leading to some of the tissue-specific differences seen in levels of NAE species in $FAAH^{-/-}$ mice. The higher levels and distinctive composition of NAPE may suggest additional brain NAPE roles, such as maintenance of physical properties of membrane domains [41] and influence on signaling processes in the brain [42], in addition to serving as the precursor for NAE synthesis.

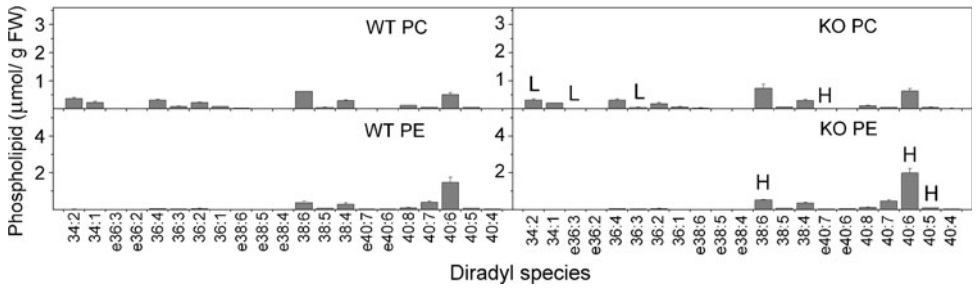

Fig. 13 PC and PE species from heart tissue of wild-type (WT) and $FAAH^{-/-}$ (KO) mice. Designations for diradyl molecular species are: numbers only represent diacyl species as total acyl carbons: total carbon–carbon double bonds; e before a number indicates an ether-linked (alk(en)yl,acyl) species as total alk(en)yl + acyl carbons: total carbon–carbon double bonds, including any vinyl ether bonds present. $N = 4$ or $5 \pm$ SD. Significance ($P < 0.05$) was determined by unpaired Student's t test for KO vs. WT. "H" indicates that the KO level is significantly higher and "L" indicates that the KO level is significantly lower than the wild-type value

Comparative analysis of major and minor phospholipids revealed higher levels of most phospholipids in brain tissue compared to heart, as expected, perhaps due to overall higher lipid content in the brain (Fig. 7). However, in $FAAH^{-/-}$ mice, brain tissue showed accumulation only in the PE and NAE contents, as discussed earlier. On the other hand, $FAAH^{-/-}$ heart tissue showed an increase not only in PE, but also in phosphatidylinositol (PI) and lysoPC. In fact lysoPC content was higher in wild-type heart tissue than in brain (Fig. 7). LysoPC is a byproduct of the *trans*-acylase reaction and might serve, together with other 1-lyso-phospholipids, as a precursor for the formation of 2-arachidonoylglycerol (2-AG) [43]. Additionally, hydrolysis of PI by a PI-specific phospholipase A_1 can also generate 2-AG [44]. Even though elimination of FAAH activity did not directly affect the NAE metabolites in heart tissue of mice, it may have influenced alternate endocannabinoid metabolic pathways by affecting the phospholipid composition.

Collectively, our targeted lipidomics results imply a metabolic *N*-acylation-phosphodiesterase pathway for acylethanolamides that is dominated by major cellular lipid constituents, but in which minor metabolites also play roles. Perturbation of FAAH may influence metabolite pools in this entire pathway, beyond simply the direct substrates for this enzyme; however, this influence by FAAH on NAPE and PE molecular species content is tissue-specific. Metabolic profiling tools like these developed here, applied to different physiological or pathological situations that have been attributed to endocannabinoid function, may help to reveal important new tissue-specific metabolic targets for therapeutic intervention at points of control not yet discovered.

Acknowledgments We would like to thank Mary R. Roth for expert technical assistance. This work was supported by a seed grant from the University of North Texas and by a grant from the US Department of Energy, Office of Basic Energy Sciences (DE-FG02-05ER15647). This study was supported in part by NIH grants MD001633 from NCMHD (R.S.D.), EY014227, AG010485, AG022550, and AG027956 (P.K.) as well as by The Garvey Texas Foundation and the Felix and Carmen Sabates Missouri Endowed Chair in Vision Research (P.K.). Instrument acquisition and method development at the Kansas Lipidomics Research Center were supported by NSF grants MCB 0455318 and DBI 0521587, K-INBRE (NIH Grant P20 RR16475 from the INBRE program of the National Center for Research Resources), and NSF EPSCoR grant EPS-0236913 with matching support from the State of Kansas through Kansas Technology Enterprise Corporation and Kansas State University.

References

1. De Petrocellis L, Di Marzo V (2009) An introduction to the endocannabinoid system: from the early to the latest concepts. Best Pract Res Clin Endocrinol Metab 23(1):1–15. doi: 10.1016/j.beem.2008.10.013
2. Di Marzo V, Bisogno T, De Petrocellis L (2000) Endocannabinoids: new targets for drug development. Curr Pharm Des 6(13): 1361–1380
3. Devane WA, Hanus L, Breuer A, Pertwee RG, Stevenson LA, Griffin G, Gibson D, Mandelbaum A, Etinger A, Mechoulam R (1992) Isolation and structure of a brain constituent that binds to the cannabinoid receptor. Science 258(5090):1946–1949
4. Schmid HH, Schmid PC, Natarajan V (1996) The n-acylation-phosphodiesterase pathway and cell signalling. Chem Phys Lipids 80(1–2):133–142
5. Schmid HH, Schmid PC, Natarajan V (1990) N-acylated glycerophospholipids and their derivatives. Prog Lipid Res 29(1):1–43
6. Giang DK, Cravatt BF (1997) Molecular characterization of human and mouse fatty acid amide hydrolases. Proc Natl Acad Sci USA 94(6):2238–2242
7. Cravatt BF, Giang DK, Mayfield SP, Boger DL, Lerner RA, Gilula NB (1996) Molecular characterization of an enzyme that degrades neuromodulatory fatty-acid amides. Nature 384(6604):83–87
8. Ahn K, McKinney MK, Cravatt BF (2008) Enzymatic pathways that regulate endocannabinoid signaling in the nervous system. Chem Rev 108(5):1687–1707
9. Piomelli D (2003) The molecular logic of endocannabinoid signalling. Nat Rev Neurosci 4(11):873–884
10. Wilson RI, Nicoll RA (2002) Endocannabinoid signaling in the brain. Science 296(5568):678–682
11. Natarajan V, Schmid PC, Schmid HH (1986) N-acylethanolamine phospholipid metabolism in normal and ischemic rat brain. Biochim Biophys Acta 878(1):32–41
12. Natarajan V, Reddy PV, Schmid PC, Schmid HH (1981) On the biosynthesis and metabolism of n-acylethanolamine phospholipids in infarcted dog heart. Biochim Biophys Acta 664(2):445–448

13. Epps DE, Natarajan V, Schmid PC, Schmid HO (1980) Accumulation of *N*-acylethanolamine glycerophospholipids in infarcted myocardium. Biochim Biophys Acta 618(3):420–430
14. Epps DE, Schmid PC, Natarajan V, Schmid HH (1979) N-Acylethanolamine accumulation in infarcted myocardium. Biochem Biophys Res Commun 90(2):628–633
15. Walker JM, Krey JF, Chen JS, Vefring E, Jahnsen JA, Bradshaw H, Huang SM (2005) Targeted lipidomics: fatty acid amides and pain modulation. Prostaglandins Other Lipid Mediat 77(1–4):35–45
16. Astarita G, Geaga J, Ahmed F, Piomelli D (2009) Chapter 4: Targeted lipidomics as a tool to investigate endocannabinoid function. Int Rev Neurobiol 85:35–55
17. Astarita G, Piomelli D (2009) Lipidomic analysis of endocannabinoid metabolism in biological samples. J Chromatogr B Analyt Technol Biomed Life Sci 877(26):2755–2767
18. Cravatt BF, Demarest K, Patricelli MP, Bracey MH, Giang DK, Martin BR, Lichtman AH (2001) Supersensitivity to anandamide and enhanced endogenous cannabinoid signaling in mice lacking fatty acid amide hydrolase. Proc Natl Acad Sci USA 98(16): 9371–9376
19. Fontana A, Di Marzo V, Cadas H, Piomelli D (1995) Analysis of anandamide, an endogenous cannabinoid substance, and of other natural n-acylethanolamines. Prostaglandins Leukot Essent Fatty Acids 53(4):301–308
20. Clement AB, Hawkins EG, Lichtman AH, Cravatt BF (2003) Increased seizure susceptibility and proconvulsant activity of anandamide in mice lacking fatty acid amide hydrolase. J Neurosci 23(9):3916–3923
21. Venables BJ, Waggoner CA, Chapman KD (2005) N-acylethanolamines in seeds of selected legumes. Phytochemistry 66(16):1913–1918. doi:10.1016/j.phytochem.2005.06.014
22. Devaiah SP, Roth MR, Baughman E, Li M, Tamura P, Jeannotte R, Welti R, Wang X (2006) Quantitative profiling of polar glycerolipid species from organs of wild-type arabidopsis and a phospholipase Dalpha1 knockout mutant. Phytochemistry 67(17):1907–1924. doi:10.1016/j.phytochem.2006.06.005
23. Astarita G, Ahmed F, Piomelli D (2008) Identification of biosynthetic precursors for the endocannabinoid anandamide in the rat brain. J Lipid Res 49(1):48–57. doi:10.1194/jlr.M700354-JLR200
24. Welti R, Li M, Li W, Sang Y, Biesiada H, Zhou H-E, Rajashekar C, Williams T, Wang X (2002) Profiling membrane lipids in plant stress response. J Biol Chem 277:31994–32002
25. Ames BN (1966) Assay of inorganic phosphate, total phosphate and phosphatases. In: Elizabeth FN, Victor G (eds) Methods in enzymology, vol 8. Academic Press, New York, pp 115–118
26. Shoemaker DP, Garland CW, Steinfeld JI (1974) Experiments in physical chemistry, 3rd edn. McGraw-Hill, New York
27. Welti R, Shah J, Li W, Li M, Chen J, Burke JJ, Fauconnier ML, Chapman K, Chye ML, Wang X (2007) Plant lipidomics: discerning biological function by profiling plant complex lipids using mass spectrometry. Front Biosci 12:2494–2506
28. Cravatt BF, Lichtman AH (2004) The endogenous cannabinoid system and its role in nociceptive behavior. J Neurobiol 61(1):149–160. doi:10.1002/neu.20080
29. Muccioli GG, Stella N (2008) An optimized GC-MS method detects nanomolar amounts of anandamide in mouse brain. Anal Biochem 373(2):220–228. doi:10.1016/j.ab.2007.09.030
30. Schmid HH, Schmid PC, Berdyshev EV (2002) Cell signaling by endocannabinoids and their congeners: questions of selectivity and other challenges. Chem Phys Lipids 121(1–2):111–134
31. Schmid HH, Berdyshev EV (2002) Cannabinoid receptor-inactive n-acylethanolamines and other fatty acid amides: metabolism and function. Prostaglandins Leukot Essent Fatty Acids 66(2–3): 363–376
32. Hansen HS, Moesgaard B, Hansen HH, Petersen G (2000) *N*-Acylethanolamines and precursor phospholipids—relation to cell injury. Chem Phys Lipids 108(1–2):135–150
33. McKinney MK, Cravatt BF (2005) Structure and function of fatty acid amide hydrolase. Annu Rev Biochem 74:411–432
34. Duncan RS, Chapman KD, Koulen P (2009) The neuroprotective properties of palmitoylethanolamine against oxidative stress in a neuronal cell line. Mol Neurodegener 4:50. doi:10.1186/1750-1326-4-50
35. Garg P, Duncan RS, Kaja S, Koulen P (2010) Intracellular mechanisms of n-acylethanolamine-mediated neuroprotection in a rat model of stroke. Neuroscience 166(1):252–262. doi:10.1016/j.neuroscience.2009.11.069
36. Astarita G, Geaga J, Ahmed F, Piomelli D (2009) Targeted lipidomics as a tool to investigate endocannabinoid function. Int Rev Neurobiol 85:35–55. doi:10.1016/S0074-7742(09)85004-6
37. Astarita G, Piomelli D (2009) Lipidomic analysis of endocannabinoid metabolism in biological samples. J Chromatogr B Analyt Technol Biomed Life Sci 877(26):2755–2767. doi:10.1016/j.jchromb.2009.01.008
38. Bisogno T, De Petrocellis L, Di Marzo V (2010) Methods for measuring endocannabinoid production and expression and activity of enzymes involved in the endocannabinoid system. In: Murphy EJ, Rosenberger TA (eds) Lipid mediated signaling. Methods in signal transduction series, March 2010 edn. CRC Press, Boca Raton, FL, pp 109–150
39. Ueda N, Puffenbarger RA, Yamamoto S, Deutsch DG (2000) The fatty acid amide hydrolase (FAAH). Chem Phys Lipids 108(1–2): 107–121
40. Tsuboi K, Sun YX, Okamoto Y, Araki N, Tonai T, Ueda N (2005) Molecular characterization of *N*-acylethanolamine-hydrolyzing acid amidase, a novel member of the choloylglycine hydrolase family with structural and functional similarity to acid ceramidase. J Biol Chem 280(12):11082–11092. doi:10.1074/jbc.M413473200
41. Brites P, Waterham HR, Wanders RJ (2004) Functions and biosynthesis of plasmalogens in health and disease. Biochim Biophys Acta 1636(2–3):219–231. doi:10.1016/j.bbalip.2003.12.010
42. Terova B, Heczko R, Slotte JP (2005) On the importance of the phosphocholine methyl groups for sphingomyelin/cholesterol interactions in membranes: a study with ceramide phosphoethanolamine. Biophys J 88(4):2661–2669. doi:10.1529/biophysj.104.058149
43. Di Marzo V, De Petrocellis L, Sugiura T, Waku K (1996) Potential biosynthetic connections between the two cannabimimetic eicosanoids, anandamide and 2-arachidonoyl-glycerol, in mouse neuroblastoma cells. Biochem Biophys Res Commun 227(1):281–288. doi:10.1006/bbrc.1996.1501
44. Sugiura T, Kondo S, Sukagawa A, Nakane S, Shinoda A, Itoh K, Yamashita A, Waku K (1995) 2-Arachidonoylgylcerol—a possible endogenous cannabinoid receptor-ligand in brain. Biochem Biophys Res Commun 215(1):89–97

Lipids (2010) 45:877–887
DOI 10.1007/s11745-010-3460-x

ORIGINAL ARTICLE

*t*10,*c*12-18:2-Induced Milk Fat Depression is Less Pronounced in Cows Fed High-Concentrate Diets

Frédéric Glasser · Anne Ferlay · Michel Doreau · Juan J. Loor · Yves Chilliard

Received: 22 December 2009 / Accepted: 16 July 2010 / Published online: 28 August 2010

Abstract In intensively reared dairy cows, milk fat secretion is reduced in response to high-concentrate diets and it is often referred to as the "milk fat depression" (MFD) syndrome. Some *trans* fatty acid (FA) isomers produced in the rumen of the cows, including *t*10,*c*12-18:2, are known for their inhibitory effect on mammary lipogenesis. To study whether this effect depends on the basal diet, duodenal infusions of *t*10,*c*12-18:2 were performed on cows fed four different diets (a factorial arrangement of forage:concentrate ratio and linseed oil supplementation). The overall response obtained with *t*10,*c*12-18:2 infusion was consistent with previous studies: a decrease in milk fat content and yield without significant variations in milk yield. Mean transfer efficiency of infused *t*10,*c*12-18:2 was 19.6%. However, the decrease in milk fat and FA yields (both de novo synthesis and preformed long-chain FA) was less pronounced in cows fed high-concentrate diets (−27% of the initial level), compared with cows fed low-concentrate diets (−42% of initial level). This difference was independent of dietary oil supplementation and milk FA yield before infusion. Results pertaining to effects of dietary forage:concentrate ratio were confirmed by statistical meta-analysis of data from previously published *t*10,*c*12-18:2 infusion experiments. This study shows that in cows fed MFD diets the mammary gland becomes more resistant to or experiences a lower response potential to further inhibition of lipogenesis and/or delta-9 desaturation of FA.

Keywords Dairy cow · Milk fatty acids · t10 · c12-CLA · Milk fat depression

Abbreviations

BHBA	Beta-hydroxy butyric acid
C16	16-Carbon fatty acids
C18	18-Carbon fatty acids
CLA	Conjugated linoleic acid
DMI	Dry matter intake
FA	Fatty acid
MFD	Milk fat depression
NDF	Neutral detergent fibre
NEFA	Nonesterified fatty acids
VFA	Volatile fatty acid

Introduction

Milk fat contributes to the value of milk for the dairy producer and is easily modified in quantity and quality by the cow's diet [1]. In intensively reared dairy cows, milk fat secretion is reduced in response to high-concentrate diets and it is often referred to as the "milk fat depression" (MFD) syndrome. For several decades, the physiological determinants of this phenomenon have been studied and has led to the current mainstream concept referred to as "biohydrogenation theory", supposedly explaining most, if not all, cases of MFD [2–4]. According to this theory, MFD is caused by some fatty acid (FA) isomers produced by

F. Glasser · A. Ferlay · M. Doreau · J. J. Loor · Y. Chilliard (✉)
INRA, UR1213 Herbivores, Site de Theix, 63122 Saint-Genès-Champanelle, France
e-mail: yves.chilliard@clermont.inra.fr

Present Address:
J. J. Loor
Mammalian NutriPhysioGenomics, Division of Nutritional Sciences, Department of Animal Sciences, University of Illinois, Urbana 61801, USA

rumen microorganisms during the biohydrogenation of dietary polyunsaturated FA. To date, three isomers of conjugated linoleic acid (CLA) have been identified for their inhibitory role on mammary lipogenesis: *t*10,*c*12-18:2, *t*9,*c*11-18:2 and *c*10,*t*12-18:2 [5–7]. Exogenous infusions of these CLA decrease the yield of both preformed FA [mainly 16- and 18-carbon (C16 and C18) FA taken up by the mammary gland from the plasma] and short- and medium-chain FA (C4-C16) from mammary de novo synthesis, with generally greater depression in the de novo synthesized FA than the preformed FA.

Many studies with duodenal infusions of *t*10,*c*12-18:2 (the only commercially available inhibitory isomer) have demonstrated its inhibitory role on mammary lipogenesis, and the response of milk fat to increasing amounts of this isomer have been published [8]. However, duodenal flows of *t*10,*c*12-18:2 (and other inhibitory isomers) measured in vivo are far too low to explain the extent of diet-induced MFD. Most authors hypothesize that this discrepancy may be due to other inhibiting *trans* 18:1 or 18:2 isomers (still unidentified) [4, 9]. The isomer *t*10-18:1 is correlated with MFD [4, 10], but short-term abomasal infusions of this isomer suggest an inhibition of milk fat secretion only when infused at high doses (>50 g/day) [11, 12].

The biohydrogenation theory is accepted by most authors as the main mechanism explaining MFD. However, milk fat depressing diets (high concentrate, high starch, polyunsaturated fats, pasture sometimes) also alter ruminal environment (decrease in pH with high concentrate) and fermentation products (increased propionate production). MFD diets, thus, lead to a simultaneous increase of numerous FA isomers and other energetic nutrients, complicating the elucidation of related mechanisms. It is possible that components other than 18:2 isomers may contribute to MFD. To test this hypothesis, we compared the effect of *t*10,*c*12-18:2 duodenal infusions (mimicking one player of the "biohydrogenation theory" component of MFD) in cows fed diets with contrasting forage:concentrate ratio and supplemental oil content. The effect of *t*10,*c*12-18:2 on milk fat synthesis has indeed never been compared in different nutritional conditions in the same study, and this comparison could provide new insights on the regulation of milk fat yield.

Experimental Procedure

Animals, Diets and Treatments

Four lactating multiparous Holstein cows (55–87 DIM) with cannulas in the rumen and proximal duodenum were used in a 4 × 4 Latin square design with factorial arrangement of treatments (four diets differing in their forage:concentrate ratio and level of oil supplementation) during four 5-week periods to evaluate responses to duodenal *t*10,*c*12-18:2 infusions. The cows were fed a high-concentrate diet (HC, forage:concentrate ratio 35:65) or low-concentrate diet (LC, forage:concentrate 65:35) without added linseed oil (diets HC and LC) or with linseed oil supplemented at 3% of DM (diets HCO and LCO). This infusion study was part of a previously published experiment [10, 13, 14], during which a pre-infusion period (the first 4 weeks of each 5-week period) was used to study the cows' response to the diets. Experimental procedures are described in [10, 13, 14]. The sole forage was long-cut grass hay and the concentrate mixture was based primarily on ground wheat, rapeseed, sunflower meal, and wheat bran. Details of ingredient, chemical composition, and FA profiles of the diet have been presented previously [13]. The experimental protocol was approved by the Animal Care and Use Committee of INRA. All experimental procedures were conducted in accordance with the Use of Vertebrates for Scientific Purposes Act 1985. Cows were housed in a tie-stall barn during the experiment. The concentrate mixtures with or without linseed oil were prepared daily and, along with the forage, were offered in equal amounts at 0900, 1330, and 1700 hours for ad libitum consumption. Cows were milked at 0600 and 1630 hours. During the fifth week of each experimental period, the cows received *t*10,*c*12-18:2 from a duodenum infusion of 5 g/day of a commercial CLA source (t10c12-CLA 95%-FFA; Natural Lipids, Hovdebygda, Norway). The CLA mixture was composed of 0.20% *c*9-18:1, 0.95% *c*9,*t*11-18:2, 94.55% *t*10,*c*12-18:2 and 2.25% *t*9,*t*11 + *t*10,*t*12-18:2.

The CLA mixture was emulsified in skim milk to ensure a uniform supply during the infusion. Emulsions were prepared in the morning of each day prior to infusion by combining 5 g of CLA with 2 g glycerol (Sigma, G6279, Saint-Quentin Fallavier, France) and 1.1 g lecithin powder (Sigma, P5394, Saint-Quentin Fallavier, France) in 991.9 g skim milk at room temperature. The mixture was homogenized at 10,000 rpm for 2 min with a Polytron homogenizer (PT-HR 3000, Fisher Scientific Bioblock, France), and checked for the presence of clumps before stirring at medium-to-high speed for 30 min at room temperature. Emulsions were dispensed into 5-L plastic bags and stored at 4 °C until infusion. Duodenal infusion of CLA began at 1400 hours on day 0 and continued for 4 days. After 24 h, the empty bag was replaced with another bag containing 1 L of emulsion. Duodenal infusates were delivered via polyvinyl chloride tube (0.5 cm i.d.), that passed through the duodenum fistula. Peristaltic pumps (STA-131900; Desaga, Heidelberg, Germany) delivered the infusate continuously over 24 h. Infusion equipment was checked daily during treatment periods to ensure correct placement in the duodenum cannula.

Sampling, Measurements and Analyses

Milk production and dry matter intake (DMI) were recorded daily throughout the infusion period. Milk was sampled at each milking and pooled each day. Fatty acids in lyophilized milk were directly methylated with 1 mL of 2 N methanolic $NaOCH_3$ at room temperature for 20 min, followed by 1 mL of 14% boron trifluoride in methanol at room temperature for 20 min [15]. Fatty acids in plasma lipids were methylated with 2 mL of 0.5 N $NaOCH_3$ at 50 °C for 30 min, followed by 2 mL of 14% boron trifluoride in methanol at 50 °C for 30 min [16, 17]. In all cases, FA methyl esters were recovered in 1 mL of hexane. Tricosanoate (Sigma, Saint-Quentin Fallavier, France) was used as the internal standard. Samples were injected by autosampler into a Trace-GC 2000 Series gas chromatograph equipped with a flame ionization detector (Thermo Finnigan, Les Ulis, France). Methyl esters from all samples were separated on a 100 m × 0.25 mm i.d. fused silica capillary column (CP-Sil 88, Chrompack, Middelburg, The Netherlands). Identification of fatty acids and detailed analytical procedure have been previously described in [10].

Calculations and Statistical Analyses

Desaturation ratios were computed for 14:0, 16:0, 18:0, *t*11-18:1 and *t*13-18:1, using their respective monounsaturated counterparts (e.g. for 18:0 the ratio is *c*9-18:1/(18:0 + *c*9-18:1) × 100). For all data, individual cow responses to CLA infusion were computed for each period (data for d4, after 4 days of infusion, minus data for d0). The statistical analyses were conducted on these responses, analysed as a Latin square with factorial arrangement of treatments using the MIXED procedure of SAS (SAS Inst., Inc., Cary, NC, USA). The statistical model included: cow, period, concentrate level, oil level, concentrate × oil interaction, and residual error. Cow was the random effect. The overall response to CLA infusion (across all diets) was also tested against zero. The responses to CLA infusion for each diet were compared to zero, and multiple comparisons of means (between diets) were performed using Tukey tests. The initial values (before infusion) are reported in the tables for comparison only, because they differed between diets, but were not subject to statistical analyses (only responses to CLA infusion were).

To determine whether the differences in responses were due to the diet or to the initial values of milk fat, we used two approaches: (1) the response to CLA infusion was expressed as a percentage of the initial value and (2) we performed a meta-analysis of the CLA infusion experiments already published. For this meta-analysis, we reviewed the published experiments of *t*10,*c*12-18:2 infusions [5–8, 11, 12, 18–25]. We excluded the experiment of Bell and Kennelly [21], in which the infusion of 45 g/day of *t*10,*c*12-18:2 probably elicited different mechanisms than studies with lower doses [26]. From these data, we calculated the response to CLA infusions and then performed nonlinear regression analyses on these responses, including the effect of CLA dose, and other putative variables (chemical composition of the diet, initial values of milk fat yield and content, milk yield, etc.). The models used were exponential decrease models: $Y = a \times (1-e^{(-b \times \text{CLA dose})})$, parameters a and b being the maximal decrease and the slope of decrease respectively. The different models were compared using AICc criteria (Akaike Information Criteria, corrected for small samples, the model with the lowest AICc value is selected).

Results

DMI and Milk Production and Composition

Average DMI did not differ between basal diets, and was not affected by *t*10,*c*12-18:2 infusion (Table 1), except for the HCO diet, due to a drop in DMI for one cow (without affecting milk production). Milk production, initially lower for the LC diet, was not affected by *t*10,*c*12-18:2 infusion. Overall, after 4 days of infusion, the milk fat percentage and yield were markedly decreased by *t*10,*c*12-18:2 infusion, and the decrease was greater ($P < 0.05$) for low-concentrate diets, irrespective of the dietary oil content (Table 1). The other production variables were not affected by *t*10,*c*12-18:2 infusion (Table 1).

Plasma Composition

Among the metabolites measured in jugular and mammary veins, mammary concentrations of acetate and glucose were significantly increased and jugular–mammary differences of acetate were significantly decreased by *t*10,*c*12-18:2 infusion (Table 1). The other plasma components (beta-hydroxybutyrate, NEFA, free cholesterol, total cholesterol, free glycerol, lactate, phospholipids, triglycerides, urea, insulin) were not significantly altered by *t*10,*c*12-18:2 infusion (some data not shown). When the J–M difference was expressed as an apparent extraction rate (as a percent of the jugular level, data not shown), *t*10,*c*12-18:2 significantly decreased ($P < 0.05$) the apparent extraction rates of acetate (48.5% after infusion vs. 68.9% before), glucose (17.8 vs. 22.3%) and BHBA (31.5 vs. 45.6%), irrespective of the basal diet.

The concentrations and the percentages of FAs in the jugular plasma were not affected by *t*10,*c*12-18:2 infusion

Table 1 Selected variables in cows fed a low-concentrate (LC) or high-concentrate (HC) diet, without (LC, HC) or with supplemental linseed oil (LCO, HCO) at 3% of DM

	Initial values				Responses to CLA infusion[A]					Overall response[B]	Effects on the response[B]		
	LC	LCO	HC	HCO	LC	LCO	HC	HCO	SEM		Conc	Oil	Conc × oil
DMI	20.1	19.7	20.9	21.1	+0.1	−0.1	+0.1	−2.1*	0.7				
Milk													
Milk yield (kg/day)	23.3	28.8	29.7	29.9	+0.03	−0.93	+0.90	+0.38	0.68				
Protein (%)	3.11	2.96	3.05	3.25	+0.07	0.16	+0.04	−0.08	0.07				
Lactose (%)	4.76	4.88	4.89	4.85	−0.14	−0.11	−0.09	−0.03	0.06				
Fat (%)	3.28	3.82	2.73	2.43	−1.35*[ab]	−1.58*[b]	−0.82*[ab]	−0.69*[a]	0.27	<0.01	<0.05		
Protein (kg/day)	0.72	0.85	0.91	0.96	+0.02	+0.02	+0.04	−0.01	0.03				
Lactose (kg/day)	1.11	1.41	1.46	1.45	−0.03	−0.08	+0.01	+0.01	0.04				
Fat (kg/day)	0.76	1.11	0.81	0.72	−0.31*[ab]	−0.49*[b]	−0.21*[a]	−0.20[a]	0.08	<0.01	<0.05		
Plasma													
Jugular BHBA (mM)	0.36	0.31	0.26	0.18	−0.07	+0.03	−0.06	0.00	0.04				
Mammary BHBA (mM)	0.21	0.18	0.13	0.09	−0.02	+0.04	−0.01	+0.05	0.02			<0.05	
J–M BHBA (mM)	0.15	0.14	0.12	0.09	−0.06	−0.01	−0.05	−0.05	0.03				
Jugular C2 (mM)	0.94	1.01	0.43	0.40	−6.59	−18.91*	−2.78	−2.63	4.89				
Mammary C2 (mM)	0.34	0.24	0.16	0.12	+3.80	+5.87*	+2.18	+4.32	2.11	<0.05			
J–M C2 (mM)	0.60	0.76	0.27	0.28	−10.39[a]	−24.78*[b]	−4.96[a]	−6.94[a]	4.45	<0.05	<0.05		
Jugular Gluc (mM)	0.6	0.61	0.64	0.66	+0.02	0.00	−0.01	−0.01	0.02				
Mammary Gluc (mM)	0.49	0.47	0.48	0.52	+0.03	+0.04	+0.02	+0.02	0.02	<0.05			
J–M Gluc (mM)	0.11	0.15	0.17	0.14	−0.02	−0.04*	−0.03	−0.03	0.02				
Jugular NEFA (mM)	0.08	0.09	0.12	0.12	0.00	+0.04*	0.00	+0.02	0.02				
Mammary NEFA (mM)	0.08	0.11	0.13	0.2	+0.03	+0.07*	0.00	+0.03	0.02				
J–M NEFA (mM)	−0.01	−0.03	−0.01	−0.08	−0.02	−0.03	0.00	−0.01	0.02				
Jugular t10c12-18:2 (g/100 g total FA)	0.00	0.00	0.00	0.00	+0.12*[a]	+0.10*[a]	+0.10*[a]	+0.09*[a]	0.02	<0.01			

The values before *t*10,*c*12-18:2 infusion into the duodenum are reported, as well as the responses after 4 days of infusion

Mean values within a row with unlike lowercase superscript letters were significantly different (Tukey test, $P < 0.05$)

BHBA beta-hydroxy-butyrate, *C2* acetate, *Gluc* glucose *J-M* jugular-mammary difference, *NEFA* non-esterified FA

* LSmeans that are significantly different from zero ($P < 0.05$)

[A] LSmeans of the individual cow responses to t10,c12-18:2 infusion

[B] *P* values of the overall response to CLA infusion (across all diets) and the main effects of dietary concentrate level, oil, and their interaction on the response to CLA infusion. Only *P* values <0.05 are mentioned

(results not shown), except *t*10,*c*12-18:2 (Table 1), which reached a mean of 0.10 g/100 g FA, irrespective of the basal diet.

Milk FA Composition

Milk content of *t*10,*c*12-18:2 was not detectable at day 0 and progressively increased until day 3–4 (Fig. 1). Most of the short- and medium-chain FA percentages were significantly decreased by *t*10,*c*12-18:2 infusion (Table 2). Some FA were not significantly affected: 4:0, the odd- and branched-chain FA. The C14 and C16 FA were only slightly affected ($0.05 < P < 0.10$). The sum of C4–C16 was significantly decreased, whereas the sum of C18 FA was increased. Most individual C18 FA percentages were numerically increased (Table 3 for 18:0 and monounsaturated C18, Table 4 for polyunsaturated C18), but only some were significantly affected (18:0, *t*13-18:1, *c*14 + *t*16-18:1, *t*10,*c*12-18:2). *T*10,*c*12-18:2 reached the highest value with the LC diet (0.27 g/100 g FA) compared with all other diets (0.17–0.19 g/100 g FA). However, *t*10,*c*12-18:2 infusion did not modify the content of most C18 FA when expressed as a percentage of total C18 (data not shown).

Among the desaturation ratios, only those of C18 FA were significantly decreased by CLA infusion: 18:0 (from 66.1 to 62.8%), *t*11-18:1 (from 33.4 to 27.6%) and *t*13-18:1 (from 24.5 to 20.2%). These desaturation ratios decreased more with diets devoid of oil. Those of 14:0 and 16:0 were not significantly affected (Table 5).

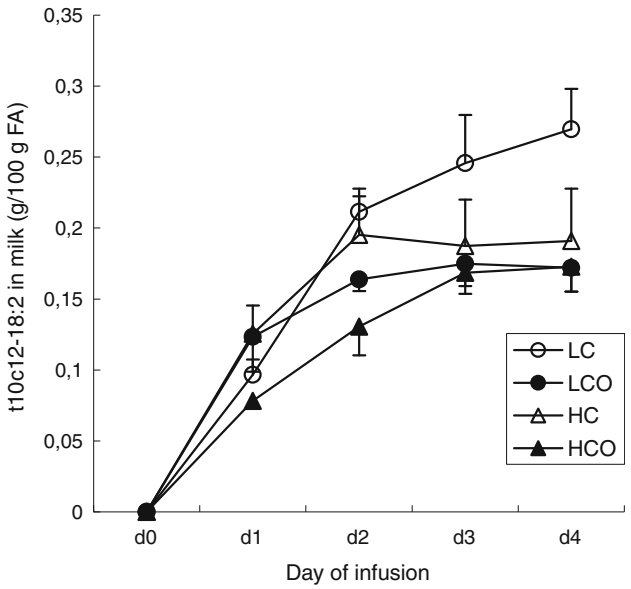

Fig. 1 Milk *t*10,*c*12-18:2 content (in g/100 g total FA) in cows fed a low- (*LC*) or high-concentrate (*HC*) diet, without (*LC, HC*) or with supplemental linseed oil (*LCO, HCO*) at 3% of DM, before the infusion (*d0*) and during 4 days of *t*10,*c*12-18:2 infusion into the duodenum

Milk Fat and FA Yields

The milk fat content and yield were decreased by *t*10,*c*12-18:2 infusion. The mean decrease over the four diets was −35.4%. The decrease was lower with high-concentrate diets than low-concentrate diets, independently of the initial yield and of oil supplementation (Table 6; Fig. 2).

The FA were grouped by chain length to discriminate between the effect of *t*10,*c*12-18:2 infusion on milk de novo synthesis and on preformed FA (C18) yield (Table 6). All the C4–C16 FA yields decreased to a greater extent than C18 yield across all diets. For all FA groups, the decrease in yield was lower with high-concentrate diets than low-concentrate diets (Table 6) independently of the initial yield (see Table 1) and of oil supplementation (except for C4–C8). The mean decrease of fat yield with high-concentrate diets was 27.5% of the initial yield, compared with 41.5% with the low-concentrate diets.

After 4 days of infusion, milk yield of *t*10,*c*12-18:2 varied between 0.85 g/day (HCO diet) and 1.13 g/day (LC diet), corresponding to a transfer efficiency of 17–23% of the amount infused daily at duodenum (mean 19.6%, no significant difference between diets).

Meta-Analysis of Published *t*10,*c*12-18:2 Infusion Studies

The database of the published data of *t*10,*c*12-18:2 infusion studies (including the present experiment) included 23 comparisons between a control and an infused groups. Several exponential decrease models were run and compared on these data. Models were adjusted on actual or percentage decrease data, and using diet composition data as additional factors on the *a* (maximal decrease) and *b* (slope of the decrease) parameters of the exponential models. The best model, based on the lowest AICc value, was the exponential model of percentage decrease with an effect of a proxy of the dietary forage/concentrate ratio (dietary neutral detergent fiber [NDF] content) on the *b* parameter:

$$\text{Milk fat content decrease (\% of initial)} = -43.9(\pm 3.6) \times \left(1 - e^{-0.00755 \times \text{NDF} \times \text{CLAdose}}\right)$$
(NDFin %DM and CLA dose in g/day, $n = 23$, $R^2 = 0.97$)

$$\text{Milk fat yield decrease (\% of initial)} = -47.2(\pm 4.4) \times \left(1 - e^{-0.00632 \times \text{NDF} \times \text{CLAdose}}\right)$$
(NDFin %DM and CLA dose in g/day, $n = 23$, $R^2 = 0.97$)

When the effect of the dose of *t*10,*c*12-18:2 was accounted for, the slope of the response was more pronounced with diets high in NDF: there is a linear effect of dietary NDF content on the slope of the response to *t*10,*c*12-18:2. The resulting model for milk fat content, computed for two NDF levels (25 and 45% of the diet, corresponding to the extreme values reported in published studies used are indicated as two lines on Fig. 3. None of the other variable tested (initial milk yield, milk yield response, initial fat yield) was significant when introduced in this model.

Discussion

The overall responses observed in the present experiment with *t*10,*c*12-18:2 infusions are consistent with the results of previous infusion experiments (reviews in [3, 26, 27]): a decrease in milk fat content and yield (−27 to −42% of the initial level), without significant variations in milk yield; the decrease was more pronounced for short- and medium chain FA, leading to milk richer in long-chain FA following infusions. The transfer efficiencies of *t*10,*c*12-18:2 (17–23%) were very close to the mean of 22% observed in previous infusion studies [8], and were not influenced by the basal diet. Transfer efficiencies of duodenal *t*10,*c*12-18:2 estimated from dietary studies with measurements of duodenal FA flows are highly variable, and were estimated to be between 50 and 100% (average 75%) in three studies [10, 28, 29], ca. 15% in one study [30], and higher than

Table 2 Percentages of selected FA (expressed as g/100 g total FA) in milk of cows fed a low- (LC) or high-concentrate (HC) diet, without (LC, HC) or with supplemental linseed oil (LCO, HCO) at 3% of DM

	Initial values				Responses to CLA infusion[A]					Overall response[B]	Effects on the response[B]		
	LC	LCO	HC	HCO	LC	LCO	HC	HCO	SEM		Conc	Oil	Conc × oil
4:0	4.01	4.39	3.80	3.01	+0.30[a]	−0.74*[b]	+0.30[a]	−0.40[b]	0.21			<0.01	
6:0	2.48	2.25	2.39	1.51	−0.25[a]	−0.79*[b]	−0.22[a]	−0.16[a]	0.12	<0.01	<0.05		*
8:0	1.49	1.21	1.53	0.81	−0.28*[a]	−0.47*[b]	−0.27*[a]	−0.17*[a]	0.06	<0.01	<0.05		*
10:0	3.33	2.33	3.68	1.77	−0.59*	−0.82*	−0.69*	−0.33	0.14	<0.01			
10:1	0.30	0.21	0.32	0.16	−0.13*	−0.11*	−0.13*	−0.06*	0.02	<0.01			
11:0	0.06	0.04	0.15	0.07	−0.02	−0.02	−0.04*	−0.02	0.01				
12:0	3.69	2.41	4.09	2.13	−0.28	−0.51*	−0.50*	−0.19	0.18	<0.01			
13:0	0.22	0.14	0.34	0.21	−0.03	−0.03	−0.07*	−0.04	0.02	<0.01			
iso-14	0.15	0.12	0.10	0.08	+0.03*[a]	−0.01[b]	0.00[b]	0.00[b]	0.01			<0.05	<0.05
14:0	11.99	8.85	11.72	7.82	−0.02[a]	−1.33*[b]	−0.67[ab]	−0.75[ab]	0.32			<0.05	<0.05
iso-15:0	0.45	0.35	0.26	0.21	−0.02	−0.06*	−0.03	+0.01	0.02				
anteiso-15:0	0.82	0.73	0.79	0.61	−0.06	−0.09	0.05	+0.03	0.06				
*c*9-14:1	1.29	0.57	1.02	0.81	+0.05[a]	−0.06[ab]	−0.24*[b]	−0.18*[ab]	0.07	<0.05	<0.05		
15:0	1.33	1.08	1.75	1.31	+0.14[a]	+0.03[a]	−0.21*[b]	0.00[a]	0.06		<0.05		<0.05
iso-16	0.35	0.28	0.30	0.22	+0.08*	0.00	+0.03	+0.02	0.02				
16:0	27.74	17.17	24.49	16.74	−3.75*[a]	−1.39[a]	−3.15*[a]	−0.78[a]	1.06			<0.05	
*t*16:1	0.64	0.63	0.66	0.87	+0.07	+0.09	−0.13	+0.11	0.10				
*c*9-16:1	1.32	0.74	0.98	1.21	−0.36*	−0.12	−0.19	−0.34*	0.13				
17:0	0.82	0.58	0.92	0.65	+0.07*	+0.05	−0.01	+0.07*	0.03				
17:1	0.26	0.15	0.29	0.24	−0.02[a]	+0.02[a]	−0.03[a]	+0.02[a]	0.02			<0.05	
Sum of C4 to C16	58.27	40.75	54.67	36.84	−5.26*	−6.27*	−5.89*	−3.25	1.54	<0.05			
Sum of C18	34.74	52.83	37.07	56.01	+5.03*	+6.27*	+6.06*	+2.99	1.42	<0.05			

The values before *t*10,*c*12-18:2 infusion into the duodenum are reported, as well as the responses after 4 days of infusion

Mean values within a row with unlike lowercase superscript letters were significantly different (Tukey test, $P < 0.05$)

* LSmeans that are significantly different from zero ($P < 0.05$)

[A] LSmeans of the individual cow responses to t10,c12-18:2 infusion

[B] *P* values of the overall response to CLA infusion (across all diets) and the main effects of dietary concentrate level, oil, and their interaction on the response to CLA infusion. Only *P* values <0.05 are mentioned

100% in two additional studies probably due to analytical inaccuracies [31, 32]. Thus, the transfer efficiency observed in infusion studies is three to four times lower than that estimated in dietary studies. This may be attributed to analytical biases in the analysis of *t*10,*c*12-18:2 duodenal flows and/or content in milk, or, more likely, to a low efficiency of infusions (lower absorption of infused lipid, due to supra-physiological dose or mode of infusion). Milk FA desaturation was only slightly affected by *t*10,*c*12-18:2 infusion, with only the desaturation ratios of C18 FA (the preferred substrates of delta-9 desaturase) being significantly affected. Indeed, alterations in milk fat desaturation ratios are not always observed when low amounts of *t*10,*c*12-18:2 are infused [3, 8, 18], suggesting that desaturation inhibition is not a major mechanism of action of *t*10,*c*12-18:2 at low doses.

The comparison of the responses to infusion between diets showed that, with the same dose of *t*10,*c*12-18:2, the decrease in milk FA yield relative to initial levels was less pronounced with high-concentrate than low-concentrate diets. This was not due to differences in initial levels of FA yield because relative decreases were not significantly related to initial levels. This was probably neither due to the duodenal flow of non-infused 18:2-inhibitory isomers if we compare the duodenal flows of FA corresponding to the four diets without infusion that have already been published [13]. Indeed, the sum of *t*10,*c*12 + *c*10,*t*12 + *t*9,*c*11 (the three inhibitory isomers identified to date) was higher with LC and HCO diets (0.52 and 0.41 g/day, respectively) and lower with LCO and HC diets (0.29 g/day), amounts that were very low compared to those infused (5 g/day). Thus, the observed differences between diets in decreases in milk FA yields were likely not linked to duodenal flows of inhibitory CLA isomers. Moreover, the amounts of *t*10,*c*12-18:2 secreted in milk following infusions were similar between diets (0.85–1.13 g/day), ruling out a

Table 3 Monounsaturated C18 FA and 18:0 (expressed as g/100 g total FA) in milk of cows fed a low- (LC) or high-concentrate (HC) diet, without (LC, HC) or with supplemental linseed oil (LCO, HCO) at 3% of DM

	Initial values				Responses to CLA infusion[A]					Overall response[B]	Effects on the response[B]		
	LC	LCO	HC	HCO	LC	LCO	HC	HCO	SEM		Conc	Oil	Conc × oil
18:0	9.00	15.42	7.40	8.44	+2.99*^{a}	+1.61^{a}	+1.90^{a}	+1.71^{a}	0.89	<0.05			
*t*4	0.01	0.05	0.03	0.05	0.00^{ab}	0.00^{b}	+0.02*^{a}	+0.01*^{ab}	0.01		<0.05		
*t*5	0.01	0.03	0.03	0.05	−0.01^{c}	0.00^{bc}	+0.02*^{a}	+0.01^{ab}	0.01		<0.01		
*t*6 + 7+8	0.23	0.54	0.38	0.78	+0.08^{a}	+0.09^{a}	+0.20*^{a}	+0.01^{a}	0.06				
*t*9	0.16	0.32	0.25	0.53	+0.03^{ab}	+0.06^{ab}	+0.10^{a}	−0.06^{b}	0.04				
*t*10	0.37	0.76	1.14	2.76	+0.05^{ab}	−0.29^{b}	+0.66*^{a}	−0.31^{b}	0.25			<0.05	
*t*11	1.32	3.19	1.51	5.35	+0.51^{a}	+0.69^{a}	+0.64^{a}	+0.75^{a}	0.40				
*t*12	0.23	0.69	0.37	0.79	+0.01^{a}	+0.07^{a}	+0.14*^{a}	+0.01^{a}	0.05				
*t*13 + 14	0.39	1.69	0.69	2.3	+0.11^{a}	+0.28*^{a}	+0.32*^{a}	+0.30*^{a}	0.08	<0.01			
Σ*t*18:1	3.18	13.20	4.33	15.67	+0.88^{ab}	+1.42^{ab}	+2.19*^{a}	+0.53^{b}	0.64				<0.05
*c*9	17.98	21.32	17.71	18.47	+0.09^{b}	+3.24*^{a}	+0.16^{b}	+0.88^{ab}	0.85				
*c*10	0.44	0.98	0.74	1.08	−0.01^{a}	+0.05^{a}	−0.10^{a}	+0.07^{a}	0.10				
*c*11	0.88	0.69	1.21	1.46	+0.07^{b}	+0.05^{b}	+0.26*^{a}	+0.01^{b}	0.08			<0.05	<0.05
*c*12	0.16	0.33	0.42	0.74	+0.02^{a}	+0.02^{a}	+0.06^{a}	−0.05^{a}	0.07				
*c*13	0.06	0.12	0.11	0.22	+0.01^{a}	0.00^{a}	−0.01^{a}	0.00^{a}	0.02				
*c*14 + *t*16	0.18	0.75	0.28	0.64	+0.05^{a}	+0.10*^{a}	+0.11*^{a}	+0.11*^{a}	0.03	<0.05			
*c*15	0.09	0.46	0.23	1.24	0.00^{a}	+0.09^{a}	−0.02^{a}	−0.03^{a}	0.08				
Σ*c*18:1	18.62	18.09	19.96	19.96	+0.23^{b}	+2.70*^{a}	+0.56^{b}	+1.13^{ab}	0.56	<0.05		<0.05	

The values before *t*10,*c*12-18:2 infusion into the duodenum are reported, as well as the responses after 4 days of infusion

Mean values within a row with unlike lowercase superscript letters were significantly different (Tukey test, $P < 0.05$)

* LSmeans that are significantly different from zero ($P < 0.05$)

[A] LSmeans of the individual cow responses to t10,c12-18:2 infusion

[B] *P* values of the overall response to CLA infusion (across all diets) and the main effects of dietary concentrate level, oil, and their interaction on the response to CLA infusion. Only *P* values <0.05 are mentioned

difference between diets due to different amounts of this isomer taken up by the mammary gland. The lower response to *t*10,*c*12-18:2 with high-concentrate diets was observed in the present study irrespective of whether the decrease was expressed in actual amounts (Table 1) or as percentage of initial value (Table 6). It was observed for all FA chain lengths (Table 6) and was also found in a meta-analysis of the published infusions of *t*10,*c*12-18:2 (Fig. 3). The coefficients found in the meta-analysis are very close to those reported in earlier studies from a smaller dataset [8] (for a NDF content of 40% DM, our slope for milk fat yield is calculated at −0.25, compared to a mean slope of −0.28 in [8]). Within the published studies involving CLA doses between 3 and 4.5 g/day, the studies using basal diets low in NDF (NDF < 36% DM in [6, 11, 18]) report decreases in milk fat content comprised between −20 and −27%, whereas the studies using basal diets higher in NDF (around 45% DM in [8, 33]) report decreases in milk fat between −35 and −39%, with similar initial milk fat.

We cannot totally exclude some saturation of the milk fat decrease, because a 50%-decrease seems to be the maximal response reported for *trans*10,*cis*12-18:2 infusions, as discussed previously in [34]. Our high-concentrate diets were already somewhat depressed compared to a standard diet, and the differences observed in the decrease could be interpreted as consequences of the initial situation. However, we argue for a specific effect of the basal diet on the response to CLA infusion, independent of the initial milk fat before infusion (see Fig. 2). The various modes of expression in this study (actual decrease, percentage decrease), together with the significant effect of dietary NDF content in the published responses from the database, advocate for an effect of the dietary forage:concentrate ratio, which modulates the main response driven by *trans*10,*cis*12-18:2 infusions. Thus, a less pronounced decrease in milk fat yield in cows fed high-concentrate diets is observed from the *t*10,*c*12-18:2 infusions published to date (the relationship is very similar for both milk fat yield and milk fat content, because milk yield is almost unaffected by *t*10,*c*12-18:2 infusions). However, it is difficult to develop hypotheses to explain this phenomenon, because data on intermediary metabolism (e. g. plasma composition) related to *t*10,*c*12-18:2 infusion are very scarce. Molecular mechanisms of MFD induced by

Table 4 Polyunsaturated C18 FA (expressed as g:100 g total FA) in milk of cows fed a low- (LC) or high-concentrate (HC) diet, without (LC, HC) or with supplemental linseed oil (LCO, HCO) at 3% of DM

	Initial values				Responses to CLA infusion[A]					Overall response[B]	Effects on the response[B]		
	LC	LCO	HC	HCO	LC	LCO	HC	HCO	SEM		Conc	Oil	Conc × oil
*t*9,*t*12	0.01	0.04	0.03	0.44	−0.01	0.00	+0.01	−0.02	0.03				
*c*9,*t*13	0.13	0.54	0.26	0.73	−0.01	+0.03	−0.01	−0.08*	0.03				
*c*9,*t*12	0.06	0.17	0.1	0.34	0.00	+0.02	+0.00	−0.02	0.03				
*t*9,*c*12	0.03	0.07	0.05	0.23	+0.01	0.00	+0.02	−0.02	0.02				
*t*11,*c*15	0.09	0.89	0.19	2.73	+0.01	+0.01	+0.02	−0.47	0.21				
*c*9,*c*12	1.78	1.44	2.73	2.47	+0.40	+0.24	+0.89*	+0.26	0.22				
*c*9,*c*15	0.18	0.15	0.18	0.16	+0.01	+0.01	+0.06	+0.03	0.03				
*c*9,*t*11	0.66	1.36	0.86	2.74	−0.03	+0.02	0.00	−0.34	0.25				
*t*9,*c*11	0.01	0.02	0.03	0.08	−0.01	−0.01	−0.01	−0.04*	0.02				
*t*10,*c*12	<0.01	<0.01	<0.01	<0.01	+0.27*	+0.17*	+0.19*	+0.17*	0.03	<0.01			
*c*9,*c*11	0.02	0.07	0.01	0.05	−0.02*[c]	+0.01[ab]	−0.01[bc]	+0.03*[a]	0.01			<0.01	
*c*10,*c*12	0.02	0.04	0.04	0.06	−0.01	−0.02	−0.01	−0.03	0.02				
*c*11,*c*13	0.02	0.00	0.00	0.00	0.00	0.00	0.00	0.00	0.01				
*t*11,*t*13	0.01	0.10	0.01	0.07	+0.02	+0.01	+0.01	+0.02	0.01				
*tt*CLA	0.02	0.03	0.02	0.04	+0.01	+0.00	+0.01	+0.01	0.01				
ΣCLA	0.77	1.61	0.97	3.05	+0.23	+0.18	+0.19	−0.19	0.23				
18:3*n*-3	0.83	1.01	0.8	1.65	+0.27*	+0.06	+0.26*	+0.11	0.09			<0.05	
Σ18:3	0.90	1.21	0.86	1.79	+0.29*	+0.05	+0.23	+0.14	0.10				

The values before t10,c12-18:2 infusion into the duodenum are reported, as well as the responses after 4 days of infusion

Mean values within a row with unlike lowercase superscript letters were significantly different (Tukey test, $P < 0.05$)

* LSmeans that are significantly different from zero ($P < 0.05$)

[A] LSmeans of the individual cow responses to t10,c12-18:2 infusion

[B] *P* values of the overall response to CLA infusion (across all diets) and the main effects of dietary concentrate level, oil, and their interaction on the response to CLA infusion. Only *P* values<0.05 are mentioned

Table 5 Desaturation ratios (in %) in milk of cows fed a low- (LC) or high-concentrate (HC) diet, without (LC, HC) or with supplemental linseed oil (LCO, HCO) at 3% of DM

	Initial values				Responses to CLA infusion[A]					Overall response[B]	Effects on the response[B]		
	LC	LCO	HC	HCO	LC	LCO	HC	HCO	SEM		Conc	Oil	Conc × oil
14:0[C]	9.7	6.1	8	9.4	+0.3	+0.3	−1.4	−1.0	0.6		<0.05		
16:0[C]	4.6	4.2	3.8	6.8	−0.7	−0.4	−0.3	−1.8*	0.7				
18:0[C]	66.3	57.9	70.6	69.6	−6.1*[b]	+0.8[a]	−4.6*[ab]	−3.3[ab]	1.8	<0.05		<0.05	
*t*11-18:1[C]	33.4	29.8	36.6	33.8	−7.5*	−3.3*	−7.5*	−4.7*	1.4	<0.01		<0.05	
*t*13-18:1[C]	23.9	23.9	27	23.3	−5.1*[ab]	−1.7[a]	−6.9*[b]	−3.6*[ab]	1.3	<0.01		<0.05	

The values before t10,c12-18:2 infusion into the duodenum are reported, as well as the responses after 4 days of infusion

Mean values within a row with unlike lowercase superscript letters were significantly different (Tukey test, $P < 0.05$)

* LSmeans that are significantly different from zero ($P < 0.05$)

[A] LSmeans of the individual cow responses to t10,c12-18:2 infusion

[B] *P* values of the overall response to CLA infusion (across all diets) and the main effects of dietary concentrate level, oil, and their interaction on the response to CLA infusion. Only *P* values <0.05 are mentioned

[C] Desaturation ratios are calculated as: 100 × desaturated/(desaturated + saturated), see "Experimental Procedure"

*t*10,*c*12-18:2 infusions at the mammary level have been described [3, 4], but this information is of limited help to explain the effect of dietary concentrate.

In the present experiment, low-concentrate diets resulted in higher ruminal acetate and lower propionate, with similar ruminal digestibilities of dietary components across

Table 6 Variation in milk yield, fat and FA, induced by *t*10,*c*12-18:2 infusion into the duodenum, in Holstein cows fed a low- (LC) or high-concentrate (HC) diet, without (LC, HC) or with supplemental linseed oil (LCO, HCO) at 3% of DM

	Responses to CLA infusion (% of initial value)[A]					Overall response[B]	Effects on the response[B]		
	LC	LCO	HC	HCO	SEM		Conc	Oil	Conc × oil
Milk yield (kg/day)	−0.2	−3.1	3.3	1.0	2.8				
Fat (%)	−40.9*[b]	−40.2*[b]	−29.4*[a]	−28.5*[a]	5.4	<0.01	<0.01		
Fat (kg/day)	−41.2*[b]	−41.8*[b]	−27.2*[a]	−27.9*[a]	5.5	<0.01	<0.01		
C4–C8 yield (g/day)	−41.8*[b]	−57.8[c]	−28.2*[a]	−37.5*[ab]	6.0	<0.01	<0.01	<0.01	
C10–C14 yield (g/day)	−43.1*[ab]	−53.8*[b]	−34.8*[a]	−36.7*[a]	6.7	<0.01	<0.05		
C16 yield (g/day)	−48.6*[c]	−45.9*[bc]	−36.2*[ab]	−31.2*[a]	7.2	<0.01	<0.01		
C18 yield (g/day)	−32.9*[b]	−34.9*[b]	−15.4*[a]	−24.1*[ab]	4.8	<0.01	<0.05		

Values are differences between after and before infusion, expressed as % of initial value

Mean values within a row with unlike lowercase superscript letters were significantly different (Tukey test, $P < 0.05$)

* LSmeans that are significantly different from zero ($P < 0.05$)

[A] LSmeans of the individual cow responses to t10,c12-18:2 infusion

[B] *P* values of the overall response to CLA infusion (across all diets) and the main effects of dietary concentrate level, oil, and their interaction on the response to CLA infusion. Only *P* values <0.05 are mentioned

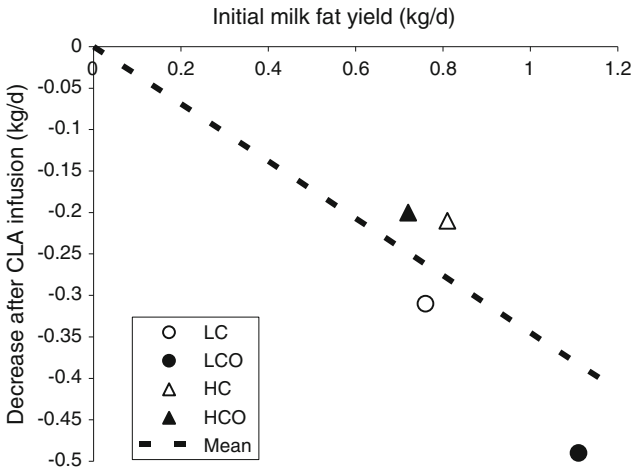

Fig. 2 Actual decrease in milk fat yield induced by t10,c12-18:2 infusion into the duodenum in Holstein cows fed a low- (*LC*) or high-concentrate (*HC*) diet, without (*LC, HC*) or with supplemental linseed oil (*LCO, HCO*) at 3% of DM. The *dotted line* indicates the mean response across all diets

diets [14]. High-concentrate diets probably induce higher ruminal propionate production and availability in cows [35]. From the present experiment, the only plasma characteristic with an interaction between *t*10,*c*12-18:2 infusion and basal diet was the jugular–mammary difference of acetate. Jugular acetate was higher with the low-concentrate diets irrespective of oil supplementation. Following *t*10,*c*12-18:2 infusion, mammary acetate increased, leading to a global decrease in jugular–mammary differences of acetate, which is consistent with the inhibition of mammary de novo synthesis by *t*10,*c*12-18:2. Moreover, this decrease was more pronounced for low-concentrate diets (Table 1) consistent with a more pronounced decrease in milk fat yield, including de novo synthesis (Table 6). No such phenomenon was observed with plasma triglyceride jugular–mammary difference (data not shown), the main source of preformed FA for the mammary gland, which did not change according to either diet or *t*10,*c*12-18:2 infusion.

A decrease in acetate mammary uptake could be the cause or the consequence of a decrease in mammary FA synthesis. Early theories of MFD encompassed variations in VFA, namely the acetate deficiency theory (acetate deficiency would be a limiting factor of mammary lipogenesis) and the 'glucogenic-insulin theory', according to which propionate and/or glucose from high-concentrate diets would increase circulating insulin and result in a shortage of lipogenic precursors for the mammary gland [36]. Indeed, VFA infusions in dairy cows induce variations in milk fat content and yield (increase following acetate infusions and decrease following propionate infusions) [37]. However, these theories have been dismissed because there is no reduction in ruminal acetate production with high-concentrate diets (but rather an increase in propionate production) [35], and the changes in FA composition following insulin-induced MFD are opposite to those observed following diet-induced MFD [36].

With the above discussion in mind, we hypothesize that cows fed high-concentrate diets are in a metabolic state that is already "detrimental" to lipogenesis: higher propionate, lower circulating acetate, and possibly higher *trans* 18:1 and 18:2 isomers. In particular, before infusions in the present experiment, the duodenal flow of *t*10-18:1 was higher with the HC and HCO (20–51 g/day) than LC and LCO diets (1–7 g/day) [13], which could have contributed to an inhibition of mammary lipogenesis [27] even before

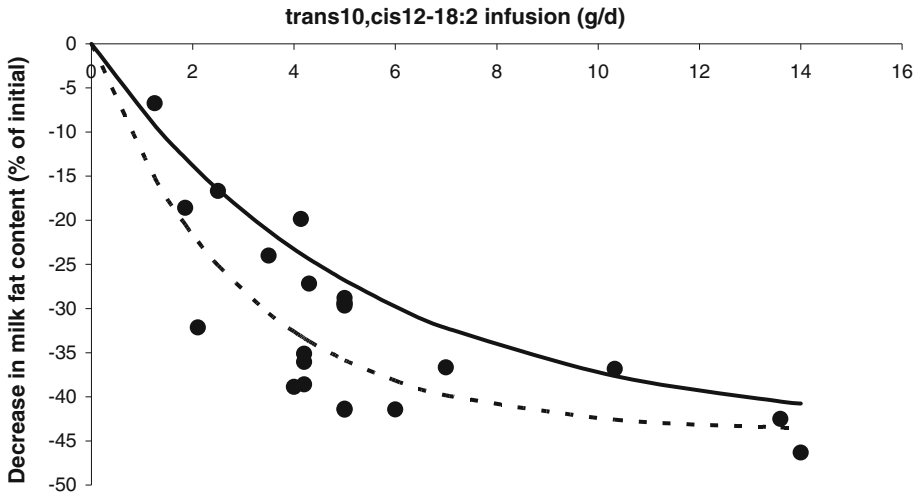

Fig. 3 Decrease in milk fat content following *t*10,*c*12-18:2 duodenal infusions in 23 groups of cows from 13 published experiments [5–8, 11, 12, 18–20, 22–25] and the present study. The *lines* show the exponential decrease model adjusted on these data, and computed for a basal diet containing 25% NDF (*solid line*) or 45% NDF (*dotted line*)

*t*10,*c*12-18:2 infusion. In this metabolic context, the mammary gland might have been more resistant to or might have experienced a lower response potential to further inhibition of lipogenesis and/or FA delta-9 desaturation. Taken together, all these events could explain the blunted response of cows fed a high-concentrate diet to *t*10,*c*12-18:2 infusion.

This experiment is the first published study comparing the impact of *t*10,*c*12-18:2 infusions on cows fed diets differing in concentrate and supplemental oil contents. Results reveal that the inhibition of mammary lipogenesis (both de novo synthesis and incorporation of long-chain FA) was less pronounced in cows fed high-concentrate diets. This response is independent of oil supplementation and milk FA yield before infusion. The impact of dietary concentrate on the milk fat yield response to *t*10,*c*12-18:2 infusion in our study has been confirmed by a meta-analysis of the previously published *t*10,*c*12-18:2 infusion experiments.

Acknowledgments We acknowledge the assistance of J.P. Pezant and the team of Les Cèdres Experimental Unit for feeding, milking, blood sampling, and caring for the cows, as well as P. Capitan, M. Tourret, and C. Delavaud for help in laboratory analyses.

This research received no specific grant and the authors declare no conflict of interest.

References

1. Chilliard Y, Glasser F, Ferlay A, Bernard L, Rouel J, Doreau M (2007) Diet, rumen biohydrogenation and nutritional quality of cow and goat milk fat. Eur J Lipid Sci Technol 109:828–855
2. Griinari JM, Bauman DE (2006) Milk fat depression: concepts, mechanisms and management applications. In: Sejrsen K, Hvelplund T, Nielsen MO (eds) Ruminant physiology digestion, metabolism and impact of nutrition on gene expression, immunology and stress. Wageningen Academic Publishers, Wageningen, pp 389–417
3. Harvatine KJ, Boisclair YR, Bauman DE (2009) Recent advances in the regulation of milk fat synthesis. Animal 3:40–54
4. Shingfield KJ, Bernard L, Leroux C, Chilliard Y (2010) Role of *trans* fatty acids in the nutritional regulation of mammary lipogenesis in ruminants. Animal 4:1140–1166
5. Perfield JW II, Lock AL, Griinari JM, Saebo A, Delmonte P, Dwyer DA, Bauman DE (2007) *Trans*-9, *cis*-11 conjugated linoleic acid reduces milk fat synthesis in lactating dairy cows. J Dairy Sci 90:2211–2218
6. Saebo A, Saebo PC, Griinari JM, Shingfield KJ (2005) Effect of abomasal infusions of geometric isomers of 10, 12 conjugated linoleic acid on milk fat synthesis in dairy cows. Lipids 40:823–832
7. Baumgard LH, Corl BA, Dwyer DA, Saebo A, Bauman DE (2000) Identification of the conjugated linoleic acid isomer that inhibits milk fat synthesis. Am J Physiol Regul Integr Comp Physiol 278:R179–R184
8. de Veth MJ, Griinari JM, Pfeiffer AM, Bauman DE (2004) Effect of CLA on milk fat synthesis in dairy cows: comparison of inhibition by methyl esters and free fatty acids, and relationships among studies. Lipids 39:365–372
9. Peterson DG, Matitashvili EA, Bauman DE (2003) Diet-induced milk fat depression in dairy cows results in increased *trans*-10, *cis*-12 CLA in milk fat and coordinate suppression of mRNA abundance for mammary enzymes involved in milk fat synthesis. J Nutr 133:3098–3102
10. Loor JJ, Ferlay A, Ollier A, Doreau M, Chilliard Y (2005) Relationship among *trans* and conjugated fatty acids and bovine milk fat yield due to dietary concentrate and linseed oil. J Dairy Sci 88:726–740
11. Lock AL, Tyburczy C, Dwyer DA, Harvatine KJ, Destaillats F, Mouloungui Z, Candy L, Bauman DE (2007) *Trans*-10 octadecenoic acid does not reduce milk fat synthesis in dairy cows. J Nutr 137:71–76
12. Shingfield KJ, Saebo A, Saebo P-C, Toivonen V, Griinari JM (2009) Effect of abomasal infusions of a mixture of octadecenoic acids on milk fat synthesis in lactating cows. J Dairy Sci 92:4317–4329
13. Loor JJ, Ueda K, Ferlay A, Chilliard Y, Doreau M (2004) Biohydrogenation, duodenal flow, and intestinal digestibility of *trans* fatty acids and conjugated linoleic acids in response to dietary forage: concentrate ratio and linseed oil in dairy cows. J Dairy Sci 87:2472–2485
14. Ueda K, Ferlay A, Chabrot J, Loor JJ, Chilliard Y, Doreau M (2003) Effect of linseed oil supplementation on ruminal digestion

in dairy cows fed diets with different forage: concentrate ratios. J Dairy Sci 86:3999–4007
15. Christie WW, Sebedio JL, Juaneda P (2001) A practical guide to the analysis of conjugated linoleic acid. INFORM 12:147–152
16. Loor JJ, Herbein JH, Polan CE (2002) *Trans* 18:1 and 18:2 isomers in blood plasma and milk fat of grazing cows fed a grain supplement containing solvent-extracted or mechanically extracted soybean meal. J Dairy Sci 85:1197–1207
17. Loor JJ, Quinlan LE, Bandara ABPA, Herbein JH (2002) Distribution of *trans*-vaccenic acid and *cis*9, *trans*11-conjugated linoleic acid (rumenic acid) in blood plasma lipid fractions and secretion in milk fat of jersey cows fed canola or soybean oil. Anim Res 51:119–134
18. Baumgard LH, Sangster JK, Bauman DE (2001) Milk fat synthesis in dairy cows is progressively reduced by increasing supplemental amounts of *trans*-10, *cis*-12 conjugated linoleic acid (CLA). J Nutr 131:1764–1769
19. Baumgard LH, Matitashvili EA, Corl BA, Dwyer DA, Bauman DE (2002) *Trans*-10, *cis*-12 conjugated linoleic acid decreases lipogenic rates and expression of genes involved in milk lipid synthesis in dairy cows. J Dairy Sci 85:2155–2163
20. Perfield JW II, Lock AL, Pfeiffer AM, Bauman DE (2004) Effects of amide-protected and lipid-encapsulated conjugated linoleic acid (CLA) supplements on milk fat synthesis. J Dairy Sci 87:3010–3016
21. Bell JA, Kennelly JJ (2003) Short communication: postruminal infusion of conjugated linoleic acids negatively impacts milk synthesis in Holstein cows. J Dairy Sci 86:1321–1324
22. Perfield JW II, Delmonte P, Lock AL, Yurawecz MP, Bauman DE (2006) *Trans*-10, *trans*-12 conjugated linoleic acid does not affect milk fat yield but reduces delta 9-desaturase index in dairy cows. J Dairy Sci 89:2559–2566
23. Peterson DG, Baumgard LH, Bauman DE (2002) Short communication: milk fat response to low doses of *trans*-10, *cis*-12 conjugated linoleic acid (CLA). J Dairy Sci 85:1764–1766
24. Saebo A, Perfield J, Delmonte P, Yurawecz M, Lawrence P, Brenna J, Bauman D (2005) Milk fat synthesis is unaffected by abomasal infusion of the conjugated diene 18:3 isomers *cis*-6, *trans*-10, *cis*-12 and *cis*-6, *trans*-8, *cis*-12. Lipids 40:89–95
25. Maxin G, Glasser F, Rulquin H (2010) Additive effects of *trans*-10, *cis*-12 conjugated linoleic acid and propionic acid on milk fat content and composition in dairy cows. J Dairy Res 77:295–301
26. Bauman DE, Perfield JW II, Harvatine KJ, Baumgard LH (2008) Regulation of fat synthesis by conjugated linoleic acid: lactation and the ruminant model. J Nutr 138:403–409
27. Shingfield KJ, Griinari JM (2007) Role of biohydrogenation intermediates in milk fat depression. Eur J Lipid Sci Technol 109:799–816
28. Loor JJ, Ferlay A, Ollier A, Ueda K, Doreau M, Chilliard Y (2005) High-concentrate diets and polyunsaturated oils alter *trans* and conjugated isomers in bovine rumen, blood, and milk. J Dairy Sci 88:3986–3999
29. Piperova LS, Sampugna J, Teter BB, Kalscheur KF, Yurawecz MP, Ku Y, Morehouse KM, Erdman RA (2002) Duodenal and milk *trans* octadecenoic acid and conjugated linoleic acid (CLA) isomers indicate that postabsorptive synthesis is the predominant source of *cis*-9-containing CLA in lactating dairy cows. J Nutr 132:1235–1241
30. Shingfield KJ, Ahvenjarvi S, Toivonen V, Arola A, Nurmela KVV, Huhtanen P, Griinari JM (2003) Effect of dietary fish oil on biohydrogenation of fatty acids and milk fatty acid content in cows. Anim Sci 77:165–179
31. Flachowsky G, Erdmann K, Huther L, Jahreis G, Mockel P, Lebzien P (2006) Influence of roughage/concentrate ratio and linseed oil on the concentration of *trans*-fatty acids and conjugated linoleic acid in duodenal chyme and milk fat of late lactating cows. Arch Anim Nutr 60:501–511
32. Moorby JM, Dewhurst RJ, Evans RT, Danelon JL (2006) Effects of dairy cow diet forage proportion on duodenal nutrient supply and urinary purine derivative excretion. J Dairy Sci 89:3552–3562
33. Perfield JW II, Saebo A, Bauman DE (2004) Use of conjugated linoleic acid (CLA) enrichments to examine the effects of *trans*-8, *cis*-10 CLA, and *cis*-11, *trans*-13 CLA on milk-fat synthesis. J Dairy Sci 87:1196–1202
34. Kadegowda AKG, Piperova LS, Erdman RA (2008) Principal component and multivariate analysis of milk long-chain fatty acid composition during diet-induced milk fat depression. J Dairy Sci 91:749–759
35. Sutton JD, Dhanoa MS, Morant SV, France J, Napper DJ, Schuller E (2003) Rates of production of acetate, propionate, and butyrate in the rumen of lactating dairy cows given normal and low-roughage diets. J Dairy Sci 86:3620–3633
36. Bauman DE, Griinari JM (2001) Regulation and nutritional manipulation of milk fat: low-fat milk syndrome. Livest Prod Sci 70:15–29
37. Rulquin H, Hurtaud C, Lemosquet S, Peyraud JL (2007) Effet des nutriments énergétiques sur la production et la teneur en matière grasse du lait de vache. Prod Animales 20:163–176

Lipids (2010) 45:889–890
DOI 10.1007/s11745-010-3473-5

EDITORIAL

NIH, Science, and Baseball: Time for Reform?

Eric J. Murphy

Published online: 22 September 2010

Last fall I was reflecting on the state of science and the funding rate at the National Institutes of Health. Baseball was winding down for most teams, while again the World Series featured two teams from the east coast, while teams in the middle of America were again amazingly absent. There are all kinds of reasons why these teams are not as competitive, but in the end it comes down to money and components like market share. Yet unlike other professional sports in America, where salary caps have been used to level the playing field and to make small market teams more competitive, no such cap exists in baseball. While major league baseball has tried revenue-leveling plans (a luxury tax), in the end the wealthier teams get the better (higher-priced) players and the less-wealthy teams get to develop the players who end up going to the wealthier teams. The end result is diminished revenue for one set of teams as fans just stop showing up to the ballpark. Quite the opposite occurs for the wealthier teams as the fans come in droves to watch their stars come out at night. So what in the world does this have to do with science?

Well, many see baseball as a pure game. There are dimensions for the diamond, but every field is unique beyond the actual diamond. There is no time limit for the game, something unique in nearly all professional sports. There is a one-on-one component as there is the constant battle between the hitter and the pitcher. Yet despite this very individual aspect of the game, baseball is a team sport in which team work is essential for success. To me, academic science is a pure pursuit, but like baseball it contains a number of polar opposites, somewhat like what Hegel described in his version of the dialectic theory.

Science is a pursuit that requires a tremendous amount of personal drive and utilization of one's intellect. Meanwhile, despite this individual effort, we work in a "team" environment, sharing our thoughts and work with others through publications and interactions at scientific congresses as well as other outlets that provide for exchange of ideas. We collaborate on projects with colleagues, maximizing the potential for success by bringing many different talents to bear on the project. Similar to baseball being a game where singles and doubles win games, science is a pursuit where all of our collective progress on a particular topic is additive and that is what often shifts our understanding of the underlying biology of a particular problem. Just like a home run is exciting and gets the fans cheering for more, big significant discoveries in science are also exciting. But in the end, like in baseball, it is the summation of incremental successes that move a field forward. As an industry colleague has routinely noted, academic scientists often work on their own time scale, yet we all work within the time frame of our grants. So many of the attributes of baseball are seen in science, but again, so are many of the disparities.

So how does NIH fit into this paradigm? Simply put, certain institutions and laboratories continue to get rich, while others seek the equivalent of science life support. Institutions on the right and left coasts have more faculty, more "stars", and ultimately more infrastructure to support an enhanced research enterprise. As in baseball, this deepens the divide between the haves and the have-nots. Those of us at institutions in the middle of America who succeed, can transition to the coasts, like a rising star in baseball. Hence, the ultimate impact is a reduction in the small market institutions' capacity to compete as they lose

E. J. Murphy (✉)
Department of Pharmacology, Physiology, and Therapeutics, University of North Dakota, 501 N. Columbia Rd., Room 3700, Grand Forks, ND 58202-9037, USA
e-mail: emurphy@medicine.nodak.edu

their intellectual infrastructure. This reduces the institutional ability to compete for grants, while enhancing the ability of the large market institutions.

In the end, NIH must reform how it allocates funds. While baseball has avoided the dreaded salary cap, is it time for NIH to institute an institutional and investigator grant dollar cap? If so, would this cap help to redistribute funds, permitting small market institutions to be in a better position to compete for grants and ultimately build infrastructure and retain "star" faculty? This would force institutions to triage grants internally, rather than the submission-in-mass process that currently exists, thereby reducing the load of already overworked study sections. If a cap is not the answer, what are other options?

In an abbreviated letter published in *The Scientist* (23(4):18, 2009), I briefly laid out a radical new funding method for the NIH. My proposed model rewards successful scientists across the country and across disciplines with a single, lifetime grant. The grant is a single award on the order of $15 million and the investigator's institution would be required to invest the principal of the grant in various investments to provide a safe, constant source of income from the investment. In doing so, the investigator can only use the investment income from the grant, which in most years would be between $500,000 and $750,000. Because our institutions use and rely on a federal subsidy called indirect costs (F&A), an additional $5 million is given to the institution to invest, with the investment income used as the indirect costs payment. Again, neither party can use the principal, which means upon retirement of the scientist, the money then becomes available for another investigator at another institution, in short a sustainable means of funding biomedical science efforts in the US. The catch is that any investigator receiving one of these awards is not permitted to apply for any other federal funding, but rather must use the investment income provided to fund their laboratory. Because nearly all institutions in America have endowments that are invested and managed locally, the overall infrastructure exists within academia and within research institutes to implement this model.

What are the advantages? Because NIH study sections appear to fund safe science and repeatedly demonstrate risk aversion, reducing the likelihood that riskier projects are funded, one clear advantage to this radical funding vehicle is a shift in the aversion to risk. We all know that risk is equal to a potential for high yield, which in science speak translates into discoveries. By eliminating the need of a scientist to secure grant funding for every idea, my proposal promotes an environment in which risk aversion is low, a polar opposite to what we currently have in place. An additional advantage is an elimination of the money raising aspects of academic science. Academic scientists spend upwards to 30–40% of their time chasing money in one form or another. Eliminating this activity will enhance the overall quality of science as investigators put more time into their creative efforts, thereby increasing the likelihood of progress and novel discoveries. Another advantage is promoting a stable work environment for students, postdoctoral fellows, and technical staff. This more-stable environment includes more time devoted by the investigator to interacting with each individual in the laboratory, enhancing the overall training of the next generation of scientists. Lastly, by taking more seasoned and experienced scientists out of the normal R01 and R21 funding mechanisms, the success rate for junior faculty will increase, ensuring a vibrant research community across disciplines and providing a sustainable scientific base for the US.

Of course there are disadvantages to this program as well. Scientist could become rather lazy and reduce their efforts in the field. While this could occur with some individuals, I doubt it would be too common of an occurrence. A 5-year review process, in which investigators would be required to provide an update on their progress, primarily by demonstrating the number and quality of publications, would mitigate these concerns. For individuals with 5–7 R01 grants in their laboratories, the amount of money provided is insufficient to run one of these so-called mega-labs, which often resemble a small biotech company in its management structure rather than an academic laboratory. Hence, there is a clear disadvantage for scientists who manage one of these mega-labs as they would have to potentially reduce staff commensurate with a reduction in financial resources. However, more importantly, market fluctuations could cause a temporary reduction in investment income and portfolio value. To minimize this risk, investigators will have to save in good years to buffer against the down years in the market, however we all know that rapid loses in the market are also followed by rapid gains. Again, while there are undoubtedly other disadvantages, I will limit my discussion to these.

Hence, if NIH would be willing to fund 500–1,000 of these grants per year for the next 5–10 years, there would be a tremendous reduction in the individuals competing in the traditional grant cycles. Risk aversion would be significantly reduced, enhancing the ability of scientists to study problems that frankly have limited chance of being funded in today's environment. By freeing up investigators' time, we are enhancing their ability to focus on projects and to formulate new, exciting ideas to test. Overall, this new model eliminates many of the problems associated with our current system and for those who qualify, it would produce a more stable and rewarding career. I believe that this model offers a sustainable system that will reward success while promoting risk, yet ensuring that funds would be available now and in the future to enhance the likelihood of success for our younger generation of scientists and provide the US with the capacity to continue our leadership in biomedical research.

Lipids (2010) 45:891–892
DOI 10.1007/s11745-010-3446-8

LETTER TO THE EDITOR

Saturated Fat and Health: Recent Advances in Research

Richard D. Feinman

Received: 26 April 2010 / Accepted: 25 May 2010 / Published online: 9 September 2010

Saturated fat of plant or animal origin has been an important ingredient in Western and non-Western diets for centuries. For the past 30 or 40 years, dietary saturated fats have attained a poor reputation especially in relation to cardiovascular health; recommendations to reduce consumption persist even in the face of equivocal or contradictory evidence. This special theme issue of Lipids on saturated fat and health presents contributions from a "hot topic" session at the 100th AOCS annual meeting in Orlando Florida, in May 2009.

Two recent publications highlight the importance of this issue. A meta-analysis by Siri-Tarino et al. [1] showed that there was no significant evidence for concluding that dietary saturated fat is associated with an increased risk of cardiovascular disease (CVD). In addition, whereas some dairy products contribute to the intake of dietary saturated fat, a meta-analysis in this theme issue of the available prospective studies showed that dairy consumption is associated with decreases in CVD risk. The latest prospective cohort study confirms this conclusion for full fat dairy [2].

Although some long chain saturated fatty acids raise low-density (LDL) cholesterol in specific dietary interventions, these fatty acids may have a positive effect on the complex of other markers referred to as atherogenic dyslipidemia: increased concentrations of small, dense LDL particles, decreased high-density lipoprotein (HDL) particles and increased triglycerides, which may be a more important risk factor for myocardial infarction and CVD. Several authors in this theme issue have pointed out that even replacement of saturated fat with polyunsaturates may have a limited effect and low omega-3 fatty acid intake may carry a much larger CVD burden. Replacement with carbohydrates is likely to be detrimental.

Entries in this publication make the point that all mammalian newborns rely on milk, which typically contains 50% of its total fat as saturated fat. Newborns and adults have the machinery to manufacture saturated fatty acids when not present in the diet. In particular, the entry by Bruce German, points out that the brain makes a large amount of saturated fatty acid during myelination. Other work presented in this issue shows that a diet high in saturated fat has very different effects in the presence of carbohydrates than in their absence. A low carbohydrate diet that is high in saturated may actually lead to a reduction in plasma saturated fat compared to one that is also high in carbohydrate, a consequence of reduction of triglycerides in the low carbohydrate diet and persistent de novo fatty acid synthesis in the high carbohydrate diet.

From a metabolic standpoint, the existence of desaturases indicates the need to have direct experimental evidence on the role of dietary lipid intake on the circulating species and biological endpoints. Finally, it is clear that regarding saturated fatty acids as one group is an oversimplification. Individual saturated fatty acids have specific functions depending on chain length. The relation between dietary intake of fats and health is complicated and the current publications point to the need to reduce oversimplification. Is it possible that evolution found benefits to saturated fatty acids that current recommendations do not consider? Whereas diets inordinately high in any component, including saturated fat, are likely to be deleterious, finite quantities of a variety of saturated fatty acids may provide distinct benefits to various metabolic processes and overall health.

R. D. Feinman (✉)
Department of Cell Biology, SUNY Downstate Medical Center,
450 Clarkson Ave, Box 8, Brooklyn, NY 11203, USA
e-mail: RFeinman@downstate.edu

References

1. Siri-Tarino PW, Sun Q, Hu FB, Kraus RM (2010) Meta-analysis of prospective cohort studies evaluating the association of saturated fat with cardiovascular disease. Am J Clin Nutr 91:535–546

2. Bonthuis M, Hughes MCB, Ibiebele TI, Green AC, van der Pols JC (2010) Dairy consumption and patterns of mortality of Australian adults. Eur J Clin Nutr (Advance online publication)

Lipids (2010) 45:893–905
DOI 10.1007/s11745-010-3393-4

REVIEW

Saturated Fat and Cardiometabolic Risk Factors, Coronary Heart Disease, Stroke, and Diabetes: a Fresh Look at the Evidence

Renata Micha · Dariush Mozaffarian

Received: 3 December 2009 / Accepted: 27 January 2010 / Published online: 31 March 2010

Abstract Dietary and policy recommendations frequently focus on reducing saturated fatty acid consumption for improving cardiometabolic health, based largely on ecologic and animal studies. Recent advances in nutritional science now allow assessment of critical questions about health effects of saturated fatty acids (SFA). We reviewed the evidence from randomized controlled trials (RCTs) of lipid and non-lipid risk factors, prospective cohort studies of disease endpoints, and RCTs of disease endpoints for cardiometabolic effects of SFA consumption in humans, including whether effects vary depending on specific SFA chain-length; on the replacement nutrient; or on disease outcomes evaluated. Compared with carbohydrate, the TC:HDL-C ratio is nonsignificantly affected by consumption of myristic or palmitic acid, is nonsignificantly decreased by stearic acid, and is significantly decreased by lauric acid. However, insufficient evidence exists for different chain-length-specific effects on other risk pathways or, more importantly, disease endpoints. Based on consistent evidence from human studies, replacing SFA with polyunsaturated fat modestly lowers coronary heart disease risk, with ~10% risk reduction for a 5% energy substitution; whereas replacing SFA with carbohydrate has no benefit and replacing SFA with monounsaturated fat has uncertain effects. Evidence for the effects of SFA consumption on vascular function, insulin resistance, diabetes, and stroke is mixed, with many studies showing no clear effects, highlighting a need for further investigation of these endpoints. Public health emphasis on reducing SFA consumption without considering the replacement nutrient or, more importantly, the many other food-based risk factors for cardiometabolic disease is unlikely to produce substantial intended benefits.

Keywords Cardiovascular disease · Diabetes mellitus · Diet · Nutrition · Saturated fatty acids · Fatty acids

Abbreviations

BMI	Body mass index
CHD	Coronary heart disease
CHO	Carbohydrate
CRP	C-reactive protein
CVD	Cardiovascular disease
FMD	Flow-mediated dilatation
FSIGTT	Frequently sampled intravenous glucose tolerance test
GLP-1	Glucagon-like peptide-1
HBA1c	Glycosylated hemoglobin
HDL	High-density lipoprotein
HOMA	Homeostasis model assessment
IL	Interleukin
LA	Linoleic acid
LDL	Low-density lipoprotein
MCP	Monocyte chemoattractant protein
MUFA	Monounsaturated fatty acids
PUFA	Polyunsaturated fatty acids
PWV	Pulse wave velocity
RCT	Randomized controlled trial
SFA	Saturated fatty acids
TC	Total cholesterol

R. Micha · D. Mozaffarian
Department of Epidemiology, Harvard School of Public Health, Boston, MA, USA

D. Mozaffarian (✉)
Division of Cardiovascular Medicine, Department of Medicine, Brigham and Women's Hospital, Harvard Medical School, 665 Huntington Ave Bldg 2-319, Boston, MA 02115, USA
e-mail: dmozaffa@hsph.harvard.edu

TFA	Trans fatty acids
TNF	Tumor necrosis factor
USFA	Unsaturated fatty acids
WHI	Women's Health Initiative
%E	Percentage of total energy intake

Introduction

Reducing the consumption of saturated fatty acids (SFA) is a pillar of international dietary recommendations to reduce the risk of cardiovascular disease (CVD) [1–3]. The World Health Organization and the US Dietary Guidelines recommend consuming less than 10%E (percentage of total energy intake) from SFA [4], and the American Heart Association less than 7%E [3]. The strong focus on SFA as a risk factor for CVD originated in the 1960s and 1970s from lines of evidence including ecologic studies across nations, short-term metabolic trials in generally healthy adults assessing total cholesterol (TC) and low-density lipoprotein cholesterol (LDL-C), and animal experiments that together appeared to provide consistent support that SFA intake increased the risk of coronary heart disease (CHD).

However, several critical questions have remained about the relationship between SFA consumption and CVD risk. First, do health effects of reducing SFA consumption vary depending on whether the replacement nutrient is carbohydrate (CHO), monounsaturated fat (MUFA), or polyunsaturated fat (PUFA)? A historical emphasis on low fat diets has produced drops in SFA consumption in the US and many other nations, but with concomitant increases in CHO, rather than MUFA or PUFA, as the replacement nutrient [1]. Is there strong evidence to support this dietary strategy? Second, do health effects of SFA vary depending on the chain-length, i.e. comparing 12-, 14-, 16-, and 18-carbon SFA? Current dietary recommendations generally focus on overall SFA consumption, without strong attention on specific SFA. Third, what is the relationship between SFA consumption and risk of stroke and type 2 diabetes mellitus? Historically, research on SFA has focused largely on CHD.

Advances in nutritional science in the last two decades now provide a substantial body of evidence to answer these questions (Fig. 1). These include well-conducted randomized controlled trials (RCTs) of SFA nutrient substitutions and multiple risk pathways as endpoints, including multiple lipid and also non-lipid risk factors (rather than only TC and LDL-C); and large prospective cohort studies and meta-analyses of RCTs of SFA consumption and clinical disease endpoints, that provide more direct evidence for

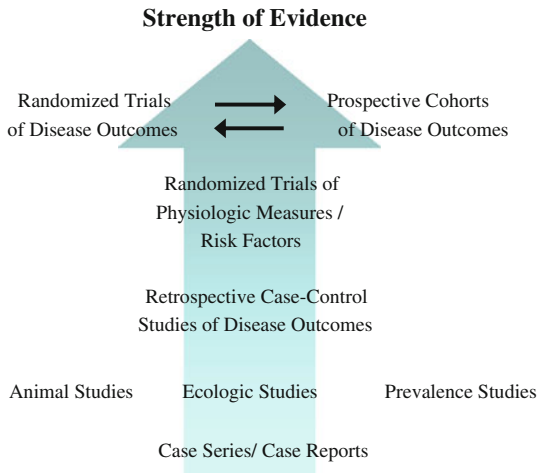

Fig. 1 Advances in nutritional science research paradigms. For causal inference about how dietary habits affect chronic disease, the best evidence is derived from randomized controlled trials (RCTs) of multiple risk pathways, observed differences in disease endpoints in prospective cohort studies, and effects on disease endpoints in RCTs. Conclusions can be considered most robust when these complementary lines of evidence provide concordant results. Adapted with permission from Harris, Mozaffarian, et al. 2009 [90]

effects on disease compared with changes in risk factors alone. Given the complementary strengths and limitations of these newer research paradigms, conclusions can be considered most robust when studies from each paradigm provide concordant evidence for health effects of SFA consumption. Together these research advances provide much stronger evidence for causal inference than data from prior available ecologic studies, limited metabolic studies, and animal experiments.

To elucidate the effects of SFA consumption on CVD risk based on the most current evidence, we reviewed the data from RCTs of multiple risk factors, large prospective cohort studies of disease endpoints, and RCTs of disease endpoints. When sufficient evidence was available, we particularly focused on the potentially different health effects of varying the replacement nutrient; of different chain-length SFA; and of specific effects on CHD, stroke, and diabetes.

Methods

Two investigators independently reviewed the literature for English-language articles published through Sep 2009 by performing searches of Medline, hand-searching of citation lists, and direct contact with experts. Inclusion criteria were any RCT or observational study in adults evaluating SFA consumption and the risk of CHD, stroke, or type 2 diabetes and related risk pathways, including lipids and lipoproteins, systemic inflammation, vascular function, and

insulin resistance (1,254 identified articles). Search terms included "saturated fat(s)", "lipoproteins", "inflammation", "blood pressure", "vascular function", "insulin resistance", "cardiovascular diseases", and "diabetes mellitus". We focused on identifying RCTs of major risk factors, large prospective cohort studies of disease endpoints, and RCTs of disease endpoints, given strengths of these designs and their complementary limitations. We excluded a priori animal experiments, ecological studies, commentaries, general reviews, and case reports. Studies were independently considered by the two investigators for inclusion; rare differences were resolved by consensus.

Effects on Cardiovascular Risk Factors

Lipids and Lipoproteins

RCTs have established clear multiple effects of SFA consumption on circulating lipids and lipoproteins [5, 6]. Each of these effects varies depending on the comparison nutrient, i.e., the nutrient isocalorically replaced for SFA (Fig. 2). Compared with CHO, SFA intake raises TC and LDL-C, but also lowers triglycerides and raises high-density lipoprotein cholesterol (HDL-C). Given these conflicting directions of effects, effects on apolipoproteins or, even better, a more global risk marker such as the TC:HDL-C ratio may provide the best overall indication of potential effects on CHD risk. Compared with CHO, SFA intake has no significant effects on the TC:HDL-C ratio or ApoB levels, and raises ApoA1 levels. In contrast, consumption of PUFA or MUFA in place of SFA leads to lowering of TC, LDL-C, and ApoB; slight lowering (for PUFA) of HDL-C and ApoA1; little effect on triglycerides; and lowering of the TC:HDL-C ratio. Compared with trans fatty acids (TFA), SFA intake has minimal effects on LDL-C but raises HDL-C and lowers triglycerides and lipoprotein(a), with improvement in the TC:HDL-C ratio [7]. Thus, consideration of which nutrient is being replaced is essential when considering lipid effects or designing dietary guidelines or policy measures related to SFA consumption. Overall, the changes in lipid and apolipoprotein levels predict minimal effects on CHD risk when CHO replaces SFA, benefits when PUFA or MUFA replace SFA, and harms when TFA replace SFA.

Effects of SFA consumption on serum lipids and lipoproteins further vary according to which specific SFA is consumed (Fig. 3) [5]. With CHO consumption as the reference, lauric (12:0), myristic (14:0), and palmitic (16:0) acid raise TC and LDL-C, whereas stearic acid (18:0) does

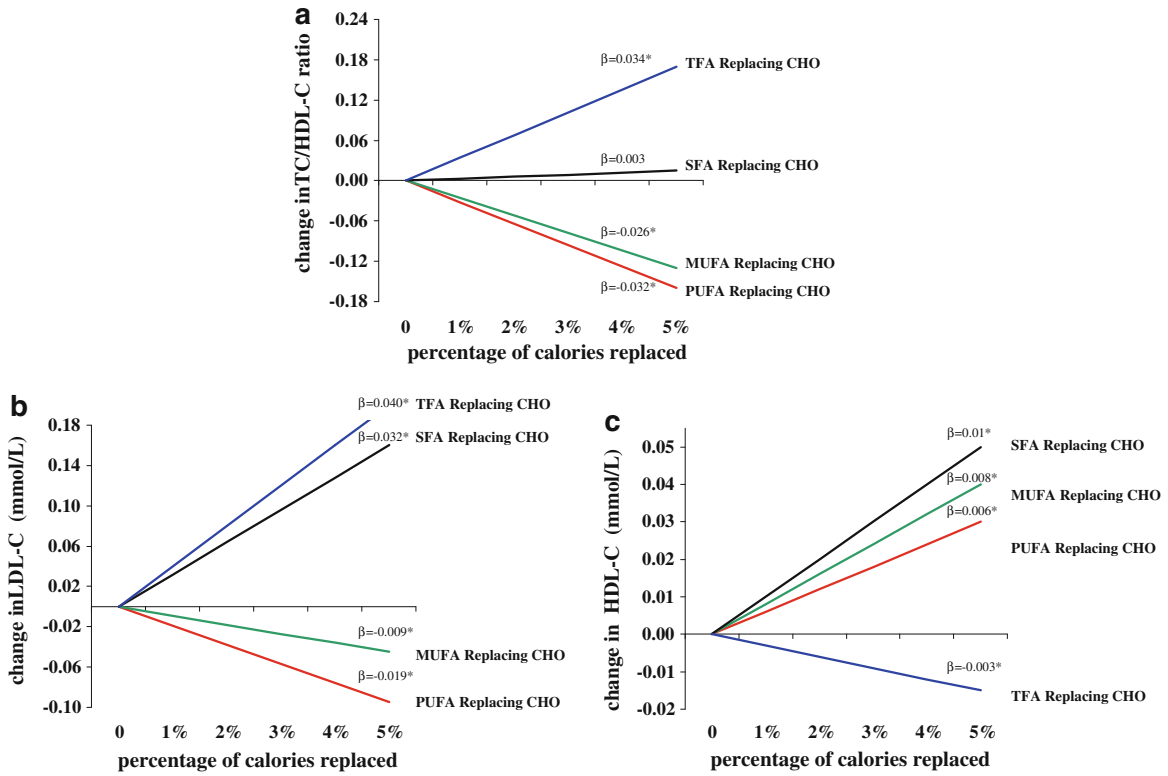

Fig. 2 Changes in blood lipid levels for consumption of saturated fatty acids (SFA), monounsaturated fatty acids (MUFA), polyunsaturated fatty acids (PUFA), or trans fatty acids (TFA) as an isocaloric replacement for carbohydrate (CHO) as a reference, based on two meta-analyses of randomized controlled feeding trials [5, 6]. β reflects the change for each 1% energy isocaloric replacement; $^*P < 0.05$

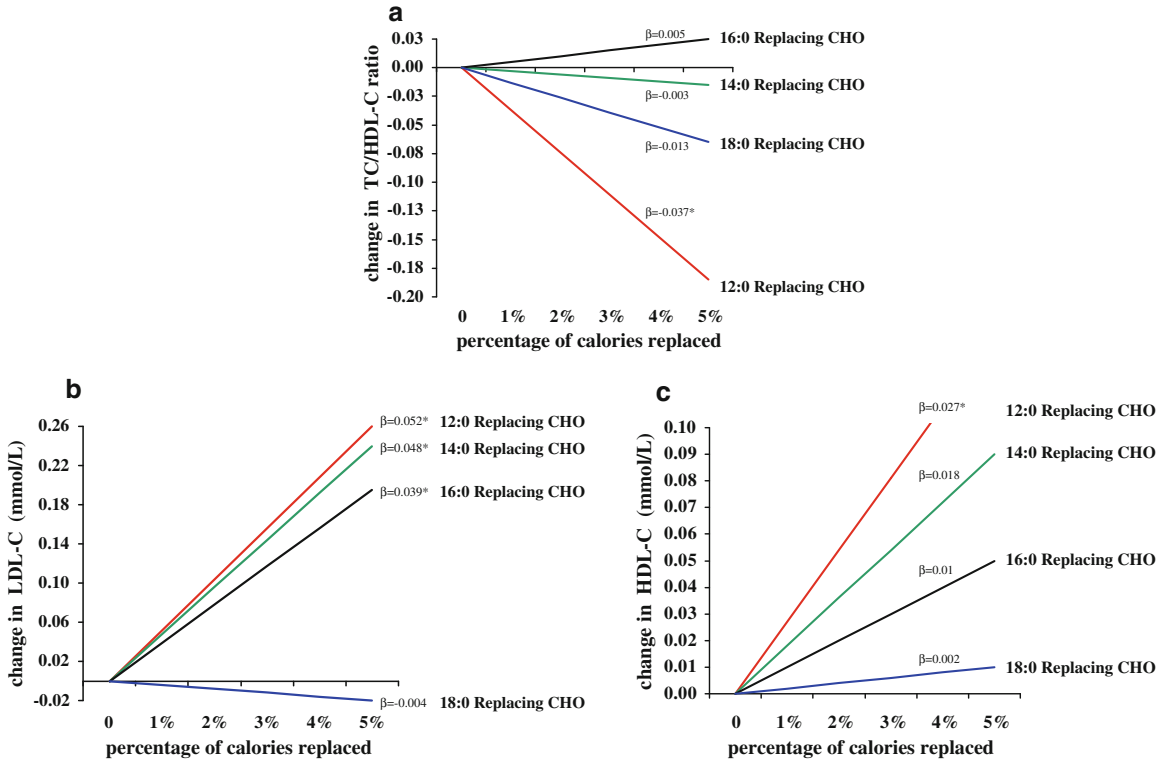

Fig. 3 Changes in blood lipid levels for consumption of different chain-length saturated fatty acids (SFA) as an isocaloric replacement for carbohydrate (CHO), based on meta-analysis of randomized controlled feeding trials [5]. β reflects the change for each 1% energy isocaloric replacement; $^*P < 0.05$

not. All SFA raise HDL-C, but HDL-raising effects are greater as chain-length decreases. Overall, the TC:HDL-C ratio is not significantly affected by myristic or palmitic acid consumption, is nonsignificantly decreased by stearic acid consumption, and is significantly decreased by lauric acid consumption (Fig. 3). These effects suggest little CHD benefit of replacing myristic, palmitic, or stearic acid with CHO, and potential harm of replacing lauric acid with CHO.

Systemic Inflammation

Inflammation independently increases risk of CVD and diabetes [8–11]. Compared with lipid effects, the influence of SFA consumption on inflammation is less well investigated, with mixed results. In a randomized cross-over trial, 20 healthy men consumed a high SFA (22%E SFA), a high MUFA (24%E MUFA), and a high CHO high PUFA (55%E CHO, 8%E PUFA) diet for 4 weeks [12]. At the end of each intervention period, participants were given a fat-rich breakfast (60%E fat) with similar fat composition to that of each diet. Consumption of a butter-rich breakfast (35%E SFA) had no effect on postprandial plasma levels of tumor necrosis factor (TNF)-α, interleukin (IL)-6 or monocyte chemoattractant protein (MCP)-1, compared with an olive oil-rich breakfast (36%E MUFA) or a walnut-rich breakfast (16%E PUFA) [12]. In another cross-over trial of 50 healthy men, consumption of low-chain SFA (12:0–16:0) for 5 weeks (8%E) had no effect on fibrinogen, C-reactive protein (CRP), or IL-6 levels; similar consumption of stearic acid (18:0) increased plasma levels of fibrinogen, but not of CRP or IL-6, compared with CHO [13]. Among hypercholesterolemic subjects ($n = 18$), a one-month diet with 16.7%E from SFA (butter), compared with 12.5%E from PUFA (soybean oil), resulted in a trend toward higher macrophage production of TNF-α, without effects on IL-6 [14].

Observational studies investigating associations between SFA intake and markers of inflammation are limited [15, 16]. Among 4,900 US adults, dietary SFA intake was not cross-sectionally associated with CRP levels, after adjusting for other risk factors and lifestyle behaviors [15]. Other cross-sectional studies have been very small and/or not multivariable-adjusted [16]. Observational studies of circulating (e.g., plasma) or tissue (e.g., adipose) SFA levels [17, 18] are helpful for investigating effects of metabolism but not of SFA consumption, as circulating and tissue SFA are poorly reflective of dietary SFA due to endogenous synthesis and regulation by lipolysis, lipogenesis, and beta-oxidation [19–22]. Overall, the limited and mixed evidence

Table 1 Effects of saturated fatty acids on blood pressure, endothelial function, and arterial stiffness in human feeding trials

Study	Outcome	*N*	Duration	Design	Comparison	SFA replaced by			
						PUFA	MUFA	TFA	CHO
Margetts et al. [26]	Blood pressure	54	6 weeks	Cross-over	18%E SFA versus 15%E PUFA	↔			
Puska et al. [27]	Blood pressure	84	12 weeks	Parallel	11%E SFA versus 8%E PUFA	↔			
Sacks et al. [28]	Blood pressure	21	6 weeks	Cross-over	16%E SFA versus 14%E PUFA or 52%E CHO	↔			↔
Storm et al. [29]	Blood pressure	15	3 weeks	Cross-over	13%E 18:0 SFA versus 16%E 16:0 SFA or 51%E CHO				↔
Piers et al. [30]	Blood pressure	8	4 weeks	Cross-over	24%E SFA versus 23%E MUFA		↔		
Sanders et al. [31]	Blood pressure	110	6 months	Parallel	17%E SFA versus 17%E MUFA or CHO[a]		↔		↔
Uusitupa et al. [33]	Blood pressure	159	6 months	Parallel	14%E SFA vs. 8%E PUFA, 11%E MUFA, or 53%E CHO	↔	↔		↔
Lahoz et al. [32]	Blood pressure	42	5 weeks	Consecutive diets-non randomized	17%E SFA versus 21%E MUFA or 13%E PUFA	↓	↓		
Rasmussen et al. [34]	Blood pressure	162	3 months	Parallel	18%E SFA versus 21%E MUFA		↓		
de Roos et al. [35]	Endothelial function – FMD	29	4 weeks	Cross-over	23%E SFA versus 9%E TFA			↓	
Fuentes et al. [36]	Endothelial function – FMD	22	4 weeks	Cross-over	20%E SFA versus 22%E MUFA or 57%E CHO		↑		↔
Keogh et al. [37]	Endothelial function – FMD	40	3 weeks	Cross-over	19%E SFA versus 19%E MUFA, 10%E PUFA, or 65%E CHO	↑	↑		↑
Sanders et al. [31]	Endothelial function – FMD	110	6 months	Parallel	17%E SFA versus 17%E MUFA or CHO[a]		↔		↔
Keogh et al. [37]	Arterial stiffness – PWV	40	3 weeks	Cross-over	19%E SFA versus 19%E MUFA, 10%E PUFA, or 65%E CHO	↔	↔		↔
Sanders et al. [31]	Arterial stiffness – PWV	110	6 months	Parallel	17%E SFA versus 17%E MUFA or CHO[a]		↔		↔

Direction of effect on reported outcome (↑ increased; ↓ decreased; ↔ no effect)

CHO carbohydrate, *MUFA* monounsaturated fatty acids, *FMD* brachial artery flow-mediated dilatation, *PUFA* polyunsaturated fatty acids, *PWV* pulse wave velocity, *SFA* saturated fatty acids, *TFA* trans fatty acids, *%E* percentage of total energy intake

[a] %E not reported

precludes strong conclusions about potential pro-inflammatory effects of SFA consumption.

Blood Pressure, Endothelial Function, and Arterial Stiffness

Effects of dietary SFA on markers of vascular function including blood pressure, endothelial function, and arterial stiffness are similarly not well characterized [23]. A few observational studies have evaluated SFA intake and incidence of hypertension, with mixed results [24, 25]. Among 30,681 US men followed for 4 years, no significant associations were seen between SFA intake and incident hypertension, after adjusting for age, body mass index, and alcohol consumption [24]. In contrast, among 11,342 US men in the MRFIT study, SFA intake was cross-sectionally positively associated with systolic and diastolic blood pressure, after adjusting for risk factors and lifestyle behaviors, although no adjustments were made for other dietary fats, CHO, or protein [25].

Randomized controlled feeding trials ranging in duration from 3 weeks to 6 months have demonstrated mixed results of SFA intake compared with MUFA, PUFA, TFA, or CHO on measures of blood pressure, endothelial dysfunction, and/or arterial stiffness [23] (Table 1). Among nine trials assessing blood pressure, seven observed no differences between the different diets [26–34]. These trials evaluated a range of SFA consumption levels and replacement nutrients (Table 1). Improvements in BP were seen in two of five RCTs including a comparison to

MUFA, one of five RCTs including a comparison to PUFA, and zero of four RCTs including a comparison to CHO. Among four trials assessing indices of endothelial function, three observed differences in brachial artery flow-mediated dilatation (FMD) between the different diets [31, 35–37]. Improvements in endothelial function were seen in two of three RCTs including a comparison to MUFA, one RCT including a comparison to PUFA, and one of three RCTs including a comparison to CHO; endothelial function was worsened in one RCT replacing SFA with TFA. In two trials evaluating arterial stiffness as assessed by pulse wave velocity (PWV) [31, 37], no effects of reducing SFA consumption were seen, including two RCTs including a comparison to MUFA, one RCT including a comparison to PUFA, and two RCTs including a comparison to CHO. Thus, evidence for effects of SFA consumption on vascular function is mixed, with no clear pattern based on underlying population characteristics, SFA consumption levels, or the comparison nutrient, and with most studies suggesting no effects.

Insulin Resistance and Diabetes

SFA has been considered a risk factor for insulin resistance and diabetes mellitus [38], but review of the current evidence indicates surprisingly equivocal findings. SFA consumption inconsistently affects insulin resistance in controlled trials (Table 2) and has not been associated with incident diabetes in prospective cohort studies (Fig. 4) [39–52]. Among generally healthy individuals, most RCTs show no differences in markers of glucose-insulin homeostasis comparing different intakes of SFA versus MUFA, PUFA, or CHO. Findings are more mixed among individuals having or predisposed to insulin resistance. In these individuals, improvements in markers of glucose-insulin homeostasis were seen in three of five RCTs including a comparison to MUFA, one of three RCTs including a comparison to PUFA, and one RCT including a comparison to CHO. Among all these trials, the great majority were short-term (up to several weeks) and surprisingly small (<20 subjects). The two largest trials ($n = 162$, $n = 59$) found SFA to worsen several indices of glucose-insulin homeostasis in comparison to MUFA (two trials) or CHO (one trial).

Significant additional insight into effects of dietary fats on glucose-insulin homeostasis can be gained from long-term studies evaluating actual onset of diabetes. Among four large prospective cohort studies, none found independent associations between consumption of either SFA (Fig. 4) or MUFA and onset of diabetes [53–56]. In contrast, three of four cohorts [54] observed lower incidence of diabetes with greater consumption of PUFA and/or vegetable fat [53, 55, 56]. In the large Women's Health Initiative trial ($n = 45{,}887$), SFA intake was reduced in the intervention group from 12.7 to 9.5%E over 8 years as part of overall total fat reduction, largely replaced with CHO [57]. In this large RCT, this significant reduction in SFA consumption had no effect on fasting glucose, fasting insulin, homeostasis model assessment (HOMA) insulin resistance, or incident diabetes (RR = 0.95, 95% CI = 0.90–1.03).

Thus, some evidence from short-term RCTs suggests that SFA consumption in place of MUFA may worsen glucose-insulin homeostasis, especially among individuals predisposed to insulin resistance. However, several long-term observational studies and one large RCT suggest no effect of SFA consumption on onset of diabetes. Further confirmatory results of either harm or no effect in additional appropriately powered studies are needed given the present inconsistency of effects across all studies.

Weight Gain and Adiposity

The role of total dietary fat in obesity has been widely studied due to its high energy content (9 kcal/g) and subsequent potential for weight gain [58–60]. Based on RCTs of weight loss with balanced-intensity interventions (i.e., all individuals receiving similar guidance and follow-up, with only the specific dietary advice varying) and prospective observational studies of weight gain, the %E from total fat does not have strong effects on adiposity compared with overall quality and quantity of foods consumed. Evidence for independent effects of specific dietary fats such as SFA on weight gain or adiposity are much more limited. In two large prospective cohort studies, increases in SFA consumption were associated with very small increases in abdominal circumference [61] or body weight during 8–9 years follow-up [62] compared with CHO, after adjusting for other risk factors and lifestyle and dietary behaviors.

Relationships with Cardiovascular Events

Coronary Heart Disease—Prospective Cohort Studies

Most individual prospective cohort studies have not observed an independent relationship between SFA consumption and incident CHD [63–67]. The relatively small number of published studies, among the many available international cohorts, also raises concern for potential publication bias (i.e., additional unreported null studies). Two recent systematic reviews and meta-analyses, the first including 9 cohorts (11 estimates) evaluating 160,673 individuals [64], and the second including 16 cohorts among 214,182 individuals [68], found no significant

Table 2 Effects of saturated fatty acids on insulin resistance in human feeding trials

Study	Subjects	*N*	Duration	Design	Comparison	Outcomes and results	SFA replaced by			
							PUFA	MUFA	TFA	CHO
Individuals Predisposed to Insulin Resistance										
Christiansen et al. [42]	Obese (BMI 33.5 ± 1.2 kg/m^2), type 2 diabetic, age 55 ± 3 years	Nine men; seven women	6 weeks	Cross-over	Three isocaloric diets: all 30%E fat, with 20%E from SFA, MUFA, or TFA	SFA versus MUFA: ↑ postprandial insulin by 78.9% and ↑ postprandial C-peptide by 41.8% ($P < 0.05$ for each) SFA versus TFA: no significant effects on postprandial insulin and C-peptide No significant effects on fasting insulin, fasting C-peptide, or fasting and postprandial glucose with any diet		↓	↔	
Vessby et al. [43]	Moderately overweight (BMI 26.5 ± 3 kg/m^2), age 48.5 ± 7.8 years	86 men, 76 women	3 months	Parallel	Two isocaloric diets: both ~37%E fat, with 17.6%E SFA, or 21.2%E MUFA; each group was further randomized to 3.6 g of either omega-3 fatty acids or olive oil	SFA versus MUFA: ↓ insulin sensitivity by 23.8% ($P = 0.05$), and ↑ insulin levels by 30.3% ($P = 0.06$) during a FSIGTT No significant effects on acute insulin response, or glucose levels during a FSIGTT with either diet		↓		
Summers et al. [44]	Obese (BMI 37 ± 6 kg/m^2), type 2 diabetic, age 53.7 ± 11 years	Eight men; nine women	5 weeks	Cross-over	Two diets: 42%E fat in SFA diet with 21%E from SFA, and 34%E fat in PUFA diet with 9%E from PUFA	SFA versus PUFA: ↓ insulin sensitivity by 20.3% ($P = 0.02$) during an euglycemic clamp No significant effects on fasting glucose insulin, or triglycerides with either diet	↓			
Vega-Lopez et al. [45]	Hyperlipidemic (LDL-cholesterol ≥ 130 mg/dl), moderately overweight (BMI 26 ± 2.4 kg/m^2), age 63.9 ± 5.7 years	Five men; ten women	5 weeks	Cross-over	Four isocaloric diets: all ~30%E fat, with 20%E from partially hydrogenated soybean (4.2%E TFA), soybean (12.5%E PUFA), palm (14.8%E SFA), or canola (15.4%E MUFA)	SFA versus PUFA, MUFA, or TFA: no significant effects on fasting insulin, fasting glucose, or HOMA	↔	↔	↔	
Paniagua et al. [46]	Obese (BMI 32.6 ± 7.8 kg/m^2), insulin resistant (as assessed by OGTT), age 62.3 ± 9.4 years	Four men; seven women	28 days	Cross-over	Three isocaloric diets: 38%E fat and 47%E CHO in the two high-fat diets, with 23%E from SFA or MUFA, and 20%E fat and 65%E CHO in the low-fat diet (the latter as a replacement of SFA)	SFA versus MUFA: ↑ HBA1c ($P < 0.01$), ↑ fasting glucose by 9.6% ($P < 0.05$), ↑ HOMA by 17.2% ($P < 0.01$), ↑ fasting proinsulin by 26.1% ($P < 0.05$), no significant effects on postprandial glucose, postprandial insulin, or postprandial GLP-1 SFA vs. CHO: ↑ HBA1c by 6.3% ($P < 0.01$), ↑ fasting glucose by 9.3% ($P < 0.05$), ↓ postprandial glucose by 51% ($P < 0.05$), ↓ postprandial insulin by 53% ($P < 0.05$), ↑ postprandial GLP-1 by 134.6% ($P < 0.05$), no significant effects on HOMA or fasting proinsulin No significant effects on fasting insulin or GLP-1, or the 60 min proinsulin:insulin ratio with any diet		↓		↓

Table 2 continued

Study	Subjects	*N*	Duration	Design	Comparison	Outcomes and results	SFA replaced by			
							PUFA	MUFA	TFA	CHO
Lithander et al. [47]	Hyperlipidemic (LDL 3.0–5.0 mmol/L), moderately overweight (BMI 25.9 ± 4.2 kg/m^2), age 39.7 ± 13.9 years	18 men	3 weeks	Cross-over	Two isocaloric diets, both 38%E fat: 18%E SFA, 10%E MUFA and 7%E PUFA in the high SFA:USFA diet, and 13%E SFA, 12%E MUFA and 8%E PUFA in the low SFA:USFA diet	SFA versus PUFA + MUFA: No significant effects on fasting adiponectin	↔	↔		
Healthy individuals										
Schwab et al. [48]	Healthy, normal weight (BMI 21.4 ± 0.5 kg/m^2), age 23.9 ± 1.2 years	11 women	4 weeks	Cross-over	Two isocaloric diets: all ~38%E fat, with 5%E from lauric acid (12:0 SFA), or 11.4%E from palmitic acid (16:0 SFA)	12:0 SFA versus 16:0 SFA: no significant effects on insulin, glucose, acute insulin response, or insulin sensitivity index during a FSIGTT with either diet				
Fasching et al. [49]	Healthy, normal weight (BMI 22.4 ± 1.8 kg/m^2), age 26 ± 3.5 years	8 men	1 week	Cross-over	Four isocaloric diets: 54%E fat and 35%E CHO in the three high-fat diets with 31.5%E from SFA, 28%E from PUFA and 22%E from MUFA, and 25%E fat and 64%E CHO in the high CHO diet	SFA versus PUFA, MUFA, or CHO: no significant effects on insulin, glucose, acute insulin response, or insulin sensitivity index during a FSIGTT with any diet	↔	↔		↔
Louheranta et al. [50]	Healthy, normal weight (BMI 22.6 ± 0.6 kg/m^2), age 22 ± 0.6 years	14 women	4 weeks	Cross-over	Two isocaloric diets: both ~38%E fat, with 18.5%E from SFA or MUFA	SFA versus MUFA: no significant effects on insulin, glucose, acute insulin response, or insulin sensitivity index during a FSIGTT with either diet		↔		
Perez-Jimenez et al. [52]	Healthy, normal weight (BMI 22.87 ± 2.45 kg/m^2), age 23.1 ± 1.8 years	30 men, 29 women	28 days	Cross-over	Baseline 28-day high SFA diet followed by Two randomized cross-over periods; all isocaloric diets: 38%E fat and 47%E CHO in the two high-fat diets, with 20%E from SFA or 22%E from MUFA, and 28%E fat and 57%E CHO in the low-fat diet (the latter as a replacement of SFA)	SFA versus MUFA: ↑ fasting insulin by 134%, ↑ fasting free fatty acids by 40.5%, ↑ mean steady-state plasma glucose by 21.9%, ↓ in vitro basal glucose uptake by 61.3%, and ↓ in vitro insulin-stimulated glucose uptake by 55.3% ($P < 0.001$ for each)		↓		↓
						SFA versus CHO: ↑ fasting insulin by 119.7%, ↑ fasting free fatty acids by 40.5%, ↑ mean steady-state plasma glucose by 29%, ↓ in vitro basal glucose uptake by 57.1% %, and ↓ in vitro insulin-stimulated glucose uptake by 55.9% ($P < 0.001$ for each)				
						No significant effects on fasting glucose with any diet				
Lovejoy et al. [51]	Healthy, normal weight (BMI 23.5 ± 0.5 kg/m^2), age 28 ± 2 years	12 men; 13 women	4 weeks	Cross-over	Three isocaloric diets: all 30%E fat, with 9%E from elaidic acid (TFA), oleic acid (MUFA), or palmitic acid (SFA)	SFA versus MUFA or TFA: no significant effects on insulin, glucose, acute insulin response, or insulin sensitivity index during a FSIGTT with any diet		↔	↔	

Direction of effect on biomarkers of insulin resistance (↑increased; ↓ decreased; ↔ no effect). If even one biomarker was affected, this was considered an effect; this might overestimate the effects of these dietary changes as often many other biomarkers were unaffected (detailed results are also provided)

BMI body mass index, *CHO* carbohydrate, *FSIGTT* frequently sampled intravenous glucose tolerance test, *GLP-1* glucagon-like peptide-1, *HBA1c* glycosylated hemoglobin, *HOMA* homeostasis model assessment, *MUFA* monounsaturated fatty acids, *PUFA* polyunsaturated fatty acids, *SFA* saturated fatty acids, *TFA* trans fatty acids, *USFA* unsaturated fatty acids, *%E* percentage of total energy intake

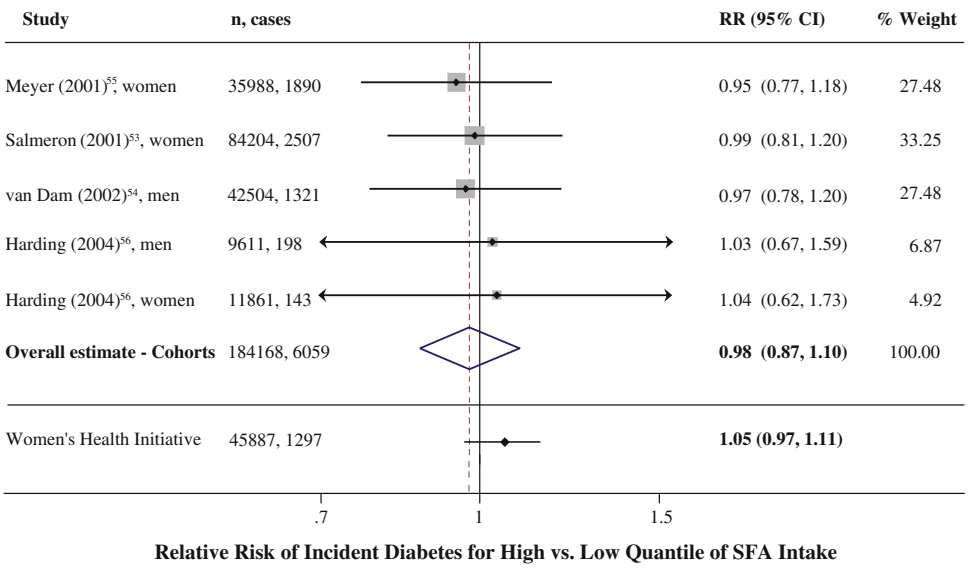

Fig. 4 Relative risk of incident diabetes associated with consumption of saturated fat (SFA). Multivariable-adjusted results from prospective cohort studies and the overall pooled result using fixed-effects meta-analysis are shown. Results from the Women's Health Initiative randomized controlled trial are also shown comparing controls (higher SFA intake) to the intervention group in which SFA was reduced by ~3.2%E over 8 years [79]. CI's for Harding et al.[56] were estimated based on the numbers of cases

association between SFA intake and CHD risk. Comparing the highest to the lowest category of consumption, the pooled RRs in these two meta-analyses were 1.06 (95% CI = 0.96–1.15) and 1.07 (95% CI = 0.96–1.19), respectively. These meta-analyses suggest no overall effect of SFA consumption on CHD events. However, these studies were unable to separately evaluate whether consuming SFA might have different effects on CHD events depending on the nutrient replaced, as would be suggested by differing effects of SFA, depending on the comparison nutrient, on blood lipids and apolipoproteins (Fig. 2).

The best observational evidence to-date of this question is a recent pooled analysis of individual-level data from 11 prospective cohort studies across three continents, including 344,696 individuals with 5,249 CHD events over 4–10 years of follow-up [69]. In fully multivariable-adjusted analyses, SFA consumption was associated with higher CHD risk only in comparison to PUFA. In other words, only consumption of PUFA in place of SFA was associated with lower CHD risk, whereas in fact consumption of CHO or MUFA in place of SFA was associated with higher CHD risk or trends toward higher CHD risk (Fig. 5). These associations were similar when analyses were restricted to CHD deaths only, and were not different in subgroups stratified by either sex or age.

Coronary Heart Disease—Randomized Controlled Trials

Eight RCTs have investigated the effects of consuming PUFA (either total or linoleic acid, LA) in place of SFA on CHD events [70–77]. Most of these trials individually found no significant effects. A recent meta-analysis of these RCTs, including a total of 13,614 participants with 1,042 CHD events, found that CHD risk was lowered by 10% for each 5%E greater PUFA intake replacing SFA [78] (Fig. 5). Many of these trials have important limitations, including for example not being double-blind; incompletely assessing compliance; randomizing sites rather than individuals and having open enrollment and drop-out; and/or including vegetable oils that contained omega-3 PUFA of plant origin that may provide cardiovascular benefits unrelated to decreased SFA intake. Nonetheless, the overall findings from these RCTs of CHD endpoints are consistent with the results from prospective cohorts (Fig. 5).

One large RCT has tested the effect of reducing SFA consumption, replaced largely with CHO, on CHD events. As described, the Women's Health Initiative trial randomized 46,558 women to lower total fat consumption, that included lowering of SFA consumption by ~3%E over 8 years, and largely replaced with CHO. Even though this was an unbalanced intervention (i.e., the intervention group received extensive dietary counseling, whereas the control group received usual care) that would generally bias toward risk-reduction in the intervention group, there were no significant effects on either incident CHD (RR = 0.93, 95%CI = 0.83–1.05) or total CVD (RR = 0.96, 95%CI = 0.89–1.03) [79]. This absence of benefit for substituting SFA with CHO is consistent with expected effects based on lipid changes (TC:HDL ratio) or observed relationships in prospective cohort studies (Fig. 5).

Stroke: Prospective Cohorts and Randomized Controlled Trials

Among five prospective cohort studies evaluating SFA consumption and incidence of stroke, one of three found

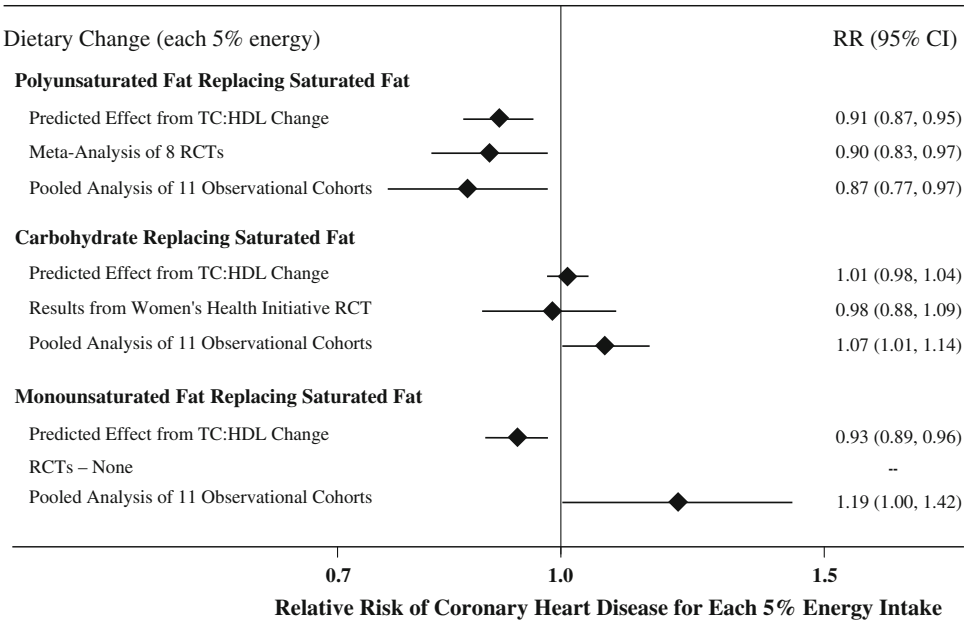

Fig. 5 Effects on coronary heart disease (CHD) risk of consuming polyunsaturated fat (PUFA), carbohydrate (CHO), or monounsaturated fat (MUFA) in place of saturated fat (SFA). Predicted effects are based on changes in the TC:HDL-C ratio in short-term trials [5], coupled with observed associations between the TC:HDL-C ratio and CHD disease events in middle-aged adults [91]. Evidence for effects of dietary macronutrients on actual CHD events comes from a meta-analysis of eight randomized controlled trials (RCTs) for PUFA replacing SFA, including 13,614 participants with 1,042 CHD events [78]; and from the Women's Health Initiative (WHI) RCT for CHO replacing SFA, including 46,558 individuals with 1,185 CHD events and ~3.2%E reduction in SFA over 8 years [79]. Evidence for observed relationships of usual dietary habits with CHD events comes from a pooled analysis of 11 prospective cohort studies, including 344,696 individuals with 5,249 CHD events [69]. Reproduced with permission from Mozaffarian et al., in press [78]

SFA to be associated with lower risk of ischemic stroke [80–82], and one of three found SFA to be associated with lower risk of hemorrhagic stroke [80, 83, 84]. Four prospective cohorts have also observed protective associations between animal protein intake, that is often consumed together with SFA, and risk of hemorrhagic stroke [85]. A recent systematic review and meta-analysis of eight prospective cohorts also found that SFA consumption was associated with trends toward lower risk of stroke: comparing the highest to the lowest category of SFA intake, the RR was 0.81 (95% CI = 0.62–1.05) [68]. In the Women's Health Initiative trial, reduction in SFA consumption did not have a significant effect on incident stroke over 8 years (RR = 1.02, 95% CI = 0.90–1.17) [79]. Thus, overall, SFA consumption does not appear to increase the risk of stroke, and in fact some studies suggest a protective effect. Further investigation of these effects, including independence from potential benefits of animal protein intake, is warranted.

Future Research Directions

The multiple well-designed studies reviewed herein provide substantial evidence for health effects of SFA consumption. However, important questions remain. Although replacement of SFA with CHO appears to provide no overall CVD benefit, indirect lines of evidence suggest that effects could vary depending on overall CHO quality [86–88]. For example, replacing SFA with less processed, higher fiber, lower glycemic index CHO could provide benefit, whereas replacing SFA with more processed, lower fiber, higher glycemic index CHO might have no effects or even be harmful. Effects of replacing SFA with CHO could also vary with an individual's susceptibility to insulin resistance/metabolic syndrome, in whom adverse metabolic effects of highly refined CHO may be more pronounced. Evidence for effects of replacing SFA with MUFA is mixed. Such effects could vary depending on other constituents in MUFA-containing foods (e.g., animal fats vs. vegetable oils), for example due to potentially beneficial phytochemicals and flavanols contained in the latter but not the former. Each of these issues requires direct investigation. Additionally, whereas the substantial differences in blood lipid effects of different chain-length SFA are clear, blood lipids represent only one set of intermediate risk markers. Investigation of the effects of different chain-length SFA on other risk pathways and, more importantly, on disease endpoints is urgently needed to determine the extent to which dietary and policy

recommendations should focus on specific SFA rather than overall SFA consumption. Additional investigation of effects of SFA consumption on blood pressure, endothelial function, insulin resistance, diabetes, and stroke (plus stroke subtypes) is also needed, including consideration of potential variation depending on both the replacement nutrients and specific chain-length SFA under consideration. Future research should also evaluate the health effects of specific foods consumed, i.e., SFA intake from different meats versus dairy versus tropical fats, as well as how individual factors, such as age, sex, lifestyle factors, predisposition to insulin resistance, or genetic variation, may alter such responses.

Conclusions

Current public health dietary recommendations often prioritize the reduction of SFA consumption to prevent CVD. A review of the current evidence, particularly findings from well-performed RCTs of risk pathways, large prospective cohorts of disease endpoints, and RCTs of disease endpoints, suggests that this focus may not produce the intended benefits. First of all, substantial evidence indicates that health effects of reducing SFA vary depending on the replacement nutrient. Based on the best evidence from human studies, replacing SFA with PUFA (e.g., vegetables, vegetable oils) lowers CHD risk, whereas replacing SFA with CHO has no benefits. Replacing SFA with MUFA has uncertain effects, based on mixed evidence within and across different research paradigms. Of note, the effects of replacing SFA with PUFA or CHO, but not MUFA, on clinical CHD endpoints could be relatively predicted from the effects of these nutrient substitutions on the TC:HDL-C ratio. Thus, policies that prioritize the reduction of SFA consumption without specifically considering the replacement nutrient may have little or no effects on disease risk, especially as the most common replacement in populations is often CHO.

Second, even under optimal replacement scenarios of SFA for PUFA, the magnitude of likely benefit warrants attention. RCTs of the blood TC:HDL-C ratio, prospective cohorts of disease endpoints, and RCTs of disease endpoints each converge on $\sim$10% reduction in CHD events for 5%E substitution of SFA with PUFA. This approaches the maximal plausible risk reduction in most populations; in the US, for example, such benefit would require overall population decrease from the current 11.5 to 6.5%E SFA consumption. Thus, although recommendations to replace SFA with PUFA appear appropriate, the much larger CVD burdens caused by other dietary factors (e.g., low omega-3, low fruits and vegetables, high trans fat, and high salt) [89] appear to warrant much more attention. Finally, although investigation of individual nutrients provides important information on potential underlying mechanisms of health effects, people make decisions about eating whole foods that contain multiple macro- and micronutrients in various amounts. Thus, food-based scientific research and policy recommendations may be most relevant in the modern era to understand and reduce the pandemics of chronic disease occurring in nearly all nations.

Acknowledgments Supported by the Searle Funds at The Chicago Community Trust and the Bill & Melinda Gates Foundation/World Health Organization Global Burden of Diseases, Injuries, and Risk Factors Study. The founders had no role in the design or conduct of the study; collection, management, analysis, or interpretation of the data; or preparation, review, or approval of the manuscript.

Conflict of interest statement R. Micha has no conflicts of interest to declare. D. Mozaffarian received ad hoc consulting honoraria (modest) from Nutrition Impact, Unilever, and SPRIM.

References

1. Centers for disease control, prevention (2004) Trends in intake of energy and macronutrients: United States, 1971–2000. Morb Mortal Wkly Rep 53(04):80–82
2. World Health Organization (2003) Diet, nutrition and the prevention of chronic diseases: report of a joint WHO/FAO expert consultation. World Health Org Tech Rep 916(i–viii):1–149 (Geneva)
3. Lichtenstein AH et al (2006) Diet and lifestyle recommendations revision 2006: a scientific statement from the American Heart Association Nutrition Committee. Circulation 114(1):82–96
4. Dietary Guidelines Advisory Committee (2005) Dietary Guidelines Advisory Committee report. http://www.health.gov/dietaryguidelines/dga2005/report/
5. Mensink RP et al (2003) Effects of dietary fatty acids and carbohydrates on the ratio of serum total to HDL cholesterol and on serum lipids and apolipoproteins: a meta-analysis of 60 controlled trials. Am J Clin Nutr 77(5):1146–1155
6. Mozaffarian D, Clarke R (2009) Quantitative effects on cardiovascular risk factors and coronary heart disease risk of replacing partially hydrogenated vegetable oils with other fats and oils. Eur J Clin Nutr 63(Suppl 2):S22–S33
7. Micha R, Mozaffarian D (2009) Trans fatty acids: effects on metabolic syndrome, heart disease and diabetes. Nat Rev Endocrinol 5(6):335–344
8. Libby P, Ridker PM, Maseri A (2002) Inflammation and atherosclerosis. Circulation 105(9):1135–1143
9. Albert CM et al (2002) Prospective study of C-reactive protein, homocysteine, and plasma lipid levels as predictors of sudden cardiac death. Circulation 105(22):2595–2599
10. Pickup JC (2004) Inflammation and activated innate immunity in the pathogenesis of type 2 diabetes. Diabetes Care 27(3):813–823
11. Vasan RS et al (2003) Inflammatory markers and risk of heart failure in elderly subjects without prior myocardial infarction: the Framingham Heart Study. Circulation 107(11):1486–1491

12. Jimenez-Gomez Y et al (2009) Olive oil and walnut breakfasts reduce the postprandial inflammatory response in mononuclear cells compared with a butter breakfast in healthy men. Atherosclerosis 204(2):e70–e76
13. Baer DJ et al (2004) Dietary fatty acids affect plasma markers of inflammation in healthy men fed controlled diets: a randomized crossover study. Am J Clin Nutr 79(6):969–973
14. Han SN et al (2002) Effect of hydrogenated and saturated, relative to polyunsaturated, fat on immune and inflammatory responses of adults with moderate hypercholesterolemia. J Lipid Res 43(3):445–452
15. King DE, Egan BM, Geesey ME (2003) Relation of dietary fat and fiber to elevation of C-reactive protein. Am J Cardiol 92(11):1335–1339
16. Lennie TA et al (2005) Dietary fat intake and proinflammatory cytokine levels in patients with heart failure. J Card Fail 11(8):613–618
17. Petersson H et al (2009) Relationships between serum fatty acid composition and multiple markers of inflammation and endothelial function in an elderly population. Atherosclerosis 203(1):298–303
18. Fernandez-Real JM et al (2003) Insulin resistance, inflammation, and serum fatty acid composition. Diabetes Care 26(5):1362–1368
19. Poppitt SD et al (2005) Assessment of erythrocyte phospholipid fatty acid composition as a biomarker for dietary MUFA, PUFA or saturated fatty acid intake in a controlled cross-over intervention trial. Lipids Health Dis 4:30
20. Sun Q et al (2007) Comparison between plasma and erythrocyte fatty acid content as biomarkers of fatty acid intake in US women. Am J Clin Nutr 86(1):74–81
21. Baylin A, Campos H (2006) The use of fatty acid biomarkers to reflect dietary intake. Curr Opin Lipidol 17(1):22–27
22. Hodson L, Skeaff CM, Fielding BA (2008) Fatty acid composition of adipose tissue and blood in humans and its use as a biomarker of dietary intake. Prog Lipid Res 47(5):348–380
23. Hall WL (2009) Dietary saturated and unsaturated fats as determinants of blood pressure and vascular function. Nutr Res Rev 22(1):18–38
24. Ascherio A et al (1992) A prospective study of nutritional factors and hypertension among US men. Circulation 86(5):1475–1484
25. Stamler J et al (1996) Relationship to blood pressure of combinations of dietary macronutrients: findings of the multiple risk factor intervention trial (MRFIT). Circulation 94(10):2417–2423
26. Margetts BM et al (1985) Blood pressure and dietary polyunsaturated and saturated fats: a controlled trial. Clin Sci (Lond) 69(2):165–175
27. Puska P et al (1985) Dietary fat and blood pressure: an intervention study on the effects of a low-fat diet with two levels of polyunsaturated fat. Prev Med 14(5):573–584
28. Sacks FM et al (1987) Effect of dietary fats and carbohydrate on blood pressure of mildly hypertensive patients. Hypertension 10(4):452–460
29. Storm H et al (1997) Comparison of a carbohydrate-rich diet and diets rich in stearic or palmitic acid in NIDDM patients: effects on lipids, glycemic control, and diurnal blood pressure. Diabetes Care 20(12):1807–1813
30. Piers LS et al (2003) Substitution of saturated with monounsaturated fat in a 4-week diet affects body weight and composition of overweight and obese men. Br J Nutr 90(3):717–727
31. Sanders T, Lewis F, Frost G (2009) Impact of the amount and type of fat and carbohydrate on vascular function in the RISCK study. Proc Nutr Soc, vol 68 (in press)
32. Lahoz C et al (1997) Effects of dietary fat saturation on eicosanoid production, platelet aggregation and blood pressure. Eur J Clin Invest 27(9):780–787
33. Uusitupa MI et al (1994) Long-term effects of four fat-modified diets on blood pressure. J Hum Hypertens 8(3):209–218
34. Rasmussen BM et al (2006) Effects of dietary saturated, monounsaturated, and n-3 fatty acids on blood pressure in healthy subjects. Am J Clin Nutr 83(2):221–226
35. de Roos NM, Bots ML, Katan MB (2001) Replacement of dietary saturated fatty acids by trans fatty acids lowers serum HDL cholesterol and impairs endothelial function in healthy men and women. Arterioscler Thromb Vasc Biol 21(7):1233–1237
36. Fuentes F et al (2001) Mediterranean and low-fat diets improve endothelial function in hypercholesterolemic men. Ann Intern Med 134(12):1115–1119
37. Keogh JB et al (2005) Flow-mediated dilatation is impaired by a high-saturated fat diet but not by a high-carbohydrate diet. Arterioscler Thromb Vasc Biol 25(6):1274–1279
38. Eyre H et al (2004) Preventing cancer, cardiovascular disease, and diabetes: a common agenda for the American Cancer Society, the American Diabetes Association, and the American Heart Association. Circulation 109(25):3244–3255
39. Galgani JE et al (2008) Effect of the dietary fat quality on insulin sensitivity. Br J Nutr 100(3):471–479
40. Riserus U, Willett WC, Hu FB (2009) Dietary fats and prevention of type 2 diabetes. Prog Lipid Res 48(1):44–51
41. Feskens EJ et al (1995) Dietary factors determining diabetes and impaired glucose tolerance: a 20-year follow-up of the Finnish and Dutch cohorts of the seven countries study. Diabetes Care 18(8):1104–1112
42. Christiansen E et al (1997) Intake of a diet high in trans monounsaturated fatty acids or saturated fatty acids: effects on postprandial insulinemia and glycemia in obese patients with NIDDM. Diabetes Care 20(5):881–887
43. Vessby B et al (2001) Substituting dietary saturated for monounsaturated fat impairs insulin sensitivity in healthy men and women: the KANWU study. Diabetologia 44(3):312–319
44. Summers LK et al (2002) Substituting dietary saturated fat with polyunsaturated fat changes abdominal fat distribution and improves insulin sensitivity. Diabetologia 45(3):369–377
45. Vega-Lopez S et al (2006) Palm and partially hydrogenated soybean oils adversely alter lipoprotein profiles compared with soybean and canola oils in moderately hyperlipidemic subjects. Am J Clin Nutr 84(1):54–62
46. Paniagua JA et al (2007) A MUFA-rich diet improves postprandial glucose, lipid and GLP-1 responses in insulin-resistant subjects. J Am Coll Nutr 26(5):434–444
47. Lithander FE et al (2008) No evidence of an effect of alterations in dietary fatty acids on fasting adiponectin over 3 weeks. Obesity (Silver Spring) 16(3):592–599
48. Schwab US et al (1995) Lauric and palmitic acid-enriched diets have minimal impact on serum lipid and lipoprotein concentrations and glucose metabolism in healthy young women. J Nutr 125(3):466–473
49. Fasching P et al (1996) No effect of short-term dietary supplementation of saturated and poly- and monounsaturated fatty acids on insulin secretion and sensitivity in healthy men. Ann Nutr Metab 40(2):116–122
50. Louheranta AM et al (1998) A high-stearic acid diet does not impair glucose tolerance and insulin sensitivity in healthy women. Metabolism 47(5):529–534
51. Lovejoy JC et al (2002) Effects of diets enriched in saturated (palmitic), monounsaturated (oleic), or trans (elaidic) fatty acids on insulin sensitivity and substrate oxidation in healthy adults. Diabetes Care 25(8):1283–1288
52. Perez-Jimenez F et al (2001) A Mediterranean and a high-carbohydrate diet improve glucose metabolism in healthy young persons. Diabetologia 44(11):2038–2043

53. Salmeron J et al (2001) Dietary fat intake and risk of type 2 diabetes in women. Am J Clin Nutr 73(6):1019–1026
54. van Dam RM et al (2002) Dietary fat and meat intake in relation to risk of type 2 diabetes in men. Diabetes Care 25(3):417–424
55. Meyer KA et al (2001) Dietary fat and incidence of type 2 diabetes in older Iowa women. Diabetes Care 24(9):1528–1535
56. Harding AH et al (2004) Dietary fat and the risk of clinical type 2 diabetes: the European prospective investigation of Cancer-Norfolk study. Am J Epidemiol 159(1):73–82
57. Tinker LF et al (2008) Low-fat dietary pattern and risk of treated diabetes mellitus in postmenopausal women: the Women's Health Initiative randomized controlled dietary modification trial. Arch Intern Med 168(14):1500–1511
58. Willett WC, Leibel RL (2002) Dietary fat is not a major determinant of body fat. Am J Med 113(Suppl 9B):47S–59S
59. Pirozzo S et al (2003) Should we recommend low-fat diets for obesity? Obes Rev 4(2):83–90
60. Lissner L, Heitmann BL (1995) Dietary fat and obesity: evidence from epidemiology. Eur J Clin Nutr 49(2):79–90
61. Koh-Banerjee P et al (2003) Prospective study of the association of changes in dietary intake, physical activity, alcohol consumption, and smoking with 9-y gain in waist circumference among 16,587 US men. Am J Clin Nutr 78(4):719–727
62. Field AE et al (2007) Dietary fat and weight gain among women in the nurses' health study. Obesity (Silver Spring) 15(4):967–976
63. Mozaffarian D (2005) Effects of dietary fats versus carbohydrates on coronary heart disease: a review of the evidence. Curr Atheroscler Rep 7(6):435–445
64. Mente A et al (2009) A systematic review of the evidence supporting a causal link between dietary factors and coronary heart disease. Arch Intern Med 169(7):659–669
65. Oh K et al (2005) Dietary fat intake and risk of coronary heart disease in women: 20 years of follow-up of the nurses' health study. Am J Epidemiol 161(7):672–679
66. Leosdottir M et al (2005) Dietary fat intake and early mortality patterns–data from The Malmo Diet and Cancer Study. J Intern Med 258(2):153–165
67. Pietinen P et al (1997) Intake of fatty acids and risk of coronary heart disease in a cohort of Finnish men: the alpha-tocopherol, beta-carotene cancer prevention study. Am J Epidemiol 145(10):876–887
68. Siri-Tarino P et al (2010) A meta-analysis of prospective cohort studies evaluating the association of saturated fat with cardiovascular disease. Am J Clin Nutr 91(3):535–546
69. Jakobsen MU et al (2009) Major types of dietary fat and risk of coronary heart disease: a pooled analysis of 11 cohort studies. Am J Clin Nutr 89(5):1425–1432
70. Dayton S et al (1968) Controlled trial of a diet high in unsaturated fat for prevention of atherosclerotic complications. Lancet 2(7577):1060–1062
71. Leren P (1970) The Oslo diet-heart study: eleven-year report. Circulation 42(5):935–942
72. Turpeinen O et al (1979) Dietary prevention of coronary heart disease: the Finnish mental hospital study. Int J Epidemiol 8(2):99–118
73. Burr ML et al (1989) Diet and reinfarction trial (DART): design, recruitment, and compliance. Eur Heart J 10(6):558–567
74. Watts GF et al (1992) Effects on coronary artery disease of lipid-lowering diet, or diet plus cholestyramine, in the St Thomas' Atherosclerosis Regression Study (STARS). Lancet 339(8793):563–569
75. Miettinen M et al (1983) Dietary prevention of coronary heart disease in women: the Finnish mental hospital study. Int J Epidemiol 12(1):17–25
76. Frantz ID Jr et al (1989) Test of effect of lipid lowering by diet on cardiovascular risk. the Minnesota Coronary Survey. Arteriosclerosis 9(1):129–135
77. Council Medical Research (1968) Controlled trial of soya-bean oil in myocardial infarction. Lancet 2(7570):693–699
78. Mozaffarian D, Micha R, Wallace SK (2010) Effects on coronary heart disease of increasing polyunsaturated fat in place of saturated fat: a systematic review and meta-analysis of randomized controlled trials. PLoS Med (in press)
79. Howard BV et al (2006) Low-fat dietary pattern and risk of cardiovascular disease: the Women's Health Initiative Randomized Controlled Dietary Modification Tria. JAMA 295(6):655–666
80. He K et al (2003) Dietary fat intake and risk of stroke in male US healthcare professionals: 14 year prospective cohort study. BMJ 327(7418):777–782
81. Seino F et al (1997) Dietary lipids and incidence of cerebral infarction in a Japanese rural community. J Nutr Sci Vitaminol 43(1):83–99
82. Gillman MW et al (1997) Inverse association of dietary fat with development of ischemic stroke in men. JAMA 278(24):2145–2150
83. Iso H et al (2001) Prospective study of fat and protein intake and risk of intraparenchymal hemorrhage in women. Circulation 103(6):856–863
84. Iso H et al (2003) Fat and protein intakes and risk of intraparenchymal hemorrhage among middle-aged Japanese. Am J Epidemiol 157(1):32–39
85. Ding EL, Mozaffarian D (2006) Optimal dietary habits for the prevention of stroke. Semin Neurol 26(1):11–23
86. Jacobs DR, Gallaher DD Jr (2004) Whole grain intake and cardiovascular disease: a review. Curr Atheroscler Rep 6(6):415–423
87. Thomas D, EJ Elliott (2009) Low glycaemic index, or low glycaemic load, diets for diabetes mellitus. Cochrane Database Syst Rev (1):CD006296
88. Livesey G et al (2008) Glycemic response and health–a systematic review and meta-analysis: relations between dietary glycemic properties and health outcomes. Am J Clin Nutr 87(1):258S–268S
89. Danaei G et al (2009) The preventable causes of death in the United States: comparative risk assessment of dietary, lifestyle, and metabolic risk factors. PLoS Med 6(4):e1000058. doi: 10.1371/journal.pmed.1000058
90. Harris WS et al (2009) Towards establishing dietary reference intakes for eicosapentaenoic and docosahexaenoic acids. J Nutr 139(4):804S–819S
91. Lewington S et al (2007) Blood cholesterol and vascular mortality by age, sex, and blood pressure: a meta-analysis of individual data from 61 prospective studies with 55,000 vascular deaths. Lancet 370(9602):1829–1839

Lipids (2010) 45:907–914
DOI 10.1007/s11745-010-3408-1

REVIEW

Atherogenic Dyslipidemia: Cardiovascular Risk and Dietary Intervention

Kiran Musunuru

Received: 31 December 2009 / Accepted: 22 March 2010 / Published online: 4 June 2010

Abstract Atherogenic dyslipidemia comprises a triad of increased blood concentrations of small, dense low-density lipoprotein (LDL) particles, decreased high-density lipoprotein (HDL) particles, and increased triglycerides. A typical feature of obesity, the metabolic syndrome, insulin resistance, and type 2 diabetes mellitus, atherogenic dyslipidemia has emerged as an important risk factor for myocardial infarction and cardiovascular disease. A number of genes have now been linked to this pattern of lipoprotein changes. Low-carbohydrate diets appear to have beneficial lipoprotein effects in individuals with atherogenic dyslipidemia, compared to high-carbohydrate diets, whereas the content of total fat or saturated fat in the diet appears to have little effect. Achieving a better understanding of the genetic and dietary influences underlying atherogenic dyslipidemia may provide clues to improved interventions to reduce the risk of cardiovascular disease in high-risk individuals.

Keywords Lipids · Lipoproteins · Cardiovascular diseases · Genetics

Definition of Atherogenic Dyslipidemia

Prospective epidemiologic studies have shown that blood levels of low-density lipoprotein cholesterol (LDL-C) significantly predict incident atherosclerotic cardiovascular disease (CVD), and LDL-C-lowering therapy has been repeatedly demonstrated in many populations to reduce CVD risk. This has led to the formulation of risk prediction algorithms for identification of high-risk individuals and specific LDL-C goals to be achieved with lifestyle and pharmacological interventions [1]. Many individuals with normal LDL-C levels nevertheless develop CVD [2], particularly in older age groups.

There is considerable heterogeneity among low-density lipoproteins (LDL), ranging from small, dense, lipid-depleted particles to large, buoyant cholesterol-enriched particles [3]. These particles have typically been grouped into four categories ranging from LDL1 (largest) to LDL4 (smallest) and subdivided even further into as many as eight subfractions. A number of studies have suggested that small LDL particles carry disproportionate atherogenic risk [4–7]. This suggests that treatment based on LDL-C levels alone potentially provides a suboptimal treatment for a significant proportion of at-risk individuals.

High-density lipoprotein cholesterol (HDL) also has a strong epidemiological relationship with CVD, with increased HDL-C levels protective against disease, and is divided into two to three subfractions. As with LDL-C, some studies suggest that specific HDL subfractions are more predictive of CVD than HDL-C [8], whereas others suggest no distinction [9–13].

Austin et al. first described a risk-conferring lipid/lipoprotein profile, termed "atherogenic dyslipidemia" or the "atherogenic lipoprotein phenotype," that comprises a higher proportion of small LDL particles, reduced HDL-C, and increased triglycerides [14]. Atherogenic dyslipidemia is characteristically seen in patients with obesity, the metabolic syndrome, insulin resistance, and type 2 diabetes mellitus [15, 16] and has emerged as an important marker for the increased CVD risk observed in these populations. Herein we review the present understanding of the

K. Musunuru (✉)
Cardiology Division, Cardiovascular Research Center and Center for Human Genetic Research, Massachusetts General Hospital, 185 Cambridge St CPZN 5th floor, Boston, MA 02114, USA
e-mail: kmusunuru@partners.org

contribution of atherogenic dyslipidemia to CVD, as well as the genetic and dietary influences underlying atherogenic dyslipidemia.

Small LDL Particles, Total LDL Particles, and CVD Risk

Besides the traditional blood lipid measurements of LDL-C, HDL-C, and triglycerides, there now exist a number of alternative measures that assess lipoprotein subfractions in some way. The best established is the measurement of the blood concentration of apolipoprotein B (apoB). Each non-HDL particle—including LDL particles, intermediate-density lipoprotein (IDL) particles, very-low-density lipoprotein (VLDL) particles, chylomicrons, and their remnants—typically harbors one apoB molecule. Thus, the apoB measure represents a count of non-HDL particles circulating in the bloodstream. More sophisticated techniques can quantify the numbers of particle within each lipoprotein class, as well as within subfractions of each lipoprotein class; in addition, peak particle size within a class (e.g., LDL peak particle diameter) can be calculated. These techniques include analytical ultracentrifugation, gradient gel electrophoresis, nuclear magnetic resonance (NMR), and a relatively new gas-phase differential electrophoretic macromolecular mobility-based method (termed as the ion mobility method).

A number of studies have now used one of the lipoprotein subfraction measurement techniques to assess whether any of the subfractions have prognostic power for CVD or intermediate endpoints for CVD such as coronary calcium score or carotid intima-media thickness. Notably, many of these studies find that the small LDL particle concentration predicts cardiovascular endpoints comparably to if not better than LDL-C [7, 17–21].

There is biological plausibility for a causal role of small LDL particles in atherosclerotic disease, with evidence that small, dense, lipid-poor LDL particles may be inherently more atherogenic than large LDL particles [6]. They have greater susceptibility to oxidation than larger particles and thus may be more likely to instigate the inflammatory processes in vascular endothelium that underlie atherosclerotic disease. They bind more tightly to arterial proteoglycans and may penetrate into the arterial wall more easily. Finally, small LDL particles have relatively lower affinity for the LDL receptor compared to mid-size particles, resulting in decreased cellular uptake and increased time spent circulating in the bloodstream, where the particles would have prolonged influence on the atherosclerotic process.

However, each of the studies that have demonstrated that small LDL particle concentrations are predictive of cardiovascular endpoints also showed that the total LDL particle number (LDL-P) is similarly predictive [7, 17–21]. This is because the small LDL particle number is highly correlated with LDL-P. Intuitively, this can be explained by the reasoning that among individuals with equal LDL-C levels, the same of amount of cholesterol distributed among a larger number of particles implies that the particles must be of smaller size on average. It is possible, then, that all LDL particles are similarly atherogenic and the association of increased small LDL particle concentrations with disease is simply the result of the increased number of LDL particles, rather than small LDL particles being uniquely atherogenic. Epidemiological studies to date have not been able to unequivocally distinguish between these two possibilities.

Regardless of whether the small LDL particle number or LDL-P is used, either offers prognostic information distinct from the standard LDL-C measure obtained with a fasting lipid profile. Reinforcing this point was the finding in the Framingham Offspring Study that when participants were divided into four groups—low LDL-C + low LDL-P, low LDL-C + high LDL-P, high LDL-C + low LDL-P, high LDL-C + high LDL-P—stratification by LDL-P markedly discriminated by CVD event-free survival, whereas there was no difference seen with stratification by LDL-C [22].

Given the data suggesting a particular role for small LDL particles in CVD, and the epidemiological observation of the "atherogenic lipoprotein phenotype" of increased small LDL particle numbers, decreased HDL-C, and increased triglycerides, some lipoprotein assays have defined cutoffs for LDL peak particle size, with high particle sizes designated as "pattern A" (normal; defined as >25.5 nm when measured by gradient gel electrophoresis [3]) and low particle sizes designated as "pattern B" (having an increased proportion of small LDL particles and, thus, more likely to have atherogenic dyslipidemia; defined as ≤ 25.5 nm when measured by gradient gel electrophoresis) to aid clinicians in categorizing patients at risk for CVD.

Principal Component Analysis of Lipoprotein Subfractions

Although numerous studies have demonstrated that some lipoprotein subfractions are predictive of CVD, none of these studies systematically analyzed the interrelationships among all of the various lipoprotein subfractions to determine whether there are distinct combinations of subfractions that independently confer cardiovascular risk. To address this question, we have applied the technique of principal component analysis to identify interrelated combinations of subfractions and determine their relationship

with CVD in a large prospective cohort study, the Malmö Diet and Cancer-Cardiovascular Cohort (MDC-CC) [23]. Principal component analysis is a statistical method that analyzes the interrelationships between numerous variables and yields a fewer number of components that explain most of the correlation information of the original variables. Each of the resulting components is an independent linear combination of the original variables; furthermore, the components are fully independent of one another, i.e., they have zero correlation.

When we applied principal component analysis to eleven lipoprotein subfractions measured by ion mobility analysis of samples from more than 4,500 individuals in MDC-CC, we identified three major independent components, all of which were associated with incident CVD in the cohort [23, 24]. Notably, one of the three components represented a pattern of increased small and medium LDL particle concentrations, decreased large HDL particle concentrations, and increased triglycerides—corresponding to atherogenic dyslipidemia. This component was much more highly associated with incident CVD events (hazard ratio of 1.22 per 1 standard deviation) than LDL-C (hazard ratio of 1.10 per 1 standard deviation), indicating it to be a superior predictor of disease [23]. The other two principal components represented LDL-associated CVD risk (hazard ratio of 1.10 per 1 standard deviation) and HDL-associated CVD protection (hazard ratio of 0.81 per 1 standard deviation). Thus, our analysis established that atherogenic dyslipidemia is an epidemiologically distinct risk factor for CVD than the traditional risk factors of LDL-C and HDL-C and represents an independent mechanistic pathway contributing to the pathogenesis of CVD. Accordingly, there is a strong rationale to explore genetic and dietary modifiers of this pathway in order to better craft targeted interventions to reduce CVD risk.

Genetics and Atherogenic Dyslipidemia

Family-based segregation analyses suggest that the atherogenic lipoprotein phenotype has a strong genetic basis that likely reflects contributions from numerous genes [14, 25, 26]. Candidate genes include those that influence LDL peak particle size; family-based and twin studies indicate a large heritable component of LDL size, ranging from 40 to 60% of the trait. Genes with variants that have been reported to be associated with LDL size include: *CETP*, encoding cholesteryl ester transfer protein, which exchanges cholesteryl esters and triglycerides from HDL lipoprotein particles to LDL particles; *LDLR*, encoding the LDL receptor, which is responsible for cellular uptake of LDL particles from the bloodstream; *LPL*, encoding lipoprotein lipase, which hydrolyzes triglycerides in chylomicrons and VLDL particles, converting the latter to LDL particles, as well facilitating cellular lipoprotein uptake; *MTP*, encoding microsomal triglyceride transfer protein, which transfers triglycerides to nascent VLDL particles in hepatocytes; and the apolipoprotein genes *APOA5*, *APOB*, *APOC3*, and *APOE*, which are important constituents of varied lipoprotein particles [25–35]. All of these genes play credible roles in determining the size and lipid content of LDL particles as well as other lipoprotein particles and so might directly contribute to atherogenic dyslipidemia.

By applying principal component analysis in the MDC-CC, we were able to define a component representing atherogenic dyslipidemia. This enabled us to perform genetic analyses on this specific component and thereby identify gene variants directly linked to the dyslipidemia profile, rather than a property of an individual lipoprotein (such as LDL size). We took advantage of data from a recent genome-wide association study on lipid traits, which identified 30 genetic loci strongly linked to one or more of the blood LDL-C, HDL-C, and triglyceride levels [36]. We assessed the strength of association between SNPs in each of these genetic loci and the atherogenic dyslipidemia component. We found that variants in six loci, harboring the *CETP*, *LPL*, *APOA5*, *LIPC*, *GALNT2*, and *MLXIPL* genes, were highly associated with this component. In confirmation, each of the SNPs at these genes was also associated with small/medium LDL particle concentrations and—in the opposite direction—large HDL particle concentrations as well as HDL-C and/or triglycerides [23]. Interestingly, the variants at all but two of the six genes (*CETP* and *APOA5*) were not associated with LDL-C.

Thus, the MDC-CC study validated several of the genes previously linked to LDL size as also having variants associated with atherogenic dyslipidemia, as well as identifying a few novel candidate genes. The implicated genes may interact in biological pathways that regulate the different components of the dyslipidemia profile; conceivably, interventions targeting one or more of these specific genes may modulate an individual's lipid/lipoprotein profile in a clinically favorable way and reduce the risk of CVD, even if they do not affect blood LDL-C levels.

Effects of Diet on Atherogenic Dyslipidemia

An important question is whether alterations in diet—whether in regard to carbohydrate, fat, or saturated fat content—have predictable effects on lipoprotein profiles and, specifically, atherogenic dyslipidemia. This has implications for nutritional counseling for patients at risk for CVD: which diets are likely to induce or worsen atherogenic dyslipidemia and thereby increase CVD risk, and

thus should be avoided, and which diets may reverse the dyslipidemia and should be recommended. A related question is whether particular diets are of greater or less benefit in individuals with atherogenic dyslipidemia compared to those without it.

In one study, 105 healthy middle-age men were placed on high-fat (46% of calories from fat), low-carbohydrate and low-fat (24% of calories from fat), high-carbohydrate diets in a crossover design in which they experienced 6 weeks on each diet [37]. To simplify the interpretation of the study results, the proportions of types of fat (unsaturated vs. saturated, 1:1 ratio) and types of carbohydrates (simple vs. complex, 1:1) remained fixed in these diets. Across all subjects, there were significantly higher levels of triglycerides and the LDL3/LDL4 subfractions (small and very small LDL particle concentrations), as well as lower HDL-C levels, while on the low-fat diet compared to the high-fat diet. Thirty-six subjects who were pattern A or intermediate (as judged by LDL peak particle diameter) when on the high-fat diet converted to pattern B on the low-fat diet; all of the individuals who were pattern B on the high-fat diet remained pattern B on the low-fat diet. In a follow-up study, the individuals who had been pattern A on both the high-fat and low-fat diets were subjected to a very-low-fat diet (10% of calories from fat, with replacement by carbohydrates) [38]. One-third of the subjects converted to pattern B on this diet. Thus, reduction of fat along with increased carbohydrate intake altered lipoprotein profiles towards atherogenic dyslipidemia.

Of interest, individuals who were pattern B on a high-fat diet, when compared to those who were pattern A on a high-fat diet, experienced a much larger reduction in LDL-C when on a low-fat diet [37]. This was confirmed in both men and in pre-menopausal women, with a two- to threefold greater reduction in LDL-C observed [39, 40]. This phenomenon appeared to be the consequence of differential effects on lipoprotein profiles. Pattern A individuals experienced a larger decrease in LDL1 (large LDL particle concentrations) and an increase in LDL3 (small LDL particle concentrations) with little change in LDL2 (medium-large particle concentrations), whereas pattern B individuals displayed a decrease in LDL2 with a smaller decrease in LDL1 and no change in LDL3. Besides explaining the discrepancy in LDL-C alteration, these observations also explain why many pattern A individuals converted to pattern B (35%) but not vice versa (6%).

Extrapolating across all of these studies, the prevalence of pattern B increases with the amount of dietary carbohydrate and decreases with the amount of dietary fat. However, in these studies the changes in the proportions of calories derived from fat were largely balanced by reciprocal changes in calories from carbohydrates, making it difficult to determine whether dietary fat or carbohydrates are the major influence on atherogenic dyslipidemia. A study in 178 overweight men shed some light on this question. When compared on a higher-carbohydrate diet (54% of calories from carbohydrates, 1:1 simple:complex) versus a lower-carbohydrate diet (39% of calories from carbohydrates, 1:1 simple:complex), between which the difference was made up of protein calories (15 vs. 29%) rather than fat (minimal change), the subjects had a higher prevalence of pattern B when on the higher-carbohydrate diet [41]. This observation suggests that dietary carbohydrates are the principal driver of atherogenic dyslipidemia.

A more complete analysis with the 178 overweight men was highly informative as to the effects of varying carbohydrates and saturated fat, as well as weight loss, on lipoprotein profiles [42]. Four diets were compared: (1) 54% of calories from carbohydrates (1:1 simple:complex) with low saturated fat, (2) 39% of calories from carbohydrates (1:1 simple:complex) with low saturated fat, (3) 26% of calories from carbohydrates (1:1 simple:complex) with low saturated fat, and (4) 26% of calories from carbohydrates (1:1 simple:complex) with high saturated fat. Diets (1) and (2) had equal fat content, diets (3) and (4) had equal fat content that was higher than that of diets (1) and (2). The subjects underwent a weight-maintenance phase of 3 weeks on the assigned diets, followed by a weight-loss phase of 5 weeks (with a subsequent four-week weight stabilization period) on the same diets.

During the weight-maintenance phase, the subjects on the low-carbohydrate diets [(3) and (4)] experienced significant decreases in their triglyceride levels as well as their LDL3 and LDL4 levels (small and very small LDL particle concentrations); the individuals on the higher-carbohydrate diets displayed only modest changes. In contrast, during the weight-loss phase, the individuals on higher-carbohydrate diets experienced larger decreases in triglycerides and small LDL particle concentrations than did those on low-carbohydrate diets. Thus, by the end of the study, the higher-carbohydrate subjects had "caught up" with the low-carbohydrate subjects. The lower the dietary carbohydrate content, the lower the prevalence of pattern B, both after the weight-maintenance phase and after the weight-loss phase, although the differences in the prevalence of pattern B were smaller after weight loss, again pointing to a "catch-up" phenomenon.

Comparing the low-saturated-fat and high-saturated-fat low-carbohydrate diets [(3) vs. (4)], there were essentially no differences in changes in triglycerides, small LDL particle concentrations, or prevalence of pattern B, either in the weight-maintenance or weight-loss phases [42]. This finding indicates that dietary saturated fat content has little influence on the components of the atherogenic lipoprotein phenotype. This agrees with the results of a study that compared the effects of four-week treatments with a

high-saturated-fat diet (38% of calories from fat, with 20% of calories from saturated fat), a monounsaturated fatty acid (MUFA) olive oil-rich diet (38% of calories from fat, with 22% of calories from MUFA), and a high-carbohydrate diet (30% of calories from fat, with <10% of calories from saturated fat, and 55% of calories from carbohydrates) in 84 individuals [43]. (In all diets, ~40% of the carbohydrate calories came from simple carbohydrates, the remainder from complex carbohydrates.) There were no differences in triglycerides, LDL size, or prevalence of pattern B between the high-saturated-fat and high-MUFA diets; in contrast, both high-fat diets yielded higher LDL sizes than the high-carbohydrate diet, with one-third of the subjects converting from pattern A to pattern B with the high-carbohydrate diet. The lack of difference in LDL size seen between the two high-fat diets is consistent with two earlier studies, one of which noted a minimal increase in LDL size with a high-MUFA diet compared to a high-saturated-fat diet [44], the other of which reported no difference [45].

Finally, analysis of a prospective cohort study (the Framingham Heart Study) confirmed that fat content in the diet, after multivariable adjustment for carbohydrate intake and a variety of other potential confounders, did not significantly affect LDL size or triglyceride levels in either men or women [46]. This was true regardless of the quality of fat studied—total fat, saturated fat, MUFA, or polyunsaturated fatty acid (PUFA) content. Thus, it appears that both the quantity and quality of fat consumed (assuming no change in the number of calories obtained from carbohydrates) have minimal effects on the atherogenic lipoprotein phenotype.

Although it is possible that different types of carbohydrates may have different effects on lipoproteins, none of the discussed studies were able to shed light on this question, since in all cases the ratio of simple to complex carbohydrates was kept constant among the experimental diets. Given that carbohydrate intake appears to be the primary driver of atherogenic dyslipidemia, it would be desirable for future studies to directly compare diets in which the proportions of different types of carbohydrates are varied, with the overall number of calories coming from carbohydrates being held constant.

In conclusion, either lowering the dietary carbohydrate content or losing weight appears to attenuate atherogenic dyslipidemia (although there does not appear to be an additive effect of the two), whereas altering the total fat or saturated fat content has little influence. However, being placed on a lower-fat, higher-carbohydrate diet appears to result in lower LDL-C levels than a higher-fat, lower-carbohydrate diet, particularly for individuals starting with pattern B. Thus, it remains unclear whether having high or low dietary carbohydrate content is more beneficial for cardiovascular health. It should be noted that the intervention studies described above were all short-term (weeks) and so were not able to compare long-term CVD outcomes resulting from the various diets. Thus, we await long-term studies before these data can be used to help shape nutritional recommendations for patients at CVD risk.

Interactions of Genetics and Dietary Interventions

Given that both genetics and diet contribute to the atherogenic lipoprotein phenotype, it is natural to expect that there may be interactions between the two factors. For example, individuals with specific variants in a gene may experience changes in lipoprotein concentrations when placed on a particular diet, whereas individuals with other variants in the gene may be resistant to the effects of that diet. Another possibility is that individuals with one set of genetic variants may experience different types of lipoprotein changes than individuals with a different set of genetic variants, when all are placed on the same diet. This might manifest, for instance, as some individuals being more prone than others to developing atherogenic dyslipidemia on a high-carbohydrate diet. Although data is sparse in regard to whether such interactions exist, some limited work suggests that interactions may play an important role in determining lipoprotein profiles and may thus be informative for CVD risk prediction. For example, knowledge of a patient's genetic information may allow medical providers and nutritional counselors to predict what lipoprotein changes are likely to occur if the patient starts a particular dietary intervention and, thus, better advise the patient regarding lifestyle changes.

In one study, 50 individuals with pattern A lipoprotein profiles, offspring of 29 sets of parents, were tested for induction of pattern B with a very-high-carbohydrate diet [47]. Notably, all six of the subjects who converted to pattern B were descended from two pattern B parents. Quantitatively, LDL peak particle size decreased to a greater degree in offspring of two pattern B parents than in offspring of two pattern A parents. These findings suggest that there is a heritable basis for the induction of atherogenic dyslipidemia by a carbohydrate-rich diet.

A more detailed study was performed to examine the interaction of varied dietary fat content and variation in the *APOA5* gene, one of the genes previously linked to atherogenic dyslipidemia [39, 48]. An uncommon DNA sequence variant in *APOA5* (~6% frequency in individuals of European descent) that alters the 19th amino acid of the apoA-V protein from serine to tryptophan, termed *APOA5*3*, was compared to the usual variant at the DNA base, termed *APOA5*1*. Individuals who had a genotype of

*1/*3 (one of each variant), when compared to individuals with *1/*1 (two copies of the usual variant) had higher small LDL particle concentrations and triglycerides, as well as higher prevalence of pattern B, regardless of whether they were on a low-fat or high-fat diet. Also, there were higher small LDL particle concentrations and triglycerides and higher prevalence of pattern B when comparing all individuals on a low-fat diet compared to those on a high-fat diet. However, there were no differences in the relative changes of small LDL particle concentrations and triglycerides—or relative rates of pattern B—between *1/*3 and *1/*1 individuals on low-fat versus high-fat diets.

Thus, while both the *3 allele and, separately, a low-fat diet influenced the lipoprotein profile towards atherogenic dyslipidemia, there was no evidence for an interaction between genotype and diet. Interestingly, the only significant difference seen in the relative changes of lipoproteins between the two genotype groups on fat-varied diets was with the LDL2 subfraction (corresponding to medium-large LDL particle concentrations), where *1/*3 subjects experienced a threefold greater decrease in LDL2 than *1/*1 subjects when on a low-fat diet versus a high-fat diet [39]. Thus, *APOA5* did not appear to affect dietary induction of atherogenic dyslipidemia, though it did modulate dietary effects on some lipoproteins.

A somewhat different analysis in the Framingham Heart Study examined both the *APOA5*3* variant as well as a different variant that alters a DNA base in the *APOA5* promoter (–1131T > C, termed *APOA5*2*) with respect to potential interactions with dietary fat intake in modulating lipoproteins [46]. Individuals with the *APOA5*2* variant displayed increased triglycerides and smaller LDL size when the dietary PUFA content was >6% (by calories); individuals without the variant showed no differences with varied PUFA intake. There were no interactions of the *APOA5*2* variant with total fat, saturated fat, or MUFA intake, nor were there any interactions of the *APOA5*3* variant with any type of fat.

Thus, while both of the *APOA5* studies discussed here suggest that *APOA5* does influence the dietary effects of fat intake on lipoproteins, they disagree on the effects of specific gene variants. This highlights a critical problem in the study of gene-diet interactions, the lack of consistency between studies. In this example, the two studies differed in study design (one was a short-term interventional study, the other an observational prospective cohort study), the types of diets examined (one focused only on total fat intake, the other on total fat as well as specific types of fat), the variants examined (one focused only on *APOA5*3*, the other on both *APOA5*2* and *APOA5*3*), the measurement of lipoproteins (one assessed each of the LDL subfractions, the other only LDL size), and the populations studied (one focused on overweight men, the other on a population-based sample).

As such, it is difficult to draw any firm conclusions from any one gene-diet study in the absence of replication by another study that examined the same question using similar methodologies. For example, one study demonstrated that a Mediterranean-style, MUFA-rich diet compared to a high-carbohydrate diet increased LDL size in individuals with certain *APOE* gene variants but decreased LDL size in those with other *APOE* variants; [43] this is potentially a clinically important observation, but no confirmatory study has yet emerged, calling this observation into doubt. As pointed out by others, the field would greatly benefit from increased collaboration and coordination of studies among international nutrition researchers [49].

Conclusion

Atherogenic dyslipidemia appears to be an important independent risk factor for CVD, confirmed by principal component analysis of lipoprotein subfractions in a large prospective cohort study. As the genetic basis of lipoprotein metabolism becomes better understood, gene variants contributing to atherogenic dyslipidemia are being identified; these genes may serve as therapeutic targets to modulate the adverse effects of the dyslipidemia. It is clear that either reduction of dietary carbohydrate content or weight loss will improve an atherogenic dyslipidemic profile, whereas specifically altering fat or saturated fat content may have little influence. We await long-term clinical trials to assess whether genetic and/or dietary interventions with the intent of modifying the dyslipidemia will ultimately translate into reduction of CVD risk.

References

1. National Cholesterol Education Program (NCEP) Expert Panel on Detection, Evaluation, Treatment of High Blood Cholesterol in Adults (Adult Treatment Panel III) (2002) Third Report of the National Cholesterol Education Program (NCEP) Expert Panel on Detection, Evaluation, and Treatment of High Blood Cholesterol in Adults (Adult Treatment Panel III) final report. Circulation 106:3143–3421
2. Genest J Jr, McNamara JR, Ordovas JM, Jenner JL, Silberman SR, Anderson KM, Wilson PW, Salem DN, Schaefer EJ (1992) Lipoprotein cholesterol, apolipoprotein A-I and B and lipoprotein (a) abnormalities in men with premature coronary artery disease. J Am Coll Cardiol 19:792–802

3. Krauss RM, Burke DJ (1982) Identification of multiple subclasses of plasma low density lipoproteins in normal humans. J Lipid Res 23:97–104
4. Lamarche B, Tchernof A, Moorjani S, Cantin B, Dagenais GR, Lupien PJ, Despres JP (1997) Small, dense low-density lipoprotein particles as a predictor of the risk of ischemic heart disease in men. Prospective results from the Quebec Cardiovascular Study. Circulation 95:69–75
5. St-Pierre AC, Ruel IL, Cantin B, Dagenais GR, Bernard PM, Despres JP, Lamarche B (2001) Comparison of various electrophoretic characteristics of LDL particles and their relationship to the risk of ischemic heart disease. Circulation 104:2295–2299
6. Berneis KK, Krauss RM (2002) Metabolic origins and clinical significance of LDL heterogeneity. J Lipid Res 43:1363–1379
7. Rosenson RS, Otvos JD, Freedman DS (2002) Relations of lipoprotein subclass levels and low-density lipoprotein size to progression of coronary artery disease in the pravastatin limitation of atherosclerosis in the coronary arteries (PLAC-I) trial. Am J Cardiol 90:89–94
8. Asztalos BF, Collins D, Cupples LA, Demissie S, Horvath KV, Bloomfield HE, Robins SJ, Schaefer EJ (2005) Value of high-density lipoprotein (HDL) subpopulations in predicting recurrent cardiovascular events in the veterans affairs HDL intervention trial. Arterioscler Thromb Vasc Biol 25:2185–2191
9. Gofman JW, Young W, Tandy R (1966) Ischemic heart disease, atherosclerosis, and longevity. Circulation 34:679–697
10. Stampfer MJ, Sacks FM, Salvini S, Willett WC, Hennekens CH (1991) A prospective study of cholesterol, apolipoproteins, and the risk of myocardial infarction. N Engl J Med 325:373–381
11. Sweetnam PM, Bolton CH, Yarnell JW, Bainton D, Baker IA, Elwood PC, Miller NE (1994) Associations of the HDL2 and HDL3 cholesterol subfractions with the development of ischemic heart disease in British men. The Caerphilly and Speedwell collaborative heart disease studies. Circulation 90:769–774
12. Fujimoto WY, Bergstrom RW, Boyko EJ, Chen KW, Leonetti DL, Newell-Morris L, Shofer JB, Wahl PW (1999) Visceral adiposity and incident coronary heart disease in Japanese-American men. The 10-year follow-up results of the Seattle Japanese-American community diabetes study. Diabetes Care 22:1808–1812
13. Sharrett AR, Ballantyne CM, Coady SA, Heiss G, Sorlie PD, Catellier D, Patsch W, Atherosclerosis Risk in Communities Study Group (2001) Coronary heart disease prediction from lipoprotein cholesterol levels, triglycerides, lipoprotein(a), apolipoproteins A-I and B, and HDL density subfractions: the Atherosclerosis Risk in Communities (ARIC) Study. Circulation 104:1108–1113
14. Austin MA, King MC, Vranizan KM, Krauss RM (1990) Atherogenic lipoprotein phenotype. A proposed genetic marker for coronary heart disease risk. Circulation 82:495–506
15. Reaven GM, Chen YD, Jeppesen J, Maheux P, Krauss RM (1993) Insulin resistance and hyperinsulinemia in individuals with small, dense low density lipoprotein particles. J Clin Invest 92:141–146
16. Kathiresan S, Otvos JD, Sullivan LM, Keyes MJ, Schaefer EJ, Wilson PW, D'Agostino RB, Vasan RS, Robins SJ (2006) Increased small low-density lipoprotein particle number: a prominent feature of the metabolic syndrome in the Framingham Heart Study. Circulation 113:20–29
17. Blake GJ, Otvos JD, Rifai N, Ridker PM (2002) Low-density lipoprotein particle concentration and size as determined by nuclear magnetic resonance spectroscopy as predictors of cardiovascular disease in women. Circulation 106:1930–1937
18. Otvos JD, Collins D, Freedman DS, Shalaurova I, Schaefer EJ, McNamara JR, Bloomfield HE, Robins SJ (2006) Low-density lipoprotein and high-density lipoprotein particle subclasses predict coronary events and are favorably changed by gemfibrozil therapy in the veterans affairs high-density lipoprotein intervention trial. Circulation 113:1556–1563
19. Mora S, Szklo M, Otvos JD, Greenland P, Psaty BM, Goff DC Jr, O'Leary DH, Saad MF, Tsai MY, Sharrett AR (2007) LDL particle subclasses, LDL particle size, and carotid atherosclerosis in the Multi-Ethnic Study of Atherosclerosis (MESA). Atherosclerosis 192:211–217
20. Kuller L, Arnold A, Tracy R, Otvos J, Burke G, Psaty B, Siscovick D, Freedman DS, Kronmal R (2002) Nuclear magnetic resonance spectroscopy of lipoproteins and risk of coronary heart disease in the cardiovascular health study. Arterioscler Thromb Vasc Biol 22:1175–1180
21. Mackey RH, Kuller LH, Sutton-Tyrrell K, Evans RW, Holubkov R, Matthews KA (2002) Lipoprotein subclasses and coronary artery calcium in postmenopausal women from the Healthy Women Study. Am J Cardiol 90:71i–76i
22. Cromwell WC, Otvos JD, Keyes MJ, Pencina MJ, Sullivan L, Vasan RS, Wilson PW, D'Agostino RB (2007) LDL particle number and risk of future cardiovascular disease in the Framingham Offspring Study—implications for LDL management. J Clin Lipidol 1:583–592
23. Musunuru K, Orho-Melander M, Caulfield MP, Li S, Salameh WA, Reitz RE, Berglund G, Hedblad B, Engstrom G, Williams PT, Kathiresan S, Melander O, Krauss RM (2009) Ion mobility analysis of lipoprotein subfractions identifies three independent axes of cardiovascular risk. Arterioscler Thromb Vasc Biol 29:1975–1980
24. Caulfield MP, Li S, Lee G, Blanche PJ, Salameh WA, Benner WH, Reitz RE, Krauss RM (2008) Direct determination of lipoprotein particle sizes and concentrations by ion mobility analysis. Clin Chem 54:1307–1316
25. Rotter JI, Bu X, Cantor RM, Warden CH, Brown J, Gray RJ, Blanche PJ, Krauss RM, Lusis AJ (1996) Multilocus genetic determinants of LDL particle size in coronary artery disease families. Am J Hum Genet 58:585–594
26. Allayee H, Aouizerat BE, Cantor RM, Dallinga-Thie GM, Krauss RM, Lanning CD, Rotter JI, Lusis AJ, de Bruin TW (1998) Families with familial combined hyperlipidemia and families enriched for coronary artery disease share genetic determinants for the atherogenic lipoprotein phenotype. Am J Hum Genet 63:577–585
27. Austin MA, Talmud PJ, Luong LA, Haddad L, Day IN, Newman B, Edwards KL, Krauss RM, Humphries SE (1998) Candidate-gene studies of the atherogenic lipoprotein phenotype: a sib-pair linkage analysis of DZ women twins. Am J Hum Genet 62:406–419
28. Hokanson JE, Brunzell JD, Jarvik GP, Wijsman EM, Austin MA (1999) Linkage of low-density lipoprotein size to the lipoprotein lipase gene in heterozygous lipoprotein lipase deficiency. Am J Hum Genet 64:608–618
29. Dart AM, Cooper B (1999) Independent effects of Apo E phenotype and plasma triglyceride on lipoprotein particle sizes in the fasting and postprandial states. Arterioscler Thromb Vasc Biol 19:2465–2473
30. Ordovas JM, Cupples LA, Corella D, Otvos JD, Osgood D, Martinez A, Lahoz C, Coltell O, Wilson PW, Schaefer EJ (2000) Association of cholesteryl ester transfer protein-TaqIB polymorphism with variations in lipoprotein subclasses and coronary heart disease risk: the Framingham Study. Arterioscler Thromb Vasc Biol 20:1323–1329
31. Talmud PJ, Edwards KL, Turner CM, Newman B, Palmen JM, Humphries SE, Austin MA (2000) Linkage of the cholesteryl ester transfer protein (CETP) gene to LDL particle size: use of a novel tetranucleotide repeat within the CETP promoter. Circulation 101:2461–2466
32. Humphries SE, Berglund L, Isasi CR, Otvos JD, Kaluski D, Deckelbaum RJ, Shea S, Talmud PJ (2002) Loci for CETP, LPL,

LIPC, and APOC3 affect plasma lipoprotein size and subpopulation distribution in Hispanic and non-Hispanic white subjects: the Columbia University BioMarkers Study. Nutr Metab Cardiovasc Dis 12:163–172
33. Skoglund-Andersson C, Ehrenborg E, Fisher RM, Olivecrona G, Hamsten A, Karpe F (2003) Influence of common variants in the CETP, LPL, HL and APO E genes on LDL heterogeneity in healthy, middle-aged men. Atherosclerosis 167: 311–317
34. Austin MA, Talmud PJ, Farin FM, Nickerson DA, Edwards KL, Leonetti D, McNeely MJ, Viernes HM, Humphries SE, Fujimoto WY (2004) Association of apolipoprotein A5 variants with LDL particle size and triglyceride in Japanese Americans. Biochim Biophys Acta 1688:1–9
35. Mar R, Pajukanta P, Allayee H, Groenendijk M, Dallinga-Thie G, Krauss RM, Sinsheimer JS, Cantor RM, de Bruin TW, Lusis AJ (2004) Association of the APOLIPOPROTEIN A1/C3/A4/A5 gene cluster with triglyceride levels and LDL particle size in familial combined hyperlipidemia. Circ Res 94:993–999
36. Kathiresan S, Willer CJ, Peloso GM, Demissie S, Musunuru K, Schadt EE, Kaplan L, Bennett D, Li Y, Tanaka T, Voight BF, Bonnycastle LL, Jackson AU, Crawford G, Surti A, Guiducci C, Burtt NP, Parish S, Clarke R, Zelenika D, Kubalanza KA, Morken MA, Scott LJ, Stringham HM, Galan P, Swift AJ, Kuusisto J, Bergman RN, Sundvall J, Laakso M, Ferrucci L, Scheet P, Sanna S, Uda M, Yang Q, Lunetta KL, Dupuis J, de Bakker PI, O'Donnell CJ, Chambers JC, Kooner JS, Hercberg S, Meneton P, Lakatta EG, Scuteri A, Schlessinger D, Tuomilehto J, Collins FS, Groop L, Altshuler D, Collins R, Lathrop GM, Melander O, Salomaa V, Peltonen L, Orho-Melander M, Ordovas JM, Boehnke M, Abecasis GR, Mohlke KL, Cupples LA (2009) Common variants at 30 loci contribute to polygenic dyslipidemia. Nat Genet 41:56–65
37. Krauss RM, Dreon DM (1995) Low-density-lipoprotein subclasses and response to a low-fat diet in healthy men. Am J Clin Nutr 62:478S–487S
38. Dreon DM, Fernstrom HA, Williams PT, Krauss RM (1999) A very low-fat diet is not associated with improved lipoprotein profiles in men with a predominance of large, low-density lipoproteins. Am J Clin Nutr 69:411–418
39. Krauss RM (2005) Dietary and genetic probes of atherogenic dyslipidemia. Arterioscler Thromb Vasc Biol 25:2265–2272
40. Dreon DM, Fernstrom HA, Williams PT, Krauss RM (1997) LDL subclass patterns and lipoprotein response to a low-fat, high-carbohydrate diet in women. Arterioscler Thromb Vasc Biol 17:707–714
41. Krauss RM, Blanche PJ, Rawlings RS, Holl LG, Orr JR, Fernstrom HS (2003) Both low dietary carbohydrate and weight loss reduce expression of atherogenic lipoprotein phenotype. Circulation 108(Suppl IV):IV-784
42. Krauss RM, Blanche PJ, Rawlings RS, Fernstrom HS, Williams PT (2006) Separate effects of reduced carbohydrate intake and weight loss on atherogenic dyslipidemia. Am J Clin Nutr 83:1025–1031
43. Moreno JA, Pérez-Jiménez F, Marín C, Gómez P, Pérez-Martínez P, Moreno R, Bellido C, Fuentes F, López-Miranda J (2004) The effect of dietary fat on LDL size is influenced by apolipoprotein E genotype in healthy subjects. J Nutr 134:2517–2522
44. Kratz M, Gülbahçe E, von Eckardstein A, Cullen P, Cignarella A, Assmann G, Wahrburg U (2002) Dietary mono- and polyunsaturated fatty acids similarly affect LDL size in healthy men and women. J Nutr 132:715–718
45. Rivellese AA, Maffettone A, Vessby B, Uusitupa M, Hermansen K, Berglund L, Louheranta A, Meyer BJ, Riccardi G (2003) Effects of dietary saturated, monounsaturated and n-3 fatty acids on fasting lipoproteins, LDL size and post-prandial lipid metabolism in healthy subjects. Atherosclerosis 167:149–158
46. Lai CQ, Corella D, Demissie S, Cupples LA, Adiconis X, Zhu Y, Parnell LD, Tucker KL, Ordovas JM (2006) Dietary intake of n-6 fatty acids modulates effect of apolipoprotein A5 gene on plasma fasting triglycerides, remnant lipoprotein concentrations, and lipoprotein particle size: the Framingham Heart Study. Circulation 113:2062–2070
47. Dreon DM, Fernstrom HA, Williams PT, Krauss RM (2000) Reduced LDL particle size in children consuming a very-low-fat diet is related to parental LDL-subclass patterns. Am J Clin Nutr 71:1611–1616
48. Pennacchio LA, Olivier M, Hubacek JA, Krauss RM, Rubin EM, Cohen JC (2002) Two independent apolipoprotein A5 haplotypes influence human plasma triglyceride levels. Hum Mol Genet 11:3031–3038
49. Kaput J, Ordovas JM, Ferguson L, van Ommen B, Rodriguez RL, Allen L, Ames BN, Dawson K, German B, Krauss R, Malyj W, Archer MC, Barnes S, Bartholomew A, Birk R, van Bladeren P, Bradford KJ, Brown KH, Caetano R, Castle D, Chadwick R, Clarke S, Clément K, Cooney CA, Corella D, Manica da Cruz IB, Daniel H, Duster T, Ebbesson SO, Elliott R, Fairweather-Tait S, Felton J, Fenech M, Finley JW, Fogg-Johnson N, Gill-Garrison R, Gibney MJ, Gillies PJ, Gustafsson JA, Hartman Iv JL, He L, Hwang JK, Jais JP, Jang Y, Joost H, Junien C, Kanter M, Kibbe WA, Koletzko B, Korf BR, Kornman K, Krempin DW, Langin D, Lauren DR, Ho Lee J, Leveille GA, Lin SJ, Mathers J, Mayne M, McNabb W, Milner JA, Morgan P, Muller M, Nikolsky Y, van der Ouderaa F, Park T, Pensel N, Perez-Jimenez F, Poutanen K, Roberts M, Saris WH, Schuster G, Shelling AN, Simopoulos AP, Southon S, Tai ES, Towne B, Trayhurn P, Uauy R, Visek WJ, Warden C, Weiss R, Wiencke J, Winkler J, Wolff GL, Zhao-Wilson X, Zucker JD (2005) The case for strategic international alliances to harness nutritional genomics for public and personal health. Br J Nutr 94:623–632

Lipids (2010) 45:915–923
DOI 10.1007/s11745-010-3445-9

REVIEW

Saturated Fats: A Perspective from Lactation and Milk Composition

J. Bruce German · Cora J. Dillard

Received: 18 March 2010 / Accepted: 24 June 2010 / Published online: 23 July 2010

Abstract For recommendations of specific targets for the absolute amount of saturated fat intake, we need to know what dietary intake is most appropriate? Changing agricultural production and processing to lower the relative quantities of macronutrients requires years to accomplish. Changes can have unintended consequences on diets and the health of subsets of the population. Hence, what are the appropriate absolute amounts of saturated fat in our diets? Is the scientific evidence consistent with an optimal intake of zero? If not, is it also possible that a finite intake of saturated fats is beneficial to overall health, at least to a subset of the population? Conclusive evidence from prospective human trials is not available, hence other sources of information must be considered. One approach is to examine the evolution of lactation, and the composition of milks that developed through millennia of natural selective pressure and natural selection processes. Mammalian milks, including human milk, contain 50% of their total fatty acids as saturated fatty acids. The biochemical formation of a single double bond converting a saturated to a monounsaturated fatty acid is a pathway that exists in all eukaryotic organisms and is active within the mammary gland. In the face of selective pressure, mammary lipid synthesis in all mammals continues to release a significant content of saturated fatty acids into milk. Is it possible that evolution of the mammary gland reveals benefits to saturated fatty acids that current recommendations do not consider?

J. B. German (✉) · C. J. Dillard
Department of Food Science and Technology,
University of California, Davis, CA 95616, USA
e-mail: jbgerman@ucdavis.edu

Keywords Saturated fat · Milk fat · Dietary intake · Lipoproteins

Abbreviations

LDL	Low-density lipoprotein
HDL	High-density lipoprotein
PPAR	Peroxisome proliferator activated receptor
PGC-1	PPAR gene transcription coactivator
LPS	Lipopolysaccharide

Introduction

Diet, Fatty Acids, and Lipoproteins

Lipids and their simplest structural elements, the fatty acids, provide myriad functions at all levels of cellular life. Nutritional scientists are still wrestling to develop a rudimentary understanding of the roles that dietary lipids exert. Lipids as simple fats are the most concentrated energy source in the diet. Until recently, this fact alone made lipids a valuable food component; however, a global epidemic of caloric imbalance and obesity has undermined this one aspect of lipid nutrition. Nonetheless, dietary lipids are well recognized as providing the essential fatty acids and to dissolve and aid in the absorption of fat-soluble vitamins. Fats also produce a broad range of effects to whole body metabolism when consumed in foods. These effects, although not yet fully understood, are a complex consequence of the absolute and relative fat content, the fatty acid composition, the structure of other components in the foods, the timing of consumption and individual variations among those consuming them. Once ingested, lipids

provide a diverse range of molecular functions and actions within cells and tissues beyond providing simple energy. Fatty acids are required for membrane synthesis, modifications of proteins and carbohydrates, construction of various structural elements in cells and tissues, production of signaling compounds and for oxidative fuel. The ability of lipids to associate spontaneously into multi-molecular structures of non-polar substituents provides a unique domain structure to biology (vesicles, globules, lipoproteins). These structures solubilize a variety of non-polar and poorly soluble cellular and extracellular constituents and transport such molecules within and between cells and tissues.

Given these various roles, why would saturated fats be so poorly thought of nutritionally? In one sense, saturated fats in the diet are unnecessary. All organisms, including humans, are fully capable of synthesizing saturated fatty acids. In the absence of sufficient dietary fat, the body is apparently capable of synthesizing all of the saturated fatty acids that it needs from the ubiquitous precursor building block acetate. This does not mean to infer that all saturated fatty acids are biologically indistinguishable. In fact, cells produce a remarkable diversity of saturated fatty acids under particular conditions, and although not all of their functions are known, they are clearly not simply interchangeable. Compositional analyses reveal remarkable specificities for particular saturated fatty acids in different lipid classes, cellular compartments and tissues [1]. Stubbs and Smith [2] reviewed studies aimed at understanding the requirement of membranes for specific fatty acid compositions. Interestingly, although composition is sensitive to polyunsaturated fatty acids, the content of saturated fatty acids in rat tissue membrane phospholipids is relatively constant at $\sim$40% regardless of dietary fat source, indicating a control mechanism at some level. The de novo synthesis of saturated fatty acids is inhibited by feeding a high-fat diet [3], and membrane fragility resulting from feeding a low dietary saturated fatty acid diet is overcome by feeding a diet rich in fat [4].

The complexity of structure and the diversity of functions of fatty acids, both unsaturated and saturated, remain poorly understood, and in only a few biological situations have distinct actions of fatty acids been described. The majority of research on fatty acids consumed in the diet has focused principally on their role in lipoprotein metabolism. Authors of a recent meta-analysis of prospective studies on dairy food consumption and incident vascular disease and Type 2 diabetes concluded that it is not possible to estimate quantitative relationships with disease incidence with any confidence. The authors also point out that apart from the effects of dairy foods on plasma lipids and on blood pressure, very little is known about the biological mechanisms underlying such relationships [5]. Even for lipoprotein metabolism, for which literally billions of dollars have been invested in research, little is actually known. For example, only in 2005 was the basic mechanistic link between saturated fatty acids and cholesterol metabolism revealed [6]. This relationship between saturated fat in the diet and cholesterol metabolism was one of the most baffling scientific challenges of the twentieth century. How could such a ubiquitous, non-essential component of diets and tissues—saturated fat—cause an increase in the accumulation of cholesterol-rich LDL in blood? As scientific research on cholesterol metabolism proceeded through the twentieth century, the question became even more perplexing. Brown and Goldstein [7] won the Nobel prize for identifying the LDL receptor on the liver as being what controlled the concentration of serum cholesterol. What then regulates the expression of the LDL receptor on the surface of liver cells? Cellular cholesterol levels within the liver cell simultaneously control cholesterol synthesis and uptake by regulating the expression of the genes for the proteins that make cholesterol in the cell and for the proteins that take up cholesterol from blood as LDL. Not surprisingly, when cholesterol levels in the cell are adequate, the genes are not turned on. However, when cholesterol levels are low, all of these genes are turned on using the identical transcription factor protein—sterol response factor binding protein [8]. Although these studies made sense of cellular cholesterol regulation—if the cell needs more cholesterol, it simultaneously turns on the genes to make more via cholesterol biosynthetic enzymes and takes more from blood via the LDL receptor—they failed to explain the role of diet in these processes.

If the same transcription factor turns on both cholesterol biosynthesis and the LDL receptor, how can saturated fat uncouple these two processes, simultaneously making more cholesterol and yet shutting down the receptor? Puigserver and Spiegelman [9] found that the liver contains an additional gene control system, the peroxisome proliferator activating receptor (PPAR), and it is in turn controlled by a higher order protein complex termed (logically) the PPAR gene transcription coactivator (PGC-1). This transcription factor coactivator family recruits entire complexes of proteins into transcriptional regulatory units controlling such multi-faceted properties as mitochondrial biogenesis [10]. In a striking result, Lin et al. [6] discovered that, when exposed to high levels of saturated fatty acids, liver cells both in vivo and in vitro actively turned on PGC-1b, and even more astonishingly, this coactivator simultaneously turned on cholesterol biosynthesis and turned off the LDL receptor. Thus, in one bold study, the basic target linking dietary saturated fat and serum cholesterol was revealed. This mechanism would account for the tendency of diets very high in saturated fat to raise total cholesterol in blood.

For some individuals, such a response could raise one of the risk factors for heart disease if they consumed diets high in saturated fat. An obvious question is what are the benefits to this biochemical response that would have caused it to be selected through evolution? Scientists are only now beginning to address the basic biological value of this regulatory control system. Nonetheless, diets very high in saturated fat would not seem prudent, as would any diet high in any food component.

Recommendations that the population decrease their intake of saturated fats was based not on a mechanistic understanding, but on years of observational evidence that dietary saturated fats generally increase blood cholesterol concentrations in animals and humans [11]. This alteration of risk factors does not necessarily lead to increases in heart disease and is certainly not universally true in all populations studied. Some studies of human populations evaluating the effects of saturated fat diets do not show the predicted elevation in heart disease; in fact, some studies see the reverse effect [12]. Recent studies are beginning to assign genetic or physiological explanations to these varying outcomes; for example, low birth weight appears to have an effect on subsequent responses to dietary fat [13]. Beare-Rogers [14] suggested that the saturated fatty acid requirements are also related to the stage of development. For example, saturated fatty acids appear to be essential for the newborn, the young and during rapid growth as they are required for the synthesis of membranes and lipoprotein.

Are Recommendations to Lower Total Fat Intakes Justified for Everyone?

Is the justification for broad recommendations to lower total fat intakes in all individuals supported by scientific evidence? In 1977, the US population was first recommended to reduce the intake of fat, with some recommendations being to reduce total fat to below 30% of calories [15]. The American Heart Association recommended that the percentage of calories be 28.6 and 25.3% total fat, respectively, and 9 and 6.1% saturated fat, respectively, in Step 1 and Step 2 diets for treatment of high blood cholesterol. This recommendation had unanticipated effects. Framingham Heart Study data showed that people with high triacylglycerol concentrations (>1.7 mmol/l) and low HDL cholesterol concentrations (<1.03 mmol/l) run a significantly higher risk of coronary artery disease [16]. The long-term health benefits of consuming a low-fat diet—particularly taking into account the variation in human responses—have not been proven and, to the contrary, some individuals move their risk profile, even for heart disease, in an adverse direction [17, 18]. In one study, healthy, non-diabetic volunteers consumed diets that contained, as a percentage of total calories, either 60% carbohydrate, 25% fat and 15% protein, or 40% carbohydrate, 45% fat and 15% protein [19]. Those consuming the 60% carbohydrate diet had higher fasting plasma triacylglycerol, remnant lipoprotein and remnant lipoprotein triacylglycerol, and lower HDL cholesterol without changing LDL cholesterol concentration. The low-fat diet lowered HDL cholesterol and caused a persistent elevation in remnant lipoproteins [19], both factors that are increasingly recognized to be important independent risk factors for heart disease and other metabolic diseases. These findings led the investigators to publish the question whether it is wise to recommend that all Americans replace dietary saturated fat with carbohydrate. It is important to point out that dietary carbohydrates have been associated with dyslipidemia [20], and lipoprotein risk factors are similar whether diets are high in fat and saturated fat or low in fat and high in sugar. Elevated triglyceride concentrations are related to increased hepatic secretion and impaired clearance of VLDL lipoprotein [21, 22]. Triglyceride response to dietary sugar may vary with the amount of sugar and the presence of other nutrients. Stanhope and Havel [23] reported that a high-fructose diet led to visceral adiposity, dyslipidemia and insulin resistance, and insulin resistance upregulates VLDL production. Perhaps the study most devastating to the basic principle that a lower fat diet improves the health of the entire population was a prospective study (The Women's Health Initiative Randomized Controlled Dietary Modification Trial) that selected approximately 49,000 women to compare a group of women consuming low-fat diets and increased fruit and vegetable consumption with a group receiving only diet-related education materials. After 8.1 years, there were no statistical differences in heart disease outcomes [24]. Two possible interpretations could be drawn from this study: first, that lower fat intakes have no effect on any women, and second, that individuals vary in their response to fat and some women are benefitted and some are adversely affected and the net numbers of each are relatively close, leading to a conclusion in this trial of no effect of a low-fat diet.

Individual Response to Dietary Fat Intakes

Ordovas [25] reviewed key factors in lipid metabolism and obesity that indicate an interplay among genes, gender, and environmental factors that modulate disease susceptibility. Studies of response to dietary fats have found variation among individuals [26] and differences between men and women [27] in their response to dietary fat changes. Studies of individual sensitivity to changes in dietary saturated fats showed groups of consistent hyper-responders and minimal responders within a population of

hypercholesterolaemic individuals [26]. Measurements of serum cholesterol in response to a decrease in dietary saturated fat showed that total cholesterol decreased to a greater extent in men than in women [27]. There are also differential responses in individuals that consume low-fat diets [28]. A series of studies showed that very-low-fat (10%), high-carbohydrate diets enriched in simple sugars increased the synthesis of fatty acids, especially palmitate, and that the individual differences in increased blood triglyceride concentrations varied considerably [29]. These fluctuations observed time after time have given impetus to the field of Nutrigenomics, and scientists are now pursuing more detailed analyses of individuals, their responses to diet and the mechanistic basis for variations in diet and health risk [30].

Controversy still remains high as to the roles that dietary fat and cholesterol play in the risk of heart disease, and the wealth of confounding factors demonstrate that saturated fat is not an overwhelming input variable for any population studied to date. Dietary saturated fats are not the only variables associated with heart disease—the causes are multi-factorial. The results of studies on the etiology of heart disease are inclusive and sometimes contradictory. It is time to take a broader view to the multiple actions and functions of each of the different saturated fats and a more individual view to assessment of diet and risk.

Biological Activities of Saturated Fatty Acids

The overwhelming emphasis on the role of saturated fats in the diet and risk of coronary heart disease has distracted investigators from studying other effects that individual saturated fatty acids may have in the body. This omission is perhaps important considering the abundance in mammalian milks of a wide range of saturated fatty acids with different chain lengths. In the context of evolution and the obvious natural selective pressure on the development of milk and all of its constituents, how do saturated fatty acids affect growth, development and survival of mammalian offspring?

Fatty acids are present in all body tissues, where they are a major part of the phospholipid component of the cell membrane. They contribute to the structural diversity within the membrane, which is now recognized to be a key aspect of membrane functions [31]. Fatty acids anchor proteins to particular regions of cell membranes, participate in signaling activities, transport cellular components and provide fuel. Saturated fatty acids have been suggested as being the preferred fuel for the heart [32]. In the absence of sufficient fat from the diet, the body synthesizes fatty acids, typically from carbohydrates. An interesting observation has been made that in adult rat liver, erucic acid (22:1)—a fatty acid that has been associated with heart disease and that is present in rapeseed oil—is rapidly converted to 18:0, demonstrating the conservation of carbons by chain-shortening of a monounsaturated fatty acid to an unsaturated fatty acid [33]. Even though all fatty acids present in the diet can be broken down and resynthesized into saturated fats, they have discrete effects. Different structures of fatty acids appear to have differing effects on a variety of metabolic and physiological processes when they are ingested.

Short-chain fatty acids are hydrolyzed preferentially from triacylglycerols and absorbed from the intestine into the portal circulation without resynthesis of triacylglycerols. These fatty acids serve as a ready source of energy. Butyric acid (4:0) is the shortest saturated fatty acid and is present in ruminant milk fat at 2–5% by weight [34], which on a molar basis is about one-third the amount of palmitic acid (16:0). Human milk contains a lower percentage (ca. 0.4%) of butyric acid. No other common food fat contains this fatty acid directly; however, the consumption of a wide range of fermentable carbohydrates can lead to the synthesis of butyric acid by endogenous microflora in the lower intestine. Butyrate is a well-known modulator of genetic regulation, and its ability to promote differentiation has led various investigators to pursue this mechanism as a means to alter the risk and development of cancer [35, 36]. This fatty acid also lowers processes of inflammation in the intestine, acting through short-chain fatty acid-binding receptors [37].

In bovine and human milk, caproic acid (6:0) is present at ca. 1 and 0.1%, respectively, and caprylic acid (8:0) and capric acid (10:0) are present at ca. 0.3 and 1.2%, respectively, of the milk fat. Not surprisingly from its nomenclature, goat milk contains the highest percentage of caprylic acid, at 2.7% of milk fat. Studies to date have documented that these three fatty acids have similar biological activities when tested as antimicrobial agents. Caprylic acid lowers salmonella infection in chickens [38]. Caprylic and capric acid have antiviral activity. The monoglyceride form, monocaprin, has been shown in vivo in animals to possess antiviral activity against retrovirus infection [39].

Lauric acid (12:0) is present in human and bovine milk at ca. 5.8 and 2.2%, respectively, of the milk fat. Studies have shown antiviral and antibacterial activities of lauric acid [40, 41]. Release of lauric acid in the stomach may have direct antimicrobial activities towards *Helicobacter pylori*, either as the fatty acid or monoacylglycerols produced by lingual lipase(s) acting on the triacylglycerols present milk fat [42, 43]. These antibacterial actions of lauric acid have been proposed to provide anticaries and antiplaque activities [44]. The overall antimicrobial effects of the medium-chain saturated fatty acids and their monoacylglycerol derivatives on various microorganisms,

including bacteria, yeast, fungi and enveloped viruses, were originally suggested to be acting through the lipid membranes of the organisms [45]. Support for this deactivation process has been shown using human and bovine milk [46]. Monolaurin released from milk lipids by lipases may account for milk's anti-protozoal activities [47]. The biological activity of laurate has been interesting in other aspects not related to the diet. For example, a remarkable experiment showed that monolaurate provided considerable protection from HIV infection when used topically on reproductive tissues in primates [48].

Bovine milk fat contains 8–14% myristic acid (14:0) and in human milk, it averages 8.6% of the milk fat. Human epidemiological studies have shown that myristic acid and lauric acid were the saturated fatty acids most strongly related to the average serum cholesterol concentrations in humans [49]. Nonetheless, several studies have shown that myristic acid increases HDL cholesterol at least as much as LDL cholesterol, and further studies have demonstrated that the unique positional distribution of myristic acid in the *sn*-2 position of triglycerides in milk fat is responsible for its tendency to raise HDL [50].

Palmitic acid is present in human and bovine milk at 22.6 and 26.3%, yet almost exclusively esterified at the *sn*-2 position of the triglyceride. This unusual stereospecific distribution appears to have important nutritional and biological implications. Human infants consuming a formula containing triacylglycerides similar to those in human milk (16% palmitic acid esterified predominantly to the *sn*-2 position) have improved intestinal absorption not just of the palmitic acid but calcium as well [51, 52]. Recently, Speigelman's group showed that palmitic acid stimulated the expression and activities of the transcription coactivator PGC-1b and by so doing promoted the transcriptional regulation of biosynthesis of lipoproteins from the liver [6]. This finding places a mechanistic understanding of the cellular actions of saturated fatty acids, particularly palmitic acid. In the context of milk, this mechanism implies that palmitic acid may have an important role in promoting successful lipoprotein metabolism in infants. This same transcription coactivator PGC-1b was also found to promote myocardial development [53]. Finally, PGC-1b was shown to increase biogenesis of mitochondria in neurons [54], further implying that this mechanism could well be involved in diverse aspects of metabolic regulation and its saturated fatty acid-appropriate development throughout the body in infants. It is not known if the presence of palmitic acid in human milk is important in the coordinate regulation and activity of PGC-1b in any of these activities.

Stearic acid (18:0) is an abundant fatty acid in milk, present in human and bovine milk fat at 7.7 and 13.2% of fat, respectively. Stearic acid is synthesized from palmitate via the elongase enzyme, either in the mammary gland by the same enzyme that is active in liver, coded by gene ELOV5 [55, 56], or by ELOV1, whose expression is induced in the mammary gland during lactation [57, 58]. Both of these genes are regulated by diet, hence the net production of stearic acid is under various aspects of metabolic control. Surprisingly, little research has pursued the specific actions of stearic acid when consumed in milk by infants, in spite of its abundance and obvious regulation within the mammary gland during fat synthesis. In adults, stearic acid does not appear to raise serum cholesterol, hence it is considered neutral to heart disease risk. This fatty acid may exert other effects also consistent with protection from heart disease via separate mechanisms. Healthy males who consumed dietary stearic acid (19 g/d) for 4 weeks exhibited beneficial effects on thrombogenic and atherogenic risk factors as compared with the effects of dietary palmitic acid [59].

Delivery of Fat-Soluble Nutrients

Fat-soluble nutrients include the essential nutrients vitamins A, D, E and K, carotenoids as vitamin A precursors, essential polyunsaturated fatty acids, and non-essential nutrients such as various tocopherols, phenolics, carotenoids (e.g., lycopene, lutein and zeaxanthin) and conjugated linoleic acid isomers that cannot be made by humans. Fat-soluble nutrients are increasingly recognized as pleotrophic nutrients with several discrete actions in addition to the direct functions for which their essentiality has been established. As a result, consumption of these components is considered to have biological activities beyond the simple prevention of deficiency and is consistent with many aspects of health [60–62]. In epidemiological studies, the abundance of fat-soluble nutrients in tissues is frequently reported to be inversely correlated with a variety of chronic and degenerative diseases, including cancers [63, 64], cardiovascular diseases [65, 66], diabetes [67] and specific tissue degeneration such as macular degeneration [68] [58, 59]. With the recognition that there are potential health values associated with the presence of fat-soluble nutrients in tissues, their absorption from the diet has become a key issue. In general, non-polar molecules are poorly absorbed, and it is not certain that the presence of a component in a food means that it will be absorbed and delivered to particular tissues in which it might be active [69]. The lipid-soluble components of milk appear to be well absorbed into and accumulated in tissues, although the basic mechanisms by which such a net delivery is accomplished are not known [70, 71].

Milkfat and HDL

Breast feeding stimulates the production of serum lipids and lipoproteins [72, 73]. Interestingly, this increase in

serum lipids in infancy is reversed in adulthood [74]. Nonetheless, throughout life, when compared with either carbohydrates or polyunsaturated fatty acids, the consumption of bovine milk fat results in the elevation of circulating HDL cholesterol. Decades of research have documented that blood HDL cholesterol concentrations are a very strong and independent predictor of heart disease [75]. This relationship has not been as successfully exploited therapeutically as lowering LDL, however, because HDL concentrations are not as responsive to diet and drugs as those of LDL. A major pharmacologic effort has pursued an increase in HDL cholesterol concentrations in humans as a means to reduce cardiovascular risk. This research is based on the extensive evidence of the associations of high HDL with protection from heart disease, even in the face of elevated LDL. There is also evidence of an opposite relationship, that low HDL is associated with increased risk, with or without elevated triglycerides. However, it has not been possible to assign independent variables to HDL differences, and studies have largely been based on HDL concentrations that are presumably high or low based on genetic rather than dietary determinants [76, 77].

HDL exert beneficial effects on overall health by myriad mechanisms, including binding and eliminating toxins, delivering bioactive compounds, protecting various cells and lipoproteins from damage and participating in their repair [78–80]. HDL is particularly important in the successful response to infection by binding and clearing bacterial endotoxin or lipopolysaccharide (LPS). LPS is the major glycolipid component of gram-negative bacterial outer membranes and is responsible for pathophysiological symptoms characteristic of infection. A wide variety of studies have documented that LPS is associated with plasma lipoproteins, suggesting that sequestering of LPS by lipid particles may form an integral part of a humoral detoxification mechanism [81, 82]. The binding of LPS to lipoproteins is highly specific under simulated physiological conditions, and HDL has the highest binding capacity for LPS [83, 84]. This basic protection mechanism may be particularly important for children [85] and for intestinally derived endotoxin. Thus, lipoprotein-binding protein–lipoprotein complexes may be part of a local defense mechanism of the intestine against translocated bacterial toxin. Because milk fats enhance HDL concentrations, they are of potential importance in protection against bacterial LPS toxicity.

Conclusions

The genes and biochemical processes of lactation that produce milk fat evolved under the constant selective pressure of nourishing mammalian infants. Lipids in milk are a source of energy for the neonate of each species. The composition and structures of lipids in milk provide bioactive components that, although not identified as "essential" nutrients by standard definitions, none-the-less serve important functions as structural building blocks, fuels, transport systems, anti-inflammatory, anti-bacterial and antiviral agents in the intestine. These lipids include triacylglycerols—which are metabolized to monoacyl- and diacylcerides and fatty acids—and phospholipids such as sphingomyelin. The lipids in milk are also carriers of important fat-soluble vitamins such as vitamin E, vitamin A and vitamin D.

The absolute quantities and proportionate balance of the various macronutrients in human diets remains the subject of both scientific research and public health speculation. Although unquestionably evolved to nourish infants, detailed examinations of milk and lactation in humans and other mammals are revealing new insights into structures and functions of different components in the diet, including fat. The gene set responsible for the production of lipids is a conspicuously retained subset of the genome throughout mammalian lactation, implying that milk is, in many respects, a lipid delivery system [86]. Saturated fatty acids are a significant component of all mammalian milks examined, including human milk. Thus, whereas diets inordinately high in any component are likely to be net deleterious, finite quantities of saturated fatty acids may provide distinct mechanistic benefits to various metabolic processes. Recognizing that different humans with different lifestyles respond differently to fat intakes and compositions implies that in the future, diets will be designed for individuals not populations. In such a future, finite intakes of specific saturated fats may actually be recommended.

References

1. Watkins SM, Reifsnyder PR, Pan HJ, German JB, Leiter EH (2002) Lipid metabolome-wide effects of the PPARgamma agonist rosiglitazone. J Lipid Res 43:1809–1817
2. Stubbs CD, Smith AD (1984) The modification of mammalian membrane polyunsaturated fatty acid composition in relation to membrane fluidity and function. Biochim Biophys Acta 779: 89–137
3. Iritani N, Fukuda E (1980) Effect of corn oil feeding on triglyceride synthesis in the rat. J Nutr 110:1138–1143
4. Kramer JK, Farnworth ER, Thompson BK, Corner AH, Trenholm HL (1982) Reduction of myocardial necrosis in male albino rats by manipulation of dietary fatty acid levels. Lipids 17:372–382

5. Elwood PC, Pickering JE, Givens DI, Gallacher JE (2010) The consumption of milk and dairy foods and the incidence of vascular disease and diabetes: an overview of the evidence. Lipids. doi:10.1007/s11745-010-3412-5
6. Lin J, Yang R, Tarr PT, Wu PH, Handschin C, Li S, Yang W, Pei L, Uldry M, Tontonoz P, Newgard CB, Spiegelman BM (2005) Hyperlipidemic effects of dietary saturated fats mediated through PGC-1beta coactivation of SREBP. Cell 120:261–273
7. Brown MS, Goldstein JL (1986) A receptor-mediated pathway for cholesterol homeostasis. Science 232:34–47
8. Brown MS, Goldstein JL (1997) The SREBP pathway: regulation of cholesterol metabolism by proteolysis of a membrane-bound transcription factor. Cell 89:331–340
9. Puigserver P, Spiegelman BM (2003) Peroxisome proliferator-activated receptor-gamma coactivator 1 alpha (PGC-1 alpha): transcriptional coactivator and metabolic regulator. Endocr Rev 24:78–90
10. Wu Z, Puigserver P, Andersson U, Zhang C, Adelmant G, Mootha V, Troy A, Cinti S, Lowell B, Scarpulla RC, Spiegelman BM (1999) Mechanisms controlling mitochondrial biogenesis and respiration through the thermogenic coactivator PGC-1. Cell 98:115–124
11. Food and Nutrition Board (2002) Dietary reference intakes for energy, carbohydrate, fiber, fat, fatty acids, cholesterol, protein, and amino acids (Macronutrients). National Academies Press, Washington, DC
12. Mozaffarian D, Rimm EB, Herrington DM (2004) Dietary fats, carbohydrate, and progression of coronary atherosclerosis in postmenopausal women. Am J Clin Nutr 80:1175–1184
13. Robinson SM, Batelaan SF, Syddall HE, Sayer AA, Dennison EM, Martin HJ, Barker DJ, Cooper C, Hertfordshire Cohort Study (2006) Combined effects of dietary fat and birth weight on serum cholesterol concentrations: the Hertfordshire Cohort Study. Am J Clin Nutr 84:237–244
14. Beare-Rogers JL (1998) Dietary fatty acids, where are we going? J Food Lipids 5:135–140
15. US Senate Select Committee on Nutrition and Human Needs (1977) Dietary goals for the United States, 2nd edn. US Government Printing Office, Washington, DC
16. Castelli WP (1992) Epidemiology of triglycerides: a view from Framingham. Am J Cardiol 70:3H–9H
17. Dreon DM, Fernstrom HA, Miller B, Krauss RM (1994) Low-density lipoprotein subclass patterns and lipoprotein response to a reduced-fat diet in men. FASEB J 8:121–126
18. Krauss RM, Dreon DM (1995) Low-density-lipoprotein subclasses and response to a low-fat diet in healthy men. Am J Clin Nutr 62:478S–487S
19. Abbasi F, McLaughlin T, Lamendola C, Kim HS, Tanaka A, Wang T, Nakajima K, Reaven GM (2000) High carbohydrate diets, triglyceride-rich lipoproteins, and coronary heart disease risk. Am J Cardiol 85:45–48
20. Welsh JA, Sharma A, Abramson JL, Vaccarino V, Gillespie C, Vos MB (2010) Caloric sweetener consumption and dyslipidemia among US adults. JAMA 303:1490–1497
21. Frayn KN, Kingman SM (1995) Dietary sugars and lipid metabolism in humans. Am J Clin Nutr 62:250S–261S (discussion 261S–263S)
22. Parks EJ, Hellerstein MK (2000) Carbohydrate-induced hypertriacylglycerolemia: historical perspective and review of biological mechanisms. Am J Clin Nutr 71:412–433
23. Stanhope KL, Havel PJ (2008) Fructose consumption: potential mechanisms for its effects to increase visceral adiposity and induce dyslipidemia and insulin resistance. Curr Opin Lipidol 19:16–24
24. Howard BV, Van Horn L, Hsia J, Manson JE, Stefanick ML et al (2006) Low-fat dietary pattern and risk of cardiovascular disease: the Women's Health Initiative Randomized Controlled Dietary Modification Trial. JAMA 295:655–666
25. Ordovas JM (2007) Gender, a significant factor in the cross talk between genes, environment, and health. Gend Med 4(Suppl B):S111–S122
26. Cox C, Mann J, Sutherland W, Ball M (1995) Individual variation in plasma cholesterol response to dietary saturated fat. BMJ 311:1260–1264
27. Weggemans R, Zock P, Urgert R, Katan M (1999) Differences between men and women in the response of serum cholesterol to dietary changes. Eur J Clin Invest 29:827–834
28. Asztalos B, Lefevre M, Wong L, Foster T, Tulley R, Windhauser M, Zhang W, Roheim PS (2000) Differential response to low-fat diet between low and normal HDL-cholesterol subjects. J Lipid Res 41:321–328
29. Hudgins LC (2000) Effect of high-carbohydrate feeding on triglyceride and saturated fatty acid synthesis. Proc Soc Exp Biol Med 225:178–183
30. Ordovas JM (2004) The quest for cardiovascular health in the genomic era: nutrigenetics and plasma lipoproteins. Proc Nutr Soc 63:145–152
31. Fielding CJ (2004) Lipid rafts and caveolae: from membrane biophysics to cell biology. Wiley-VCH, Weinheim
32. Lawson L, Kummerow F (1979) [beta]-Oxidation of the coenzyme a esters of elaidic, oleic, and stearic acids and their full-cycle intermediates by rat heart mitochondria. Biochim Biophys Acta 573:245–254
33. Murphy CC, Murphy EJ, Golovko MY (2008) Erucic acid is differentially taken up and metabolized in rat liver and heart. Lipids 43:391–400
34. Smith J, German J (1995) Molecular and genetic effects of dietary derived butyric acid. Food Tech 49:87–90
35. Smith JG, Yokoyama WH, German JB (1998) Butyric acid from the diet: actions at the level of gene expression. Crit Rev Food Sci Nutr 38:259–297
36. Young GP, Hu Y, Le Leu RK, Nyskohus L (2005) Dietary fibre and colorectal cancer: a model for environment–gene interactions. Mol Nutr Food Res 49:571–584
37. Maslowski KM, Vieira AT, Ng A, Kranich J, Sierro F, Yu D, Schilter HC, Rolph MS, Mackay F, Artis D, Xavier RJ, Teixeira MM, Mackay CR (2009) Regulation of inflammatory responses by gut microbiota and chemoattractant receptor GPR43. Nature 461:1282–1286
38. Johny A, Baskaran S, Charles A, Amalaradjou M, Darre M, Khan MI, Hoagland TA, Schreiber DT, Donoghue AM, Donoghue DJ (2009) Prophylactic supplementation of caprylic acid in feed reduces *Salmonella enteritidis* colonization in commercial broiler chicks. J Food Prot 72:722–727
39. Neyts J, Kristmundsdottir T, De Clercq E, Thormar H (2000) Hydrogels containing monocaprin prevent intravaginal and intracutaneous infections with HSV-2 in mice: impact on the search for vaginal microbicides. J Med Virol 61:107–110
40. Hornung B, Amtmann E, Sauer G (1994) Lauric acid inhibits the maturation of vesicular stomatitis virus. J Gen Virol 75:353–361
41. Batovska D, Todorova I, Tsvetkova I, Najdenski H (2009) Antibacterial study of the medium chain fatty acids and their 1-monoglycerides: individual effects and synergistic relationships. Pol J Microbiol 58:43–47
42. Sun CQ, O'Connor CJ, Roberton AM (2003) Antibacterial action of fatty acids and monoglycerides against *Helicobacter pylori*. FEMS Immunol Med Microbiol 36:9–17
43. Sun CQ, O'Connor CJ, Roberton AM (2002) The antimicrobial properties of milkfat after partial hydrolysis by calf pregastric lipase. Chem Biol Interact 140:185–198

44. Schuster GS, Dirksen TR, Ciarlone AE, Burnett GW, Reynolds MT, Lankford MT (1980) Anticaries and antiplaque potential of free-fatty acids in vitro and in vivo. Pharmacol Ther Dent 5:25–33
45. Thormar H, Isaacs C, Brown H, Barshatzky M, Pessolano T (1987) Inactivation of enveloped viruses and killing of cells by fatty acids and monoglycerides. Antimicrob Agents Chemother 31:27–31
46. Isaacs CE, Litov RE, Thormar H (1995) Antimicrobial activity of lipids added to human milk, infant formula, and bovine milk. J Nutr Biochem 6:362–366
47. Reiner DS, Wang CS, Gillin FD (1986) Human milk kills *Giardia lamblia* by generating toxic lipolytic products. J Infect Dis 154:825–832
48. Li Q, Estes JD, Schlievert PM, Duan L, Brosnahan AJ, Southern PJ, Reilly CS, Peterson ML, Schultz-Darken N, Brunner KG, Nephew KR, Pambuccian S, Lifson JD, Carlis JV, Haase AT (2009) Glycerol monolaurate prevents mucosal SIV transmission. Nature 458:1034–1038
49. Kromhout D, Menotti A, Bloemberg B, Aravanis C, Blackburn H, Buzina R, Dontas AS, Fidanza F, Giampaoli S, Jansen A, Martti K, Martijn K, Aulikki N, Srecko N, Juha P, Maija P, Sven P, Leena R, Bozidar S, Hironori T (1995) Dietary saturated and *trans*fatty acids and cholesterol and 25-year mortality from coronary heart disease: the seven countries study. Prev Med 24:308–315
50. Dabadie H, Peuchant E, Bernard M, LeRuyet P, Mendy F (2005) Moderate intake of myristic acid in *sn*-2 position has beneficial lipidic effects and enhances DHA of cholesteryl esters in an interventional study. J Nutr Biochem 16:375–382
51. Carnielli VP, Luijendijk IH, van Goudoever JB, Sulkers EJ, Boerlage AA, Degenhart HJ, Sauer PJ (1995) Feeding premature newborn infants palmitic acid in amounts and stereoisomeric position similar to that of human milk: effects on fat and mineral balance. Am J Clin Nutr 61:1037–1042
52. Carnielli VP, Luijendijk IH, Van Goudoever JB, Sulkers EJ, Boerlage AA, Degenhart HJ, Sauer PJ (1996) Structural position and amount of palmitic acid in infant formulas: effects on fat, fatty acid, and mineral balance. J Pediatr Gastroenterol Nutr 23:553–560
53. Lai L, Leone TC, Zechner C, Schaeffer PJ, Kelly SM, Flanagan DP, Medeiros DM, Kovacs A, Kelly DP (2008) Transcriptional coactivators PGC-1alpha and PGC-lbeta control overlapping programs required for perinatal maturation of the heart. Genes Dev 22:1948–1961
54. Wareski P, Vaarmann A, Choubey V, Safiulina D, Liiv J, Kuum M, Kaasik A (2009) PGC-1 and PGC-1 regulate mitochondrial density in neurons. J Biol Chem 284:21379–21385
55. Moon YA, Shah NA, Mohapatra S, Warrington JA, Horton JD (2001) Identification of a mammalian long chain fatty acyl elongase regulated by sterol regulatory element-binding proteins. J Biol Chem 276:45358–45366
56. Moon Y, Hammer R, Horton J (2009) Deletion of ELOVL5 leads to fatty liver through activation of SREBP-1c in mice. J Lipid Res 50:412–423
57. Rudolph MC, Neville MC, Anderson SM (2007) Lipid synthesis in lactation: diet and the fatty acid switch. J Mammary Gland Biol Neoplasia 12:269–281
58. Russell TD, Palmer CA, Orlicky DJ, Fischer A, Rudolph MC, Neville MC, McManaman JL (2007) Cytoplasmic lipid droplet accumulation in developing mammary epithelial cells: roles of adipophilin and lipid metabolism. J Lipid Res 48:1463–1475
59. Kelly FD, Sinclair AJ, Mann NJ, Turner AH, Abedin L, Li D (2001) A stearic acid-rich diet improves thrombogenic and atherogenic risk factor profiles in healthy males. Eur J Clin Nutr 55:88–96
60. Giovannucci E, Ascherio A, Rimm E, Stampfer M, Colditz G, Walter C, Willett WC (1995) Intake of carotenoids and retinol in relation to risk of prostate cancer. J Nat Cancer Inst 87:1767–1776
61. Traber MG, Packer L (1995) Vitamin E: beyond antioxidant function. Am J Clin Nutr 62:1501S–1509S
62. Dietrich M, Traber MG, Jacques PF, Cross CE, Hu Y, Block G (2006) Does gamma-tocopherol play a role in the primary prevention of heart disease and cancer? A review. J Am Coll Nutr 25:292–299
63. Zhu Z, Parviainen M, Männistö S, Pietinen P, Eskelinen M, Syrjänen K, Uusitupa M (1996) Vitamin E concentration in breast adipose tissue of breast cancer patients (Kuopio, Finland). Cancer Causes Control 7:591–595
64. Ahmed M, Fayed S, Hossein H, Tash F (1999) Lipid peroxidation and antioxidant status in human cervical carcinoma. Dis Markers 15:283–291
65. Palace VP, Khaper N, Qin Q, Singal PK (1999) Antioxidant potentials of vitamin A and carotenoids and their relevance to heart disease. Free Radic Biol Med 26:746–761
66. Palace VP, Hill MF, Khaper N, Singal PK (1999) Metabolism of vitamin A in the heart increases after a myocardial infarction. Free Radic Biol Med 26:1501–1507
67. Haffner SM (2000) Coronary heart disease in patients with diabetes. N Engl J Med 342:1040–1042
68. Belda JI, Roma J, Vilela C, Puertas FJ, Diaz-Llopis M, Bosch-Morell F, Romero FJ (1999) Serum vitamin E levels negatively correlate with severity of age-related macular degeneration. Mech Ageing Dev 107:159–164
69. Papas AM (1996) Determinants of antioxidant status in humans. Lipids 31(Suppl):S77–S82
70. Jeanes YM, Hall WL, Ellard S, Lee E, Lodge JK (2004) The absorption of vitamin E is influenced by the amount of fat in a meal and the food matrix. Br J Nutr 92:575–579
71. Lodge JK, Hall WL, Jeanes YM, Proteggente AR (2004) Physiological factors influencing vitamin E biokinetics. Ann N Y Acad Sci 1031:60–73
72. Harit D, Faridi MM, Aggarwal A, Sharma SB (2008) Lipid profile of term infants on exclusive breastfeeding and mixed feeding: a comparative study. Eur J Clin Nutr 62:203–209
73. Fujita H, Okada T, Inami I, Makimoto M, Hosono S, Minato M, Takahashi S, Mugishima H, Yamamoto T (2008) Low-density lipoprotein profile changes during the neonatal period. J Perinatol 28:335–340
74. Owen CG, Whincup PH, Odoki K, Gilg JA, Cook DG (2002) Infant feeding and blood cholesterol: a study in adolescents and a systematic review. Pediatrics 110:597–608
75. Chapman MJ (2006) Therapeutic elevation of HDL-cholesterol to prevent atherosclerosis and coronary heart disease. Pharmacol Ther 111:893–908
76. Wang N, Lan D, Chen W, Matsuura F, Tall AR (2004) ATP-binding cassette transporters G1 and G4 mediate cellular cholesterol efflux to high-density lipoproteins. Proc Natl Acad Sci USA 101:9774–9779
77. Wang X, Paigen B (2005) Genetics of variation in HDL cholesterol in humans and mice. Circ Res 96:27–42
78. Argraves KM, Argraves WS (2007) HDL serves as a S1P signaling platform mediating a multitude of cardiovascular effects. J Lipid Res 48:2325–2333
79. Rader DJ (2006) Molecular regulation of HDL metabolism and function: implications for novel therapies. J Clin Invest 116:3090–3100
80. Canturk NZ, Canturk Z, Okay E, Yirmibesoglu O, Eraldemir B (2002) Risk of nosocomial infections and effects of total

cholesterol, HDL cholesterol in surgical patients. Clin Nutr 21:431–436
81. Feingold KR, Funk JL, Moser AH, Shigenaga JK, Rapp JH, Grunfeld C (1995) Role for circulating lipoproteins in protection from endotoxin toxicity. Infect Immun 63:2041–2046
82. Pajkrt D, Doran JE, Koster F, Lerch PG, Arnet B, van der Poll T, ten Cate JW, van Deventer SJ (1996) Antiinflammatory effects of reconstituted high-density lipoprotein during human endotoxemia. J Exp Med 184:1601–1608
83. van Leeuwen HJ, van Beek AP, Dallinga-Thie GM, van Strijp JA, Verhoef J, van Kessel KP (2001) The role of high density lipoprotein in sepsis. Neth J Med 59:102–110
84. Levels JH, Abraham PR, van den Ende A, van Deventer SJ (2001) Distribution and kinetics of lipoprotein-bound endotoxin. Infect Immun 69:2821–2828
85. Liuba P, Persson J, Luoma J, Yla-Herttuala S, Pesonen E (2003) Acute infections in children are accompanied by oxidative modification of LDL and decrease of HDL cholesterol, and are followed by thickening of carotid intima-media. Eur Heart J 24:515–521
86. Lemay DG, Lynn DJ, Martin WF, Casey TM, Kriventseva EV, Rincon G, Barris WC, Hinrichs AS, Molenaar AJ, Pollard KS, Neville MC, Maqbool NJ, Zdobnov EM, Tellam RL, Medrano JF, German JB, Rijnkels M (2009) The bovine lactation genome: insights into the evolution of mammalian milk. Genome Biol 10:R43

Lipids (2010) 45:925–939
DOI 10.1007/s11745-010-3412-5

ORIGINAL ARTICLE

The Consumption of Milk and Dairy Foods and the Incidence of Vascular Disease and Diabetes: An Overview of the Evidence

Peter C. Elwood · Janet E. Pickering · D. Ian Givens · John E. Gallacher

Received: 17 February 2010 / Accepted: 22 March 2010 / Published online: 16 April 2010

Abstract The health effects of milk and dairy food consumption would best be determined in randomised controlled trials. No adequately powered trial has been reported and none is likely because of the numbers required. The best evidence comes, therefore, from prospective cohort studies with disease events and death as outcomes. Medline was searched for prospective studies of dairy food consumption and incident vascular disease and Type 2 diabetes, based on representative population samples. Reports in which evaluation was in incident disease or death were selected. Meta-analyses of the adjusted estimates of relative risk for disease outcomes in these reports were conducted. Relevant case–control retrospective studies were also identified and the results are summarised in this article. Meta-analyses suggest a reduction in risk in the subjects with the highest dairy consumption relative to those with the lowest intake: 0.87 (0.77, 0.98) for all-cause deaths, 0.92 (0.80, 0.99) for ischaemic heart disease, 0.79 (0.68, 0.91) for stroke and 0.85 (0.75, 0.96) for incident diabetes. The number of cohort studies which give evidence on individual dairy food items is very small, but, again, there is no convincing evidence of harm from consumption of the separate food items. In conclusion, there appears to be an enormous mis-match between the evidence from long-term prospective studies and perceptions of harm from the consumption of dairy food items.

Keywords Dairy · Milk · Butter · Cheese · Heart disease · Stroke · Diabetes · Cohort studies

P. C. Elwood (✉) · J. E. Gallacher
Department of Primary Care and Public Health, Cardiff University, University Hospital of Wales, Cardiff CF14 4YS, UK
e-mail: pelwood@doctors.org.uk

J. E. Pickering
MRC Epidemiology Unit, Cardiff, UK

D. I. Givens
Nutritional Sciences Research Unit, School of Agriculture, Policy and Development, University of Reading, Reading, Berkshire, UK

Introduction

Milk and dairy foods contain saturated fats, and their consumption often leads to a rise in plasma cholesterol level. This, together with the belief that milk is 'fattening', appears to have led to the widespread conviction that milk and dairy foods are a factor in obesity and in heart disease, and that their consumption should be limited.

At least ten hypotheses have been defined in attempts to explain the supposed harm from milk and dairy consumption [1]. The mechanism most frequently quoted is, undoubtedly, a rise in plasma cholesterol concentration following the ingestion of milk or a dairy food item. The drawing of conclusions about milk from its effect upon a single 'intermediate' variate, such as cholesterol level, is, however, quite unreasonable, as it ignores the fact that milk, being a complex food with a host of nutrients, is likely to affect many mechanisms relevant to the development of vascular and other diseases. The only valid basis for conclusions about a food item and health or survival comes from long-term studies of the consumption of that food and the incidence of disease or death.

Archie Cochrane was one of the first to urge that conclusions in clinical practice and in medical research are evidence-based, and that the evidence considered comes from all of the available, bias-free relevant studies [2]. The urgings of Cochrane and others have led to 'evidence-based

medicine' within the whole field of clinical and public health practice. Alvarez-León et al. [3] have, however, pointed out that statements about the benefits and risks of dairy product consumption appear to be based on selected physio-pathological data, such as relationships with cholesterol level, and not on valid epidemiological evidence, indeed, as Alvarez-León et al. commented: "Public health nutrition should not be unaware of the need for evidence-based conclusions."

The most convincing evidence on a food item and health would come from randomised controlled trials, but no adequately powered trials of milk or dairy consumption have been reported, nor are any likely to be conducted because of the numbers of participants required and the compliance that would be necessary from each participant. By default, the best evidence on dairy food consumption, health and survival comes, therefore, from long-term cohort studies with disease events and death as the outcomes.

We report the results of a literature search and meta-analyses of prospective cohort studies of milk and dairy food consumption as predictors, and death, vascular disease and diabetes as outcomes. We also summarise evidence from relevant retrospective case–control studies.

Experimental Procedure

As far as possible, the procedures in the review and meta-analyses which we conducted are those outlined by Egger et al. [4] and Moher et al. [5] using the statistical programmes available at http://www.systematicreviews.com.

Search Strategy

A number of searches were conducted using Medline, PubMed and ISI Web of Science, and four researchers were involved. Using the search terms for predictors: milk, dairy, dairy products, cheese, butter, cream and yoghurt, together with the terms for outcomes: death, heart disease and stroke, 138 papers were identified and limiting these to 'adult' gave 47 papers. The predictors together with the outcome terms diabetes and diabetes mellitus Type 2 gave 330 papers. From these, five papers were selected. Papers which used a composite of foods including dairy items as a predictor were not selected. A further three papers with relevant results, which had not been detected in the electronic searches but which had been identified by the lead author during extensive reading over the past ten and more years, were included.

In the end, a total of 38 reports of cohort studies were selected and used in the analyses presented. Five case–control retrospective studies which gave relevant data are described in what follows, but are not examined by meta-analyses. In an attempt to clarify uncertainties, and/or to obtain further data, letters were sent to 14 authors, but responses were obtained from only a very few.

Meta-Analyses

The results of a test of homogeneity between studies is given for each dairy food, together with estimates of the overall relative risk. Difficulties arose from the fact that the results of individual studies were reported in terms of relative risk, odds ratio or hazard ratio. These three measures of risk are not entirely equivalent. However, in almost all of the studies, the event rate is well below 10% and, in this situation, the odds ratio can be considered as a good approximation for the relative risk [4]. The hazard ratio is a comparison of time-to-event and, so, is not an approximation for the relative risk. However, repeating the summary calculations with and without the studies which reported a hazard ratio produced only a trivial difference in the results.

The summary statistic was calculated using the 'meta' command in the Stata statistical software package [4]. This uses an inverse-variance weighting to calculate fixed and random effects summary statistics. The 'meta' command was convenient as it calculates the variance using the confidence intervals of the risk estimate. Homogeneity was assessed using the Q statistic, which tests the null hypothesis that the variation between trials is compatible with chance. It follows a Chi-squared distribution with $n - 1$ degrees of freedom, where n is the number of studies being investigated. In many of our groupings, there was significant heterogeneity. The heterogeneity led to the choice of random effects models for the summary statistics. The adjusted relative risks (RR) given in each individual report were noted, and pooled estimates were obtained from these by weighting the natural logs of each reported RR by the inverse of the variance, as described by Gao et al. [6].

In addition to all of the above, data from relevant retrospective case–control studies are described in the text.

Results

Dairy Foods

Eight long-term cohort studies have reported on all-cause deaths in relation to dairy food consumption (Table 1). Unfortunately, two of the studies [7, 8] do not include sufficient data for inclusion in a meta-analysis. There is no significant heterogeneity between the results for the six studies ($P = 0.427$) and a meta-analysis suggests a small but significant reduction in total mortality in the subjects with the highest dairy consumption, relative to the risk in

Table 1 Dairy foods and all-cause mortality. Details of cohort studies in which the consumption of 'dairy foods' (see text) was related to the risk of death, with an estimate of homogeneity between the studies and the results of a meta-analysis

Study	Number in cohort (length of follow-up)	Number of deaths	Factors adjusted for	Adjusted estimate of risk (95% CI)	Predictive factor and subgroups compared
Kahn et al. [7] An Adventists cohort	22,033 subjects (21 years)	6,075	Age, sex, smoking, history of vascular disease, hypertension, diabetes	0.98 (NS)	3+ glasses/week vs <1 glass of whole milk
van der Vijver et al. [8] Dutch Civil Servants cohort	2,605 subjects (28 years)	Numbers not stated	Age, smoking, BMI, systolic BP, cholesterol, energy, alcohol	1.0 (0.7–1.4) men 0.8 (0.5–1.3) women	Top third of total calcium intake vs lowest third
Kelemen et al. [45] Iowa Women's cohort	29,017 subjects (15 years)	3,978	Age, BMI, smoking, energy, education, hypertension, post-menopausal, vitamins, fat intake, fruit, vegetables, fibre	1.10 (0.97–1.24)	A simulation study substituting a composite of milk, cream, ice cream yoghurt and cheese protein
Mann et al. [46] Oxford Vegetarian cohort	10,802 subjects (13.3 years)	383	Age, sex, smoking, social class	0.87 (0.68–1.13)	More than 1/2 pint milk/day vs less than 1/2
Ness et al. [30] Scottish Men cohort	5,765 men (25 years)	2,350	Age, social class, health behaviour and health status	0.81 (0.61–1.09)	1 pint+ milk/day vs no milk
Elwood et al. [31] Caerphilly cohort	2,512 men (20–24 years)	811	Age, smoking, social class, IHD, BMI, energy, alcohol, fasting cholesterol HDL cholesterol and triglycerides	1.20 (0.80–1.80)	1 pint+ /milk/day vs little or no milk
Trichopoulou et al. [47] A Greek cohort	1,013 diabetic subjects (4.5 years)	80	Age, gender, smoking, education weight and height, hip circum., insulin, hypertension, hyperchol., food groups	0.92 (0.71–1.19)	Increase in dairy foods by 1 SD/day
van der Pols et al. [48] Carnegie cohort	4,374 subjects (66–68 years)	1,468	Age, sex, area, energy, fruit, vegetables, eggs, protein, fat, energy	0.77 (0.61–0.98)[a] 0.77 (0.61–0.97)[a]	Top vs bottom quartile dairy Top vs bottom quartile milk

Data from Kahn et al. [7] omitted because of the absence of detailed data; van der Vijver et al. [8] omitted because it was based on the total dietary calcium; Kelemen et al. [45] omitted because it is a test of dietary substitution

0.64M person years; 5,092 deaths: heterogeneity between studies $P = 0.427$

Meta-analysis (random effects) RR (95% CI) for highest intake groups 0.87 (0.77–0.98)

vs = compared with, or relative to; 1 pint = 0.568 l

[a] In van der Pols et al. [48], the estimate for dairy intake was included in the above meta-analysis. This is reported as a hazard ratio and if it is omitted from the meta-analysis, the heterogeneity is $P = 0.470$ and the overall RR = 0.91 (0.78–1.05)

the subjects with the lowest consumption (RR) 0.87; 95% confidence limits (0.77, 0.98).

Milk

Table 2 summarises data from 11 cohort studies of milk consumption and ischaemic heart disease (IHD). Again, two do not include adequate data for inclusion in a meta-analysis. The results of the other nine cohorts show no significant heterogeneity ($P = 0.570$) and the overall risk of incident heart disease in the subjects with the highest milk intake, relative to those within each cohort with the lowest milk intakes, is 0.92 (0.80, 0.99).

As indicated in a footnote to Table 2, the result reported by Hu et al. [9] for whole milk (1.67; 1.14, 1.90) shows marked heterogeneity with all the other estimates of risk for milk. We have, therefore, used the estimate of Hu et al. [9] for skimmed milk in our meta-analysis. If, however, it is assumed that 20% of women in that cohort had been drinking whole milk and 80% skimmed milk, then an overall estimate of IHD risk in the cohort studied by Hu et al. [9] is 0.96 (0.74, 1.15), and putting this estimate into

Table 2 Milk and dairy consumption and incident ischaemic heart disease (IHD). Details of cohort studies in which the consumption milk and dairy foods was related to incident heart disease, with the results of a meta-analysis

Study	Number of subjects (length of follow-up)	Number of heart disease events	Factors adjusted for	Adjusted estimate of risk (95% CI)	Predictive factor
Snowdon et al. [33] An Adventists cohort	8,725 males 15,048 females (20 years)	758 841 IHD deaths	Age, smoking and other food items, weight, marital status	0.94 1.11	Two glasses of milk/day vs none
van der Vijver et al. [8] Dutch Civil Servants cohort	1,340 males 1,265 females	366 178 CHD deaths	Age, smoking, BMI, systolic BP, cholesterol, energy, alcohol	0.77 (0.53–1.11) 0.91 (0.55–1.50)	Top and bottom tertile of dietary calcium intake
Fraser [49] An Adventists cohort	26,473 subjects (duration not stated)	Total CHD no. not stated	None	1.33 ($P < 0.07$)	One glass or more whole milk vs none
Kelemen et al. [45] Iowa Women's cohort	29,017 subjects (15 years)	739 CHD deaths	Age, BMI, smoking, energy, education, hypertension, post-menopausal, vitamins, fat intake, fruit, vegetables, fibre	1.41 (1.07–1.87)	A simulation study substituting a composite of milk, cream, ice cream yoghurt and cheese for protein
Nettleton et al. [50] ARIC cohort	14,153 subjects (13 years)	1,140 incident heart failure	Age, sex, race, smoking, alcohol, prevalent disease, education, activity	1.08 (1.01–1.16)[a]	High-fat dairy: whole milk, cheese and ice cream
Shaper et al. [37] UK RHS cohort	7,735 subjects (9.5 years)	608 IHD events	Age, social class, smoking, cholesterol, blood pressure and diabetes	0.88 (0.55–1.40)	Milk drunk and taken on cereals vs 'none'
Mann et al. [46] Oxford Vegetarian cohort	10,802 subjects (13.3 years)	63 IHD deaths	Age, sex, smoking, social class	1.50 (0.81–2.78)	More than 1/2 pint milk per day vs less than 1/2 pint
Bostick et al. [51] Iowa women cohort	34,486 women (8 years)	387 IHD deaths	Age, energy, BMI, waist–hip ratio, diabetes, smoking, vit. E, saturated fat, oestrogen, alcohol, education, activity	0.94 (0.66–1.35)	Top and bottom quartile of milk products
Hu et al. [9] Health Prof. cohort	80,082 women (14 years)	939 total CHD	Age, BMI, menopause, HRT, smoking, alcohol, family history, hypertension, aspirin, exercise, vit. E	1.67 (1.14–1.90)[a] 0.78 (0.63–0.96)[a] 1.04 (0.96–1.12)[a] 0.93 (0.85–1.02)[a]	More than two glasses milk/day vs less than one/week: whole milk, skimmed milk, one serving per day high-fat dairy, one serving per day low-fat dairy
Ness et al. [30] Scottish Men cohort	5,765 men (25 years)	892 CHD deaths	Age, social class, health behaviour and health status	0.68 (0.40–1.13)	More than one pint milk/day vs less than one-third/day
Elwood et al. [31] Caerphilly cohort	2,512 men (20–24 years)	493 total IHD	Age, smoking, social class, IHD, BMI, energy, alcohol, fasting cholesterol, HDL cholesterol and triglycerides	0.71 (0.40–1.26)	One or more pint/day vs little or no milk/day
Al Delaimy et al. [52] Health Prof. cohort	39,800 subjects (12 years)	1,458 total IHD	Age, BMI, time period, smoking, alcohol, energy and vit E intake, activity, diabetes, hyperchol, family history, aspirin	1.03 (0.86–1.26) 1.01 (0.83–1.23)	Top and bottom quintile of dairy calcium intake Total dairy product intake
Larmarche [53] Quebec Cardiovasc. Cohort	2,000 men (13 years)	217 total CHD	Age, smoking, BMI, diabetes	0.73 (0.56–0.93)	Above and below average intake of dairy products

Table 2 continued

Study	Number of subjects (length of follow-up)	Number of heart disease events	Factors adjusted for	Adjusted estimate of risk (95% CI)	Predictive factor
Trichopoulou et al. [47] A Greek cohort	1,013 subjects (4.5 years)	46 CVD deaths	Age, gender, smoking, education, weight and height, hip circum., insulin, hypertension, hyperchol., food groups	0.95 (0.68–1.31)	150 g (one SD) increase in dairy products
Umesawa et al. [54] JACC cohort	21,068 men 32,319 women (10 years)	135 99 Total CHD	Age, sex, BMI, smoking, alcohol, sodium, potassium, fatty acids, area, menopause, hyperchol., diabetes	0.80 (0.45–1.44) 1.06 (0.50–2.25)	Top and bottom quintile of dairy calcium intake
Umesawa et al. [32] JPHC cohort	41,526 (13 years)	322 total CHD	Age, sex, BMI, smoking, alcohol, sodium, potassium, fatty acids, area, menopause, hyperchol., diabetes	1.09 (0.74–1.61)	Top and bottom quintile of dairy calcium intake
van der Pols et al. [48] Carnegie cohort[c]	4,374 subjects (66–68 years)	378 CHD deaths	Age, sex, area, energy, fruit, vegetables, eggs, protein, fat, energy	0.74 (0.45–.22)[a, b] 1.06 (0.49 1.31)[a, b]	Top and bottom quintile of dairy products Top and bottom quintile of milk

Data from Snowdon et al. [33] and Fraser [49] omitted because of the absence of detailed data; van der Vijver et al. [8] omitted because it was based on the total dietary calcium; Kelemen et al. [45] omitted because it is a test of dietary substitution; Nettleton et al. [50] omitted because the outcome is heart failure

4.3M person years; 16,212 IHD events: heterogeneity between studies $P = 0.570$

Meta-analysis: risk of a heart disease event in the subjects with the highest milk/dairy intake, relative to that in the subjects with the lowest intake: 0.92 (0.80–0.99)

[a] If Nettleton et al. [50] is included, the heterogeneity between studies $P = 0.033$; RR = 0.92 (0.82–1.03)

[b] An estimate for Hu et al. [9] based on the data for milk, assuming 20% of women had been on whole milk, 80% on skimmed, the heterogeneity is $P = 0.454$; overall RR = 0.88 (0.80, 0.97) and when van der Pols et al. is omitted (because an HR is stated), the heterogeneity is $P = 0.408$; RR = 0.88 (0.80–0.98). When the estimates of Hu et al. [9] for dairy is used, $P = 0.570$; RR = 0.92 (0.86–0.99)

[c] In van der Pols et al. [48], risk estimates which had been adjusted for calcium are not used because the inclusion of calcium may have led to over-adjustment

the meta-analysis gives an overall estimate for milk and heart disease of 0.91 (0.77–1.07). A similar problem arose with estimates derived from the same cohort of the US Nurses Health Study by Sun et al. [10]. They used plasma pentadecanoic acid as a surrogate for dairy fat consumption, though it can also be obtained from beef, lamb and venison. The estimate of risk for heart disease that they obtained is statistically inconsistent with estimates derived from other populations in which the same surrogate approach had been used [11]. It could possibly be that the women within the Nurses' Cohort who drank whole milk had become so highly selected with reference to a range of health-related behaviours that they may have become unrepresentative of any meaningful population group.

In a report based on 27,529 Adventists, Snowdon [12] states that milk was not related to all-cause mortality, but he gives no data. Likewise, Jacobsen and Stensvold [13] refer to "a large prospective study with more than 17,000 men and women followed for 11.5 years (which) showed an inverse relationship between milk drinking (predominantly full-fat milk) and the risk of cardiovascular death." One of the authors (BKJ) was contacted and details requested, but these are not now available.

A number of cross-sectional studies have been reported in which the past milk consumption of patients admitted to hospital with a myocardial infarct was compared with the past consumption by control subjects without evidence of vascular disease. This research strategy has uncertainties because only a proportion of patients survive an infarct and are questioned, and because the estimation of milk intake prior to the infarct is dependent upon memory. Four such studies have been reviewed elsewhere [14] and a meta-analysis yielded an overall relative risk of milk consumption and incident heart disease of 0.83 (0.66, 0.99). A further, unusual case–control study of 144 diabetic patients with peripheral vascular disease matched with 288 control diabetic patients reported an odds ratio of 0.71 (0.42, 1.19) for peripheral vascular disease in those who consumed milk more than seven times a week relative to those who took milk twice or less per week [15].

The estimates of risk for milk consumption and stroke incidence in the 11 cohorts summarised in Table 3 show

Table 3 Milk and dairy consumption and incident stroke. Details of cohort studies in which the consumption of milk and dairy foods was related to incident stroke events, with the results of a meta-analysis

Study	Number of subjects (length of follow-up)	Number and type of stroke	Factors adjusted for	Predictive factor	Adjusted estimate of risk (95% CI)
Iso et al. [19] Nurses Health cohort	85,764 women (14 years)	347 ischaemic	Age, smoking, time interval, BMI, alcohol, menopause, hormone use, exercise, multivitamins, fatty acid intake, history of hypertension, diabetes and cholesterol	Top and bottom quintile of dairy calcium	0.70 (0.51–0.97)
Kinjo et al. [55] A Japanese cohort	223,170 subjects (16 years)	3,084 thromboembolic	Age, sex, area, smoking, alcohol, occupation	Milk four or more times/week vs less than once/week	0.85 (0.77–0.92)
Ness et al. [30] Scottish Men cohort	5,765 men (25 years)	196 stroke deaths	Age, social class, health behaviour and health status	More than one pint/day vs less than one-third/day	0.84 (0.31–2.30)
Sauvaget et al. [56] Life span cohort	40,349 subjects (16 years)	1,462 stroke deaths	Sex, age, area, BMI, smoking, alcohol, education, diabetes, hypertension, radiation history	Milk almost daily vs none dairy products almost daily vs none	0.94 (0.79–1.12)[a] 0.73 (0.57–0.94)
He et al. [57] Health Prof. cohort	43,732 men (14 years)	451 ischaemic	Smoking, alcohol, BMI, activity, hyperchol., hypertension, aspirin, potassium, multivitamins, vit E, fruit and veg, energy	High-fat dairy once a day+ vs less than once a week	1.23 (0.74–2.03)
Elwood et al. [31] Caerphilly cohort	2,512 men (22–25 years)	185 ischaemic	Age, smoking, social class, IHD, BMI, energy, alcohol, fasting cholesterol, HDL cholesterol and triglycerides	One or more pint/day vs little or no milk	0.66 (0.24–1.81)
Abbott et al. [58] Honolulu heart cohort	3,150 men (22 years)	229 thromboembolic	Age, dietary K and Na, alcohol, smoking, activity, BP, glucose, cholesterol, glucose, uric acid, Hct	16 oz/day milk drunk vs non-drinkers	0.67 (0.45–1.00)
Larsson et al. [23] ATBC cohort	26,556 men (13.6.years)	2,702 cerebral infarcts	Age, smoking, alcohol, BMI, education, total cholesterol, diabetes, IHD, energy intake and activity, intake of various foods and original randomisation	Top quintile of a composite of low-fat, whole and sour milk vs lowest quintile	1.03 (0.96–1.10)
Umesawa et al. [54] JACC cohort	110,792 subjects (12.9 years)	284 stroke deaths	Age, sex, BMI, smoking, alcohol, sodium, potassium, fatty acids, area, menopause, hyperchol., diabetes	Top and bottom quintile of dairy calcium intake	0.53 (0.34–0.81)
Umesawa et al. [32] JPHC cohort	41,526 subjects (12.9 years)	664 ischaemic	Age, sex, BMI, smoking, alcohol, sodium, potassium, fatty acids, area, menopause, hyperchol., diabetes	Top and bottom quintile of dairy calcium intake	0.70 (0.52–0.94)
van der Pols et al. [48] Carnegie cohort	4,374 subjects (66–68 years)	121 stroke deaths	Age, sex, area, energy, fruit, vegetables, eggs, protein, fat, energy	Top and lowest quartiles of dairy Top and bottom quartile of milk	0.61 (0.27–1.38)[a] 0.60 (0.28, 1.33)

8.4M person years; 9,725 strokes: heterogeneity between studies $P < 0.000$

Meta-analysis: risk of a stroke in the subjects with the highest milk/dairy intake, relative to that in the subjects with the lowest intake: 0.79 (0.68–0.91)

[a] For both Sauvaget et al. [56] and van der Pols et al. [48], the results for 'dairy' are used in the meta-analysis

Table 4 Dairy foods, haemorrhagic stroke and sub-arachnoid bleeds. Details of cohort studies in which the consumption of dairy food was related to the risk of haemorrhagic stroke, or a sub-arachnoid bleed, with estimates of homogeneity between the studies and the results of meta-analyses

Study	Number of subjects (length of follow-up)	Number and type of disease event	Factors adjusted for	Adjusted RR (95% CI)	Predictive factor and subgroups compared
Kinjo et al. [55] A Japanese cohort	223,170 subjects (16 years)	4,773 haemorrhagic stroke deaths	Sex, age, area, smoking, alcohol, occupation	0.74 (0.68–0.80)	Milk four or more times/week vs once/week
He et al. [57] Health Prof. cohort	43,732 men (14 years)	124 haemorrhagic strokes	Smoking, alcohol, BMI, activity, hyperchol., hypertension, aspirin, potassium, multivitamins, vit E, fruit and veg., energy	1.22 (0.47–3.16)	High-fat dairy once a day or more vs less than once a week
Umesawa et al. [54] JACC cohort	21,068 men 32,319 women (10 years)	113 haemorrhagic strokes 128 haemorrhagic strokes	Age, sex, BMI, smoking, alcohol, sodium, potassium, fatty acids, area, menopause, hyperchol., diabetes	0.46 (0.23–0.91) 0.51 (0.28–0.94)	Top and bottom quintile of dairy calcium intake
Umesawa et al. [32] JPHC cohort	41,526 subjects (12.9 years)	425 haemorrhagic strokes	Age, sex, BMI, smoking, alcohol, sodium, potassium, fatty acids, area, menopause, hyperchol., diabetes	0.65 (0.43–0.97)	Top quintile of dairy calcium vs lowest quintile
Larsson et al. [23] ATBC cohort	26,556 men (13.6 years)	383 haemorrhagic strokes	Age, smoking, alcohol, BMI, education, total cholesterol, diabetes, IHD, energy intake and activity, intake of various foods and original randomisation	1.01 (0.82–1.20)[a] 1.32 (0.89–1.94)[a]	Top quintile of a composite of low-fat, whole and sour milk vs lowest quintile Top and lowest quintile of dairy products vs lowest quintile
0.36M person years: 5,946 haemorrhagic strokes: heterogeneity between studies $P = 0.014$					
Meta-analysis (random effects) RR (95% CI) for highest intake groups 0.75 (0.60–0.94)					
Umesawa et al. [54] JACC cohort	21,068 men 32,319 women (10 years)	37 sub-arachnoid bleeds 34 sub-arachnoid bleeds	Age, sex, BMI, smoking, alcohol, sodium, potassium, fatty acids, area, menopause, hyperchol., diabetes	0.19 (0.04–0.87) 0.41 (0.17–0.97)	Top and bottom quintile of dairy calcium intake
Umesawa et al. [32] JPHC cohort	41,526 subjects 12.9 years	217 sub-arachnoid bleeds	Age, sex, BMI, smoking, alcohol, sodium, potassium, fatty acids, area, menopause, hyperchol., diabetes	0.74 (0.46–1.61)	Top quintile of dairy calcium vs lowest quintile
Larsson et al. [23] ATBC cohort	26,556 men 13.6 years	196 sub-arachnoid bleeds	Age, smoking, alcohol, BMI, education, total cholesterol, diabetes, IHD, energy intake and activity, intake of various foods and original randomisation	1.26 (1.00–1.52)	Top and bottom quintile: dairy products, all milks (whole + low-fat + sour)
0.96M person years: 484 sub-arachnoid bleeds: heterogeneity between studies $P = 0.004$					
Meta-analysis (random effects) RR (95% CI) for highest intake groups 0.65 (0.32–1.31)					

vs = compared with, or relative to

[a] The results for haemorrhagic stroke are based on Larsson et al. [23] for milk. Using Larsson et al. [23] for dairy gives $P = 0.022$, RR = 0.76 (0.58–1.00)

significant heterogeneity, and although the overall estimate of risk is significant (0.78; 0.68, 0.91), this cannot be interpreted with confidence. However, the data on stroke in Table 3 relate, as far as is possible, to ischaemic stroke and in Table 4, reports on haemorrhagic strokes and sub-arachnoid bleeds are summarised. Five studies give evidence on haemorrhagic stroke, and, again, there is significant heterogeneity, but the overall risk in relation to dairy intake is 0.75; (0.60, 0.94). Only three studies give evidence on sub-arachnoid bleeds and, ignoring significant heterogeneity, the overall risk in those with the highest dairy intake is 0.65 (0.32, 1.31).

Butter and Cheese

Table 5 summarises the data from studies in which butter and cheese consumption were examined as possible predictors of vascular disease. For butter, the literature search identified only five cohort studies with incident vascular disease as the outcome. Only three of these give sufficient data to enable inclusion in a meta-analysis. The results are homogeneous, but the overall relationship between butter consumption and vascular events (0.93; 0.84, 1.02) is not statistically significant. In another early cohort study [16], 832 men were followed for 21 years. There were 267 incident CHD events and the authors commented: 'butter intake did not predict CHD incidence,' but no original data are given.

Several case–control studies of butter and vascular disease have been reported. In one, the previous diets of 106 patients with a myocardial infarct were compared with the diets of 105 controls, and an adjusted odds ratio of an infarct was reported as 2.80 (1.14, 6.85) for 'butter and margarine' [17]. In another, the use of butter by 287 women with an acute myocardial infarct was compared with that of 649 control women and an odds ratio in the upper third, adjusted for age alone, of 2.3 was reported [18]. In a study of diabetic patients, 144 with peripheral arterial disease were compared with 288 matched control patients and an odds ratio of 2.06 (1.15. 3.68) reported for the consumption of butter [15].

Evidence on cheese and vascular disease is also limited. Results have been reported from six cohort studies (Table 5), but sufficient data for a meta-analysis are given in only two. A difficulty arises here because, while random effects meta-analysis seems to be appropriate throughout the work in this paper, in the case of the two studies with cheese, there is a massive difference in the numbers of events and, hence, in the power of the two studies, with conclusions in one being based on only 64 vascular events and on 2,702 disease events in the other. It seems reasonable, therefore, for this one dairy item, to use a fixed effects model, thus, weighting the studies appropriately. This gives an overall estimate of risk from cheese of 0.90 (0.79, 1.03).

Other studies on cheese include a follow-up of 27,529 seventh-day Adventists over 20 years, in which it is stated that "…cheese… consumption (was) unrelated to stroke mortality" but no data are given [12]. In a report based on the 85,764 women in the US Nurses Health Study, the authors comment that the inverse association observed for stroke with dairy calcium was not restricted to milk, but was also observed for hard cheese [19], but, again, no data are given. Finally, in a wide-ranging review of studies of cheese consumption, Tholstrup [20] found "no convincing evidence of harm," and wrote of the 'neutral' effect of cheese on coronary heart disease.

A number of studies based on retrospective case–control comparisons examined cheese consumption and vascular disease. A comparison of the past diets of 106 patients with myocardial infarction and 105 control subjects [17] gave an adjusted odds ratio for cheese and yoghurt of 0.42 (0.18–1.03). In another case–control study of 111 myocardial infarction patients and 107 controls [21], an estimated odds ratio in the highest quartile of cheese intake of 0.34 (0.13, 0.91) was reported. In yet other case–control studies, estimates of 0.77 (0.54–1.11) [22] and 1.0 (no CIs stated) [18] were made for cheese consumption. Finally, Ciccarone et al. [15] reported an odds ratio for cheese consumption in 144 diabetic patients with peripheral vascular disease compared with 288 matched control diabetic patients of 0.61 (0.26–1.45).

Other Dairy Foods

Evidence on other individual dairy food items is very sparse indeed. The large ATBS cohort of Finnish male smokers originally enlisted for a randomised trial of antioxidant prophylaxis [23] yielded adjusted odds ratios for the quintile of subjects with the largest intake of cream (0.81; 0.72–0.92 for cerebral infarction and 0.72; 0.52–1.00 for intra-cerebral haemorrhage), yoghurt (1.08; 0.95–1.24 and 1.08; 0.58–1.28) and ice cream (0.92; 0.81–1.03 and 1.21; 0.89–1.63), none of which are significant. In the report on the US Nurses Health Study, Iso et al. [19] commented that the inverse association observed for stroke with dairy calcium was not restricted to milk, but was also shown for yoghurt and for ice cream.

Evidence from cross-sectional retrospective studies of these items comes from Tavani et al. [22], who reported an odds ratio for yoghurt in a case–control study based on 507 patients with an acute myocardial infarction of 0.55 (0.32–0.95). Biong et al. [21] based a study on 111 myocardial infarction patients and 107 controls and estimated an odds ratio in the highest quartile of ice cream of 0.99 ($P = 0.21$, no CIs stated). Finally, a case–control study of cream consumption in 432 diabetic patients yielded an odds ratio of 2.79 (0.93–8.35) for peripheral vascular disease [15].

Dairy Foods and Diabetes

Elsewhere [24], we have reported a meta-analysis of cross-sectional studies of milk and/or dairy consumption and the metabolic syndrome (RR in the highest consumers of milk and dairy: 0.74; 0.64–0.84). Five studies have now reported on dairy consumption and incident Type 2 diabetes (Table 6). The results of these studies (Table 6) are homogeneous, and the estimated overall relative risk for diabetes is 0.85 (0.75–0.96).

Table 5 Butter, cheese, and vascular disease and death. Details of cohort studies in which the consumption of cheese and of butter was related to a disease outcome or death, with estimates of homogeneity between the studies and the results of a meta-analyses

Study	Number of subjects (length of follow-up)	Number and type of disease event	Factors adjusted for	Adjusted estimate of risk (95% CI)	Predictive factor and subgroups compared
Kahn et al. [7] An Adventists cohort	22,033 subjects (21 years)	5,627 deaths	Age, sex, smoking, history of vascular disease, hypertension, diabetes	1.03 NS (1)	Butter daily cf less than once/week
Gartside et al. [59] NHANES I	5,811 (16 years)	CHD events Number not stated	Age, sex, race, poverty, region, BMI, smoking, education, activity, cholesterol	Increase in CHD events as butter intake rose $P = 0.026$	Use of butter
Shaper et al. [37] UK RHS cohort	7,735 subjects (9.5 years)	608 IHD events	Age, social class, smoking, cholesterol, blood pressure and diabetes	0.87 (0.79–1.06)	Use of butter cf margarine
Elwood et al. reported in Shaper et al. Caerphilly cohort	2,187 men (20–24 years)	605 vascular events	Age, smoking, social class, IHD, BMI, alcohol, total fat intake, systolic BP, diabetes	0.87 (0.69–1.11)	Use of butter cf margarine use
Larsson et al. [23] ATBC cohort	26,556 men (13.6 years)	2,702 cerebral infarcts 383 haemorrhagic 196 sub-arachnoid	Age, smoking, alcohol, BMI, education, total cholesterol, diabetes, IHD, energy intake and activity, intake of various foods and original randomisation	1.00 (0.87–1.14)[a] 1.44 (1.01–2.07) 0.98 (0.59–1.64)	Top quintile of butter cf lowest quintile
Data from Kahn et al. [7] and Gartside et al. [59] omitted because of absence of detailed data					
0.36M person years: 3,310 vascular disease events: heterogeneity between studies $P = 0.333$					
Meta-analysis (random effects) RR (95% CI) for highest intake groups 0.93 (0.84–1.02)					
Kahn et al. [7] An Adventists cohort	22,033 subjects (21 years)	6,075 deaths	Age, sex, smoking, history of vascular disease, hypertension, diabetes	0.96 NS[b]	Cheese on 5–7 days/week cf less than one
Snowdon et al. [33] An Adventists cohort	25,153 subjects (20 years)	758 male IHD deaths 841 female IHD deaths	Age, smoking and other food items, weight, marital status	0.95 ($P > 0.05$)[b] 0.91 ($P > 0.05$)[b]	Cheese daily cf none
Fraser [49] An Adventists cohort	26,473 (duration not stated)	Coronary events Number not stated	Not stated	0.97 NS	Three or more times/week cf less than once
Gartside et al. [59] NHANES I	5,811 (16 years)	CHD events	Age, sex, race, poverty, region, BMI, smoking, education, activity, cholesterol	0.88 ($P < 0.002$)	Once or more/day cf none
Mann et al. [46] A vegetarian cohort	10,802 subjects (13.3 years)	64 IHD deaths	Age, sex, smoking, social class	2.47 (0.97–6.26)	Cheese 5 or more times/week cf less than once
Larsson et al. [23] ATBC cohort	26,556 men (13.6 years)	2,702 cerebr. infarcts 383 haemorrhagic 196 sub-arachnoid	Age, smoking, alcohol, BMI, education, total cholesterol, diabetes, IHD, energy intake and activity, intake of various foods and original randomisation	0.88 (0.77–1.01)[a] 1.01 (0.72–1.41) 1.07 (0.66–1.72)	Top quintile of cheese cf lowest quintile
Data from Kahn et al. [7], Snowdon et al. [33], Fraser [49] and Gartside et al. [59] omitted because ofabsence of detailed data					
0.4M person years: 2,766 vascular disease events: heterogeneity between studies $P = 0.032$					
Meta-analysis (random effects) RR (95% CI) for highest intake groups 1.32 (0.49–3.56)					
Meta-analysis (fixed effects) RR (95% CI) for highest intake groups 0.90 (0.79–1.03)					

cf = compared, or, relative to

[a] Elwood et al. here represents data from the Caerphilly Cohort Study reported in Shaper et al. [15], re-analysed by us and updated

[b] The studies of cheese intake by Snowdon et al. [58], by Kahn et al. [7] and by Fraser [23] may be on the same cohort. None of these, nor Gartside et al. [20], could be included in the meta-analysis, as no estimates of error are given

[c] For Larsson et al. [10], only the results for cerebral infarction were included in the meta-analysis

Table 6 Milk and dairy consumption and diabetes. Details of cohort studies in which the consumption of milk and dairy foods was related to new cases of diabetes, with the results of a meta-analysis

Study	Number of subjects (length of follow-up)	Number of new diabetes	Factors adjusted for	Adjusted estimate of risk (95% CI)	Predictive factor
Choi et al. [60] Health Prof. Cohort	41,254 males (12 years)	1,243	Age, smoking, alcohol, energy, family history, hyperchol., hypertension, energy intake and activity	0.91 (0.85–0.97)	Increase of one serving of dairy foods/day
Liu et al. [61] Women's Health cohort	37,183 females (10 years)	1,603	Age, smoking, alcohol, BMI, hypertension, hyperchol, HRT, family history, energy and activity, dietary intakes randomisation	0.79 (0.67–0.94)[a] 1.04 (0.84–1.30) 0.92 (0.78–1.09)	Top and bottom quintile of all dairy foods Whole milk twice+/week vs <1/month Skim milk twice+/week vs <1/month
van Dam et al. [62] Caerphilly cohort	41,186 females (8 years)	1,964	Age, BMI, smoking, alcohol, education, family history, activity, energy, coffee, sugar, meat, whole grain consumption	0.93 (0.75–1.15)	Highest vs lowest quintile of total dairy intake
Elwood et al. [24] Caerphilly cohort	640 males (22–25 years)	41	Age, smoking, social class, IHD, BMI, alcohol, total fat intake, systolic BP	0.57 (0.20–1.63)	Highest and lowest quartile of milk intake
Villegas et al. [63] Shanghai women cohort	64,191 women (6.9 years)	2,270	Age, BMI, smoking, alcohol, waist–hip ratio, activity, income, education, occupation, hypertension, energy	0.60 (0.41–0.88)	>200 g milk/day vs none

1.7M person years: 7,121 new diabetic patients: heterogeneity between studies $P = 0.122$

Meta-analysis (fixed effects) RR (95% CI) for highest intake groups: 0.85 (0.75–0.96)

[a] The result from Liu et al. [61] for dairy is used in the meta-analysis

Discussion

Much has been written on the associations between the consumption of milk and dairy products and individual vascular risk factors, and, in particular, effects on plasma cholesterol level. An evaluation based upon a single risk factor for a disease can, however, be misleading. At the same time as affecting lipid markers of heart disease, the consumption of milk and dairy produce is associated with an increase in the level of high-density lipoprotein cholesterol [25, 26] and with a reduction in blood pressure [27, 28], and, furthermore, milk and dairy food items are likely to have effects upon many other biological mechanisms and disease processes. Even studies which have examined relationships with a cluster of risk factors for disease, such as the metabolic syndrome [24], cannot possibly give a valid estimate of the overall effect of a complex food such as milk on disease incidence.

Most concern appears to focus on milk consumption and heart disease, and the evidence we present on this is substantial. The studies are homogeneous and the meta-analysis of all of the available evidence suggests that there is a small but worthwhile reduction in risk of coronary heart disease (0.92; 0.80, 0.99) in the subjects who drink the most milk. The evidence which we present on milk and the risk of stroke is also substantial and suggests a reduction in both all stroke (0.79; 0.68–0.91) and in haemorrhagic lesions in those with the highest consumption of milk. A reduction in sub-arachnoid haemorrhage was unexpected, as the aetiology of this condition is totally different to that of thrombo-embolic or haemorrhagic stroke, but benefit from a reduction in blood pressure would be common to all of these events.

All-cause mortality also shows a reduction associated with dairy food consumption (0.87; 0.77–0.98). The evidence of a reduction in diabetes is also substantial, the results of the separate studies are homogeneous ($P = 0.122$) and the risk reduction in the highest consumers of dairy foods is statistically significant (0.85; 0.75–0.96).

The literature on milk and dairy consumption and cancer is extensive. A detailed examination of the evidence is beyond the scope of this review, but it has been reviewed by the World Cancer Research Fund and the American

Institute for Cancer Research [29]. The consumption of milk or dairy foods is associated with a significant reduction in colon cancer (the pooled RR from ten cohort studies is 0.78; 0.69–0.88 and for bladder cancer in four cohorts, the RR is 0.82; 0.67–0.99). There may, however, be an increased risk of prostate cancer, the relative risk estimated from eight cohorts being 1.05; 0.98–1.14. No relationship of importance with milk or dairy consumption was reported for any other cancer.

Apart, perhaps, from milk, no firm conclusions can, however, be drawn on the individual dairy food items. In fact, there is an extreme paucity of studies relating to individual dairy food items. We find this quite remarkable, given the strength of the beliefs about the undesirable effects of butter in particular. The disparity between the results on butter from cohort and from retrospective case–control studies is of concern. Thus, the overview of three cohort studies suggests a possible reduction in vascular disease risk (0.93; 0.84–1.02), while two cross-sectional studies suggested an increase and one an increase in peripheral arterial disease from the consumption of butter. This kind of inconsistency between evidence collected prospectively and evidence dependent upon the memory of patients is, however, not unknown in epidemiological research, and, perhaps, the main message of these data relates to the inadequacy of the evidence on butter and the other dairy items, rather than whether or not there is evidence of harm.

Unfortunately, it is not possible to estimate quantitative relationships with disease incidence for the consumption of a dairy item with any confidence. For example, within the studies reporting milk consumption, the quantity defined as 'high' varied in the different studies. Most studies used quartiles or quintiles of the distribution of intakes, while others defined milk intake in terms of the number of occasions on which milk or dairy foods were consumed. Nevertheless, several studies defined a 'high' intake as the consumption of one pint (568 ml) or more per day [30–32], in others two or more 'glasses' per day [19, 33], while in a study based on weighed dietary intakes [34], the mean daily consumption of milk in the subjects who showed a reduction in vascular disease and diabetes was a pint (568 ml) or more.

A number of systematic reviews of dairy foods have already been published and are consistent with what we present. Gibson et al. [35] identified 12 cohort studies and, from them, drew the conclusion that their review showed "no consistent findings to support the concept that dairy food consumption is associated with a higher risk of coronary heart disease." Mente et al. [36] looked at a number of foods, including milk. Their conclusion, based on five cohort studies, was that milk has "no significant association with coronary heart disease" (0.91; 0.73–1.00). Two earlier overview studies by us [14, 31] examined associations with milk, and, although based on smaller numbers of cohorts, the results of both are in close agreement with those which we now report.

There are, of course, serious limitations in the evidence we present. The cohort strategy is powerful, but it still has uncertainties and possible biases. In particular, estimates of risk for one item can be confounded by the effects of dietary and other factors apart from milk and dairy consumption. Then, there are differences in social class, smoking and other factors between subjects who drink milk and those who drink little or none, and some of the studies comment upon these [31, 37]. While all of the estimates upon which we have based our overall meta-analyses have each been adjusted for a number of confounding factors, as listed in the tables (age, social class, smoking, alcohol, activity etc.), residual confounding by unknown factors is still possible. While it is possible that this could possibly explain the observed reductions in vascular disease, diabetes and all-cause mortality, it seems highly unlikely that a true harmful effect of milk/dairy consumption on the diseases considered could have been missed simply because of some important, but as yet unknown, confounding factor(s). It is also possible, but again extremely unlikely, that publication bias has led to studies which showed harm from dairy consumption have been preferentially withheld from publication.

The issue of fat-reduced, skimmed milk and other fat-reduced dairy products remains. Despite the widespread beliefs that whole milk increases the risk of vascular disease, and is 'fattening', the appropriate question to ask is: do fat-reduced milks provide any advantage further to the benefits conferred by the consumption of whole dairy foods or milk, or does the removal of fat reduce the benefit of the whole items? Low-fat milks were not widely used in the US until about 1989 and about 2000 in the UK, and a large part of the follow-up periods of most of the cohort studies which we have included in the meta-analyses relate, therefore, to times when the milk and dairy items consumed were the full-fat items. Epidemiological studies are of necessity long term and, therefore, the data which we have summarised and the conclusion we have drawn relate overwhelmingly to whole milk and full-fat dairy items.

Given the promotion of fat-reduced milks by many authorities and the large increase in the consumption of fat-reduced milks and dairy items throughout the Western world, this is an area requiring critical study. A number of reports do give evidence on the incidence of disease events in subjects within the same cohort who drank whole milk and others who drank fat-reduced milk, and we have summarised some of these data elsewhere [14]. However, it is most important to accept that persons who

Table 7 Summary of the relative risk for milk and/or dairy food consumption and various diseases, together with the total numbers of deaths in England and Wales in 2008 from those causes

Cause of death[a]	Number of cohort studies (no. in analyses)	Estimate of the risk ratio for milk or dairy food consumption[b] (significance of heterogeneity between studies)	Number of deaths in England and Wales in 2008
All-cause deaths	8 (5)	0.87; 0.77–0.98 ($P = 0.427$)	509,090
Ischaemic heart disease (I20–I25)[a]	17 (13)	0.92; 0.80–0.99 ($P = 0.570$)	76,985
Stroke (I60–I69)[a]			
Thrombo-embolic	11 (11)	0.79; 0.68–0.91 ($P < 0.000$)	46,446
Haemorrhagic	5 (3)	0.75; 0.60–0.94 ($P = 0.014$)	7,497
Sub-arachnoid	3 (3)	0.65; 0.32–1.31 ($P = 0.004$)	8,000[c]
Type 2 diabetes (E10-15)[a]	5 (5)	0.85; 0.75–0.96 ($P = 0.122$)	5,541

[a] Causes of death as defined in the short list used in the classification of causes of death by the Office of National Statistics UK (Office for National Statistics: mortality statistics: cause (series DH2 No.32). London: The Stationery Office, 2008)

[b] Estimate of the risk of each disease in subjects with the highest consumption of milk/dairy, relative to the risk in the subjects with the lowest risk (usually the top and the bottom fifths in subjects ranked by consumption)

[c] This is an estimate of the total incidence and not the number of deaths

choose to drink fat-reduced milks will almost certainly have adopted other 'healthy' behaviours, and these will confound any differences in disease outcome within groups of persons defined by the type of milk consumed. It has to be accepted that these other confounding factors cannot all be known, but they will be responsible for biases which cannot possibly be estimated or allowed for. In the absence of evidence from large long-term randomised trials, the statement of German and Dillard [38] is, therefore, most apposite: "Such hypotheses (about fat-reduced milks) are the basis of sound scientific debate; however they are not the basis of sound public health policy."

On a priori grounds, milk would be expected to be beneficial to health. Calcium has many biological actions, including a reduction in fat absorption through the forming of soaps in the intestine and the binding of cholesterol and bile acids in the gut [39]. Of greater importance is a reduction of blood pressure by dietary calcium, and in a 6-year study of 2,245 older subjects in the Rotterdam Cohort Study, a 20% reduction in incident hypertension was attributed to dairy food consumption [40]. While calcium, magnesium and potassium are all required to prevent hypertension, dairy products are unique in providing a balanced supply of these elements [3, 41]. This may be why milk appears to have a greater effect on blood pressure than dietary calcium supplements [27]. Furthermore, in addition to the minerals provided by milk, certain peptides released on the digestion of milk proteins may have a beneficial effect on blood pressure by inhibiting the angiotension-1-converting enzyme, thus, modulating endothelial function [42].

Renaud et al. [43] described further effects of dietary calcium on thrombo-embolic mechanisms. They fed butter to rabbits and to half, they also gave high levels of calcium. The calcium led to a reduction in platelet aggregation, and a reduction in the severity of atherosclerosis. However, an examination of extensive platelet-related tests in 1,433 older men in the Caerphilly Cohort Study [44] gave no confirmatory evidence in terms of an association between milk consumption and platelet aggregation to adenosine phosphate ($P = 0.41$), or stressed template bleeding times ($P = 0.91$) (unpublished data).

The results of the literature search and meta-analyses presented here are summarised in Table 7 and in Fig. 1. The similarity of the estimates of risk is remarkable and, although conclusions have to be tentative, it seems not unreasonable to conclude that there is no evidence that dairy foods as a total group are associated with harm to health either in terms of death, heart disease, stroke or diabetes, but are probably beneficial in relation to these disease outcomes.

Apart from their effects on plasma lipids and on blood pressure, very little is known about the biological mechanisms likely to be involved in the relationships of milk and dairy foods with human diseases or, indeed, whether milk can be modified to provide increased health advantages. Clearly, more work should be done.

Due to a focus on the small rise in blood cholesterol with milk drinking, the debate on milk has never achieved a reasonable balance in the evaluation of risks and benefits. We believe that the debate about the health risks and benefits of milk and dairy consumption in Western communities should focus on evidence of direct relevance to

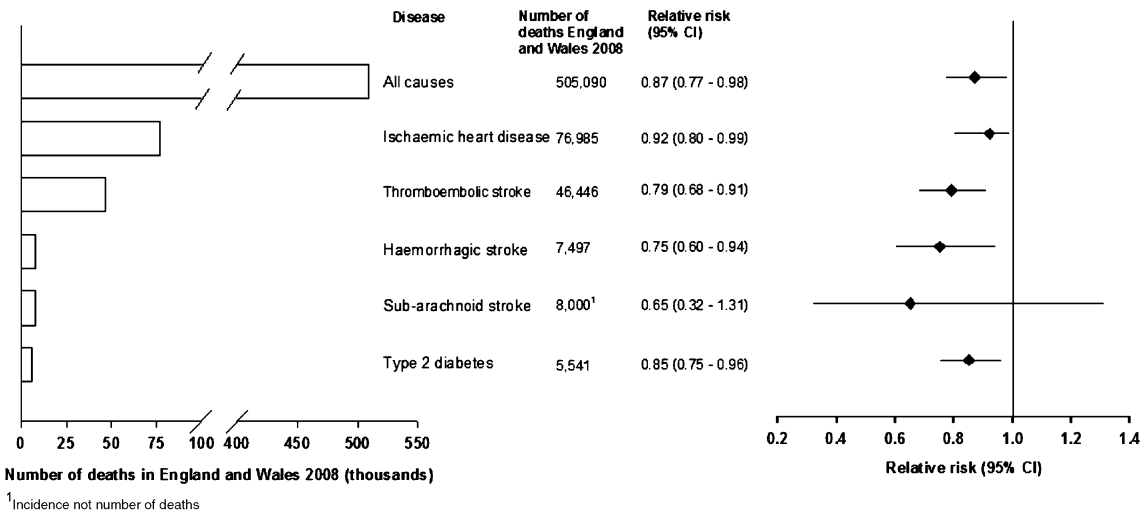

Fig. 1 The numbers of deaths in England and Wales in 2008 from various causes, and the risks for these causes in the subjects with the highest milk/dairy consumption, relative to the risk in the subjects with the lowest milk/dairy consumption

health and survival, such as we have presented in this review, and this would benefit greatly if it were supported by a concerted and targeted research effort to understand the underlying mechanisms.

Acknowledgements Janie Hughes, research assistant, gave considerable help in the literature searches.

Funding The authors have no vested interest and no special funding was received for the work described. The author has the right to grant, and does grant, an exclusive licence on a worldwide basis, to permit this article to be published and to exploit all subsidiary rights as set out in the appropriate license.

References

1. Elwood PC (2001) Milk, coronary disease and mortality. J Epidemiol Community Health 55:375
2. Cochrane AL (1972) Effectiveness and efficiency. Random reflections on health services. Nuffield Provincial Hospitals Trust, London
3. Alvarez-León E-E, Román-Viñas B, Serra-Majem LS (2006) Dairy products and health: a review of the epidemiological evidence. Br J Nutr 96:S94–S99
4. Egger M, Davey Smith G, Altman DG (2001) Systematic reviews in health care: meta-analysis in context. BMJ Books, London
5. Moher D, Liberati A, Tetzlaff J, Altman DG; PRISMA Group (2009) Preferred reporting items for systematic reviews and meta-analyses: the PRISMA statement. BMJ 339:b2535
6. Gao X, LaValley MP, Tucker KL (2005) Prospective studies of dairy product and calcium intakes and prostate cancer risk: a meta-analysis. J Natl Cancer Inst 97:1769–1777
7. Kahn HA, Phillips RL, Snowdon DA, Choi W (1984) Association between reported diet and all-cause mortality. Twenty-one-year follow-up on 27,530 adult Seventh-Day Adventists. Am J Epidemiol 119:775–787
8. van der Vijver LPL, van der Waal MAE, Weterings KGC, Dekker JM, Schouten EG, Kok F (1992) Calcium intake and 28-year cardiovascular and coronary heart disease mortality in Dutch civil servants. Int J Epidemiol 21:36–39
9. Hu FB, Stampfer MJ, Manson JE, Ascherio A, Colditz GA, Speizer FE, Hennekens CH, Willett WC (1999) Dietary saturated fats and their food sources in relation to the risk of coronary heart disease in women. Am J Clin Nutr 70:1001–1008
10. Sun Q, Ma J, Campos H, Hu FB (2007) Plasma and erythrocyte biomarkers of dairy fat intake and risk of ischemic heart disease. Am J Clin Nutr 86:929–937
11. Elwood P, Fehily A, Pickering J, Givens I (2008) Pentadecanoic acid (15:0), milk, and ischemic heart disease. Am J Clin Nutr 87:1540–1541
12. Snowdon DA (1998) Animal product consumption and mortality because of all causes combined, coronary heart disease, stroke, diabetes, and cancer in Seventh-day Adventists. Am J Clin Nutr 48:739–748
13. Jacobsen BK, Stensvold I (1992) Milk—a better drink? Relationships with total serum cholesterol in a cross-sectional survey. The Nordland Health Study. Scand J Soc Med 20:204–208
14. Elwood PC, Givens DI, Beswick AD, Fehily AM, Pickering JE, Gallacher JE (2008) The survival advantage of milk and dairy consumption: an overview of evidence from cohort studies of vascular diseases, diabetes and cancer. J Am Coll Nutr 27:723S–734S
15. Ciccarone E, Di Castelnuovo A, Salcuni M, Siani A, Giacco A, Donati MB, de Gaetano G, Capani F, Iacoviello L (2003) A high-score Mediterranean dietary pattern is associated with a reduced risk of peripheral arterial disease in Italian patients with Type 2 diabetes. J Thromb Haemost 1:1744–1752
16. Gillman MW, Cupples LA, Gagnon D, Millen BE, Ellison RC, Castelli WP (1997) Margarine intake and subsequent coronary heart disease in men. Epidemiology 8:144–149
17. Lockheart MSK, Steffen LM, Rebnord HM, Fimreite RL, Ringstad J, Thelle DS, Pedersen JI, Jacobs DR (2007) Dietary

patterns, food groups and myocardial infarction: a case–control study. Br J Nutr 98:380–387
18. Gramenzi A, Gentile A, Fasoli M, Negri E, Parazzini F, La Vecchia C (1990) Association between certain foods and risk of acute myocardial infarction in women. BMJ 300:771–773
19. Iso H, Stampfer MJ, Manson JE, Rexrode K, Hennekens CH, Colditz GA, Speizer FE, Willett WC (1999) Prospective study of calcium, potassium, and magnesium intake and risk of stroke in women. Stroke 30:1772–1779
20. Tholstrup T (2006) Dairy products and cardiovascular disease. Curr Opin Lipidol 17:1–10
21. Biong AS, Rebnord HM, Fimreite RL, Trygg KU, Ringstad J, Thelle DS, Pedersen JI (2008) Intake of dairy fat and dairy products, and risk of myocardial infarction: a case–control study. Int J Food Sci Nutr 59:155–165
22. Tavani A, Gallus S, Negri E, La Vecchia C (2002) Milk, dairy products, and coronary heart disease. J Epidemiol Com Health 56:471–472
23. Larsson SC, Männistö S, Virtanen MJ, Kontto J, Albanes D, Virtamo J (2009) Dairy foods and risk of stroke. Epidemiology 20:355–360
24. Elwood PC, Pickering JE, Fehily AM (2007) Milk and dairy consumption, diabetes and the metabolic syndrome: the Caerphilly prospective study. J Epidemiol Community Health 61(8):695–698
25. Temme EHM, Mensink RP, Hornstra G (1996) Comparison of the effects of diets enriched in lauric, palmitic, or oleic acids on serum lipids and lipoproteins in healthy women and men. Am J Clin Nutr 63:897–903
26. Mensink RP, Zock PL, Kester AD, Katan MB (2003) Effects of dietary fatty acids and carbohydrates on the ratio of serum total to HDL cholesterol and on serum lipids and apolipoproteins: a meta-analysis of 60 controlled trials. Am J Clin Nutr 77:1146–1155
27. Griffith LE, Guyatt GH, Cook RJ, Bucher HC, Cook DJ (1999) The influence of dietary and nondietary calcium supplementation on blood pressure: an updated metaanalysis of randomized controlled trials. Am J Hypertens 12:84–92
28. Garcia-Palmieri MR, Costas R Jr, Cruz-Vidal M, Sorlie PD, Tillotson J, Havlik RJ (1984) Milk consumption, calcium intake, and decreased hypertension in Puerto Rico. Puerto Rico Heart Health Program study. Hypertension 6:322–328
29. World Cancer Research Fund/American Institute for Cancer Research (2007) Food, nutrition, physical activity, and the prevention of cancer: a global perspective. American Institute of Cancer Research (AICR), Washington, pp 129–132
30. Ness AR, Davey Smith G, Hart C (2001) Milk, coronary heart disease and mortality. J Epidemiol Community Health 55:379–382
31. Elwood PC, Pickering JE, Fehily AM, Hughes J, Ness AR (2004) Milk drinking, ischaemic heart disease and ischaemic stroke I. Evidence from the Caerphilly cohort. Eur J Clin Nutr 58:711–717
32. Umesawa M, Iso H, Ishihara J, Saito I, Kokubo Y, Inoue M, Tsugane S, JPHC Study Group (2008) Dietary calcium intake and risks of stroke, its subtypes, and coronary heart disease in Japanese: the JPHC Study Cohort I. Stroke 39:2449–2456
33. Snowdon DA, Phillips RL, Fraser GE (1984) Meat consumption and fatal ischemic heart disease. Prev Med 13:490–500
34. Elwood PC, Strain JJ, Robson PJ, Fehily AM, Hughes J, Pickering J, Ness A (2005) Milk consumption, stroke, and heart attack risk: evidence from the Caerphilly cohort of older men. J Epidemiol Com Health 59:502–505
35. Gibson RA, Makrides M, Smithers LG, Voevodin M, Sinclair AJ (2009) The effect of dairy foods on CHD: a systematic review of prospective cohort studies. Br J Nutr 102:1267–1275
36. Mente A, de Koning L, Shannon HS, Anand SS (2009) A systematic review of the evidence supporting a causal link between dietary factors and coronary heart disease. Arch Intern Med 169:659–669
37. Shaper AG, Wannamethee G, Walker M (1991) Milk, butter, and heart disease. Br Med J 302:785–786
38. German JB, Dillard CJ (2004) Saturated fats: what dietary intake? Am J Clin Nutr 80:550–559
39. Ditscheid B, Keller S, Jahreis G (2005) Cholesterol metabolism is affected by calcium phosphate supplementation in humans. J Nutr 135:1678–1682
40. Engberink MF, Hendriksen MA, Schouten EG, van Rooij FJA, Hofman A, Witteman JC, Geleijnse JM (2009) Inverse association between dairy intake and hypertension: the Rotterdam Study. Am J Clin Nutr 89:1877–1883
41. Massey LK (2001) Dairy food consumption, blood pressure and stroke. J Nutr 131:1875–1878
42. Clare DA, Swaisgood HE (2000) Bioactive milk peptides: a prospectus. J Dairy Sci 83:1187–1195
43. Renaud S, Ciavatti M, Thevenon C, Ripoll JP (1983) Protective effects of dietary calcium and magnesium on platelet function and atherosclerosis in rabbits fed saturated fat. Atherosclerosis 47:187–198
44. Elwood PC, Beswick A, Pickering J, McCarron P, O'Brien JR, Renaud SR, Flower RJ (2001) Platelet tests in the prediction of myocardial infarction and ischaemic stroke: evidence from the Caerphilly Prospective study. Br J Haematol 113:514–520
45. Kelemen LE, Kushi LH, Jacobs DR Jr, Cerhan JR (2005) Associations of dietary protein with disease and mortality in a prospective study of postmenopausal women. Am J Epidemiol 161:239–249
46. Mann JI, Appleby PN, Key TJ, Thorogood M (1997) Dietary determinants of ischaemic heart disease in health conscious individuals. Heart 78:450–455
47. Trichopoulou A, Psaltopoulou T, Orfanos P, Trichopoulos D (2006) Diet and physical activity in relation to overall mortality amongst adult diabetics in a general population cohort. J Intern Med 259:583–591
48. van der Pols JC, Gunnell D, Williams GM, Holly JM, Bain C, Martin RM (2009) Childhood dairy and calcium intake and cardiovascular mortality in adulthood: 65-year follow-up of the Boyd Orr cohort. Heart 19:1600–1606
49. Fraser GE (1994) Diet and coronary heart disease: beyond dietary fats and low-density-lipoprotein cholesterol. Am J Clin Nutr 59:1117S–1123S
50. Nettleton JA, Steffen LM, Loehr LR, Rosamond WD, Folsom AR (2008) Incident heart failure is associated with lower whole-grain intake and greater high-fat dairy and egg intake in the Atherosclerosis Risk in Communities (ARIC) study. J Am Diet Assoc 108:1881–1887
51. Bostick RM, Kushi LH, Wu Y, Meyer KA, Sellers TA, Folsom AR (1999) Relation of calcium, vitamin D, and dairy food intake to ischemic heart disease mortality among postmenopausal women. Am J Epidemiol 149:151–161
52. Al-Delaimy WK, Rimm E, Willett WC, Stampfer MJ, Hu FB (2003) A prospective study of calcium intake from diet and supplements and risk of ischemic heart disease among men. Am J Clin Nutr 77:814–818
53. Larmarche B (2004) Dairy products—the metabolic syndrome and cardiovascular disease: lessons from Canada. Paper given at the World Dairy Summit, Melbourne, Australia, November 2004
54. Umesawa M, Iso H, Date C, Yamamoto A, Toyoshima H, Watanabe Y, Kikuchi S, Koizumi A, Kondo T, Inaba Y, Tanabe N, Tamakoshi A (2006) Dietary intake of calcium in relation to mortality from cardiovascular disease: the JACC study. Stroke 37:20–26
55. Kinjo Y, Beral V, Akiba S, Key T, Mizuno S, Appleby P, Yamaguchi N, Watanabe S, Doll R (1999) Possible protective

effect of milk, meat and fish for cerebrovascular disease mortality in Japan. J Epidemiol 9:268–274
56. Sauvaget C, Nagano J, Allen N, Grant EJ, Beral V (2003) Intake of animal products and stroke mortality in the Hiroshima/Nagasaki Life Span Study. Int J Epidemiol 32:536–543
57. He K, Merchant A, Rimm EB, Rosner BA, Stampfer MJ, Willett WC, Ascherio A (2003) Dietary fat intake and risk of stroke in male US healthcare professionals: 14 year prospective cohort study. BMJ 327:777–782
58. Abbott RD, Curb JD, Rodriguez BL, Sharp DS, Burchfiel CM, Yano K (1996) Effect of dietary calcium and milk consumption on risk of thromboembolic stroke in older middle-aged men. The Honolulu Heart Program. Stroke 27:813–818
59. Gartside PS, Wang P, Glueck CJ (1998) Prospective assessment of coronary heart disease risk factors: the NHANES I epidemiologic follow-up study (NHEFS) 16-year follow-up. J Am Coll Nutr 17:263–269
60. Choi HK, Willett WC, Stampfer MJ, Rimm E, Hu FB (2005) Dairy consumption and risk of type 2 diabetes mellitus in men: a prospective study. Arch Intern Med 165:997–1003
61. Liu S, Song Y, Ford ES, Manson JE, Buring JE, Ridker PM (2005) Dietary calcium, vitamin D, and the prevalence of metabolic syndrome in middle-aged and older U.S. women. Diabetes Care 28:2926–2932
62. van Dam RM, Hu FB, Rosenberg L, Krishnan S, Palmer JR (2006) Dietary calcium and magnesium, major food sources, and risk of type 2 diabetes in U.S. black women. Diabetes Care 29:2238–2243
63. Villegas R, Gao Y-T, Dai Q, Yang G, Cai H, Li H, Zheng W, Shu XO (2009) Dietary calcium and magnesium intakes and the risk of type 2 diabetes: the Shanghai Women's Health Study. Am J Clin Nutr 89:1059–1067

Lipids (2010) 45:941–946
DOI 10.1007/s11745-010-3444-x

ORIGINAL ARTICLE

The Complex and Important Cellular and Metabolic Functions of Saturated Fatty Acids

Philippe Legrand · Vincent Rioux

Received: 16 February 2010 / Accepted: 21 June 2010 / Published online: 13 July 2010

Abstract This review summarizes recent findings on the metabolism and biological functions of saturated fatty acids (SFA). Some of these findings show that SFA may have important and specific roles in the cells. Elucidated biochemical mechanisms like protein acylation (N-myristoylation, S-palmitoylation) and regulation of gene transcription are presented. In terms of physiology, SFA are involved for instance in lipogenesis, fat deposition, polyunsaturated fatty acids bioavailability and apoptosis. The variety of their functions demonstrates that SFA should no longer be considered as a single group.

Keywords Dietary saturated fatty acids · Myristic acid · Metabolism · N-myristoylation

Abbreviations

FA	Fatty acids
NMT	Myristoyl–CoA: protein N-myristoyltransferase
PL	Phospholipids
PUFA	Polyunsaturated fatty acids
SCD	Stearoyl–CoA desaturase
SFA	Saturated fatty acids
TAG	Triglycerides

Introduction

Observational studies have shown that high intake of saturated fatty acids (SFA) is positively associated with increased levels of blood cholesterol and high coronary heart disease mortality rates [1, 2]. However, more recent studies have shown inverse association [3, 4], and the meta-analysis by Siri-Tarino et al. [5] reopened the debate when writing that "there is no significant evidence for concluding that dietary saturated fat is associated with an increased risk of CHD or CVD". Without entering this interesting epidemiological debate on the deleterious effects of some of saturated fatty acids, it seems that they can be no longer considered as a single group in terms of structure, metabolism [6, 7] and cellular function. In this context, this review will focus only on recent findings suggesting that individual SFA possess specific properties associated with important biological functions.

P. Legrand (✉) · V. Rioux
Laboratoire de Biochimie-Nutrition Humaine, Agrocampus Rennes, INRA USC 2012, 65 rue de Saint-Brieuc, CS 84215, 35042 Rennes Cedex, France
e-mail: philippe.legrand@agrocampus-ouest.fr

New Aspects on the Metabolism of Saturated Fatty Acids

Cellular Origin of Saturated Fatty Acids

SFA usually account for 30–40% of total FA in animal tissues, distributed in palmitic acid (15–25%), stearic acid (10–20%), myristic acid (0.5–1%) and lauric acid (less than 0.5%). Palmitic and stearic acids are universally found in natural fats. Lauric acid is specifically abundant in copra (39–54%) and palmist oils (44–51%). Myristic acid and short-chain fatty acids (including butyric acid) represent each about 10% of FA in milk fat. Apart from the dietary sources, it is well known that the body is capable of synthesizing SFA. Because of their multiple potential origins, it has been difficult to quantify the real importance of dietary SFA when compared with endogenous SFA, especially for palmitic acid. Adipose tissue concentrations of C15:0, C17:0 but also C14:0 have been used as quantitative

markers of dairy consumption [8]. With regard to myristic acid, the amount of its endogenous biosynthesis [9] is indeed far smaller than the amounts consumed from dietary sources (4 g/day in a Swedish population) [10].

Desaturation of Saturated Fatty Acids

Recent findings on SFA concern their respective capacities to be desaturated. Every SFA from C12:0 to C18:0 is converted to its respective monounsaturated product through the action of Δ9-desaturase (Stearoyl–CoA desaturase, SCD) but with varying efficiency. In the rat [11], a clear increase in hepatic Δ9-desaturase activity is related to the carbon chain length, from C12:0 to C18:0. Evidence was also recently presented that palmitic acid, already known as a substrate of Δ9-desaturase, can also be desaturated by the mammalian Δ6-desaturase (Fatty acid desaturase 2: FADS2) [12]. Palmitic acid Δ6-desaturation produces sapienic acid (C16:1n-10) in the preputial gland of SCD1−/− mice [13] and in human sebaceous glands in which the expression of SCD is low [14]. The importance of this human physiological specificity remains to be determined.

Specific Biochemical Functions of Individual SFA

Regulation of Protein Activation by N-terminal Myristoylation

Myristic and palmitic acids are directly involved in the two classes of protein fatty acid acylation, N-terminal myristoylation and side-chain palmitoylation [15]. Protein N-myristoylation (Fig. 1) refers to the highly specific covalent attachment of myristic acid, by an amide linkage, to the NH_2-terminal glycine residue of increasing number of eukaryotic and viral proteins [16]. Myristoyl–CoA: protein N-myristoyltransferase (NMT, EC 2.3.1.97), the enzyme catalyzing this stable acylation, has been identified in many organisms. Genetic advances have revealed that mammals possess two distinct NMT genes, named type 1 and 2 [17–19]. The contribution of each gene transcript to NMT expression and activity in vivo, and the specific role of each NMT isoform in cellular replication, proliferation, and other cellular processes, is still under investigation [20–22]. They both seem to have a similar high substrate selectivity for myristic acid [17, 19]. The myristoyl moiety has been shown to mediate protein subcellular localization, protein–protein interaction or protein–membrane interactions (Fig. 1) required for the biological activities of the myristoylated proteins [16]. In the myristoylation pathway, myristic acid therefore exhibits a specific and important role for protein activation.

The proteins that are substrates of NMT include key components in intracellular signaling pathways, oncogenes, structural viral proteins, and common constitutive eukaryotic proteins. Computational prediction recently suggested that about 0.5% of all proteins in the human genome could be myristoylated [23]. New protein substrates identified recently in mammals are the tumor suppressor Fus1 [24], TRIF [25], the sphingolipid Δ4-desaturases type 1 and 2 [26], and truncated protein forms that become substrates after post-translational cleavage by caspases that reveals an internal myristoylation motif: BID [27], actin [28], gelsolin [29], and p21-activated protein kinase 2 [30].

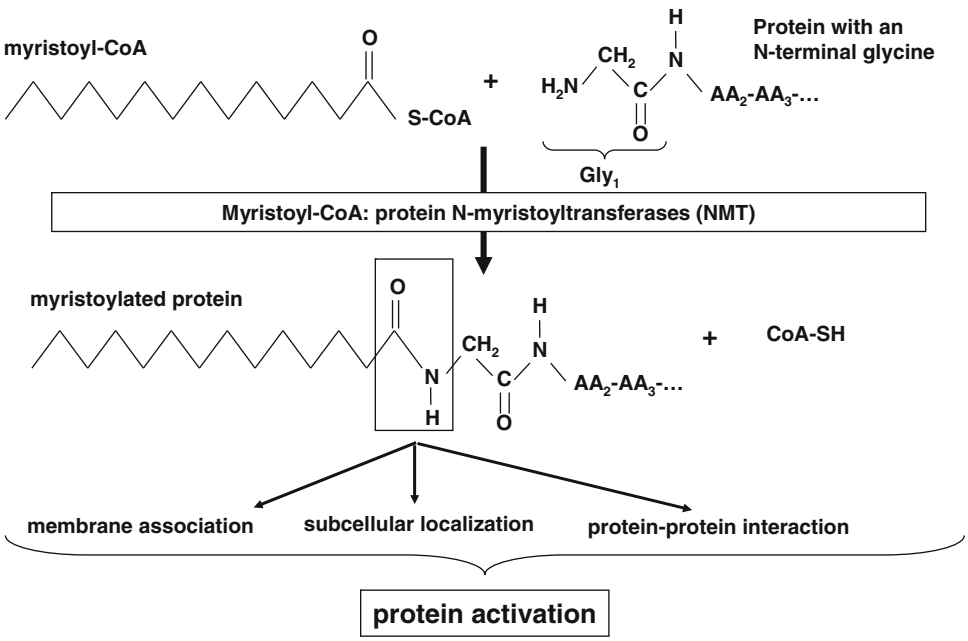

Fig. 1 N-terminal myristoylation of proteins with myristic acid by myristoyl–CoA: protein N-myristoyltransferases (*NMT*) and biological consequences for the myristoylated proteins

Can Myristic Acid be the Rate-Limiting Molecule in the Myristoylation Pathway?

Since endogenous biosynthesis of C14:0 [9] is very low as compared with dietary sources [10], one can ask if the amount of free myristic acid could be insufficient to provide myristoyl–CoA: protein N-NMT with enough co-substrate. In yeast, studies analyzing the activity of NMT have suggested that the enzyme was able to use both exogenous and endogenous myristic acid as the substrate [31–33]. During the process of the maturation of one protein, the pool of endogenous free myristoyl–CoA would probably be sufficient [34]. However, when considering the pool of myristoylable proteins or the specific process for the maturation of viral proteins like Gag or Nef during the course of a viral, retroviral or lentiviral infection, the amount of myristoyl–CoA co-substrate needed is considerable [35]. The requirement for myristic acid suggests that in certain cases, it could be the rate-limiting molecule in this mechanism or that competition could occur. In addition, the mechanism by which myristic acid initially esterified in the TAG or PL is used for myristoylation is unknown, too. The available evidence indicates that the intracellular concentration of free myristic acid in endothelial cells is crucial for the activation of thrombospondin-1 and could be modulated by its uptake from the medium through CD36 [36].

Regulation of Protein–Membrane Interactions by Palmitoylation

Protein palmitoylation refers to the post-translational formation of a thioester linkage between the side-chain of cysteine and palmitic acid, mainly [37], or other saturated fatty acids, like myristic and lauric acids [38]. A long time ago, the ester linkage between saturated fatty acids and serine or threonine residues was also reported [39], but since then, this type of linkage has not been described again.

Palmitoylation is involved in regulatory mechanisms because the association of the protein with the palmitoyl moiety is reversible and facilitates protein–membrane interactions and subcellular trafficking of proteins. Several signal transductions depend therefore on palmitic acid, including proteins that have been shown to undergo successive myristoylation and palmitoylation, like the α subunit of many heterotrimeric G proteins [40]. Mammalian protein palmitoyltransferases (also named Protein S-AcylTransferases PAT) are still under investigation [37]. The recent biochemical evidence of the PAT activity of a family of proteins that share a DHHC motif in yeast [41–43] has opened a new field of investigation.

Regulation of Gene Transcription by Saturated Fatty Acids

While dietary PUFA are known to regulate gene expression through their influence on transcription factors (PPAR, SREBP), the effect of SFA on gene transcription has been less explored. Lin et al. [44] have shown that SFA (C10:0–C18:0) strongly elevate the PGC-1β mRNA level, that co-activates the action of SREBP family of transcription factors, and consequently increase the transcription of lipogenic target genes (*FAS*, *SCD-1*). Co-activation of the nuclear receptor LXR/RXR also promotes VLDL secretion. SFA (but also monounsaturated FA) are known to bind hepatocyte nuclear factor 4 (HNF4). In liver cells, palmitate and oleate both enhanced the transcription of glucose-6-phosphatase gene. Palmitate also induced the recruitment of several transcription factors like NF-κB, HNF4, CEBPα, and PPARα [45]. SFA, when linked to the lipid A moiety of lipopolysaccharides, or free, also indirectly induce NF-κB nuclear translocation, activation and expression of COX-2, and other pro-inflammatory cytokines, through the recently described toll-like receptor 4-derived signaling pathways [46, 47]. Finally, because it is an inhibitor of the histone deacetylase activity, butyric acid regulates the expression of several genes, like *IL5*, by altering the histone acetylating status of their promoter regions, with consequences for the structure of chromatin [48, 49].

New Demonstrated or Putative Physiological Roles of SFA

Stearic Acid is Neutral for Cholesterol but Could be Pro-Lipogenic

As for the other long-chain saturated fatty acids, the health impact of stearic acid has been studied, showing no deleterious effect on cardiovascular disease risk [50, 51]. The high rate of C18:0 conversion to C18:1n-9 by Δ9-desaturation was suggested to explain this neutral effect on cholesterol metabolism, compared to the other SFA [52]. On the other hand, the desaturation of dietary stearate to endogenous oleate has been described as a stimulating factor for VLDL–TAG secretion in hepatocytes [53], and an essential step mediating the induction of lipogenesis [54] and the promotion of obesity [55], showing the very important role of SCD. The evidence concerning the putative effect of stearic acid on thrombotic tendency appears inconsistent [56, 57].

Myristic Acid Could Regulate PUFA Bioavailability

It has recently been suggested that myristic acid may be an activator of the conversion of α-linolenic acid to

docosahexaenoic acid (DHA). In cultured rat hepatocytes, myristic acid had a specific and dose-dependent effect on Δ6-desaturase activity [58]. In vivo, when myristic acid was supplied for 2 months in the diet of rats (from 0.2 to 1.2% of dietary energy), with similar level of dietary α-linolenic acid (1.6% of FA, 0.3% of energy), a dose–response accumulation of eicosapentaenoic acid (EPA) was shown in the liver and plasma [59].

In addition, in humans, compared with a diet containing 0.6% of myristic acid mainly in the *sn*-2 position in the TAG, a diet containing 1.2% of myristic acid during a 5-week consumption period significantly enhanced EPA and DHA levels in the plasma PL and DHA level in the plasma cholesteryl esters [60]. When the intake of myristic acid increased from 1.2 to 1.8% energy in the same population, EPA, DPA and DHA decreased significantly in plasma PL and EPA also decreased in cholesteryl esters [61]. This result suggest that, in humans, the effect of myristic acid on circulating (n-3) PUFA follows a U-shaped curve with a favorable turning point at around 1.2% of total daily energy.

So far as potential mechanism(s) of action are concerned, the increase in the activity of Δ6-desaturase by myristic acid was first postulated to be mediated by N-myristoylation (see below) because this enzyme exhibits an N-terminal glycine residue. However, we recently demonstrated that Δ6-desaturase is not myristoylated in vivo [26]. The hypothesis has been proposed that myristoylation of another protein of the whole complex of Δ6-desaturation, NADH cytochrome *b*5 reductase [62], could account for this increased activity.

Lauric Acid Could be a Precursor for ω3 Fatty Acid Biosynthesis

The low level of C12:0 conversion to C12:1n-3 in the liver of rats has led to the hypothesis that this monounsaturated fatty acid of the (n-3) series might be, under extreme physiological circumstances [for example animals deprived of (n-3) PUFA in the diet during a long period], an unusual precursor for the biosynthesis of α-linolenic acid, by successive Δ6-desaturation, elongation, Δ5-desaturation and two final elongations [11].

SFA May Play Multiple Roles in Early Events of Apoptosis

Specific histone deacetylase inhibitors, like butyric acid, selectively induce cellular differentiation, growth arrest and apoptosis in a variety of cancer cells [63]. Although contradictory effects have been reported [64], it seems that delivery of an adequate amount of butyrate to the appropriate site could protect against early tumorigenic events [65].

Several SFA may induce apoptosis via different ways. First, as already suggested above, butyrate and short-chain SFA may also have an effect on apoptosis [66]. Second, the pro-apoptotic effect of non-esterified palmitate and stearate was shown to require acyl–CoA formation and NF-κB activation [67]. Third, SFA may also influence apoptosis via the ceramide pathway by inducing ceramide de novo synthesis at several steps [68–70]. The first step catalyzed by the serine palmitoyltransferase involves serine condensation with palmitoyl–CoA [71]. The last step is catalyzed by dihydroceramide Δ4-desaturase (DES). We recently showed that both DES1 and DES2 isoforms are myristoylated and that this N-terminal modification significantly increased the activity of recombinant DES1 in COS-7 cells [26]. Compared with a recombinant unmyristoylable mutant form of DES1 (N-terminal glycine replaced by an alanine), the desaturase activity of the myristoylable wild-type DES1 was two times higher, in the presence of myristic acid incubated with the cells [26]. The description of this regulatory mechanism highlighted a new potential relationship between myristic acid, the saturated fatty acid capable of binding and activating the enzyme involved in the final de novo ceramide biosynthesis step, and lipoapoptosis induced through the ceramide pathway. Therefore, we subsequently hypothesized and showed that the myristoylation of recombinant DES 1 can target part of the enzyme to the mitochondria, leading to an increase in ceramide levels (specifically in the mitochondria) which in turn leads to apoptosis in the COS-7 cell model [72].

Medium-Chain Fatty Acids and Fat Deposition

A point of interest is the specific role played by medium-chain SFA. It has been reported that overfeeding with a medium-chain TAG diet in rats results in a diminished deposition of fat, when compared with rats overfed with isocaloric long-chain TAG [73]. This suggests an obligatory oxidation of medium-chain SFA in the liver, after transport via the portal vein, leaving no medium-chain TAG for accumulation in adipose tissue [73]. Another hypothesis for medium-chain TAG effect is their inhibitory effect on apoB synthesis, reducing the VLDL secretion by hepatocytes. This has been observed with octanoate in chicken hepatocytes [74].

Conclusion

We have reported here new knowledge on cellular and physiological functions of the different SFA. For this reason, SFA should no longer be considered as a single group in terms of structure, metabolism, and function.

References

1. Keys A (1970) Coronary heart disease in seven countries. Circulation 41:1–211
2. Kromhout D, Bloemberg B, Feskens E, Menotti A, Nissinen A (2000) Saturated fat, vitamin C and smoking predict long-term population all-cause mortality rates in the seven countries study. Int J Epidemiol 29:260–265
3. Gillman MW, Cupples LA, Millen BE, Ellison RC, Wolf PA (1997) Inverse association of dietary fat with development of ischemic stroke in men. JAMA 278:2145–2150
4. Mozaffarian D, Rimm EB, Herrigton DM (2004) Dietary fats, carbohydrate, and the progression of coronary atherosclerosis in post menopausal women. Am J Clin Nutr 80:1175–1184
5. Siri-Tarino PW, Sun Q, Hu FB, Krauss RM (2010) Meta-analysis of prospective cohort studies evaluating the association of saturated fat with cardiovascular disease. Am J Clin Nutr 91:535–546
6. Hughes TA, Heimberg M, Wang X, Wilcox H, Hughes SM, Tolley EA, Desiderio DM, Dalton JT (1996) Comparative lipoprotein metabolism of myristate, palmitate, and stearate in normolipidemic men. Metabolism 45:1108–1118
7. Rioux V, Lemarchal P, Legrand P (2000) Myristic acid, unlike palmitic acid, is rapidly metabolized in cultured rat hepatocytes. J Nutr Biochem 11:198–207
8. Warensjö E, Jansson JH, Berglund L, Boman K, Ahren B, Weinehall L, Lindahl B, Hallmans G, Vessby B (2004) Estimated intake of milk fat is negatively associated with cardiovascular risk factors and does not increase the risk of a first acute myocardial infarction. A prospective case-control study. Br J Nutr 91:635–642
9. Rioux V, Catheline D, Legrand P (2007) In rat hepatocytes, myristic acid occurs through lipogenesis, palmitic acid shortening and lauric acid elongation. Animal 1:820–826
10. Wolk A, Furuheim M, Vessby B (2001) Fatty acid composition of adipose tissue and serum lipids are valid biological markers of dairy fat intake in men. J Nutr 131:828–833
11. Legrand P, Catheline D, Rioux V, Durand G (2002) Lauric acid is desaturated to C12:1n-3 by rat liver homogenate and hepatocytes. Lipids 37:569–572
12. Guillou H, Rioux V, Catheline D, Thibault JN, Bouriel M, Jan S, D'Andrea S, Legrand P (2003) Conversion of hexadecanoic acid to hexadecenoic acid by rat Δ6-desaturase. J Lipid Res 44:450–454
13. Miyazaki M, Gomez FE, Ntambi JM (2002) Lack of stearoyl–CoA desaturase-1 function induces a palmitoyl-CoA delta-6 desaturase and represses the stearyl–CoA desaturase-3 gene in the preputial glands of the mouse. J Lipid Res 43:2146–2154
14. Ge L, Gordon JS, Hsuan C, Stenn K, Prouty SM (2003) Identification of the delta-6 desaturase of human sebaceous glands: expression and enzyme activity. J Invest Dermatol 120:707–714
15. Towler DA, Gordon JI, Adams SP, Glaser L (1988) The biology and enzymology of eukaryotic protein acylation. Annu Rev Biochem 57:69–99
16. Johnson DR, Bhatnagar RS, Knoll LJ, Gordon JI (1994) Genetic and biochemical studies of protein N-myristoylation. Annu Rev Biochem 63:869–914
17. Giang DK, Cravatt BF (1998) A second mammalian N-myristoyltransferase. J Biol Chem 273:6595–6598
18. Rundle DR, Rajala RVS, Anderson RE (2002) Characterization of type I and type II myristoyl–CoA: protein N-myristoyltransferase with the acyl–CoAs found on heterogeneously acylated retinal proteins. Exp Eye Res 75:87–97
19. Rioux V, Beauchamp E, Pedrono F, Daval S, Molle D, Catheline D, Legrand P (2006) Identification and characterization of recombinant and native rat myristoyl–CoA: protein N-myristoyltransferases. Mol Cell Biochem 286:161–170
20. Yang SH, Shrivastav A, Kosinski C, Sharma RK, Chen MH, Berthiaume LG, Peters LL, Chuang PT, Young SG, Bergo MO (2005) N-myristoyltransferase 1 is essential in early mouse development. J Biol Chem 280:18990–18995
21. Ducker CE, Upson JJ, French KJ, Smith CD (2005) Two N-myristoyltransferase isozymes play unique roles in protein myristoylation, proliferation, and apoptosis. Mol Cancer Res 3:463–476
22. Selvakumar P, Smith-Windsor E, Bonham K, Sharma RK (2006) N-myristoyltransferase 2 expression in human colon cancer: cross-talk between the calpain and caspase system. FEBS Lett 580:2021–2026
23. Maurer-Stroh S, Gouda M, Novatchkova M, Schleiffer A, Schneider G, Sirota FL, Wildpaner M, Hayashi N, Eisenhaber F (2004) MYRbase: analysis of genome-wide glycine myristoylation enlarges the functional spectrum of eukaryotic myristoylated proteins. Genome Biol 5:1–16
24. Uno F, Sasaki J, Nishizaki M, Carboni G, Xu K, Atkinson EN, Kondo M, Minna JD, Roth JA, Ji L (2004) Myristoylation of Fus1 protein is required for tumor suppression in human lung cancer cells. Cancer Res 64:2969–2976
25. Rowe DC, McGettrick AF, Latz E, Monks BG, Gay NJ, Yamamoto M, Akira S, O'Neill LA, Fitzgerald KA, Golenbock DT (2006) The myristoylation of TRIF-related molecule is essential for toll-like receptor 4 signal transduction. Proc Natl Acad Sci USA 103:6399–6404
26. Beauchamp E, Goenaga D, Le Bloc'h J, Catheline D, Legrand P, Rioux V (2007) Myristic acid increases the activity of dihydroceramide Δ4-desaturase 1 through its N-terminal myristoylation. Biochimie 89:1553–1561
27. Zha J, Weiler S, Oh KJ, Wei MC, Korsmeyer SJ (2000) Posttranslational N-myristoylation of BID as a molecular switch for targeting mitochondria and apoptosis. Science 290:1761–1765
28. Utsumi T, Sakurai N, Nakano K, Ishisaka R (2003) C-terminal 15 kDa fragment of cytoskeletal actin is posttranslationally N-myristoylated upon caspase-mediated cleavage and targeted to mitochondria. FEBS Lett 539:37–44
29. Sakurai N, Utsumi T (2006) Posttranslational N-myristoylation is required for the anti-apoptotic activity of human tGelsolin, the C-terminal caspase cleavage product of human gelsolin. J Biol Chem 281:14288–14295
30. Vilas GL, Corvi MM, Plummer GJ, Seime AM, Lambkin GR, Berthiaume LG (2006) Posttranslational myristoylation of caspase-activated p21-activated protein kinase 2 (PAK2) potentiates late apoptotic events. Proc Natl Acad Sci USA 103:6542–6547
31. Duronio RJ, Rudnick DA, Johnson RL, Johnson DR, Gordon JI (1991) Myristic acid auxotrophy caused by mutation of *S. cerevisiae* myristoyl–CoA: protein N-myristoyltransferase. J Cell Biol 113:1313–1330
32. Duronio RJ, Reed SI, Gordon JI (1992) Mutations of human myristoyl–CoA: protein N-myristoyltransferase cause temperature-sensitive myristic auxotrophy in *Saccharomyces cerevisiae*. Proc Natl Acad Sci USA 89:4129–4133
33. Johnson DR, Knoll LJ, Levin DE, Gordon JI (1994) *Saccharomyces cerevisiae* contains four fatty acid activation (FAA) genes: an assessment of their role in regulating protein N-myristoylation and cellular lipid metabolism. J Cell Biol 127:751–762
34. Boutin JA (1997) Myristoylation. Cell Signal 9:15–35
35. Hill BT, Skowronski J (2005) Human N-myristoyltransferases form stable complexes with lentiviral nef and other viral and cellular substrate proteins. J Virol 79:1133–1141
36. Isenberg JS, Jia Y, Fukuyama J, Switzer CH, Wink DA, Roberts DD (2007) Thrombospondin-1 inhibits nitric oxide signaling via CD36 by inhibiting myristic acid uptake. J Biol Chem 282:15404–15415

37. Mitchell DA, Vasudevan A, Linder ME, Deschenes RJ (2006) Protein palmitoylation by a family of DHHC protein *S*-acyltransferases. J Lipid Res 47:1118–1127
38. Rioux V, Galat A, Jan G, Vinci F, d'Andrea S, Legrand P (2002) Exogenous myristic acid acylates proteins in cultured rat hepatocytes. J Nutr Biochem 13:66–74
39. Grand RJA (1989) Acylation of viral and eukaryotic proteins. Biochem J 258:625–638
40. Chen CA, Manning DR (2001) Regulation of G proteins by covalent modification. Oncogene 20:1643–1652
41. Lobo S, Greentree WK, Linder ME, Deschenes RJ (2002) Identification of a Ras palmitoyltransferase in *Saccharomyces cerevisiae*. J Biol Chem 277:41268–41273
42. Roth AF, Feng Y, Chen L, Davis NG (2002) The yeast DHHC cysteine-rich domain protein Akr1p is a palmitoyl transferase. J Cell Biol 159:23–28
43. Smotrys JE, Schoenfish MJ, Stutz MA, Linder ME (2005) The vacuolar DHHC-CRD protein Pfa3p is a protein acyltransferase for Vac8p. J Cell Biol 170:1091–1099
44. Lin J, Yang R, Tarr PT, Wu PH, Handschin C, Li S, Yang W, Pei L, Uldry M, Tontonoz P, Newgard CB, Spiegelman BM (2005) Hyperlipidemic effects of dietary saturated fats mediated through PGC-1beta coactivation of SREBP. Cell 120:261–273
45. Xu C, Chakravarty K, Kong X, Tuy TT, Arinze IJ, Bone F, Massillon D (2007) Several transcription factors are recruited to the glucose-6-phosphatase gene promoter in response to palmitate in rat hepatocytes and H4IIE cells. J Nutr 137:554–559
46. Lee JY, Sohn KH, Rhee SH, Hwang D (2001) Saturated fatty acids, but not unsaturated fatty acids, induce the expression of cyclooxygenase-2 mediated through Toll-like receptor 4. J Biol Chem 276:16683–16689
47. Lee JY, Ye J, Gao Z, Lee WH, Zhao L, Sizemore L, Hwang DH (2003) Reciprocal modulation of toll-like receptor-4 signaling pathways involving My88 and phosphatidyinositol 3-kinase/AKT by saturated and polyunsaturated fatty acids. J Biol Chem 278:37041–37051
48. Smith JG, Yokoyama WH, German JB (1998) Dietary butyric acid: implications for gene expression. Crit Rev Food Sci Nutr 38:259–297
49. Han S, Lu J, Zhang Y, Cheng C, Li L, Han L, Huang B (2007) HDAC inhibitors TSA and sodium butyrate enhanced the human IL-5 expression by altering histone acetylation status at its promoter region. Immunol Lett 108:143–150
50. Yu S, Derr J, Etherton TD, Kris-Etherton PM (1995) Plasma cholesterol-predictive equations demonstrate that stearic is neutral and monounsaturated fatty acids are hypocholesterolemic. Am J Clin Nutr 61:1129–1139
51. Hunter JE, Zhang J, Kris-Etherton PM (2010) Cardiovascular disease risk of dietary stearic acid compared with *trans*, other saturated and unsaturated fatty acids : a systematic review. Am J Clin Nutr 91:46–63
52. Bonanome A, Grundy SM (1988) Effect of dietary stearic acid on plasma cholesterol and lipoprotein levels. N Engl J Med 318:1244–1248
53. Legrand P, Catheline D, Fichot MC, Lemarchal P (1997) Inhibiting delta9-desaturase activity impairs triacylglycerol secretion in cultured chicken hepatocytes. J Nutr 127:249–256
54. Sampath H, Miyazaki M, Dobrzyn A, Ntambi JM (2007) Stearoyl–CoA desaturase-1 mediates the pro-lipogenic effects of dietary saturated fatty acids. J Biol Chem 282:2483–2493
55. Paillard F, Catheline D, Le Duff F, Bouriel M, Pouchard M, Deugnier Y, Daubert JC, Legrand P et al (2008) Δ9-desaturase, new candidate implied in the expression of triglyceridemia and abdominal adiposity. Nutr Metab Cardiovasc Dis 18:436–440
56. Tholstrup T, Miller GJ, Bysted A, Sandstrom B (2003) Effect of individual dietary fatty acids on postprandial activation of blood coagulation factor VII and fibrinolysis in healthy young men. Am J Clin Nutr 77:1125–1132
57. Thijssen MA, Hornstra G, Mensink RP (2005) Stearic, oleic and linoleic acids have comparable effects on markers of thrombotic tendency in healthy human subjects. J Nutr 135:2805–2811
58. Jan S, Guillou H, D'Andréa S, Daval S, Bouriel M, Rioux V, Legrand P (2004) Myristic acid increases Δ6-desaturase activity in cultured rat hepatocytes. Reprod Nutr Dev 44:131–140
59. Rioux V, Catheline D, Bouriel M, Legrand P (2005) Dietary myristic acid at physiologically relevant levels increases the tissue content of C20:5n-3 and C20:3n-6 in the rat. Reprod Nutr Dev 45:599–612
60. Dabadie H, Peuchant E, Bernard M, Le Ruyet P, Mendy F (2005) Moderate intake of myristic acid in *sn*-2 position has beneficial lipidic effects and enhances DHA of cholesteryl esters in an interventional study. J Nutr Biochem 16:375–382
61. Dabadie H, Motta C, Peuchant E, Le Ruyet P, Mendy F (2006) Variations in daily intakes of myristic and α-linolenic acids in *sn*-2 position modify lipid profile and red blood cell membrane fluidity. Br J Nutr 96:283–289
62. Borgese N, Aggujaro D, Carrera P, Pietrini G, Bassetti M (1996) A role for N-myristoylation in protein targeting: NADH-cytochrome *b*5 reductase requires myristic acid for association with outer mitochondrial but not ER membranes. J Cell Biol 135:1501–1513
63. Chen J, Ghazawi FM, Bakkar W, Li Q (2006) Valproic acid and butyrate induce apoptosis in human cancer cells through inhibition of gene expression of Akt/protein kinase B. Mol Cancer 5:71
64. Stempelj M, Kedinger M, Augenlicht L, Klampfer L (2007) Essential role of the JAK/STAT1 signaling pathway in the expression of inducible nitric-oxide synthase in intestinal epithelial cells and its regulation by butyrate. J Biol Chem 282:9797–9804
65. Sengupta S, Muir JG, Gibson PR (2006) Does butyrate protect from colorectal cancer? J Gastroenterol Hepatol 21:209–218
66. Belakavadi M, Prabhakar BT, Salimath BP (2007) Purification and characterization of butyrate-induced protein phosphatase involved in apoptosis of Ehrlich ascites tumor cells. Biochim Biophys Acta 1770:39–47
67. Staiger K, Staiger H, Weigert C, Haas C, Haring HU, Kellerer M (2006) Saturated, but not unsaturated, fatty acids induce apoptosis of human coronary artery endothelial cells via nuclear factor-κB activation. Diabetes 55:3121–3126
68. Andrieu-Abadie N, Gouaze V, Salvayre R, Levade T (2001) Ceramide in apoptosis signaling: relationship with oxidative stress. Free Radic Biol Med 31:717–728
69. Siskind LJ (2005) Mitochondrial ceramide and the induction of apoptosis. J Bioenerg Biomembr 37:143–153
70. Stiban J, Fistere D, Colombini M (2006) Dihydroceramide hinders ceramide channel formation: implications on apoptosis. Apoptosis 11:773–780
71. Paumen MB, Ishida Y, Muramatsu M, Yamamoto M, Honjo T (1997) Inhibition of carnitine palmitoyltransferase I augments sphingolipid synthesis and palmitate-induced apoptosis. J Biol Chem 272:3324–3329
72. Beauchamp E, Tekpli X, Marteil G, Lagadic-Gossmann D, Legrand P, Rioux V (2009) N-Myristoylation targets dihydroceramide Delta4-desaturase 1 to mitochondria: partial involvement in the apoptotic effect of myristic acid. Biochimie 91:1411–1419
73. Geliebter A, Torbay N, Bracco ET, Hashim SA, Van Itallie TB (1983) Overfeeding with medium chain triglyceride diet results in diminished deposition of fat. Am J Clin Nutr 37:1–4
74. Tachibana S, Sato K, Cho Y, Chiba T, Schneider WJ, Akiba Y (2005) Octanoate reduces very low-density lipoprotein secretion by decreasing the synthesis of apolipoprotein B in primary cultures of chicken hepatocytes. Biochim Biophys Acta 1737:36–43

Lipids (2010) 45:947–962
DOI 10.1007/s11745-010-3467-3

ORIGINAL ARTICLE

Limited Effect of Dietary Saturated Fat on Plasma Saturated Fat in the Context of a Low Carbohydrate Diet

Cassandra E. Forsythe · Stephen D. Phinney · Richard D. Feinman · Brittanie M. Volk · Daniel Freidenreich · Erin Quann · Kevin Ballard · Michael J. Puglisi · Carl M. Maresh · William J. Kraemer · Douglas M. Bibus · Maria Luz Fernandez · Jeff S. Volek

Received: 6 January 2010 / Accepted: 22 August 2010 / Published online: 7 September 2010

Abstract We recently showed that a hypocaloric carbohydrate restricted diet (CRD) had two striking effects: (1) a reduction in plasma saturated fatty acids (SFA) despite higher intake than a low fat diet, and (2) a decrease in inflammation despite a significant increase in arachidonic acid (ARA). Here we extend these findings in 8 weight stable men who were fed two 6-week CRD (12%en carbohydrate) varying in quality of fat. One CRD emphasized SFA (CRD-SFA, 86 g/d SFA) and the other, unsaturated fat (CRD-UFA, 47 g SFA/d). All foods were provided to subjects. Both CRD decreased serum triacylglycerol (TAG) and insulin, and increased LDL-C particle size. The CRD-UFA significantly decreased plasma TAG SFA (27.48 ± 2.89 mol%) compared to baseline (31.06 ± 4.26 mol%). Plasma TAG SFA, however, remained unchanged in the CRD-SFA (33.14 ± 3.49 mol%) despite a doubling in SFA intake. Both CRD significantly reduced plasma palmitoleic acid (16:1n-7) indicating decreased de novo lipogenesis. CRD-SFA significantly increased plasma phospholipid ARA content, while CRD-UFA significantly increased EPA and DHA. Urine 8-iso $PGF_{2\alpha}$, a free radical-catalyzed product of ARA, was significantly lower than baseline following CRD-UFA (−32%). There was a significant inverse correlation between changes in urine 8-iso $PGF_{2\alpha}$ and PL ARA on both CRD ($r = -0.82$ CRD-SFA; $r = -0.62$ CRD-UFA). These findings are consistent with the concept that dietary saturated fat is efficiently metabolized in the presence of low carbohydrate, and that a CRD results in better preservation of plasma ARA.

Keywords Saturated fat · Palmitic acid · Palmitoleic acid · Plasma fatty acid composition · Ketogenic diet · Omega-3 eggs · Metabolic syndrome · Insulin sensitivity · Controlled human feeding study · EPA · DHA · LDL/HDL ratio

Abbreviations

ALA	α-Linoleic acid
ARA	Arachidonic acid
BMI	Body mass index
CRD	Carbohydrate restricted diet
CVD	Cardiovascular disease
CE	Cholesteryl ester
D6D	Delta-6-desaturase
DHA	Docosahexaenoic acid
EPA	Eicosapentaenoic acid
FM	Fat mass
hs-CRP	High sensitivity C-reactive protein
HOMA-IR	Homeostasis model assessment insulin resistance index

C. E. Forsythe · B. M. Volk · D. Freidenreich · E. Quann · K. Ballard · M. J. Puglisi · C. M. Maresh · W. J. Kraemer · J. S. Volek (✉)
Department of Kinesiology, University of Connecticut, 2095 Hillside Road, Unit 1110, Storrs, CT 06269-1110, USA
e-mail: jeff.volek@uconn.edu

M. J. Puglisi · M. L. Fernandez
Department of Nutritional Science, University of Connecticut, Storrs, CT, USA

R. D. Feinman
Department of Cell Biology, SUNY Downstate Medical Center, Brooklyn, NY, USA

S. D. Phinney
School of Medicine (Emeritus), University of California, Davis, Davis, CA, USA

D. M. Bibus
University of Minnesota and Lipid Technologies, LLC, Austin, MN, USA

IL	Interleukin
LA	Linoleic acid
MCP-1	Monocyte chemotactic protein-1
MUFA	Monounsaturated fatty acids
MI	Myocardial infarction
NA	Not available
%en	Percent total energy
PUFA	Polyunsaturated fatty acids
TAG	Triacylglycerol
PL	Phospholipid
ROS	Reactive oxygen species
RDA	Recommended daily allowance
SFA	Saturated fatty acids
TNF-α	Tumor necrosis factor-α

Introduction

The rationale for using carbohydrate-restricted diets (CRD) in an experimental setting is that dietary carbohydrate is the major stimulus of the glucose-insulin axis which, in turn has profound effects on several metabolic processes. The shift away from an anabolic state leads to an increase in fat oxidation thereby altering lipoprotein metabolism and cardio-metabolic profile [1]. Low carbohydrate diets consistently decrease fasting and postprandial plasma triacylglycerol (TAG), increase HDL-cholesterol (HDL-C), lower plasma insulin, and improve insulin sensitivity [2]. While LDL-cholesterol (LDL-C) responses are more variable, there is a consistent shift from small to larger particles [3]. These responses to carbohydrate restriction have been shown to occur in isocaloric experiments [4–6] indicating that the effects are not solely due to weight loss.

In our previous study of overweight men and women consuming a hypocaloric CRD, one of the most striking responses was a significantly greater reduction in plasma SFA levels in response to a CRD compared to a low fat diet, despite a threefold greater presence of *dietary* SFA in the carbohydrate-reduced diet [7]. Control of lipid metabolism, particularly SFA availability, is of current interest because of a recent meta-analysis showing that dietary SFA is not a risk factor for cardiovascular disease [8] and the indication that replacement by carbohydrate, in particular, may increase risk [9]. The extent to which plasma SFA reflects dietary saturated fat consumption is not clear-cut and is significantly affected by the presence of carbohydrate [3, 7]. Cassady et al. [10], for example, found that plasma palmitic and stearic acids did not depend on the saturated fat content of two different CRD. Two other studies reported lower plasma levels of SFA in response to diets that contained two to threefold greater intake of SFA but were lower in carbohydrate than standard intakes [11, 12].

The other remarkable finding in our previous investigation was a significant decrease in inflammatory markers despite a marked increase in plasma arachidonic acid (ARA) [7]. The metabolic intermediates in the production of ARA were decreased suggesting that synthesis was not increased. We proposed rather that the increase was due to better preservation of ARA. This idea was supported indirectly by the observation of significant reductions in several inflammatory cytokines that were also inversely correlated with changes in ARA. The ratio of n-6 to n-3 highly unsaturated fatty acids in phospholipids (PL) has received significant attention due to their conversion to eicosanoids of different biologic effects. The n-6 ARA (20:4n-6) more readily promotes inflammation when converted enzymatically or non-enzymatically to pro-inflammatory eicosanoids and F_2-isoprostanes [13, 14], whereas an increase in membrane eicosapentaenoic acid (EPA; 20:5n-3), an n-3 PUFA has anti-inflammatory effects and decreases risk of cardiovascular disease [15, 16]. Increasing ARA in membranes, however, does not inevitably lead to greater inflammation and may in fact have the opposite effect [15, 17]. The proinflammatory effects of ARA are due to metabolites produced subsequent to its release from membranes rather than the proportion of the intact fatty acid. Enzymatic metabolism of free ARA results in production of eicosanoids, and free radical-induced peroxidation of ARA results in the formation of isoprostanes. Measurement of isoprostanes is considered an accurate marker of oxidative stress, but it also represents a unique non-enzymatic degradation product of ARA [18].

Here, we extend the findings of our previous study by assessing plasma fatty acid composition responses in men who participated in two 6-week weight maintenance CRD feeding periods varying only in fatty acid composition. One CRD was designed to be high in SFA (emphasizing dairy fat and eggs), and the other was designed to be lower in saturated fat and consequently higher in unsaturated fat from both polyunsaturated (PUFA) and monounsaturated (MUFA) fatty acids (emphasizing fish, nuts, omega-3 enriched eggs, and olive oil). The objectives were to: (1) establish whether the disconnect between dietary and plasma SFA levels persists under isocaloric conditions, (2) determine if a weight stable CRD increases plasma ARA and the association with inflammatory markers and isoprostanes, and (3) determine whether an increase in dietary EPA and docosahexaenoic acid (DHA; 22:6n-3) on a CRD mitigates the increase in plasma ARA and its association with inflammatory markers and isoprostanes.

Experimental Procedures

Study Participants

Eight men, aged 38–58 years old, with BMI of 25–35 kg/m^2 participated in this controlled dietary intervention. Medical history, family history, and dietary intake from a 3 day diet record were collected at baseline. Exclusion criteria were abnormal glucose levels, hypercholesterolemia, a diagnosis of Type I or II diabetes, liver or other metabolic or endocrine dysfunction, hypertension, or use of cholesterol or diabetic medications. Subjects were also excluded if they were taking any supplements known to affect serum lipoprotein levels (i.e. fish oil, niacin, psyllium fiber) or inflammation (i.e. aspirin). Subjects were not excluded if they were already following a CRD, but were excluded if they were trying to lose weight or had a body mass that changed ±3 kg in the last 3 months. Subjects were asked to maintain their same activity level during the experimental period (verified by activity records) and sedentary individuals were not allowed to start a new exercise program in order to account for possible confounding effects on the dependant variables.

Study Design and Dietary Intervention

In a randomized, cross-over, controlled design, an isocaloric carbohydrate restricted high saturated fat diet (CRD-SFA) was compared to a CRD higher in unsaturated fat (CRD-UFA). Each dietary feeding period was 6 weeks in duration, based on previous research showing that the fatty acid composition of plasma PL stabilizes within 4–6 weeks of dietary change [19] and blood lipids stabilize within 6 weeks of a CRD [20]. Three weeks prior to starting each of the 6 week dietary feeding periods, all subjects were counseled to consume a run-in free-living weight-maintaining CRD (~10%en from carbohydrate, 65%en from fat, and 25%en from protein), using standardized procedures from our research laboratory. The purpose of this run-in period was to: aide in determining an appropriate energy level to maintain body weight; standardize subject's physiologic state before each diet; and initiate metabolic adaptations to carbohydrate restriction. Urinary ketones were monitored throughout the entire CRD run-in period and intervention using reagent strips (Bayer Corporation, Elkart, IN) to ensure compliance and to assure the presence of nutritional ketosis. After the run-in period, subjects were randomized to one of two dietary arms as described above. Following the 6 week feeding period, subjects returned to their individual baseline diet for 4 weeks. Once washed out, they returned to the same run-in CRD for another 3 weeks, and then crossed over to the next 6 week controlled CRD feeding arm.

Dietary energy for each subject was prescribed to maintain body weight, estimated using the Harris-Benedict equation and multiplied by an activity factor from 1.2 to 1.55 depending on individual activity level. This was averaged with their caloric intake during their baseline dietary intake and run-in CRD period. Composition of the experimental diets was developed using nutrient analysis software consisting of normal foods that differed only in the relative amount of saturated and unsaturated fatty acids, but were matched for food type, energy, total fat, dietary fiber, *trans* fat, and cholesterol (Food Processor 7.71, ESHA Research, Salem, OR). Validation of the daily nutrient composition was confirmed by chemical analysis (Covance Inc, Princeton, NJ). Table 1 shows the average nutrient intake for 3 days of the 7-day rotational menu via chemical analysis. A daily multi-vitamin and mineral

Table 1 Nutritional analysis of habitual and experimental diets

Nutrient	Baseline	CRD-SFA	CRD-UFA
Energy (kcal/d)	2,072 ± 498	2,513 ± 214	2,513 ± 214
Protein (%)	24.6 ± 7.3	28.5 ± 2.7	29.8 ± 1.5
Protein (g)	128.3 ± 45	179.1 ± 15	187.2 ± 15
Carbohydrates (%)	34.2 ± 18	13.4 ± 2.6	12.3 ± 2.5
Carbohydrates (g)	174.2 ± 99	84.9 ± 7.1	77.3 ± 6.6
Fiber (g)	12.4 ± 5.1	19.2 ± 4.8	18.5 ± 1.2
Fat (%)	41.3 ± 12.0	58.6 ± 3.7	57.9 ± 3.9
Fat (g)	94.1 ± 35.0	163.6 ± 11.9	161.3 ± 7.5
SFA (%)	17.2 ± 5.0	30.8 ± 4.3	17.0 ± 2.0
SFA (g)	39.8 ± 11.9	85.6 ± 6.9	47.2 ± 2.8
14:0	NA	9.45 ± 2.4	4.02 ± 1.8
16:0 (g)	NA	46.1 ± 3.4	23.2 ± 4.9
18:0 (g)	NA	22.9 ± 1.9	13.1 ± 2.1
MUFA (%)	16.4 ± 5.8	20.9 ± 0.8	24.7 ± 3.1
MUFA (g)	37.0 ± 13.4	58.1 ± 2.1	68.6 ± 8.7
18:1 (g)	NA	56.6 ± 1.4	64.3 ± 6.9
PUFA (%)	7.4 ± 2.4	4.5 ± 0.3	14.7 ± 3.0
PUFA (g)	16.3 ± 6.5	12.4 ± 1.9	40.8 ± 8.1
n-3 PUFA (%)	NA	0.6 ± 0.1	2.9 ± 0.3
n-6 PUFA (%)	NA	3.8 ± 0.8	10.8 ± 2.0
18:2n-6 (g)	NA	9.9 ± 2.6	27.9 ± 6.3
18:3n-3 (g)	NA	1.2 ± 0.3	7.5 ± 1.4
20:4n-6 (g)	NA	0.5 ± 0.1	0.5 ± 0.2
20:5n-3 (g)	NA	0.2 ± 0.0	0.6 ± 0.2
22:6n-3 (g)	NA	0.2 ± 0.1	0.9 ± 0.1
Trans fatty acids (g)	1.7 ± 1.9	2.4 ± 0.3	1.4 ± 0.1
Cholesterol (mg)	426.4 ± 267.4	854 ± 97.3	849 ± 41.9

Values are mean percentages of total energy ± SD. *NA* data not available from habitual diet records. Habitual diets calculated from baseline 3-day food records of each participant. Habitual diets analyzed by Food Processor, ESHA Research, Salem, OR. Experimental diets analyzed by Covance Laboratories, Inc, Princeton, NJ

supplement at levels ≥100% of the RDA was also given to subjects and consumed throughout the entire intervention to ensure adequate micronutrient status.

In each 6-week feeding period, all food and beverages were provided for subjects in a 7-day rotational menu, and no other foods or beverages were allowed, unless they were calorie-free or very-low-calorie (i.e., tea, water, diet soda). Predominant foods in the CRD-SFA were high-fat dairy (cream, butter, cheese, and low-carbohydrate milk), eggs, meat, poultry, and white fish, and a few low omega-3 nuts and seeds (such as almonds). In the CRD-UFA, predominant foods were liquid omega-3 PUFA eggs (Egg Creations, Burnbrae Farms Ltd, ON, Canada. Containing EPA, DPA and DHA), hard shell omega-3 eggs (high in ALA and DHA), salmon, sardines, meat, poultry, olive oil, canola oil, low-fat low-carbohydrate dairy, walnuts, and seeds. Subjects picked up prepared, packaged food every Monday, Wednesday and Friday. All take-out food containers were returned unwashed and inspected to ensure that all food and fat had been consumed.

Anthropometrics

Body weight was measured weekly in the morning before food consumption and maintained within ±2 kg during the dietary intervention. Adjustments in caloric intake were made to maintain body weight within these parameters. Body composition was measured by dual-energy X-ray absorptiometry (Prodigy, Lunar Corporation, Madison, WI) at baseline, and at the start and end of each diet feeding intervention. Analyses were performed by the same blinded technician.

Blood Collection and Analysis

Blood samples were obtained at baseline, pre-dietary intervention and post-dietary intervention for both feeding periods. The sample was obtained from an arm vein after subjects rested quietly for 10 min in the supine position. Whole blood was collected into tubes with no preservative or EDTA and centrifuged at 1,500×*g* for 15 min and 4 °C, and promptly aliquoted into separate storage tubes which were stored at −75 °C until analyzed. A portion of serum (~3 ml) was immediately sent to a certified medical laboratory (Quest Diagnostics, Wallingford, CT) for determination of total cholesterol (TC), HDL-C, TAG, and calculated LDL-C concentrations using automated enzymatic procedures (Olympus America Inc., Melville, NY).

Glucose and insulin concentrations were analyzed in serum in duplicate (YSI 2300 STAT, Yellow Springs, OH, CV 0.5%) and radioimmunoassay (Diagnostic Systems Laboratory, Webster, TX, CV 4.3%), respectively, and used to calculate an index of insulin resistance [HOMA-IR; calculated as Glucose (mmol/l) Insulin (μIU/ml/22.5)]. The 75th percentile cut-off value for insulin resistance in non-diabetic individuals has been determined to correspond to a value of 2.29 [17]. Lipoprotein particle size of LDL-C was determined in serum using non-gradient polyacrylamide gel electrophoresis (Lipoprint LDL System, Quantimetrix Co., Redondo Beach, CA) as previously described [21]. Serum total ketone bodies were determined by a cyclic enzymatic method that measures both acetoacetate (AcAc) and 3-hydroxybutyrate (3-HB) (Wako Chemicals USA Inc, Richmond, VA). Absorbance was read at a wavelength of 404 nm on a microplate reader (Versa Max Molecular Devices Corp. Sunnyvale, CA, USA) and analyzed with associated SoftMax Pro software (CV 4.2%). Serum IL-6, IL-8, MCP-1, TNF-α, and leptin were measured using xMAP® technology on a Luminex® IS 200 system with antibodies to these analytes from LINCO Research (St. Charles, MO). Assays were completed in duplicate according to manufacturer's instructions (IL-6 CV 12.7%, IL-8 CV 10.4%, MCP-1 CV 7.3%, TNF-α CV 9.7%, Leptin CV 10.2%). High Sensitivity C-reactive protein (hs-CRP) was determined in serum on an IMMULITE Automated Analyzer using the commercially available immulite chemiluminescent enzyme immunometric assay (Immulite®, Diagnostic Products Corp., Los Angeles, CA, USA).

A 24-h urine collection was performed at baseline and post-dietary intervention. A 10-ml aliquot of urine was stored at −75 °C for subsequent analysis of F_2-Isoprostane (8-iso $PGF_{2\alpha}$) concentrations. All samples were analyzed in triplicate using column extraction followed by an ACE™ Competitive Enzyme Immunoassay with 8-Isoprostane enzyme-linked immunosorbent assay (EIA) kit (Cayman Chemicals, Ann Arbor, MI). Briefly, 2 ml frozen thawed urine was purified through an 8-Isoprostane Affinity Column (Caymen Chemicals), washed with column buffer and ultra pure water, and eluted with ethanol:water (95:5). Elution was dried with nitrogen; the volume of the dried sample was brought to 2 ml with enzyme immunoassay buffer in a 1:10 dilution. Absorbance was read at 420 nm and data was analyzed with a log-logit curve fit (CV 5.7%). The results were expressed relative to creatinine concentrations determined using Jaffe's colorimetric method (Cayman Chemicals) read at an absorbance of 490 nm (CV 3.2%).

Fatty Acid Composition

Plasma was shipped on dry ice to Lipid Technologies LLC (Austin, MN) and analyzed for plasma fatty acid composition in circulating PL, TAG and CE using capillary gas chromatography as previously described [7]. Lipids were extracted according to the method of Bligh/Dyer whereby

mixtures of plasma, methanol, chloroform and water were prepared such that lipid is recovered in a chloroform layer. The resulting lipid extracts were maintained under an atmosphere of nitrogen following extraction and kept frozen prior to additional processing. Immediately prior to lipid class separation, lipid samples were dried under a gentle stream of nitrogen, rediluted in 50 μl of chloroform and prepared for lipid class separation. Lipid classes were separated on commercial silica gel G plates (AnalTech, Newark, DE). The chromatographic plates were developed in a solvent system consisting of distilled petroleum ether (b.p.30–60 °C): diethyl ether: acetic acid (80:20:1, by vol). Following development, the silica gel plates were sprayed with a methanolic solution containing 0.5% 2,7-dichlorofluorescein which was then used to visualize lipid classes under ultraviolet light. Desired corresponding lipid bands were then scraped into Teflon-lined screw cap tubes. The samples were then transesterified with boron trifluoride (10%) in excess methanol (Supelco, Bellefonte, PA) in an 80 °C water bath for 90 min. Resulting fatty acid methyl esters were extracted with water and petroleum ether and stored frozen until gas chromatographic analysis was performed.

Lipid class fatty acid methyl ester composition was determined by capillary gas chromatography. Methyl ester samples were blown to dryness under nitrogen and resuspended in hexane. Resulting fatty acid methyl esters were separated and quantified with a Shimadzu capillary gas chromatograph (GC17) utilizing a 30 m Restek free fatty acid phase (FFAP) coating and EZChrom software. The instrument temperature was programmed from 190 to 240° at 7 °C/min with a final hold of 10 min, separating and measuring fatty acid methyl esters ranging from 12:0 to 24:1. The detector temperature was 250 °C. Helium carrier gas was used at a flow rate of 1.4 ml/min. and a split ratio of 1:25. Chromatographic data was collected and processed with EZChrom software (Scientific Products, CA). Fatty acids were identified by comparison to authentic fatty acid standards and quantitated with peak area and internal standard. Individual peaks, representing as little as 0.05% of the fatty acid methyl esters, were distinguished. Fatty acid data are expressed in relative (mol%) and absolute (nmol/ml) terms.

Statistics

ANOVA with repeated measures was used to evaluate changes from baseline across diets. Data that was not normally distributed was log transformed. Significant main effects were further analyzed using a Tukey post hoc test. Differences between values following CRD-SFA and CRD-UFA were evaluated using paired student's *t* test. The alpha level for significance was <0.05.

Results

Dietary Intake

Nutrient intake estimated at baseline from dietary records showed a lower than expected energy, 2,072 kcal/d compared to 2,513 kcal/d for the feeding periods. This was likely due to under-reporting at baseline (Table 1) [22] although it has been argued that the demands of gluconeogenesis and other processes require more energy for weight maintenance [23]. Habitual carbohydrate intake was also lower than the average American diet at 32%en reflecting two subjects who were habitually consuming a lower-carbohydrate diet. Both CRD were well tolerated and compliance was excellent as assessed by verbal feedback and inspection of returned food containers throughout the intervention. There was no consistent preference for one diet treatment over the other by subjects. Briefly, the main difference between the two low carbohydrate diets was in the relative amount of SFA, MUFA, PUFA (CRD-SFA = 31, 21, and 5%; CRD-UFA = 17, 25, and 15%). Although the CRD-UFA contained higher amounts of both n-6 and n-3 PUFA, the ratio of n-6/n-3 PUFA was lower in the CRD-UFA. Other nutrients, including cholesterol, were matched with the exception of (naturally occurring) *trans* fatty acids which were inherently higher on the CRD-SFA diet due to the higher intake of high-fat dairy. Compared to baseline, the CRD-SFA diet provided more than twice as much dietary SFA (86 vs. 40 g) while in the CRD-UFA, intake of SFA was 47 grams. Compared to baseline, the CRD-UFA provided more total PUFA (41 vs. 16 g), n-3 PUFA (3%en vs. 0.7%en), and n-6 PUFA (11%en vs. 7%en). Cholesterol intake in both diets was about twofold higher than baseline intake.

Body Weight and Composition

Body fat percentage and body mass of subjects after the two experimental diets were not significantly different from baseline. A small, but significant ($P < 0.05$) decrease in body mass (difference: 0.94 ± 0.13 kg) occurred following the CRD-UFA diet compared to the CRD-SFA diet (Table 2).

Blood Markers

Blood lipid, metabolic, and inflammatory markers are presented in Table 2. Serum ketones were moderately elevated as a result of carbohydrate restriction. Fasting plasma TC and LDL-C were variable but were higher on average following CRD-SFA compared to CRD-UFA. The increase in HDL-C following CRD-SFA (14%) and CRD-UFA (8%) from baseline resulted in no significant change in the TC/HDL or LDL/HDL ratios.

Table 2 Body composition and blood marker responses of subjects at baseline and following the two low carbohydrate diets

Characteristic	Baseline	CRD-SFA	CRD-UFA	ANOVA
Age (year)	45 ± 7.9			
BMI (kg/m^2)	30.0 ± 4.0	29.6 ± 3.7	29.3 ± 3.7†	0.190
Body weight (kg)	95.4 ± 13.5	94.1 ± 13.7	93.1 ± 13.8†	0.180
Body fat (%)	28.4 ± 6.5	26.8 ± 5.7$^{£}$	26.8 ± 5.7$^{£}$	0.075
Fat mass (kg)	26.6 ± 9.0	25.0 ± 7.8	24.5 ± 7.9	0.175
Lean body mass (kg)	65.2 ± 7.4	65.6 ± 7.7	65.2 ± 8.0	0.600
Total cholesterol (mg/dl)	191.0 ± 32.6	215.6 ± 46.5	192.9 ± 27.5†	0.145
LDL-C (mg/dl)	118 ± 29.8	144.1 ± 42.9	125.1 ± 29.1†	0.119
HDL-C (mg/dl)	47.8 ± 10.4	54.5 ± 12.0	51.6 ± 9.4	0.080
TAG (mg/dl)	122.0 ± 55.9	85.1 ± 34.3*	80.4 ± 17.5*	0.047
Total cholesterol/HDL-C	4.1 ± 1.0	4.1 ± 1.1	3.9 ± 0.9	0.467
LDL/HDL	2.6 ± 0.8	2.7 ± 0.9	2.5 ± 0.8	0.526
TAG/HDL-C	2.8 ± 1.9	1.7 ± 0.9*	1.6 ± 0.6*	0.041
LDL mean size (nm)	270.1 ± 3.8	273.4 ± 2.6*	273.3 ± 1.58*	0.023
LDL peak size (nm)	274.3 ± 6.3	279.0 ± 4.8$^{£}$	279.8 ± 2.6*	0.031
Glucose (mmol/l)	5.96 ± 0.4	6.14 ± 0.5	6.12 ± 0.4	0.443
Insulin (pmol/l)	52.5 ± 32.5	41.6 ± 14.0	40.2 ± 15.7	0.256
HOMA-IR	2.0 ± 1.2	1.6 ± 0.5	1.6 ± 0.6	0.383
Ketones (μmol/l)	106 ± 42	200 ± 130	267 ± 155*	0.020
Leptin (ng/ml)	11.6 ± 6.5	8.7 ± 5.2	7.6 ± 3.5	0.062
hs-CRP (mg/dl)	2.7 ± 2.3	1.8 ± 0.9	2.7 ± 1.8	0.509
IL-6 (pg/ml)	1.3 ± 1.1	0.9 ± 0.9	1.1 ± 1.2	0.065
IL-8 (pg/ml)	1.7 ± 0.6	1.5 ± 0.9	1.9 ± 1.1	0.333
TNF-α (pg/ml)	3.8 ± 1.5	3.4 ± 1.4	3.6 ± 1.6	0.531
MCP-1 (pg/ml)	251 ± 81	234 ± 94	269 ± 123	0.670
8-iso $PGF_{2\alpha}$ (pg/mg creatinine)	629 ± 262	524 ± 146	425 ± 61	0.053

Values are means ± SD

HOMA-IR homeostasis model assessment insulin resistance index

* $P < 0.05$ from baseline based on repeated measures ANOVA and Tukey post hoc

† $P < 0.05$ from CRD-SFA diet (dependent *t* test)

$^{£}$ $P < 0.08$ from baseline

Consistent with numerous studies on CRD even in the absence of weight loss, a dramatic decrease in plasma TAG was seen. TAG fell from baseline by 39% after the CRD-SFA and by 34% on the CRD-UFA. There was also a decrease in TAG/HDL ratio for both the CRD-SFA (−39%) and CRD-UFA (−43%). LDL mean and peak particle size following the two diets were both significantly higher than baseline.

Blood glucose, insulin, and HOMA-IR were not significantly different from baseline or between diets. Using 2.29 as the cut-off point to define insulin resistance [21], two subjects were insulin resistant (HOMA-IR = 3.06 and 5.53) at baseline. HOMA-IR values were <2.29 for both subjects after the CRD-UFA and for one of the insulin resistant subjects after the CRD-SFA.

There were no significant differences in any of the serum inflammatory markers (hs-CRP, IL-6, IL-8, TNF-α, MCP-1, leptin) between the two interventions. Compared to baseline levels of urinary 8-iso $PGF_{2\alpha}$ (629 ± 262 pg/Creatinine mg), concentrations were reduced by 17% after the CRD-SFA (524 ± 146 pg/Creatinine mg; $P = 0.253$) and by 32% after the CRD-UFA (425 ± 61 pg/Creatinine mg; $P = 0.018$). After the CRD-UFA, all 8 subjects had lower urine 8-iso $PGF_{2\alpha}$ than baseline and 7 out of 8 had lower concentrations compared to the CRD-SFA.

Plasma Saturated and Monounsaturated Fatty Acids

The major changes in plasma SFA and MUFA were in the plasma TAG fraction. The mol% of total SFA in TAG was significantly lower following CRD-UFA compared to CRD-SFA (Table 3). At the same time, the effect was less than might be expected given the nearly two-fold difference in dietary saturated fat suggesting that the reduction in carbohydrate was the major determinant; there was, in fact, no difference in total SFA in TAG between baseline and CRD-SFA. The lower total SFA after the CRD-UFA was mainly attributed to a decrease in 16:0, the predominant SFA in plasma TAG although, again, the magnitude of the effect was small. Compared to baseline, 16:1n-7 mol% in plasma TAG was significantly lower following both CRD, but not different between CRD. A comprehensive list of fatty acids from TAG, PL and CE fractions is provided in Table 3.

Plasma Polyunsaturated Fatty Acids

The major changes in plasma PUFA were in the PL fraction. There were distinct differences between the CRD in plasma PL long chain n-6 and n-3 PUFA (Table 3). Compared to baseline, all subjects had an increase in 20:4n-6 after the CRD-SFA, and those values were higher than 20:4n-6 after the CRD-UFA in all but one subject. Interestingly, despite an increase in 20:4n-6 in response to the CRD-SFA the immediate precursor 20:3n-6 was not increased and was in fact lower than baseline. Total n-3 PUFA was significantly higher following the CRD-UFA than baseline and CRD-SFA values primarily due to greater increases in 20:5n-3 (EPA) and 22:6n-3 (DHA). The PL n-6/n-3 ratio (calculated as the sum of all n-6 PUFA divided by the sum of all n-3 PUFA), was significantly lower following CRD-UFA than CRD-SFA and baseline. Compared to baseline, the ARA/EPA ratio was significantly increased after the CRD-SFA whereas it was decreased after the CRD-UFA. Compared to baseline the ARA/EPA ratio was decreased after the CRD-UFA in all subjects, and it was higher during the CRD-SFA than the CRD-UFA in all subjects.

Intuitively, one might presume an increase in PL ARA would result in a corresponding increase in 8-iso $PGF_{2\alpha}$, yet we observed the opposite. There was a significant inverse correlation between changes in urine 8-iso $PGF_{2\alpha}$ and PL ARA on both low carbohydrate diets ($r = -0.82$ CRD-SFA, $P = 0.007$; $r = -0.62$ CRD-UFA, $P = 0.05$) indicating that those subjects who showed greater increases in plasma ARA had greater reductions in 8-iso $PGF_{2\alpha}$.

Discussion

Dietary saturated fat has been the focus of nutritional recommendations since the 1970 study of Ancel Keys [24]. Current recommendations are as low as 7% [25] although the subject has always generated some controversy. The biologic effect of dietary SFA is presumed to rest with its effect on plasma SFA and other lipid fractions but a number of reports in the literature suggest that this needs to be experimentally established [7, 11, 12]. In the current study, we used a controlled-feeding design to examine responses in plasma fatty acids, lipoproteins, isoprostanes and inflammatory markers in men who switched from their habitual diet to a CRD either high in SFA (CRD-SFA) or unsaturated fat (CRD-UFA) including eggs with long chain n-3 PUFA. The primary findings were that: (1) there is limited effect of dietary SFA on plasma SFA in the context of a weight maintenance low carbohydrate diet, (2) a weight maintenance CRD high in SFA (representing the typical nutrient composition of CRD we have studied in our many previous investigations) resulted in a significant increase in plasma ARA without an accompanying increase in inflammation or oxidative stress, (3) a weight maintenance CRD higher in unsaturated fat (CRD-UFA) including EPA and DHA (CRD-UFA) prevented the increase in plasma ARA while increasing plasma EPA and DHA content and significantly decreasing urine 8-iso $PGF_{2\alpha}$, a degradation breakdown product of ARA, and, (4) the changes in plasma ARA and urine 8-iso $PGF_{2\alpha}$ were inversely correlated on both CRD independent of fat composition supporting and strengthening our hypothesis of less catabolism of ARA (i.e., better preservation of ARA) on a CRD.

Saturated Fat

The most striking finding was the lack of association between dietary SFA intake and plasma SFA concentrations. Compared to baseline, a doubling of saturated fat intake on the CRD-SFA did not increase plasma SFA in any of the lipid fractions, and when saturated fat was only moderately increased on the CRD-UFA, the proportion of SFA in plasma TAG was reduced from 31.06% to 27.48 mol%. Since plasma TAG was also reduced, the total SFA concentration in plasma TAG was decreased by 47% after the CRD-UFA, similar to the 57% decrease we observed in overweight men and women after 12 week of a hypocaloric CRD [7]. These results can best be explained by the metabolic adaptations induced by carbohydrate restriction [1], notably less stimulation of insulin. Lower insulin levels result in increased lipolysis and fatty acid oxidation while simultaneously decreasing activity of key enzymes in de novo lipogenesis. From a mechanistic standpoint, restriction in dietary carbohydrate is the dominant dietary manipulation that accelerates fat mobilization and oxidation [26]. The lipid fraction most responsive to carbohydrate restriction was TAG. Higher incorporation of SFA into VLDL TAG is correlated with insulin resistance and adiposity [27], probably reflecting accelerated hepatic *de novo* lipogenesis. Plasma TAG transports the greatest amount of fatty acids that are actively involved in energy exchange. Therefore a decrease in plasma SFA, from reduced hepatic fatty acid synthesis or increased beta-oxidation, may attenuate atherogenic cell-signaling even in the presence of higher dietary SFA. The limited change in SFA in PL may be due to lower turnover in this fraction (the sn-1 position almost always carries a SFA), or to the short duration of this study. Previous studies have shown that increased plasma PL and CE SFA levels predict development of cardiovascular disease (CVD) [28, 29].

The presence of palmitoleic acid (16:1n-7) is an indicator of *de novo* fatty acid synthesis [30] since the compound is limited in the diet. Both isocaloric CRD feeding

Table 3 Plasma TAG, PL and CE fatty acid responses at baseline and following the two low carbohydrate diets

	Baseline	CRD-SFA	CRD-UFA	ANOVA
TAG (nmol/ml)				
SFA				
14:0	66.5 ± 48.3	32.8 ± 15.7	23.9 ± 10.1*	0.023
15:0	10.5 ± 5.3	7.8 ± 3.5	6.4 ± 1.8	0.090
16:0	915.8 ± 585.7	540.8 ± 157.9	482.1 ± 167.8*	0.036
18:0	126.0 ± 72.9	98.3 ± 32.8	83.5 ± 21.3	0.216
20:0	1.8 ± 0.6	1.4 ± 0.5	1.4 ± 0.3	0.222
22:0	0.9 ± 0.7	0.6 ± 0.9	0.9 ± 0.7	0.711
24:0	1.1 ± 0.7	1.1 ± 0.6	1.7 ± 1.5	0.392
Total SFA	1122 ± 707	683 ± 203	600 ± 200*	0.043
MUFA				
14:1	3.9 ± 5.3	1.7 ± 2.0	0.1 ± 0.3	0.105
15:1	1.4 ± 0.6	1.0 ± 0.3	1.1 ± 0.6	0.280
16:1	147.4 ± 113.7	55.9 ± 20.1*	58.4 ± 25.1*	0.014
17:1	9.7 ± 5.9	6.7 ± 2.8	6.3 ± 2.7	0.132
18:1n9	1233.6 ± 562.6	772.8 ± 203.7*	821 ± 271.8*	0.018
20:1n7	4.5 ± 3.4	2.9 ± 2.3	1.6 ± 1.6	0.085
20:1n9	7.7 ± 2.6	5.8 ± 1.7	7.6 ± 3.3	0.177
22:1n9	2.7 ± 1.6	2.2 ± 1.6	2.4 ± 1.5	0.731
24:1	0.0 ± 0.0	0.1 ± 0.3	0.6 ± 1.2	–
Total MUFA	1411 ± 687	849 ± 227*	899 ± 302*	0.017
PUFA				
18:3n3	37.8 ± 16.6	16.8 ± 7.9*	39.0 ± 21.0†	0.014
18:4n3	5.6 ± 4.4	3.6 ± 2.5	3.7 ± 3.2	0.283
20:3n3	0.7 ± 0.8	0.2 ± 0.3	0.3 ± 0.5	0.245
20:4n3	1.5 ± 1.6	0.8 ± 0.9	1.3 ± 1.8	0.548
20:5n3	8.9 ± 5.7	4.2 ± 2.5	32.7 ± 49.6	0.148
22:5n3	12.9 ± 7.5	7.7 ± 3.1	15.9 ± 10.6	0.111
22:6n3	15.2 ± 6.7	12.2 ± 6.9	53.6 ± 75.1	0.128
18:2n6	712.0 ± 330.7	382.9 ± 146.7*	469.1 ± 170.9*	0.007
18:3n6	16.4 ± 10.1	8.5 ± 7.4	5.6 ± 2.1*	0.026
20:2n6	6.2 ± 3.6	3.1 ± 1.1*	2.7 ± 1.1*	0.007
20:3n6	10.3 ± 6.6	4.8 ± 2.0*	3.6 ± 1.6*	0.009
20:4n6	43.4 ± 14.3	40.0 ± 15.4	34.1 ± 15.0	0.169
22:4n6	4.7 ± 2.2	3.6 ± 1.7	1.9 ± 0.7*	0.005
22:5n6	2.7 ± 1.3	2.9 ± 1.5	2.0 ± 1.6	0.150
20:3n9	2.4 ± 0.9	2.8 ± 1.5	1.4 ± 0.4†	0.009
Total PUFA	881 ± 377	494 ± 189*	667 ± 307	0.010
Total n3	82.6 ± 21.0	45.4 ± 19.9	46.5 ± 151.9	0.087
Total n6	796 ± 362	455 ± 170*	519 ± 186*	0.008
n6/n3	9.5 ± 3.2	10.3 ± 2.3	5.1 ± 2.2*,†	0.003
AA/EPA	6.6 ± 3.8	10.5 ± 3.2	2.3 ± 1.6†	0.001
TAG (mol%)				
SFA				
14:0	1.75 ± 0.59	1.55 ± 0.45	1.09 ± 0.26*	0.018
15:0	0.31 ± 0.06	0.37 ± 0.10	0.30 ± 0.07	0.074
16:0	25.22 ± 3.72	26.20 ± 2.09	21.99 ± 2.39†	0.023
18:0	3.65 ± 0.78	4.86 ± 1.24*	3.92 ± 0.59†	0.008

Table 3 continued

	Baseline	CRD-SFA	CRD-UFA	ANOVA
20:0	0.06 ± 0.02	0.07 ± 0.03	0.07 ± 0.02	0.605
22:0	0.03 ± 0.03	0.03 ± 0.04	0.04 ± 0.02	0.624
24:0	0.04 ± 0.04	0.06 ± 0.04	0.07 ± 0.04	0.570
Total SFA	31.06 ± 4.26	33.14 ± 3.49	27.48 ± 2.89†	0.022
MUFA				
14:1	0.08 ± 0.09	0.07 ± 0.07	0.00 ± 0.01	0.057
15:1	0.04 ± 0.03	0.05 ± 0.02	0.06 ± 0.04	0.553
16:1	3.78 ± 1.22	2.66 ± 0.36*	2.59 ± 0.37*	0.006
17:1	0.27 ± 0.04	0.32 ± 0.07	0.28 ± 0.05	0.167
18:1n9	36.15 ± 2.77	37.41 ± 1.89	37.40 ± 2.98	0.512
20:1n7	0.12 ± 0.06	0.14 ± 0.08	0.06 ± 0.06	0.095
20:1n9	0.25 ± 0.07	0.29 ± 0.09	0.34 ± 0.07	0.068
22:1n9	0.10 ± 0.07	0.12 ± 0.10	0.12 ± 0.08	0.360
24:1	0.00 ± 0.00	0.01 ± 0.02	0.02 ± 0.04	–
Total MUFA	40.79 ± 2.60	41.07 ± 1.66	40.89 ± 2.97	0.971
PUFA				
18:3n3	1.12 ± 0.22	0.79 ± 0.22	1.70 ± 0.45*,†	0.000
18:4n3	0.17 ± 0.09	0.17 ± 0.12	0.16 ± 0.09	0.913
20:3n3	0.02 ± 0.03	0.01 ± 0.01	0.01 ± 0.02	0.555
20:4n3	0.04 ± 0.06	0.04 ± 0.04	0.06 ± 0.09	0.800
20:5n3	0.36 ± 0.38	0.20 ± 0.08	1.25 ± 1.40	0.058
22:5n3	0.49 ± 0.49	0.36 ± 0.10	0.69 ± 0.25	0.116
22:6n3	0.57 ± 0.47	0.55 ± 0.20	2.07 ± 2.07	0.040
18:2n6	20.97 ± 3.17	18.19 ± 4.15	21.41 ± 2.48	0.139
18:3n6	0.46 ± 0.14	0.39 ± 0.28	0.25 ± 0.05	0.065
20:2n6	0.18 ± 0.04	0.15 ± 0.03	0.12 ± 0.03	0.051
20:3n6	0.28 ± 0.06	0.23 ± 0.05	0.16 ± 0.05*	0.005
20:4n6	1.40 ± 0.44	1.87 ± 0.36*	1.58 ± 0.42	0.019
22:4n6	0.14 ± 0.05	0.17 ± 0.06	0.09 ± 0.02*,†	0.001
22:5n6	0.10 ± 0.07	0.13 ± 0.04	0.09 ± 0.04	0.084
20:3n9	0.08 ± 0.04	0.13 ± 0.04	0.07 ± 0.02†	0.001
Total PUFA	26.38 ± 3.83	23.38 ± 4.97	29.71 ± 4.12*	0.019
Total n3	2.78 ± 1.22	2.12 ± 0.52	5.94 ± 3.91*,†	0.014
Total n6	23.52 ± 3.32	21.13 ± 4.61	23.70 ± 2.61	0.284
n6/n3	9.52 ± 3.24	10.25 ± 2.28	5.09 ± 2.18*,†	0.003
AA/EPA	6.58 ± 3.83	10.49 ± 3.22	2.29 ± 1.61†	0.001
PL (nmol/ml)				
SFA				
14:0	19.0 ± 5.8	23.0 ± 5.2	18.4 ± 8.0	0.322
15:0	7.3 ± 1.3	10.1 ± 2.7*	7.3 ± 1.4†	0.006
16:0	1159.4 ± 120.3	1235.3 ± 217.0	1170.5 ± 160.1	0.604
18:0	596.5 ± 85.7	552.0 ± 114	534.0 ± 60.8	0.450
20:0	17.0 ± 3.4	18.3 ± 4.2	16.7 ± 2.7	0.461
22:0	46.2 ± 10.6	47.6 ± 14.6	37.4 ± 8.0	0.070
24:0	37.5 ± 9.2	41.2 ± 13.2	28.4 ± 8.0†	0.020
Total SFA	1,882.8 ± 210.9	1,927.4 ± 349.4	1,812.8 ± 216.5	0.688
MUFA				
14:1	3.3 ± 4.7	3.7 ± 3.4	4.9 ± 3.9	0.707

Table 3 continued

	Baseline	CRD-SFA	CRD-UFA	ANOVA
15:1	19.6 ± 14.4	32.1 ± 20.4	25.2 ± 11.6	0.299
16:1	35.3 ± 14.1	28.5 ± 4.7	25.0 ± 7.7	0.137
17:1	14.6 ± 8.3	25.1 ± 14.6	18.9 ± 7.8	0.186
18:1n9	426.3 ± 56.1	420.4 ± 82.0	386.7 ± 73.6	0.363
20:1n7	2.8 ± 2.2	2.5 ± 1.6	1.5 ± 1.6	0.281
20:1n9	5.6 ± 1.6	5.9 ± 2.4	7.7 ± 3.1	0.129
22:1n9	4.9 ± 2.6	5.2 ± 2.1	5.2 ± 2.3	0.863
24:1	41.1 ± 11.6	45.0 ± 15.2	48.3 ± 10.1	0.291
Total MUFA	553.5 ± 73.4	568.5 ± 119.2	523.3 ± 84.2	0.549
PUFA				
18:3n3	9.0 ± 1.4	9.1 ± 3.6	10.3 ± 3.3	0.644
18:4n3	3.8 ± 1.8	5.1 ± 1.7	3.3 ± 1.5	0.124
20:3n3	0.4 ± 0.6	0.0 ± 0.0	0.1 ± 0.2	–
20:4n3	3.3 ± 2.3	2.4 ± 1.5	3.0 ± 1.6	0.719
20:5n3	36.2 ± 23.1	27.4 ± 12.5	148.8 ± 110.5*,†	0.005
22:5n3	32.3 ± 5.5	32.8 ± 11.2	34.3 ± 7.6	0.786
22:6n3	126.6 ± 39.3	122.6 ± 30.1	201.2 ± 46.7*,†	0.000
18:2n6	951.5 ± 141.3	986.7 ± 184.8	917.8 ± 208.1	0.567
18:3n6	6.9 ± 2.8	5.6 ± 1.4	4.4 ± 1.3*,†	0.104
20:2n6	12.3 ± 2.5	11.4 ± 2.2	9.6 ± 2.7	0.113
20:3n6	122.7 ± 38.9	102.7 ± 31.7	62.4 ± 28.2*	0.016
20:4n6	464.5 ± 62.1	580.2 ± 110.7*	462.8 ± 59.0†	0.010
22:4n6	16.5 ± 4.0	17.7 ± 5.2	8.1 ± 1.7*,†	0.000
22:5n6	10.4 ± 3.4	12.1 ± 7.3	4.3 ± 1.5*,†	0.008
20:3n9	5.9 ± 6.0	8.2 ± 13.4	3.9 ± 2.6	0.459
Total PUFA	1802.2 ± 158.9	1924.1 ± 365.5	1874.4 ± 354.9	0.657
Total n3	211.6 ± 60.3	199.4 ± 51.4	401.1 ± 155.3*,†	0.001
Total n6	1584.8 ± 155.8	1716.4 ± 321.7	1469.4 ± 280.2	0.124
n6/n3	8.0 ± 2.4	8.8 ± 1.2	4.1 ± 1.6*,†	0.000
AA/EPA	16.4 ± 7.2	23.9 ± 7.2	4.8 ± 3.3*,†	0.000
PL (mol%)				
SFA				
14:0	0.45 ± 0.14	0.54 ± 0.18	0.43 ± 0.17	0.367
15:0	0.17 ± 0.04	0.23 ± 0.04*	0.17 ± 0.01†	0.002
16:0	27.19 ± 0.64	28.02 ± 0.90	27.86 ± 0.92	0.120
18:0	13.96 ± 1.06	12.46 ± 0.81	12.81 ± 1.39	0.048
20:0	0.40 ± 0.06	0.42 ± 0.07	0.40 ± 0.05	0.656
22:0	1.08 ± 0.22	1.07 ± 0.21	0.89 ± 0.17	0.033
24:0	0.88 ± 0.19	0.92 ± 0.19	0.68 ± 0.18*,†	0.008
Total SFA	44.13 ± 1.18	43.66 ± 1.17	43.24 ± 1.93	0.452
MUFA				
14:1	0.08 ± 0.12	0.09 ± 0.09	0.12 ± 0.10	0.744
15:1	0.46 ± 0.34	0.67 ± 0.37	0.62 ± 0.32	0.397
16:1	0.82 ± 0.27	0.67 ± 0.20	0.59 ± 0.14*	0.043
17:1	0.34 ± 0.19	0.54 ± 0.26	0.46 ± 0.22	0.240
18:1n9	9.99 ± 0.73	9.53 ± 0.76	9.15 ± 0.67*	0.050
20:1n7	0.07 ± 0.05	0.06 ± 0.03	0.04 ± 0.04	0.372
20:1n9	0.13 ± 0.04	0.14 ± 0.07	0.18 ± 0.07	0.238

Table 3 continued

	Baseline	CRD-SFA	CRD-UFA	ANOVA
22:1n9	0.11 ± 0.06	0.12 ± 0.05	0.12 ± 0.05	0.901
24:1	0.96 ± 0.24	1.03 ± 0.35	1.16 ± 0.25	0.237
Total MUFA	12.96 ± 0.69	12.84 ± 0.94	12.45 ± 1.04	0.397
PUFA				
18:3n3	0.21 ± 0.03	0.20 ± 0.05	0.25 ± 0.08	0.278
18:4n3	0.09 ± 0.04	0.11 ± 0.03	0.08 ± 0.05	0.203
20:3n3	0.01 ± 0.02	0.00 ± 0.00	0.00 ± 0.01	–
20:4n3	0.08 ± 0.05	0.05 ± 0.03	0.07 ± 0.03	0.568
20:5n3	0.87 ± 0.59	0.61 ± 0.23	3.44 ± 2.23*,†	0.002
22:5n3	0.76 ± 0.12	0.73 ± 0.15	0.81 ± 0.13	0.097
22:6n3	2.97 ± 0.84	2.77 ± 0.46	4.79 ± 0.92*,†	0.000
18:2n6	22.36 ± 2.79	22.32 ± 1.14	21.63 ± 2.24	0.493
18:3n6	0.16 ± 0.05	0.13 ± 0.02	0.10 ± 0.02*	0.031
20:2n6	0.29 ± 0.05	0.26 ± 0.05	0.23 ± 0.06	0.110
20:3n6	2.86 ± 0.77	2.31 ± 0.53	1.49 ± 0.58*	0.002
20:4n6	10.96 ± 1.63	13.14 ± 0.78*	11.03 ± 0.51†	0.002
22:4n6	0.38 ± 0.07	0.40 ± 0.10	0.19 ± 0.04*,†	0.000
22:5n6	0.25 ± 0.08	0.27 ± 0.14	0.10 ± 0.03*,†	0.002
20:3n9	0.14 ± 0.13	0.19 ± 0.32	0.09 ± 0.06	0.496
Total PUFA	42.37 ± 2.45	43.49 ± 1.71	44.32 ± 1.93	0.153
Total n3	4.98 ± 1.42	4.47 ± 0.60	9.45 ± 2.89*,†	0.000
Total n6	37.25 ± 2.58	38.83 ± 1.61	34.78 ± 2.50†	0.002
n6/n3	8.04 ± 2.42	8.81 ± 1.23	4.08 ± 1.56*,†	0.000
AA/EPA	16.04 ± 7.22	23.85 ± 7.22	4.82 ± 3.31*,†	0.000
CE (nmol/ml)				
SFA				
14:0	36.59 ± 7.9	51.16 ± 25.0	30.46 ± 9.7†	0.047
15:0	10.52 ± 7.1	15.57 ± 6.9	9.16 ± 6.9	0.099
16:0	608.76 ± 51.4	720.01 ± 213.0	611.48 ± 66.2	0.138
18:0	95.77 ± 109.6	71.97 ± 20.9	54.75 ± 12.2	0.512
20:0	5.13 ± 4.8	10.28 ± 13.5	3.50 ± 5.2	0.241
22:0	0.69 ± 1.3	5.44 ± 9.6	2.76 ± 2.8	0.273
24:0	0.41 ± 0.8	1.18 ± 2.3	0.76 ± 1.7	0.672
Total SFA	757.87 ± 106.3	875.61 ± 263.2	712.87 ± 65.6	0.208
MUFA				
14:1	0.55 ± 1.0	2.25 ± 2.6	1.88 ± 1.3	0.110
15:1	1.52 ± 3.0	1.29 ± 1.2	1.07 ± 1.5	0.924
16:1	123.62 ± 64.5	119.63 ± 32.8	85.55 ± 5.5	0.221
17:1	10.47 ± 1.7	16.90 ± 9.7	10.37 ± 1.6	0.071
18:1n9	878.74 ± 120.6	1063.96 ± 362.2	925.07 ± 181.7	0.146
20:1n7	0.00 ± 0.0	0.00 ± 0.0	0.00 ± 0.0	–
20:1n9	0.00 ± 0.0	0.00 ± 0.0	0.00 ± 0.0	–
22:1n9	9.54 ± 9.4	18.09 ± 33.0	6.00 ± 4.9	0.383
24:1	13.58 ± 20.1	6.84 ± 16.7	6.39 ± 8.9	0.615
Total MUFA	11038.03 ± 158.0	228.97 ± 400.1	1036.33 ± 176.4	0.189
PUFA				
18:3n3	22.23 ± 6.2	24.61 ± 15.3	34.74 ± 10.8*,†	0.013
18:4n3	12.89 ± 8.6	8.80 ± 7.8	3.50 ± 3.6*	0.039

Table 3 continued

	Baseline	CRD-SFA	CRD-UFA	ANOVA
20:3n3	0.00 ± 0.0	0.00 ± 0.0	0.00 ± 0.0	–
20:4n3	0.00 ± 0.0	0.00 ± 0.0	0.00 ± 0.0	–
20:5n3	31.14 ± 9.4	35.27 ± 22.4	151.52 ± 81.0*,†	0.000
22:5n3	4.23 ± 3.6	3.08 ± 3.7	1.85 ± 1.7	0.311
22:6n3	29.92 ± 9.2	28.29 ± 10.0	41.53 ± 9.3*,†	0.003
18:2n6	2846.45 ± 493.33	283.30 ± 862.9	3026.10 ± 464.9	0.140
18:3n6	45.83 ± 22.5	33.73 ± 12.7	20.67 ± 8.2*	0.029
20:2n6	2.40 ± 2.5	4.44 ± 5.8	1.35 ± 1.3	0.252
20:3n6	33.35 ± 11.1	33.40 ± 12.8	18.48 ± 5.8*,†	0.026
20:4n6	362.54 ± 97.3	502.29 ± 136.6*	381.07 ± 56.3†	0.007
22:4n6	0.00 ± 0.0	0.00 ± 0.0	0.00 ± 0.0	0.252
22:5n6	0.00 ± 0.0	0.00 ± 0.0	0.00 ± 0.0	–
20:3n9	3.59 ± 4.8	4.48 ± 4.6	0.76 ± 0.9	0.217
Total PUFA	3394.56 ± 586.7	3961.70 ± 1045.3	3681.58 ± 536.2	0.110
Total n3	100.41 ± 14.5	100.05 ± 43.8	233.14 ± 92.2*,†	0.000
Total n6	3290.56 ± 588.1	3857.17 ± 1010.6	3447.68 ± 483.1	0.094
n6/n3	33.65 ± 8.5	42.73 ± 12.0	16.61 ± 5.9*,†	0.000
AA/EPA	11.91 ± 2.9	19.06 ± 10.7	3.15 ± 1.5*,†	0.001
CE (mol%)				
SFA				
14:0	0.69 ± 0.12	0.79 ± 0.27	0.56 ± 0.20	0.086
15:0	0.20 ± 0.13	0.25 ± 0.13	0.18 ± 0.16	0.115
16:0	11.51 ± 0.80	11.52 ± 0.57	11.14 ± 0.39	0.381
18:0	1.97 ± 2.59	1.16 ± 0.23	1.00 ± 0.21	0.422
20:0	0.10 ± 0.09	0.16 ± 0.19	0.06 ± 0.09	0.280
22:0	0.01 ± 0.02	0.08 ± 0.13	0.05 ± 0.06	0.302
24:0	0.01 ± 0.01	0.02 ± 0.05	0.02 ± 0.03	0.680
Total SFA	14.49 ± 3.26	13.98 ± 0.90	13.02 ± 0.69	0.361
MUFA				
14:1	0.01 ± 0.02	0.03 ± 0.04	0.03 ± 0.02	0.225
15:1	0.03 ± 0.07	0.02 ± 0.02	0.02 ± 0.03	0.764
16:1	2.30 ± 1.01	1.93 ± 0.22	1.57 ± 0.17	0.084
17:1	0.20 ± 0.04	0.26 ± 0.10	0.19 ± 0.02	0.129
18:1n9	16.68 ± 2.69	16.97 ± 1.54	16.74 ± 1.42	0.910
20:1n7	0.00 ± 0.00	0.00 ± 0.00	0.00 ± 0.00	–
20:1n9	0.00 ± 0.00	0.00 ± 0.00	0.00 ± 0.00	–
22:1n9	0.19 ± 0.19	0.27 ± 0.46	0.12 ± 0.10	0.460
24:1	0.27 ± 0.41	0.11 ± 0.28	0.12 ± 0.17	0.529
Total MUFA	19.68 ± 3.19	19.59 ± 1.19	18.80 ± 1.25	0.538
PUFA				
18:3n3	0.42 ± 0.10	0.37 ± 0.16	0.62 ± 0.12*,†	0.000
18:4n3	0.25 ± 0.20	0.14 ± 0.11	0.06 ± 0.07*	0.022
20:3n3	0.00 ± 0.00	0.00 ± 0.00	0.00 ± 0.00	–
20:4n3	0.00 ± 0.00	0.00 ± 0.00	0.00 ± 0.00	–
20:5n3	0.59 ± 0.17	0.55 ± 0.32	2.70 ± 1.23*,†	0.000
22:5n3	0.08 ± 0.07	0.05 ± 0.06	0.03 ± 0.03	0.273
22:6n3	0.57 ± 0.20	0.46 ± 0.12	0.76 ± 0.18*,†	0.000
18:2n6	53.36 ± 6.44	53.04 ± 2.73	54.87 ± 1.91	0.591

Table 3 continued

	Baseline	CRD-SFA	CRD-UFA	ANOVA
18:3n6	0.85 ± 0.35	0.55 ± 0.18	0.39 ± 0.16*	0.009
20:2n6	0.04 ± 0.05	0.07 ± 0.08	0.03 ± 0.02	0.376
20:3n6	0.62 ± 0.15	0.53 ± 0.08	0.35 ± 0.13*,†	0.003
20:4n6	6.75 ± 1.50	8.13 ± 0.83*	6.97 ± 1.04	0.045
22:4n6	0.00 ± 0.00	0.00 ± 0.00	0.00 ± 0.00	–
22:5n6	0.00 ± 0.00	0.00 ± 0.00	0.00 ± 0.00	–
20:3n9	0.06 ± 0.08	0.07 ± 0.07	0.01 ± 0.02	0.248
Total PUFA	63.60 ± 7.11	63.95 ± 2.74	66.79 ± 0.94	0.281
Total n3	1.91 ± 0.34	1.57 ± 0.46	4.18 ± 1.34*,†	0.000
Total n6	61.62 ± 7.40	62.31 ± 2.94	62.60 ± 1.69	0.903
n6/n3	33.65 ± 8.52	42.73 ± 11.98	16.61 ± 5.95*,†	0.000
AA/EPA	11.91 ± 2.93	19.06 ± 10.67	3.15 ± 1.49*,†	0.001

Values are means ± SD. Repeated measures ANOVA and Tukey post hoc

* $P < 0.05$ from baseline

† $P < 0.05$ from CRD-SFA

periods in this study significantly decreased TAG 16:1n-7, suggesting that similar reductions in our previous experiments using a hypocaloric CRD [3, 7], were a consequence of carbohydrate restriction rather than calorie reduction or weight loss. Lower 16:1n-7 also provides an explanation for the lack of association between dietary and plasma SFA since the 16:0 species is the primary product of fatty acid synthesis. Parallel reduction in 16:0 and 16:1n-7 suggests that stearoyl-CoA desaturase-1 (SCD-1), the enzyme responsible for desaturating 16:0, was not down-regulated independent of lipogenesis, since, in that case, the proportion of 16:0 would be expected to rise. Increased plasma levels of SFA and 16:1n-7 have been reported in obese adolescents [31] and adults with MetSyn [32] and higher 16:1n-7 is associated with increased abdominal obesity, lipogenesis, and hypertriglyceridemia [33, 34].

Highly Unsaturated Fatty Acids

The increase in PL ARA in weight stable men after the CRD-SFA (order of 2 units expressed as mol%) is similar to the previously reported effect in overweight men on a hypocaloric diet [7] indicating that the latter was not due to weight loss. Replacing SFA with unsaturated fat including n-3 PUFA prevented the increase in plasma ARA, and also resulted in a marked increase in plasma EPA and DHA, likely a result of higher dietary intake on the CRD-UFA (1.5 g vs. 0.4 g/day). Previous studies have shown close association between dietary EPA and DHA and plasma EPA and DHA [35]. Increased plasma ARA following CRD-SFA may have resulted from less competition from n-3 PUFA for preferential acyl incorporation into the sn-2 position of phospholipids [36]. Dietary intakes of ARA were high in both CRD-UFA and CRD-SFA. Competition among n-3 and n-6 PUFA at the level of desaturation and chain elongation steps of fatty acid biosynthesis may also be important.

An increase in phospholipid ARA mol% and PL ARA/EPA ratio is commonly viewed as contributing to a pro-inflammatory and pro-oxidative state. These effects following CRD-SFA, however, were not accompanied by elevation of any of the inflammatory markers or 8-iso $PGF_{2\alpha}$. Along these lines, a meta-analysis of 14 case–control and prospective cohort studies found that increased ARA in plasma PL or triglycerides was not associated with coronary events [37], while a recent case-controlled study of acute coronary syndrome (ACS) found a U-shaped relationship between odds ratio for ACS and erythrocyte ARA content [38]. Ferrucci L et al. [15] demonstrated and inverse relation between plasma ARA and pro-inflammatory markers, in agreement with the current study. A CRD that resulted in an increased ARA/EPA ratio also decreased C-reactive protein (CRP) [17]. A number of other studies have failed to link increased ARA in plasma lipids with deleterious outcomes [39–43]. The lack of association between plasma PL ARA and plasma PL ARA/EPA ratio and inflammation following CRD-SFA supports the idea that ARA in plasma membranes is not pro-inflammatory, especially in the context of low dietary carbohydrate. In fact, there was a trend ($P < 0.08$) for an anti-inflammatory effect on the adipocytokine leptin. Although leptin is not a classic cytokine, several immune cells (including polymorphonuclear leukocytes, monocytes, macrophages and lymphocytes) have leptin receptors and their activity can be modulated by leptin. Leptin has also been shown to stimulate production of ROS by activated monocytes in vitro [44].

Previous CRD investigations indicate significant reductions in response to a low carbohydrate diet even when normalizing for changes in body or fat mass [3].

The isoprostane 8-iso $PGF_{2\alpha}$ is a free radical-catalyzed product of ARA measured as a general indicator of oxidative stress [18]. We found no change in 8-iso $PGF_{2\alpha}$ after the CRD-SFA despite a significant increase in plasma ARA. Similarly, a significant decrease in 8-iso $PGF_{2\alpha}$ was observed after the CRD-UFA where there was no change in plasma ARA. The inverse correlation between changes in plasma PL ARA and 8-iso $PGF_{2\alpha}$ indicates better preservation of ARA in response to a CRD. The fat sources in this diet, olive oil and lipid from fish and liquid omega-3 eggs, may have contributed to lower urinary 8-iso $PGF_{2\alpha}$ following CRD-UFA. Urinary excretion has been shown to be reduced by extra virgin olive oil [45], moderate fish oil supplementation (3.6 g/d n-3 PUFA), [46] and one daily fish meal (providing 3 g n-3 PUFA) reduced urinary F_2-isoprostane levels in dyslipidemic non-insulin-dependent diabetic patients [47].

Insulin Resistance Syndrome

Saturated fatty acids are often implicated in the worsening of insulin resistance [48], but the effect is contingent upon the presence of ample carbohydrate. Carbohydrate restriction in the presence of high saturated fat leads to improvement in insulin sensitivity despite increased lipolytic rates and release of fatty acids into the circulation [49]. In the current study, the two subjects who had insulin resistance at baseline improved after restricting carbohydrate. The TAG/HDL-C ratio is strongly correlated with insulin resistance and levels >3.5 are indicative of increased CVD risk [50]. All subjects showed TAG/HDL-C values less than this value after the CRD consistent with the HOMA-IR results. Carbohydrate restrictions thus improved insulin sensitivity independent of dietary fatty acid composition. Many factors can influence serum cholesterol responses to saturated fat [51] including genetic variations [52] and the current study showed high variability in LDL-C. Independent of LDL-C concentration, however, individuals with a predominance of small LDL particles (pattern B) have >threefold risk of CVD [53]. In the current study, the variable LDL response was accompanied by uniform increase in LDL particle size.

Dietary Recommendations

The current findings further challenge the broad recommendation to restrict saturated fat especially since those calories are likely to be replaced with carbohydrate. The many factors that contribute to the relation of fat intake and fatty acid composition have been reviewed [54], and our results emphasize the substantial impact of a low carbohydrate intake in regulating the connection between dietary and plasma SFA. A higher saturated fat intake can be efficiently metabolized in the presence of low carbohydrate and lead to consistent improvements in markers of CVD risk. Whereas studies of benefits of carbohydrate restriction are rarely cited in the literature, responses of even a single meal high in saturated fat are taken as convincing evidence even if done in the presence of high carbohydrate. Ultimately, however, long term studies show that replacement of saturated fat with carbohydrate is at best neutral [55, 56]. Persistence of recommendations in the face of continued failure of large trials to show an effect of saturated fat remains one of the strange anomalies in current medical science.

Substitution of a portion of the SFA within a CRD with UFA including a combination of both MUFA and n-6 and n-3 PUFA had a profound effect on plasma fatty acid composition, reduced oxidative stress, but did not alter the positive effects on features of metabolic syndrome (e.g., insulin, TAG, LDL particle size). As low carbohydrate diets become more widely prescribed and used, it will be important to determine the range of dietary fatty acids most conducive to improving long-term health. Our results point to a suitable diet that had an emphasis on low carbohydrate foods with fat sources emphasizing MUFA and n-3 PUFA (e.g., omega-3 eggs, avocado, salmon, sardines, meat, poultry, olive oil, canola oil, nuts and seeds) although there was little if any detriment in a higher saturated fat approach.

Acknowledgments This work was supported by the American Egg Board-Egg Nutrition Center Dissertation Fellowship in Nutrition Award. The funding agency had no input to the design and conduct of the study, the interpretation of the data, or preparation and approval of manuscripts.

References

1. Volek JS, Fernandez ML, Feinman RD, Phinney SD (2008) Dietary carbohydrate restriction induces a unique metabolic state positively affecting atherogenic dyslipidemia, fatty acid partitioning, and metabolic syndrome. Prog Lipid Res 47:307–318
2. Volek JS, Feinman RD (2005) Carbohydrate restriction improves the features of metabolic syndrome. Metabolic syndrome may be defined by the response to carbohydrate restriction. Nutr Metab (Lond) 2:31
3. Volek JS, Phinney SD, Forsythe CE et al (2009) Carbohydrate restriction has a more favorable impact on the metabolic syndrome than a low fat diet. Lipids 44:297–309
4. Krauss RM, Blanche PJ, Rawlings RS, Fernstrom HS, Williams PT (2006) Separate effects of reduced carbohydrate intake and weight loss on atherogenic dyslipidemia. Am J Clin Nutr 83:1025–1031
5. Sharman MJ, Kraemer WJ, Love DM et al (2002) A ketogenic diet favorably affects serum biomarkers for cardiovascular disease in normal-weight men. J Nutr 132:1879–1885

6. Volek JS, Sharman MJ, Gomez AL, Scheett TP, Kraemer WJ (2003) An isoenergetic very low carbohydrate diet improves serum HDL cholesterol and triacylglycerol concentrations, the total cholesterol to HDL cholesterol ratio and postprandial lipemic responses compared with a low fat diet in normal weight, normolipidemic women. J Nutr 133:2756–2761
7. Forsythe CE, Phinney SD, Fernandez ML et al (2008) Comparison of low fat and low carbohydrate diets on circulating fatty acid composition and markers of inflammation. Lipids 43:65–77
8. Siri-Tarino PW, Sun Q, Hu FB, Krauss RM (2010) Meta-analysis of prospective cohort studies evaluating the association of saturated fat with cardiovascular disease. Am J Clin Nutr 91(3):535–546
9. Siri-Tarino PW, Sun Q, Hu FB, Krauss RM (2010) Saturated fat, carbohydrate, and cardiovascular disease. Am J Clin Nutr 91(3):502–509
10. Cassady BA, Charboneau NL, Brys EE, Crouse KA, Beitz DC, Wilson T (2007) Effects of low carbohydrate diets high in red meats or poultry, fish and shellfish on plasma lipids and weight loss. Nutr Metab (Lond) 4:23
11. King IB, Lemaitre RN, Kestin M (2006) Effect of a low-fat diet on fatty acid composition in red cells, plasma phospholipids, and cholesterol esters: investigation of a biomarker of total fat intake. Am J Clin Nutr 83:227–236
12. Raatz SK, Bibus D, Thomas W, Kris-Etherton P (2001) Total fat intake modifies plasma fatty acid composition in humans. J Nutr 131:231–234
13. Hjelte LE, Nilsson A (2005) Arachidonic acid and ischemic heart disease. J Nutr 135:2271–2273
14. Lands B (2008) A critique of paradoxes in current advice on dietary lipids. Prog Lipid Res 47:77–106
15. Ferrucci L, Cherubini A, Bandinelli S, Bartali B, Corsi A, Lauretani F, Martin A, Andres-Lacueva C, Senin U, Guralnik JM (2006) Relationship of plasma polyunsaturated fatty acids to circulating inflammatory markers. J Clin Endocrinol Metab 91:439–446
16. von Schacky C, Harris WS (2007) Cardiovascular risk and the omega-3 index. J Cardiovasc Med (Hagerstown) 8(Suppl 1): S46–S49
17. Johnston CS, Tjonn SL, Swan PD, White A, Hutchins H, Sears B (2006) Ketogenic low-carbohydrate diets have no metabolic advantage over nonketogenic low-carbohydrate diets. Am J Clin Nutr 83:1055–1061
18. Morrow JD, Roberts LJ (1997) The isoprostanes: unique bioactive products of lipid peroxidation. Prog Lipid Res 36:1–21
19. Harris WS, Pottala JV, Sands SA, Jones PG (2007) Comparison of the effects of fish and fish-oil capsules on the n 3 fatty acid content of blood cells and plasma phospholipids. Am J Clin Nutr 86:1621–1625
20. Volek JS, Gomez AL, Kraemer WJ (2000) Fasting lipoprotein and postprandial triacylglycerol responses to a low-carbohydrate diet supplemented with n-3 fatty acids. J Am Coll Nutr 19:383–391
21. Radikova Z, Koska J, Huckova M et al (2006) Insulin sensitivity indices: a proposal of cut-off points for simple identification of insulin-resistant subjects. Exp Clin Endocrinol Diab 114:249–256
22. Hoidrup S, Andreasen AH, Osler M et al (2002) Assessment of habitual energy and macronutrient intake in adults: comparison of a seven day food record with a dietary history interview. Eur J Clin Nutr 56:105–113
23. Feinman RD, Fine EJ (2004) "A calorie is a calorie" violates the second law of thermodynamics. Nutr J 3(9)
24. Keys A (1970) Coronary heart disease in seven countries 41(Suppl): 1–211
25. American Diabetes Association (2008) Nutrition recommendations and interventions for diabetes—2008. Diabetes Care 31(Suppl 1):S61–S78
26. Klein S, Wolfe RR (1992) Carbohydrate restriction regulates the adaptive response to fasting. Am J Physiol 262:E631–E636
27. Kotronen A, Velagapudi VR, Yetukuri L et al (2009) Serum saturated fatty acids containing triacylglycerols are better markers of insulin resistance than total serum triacylglycerol concentrations. Diabetologia 52:684–690
28. Miettinen TA, Naukkarinen V, Huttunen JK, Mattila S, Kumlin T (1982) Fatty-acid composition of serum lipids predicts myocardial infarction. Br Med J (Clin Res Ed) 285:993–996
29. Wang L, Folsom AR, Eckfeldt JH (2003) Plasma fatty acid composition and incidence of coronary heart disease in middle aged adults: the atherosclerosis risk in communities (ARIC) study. Nutr Metab Cardiovasc Dis 13:256–266
30. Aarsland A, Wolfe RR (1998) Hepatic secretion of VLDL fatty acids during stimulated lipogenesis in men. J Lipid Res 39:1280–1286
31. Klein-Platat C, Drai J, Oujaa M, Schlienger JL, Simon C (2005) Plasma fatty acid composition is associated with the metabolic syndrome and low-grade inflammation in overweight adolescents. Am J Clin Nutr 82:1178–1184
32. Warensjo E, Riserus U, Vessby B (2005) Fatty acid composition of serum lipids predicts the development of the metabolic syndrome in men. Diabetologia 48:1999–2005
33. Kunesova M, Hainer V, Tvrzicka E et al (2002) Assessment of dietary and genetic factors influencing serum and adipose fatty acid composition in obese female identical twins. Lipids 37:27–32
34. Paillard F, Catheline D, Duff FL et al (2008) Plasma palmitoleic acid, a product of stearoyl-coA desaturase activity, is an independent marker of triglyceridemia and abdominal adiposity. Nutr Metab Cardiovasc Dis 18:436–440
35. Vidgren HM, Agren JJ, Schwab U, Rissanen T, Hanninen O, Uusitupa MI (1997) Incorporation of n-3 fatty acids into plasma lipid fractions, and erythrocyte membranes and platelets during dietary supplementation with fish, fish oil, and docosahexaenoic acid-rich oil among healthy young men. Lipids 32:697–705
36. Lands WE, Libelt B, Morris A, Kramer NC, Prewitt TE, Bowen P, Schmeisser D, Davidson MH, Burns JH (1992) Maintenance of lower proportions of (n-6) eicosanoid precursors in phospholipids of human plasma in response to added dietary (n-3) fatty acids. Biochim Biophys Acta 1180:147–162
37. Harris WS, Poston WC, Haddock CK (2007) Tissue n-3 and n-6 fatty acids and risk for coronary heart disease events. Atherosclerosis 193:1–10
38. Block RC, Harris WS, Reid KJ, Spertus JA (2008) Omega-6 and trans fatty acids in blood cell membranes: a risk factor for acute coronary syndromes? Am Heart J 156:1117–1123
39. Nelson GJ, Schmidt PC, Bartolini G, Kelley DS, Phinney SD, Kyle D, Silbermann S, Schaefer EJ (1997) The effect of dietary arachidonic acid on plasma lipoprotein distributions, apoproteins, blood lipid levels, and tissue fatty acid composition in humans. Lipids 32:427–433
40. Nelson GJ, Schmidt PC, Bartolini G, Kelley DS, Kyle D (1997) The effect of dietary arachidonic acid on platelet function, platelet fatty acid composition, and blood coagulation in humans. Lipids 32:421–425
41. Kelley DS, Taylor PC, Nelson GJ, Schmidt PC, Mackey BE, Kyle D (1997) Effects of dietary arachidonic acid on human immune response. Lipids 32:449–456
42. Kelley DS, Taylor PC, Nelson GJ, Mackey BE (1998) Arachidonic acid supplementation enhances synthesis of eicosanoids without suppressing immune functions in young healthy men. Lipids 33:125–130
43. Calder PC (2007) Dietary arachidonic acid: harmful, harmless or helpful? Br J Nutr 98:451–453

44. Guzik TJ, Mangalat D, Korbut R (2006) Adipocytokines—novel link between inflammation and vascular function? J Physiol Pharmacol 57:505–528
45. Visioli F, Caruso D, Galli C, Viappiani S, Galli G, Sala A (2000) Olive oils rich in natural catecholic phenols decrease isoprostane excretion in humans. Biochem Biophys Res Commun 278:797–799
46. Nalsen C, Vessby B, Berglund L, Uusitupa M, Hermansen K, Riccardi G, Rivellese A, Storlien L, Erkkila A, Yla-Herttuala S, Tapsell L, Basu S (2006) Dietary (n-3) fatty acids reduce plasma F2-isoprostanes but not prostaglandin F2alpha in healthy humans. J Nutr 136:1222–1228
47. Mori TA, Dunstan DW, Burke V, Croft KD, Rivera JH, Beilin LJ, Puddey IB (1999) Effect of dietary fish and exercise training on urinary F2-isoprostane excretion in non-insulin-dependent diabetic patients. Metabolism 48:1402–1408
48. Vessby B, Unsitupa M, Hermansen K et al (2001) Substituting dietary saturated for monounsaturated fat impairs insulin sensitivity in healthy men and women: the KANWU study. Diabetologia 44:312–319
49. Kirk E, Reeds DN, Finck BN, Mayurranjan SM, Patterson BW, Klein S (2009) Dietary fat and carbohydrates differentially alter insulin sensitivity during caloric restriction. Gastroenterology 136:1552–1560
50. McLaughlin T, Reaven G, Abbasi F et al (2005) Is there a simple way to identify insulin-resistant individuals at increased risk of cardiovascular disease? Am J Cardiol 96:399–404
51. Wilke MS, Clandinin MT (2005) Influence of dietary saturated fatty acids on the regulation of plasma cholesterol concentration. Lipids 40:1207–1213
52. Mata P, Lopez-Miranda J, Pocovi M et al (1998) Human apolipoprotein A-I gene promoter mutation influences plasma low density lipoprotein cholesterol response to dietary fat saturation. Atherosclerosis 137:367–376
53. Austin MA, King MC, Vranizan KM, Krauss RM (1990) Atherogenic lipoprotein phenotype. A proposed genetic marker for coronary heart disease risk. Circulation 82:495–506
54. Lands WEM (1995) Long-term fat intake and biomarkers. Am J Clin Nutr 61:721S–725S
55. Howard BV, Van Horn L, Hsia J et al (2006) Low-fat dietary pattern and risk of cardiovascular disease: the women's health initiative randomized controlled dietary modification trial. JAMA 295:655–666
56. Jakobsen MU, O'Reilly EJ, Heitmann BL et al (2009) Major types of dietary fat and risk of coronary heart disease: a pooled analysis of 11 cohort studies. Am J Clin Nutr 89:1425–1432

Lipids (2010) 45:963–973
DOI 10.1007/s11745-010-3476-2

ORIGINAL ARTICLE

Bovine Adipose Triglyceride Lipase is Not Altered and Adipocyte Fatty Acid-Binding Protein is Increased by Dietary Flaxseed

Jeffrey Deiuliis · Jonghyun Shin · Eric Murphy · Scott L. Kronberg · Maurice L. Eastridge · Yeunsu Suh · Jong-Taek Yoon · Kichoon Lee

Received: 11 May 2010 / Accepted: 14 September 2010 / Published online: 1 October 2010

Abstract In this paper, we report the full-length coding sequence of bovine ATGL cDNA and analyze its expression in bovine tissues. Similar to human, mouse, and pig ATGL sequences, bovine ATGL has a highly conserved patatin domain that is necessary for lipolytic function in mice and humans. This suggests that ATGL is functionally intact as a triglyceride lipase in cattle. Tissue distribution of ATGL gene expression was highest in fat and muscle (skeletal and cardiac) tissue, while protein expression was solely detectible in the adipose tissue. The effect of 109 days of flaxseed supplementation on ATGL and adipocyte fatty acid-binding protein (FABP4 or A-FABP, E-FABP or FABP5) expression was examined in Angus steers. Supplemented steers had greater triacylglycerol (TAG) content in the muscle compared with unsupplemented ones. Additionally, supplementation increased A-FABP expression and decreased stearoyl-CoA desaturase 1 (SCD-1) expression in muscle, while total ATGL expression was unaffected. In summary, supplementation of cattle rations with flaxseed increased muscle TAG concentrations attributed in part to increased expression of key enzymes involved in lipid trafficking (A-FABP) and metabolism (SCD-1).

Keywords Lipolysis · Adipose triglyceride lipase · Bovine · Flaxseed

J. Deiuliis · J. Shin · M. L. Eastridge · Y. Suh · K. Lee
Department of Animal Sciences and The Ohio State University Interdisciplinary Human Nutrition Program, The Ohio State University, Columbus, OH, USA

E. Murphy
Department of Pharmacology, Physiology, and Therapeutics and Department of Chemistry, School of Medicine and Health Sciences, University of North Dakota, 501N. Columbia Road, Room 3700, Grand Forks, ND 58202-9037, USA

S. L. Kronberg
USDA, ARS, Northern Great Plains Research Laboratory, Mandan, ND 58554, USA

J.-T. Yoon
Department of Animal Life Resources, HanKyung National University, Kyunggi-do 456-749, Korea

K. Lee (✉)
Department of Animal Sciences, The Ohio State University, 2029 Fyffe Rd, Columbus, OH 43210, USA
e-mail: lee.2626@osu.edu

Abbreviations

AA	Amino acid
A-FABP	Adipocyte-type fatty acid-binding protein
ATGL	Adipose triglyceride lipase
E-FABP	Epidermal fatty acid-binding protein
FS	Flaxseed supplementation
H-FABP	Heart-type fatty acid binding protein
HRP	Horse radish peroxidase
HSL	Hormone sensitive lipase
LPL	Lipoprotein lipase
M-MLV	Moloney murine leukemia virus
PKA	Protein kinase A
PMSF	Phenylmethylsulfonyl fluoride
PPARγ	Peroxisome proliferator-activated receptor gamma
PVDF	Polyvinylidene fluoride
SCD-1	Stearoyl-CoA desaturase 1
TBST	Tris-buffered saline with Tween twenty
TAG	Triacylglycerol

Introduction

Altering the fatty acid composition of beef products for human consumption adds value, creating a functional food which may enhance the overall health of meat-consuming individuals. In the Western diet, the consumption of n-3 fatty acids via dietary intake is low because of relatively low rates of fish consumption and the industrial production of animal feeds rich in grains containing n-6 fatty acids, leading to production of meat rich in n-6 and low in n-3 fatty acids [1]. In addition, it is important to mention that beef fat has a high degree of saturation due to the biohydrogenation of unsaturated dietary fatty acids by rumen microorganisms, though there is a variation in the n-6/n-3 ratio between breeds and production systems. It has been demonstrated that feeding diets high in flaxseed increases n-3 fatty acid content in beef and poultry [2–4]. We have previously shown that n-3 levels in Angus beef increased from 27 to 45 mg per 100 g [2]. The acceptable macronutrient distribution range set by the National Academy of Sciences, Institute of Medicine, Food and Nutrition Board in 2005 for total n-3 fatty acids is 0.6–1.2% of energy, 1.3–2.6 g for a person consuming 2,000 kilocalories per day. Studies indicate that in humans, a high intake of n-6 fatty acids shifts the physiologic state to one that is prothrombotic and proaggregatory, characterized by increases in blood viscosity and vasoconstriction, and reduced bleeding time, while high intake of n-3 fatty acids have anti-inflammatory, anti-thrombotic, anti-hypertensive, and anti-arrhythmic properties, while also improving arterial compliance, vasodilation, and serum lipid profiles [5–8]. The average Western diet has an n-6 to n-3 fatty acid ratio of approximately 20–30:1 [5], hence large scale production of n-3 enriched meats would provide alternative sources of n-3 fatty acids for consumers.

Supplementation with flaxseed changes not only the fatty acid composition of skeletal muscle of Angus steers [2], but may also affect lipid metabolism within the muscle altering total fat concentration. Because dietary n-3 fatty acids increase the expression of PPARγ in flax-supplemented cattle [2], the impact of this dietary regimen on the expression of adipose triglyceride lipase (ATGL) and on adipocyte fatty acid-binding protein (A-FABP, FABP-4) was examined in this study. ATGL is a newly discovered lipase which hydrolyzes the first ester bond of stored triacylglycerols, releasing nonesterified free fatty acids [9]. It is associated with lipid droplets and is found at high concentrations in adipose tissue, though it is present in tissues with lipid stores [10]. ATGL activity is required for PKA-stimulated fatty acid and glycerol release in murine embryonic fibroblast adipocytes [11] and is the rate-limiting step in hormone-induced lipolysis [9, 12]. The product, diacylglycerol, is then hydrolyzed by activated hormone sensitive lipase (HSL), which has a higher substrate affinity for diacylglycerol than triacylglycerol (TAG) [12]. A direct interaction between A-FABP and HSL promotes the hydrolysis of lipid droplet stored TAG, thus it is thought that A-FABP may be involved in fatty acid trafficking from the lipid droplet to the adipocyte membrane where the fatty acid leaves the cell [13, 14]. Thus, ATGL, HSL, and A-FABP work in concert to mobilize esterified fatty acids stores from lipid storing tissues, although the impact of n-3 fatty acid supplementation on expression of these key proteins in cattle is not fully characterized.

To address this question, we examined the expression of these proteins in longissimus muscle of Angus steers finished on a diet containing flaxseed rations. In addition, while the sequences of ATGL for mouse, swine, human, and avian species are known [9, 15, 16], the sequence of bovine ATGL and its response to dietary manipulation is not known. Herein, we report for the first time the sequence for bovine ATGL and characterize ATGL gene expression in cattle. We also demonstrate that ATGL gene expression was not influenced by dietary n-3 fatty acids in cattle, although the expression of A-FABP was increased, consistent with our previous work demonstrating an increase in PPARγ expression in these cattle [2].

Materials and Methods

Feeding Regimen for Angus Cattle

The experimental methods for the feeding of Angus steers were described in our previous report [2]. Briefly, 20 Angus steers that were 16 months old with a mean body weight of 414 kg (SD = 39 kg) at the start of the study were divided into two groups: flaxseed supplement (907 g/day) and control groups (10 steers per group). The basal diet of the grazing steers was forage during the first 2.5 months of the trial, then a combination of forage and concentrate for the next month and primarily concentrate for the final month [2]. Intake of feedstuffs for the basal diet of grazing steers was ad libitum and the percentage of their diet from flaxseed (907 g/day for final 107 days of supplementation) was therefore not determined. At the end of the flaxseed supplementation period, the steers were slaughtered and cross-sectional pieces of longissimus dorsi muscles (ribeye steaks) between the 12th and 13th ribs were collected from each carcass. Muscle tissues were stored at −80°C for later use.

Four Angus cattle with about 460 kg of body weight (~550 day old) were euthanized by captive bolt stunning and exsanguination at the Ohio State University's Meat Science Laboratory located in the Department of Animal Sciences, Columbus, OH, USA. Adipose tissue, heart, muscle, lung, liver, and kidney were collected immediately

after euthanization, snap-frozen in liquid nitrogen and stored at −80°C before total RNA and protein isolations to examine tissue distribution of ATGL expression. Animal care and procedures were approved by the OSU Institutional Animal Care and Use Committee.

RNA Isolation

RNA was isolated from bovine tissue samples using Trizol™ (Invitrogen, Carlsbad, CA, USA) according to the manufacturer's instructions. RNA quality was assessed by agarose gel electrophoresis. Approximately 1 μg of total RNA was reverse transcribed according to the manufacturer's instructions (Invitrogen Life Technologies—M-MLV reverse transcriptase).

Cloning of Bovine ATGL

Subcutaneous dorsal back adipose (100 mg) was sampled within 3 min of euthanization, snap-frozen in liquid nitrogen, and stored at −80°C before total RNA isolation. Complementary DNA from subcutaneous adipose tissue of Angus cattle was used as a template for PCR. Primers were designed according to several partial bovine DNA sequences that contain conserved sequence homology among human (Genbank accession numbers: AY894804, NM_020376) and mouse (AJ278476, AK031609) sequences. A MJ Research PTC-200 thermal cycler (MJ Research Inc., South San Francisco, CA, USA) and DNA Taq polymerase (Invitrogen) were used for all PCR. The PCR products were separated by electrophoresis on a 1% agarose gel and the appropriate band(s) excised and gel extracted using the Qiagen Gel Extraction kit (Qiagen, Alameda City, CA, USA). The product was then ligated to the pCR 2.1-TOPO vector using the TOPO TA Cloning Kit (Invitrogen). Positive clones were sequenced by The Ohio State University sequencing core facility using an Applied Biosystems 3730 DNA Analyzer (Foster City, CA, USA). The resulting sequences confirmed bovine ATGL by homology to the mouse, human, and pig and by identification of characteristic enzyme domains. Real-time primers were then designed to measure ATGL gene expression ("F2" 5′-GTGGACGGTGGCATCTCAGA-3′, "R2" 5′-TACAGGGATGGCCTCCGCTT-3′). Primers were designed to span genomic introns, thus allowing for detection of genomic DNA contamination. PCR using F2/R2 primers were optimized for use in real-time PCR.

Quantitative Real-Time PCR Detection of Total Gene Expression

Real-time PCR was performed using SYBR green I nucleic acid dye (Molecular Probes Invitrogen detection technologies) on an ABI 7300 (Applied Biosystems). AmpliTaq Gold™ (Applied Biosystems) was used in all real-time reactions as was the following thermal profile: 95°C 10 m, 40 cycles of 94°C 30 s, 58°C 60 s, 82°C 30 s. The C_T values for the internal control (cyclophilin) and target genes, as determined by the ABI software, were used to calculate gene expression using the $2^{-\Delta\Delta Ct}$ method. All target genes were normalized to cyclophilin and changes were calculated as relative fold-change to cyclophilin. Randomly selected samples from all real-time runs were resolved by agarose gel electrophoresis to ensure the amplification of one product. In addition, dissociation/melting curves yielded single peaks, indicating a single product with lack of primer dimers or genomic DNA contamination. "No template" negative controls were included in all PCR to detect contamination. Primer sequences used for the quantitative real-time PCR are shown in Table 1.

Protein Isolation and Immunoblotting

Approximately 80 mg of tissue was homogenized in 800 μl of lysis buffer (1% Triton X-100, 150 mM NaCl, 20 mM HEPES pH 7.5, 10% glycerol, 1 mM EDTA, 100 mM NaF, 100 μM sodium orthovanadate, 1 mM PMSF, and 10 μL/mL protease inhibitor cocktail (Sigma–Aldrich, P8340). The protein content of cell lysate was determined using the bicinchoninic acid (BCA) Protein Assay Kit (Pierce Chemical Co., Rockfold, IL, USA). Samples were separated by SDS-PAGE using the mini-Protean system (Bio-RadHer). The protein was wet-transferred to a PVDF membrane (Amersham Biosciences Hybond-P™), blocked in 5% non-fat dry milk in 1x-TBST (0.1% Tween 20) and incubated overnight at 4°C with primary antibody (1:3,000) specific to ATGL (Cell Signaling Technology, Inc., Danvers. MA, USA) in 5% non-fat dry milk. After washing in 1x-TBST, blots were incubated with the appropriated HRP-conjugated secondary antibody for 1 h at room temperature. Blots were washed before addition of ECL plus™ (Amersham Biosciences) and bands were detected with Hyperfilm™ (Amersham Biosciences).

Analysis of Triacylglycerol Mass

Samples were taken from visibly lean portions of frozen ribeye steak and immersed in liquid nitrogen. These samples were then pulverized at liquid nitrogen temperatures to a fine homogeneous powder. Pulverized muscle tissue from flaxseed-supplemented and non-supplemented Angus steers was weighed, homogenized in hexane: 2-propanol (3:2 by vol) using a Polytron tissue homogenizer, and the lipids were extracted [17]. The samples were subjected to centrifugation (2,750*g*, 4°C, 10 min) and the lipid containing solvent removed from the pellet. The samples were

Table 1 Primer sequences for quantitative real-time polymerase chain reaction

Primer	Sequence	Product size (bp)	GenBank accession #
ATGL-F1	5′-CCGCGATGTTCCCCAAGGAGA-3′	742	FJ897536
ATGL-R1	5′-AAGCGGAGGCCATCCCTGTA-3′		
ATGL-F2	5′-GTGGACGGTGGCATCTCAGA-3′	983	FJ897536
ATGL-R2	5′-CCTTAGCAAGGGGGCGAGCT-3′		
ATGL-F2	5′-GTGGACGGTGGCATCTCAGA-3′	251	FJ897536
ATGL-R1	5′-AAGCGGAGGCCATCCCTGTA-3′		
LPL-F	5′-ACTGTGGCTGAGAGCGAGAACA-3′	310	NM_001075120
LPL-R	5′-TATTCAGGGACTTGTCATGGCAT-3′		
HSL-F	5′-AGTCCCACCTGAAATCAGTGT-3′	226	NM_001080220
HSL-F	5′-CCAAGTAAGAAGTTGATGGTT-3′		
CYC-F	5′-GTGGTCATCGGTCTCTTTGG-3′	184	NM_174152
CYC-R	5′-CACCGTAGATGCTCTTACCTC-3′		
A-FABP-F	5′-CAGTGAAAACTTTGATGATTA-3′	191	NM_174314
A-FABP-R	5′-CTGGAGTGATTTCATCAAATT-3′		
SCD-1-F	5′-AAGAGCCGAGAAGCTGGTGAT-3′	362	AY241933
SCD-1-R	5′-AATCAATGA AGAACGTGGTAAA-3′		
E-FABP-F	5′-GAGAAGTTTGAAGAGACCACAGCTG-3′	248	NM_174315.3
E-FABP-R	5′-AGCTTGTTCATCCTCGCAGCT-3′		

ATGL adipose triglyceride lipase, *LPL* lipoprotein lipase, *HSL* hormone sensitive lipase, *CYC* cyclophilin, *A-* or *E-FABP* adipocyte- or epidermal-fatty acid binding protein, *SCD*-1 stearoyl-CoA desaturase (delta-9-desaturase), *F* forward, *R* reverse

reduced in volume using nitrogen evaporation and the lipid redissolved in a known volume of hexane:2-propanol (3:2 by vol). To analyze TAG mass, the samples were quantitatively applied to a thin layer chromatography plate (silica gel G, Analtech, Newark, DE, USA) and the neutral lipids separated using petroleum ether:diethyl ether:acetic acid (75:25:1.3 by vol). This method separates TAG from cholesteryl esters as well as from other neutral lipids, such as cholesterol and unesterified fatty acids [8]. The TAG was removed from the plate by scrapping and the sample placed into an acid-washed test tube to which concentrated sulfuric acid was added [18]. The tube was heated at 200°C for 15 min in a heating block and the sample subjected to centrifugation (2,500 *g* for 10 min) to pellet the silica. The absorbance at 375 nm was measured in a quartz cuvette using a Beckman DU-640 spectrophotometer (Fullerton, CA, USA). Absorbance was converted to mass using triolein glycerol (MW 882, Nuchek Prep, Elysian, MN, USA) and the values are expressed as μg/g wet weight (ww).

Bioinformatics, Sequence Analysis, and Statistical Analysis

Bioinformatics and sequence analysis were performed as previously described [11]. The sequence Scanner (v 1.0) was used to generate the chromatogram of cloned bovine ATGL cDNA by using Applied Biosystems genetic analyzer instruments. ATGL nucleotide and putative protein sequences of pig [15] and avian [16] were already reported and used for sequence analysis and comparison. Mouse and human ATGL nucleotide and putative protein sequences were obtained from NCBI. The alignment and comparison of nucleotide or protein sequences were done using ClustalX and GeneDoc™ software. The phylogenic tree was constructed by CLUSTAL W (Version 1.83) and MEGA 4 software (neighbor joining method) [19] using the putative ATGL protein sequences of various species. The neighbor joining method is a simplified version of the minimum evolution (ME) method using distance measures to correct for multiple hits at the same sites, and chooses a topology showing the smallest value of the sum of all branches as an estimate of the correct tree [19].

With the exception of the phylogenic branch lengths, all results are presented as mean ± SEM. Comparison of two means was accomplished by a Student's *t* test at $P \leq 0.05$ and 0.01. Comparisons among gene expression data were performed using one-way analysis of variance (ANOVA) followed by the Tukey's test at $P \leq 0.05$. Statistical analysis was performed using Minitab software (version 15.0).

Results

We identified several partial bovine DNA sequences in The Institute for Genomic Research (TIGR) database that were homologous to the human ATGL sequence. Primers were designed based on these sequences to clone a full length sequence of bovine ATGL. Soon after we cloned this sequence, another group submitted a bovine ATGL

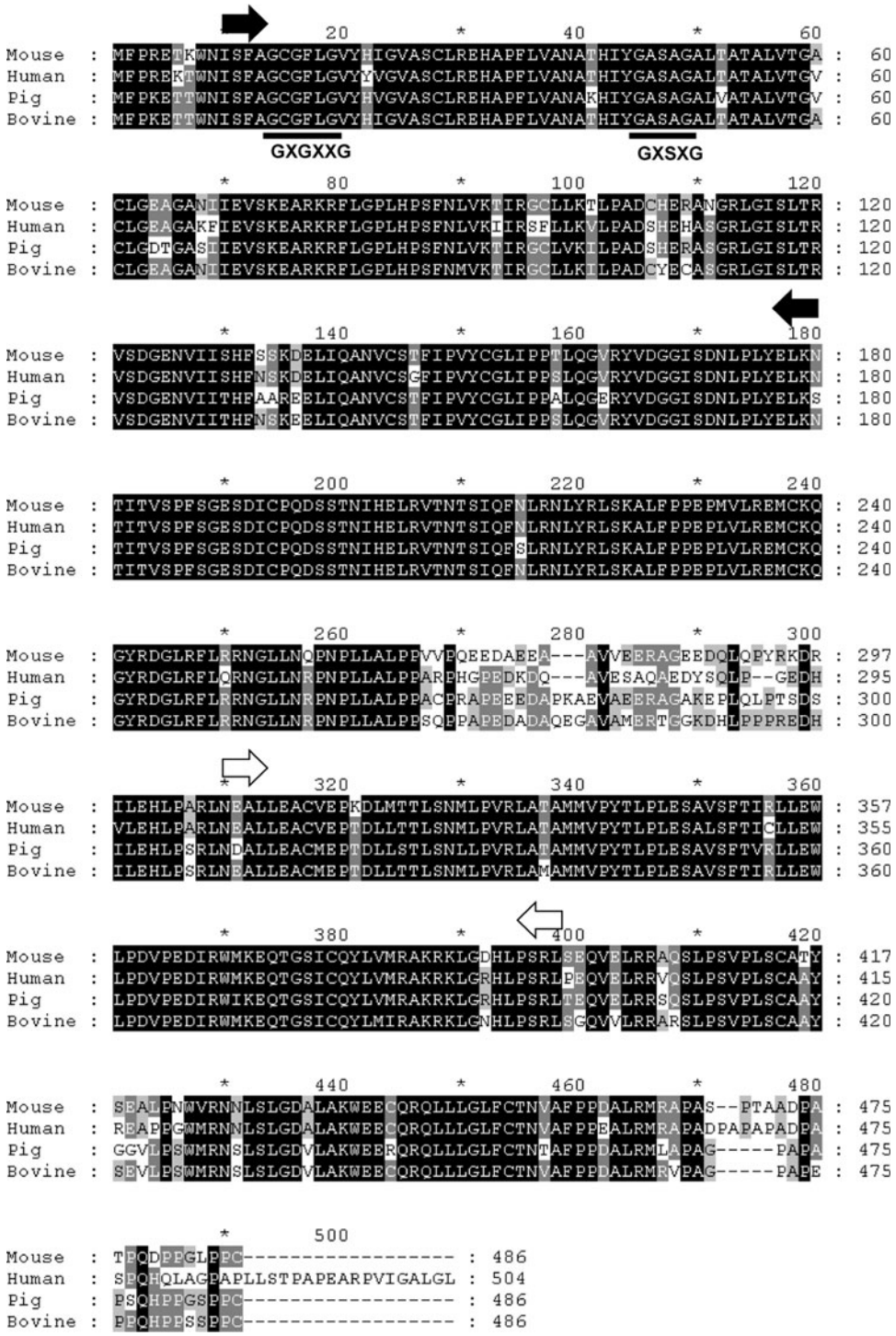

Fig. 1 Amino acid sequence alignment of cow, human, and mouse ATGL. *Black shading* indicates identical aa and *gray shading* indicates aa in the same R groups. The 10–180 aa at the N-terminal indicated as the *filled arrows* were identified as a patatin domain in the Pfam protein family data base. The conserved glycine-rich motif (G*X*G*XX*G) and the serine hydrolase motif (G*X*S*X*G) are shown at the N-terminus. The aa (310–400) indicated as *unfilled arrows* are hydrophobic domain

sequence to Genbank (XM_864571). Our sequence (Genbank FJ897536) and XM_864571 are identical except for a 1 bp mismatch which does not result in an altered amino acid sequence and may represent a polymorphism within the gene. Bovine and porcine ATGL share a great deal of homology. Like porcine ATGL, computer-generated translation analysis of the bovine ATGL cDNA yielded open reading frames of 486 aa (Fig. 1). In addition, there were additions of 3 aa (278–280) and deletions of 5 aa (467–471) in both cattle and pigs compared to human ATGL. Phylogenic analysis revealed that bovine and porcine ATGL proteins share greater homology to human than to mouse, quail, chicken, or turkey (Fig. 2). Bovine ATGL coding sequence has a 90% sequence homology to the human sequence (AY894804). The first 180 aa of the ATGL protein represent the patatin domain which is

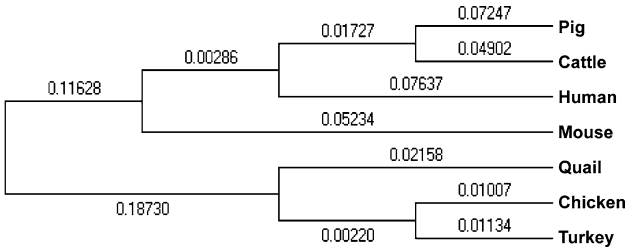

Fig. 2 A phylogenetic analysis of ATGL protein. A phylogenetic tree was constructed to determine the evolutionary relationship of ATGL proteins among various species. Mammalian ATGL proteins form a hierarchical structure distinct from the avian cluster demonstrating relatedness of the species by ATGL sequence. The values, representing branch lengths, are determined by the neighbor joining algorithm (see "Materials and Methods")

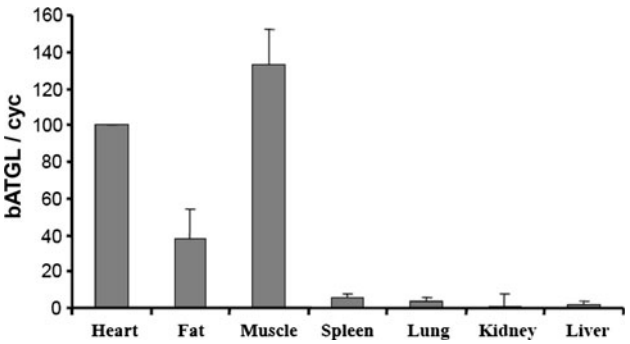

Fig. 3 Tissue distribution of bovine ATGL gene expression. Total RNA was isolated from various bovine tissues. The mRNA expression of bovine ATGL gene was determined by quantitative real-time RT-PCR and expressed as a ratio to cyclophilin expression. Data reported as means ± SEM ($n = 4$)

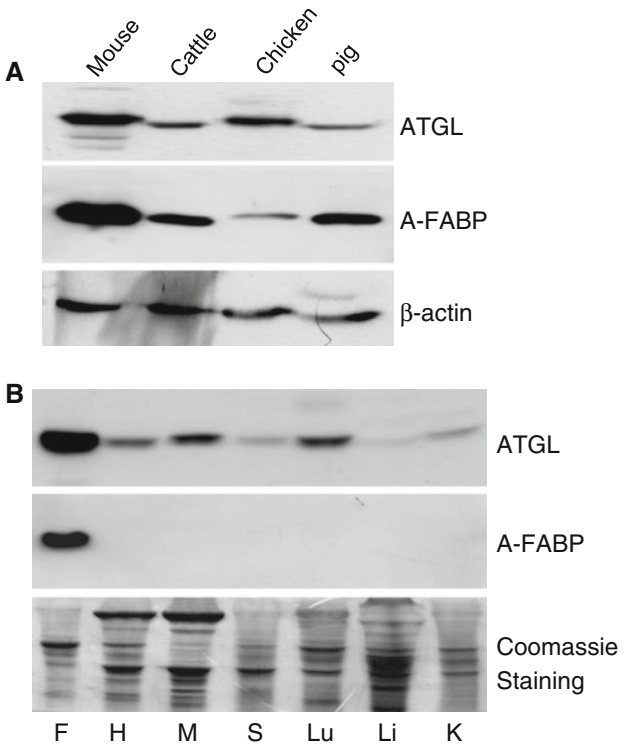

Fig. 4 The predominant expressions of adipose triglyceride lipase (ATGL) protein in bovine tissues. **a** Protein lysates from adipose tissues of mouse, cattle, chicken, and pig were separated by SDS-PAGE and immunoprobed with the ATGL antibodies as described in "Materials and Methods". The same protein lysates were subjected to Western blot analysis for A-FABP protein. β-actin was used as an internal control. **b** Equal amount of protein extracted from the subcutaneous adipose tissue (*F*), heart (*H*), muscle (*M*), spleen (*S*), lung (*Lu*), liver (*Li*), and kidney (*K*) were separated by SDS-PAGE and bovine ATGL protein was determined by Western blot analysis. The same protein lysates were also subjected to Western blot analysis for A-FABP protein. Commassie staining was assessed to verify similar levels of protein loading between samples

responsible for the lipolytic activity of ATGL (Fig. 1). The hydrophobic domain indicated in open arrows (310–398 aa) is conserved across human, cattle, pig, and mouse sequences with significant interspecies variations only occurring up and downstream of the domain.

ATGL gene expression in analyzed tissues revealed that the cardiac and skeletal muscle exhibited higher expression than the subcutaneous adipose tissue (Fig. 3). This may be unique to cattle, as expression of this gene in mouse and pig is highest in subcutaneous adipose tissue [15]. Expression in the spleen, lung, kidney, and liver were many fold lower than heart, muscle or adipose (Fig. 3).

To compare relative amounts of ATGL protein in different tissues, Western blot analysis for ATGL protein was performed using antibodies that recognize a conserved sequence around Pro186 of human ATGL. The molecular weight of ATGL protein as calculated by the Protein Molecular Weight program in Sequence Manipulation Suite [20] showed that mouse ATGL (486 aa) is 53.66 kDa, cattle (486 aa) is 53.35 kDa, chicken ATGL (483 aa) is 53.59 kDa, and pig ATGL (486 aa) is 53.19 kDa. Western blot analysis showed a single band (53 kDa) of ATGL proteins for the mouse, cattle, chicken, and pig (Fig. 4a), which is consistent with predicted molecular weights of ATGL. Therefore, we concluded that the antibodies were usable for the study of bovine ATGL protein expression. Western blot analysis for tissue distribution of ATGL protein showed that a strong single band of the expected size of the bovine ATGL protein was detected in adipose tissues, but other tissues expressed very low amounts of ATGL protein in cattle (Fig. 4b). When the membrane was probed with adipocyte-fatty acid-binding protein (A-FABP) antibody, A-FABP was detected only in adipose tissue at a short exposure time. Due to variation in amount of beta-actin among different tissues, Coomassie staining was assessed to verify similar amounts of protein loading among samples.

In order to determine if flaxseed supplementation (FS) altered muscle TAG mass, we analyzed the TAG content in the skeletal muscle. We found that the FS group exhibited a

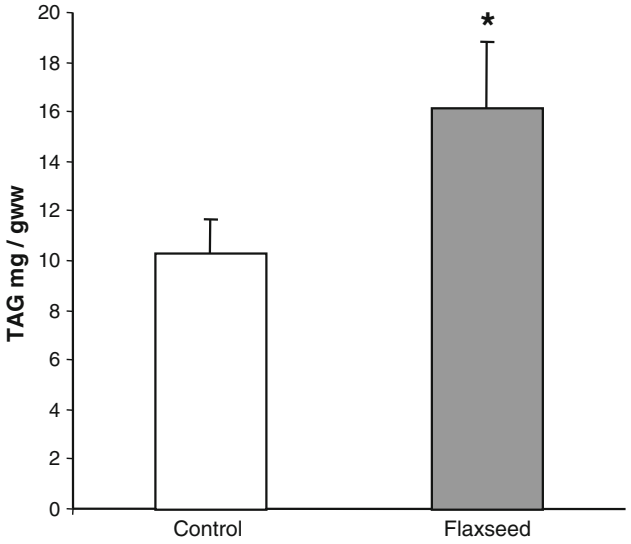

Fig. 5 Triacylglycerols (TAG) contents in the longissimus muscle of Angus steers with or without supplemental flaxseed. TAG content is reported as mg of TAG per g of wet weight ($n = 7$)

significant ($P < 0.05$) 1.5-fold increase in TAG per g of tissue over the control group (Fig. 5). This increase in TAG content was not the result of a net gain in lipid synthesis as the total phospholipid mass was not significantly different between groups (4.1 ± 0.4 nmol/g ww in control vs. 4.7 ± 0.6 nmol/g ww in FS group). Thus, the increased TAG content was due to not only synthesis, but also to accretion of dietary fatty acids.

To better understand how flaxseed supplementation specifically modulates TAG content, we focused on the expression of pertinent genes involved with fatty acid metabolism within the skeletal muscle. We found that flaxseed supplementation did not affect ATGL gene expression and protein content in skeletal muscle of the steers compared to control animals (Fig. 6a, b) when normalized to housekeeping genes/loading controls. Gene expression of HSL and lipoprotein lipase in the muscle were also unaffected by flaxseed supplementation. However, we examined the expression of adipose specific fatty acid binding proteins (A-FABP and E-FABP) as possible molecular indicators for increased muscle TAG accumulation. Both A-FABP and E-FABP were examined as these proteins are found in the adipocyte; In the A-FABP gene-ablated mouse, E-FABP expression demonstrates a compensatory increase in its expression [21]. A-FABP significantly ($P < 0.05$) increased with flaxseed supplementation (Fig. 6d), while E-FABP expression was unaltered (Fig. 6e). Stearoyl-CoA desaturase-1 (SCD-1) expression, the rate limiting enzyme catalyzing the desaturation of saturated fatty acids, was significantly ($P < 0.05$) decreased in muscle tissue by flaxseed supplementation ($P \leq 0.05$) (Fig. 6g).

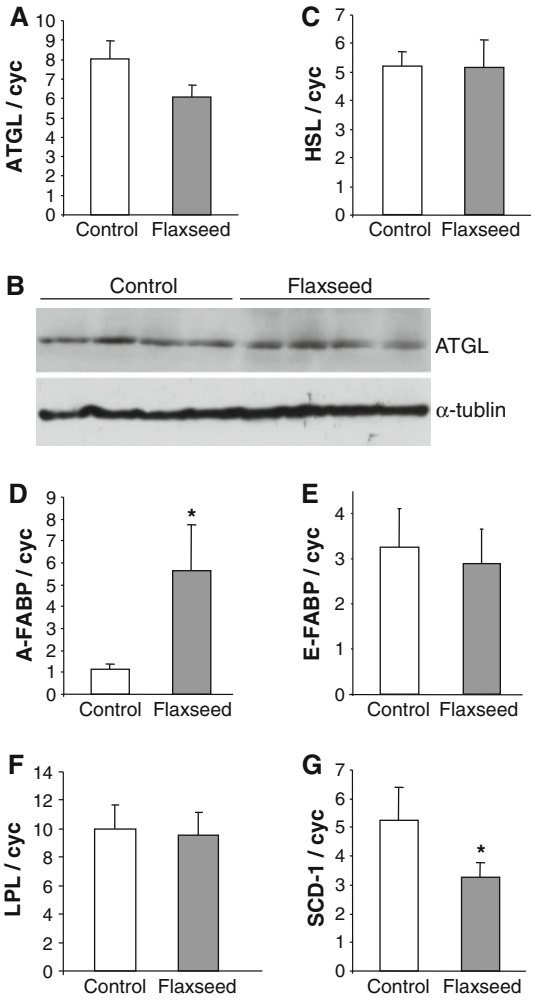

Fig. 6 Expression of genes involved in lipid metabolism in the longissimus muscle of Angus steers with or without supplemental flaxseed. Expression of ATGL (**a**), HSL (**c**), A-FABP (**d**), E-FABP (**e**), LPL (**f**), and SCD-1 (**g**) genes were measured by quantitative real-time PCR ($n = 9$–10). * Mean differences ($P < 0.05$). **b** The protein lysates were subjected to Western blot analysis for ATGL protein. α-tubulin was used as an internal control

Discussion

In this study, we cloned the cDNA encoding for bovine ATGL and compared its amino acid sequence with other species to determine interspecies variations and to examine interspecies conservation of lipase enzyme motifs. Comparison analysis of amino acid sequences of putative cattle ATGL protein with mouse, human, and pig revealed that two major domains; a patatin domain (1–180) and a hydrophobic domain (309–396) are conserved in these mammals. In the patatin domains, the active serine hydrolase motif (*GXSXG*) was GASAG and the glycine-rich motif (*GXGXXG*) was GCGFLG in all four species compared. These motives are conserved from yeast to mammals [22], suggesting functional importance for

ATGL activity across species. The hydrophobic domain of ATGL is responsible for the localization of ATGL protein on the surface of lipid droplets called the adiposome [23]. Point mutations and deletion of the hydrophobic domain in the human population cause neutral lipid storage disorder with cardiomyopathy due to inability of mutant ATGL to access the TAG substrate stored in the adiposomes [23]. However, mutations of the ATGL protein at the hydrophobic domain maintained lipase activities [23]. Conservation of two important domains in bovine ATGL suggests the evolutionary importance in maintaining the lipase activities as well as association with the surface of the adiposome.

ATGL is associated with the lipid droplet [10]. Therefore, it is logical to assume that tissues with a greater abundance of accumulated TAG, and thus a larger lipid droplet, will have increased expression of ATGL as seen in tissue distribution (Fig. 3). High relative expression of ATGL in adipose tissue is consistent with expression in mice; however, ATGL gene expression in cattle skeletal muscle seems to be high relative to most tissues tested, a pattern that was also observed in pig [15, 24]. Although ATGL gene expression in muscle was high, ATGL protein was not. The reasons for this observation are unclear; however, it might be explained by differences in translation efficiencies or degradation rates among the tissues. Again, this pattern is also observed in pig [15]. Cattle muscle ATGL expression is probably due to the presence of lipid droplets (adiposomes) in the myocytes within the muscle fibers themselves, as well as the presence of intramuscular adipocytes. Recent studies have shown that the disruption of the ATGL gene in mice and mutations of ATGL gene in the human resulted in excessive lipid accumulation in the muscle and heart, causing myocardial dysfunction [23, 25]. Recent studies showing the negative association of intramuscular fat with ATGL expression strongly suggest the involvement of ATGL in lipid metabolism in muscle [26, 27].

Others have shown that flaxseed supplementation during the finishing stage of beef cattle improved carcass quality with increased marbling scores (amount of intramuscular fat) and percentage of carcasses grading USDA Choice or greater [4, 28]. Increased TAG contents in the muscle of Angus beef cattle in the current study agree with these previous studies. The amount of TAG in the muscle can be largely attributed to intramuscular adipocytes with a minor contribution from lipid droplets within myofibers [29]. Therefore, increased TAG content in the muscle by flaxseed supplementation may be due to hypertrophy and/or hyperplasia of intramuscular adipocytes. A-FABP, an adipogenic marker, is expressed during adipocyte differentiation and maturation [30]. In fact, increased A-FABP expression is associated with increased marbling in cattle and increased TAG content [31], similar to what we have reported herein. In addition, elevated A-FABP expression is associated with increased intramuscular fat content in ducks [32], chickens [33, 34], and hogs [35, 36], suggesting that it is a broad biomarker for increased intramuscular fat deposition. Increased A-FABP expression in the muscle by flaxseed supplementation further supports the supposition that increased TAG is associated with increased adipogenic activities in the muscle.

PPARγ is a major transcription factor, promoting adipogenesis [30]. Our previous study showed that flaxseed supplementation in Angus steers increased PPARγ mRNA expression by 2.7-fold in the muscle compared with the control [2]. Comparative analysis of mammalian A-FABP promoters revealed that two PPAR binding sites are conserved in A-FABP promoters in mammals, including human, mouse, dog, pig, and cattle, and that PPAR agonists are strong transcription activators of A-FABP genes in mammals [37, 38]. Therefore, because A-FABP is a putative PPARγ-regulated gene, the effects of n-3 PUFA, alpha-linolenic acid on A-FABP expression may be attributable to PPAR agonism. This conclusion is supported by the findings that the n-3 long chain fatty acids alpha-linolenic acid and docosahexaenoic acids [39] as well as synthetic PPAR agonists (thiazolidinedione/glitazone class of compounds) acting as PPARγ ligands modulate PPAR binding activity, regulating expression of responsive genes. There is also evidence that A-FABP plays a role in regulating PPARγ activity by binding PPARγ directly and by channeling fatty acid ligands directly to PPARγ [40]. These findings support a role for regulation of a FABP-PPAR axis by dietary fatty acid ligands. Also, it should be noted that PPARγ activation in muscle cells of mouse, pigs, cattle, and humans results in transdifferentiation to adipocytes [41–46]. It is important to note that PPARγ expression is significantly elevated in these same cattle [2], consistent with the elevated expression of A-FABP. Thus, it is possible that enhancement of PPARγ activation/expression in the muscle by flaxseed supplementation may increase adipogenic activities as evidenced by increased TAG concentration and A-FABP expression.

Higher gene expression of ATGL was found in the adipocyte fraction in mice, pigs, and chickens compared to the stromal-vascular fraction which is partially composed of preadipocytes [15, 16, 47]. Localization of ATGL protein on the surface of lipid droplets and induction of ATGL expression during adipocyte differentiation further indicate association of ATGL expression with TAG content [10, 47]. In the current study, TAG content and A-FABP gene expression increased in the muscle with flaxseed supplementation, although ATGL expression was not different between groups. If ATGL expression were normalized to

TAG content, then ATGL expression would be lower in the FS group than the control. Though A-FABP is known to bind to HSL [13, 14, 48], we did not observe a difference in HSL gene expression between groups. A-FABP has an important role in modulating HSL activity by acting as a chaperone protein and directing HSL to the lipid droplet [14] where it may have a role in fatty acid efflux from the lipid droplet and out of the adipocyte. However, it is important to note that elevated A-FABP expression did not result in a change in muscle tissue E-FABP expression (Fig. 6d, e), though in A-FABP gene-ablated mice there was a compensatory increase in E-FABP expression [21]. In addition, muscle tissue H-FABP expression was not enhanced by dietary flaxseed supplementation [2], indicating that the elevation of A-FABP expression following flaxseed supplementation is specific to A-FABP and does not result in the overall increased expression of FABP found in muscle tissue. Hence, A-FABP is an important regulator of adipocyte lipid metabolism and is a consistent marker across species for intramuscular fat deposition, which is consistent with our results.

SCD-1 is a lipogenic enzyme that catalyzes desaturation resulting in the synthesis of monounsaturated fatty acids. SCD-1 gene expression is largely controlled by the transcription factors PPARα and SREBP-1c [49, 50]. Dietary PUFA decreases the expression of SCD-1 in the liver and adipose of diabetic mice [51, 52], which is consistent with our observations. More applicably, supplementation of beef cattle with n-3 PUFA in the form of fish oil also decreases SCD-1 mRNA expression in the muscle [53]. Archibeque et al. [54] reported that flaxseed supplementation at 10% of daily dry matter intake, which amounted to 1,096 g/day compared to 907 g/day for the present study, did not affect SCD-1 enzyme activities in the muscle of Angus steers; however, they did not report fatty acid composition or content of muscle. Herein, we demonstrate reduction of SCD-1 mRNA expression in skeletal muscle by flaxseed supplementation. This reduction is further supported by a 40% reduction in oleic acid content, the end product of SCD-1 enzyme aczivity, in the muscle of Angus beef with flaxseed supplementation [2], thereby mechanistically accounting for our previous observations in these cattle. Therefore, our data indicate that flaxseed supplementation decreases oleic acid content in the muscle via a reduction in SCD-1 expression.

In summary, bovine ATGL cDNA was cloned and sequenced for the first time. We showed that expression of bovine ATGL protein is adipose tissue specific among various tissues. Comparative analysis revealed that bovine ATGL protein also contained two conserved domains that are important for ATGL functioning. Flaxseed supplementation for approximately 3.5 months before slaughter increased muscle TAG concentration in Angus steers compared to unsupplemented animals. We attribute the increased muscle TAG content in part to the effects of flaxseed supplementation-derived alpha-linolenic acid on A-FABP expression via PPARγ agonism and our previously reported finding of elevated PPARγ expression. Although flaxseed supplementation did not alter expression of HSL or ATGL, it did decrease the expression of SCD-1, consistent with a reduction in oleic acid content in these cattle [2]. Flaxseed supplementation may have beneficial effects on marbling characteristics due to the altered expression of key genes associated with marbling in cattle and TAG content.

Acknowledgments This work was supported by the Ohio Agricultural Research and Development Center Interdisciplinary research funding (K. Lee), and partially supported by the National Research Foundation of Korea Grant funded by the Korean Government [NRF-2009-352-F00029].

References

1. Crawford MA (1968) Fatty-acid ratios in free-living and domestic animals. Possible implications for atheroma. Lancet 1:1329–1333
2. Kronberg SL, Barcelo-Coblijn G, Shin J, Lee K, Murphy EJ (2006) Bovine muscle n-3 fatty acid content is increased with flaxseed feeding. Lipids 41:1059–1068
3. Betti M, Schneider BL, Wismer WV, Carney VL, Zuidhof MJ, Renema RA (2009) Omega-3-enriched broiler meat: 2 Functional properties, oxidative stability, and consumer acceptance. Poult Sci 88:1085–1095
4. Maddock TD, Bauer ML, Koch KB, Anderson VL, Maddock RJ, Barcelo-Coblijn G, Murphy EJ, Lardy GP (2006) Effect of processing flax in beef feedlot diets on performance, carcass characteristics, and trained sensory panel ratings. J Anim Sci 84:1544–1551
5. Simopoulos AP (1999) Essential fatty acids in health and chronic disease. Am J Clin Nutr 70:560S–569S
6. Micallef MA, Munro IA, Garg ML (2009) An inverse relationship between plasma n-3 fatty acids and C-reactive protein in healthy individuals. Eur J Clin Nutr 63:1154–1156
7. Kris-Etherton PM, Harris WS, Appel LJ (2002) Fish consumption, fish oil, omega-3 fatty acids, and cardiovascular disease. Circulation 106:2747–2757
8. Barceló-Coblijn G, Murphy EJ (2009) Alpha-linolenic acid and its conversion to longer chain n-3 fatty acids: benefits for human health and a role in maintaining tissue n-3 fatty acid levels. Prog Lipid Res 48(6):355–374
9. Zimmermann R, Strauss JG, Haemmerle G, Schoiswohl G, Birner-Gruenberger R, Riederer M, Lass A, Neuberger G, Eisenhaber F, Hermetter A, Zechner R (2004) Fat mobilization in adipose tissue is promoted by adipose triglyceride lipase. Science 306:1383–1386
10. Smirnova E, Goldberg EB, Makarova KS, Lin L, Brown WJ, Jackson CL (2006) ATGL has a key role in lipid droplet/adiposome degradation in mammalian cells. EMBO Rep 7:106–113
11. Miyoshi H, Perfield JW 2nd, Souza SC, Shen WJ, Zhang HH, Stancheva ZS, Kraemer FB, Obin MS, Greenberg AS (2007) Control of adipose triglyceride lipase action by serine 517 of perilipin A globally regulates protein kinase A-stimulated lipolysis in adipocytes. J Biol Chem 282:996–1002

12. Haemmerle G, Zimmermann R, Hayn M, Theussl C, Waeg G, Wagner E, Sattler W, Magin TM, Wagner EF, Zechner R (2002) Hormone-sensitive lipase deficiency in mice causes diglyceride accumulation in adipose tissue, muscle, and testis. J Biol Chem 277:4806–4815
13. Smith AJ, Thompson BR, Sanders MA, Bernlohr DA (2007) Interaction of the adipocyte fatty acid-binding protein with the hormone-sensitive lipase: regulation by fatty acids and phosphorylation. J Biol Chem 282(44):32424–32432
14. Smith AJ, Sanders MA, Thompson BR, Londos C, Kraemer FB, Bernlohr DA (2004) Physical association between the adipocyte fatty acid-binding protein and hormone-sensitive lipase: a fluorescence resonance energy transfer analysis. J Biol Chem 279(50):52399–52405
15. Deiuliis JA, Shin J, Bae D, Azain MJ, Barb R, Lee K (2008) Developmental, hormonal, and nutritional regulation of porcine adipose triglyceride lipase (ATGL). Lipids 43:215–225
16. Lee K, Shin J, Latshaw JD, Suh Y, Serr J (2009) Cloning of adipose triglyceride lipase complementary deoxyribonucleic acid in poultry and expression of adipose triglyceride lipase during development of adipose in chickens. Poult Sci 88:620–630
17. Hara A, Radin NS (1978) Lipid extraction of tissues with a low-toxicity solvent. Anal Biochem 90:420–426
18. Marzo A, Ghirardi P, Sardini D, Meroni G (1971) Simplified measurement of monoglycerides, diglycerides, triglycerides, and free fatty acids in biological samples. Clin Chem 17(3):145–147
19. Tamura K, Dudley J, Nei M, Kumar S (2007) MEGA4: molecular evolutionary genetics analysis (MEGA) software version 4.0. Mol Biol Evol 24:1596–1599
20. Stothard P (2000) The sequence manipulation suite: JavaScript programs for analyzing and formatting protein and DNA sequences. Biotechniques 28:1102–1104
21. Hertzel AV, Smith LA, Berg AH, Cline GW, Shulman GI, Scherer PE, Bernlohr DA (2006) Lipid metabolism and adipokine levels in fatty acid-binding protein null and transgenic mice. Am J Physiol Endocrinol Metab 290(5):E814–E823
22. Kurat CF, Natter K, Petschnigg J, Wolinski H, Scheuringer K, Scholz H, Zimmermann R, Leber R, Zechner R, Kohlwein SD (2006) Obese yeast: triglyceride lipolysis is functionally conserved from mammals to yeast. J Biol Chem 281:491–500
23. Fischer J, Lefevre C, Morava E, Mussini JM, Laforet P, Negre-Salvayre A, Lathrop M, Salvayre R (2007) The gene encoding adipose triglyceride lipase (PNPLA2) is mutated in neutral lipid storage disease with myopathy. Nat Genet 39:28–30
24. Kim JY, Tillison K, Lee JH, Rearick DA, Smas CM (2006) The adipose tissue triglyceride lipase ATGL/PNPLA2 is downregulated by insulin and TNF-alpha in 3T3–L1 adipocytes and is a target for transactivation by PPARgamma. Am J Physiol Endocrinol Metab 291:E115–E127
25. Haemmerle G, Lass A, Zimmermann R, Gorkiewicz G, Meyer C, Rozman J, Heldmaier G, Maier R, Theussl C, Eder S, Kratky D, Wagner EF, Klingenspor M, Hoefler G, Zechner R (2006) Defective lipolysis and altered energy metabolism in mice lacking adipose triglyceride lipase. Science 312:734–737
26. Jocken JW, Blaak EE (2008) Catecholamine-induced lipolysis in adipose tissue and skeletal muscle in obesity. Physiol Behav 94:219–230
27. Watt MJ, Steinberg GR (2008) Regulation and function of triacylglycerol lipases in cellular metabolism. Biochem J 414:313–325
28. LaBrune HJ, Reinhardt CD, Dikeman ME, Drouillard JS (2008) Effects of grain processing and dietary lipid source on performance, carcass characteristics, plasma fatty acids, and sensory properties of steaks from finishing cattle. J Anim Sci 86:167–172
29. Pethick DW, Harper GS, Oddy VS (2004) Growth, development and nutritional manipulation of marbling in cattle: a review. Aust J Exp Agric 44:705–715
30. Baillie RA, Sha X, Thuillier P, Clarke SD (1998) A novel 3T3-L1 preadipocyte variant that expresses PPARgamma2 and RXRalpha but does not undergo differentiation. J Lipid Res 39:2048–2053
31. Jurie C, Cassar-Malek I, Bonnet M, Leroux C, Bauchart D, Boulesteix P, Pethick DW, Hocquette JF (2007) Adipocyte fatty acid-binding protein and mitochondrial enzyme activities in muscles as relevant indicators of marbling in cattle. J Anim Sci 85(10):2660–2669
32. Saez G, Davail S, Gentès G, Hocquette JF, Jourdan T, Degrace P, Baéza E (2009) Gene expression and protein content in relation to intramuscular fat content in Muscovy and Peking ducks. Poult Sci 88(11):2382–2391
33. Li WJ, Li HB, Chen JL, Zhao GP, Zheng MQ, Wen J (2008) Gene expression of heart-and adipocyte-fatty acid-binding protein and correlation with intramuscular fat in Chinese chickens. Anim Biotechnol 19(3):189–193
34. Ye MH, Chen JL, Zhao GP, Zheng MQ, Wen J (2010) Associations of A-FABP and H-FABP markers with the content of intramuscular fat in Beijing-You chicken. Anim Biotechnol 21(1):14–24
35. Gardan D, Louveau I, Gondret F (2007) Adipocyte- and heart-type fatty acid binding proteins are both expressed in subcutaneous and intramuscular porcine (Sus scrofa) adipocytes. Comp Biochem Physiol B Biochem Mol Biol 148(1):14–19
36. Zhao SM, Ren LJ, Chen L, Zhang X, Cheng ML, Li WZ, Zhang YY, Gao SZ (2009) Differential expression of lipid metabolism related genes in porcine muscle tissue leading to different intramuscular fat deposition. Lipids 44(11):1029–1037
37. Hausman GJ, Poulos SP, Pringle TD, Azain MJ (2008) The influence of thiazolidinediones on adipogenesis in vitro and in vivo: potential modifiers of intramuscular adipose tissue deposition in meat animals. J Anim Sci 86:E236–E243
38. Shin J, Li B, Davis ME, Suh Y, Lee K (2009) Comparative analysis of fatty acid binding protein 4 promoters: conservation of PPAR binding sites. J Anim Sci 87:3923–3934
39. Kaplins'kyi SP, Shysh AM, Nahibin VS, Dosenko V, Klimashevs'kyi VM, Moibenko OO (2009) Omega-3 polyunsaturated fatty acids stimulate the expression of PPAR target genes. Fiziol Zh 55:37–43
40. Adida A, Spener F (2006) Adipocyte-type fatty acid-binding protein as inter-compartmental shuttle for peroxisome proliferator activated receptor gamma agonists in cultured cell. Biochim Biophys Acta 1761:172–181
41. Hu E, Tontonoz P, Spiegelman BM (1995) Transdifferentiation of myoblasts by the adipogenic transcription factors PPAR gamma and C/EBP alpha. Proc Natl Acad Sci USA 92:9856–9860
42. Yu YH, Liu BH, Mersmann HJ, Ding ST (2006) Porcine peroxisome proliferator-activated receptor gamma induces transdifferentiation of myocytes into adipocytes. J Anim Sci 84:2655–2665
43. De Coppi P, Milan G, Scarda A, Boldrin L, Centobene C, Piccoli M, Pozzobon M, Pilon C, Pagano C, Gamba P, Vettor R (2006) Rosiglitazone modifies the adipogenic potential of human muscle satellite cells. Diabetologia 49:1962–1973
44. Poulos SP, Hausman GJ (2006) A comparison of thiazolidinedione-induced adipogenesis and myogenesis in stromal-vascular cells from subcutaneous adipose tissue or semitendinosus muscle of postnatal pigs. J Anim Sci 84:1076–1082
45. Singh NK, Chae HS, Hwang IH, Yoo YM, Ahn CN, Lee SH, Lee HJ, Park HJ, Chung HY (2007) Transdifferentiation of porcine satellite cells to adipoblasts with ciglitizone. J Anim Sci 85:1126–1135
46. Torii SI, Kawada T, Matsuda K, Matsui T, Ishihara T, Yano H (1998) Thiazolidinedione induces the adipose differentiation of fibroblast-like cells resident within bovine skeletal muscle. Cell Biol Int 22:421–427

47. Villena JA, Roy S, Sarkadi-Nagy E, Kim KH, Sul HS (2004) Desnutrin, an adipocyte gene encoding a novel patatin domain-containing protein, is induced by fasting and glucocorticoids: ectopic expression of desnutrin increases triglyceride hydrolysis. J Biol Chem 279:47066–47075
48. Jenkins-Kruchten AE, Bennaars-Eiden A, Ross JR, Shen WJ, Kraemer FB, Bernlohr DA (2003) Fatty acid-binding protein-hormone-sensitive lipase interaction. Fatty acid dependence on binding. J Biol Chem 278(48):47636–47643
49. Tang C, Cho HP, Nakamura MT, Clarke SD (2003) Regulation of human delta-6 desaturase gene transcription: identification of a functional direct repeat-1 element. J Lipid Res 44:686–695
50. Matsuzaka T, Shimano H, Yahagi N, Amemiya-Kudo M, Yoshikawa T, Hasty AH, Tamura Y, Osuga J, Okazaki H, Iizuka Y, Takahashi A, Sone H, Gotoda T, Ishibashi S, Yamada N (2002) Dual regulation of mouse delta(5)- and delta(6)-desaturase gene expression by SREBP-1 and PPARalpha. J Lipid Res 43:107–114
51. Waters KM, Ntambi JM (1996) Polyunsaturated fatty acids inhibit hepatic stearoyl-CoA desaturase-1 gene in diabetic mice. Lipids 31(Suppl):S33–S36
52. Jones BH, Maher MA, Banz WJ, Zemel MB, Whelan J, Smith PJ, Moustaid N (1996) Adipose tissue stearoyl-CoA desaturase mRNA is increased by obesity and decreased by polyunsaturated fatty acids. Am J Physiol 271:E44–E49
53. Waters SM, Kelly JP, O'Boyle P, Moloney AP, Kenny DA (2009) Effect of level and duration of dietary n-3 polyunsaturated fatty acid supplementation on the transcriptional regulation of Delta9-desaturase in muscle of beef cattle. J Anim Sci 87:244–252
54. Archibeque SL, Lunt DK, Gilbert CD, Tume RK, Smith SB (2005) Fatty acid indices of stearoyl-CoA desaturase do not reflect actual stearoyl-CoA desaturase enzyme activities in adipose tissues of beef steers finished with corn-, flaxseed-, or sorghum-based diets. J Anim Sci 83:1153–1166

Lipids (2010) 45:975–986
DOI 10.1007/s11745-010-3481-5

ORIGINAL ARTICLE

Short Chain Saturated Fatty Acids Decrease Circulating Cholesterol and Increase Tissue PUFA Content in the Rat

Philippe Legrand · Erwan Beauchamp · Daniel Catheline · Frédérique Pédrono · Vincent Rioux

Received: 19 January 2010 / Accepted: 20 September 2010 / Published online: 6 October 2010

Abstract This study investigates the effect of various dietary saturated fatty acid (SFA) profiles on plasma lipid parameters and tissue fatty acid composition in rats. The experiment was designed to monitor polyunsaturated fatty acids (PUFA) levels, while examining different amounts and types of SFA. Four isocaloric diets were prepared, containing 10–11 mol% of fatty acids (FA) as linoleic acid (LNA) and 2.5 mol% as α-linolenic acid (ALA), leading to an identical and well-balanced LNA/ALA ratio. The initial rapeseed oil/corn oil mixture providing ALA and LNA was enriched with olive oil to prepare the olive oil diet. The butterfat diet was supplemented with butterfat, containing short-chain SFA (C4:0–C10:0, 17 mol% of FA), lauric acid (C12:0, 3.2 mol%), myristic acid (C14:0, 10.5 mol%) and palmitic acid (C16:0, 14.5 mol%). The saturates diet was supplemented with trilaurin, trimyristin and tripalmitin to obtain the same level of lauric, myristic and palmitic acids as the butterfat diet, without the short-chain SFA. The trimyristin diet was enriched with trimyristin only. The results showed that the butterfat diet contributed to specific effects, compared to the olive oil diet and the saturates and trimyristin diets: a decrease in plasma total, LDL- and HDL-cholesterol, higher tissue storage of ALA and LNA, and a higher level of (n-3) highly unsaturated fatty acids in some tissues. This study supports the hypothesis that in diets with identical well-balanced LNA/ALA ratios, short chain SFA may decrease circulating cholesterol and increase tissue polyunsaturated fatty acid content in the rat.

Keywords Dietary saturated fatty acids · Plasma cholesterol · (n-3) Polyunsaturated fatty acids · Rat

Abbreviations

ALA	α-Linolenic acid
ARA	Arachidonic acid
DHA	Docosahexaenoic acid
DPA	Docosapentaenoic acid
EPA	Eicosapentaenoic acid
FA	Fatty acid(s)
HUFA	Highly unsaturated fatty acids
LNA	Linoleic acid
PL	Phospholipids
PUFA	Polyunsaturated fatty acids
SFA	Saturated fatty acids
TAG	Triacylglycerol(s)

Introduction

Observational studies have shown that a high intake (more than 15% of daily energy intake) of saturated fatty acids (SFA) is positively associated with increased levels of blood cholesterol and high coronary heart disease mortality rates [1, 2]. Dietary SFA are therefore usually associated with negative consequences for human health. However, a recent meta-analysis of prospective epidemiologic studies suggested that there is no significant evidence for concluding that dietary saturated fat is

P. Legrand · E. Beauchamp · D. Catheline · F. Pédrono · V. Rioux (✉)
Laboratoire de Biochimie-Nutrition Humaine,
Agrocampus Ouest, INRA USC 2012,
65 rue de Saint-Brieuc, CS 84215,
35042 Rennes Cedex, France
e-mail: Vincent.Rioux@agrocampus-ouest.fr

associated with increased risk of coronary heart disease or cardiovascular disease [3]. In addition, several other recent works have contributed to the emerging evidence that all dietary SFA are not necessarily associated with a negative impact on atherosclerosis biomarkers and that their specific identity, individual intake level and dietary origin must be considered [4–7]. For instance, short and medium chain SFA have been shown to have no increasing effect on plasma cholesterol in humans [8]. Myristic acid has deleterious effects on blood cholesterol level in animals and humans when provided at high level exceeding 4% of dietary energy [9, 10], but these negative effects disappear when its dietary level is moderate (1.0–2.5% of dietary energy) [11–14]. Stearic acid has also been demonstrated to be neutral on plasma cholesterol concentrations [15] and to have no negative effect on thrombotic markers in humans [16]. Furthermore, an increasing number of studies have shown that some SFA have important and specific biological roles in the cells [4]. Among SFA, specific biochemical functions can be assigned to myristic acid (C14:0) and palmitic acid (C16:0) that are directly involved in the two classes of protein fatty acid acylation, N-myristoylation and side-chain palmitoylation [17]. Butyric acid is also known to regulate the expression of several genes because it is an inhibitor of histone deacetylase activity [18].

In this context, the present study was aimed at investigating the impact of the saturated fat part of four isocaloric diets on plasma lipid parameters and tissue fatty acid composition in the rat. The experiment was designed to monitor PUFA levels, while examining different amounts and types of saturated fatty acids. The four diets contained equal amounts of α-linolenic acid (ALA, 2.5 mol% of FA, i.e. 0.55% of dietary energy) and linoleic acid (LNA, 10–11 mol% of FA, i.e. 2.6% of dietary energy), provided by a mixture of rapeseed and corn oils, and were supplemented respectively (i) with olive oil (olive oil diet), containing therefore low saturated fat; (ii) with butterfat (butterfat diet), containing short-chain SFA (C4:0–C10:0, 17 mol% of FA), lauric acid (C12:0, 3.2 mol%), myristic acid (C14:0, 10.5 mol%) and palmitic acid (C16:0, 14.5 mol%); (iii) with a mixture of trilaurin, trimyristin and tripalmitin (saturates diet) to obtain the same level of lauric, myristic and palmitic acids as the butterfat diet and (iv) with trimyristin only (trimyristin diet). Plasma lipid parameters and tissue fatty acid composition were measured in rats after a 8-week diet period, showing that the butterfat diet contributed to specific effects, compared with the olive oil diet and the two synthetic saturated fat diets: a decrease in plasma total, LDL- and HDL-cholesterol, a higher tissue storage of both ALA and LNA and a higher level of (n-3) highly unsaturated fatty acids (HUFA) in some tissues.

Materials and Methods

Chemicals

Solvents and chemicals were obtained from Fisher (Elancourt, France) or Sigma (St-Quentin Fallavier, France). Kits for measuring plasma cholesterol and triacylglycerols (TAG) were purchased from Bio-Mérieux (Lyon, France). Fractionated butterfat was given by Lactalis (Retiers, France). Tripalmitin and trilaurin were from Sigma. Trimyristin was extracted from powdered nutmeg by refluxing with diethyl ether (250 mL/100 g of nutmeg) for 5 h [19]. After filtration and concentration, the solution was cooled down to 0 °C. TAG were collected by filtration, washed twice with cold ethanol and re-crystallized from acetone. The purified nutmeg TAG extract contained 92.9% of myristic acid, 1.3% of lauric acid, 5.7% of palmitic acid, and traces of oleic acid and linoleic acid.

Diets

Diets were prepared at the Unité de Production d'Aliments Expérimentaux (UPAE, INRA, Jouy-en-Josas, France). They were isocaloric and varied only in the type of fat used. The composition was as follows (g/100 g): 42.6 corn starch, 19.8 casein, 21.3 sucrose, 0.9 cellulose, 3.6 mineral mix, 0.9 vitamin mix, 0.9 agar–agar and 10.0 lipid. Fat provided 22% of total energy. Lipid fractions of the diets were made by mixing natural and synthetic fats. Dietary fatty acids were carefully controlled with respect to LNA and ALA levels (Table 1), while examining different amounts and types of SFA. The olive oil diet was prepared by mixing rapeseed oil (19%), corn oil (5%) and olive oil (76%). The butterfat diet was obtained by mixing rapeseed oil (18%), corn oil (12%), fractionated butterfat (66.5%) and a small portion of trimyristin (3.5%). The saturates diet was a mix of rapeseed oil (21%), corn oil (8%) and olive oil (47%) supplemented with trilaurin (10%), trimyristin (11%) and tripalmitin (3%) to obtain the same exact level of lauric acid, myristic acid and palmitic acid as the butterfat diet (Table 1).

The trimyristin diet was prepared by mixing rapeseed oil (20%), corn oil (6%) and olive oil (63%) supplemented with trimyristin only to obtain the required level of C14:0 (12 mol% of FA). Finally, cholesterol in the butterfat diet amounted to 0.09 g/100 g and was not detected in the other three diets.

Animals

The experimental procedure was in compliance with recommendations of the 2003/65/CEE European directive for animal experimentation. Sprague–Dawley male rats

Table 1 Fatty acid (FA) composition (mol% of total FA) of the experimental diets

Fatty acid	Olive oil	Butterfat	Saturates	Trimyristin
C4:0		8.54		
C6:0		3.61		
C8:0		1.82		
C10:0		3.37		
C12:0		3.23	4.14	0.18
C14:0	0.01	10.56	12.04	12.23
C16:0	8.49	14.50	16.68	7.89
C17:0	0.15	0.25	0.10	0.12
C18:0	3.00	4.13	2.33	2.56
C20:0	0.39	0.14	0.29	0.34
C22:0	0.23		0.14	0.19
Other SFA (odd, iso, anteiso…) < 0.5% each		1.92		
ΣSFA	12.27	52.07	35.72	23.51
C10:1		0.31		
C14:1 n-5		0.97		
C16:1 n-9	0.13	0.30	0.08	0.11
C16:1 n-7	0.36	1.42	0.24	0.31
C18:1 n-9	70.48	28.27	48.17	59.98
C18:1 n-7	2.46	1.32	1.86	2.17
C18:1 n-9 *trans*		0.30		
C18:1 n-7 *trans*		1.51		
C20:1 n-9		0.20		
ΣMUFA	73.43	34.60	50.35	62.57
C18:2 n-6	11.76	10.31	11.45	11.41
C18:2 *cis*-9 *trans*-11		0.69		
C20:4 n-6		0.04		
Σ n-6 PUFA	11.76	11.04	11.45	11.41
C18:3 n-3	2.54	2.23	2.48	2.51
C22:5 n-3		0.06		
Σ n-3 PUFA	2.54	2.29	2.48	2.51
C18:2/C18:3 M ratio	4.6	4.6	4.6	4.5

(60 g body weight, 6 weeks old at the beginning of the experiment) were obtained from the breeding center R. Janvier (Le Genest-St-Isle, France) and maintained on rat chow (nutriment A04, Scientific Animal Food and Engineering, Augy, France) with free access to water for one week before the study. Then, the rats were randomly assigned to four groups ($n = 6$ per group) and fed ad libitum with the four diets described above (olive oil, butterfat, saturates and trimyristin diets) for 8 weeks. At the end of this period, the rats were fasted overnight. On the following morning, they were anaesthetized with an intraperitoneal injection of pentobarbital (7.5 mg/100 g body weight) [13]. Blood samples were drawn into heparinized tubes by cardiac puncture. The tissues (liver, brain, epididymal fat, heart, testis, eyes) were removed, weighed, snap-frozen in liquid nitrogen and stored at −80 °C. The plasma was separated from the blood cells by centrifugation (2,500 g, 10 min, 4 °C). Plasma cholesterol and TAG were assayed with commercial enzymatic kits, according to the manufacturer's instructions.

Lipid Extraction and FA Analysis

Lipids from all the tissues except plasma and red blood cells were extracted using a mixture of dimethoxymethane/methanol (4:1 v/v) [20]. Lipids from the plasma and red blood cells were extracted from 1 mL-samples with a mixture of hexane/isopropanol (3:2 v/v), after acidification with 1 mL HCl 3 mol/L [21]. Lipid species (from liver and heart) were separated by thin-layer chromatography using silicagel H plates and a mixture of hexane:diethyl-ether:acetic acid (85:15:1 v/v/v). Phospholipids (PL) and TAG were scraped off the plate and extracted with 2 mL of diethyl ether for TAG, or 2 mL of methanol for PL, as described previously [13]. Total lipid extracts or lipid species were saponified for 30 min at 70 °C with 1 mL of

0.5 mol/L NaOH in methanol and methylated with 1 mL BF_3 (14% in methanol) for 15 min at 70 °C. FA methyl esters were extracted twice with pentane and analyzed by gas chromatography using an Agilent Technologies 6890N (Bios Analytic, Toulouse, France) with a split injector (40:1) at 250 °C and a bonded silica capillary column (30 m × 0.25 mm; BPX 70; SGE, Villeneuve-St-Georges, France) with a polar stationary phase of 70% cyanopropylpolysilphenylene-siloxane (0.25 µm film thickness). Helium was used as the carrier gas (average velocity 24 cm/s). The column temperature program started at 150 °C, was ramped at 2 °C/min to 220 °C, and held at 220 °C for 10 min. The flame ionization detector temperature was 250 °C.

Results Expression and Statistical Analysis

The results are expressed as means ± SD ($n = 6$). Data were analyzed by analysis of variance with the R statistical software followed by Tukey's multiple comparison tests. A value of $P < 0.05$ was considered to be statistically significant.

Results

Physiological Status and Plasma Lipid Parameters

Rats ($n = 6$ in each group) were fed the olive oil, butterfat, saturates and trimyristin diets (Table 1) for 8 weeks. The diets were designed to contain different amounts and types of SFA. The dietary consumption was identical in the four groups. At the end of this period, body weights, plasma lipid concentrations (Table 2), and total FA content of the tissues (Tables 3–7 and Supplemental Tables) were analyzed. The body weight of the animals was similar in the four groups. Significant differences between groups were found in the plasma lipid parameters of the rats (Table 2). Total cholesterol was significantly lower in the butterfat group than in the olive oil, saturates and trimyristin groups. Total cholesterol was also significantly lower in animals of the saturates group than in animals of the olive oil group. The low total cholesterol level of the butterfat group resulted both from significantly lower LDL-cholesterol than the olive oil and trimyristin groups and significantly lower HDL-cholesterol than the olive oil and saturates groups (Table 2). Consequently, the total cholesterol/HDL-cholesterol ratio was also significantly lower in the butterfat and saturates groups than in the olive oil and trimyristin groups. Plasma TAG (Table 2) and plasma total FA (Table 5) were significantly lower in the trimyristin group than in the saturates group. Finally, the total FA content in adipose tissue (Table 3), liver (Table 4), red blood cells (Table 6) and heart (Table 7), expressed as mol FA/g tissue, was similar.

Saturated FA Profiles of the Tissues

The composition of SFA in lipids of adipose tissue, liver, plasma, red blood cells, heart (Tables 3–7) and brain, testis, retina (Supplemental Tables 1–3) was first analyzed. The composition of SFA in lipid species (TAG and PL) was analyzed only in the liver and heart (Supplemental Tables 4–7). Although short-chain SFA (C4:0-C10:0) were present in the butterfat diet, they were not detected after feeding animals for 8 weeks with this diet, whatever the tissue analyzed. Lauric acid, which was present (3.2–4.1 mol% of FA) in the butterfat and saturates diets, was detected only in adipose tissue (1.3 mol% of FA) and liver (0.08 mol% of FA) of these two groups (Tables 3, 4). An expected increase in C14:0 level (Tables 3–7), with preferential incorporation into TAG rather than into PL as shown in the liver and heart (Supplemental Tables 4–7), was detected in all the tissues of the rats fed the butterfat, saturates and trimyristin diets (containing 10–12 mol% myristic acid) compared with olive oil diet (deprived of

Table 2 Effect of the diets on the body weight and plasma lipid concentrations of the rats fed for 8 weeks

	Olive oil	Butterfat	Saturates	Trimyristin
Weight				
Body (g)	531.7 ± 44.1	530.7 ± 48.1	527.5 ± 46.2	487.5 ± 42.2
Plasma lipids				
Total cholesterol (mg/mL)	2.24 ± 0.51[a]	1.38 ± 0.39[c]	1.76 ± 0.24[b]	1.89 ± 0.45[a,b]
HDL-cholesterol (mg/mL)	0.52 ± 0.04[a]	0.40 ± 0.08[b]	0.55 ± 0.06[a]	0.43 ± 0.09[b]
Total cholesterol/HDL-cholesterol	4.28 ± 0.70[a]	3.49 ± 0.84[b]	3.20 ± 0.51[b]	4.43 ± 1.06[a]
Triacylglycerols (mg/mL)	1.57 ± 0.57[a,b]	1.32 ± 0.66[a,b]	1.78 ± 0.77[a]	1.12 ± 0.33[b]
Calculated LDL-cholesterol (mg/mL)[A]	1.40 ± 0.40[a]	0.72 ± 0.26[b]	0.85 ± 0.26[b]	1.23 ± 0.39[a]

All data are means ± SD ($n = 6$ in each group). Different superscripts letters in the same row indicate a significant difference among the data ($P < 0.05$)

[a] LDL-cholesterol was calculated with the following formula LDL-cholesterol = (Total cholesterol) − (HDL-cholesterol) – (TG/5)

Table 3 Fatty acid composition (mol% of total FA) of adipose tissue total lipids of the rats

Fatty acid	Olive oil	Butterfat	Saturates	Trimyristin
C12:0	0.11 ± 0.06^{c}	1.39 ± 0.11^{a}	1.22 ± 0.20^{a}	0.20 ± 0.05^{b}
C14:0	1.00 ± 0.14^{c}	6.77 ± 0.34^{a}	5.67 ± 0.36^{b}	5.85 ± 0.29^{b}
C16:0	17.34 ± 1.31^{c}	23.17 ± 1.22^{a}	21.37 ± 1.44^{b}	18.10 ± 1.65^{c}
C18:0	2.08 ± 0.09^{b}	2.31 ± 0.26^{a}	1.68 ± 0.16^{c}	1.83 ± 0.23^{c}
ΣSFA	20.77 ± 1.40^{d}	34.97 ± 0.89^{a}	30.16 ± 1.30^{b}	26.21 ± 1.57^{c}
C16:1 n-7	3.62 ± 0.78^{c}	7.03 ± 1.50^{a}	5.12 ± 0.94^{b}	4.73 ± 0.50^{b}
C18:1 n-9	60.42 ± 2.01^{a}	38.67 ± 1.62^{d}	48.79 ± 1.51^{c}	54.02 ± 1.25^{b}
C18:1 n-7	4.59 ± 0.40	4.77 ± 0.37	4.65 ± 0.41	4.39 ± 0.20
C18:1 n-9 *trans*	0.06 ± 0.01^{b}	0.24 ± 0.01^{a}	0.05 ± 0.01^{b}	0.06 ± 0.01^{b}
C18:1 n-7 *trans*	ND	0.81 ± 0.08	ND	ND
ΣMUFA	69.71 ± 1.01^{a}	53.05 ± 0.75^{d}	59.59 ± 0.87^{c}	64.33 ± 0.87^{b}
C18:2 n-6	8.14 ± 0.43^{b}	10.28 ± 0.71^{a}	8.85 ± 0.77^{b}	8.15 ± 0.65^{b}
Σ n-6 PUFA	8.33 ± 0.41^{b}	10.48 ± 0.68^{a}	9.02 ± 0.79^{b}	8.32 ± 0.68^{b}
Σ n-6 HUFA	0.19 ± 0.02	0.20 ± 0.04	0.17 ± 0.04	0.17 ± 0.03
C18:3 n-3	1.09 ± 0.07^{b}	1.37 ± 0.06^{a}	1.14 ± 0.14^{b}	1.05 ± 0.11^{b}
C20:5 n-3	0.01 ± 0.00^{b}	0.05 ± 0.01^{a}	0.01 ± 0.01^{b}	0.01 ± 0.01^{b}
Σ n-3 PUFA	1.13 ± 0.07^{b}	1.46 ± 0.08^{a}	1.18 ± 0.16^{b}	1.09 ± 0.13^{b}
Σ n-3 HUFA	0.04 ± 0.02^{b}	0.09 ± 0.03^{a}	0.04 ± 0.02^{b}	0.04 ± 0.02^{b}
Total FA (mmol/g tissue)	2.06 ± 0.11	2.02 ± 0.18	2.08 ± 0.26	2.25 ± 0.24

All data are means ± SD ($n = 6$). Different superscripts letters in the same row indicate a significant difference among the data ($P < 0.05$). n-6 PUFA include C18:2 n-6, C18:3 n-6, C20:2 n-6, C20:3 n-6, C20:4 n-6, C22:4 n-6 here; n-6 HUFA include C18:3 n-6, C20:2 n-6, C20:3 n-6, C20:4 n-6, C22:4 n-6 here; n-3 PUFA include C18:3 n-3, C20:5 n-3, C22:5 n-3, C22:6 n-3 here; HUFA include C20:5 n-3, C22:5 n-3, C22:6 n-3 here.

ND not detected

myristic acid). Interestingly, the rats fed the butterfat diet had a significantly higher C14:0 amount in adipose tissue than the saturates and trimyristin animals (Table 3), although these three diets contained exactly the same amount of myristic acid (Table 1). Concerning C16:0, the butterfat and saturates diets contained 2 times more palmitic acid (14–16 mol%) than the olive oil and trimyristin diets (7–8 mol%) and its level in adipose tissue, liver and plasma (Tables 3–5) was related to its dietary level. Differences in C18:0 levels shown in adipose tissue, plasma and red blood cells, were also related to its higher dietary level in the butterfat diet (Table 1).

Monounsaturated FA Profiles of the Tissues

Oleic acid content was significantly higher in all the tissues of the olive oil group (70 mol% of oleic acid in the diet) compared to the butterfat group (34 mol% of oleic acid in the diet), except in the brain (Supplemental Table 1), with intermediate levels in the tissues of the trimyristin and saturates groups (Tables 3–7). Conversely, *trans* monounsaturated FA (C18:1 n-9 and n-7 *trans*) from the butterfat diet were detected in adipose tissue, liver and heart of the butterfat animals (Tables 3, 4, 7).

(n-3) PUFA Profiles of the Tissues

The 4 diets were designed to contain strictly equal amounts of ALA (2.5 mol% of FA) (Table 1). However, significantly higher amounts of ALA were found in the adipose tissue of the butterfat group compared to the olive oil, saturates and trimyristin groups (Table 3), in the liver of the butterfat group compared to the olive oil and saturates groups (Table 4) and plasma of the butterfat group compared to the olive oil and trimyristin groups (Table 5). Similar results were shown in the TAG fraction of liver (Supplemental Table 5). Among detected (n-3) HUFA, EPA (C20:5 n-3) was significantly higher in adipose tissue (Table 3) and red blood cells (Table 6) of butterfat animals compared to olive oil, saturates and trimyristin animals, and significantly higher in the heart of the butterfat group than in the saturates and trimyristin groups (Table 7). DPA (C22:5 n-3) was also significantly higher in the liver of the butterfat animals compared with the olive oil animals (Table 4), and in the heart (Table 7) and retina (Supplemental Table 3) of the butterfat animals compared with the olive oil, saturates and trimyristin animals. Similar results on DPA levels were shown in the PL fractions of liver and heart (Supplemental Tables 4 and 6). DHA was not

Table 4 Fatty acid composition (mol% of total FA) of liver total lipids of the rats

Fatty acid	Olive oil	Butterfat	Saturates	Trimyristin
C12:0	0.02 ± 0.01[b]	0.09 ± 0.02[a]	0.08 ± 0.03[a]	0.03 ± 0.01[b]
C14:0	0.54 ± 0.09[b]	1.31 ± 0.14[a]	1.47 ± 0.31[a]	1.30 ± 0.27[a]
C16:0	22.13 ± 0.92[b]	24.74 ± 1.18[a]	24.63 ± 0.73[a]	22.83 ± 1.63[b]
C18:0	9.98 ± 2.09	9.70 ± 1.46	9.49 ± 1.88	10.31 ± 1.67
ΣSFA	32.86 ± 1.70[b]	36.49 ± 1.37[a]	35.84 ± 1.31[a]	34.64 ± 1.64[a,b]
C16:1 n-7	3.04 ± 0.49[b]	4.79 ± 1.30[a]	3.54 ± 0.72[a,b]	3.34 ± 0.98[a,b]
C18:1 n-9	34.15 ± 4.90[a]	25.91 ± 2.50[b]	29.55 ± 4.27[a,b]	30.51 ± 2.91[a]
C18:1 n-7	3.71 ± 0.33[a,b]	3.55 ± 0.41[b]	4.12 ± 0.34[a]	3.39 ± 0.34[b]
C18:1 n-9 *trans*	0.11 ± 0.04	0.12 ± 0.05	0.10 ± 0.01	0.10 ± 0.04
C18:1 n-7 *trans*	ND	0.32 ± 0.11	ND	ND
ΣMUFA	41.77 ± 5.65	35.47 ± 2.80	38.01 ± 4.96	38.05 ± 3.59
C18:2 n-6	7.03 ± 0.80[c]	10.51 ± 2.19[a]	8.18 ± 0.46[b]	8.52 ± 1.62[a,b,c]
C20:3 n-6	0.48 ± 0.17	0.48 ± 0.13	0.42 ± 0.14	0.42 ± 0.12
C20:4 n-6	12.45 ± 2.76	11.50 ± 1.57	11.95 ± 2.67	12.92 ± 1.88
C22:4 n-6	0.13 ± 0.03	0.14 ± 0.01	0.14 ± 0.03	0.15 ± 0.03
C22:5 n-6	0.11 ± 0.02	0.11 ± 0.03	0.11 ± 0.03	0.13 ± 0.04
Σ n-6 PUFA	20.38 ± 3.44	23.36 ± 1.79	22.22 ± 2.40	22.31 ± 2.23
Σ n-6 HUFA	13.35 ± 2.93	12.42 ± 1.61	12.78 ± 2.80	13.80 ± 1.95
C18:3 n-3	0.37 ± 0.06[b]	0.72 ± 0.26[a]	0.45 ± 0.08[b]	0.46 ± 0.21[a,b]
C20:5 n-3	0.17 ± 0.08	0.25 ± 0.10	0.17 ± 0.05	0.19 ± 0.05
C22:5 n-3	0.30 ± 0.08[b]	0.41 ± 0.08[a]	0.35 ± 0.08[a,b]	0.33 ± 0.06[a,b]
C22:6 n-3	3.88 ± 0.68	3.54 ± 0.87	4.03 ± 0.85	3.70 ± 0.77
Σ n-3 PUFA	4.72 ± 0.80	4.93 ± 0.89	5.00 ± 0.89	4.68 ± 0.72
Σ n-3 HUFA	4.35 ± 0.80	4.20 ± 0.94	4.55 ± 0.93	4.22 ± 0.79
Total FA (μmol/g tissue)	147.1 ± 29.5	143.6 ± 24.7	146.8 ± 29.2	135.1 ± 29.4

All data are means ± SD ($n = 6$). Different superscripts letters in the same row indicate a significant difference among the data ($P < 0.05$). n-6 PUFA include C18:2 n-6, C18:3 n-6, C20:2 n-6, C20:3 n-6, C20:4 n-6, C22:4 n-6 and C22:5 n-6 here; n-6 HUFA include C18:3 n-6, C20:2 n-6, C20:3 n-6, C20:4 n-6, C22:4 n-6 and C22:5 n-6 here; n-3 PUFA include C18:3 n-3, C20:5 n-3, C22:5 n-3 and C22:6 n-3 here; n-3 HUFA include C20:5 n-3, C22:5 n-3 and C22:6 n-3 here.

ND not detected

significantly different between the 4 groups, whatever the tissue analyzed. Concerning longer HUFA (C24:5 n-3 and C24:6 n-3), they were detected only in the retina (Supplemental Table 3), they were higher in the butterfat group. All these increases in individual HUFA resulted in a significantly higher level of total (n-3) HUFA and total (n-3) PUFA (ALA + n-3 HUFA) in adipose tissue of the butterfat group compared to the olive oil, saturates and trimyristin groups (Table 3), in the heart in the butterfat group compared to the olive oil and trimyristin groups (Table 7) and in the retina in the butterfat group compared to the olive oil group (Supplemental Table 3).

(n-6) PUFA Profiles of the Tissues

The 4 diets were designed to contain equal amounts of LNA (10-11 mol% of FA) (Table 1). However, significantly higher amounts of LNA were found in adipose tissue, plasma, heart and brain of the butterfat group compared to the 3 other groups (Tables 3, 5, 7 and Supplemental Table 1), in the liver of the butterfat group compared to the olive oil and saturates groups (Table 4) and in red blood cells of the butterfat group compared to the saturates and trimyristin groups (Table 6). Similar higher levels of LNA in the butterfat group were shown in the TAG and PL fractions of liver and heart (Supplemental Tables 4–7). Among detected (n-6) HUFA, C20:3 n-6 was significantly higher in red blood cells and heart of butterfat animals compared to saturates and trimyristin animals (Tables 6–7) and in the liver TAG and heart PL of the butterfat group compared to the olive oil group (Supplemental Tables 5–6). Higher levels of C20:4 n-6 appeared in the liver TAG of the butterfat group compared to the olive oil group (Supplemental Table 5). Conversely, C22:5 n-6 was significantly lower in red blood cells of butterfat animals compared to olive oil, saturates and trimyristin animals (Table 6) and significantly lower in the heart of the butterfat group compared with the trimyristin animals

Table 5 Fatty acid composition (mol% of total FA) of plasma total lipids of the rats

Fatty acid	Olive oil	Butterfat	Saturates	Trimyristin
C14:0	0.51 ± 0.13^{b}	1.74 ± 0.46^{a}	1.50 ± 0.29^{a}	1.72 ± 0.52^{a}
C16:0	$19.67 \pm 1.29^{a,b}$	21.84 ± 2.02^{a}	21.33 ± 1.50^{a}	19.42 ± 1.16^{b}
C18:0	2.84 ± 0.40^{b}	3.73 ± 0.87^{a}	$3.04 \pm 0.63^{a,b}$	$3.37 \pm 0.66^{a,b}$
ΣSFA	23.39 ± 1.33^{c}	27.99 ± 1.42^{a}	26.20 ± 1.03^{b}	$24.99 \pm 1.38^{b,c}$
C16:1 n-7	2.53 ± 0.39^{c}	4.68 ± 1.38^{a}	3.22 ± 0.48^{b}	$3.32 \pm 0.72^{a,b}$
C18:1 n-9	39.56 ± 1.40^{a}	27.08 ± 2.68^{c}	32.35 ± 2.14^{b}	34.48 ± 2.34^{b}
C18:1 n-7	3.38 ± 0.16^{b}	3.81 ± 0.34^{a}	$3.57 \pm 0.36^{a,b}$	3.30 ± 0.21^{b}
ΣMUFA	46.18 ± 1.57^{a}	36.06 ± 3.91^{c}	$39.66 \pm 2.72^{b,c}$	42.01 ± 2.71^{b}
C18:2 n-6	10.35 ± 0.69^{c}	13.43 ± 1.59^{a}	11.70 ± 0.93^{b}	$10.76 \pm 0.64^{b,c}$
C20:3 n-6	0.23 ± 0.03	0.29 ± 0.08	0.24 ± 0.04	0.22 ± 0.04
C20:4 n-6	15.39 ± 2.81	17.33 ± 5.82	17.25 ± 4.34	17.92 ± 2.70
C22:4 n-6	0.26 ± 0.13	0.19 ± 0.06	0.28 ± 0.14	0.18 ± 0.05
C22:5 n-6	0.19 ± 0.04	0.22 ± 0.05	0.20 ± 0.04	0.21 ± 0.07
Σ n-6 PUFA	26.64 ± 2.75	31.04 ± 7.21	30.17 ± 4.71	29.56 ± 2.50
Σ n-6 HUFA	16.29 ± 2.74	18.31 ± 5.85	18.21 ± 4.36	18.80 ± 2.81
C18:3 n-3	0.80 ± 0.12^{b}	1.12 ± 0.33^{a}	$0.89 \pm 0.22^{a,b}$	0.74 ± 0.11^{b}
C20:5 n-3	0.53 ± 0.10	0.73 ± 0.34	0.60 ± 0.13	0.56 ± 0.13
C22:5 n-3	0.33 ± 0.06	0.38 ± 0.15	0.41 ± 0.13	0.29 ± 0.08
C22:6 n-3	1.65 ± 0.15	1.76 ± 0.58	1.94 ± 0.33	1.40 ± 0.45
Σ n-3 PUFA	$3.31 \pm 0.30^{a,b}$	3.99 ± 0.87^{a}	3.85 ± 0.76^{a}	2.99 ± 0.34^{b}
Σ n-3 HUFA	2.52 ± 0.22	2.87 ± 0.95	2.96 ± 0.55	2.25 ± 0.48
Total FA (μmol/mL tissue)	$5.72 \pm 1.97^{a,b}$	$4.16 \pm 1.88^{a,b}$	5.28 ± 1.06^{a}	3.55 ± 1.47^{b}

All data are means ± SD ($n = 6$). Different superscripts letters in the same row indicate a significant difference among the data ($P < 0.05$). n-6 PUFA include C18:2 n-6, C18:3 n-6, C20:2 n-6, C20:3 n-6, C20:4 n-6, C22:4 n-6 and C22:5 n-6 here; n-6 HUFA include C18:3 n-6, C20:2 n-6, C20:3 n-6, C20:4 n-6, C22:4 n-6 and C22:5 n-6 here; n-3 PUFA include C18:3 n-3, C20:5 n-3, C22:5 n-3 and C22:6 n-3 here; n-3 HUFA include C20:5 n-3, C22:5 n-3 and C22:6 n-3 here

(Table 7). These opposite differences in individual (n-6) HUFA did not result in any significant difference of total (n-6) HUFA in the tissues. However, the total (n-6) PUFA (LNA + n-6 HUFA) was significantly higher, due to the increase in LNA, in adipose tissue and heart of the butterfat group compared to the olive oil, saturates and trimyristin groups (Tables 3 and 7).

Discussion

This study was aimed at investigating the impact of the specific SFA composition of 4 diets with identical well-balanced LNA/ALA ratio on plasma lipid parameters and tissue fatty acid composition in rats. The rats were fed with these four diets for 8 weeks, as already done in two previous studies investigating more specifically the physiological effects of dietary myristic acid [13, 19].

First, the results on plasma lipid concentrations (Table 2) show that rats fed with the butterfat diet (LNA and ALA diet enriched with butterfat) have a lower level of plasma total cholesterol than the 3 other groups. Total cholesterol was also significantly lower in animals of the saturates group than in animals of the olive oil group. Therefore, the diet containing the highest level of SFA (about 52 mol% of FA; Table 1), coming from butterfat, led to the lowest level of plasma cholesterol. However, an extrapolation of this interesting result to humans is not easy since rats exhibit a low cholesterol ester transfer protein (CETP) activity and high HDL-cholesterol/total cholesterol ratio [22]. Moreover, the present study design uses test diets which can be considered as low fat in terms of dietary energy (22% of total energy from fat) when compared with typical human diet (30–35% of total energy from fat). However, usual fat for rat maintenance is about 8% of total energy from fat and the present study using 22% of energy from fat can therefore be considered as high fat in rodent models. In terms of saturated fat supply, the diets can be considered as moderate, varying from 12 to 52 mol% of total FA (i.e. 2.4–9.7% of total energy from saturated fat). Finally, a low amount of cholesterol (0.09 g/100 g diet) was present in the butterfat diet and no cholesterol was

Table 6 Fatty acid composition (mol% of total FA) of red blood cell total lipids of the rats

Fatty acid	Olive oil	Butterfat	Saturates	Trimyristin
C14:0	0.48 ± 0.09[b]	0.84 ± 0.19[a]	0.77 ± 0.15[a]	0.95 ± 0.20[a]
C16:0	20.40 ± 0.61	21.53 ± 1.40	21.82 ± 1.33	20.52 ± 0.66
C18:0	14.60 ± 0.74[b]	16.53 ± 1.27[a]	15.67 ± 1.32[a,b]	14.59 ± 0.86[b]
ΣSFA	36.19 ± 0.69[a]	39.78 ± 2.81[b]	38.95 ± 1.97[b]	36.91 ± 0.37[a,b]
C16:1 n-7	1.59 ± 0.36	1.84 ± 0.67	1.42 ± 0.53	1.79 ± 0.44
C18:1 n-9	17.02 ± 1.55[a]	11.74 ± 0.81[c]	13.30 ± 1.39[b,c]	15.60 ± 1.88[a,b]
C18:1 n-7	3.97 ± 0.19	3.73 ± 0.20	3.81 ± 0.26	3.76 ± 0.17
ΣMUFA	23.52 ± 1.69[a]	18.05 ± 1.37[b]	19.27 ± 1.79[b]	22.01 ± 1.52[a]
C18:2 n-6	6.01 ± 0.93[a,b]	6.73 ± 0.40[a]	5.66 ± 0.53[b]	5.87 ± 0.67[b]
C20:3 n-6	0.82 ± 0.09[a,b]	0.97 ± 0.13[a]	0.76 ± 0.09[b]	0.70 ± 0.09[b]
C20:4 n-6	27.28 ± 1.79	27.15 ± 2.92	27.90 ± 1.54	27.80 ± 2.72
C22:4 n-6	0.88 ± 0.10	0.88 ± 0.18	1.00 ± 0.13	0.98 ± 0.21
C22:5 n-6	0.51 ± 0.19[a]	0.31 ± 0.14[b]	0.61 ± 0.28[a]	0.57 ± 0.18[a]
Σ n-6 PUFA	35.50 ± 1.43	35.16 ± 3.34	35.59 ± 1.77	36.37 ± 2.31
Σ n-6 HUFA	29.49 ± 2.04	29.71 ± 2.95	30.70 ± 1.75	30.49 ± 2.95
C18:3 n-3	0.31 ± 0.08	0.34 ± 0.08	0.28 ± 0.04	0.31 ± 0.09
C20:5 n-3	0.43 ± 0.06[b]	0.59 ± 0.08[a]	0.39 ± 0.05[b]	0.41 ± 0.06[b]
C22:5 n-3	1.00 ± 0.20	1.44 ± 0.46	1.21 ± 0.18	1.09 ± 0.20
C22:6 n-3	2.96 ± 0.50	3.13 ± 0.54	3.27 ± 0.52	2.75 ± 0.38
Σ n-3 PUFA	4.71 ± 0.65[a,b]	5.49 ± 0.74[a]	5.15 ± 0.62[a,b]	4.56 ± 0.47[b]
Σ n-3 HUFA	4.40 ± 0.70	5.15 ± 0.75	4.87 ± 0.66	4.25 ± 0.54
Total FA (μmol/mL tissue)	20.50 ± 4.69	14.71 ± 3.71	16.10 ± 3.82	17.32 ± 2.99

All data are means ± SD ($n = 6$). Different superscripts letters in the same row indicate a significant difference among the data ($P < 0.05$). n-6 PUFA include C18:2 n-6, C18:3 n-6, C20:2 n-6, C20:3 n-6, C20:4 n-6, C22:4 n-6 and C22:5 n-6 here; n-6 HUFA include C18:3 n-6, C20:2 n-6, C20:3 n-6, C20:4 n-6, C22:4 n-6 and C22:5 n-6 here; n-3 PUFA include C18:3 n-3, C20:5 n-3, C22:5 n-3 and C22:6 n-3 here; n-3 HUFA include C20:5 n-3, C22:5 n-3 and C22:6 n-3 here

detected in the three other diets, but it is now generally accepted that dietary cholesterol is not a significant factor in determining blood cholesterol levels in the general human population [23].

We found in the present study that plasma total cholesterol level was inversely correlated with dietary SFA level. The total cholesterol/HDL-cholesterol ratio, which is considered to be a better predictor of coronary heart disease risk (in humans) than LDL- and HDL-cholesterol themselves [24], was also significantly lower in the butterfat group than in the olive oil and trimyristin animals. In the literature, such a significant inverse correlation was found in postmenopausal women with relatively low total fat intake, showing that a greater saturated fat intake was associated with less progression of coronary atherosclerosis [25]. Another inverse correlation was also found between the dietary content of SFA from milk fat and serum concentration of cholesterol in 15-year-old Swedish adolescents [26]. A possible explanation was that milk fat may reduce the risk of cardiac diseases through reduced formation of small dense LDL particles [27]. As recently described in healthy men and women [24], our results suggest not only that a moderate consumption of dairy products does not increase the risk of cardiovascular diseases [12, 28], but also that it can be better in term of prevention than a diet deprived of SFA, like the olive oil diet in the present study.

Second, the other major interesting result of this study is the differential influence of the diets on tissue (n-3) and (n-6) PUFA concentrations (Tables 3–7). In order to compare their effects on PUFA composition, the diets were designed to contain strictly equal amounts of ALA (2.5 mol% of FA, i.e. 0.55% of dietary energy) and LNA (10–11 mol% of FA, i.e. 2.6% of dietary energy) in a ratio of 4.6 that meets human essential FA requirements [29]. The results showed an increased accumulation of both ALA and LNA in several tissues of butterfat animals compared to olive oil, saturates and trimyristin animals. Concerning the essential (n-6) and (n-3) HUFA, an effect of the butterfat diet was shown on the level of EPA and DPA (n-3). Although there were traces of DPA (n-3) in the butterfat diet, it seems that the increase shown in tissue EPA and DPA (n-3) is not

Table 7 Fatty acid composition (mol% of total FA) of heart total lipids of the rats

Fatty acid	Olive oil	Butterfat	Saturates	Trimyristin
C14:0	0.20 ± 0.05[b]	0.42 ± 0.16[a]	0.44 ± 0.15[a]	0.52 ± 0.07[a]
C16:0	11.74 ± 0.59	12.30 ± 0.89	12.23 ± 0.70	11.99 ± 0.41
C18:0	20.07 ± 0.83	20.09 ± 0.70	20.65 ± 0.36	20.29 ± 0.52
ΣSFA	32.27 ± 1.11[b]	33.06 ± 0.94[a,b]	33.55 ± 0.52[a]	33.08 ± 0.94[a,b]
C16:1 n-7	0.62 ± 0.10	0.84 ± 0.28	0.58 ± 0.15	0.64 ± 0.07
C18:1 n-9	14.21 ± 1.03[a]	9.04 ± 0.87[d]	10.21 ± 0.65[c]	12.43 ± 0.95[b]
C18:1 n-7	4.79 ± 0.34	4.56 ± 0.27	4.81 ± 0.19	4.69 ± 0.13
C18:1 n-9 *trans*	0.11 ± 0.02[b]	0.28 ± 0.04[a]	0.11 ± 0.02[b]	0.12 ± 0.04[b]
ΣMUFA	20.17 ± 0.82[a]	15.01 ± 1.09[c]	16.07 ± 0.73[c]	18.34 ± 0.94[b]
C18:2 n-6	14.61 ± 2.14[b]	17.61 ± 0.73[a]	15.74 ± 0.76[b]	15.79 ± 1.33[b]
C20:3 n-6	0.53 ± 0.06[b]	0.63 ± 0.06[a]	0.51 ± 0.04[b]	0.50 ± 0.06[b]
C20:4 n-6	20.17 ± 0.91	20.68 ± 1.04	21.14 ± 0.64	20.17 ± 0.58
C22:4 n-6	0.53 ± 0.05	0.50 ± 0.06	0.58 ± 0.07	0.54 ± 0.05
C22:5 n-6	0.67 ± 0.16[a,b]	0.54 ± 0.06[b]	0.69 ± 0.19[a,b]	0.70 ± 0.17[a]
Σ n-6 PUFA	36.63 ± 1.23[c]	40.07 ± 0.92[a]	38.40 ± 0.37[b]	37.81 ± 1.17[b,c]
Σ n-6 HUFA	22.03 ± 1.08	22.44 ± 1.08	23.83 ± 0.77	22.03 ± 0.79
C18:3 n-3	0.19 ± 0.03	0.20 ± 0.03	0.18 ± 0.02	0.17 ± 0.02
C20:5 n-3	0.16 ± 0.02[a,b]	0.20 ± 0.04[a]	0.13 ± 0.02[b]	0.14 ± 0.04[b]
C22:5 n-3	1.05 ± 0.07[c]	1.61 ± 0.12[a]	1.26 ± 0.16[b]	1.11 ± 0.09[b,c]
C22:6 n-3	9.13 ± 0.86	9.54 ± 0.52	9.65 ± 0.65	8.95 ± 0.99
Σ n-3 PUFA	10.69 ± 0.89[b]	11.74 ± 0.45[a]	11.41 ± 0.73[a,b]	10.52 ± 0.97[b]
Σ n-3 HUFA	10.50 ± 0.90[b]	11.54 ± 0.47[a]	11.23 ± 0.73[a,b]	10.35 ± 0.98[b]
Total FA (μmol/g tissue)	199.3 ± 11.8	200.7 ± 13.0	194.4 ± 7.9	185.9 ± 46.5

All data are means ± SD ($n = 6$). Different superscripts letters in the same row indicate a significant difference among the data ($P < 0.05$). n-6 PUFA include C18:2 n-6, C20:2 n-6, C20:3 n-6, C20:4 n-6, C22:4 n-6 and C22:5 n-6 here; n-6 HUFA include C20:2 n-6, C20:3 n-6, C20:4 n-6, C22:4 n-6 and C22:5 n-6 here; n-3 PUFA include C18:3 n-3, C20:3 n-3, C20:5 n-3, C22:5 n-3, and C22:6 n-3 here; n-3 HUFA include C20:3 n-3, C20:5 n-3, C22:5 n-3, and C22:6 n-3 here

linked to the presence of these traces but more likely to other mechanisms (increased conversion from ALA, increased incorporation in specific tissues, lower β-oxidation) since no effect of ARA traces in the butterfat diet is shown on the level of tissue ARA. Therefore, the butterfat diet increased the level of tissue (n-3) HUFA, especially in the heart (Table 7) where these derivatives have been suggested to have cardio-protective effects [30] and in the retina (Supplemental Table 3) where they have been described to be important for neural development [31]. Altogether, these results show beneficial effects in the measured physiological parameters (circulating cholesterol and level of tissue (n-3) PUFA) of the butterfat diet (LNA and ALA diet enriched with butterfat) compared with the olive oil diet (LNA and ALA diet enriched with olive oil), with intermediate levels of the saturates diet (LNA and LA diet enriched with synthetic saturated TAG).

These results led us to wonder what can explain these differential effects, when considering the FA composition of the four diets (Table 1). The comparison of the dietary FA composition suggests firstly that some effects can be attributed to the presence of short and medium chain SFA (C4:0–C10:0) in the butterfat diet. Indeed, this diet is characterized by its high level in SFA from butterfat (about 52 mol% of total FA), including specifically short and medium chain SFA (C4:0–C10:0; 17 mol% of total FA) (Table 1). In the literature, dietary short and medium-chain SFA have been shown to have no increasing effect on plasma cholesterol in humans [8]. Moreover, C8:0 and C10:0 were hypocholesterolemic in the rat [32], in the dog [33], and C8:0 has an inhibitory effect on the synthesis of apoprotein B in the liver which is necessary for VLDL secretion [34]. An hypothesis for the beneficial effect of dietary short and medium-chain SFA is that they are directly absorbed through the portal vein leading to their preferential β-oxidation in the liver [35] whereas long-chain fatty acids are secreted as chylomicrons in the lymph and plasma, leading likely to an increased storage in adipose and other tissues. This metabolic specificity may explain not only the total absence of short and medium

chain fatty acids in every tissue but also their increased substrate competition with ALA and LNA for the β-oxidation pathway, leading to the sparing and increased storage of these two PUFA.

A 2nd difference between the olive oil and butterfat diets is the presence of myristic acid (Table 1), which is a characteristic of dairy fat. The saturates and trimyristin diets were therefore designed to answer the question of the relative effects of myristic acid versus short and medium chain saturated fatty acids. The results showed that the saturates diet lowered the plasma cholesterol level (Table 2) compared with the olive oil diet, but to a lesser extent than the butterfat diet. For instance, total cholesterol was significantly higher in the saturates group than in the butterfat group. Myristic acid has long been considered as having played a major role in the increase in blood cholesterol level in animals and humans, when provided at high level, exceeding 4% of dietary energy [9, 10]. However, when its dietary level is moderate (1.0–2.5% of dietary energy) no evidence of deleterious effects of this specific fatty acid has been reported [11–14, 25]. In humans, a moderate supply of myristic acid (1.8% of daily energy) was shown to improve lecithin cholesterol acyltransferase (LCAT) activity, which is considered beneficial in terms of HDL cholesterol concentration and reverse cholesterol transport [36]. Concerning now LNA, ALA and (n-3) HUFA concentrations, the effects shown after the butterfat diet (compared with olive oil diet) were less significant or disappeared in saturates animals (Tables 3–7). In addition, the trimyristin diet did not cause any differences in tissue n-6 and n-3 PUFA profiles (Tables 3–7), nor in plasma lipid parameters (except in HDL-cholesterol) in comparison to the olive oil diet (Table 2), which suggests that myristic acid alone, when provided as trimyristin at least, does not appear as responsible for the effects seen with the butterfat diet. However, we have also to take into account that myristic acid is mainly in the *sn*-2 position in dairy TAG of the butterfat diet, whereas it is equally distributed in the 3 positions in the synthetic saturated TAG of the two other saturated fat diets (saturates and trimyristin diets) [37]. It has been suggested that fatty acids in the *sn*-2 position are better absorbed in enterocytes [38], but there are still controversies about the real physiological impact of fatty acids when located in the *sn*-2 position [39, 40]. In our study, when analyzing the effect of the 3 diets containing 10-12 mol% myristic acid (butterfat, saturates and trimyristin), myristic acid was found significantly higher in adipose tissue of the rats fed the butterfat diet (Table 3), suggesting that myristic acid in *sn*-2 position is indeed better absorbed or better stored. Concerning the plasma lipid parameters, it remains difficult to relate the *sn*-2 position of myristic acid in dairy fat to the beneficial effect of the butterfat diet. Concerning the effect on (n-3) HUFA derivatives, we can suppose that myristic acid in *sn*-2 position and its subsequent increased bioavailability could increase Δ6-desaturase activity and long chain (n-3) HUFA tissue concentration, as already shown in cultured rat hepatocytes incubated with myristic acid [41].

A third specific characteristic of the butterfat diet, compared to the three other diets, is the presence of *trans* FA and conjugated linoleic acids (CLA) with possible biological effects. It has been shown that feeding rumenic acid (*cis* 9, *trans* 11 CLA) may beneficially affect lipoprotein profile in hamster [42]. However, CLA did not modify LNA and ALA metabolism in healthy human subjects consuming a diet with adequate intake of essential fatty acids [43].

Finally, one could consider that the high level of oleic acid in the olive oil diet (70 mol% of dietary FA) could be involved in the effects shown in this study, when compared to the butterfat and saturates diets. However, oleic acid is considered to be neutral in plasma lipid metabolism, when provided in the range 15–21% of total dietary energy [44, 45], which is the case in the present study (15.6% of total dietary energy). Olive oil is also known to contain high level of squalene (300–700 mg/100 g) and this phytosterol precursor has been shown to be at least partly absorbed and then quantitatively converted to cholesterol. The squalene content of olive oil could therefore contribute to an increase in plasma cholesterol concentration [46]. Concerning the effects on n-3 and n-6 PUFA, oleic acid is known to be a substrate of the Δ6-desaturase, and high level of tissue C18:1 n-9 could compete with LNA and ALA for the biosynthesis of HUFA of the n-9 series rather than HUFA of the n-6 and n-3 series. This hypothesis could explain some of the difference between the olive oil and butterfat diets regarding n-3 HUFA levels.

As a conclusion, the results show that in diets with identical well-balanced LNA/ALA ratio, the specific SFA composition has an impact on plasma cholesterol parameters and tissue PUFA content.

Acknowledgments The authors thank ARILAIT RECHERCHES (France) for constructive scientific discussion and financial support. We are grateful to Dr. Le Ruyet (Lactalis) for providing the fractionated butterfat and X. Blanc (UPAE, INRA, Jouy en Josas, France) for the preparation of the diets. We thank N. Monthéan and R. Marion for able technical assistance and animal care. The authors declare that this work was supported by research grants from the French Dairy Council.

References

1. Keys A, Menotti A, Aravanis C, Blackburn H, Djordevic BS, Buzina R, Dontas AS, Fidanza F, Karvonen MJ, Kimura N et al (1984) The seven countries study: 2, 289 deaths in 15 years. Prev Med 13:141–154

2. Kromhout D, Bloemberg B, Feskens E, Menotti A, Nissinen A (2000) Saturated fat, vitamin C and smoking predict long-term population all-cause mortality rates in the Seven Countries Study. Int J Epidemiol 29:260–265
3. Siri-Tarino PW, Sun Q, Hu FB, Krauss RM (2010) Meta-analysis of prospective cohort studies evaluating the association of saturated fat with cardiovascular disease. Am J Clin Nutr 91:535–546
4. Rioux V, Legrand P (2007) Saturated fatty acids: simple molecular structures with complex cellular functions. Curr Opin Clin Nutr Metab Care 10:752–758
5. Kris-Etherton PM, Griel AE, Psota TL, Gebauer SK, Zhang J, Etherton TD (2005) Dietary stearic acid and risk of cardiovascular disease: intake, sources, digestion, and absorption. Lipids 40:1193–1200
6. Ravnskov U (1998) The questionable role of saturated and polyunsaturated fatty acids in cardiovascular disease. J Clin Epidemiol 51:443–460
7. Parodi PW (2009) Has the association between saturated fatty acids, serum cholesterol and coronary heart disease been over emphasized? Int Dairy J 19:345–361
8. Hu FB, Stampfer MJ, Manson JE, Ascherio A, Colditz GA, Speizer FE, Hennekens CH, Willett WC (1999) Dietary saturated fats and their food sources in relation to the risk of coronary heart disease in women. Am J Clin Nutr 70:1001–1008
9. Salter AM, Mangiapane EH, Bennett AJ, Bruce JS, Billett MA, Anderton KL, Marenah CB, Lawson N, White DA (1998) The effect of different dietary fatty acids on lipoprotein metabolism: concentration-dependent effects of diets enriched in oleic, myristic, palmitic and stearic acids. Br J Nutr 79:195–202
10. Hayes KC, Khosla P (1992) Dietary fatty acid thresholds and cholesterolemia. FASEB J 6:2600–2607
11. Loison C, Mendy F, Serougne C, Lutton C (2002) Dietary myristic acid modifies the HDL-cholesterol concentration and liver scavenger receptor BI expression in the hamster. Br J Nutr 87:199–210
12. Tholstrup T, Vessby B, Sandstrom B (2003) Difference in effect of myristic and stearic acid on plasma HDL cholesterol within 24 h in young men. Eur J Clin Nutr 57:735–742
13. Rioux V, Catheline D, Bouriel M, Legrand P (2005) Dietary myristic acid at physiologically relevant levels increases the tissue content of C20:5 n-3 and C20:3 n-6 in the rat. Reprod Nutr Dev 45:599–612
14. Dabadie H, Motta C, Peuchant E, LeRuyet P, Mendy F (2006) Variations in daily intakes of myristic and alpha-linolenic acids in *sn*-2 position modify lipid profile and red blood cell membrane fluidity. Br J Nutr 96:283–289
15. Yu S, Derr J, Etherton TD, Kris-Etherton PM (1995) Plasma cholesterol-predictive equations demonstrate that stearic acid is neutral and monounsaturated fatty acids are hypocholesterolemic. Am J Clin Nutr 61:1129–1139
16. Thijssen MA, Hornstra G, Mensink RP (2005) Stearic, oleic, and linoleic acids have comparable effects on markers of thrombotic tendency in healthy human subjects. J Nutr 135:2805–2811
17. Towler DA, Gordon JI, Adams SP, Glaser L (1988) The biology and enzymology of eukaryotic protein acylation. Annu Rev Biochem 57:69–99
18. Coradini D, Speranza A (2005) Histone deacetylase inhibitors for treatment of hepatocellular carcinoma. Acta Pharmacol Sin 26:1025–1033
19. Rioux V, Catheline D, Beauchamp E, Le Bloc'h J, Pédrono F, Legrand P (2008) Substitution of dietary oleic for myristic acid increases the tissue storage of alpha-linolenic acid and the concentration of docosahexaenoic acid in brain, red blood cells and plasma in the rat. Animal 2:636–644
20. Guillou H, Martin P, Jan S, D'Andrea S, Roulet A, Catheline D, Rioux V, Pineau T, Legrand P (2002) Comparative effect of fenofibrate on hepatic desaturases in wild-type and peroxisome proliferator-activated receptor alpha-deficient mice. Lipids 37:981–989
21. Rioux V, Lemarchal P, Legrand P (2000) Myristic acid, unlike palmitic acid, is rapidly metabolized in cultured rat hepatocytes. J Nutr Biochem 11:198–207
22. Tsutsumi K, Hagi A, Inoue Y (2001) The relationship between plasma high density lipoprotein cholesterol levels and cholesteryl ester transfer protein activity in six species of healthy experimental animals. Biol Pharm Bull 24:579–581
23. Fernandez ML, Calle M (2010) Revisiting dietary cholesterol recommendations: does the evidence support a limit of 300 mg/d? Curr Atheroscler Rep doi:10.1007/s11883-010-0130-7
24. Tholstrup T (2006) Dairy products and cardiovascular disease. Curr Opin Lipidol 17:1–10
25. Mozaffarian D, Rimm EB, Herrington DM (2004) Dietary fats, carbohydrate, and progression of coronary atherosclerosis in postmenopausal women. Am J Clin Nutr 80:1175–1184
26. Samuelson G, Bratteby LE, Mohsen R, Vessby B (2001) Dietary fat intake in healthy adolescents: inverse relationships between the estimated intake of saturated fatty acids and serum cholesterol. Br J Nutr 85:333–341
27. Sjogren P, Rosell M, Skoglund-Andersson C, Zdravkovic S, Vessby B, de Faire U, Hamsten A, Hellenius ML, Fisher RM (2004) Milk-derived fatty acids are associated with a more favorable LDL particle size distribution in healthy men. J Nutr 134:1729–1735
28. Dabadie H, Peuchant E, Bernard M, LeRuyet P, Mendy F (2005) Moderate intake of myristic acid in sn-2 position has beneficial lipidic effects and enhances DHA of cholesteryl esters in an interventional study. J Nutr Biochem 16:375–382
29. Simopoulos AP, Leaf A, Salem N Jr (1999) Essentiality of and recommended dietary intakes for omega-6 and omega-3 fatty acids. Ann Nutr Metab 43:127–130
30. Harper CR, Edwards MJ, DeFilippis AP, Jacobson TA (2006) Flaxseed oil increases the plasma concentrations of cardioprotective (n-3) fatty acids in humans. J Nutr 136:83–87
31. Alessandri JM, Poumes-Ballihaut C, Langelier B, Perruchot MH, Raguenez G, Lavialle M, Guesnet P (2003) Incorporation of docosahexaenoic acid into nerve membrane phospholipids: bridging the gap between animals and cultured cells. Am J Clin Nutr 78:702–710
32. Kaunitz H, Slanetz CA, Johnson RE, Babayan VK (1960) Medium-chain and long-chain saturated triglycerides and linoleic acid requirements. J Nutr 71:400–404
33. Grande F (1962) Dog serum lipid responses to dietary fats differing in the chain length of the saturated fatty acids. J Nutr 76:255–264
34. Tachibana S, Sato K, Cho Y, Chiba T, Schneider WJ, Akiba Y (2005) Octanoate reduces very low-density lipoprotein secretion by decreasing the synthesis of apolipoprotein B in primary cultures of chicken hepatocytes. Biochim Biophys Acta 1737:36–43
35. Bach AC, Babayan VK (1982) Medium-chain triglycerides: an update. Am J Clin Nutr 36:950–962
36. Vaysse-Boue C, Dabadie H, Peuchant E, Le Ruyet P, Mendy F, Gin H, Combe N (2007) Moderate dietary intake of myristic and alpha-linolenic acids increases lecithin-cholesterol acyltransferase activity in humans. Lipids 42:717–722
37. Jensen RG, Ferris AM, Lammi-Keefe CJ, Henderson RA (1990) Lipids of bovine and human milks: a comparison. J Dairy Sci 73:223–240
38. Innis SM, Dyer R, Nelson CM (1994) Evidence that palmitic acid is absorbed as *sn*-2 monoacylglycerol from human milk by breast-fed infants. Lipids 29:541–545
39. Porsgaard T, Xu X, Gottsche J, Mu H (2005) Differences in the intramolecular structure of structured oils do not affect pancreatic

lipase activity in vitro or the absorption by rats of (n-3) fatty acids. J Nutr 135:1705–1711
40. Emken EA, Adlof RO, Duval SM, Shane JM, Walker PM, Becker C (2004) Effect of triacylglycerol structure on absorption and metabolism of isotope-labeled palmitic and linoleic acids by humans. Lipids 39:1–9
41. Jan S, Guillou H, D'Andrea S, Daval S, Bouriel M, Rioux V, Legrand P (2004) Myristic acid increases delta6-desaturase activity in cultured rat hepatocytes. Reprod Nutr Dev 44:131–140
42. LeDoux M, Laloux L, Fontaine JJ, Carpentier YA, Chardigny JM, Sebedio JL (2007) Rumenic acid significantly reduces plasma levels of LDL and small dense LDL cholesterol in hamsters fed a cholesterol- and lipid-enriched semi-purified diet. Lipids 42:135–141
43. Turpeinen AM, Barlund S, Freese R, Lawrence P, Brenna JT (2006) Effects of conjugated linoleic acid on linoleic and linolenic acid metabolism in man. Br J Nutr 95:727–733
44. Carmena R, Ascaso JF, Camejo G, Varela G, Hurt-Camejo E, Ordovas JM, Martinez-Valls J, Bergstom M, Wallin B (1996) Effect of olive and sunflower oils on low density lipoprotein level, composition, size, oxidation and interaction with arterial proteoglycans. Atherosclerosis 125:243–255
45. Mensink RP, Katan MB (1989) Effect of a diet enriched with monounsaturated or polyunsaturated fatty acids on levels of low-density and high-density lipoprotein cholesterol in healthy women and men. N Engl J Med 321:436–441
46. Ostlund RE, Racette SB, Stenson WF (2002) Effects of trace components of dietary fat on cholesterol metabolism: phytosterols, oxysterols, and squalene. Nutr Rev 60:349–359

Lipids (2010) 45:987–995
DOI 10.1007/s11745-010-3470-8

ORIGINAL ARTICLE

Liver-Specific Pyruvate Dehydrogenase Complex Deficiency Upregulates Lipogenesis in Adipose Tissue and Improves Peripheral Insulin Sensitivity

Cheol Soo Choi · Pushpankur Ghoshal · Malathi Srinivasan · Sheene Kim · Gary Cline · Mulchand S. Patel

Received: 26 April 2010 / Accepted: 25 August 2010 / Published online: 12 September 2010

Abstract The pyruvate dehydrogenase complex (PDC) plays a critical role in lipid synthesis and glucose homeostasis in the fed and fasting states. The central role of the liver in the maintenance of glucose homeostasis has been established by studying changes in key enzymes (including PDC) and the carbon-flux via several pathways under different metabolic states. In the present study we have developed a murine model of liver-specific PDC deficiency using Cre-loxP technology to investigate its consequences on lipid and carbohydrate metabolism. There was no incorporation of glucose-carbon into fatty acids by liver in vitro from liver-specific *Pdha1* knockout (L-PDHKO) male mice due to absence of hepatic PDC activity. Interestingly, there was a compensatory increase in lipogenic capacity in epididymal adipose tissue from L-PDHKO mice. Both fat and lean body mass were significantly reduced in L-PDHKO mice, which might be explained by an increase in total energy expenditure compared with wild-type littermate mice. Furthermore, both liver and peripheral insulin sensitivities measured during a hyperinsulinemic-euglycemic clamp were improved in L-PDHKO mice. The findings presented here demonstrate (i) the indispensable role of PDC for lipogenesis from glucose in liver and (ii) specific adaptations in lipid and glucose metabolism in the liver and adipose tissue to compensate for loss of PDC activity in liver only.

Keywords PDC deficiency · *Pdha1* deletion · Lipogenesis · Glucose homeostasis · Liver glycogen · Liver · Adipose tissue · Hyperinsulinemic clamp

Abbreviations

PDC	Pyruvate dehydrogenase complex
L-PDHKO	Liver-specific pyruvate dehydrogenase knockout
PDH	Pyruvate dehydrogenase
FFA	Free fatty acid
TCA	Tricarboxylic acid

Introduction

The liver plays the central role in the maintenance of glucose homeostasis in mammals. Liver has the full complement of enzymes for the synthesis of glycogen, lipids (secreted as part of very low density lipoproteins) and other molecules from dietary carbohydrates in the fed state and for the synthesis of glucose from gluconeogenic precursors during the fasting state [1, 2]. Glucose from the dietary carbohydrates is initially converted into liver glycogen via both the direct and indirect pathways, the latter involving the following sequence: glucose to three carbon intermediates to glycogen [1, 3]. Lactate appears to be the major three-carbon precursor because it is readily produced from glucose by extrahepatic tissues [4]. The availability of substrate supply for the indirect pathway is supported by demonstration of a delayed activation by dephosphorylation

C. S. Choi and P. Ghoshal contributed equally to this work.

P. Ghoshal · M. Srinivasan · M. S. Patel (✉)
Department of Biochemistry, School of Medicine and Biomedical Sciences, University at Buffalo, The State University of New York, Buffalo, NY 14214, USA
e-mail: mspatel@buffalo.edu

C. S. Choi · S. Kim · G. Cline
Department of Internal Medicine, Yale University School of Medicine, New Haven, CT 06510, USA

of the pyruvate dehydrogenase complex (PDC) in several mammalian tissues (including liver) in the immediate postprandial period [5, 6].

PDC is located at the cross-roads of glucose and fatty acid metabolism and hence the flux through mammalian PDC is tightly regulated by a phosphorylation (inactivation)/dephosphorylation (activation) mechanism catalyzed by a dedicated group of kinases and phosphatases [5, 7, 8]. In the fasting state PDC, in most tissues except the brain, is readily phosphorylated and inactivated inhibiting glucose oxidation. In the fed state PDC is reactivated by its dephosphorylation resulting in increased oxidative utilization of glucose in most tissues and lipid biosynthesis in the liver and adipose tissue [5, 7, 8]. Only after PDC reactivation (after an initial delay) in the liver and other tissues, can the oxidative metabolism of glucose support energy production and the biosynthesis of lipids from acetyl-CoA generated from glucose-derived pyruvate via the action of PDC [6, 9]. Thus, the timing and degree of reactivation of PDC in the liver plays a pivotal role in directing carbon flow from dietary carbohydrates to the synthesis of hepatic glycogen and lipids.

PDC deficiency is one of the major genetic disorders of oxidative metabolism resulting in congenital lactic acidosis and neurological dysfunctions [10, 11]. Although the majority of the genetic defects in human PDC is identified in the pyruvate dehydrogenase (PDH) α subunit gene (*PDHA1*) localized on chromosome X [12], the defects in the other component genes of the complex are also reported to cause similar clinical complications [11, 13]. To gain insight into the pathophysiology of PDC deficiency, we have developed a line of mice carrying an inducible null mutation in the *Pdha1* gene localized on chromosome X using the Cre-loxP system [14]. The *Pdha1* gene in mice encodes the α subunit of the pyruvate dehydrogenase (PDH) component of PDC in somatic cells [15]. Generation of a generalized null mutation in mice has proven to be lethal at an early embryonic stage in male mice in this model [14]. However, tissue-specific or cell-specific deletion of the *Pdha1* gene encoding the α subunit of PDH can allow fetal development and postnatal survival of males to enable investigation of its impact on glucose and lipid metabolism [16, 17].

In the present study, we generated liver-specific deletion of the *Pdha1* gene by breeding females ($Pdha1^{flox8/flox8}$ genotype) with liver-specific albumin/Cre expressing transgenic males [18] to create liver-specific PDC deficiency. The consequences of loss of liver PDC activity on whole body and tissue-specific carbohydrate and lipid metabolism in affected male mice were investigated using complementary in vitro and in vivo approaches. The results presented here show that whole body insulin sensitivity was increased and there are specific alterations in glucose and lipid metabolism in both the liver and adipose tissue in male mice with near complete PDC deficiency in the liver only.

Materials and Methods

Animals

All experiments were conducted in accordance with the *Guide for the Use and Care of Laboratory Animals* and approved by the Institutional Animal Care and Use Committee of University at Buffalo. Mice were housed under controlled temperature (22 ± 2°C) and lighting (12-h light; 0700–1900 h, 12-h dark; 1900–0700 h) with free access to water and a standard rodent laboratory diet (Harlan Teklad, Madison, WI). Generation of male and female mice harboring the $Pdha1^{flox8}$ allele(s) were done as described previously [14]. Briefly, two loxP sites were introduced into intronic sequences flanking exon 8 to generate the $Pdha1^{flox8}$ allele. Progeny carrying the $Pdha1^{flox8}$ allele was intrabred to produce a line of animals that carried only the $Pdha1^{flox8}$ allele. To initiate deletion of exon 8 in vivo in liver, homozygous $Pdha1^{flox8/flox8}$ females were bred with males from C57BL/6-TgN9AlbCre)21Mgn transgenic line obtained from the Jackson Laboratory which carried an autosomally integrated C*re* gene with liver-specific (hepatocyte-specific) albumin promoter [18]. For in vivo studies including body composition, energy balance and hyperinsulinemic euglycemic clamp study, male mice were maintained and studied in accordance with the Institutional Animal Care and Use Committee of Yale University School of Medicine. All of the experiments in this study were performed with 3–4 month-old male mice, and unless otherwise indicated all studies were performed in fed mice.

Genotype Analysis

Tail DNA from progeny were isolated as per manufacturer's protocol (Omniprep^{TM}I, Genotechnolgy, Inc.) and amplified using a *Pdha1* sense primer 5′ AGCAGCCAGCACGGA CTACT 3′ and antisense primer 5′ GCAGCCAAACAGA TTACACC 3′ and *Cre* primers sense 5′ GCATTTCTGG GGATTGCTTA 3′ and an antisense 5′ CCCGGCAAAAC AGGTAGTTA 3′ [14]. Animals in the fed state were deeply anesthetized, killed by decapitation, the livers were quickly removed, frozen in liquid nitrogen and stored at −70°C. A portion of the liver was processed for isolation of genomic DNA and polymerase chain reaction was carried out as described [14]. Thermal cycle consisted of initial denaturation at 95°C for 10 min, followed by 35 cycles of 1 min denaturation at 95°C, 1 min annealing at 68°C, 1.5 min extension at 72°C after a final extension at 72°C for 10 min,

25 µl of the final reaction was mixed with 15 µl of gel loading buffer and electrophoresed on 1% agarose gel stained with ethidium bromide.

Enzyme Activities and Protein Detection

For the assay of 'total' PDC activity, tissues from fed male mice were homogenized in KCl-MOPS buffer containing protease inhibitors. After three freeze–thaw cycles and centrifugation, samples were dephosphorylated with recombinant rat phospho-PDH phosphatase [19, 20], and stored at −80°C. Total PDC activity was determined by the production of $^{14}CO_2$ from [1-^{14}C]pyruvate [19]. PDC activity is expressed as munits/mg protein. For measurement of glycogen synthase activities, tissues were homogenized in ice-cold 50 mM Tris–HCl, pH 7.8 containing 100 mM NaF, 10 mM EDTA and a cocktail of the protease inhibitors and centrifuged at 1500×*g* for 5 min. Glycogen synthase activities (active and total forms) were measured in the supernatants using UDP-[U-^{14}C]glucose [21] and are expressed as nmol of UDP-glucose incorporated/min/mg soluble protein. Activity ratio is ratio of the 'active' to 'total' form of glycogen synthase activity. Tissue glycogen content was measured according to Lo et al. [22]. Proteins were measured using BioRad kit (Bio-Rad, Hercules, CA). To detect pyruvate dehydrogenase (PDH) proteins (α and β subunits) in solubilized tissue extracts, aliquots (20 µg of protein) were size fractionated on SDS-PAGE, transferred to nitrocellulose membrane, probed with a polyclonal anti-PDH rabbit primary antibody [19] and goat anti-rabbit IgG (H + L)-horse radish peroxidase conjugate secondary antibody. A purified mammalian PDH preparation was used as an internal molecular weight marker. Proteins bands were visualized by chemiluminescence method.

Body Composition and Whole Body Energy Balance

Fat and lean body masses were assessed by ^{1}H magnetic resonance spectroscopy (Bruker BioSpin, Billerica, MA). Metabolic measurements of unrestrained activity, energy expenditure, and food consumption were determined using a Comprehensive Animal Metabolic Monitoring System (CLAMS: Columbus instruments, Columbus, OH). Energy expenditure and food consumption data were normalized with respect to body weight. Energy expenditure was calculated from the gas exchange data using the following formula: Energy expenditure = (3.815 + 1.232 * RQ) * VO_2. Respiratory quotient (RQ) is the ratio of VCO_2 to VO_2, which changes depending on the energy source the animal is using. Locomotor activity was measured on *x* and *z*-axis using infrared beams to count the amount of beam breaks during the specified measurement period. Feeding was calculated from the change in the weight of chow in the Center-Feeder with respect to time.

In Vitro Synthesis of Fatty Acids

For study of lipogenesis in vitro, 3–4 month-old male mice were first fasted for 24 h and then refed for 24 h. Liver slices and pieces of adipose tissue (about 100 mg) were incubated in a sealed flask containing 3 ml of Krebs–Ringer bicarbonate buffer, pH 7.4, containing 0.5 mM $CaCl_2$, 0.3 U insulin and 50 mM glucose (3 µCi D-[U-^{14}C]glucose) or 10 mM [U-^{14}C]acetate plus 50 mM glucose at 37°C for 3 h. $^{14}CO_2$ was trapped and radioactivity was determined using a Beckman LS 6500 counter [23, 24]. Lipids from liver slices and pieces of adipose tissue were extracted with chloroform–methanol (2:1, v/v), saponified with alcoholic KOH, fatty acids fraction extracted with petroleum ether, and radioactivity was determined [23].

Hyperinsulinemic-Euglycemic Clamp

Seven days prior to the hyperinsulinemic-euglycemic clamp studies, indwelling catheters were placed into the right internal jugular vein extending to the right atrium. After an overnight fast, [3-^{3}H]glucose (high pressure liquid chromatography purified; Perkin Elmer, Boston, MA) was infused at a rate of 0.05 µCi/min for 2 h to assess the basal glucose turnover. Following the basal period, hyperinsulinemic-euglycemic clamp was conducted for 120 min with a primed/continuous infusion of human insulin (126 pmol/kg prime, 18 pmol/kg/min infusion) [25]. To estimate insulin-stimulated whole body glucose fluxes, [3-^{3}H]glucose was infused at a rate of 0.1 µCi/min throughout the clamps [25]. Rates of basal and insulin-stimulated whole-body glucose turnover and hepatic glucose production were determined as described [26]. Whole body glycolysis was calculated from the rate of increase in plasma ^3H_2O concentration divided by the specific radioactivity of plasma D-[3-^{3}H]glucose [26]. Whole body glycogen synthesis was estimated by subtracting whole body glycolysis from whole body glucose uptake, assuming that glycolysis and glycogen synthesis account for the majority of insulin-stimulated glucose uptake [27]. Additional blood samples were obtained for the measurement of plasma insulin and free fatty acid (FFA) concentrations at the end of basal and clamp periods.

Data Analysis and Presentation of Results

All results are expressed as means ± SEM of 'n' observations. Statistical differences between the means were accessed by Student's *t*-test.

Results

Characterization of Liver-Specific Pdha1 Knockout Mice

Breeding of targeted homozygous females ($Pdha1^{flox8}/^{flox8}$) with liver-specific wild-type alb-Cre^{+} ($Pdha1^{wt}/Y$; Cre^{liver+}) transgenic males resulted in male mice in the progeny with two different genotypes: $Pdha1^{flox8}$/Y, Cre^{liver-} (wild-type control mice) and $Pdha1^{\Delta ex8}/Y$, Cre^{liver+} [liver-specific PDH knockout (L-PDHKO) mice]. Only male progeny was used in this study because females carrying the *Cre* transgene would have variable expression of the normal allele due to Lyonization (random inactivation of the one of the two chromosome X). Initially the presence or absence of the *Cre* transgene in these mice was determined by PCR method using the tail DNA, and later it was confirmed by the same method using liver DNA. Polymerase chain reaction analysis of liver DNA from L-PDHKO mice ($Pdha1^{\Delta ex8}/Y$, Cre^{liver+}) showed near complete deletion (>95%) of the *Pdha1* gene compared to that from the wild-type control mice (Fig. 1a). Deletion of the loxP-flanked exon 8 by Cre recombinase resulted in the amplification of a 400 base pair product in the L-PDHKO mice whereas a 800 base pair amplification product was generated from the targeted $Pdha1^{flox8}$ allele of the wild-type control mice (Fig. 1a). As expected, there was no deletion in the $Pdha1^{flox8}$ allele in the skeletal muscle, heart and epididymal adipose tissue from the L-PDHKO mice (Fig. 1b).

There was no noticeable embryonic lethality (as evident from normal litter size) and the L-PDHKO mice were obtained with the expected frequency among male progeny. Newborn male L-PDHKO mice were indistinguishable from other littermates.

As predicted based on the results of polymerase chain reaction analysis, there was near complete loss of 'total' PDC activity in livers from L-PDHKO male mice compared to wild-type control male mice (Table 1). To further investigate the effect of deletion of the liver *Pdha1* allele in the knockout mice on the α and β subunits of the PDH component of the PDC, liver extracts were subjected to Western blot analysis using anti-PDH antibodies. Levels of both the α and β subunits of the PDH component were reduced to undetectable level in the liver extracts from the L-PDHKO male mice compared with wild-type control mice (Fig. 2). This finding is consistent with our previous observations that patients with genetic defects in the *PDHA1* gene only showed the loss of both the α and β subunit proteins of PDH due to instability of the β subunit in the absence of the α subunit in the mitochondrial preparations [13]. As expected, the levels of these two proteins in skeletal muscle, heart and epididymal adipose tissue

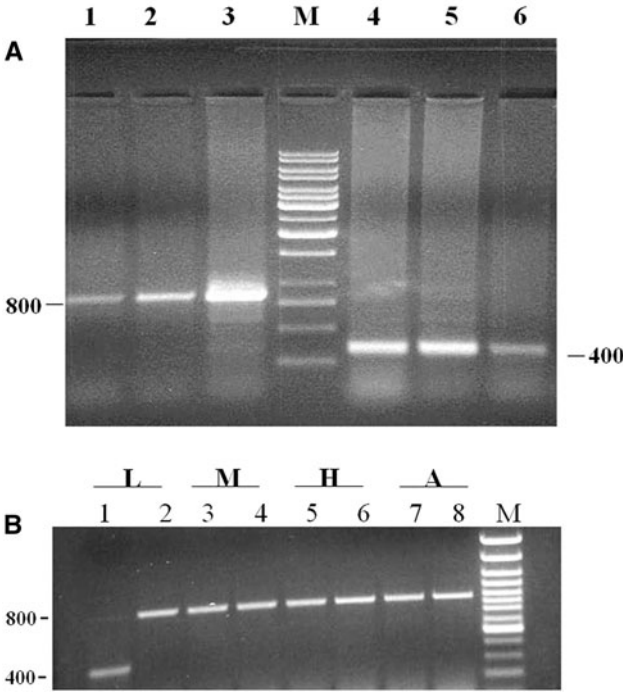

Fig. 1 Polymerase chain reaction amplification of chromosomal DNA of wild-type control ($Pdha1^{flox8}/Y$, Cre^{liver-}) and L-PDHKO ($Pdha1^{\Delta ex8}/Y$, Cre^{liver+}) male mice in the fed state. **a** In case of liver DNA from the controls, the *Pdha1* primers produced a 800 bp product (*lanes 1–3* for three different control littermate male mice) whereas the same primers produced a 400 bp product (*lanes 4–6*) with liver DNA from three L-PDHKO male mice indicating deletion of exon 8 in the *Pdha1* gene. **b** Polymerase chain reaction amplification of DNA from different tissues. Lanes with odd numbers are for a L-PDHKO mouse and even numbers are for a wild-type control mouse. Liver (*L lanes 1 and 2*), skeletal muscle (*M lanes 3 and 4*), heart (*H lanes 5 and 6*), and adipose tissue (*A lanes 7 and 8*). *M* indicates DNA ladder lane in both the gels

extracts from the two groups of mice were very similar (results not shown), indicating no effect of liver-specific deletion of the *Pdha1* on the levels of PDH proteins in other tissues.

Liver-Specific PDC Deficiency on Fat Mass, Energy Expenditure and Glycogen Stores

Adult L-PDHKO mice had lower whole body weight (by 12%) compared with wild-type control mice. Nuclear magnetic resonance analysis of body composition suggested that this was a consequence of a reduction in fat and lean mass by 33 and 9%, respectively (Table 1), compared with age-matched wild-type control mice. In order to further evaluate the reduction in body weight and fat mass [despite increased food intake], energy balance of the mice was assessed in an animal metabolic monitoring system for 4 days (2 days of acclimation followed by 2 days of measurements). L-PDHKO mice showed increased energy expenditure by 10% ($p < 0.05$) while locomotor activity

Table 1 Body weights and basal energy metabolic parameters from littermate wild-type control and L-PDHKO mice

Parameter	Wild-type	L-PDHKO
Body weight (g)	36.3 ± 1.4 (11)	31.8 ± 1.1 (10)*
Fat mass (g)	5.04 ± 0.66 (11)	3.36 ± 0.29 (10)*
Lean body mass (g)	26.14 ± 0.77 (11)	23.67 ± 0.84 (10)*
Energy expenditure (kcal/kg/h)	14.5 ± 0.4 (6)	16.0 ± 0.5 (6)*
Food intake (g/kg/h)	5.2 ± 0.4 (6)	5.8 ± 0.5 (6)*
Locomotor activity (counts)	73.1 ± 16.2 (6)	46.8 ± 4.9 (6)
Liver PDC (total) activity (mU/mg protein)	5.8 ± 0.2 (8)	0.08 ± 0.02 (8)***
Liver glycogen (mg/g)	55.2 ± 3.9 (9)	74.9 ± 4.4 (11)**
Muscle glycogen (mg/g)	7.9 ± 1.3 (4)	9.5 ± 1.0 (4)
Liver glycogen synthase active (mU/mg protein)	191 ± 2 (5)	175 ± 16 (5)
Liver glycogen synthase activity ratio (active/total)	0.60	0.66

The results are means ± SEM (n as shown)

*$p < 0.05$, **$p < 0.01$, ***$p < 0.001$ versus wild-type

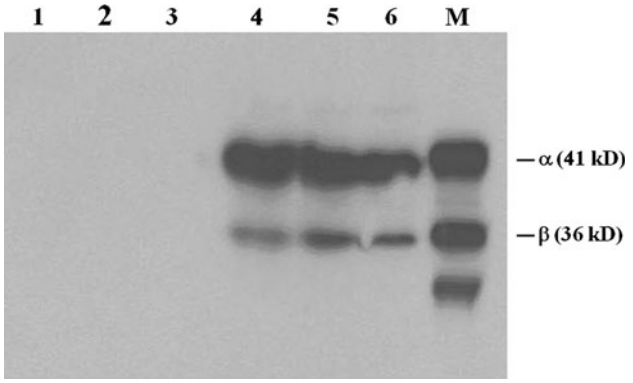

Fig. 2 Western blot analysis of PDH proteins in solubilized liver homogenates from wild-type control and L-PDHKO male mice in the fed state. Immunoblot analysis of liver homogenates indicating lack of PDH proteins (α and β subunits) in livers from three L-PDHKO male mice. (*Pdha1*$^{\Delta ex8}$*/Y Cre*$^{liver+}$; *lanes 1–3*) in comparison to three wild-type male mice (*Pdha1*^{flox8}*/Y Cre*$^{liver-}$; *lanes 4–6*). *M* purified PDH proteins [α (41 kDa) and β (36 kDa) subunits with a degraded lower molecular weight immunoreactive product]

did not differ in both groups ($p = 0.1$) (Table 1). However, when recalculated with respect to lean body mass, there was no difference in energy expenditure and food intake between groups (energy expenditure: 19.0 ± 1.1 vs. 20.0 ± 1.7 (WT vs. KO, $p = 0.624$) and food intake: 6.68 ± 0.29 vs. 7.69 ± 0.68 (WT vs. KO, $p = 0.1997$).

Interestingly, the glycogen content in the liver was significantly higher in L-PDHKO mice compared with wild-type control mice (Table 1) despite no change in the activity level of active glycogen synthase as well as percent active form of the enzyme in livers of L-PDHKO mice (Table 1). In contrast to the liver, the levels of glycogen in skeletal muscle from both the groups did not differ significantly (Table 1).

In Vitro Analysis of Lipogenesis

To investigate the consequence of L-PDHKO (and hence PDC function) on in vitro fatty acid biosynthesis, the incorporation of radioactive two-carbon fragments derived from D-[U-^{14}C]glucose or [U-^{14}C]acetate by liver slices was measured. The oxidation of either of these two labeled substrates to $^{14}CO_2$ by liver slices was not significantly different between the two groups of mice (Table 2). As predicted based on nearly complete absence of PDC activity, the incorporation of labeled two-carbon fragments generated from D-[U-^{14}C]glucose via the action of PDC into fatty acids was completely absent in liver slices from L-PDHKO mice compared with wild-type control mice (Table 2). As expected, the oxidation of [U-^{14}C]acetate to $^{14}CO_2$ and its incorporation into fatty acids by liver slices were similar between the two groups of mice, indicating that the pathway involving the biosynthesis of fatty acids from acetyl-CoA was not affected in the livers from L-PDHKO mice.

Since liver and adipose tissue are two major organs responsible for fatty acid synthesis, we speculated if there would be a compensatory increase in fatty acid synthesis in adipose tissue of L-PDHKO mice. Indeed, there was a marked increase in the incorporation of two-carbon fragments from both D-[U-^{14}C]glucose (about 2.5-fold) and [U-^{14}C]acetate (about fourfold) into fatty acids by epididymal adipose tissue from L-PDHKO male mice compared with wild-type control mice. There was also a significant increase in the oxidation of [U-^{14}C]acetate only to $^{14}CO_2$ by adipose tissue from L-PDHKO mice compared with wild-type control mice (Table 2), and could account for increased energy needs for increased lipid biosynthesis which cannot be obtained from glucose oxidation.

Hyperinsulinemic-Euglycemic Clamp in Liver-PDHKO Mice

In the fed and fasting conditions, the plasma levels of glucose and insulin in the L-PDHKO mice were not different from that of the littermate control male mice (Table 3). To further evaluate the role of hepatic PDC

Table 2 In vitro oxidation to $^{14}CO_2$ and incorporation into fatty acids of [U-^{14}C]glucose and [U-^{14}C]acetate in liver slices and pieces of epididymal adipose tissue from wild-type control and L-PDHKO male mice

Tissue	Substrates	Animals	$^{14}CO_2$	^{14}C-fatty acids
Liver	[U-^{14}C]Glucose	Wild-type	307 ± 3 (8)	49.8 ± 12.5 (8)
		L-PDHKO	335 ± 66 (8)	0 (8)**
Liver	[U-^{14}C]Acetate+Glucose	Wild-type	255 ± 67 (6)	23.1 ± 8.4 (6)
		L-PDHKO	202 ± 28 (6)	17.8 ± 2.7 (6)
Adipose tissue	[U-^{14}C]Glucose	Wild-type	3375 ± 300 (8)	635 ± 106 (6)
		L-PDHKO	3717 ± 308 (8)	1575 ± 457 (6)*
Adipose tissue	[U-^{14}C]Acetate+Glucose	Wild-type	329 ± 34 (6)	334 ± 143 (6)
		L-PDHKO	615 ± 89 (5)*	1281 ± 334 (6)*

The results (nmol/g wet wt/3 h) are means ± SEM (*n* as shown)

*$p < 0.01$, **$p < 0.001$

Table 3 Plasma glucose, insulin and free fatty acid from wild-type control (WT) and L-PDHKO mice

Parameter	Fasted		Fed		Clamp	
	WT	L-PDHKO	WT	L-PDHKO	WT	L-PDHKO
Glucose (mg/dl)	137 ± 4 (9)	133 ± 9 (9)	218 ± 7 (9)	205 ± 11 (11)	122 ± 3 (6)	112 ± 3 (10)
Insulin (μU/ml)	16.6 ± 1.6 (9)	14.4 ± 1.2 (10)	24.3 ± 9.3 (4)	19.8 ± 3.0 (4)	59.6 ± 6.8 (8)	61.0 ± 3.8 (9)
Fatty acids (mequiv/l)	0.93 ± 0.09 (9)	0.82 ± 0.09 (10)	nd	nd	0.56 ± 0.08 (8)	0.47 ± 0.06 (9)

The results are means ± SEM (*n* as shown)

nd not determined

deficiency on insulin action of glucose metabolism in vivo, we performed a 2-h hyperinsulinemic-euglycemic clamp in awake mice. During the clamp, plasma insulin was raised to ~360 pM (Table 3) and plasma glucose was clamped at ~6.5 mM in both groups (Fig. 3a). Plasma free fatty acid (FFA) concentrations were suppressed similarly in both groups by the insulin infusion (Fig. 3e, Table 3). L-PDHKO mice had increased whole body insulin sensitivity, as reflected by 60% higher glucose infusion rates required to maintain plasma glucose during the steady state of clamp as compared with the wild-type control group (Fig. 3b). This was accounted for by a 70% increase in insulin-induced suppression of hepatic glucose production (Fig. 3c) and a 23% increase in insulin-stimulated whole body glucose uptake (Fig. 3d). The increased whole body glucose uptake in the L-PDHKO group was accompanied by 45% increased glycogen synthesis rate, as compared with the wild-type control group (Fig. 3d).

Discussion

Our current understanding of the PDC regulatory mechanisms has been derived from both purified PDC preparations as well as by a variety of in vitro and in vivo experimental techniques employed for investigations of the carbon-flux via PDC in the liver under different dietary and/or hormonal conditions. In the present study, the generation of L-PDHKO mice has allowed us to reassess the known role of PDC in the disposal of glucose-carbons for energy production and lipid biosynthesis in the liver during the absorptive state and to uncover an unexpected compensatory effect on lipid synthesis in adipose tissue. Furthermore, L-PDHKO male mice showed improved insulin sensitivity in both the liver and peripheral tissues.

Since PDC is the only known reaction to generate acetyl-CoA from pyruvate, there was, as expected, no incorporation of ^{14}C from D-[U-^{14}C]glucose into long-chain fatty acids by liver slices from the L-PDHKO mice. Unexpectedly, there was a compensatory increase in lipogenesis from glucose in epididymal adipose tissue from the L-PDHKO mice. The mechanism by which this adaptive increase in lipogenic capacity is increased in adipose tissue in the L-PDHKO mice remains to be investigated. Under in vitro conditions, the oxidation of D-[U-^{14}C]glucose to $^{14}CO_2$ was not reduced in liver slices from the L-PDHKO mice compared to the controls largely due to (i) the use of D-[U-^{14}C]glucose (1-^{14}C of glucose can be converted to $^{14}CO_2$ via the pentose phosphate pathway) and (ii) possibly an increased flux of [U-^{14}C]pyruvate (derived from

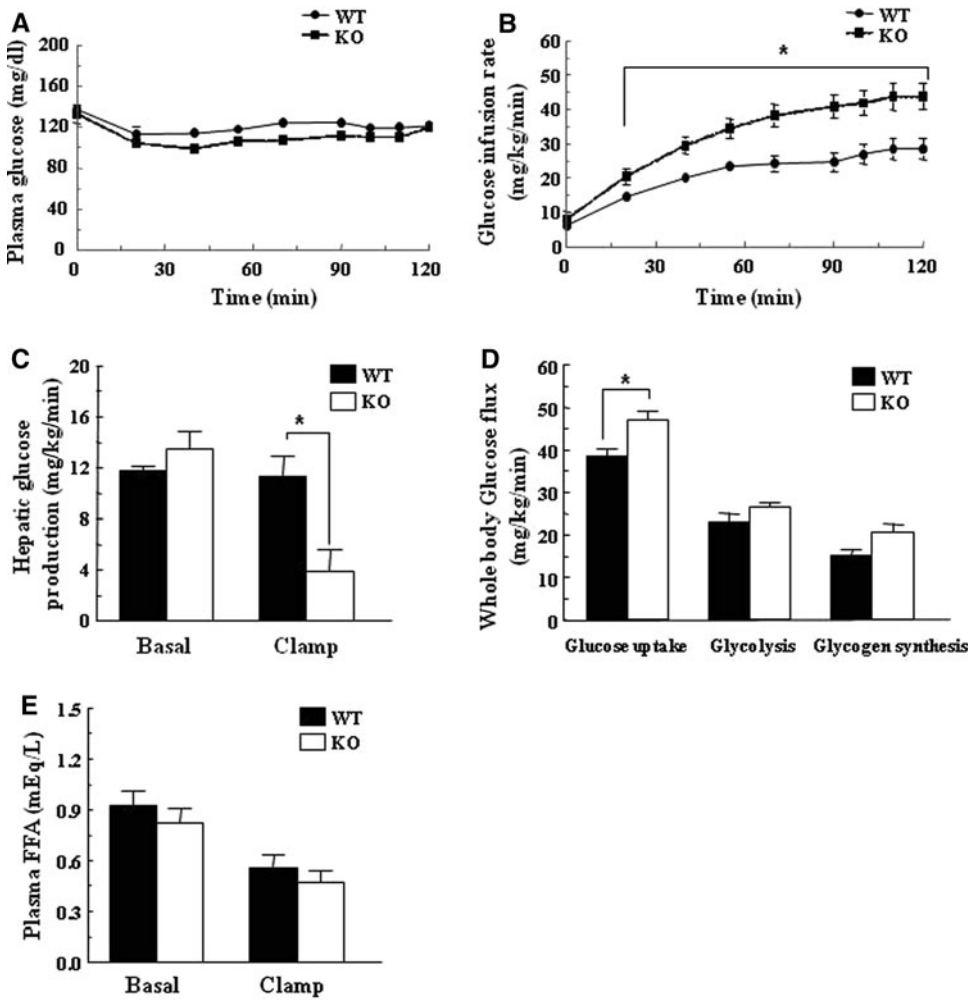

Fig. 3 Hepatic and peripheral insulin sensitivity in wild-type control and L-PDHKO male mice after an overnight fast. Hepatic and peripheral insulin sensitivities were assessed by means of hyperinsulinemic-euglycemic clamps. **a** Plasma glucose levels during the clamp, **b** Glucose infusion rates, **c** Hepatic glucose production, **d** Whole body glucose uptake, whole body glycolysis and whole body glycogen synthesis, **e** Plasma free fatty acid levels. The results are expressed as means ± SEM for 6 wild-type (WT) and 8-9 L-PDHKO (KO) mice. $*p < 0.05$ vs. wild-type

D-[U-^{14}C]glucose) for carboxylation via pyruvate carboxylase and subsequent cycling in the tricarboxylic acid (TCA) cycle.

Hepatic glycogen can be formed either by a direct pathway or by an indirect pathway from gluconeogenic precursors [1, 3, 4]. In the fed state, glucose produced via gluconeogenesis is shunted into glycogen synthesis rather than being released by glucose-6-phosphatase and can also contribute to the measured "indirect pathway" [4]. Evidence indicates that a delayed reactivation of PDC in several extrahepatic tissues as well as in the liver is important for the provision of carbon-precursors for hepatic gluconeogenesis (primarily for glycogen deposition) and also for restricting hepatic lipogenesis from dietary carbohydrates during the immediate absorptive period after a glucose load to 48-h starved rats [5, 6, 9]. A gradual reactivation of PDC in the liver as well as in other tissues after feeding allows the utilization of diet-derived glucose for the biosynthesis of lipids and/or energy production. Even a low rate of decarboxylation of pyruvate via PDC (due to a delayed reactivation) during the first 2 h after refeeding of fasted normal rats can reduce the availability of pyruvate for gluconeogenesis plus glycogenesis in the liver. This diversion of pyruvate via PDC, however, could not occur in the L-PDHKO mice in this study and hence may explain an increased hepatic glycogen level observed in the L-PDHKO mice in fed condition.

Liver-specific *Pdha1* deletion resulted in significant changes in metabolic fuel regulation in the liver and adipose tissue. As anticipated, the blood glucose levels in L-PDHKO mice were not different from that of control mice in the fed condition because glucose utilization by the liver represents only a small fraction of the total glucose metabolism in vivo. To maintain TCA cycle flux and to compensate for this loss of PDC-derived acetyl-CoA in the liver of L-PDHKO mice, it is suggested that a comparable increase in acetyl-CoA production from fatty acids and possibly some amino acids must occur to support energy need for other biosynthetic processes in the liver. At the whole body level, the increased rates of fatty acid synthesis in the adipose tissue of L-PDHKO mice may be a compensatory mechanism to adjust to the need to increase the

hepatic flux of fatty acids into the TCA cycle. The similar levels of plasma FFA levels, as well as decreased whole-body fat mass, suggests that the increased adipose FFA synthesis rates are balanced possibly by the increased rates of hepatic FFA utilization.

The complete loss of hepatic PDC activity resulted in elimination of de novo hepatic FFA synthesis from glucose-carbon (Table 2), and possibly combined with an increased flux of FFA into acetyl-CoA as an alternate source may explain the increased insulin sensitivity of the liver in the L-PDHKO mice, as reflected in the greater suppression of hepatic glucose production. Recently, it has been shown that fatty acid-induced hepatic insulin resistance is associated with increased diacylglycerol concentrations and activation of *PKCε* by diacylglycerol [28, 29]. The increased demand by the L-PDHKO mice for circulating FFA to maintain normal rates of hepatic mitochondrial oxidative phosphorylation could lead to a decrease in FFA metabolites that are thought to activate PKCε and lead to changes in hepatic insulin sensitivity. At the whole-body level, we also observed an increase in insulin-stimulated peripheral glucose metabolism in the L-PDHKO mice. Under these clamp conditions, increases in oxidative and non-oxidative glucose disposal are chiefly by muscle and adipose tissue. The 23% increase in glucose uptake may be accounted for by the ~twofold increase in lipogenesis from glucose in adipose tissue and the 45% increase in whole body glycogen synthesis. In summary, it is suggested that the increased utilization of FFA by the liver to maintain normal rates of oxidative phosphorylation led to increased insulin sensitivity in peripheral tissues as well as liver.

Acknowledgments This work was supported by grants from the U.S. Public Health Service [DK20478 (MSP), DK71071 (GWC) and U24 DK59635 (CSC and GWC)] and the National Organization of Rare Disorders (MSP). We thank Dr. Gail Willsky of University at Buffalo for critical reading of this manuscript.

References

1. Katz J, McGarry JD (1984) The glucose paradox: Is glucose a substrate for liver metabolism? J Clin Invest 74:1901–1909
2. Granner D, Pilkis S (1990) The genes of hepatic glucose metabolism. J Biol Chem 265:10173–11017
3. Newgard CB, Hirsch LJ, Foster DW, McGarry JD (1983) Studies on the mechanism by which exogenous glucose is converted into liver glycogen in the rat: a direct or an indirect pathway? J Biol Chem 258:8046–8052
4. Shulman GI, Rossetti L, Rothman DL, Blair JB, Smith D (1987) Quantitative analysis of glycogen repletion by nuclear magnetic resonance spectroscopy in the conscious rat. J Clin Invest 80:387–393
5. Sugden MS, Holness MJ (2003) Recent advances in mechanisms regulating glucose oxidation at the level of the pyruvate dehydrogenase complex by PDKs. Am J Physiol Endocrinol Metab 284:E855–E862
6. Holness MJ, French TJ, Sugden MC (1986) Hepatic glycogen synthesis on carbohydrate re-feeding after starvation. Biochem J 235:441–445
7. Harris RA, Bowker-Kinley MM, Huang B, Wu P (2002) Regulation of the activity of the pyruvate dehydrogenase complex. Adv Enzyme Regul 42:249–259
8. Patel MS, Korotchkina LG (2003) The biochemistry of the pyruvate dehydrogenase complex. Biochem Mol Biol Educ 1:5–15
9. Schummer CM, Werner U, Tennagels N, Schmoll D, Haschke G, Juretschke H-P, Patel MS, Gerl M, Kramer W, Herling AW (2008) Dysregulated pyruvate dehydrogenase complex in Zucker diabetic fatty rats. Am J Physiol Endocrinol Metab 294:E88–E96
10. Lissens W, De Meirleir L, Seneca S, Liebaers I, Brown GK, Brown RM, Ito M, Naito E, Kuroda Y, Kerr DS, Wexler ID, Patel MS, Robinson BH, Seyda A (2000) Mutations in the X-linked pyruvate dehydrogenase (E1) alpha subunit gene (PDHA1) in patients with a pyruvate dehydrogenase complex deficiency. Hum Mutat 15:209–219
11. Robinson BH (2001) Lacticacidemia: disorders of pyruvate carboxylase and pyruvate dehydrogenase. In: Scriver CR, Sly WS, Valle D, Beaudet AL (eds) Metabolic and molecular basis of the inherited disease, 7th edn. McGraw-Hill, New York, pp 2275–2295
12. Brown RM, Dahl HHM, Brown GK (1989) X-chromosome location of the functional gene for the E1α submit of the human pyruvate dehydrogenase complex. Genomics 4:174–181
13. Patel MS, Harris RA (1995) α-Ketoacid dehydrogenase complexes: gene regulation and genetic defects. FASEB J 9:1164–1172
14. Johnson MT, Mahmood S, Hyatt SL, Yang HS, Soloway PD, Hanson RW, Patel MS (2001) Inactivation of the murine pyruvate dehydrogenase (*Pdha1*) gene and its effect on early embryonic development. Mol Genet Metab 74:293–302
15. Takakubo F, Dahl HH (1992) The expression pattern of the pyruvate dehydrogenase E1 alpha subunit genes during spermatogenesis in adult mouse. Expt Cell Res 199:39–49
16. Pliss L, Pentney RJ, Johnson MT, Patel MS (2004) Biochemical and structural brain alterations in female mice with "cerebral" pyruvate dehydrogenase deficiency. J Neurochem 91:1082–1091
17. Sidhu S, Gangasani A, Korotchkina LG, Suzuki G, Fallavollita JA, Canty JM Jr, Patel MS (2008) Tissue-specific pyruvate dehydrogenase complex deficiency causes cardiac hypertrophy and sudden death of weaned male rats. Am J Physiol Heart Circ Physiol 295:H946–H952
18. Postic C, Shiota M, Niswender KD, Jetton TL, Chen Y, Moates M, Shelton KD, Linder J, Cherrington AD, Magnuson MA (1999) Dual roles for glucokinase in glucose homeostasis as determined by liver and pancreatic beta cell-specific gene knock-outs using Cre recombinase. J Biol Chem 274:305–315
19. Kerr DS, Ho L, Berlin CM, Lanoue KF, Towfighi J, Hoppel CL, Lusk MM, Gondek CM, Patel MS (1987) Systemic deficiency of the first component of the pyruvate dehydrogenase complex. Pediatr Res 22:312–318
20. Korotchkina LG, Sidhu S, Patel MS (2006) Characterization of testis-specific isoenzyme of human pyruvate dehydrogenase. J Biol Chem 281:9688–9696
21. Thomas JA, Schlender KK, Larner J (1968) A rapid filter paper assay for UDP-glucose glycogen glucosyltransferase, including an improved biosynthesis of UDP-^{14}C-glucose. Anal Biochem 25:486–499
22. Lo S, Russel JC, Taylor AW (1970) Determination of glycogen in small tissue samples. J Applied Physiol 28:234–236
23. Patel MS, Jomain-Baum M, Ballard FJ, Hanson RW (1971) Pathway of carbon flow during fatty acid synthesis from lactate and pyruvate in rat adipose tissue. J Lipid Res 12:179–191

24. Kaplan ML, Leveille GA (1981) Development of lipogenesis and insulin sensitivity in tissues of the *ob/ob* mouse. Am J Physiol Endocrinol Metab 240:E101–E107
25. Samuel VT, Choi CS, Phillips TG, Romanelli AJ, Geisler JG, Bhanot S, McKay R, Monia B, Shutter JR, Lindberg RA, Shulman GI, Veniant MM (2006) Targeting foxo1 in mice using antisense oligonucleotide improves hepatic and peripheral insulin action. Diabetes 55:2042–2050
26. Choi CS, Fillmore JJ, Kim JK, Liu Z, Kim S, Kulkarni A, Distefano A, Hwang Y, Kahn M, Chen Y, Yu C, Moore IK, Reznick RM, Higashimori T, Collier EF, Shulman GI (2007) Overexpression of uncoupling protein 3 in skeletal muscle protects against fat-induced insulin resistance. J Clin Invest 117:1995–2003
27. Rossetti L, Giaccari A (1990) Relative contribution of glycogen synthesis and glycolysis to insulin-mediated glucose uptake. A dose-response euglycemic clamp study in normal and diabetic rats. J Clin Invest 85:1785–1792
28. Samuel VT, Liu ZX, Qu X (2004) Mechanism of hepatic insulin resistance in non-alcoholic fatty liver disease. J Biol Chem 279:32345–32353
29. Neschen S, Morino K, Hammond LE, Zhang D, Liu ZX, Romanelli AJ, Cline GW, Pongratz RL, Zhang XM, Choi CS, Coleman RA, Shulamn GI (2005) Prevention of hepatic steatosis and hepatic insulin resistance in mitochondrial acyl-CoA:glycerol-sn-3-phosphate acyltransferase 1 knockout mice. Cell Metab 2:55–63

Lipids (2010) 45:997–1009
DOI 10.1007/s11745-010-3465-5

ORIGINAL ARTICLE

Inhibition of Insulin and T_3-Induced Fatty Acid Synthase by Hexanoate

Murielle M. Akpa · Floriane Point · Sabine Sawadogo · Anne Radenne · Catherine Mounier

Received: 8 April 2010 / Accepted: 6 August 2010 / Published online: 1 September 2010

Abstract Fatty acid synthase (FAS) is responsible for the de novo synthesis of palmitate and stearate. This enzyme is activated by insulin and T_3, and inhibited by fatty acids. In this study, we show that insulin and T_3 have an inducing effect on FAS enzymatic activity, which is synergetic when both hormones are present. Octanoate and hexanoate specifically inhibit this hormonal effect. A similar inhibitory effect is observed at the level of protein expression. Transient transfections in HepG2 cells revealed that hexanoate inhibits, at least in part, FAS at a transcriptional level targeting the T_3 response element (TRE) on the FAS promoter. The effect of C6 on FAS expression cannot be attributed to a modification of insulin receptor activation or to a decrease in T_3 entry in the cells. Using bromo-hexanoate, we determined that hexanoate needs to undergo a transformation in order to have an effect. When incubating cells with triglyceride–hexanoate or carnitine–hexanoate, no effect on the enzymatic activity induced by insulin and T_3 is observed. A similar result was obtained when cells were incubated with betulinic acid, an inhibitor of the diacylglycerol acyltransferase. However, the incubation of cells with Triacsin C, a general inhibitor of acyl-CoA synthetases, completely reversed the inhibitory effect of hexanoate. Our results suggest that in hepatic cells, hexanoate needs to be activated into a CoA derivative in order to inhibit the insulin and T_3-induced FAS expression. This effect is partially transcriptional, targeting the TRE on the FAS promoter.

Keywords Fatty acid synthase · Insulin · T_3 · Medium chain fatty acids · Hexanoate · Acylation · Transcription

Abbreviations

CEH	Chick embryo hepatocyte
CPT1	Carnitine palmitoyl transferase 1
C6	Hexanoate
C8	Octanoate
DGAT	Diacylglycerol transferase
ERK	Extracellular signal regulated kinase
FAS	Fatty acid synthase
IR	Insulin receptor
IRE	Insulin response element
KPi	Potassium phosphate
MAPK	Mitogen activated protein kinase
MCFA	Medium chain fatty acid(s)
NADPH	Nicotinamide adenine dinucleotide phosphate
PI3-Kinase	Phosphatidyl-inositol-3 phosphate kinase
PUFA	Polyunsaturated fatty acid(s)
PY	Phospho-tyrosine
SREBP-1c	Sterol regulatory element binding protein
T_3	Triiodothyronine
TBS	Tris-buffered saline
TBST	Tris-buffered saline Tween-20
TG	Triglyceride
TK	Thymidine kinase
TR	Thyroid hormone receptor
TRE	T_3 response element

M. M. Akpa · F. Point · S. Sawadogo · A. Radenne · C. Mounier (✉)
Département des Sciences Biologiques,
Centre de Recherche BioMed, Université du Québec à Montréal,
C.P. 8888, Succursale Centre-ville, Montréal H3C 3P8, Canada
e-mail: mounier.catherine@uqam.ca

Introduction

Most fatty acids found in the diet have 14 or more carbons while medium chain fatty acids (MCFA) have a 6–10 carbon-chain. Large amounts of MCFA are found in coconut and palm kernel oil, representing more than 50% of the fatty acids [1]. They are also present in bovine milk, representing 4–12% of the total lipid content. However, their presence in milk depends on the genetic background, the stage of lactation and the diet of the animal [2]. Metabolism of MCFA in the liver is quite different from longer chain fatty acids. MCFA rapidly cross the mitochondrial barrier and do not required the carnitine palmitoyl transferase I (CPTI) for this transport. Subsequently, MCFA are activated by medium-chain acyl CoA synthase, forming CoA derivatives [3]. Their esterification is limited [4]. They are mainly oxidized, behaving more like glucose than fat [5]. However, in humans, they not only served as a source of energy, but can also be reesterified and deposited in the adipose tissue [6]. In addition, a study performed in rat showed that animals fed with medium chain triglycerides show a large number of triglycerides and phospholipids containing MCFA in adipose tissue [7].

Medium chain fatty acids have been used for more than 50 years in clinical nutrition to treat pancreatic insufficiency and fat malabsorption [8]. They have also been added to infant formulas, improving the energy intake that can be metabolized [6]. MCFA may have several implications in human health, including a decrease in fasting [9] and postprandial plasma lipid concentration [10], and in body weight [11], as well as an increase in insulin sensitivity [12]. In rats, the effect of MCFA on body weight appears to be mediated, by down regulation of adipogenic genes and PPARγ, as well as by inhibition of lipogenesis in adipocytes [7]. The effect on hepatic de novo lipid synthesis remains, however, to be demonstrated.

In contrast to rodents, lipogenesis in humans as in birds takes place mainly in the liver [13]. There are two central lipogenic enzymes that are tightly regulated by hormones and nutrients. Acetyl-CoA carboxylase (ACC) synthesizes malonyl-CoA from acetyl-CoA, which is in turn converted by fatty acid synthase (FAS) (EC.2.3.1.85) into long chain saturated fatty acids. FAS is expressed mainly in the liver and the brain. In vertebrates, FAS is a homodimer made of two peptide chains of about 260 kDa each [14, 15]. It is located in the cytoplasm of the cell [16]. In the presence of nicotinamide adenine dinucleotide phosphate (NADPH), this multifunctional enzymatic complex is responsible for the production of palmitate, a long chain saturated fatty acid, using acetyl-CoA and malonyl-CoA as building blocks. A single gene that gives rise to one mRNA in mouse and two in chicken and rat, due to alternative splicing, encodes FAS [17, 18].

In the liver, the activity of FAS, like most lipogenic enzymes [19], is regulated through nutrients and hormones. Starvation causes decreased activity of the enzyme, and refeeding restores it [20, 21]. A similar effect of refeeding is also observed on the mRNA expression level and stability, as well as on transcription [17, 21–24]. Insulin [25], triiodothyronine (T_3) [19, 26] and glucose stimulate FAS activity, whereas glucagon [25], medium chain fatty acids (MCFA) [27] and polyunsaturated fatty acids (PUFA) decrease it [28–31]. Insulin increases FAS activity by enhancing transcription through the modification of transcription factors' binding on the insulin response element (IRE) located on the promoter [25]. We recently demonstrated that insulin is also able to modulate FAS transcription through a specific T_3 response element (TRE) [32]. In the same study, we not only demonstrated that T_3 regulates FAS through a direct genomic action on the TRE, but also via a non-genomic action involving the activation of the PI3-kinase-ERK1/2 MAPK signaling pathway. MCFA specifically inhibit insulin and T_3-induced FAS activity by a still unknown mechanism [27]. The inhibition of FAS through MCFA is selective and specific, since they do not inhibit β-actin transcription and longer or shorter fatty acids have no effect whatsoever [27]. It was suggested that the active inhibitor is a derivative of the MCFA [27].

In the present study, we have shown that hexanoate and octanoate specifically inhibit insulin and T_3-induced FAS enzymatic activity in hepatocytes. We also showed that hexanoate works by modulating the level of FAS protein expression. This effect is partially due to transcriptional targeting of the TRE on the FAS promoter. The hexanoate is rapidly taken up by the cells and mainly metabolized into triglycerides and cholesterol esters. Hexanoate does not modify the activation of the insulin receptor, nor the entrance of T_3 in the cells. Using specific inhibitors of MCFA metabolism, it appears that acyl-CoA hexanoate, which is rapidly formed after the cellular uptake, needs to be generated in order to inhibit the insulin and T_3-induced FAS activity and expression.

Methods

Materials

Eggs from white Leghorn chickens were purchased from Couvoir Simentin (Mirabel, QC). Waymouth medium, 3,5,3-L-triiodothyronine, insulin, hexanoate, octanoate, etomoxir, betulinic acid, acetyl-CoA, malonyl-CoA, NADPH, and [^{14}C]-hexanoate were obtained from Sigma Aldrich (Saint Louis, MO). Fugene HD transfecting agent was obtained from Roche Diagnostic (Laval, QC). Triacsin C was obtained from Biomol Research Laboratories

(Cedarlane Laboratories limited, Hornby, ON). Collagenase H was obtained from Roche Diagnostic (Laval, QC). Anti-FAS, anti-GAPDH and anti-PY (PY99) antibodies were obtained from Santa Cruz Biotechnology (Santa Cruz, CA). The FITC-labelled goat anti rabbit IgG was purchased from Invitrogen. The anti-IR (α-960) was a generous gift of Dr. B. I. Posner (McGill University, QC). Unless otherwise specified in the text, all other chemicals including the anti-T_3 antibody were purchased from Sigma.

Cell Culture and Transfection Procedure

Chick embryo hepatocytes (CEH) were isolated from livers of 19-day-old chick embryos [13] (protocol # 590 approved by the University animal care committee). Briefly, 12 chick livers were removed rapidly and placed in iced Krebs–Ringer bicarbonate buffer, pH 7.4. Chopped livers were then digested by Collagenase H and the resulting suspension was filtered through two layers of nylon mesh. The cells were collected by centrifugation and washed twice in Krebs–Ringer bicarbonate buffer. 2.5×10^6 cells were plated in 35 mm tissue dishes and cultured at 40°C under 5% CO_2 in Waymouth medium supplemented with streptomycin and penicillin. After 24 h, the medium was removed by aspiration and replaced by medium supplemented with 1.6 μM of T_3 and/or 100 nM of insulin, and incubated for an additional 24 h. The respective concentrations used in the experiments for T_3 and insulin were determined using a dose-response curve and from previously published studies [32]. The incubation was also performed in presence of 1 μM MCFA (hexanoate or octanoate resuspended in 1× PBS as a vehicle), triglycerides, carnitine–hexanoate or carnitine–octanoate. The triglycerides were coupled to bovine serum albumin (BSA) at a 1:4 ratio in order to facilitate their entry into the cell [33]. The experiments using radio-labeled compounds were performed with [^{14}C]-hexanoate that was added to the medium after a 24 h pre-incubation period with the various hormones, for either 1 or 24 h. For the experiments using inhibitors, the CEH were pre-incubated for 30 min with either DMSO 0.5%, 1 μM Etomoxir, 1 μM Betulinic acid or 5 μM Triascin C, followed by the hormonal treatment for 24 h.

The human hepatocarcinoma cells (HepG2) were cultured in modified Eagle medium (MEM) supplemented with streptomycin (100 μg/mL), penicillin (60 μg/mL), FBS (10%) and glutamine (4 mM final). The day before, cells were plated at 80% confluence (about 1×10^6 cells per well) in 12 well plates. They were then incubated for 24 h with 3.5 μL of Fugene HD, 0.75 μg of the DNA construct and 0.25 μg of pRSV-β-galactosidase, without serum nor antibiotics. The medium was then replaced with one containing hormones and fatty acid at the concentrations indicated on the figure legend. After 24 h of culture, the cells were harvested and the different cellular extracts were prepared.

Analysis of Cell Extracts

HepG2 cells were lysed at room temperature in CAT Elisa lysis buffer (Roche Diagnostics, Laval, PQ), and protein concentration [34], luciferase [35] and β-galactosidase [36] activities were measured. The results were expressed as luciferase activity per milligram of soluble protein and then normalized for transfection efficiency using the β-galactosidase activity. Transcriptional rates were expressed as a percentage of the standardized activity measured in the untreated cells.

FAS Activity

Fatty acid synthase activity was measured by tracking the decrease of absorbance at 340 nm as a result of NADPH disappearance due to the conversion of malonyl-CoA and acetyl-CoA into long chain fatty acids [37]. Following hormonal stimulation, 2–3 plates of treated cells (about 10×10^6 cells prepared from a pool of 12 chicks' livers) were harvested in 1× PBS. After a short centrifugation, the cells were re-suspended in ice-cold homogenization buffer. The cytosolic extracts were prepared through homogenization of the cells with a Dounce homogenizer. The lysates were subsequently centrifuged at 3,000 rpm for 15 min at 4°C. FAS activities were evaluated by mixing, in a Quartz cuvette, 50 μL of cell lysate, 0.5 M Kpi, pH 7; 25 μM acetyl-CoA; 100 μM NADPH; 3 mM EDTA and 1 mM DTT [38, 39]. The reaction was initialized by adding malonyl-CoA (0.1 mM final). The optical density (OD) at 340 nm was then monitored for 15 min at 40°C in a Cary-100 spectrophotometer (Varian, QC).

Western Blot Analysis

After treatment with various test agents at the times and concentrations indicated in the figure legends, HepG2 cells were rinsed twice with ice-cold 1× PBS (pH 7.4) and solubilized with lysis buffer (50 mM Hepes, pH 7.5, 150 mM NaCl, 10 mM sodium pyrophosphate, 100 mM sodium fluoride, 1.5 mM $MgCl_2$, 1 mM EGTA, 200 μM sodium orthovanadate, 1 mM phenylmethylsulfonyl fluoride, 10 μg/mL leupeptin, 10 μg/mL aprotinin, 10% glycerol, and 1% Triton X-100). Cell lysates were clarified by centrifugation at 10,000×g for 20 min at 4°C, and protein concentration in the resulting supernatants was determined using the BioRad protein assay (BioRad, Mississauga, ON). 20–100 μg of protein were mixed with 4 μL of 3× Laemmli sample buffer (2% SDS, 2% β-mercaptoethanol,

10% v/v glycerol and 50 mg/L bromophenol blue in 0.1 M Tris–HCl buffer, pH 6.8), heated at 100°C for 5 min, subjected to SDS-PAGE and then transferred to Immobilon-P membranes for immunoblotting. Membranes were incubated for 1 h in blocking buffer (1× TBS, 0,1% Tween-20: TBST) containing 5% milk and then overnight in 1× TBST containing 5% BSA and with the various antibodies: FAS (1:1,000), GADPH (1:1,000), Phosphotyrosine (1/1,000) and IR-α960 (1/1,000). After three successive washes in 1× TBST, membranes were incubated for 1 h at room temperature in 1× TBST in the presence of an anti-Rabbit IgG or an anti-Mouse IgG bound to the horseradish peroxidase (1/10,000). Signals were revealed using the ECL plus Western blotting detection reagent according to the manufacturer instructions (Roche Diagnostics, Laval, QC). The appropriate bands were quantified using the phospho-imager system (Molecular imager FX, Biorad, Mississauga, ON).

Flow Cytometric Analysis of T_3 Content

After 24 h starvation, HepG2 cells were treated for 1 h with T_3 or insulin and T_3 with or without hexanoate. Cells were rinsed with 1× PBS and fixed for 1 h in 0.25% of paraformaldehyde. Thereafter, the cells were permeabilized with 0.05% Tween 20 in 1× PBS containing 1% FBS. The hormone content was detected using a T_3 antibody (1/1,000) as a primary antibody and FITC-labelled goat anti rabbit IgG (1/1,000) as a secondary antibody. To control for the specificity of the signal, cell fluorescence was measured in the absence of both antibodies or only in the presence of the secondary antibody. The measurement was done in a FACS flow cytometer (Becton Dickinson) using 1×10^6 cells for each measurement. For the analysis of the result, a cellquest program was used.

Fatty Acid Uptake

Chick embryo hepatocytes were incubated in serum free Waymouth medium supplemented with hormones, inhibitors and [^{14}C]-hexanoate for 24 h as indicated on the figure legends. The uptake was then stopped, after removal of the culture medium, with a pre-heated solution (37°C) containing 0.5% BSA prepared in 1× PBS and 0.9% NaCl. The naked cells were then stripped and lysed in 0.1 M NaOH overnight at 4°C. Cell lysates were subsequently quantified by β-scintillation with the Liquid scintillation analyzer Tri-carb 2800 TR (Perkin Elmer, Quebec).

Lipid Profile

Chick embryo hepatocytes were incubated in serum free Waymouth medium supplemented with hormones, inhibitors and [^{14}C]-hexanoate for 24 h as indicated on the figure legends. The uptake was stopped with 0.2% BSA in 1× PBS. Lipids were extracted from the cells for 1 h in a hexane:isopropanol mix (3:2, v/v). The lysates were subsequently evaporated under nitrogen and re-suspended in 50 μL of chloroform. The samples and standards (cholesterol and cholesteryl oleate) were then migrated on a TLC silicate plate in a solution containing petroleum ether, anhydrous ether and glacial acetic acid (90:10:1), and revealed in an iodide saturated chamber. The strips were then cut, scraped and read by scintillation using the Liquid scintillation analyzer Tri-carb 2800 TR (Perkin Elmer, Quebec).

Results

Role of insulin, T_3 and Medium Chain Fatty Acids on FAS Enzymatic Activity

In the present study, we used CEH to measure FAS activity. Incubation of CEH with 100 nM insulin or 1.6 μM T_3 increases FAS enzymatic activity about threefold (Fig. 1a) and in the presence of both hormones, an important synergistic effect is observed, increasing the activity 14-fold. Similar hormonal effects were observed on the promoter activity demonstrating that this hormonal regulation is transcriptional [32]. We subsequently tested the effect of medium chain fatty acids (MCFA) on FAS enzymatic activity. Addition of 1 μM hexanoate or octanoate does not modify basal, insulin or T_3-induced FAS enzymatic activity. On the other hand, when MCFA were used in concordance with insulin and T_3, they had an inhibitory effect on FAS enzymatic activity of about half (Fig. 1b, c). The inhibition was even more effective when hexanoate was used (50%) compared to the effect of octanoate (40%).

Effect of Hormonal Treatment on Hexanoate Uptake

Our previous data demonstrated that hexanoate only inhibits FAS activity in the presence of both insulin and T_3. However, we could not exclude that in the absence of both hormones, the MCFA may not efficiently penetrate into the cell. In order to evaluate this hypothesis, we measured the uptake of [^{14}C]-hexanoate at each hormonal condition. In the absence of any hormonal treatment, hexanoate efficiently enters the cell. However, this uptake is significantly increased by the presence of either insulin, T_3 or both hormones (Fig. 2a). We have to note that regardless of the hormonal treatment used, the radio-labeled hexanoate was able to enter the cell unhindered and this in a very short time lapse. The results show that only after 1 h, the levels

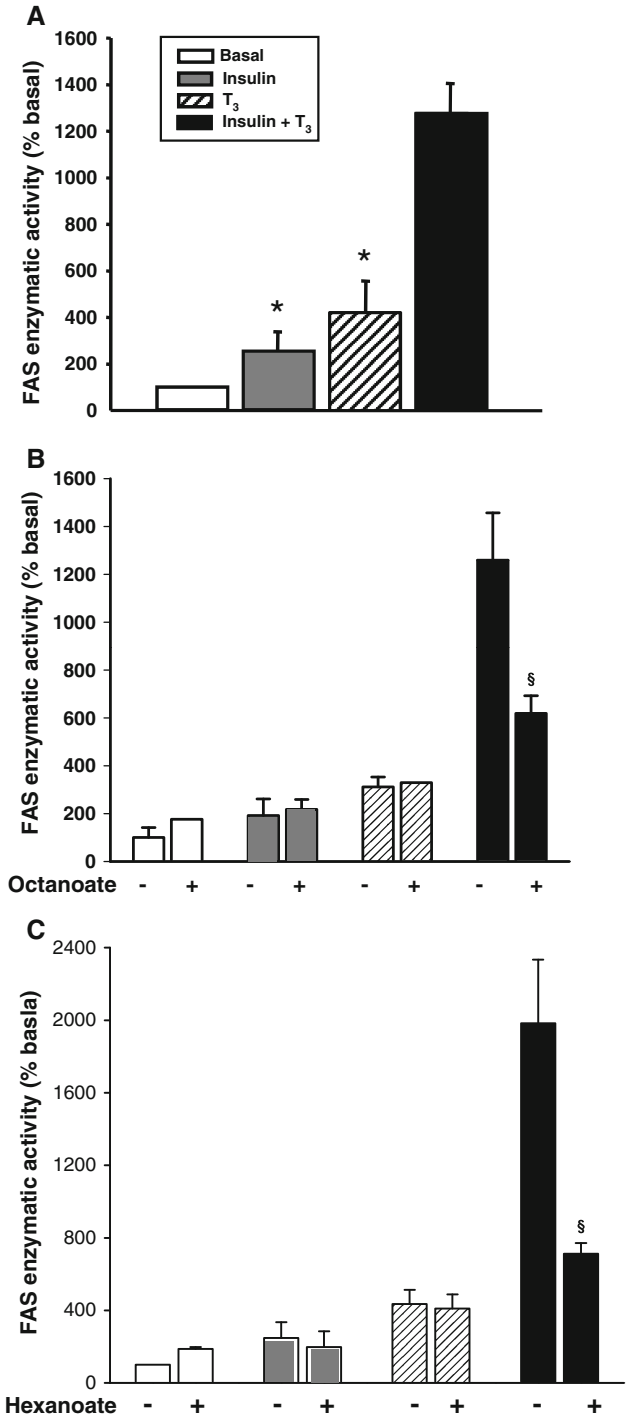

◀ **Fig. 1** Effect of MCFA on FAS enzymatic activity. The CEH were incubated for 24 h in Waymouth media (*white bars*), in the presence of either 100 nM insulin (*grey bars*), 1.6 μM T_3 (*hatched bars*) or with both hormones (*black bars*). FAS activity was evaluated as indicated in "Methods". **a** Results represent FAS activities and are the mean of at least three independent experiments representing three different preparations of hepatocytes. They are expressed in function of the value obtained in untreated samples. The *bars* indicate the standard deviation (SD). $^{*}P < 0.001$ for insulin or T_3 treated versus untreated cells. Cells were treated as described above except that 1 μM of hexanoate (**b**) or octanoate (**c**) was added to the media. Results are expressed as described above and are the mean of three independent experiments. The *bars* indicate the SD. $^{\S}P < 0.01$ for insulin and T_3 treated cells versus insulin, T_3 and MCFA treated cells

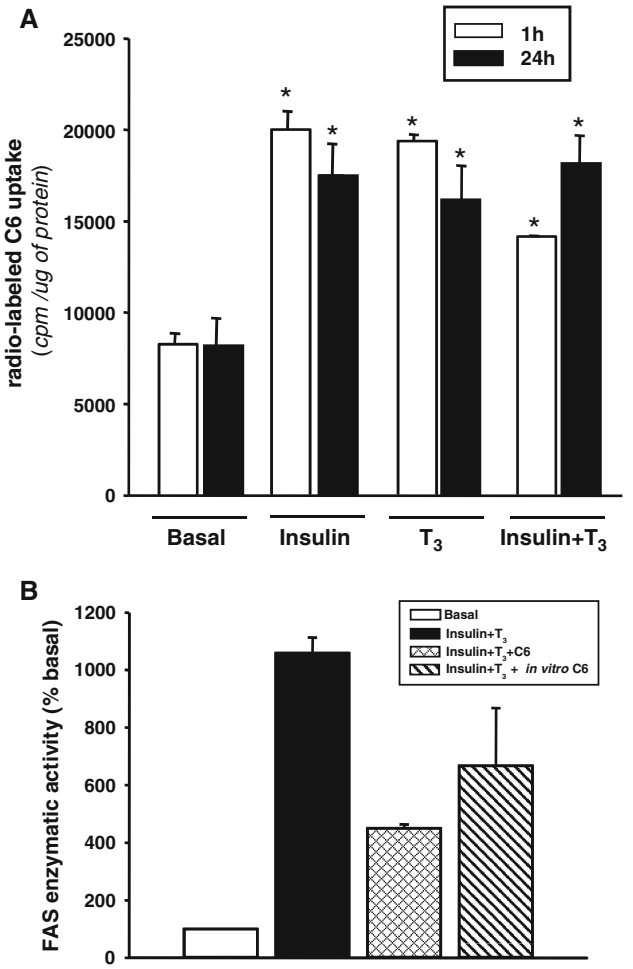

Fig. 2 Effect of hormonal treatment on hexanoate uptake. **a** The CEH were incubated for either 1 h (*white bars*) or 24 h (*black bars*) in the presence or absence of 100 nM insulin, 1.6 μM T_3 or with both hormones. In each condition, 1 μCi of [^{14}C]-hexanoate was also added. The C6 uptake was evaluated as indicated in "Methods". Results are expressed in cpm per milligram of protein and are the mean of three independent experiments. The *bars* indicate the SD. $^{*}P < 0.05$ for insulin and/or T_3 treated versus untreated cells. **b** FAS activity was measured as described in "Methods", using cell lysate from untreated (*white bars*) or treated with 100 nM insulin and 1.6 μM T_3-treated cells for 24 h (*black bars*) with addition of 1 μM hexanoate in the media (*crossed bar*) or in the enzymatic reaction buffer (*hatched bar*)

of [^{14}C]-hexanoate found in the cells are comparable to those found in cells exposed for 24 h.

Post-Translational Effect of Hexanoate on FAS Activity

In order to evaluate whether the inhibition by hexanoate was due to an allosteric competition, we added the MCFA

in the reaction buffer just before measuring the enzymatic activity. As depicted in Fig. 2b, the hexanoate needs to be present in the cell in order to efficiently inhibit the insulin and T_3-induced FAS activity (Fig. 2b), while the presence of hexanoate in the reaction buffer has no effect. In agreement with previous data, our results suggest that the MCFA regulates the level of FAS activity probably by modulating the level of FAS expression and not by acting at a post-translational level.

Effects of T_3, insulin, and hexanoate on FAS expression

In order to evaluate the effect of hexanoate on FAS expression, we measured the level of FAS protein in cells treated with various combinations of T_3, insulin and hexanoate by Western blot. As shown in Fig. 3a, hexanoate inhibits insulin and T_3-induced FAS protein expression by about 50%. This level correlates to the one observed on FAS activity, suggesting that hexanoate inhibits FAS activity by modulating its level of expression.

We next evaluated the effect of hexanoate on FAS transcription. We had previously demonstrated that T_3 and insulin target a specific TRE on the FAS promoter [20]. We cloned this TRE upstream of the minimal promoter of thymidine kinase and the luciferase reporter gene and transiently transfected the DNA construct into HepG2 cells. Luciferase activity was then measured in presence of T_3, insulin and hexanoate. As expected, in presence of T_3 or insulin, the luciferase activity was increased about 1.3-fold through the TRE whereas in presence of both hormones, the transcription increases more than 2-fold (Fig. 3b). When the cells are incubated with hormones and hexanoate, the transcriptional activity is inhibited by more than 25%. These results suggest that hexanoate regulates at least in part, FAS transcription via the TRE located on the FAS promoter.

Effect of C6 on Insulin Receptor Phosphorylation and T_3 Uptake

In order to evaluate the effect of C6 directly on the hormonal response, we measured the level of phosphorylation of the insulin receptor in HepG2 cells as well as the T_3 uptake. As expected, the tyrosine phosphorylation of the insulin receptor is only detected in the presence of insulin (Fig. 4a). The addition of C6 does not modify the phosphorylation state of the receptor with or without T_3.

Using flow cytometry, we evaluated the uptake of T_3 under various conditions. Incubation of cells only with the secondary antibody revealed a lower fluorescence than the one observed in the presence of both antibodies ($*P < 0.05$ comparing lane 1 to untreated and T_3-treated cells). Incubation of the cells with T_3 increases the detected fluorescence compared to untreated cells ($**P = 0.001$ comparing untreated to T_3-treated cells). This demonstrates the specificity of the fluorescence detection in our

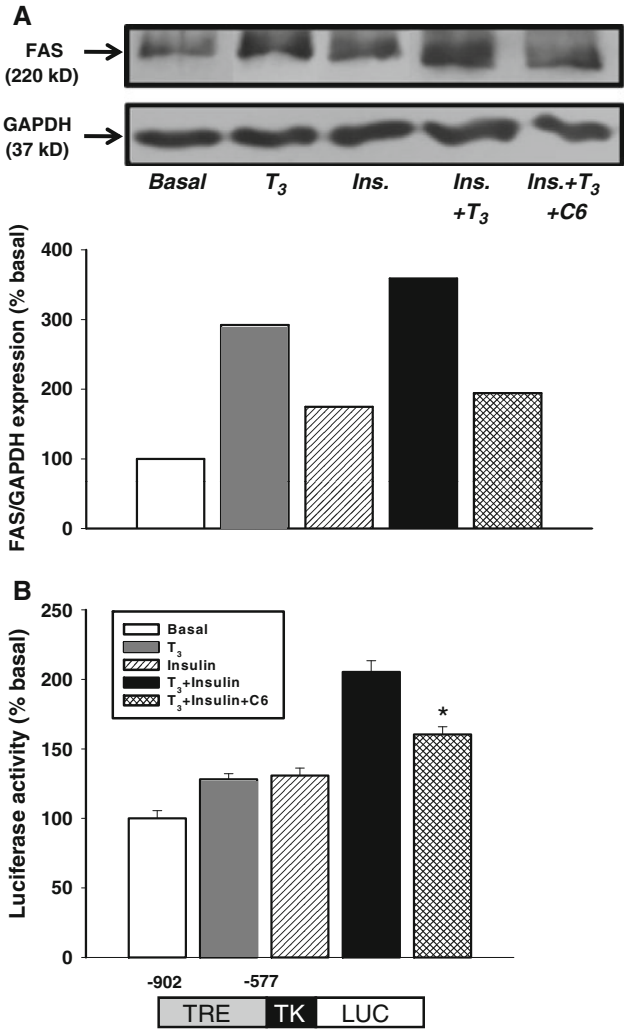

Fig. 3 Effect of hexanoate on FAS expression. **a** HepG2 cells were incubated for 24 h with T_3 (1.6 μM), insulin (100 nM) and/or C6 (1 μM). The cells were lysed; extracted proteins were resolved on 10% SDS-PAGE and then immunoblotted with either an anti-FAS antibody (*top panel*) or an anti-GAPDH antibody (*bottom panel*). The Western blot signals were quantified by densitometry and normalized to GAPDH. The results presented in the graph are expressed as a percentage of the signal intensity observed in untreated (*basal*) cells. **b** HepG2 cells were transiently transfected with the TRE-TK-LUC DNA construct (0.75 μg/well) and pRSV-βgal (0.25 μg/well) as described in "Methods". After removing the transfection medium, the hepatocytes were incubated for 24 h in MEM or in the same medium containing 1.6 μM of T_3, 100 nM of insulin or both hormones without or with 1 μM of C6. Results are expressed as luciferase activities normalized by β-galactosidase activity per milligram of soluble protein. They are represented as a percentage of the activity measured in the untreated sample and are the mean of at least three independent experiments. The *bars* indicate the standard deviation (SD). $*P = 0.02$ compared to insulin and T_3 treated cells. Schematic representation of the DNA construct is depicted in the bottom of the graph

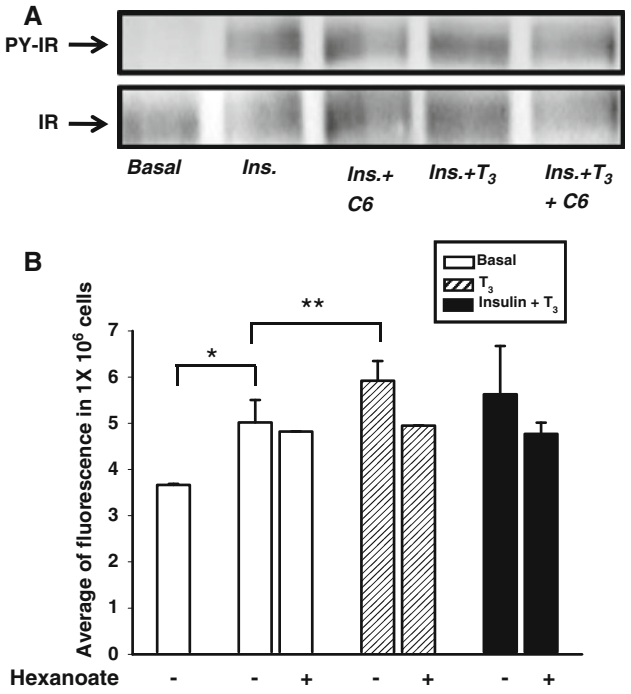

Fig. 4 **a** Effect of hexanoate on insulin receptor phosphorylation and T_3 uptake. HepG2 cells were incubated for 24 h with T_3 (1.6 μM), insulin (100 nM) and/or C6 (1 μM). The cells were lysed; 100 μg of extracted proteins were resolved on 10% SDS-PAGE and then immunoblotted with either an anti-phosphotyrosine antibody (*top panel*) or an anti-insulin receptor antibody (*bottom panel*). **b** HepG2 cells were incubated for 1 h with T_3 (1.6 μM), insulin (100 nM) and/or C6 (1 μM). Cells were fixed and permeabilized as described in "Methods". The T_3 content was measured by labeling the cells with an anti-T_3 antibody (1/1,000) and anti FITC goat anti-rabbit (1/1,000) except for the first condition (*first bar*) where a primary antibody was omitted. Fluorescence was then measured by flow cytometry. The results represent the average of three independent experiments and are expressed as the average of fluorescence detected in 1×10^6 cells. $^*P < 0.05$, $^{**}P = 0.001$

experiment. Addition of C6 does not modify the uptake of T_3, despite a tendency to decrease. However, these values did not reach the level of significance (Fig 4b). Taken together, our results show that C6 inhibits FAS activity and expression, but not by influencing the linkage between insulin and its receptor or the entrance of T_3 in the cells.

Effect of MCFA Metabolites on FAS Enzymatic Activity

As MCFA taken up by the cells are rapidly metabolized [40], we analyzed the cellular lipid profile after incubating the cells for 24 h with [^{14}C]-hexanoate. As depicted in Table 1, we showed that about 60% of the ^{14}C is now found in the triacylglycerol fraction. The presence of both insulin and T_3 even increases it to almost 66%. The rest of the ^{14}C end up in the cholesterol ester (around 25%) and phospholipids fractions (around 10%). However, the presence of both hormones appears to decrease this conversion, orienting the MCFA towards the esterification pathway.

Table 1 Hormonal effect on CEH lipid profile

	Basal	Insulin	T_3	Insulin + T_3
Phospholipids	11.6 ± 7.2	10.4 ± 5.0	12.2 ± 8.6	7.5 ± 3.2
Free cholesterol	1.0 ± 0.9	0.9 ± 0.8	0.9 ± 0.5	0.5 ± 0.3
Diacylglycerol	7.1 ± 3.2	4.5 ± 2.1	8.7 ± 5.6	5.0 ± 2.3
Triacylglycerol	55.7 ± 8.8	58.0 ± 7.4	50.8 ± 14.8	65.6 ± 3.0*
Cholesterol ester	24.6 ± 4.0	26.2 ± 5.1	27.4 ± 5.6	21.4 ± 4.3§

Cells were incubated for 24 h with hexanoate in presence or not of 100 nM insulin and/or 1.6 μM T_3. The lipid profile was revealed as indicated in "Methods". Results are expressed as percentage of the total radioactive content. Data are the mean of three independent experiments, ±SD

* $P = 0.001$ versus basal

§ $P = 0.01$ versus basal

Even if the hexanoate entering the cell appears to be mostly metabolized into triacylglycerol, we devised a strategy that should enable us to determine if hexanoate needs to be modified in order to inhibit FAS enzymatic activity (Fig. 5a). If it acts unchanged, we should see the same effect when bromo-hexanoate, a form of hexanoate that cannot be metabolized, is used. On the other hand, if bromo-hexanoate fails to inhibit FAS enzymatic activity, it strongly suggests that a metabolite is involved in the inhibitory process, be it through esterification or *β*-oxidation. In Fig. 5b, we observed that bromo-hexanoate has no inhibitory effect on insulin and T_3-induced FAS enzymatic activity, thus suggesting the implication of a metabolite. Incubation of cells with either glycerol–hexanoate (Fig. 5c) or carnitine–hexanoate (Fig. 5d) does not reveal any inhibition of FAS enzymatic activity. Taken together, our results suggest that after 24 h, the MCFA is metabolized, probably *β*-oxidized, but glycerol–hexanoate and carnitine–hexanoate are not directly responsible for the modulation of the FAS enzymatic activity.

Role of Fatty Acids Metabolism Inhibitors on the Effect of Hexanoate on FAS Enzymatic Activity

In order to validate our previous data showing that neither glycerol–hexanoate (Fig. 5c) nor carnitine–hexanoate (Fig. 5d) directly inhibit insulin and T_3-induced FAS enzymatic activity, we used specific pharmaceutical inhibitors to evaluate the role of each lipid metabolic pathway. In Fig. 6a, we can see that the inhibitory effect of hexanoate on insulin and T_3-induced FAS enzymatic

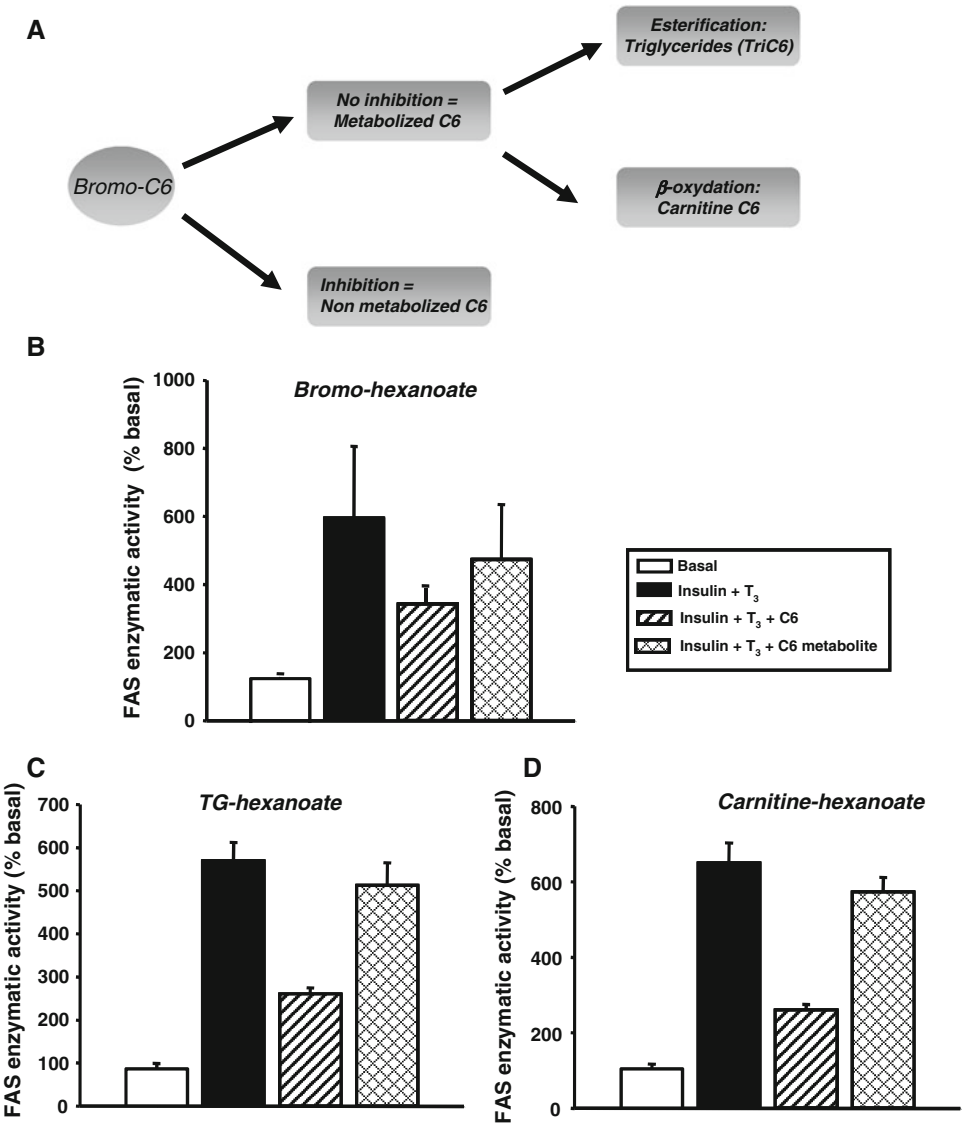

Fig. 5 Effects of the hexanoate metabolites on FAS enzymatic activity. **a** Schematic representation of C6 metabolism in CEH cells. CEH were incubated for 24 h in Waymouth media (*white bars*) or with addition of 100 nM insulin and 1.6 μM T_3 (*black bars*) supplemented with 1 μM of hexanoate (*hatched bars*). The effect of 1 μM bromo-hexanoate (**b**), 1 μM TG-hexanoate (**c**) or 1 μM carnitine–hexanoate (**d**) (*crossed bars*) was also evaluated. FAS activity was evaluated as indicated in "Methods". Results are the mean of at least three independent experiments and are expressed as a function of the value obtained in untreated samples. The bars indicate the SD

activity remained when the cells were treated with Etomoxir, an inhibitor of the CPT1. The same is true as shown in Fig. 6b, depicting the cells that were treated with Betulinic acid, a specific inhibitor of the diacylglycerol transferase (DGAT). We have to note that the presence of these inhibitors does not affect the uptake of hexanoate (Fig. 6d, crossed bars). These results confirm our previous observations suggesting that hexanoate is neither esterified nor *β*-oxidized in order to inhibit FAS enzymatic activity in the presence of insulin and T_3. However, the use of bromo-hexanoate demonstrated that hexanoate needs to be metabolized. It had previously been demonstrated that as soon as the MCFA enters the cell, it is rapidly transformed into an acyl-CoA derivative, reaction catalyzed by the octanoyl-CoA synthetase [1]. In order to test this hypothesis, we evaluated the effect of Triacsin C, a general inhibitor of acyl-CoA synthetases [41], on the inhibitory effect of hexanoate. Under those conditions, we saw a total abolition of the inhibitory effect induced by hexanoate, and recovered the synergic effect seen when the cells are stimulated with insulin and T_3 (Fig. 6c). The MCFA effect on FAS appears to be specific to hexanoyl-CoA, as the presence of Triascin C in the culture media in absence of C6 does not modify the insulin and T_3-induced FAS activity (Fig. 6c, grey bar). As observed for Etomoxir and Betulinic Acid, the Triacsin C has no effect on the uptake of hexanoate (Fig. 6d, crossed bars). Finally, we showed that hexanoyl-CoA is behaving like hexanoate on FAS activity as incubation of cells with this compound efficiently inhibits the insulin and T_3-induced FAS activity (Fig. 6e). As previously observed for C6 (Fig. 2b), the presence of hexanoyl-CoA in the reaction buffer does not modify the insulin and T_3-induced FAS activity (Fig 6e).

Taken together, our results suggest that in hepatocytes, hexanoate needs to be converted to an acyl-CoA derivative in order to inhibit the insulin and T_3-induced FAS

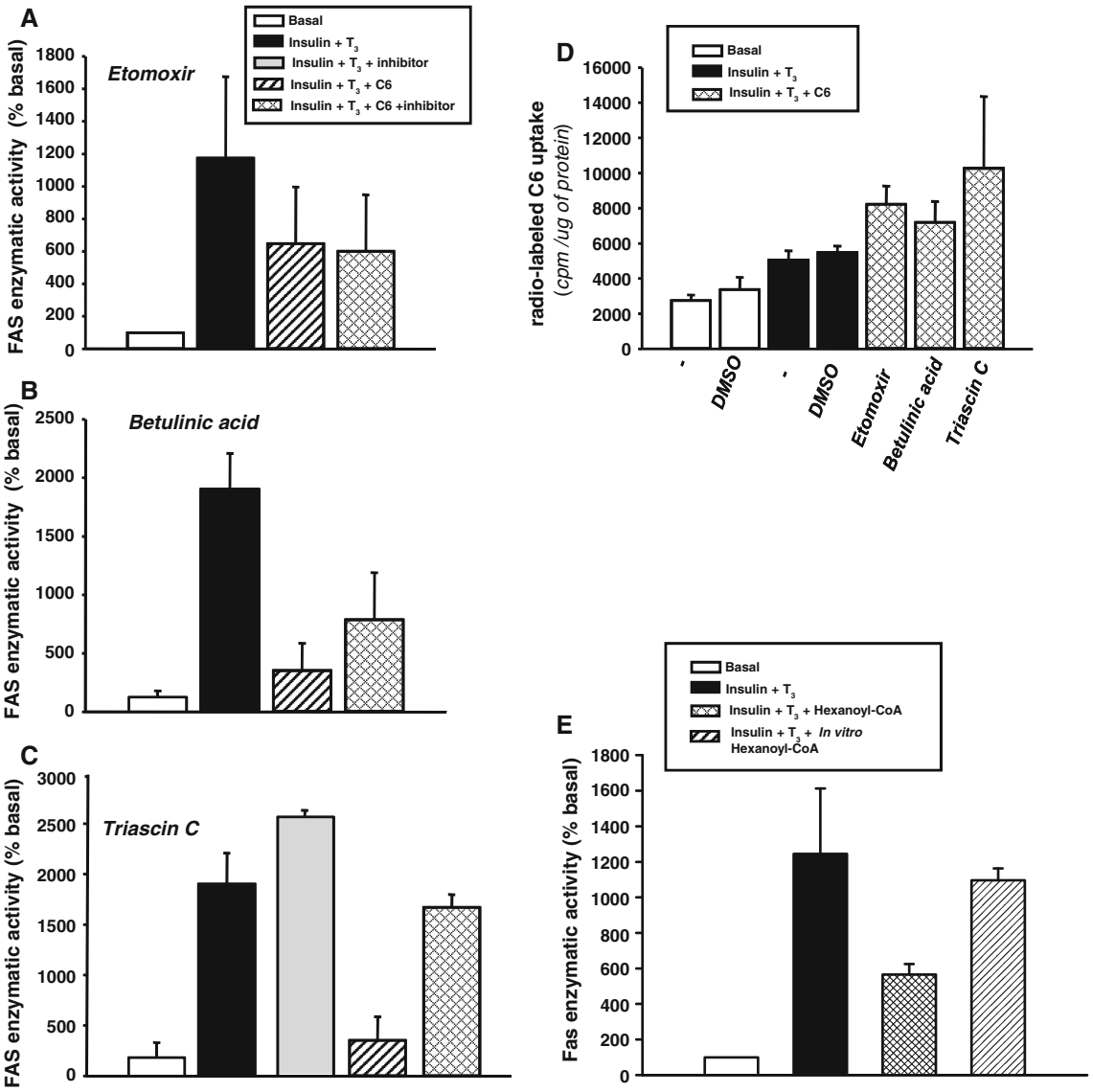

Fig. 6 Effects of lipid metabolic pathways inhibitors on FAS activity and C6 uptake. The CEH were incubated for 24 h in Waymouth media (*white bars*) or with addition of 100 nM insulin and 1.6 μM T_3 (*black bars*) in the presence or absence of hexanoate (*hatched bars*). The effects of (**a**) 1 μM Etomoxir, (**b**) 1 μM Betulinic acid and (**c**) 5 μM Triascin C (*crossed bars*) on insulin and T_3-induced FAS activity and C6 inhibition were also tested. For (**b**) and (**c**), 5% of DMSO was added to each treatment. FAS activity was evaluated as indicated in "Methods". Results are the mean of at least three independent experiments and are expressed as a function of the value obtained in untreated samples. The *bars* indicate SD. $^*P = 0.0065$ compared to Insulin/T_3/C6 treated cells. **d** CEH were incubated for 24 h with 1 μCi of [^{14}C]-hexanoate (*white bars*) and in presence of 100 nM insulin and 1.6 μM T_3 (*black bars*). DMSO was added as indicated in the figure. In addition, 1 μM Etomoxir, 1 μM Betulinic acid or 5 μM Triascin C were added (*crossed bars*) and the C6 uptake was evaluated as indicated in "Methods". Results are expressed in absolute values and are the mean of three independent experiments. The *bars* indicate SD. **e** FAS activity was measured as described in "Methods", using cell lysate from untreated (*white bars*) or treated with 100 nM insulin and 1.6 μM T_3-treated cells for 24 h (*black bars*) with addition of 1 μM hexanoyl-CoA in the media (*crossed bar*) or in the enzymatic reaction buffer (*hatched bar*)

enzymatic activity. Hexanoate acts at the transcriptional level, targeting a TRE on the FAS promoter and modulating its transcriptional activation in response to insulin and T_3. This inhibitory effect cannot be attributed to a modification of insulin receptor activation nor to a decrease in T_3 entry in the cells.

Discussion

Our findings show that hexanoate only inhibits FAS when the enzyme is stimulated by insulin and T_3. These two hormones are strongly secreted during the postprandial state, increasing de novo lipid synthesis. This allows

glucose and, to a lower extent, fatty and amino acids to be transformed into triglycerides and subsequently stored in adipose tissues. Decreasing insulin and T_3-induced FAS activity by hexanoate will probably decrease the amount of TG formed and subsequently the amount of VLDL secreted. This is in agreement with a study showing that incubation of hepatocytes with MCFA decreases VLDL secretion [42]. In addition, several studies have shown that diets containing MCFA can induce weight loss [8]. They attributed the weight loss to increased energy expenditure but also, as shown in our study, by decreased hepatic lipogenesis. The effects of MCFA are of great interest when looking at the inhibition of the postprandial state of de novo lipogenesis, which is associated with an increased secretion of insulin and T_3.

Previous studies have been shown that FAS is regulated at the transcriptional level [17, 43, 44], and that medium chain fatty acids, such as hexanoate and octanoate have an inhibitory effect [27]. This effect was only observed when FAS was stimulated with insulin and T_3. Recently, the need for hormone involvement in the MCFA action has also been observed on the inhibition of adipogenesis in 3T3-LI adipocytes [45]. In the same study, the authors also showed that in the absence of hormones, MCFA increase adipogenesis. As depicted in Fig. 1b, c, MCFA treatment in absence of any hormones leads to an increase in FAS activity. However, the difference does not reach statistical significance and needs to be further confirmed.

We and others have observed that hexanoate and octanoate, but not decanoate nor butanoate (data not shown, [27]), can inhibit FAS enzymatic activity. This inhibition is very specific to these two fatty acids, and more pronounced with hexanoate (about 50%) than with octanoate (about 40%) (Fig. 1b, c). In addition, the inhibitory effect of hexanoate appears to be targeted to lipogenic genes in as so far as FAS, malic enzyme and acetyl CoA carboxylase are concerned [46], because DNA content and transcription of the glyceraldehyde-3-phosphate dehydrogenase and beta-actin genes were not inhibited [27].

It has been previously demonstrated that hexanoate inhibits some lipogenic genes at the transcriptional level [27]. This was confirmed by our experiment showing that MCFA inhibition was not due to allosteric competition. In addition, we showed that hexanoate inhibits FAS through the inhibition of protein expression and transcriptional activity of the TRE. Roncero and collaborators [27] demonstrated that hexanoate and octanoate inhibit lipogenic enzymes activities at a transcriptional step, and did so within 30 min. This is in agreement with our observations showing that hexanoate was able to enter the cell unhindered in just 1 h.

We had previously demonstrated that the FAS TRE is targeted by insulin and T_3 [32]. As previously demonstrated for the malic enzyme promoter [47], we showed that hexanoate targets the TRE on the FAS promoter (Fig. 3b), inhibiting its transcriptional activity in the presence of insulin and T_3. The level of inhibition on the transcriptional activity of the FAS TRE is, however, lower than that observed at the FAS protein and activity levels (25 vs. 50%). It has been previously published that MCFA are able to modulate transcription by inhibiting the accumulation of mature SREBP-1c caused by T_3 and insulin [48]. We know that SREBP-1c regulates FAS transcription by binding an element located outside of the TRE used in our present study [49]. Therefore, the difference observed between the inhibition by C6 of FAS activity and the inhibition at the transcriptional level may be attributed to an effect of C6 on SREBP. This is currently under investigation.

The precise molecular mechanism of MCFA action on the TRE is still unknown. On the malic enzyme promoter, hexanoate does not modify the binding of T_3 to its nuclear receptor TR, neither does it modify the TR binding on the TRE [47]. Previous studies performed in mice have suggested that MCFA decrease PPARγ and SREBP-1c expression. A role of SREBP-1c cannot explain the effect of MCFA on the FAS promoter as in our experiment, the MCFA effect is observed when we use the sequence only including the TRE. The SREBP-1c binding site is not included in the tested DNA promoter fragment.

A previous study in chick embryo hepatocytes demonstrated that MCFA also act on the estrogen receptor (ER) [47]. On promoters, ER dimerizes with itself and not with one of its heterodimerization partners: RXR and PPAR. As the mechanism of MCFA on estrogen and T_3-induced transcription is probably the same, RXR and PPAR are probably not the target of MCFA on the FAS promoter.

In the present study, we showed that hexanoate does not modify the linkage between insulin and its receptor nor the entrance of T_3 in the cells (Fig. 4). However, we cannot exclude that C6 may affect downstream events on the insulin and T_3-activated signaling pathways. In neurons, MCFA are able to modulate intracellular MAPK pathways [50, 51]. We have recently demonstrated that insulin and T_3 mediate their effect on the TRE of the FAS promoter through the activation of a ERK1/2 MAPK pathway [32]. MCFA may modulate the activation of ERK1/2 leading to inhibition of FAS transcription. Finally, MCFA may act on GPCR, activating downstream signaling cascades [52], leading to the phosphorylation of transcription factors bound to the TRE, and modulation of FAS transcription [53]. The exact molecular mechanism of MCFA action on the FAS TRE is currently under investigation.

Our data show that the MCFA enters the cell rapidly. It is well established that MCFA uptake occurs by simple

diffusion without the implication of specific transporters [54, 55]. It is rapidly transformed into an acyl-CoA derivative through the action of a specific acyl-CoA synthetase [1]. This acylation occurs in the mitochondria as the MCFA easily crosses the double mitochondrial membrane and, unlike long-chain fatty acids, they do not require the presence of carnitine palmityl transferases [56]. This is in agreement with the fact that neither carnitine–hexanoate nor Etomoxir (inhibitor of CTPI) affect insulin and T_3-induced FAS enzymatic activity.

The CoA-derivative of MCFA can be transformed into ketone bodies through the β-oxidation pathway. However, this does not appear to be the case in CEH as most of the [^{14}C]-hexanoate taken up by the cells is now found in the triglyceride fraction (more than 60%; Table 1). Therefore, most of the Acyl-CoA hexanoate must be transformed into acetyl-CoA, becoming a carbon source for de novo lipid synthesis ending with the formation of new triglycerides and cholesterol derivatives [56]. This is supported by the fact that in the presence of insulin and T_3, the amount of [^{14}C]-TG is increased compared to the level measured in the absence of any hormonal stimulation (Table 1). Indeed, it is well known that insulin stimulates hepatic triacylglycerol secretion through the general activation of de novo lipid synthesis [57]. It is also well established that T_3 stimulates de novo lipid synthesis in the liver, increasing synthesis of TG [58, 59]. However, the use of betulinic acid, an inhibitor of DGAT, a rate limiting step in the esterification pathway (Fig. 6b) or the incubation of cells with TG-hexanoate (Fig. 5c) did not reveal any abolition of the inhibitory effect of hexanoate on insulin and T_3-induced FAS activity. The incubation of cells with Triacsin C, a general inhibitor of acyl-CoA synthetases [41], completely reversed the inhibitory effect of hexanoate on insulin and T_3-induced FAS activity. Therefore, our data strongly suggest that only the Acyl-CoA hexanoate, which is very rapidly formed after the uptake of the fatty acid by the cell [56], is able to modulate the FAS enzymatic activity. This is also in agreement with the fact that hexanoate is able to inhibit FAS transcription after only 30 min of incubation [27] and that direct incubation of cells with hexanoyl-CoA also abolished insulin and T_3-induced FAS activity (Fig. 6e).

In conclusion, in the present study we have shown that hexanoate is rapidly taken up by the chick embryo hepatocytes. It is subsequently metabolized into an acyl-CoA derivative that is able to specifically inhibit insulin and T_3-induced FAS activity. This inhibition results in decreased FAS protein expression levels. Hexanoate targeting the TRE on the FAS promoter is responsible for part of the inhibition observed at the protein level. We also showed that the C6 effect on FAS expression cannot be attributed to a modification of insulin receptor activation or to a decrease in T_3 entry in the cells.

Acknowledgments This study was supported by a grant from NSERC.

References

1. Bach AC, Babayan VK (1982) Medium-chain triglycerides: an update. Am J Clin Nutr 36:950–962
2. Jensen RG (2002) The composition of bovine milk lipids: January 1995 to December 2000. J Dairy Sci 85:295–350
3. Ikeda Y, Hine DG, Okamura-Ikeda K, Tanaka K (1985) Mechanism of action of short-chain, medium-chain, and long-chain acyl-CoA dehydrogenases. Direct evidence for carbanion formation as an intermediate step using enzyme-catalyzed C-2 proton/deuteron exchange in the absence of C-3 exchange. J Biol Chem 260:1326–1337
4. Papamandjaris AA, MacDougall DE, Jones PJ (1998) Medium chain fatty acid metabolism and energy expenditure: obesity treatment implications. Life Sci 62:1203–1215
5. Babayan VK (1987) Medium chain triglycerides and structured lipids. Lipids 22:417–420
6. Sarda P, Lepage G, Roy CC, Chessex P (1987) Storage of medium-chain triglycerides in adipose tissue of orally fed infants. Am J Clin Nutr 45:399–405
7. Han J, Hamilton JA, Kirkland JL, Corkey BE, Guo W (2003) Medium-chain oil reduces fat mass and down-regulates expression of adipogenic genes in rats. Obes Res 11:734–744
8. Marten B, Pfeuffer M, Schrezenmeir J (2006) Medium-chain triglycerides. Int Dairy J 16:1374–1382
9. Sato K, Cho Y, Tachibana S, Chiba T, Schneider WJ, Akiba Y (2005) Impairment of VLDL secretion by medium-chain fatty acids in chicken primary hepatocytes is affected by the chain length. J Nutr 135:1636–1641
10. Kalogeris TJ, Monroe F, Demichele SJ, Tso P (1996) Intestinal synthesis and lymphatic secretion of apolipoprotein A-IV vary with chain length of intestinally infused fatty acids in rats. J Nutr 126:2720–2729
11. St-Onge MP, Jones PJ (2002) Physiological effects of medium-chain triglycerides: potential agents in the prevention of obesity. J Nutr 132:329–332
12. Eckel RH, Hanson AS, Chen AY, Berman JN, Yost TJ, Brass EP (1992) Dietary substitution of medium-chain triglycerides improves insulin-mediated glucose metabolism in NIDDM subjects. Diabetes 41:641–647
13. Goodridge AG (1973) Regulation of fatty acid synthesis in isolated hepatocytes. Evidence for a physiological role for long chain fatty acyl coenzyme A and citrate. J Biol Chem 248:4318–4326
14. Stoops JK, Arslanian MJ, Oh YH, Aune KC, Vanaman TC, Wakil SJ (1975) Presence of two polypeptide chains comprising fatty acid synthetase. Proc Natl Acad Sci USA 72:1940–1944
15. Wakil SJ (1989) Fatty acid synthase, a proficient multifunctional enzyme. Biochemistry 28:4523–4530
16. Gibson DM, Titchener EB, Wakil SJ (1958) Studies on the mechanism of fatty acid synthesis. V. Bicarbonate requirement for the synthesis of long-chain fatty acids. Biochim Biophys Acta 30:376–383
17. Back DW, Goldman MJ, Fisch JE, Ochs RS, Goodridge AG (1986) The fatty acid synthase gene in avian liver. Two mRNAs are expressed and regulated in parallel by feeding, primarily at the level of transcription. J Biol Chem 261:4190–4197

18. Amy CM, Williams-Ahlf B, Naggert J, Smith S (1992) Intron-exon organization of the gene for the multifunctional animal fatty acid synthase. Proc Natl Acad Sci USA 89:1105–1108
19. Wilson SB, Back DW, Morris SM Jr, Swierczynski J, Goodridge AG (1986) Hormonal regulation of lipogenic enzymes in chick embryo hepatocytes in culture. Expression of the fatty acid synthase gene is regulated at both translational and pretranslational steps. J Biol Chem 261:15179–15182
20. Back DW, Wilson SB, Morris SM Jr, Goodridge AG (1986) Hormonal regulation of lipogenic enzymes in chick embryo hepatocytes in culture. Thyroid hormone and glucagon regulate malic enzyme mRNA level at post-transcriptional steps. J Biol Chem 261:12555–12561
21. Morris SM Jr, Winberry LK, Fisch JE, Back DW, Goodridge AG (1984) Developmental and nutritional regulation of the messenger RNAs for fatty acid synthase, malic enzyme and albumin in the livers of embryonic and newly-hatched chicks. Mol Cell Biochem 64:63–68
22. Kurokawa R, Yu VC, Naar A, Kyakumoto S, Han Z, Silverman S, Rosenfeld MG, Glass CK (1993) Differential orientations of the DNA-binding domain and carboxy-terminal dimerization interface regulate binding site selection by nuclear receptor heterodimers. Genes Dev 7:1423–1435
23. Laux T, Schweizer M (1990) Dietary-induced pre-translational control of rat fatty acid synthase. Biochem J 266:793–797
24. Iritani N (1992) Nutritional and hormonal regulation of lipogenic-enzyme gene expression in rat liver. Eur J Biochem 205:433–442
25. Paulauskis JD, Sul HS (1989) Hormonal regulation of mouse fatty acid synthase gene transcription in liver. J Biol Chem 264:574–577
26. Stapleton SR, Mitchell DA, Salati LM, Goodridge AG (1990) Triiodothyronine stimulates transcription of the fatty acid synthase gene in chick embryo hepatocytes in culture. Insulin and insulin-like growth factor amplify that effect. J Biol Chem 265:18442–18446
27. Roncero C, Goodridge AG (1992) Hexanoate and octanoate inhibit transcription of the malic enzyme and fatty acid synthase genes in chick embryo hepatocytes in culture. J Biol Chem 267:14918–14927
28. Blake WL, Clarke SD (1990) Suppression of rat hepatic fatty acid synthase and S14 gene transcription by dietary polyunsaturated fat. J Nutr 120:1727–1729
29. Jump DB, Clarke SD, Thelen A, Liimatta M, Ren B, Badin M (1996) Dietary polyunsaturated fatty acid regulation of gene transcription. Prog Lipid Res 35:227–241
30. Clarke SD, Jump DB (1994) Dietary polyunsaturated fatty acid regulation of gene transcription. Annu Rev Nutr 14:83–98
31. Moon YS, Latasa MJ, Griffin MJ, Sul HS (2002) Suppression of fatty acid synthase promoter by polyunsaturated fatty acids. J Lipid Res 43:691–698
32. Radenne A, Akpa M, Martel C, Sawadogo S, Mauvoisin D, Mounier C (2008) Hepatic regulation of fatty acid synthase by insulin and T3: evidence for T3 genomic and nongenomic actions. Am J Physiol Endocrinol Metab 295:E884–E894
33. Kuhl WE, Spector AA (1970) Uptake of long-chain fatty acid methyl esters by mammalian cells. J Lipid Res 11:458–465
34. Bradford MM (1976) A rapid and sensitive method for the quantitation of microgram quantities of protein utilizing the principle of protein–dye binding. Anal Biochem 72:248–254
35. de Wet JR, Wood KV, DeLuca M, Helinski DR, Subramani S (1987) Firefly luciferase gene: structure and expression in mammalian cells. Mol Cell Biol 7:725–737
36. Sambrook J, Russell DW (2000) Molecular cloning: a laboratory manual. Cold Spring Harbor, New York
37. Goodridge AG (1972) Regulation of the activity of acetyl coenzyme A carboxylase by palmitoyl coenzyme A and citrate. J Biol Chem 247:6946–6952
38. Fischer PW, Goodridge AG (1978) Coordinate regulation of acetyl coenzyme A carboxylase and fatty acid synthetase in liver cells of the developing chick in vivo and in culture. Arch Biochem Biophys 190:332–344
39. Hsu RY, Yun SL (1970) Stabilization and physicochemical properties of the fatty acid synthetase of chicken liver. Biochemistry 9:239–245
40. Aoyama T, Nosaka N, Kasai M (2007) Research on the nutritional characteristics of medium-chain fatty acids. J Med Invest 54:385–388
41. Gauthier MS, Miyoshi H, Souza SC, Cacicedo JM, Saha AK, Greenberg AS, Ruderman NB (2008) AMP-activated protein kinase is activated as a consequence of lipolysis in the adipocyte: potential mechanism and physiological relevance. J Biol Chem 283:16514–16524
42. Tachibana S, Sato K, Cho Y, Chiba T, Schneider WJ, Akiba Y (2005) Octanoate reduces very low-density lipoprotein secretion by decreasing the synthesis of apolipoprotein B in primary cultures of chicken hepatocytes. Biochim Biophys Acta 1737:36–43
43. Goodridge AG, Fantozzi DA, Klautky SA, Ma XJ, Roncero C, Salati LM (1991) Nutritional and hormonal regulation of genes for lipogenic enzymes. Proc Nutr Soc 50:115–122
44. Semenkovich CF (1997) Regulation of fatty acid synthase (FAS). Prog Lipid Res 36:43–53
45. Yang JY, Della-Fera MA, Rayalam S, Park HJ, Ambati S, Hausman DB, Hartzell DL, Baile CA (2009) Regulation of adipogenesis by medium-chain fatty acids in the absence of hormonal cocktail. J Nutr Biochem 20:537–543
46. Yonezawa T, Yonekura S, Sanosaka M, Hagino A, Katoh K, Obara Y (2004) Octanoate stimulates cytosolic triacylglycerol accumulation and CD36 mRNA expression but inhibits acetyl coenzyme A carboxylase activity in primary cultured bovine mammary epithelial cells. J Dairy Res 71:398–404
47. Thurmond DC, Baillie RA, Goodridge AG (1998) Regulation of the action of steroid/thyroid hormone receptors by medium-chain fatty acids. J Biol Chem 273:15373–15381
48. Zhang Y, Yin L, Hillgartner FB (2003) SREBP-1 integrates the actions of thyroid hormone, insulin, cAMP, and medium-chain fatty acids on ACCalpha transcription in hepatocytes. J Lipid Res 44:356–368
49. Griffin MJ, Sul HS (2004) Insulin regulation of fatty acid synthase gene transcription: roles of USF and SREBP-1c. IUBMB Life 56:595–600
50. Watters JJ, Campbell JS, Cunningham MJ, Krebs EG, Dorsa DM (1997) Rapid membrane effects of steroids in neuroblastoma cells: effects of estrogen on mitogen activated protein kinase signalling cascade and c-fos immediate early gene transcription. Endocrinology 138:4030–4033
51. Kamata Y, Shiraga H, Tai A, Kawamoto Y, Gohda E (2007) Induction of neurite outgrowth in PC12 cells by the medium-chain fatty acid octanoic acid. Neuroscience 146:1073–1081
52. Brown AJ, Jupe S, Briscoe CP (2005) A family of fatty acid binding receptors. DNA Cell Biol 24:54–61
53. Yen PM (2001) Physiological and molecular basis of thyroid hormone action. Physiol Rev 81:1097–1142
54. Hamilton JA, Kamp F (1999) How are free fatty acids transported in membranes? Is it by proteins or by free diffusion through the lipids? Diabetes 48:2255–2269
55. Kamp F, Hamilton JA (2006) How fatty acids of different chain length enter and leave cells by free diffusion. Prostaglandins Leukot Essent Fatty Acids 75:149–159

56. Bremer J (1980) Carnitine and its role in fatty acid metabolism. Trends Biochem Sci 2:207–209
57. Zammit VA (2002) Insulin stimulation of hepatic triacylglycerol secretion in the insulin-replete state: implications for the etiology of peripheral insulin resistance. Ann N Y Acad Sci 967:52–65
58. Dayton S, Dayton J, Drimmer F, Kendall FE (1960) Rates of acetate turnover and lipid synthesis in normal, hypothyroid and hyperthyroid rats. Am J Physiol 199:71–76
59. Diamant S, Gorin E, Shafrir E (1972) Enzyme activities related to fatty-acid synthesis in liver and adipose tissue of rats treated with triiodothyronine. Eur J Biochem 26:553–559

Lipids (2010) 45:1011–1023
DOI 10.1007/s11745-010-3471-7

ORIGINAL ARTICLE

Dietary Lecithin Source Affects Growth Potential and Gene Expression in *Sparus aurata* Larvae

Dulce Alves Martins · Alicia Estévez · Neil C. Stickland · Bigboy H. Simbi · Manuel Yúfera

Received: 4 June 2010 / Accepted: 25 August 2010 / Published online: 10 September 2010

Abstract Soybean lecithin (SBL), used as a phospholipid source in larval fish diets, may compromise growth and survival in marine species, and affect gene expression, due to differences in fatty acid composition relative to marine lecithins (ML). The potential of SBL as a phospholipid source in gilthead seabream microdiets as compared to ML was evaluated. Two stocking densities were tested in order to exacerbate possible dietary effects: 5 and 20 larvae L^{-1}. Larvae reflected dietary fatty acid profiles: linoleic acid was higher, whereas eicosapentaenoic and arachidonic acids were lower in SBL fed groups than in ML fed larvae. Highest stocking density decreased survival, and led to elevated saturates and lower docosahexaenoic acid levels in polar lipid. Muscle histology observations showed hindered growth potential in SBL fed larvae. Despite similar cortisol levels between treatments, higher glucocorticoid receptor (GR), as well as hormone-sensitive lipase (HSL) mRNA levels in SBL fed groups revealed a role for fatty acids in gene regulation. Further analysed genes suggested these effects were independent from the hypothalamus-pituitary-interrenal axis control and the endocannabinoid system. Cyclooxygenase-2 and gluconeogenesis seemed unaffected. For the first time in fish, a link between dietary lecithin nature and HSL gene transcription, perhaps regulated through GR fatty acid-induced activation, is suggested. Enhanced lipolytic activity could partly explain lower growth in marine fish larvae when dietary ML is not provided.

Keywords Dietary lipid · Stocking density · Gilthead seabream · Larvae · Fatty acids · Stress · Gene expression

Abbreviations

SBL	Soybean lecithin
ML	Marine lecithin
SAFA	Saturated fatty acids
MUFA	Monounsaturated fatty acids
PUFA	Polyunsaturated fatty acids
HUFA	Highly unsaturated fatty acids
TFA	Total fatty acids
PLA2	Phospholipase A2
COX-2	Cyclooxygenase-2
ACTH	Adrenocorticotropic hormone
POMC	Pro-opiomelanocortin
GR	Glucocorticoid receptors
FBPase	Fructose-1, 6-bisphosphatase
PKC	Protein kinase C
HSL	Hormone-sensitive lipase
GH	Growth hormone
CB1 receptor	Cannabinoid 1 receptor
ARA	Arachidonic acid

D. Alves Martins · M. Yúfera
Instituto de Ciencias Marinas de Andalucía (CSIC), Apartado Oficial E-11510, Puerto Real, Cádiz, Spain

D. Alves Martins (✉)
Centro de Ciências do Mar do Algarve, Universidade do Algarve, Campus de Gambelas, 8005-139 Faro, Portugal
e-mail: dimartins@ualg.pt

A. Estévez
Centro de Acuicultura, IRTA and Centro de Referencia en Acuicultura, Generalitat de Cataluña, 43540 San Carlos de la Rápita, Tarragona, Spain

N. C. Stickland · B. H. Simbi
Department of Veterinary Basic Sciences, The Royal Veterinary College, University of London, London NW1 0TU, UK

DHA	Docosahexaenoic acid
EPA	Eicosapentaenoic acid
DAH	Days after hatching
RGR	Relative growth rate
GRE	Glucocorticoid responsive element
11βHSD1	11-β hydroxysteroid dehydrogenase type 1
NF-κB	Nuclear factor-kappa B
PPAR	Peroxisome proliferator-activated receptor
HPI	Hypothalamus–pituitary–interrenal
2-AG	2-Arachidonoylglycerol
HPA	Hypothalamus–pituitary–adrenal
PEPCK	Phosphoenolpyruvate carboxykinase

Introduction

A dietary phospholipid source, particularly of marine origin, is generally recognised to promote growth and survival, as well as skeletal development, and perhaps stress resistance in fish larvae [1, 2]. Phospholipids are key cell membrane constituents, and have a relevant role in lipid transportation from the intestine which seems to be of utmost importance in larvae; they are also thought to influence dietary palatability [1]. Commercially available lecithins are mixtures of phospholipids obtained from oils of either vegetable or animal nature. Due to its market availability and relatively stable composition, soybean lecithin (SBL) is generally included as a phospholipid providing ingredient in larval diets, although its fatty acid composition differs greatly from that of marine lecithin (ML). Typically, SBL presents elevated linoleic acid levels and does not contain highly unsaturated fatty acids (HUFA) which characterize ML. Despite the abundance of HUFA under the triacylglyceride form in larval diets provided mostly through fish oil ingredients, some supply under the phospholipid form seems necessary to sustain growth in marine fish larvae [3, 4]. The reasons underlying this requirement are still poorly understood and further research is needed for the optimisation of larval diets. It would be plausible to hypothesise that deleterious effects of dietary SBL as compared with ML on growth and development in fish larvae could be due, at least partly, to changes in cell content of certain fatty acids and their metabolites which can play key roles in many cellular events, such as gene expression regulation [5–7].

Stress coping ability, which requires energy expenditure, has been increasingly recognised as a valuable parameter for the evaluation of physiological condition in fish. Eicosanoid production, their type and relative amounts, is supposedly influenced by the dietary supply of certain fatty acids and believed to play a major role on the success of the stress response in larvae, although seldom explored in fish stress studies [8, 9]. Eicosanoids are generated by the activity of phospholipase A2 (PLA2) and other enzymes, such as cyclooxygenase-2 (COX-2), over fatty acids derived from cell membrane phospholipids [10]. Other enzymes (lipoxygenase, epoxygenase) also contribute to eicosanoid production which may stimulate adrenocorticotropic hormone (ACTH) and modify induced cortisol release [8, 11]. The ability to recover homeostatic balance in response to stress is determined by a response system in which a variety of transcription factors and nuclear receptors are implied, possibly under direct or indirect influence of fatty acids or their metabolites [12]. Besides, the issue of cell membrane composition is also relevant for genomic steroid actions since the ability of a substance to partition into the membrane is critical for its bioavailability to intracellular receptors [13, 14].

This study was designed to test two diets differing in the phospholipid source, in seabream larvae. A relatively high stocking density was used as a chronic stressor with the aim of possibly intensifying effects of the diets on growth, survival, and stress associated parameters. Exploring effects of dietary lecithin source on aspects related to stress physiology was expected to provide clues for its metabolic regulation by dietary fatty acids. As such, the gene expressions of pro-opiomelanocortin (POMC, a precursor for ACTH), glucocorticoid receptors (GR, cortisol signaling mediators), COX-2, and fructose-1,6-bisphosphatase (FBPase, involved in stress-induced gluconeogenesis) were analysed. Furthermore, the expression of protein kinase C (PKC) gene was studied as a potential intermediary in steroidogenesis, and responsive to cellular ARA abundance [15, 16]. Other genes targeted were those for the rate-limiting enzyme hormone-sensitive lipase (HSL), growth hormone (GH), and cannabinoid 1 receptor (CB1 receptor). CB1 receptors are distributed within the central nervous system [17, 18] and their expression could reflect changes in dietary fatty acid supply, especially arachidonic acid (ARA). Also, histological analyses of the muscle were conducted in order to identify short-term effects of the experimental conditions on the growth potential of the larvae, which is believed to be related with the number of small sized muscle fibres in fish [19–21].

Experimental Procedure

Experimental Conditions

A bifactorial experiment was conducted during 7 days on gilthead seabream larvae. Eggs were obtained from the "Planta de Cultivos Marinos" of the University of Cádiz (Puerto Real, Spain) and placed in 200-L incubator tanks in

a flow-through system, with constant aeration. After hatching, the larvae were transferred into 300-L tanks and fed on *Nannochloropsis gaditana* (Fitoplancton marino, EasyAlgae) enriched rotifers (*Brachionus rotundiformis* and *B. plicatilis*; 5–15 per ml of tank water) from 5 to 25 days after hatching (DAH), according to the feeding protocols established by Polo et al. [22]. After 14 DAH, *N. gaditana* and *Isochrysis galvana* (T-Iso) enriched *Artemia nauplii* were also provided at 1–2 nauplii per ml. From 32 DAH onwards, fish were fed exclusively on microencapsulated diets (200–400 μm size), prepared according to the method described by Yúfera et al. [23], and containing commercial phospholipid mixtures (lecithins) of either marine (ML) or soybean (SBL) origin (Table 1). Both diets were formulated to present phosphatidylcholine and phosphatidylinositol, thought to be main growth-promoting fractions in lecithin for fish larvae, in a total content of approximately 1% of the diet as suggested by Coutteau et al. [24]. The ratio phosphatidylcholine/(phosphatidylinositol + phosphatidylserine) was maintained at 2.5 in both diets.

During the one-week inert feeding period, larvae were kept in a flow-through system consisting of eight cylindro-conical baskets (43 L) with a plankton net bottom immersed in one tank. Four of the baskets held seabream groups at a low density ("L" groups) of 5 larvae L^{-1} and other four held groups kept at the higher stocking density ("H" groups) of 20 larvae L^{-1}. The experimental diets were assigned so that each treatment was tested in duplicate (ML-L, ML-H, SBL-L, SBL-H). Feed was supplied in excess, manually during the day and with automatic feeders at night. Constant aeration was provided so as to maintain dissolved oxygen levels around 6 mg L^{-1}, water temperature was kept at 20 ± 0.5 °C and a light:dark photoperiod of 14:10 h was used. Water salinity was 33 g L^{-1}. Tank maintenance, removal of dead fish and uneaten feed were performed daily.

Sampling procedures

Initial fish samples were taken for determination of individual dry weight and total length at 32 DAH ($n = 10$). At the end of the experiment (39 DAH), fish samples were collected from all treatments for dry weight and total length determination ($n = 10$), muscle histology ($n = 6$), gene expression analyses through mRNA quantification ($n = 12$), whole-body cortisol ($n = 14$), and lipid quantification (minimum 100 mg body mass per tank). All larvae sampled were anaesthetised with an overdose of ethyl-4-amino-benzoate and washed with distilled water before storage or measurements, with the exception of animals used for gene expression analysis. These were immediately stored in an RNA stabilizing solution, RNA*Later*™

Table 1 Formulation and proximate composition of microencapsulated diets prepared by internal gelation (g kg^{-1}), for gilthead seabream larvae

Ingredients	ML	SBL
Fish meal[a]	50	50
Fish hydrolysate[b]	100	100
Cuttlefish meal[c]	450	450
Casein[d]	50	50
Sodium alginate[e]	70	70
Baker yeast[f]	30	30
Dextrin[g]	40	40
Fish oil[h]	73.5	80
Soybean lecithin[i]	–	50
Marine lecithin[j]	56.5	–
Vitamin premix[k]	20	20
Vitamin C[l]	30	30
Vitamin E[m]	10	10
Mineral premix[n]	20	20
Proximate composition		
Moisture (%)	7.1	8.2
Protein (% DM)	69.9	69.1
Lipid (% DM)	16.9	18.5
Carbohydrates[o] (% DM)	8.7	7.8
Ash (% DM)	4.6	4.7

[a] AGLONORSE MICROFEED, Norsildmel Innovation AS, Bergen, Norway

[b] CPSP-90, Soprepêche, France

[c] SQUID POWDER 0278, Rieber & Søn ASA, Bergen, Norway

[d] VWR International, Fontenay sous Bois, France

[e] ICN 154724

[f] Commercial bread yeast

[g] Commercial grade type I, MP Biomedicals, LLC, Illkirch, France

[h] Cod liver oil, José M. Vaz Pereira, S.A., Sintra, Portugal

[i] Lecithin Soy Refined, MP Biomedicals, LLC, Illkirch, France containing (% total lipid): phosphatidylcholine 25.8%, phosphatidylethanolamine 20.1%, phosphatidylserine 12.0%, phosphatidylinositol 5.5%, sphingolipids 5.6%, cholesterol 10.0%, free fatty acids 17.5%, sphingomyelin 2.6%, phosphatidic acid/cardiolipin 1.0%

[j] Marine natural lecithin LC 40, PhosphoTech Laboratories, Saint-Herblain, France containing (% total lipid): phosphatidylcholine 21.0%, phosphatidylethanolamine 8.9%, phosphatidylserine 3.2%, phosphatidylinositol 4.8%, cholesterol 40.5%, free fatty acids 18.0%, sphingomyelin 3.6%

[k] Vitamin premix supplied the following (per kg of diet): vitamin A/D_3 500/100, 1,000 mg; vitamin D_3 500, 40 mg; vitamin E 50, alpha-tocopherol acetate, 3,000 mg; vitamin K_3 23%, 220 mg; thiamine HCl, 50 mg; riboflavin 80, 250 mg; d-Ca pantothenate, 1,100 mg; niacin, 500 mg; pyridoxine, 150 mg; folic acid, 50 mg; vitamin B_{12} 0.1, 500 mg; biotin 20, 38 mg; ascorbic acid polyphosphate 35%, 57.2 g; choline chloride 60%, 100 g; inositol, 15 g; antioxidants, 1.25%

[l] Sodium, calcium ascorbyl-2-phosphate, ROVIMIX STAY-C 35, DSM Nutritional Products, Inc

[m] DL-alpha-tocopherol acetate, MP Biomedicals, LLC, Eschwege, Germany

[n] Mineral premix supplied the following (per kg of diet): monocalcium phosphate 35.2%, calcium carbonate 11.5%, sodium chloride 20.0%, potassium chloride 26.0%, copper sulphate 0.024%, magnesium sulphate 5.0%, ferrous sulphate 0.6%, manganous sulphate 0.81%, zinc sulphate 0.17%, potassium iodide 0.0031%, sodium selenite, 0.6%

[o] Carbohydrates = 100 − (protein + lipid + ash)

(Ambion, Austin, TX, USA), at 4 °C overnight, then at −20 °C until analytical work was conducted. Whole larvae samples for histological analyses were fixated in a 0.1 M phosphate buffer containing 3% glutaraldehyde 25% EM and stored at 4 °C. Both cortisol determination and fatty acid analysis samples were stored in a −80 °C freezer to avoid material degradation and peroxidation until further analyses.

Analytical Methods

Experimental diets were analysed for proximate composition according to the following procedures: dry matter determined gravimetrically by drying in an oven at 105 °C for 24 h; crude ash by incineration in a muffle furnace at 500 °C for 5 h; crude protein (% N × 6.25) determined using an elemental analyzer (Thermoquest Flash 1112, Rodano, Italy) with sulphanilamide as a standard; total lipid extracted in chloroform:methanol (2:1, v/v) according to Folch et al. [25] and quantified gravimetrically after evaporation of the solvent under a stream of nitrogen followed by overnight vacuum desiccation. Total lipid was stored in chloroform:methanol (2:1, 20 mg ml^{-1}) with 0.01% butylated hydroxytoluene (BHT) at −20 °C until final analysis. Fatty acid composition of total lipid and polar lipid fraction of the diets was also determined following an acid catalyzed transmethylation [26]. Fatty acid methyl esters were extracted twice using isohexane:diethyl ether (1:1, v/v), purified on TLC plates and analysed by gas–liquid chromatography on a Thermo TraceGC (Thermo Fisher Scientific, Waltham, MA, USA) instrument fitted with a BPX70 capillary column (30 m–0.25 mm id, SGE), using a two-stage thermal gradient from 50 °C (injection temperature) to 150 °C after ramping at 40 °C min^{-1} and holding at 250 °C after ramping at 2 °C min^{-1}, using helium (1.2 ml min^{-1} constant flow rate) as the carrier gas, on-column injection, and flame ionisation detection. Peaks were identified by comparison with known standards (Supelco, Madrid, Spain) and a well characterised fish oil, and quantified by means of the response factor to the internal standard, 21:0 fatty acid, added prior to transmethylation, using a Chrompack program (Thermo Finnigan, San Jose, CA, USA). To carry out fatty acid composition analysis of the polar lipid fraction, total lipid extract was evaporated to dryness, diluted in chloroform (about 30 mg of lipids in 500 µl of solvent) and injected on a Sep-Pack silica cartridge (Waters S.A., Milford, MA, USA; [27]). After adsorption of the sample, 20 ml of chloroform were pushed through the cartridge with a syringe avoiding the formation of air bubbles and the non-polar fraction discarded. The fraction containing the polar lipids was eluted through the cartridge with 30 ml of methanol, collected and subjected to acid catalysed transmethylation as indicated above. Lipid class composition of the lecithins and diets was determined by high-performance thin-layer chromatography (HPTLC). Approximately 10 µg of lipid was applied as a 2 mm streak and the plate developed to two-thirds distance with methyl acetate/isopropanol/chloroform/methanol/0.25% aqueous KCl (25:25:25:10:9, v/v), to separate polar lipid classes, and then fully developed with isohexane:diethyl ether:acetic acid (85:15:1, v/v). Lipid classes were visualised by charring at 160 °C for 15 min after spraying with 3% (w/v) aqueous cupric acetate containing 8% (v/v) phosphoric acid, and quantified by densitometry using a Bio-Rad GS-800 densitometer (Bio-Rad Laboratories, Spain) and the software QuantityOne (Bio-Rad Laboratories, Spain). The identities of individual lipid classes were confirmed by comparison with authentic standards.

The total length of the larvae was measured with a micrometer eye piece and whole body dry weight was determined by drying samples at 70 °C for several days until constant weight was attained. At the end of the trial, relative growth rate (RGR; [28]) was calculated for all treatment groups, as well as survival. Theoretical biomass was calculated as the product of survival by the mean weight of the larvae.

For muscle histology analyses complete transverse sections were cut from each fish at the level of the anal vent, washed in the fixation buffer, post-fixed in 1% osmium tetroxide, dehydrated, and embedded in TAAB resin according to Stickland et al. [29]. Transverse sections of 1 µm thickness were obtained using a Reichert ultramicrotome and stained with 1% toluidine blue. Slides were examined using a Zeiss image analysis system (KS 300, Kontron, Munich, Germany). White-muscle cross-sectional areas, small (less than 25 μm^2), and large (more than 25 μm^2) fibre numbers from a quadrant of each transverse section were quantified (as in 29).

Total lipid from larval tissues was extracted [25]. Separation of the polar lipid fraction and determination of its fatty acid profile in larvae samples were carried out as previously described.

A commercial cortisol enzyme-linked immunosorbent assay kit (ELISA; Neogen Corporation, Lexington, KY, USA) was used to assess whole-body cortisol levels in pooled larvae samples of about 20 mg (7 fish per sample). This was preceded by sample homogenisation in a phosphate buffered saline solution (PBS) and extraction with diethyl ether. The latter was performed following recommendations by Sink et al. [30] involving the addition of 100 µL of a food-grade vegetable oil per gram of sample body weight. Olive oil was used and previously assayed for cortisol to ensure no cross contamination would occur from animal fats. After extraction and solvent evaporation under a stream of nitrogen, lipid extracts containing cortisol were

reconstituted in the kit's extraction buffer, diluted to an appropriate factor and analysed according to the kit manufacturer's instructions. All samples and standards were run in duplicate. Intra- and inter-assay variation values were checked and a % CV of $\leq$20.0 was set as acceptable. Parallelism and linearity (passing limit $r^2 > 0.90$) were tested using serial dilutions of sample extracts.

For molecular analyses six larvae sampled from each tank were pooled, homogenised in Tri Reagent (Sigma, Poole, Dorset, UK) with an ultra-turrax (IKA, Werke GmbH & Co. KG, Staufen, Germany), and RNA extracted with chloroform followed by ethanol precipitation. Qiagen RNeasy columns (Qiagen, Crawley, UK) were used for DNase treatment and sample purification. Samples were eluted with Sigma Pure water (Sigma) and RNA concentration measured spectrophotometrically using a Nanodrop N-1000 system (Nanodrop Technologies, Wilmington, DE, USA). Formaldehyde gel electrophoresis was performed to determine the integrity of total RNA by analysing bands under UV light. Reverse transcription of sample RNA was performed with Quantitect Reverse Transcription Kit (Qiagen, Valencia, CA, USA) according to the manufacturer's instructions, using half a microgram of total RNA. The primers used were designed with the support of the Primer-3 Web-Software (Whitehead Institute for Biomedical Research, Cambridge, MA, USA) and synthesised by Eurofins MWG Operon (Ebersberg, Germany). Primer sequences and Accession numbers for the mRNAs analysed are described in Table 2. Genes analysed were GH, POMC, CB1 receptor, GR, HSL, FBPase, COX-2, and PKC. Real-time PCR, based on Quantitect Sybr Green detection (Qiagen), was performed on 2 µl cDNA samples, using a Chromo-4 Thermal Cycler (MJ Research Inc., Waltham, MA, USA). The relative concentrations of the target amplicons were calculated by the cycler's software (Bio-Rad, Hercules, CA, USA) from a standard curve created with serial dilutions of standard DNA. The relative concentrations of target sequences in each run were expressed as numbers of copies and normalised to 0.5 µg of total RNA. All PCR products were checked for specificity and purity from a melting curve produced by the thermal cycler software at the end of each run.

Statistical Analysis

Data were analysed by a two-way ANOVA with SPSS 16.0 software package using diet and stocking density as fixed factors. For data not presenting a normal distribution and/or variance homogeneity, log-transformation was applied. Differences were considered significant at an alpha level of 0.10 due to both small sample sizes caused by feasibility constraints, and the exploratory character of this experiment, as recommended by Rubin [31].

Table 3 Fatty acid composition (% total fatty acids, TFA) of the experimental diets

Total fatty acids (mg g^{-1} lipids)	ML		SBL	
	500.6		534.5	
	Total lipid	Polar fraction	Total lipid	Polar fraction
Fatty acid (% TFA)				
16:0	18.7	17.5	15.9	12.5
18:0	3.4	5.8	3.2	7.6
Σ SAFA	27.1	24.1	23.2	20.6
16:1n-7	4.7	0.5	4.6	0.5
18:1*	20.1	20.7	19.6	22.1
20:1n-9	6.5	5.2	5.5	2.3
Σ MUFA	31.3	26.4	29.8	24.8
18:2n-6	2.2	1.6	11.0	18.6
20:4n-6	0.9	0.7	0.6	0.4
Σ n-6 PUFA	3.5	2.5	12.2	19.1
18:3n-3	0.9	0.3	1.9	2.6
20:5n-3	12.0	15.4	10.3	11.2
22:5n-3	0.7	0.4	0. 8	0.4
22:6n-3	21.8	29.8	17. 6	20.7
Σ n-3 PUFA	38.0	46.5	34.9	35.3
Σ PUFA	41.5	49.0	51.0	54.4

* Sum of 18:1n-7 and 18:1n-9

Table 2 Primers in the 5′–3′ direction used for the real-time PCR analysis

Primer	Forward	Reverse	Product size (bp)	Accession number
GH	GCTCAGTGTTGAAGCTGCTG	TGGGTGAAATCTGGTTCCTC	108	S54890
POMC	GAGGAGTCAGCCGAGGTCTT	GCCTTCTCCTCCTCCTCCT	101	AY714372
CB1 receptor	AGCGTGCTGGTTCTTTTCAT	ACAAGGCTCTTCTGGGAGGT	104	EF051620
COX-2	TGATCGAGGACTACGTGCAG	AGTGGGTGCCAGTGGTAAAG	139	AB292357
PKC	GACAGTTTGCCCTGTCTGGT	GAGAAAGCCACGCTCAAAAC	118	DQ111989
GR	CGGTCACTGCTACGTCTTCA	CCTCCCAGCACACAGGTAAT	170	DQ486890
HSL	GTTGCAGCCAGCTCTTTCTT	TCGGTTTCAGTGATGTTCCA	134	EU781499
FBPase	CTCTGCAGCCTGGAAGAAAC	TCCAGCATGAAGCAGTTGAC	106	AF427867

Table 4 Growth performance of seabream larvae fed different phospholipid sources and stocked under different densities

	Experimental treatment				Significance level		
	ML-L	ML-H	SBL-L	SBL-H	Diet	Density	Diet × density
Dry weight (mg per larva)	0.5 ± 0.1	0.4 ± 0.0	0.3 ± 0.0	0.3 ± 0.0	*	NS	NS
Total length (mm)	8.5 ± 0.7	8.8 ± 0.1	8.1 ± 0.3	7.8 ± 0.2	*	NS	NS
RGR (% per day)	3.8 ± 3.8	3.6 ± 0.6	−0.4 ± 2.3	−0.2 ± 0.8	*	NS	NS
Survival (%)	77.5 ± 1.8	59.5 ± 2.8	80.8 ± 6.6	54.2 ± 5.6	NS	*	NS
Theoretical biomass (mg)	35.4 ± 9.8	26.4 ± 2.4	27.3 ± 2.1	18.5 ± 0.8	*	*	NS

Values are means ± SD. Significant effects determined by two-way analysis of variance indicated by $^*P < 0.10$ or *NS* not significant

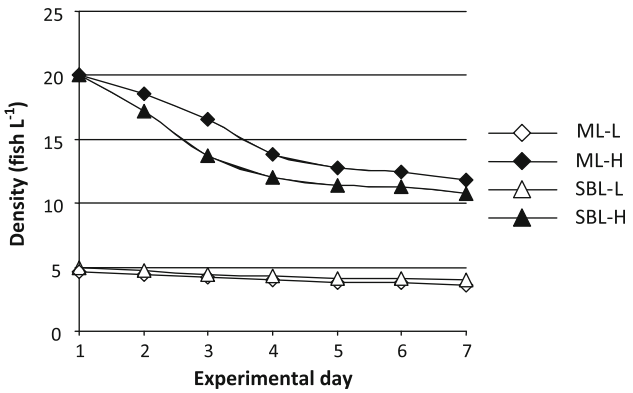

Fig. 1 Stocking density changes estimated during the experimental period in all treatment groups

Results

Proximate composition of the experimental diets (dry matter basis) showed high protein content (69–70%) and lipid levels around 17–18% (Table 1). Saturated fatty acids and n-3 series polyunsaturates, particularly docosahexaenoic acid (DHA, 22:6n-3), were higher in the ML diet, whereas the SBL diet contained higher levels of linoleic (18:2n-6) and linolenic (18:3n-3) acids, as shown in Table 3. Concerning dietary polar lipid fractions, the levels of palmitic (16:0), eicosenoic (20:1n-9), and eicosapentaenoic (EPA, 20:5n-3) acids, as well as DHA, were more elevated in the ML diet than in the SBL treatment, whereas the latter presented a considerably higher content in linoleic acid than the ML diet.

At 32 DAH, larvae weighed 0.3 ± 0.0 mg and were about 7.9 ± 0.2 mm long. Although classic growth performance analysis was not a main objective of this study due to its short duration, data relative to larval dry weight, total length and relative growth rate (RGR) at the end of the experiment are presented (Table 4), along with survival and theoretical biomass results. No significant interaction effects between diet and stocking density were detected for these parameters. Statistical analyses revealed dietary effects on dry weight, total length and RGR, such that values obtained for ML fed larvae were higher than those presented by SBL fed groups. Groups offered the SBL treatment showed actual weight loss during the one-week period whereas animals fed on the ML diet grew at about 3.6–3.8% per day. Nonetheless, high variation was observed between replicate tanks with the ML-L treatment. Although the SBL diet seemed to compromise growth,

Table 5 Histological analysis of a muscle quadrant area, fibre number, small:large fibre ratio and fibre density (per mm^2) in gilthead seabream larvae fed the experimental diets and stocked under two different densities

	Experimental treatment				Significance level		
	ML-L	ML-H	SBL-L	SBL-H	Diet	Density	Diet × density
Total							
Area (mm^2)	42.1 ± 5.9	30.8 ± 5.4	37.4 ± 4.7	33.6 ± 5.0	NS	NS	NS
Small fibres	255.3 ± 18.7	239.0 ± 24.4	196.3 ± 19.2	159.8 ± 16.8	*	NS	NS
Large fibres	315.7 ± 29.6	272.5 ± 28.6	298.2 ± 27.1	257.2 ± 25.3	NS	NS	NS
Small:large fibres	0.8 ± 0.0	0.9 ± 0.1	0.7 ± 0.1	0.6 ± 0.0	*	NS	NS
Density							
Small fibres	6.3 ± 0.8	8.4 ± 1.0	5.5 ± 0.5	5.0 ± 0.5	*	NS	NS
Large fibres	7.6 ± 0.5	9.3 ± 0.7	8.2 ± 0.4	8.1 ± 0.8	NS	NS	NS

Values are means ± SE. Significant effects determined by two-way analysis of variance indicated by $^*P < 0.10$ or *NS* not significant

survival was not affected. Mortality occurred in all treatments, especially until around day 5 in "H" groups which resulted in lower stocking densities at the end of the experiment than initially established (Fig. 1). Overall, survival was lower in groups kept at the higher stocking density (54.2–59.5%) than in "L" groups (77.5–80.8%). Theoretical biomass decreased with both larval density ($P = 0.072$) and the SBL regime ($P = 0.092$).

Results from muscle histology analysis are shown in Table 5 and revealed no significant interaction effects between diet and stocking density for any of the measured parameters. Measurements of the cross-sectional area of a quadrant of fish muscle (Fig. 2) did not reveal statistical differences between treatments. Nonetheless, average values were between 37.4 and 42.1 mm^2 for fish stocked at low density, whereas those at high density showed average areas of 30.8–33.6 mm^2. Histological analysis of white muscle showed dietary effects on the total number and density of small fibres but not of large fibres. As such, fish fed the SBL diet showed about 28% less small fibre number and density compared to those fed the ML diet. Overall, histological analysis pointed to a higher growth potential in seabream supplied with ML as compared to SBL groups.

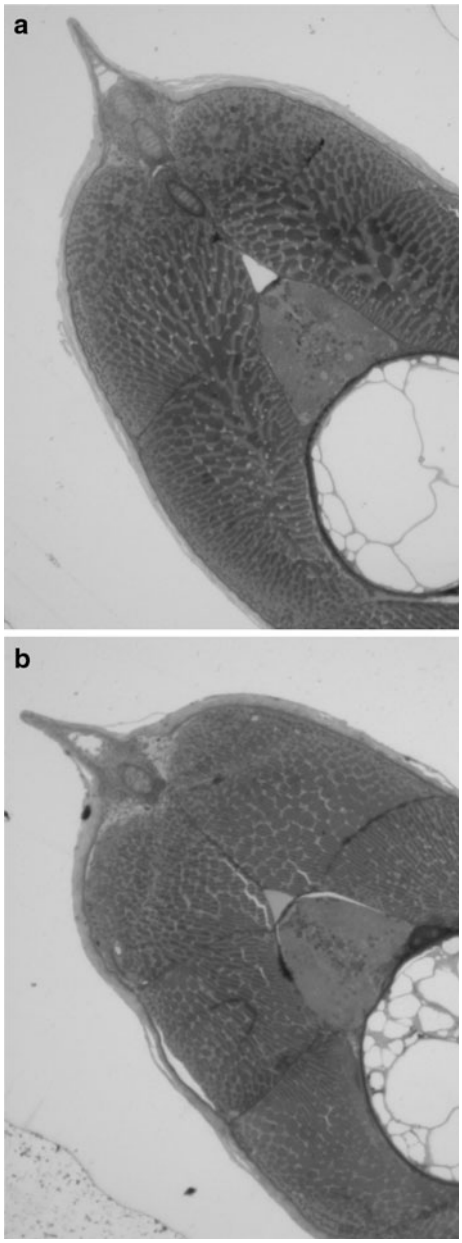

Fig. 2 Transverse sections through gilthead seabream larvae from ML-L (**a**) and SBL-L (**b**) experimental groups stained with 1% toluidine blue (20×)

Lipid content and total fatty acid composition of the larvae are described in Table 6. Total lipid content revealed a significant interaction effect between diet and stocking conditions such that slightly higher levels were found in SBL-H than SBL-L fish, whereas values were very similar between ML diet groups. Deposition of 18:2n-6 was higher in fish fed SBL than in ML fed groups. Also, slightly higher levels of 18:1n-9, 18:1n-7 and 18:3n-3 were detected in SBL fed animals, whereas ML fed fish showed larger accumulation of arachidonic acid (ARA, 20:4n-6) and EPA than SBL groups. Analyses of the polar lipid showed statistically significant interaction effects between diet and stocking density for 18:0, 20:1n-9, and 18:3n-3. Higher stocking density conditions resulted in increased total saturated fatty acid (SAFA) levels, particularly 18:0 in SBL fed groups (Table 7), and a reduction of total PUFA, especially DHA. Differences were also found due to dietary treatments. Linoleic and linolenic acids were higher in the polar lipid of SBL than ML fed animals, whereas ARA remained highest in ML fed fish. Contrary to findings in the total lipid fatty acid profile, EPA was kept at similar levels in all treatment groups. Besides, unlike the trend observed in dietary composition, DHA deposition in the larvae was apparently unaffected by its dietary content.

Whole-body cortisol analysis did not show a significant interaction effect between diet and stocking density or statistical differences between treatments. Results are presented in Fig. 3. Average values were about 8.0 ng g^{-1} (larval wet weight) in fish stocked at high density. In ML-L and SBL-L groups, average cortisol levels were 12.4 and 9.0 ng g^{-1}, respectively. Displacement curves for cortisol standards and sample serial dilutions are presented (Fig. 4a). Validation tests for the ELISA involving a vegetable oil volume-boosting method showed values of 5.07% for intra-assay coefficient of variation (% CV) and 18.7% for inter-assay CV. Linearity r^2 value was 0.9997 and parallelism was confirmed (Fig. 4b).

Results of the molecular analyses of gene expression are presented in Fig. 5. No significant interaction effects between diet and stocking density were identified for any

Table 6 Total lipid content and fatty acid composition (% TFA) of whole-body gilthead seabream larvae fed the experimental diets and stocked under two different densities

	Initial	Experimental treatment				Significance level		
		ML-L	ML-H	SBL-L	SBL-H	Diet	Density	Diet × density
Total lipids (mg g^{-1} DW)	–	20.7 ± 2.3	19.8 ± 1.0	16.2 ± 2.3	21.8 ± 0.5	NS	*	*
Total fatty acids (mg g^{-1} lipids)	–	433.8 ± 15.4	420.4 ± 50.8	449.1 ± 15.6	427.4 ± 38.3	NS	NS	NS
Fatty acid (% TFA)								
16:0	20.1	23.0 ± 1.2	20.9 ± 2.7	22.1 ± 0.6	20.5 ± 0.9	NS	NS	NS
18:0	5.2	9.1 ± 0.0	9.2 ± 1.5	9.3 ± 0.4	8.2 ± 0.8	NS	NS	NS
Σ SAFA	30.1	36.5 ± 2.3	31.5 ± 4.3	33.2 ± 0.8	31.2 ± 2.1	NS	NS	NS
16:1n-7	5.5	3.2 ± 0.2	3.4 ± 0.7	3.5 ± 0.8	4.0 ± 1.0	NS	NS	NS
18:1n-9	12.3	13.1 ± 0.1	12.7 ± 0.9	13.9 ± 0.5	13.8 ± 0.1	*	NS	NS
18:1n-7	2.8	1.6 ± 0.2	1.8 ± 0.4	2.2 ± 0.0	2.1 ± 0.3	*	NS	NS
20:1n-9	0.9	1.7 ± 0.4	1.6 ± 0.6	1.7 ± 0.1	0.7 ± 0.9	NS	NS	NS
Σ MUFA	22.1	19.9 ± 0.7	19.8 ± 2.5	21.6 ± 0.2	20.8 ± 0.3	NS	NS	NS
18:2n-6	2.2	1.6 ± 0.0	1.7 ± 0.3	6.1 ± 0.3	6.6 ± 0.0	*	NS	NS
20:4n-6	1.5	4.0 ± 0.1	4.3 ± 0.5	3.6 ± 0.1	3.8 ± 0.2	*	NS	NS
Σ n-6 PUFA	5.2	6.4 ± 0.2	7.0 ± 1.2	10.2 ± 0.3	11.1 ± 0.2	*	NS	NS
18:3n-3	0.4	0.3 ± 0.1	0.3 ± 0.0	0.5 ± 0.0	0.6 ± 0.0	*	*	NS
20:5n-3	7.3	9.2 ± 0.2	10.5 ± 1.2	8.2 ± 0.4	8.8 ± 0.5	*	NS	NS
22:5n-3	2.6	5.6 ± 0.2	6.7 ± 1.0	5.9 ± 0.0	6.0 ± 0.5	NS	NS	NS
22:6n-3	30.1	21.8 ± 2.0	23.6 ± 3.6	20.0 ± 0.3	21.0 ± 1.1	NS	NS	NS
Σ n-3 PUFA	41.8	37.2 ± 1.9	41.7 ± 5.6	35.0 ± 0.7	36.8 ± 2.2	NS	NS	NS
Σ PUFA	47.0	43.6 ± 1.6	48.7 ± 6.8	45.3 ± 1.0	47.9 ± 2.4	NS	NS	NS

Values are means ± SD. Significant effects determined by two-way analysis of variance indicated by $*P < 0.10$ or *NS* not significant. Values referred for larvae initial fatty acid composition were based on typical values reported by Robin and Vincent [60] for 3 dph gilthead seabream

of the genes analysed. Quantification of mRNA for GH, POMC, CB1 receptor, FBPase, COX-2, and PKC showed no significant differences under the experimental conditions tested. Nonetheless, the expression of HSL and GR genes was up-regulated in SBL groups compared to ML fed larvae, whereas no statistical differences were found due to stocking density.

Discussion

Early life stages in gilthead seabream are characterised by hyperplastic growth of white myofibres [32, 33]. Small muscle fibres are evidence of ongoing fibre hyperplasia in fish muscle. This appears to have been less in fish fed the SBL diet than in those supplied with ML, which indicates hindered growth potential in the former although essential fatty acid requirements were met for the species, according to recommendations by Sargent et al. [34] and Castell et al. [35]. These authors point at n-3 HUFA requirements of about 1.5% of the diet when the ratio DHA/EPA is about 2, and ARA levels between 0.5 and 1.0% of total dietary fatty acids, respectively. On the other hand, survival was not affected by dietary lecithin source. Instead, high stocking density increased mortality, which was also related to higher levels of saturated fatty acids, particularly stearic acid (18:0), and lower DHA in the polar lipid fraction than found in "L" groups. Thus, we hypothesise that membrane fluidity might have been affected in "H" groups which could have disturbed the activity of membrane-bound enzymes, ion channels, or receptors and led to higher mortality. The reasons why high density stocking would cause the observed changes in polar lipid fatty acids are unclear but results suggested that seabream larvae might have a higher requirement for DHA under such rearing conditions.

In gilthead seabream larvae, 5% dietary SBL inclusion as provided in the present study was reported to increase microdiet consumption rates perhaps due to an attractant effect [36]. In another study, elevation of dietary polar lipid levels improved microdiet ingestion in seabream, regardless of its soybean or marine origin [37]. Although feed consumption was not determined in this experiment, similar survival between dietary treatments and the fact that whole-body fatty acid composition mirrored differences between diets indicated the acceptance of the experimental

Table 7 Fatty acid composition of the polar lipid fraction (% TFA) of whole-body gilthead seabream larvae fed the experimental diets and stocked under two different densities

	Experimental treatment				Significance level		
	ML-L	ML-H	SBL-L	SBL-H	Diet	Density	Diet × density
Total PL (mg g^{-1} DW)	570.0 ± 155.6	495.0 ± 49.5	665.0 ± 91.9	360.0 ± 84.9	NS	NS	NS
Total fatty acids (mg g^{-1} polar lipids)	481.7 ± 103.3	540.9 ± 114.2	505.1 ± 48.8	558.1 ± 83.3	NS	NS	NS
Fatty acid (% TFA)							
16:0	16.2 ± 0.9	17.4 ± 1.6	15.3 ± 2.4	16.2 ± 3.6	NS	NS	NS
18:0	11.3 ± 0.4	12.2 ± 1.3	10.7 ± 0.2	15.3 ± 0.8	*	*	*
Σ SAFA	28.8 ± 1.7	30.5 ± 0.2	26.2 ± 2.1	32.0 ± 2.4	NS	*	NS
16:1n-7	0.9 ± 0.2	0.8 ± 0.1	0.8 ± 0.2	0.6 ± 0.2	NS	NS	NS
18:1	10.7 ± 0.6	11.0 ± 0.2	11.2 ± 0.9	11.1 ± 0.2	NS	NS	NS
20:1n-9	2.4 ± 0.3	2.2 ± 0.2	1.7 ± 0.1	2.4 ± 0.2	NS	NS	*
Σ MUFA	13.9 ± 0.7	14.0 ± 0.3	13.7 ± 1.2	14.0 ± 0.2	NS	NS	NS
18:2n-6	1.7 ± 0.6	1.5 ± 0.1	4.6 ± 0.6	4.3 ± 0.4	*	NS	NS
20:4n-6	5.3 ± 0.5	5.7 ± 0.3	4.7 ± 0.3	4.3 ± 0.0	*	NS	NS
Σ n-6 PUFA	7.2 ± 1.3	7.4 ± 0.2	9.5 ± 1.0	8.9 ± 0.2	*	NS	NS
18:3n-3	0.2 ± 0.0	0.2 ± 0.0	0.3 ± 0.1	0.5 ± 0.1	*	NS	*
20:5n-3	11.0 ± 0.3	11.0 ± 0.7	10.7 ± 0.9	10.0 ± 0.2	NS	NS	NS
22:5n-3	7.0 ± 0.3	7.4 ± 0.6	7.2 ± 0.3	6.8 ± 0.5	NS	NS	NS
22:6n-3	30.4 ± 2.4	28.0 ± 0.3	31.2 ± 3.2	26.8 ± 1.1	NS	*	NS
Σ n-3 PUFA	49.1 ± 2.3	47.1 ± 0.3	49.9 ± 4.1	44.5 ± 1.7	NS	NS	NS
Σ PUFA	56.3 ± 1.0	54.4 ± 0.5	59.4 ± 3.1	53.4 ± 1.9	NS	*	NS

Values are means ± SD. Significant effects determined by two-way analysis of variance indicated by $*P < 0.10$ or *NS* not significant

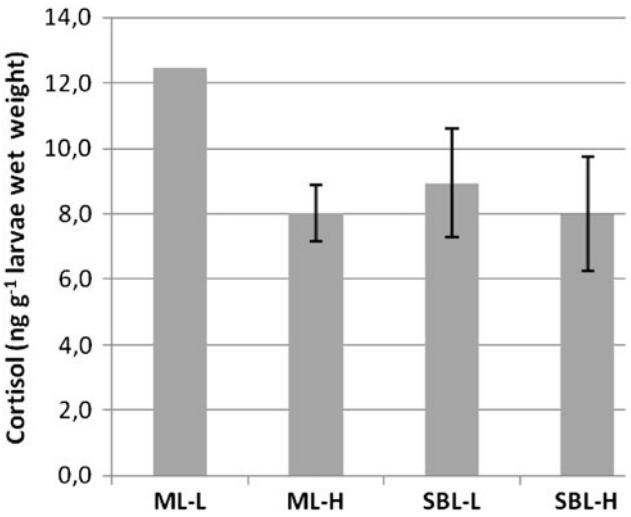

Fig. 3 Whole-body basal cortisol levels in seabream larvae fed different phospholipid sources and stocked under different densities. Values are means ± SE. Absence of *letters* means no statistical differences ($p > 0.10$)

diets. Therefore, the detrimental effects observed on growth performance could be attributed to dietary lecithin origin. Surprisingly, despite numerous publications reporting the importance of dietary phospholipids for fish larvae, no studies have been published on the viability of SBL use as compared to ML containing diets in marine species. The efficiency of HUFA supplied through diet under the phospholipid form in sustaining growth, as exemplified in this study, is generally recognised [2]. However, the reasons for this are yet unclear. Perhaps due to improved digestibility, marine phospholipids tend to be more efficient in supplying essential fatty acids than neutral lipids, although in freshwater fish SBL seems to satisfy larval phospholipid requirements [1].

As expected, dietary fatty acid composition was reflected in fish tissues. In SBL diet fed groups a significant increase in linoleic acid was noted in both total and polar lipids, concurrent with a decrease in ARA, relative to ML fed larvae. Besides potential effects on cell membrane lipid composition and function, dietary fat has profound effects on gene expression. Polyunsaturated fatty acids and their metabolites can act in conjunction with nuclear receptors and transcription factors to affect the transcription of a variety of genes [7] leading to changes in metabolism, growth and cell differentiation [6]. Thus, diet induced changes in gene expression could provide indications as to mechanisms by which dietary fatty acids could have regulated metabolism in larvae fed distinct lecithins.

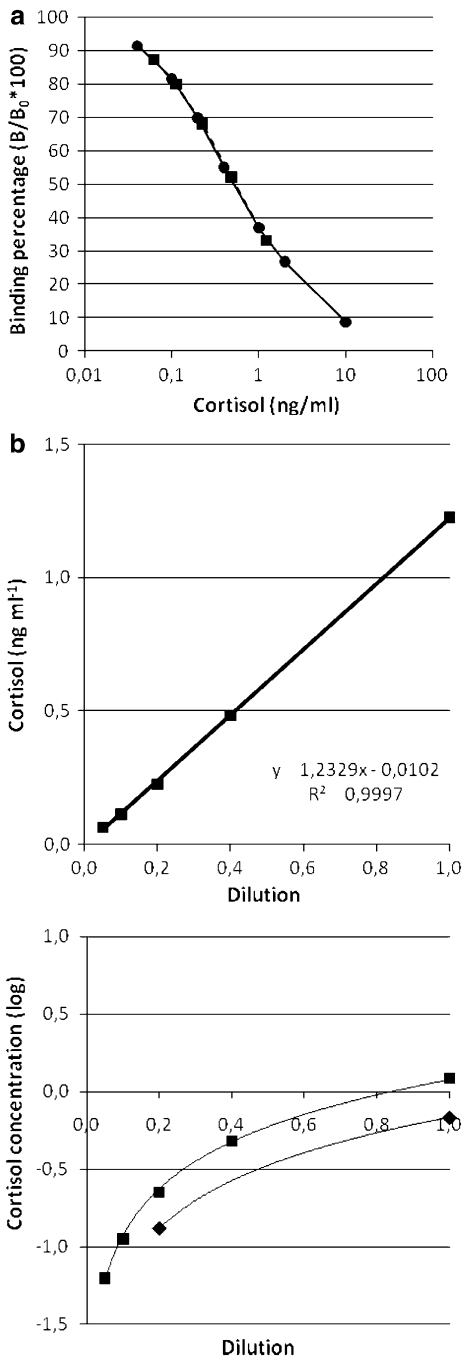

Fig. 4 **a** Displacement curves for cortisol standards (*black circles*) and serial dilutions of a gilthead seabream sample (*black squares*). *B* absorbance reading of the sample or standard. B_0 absorbance reading of blank. Each point is the mean of duplicate determinations. **b** Linearity and parallelism of the ELISA cortisol analysis method. Each point is the mean of duplicate determinations

Despite the absence of differences between treatments for whole-body cortisol concentrations, which were in accordance with values reported by Szisch et al. [1] for seabream, GR mRNA levels were higher in SBL diet fed fish. A similar trend was noted for HSL which has been identified as a glucocorticoid-sensitive gene in mammals [38], containing glucocorticoid responsive elements (GREs) in its promoter [39, 40]. This is also likely in fish as enhanced lipolytic activity and increased free fatty acid levels in the plasma are generally associated to the stress response (reviewed by Mommsen et al. [12]). HSL catalyses the rate-limiting step in fatty acid mobilization from stored triglycerides, determining the supply of energy substrates in the body [41]. A relative up-regulation of this enzyme in SBL fed fish could hinder or even impair growth as observed due to energy deviation away from anabolic metabolism. The observed effects on larval growth were not determined by differences in the gene expression of GH, the main regulator of postnatal somatic growth stimulating cell division, skeletal growth, and protein synthesis. GH can also enhance lipolysis in starved fish, as seen in seabream adipocytes [42]; however, feeding conditions did not differ among experimental groups and HSL results did not appear to be influenced by GH as its mRNA levels indicated.

Although GR mRNA and protein expression are not always correlated, as seen in rainbow trout [43] no such information is currently available for gilthead seabream. Present results suggested an effect of dietary fatty acid supply on the regulation of GR gene expression regardless of values detected by whole-body total cortisol analyses. Indeed, cortisol plasma concentrations may not always be correlated to cytosolic GRs [44], and increased intracellular concentrations of glucocorticoids can result from overexpression of 11-β hydroxysteroid dehydrogenase type 1 (11βHSD1; [45]) which converts cortisone to cortisol. Thus, both protein levels of this enzyme and GRs can determine the physiological activity of glucocorticoids. Several possible pathways for the modulation of GR gene expression by fatty acids may exist. Nuclear factor-kappa B (NF-κB), a GR transcription factor [46], can be activated in the presence of linoleic and oleic acids, as seen in rats [47], and may have contributed for the enhancement of GR expression in larvae fed the SBL diet. Peroxisome proliferator-activated receptors (PPARs), probably the best known factors in fatty acid regulation of gene transcription, also interact with NF-κB and AP-1 [48], both transcription factors for GRs (reviewed by Yudt and Cidlowski [49]). Indeed, linoleic acid was reported to be a potent PPAR activator relative to other fatty acids [50]. Another hypothesis for GRs fatty acid modulation is that ARA could bind these receptors at sites different from those bound by steroids, hence inhibiting their activity [51]. Dose-dependent suppression of GR binding has been reported for various unsaturated fatty acids likely as part of a negative feedback mechanism [52]. Nonetheless, in this study, seabream larvae showing lower GR and HSL transcripts presented only slightly higher ARA levels in body lipid.

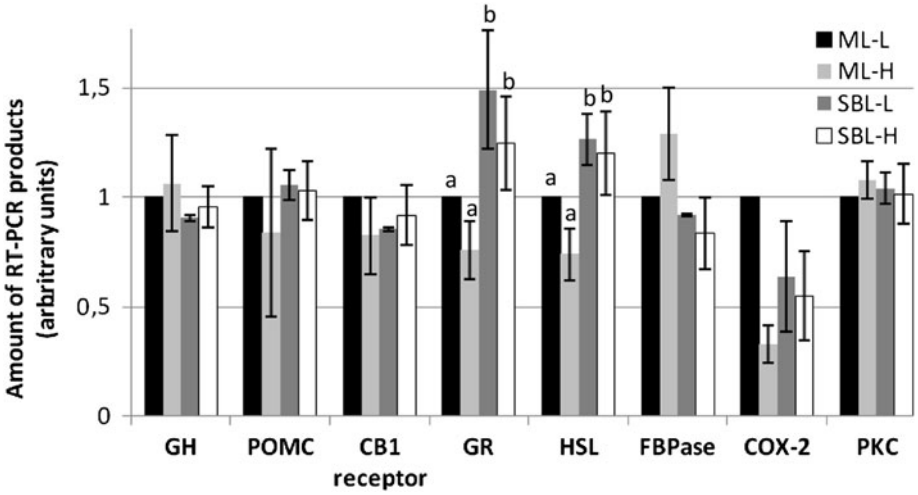

Fig. 5 Expression of genes using real-time PCR and SyBR green detection in gilthead seabream larvae submitted to the experimental conditions. The mRNA levels relative to ML-L treatment were arbitrarily defined as 1 unit. Data are expressed as means ± SE. Different letters mean significant differences ($P < 0.10$). *GH* growth hormone, *POMC* pro-opiomelanocortin, *CB1 receptor* cannabinoid CB1 receptor, *GR* glucocorticoid receptor, *HSL* hormone-sensitive lipase, *FBPase* fructose-1,6-bisphosphatase, *COX-2* cyclooxygenase-2, *PKC* protein kinase C

The gene expression of POMC which encodes for ACTH in gnathostomes was analysed due to the central role of ACTH on cortisol production. POMC gene expression results corroborated those obtained from cortisol measurements, further suggesting that the differential expression of the GR gene was not determined by fatty acids at the hypothalamus–pituitary–interrenal (HPI) axis level.

PKC has important roles in various biological processes (e.g., signal transduction, cell proliferation) including the tonic inhibitor control of steroidogenesis as reported in mammal cells stimulated by intracellular ARA [15, 16, 53]. In this study, results do not indicate that PKC was involved in maintaining similar cortisol levels between groups. In fact, PKC gene expression was so identical among samples and experimental conditions that it could potentially be used as a control gene in future studies with seabream, as suggested in humans [54].

An acute stress challenge could be required for the release of ARA in the cells and further evidencing effects of dietary fatty acid supply on the expression of stress response related genes. This could be underlying the lack of differences regarding PKC as well as COX-2 gene expression between treatments which did not appear to relate to the observed results regarding both GR and HSL genes. In fish, the endocannabinoid system is thought to be involved in the modulation of adaptive responses to environmental conditions [55]. For example, under non-stressful conditions, production of 2-AG (2-arachidonoylglycerol) is higher than in stressed animals, leading to CB1 receptor up-regulation, which depresses hypothalamus–pituitary–adrenal (HPA) axis activity in mammals [56]. Several lines of evidence indicate that, through CB1 receptor activation, endocannabinoids can also regulate NF-κB and AP-1 activities [57, 58], thus potentially interfering with GR activity and the stress response. The lack of differences between experimental groups was in accordance with results obtained for other analysed genes, like COX-2 and PKC further suggesting that the influence of dietary lecithin on GR and HSL genes was exerted, in non-acutely stressed larvae, at the level of GR activation through factors independent from the classic HPI axis regulation.

Gluconeogenesis, in which FBPase is a key enzyme, is responsible for glucose production in response to cortisol [12]. It is assumed that glucocorticoids stimulate gluconeogenesis by increasing PEPCK (phosphoenolpyruvate carboxykinase) gene transcription which contains a GRE, or by stimulating the supply of hepatic precursors (reviewed by Mommsen et al. [12]). Thus, both higher GR expression and lipolytic activity could have contributed to enhance gluconeogenesis; instead, statistically similar FBPase mRNA levels found between groups suggested a more dramatic increase in GR activity could be required to affect gluconeogenesis enzyme activities, as this is usually associated with a rise in plasma cortisol levels.

In summary, changes induced in body fatty acid phenotype through dietary SBL supply exerted a lipolytic effect, compared to ML fed fish, possibly mediated by GR activity, which could have contributed importantly for the detrimental effects observed on growth with the SBL diet. Furthermore, the proposed regulation of GR activity by fatty acids seems to have been independent from the action of the HPI axis, the endocannabinoid system, COX-2

activity, and did not appear to affect gluconeogenesis. On the other hand, no effects of rearing density were found in terms of the expression of genes analysed in this study, although rearing conditions are generally known to interfere with neuroendocrine homeostasis in fish.

The importance of dietary fatty acids on stress coping ability has been repeatedly demonstrated in fish larvae although with limited understanding of the physiological mechanisms involved. Studies regarding fatty acid control over fish GRs are scarce [59] despite their major role in linking and integrating signaling pathways and regulatory processes in cells, tissues, and whole organisms [49]. This aspect is not only relevant in marine fish larval nutrition but should be considered in dietary fish oil replacement research, a recognised priority for the sustainable production of farmed fish.

Acknowledgments The authors wish to thank Ms. Rosa Vázquez (Marine cultures service, University of Cádiz, Spain) for supplying the seabream eggs, Dr. Luísa Valente (Centro Interdisciplinar de Investigação Marinha e Ambiental, Portugal) and Mr. Manuel Arjonilla Medina (Analysis service of Instituto de Ciencias Marinas de Andalucía, CSIC, Spain) for kindly assisting in dietary composition analysis, and Dr. Gonzalo Martínez-Rodríguez (Instituto de Ciencias Marinas de Andalucía, CSIC, Spain) for the help provided during the experimental system set-up. Also, the authors acknowledge Noelia Gras and Marta Sastre (Centro de Acuicultura, IRTA, Spain) for the help provided in lipid extraction, lipid class and fatty acid analysis of the samples. Dulce Alves Martins was funded by Fundação para a Ciência e a Tecnologia, Portugal (SFRH/BPD/32469/2006). This study was funded by Consejería Innovación, Ciencia y Empresa, Junta de Andalucía (Spain) which is co-financed by FEDER (project P06-AGR-01697 to M. Yúfera). Publication benefits from participation in LARVANET COST action FA0801.

References

1. Szisch V, Papandroulakis N, Fanouraki E, Pavlidis M (2005) Ontogeny of the thyroid hormones and cortisol in the gilthead sea bream, *Sparus aurata*. Gen Comp Endocrinol 142:186–192
2. Cahu CL, Gisbert E, Villeneuve LAN, Morais S, Hamza N, Wold PA, Zambonino Infante JL (2009) Influence of dietary phospholipids on early ontogenesis in fish. Aquacult Res 40:989–999
3. Bell JG, McEvoy LA, Estévez A, Shields RJ, Sargent JR (2003) Optimising lipid nutrition in first-feeding flatfish larvae. Aquaculture 227:211–220
4. Gisbert E, Villeneuve L, Zambonino-Infante JL, Quazuguel P, Cahu CL (2005) Dietary phospholipids are more efficient than neutral lipids for long-chain polyunsaturated fatty acid supply in European sea bass *Dicentrarchus labrax* larval development. Lipids 40:609–618
5. Sessler AM, Ntambi JM (1998) Polyunsaturated fatty acid regulation of gene expression. J Nutr 128:923–926
6. Jump DB, Clarke SD (1999) Regulation of gene expression by dietary fat. Annu Rev Nutr 19:63–90
7. Sampath H, Ntambi JM (2005) Polyunsaturated fatty acid regulation of genes of lipid metabolism. Annu Rev Nutr 25:317–340
8. Van Anholt RD, Spanings FAT, Koven WM, Nixon O, Wendelaar Bonga SE (2004) Arachidonic acid reduces the stress response of gilthead seabream *Sparus aurata* L. J Exp Biol 207:3419–3430
9. Gjøen T, Obach A, Rosjo C, Helland BG, Rosenlund G, Hvattum E, Ruyter B (2004) Effect of dietary lipids on macrophage function, stress susceptibility and disease resistance in Atlantic salmon (*Salmo salar*). Fish Physiol Biochem 30:149–161
10. Lands WEM (1991) Biosynthesis of prostaglandins. Annu Rev Nutr 11:41–60
11. Hirai A, Tahara K, Tamura Y, Saito H, Terano T, Yoshida S (1985) Involvement of 5-lipoxygenase metabolites in ACTH stimulated corticosteroids in rat adrenal glands. Prostaglandins 30:749–767
12. Mommsen TP, Vijayan MM, Moon T (1999) Cortisol in teleosts: dynamics, mechanisms of action, and metabolic regulation. Rev Fish Biol Fisher 9:211–268
13. Golden GA, Rubin RT, Mason RP (1998) Steroid hormones partition to distinct sites in a model membrane bilayer: direct demonstration by small-angle X-ray diffraction. Biochim Biophys Acta 1368:161–166
14. Mason RP, Golden GA, Mason PE, Rubin RT (1996) Steroid effects on cell membrane structure: implications for depressive illness. Biol Psychiatry 39:585
15. McPhail L, Clayton CC, Snyderman R (1984) A potential second messenger role for unsaturated fatty acids: activation of Ca^{2+}-dependent protein kinase. Science 224:622–625
16. Farooqui AA, Horrocks LA (2006) Phospholipase A2-generated lipid mediators in brain: the good, the bad, and the ugly. Neuroscientist 12:245–260
17. Cottone E, Forno S, Campantico E, Guastalla A, Viltono L, Mackie K, Franzoni MF (2005) Expression and distribution of CB1 cannabinoid receptors in the central nervous system of the African cichlid fish *Pelvichromis pulcher*. J Comp Neurol 485:293–303
18. Valenti M, Cottone E, Martinez R, De Pedro N, Viveros MP, Franzoni MF, Delgado MJ, Di Marzo V (2005) The endocannabinoid system in the brain of *Carassius auratus* and its possible role in the control of food intake. J Neurochem 95:662–672
19. Higgins PJ, Thorpe JE (1990) Hyperplasia and hypertrophy in the growth of skeletal muscle in juvenile Atlantic salmon, *Salmo salar* L. J Fish Biol 37:505–519
20. Galloway TF, Kjørsvik E, Kryvi H (1999) Muscle growth and development in Atlantic cod larvae (*Gadus morhua* L.) related to different somatic growth rates. J Exp Biol 202:2111–2120
21. Pitkänen TI, Xie SQ, Krasnov A, Mason PS, Mölsä H, Stickland NC (2001) Changes in tissue cellularity are associated with growth enhancement in genetically modified Arctic char (*Salvelinus alpinus* L.) carrying recombinant growth hormone gene. Mar Biotechnol 3:188–197
22. Polo A, Yúfera M, Pascual E (1992) Feeding and growth of gilthead seabream (*Sparus aurata* L.) larvae in relation to the size of the rotifer strain used as food. Aquaculture 103:45–54
23. Yúfera M, Fernández-Diaz C, Pascual E (2005) Food microparticles for larval fish prepared by internal gelation. Aquaculture 248:253–262
24. Coutteau P, Geurden I, Camara MR, Bergot P, Sorgeloos P (1997) Review on the dietary effects of phospholipids in fish and crustacean larviculture. Aquaculture 155:149–164
25. Folch JM, Lees M, Sloane Standley GH (1957) A simple method for the isolation and purification of total lipids from animal tissues. J Biol Chem 226:497–509
26. Christie WW (1982) Lipid analysis, Pergamon Press, Oxford
27. Juaneda P, Rocquelin G (1985) Rapid and convenient separation of phospholipids and non phosphorus lipids from rat heart using silica cartridges. Lipids 20:40–41
28. Ricker WE (1958) Handbook of computations for biological statistics of fish populations. Can J Fish Aquat Sci 119:1–300

29. Stickland NC, White RN, Mescall PE, Crook AR, Thorpe JE (1988) The effect of temperature on myogenesis in embryonic development of the Atlantic salmon (*Salmo salar* L.). Anat Embryol 178:253–257
30. Sink TD, Kumaran S, Lochmann RT (2007) Development of a whole-body cortisol extraction procedure for determination of stress in golden shiners, *Notemigonus crysoleucas*. Fish Physiol Biochem 33:189–193
31. Rubin A (2010) Statistics for Evidence-Based Practice and Evaluation, 2nd edn Wadsworth Cengage Learning
32. Patruno M, Radaelli G, Mascarello F, Candia Carnevali MD (1998) Muscle growth in response to changing demands of functions in the teleost *Sparus aurata* (L.) during development from hatching to juvenile. Anat Embryol 198:487–504
33. Koumoundouros G, Ashton C, Xenikoudakis G, Giopanou I, Georgakopoulou E, Stickland N (2009) Ontogenetic differentiation of swimming performance in gilthead seabream (*Sparus aurata*, L. 1758) during metamorphosis. J Exp Mar Biol Ecol 370:75–81
34. Sargent JR, Tocher DR, Bell JG (2002) The Lipids. In: Halver JE, Hardy RW (eds) Fish Nutrition, 3rd edn, Academic Press, San Diego
35. Castell JD, Bell JG, Tocher DR, Sargent JR (1994) Effects of purified diets containing different combinations of arachidonic and docosahexaenoic acid on survival, growth and fatty acid composition of juvenile turbot (*Scophthalmus maximus*). Aquaculture 128:315–333
36. Koven WM, Kolkovski S, Tandler A, Kissil GW, Sklan D (1993) The effect of dietary lecithin and lipase as a function of age, on n-9 fatty acid incorporation in the tissue lipids of *Sparus aurata* larvae. Fish Physiol Biochem 10:357–364
37. Izquierdo MS, Tandler A, Salhi M, Kolkovski S (2001) Influence of dietary polar lipids' quantity and quality on ingestion and assimilation of labelled fatty acids by larval gilthead seabream. Aquacult Nutr 7:153–160
38. Slavin BG, Ong JM, Kern PA (1994) Hormonal regulation of hormone-sensitive lipase activity and mRNA levels in isolated rat adipocytes. J Lipid Res 35:1535–1541
39. Lampidonis AD, Stravopodis DJ, Voutsinas GE, Messini-Nikolaki N, Stefos GC, Margaritis LH, Argyrokastritis A, Bizelis I, Rogdakis E (2008) Cloning and functional characterization of the 5′ regulatory region of ovine hormone sensitive lipase (HSL) gene. Gene 427:65–79
40. Le PP, Friedman JR, Schug J, Brestelli J, Parker JB, Bochkis IM, Kaestner KH (2005) Glucocorticoid receptor-dependent gene regulatory networks. PLoS Genet 1:159–170
41. González-Yanes C, Sánchez-Margalet V (2006) Signalling mechanisms regulating lipolysis. Cell Signal 18:401–408
42. Albalat A, Gómez-Requeni P, Rojas P, Médale F, Kaushik S, Vianen GJ, Van den Thillart G, Gutiérrez J, Pérez-Sánchez J, Navarro I (2005) Nutritional and hormonal control of lipolysis in isolated gilthead seabream (*Sparus aurata*) adipocytes. Am J Physiol Regul Integr Comp Physiol 289:259–265
43. Singer TD, Raptis S, Sathiyaa R, Nichols JW, Playle RC, Vijayan MM (2007) Tissue-specific modulation of glucocorticoid receptor expression in response to salinity acclimation in rainbow trout. Comp Biochem Physiol B 146:271–278
44. Weisbart M, Charkraborti PK, Gallivan G, Eales JG (1987) Dynamics of cortisol-receptor activity in the gills of the brook trout, *Salvelinus fontinalis*, during seawater adaptation. Gen Comp Endocrinol 68:440–448
45. Masuzaki H, Paterson J, Shinyama H, Morton NM, Mullins JJ, Seckl JR, Flier JS (2001) A transgenic model of visceral obesity and the metabolic syndrome. Science 294:2166–2170
46. Webster JC, Oakley RH, Jewell CM, Cidlowski JA (2001) Proinflammatory cytokines regulate human glucocorticoid receptor gene expression and lead to the accumulation of the dominant negative β isoform: a mechanism for the generation of glucocorticoid resistance. Proc Natl Acad Sci USA 98:6865–6870
47. Dichtl W, Nilsson L, Gonçalves I, Ares MPS, Banfi C, Calara F, Hamsten A, Eriksson P, Nilsson J (1999) Very low-density lipoprotein activates nuclear factor-κB in endothelial cells. Circ Res 84:1085–1094
48. Delerive P, De Bosscher K, Besnard S, Berghe WV, Peters JM, Gonzalez FJ, Fruchart JC, Tedgui A, Haegeman G, Staels B (1999) Peroxisome proliferator-activated receptor α negatively regulates the vascular inflammatory gene response by negative cross-talk with transcription factors NF-κB and AP-1. J Biol Chem 274:32048–32054
49. Yudt MR, Cidlowski JA (2002) The glucocorticoid receptor: coding a diversity of proteins and responses through a single gene. Mol Endocrinol 16:1719–1726
50. Göttlicher M, Widmarkt E, Li Q, Gustafsson J (1992) Fatty acids activate a chimera of the clofibric acid-activated receptor and the glucocorticoid receptor. Proc Natl Acad Sci USA 89:4653–4657
51. Kato J, Takano A, Mitsuhashi N, Koike N, Yoshida K, Hirata S (1987) Modulation of brain progestin and glucocorticoid receptors by unsaturated fatty acid and phospholipid. J Steroid Biochem 27:641–648
52. Viscardi RM, Max SR (1993) Unsaturated fatty acid modulation of glucocorticoid receptor-binding in L2-cells. Steroids 58:357–361
53. Lopez-Ruiz MP, Choi MS, Rose MP, West AP, Cooke BA (1992) Direct effect of arachidonic acid on protein kinase C and LH-stimulated steroidogenesis in rat Leydig cells; evidence for tonic inhibitory control of steroidogenesis by protein kinase C. Endocrinology 130:1122–1130
54. Eisenberg E, Levanon EY (2003) Human housekeeping genes are compact. Trends Genet 19:362–365
55. Palermo FA, Ruggeri B, Mosconi G, Virgili M, Polzonetti-Magni AM (2008) Partial cloning of CB1 cDNA and CB1 mRNA changes in stress responses in the *Solea solea*. Mol Cell Endocrinol 286:52–59
56. Patel S, Roelke CT, Rademacher DJ, Cullinan WE, Hillard CJ (2004) Endocannabinoid signaling negatively modulates stress-induced activation of the hypothalamic–pituitary–adrenal axis. Endocrinology 145:5431–5438
57. Daaka Y, Zhu W, Friedman H, Klein TW (1997) Induction of interleukin-2 receptor alpha gene by Δ9-tetrahydrocannabinol is mediated by nuclear factor κB and CB1 cannabinoid receptor. DNA Cell Biol 16:301–309
58. Zhao Q, He Z, Chen N, Cho YY, Zhu F, Lu C, Ma W, Bode AM, Dong Z (1992) 2-Arachidonoylglycerol stimulates activator protein-1-dependent transcriptional activity and enhances epidermal growth factor-induced cell transformation in JB6 P^+ cells. J Biol Chem 280:26735–26742
59. Lee PC, Struve M (1992) Unsaturated fatty acids inhibit glucocorticoid receptor-binding of trout hepatic cytosol. Comp Biochem Physiol B 102:707–711
60. Robin JH, Vincent B (2003) Microparticulate diets as first food for gilthead seabream larva (*Sparus aurata*): study of fatty acid incorporation. Aquaculture 225:463–474

with enlargement (hypertrophy) of adipocytes, macrophage accumulation and subsequent changes in the production of bioactive proteins or adipokines to favor a more pro-inflammatory profile [3–5]. These changes are associated with obesity-related health problems, the development of metabolic syndrome and an increased risk of cardiovascular disease [6–8]. Some of the pro-inflammatory adipokines involved in pathogenesis of these diseases include angiotensinogen, tumor necrosis factor (TNF)-α and interleukin (IL)-6.

All components of the renin–angiotensin system (RAS), including angiotensin II (AngII) and its precursor angiotensinogen, are present in adipose tissue and this local RAS has been implicated in the regulation of adipose growth as well as the regulation of blood pressure [9, 10]. In support of this argument, mice that selectively over-express angiotensinogen in adipose tissue exhibit an increase in circulating angiotensinogen and are hypertensive [9]. Upon binding to its receptor, AngII also stimulates pro-inflammatory cytokines through the activation of nuclear factor-κB (NF-κB) [11], which further contributes to the pathogenesis of cardiovascular complications [12].

Due to the large increases in obesity-related cardiovascular complications, the need for preventative strategies is at an all time high. The use of dietary compounds to prevent or treat obesity-related cardiovascular risk factors may be an attractive idea for some. Conjugated linoleic acid (CLA) is a fatty acid derived from ruminant animals that is being examined for its potential health benefits [13]. Our laboratory has shown that feeding a mixture of CLA isomers to obese *fa/fa* Zucker rats favorably alters levels of adipokines in serum and epididymal adipose tissue, and at the same time reduces adipocyte size [14]. A recent study by Martins et al. [15] also showed increased serum adiponectin levels in obese Zucker rats given a mixture of CLA isomers and the potential for other cardiovascular benefits such as lowered plasminogen activated inhibitor-1 levels. At this time, however, it remains unclear which CLA isomer is responsible for reducing adipocyte size in an obese model and if other adipose-derived proteins may be affected. Research from other groups suggest that the t10,c12-CLA isomer may be responsible for the cardiovascular benefits, such as improving blood pressure by reducing adipose angiotensinogen mRNA [16]. At this point, however, it remains unclear whether these changes in angiotensinogen mRNA will affect angiotensinogen protein levels or if CLA would have an effect on AngII receptors. Additionally, previous studies examining CLA and NF-κB have primarily been carried out in culture models [17, 18], leaving the effects of CLA isomers in vivo on NF-κB activation in tissues still to be determined. This study was therefore designed to investigate the effects of individual CLA isomers on epididymal adipocyte size and to examine the relationship with the local adipose RAS in obesity. The study focused on epididymal adipose tissue as a visceral adipose depot because visceral adiposity is associated with metabolic complications of obesity and cardiovascular disease and is strong predictor of obesity-related risk factors and mortality [19, 20].

Materials and Methods

Animals and Diet

During an 8-week experimental period, 6-week old male *fa/fa* Zucker rats ($n = 6$/group; Harlan, Indianapolis, IN, USA) received diets based on the AIN-93 formula differing in the amounts of CLA isomers as previously published [21]. There were three groups (a) control diet (b) 0.4% (w/w) *cis*(c)9,*trans*(t)11-CLA diet, and (c) 0.4% (w/w) t10,c12-CLA diet. At the end of the feeding period, rats were euthanized by CO_2 asphyxiation and epididymal adipose tissue was dissected, frozen in liquid nitrogen or Cryogel embedding medium and subsequently stored at −80 °C until analyzed. The University of Manitoba Protocol Management and Review Committee approved the animal protocol which was in agreement with the Canadian Council on Animal Care Guidelines [22].

Morphometry

Tissues sections (10 μm thick) were cut on a cryotome and mounted on SuperFrost Plus glass slides. Sections were fixed in formaldehyde and assessed under a light microscope (BH2-RFCA; Olympus) equipped with a camera (Q-Imaging). Using Image J software as previously described [14], a continuous block of 25 cells was measured in every field to determine average cell size (μm^2) and mean adipocyte size per group was calculated. Based on Sturges' rule [23], 10 different classes of adipocyte area were determined and the cell size distribution for each treatment group was expressed as a percentage. The number of adipocyte was assessed by counting a 160 μm^2 area in the centre of each field/section and the mean number per group was calculated.

RT-PCR Analysis

Total RNA was isolated from epididymal adipose tissue using TRIzol reagent. The concentration of RNA and the purity of the samples were assessed spectrophotometrically. RNA was digested with DNase, reverse transcribed into cDNA and amplified with an Access RT-PCR system kit (Promega). Primer sequences for detection of angiotensinogen, AngII receptor1a, AngII receptor1b, TNF-α, IL-6,

Table 1 Primer sequences for RT-PCR

Gene name	Primer sequence
Angiotensinogen	F: 5′-CAC GGA CAG CAC CCT ATT TT-3′
	R: 5′-GCT GTT GTC CAC CCA GAA CT-3′
TNF-α	F: 5′-GTC AGC CGA TTT TGC CAT TTC-3′
	R: 5′-AAC GAT GAA CAC GCC AGT-3′
IL-6	F: 5′-CCC AAC TTC CAA TGC TCT CCT AAT G-3′
	R: 5′-GCA CAC TAG GTT TGC CGA GTA GAC C-3′
IL-10	F: 5′-GGC TCA GCA CTG CTA TGT TGC C-3′
	R: 5′-AGC ATG TGG GTC TGG CTG ACT G-3′
rpL32	F: 5′-TAA GCG AAA CTG GCG GAA AC-3′
	R: 5′-GCT CGT CTT TCT ACG ATG GCT T-3′
AngII receptor type 1a	F: 5′-CTC AAG CCT GTC TAC GAA AAT GAG-3′
	R: 5′-TAG ATC CTG AGG CAG GGT GGA T-3′
AngII receptor type 1b	F: 5′-CTT TCC TAC CGC CCT TCA GAT A-3′
	R: 5′-TGA GTG CTT TCT CTG CTT CAA C-3′

F Forward primer, *R* reverse primer

IL-10 and ribosomal protein L32 (rpL32) mRNA can be found in Table 1. In view of the fact that high levels of pro-inflammatory mediators have been linked to obesity and CLA is considered effective against obesity [24], we also examined the anti-inflammatory mediator IL-10. cDNA products were run on an agarose gel, visualized with Vista Green Nucleic Acid Stain and relative intensity of the bands was quantified by densitometry. Results are expressed as arbitrary units after normalization to rpL32 expression.

Protein Extraction and Western Blotting

The bicinchoninic acid assay (Pierce) was used to determine total protein in samples isolated from adipose tissue using a mortar and pestle and 3× sodium dodecyl sulfate sample buffer. Adipose samples (15 μg protein) were analyzed by Western blotting as described previously [25] with antibodies (diluted 1:1,000) for angiotensinogen (Fitzgerald), AngII receptor 2 (Santa Cruz), TNF-α (Cell Signaling), IL-6 (Biosource), IL-10 (Biosource), NF-κB (Cell Signaling), F4/80 (Abcam) and total mitogen-activated protein kinase (MAPK) (Cell Signaling). The latter was used to account for possible variability in sample loading. Autoradiography and scanning densitometry with Quantity One image analysis software (BioRad) were used to capture and quantify band intensities.

NF-κB Activation

Nuclear extracts from epididymal adipose tissue samples were prepared using a Nuclear Extract Kit according to manufacturer's instructions (Active Motif). NF-κB binding activity was determined using a TransAM NF-κB Transcription Factor ELISA Kit according to manufacturer's instructions (Active Motif).

Statistical Analysis

Data were analyzed with Statistical Analysis Software (SAS 6.04; SAS Institute, Cary, NC, USA) to examine the effect of diet on cell size, mRNA and protein levels by a one-way analysis of variance (ANOVA) followed by Duncan's multiple range test. Differences were considered significant at $P < 0.05$ and all results are expressed as means ± standard error (SEM).

Results

Growth Performance and Feed Intake

There were no significant differences in body weight gained (control 433 ± 10 g; c9,t11-CLA 452 ± 9 g; t10,c12-CLA 453 ± 8 g) or epididymal adipose mass (data not shown) among groups. Likewise, daily food intake was similar among groups (control 27.2 ± 0.5 g/day; c9,t11-CLA 28.8 ± 0.6 g/day; t10,c12-CLA 28.9 ± 0.4 g/day).

Adipocyte Size

Previously we reported that a mixture of CLA isomers reduced adipocyte size [14], however, the contribution of the individual CLA isomers was not investigated. Therefore, the current study was designed to examine the effect of individual CLA isomers on adipocyte size. The group receiving the t10,c12-CLA isomer had 60% smaller adipocytes compared to the control and c9,t11-CLA groups (Fig. 1a, b). The distribution pattern of cell size shows that 80% of adipocytes in the t10,c12-CLA isomer group were <2,000 μm^2, with less than 2% of cells >5,000 μm^2, whereas the control group and the c9,t11-CLA group had a

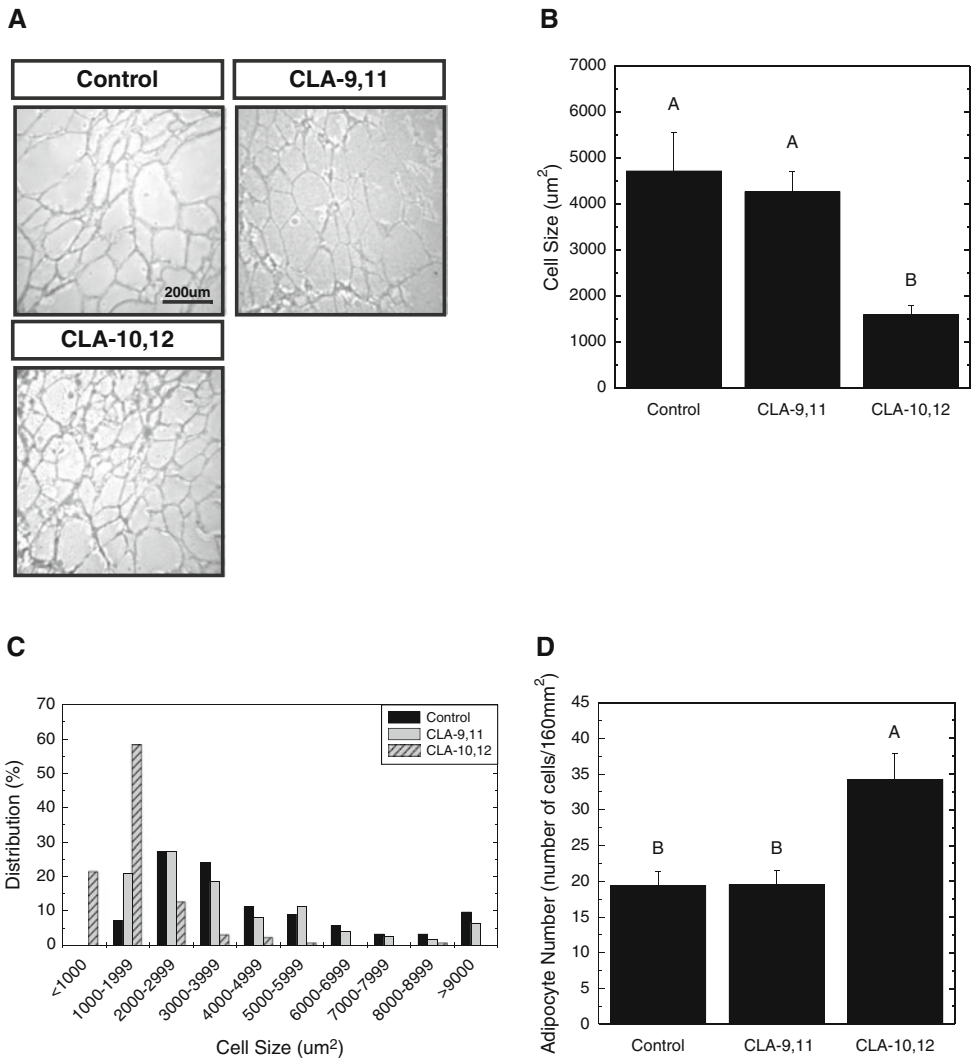

Fig. 1 Morphometry of epididymal adipose tissue from *fa/fa* Zucker rats fed CLA isomers for 8 weeks (n = 5/group). Adipocyte size (**a**) was quantified for each treatment group and cell size (**b**) is reported in μm^2 for the overall mean ± SEM. The distribution of adipocyte size (**c**) in each treatment group is also shown. Number of adipocytes (**d**) for each treatment group is reported as overall mean number of cells ± SEM per 160 mm^2. Means with different letters are significantly different ($P \leq 0.05$) as determined by Duncan's multiple range test. Control, *fa/fa* Zucker rats fed 0% CLA; CLA-9,11, *fa/fa* Zucker rats fed 0.4% c9,t11-CLA; CLA-10,12, *fa/fa* Zucker rats fed 0.4% t10,c12-CLA

53–63% of cells in the 2,000–5,000 μm^2 range and more than 25% of the cells were in excess of 5,000 μm^2 (Fig. 3c). The group receiving the t10,c12-CLA isomer also had 43% more adipocytes compared to the control and c9,t11-CLA groups (Fig. 1d).

Adipokines in Adipose Tissue

It is suggested that adipocyte size alters the production of adipokines [3–5] and because the t10,c12-CLA isomer reduced adipocyte size we decided to explore the adipokine status in the adipose tissue. Unexpectedly, the AngII precursor angiotensinogen was not changed at the gene (Fig. 2a) or protein level (Fig. 3a) in the adipose tissue of the rats fed CLA isomers. There was also no change in AngII receptors (Figs. 2e, f, 3b). Similarly, TNF-α, IL-6 and IL-10 mRNA were unchanged with CLA isomers (Fig. 2b–d). Likewise, protein levels of TNF-α, IL-6 and IL-10 were similar among all groups (Fig. 3c–e). Because macrophage infiltration occurs in obesity and contributes to the pro-inflammatory state of adipose tissue [5], the macrophage marker F4/80 was examined. None of the diets influenced the levels of macrophages within the adipose tissue (Fig. 4a).

NF-κB Activation

Given that NF-κB regulates many genes involved in inflammation [11], we next examined the levels of phosphorylated NF-κB and its promoter binding activity in epididymal adipose tissue. Neither CLA isomer affected either NF-κB phosphorylation (Fig. 4b) or DNA binding (Fig. 4c).

Discussion

The current study has demonstrated that feeding t10,c12-CLA to obese *fa/fa* Zucker rats reduces epididymal adipocyte size and increases cell number. The effect of CLA

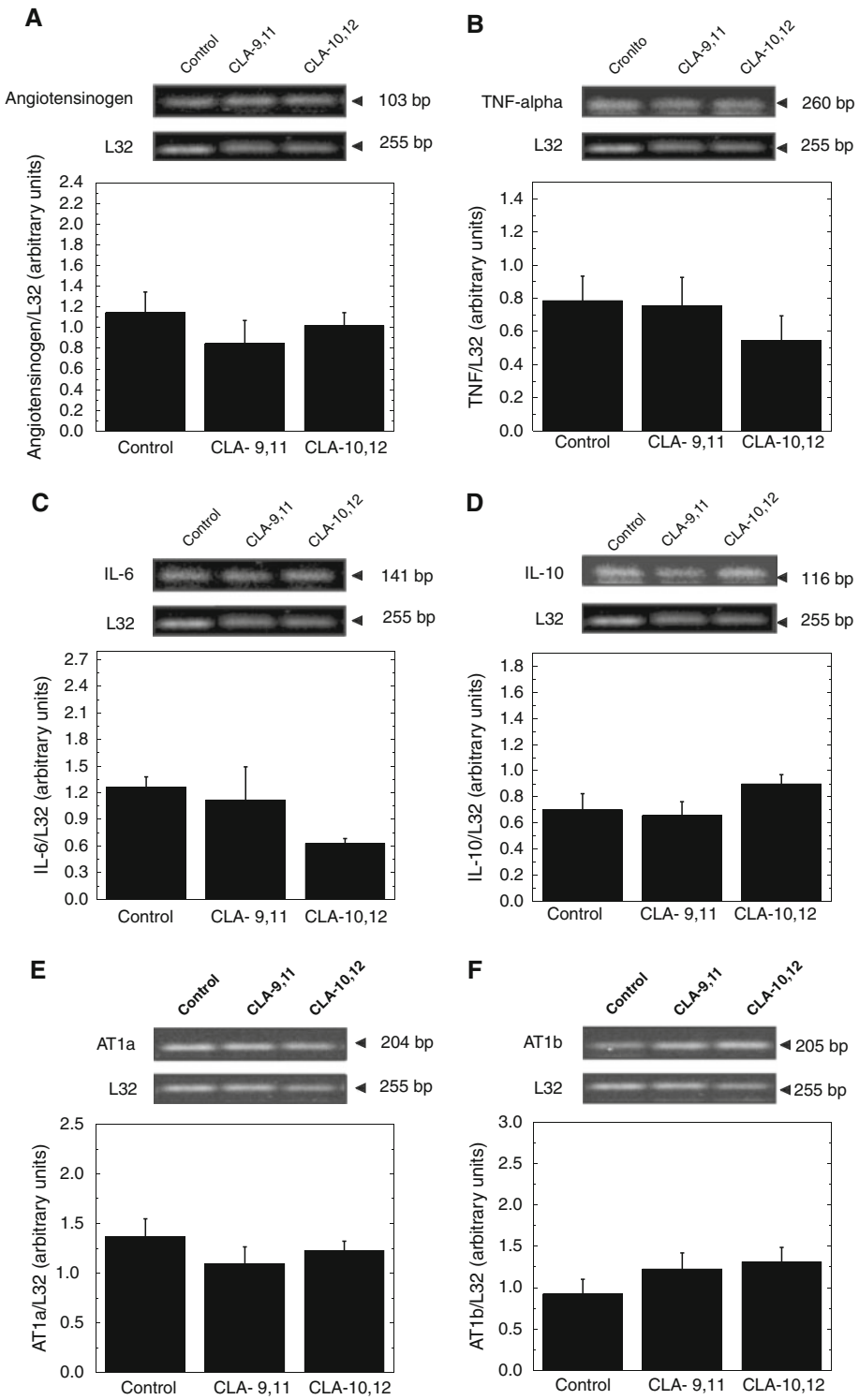

Fig. 2 Epididymal adipose tissue mRNA levels of angiotensinogen (**a**), TNF-α (**b**), IL-6 (**c**), IL-10 (**d**), AT1a (**e**) and AT1b (**f**) in *fa/fa* Zucker rats ($n = 6$/group). mRNA was analyzed using RT-PCR. The relative intensity of the bands was quantified by densitometry and normalized to that of ribosomal protein L32. Representative gels are shown for each plot. Data are presented as means ± SEM. No significant differences ($P > 0.05$) were detected by ANOVA. Control, *fa/fa* Zucker rats fed 0% CLA; CLA-9,11, *fa/fa* Zucker rats fed 0.4% c9,t11-CLA; CLA-10,12, *fa/fa* Zucker rats fed 0.4% t10,c12-CLA; AT1a, AngII receptor type 1a; AT1b, AngII receptor type 1b; L32, ribosomal protein L32; bp, base pair

on adipocyte size in rats has previously been examined with either a mixture of CLA isomers [14, 26] or single isomers in a non-obese model [27]. Earlier work examining the effects of CLA mixtures on adipocyte size revealed that other types of fat in the diet may influence the effects of CLA [14, 26, 27]. For example, rats consuming diets based on a soybean oil background and supplemented with a mixture of CLA isomers have reduced cell size [14, 26], whereas the effects of CLA are lost when the background consists of saturated palm oil [27]. In the same study that used palm oil, isomer specific effects were also examined and the c9,t11-CLA isomer increased adipocyte size and

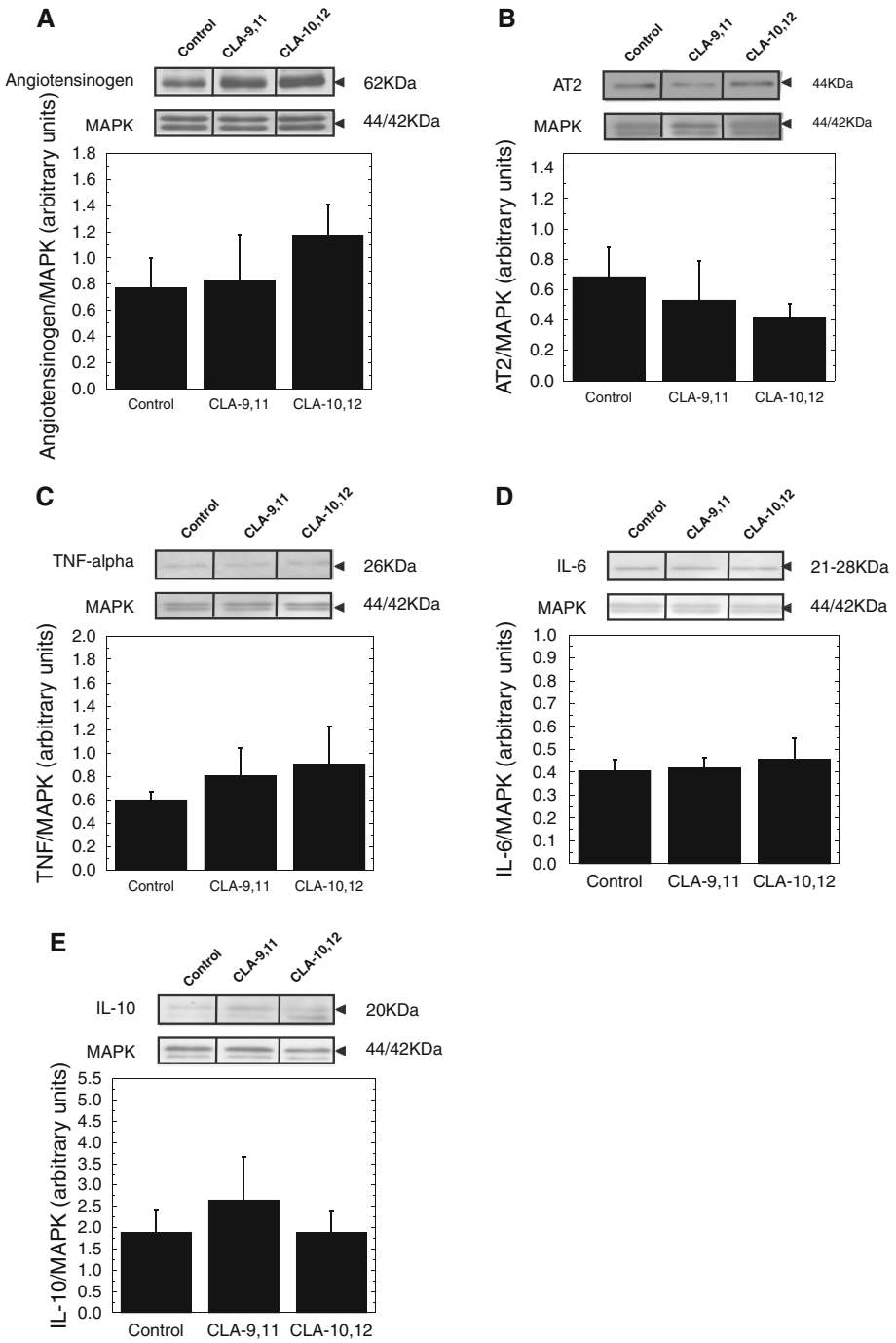

Fig. 3 Epididymal adipose tissue protein levels of angiotensinogen (**a**), AngII receptor type 2 (**b**), TNF-α (**c**), IL-6 (**d**) and IL-10 (**e**) in *fa/fa* Zucker rats ($n = 4$–6/group). Protein levels were measured using Western blot analysis. The relative intensity of the protein bands was quantified by densitometry and normalized to that of MAPK. Representative Western blots are shown for each plot. Data are presented as means ± SEM. No significant differences ($P > 0.05$) were detected by ANOVA. Control, *fa/fa* Zucker rats fed 0% CLA; CLA-9,11, *fa/fa* Zucker rats fed 0.4% c9,t11-CLA; CLA-10,12, *fa/fa* Zucker rats fed 0.4% t10,c12-CLA; AT2, AngII receptor type 2

consequently decreased the number of adipocytes per unit of area in the inguinal and retroperitoneal depots of Wistar rats [27]. The increase observed with the c9,t11-CLA isomer was abolished when a mixture of CLA isomers was provided [27], suggesting t10,c12-CLA may have beneficial effects for reducing cell size. Lopes et al [27] also showed rats receiving the t10c12-CLA isomer had significantly more adipocytes per unit area compared to the group receiving the c9,t11-CLA isomer. In agreement with this hypothesis, our study demonstrated that the t10,c12-CLA isomer is responsible for reducing cell size and increasing adipocyte number. Additionally, because earlier work in *fa/fa* Zucker rats fed a mixture of CLA isomers demonstrated that reduced adipocyte size was associated with altered adipokines, we wanted to test if the beneficial changes in adipocytes size observed with the t10,c12-CLA isomer also produce changes in local adipose RAS and cellular adipokine status.

Evidence suggests that obesity-related complications may be due in part to the activation of a local RAS in

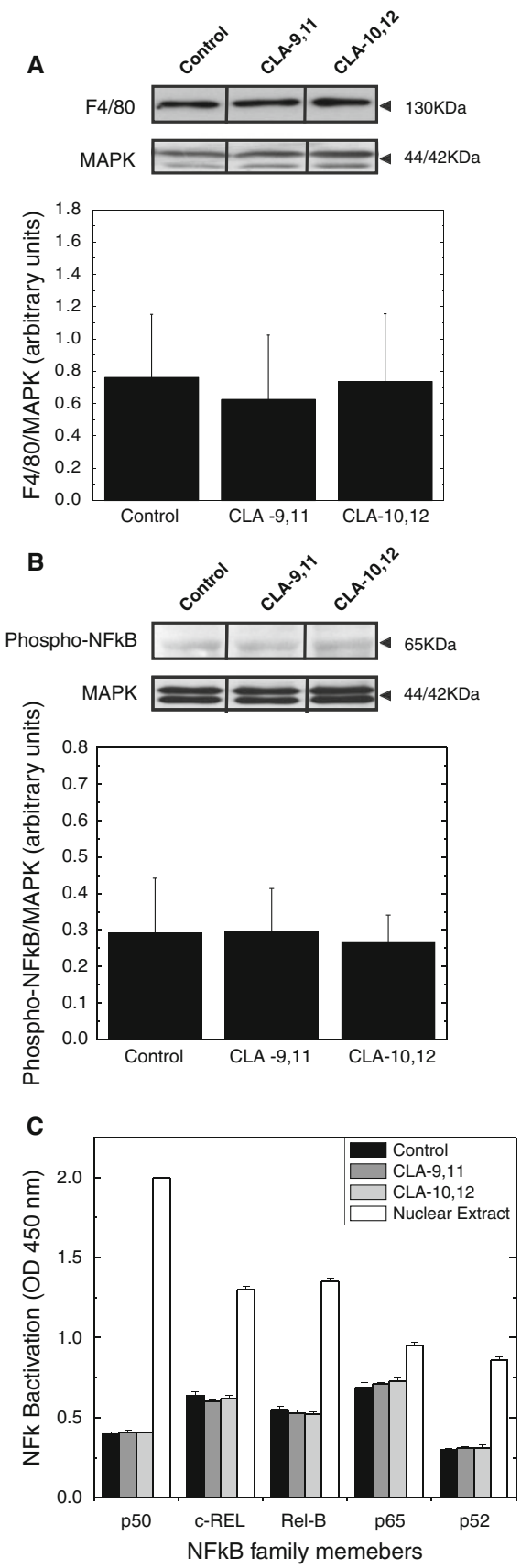

◀ **Fig. 4** Epididymal adipose tissue F4/80 (**a**), phosphorylated NF-κB levels (**b**) and NF-κB binding activity (**c**) in *fa/fa* Zucker rats ($n = 6$/group). Protein levels were measured using Western blot analysis. Relative intensity of the protein bands was quantified by densitometry and normalized to that of MAPK. A representative Western blot is shown. Activation of NF-κB was measured with TransAM ELISA kits (Active Motif). Data are presented as means ± SEM. No significant differences ($P > 0.05$) were detected by ANOVA. Control, *fa/fa* Zucker rats fed 0% CLA; CLA-9,11, *fa/fa* Zucker rats fed 0.4% c9,t11-CLA; CLA-10,12, *fa/fa* Zucker rats fed 0.4% t10,c12-CLA; nuclear extract, positive control

adipose tissue [9, 28, 29], however, in the current study, no significant differences were detected in adipose angiotensinogen levels or AngII receptors of CLA fed rats. To our knowledge this is the first report describing the effect of CLA isomers on AngII receptors. In contrast, previous work showed OLETF rats fed the t10,c12-CLA isomer had suppressed angiotensinogen gene expression in peri-renal adipose tissue [16]. Furthermore, Hainault et al. [30] showed angiotensinogen levels were greater in inguinal adipocytes isolated from obese compared to lean Zucker rats. Perhaps assessment of angiotensinogen mRNA or protein levels in different adipose depots or different models may be responsible for the varying results. Epididymal adipose tissue was investigated in this study because alterations in adipokine levels in epididymal adipose tissue have been noted in this animal model [14]. We measured angiotensinogen protein levels in epididymal adipose tissue as well as peri-renal adipose tissue (data not shown), however, we were unable to detect any dietary effects on angiotensinogen levels in either depot. Additionally, it may be that a reduction in fat mass is required in rats to achieve changes in angiotensinogen mRNA [31, 32].

Despite observing changes in adipocyte size, we did not note any changes in adipokine status or macrophage inflammation in the epididymal adipose tissue. However, it is still possible that the inflammatory mediators produced in liver, spleen, or other tissues could affect changes observed with CLA supplementation. Gollisch et al. [33] examined exercise as a means to reduce cell size and inflammatory cytokines in Sprague Dawley rats, however, results showed that maintenance of a small adipocyte size by exercise did not alter IL-6 or TNF-α mRNA compared to sedentary rats with increased adipocyte size. Thus, lifestyle interventions aimed at altering adipocyte size to improve inflammatory adipokine status of rats require more investigation before conclusions can be drawn. In contrast, studies in mice and isolated human adipocytes have clearly demonstrated that the t10,c12-CLA isomer increases mRNA levels of IL-6 and TNF-α in adipose tissue [17, 34]. Unlike the rat model used in the current study, mice

(irrespective of their metabolic state) also display increased macrophage infiltration when given t10,c12-CLA or a mixture of CLA isomers [17, 35–37]. This study thus adds to the literature that has demonstrated differences in the inflammatory response between mice and rats when given the t10,c12-CLA isomer.

Previous work using cell culture models suggests that CLA isomers may be able to modulate NF-κB activity [18, 38, 39], thus to our knowledge this is the first study to examine phosphorylation and binding activity of NF-κB in adipose tissue after dietary intervention. Our results in obese rats show no effect of either CLA isomer on NF-κB phosphorylation or binding activity, however, these results were not unexpected given that levels of the inflammatory adipokines examined were unchanged by the treatments. In contrast to the current study, isolated human adipocytes treated directly with t10,c12-CLA isomer have increased TNF-α and IL-6 mRNA and this was associated with an increase in IκBα phosphorylation and NF-κB binding activity [18]. Likewise, increased NF-κB binding activity was demonstrated in human umbilical vein endothelial cells treated with either the c9,t11-CLA or t10,c12-CLA isomer [38]. In a mouse macrophage cell line (RAW264.7), however, a mixture of CLA isomers reduced phosphorylated IκBα and NF-κB binding activity [39]. Additionally, a significant increase in NF-κB activity is observed in murine myotubes treated with t10,c12-CLA isomer but not murine myoblasts [40]. Thus, it appears that differing results occur not only between obese rat and mouse models but also different cell types, emphasizing the need for more research in this area. Future work is necessary to determine cell and species-specific effects of CLA isomers, as well as determine if therapeutic strategies that reduce adipocyte size can directly alter adipokine production and secretion.

In conclusion, this study demonstrates that t10,c12-CLA is the isomer responsible for the reduction in adipocyte size that was observed in an earlier study using a mixture of CLA isomers in *fa/fa* Zucker rats [14]. The reduction in adipocyte size, however, did not alter components the local adipose RAS such as angiotensinogen and AngII receptors, or associated adipokines such as TNF-α, IL-6 and IL-10. Furthermore, CLA isomers have no influence on macrophage infiltration or NF-κB activity in the adipose tissue of obese Zucker rats. Therefore, further work is needed to determine if there are any functional changes in the adipocyte as a result of reduced cell size via t10,c12-CLA isomer treatment.

Acknowledgments We would like to thank Danielle Stringer and Lisa Rigaux for help with the animal care and the contribution of the St. Boniface Hospital and Research Foundation towards infrastructure support. Financial support for this study was provided by grants from Dairy Farmers of Canada (C.T. and P.Z.) and Canada-Manitoba Agri-Food Research and Development Initiative (C.T. and P.Z.), and a Natural Sciences and Engineering Research Council of Canada as postgraduate scholarship (V.D.).

Conflict of interest None.

References

1. Ahima RS (2006) Adipose tissue as an endocrine organ. Obesity (Silver Spring) 14(Suppl 5):242S–249S
2. Athyros VG, Tziomalos K, Karagiannis A, Anagnostis P, Mikhailidis DP (2010) Should adipokines be considered in the choice of the treatment of obesity-related health problems? Curr Drug Targets 11:122–135
3. Jo J, Gavrilova O, Pack S, Jou W, Mullen S, Sumner AE, Cushman SW, Periwal V (2009) Hypertrophy and/or hyperplasia: dynamics of adipose tissue growth. PLoS Comput Biol 5:e1000324
4. Skurk T, Alberti-Huber C, Herder C, Hauner H (2007) Relationship between adipocyte size and adipokine expression and secretion. J Clin Endocrinol Metab 92:1023–1033
5. Weisberg SP, McCann D, Desai M, Rosenbaum M, Leibel RL, Ferrante AW Jr (2003) Obesity is associated with macrophage accumulation in adipose tissue. J Clin Invest 112:1796–1808
6. Inadera H (2008) The usefulness of circulating adipokine levels for the assessment of obesity-related health problems. Int J Med Sci 5:248–262
7. Berg AH, Scherer PE (2005) Adipose tissue, inflammation, and cardiovascular disease. Circ Res 96:939–949
8. Matsuzawa Y (2005) White adipose tissue and cardiovascular disease. Best Pract Res Clin Endocrinol Metab 19:637–647
9. Massiera F, Bloch-Faure M, Ceiler D, Murakami K, Fukamizu A, Gasc JM, Quignard-Boulange A, Negrel R, Ailhaud G, Seydoux J, Meneton P, Teboul M (2001) Adipose angiotensinogen is involved in adipose tissue growth and blood pressure regulation. FASEB J 15:2727–2729
10. Kouyama R, Suganami T, Nishida J, Tanaka M, Toyoda T, Kiso M, Chiwata T, Miyamoto Y, Yoshimasa Y, Fukamizu A, Horiuchi M, Hirata Y, Ogawa Y (2005) Attenuation of diet-induced weight gain and adiposity through increased energy expenditure in mice lacking angiotensin II type 1a receptor. Endocrinology 146:3481–3489
11. Sanz-Rosa D, Oubina MP, Cediel E, de Las Heras N, Vegazo O, Jimenez J, Lahera V, Cachofeiro V (2005) Effect of AT1 receptor antagonism on vascular and circulating inflammatory mediators in SHR: role of NF-kappaB/IkappaB system. Am J Physiol Heart Circ Physiol 288:H111–H115
12. Rodriguez-Iturbe B, Sindhu RK, Quiroz Y, Vaziri ND (2005) Chronic exposure to low doses of lead results in renal infiltration of immune cells, NF-kappaB activation, and overexpression of tubulointerstitial angiotensin II. Antioxid Redox Signal 7:1269–1274
13. Benjamin S, Spener F (2009) Conjugated linoleic acids as functional food: an insight into their health benefits. Nutr Metab (Lond) 6:36
14. Noto A, Zahradka P, Yurkova N, Xie X, Truong H, Nitschmann E, Ogborn MR, Taylor CG (2007) Dietary conjugated linoleic acid decreases adipocyte size and favorably modifies adipokine status and insulin sensitivity in obese, insulin-resistant rats. Metabolism 56:1601–1611

15. Martins SV, Lopes PA, Alfaia CM, Rodrigues PO, Alves SP, Pinto RM, Castro MF, Bessa RJ, Prates JA (2010) Serum adipokine profile and fatty acid composition of adipose tissues are affected by conjugated linoleic acid and saturated fat diets in obese Zucker rats. Br J Nutr 103:869–878
16. Nagao K, Inoue N, Wang YM, Hirata J, Shimada Y, Nagao T, Matsui T, Yanagita T (2003) The 10*trans*, 12*cis* isomer of conjugated linoleic acid suppresses the development of hypertension in Otsuka Long-Evans Tokushima fatty rats. Biochem Biophys Res Commun 306:134–138
17. Poirier H, Shapiro JS, Kim RJ, Lazar MA (2006) Nutritional supplementation with *trans*-10, *cis*-12-conjugated linoleic acid induces inflammation of white adipose tissue. Diabetes 55:1634–1641
18. Chung S, Brown JM, Provo JN, Hopkins R, McIntosh MK (2005) Conjugated linoleic acid promotes human adipocyte insulin resistance through NFkappaB-dependent cytokine production. J Biol Chem 280:38445–38456
19. Cameron AJ, Dunstan DW, Owen N, Zimmet PZ, Barr EL, Tonkin AM, Magliano DJ, Murray SG, Welborn TA, Shaw JE (2009) Health and mortality consequences of abdominal obesity: evidence from the AusDiab study. Med J Aust 191:202–208
20. Despres JP, Arsenault BJ, Cote M, Cartier A, Lemieu I (2008) Abdominal obesity: the cholesterol of the 21st century? Can J Cardiol 24(Suppl D):7D–12D
21. Ruth MR, Taylor CG, Zahradka P, Field CJ (2008) Abnormal immune responses in *fa/fa* Zucker rats and effects of feeding conjugated linoleic acid. Obesity (Silver Spring) 16:1770–1779
22. Canadian Council on Animal Care (CCAC) (1993) Guide to the care and use of experimental animals. http://www.ccac.ca/en/CCAC_Programs/Guidelines_Policies/GUIDES/ENGLISH/toc_v1.htm. Accessed 07/22 2009
23. Sturges HA (1926) The choice of a class interval. J Am Stat Assoc 21:65–66
24. Benjamin S, Spener F (2009) Conjugated linoleic acids as functional food: an insight into their health benefits. Nutr Metab (Lond) 6:36
25. Yau L, Elliot T, Lalonde C, Zahradka P (1998) Repression of phosphoenolpyruvate carboxykinase gene activity by insulin is blocked by 3-aminobenzamide but not by PD128763, a selective inhibitor of poly(ADP-ribose) polymerase. Eur J Biochem 253:91–100
26. Azain MJ, Hausman DB, Sisk MB, Flatt WP, Jewell DE (2000) Dietary conjugated linoleic acid reduces rat adipose tissue cell size rather than cell number. J Nutr 130:1548–1554
27. Lopes PA, Martins SV, Pinho MS, Alfaia CM, Fontes CM, Rodrigues PO, Morais GS, Castro MF, Pinto R, Prates JA (2008) Diet supplementation with the *cis*-9, *trans*-11 conjugated linoleic acid isomer affects the size of adipocytes in Wistar rats. Nutr Res 28:480–486
28. Engeli S, Negrel R, Sharma AM (2000) Physiology and pathophysiology of the adipose tissue renin–angiotensin system. Hypertension 35:1270–1277
29. Boustany CM, Bharadwaj K, Daugherty A, Brown DR, Randall DC, Cassis LA (2004) Activation of the systemic and adipose renin–angiotensin system in rats with diet-induced obesity and hypertension. Am J Physiol Regul Integr Comp Physiol 287: R943–R949
30. Hainault I, Nebout G, Turban S, Ardouin B, Ferre P, Quignard-Boulange A (2002) Adipose tissue-specific increase in angiotensinogen expression and secretion in the obese (*fa/fa*) Zucker rat. Am J Physiol Endocrinol Metab 282:E59–E66
31. Engeli S, Bohnke J, Gorzelniak K, Janke J, Schling P, Bader M, Luft FC, Sharma AM (2005) Weight loss and the renin–angiotensin–aldosterone system. Hypertension 45:356–362
32. Nagao K, Inoue N, Wang YM, Hirata J, Shimada Y, Nagao T, Matsui T, Yanagita T (2003) The 10*trans*, 12*cis* isomer of conjugated linoleic acid suppresses the development of hypertension in Otsuka Long-Evans Tokushima fatty rats. Biochem Biophys Res Commun 306:134–138
33. Gollisch KS, Brandauer J, Jessen N, Toyoda T, Nayer A, Hirshman MF, Goodyear LJ (2009) Effects of exercise training on subcutaneous and visceral adipose tissue in normal- and high-fat diet-fed rats. Am J Physiol Endocrinol Metab 297:E495–E504
34. Martinez K, Kennedy A, West T, Milatovic D, Aschner M, McIntosh M (2010) *trans*-10, *cis*-12-Conjugated linoleic acid instigates inflammation in human adipocytes compared with preadipocytes. J Biol Chem 285:17701–17712
35. Wendel AA, Purushotham A, Liu LF, Belury MA (2008) Conjugated linoleic acid fails to worsen insulin resistance but induces hepatic steatosis in the presence of leptin in ob/ob mice. J Lipid Res 49:98–106
36. LaRosa PC, Miner J, Xia Y, Zhou Y, Kachman S, Fromm ME (2006) *Trans*-10, *cis*-12 conjugated linoleic acid causes inflammation and delipidation of white adipose tissue in mice: a microarray and histological analysis. Physiol Genomics 27: 282–294
37. Liu LF, Purushotham A, Wendel AA, Belury MA (2007) Combined effects of rosiglitazone and conjugated linoleic acid on adiposity, insulin sensitivity, and hepatic steatosis in high-fat-fed mice. Am J Physiol Gastrointest Liver Physiol 292:G1671–G1682
38. Nakamura YK, Omaye ST (2009) Conjugated linoleic acid isomers' roles in the regulation of PPAR-gamma and NF-kappaB DNA binding and subsequent expression of antioxidant enzymes in human umbilical vein endothelial cells. Nutrition 25:800–811
39. Cheng WL, Lii CK, Chen HW, Lin TH, Liu KL (2004) Contribution of conjugated linoleic acid to the suppression of inflammatory responses through the regulation of the NF-kappaB pathway. J Agric Food Chem 52:71–78
40. Hommelberg PP, Plat J, Remels AH, van Essen AL, Kelders MC, Mensink RP, Schols AM, Langen RC (2010) *Trans*-10, *cis*-12 conjugated linoleic acid inhibits skeletal muscle differentiation and GLUT4 expression independently from NF-kappaB activation. Mol Nutr Food Res

morphologic alterations, including impaired body-weight gain, changes in body composition, hepatic steatosis and lipid changes, both in animals and humans [1]. In order to reverse the negative consequences of protein depletion, it is important to supply an adequate equilibrium of nutrients. In this regard, Kern et al. [2] have recently reported that it is not recommended to provide a high protein diet, and that the type and amount of dietary fat might play an important role in the nutritional intervention to overcome the protein deficit stage.

Conjugated linoleic acid is a group of positionally and geometrically conjugated dienoic isomers of linoleic acid produced by the biological and/or industrial hydrogenation/isomerization of fatty acids (FA) [3]. In natural fats, *c*9,*t*11-CLA is the main CLA isomer, while synthetic products commercially available for human consumption are composed of an equimolecular mixture of *c*9,*t*11-CLA and *t*10,*c*12-CLA as main sources of FA isomers. *c*9,*t*11-CLA has called the attention of many researchers for its anti-carcinogenic properties [4] and today there is evidence of the beneficial and detrimental effects of both isomers on humans and experimental animals [5–7]. Although it is well known that the effects of the individual isomers are different, most clinical studies were carried out with different commercial mixtures containing predominantly *c*9,*t*11-CLA and *t*10,*c*12-CLA [8]. Considering that the FDA has recently approved CLA as a 'Generally Recognized as Safe' (GRAS) category [9] (http://www.fda.gov/Food/FoodIngredientsPackaging/GenerallyRecognizedasSafeGRAS/GRASListings/ucm153908.htm), a measure that will foster the commercial production of food and beverages with CLA supplementation, we believe that the study of its functional properties is relevant. In terms of functional impact, these FA have displayed several bioactive properties such as decrease of body fat, increase of lean body mass and protection against muscle catabolism induced by endotoxins [10], mainly in animal models. In well-nourished animals, CLA can be incorporated into tissues [11] and metabolized [12]. By means of different biochemical mechanisms, CLA modulates the concentration of triacylglycerol (TAG) in liver, adipose tissue and plasma [13], regulates the oxidative status [14], affects some enzyme activities [15] and changes the hormonal and mediators milieu [16] in different species.

Many of the effects attributed to CLA, such as increase in lean body mass and regulation of lipid metabolism, suggest that CLA could play an important role in the recovery of the catabolic status, as reported in animals injected with lipopolysaccharide [17]. We have reported elsewhere [18] the potential beneficial effect of CLA on the recovery of protein malnutrition. Another factor benefitting recovery after protein depletion could be the intake of high-energy-density diets [1] by increasing the amount of dietary fat. In this sense, previous work from our laboratory [18] demonstrated that the intake of a commercially available CLA oil showed preventive effects on liver and adipose tissue lipid accumulation when administered in protein repletion diets with high (20%, w/w) fat content, although no effects were observed on nitrogen retention. Given these findings, the first aim of the present study was to investigate the effect of CLA oil at two different amounts of dietary fat on parameters related to TAG regulation in rats during protein repletion, specifically hepatic TAG secretion and circulating TAG removal. As these changes could be related to alterations in the FA profile of plasma and different tissues, the second objective of this study was to assess the incorporation of CLA and the potential alterations on FA composition in plasma, liver and epididymal white adipose tissue (EWAT) of protein repleted rats. On the other hand, it has been suggested that protein depletion could lead to an increase in oxidative damage by diminishing antioxidant defenses [19]. Free radicals have been implicated in the development of several nutritional and metabolic diseases such as dyslipidemia and obesity [20], and hepatic steatosis has also been related to the onset of liver lipid peroxidation [21]. Since polyunsaturated FA and CLA intake has been previously reported to influence the oxidative status [14, 20], the modifications of lipid profile and/or FA metabolism could impact on liver lipid peroxidation. Therefore, our third aim was to investigate the effect of CLA on the liver oxidative status in rats fed CLA at two different amounts of dietary fat in protein repletion.

Materials and Methods

Materials

Most nutrient compounds, including vitamins and minerals for diet preparations were chemical grade or better, with the exception of corn oil (Mazola, Argentina), sucrose, cellulose, and corn starch which were obtained from local sources. CLA rich oil was kindly provided by Lipid Nutrition B.V. (Wormerveer, The Netherlands). Standards, biochemical reagents and enzymes were obtained from Sigma Chemical Co. (St. Louis, MO, USA). ^{3}H-Triolein was acquired from Perkin Elmer (Boston, USA). The plasma TAG kit was purchased from Wiener Co. (Rosario, Argentina). All solvents and reagents used for the FA quantification were of chromatography grade and all the other chemicals used were at least ACS purity.

Preparation of Diets

The composition of diets is shown in Table 1 and was based on the American Institute of Nutrition Ad Hoc

Table 1 Composition of the experimental diets (g/kg diet)

Ingredient	LP	C	C + CLA	HF	HF + CLA
Corn starch	679.5	529.5	529.5	399.5	399.5
Casein	50	200	200	200	200
Sucrose	100	100	100	100	100
Corn oil	70	70	–	200	–
Oil mixture[a]	–	–	70	–	200
Fibre	50	50	50	50	50
Mineral mixture[b]	35	35	35	35	35
Vitamin mixture[b]	10	10	10	10	10
L-Cystine + L-methionine	3.0	3.0	3.0	3.0	3.0
Choline	2.5	2.5	2.5	2.5	2.5

LP Low protein, *C* control, *C + CLA* C supplemented with CLA, *HF* high fat diet, *HF + CLA* HF supplemented with CLA

[a] Oil mixture contained 85% of corn oil and 15% of CLA rich oil

[b] Vitamin and mineral mixtures were formulated according to Reeves [22]

Table 2 Fatty acid composition of dietary oils

Fatty acids	Corn oil	Oil mixture
14:0	0.05	0.04
16:0	12.29	11.23
16:1	0.11	0.09
17:0	0.07	0.06
18:0	1.90	1.96
18:1	30.39	27.67
18:1n-7	1.15	1.12
18:2n-6	52.34	44.72
*c*9,*t*12-18:2	0.06	0.11
*t*9,*c*12-18:2	0.04	0.03
*c*9,*t*11-CLA	ND	5.71
*c*11,*t*13-CLA	ND	0.14
*t*10,*c*12-CLA	ND	5.71
18:3n-3	0.96	0.82
20:0	0.45	0.43
20:1	0.20	0.17

Values are means as weight percentage (w/w) of the total fatty acid methyl esters

ND Not detected

Committee recommendation (AIN-93G) [22]. The control (C) diet (1656.9 KJ/100 g) contained 20% of casein as protein source and 7% of corn oil (20% of energy) as dietary fat source. The LP diet contained 5% of casein, isocalorically balancing the protein with carbohydrates. High energy diets were achieved by increasing 2.86-fold the total dietary fat content. Therefore, in the HF diet, 13% of oil replaced an identical amount of carbohydrates, obtaining a hypercaloric diet (1928.8 KJ/100 g and 38.5% of energy as fat). CLA was included in an "oil mixture", which contained 85% of corn oil and 15% of CLA rich oil. Thus, CLA represented 1% (w/w) in the C + CLA diet and 2.86% (w/w) in the HF + CLA diet, securing a constant ratio between CLA and the linoleic acid (18:2n-6) provided by corn oil, given the fact that the competition between CLA and this FA could affect the action of the former [11]. Corn oil was replaced by this "oil mixture" in both the C + CLA and HF + CLA diets. The CLA rich oil chosen for the present study is commercially available for human consumption, composed of an equimolecular mixture of *c*9,*t*11-CLA and *t*10,*c*12-CLA as main sources of isomeric FA. All diets exceeded the essential FA recommendations. The FA composition of corn oil and the "oil mixture" as methyl esters was determined by gas chromatography (GC) using the same procedure indicated below, as shown in Table 2. Each diet was freshly prepared every 3 days throughout the experimental period.

Animals and General Protocol

All the studies were conducted in agreement with the regulations of the School of Biochemistry, Guide to the Care and Use of Experimental Animals of Laboratory [23]. Experiments were carried out on male Wistar rats provided by the "Comisión Nacional de Energía Atómica" (Buenos Aires, Argentina) which were housed in the animal quarters. During the experimental period, they were kept under controlled conditions (23 ± 2°C and a 12-h light–dark cycle). For 2 weeks, the animals had free access to water and to the control (C) diet with recommended levels of nutrients [22], until they reached 100–110 g of body weight. A basal (B) group was formed with six of these animals. In order to obtain the basal values of some metabolic parameters, they were then weighed and sacrificed (9.00–11.00 a.m.) under anaesthesia (1 + 100 mg of azepromazine and ketamine/ kg b.w., respectively), to collect blood and dissected tissues according to the assay proposed or to perform the in vivo hepatic TAG secretion test. Blood samples were centrifuged at 4°C and plasma was immediately used or frozen and stored at −80 °C until analyzed. Liver, gastrocnemius muscle and EWAT were frozen, weighed and stored at −80°C until processed.

The rest of the animals were fed ad libitum an isocaloric low protein (LP) diet for 14 days. After this partial protein depletion period, six rats were weighed and killed following the procedure mentioned above, and the remaining animals were divided into four groups ($n = 6$) and fed ad libitum during a 30-day period with normal (20%, w/w) levels of casein, and 7% (w/w) or 20% (w/w) (high fat, HF) of dietary fat, supplemented or not with CLA; thus, the protein repletion dietary groups were identified C + CLA, C, HF + CLA and HF, respectively. At the end of the

protein repletion with the four recovery diets, all the animals were weighed and killed as previously mentioned.

Determination of Muscle Triacylglycerol Concentration

Portions of frozen muscle were powdered, homogenized in saline (10% w/v) and their TAG concentration was quantified by a spectrophotometric method [24].

Analysis of Lipoprotein Lipase Activities

Since skeletal muscle and adipose tissue are the main tissues involved in the removal of plasma TAG-rich lipoproteins by the lipoprotein lipase (LPL) enzyme, gastrocnemius muscle and EWAT were chosen to measure the LPL activities using ^{3}H-Triolein as a substrate, according to the technique described by Nilsson-Ehle and Schotz [25]. In the case of EWAT, the results were expressed as miliUnits (mU) per gram of EWAT (mU/g EWAT) and mU per whole pad of EWAT (mU/EWAT) (1 mU = 1 n-mol/min). In the gastrocnemius muscle, enzyme activity was expressed as mU/g gastrocnemius.

Estimation of In Vivo Hepatic Triacylglycerol Secretion

Another set of animals ($n = 36$) submitted to the same dietary treatments was fasted overnight and anaesthetized, as indicated above. 600 mg/kg of body weight of Triton WR 1339 in saline solution, an agent known to inhibit peripheral removal of TAG-rich lipoproteins, was injected i.v. [26]. Blood samples were taken immediately before and 120 min after the injection of Triton solution for the estimation of TAG accumulation in plasma. Since the weight of the animals was different between the experimental groups (especially between LP and C), the hepatic TAG secretion was calculated taking into account the TAG accumulation in plasma using the following formula:

$$\text{Hepatic TAG secretion}(\text{nmol}/\text{ml}/\text{min}) = [\text{TAG}_{120} - \text{TAG}_{0}]/120,$$

where TAG_0 and TAG_{120} were the plasma TAG concentration (nmol/ml) at 0 and 120 min after Triton WR 1339 administration and 120 was the experimental time in minutes.

Lipid Extraction and Fatty Acid Analysis

Total lipids were extracted from liver, EWAT and plasma samples collected at 0 and 120 min of the in vivo hepatic TAG secretion estimation test using the Bligh and Dyer [27] method. Extracted FA were methylated using sodium methoxide, and FA methyl esters (FAME) were analyzed by GC using a Shimadzu 2014 chromatograph equipped with a flame ionization detector. FAME were identified by comparison of their retention times relative to those of commercial standards (AccuStandard, New Haven, USA and Sigma, St. Louis, MO, USA). Another set of standards was provided by CYTED network 208RT0343. Chromatographic data processing was performed with GC Solutions software. All individual FA results were expressed as mol/100 mol of total FAME. FA with concentrations lower than 0.5 wt% were considered minor, and were not shown unless they were CLA isomers. FA composition of the lipids secreted by the liver was estimated considering plasma FA composition and lipid content at 0 and 120 min of the in vivo hepatic TAG secretion test.

Analysis of Liver Oxidative Stress Parameters

To quantify the liver lipid peroxidation (LPO), malondialdehyde was measured using the thiobarbituric acid method reported by Ohkawa et al. [28]. LPO was expressed as nmol malondialdehyde equivalents/g of liver.

Total liver glutathione (GSH) concentration, as the main non-protein sulfhydryl compound, was measured according to the method reported by Ellman et al. [29]. GSH concentration was expressed as μmol GSH/g of liver.

Catalase and glutathione peroxidase (GSH-Px) activities were assessed in liver by the method reported by Aebi [30] and Paglia and Valentine [31], respectively. CAT and GSH-Px activities were expressed as U (μmol/min)/mg protein. Protein concentrations in each fraction were determined by the method proposed by Lowry et al. [32].

Statistics

Values were expressed as the means ± standard errors of six animals per group. Statistical differences between the LP and B group mean, and between the C and LP group mean were established by unpaired Student's t test. The data to compare the effect of different diets during protein repletion was statistically analyzed by two-way ANOVA (2×2) using CLA supplementation and amount of dietary fat as independent variables. All post hoc multiple comparisons were made using Scheffe's critical range test. Significant differences were considered at $P < 0.05$.

Results

We found a significantly decreased hepatic TAG secretion in circulation (−26%) and a higher EWAT LPL activity (Table 3), which could be two of the biochemical mechanisms involved in the decrease of plasma TAG and the increase of hepatic TAG concentration previously observed

Table 3 Parameters related to TAG regulation

	B	LP	Protein repletion				ANOVA
			C	C + CLA	HF	HF + CLA	
Hepatic TAG secretion (nmol/ml/min)	49.89 ± 2.16	36.9 ± 2.70*	49.05 ± 2.01$^{\#,a}$	57.48 ± 2.99^{b}	37.86 ± 2.28^{c}	53.28 ± 2.67^{b}	Fat, CLA
LPL activities							
mU/g gastrocnemius	71.8 ± 4.8	43.6 ± 2.4*	49.7 ± 1.9	43.2 ± 3.1	52.1 ± 4.5	54.4 ± 4.2	NS
mU/g EWAT	407.2 ± 32.7	496.8 ± 25.0	171.1 ± 14.8$^{\#}$	205.0 ± 15.5	195.0 ± 23.3	210.9 ± 15.1	NS
mU/EWAT	160.0 ± 14.5	328.1 ± 13.3*	319.8 ± 34.7	354.6 ± 29.6	480.5 ± 39.7	465.2 ± 41.0	NS

Values are means ± standard errors of the mean ($n = 6$)

B Basal, *LP* low protein, *C* control, *C + CLA* C supplemented with CLA, *HF* high fat, *HF + CLA* HF supplemented with CLA, *TAG* triacylglycerol, *LPL* lipoprotein lipase, *mU/g EWAT* miliUnits per gram of epididymal white adipose tissue, *mU/EWAT* miliUnits per whole pad of epididymal white adipose tissue, *NS* not significant

*$P < 0.05$ versus B. $^{\#}P < 0.05$ versus LP. Different superscript letters indicate significant differences at $P < 0.05$ by Scheffe's test after ANOVA (2 × 2) between protein repletion groups

during protein depletion [18]. In addition, gastrocnemius LPL activity was decreased, matching with the significantly reduced TAG concentration (μmol/g; LP 3.33 ± 0.33 vs B 5.35 ± 0.51, $P < 0.05$).

Protein repletion with 7% (w/w) of dietary fat (C group) restored hepatic TAG secretion. EWAT LPL activity (mU/g EWAT) was decreased in this dietary group, but as the weight of this tissue was increased, its contribution to the circulating TAG removal (mU/EWAT) was not changed. In addition, LPL activity, as well as the TAG concentration in gastrocnemius muscle remained unchanged when compared to the LP diet (μmol/g; C 3.95 ± 0.69 vs LP 3.33 ± 0.33, not significant).

Conjugated linoleic acid at 7% (w/w) of dietary fat increased the hepatic TAG secretion 15% without affecting LPL activity in both EWAT and muscle. In addition, muscle TAG concentration remained unchanged by CLA (μmol/g; C + CLA 3.22 ± 0.33 vs C 3.95 ± 0.69, NS). However, protein repletion with HF diets strikingly decreased TAG secretion by the liver (−23% vs C group) (Table 3). This fact was related to the low plasma TAG concentration and to the lack of normalization of hepatic TAG concentration. In contrast, the HF diet did not induce changes in LPL activity in EWAT or in muscle. The HF diet in the presence and in the absence of CLA showed higher muscular TAG concentration (μmol/g; HF 5.23 ± 0.52 and HF + CLA 4.44 ± 0.47 vs C 3.95 ± 0.69 and C + CLA 3.22 ± 0.33, $P < 0.05$, respectively), related to a slight but not significant increase in muscular LPL activity (Table 3).

All these alterations in the lipid metabolism were accompanied by modifications in FA composition in plasma, liver and EWAT. In plasma (Table 4), protein depletion mainly raised the levels of 16:0, 16:1n-9, 18:1n-9, 22:4n-6 and 22:5n-6, while it decreased the level of 18:0 FA. Protein repletion with 7% (w/w) of dietary fat tended to normalize these changes, even though not completely. On the other hand, protein repletion with HF diets decreased the levels of 16:0 and more markedly that of 16:1n-9, as well as it increased the levels of 18:0 and 18:2n-6. Dietary CLA was significantly incorporated into plasma lipids in C + CLA and HF + CLA groups, not linked to the amount ingested. The levels of *t*10,*c*12-CLA were much smaller than those of *c*9,*t*11-CLA, although both isomers were equimolecularly present in both CLA containing diets. CLA incorporation was associated to decreased 16:0 levels.

The FA composition of the lipids secreted by the liver during the TAG secretion test was shown in Table 5. Protein depletion increased the levels of 16:0 and 18:1n-9 and reduced 18:0 and 20:4n-6. In protein repletion, most of the FA alterations induced by the LP diet were normalized. As observed in basal plasma, dietary CLA was incorporated into the TAG secreted by the liver, not linked to the amount ingested. It can be assumed that the lipids secreted by the liver were more affected by CLA than by the amount of dietary fat. Mainly, CLA supplementation reduced MUFA and increased the 18:0 of the lipids secreted by the liver. With respect to 18:2n-6, besides the increase exerted by HF, CLA intake decreased its level, and this led to its normalization in the HF + CLA group.

Liver FA composition (Table 6) showed that protein depletion reduced the levels of 20:4n-6, 22:5n-3 and 22:6n-3 PUFA. Protein repletion with 7% (w/w) of dietary fat did not reverse these alterations. On the other hand, protein repletion with HF diets markedly increased the 18:2n-6 level, and it also decreased the level of C16 FA. In the liver of CLA fed rats, both CLA isomers were incorporated; however, the level of *t*10,*c*12-CLA was lower than that of *c*9,*t*11-CLA. In addition, mainly *t*10,*c*12-CLA level was higher in liver than in plasma, increasing the *t*10,*c*12-CLA/*c*9,*t*11-CLA ratio. The SCD-1 indexes were calculated in

Table 4 Plasma FA composition (wt%) as methyl esters

	B	LP	Protein repletion				ANOVA
			C	C + CLA	HF	HF + CLA	
SFA							
16:0	22.73 ± 2.20	31.69 ± 1.58*	26.73 ± 0.46$^{\#,a}$	25.64 ± 0.27^{a,b}	24.06 ± 0.49^{b,c}	22.68 ± 0.48^{c}	Fat, CLA
18:0	19.76 ± 0.70	12.46 ± 0.12*	14.78 ± 0.03$^{\#,a}$	14.63 ± 0.35^{a}	16.47 ± 0.10^{b}	15.76 ± 0.66^{b}	Fat
MUFA							
16:1n-9	0.54 ± 0.02	1.29 ± 0.11*	0.87 ± 0.31^{a}	1.38 ± 0.07^{a}	0.26 ± 0.01^{b}	0.37 ± 0.08^{b}	Fat
18:1n-9	8.81 ± 0.65	14.83 ± 1.42*	12.55 ± 0.50	13.05 ± 0.43	11.49 ± 0.09	12.34 ± 0.91	NS
18:1n-7	1.25 ± 0.05	1.22 ± 0.12	1.48 ± 0.52	1.96 ± 0.02	1.20 ± 0.01	1.29 ± 0.04	NS
PUFA							
18:2n-6	21.71 ± 1.13	21.40 ± 2.39	19.61 ± 0.53^{a}	20.53 ± 0.08^{a}	22.14 ± 0.06^{b}	23.08 ± 0.36^{b}	Fat
*c*9,*t*11-CLA	ND	ND	ND^{a}	0.74 ± 0.03^{b}	ND^{a}	0.77 ± 0.10^{b}	CLA
*t*10,*c*12-CLA	ND	ND	ND^{a}	0.19 ± 0.02^{b}	ND^{a}	0.13 ± 0.04^{b}	CLA
20:4n-6	23.07 ± 4.28	15.10 ± 1.54	19.58 ± 1.30	16.25 ± 0.50	19.51 ± 0.69	19.45 ± 0.98	NS
22:4n-6	ND	0.45 ± 0.02*	0.25 ± 0.10^{a}	0.52 ± 0.05^{a,b}	0.63 ± 0.07^{b}	0.35 ± 0.05^{a,b}	CLA × fat
22:5n-6	ND	0.42 ± 0.24*	0.44 ± 0.19	0.79 ± 0.09	1.06 ± 0.25	0.69 ± 0.12	NS
22:6n-3	0.59 ± 0.42	0.61 ± 0.10	0.27 ± 0.10	0.51 ± 0.02	0.52 ± 0.04	0.53 ± 0.10	NS
Minor/unknown	1.54	0.55	3.42	3.80	2.66	2.56	

Values are means ± standard errors of the mean ($n = 6$)

B Basal, *LP* low protein, *C* control, *C + CLA* C supplemented with CLA, *HF* high fat, *HF + CLA* HF supplemented with CLA, *NS* not significant, *FA* fatty acid, *SFA* saturated FA, *MUFA* monounsaturated FA, *PUFA* polyunsaturated FA

*$P < 0.05$ versus B. $^{\#}P < 0.05$ versus LP. Different superscript letters indicate significant differences at $P < 0.05$ by Scheffe's test after ANOVA (2 × 2) between protein repletion groups

Table 5 Fatty acid composition of the lipids secreted by the liver (wt%) as methyl esters

	B	LP	Protein repletion				ANOVA
			C	C + CLA	HF	HF + CLA	
SFA							
16:0	22.75 ± 1.23	28.31 ± 0.51*	25.96 ± 0.53$^{\#,a}$	24.44 ± 0.25^{b}	24.27 ± 0.13^{b}	22.26 ± 0.21^{c}	Fat, CLA
18:0	15.39 ± 1.10	10.50 ± 0.41*	11.83 ± 0.54^{a}	13.76 ± 0.11^{a}	12.05 ± 0.31^{a}	18.44 ± 0.56^{b}	Fat, CLA, CLA × fat
MUFA							
16:1n-9	0.84 ± 0.06	1.21 ± 0.35	2.19 ± 0.33^{a}	1.35 ± 0.23^{a,b}	1.10 ± 0.19^{b,c}	0.31 ± 0.03^{c}	Fat, CLA
18:1n-9	13.13 ± 1.20	17.82 ± 0.59*	13.16 ± 0.51$^{\#,a}$	10.47 ± 0.61^{b}	14.87 ± 0.73^{a}	9.64 ± 0.72^{b}	CLA
18:1n-7	1.71 ± 0.19	1.54 ± 0.20	1.81 ± 0.17^{a}	1.29 ± 0.16^{b}	1.56 ± 0.21^{a}	0.95 ± 0.01^{b}	CLA
PUFA							
18:2n-6	21.82 ± 1.00	20.50 ± 2.14	22.14 ± 0.36^{a}	20.70 ± 0.31^{a}	28.21 ± 0.36^{b}	22.03 ± 0.61^{a}	Fat, CLA, CLA × fat
*c*9,*t*11-CLA	ND	ND	ND^{a}	0.62 ± 0.01^{b}	ND^{a}	0.58 ± 0.10^{b}	CLA
*t*10,*c*12-CLA	ND	ND	ND^{a}	0.10 ± 0.06^{b}	ND^{a}	0.37 ± 0.03^{b}	CLA
20:4n-6	16.93 ± 0.78	12.37 ± 0.78*	17.62 ± 0.57^{a}	18.62 ± 0.89^{a,b}	14.26 ± 0.33^{c}	20.74 ± 0.34^{b}	CLA, CLA × fat
22:4n-6	ND	0.63 ± 0.07*	0.28 ± 0.06^{a}	0.68 ± 0.03^{b}	0.39 ± 0.01^{a}	0.49 ± 0.03^{a,b}	CLA, CLA × fat
22:5n-6	ND	0.72 ± 0.13*	1.13 ± 0.09^{a}	1.41 ± 0.06^{a}	0.63 ± 0.01^{b}	1.04 ± 0.16^{a,b}	Fat, CLA
22:6n-3	1.96 ± 0.71	0.50 ± 0.28	0.92 ± 0.11	1.14 ± 0.04	0.87 ± 0.07	1.19 ± 0.17	NS
Minor/unknown	5.47	5.90	2.96	5.42	1.79	1.98	

Values are means ± standard errors of the mean ($n = 6$)

B Basal, *LP* low protein, *C* control, *C + CLA* C supplemented with CLA, *HF* high fat, *HF + CLA* HF supplemented with CLA, *NS* not significant, *FA* fatty acid, *SFA* saturated FA, *MUFA* monounsaturated FA, *PUFA* polyunsaturated FA

*$P < 0.05$ versus B. $^{\#}P < 0.05$ versus LP. Different superscript letters indicate significant differences at $P < 0.05$ by Scheffe's test after ANOVA (2 × 2) between protein repletion groups

Table 6 Liver FA composition (wt%) as methyl esters

	B	LP	Protein repletion				ANOVA
			C	C + CLA	HF	HF + CLA	
SFA							
16:0	19.91 ± 1.25	24.09 ± 1.45	21.11 ± 1.43[a]	20.60 ± 0.97[a]	16.51 ± 0.36[b]	15.44 ± 0.45[b]	Fat
18:0	15.11 ± 1.65	11.35 ± 0.88	11.24 ± 1.51	15.20 ± 0.30	12.52 ± 0.70	12.85 ± 1.23	NS
MUFA							
16:1n-9	1.35 ± 0.77	1.61 ± 0.33	1.53 ± 0.52[a]	1.23 ± 0.32[a]	0.39 ± 0.08[b]	0.10 ± 0.04[b]	Fat
18:1n-9	11.19 ± 1.83	16.80 ± 1.98	15.00 ± 3.56	11.26 ± 0.83	13.45 ± 0.88	12.19 ± 1.06	NS
18:1n-7	2.24 ± 0.38	2.20 ± 0.34	3.21 ± 0.55	1.44 ± 0.83	1.14 ± 0.39	1.19 ± 0.40	NS
PUFA							
18:2n-6	19.30 ± 0.82	19.15 ± 1.52	19.98 ± 1.32[a]	17.71 ± 0.92[a]	26.82 ± 1.02[b]	26.93 ± 1.24[b]	Fat
*c*9,*t*11-CLA	0.03 ± 0.01	0.01 ± 0.01	0.09 ± 0.02[a]	0.79 ± 0.12[b]	ND[a]	1.20 ± 0.16[b]	CLA
*t*10,*c*12-CLA	ND	ND	ND[a]	0.40 ± 0.08[b]	ND[a]	0.83 ± 0.14[c]	CLA, CLA × fat
18:3n-3	0.36 ± 0.07	0.18 ± 0.06	0.28 ± 0.04	0.24 ± 0.02	0.26 ± 0.02	0.30 ± 0.02	NS
20:2n-6	0.44 ± 0.05	0.29 ± 0.11	0.47 ± 0.08[a]	0.66 ± 0.10[a]	1.05 ± 0.15[b]	1.19 ± 0.17[b]	Fat
20:3n-6	0.43 ± 0.02	0.55 ± 0.19	0.57 ± 0.04	0.54 ± 0.06	0.66 ± 0.07	0.55 ± 0.07	NS
20:4n-6	21.80 ± 0.54	14.46 ± 2.25*	17.06 ± 3.49	20.35 ± 1.18	19.59 ± 0.79	18.79 ± 1.38	NS
20:5n-3	0.11 ± 0.03	0.08 ± 0.02	0.05 ± 0.02	0.03 ± 0.02	0.04 ± 0.02	0.07 ± 0.03	NS
22:4n-6	0.94 ± 0.16	1.39 ± 0.02*	1.40 ± 0.18[a]	1.19 ± 0.12[b]	1.70 ± 0.16[a]	1.12 ± 0.09[b]	CLA
22:5n-6	1.83 ± 0.48	1.97 ± 0.31	1.91 ± 0.33	2.62 ± 0.42	1.71 ± 0.27	1.64 ± 0.18	NS
22:5n-3	0.80 ± 0.09	0.49 ± 0.04*	0.32 ± 0.12	0.61 ± 0.10	0.48 ± 0.03	0.42 ± 0.02	NS
22:6n-3	2.98 ± 0.40	1.49 ± 0.28*	1.51 ± 0.39	1.81 ± 0.09	1.67 ± 0.17	1.73 ± 0.16	NS
Minor/unknown	5.55	3.89	4.27	3.31	2.01	3.45	
Ratios							
16:1/16:0	0.061 ± 0.029	0.066 ± 0.011	0.071 ± 0.023[a]	0.058 ± 0.013[a]	0.023 ± 0.004[b]	0.007 ± 0.002[c]	Fat, CLA, CLA × fat
18:1/18:0	0.85 ± 0.27	1.54 ± 0.28	1.52 ± 0.55[a]	0.74 ± 0.06[b]	1.10 ± 0.13[a,b]	0.99 ± 0.15[a,b]	Fat, CLA, CLA × fat
SFA/unsaturated FA	0.62 ± 0.04	0.61 ± 0.03	0.54 ± 0.02[a]	0.61 ± 0.02[a]	0.43 ± 0.02[b]	0.43 ± 0.03[b]	Fat

Values are means ± standard errors of the mean ($n = 6$)

B Basal, *LP* low protein, *C* control, *C + CLA* C supplemented with CLA, *HF* high fat, *HF + CLA* HF supplemented with CLA, *NS* not significant, *FA* fatty acid, *SFA* saturated FA, *MUFA* monounsaturated FA, *PUFA* polyunsaturated FA

*$P < 0.05$ versus B. #$P < 0.05$ versus LP. Different superscript letters indicate significant differences at $P < 0.05$ by Scheffe's test after ANOVA (2 × 2) between protein repletion groups

liver by determining the amount of conversion of SFA (16:0 and 18:0) to MUFA (16:1 and 18:1). The 16:1/16:0 and 18:1/18:0 ratios served as a surrogate markers for SCD-1 activity as 16:0 and 18:0 were the predominant substrates for the SCD-1 enzyme. The changes on MUFA/SFA ratios exerted by the HF diets reduced both SCD-1 indexes. Although CLA incorporation was not associated with statistically significant changes in MUFA and SFA, the 16:1/16:0 ratio was decreased in 70% in HF + CLA versus HF group, while the 18:1/18:0 ratio was reduced 50% in C + CLA versus C group.

In EWAT, protein depletion decreased the level of 18:2n-6 and its derivatives, as well as it increased 18:0, 18:3n-3 and 22:5n-3 FA (Table 7). Protein repletion with 7% (w/w) of dietary fat normalized most of the changes in the FA profile induced by the LP diet. Recovery with the HF diets increased the level of 18:2n-6 and decreased that of 16:1n-9, reaching statistical significance in the presence of CLA. In EWAT, the incorporation of both isomers was higher than in liver and plasma, being 40% higher in HF + CLA than in C + CLA. In addition, the incorporation of *c*9,*t*11-CLA was around 70% higher than that of *t*10,*c*12-CLA.

The changes in hepatic TAG accumulation previously reported in this animal model and the alterations in the FA profile currently observed were accompanied by mild alterations in the oxidative stress related parameters, as can be seen in Table 8. Protein depletion increased LPO levels,

Table 7 Epididymal adipose tissue FA composition (wt%) as methyl esters

	B	LP	Protein repletion				ANOVA
			C	C + CLA	HF	HF + CLA	
SFA							
16:0	21.32 ± 1.73	23.69 ± 0.77	20.68 ± 0.79$^{\#,a,b}$	23.54 ± 0.05^{a}	22.06 ± 3.69^{a,b}	14.05 ± 0.23^{b}	CLA × fat
18:0	2.53 ± 0.07	4.43 ± 0.27*	2.79 ± 0.04$^{\#}$	2.60 ± 0.06	2.78 ± 0.09	2.71 ± 0.01	NS
MUFA							
16:1n-9	4.86 ± 1.04	3.46 ± 0.69	3.85 ± 0.49^{a}	2.90 ± 0.02^{a}	3.17 ± 0.90^{a}	0.53 ± 0.03^{b}	Fat, CLA
18:1n-9	30.29 ± 0.59	29.61 ± 0.80	31.67 ± 0.82	27.56 ± 0.43	29.60 ± 1.74	29.27 ± 0.05	NS
*t*11-18:1	0.12 ± 0.07	0.13 ± 0.08	0.24 ± 0.09	0.25 ± 0.14	0.13 ± 0.03	0.45 ± 0.01	NS
*c*11-18:1	1.39 ± 0.80	1.14 ± 0.63	1.64 ± 0.94^{a,b}	3.43 ± 0.07^{a}	0.03 ± 0.00^{b}	0.81 ± 0.47^{b}	Fat, CLA
PUFA							
18:2n-6	33.11 ± 3.73	30.70 ± 0.68	33.20 ± 1.18^{a,b}	29.35 ± 0.07^{a}	36.83 ± 3.61^{a,b}	41.91 ± 0.29^{b}	Fat, CLA × fat
*c*9,*t*11-CLA	0.34 ± 0.04	0.35 ± 0.12	0.16 ± 0.03^{a}	2.74 ± 0.08^{b}	0.28 ± 0.03^{a}	3.59 ± 0.04^{c}	Fat, CLA, CLA × fat
*t*10,*c*12-CLA	ND	ND	ND^{a}	1.49 ± 0.06^{b}	ND^{a}	2.22 ± 0.18^{c}	Fat, CLA, CLA × fat
18:3n-3	0.71 ± 0.00	0.88 ± 0.01*	0.67 ± 0.03	0.58 ± 0.01	0.57 ± 0.04	0.64 ± 0.02	NS
20:2n-6	0.19 ± 0.01	0.11 ± 0.03	ND^{a}	0.24 ± 0.02^{b,c}	0.14 ± 0.01^{b}	0.24 ± 0.03^{c}	Fat, CLA, CLA × fat
20:3n-6	0.12 ± 0.02	0.05 ± 0.03	0.11 ± 0.00$^{\#,a}$	0.04 ± 0.00^{b}	0.11 ± 0.00^{a}	0.06 ± 0.02^{b}	CLA
20:4n-6	0.84 ± 0.03	0.31 ± 0.17*	0.75 ± 0.02$^{\#,a}$	0.29 ± 0.04^{b}	0.64 ± 0.06^{a}	0.50 ± 0.09^{a,b}	CLA, CLA × fat
22:4n-6	0.19 ± 0.01	0.10 ± 0.03*	0.18 ± 0.01$^{\#,a}$	0.06 ± 0.01^{b}	0.15 ± 0.03^{a,c}	0.10 ± 0.01^{b,c}	CLA, CLA × fat
22:5n-6	0.12 ± 0.02	0.06 ± 0.01*	0.13 ± 0.02$^{\#,a}$	0.04 ± 0.01^{b}	0.07 ± 0.01^{b}	0.03 ± 0.02^{b}	Fat, CLA, CLA × fat
22:5n-3	0.04 ± 0.01	0.11 ± 0.02*	0.03 ± 0.00$^{\#,a}$	ND^{b}	0.02 ± 0.00^{a}	ND^{b}	CLA
22:6n-3	0.04 ± 0.01	0.03 ± 0.02	0.03 ± 0.00^{a}	ND^{b}	0.01 ± 0.00^{c}	ND^{b}	Fat, CLA, CLA × fat
Minor/unknown	3.77	4.78	3.86	3.40	4.90	2.90	

Values are means ± standard errors of the mean ($n = 6$)

B Basal, *LP* low protein, *C* control, *C + CLA* C supplemented with CLA, *HF* high fat, *HF + CLA* HF supplemented with CLA, *NS* not significant, *FA* fatty acid, *SFA* saturated FA, *MUFA* monounsaturated FA, *PUFA* polyunsaturated FA

*$P < 0.05$ versus B. $^{\#}P < 0.05$ versus LP. Different superscript letters indicate significant differences at $P < 0.05$ by Scheffe's test after ANOVA (2 × 2) between protein repletion groups

Table 8 Oxidative stress parameters

	B	LP	Protein repletion				ANOVA
			C	C + CLA	HF	HF + CLA	
LPO (nmol/g)	110.94 ± 6.92	179.26 ± 23.83*	113.47 ± 13.21$^{\#}$	114.39 ± 11.94	105.70 ± 8.28	114.33 ± 17.54	NS
GSH (μmol/g)	2.26 ± 0.14	3.47 ± 0.51*	3.54 ± 0.46	4.18 ± 0.57	4.47 ± 0.56	3.90 ± 0.34	NS
Enzymatic activity (U/mg protein)							
GSH-Px	0.104 ± 0.022	0.113 ± 0.011	0.078 ± 0.005$^{\#}$	0.079 ± 0.011	0.094 ± 0.017	0.096 ± 0.019	NS
CAT	87.69 ± 2.07	61.75 ± 6.26*	85.84 ± 5.53$^{\#}$	85.73 ± 4.86	76.53 ± 4.99	79.78 ± 4.11	NS

Values are means ± standard errors of the mean ($n = 6$)

B Basal, *LP* low protein, *C* control, *C + CLA* C supplemented with CLA, *HF* high fat, *HF + CLA* HF supplemented with CLA, *NS* not significant, *LPO* lipoperoxidation, *GSH* reduced glutathione, *GSH-Px* glutathione peroxidase, *CAT* catalase

*$P < 0.05$ versus B. $^{\#}P < 0.05$ versus LP

and this was related to a reduction in CAT activity despite a higher hepatic GSH concentration. Protein repletion normalized LPO levels and CAT activity. The presence of CLA, as well as HF diet intake, did not generate further modifications in the liver oxidative stress parameters.

Discussion

To the best of our knowledge, this is the first study to investigate the potential effect of CLA at two different amounts of dietary fat on the contribution of both hepatic

TAG secretion and capability of TAG removal by gastrocnemius muscle and EWAT, and its possible associations with changes in the FA composition in plasma, liver and epididymal white adipose tissue and the hepatic oxidative status in protein repleted rats. However, it is widely known that *c*9,*t*11-CLA and *t*10,*c*12-CLA have different effects on tissue FA metabolism and composition [11, 33, 34]. Therefore, an equimolecular mixture of both isomers was chosen in this study. Although the animal model seemed to be limited, it provided information about the effects of the CLA oil commercially available for human consumption.

The partial depletion of dietary proteins (5% casein) in the animal model under study was characterized by hypotriglyceridemia, hepatomegaly and steatosis [18, 35, 36]. The decreased hepatic TAG secretion and high EWAT LPL activity observed could explain, at least in part, the low plasma TAG concentrations previously found in this animal model [18]. In addition to changes in VLDL composition, assembly and secretion, associated with the decrease of VLDL apolipoprotein, phospholipids and TAG contents reported by other authors [35], our results of the low hepatic TAG secretion also correlated with the hepatic steatosis. Furthermore, in agreement with other studies [37], we also found that partial protein depletion decreased the muscle LPL activity and this was consistent with the decreased TAG concentrations observed in the gastrocnemius muscle. The alterations observed in the lipid metabolism were accompanied by modifications in FA composition in plasma, liver and EWAT. In plasma, protein depletion increased MUFA and 16:0 and decreased 18:0 levels. In liver, these changes were less pronounced without reaching statistical differences. The decrease observed in liver 20:4n-6 and n-3 FA was in agreement with that reported by other authors [36, 38]. As PUFA are more prone to oxidation than MUFA and SFA, the reduction in total PUFA and the increase in SFA might also explain the hepatic steatosis observed in the LP group. The TAG secreted by the liver presented FA compositional changes, similar to those observed in liver. On the other hand, EWAT showed an increase in n-3 FA, perhaps as a compensatory mechanism, storing these FA that were deficient in liver.

The hepatic steatosis observed in protein depleted animals could be an important factor in the induction of oxidative stress, reflected by the high LPO values. This action could be mediated, at least in part, by a decrease in the activity of a key antioxidant enzyme, such as CAT, and not completely counteracted by the increase in liver GSH concentration.

Normalization of hepatic TAG secretion in protein repletion with 7% (w/w) of dietary fat could be the main mechanism involved in the reversion of hepatic steatosis and decreased circulating TAG reported elsewhere [18]. This effect normalized most of the changes observed in the FA profile of plasma, EWAT, liver and TAG exported from liver. This mechanism could have more influence than certain enzymes involved in FA metabolism such as liver SCD-1, since 16:1/16:0 and 18:1/18:0 ratios remained unchanged in protein depletion and repletion.

Dietary CLA prevented hepatic lipid accumulation in partial protein repletion with a high amount of dietary fat [18]. The present study shows that hepatic TAG secretion was the most important mechanism involved in protein repletion when HF diets were used. Thus, while HF diets without CLA showed a low liver TAG secretion contributing to maintain the hepatic TAG accumulation, the presence of CLA prevented hepatic steatosis from increasing hepatic TAG secretion, and it also altered the FA profile of the lipids secreted by the liver. In addition, CLA was incorporated to the TAG secreted by the liver, concurrent with a decrease in MUFA and higher levels of n-6 PUFA. This evidence does not preclude the fact that changes in the composition and size of lipoproteins secreted by the liver could be modified by CLA, as shown in an in vitro study [39].

The presence of CLA did not affect muscular and EWAT LPL activity and this could also contribute to the lack of changes in plasma and muscle TAG concentration. Several authors [40, 41] reported contrasting results in hamsters and diabetic rats fed CLA without previous protein depletion. Clearly, the sensitivity and condition of the animals could be determining as well as the type of isomer used. The effects of CLA on LPL activity in EWAT and culture adipocytes are controversial [6], and the differences with our results might be related to experimental conditions. Furthermore, the increased muscle TAG concentration in protein repletion with HF diet was associated with a slight and not significant raise of muscle LPL activity. This fact could also be related to the high FA and energy availability provided by the diet.

Both CLA isomers were incorporated into liver, EWAT, plasma and lipids secreted by the liver. In all the samples, the level of *t*10,*c*12-CLA was much smaller than that of *c*9,*t*11-CLA, in agreement with the results from Kelley et al. [11] in different tissues of mice. This effect could be most likely due to a higher β-oxidation of *t*10,*c*12-CLA [42]. The CLA level was higher in EWAT, followed by liver, and then by plasma. In EWAT, both isomers were more abundantly incorporated in the HF + CLA diet than in the C + CLA diet, reflecting the higher level of CLA in the former. On the other hand, dietary CLA were similarly incorporated in plasma lipids in C + CLA and HF + CLA groups, reflecting that in both diets the total amount of CLA represented equal proportions of the dietary fat (15% of the total fat).

The tissue ratios between the level of SFA and MUFA of C16 and C18 FA can be used as SCD-1 indexes reflecting the enzyme activity [43]. Different levels of SCD-1 activity, index and/or expression have been associated with liver steatosis. For instance, Gutierrez-Juárez et al. [44] reported liver steatosis in a model of reduced SCD-1 expression. In our case, lower C16 and C18 FA SCD-1 indexes were associated with high fat intake, as expected, given the fact that the Scd1 mRNA expression was reported to be lower in animals fed 20% corn oil [45]. On the other hand, the effect of CLA on liver SCD-1 expression and activity has been studied in vitro [46, 47], but few studies of these parameters in animal models have been published in the literature [48]. These reports mainly concur in the fact that *t*10,*c*12-CLA decreases both enzyme expression and activity, in agreement with our results. Even though decreasing the SCD index, CLA was not related to higher hepatic TAG concentration. On the contrary, CLA intake with 20% (w/w) of dietary fat prevented hepatic lipid accumulation. In agreement with our results, Purushotham et al. [43] reported that CLA intake could reduce hepatic steatosis when it was produced by the previous intake of a HF diet instead of protein depletion. The apparent liver protective effect of CLA observed in previously malnourished rats was clearly opposite to that observed in well-nourished mice fed HF diets [49], where CLA drastically increased liver TAG concentration.

Protein repletion restored the liver oxidative status independently of the amount of dietary fat or the presence of CLA. The present results differed from those previously reported by our group [49], showing that HF diet intake induced LPO, and the presence of CLA in the diet could prevent this effect by increasing hepatic GSH concentration in a mouse model with no previous protein depletion.

In sum, this work provided further insight into the plausible role of commercially available CLA on the recovery from protein depletion with 7% (w/w) and high (20%, w/w) dietary fat content. Protein repletion only in the presence of CLA normalized plasma and liver TAG concentration independently of the amount of dietary fat through an increase of hepatic TAG secretion. In addition, CLA in protein repletion was incorporated into the plasma and tissues, its levels in EWAT being > liver > plasma, and that of *c*9,*t*11-CLA being >*t*10,*c*12-CLA. This was accompanied by alterations in FA composition. The determination of the mechanisms by which CLA and/or the content of dietary fat could regulate metabolic disorders associated with lipid metabolism might greatly contribute to understanding the development and intervention of diet-induced chronic disorders.

Acknowledgments We wish to thank Walter DaRú for his technical assistance with the animals. This work was financed by ANPCyT (Agencia Nacional Científica y Tecnológica, PICT # 25750, PICTO # 36181) and Universidad Nacional del Litoral-Cursos de Acción para la Investigación y Desarrollo (CAI+D 2006 No. 12/B616). We are also grateful to CYTED (Programa de Ciencia y Tecnología para el Desarrollo-Ministerio Español de Ciencia y Tecnología—BFI2002-00218) for the financial support of the Network 208RT0343, where this research was integrated

References

1. Waterlow J (1996) Malnutrición proteico-energética. Organización Panamericana de la Salud Press, Washington DC
2. Kern M, Beuttenmuller D, Diehl S, McCormick C, Ambrose M (2002) The effects of protein repletion at varied levels on the growth and nutritional status of protein restricted rats. Nutr Res 22:957–963
3. Chin SF, Liu W, Storkson JM, Ha YL, Pariza MW (1992) Dietary sources of conjugated dienoic isomers of linoleic acid, a newly recognized class of anticarcinogens. J Food Compos Anal 5:185–197
4. Ip C, Jiang C, Thompson HJ, Scimeca JA (1997) Retention of conjugated linoleic acid in the mammary gland is associated with tumor inhibition during the post-initiation phase of carcinogenesis. Carcinogenesis 18:755–759
5. Parra P, Serra F, Palou A (2010) Moderate doses of conjugated linoleic acid isomers mix contribute to lowering body fat content maintaining insulin sensitivity and a noninflammatory pattern in adipose tissue in mice. J Nutr Biochem 21:107–115
6. Salas-Salvadó J, Márquez-Sandoval F, Bulló M (2006) Conjugated linoleic acid intake in humans: a systematic review focusing on its effect on body composition, glucose, and lipid metabolism. Crit Rev Food Sci Nutr 46:479–488
7. Silveira MB, Carraro R, Monereo S, Tébar J (2007) Conjugated linoleic acid (CLA) and obesity. Public Health Nutr 10:1181–1186
8. Bhattacharya A, Banu J, Rahman M, Causey J, Fernandes G (2006) Biological effects of conjugated linoleic acids in health and disease. J Nutr Biochem 17:789–810
9. US Food and Drug Administration (accessed Oct 2009) Agency response letter GRAS Notice No. GRN 000232 http://www.fda.gov/Food/FoodIngredients Packaging/GenerallyRecognizedasSafeGRAS/GRASListings/ucm153908.htm
10. Butz DE, Li G, Cook ME (2006) t10,c12 Conjugated linoleic acid induces compensatory growth after immune challenge. J Nutr Biochem 17:735–741
11. Kelley DS, Bartolini GL, Newman JW, Vemuri M, Mackey BE (2006) Fatty acid composition of liver, adipose tissue, spleen, and heart of mice fed diets containing t10, c12-, and c9, t11-conjugated linoleic acid. Prostaglandins Leukot Essent Fatty Acids 74:331–338
12. Banni S, Petroni A, Blasevich M, Carta G, Cordeddu L, Murru E et al (2004) Conjugated linoleic acids (CLA) as precursors of a distinct family of PUFA. Lipids 39:1143–1146
13. Liu LF, Purushotham A, Wendel AA, Belury MA (2007) Combined effects of rosiglitazone and conjugated linoleic acid on adiposity, insulin sensitivity, and hepatic steatosis in high-fat-fed mice. Am J Physiol Gastrointest Liver Physiol 292:G1671–G1682
14. Kim HK, Kim SR, Ahn JY, Cho IJ, Yoon CS, Ha TY (2005) Dietary conjugated linoleic acid reduces lipid peroxidation by increasing oxidative stability in rats. J Nutr Sci Vitaminol (Tokyo) 51:8–15
15. Takahashi Y, Kushiro M, Shinohara K, Ide T (2003) Activity and mRNA levels of enzymes involved in hepatic fatty acid synthesis

and oxidation in mice fed conjugated linoleic acid. Biochim Biophys Acta 1631:73–265
16. Poirier H, Niot I, Clement L, Guerre-Millo M, Besnard P (2005) Development of conjugated linoleic acid (CLA)-mediated lipoatrophic syndrome in the mouse. Biochimie 87:73–79
17. Miller CC, Park Y, Pariza MW, Cook ME (1994) Feeding conjugated linoleic acid to animals partially overcomes catabolic responses due to endotoxin injection. Biochem Biophys Res Commun 198:1107–1112
18. Andreoli MF, Scalerandi MV, Borel IM, Bernal CA (2007) Effects of CLA at different dietary fat levels on the nutritional status of rats during protein repletion. Nutrition 23:827–835
19. Li J, Wang H, Stoner GD, Bray TM (2002) Dietary supplementation with cysteine prodrugs selectively restores tissue glutathione levels and redox status in protein-malnourished mice. J Nutr Biochem 13:625–633
20. Saiki R, Okazaki M, Iwai S, Kumai T, Kobayashi S, Oguchi K (2007) Effects of pioglitazone on increases in visceral fat accumulation and oxidative stress in spontaneously hypertensive hyperlipidemic rats fed a high-fat diet and sucrose solution. J Pharmacol Sci 105:157–167
21. Grattagliano I, Caraceni P, Portincasa P, Domenicali M, Palmieri VO, Trevisani F et al (2003) Adaptation of subcellular glutathione detoxification system to stress conditions in choline-deficient diet induced rat fatty liver. Cell Biol Toxicol 19:355–366
22. Reeves PG, Nielsen FH, Fahey GC Jr (1993) AIN-93 purified diets for laboratory rodents: final report of the American Institute of Nutrition ad hoc writing committee on the reformulation of the AIN-76A rodent diet. J Nutr 123:1939–1951
23. Bayne K (1996) Revised guide for the care and use of laboratory animals available. American Physiological Society. Physiologist 39(199):208–211
24. Laurell S (1966) A method for routine determination of plasma triglycerides. Scand J Clin Lab Invest 18:668–672
25. Nilsson-Ehle P, Schotz MC (1976) A stable, radioactive substrate emulsion for assay of lipoprotein lipase. J Lipid Res 17:536–541
26. Otway S, Robinson DS (1967) The use of a non-ionic detergent (Triton WR 1339) to determine rates of triglyceride entry into the circulation of the rat under different physiological conditions. J Physiol 190:321–332
27. Bligh EG, Dyer WJ (1959) A rapid method of total lipid extraction and purification. Can J Biochem Physiol 37:911–917
28. Ohkawa H, Ohishi N, Yagi K (1979) Assay for lipid peroxides in animal tissues by thiobarbituric acid reaction. Anal Biochem 95:351–358
29. Ellman G, Lysko H (1979) A precise method for the determination of whole blood and plasma sulfhydryl groups. Anal Biochem 93:98–102
30. Aebi H (1984) Catalase in vitro. Methods Enzymol 105:121–126
31. Paglia DE, Valentine WN (1967) Studies on the quantitative and qualitative characterization of erythrocyte glutathione peroxidase. J Lab Clin Med 70:158–169
32. Lowry OH, Rosebrough NJ, Farr AL, Randall RJ (1951) Protein measurement with the Folin phenol reagent. J Biol Chem 193:265–275
33. Bissonauth V, Chouinard Y, Marin J, Leblanc N, Richard D, Jacques H (2006) The effects of t10, c12 CLA isomer compared with c9, t11 CLA isomer on lipid metabolism and body composition in hamsters. J Nutr Biochem 17:597–603
34. Zabala A, Portillo MP, Macarulla MT, Rodriguez VM, Fernandez-Quintela A (2006) Effects of *cis*-9, *trans*-11 and *trans*-10, *cis*-12 CLA isomers on liver and adipose tissue fatty acid profile in hamsters. Lipids 41:993–1001
35. Bouziane M, Prost J, Belleville J (1992) Changes in serum and lipoprotein fatty acids of growing rats fed protein-deficient diets with low or adequate linolenic acid concentrations. J Nutr 122:2037–2046
36. Narce M, Poisson JP, Belleville J, Chanussot B (1992) Depletion of delta 9 desaturase (EC 1.14.99.5) enzyme activity in growing rat during dietary protein restriction. Br J Nutr 68:627–637
37. Boualga A, Bouchenak M, Belleville J (2000) Low-protein diet prevents tissue lipoprotein lipase activity increase in growing rats. Br J Nutr 84:663–671
38. Bouziane M, Prost J, Belleville J (1994) Changes in fatty acid compositions of total serum and lipoprotein particles, in growing rats given protein-deficient diets with either hydrogenated coconut or salmon oils as fat sources. Br J Nutr 71:375–387
39. Mitmesser SH, Carr TP (2005) Trans fatty acids alter the lipid composition and size of apoB-100-containing lipoproteins secreted by HepG2 cells. J Nutr Biochem 16:178–183
40. Henriksen EJ, Teachey MK, Taylor ZC, Jacob S, Ptock A, Kramer K et al (2003) Isomer-specific actions of conjugated linoleic acid on muscle glucose transport in the obese Zucker rat. Am J Physiol Endocrinol Metab 285:E98–E105
41. Zabala A, Fernandez-Quintela A, Macarulla MT, Simon E, Rodriguez VM, Navarro V et al (2006) Effects of conjugated linoleic acid on skeletal muscle triacylglycerol metabolism in hamsters. Nutrition 22:528–533
42. de Deckere EAM, van Amelsvoort JMM, McNeill GP, Jones P (1999) Effects of conjugated linoleic acid (CLA) isomers on lipid levels and peroxisome proliferation in the hamster. Br J Nutr 82:309–317
43. Purushotham A, Shrode GE, Wendel AA, Liu LF, Belury MA (2007) Conjugated linoleic acid does not reduce body fat but decreases hepatic steatosis in adult Wistar rats. J Nutr Biochem 18:676–684
44. Gutierrez-Juárez R, Pocai A, Mulas C, Ono H, Bhanot S, Monia BP et al (2006) Critical role of stearoyl-CoA desaturase-1 (SCD1) in the onset of diet-induced hepatic insulin resistance. J Clin Invest 116:1686–1695
45. Park EI, Paisley EA, Mangian HJ, Swartz DA, Wu MX, O'Morchoe PJ et al (1997) Lipid level and type alter stearoyl CoA desaturase mRNA abundance differently in mice with distinct susceptibilities to diet-influenced diseases. J Nutr 127:566–573
46. Bretillon L, Chardigny JM, Gregoire S, Berdeaux O, Sebedio JL (1999) Effects of conjugated linoleic acid isomers on the hepatic microsomal desaturation activities in vitro. Lipids 34:965–969
47. Pariza MW, Park Y, Cook ME (2000) Mechanisms of action of conjugated linoleic acid: evidence and speculation. Proc Soc Exp Biol Med 223:8–13
48. Lee KN, Pariza MW, Ntambi JM (1998) Conjugated linoleic acid decreases hepatic stearoyl-CoA desaturase mRNA expression. Biochem Biophys Res Commun 248:817–821
49. Andreoli MF, Gonzalez MA, Martinelli MI, Mocchiutti NO, Bernal CA (2009) Effects of dietary conjugated linoleic acid at high-fat levels on triacylglycerol regulation in mice. Nutrition 25:445–452

volunteers who had previously consumed pure unlabeled isomers during 24 weeks [3].

Methods

Materials

Unlabeled CLA isomers were provided by Natural Lipids Ltd. (Hovdebygda, Norway). [1-^{13}C]-9*c*,11*t* and [1-^{13}C]-10*t*,12*c* were synthesized as already described [4]. [1-^{13}C]-9*c*-18:1 was purchased (Isotec Inc. OH, USA). The chemical purity was ≥98% with isotopic purity 98.2% 9*c*-18:1, 99% 9*c*,11*t* and 98% 10*t*,12*c* by GC–MS. The triacylglycerol (TAG) form, containing two molecules of labeled fatty acid (positions 1(3) and 2) and one molecule of unlabeled 9*c*-18:1 (position 3(1)) was synthesized as published elsewhere [5] and packaged into individual doses of approximately 1 g of pure TAG in 30 g high oleic sunflower oil (Lesieur, Coudekerque, France). To maintain blinding, individual doses were labeled with the same code as during the 24 week clinical trial. Only Danone (Danone Research Center, Palaiseau, France) could unblind the study.

Study Protocol

This study was part of a placebo-controlled, double-blind, randomized intervention trial to compare the effects of 9*c*-18:1 (control), 9*c*,11*t*- and 10*t*,12*c*-CLA on body composition in healthy overweight men and women. Details of this study have been described elsewhere [3]. The isotope study followed 24 weeks of CLA/9*c*-18:1 treatment. The ^{13}C-labeled substrates were given as TAG to ensure high bioavailability [1, 6]. Twenty-four subjects among the group receiving 3 g/day of 9*c*-18:1 or 9*c*,11*t*- or 10*t*, 12c-CLA were randomly chosen and blinding preserved. Volunteer numbers per group ($n = 8$) were calculated based on our previous experience [7]. However, 2 volunteers from Maastricht withdrew and 22 subjects successfully completed the study: 8 from the 9*c*-18:1 (control) group (4 females, 4 males) and the 9*c*,11*t*-CLA group (3 females, 5 males), and 6 subjects from the 10*t*,12*c*-CLA group (2 females, 4 males). The study protocol was approved by the Ethical Committees in France and the Netherlands. Informed written consent of all the subjects was obtained prior to entering the study.

The study design (Fig. 1) was standardized between Clermont-Ferrand and Maastricht. Briefly, after an overnight (12 h) fast, O_2 consumption (vO_2) and CO_2 production (vCO_2) were measured for 30 min using a ventilated-hood indirect calorimeter (Deltatrac, Datex, Helsinki, Finland). The respiratory quotient (RQ, the ratio of vCO_2:vO_2) and energy expenditure (EE) were calculated at baseline and 2, 3, 5, and 8 h after ingestion of the tracers. Energy expenditure (EE) was calculated using Weir's equation [8] whereas, non-protein respiratory quotient (NPRQ) and substrate oxidation rates were calculated using equations from Ferranini [9].

Breath samples were collected into tubes (Vacutainer, Becton–Dickinson, Grenoble, France) at baseline to determine the basal ^{13}C abundance of breath CO_2, hourly for a period of 8, 24 and 48 h post-dose. Rate of expiration of $^{13}CO_2$ in breath was calculated by multiplying the vCO_2 by the enrichment of the breath CO_2 pool.

Subjects stayed fasted at the laboratory during these 8 h and were requested to remain in a resting, but not sleeping, state and to refrain from talking. Before leaving, they ate a meal without ^{13}C rich foods (e.g. maize and sugar cane). They also received advice to avoid these foods for the next 48 h.

Analytical Procedures

Breath $^{13}CO_2$ enrichments were analyzed by isotope ratio mass spectrometry (IRMS) (mGas system, Fisons Instruments, Middlewich, England). The CO_2 was introduced into the IRMS to measure the ^{13}C to ^{12}C isotopic ratio of the sample and calculate the isotopic abundance relative to the Vienna-PDB international standard (δ^{13}C in % vs. PDB) [10]. The rate of $^{13}CO_2$ production was calculated by multiplying $^{13}CO_2$ enrichment by CO_2 production (measured using indirect calorimetry) as previously published [10]. Cumulative $^{13}CO_2$ production, i.e. the area under the curve (AUC), was calculated using the trapezium rule [10].

Statistical Analysis

Results are given as means ± SD. Treatment effects were examined using ANOVA following by a non-parametric test

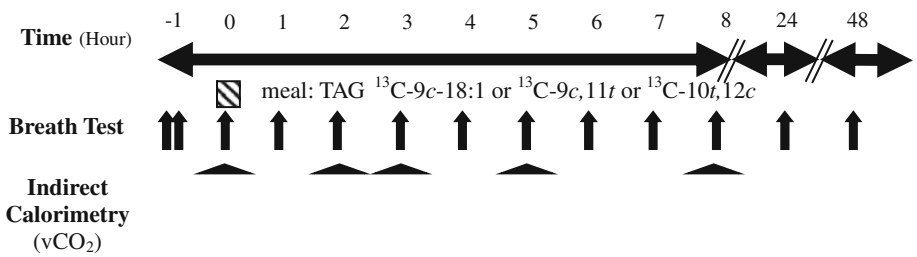

Fig. 1 Experimental design. Twenty-two subjects ingested labeled 1 g of TAG (9*c*-18:1 (control) or 9*c*,11*t* or 10*t*,12*c* isomer) mixed with 30 g of a high oleic sunflower oil

Table 1 Anthropometric variables of the subjects in control, 9*c*,11*t*, and 10*t*,12*c* groups at the end of the intervention period

	9*c*-18:1 (Control)	9*c*,11*t*	10*t*,12*c*	ANOVA
N	8	8	6	
Gender (M/F)	M = 4/F = 4	M = 5/F = 3	M = 4/F = 2	
Age (year)	54.3 ± 7.3	47.3 ± 8.9	47.3 ± 8.3	0.204
Height (cm)	169.1 ± 10.0	175.6 ± 8.9	170.9 ± 7.4	0.355
BMI (kg/m^2)	28.1 ± 1.7	26.9 ± 1.4	26.9 ± 1.0	0.200
Waist/Hip	0.90 ± 0.10	0.93 ± 0.09	0.90 ± 0.07	0.756
Body fat mass (%)	30.2 ± 8.3	28.1 ± 4.5	27.4 ± 6.7	0.713
Lean body mass (LBM) (kg)	56.8 ± 12.9	60.0 ± 9.6	57.3 ± 8.2	0.805
RQ (respiratory quotient)	0.86 ± 0.04	0.86 ± 0.03	0.82 ± 0.04	0.113
NPRQ (non-protein respiratory quotient)	0.81 ± 0.06	0.78 ± 0.03	0.77 ± 0.06	0.305
EE (energy expenditure) (kcal/8 h)	613 ± 108	579 ± 99	609 ± 98	0.771
Fat oxidation (g/kg LBM/8 h)	0.70 ± 0.20	0.63 ± 0.18	0.64 ± 0.24	0.859
Carbohydrate oxidation (g/kg LBM/8 h)	1.96 ± 0.61	1.81 ± 0.34	1.83 ± 0.24	0.993

Values are means ± SD

(Fisher PLSD test) to compare the treatments pairwise, when a significant treatment effect was observed. Moreover, repeated-measures ANOVA were used to look for possible interactions between treatment and time. A two-way ANOVA analysis was performed to look for possible gender effects and a possible interaction between treatment and gender interaction. Statistics were performed by using Statview 5.0 (SAS Institute Inc., Cary, NC, USA).

Results

Mean values for age, height, BMI, waist/hip ratio, fat free mass, percentage body fat, and respiratory quotient (RQ) at the start of this study did not differ significantly between groups (Table 1). None of the parameters related to energy expenditure varied between groups (Table 1).

Excretion of $^{13}CO_2$ in the breath measured over 48 h followed a similar pattern in the three groups. Labeled fatty acid oxidation peaked between 5 and 6 h post-dose for all tracers and decreased thereafter to reach the basal ^{13}C-level at 24 and 48 h (Fig. 2). However, cumulative fatty acid oxidation determined from AUC results, was significantly higher for ^{13}C-9*c*,11*t*-CLA than for ^{13}C-9*c*-18:1 ($P < 0.01$) or ^{13}C-10*t*,12*c*-CLA ($P = 0.01$). There was no difference between 10*t*,12*c*-CLA and 9*c*-18:1 ($P = 0.66$).

The oxidation of CLAs was not affected by gender ($P = 0.73$) (data not shown). Oxidation rate of 9*c*,11*t*-CLA amounted for 31.0 ± 3.6% of the oral dose for 8 h. It was significantly higher than for 9*c*-18:1 (22.2 ± 8.0%) ($P = 0.02$) and 10*t*,12*c*-CLA (21.6 ± 8.7%) ($P = 0.02$).

Discussion

In the present study, we have assessed the oxidation of CLA isomers using a similar method to one previously published with n-3 fatty acids [7]. Our results show that

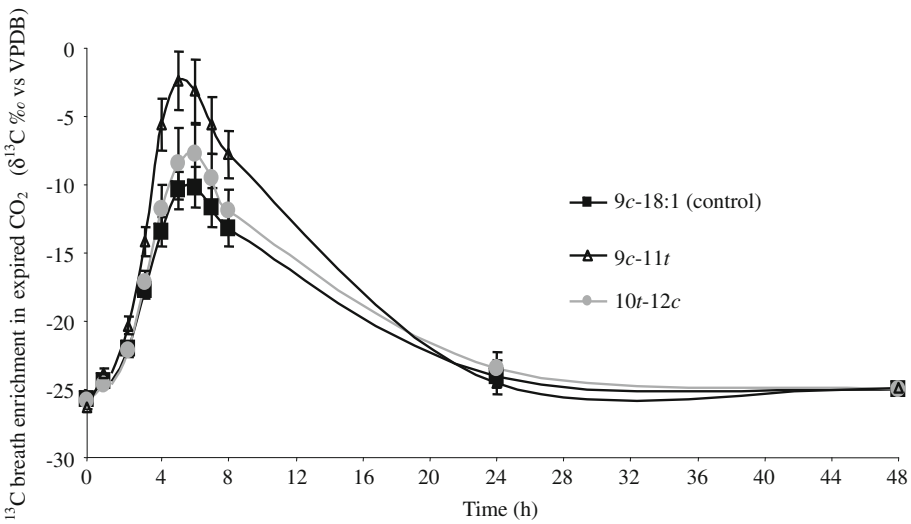

Fig. 2 Time course of the ^{13}C enrichment in breath $^{13}CO_2$ (vs. VPDB) after an oral dose of 1 g of TAG containing each [1-^{13}C]-9*c*-18:1 (control), [1-^{13}C]-9*c*,11*t* and [1-^{13}C]-10*t*,12*c* isomers given to 8, 8, and 6 volunteers in 9*c*-18:1, 9*c*,11*t* and 10*t*,12*c* groups, respectively. Values are means ± SEM

postprandial β-oxidation of 9*c*,11*t*-CLA is higher than that of 9*c*-18:1 and 10*t*,12*c*-CLA, contrary to our expectation. Results obtained in rodents and in vitro suggested that the 10*t*,12*c* isomer is more oxidized than the 9*c*,11*t* [1]. In addition, the reduced percentage of body fat observed in animals and the enhanced energy metabolism after administration of a CLA mixture has been attributed to the 10*t*,12*c* isomer [11, 12]. However, in mitochondria from liver homogenates, 10*t*,12*c*-CLA was less oxidized than 9*c*,11*t*-CLA, possibly because of its higher esterification rate which possibly prevented its entrance into β-oxidation [13]. Our present finding combined with the latter data suggest that the lower metabolic effect of 9*c*,11*t*-CLA may be attributed to its higher mitochondrial oxidation, but we did not investigate further the potential mechanisms related to our observation. A recent study by Goedecke et al. [14] demonstrated a greater incorporation of 10*t*,12*c*-CLA into adipose and muscle tissues compared with 9*c*,11*t*-CLA in healthy non-obese volunteers, perhaps for similar reasons.

Despite differences in postprandial oxidation between the two CLA isomers, we found that energy expenditure, RQ, NPRQ and fat oxidation were similar between the three groups (Table 1). These results are in accordance with two other studies. In the first one [15], resting RQ, fat oxidation, and energy expenditure were unchanged after a daily supplement containing 3 g of a mixture of CLA-isomers (11*c*,13*t*: ~23% (w/w), 10*t*,12*c*: ~23% (w/w) and 9*c*,11*t*: 18%) for 64 days in healthy normal-weight women. Body composition measured with DEXA-method, indicated that CLA had no effect on body fat mass. Moreover, Watras et al. [16] demonstrated that a 6 month CLA supplementation was associated with fat mass loss compared to placebo (-1.0 ± 2.2 and 0.7 ± 3 kg, respectively, $P = 0.02$), but without any effect on resting metabolic rate. These and our results are however in marked contrast with two other intervention studies. Consumption of a CLA supplement (50:50 9*c*,11*t* and 10*t*,12*c*) as TAG (3.76 g) for 98 days significantly increased basal energy expenditure in overweight men and women [17]. Similarly, with 3.2 g/day of CLA mixture (39.2% 9*c*,11*t* and 38.5% 10*t*,12*c*), energy expenditure and fat oxidation were enhanced during sleep in overweight men and women [18]. In addition, RQ during the 24 h period tended to decrease. This was, however, not associated with changes in the oxidation of dietary fat as monitored by labeled oleate and palmitate administered during a breakfast meal [18]. These discrepancies require additional exploration on the effect of CLA isomers on whole body energy metabolism.

Our study is the first that has examined the in-vivo metabolic behavior of pure CLA-isomers in humans. It has, however, some limitations. First, the sample size with six to eight volunteers per group is small, even if statistical significance between the groups was reached. Secondly, oxidation was measured at rest, while physical exercise may modify fatty acids utilization [15]. Thirdly, we only studied oxidation within a time frame of 48 h and do not know what happened with the remaining label. Despite these limitations, we can conclude that 9*c*,11*t* is more rapidly oxidized compared than 10*t*,12*c* CLA.

Acknowledgments We are grateful to Asgeir Saebo (Natural ASA, Norway) for providing the CLA isomers. For their invaluable help, we are most grateful to the participants. C. Giraudet (Clermont) and P. Rousset (Clermont) are acknowledged for the analyses of the $^{13}CO_2$ isotopic enrichments. Supported by The European Commission: conjugated linoleic acid (CLA) in functional food: a potential benefit for overweight middle-aged Europeans, Fifth (EC) framework program QLK1-1999-00076.

References

1. Park Y, Storkson JM, Albright KJ, Liu W, Pariza MW (1999) Evidence that the *trans*-10, *cis*-12 isomer of conjugated linoleic acid induces body composition changes in mice. Lipids 34:235–241
2. Hargrave KM, Li C, Meyer BJ, Kachman SD, Hartzell DL, Della-Fera MA, Miner JL, Baile CA (2002) Adipose depletion and apoptosis induced by *trans*-10, *cis*-12 conjugated linoleic acid in mice. Obes Res 10:1284–1290
3. Malpuech-Brugere C, Verboeket-van de Venne WP, Mensink RP, Arnal MA, Morio B, Brandolini M, Saebo A, Lassel TS, Chardigny JM, Sebedio JL, Beaufrere B (2004) Effects of two conjugated linoleic acid isomers on body fat mass in overweight humans. Obes Res 12:591–598
4. Loreau O, Maret A, Chardigny JM, Sebedio JL, Noel JP (2001) Sequential substitution of 1, 2-dichloro-ethene: a convenient stereoselective route to (9Z, 11E)- (10E, 12Z)- and (10Z, 12Z). Chem Phys Lipids 110:57–67
5. Redden PR, Lin X, Horrobin DF (1996) Comparison of the grignard deacylation TLC and HPLC methods and high resolution 13C-NMR for the sn-2 positional analysis of triacylglycerols containing gamma-linolenic acid. Chem Phys Lipids 79:9–19
6. Navarro V, Zabala A, Macarulla MT, Fernandez-Quintela A, Rodriguez VM, Simon E, Portillo MP (2003) Effects of conjugated linoleic acid on body fat accumulation and serum lipids in hamsters fed an atherogenic diet. J Physiol Biochem 59: 193–199
7. Bretillon L, Chardigny JM, Sebedio JL, Noel JP, Scrimgeour CM, Fernie CE, Loreau O, Gachon P, Beaufrere B (2001) Isomerization increases the postprandial oxidation of linoleic acid but not alpha-linolenic acid in men. J Lipid Res 42:995–997
8. Weir JB (1949) New methods for calculating metabolic rate with special reference to protein metabolism. J Physiol 109:1–9
9. Ferrannini E (1988) The theoretical bases of indirect calorimetry: a review. Metabolism 37:287–301
10. Dangin M, Desport JC, Gachon P, Beaufrere B (1999) Rapid and accurate $^{13}CO_2$ isotopic measurement in whole blood: comparison with expired gas. Am J Physiol 276:E212–E216
11. Ohnuki K, Haramizu S, Ishihara K, Fushiki T (2001) Increased energy metabolism and suppressed body fat accumulation in mice by a low concentration of conjugated linoleic acid. Biosci Biotechnol Biochem 65:2200–2204
12. Nagao K, Wang YM, Inoue N, Han SY, Buang Y, Noda T, Kouda N, Okamatsu H, Yanagita T (2003) The 10*trans*, 12*cis* isomer of conjugated linoleic acid promotes energy metabolism in OLETF rats. Nutrition 19:652–656

13. Demizieux L, Degrace P, Gresti J, Loreau O, Noel JP, Chardigny JM, Sebedio JL, Clouet P (2002) Conjugated linoleic acid isomers in mitochondria: evidence for an alteration of fatty acid oxidation. J Lipid Res 43:2112–2122
14. Goedecke JH, Rae DE, Smuts CM, Lambert EV, O'Shea M (2009) Conjugated linoleic acid isomers, *t*10*c*12 and *c*9*t*11, are differentially incorporated into adipose tissue and skeletal muscle in humans. Lipids 44:983–988
15. Zambell KL, Keim NL, Van Loan MD, Gale B, Benito P, Kelley DS, Nelson GJ (2000) Conjugated linoleic acid supplementation in humans: effects on body composition and energy expenditure. Lipids 35:777–782
16. Watras AC, Buchholz AC, Close RN, Zhang Z, Schoeller DA (2007) The role of conjugated linoleic acid in reducing body fat and preventing holiday weight gain. Int J Obes (Lond) 31:481–487
17. Nazare JA, de la Perriere AB, Bonnet F, Desage M, Peyrat J, Maitrepierre C, Louche-Pelissier C, Bruzeau J, Goudable J, Lassel T, Vidal H, Laville M (2007) Daily intake of conjugated linoleic acid-enriched yoghurts: effects on energy metabolism and adipose tissue gene expression in healthy subjects. Br J Nutr 97:273–280
18. Close RN, Schoeller DA, Watras AC, Nora EH (2007) Conjugated linoleic acid supplementation alters the 6-mo change in fat oxidation during sleep. Am J Clin Nutr 86:797–804

remove lipids from the cells, followed by quantification by weighing or chromatography [4–13]. Solvent extractions from microalgae are typically based on the methods using chloroform and methanol published in the 1950s by Folch et al. [14] and Bligh and Dyer [15]. It is well recognised that solvent extraction often extracts lipids incompletely, particularly free fatty acids, and can extract significant quantities of non-nutritive, non-saponifiable material such as pigments [16–18]. Small modifications in the protocol can have a large effect on extraction efficiency [19]. Smedes and Askland [20] tested various ratios of chloroform and methanol, described by the Bligh and Dyer method, and suggested that the yield of lipid could be increased by using a higher methanol content. This implied that the original Bligh and Dyer method resulted in incomplete extraction. Iverson et al. [19] compared the Bligh and Dyer and the Folch methods for a range of marine tissues, and concluded that the Bligh and Dyer method significantly underestimated the lipid content of samples containing more than 2% lipids. The effect was aggravated by increasing lipid content, resulting in an underestimation of 50% compared to the Folch method in the samples with the highest lipid content.

Gas chromatography (GC) can be used to quantify individual fatty acids as well as the total fatty acid present in a lipid extract. GC of lipids requires derivatisation to volatilise the samples [21]. This is normally achieved by converting saponifiable lipids [in biological samples, mainly triacylglycerols (TAG) and phospholipids] to FAME by addition of an excess of methanol and a catalyst, in a reaction known as transesterification [21, 22]. This eliminates the problem of extraction of non-fatty acid substances, such as pigments, as these are not detected by GC, but the accuracy of quantification is still dependent on the completeness of the extraction.

Instead of improving extraction methods, some investigators have eliminated extraction completely by transesterifying lipids in situ. Direct transesterification (DT) was first successfully performed in 1963 by Abel and co-workers [23]. Since then, it has been verified by numerous researchers in a variety of tissues, as a simple and rapid method of quantifying fatty acids by combining extraction and transesterification into one step. Diverse methods have been used for DT, but most involve the addition of an organic solvent, methanol, catalyst and heat to a small amount of dried sample (see [21] and [22] for comprehensive reviews of this). DT has previously, although infrequently, been applied to the quantification of fatty acids in microalgae [24–31], however, no evaluation or comparison to alternative methods has been made.

Transesterification involves the cleaving of an ester bond by an alcohol and can be catalysed by either a base or an acid. Usually a single catalyst is used and the choice is determined by the characteristics of the different catalysts. Alkaline catalysts, such as sodium methoxide (SM), or sodium or potassium hydroxide in methanol, transesterify complex lipids quickly and at lower temperatures than required by acid catalysts, but they do not esterify free fatty acids [21]. Acid catalysts, such as hydrochloric or sulphuric acid in methanol or boron trifluoride (BF_3) methanol, require heating and longer reaction times than basic catalysts [22], but can transesterify complex lipids as well as esterifying free fatty acids [21]. Considering the different capacities of acid and base catalysts, some investigators have used a combination of a basic catalyst or alkaline hydrolysis with NaOH or KOH in methanol, followed by an acid catalyst [21, 22, 32]. This study investigated whether the sequential use of two catalysts would improve the efficiency of DT in microalgae, particularly in the presence of water.

Water is known to interfere with the transesterification reaction [21, 22]. It is a stronger electron donor than methanol and the presence of water in the reaction system can cause hydrolysis, the opposite of esterification. To avoid interference by water, it has been suggested that the sample be dried, or a water scavenger such as 2,2-dimethoxypropane be added [22], however, there are reports which dispute the need for these practices below a critical water content. Lepage and Roy [33], using the catalyst acetyl chloride, found recoveries (>95%) to be unaffected by the presence of water up to 5% of the total reaction volume, while a water content of 10–15% significantly impaired the reaction. Most studies using DT for quantification of fatty acids in microalgae have used freeze-dried biomass, although there has been no investigation as to whether this is necessary.

This study tested and compared the effectiveness of DT to alternative methods of quantifying total fatty acid content in microalgae. The results of DT on three algal species were compared to those obtained by extraction using the Folch, the Bligh and Dyer, and the Smedes and Askland methods. The effects of using a sequential combination of base and acid catalysts, as well as the influence of water, on transesterification efficiency were investigated.

Experimental Procedure

Analytical Reagents

All reagents used were of chromatography standard. Toluene (99.9%) and chloroform (99.8%) were from Sigma-Aldrich (USA) and hexane (98%) and methanol (99.9%) from Merck (Germany). Methanolic base (0.5N), also known as sodium methoxide (SM), and boron trifluoride (BF_3) methanol solution (14%) were obtained from Sigma-Aldrich (USA). Distilled water (dH_2O) from a

Millipore system was used for all analyses. Internal standards used were glyceryl triheptadecanoate (C17-TAG) and methyl nonadecanoate (C19-ME) from Sigma-Aldrich (USA).

Algal Culture and Preparation

Two freshwater Chlorophyta (green algae), *Chlorella vulgaris* (*Cv*) (UTEX 395) and *Scenedesmus* sp. (*Sc*) (obtained from algal culture ponds near Upington, South Africa) and a marine Eustigmatophyte, *Nannochloropsis* sp. (*Nan*) were tested. Culture media for the freshwater species was 3N BBM medium, while the marine alga was grown in F2 medium (UTEX: http://www.sbs.utexas.edu/utex). Airlift reactors with a working volume of 3.2 L were sparged with air (*Cv* and *Sc*) or 4,400 ppm (0.44%) CO_2 (*Nan*) at a gas flow rate of 2 L min^{-1}. Light (80–160 μmol s^{-1} m^{-2}) was provided by three 18 W cool white fluorescent bulbs (Osram). Cells were harvested by centrifugation at 4,000 rpm for 10 min, rinsed in either distilled water (for freshwater cultures) or sterile seawater (marine cultures) and re-centrifuged. Biomass used in the experiments was from a single batch of each species.

Determination of Biomass Water Content

The wet pellet, following centrifugation, was weighed and resuspended in a known volume of distilled water or sterile seawater. A sample of this biomass concentrate corresponding to 0.1 g wet weight was filtered through a pre-weighed 0.45 μm Millipore filter and dried at 80 °C overnight. After cooling to room temperature in a desiccator, filters were weighed to determine the relative dry biomass and water content. The 0.1 g wet weight samples of *Cv*, *Sc* and *Nan* corresponded to 19.6 ± 0.31, 19.8 ± 0.12, and 27.4 ± 0.85 mg dry weight, respectively.

Extraction

All extractions and DTs were performed in triplicate, using samples of 0.1 g wet weight algal biomass. The control for each experiment was 80 μl dH_2O. Total lipid was extracted by the Bligh and Dyer method [15], the Smedes and Askland method [20] and the Folch method [14]. Each sample was extracted three times and the resulting solvent volumes combined. The combined extract was dried at room temperature overnight, transesterified and subjected to GC analysis for quantification of fatty acids. The residual biomass from each extraction was recovered and tested for any remaining fatty acids by DT.

The original protocols were followed as closely as possible, with the following two modifications:

- Sample size was scaled down by a factor of 1,000, with extraction volumes scaled accordingly.
- Homogenisation was replaced by vortexing at maximum speed for 3 min.

According to Folch et al. [14]: "the procedure can be run on any scale that is otherwise technically feasible". In order to verify that the scale of the reaction did not affect the results, the three extraction techniques and DT were repeated in triplicate using 1 g of *Sc* biomass (i.e. volumes scaled down by a factor of 100). Results were found to be very similar to extractions from 0.1 g (data not shown).

Transesterification

For DT, reagents were added directly to either internal standards, olive oil, or algal biomass. For DT of wet algal biomass, negative controls of 80 μl water were included, as well as a control for each algal species containing biomass but no internal standards, to test for the presence of C17 or C19 compounds in the algal cells. For extraction-transesterification, reagents were added to the dried extract or residual biomass from lipid extractions. Two internal standards were used: glyceryl triheptadecanoate (C17-TAG) was added prior to the reaction as a quantitative internal standard, and methyl nonadecanoate (C19-ME) was added in the final solvent extraction step to verify the completeness of the transesterification and efficiency of extraction into the hexane layer. A combination of base followed by acid catalysis was performed as follows: samples were dissolved in 500 μl toluene containing 0.1 mg C17-TAG in glass test tubes with silicon-lined screw-cap lids. One hundred microliters of 2,2-dimethoxypropane (water scavenger) was added. Sodium methoxide (1 ml) was then added and the samples mixed briefly by vortexing before being placed in an incubator at 80 °C, with shaking at 300 rpm for 20 min. Samples were cooled for 5 min to room temperature and 1 ml BF_3 methanol was added before repeating the incubation. After cooling for 5 min to room temperature, 400 μl dH_2O and 400 μl hexane containing 0.1 mg C19-ME were added and tubes mixed by vortexing. Samples were centrifuged at 4,000 rpm for 1 min and the upper hexane-toluene layer, containing the FAME extract, was transferred to vials for GC.

Gas Chromatography

The FAME extract (1 μl), containing internal standards, was injected into a Varian 3900 GC equipped with a flame ionisation detector and SupelcoWax 10 column (30 m × 320 mm × 1.0 μm film thickness) (Supelco, USA). Standard split/splitless injection was used with a split of 100 and an injector temperature of 270 °C. The column

temperature was increased from 180 °C to 260 °C at 2 °C min^{-1}. Nitrogen (2 ml min^{-1}) was used as the carrier gas and the detector temperature was 260 °C. Peaks were identified by retention time using Supelco 37 Component FAME and C14:0 to C22:0 FAME mixtures. Peak areas were used to quantify each FAME relative to the internal standards. Differences in the response factor of the detector to the range of FAMEs in the samples were negligible. The total fatty acid content was calculated by adding all the individual FAME peak areas.

Catalyst Tests

To test the efficiency of transesterification using a single catalyst, as opposed to a combination, C17-TAG samples (0.1 mg) were transesterified with either 1 ml SM, 1 ml BF_3 methanol, or a combination of the two catalysts. The tests were repeated with the addition of 80 µl water (equivalent to the amount of water in the algal pellets), with and without 100 µl of the water scavenger 2,2-dimethoxypropane. The efficiency of transesterification was calculated by dividing the peak area of the resulting C17-ME, by the peak area of the C19-ME added post-reaction. As equal quantities of these two standards were added (the mass of the three methyl esters formed is very similar to that of the TAG), their ratio gave an indication of how much of the C17-TAG was converted to fatty acid methyl esters.

Accuracy, Precision, and Limits of Detection and Quantification

To test the accuracy, precision, linearity, and limits of detection (LOD) and quantification (LOQ) of the assay, triplicate samples of 10, 5, 2.5, 1, 0.5, 0.1, 0.05, 0.01, 0.005 and 0.001 mg 100% extra virgin olive oil (Borges, Spain) were made up in toluene. Negative controls containing no olive oil were included. All samples were transesterified and quantified by GC. To estimate inter-experimental error, fresh 5 and 2.5 mg samples were analysed on three consecutive days. The LOD was defined as the minimum concentration at which distinct peaks could still be discerned above the baseline noise. The LOQ was defined as the lowest concentration of fatty acid that could be quantified with an accuracy and precision (calculated according to Wu et al. [34]) within 15%.

Sensitivity to Water

The effect of water on the two-catalyst reaction was tested using 0.1 mg of the C17-TAG internal standard as substrate, with dH_2O addition up to 50% of the final total reaction volume. Transesterification was carried out using C19-ME as the internal standard, with or without 100 µl of the water scavenger 2,2-dimethoxypropane. Reactions were done in duplicate.

Results

Direct Transesterification Versus Extraction-Transesterification

Total fatty acid content determined by DT and by the three extraction-transesterification methods in *Cv*, *Sc* and *Nan* are shown in Fig. 1. For all three species, DT yielded a higher estimation of fatty acid content than any of the extraction-transesterification methods. Of the extraction methods, the Folch method yielded higher results (77–93% of DT values) than the Smedes and Askland (23–73%) and the Bligh and Dyer (19–63%) methods. The Smedes and Askland method recovered more fatty acid from *Cv* and *Sc* than the Bligh and Dyer method.

DT on the residual biomass after the solvent extractions yielded additional fatty acid, indicating that the extraction procedures did not extract all the fatty acid. The sum of fatty acid extracted plus fatty acid remaining in the residual biomass was similar to that obtained by DT.

Single Catalyst Versus Sequential Combination of Catalysts

The ratio of C17-ME to C19-ME following the sequential combination of a basic catalyst followed by an acid catalyst demonstrated the degree to which C17-TAG was transesterified (Fig. 2). Values greater than 100% were obtained when the area of the C17-TAG peak was greater than that of the C19-ME peak. This could have been due to minor errors in dilution or pipetting of standard solutions.

When the two reagents were used sequentially, 100% conversion of TAG to FAME was obtained in the presence or absence of water. In the absence of water, the acid BF_3 catalyst alone produced an equivalent degree of transesterification to both reagents together, but the basic SM catalyst resulted in only 67% conversion. In the presence of water, no transesterification occurred with SM, while with BF_3 32% conversion was obtained. The addition of a water scavenger to the reaction containing 80 µl water improved the conversion with BF_3 to 55%, but did not improve SM conversion.

Accuracy, Precision and Limits of Detection and Quantification

To test the accuracy, scalability and reproducibility of the DT assay, serial dilutions of olive oil in toluene were

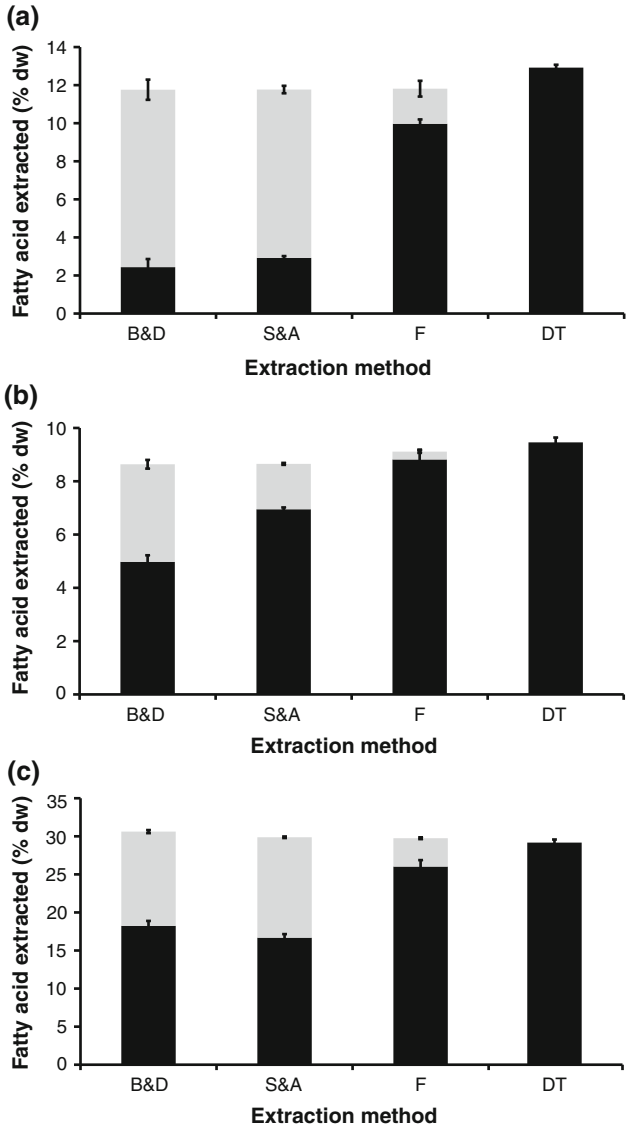

Fig. 1 Fatty acid content (as a percentage of the algal biomass dry weight) of **a** *Chlorella vulgaris*, **b** *Scenedesmus* sp. and **c** *Nannochloropsis* sp. measured by extraction with the Bligh and Dyer (B&D), Smedes and Askland (S&A) or Folch (F) methods, followed by transesterification and GC, or DT of the wet algal pellet. *Black bars* are the fatty acid content measured by the four different methods. *Light grey bars* are the fatty acid obtained by the DT carried out on the biomass residue from the extractions

directly transesterified and quantified by GC. The correlation coefficient of fatty acid concentration determined from the assay to that added to the samples was 0.96 with a linear regression coefficient of 0.9999. The LOD was 5 μg fatty acid, and the LOQ was 50 μg. For olive oil samples between 500 μg and 10 mg, the accuracy and precision of the assay were within 5 and 2.5%, respectively. The inter-experimental accuracy and precision were both within 5%.

Sensitivity to Water

The addition of water up to 10% of the total reaction volume had little effect on the efficiency of the reaction (Fig. 3). With the addition of larger volumes of water, the efficiency decreased dramatically and recovery was variable, as shown by the large error bars with between 20 and 50% water. Results with and without the water scavenger below 10% water were similar. Above 30% water, reactions containing the water scavenger resulted in an increase in the efficiency of transesterification, however, this still represented a substantial under-estimation of the fatty acid content and there was a high degree of variation between samples.

Discussion

This paper presented a rigorous comparison of DT to the most common alternative methods of lipid quantification in microalgae. It was shown, across three algal species, that DT was a simple, accurate and reliable method, capable of determining total fatty acid content more efficiently than traditional solvent extraction methods.

The commonly used extraction method of Bligh and Dyer was the least effective extraction method tested. It significantly underestimated fatty acid content (by up to 81% in the case of *Cv*), accounting for 19–63% of fatty acids quantified by DT. Smedes and Askland [20] investigated the solvent ratios used by Bligh and Dyer and proposed that a greater proportion of methanol would result in a better recovery of lipids. This was true for the green algal species, as the Smedes and Askland method yielded 17–28% more fatty acids than the Bligh and Dyer method (although 6% less fatty acid than the Bligh and Dyer method for *Nan*). However, the Smedes and Askland method still underestimated lipid content, measuring 23–73% of the fatty acid content measured by DT. The Folch extraction method was the most effective, yielding 77–94% of the total extracted by DT. These findings are in agreement with Lepage and Roy [35] who reported that fatty acid recovery from milk and adipose tissue was improved by DT due to the elimination of multiple extraction and purification steps. Fatty acid recoveries from samples of human milk and adipose tissue were 11–16% better than the Folch extraction. Iverson et al. [19] also showed that the Bligh and Dyer method greatly underestimated lipid content compared to the Folch method in fish samples.

DT completely eliminates the need for lipid extraction and purification and can be performed on small sample volumes. Classical lipid extraction techniques are lengthy and involve multiple steps, while DT is rapid and can be

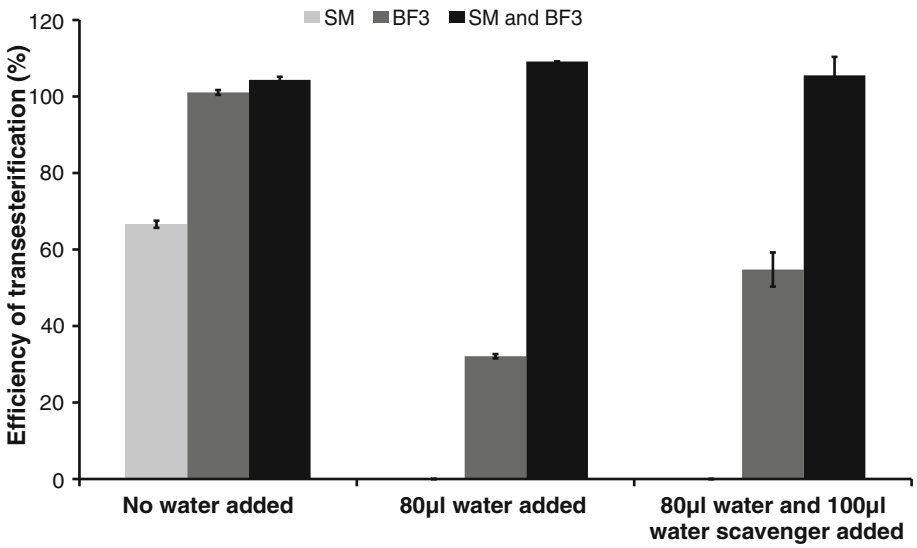

Fig. 2 The efficiency of transesterification of glyceryl triheptadecanoate (C17-TAG) by the basic catalyst sodium methoxide (SM), the acid catalyst boron trifluoride-methanol (BF_3) and a combination of the two (SM and BF_3), compared under three different reaction conditions: anhydrous, with 80 µl water, and with 80 µl water and 100 µl water scavenger

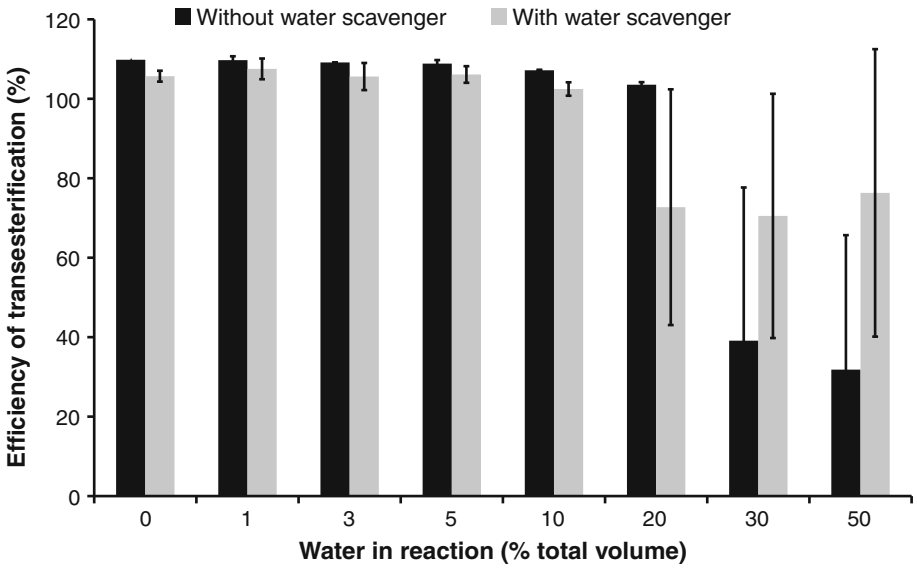

Fig. 3 Efficiency of transesterification, measured by conversion of C17-TAG to C17-ME, as a function of reaction water content, with and without addition of a water scavenger

performed in a single tube, minimising sample losses. The assay was found to be accurate and reproducible to 5% above 0.5 mg and 15% (defined as the LOQ) above 0.05 mg. Assuming a relatively low fatty acid content of 10% dry weight and a biomass concentration of 1 g L^{-1}, this LOQ equates to an algal sample of 0.5 mg dry weight or 2.5 mg wet weight.

The sequential addition of a basic and acid catalyst improved the efficiency of DT, particularly when there was water present in the reaction. With the addition of an amount of water equivalent to that in the centrifuged microalgal samples (80 µl), the basic catalyst SM was completely inhibited and the activity of BF_3 was reduced, while the combination of catalysts yielded complete conversion. This might have been due to the basic catalyst, in the presence of water, resulting in saponification (or alkaline hydrolysis) and cleaving the ester bonds between fatty acids and glycerol. This removed the water and allowed the acid catalyst to esterify the free fatty acids at a faster rate [21]. If dry samples are used, BF_3 on its own is as effective as a combination of catalysts. However, under conditions where there is water present in the reaction, a combination of base and acid catalysts should be used, or alkaline hydrolysis should be performed before methylation.

The majority of previously reported DT protocols for microalgae used lyophilised biomass and a single acid catalyst [25–31]. This study has shown that drying of centrifuged algal biomass was not necessary if a sequential combination of basic and acid catalysts were used. The two-reagent transesterification reaction was unaffected by water up to 10% of the total reaction volume (290 µl). The water content of the algal samples contributed 80 µl of water (3% of total reaction volume) and was well within the acceptable range, thus centrifuged samples could be

processed immediately without drying. It was not necessary to add a water scavenger at water contents less than 10%, although this may have been beneficial at high water contents (>30%). As additional reactants such as 2,2-dimethoxypropane can cause extra peaks in the chromatogram, it is recommended that water scavengers not be used at low water contents (<10%).

The major limitation of this method is that by converting all lipids directly into FAME, lipids can no longer be separated and evaluated as different classes, e.g. polar phospholipids and glycolipids versus non-polar or neutral triacylglycerols. If a study requires the differentiation of lipid classes, solvent extraction of the tissue may be necessary.

As FAME are the components of biodiesel and transesterification is the major method of biodiesel production, DT has potential large-scale application in the rapid, low cost production of biodiesel directly from microalgal cells without the need for oil extraction. Johnson and Wen [36] showed that a one-step method of DT resulted in a higher FAME yield from *Schizochytrium limacinum* (a Thraustochytrid, taxonomically aligned with heterokont microalgae [37]) than oil extraction followed by transesterification, and could produce biodiesel where 8 out of 11 parameters met ASTM fuel standards. Eliminating the step of oil extraction could make the process cheaper, but does not eliminate the need for harvesting and dewatering of the biomass to less than 10%. The analytical procedure described here would need to be further developed to use cheaper and less toxic transesterification reagents, and allow recycling of the solvents. Preliminary data has indicated that sodium hydroxide in methanol (0.5N) and hydrochloric acid in methanol (5%) can be substituted for sodium methoxide and BF_3 methanol, respectively (data not shown).

Acknowledgments This work is based upon research supported by the South African National Energy Research Institute (SANERI), the South African Research Chairs Initiative (SARChI) of the Department of Science and Technology and the National Research Foundation (NRF). The financial assistance of these organisations towards this research is hereby acknowledged. Opinions expressed and conclusions arrived at are those of the authors and are not necessarily to be attributed to SANERI, SARChI or the NRF.

References

1. Pulz O, Gross W (2004) Valuable products from biotechnology of microalgae. Appl Microbiol Biotechnol 6:635–648
2. Spolaore P, Joannis-Cassan C, Duran E, Isambert A (2006) Commercial applications of microalgae. J Biosci Bioeng 2:87–96
3. Apt KE, Behrens PW (1999) Commercial developments in microalgal biotechnology. J Phycol 2:215–226
4. Shifrin NS, Chisholm SW (1981) Phytoplankton lipids: interspecific differences and effects of nitrate, silicate and light-dark cycles. J Phycol 4:374–384
5. Ben-Amotz A, Tornabene TG, Thomas WH (1985) Chemical profile of selected species of microalgae with emphasis on lipids. J Phycol 1:72–81
6. Suen Y, Hubbard JS, Holzer G, Tornabene TG (1987) Total lipid production of the green alga *Nannochloropsis* sp. QII under different nitrogen regimes. J Phycol 23(2):289–296
7. Volkman JK, Jeffrey SW, Nichols PD, Rogers GI, Garland CD (1989) Fatty acid and lipid composition of 10 species of microalgae used in mariculture. J Exp Mar Biol Ecol 3:219–240
8. Renaud SM, Parry DL, Thinh LV (1994) Microalgae for use in tropical aquaculture I: gross chemical and fatty acid composition of twelve species of microalgae from the Northern Territory. Australia. J Appl Phycol 3:337–345
9. Reitan KI, Rainuzzo JR, Olsen Y (1994) Effect of nutrient limitation on fatty acid and lipid content of marine microalgae. J Phycol 6:972–979
10. Pratoomyot J, Srivilas P, Noiraksar T (2005) Fatty acids composition of 10 microalgal species. Songklanakarin. J Sci Technol 6:1179–1187
11. Mansour MP, Frampton DMF, Nichols PD, Volkman JK, Blackburn SI (2005) Lipid and fatty acid yield of nine stationary-phase microalgae: applications and unusual C24–C28 polyunsaturated fatty acids. J Appl Phycol 4:287–300
12. Patil V, Källqvist T, Olsen E, Vogt G, Gislerød HR (2007) Fatty acid composition of 12 microalgae for possible use in aquaculture feed. Aquacult Int 1:1–9
13. Widjaja A, Chien CC, Ju YH (2009) Study of increasing lipid production from fresh water microalgae *Chlorella vulgaris*. J Taiwan Inst Chem Eng 1:13–20
14. Folch J, Lees M, Sloane Stanley GH (1957) A simple method for the isolation and purification of total lipids from animal tissues. J Biol Chem 226(1):497–509
15. Bligh EG, Dyer WJ (1959) A rapid method of total lipid extraction and purification. Can J Biochem Physiol 8:911–917
16. Palmquist DL, Jenkins TC (2003) Challenges with fats and fatty acid methods. J Anim Sci 12:3250–3254
17. Pruvost J, Van Vooren G, Cogne G, Legrand J (2009) Investigation of biomass and lipids production with *Neochloris oleoabundans* in a photobioreactor. Bioresour Technol 23:5988–5995
18. Ratledge C (1987) Lipid Biotechnology: a wonderland for the microbial physiologist. J Am Oil Chem Soc 12:1647–1656
19. Iverson SJ, Lang SLC, Cooper MH (2001) Comparison of the Bligh and Dyer and Folch methods for total lipid determination in a broad range of marine tissue. Lipids 11:1283–1287
20. Smedes F, Askland TK (1999) Revisiting the development of the Bligh and Dyer total lipid determination method. Mar Pollut Bull 3:193–201. doi:10.1016/S0025-326X(98)00170-2
21. Liu KS (1994) Preparation of fatty acid methyl esters for gas-chromatographic analysis of lipids in biological materials. J Am Oil Chem Soc 11:1179–1187
22. Carrapiso AI, García C (2000) Development in lipid analysis: some new extraction techniques and in situ transesterification. Lipids 11:1167–1177
23. Abel K, Deschmertzing H, Peterson JI (1963) Classification of microorganisms by analysis of chemical composition. I. Feasibility of utilizing gas chromatography. J Bacteriol 85(5):1039–1044
24. Montaini E, Chini Zittelli G, Tredici MR, Molina Grima E, Fernandez Sevilla JM, Sanchez Perez JA (1995) Long-term preservation of *Tetraselmis suecica*: Influence of storage on viability and fatty acid profile. Aquaculture 1–2:81–90
25. Rodríguez-Ruiz J, Belarbi EH, Sánchez JLG, Alonso DL (1998) Rapid simultaneous lipid extraction and transesterification for fatty acid analyses. Biotechnol Tech 9:689–691

26. Wen ZY, Chen F (2001) Optimization of nitrogen sources for heterotrophic production of eicosapentaenoic acid by the diatom *Nitzschia laevis*. Enzyme Microb Technol 6–7:341–347
27. Blokker P, Pel R, Akoto L, Brinkman UAT, Vreuls RJJ (2002) At-line gas chromatographic–mass spectrometric analysis of fatty acid profiles of green microalgae using a direct thermal desorption interface. J Chromatogr A 1–2:191–201
28. Carvalho AP, Pontes I, Gaspar H, Malcata FX (2006) Metabolic relationships between macro-and micronutrients, and the eicosapentaenoic acid and docosahexaenoic acid contents of *Pavlova lutheri*. Enzyme Microb Technol 3–4:358–366
29. Fajardo AR, Cerdán LE, Medina AR, Fernández FGA, Moreno PAG, Grima EM (2007) Lipid extraction from the microalga *Phaeodactylum tricornutum*. Lipid-Fett 2:120–126
30. Armenta RE, Scott SD, Burja AM, Radianingtyas H, Barrow CJ (2009) Optimization of fatty acid determination in selected fish and microalgal oils. Chromatographia 3:629–636
31. Hsieh CH, Wu WT (2009) Cultivation of microalgae for oil production with a cultivation strategy of urea limitation. Bioresour Technol 17:3921–3926
32. Metcalfe LD, Schmitz AA, Pelka JR (1966) Rapid preparation of fatty acid esters from lipids for gas-chromatographic analysis. Anal Chem 38:514–515
33. Lepage G, Roy C (1986) Direct transesterification of all classes of lipids in a one-step reaction. J Lipid Res 1:114–120
34. Wu YT, Lin LC, Tsai TH (2009) Measurement of free hydroxytyrosol in microdialysates from blood and brain of anesthetized rats by liquid chromatography with fluorescence detection. J Chromatogr A 16:3501–3507
35. Lepage G, Roy C (1984) Improved recovery of fatty acid through direct transesterification without prior extraction or purification. J Lipid Res 12:1391–1396
36. Johnson MB, Wen Z (2009) Production of biodiesel fuel from the microalga *Schizochytrium limacinum* by direct transesterification of algal biomass. Eng Fuel 23(10):5179–5183
37. Lewis TE, Nichols PD, McMekin TA (1999) The biotechnological potential of Thraustochytrids. Mar Biotechnol 6:580–587

decomposed to aldehydes during the digestion and absorption processes. Giuffrida et al. [3] detected that low pH promotes breakdown of epoxidized lipids to diols in simulated gastric conditions. Low pH also promotes oxidation of double bonds and as oxygen is present in the stomach in excess, it is likely that the stomach acts as an oxidative bioreactor [4, 5]. Moreover, the ferrous ions that are formed during the digestion of meat products can readily act as catalysts in the oxidation reactions in the stomach [6, 7]. It is difficult to study lipid oxidation during digestion processes, because of the necessity of using animal models and because such research requires complex analytical procedures. However, there are alternatives to animal models. In the current experiment, an artificial digestion model was adopted to analyze the progression of lipolysis and the presence of oxidized lipids [8, 9].

During digestion, triacylglycerols (TAG), which are the main molecular species of refined oils, are hydrolyzed by different enzymes to form free fatty acids (FFA) and monoacylglycerols (MAG). Diacylglycerols (DAG) are also formed in the stomach and in the first part of the small intestine. Lingual lipase and gastric lipase are both active in the acidic environment in the stomach and can hydrolyze from 10 to 30% of the TAG present in the stomach to FFA and DAG [10, 11]. Generally, short and medium-length fatty acids are hydrolyzed more efficiently by gastric lipase than long ones, and the *sn*-3 position is preferred over the *sn*-1 position while the *sn*-2 position is left mostly intact [12]. Different polarities and dipole properties of FFA, MAG, DAG, and TAG result in different distributions inside the lipid droplets formed during digestion. As digestion proceeds, lipid droplets become smaller in size and eventually form mixed micelles with phospholipids, cholesterol, cholesteryl esters and bile salts in the intestine. FFA and MAG are released from the mixed micelles in the duodenum and absorption takes place. Some absorption of FFA also takes place in the stomach [13].

Among the various methods developed to analyze these nonvolatile lipids is high performance liquid chromatography (HPLC) coupled with mass spectrometry (MS). Atmospheric pressure chemical ionization (APCI)–MS [14–18] and electrospray ionization (ESI)–MS [19, 20] have been used to determine e.g. the TAG composition of low erucic acid rapeseed oil. APCI–MS [18] and ESI–MS [21] have also been used to analyze oxidized TAG species of low erucic acid rapeseed oil as ammonium adducts. Simultaneous analysis of different lipid classes is usually performed in a less specific manner e.g. with thin layer chromatography (TLC) [22]. Furthermore, normal phase (NP)-HPLC is frequently used in the crude separation of FFA, MAG, DAG, TAG, phospholipids, and different cholesterol species, followed by more detailed gas chromatography (GC) or HPLC analysis. More specialized NP-HPLC–ESI–MS^n analysis of different lipid classes has recently been developed [23]. Solid phase extraction (SPE) is often used to separate major lipid classes from each other prior to more specific analysis of different molecular species [22].

Once isolated, fatty acids are routinely analyzed by GC as methyl esters. NP-HPLC analysis of fatty acids is usually performed after derivatization to picolinyl or methyl esters, but some work has also been done with underivatized free fatty acids [24, 25]. Orellena-Coca analyzed epoxidized free fatty acids with a reversed phase (RP)-HPLC-evaporative light scattering detector (ELSD)–MS and MS/MS with good resolution between individual molecular species [26]. However, the handling and derivatization of the sample takes time and possibly exposes the sample to further oxidation or other deterioration. Moreover, GC analysis involves elevated temperatures that may affect some of the oxidized molecules such as unstable hydroperoxides.

The purpose of the current study was to develop a method for the simultaneous analysis of FFA, MAG, DAG, and TAG molecular species and their oxidation products from lipid digestion samples. In particular, the aims were to (a) achieve adequate resolution among individual molecular species while reducing the overall workload significantly and (b) reduce the risk of sample oxidation during handling. The developed HPLC–ELSD–ESI–MS method was applied to study lipid digestion and oxidation in an artificial digestion model.

Experimental Procedures

Materials and Methods

All solvents were of HPLC grade or when adequate, *p.a.* grade. HPLC grade water was prepared with Millipore Milli-Q water purification system (Millipore SA, Molsheim, France). Porcine pepsin, lipase, pancreatin, α-amylase from *Aspergillus oryzae*, and bovine serum type II albumin were purchased from Sigma-Aldrich Co. (St. Louis, MO, USA). Mucin was purchased from Carl Roth GmbH (Karlsruhe, Germany). 12-hydroxyoctadecanoic acid (>98%), 1(3)-monopalmitoyl-*sn*-glycerol (>99%), 1(3)-monostearoyl-*sn*-glycerol (>99%), 1(3)-monooleoyl-*sn*-glycerol (>99%), 1(3)-monolinoleoyl-*sn*-glycerol (>99%), 1(3)-monolinoleoyl-*sn*-glycerol (>98%), 1,2(2,3)-dipalmitoyl-*sn*-glycerol (>99%), 1,3-dipalmitoyl-*sn*-glycerol (>99%), 1,3-dioleoyl-*sn*-glycerol (>99%), 1,3-dilinoleoyl-*sn*-glycerol (>99%), and 1,3-dilinolenoyl-*sn*-glycerol (>99%) were purchased from Larodan Fine Chemicals AB (Malmö, Sweden). Saturated even carbon number free fatty acids (C_{10}–C_{24}), and palmitoleic, oleic, linoleic, and α-linolenic

acids, and trinonadecanoyl-*sn*-glycerol were purchased from Sigma-Aldrich Co. A triacylglycerol mixture (GLC HPLC # G-1) was purchased from Nu-Check Prep Inc. (Elysian, MN, USA). The mixture was composed of saturated TAG from tricaprin to tristearin, and also included tripalmitolein, triolein, trilinolein, and trilinolenin (see Table 2). Oxidized triacylglycerols (1,3-distearoyl-2-(monohydroperoxy)stearoyl-*sn*-glycerol, 1,3-dibehenoyl-2-(monohydroperoxy) oleoyl-*sn*-glycerol, 1,3-distearoyl-2-(monohydroperoxy) oleoyl-*sn*-glycerol, 1,3-dibehenoyl-2-(monoepoxy)stearoyl-*sn*-glycerol, 1,3-distearoyl-2-(diepoxy)stearoyl-*sn*-glycerol, 1,2-(monoepoxy)distearoyl-3-stearoyl-*sn*-glycerol, 1,3-distearoyl-2-(monohydroperoxy)linoleoyl-*sn*-glycerol, and 1,3-dibehenoyl-2-(9-oxo)nonanoyl-*sn*-glycerol) were used from previous experiments [27]. Rapeseed oil (Kultasula, Raisio plc, Finland), milk protein isolate (MAITO90, Func Food Finland Oy, Finland), potato starch (Pirkka, Kesko Corporation, Finland), and fiber preparation (Kuidukas, Myllyn Paras Oy, Finland) were purchased from a grocery store. 3-chloroperoxybenzoic acid and methylene blue were obtained from Sigma-Aldrich Co. Hydrogen peroxide (30%) and formic acid (99%) were obtained from Riedel-de Haën (Riedel-de Haën AG, Seelze, Germany).

Oil Oxidation and Synthesis of Oxidized Reference Compounds

Low erucic acid rapeseed oil was oxidized in a convection oven at 100°C for 48 h. As epoxides are reported to break down to diols in acidic conditions, hydroxylated oil was selected as the second oxidized oil for the digestive experiments [3]. The hydroxylated oil was prepared by chemical oxidation according to Harry-O'Kuru and Carriere from rapeseed oil [28]. Formic acid (370 μL) was mixed with rapeseed oil (3.0 g) while gently mixing with a magnetic stirrer in test tubes. Hydrogen peroxide (3.8 mL) was added slowly while mixing and the temperature was raised to 70°C for 15 h. H_2O (1.8 mL) was added with HCl (250 μL). Mixing was continued for an additional 15 h at 70°C. The mixture was transferred to a separatory funnel with ethyl acetate. The chemically oxidized oil was first washed with saturated NaCl solution, then with saturated $NaHCO_3$ solution, and finally with MQ water. Ethanol (97%) was added to separate the water from the chemically oxidized oil. A rotary evaporator (50°C) was used to dry the oil.

Additionally, linoleic and linolenic acids were oxidized by a photosensitizing method according to Neff et al. [29] and epoxy derivatives were prepared according to Deffense [30]. Briefly, 15 mg of linoleic and linolenic acids in dichloromethane (400 μL) were mixed separately with 3-chloroperoxybenzoic acid (40 mg) to form epoxy derivatives, and linoleic and linolenic acids (30 mg each) in dichloromethane (400 μL) were photo-oxidized in 0.1 mM methylene blue solution (3 mL) under a 250 W UV light (distance from light 20 cm for 15 h) to form hydroperoxides. The solutions in test tubes were kept in an ice bath during the photo-oxidation. In addition, hydroperoxidized monoacylglycerols and diacylglycerols were produced by photo-oxidation from 1(3)-monooleoyl-*sn*-glycerol, 1(3)-monolinoleoyl-*sn*-glycerol, 1(3)-monolinolenoyl-*sn*-glycerol, 1,2(2,3)-dioleoyl-*sn*-glycerol, and 1,2(2,3)-dilinoleoyl-*sn*-glycerol. Peroxide values were measured from the oxidized rapeseed oils according to AOCS method Cd 8-53 [31].

Standard Meal

A standard meal was prepared for the digestion experiments. Potato starch was used as the carbohydrate source, milk protein isolate as the protein source, and fiber was obtained from a bran mixture of oat, rye, and wheat. The carbohydrate, protein, and fiber contents of the standard meal were calculated from the composition information given by the manufacturers. The Finnish nutritional recommendations from the National Nutrition Council [32] and the National FINDIET 2002 survey [33] were used as the basis for the calculations of the macronutrient composition of the standard meal. 50.0% of the energy of the standard meal came from carbohydrates, 16.5% from proteins, and 33.5% from separately added lipids. Three grams of fiber were added for each MJ of energy. Lipids were removed from the milk protein isolate and from the fiber preparation by a exhaustive (40 h) Soxhlet extraction with chloroform and methanol (2:1, v/v). Lipid-free ingredients were dried in a convection oven (60°C) overnight, weighed, and mixed together. The dry standard meal base was stored in a desiccator. The standard meal was prepared from the dry base by adding water and consecutively heating the mixture (100°C for 20 min.) to hydrate the starch. The lipid component was added separately.

Artificial Digestion Model

The artificial digestion model to be developed was based on the Versantvoort et al. [8, 9] comprehensive study on simulation of human digestive processes. The compositions of digestive fluids used here were based on the fed state, in contrast to the fasted state, simulating the conditions during and after meal consumption and digestion. The main differences to Versantvoort's model were the scale and scope and the collection of saliva from volunteers instead of artificially making it. Inorganics were weighed and diluted in 25-mL volumetric flasks which were stored in a refrigerator. Organic fluids were prepared on the same day the digestion model was used. Appropriate amounts were

Table 1 Volumetric composition of the artificial digestion model

Component	Volume (mL)
Food	0.9
Saliva	0.6
Gastric fluid	1.2
Bicarbonate (1 M)	0.2
Bile	0.6
Intestinal fluid	1.2
Total volume	4.7

weighed into 25-mL volumetric flasks and dissolved in deionized water. The collected saliva was centrifuged (1,100×*g*) and the supernatant was used as is on the same day. Saliva was stored refrigerated for a short period of time. The simulated gastric fluid, bile, and intestinal fluid were prepared from organic and inorganic fluids according to Versantvoort et al. [9]. All the liquids were heated to 37°C before use in the artificial digestion model.

The standard meal (900 mg) was weighed in test tubes and the appropriate oil (35 mg) was added, together with an internal standard (5 mg of 12-hydroxystearic acid). Saliva and gastric fluid were added (see Table 1), the test tubes were capped and incubated (pH 2–3) in a shaker for 2 h (700 U/min, 37°C). Finally, bicarbonate, bile, and intestinal fluid were added and the test tubes were incubated for an additional 2 h (pH 6.5–7). Samples (200 μL) were taken for extraction. The pH of the food and digestive fluid mixtures in different digestive phases were checked with a pH meter (WTW inoLab Ph Level 1, Wissenschaftlich-Technische Werkstätten GmbH, Weilheim, Germany).

Extraction

Samples after digestion were extracted according to Folch et al. [34] with minor adjustments. Nitrogen gas was used as an inert atmosphere during the extraction procedures. Samples (200 μL) of digestion fluid were added to disposable glass test tubes and MeOH (1.5 mL) was added. The test tubes were mixed thoroughly and chloroform (3 mL) was added. The test tubes were incubated in a shaker (700 U/min) at room temperature for 1 h. H_2O (1.25 mL) was added, mixed and left to stand. The test tubes were centrifuged at 1,000×*g* for 10 min and the lower phase was carefully transferred into a clean tube. For quantitative extraction, clean lower phase (2 mL) was added to the remaining upper phase, and the test tubes were remixed and centrifuged. The lower phases were combined avoiding any precipitates, evaporated to dryness, and dissolved in isopropanol (1 mL). The samples were not filtered prior to analysis. Extracted samples were stored in a deep freezer (−80°C) for a short period of time until analyzed.

GC Analysis of Fatty Acid Methyl Esters

The fatty acid composition of native rapeseed oil was determined using a GC–flame ionization detector (FID) by comparison to authentic reference compounds. Briefly, 0.3 mg of oil were transferred into test tubes and spiked with 0.1 mg of internal standard trinonadecanoin. Toluene (100 μL) and boron trifluoride in methanol (0.5 mL) were added and the capped test tubes were incubated for 1 h (90°C). After extraction with hexane (0.8 mL) and H_2O (1 mL), the samples were analyzed with a Perkin-Elmer Auto-System Gas Chromatograph (Waltham, MA, USA) with an autosampler and a 60 m × 0.25 mm i.d., 0.25 μm film thickness, J.W. Scientific DB-23 column (Agilent Technologies Inc., Santa Clara, CA, USA). The following temperature program was used. An initial 130°C oven temperature was held for 1 min, then increased to 170°C (6.5°C/min), then to 215°C (2.8°C/min) and held for 12 min, and finally to 230°C (40°C/min) and held for 3 min. The injector was held at 270°C and the detector at 290°C. The injection volume was 1 μL and four replicates were injected per sample.

HPLC–ELSD–ESI–MS Analysis

A Waters Acquity UPLC™ was used as an LC inlet (Milford, MA, USA), and a Macherey-Nagel C18 Nucleodur ISIS column (250 mm × 4.6 mm i.d., 5 μm particle size, Macherey-Nagel inc., Bethlehem, PA, USA) was used for the separation of lipid components. An evaporative light scattering detector (Sedex LT-75, Sedere Inc., Lawrenceville, NJ, USA) was used to detect the separated sample components simultaneously with a Waters Quattro Premier tandem quadruple mass spectrometer used in positive ESI mode. A solvent gradient program was used for the HPLC separation. Solvent A was composed of acetonitrile, H_2O, and formic acid (50:50:0.1, by vol). Solvent B was composed of isopropanol, acetone, and formic acid (90:10:0.1, by vol). Solvent B was increased from an initial level of 10 to 60% in 40 min and to 95% in 85 min. The total flow rate was 1.0 mL/min of which 20% was directed to the mass spectrometer. The ELSD was operated at 40 psi and 70°C.

High water and isopropanol contents of the mobile phases resulted in very high operating pressures. 250 mm × 4.6 mm i.d. columns with 5 μm silica particles can withstand around 5,000 psi of back pressure. Acetone could have been used as pure B solvent but the increase in the low *m/z* background noise in MS was excessive. Instead we modified the existing column oven of the Acquity UPLC system to hold a 250 mm × 4.6 mm i.d. column. After careful insulation, it was possible to decrease the back pressure significantly (approx. to half) by warming up

the column to 60°C. A more modest temperature (30°C) was, however, selected to minimize possible in-column oxidation during the 90 min analysis. This small increase in column temperature when combined with 10% acetone in solvent B was enough to keep the maximum back pressure at less than 5,000 psi.

Free fatty acids can partially ionize during chromatography, resulting in peak broadening and tailing. Different ionization suppressors were tested during optimization. 0.05% trifluoroacetic acid (TFA) gave the sharpest peaks for FFA but resulted in excess noise in the MS detector. Acetic acid and formic acid (0.1%) were similar in the efficiency of ionization suppression during chromatography but not as effective as TFA. Formic acid was selected because of the lowest noise in MS, although some peak broadening still occurred.

Mass calibration of the mass spectrometer was done automatically by Waters MassLynx 4.1 control software. Preliminary calibration was done by infusion of a NaCsI solution. This, however, resulted in small systematic mass error in the higher mass region which was corrected by recalibrating the instrument and all the acquired data. The new calibration was done with the aid of water clusters [35]. Three types of calibrations were performed on each quadrupole: a static scan calibration (50–1,800 Da), a scanning calibration (50–1,800 Da), and a scan speed compensation calibration (200–5,000 amu/s). 31 peaks obtained by the infusion of 0.1% TFA solution were compared to a reference file (calculated monoisotopic cluster peaks of water, $[H_3O + nH_2O]^+$) and calibration curves were obtained. The maximum acceptable deviation of mass differences was set at 0.2, which was not exceeded during the calibration. The mass precision remained good throughout the analyses, and therefore, all the recalibrated data were considered accurate. Tuning was performed by introducing reference compounds via a syringe pump to a tee leading into the ion source, while the solvent flow from the inlet was set at 150 μL/min. Mass spectra from 150 to 1,100 *m/z* were collected in the positive ionization mode. Tuning was optimized for simultaneous analysis of FFA, MAG, DAG, and TAG. The ESI capillary voltage was set at 3.00 kV, the cone voltage at 300 V, the extractor voltage at 2 V, the source temperature at 120°C, the desolvation temperature at 170°C, the desolvation gas (N_2) flow at 600 L/h, and the cone gas flow at 500 L/h. The cone voltage was set at 300 V, because less background noise was observed compared to a smaller and more typical setting of 10–60 V.

Quantitative Calculations

Quantitative calculations were performed from calibration and sample runs. MassLynx 4.1 was used for ELSD and MS data collection and analysis. Origin 8 SR4 (OriginLab Co., Northampton, MA, USA) was used for calibration curve fittings. The quantification was based on calibration curves that were formed by linear fitting of the area of extracted single ion mass chromatogram peaks versus concentration. An internal standard (12-hydroxyoctadecanoic acid) was used to correct for any sample loss during sampling or Folch extraction. Duplicate runs of five different levels of reference compounds were performed to obtain calibration curves. 10, 5, 2.5, 1.25, 0.625 μg loads to column were used for FFA, and one tenth of the amount of FFA for MAG, DAG, and TAG. The saturation of the MS signal limited the accuracy of quantification at higher concentrations. No reliable quantification was performed on the oxidized compounds because the reference compounds acquired were not sufficiently pure.

Results and Discussion

Development of HPLC–ELSD–ESI–MS Method

To develop a comprehensive HPLC method that would be capable of separating FFA, MAG, DAG, TAG, and their oxidized equivalents, a large number of reference compounds was used. Figure 1 shows ELSD and MS chromatograms, as well as a combined full scan mass spectrum of 0–90 min of the unoxidized reference compounds analyzed by the developed method. Analogous chromatograms and a spectrum of oxidized reference compounds are presented in Fig. 2. In addition, oxidized reference compounds were analyzed individually. The assignments, the retention times of the unoxidized and oxidized reference compounds, and the most abundant positive ions formed in ESI–MS are given in Tables 2 and 3, respectively (oxidized molecules are numbered with apostrophes and unoxidized with plain numbers.) Linear fitting equations used in the quantification of some of the MAG, and DAG are shown in Table 4, along the coefficients of determination.

The ELSD served as an auxillary detector and produced similar response profiles as the MS detector for the unoxidized lipids. However, the relative signal intensities of FFA (e.g. peaks 6 and 17 in Fig. 1a) compared to MAG, DAG and TAG were much higher in the ELSD signal compared with the ESI–MS signal in the positive ionization mode (see Fig. 1b). This indicates poor ionization of the FFA in the positive ionization ESI–MS. Also, epoxidized FFA (peaks 1′, 2′, and 4′ in Fig. 2a) had a much higher relative signal intensity in the ELSD. Diacylglycerols formed $[M+23]^+$ ions (sodium adducts) efficiently which corresponded to higher MS signal intensity of DAG (e.g. peaks 19, 22, and 26 in Fig. 1b) compared with MAG (e.g. peak 14 in Fig. 1b). It is worth noting that the flowrate into the ELSD was higher as only 20% of the total flow was

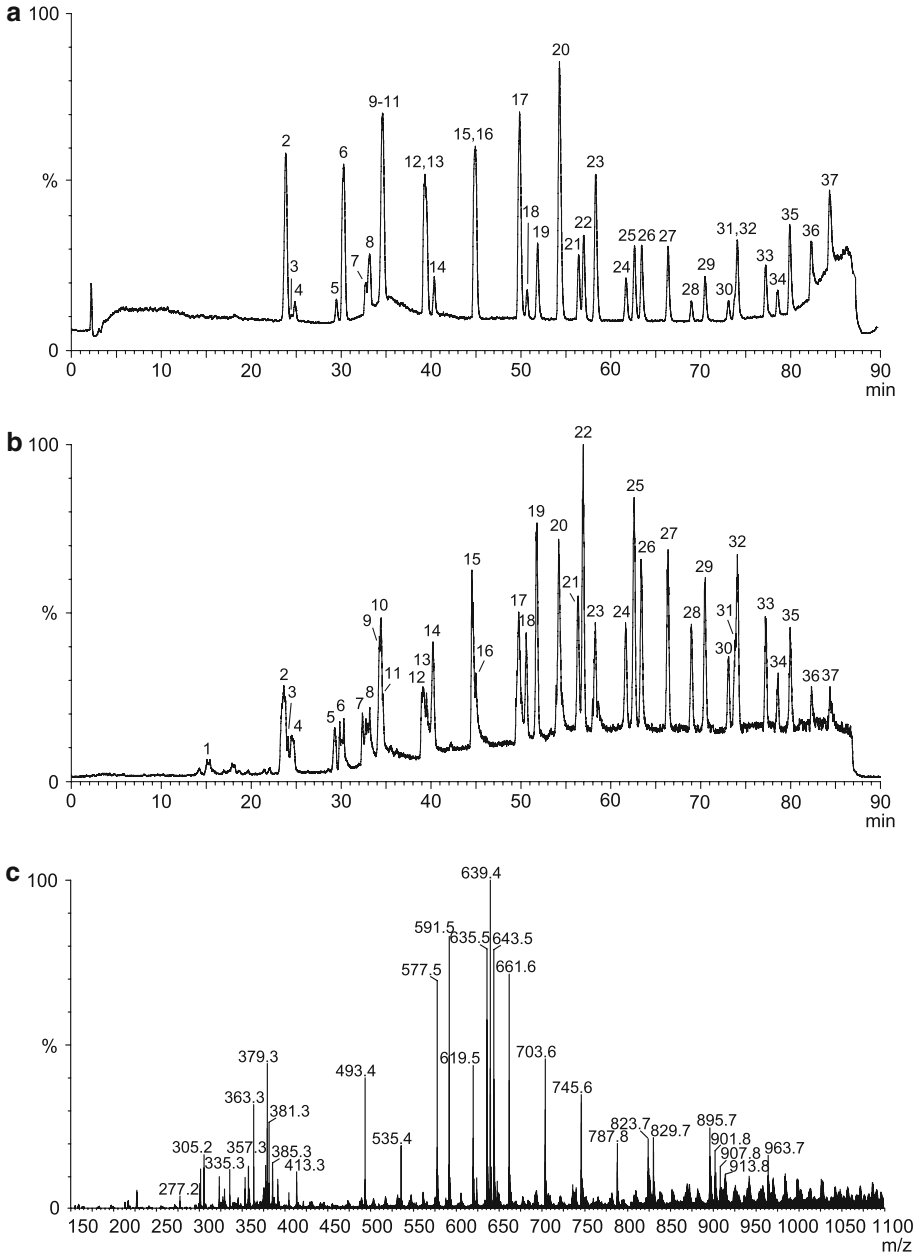

Fig. 1 ELSD chromatogram (**a**), full scan total ion MS chromatogram (**b**), and a combined full scan mass spectrum of 0–90 min (**c**) of unoxidized reference compound mixture. Analyzed as explained in experimental procedures. The amount injected was 5.0 μg of each FFA, 0.5 μg MAG, DAG, and most of the TAG. Refer to Table 2 for peak numbering

directed into the MS detector, and that the amount of FFA injected was ten times the amount of MAG, DAG, and TAG. As expected, the linear range of the response was higher with the ELSD. The total ion current chromatograms include much information that can be extracted and enables the study of closely eluting and unresolved peaks.

As expected, free fatty acids displayed negative $[M-H]^-$ ions when negative ionization mode was used, but as oxidized FFA did not readily form negative ions and since MAG, DAG or TAG did not form negative ions at all, negative ionization was not used. Protonated molecules $[M+H]^+$ were not observed by ESI–MS during analysis, as previously noted by others [17, 18], but instead the analytes formed sodium adducts $[M+23]^+$ and clusters of adducts $[2*M+23]^+$, $[2*M+45]^+$, $[2*M+67]^+$, and $[3*M+89]^+$. Water adducts $[M+18]^+$ were mainly observed with epoxidized FFA. Some protonated molecules and more intense water adducts were seen during tuning, but the flow rate was lower than in actual analyses. Medium length (10:0–16:0) FFA formed mainly $[M+45]^+$ ions and clusters of adducts with minimal $[M+23]^+$ ions. The $[M+45]^+$ ion is probably an adduct of a deprotonated molecule and two sodium atoms. Similarly, ions $[2*M+67]^+$ and $[3*M+89]^+$ probably correspond to clusters of two and

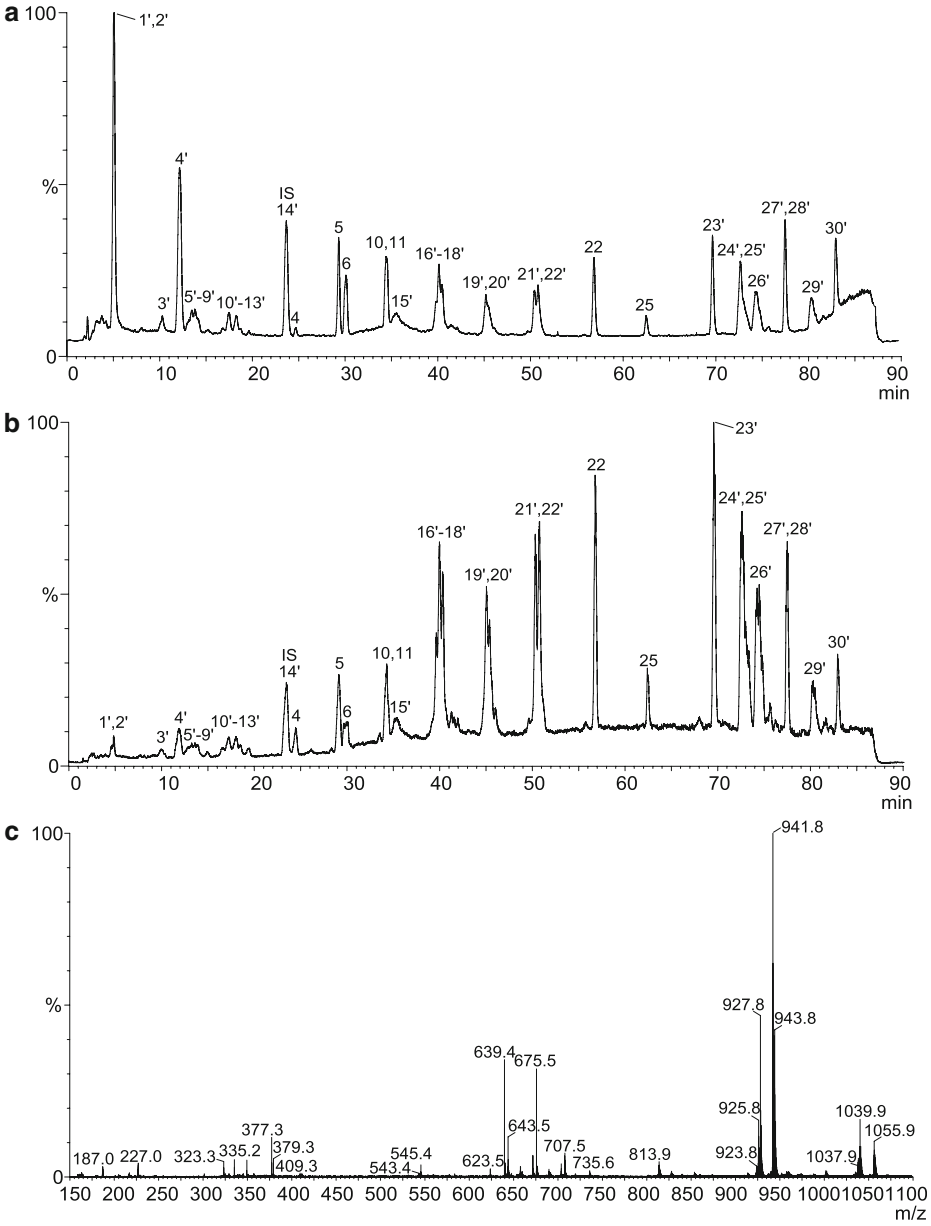

Fig. 2 ELSD chromatogram (**a**), full scan total ion MS chromatogram (**b**), and a combined full scan mass spectrum of 0–90 min (**c**) of oxidized reference compound mixture. Analyzed as explained in experimental procedures. Refer to Tables 2 and 3 for peak numbering

three deprotonated molecules plus three and four sodium atoms. Longer (>18:0) free fatty acids formed more of $[M+23]^+$ adducts. The amount of cluster ions was reduced when the cone gas flow rate was increased to 500 L/h. Possibly conditions in the ion source, such as high cone voltage, facilitated the formation of these somewhat undesirable clusters. Higher weight clusters, however, were of aid in the assignments of some ions.

MAG, DAG, and TAG formed predominantly sodium adducts. Owing to the upper limit of the scanning range (150–1,100 *m/z*), higher molecular weight clusters were observed from glycerolipids only if the $[M+23]^+$ ion was less than *m/z* 538. A distinctive $[M-H_2O+Na]^+$ ion formed from dehydration of the hydroperoxide group was seen in hydroperoxidized MAG, DAG, and TAG when analyzed by ESI–MS. This dehydration phenomenon has also been observed by others [18, 36]. The intensity of the $[M-H_2O+Na]^+$ ion varied from nearly 0% up to 65% compared to $[M+Na]^+$. Hydroperoxidized FFA, instead, formed $[M-H_2O+45]^+$ ions. Synthesized hydroperoxides of FFA, MAG and DAG clearly formed different geometric isomers with different retention times (see Fig. 2). Our RP-HPLC method can separate some of them, but some co-elution still occurred. In order to identify molecular species more reliably, purification by preparative HPLC and consecutive MS/MS and NMR analyses would be needed.

Table 2 Retention times and most abundant positive ions of the unoxidized reference compounds

Peak no.	Compound	ACN:DBN[a]	t_R (min)	RRT[b]	M_{mono} (Da)[c]	$[M+18]^+$ (m/z)[d]	$[M+23]^+$ (m/z)[d]	$[M+45]^+$ (m/z)[d]	$[2*M+23]^+$ (m/z)[d]	$[2*M+45]^+$ (m/z)[d]	$[2*M+67]^+$ (m/z)[d]	$[3*M+89]^+$ (m/z)[d]
1	Capric acid	10:0	15.2	0.64	172.1		195.1	217.1		389.3	411.3	605.4
2	12-Hydroxystearic acid	18:0	23.6	1.00	300.3		323.3	345.3	623.5	645.5	667.6	989.7
3	Myristic acid	12:0	24.2	1.03	200.2		223.2	245.2		445.3	467.3	689.4
4	1(3)-Monolinolenoyl-*sn*-glycerol	18:3	24.7	1.05	352.3		375.3					
5	1(3)-Monolinoleoyl-*sn*-glycerol	18:2	29.3	1.24	354.3		377.3					
6	α-Linolenic acid	18:3	30.1	1.28	278.2	296.2	301.2	323.2		601.4	623.4	923.6
7	Lauric acid	14:0	32.4	1.37	228.2		251.2	273.2		501.4	523.4	773.5
8	Palmitoleic acid	16:1	33.0	1.40	254.2		277.2	299.2		553.4	575.4	851.6
9	1(3)-Monopalmitoyl-*sn*-glycerol	16:0	34.2	1.45	330.3		353.3		683.5			
10	1(3)-Monooleoyl-*sn*-glycerol	18:1	34.4	1.46	356.3		379.3		735.6			
11	Linoleic acid	18:2	34.5	1.46	280.2	298.3	303.1	325.2			627.4	929.7
12	Oleic acid	18:1	39.1	1.66	282.3	300.3	305.2	327.3	587.5	609.5	631.5	935.8
13	Palmitic acid	16:0	39.4	1.67	256.2		279.2	301.3	535.4	557.5	579.4	857.7
14	1(3)-Monostearoyl-*sn*-glycerol	18:0	40.2	1.70	358.3		381.3		739.6			
15	Tricapryloyl-*sn*-glycerol	24:0	44.6	1.89	470.4		493.4		963.7			
16	Stearic acid	18:0	45.0	1.91	284.3		307.2	329.2	591.5	613.5	635.5	941.8
17	Arachidic acid	20:0	49.7	2.11	312.3	330.3	335.3	357.3	647.6	669.6	691.6	1,025.9
18	Trinonanoyl-*sn*-glycerol	27:0	50.6	2.14	512.4		535.4					
19	1,3-Diolinolenoyl-*sn*-glycerol	36:6	51.8	2.19	612.5		635.5					
20	Behenic acid	22:0	54.2	2.30	340.3		363.3	385.3	703.7	725.6	747.6	
21	Tricaproyl-*sn*-glycerol	30:0	56.4	2.39	554.5		577.5					
22	1,3-Dilinoleoyl-*sn*-glycerol	36:4	56.9	2.41	616.5		639.4					
23	Lignoceric acid	24:0	58.3	2.47	368.4		391.4	413.3	759.7		803.8	
24	Triundecanoyl-*sn*-glycerol	33:0	61.7	2.61	596.5		619.5					
25	1,3-Dioleoyl-*sn*-glycerol	36:2	62.6	2.65	620.5		643.5					
26	1,3-Dipalmitoyl-*sn*-glycerol	32:0	63.4	2.69	568.5		591.5					
27	Trilauroyl-*sn*-glycerol	36:0	66.4	2.81	638.5		661.6					
28	Trilinolenoyl-*sn*-glycerol	54:9	68.9	2.92	872.7		895.7					
29	Tritridecanoyl-*sn*-glycerol	39:0	70.5	2.99	680.6		703.6					
30	Tripalmitoleoyl-*sn*-glycerol	48:3	73.1	3.10	800.7		823.7					
31	Trilinoleoyl-*sn*-glycerol	54:6	73.8	3.13	878.7		901.8					
32	Trimyristoyl-*sn*-glycerol	42:0	74.1	3.14	722.6		745.6					
33	Tripentadecanoyl-*sn*-glycerol	45:0	77.2	3.27	764.7		787.7					
34	Trioleoyl-*sn*-glycerol	54:3	78.6	3.33	884.8		907.8					

Table 2 continued

Peak no.	Compound	ACN:DBN[a]	t_R (min)	RRT[b]	M_{mono} (Da)[c]	$[M+18]^+$ (m/z)[d]	$[M+23]^+$ (m/z)[d]	$[M+45]^+$ (m/z)[d]	$[2*M+23]^+$ (m/z)[d]	$[2*M+45]^+$ (m/z)[d]	$[2*M+67]^+$ (m/z)[d]	$[3*M+89]^+$ (m/z)[d]
35	Tripalmitoyl-*sn*-glycerol	48:0	80.0	3.39	806.7		829.7					
36	Triheptadecanoyl-*sn*-glycerol	51:0	82.3	3.49	848.8		871.7					
37	Tristearoyl-*sn*-glycerol	54:0	84.4	3.58	890.8		913.8					

[a] Acyl carbon number:double bond number of fatty acid moieties

[b] Relative retention time to internal standard (12-hydroxystearic acid)

[c] Monoisotopic mass (calculated from the most abundant atom isotope masses)

[d] Measured mass of the ion

Analysis of Native, Thermally Oxidized, and Chemically Oxidized Rapeseed Oils

Fatty acid composition of the native low erucic acid rapeseed oil determined by GC–FID is shown in Table 5. The FA composition is similar to rapeseed oils used in Sweden [19], the Czech Republic [16], and North America [14], although oils of some Canola varieties have more oleic acid (72%) and much less linoleic (<2%) and α-linolenic (<2%) acids [21]. Typical low erucic acid rapeseed oil is susceptible to autoxidation, as 35% of the fatty acids are polyunsaturated and nearly 60% are monounsaturated. The peroxide values of the oxidized oils were 100 mequiv O_2/kg for the oven-oxidized rapeseed oil and 20 mEq O_2/kg for the chemically oxidized oil. Full scan total ion MS chromatograms of the undigested oils analyzed by the developed HPLC–ELSD–ESI–MS method are presented in Fig. 3 and fingerprint-like, diagnostic, combined spectra of the different oils are given in Fig. 4. Peak assignments and the most abundant positive ions, formed in ESI–MS from undigested native rapeseed, chemically oxidized rapeseed, and oven-oxidized rapeseed oils, are presented in Table 6.

The combined full scan spectra of different oils (Fig. 4) showed that thermally oxidized rapeseed oil and chemically oxidized rapeseed oil clearly differ from each other and from natural unoxidized rapeseed oil. Much of the UFA oxidized to higher molecular weight products but some were also converted to smaller molecular weight molecules, as in oven-oxidized rapeseed oil. These smaller molecular weight oxidation products are probably secondary oxidation products such as core aldehydes as described by Sjövall et al. and others [37–41]. Confirmation of the core aldehydes would have required derivatization with 2,4-dinitrophenylhydrazine and consecutive negative ESI–MS analysis [39, 40]. Moreover, the high temperature during oven oxidation may produce some dimers, trimers and various other oligomers of triacylglycerols as determined by Byrdwell et al. [41] Our HPLC method was not optimized for separating these high molecular weight oxidation products. Chemically oxidized oil contains, as expected, mainly hydroxy triacylglycerols, whereas hydroperoxides [20] are present mainly in the oven-oxidized rapeseed oil.

Artificial Digestion Model and Progression of Lipolysis

Figure 5 represents the full scan MS chromatograms of the digestion products of different oils used in the study. Only small amounts of diacylglycerols and even less triacylglycerols were detected in the model chyme 2 h after the addition of lipases. After 1 h of digestion with lipases, there were still significant amounts of DAG present along

Table 3 Retention times and most abundant positive ions of the oxidized reference compounds

Peak no.	Assignments of the reference compounds	ACN:DBN[a]	t_R (min)	RRT[b]	M_{mono} (Da)[c]	$[M-H_2O+23]^+$ (m/z)[d]	$[M-H_2O+45]^+$ (m/z)[d]	$[M+18]^+$ (m/z)[d]	$[M+23]^+$ (m/z)[d]	$[2*M+23]^+$ (m/z)[d]
1′	Dihydroperoxylinolenic acid	18:3	4.6	0.19	342.2		369.2		365.2	
2′	(9,12,15)Triepoxystearic acid	18:0	4.9	0.21	326.2			344.2	349.2	
3′	1(3)-(Hydroperoxy)monolinolenoyl-*sn*-glycerol	18:3	10.0	0.42	384.3				407.2	
4′	(9,12)Diepoxystearic acid	18:0	12.0	0.51	312.2			330.5	335.2	647.5
5′	1(3)-(Hydroperoxy)monolinoleoyl-*sn*-glycerol	18:2	12.9	0.55	386.3	391.3			409.3	
6′	1(3)-(Hydroperoxy)monolinoleoyl-*sn*-glycerol	18:2	13.3	0.57	386.3	391.3			409.3	
7′	1(3)-(Hydroperoxy)monolinoleoyl-*sn*-glycerol	18:2	13.6	0.58	386.3	391.3			409.3	
8′	1(3)-(Hydroperoxy)monolinoleoyl-*sn*-glycerol	18:2	13.9	0.59	386.3	391.3			409.3	
9′	Monohydroperoxylinolenic acid	18:3	13.9	0.59	310.2		337.2		333.2	
10′	1(3)-(Hydroperoxy)monooleoyl-*sn*-glycerol	18:1	17.3	0.73	388.3	393.3			411.3	
11′	1(3)-(Hydroperoxy)monooleoyl-*sn*-glycerol	18:1	18.1	0.77	388.3	393.3			411.3	
12′	Monohydroperoxylinoleic acid	18:2	18.4	0.78	312.2		339.2		335.2	
13′	Monohydroperoxylinoleic acid	18:2	19.3	0.82	312.2		339.2		335.2	
14′	12-Hydroxystearic acid	18:0	23.5	1.00	300.3				323.3	
15′	1,3-(Dihydroperoxy)dilinoleoyl-*sn*-glycerol	36:4	35.3	1.50	680.5	685.4			703.5	
16′	1,3-(Dihydroperoxy)dioleoyl-*sn*-glycerol	36:2	39.7	1.69	684.5	689.5			707.5	
17′	1,3-(Dihydroperoxy)dioleoyl-*sn*-glycerol	36:2	40.0	1.70	684.5	689.5			707.5	
18′	1,3-(Dihydroperoxy)dioleoyl-*sn*-glycerol	36:2	40.4	1.72	684.5	689.5			707.5	
19′	1,3-(Monohydroperoxy)dilinoleoyl-*sn*-glycerol	36:4	45.1	1.92	648.5	653.5			671.5	
20′	1,3-(Monohydroperoxy)dilinoleoyl-*sn*-glycerol	36:4	45.4	1.93	648.5	653.5			671.5	
21′	1,3-(Monohydroperoxy)dioleoyl-*sn*-glycerol	36:2	50.4	2.14	652.5	657.5			675.5	
22′	1,3-(Monohydroperoxy)dioleoyl-*sn*-glycerol	36:2	50.7	2.16	652.5	657.5			675.5	
23′	1,2-Di(monoepoxy)stearoyl-3-stearoyl-*sn*-glycerol	54:0	69.6	2.97	918.8				941.8	
24′	1,3-Distearoyl-2-(diepoxy)stearoyl-*sn*-glycerol	54:0	72.7	3.09	918.8				941.8	
25′	1,3-Distearoyl-2-(monohydroperoxy)linolenoyl-*sn*-glycerol	54:2	72.7	3.09	918.8	923.8			941.9	
26′	1,3-Distearoyl-2-(monohydroperoxy)linoleoyl-*sn*-glycerol	54:1	74.3	3.16	920.8	925.8			943.8	
27′	1,3-Distearoyl-2-(monoepoxy)stearoyl-*sn*-glycerol	54:0	77.5	3.30	904.8				927.8	
28′	1,3-Dibehenoyl-2-(9-oxo)nonanoyl-*sn*-glycerol	53:0	77.5	3.30	890.8				913.8	

Table 3 continued

Peak no.	Assignments of the reference compounds	ACN:DBN[a]	t_R (min)	RRT[b]	M_{mono} (Da)[c]	$[M-H_2O+23]^+$ $(m/z)^d$	$[M-H_2O+45]^+$ $(m/z)^d$	$[M+18]^+$ $(m/z)^d$	$[M+23]^+$ $(m/z)^d$	$[2*M+23]^+$ $(m/z)^d$
29′	1,3-Dibehenoyl-2-(monohydroperoxy)oleoyl-*sn*-glycerol	62:1	80.4	3.43	1,032.9	1,037.9			1,055.9	
30′	1,3-Dibehenoyl-2-(monoepoxy)stearoyl-*sn*-glycerol	62:0	82.9	3.53	1,016.9				1,039.9	

[a] Acyl carbon number:double bond number of fatty acid moieties

[b] Relative retention time to internal standard (12-hydroxystearic acid)

[c] Monoisotopic mass (calculated from the most abundant atom isotope masses)

[d] Measured mass of the ion

Table 4 Linear fitting equations and R^2 values of calibration plots of some reference compounds

Compound	Equation	R^2
18:1-MAG[a]	1.708E−5x + 1.137	0.9831
18:2-MAG[a]	5.399E−5x + 8.652	0.9864
18:3-MAG[a]	9.018E−5x + 8.544	0.9917
36:2-DAG	1.032E−5x + 3.438	0.9922
36:4-DAG	8.780E−6x + 2.616	0.9929
36:6-DAG	1.088E−5x + 2.858	0.9923

[a] *Sn*-1(3) and *sn*-2 regioisomers assumed identical response

Table 5 Fatty acid composition of low erucic acid rapeseed oil (*Brassica napus*)

FA	(% Weight)	SD (%)
14:0	<0.1	–
16:0	3.3	0.02
16:1	0.2	0.00
18:0	1.6	0.02
18:1(n-7)	2.7	0.01
18:1(n-9)	55.6	0.01
18:2(n-6)	22.4	0.02
18:3(n-6)	0.3	0.02
18:3(n-3)	12.4	0.02
20:0	0.5	0.03
20:1(n-9)	1.0	0.02
20:2(n-6)	<0.1	–
22:0	<0.1	–
22:1(n-9)	<0.1	–
24:0	<0.1	–
SFA	5.5	
MUFA	59.5	
PUFA	35.0	

Fatty acid composition was analyzed by GC as methyl esters, $n = 4$

SFA Saturated fatty acids, *MUFA* monounsaturated fatty acids, *PUFA* Polyunsaturated fatty acids

with TAG as well as some MAG and FFA (data not shown). These observations indicate that the overall digestion process was simulating the efficacy of the human digestive system quite well, even though there was no gastric lipase present. It is also worth observing that oxidized oils were digested as efficiently as unoxidized. No substrate specificity in favor of unoxidized oils was detected in the enzymatic processes. Table 7 summarizes the observed and identified digestion products of different oils. Several molecules remained unidentified due to the lack of authentic reference compounds, but some conclusions can be drawn from the mass spectra. Molecules with intense *m/z* 341 and 343 ions are likely to be hydroxylated and epoxidized linoleic and linolenic acids, since the

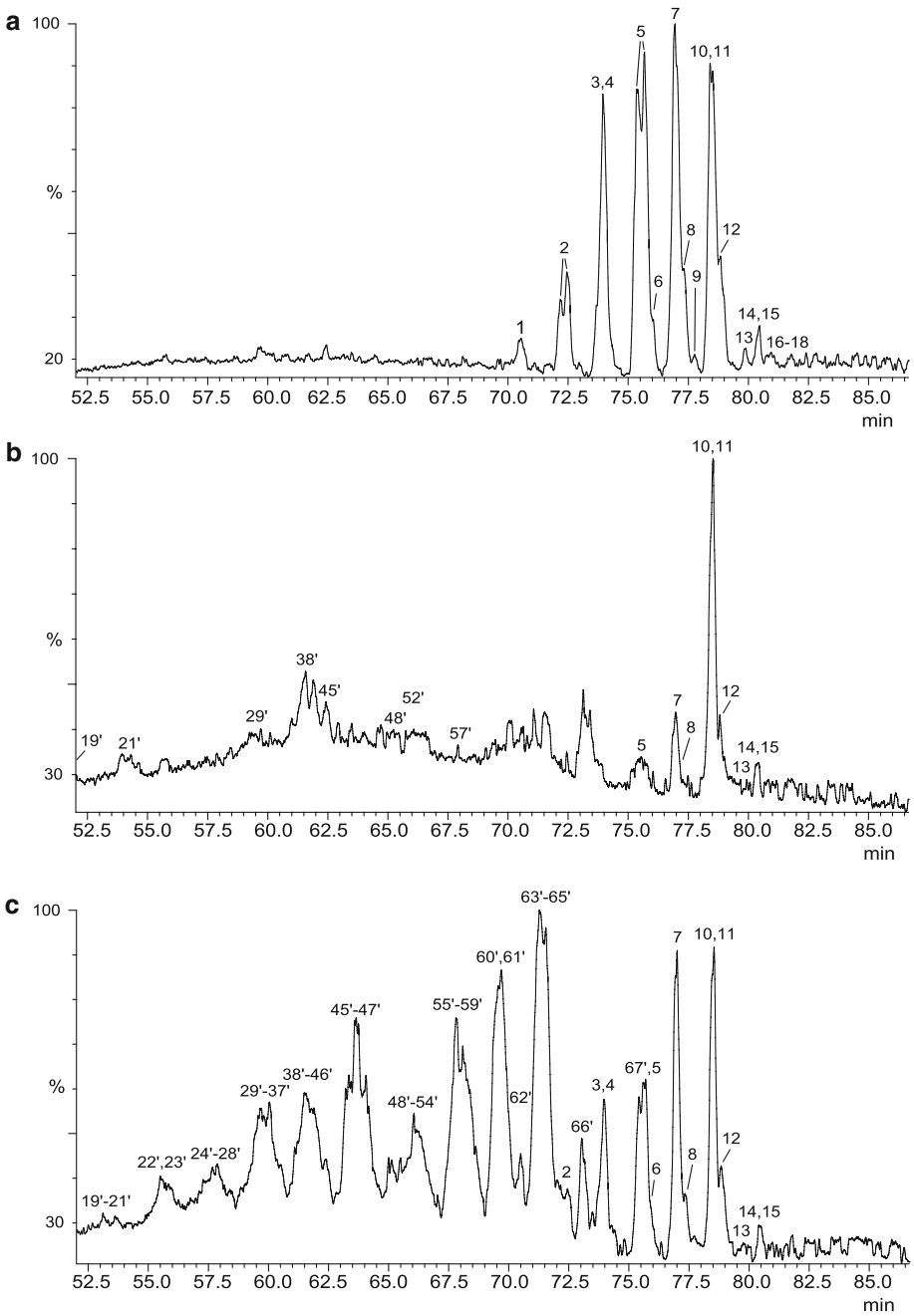

Fig. 3 Full scan total ion MS chromatograms of undigested rapeseed oil (**a**), oven-oxidized rapeseed oil (**b**), and chemically oxidized oil (**c**). Analyzed as indicated in experimental procedures. Refer to Table 6 for peak numbering

calculated values would fit if the formed ion is the expected $[M+45]^+$.

The proportional amounts of regioisomeric *sn*-2 and *sn*-1(3) monoacylglycerol pairs following digestion for 4 h (2 h with lipases) were quite unexpected (Table 8). After the artificial digestion of regular rapeseed oil, 35% of monoolein, 25% of monolinolein and 15% monolinolenin were in the *sn*-1(3) configuration. In the chemically oxidized oil the relative amounts were 30, 21, 20% and in the oven-oxidized oil 13, 0, 0%, respectively. Since pancreatic lipase is thought to be exclusively *sn*-1(3) specific, only the *sn*-2 regioisomer should have been present abundantly. The stereoselectivity of pancreatic lipase has been studied in the past but with limited focus on the formed monoacylglycerol identities in vivo or ex vivo [42]. Constantine et al. [43] observed that some free glycerol was formed when TAG were incubated for extended time. This could be explained by acyl migration of *sn*-2-MAG to *sn*-1(3) and subsequent hydrolysis to FFA and free glycerol. The chemically oxidized oil contained 28% and oven-oxidized oil 11% of the native TAG species present in unoxidized rapeseed oil. This partially explains the smaller amount of

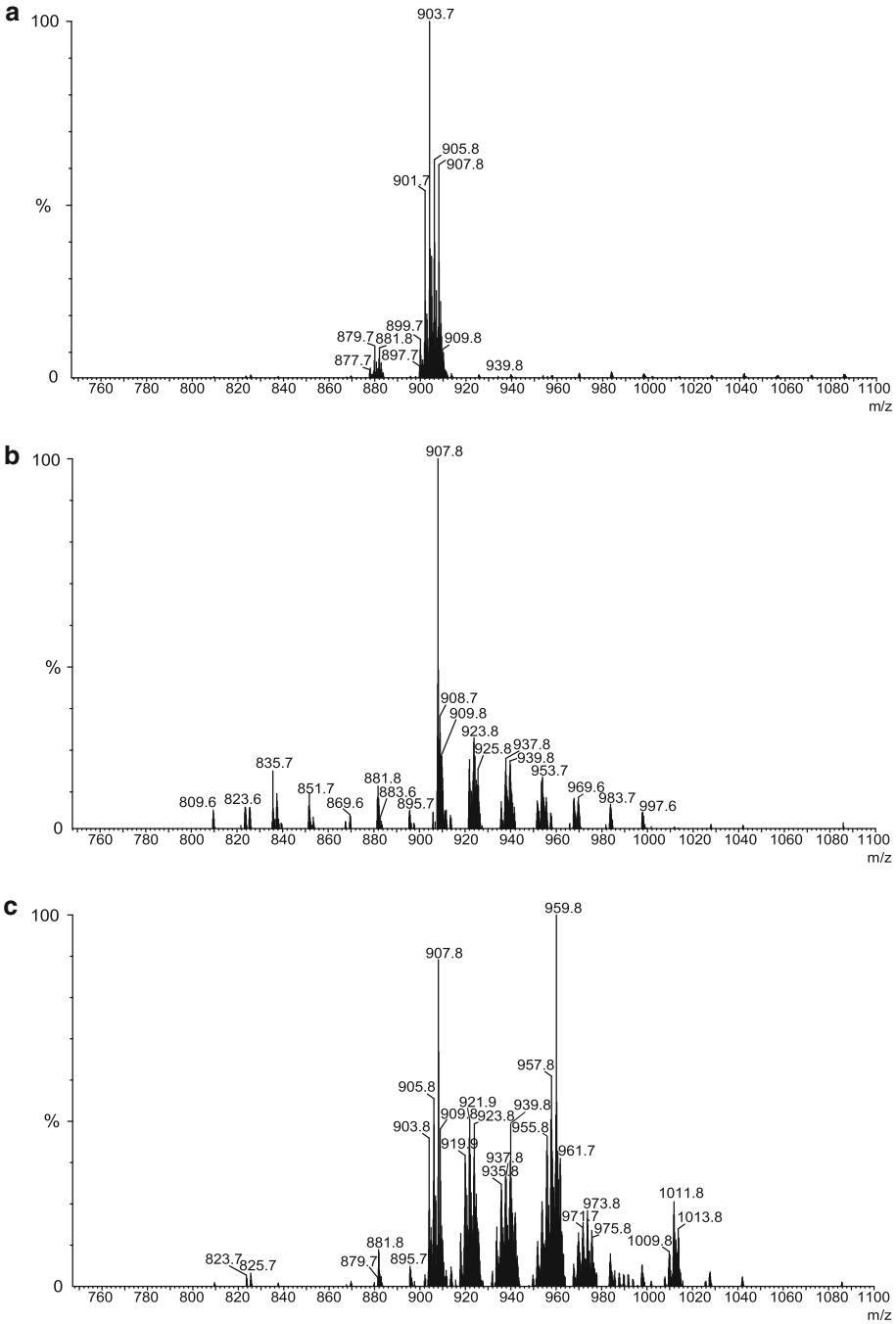

Fig. 4 Combined mass spectra of 50–85 min of undigested rapeseed oil (**a**), oven-oxidized rapeseed oil (**b**), and chemically oxidized oil (**c**). Analyzed as indicated in experimental procedures. Refer to Table 6 for peak listings

sn-1(3)-MAG present in the digested oxidized oils compared to the unoxidized oil.

If the only explanation of the presence of *sn*-1(3)-MAG is nonenzymatic acyl migration, it occurred at a clearly higher rate than previously thought. Although the low pH of the stomach facilitates acyl migration, such a high isomerization was not anticipated due to the addition of bicarbonate to the chyme in the intestinal phase of the artificial digestion model. Furthermore, the substrate specificity of pancreatic lipase should be considered. Again, if only acyl migration was the explanation, the *sn*-1(3)-MAG should have been hydrolyzed to free fatty acids and glycerol by the pancreatic lipase. It is possible that *sn*-1(3)-MAG have a very different affinity to pancreatic lipase as opposed to *sn*-1,2(2,3)-DAG. On-column acyl migration cannot explain the observed *sn*-1(3)-MAG because it would show as a broadening of the observed peaks. Also, sample treatment is minimized and only Folch extraction is done after the artificial digestion. Future experiments should address this interesting observation.

Table 6 Retention times and most abundant positive ions of oxidized and unoxidized triacylglycerols found in the undigested oils

Peak no.	Postulated structures or functional groups	Oxygen atoms[a]	ACN:DBN[b]	t_R (min)	RRT[c]	M_{mono} (Da)[d]	$[M+23]^+$ (m/z)[e]	Abundance		
								Rapeseed oil	Chemically oxidized oil	Oven oxidized oil
1	18:3–18:3–18:2	0	54:8	70.5	3.00	874.7	897.7	150,000	–	–
2	18:2–18:3–18:2/18:3–18:3–18:1	0	54:7	72.3	3.08	876.7	899.7	1,732,000	53,000	–
3	18:3–18:3–18:0/18:2–18:3–18:1/18:2–18:2–18:2	0	54:6	74.0	3.15	878.7	901.7	4,414,000	512,000	–
4	16:1–18:3–18:1/16:1–18:2–18:2/16:0–18:3–18:2	0	52:5	74.3	3.16	852.7	875.7	229,000	26,000	–
5	18:2–18:3–18:0/18:1–18:3–18:1/18:2–18:2–18:1	0	54:5	75.5	3.21	880.8	903.7	7,256,000	1,687,000	48,000
6	16:0–18:3–18:1/16:1–18:3–18:0/16:0–18:2–18:2/16:1–18:2–18:1	0	52:4	75.9	3.23	854.7	877.7	771,000	138,000	–
7	18:1–18:2–18:1/18:1–18:3–18:0/18:2–18:2–18:0	0	54:4	77.0	3.28	882.8	905.8	5,477,000	2,099,000	484,000
8	16:1–18:1–18:1/16:0–18:2–18:1/16:0–18:3–18:0	0	52:3	77.4	3.29	856.8	879.7	9,150,00	264,000	46,000
9	16:0–18:2–16:0/16:1–18:1–16:0	0	50:2	77.7	3.30	830.7	853.7	24,000	–	–
10	20:1–18:3–18:0/20:1–18:2–18:1	0	56:4	78.4	3.33	910.8	933.8	184,000	87,000	28,000
11	18:1–18:1–18:1/18:1–18:2–18:0/18:0–18:3–18:0/20:1–18:1–16:1/20:1–18:2–16:0	0	54:3	78.5	3.34	884.8	907.8	3,381,000	1,734,000	1,695,000
12	16:1–18:1–18:0/16:0–18:2–16:0	0	52:2	78.9	3.36	858.8	881.8	898,000	389,000	370,000
13	20:1–18:1–18:1/20:1–18:2–18:0/20:0–18:3–18:0/20:0–18:2–18:1	0	56:3	79.8	3.40	912.8	935.8	239,000	71,000	58,000
14	18:1–18:1–18:0/18:0–18:2–18:0	0	54:2	80.4	3.42	886.8	909.8	280,000	130,000	126,000
15	20:0–18:2–18:1/20:0–18:3–18:0	0	56:3	80.5	3.43	912.8	935.8	Trace	–	–
16	20:1–18:1–18:0/20:0–18:2–18:0	0	56:2	81.9	3.49	914.8	937.8	Trace	–	–
17	20:1–18:2–20:0/20:1–18:1–20:1	0	58:3	81.9	3.49	940.8	963.8	Trace	–	–
18	20:1–18:3–22:0/20:0–18:3–22:1/20:0–18:3–22:1	0	60:4	81.9	3.49	966.9	989.9	Trace	–	–
19’	–	–	–	51.8	2.20	–	849.6	–	–	151,000
20’	Tetrahydroxide	4	58:4	53.0	2.26	1,002.8	1,025.7	–	68,000	–
21′	–	–	–	53.9	2.29	–	851.7	–	–	197,000
22′	Dihydroxide	2	58:5	55.5	2.36	968.8	991.8	–	185,000	–
23′	Tetrahydroxide	4	58:4	55.6	2.37	1,002.8	1,025.7	–	80,000	–
24′	Dihydroxide	2	54:6	57.4	2.44	910.7	933.7	–	242,000	–
25′	Tetrahydroxide	4	58:4	57.5	2.45	1,002.8	1,025.7	–	94,000	–
26′	Tetrahydroxide/monohydroxide	4/1	56:0/60:4	57.8	2.46	982.8	1,005.8	–	102,000	–
27′	Dihydroxide	2	58:5	57.8	2.46	968.8	991.8	–	206,000	–
28′	Dihydroxide	2	56:2	57.9	2.47	946.8	969.8	–	192,000	–
29′	–	–	–	59.3	2.52	–	833.5	–	–	122,000
30′	Dihydroxide	2	54:6	59.7	2.54	910.7	933.7	–	267,000	–
31′	Dihydroxide	2	54:5	59.7	2.54	912.7	935.7	–	590,000	–
32′	Tetrahydroxide	4	54:3	59.7	2.54	948.8	971.7	–	387,000	–
33′	Trihydroxide	3	58:4	59.7	2.54	986.8	1,009.8	–	336,000	–
34′	Monohydroxide/trihydroxide	1/3	60:3/58:5	59.7	2.54	984.9	1,007.8	–	350,000	–
35′	Dihydroxide	2	56:2	59.8	2.55	946.8	969.6	–	279,000	–
36′	Monohydroxide/dihydroxide	1/2	58:4/60:2	60.0	2.56	1,002.8	1,025.8	–	67,000	–
37′	Dihydroxide/tetrahydroxide	2/4	58:4/56:6	60.1	2.56	970.8	993.8	–	221,000	–
38′	–	–	–	61.6	2.62	–	835.7	–	–	538,000

Table 6 continued

Peak no.	Postulated structures or functional groups	Oxygen atoms[a]	ACN:DBN[b]	t_R (min)	RRT[c]	M_{mono} (Da)[d]	$[M+23]^+$ (m/z)[e]	Abundance		
								Rapeseed oil	Chemically oxidized oil	Oven oxidized oil
39′	Dihydroxide	2	54:4	61.6	2.62	914.8	937.8	–	753,000	–
40′	Tetrahydroxide/dihydroperoxide	4	54:2	61.6	2.62	950.8	973.1	–	380,000	–
41′	Monohydroxide/trihydroxide	1/3	60:2/58:4	61.7	2.63	986.8	1,009.8	–	331,000	–
42′	dihydroxide	2	54:6	61.8	2.63	910.7	933.7	–	288,000	–
43′	Dihydroxide	2	54:5	61.9	2.63	912.7	935.7	–	575,900	–
44′	Tetrahydroxide	4	56:1	61.9	2.64	948.8	971.8	–	438,000	
45′	Monohydroperoxide	2	54:5	62.4	2.65	912.7	935.7	–	–	309,000
46′	Dihydroxide	2	54:5	63.3	2.70	912.7	935.8	–	466,000	–
47′	Dihydroxide	2	54:3	63.7	2.71	916.8	939.8	–	974,000	–
48′	Monohydroperoxide	2	54:4	65.5	2.77	914.8	937.8	–	–	515,000
49′	Dihydroxide	2	54:3	65.0	2.78	916.8	939.8	–	362,000	–
50′	Tetrahydroxide	4	54:1	66.1	2.82	952.8	975.8	–	270,000	–
51′	Trihydroxide	3	54.4	66.1	2.82	930.8	953.7	–	365,000	–
52′	Monohydroperoxide	2	54:3	66.2	2.81	916.8	939.8	–	–	956,000
53′	Dihydroxide/monohydroxide + epoxide	2	54:3/54:2	66.3	2.82	916.8	939.7	–	608,170	–
54′	Dihydroxide	2	52:0	66.2	2.82	894.8	917.8	–	327,000	–
55′	Monohydroxide	1	56:1	67.9	2.89	932.8	955.8	–	1,312,500	–
56′	Dihydroxide	2	52:0	67.9	2.89	894.8	917.8	–	780,000	–
57′	Monohydroxide	1	54:6	68.0	2.90	894.8	917.8	–	774,000	34,000
58′	Dihydroxide	2	52:0	68.1	2.90	894.8	917.8	–	744,000	–
59′	Dihydroxide	2	54:2	68.4	2.91	918.8	941.8	–	818,000	–
60′	Trihydroxide	3	54:2	69.7	2.97	934.8	957.8	–	1,797,000	–
61′	Monohydroxide	1	54:5	69.7	2.97	896.7	919.7	–	1,248,000	–
62′	Monohydroxide	1	54:5	70.0	2.98	896.7	919.9	–	1,696,000	2,67,000
63′	Monohydroxide	1	54:4	71.3	3.04	898.8	921.9	–	1,630,000	968,000
64′	Trihydroxide	3	54:1	71.3	3.04	936.8	959.8	–	2,770,000	–
65′	Monohydroxide	1	54:3	73.1	3.11	900.8	923.8	–	768,000	766,000
66′	Monohydroxide	1	54:2	75.4	3.21	902.8	925.8	–	181,000	64,000

Concentration of the oils injected 1.00 mg/mL (10 μL)

[a] Oxygen atoms added by oxidation

[b] Acyl carbon number: double bond number of fatty acid moieties

[c] Relative retention time to internal standard (12-hydroxystearic acid)

[d] Monoisotopic mass (calculated from the most abundant atom isotope masses)

[e] Measured mass of the most abundant ion

The developed HPLC–ELSD–ESI/MS method was shown to be very useful in the survey of digestion processes of glycerolipids present in an artificial digestion model. The method was capable of separating free fatty acids, monoacylglycerols, diacylglycerols and triacylglycerols and their oxidized equivalents with adequate resolution and, in case of MAG with good resolution, enabling the quantitation of regioisomeric pairs of MAG. Compared to other total lipid profiling techniques, such as capillary gas-liquid chromatography with FID that require derivatization and sample heating [44], this HPLC method has the advantage of minimal sample degradation during analysis. Unprotected hydroperoxy groups are known to isomerize and decompose when heated to high temperatures [45]. Acid-catalyzed methylation techniques have a tendency to isomerize conjugated diene structures and form artifacts [46]. On the other hand, base-catalyzed transesterification is a milder reaction, but cannot derivatize free fatty acids. Shotgun lipidomics with time of flight (TOF) mass spectrometry offers a different route to lipid profiling, but lacks the

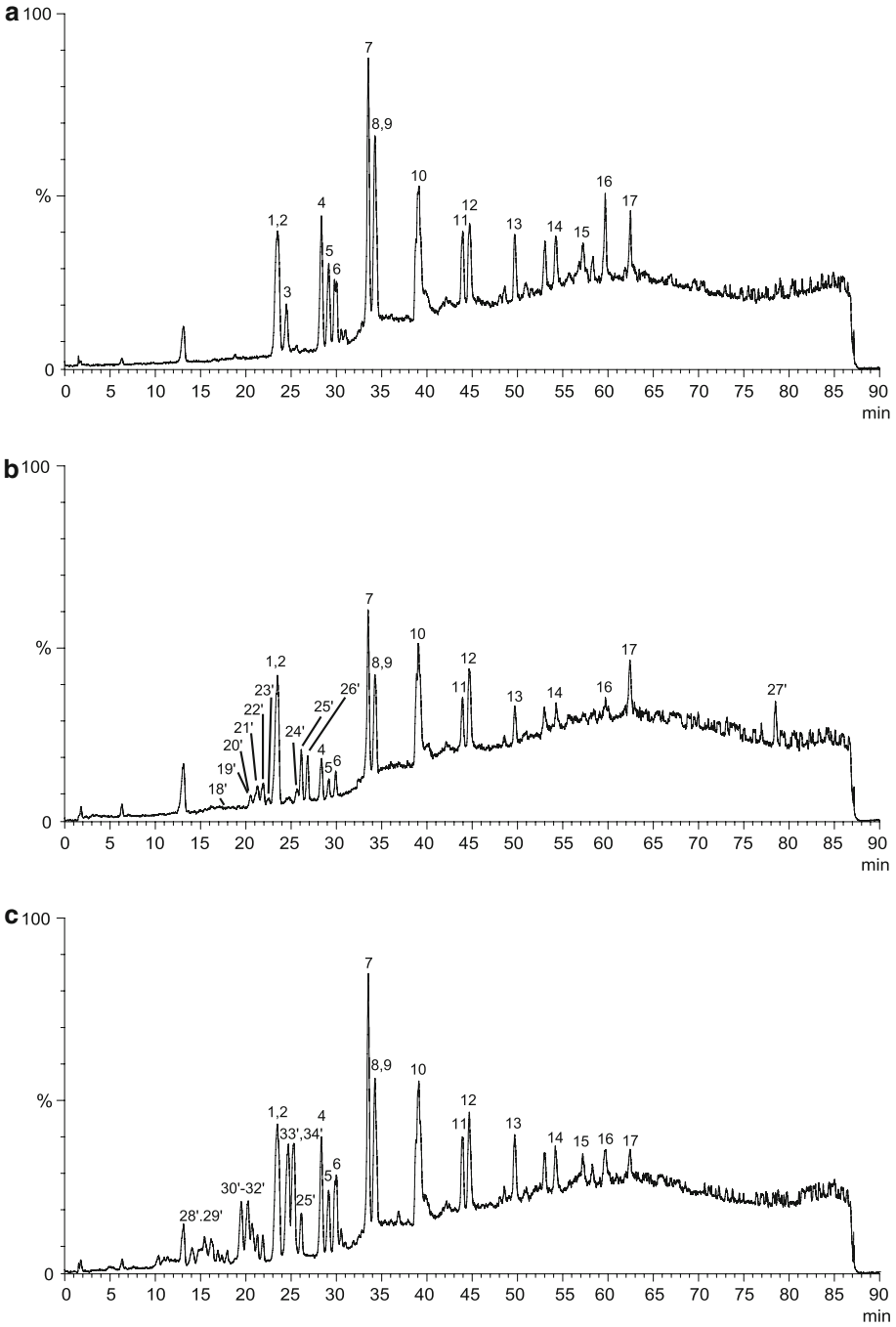

Fig. 5 Full scan total ion MS chromatograms of digested rapeseed oil (**a**), digested oven-oxidized rapeseed oil (**b**), and digested chemically oxidized oil (**c**). Analyzed as indicated in experimental procedures. Refer to Table 7 for peak numbering

separation specificity of liquid chromatography [47]. Ion suppression can be a problem when performing a direct infusion MS analysis. TLC–FID can be used for the quantitative assessment of FFA, MAG, DAG, and TAG species, but the method lacks the specificity of liquid chromatographic separation coupled with mass spectrometric detection [48].

The limitations of the developed method were sensitivity and resolution between some close eluting peaks. Even so, this method does offer a comprehensive view of the molecular structures found in complex lipid samples. If only sensitivity for known molecular species is sought, then selected ion monitoring (SIM) could be used, as full scan mass analysis from 150 to 1,100 *m/z* lowers the sensitivity compared to a narrower mass window. The length of single analysis is also a limiting factor. The chromatography time of 90 min should be shortened to speed up the analysis as a whole. Modern fast LC, UPLC™ and similar ultra high performance LC methods offer the possibility of shortening the time needed for analysis and

Table 7 Retention times and most abundant positive ions of the digested oils

Peak no.	Compound or postulated structure	ACN:DBN[a]	t_R (min)	RRT[b]	M_{mono} (Da)[c]	$[M+23]^+$ (m/z)[d]	$[M+45]^+$ (m/z)[d]	$[2*M+23]^+$ (m/z)[d]	$[2*M+67]^+$ (m/z)[d]	$[3*M+89]^+$ (m/z)[d]
1	12-Hydroxystearic acid	18:0	23.5	1.00	283.3	323.4	345.4	623.7		
2	2-Monolinolenoyl-*sn*-glycerol	18:3	23.6	1.00	352.3	375.4				
3	1(3)-Monolinolenoyl-*sn*-glycerol	18:3	24.5	1.04	352.3	375.4				
4	2-Monolinoleoyl-*sn*-glycerol	18:2	28.4	1.21	354.3	377.4		731.8		
5	1(3)-Monolinoleoyl-*sn*-glycerol	18:2	29.1	1.24	354.3	377.4		731.8		
6	α-Linolenic acid	18:3	29.8	1.27	278.2		323.3		623.6	923.6
7	2-Monooleoyl-*sn*-glycerol	18:1	33.5	1.43	356.3	379.4		735.8		
8	1(3)-Monooleoyl-*sn*-glycerol	18:1	34.3	1.46	356.3	379.4		735.8		
9	Linoleic acid	18:2	34.5	1.47	280.2		325.4		627.6	929.9
10	Oleic acid	18:1	39.1	1.66	282.3	305.4				
11	Erucic acid	20:1	44.0	1.87	310.3		355.3		687.4	1,019.8
12	Stearic acid	18:0	44.7	1.90	284.3		329.3		635.8	942.0
13	Arachidic acid	20:0	49.8	2.12	312.3		357.4			1,026.2
14	Behenic acid	22:0	54.2	2.31	340.3		385.3			
15	Dilinoleoyl-*sn*-glycerol	36:4	57.3	2.44	616.5	639.5				
16	Monooleoyl-monolinoleoyl-*sn*-glycerol	36:3	59.7	2.54	618.5	641.7				
17	Dioleoyl-*sn*-glycerol	36:2	62.5	2.66	620.5	643.6				
18′	Monohydroxide	18:3	17.8	0.76	294		339.3			
19′	Monohydroxide	18:2	20.5	0.87	296		341.5			
20′	Monoepoxide	18:1	20.5	0.87	298		343.4			
21′	–	–	21.3	0.91	296		341.4			
22′	–	–	21.9	0.93	296		341.2			
23′	–	–	22.4	0.95	296		341.2			
24′	–	–	25.6	1.09	298		343.3		663.3	983.5
25′	–	–	26.1	1.11	298		343.3			
26′	–	–	26.8	1.14	298		343.3			
27′	Trioleyl-*sn*-glycerol	–	78.5	3.34	884.8	908.2				
28′	–	–	19.5	0.83	296		341.1			
29′	–	–	19.5	0.83	408	431.3				
30′	–	–	20.2	0.86	296		341.2			
31′	–	–	20.2	0.86	408	431.4				
32′	–	–	20.7	0.88	296		341.5			
33′	–	–	24.7	1.05	298		343.4			
34′	–	–	25.1	1.07	298		343.4			

[a] Acyl carbon number:double bond number of fatty acid moieties

[b] Relative retention time to internal standard (12-hydroxystearic acid)

[c] Monoisotopic mass (calculated from the most abundant atom isotope masses). Values without decimals are speculated nominal weights

[d] Measured mass of the ion

Table 8 Absolute and relative amounts of *sn*-1(3) and *sn*-2-monoacylglycerols after artificial digestion of oils with different oxidative status

Compound	Rapeseed oil[a]			Chemically oxidized oil[a]			Oven oxidized oil[a]		
	wt% of oil	(%)	SD (%)	wt% of oil	(%)	SD (%)	wt% of oil	(%)	SD (%)
sn-2-18:1-MAG	10.6	65	7.61	5.5	70	4.49	2.7	87	1.88
sn-1(3)-18:1-MAG	5.6	35	7.61	2.1	30	4.49	0.3	13	1.88
sn-2-18:2-MAG	16.1	75	2.43	7.1	79	1.29	1.5	100	–
sn-1(3)-18:2-MAG	5.3	25	2.43	1.9	21	1.29	nd	nd	–
sn-2-18:3-MAG	13.6	85	0.76	7.6	80	0.23	1.8	100	–
sn-1(3)-18:3-MAG	2.4	15	0.76	1.9	20	0.23	nd	nd	–
Sum (Σ)	53.5			25.9			6.3		

nd Not detected

[a] $N = 2$

simultaneously maintaining or even enhancing resolution and sensitivity. Combined full scan spectra after proper chromatographic separation can produce fingerprint-like, diagnostic profiles of different kinds of samples for such uses as lipid oxidation monitoring, monitoring of lipolysis, and other metabolomic and lipidomic studies. The HPLC solvent gradient separation developed can easily be applied to preparative HPLC to isolate and purify oxidized fractions from different kinds of lipid samples. Nuclear magnetic resonance analysis of different fractions of digestion products could provide accurate information on the structures of oxidized lipid molecules.

Acknowledgments This work has been funded by the Academy of Finland. Aleksandra Phuphusit is thanked for the preparation of some of the reference compounds.

References

1. Kanazawa K, Ashida H (1998) Catabolic fate of dietary trilinoleoyl hydroperoxides in rat gastrointestines. Biochim Biophys Acta 1393:336–348
2. Kanazawa K, Ashida H (1998) Dietary hydroperoxides decompose to aldehydes in stomach before being absorbed into the body. Biochim Biophys Acta 1393:349–361
3. Giuffrida F, Destaillats F, Robert F, Skibsted LH, Dionisi F (2004) Formation and hydrolysis of triacylglycerol and sterol epoxides: role of unsaturated triacylglycerol peroxyl radicals. Free Radic Biol Med 37:104–114
4. Kanner J, Lapidot T (2001) The stomach as a bioreactor: dietary lipid peroxidation in the gastric fluid and the effects of plant-derived antioxidants. Free Radic Biol Med 31:1388–1395
5. Gorelik S, Lapidot T, Shaham I, Granit R, Ligumsky M, Kohen R, Kanner J (2005) Lipid peroxidation and coupled vitamin oxidation in simulated and human gastric fluid inhibited by dietary polyphenols: health implications. J Agric Food Chem 53:3397–3402
6. Lapidot T, Grant R, Kanner J (2005) Lipid hydroperoxidase activity of myoglobin and phenolic antioxidants in simulated gastric fluid. J Agric Food Chem 53:3391–3396
7. Lapidot T, Grant R, Kanner J (2005) Lipid peroxidation by "free" iron ions and myoglobin as affected by dietary antioxidants in simulated gastric fluid. J Agric Food Chem 53:3383–3390
8. Versantvoort CHM, Van de Kamp E, Rompelberg CJM (2004) Development and applicability of an in vitro digestion model in assessing the bioaccessibility of contaminants from food, RIVM report 32102002/2004
9. Versantvoort CHM, Oomen AG, Van de Kamp E, Rompelberg CJM, Sips AJAM (2005) Applicability of an in vitro digestion model in assessing the bioaccessibility of mycotoxins from food. Food Chem Toxicol 43:31–40
10. Bernbäck S, Bläckberg L, Hernell O (1990) The complete digestion of human milk triacylglycerol in vitro requires gastric lipase, pancreatic colipase-dependent lipase and bile salt-stimulated lipase. J Clin Invest 85:1221–1226
11. Carey M, Small D, Bliss C (1983) Lipid digestion and absorption. Ann Rev Physiol 45:651–677
12. Rogalska E, Rausac S, Verger R (1990) Stereoselectivity of lipases. II. Stereoselective hydrolysis of triglycerides by gastric and pancreatic lipases. J Biol Chem 265:20271–20276
13. Carey MC, Small DM, Bliss CM (1983) Lipid digestion and absorption. Ann Rev Physiol 45:651–677
14. Byrdwell WC, Neff WE, List GR (2001) Triacylglycerol analysis of potential margarine base stocks by high-performance liquid chromatography with atmospheric pressure chemical ionization mass spectrometry and flame ionization detection. J Agric Food Chem 49:446–457
15. Beermann C, Winterling N, Green A, Möbius M, Schmitt JJ, Boehm G (2007) Comparison of the structures of triacylglycerols from native and transgenic medium-chain fatty acid-enriched rape seed oil by liquid chromatography–atmospheric pressure chemical ionization ion-trap mass spectrometry (LC–APCI–ITMS). Lipids 42:383–394
16. Lisa M, Holčapek M (2008) Triacylglycerol profiling in plant oils important in food industry, dietics and cosmetics using high-performance liquid chromatography–atmospheric pressure chemical ionization mass spectrometry. J Chromatogr A 1198–1999:115–130
17. Holčapek M, Jandera P, Zderadička P, Hrubá L (2003) Characterization of triacylglycerol and diacylglycerol composition of plant oils by using high-performance liquid chromatography–atmospheric pressure chemical ionization mass spectrometry. J Chromatogr A 1010:195–215
18. Byrdwell WC, Neff WE (2004) Dual parallel electrospray ionization and atmospheric pressure chemical ionization mass spectrometry (MS), MS/MS and MS/MS/MS for the analysis of triacylglycerols and triacylglycerol oxidation products. Rapid Commun Mass Spectrom 16:300–319

19. Svensson J, Adlercreutz P (2008) Identification of triacylglycerols in the enzymatic transesterification of rapeseed and butter oil. Eur J Lipid Sci 110:1007–1013
20. Neff WE, Byrdwell WC (1998) Characterization of model triacylglycerol (triolein, trilinolein and trilinolenin) autoxidation products via high-performance liquid chromatography coupled with atmospheric pressure chemical ionization mass spectrometry. J Chromatogr A 818:169–186
21. Byrdwell WC, Neff WE (2001) Autoxidation products of normal and genetically modified canola oils determined using liquid chromatography with mass spectrometric detection. J Chromatogr A 905:85–102
22. Christie WW (1992) Advances in lipid methodology. Oily Press, Ayr, pp 1–17
23. Kalo PJ, Ollilainen V, Rocha JM, Malcata FX (2006) Identification of molecular species of simple lipids by normal phase liquid chromatography–positive electrospray tandem mass spectrometry, and application of developed methods in comprehensive analysis of low erucic acid rapeseed oil lipids. Int J Mass Spectrom 254:106–121
24. Gladovič N, Zupančič-Kralj L, Plavec J (1997) Determination of primary oxidation products of linoleic acid and triacylglycerols. J Chromatogr A 767:63–68
25. Aveldano MI, VanRollins M, Horrocks L (1983) Separation and quantitation of free fatty acids and fatty acid methyl esters by reverse phase high pressure liquid chromatography. J Lipid Res 24:83–93
26. Orellena-Coca C, Adlercreutz D, Andersson MM, Mattiasson B, Hatti-Kaul R (2005) Analysis of fatty acid epoxidation by high performance liquid chromatography coupled with evaporative light scattering detection and mass spectrometry. Chem Phys Lipids 135:189–199
27. Suomela JP, Ahotupa M, Sjövall O, Kurvinen JP, Kallio H (2004) New approach to the analysis of oxidized triacylglycerols in lipoproteins. Lipids 39:507–512
28. Harry-O'kuru R, Carriere C (2002) Synthesis, rheological characterization, and constitutive modelling of polyhydroxy triglycerides derived from milkweed oil. J Agric Food Chem 50:3214–3221
29. Neff WE, Frankel EN, Weisleder D (1982) Photosensitized oxidation of methyl linolenate. Secondary Products. Lipids 17:780–790
30. Deffense E (1993) Nouvelle méthode d'analyse pour séparer, via HPLC, les isoméres de position 1–2 et 1–3 des triglycérides mono-insaturés des graisses végétales. Rev Fr Corps Grass 40:33–39
31. AOCS (1997) Standard methods and the recommended practices of the AOCS, 5th edn. AOCS press, Champaign
32. National Nutrition Council (2005) Suomalaiset ravitsemussuositukset–ravinto ja liikunta tasapainoon. Edita Publishing, Oy Helsinki
33. Männistö S, Reinivuo H, Korhonen T, Pakkala H, Tapanainen H (2003) The National FINDIET 2002 Study. Kansanterveyslaitoksen julkaisuja B3/2003. National Public Health Institute, Ravitsemusyksikkö, Helsinki
34. Folch J, Lees M, Sloane Stanley GH (1956) A simple method for the isolation and purification of total lipids from animal tissues. J Biol Chem 226:497–509
35. Ledman DW, Fox RO (1997) Water cluster calibration reduces mass error in electrospray ionization mass spectrometry of proteins. J Am Soc Mass Spectrom 8:1158–1164
36. Giuffrida F, Skibsted LH, Dionisi F (2004) Structural analysis of hydroperoxy- and epoxy-triacylglycerols by liquid chromatography mass spectrometry. Chem Phys Lipids 131:41–49
37. Sjövall O, Kuksis A, Kallio H (2001) Reversed-phase high-performance liquid chromatographic separation of *tert*-butyl hydroperoxide oxidation products of unsaturated triacylglycerols. J Chromatogr A 905:119–132
38. Sjövall O, Kuksis A, Kallio H (2001) Analysis of molecular species of peroxide adducts of triacylglycerols following treatment of corn oil with *tert*-butyl hydroperoxide. Lipids 36:1347–1356
39. Sjövall O, Kuksis A, Kallio H (2002) Formation of triacylglycerol core aldehydes during rapid oxidation of corn and sunflower oils with *tert*-butyl hydroperoxide/Fe^{2+}. Lipids 37:81–94
40. Sjövall O, Kuksis A, Kallio H (2003) Tentative identification and quantification of TAG core aldehydes as dinitrophenylhydrazones in autoxidized sunflower seed oil using reversed-phase HPLC with electrospray ionization MS. Lipids 38:1179–1190
41. Byrdwell WC, Neff WE (2004) Electrospray ionization MS of high M.W. TAG oligomers. JAOCS 81:13–26
42. Lykidis A, Mougios V, Arzoglou P (1995) Kinetics of the two-step hydrolysis of triacylglycerol by pancreatic lipases. Eur J Biochem 230:892–898
43. Constatin MJ, Pasero L, Desnuelle P (1960) Quelques remarques complémentaires sur l'hydrolyse des triglycerides par la lipase pancréatique. Biochim Biophys Acta 43:103–109
44. Myher JJ, Kuksis A (1984) Determination of plasma total lipid profiles by capillary gas-liquid chromatography. J Biochem Biophys Meth 10:13–23
45. Lercker G, Bortolomeazzi R, Pizzale L (1998) Thermal degradation of single methyl oleate hydroperoxides obtained by photosensitized oxidation. JAOCS 75:1115–1120
46. Kramer JKG, Fellner V, Dugan MER, Sauer FD, Mossoba MM, Yurawecz MP (1997) Evaluating acid and base catalysts in the methylation of milk and rumen fatty acids with special emphasis on conjugated dienes and total *trans* fatty acids. Lipids 32:1219–1228
47. Ståhlmana M, Ejsingb CS, Tarasovc K, Permana J, Boréna J, Ekroosc K (2009) High-throughput shotgun lipidomics by quadrupole time-of-flight mass spectrometry. J Chromatogr B 877:2664–2672
48. Abdelkafi S, Fouquet B, Barouh N, Durner S, Pina M, Scheirlinckx F, Villeneuve P, Carrière F (2009) In vitro comparison between Carica papaya and pancreatic lipases during meal lipolysis: potential use of CPL in enzyme replacement therapy. Food Chem 115:488–494

Structural information organized by the SC components is essential for knowing the detailed diffusion mechanisms of SC. The role of the intercellular SC lipid bilayer in relation to the barrier function has been investigated by infrared (IR) spectroscopy [7–9] and X-ray diffraction [10, 11]. IR examination showed that the outer layers were less cohesive and the intercellular lipids are disordered compared with the deeper membrane, based on the C–H stretching absorbance of the methyl groups of the lipid acyl chains. The effects of UV irradiation and ethanol perturbations on the SC organization were studied by FTIR and IR imaging microspectroscopy. The X-ray approach is somewhat limited to model lipid membranes containing water or in-vitro SC specimens. Moreover, these methods are have difficulty to obtain information about depth-related changes of the SC.

On the other hand, EPR is a sensitive and nondestructive technique to measure the probe moieties in the lipid bilayers at ambient temperature [1–6]. The EPR probe method can provide an insight into the SC lipid organization as well as its dynamics. Detailed studies of EPR line intensities, linewidths, and line separations with various spin probes may provide the following information: (1) changes in the spin probe's molecular environment as well as nano- to micro-molar probe concentrations, (2) relative reorientation, and (3) lipid structure. The EPR spectroscopic technique could provide more interpretable information, which would allow us to understand the actual SC system further.

In addition, the EPR simulation can potentially provide further insight into skin-lipid structures. The order parameter (S_0) of the spin probe will provide a useful index about structural dependence as a function of the SC depth. The value obtained by the simulation will change by the signal intensity of the sebum secretion and other contribution of SC materials. However, the relative value of the particular SC sample as a function of the depth could provide a useful index of the SC.

In this report, we investigated the lipid structure of hairless mouse SC using aliphatic spin probes together with an EPR slow-tumbling simulation. Hairless mouse SC was used to find the spin-probe permeation effect of terpenes on the SC lipid. EPR spectra were analyzed by a slow-tumbling simulation. The values obtained for the lipid structure are discussed in terms of EPR spectral changes as well as the SC treated with chemical enhancers.

Experimental Sections

SC Cyanoacrylate Glue Stripping

The Institutional Animal Care and Use Committee of NIRS (National Institute of Radiological Sciences) approved the protocols used herein. The sampling method was first utilized by Marks and Dawber [12] to obtain SC sheets. Recently, Yagi et al. [5, 6] developed a process to study SC properties.

A glass plate (7 × 37 mm; Matsunami Glass Ind. Ltd., Tokyo, Japan) was used to strip the SC sheet. A single drop (~12 mg) of a commercially available cyanoacrylate resin had been uniformly spread on the plate. The glass plate was pasted on the back of the hairless mouse (HOS:HR-1, 8-week-old male). The SC specimens were successively removed from the back of the hairless mouse under anesthesia. The SC was stripped consecutively from one to three or four times. Approximately 1 mg of SC sample is required for the measurements.

Once the glue has solidified, no significant signal arises from the cured resin or from the spin probe dissolved in the resin [13]. The only signal observed arises from the spin probe in the attached SC sheet. This method has the advantage of avoiding prior exposure of the SC to enzymes [14]. The EPR signal intensity may depend to a slight degree on how thick a sample is removed by each stripping, but the dependence can be minimized by the amount and area of glue on the glass plate.

Preparation of SC Sheets

The spin probe reagents, 5-doxylstearic acid (5-DSA) and 3β-doxyl-5α-cholestane (CHL), were purchased from Aldrich-Sigma Chemical Co. Inc. and used as received. The molecular structures and coordination of spin probes used in this study of a slow-tumbling simulation are depicted in Fig. 1.

The terpenes, α-terpineol and (+)-limonene, were purchased from Sigma-Aldrich and used as received. The original solution of α-terpineol and (+)-limonene were separately applied on the back of the hairless mouse for 5 min and then the chemicals were wiped off. Then, one piece of stripped SC (~7 × 22 mm^2) was incubated in ~50 μM 5-DSA or CHL aqueous solutions for about 60 min at 37 °C. The probe solution was dropped onto the SC sheet. The SC sheet repels the aqueous solution but the probe goes into the lipid phase during the incubation. After rinsing with deionized water to remove excess spin probe, the SC sample was mounted on an EPR cell. The detailed sample preparations are described elsewhere [6].

EPR Measurements

A JEOL JES-FR30 X-band (9 GHz) EPR spectrometer was used to measure the SC samples at NIRS and analyses of EPR results were mainly performed by Nakagawa. Typical spectrometer settings were as follows: microwave power, 10 mW; time constant, 1 s; sweep time, 8 min;

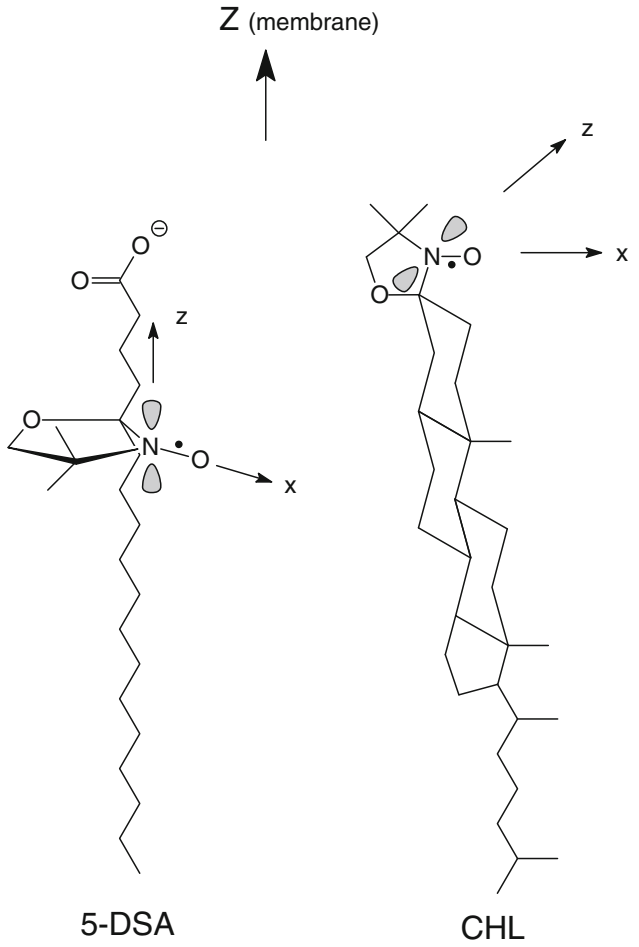

Fig. 1 Coordination of the spin probes, 5-DSA and CHL, for the slow-tumbling calculations are presented. The z-axis is the membrane director

modulation, 0.2 mT; sweep width, 15 mT. All measurements were performed at ambient temperature. The EPR spectra of the SC samples were analyzed using a quantitative simulated order parameter (S_0) [5, 6].

EPR Slow-Tumbling Simulation Analysis

The slow-tumbling motions on the order of 10^{-7} s of the aliphatic spin probes in membranes were evaluated by using the nonlinear least-squares fitting program NLLS to calculate the EPR spectra based on the stochastic Liouville equation [15, 16]. The lipid and 5-DSA molecules in the lipid bilayer experience ordering potentials, which restrict the amplitude of the rotational motion. The ordering potential in a lipid bilayer determines the orientational distribution of molecules with respect to the local ordering axis of the bilayer [17]. The overall orientation of the probe can be expressed by the order parameter (S_0), which is defined as follows [16, 18],

$$S_0 = \left\langle \frac{1}{2}\left(3\cos^2\gamma - 1\right)\right\rangle = \frac{\int d\Omega \exp(-U/kT) D^2_{00}}{\int d\Omega \exp(-U/kT)}, \quad (1)$$

which measures the angular extent of the rotational diffusion of the nitroxide probe moiety. Gamma (γ) is the angle between the rotational diffusion symmetry axis and the z-axis of the nitroxide axis system as shown in Fig. 2. The $\Omega = (\alpha, \beta, \gamma)$ are the Euler angles between the molecular frame of the rotational diffusion tensor, U is the ordering potential, and D is a Winger rotation matrix element.

In calculation based on the experimental spectra, the following principal components, A_{XX}, A_{YY}, A_{ZZ} = (0.66, 0.55, 3.45) mT and g_{XX}, g_{YY}, g_{ZZ} = (2.0086, 2.0063, 2.0025), were used for 5-DSA [19]. The components, A_{XX}, A_{YY}, A_{ZZ} = (0.49, 0.55, 3.31) mT and g_{XX}, g_{YY}, g_{ZZ} = (2.0087, 2.0057, 2.0021), were used for CHL [20].

The local or microscopic ordering of the nitroxide probe in the multilamellar lipid bilayer is characterized by the S_0 value. A larger S_0 value indicates highly ordered structure and a smaller S_0 shows less ordered structure. The modern simulation takes into account EPR intensities, linewidths, and hyperfine coupling values and provides the quantitative information regarding the probe environment. Therefore, S_0-value reflects the local ordering of the lipid structure in the membrane. The error of the spectral simulation is a few percentage points in the case of the dipalmitoylphosphatidylcholine membrane [17].

Results

First, we examined the probe stock solutions. Figure 3 shows EPR spectra of the probe aqueous solutions which were used for incubation of SC sheets. The left-hand EPR spectrum is of a 5-DSA solution and the right-hand

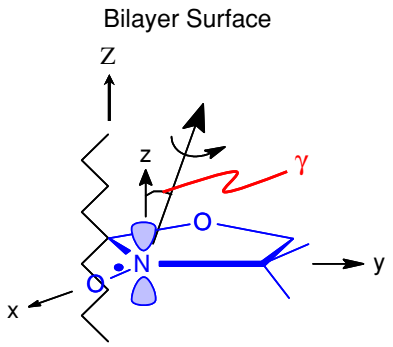

Fig. 2 A schematic representation of a conformation of DSA spin probe in the SC membrane, where the z-axis of the acyl chain is parallel to the z-axis of the nitrogen $2P_z$ orbital

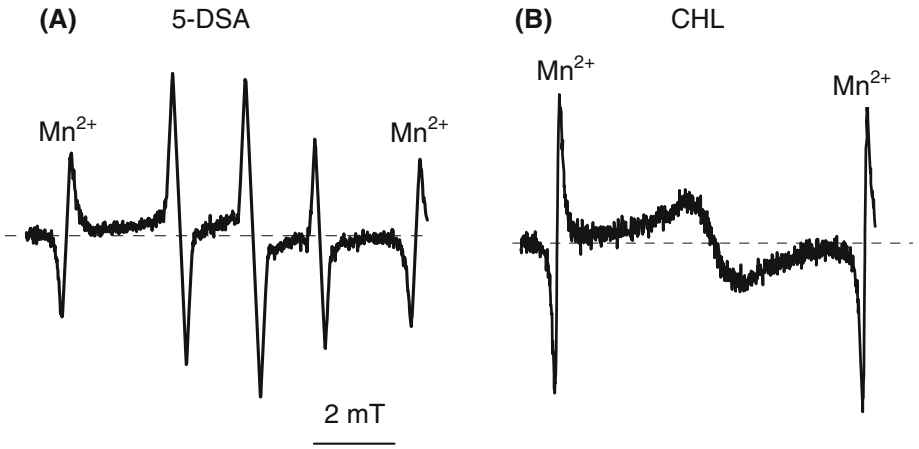

Fig. 3 EPR spectra of spin probes, **a** 5-DSA and **b** CHL, aqueous stock solutions are presented. The EPR spectra were obtained with a single scan

spectrum is of a CHL solution with reference signals for MnO^{2+} (8.69 mT at the distance of the third and the forth peaks). The three-line signal of the 5-DSA aqueous solution was observed. The sharp pattern indicates that 5-DSA is in free tumbling motion in the solution. The one-line signal was observed for CHL aqueous solution.

Figure 4 shows the experimental and simulated EPR spectra of 5-DSA in the SC. The EPR spectra obtained were very stable. The arrow in the spectrum indicates the characteristic peak, which is prominent for the first strip. This peak diminishes in intensity with increasing depth in the SC. It is noteworthy that one can observe the same signal intensity and line-shape at least few hours. The probe may be stable in the lipid bilayer of SC. The top spectrum is the first strip of the SC.

The marked peak appears near the center of the spectrum because the probe embedded in the first sample stripped has greater freedom of motion. The other two lines of the nitroxide probe overlaid the central region of the spectrum. The results imply that signals can originate from sebaceous secretion [6].

Next, we examined the effect of penetration enhancers (terpenes) on the SC lipid. Figure 5 presents the chemical structures of the terpenes, (+)-limonene, and α-terpineol. Figure 6 shows EPR spectra of a terpineol treated SC sheet as a function of depth. The spectra indicate the first and the third stripped SC treated with terpineol. The EPR intensity was very prominent for the first one. The signal intensity of the third stripped SC is a little smaller than that of the first strip.

In addition, we examined the spin probe CHL. Figure 7 shows EPR spectra of CHL from the hairless mouse SC. A relatively broad signal pattern was obtained. The spectral pattern for the second strip was very similar to that of the first strip, except for the intensity. The amplitude of the derivative spectrum for the second strip was about one-half of the amplitude of the first strip.

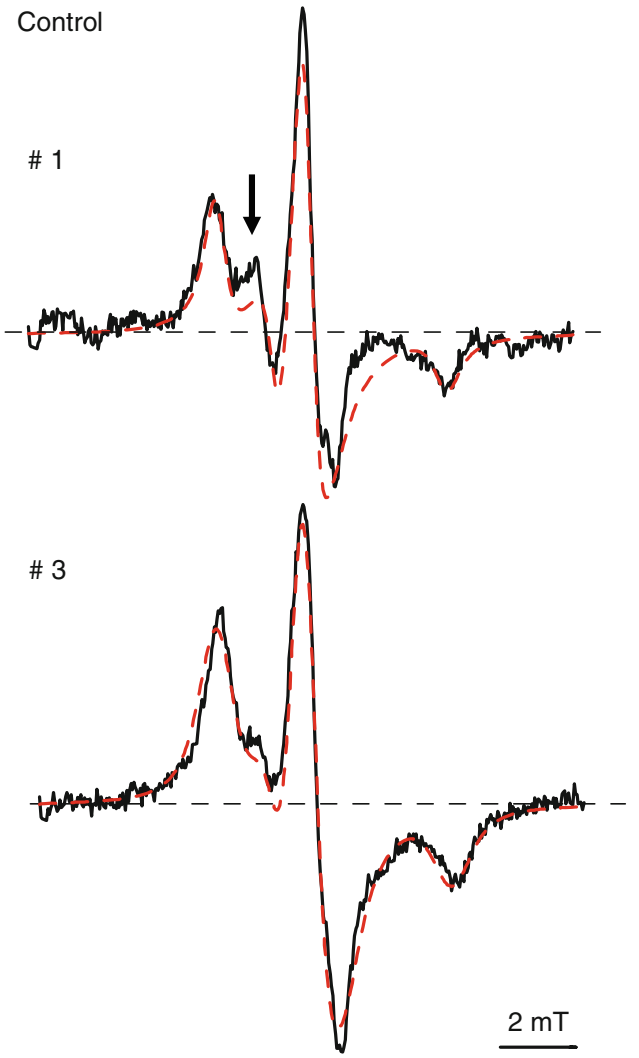

Fig. 4 Experimental (*solid line*) and simulated (*dashed line*) EPR spectra of 5-DSA probe are shown. Stripping numbers show consecutively stripped SC from the surface downwards. The *arrow* of stripping number *1* indicates the characteristic peak. The EPR spectra were obtained with the single scan. The *y*-axes for both spectra range from −800 to +1,200

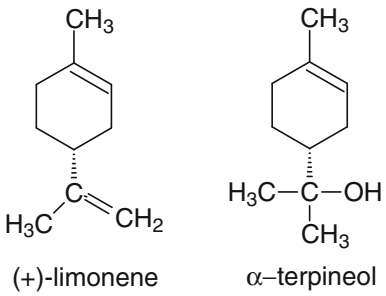

Fig. 5 Chemical structures of the terpenes used in this investigation

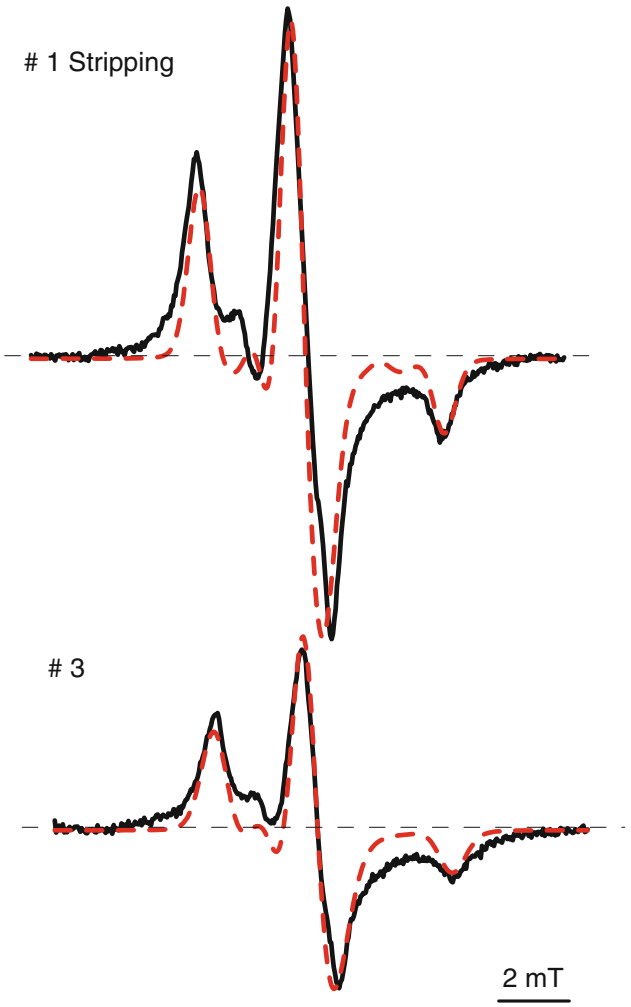

Fig. 6 Experimental (*solid line*) and simulated (*dashed line*) EPR spectra of 5-DSA probe for SC treated with α-terpineol are presented. Stripping numbers show consecutively stripped SC from the surface downwards. The *y*-axes for both spectra range from −2,000 to +2,000

Discussion

Changes in the lipid structural ordering (S_0) of SC can be monitored using the aliphatic probes. The orientation of the spin probe reflects the local molecular environment and the ordering should serve as indicator of conformational changes in the lipid bilayers of the SC. The higher value of the ordering indicates the rigid structure of the SC lipid.

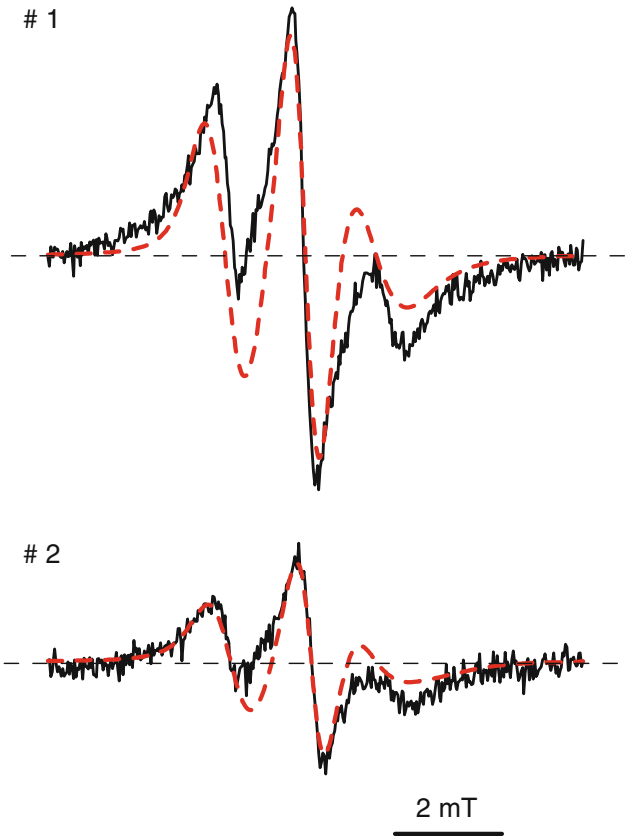

Fig. 7 Experimental (*solid line*) and simulated (*dashed line*) EPR spectra of CHL probe are presented. Stripping numbers show consecutively stripped SC from the surface downwards. The *y*-axes for both spectra range from −1,500 to +1,500

The asymmetric spectral pattern for 5-DSA suggests that 5-DSA is immobile in the SC. The reasonable agreement between the experimental and simulated spectra was obtained as shown in Fig. 4. The simulated S_0 values for the first and third stripped SC were 0.20 and 0.56, respectively. The reasonable agreement suggests that simulation analysis can provide information regarding the quantitative ordering structure of the SC lipids. It is noted that the deviation of the simulated spectrum from the observed spectrum may affect the S_0 value.

One can calculate the angle (γ in Eq. 1 and Fig. 2) between the rotational diffusion symmetry axis (the lipid in SC) and the *z*-axis of the nitroxide axis system [21]. Figure 8 represents the schematic illustration of the bilayer distance in relation to the angle. The simulated S_0 value of 0.20 can be the angle of 69°. The value of 0.55 is the angle of 33°. The angle suggests that the lipids align nearly 33° to the bilayer surface (Fig. 8). Thus, the distance within the bilayer will change because of the S_0 change.

Figure 9 shows a comparison of EPR spectra for control, limonene, and terpineol. The spectra were the first strip. The signal intensity of limonene treated SC is ~1.8 times stronger than that of the control. The signal intensity of terpineol treated SC is ~3.0 times stronger than that of the control. There is significant 5-DSA permeation effect of terpineol on the SC. In the 5-DSA case, the EPR intensity is proportional to the 5-DSA concentration in the SC because of the same EPR linewidth. Thus, the present results suggest that the α-terpineol having an OH-group is more effectively incorporated into the SC lipid than that of limonene.

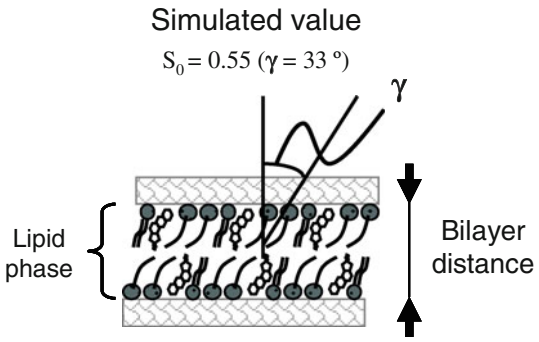

Fig. 8 Schematic illustration of the SC lipid bilayer is presented. The value of simulated order parameter (S_0) related to the angle (γ) between the bilayer surface and the single-chain probe is shown

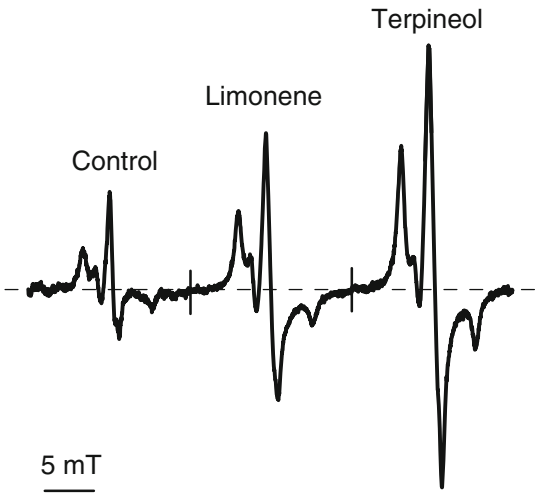

Fig. 9 A comparison of 5-DSA EPR spectra for control, limonene treated, and α-terpineol treated SC is presented. The EPR spectra were obtained for the first stripping of the SC

The simulated S_0 values for the first and the second strip (Fig. 6) were 0.81 and 0.80, respectively. The value for the first one is high even though the discrepancy between the experimental base line and simulated base line. Moreover, the amplitude of the derivative spectrum for the first strip was about two times stronger than that of the third strip (Fig. 6). The permeation of 5-DSA in SC was significant for the first strip. It was also suggested that 5-DSA penetrated the lipids of SC with other penetration enhancers [22]. The EPR spectra were drastically changed by the application of laurocapram in SC after 5–6 h [22] (laurocapram is an unfamiliar chemical in Japan. It was not available commercially at the time of the experiments). The present EPR results showed that EPR intensities increased within 5 min after application of the terpenes.

For CHL, the broad signal without detailed hyperfine splitting was observed. The dotted line is the slow-tumbling simulation of the observed spectra. There is a clear difference between the observed and simulated spectra. The simulated value (e.g. $S_0 \sim 0.3$) may not be reliable because of the discrepancy. The three-line pattern suggests that CHL is probably mobile in the SC.

Moreover, the three-line pattern (the three-line stick spectrum) and the weak outer side peaks were obtained for terpineol treated SC as shown in Fig. 10. The simulation discrepancy and the EPR signal for the terpineol were very different from the results of 5-DSA. Thus, EPR results imply that CHL probe may locate in different parts of the SC.

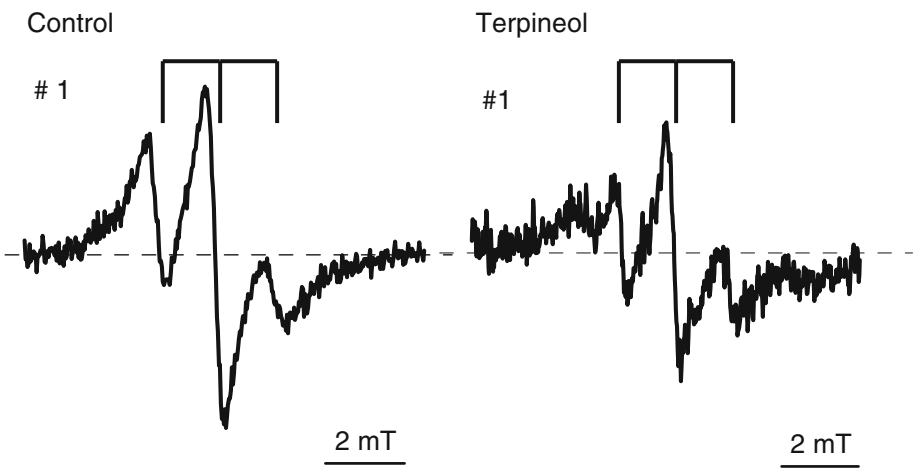

Fig. 10 A comparison of EPR spectra of CHL probe for control (*left side*) and α-terpineol treated SC (*right side*) is shown. The EPR spectra were the first stripping. The *three-line* stick spectrum indicates the signals due to the fast motion of the probe. The *y*-axis for control ranges from −1,500 to +1,500. The *y*-axis for terpineol ranges from −500 to +500

Finally, we made the quantitative evaluation of the effect of terpenes on intercellular lipid structure in SC as a function of skin depth. EPR along with a modern computational analysis provides structural changes of the SC. It was found that α-terpineol significantly enhanced the permeation of the 5-DSA in the SC. Moreover, the bulky CHL molecule showed a quite different behavior to that of 5-DSA in the SC. Therefore, the EPR technique could in turn provide more comprehensive information, which would further the understanding of various SC states. The present results could be useful for percutaneous absorption of drugs.

Acknowledgments Part of this research was supported by a Grant-in-Aid for Scientific Research (C) (21500410) from JSPS (K.N.).

References

1. Kawasaki Y, Quan D, Sakamoto K, Cooke R, Maibach HI (1999) Influence of surfactant mixtures on intercellular lipid fluidity and skin barrier function. Skin Res Technol 5:96–101
2. Mizushima J, Kawasaki Y, Tabohashi T, Maibach HI (2000) Effect of surfactants on human stratum corneum: electron paramagnetic resonance. Int J Pharm 197:193–202
3. Alonso A, Meirelles NC, Yushmanov VE et al (1996) Water increases the fluidity of intercellular membranes of stratum corneum: correlation with water permeability, elastic and electrical resistance properties. J Invest Dermatol 106:1058–1063
4. Kitagawa S, Ikarashi A (2001) Analysis of electron spin resonance spectra of alkyl spin labels in excised guinea pig dorsal skin, its stratum corneum, delipidized skin and stratum corneum model lipid liposomes. Chem Pharm Bull 49:165–168
5. Nakagawa K, Mizushima J, Takino Y, Kawashima T, Maibach HI (2006) Chain ordering of stratum corneum lipids investigated by EPR slow-tumbling simulation. Spectrochim Acta A Mol Biomol Spectrosc 63:816–820
6. Yagi E, Sakamoto K, Nakagawa K (2007) Depth dependence of stratum corneum lipid ordering: a slow-tumbling simulation for electron paramagnetic resonance. J Invest Dermatol 127:895–899
7. Bommannan D, Potts RO, Guy RH (1990) Examination of stratum corneum barrier function in vivo by infrared spectroscopy. J Invest Dermatol 95:403–408
8. Zhang G, Moore DJ, Mendelsohn R, Flach CR (2006) Vibrational microspectroscopy and imaging of molecular composition and structure during human corneocytes maturation. J Invest Dermatol 126:1088–1094
9. Merle C, Baillet-Guffroy A (2009) Physical and chemical perturbations of the supramolecular organization of the stratum corneum lipids: In vitro to ex vivo study. Biochim Biophys Acta 1788:1092–1098
10. Cornwell PA, Barry BW, Bouwstra JA, Gooris GS (1996) Modes of action of terpene penetration enhancers in human skin; differential scanning calorimetry, small-angle X-ray diffraction and enhancer uptake studies. Int J Pharm 127:9–26
11. Pilgram GSK, Engelsma-Van Pelt AM, Bouwstra JA, Koerten HK (1999) Electron diffraction provides new information on human stratum corneum lipid organization studied in relation to depth and temperature. J Invest Dermatol 113:403–409
12. Marks R, Dawber RP (1971) Skin surface biopsy: an improved technique for the examination of the horny layer. Br J Dermatol 84:117–123
13. Yagi E, Nakagawa K, Sakamoto K (2008) Establishment of ex vivo stratum corneum lipid ordering analysis by electron spin resonance. J Soc Cosmet Chem Jpn 42:231–236
14. Hou SY, Rehfeld SJ, Plachy WZ (1991) X-ray diffraction and electron paramagnetic resonance spectroscopy of mammalian stratum corneum lipid domains. In: Elias PM (ed) Advances in lipids research, vol 24. Academic Press, New York, pp 141–171
15. Schneider DJ, Freed JH (1989) Calculating slow motional magnetic resonance spectra. In: Berliner LJ, Reuben J (eds.) Biological magnetic resonance, vol 8. Plenum Press, New York, pp 1–76
16. Budil DE, Lee S, Saxena S, Freed JH (1996) Nonlinear-least-squares analysis of slow-motion EPR spectra in one and two dimensions using a modified Levenberg–Marquardt algorithm. J Magn Reson Ser A 120:155–189
17. Ge M, Freed JH (1998) Polarity profiles in oriented and dispersed phosphatidylcholine bilayers are different: an ESR study. Biophys J 74:910–917
18. Crepeau RH, Saxena S, Lee S, Patyal BR, Freed JH (1994) Studies on lipid membranes by two-dimensional Fourier transform ESR: enhancement of resolution to ordering and dynamics. Biophys J 66:1489–1504
19. Ge M, Rananavare SB, Freed JH (1990) ESR studies of stearic acid binding to bovine serum albumin. Biochim Biophys Acta 1036:228–326
20. Barnes JP, Freed JH (1998) Dynamics and ordering in mixed model membranes of dimyristoylphosphatidylcholine and dimyristoylphosphatidylserine: a 250-GHz electron spin resonance study using cholestane. Biophys J 75:2532–2546
21. Nakagawa K (2010) Electron paramagnetic resonance investigation of stratum corneum lipid structure. Lipids 45:91–96
22. Quan D, Maibach HI (1994) An electron paramagnetic resonance study. I. Effect of Azone on 5-doxyl stearic acid-labeled human stratum corneum. Int J Pharm 104:61–72

GβL	G protein β subunit-like protein also known as mLST8
GLUT 4	Glucose transporter 4
IRS	Insulin receptor substrate
LKB	Tumor suppressor protein
LPAAT	Lysophosphatidic acid acyl transferase
MEFs	Mouse embryonic fibroblasts
MGL	Monoacylglycerol lipase
mTOR	Mammalian target of rapamycin (TOR)
mTOR P-S2481	mTOR phosphorylated on serine 2481
mTORC1	Mammalian target of rapamycin complex 1
mTORC2	Mammalian target of rapamycin complex 2
NCS	Newborn calf serum
NEFA	Nonesterified fatty acids
RAPA	Rapamycin
Raptor	Regulatory associated protein of mammalian target of rapamycin
Rheb	Ras homolog enriched in brain
Rictor	Rapamycin-insensitive companion of mTOR
RII	Regulatory subunit II of PKA
TOS	TOR signaling motif
PA	Phosphatidic acid
PDE	Phosphodiesterase
PLD	Phospholipase D
PI3K	Phosphatidylinositol 3-OH kinase
Pol I	Polymerase I
PKA	Protein kinase A
PKB/AKT	Protein kinase B
PPAR γ	Peroxisome proliferator-activated receptor-γ
PTEN	Phosphatase and tensin homologue deleted on chromosome 10
S6K1	p70 ribosomal protein S6 kinase 1
S6K1 P-T389	S6K1 phosphorylated on threonine 389
TAG	Triacylglycerol
TSC	Tuberous sclerosis complex
VLDL	Very low density lipoprotein

Introduction

The mammalian target of rapamycin (mTOR), an evolutionarily conserved Ser/Thr protein kinase, coordinates a signal transduction network that controls a plethora of fundamental cellular functions [1–3]. mTOR forms the catalytic core of at least two functionally distinct signaling complexes, mTOR complex 1 (mTORC1) and mTOR complex 2 (mTORC2) [3]. The better-understood complex, mTORC1, functions as an environmental sensor to promote anabolic cellular processes such as ribosomal gene transcription, protein synthesis, lipid synthesis, cell growth/size, and cell proliferation in response to sufficient levels of growth factors, nutrients, and hormones [2, 3]. Conversely, adverse cellular conditions rapidly downregulate mTORC1 signaling to promote catabolic functions such as autophagy [4]. mTORC1 and mTORC2 contain shared and unique partner proteins, possess unique cellular functions, and exhibit differing sensitivities to rapamycin, a clinically employed immunosuppressive drug [3]. Rapamycin (clinically known as sirolimus) associates with a cellular protein called FKBP12 [5]. Upon entering the cell, the rapamycin/FKBP12 complex directly binds to the mTOR FRB (FKBP12-rapamycin binding) domain, which lies immediately N-terminal to the kinase domain [5]. Rapamycin/FKBP12 binds assembled mTORC1 but not assembled mTORC2 [5]. Thus, rapamycin acutely inhibits mTORC1 but not mTORC2 signaling. While the mechanisms by which rapamycin allosterically inhibits mTORC1 signaling remain incompletely defined, the drug reduces the affinity between mTOR and raptor, a critical mTORC1 partner protein [5, 6]. Additionally, rapamycin reduces mTORC1 intrinsic kinase activity, as monitored by mTOR S2481 autophosphorylation [7]. The use of rapamycin in clinical medicine underscores the importance of mTORC1 for organismal physiology. Not only does rapamycin reduce organ transplant rejection [8], it reduces the intimal de-differentiation and hyperplasia of vascular smooth muscle cells that often follows coronary artery stent restenosis [9]. Strikingly, rapamycin extends rodent lifespan [10]. Rapamycin analogs and second-generation mTOR catalytic inhibitors also hold therapeutic promise as anti-cancer agents [5].

Rapamycin administration incurs adverse side effects, however. Various clinical trials have documented the development of hypertriglyceridemia or hypercholesterolemia in renal, hepatic, cardiac, and islet transplant patients [11, 12]. Additionally, rapamycin has also been shown to elevate serum free fatty acid (FFA) levels and induce glucose intolerance [13] in transplant patients as well as in mice lacking the mTORC1 downstream target S6K1 [14]. Clinical trials have also documented the occurrence of hyperlipidemia upon the administration of the rapamycin analog CCI-779 (also known as temsirolimus; Wyeth) in the treatment of metastatic melanoma and glioblastoma multiforme [15]. Consistent with rapamycin increasing levels of circulating FFAs and inducing hyperlipidemia, mice lacking S6K1 globally or lacking raptor in adipose are lean with reduced adipose mass and exhibit resistance to diet-induced obesity [14]. Thus, mTORC1 inhibition induced by pharmacological or genetic ablation disrupts lipid homeostasis in vivo.

In this study we set out to better understand how mTORC1 signaling impacts lipid metabolism in cultured adipocytes. Adipose tissue, once considered an inert energy storage depot, is now recognized as an important metabolic and endocrine organ that coordinates energy intake and expenditure critical for energy homeostasis [16]. Adipose tissue removes glucose from the circulation (via the action of the insulin-responsive glucose transporter GLUT4) and stores surplus energy in the form of triacylglycerol (TAG) within lipid droplets. The tissue releases energy as needed via the action of lipolysis, the process by which enzymes known as lipases break down TAG into FFA and glycerol, which are then released into the circulation. Diverse extracellular stimuli regulate lipolysis. Catecholamines (e.g., epinephrine) and glucocorticoids (e.g., cortisol) promote lipolysis while insulin and FFA themselves suppress lipolysis [17]. Starvation or stress triggers the release of catecholamines, which promote lipolysis by activating G protein-coupled adrenergic receptors that activate adenylate cyclase (AC), which lead to increased production of cAMP and activation of protein kinase A (PKA). Several laboratories have established that PKA phosphorylates two lipolytic proteins, perilipin and hormone sensitive lipase (HSL) [18]. Perilipin functions as a master regulator of lipolysis [19, 20]. Under basal conditions, perilipin coats and protects lipid storage droplets. Upon agonist stimulation, PKA phosphorylates perilipin A, which induces a conformational change in the perilipin coating that enables the recruitment of HSL from the cytoplasm to the surface of the lipid droplet [21, 22]. Indeed, perilipin knockout mice have reduced adipose tissue mass and exhibit elevated basal lipolysis with resistance to β-adrenergic-stimulated lipolysis; moreover, the mice display resistance to diet-induced and genetic obesity [18, 22–24].

Our previous work demonstrated that rapamycin administration induces hypertriglyceridemia in organ transplant patients [11], and increases TAG and plasma FFA in guinea pigs [25]. Here, we test the hypothesis that rapamycin promotes TAG lipolysis in cultured murine 3T3-L1 adipocytes. We found that inhibition of mTORC1 signaling with rapamycin augments lipolysis promoted by the β-adrenergic agonist isoproterenol without augmenting cellular cAMP levels. Additionally, we found that rapamycin enhances isoproterenol-induced phosphorylation of HSL. These data indicate that mTORC1 inhibition synergizes with the PKA pathway to promote lipolysis by modulating HSL function. Improved understanding of how mTORC1 inhibition promotes lipolysis to disrupt lipid metabolism may assist clinicians in the future to better handle the deleterious side effects incurred by therapeutic rapamycin treatment during immunosuppression, cancer chemotherapy, or following coronary artery angioplasty.

Experimental Procedures

Materials

Reagents were obtained from the following sources: CHAPS (3-[(3-cholamidopropyl)- dimethylammonio]-1-propanesulfonate) was from Pierce (Rockford, IL, USA); nitrocellulose membrane (0.45 microns) was from Schleicher and Schuell Bioscience Inc. (Keene, NH, USA); autoradiography film (HyBlot CL) was from Denville Scientific Inc. (Metuchen, NJ, USA); reagents for enhanced chemiluminescence (ECL) (Immobilon Western-Chemiluminescent HRP Substrate) were from Upstate/Millipore (Billerica, MA, USA); all standard chemicals were from either Fisher Chemicals (Pittsburgh, PA, USA), Calbiochem/EMD Chemicals (Gibbstown, NJ, USA), or Sigma-Aldrich (St. Louis, MI, USA).

Antibodies

The following antibodies were purchased from Cell Signaling Technology (Danvers, MA, USA): P-S6K1-T389 (rabbit monoclonal 108D2); P-mTOR-S2481, HSL, ATGL, MGL. The perilipin antibody was from Chemicon/Millipore (Billerica, MA, USA) (#AB10200), and the β-actin monoclonal antibody was from Sigma-Aldrich (St. Louis, MI, USA). Antibodies to detect the phosphorylation of PKA on its regulatory subunits RIIα (S96) and RIIβ (S114) were from Upstate/Millipore (Billerica, MA, USA). Custom, affinity-purified anti-peptide antibodies against mTOR and S6K1 were generated in rabbits, as described [7]. Sheep anti-mouse antibodies and donkey anti-rabbit HRP secondary antibodies were from GE-Healthcare (Piscataway, NJ, USA).

Differentiation of 3T3-L1 Fibroblasts into Adipocytes

3T3-L1 fibroblasts (kindly provided by Dr. Ormond MacDougald; University of Michigan Medical School) were cultured in Dulbecco's Modified Eagle Medium (DMEM) that contained high glucose (4.5 g/L), glutamine (584 mg/L), and sodium pyruvate (110 mg/L) supplemented with 10% newborn calf serum (NCS) (Gibco/Invitrogen; Carlsbad, CA, USA) and maintained at 37 °C in 5% CO_2. 3T3-L1 fibroblasts were differentiated into adipocytes by a standard protocol. Briefly, differentiation was induced 2 days post confluency by the addition of DMEM containing 10% fetal bovine serum (FBS) (Hyclone) and dexamethasone (1 μM) (Sigma-Aldrich; St. Louis, MO, USA), 3-isobutyl-1-methylxanthine IBMX (0.5 mM) (Sigma-Aldrich; St. Louis, MI, USA) and insulin (100 nM) (Gibco/Invitrogen; Carlsbad, CA, USA) for 2 days. The cells were further incubated with DMEM/FBS supplemented with

insulin for an additional 2 days. Fully differentiated adipocytes were maintained in DMEM/FBS at 37 °C in a humidified atmosphere containing 5% CO_2 and used 9–14 days after the initiation of differentiation.

Cell Culture, Drug Treatment, Cell Lysis and Western Immunoblotting

3T3-L1 adipocytes were serum deprived for 20 h via incubation in DMEM supplemented with 20 mM Hepes (pH 7.2). Following serum deprivation, adipocytes were drug treated for 30 min by the addition of rapamycin (20 ng/mL) (22 nM) (Calbiochem/EMD Chemicals; Gibbstown, NJ, USA), or wortmannin (100 nM) (Upstate/Millipore; Billerica, MA, USA) prior to the addition of the β-adrenergic agonist isoproterenol (10 μM) (Chemicon/Millipore; Billerica, MA, USA) unless indicated otherwise, insulin (100 nM) (Invitrogen; Carlsbad, CA, USA), or both for 30 min. For cell lysis, adipocytes were washed 2× with ice cold PBS [pH 7.4] and collected in ice cold lysis Buffer A (10 mM KPO_4 [pH 7.2]; 1 mM EDTA; 5 mM EGTA; 10 mM $MgCl_2$; 50 mM β-glycerophosphate; 1 mM sodium orthovanadate (Na_3VO_4); 5 μg/mL pepstatin A; 10 μg/mL leupeptin; 40 μg/mL PMSF) containing the detergent CHAPS (0.3%). Lysates were spun at 13,200 rpm for 5 min at 4 °C, and the post-nuclear supernatants were collected. Bradford assay was used to normalize protein levels for the measurement of triacylglycerol content, lipolysis, cAMP levels, and Western immunoblot analyses. For immunoblots, whole cell lysates were resuspended in 1× sample buffer (50 mM Tris–HCl pH 6.8, 10% glycerol, 2% SDS, 2% β-mercaptoethanol, 0.02% bromophenol blue). Samples were heated at 95 °C for 5 min, resolved on SDS–PAGE gels, and transferred to nitrocellulose membrane using Towbin transfer buffer (25 mM Tris; 192 mM glycine; 10% methanol; 0.02% SDS). Immunoblotting was performed by blocking membranes in TBST (40 mM Tris–HCl pH 7.5; 0.9% NaCl; 0.1% Tween-20) containing 3% nonfat milk and incubating the membranes in TBST with 2% BSA containing primary antibodies or secondary HRP-conjugated antibodies. Blots were developed by enhanced chemiluminescence (ECL).

Measurement of Cellular Triacylglycerol Content

Adipocyte triacylglycerol concentrations were measured by enzymatic methods following manufacturer instructions (Wako Chemicals, Inc.; Richmond, VA, USA) following cellular lysis and normalization of protein content. Briefly, samples and a set of triolein standards were incubated with triacylglycerol reagent A at 37 °C for 5 min followed by addition of triacylglycerol reagent B for 5 min at 37 °C. The colorimetric reaction was then measured at wavelength 590 nm and expressed as mg/mg protein.

Lipolysis Assays

Following serum deprivation and drug treatment, differentiated 3T3-L1 adipocytes were stimulated with isoproterenol for either 1 h or 4 h, as indicated in the figure legends. The media was collected and analyzed for free fatty acid release in the culture media using a NEFA C assay (Wako Chemicals; Richmond, VA, USA) and read by a spectrophotometer at wavelength 540 nm. Free fatty acid release was measured in millimole per microgram protein (mmol/ug) and expressed as relative free fatty acid percent. Glycerol release in the media was measured by colorimetric assay at wavelength 540 nm using a Chemicon lipolysis kit, following the manufacturer's instructions (Chemicon/Millipore; Billerica, MA, USA).

Measurement of Cellular cAMP Levels

Following serum deprivation, drug treatment, and isoproterenol stimulation, cAMP levels were measured using a HitHunter cAMP EFC (enzyme fragment complementation) assay (Amersham/GE-Healthcare; Piscataway, NJ, USA) following the manufacturer's instructions. All samples and standards were run in triplicates, and luminescence was detected using a multimode microplate reader (PerkinElmer, VICTOR 3; Waltham, MA, USA).

Statistics

ANOVA (Analysis of Variance) was used to determine overall statistical significance among various treatment groups. If significance was achieved at $P < 0.05$, then post-hoc secondary LSD (Least Significant Difference) tests were performed.

Results

Insulin-Mediated Activation of mTORC1 Promotes Triacylglycerol Accumulation in 3T3-L1 Adipocytes

To determine whether mTORC1 signaling controls triacylglycerol (TAG) content in adipocytes, we differentiated 3T3-L1 fibroblasts into adipocytes and treated them with insulin in the absence or presence of rapamycin for 18 h after a period of serum deprivation. As expected, chronic insulin treatment promoted triacylglycerol storage (Fig. 1a). We found that rapamycin treatment reduced insulin-stimulated TAG accumulation ~50% in a statistically significant manner ($P < 0.05$), thus demonstrating

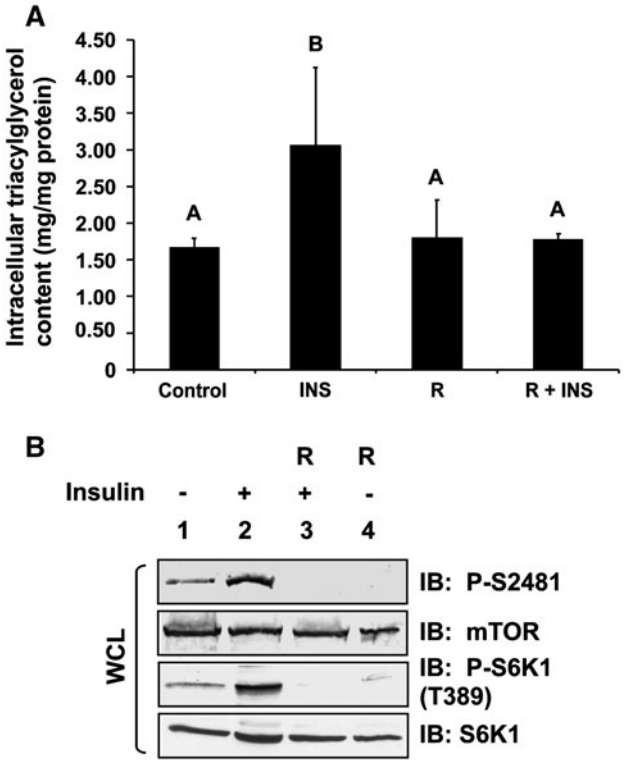

Fig. 1 Insulin-stimulated triacylglycerol (TAG) accumulation in 3T3-L1 adipocytes requires mTORC1 signaling. **a** 3T3-L1 adipocytes were serum-deprived for 20 h (*Control*) and then pre-treated without or with rapamycin (20 ng/mL) for 30 min. Cells were stimulated without (*Control*) or with insulin (INS) (100 nM) in the absence (*R*) or continued presence of rapamycin (*R* + *INS*) for 18 h. Whole cell lysates were analyzed for triacylglycerol content (mg/mg protein) via a colorimetric assay (see "Experimental Procedures") after normalization for protein content. The *graph* represents the mean ± SD of triplicate samples from one experiment but is representative of three independent experiments; thus, each *bar* represents $n = 3$. Differences between treatment groups were analyzed using ANOVA, and differences were considered statistically different at a level of 0.05. *Bars* with different letters are statistically significant. **b** The whole cell lysates analyzed in (**a**) were resolved on SDS–PAGE and immunoblotted with the indicated antibodies to confirm the expected activation and/or inhibition of mTORC1 signaling

that mTORC1 signaling is required for insulin-stimulated TAG storage. To confirm that insulin mediated the activation of mTORC1 and downstream signaling in a rapamycin-sensitive manner in this experiment, we immunoblotted whole cell lysates with mTOR P-S2481 and S6K1 P-T389 antibodies (Fig. 1b). Upon activation, mTOR autophosphorylates on S2481; thus, mTOR P-S2481 immunoblotting monitors intrinsic mTOR catalytic activity [7]. Activated mTORC1 then directly phosphorylates S6K1 on T389 [26]; thus, S6K1 P-T389 immunoblotting monitors mTORC1 downstream signaling. As rapamycin inhibited insulin-stimulated autophosphorylation of mTOR on S2481 and the phosphorylation of S6K1 on T389, these data indicate that rapamycin indeed inhibited the insulin-stimulated activation of mTORC1.

Rapamycin Augments β-Adrenergic-Stimulated Lipolysis in 3T3-L1 Adipocytes

As we found that rapamycin-mediated inhibition of mTORC1 signaling reduces cellular TAG content, we next asked whether rapamycin reduces TAG content by promoting lipolytic rate. As the insulin/PI3K pathway promotes mTORC1 signaling and also suppresses lipolysis (via Akt-mediated activation of phosphodiesterase [PDE], an enzyme that hydrolyzes cAMP to AMP) [27], we measured adipocyte lipolysis in the absence of serum growth factors in order to study lipolysis independently of PDE action. To stimulate lipolysis, we employed the catecholamine isoproterenol, a synthetic β2-adrenergic agonist. By treating serum deprived 3T3-L1 adipocytes with isoproterenol in the absence or presence of rapamycin, we found that inhibition of mTORC1 signaling augments isoproterenol stimulated lipolysis in a statistically significant manner, as measured by the release of FFA (Fig. 2a) into the cell culture media after 1 h of incubation. Based on our preliminary kinetic data (data not shown) as well as reported literature [28], a 1-h time point was optimal for measurements of glycerol release (Fig. 2b) while a 4-h time point was optimal for measurements of FFA release. We thus next measured FFA release utilizing a 4-h time point to determine whether mTORC1 inhibition with rapamycin augments basal lipolysis, whether insulin suppresses isoproterenol-stimulated lipolysis, and whether mTORC1 inhibition using the PI3K inhibitor wortmannin augments isoproterenol-stimulated lipolysis (similar to rapamycin). We found that rapamycin had no effect on basal lipolysis after 4 h of incubation, while, insulin indeed suppressed isoproterenol-stimulated lipolysis, as expected (Fig. 2c). Interestingly, mTORC1 inhibition with rapamycin rescued the suppression of lipolysis caused by insulin, suggesting a novel role for mTORC1 in suppression of lipolysis via the insulin/Akt/PDE pathway (Fig. 2c). Similar to rapamycin, wortmannin treatment augmented isoproterenol-stimulated lipolysis, suggesting a novel role for PI3K as well as mTORC1 in suppression of lipolysis (Fig. 2c). The finding that inhibition of PI3K with wortmannin phenocopies rapamycin treatment to augment isoproterenol-stimulated lipolysis is consistent with the well-known regulation of mTORC1 by PI3K [3]. These data suggest that the PI3K/mTORC1 pathway mediates lipolytic suppression.

Rapamycin Does Not Modulate Cellular cAMP Levels

To begin to understand the mechanism by which mTORC1 inhibition augments isoproterenol-stimulated lipolysis, we

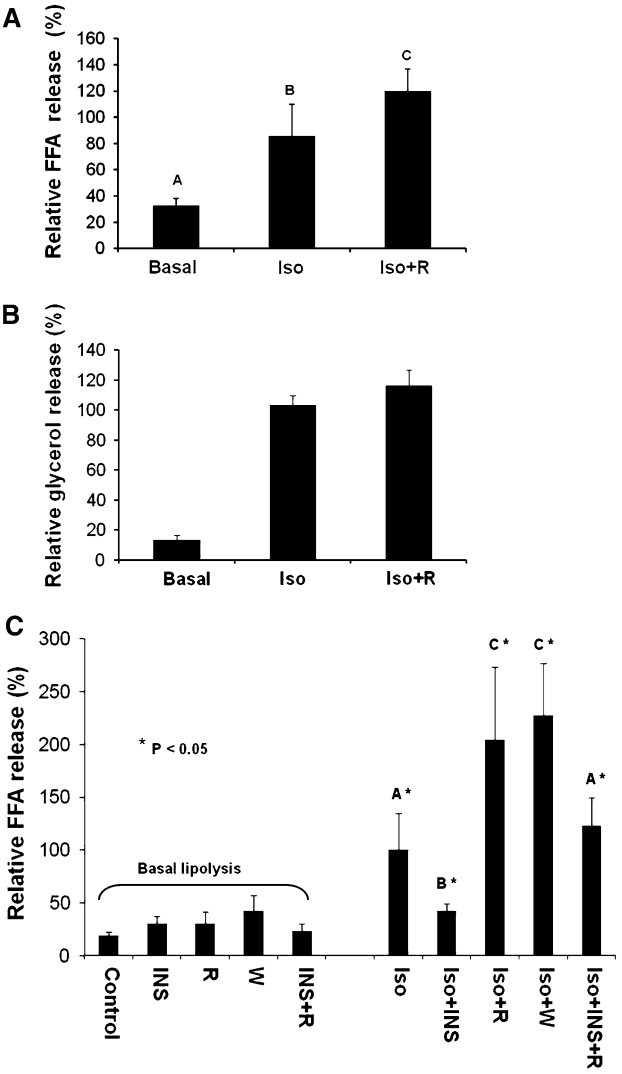

Fig. 2 Inhibition of mTORC1 with rapamycin augments β-adrenergic-activated lipolysis in 3T3-L1 adipocytes. **a, b** 3T3-L1 adipocytes were serum-deprived for 20 h and then pre-treated without or with rapamycin (*R*) (20 ng/mL) for 30 min. Cells were then incubated in the absence (*Basal*) or presence of isoproterenol (*Iso*) (10 μM) for 1 h in the absence or continued presence of rapamycin (*Iso* + *R*). Relative free fatty acid (FFA) release was measured in (**a**) and relative glycerol release was measured in (**b**). In graphs (**a**, **b**) each *bar* represents the mean value ± SD of 5 samples from three independent experiments; thus, each *bar* represents $n = 5$. The value from cells treated with Iso alone was set to 100%, and all other values were normalized to this value. **c** 3T3-L1 adipocytes were treated similarly as in (**a**, **b**) with minor modifications, and relative free fatty acid (FFA) release was measured, as in (**a**). Briefly, serum-deprived cells were pre-treated without or with rapamycin (20 ng/mL) or wortmannin (100 nM) for 30 min. Cells were then incubated in the absence (*Basal lipolysis*) or presence of isoproterenol (10 μM) for 4 h without (*Iso*) or with insulin (100 nM) (*Iso* + *INS*), rapamycin (*Iso* + *R*), wortmannin (*Iso* + *W*), or both insulin and rapamycin (*Iso* + *INS* + *R*), as indicated in the graph. Cells incubated in the absence of isoproterenol (*Basal lipolysis*) were also incubated with insulin (*INS*), rapamycin (*R*), wortmannin (*W*), and insulin and rapamycin (*INS* + *R*) for 4 h. In graph (**c**), each *bar* represents the mean value ± SD of nine samples from three independent experiments; thus, each *bar* represents $n = 9$. As in graphs (**a**, **b**), the value of Iso alone was set to 100%, and all other values were normalized to this value. Differences between treatment groups were analyzed using ANOVA, and differences were considered statistically different at a level of 0.05. *Bars* with different letters are statistically significant

determined whether rapamycin augments isoproterenol-stimulated production of cAMP. Studies in yeast have shown that TOR may function upstream of PKA [29], thus lending support to such a hypothesis. We thus measured cellular levels of cAMP in adipocytes stimulated with isoproterenol in the absence or presence of rapamycin for 15 min (Fig. 3a) and 30 min (Fig. 3b). We found that rapamycin treatment had no effect on cAMP levels during basal or catecholamine-stimulated lipolysis. Thus, these data suggest that mTORC1 inhibition does not augment catecholamine-stimulated lipolysis by leading to increased levels of cAMP.

Rapamycin Does Not Affect PKA Phosphorylation

To begin to study the regulation of PKA activity in intact cells, we investigated the phosphorylation of PKA on its regulatory subunits, RIIα (S96) and RIIβ (S114), utilizing phospho-specific antibodies. Studies have shown that autophosphorylation of S96 on the regulatory subunit RIIα promotes local PKA activity in cardiac muscle [30]. Additionally, point mutation of the S114 autophosphorylation site on RIIβ has been shown to block the nuclear localization of PKA and to inhibit PKA function in T cells both in vitro [31] and in vivo [32]. We found that isoproterenol-stimulated PKA phosphorylation on regulatory subunit RIIα (S96) or regulatory subunit RIIβ (S114) was not altered by rapamycin treatment at various isoproterenol concentrations (Fig. 4a). While by no means conclusive, these data suggest that mTORC1 inhibition may promote isoproterenol-stimulated lipolysis downstream of PKA. Alternatively, it remains possible that mTORC1 inhibition inhibits PKA activity via a mechanism independent of regulatory subunit phosphorylation.

Rapamycin Modestly Augments the Phosphorylation of HSL

To determine whether PKA signaling and mTORC1 inhibition synergistically modulate the activation state of lipolytic targets, we assayed the phosphorylation of two well known PKA dependent targets, hormone sensitive lipase (HSL) and perilipin. In response to starvation and stress, catecholamine induced activation of the cAMP/PKA pathway leads to PKA-mediated phosphorylation of both perilipin and HSL [23]. PKA-induced phosphorylation of perilipin on at least 6 sites triggers a conformational change

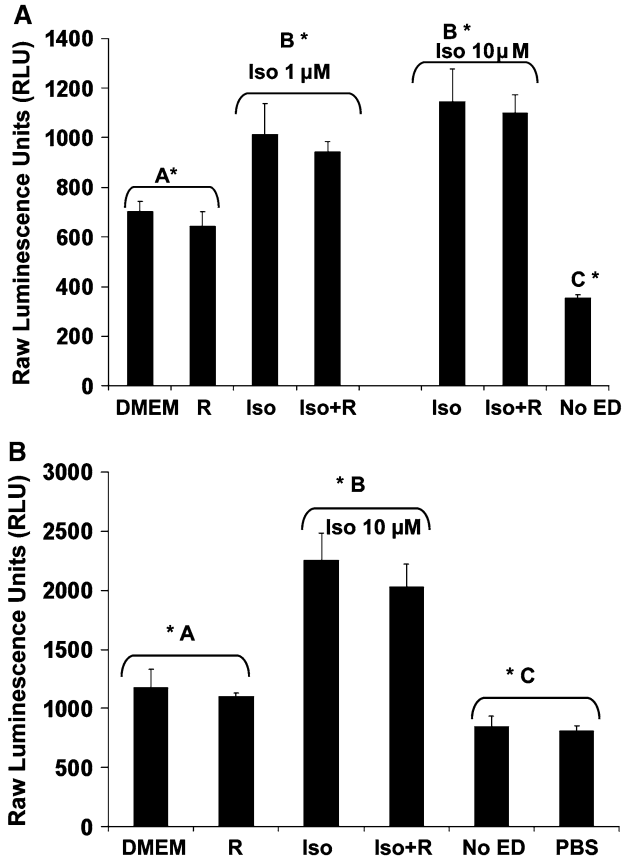

Fig. 3 Rapamycin does not augment cAMP levels over β-adrenergic agonist alone. cAMP levels were measured using the HitHunter cAMP EFC chemiluminescent detection assay (Amersham, Inc.), according to manufacturer's directions. Briefly, 3T3-L1 adipocytes were serum deprived 20 h and pre-treated without or with rapamycin (*R*) (20 ng/mL) for 30 min. Cells were then incubated in the absence (*DMEM*) or presence of isoproterenol (*Iso*) (1 µM or 10 µM) for 15 min (**a**) or (10 µM) 30 min (**b**) in the absence or presence of rapamycin (*Iso* + *R*). "*No ED*" (without enzyme donor) and "*PBS*" represent negative controls for this assay. *Bars* with different letters are statistically significant at a level of 0.05

that disassembles the perilipin protective coat and induces the translocation of HSL from the cytoplasm to the surface of lipid droplet, whereby HSL docks to phosphorylated perilipin [23, 33]. To determine whether rapamycin augments isoproterenol-stimulated phosphorylation of perilipin, we employed a commonly used SDS–PAGE mobility shift assay to determine the phosphorylation state of perilipin. Serum deprived 3T3-L1 adipocytes were pretreated with rapamycin and then stimulated in the absence of isoproterenol or with a series of isoproterenol concentrations ranging from maximal to sub-maximal (10 µM down to 1 nM). As expected, isoproterenol strongly promoted the phosphorylation of perilipin in a dose-dependent manner, as shown by decreased electrophoretic mobility on SDS–PAGE (Fig. 4b). Rapamycin treatment had no effect on isoproterenol-induced perilipin phosphorylation, even at sub-maximal doses (0.1 µM, 10 nM). At the limited resolution of this assay, these data suggest that mTORC1 inhibition with rapamycin does not synergize with catecholamine induced PKA signaling to promote significant phosphorylation of perilipin. Although mobility shift is a commonly used method in detection of perilipin phosphorylation state, we acknowledge the possibility that rapamycin could promote the phosphorylation of individual sites on perilipin whose phosphorylation state may not be measurable by mobility shift. We next investigated the phosphorylation of the lipase HSL, which functions as the rate-limiting enzyme in the lipolytic cascade. To date, three PKA-mediated phosphorylation sites (Ser^{563}; Ser^{659}; Ser^{660}) and one AMPK-mediated phosphorylation site (Ser^{565}) have been identified on rat HSL, as illustrated in Fig. 4c [34, 35]. Phosphorylation of HSL on Ser^{563} by PKA is thought to promote the intrinsic catalytic activity of HSL [36], while phosphorylation of HSL on Ser^{659} and Ser^{660} by PKA are thought to promote the translocation of cytosolic HSL to the surface of the lipid droplet [23]. Conversely, phosphorylation of HSL on Ser^{565} by AMPK is thought to inhibit HSL activity [37]. By treating 3T3-L1 adipocytes with various concentrations of isoproterenol in the absence and presence of rapamycin, we found that rapamycin augmented HSL Ser^{563} phosphorylation (Fig. 4c). On the contrary, there was no additional effect of rapamycin on isoproterenol-stimulated phosphorylation of HSL Ser^{660} (Fig. 4c). Neither isoproterenol nor rapamycin modulated AMPK Ser^{565} phosphorylation, which appears to be constitutively activated under basal conditions [37]. Taken together, these data indicate that mTORC1 inhibition with rapamycin synergizes with PKA signaling to augment the phosphorylation of HSL on Serine 563, which may accelerate lipolysis by augmenting HSL catalytic activity.

Rapamycin Has No Effect on ATGL, HSL, or MGL Protein Expression

To determine whether mTORC1 inhibition with rapamycin additionally promotes lipolysis by modulating the expression of the lipases critical for the breakdown of TAG into FFAs and glycerol, we examined the protein expression of adipose triacylglycerol lipase (ATGL), hormone sensitive lipase (HSL), and monoacyl lipase (MGL). It is currently believed that ATGL initiates basal as well as hormone sensitive lipolysis of triacylglycerol [38, 39] to FFA and diacylglycerol. Subsequently, HSL acts on diacylglycerol particles to release FFA and monoacylglycerol. The final step in lipolysis is catalyzed by the hormone-insensitive MGL, which acts on monoacylglycerol to release FFA and glycerol [39]. Some investigators [40] also suggest a role for triacylglycerol hydrolase (TGH) in lipolysis; the relative contribution of TGH in the lipolytic cascade within the

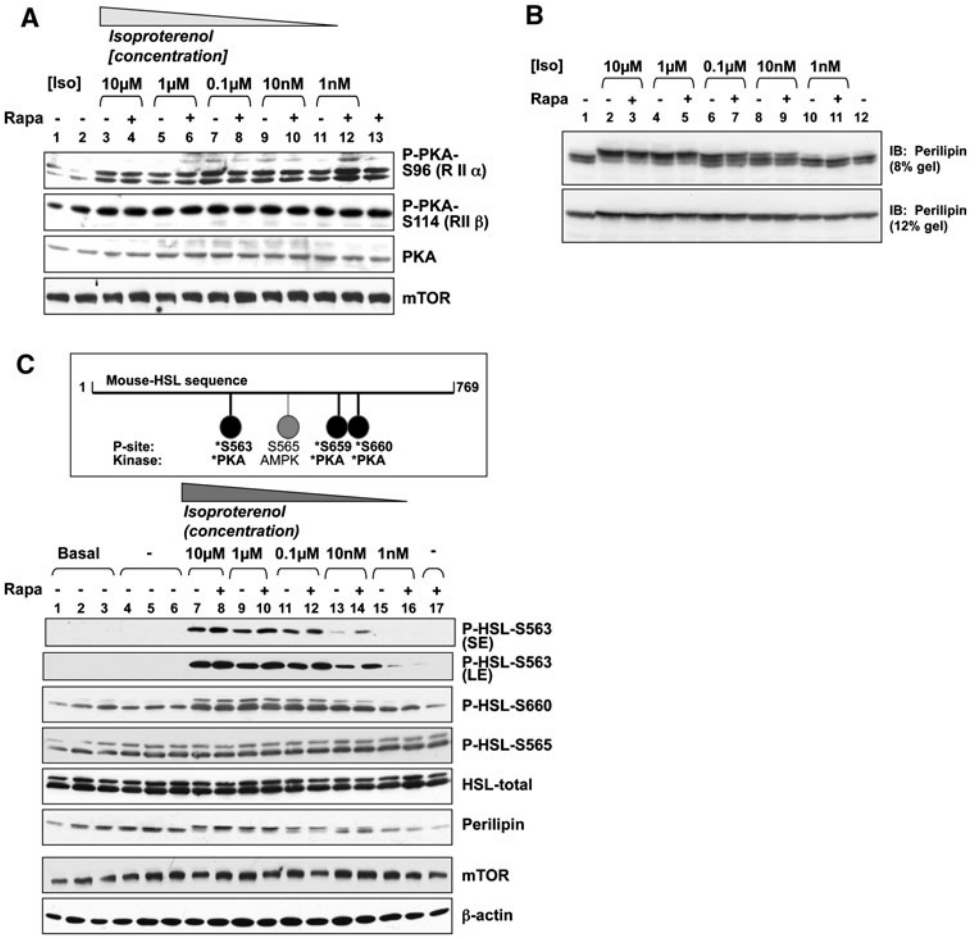

Fig. 4 Rapamycin augments isoproterenol-stimulated phosphorylation of HSL on S563 in the absence of effects on PKA regulatory subunit or perilipin phosphorylation. **a** Rapamycin does not modulate the phosphorylation of PKA on the regulatory subunits RIIα (S196) or RII*β* (S114): 3T3-L1 adipocytes were serum-deprived for 20 h and then pre-treated without (−) or with (+) rapamycin (20 ng/mL) for 30 min. Cells were incubated in the absence (−) or presence of various concentrations of isoproterenol (*Iso*) ranging from 10 μM to 1 nM for 15 min, as indicated. After lysis, whole cell lysate was resolved on SDS–PAGE and immunoblotted with the indicated antibodies. **b** Rapamycin does not augment isoproterenol-stimulated phosphorylation of perilipin: 3T3-L1 adipocytes were serum-deprived for 20 h and pre-treated without (−) or with (+) rapamycin (*Rapa*) (20 ng/mL) for 30 min. Cells were then incubated in the absence (−) or presence (+) of isoproterenol (*Iso*) (10 μM) in the absence or presence of rapamycin for 15 min. After lysis, whole cell lysate was resolved on SDS–PAGE and immunoblotted with perilipin antibodies. Note: To observe perilipin electrophoretic mobility shift, a measure of perilipin phosphorylation, a 21 cm long 8% gel was run for 3:30 h. To visualize total perilipin, a 13-cm long 12% gel was run for 1:45 h. **c** Rapamycin augments isoproterenol-stimulated phosphorylation of HSL on S563 (a PKA phosphorylation site) but not on S565 (an AMPK phosphorylation site): *Upper panel*: Schematic of the HSL sites phosphorylated by PKA and AMPK. *Lower panel*: 3T3-L1 adipocytes were serum-deprived and pre-treated without (−) or with (+) rapamycin, as in (**a**, **b**) above. Cells were then incubated in the absence (−) or presence of various concentrations of isoproterenol (Iso) ranging from 10 μM to 1 nM for 15 min, as indicated. After lysis, whole cell lysates were resolved on SDS–PAGE and immunoblotted with the indicated antibodies. Cells were also lysed immediately after serum deprivation (*Basal*). Two P-HSL-S563 film exposures are shown (SE-short exposure, LE-long exposure)

adipocyte remains unclear, however. We treated 3T3-L1 adipocytes with isoproterenol in the absence or presence of rapamycin for 18 h and measured the protein expression of ATGL, HSL, and MGL by immunoblot (Fig. 5). We found no differences in the abundance of these 3 important lipases under any treatment condition. Thus, these data indicate that mTORC1 inhibition with rapamycin does not augment lipolytic rate by increasing the expression of a critical lipase.

Discussion

Here, we investigated the biochemical mechanism by which mTORC1 inhibition via the immunosuppressive drug rapamycin induces hypertriglyceridemia and increases circulating free FFAs in organ transplant patients [11] as well as in guinea pigs [25]. We report that treatment of 3T3-L1 adipocytes with the mTORC1 inhibitor rapamycin decreases TAG storage by augmenting lipolysis induced by

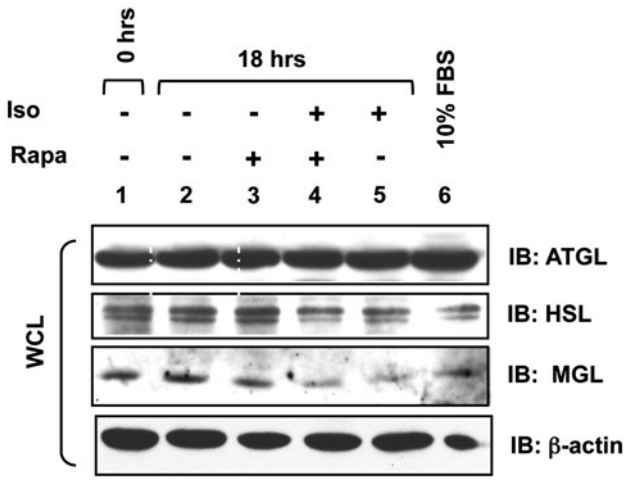

Fig. 5 Rapamycin does not modulate the protein expression of ATGL, HSL, or MGL. 3T3-L1 adipocytes were serum-deprived for 20 h (*lanes 1–5*) and pre-treated without (*lanes 1–2, 5*) or with (*lanes 3, 4*) rapamycin (R) (20 ng/mL) for 30 min. Cells were then incubated in the absence (−) (*lanes 2–3*) or presence (+) (*lanes 4–5*) of isoproterenol (10 μM) for 18 h in the absence or continued presence of rapamycin, as indicated. In lane 1, cells were lysed after the 20 h serum deprivation period ($t = 0$). In *lane 6*, cells were cultured in DMEM/10% FBS (steady-state, non-starved conditions). After lysis, whole cell lysate was resolved on SDS–PAGE and immunoblotted with the indicated antibodies

isoproterenol, a *β*-adrenergic agonist, without altering basal lipolysis. While, the measured effect of rapamycin on hormone-induced lipolysis was modest, the combined effect of increased lipolysis and decreased TAG synthesis incurred by mTOR inhibition likely has a more significant impact on TAG metabolism. Our data further elucidate the mechanism by which mTORC1 inhibition cooperates with PKA signaling to promote lipolysis: We found that rapamycin augments isoproterenol-induced phosphorylation of HSL (on S563) via a mechanism that does not involve increased production of cAMP. These data indicate that mTORC1 inhibition and PKA signaling synergize either downstream of PKA or at the level of PKA to promote lipolysis (Fig. 6). Whether, mTORC1 inhibition and PKA converge on common lipolytic targets (e.g. HSL, ATGL) via parallel pathways or, whether mTORC1 inhibition converges on PKA itself to enhance its function (via increased enzymatic activity, altered subcellular localization, etc.) remains currently unknown (see model in Fig. 6). In support of the former model, TOR and PKA signal via parallel pathways in budding yeast to regulate the transcriptional expression of ribosomal protein genes and stress-responsive genes [41]. In support of the latter model, TORC1 signaling in budding yeast was reported recently to regulate PKA activity [42]. Lastly, we found that rapamycin treatment (18 h) had no effect on the expression of various lipases, including ATGL, HSL, or MGL under basal or isoproterenol-stimulated conditions.

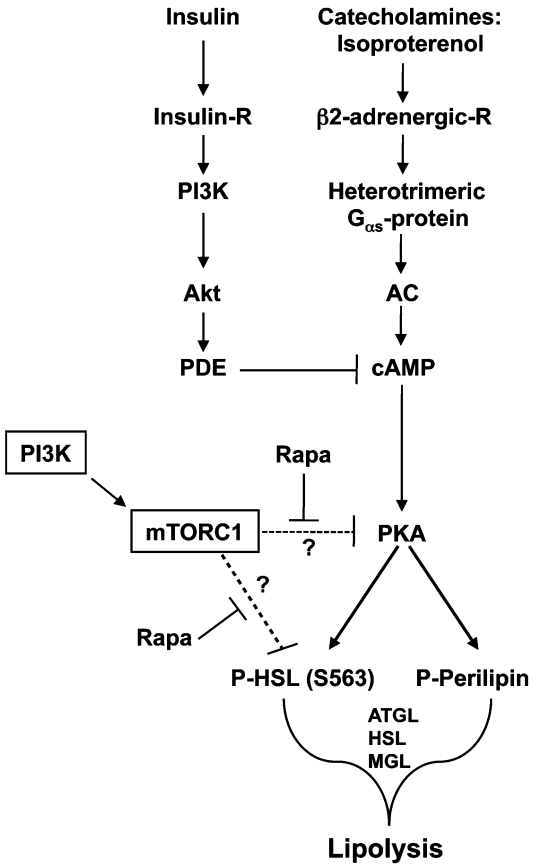

Fig. 6 Model for the role of mTORC1 signaling in suppression of lipolysis in adipocytes. The *β*-adrenergic agonist isoproterenol, a synthetic catecholamine, promotes triacylglycerol (TAG) breakdown (lipolysis) by activating a large heterotrimeric $G_{\alpha s}$-protein that activates adenylate cyclase (*AC*), which converts ATP into cAMP. cAMP binds the regulatory subunits of protein kinase (*PKA*), thus dissociating the repressive regulatory subunits from the catalytic subunits. Catalytically active PKA phosphorylates downstream targets, including perilipin and hormone sensitive lipase (*HSL*), which contribute to initiation of lipolysis together with several other lipases including *ATGL* (adipose triacylglycerol lipase) and MGL (monoacyl lipase), ultimately leading to the breakdown of TAG into free fatty acids (*FFA*) and glycerol. mTORC1 signaling suppresses lipolysis by either acting on common lipolytic targets (e.g., HSL, others?) via a pathway parallel to PKA or by converging on PKA to inhibiting its function. By inhibiting mTORC1 signaling, rapamycin synergizes with the PKA pathway to promote lipolysis, thus reducing TAG storage; therefore, mTORC1 signaling suppresses lipolysis, thus augmenting TAG storage

Our data are consistent with the recent work of Chakrabarti et al., who showed that inhibition of mTORC1 signaling via rapamycin or knockdown of the critical mTORC1 partner raptor decreases TAG storage by increasing lipolysis in 3T3-L1 adipocytes [43]. Consistently, this work demonstrated that overexpression of the mTORC1 activator Rheb augments TAG storage and suppresses lipolysis [43]. Our data differ in that Chakrabarti et al. found that rapamycin also modestly augments

basal lipolysis and modestly reduces the mRNA and protein expression of the lipase ATGL [43]. We found no evidence for alterations in basal lipolytic rate or ATGL expression upon rapamycin treatment. Perhaps differences in experimental conditions account for these apparent discrepancies.

Emerging data identify mTORC1 an important novel controller of both anabolic and catabolic lipid metabolism by regulating lipogenesis and lipolysis, respectively [44, 45]. mTORC1 signaling induces adipogenic differentiation and maintains the adipogenic program by promoting the expression and activation state of the transcription factor PPARγ (peroxisome proliferator-activated receptor-γ), a nuclear hormone receptor that induces the expression of genes that promote fatty acid uptake, synthesis, esterification, and storage [46]. Moreover, mTORC1 signaling promotes lipid biosynthesis by cleaving the transcription factor SREBP-1 (sterol regulatory element binding protein-1) into a mature form that translocates to the nucleus to induce the expression of lipogenic genes that promote fatty acid and TAG synthesis [45, 47].

As increased levels of circulating FFA are well documented as an etiological factor in the development of insulin resistance, the cumulative data suggest that rapamycin administration to patients may exacerbate insulin resistance by promoting TAG lipolysis [48]. Indeed, studies in a diabetic rodent model showed that injection of rapamycin led to worsened hyperglycemia and diabetes [48]. Impaired TOR signaling also appears to promote lipolysis in model organisms. For example, in Drosophila, loss-of-function mutations in *melted* leads to decreased dTOR signaling and a 10% decrease in animal size, consistent with a role of mTOR in cell growth control; strikingly, *melted* flies possess 40% less fat relative to control animals in the fat body, the primary energy storage organ [49]. This phenotype is fat-body autonomous, as re-expression of wild type *melted* in the fat body rescues the leanness of *melted* mutants [49]. Additionally, global knockout of the mTORC1 substrate S6K1 in mice produces animals with increased levels of plasma FFA that exhibit mild glucose intolerance and resistance to diet-induced obesity [14, 50]. Consistently, increased mTORC1 signaling to eukaryotic initiation factor 4E (eIF4E) via global knockout of the eIF4E inhibitors 4EBP-1 and 4EBP-2 leads to increased adipogenesis, decreased lipolysis, and increased FFA re-esterification, which cooperatively induce obesity [51].

In conclusion, these data demonstrate that cellular inhibition of mTORC1 signaling with rapamycin, as well as inhibition of PI3K with wortmannin, synergizes with the PKA pathway to augment the phosphorylation of HSL leading to enhanced hormone-induced lipolysis. Thus, mTORC1 signaling antagonizes the PKA pathway to suppress hormone-induced lipolysis. Many questions remain regarding the molecular mechanism by which mTORC1 signaling impacts lipolytic targets. Does mTORC1 directly or indirectly (via downstream substrates) antagonize PKA signaling? Does mTORC1 signaling suppress PKA activity or does mTORC1 signal along a parallel pathway that converges on a common lipolytic target that lies downstream of PKA? Our data and that of others reveal a novel role for PI3K/mTORC1 signaling in control of cellular TAG and FFA metabolism: mTORC1 signaling reduces lipolytic rate, thus promoting TAG storage. Elucidating the molecular mechanisms by which mTORC1 signaling modulates lipid metabolism may enable clinicians in the future to better manage the deleterious side effects incurred by therapeutic rapamycin or analog treatment employed for immunosuppression, stent restenosis, and cancer. Additionally, as altered lipid homeostasis contributes to diverse human diseases including type II diabetes, obesity, cancer, and cardiovascular disease, elucidation of the biochemical mechanisms by which mTORC1 signaling modulates lipid metabolism is important both biologically and clinically.

Acknowledgments The authors would like to express their gratitude to Drs. Nancy Weigel (Baylor College of Medicine) and Victoria Knutson (University of Texas) for sharing reagents, encouragement, support, and advice. Funding: This work was funded by grants from the National Institutes of Health (K01 DK60654) and the American Heart Association (0750060Z) to GS and NIH-R01 (DK-078135) to DCF.

Conflict of interest Nothing to disclose; there are no commercial or other associations that may pose a conflict of interest.

References

1. Fingar DC, Blenis J (2004) Target of rapamycin (TOR): an integrator of nutrient and growth factor signals and coordinator of cell growth and cell cycle progression. Oncogene 23:3151–3171
2. Soliman GA (2005) The mammalian target of rapamycin signaling network and gene regulation. Curr Opin Lipidol 16:317–323
3. Foster KG, Fingar DC (2010) Mammalian target of rapamycin (mTOR): conducting the cellular signaling symphony. J Biol Chem 285:14071–14077
4. Jung CH, Ro SH, Cao J, Otto NM, Kim DH (2010) mTOR regulation of autophagy. FEBS Lett 584:1287–1295
5. Guertin DA, Sabatini DM (2009) The pharmacology of mTOR inhibition. Sci Signal 2:pe24
6. Oshiro N, Yoshino K, Hidayat S, Tokunaga C, Hara K, Eguchi S, Avruch J, Yonezawa K (2004) Dissociation of raptor from mTOR is a mechanism of rapamycin-induced inhibition of mTOR function. Genes Cells 9:359–366
7. Soliman GA, Acosta-Jaquez HA, Dunlop EA, Ekim B, Maj NE, Tee AR, Fingar DC (2010) mTOR Ser-2481 autophosphorylation monitors mTORC-specific catalytic activity and clarifies rapamycin mechanism of action. J Biol Chem 285:7866–7879

8. Kahan BD (2004) Sirolimus: a ten-year perspective. Transplant Proc 36:71–75
9. Morice MC, Serruys PW, Sousa JE, Fajadet J, Ban Hayashi E, Perin M, Colombo A, Schuler G, Barragan P, Guagliumi G, Molnar F, Falotico R (2002) A randomized comparison of a sirolimus-eluting stent with a standard stent for coronary revascularization. N Engl J Med 346:1773–1780
10. Harrison DE, Strong R, Sharp ZD, Nelson JF, Astle CM, Flurkey K, Nadon NL, Wilkinson JE, Frenkel K, Carter CS, Pahor M, Javors MA, Fernandez E, Miller RA (2009) Rapamycin fed late in life extends lifespan in genetically heterogeneous mice. Nature 460:392–395
11. Morrisett JD, Abdel-Fattah G, Hoogeveen R, Mitchell E, Ballantyne CM, Pownall HJ, Opekun AR, Jaffe JS, Oppermann S, Kahan BD (2002) Effects of sirolimus on plasma lipids, lipoprotein levels, and fatty acid metabolism in renal transplant patients. J Lipid Res 43:1170–1180
12. Mathe D, Adam R, Malmendier C, Gigou M, Lontie JF, Dubois D, Martin C, Bismuth H, Jacotot B (1992) Prevalence of dyslipidemia in liver transplant recipients. Transplantation 54:167–170
13. Teutonico A, Schena PF, Di Paolo S (2005) Glucose metabolism in renal transplant recipients: effect of calcineurin inhibitor withdrawal and conversion to sirolimus. J Am Soc Nephrol 16:3128–3135
14. Um SH, Frigerio F, Watanabe M, Picard F, Joaquin M, Sticker M, Fumagalli S, Allegrini PR, Kozma SC, Auwerx J, Thomas G (2004) Absence of S6K1 protects against age- and diet-induced obesity while enhancing insulin sensitivity. Nature 431:200–205
15. Margolin K, Longmate J, Baratta T, Synold T, Christensen S, Weber J, Gajewski T, Quirt I, Doroshow JH (2005) CCI-779 in metastatic melanoma: a phase II trial of the California Cancer Consortium. Cancer 104:1045–1048
16. Ahima RS (2006) Adipose tissue as an endocrine organ. Obesity (Silver Spring) 14(Suppl 5):242S–249S
17. Cawthorn WP, Sethi JK (2008) TNF-alpha and adipocyte biology. FEBS Lett 582:117–131
18. Egan JJ, Greenberg AS, Chang MK, Wek SA, Moos MC Jr, Londos C (1992) Mechanism of hormone-stimulated lipolysis in adipocytes: translocation of hormone-sensitive lipase to the lipid storage droplet. Proc Natl Acad Sci USA 89:8537–8541
19. Wang S, Soni KG, Semache M, Casavant S, Fortier M, Pan L, Mitchell GA (2008) Lipolysis and the integrated physiology of lipid energy metabolism. Mol Genet Metab 95:117–126
20. Cohen AW, Razani B, Schubert W, Williams TM, Wang XB, Iyengar P, Brasaemle DL, Scherer PE, Lisanti MP (2004) Role of caveolin-1 in the modulation of lipolysis and lipid droplet formation. Diabetes 53:1261–1270
21. Su CL, Sztalryd C, Contreras JA, Holm C, Kimmel AR, Londos C (2003) Mutational analysis of the hormone-sensitive lipase translocation reaction in adipocytes. J Biol Chem 278:43615–43619
22. Saha PK, Kojima H, Martinez-Botas J, Sunehag AL, Chan L (2004) Metabolic adaptations in the absence of perilipin: increased beta-oxidation and decreased hepatic glucose production associated with peripheral insulin resistance but normal glucose tolerance in perilipin-null mice. J Biol Chem 279: 35150–35158
23. Brasaemle DL, Rubin B, Harten IA, Gruia-Gray J, Kimmel AR, Londos C (2000) Perilipin A increases triacylglycerol storage by decreasing the rate of triacylglycerol hydrolysis. J Biol Chem 275:38486–38493
24. Martinez-Botas J, Anderson JB, Tessier D, Lapillonne A, Chang BH, Quast MJ, Gorenstein D, Chen KH, Chan L (2000) Absence of perilipin results in leanness and reverses obesity in Lepr(db/db) mice. Nat Genet 26:474–479
25. Aggarwal D, Fernandez ML, Soliman GA (2006) Rapamycin, an mTOR inhibitor, disrupts triglyceride metabolism in guinea pigs. Metabolism 55:794–802
26. Burnett PE, Barrow RK, Cohen NA, Snyder SH, Sabatini DM (1998) RAFT1 phosphorylation of the translational regulators p70 S6 kinase and 4E-BP1. Proc Natl Acad Sci USA 95:1432–1437
27. Holm C (2003) Molecular mechanisms regulating hormone-sensitive lipase and lipolysis. Biochem Soc Trans 31:1120–1124
28. Kishida K, Kuriyama H, Funahashi T, Shimomura I, Kihara S, Ouchi N, Nishida M, Nishizawa H, Matsuda M, Takahashi M, Hotta K, Nakamura T, Yamashita S, Tochino Y, Matsuzawa Y (2000) Aquaporin adipose, a putative glycerol channel in adipocytes. J Biol Chem 275:20896–20902
29. Chen JC, Powers T (2006) Coordinate regulation of multiple and distinct biosynthetic pathways by TOR and PKA kinases in *S. cerevisiae*. Curr Genet 49:281–293
30. Manni S, Mauban JH, Ward CW, Bond M (2008) Phosphorylation of the cAMP-dependent protein kinase (PKA) regulatory subunit modulates PKA-AKAP interaction, substrate phosphorylation, and calcium signaling in cardiac cells. J Biol Chem 283:24145–24154
31. Budillon A, Cereseto A, Kondrashin A, Nesterova M, Merlo G, Clair T, Cho-Chung YS (1995) Point mutation of the autophosphorylation site or in the nuclear location signal causes protein kinase A RII beta regulatory subunit to lose its ability to revert transformed fibroblasts. Proc Natl Acad Sci USA 92:10634–10638
32. Elliott MR, Shanks RA, Khan IU, Brooks JW, Burkett PJ, Nelson BJ, Kyttaris V, Juang YT, Tsokos GC, Kammer GM (2004) Down-regulation of IL-2 production in T lymphocytes by phosphorylated protein kinase A-RIIbeta. J Immunol 172:7804–7812
33. Sztalryd C, Xu G, Dorward H, Tansey JT, Contreras JA, Kimmel AR, Londos C (2003) Perilipin A is essential for the translocation of hormone-sensitive lipase during lipolytic activation. J Cell Biol 161:1093–1103
34. Garton AJ, Campbell DG, Cohen P, Yeaman SJ (1988) Primary structure of the site on bovine hormone-sensitive lipase phosphorylated by cyclic AMP-dependent protein kinase. FEBS Lett 229:68–72
35. Anthonsen MW, Ronnstrand L, Wernstedt C, Degerman E, Holm C (1998) Identification of novel phosphorylation sites in hormone-sensitive lipase that are phosphorylated in response to isoproterenol and govern activation properties in vitro. J Biol Chem 273:215–221
36. Shen WJ, Patel S, Natu V, Kraemer FB (1998) Mutational analysis of structural features of rat hormone-sensitive lipase. Biochemistry 37:8973–8979
37. Donsmark M, Langfort J, Holm C, Ploug T, Galbo H (2004) Contractions induce phosphorylation of the AMPK site Ser565 in hormone-sensitive lipase in muscle. Biochem Biophys Res Commun 316:867–871
38. Donsmark M, Langfort J, Holm C, Ploug T, Galbo H (2004) Regulation and role of hormone-sensitive lipase in rat skeletal muscle. Proc Nutr Soc 63:309–314
39. Zechner R, Kienesberger PC, Haemmerle G, Zimmermann R, Lass A (2009) Adipose triglyceride lipase and the lipolytic catabolism of cellular fat stores. J Lipid Res 50:3–21
40. Wei E, Gao W, Lehner R (2007) Attenuation of adipocyte triacylglycerol hydrolase activity decreases basal fatty acid efflux. J Biol Chem 282:8027–8035
41. Zurita-Martinez SA, Cardenas ME (2005) Tor and cyclic AMP-protein kinase A: two parallel pathways regulating expression of genes required for cell growth. Eukaryot Cell 4:63–71
42. Soulard A, Cremonesi A, Moes S, Schutz F, Jeno P, Hall MN (2010) The rapamycin-sensitive phosphoproteome reveals that

TOR controls protein kinase A toward some but not all substrates. Mol Biol Cell 21:3475–3486
43. Chakrabarti P, English T, Shi J, Smas CM, Kandror KV (2010) Mammalian target of rapamycin complex 1 suppresses lipolysis, stimulates lipogenesis, and promotes fat storage. Diabetes 59: 775–781
44. Laplante M, Sabatini DM (2009) mTOR signaling at a glance. J Cell Sci 122:3589–3594
45. Porstmann T, Santos CR, Griffiths B, Cully M, Wu M, Leevers S, Griffiths JR, Chung YL, Schulze A (2008) SREBP activity is regulated by mTORC1 and contributes to Akt-dependent cell growth. Cell Metab 8:224–236
46. Kim JE, Chen J (2004) regulation of peroxisome proliferator-activated receptor-gamma activity by mammalian target of rapamycin and amino acids in adipogenesis. Diabetes 53: 2748–2756
47. Laplante M, Sabatini DM (2010) mTORC1 activates SREBP-1c and uncouples lipogenesis from gluconeogenesis. Proc Natl Acad Sci USA 107:3281–3282
48. Leibowitz G, Cerasi E, Ketzinel-Gilad M (2008) The role of mTOR in the adaptation and failure of beta-cells in type 2 diabetes. Diabetes Obes Metab 10(Suppl 4):157–169
49. Teleman AA, Chen YW, Cohen SM (2005) Drosophila Melted modulates FOXO and TOR activity. Dev Cell 9:271–281
50. Pende M, Kozma SC, Jaquet M, Oorschot V, Burcelin R, Le Marchand-Brustel Y, Klumperman J, Thorens B, Thomas G (2000) Hypoinsulinaemia, glucose intolerance and diminished beta-cell size in S6K1-deficient mice. Nature 408:994–997
51. Le Bacquer O, Petroulakis E, Paglialunga S, Poulin F, Richard D, Cianflone K, Sonenberg N (2007) Elevated sensitivity to diet-induced obesity and insulin resistance in mice lacking 4E-BP1 and 4E-BP2. J Clin Invest 117:387–396

lipoproteins and bile components, the liver regulates the quantity and quality of lipids available to peripheral tissues. The liver has not evolved as a triacylglycerol (TAG) storage organ, however, hepatocytes transiently or chronically, for physiological or pathological reasons, may sometimes store increased amounts of lipids.

In addition, the liver has remarkable regenerative potential. Liver regeneration after 70% partial hepatectomy (PH) in rodents is considered a paradigm to study the proliferative process that involves multiple intra- and extrahepatic signalling pathways (reviewed in [1–4]). After PH, around 90% of the remaining liver parenchymal cells synchronously re-enter the cell cycle contributing to organ growth. In parallel, there is a rapid accumulation of TAG, possibly linked to the metabolic and structural requirements for hepatocyte proliferation [5, 6]. While the association of liver regeneration after PH with transient steatosis is recognized, there seems to be no agreement concerning whether manipulations of lipid availability and metabolism can alter hepatocyte proliferation and the outcome of liver regeneration [7–10].

Lipids are stored in lipid droplets (LD), dynamic organelles in the cytoplasm of cells. These LD are composed of a hydrophobic core of neutral lipids, mainly TAG and cholesteryl esters (CE), surrounded by a monolayer of phospholipids (PL) and unesterified (free) cholesterol (C), with associated proteins. The lipid composition of LD seems to depend on the cell type and to adapt to the cell environment and pathophysiological context [11]. Such molecular heterogeneity would help provide complexity and plasticity to the organelle, characteristics that enable LD to carry out a range of specific functions in cellular lipid metabolism. There is a high diversity even among the minor lipids in LD. For example, phospholipids are represented by more than 160 different molecular species in CHO cells [12]. Moreover, the dramatic variability in the LD-associated proteins (reviewed in [13]) seems to be related to various aspects of lipid droplet biology, including their biogenesis and regression, the metabolism of stored lipids, interactions with membrane systems for exchange of components, intracellular transport, and structural stabilization in fusion processes [14–20]. It is then logical to expect that LD have cell- and stored lipid-specific functions (reviewed in [21]).

Two paradigms concerning lipid droplets are recognized in animal cells: LD in steroidogenic cells, which are rich in CE and supply a ready source of cholesterol for steroid hormone synthesis [22]; and LD in adipocytes, which are rich in TAG and provide fatty acid substrates for the production of energy and intracellular signalling [14, 23]. As far as we know no data on lipid metabolism of LD in post-PH liver has been reported in the literature. The aim of our work was to evaluate the hypothesis that quiescent and regenerating liver after PH contain LD populations of different sizes and densities with specific characteristic lipid compositions. In addition, we attempted to determine whether liver LD pertained to one of the aforementioned paradigms.

Materials and Methods

Animals and Partial Hepatectomy

Animal care and surgical procedures were approved by the University of the Basque Country Animal Care and Use Committee. Female Sprague–Dawley rats weighing 175–200 g were fed with low fat chow (A04 Panlab, Spain). Animals ($n = 3$) were subjected to 70% PH [24], with removal of the median and left lobes. The resected tissue (quiescent liver) was used as the control sample. The remaining tissue mass (regenerating liver) was removed 24 h later. Tissue pieces were always individually processed.

Histological Staining

Newly obtained liver pieces were frozen in liquid nitrogen-cooled isopentane and 12 μm thick sections were obtained in a cryostat (Microm, HM550) at −25 °C. Sections were rinsed with 60% isopropanol and stained for 15 min with freshly prepared Oil Red O (Sigma) solution (0.5% in isopropanol followed by dilution to 60% with distilled water and filtered). After several rinses in 60% isopropanol and distilled water, slides were counterstained with hematoxylin for 2 min, rinsed with water and mounted (Glycergel, Dako). Digital images were taken with a ProgRes (Jenoptik) camera coupled to a Nikon (Eclipse 50i) microscope.

Isolation of Lipid Droplet Populations from Quiescent and Regenerating Liver Tissue

Liver homogenates were obtained at 4 °C as described previously [25]. Pieces of freshly extracted quiescent and regenerating liver tissue were homogenized using a Potter homogenizer in four volumes of 20 mM Tris–HCl buffer pH 7.4, containing 1 mM EDTA, and protease inhibitors (Roche). LD populations were isolated and characterized separately for each animal as described elsewhere [26]. Briefly, the nuclei were sedimented and the post-nuclear supernatant (PNSN) was adjusted to 20% (wt/vol) sucrose. Then, 1.5 ml PNSN was loaded onto a discontinuous sucrose gradient composed of four phases (1.5 ml each) ranging from 40 to 25% sucrose, and overlaid with three more 1.5 ml phases of 15, 10 and 5% sucrose. The tubes

were centrifuged at 150,000*g* in a TST 41.14 rotor (Kontron) for 4 h. Eight fractions (F1–F8) were harvested from the top of the gradient (Fig. 2). The upper, semisolid, fraction F1 was collected by adsorption on a hydrophobic spatula and dissolved in 60 mM Tris–HCl buffer pH 6.8, containing 10% SDS and 50% sucrose. Fractions F2–F8 was collected by pipetting. Western blot analysis showed that the harvested fractions (F1–F8) were enriched in the LD marker adipophilin and that there was no cross-contamination with endoplasmic reticulum or Golgi marker proteins (Supplementary Fig. 1).

Assessment of Lipid Composition of Lipid Droplets

Lipids were exhaustively extracted from each isolated LD population following the method of Folch et al. [27]. Briefly, a portion of each fraction was mixed with eight volumes of chloroform/methanol/water (2:1:0.0075, v:v:v) and the methanol phase was re-extracted with four volumes of the same mixture. The chloroform phases were aspirated, combined, and washed with 1.5 ml of 0.88% KCl. After centrifugation, the aqueous phase was discarded and the chloroform evaporated. The lipid extract was dissolved in toluene and cholesteryl formate (internal standard) was added.

Lipids were separated using a thin-layer chromatography system composed of six sequential mobile phases as described by Ruiz and Ochoa [28]. Standard curves for all lipid classes were run in each plate. Development allowed sphingomyelin (CerPCho), phosphatidylcholine (PtdCho), phosphatidylinositol (PtdIns), phosphatidylserine (PtdSer), phosphatidylethanolamine (PtdEtn), C, TAG and CE to be separated. The lipid spots were quantified as detailed previously [28] using Quantity One software (Bio-Rad). Analysis was carried out at least twice per extract.

Statistics

Statistical analysis was performed using GraphPad Prism version 5.02 (GraphPad Software, San Diego, CA). Trends along the gradient for each condition were evaluated by one-way analysis of variance (ANOVA) and differences between trends using two-way ANOVA followed by the Bonferroni multiple comparison test. Light and dense fractions were compared by the unpaired Student's *t* test, while correlations between lipid classes were assessed using the Pearson correlation coefficient. A $p \leq 0.05$ was considered statistically significant.

Results

The regenerating liver after 70% PH in rodents is a paradigm of physiological liver steatosis characterized by a massive, transient accumulation of LD [6, 29]. Figure 1 shows Oil Red O-stained sections of rat liver tissue either resected at the time of PH (quiescent, control condition) or 24 h post-PH (regenerating, steatotic condition). In the upper panels, captured at ×400 optical magnifications, the proliferation of LD in regenerating liver can be seen. Lower images (×1000) illustrate the heterogeneity in the LD size distribution in regenerating tissue. In order to analyze the differential lipid composition of LD from quiescent and regenerating liver, and to evaluate if lipid

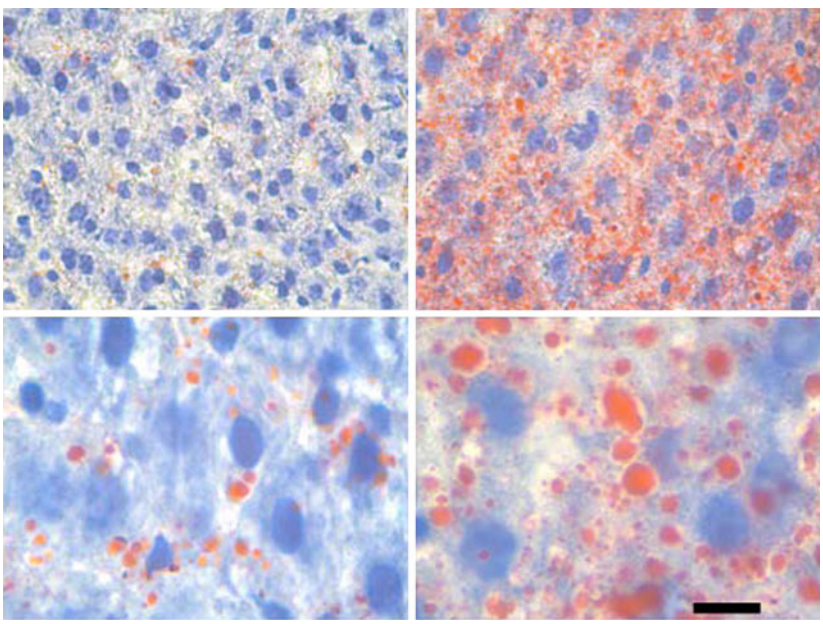

Fig. 1 Lipid droplet distribution in quiescent (*left*) and regenerating (*right*) liver tissue. Frozen liver sections (12 μm) were stained with Oil Red O to visualize lipid inclusions and counterstained with hematoxylin. *Upper* and *lower* images were captured at ×400 and ×1000 magnification, respectively. The *bar* corresponds to 10 μm at ×1000

profiles depend on the size of the particles, we isolated eight LD fractions of different densities, and compared the lipid composition of fractions within each condition and of matched density fractions between the conditions. Western blot analysis, using antibodies against the LD marker adipophilin, the endoplasmic reticulum marker calregulin and the Golgi marker GM-130, confirmed that fractions F1–F8, which float at different sucrose percentage solutions over the sample loading layer, were LD-rich and free of contamination with microsomes (Supplementary Fig. 1).

Of the density-matched LD populations, only F1 differed markedly ($p \leq 0.001$) between tissue conditions (Fig. 2a). The absolute amount of lipids is given in Table 1. Notably, low density LD concentrated in F1, floating above 5% sucrose and with a density <1.02 g/ml, were responsible for the characteristic rise in lipid levels observed after PH.

The molar ratio between the major hydrophobic lipids in the core of the organelle (TAG + CE) and the major amphipathic lipids on the surface (PL + C) is a surrogate index of LD volume (Fig. 2b). The trends in the LD apparent volume across the density gradient fractions differed between quiescent and regenerating liver ($p \leq 0.005$). With the exception of F1 droplets, which were substantially larger in regenerating tissue, the apparent volume of LD was lower in the steatotic than in the control samples.

We determined the molar fraction of each lipid class in LD populations from quiescent (Fig. 3a) and from regenerating liver (Fig. 3b, the grey intensity of *bars* increases with LD density). A one-way ANOVA and linear trend test showed a fall in the molar proportion of TAG as LD population density increased (a, $p \leq 0.05$) in both tissue conditions, more pronounced in regenerating tissue. Furthermore, a significant positive correlation between the increase in the PtdEtn molar fraction and LD density (a, $p \leq 0.05$) was observed in LD populations from the steatotic samples.

There was a negative correlation ($p \leq 0.05$) between the contents of TAG and all of the membrane lipids in LD populations from regenerating liver (Fig. 3b). In addition, positive correlations were found within the phospholipids (at least $p \leq 0.05$) and between them and the C molar fraction ($p \leq 0.05$); however, none of the lipids were found to have significant correlations with the molar ratio of the highly hydrophobic CE. These findings indicate that the density of LD populations isolated from liver tissue is more closely related to TAG than to CE content, especially in conditions of regeneration.

To simplify comparisons isolated LD populations were classified according to the lipid composition. Two LD types were defined in each tissue type, i.e., in quiescent and in regenerating liver tissue: fractions 1–3, corresponding to

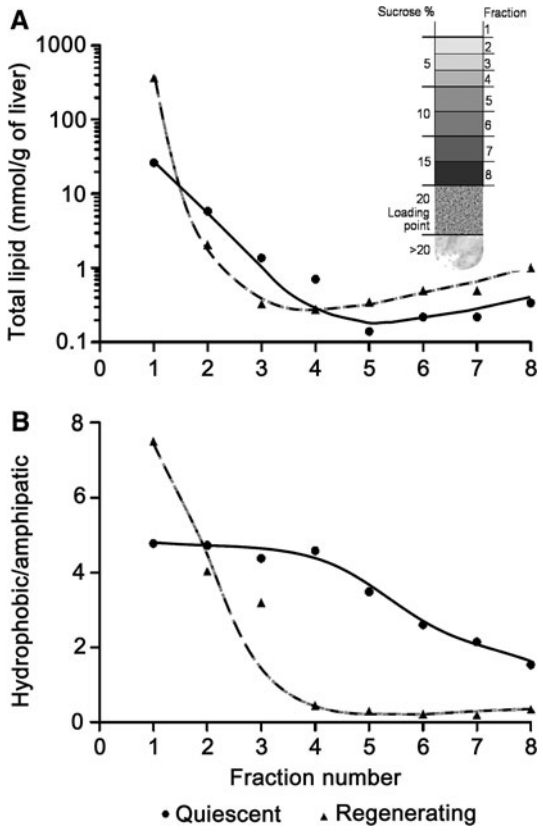

Fig. 2 Basic features of lipid droplet populations from quiescent and regenerating liver tissue. Quiescent and regenerating liver pieces were homogenized, and the post-nuclear supernatant adjusted to 20% sucrose and centrifuged in a density gradient. Fractions 1–8 (F1–F8) above the loading point, ranging from 0 to 15% sucrose (schematized in the insert of panel A), were identified as adipophilin(+) lipid droplets (LD) (Supplementary Fig. 1). **a** Graph showing the total lipid content in F1–F8 from quiescent and regenerating liver is plotted (the individual values are given in Table 1). Note a logarithmic scale is used to make differences between tissues readily visible. **b** The hydrophobic/amphipathic lipid ratio was calculated for each LD population, and represented separately for quiescent and for regenerating liver

LD floating at sucrose ≤5% (density ≤1.02 g/ml) and fractions 5–8, corresponding to sucrose solutions of density ≥1.06 g/ml, were grouped; we refer to these groups as light and dense LD, respectively. Fraction four was not included in either of the groups. This grouping and the exclusion of F4 are in line with the greatest statistically significant differences (Student's t test) in terms of the density between light and dense LD and minimum variance analyzed for both physiological conditions. The mean molar ratios for each lipid class in the two subtypes for quiescent and regenerating tissues are shown in Fig. 3c.

A specific lipid composition pattern was observed for each LD group. Accordingly, it was possible to define four phenotypes of lipid droplets, which do not necessarily coexist in the healthy liver. The main features of these

Table 1 Lipid content of the lipid droplet density fractions F1–F8 isolated from quiescent and regenerating liver

Fraction	Hydrophobic lipids				Amphipathic lipids			
	Triacylglycerols (mmol/g of liver)		Cholesteryl esters (μmol/g of liver)		Phospholipids (μmol/g of liver)		Free cholesterol (μmol/g of liver)	
	Quiescent liver	Regenerating liver	Quiescent liver	Regenerating liver	Quiescent liver	Regenerating liver	Quiescent liver	Regenerating liver
1	18.42 ± 11.18	319.9 ± 185.9	3,075 ± 1,589	3,453 ± 1,532	1,459 ± 600	18,839 ± 11,456	3,487 ± 1,757	22,993 ± 16,317
2	3.62 ± 2.58	0.13 ± 0.26	126.9 ± 81.4	23.2 ± 11.3	1,929 ± 1,513	467.0 ± 168.2	164.9 ± 65.3	77.2 ± 20.7
3	0.87 ± 0.64	0.01 ± 0.01	46.5 ± 26.7	*	430.4 ± 337.9	105.0 ± 47.6	34.1 ± 14.8	23.2 ± 4.7
4	0.45 ± 0.32	0.02 ± 0.04	38.2 ± 18.8	*	203.4 ± 159.1	159.6 ± 63.4	21.7 ± 11.5	30.1 ± 10.7
5	0.07 ± 0.05	0.04 ± 0.03	14.4 ± 2.9	*	41.4 ± 31.7	240.5 ± 111.5	11.9 ± 5.1	38.9 ± 12.2
6	0.09 ± 0.06	0.06 ± 0.03	14.4 ± 2.8	*	107.6 ± 83.1	333.7 ± 126.9	14.1 ± 5.7	76.1 ± 34.1
7	0.07 ± 0.03	0.06 ± 0.03	38.8 ± 6.8	*	94.2 ± 71.6	325.2 ± 123.1	24.5 ± 4.2	85.1 ± 34.1
8	0.13 ± 0.03	0.12 ± 0.12	51.4 ± 7.4	*	122.8 ± 89.2	567.6 ± 231.3	52.3 ± 10.7	157.9 ± 68.9

Data are the means ± SE of three independent experiments

* Below the detection limit (0.05 nmol) in two of three samples

phenotypes, in terms of lipid molar fractions and apparent volumes, are illustrated schematically in Fig. 4. Light particles seem to constitute the LD structures used for fuel storage, and although proportions of TAG in non-steatotic and steatotic livers did not differ statistically their quantity increased considerably during regeneration (Figs. 3c, 4). The two forms of cholesterol are more abundant in the quiescent liver tissue. Results shown in Figs. 2, 4 indicate that there are only moderate differences in apparent volume between light and dense liver LD in the quiescent tissue but that the volumes are dramatically affected by regeneration. Quiescent dense LD (F5–F8) were found to have an apparent volume nearly ten times larger than their counterparts of equal density from regenerating tissue, which corresponds to a hydrophobic/amphipathic ratio up to 20-fold lower. An explanation for such an effect may reside in notably large quantities of CE in the lipid core of the quiescent dense particles.

Discussion

Resection of 70% of a healthy adult liver triggers regenerative mechanisms that result in complete restoration of liver mass and function within a week or so in adult rodents. During this process, the residual mature hepatocytes proliferate [30] and have the capacity to accumulate substantial amounts of lipids in cytoplasmic LD (see liver sections in Fig. 1). By fractionation of quiescent and regenerating rat liver in a discontinuous sucrose gradient, we isolated LD populations from each condition. LD, defined as adipophilin-positive organelles, were localized in a range of fractions lying above the loading point (Supplementary Fig. 1). The scheme in Fig. 4 summarize the features of the four models of LD phenotypes defined in this work considering the lipid composition. The micrographs in Fig. 1 show high heterogeneity in the LD sizes in regenerating tissue consistent with the analysis of lipid composition.

LD are composed of a core of neutral lipids, TAG and CE, surrounded by a coating of amphipathic cholesterol and phospholipids with which specific proteins can be associated permanently or transiently. Our results show that the TAG accumulated in regenerating tissue mostly corresponded to densities below 1.02 g/ml (F1) and probably to the large-sized LD observed in micrographs of stained tissue (Fig. 1). This accumulation seems to be essential to accomplish timely liver regeneration [31], probably providing precursors for membranes and intracellular signalling, and fatty acids for energy production by mitochondrial and peroxisomal oxidation.

Characterization of LD sub-populations was first described by Ontko et al. [32], who showed that the lipid composition of lipid droplets in rat liver varied. The analysis of fibroblasts, lymphocytes and CHO cells by Bartz et al. [12] revealed differences between LD in their lipid composition. These differential characteristics could be connected with specialized behaviors of LD. The lipid content has been related to cell function in hepatic stellate cells that store retinoids for the whole body in their LD [33]; macrophages and neutrophils are important storage sites for arachidonic acid that is a building block for numerous biological mediators, and muscles and plant seeds store TAG for the supply of energy in periods of scarcity [for a review, see [34]).

LD from regenerating tissue, especially those from F1, are similar to adipocyte LD, large and TAG-enriched [14, 35], and practically devoid of cholesteryl esters, lipids

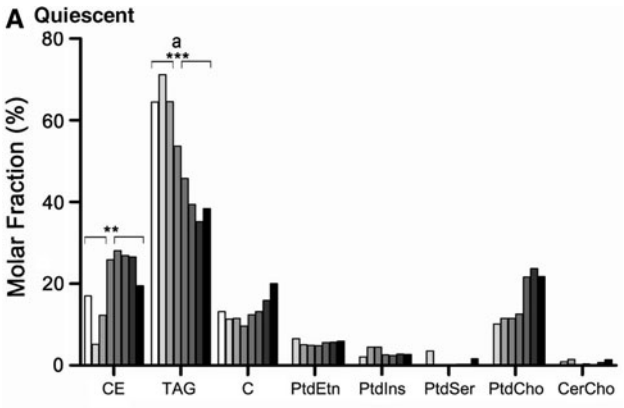

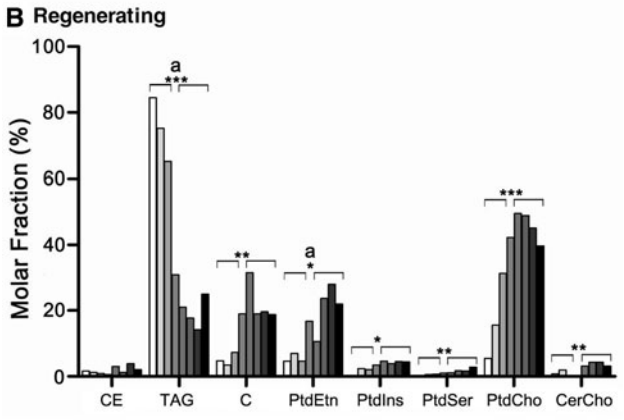

C

	QUIESCENT		REGENERATING	
	Fractions		Fractions	
	1-3	5-8	1-3	5-8
CE	7.54**	25.32	1.35#	2.57#
TAG	66.79***	39.71	74.95	19.5###
C	12.06	15.42	5.22#,**	22.26
PtdEtn	5.81	5.60	5.45*	22.05#
PtdIns	2.95	2.67	2.25*	4.39
PtdSer	3.57	0.81	0.52**	2.41#
PtdCho	10.87	19.98	17.53***	45.78###
CerPCho	1.09	0.72	1.77***	7.48###

Fig. 3 Lipid composition of lipid droplet populations from quiescent and regenerating liver tissue. Lipid composition was analyzed in lipid droplet (LD) fractions 1–8 (F1–F8) after separation of lipid classes as described in "Materials and Methods". The average molar fraction of neutral and amphipathic lipids in LD fractions from quiescent (**a**) and regenerating (**b**) liver is shown. For each lipid class, fractions 1–8 of increasing density are represented as *bars* of increasing *grey* intensity from left to right. Data were analyzed using the Student's *t* test. $^{*}p < 0.05$; $^{**}p < 0.01$; $^{***}p < 0.001$: light (F1–F3, taken together) versus dense (F5–F8, taken together) fractions. Statistical analysis of the trends as a function of the gradient for each lipid class was performed by one-way ANOVA: "*a*" indicates $p \leq 0.05$. (**c**) Molar fractions of lipid classes in light (F1–F3) and dense (F5–F8) fractions. Data were analyzed using the Student's *t* test: $^{*}p < 0.05$; $^{**}p < 0.01$; $^{***}p < 0.001$, as compared to dense fractions within the same condition; and $^{\#}p < 0.05$; $^{\#\#}p < 0.01$; $^{\#\#\#}p < 0.001$, as compared to counterpart fractions of quiescent liver

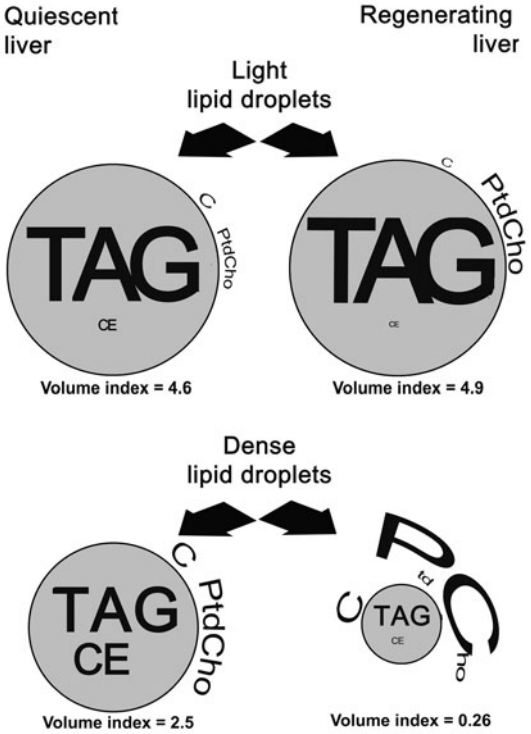

Fig. 4 Schematic representation of light and dense lipid droplets in both quiescent and regenerating livers. We propose four phenotypes of lipid droplets (LD) that occur under physiological conditions on the basis of the molar proportions of the major lipid components. The diameter of the circle representing the LD has been scaled according to the apparent volume calculated by the ratio hydrophobic/amphipathic lipids. The font size of the lipid acronym is proportional to the assessed relative abundance of each lipid (shown in Fig. 3). *TAG* triacylglycerol, *CE* cholesteryl ester, *C* free cholesterol, *PtdCho* phosphatidylcholine

that were found at high levels in all densities LD of quiescent tissue. LD from quiescent liver tissue resemble those of steroidogenic cells, characterized by their high CE content to provide the supply of cholesterol needed for steroid hormone synthesis [34]. In liver parenchymal cells, cholesterol is required for bile acid synthesis and its biliary secretion and also for the assembly of very low density lipoproteins, the secretion rate of which, like that of TAG, is highly dependent on cholesterol availability [36–38]. After PH, the proliferative state is accompanied by profound changes in cholesterol homeostasis [39, 40]. During regeneration, cholesterol metabolism is focused on increasing its cellular availability, which would sustain the formation of new membranes. Limitation of the rate of degradation and secretion of cholesterol, and the activation of its biosynthesis, lead to the maintenance of liver cholesterol levels [40]. Our results suggest that these adaptative changes are accompanied by the mobilization of the CE stored in the LD.

It is well known that metabolic profile changes occur after PH, because of changes in the availability of precursors and enzymatic activities, leading to an increase in the capacity of TAG, PtdCho and PtdEtn synthesis [41–43].

In parallel with the rise of TAG content, these metabolic changes trigger a dramatic increase in the amount of PtdEtn in the liver. Our results show that this is reflected in the percentage of PtdEtn in dense LD only. Such a rise could be related to the need for rapid structural and functional changes involved in LD formation and utilization, for example, to facilitate interactions with proteins. Our data show that the dense LD after PH also became enriched in CerPCho (accounting for 9% of the membrane lipids; data not shown), which is a lipid that tends to segregate forming disordered membrane domains potentially important for lipid–protein specific interactions [44].

In summary, we propose two models of LD in each of the physiological conditions of hepatic tissue analyzed (quiescence and regeneration): one corresponding to light (density $\leq$1.02 g/ml) and one to dense (density $\geq$1.06 g/ml) particles, on the basis of their specific lipid profiles. Our findings provide evidence that hepatic lipid droplets are multifunctional and adaptative structures and support the notion that LD in the liver are complex organelles with probably still unknown roles in lipid metabolism.

Acknowledgments Research was supported by grants from the Spanish National Ministry for Education and Science (SAF2007/60211) and the Basque Government (Saiotek program and IT-325-07). I.G-A. was recipient of a research training fellowship from the Basque Government.

References

1. Fausto N (2000) Liver regeneration. J Hepatol 32:19–31
2. Michalopoulos GK (2007) Liver regeneration. J Cell Physiol 213:286–300
3. Michalopoulos GK (2009) Liver regeneration: alternative epithelial pathways. Int J Biochem Cell Biol. doi:10.1016/j.biolcel.209.09.014
4. Taub R (2004) Liver regeneration: from myth to mechanism. Nat Rev Mol Cell Biol 5:836–847
5. Newberry EP, Kennedy SM, Xie Y, Luo J, Stanley SE, Semenkovich CF, Crooke RM, Graham MJ, Davidson NO (2008) Altered hepatic triglyceride content after partial hepatectomy without impaired liver regeneration in multiple murine genetic models. Hepatology 48:1097–1105
6. Shteyer E, Liao Y, Muglia LJ, Hruz PW, Rudnick DA (2004) Disruption of hepatic adipogenesis is associated with impaired liver regeneration in mice. Hepatology 40:1322–1332
7. DeAngelis RA, Markiewski MM, Taub R, Lambris JD (2005) A high-fat diet impairs liver regeneration in C57BL/6 mice through overexpression of the NF-kappaB inhibitor, IkappaBalpha. Hepatology 42:1148–1157
8. Fernandez MA, Albor C, Ingelmo-Torres M, Nixon SJ, Ferguson C, Kurzchalia T, Tebar F, Enrich C, Parton RG, Pol A (2006) Caveolin-1 is essential for liver regeneration. Science 313:1628–1632
9. Leclercq IA, Field J, Farrell GC (2003) Leptin-specific mechanisms for impaired liver regeneration in ob/ob mice after toxic injury. Gastroenterology 124:1451–1464
10. Yamauchi H, Uetsuka K, Okada T, Nakayama H, Doi K (2003) Impaired liver regeneration after partial hepatectomy in db/db mice. Exp Toxicol Pathol 54:281–286
11. Rinia HA, Burger KN, Bonn M, Muller M (2008) Quantitative label-free imaging of lipid composition and packing of individual cellular lipid droplets using multiplex CARS microscopy. Biophys J 95:4908–4914
12. Bartz R, Li WH, Venables B, Zehmer JK, Roth MR, Welti R, Anderson RG, Liu P, Chapman KD (2007) Lipidomics reveals that adiposomes store ether lipids and mediate phospholipid traffic. J Lipid Res 48:837–847
13. Hodges BD, Wu CC (2010) Proteomic insights into an expanded cellular role for cytoplasmic lipid droplets. J Lipid Res 51:262–273
14. Brasaemle DL, Barber T, Wolins NE, Serrero G, Blanchette-Mackie EJ, Londos C (1997) Adipose differentiation-related protein is a ubiquitously expressed lipid storage droplet-associated protein. J Lipid Res 38:2249–2263
15. Brasaemle DL, Dolios G, Shapiro L, Wang R (2004) Proteomic analysis of proteins associated with lipid droplets of basal and lipolytically stimulated 3T3–L1 adipocytes. J Biol Chem 279:46835–46842
16. Cermelli S, Guo Y, Gross SP, Welte MA (2006) The lipid-droplet proteome reveals that droplets are a protein-storage depot. Curr Biol 16:1783–1795
17. Dugail I, Hajduch E (2007) A new look at adipocyte lipid droplets: towards a role in the sensing of triacylglycerol stores? Cell Mol Life Sci 64:2452–2458
18. Fujimoto Y, Itabe H, Kinoshita T, Homma KJ, Onoduka J, Mori M, Yamaguchi S, Makita M, Higashi Y, Yamashita A, Takano T (2007) Involvement of long chain acyl-CoA synthetase in local synthesis of neutral lipids in cytoplasmic lipid droplets in human hepatocyte HuH7. J Lipid Res 48:1280–1292
19. Umlauf E, Csaszar E, Moertelmaier M, Schuetz GJ, Parton RG, Prohaska R (2004) Association of stomatin with lipid bodies. J Biol Chem 279:23699–23709
20. Welte MA (2007) Proteins under new management: lipid droplets deliver. Trends Cell Biol 17:363–369
21. Murphy DJ, Vance J (1999) Mechanisms of lipid-body formation. Trends Biochem Sci 24:109–115
22. Mendis-Handagama SM, Aten RF, Watkins PA, Scallen TJ, Berhman HR (1995) Peroxisomes and sterol carrier protein-2 in luteal cell steroidogenesis: a possible role in cholesterol transport from lipid droplets to mitochondria. Tissue Cell 27:483–490
23. Igal RA, Coleman RA (1998) Neutral lipid storage disease: a genetic disorder with abnormalities in the regulation of phospholipid metabolism. J Lipid Res 39:31–43
24. Waynforth HB, Flecknell PA (1992) Experimental and surgical technique in the rat. Academic Press, London, pp 241–245
25. Palacios L, Ochoa B, Jose Gomez-Lechon M, Vicente CJ, Fresnedo O (2006) Overexpression of SND p102, a rat homologue of p100 coactivator, promotes the secretion of lipoprotein phospholipids in primary hepatocytes. Biochim Biophys Acta 1761:698–708
26. García-Arcos I, Rueda Y, González-Kother P, Palacios L, Ochoa B, Fresnedo O (2010) Association of SND1 protein with low density lipid droplets in hepatic steatosis. J Physiol Biochem 66:73–83
27. Folch J, Lees M, Sloane Stanley GH (1957) A simple method for the isolation and purification of total lipids from animal tissues. J Biol Chem 226:497–509
28. Ruiz JI, Ochoa B (1997) Quantification in the subnanomolar range of phospholipids and neutral lipids by monodimensional thin-layer chromatography and image analysis. J Lipid Res 38:1482–1489

29. Brasaemle DL (2006) A metabolic push to proliferate. Science 313:1581–1582
30. Grisham JW (1962) A morphologic study of deoxyribonucleic acid synthesis and cell proliferation in regenerating rat liver; autoradiography with thymidine-H3. Cancer Res 22:842–849
31. Farrell GC (2004) Probing Prometheus: fat fueling the fire? Hepatology 40:1252–1255
32. Ontko JA, Perrin LW, Horne LS (1986) Isolation of hepatocellular lipid droplets: the separation of distinct subpopulations. J Lipid Res 27:1097–1103
33. Blaner WS, O'Byrne SM, Wongsiriroj N, Kluwe J, D'Ambrosio DM, Jiang H, Schwabe RF, Hillman EM, Piantedosi R, Libien J (2008) Hepatic stellate cell lipid droplets: a specialized lipid droplet for retinoid storage. Biochim Biophys Acta 1791:408–418
34. Murphy DJ (2001) The biogenesis and functions of lipid bodies in animals, plants and microorganisms. Prog Lipid Res 40:325–438
35. Jump DB, Clarke SD (1999) Regulation of gene expression by dietary fat. Annu Rev Nutr 19:63–90
36. Fuki IV, Preobrazhensky SN, Misharin AY, Bushmakina NG, Menschikov GB, Repin VS, Karpov RS (1989) Effect of cell cholesterol content on apolipoprotein B secretion and LDL receptor activity in the human hepatoma cell line, HepG2. Biochim Biophys Acta 1001:235–238
37. Isusi E, Aspichueta P, Liza M, Hernandez ML, Diaz C, Hernandez G, Martinez MJ, Ochoa B (2000) Short- and long-term effects of atorvastatin, lovastatin and simvastatin on the cellular metabolism of cholesteryl esters and VLDL secretion in rat hepatocytes. Atherosclerosis 153:283–294
38. Temel RE, Hou L, Rudel LL, Shelness GS (2007) ACAT2 stimulates cholesteryl ester secretion in apoB-containing lipoproteins. J Lipid Res 48:1618–1627
39. Field FJ, Mathur SN, LaBrecque DR (1985) Cholesterol metabolism in regenerating liver of the rat. Am J Physiol 249:G679–G684
40. Lo Sasso G, Celli N, Caboni M, Murzilli S, Salvatore L, Morgano A, Vacca M, Pagliani T, Parini P, Moschetta A (2010) Down-regulation of the LXR transcriptome provides the requisite cholesterol levels to proliferating hepatocytes. Hepatology 51:1334–1344
41. Delahunty TJ, Rubinstein D (1970) Accumulation and release of triglycerides by rat liver following partial hepatectomy. J Lipid Res 11:536–543
42. Houweling M, Tijburg LB, Vaartjes WJ, Van Golde LM (1992) Phosphatidylethanolamine metabolism in rat liver after partial hepatectomy. Control of biosynthesis of phosphatidylethanolamine by the availability of ethanolamine. Biochem J 283(Pt 1):55–61
43. Tijburg LB, Nyathi CB, Meijer GW, Geelen MJ (1991) Biosynthesis and secretion of triacylglycerol in rat liver after partial hepatectomy. Biochem J 277(Pt 3):723–728
44. Vance DE, Vance JE (2008) Biochemistry of lipids, lipoproteins and membranes. Elsevier, Amsterdam

resistance is mainly determined by the response of skeletal muscle to insulin. Lipid oversupply is known to play a causative role in the generation of muscle insulin resistance, and lipid signaling molecules derived from free fatty acid (FFA) such as diacylglycerol (DAG) and ceramide were reported to interfere with insulin signal transduction in skeletal muscle (reviewed in [1]).

Recently, dietary monounsaturated fatty acids (MUFA) has been known to have beneficial effect on insulin sensitivity, as compared to a saturated fatty acids (SFA) [2–5]. The associations of dietary SFA with insulin resistance and the development of metabolic syndrome or diabetes were elucidated in several studies [6–9]. Recent studies reported that, compared with unsaturated fatty acids, SFA increased intramuscular accumulation of lipid metabolites (DAG or ceramide) and attenuated insulin-stimulated glucose uptake of skeletal muscle [9, 10].

Insulin receptor substrates (IRS)-1 and -2 are the docking proteins of the insulin receptor; these proteins are recruited to the receptor after insulin binding and play a central role in the translocation of glucose transporter type 4 (GLUT4) through the activation of the phosphoinositol 3-kinase (PI3K) pathway (reviewed in [1]). Although intramuscular lipid metabolites are known to affect the IRS/PI3K pathway, to our knowledge there are few in vivo studies investigating the effect of dietary SFA and MUFA on this pathway. In this study, we compared the effect of dietary SFA and MUFA on the IRS/PI3K pathway and GLUT4 membrane translocation in the skeletal muscle of a type 2 diabetic animal model. The results of this study might provide clues to understanding the mechanism through which dietary fatty acid composition affect skeletal muscle insulin sensitivity and could provide the theoretical background for nutritional advice for T2DM patients.

Materials and Methods

Animals and Experimental Diet

Twenty-nine-week-old male Otsuka Long-Evans Tokushima fatty (OLETF) rats (Otsuka Pharmaceutical, Tokushima, Japan) were kept at ambient temperature (22°C ± 1°C) on a 12-h light–dark cycle with free access to water and diet. Before any experimental intervention, animals were fed a standard rodent chow (Samtako, Osan, Korea). After 1 week, rats were divided into three experimental diet groups. Rats in the control group (chow, $n = 10$) were fed standard rat chow (61.8% carbohydrate, 15.7% fat, 22.5% protein expressed as percentages of the total caloric intake, chow diet) purchased from Samtako; the SFA group (SFA, $n = 10$) was fed a high-fat diet that primarily consisted of saturated fatty acids (24.3% carbohydrate, 52.8% fat, 22.9% protein, lard oil as 79.1% of total fat, SFA diet); and the MUFA group (MUFA, $n = 10$) was fed a high-fat diet that consisted primarily of monounsaturated fatty acids (24.3% carbohydrate, 52.8% fat, 22.9% protein, olive oil as 79.1% of total fat, MUFA diet). We made the high-fat diet by adding olive oil or lard oil to the purchased normal chow diet, and the ingredients of chow diet were as follows; ground corn, dehulled soybean meal, wheat middlings, ground wheat, fish meal, cane molasses, wheat germ, dried beet pulp, brewers dried yeast, dehydrated alfalfa meal, ground oats, dried whey, soybean oil, vitamin premix, and mineral premix. Animals were provided with food and water ad libitum throughout the experimental period. Animals were maintained on their diets for 3 weeks before testing. The animals were euthanized at the end of a dark cycle after overnight fasting for tissue sampling. Blood was collected by cardiac puncture and the vastus lateralis muscle was rapidly dissected out, immediately frozen in liquid nitrogen, and stored at −80°C until analysis. All procedures were approved by the Institutional Animal Care and Use Committee of the Yonsei University College of Medicine.

Insulin Tolerance Test (ITT)

After 3 weeks of experimental diet feeding, an ITT was performed. After a 6-h fast, rats were intraperitoneally injected with 0.75 U/kg human regular insulin (Humulin-R®, Eli Lilly and Company, Indianapolis, IN, USA). Blood samples were obtained at the indicated time by tail snipping, and blood glucose levels were measured with a glucose analyzer (Accu-Check; Roche Diagnostics, Basel, Switzerland).

Oral Glucose Tolerance Test (OGTT)

An OGTT was performed in rats after forced oral administration of a 20% glucose solution (2 g/kg) with a 10-ml syringe followed by an overnight fast. Blood samples were obtained at the indicated time by tail snipping, and blood glucose levels were measured with a glucose analyzer (Accu-Check; Roche Diagnostics).

RNA and cDNA Preparation

Total RNA was isolated from rat skeletal muscle tissue using Trizol reagent (Invitrogen, Carlsbad, CA, USA) and quantified by nano drop (ND-1000, DM Science, Seoul, Korea). Following RNA extraction, 4 μl RNA was treated with 1 U DNase I to remove all contaminating genomic DNA. DNase-treated RNA was subsequently used for cDNA synthesis using MMLV reverse transcriptase (Promega, Madison, WI, USA): 1 μl oligo dT primer was added to 4 μl RNA with 5× MMLV reaction buffer,

2.5 mM each dNTP, 1 U RNasin ribonuclease inhibitor and MMLV reverse transcriptase (200 units). cDNA was stored at −20°C.

Semi-Quantitative RT-PCR

The mRNA levels of IRS-1 and -2 were assessed by semi-quantitative RT-PCR analysis using glyceraldehyde-3-phosphate dehydrogenase (GAPDH) as a control. PCR primers were designed as follows: IRS-1 sense, 5′-ggttttg gtcaaggatgtta-3′; IRS-1 anti-sense, 5′-tgctgaggtcatttaggtc t-3′; IRS-2 sense, 5′-cttttctcccctccacaagc-3′; IRS-2 anti-sense, 5′-caagaacggttgaggagcaa-3′; GAPDH sense, 5′-catt gacctcaactacatggt-3′; and GAPDH anti-sense, 5′-gtgaagac gccagtagactc-3′. RT-PCR products were electrophoresed on a 1% (w/v) agarose gel, stained with ethidium bromide and visualized by UV light.

Plasma Membrane Protein Extraction

The extraction of sarcolemmal membrane protein from skeletal muscle tissue was performed using a commercially available plasma membrane protein extraction kit (#k268-50, BioVision, Mountain View, CA, USA) according to the manufacturer's instructions [11, 12]. For membrane fractionation, skeletal muscle samples of each experimental group were homogenized and processed for extraction of sarcolemmal membrane protein. The protein content in the sarcolemmal membrane fraction was measured by Bradford reagent (Bio-Rad, Hercules, CA, USA). The α1 subunit of the Na^+/K^+-ATPase, a sarcolemmal membrane marker, was measured by immunoblot to document adequate enrichment of membrane fractions.

Immunoblot Analysis

Aliquots of tissue homogenates were denatured under reducing conditions (1.75% SDS, 15 mM 2-mercaptoethanol; 5 min at 100°C), then subjected to SDS-PAGE and immunoblot analyses. To detect IRS-1, nitrocellulose membranes were incubated overnight at 4°C with anti-IRS-1 antibody (rabbit polyclonal IgG, 1:100, Millipore, Billerica, MA, USA) then with goat anti-rabbit IgG conjugated to horseradish peroxidase (1:5,000, Santa Cruz Biotechnology, Santa Cruz, CA, USA) for 1 h. Immunolabeling was detected with the ECL Western Blotting Analysis System (Thermo Fischer Scientific, Waltham, MA, USA). All immunoreactivity was normalized to total protein as determined by Bradford assay (Sigma-Aldrich, St. Louis, MO, USA). We used following reagents to detect specific protein we investigated; for phosphorylated IRS-1 (p-IRS-1, Tyr896), anti-p-IRS-1 antibody (rabbit monoclonal IgG, 1:100, Epitomics, Burlingame, CA, USA) and goat anti-rabbit IgG secondary antibody conjugated to horseradish peroxidase (1:5,000, Santa Cruz Biotechnology); for IRS-2, anti-IRS-2 antibody (rabbit polyclonal IgG, 1:250, Sigma-Aldrich) and goat anti-rabbit IgG secondary antibody conjugated to horseradish peroxidase (1:5,000, Santa Cruz Biotechnology); for phosphorylated IRS-2 (p-IRS-2, Ser731), anti-p-IRS-2 antibody (rabbit polyclonal IgG, 1:1,000, Abbomax, San Jose, CA, USA) and goat anti-rabbit IgG secondary antibody conjugated to horseradish peroxidase (1:5,000, Santa Cruz Biotechnology); for phosphorylated p85 subunit of PI3K (p-PI3K p85, Tyr458), anti-p-PI3K p85 antibody (rabbit polyclonal IgG, 1:1,500; Cell Signaling Technology, Danvers, MA, USA) and goat anti-rabbit IgG secondary antibody conjugated to horseradish peroxidase (1:5,000, Santa Cruz Biotechnology); for phosphorylated extracellular signal-regulated kinase 1/2 (p-ERK1/2, Tyr204), anti-p-ERK1/2 antibody (mouse monoclonal IgG, 1:1,500, Santa Cruz Biotechnology) and goat anti-mouse IgG secondary antibody conjugated to horseradish peroxidase (1:5,000, Santa Cruz Biotechnology); for GLUT4, anti-GLUT4 antibody (mouse monoclonal IgG, 1:500, Cell Signaling Technology) and goat anti-mouse IgG secondary antibody conjugated to horseradish peroxidase (1:5,000, Santa Cruz Biotechnology); for Na^+/K^+-ATPase, anti-Na^+/K^+-ATPase antibody (rabbit monoclonal IgG, 1:2,000, Epitomics) and goat anti-rabbit IgG secondary antibody conjugated to horseradish peroxidase (1:5,000, Santa Cruz Biotechnology). β-actin immunoreactivity, detected with monoclonal anti-β-actin antibody (1:5,000, Sigma-Aldrich) and goat anti-mouse IgG secondary antibody conjugated to horseradish peroxidase (1:5,000, Santa Cruz Biotechnology), was used as a loading control.

Statistical Analysis

All statistical analyses were performed with SPSS software (version 15.0; SPSS Inc, Chicago, IL, USA). Values were expressed as means ± SD. Statistical analyses were performed using the unpaired Student's t test or one way ANOVA. Data with a p value <0.05 were considered statistically significant.

Results

Insulin Sensitivity was Impaired in OLETF Rats Fed the SFA Diet and Maintained in Those Fed the MUFA Diet

To evaluate the extent of insulin resistance developed in OLETF rats from each group, we performed ITT and OGTT. The glucose disposal rate between 15 and 30 min after insulin administration was significantly reduced in

rats fed the SFA diet, as compared with rats fed the chow diet or the MUFA diet (Fig. 1a). OGTT showed that the blood glucose levels of rats fed the SFA diet were significantly higher than those of rats fed the chow diet or the MUFA diet for all time intervals tested (Fig. 1b).

Dietary SFA Altered the IRS-1/PI3K Pathway and IRS-2 and ERK1/2 Activity

To investigate the effect of dietary fatty acid composition on insulin signal transduction in skeletal muscle, we evaluated the mRNA expression of IRS-1 and -2 in vastus lateralis muscle from OLETF rats in each group. Muscle IRS-1 mRNA expression was significantly reduced in rats fed the SFA diet, as compared with those fed the normal chow diet; however, the MUFA diet did not change the mRNA expression of muscle IRS-1, as compared with the chow diet (chow vs. SFA vs. MUFA, 1.00 ± 0.06 vs. 0.46 ± 0.03 vs. 0.96 ± 0.05 AU, $p < 0.001$) (Fig. 2a). The protein abundance of IRS-1 and phosphorylated IRS-1 in the whole homogenate of skeletal muscle sample showed the same tendency with mRNA expression(IRS-1, chow vs. SFA vs. MUFA, 1.00 ± 0.17 vs. 0.36 ± 0.16 vs. 0.96 ± 0.20 AU, $p < 0.001$; p-IRS-1, chow vs. SFA vs. MUFA, 1.00 ± 0.15 vs. 0.17 ± 0.09 vs. 0.87 ± 0.19 AU, $p < 0.001$) (Fig. 2a and 2b). On the contrary, muscle IRS-2 mRNA expression and protein abundance of IRS-2 and phosphorylated IRS-2 increased in rats fed the SFA diet, as compared with rats fed the chow diet, whereas there was no difference in muscle IRS-2 expression between rats fed the MUFA diet and the chow diet (mRNA, chow vs. SFA vs. MUFA, 1.00 ± 0.05 vs. 1.77 ± 0.04 vs. 1.08 ± 0.08 AU, $p < 0.001$; protein, IRS-2, chow vs. SFA vs. MUFA, 1.00 ± 0.14 vs. 1.72 ± 0.33 vs. 0.87 ± 0.26 AU, $p < 0.001$; protein, p-IRS-2, chow vs. SFA vs. MUFA, 1.00 ± 0.36 vs. 3.97 ± 0.58 vs. 0.57 ± 0.45 AU, $p < 0.001$) (Fig. 3). To investigate the activation of PI3K and ERK1/2, the downstream protein kinases of IRS-1 and -2, we also measured the protein abundance of phosphorylated p85 subunit of PI3K and phosphorylated ERK1/2 in the whole homogenate of skeletal muscle sample. In OLETF rats fed the SFA diet, the level of p-PI3K p85 was decreased and the level of p-ERK1/2 was significantly increased, as compared with rats fed the chow diet, whereas there was no difference in p-PI3K p85 and p-ERK1/2 between rats fed the chow diet and the MUFA diet (p-PI3K p85, chow vs. SFA vs. MUFA, 1.00 ± 0.06 vs. 0.36 ± 0.06 vs. 0.97 ± 0.07 AU, $p < 0.001$; p-ERK1/2, chow vs. SFA vs. MUFA, 1.00 ± 0.08 vs. 5.59 ± 0.54 vs. 1.11 ± 0.16 AU, $p < 0.001$) (Fig. 4).

Dietary SFA Reduced GLUT4 Membrane Translocation in Rat Skeletal Muscle

We investigated the whole cell and sarcolemmal membrane expression of GLUT4 in vastus lateralis muscle from OLETF rats in each group to investigate whether alteration in the IRS-1/PI3K pathway by dietary SFA affected GLUT4 membrane translocation. There was no difference in GLUT4 protein abundance in whole cell lysates of muscle samples from each experimental diet group (Fig. 5a). However, GLUT4 protein abundance in the muscle plasma membrane was significantly reduced by the SFA diet, compared to the normal chow diet (chow vs.

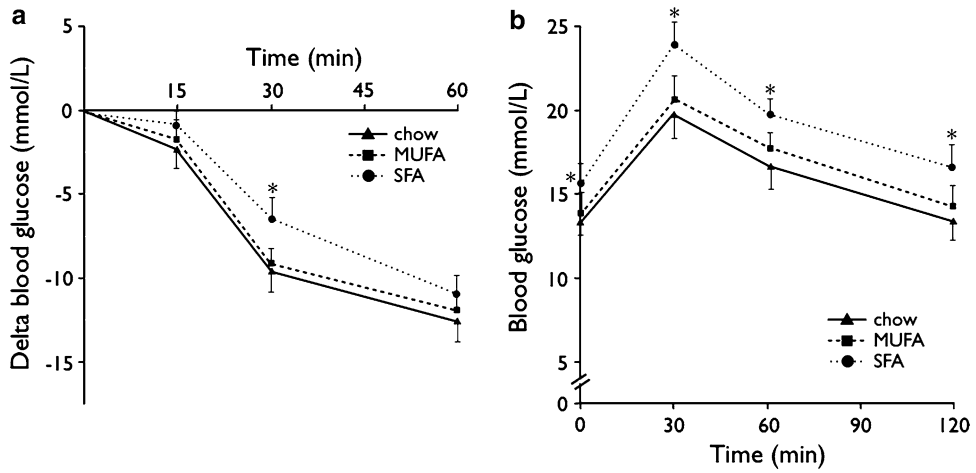

Fig. 1 The effect of dietary fatty acid composition on intraperitoneal insulin tolerance test and oral glucose tolerance test. **a** Intraperitoneal insulin tolerance test in OLETF rats fed the 3 experimental diets for 3 weeks ($n = 10$ in each group). The change in blood glucose above the basal level is depicted. **b** Oral glucose tolerance test in OLETF rats fed the 3 experimental diets for 3 weeks ($n = 10$ in each group). *chow* normal chow diet, *MUFA* monounsaturated fatty acid (olive oil) enriched high-fat diet, *SFA* saturated fatty acid (lard oil) enriched high-fat diet, *$p < 0.05$ versus chow

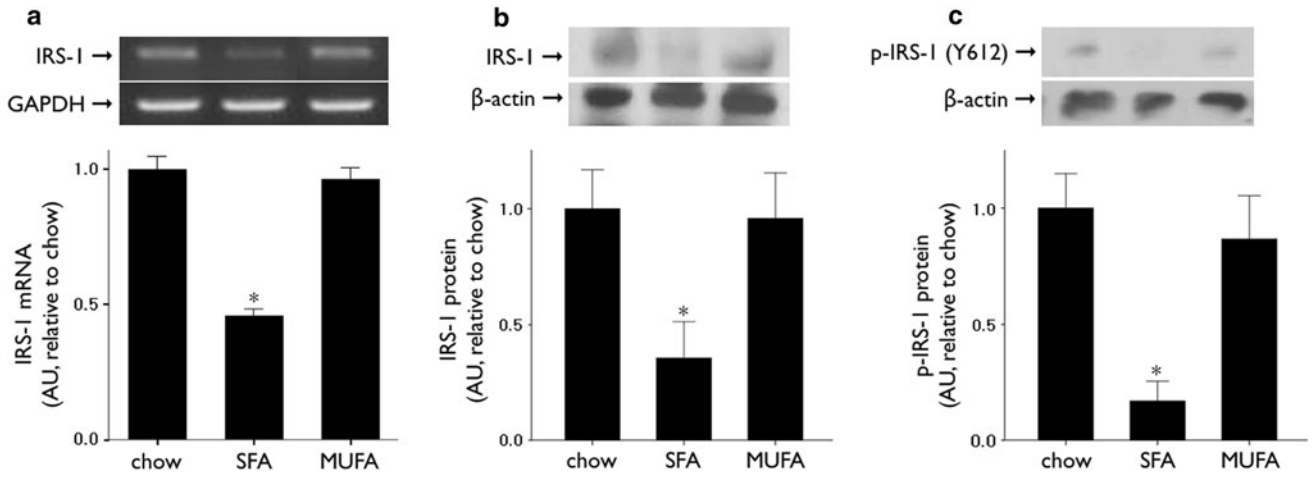

Fig. 2 The effect of dietary fatty acid composition on IRS-1 expression in skeletal muscle. RT-PCR and western blot analysis were performed on vastus lateralis muscle samples of OLETF rats fed the 3 experimental diets for 3 weeks ($n = 10$ in each group). **a** Semi-quantitative RT-PCR for IRS-1. **b** Western blot showing total IRS-1 protein level. **c** Western blot showing phosphorylated IRS-1 (Tyr896) protein level. *IRS-1* insulin receptor substrate-1, *p-IRS-1* phosphorylated IRS-1, *GAPDH* glyceraldehyde-3-phosphate dehydrogenase, *AU* arbitrary unit, *chow* normal chow diet, *SFA* saturated fatty acid (lard oil) enriched high-fat diet, *MUFA* monounsaturated fatty acid (olive oil) enriched high-fat diet, $*p < 0.05$ versus chow

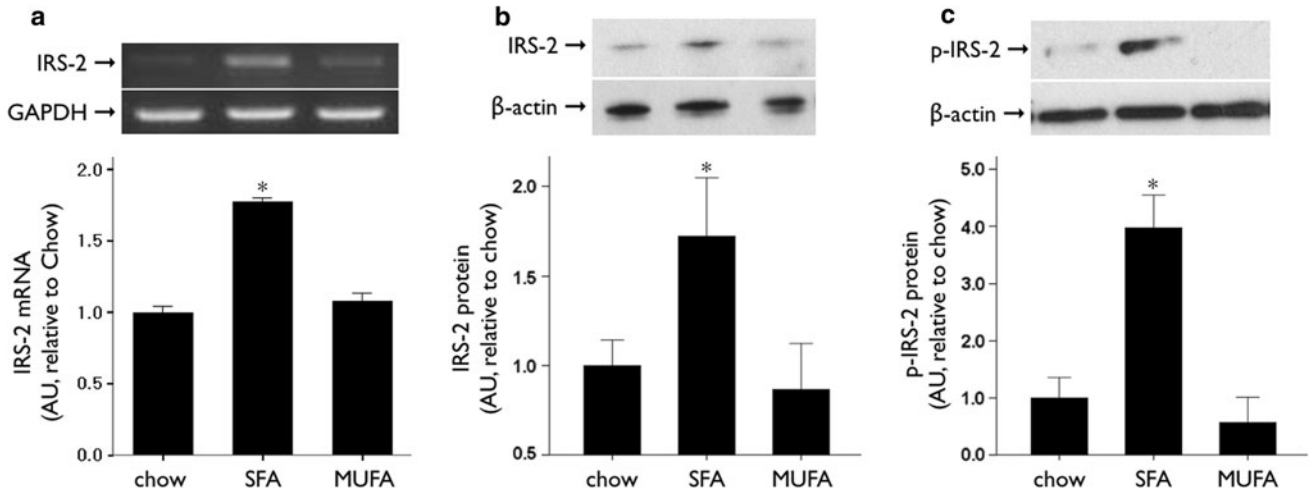

Fig. 3 The effect of dietary fatty acid composition on IRS-2 expression in skeletal muscle. RT-PCR and western blot analysis were performed on vastus lateralis muscle samples of OLETF rats fed the 3 experimental diets for 3 weeks ($n = 10$ in each group). **a** Semi-quantitative RT-PCR for IRS-2. **b** Western blot showing total IRS-2 protein level. **c** Western blot showing phosphorylated IRS-2 (Ser731) protein level. *IRS-2* insulin receptor substrate-2, *p-IRS-2* phosphorylated IRS-2, *GAPDH* glyceraldehyde-3-phosphate dehydrogenase, *AU* arbitrary unit, *chow* normal chow diet, *SFA* saturated fatty acid (lard oil) enriched high-fat diet, *MUFA* monounsaturated fatty acid (olive oil) enriched high-fat diet, $*p < 0.05$ versus chow

SFA, 1.00 ± 0.23 vs. 0.34 ± 0.15 AU, $p < 0.001$) (Fig. 5b). In contrast, GLUT4 protein abundance in muscle plasma membrane of rats fed the MUFA diet was not different from that in rats fed the chow diet.

Discussion

In this study, we observed the effect of dietary fatty acid composition of a high-fat diet on the insulin signaling pathway and GLUT4 membrane translocation in skeletal muscle of OLETF rats, a type 2 diabetic animal model. Insulin sensitivity measured by ITT was attenuated in the SFA group, whereas the MUFA group showed improved insulin sensitivity, compared with the SFA group. We focused on the insulin sensitivity of skeletal muscle for this study because the skeletal muscle is the major site of insulin-stimulated glucose disposal (reviewed in [1]).

First, we investigated the effect of dietary SFA on the insulin signaling pathway in vastus lateralis muscle of OLETF rats. The association of dietary SFA and insulin resistance of skeletal muscle can be explained by several

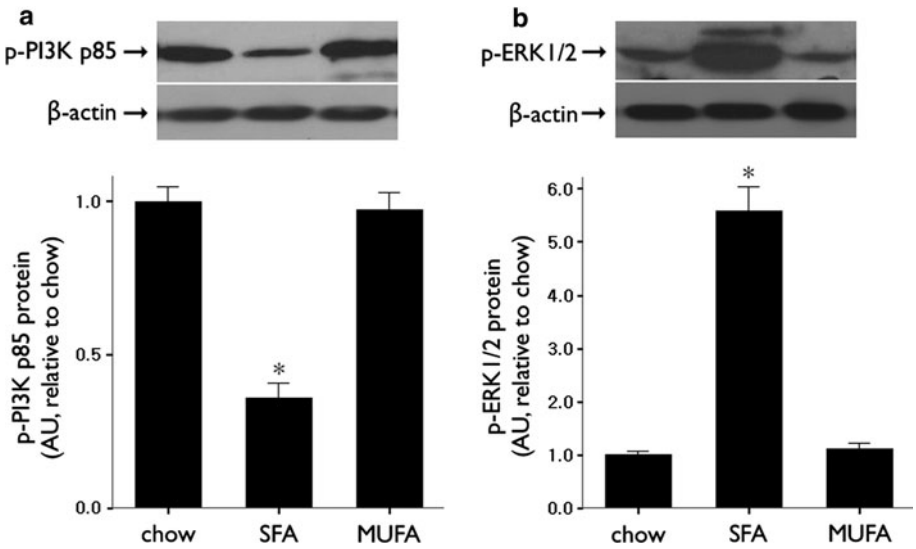

Fig. 4 The effect of dietary fatty acid composition on the phosphorylation of PI3K and ERK1/2 in skeletal muscle. Western blot analysis of vastus lateralis muscle from OLETF rats fed the 3 experimental diets for 3 weeks ($n = 10$ in each group). **a** Western blot showing phosphorylated p85 subunit of PI3K (Tyr458) protein level. **b** Western blot showing phosphorylated ERK1/2 (Tyr204) protein level. *p-PI3K p85* phosphorylated p85 subunit of phosphoinositol 3-kinase, *p-ERK1/2* phosphorylated extracellular signal-regulated kinase 1/2, *AU* arbitrary unit, *chow* normal chow diet, *SFA* saturated fatty acid (lard oil) enriched high-fat diet, *MUFA* monounsaturated fatty acid (olive oil) enriched high-fat diet, $*p < 0.05$ versus chow

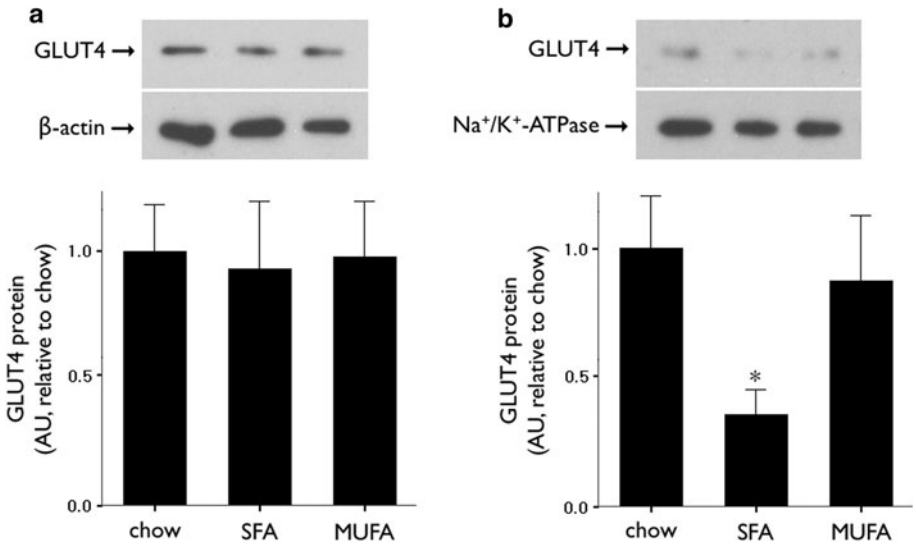

Fig. 5 The effect of dietary fatty acid composition on GLUT4 membrane translocation in skeletal muscle. Western blot analysis of vastus lateralis muscle from OLETF rats fed the 3 experimental diets for 3 weeks ($n = 10$ in each group). **a** Western blot showing GLUT4 protein level in whole cell lysate. **b** Western blot showing GLUT4 protein level in plasma membrane. *GLUT4* glucose transporter type 4, *AU* arbitrary unit, *chow* normal chow diet, *SFA* saturated fatty acid (lard oil) enriched high-fat diet, *MUFA* monounsaturated fatty acid (olive oil) enriched high-fat diet, $*p < 0.05$ versus chow

mechanisms. The traditional explanation proposes that dietary fatty acid composition affects the composition of cell membranes and membrane function such as GLUT4 translocation or insulin receptor affinity [13]. Recently, several studies reported a direct effect of dietary fatty acid composition or lipid oversupply on gene expression, enzyme activity, and signal transduction associated with insulin sensitivity (reviewed in [1]). Accumulation of lipid metabolites and mitochondrial dysfunction were also reported as possible mechanisms of the SFA-induced insulin resistance [9, 10, 14, 15]. Our results showed that the SFA-rich high-fat diet reduced IRS-1 mRNA expression and protein abundance of total IRS-1 and activated IRS-1, whereas this diet increased IRS-2 and activated IRS-2. IRS-1 and -2 are the docking proteins of the insulin receptor; the proteins are recruited to the receptor after

insulin binding and play a central role in the translocation of GLUT4. In skeletal muscle, IRS-1, and to a lesser extent, IRS-2, appear to be particularly important in the control of glucose metabolism through activation of the PI3K pathway (reviewed in [1]). Recent studies have reported that IRS-1 and IRS-2 have distinct regulatory functions in insulin signaling pathway [16, 17]. Zheng et al. [16] reported that dexamethasone treatment reduced IRS-1 protein and PI3K/Akt signaling and increased IRS-2 protein and MEK/ERK signaling in rat L6 myotubes. Piro et al. reported that palmitate treatment reduced IRS-1/PI3K/Akt signaling and increased IRS-2/ERK signaling in pancreatic α-cell line. Considering that dexamethasone, palmitate and the SFA-rich high-fat diet are responsible for insulin resistance, as well as on the basis of our results showing the different effect of the SFA-rich high-fat diet on skeletal muscle IRS-1 and -2 expressions, we hypothesized that dietary SFA might reduce IRS-1/PI3K signaling and increase IRS-2/ERK signaling in rat skeletal muscle. As expected, our data were consistent with previous studies mentioned above; the protein abundance of activated PI3K was reduced in the skeletal muscle of the SFA group, whereas activated ERK1/2 was increased by dietary SFA. Altogether, our results suggest that the alteration in the IRS-1/PI3K pathway plays a crucial role in SFA-induced insulin resistance in skeletal muscle. In addition, IRS-2 might play a minor role in SFA-induced insulin resistance and the downstream effect of increased IRS-2 appears to be limited to increasing ERK1/2-mediated mitogenic properties, not affecting PI3K-mediated insulin-induced glucose disposal in skeletal muscle. The mechanism underlying this difference in SFA-induced changes in IRS-1 and IRS-2 expression is unclear. Although some clues may be provided by studies showing that Forkhead box O3a (FOXO3a) mediates signaling crosstalk between IRS-1 and -2 during glucocorticoid-induced skeletal muscle atrophy [16], further investigation is needed. We also demonstrated that GLUT4 membrane translocation in skeletal muscle was decreased in SFA diet-fed rats, as compared with those fed the chow diet. This result shows that the alteration in the IRS-1/PI3K pathway by dietary SFA affects the GLUT4 membrane translocation and might, therefore, reduce insulin-stimulated glucose disposal in skeletal muscle.

We also investigated the effect of dietary MUFA in the high-fat diet condition on the insulin signaling pathway in skeletal muscle of OLETF rats. The changes in IRS-1/-2, p-PI3K p85, and p-ERK1/2 induced by dietary SFA completely disappeared when SFA was substituted by MUFA; there was no difference in IRS-1 and -2 expression or in levels of activated PI3K and ERK1/2 between rats fed the MUFA-rich high-fat diet and those fed the chow diet. Our results are consistent with previous findings that the prevention of palmitate-induced insulin resistance by oleate in L6 muscle cells is associated with the ability of oleate to maintain insulin signaling through PI3K [18]. GLUT4 membrane translocation was also preserved in skeletal muscle of the MUFA group. Thus, despite their high-fat diet, the MUFA group had an intact IRS-1/PI3K pathway and maintained GLUT4 membrane translocation and insulin-stimulated glucose disposal in skeletal muscle. Our results are consistent with several randomized controlled clinical studies showing that dietary MUFA improves insulin sensitivity, compared with the SFA-rich diet [2–5]. According to a recent review, consumption of SFA instead of MUFA may worsen glucose-insulin homeostasis, especially among individuals predisposed to insulin resistance [19]. We used a type 2 diabetic animal model for this study; thus, the results of the present study suggest a possible mechanism for the beneficial effect of dietary MUFA, especially in type 2 diabetic patients consuming high-fat diet.

One limitation of this study is that we did not measure the insulin-stimulated glucose disposal of skeletal muscle using radioisotopes. However, to our knowledge, this is the first in vivo study to investigate the effect of dietary fatty acid composition on the insulin signaling pathway and subsequent GLUT4 translocation in skeletal muscle for a type 2 diabetic status under conditions of a high-fat diet. Considering the reality that the majority of diabetic patients fail to reduce the amount of fat or calories in their diet [20–22], this study provides meaningful information that a MUFA-enriched diet could allow diabetic patients to maintain insulin sensitivity even if they continue to consume a high-fat diet.

In conclusion, we showed a beneficial effect of dietary MUFA on insulin sensitivity in a type 2 diabetic model with high-fat diet conditions. This beneficial effect of dietary MUFA, as compared with SFA, is associated with an intact insulin signaling pathway through IRS-1/PI3K and maintenance of GLUT4 membrane translocation in skeletal muscle, both of which were altered by dietary SFA. This study might provide an experimental rationale for dietary advice for type 2 diabetic patients.

Acknowledgments This work was supported by a National Research Foundation grant awarded by the Korea government (MEST) (No. 2009-0091380).

Conflict of interest None.

References

1. Schmitz-Peiffer C (2000) Signalling aspects of insulin resistance in skeletal muscle: mechanisms induced by lipid oversupply. Cell Signal 12(9–10):583–594

2. Vessby B, Uusitupa M, Hermansen K, Riccardi G, Rivellese AA, Tapsell LC, Nalsen C, Berglund L, Louheranta A, Rasmussen BM, Calvert GD, Maffetone A, Pedersen E, Gustafsson IB, Storlien LH (2001) Substituting dietary saturated for monounsaturated fat impairs insulin sensitivity in healthy men and women: the KANWU Study. Diabetologia 44(3):312–319
3. Perez-Jimenez F, Lopez-Miranda J, Pinillos MD, Gomez P, Paz-Rojas E, Montilla P, Marin C, Velasco MJ, Blanco-Molina A, Jimenez Pereperez JA, Ordovas JM (2001) A Mediterranean and a high-carbohydrate diet improve glucose metabolism in healthy young persons. Diabetologia 44(11):2038–2043
4. Lovejoy JC, Smith SR, Champagne CM, Most MM, Lefevre M, DeLany JP, Denkins YM, Rood JC, Veldhuis J, Bray GA (2002) Effects of diets enriched in saturated (palmitic), monounsaturated (oleic), or trans (elaidic) fatty acids on insulin sensitivity and substrate oxidation in healthy adults. Diabetes Care 25(8):1283–1288
5. Paniagua JA, Gallego de la Sacristana A, Romero I, Vidal-Puig A, Latre JM, Sanchez E, Perez-Martinez P, Lopez-Miranda J, Perez-Jimenez F (2007) Monounsaturated fat-rich diet prevents central body fat distribution and decreases postprandial adiponectin expression induced by a carbohydrate-rich diet in insulin-resistant subjects. Diabetes Care 30(7):1717–1723
6. Maron DJ, Fair JM, Haskell WL (1991) Saturated fat intake and insulin resistance in men with coronary artery disease. The Stanford Coronary Risk Intervention Project Investigators and Staff. Circulation 84(5):2020–2027
7. Parker DR, Weiss ST, Troisi R, Cassano PA, Vokonas PS, Landsberg L (1993) Relationship of dietary saturated fatty acids and body habitus to serum insulin concentrations: the Normative Aging Study. Am J Clin Nutr 58(2):129–136
8. Chavez JA, Summers SA (2003) Characterizing the effects of saturated fatty acids on insulin signaling and ceramide and diacylglycerol accumulation in 3T3–L1 adipocytes and C2C12 myotubes. Arch Biochem Biophys 419(2):101–109
9. Montell E, Turini M, Marotta M, Roberts M, Noe V, Ciudad CJ, Mace K, Gomez-Foix AM (2001) DAG accumulation from saturated fatty acids desensitizes insulin stimulation of glucose uptake in muscle cells. Am J Physiol Endocrinol Metab 280(2):E229–E237
10. Lee JS, Pinnamaneni SK, Eo SJ, Cho IH, Pyo JH, Kim CK, Sinclair AJ, Febbraio MA, Watt MJ (2006) Saturated, but not n-6 polyunsaturated, fatty acids induce insulin resistance: role of intramuscular accumulation of lipid metabolites. J Appl Physiol 100(5):1467–1474
11. Banerjee SK, Wang DW, Alzamora R, Huang XN, Pastor-Soler NM, Hallows KR, McGaffin KR, Ahmad F (2010) SGLT1, a novel cardiac glucose transporter, mediates increased glucose uptake in PRKAG2 cardiomyopathy. J Mol Cell Cardiol 49(4):683–692
12. Wu KY, Zhou XP, Luo ZG (2010) Geranylgeranyl transferase I is essential for dendritic development of cerebellar Purkinje cells. Mol Brain 3:18
13. Storlien LH, Pan DA, Kriketos AD, O'Connor J, Caterson ID, Cooney GJ, Jenkins AB, Baur LA (1996) Skeletal muscle membrane lipids and insulin resistance. Lipids 31(Suppl):S261–S265
14. Hirabara SM, Curi R, Maechler P (2010) Saturated fatty acid-induced insulin resistance is associated with mitochondrial dysfunction in skeletal muscle cells. J Cell Physiol 222(1):187–194
15. Abdul-Ghani MA, Muller FL, Liu Y, Chavez AO, Balas B, Zuo P, Chang Z, Tripathy D, Jani R, Molina-Carrion M, Monroy A, Folli F, Van Remmen H, DeFronzo RA (2008) Deleterious action of FA metabolites on ATP synthesis: possible link between lipotoxicity, mitochondrial dysfunction, and insulin resistance. Am J Physiol Endocrinol Metab 295(3):E678–E685
16. Zheng B, Ohkawa S, Li H, Roberts-Wilson TK, Price SR (2010) FOXO3a mediates signaling crosstalk that coordinates ubiquitin and atrogin-1/MAFbx expression during glucocorticoid-induced skeletal muscle atrophy. FASEB J 24(8):2660–2669
17. Piro S, Maniscalchi ET, Monello A, Pandini G, Mascali LG, Rabuazzo AM, Purrello F (2010) Palmitate Affects Insulin Receptor Phosphorylation and Intracellular Insulin Signal in a Pancreatic {alpha}-Cell Line. Endocrinology 151:4197–4206
18. Gao D, Griffiths HR, Bailey CJ (2009) Oleate protects against palmitate-induced insulin resistance in L6 myotubes. Br J Nutr 102(11):1557–1563
19. Micha R, Mozaffarian D (2010) Saturated Fat and Cardiometabolic Risk Factors, Coronary Heart Disease, Stroke, and Diabetes: a Fresh Look at the Evidence. Lipids (in press)
20. Lee H, Kim M, Daly BJ (2008) Nutritional patterns of Korean diabetic patients: an exploratory study. Int Nurs Rev 55(4): 442–446
21. Geiss LS, James C, Gregg EW, Albright A, Williamson DF, Cowie CC (2010) Diabetes risk reduction behaviors among U.S. adults with prediabetes. Am J Prev Med 38(4):403–409
22. Zilli F, Croci M, Tufano A, Caviezel F (2000) The compliance of hypocaloric diet in type 2 diabetic obese patients: a brief-term study. Eat Weight Disord 5(4):217–222

address its underlying causes is an important public health priority. Dysregulated lipid metabolism leading to elevated low density lipoprotein (LDL)-cholesterol (C) and low plasma high density lipoprotein (HDL)-C are important CVD risk factors [1–6]. With wider use of the statins, low HDL-C has emerged as the most important lipoprotein disorder for which current therapies are inadequate. The need for new approaches is highlighted by the failed trial of a cholesteryl ester transfer protein (CETP) inhibitor [7]. Although hypertriglyceridemia and low HDL-C are mechanistically linked, the latter is more strongly correlated with CVD mortality [2]. HDL-C and cardioprotection are mechanistically linked by reverse cholesterol transport (RCT), the transfer of cholesterol from macrophages in the subendothelial space to the liver for disposal [8]. The first two RCT steps are macrophage cholesterol efflux and cholesterol esterification in plasma [8]. Thus, an intervention that enhances both of these steps could be a therapeutically useful new approach to improve RCT.

A recombinant (r) virulence determinant from *Streptococcus pyogenes* [9], serum opacity factor (SOF), delipidates human HDL yielding a cholesteryl ester-rich microemulsion (CERM), lipid-free apo A-I and a "neo HDL" [10–12]. Given that neo HDL is more phospholipid-rich than HDL and that cholesterol efflux and esterification are increased by increased phospholipid content of acceptors and substrates, respectively [13–16], we tested the effects of SOF-mediated conversion of HDL in whole plasma to neo HDL on efflux and esterification.

Experimental Procedures

Materials

Total lipoproteins (TLP) and HDL were isolated from human plasma obtained from The Methodist Hospital Blood Donor Center by addition of KBr to $d = 1.21$ g/mL and flotation (48 h at 40,000 rpm, Beckman Ti 50.2 rotor). VLDL, LDL, HDL and lipoprotein-deficient serum (LPDS) were isolated by sequential flotation at $d = 1.012$, 1.063 and 1.21 g/mL, respectively. Lipoprotein purity was verified by size exclusion chromatography (SEC) and SDS-PAGE. Protein was determined with a kit (BioRad DC assay) using BSA as a standard. LDL was stored at 4 °C under nitrogen gas and used within 14 days. OxLDL was prepared by exposing LDL to 5 μmol/L CuSO4 for 24 h at 37 °C [17]. Lipid oxidation was verified by an assay for thiobarbituric acid-reactive substances; precautions were taken to exclude endotoxin. Neo HDL was prepared by incubating HDL (~2 mg/mL) and rSOF (1 μg/mL) in 47.5 mL overnight at 37 °C. The reaction mixture was adjusted to a $d = 1.063$ g/mL with KBr and centrifuged for 18 h at 45,000 rpm (Beckman Ti 50.2 rotor). The upper half of the tube was removed by aspiration. The bottom half was adjusted to a $d = 1.24$ g/mL with KBr and centrifuged as above for 40 h. The neo HDL removed from the top was pure as assessed by SEC [12]. Tris-buffered saline (TBS = 10 mM Tris, 100 mM NaCl, 1 mM EDTA, pH 7.4) was used throughout unless otherwise specified. [^{3}H]Cholesterol was from Amersham Biosciences (Piscataway, NJ, USA). Buffer salts were from Fisher Scientific, Inc., (Rockville, MD, USA). A recombinant polyhistidine-tagged, truncated form of *sof2*, encoding amino acids 38–843 (rSOF) was cloned and expressed in *Escherichia coli* and purified by metal affinity chromatography [10].

Effect of rSOF on LCAT Cholesterol Esterification

HDL was labeled with [^{3}H]cholesterol (~100 μCi) by injection of an ethanolic solution [15] and split into two equal aliquots; rSOF (1 μg/mL) was added to one and an equal volume of saline was added to the other and incubated overnight at 37 °C. On ice, the fractions were recombined as follows: (a) [^{3}H]HDL + (LDL + VLDL) + LPDS, (b) rSOF-treated [^{3}H]HDL + (LDL + VLDL) + LPDS, (c) [^{3}H]HDL + LPDS, and (d) rSOF-treated [^{3}H]HDL + LPDS. TBS was added to each sample to give equal volumes. The samples were incubated at 37 °C for 30 min and transferred to ice. Triplicate aliquots (100 μL) of each incubation were β-counted. Another set of triplicate aliquots were extracted with 4 mL hexane and the phases separated by low speed centrifugation for 5 min; 3-mL aliquots of the upper layer were evaporated under nitrogen and the residue dissolved in 30 μL chloroform. CE and FC were resolved by thin layer chromatography (Whatman TLC silica gel 60A plates) in hexane/diethyl ether/acetic acid (75:35:1, by volume). After spraying the plates with Primuline dye (Sigma–Aldrich, St. Louis, MO, USA), FC and CE bands were identified by comparison with standards. The FC and CE were collected and quantified by β-counting. A 200-μL aliquot of each incubation mixture was analyzed by SEC to determine the distribution of radiolabel into CERM, VLDL, LDL, HDL and neo HDL. SEC profiles of the LCAT reaction products were determined essentially as described [11] using an Amersham Pharmacia ÄKTA chromatography system equipped with two Superose HR6 columns in tandem. Samples were injected into the chromatograph using a 0.2-mL sample loop, and eluted with TBS; 1-mL fractions were collected and analyzed by β-counting.

Effects of rSOF Activity Against Lipoproteins on Cellular Cholesterol Efflux

Plasma, TLP, HDL, and the products of their reactions with rSOF were extensively dialyzed at 4 °C against TBS and

tested as acceptors of cholesterol from the human monocyte-derived macrophage cell line, THP-1 (American Type Culture Collection). THP-1 cells were maintained in RPMI 1640 with 10% FBS, 100 U/mL penicillin, 100 mg/mL streptomycin, 1 mM sodium pyruvate and 2 mM glutamine. Cholesterol efflux was assayed as described previously [15, 16, 18]. In brief, THP-1 cells were seeded and activated with 0.1 μg/mL phorbol 12-myristate 13-acetate for 24 h. Cells were then labeled in serum-containing medium with [1α, 2α(n)-^{3}H]cholesterol (specific radioactivity 1.81 TBq/mmol, final radioactivity 74 KBq/mL) at 37 °C for 48 h in a CO_2 incubator at which time they were ~80% confluent. After labeling, cells were washed twice to remove excess label, and incubated for an additional 18 h in serum-free medium to ensure equilibration of labeled cholesterol into all intracellular pools. During this phase, the THP-1 medium contained the LXR agonist T0901317 (1 μM) to activate the macrophage in a way that increased the activities of ABCA1 and ABCG1 in cells that were not cholesterol-loaded. To initiate the efflux assay, cells were washed and incubated for 0–2 h at 37 °C in serum-free medium containing various concentrations of human plasma (0–8%), TLP, HDL, or neo HDL (10–200 μg/mL). After incubation, the medium was collected, centrifuged, and the supernatant analyzed by β-counting. Cell lipids were extracted with isopropanol and analyzed by β-counting. Cholesterol efflux ($\%E$) was expressed as the percentage of total labeled cholesterol transferred from cells to the medium. Efflux was compared on the basis of acceptor-protein concentration and the data were fitted to the equation $\%E = E_{max} \times (LP)/[K_m + (LP)]$, where LP was the lipoprotein concentration as protein, E_{max} was the maximum efflux and K_m was the lipoprotein concentration at half E_{max} using Systat-Sigma Plot (Point Richmond, CA, USA).

Efflux via ABCA1 and ABCG1

Efflux from ABCA1 and ABCG1-expressing BHK cells under a mifepristone-inducible promoter and MOCK cells transfected with the pGene V5 His plasmid alone were tested as reported by Vaughan and Oram [19]. ABCA1- and ABCG1-expressing BHK cells were labeled with [^{3}H]cholesterol to equilibrium 1 day prior to mifepristone treatment. ABCA1 and ABCG1 receptors were induced by incubating cells for 18–20 h in DMEM with 1 mg/mL fatty acid free bovine serum albumin and 10 nM mifepristone. Unactivated cells (no mifepristone) were used as a negative controls. Transporter-specific efflux was calculated as the difference between efflux from ABCA1 and ABCG1-expressing cells with and without activation.

Comparison of the Effects of HDL and Neo HDL on Inflammatory IL-6 and TNF-α

Mouse peritoneal macrophages were collected from C57Bl/6 J mice 2 days after mineral oil injection and seeded in RPMI-1640 medium supplemented with 5% BSA in 96-well plates at ~10^5cells/well and cultured for 1 day. HDL and neo HDL were preincubated with OxLDL at ratio of 1:1 protein for 1 h at 37 °C. Cells were treated with OxLDL(100 μg/mL), HDL(100 μg/mL) and neo HDL(100 μg/mL), HDL-OxLDL (100 μg/mL each), and neo HDL-OxLDL(100 μg/mL each), respectively. IL-6 and TNF-α concentrations in the media were measured by ELISA kits (BD Bioscience) 18 h after treatment.

Statistical Tests

Statistical analysis of data was done as indicated in the figure legends, using the t test for pairs of means, one-way ANOVA with Tukey's post hoc test for multiple comparisons, and two-way ANOVA with Bonferroni post tests for regression plots, using SPSS and GraphPad Prism statistical software.

Results

Macrophage Cholesterol Efflux

Cholesterol efflux from THP-1 macrophages to plasma (1%) and TLP (25 μg/mL) were linear with time and increased by preincubation with rSOF; efflux to neo HDL formed from treatment of HDL with rSOF was also higher than that to HDL (Fig. 1a–c). The respective ratios of the rates of efflux to the rSOF-derived acceptors to controls were 2.4, 3.3, and 2.6. Increasing the rSOF pre incubation time increased cholesterol efflux and the production of neo HDL and CERM (Supplementary Figs. 1, 2).

[^{3}H]Cholesterol efflux kinetics from THP-1 macrophages to various acceptors with and without rSOF treatment were also measured. The acceptors were, respectively, plasma ± rSOF, TLP ± rSOF, HDL ± rSOF reaction mixtures and isolated HDL and neo HDL (Fig. 2a–d). Efflux from cholesterol-loaded macrophages to plasma was also measured (Fig. 2a, insert). rSOF treatment improved the global parameter of cholesterol efflux, $Cat_{eff} = V_{max}/K_m$(Supplementary Table 1). The Cat_{eff} for acceptors that were rSOF-derived were 2–3 times higher than those of the acceptors from which they were formed (Supplementary Table 1). When measured as mass, macrophage cholesterol efflux to HDL after incubation with rSOF increased with the addition of the LXR agonist

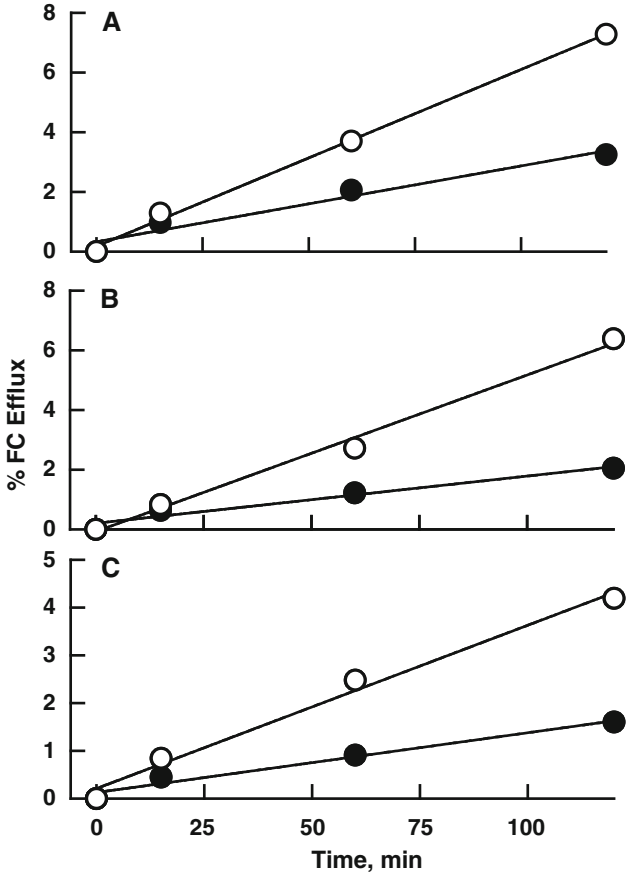

Fig. 1 Time-dependence of cholesterol efflux from THP-1 macrophages. **a** Plasma (1%) and plasma (1%) after overnight incubation with rSOF (1 μg/mL) were incubated with [^{3}H]cholesterol-labeled macrophages for 0–2 h and the amount of radiolabel transferred to media determined. **b** Similar data were collected for TLP (25 μg/mL) and TLP (25 μg/mL) after incubation overnight with rSOF. **c** Similar data for transfer of radiolabel to isolated HDL and neo HDL (both 25 μg/mL). The ratios of the slopes of rSOF derived acceptors to controls in **a**–**c** were 2.4, 3.3, and 2.6, respectively. $r^2 > 0.95$ for all plots. *Closed circles* **a** control plasma, **b** control TLP, **c** HDL. *Open circles* **a** Plasma + rSOF, **b** TLP + rSOF, **c** neo HDL. The efflux values were means ± SD of two experiments in triplicate. In **a**–**c** the error *bars* were smaller than the symbols

(TO-901317) both with and without cholesterol loading (Supplementary Fig. 3).

We identified the plasma acceptors of cellular [^{3}H]cholesterol after 15 min and 2 h efflux times by SEC. After a 15-min incubation of 3% plasma with cells, most of the cell-derived [^{3}H]cholesterol co-eluted with HDL and VLDL (Fig. 3a). In contrast, [^{3}H]cholesterol effluxed to 3% plasma pre-treated for 3 h with rSOF co-eluted with neo HDL and CERM + VLDL (Fig. 3a). After longer incubation (2 h) with macrophages the SEC profiles indicated more transfer to CERM and LDL for rSOF-treated plasma than to VLDL and LDL for control (Fig. 3b). Similar experiments were conducted with TLP, which

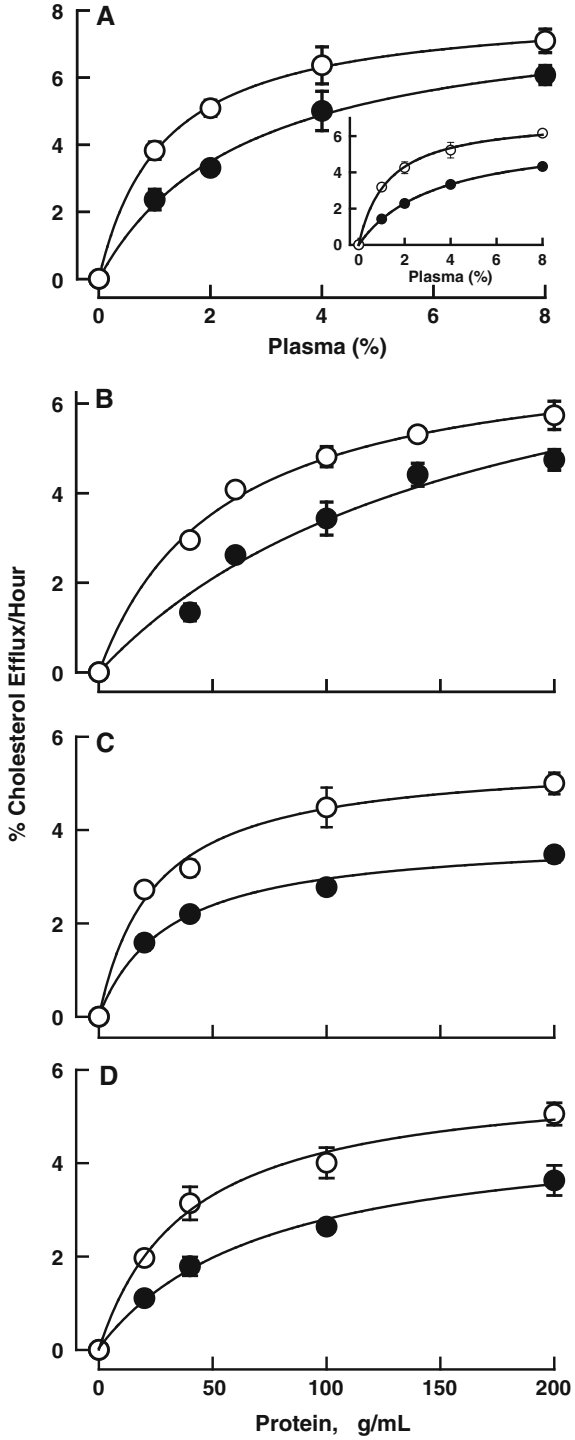

Fig. 2 [^{3}H]Cholesterol efflux from THP-1 macrophages to various acceptors. The acceptors were plasma (**a**), TLP (**b**), and HDL (**c**) each with (*open circles*) and without (*closed circles*) preincubation with rSOF for 18 h. Efflux to isolated HDL (*closed circles*) and neo HDL formed from rSOF + HDL (*open circles*) is shown in (**d**). Insert in **a** shows efflux from cholesterol-loaded macrophages to plasma. Other details are in "Materials" and Fig. 1. Two-way ANOVA analysis of the regression plots indicated that rSOF pretreatment significantly increased efflux to all of the acceptors ($p < 0.001$), and Bonferroni post tests indicated this was true for all the concentrations tested ($p < 0.01$)

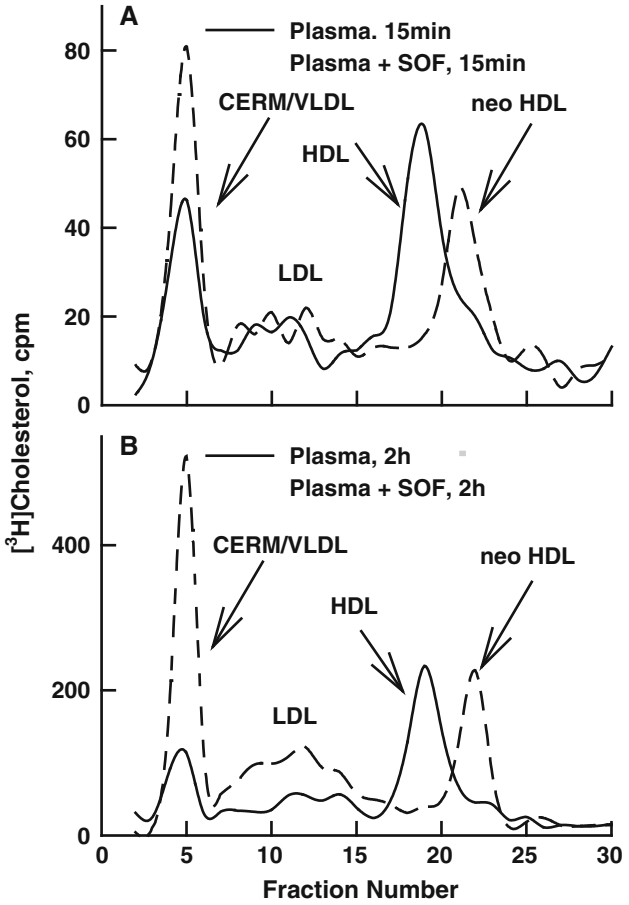

Fig. 3 SEC of 3% plasma, with and without rSOF pretreatment (3 h), after incubation with [^{3}H]cholesterol-labeled THP-1 macrophages. Cells were labeled and treated as in Fig. 1. **a** Fifteen min incubation, **b** 2 h incubation. Plasma (*continuous lines*), plasma post-rSOF (*dashed lines*). Media were transferred to tubes in wet ice and immediately analyzed by SEC in which the effluent was monitored by absorbance at 280 nm (not shown) and by the radioactivity of collected fractions. The peak elution fractions for CERM/VLDL, LDL, HDL, and neo were 4, 12, 19, and 22 mL, respectively

lacks lipid transfer protein and LCAT activities. At 15 min, [^{3}H]cholesterol appeared in all lipoprotein subclasses but at 2 h, a greater fraction was in LDL. (Supplementary Fig. 4). Similarly, SEC showed that cell-derived cholesterol associates with HDL and neo HDL when they were used as acceptors (Supplementary Fig. 5a, c), and efflux to all acceptors was greater at 2 h than at 15 min. When the total rSOF-HDL reaction mixture was used as acceptor, [^{3}H]cholesterol was found in both the neo HDL and the CERM (Supplementary Fig. 5b), and the presence of CERM promoted more total efflux than neo HDL alone at both 15 min and 2 h. Finally, macrophage cholesterol efflux to plasma depleted of apo B-containing lipoproteins increased when the preincubation time with rSOF was increased from 15 to 120 min. With the longer preincubation time, more neo HDL and CERM were formed, and there was a corresponding increase in association of

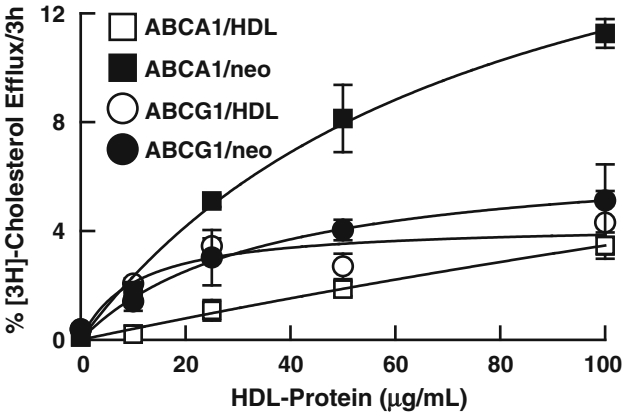

Fig. 4 [^{3}H]Cholesterol efflux from ABCA1- and ABCG1-transfected BHK cells to various protein concentrations of HDL and neo HDL. HDL and neo HDL were incubated with radiolabeled, mifepristone-induced cells for 3 h and the amount of the radiolabel transferred to media determined. The control assays were done with non-induced cells. The efflux values are means ± SD of two experiments in triplicate. Two-way ANOVA analysis of the regression plots indicated that efflux to neo HDL was significantly greater than to HDL for the ABCA1 cells ($p = 0.002$) but that efflux to neo HDL and HDL was not significantly different for the ABCG1 cells

[3H]cholesterol with CERM and neo HDL instead of HDL (Supplementary Fig. 6).

Efflux via ABCA1 and ABCG1

FC efflux from ABCG1-expressing BHK cells to neo HDL and HDL were not significantly different (Fig. 4). In contrast, FC efflux from ABCA1-expressing BHK cells to neo HDL was higher than that to HDL (Fig. 4).

Remodeling of HDL and Neo HDL

HDL-[^{3}H]cholesterol and neo HDL-[^{3}H]cholesterol were incubated with HDL-deficient plasma in amounts that restored the original plasma protein compositions. The LCAT reactivity of neo HDL was higher (+68%) than that of HDL (Fig. 5, left bars). Comparison of the LCAT reactivity of neo HDL and HDL (Fig. 5, right bars), showed CE production from neo HDL was higher than that from HDL (+165%). These samples were also analyzed by SEC, which showed that association of radiolabel with lipoproteins decreased as LDL > HDL > VLDL (Fig. 6a). When the HDL was replaced by rSOF-treated HDL the distribution decreased as LDL > CERM > neo HDL. The experiment with HDL and neo HDL without the apo B-containing lipoproteins showed that most remodeled neo HDL-[^{3}H]cholesterol was associated with CERM while most HDL-[^{3}H]cholesterol remained in the HDL peak (Fig. 6b). The enhancement of cholesterol esterification increased with rSOF dose (Supplementary Fig. 7).

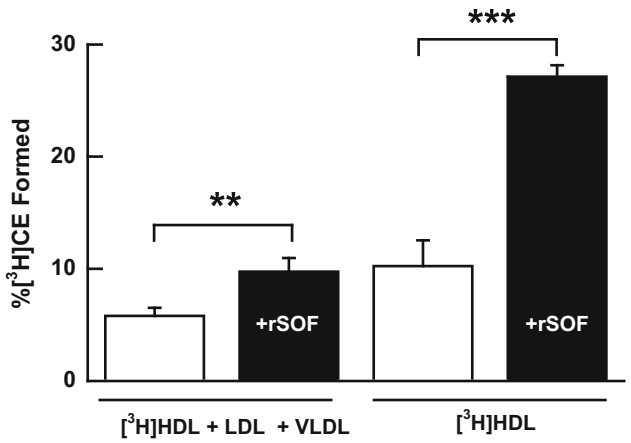

Fig. 5 Effect of rSOF reaction on cholesterol esterification via LCAT. Isolated HDL was labeled with [^{3}H]FC as described in "Materials" and recombined with (LDL + VLDL) and LPDS using amounts that returned all components to their original plasma concentrations. The incubations were for 30 min at 37 °C. The esterification rates are means ± SD of two experiments in triplicate. Statistical analysis by *t* test of HDL versus neo HDL under the same conditions, $^{**}p < 0.01$, $^{***}p < 0.001$

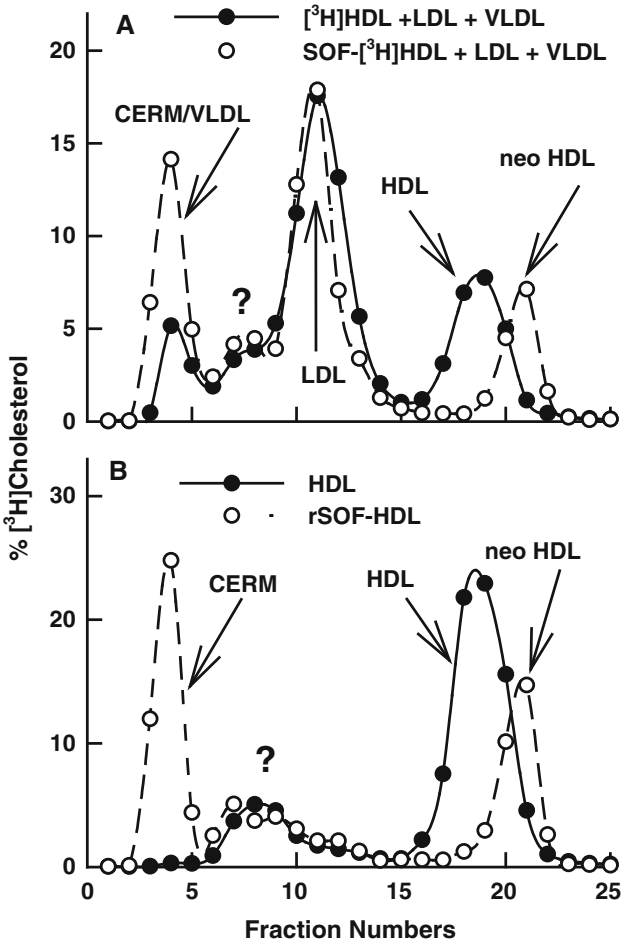

Fig. 6 Distribution of [^{3}H]cholesterol among lipoprotein subclasses after incubation with LPDS for 30 min. Labeling is as in "Materials". **a** Reconstituted whole plasma. SOF treatment of plasma TLP increased non HDL-associated cholesterol from 69 to 86%. **b** HDL or rSOF-HDL plus LPDS. Subtracting the radiolabel in HDL or neo HDL showed that SOF treatment increased the non HDL-associated cholesterol from 22 to 65%. A similar pattern was observed when the incubation with LPDS was reduced to 15 min. Some [^{3}H]cholesterol associated with a peak labeled "?" that was not identified but was likely a component of LPDS because it appears both **a** and **b**

The major fractions from Fig. 6 were used to determine the fraction of cholesterol as ester. HDL-[^{3}H]cholesterol and rSOF-treated HDL-[^{3}H]cholesterol, which contains CERM, neo HDL and lipid-free apo A-I [11], were incubated with HDL-deficient plasma and the distribution of [^{3}H]cholesterol into CE determined (Supplementary Fig. 8a). With rSOF treatment the formation of [^{3}H]CE increases and shifts to the non HDL fractions. The fractions of [^{3}H]CE in the neo HDL and the CERM/VLDL fraction were highest. A similar experiment in which LPDS was incubated with HDL-[^{3}H]cholesterol at their original plasma concentrations showed that at 30 min ~40% of the total cholesterol in HDL was CE (Supplementary Fig. 8b). When HDL-[^{3}H]cholesterol was replaced by rSOF-treated HDL-[^{3}H]cholesterol only 20% of the total cholesterol in neo HDL was esterified. However, more than 60% of the total cholesterol in the coexisting CERM fraction was esterified. Thus, most of the [^{3}H]cholesterol in the CERM peak in Fig. 6a was CE.

Comparative Attenuation of OxLDL-Induced Cytokine Secretion by Mouse Peritoneal Macrophages by HDL and Neo HDL

The effects of HDL and neo HDL on the secretion of the cytokines, IL-6 and TNF-α, by mouse peritoneal macrophages exposed to OxLDL were compared. Both lipoproteins elicited a dose-dependent reduction in IL-6 and TNF-α secretion that was greater for neo HDL (Supplementary Fig. 9). The effects at a single concentration were compared in detail (Fig. 7). These data showed that neither HDL nor neo HDL alone affected cytokine secretion elicited by LDL. In contrast, TNF-α and IL-6 secretion elicited by incubation of macrophages with OxLDL was reduced by coincubation with either HDL or neo HDL, with the effect of the latter being 96 and 103% greater ($p < 0.05$ for both).

Discussion

To simulate a physiological setting, we compared efflux to plasma with and without preincubation with rSOF and found that the parameters for efflux were improved by rSOF treatment and that efflux increased with longer

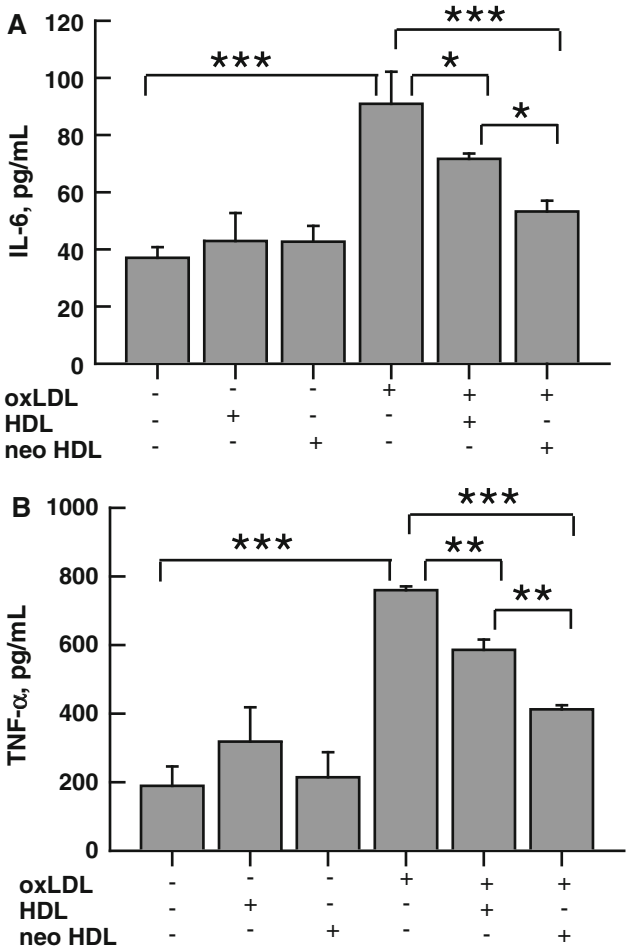

Fig. 7 Comparative attenuation of OxLDL-induced secretion of cytokines by HDL and neo HDL. HDL and neo HDL attenuated OxLDL-induced IL-6 and TNF-α production in a dose-dependent manner (Supplemental Fig. 9). For the data shown here, OxLDL (100 μg/mL) was preincubated with 100 μg/mL of HDL or neo HDL for 1 h at 37 °C. Cells were then incubated with OxLDL, HDL, neo HDL, HDL + OxLDL and neo HDL + OxLDL for 16 h. IL-6 and TNF-α secretion were measured by ELISA. One-way ANOVA analysis with Tukey's post-test indicated the means were significant as indicated ***$p < 0.001$, **$p < 0.01$, *$p < 0.05$

incubation times. Kinetic parameters for efflux to TLP, which lacks the lipid transfer proteins and LCAT of plasma, were similarly improved. In both plasma and TLP, the initial acceptor with and without rSOF-treatment, respectively, appears to be neo HDL and HDL because the fraction of [^{3}H]cholesterol in these particles was higher at 15 min than at 2 h (Fig. 3 and Supplemental Fig. 4). At both 15 min and 2 h, the distribution of [^{3}H]cholesterol was different for plasma and TLP. With plasma as the acceptor, more of the radiolabel was in the VLDL/CERM fraction, while with the TLP acceptor, more radiolabel was in LDL, an effect that was more profound at 2 h than at 15 min. This difference was likely due to the presence of CETP and LCAT activities in plasma but not in TLP. In the absence of LCAT activity, [^{3}H]cholesterol remained unesterified and was spontaneously transferred from HDL or neo HDL to other lipoproteins. In contrast, in plasma [^{3}H]cholesterol was converted to its ester, which requires CETP for transfer to other lipoproteins, a process that was much slower than that of spontaneous [^{3}H]cholesterol transfer from HDL [20–23].

[^{3}H]Cholesterol efflux to rSOF-treated HDL and isolated neo HDL was greater than that to HDL. This finding further supports the hypothesis that the increased efflux to plasma and TLP post-rSOF treatment is due to a more rapid initial transfer to neo HDL than to HDL (Supplementary Fig. 5a, c). Notably, a large fraction of the [^{3}H]cholesterol efflux to rSOF-treated HDL appeared in the CERM fraction (Supplementary Fig. 5b). As with TLP, the fraction of [^{3}H]cholesterol in the CERM was greater at 2 h than at 15 min. This further supported our hypothesis that [^{3}H]cholesterol transfer to non-neo HDL fractions in TLP was spontaneous free cholesterol transfer and that cholesterol desorbs more rapidly from neo HDL than from HDL. This was consistent with data showing that spontaneous lipid transfer rates increase with decreasing particle size according to the Kelvin equation [21].

Differences in the size, charge, apo composition and PL content of neo HDL and HDL might be mechanistically linked to differences in cholesterol efflux. Size probably does not play an important role in the rate differences. When normalized to PL content, there was no difference in efflux to rHDL of varying size and when normalized to particle number at constant PL concentration, cellular FC efflux to larger particles was more efficient [22], the opposite of our observations. Although HDL can have either α or pre β mobility and the latter was a preferred plasma acceptor of cholesterol, there was little evidence that charge was an important efflux discriminator. In contrast, the higher PL and apo A-II content of neo HDL compared to HDL [10, 11] could underlie the differences. Other studies support this; normalized to PL content ABCG1-mediated FC to rHDL efflux is more highly correlated with apo A-II ($r^2 = 0.7$) than with apoA-I ($r^2 = 0.5$); the underlying mechanism for this has not been identified. On the other hand, both spontaneous and ABCG1-mediated efflux increases with HDL-PL [24, 25]. This is supported by numerous studies with both rHDL and modified plasma HDL [13–16]. Indeed, the similar increases in efflux to neo HDL and to rSOF-treated plasma versus HDL and untreated plasma, respectively, are compelling evidence that neo HDL and not lipid-free apo A-I, which is also formed by rSOF [10], is the mechanistic link to increased efflux in plasma.

The studies of efflux from cells expressing ABCA1 and ABCG1 provide clues to the source of the increased efflux to neo HDL (Fig. 4). The higher efflux to neo HDL versus

HDL again showed that neo HDL was a superior acceptor. More importantly, the higher efflux from the ABCA1-expressing cells suggests that this transporter mediates the efflux to neo HDL. A role for lipid-free apo A-I cannot be excluded in the efflux from plasma and TLP. However, the similar increases in Cat_{eff} for efflux to plasma, TLP and isolated neo HDL, which contains no lipid-free apo A-I, suggests that neo HDL and not lipid-free apo A-I was the major acceptor. Although it has been suggested that ABCG1 is an important mediator of efflux to lipidated species [26], other studies have not supported this and have shown that pre β_1-HDL is an efficient FC acceptor via ABCA1 [27]. Given the similarity between neo HDL and pre β_1-HDL particles with respect to size, smaller than HDL, efficient efflux via ABCA1 was not unexpected. This finding was interesting in the context of the report that cholesterol efflux to plasma correlates better with the concentration of pre β_1-HDL than with that of HDL [28].

LCAT Reactivity of HDL and Neo HDL

CE formation via LCAT was higher (+68%) in plasma treated with rSOF than in untreated control plasma. LCAT catalyzed CE formation in neo HDL, the product of rSOF, was even higher (+165%) than that of HDL. The smaller increase in whole plasma may be due to some binding of LCAT to other lipoproteins such as LDL which is a poorer substrate [29]. Similarly, the higher rate of CE formation from neo HDL than from HDL suggests that higher neo HDL-reactivity underlies the differences observed in plasma. The higher rate of esterification in both rSOF-treated plasma versus control plasma and isolated HDL versus neo HDL, may be due to the higher PL content of neo HDL versus HDL [10, 11] and the transfer of CE to CERM which could produce some modest relief of product inhibition. The more likely explanation is that neo HDL has a lower FC/PL ratio than HDL and that high cholesterol concentrations are inhibitory; the optimal FC/PL ratio for LCAT activity is 12.5 mol%, above which activity declines [30]. This optimum is considerably lower than the FC/PL ratio of native HDL, ~25 mol% [31].

According to SEC of the respective products of the LCAT reaction against HDL and rSOF-treated HDL in whole plasma, most of the radiolabel occurs with LDL + VLDL and LDL + VLDL/CERM. However, the radiolabel in the VLDL/CERM fractions was higher than that of the VLDL (Fig. 6a). A similar experiment in which the reaction mixture does not contain VLDL or LDL also showed increased radiolabel in the CERM (Fig. 6b) suggesting that the increased radiolabel seen in the void volume of Fig. 6a was bound to CERM as CE and not to VLDL (Fig. 6). Whether the appearance of additional cholesterol in apo B lipoproteins is beneficial cannot be stated with certainty. One view is that any increase in cholesterol in VLDL and LDL is atherogenic. However, others opine that transfer to the apo B lipoproteins helps clear more cholesterol via the non-HDL receptors. New work in our laboratory shows that the CE transferred from HDL to CERM by rSOF is rapidly taken up by hepatocytes in vitro [32] and in vivo in mice, cleared from plasma into the liver (Rosales et al., unpublished work).

Enhanced Reduction of Cytokine Secretion by Neo HDL Versus HDL

Hypercholesterolemia is associated with increased numbers of arterial macrophage foam cells, a hallmark of an inflammatory state. HDL has anti inflammatory properties that oppose the inflammatory properties of OxLDL, an effect that may be due to enhanced cholesterol efflux to HDL [33, 34]. Our data, which compare the effects of HDL and neo HDL on the OxLDL-induced secretion of TNF-α and IL-6, show neo HDL producing nearly twice the suppression of these two markers of inflammation. Thus, the rSOF reaction has the potential to reduce inflammation via the formation of neo HDL.

rSOF: A Path to Improved RCT

Thus, rSOF activity against plasma might improve key steps in RCT, which comprises macrophage cholesterol efflux that forms nascent HDL and esterification of nascent HDL-cholesterol by LCAT. First, rSOF treatment increased cholesterol efflux under all conditions, plasma, TLP, and isolated HDL. Cholesterol accumulation in macrophage foam cells induces an inflammatory response, apoptosis, and other adverse effects associated with atherogenesis [35]. Cholesterol efflux from macrophages to HDL and apoA-I is one mechanism of atheroprotection [36, 37].

Second, neo HDL was a better LCAT substrate than HDL even in whole plasma. Although recent studies have shown that LCAT may be less important in RCT than once thought [38], in the context of rSOF the LCAT reaction may be important to the final RCT step, hepatic CE uptake, because a major fraction of HDL-cholesterol was transferred to the CERM mostly as its ester. Future studies in vivo will determine the feasibility of an SOF-based therapy, and provide a rationale for finding small molecules or peptides that catalyze the SOF reaction.

Acknowledgments Dr. Urbain Tchoua dedicates this publication to his father, Jean-Pierre Tchoua, who passed away during its preparation. We thank Dr. Joshua S. Wooten for help with statistical analyses. Supported by grants-in-aid from the National Institutes of Health (HJP, HL-30914 and HL-56865), the Merck-UNCF Science Inititative (UT) and the Department of Veterans Affairs (HSC).

References

1. Frick MH, Elo O, Haapa K, Heinonen OP, Heinsalmi P, Helo P, Huttunen JK, Kaitaniemi P, Koskinen P, Manninen V (2003) Helsinki heart study: primary-prevention trial with gemfibrozil in middle-aged men with dyslipidemia safety of treatment, changes in risk factors, and incidence of coronary heart disease. N Engl J Med 317:1237–1245
2. Manninen V, Elo MO, Frick M, Haapa K, Heinonen OP, Heinsalm P, Helo P, Huttunen JK, Kaitaniem P, Koskinen P (1988) Lipid alterations and decline in the incidence of coronary heart disease in the Helsinki heart study. JAMA 260:641–651
3. Rhoads GG, Gulbrandsen CL, Kagan A (1976) Serum lipoproteins and coronary heart disease in a population study of Hawaii Japanese men. N Engl J Med 294:293–298
4. Gordon T, Castelli WP, Hjortland MC, Kannel WB, Dawber TR (1977) High density lipoprotein as a protective factor against coronary heart disease: the Framingham study. Am J Med 66:707–714
5. Miller NE, Thelle DS, Førde OH, Mjøs OD (1977) The Tromsø heart study: high-density lipoprotein and coronary heart-disease: a prospective case–control study. Lancet 1:964–968
6. Jacobs DR Jr, Mebane IL, Bangdiwala SI, Criqu MH, Tyroler HA (1990) High density lipoprotein cholesterol as a predictor of cardiovascular disease mortality in men and women: the follow-up study of the lipid research clinics prevalence study. Am J Epidemiol 131:32–47
7. Barter PJ, Caulfield M, Eriksson M, Grundy SM, Kastelein JJ, Komajda M, Lopez-Sendon J, Mosca L, Tardif JC, Waters DD, Shear CL, Revkin JH, Buhr KA, Fisher MR, Tall AR, Brewer HB (2007) Effects of torcetrapib in patients at high risk for coronary events. N Engl J Med 357L:2109–2122
8. Cuchel M, Rader DJ (2006) Macrophage reverse cholesterol transport: key to the regression of atherosclerosis? Circulation 113:2548–2555
9. Courtney HS, Zhang YM, Frank MW, Rock CO (2006) Serum opacity factor, a streptococcal virulence factor that binds to apolipoproteins A-I and A-II and disrupts high density lipoprotein structure. J Biol Chem 281:5515–5521
10. Gillard BK, Courtney HS, Massey JB, Pownall HJ (2007) Serum opacity factor unmasks human plasma high density lipoprotein instability via selective delipidation and apolipoprotein A-I desorption. Biochemistry 46:12968–12978
11. Pownall HJ, Courtney HS, Gillard BK, Massey JB (2008) Properties of the products formed by the activity of serum opacity factor against human plasma high density lipoproteins. Chem Phys Lipids 156:45–51
12. Han M, Gillard BK, Courtney HS, Ward K, Rosales C, Khant H, Ludtke SJ, Pownall HJ (2009) Disruption of human plasma high density lipoproteins by streptococcal serum opacity factor requires labile apolipoprotein A-I. Biochemistry 48:1481–1487
13. Picardo M, Massey JB, Kuhn DE, Gotto AM Jr, Gianturco SH, Pownall HJ (1986) Partially reassembled high density lipoproteins effects on cholesterol flux, synthesis, and esterification in normal human skin fibroblasts. Arteriosclerosis 6:434–441
14. Yancey PG, De la Llera-Moya M, Swarnakar S, Monzo P, Klein SM, Connelly MA, Johnson WJ, Williams DL, Rothblat GH (2000) High density lipoprotein phospholipid composition is a major determinant of the bi-directional flux and net movement of cellular free cholesterol mediated by scavenger receptor BI. J Biol Chem 275:36596–36604
15. Tchoua U, Gillard BK, Pownall HJ (2010) HDL superphospholipidation enhances key steps in reverse cholesterol transport. Atherosclerosis 209:430–435
16. Pownall HJ (2006) Detergent-mediated phospholipidation of plasma lipoproteins increases HDL cholesterophilicity and cholesterol efflux via SR-BI. Biochemistry 45(38):11514–11522
17. Steinbrecher UP (1987) Oxidation of human low density lipoprotein results in derivatization of lysine residues of apolipoprotein B by lipid peroxide decomposition products. J Biol Chem 262:3603–3608
18. Mukhamedova N, Escher G, D'Souza W, Tchoua U, Grant A, Krozowski Z, Bukrinsky M, Sviridov D (2008) Enhancing apolipoprotein A-I-dependent cholesterol efflux elevates cholesterol export from macrophages in vivo. J Lipid Res 49:2312–2322
19. Vaughan AM, Oram JF (2006) ABCA1 and ABCG1 or ABCG4 act sequentially to remove cellular cholesterol and generate cholesterol-rich HDL. J Lipid Res 47:2433–2443
20. Lund-Katz S, Hammerschlag B, Phillips MC (1982) Kinetics and mechanism of free cholesterol exchange between human serum high- and low-density lipoproteins. Biochemistry 21:2964–2969
21. Massey JB, Hickson D, She HS, Sparrow JT, Via DP, Gotto AM Jr, Pownall HJ (1984) Measurement and prediction of the rates of spontaneous transfer of phospholipids between plasma lipoproteins. Biochim Biophys Acta 794:274–280
22. Pownall HJ, Bick DL, Massey JB (1991) Spontaneous phospholipid transfer: development of a quantitative model. Biochemistry 30:5696–5700
23. Pownall HJ, Brauchi D, Kilinç C, Osmundsen K, Pao Q, Payton-Ross C, Gotto AM, Ballantyne CM (1999) Correlation of serum triglyceride and its reduction by ω-3 fatty acids with lipid transfer activity and the neutral lipid compositions of high-density and low-density lipoproteins. Atherosclerosis 143:285–297
24. Davidson WS, Rodriguez WV, Lund-Katz S, Johnson WJ, Rothblat GH, Phillips MC (1995) Effects of acceptor particle size on the efflux of cellular free cholesterol. J Biol Chem 270:17106–17113
25. Sankaranarayanan S, Oram JF, Asztalos BF, Vaughan AM, Lund-Katz S, Adorni MP, Phillips MC, Rothblat GH (2009) Effects of acceptor composition and mechanism of ABCG1-mediated cellular free cholesterol efflux. J Lipid Res 50:275–284
26. Wang N, Lan D, Chen W, Matsuura F, Tall AR (2004) ATP-binding cassette transporters G1 and G4 mediate cellular cholesterol efflux to high-density lipoproteins. Proc Natl Acad Sci USA 101:9774–9779
27. Duong PT, Weibel GL, Lund-Katz S, Rothblat GH, Phillips MC (2008) Characterization and properties of pre beta-HDL particles formed by ABCA1-mediated cellular lipid efflux to apo A-I. J Lipid Res 49:1006–1014
28. de la Llera-Moya M, Drazul-Schrader D, Asztalos BF, Cuchel M, Rader DJ, Rothblat GH (2010) The ability to promote efflux via ABCA1 determines the capacity of serum specimens with similar high-density lipoprotein cholesterol to remove cholesterol from macrophages. Arterioscler Thromb Vasc Biol 30:796–801
29. Chen CH, Albers JJ (1982) Distribution of lecithin–cholesterol acyltransferase (LCAT) in human plasma lipoprotein fractions evidence for the association of active LCAT with low density lipoproteins. Biochem Biophys Res Commun 107:1091–1096
30. Aron L, Jones S, Fielding CJ (1978) Human plasma lecithin-cholesterol acyltransferase: characterization of cofactor-dependent phospholipase activity. J Biol Chem 253:7220–7226
31. Havel RJ, Goldstein JL, Brown MS, Bondy PK, Rosenberg LE (1980) Lipoproteins and lipid transport in the context of metabolic disease. Saunders Publishing, Philadelphia, pp 393–494
32. Gillard BK, Rosales C, Lin H-Y, Courtney HS, Pownall HJ (2010) Treatment of human HDL with serum opacity factor increases the rate of cholesterol ester uptake by human hepatoma cells. Biochemistry (in press)

33. Barter PJ, Nicholls S, Rye KA, Anantharamaiah GM, Navab M, Fogelman AM (2004) Antiinflammatory properties of HDL. Circ Res 95(8):764–772
34. Robbesyn F, Garcia V, Auge N, Vieira O, Frisach MF, Salvayre R, Negre-Salvarye A (2003) HDL counterbalance the proinflammatory effect of oxidized LDL by inhibiting intracellular reactive oxygen species rise, proteasome activation, and subsequent NF-kappaB activation in smooth muscle cells. FASEB J 17(6):743–745
35. Tall AR (2008) Cholesterol efflux pathways and other potential mechanisms involved in the athero-protective effect of high density lipoproteins. J Intern Med 263(3):256–273
36. Rader DJ (2007) Mechanisms of disease: HDL metabolism as a target for novel therapies. Nat Clin Pract Cardiovasc Med 4:102–109
37. Tabas I (2005) Consequences and therapeutic implications of macrophage apoptosis in atherosclerosis: the importance of lesion stage and phagocytic efficiency. Arterioscler Thromb Vasc Biol 25:2255–2264
38. Tanigawa H, Billheimer JT, Tohyama J, Fuki IV, Ng DS, Rothblat GH, Rader DJ (2009) Lecithin-cholesterol acyltransferase expression has minimal effects on macrophage reverse cholesterol transport in vivo. Circulation 120:160–169

Keywords Phytoestrogens · Isoflavones · Isoflavone-rich soy · Soy protein · Milk protein · Postprandial metabolism · Postprandial lipemia · Hypertriacylglycerolemia · Cardiovascular disease risk · Triglycerides · Lipid profile

Abbreviations

CVD	Cardiovascular disease
Milk	Milk protein
Soy−	Isoflavone-poor soy
Soy+	Isoflavone-rich soy
TC	Total cholesterol
TAG	Triacylglycerol
Apo B-100	Apolipoprotein B-100
Apo A-I	Apolipoprotein A-I
FDA	Food and Drug Administration
VLDL	Very-low density lipoprotein
AUC	Area under the curve
BMI	Body mass index
HDL-C	High density lipoprotein cholesterol constituent
NEFA	Non-esterified fatty acids
ANOVA	Analysis of variance
LDL-C	Low density lipoprotein cholesterol constituent
RLP-C	Remnant-like particle-cholesterol
TRL	Triacylglycerol rich lipoprotein
LDL	Low density lipoprotein
HDL	High density lipoprotein
LCAT	Lecithin:cholesterol acyltransferase

Introduction

The efficacy of soy product consumption in reducing the risk factors for cardiovascular disease (CVD) owing to constituents beyond vegetarian diet benefits, such as fiber content and the degree of saturation of fat, has recently been questioned [44]. The US Food and Drug Administration (FDA) used a meta-analysis by Anderson et al. [4] as the basis for the food labeling health claim that: "Diets low in saturated fat and cholesterol that include 25 g of soy protein a day may reduce the risk of heart disease". According to the US FDA's health claim report card, this claim receives a letter grade of "A" on account of "significant scientific agreement". While a plethora of randomized control trials demonstrate a salubrious effect of soy protein [3, 32, 57, 62], other studies controvert these benefits [20, 30, 31]. Of particular interest and for comparison are the limited findings in recent meta-analyses regarding the efficacy of soy protein and isoflavone constituents in altering the traditional blood lipid profile (i.e., total cholesterol, low-density lipoprotein cholesterol, high-density lipoprotein cholesterol, and triacylglycerol) [42, 53, 61]. Furthermore, it is not clear whether these modest findings are due to the isoflavone constituents as once postulated, or to other innate components of *Glycine max* (Linnaeus) Merrill such as phytate, saponins, and storage proteins (i.e., conglycinin and glycinin; 7s and 11s globulins, respectively) [13, 18, 21, 28, 55]. Other complications in the soy controversy include differences in the method employed to extract soy protein and processing techniques on the bioavailability of soy constituents (e.g., isoflavones, fiber, saponins, and fat), study design (e.g., parallel vs. crossover), population studied (e.g., normo- vs. hyper-cholesterolemic; ethnicity), geographic area of cultivation, cultivar used, and length of intervention [6, 11, 15, 29, 41, 50, 53]. Moreover, the inter-individual contradistinction of gastrointestinal microflora conversion of daidzein to a more potent isoform, equol, affects the bioavailability and potency (e.g., responders vs. non-responders) of ingested isoflavones [29, 46, 50]. However, this intimation has recently been challenged [7, 16, 54].

Conventional laboratory analysis of blood lipids requires the patient to fast for 8–12 h prior to drawing blood, however, most individuals spend their time ostensibly in a postprandial state, which may partially explain the disparities regarding the salubrious effect of soy [1]. Zilversmit [63] first postulated that the etiology of atherogenesis may be more wholly explained by analyzing triacylglycerol-rich lipoproteins (i.e., chylomicrons + VLDL) and subsequent metabolic remnants. Three decades later, research has progressively expounded upon this intimation by demonstrating that the postprandial state may be an over-looked, independent risk factor for future cardiac events [5, 8, 22, 26, 35, 36, 52]. Intriguingly, several studies have found that triacylglycerol-rich lipoproteins and apolipoprotein B-48 (a constituent protein marker identifying fats that are intestinally derived) are elevated in patients with normal fasting concentrations of TAG but who present with CVD compared with matched healthy subjects after ingesting a high-fat meal (i.e., lipid challenge) [17, 23, 39, 47]. Thus, studies involving soy consumption and its effect on the traditional lipid profile may be missing a more favorable, metabolic processing of exogenous lipids. The first study to evaluate the effect of a soy protein isolate on postprandial remnant-like particles showed no change in fasting lipid concentrations but a significant and more favorable decrease in postprandial, remnant-like cholesterol concentration and area under the curve (AUC) compared with an atherogenic control (i.e., casein); after 3 weeks of supplementation in 11 Japanese males [48]. It is plausible then, that the salubrious effect of soy may be more detectable during the postprandial state rather than following an overnight fast and may be more representative of an individual's normal metabolic state. Therefore, postprandial concentrations of lipoprotein

constituents may be more sensitive and more indicative factors of CVD risk.

The primary purpose of this study was to determine if measuring postprandial concentrations of lipoprotein constituents were more sensitive than the traditional lipid profile for detecting any salubrious effects of consuming soy protein with and without isoflavones. A secondary purpose was to evaluate apolipoprotein B-100 and A-I concentrations as potential mechanisms responsible for any beneficial effects. Since soy studies have mostly been myopic with respect to gender, we sought to describe the effects of Soy− and Soy+ in normolipidemic, sedentary males.

Materials and Methods

Participants

This study was approved by the University at Buffalo's Human Subject's Review Committee. Thirty-five men, with mean ± SD values of 24.2 ± 2.3 years, 175.7 ± 6.6 cm, 73.9 ± 14.6 kg, and 23.8 ± 3.7 kg/m^2 for age, height, weight, and body mass index (BMI), respectively, were recruited to participate voluntarily in a study investigating the effects of soy on CVD risk factors from the Western New York community. Informed consent was obtained prior to participation in the screening process. Participants were included in the study if they met the following criteria: not taking cholesterol reducing medications, BMI between 18 and 26 kg/m^2, non-habitual soy consumers, non-extremist dietary practitioners (i.e., high protein and/or fat intakes), and non-smokers. Participants were also screened for fasting lipid (TC, HDL-C, and TAG) and glucose concentrations using the Cholestech L·D·X® (Cholestech Corporation, Hayward, CA) and Accu-Chek Advantage Analyzers (Roche Diagnostics Corporation, Indianapolis, IN), respectively. A physician recorded the participant's medical history and performed a physical examination to exclude those participants with a known history of cardiovascular, pulmonary, and metabolic diseases.

Anthropometric Measurements

Data for age, height, weight, BMI, body composition, circumferences, and blood pressure were recorded and previously published [45].

Dietary Procedures and Analyses

A double-blind, parallel-arm design was used to compare the effects of a milk protein isolate (Milk, as the control group; atherogenic equivalent) an isoflavone-poor soy protein isolate (Soy−), and an isoflavone-rich soy protein isolate (Soy+) on postprandial lipid and glucose concentrations. Each participant was randomly assigned by a trained research assistant to one of the three protein supplement groups: Milk, Soy− or Soy+. The supplements were donated by The Solae Company (St. Louis, MO, USA) and consisted of 25 g of powdered protein isolate packaged in a vacuum sealed envelope; constituents have previously been reported [45]. The protein powder was mixed with a beverage of the participant's choice (including milk) and taken daily for 28 days. All unused and/or empty packets were returned in the large envelopes to the lab as an indicator of compliance.

A registered dietitian collected 3-day diet records and analyzed them using Nutritionist Pro Software (First Databank, San Bruno, CA, USA); data have been previously published [45].

Test Meal

Participants visited the laboratory, at baseline and approximately 28 days later, and were given a 998.6 kcal (239.5 kJ) liquid meal consisting of approximately 40.0% carbohydrate, 40.2% fat, and 19.8% protein. Ingredients were mixed together in a blender on "liquefy" for 2 min and included 350.6 g of skim milk, 141.034 g of Hershey's Lite Chocolate Syrup© (The Hershey Company, Hershey, PA, USA), 82.775 g of Wegmans' Natural Creamy Peanut Butter© (Wegmans Food Markets, Rochester, NY, USA), and 11.84 g of Optimum Nutrition's chocolate-flavored Whey protein© (Optimum Nutrition, Inc., Aurora, IL, USA). Subjects were given approximately 15 min to consume the liquid meal.

Fasting and Postprandial Blood Draws

Fasting and postprandial blood samples were taken at baseline and approximately 28 days later. Participants visited the laboratory after a 12-h fast and a registered nurse placed an IV-catheter in an antecubital vein. A 7-mm microbore extension was connected to the catheter and secured with sterile Tegaderm™ (3M Health Care, St. Paul, MN). These collectively remained in place for the duration of the laboratory visit (i.e., ~6.5 h). For blood draws, an 18-gauge needle was attached to a 10-mL syringe and approximately 3 mL of blood was placed into a 5-mL serum vacutainer tube; allowed to clot at room temperature. 3 mL of 0.9% saline solution was used between blood draw samples as a flush to prevent coagulation in the microbore extension/catheter setup. 5 mL of blood/saline was drawn and discarded before each blood draw to minimize contamination of the sample from the flush. Serum samples were centrifuged within 30 min of collection at

3,000 r/min (1,875*g*) for 30 min at 4°C (Sorvall RT60000B Refrigerated Centrifuge, Newton, CT). Serum samples were stored at −80 °C until analysis. After participants ingested the test meal, postprandial blood samples were taken at 30, 60, 120, 240, and 360 min using the blood draw procedures aforementioned. Participants were instructed not to consume any food or participate in any moderate to vigorous physical activity during the 6 h of postprandial blood draws. Water was provided ad libitum.

Blood Sample Analysis (Lipids and Glucose)

Blood was analyzed for triacylglycerol (TAG), total cholesterol (TC), non-esterified fatty acids (NEFA), apolipoproteins B-100 and A-I (Apo B-100 and Apo A-I, respectively), and glucose using commercially available kits from Wako Chemicals USA, Inc. (Richmond, VA). In addition, all procedures were followed as directed in the application parameters obtained from Wako for the Cobas Fara centrifugal analyzer for Automated Chemistry Analysis (Model # 22-2081, Roche Diagnostic Systems, Nutley, NJ). All assays for each participant were run in duplicate on the same day with the same reagent batch. External calibrators were included on all assays on every run, and the range of concentrations in the calibration curves encompassed the range of expected sample values. Two controls were used, Accutrol and Cardiolipid, that were run ten times throughout the duration of each test to ensure intra-assay reproducibility.

Triacylglycerol

TAG was measured by the enzymatic colorimetric endpoint method (Kit #s 999-37491 and 995-37591). Serum plasma samples were first combined with the Enzyme color A reagent (50 mmol/L Good's buffer, pH 7.0 containing 0.45 mmol/L *N*-(2-hydroxy-3-sulfopropyl)-3,5-dimethoxyaniline, 30 IU/mL glycerol kinase from *Cellulomonas* sp., 4.0 mmol/L adenosine-5′-triphosphate, 3.8 IU/mL glycerol-3-phosphate oxidase from *Streptococcus* sp., 200 IU/mL catalase from bovine liver and 2.4 IU/mL ascorbate oxidase from *Acremonium* sp.) to decompose free glycerol so as not to interfere with the assay. Enzyme color B reagent (50 mmol/L Good's buffer, pH 7.1 containing 150 IU/mL lipoprotein lipase (LPL) from *Pseudomonas* sp., 13.5 IU/mL peroxidase from horseradish, 3.4 mmol/L 4-aminoantipyrine and 0.1% sodium azide) was then added to hydrolyze TAG into glycerol and free fatty acids by LPL. The liberated glycerol was phosphorylated by adenosine-5′-triphosphate and underwent oxidation by glycerol-3-phosphate oxidase which resulted in the release of hydrogen peroxide. *N*-(2-hydroxy-3-sulfopropyl)-3,5-dimethoxyaniline and 4-aminoantipyrine underwent quantitative oxidative condensation catalyzed by peroxidase due to the presence of hydrogen peroxide. The resultant blue pigment from these reactions was measured for absorbance and was directly correlated with TAG concentrations.

Total Cholesterol

TC concentrations were measured by using the enzymatic colorimetric method (Kit # 276-64909). Serum samples were combined with a working color reagent (0.15/150 M Tris buffer solution, 0.13 U/mL cholesterol oxidase, 0.13 U/mL cholesterol ester hydrolase, 2.4 U/mL peroxidase, and 0.015% 4-aminoantipyrine) and allowed to incubate for 5 min at 37°C. The cholesterol esters in the serum were hydrolyzed to free cholesterol and fatty acids in a reaction catalyzed by cholesterol ester hydrolase. The cholesterol produced and the free cholesterol already present in the serum were oxidized in a reaction catalyzed by cholesterol oxidase that generated hydrogen peroxide. The hydrogen peroxide formed participated in quantitative oxidative condensation between *p*-chlorophenol and 4-aminoantipyrine in the presence of peroxidase. The product of the reaction was a red quinone pigment. The total amount of cholesterol in the test sample was determined by measurement of the absorbance of the red color at its maximal absorption wavelength of 505 nm.

Non-esterified Fatty Acids

NEFA was measured using the enzymatic colorimetric method (Kit # 994-75409E). Serum samples were first combined with color reagent A (acyl-coenzyme A synthetase, ascorbate oxidase, coenzyme A (CoA), adenosine triphosphate, 4-aminoantipyrine, 0.05 mol/L phosphate buffer, 3 mmol/L magnesium chloride, surfactant, and stabilizers) and incubated for 10 min at 37 °C. NEFA in serum, when treated with acyl-CoA synthetase in the presence of adenosine triphosphate, magnesium cations and CoA, formed the thiol esters of CoA known as acyl-CoA as well as the byproducts adenosine monophosphate and pyrophosphate. The samples/solutions were then mixed with color reagent B [acyl-coenzyme A oxidase, peroxidase and 1.2 mmol/L 3-methyl-*N*-ethyl-*N*-(*β*-hydroxy- ethyl)-aniline] and incubated for 10 min at 37 °C. In the second portion of the procedure, the acyl-CoA was oxidized by added acyl-CoA oxidase to produce hydrogen peroxide which in the presence of added peroxidase allowed the oxidative condensation of 3-methyl-*N*-ethyl-*N*-(*β*-hydroxy-ethyl)-aniline with 4-aminoantipyrine to form a purple colored adduct with an absorption maximum at 550 nm. Hence, the amount of NEFA in the sample was determined from the optical density measured at 550 nm.

Ascorbic acid existing in the sample would be expected to cause significant interference due to its biological role as an antioxidant and known ability to react with hydrogen peroxide. Therefore, ascorbate oxidase was added to the reaction mixture at the outset to remove all ascorbic acid from the sample.

Apolipoprotein B-100

Apolipoprotein B-100 was measured by a turbidimetric immunoassay procedure (Kit # 993-27401). Serum samples were mixed with a buffer (100 mmol/L phosphate buffer and 0.1% sodium azide) and an anti-human antibody (11.5 mg Ag/mL anti-human apolipoprotein B isolated from goat and 0.1% sodium azide) specific for apo B-100. The binding of apo B-100 to the anti-human antibody yielded an insoluble aggregate that caused increased turbidity. The degree of turbidity was measured optically and was proportional to the amount of apo B-100 in the sample.

Apolipoprotein A-I

Apolipoprotein A-I was measured by a turbidimetric immunoassay procedure (Kit # 991-27201). Serum samples were combined with a buffer (100 mmol/L phosphate buffer and 0.1% sodium azide) and an anti-human apo A-I antibody (1.15 mg Ag/mL prepared from goat and 0.1% sodium azide) that yielded an insoluble aggregate that caused increased turbidity. The extent of the turbidity was then measured optically and was proportional to the amount of apo A-I in the sample.

Glucose

Glucose was measured by using an enzymatic colorimetric method (Kit # 994-90902). Serum samples were combined with the working reagent (60 mmol/L phosphate buffer, 5.3 mmol/L phenol, 0.13 U/mL mutarotase, 9.0 U/mL glucose oxidase, 0.65 U/mL peroxidase, 0.50 mmol/L 4-aminoantipyrine, and 2.7 U/L ascorbate oxidase) and incubated for 5 min at 37 °C. The equilibrium of D-glucose in solution was maintained in the ratio of α-D-glucose 36.5% and β-D-glucose 63.5%. Glucose oxidase reacted only with β-D-glucose. The existing α-D-glucose in the sample was converted rapidly to the β-isomer by the action of mutarotase and was then oxidized by glucose oxidase to produce hydrogen peroxide. In the absence of mutarotase, the reaction proceeded slowly because β-D-glucose was first consumed by glucose oxidase as α-D-glucose was gradually converted to β-D-glucose. When mutarotase was added, α-D-glucose was rapidly converted to β-D-glucose, so that glucose oxidase action was facilitated. The hydrogen peroxide produced induced oxidative condensation between phenol and 4-aminoantipyrine in the presence of peroxidase, so that a red color was produced. The amount of glucose contained in the test sample was determined by measuring the absorbance of the red color.

Area Under the Curve

AUC was calculated in increments to determine temporal differences. The summation of intervals (i.e., 0 + 30 min; 30 + 60 min; 60 + 120 min; 120 + 240 min; 240 + 360 min) was divided by two followed by the subtraction of fasting values to normalize the data. To normalize the data for hours, incremental AUC values were multiplied by 0.5, 1.0, and 2.0 for the 0 + 30 min and 30 + 60 min intervals, the 60 + 120 min interval, and the 120 + 240 min and 240 + 360 min intervals, respectively. The total AUC was calculated as the summation of normalized intervals.

Statistics

A general linear model, two-way repeated measures analysis of variance (ANOVA) was used to determine significant differences in variables listed in Table 1 and Figs. 1, 2, and 3 after protein supplementation. The Bonferroni (all pair-wise) multiple comparison test was used to determine the main effects of diet collapsed across time (Milk pre plus Milk post vs. Soy− pre plus Soy− post vs. Soy+ pre plus Soy+ post) and time collapsed across diet (Milk pre plus Soy− pre plus Soy+ pre vs. Milk post plus Soy− post plus Soy+ post) and to determine any diet by time interactions (pre vs. post within groups). A p value <0.05 was considered statistically significant. The data were analyzed with Number Cruncher Statistical Systems software (NCSS 2000, Kaysville, UT). Protein group identification was not revealed to the principle investigator until after they performed all biochemical and statistical analyses.

Results

Participants

Owing to poor study compliance and subsequent data outliers, 5 participants were eliminated leaving 9, 11, and 10 participants for the Milk, Soy−, and Soy+ groups, respectively.

Postprandial Serum Concentrations

Baseline and post-intervention data are presented in Table 1 and Figs. 1, 2, and 3. After 4 weeks of supplementation with 25 g/day of Soy− protein, TAG increased by 90.7 mg/dL at 240 min and TAG total AUC increased

Table 1 Mean ± SEM values for blood lipid and glucose analyses in 30 sedentary males

	Milk ($n = 9$)		Soy− ($n = 11$)		Soy+ ($n = 10$)	
	Pre (M ± SEM)	Post (M ± SEM)	Pre (M ± SEM)	Post (M ± SEM)	Pre (M ± SEM)	Post (M ± SEM)
Triacylglycerol (TAG) (mg/dL)						
Fasting	100.0 ± 23.1	92.4 ± 16.4	115.6 ± 24.5	125.1 ± 23.8	91.1 ± 11.9	95.3 ± 25.2
30-min	112.4 ± 22.9	112.3 ± 19.8	108.0 ± 23.8	135.3 ± 28.5	115.4 ± 15.9	110.7 ± 23.6
60-min	122.2 ± 21.0	137.6 ± 26.3	144.0 ± 31.9	157.3 ± 26.6	122.9 ± 14.2	119.8 ± 22.0
120-min	192.2 ± 32.3	174.8 ± 28.4	183.2 ± 26.0	216.4 ± 19.9	185.4 ± 24.6	171.2 ± 23.8
240-min	217.1 ± 51.5^{ab}	221.7 ± 53.9^{ab}	202.5 ± 38.1^{a}	293.2 ± 42.3^{b}	253.3 ± 30.6^{ab}	211.4 ± 33.3^{ab}
360-min	140.4 ± 40.9	151.3 ± 45.1	149.5 ± 48.7	220.2 ± 44.4	174.8 ± 28.6	140.4 ± 31.8
Total AUC	435.5 ± 101.2^{ab}	484.7 ± 131.5^{ab}	326.3 ± 77.0^{a}	597.3 ± 69.1^{b}	564.4 ± 89.5^{ab}	417.3 ± 54.7^{ab}
Total cholesterol (TC) (mg/dL)						
Fasting	182.5 ± 15.0	165.1 ± 9.7	189.6 ± 18.1	189.7 ± 13.1	166.9 ± 24.0	194.0 ± 13.9
30-min	194.1 ± 19.1	170.4 ± 14.0	165.0 ± 19.6	185.0 ± 14.0	182.2 ± 16.4	187.9 ± 11.1
60-min	176.5 ± 15.7	183.0 ± 17.5	179.8 ± 16.9	187.4 ± 13.1	169.8 ± 14.2	189.2 ± 16.6
120-min	194.7 ± 18.6	161.8 ± 9.7	179.6 ± 13.4	176.6 ± 14.8	175.9 ± 18.5	199.3 ± 16.7
240-min	192.7 ± 21.1	182.8 ± 13.8	167.8 ± 13.1	165.7 ± 15.9	191.0 ± 21.3	203.4 ± 11.1
360-min	192.1 ± 19.5	188.1 ± 14.5	175.0 ± 14.9	184.1 ± 12.5	188.6 ± 19.1	188.3 ± 12.9
Non-esterified fatty acids (NEFA) (mg/dL)^{A}						
Fasting	0.31 ± 0.05	0.37 ± 0.09	0.57 ± 0.13	0.55 ± 0.14	0.38 ± 0.08	0.36 ± 0.06
30-min	0.35 ± 0.08	0.24 ± 0.05	0.33 ± 0.05	0.28 ± 0.04	0.27 ± 0.05	0.32 ± 0.06
60-min	0.27 ± 0.04	0.23 ± 0.03	0.21 ± 0.03	0.19 ± 0.03	0.21 ± 0.03	0.24 ± 0.04
120-min	0.31 ± 0.03	0.31 ± 0.05	0.30 ± 0.03	0.28 ± 0.05	0.24 ± 0.03	0.28 ± 0.03
240-min	0.49 ± 0.05	0.36 ± 0.05	0.44 ± 0.06	0.49 ± 0.08	0.43 ± 0.05	0.40 ± 0.06
360-min*	0.65 ± 0.07	0.53 ± 0.06	0.61 ± 0.07	0.60 ± 0.09	0.64 ± 0.08	0.47 ± 0.05
Apolipoprotein B-100 (mg/dL)						
Fasting	79.6 ± 8.0	69.5 ± 7.2	70.3 ± 3.4	71.2 ± 2.6	79.4 ± 5.6	75.9 ± 4.1
30-min	79.6 ± 8.4	70.2 ± 7.1	68.0 ± 4.4	67.8 ± 3.9	79.1 ± 6.2	76.2 ± 5.9
60-min	80.4 ± 7.6	76.4 ± 6.2	70.9 ± 3.6	68.9 ± 4.3	77.3 ± 5.6	68.1 ± 7.6
120-min	81.3 ± 8.1	77.3 ± 5.6	69.1 ± 3.6	73.6 ± 2.2	76.8 ± 6.1	77.5 ± 5.5
240-min	81.2 ± 7.4^{b}	69.0 ± 7.0^{ab}	66.0 ± 2.7^{a}	73.1 ± 2.7^{ab}	77.7 ± 5.9^{b}	79.6 ± 5.0^{b}
360-min	80.9 ± 7.2	74.1 ± 6.0	70.0 ± 5.2	71.4 ± 3.6	77.8 ± 4.8	73.5 ± 4.8
TAG/apolipoprotein B-100 ratio						
Fasting	1.2 ± 0.2	1.3 ± 0.3	1.6 ± 0.3	1.7 ± 0.3	1.2 ± 0.1	1.3 ± 0.3
30-min	1.4 ± 0.2	1.6 ± 0.4	1.6 ± 0.3	2.0 ± 0.3	1.5 ± 0.2	1.4 ± 0.3
60-min	1.5 ± 0.2	1.8 ± 1.1	2.0 ± 0.3	2.3 ± 0.3	1.7 ± 0.2	2.5 ± 0.3
120-min	2.4 ± 0.3	2.3 ± 0.3	2.6 ± 0.2	2.9 ± 0.3	2.5 ± 0.2	2.2 ± 0.2
240-min	2.5 ± 0.4	3.1 ± 0.6	3.0 ± 0.5	3.9 ± 0.5	3.4 ± 0.3	2.7 ± 0.5
360-min	1.6 ± 0.4	1.9 ± 0.4	2.1 ± 0.6	3.0 ± 0.5	2.1 ± 0.2	1.8 ± 0.4
Apolipoprotein A-I (mg/dL)^{B}						
Fasting	170.7 ± 7.6	170.1 ± 7.9	174.0 ± 7.7	180.1 ± 6.6	188.7 ± 7.5	183.9 ± 10.2
120-min	177.9 ± 4.7	182.8 ± 7.0	171.6 ± 5.6	180.6 ± 7.2	182.4 ± 3.9	187.0 ± 9.6
240-min	178.1 ± 7.5^{ab}	149.8 ± 7.2^{a}	166.8 ± 6.1^{ab}	179.2 ± 5.1^{ab}	185.5 ± 6.5^{ab}	189.7 ± 11.4^{b}
360-min	171.7 ± 5.3	176.5 ± 6.6	169.6 ± 6.4	180.6 ± 8.1	182.1 ± 6.4	181.0 ± 6.4
Glucose (mg/dL)						
Fasting	97.0 ± 3.8	96.4 ± 6.0	94.4 ± 4.2	94.5 ± 3.1	83.1 ± 4.8	93.8 ± 3.1
30-min	109.6 ± 4.3	89.2 ± 5.7	88.8 ± 6.5	97.8 ± 8.3	107.6 ± 6.2	100.1 ± 4.8
60-min	91.2 ± 3.7	90.1 ± 5.6	86.1 ± 5.3	91.2 ± 6.4	89.9 ± 7.0	87.2 ± 5.3
120-min	98.6 ± 3.3	86.3 ± 6.2	90.1 ± 5.6	95.1 ± 4.8	92.1 ± 3.7	100.6 ± 5.0

Table 1 continued

	Milk ($n = 9$)		Soy− ($n = 11$)		Soy+ ($n = 10$)	
	Pre (M ± SEM)	Post (M ± SEM)	Pre (M ± SEM)	Post (M ± SEM)	Pre (M ± SEM)	Post (M ± SEM)
240-min	101.4 ± 6.2	96.1 ± 6.7	97.5 ± 3.6	98.0 ± 3.4	103.3 ± 3.8	108.1 ± 6.5
360-min	94.4 ± 3.3	95.1 ± 4.6	98.0 ± 6.5	96.6 ± 3.3	95.8 ± 5.7	95.1 ± 3.9

Values with the same letters are not significantly different ($p < 0.05$)

Soy− Isoflavone-poor soy protein isolate, *Soy*+ Isoflavone-rich soy protein isolate

[A] Values with an * are significantly different from pre values; main effect of time ($p < 0.05$)

[B] Data for the 30 and 60 min time points are unavailable

by 271.1 mg/dL ($p = 0.012648$ and $p = 0.007190$, respectively; pre vs. post within group). NEFA decreased by 0.1 mg/dL at 360 min after protein supplementation ($p = 0.025743$; main effect of time collapsed across diet). Soy+ supplementation resulted in higher apo A-I at 240 min compared with the Milk group (189.7 vs. 149.8 mg/dL; $p = 0.044964$; post vs. post between groups).

Discussion

This study examined the effect of 28 days of Milk, Soy−, and Soy+ supplementation on select fasting and postprandial blood lipid and glucose concentrations in normocholesterolemic, sedentary males. Our data support the hypothesis that the postprandial state is more sensitive than the traditional lipid profile for detecting changes associated with soy consumption in this study population, which is in concurrence with previous data [48]. While fasting blood lipid and glucose concentrations did not change significantly, postprandial TAG concentration was surprisingly higher after Soy− consumption. In addition, there was a trend for reduced postprandial TAG concentration after Soy+ consumption. These data suggest that the dearth of isoflavones in Soy− may deleteriously alter postprandial processing of TAG such that over time risk for CVD potentially increases. Together, with a previous report, our data show support for measuring blood lipids in a postprandial state in order to detect changes with soy ingestion [48]. However, these changes are minimal at best in the normocholesterolemic, sedentary male, which provides credence to a recent statement by the American Heart Association; which iterated that the ingestion of soy products provides little additional, salubrious benefit beyond the typical vegetarian diet [44].

Postprandial metabolism has been increasingly recognized as an important, but crudely defined tool in the assessment of CVD risk factors. The well-established traditional lipid profile standardizes CVD risk factors by utilizing a fasting blood sample which controls for diurnal flux in plasma lipids, utilizes the Friedewald formula for LDL-C estimation, and compares patient samples to population norms [8]. While these analytical attributes are desirable, most individuals spend the majority of their day processing exogenous nutrients, which supports the ideology that postprandial metabolism may be more sensitive to their usual metabolic state and therefore might allude to occult CVD risk factors. Recent large, prospective studies and others support the foregoing intimation by demonstrating that postprandial TAG concentration was associated with an increased risk for CVD and a subsequent cardiovascular incident independent of the traditional lipid profile [5, 14, 22, 33, 35]. In contrast to fasting studies evaluating TAG's role in CVD risk factor assessment, postprandial TAG concentration maintained a strong, prognostic relationship with CVD despite adjusting for fasting TC and HDL-C concentrations [5, 10, 25, 33]. In the first study to analyze the postprandial state in conjunction with a soy treatment, Shige et al. [48] reported that remnant-like particle-cholesterol (RLP-C) was significantly reduced compared with a casein treatment after 3 weeks of supplementation in 11 Japanese males. Additionally, AUC for RLP-C decreased by 7.7 mg/dL (0.20 mmol/L) after the soy protein treatment compared to the casein treatment which increased significantly by 5.4 mg/dL (0.14 mmol/L). Since RLP-C has been demonstrated to be an independent predictor of future cardiac events, these data suggest that soy protein may reduce this innate risk [24]. In the present study, we did not observe any significant changes in fasting or postprandial cholesterol concentrations. However, it is important to note that we did not discern between TRLs containing Apo B-48 (intestinally derived) and Apo B-100 (hepatically derived) lipoproteins, which limits the analytical density range of these lipoproteins and thus may ameliorate our sensitivity to the favorable changes observed by Shige [24]. In contrast to Shige, we observed a significant increase of 83% from baseline values in AUC postprandial TAG concentration after Soy− consumption but not in the Milk or Soy+ fed groups; suggesting that the absence of isoflavones in this supplement leads to undesirable changes in TAG and may have clinical implications for CVD. It is noteworthy that the Soy+ group

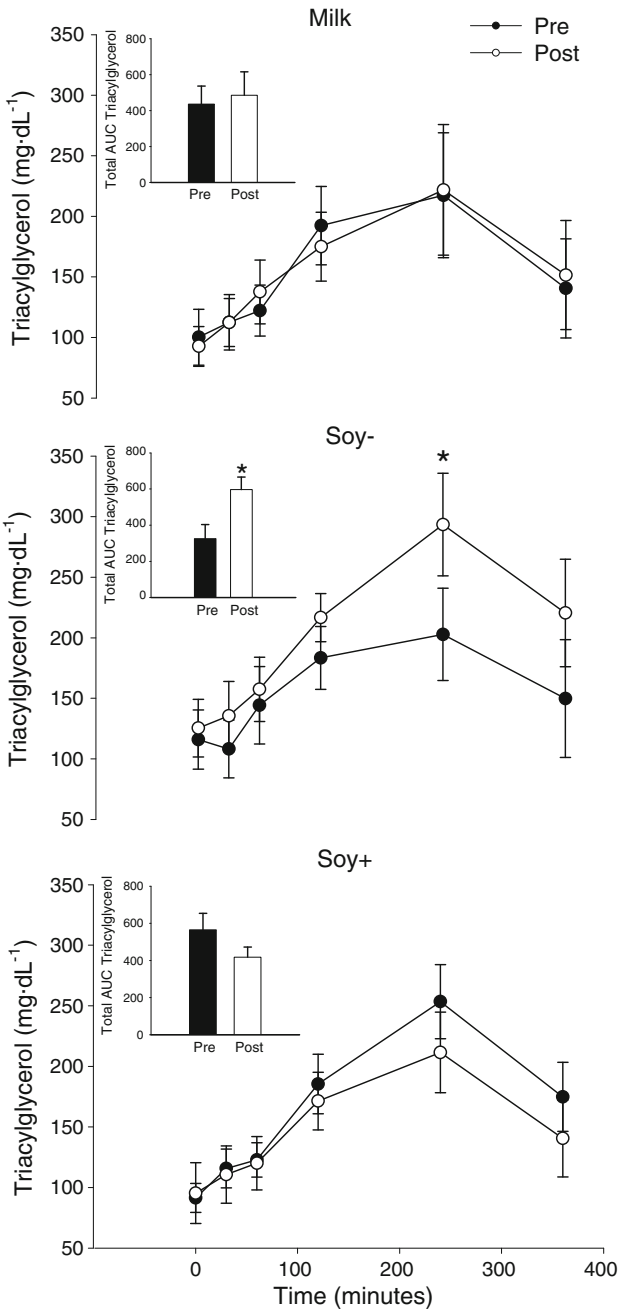

Fig. 1 Triacylglycerol serum concentration after a 12-h fast and ingestion of a high calorie mixed meal before and after 28 days of supplementation with a milk protein isolate (*Milk*), isoflavone-poor soy protein isolate (*Soy*−) or an isoflavone-rich soy protein isolate (*Soy*+) ($n = 9$, $n = 11$, and $n = 10$, respectively). Values are the average of 30 sedentary males ± the standard error of the mean. Significant difference between pre and post values ($^*p < 0.05$)

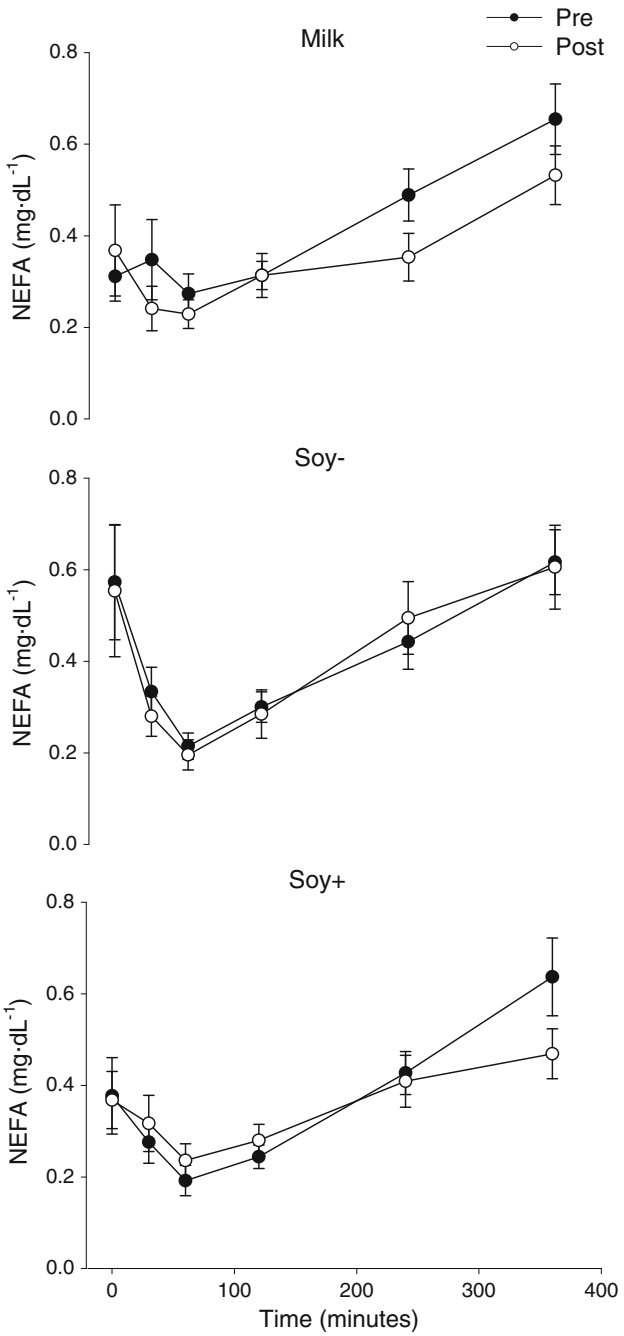

Fig. 2 Non-esterified fatty acid (*NEFA*) serum concentration after a 12-h fast and ingestion of a high calorie mixed meal before and after 28 days of supplementation with a milk protein isolate (*Milk*), isoflavone-poor soy protein isolate (*Soy*−) or an isoflavone-rich soy protein isolate (*Soy*+) ($n = 9$, $n = 11$, and $n = 10$, respectively). Values are the average of 30 sedentary males ± the standard error of the mean

showed a decreasing trend of 26% in AUC postprandial TAG concentration. Although not statistically significant, these data are suggestive of a modulating role for soy isoflavones as previously reported [7]. Furthermore, these differences were significantly greatest 240 min after ingestion of the test meal with a similar trend at 360 min. Cohn et al. [9] reported that TAG concentration peaks approximately 3–4 h post-absorption of a singular meal and returns to fasting concentrations within 6–8 h in disease-free individuals, which was nearly observed in the present study.

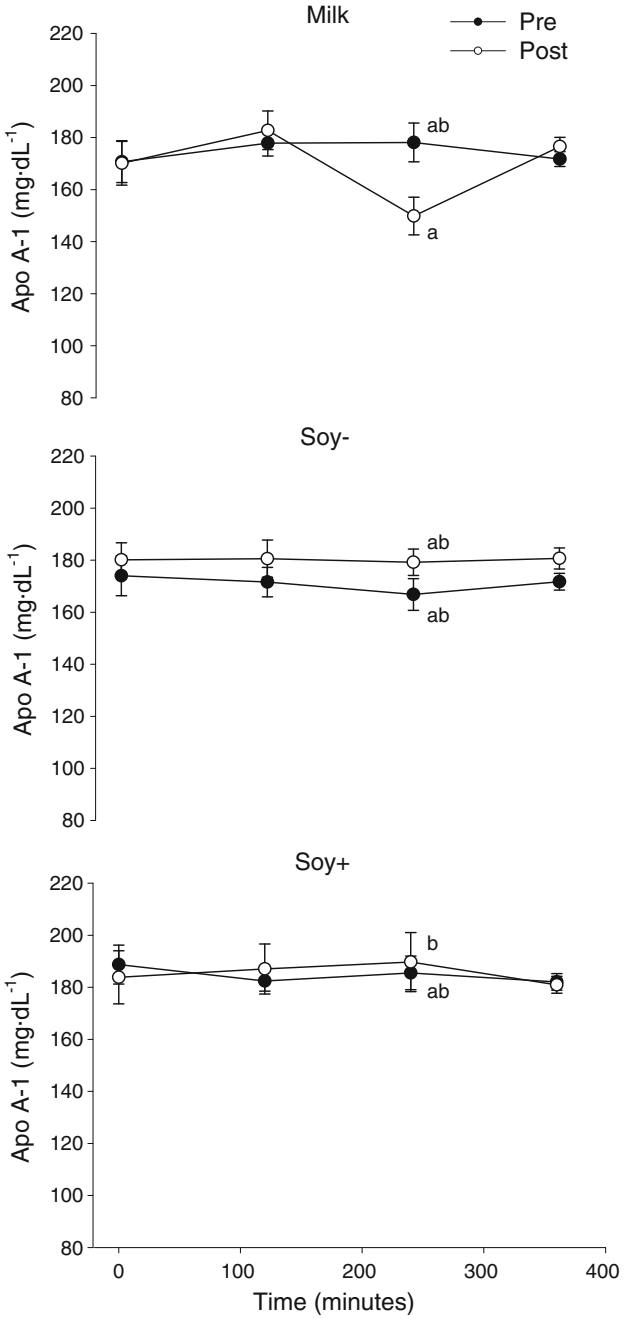

Fig. 3 Apolipoprotein A-I serum concentration after a 12-h fast and ingestion of a high calorie mixed meal before and after 28 days of supplementation with a milk protein isolate (*Milk*), isoflavone-poor soy protein isolate (*Soy*−) or an isoflavone-rich soy protein isolate (*Soy*+) ($n = 9$, $n = 11$, and $n = 10$, respectively). Values are the average of 30 sedentary males ± the standard error of the mean. Values with the same letters are not statistically significant ($p < 0.05$)

It is interesting to note that we observed a significant decrease of 15.5% in NEFA at 360 min after protein consumption regardless of the protein source. Interpretation of this observation is not clear, however, a discussion regarding dietary intake may partially explain this finding. Collection of dietary data in free-living participants is desirable but presents an immutable challenge of study compliance. Previously, we reported dietary analysis data on the current study population and the difficulty in interpretation owing to poor study compliance with recording data; thus, we were forced to analyze our results with ten fewer participants compared with other reported data [45]. Despite this limitation, it is interesting to note that Soy− increased their saturated fat intake by 14.2%, as a percentage of the total identifiable lipid, and 3.0%, if calculated as a percentage of total kilocalories after supplementation. It is putative that a higher than recommended chronic ingestion of saturated fat results not only in higher fasting levels of TAG but also exacerbates the postprandial response in TAG [12, 19, 27, 34, 56, 58]. Therefore, it is plausible that the significant increase observed in postprandial TAG in Soy− may be due to higher exogenous consumption of foods containing a greater proportion of saturated fat. We also reported that saturated fat intake, calculated as a percentage of the total identifiable lipid, increased by 4.0% after protein supplementation regardless of the protein source in the current study population. These data may imply that the release of NEFA from adipose tissue (i.e., lipolysis) was reduced at 360 min owing to greater amounts of available exogenous fats. It is important to reiterate that these interpretations and any subsequent clinical significance are mere hypotheses based on the available literature to date and warrant better control for future investigation.

Apolipoproteins B-48 and B-100 are substantive constituents of chylomicrons and VLDL and LDL particles, respectively. Chylomicrons are intestinally derived lipoproteins that contain one apolipoprotein B-48 per chylomicron particle and serves as the hepatic cell receptor ligand [38]. Similarly, one apolipoprotein B-100 is found per VLDL and LDL particle and functions as a cell receptor ligand [38]. As such, studies have used apolipoprotein B-48 and B-100 as direct measurement of the number of chylomicron, VLDL and LDL particles in circulation [40, 51]. Since the penetration of the endothelium by lipoprotein particles is a gradient-driven process, fewer, potentially atherogenic particles would succumb to oxidation and therefore subsequent vascular damage and succeeding risk for CVD diminished [59]. In the present study we did not observe any clinically remarkable changes in apolipoprotein B-100, which is in agreement with our previously published nuclear magnetic resonance (NMR) data [45].

TAG concentration during the postprandial state is dependent upon the total amount of ingested lipid, hepatic and lipoprotein lipase activity, and LDL receptor expression [38]. As previously discussed, TRLs contain one apolipoprotein ligand per lipoprotein particle which binds

to the LDL receptor and results in the physical removal of the particle from circulation [37, 43]. Hepatic and lipoprotein lipase serve to reduce the size of these particles in circulation by hydrolyzing the TAG into its constituents, glycerol and fatty acids, and subsequently results in the delivery of the fatty acids to tissues such as muscle and adipose [60]. While direct measurement of lipoprotein particle size and number is highly desirable, the size of TRL particles can be inferred via the TAG to apolipoprotein ratio [2]. In the present study, we did not observe a significant difference in the TAG/apolipoprotein B-100 ratio but a decreasing trend was apparent 240 min postprandially. We speculate that hepatic and lipoprotein lipase activities may have been altered owing to Soy− and Soy+ consumption resulting in the respective, observed TAG concentrations. Unfortunately, it is difficult to quantify TAG concentration and lipase activity concomitantly without introducing analytical error and therefore we were unable to do so in the present study. Previously, we reported that hepatic lipase concentration increased by 19.2% after Soy− consumption in a fasted state which resulted in an increase in the number of small, dense HDL particles (TAG-rich from interacting with TRLs) which would theoretically increase CVD risk [45]. It is plausible that hepatic and/or lipoprotein lipase activity may be altered as a result of isoflavone presence in products containing soy protein resulting in changes similar to those observed in the present study. The dearth of information regarding isoflavone effect on lipid remodeling via hepatic and lipoprotein lipase activity warrants further investigation as a potential mechanism.

Apolipoproteins A-I and A-II constitute the major structural protein of HDL particles and play a key role in HDL metabolism. In particular, apolipoprotein A-I serves as the select acceptor of cell cholesterol, as a lecithin:cholesterol acyltransferase (LCAT) cofactor, as a promoter of reverse cholesterol transport, and as a ligand for the HDL receptor [49]. Although we did not see any fasting or postprandial changes in total cholesterol, we did observe that apolipoprotein A-I was significantly higher by 21% in Soy+ post supplementation compared with Milk post supplementation at 240 min after the test meal ingestion. Furthermore, apolipoprotein A-I concentration after Milk supplementation showed a non-significant decreasing trend of 27.7% at 240 min after the test meal ingestion (i.e., pre vs. post within group difference). We speculate that these data may indicate lower HDL particle concentration and subsequent cholesterol constituent, which is in agreement with the atherogenic diet. It is noteworthy that TC showed a non-significant decreasing trend after Milk supplementation, which seemingly supports our data; however, caution is warranted in this interpretation as we did not measure HDL-C or HDL particle size and number in the postprandial state. Future studies are needed to elucidate lipoprotein particle remodeling in the postprandial state as a result of soy consumption utilizing NMR analysis of lipoprotein particle size and number.

In summary, we have demonstrated that the postprandial state is a viable and more sensitive indicator of CVD risk compared with the traditional lipid profile with respect to the potential salubrious effects of consuming soy protein for 28 days in sedentary, normocholesterolemic males. Our data suggest that soy isoflavones may play a role in postprandial TAG processing and that removing these phytochemicals from soy products may obviate any cardioprotective effect and may even have a deleterious consequence if ingested chronically. However, these data and subsequent interpretations are limited and should be viewed as preliminary data owing to the low number subjects within each group. Further research is warranted to clarify the use of the postprandial state as a means of investigating potential cardio-protective effects of soy protein consumption on TAG processing after ingestion of a test meal.

Acknowledgments The authors would like to thank The Solae Company (St. Louis, MO, USA) for donating the protein supplements used in this study. Special gratitude is warranted to our colleagues Amy Miracle and Jack Young for their input in the final review of this manuscript.

References

1. (2002) National Cholesterol Education Program (NCEP) Expert Panel on detection, evaluation, and treatment of high blood cholesterol in adults (Adult Treatment Panel III). Third report of the national cholesterol education program (NCEP) Expert Panel on detection, evaluation, and treatment of high blood cholesterol in adults (Adult Treatment Panel III) final report. Circulation 106:3143–3421
2. Adiels M, Packard C, Caslake MJ, Stewart P, Soro A, Westerbacka J, Wennberg B, Olofsson S-O, Taskinen M-R, Borén J (2005) A new combined multicompartmental model for apolipoprotein B-100 and triglyceride metabolism in VLDL subfractions. J Lipid Res 46:58–67
3. Allen JK, Becker DM, Kwiterovich PO, Lindenstruth KA, Curtis C (2007) Effect of soy protein-containing isoflavones on lipoproteins in postmenopausal women. Menopause 14:106–114
4. Anderson JW, O'Neal DS, Riddell-Mason S, Floore TM, Dillom DW, Oeltgen PR (1995) Postprandial serum glucose, insulin, and lipoprotein responses to high- and low-fiber diets. Metabolism 44:848–854
5. Bansal S, Buring JE, Rifai N, Mora S, Sacks FM, Ridker PM (2007) Fasting compared with nonfasting triglycerides and risk of cardiovascular events in women. J Am Med Assoc 298:309–316
6. Caldwell CR, Britz SJ, Mirecki RM (2005) Effect of temperature, elevated carbon dioxide, and draught during seed development on the isoflavone content of dwarf soybean [*Glycine max* (L.) Merrill] grown in controlled environments. J Agric Food Chem 53:1125–1129
7. Cederroth CR, Nef S (2009) Soy, phytoestrogens and metabolism: a review. Mol Cell Endocrinol 304:30–42

8. Cohn JS (2006) Postprandial lipemia and remnant lipoproteins. Clin Lab Med 26:773–786
9. Cohn JS, McNamara JR, Cohn SD, Ordovas JM, Schaefer EJ (1988) Postprandial plasma lipoprotein changes in human subjects of different ages. J Lipid Res 29:469–479
10. Collaboration APCS (2004) Serum triglycerides as a risk factor for cardiovascular diseases in the Asia-Pacific Region. Circulation 110:2678–2686
11. Coward L, Smith M, Kirk M, Barnes S (1998) Chemical modification of isoflavones in soy foods during cooking and processing. Am J Clin Nutr 68:1486s–1491s
12. De Bruin TWA, Brouwer B, Trip ML, Jansen H, Erkelens DW (1993) Different postprandial metabolism of olive oil and soybean oil: a possible mechanism of the high-density lipoprotein conserving effect of olive oil. Am J Clin Nutr 58:477–483
13. Dewell A, Hollenbeck PL, Hollenbeck CB (2006) Clinical review: a critical evaluation of the role of soy protein and isoflavone supplementation in the control of plasma cholesterol concentrations. J Clin Endocrinol Metab 91:772–780
14. Freiberg JJ, Tybjaerg-Hansen A, Jensen JS, Nordestgaard BG (2008) Nonfasting triglycerides and risk of ischemic stroke in the general population. J Am Med Assoc 300:2142–2152
15. Friedman M, Brandon DL (2001) Nutritional and health benefits of soy proteins. J Agric Food Chem 49:1069–1086
16. Gardner CD, Messina M, Kiazand A, Morris JL, Franke AA (2007) Effect of two types of soy milk and dairy milk on plasma lipids in hypercholesterolemic adults: a randomized trial. J Am Coll Nutr 26:669–677
17. Ginsberg HN, Jones J, Blaner WS, Thomas A, Karmally W, Fields L, Blood D, Beg MD (1995) Association of postprandial triglyceride and retinyl palmitate responses with newly diagnosed exercise-induced myocardial ischemia in middle-aged men and women. Arterioscler Thromb Vasc Biol 15:1829–1838
18. Hanson LN, Engelman HM, Alekel DL, Schalinske KL, Kohut ML, Reddy MB (2006) Effects of soy isoflavones and phytate on homocysteine, C-reactive protein, and iron status in postmenopausal women. Am J Clin Nutr 84:774–780
19. Harris WS, Connor WE, Alam N, Illingworth DR (1988) Reduction of postprandial triglyceridemia in humans by dietary n-3 fatty acids. J Lipid Res 29:1451–1460
20. Ho SC, Chen YM, Ho SS, Woo JL (2007) Soy isoflavone supplementation and fasting serum glucose and lipid profile among postmenopausal Chinese women: a double-blind, randomized, placebo-controlled trial. Menopause 14:905–912
21. Hooper L, Kroon PA, Rimm EB, Cohn JS, Harvey I, Le Cornu KA, Ryder JJ, Hall WL, Cassidy A (2008) Flavonoids, flavonoid-rich foods, and cardiovascular risk: a meta-analysis of randomized controlled trials. Am J Clin Nutr 88:38–50
22. Kannel WB, Vasan RS (2009) Triglycerides as vascular risk factors: new epidemiologic insights. Curr Opin Cardiol 24:345–350
23. Karpe F, Steiner G, Uffelman K, Olivecrona T, Hamsten A (1994) Postprandial lipoprotein and progression of coronary atherosclerosis. Atherosclerosis 106:83–97
24. Kolovou GD, Anagnostopoulou KK, Daskalopoulou SS, Mikhailidis DP, Cokkinos DV (2005) Clinical relevance of postprandial lipaemia. Curr Med Chem 12:1931–1945
25. Langsted A, Freiberg JJ, Nordestgaard GB (2008) Fasting and nonfasting lipid levels: influence of normal food intake on lipids, lipoproteins, apolipoproteins, and cardiovascular risk prediction. Circulation 118:2047–2056
26. Le N-A, Walter MF (2007) The role of hypertriglyceridemia in atherosclerosis. Curr Atheroscler Rep 9:110–115
27. Levy E, Roy CC, Goldstein R, Bar-On H, Ziv E (1991) Metabolic fate of chylomicrons obtained from rats maintained on diets varying in fatty acid composition. J Am Coll Nutr 10:69–78
28. Lovati MR, Manzoni C, Corsini A, Granata A, Frattinin R, Fumagalli R, Sirtori CR (1992) Low density lipoprotein receptor activity is modulated by soybean globulins in cell culture. J Nutr 122:1971–1978
29. Lu LW, Anderson K (1998) Sex and long-term soy diets affect the metabolism and excretion of soy isoflavones in humans. Am J Clin Nutr 68:1500s–1504s
30. Ma Y, Chiriboga D, Olendzki BC, Nicolosi R, Merriam PA, Ockene IS (2005) Effect of soy protein containing isoflavones on blood lipids in moderately hypercholesterolemic adults: a randomized controlled trial. J Am Coll Nutr 24:275–285
31. Matthan NR, Jalbert SM, Ausman LM, Kuvin JT, Karas RH, Lichenstein AH (2007) Effect of soy protein from differently processed products on cardiovascular disease risk factors and vascular endothelial function in hypercholesterolemic subjects. Am J Clin Nutr 85:960–966
32. McVeigh BL, Dillingham BL, Lampe JW, Duncan AM (2006) Effect of soy protein varying in isoflavone content on serum lipids in healthy young men. Am J Clin Nutr 83:244–251
33. Mora S, Rifai N, Buring JE, Ridker PM (2008) Fasting compared with nonfasting lipids and apolipoproteins for predicting incident cardiovascular events. Circulation 118:993–1001
34. Muesing RA, Griffin P, Mitchell P (1995) Corn oil and beef tallow elicit different postprandial responses in triglycerides and cholesterol, but similar changes in constituents of high-density lipoprotein. J Am Coll Nutr 14:53–60
35. Nordestgaard BG, Benn M, Schnohr P, Tybjaerg-Hansen A (2007) Nonfasting triglycerides and risk of myocardial infarction, ischemic heart disease, and death in men and women. J Am Med Assoc 298:299–308
36. O'Keefe JH, Bell DSH (2007) Postprandial hyperglycemia/hyperlipidemia (postprandial dysmetabolism) is a cardiovascular risk factor. Am J Cardiol 100:899–904
37. Otvos JD, Jeyarajah EJ, Cromwell WC (2002) Measurement issues related to lipoprotein heterogeneity. Am J Cardiol 90:22i–29i
38. Parks EJ (2001) Recent findings in the study of postprandial lipemia. Curr Atheroscler Rep 3:462–470
39. Patsch JR, Miesenbock G, Hopferwieser T, Muhlberger V, Knapp E, Dunn JK, Gotto AM, Patsch W (1992) Relation of triglyceride metabolism and coronary disease. Arterioscler Thromb 12:1336–1345
40. Pischon T, Girman CJ, Sacks FM, Rifai N, Stampfer MJ, Rimm EB (2005) Non-high-density lipoprotein cholesterol and apolipoprotein B in the prediction of coronary heart disease in men. Circulation 112:3375–3383
41. Potter SM (1998) Soy protein and cardiovascular disease: the impact of bioactive components in soy. Nutr Rev 56:231–235
42. Reynolds K, Chin A, Lees KA, Nguyen A, Bujnowski D, He J (2006) A meta-analysis of the effect of soy protein supplementation on serum lipids. Am J Cardiol 98:633–640
43. Sacks FM (2006) The apolipoprotein story. Atheroscler Suppl 7:23–27
44. Sacks FM, Lichenstein A, Horn LV, Harris W, Kris-Etherton P, Winston M (2006) Soy protein, isoflavones, and cardiovascular health: an American Heart Association Science Advisory for health professionals from the Nutrition Committee. Circulation 113:1034–1044
45. Santo AS, Cunningham AM, Alhassan S, Browne RW, Burton H, Leddy JJ, Grandjean PW, Horvath SM, Horvath PJ (2008) NMR analysis of lipoprotein particle size does not increase sensitivity to the effect of soy protein on CVD risk when compared with the traditional lipid profile. Appl Physiol Nutr Metab 33:489–500
46. Setchell K (1998) Phytoestrogens: the biochemistry, physiology, and implications for human health of soy isoflavones. Am J Clin Nutr 68:1333–1346

47. Sharret AR, Chambless LE, Heiss G, Paton CC, Patsch W (1995) Association of postprandial triglyceride and retinyl palmitate responses with asymptomatic carotid artery atherosclerosis in middle-aged men and women. Arterioscler Thromb Vasc Biol 15:2122–2129
48. Shige H, Ishikawa T, Higashi K, Yamashita T, Tomiyasu K, Yoshida H, Hosoai H, Ito T, Nakajima K, Ayaori M, Yonemura A, Suzukawa M, Nakamura H (1998) Effects of soy protein isolate (SPI) and casein on the postprandial lipemia in normolipidemic men. J Nutr Sci Vitaminol 44:113–127
49. Sirtori CR, Calabresi L, Franceschini G (1999) Recombinant apolipoproteins for the treatment of vascular diseases. Atherosclerosis 142:29–40
50. Slavin JL, Karr SC, Hutchins AM, Lampe JW (1998) Influence of soybean processing, habitual diet, and soy dose on urinary isoflavonoid excretion. Am J Clin Nutr 68:1492s–1495s
51. Sniderman AD, Furberg CD, Keech A, JERv Lennep, Frohlich J, Jungner I, Walldius G (2003) Apolipoproteins versus lipids as indices of coronary risk and as targets for statin treatment. Lancet 361:777–780
52. Stalenhoef AFH, Graaf Jd (2008) Association of fasting and nonfasting serum triglycerides with cardiovascular disease and the role of remnant-like lipoproteins and small dense LDL. Curr Opin Lipidol 19:355–361
53. Taku K, Umegaki K, Sato Y, Endoh K, Watanabe S (2007) Soy isoflavones lower serum total and LDL cholesterol in humans: a meta-analysis of 11 randomized controlled trials. Am J Clin Nutr 85:1148–1156
54. Thorp A, Howe PRC, Mori TA, Coates AM, Buckley JD, Hodgson J, Mansour J, Meyer BJ (2008) Soy food consumption does not lower LDL cholesterol in either equol or nonequol producers. Am J Clin Nutr 88:298–304
55. Torres N, Torre-Villalvazo I, Tovar AR (2006) Regulation of lipid metabolism by soy protein and its implication in diseases mediated by lipid disorders. J Nutr Biochem 17:365–373
56. Van Heek M, Zilversmit DB (1990) Postprandial lipemia and lipoprotein lipase in the rabbit are modified by olive and coconut oil. Arteriosclerosis 10:421–429
57. Wangen KE, Duncan AM, Xu X, Kurzer MS (2001) Soy isoflavones improve plasma lipids in normocholesterolemic and mildly hypercholesterolemic postmenopausal women. Am J Clin Nutr 73:225–231
58. Weintraub MS, Zechner R, Brown A, Eisenberg S, Breslow JL (1988) Dietary polyunsaturated fats of the w-6 and w-3 series reduce postprandial lipoproteins levels. J Clin Invest 82:1884–1893
59. Weissberg PL, Rudd JH (eds) (2002) Atherosclerotic biology and epidemiology of disease textbook of cardiovascular medicine. Lippincott Williams & Wilkins, Philadelphia
60. Yu KC-W, Cooper AD (2001) Postprandial lipoproteins and atherosclerosis. Front Biosci 6:d332–d354
61. Zhan S, Ho SC (2005) Meta-analysis of the effects of soy protein containing isoflavones on the lipid profile. Am J Clin Nutr 81:397–408
62. Zhuo X-G, Melby MK, Watanabe S (2004) Soy isoflavone intake lowers serum LDL cholesterol: a meta-analysis of 8 randomized controlled trials in humans. J Nutr 134:2395–2400
63. Zilversmit DB (1979) Atherogenesis: a postprandial phenomenon. Circulation 60:473–485

fasting serum TAG concentration is very important for patients with HTG, atherosclerosis, cardiovascular disease or T2DM, etc.

1,3-Diacylglycerol (DAG), which has been consumed for many years, is a natural component (2–10%) of some edible fats and oils [6]. A cooking oil product manufactured by Kao Corporation containing about 83% (w/w) DAG has been approved as a "Food for Specified Health Use" by the Ministry of Health, Labour and Welfare of Japan since 1999 [7]. In 2000, the Food and Drug Administration also granted this product a status of generally recognized as safe [8].

DAG supplementation was previously reported to reduce the fasting serum TAG concentration compared with TAG [9, 10]. However, this efficacy was not consistently accepted by all past studies. In a study conducted by Nagao et al., after 16 weeks supplementation, the fasting serum TAG concentration of DAG group decreased from 1.16 to 1.04 mmol/L while that of TAG group decreased from 1.31 to 1.10 mmol/L [11]. So it is still in doubt whether DAG is efficacious for reducing the fasting serum TAG concentration.

Meta-analysis is a statistical technique in which results of separate studies are combined to increase statistical power and clarity, and to estimate the size of treatment effects more accurately. This method has some inherent weaknesses such as the sources of bias are not controlled and the heavy reliance on published studies [12]. Despite these weaknesses, meta-analysis is still employed in many clinical settings to evaluate the efficacy and safety of a variety of therapeutic interventions due to its advantages [13, 14]. We have already examined the effects of DAG on body weight control and the postprandial serum TAG concentration in our previous studies [13, 14]. In this study, we performed a meta-analysis of randomized controlled trials to assess the association between DAG intake and the fasting serum TAG concentration.

Methods

Selection of Studies

Potential papers were initially searched from electronic databases of Medline (1966–2010), Embase (1984–2010) and Cochrane library using the standardized subject terms and search strategy in Table 1. The references of all located papers were searched for further studies.

Inclusion Criteria

A trial was included if it was randomized controlled designed in humans, used DAG supplementation as the only intervention and used the fasting serum TAG concentration as one of the endpoints. No restrictions were imposed on the daily dose of test oil and the physiological conditions of subjects.

Table 1 Search strategy and search terms used to identify studies on diacylglycerol supplementation and fasting serum triacylglycerol concentration

(1)	Diacylglycerol
(2)	Diacylglycerols
(3)	Diglyceride
(4)	Diglycerides
(5)	DAG
(6)	(1) or (2) or (3) or (4) or (5)
(7)	Fasting
(8)	Lipid
(9)	Hypertriglyceridemia
(10)	Hyperlipidemia
(11)	(7) or (8) or (9) or (10)
(12)	(6) and (11)

Validity Assessment

The methodological quality of included papers was evaluated using the scoring system developed by Jadad (Table 2) [15].

Information Extraction

The detailed information was extracted independently by two reviewers in a standardized manner according to the predefined protocol. Any discrepancies were resolved by discussing them with an additional reviewer. The extracted characteristics included the study design (i.e., parallel or crossover, open, single- or double-blinded), number of subjects, daily dose of test oil, duration of supplementation, fasting serum TAG concentrations at baseline and final, the net change of concentration in along with corresponding standard deviations (SD). For studies that reported multiple time points for the same subjects, only the last points of the supplementation were extracted for analysis.

In the study conducted by Yasunaga et al., the safety aspects of high-dose dietary DAG were separately tested in males and females, so the data of the males and that of the females were extracted and included as two independent studies. The influence of these two studies on the overall results was tested by sensitivity analysis [16]. Similar extraction methods were also used in meta-analysis conducted by He et al. [17] in which two separate studies from study conducted by Joshipura et al. were extracted and included as independent trial [18]. In the study conducted by Yanagisawa et al., TAG concentration was reported as

Table 2 Quality of included studies

Studies	Generation of allocation sequence	Allocation concealment	Investigator blindness	Description of withdrawals and drop-outs	Score
Yamamoto 2006 [9]	1	1	1	0	3
Yamamoto 2001 [10]	1	1	1	0	3
Nagao 2000 [11]	1	1	1	0	3
Yasunaga 2004 (M) [16]	1	1	1	1	4
Yasunaga 2004 (F) [16]	1	1	1	1	4
Yanagisawa 2003 [19]	1	1	1	0	3
Li 2008 [28]	1	1	1	1	4

mg/dL which was transformed to mmol/L according to the formula mg/dL $\times$ 0.01129 = mmol/L [19]. In the study conducted by Yanagisawa et al., TAG concentrations were reported in the form of figures, so the specific data were obtained by measuring the corresponding figures and sensitivity analysis was performed to test the influence of this study on the overall results [19]. In the study conducted by Nagao et al., the concentrations were reported as means $\pm$ standard errors (SE) which were transformed to means $\pm$ SDs. In some studies, the SDs of mean change in fasting serum TAG concentration were not reported. The authors were contacted for detailed data but no reply was received. Therefore, the missing SDs were imputed using methods provided by the Cochrane Handbook [20].

Statistical Analysis

The validity of random design was tested by meta-analysis in advance. The net change of fasting serum TAG concentration was used as the endpoint to assess the effect of DAG supplementation. The influence of each study on the result of meta-analysis was weighted by the inverse of variance, and studies with narrower confidence intervals (CI) were given more weight. A random effect model was adopted to calculate the weighted mean difference (WMD) and 95% CI because of the heterogeneity in daily dose, duration of supplementation and initial characteristics of subjects among all studies. Meta-analysis was conducted using the software of Review Manager 4.2 (Update Software Ltd, Oxford, England). Sensitivity analysis was conducted to determine whether conclusions were robust to decisions made during the review process [20]. In this study, sensitivity analysis was performed to test the robustness of the overall result during the inclusion/exclusion of paper in which TAG concentrations were reported in the form of figure and paper in which two independent studies were extracted. A funnel plot was used to test the possibility of publication bias and fail-safe number analysis was used to determine the number of studies with null effects that would have to exist to nullify the reported reduction efficacy [14, 21]. All studies were divided into three groups (healthy, diabetic and diabetic with HTG groups) according to the physiological conditions of subjects. Sub-group analysis was performed to determine whether the physiological conditions influence the effect of DAG. The influences of daily dosage and the initial fasting serum TAG concentration on the effect of DAG were assessed using weight estimation in SPSS 12.0.

Results

Of the 13 publications identified after title and abstract evaluation, one did not provide the detailed data [22], two did not take DAG as the only intervention [23, 24], three were designed without placebo control [25–27], one lasted only for 2 days [28]. Finally, six papers with seven independent studies (298 subjects) were included into the statistic pooling [9–11, 16, 19, 29] (Fig. 1). Validity assessment showed that three studies got 4 points and four studies got 3 points (Table 2). The detailed information of included studies is shown in Table 3. The preparations of test oil are shown in Table 4 and there were no significant differences in the fatty acid composition between two test

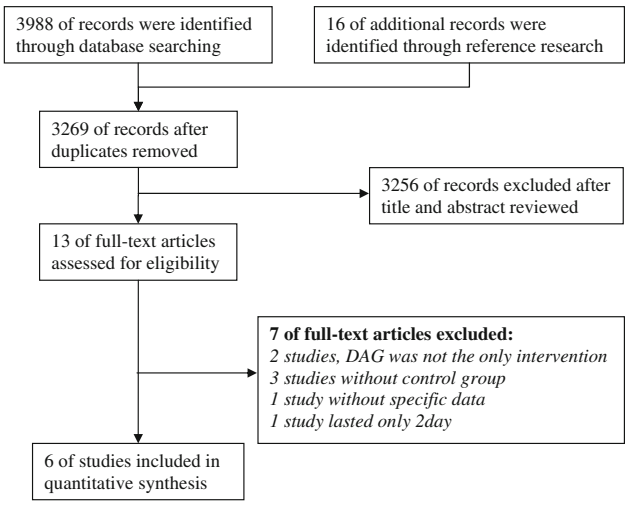

Fig. 1 Flow of study selection

Table 3 Study characteristics

First author and publication year	Design	Duration	Subjects	Sample size DAG/TAG	Age DAG/TAG	Concentration of TAG (mmol/L) baseline/final		Dose (g/d)
						DAG group	TAG group	
Yamamoto 2006 [9]	RSBCP	3 months	T2DM&HTG	(4:7)/(7:6)	61.5 ± 6.2/54.3 ± 13.1	2.55 ± 1.65/1.98 ± 1.14	1.91 ± 1.07/1.83 ± 0.95	10
Yamamoto 2001 [10]	RSBCP	12 weeks	T2DM&HTG	(3:5)/(4:4)	56.8 ± 7.3/54.1 ± 18.8	2.51 ± 0.75/1.52 ± 0.28	3.22 ± 2.13/3.59 ± 1.70	10
Nagao 2000 [11]	RDBCP	16 weeks	H	(19:0)/(19:0)	27–49	1.16 ± 0.39/1.04 ± 0.39	1.31 ± 0.70/1.10 ± 0.52	10
Yasunaga 2004 (M) [16]	RDBCP	12 weeks	H	(21:0)/(21:0)	34.7 ± 6.1/34.6 ± 6.90	1.07 ± 0.84/1.10 ± 0.82	0.95 ± 0.52/1.04 ± 0.72	34
Yasunaga 2004 (F) [16]	RDBCP	12 weeks	H	(0:18)/(0:21)	31.1 ± 6.8/32.0 ± 6.10	0.66 ± 0.35/0.60 ± 0.26	0.67 ± 0.24/0.55 ± 0.16	25
Yanagisawa 2003 [19]	RDBCP	8 weeks	H	(0:13)/(0:14)	20.3 ± 2.1	0.56 ± 0.27/0.70 ± 0.34	0.55 ± 0.17/0.72 ± 0.29	20
Li 2008 [29]	RDBCP	120 days	T2DM	(24:36)/(23:29)	54.1 ± 6.7/53.9 ± 6.00	1.51 ± 1.07/1.64 ± 1.07	1.45 ± 0.77/1.75 ± 1.19	25

RD(S)BCP Random double (single)-blind control parallel design, *H* healthy; *T2DM* Type 2 diabetes mellitus; *HTG* Hypertriglyceridemia, *Sample size* (M:F) of the DAG group/(M:F) of the TAG group, Data were reported in mean ± SD

oils in all studies. Three studies reported whether the supplementation of DAG can induce adverse effect to subjects [9, 16, 29]. In the study conducted by Yamamoto et al. [9] and the study conducted by Li et al. [29], no aggravation of physical conditions or adverse reaction were noted after ingestion of the test oils throughout the study period. In the study conducted by Yasunaga et al., some adverse effects were reported during the treatment period. However, there was no significant change in any group when compared with background records. In addition, the number of definite complaints in DAG group was smaller than that of the TAG group and no serious adverse effects were reported during the treatment [16].

Meta-analysis showed that there was no significant difference in the initial fasting serum TAG concentration between DAG and TAG groups (WMD: 0 mmol/L; 95% CI: −0.11 to 0.11 mmol/L; $P = 0.95$) (Fig. 2).

Meta-analysis with random effect model showed that there was no significant difference in the net change of fasting serum TAG concentration between DAG and TAG groups after test oil supplementation (WMD: −0.07 mmol/L; 95% CI: −0.21 to 0.08 mmol/L; $P = 0.37$) (Fig. 3). Funnel plot analysis showed that all studies distributed in the 95% CI except for the study conducted by Yamamoto et al. (Fig. 4) [10]. Fail-safe number analysis indicated that 18 studies with positive effect were necessary to reverse the reported non-significant efficacy of DAG.

Sensitivity analysis was performed to determine the robustness of meta-analysis. The first tested whether the removal of two studies extracted from the paper conducted by Yasunaga et al affect the overall outcome. Results showed that there still was no significant difference between two groups (WMD: −0.15 mmol/L; 95% CI: −0.38 to 0.08 mmol/L; $P = 0.20$) [16]. The second showed that the removal of study in which the data was reported in the form of figure did not affect the overall results significantly (WMD: −0.10 mmol/L; 95% CI: −0.30 to 0.10 mmol/L; $P = 0.31$) [19]. In the third one, the removal of study which distributed out of the 95% CI did not affect the overall result (WMD: −0.02 mmol/L; 95% CI: −0.10 to 0.07 mmol/L; $P = 0.74$) [10]. Finally, the removal of all above studies did not change the direction of the overall results (WMD: −0.10 mmol/L; 95% CI: −0.34 to 0.14 mmol/L; $P = 0.41$) [10, 16, 19].

Sub-group analysis showed that DAG reduced the fasting serum TAG concentration in diabetic subjects with HTG (WMD: −0.87 mmol/L; 95% CI: −1.71 to −0.02 mmol/L; $P = 0.04$) [9, 10], but not in healthy (WMD: 0.02 mmol/L; 95% CI: −0.06 to 0.11 mmol/L; $P = 0.58$) [11, 16, 19] and diabetic subjects (WMD: −0.17 mmol/L; 95% CI: −0.39 to 0.05 mmol/L; $P = 0.12$) [29] (Fig. 3). However, as far as the sub-group of

Table 4 Preparation of test oil

Studies	DAG oil	TAG oil
Yamamoto 2006 [9]	Prepared from rapeseed and soy oil with lipase	Mixture of rapeseed, soybean and safflower oil
Yamamoto 2001 [10]	Provided by the kao corporation	Provided by the kao corporation
Nagao 2000 [11]	Esterifying glycerol with fatty acids from rapeseed oil	Mixture of rapeseed, soybean and safflower oil
Yasunaga 2004 (M) [16] Yasunaga 2004 (F) [16]	Etherification reaction of fatty acids derived from natural plant oil with monoacylglycerol or glycerin with lipase	Mixture of rapeseed, soybean and safflower oil
Yanagisawa 2003 [19]	Prepared from the mixture of rapeseed and soy oil	Prepared from the mixture of rapeseed and soy oil
Li 2008 [29]	Provided by the kao corporation	Provided by the kao corporation

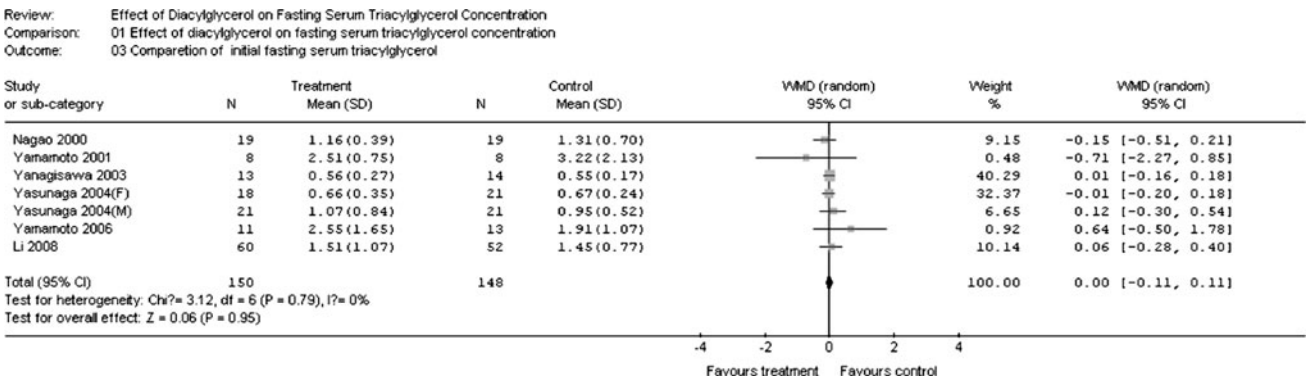

Fig. 2 Comparison in initial fasting serum TAG concentration between DAG and TAG groups (random effect model)

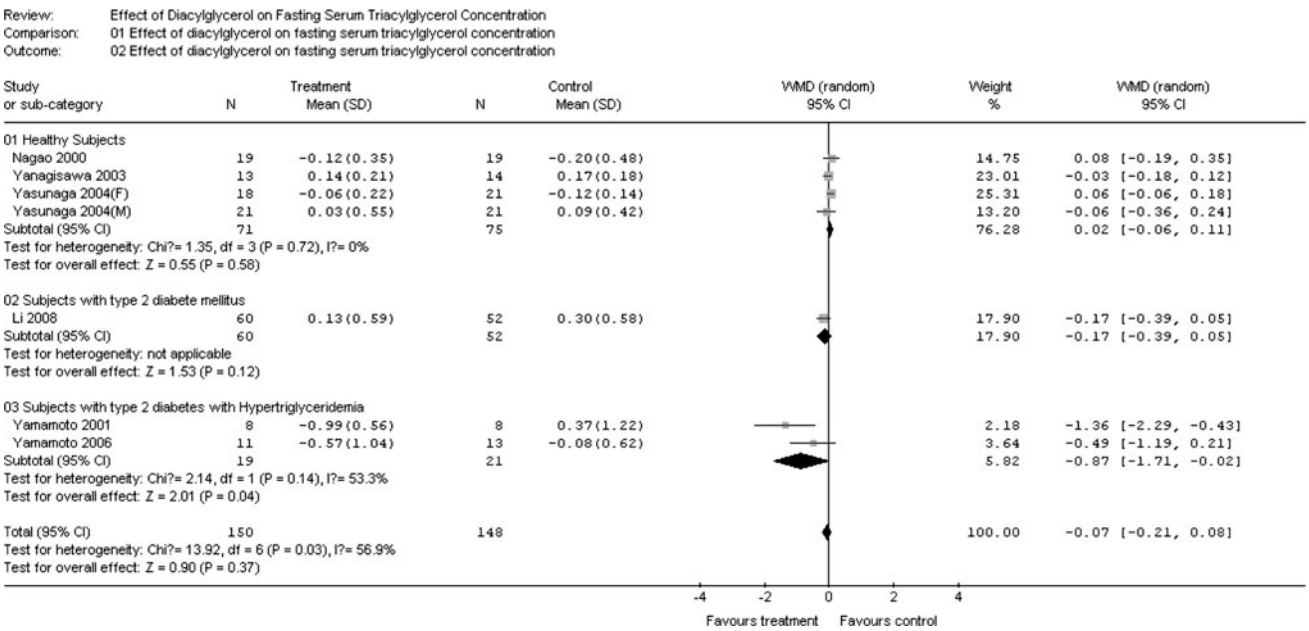

Fig. 3 Sub-group analysis of the effect of DAG on fasting serum TAG concentration (random effect model). All studies were divided into three groups according to the physiological conditions of subject (healthy, diabetic, diabetic with HTG groups)

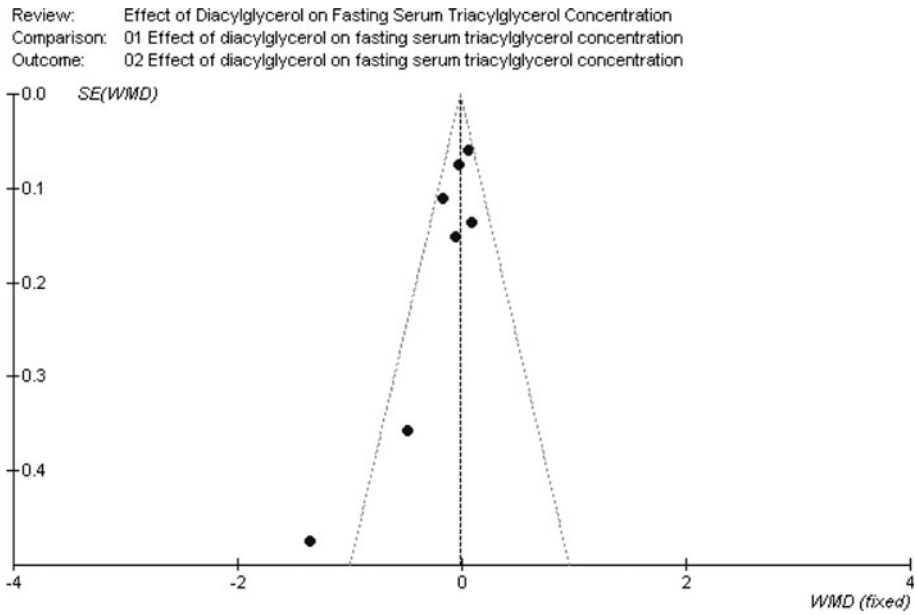

Fig. 4 Funnel plot of the mean difference in fasting serum TAG concentration reduction plotted against 1/SE. The distribution of studies was relatively symmetric except for the study conducted by Yamamoto et al. which means the possibility of publication bias [10]

T2DM patients with HTG concerned, analysis was based only on 40 patients and a moderate I square had been obtained.

Weight estimation analysis of all the studies included indicated that the effect of DAG was influenced to some extent by the initial fasting serum TAG concentration, although this trend did not reach the significant level ($P = 0.328$). However, this efficacy was not influenced by the daily dose ($P = 0.996$).

Discussion

In meta-analysis of continuous outcomes, the influences of initial values on the overall results were usually not taken into account because all included studies were randomly designed. But evidence shows that although the subjects were assigned into two groups randomly at the beginning of experiments, there is significant difference incidentally in some variables between two groups [11]. The effect of dietary intervention might be correlated with the initial values, such as subjects with abundance of visceral fat area tended to achieve larger reduction in visceral fat after body weight loss [30]. In fact, a weak but significant correlation between the initial values and the losses of visceral fat have been already observed in the study conducted by Nagao et al. [11]. So whether there were significant differences in initial values of tested variables should be examined. As far as current study concerned, the differences in initial fasting serum TAG concentration were relatively great in two studies conducted by Yamamoto et al., although all subjects were assigned into two groups randomly [9, 10]. However, these two studies were given small weights (0.48 and 0.92%, respectively) during the meta-analysis because of their great SDs. Their influences on the overall result were reduced greatly and non-significant result was obtained (Fig. 2).

Meta-analysis indicated that DAG oil supplementation did not reduce the fasting serum TAG concentration significantly compared with TAG oil. This result was consistent with four papers that had been included [11, 16, 19, 29] but not consistent with two papers published by Yamamoto et al. [9, 10]. In these two studies, the fasting serum TAG concentrations of DAG groups decreased 0.99 mmol/L and 0.57 mmol/L respectively which were significantly greater than those of TAG group (−0.37 and 0.08 mmol/L, respectively) after test oil supplementation. However, these two studies were given small weights (2.18 and 3.64%, respectively) because of their great SDs. Their influences on the overall result were reduced greatly and non-significant result had been obtained (Fig. 2).

Positive results were reported in two studies [9, 10] and negative results were reported in five studies [11, 16, 19, 29]. This inconsistency might be caused by the differences in initial physiological conditions of subjects. So all studies were divided into three groups (healthy, diabetic and diabetic with HTG groups) and sub-group analysis was used to determine the effect of DAG in each group. Results showed that DAG did not reduce the fasting serum TAG concentration significantly in healthy group compared with TAG. In the diabetic group in which the initial fasting serum TAG concentrations were higher than those of healthy group, the effect of DAG seemed to be enhanced to some extent according to the greater WMD and lower P value. In the diabetic with HTG group, the effect of DAG was increased furthermore and reached significant level. These

results indicated that effect of DAG might be influenced by the initial fasting serum TAG concentration of subjects. Furthermore, weight estimation analysis showed that the effect of DAG was influenced to some extent by the initial fasting serum TAG concentration, although this influence did not reach the significant level. All these results indicated that DAG supplementation was more efficacious in reducing the fasting serum TAG concentration in subjects with higher initial concentrations.

It was conceived that DAG supplementation could reduce the increment of postprandial TAG concentration compared with TAG supplementation. The different structure of DAG from TAG was regarded as the major contribution. The initial products of digested TAG are free fatty acids (FFA) and 2-monoacylglycerol (MAG) and those for 1,3-DAG are mainly FFA and 1(3)-MAG [31]. The resynthesis of TAG in small intestinal epithelial cells from 2-MAG is faster than that from 1(3)-MAG because the later involves the phosphatidic acid pathway, a slow turnover pathway than 2-MAG pathway, which interpreted the less increment of postprandial TAG concentration after DAG consumption compared with TAG [32]. This effect of DAG has also been proved in our former meta-analysis in which DAG supplementation reduced the increment of TAG concentration at postprandial 2, 4 and 6 h [14]. However, more studies are needed to elucidate whether DAG supplementation affect the fasting serum TAG concentration.

There were several limitations in this study. Firstly, it was conceivable that some trials were not uncovered although systematic efforts were made to locate and retrieve them. In this study, the fail-safe number indicated the light possibility of publication bias. The distorting effects arising from publication bias and location bias have repeatedly been reported [33–35]. Secondly, there was great heterogeneity among all included studies, especially in the initial fasting serum TAG concentration. Although the validity of random design was verified beforehand and random effect model was adapted to reduce the influence of heterogeneity, the great differences in initial fasting serum TAG concentrations might have influenced the result of meta-analysis [9, 10]. Thirdly, all located studies were conducted with Asian subjects. This restriction limits the application of current study to American and European people. So, more studies are needed with Western subjects. Finally, the number of patients included in this meta-analysis is very small which might due to the specialism of this topic. The subsequent sub-group analysis was performed based even smaller number of patients. As far as the T2DM patients with HTG sub-group concerned, the analysis was performed based on only 40 patients and had a moderate I square statistic although a significant result had been obtained. This significant effect should be viewed with caution and more studies are needed to establish this efficacy. In spite of these limitations, the high methodological quality of all the studies included (such as randomized, double-blind, TAG controlled design) and the high consistency of sensitivity analysis indicated the robustness of this meta-analysis.

Compared with TAG oil, supplementation of DAG oil did not cause significant adverse reactions which might be due to the similarity in fatty acids composition, energy values and bioavailability between them [36].

In conclusion, DAG supplementation did not reduce the fasting serum TAG concentration significantly compared with TAG in this meta-analysis of seven randomized controlled trials, but some effects were suggested in diabetic patients with HTG.

Acknowledgments This work was supported by the Shandong Provincial Key Special Projects of Transformation of Independent Innovative Achievement, China (2009ZHZX1A1303) and the Ministry of Agriculture' Special Funds for Scientific Research on Public Causes, China (200903043-3-2).

References

1. Tada N, Yoshida H (2003) Diacylglycerol on lipid metabolism. Curr Opin Lipidol 14:29–33
2. Codario RA (2007) Hypertriglyceridemia and cardiovascular disease management. J Am Acad Nurse Pract 19:7–10
3. Fried SK, Rao SP (2003) Sugars, hypertriglyceridemia, and cardiovascular disease. Am J Clin Nutr 78:873S–880S
4. Eberting CL, Javor E, Gorden P, Turner ML, Cowen EW (2005) Insulin resistance, acanthosis nigricans, and hypertriglyceridemia. J Am Acad Dermatol 52:341–344
5. Lin CY, Chen MF, Lin LY, Liau CS, Lee YT, Su TC (2008) Insulin resistance is the major determinant for microalbuminuria in severe hypertriglyceridemia: implication for high-risk stratification. Intern Med 47:1091–1097
6. Dalanzo R, Kozerek W, Wade R (1982) Glyceride composition of processed fats and oils as determined by glass capillary gas chromatography. J Am Oil Chem Soc 49:292–295
7. Saito S, Tomonobu K, Hase T, Tokimitsu I (2006) Effects of diacylglycerol on postprandial energy expenditure and respiratory quotient in healthy subjects. Nutrition 22:30–35
8. Takase H (2007) Metabolism of diacylglycerol in humans. Asia Pac J Clin Nutr 16(Suppl 1):398–403
9. Yamamoto K, Takeshita M, Tokimitsu I, Watanabe H, Mizuno T, Asakawa H, Tokunaga K, Tatsumi T, Okazaki M, Yagi N (2006) Diacylglycerol oil ingestion in type 2 diabetic patients with hypertriglyceridemia. Nutrition 22:23–29
10. Yamamoto K, Asakawa H, Tokunaga K, Watanabe H, Matsuo N, Tokimitsu I, Yagi N (2001) Long-term ingestion of dietary diacylglycerol lowers serum triacylglycerol in type II diabetic patients with hypertriglyceridemia. J Nutr 131:3204–3207
11. Nagao T, Watanabe H, Goto N, Onizawa K, Taguchi H, Matsuo N, Yasukawa T, Tsushima R, Shimasaki H, Itakura H (2000) Dietary diacylglycerol suppresses accumulation of body fat compared to triacylglycerol in men in a double-blind controlled trial. J Nutr 130:792–797
12. Gibaldi M (1993) Meta-analysis. A review of its place in therapeutic decision making. Drugs 46:805–818
13. Xu T, Li X, Zhang Z, Ma X, Li D (2008) Effect of diacylglycerol on body weight: a meta-analysis. Asia Pac J Clin Nutr 17: 415–421

14. Xu T, Li X, Ma X, Zhang Z, Zhang T, Li D (2009) Effect of diacylglycerol on postprandial serum triacylglycerol concentration: a meta-analysis. Lipids 44:161–168
15. Jadad AR, Moore RA, Carroll D, Jenkinson C, Reynolds DJ, Gavaghan DJ, McQuay HJ (1996) Assessing the quality of reports of randomized clinical trials: is blinding necessary? Control Clin Trials 17:1–12
16. Yasunaga K, Glinsmann WH, Seo Y, Katsuragi Y, Kobayashi S, Flickinger B, Kennepohl E, Yasukawa T, Borzelleca JF (2004) Safety aspects regarding the consumption of high-dose dietary diacylglycerol oil in men and women in a double-blind controlled trial in comparison with consumption of a triacylglycerol control oil. Food Chem Toxicol 42:1419–1429
17. He FJ, Nowson CA, MacGregor GA (2006) Fruit and vegetable consumption and stroke: meta-analysis of cohort studies. Lancet 367:320–326
18. Joshipura KJ, Ascherio A, Manson JE, Stampfer MJ, Rimm EB, Speizer FE, Hennekens CH, Spiegelman D, Willett WC (1999) Fruit and vegetable intake in relation to risk of ischemic stroke. JAMA 282:1233–1239
19. Yanagisawa Y, Kawabata T, Tanaka O, Kawakami M, Hasegawa K, Kagawa Y (2003) Improvement in blood lipid levels by dietary sn-1, 3-diacylglycerol in young women with variants of lipid transporters 54T-FABP2 and -493 g-MTP. Biochem Biophys Res Commun 302:743–750
20. Higgins J, Green S (2006) Cochrane handbook for systematic reviews of interventions 4.2.6. John Wiley & Sons, Chichester, pp 119–122
21. Rosenthal R (1979) The 'fail-drawer problem' and tolerance of null result. Psychol Bull 86:638–641
22. Maki KC, Davidson MH, Tsushima R, Matsuo N, Tokimitsu I, Umporowicz DM, Dicklin MR, Foster GS, Ingram KA, Anderson BD, Frost SD, Bell M (2002) Consumption of diacylglycerol oil as part of a reduced-energy diet enhances loss of body weight and fat in comparison with consumption of a triacylglycerol control oil. Am J Clin Nutr 76:1230–1236
23. Meguro S, Higashi K, Hase T, Honda Y, Otsuka A, Tokimitsu I, Itakura H (2001) Solubilization of phytosterols in diacylglycerol versus triacylglycerol improves the serum cholesterol-lowering effect. Eur J Clin Nutr 55:513–517
24. Saito S, Takeshita M, Tomonobu K, Kudo N, Shiiba D, Hase T, Tokimitsu I, Yasukawa T (2006) Dose-dependent cholesterol-lowering effect of a mayonnaise-type product with a main component of diacylglycerol-containing plant sterol esters. Nutrition 22:174–178
25. Matsuyama T, Shoji K, Watanabe H, Shimizu M, Saotome Y, Nagao T, Matsuo N, Hase T, Tokimitsu I, Nakaya N (2006) Effects of diacylglycerol oil on adiposity in obese children: initial communication. J Pediatr Endocrinol Metab 19:795–804
26. Katsuragi Y, Takeda Y, Abe C, Mori K, Toi T, Takei A, Shimasaki H, Itakura H (2001) Effects of dietary α-linolenic acid-rich diacylglycerol on body fat in man (2) effects on resting metabolism and fat metabolism. J Oleo Sci 50:747–752
27. Teramoto T, Watanabe H, Ito K, Omata Y, Furukawa T, Shimoda K, Hoshino M, Nagao T, Naito S (2004) Significant effects of diacylglycerol on body fat and lipid metabolism in patients on hemodialysis. Clin Nutr 23:1122–1126
28. Kamphuis MM, Mela DJ, Westerterp-Plantenga MS (2003) Diacylglycerols affect substrate oxidation and appetite in humans. Am J Clin Nutr 77:1133–1139
29. Li D, Xu T, Takase H, Tokimitsu I, Zhang P, Wang Q, Yu X, Zhang A (2008) Diacylglycerol-induced improvement of whole-body insulin sensitivity in type 2 diabetes mellitus: a long-term randomized, double-blind controlled study. Clin Nutr 27:203–211
30. Leenen R, van der Kooy K, Deurenberg P, Seidell JC, Weststrate JA, Schouten FJ, Hautvast JG (1992) Visceral fat accumulation in obese subjects: relation to energy expenditure and response to weight loss. Am J Physiol 263:E913–E919
31. Kondo H, Hase T, Murase T, Tokimitsu I (2003) Digestion and assimilation features of dietary DAG in the rat small intestine. Lipids 38:25–30
32. Taguchi H, Watanabe H, Onizawa K, Nagao T, Gotoh N, Yasukawa T, Tsushima R, Shimasaki H, Itakura H (2000) Double-blind controlled study on the effects of dietary diacylglycerol on postprandial serum and chylomicron triacylglycerol responses in healthy humans. J Am Coll Nutr 19:789–796
33. Dickersin K (1990) The existence of publication bias and risk factors for its occurrence. JAMA 263:1385–1389
34. Easterbrook PJ, Berlin JA, Gopalan R, Matthews DR (1991) Publication bias in clinical research. Lancet 337:867–872
35. Egger M, Smith GD (1998) Bias in location and selection of studies. BMJ 316:61–66
36. Taguchi H, Nagao T, Watanabe H, Onizawa K, Matsuo N, Tokimitsu I, Itakura H (2001) Energy value and digestibility of dietary oil containing mainly 1, 3-diacylglycerol are similar to those of triacylglycerol. Lipids 36:379–382

fish and marine mammals of different species, brands and grades by using the FAME profiles and PCA. The GC FAME profiles from plant oils such as rapeseed, linseed and soy oils and seven different brands of n-3 supplements are also used in the discrimination process. The discrimination between and within animal oils is studied by using three different data analysis strategies: firstly, the analysis of the full FAME profiles from plant, supplement and animal oils; secondly, the analysis of selected FAME profiles from plant, supplement and animal oils with levels higher than 0.5% of the total composition; thirdly, the analysis of the full FAME profiles from animal oils. It must be mentioned that discrimination studies of n-3 rich oils derived from fish and marine mammals have not been previously reported.

Experimental

Reagents and Samples

Sodium hydroxide, hexane, methanol, boron trifluoride in methanol (20% w/v) and chloroform were purchased from Merck (Darmstadt, Germany). Butylated hydroxytoluene (BHT) and boron trichloride in methanol (14%) were purchased from Sigma–Aldrich Co., USA. FAME pure standards and also model mixture standards 2A and 2B (18:0, 18:1n-9, 18:2n-6, 18:3n-3, 20:4n-6), 3A (18:2n-6, 18:3n-3, 20:4n-6, 22:6n-3), 4A (6:0, 8:0, 10:0, 12:0, 14:0) 6A (16:0, 18:0, 20:0, 22:0, 24:0), 7A (16:1n-7, 16:1n-9, 20:1n-9, 22:1n-11, 24:1n-9) and 14A (13:0, 15:0, 17:0, 19:0, 21:0) were purchased from Nu-Chek Prep (Elysian, MN, USA). Nonadecanoic acid methyl ester (19:0) internal standard was from Fluka (Buchs, Switzerland). De-ionized water was purified in a Milli-Q system (Milli-Q system Millipore, Milford, MA, USA). The fish oils were cod liver oil from Peter Möller, Lysaker, Norway and salmon oil from Havnegater, Sortland, Norway. The two brands of harp seal oils (*Pagophilus groenlandicus*) were from Rieber Skinn A/S, Bergen, Norway (two refined samples from different batches, designated as RSA1 and RSA2, and one crude sample designated as CSA were provided) and from JFM Sunile A/S, Os, Norway (one refined sample designated as RSB was provided). Whale oil (*Balaenoptera acutorostrata*) conventionally (WC) and molecularly (WM) distilled were from Myklebust Trading AS, Myklebost, Norway. The plant oils analyzed were soy oil (Mills DA, Sofienberg, Norway), linseed and rapeseed oils (Kinsarvik Naturkost, Bergen, Norway). The seven commercial n-3 supplements obtained from a local pharmacy were Fri Flyt (Vesterålens Naturprodukter AS, Sortland, Norway), Natur-Omega (Naturhuset AS, Vøyenenga, Norway), Møllers dobbel (Peter Möller, Lysaker, Norway), Pikasol (Axellus A/S, Oslo, Norway), Omega-3 Forte (Vitamed, Sarpsborg, Norway), Omega-3 høykonsentrert (Sunkost, Oslo, Norway), El Dorado (Probio Nutraceuticals, Tromsø, Norway). The supplements were designated as K1, K2, K3, K4, K5, K6 and K7, respectively.

FAME Preparation

The FAME preparation protocol has been published elsewhere [48]. Briefly, 50 mg of the sample are mixed with 2 ml BF_3/CH_3OH and 5 mg of the 19:0 internal standard. The mixture is heated at 100 °C for 1 h and cooled down to room temperature. Aliquots of 1 ml of hexane and 2 ml of H_2O are added, vortex-mixed for 15 s, placed in a centrifuge at 3,000 rpm for 2 min and the FAME are then extracted from the upper hexane phase. Depending on the fat content the sample is either concentrated under nitrogen or diluted with hexane and subsequently subjected to GC analysis.

The FAME for every kind of oil (fish, marine mammal and plant) were prepared in triplicate and for the n-3 supplements in duplicate.

Gas Chromatography Instrumentation

Analysis of the FAME was performed on a Perkin-Elmer AutoSystem XL gas chromatograph (Perkin-Elmer, Norwalk, Connecticut) equipped with a liquid autosampler and a flame ionization detector. The FAME samples were analyzed on a CP-Sil 88 capillary column (50 m × 0.32 mm ID 0.2 μm film thickness, Varian, Courtaboeuf, France). Data collection was performed by the Perkin-Elmer TotalChrom Data System software version 6.3. The temperature program was as follows: the oven temperature was held at 60 °C for 1 min, ramped to 160 °C at 25 °C/min, held at 160 °C for 28 min, ramped to 190 °C at 25 °C/min, held at 190 °C for 17 min, ramped to 220 °C at 25 °C/min and finally held at 220 °C for 10 min. Direct on-column injection was used. The injector port temperature was ramped instantaneously from 50 to 250 °C and the detector temperature was 250 °C. The carrier gas was ultra-pure helium at a pressure of 82 KPA. The analysis time was 60 min. This time interval was sufficient to detect FAME with chains from 10 to 24 carbons in length. The FAME peaks were identified by comparison of their retention times with the retention times of highly purified FAME standards. Since the concentration of the internal standard (19:0) is known and its recovery in the different oils was constant, the comparison of the various FAME peak areas with 19:0 peak area is used to calculate the concentration of the FAME in the various oils and supplements.

Table 1 FAME concentrations (mg/g) for different brands and grades of seal oils

Sample	Seal oil											
Manufacturer	A									B		
Quality	Crude			Refined						Refined		
Designation	CSA			RSA1 (batch 1)			RSA2 (batch 2)			RSB		
Replicate	i	ii	iii	i	ii	iii	i	ii	iii	i	ii	iii
14:0	42.8	44.3	41.5	42.2	42.5	41.6	45.4	45.9	45.9	40.2	40.3	40.1
15:0	2.5	2.7	2.5	2.6	2.7	2.4	2.8	2.9	2.8	2.8	2.9	2.9
16:0	72.8	75.5	70.4	69.6	70.4	68.5	66.2	66.7	65.9	75.5	75.8	75.3
17:0	0.5	0.5	0.5	0.4	0.4	0.4	0.7	0.7	0.7	1.7	1.7	1.7
18:0	10.5	10.8	10.1	10.0	10.0	9.7	8.4	8.8	8.5	12.2	12.6	11.9
20:0	0.3	0.3	0.3	0.0	0.0	0.0	0.0	0.0	0.0	0.0	0.0	0.0
Total SFA	129.4	134.1	125.3	124.8	126.0	122.6	123.5	125.0	123.8	132.4	133.3	131.9
14:1n-9	6.3	6.7	6.2	6.9	7.1	6.6	7.1	7.3	7.0	6.0	6.0	6.0
16:1n-9	3.5	3.8	3.5	4.3	4.3	4.0	3.8	3.9	3.9	4.6	4.8	4.5
16:1n-7	143.5	148.6	138.5	149.9	151.0	148.7	155.9	157.1	155.7	147.8	148.3	147.5
18:1n-11	30.2	32.0	29.6	39.9	41.3	38.3	39.7	40.5	39.1	44.8	45.1	44.7
18:1n-9	158.0	163.5	152.3	153.1	156.2	149.8	149.6	150.1	149.1	152.6	153.3	152.0
18:1n-7	38.3	38.4	38.2	38.5	38.6	38.2	35.5	35.9	35.2	42.4	42.7	42.5
20:1n-11	17.2	17.8	16.4	21.0	21.8	20.2	18.9	19.4	18.8	25.8	26.0	25.8
20:1n-9	85.2	89.1	81.1	85.5	86.4	84.4	70.5	72.3	69.8	99.6	100.3	99.9
20:1n-7	5.4	5.5	5.0	5.2	5.3	5.1	4.2	4.4	4.2	6.2	6.5	6.0
22:1n-11	18.9	19.5	18.2	19.7	20.5	18.8	17.2	17.6	17.1	23.5	23.6	23.2
22:1n-9	4.7	4.7	4.2	4.7	4.8	4.4	4.0	4.1	4.0	6.1	6.2	5.9
24:1n-9	4.7	4.8	4.4	4.8	4.9	4.6	5.0	5.1	5.0	4.3	4.3	4.3
Total MUFA	515.9	534.4	497.6	533.5	542.2	523.1	511.4	517.7	508.9	563.7	567.1	562.3
16:2n-4	6.5	6.8	6.4	5.7	5.8	5.4	5.7	5.7	5.7	4.6	4.7	4.6
16:3n-3	2.4	2.6	2.4	2.0	2.1	2.0	2.0	2.1	2.0	1.6	1.6	1.6
16:4n-3	4.3	4.5	4.2	3.0	3.0	2.8	3.8	4.0	3.8	3.4	3.6	3.4
18:2n-6	17.5	17.8	16.4	16.5	16.7	16.6	18.0	18.2	17.9	15.4	15.8	15.1
18:3n-3	5.0	5.1	4.7	4.6	4.7	4.5	5.0	5.0	5.0	4.5	4.7	4.4
18:4n-3	13.0	13.3	12.4	11.6	12.0	10.9	12.4	13.0	12.9	9.3	9.4	9.3
20:2n-6	1.7	1.8	1.6	1.7	1.8	1.7	1.6	1.6	1.6	2.1	2.1	2.0
20:4n-6	4.9	5.1	4.7	4.2	4.5	4.2	4.9	5.0	4.8	3.6	3.7	3.5
20:4n-3	4.5	4.6	4.2	4.3	4.3	4.0	4.6	4.7	4.6	3.8	3.9	3.8
20:5n-3	67.2	70.7	65.7	61.3	64.5	58.2	64.5	64.9	64.3	53.7	54.8	53.5
22:5n-3	38.1	40.3	37.2	38.6	40.0	37.0	38.1	38.5	37.9	36.6	36.8	36.5
22:6n-3	82.7	86.4	78.6	76.8	81.5	74.1	88.2	90.6	86.9	57.5	58.3	57.6
Total n-3	217.2	227.5	209.4	202.2	212.1	193.5	218.6	222.8	217.4	170.4	173.1	170.1
Total n-6	24.1	24.7	22.7	22.4	23.0	22.5	24.5	24.8	24.3	21.1	21.6	20.6
Total PUFA	247.8	259.0	238.5	230.3	240.9	221.4	248.8	253.3	247.4	196.1	199.4	195.3

SFA saturated fatty acids, *MUFA* monounsaturated fatty acids, *PUFA* polyunsaturated fatty acids

Principal Component Analysis

Principal component analysis (PCA) is a well documented multivariate method for reducing the dimensionality of a data set by rotating and constructing orthogonal linear combinations of the original variables and projecting the maximum variability onto a new axis also known as principal components (PCs). The results are classified according to the level of information produced by the various combinations of the original variables in a way that the first component (PC1) is the major axis of the points in the p-dimensional space that accounts for the largest variation

Table 2 FAME concentrations (mg/g) for whale (different grades) and fish (different species) oils

Sample	Whale oil						Fish oil					
Quality	Conventionally distilled			Molecularly distilled			Cod liver			Salmon		
Designation	WC			WM			CL			SA		
Replicate	i	ii	iii	i	ii	iii	i	ii	iii	i	ii	iii
14:0	50.5	50.6	50.4	47.8	48.1	47.5	33.7	33.6	33.6	41.1	41.8	40.5
15:0	3.4	3.5	3.3	3.6	3.7	3.3	3.1	3.2	3.0	3.9	3.9	3.8
16:0	74.5	75.2	72.7	95.3	95.8	94.6	91.9	92.6	91.0	130.5	133.4	127.5
17:0	4.9	5.0	4.8	3.7	4.0	3.7	5.8	5.8	5.7	2.7	2.8	2.5
18:0	16.4	16.1	15.6	23.5	23.9	23.4	18.5	19.1	17.8	30.5	31.4	29.8
20:0	0.5	0.5	0.5	0.7	0.7	0.6	0.0	0.0	0.0	1.8	1.9	1.7
22:0	0.0	0.0	0.0	0.0	0.0	0.0	0.0	0.0	0.0	1.7	1.8	1.7
24:0	0.0	0.0	0.0	0.0	0.0	0.0	1.7	1.8	1.6	0.0	0.0	0.0
Total SFA	150.2	150.9	147.3	174.6	176.2	173.1	154.7	156.1	152.7	212.2	217.0	207.5
14:1n-9	3.9	3.8	3.9	3.5	3.7	3.4	0.0	0.0	0.0	0.0	0.0	0.0
16:1n-9	3.2	3.2	3.1	3.5	3.6	3.5	4.3	4.6	4.3	2.8	2.9	2.6
16:1n-7	74.0	75.2	71.8	65.1	65.7	64.6	60.7	62.8	58.6	39.6	39.9	39.1
18:1n-11	18.2	18.0	17.4	19.7	19.8	19.4	13.6	13.7	13.6	3.9	4.0	3.8
18:1n-9	147.0	147.3	146.1	136.6	137.1	135.9	122.7	123.8	121.4	242.1	243.2	240.9
18:1n-7	21.4	21.3	20.9	25.5	25.6	25.3	34.9	35.1	34.5	29.5	30.2	28.6
20:1n-11	20.9	21.6	20.2	21.7	21.8	21.4	10.2	10.3	10.0	4.6	4.8	4.6
20:1n-9	96.9	98.1	94.8	128.4	129.1	127.6	77.9	78.2	77.7	43.1	43.5	42.7
20:1n-7	2.1	2.1	2.0	2.7	2.8	2.7	3.2	3.3	3.2	2.5	2.7	2.4
22:1n-11	94.4	96.6	91.3	120.8	122.1	119.4	50.0	50.0	49.9	39.2	39.9	38.8
22:1n-9	7.0	7.1	6.7	10.5	10.9	10.1	6.0	6.1	5.9	7.5	7.9	7.3
24:1n-9	6.9	7.1	6.8	6.5	7.0	6.4	7.9	7.9	7.9	8.1	8.4	7.8
Total MUFA	495.9	501.4	485.0	544.5	549.2	539.7	391.4	395.8	387.0	422.9	427.4	418.6
16:2n-4	3.6	3.6	3.5	2.8	3.0	2.8	4.2	4.3	4.0	3.7	3.9	3.7
16:3n-3	0.0	0.0	0.0	0.0	0.0	0.0	3.4	3.4	3.4	1.9	2.0	1.8
16:4n-3	2.6	2.6	2.5	0.0	0.0	0.0	4.6	4.7	4.3	3.2	3.3	3.0
18:2n-6	19.4	19.7	19.2	17.4	17.6	17.0	18.5	18.5	18.4	81.4	82.3	80.4
18:3n-3	12.6	12.7	12.4	10.9	11.1	10.7	7.8	7.8	7.5	30.4	31.0	29.9
18:4n-3	27.6	27.9	26.3	19.4	19.8	18.7	24.5	25.1	23.7	9.2	9.3	8.8
20:3n-3	0.0	0.0	0.0	0.0	0.0	0.0	0.0	0.0	0.0	3.3	3.4	3.2
20:2n-6	3.0	3.1	2.8	3.5	3.6	3.4	2.6	2.6	2.5	6.9	7.1	6.6
20:3n-6	0.0	0.0	0.0	0.0	0.0	0.0	0.0	0.0	0.0	1.6	1.7	1.5
20:4n-6	3.8	3.9	3.6	2.8	3.0	2.8	6.5	6.5	6.5	3.4	3.6	3.4
20:4n-3	14.1	14.1	14.0	11.1	11.3	10.7	8.0	8.0	7.9	10.7	11.4	10.3
20:5n-3	46.5	47.2	45.3	35.1	36.1	33.9	106.7	108.1	105.1	39.1	40.7	37.7
22:5n-3	23.0	23.0	22.9	20.5	21.1	20.3	16.4	16.6	16.0	21.9	22.4	21.3
22:6n-3	76.7	76.3	75.1	48.3	50.7	47.3	145.6	149.6	141.2	52.3	54.0	50.4
Total n-3	203.1	203.8	198.5	145.3	150.1	141.6	317.0	323.3	309.1	172.0	177.5	166.4
Total n-6	26.2	26.7	25.6	23.7	24.2	23.2	27.6	27.6	27.4	93.3	94.7	91.9
Total PUFA	232.9	234.1	227.6	171.8	177.3	167.6	348.8	355.2	340.5	269.0	276.1	262.0

SFA saturated fatty acids, *MUFA* monounsaturated fatty acids, *PUFA* polyunsaturated fatty acids

in the data and consequently it contains the most possible information. The second component (PC2) is perpendicular to PC1 and it defines the next largest amount of variation.

The results as presented in the various tables (Tables 1, 2, 3, 4 and 5) were combined (according to the various approaches to be discussed) and arranged in $m \times n$ data

Table 3 FAME concentrations (mg/g) for different brands of n-3 supplements

Sample	Supplements													
Designation	K1		K2		K3		K4		K5		K6		K7	
Replicate	i	ii	i	ii	i	ii	i	ii	i	ii	i	ii	i	ii
14:0	2.6	2.5	0.0	0.0	22.2	22.2	1.3	1.2	3.0	3.1	2.5	2.6	2.7	1.2
15:0	0.0	0.0	0.0	0.0	1.4	1.5	0.0	0.0	0.0	0.0	0.0	0.0	0.0	0.0
16:0	22.2	22.4	44.7	44.4	58.5	58.8	24.2	23.9	22.7	22.7	12.4	12.6	22.7	15.3
17:0	0.0	0.0	0.0	0.0	0.0	0.0	0.0	0.0	0.0	0.0	0.0	0.0	2.7	2.1
18:0	29.7	29.9	22.8	22.7	18.8	19.2	31.6	31.5	27.0	26.5	14.2	14.6	29.8	22.1
20:0	3.3	3.4	1.9	2.0	2.5	2.3	4.8	4.8	9.3	9.2	4.3	4.3	3.4	6.6
22:0	1.0	0.9	0.0	0.0	0.9	0.8	0.0	0.0	2.4	2.4	0.0	0.0	0.0	1.2
24:0	0.0	0.0	0.0	0.0	1.1	1.2	0.0	0.0	0.0	0.0	0.0	0.0	0.0	0.0
Total SFA	58.8	59.1	69.4	69.1	105.4	106.0	61.9	61.4	64.4	63.9	33.4	34.1	58.8	59.1
16:1n-9	0.0	0.0	0.0	0.0	1.2	1.1	0.0	0.0	0.0	0.0	0.0	0.0	0.0	0.0
16:1n-7	8.7	8.5	0.0	0.0	26.3	25.9	8.6	8.3	8.4	8.4	7.2	7.4	8.7	7.9
18:1n-9	62.2	62.6	175.0	174.1	46.3	45.4	60.1	59.3	51.9	51.0	39.5	40.0	62.7	50.7
18:1n-7	18.3	18.4	8.5	8.6	14.5	13.9	21.9	21.5	20.2	19.9	13.7	13.7	18.7	16.5
20:1n-11	1.8	1.7	2.9	2.8	2.0	1.9	2.5	2.4	1.2	1.1	1.4	1.3	1.8	1.1
20:1n-9	13.5	13.5	0.0	0.0	13.9	13.7	24.2	23.8	23.2	23.0	19.2	19.5	13.9	23.7
20:1n-7	4.5	4.5	0.0	0.0	3.0	3.1	4.3	4.3	3.2	3.1	3.4	3.5	4.5	2.8
22:1n-11	11.2	11.6	0.0	0.0	20.6	19.4	15.5	15.3	8.9	8.5	10.8	10.7	11.5	8.2
22:1n-9	1.5	1.5	0.0	0.0	2.8	2.6	3.3	3.2	5.2	5.1	4.7	4.6	1.5	5.5
24:1n-9	9.3	9.4	0.0	0.0	5.0	5.6	11.4	11.3	12.2	12.1	16.3	17.2	11.9	14.5
Total MUFA	131.0	131.7	186.4	185.5	135.6	132.6	151.8	149.4	134.4	132.2	116.2	117.9	131.0	131.7
16:2n-4	1.6	1.6	0.0	0.0	4.4	4.8	1.0	1.1	1.1	1.1	1.1	1.2	1.9	1.0
16:3n-3	2.4	2.3	0.0	0.0	6.2	6.0	1.5	1.6	1.7	1.6	1.5	1.4	2.0	1.2
18:2n-6	6.9	7.0	259.9	258.8	5.7	5.3	8.2	8.2	7.0	6.7	5.0	5.4	7.2	7.2
18:3n-3	3.7	3.7	312.5	312.5	3.5	3.3	5.8	5.7	4.5	4.5	3.3	3.1	3.7	3.9
18:4n-3	16.4	16.5	0.0	0.0	13.7	13.6	21.1	21.0	20.6	20.3	13.1	12.8	16.4	16.7
20:2n-6	2.1	2.1	0.0	0.0	1.6	1.6	2.5	2.6	2.1	2.2	2.1	2.2	2.2	2.0
20:3n-6	1.8	2.0	0.0	0.0	1.4	1.5	2.3	2.3	2.5	2.5	2.4	2.6	1.8	2.2
20:4n-6	12.9	13.1	0.0	0.0	9.4	8.9	17.7	17.6	15.7	15.4	15.3	14.9	12.9	14.0
20:4n-3	10.5	10.5	0.0	0.0	7.7	8.0	14.7	14.5	16.2	16.0	14.7	14.5	10.5	15.1
20:5n-3	242.6	245.0	0.0	0.0	174.9	174.2	283.8	281.5	276.4	273.1	260.3	250.1	239.8	238.1
22:5n-3	24.9	25.2	0.0	0.0	25.6	26.9	28.9	28.7	35.8	35.2	42.1	40.8	24.7	36.6
22:6n-3	168.0	169.4	0.0	0.0	167.8	182.4	175.1	173.6	175.3	173.0	198.6	182.9	162.8	172.4
Total n-3	468.5	472.6	312.5	312.5	399.4	414.4	530.9	526.6	530.5	523.7	533.6	505.6	459.9	484.0
Total n-6	23.7	24.2	259.9	258.8	18.1	17.3	30.7	30.7	27.3	26.8	24.8	25.1	24.1	25.4
Total PUFA	493.8	498.4	572.4	571.3	421.9	436.5	562.6	558.4	558.9	551.6	559.5	531.9	493.8	498.4

SFA saturated fatty acids, *MUFA* monounsaturated fatty acids, *PUFA* polyunsaturated fatty acids

matrices where *m* represents every prepared oil sample and *n* represents every analyzed fatty acid. The matrices submitted to PCA are standardized by subtracting their means and dividing by their standard deviations in order to construct linear combinations of the predictor variables *n* that contains the greatest variance. The PCA score and loading plots of the FAME profiles from the various oils were computed with the software package Statgraphics Plus 5.1 (Statistical Graphics Corp.).

Results

The fish, marine mammal and plant oils were prepared in triplicate and the n-3 supplements in duplicate. The triplicate and duplicate lipid profiles from the various injected oil samples, expressed as mg FAME/g sample, are presented in Tables 1, 2, 3, 4 and 5. The individual profiles were arranged in a data matrix consisting of 47 rows representing the various analyzed oils with their respective

Table 4 FAME concentrations (mg/g) for different plant oils

Sample	Plant oil								
Name	Soy			Rapeseed			Linseed		
Designation	SO			RP			LN		
Replicate	i	ii	iii	i	ii	iii	i	ii	iii
16:0	89.5	90.3	89.0	35.8	36.2	34.5	40.5	41.3	39.7
18:0	28.2	28.5	27.9	15.0	15.4	14.5	33.9	34.9	32.9
20:0	4.5	4.6	4.5	5.4	5.5	5.2	3.1	3.1	3.0
22:0	4.4	4.4	4.4	2.7	2.8	2.7	0.9	0.9	0.9
24:0	1.5	1.6	1.5	0.0	0.0	0.0	0.0	0.0	0.0
Total SFA	128.1	129.4	127.3	58.9	59.9	56.9	78.4	80.2	76.5
16:1n-7	0.0	0.0	0.0	1.7	1.7	1.6	0.0	0.0	0.0
18:1n-9	225.4	225.6	225.4	565.3	567.5	563.0	194.6	195.8	193.3
18:1n-7	13.6	13.7	13.4	24.7	25.2	24.1	5.5	5.5	5.4
20:1n-9	2.1	2.1	2.0	10.1	10.4	9.7	0.0	0.0	0.0
Total MUFA	241.1	241.4	240.8	601.8	604.8	598.4	200.1	201.3	198.7
18:2n-6	494.0	496.1	494.0	172.7	176.8	168.4	133.4	134.3	132.5
18:3n-3	51.9	52.0	51.9	84.6	85.5	83.6	506.1	507.3	504.9
Total n-3	51.9	52.0	51.9	84.6	85.5	83.6	506.1	507.3	504.9
Total n-6	494.0	496.1	494.0	172.7	176.8	168.4	133.4	134.3	132.5
Total PUFA	545.9	548.1	545.9	257.3	262.3	252.0	639.5	641.6	637.4

SFA saturated fatty acids, *MUFA* monounsaturated fatty acids, *PUFA* polyunsaturated fatty acids

replicates and 34 columns representing the individual FAME detected by GC. The 34 individual FAME profiles were: 14:0, 14:1n-9, 15:0, 16:0, 16:1n-9, 16:1n-7, 17:0, 16:2n-4, 18:0, 16:3n-3, 18:1n-11, 18:1n-9, 18:1n-7, 16:4n-3, 18:2n-6, 20:0, 18:3n-3, 20:1n-11, 20:1n-9, 20:1n-7, 18:4n-3, 20:2n-6, 20:3n-6, 22:0, 20:3n-3, 20:4n-6, 22:1n-11, 22:1n-9, 20:4n-3, 20:5n-3, 24:0, 24:1n-9, 22:5n-3, 22:6n-3.

Discrimination by Using the Full FAME Profiles from Plant, Supplement and Marine Animal Oils

The 47 × 34 matrix was submitted to PCA as a data exploration technique and a total of six components (PCs) were extracted and grouped in decreasing order of variance. The first component (PC1) which explains 41.91% of the total variation can be used to discriminate the oils according to their nature as is shown in Fig. 1. A plot of the scores of the two first components (Fig. 2), which explain 66.35% of the data variation, differentiates basically the same number of groups and sub-groups found in Fig. 1. Besides, the loadings of the two first components, were plotted to investigate the relationship between the various FAME (Fig. 3).

The six PCs computed by using the 47 × 34 matrix were plotted against each other to produce two and three dimensional PC scores graphs and consequently explore the capability of these PCs to discriminate confidently within the marine animal oils. Unfortunately, clear and well-defined patterns that allow one to differentiate the various oils and grades were not observed in any of the graphical representations, hence a data reduction, based on selected FAME profiles, was implemented.

Discrimination by Using Selected FAME Profiles from Plant, Supplement and Marine Animal Oils

FAME data reduction has been used in the discrimination of oils derived from one fish species (cod liver oil) by selecting the 15 FAME with levels higher than 1% of the total composition [42]. Considering that in the present study the 34 FAME or variables are given in mg/g and arranged in columns for PCA purposes (47 × 34), it was decided to discard all the FAME columns with average values <5 mg/g (<0.5% of the total averaged FAME profile), in that way 19 FAME profiles were retained (14:0, 16:0, 16:1n-7, 18:0, 18:1n-11, 18:1n-9, 18:1n-7, 18:2n-6, 18:3n-3, 20:1n-11, 20:1n-9, 18:4n-3, 20:4n-6, 22:1n-11, 20:4n-3, 20:5n-3, 24:1n-9, 22:5n-3, 22:6n-3). A new data matrix of size 47 × 19 was submitted to PCA and three PCs, explaining 85.29% of the total data variability, were computed. The three PCs were used to generate various two and pseudo-three dimensional score plots which essentially showed a clear

Table 5 FAME concentrations (mg/g) for conventionally distilled whale oil (WC) adulterated with of cod liver oil (CL)

Sample	Mixtures of conventional distilled whale oil (WC) and cod liver oil (CL)								
WC:CL (%)	90:10			80:20			50:50		
Replicate	i	ii	iii	i	ii	iii	i	ii	iii
14:0	48.0	48.1	48.1	47.5	47.4	47.9	42.5	42.3	41.9
15:0	3.4	3.4	3.3	3.3	3.4	3.3	3.3	3.3	3.2
16:0	77.0	77.0	76.1	78.0	78.1	77.9	83.2	83.4	83.2
17:0	5.1	5.1	5.1	5.1	5.2	5.1	5.4	5.4	5.4
18:0	16.3	16.4	16.2	16.5	16.6	16.5	17.2	17.4	17.2
20:0	0.5	0.5	0.5	0.4	0.4	0.4	0.3	0.3	0.3
24:0	0.2	0.2	0.2	0.4	0.4	0.4	0.9	0.9	0.9
Total SFA	150.5	150.7	149.5	151.2	151.5	151.5	152.8	153.0	152.1
14:1n-9	3.3	3.3	3.3	3.1	3.1	3.0	1.9	1.9	1.9
16:1n-9	3.3	3.4	3.3	3.5	3.5	3.5	3.8	3.8	3.8
16:1n-7	72.1	72.1	71.8	71.6	71.8	71.1	67.1	67.9	68.2
18:1n-11	17.6	17.6	17.5	17.1	17.2	17.1	15.8	15.9	15.9
18:1n-9	144.5	145.9	142.8	142.7	143.5	142.2	135.0	136.3	136.3
18:1n-7	22.5	22.7	22.5	23.9	24.1	23.8	27.9	28.1	27.9
20:1n-11	19.9	19.9	19.9	18.8	18.8	18.8	15.6	15.6	15.6
20:1n-9	95.2	95.4	95.2	93.4	93.5	93.3	87.7	87.9	87.7
20:1n-7	2.2	2.2	2.2	2.3	2.3	2.3	2.7	2.7	2.7
22:1n-11	89.7	90.1	89.5	85.3	85.7	85.1	71.8	72.4	71.8
22:1n-9	6.9	6.9	6.8	6.8	6.8	6.7	6.5	6.5	6.5
24:1n-9	7.0	7.1	7.0	7.1	7.2	7.1	7.4	7.5	7.4
Total MUFA	484.2	486.6	481.8	475.6	477.5	474.0	443.2	446.5	445.7
16:2n-4	3.6	3.6	3.6	3.7	3.7	3.7	3.9	3.9	3.9
16:3n-3	0.3	0.3	0.3	0.7	0.7	0.7	1.7	1.7	1.7
16:4n-3	2.8	2.8	2.7	3.0	3.0	2.9	3.5	3.6	3.5
18:2n-6	19.4	19.4	19.4	19.3	19.3	19.3	19.0	19.0	19.0
18:3n-3	12.0	12.2	12.0	11.6	11.7	11.5	10.0	10.3	10.0
18:4n-3	27.2	27.4	27.0	26.9	27.1	26.7	25.9	26.3	25.9
20:2n-6	2.9	2.9	2.9	2.9	2.9	2.9	2.8	2.8	2.8
20:4n-6	4.0	4.0	4.0	4.3	4.3	4.3	5.1	5.2	5.1
20:4n-3	13.5	13.5	13.4	12.9	12.9	12.8	11.0	11.1	11.0
20:5n-3	53.2	53.5	53.1	59.3	59.5	59.1	77.2	77.6	77.2
22:5n-3	22.3	22.4	22.3	21.7	21.7	21.6	19.6	19.7	19.6
22:6n-3	83.8	84.6	83.5	90.8	91.5	90.4	111.3	112.3	109.2
Total n-3	215.1	216.7	214.3	226.9	228.1	225.7	260.2	262.6	258.1
Total n-6	26.3	26.3	26.3	26.5	26.5	26.5	26.9	27.0	26.9
Total PUFA	245.0	246.6	244.2	257.1	258.3	255.9	291.0	293.5	288.9

SFA saturated fatty acids, *MUFA* monounsaturated fatty acids, *PUFA* polyunsaturated fatty acids

discrimination between plant, supplements and marine animal oils as already observed in Figs. 1, 2.

Discrimination by Using Full FAME Profiles from Marine Animal Oils

The contribution of the supplement and plant oils was removed as an alternative approach to discriminate the various marine oils. A 24 × 34 matrix was constructed by using the data presented in Tables 1, 2 and submitted to PCA. A considerable percentage of the variability of this matrix (97.58%) was explained by four extracted PCs (49.80, 22.65, 20.08 and 5.05%). The score plot of PC1 and PC4 (Fig. 4) indicates that it is possible to discriminate within the four different types of animal oils by using these two components.

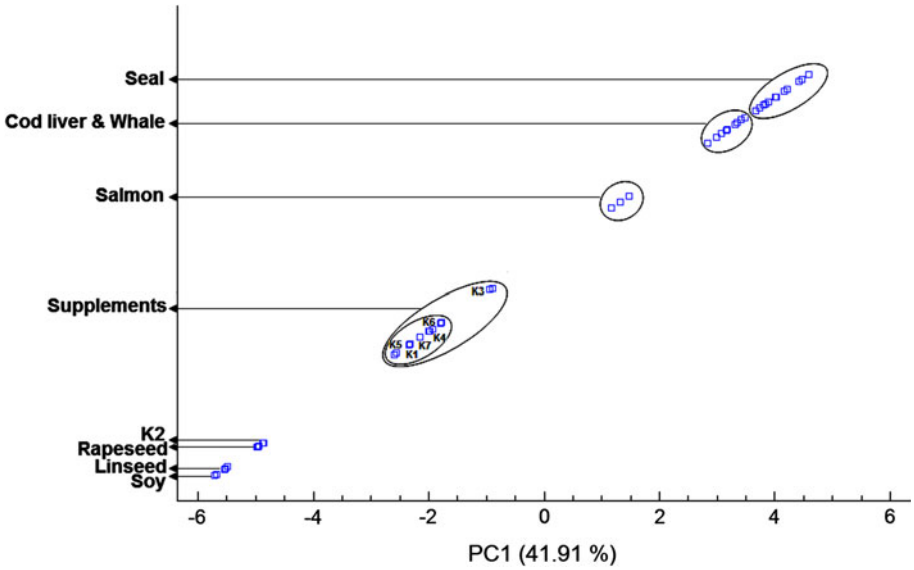

Fig. 1 PC1 score plot for the different kinds of oils obtained after computing a 47 × 34 (samples × FAME profiles) data matrix. The different supplements and providers are designated by *numbered letter Ks*. For details regarding the providers see "Experimental"

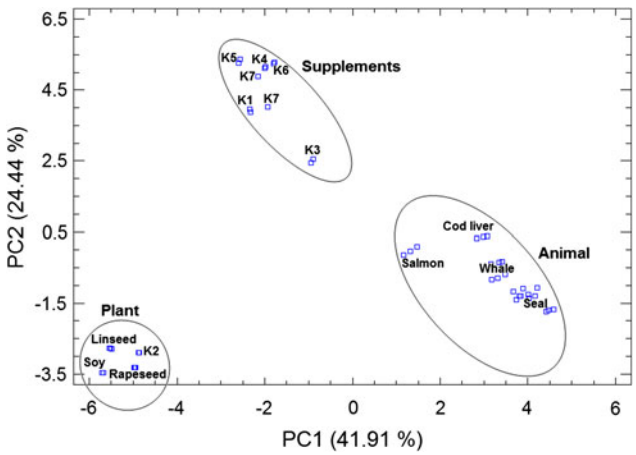

Fig. 2 PC1 and PC2 score plot for the different kinds of oils obtained after computing a 47 × 34 (samples × FAME profiles) data matrix. The different supplements and providers are designated by *numbered letter Ks*. For details regarding the providers see "Experimental"

Discrimination Between Genuine and Adulterated Oils

Further assessment of the capability of GC for discriminating between pure and adulterated oils, was achieved using conventionally distilled whale oil (WC) debased by cod liver oil in the proportions 90:10, 80:20 and 50:50. The FAME profiles of the mixtures prepared in triplicate (Table 5) along with the profiles of the marine animal oils described in Tables 1 and 2 were submitted to PCA and four PCs extracted, explaining 47.05, 25.08, 20.19 and 5.36% of the data variability, respectively.

Discussion

Discrimination by Using the Full FAME Profiles from Plant, Supplement and Marine Animal Oils

A graph of PC1 for the various oil samples (Fig. 1) shows that different kinds of oils can be basically differentiated along the PC1 axis. Specifically, the scores of the analyzed plant and animal oils grouped themselves at opposite ends of the PC1 axis while the scores of six supplements (K1 and K3–7) in the middle of this axis. The scores for K2 overlaps those from rapeseed oil, hence it is likely that this supplement contains this particular oil. In addition, the supplements as well as the animals exhibit some subgroups which discriminate supplement K3 in the former and salmon oil in the latter. These latent sub-structures are attributed to the consistently high levels of 16:0 and 16:1n-7 in supplement K3 (on average three times higher compared to the others supplements of this group) and the high levels of 18:1n-9, 18:2n-6 and 18:3n-3 in the salmon oil (on average 1.7, 4.7 and 5.0 times higher than the rest of marine animal oils, respectively).

The score plot of the first two PC (Fig. 2) which explained 41.91 and 24.44%, respectively, of the total variability of the different types of oil FAME profiles allowed concluding that PC1 discriminates in effect between animal and plant oils while PC2 differentiates between supplements and plant oils. Besides, this score plot revealed that in addition to rapeseed oil, supplement K2 also contains linseed oil due to the proximity of their scores. This proximity was constantly observed when the scores of any of the six PCs were plotted against each

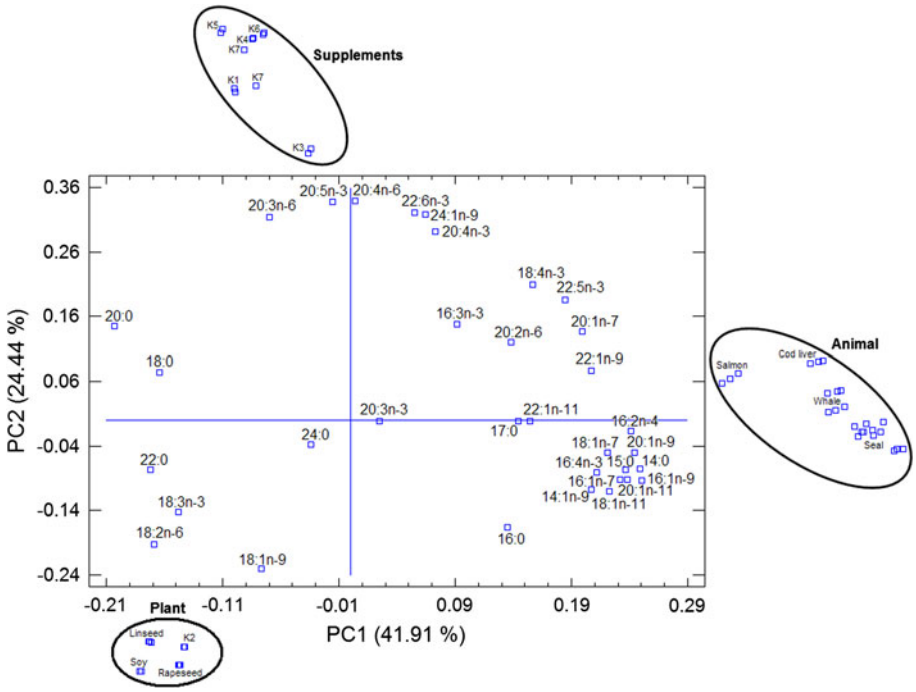

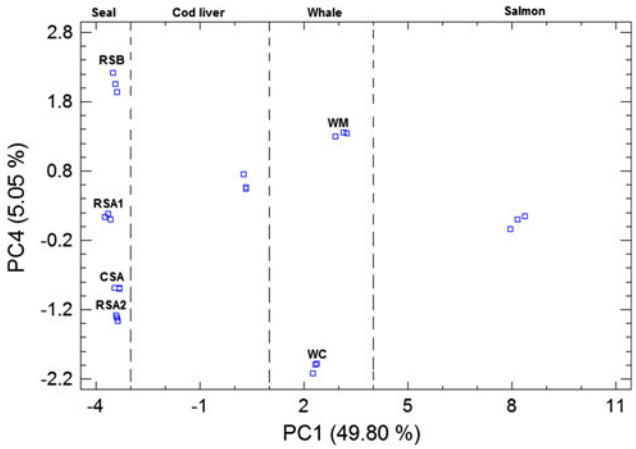

Fig. 4 PC1 and PC4 score plot for the fish and marine mammal oils obtained after computing a 24 × 34 (samples × FAME profiles) data matrix. RSA1 and RSA2 are refined seal oils from provider A and from different batches. CSA is crude seal oil from provider A. RSB is refined seal oil from provider B. WM and WC are molecularly and conventionally distilled whale oils from the same provider. For details regarding the providers see "Experimental"

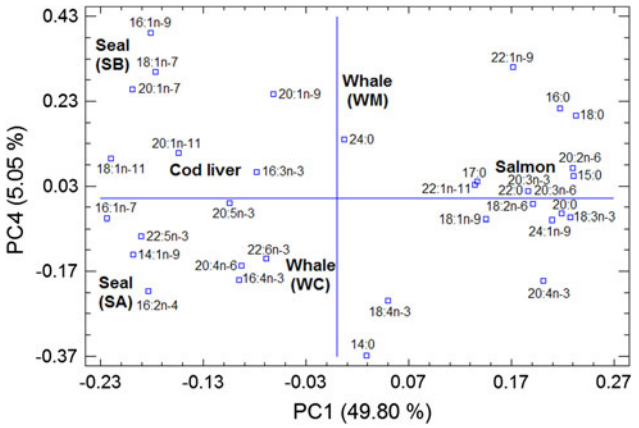

Fig. 5 FAME loading plot for PC1 and PC4 and its relationship to the scores portrayed in Fig. 4

other. The presence of rapeseed and linseed oils in the composition of K2 was confirmed by searching the webpage of the manufacturer of this particular supplement. The PC1 versus PC2 plot (Fig. 2) revealed some variability in the individual scores for K7 which could be attributed to experimental errors, indicating the importance of replication in discrimination studies.

The plot of the loadings of the two first components, expressing the relationship between the various FAME (Fig. 3) showed the lack of correlation between 20:5n-3 and 18:1n-9 on the PC2 axis, indicating that none of the plant oils studied in the present investigation are present in the composition of supplements K1, K3, K4, K5, K6 and K7. These observations are in agreement with the various manufacturers who have reported some special developed oils (name not disclosed), refined fish oil (from non-specified origin), gelatin from pork, etc. among the various constituents of their supplements rather than plant oils.

The superimposition of the three main clusters from Fig. 2 on the loading plot (Fig. 3) demonstrates unequivocally that the observed inverse correlation between 20:5n-3 (positive PC2 loading value) and 18:1n-9 (negative PC2 loading value) is responsible for the discrimination between supplements (with scores highly associated to

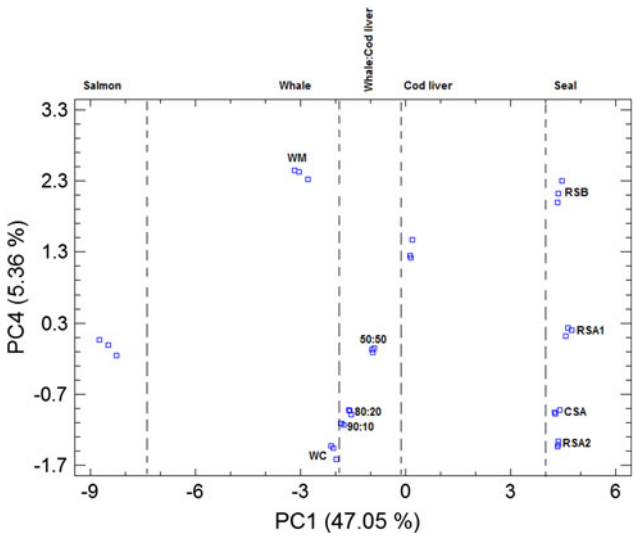

Fig. 6 PC1 and PC4 score plot for the various genuine marine oils and three samples of adulterated whale oil (WC) with cod liver oil at different proportions (90:10, 80:20 and 50:50). The PCs were obtained after computing a 33 × 34 data matrix. RSA1 and RSA2 are refined seal oils from provider A and from different batches. CSA is crude seal oil from provider A. RSB is refined seal oil from provider B. WM and WC are molecularly and conventionally distilled whale oils from the same provider. For details regarding the providers see "Experimental". PC1 and PC4 score plot for genuine and adulterated fish and marine mammal oils by using the full FAME profiles

20:5n-3) and plant oils (with scores highly associated to 18:1n-9). Similarly, the lack of correlation between 16:1n-9, 14:0, 20:1n-9, 16:2n-4 (positive PC1 loading values) and 22:0, 18:2n-6 (negative PC1 loading values) is responsible for discriminating between animal and plant oils.

Discrimination by Using Selected FAME Profiles from Plant, Supplement and Marine Animal Oils

The discrimination patterns of the various two and pseudo-three dimensional score plots obtained after performing PCA on selected FAME profiles were basically similar to those obtained by using the full FAME profiles (Figs. 1, 2). However, the graphs consistently misclassified supplement K2 as containing a mixture of the three plant oils (soy, linseed and rapeseed oil) while in fact only linseed and rapeseed oil are present in this particular supplement. This result indicates that PCA on full FAME profiles outperforms the proposed data reduction approach for supplement classification. The various plots generated with the aforementioned three PCs were also unable to establish a clear distinction between the various species, brands and grades of animal oils; hence a further discrimination study was carried out by using only the full FAME profiles derived from marine oils.

Discrimination by Using Full FAME Profiles from Marine Animal Oils

The PC1 and PC4 score plot (Fig. 4) shows that PC1 can discriminate between the four different types of animal oils, namely seal oil, cod liver oil, whale oil and salmon oil and that PC4 can discriminate effectively within every animal oil species and their alleged qualities. For instance, it is observed that the two different batches of refined seal oils from manufacturer-A (designated as RSA1 and RSA2 in Fig. 4) display positive and negative PC4 score values, respectively, indicating some differences between them. In addition, the crude and the refined seal oils from the same manufacturer and designated as CSA and RSA2 in Fig. 4, exhibit negative scores values, indicating a correlation between these two oils regardless their alleged qualities. The discrimination between the seal oils from different manufacturers namely Rieber Skinn (SA) and JFM Sunile (SB) is observed in Fig. 4. The variables responsible for the discrimination between the manufactures are visualized by means of the PC1 and PC4 loading plot (Fig. 5). The higher contents of 16:1n-9, 18:1n-7, 20:1n-7 and the lower contents of 16:2n-4 in SB compared to SA are the main fatty acids that contribute to distinguish SA from SB. Similarly, Fig. 4 shows the unmistakably differentiation between molecularly distilled whale oil (WM) from conventionally distilled whale oil (WC) which is mainly due to the slightly higher levels of 20:1n-9, the lower levels of 22:6n-3 and 18:4n-3 as well as the lack of 16:4n-3 in WM compared to WC. The clear-cut distinction between cod liver and salmon oil along the PC1 axis (Fig. 4) is mainly attributed to the contribution of several fatty acids such as 18:1n-11 and 16:1n-7 at negative PC1 values and 20:2n-6 and 18:3n-3 at positive PC1 values as indicated in Fig. 5.

Discrimination Between Genuine and Adulterated Oils

The PC1and PC4 score plot (Fig. 6) demonstrates that it is possible to discriminate adulterated from genuine whale oil samples. The information retained by PC1 is mainly connected with the nature of the various oils. For instance, five specific regions can be visualized along the PC1 axis (salmon, whale, whale + cod liver, cod liver and seal) while the information retained by PC4 is mainly connected with the discrimination within animal oil species, their alleged qualities and the various proportions of cod liver oil used to adulterate genuine whale oil.

In conclusion, the different approaches used in the discrimination process indicated that PCA on the full FAME profiles is the best strategy to discriminate between the various oils considered in this study. Considering that n-3 rich oils derived from animals are highly regarded as alternative medicines worldwide, the potentiality of

unexplored single or coupled techniques for authentication and discrimination of these kinds of oils should be investigated to prevent fraudulent practices.

Acknowledgments The European Commission in the context of the Erasmus Mundus Program and The Norwegian Research Council (SIP project NRF 173534/I30) are gratefully acknowledged for financial support of Y.Z and Z.D, respectively.

References

1. Parry EJ (1904) The adulteration of cod liver oil. Lancet 163:378
2. Carter OCS (1885) On the detection of adulterations in oils. Am Philos Soc 22:296–299
3. Jakab A, Heberger K, Forgacs E (2002) Comparative analysis of different plant oils by high-performance liquid chromatography-atmospheric pressure chemical ionization mass spectrometry. J Chromatogr A 976:255–263
4. Holčapek M, Jandera P, Zderadička P, Hrubá L (2003) Characterization of triacylglycerol and diacylglycerol composition of plant oils using high-performance liquid chromatography-atmospheric pressure chemical ionization mass spectrometry. J Chromatogr A 1010:195–215
5. Park JR, Lee DS (2003) Detection of adulteration in olive oils using triacylglycerols compositions by high temperature gas chromatography. Bull Korean Chem Soc 24:527–530
6. Lísa M, Holčapek M (2008) Triacylglycerols profiling in plant oils important in food industry, dietetics and cosmetics using high-performance liquid chromatography-atmospheric pressure chemical ionization mass spectrometry. J Chromatogr A 1198:115–130
7. Christopoulou E, Lazaraki M, Komaitis M, Kaselimis K (2004) Effectiveness of determinations of fatty acids and triglycerides for the detection of adulteration of olive oils with vegetable oils. Food Chem 84:463–474
8. Ruth SM, Villegas B, Akkermans W, Rozijn M, van der Kamp H, Koot A (2010) Prediction of the identity of fats and oils by their fatty acid, triacylglycerol and volatile compositions using PLS-DA. Food Chem 118:948–955
9. Woodbury SE, Evershed RP, Rossell JB, Griffith RE, Farnell P (1995) Detection of vegetable oil adulteration using gas-chromatography combustion isotope ratio mass-spectrometry. Anal Chem 67:2685–2690
10. Kelly S, Parker I, Sharman M, Dennis J, Goodall I (1997) Assessing the authenticity of single seed vegetable oils using fatty acid stable carbon isotope ratios ($^{13}C/^{12}C$). Food Chem 59:181–186
11. Vigli G, Philippidis A, Spyros A, Dais P (2003) Classification of edible oils by employing ^{31}P and ^{1}H NMR spectroscopy in combination with multivariate statistical analysis. A proposal for the detection of seed oil adulteration in virgin olive oils. J Agric Food Chem 51:5715–5722
12. Wang L, Lee FSC, Wang XR, He Y (2006) Feasibility study of quantifying and discriminating soybean oil adulteration in camellia oils by attenuated total reflectance MIR and fiber optic diffuse reflectance NIR. Food Chem 95:529–536
13. Tay A, Singh RK, Krishnan SS, Gore JP (2002) Authentication of olive oil adulterated with vegetable oils using Fourier transform infrared spectroscopy. Lebenson Wiss Technol 35:99–103
14. Gurdeniz G, Ozen B (2009) Detection of adulteration of extra-virgin olive oil by chemometric analysis of mid-infrared spectral data. Food Chem 116:519–525
15. Tarandjiiska RB, Marekov IN (1998) Precise classification of virgin olive oils with various linoleic acid contents based on triacylglycerol analysis. Anal Chim Acta 364:83–91
16. Mildner-Szkudlarz S, Jelen HH (2008) The potential of different techniques for volatile compounds analysis coupled with PCA for the detection of the adulteration of olive oil with hazelnut oil. Food Chem 110:751–761
17. Dourtoglou VG, Dourtoglou Th, Antonopoulos A, Stefanou E, Lalas S, Poulos C (2003) Detection of olive oil adulteration using principal component analysis applied on total and regio FA content. J Am Oil Chem Soc 80:203–208
18. Jakab A, Jablonkai I, Forgács E (2003) Quantification of the ratio of positional isomer dilinoleoyl-oleoyl glycerols in vegetable oils. Rapid Commun Mass Spectrom 17:2295–2302
19. Goodacre R, Vaidyanathan S, Bianchi G, Kell DB (2002) Metabolic profiling using direct infusion electrospray ionisation mass spectrometry for the characterisation of olive oils. Analyst 127:1457–1462
20. Ollivier D, Artaud J, Pinatel C, Durbec JP, Guérère M (2006) Differentiation of French virgin olive oil RDOs by sensory characteristics, fatty acid and triacylglycerol compositions and chemometrics. Food Chem 97:382–393
21. Gómez-Ariza JL, Arias-Borrego A, García-Barrera T, Beltran R (2006) Comparative study of electrospray and photospray ionization sources coupled to quadrupole time-of-flight mass spectrometer for olive oil authentication. Talanta 70:859–869
22. Sikorska E, Górecki T, Khmelinskii IV, Sikorski M, Koziol J (2005) Classification of edible oils using synchronous scanning fluorescence spectroscopy. Food Chem 89:217–225
23. Mannina L, Patumi M, Fiordiponti P, Emanuele MC, Segre AL (1999) Olive and hazelnut oils: a study by high field ^{1}H-NMR and gas chromatography. Ital J Food Sci 2:139–149
24. Fauhl C, Reniero F, Guillou C (2000) ^{1}H NMR as a tool for the analysis of mixtures of virgin olive oil with oils of different botanical origin. Magn Reson Chem 38:436–443
25. Armenta S, Garrigues S, de la Guardia M (2007) Determination of edible oil parameters by near infrared spectrometry. Anal Chim Acta 596:330–337
26. Diaz TG, Merás ID, Casas JS, Franco MFA (2005) Characterisation of virgin olive oils according to its triglycerides and sterols composition by chemometric methods. Food Control 16:339–347
27. Brodnjak-Vončina D, Kodba ZC, Novič M (2005) Multivariate data analysis in classification of vegetable oils characterized by the content of fatty acids. Chemom Intell Lab Syst 75:31–43
28. Peña F, Cárdenas S, Gallego M, Valcárcel M (2005) Direct olive oil authentication: Detection of adulteration of olive oil with hazelnut oil by direct coupling of headspace and mass spectrometry, and multivariate regression techniques. J Chromatogr A 1074:215–221
29. Krist S, Stuebiger G, Bail S, Unterweger H (2006) Detection of adulteration of poppy seed oil with sunflower oil based on volatiles and triacylglycerol composition. J Agric Food Chem 54:6385–6389
30. Cunha SC, Oliveira MBPP (2006) Discrimination of vegetable oils by triacylglycerols evaluation of profile using HPLC/ELSD. Food Chem 95:518–524
31. Dugo P, Favoino O, Tranchida PQ, Dugo G, Mondello L (2004) Off-line coupling of non-aqueous reversed-phase and silver ion high-performance liquid chromatography-mass spectrometry for the characterization of rice oil triacylglycerol positional isomers. J Chromatogr A 1041:135–142

32. Asbury GR, Al-Saad K, Siems WF, Hannan RM, Hill HH (1999) Analysis of triacylglycerols and whole oils by matrix-assisted laser desorption/ionization time of flight mass spectrometry. J Am Soc Mass Spectrom 10:983–991
33. Beermann C, Winterling N, Green A, Möbius M, Schmitt J, Boehm G (2007) Comparison of the structures of triacylglycerols from native and transgenic medium-chain fatty acid-enriched rape seed oil by liquid chromatography–atmospheric pressure chemical ionization ion-trap mass spectrometry (LC–APCI-ITMS). Lipids 42:383–394
34. Lee DS, Lee ES, Kim HJ, Kim SO, Kim K (2001) Reversed phase liquid chromatographic determination of triacylglycerol composition in sesame oils and the chemometric detection of adulteration. Anal Chim Acta 429:321–330
35. Webster L, Simpson P, Shanks AM, Moffat CF (1999) The authentication of olive oil on the basis of hydrocarbon concentration and composition. Analyst 125:97–104
36. Apetrei C, Rodríguez-Méndez ML, de Saja JA (2005) Modified carbon paste electrodes for discrimination of vegetable oils. Sens Actuators B 111:403–409
37. Christy AA, Kasemsumran S, Du YP, Ozaki Y (2004) The detection and quantification of adulteration in olive oil by near-infrared spectroscopy and chemometrics. Anal Sci 20: 935–940
38. Zou MQ, Zhang XF, Qi XH, Ma HL, Dong Y, Liu CW, Guo X, Wang H (2009) Rapid authentication of olive oil adulteration by Raman spectrometry. J Agric Food Chem 57:6001–6006
39. Møller JKS, Catharino RR, Eberlin MN (2007) Electrospray ionization mass spectrometry fingerprinting of essential oils: Spices from the Labiatae family. Food Chem 100:1283–1288
40. Obeidat SM, Khanfar MS, Obeidat WM (2009) Classification of edible oils and uncovering adulteration of virgin olive oil using FTIR with the aid of chemometrics. Aust J Basic Appl Sci 3:2048–2053
41. Kurata S, Yamaguchi K, Nagai M (2005) Rapid discrimination of fatty acid composition in fats and oils by electrospray ionization mass spectrometry. Anal Sci 21:1457–1465
42. Standal IB, Praël A, McEvoy L, Axelson DE, Aursand M (2008) Discrimination of cod liver oil according to Wild/Farmed and geographical origins by GC and ^{13}C NMR. J Am Oil Chem Soc 85:105–112
43. Rohman A, Man YBC (2009) Analysis of cod-liver oil adulteration using Fourier transform infrared (FTIR) spectroscopy. J Am Oil Chem Soc 86:1149–1153
44. Cozzolino D, Murray I, Chree A, Scaife JR (2005) Multivariate determination of free fatty acids and moisture in fish oils by partial least-squares regression and near-infrared spectroscopy. LWT-Food Sci Technol 38:821–828
45. Aursand M, Jørgensen L, Grasdalen H (1995) Positional distribution of ω3 fatty acids in marine lipid triacylglycerols by high-resolution ^{13}C nuclear magnetic resonance spectroscopy. J Am Oil Chem Soc 72:293–297
46. Standal IB, Axelson DE, Aursand M (2009) Differentiation of fish oils according to species by ^{13}C-NMR regiospecific analyses of triacyglycerols. J Am Chem Soc 86:401–407
47. Martinez I, Standal IB, Axelson DE, Finstad B, Aursand M (2009) Identification of the farm origin of salmon by fatty acid and HR ^{13}C NMR profiling. Food Chem 116:766–773
48. Araujo P, Nguyen TT, Frøyland L, Wang JD, Kang JX (2008) Evaluation of a rapid method for the quantitative analysis of fatty acids in various matrices. J Chromatogr A 1212:106–113